

ROBERT ALEXANDER CHALMERS

MARY R. MASSON

Department of Chemistry, University of Aberdeen, Meston Walk, Old Aberdeen, Scotland

Robert Alexander Chalmers was born (on 17 June, 1920) and brought up in Birmingham. When he left school at the age of 16, he became an apprentice "lab-boy" in the laboratories of a well-known motor component manufacturer. A major function of these laboratories was the analytical control of the electroplating process, which involved a wide range of analyses, and therefore offered a first-class training for a prospective analytical chemist. An important part of the work was the sampling, which involved balancing on planks above large cyanide-containing plating baths—so Chalmers' introduction to analytical work was much more exciting than usual.

After nearly 5 years, Chalmers moved to Coventry to the laboratory of Humber-Hillman, as analyst, but it was now war-time, and he was soon afterwards called up into the Royal Engineers. He spent 3 months of "basic training" learning to drill, to dig trenches, to demolish trees, bridges and railway lines, and to run with and deliver poison-gas cylinders. For his next 3 months of service, he was sent to the anti-gas-warfare laboratories at Porton Down, where much of the work involved analyses concerned with the testing of the bursting patterns of mustard-gas shells containing arsenic as a non-volatile marker element. Another duty was to prepare test papers for use in gas-detection apparatus.

After his time at Porton, Chalmers was discharged to the reserves, and returned to Humber-Hillman, where he remained until called up again towards the end of the war, this time into Intelligence. He served mainly in India, where he acquired his liking for Indian food, especially curry (and learned to cook it to perfection). (Someone once asked him for a definition of good food. He replied "If you can see perspiration on my head when I am eating it, it means it is good food".)

During this second period in the army, Chalmers had decided not to return to his old job when he was demobbed, but instead to study for a degree at Manchester University. He managed to secure a grant for the latter part of the B.Sc. course, but for the first year he had to work in his spare time. One of his jobs was at the dog-racing track, where he sharpened his ability to do mental arithmetic by working on the Totalizer. At the University, in view of his extensive previous experience, he was excused some of the ordinary laboratory classes and given special projects to work on, one of which involved the separation by ion-exchange of "didymium" into neodymium and praseodymium. He spent a great deal of

time in the basement of the building among the rats (from an adjacent brewery) practising his micro-analytical technique, and he was allowed to use the precious "Spekker" absorptiometer, since he had previously used one at Porton.

Despite much time spent playing cards, snooker, and taking part in other non-academic pursuits, in 1950 Chalmers gained the degree of B.Sc. in chemistry with First Class Honours. Since there was no research done in analytical chemistry at Manchester, he moved to Edinburgh to work under Dr. Christina Miller. Dr. Miller had many interests in analytical and inorganic chemistry, but the field Chalmers worked on with her was the microanalysis of rocks. He was successful in developing methods for micro-determination of iron, silica, phosphoric oxide and alumina, and in 1953 was awarded the degree of Ph.D.

Chalmers then moved to Durham, as I.C.I. fellow in the Department of Geology, where he further developed his interest in rock analysis, and in collaboration with the electrical engineering department at Newcastle, he built a recording spectrophotometric titrimeter. (This required regular transporting of a Unicam SP600 between Durham and Newcastle, and the project certainly proved the robustness of that instrument, still in working order now, more than 30 years later.) It was during Chalmers' time at Durham that he first did any editorial work. On the suggestion of Dr. Miller, he was invited to edit and revise "Quantitative Chemical Analysis", by Cumming and Kay, which he did to produce a successful 11th edition.

In 1956 Chalmers moved to Aberdeen to take up an appointment as lecturer in chemistry. There was no analytical section at Aberdeen at that time, but Chalmers wasted no time in establishing analytical chemistry as part of the curriculum, and in building up a research group. He was appointed Senior Lecturer in 1965 and Reader in 1970, in recognition of his being regarded as a first-rate member of staff, with teaching ability of a very high order, and of his steady high-quality research output. His standing as an analytical chemist was again recognized by his election in 1978 as a Fellow of the Royal Society of Edinburgh.

Thanks to Chalmers, Aberdeen came to be recognized as one of the few centres of excellence in analytical chemistry in the U.K., and a special feature was that most of the analytical chemistry teaching was given to all the undergraduate chemists in the

third year of a 4-year course, and not just to final-honours-year specialists, or M.Sc. or Ph.D. students. Many of Chalmers' former students testify to his excellence as a teacher, and remember with pleasure the lecture-demonstrations he delighted in giving. He used to swap ideas for these with colleagues at other universities, and one such colleague recalls a spectacular experiment involving the use of potassium cyanide, which was quite safe provided that all the reagents were added in the correct order, but which did have the added excitement for students that the lecturer might kill himself if he did anything wrong. Chalmers did this demonstration "with panache and conviction", but the unfortunate colleague had a disaster. "The lecture theatre was evacuated, I went for an emetic, and vowed never to die in the cause of educating or amusing students."

Although the lectures were a very important part of Chalmers' teaching, he was really at his best in the laboratory classes. There, he would wander round the benches of students, glass wash-bottle in hand, always ready to demonstrate a laboratory technique, or a correct end-point, or how to use an instrument. Periodically, he would gather a small group of students around him, and make sure they understood every bit of the chemistry of the determination they were doing. Analytical chemistry could never be likened to following recipes in a cookery book in Chalmers' laboratory classes. He took great pleasure in telling each new batch of students that they must be certain to write everything straight into their lab notebooks, and not onto any small scraps of paper (or sometimes "wee orra bitties o' paper"), because he was sure to pick up any such piece of paper and use it to light a bunsen burner (but he was never known to actually do this).

Over the years Chalmers kept up a varied research programme, as is shown by his publication list. However, he had many more research students than this list reveals, because he preferred to encourage independent work by his students, only stepping in if the research seemed to be getting off course, or if the student asked for help; and he would not have his name attached to papers unless he had made a significant contribution either to the research or to the writing of the paper. A recent student recalls being told "Never believe what I tell you. Check it yourself—that is what laboratories are for."

In recent years, Chalmers has gained the reputation of being an advocate of classical methods, both among the students at Aberdeen University, and in a wider context; and it is true that he always emphasized the importance of these methods for standardizing instruments, and in situations where great accuracy is required. Among students, and perhaps others too, this somehow came to be interpreted as meaning that Chalmers thought all instrumental methods to be useless. It is to be hoped that readers of *Talanta* will realise that Chalmers knows more about most instrumental methods than the

majority of analytical chemists. Indeed, he has often during his career worked with instrumental methods in their infancy, and given lectures on them before most folk knew they existed. However, he has always been very aware of a tendency for people to have blind faith in meters (or digital displays) and black boxes, and felt, correctly I think, that it was important to give continual reminders of the failings of instrumental methods.

In his younger days, Chalmers had many interests and hobbies. As a small boy, he was interested in wild life, especially butterflies, and even nowadays, he returns from holiday eager to consult his books in the hope of identifying some new species. Books are another passion, and he likes all sorts but perhaps especially humerous ones, like Hašek's "The Good Soldier Svejk", "Archy and Mehitabel", "Cloche-merle", or the works of James Thurber and A. P. Herbert. He took part in many sporting activities, such as snooker, squash, golf, and especially hill-walking and rock-climbing (but not, as another Pergamon editor once became convinced, pole-vaulting). He was always fond of dog-racing, and he played a large variety of card games. As Editor of *Talanta*, he has had very much less free time for such activities, but he does still manage a bit of gardening, painting and decorating, and, with the aid of his old climbing ropes, roof-repairing.

Chalmers probably did not realise in 1966, when he assumed the editorship of *Talanta*, in succession to (the late) Professor Cecil Wilson and Dr. Mo Williams, the extent to which the journal would take over his life. Would he have taken it on if he had? We will never know, but all who are associated with *Talanta* in any way must be grateful to him for the great amount of time and energy that he has devoted over the past 20 years, and continues to devote, to ensuring that everything about *Talanta* is of the highest standard.

As if he did not spend enough time editing for *Talanta*, Chalmers has also long been involved in the editing of books, first for Van Nostrand Ltd. and later for Ellis Horwood Ltd. The most recent book published in the Horwood series was the fiftieth book Chalmers has edited. He is just as thorough an editor of books as he is of *Talanta*, unlike some book-series editors, who seem to make very few if any changes to manuscripts which pass through their hands. He is also a Regional Editor, and Chairman of the Editorial Board, of *Mikrochimica Acta*, Vienna.

The large amount of time Chalmers has spent editing has undoubtedly had some effect on the amount of original research he has been able to do in recent years. However, he feels, and many will agree with him, that he is probably making a greater contribution to the quality of the literature by spending his time on editorial work, than he could hope to if he were to do more research.

Chalmers was a keen member of the Society for Analytical Chemistry for many years, and in 1963–64

he was Chairman of the Scottish Section, and served on Council. However, he had had a disagreement with the Chemical Society at some time, and strongly disapproved of the amalgamation of the SAC with the other chemical bodies—to the extent that from 1972 to 1974 he was the only member of the SAC, and when the amalgamation was completed at the start of 1975, he refused to relent and join the CS. However, later in a rash moment, he promised to join if (the late) Professor Ronald Belcher, then Chairman of the *Talanta* Editorial Board, was elected President of the Analytical Division, and he was not allowed to forget his promise when that occurred. However, he still did not often get around to going to conferences in Britain. Many of his friends in the U.K. recall with amusement that they first met Chalmers in Budapest, or Prague, or Helsinki. He was persuaded to come to SAC83 in Edinburgh, as Overseas Delegates Officer, to the amazement and pleasure of many.

A friend recalls exhibiting a poster there, only to be approached by Chalmers, who ran a practised eye over the subject matter. In about 5 seconds flat, he said “There’s a small grammatical error in your penultimate sentence”. He was right, but it took the friend 5 minutes to work out what the error was.

Many readers of *Talanta* will be unaware of Chalmers’ sense of fun and love of jokes. Dr. Miller recalls his “puckish sense of humour”. Professor Marzenko refers to “his high sense of humour, his cheerful disposition and friendliness for people”, and his old friend Dr. Rudolf Přibil writes “Bob for me is a very attractive man, absolutely unformal, who likes jokes, anecdotes, and funny gossips”. Indeed, Chalmers has an amazing store of jokes and stories (some culled from his wife’s medical trade magazines) which with a bit of prodding he will start telling at parties and such occasions.

It is probably true, as Chalmers has told friends apparently in jest, that with a Scottish father and an English mother, he thinks of himself as not Scottish or English, but rather as a European. He certainly has many good friends in the continent of Europe. Professor Inczédy recalls that “the very first visit of Bob to Hungary was in 1960, when he attended the Analytical Conference in Budapest. The conference was international with many foreign participants. At that time, Scotland was maybe farther away than now, and there was also the iron curtain; anyway it was very surprising when Bob arrived dressed fully in tourist clothes, with rucksack and heavy walking boots. Nevertheless, despite his peculiar clothing, he won very quickly the strong sympathy of all the Hungarian colleagues and friends.”

Professor Inczédy recalls that on another occasion, when Chalmers was visiting Veszprém University, he was to be taken to a concert that started very early. His hosts took him to the University canteen for a short dinner, “but accidentally and unfortunately, there was a very poor meal served there that night—

the poorest ever served there—some cocoa with bread or so. We were all very much worried about it, but he said to us very quietly and politely—in his well known manner—it was completely O.K.”

Dr. Přibil has sent us a number of stories about Chalmers.

“Bob likes travelling abroad. During the past 25 years he has visited Czechoslovakia many times. Once, when he was still single, he arrived in a very strange, small, and very delapidated-looking car. We stopped in front of a hotel in the centre of Prague where Bob had booked accommodation. Immediately, a crowd of onlookers gathered and stared with amusement at the car. Bob opened the boot and pulled out dirty garments and handed them to my wife, who promised to do the washing. A man in the crowd said in a loud voice ‘Is it possible that such cars are used in Britain and that they even dare to travel abroad in them?’ Bob looked absolutely unmoved by the jokes and laughs of the crowd. I tried to save the situation by saying that he normally used a big nice car in Britain but it wouldn’t squeeze into our narrow streets.

“With this car we made a trip to a small village in northern Bohemia where my family used to spend our holidays. The car attracted a great deal of attention there as well. Bob had to open the bonnet to allow the local car experts to examine the engine. One of them, a friend of mine, wished to see the spark plugs, but everything was so rusty that human strength was insufficient to unscrew them. Bob explained that he always bought cars that had done at least 100,000 miles. ‘After such a test, real quality shows’, he said. Eventually the original ridicule changed into admiration of British materials and workmanship.”

In Aberdeen, too, Chalmers’ various cars have caused amusement. His first car was a pre-war Morris Tourer, which is probably the car that Dr. Přibil recalls. He then had two Rileys, first a green one, then an old black one, inside which very little of Chalmers was visible when he was driving, apart from his beret. (His berets have usually been black, but on one occasion a green beret apparently caused him to be regarded with great suspicion by the security staff at the Laboratory of the Government Chemist—they thought he might be an I.R.A. sympathiser.) The black Riley is reported to have exceeded 80 m.p.h. on the Nairn-to-Inverness road, so it was obviously not a bad car! When Chalmers bought his grey Saab in 1971, it was nearly new: everyone was amazed—but a little disappointed at his loss of faith in British automobile engineering. However, he drove that car for so long—over 13 years—that it became as notorious as his previous ones. Chalmers has recently bought a new Peugeot, but his student son Martin still drives the Saab.

Dr. Přibil’s second story is reminiscent of one of Professor Inczédy’s.

“Once Bob arrived in Prague by train from Vienna, with a rather worn rucksack as his only piece of

luggage. He noticed my surprise at the railway station and said 'The rucksack is best for travel; you have both hands free.' Bob had booked accommodation in the best hotel in the very centre of Prague. In the reception hall, I had the following conversation in Czech with the head of reception: 'Where is this gentleman's luggage?' asked the receptionist. 'He has only the rucksack' I answered. His face darkened, and he said 'Frankly speaking, we do not like this here. We have luggage boys to carry the luggage up and down as required. You understand, it gives us a certain control over our guests' movements. A man with a rucksack can easily disappear without paying. This is rather risky for us.' I said 'Oh no, you don't need to worry. This gentleman is a very close friend of mine—he is a professor from Aberdeen in Scotland'. 'From Aberdeen' exclaimed the receptionist, 'it is even more risky'.

When Dr. Příbil came to Britain on a lecturing tour, he stayed with Chalmers, and apparently was introduced to that Scottish culinary delicacy, haggis, served sliced (which is a most unusual manner). He recalls also "One day we were watching T.V. Bob was sitting comfortably in an easy chair with some *Talanta* manuscripts, from time to time glancing at the T.V. but after a while, he dozed off. I said to myself: this is the time to have a good gulp of whisky. I got up and slowly and carefully I reached his bar. To my great alarm, I heard Bob's low voice: 'If I am expecting a drinker like you, Rudla, as a visitor, I leave less than 1 inch in every bottle. The rest I keep in the basement.'"

The other side to that tale is that Chalmers was greatly concerned about the state of his friend's liver and digestive system, and did not want to be responsible for any further deterioration. Chalmers is not really a true citizen of his adopted city. (ABERDEEN PROVERB: Dinna spend money on drink, but aye keep a corkscrew.)

Dr. Stan Kotrlý has sent an account of Chalmers attending an analytical conference: he warns "there is only a little grain of truth in it", but it seems remarkably authentic.

"Bob's friends may tell you crack stories about his witty comments on various vices of scientific paper writers, or about the latest record in brevity of his editorial letters, but they all agree that it is always a jolly event to meet Bob at a conference. It is easy to find him after a morning lecture. If he is not arguing hotly with a blushing *Talanta* contributor over a cup of coffee, he will surely be found in the lounge. Undisturbed by the surrounding turmoil, he sits there at a corner table, high shiny forehead bent over a manuscript, and his keen eye and hand running down a page, leaving behind them a red mass of editorial corrections. And of course, his lecture is awaited by an audience eager to hear a new funny opening to his paper, which is then spiced with impromptu sagacious remarks. See for yourself how effectively the attention of an international audience can be tuned

in to Scottish accents of a slightly hoarse voice, by an introduction like this one.

"Mr. Chairman, before I begin to discuss some of our results, I should like to draw your attention to the interesting correlation between the level of fish consumption and the development of brains in Scotland. It was actually revealed by chance. Once a Northumberland farmer met his friend, a Scottish fisherman. 'Why', he asked, 'are you Scots so shrewd.' 'That's simple', was the reply. 'You have to eat fish.' And so special deliveries of fish from the river Tweed were arranged, for a special price, of course. After some time, the farmer grew impatient. 'So much money spent on bones of your wee fishes! All my mouth aches and there's no improvement!' 'On the contrary', the fisherman grinned broadly with a glance in the direction of his new boat. 'You can just see the result, old man, can't you?' . . .

"Such lecture openings evidently had a catalytic effect on inventive minds, since in due course, various funny stories with Bob as an essential ingredient circulated among his friends. Embellished by imagination and perfumed with alcohols of exaggeration, some of these stories became a local legend, and adornment to the colour of an academic club.

"At the memorable Second Analytical Conference at Golden Sands on the Bulgarian coast, I found Bob as usual, keeping his nose to the grindstone of the editorial work; but he was unusually subdued. 'Do read it', he implored. 'I can't make any sense of this bit of text.' I read it and saw the snag. It was an article by a big name. 'If you have on your heavy editorial boots, we may put it right quickly. I have glimpsed near the conference hall a good-looking girl who is rumoured to be a secretary of your man. Surely he will not be far away.' She was really nice to us, and willing to help. Another lady, the interpreter, well-endowed with plump proportions, was also kindly disposed, but she could not do much with the text either. The outer defences were, however, conquered and we were finally ushered to the old man. After some painfully careful reading he admitted: 'Sorry, it does not make any sense to me either. What a useless piece of translation. Anyway, I have to see my original notes.' . . . 'And authors wonder why I sometimes take a long time to edit their papers!' Bob gave vent to his indignation when we came out into the bright sun and vivid colours of the seaside scene. We went for a stroll up a wooded park, then down along wet sand splashed by waves. We found a restaurant with a terrace open to the sea, where the gentle breeze and delicious wine recharged our batteries and revived reminiscences of mutual friends, and inspired ambitious plans for the future. The baked fish was delicious."

Chalmers retired from his post at Aberdeen University on 30 September, 1985. He had originally intended to remain working until he was 70, as his contract allowed, but the cuts imposed on U.K. universities in 1981 led to many of the senior staff

agreeing to take early retirement. He will be continuing to edit *Talanta*, but it is to be hoped that he will find a little time for some of his pet retirement projects, such as the founding of a new journal, "The Journal of Useless New Knowledge" (think about the abbreviation!), or the study of the reactions of platinum with various types of wine (provided by the wine-merchants, of course). Perhaps his son Martin, at present a final-year computing science student, will be able to persuade him that computers are not just useful for drawing on (an author once referred to "curves drawn on a computer"), and introduce him to the joys of home computing. Perhaps his long-suffering wife Grace will be able to enjoy his company just a little bit more.

Let us hope, anyway, that Chalmers will have a happy, healthy, and fruitful retirement from University duties, and that he will continue to edit in his inimitable manner for many years to come.

Acknowledgements—I would very much like to thank all who sent stories, anecdotes and reminiscences for this article.

PUBLICATIONS OF R. A. CHALMERS

1. C. C. Miller and R. A. Chalmers, A critical investigation of the silver reductor in the microvolumetric determination of iron, especially in silicate rocks, *Analyst*, 1952, **77**, 2.
2. C. C. Miller and R. A. Chalmers, The precipitation of silica as 2:4-dimethylquinoline silicomolybdate and its gravimetric determination as silicomolybdic anhydride. *ibid.*, 1953, **78**, 24.
3. R. A. Chalmers, The spectrophotometric determination of phosphoric oxide in the presence of silica, *ibid.*, 1953, **78**, 32.
4. C. C. Miller and R. A. Chalmers, The determination of alumina, *ibid.*, 1953, **78**, 686.
5. F. H. Stewart, R. A. Chalmers and R. Phillips, Veatchite from the Permian evaporites of Yorkshire, *Min. Mag.*, 1954, **30**, 389.
6. R. A. Chalmers, A spectrophotometric microtitration of calcium, *Analyst*, 1954, **79**, 519.
7. R. A. Chalmers and C. A. Walley, A recording spectrophotometric titrimeter, *ibid.*, 1957, **82**, 329.
8. R. A. Chalmers and E. S. Page, The reporting of chemical analyses of silicate rocks, *Geochim. Cosmochim. Acta*, 1957, **11**, 247.
9. R. A. Chalmers and D. M. Dick, The use of alkali hydroxides for the separation of the copper and arsenic groups, *Analyst*, 1957, **82**, 652.
10. R. A. Chalmers, L. S. Dent and H. F. W. Taylor, Zeophyllite, *Min. Mag.*, 1958, **31**, 726.
11. R. A. Chalmers and D. A. Thomson, A method for the determination of phosphorus in organic compounds, *Anal. Chim. Acta*, 1958, **18**, 575.
12. K. C. Dunham, R. Phillips, R. A. Chalmers and D. A. Jones, The chromiferous ultrabasic rocks of Eastern Sierra Leone, *Overseas Geology and Mineral Resources Bulletin*, Supplement No. 3, HMSO, London, 1958.
13. R. A. Chalmers and G. A. Cheyne, Determination of sodium and potassium in serum and urine, *Unicam Methods Sheet* No. 900/2, 1959.
14. R. A. Chalmers and D. A. Thomson, A precision burette, *Analyst*, 1960, **85**, 226.
15. J. Murdoch and R. A. Chalmers, Ettringite ("Woodfordite") from Crestmore, California, *Amer. Mineral.*, 1960, **45**, 1275.
16. R. A. Chalmers, Some seldom-remembered errors in analytical chemistry, *Manuf. Chemist.*, 1962, **33**, 135.
17. R. A. Chalmers, The widening scope of organic analysis, *ibid.*, 1962, **33**, 460.
18. R. A. Chalmers, Chapter IX.3b (aluminium) in *Comprehensive Analytical Chemistry*, Vol. IC (ed. C. L. Wilson and D. W. Wilson), Elsevier, Amsterdam, 1962, p. 103.
19. R. A. Chalmers, Chapter X.5a (vanadium) *op. cit.*, p. 542.
20. R. A. Chalmers, Chapter X.6a (chromium) *op. cit.*, p. 581.
21. R. A. Chalmers, Chapter X.6b (molybdenum) *op. cit.*, p. 589.
22. R. A. Chalmers, Chapter X.6c (tungsten) *op. cit.*, p. 598.
23. R. A. Chalmers, Chapter X.8a (iron) *op. cit.*, p. 635.
24. R. A. Chalmers, A. W. Nicol and H. F. W. Taylor, The composition of nekoite, *Min. Mag.*, 1962, **33**, 70.
25. R. A. Chalmers, Oxidation potentials in qualitative analysis, *Analytical Chemistry 1962*, Elsevier, Amsterdam, 1963, p. 45.
26. R. A. Chalmers, V. C. Farmer, R. I. Harker, S. Kelly and H. F. W. Taylor, Reycrite, *Min. Mag.*, 1964, **33**, 821.
27. R. A. Chalmers and R. N. Curnow, The effect of random balance errors in the calibration of a set of weights, *Analyst*, 1964, **89**, 567.
28. R. A. Chalmers and D. M. Dick, Systematic analysis by solvent extraction methods. Part I, *Anal. Chim. Acta*, 1964, **31**, 520.
29. R. A. Chalmers and D. M. Dick, Systematic analysis by solvent extraction methods. Part II, *ibid.*, 1965, **32**, 117.
30. W. Moser, R. A. Chalmers and A. G. Fogg, The Boedeker reaction, Part I, *J. Inorg. Nucl. Chem.*, 1965, **27**, 831.
31. A. B. Carpenter, R. A. Chalmers, J. A. Gard, K. Speakman and H. F. W. Taylor, Jennite, a new mineral, *Amer. Mineral.*, 1966, **51**, 56.
32. R. A. Chalmers and A. G. Sinclair, Analytical applications of β -heteropoly acids, Part I, *Anal. Chim. Acta*, 1965, **33**, 384.
33. R. A. Chalmers and A. G. Sinclair, Analytical applications of β -heteropoly acids, Part II, *ibid.*, 1966, **34**, 412.

34. R. A. Chalmers, D. A. Edmond and W. Moser, Oxidimetry of iron(II) and the peroxide effect, *ibid.*, 1966, **35**, 404.
35. A. G. Fogg, W. Moser and R. A. Chalmers, The Boedeker reaction, Part III, *ibid.*, 1966, **36**, 248.
36. R. A. Chalmers and G. Svehla, Systematic analysis by solvent extraction methods, Part III, *Solvent Extraction Chemistry*, North-Holland, 1967, p. 600.
37. R. A. Chalmers, Chemical analysis of silicates, *The Chemistry of Cements*, H. F. W. Taylor (ed.), Vol 2, Academic Press, New York, 1964.
38. R. A. Chalmers and A. G. Sinclair, Organic molybdate complexes, *J. Inorg. Nucl. Chem.*, 1967, **29**, 2065.
39. R. A. Chalmers, The stability constants of PAR and TAR complexes, *Talanta*, 1967, **14**, 527.
40. R. A. Chalmers and M. A. Basit, A critical study of oxine as an analytical reagent, *Analyst*, 1967, **92**, 680.
41. R. A. Chalmers and G. M. Telling, A reassessment of rhodizonic acid as a qualitative reagent, *Mikrochim. Acta*, 1967, 1126.
42. R. A. Chalmers and M. Umar, Secondary standards, Part I, *Anal. Chim. Acta*, 1967, **39**, 521.
43. R. A. Chalmers and M. Umar, Secondary standards, Part II, *ibid.*, 1968, **42**, 257.
44. R. A. Chalmers and M. A. Basit, Spectrophotometric determination of alumina, *Analyst*, 1968, **93**, 629.
45. R. A. Chalmers and G. A. Wadds, Spectrofluorimetric analysis of mixtures of the principal opium alkaloids, *ibid.*, 1970, **95**, 234.
46. R. A. Chalmers, Writing, reviewing and editing in analytical chemistry, *CRC Crit. Rev. Anal. Chem.*, 1970, **1**, 217.
47. R. A. Chalmers and J. Stark, Continuous assessment of practical work in the Scottish HNC course in chemistry, *Educ. in Chem.*, 1968, **5**, 154.
48. R. A. Chalmers, Separation in organic chemistry, *Pure Appl. Chem.*, 1971, **25**, 687.
49. R. A. Chalmers and F. I. Miller, Metal-metallochromic indicator complexes as acid-base indicators, *Analyst*, 1971, **96**, 97.
50. L. Erdely, L. Pološ and R. A. Chalmers, Development and publication of new gravimetric methods of analysis, *Talanta*, 1970, **17**, 1143.
51. R. A. Chalmers and M. Umar, Secondary standards, Part III, *Chimie Analitica (Romania)*, 1971, **1**, 42.
52. A. Berka, J. Ševčík and R. A. Chalmers, Development and publication of new titrimetric methods, *Talanta*, 1972, **19**, 747.
53. R. A. Chalmers, Enrichment in trace analysis, *Pure Appl. Chem.*, 1972, **31**, 569.
54. A. C. Mehta and R. A. Chalmers, Spectrofluorimetric investigation of alkaloids, *Chem. Analit (Warsaw)*, 1972, **17**, 565.
55. R. A. Chalmers and I. L. Marr, Chemistry as a branch of analytical chemistry, *Z. Anal. Chem.*, 1973, **253**, 314.
56. R. A. Chalmers and A. F. J. Jackson, Spectrofluorimetric determination of thebaine, *Mikrochim. Acta*, 1975 **II**, 273.
57. R. A. Chalmers and A. F. J. Jackson, Critical evaluation of fluorimetric assay methods for morphine, *Rev. Roum. Chim.*, 1977, **22**, 575.
58. R. A. Chalmers, Standards and standardisation, *Comprehensive Analytical Chemistry*, G. Svehla (ed.), Vol. III, Elsevier, Amsterdam, 1975.
59. R. A. Chalmers, The analysis of a paper on analytical chemistry, *Essays on Analytical Chemistry in Memory of Professor Anders Ringbom*, E. Wänninen (ed.), Pergamon, Oxford, 1977.
60. E. Rancke-Madsen and R. A. Chalmers, Scandinavian contributions to analytical chemistry, *Talanta*, 1975, **22**, 939.
61. R. A. Chalmers, Problems in the teaching of analytical chemistry, *Pure Appl. Chem.*, 1978, **50**, 97.
62. F. Szabadváry and R. A. Chalmers, Carl Friedrich Mohr and analytical chemistry in Germany, *Talanta*, 1979, **26**, 609.
63. R. A. Chalmers and F. Szabadváry, Jöns Jakob Berzelius (1779–1848) and analytical chemistry, *Talanta*, 1980, **27**, 1029.
64. F. Szabadváry and R. A. Chalmers, On the invention of conductimetric titration, *Talanta*, 1983, **30**, 997.
65. M. I. Farooqi and R. A. Chalmers, A rapid screening test for efficiency of scale inhibitors, *Lab. Practice*, 1985, **34** (10), 104.

BOOKS

1. R. A. Chalmers, editor, *Quantitative Chemical Analysis*, Cumming and Kay, 11th edition, Oliver and Boyd, Edinburgh, 1956.
2. R. A. Chalmers, *Aspects of Analytical Chemistry*, Oliver and Boyd, Edinburgh, 1968. Czechoslovak Translation, SNTL, Prague, 1971.
3. A. K. De, S. M. Khopkar and R. A. Chalmers, *Solvent Extraction of Metals*, Van Nostrand Reinhold, London, 1970.
4. G. E. Baiulescu, C. Patroescu and R. A. Chalmers, *Education and Teaching in Analytical Chemistry*, Horwood, Chichester, 1982.

Also

Van Nostrand Series in Analytical Chemistry
 Ellis Horwood Series in Analytical Chemistry.
 R. Přibil, *Applied Complexometry*, edited by
 R. A. Chalmers, Pergamon Press, Oxford, 1982.

THE ANALYSIS OF A PAPER ON ANALYTICAL CHEMISTRY

ROBERT A. CHALMERS

Chemistry Department, University of Aberdeen, Meston Walk, Old Aberdeen, Scotland

Summary—Guidance is offered on the assessment, by authors, referees and editors, of scientific papers, before and after their submission for publication.

The remarks made in this paper refer specifically to analytical chemistry, but may also apply, *mutatis mutandis*, to other fields of chemistry. The object is to provide a working guide for the assessment of the value of contributions, both actual and potential, to the literature, and hence to assist authors in writing their papers and doing the work that is first necessary, and editors and referees in judging the results. The hoped-for result is that good papers will be even better and bad papers eliminated.

Just as there are two kinds of error in applying criteria of detection,¹ there are two kinds of error in the publication of scientific papers. The error of the "first kind" is to publish a paper that should be rejected, and the error of the "second kind" is to reject a paper when it should be accepted. The errors of the first kind are the more serious, because (a) such papers are likely to form part of a series linked by cross-references, and anything in print tends to be regarded as holy writ, especially if it is mentioned often enough in citation indexes, (b) errors of the first kind are vastly more numerous than errors of the second kind (which will usually be corrected by the author finding a more sensible vehicle for the paper). It is therefore essential that referees and editors should know how to evaluate a manuscript before its publication, and that readers of the literature should be able to assess papers already published.

It is convenient to consider this analytical procedure as applied to the sections of a paper in the usual order of their appearance.

The title

This should be sufficiently full to convey accurately the purpose and content of the work, so that readers can decide whether it interests them without having to read the summary of the whole paper. Thus "Determination of lead" is not a satisfactory title, even for a comprehensive review. The reader wants to know whether the paper is a review or an account of

research, what type of concentration is determined, what the matrix is, *etc.* The title should also be grammatically correct and readable. "Identification of bacteria using mass spectrometry" leaves one wondering about science fiction. "The geologic column" appearing in *Geotimes*, and written by Robert L. Bates, is a veritable treasurehouse of monstrosities in the title department. "Geochronobioclimatopaleo-magnetostratigraphy" illustrates the danger of compounding words (for example, what does "chromatopolarography" convey to the reader?). The increasing habit of using nouns as adjectives must surely have reached the limit with "Earth resources technology satellite data collection platform field installation, operation and maintenance manual".

As pointed out elsewhere,² language is a precise tool, and should be used as one. Those writing in languages foreign to them may be excused for lapses, but not native speakers or the editors who do not correct such faults.

The summary

Almost all journals require a precis to be written, and this must convey to the reader the important information in the paper proper, and should be understandable in itself without reference to the main text. It should not contain material that does not appear in the paper itself.

The introduction

This section usually gives a historical survey and the reasons for doing the research. The documentation should be thorough enough to cover the main points and give the reader an adequate lead-in to the literature, but it need not be so comprehensive as to mention all the work on the topic, whether it is useful and germane or not. The main purpose is to give the background to the work. It is here that the first doubts may arise in the reader's mind. Has the selection of literature been biased in any way? Has an original source been omitted either by accident or design? As hinted in a serio-comic article,³ it is easy to establish a reputation by using someone else's idea and producing rapidly a number of papers on it, only

Reprinted from E. Wänninen, ed., *Essays on Analytical Chemistry in Memory of Professor Anders Ringbom*, Pergamon, Oxford, 1977; by permission of the Publishers.

the first of these actually mentioning the originator of the idea, and the third and subsequent papers referring back to the second in the series. It is advisable for the author to *read* the papers referred to in this section. Because of the "chain reaction" effect in published work,⁴ errors may have been made and perpetuated in derivative publications. Even if the referee does not have first-hand knowledge of the relevant literature, a quick scan will usually reveal whether the author is quoting other authors or has consulted the originals (and has understood and quoted them correctly).

Experimental work

The account of the experimentation must be sufficiently complete for the work to be repeatable by someone else starting from scratch. A clear distinction should be made between the exploratory work done in arriving at the method or conclusion reached, and the practical details of any procedure recommended for application. The reason for this is simple. In the development of the technique, the amount of determinand was always known, and many of the experimental parameters could be altered with direct reference to this quantity; in a "real" application the determinand is the unknown quantity, and the parameters used should have a wide enough tolerance to cover the widest range expected for the determinand, without the need for prior knowledge of the amount present. It is not unknown for a paper on use of a spectrophotometric reagent in a mixed solvent system to specify that the reagent, dissolved in say ethanol, is to be added in fixed ratio to the amount of determinand, itself in acidic aqueous solution, and enough additional acid and ethanol added to bring their total concentrations in the final solution to some critical value. Such a procedure is of little practical use to the working analyst.

Because expertise has been unconsciously acquired during the many repetitions of experiments in the development of a method, small but vitally important points of technique may be overlooked in the writing up of the procedure; it is desirable to ask a competent analyst who is unacquainted with the new method to try it out on standard materials before the final version of the paper is written. Any inadequacies in description will often be manifested by errors in the results, and can be put right.

The details of procedures should be self-consistent (e.g., 50 ml of solution should not be diluted to 25 ml) and wherever possible the tolerances for amounts of reagents *etc.* should be stated.⁵ When specially constructed apparatus is used, the description given should be full enough for the reader to be able to have it made. When standard equipment is used it is not necessary to specify the model unless this is important for assessment of performance. Almost any spectrophotometer covering the necessary wavelength range will do for colorimetric analysis, but for measurement of constants such as molar absorptivity,

it may be necessary to say which type of instrument was used. Similarly with reagents, most chemicals of analytical-reagent grade will conform to a more or less standard specification, and it is only necessary to name the supplier if it is absolutely essential, for some reason, to use only that maker's product. An almost universal failing, for which editors (including the present writer) must take some responsibility, is to say that certain reference solutions were standardised by established methods but then to give no information about the number of standardisations done or the precision of the results. One of the few exceptions seems to be the class of papers on thermometric titrations, where the precision of the "classical" method is determined and compared (usually to its detriment) with that of the thermometric method. The only point to make here is that very often the precision reported for the classical method is much poorer than experience indicates should be the case, and a doubt is raised in the mind of the reader. Calibration of weights and apparatus also appears to be generally unheard of, although the most cursory glance at standard specifications shows that a comparatively large error can accrue from ignoring the existence of manufacturer's tolerances.⁶

Results and discussion

The first question here is whether the results mean what the author thinks they do, and whether the interpretation placed upon them is valid. Graphical and tabular presentation of results often gives a good insight into the validity of the work and the discussion, and for this reason the author should supply full details of the experimental results with the manuscript, even though some will be edited out. The first thing to look for is the number of significant figures quoted. If these exceed the number that can be justified in terms of the likely experimental error in weighing, instrument reading *etc.*, then the reader may begin to have doubts about the author's knowledge and competence. On the other hand, too few significant figures may conceal the errors associated with the method.

It is often particularly significant if an author quotes a table of results instead of drawing a graph, especially if all the other results have been presented graphically, or a statement is made about the relationship between the results, and some mathematical manipulation is needed. An example from experience is a set of Job plots which were all of normal form, and accompanied by a table of absorbances at different mole fractions for another system, which when plotted showed the formation of two complexes, only one of which was discussed in the text. Another was a table of absorbances which were said to result in a linear graph after appropriate manipulation; an actual plot turned out to be a more or less smooth curve. In another paper no fewer than six significant figures were quoted (because measurements were made to $1 \mu\text{V}$, "which is 1 part in 10^{10} "

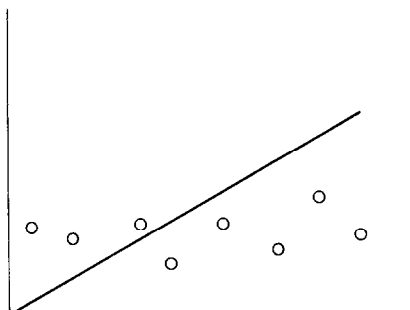


Fig. 1.

according to the author) though the results were based on only some tens of mV change in signal. The same paper had a least-squares treatment of the results; the author kindly supplied the raw data, and a statistical test for the standard deviation of the slope gave a value that was about 25% of the slope. A plot of the data showed why—there were two large errors in subtraction in the results supplied, resulting in two large discontinuities in the graph. Yet again, a plot similar to that in Fig. 1 was submitted as “evidence” of a correlation.

Another author produced a graph like that shown in Fig. 2, with the statement that the standard deviation for the distance of the points from the line had a certain value. Enquiry as to why a straight line would not do equally well produced a set of raw data which turned out to be duplicate determinations that when plotted as error bars gave Fig. 3.

In a conductometric investigation the plot of conductance *vs.* volume of titrant gave curve *a* in Fig. 4, which did not fit in with the experimenter’s preconceived ideas; it was therefore transformed into the reciprocal curve (*b*) to which tangents or segments could be fitted to prove the “theory”.

Very long extrapolations from closely spaced data are another fruitful source of dubiety in the reader’s mind, especially when accompanied by an impressively large number of significant figures. For example, no fewer than five significant figures in a

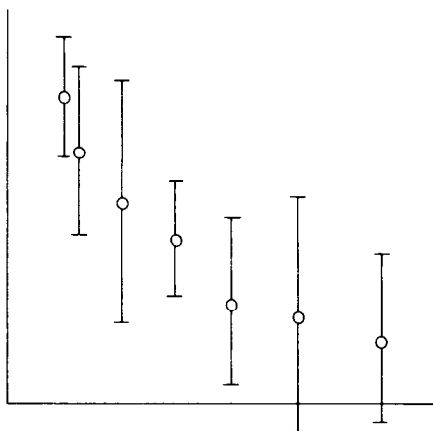


Fig. 3.

standard entropy change have been deduced from equilibrium constants measured at 25, 35 and 45 C. Again, extrapolations sometimes become almost asymptotic by the time they reach the appropriate coordinate.

Statistics may also easily be abused. Most workers seem to have heard of variance, but many still apply the “root mean square” formula to the results of two or three experiments, and very few apply Student’s *t*-test even if they have heard of it. It is true that “intuitive” inspection of the results will often lead to sound conclusions,⁷ but statistics, if used at all, should be used properly.

References

It is absolutely essential that the references given should be quoted accurately. To this end, they should all have been checked against the originals (or at least against abstracts, in which case the reference to the abstract should also be given). They should also actually have been consulted and not lifted piecemeal from a paper by someone else. There is no excuse whatever for inaccurate copying of references, nor for writing them in a style that is not that for the journal to which the paper is submitted. Failure to use

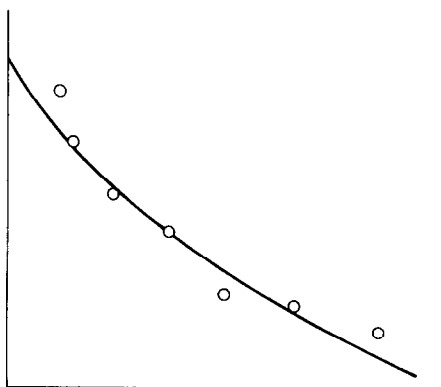


Fig. 2.

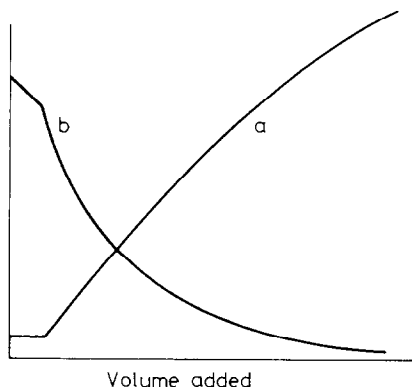


Fig. 4.

journal style may suggest that the paper has already been rejected by another journal (sometimes identifiable!). However, the editor also bears the responsibility of ensuring that authors are suitably informed of the error of their ways if they produce incorrect or inadequate references.

GENERAL ASSESSMENT OF A PAPER

Because analytical chemistry, above all other branches of chemistry, is an intensely practical branch of science, the prime criterion of a paper on analysis must be its *usefulness*. No matter how elegant a piece of work may be, if it has no conceivable application it must remain an academic curiosity. It is true that certain academic curiosities of the past have found subsequent applications, but their number is so small that it merely serves to prove the rule. Once the paper has been read as a whole, for obvious errors of chemistry and logic, the next task is to assess its value to the practising analyst.

Such value judgments must be based on a good working knowledge of the type of method dealt with, and of possible applications in industrial and research analysis. The literature is rather like the "fat lady" at a carnival sideshow. It is held together by a skeleton of bone-hard solid fact, with connective tissue of theory and muscle of useful application, the whole being overlaid by a mountain of the fat of pointless variation that is of no use to any but those who make their living from it (those academic and other professional researchers who do not have the ability or originality to strike out a new line of their own). Research has indeed become a sacred cow when the amount of trivial work is so large that a vast range of new journals has had to be created for it to achieve publication. What is the result? Long series of papers ringing the changes on reagent (how many compounds have been tested as reagents for copper, found wanting, but reported for "the sake of completeness"?), ion determined (the minimum number of papers to be expected for a new reagent is the number of metals *etc.* it will react with), method of completing the determination (one paper per method, for the same metal-reagent combination).

Many authors seem to consider it unnecessary to suggest how their work may actually be applied, deeming it enough to provide a method that works for a pure solution of the determinand, with or without addition of other species (one at a time, but scarcely ever in combination). Frequently the ratio of the tolerable level of interfering ion to determinand is so low that the method would be utterly useless unless the determinand were the major species present in the sample, and usually a few set ratios are tested without any attempt to find the true tolerance limit. Sometimes the oxidation states chosen for the interference tests do not correspond to those that

would be obtained after a decomposition procedure, and the possibility of formation of kinetically stabilised thermodynamically unstable complexes (inert complexes) is tacitly ignored. Over forty years ago, Lundell⁸ wrote some words of wisdom that are often referred to but apparently seldom read.

Methods have been concocted (no other word will do to describe their development) that are so involved and tortuous that the errors build up very quickly to an unacceptable level. Others require very exacting time schedules or very close tolerance limits on pH and other parameters. Such methods are of very limited value, and are only useful if no other exists capable of giving about the same precision and accuracy.

There are enough textbooks and papers on how to conduct research (*e.g.*, the series commissioned for *Talanta*^{9, 15}) for there to be no reason for researchers to plead ignorance of what should have been done. Referees and editors are all too often involved in giving free lessons in chemistry, logic, grammar *etc.*, and may feel obliged to spend far more time over an unacceptable paper than it is worth, simply to justify their opinion to the author.

Scientists are commonly regarded as illiterate. In the sense that they are frequently unable to communicate their thoughts and knowledge fluently and accurately, this charge has a substantial foundation in fact. It is unfortunately equally true in the sense that they sometimes seem unable to distinguish good and useful from bad and pointless science when they read it. The remedy lies in their own hands. Literacy is a skill that can be gained like any other, by precept and practice, and a more ruthless attitude on the part of referees and editors of journals would greatly improve the quality both of science and of its image in the popular mind.

REFERENCES

1. J. B. Boos, *Analyst*, 1962, **87**, 832.
2. R. A. Chalmers, *CRC Crit. Rev. Anal. Chem.*, 1970, **1**, 217.
3. "Decembrius", *Retort* (Birmingham University Student Chemistry Society), 1971, **47**, No. 1, 4.
4. A. T. Austin, E. D. Hughes, and C. K. Ingold, *Nature*, 1947, **160**, 406.
5. A. L. Wilson, *Talanta*, 1970, **17**, 21.
6. R. A. Chalmers, in *Wilson and Wilson's Comprehensive Analytical Chemistry*, Vol. 3, ed. G. Svehla, Elsevier, Amsterdam, 1975.
7. A. L. Wilson, *Talanta*, 1974, **21**, 1109.
8. G. E. F. Lundell, *Ind. Eng. Chem., Anal. Ed.*, 1933, **5**, 221.
9. G. F. Kirkbright, *Talanta*, 1966, **13**, 1.
10. L. Erdey, L. Pólos, and R. A. Chalmers, *ibid.*, 1970, **17**, 1143.
11. G. J. Moody, and J. D. R. Thomas, *ibid.*, 1972, **19**, 623.
12. A. Berka, J. Ševčík, and R. A. Chalmers, *ibid.*, 1972, **19**, 747.
13. H. B. Mark, Jr., *ibid.*, 1973, **20**, 257.
14. J. Ramírez-Muñoz, *ibid.*, 1973, **20**, 705.
15. H. S. Rossotti, *ibid.*, 1974, **21**, 809.

DETERMINATION OF BISMUTH BY ELECTROCHEMICAL STRIPPING ANALYSIS

ELIMINATION OF INTERFERENCES BY USING A MERCURY FILM ELECTRODE MODIFIED WITH TRI-*n*-OCTYLPHOSPHINE OXIDE, AND APPLICATION TO COPPER ALLOYS

JIRÍ LEXA

Chemical Laboratories, Central Research Institute, Škoda Works, 316 00 Pilsen, Czechoslovakia

KAREL ŠTULÍK*

Department of Analytical Chemistry, Charles University, Albertov 2030, 128 40 Prague 2, Czechoslovakia

(Received 12 April 1985. Revised 20 August 1985. Accepted 10 September 1985)

Summary—A mercury film electrode modified with a film consisting of tri-*n*-octylphosphine oxide in a poly(vinyl chloride) matrix is used for a galvanostatic stripping determination of bismuth in copper and copper alloys. The method can be used to determine from 0.002 to 0.5% of bismuth. It is very selective, simple and rapid. The precision and accuracy are good and the only serious interference is caused by tin(IV).

The preparation and electrochemical properties of a mercury film electrode modified with tri-*n*-octylphosphine oxide (TOPO-MFE) have been described in an earlier paper.¹ This type of electrode makes possible very selective determinations of many metals. The general procedure for electrochemical stripping determinations with the TOPO MFE involves four steps: (1) accumulation of the metal ion in the TOPO film (non-electrochemical; essentially a solvent-extraction step); (2) electrochemical deposition of the metal from the TOPO film into the mercury film (potentiostatic electrolytic reduction of the metal ion, here termed pre-electrolysis); (3) electrochemical stripping of the metal from the mercury film back into the TOPO film (galvanostatic or potentiostatic oxidative stripping as in ASV); (4) back-extraction of metal ions from the TOPO film into the solution (as with step 1, this is non-electrochemical). The highest selectivity is obtained when the sample solution is replaced by a pure base electrolyte after the extraction and accumulation of the metal ion into the TOPO film. The extraction efficiency and selectivity depend mainly on the composition and acidity of the sample solution. This paper describes the application of the TOPO MFE to the determination of bismuth in copper and copper alloys, by galvanostatic stripping analysis (GSA).

The most common methods for the determination of bismuth in copper alloys employ spectrophotometry or flame atomic-absorption spectrometry. These methods are not particularly sensi-

tive and often require preconcentration of bismuth, usually by co-precipitation with lanthanum(III) or iron(III) hydroxide. Toropova *et al.*² proposed an electrochemical stripping method better suited to the determination of low levels of bismuth in copper alloys, based on a selective preconcentration by chemical reduction of Bi³⁺ by metallic mercury in a solution containing thiourea. Later, to improve the selectivity of the method, bismuth was separated from the matrix elements by extraction of its iodo-complex into methyl isobutyl ketone.^{3,4} These methods have an advantage in the possibility of simultaneous determination of antimony.

The galvanostatic stripping method with the TOPO-MFE described in the present paper is very simple and exhibits high sensitivity and selectivity. The solution need not be deaerated. As the highest extraction distribution ratios have been obtained in hydrochloric acid media,⁵ a solution of hydrochloric acid was also used in this determination. It follows from the literature data⁵ on extraction of various elements from hydrochloric acid into 5% TOPO solution in toluene that the extraction of bismuth into the TOPO film will probably be most affected by gold, uranium, tin and zinc.

EXPERIMENTAL

For the description of the apparatus and the experimental techniques see our preceding paper.¹ The TOPO-MFE was prepared by Procedure B,¹ with the optimal parameters, *i.e.*, a TOPO film thickness of 1.6 μm and silver and mercury film thicknesses of 0.9 and 1.7 μm , respectively. The reagents used in this work were of p.a. purity (Lachema, Czechoslovakia) and were not further purified. The experimentation is described below.

*Author for correspondence.

RESULTS AND DISCUSSION

Optimization of the conditions for determination of bismuth

Preliminary experiments indicated that extraction of bismuth from 0.5M hydrochloric acid into the TOPO film is sufficiently rapid and that the bismuth is retained in the TOPO film during exchange of the base electrolyte and washing with pure 0.5M hydrochloric acid.¹ The extraction of copper is complicated by the different behaviour of Cu^{2+} and Cu^+ . Both are extracted into the TOPO film, but Cu^{2+} is partially back-extracted during washing with pure 0.5M hydrochloric acid, whereas Cu^+ is retained in the TOPO film, apparently owing to stronger solvation by TOPO (and possibly also by slower transport through the TOPO film). Janoušek⁶ observed a substantial increase in the extraction of copper from hydrochloric acid into 0.1M TOPO in methyl isobutyl ketone on addition of ascorbic acid to the solution and hence the effect of stronger solvation of cuprous chloride by TOPO apparently predominates.

A concentration of hydrochloric acid was therefore sought that would back-extract Cu^{2+} but not bismuth. A 0.5M hydrochloric acid solution containing Bi^{3+} or Cu^{2+} at concentrations of 2 or 10 $\mu\text{g/ml}$, respectively, was used to accumulate the metals on the TOPO-MFE (disconnected from the potentiostat). Then pre-electrolysis was performed for 80 sec at potentials of -0.400 V (Bi) or -0.600 V (Cu). The deposit was stripped galvanostatically at a current of 5 μA , yielding data on the relative amounts extracted. The solution was then replaced by pure hydrochloric acid of a particular concentration and this was stirred for 80 sec, with the working electrode disconnected from the potentiostat. Next the solution was replaced by pure 0.5M hydrochloric acid and the amount of the test element still contained in the TOPO film was determined by GSA under the same conditions as above. The TOPO-MFE was always regenerated by immersion for 80 sec in a stirred solution of 1M citric acid. The dependence of the fractions of Bi^{3+} and Cu^{2+} retained in the TOPO film after washing, on the hydrochloric acid concentration in the washing solution, is given in Fig. 1. It can be seen that the best separation of Cu^{2+} from Bi^{3+} is obtained by washing with hydrochloric acid at the lowest concentrations; bismuth is also somewhat back-extracted, but it can be assumed that the percentage loss of bismuth will be constant, independent of its concentration in the test solution. The percentage of Bi^{3+} retained in the TOPO film is mostly somewhat higher than 100%. This is caused by the fact that the first GSA stripping determination was carried out in the presence of the solution containing the test metals. Therefore, accumulation into the TOPO film continued during this determination. As virtually no bismuth was back-extracted during the washing step (except when the lowest hydrochloric acid concentrations were used),

the amount of bismuth determined in the second GSA determination was greater than that determined previously.

The electrode activity depends on the effectiveness of the back-extraction of interfering elements. As tin is a likely interferent the conditions for back-extraction of bismuth and tin were examined. The elements were extracted into the TOPO film from 0.5M (for Bi^{3+}) or 1M (for Sn^{4+}) hydrochloric acid containing 5 μg of bismuth or 25 μg of tin per ml. Pre-electrolysis was applied for 80 sec at potentials of -0.300 V (for Bi) or -1.20 V (for Sn) and the elements were then stripped galvanostatically at a current of 5 μA , giving data on the relative amounts extracted into the TOPO film. After two washings with water, the cell was filled with a test back-extraction solution, which was then stirred for 80 sec. The solution was removed and the cell washed twice with water and the residues of the metals in the TOPO film were determined by GSA in pure solutions of 0.5M (for Bi) and 1M (for Sn) hydrochloric acid under the same conditions as above. The back-extraction efficiencies are summarized in Table 1. The back-extraction efficiency also depends on other factors, e.g., the PVC matrix of the film, and thus the data in Table 1 must be considered as a comparison of the relative efficiencies of the solutions studied. Bismuth is most efficiently back-extracted with 3M sulphuric acid. Tin(IV) cannot be back-extracted with

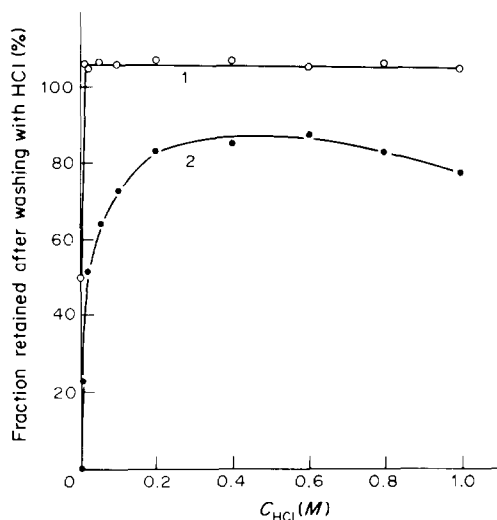


Fig. 1. Effect of hydrochloric acid concentration on the retention of bismuth (1) and copper (2) in the TOPO film. $C_{\text{Bi}} = 2 \mu\text{g/ml}$, $C_{\text{Cu}} = 10 \mu\text{g/ml}$; accumulation in the TOPO film for 80 sec from 0.5M HCl, with the working electrode disconnected; 80-sec pre-electrolysis at -0.400 V (Bi) and -0.600 V (Cu) in the same solution; GSA stripping step at 5 μA ; solution exchange for a pure HCl solution of a particular concentration; stirring for 80 sec with the working electrode disconnected; solution exchange for pure 0.5M HCl; GSA determination of the residues of the metals in the TOPO film under the same conditions as above. The fraction retained calculated as the percentage ratio of the results of the second to the first GSA determination.

Table 1. Back-extraction yields of bismuth and tin(IV)

Back-extraction solution	Back-extraction yield, %	
	Bi	Sn
H ₂ O	47	29
0.3M H ₂ SO ₄	81	21
3M H ₂ SO ₄	97	-3*
1M oxalic acid	79	29
1M citric acid	88	40
0.1M NaF	28	41
0.7M H ₃ PO ₄	68	49
7M HCl	88	—

*Because the TOPO phase was analysed for tin, and the experimental uncertainty resulted in an apparent 103% retention in the TOPO phase.

an efficiency higher than 50%, apparently owing to slow reaction of the solvate, but back-extraction with phosphoric acid is recommended, in view of the fact that increasing concentrations of tin cause an irreversible decrease in the sensitivity of the determination of bismuth, owing to gradual reduction of the extraction capacity of the TOPO film for bismuth.

Before examination of the effect of the accumulation time and electrolysis potential on the transition time for bismuth in 0.5M hydrochloric acid, the range of calibration graph linearity was found for accumulation and pre-electrolysis potentials of -0.300 V applied for 80 sec in 0.5M hydrochloric acid; it extends from zero to 6 μ g/ml bismuth concentration ($\tau = 23$ sec, $I_{\text{strip}} = 5 \mu\text{A}$). The effect of the accumulation time on the bismuth transition time was studied both for an accumulation potential of -0.300 V and for the working electrode disconnected from the potentiostat, with 1 μ g of Bi per ml in 0.5M hydrochloric acid, under the same conditions as above. The effect of pre-electrolysis time at -0.300 V on the bismuth transition time was examined, for an accumulation time of 80 sec with the working electrode disconnected (0.5M hydrochloric acid, Bi 5 μ g/ml). The three dependences are given in Fig. 2 and indicate that diffusion of bismuth through the TOPO film is the limiting factor in the overall process (see also the earlier paper¹), and that migration transport is insignificant at an electrode potential of -0.300 V. The dependence of the bismuth transition time on the accumulation and pre-electrolysis potential (Fig. 3) then shows that solvate migration is insignificant even at higher electrode potentials.

Therefore, the optimal conditions for the determination of bismuth can be summarized as follows: (1) the accumulation of bismuth is best done with the TOPO-MFE disconnected from the potentiostat, as the bismuth transport through the TOPO film is virtually unaffected by the electrode potential and in this way the highest selectivity of determination is attained; (2) the determination is then done after replacement of the sample solution by a pure base electrolyte, into which bismuth is not back-extracted from the TOPO film; (3) stripping of the elements from the TOPO film after the determination is best

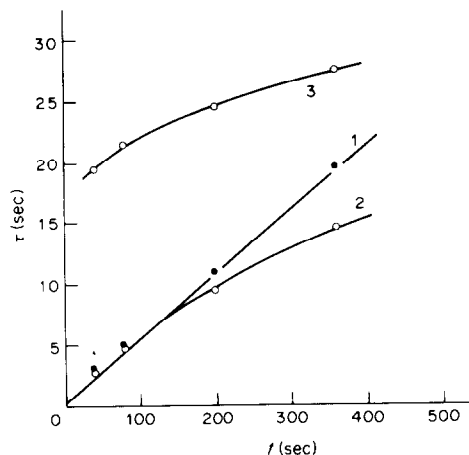


Fig. 2. Effect of accumulation time and TOPO-MFE potential on the transition time of bismuth in the GSA determination in 0.5M HCl. Accumulation: (1) $C_{\text{Bi}} = 1 \mu\text{g/ml}$, electrode potential -0.300 V. (2) $C_{\text{Bi}} = 1 \mu\text{g/ml}$, disconnected working electrode. (3) $C_{\text{Bi}} = 5 \mu\text{g/ml}$, disconnected working electrode. GSA determination: $E_e = -0.300$ V, $I_{\text{strip}} = 5 \mu\text{A}$. (1) $C_{\text{Bi}} = 1 \mu\text{g/ml}$, $t_e = 80$ sec. (2) $C_{\text{Bi}} = 0$, $t_e = 80$ sec. (3) $C_{\text{Bi}} = 0$.

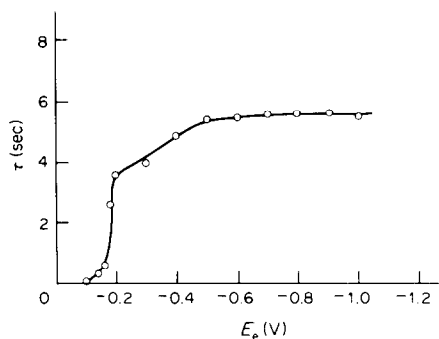


Fig. 3. Effect of TOPO-MFE potential on the transition time in the GSA determination of bismuth in 0.5M HCl. Accumulation: $C_{\text{Bi}} = 1 \mu\text{g/ml}$, $E_{\text{acc}} = E_e$, $t_{\text{acc}} = 80$ sec. GSA determination: $C_{\text{Bi}} = 1 \mu\text{g/ml}$, $t_e = 80$ sec, $I_{\text{strip}} = 5 \mu\text{A}$.

done with acid solutions without electrode polarization, to stabilize the distribution of H⁺ and A⁻ ions in the TOPO film and avoid large changes in the TOPO-MFE activity.

Determination of bismuth, and interferences from tin and zinc

On the basis of the results above, bismuth was determined as follows. The TOPO-MFE was soaked for 15 min in 3M sulphuric acid before the first measurement. Bismuth was then accumulated for 80 sec from a stirred solution of 0.5M hydrochloric acid/0.4M phosphoric acid containing 5 μ g of Bi per ml, with the TOPO-MFE disconnected from the potentiostat; the electrode was then rinsed twice with water and the galvanostatic stripping determination was done with pure 0.5M hydrochloric acid. After the measurement, bismuth was back-extracted from the electrode by an 80-sec immersion in stirred 3M sulphuric acid. The dependence of the TOPO-MFE

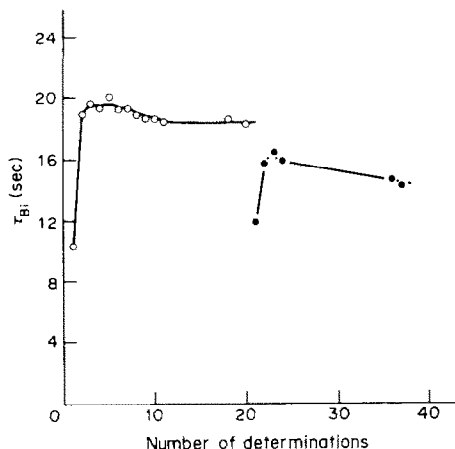


Fig. 4. Activity of the TOPO-MFE in the GSA determination of bismuth in a solution of $0.5M$ HCl + $0.4M$ H_3PO_4 , the first day (○) and the second day (●) after preparation of the TOPO-MFE. Accumulation: $0.5M$ HCl + $0.4M$ H_3PO_4 , $C_{Bi} = 5 \mu\text{g/ml}$, disconnected electrode, accumulation time, 80 sec. GSA determination: after accumulation the TOPO-MFE was rinsed twice with water and then Bi was determined in $0.5M$ HCl. $E_c = -0.300$ V, $t_c = 40$ sec, $I_{strip} = 5 \mu\text{A}$.

activity on the number of determinations is illustrated in Fig. 4. The average transition time for the bismuth stripping was $\bar{\tau}_{Bi} = 19.0$ sec during the first day (with a standard deviation of ± 0.5 sec, $n = 12$) and $\bar{\tau}_{Bi} = 15.4$ sec during the second day of use (S.D. = ± 0.9 sec, $n = 5$). These results represent only a rough estimate of the stability of the TOPO-MFE response, as different analyses were done with the electrode between these measurements. However, it is generally to be expected that the first determination will always yield an outlying result. The greatest changes in the TOPO-MFE activity were observed on polarization of the electrode at potentials of anodic mercury dissolution (see Lexa and Štulík,¹ formation of the mercury salt solvates).

The presence of phosphoric acid in the base electrolyte suppresses the accumulation of tin(IV) in the TOPO film, and back-extraction of the bismuth accumulated from this solution amounts to only about 15% during washing with the first two portions

of water; on further washing, no additional back-extraction of bismuth is observed.

Calibration curves for 0.5 – $5.0 \mu\text{g}$ of Bi per ml were obtained by GSA by the following procedure. (1) Accumulation of bismuth for 80 sec from bismuth solution in $0.5M$ hydrochloric acid/ $0.4M$ phosphoric acid, with the TOPO-MFE disconnected from the potentiostat. (2) Rinsing with water and pre-electrolysis of bismuth in pure $0.5M$ hydrochloric acid/ $0.4M$ phosphoric acid ($E_c = -0.300$ V, $t_c = 40$ sec, $I_{strip} = 5 \mu\text{A}$). (3) Electrode regeneration in stirred $3M$ sulphuric acid for 80 sec.

For the sake of comparison, calibration curves were also obtained by direct-current anodic-stripping voltammetry (DCASV) and differential-pulse anodic-stripping voltammetry (DPASV) under the same conditions, except for the times of accumulation and the electrode regeneration, which were 200 sec. The potential scan-rate was 10 mV/sec for DCASV and 5 mV/sec for DPASV; the pulse amplitude and frequency in DPASV were -12.5 mV and 1 sec. The methods of DCASV and DPASV are more sensitive than GSA and thus the respective bismuth concentration ranges were 0.05 – 0.6 and 0.005 – $0.08 \mu\text{g/ml}$. The characteristics of the calibration curves are summarized in Table 2. Back-extraction of bismuth by 200-sec immersion in $3M$ sulphuric acid at very low concentrations is not complete and two regeneration steps are required to suppress the electrode memory effect. As follows from Table 2, DCASV and especially DPASV should be used when very low concentrations of bismuth are to be determined. However, for common applications the sensitivity of GSA suffices, with the advantages of improved selectivity and the possibility of working with solutions that are not deaerated. (Solution deaeration is by far the longest stage of the whole determination).

The selectivity of the GSA determination of bismuth with respect to tin and zinc was studied with $2 \mu\text{g}$ of Bi per ml, 80-sec accumulation from $0.5M$ hydrochloric acid (disconnected electrode) and stripping step with pure $0.5M$ hydrochloric acid (no rinsing with water) at $E_c = -0.300$ V, $t_c = 40$ sec and $I_{strip} = 5 \mu\text{A}$. The electrode was regenerated for 80 sec in stirred $3M$ sulphuric acid. The results are given in

Table 2. Regression calibration straight lines, $\tau = b C_{Bi} + a$ (GSA) and $I = b C_{Bi} + a$ (DCASV and DPASV); $\alpha = 0.05$

Method	n	$b \pm s_b t_x$	$a \pm s_a t_x$	r	Limit of determination, $\mu\text{g/ml}$
GSA	6	3.67 ± 0.25 sec. $\mu\text{g}^{-1} \cdot \text{ml}$	0.3 ± 0.5 sec	0.999	0.08
DCASV	6	19.7 ± 0.5 $\mu\text{A} \cdot \mu\text{g}^{-1} \cdot \text{ml}$	0.3 ± 0.3 μA	0.999	0.01
DPASV	7	132 ± 18 $\mu\text{A} \cdot \mu\text{g}^{-1} \cdot \text{ml}$	-0.3 ± 0.8 μA	0.994	0.001

n = number of determinations, s_a , s_b = S.D. estimates, t_x = Student's coefficient, r = correlation coefficient; limit of determination was obtained as three times the S.D. value.

Table 3. Selectivity of the GSA determination of bismuth with the TOPO-MFE

Solution	Interfering ion, M ⁿ	C _M /C _{Bi}	Bi recovery, %
0.5M HCl	Zn ²⁺	1	99
		5	102
		25	97
	Sn ⁴⁺	125	85
		1	94
		5	66
0.5M HCl + 0.1M citric acid	10	50	
0.5M HCl + 0.5M citric acid	10	40	
0.5M HCl + 0.4M H ₃ PO ₄	10	49	
	100	98	
0.5M HCl + 2M H ₃ PO ₄	10	4	
	10	102	
	50	88*	
	100	56*	

*GSA determination in a solution of 0.5M HCl + 0.4M H₃PO₄, after solution exchange.

Table 3, from which it follows that when 0.5M hydrochloric acid is used as the base electrolyte in the accumulation step, interference by zinc begins at a zinc-to-bismuth weight ratio greater than 25, but tin(IV) interferes even at the same concentration as that of bismuth. In the presence of phosphoric acid in the base electrolyte, however, tin(IV) is partially masked and a tenfold ratio to bismuth can be tolerated: 0.4M phosphoric acid does not affect the accumulation of bismuth and may also mask some other cations, especially those with higher oxidation numbers. In the presence of large amounts of tin(IV) and zinc, the recovery of bismuth is low and the TOPO-MFE activity gradually decreases. Nevertheless, bismuth can still be determined (see Table 4), but the standard-addition method must be used.

The GSA method of determination of bismuth was applied to analyses of pure copper and copper alloys.

Procedure. To 0.1 g of sample in a 50-ml beaker covered with a watch-glass add 1.0 ml of hydrochloric acid (1 + 1) and 1 ml of 30% hydrogen peroxide. Allow the sample to dissolve, rinse the beaker walls with ca. 7 ml of water, add 0.1 ml of 1M iron(II) sulphate and boil briefly to destroy the peroxide completely. Add 0.5 ml of phosphoric acid (1 + 1) or

2.5 ml for samples containing high concentrations of tin), transfer the solution to a 10-ml standard flask and dilute with water to the mark. Transfer the solution to the electrolysis cell and accumulate bismuth for 80 sec with the TOPO-MFE disconnected from the potentiostat. Wash the TOPO-MFE with water and replace the test solution with pure 0.5M hydrochloric acid and perform a 40-sec pre-electrolysis at a potential of -0.300 V. Then strip the deposit galvanostatically at a stripping current of 5 μ A and measure the transition time. Obtain the bismuth concentration from a calibration curve, or, in the presence of large amounts of tin and zinc, by the standard-addition method. Before the next measurement, regenerate the TOPO-MFE by immersion in a stirred solution of 3M sulphuric acid for 80 sec.

For analyses of pure copper, with a bismuth content of less than 1 ppm, to which various amounts of bismuth were added, the calibration regression straight line, τ (sec) = c_{Bi} (176 \pm 5) (sec/%) + (0.2 \pm 0.1) (sec), was obtained, with a correlation coefficient of 0.998 and a detection limit of 0.002% Bi in Cu (three times the standard deviation; $n = 6$).

The precision and accuracy of the method were tested by analyses of standard copper alloys and by

Table 4. Accuracy and precision of the GSA determination of bismuth in copper alloys

Standard material	Certified Bi content, %	Contents of other metals, %				Bi content found, %			
		Sn	Zn	Sb	Ag	AAS*	HAAS†	<i>n</i>	GSA $L_{1,2}$ §
Škoda No. 1	—	0.009	0.01	0.01	0.006	0.005	0.005	4	0.0046 \pm 0.0005
Škoda No. 2	—	0.014	0.01	0.01	0.008	0.007	0.007	5	0.0070 \pm 0.0008
Škoda No. 3	—	0.02	0.02	0.02	0.01	0.011	0.011	5	0.0108 \pm 0.0006
Škoda No. 4	—	0.03	0.02	0.03	0.02	0.015	—	4	0.014 \pm 0.001
Škoda No. 5	—	0.05	0.02	0.05	0.01	0.022	—	4	0.022 \pm 0.001
Škoda No. 6	—	0.08	0.02	0.08	0.01	0.040	—	3	0.041 \pm 0.002
ČKD 319	0.045	6.6	2.3	0.25	—	—	—	4	0.043 \pm 0.008
ČKD 322	0.02	13.5	0.5	0.03	—	—	—	4	0.014 \pm 0.005

*After separation and preconcentration of bismuth by co-precipitation with lanthanum hydroxide.

†AAS with hydride generation.⁷

§ $L_{1,2} = \bar{x} \pm st_x/\sqrt{n}$; n = number of determinations; $\alpha = 0.05$.

comparison of the results with those obtained by AAS.⁷ The results are summarized in Table 4, from which it can be seen that the GSA method yields results that are in good agreement with those obtained by AAS and with the certified bismuth contents. Hence, the method can be used for a simple, direct, rapid and reliable determination of bismuth in copper alloys, at bismuth contents from 0.002 to 0.5%. To determine lower contents of bismuth, DPASV should be used, but the calibration curve ceases to be linear below 0.001% Bi, owing to interference from the copper.

REFERENCES

1. J. Lexa and K. Štulík, *Talanta*, 1985, **32**, 1027.
2. V. F. Toropova, Yu. N. Polyakov, L. N. Soboleva, M. M. Bazgutdinov and A. Ya. Zhdanova, *Zavodsk. Lab.*, 1976, **42**, 767.
3. V. F. Toropova, Yu. N. Polyakov and G. N. Zhdanov, *Zh. Analit. Khim.*, 1984, **39**, 1455.
4. *Idem*, *Zavodsk. Lab.*, 1984, **50**, No. 1, 4.
5. T. Ishimori, K. Kimura, T. Fujino and H. Murakami, *J. At. Energy Soc. Japan*, 1962, **4**, 117.
6. I. Janoušek, *Ph. D. Thesis*, Charles University, Prague, 1980.
7. *Idem*, private communication.

Dedication—Dedicated to Bob Chalmers in recognition of his brilliant editorship and long years of friendship.

Karel Štulík

PHOSPHORESCENCE CHARACTERISTICS OF ACETOPHENONE, BENZOPHENONE, *p*-AMINOBENZOPHENONE AND MICHLER'S KETONE IN VARIOUS ENVIRONMENTS*

G. SCHARF† and J. D. WINEFORDNER§

Department of Chemistry, University of Florida, Gainesville, FL 32611, U.S.A.

(Received 7 May 1985. Revised 26 August 1985. Accepted 5 September 1985)

Summary—The phosphorescence characteristics (excitation and emission spectra and lifetimes) of acetophenone (AP), benzophenone (BP), *p*-aminobenzophenone (PABP) and Michler's ketone (MK) adsorbed on Whatman No. 1 filter paper were measured at various temperatures, and compared with the phosphorescence characteristics in different solvent glasses at 77 K. Both AP and BP phosphoresce on filter paper only at low temperature (208 K). The phosphorescence lifetimes of AP and BP are <1 msec, indicating a $^3(n, \pi^*)$ lower triplet level for paper substrates. With PABP, the low lying triplet state in polar solvents is $^3(\text{CT})$ and in non-polar solvents is $^3(n, \pi^*)$; PABP on filter paper results in spectral characteristics similar to those of PABP in polar solvents at 77 K. The lifetime of PABP is longer than that of BP, indicating a $^3(\text{CT})$ low-lying triplet state. MK, like PABP, has strongly environment-dependent photophysical properties. MK, when adsorbed on filter paper, has an intense long-lived luminescence at room temperature, resulting in a limit of detection of 3 ng/ml or 3 pg, and a linear dynamic range of over 3 orders of magnitude. MK appears to be strongly hydrogen-bonded to the filter paper. In studies in ethanol and other solvents, MK adsorbed on filter paper shows a dramatic change in its phosphorescence spectrum when the temperature is lowered from 298 K to 208 K; the phosphorescence peak moves to longer wavelengths and the intensity decreases. The temperature effect could arise from the presence of several conformers of MK or be due to different environmental sites or *E*-type delayed fluorescence. The low-lying triplet state of MK on filter paper is most likely a $^3(\text{CT})$ state. Lowering the temperature appears to increase the phosphorescence intensity for ketones which phosphoresce in the $^3(n, \pi^*)$ triplet state, but affects it only slightly for analytes which phosphoresce in the $^3(\pi, \pi^*)$ triplet state. Room-temperature phosphorescence seems to arise for aromatic ketones and aldehydes with low-lying $^3(\pi, \pi^*)$ or $^3(\text{CT})$ triplet states.

In recent years, room-temperature phosphorescence (RTP) has become a useful analytical technique.^{1,6} It is suggested that to restrict the radiationless deactivation processes of the first excited triplet state, the phosphor should be held rigidly on the substrate.² The studies by Schulman and Walling⁷ and later by Wellons *et al.*⁸ demonstrated that aromatic ionic compounds exhibit strong RTP. On the other hand, non-ionic forms of the same compounds do not phosphoresce at room temperature when adsorbed on filter paper. These observations show the important role of dipole-dipole interactions between the phosphor and the substrate. Schulman and Parker⁹ suggested that hydrogen-bonding of the phosphor to the substrate is also very important for minimizing the non-radiative deactivations of the excited triplet state. Dalterio and Hurtubise¹⁰ have recently used several spectroscopic techniques to study the interactions of aromatic hydrocarbons and hydroxy compounds with several solid supports. They have also shown that there are hydrogen-bonding interactions

between the phosphors and the substrates. RTP has been observed from non-polar polynuclear aromatic compounds in the presence of heavy atoms. It has been suggested¹¹ that the heavy atom forms a π -complex with the analyte, thus increasing the interactions between the phosphor and the support. In view of the importance of the interactions and our previous studies¹² on RTP of aromatic ketones and aldehydes, we decided to study the nature of the interactions between several of these compounds and filter paper.

The absorption spectra of aromatic ketones are characterized by two types of electronic transitions: (i) a weak $^1(n, \pi^*)$ absorption band, (ii) a high-intensity $^1(\pi, \pi^*)$ absorption band. Polar solvents have stronger hydrogen bonding and dipole-dipole interactions with the $^1(n, \pi^*)$ ground-state than with the $^1(n, \pi^*)$ excited state. Therefore, the energy gap between the two states increases, producing a blue shift of this band. For the $^1(\pi, \pi^*)$ transitions, it has been suggested¹³ that the excited state is more polar than the ground-state. Therefore, the excited state is stabilized to a greater extent than the ground-state, and the $^1(\pi, \pi^*)$ transitions are red-shifted with increase in the polarity and hydrogen-bonding capability of the solvent.¹⁴

*Research supported by NIH-GM-11373-21.

†On leave from Institute of Chemistry, Tel-Aviv University, Tel-Aviv, Israel.

§Author to whom correspondence should be addressed.

These carbonyl compounds may be classified into three groups: (i) compounds which have a low-lying $^3(n, \pi^*)$ state in polar and non-polar solvents; (ii) ketones which have a low-lying $^3(n, \pi^*)$ state in non-polar solvents, but a low-lying $^3(\pi, \pi^*)$ state in polar media; (iii) ketones which have a low-lying $^3(\pi, \pi^*)$ state in all solvents. These characteristics affect the photochemical reactivity of aromatic carbonyls. Ketones with a low-lying $^3(n, \pi^*)$ state abstract hydrogen from the solvent in a highly efficient photochemical reaction. For a $^3(n, \pi^*)$ excited state, the carbonyl oxygen atom is electron-deficient, and the excitation energy is localized on the carbonyl group. On the other hand, ketones with low-lying $^3(\pi, \pi^*)$ states are less reactive in hydrogen-abstraction reactions, since the excitation energy is partially delocalized into the aromatic π -system.¹⁵

In singlet-excited aryl ketones having strong electron-donating groups, charge is transferred from the substituent to the carbonyl group, producing a charge-transfer excited state $^1(CT)$. These ketones belong to the highly polar D-Ar-A (D = donor, Ar = aryl, and A = acceptor) class of compounds, for which the characteristics of the absorption spectra are strongly dependent on the polarity of the solvent.¹⁴

As mentioned before, the nature of the lowest triplet state in some aromatic ketones is solvent-dependent. In non-polar solvents, such as cyclohexane, the lowest triplet has the $^3(n, \pi^*)$ configuration, and in polar solvents, such as alcohols, the lowest triplet has the $^3(\pi, \pi^*)$ or $^3(CT)$ configuration. In this work, we determined the configuration of the lowest triplet (and for PABP and MK, also the lowest singlet) of aromatic ketones adsorbed on filter paper. This gave a closer insight into the nature of the interactions between the paper substrate and the analyte in solid-surface luminescence.

EXPERIMENTAL

The instrumental system and experimental conditions, except for those detailed below, have already been described.¹⁶

Measurements in solvent matrices at liquid-nitrogen temperature were performed with the Perkin-Elmer LS-5 luminescence spectrometer equipped with the low-temperature luminescence accessory. Ultraviolet absorption spectra were obtained with a Hewlett-Packard 8450A diode-array spectrophotometer. Reflectance spectra were obtained with a Perkin-Elmer Lambda-3B spectrophotometer equipped with an integrating sphere attachment. Spectra were plotted with a Hewlett-Packard 7470A plotter.

Materials

All aromatic ketones used in the study were of analytical grade (Fluka) and recrystallized several times from ethanol (used as received). Whatman No. 1 filter paper was used for all solid-surface measurements.

RESULTS AND DISCUSSION

Acetophenone and benzophenone

Acetophenone (AP) and benzophenone (BP) are often used as triplet sensitizers because of their

high-efficiency triplet yields (quantum yield of intersystem crossing, $\Phi_{isc} \cong 1$). In addition, the phosphorescence quantum yields of AP and BP are also relatively high ($\Phi_p > 0.7$). It has been found¹⁷ that in an ethanolic glass both AP and BP phosphoresce in the $^3(n, \pi^*)$ triplet state. The phosphorescence lifetimes originating from the $^3(n, \pi^*)$ state at 77 K are usually in the msec range, whereas the phosphorescence lifetimes from the $^3(\pi, \pi^*)$ state are 10–1000 times as long. Hence the phosphorescence lifetime of the analyte adsorbed on filter paper should indicate the electronic configuration of the emitting triplet.

Phosphorescence is sometimes observed from the $^3(n, \pi^*)$ state, in fluid solutions at room temperature. On the other hand, phosphorescence from the $^3(\pi, \pi^*)$ state is rarely observed¹⁸ unless special care is taken to exclude oxygen and other triplet quenchers. It is also possible to observe phosphorescence originating from a $^3(\pi, \pi^*)$ state in the presence of heavy atoms and surfactants.¹⁹

Thus, AP and BP should be ideal compounds for room-temperature phosphorimetry. However, we have found¹² that aromatic ketones having a low-lying $^3(n, \pi^*)$ state generally give very poor RTP signals. For example, using a spectrofluorimeter equipped with a mechanical chopper, we were unable to distinguish an RTP signal from the background emission for BP and AP, even when relatively concentrated ketone solutions were used. The reason for this is probably not only the intrinsically short phosphorescence lifetime of the $^3(n, \pi^*)$ state, but also the non-rigid nature of the molecule in this state compared to that of molecules in a $^3(\pi, \pi^*)$ state.

The spectrofluorimeter used in this study was the Perkin-Elmer LS-5, which is equipped with a flash-lamp and an electronic gating system which allow use of short delay times, such as 0.05 msec.¹⁶ To obtain high ratio of analyte-to-background phosphorescence, very short delay times (0.05–0.1 msec) and short gate times (0.3–1 msec) were chosen. However, even under those fairly optimal conditions, relatively concentrated AP (6.25 mg/ml at room temperature, and 0.625 mg/ml at 208 K) and BP (240 μ g/ml at room temperature, and 24 μ g/ml at 208 K) solutions were needed. Furthermore, to obtain phosphorescence signals with good signal-to-noise ratios from AP and BP adsorbed on Whatman No. 1 filter paper, the phosphorescence spectra and lifetimes were measured¹⁶ at 208 K (Figs. 1 and 2).

In Table 1, the phosphorescence lifetimes of AP and BP in various matrices are given. The phosphorescence lifetime of BP adsorbed on filter paper is about one order of magnitude smaller than in solvent glasses. This is expected because of the difference in the temperature at which the measurements were performed. Similarly the phosphorescence lifetime of AP adsorbed on filter paper is one order of magnitude smaller than its lifetime in EPA (5:5:2 v/v diethyl ether:isopentane:ethanol). We may thus con-

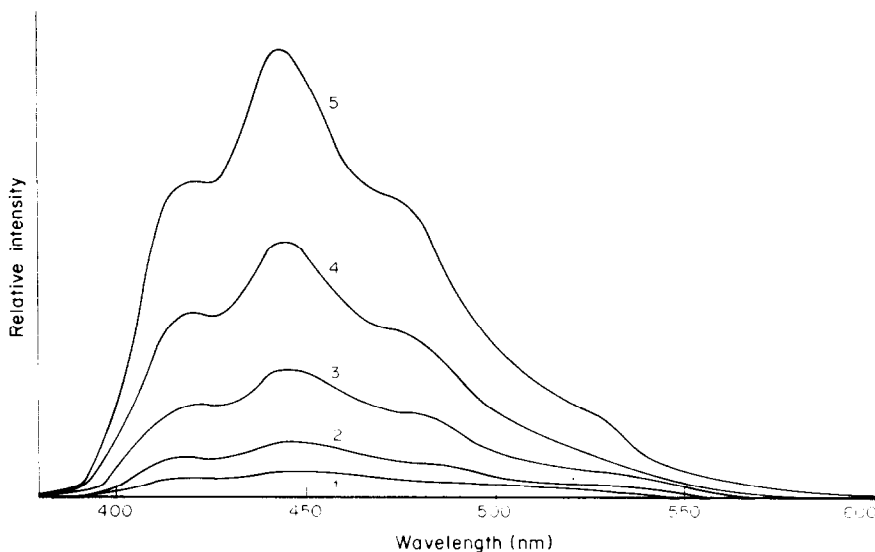


Fig. 1. Emission spectra of benzophenone adsorbed on Whatman No. 1 filter paper at various temperatures: 1, 20°C; 2, 0°C; 3, -20°C; 4, -40°C; 5, -65°C. The spectra demonstrate the relative intensities at the various temperatures.

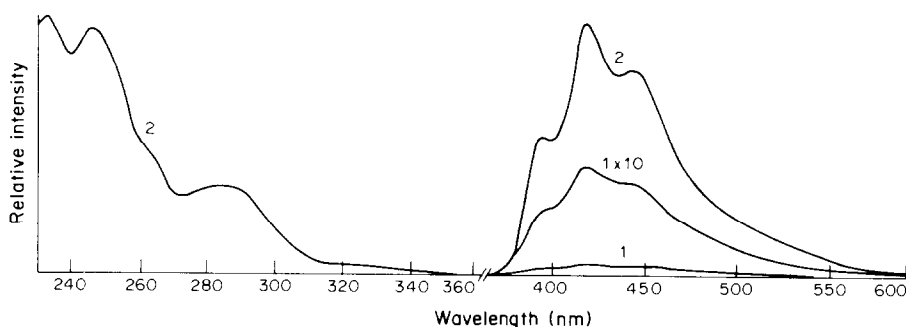


Fig. 2. Excitation and emission spectra of acetophenone adsorbed on Whatman No. 1 filter paper: 1, emission spectra at 25°C; 2, excitation and emission at -65°C. The spectra show the relative intensities.

clude that, when adsorbed on filter paper both AP and BP phosphoresce in the $^3(n, \pi^*)$ state, as in alcohol glasses, in contrast to the situation in acidic ethanol glass and methylcyclohexane-silica gel glass. It has been found^{13,20} that in these glasses the AP phosphorescence lifetime is considerably longer, indicating that the lowest triplet is the $^3(\pi, \pi^*)$ state.

The phosphorescence spectra of AP and BP adsorbed on filter paper are relatively structured, especially at 208 K, compared to those in acidic ethanol

glass (Figs. 1 and 2). The vibrational patterns which correspond to the carbonyl vibrational levels in the ground state are easily observed; such vibrational patterns are typical for phosphorescence emitted from a $^3(n, \pi^*)$ state.¹⁵

p-Aminobenzophenone

It has been suggested²⁰ that for acetophenone in ethanol solution the energy gap between T_1 $^3(n, \pi^*)$ and T_2 $^3(\pi, \pi^*)$ becomes rather small. Hence, if the

Table 1. Phosphorescence lifetimes of acetophenone and benzophenone in various matrices

Compound	Solvent/Substrate	Temperature, K	τ_p , msec
Acetophenone	EPA	77	8 ^a
Acetophenone	MCH + silica gel	77	550 ^a
Acetophenone	EtOH + HCl	77	350 ^a
Acetophenone	Whatman No. 1	208	0.8 ± 0.04 ^c
Benzophenone	Cyclohexane	77	5.1 ^b
Benzophenone	iPrOH	77	5.4 ^b
Benzophenone	Whatman No. 1	208	0.5 ± 0.05 ^c

^aData taken from Lamola.²⁰

^bData taken from Porter and Suppan.²¹

^cMeasured with Obey-Decay program.

energy of the $^3(\pi, \pi^*)$ state is lowered, the relative order of these two triplet states might be reversed. This might be achieved by substituting an electron-donating group, *e.g.*, an amino or dimethylamino group, *para* to the carbonyl group.¹⁴ Several researchers²²⁻²⁴ have postulated that this is the situation for *p*-aminobenzophenone (PABP); the low-lying triplet state in a polar protic solvent, such as 2-propanol or ethanol, is the $^3(\text{CT})$ state, and the low-lying triplet state in non-polar solvents, such as cyclohexane, is the $^3(n, \pi^*)$ state. Moreover, PABP is a D-Ar-A compound and its spectral emission properties change considerably with the polarity and hydrogen-bonding capability of the solvent or the substrate.²⁴⁻²⁶

From the data given in Table 2, it is clear that there are hydrogen-bonding interactions between the filter paper and PABP. Thus, the reflectance spectrum and the RTP excitation spectrum of PABP adsorbed on filter paper are very similar to the ultraviolet absorption spectrum of PABP in ethanol at room temperature. These absorption bands are considerably red-shifted compared to the corresponding bands in ether and cyclohexane solutions, indicating that the first excited singlet of PABP adsorbed on filter paper is the $^1(\text{CT})$ state. The phosphorescence emission spectrum of PABP in ethanol glass at 77 K is also similar to that of PABP on filter paper at room temperature, and in both spectra the emission peak is red-shifted compared to the emission bands in diethyl ether and cyclohexane medium.

Table 2. Spectroscopic data for *p*-aminobenzophenone

Solvent	Absorption	Phosphorescence	
	$\lambda_{\text{max}}, \text{nm}$	$\lambda_{\text{ex}}, \text{nm}$	$\lambda_{\text{em}}, \text{nm}$
Cyclohexane	303 ^b	— ^c	425 ^b
Ether	238, 317 ^d	— ^c	454, 484 ^e
Ethanol	244, 335 ^d	253, 354 ^d	484 ^d
Whatman No. 1	248, 336 ^{d,f}	248, 336 ^d	485 ^d

^aMeasured at room temperature.

^bData taken from Porter and Suppan.²¹

^cData taken from Porter and Suppan²¹ or Davidson and Sauthanam.²⁴

^dThis work.

^eData from Davidson and Sauthanam.²⁴

^fReflectance spectrum.

The phosphorescence excitation spectrum in ethanol at 77 K is red-shifted compared to the room-temperature excitation spectrum of PABP adsorbed on Whatman No. 1 filter paper. This is a rather rare situation, since usually^{2,6} the RTP spectra are red-shifted compared to those obtained at low temperature. This red-shift may be attributed to the enhanced hydrogen-bonding and dipole-dipole interactions at low temperatures.^{14,22,27}

The RTP spectrum of PABP does not exhibit vibrational structure, and in this sense is very similar to the phosphorescence spectrum of PABP in ethanol glass at 77 K. On the other hand, the phosphorescence spectrum of PABP in the aprotic ether glass is relatively structured.²⁴ All these observations indicate that there are strong hydrogen-bonding interactions between the paper and the adsorbed PABP molecules.

The phosphorescence lifetime of PABP at 298 K (Table 3) is about 40 times that at 208 K of benzophenone adsorbed on filter paper. In our opinion, this indicates that the RTP must originate from a $^3(\text{CT})$ triplet state rather than from a $^3(n, \pi^*)$ state. We have found that at room temperature PABP phosphoresces rather poorly. These results indicate that in ethanol solutions at room temperature the PABP triplet is not highly populated.^{22,23} In ethanol glass, PABP phosphoresces with relatively low efficiency, whereas in cyclohexane solution at room temperature the PABP triplet is quite efficiently formed ($\Phi_{\text{isc}} = 0.3$).²³

Michler's ketone

The photophysical and photochemical properties of Michler's ketone [4,4'-bis(dimethylaminobenzophenone)] (MK) have been very extensively studied.^{21,22,27-34} MK is widely used as a triplet sensitizer in many photochemical reactions, owing to its high triplet yield. However, like PABP, its photoreactivity and photophysical properties are strongly solvent-dependent.^{22,28} In non-polar solvents, *e.g.*, cyclohexane, MK is very photoreactive, and the quantum yield of intersystem crossing is very high ($\Phi_{\text{isc}} = 0.91$). On the other hand, in ethanol solutions, MK is unreactive and the quantum efficiency of triplet formation is very low ($\Phi_{\text{isc}} = 0.08$). This has been attributed^{22,28} to the fact that in non-polar

Table 3. Phosphorescence lifetimes of PABP and MK on Whatman No. 1 filter paper

Compound	Temperature, °C	$\lambda_{\text{ex}}, \text{nm}$	$\lambda_{\text{em}}, \text{nm}$	τ_p, msec
PABP	25	340	485	19.4 ± 0.9
PABP	25	340	485	2.14 ^b ± 0.15
MK	25	390	465	8.2 ± 0.26
MK	25	390	465	1.84 ^b ± 0.04
MK	-65	390	510	36.5 ± 3.6

^aMeasured on at least 4 different samples by using Obey-Decay program (correlation coefficient ≥ 0.99).

^bThe short lifetimes were obtained while using delay times shorter than 1 msec.

Table 4. Spectral properties^a of MR in various matrices at different temperatures

Solvent/Substrate	Absorption		Phosphorescence	
	λ_{max}, nm	λ_{ex}, nm	λ_{em}, nm	τ_p, sec
Hydrocarbon (303 K)	330 ^b	330 ^b 354 ^b	433, 462 ^b 440, 470 ^b	
Methyl THF (303 K)	345 ^c	370 ^c 400 ^c	455 ^c 471 ^c	0.09 ^c 0.55 ^c
Diethyl ether (303 K)	242, 338 ^d	390 ^d	475, 504 ^d	0.2 ^c , 0.14 ^b
Ethanol (303 K)	245, 366, (388 at 95 K) ^b	420 ^d	500, 520sh ^d	0.4 ^c , 0.28 ^b
Whatman No. 1 (303 K)	249, 372 ^{d,e}	392 ^d 410 ^d	465 ^d 467 ^d	
Whatman No. 1 (208 K)		390 ^d 410 ^d	510 ^d 520 ^d	
Whatman No. 1 (77 K) ^{d,f}		380 ^{d,f} 420 ^{d,f}	505 ^{d,f} 515 ^{d,f}	

^aThe underlined wavelengths indicate peak maxima.

^bData from Groenen and Koelman.^{33,34}

^cData from Klopffer.³¹

^dThis work.

^eReflectance spectrum.

^fObtained with Perkin-Elmer MBF-44B spectrophotofluorimeter.

solvents the reactive $^3(n, \pi^*)$ is the lowest triplet state, whereas in polar protic solvents the unreactive $^3(CT)$ is the low-lying triplet state.

In addition, MK exhibits unique photophysical features in solvent glasses at 77 K,^{27,31-34} namely, the phosphorescence emission spectra and decay times depend on the wavelength of excitation. These rather peculiar characteristics encouraged us to study the photophysical properties of MK adsorbed on Whatman No. 1 filter paper.

Spectral properties. MK shows a very intense long-lived luminescence at room temperature when adsorbed on Whatman No. 1 filter paper and the

detection limit is 3 ng/ml (absolute limit 3 pg, linear dynamic range >3 orders of magnitude).

Table 4 reveals that the absorption maxima of MK adsorbed on filter paper occur at longer wavelengths than for MK in other media, indicating that MK has strong hydrogen-bonding interactions with paper at room temperature. The phosphorescence excitation spectra of MK on paper at room temperature and in ethanol glass at 77 K are similar, and are red-shifted compared to the spectra in aprotic glasses. The emission spectra of MK in ethanol glass and on paper at 303, 208 and 77 K (Figs. 3-6) are also similar, and structureless, in contrast to the structured spectra of

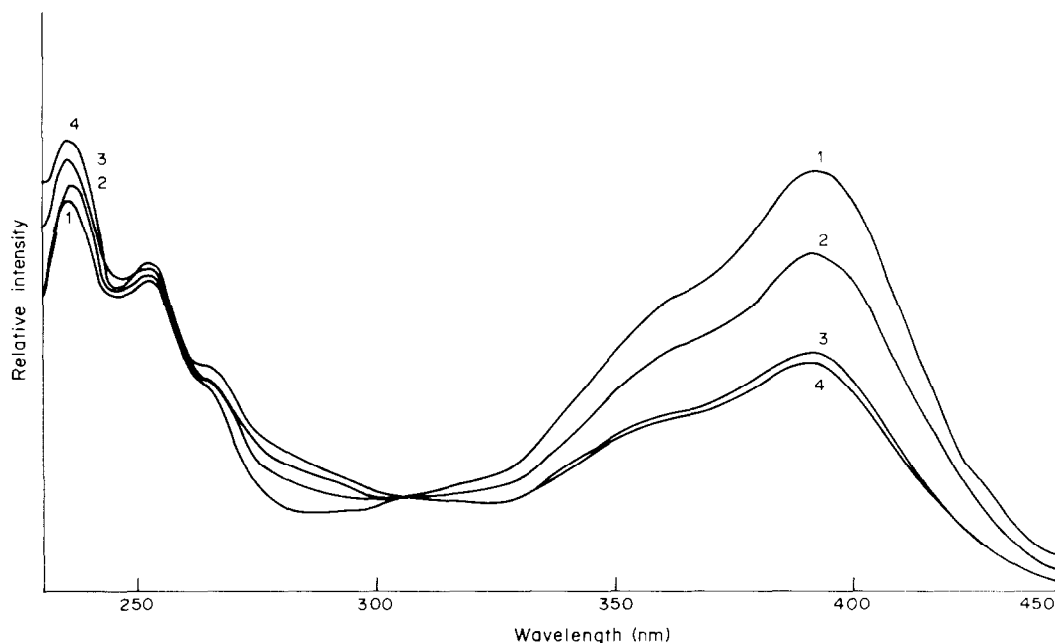


Fig. 3. Excitation spectra of MK adsorbed on Whatman No. 1 filter paper, measured at various temperatures: 1, 25°C; 2, -12°C; 3, -50°C; 4, -65°C. The spectra show that upon cooling, the peak at 392 nm decreases while the peak at 235 nm increases.

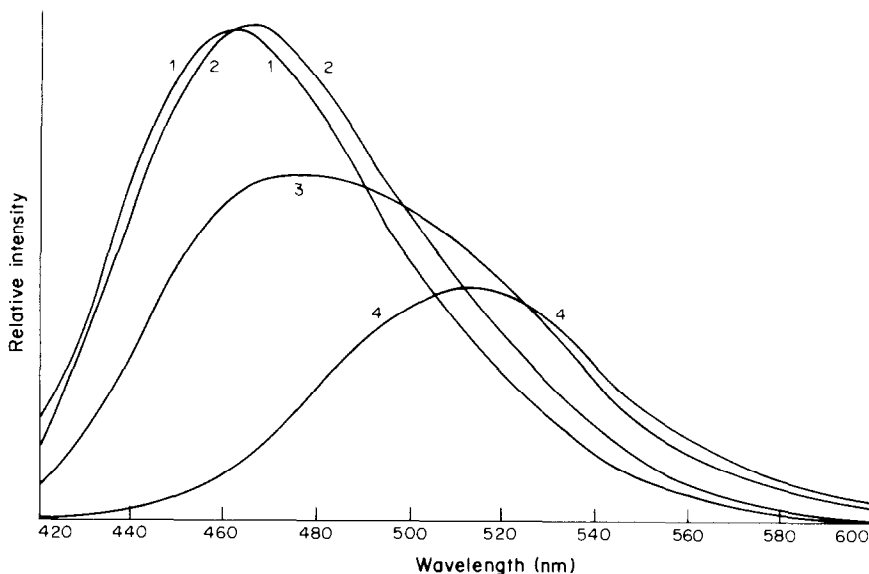


Fig. 4. The effect of lowering the temperature for MK adsorbed on Whatman No. 1 filter paper, emission spectra: 1, 71°C; 2, 36°C; 3, -9°C, 4, -65°C.

MK in alkane glass.³⁴ Moreover, in hydrocarbon glass, where its lowest excited singlet is the $^1(n, \pi^*)$ state, MK gives no fluorescence. On the other hand, MK in ethanol glass and on filter paper at 77 K exhibits both fluorescence and phosphorescence. These observations indicate that the lowest excited singlet of MK adsorbed on filter paper, as in ethanol glass, is the $^1(\text{CT})$ state. Interestingly the phosphorescence excitation peak of MK on filter paper at room temperature is red-shifted compared to the peak obtained in the reflectance spectrum (Table 4). This is in contrast to our observations for PABP (Table 2), in which the reflectance spectrum and the phosphorescence excitation spectrum are identical.

Temperature effects. Unlike the case for MK in solvent glasses at 77 K,^{20,31,34} and in ethanol solutions at room temperature,^{33,34} the emission spectrum of MK on filter paper at room temperature does not change when the excitation wavelength is varied, though the emission peak shifts slightly with change in excitation wavelength at 208 and 77 K (Table 4). However, a dramatic change in the phosphorescence spectra of MK on filter paper is observed on lowering the temperature (Figs. 3 and 4). When our Dewar sample-holder (described in detail elsewhere¹⁶) was used two major changes occurred: (i) the phosphorescence emission peak moved toward longer wavelengths; (ii) the intensity decreased considerably

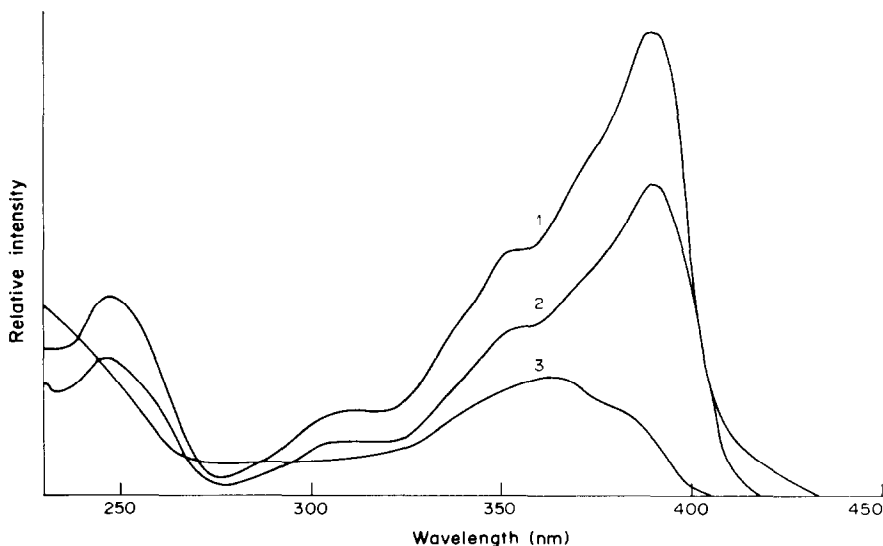


Fig. 5. Excitation spectra of MK in ethanolic glass at 80 K: 1—scanned with λ_{em} set at 475 nm (peak—389 nm); 2—scanned with λ_{em} set at 540 nm (peak—390 nm); 3—scanned with λ_{em} set at 450 nm (peak—363 nm).

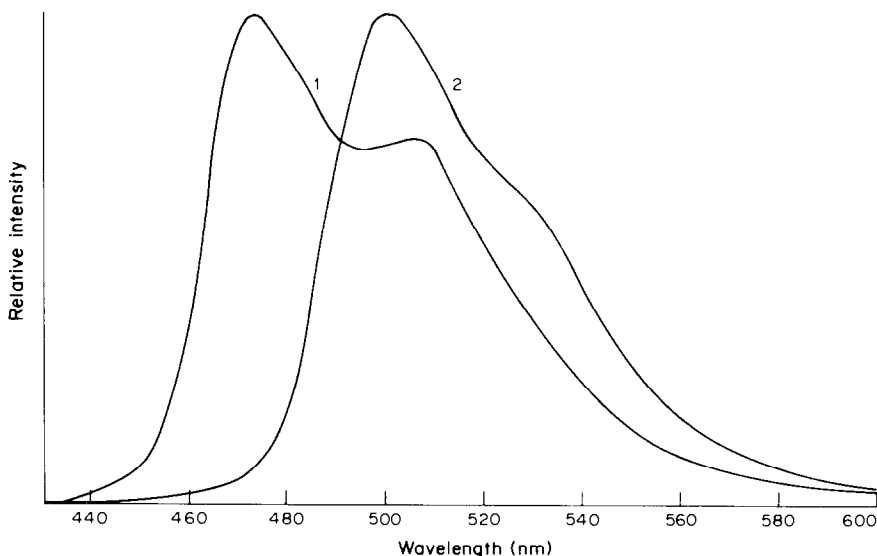


Fig. 6. Emission spectra of MK in ethanolic glass at 80 K: 1—excitation at 390 nm (peaks—475 and 504 nm); 2—excitation at 420 nm (peak—500 nm). The intensity of spectrum 1 is 20 times that of spectrum 2. On excitation at 420 nm conformer B dominates the emission spectra.³⁴

as the peak shifted to the red. Usually, lowering the temperature induces a blue-shift^{2,6,16} of the phosphorescence excitation spectrum and especially of the emission spectrum. This trend is indeed observed for most of the compounds shown in Tables 5 and 6. On the other hand, for MK only, the excitation peak is blue-shifted, but the emission peak is considerably red-shifted. This red-shift cannot be attributed to the change in background emission, since the phosphorescence of Whatman No. 1 filter paper is blue-

shifted on cooling (Table 5). In addition, it was found that when the temperature is lowered, the intensity of the excitation peak at 392 nm decreases but the intensity at 235 nm increases (Fig. 3). Here, the enhancement in the short wavelength region is due to the enhanced background emission which occurs on cooling the filter paper.

Two main explanations have been given for the dependence of the MK emission spectra on the excitation wavelength (Figs. 5 and 6). (i) There are

Table 5. Spectral properties of MK on Whatman No. 1 filter paper at various temperatures

Sample	Temperature, °C	Phosphorescence (relative intensity)	
		λ_{ex}, nm	λ_{em}, nm
MK	70	235,393	462 (100)
MK	25	234,392	465 (103)
MK	-65	234,390	515 (50)
Whatman No. 1	70	237,255	501
Whatman No. 1	25	237,255	480
Whatman No. 1	-65	237,252	450

Table 6. Spectral properties of aromatic carbonyls adsorbed on Whatman No. 1 filter paper at room temperature and at low temperature (-65°C)

Compound	RTP		LTP		$\frac{I_{LTP}}{I_{RTP}}$	Type of triplet, T_1
	λ_{em}, nm	λ_{em}, nm	λ_{ex}, nm	λ_{em}, nm		
Acetophenone	<u>247</u> , 260sh	400sh, <u>418</u> , 440sh	<u>247</u> , 287	394, <u>418</u> , 443	20	n, π^*
Benzophenone	<u>265</u>	425sh, <u>447</u> , 470sh	<u>265</u>	417, <u>445</u> , 470sh	20	n, π^*
MK	<u>392</u>	<u>465</u>	<u>390</u>	<u>510</u>	0.5	π, π^* (CT)
PAAP ^b	<u>320</u>	<u>472</u>	<u>320</u>	<u>470</u>	1.2	π, π^* (CT)
6-Chrysenecarboxylic ^c acid	<u>278</u>	<u>525</u> , 558sh	<u>278</u>	<u>522</u> , 558sh	1.3	π, π^* (CT)

^aThe underlined wavelengths were used for excitation or emission.

^bData from Scharf and Winefordner.³⁹

^cData from Scharf *et al.*¹⁶

^dCT = charge-transfer.

several species of MK molecules in discrete solvent micro-environments. In solid glasses, MK can exhibit single or multiple hydrogen bonds or none at all, each species displaying different spectral characteristics.²⁷ (ii) There are two MK conformers, A and B, which have slightly different excitation and emission spectra.^{33,34} If hydrogen bonding is the reason for the variations, at various temperatures, in the spectral features of MK adsorbed on filter paper, then since hydrogen-bonding interactions are stronger at lower temperatures^{14,27} the spectrum of highly hydrogen-bonded MK molecules should be red-shifted,²⁷ and have relatively low phosphorescence yields because of the smaller intersystem crossing rate of this species.²² On the other hand, we can also relate these observations to the formation of another MK conformer which has a relatively low phosphorescence efficiency. Thus, at room temperature, conformer A, which is highly phosphorescent, predominates in the phosphorescence spectra. Upon cooling, conformer B, which phosphoresces rather poorly at longer wavelengths, becomes the favoured conformer (Fig. 6). This also explains why the phosphorescence of MK changes only slightly at temperatures above 298 K (Fig. 4), since conformer A is already dominant at room temperature. A further possible explanation for the changes occurring on cooling MK samples on filter paper is that the long-lived luminescence observed at room temperature is composed of both *E*-type delayed fluorescence and phosphorescence. The *E*-type delayed fluorescence, which arises by thermal repopulation of the singlet excited state from the triplet,⁶ eventually decreases on cooling.

E-type delayed fluorescence has been observed at room temperature for several organic compounds adsorbed on filter paper.^{11,35,36} In these compounds, the energy gap between S_1 and T_1 is usually smaller than 10 kcal/mole.^{35,36} The energy gap for MK in ethanol glass at 77 K is 6.9–8.9 kcal/mole (the energy gap changes with the excitation wavelength). This gap is probably smaller at room temperature, since the fluorescence in ethanol at room temperature occurs at 450 nm, compared to 410 nm ($\lambda_{\text{ex}} = 390$ nm) at 77 K. This might also be the reason why separated peaks for the fluorescence and phosphorescence were not observed for MK on filter paper at room temperature.

Similarly, *E*-type delayed fluorescence and phosphorescence have been observed for benzophenone (BP) in fluid solutions,³⁷ and in polymer matrices³⁸ at room temperature. Like that of BP³⁸ the intensity of the delayed fluorescence of MK does not increase when the paper is heated from 298 to 343 K (Fig. 4 and Table 5).

Phosphorescence lifetimes. In Tables 3 and 4, the phosphorescence lifetimes of MK in various matrices at different temperatures are given. The RTP lifetime of MK is rather short compared to the lifetimes measured in solvent glasses at 77 K. However, the phosphorescence lifetime increases considerably (by a

factor of 4) on cooling to 208 K. This rather large difference^{16,39} in MK phosphorescence lifetimes at room temperature and at 208 K might indicate that these lifetimes correspond to two different species.

Nakagaki *et al.*²⁶ found that in compounds having D–Ar–A structure, increasing the electron-donating capability of the donor group increases the spin–orbit coupling in the molecule, and decreases the singlet–triplet splitting. Therefore, the phosphorescence lifetimes of these molecules become shorter. This might explain why the RTP lifetime of MK is shorter than the lifetime of PABP. In addition, the lifetime of MK at 208 K is about two orders of magnitude longer than the lifetime of benzophenone at the same temperature. This indicates that for these conditions, MK phosphoresces in a $^3(\text{CT})$ state rather than a $^3(n, \pi^*)$ state.

CONCLUDING REMARKS

Temperature effects

We have shown that in several cases the phosphorescence intensity increases quite strongly when the temperature is lowered. On the other hand, the phosphorescence intensity of MK decreases when the temperature is lowered. These observations indicate that changing the temperature can extend the versatility and selectivity of analytical solid-surface luminescence. Moreover, from the data given in Table 6, it can be deduced that lowering the temperature increases the phosphorescence intensity of ketones emitting in a $^3(n, \pi^*)$ triplet state. On the other hand, for analytes which phosphoresce in the $^3(\pi, \pi^*)$ triplet state, lowering the temperature affects the phosphorescence intensity only slightly.¹⁶ This also demonstrates the non-rigid nature of molecules in the $^3(n, \pi^*)$ state.

The changes in luminescence observed on cooling MK on filter paper are rather interesting, and may be interpreted by each of the mechanisms described. However, to differentiate between the various pathways more experiments are required. We intend to continue studies on the temperature-dependence of other compounds related to MK.

The nature of the emitting triplet

We have found¹² that aromatic ketones emitting in a $^3(n, \pi^*)$ triplet state do not exhibit appreciable RTP. On the other hand, aromatic ketones and aldehydes with low-lying $^3(\pi, \pi^*)$ or $^3(\text{CT})$ triplet states usually phosphoresce significantly at room temperature. Thus, when the RTP of a mixture of BP and MK was measured, only the phosphorescence of MK was observed, even in the presence of very high concentrations of BP, whereas in ethanolic glass at 77 K, both MK and BP phosphoresced. Interestingly, it was mentioned by Suppan²⁹ that commercial MK usually contains BP, which interferes with the photochemical and photochemical processes of the MK.

Hydrogen-bonding between the paper and the phosphor

We have shown that aromatic ketones are strongly hydrogen-bonded to the paper substrate. These interactions cause the phosphor to be rigidly held on the paper, thus minimizing radiationless deactivation of the triplet state.^{2,6} Moreover, we have also found that the hydrogen-bonding and dipole-dipole interactions between the paper and the phosphor control the nature of the excited singlet and the emitting triplet of the adsorbed phosphor.

Analytical aspects

We have demonstrated that RTP is a technique well suited to determination of aromatic ketones bearing electron-donating groups. A very low limit of detection (LOD) was obtained for MK adsorbed on Whatman No. 1 filter paper (3 ng/ml); which may be compared with the LOD of 20 ng/ml obtained for *p*-aminoacetophenone adsorbed on filter paper.³⁹

It seems that the quantum efficiency of triplet formation for MK adsorbed on filter paper is much higher than that in alcohol solution at room temperature.²² It will thus be interesting to evaluate the phosphorescence quantum efficiency of MK adsorbed on filter paper at room temperature.

REFERENCES

1. T. Vo-Dinh and J. D. Winefordner, *Appl. Spectrosc. Rev.*, 1977, **13**, 264.
2. R. T. Parker, R. S. Freedlander and R. B. Dunlap, *Anal. Chim. Acta*, 1980, **119**, 189.
3. *Idem, ibid.*, 1980, **120**, 1.
4. J. J. Aaron and J. D. Winefordner, *Anal. Chim. Acta*, 1982, **10**, 299.
5. R. J. Hurtubise, *Solid Surface Luminescence Analysis: Theory, Instrumentation, Applications*, Chapters 5 and 7. Dekker, New York, 1981.
6. T. Vo-Dinh, *Room Temperature Phosphorimetry for Chemical Analysis*, Wiley, New York, 1984.
7. E. M. Schulman and C. Walling, *J. Phys. Chem.*, 1973, **77**, 902.
8. S. L. Wellons, R. A. Paynter and J. D. Winefordner, *Spectrochim. Acta*, 1974, **30A**, 2133.
9. E. M. Schulman and R. T. Parker, *J. Phys. Chem.*, 1977, **81**, 1932.
10. R. A. Dalterio and R. J. Hurtubise, *Anal. Chem.*, 1984, **56**, 336.
11. E. L. Y. Bower and J. D. Winefordner, *Anal. Chim. Acta*, 1978, **102**, 1.
12. G. Scharf and E. Zadok, unpublished results, Tel-Aviv University, Israel.
13. C. H. Nicholls and P. A. Leermakers, *Advan. Photochem.*, 1971, **8**, 315.
14. G. Yamaguchi, Y. Kakinoki and H. Tsubomura, *Bull. Chem. Soc. Japan*, 1967, **40**, 526.
15. N. J. Turro, *Modern Molecular Photochemistry*, p. 375. Benjamin/Cummings, Menlo Park, CA, 1978.
16. G. Scharf, B. W. Smith and J. D. Winefordner, *Anal. Chem.*, 1985, **57**, 1230.
17. R. S. Becker, *Theory and Interpretation of Fluorescence and Phosphorescence*, Chapter 12. Wiley-Interscience, New York, 1969.
18. G. Favaro and F. Masetti, *J. Photochem.*, 1981, **15**, 241.
19. L. J. Cline-Love and M. Skrielec, *Anal. Chem.*, 1981, **53**, 2103.
20. A. A. Lamola, *J. Chem. Phys.*, 1967, **47**, 4810.
21. G. Porter and P. Suppan, *Trans. Faraday Soc.*, 1965, **61**, 1664.
22. D. I. Schuster, M. D. Goldstein and P. Bane, *J. Am. Chem. Soc.*, 1977, **99**, 187.
23. S. G. Cohen, M. D. Salzman and J. B. Guttenplan, *Tetrahedron. Lett.*, 1969, 4321.
24. R. S. Davidson and M. Santhanam, *Chem. Commun.*, 1971, 1114.
25. T. P. Carsey, G. L. Findley and S. P. McGlynn, *J. Am. Chem. Soc.*, 1979, **101**, 4502.
26. I. R. Nakagaki, S. Nagakura, T. Kobayashi and S. Iwata, *Bull. Chem. Soc. Japan*, 1978, **51**, 2867.
27. P. R. Callis and R. W. Wilson, *Chem. Phys. Lett.*, 1972, **13**, 417.
28. P. Suppan, *J. Chem. Soc. Faraday Trans. I*, 1975, **71**, 539.
29. R. N. Griffin, *Photochem. Photobiol.*, 1968, **7**, 159.
30. P. Suppan, *Spectrochim. Acta*, 1974, **30A**, 1939.
31. W. Klopffer, *Chem. Phys. Lett.*, 1971, **11**, 482.
32. W. Liptay, H. J. Schumann and F. Petzke, *ibid.*, 1976, **39**, 427.
33. E. J. J. Groenen and W. N. Koelman, *J. Chem. Soc. Faraday Trans. II*, 1979, **75**, 58.
34. *Idem, ibid.*, 1979, **75**, 69.
35. R. T. Parker, R. S. Freeland, E. M. Schulman and R. B. Dunlap, *Anal. Chem.*, 1979, **51**, 1921.
36. Y. Nishikawa, K. Hizaki, Y. Onoue, K. Nishikawa, Y. Yoshitake and T. Shigematsu, *Bunseki Kagaku*, 1983, **32**, E115.
37. R. E. Brown, L. A. Singer and J. H. Parks, *Chem. Phys. Lett.*, 1972, **14**, 193.
38. P. F. Jones and A. R. Calloway, *ibid.*, 1971, **10**, 438.
39. G. Scharf and J. D. Winefordner, *Spectrochim. Acta*, 1985, **41A**, 899.

Dedication—Dedicated to R. A. Chalmers.

STUDY OF pH AND SUBSTRATE EFFECTS ON ROOM-TEMPERATURE PHOSPHORIMETRY OF SOME INDOLECARBOXYLIC ACIDS*

MARTA ANDINO, J. J. AARON† and J. D. WINEFORDNER‡

Department of Chemistry, University of Florida, Gainesville, FL 32611, U.S.A.

(Received 5 March 1985. Accepted 31 July 1985)

Summary—Room-temperature phosphorescence (RTP) of eight indolecarboxylic acids has been investigated under different pH conditions, and on several ion-exchange filter papers. RTP excitation and emission wavelengths do not change significantly with pH. The largest RTP signals are obtained from neutral solutions adsorbed on DE-81 anion-exchange filter paper, while alkaline (pH ~ 13) solutions on S & S 903 filter paper treated with DTPA (diethylenetriaminepenta-acetic acid) give stronger signals than neutral or acidic (pH ~ 1.6) solutions on the same substrate. The existence of several hydrogen-bonding interactions between the various ionic indolecarboxylic acid species and the substrates is discussed. Heavy-atom enhancement factors ranging between 4 and 550, according to the compound, are obtained with iodide. Absolute limits of detection between 100 and 500 pg demonstrate the usefulness of RTP for determination of indolecarboxylic acids at the trace level.

The use of room-temperature phosphorimetry (RTP) as an analytical technique has received considerable attention in the past few years, as is shown by several reviews of the field.¹⁻⁷ Recently, Su and Winefordner,⁸ and Aaron *et al.*,⁹ found that anion-exchange filter papers, such as Whatman DE-81, gave the lowest luminescence background and the largest analyte RTP signals in the presence of heavy atoms such as iodine (as I⁻) and thallium (as Tl⁺); also, RTP had the advantage of significantly decreasing the limits of detection for a variety of organic compounds, including pesticides, aromatic hydrocarbons and indoles.^{8,9} Other solid substrates, such as silica gel,^{3-6,10} sodium acetate^{3,4} and polyacrylic acid-alkali-metal halide mixtures¹⁰⁻¹² have been tested for RTP. The influence of external heavy atoms on RTP has also been investigated by many authors.^{4,9,13}

Surprisingly, relatively little work has been reported until now on the effect of pH on RTP,^{10,14-16} although change in pH obviously determines the nature of many species, and the ways in which they can interact with the solid substrate on which they are adsorbed. Therefore, pH-related studies are very important in the understanding of the type of interactions responsible for the occurrence of RTP. Several authors have suggested that hydrogen-bonding of organic ionic molecules to the substrate increases the rigidity and, consequently, the RTP intensity of analytes adsorbed on filter paper, sodium acetate, or silica gel containing a polyacrylate

binder.^{2,6,17,18} Ramasamy and Hurtubise¹⁰ found that 0.1M hydrobromic and 0.1M hydrochloric acid made the RTP signal of most nitrogen heterocyclics and aromatic amines adsorbed on filter paper and silica gel chromatoplates much stronger than that obtained in neutral media, and alkaline solutions gave relatively weak RTP intensity in most cases. Hurtubise and Smith¹⁵ investigated the pH effect on the RTP of several aromatic carboxylic acids adsorbed on silica gel and polyacrylic acid-sodium chloride mixture. They found that terephthalic acid and coumarin-3-carboxylic acid, adsorbed on silica gel chromatoplates containing a polyacrylate salt, yielded stronger RTP signals when sorbed from hydrochloric acid than from neutral solutions and concluded that interactions between the undissociated form of the aromatic carboxylic acid and the polyacrylate were responsible for inducing the phosphorescence; hydrogen-bonding would be the main but not the only interaction in RTP.¹⁵ Reflectance and infrared spectroscopy of benzo(*f*)quinoline and quinoline adsorbed on filter paper, silica gel and polyacrylic acid-sodium chloride mixtures confirmed the existence of several hydrogen-bonding interactions of positively charged and neutral forms of these heterocycles with the different solid substrates, depending on the pH of the test solution.¹⁴

In the present study we have evaluated the pH effect on the room-temperature phosphorescence of several indolecarboxylic acids. The possible mechanisms of interaction of indolecarboxylic acids with different ion-exchange filter papers have been investigated. In addition, we have determined the RTP analytical figures of merit of these compounds by using Whatman DE-81 anion-exchange filter paper, in optimal pH and heavy-atom conditions.

*Research supported by NIH-5R01-GM11373-22.

†Present address: Departement de Chimie, Faculté des Sciences, Université de Dakar, Senegal, West Africa.

‡Author to whom correspondence should be addressed.

EXPERIMENTAL

Apparatus

All RTP spectra and intensity measurements were performed with an Aminco-Bowman spectrophotofluorometer (American Instrument Co., Silver Spring, MD, U.S.A.), fitted with an Aminco 150-W Xenon arc lamp, a potted Hamamatsu 1P21 photomultiplier tube (Hamamatsu Corp., Middlesex, NJ, U.S.A.), an MFE Plotmatic FIS X-Y recorder (MFE Corp., Salem, NJ, U.S.A.), and a laboratory-constructed phosphoroscope for use with the multiple sampling bar system.¹⁹ During all RTP measurements, the sample compartments were flushed with dry nitrogen.

Reagents

3-Indoleacetic acid, 3-indolebutyric acid, 2-indolecarboxylic acid, 5-indolecarboxylic acid, DL- β -3-indolelactic acid, 3-indoleacrylic acid, 3-indolepyruvic acid monohydrate, and 3-indoxyl acetate were purchased from Aldrich Co. (Milwaukee, WI, U.S.A.) and used as received. Diethylenetriaminepenta-acetic acid (DTPA) was obtained from Sigma Chemical Co. (St Louis, MO, U.S.A.). Potassium iodide (Fisher Scientific, Fairlawn, NJ, U.S.A.) was utilized in the heavy-atom studies. The solvents used were absolute ethanol (Florida Distillers Co., Lake Alfred, FL, U.S.A.) and "nanopure" demineralized water (Barnstead System, Sybron Co.). The filter papers used were DE-81 (Whatman Chemical Separation Inc., Clifton, NJ, U.S.A.), DTPA-treated S & S 903 (prepared as described by Bateh and Winefordner²⁰), and cation-exchange CM-23 carboxymethylcellulose resin (Whatman Chemical Separation Inc.) on S & S 903 as support.

Procedure

Portions (2 μ l) of sample solution (or solvent) and of 1M potassium iodide solution were successively introduced by means of an SMI "micropetter" (Emeryville, CA, U.S.A.) onto the 0.25-in. diameter filter-paper discs, which were held in the multiple sampling bar. Immediately afterwards, the

sampling bar was inserted into the sample compartment of the spectrophotofluorometer, where the samples were allowed to dry for about 8 min under a flow of dry nitrogen. RTP measurements were then made. The solutions of the indolecarboxylic acids were prepared in neutral, basic and acidic solvents. Neutral solutions were made up with an ethanol-water (50:50 v/v) mixture; acidic solutions were made approximately 0.1M in hydrochloric acid (pH \sim 1.6); basic solutions were made approximately 0.5M in sodium hydroxide (pH \sim 13).

RESULTS AND DISCUSSION

RTP spectral properties

All the indolecarboxylic acids under study showed RTP spectra, when adsorbed on DE-81 filter paper in the presence of 1M potassium iodide, with the exception of 3-indoleacrylic acid, which gave no detectable phosphorescence signal at a concentration of 10^{-3} M. The RTP excitation and emission wavelength maxima are given in Table 1 for neutral, basic and acidic conditions.

It can be seen that the excitation and emission maxima do not change markedly with pH (Fig. 1), although a significant blue-shift is observed on going from pH 7 to pH 13 for 5-indolecarboxylic acid and indoxyl acetate. However, the change in the phosphorescence spectrum for the latter compound is probably due to hydrolysis in basic solution; indeed we noted a rapid colour change of the basic indoxyl acetate solution, from blue to pink-orange on agitation. The absence of pH-related shifts of the emission spectra of most of the indolecarboxylic acids is in agreement with the results of Aaron *et al.*,²¹ who

Table 1. Room-temperature phosphorescence spectral properties of indolecarboxylic acids*

Compound	pH conditions	$\lambda_{ex} \dagger, nm$	$\lambda_{em} \dagger, nm$
3-Indoleacetic acid	Neutral§	286	(429), <u>450</u>
	0.5M NaOH‡	288	450
3-Indolebutyric acid	Neutral	287	448
	0.5M NaOH	286	450
2-Indolecarboxylic acid	Neutral	299	(475), 490
	0.5M NaOH	299	(473), <u>489</u>
5-Indolecarboxylic acid**	0.1M HCl#	245, 272	452
	Neutral	245, <u>272</u>	453
	0.5M NaOH	243, <u>271</u>	439
DL-3-Indolelactic acid	Neutral	288	448
3-Indolepyruvic acid	Neutral	283	442
	0.5M NaOH	286	442
3-Indoxyl acetate	Neutral	266††	466††
	0.5M NaOH	323	434

*Concentrations about 10^{-3} M in 1M potassium iodide solution in ethanol-water (50:50 v/v). All RTP spectra were determined on DE-81 filter paper with the Aminco-Bowman spectrophotofluorometer, unless otherwise noted.

†Wavelengths of the main peaks are underlined (when there are several components); wavelengths of shoulders are given in parentheses; precision of wavelength value ± 1 nm.

§Ethanol-water (50:50 v/v) solvent.

‡Approximately pH 13.

Approximately pH 1.6.

**RTP spectra were determined on DTPA-treated S & S 903 filter paper, with an LS-5 Perkin-Elmer spectrophotofluorometer.

††RTP spectra were determined with an LS-5 Perkin-Elmer spectrophotofluorometer.

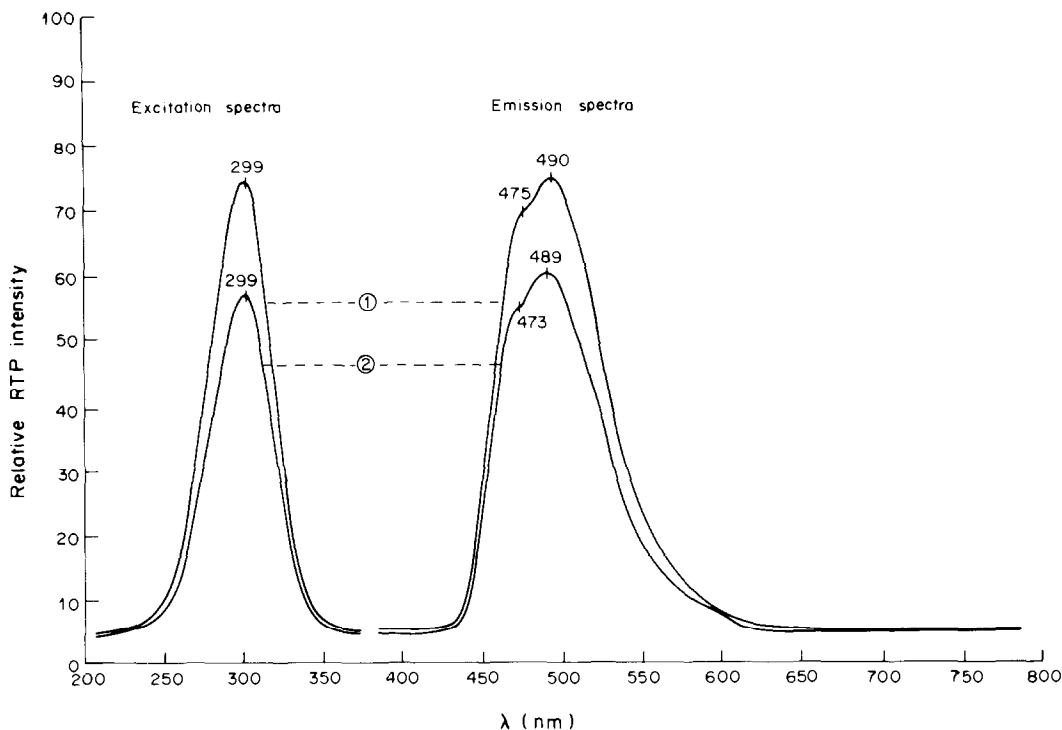


Fig. 1. Effect of pH on the RTP spectra of 2-indolecarboxylic acid ($10^{-3}M$) on DE-81 filter paper, in the presence of $1M$ KI. 1, Excitation and emission spectra of neutral water-ethanol (50:50 v/v) solution. 2, Excitation and emission spectra of basic ($0.5M$ NaOH) water-ethanol (50:50 v/v) solution.

found that the low-temperature phosphorescence (LTP) spectra of these compounds did not change significantly with pH. It is apparent that RTP and LTP emission bands occur at very similar wavelengths,²¹ although the RTP bands are broadened and show little vibrational fine structure compared to LTP spectra, as previously observed for several other compounds.^{9,22} However, our RTP results, obtained on filter paper, are in contrast to those of Hurtubise and Smith,¹⁵ who recently found that when adsorbed on aluminium-backed silica gel chromatoplates, 2-indolebutyric acid and 1-methylindole-2-carboxylic acid did not show any RTP signal, although 5-indolecarboxylic acid did. This difference in behaviour of the first two of these compounds, with the nature of the solid substrate used, seems to indicate that anion-exchange filter paper induces stronger phosphorescence signals than does silica gel in the case of indolecarboxylic acids.

pH and substrate effects on RTP intensity

The influence of pH and substrate on the RTP intensity of indolecarboxylic acids was investigated, with neutral, basic ($0.5M$ sodium hydroxide) and acidic ($0.1M$ hydrochloric acid) solutions adsorbed on DE-81, DTPA-treated S & S 903 filter papers and CM resin on paper support. In Table 2, we give the net RTP relative intensities found for the indolecarboxylic acids adsorbed on the different substrates at various pH values.

At constant pH, the RTP intensities of all the compounds tested were higher on DE-81 filter paper than on the DTPA and CM supports. In basic solutions, the enhancement of the RTP signal by DE-81 was generally less marked. DE-81 also gave larger RTP signals than other papers did, for several pesticides, drugs and substituted indoles.^{8,9} This behaviour can be explained by assuming that the carboxyl groups of the indole acids are hydrogen-bonded to hydroxide groups that are present on the anion-exchange filter paper DE-81, but not the other papers.

It can also be seen from Table 2 that the pH of the test solution has a marked but variable effect on the phosphorescence signal. On DE-81, use of neutral media yielded slightly stronger signals than those from alkaline media, and signals 2-7 times those from acidic media. In contrast, on DTPA-treated S & S 903, alkaline media ($0.5M$ sodium hydroxide) enhanced the signal for indolecarboxylic acids by a factor of 2-6 relative to that for neutral and acidic solutions, except for 3-indolelactic acid. With the cation-exchanger CM-treated S & S 903, there were relatively small differences in RTP signal from neutral and basic solutions.

pH-related interactions in RTP

The effect of pH on the RTP signals of indolecarboxylic acids suggests that various interactions occur between particular indole acid species

Table 2. Comparison of RTP intensities of indolecarboxylic acids on various substrates under various conditions*

Compound	Substrate†	pH conditions§	RTP net relative intensity‡	$I_{\text{pH}}/I_{\text{pH}13}$ #	
3-Indoleacetic acid	DE-81	Neutral	40.0	1.6	
		13	25.0	1.0	
	DPTA	Neutral	5.5	0.2	
		13	24.5	1.0	
		13	9.9	1.0	
3-Indolebutyric acid	DE-81	1.6	13.5	0.7	
		Neutral	24.3	1.2	
2-Indolecarboxylic acid	DE-81	13	20.2	1.0	
		1.6	5.5	0.2	
		Neutral	6.4	0.3	
		13	22.3	1.0	
	DTPA	Neutral	8.8	1.8	
		13	5.0	1.0	
	CM-10	DE-81	1.6	33.5	0.6
			Neutral	68.2	1.3
		13	51.6	1.0	
		1.6	4.0	0.1	
Neutral		15.1	0.5		
13		31.0	1.0		
5-Indolecarboxylic acid	DE-81	1.6	8.3	0.3	
		Neutral	26.5	0.9	
		13	29.0	1.0	
		1.6	9.6	0.5	
	DTPA	Neutral	23.1	1.3	
		13	17.6	1.0	
	CM-10	Neutral	6.1	0.4	
		13	16.5	1.0	
DL-3-Indolelactic acid	DE-81	Neutral	18.3	1.4	
		13	13.0	1.0	
		1.6	9.7	0.5	
	DTPA	Neutral	72.5	4.1	
		13	17.6	1.0	
		1.6	1.8	0.1	
3-Indolepyruvic acid	DE-81	Neutral	27.4	2.0	
		13	13.7	1.0	
	CM-10	1.6	3.4	0.5	
		13	6.4	1.0	
3-Indoxyl acetate**	DE-81	Neutral	1.0	0.4	
		13	2.2	1.0	
	CM-10	Neutral	0.2	—	
	DE-81	13	21.0	—	

*Sample volume was 3 μl for DTPA and CM-10 substrates and 2 μl for DE-81 filter paper; $[\text{KI}] = 1\text{M}$; solvent ethanol-water 50:50 v/v.

†DTPA means diethylenetriaminepenta-acetic acid-treated S & S 903 filter paper; CM-10 means carboxymethylcellulose-treated S & S 903 filter paper, with a pH of 10.0, corresponding to the pH of the filtrate obtained after rinsing the resin.

§See text for the preparation of solutions at different pH.

‡RTP net relative intensity was corrected for background phosphorescence intensity and normalized to the RTP intensity of 10^{-3}M 3-indolepyruvic acid on DE-81. RSD = 10%.

$I_{\text{pH}}/I_{\text{pH}13}$ represents the RTP relative intensity of the neutral or pH 1.6 solution compared to the relative intensity of the pH 13 solution, with the same substrate.

**RTP intensity probably corresponds to the hydrolysis product of this compound. For neutral solution, no detectable phosphorescence was observed with the Aminco-Bowman spectrophotofluorometer.

and the substrates. Since the excited triplet-state dissociation constants ($\text{p}K_{\text{a}}^{\text{T}}$) of the indole acids range between 4.5 and 6.3,²¹ only undissociated species can be present in solutions at pH 1.6. In aqueous ethanol solutions, there will be a mixture of the undissociated and anionic species, as shown by the apparent pH of 4.5 for the aqueous ethanol solution of 5-indolecarboxylic acid, for which $\text{p}K_{\text{a}}^{\text{T}}$ is 4.9.²¹

Finally, only the indolecarboxylate species will be present in solutions at pH 13.

On DE-81 filter paper, the mixture of dissociated and undissociated forms of the acid present in neutral solutions could remain on the dry surface and form various combinations of hydrogen bonds with the anion-exchange OH^- groups as well as with the neutral cellulose OH groups of the paper, which

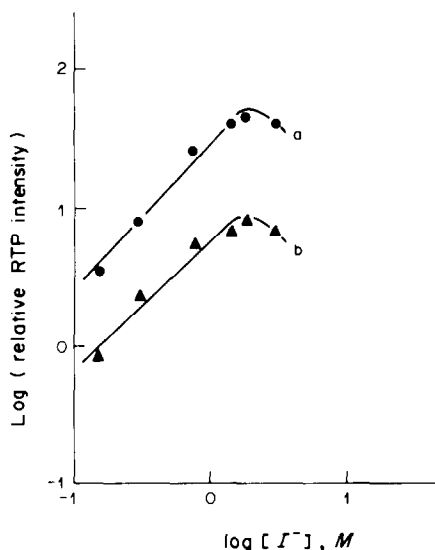


Fig. 2. Heavy-atom RTP response curves for 3-indolebutyric acid on DE-81 filter paper, in neutral water-ethanol (50:50 v/v) solutions. Concentrations of 3-indolebutyric acid: $10^{-3}M$ (curve a), $10^{-4}M$ (curve b).

would give the strongest phosphorescence signals. When acidified solutions are adsorbed, however, only undissociated species would be present in the "dry" state and give weaker hydrogen bonds with the substrate, which would explain the significantly lower phosphorescence signal. Finally, when basic test solutions are used, electrostatic repulsions between the carboxylate groups and the OH^- groups of the

DE-81 paper will diminish the overall hydrogen bonding, thus reducing the RTP intensity.

It is surprising that the phosphorescence signals from DTPA-treated S & S 903 paper were higher for alkaline solutions ($\text{pH} \sim 13$), than neutral or acidic solutions. In the high-pH test, the diethylenetriaminepenta-acetic acid should initially react with the sodium hydroxide, and on drying exist only as the pentasodium salt, since $\text{p}K_{a5}$ is 10.56;²³ electrostatic repulsion between the indolecarboxylate and DTPA acetate groups should then prevent formation of hydrogen bonds with the hydroxyl groups of the paper. However, as the sodium hydroxide content of the 2- μl sample is only 1 μmole , although the pH of the sample is >13 the composition of the dried sample spot will depend on the loading of DTPA on the paper and the degree of diffusion of the sample spot before drying. Therefore, it is not clear whether hydrogen-bonding is responsible for the increase of the RTP signals of indolecarboxylates when spotted in alkaline solutions onto DTPA-treated S & S 903, or to packing of the DTPA sodium salt into the filter paper. The latter could cause inhibition of the internal molecular motions of the phosphor, analogously to the interaction mechanism proposed by Niday and Seybold²⁴ to explain the effect, on RTP, of several salts or sugars packed into paper.

Heavy-atom effect on RTP intensity

The "heavy atom" effect of iodide on the RTP response curves ($\log I$ vs. \log concentration of heavy atom at a given analyte concentration) was studied by

Table 3. RTP net intensities of selected indolecarboxylic acids with and without heavy atom present*

Compound	Substrate†	pH conditions	Heavy atom‡	RTP net relative intensity‡	I_{-}/I_0 #
3-Indoleacetic acid	DE-81	Neutral	I^-	46.5	152
	DE-81	13	None	0.3	
3-Indolebutyric acid	DE-81	Neutral	I^-	28.5	260
	DE-81	Neutral	None	0.1	
3-Indoxyl acetate	DE-81	13	I^-	24.1	300
	DE-81	13	None	0.08	
DL-3-Indolelactic acid	DE-81	Neutral	I^-	20.6	4
	DE-81	Neutral	None	5.0	
2-Indolecarboxylic acid	DTPA	Neutral	I^-	72.5	480
	DTPA	Neutral	None	0.15	
	DTPA	Neutral	I^-	27.5	550
2-Indolecarboxylic acid	DE-81	13	I^-	0.05	
			None	51.5	16.3
	DTPA	13	I^-	3.1	
			None	31.0	8.3
			I^-	3.7	

*See first footnote in Table 2.

†DTPA stands for diethylenetriaminepenta-acetic acid-treated S & S 903 filter paper.

‡ I^- refers to 1M potassium iodide solution. None means an analyte solution without heavy atom.

‡RTP net relative intensity was corrected for background phosphorescence intensity and normalized to the RTP intensity of $10^{-3}M$ 3-indolebutyric acid on DE-81. RSD = 10%.

I_{-}/I_0 represents the heavy-atom enhancement factor, defined as the ratio of analyte RTP net relative intensity in the presence of 1M KI (I_{-}) to analyte RTP net relative intensity without heavy atom (I_0).

Table 4. RTP analytical figures of merit of selected indolecarboxylic acids*

Compound	LDR,† μg/ml	Slope‡	Correlation coefficient	Absolute LOD,‡ ng
3-Indoleacetic acid	1,000	0.87	0.994	0.2
3-Indolebutyric acid	100	0.92	0.999	0.5
DL-3-Indolelactic acid	200	0.88	0.996	0.3
2-Indolecarboxylic acid	1,000	0.85	0.996	0.1
5-Indolecarboxylic acid	1,000	0.82	0.998	0.1

*Evaluated on DE-81 filter paper, with 1M KI solution in ethanol-water (50:50 v/v).

†LDR = linear dynamic range, corresponding to the ratio of the upper concentration of linearity (within 5%) and the LOD.

‡Slope calculated from the log-log analytical calibration curve.

‡LOD = limit of detection, defined as the amount of analyte (in ng) giving a signal-to-noise ratio of 3. Absolute LOD was calculated for a 2-μl sample solution.

varying the concentration of both heavy atom and analyte on DE-81 substrate. The RTP response curves for 3-indolebutyric acid are shown in Fig. 2. They are linear over a range of about one order of magnitude, and the curves decrease for I^- concentrations $>2M$. Although RTP response curves, and therefore optimal potassium iodide concentrations for maximum sensitivity, may differ according to the analyte,⁸ a concentration of 1M was selected for the analytical quantitative RTP studies of all the indolecarboxylic acids tested.

Table 3 presents the heavy-atom enhancement factors for several indole acids. With the exception of 3-indoxyl acetate and 2-indolecarboxylic acid, the RTP signals were extremely weak in the absence of a heavy atom, but relatively strong when 1M potassium iodide was used. Therefore, heavy-atom en-

hancement factors (I_1/I_0) are generally very large, ranging between 4 and 550 according to the particular compound. Our results are in agreement with the earlier data of Meyers and Seybold²⁵ who found a heavy-atom enhancement factor of 370 for unsubstituted indole, with 1M sodium iodide.

Analytical figures of merit

The characteristics of the RTP calibration curves and the limits of detection for several indolecarboxylic acids are shown in Table 4, for optimal conditions, *i.e.*, neutral sample solution on DE-81, with addition of 1M potassium iodide. The log-log calibration plots (see Fig. 3) with slopes close to unity are linear from 10^{-6} or $10^{-5}M$ up to $10^{-3}M$ for the compounds studied, indicating linear response; there is also excellent precision. The absolute limits of detection (LOD) are particularly low, ranging between 0.1 and 0.5 ng (corresponding to a concentration of 0.1 μg/ml) for 3-indoleacetic acid, compares favourably with the literature values of 50 ng obtained by silica-gel thin-layer fluorimetry,²⁶ 0.02 μg/ml evaluated by LTP,²⁷ and 0.1 ng determined by HPLC with fluorescence detection.²⁸ Therefore, our results demonstrate that room temperature phosphorimetry constitutes a precise, simple and sensitive analytical method for determination of indolecarboxylic acids.

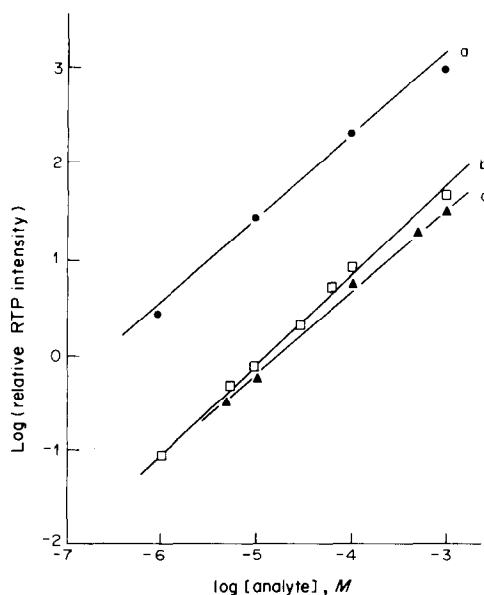


Fig. 3. Calibration curves of log (relative RTP intensity, I) vs. log (analyte concentration for DE-81 filter paper as substrate, in neutral solution). ● Curve a, 2-indolecarboxylic acid. □ Curve b, 3-indoleacetic acid. ▲ Curve c, DL-3-indolelactic acid.

REFERENCES

1. T. Vo-Dinh and J. D. Winefordner, *Appl. Spectrosc. Rev.*, 1977, **13**, 261.
2. R. T. Parker, R. S. Freedlander and R. Dunlap, *Anal. Chim. Acta*, 1980, **119**, 189.
3. *Idem, ibid.*, 1980, **120**, 1.
4. J. L. Ward, G. L. Walden and J. D. Winefordner, *Talanta*, 1981, **28**, 201.
5. R. J. Hurtubise, *Solid Surface Luminescence Analysis Theory, Instrumentation and Applications*, Chapters 3, 5, and 7. Dekker, New York, 1981.
6. J. J. Aaron and J. D. Winefordner, *Analisis*, 1982, **10**, 299.

7. T. Vo-Dinh, *Room Temperature Phosphorimetry for Chemical Analysis*, Wiley, New York, 1984.
8. S. Y. Su and J. D. Winefordner. *Can. J. Spectrosc.*, 1983, **28**, 19.
9. J. J. Aaron, M. Andino and J. D. Winefordner, *Anal. Chim. Acta*, 1984, **160**, 171.
10. R. M. Ramasamy and R. J. Hurtubise, *Anal. Chem.*, 1982, **54**, 1642.
11. R. A. Dalterio and R. J. Hurtubise, *ibid.*, 1982, **54**, 224.
12. *Idem*, *ibid.*, 1983, **55**, 1084.
13. J. J. Aaron and J. D. Winefordner, *Analisis*, 1979, **7**, 168.
14. S. M. Ramasamy and R. J. Hurtubise, *Anal. Chim. Acta*, 1983, **152**, 83.
15. R. J. Hurtubise and G. A. Smith, *ibid.*, 1982, **139**, 315.
16. R. J. Hurtubise, *Talanta*, 1981, **28**, 145.
17. C. D. Ford and R. J. Hurtubise, *Anal. Chem.*, 1980, **52**, 656.
18. J. N. Miller, *TrAC*, 1981, **1**, 31.
19. J. L. Ward, R. P. Bateh and J. D. Winefordner, *Analyst*, 1982, **107**, 335.
20. R. P. Bateh and J. D. Winefordner, *Talanta*, 1982, **29**, 713.
21. J. J. Aaron, A. Tine, M. E. Wojciechowska and C. Parkanyi, *J. Lumin.*, in the press.
22. J. J. Aaron, E. Kaleel and J. D. Winefordner, *J. Agri. Food Chem.*, 1979, **27**, 1233.
23. A. Ringbom, *Les Complexes en Chimie Analytique*, p. 328. Dunod, Paris, 1967.
24. G. T. Niday and P. G. Seybold, *Anal. Chem.*, 1978, **50**, 1577.
25. M. L. Meyers and P. G. Seybold, *ibid.*, 1979, **51**, 1609.
26. M. Hausler, J. D. McNeil, R. W. Frei and O. Hutzinger, *Mikrochim. Acta*, 1973, 43.
27. L. B. Sanders and J. D. Winefordner, *J. Agri. Food Chem.*, 1972, **20**, 167.
28. R. Buldini, S. Girotti, A. M. Pierpaoli and D. Tonelli, *Microchem. J.*, 1982, **27**, 365.

Dedication– Dedicated to R. A. Chalmers.

METHYL ISOBUTYL KETONE EXTRACTION OF IODIDE COMPLEXES FROM SULPHURIC ACID-POTASSIUM IODIDE MEDIA AND BACK-EXTRACTION INTO AN AQUEOUS PHASE

ELSIE M. DONALDSON

Mineral Sciences Laboratories, Canada Centre for Mineral and Energy Technology,
Department of Energy, Mines and Resources, Ottawa, Canada

MOHUI WANG

Chengdu Geological College, Chengdu, People's Republic of China

(Received 25 March 1985. Revised 13 June 1985. Accepted 3 September 1985)

Summary—The methyl isobutyl ketone extraction of 15 elements (Cu, Ag, Zn, Cd, In, Tl, Ge, Sn, As, Sb, Bi, Se, Te, Mo and Pd) as iodide complexes from 0.1–5*M* sulphuric acid/0.01–0.5*M* potassium iodide media has been studied. At the optimum potassium iodide concentrations, and a 1:2 v/v ratio of organic to aqueous phase, Cu(II), Ag, Cd, In(III), Tl(III), Sb(III), Bi, Te(IV) and palladium(II) are completely extracted in a single step from 1–5*M* sulphuric acid. All these elements except palladium are also quantitatively extracted from 0.05–0.5*M* iodide/2*M* sulphuric acid. Zn, Sn(IV) and As(³II) are completely extracted at high acid and iodide concentrations, and at the highest concentrations of acid and iodide investigated, Ge is partly extracted and Mo(VI) is slightly extracted. The extraction of Se(IV) is incomplete because of its reduction to the elemental state by iodide. The back-extraction of the elements has also been investigated and the forms in which they are extracted and potential analytical separations and interferences are discussed.

Two current long-term CANMET projects are the study of the behaviour of silver in hydrometallurgical zinc processes, and the certification of diverse sulphide and other ores, concentrates and related materials for major, minor and trace elements. In the course of these studies various methods have been developed for the determination of silver,^{1,3} indium,⁴ antimony,⁵ arsenic,⁶ selenium,⁷ tellurium,⁸ bismuth,⁹ tin¹⁰ and germanium.¹¹ Most of these elements can be extracted into polar organic solvents such as tributyl phosphate and ketones from acidic iodide media¹² but zinc is not appreciably extracted at high acid and iodide concentrations.¹³ Hence group extraction of some of these elements as iodides, coupled with a flame or graphite-furnace atomic-absorption spectrophotometry (AAS) finish, might provide a relatively rapid method for the determination of some five or more of these elements in the materials under consideration. The method would necessitate separation of the elements from matrix elements such as lead and iron and, particularly for graphite-furnace AAS, back-extraction from the organic phase. Extraction from sulphuric acid medium would be obligatory, partly for preliminary removal of lead as lead sulphate and also because lead iodide is co-extracted from hydrochloric acid-iodide media^{12,14} and nitric acid readily oxidizes iodide.

Methyl isobutyl ketone (MIBK) is one of the most efficient and widely used polar solvents for the extrac-

tion of iodide complexes.^{12,15,16} Non-polar solvents such as toluene and benzene extract only non-solvated molecular iodide compounds such as SbI₃, AsI₃ and SnI₄, but MIBK extracts not only these species and co-ordinatively solvated iodides such as TlI₃·S (where S represents the solvent) but also the ion-association complexes of anions such as [CdI₄]²⁻ with alkali-metal ions or protons.^{12,17,20} Several investigators^{13,21-23} have studied extraction of various elements into MIBK from sulphuric acid solutions containing alkali metal iodides, and the extraction procedure has been applied to group separation and spectrographic determination of various trace elements, including zinc, in steel.²² Various investigators have studied the extraction of individual elements^{17,20,24-26} but mostly for a limited range of conditions. A problem for many workers is that much of the information available is in Russian or Japanese,²⁷⁻³¹ with no English translation available, and often there is inadequate information in the abstracts. Furthermore, except for the work of Krivenkova *et al.*²² and Clark and Viets^{32,33} very little information is available on stripping of the elements from the MIBK extract.

Preliminary tests having shown that some of the elements mentioned above can be quantitatively extracted into MIBK in one step from sulphuric acid media at low potassium iodide concentration ($\leq 0.05M$) when the volume ratio of organic to aqueous phase is 1:2, and that zinc is $\leq 1.5\%$ co-extracted, at the 500 mg level, from solutions that are

up to $\sim 0.1M$ in potassium iodide and up to $2M$ in sulphuric acid, a comprehensive investigation of MIBK extraction of iodides seemed to us to be of considerable value in our current and future work. This paper describes the results of these studies and the stripping investigations. Their analytical application to analysis of zinc ores and related materials will be the subject of a future paper.

EXPERIMENTAL

Reagents

Working solutions of copper, silver, zinc and cadmium were prepared by dissolving the metals in dilute nitric and sulphuric acids, followed by evaporation of the solutions to dryness, dissolution of the salts in water and dilution to the required volume with water. Solutions of selenium(IV), tellurium(IV) and thallium(III) were prepared by dissolving Se, TeO_2 and Tl_2O_3 in dilute nitric acid plus sufficient sulphuric acid to give a final concentration of $1M$, evaporating the solutions to fumes of sulphur trioxide, cooling and taking up and diluting to the required volume with water. A solution of antimony(III) was made by dissolving potassium antimony tartrate in water.

Germanium, arsenic(III) and molybdenum(VI) solutions were prepared by dissolving the oxides in dilute sodium hydroxide solution. A palladium(II) solution, $1M$ in sulphuric acid, was prepared by treating an aliquot of a commercial palladium chloride solution with *aqua regia* plus the required volume of concentrated sulphuric acid and ≈ 0.5 ml of concentrated perchloric acid and evaporating the solution to fumes of perchloric acid, then cooling and diluting to the necessary volume.

Stock $1000\text{-}\mu\text{g/ml}$ indium and bismuth solutions were prepared by dissolving the metals in dilute nitric acid. Working solutions, $1M$ in sulphuric acid, were prepared by evaporating suitable aliquots of these solutions, plus the required volume of concentrated sulphuric acid, to fumes of sulphur trioxide, cooling and diluting to volume with water. A stock $1000\text{-}\mu\text{g/ml}$ tin(IV) solution, $5M$ in sulphuric acid, was prepared by dissolving the metal in the required volume of concentrated sulphuric acid, oxidizing to tin(IV) with hydrogen peroxide and evaporating to fumes of sulphur trioxide to destroy the excess of peroxide, then cooling and diluting to volume with water. A working solution, $2M$ in sulphuric acid and 0.5% in tartaric acid, was prepared by adding the required amounts of tartaric and sulphuric acids and water to a suitable aliquot of this solution.

In all these working solutions the concentration of the element of interest (assuming the starting materials were 100% pure) was $100\text{ }\mu\text{g/ml}$.

Analytical-reagent grade MIBK was used without further purification.

General extraction procedure

Five-ml aliquots of working solution were added to a series of 250-ml separatory funnels marked at 100 ml (Note 1). After addition of the required volumes of $10M$ sulphuric acid and $2M$ potassium iodide, the solutions were diluted to the mark with water, mixed and allowed to stand for 30 min. Then 50 ml of MIBK were added to each funnel and the solutions shaken vigorously for 2 min. The aqueous phases were discarded and the extracted element stripped by shaking each of the organic phases for 2–3 min with 25 ml (Notes 2 and 3) of an appropriate stripping solution, then with 10- and 5-ml portions of the stripping solution for 1 min and 30 sec, respectively, each set of aqueous phases being combined in 150-ml beakers.

Treatment of the strip solutions

Except as indicated below, about 2 ml of 50% v/v

sulphuric acid was added to each of the combined strip solutions, the beakers were covered and the solutions evaporated to ~ 20 ml. The covers were removed, the solutions were evaporated to fumes of sulphur trioxide and organic material was destroyed by repeated addition of ~ 0.5 -ml portions of concentrated perchloric acid to the hot solutions. The solutions were then evaporated to dryness and residues analysed by the methods shown in Table 1. For most of these analyses, the residues were dissolved in an appropriate acid. However, for molybdenum, the residue was dissolved in dilute ammonia solution, the excess of which was then removed by boiling, and the solutions were acidified with hydrochloric acid for the final AAS determination.^{3,4} For germanium, the residue was dissolved in dilute sodium hydroxide solution and appropriate aliquots were analysed with phenylfluorone.¹¹ For palladium, 10 ml of concentrated nitric acid were added to the strip solutions to destroy thiourea before treatment as described above, and the salts ultimately obtained were treated with *aqua regia* to dissolve any elemental palladium formed by reduction during the evaporation step. The hydrochloric acid content of the resulting solutions was adjusted to 10% v/v for the AAS determination. In the case of silver, ~ 2 mg of potassium chloride was added to the strip solution to prevent formation of a highly insoluble silver compound during the evaporation to dryness in the presence of sulphuric and perchloric acids.² Similarly, ~ 25 mg of sodium sulphate was added to the tellurium solutions before the evaporation step.⁸

For the determination of antimony, ~ 2 mg of potassium sulphate was added to the strip solution, which was then evaporated to fumes of sulphur trioxide and treated with *aqua regia* to oxidize the antimony to antimony(V). The solution was then evaporated to dryness and the residue dissolved in hot dilute potassium hydroxide solution. After addition of tartaric and hydrochloric acids, antimony(V) was reduced to antimony(III) with sulphurous acid, the excess of which was removed by boiling before the AAS determination.⁵

For the determination of arsenic, the strip solution was heated to remove the methanol, then made slightly alkaline with dilute sodium hydroxide solution. An aliquot of the resulting solution was treated with nitric acid to oxidize residual iodide (which interferes with the spectrophotometric determination) and the solution was evaporated to dryness on a water-bath. The remaining nitric acid was destroyed with formic acid, the solution was evaporated to dryness again and the residue was heated overnight at $\sim 130^\circ$ in an oven. After dissolution of the salts in dilute sodium hydroxide solution and neutralization with dilute sulphuric acid, any arsenic(III) present was oxidized with bromine water, the excess of which was removed by boiling before the final determination of arsenic.⁶

In the case of selenium, perchloric acid was added to the strip solution, which was then evaporated to fumes of perchloric acid to remove nitric acid and hydrogen peroxide before the spectrophotometric determination.⁷

Notes

1. In tests with antimony(III) and tin(IV), 5 ml of 5% tartaric acid solution were added to prevent hydrolysis.

2. When oxidizing strip solutions were used, it was sometimes necessary, particularly in tests which involved extraction at high sulphuric acid and potassium iodide concentrations, to use either a longer initial shaking time (up to ~ 4 min) or up to ~ 30 ml of strip solution to obtain a colourless aqueous phase devoid of iodine.

3. When the stripping agent was water (*viz.* for arsenic and germanium), about 2–4 ml of methanol was added after each stripping step, followed by gentle inversion of the funnel 3 or 4 times to destroy any emulsion and promote rapid separation of the layers.

Table 1. Stripping solutions employed and analytical methods used to determine the degree of extraction

Element	Stripping solution*	Method†	Wavelength, nm
Cu	10% HNO ₃ -20% H ₂ O ₂	AAS-2% HNO ₃	324.8
Ag	40% HNO ₃ -10% HCl	AAS-20% HCl-1% diethylenetriamine ^{2,3}	328.1
Zn	20% HNO ₃ -20% H ₂ O ₂	AAS-2% HNO ₃	213.9
Cd	20% HNO ₃ -20% H ₂ O ₂	AAS-2% HNO ₃ -1000 µg/ml K	228.8
In	20% HNO ₃ 20% H ₂ O ₂	AAS-4% HNO ₃ -2000 µg/ml K ⁴	303.9
Tl	40% HNO ₃	AAS 4% HNO ₃	276.8
Ge	Water	LAS phenylfluorone ¹¹	507
Sn	20% HNO ₃ -20% H ₂ O ₂	AAS-10% HCl-0.5% tartaric acid 250 µg/ml K ¹⁰	235.4
As	Water	LAS molybdenum blue ⁶	845
Sb	40% HNO ₃	AAS-10% HCl-0.25% tartaric acid-2000 µg/ml K ⁵	217.6
Bi	20% HNO ₃ -20% H ₂ O ₂	AAS 5% HNO ₃ ⁹	223.1
Se	10% HNO ₃ -10% CH ₃ COOH-70% H ₂ O ₂	LAS-3,3'-diaminobenzidine hydrochloride ⁷	420
Te	20% HNO ₃ -60% H ₂ O ₂	LAS-thiourea	330
Mo	40% HNO ₃	AAS-10% HCl-1000 µg/ml Al ¹⁴	313.3
Pd	50% HCl 1% thiourea	AAS 10% HCl 1% HNO ₃	244.8

*The concentrations refer to volume proportions for the concentrated acids and of 30% hydrogen peroxide solution in the mixture and the w/v content of thiourea.

†AAS = atomic-absorption spectrometry; LAS = light-absorption spectrophotometry.

RESULTS

The degree of extraction of various iodide complexes into MIBK from 0.1-5M sulphuric acid/0.01-0.5M potassium iodide media in a single step with a 1:2 v/v ratio of organic to aqueous phase is shown in Figs. 1-6. Higher sulphuric acid and potassium iodide concentrations were not investigated because the MIBK phase would contain so much iodine that potentially dangerous exothermic reactions could occur in stripping with nitric acid with or without hydrogen peroxide; furthermore, potassium sulphate would be deposited and interfere mechanically with the extraction. The oxidation states shown for the elements are the initial states. The extraction of gold(III) and platinum(IV) was not investigated because suitable sulphuric acid solutions of these elements could not be prepared; evaporation to fumes of sulphur trioxide to remove *aqua regia* or hydrochloric acid resulted in reduction of some gold and platinum to the elemental state. Lead was not investigated because insoluble lead sulphate is formed in sulphuric acid solutions. Initial tests were done with various potassium iodide concentrations in 2M sulphuric acid because this is a convenient acidity for analytical purposes; if extraction was quantitative over almost the whole range of iodide concentration, higher and lower acidities were not always investigated.

The stripping solutions and determination methods used are shown in Table 1. Although mixtures containing up to 10% v/v nitric acid and 67% v/v 30% hydrogen peroxide solution have been recommended for stripping halide complexes from MIBK extracts containing Alamine 336 and Aliquat 336,^{32,33} solutions containing less than 10% v/v nitric acid were ineffective for many of the iodides tested in this work. For complete stripping of most elements sufficient nitric acid alone or nitric acid plus hydrogen peroxide had to be present for the MIBK phase to become

colourless with 2-3 min of shaking. Both nitric acid and hydrogen peroxide oxidize iodide to iodate and hence destroy the iodide complexes in the extract.^{32,33} In this work, 40% v/v nitric acid and 20% v/v nitric acid/20% v/v 30% hydrogen peroxide mixture were found to be as effective stripping solutions for many of the elements studied. The use of more concentrated nitric acid is not recommended because of the exothermic reactions already mentioned. The results of the stripping tests are described in the appropriate sections below.

Copper and silver

Figure 1 shows copper is completely extracted into MIBK from 2M sulphuric acid/0.02-0.5M potassium iodide and from 0.05M potassium iodide/1-5M sulphuric acid. The copper(II) is reduced to copper(I) by the iodide and presumably extracted as ion-association complexes of anionic species such as [CuI₂]⁻ and [Cu₂I₃]⁻ with potassium ions.¹⁹ The results are in relatively good agreement with those of Kakita and Gotô²¹ who showed that, for a 1:1 volume ratio of organic to aqueous phase, up to ≈ 10 mg of copper can be quantitatively extracted from ≈ 2-4M sulphuric acid/0.5M potassium iodide. Their results, and recent work by Krivenkova *et al.*²² and Byrne,¹³ show that the degree of extraction (or distribution ratio) decreases with increasing potassium iodide concentration. Possibly this could be due to formation of less readily extracted higher iodo-complexes of copper(I). The results obtained in this work show that copper can be quantitatively extracted at considerably lower potassium iodide concentrations than those (≥ 0.25M) investigated by Kakita and Gotô.²¹ Up to at least 20 mg of copper can be completely extracted in one extraction from 2M sulphuric acid/0.1M potassium iodide. The extracted copper can be readily stripped from the MIBK extract in three stages, as described in the procedure, with either 40% nitric acid or with solutions contain-

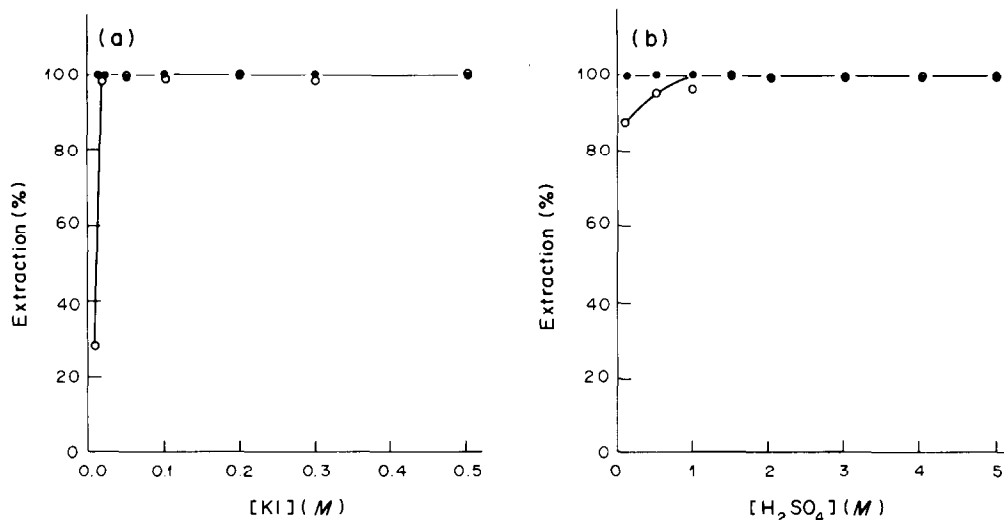


Fig. 1. Effect of H₂SO₄ and KI concentrations on the extraction of Cu and Ag. (a) ○: Cu-2M H₂SO₄; ●: Ag-2M H₂SO₄; (b) ○: Cu-0.05M KI; ●: Ag-0.02M KI.

ing 10% nitric acid and 30% hydrogen peroxide, or 20% each of nitric acid and hydrogen peroxide. Complete back-extraction of copper could not be obtained with up to 30% nitric acid alone.

Figures 1(a) and (b) show that silver is quantitatively extracted from 2M sulphuric acid/0.01–0.5M potassium iodide and from 0.02M potassium iodide/0.1–5M sulphuric acid, respectively. Recently, Semkow and Wahl²³ reported that the extraction of silver is complete in a single step with an equal volume of a mixture of 85% MIBK and 15% cyclohexanone from 0.05M sulphuric acid/0.1M potassium iodide. Depending on the iodide concentration, silver is extracted as ion-association complexes of [AgI₂]⁻ or [Ag₂I₃]⁻.^{19,35} Byrne¹³ found that, with MIBK as extractant, the distribution ratio for silver decreases as the potassium iodide concentration increases above 0.5M. Possibly this decrease may be caused by the formation of unextractable multi-charged species at high iodide concentrations. Byrne also found that prolonged shaking can lead to partial back-extraction of silver into the aqueous phase and, consequently, he recommends an extraction time of 1 min. However, no adverse effects were encountered in our work when the test solutions were shaken for 2 min. Any insoluble silver iodide formed in the aqueous phase on the addition of potassium iodide solution readily dissolves during the extraction step, presumably because the removal of the ion-association complexes by extraction shifts the equilibrium. Silver cannot be completely stripped from the MIBK phase with high concentrations of nitric acid, because insoluble silver iodide is formed under these conditions. Furthermore, it cannot be stripped with concentrated hydrochloric acid containing thiourea.² However, it is readily back-extracted with 40% nitric acid containing 10% v/v hydrochloric

acid, which prevents the formation of silver iodide by preferential formation of the AgCl₂⁻ complex.

Zinc and cadmium

Figures 2(a) and (b) show that, as found by previous investigators,^{13,22} the degree of extraction of zinc increases with increasing potassium iodide concentration. The results show also that up to at least 500 μg of zinc can be extracted in one step from 4M sulphuric acid/0.5M potassium iodide and from 5M sulphuric acid/0.4–0.5M potassium iodide, but is not appreciably extracted if the concentrations are ≤2M sulphuric acid and ≤0.1M potassium iodide. Byrne¹³ found that like silver, zinc is also partly back-extracted into the aqueous phase on prolonged shaking, particularly at low iodide concentrations (≈0.05M). Probably zinc is extracted as an ion-association complex of an anionic species such as [ZnI₃]⁻ or [ZnI₄]²⁻, since it is not extracted into non-polar solvents such as toluene.³⁶ Zinc is effectively stripped from the MIBK with 20% nitric acid/20% hydrogen peroxide solution.

Figures 2(a) and (b) show that cadmium is completely extracted from 2M sulphuric acid/0.01–0.5M potassium iodide and from 0.02M potassium iodide/1–5M sulphuric acid. These results show that it is quantitatively extracted at much lower iodide concentrations than those investigated by Byrne,¹³ Kakita and Gotô²¹ and Krivenkova *et al.*²² However, cadmium has been determined in waste water containing large amounts of zinc and manganese, by extraction into MIBK from 1M sulphuric acid/0.02M potassium iodide³¹ and has also been quantitatively extracted from solutions of moderate potassium iodide (0.1M) and low sulphuric acid content (0.05M).²³ Although no decrease in the degree of extraction of cadmium with increasing potassium

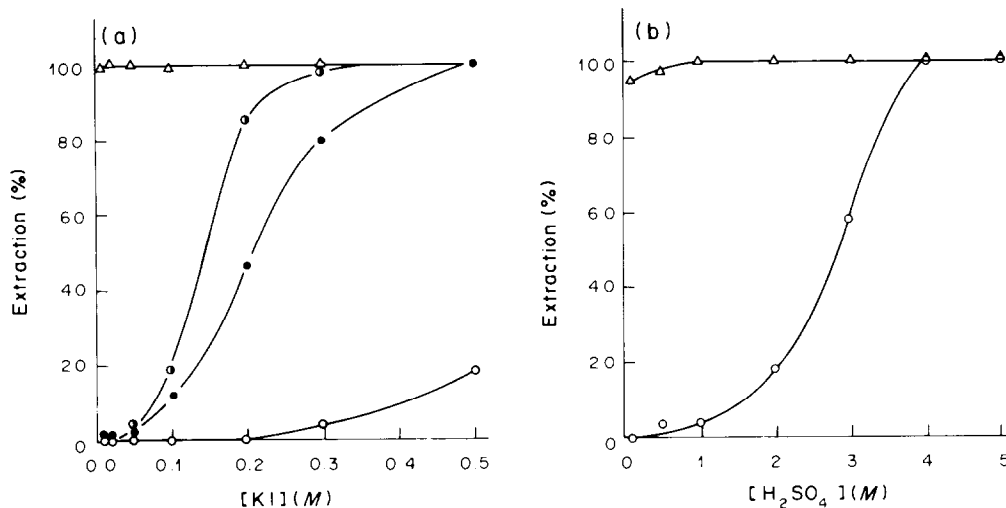


Fig. 2. Effect of H₂SO₄ and KI concentrations on the extraction of Zn and Cd. (a) ○: Zn-2M H₂SO₄; ●: Zn-4M H₂SO₄; ●: Zn-5M H₂SO₄; △: Cd-2M H₂SO₄; (b) ○: Zn-0.5M KI; △: Cd-0.02M KI.

iodide concentration was observed in the present work because of the low iodide concentrations used, Kakita and Gotô's²¹ results show that, at low sulphuric acid concentration ($\approx 0.5M$), the degree of extraction of cadmium decreases with increasing potassium iodide concentration up to $\approx 1.5M$ and then increases slightly. Byrne¹³ obtained results similar to those of Kakita and Gotô, *viz.* distribution ratio minima which shifted toward lower potassium iodide concentration as the acidity increased. However, Krivenkova *et al.*²² obtained a maximum on the plot of distribution ratio *vs.* iodide concentration. Maxima and minima for these plots have also been obtained for other polar solvents such as diethyl ether, isopentyl alcohol³⁷ and tributyl phosphate.³⁸ According to Kuchkarev *et al.*,^{20,26} MIBK extracts cadmium predominantly as neutral solvated CdI₂·4MIBK and as a solvated ion-association complex of [CdI₄]²⁻, *viz.* K₂[CdI₄] $\cdot n$ MIBK. However, Solomatin and

Kuz'min³⁷ suggest that, as the iodide concentration increases, CdI₂ is first converted into [CdI₃]⁻, which is strongly extracted, then into [CdI₄]²⁻ which is poorly extracted. This, depending on the acid concentration, causes the maxima and minima in the previously reported curves of distribution ratio *vs.* iodide concentration. Cadmium is readily stripped from the MIBK extract with 20% nitric acid/20% hydrogen peroxide solution.

Indium and thallium

Figures 3(a) and (b) show that indium(III) is quantitatively extracted from 2M sulphuric acid/0.05–0.5M potassium iodide and from 0.1M potassium iodide/0.1–5M sulphuric acid. Extraction was about 97% complete from 0.1M potassium iodide in the absence of sulphuric acid. These results are consistent with recent results obtained by Semkova and Wahl²³ who found that indium can be

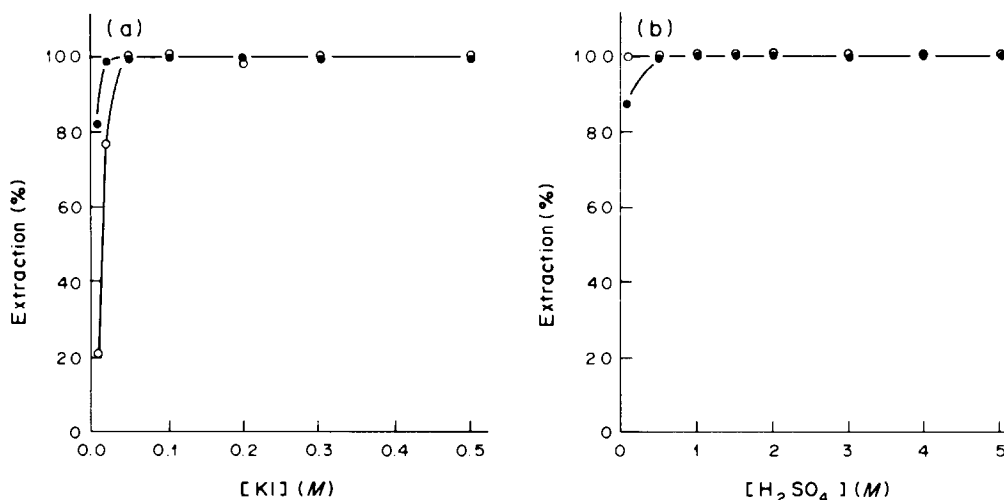


Fig. 3. Effect of H₂SO₄ and KI concentrations on the extraction of In(III) and Tl(III). (a) ○: In(III)-2M H₂SO₄; ●: Tl(III)-2M H₂SO₄; (b) ○: In(III)-0.1M KI; ●: Tl(III)-0.1M KI.

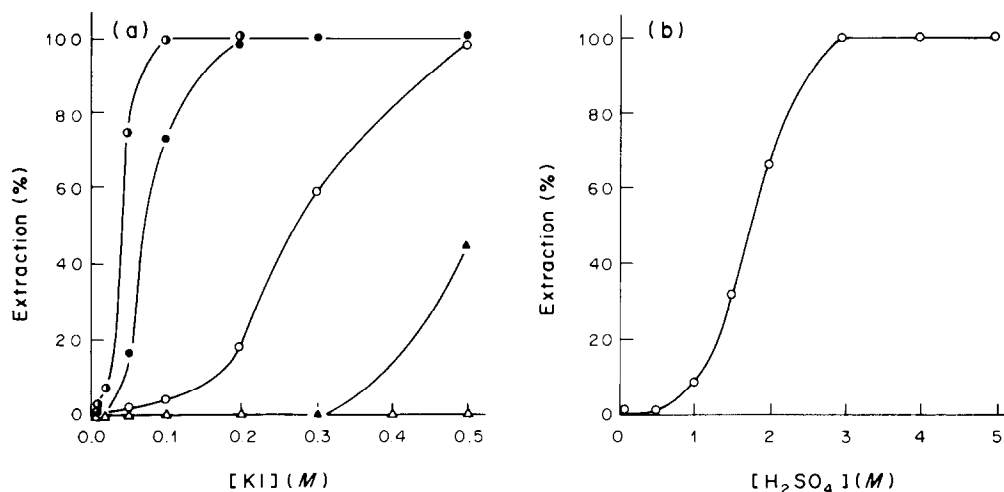


Fig. 4. Effect of H_2SO_4 and KI concentrations on the extraction of Sn(IV) and Ge(IV). (a) ○: Sn(IV)-2M H_2SO_4 ; ●: Sn(IV)-3M H_2SO_4 ; ◐: Sn(IV)-4M H_2SO_4 ; △: Ge(IV)-2M H_2SO_4 ; ▲: Ge(IV)-5M H_2SO_4 ; (b) ○: Sn(IV)-0.3M KI.

completely extracted into a mixture of 85% MIBK and 15% cyclohexanone from an equal volume of 0.025–0.15M sulphuric acid/0.1–0.3M potassium iodide. Large amounts of indium (100 mg) can also be quantitatively extracted into MIBK from an equal volume of $\leq 0.5M$ sulphuric acid/0.5–1M potassium iodide.³⁹ The distribution ratio increases with potassium iodide concentration up to at least 1M.^{13,39} MIBK extracts indium not only as the uncharged complex, InI_3 , but predominantly as an ion-pair of $[\text{InI}_4]^-$.^{15,17} In the present work, complete stripping of indium from the MIBK phase could not be obtained with 10% nitric acid, particularly from extracts obtained during extraction from $\geq 3M$ sulphuric acid. Quantitative back-extraction is readily achieved with 20% nitric acid/20% hydrogen peroxide solution.

The extraction profiles for thallium(III) [Figs. 3(a) and (b)] show that the extraction is complete from 2M sulphuric acid/0.05–0.5M potassium iodide and from 0.1M potassium iodide/0.5–5M sulphuric acid, respectively. Although no information has been found in the literature on the MIBK extraction of thallium from sulphuric acid–iodide media, previous work with cyclohexanone as solvent suggests that thallium is extracted as the solvated neutral iodide, $\text{TlI}_3 \cdot \text{S}$ (where S represents the solvent), and as the solvated ion-pair of $[\text{TlI}_4]^-$, viz. $\text{K}[\text{TlI}_4] \cdot 3\text{S}$.¹⁹ Although thallium(III) is reduced to thallium(I) by iodide, it has been stated that in the presence of excess of iodide the iodine produced can reoxidize the thallium(I) with formation of the anionic tetraiodothallate(III) complex.⁴⁰ Thallium(I) can also be extracted from iodide solutions with polar solvents.^{19,41} In the present work, thallium(III) could not be completely back-extracted from the MIBK extract (under the chosen conditions of volumes and shaking times) with 10% nitric acid containing 70% hydrogen peroxide, 20% nitric acid containing 20–50% hydrogen peroxide or 30% nitric acid containing 20%

hydrogen peroxide. With the 20–30% nitric acid/hydrogen peroxide mixtures only ~45–60% of the extracted thallium was recovered. However, 40% nitric acid was found to be effective for stripping purposes.

Germanium and tin

Figure 4(a) shows that, at the 500- μg level, germanium is not extracted from 2M sulphuric acid containing potassium iodide up to 0.5M concentration, but is about 44% extracted from 5M sulphuric acid/0.5M potassium iodide, which shows that the degree of extraction increases with increasing acidity. According to Byrne and Gorenc,³⁶ and Tanaka and Takagi,⁴² who studied the extraction of germanium into toluene and cyclohexane, respectively, from sulphuric acid media, the degree of extraction also increases with increasing iodide concentration. Although Tanaka and Takagi's results suggest that the extraction is almost quantitative from $\approx 5M$ sulphuric acid/1M sodium iodide, tests with potassium iodide showed that, at this acidity and iodide concentration, potassium sulphate deposits in the solution and interferes mechanically with the extraction. Only $\approx 62\%$ of the added germanium was recovered from the MIBK extract under these conditions. Germanium is extracted as the neutral iodide, GeI_4 ,¹² and can be readily stripped from the extract with water. However, the addition of methanol is required after each stripping step to destroy the emulsions that form.

The extraction profiles for tin(IV) [Figs. 4(a) and (b)] show that the degree of extraction increases with increasing potassium iodide and sulphuric acid concentrations up to at least 0.5 and 5M, respectively, and that the extraction is quantitative from 4M sulphuric acid/0.1–0.5M potassium iodide and from 3–5M sulphuric acid/0.3M potassium iodide. These results are consistent with those reported for the

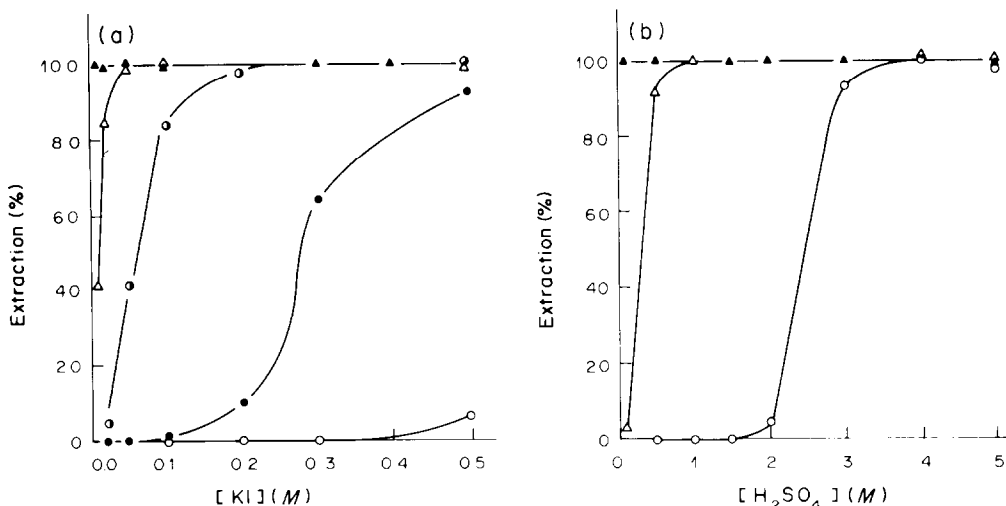


Fig. 5. Effect of H₂SO₄ and KI concentrations on the extraction of As(III), Sb(III) and Bi. (a) ○: As(III)-2M H₂SO₄; ●: As(III)-3M H₂SO₄; ○: As(III)-4M H₂SO₄; △: Sb(III)-2M H₂SO₄; ▲: Bi-2M H₂SO₄; (b) ○: As(III)-0.5M KI; △: Sb(III)-0.1M KI; ▲: Bi-0.02M KI.

extraction of tin(IV) into toluene, a non-polar solvent.³⁶ They are also consistent with those obtained by Krivenkova *et al.*,²² who found that the distribution ratio, with MIBK as extractant, increases with increasing sulphuric acid and potassium iodide concentrations up to at least 2.5 and 1.2M, respectively. Tin(II) can also be extracted into MIBK from sulphuric acid-iodide solutions containing chromous chloride as reductant.²⁵ Tin(IV) is extracted into MIBK as the unsolvated neutral iodide, SnI₄,¹² and can be readily stripped from the extract with 20% nitric acid/20% hydrogen peroxide solution. Tests showed that back-extraction of tin with 40% nitric acid/10% hydrochloric acid is incomplete. Only about half of the tin in the extract is stripped under these conditions. Conversely, in previous work¹⁰ it was found that tin(IV), extracted as the iodide into toluene, can be completely stripped from the extract with a mixture containing 50% v/v nitric acid, 10% v/v sulphuric acid and 20% v/v hydrochloric acid. Consequently, it is possible that some SnCl₄ or higher negatively charged species such as [SnCl₅]⁻ or [SnCl₆]²⁻ are formed under these conditions and that these complexes are insoluble in toluene but soluble in MIBK.

Arsenic, antimony and bismuth

Figures 5(a) and (b) show that the extraction of arsenic(III) into MIBK is quantitative only at relatively high sulphuric acid and iodide concentrations, *viz.* 4-5M sulphuric acid/≈0.3-0.5M potassium iodide, and that the extraction increases with increasing potassium iodide concentration up to at least 0.5M. These results are reasonably consistent with those reported for the extraction of arsenic into toluene from sulphuric acid-potassium iodide media.³⁶ Arsenic can also be quantitatively extracted at higher acidities and lower iodide concentrations.^{36,43}

Arsenic(V) is reduced to arsenic(III) by iodide in acid media, and this is extracted into MIBK as the neutral molecule, AsI₃,¹² and can be readily stripped from the extract with water, as described for germanium.

Antimony(III) is completely extracted from 2M sulphuric acid/0.05-0.5M potassium iodide [Fig. 5(a)] and from 0.1M potassium iodide/1-5M sulphuric acid [Fig. 5(b)]. Antimony(V) is reduced to antimony(III) by iodide in acid media. At potassium iodide concentrations greater than ≈0.5M the degree of extraction of antimony decreases; about 96% is extracted from 1M potassium iodide/2M sulphuric acid. These results are reasonably consistent with those obtained by Kakita and Gotô,²¹ who found that the degree of extraction steadily decreases as the potassium iodide concentration increases from ≈0.5 to at least 3M. Krivenkova *et al.*²² found that the distribution ratios for extraction into MIBK from ≈2M sulphuric acid decreased with potassium iodide concentration up to ≈0.8M, then increased slightly. Decreases in the degree of extraction have also been observed, but to a much greater extent, with non-polar solvents such as toluene³⁶ and benzene.^{28,43-45} This decrease has been attributed to the formation of the anionic [SbI₄]⁻ species, which does not form ion-pairs that are extractable into these solvents.^{28,43,45,46} However, because polar solvents such as MIBK extract both the uncharged SbI₃ complex and ion-pairs of [SbI₄]⁻,^{12,28,43,45,46} the effect of potassium iodide on the extraction would be considerably less with polar solvents than with non-polar solvents which extract only SbI₃. The decrease in the MIBK extraction of antimony at high iodide concentrations may be caused by the liberation of iodine and subsequent oxidation of antimony(III) to the less extractable antimony(V).⁴⁶ Possibly, this decrease in extraction may be avoided by adding ascorbic acid to the solution before the addition of potassium iodide, to

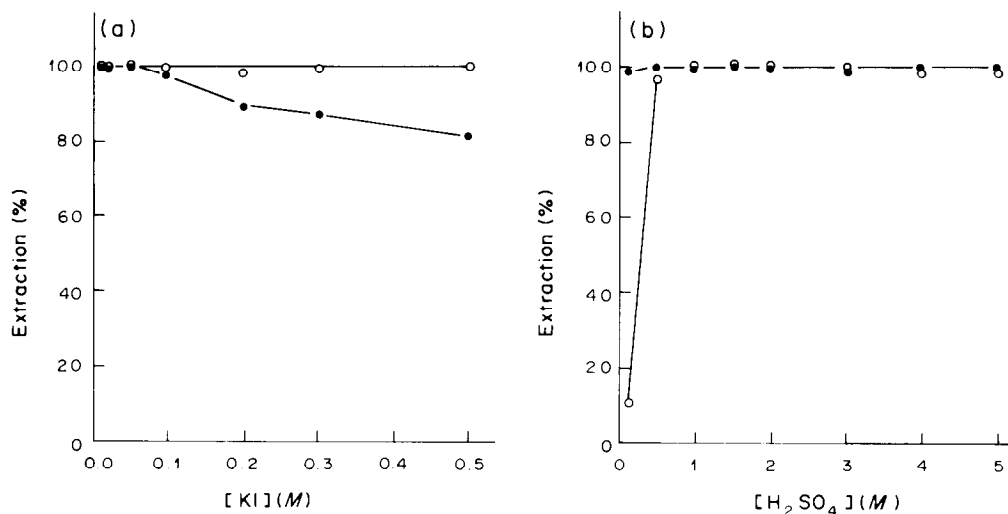


Fig. 6. Effect of H_2SO_4 and KI concentrations on the extraction of Te(IV) and Pd(II). (a) \circ : Te(IV)-2M H_2SO_4 ; \bullet : Pd(II)-2M H_2SO_4 ; (b) \circ : Te(IV)-0.02M KI; \bullet : Pd(II)-0.02M KI.

inhibit the formation of iodine. Although 40% nitric acid was used in this work to strip antimony from the MIBK extract, later work showed that $\approx 3\%$ nitric acid is equally effective. Tartaric acid was required in the test solutions to prevent hydrolysis of antimony; erratic results were obtained in its absence.

Figures 5(a) and (b) show that the extraction of bismuth is complete from 2M sulphuric acid/ ≈ 0.01 –0.5M potassium iodide and from 0.02M potassium iodide/0.1–5M sulphuric acid. Although no apparent increases or decreases in extraction were observed at the acid and iodide concentrations used in this work, previous investigators have found that the degree of extraction with oxygen-compound solvents decreases with increasing iodide concentration,^{21,22,47} presumably because of the formation of multicharged anionic $[\text{BiI}_5]^{2-}$ and $[\text{BiI}_6]^{3-}$ complexes that are not extractable into the organic phase. MIBK and other oxygen-containing solvents such as tributyl phosphate and cyclohexanone extract bismuth as the neutral iodide, BiI_3 , and as ion-pairs of $[\text{BiI}_4]^-$.^{12,47} The present work showed that it can be completely stripped from MIBK extracts with 20% nitric acid/20% hydrogen peroxide solution.

Selenium, tellurium and molybdenum

Byrne and Gorenc³⁶ found that up to $\approx 20 \mu\text{g}/\text{ml}$ concentration in the aqueous phase, selenium(IV) is $\approx 99\%$ extracted into toluene from ≈ 0.1 –6M sulphuric acid/0.05–1M potassium iodide, presumably as the amorphous form produced by reduction with hydriodic acid. However, in our work, the extraction of selenium(IV) was incomplete and very erratic because of this reduction. Only about 73–86% and 80–86% of the added selenium was extracted from 2M sulphuric acid/0.5–1M potassium iodide and from 4M sulphuric acid/0.2–1M potassium iodide. In these tests, selenium was stripped from the extract

with a mixture of nitric and acetic acids and hydrogen peroxide.^{32,33}

The extraction profiles for tellurium(IV) [Figs. 6(a) and (b)] show that it is quantitatively extracted into MIBK from 2M sulphuric acid/0.01–0.5M potassium iodide and from 0.02M potassium iodide/1–5M sulphuric acid. These results are reasonably consistent with those obtained by Kakita and Gotô,²¹ who found that the extraction is complete from 0.5–4M sulphuric acid that is at least 0.5–1.5M in potassium iodide and from 0.25–3M potassium iodide that is at least 1–2.5M in sulphuric acid. They did not investigate the extraction of tellurium at iodide concentrations less than 0.25M. It is generally considered that tellurium is extracted into oxygen-compound solvents as ion-association complexes of $[\text{TeI}_6]^{2-}$, and possibly of $[\text{TeI}_5]^-$ from dilute iodide media.¹² However, Havezov and Stoepler⁴⁸ found that, at low iodide concentrations, tellurium can be extracted into *o*-xylene, a non-polar solvent, as the neutral iodide, TeI_4 . Consequently, depending on the iodide concentration, it is probably extracted into MIBK as both TeI_4 and $[\text{TeI}_6]^{2-}$. Tellurium can be readily stripped from the extract with 20% nitric acid–60% hydrogen peroxide solution. Back-extraction with 20% nitric acid–20% hydrogen peroxide solution was incomplete from extracts obtained from $> 2\text{M}$ sulphuric acid/ $> 0.1\text{M}$ potassium iodide.

Molybdenum(VI) is $\approx 5\%$ extracted into MIBK from 5M sulphuric acid/0.5M potassium iodide. This agrees with earlier work in which $\approx 6\%$ and $< 1\%$ extraction into diethyl ether from 6.9M hydriodic acid⁴⁹ and from 0.75M sulphuric acid/–1.5M potassium iodide,⁴¹ respectively was reported. Although it has been reported that molybdenum is $\approx 43\%$ extracted into MIBK from 2.3M hydrochloric acid/0.2M potassium iodide containing ascorbic acid,⁵⁰ it is highly probable that it is largely extracted as a chloro-complex under these conditions.

Palladium

Figure 6(a) shows that palladium(II), which forms a reddish brown iodide complex, is completely extracted into MIBK from 2M sulphuric acid/0.01–0.05M potassium iodide, and that the degree of extraction decreases with increasing iodide concentration. Extraction is quantitative from 0.02M potassium iodide/0.5–5M sulphuric acid [Fig. 6(b)]. MIBK extracts palladium as ion-association complexes of $[\text{PdI}_4]^{2-}$.²⁴ The decrease in the extraction of palladium at $>0.05M$ potassium iodide concentration may be caused by the formation of unextractable higher multicharged anionic complexes.⁵¹ Palladium cannot be stripped from the extract with 30% nitric acid–30% hydrogen peroxide solution or with 40% nitric acid. It is readily stripped with 50% hydrochloric acid containing 1% thiourea as a complexing agent.²

DISCUSSION

The results of the present work show that, in general, the degree of extraction of all the elements investigated increases with increasing sulphuric acid concentration, and that copper, silver, cadmium, bismuth, tellurium and palladium can be quantitatively extracted as iodides into 50 ml of MIBK, in one extraction from 100 ml of 2M sulphuric acid containing potassium iodide at concentrations as low as 0.02M. In the absence of mutual interference effects between the extracted species,⁵² the group separation of copper, silver, cadmium, indium, thallium, antimony, bismuth and tellurium from zinc, tin and arsenic is possible by simultaneous extraction of these elements into MIBK from $\approx 2M$ sulphuric acid/ ≈ 0.05 – $0.1M$ potassium iodide. It is probable that all or most of the elements extracted can be quantitatively back-extracted from the extract by stripping first several times with 40% nitric acid containing hydrochloric acid to remove silver, then several times with 20% nitric acid–60% hydrogen peroxide solution to ensure the complete recovery of tellurium. Zinc, tin and arsenic can be included in the group separation by extracting from 5M sulphuric acid/0.4M potassium iodide or from 4M sulphuric acid/0.5M potassium iodide. Tin, but not zinc and arsenic, can be included by extracting from 4M sulphuric acid/0.1M potassium iodide. Under these conditions very little arsenic would be co-extracted, and co-extracted zinc could readily be removed from the extract by washing it with a sulphuric acid–potassium iodide solution of the same composition as that used for the extraction. If the separate recovery of zinc, tin and arsenic or of tin alone is required, copper, silver and the other elements mentioned above can be extracted from 2M sulphuric acid/0.05–0.1M potassium iodide as already described, followed by one or two washes of the extract with a solution of the same acid and iodide concentration as that used for the extraction, to recover the

co-extracted zinc, tin and arsenic. Subsequently, after adjustment of the sulphuric acid and potassium iodide concentrations of the combined aqueous phase to the required levels mentioned above, zinc, tin and arsenic, or tin alone, could be extracted, and finally stripped from the extract with water, followed by 20% nitric acid–20% hydrogen peroxide solution as described below. However, for a single stage extraction, sufficient MIBK would have to be used in this second extraction step for the volume ratio of the organic to aqueous phase to be 1:2. The extraction of tin and arsenic, or of arsenic alone, at the acid and iodide concentrations mentioned above, is not applicable in the presence of a large amount of zinc, and none of the extraction schemes already mentioned is applicable in the presence of a large amount of copper. However, in the presence of a large amount of zinc, it should be readily possible to include tin and arsenic in a separation scheme by extracting them into toluene from $\approx 5M$ sulphuric acid/0.5M potassium iodide,³⁶ after the group separation of copper and other elements from 2M sulphuric acid/0.05–0.1M potassium iodide and the recovery of any co-extracted tin and arsenic from the extract as described above.

Some preliminary tests have shown that, in the presence of 500 mg of zinc and 50 mg of iron(III), up to at least 500 μg each of copper, silver, cadmium, indium and bismuth can be simultaneously and quantitatively extracted into MIBK from 2M sulphuric acid/0.1M potassium iodide under the conditions used in this work. In these tests iron(III) was reduced to iron(II) with ascorbic acid before the addition of potassium iodide. Co-extracted zinc and residual iron were removed from the extract by washing it once with 20 ml of 2M sulphuric acid/0.1M potassium iodide and the extracted elements were stripped with 40% nitric acid–20% hydrochloric acid solution. Because of the large amount of iodide present in the extract under these conditions, more hydrochloric acid than that used during the study of the extractability of silver (*cf.* Table 1) was needed in the stripping solution to keep silver in solution during the stripping step. Subsequent work showed that if the solution to be extracted contains lead sulphate and this is removed by filtration before the extraction step, low results will be obtained for silver, bismuth and also for antimony, because of their partial occlusion by the precipitate. Calcium sulphate also occludes silver.² The occluded silver can be readily removed from lead sulphate, but not from calcium sulphate, by washing with 25% ammonia solution.^{1,2} Work is continuing to find a simple and rapid method for recovering the occluded bismuth and antimony from lead sulphate.

In the presence of moderate amounts of arsenic(III) (*e.g.*, 1 mg), low results are obtained for tin when it is stripped from the MIBK extract with 20% nitric acid–20% hydrogen peroxide solution. Low results were also obtained previously¹⁰ in similar

circumstances when tin was extracted into toluene as the iodide and stripped with 50% v/v nitric acid–10% v/v sulphuric acid. This was caused by the formation of a tin(IV)–arsenic(V) compound which, although it was completely stripped from the toluene phase, was insoluble in the stripping solution and partially remained in the funnel after the back-extraction step. This compound could be kept in solution by adding hydrochloric acid to the stripping solution. However, as found in the present work, stripping solutions containing hydrochloric acid are ineffective for stripping tin from MIBK extracts, because of the probable formation of SnCl_4 or anionic chloro-complexes which remain in the MIBK phase. Some further work showed that although tin alone is not appreciably stripped with water (only $\approx 13\%$ at the 500- μg level), it is completely stripped with water if sufficient arsenic is present during the extraction step. This suggests that under these conditions tin and arsenic are extracted in the form of a tin(IV)–arsenic(III)–iodide compound. Although this behaviour has not been investigated further, it is possible that, in the presence of both small and moderate amounts of arsenic, complete back-extraction of tin from MIBK extracts may be obtained by stripping the extract first several times with water to remove the extracted tin–arsenic compound and then with 20% nitric acid–20% hydrogen peroxide solution to ensure the recovery of any remaining tin.

Acknowledgement—The authors thank E. Mark for performing some of the extraction and stripping tests for tin.

REFERENCES

1. E. M. Donaldson, *Talanta*, 1982, **29**, 1069.
2. *Idem, ibid.*, 1984, **31**, 443.
3. E. M. Donaldson, E. Mark and M. E. Leaver, *ibid.*, 1984, **31**, 89.
4. E. M. Donaldson, *CANMET Report 83-4E*, Canada Centre for Mineral and Energy Technology, Energy, Mines and Resources Canada, Ottawa, 1983.
5. *Idem, Talanta*, 1979, **26**, 999.
6. *Idem, ibid.*, 1977, **24**, 105.
7. *Idem, ibid.*, 1977, **24**, 441.
8. *Idem, ibid.*, 1976, **23**, 823.
9. *Idem, ibid.*, 1979, **26**, 1119.
10. *Idem, ibid.*, 1980, **27**, 499.
11. *Idem, ibid.*, 1984, **31**, 997.
12. A. A. Prokoshev, L. K. Chuchalin, B. Z. Iofa and Yu. A. Zolotov, *J. Anal. Chem. USSR*, 1972, **27**, 1230 (and references therein).
13. A. R. Byrne, *Radiochem. Radioanal. Lett.*, 1979, **40**, 1.
14. C. L. Luke, *Anal. Chim. Acta*, 1967, **39**, 447.
15. H. Irving and F. J. C. Rossotti, *J. Chem. Soc.*, 1955, 1946.
16. P. W. West, P. Senise and J. K. Carlton, *Anal. Chim. Acta*, 1952, **6**, 488.
17. Y. Hasegawa, H. Takeuchi and T. Sekine, *Bull. Chem. Soc. Japan*, 1972, **45**, 1388.
18. B. Ya. Spivakov and O. M. Petrukhin, *Russ. J. Inorg. Chem.*, 1980, **25**, 132.
19. H. Specker and W. Pappert, *Z. Anorg. Allgem. Chem.*, 1965, **341**, 287.
20. E. A. Kuchkarev and E. F. Zavarzina, *J. Anal. Chem. USSR*, 1979, **34**, 1485.
21. Y. Kakita and H. Gotô, *Sci. Rep. Res. Inst. Tôhoku Univ., Ser. A*, 1963, **15**, 133.
22. N. P. Krivenkova, L. I. Pavlenko, B. Ya. Spivakov, I. A. Popova, T. S. Plotnikova, V. M. Shkinev, I. P. Karlamov and Yu. A. Zolotov, *J. Anal. Chem. USSR*, 1976, **31**, 439.
23. T. Semkow and A. C. Wahl, *J. Radioanal. Chem.*, 1983, **79**, 93.
24. J. F. Duke and W. Stawpert, *Analyst*, 1960, **85**, 671.
25. B. R. Erdal and A. C. Wahl, *J. Inorg. Nucl. Chem.*, 1968, **30**, 1985.
26. E. A. Kuchkarev, E. F. Zavarzina and A. P. Kreshkov, *Ind. Lab. (USSR)*, 1979, **45**, 1006.
27. Yu. A. Zolotov, B. Z. Iofa and L. K. Chuchalin, *Extraction of Halide Complexes of Metals*, Nauka, Moscow, 1973.
28. K. Tanaka, *Bunseki Kagaku*, 1961, **10**, 1087; *Chem. Abstr.*, 1962, **56**, 12294d.
29. F. G. Zharovskii, E. S. Sereda and E. D. Voronova, *Ukr. Khim. Zh.*, 1964, **30**, 274; *Chem. Abstr.*, 1964, **61**, 85c.
30. T. Kono and S. Kobayashi, *Bunseki Kagaku*, 1970, **19**, 1491; *Chem. Abstr.*, 1971, **74**, 94017p.
31. E. Yamada and H. Namiki, *Kogyo Yosui*, 1974, **190**, 21; *Chem. Abstr.*, 1975, **82**, 7419v.
32. J. R. Clark and J. G. Viets, *Anal. Chem.*, 1981, **53**, 65.
33. *Idem, ibid.*, 1983, **55**, 166.
34. E. M. Donaldson, *Talanta*, 1980, **27**, 79.
35. H. Specker and H. Hartkamp, *Naturwissenschaften*, 1956, **43**, 516.
36. A. R. Byrne and D. Gorenc, *Anal. Chim. Acta*, 1972, **59**, 81.
37. V. S. Solomatin and N. M. Kuz'min, *Russ. J. Inorg. Chem.*, 1970, **15**, 83.
38. P. P. Kish and I. S. Balog, *J. Anal. Chem. USSR*, 1976, **31**, 1067.
39. H. Hartkamp and H. Specker, *Talanta*, 1959, **2**, 67.
40. A. I. Busev, V. G. Tiptsova and V. M. Ivanov, *Handbook of the Analytical Chemistry of the Rare Elements*, pp. 279–280. Halsted Press, New York, 1970.
41. H. M. Irving and F. J. C. Rossotti, *Analyst*, 1952, **77**, 801.
42. K. Tanaka and N. Takagi, *Anal. Chim. Acta*, 1969, **48**, 357.
43. E. E. Rakovskii, T. D. Krylova and A. Yu. Frolova, *J. Anal. Chem. USSR*, 1981, **36**, 749.
44. R. W. Ramette, *Anal. Chem.*, 1958, **30**, 1158.
45. Yu. A. Zolotov, A. I. Fomina, N. A. Agrinskaya and I. I. Antipova-Karataeva, *J. Anal. Chem. USSR*, 1972, **27**, 2049.
46. A. Alian, A. El-Kot, M. S. El-Bassiouny and A. Haggag, *J. Radioanal. Chem.*, 1975, **24**, 271.
47. H. A. Mottoia and E. B. Sandell, *Anal. Chim. Acta*, 1961, **24**, 301.
48. I. Havezov and M. Stoeppler, *Z. Anal. Chem.*, 1972, **258**, 189.
49. S. Kitihara, *Bull. Inst. Phys. Chem. Res. (Tokyo)*, 1948, **24**, 454.
50. J. B. Headridge and J. Richardson, *Analyst*, 1970, **95**, 930.
51. E. B. Sandell, *Colorimetric Determination of Traces of Metals*, 3rd Ed., p. 715. Interscience, New York, 1959.
52. Yu. A. Zolotov and A. A. Prokoshev, *J. Anal. Chem. USSR*, 1973, **28**, 559.

Dedication—This paper is dedicated to Dr. R. A. Chalmers on the occasion of his 20th year as Editor-in-Chief of *Talanta*. For one of us (E.M.D.), who has great respect for his knowledge of analytical chemistry and his editorial capabilities, and who has benefited from his constructive criticism and advice throughout his editorship, it is a personal honour and pleasure to be a part of this tribute.

SPECIATION STUDIES BY FLOW-INJECTION ANALYSIS

M. D. LUQUE DE CASTRO

Department of Analytical Chemistry, Faculty of Sciences, University of Córdoba, Córdoba, Spain

(Received 30 April 1985. Accepted 29 August 1985)

Summary—A survey of the use of flow-injection analysis for speciation studies is presented. Comments are made about the future potential of the technique, and suggestions are made for further research.

Study of the speciation of an element involves the determination of the various individual physico-chemical forms.¹ This is of great interest, especially in environmental analysis, because the toxicity of an element depends on its chemical form. For example, As(III) is more toxic than As(V) and As(V) has higher toxicity as arsenate than as monomethylarsonic acid, which in turn is more toxic than dimethylarsonic acid.² Chromium(VI) has been associated with several diseases,³ but chromium(III) is relatively non-toxic. Such differences in toxicity are one of the main reasons for the enormous recent development of analytical methods for differentiating the various forms of an element existing in the medium of interest.^{1,4-6}

Flow-injection analysis (FIA) has been found very useful in speciation studies, but its full potential has not yet been realized. This article reviews existing FIA methods for speciation, and mentions some that have not yet been utilized but could help to overcome certain problems encountered. Methods suggested up to now have been concerned only with determination of two oxidation states of an element, but there is great potential for development of methods for more complex systems.

In this review, FIA configurations have been divided into two main groups, according to the number of detectors needed for the determination. When more than a single detector is used, subdivision is possible, by considering whether the detectors are arranged in series or parallel. Table I shows these divisions, and also a further division according to the presence or absence of a redox system.

CONFIGURATIONS WITH A SINGLE DETECTOR

Configurations with a single detector require some imagination from the designer. The methods proposed so far deal only with redox systems, and involve the use of a single indicator reaction for one of the species, and addition of a redox agent to transform the other into the one which undergoes the indicator reaction.

The simplest method uses redox pretreatment of

alternate aliquots, so that one of the forms (sample without pretreatment) or the sum of both (pretreated sample) can be determined by the same reaction. An example is the determination of NO_2^- and NO_3^- suggested by Valcárcel *et al.*⁷ in which NO_3^- is determined indirectly by AAS, through formation of an ion-pair with the Cu(I)-neocuproin complex and extraction into isobutyl methyl ketone. Prior oxidation of NO_2^- allows determination of the sum of the two anions, and the NO_2^- concentration is found by difference. A slightly more complicated approach for NO_2^- and NO_3^- employs an injection valve with two loops that are used alternately. One loop contains a microcolumn for reduction of NO_3^- to NO_2^- .^{8,9} The sum of nitrate and nitrite is thus determined by the Griess reaction (Shinn's modification), which is commonly used for photometric determination of nitrite. Sample passed through the other loop is analysed for only the nitrite originally present. The Xu and Fang manifold for determination of NO_2^- and NO_3^- in waters and soils¹⁰ uses two channels, each with its own injection valve, and one of the channels incorporates a reducing column. The two channels merge before the confluence with the reagents. Injection first into one channel and then the other allows determinations of NO_2^- and of $\text{NO}_2^- + \text{NO}_3^-$.

The use of a valve to switch between streams with and without a redox agent (Fig. 1) for sequential determination of the oxidation states of an element has been the most usual method for speciation by FIA. Applications have included determination of Fe(III) and Fe(II) [indicator reaction Fe(II)-1,10-phenanthroline; reductant ascorbic acid],¹¹ Cr(VI) and Cr(III) [indicator reaction Cr(VI)-1,5-diphenylcarbazide; oxidant Ce(IV)],¹¹⁻¹³ and AsO_4^{3-} and AsO_2^- (indicator reaction formation of molybdenum blue; oxidant IO_3^-).¹⁴ Many methods used for arsenic speciation, such as those based on detection by AAS or ICP with prior selective hydride formation,¹⁵ ion-exchange,¹⁶ volatilization¹⁷ or HPLC¹⁸ have not yet been adapted for FIA.

A method not requiring a redox agent could be based on use of selective indicator reactions for each

Table 1. FIA configurations for speciation studies

With a single detector		
<i>With sample pretreatment</i>		
<i>With redox column in sample loop or in reactor</i>		
<i>With selecting valve</i>		{ two complexing agents redox stream
<i>With two flow-cells aligned with the same optical path</i>		
<i>With splitting and confluence points</i>		
<i>With asymmetric merging zones</i>		{ series flow-cells parallel flow-cells
<i>With double-beam spectrophotometer</i>		{ open system closed system
<i>With reversed FIA</i>		
With two detectors		
series	<i>With dissolved redox agent</i>	{ optical and electrochemical detectors two optical detectors two electrochemical detectors
	<i>Without dissolved redox agent</i>	{ molecular and atomic optical detectors optical and electrochemical detectors two optical detectors two electrochemical detectors
	<i>With redox agent in column</i>	{ two identical detectors (optical or electrochemical)
parallel	<i>With dissolved redox agent</i>	{ two identical or different detectors (optical or electrochemical)
	<i>Without redox agent</i>	{ molecular and atomic optical detectors optical and electrochemical detectors two electrochemical detectors

oxidation state, with a valve to switch between the streams of the indicator reagents. The detector would have to be sensitive to both products. Such methods have not yet been described, probably because it is difficult to find suitable chemical systems.

The speciation of an element can be determined in a simultaneous manner with a single detector (the term "simultaneous" in FIA means determination of two or more species in the same injection sample)¹⁹ in several ways.

(a) Two cells are aligned in the same optical path of the detector in a manifold. The injected sample is split into two sub-plugs, both of which reach a detector cell, but at different times; each is first merged with a reagent stream (for determination of one of the oxidation states) or first with a redox

stream and later with that of the reagent (determination of the sum of the two oxidation states), as shown in Fig. 2a. This has been done for chromium with the indicator reaction already mentioned.¹³

(b) A manifold with both splitting and confluence points before the detector (Fig. 2b) can also be used for the chromium determination.¹³

(c) The merging-zones mode²⁰ is an ingenious way of performing speciation studies with a simple two-channel manifold. A large sample volume is injected along with a small amount of redox reagent, so that only the final zone of the sample plug merges with the redox agent. This channel then merges with that of the reagent. In the two-peak recording obtained, the first peak is due to one of the oxidation states and the second to the sum of the two. A somewhat more complicated configuration, but with greater possi-

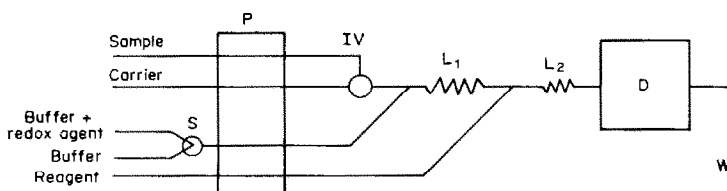


Fig. 1. FIA configuration with a single detector for study of speciation by sequential determination. S—selecting valve; IV—injection valve; P—peristaltic pump; L₁, L₂—reactors; D—detector; W—waste.

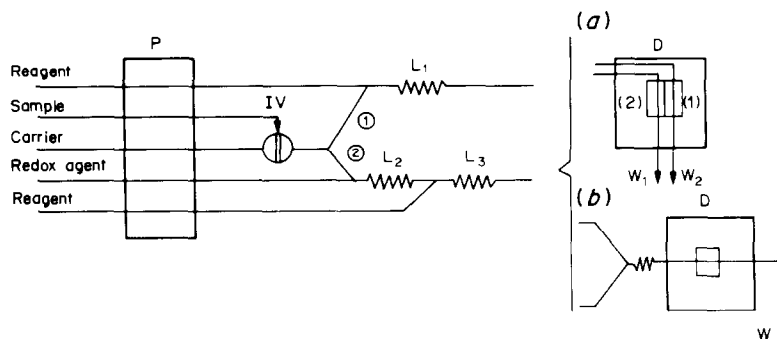


Fig. 2. FIA configurations with a single detector for study of speciation by simultaneous determination: (a) with two flow-cells aligned in the same optical path of the detector; (b) with a confluence point before the detector.

bilities, involves use of the asymmetric merging-zones mode in a closed system, to allow multidetection with a single detector.²¹ In this way, reaction rates can be studied and measurement methods unusual in FIA applied.²²

(d) A double-beam spectrophotometer can be used without or with splitting of the sample if a series (Fig. 3a) or parallel (Fig. 3b) configuration of the cells is used. The first configuration was tested for chromium speciation with diphenylcarbazide (DPC), but was unsuccessful because of the characteristics of the chemical system;¹³ it can be applied in chemical systems without this shortcoming. The second configuration gave good results with the same chemical system.¹³

(e) The potential of FIA for speciation studies is increased by use of the reversed FIA mode, rFIA.²⁰ The most serious problem of rFIA is that sample consumption is higher than in normal FIA. However, this is not a problem in studies of water samples (tap-, sea-, waste-water, etc.), which are usually abundant.

The three configurations outlined in Fig. 4 have been tested for speciation of chromium in water [indicator reaction Cr(VI)–DPC]. Configurations *a* and *b* allow the simultaneous determination of the two oxidation states; configuration *c* permits their sequential determination. In Fig. 4a continuous analysis for Cr(VI) and periodical analysis for Cr(III) is achieved, as shown. In Fig. 4b, the asymmetric confluence of a large DPC plug and a small plug of oxidant gives two peaks, the first related to the Cr(VI) concentration, and the second to the sum of the two oxidation states. In Fig. 4c, valve S is used to switch between determination of Cr(VI) (upper sub-manifold) and of [Cr(VI) + Cr(III)] (lower sub-manifold).²³

The rFIA mode has also been utilized for determination of NO_2^- and NO_3^- by the modified Griess reaction. A valve allows passage of some of the sample stream through a by-pass with a cadmium microcolumn, in an alternating manner. After this valve is a confluence point with sulphanilamide

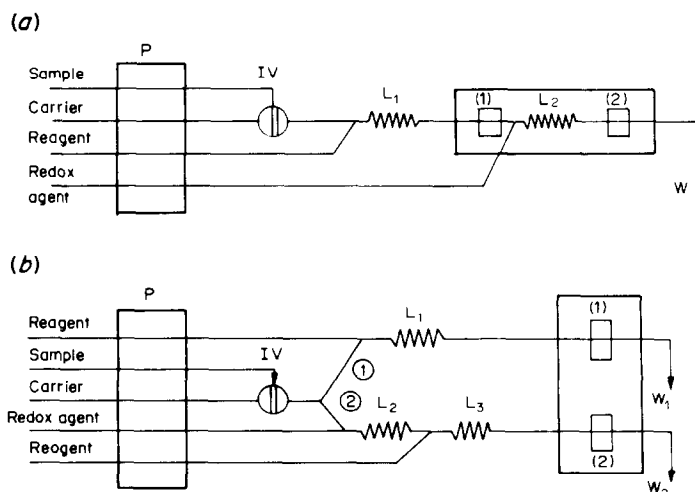


Fig. 3. FIA configurations with double-beam spectrophotometer for speciation studies (simultaneous determination): (a) series configuration of the flow-cells; (b) parallel configuration.

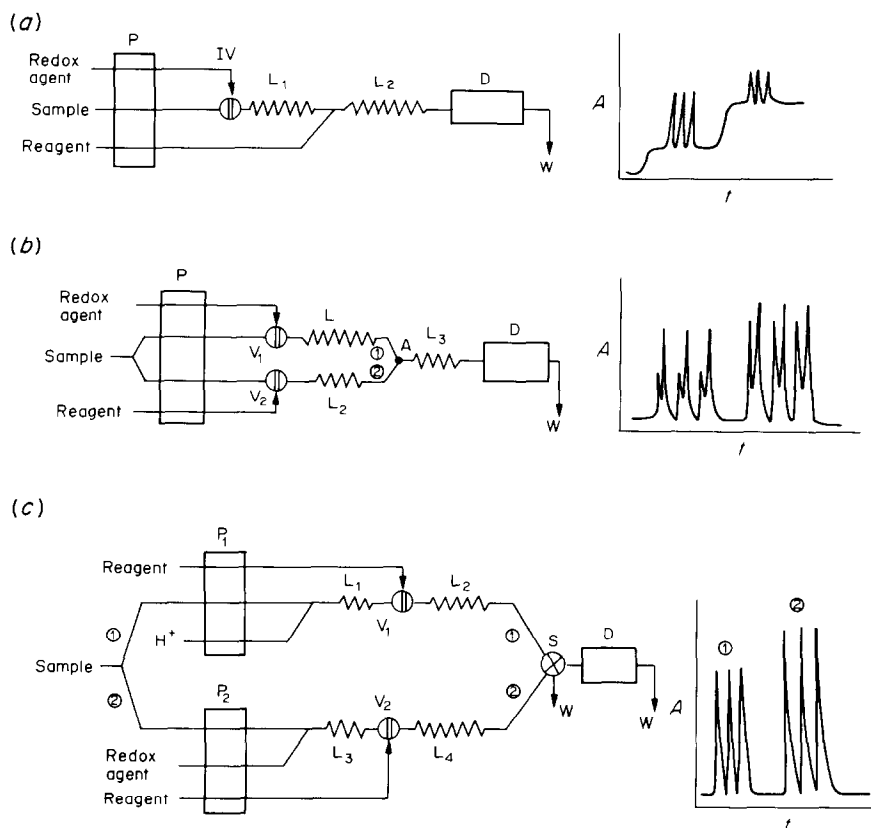


Fig. 4. Reversed FIA configurations for speciation studies, and the recordings obtained in each case: (a) with continuous determination of Cr(VI) and periodical determination of Cr(III); (b) with asymmetric merging zones; (c) sequential determination of Cr(VI) (upper sub-system) or overall chromium (lower sub-system) with the aid of a selecting valve, S.

solution, before injection of *N*-(1-naphthyl)ethylenediamine. The method has been applied to seawater.²⁴

Electrochemical detection has not been used in such a configuration, but it seems likely that it would increase the potential of FIA.

CONFIGURATIONS WITH TWO DETECTORS

Despite the greater costs, the inclusion of two detectors in FIA manifolds for speciation studies opens up many more possibilities. The use of a redox agent in the chemical system is then not necessary. The various designs are discussed in the order in which they appear in Table 1.

Series detectors

When a suitable redox agent is used, manifolds can involve (a) an optical and an electrochemical detector; (b) two identical detectors, one of which measures the concentration of one oxidation state, and the other, located after the confluence with a suitable redox agent, determines the sum of the two oxidation states; (c) two different electrochemical detectors placed as in (b). These possibilities have not yet been applied.

When no redox agent is used in the chemical system, both the chemical and the FIA systems become simpler. The methods suggested by Burguera and Burguera²⁵ and Lynch *et al.*²⁶ for determination of Fe(III)/Fe(II) and Cr(VI)/Cr(III) use optical, molecular and atomic detectors to determine one of the oxidation states (molecular detector) and the overall concentration (atomic detector) of the element concerned. It would be possible to use an optical detector to determine one of the chemical forms of the element and an electrochemical detector to determine the other or the sum of the two. The use of two potentiometric detectors (ISEs) in series has been outlined by Růžička *et al.* for nitrogen speciation studies (NO_3^- and NH_4^+).^{27,28} Voltammetry could also be applied, with working electrodes suitable for the chemical system under study and at an appropriate potential for detection of each of the oxidation states. The more negative electrode would provide the concentration of one of the species or the overall concentration, depending on whether the technique used were differential or not.

Parallel detectors

Two identical optical detectors in parallel and a solid redox agent (reducing microcolumn) have been

used to determine NO_2^- and NO_3^- . In parallel systems, there must be a splitting point after the injection port, to provide a sub-plug to each sub-system.²⁹ Confluence with a redox agent could be used instead of the column, and the optical detectors could be replaced by electrochemical ones, but neither approach has yet been realized.

Two systems with no redox agent have been proposed. (1) Use of a multichannel spectrophotometer and multiple injection for determination of NH_4^+ by formation of indophenol blue, and of nitrate by direct spectrophotometric measurement.³⁰ The sample is injected simultaneously, by the multiple valve, into each of the sub-systems, later merging with the reagent channels in the NH_4^+ sub-system. (2) Use of two spectrophotometers, one for determination of Fe(II) with 1,10-phenanthroline, and the other for determination of Fe(III) with thiocyanate. The manifold has a dual injection valve which inserts a plug into each sub-system.³¹

Possibilities that might be considered in the future again include use of an optical and an electrochemical detector, or two electrochemical detectors. Injection could be performed by a dual valve, or a single injection could be made into a manifold with a splitting point located after the injection system.

The method suggested by Burguera and Burguera³² for determination of sulphide, sulphite, sulphate and total sulphur with the aid of a molecular-emission detector is of particular interest. The method is based on the differing emission generation rates for the various anions, resulting in the sequential appearance of peaks due to S^{2-} , SO_3^{2-} and SO_4^{2-} . The use of hydrogen peroxide as carrier allows the determination of total sulphur.

A new alternative for the determination of more than two chemical forms of the same element is currently under study.³³ This makes use of some of the configurations suggested for chromium speciation studies (rFIA or normal FIA), along with a pH microelectrode located in the sample stream before the point of injection of the reagent (rFIA) or inside the loop of the injection valve if normal FIA is used. Once the sample pH is known, the use of known values for the formation constants of the various chemical forms [$\text{Cr}_2\text{O}_7^{2-}$, CrO_4^{2-} , HCrO_4^- , H_2CrO_4 and Cr(III) hydroxo-complexes] allows the concentration of these species to be calculated, along with that of total chromium.

FUTURE DEVELOPMENTS

The potential of FIA for speciation studies is not limited to the configurations and methods already described. Many more analytical methods should be amenable to adaptation for FIA. Some points deserve special attention.

(1) Separation techniques associated with continuous unsegmented flow systems may be used as a

means of eliminating interferences from other species present, and also to separate the various chemical forms of the element of interest. The following techniques have been used in conventional speciation methods: ion-exchange (in arsenic speciation¹⁶), gel filtration (aluminium speciation³⁴), Donnan dialysis (complexes of Pb, Zn, Cu and Cd with glycine and humic and nitrilotriacetic acids in lake waters³⁵), HPLC (intermediate polar coal-derivatives,³⁶ arsenic and selenium,¹⁸ organocopper complexes,³⁷ methyltins,³⁸ *etc.*), thermal vaporization (inorganic and organometallic compounds³⁹). The selective formation of hydrides can also be utilized as a separation technique.^{14,16}

(2) Many useful detection techniques (infrared spectrometry,³⁶ atmospheric-pressure ionization mass-spectrometry,⁴⁰ inductively coupled plasma spectrometry,¹⁸ ultraviolet resonance Raman spectrometry,⁴¹ *etc.*) have not yet been used for detection in FIA-speciation. Electrochemical techniques, especially potentiometry^{27,28} and voltammetry⁴³⁻⁴⁵ should also be useful since commercially available instruments are affordable even by modest laboratories. A diode-array detector has recently been used to monitor the sample plug at several wavelengths⁴⁶ and the potential of this for solving speciation problems is clear.

(3) So far FIA has been used in speciation studies of very few elements. Currently, selenium is under study⁴⁷ on account of its presence in waters and biological fluids,⁴⁸ but there are many other elements⁴⁹⁻⁵¹ of interest.

(4) Conventional analytical methods have provided interesting results in theoretical studies of speciation (*e.g.*, the work of Marinsky and co-workers^{52,53} but FIA has not yet been used for this purpose.

Acknowledgement—The CAICYT is thanked for financial support (Grant No. 2012-83).

REFERENCES

1. G. G. Leppard (ed.), *Trace Element Speciation in Surface Waters*, Plenum Press, New York, 1983.
2. S. A. Peoples, in *Arsenical Pesticides*, E. A. Woolson, (ed.), Am. Chem. Soc., Washington, 1975.
3. E. Berman, in *Toxic Metals and Their Analysis*, L. C. Thomas (ed.), Heyden, Philadelphia, 1980.
4. T. M. Florence, *Talanta*, 1982, **29**, 345.
5. G. E. Pacey and B. P. Bubnis, *Int. Lab.*, 1984, **25**, No. 9, 26.
6. T. M. Florence and G. E. Batley, *CRC Crit. Rev. Anal. Chem.*, 1980, **9**, 219.
7. M. Gallego, M. Silva and M. Valcárcel, *J. Food Sci.*, in press.
8. J. F. Van Staden, *Anal. Chim. Acta*, 1982, **138**, 403.
9. M. F. Giné, F. H. Bergamin, E. A. G. Zagatto and B. F. Reis, *ibid.*, 1980, **114**, 191.
10. Xu Shukun and Fang Zhaolun, *Fenxi Huaxue*, 1983, **93**, 11.
11. B. P. Bubnis, M. R. Straka and G. E. Pacey, *Talanta*, 1983, **30**, 841.
12. J. C. Andrade, J. C. Rocha and N. Baccan, *Analyst*, 1985, **110**, 197.

13. J. Ruz, A. Ríos, M. D. Luque de Castro and M. Valcárcel, *Anal. Chim. Acta*, in press.
14. P. Linares, M. D. Luque de Castro and M. Valcárcel, *Anal. Chem.*, in press.
15. P. Weigt and A. Sappl, *Z. Anal. Chem.*, 1983, **316**, 306.
16. J. Aggett and R. Kadwani, *Analyst*, 1983, **108**, 1495.
17. B. Sarx and K. Bächmann, *Z. Anal. Chem.*, 1983, **316**, 621.
18. J. P. McCarthy, J. A. Caruso and F. L. Fricke, *J. Chromatog. Sci.*, 1983, **21**, 389.
19. M. D. Luque de Castro and M. Valcárcel, *Analyst*, 1984, **109**, 413.
20. M. Valcárcel and M. D. Luque de Castro, *Flow Injection Analysis: Principles and Applications*, Horwood, Chichester, in the press.
21. A. Ríos, M. D. Luque de Castro and M. Valcárcel, *Anal. Chem.* 1985, **57**, 1803.
22. J. Ruz, A. Ríos, M. D. Luque de Castro and M. Valcárcel, *Talanta*, in press.
23. *Idem*, *Z. Anal. Chem.*, in press.
24. K. S. Johnson and R. L. Petty, *Limnol. Oceanog.*, 1983, **28**, 1260.
25. J. L. Burguera and M. Burguera, *Anal. Chim. Acta*, 1984, **161**, 375.
26. T. P. Lynch, N. J. Kernoghan and J. N. Wilson, *Analyst*, 1984, **109**, 839.
27. E. H. Hansen, J. Růžička and A. K. Ghose, *Int. Atomic Energy Agency*, Vienna 1980, Comm. 6, p. 77.
28. E. H. Hansen, F. J. Krug, A. K. Ghose and J. Růžička, *Analyst*, 1977, **102**, 714.
29. L. Anderson, *Anal. Chim. Acta*, 1979, **110**, 123.
30. J. Slanina, F. Bakker, A. Bruyn-Hes and J. J. Möls, *ibid.*, 1980, **113**, 331.
31. T. P. Lynch, N. J. Kernoghan and J. N. Wilson, *Analyst*, 1984, **109**, 843.
32. J. L. Burguera and M. Burguera, *Anal. Chim. Acta*, 1984, **157**, 177.
33. J. Ruz, A. Torres, A. Ríos, M. D. Luque de Castro and M. Valcárcel, *J. Autom. Chem.*, in press.
34. P. G. C. Campbell, M. Bisson, R. Bougie, A. Tessier and J. P. Villeneuve, *Anal. Chem.*, 1983, **55**, 2246.
35. J. A. Cox, K. Slonawska, D. K. Gatchell and A. G. Hiebert, *ibid.*, 1984, **56**, 650.
36. R. S. Brown and L. T. Taylor, *ibid.*, 1983, **55**, 723.
37. L. Brown, S. J. Haswell, M. M. Rhead, P. O'Neill and K. C. C. Bancroft, *Analyst*, 1983, **108**, 1511.
38. J. C. Means and K. L. Hulebak, *Neurotoxicology*, 1983, **4**, 37.
39. S. Hanamura, B. W. Smith and J. D. Winefordner, *Anal. Chem.*, 1983, **55**, 2026.
40. N. H. Hijazi and G. B. De Brou, *Trans. Tech. Sect. (Can. Pulp. Pap. Assoc.)*, 1982, **8**, 100.
41. S. A. Asher, *Anal. Chem.*, 1984, **56**, 720.
42. C. J. Kramer, G. Yu and J. C. Duinker, *Z. Anal. Chem.*, 1984, **317**, 383.
43. *Idem*, *Anal. Chim. Acta*, 1984, **164**, 163.
44. T. E. Edmonds, *Anal. Proc.*, 1984, **21**, 366.
45. H. W. Nürnberg, *Z. Anal. Chem.*, 1983, **316**, 557.
46. F. Lázaro, A. Ríos, M. D. Luque de Castro and M. Valcárcel, *Flow Analysis III*, Birmingham, 1985.
47. P. Linares, personal communication.
48. H. J. Robberecht and H. A. Deelstra, *Talanta*, 1984, **31**, 497.
49. Z. Wang and A. Peng, *Fenxi Huaxue*, 1983, **11**, 321.
50. B. Welte, N. Bles and A. Montiel, *Environ. Technol. Lett.*, 1983, **4**, 79.
51. *Idem*, *ibid.*, 1983, **4**, 223.
52. I. Merle and J. A. Marinsky, *Talanta*, 1984, **31**, 199.
53. S. Alegret, M. T. Escalas and J. A. Marinsky, *ibid.*, 1984, **31**, 683.

ANALYTICAL APPLICATIONS OF ABSORPTION SPECTROELECTROCHEMISTRY AT GRAZING INCIDENCE

JULIAN F. TYSON

Department of Chemistry, Loughborough University of Technology, Loughborough, England

(Received 12 July 1985. Accepted 28 August 1985)

Summary—Analytical applications of spectroelectrochemistry are limited by the short path-length, in the absorbing medium, that can be produced with most light-beam/electrode configurations. This disadvantage is overcome for grazing incidence. A cell fitted with glassy-carbon electrodes and used in a conventional spectrophotometer is described and applied to model systems illustrating the use of (a) homogeneous redox reactions, (b) homogeneous redox reaction followed by chemical reaction and (c) electro-deposition followed by stripping into a reagent solution. This last technique is the spectro-electrochemical analogue of anodic-stripping voltammetry.

Although many spectroscopic techniques have been used to monitor species both in the diffusion layer and on the electrode surface (during and after electrolysis), there have been few quantitative analytical applications.¹ The aim of most of such studies has been the elucidation of reaction mechanisms, measurement of rate constants, diffusion coefficients, E^0 and n values, and study of the electrode surface. As candidates for quantitative analytical application, spectroelectrochemical experiments based on the absorption of light by species in the diffusion layer after imposition of a potential step are the most interesting, because the equations which relate the absorbance to various parameters of the system are analogous to the Beer–Lambert equation for conventional solution spectrophotometry. These experiments include total internal reflection at an optically transparent electrode (OTE)² and normal transmission at an OTE.³ The limitations of the former technique are set by the path-length in the absorbing medium, which in turn depends on the extent to which the totally internally reflected beam passes into the solution at the other side of the electrode interface. The latter technique is limited by the time taken for the “equivalent path-length” to reach high enough values, the basic equation being

$$A = \epsilon_R 2 \left(\frac{D_o t}{\pi} \right)^{1/2} C_o^b \quad (1)$$

where A is the absorbance, ϵ_R the molar absorptivity of the reduced species, D_o the diffusion coefficient of the oxidized species, t time and C_o^b the bulk concentration of the oxidized species. This form of the equation is for the reaction $O + ne \rightarrow R$, namely a homogeneous reduction at the electrode surface. The “equivalent path-length” is $2(D_o t/\pi)^{1/2}$ and thus for a given system with constant ϵ_R , C_o^b and D_o , the absorbance increases with the square root of the time.

For a hypothetical value of 10^{-5} cm²/sec for D_o the change in equivalent path-length (cm) with time is given in Fig. 1. It can be seen that the path-length (and hence absorbance) increases only very slowly with time. It can readily be calculated from equation (1) that it will take something approaching 22 hr for the equivalent path-length to become 1 cm.

If the light-beam is passed at grazing incidence over the surface of the electrode the equation (1) is modified⁴ to

$$A = \epsilon_R 2(D_o t/\pi)^{1/2}(b/h)C_o^b \quad (2)$$

where b is the length of electrode surface traversed by the light-beam, h the width of the beam and the other symbols have the same meaning as before. The “equivalent path-length” in this equation is $2(D_o t/\pi)^{1/2}(b/h)$ and is shown as a function of time in Fig. 1 for values of b and h of 1 and 0.05 cm respectively. It can readily be seen that potentially useful “path-lengths” are obtained in only a few minutes.

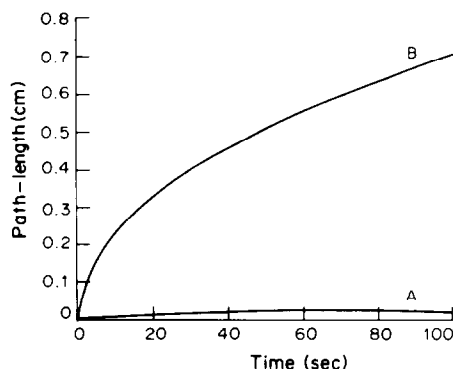


Fig. 1. Variations of “equivalent path-length” with time, for a hypothetical compound with a diffusion coefficient of 10^{-5} cm²/sec, with absorbance measured normal to (curve A) and parallel to (curve B) the electrode surface.

The quantitative analytical basis of the technique is also seen from equation (2). The absorbance is directly proportional to concentration at a given time, and furthermore, the slope of the A vs. $t^{1/2}$ plot is also proportional to concentration. The "equivalent path-length" model predicts that the absorbance will reach a maximum value when $2(D_0 t/\pi)^{1/2} = h$. For the values used here, the time for this to occur is 196 sec.

In recent years there has been an increase in the use of the parallel or near-parallel absorption method (see, for example, references 5–10) and other methods of increasing the sensitivity of the measurement, such as use of a circulating, long optical-path, thin-layer cell.¹¹

In this paper, two methods using grazing incidence and a glassy carbon electrode are reported. In the first, homogeneous reactions are used, in which the determinand species undergoes a spectral change on oxidation or reduction at the electrode surface. The possibility of producing a spectral change by a chemical reaction subsequent to the electrode reaction was also investigated. In the second method, a spectroelectrochemical analogue of anodic-stripping voltammetry is used, in which the metal to be determined is electro-deposited on the electrode surface and then stripped off into a solution of a spectrophotometric reagent.

EXPERIMENTAL

Reagents

Metal-ion solutions were prepared from analytical-reagent grade salts. Spectrophotometric and other reagent solutions were prepared from the solid reagents. All solutions were prepared with triply distilled water.

Apparatus

The cell-holder of a Pye Unicam SP600 Series 2 spectrophotometer was modified to accept a cell with two glassy-carbon plate electrodes (see Fig. 2). Slits (approximately 1 mm wide) mounted in front of and behind the cell

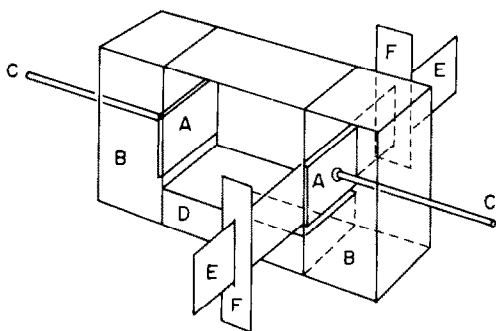


Fig. 2. Sketch of the spectroelectrochemical cell. The glassy-carbon electrodes, A (10 × 20 mm), are mounted in resin blocks, B, and connected to the external circuit by copper wires, C, joined to their backs with silver-loaded epoxy resin. The blocks are secured to a Teflon base, D, with the electrodes about 20 mm apart. The cell windows are microscope slides cut to size and glued in place. The path and dimensions of the light-beam, E, are defined by the slits, F, mounted either side of the cell assembly.

defined the light-beam and the cell was positioned by horizontal adjustment with a worm gear drive. The cell was equipped with a variety of inlets and outlets so that sample solutions *etc.* could be pumped in and out, the solution deoxygenated with oxygen-free nitrogen and a nitrogen atmosphere maintained. The spectrometer output was converted into absorbance by an SP45 unit and monitored with an $X-t$ recorder. The electrode potential was controlled by means of a manual polarograph (Southern Analytical A1650) or a potentiostat (Princeton Applied Research 174).

Procedures

The general procedure for the homogeneous reactions was to transfer the solution (in background electrolyte) to the cell, deoxygenate it, set zero and 100% transmission, start the chart recorder and apply a potential step (typically 2 V vs. the counter-electrode). For the anodic-stripping mode, after a suitable deposition time, the solution was replaced by one containing the spectrophotometric reagent (dissolved in background electrolyte), the absorbance scale was set, the chart recorder started, and a potential step applied.

RESULTS AND DISCUSSION

Homogeneous reactions

Various species were investigated, including ferroin, ferrocyanide, phosphomolybdate, methyl viologen (1,1'-dimethyl-4,4'-bipyridinium), permanganate, dichromate and iodide. The oxidation of iodide was monitored by means of the absorbance of the iodine produced or that of the blue starch-iodine compound. For all the species examined, the plots of A vs. $t^{1/2}$ had a linear region (as shown in Fig. 3), the slope of which showed a high correlation with concentration. A similar correlation between the maximum absorbance obtained and concentration was also observed. As examples, the results for phosphomolybdate and the iodide-starch system are given in Table 1.

Anodic-stripping

The following combinations of metal and spectrophotometric reagent were investigated: (a) copper and Pyrocatechol Violet (PCV), murexide, or pyridyl

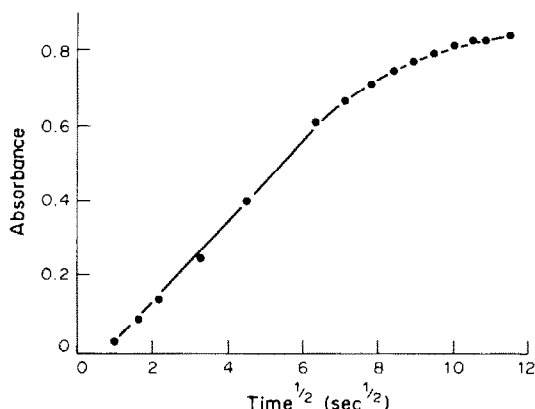


Fig. 3. Plot of absorbance (at 720 nm) against $t^{1/2}$ for phosphomolybdenum blue ($8 \times 10^{-4} M$). The applied potential was -2.0 V.

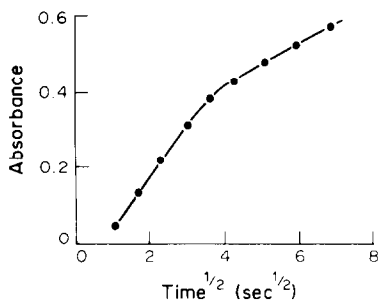


Fig. 4. Plot of absorbance (at 630 nm) against $t^{1/2}$ for the anodic redissolution of copper (at +2.0 V) into a solution of Pyrocatechol Violet.

azo resorcinol (PAR), (b) zinc and zincon or PCV, (c) cadmium and murexide or PCV, (d) silver and 1,10-phenanthroline plus tetrabromofluorescein. All these systems exhibited a linear portion in the plot of A vs. $t^{1/2}$ (see Fig. 4 for example), with a slope strongly correlated with concentration; the maximum absorbance was also correlated with concentration. Results for the copper-PVC system are given in Table 1. The best performance in terms of sensitivity and detection limit was obtained for silver, with a $3 \times 10^{-7} M$ concentration ($0.03 \mu\text{g/ml}$) being detectable after a deposition time of 15 min.

It is interesting that the linear A vs. $t^{1/2}$ relationship is obtained for systems which might be expected to be far removed from the simple case of semi-infinite linear diffusion. This shows that in the systems so far chosen for investigation, the reaction kinetics are fast compared with the diffusion-controlled movement of species in solution. The homogeneous reactions show that the electrode acts as a solid redox reagent in the system and eliminates the thermodynamic and kinetic problems that are sometimes associated with the use of conventional redox reagents. The chemistry of the molybdenum heteropoly acid species provides a good example of the difficulties that can beset a spectrophotometric procedure. At least six different reducing agents have been recommended for the production of phosphomolybdenum blue and the product of the reaction may be either the α or the β form, depending on the reaction conditions and order of addition of reagents.^{12,13} Often, as well as specifying the order of addition of reagents, a conventional procedure will specify a time period during which the absorbance should be measured. The use of the slope of the A vs.

$t^{1/2}$ plot as the quantitative parameter means that solutions more concentrated than those that can be handled by the conventional procedure can be measured without predilution. Both modes of operation can provide procedures for given analytes, as selectivity can be introduced by control of the electrode potential at the various stages, by use of masking agents, and by use of consecutive chemical reactions following the electrochemistry. At present the methods are slow and have not demonstrated any dramatic improvement in sensitivity or detection limits (this is not expected for homogeneous systems), but in principle the anodic-stripping mode could rival its voltammetric analogue, as it is not limited by the problem of distinguishing between faradaic and non-faradaic processes. It can be seen from equation (2) that the speed of the technique could be improved by reducing h , the width of the beam defined by the slits. With a conventional solution spectrophotometer, there is a limit to the reduction in beam-width that can be achieved before an unacceptable lowering of the signal to noise ratio occurs. This difficulty could be overcome by use of a laser as light-source, and the use of a slit-width as narrow as $3 \mu\text{m}$ with such a source and consequent improvement in the rise time have been reported.⁵ The electrode material, glassy carbon, appears more suitable than platinum, which was used in previous studies¹⁴ and produced OH^- in the diffusion layer on reduction after an anodic pretreatment. No special cleaning of the electrodes has been found necessary and their efficiency has been maintained for several months.

CONCLUSIONS

The results of these preliminary investigations show that spectroelectrochemistry at a glassy-carbon electrode with use of the grazing-incidence configuration has considerable promise as a quantitative analytical technique, particularly when coupled with potential-step electrochemistry. The two modes described here, homogeneous reaction and anodic stripping, have both been shown to have features capable of exploitation for achieving selective and sensitive analytical determinations. It is expected that some improvement on these preliminary results would be obtained with a better quality spectrophotometer, but a purpose-built instrument (incorporating a tunable laser source) would be ex-

Table 1. Least-squares linear regression analysis of calibration data [A_{max} is maximum absorbance on absorbance-time plot, m is slope of absorbance-time^{1/2} plot ($\text{sec}^{-1/2}$), C is concentration (M), n is number of data points, and r is Pearson's correlation coefficient]

System	A_{max} vs. C				m vs. C			
	n	slope, $l./\text{mole}$	intercept	r	n	slope, $l.\text{mole}^{-1}.\text{sec}^{-1/2}$	intercept	r
Phosphomolybdenum blue	10	8.1×10^3	0.004	0.996	9	1.1×10^3	0.014	0.999
Iodide-starch	9	8.5×10^3	-0.35	0.998	8	2.5×10^3	-0.10	0.988
Copper-Pyrocatechol Violet	7	4.6×10^2	-0.018	0.983	7	1.6×10^2	-0.003	0.993

pensive, and one of the attractive features of the technique in its present form is that it forms the basis of a low-cost accessory for an existing conventional spectrophotometer. It is expected that the analytical capability of the technique could be extended by use of fluorescence and chemiluminescence measurement.

Acknowledgement—Assistance from J. R. Erone, A. S. Khulumula and P. J. Weir with aspects of the experimental work is gratefully acknowledged.

REFERENCES

1. J. Robinson, *Specialist Periodical Report on Electrochemistry*, Vol. 9, p. 101. Royal Society of Chemistry, London, 1984.
2. T. Kuwana and N. Winograd, *Electroanalytical Chemistry*, Vol. 7, A. J. Bard (ed.), p. 9. Dekker, New York, 1974.
3. J. W. Strojek and T. Kuwana, *J. Electroanal. Chem.*, 1968, **16**, 471.
4. J. F. Tyson and T. S. West, *Talanta*, 1980, **27**, 335.
5. R. Pruiksmas and R. L. McCreery, *Anal. Chem.*, 1981, **53**, 202.
6. R. L. McCreery, R. Pruiksmas and R. Fagan, *ibid.*, 1979, **51**, 749.
7. M. J. Simone, W. R. Heineman and G. P. Kreishman, *ibid.*, 1982, **54**, 2382.
8. J. Zak, M. D. Porter and T. Kuwana, *ibid.*, 1983, **55**, 2219.
9. C. W. Anderson and M. R. Cushman, *ibid.*, 1982, **54**, 2122.
10. J. D. Brewster and J. L. Anderson, *ibid.*, 1982, **54**, 2560.
11. J. L. Anderson, *ibid.*, 1979, **51**, 2312.
12. R. A. Chalmers and A. G. Sinclair, *Anal. Chim. Acta*, 1965, **33**, 384.
13. *Idem*, *ibid.*, 1966, **34**, 412.
14. J. F. Tyson and T. S. West, *Talanta*, 1979, **26**, 117.

Dedication—As one who had the good fortune to be first made aware of the fascination of the application of chemical principles to the solving of analytical problems by Bob Chalmers, it is indeed a pleasure to have a small part in this tribute to him. In all aspects of his career as a professional analytical chemist, he sets examples of the highest standards and, in making this contribution, I am pleased to acknowledge that much of the enjoyment derived from the challenge of trying to emulate his example is due to his valued guidance, encouragement and friendship.

MATRIX MODIFICATION—THE USE OF PROTEIN-FREE SOLUTIONS IN THE DETERMINATION OF METALS IN BLOOD BY FLAME ATOMIC FLUORESCENCE AND EMISSION SPECTROMETRY

E. J. EKANEM,* C. L. R. BARNARD† and J. M. OTTAWAY

Department of Pure and Applied Chemistry, University of Strathclyde, 295 Cathedral Street, Glasgow, Scotland

G. S. FELL

Department of Clinical Biochemistry, Royal Infirmary, Glasgow, Scotland

(Received 27 June 1985. Accepted 9 September 1985)

Summary—A procedure is described for matrix modification in the determination of metals in blood by flame spectrometric methods. The protein is removed by precipitation with dilute nitric acid and centrifugation and the supernatant liquid is used for direct analysis. Nitric acid is compared with other acids as the precipitant. The technique is simple, contamination-free and provides a solution which may be directly compared with aqueous calibration standards. Its application for determination of clinically important metals by flame atomic fluorescence and emission spectrometry is demonstrated.

The direct determination of protein-bound metals in blood samples is complicated by the high matrix effect of the proteins themselves.¹ The nature of the interactions between blood and metals is the subject of much debate and numerous metals are present as complexes with blood components and to a lesser extent as the free ions.

Release of the metals from such complexes requires either the use of chelating agents or destruction of the ligand. The usual procedure for destroying organic material in blood samples involves wet oxidation² with mixtures of sulphuric and nitric acids, and/or perchloric acid. Carter and Yeoman³ have described the use of low-temperature ashing in an oxygen plasma, although this is also a time-consuming procedure. Various pressurized-bomb digestion systems have been described⁴ but there is always an appreciable decomposition time and significant risk of contamination.⁵ Use of glassy carbon instead of the traditional PTFE as the bomb material reduces contamination.⁶ Novel, contamination-free ultraviolet-irradiation techniques have been described by Batley and Farrar,⁷ but are even slower, the oxidation taking up to 12 hr.

Routine analysis for clinically important metals in blood or plasma/serum has been largely restricted to

flame emission spectrometry (FES) and atomic-absorption spectrometry (AAS). Flame atomic-fluorescence spectrometry has been described for the determination of both trace^{8,9} and major¹⁰ metals, with use of line and continuum sources respectively. There are difficulties in the determination of metals in whole blood, owing to the particulate nature and viscosity of the sample. Such problems are reduced by dilution of the sample, but this increases the lower limit of determination.

Removal of proteins from blood prior to colorimetric analysis is widely used in the biochemical laboratory.^{11,12} The protein precipitants in common use include sodium tungstate or alkaline zinc sulphate solution, and trichloroacetic and perchloric acids. Use of acids is preferred in metal analysis because they are available in high-purity grades.

The addition of acids to blood denatures the proteins, resulting in their precipitation,¹³ with dissolution and release of the metals into the supernatant fluid. This is commonly used as a matrix modification procedure when metals are determined in blood by carbon-furnace atomic-absorption spectrometry (CFAAS).¹⁴⁻¹⁸ Protein-free liquids produced in this manner by centrifugation are frequently referred to as "protein-free filtrates" but the more correct terminology "supernatant fluid" will be used throughout this article.

A comparison of several acids commonly used to deproteinate blood is presented. The characteristics of each are compared in terms of metal release and suitability for flame spectrometric analysis. The application of the technique for the AFS determination

*Now at School of Basic Studies, Ahmadu Bello University, Zaria, Nigeria.

†Now at Department of Chemistry and Metallurgy, Glasgow College of Technology, Cowcaddens, Glasgow, Scotland.

of cadmium, zinc, magnesium, calcium and iron is described, together with the flame AES determination of sodium and potassium.

EXPERIMENTAL

Apparatus

The spectrometer used for line-source atomic-fluorescence spectrometry (LSAFS) was essentially the same as that described by Michel and co-workers.^{8,10} The temperature control of the electrodeless discharge lamp (EDL) was modified by incorporation of a thermocouple feedback system to maintain a constant temperature environment for the EDL.

An Eimac xenon-arc continuum source was used at low power for background correction in LSAFS and also at higher power as a primary source in continuum-source AFS (CSAFS). In the latter case, background correction was achieved by means of a laboratory-constructed wavelength modulation device.¹⁰ The same configuration of flame, monochromator and detector was also used in the emission mode (*i.e.*, with no light source) and in this case background correction was also achieved by means of wavelength modulation. In all cases, a nitrogen-separated flame was used to reduce flame background.⁸

Reagents

Analytical-grade reagents were used for preparation of solutions and "AristaR" nitric acid was used to precipitate the blood proteins. In all cases, solutions were prepared with high-purity demineralized water.

Blood sample collection and storage

The technique was developed with out-dated whole blood samples supplied by the blood bank. Samples for evaluation of the technique were collected in accordance with the established procedure used for CFAAS determinations of blood cadmium at Glasgow Royal Infirmary.¹⁹ Whole blood was obtained by venepuncture and stored in contamination-free tubes containing anticoagulant (potassium-EDTA or lithium-heparin). All blood samples, including plasma and serum, were stored temporarily at 4° or for longer periods at -20°.

The sample containers, polypropylene centrifuge tubes and volumetric ware were all soaked overnight in nitric acid (1 + 1), then washed and rinsed with demineralized water prior to use. The containers were regularly examined for contamination, by rinsing with 2*M* nitric acid and aspirating the washings into the flame. The signals obtained were below the detection limits in all cases.

Deproteinization of the samples

A 2-ml portion of the blood sample was transferred into a centrifuge tube containing 2 ml of precipitant. The tube was stoppered and vigorously shaken, then the mixture was centrifuged at 3000 rpm for 30 sec, after which the protein-free supernatant liquid was separated for analysis. Plasma-protein precipitation was found to be complete only if the precipitant was refrigerated before mixing.

Each precipitant was considered in turn for its efficiency in releasing metal ions from the proteins in blood, and the physical properties of the deproteinized samples were compared with those of the aqueous standards used for calibration.

Evaluation of deproteinized samples for metal determination

Detection limits. The limit of detection was taken as the analyte concentration equivalent to twice the noise level associated with a deproteinized sample known to contain an analyte concentration (after appropriate dilution) about four times the detection limit for a purely aqueous solution.

Precision. To measure the precision of the entire procedure, 15 separate 2-ml portions of the same pooled blood sample were deproteinized and diluted as appropriate for each analyte. The precision was determined as the relative standard deviation for each element measured in the 15 samples.

Accuracy. The accuracy of the procedure was evaluated by direct comparison with other spectrometric methods applied to the same samples. The levels of cadmium and zinc found in the deproteinized samples were compared with those obtained by the standard CFAAS method. Similarly, flame AAS was used for checking the magnesium levels, FES for sodium and potassium and colorimetry for calcium and iron.

Analytical procedures

Calibration standards were prepared from 2000-ppm stock solutions by serial dilution and were matrix-matched to the acid concentration of the deproteinized samples. The prepared samples were directly aspirated without dilution for the determination of cadmium by LSAFS and of zinc and iron by CSAFS. The solution was diluted 50-fold before CSAFS determination of calcium and magnesium. Calcium, sodium and potassium were determined with the instrument in the wavelength-modulated FAES mode, the deproteinized samples being diluted 50-fold for calcium and 500-fold for sodium and potassium determinations.

The analytical standards and deproteinized samples were all prepared so as to contain 1000 µg of lanthanum (added as lanthanum nitrate solution) per ml to reduce anionic interferences. The 1.0*M* nitric acid concentration in the standards and deproteinized samples reduced the interferences from sodium, calcium and phosphate in the determination of iron. In the determination of sodium, it was necessary to have 3000 ppm of potassium present in the test solution, and for potassium, 2000 ppm of sodium, in order to suppress ionization effects.

RESULTS AND DISCUSSION

The four acids, hydrochloric, nitric, monochloroacetic (CA) and trichloroacetic (TCA), tested as protein precipitants, were compared in terms of the viscosity (measured as nebulizer uptake rate) and volume of the supernatant liquid produced. The release of metals from blood or plasma was assessed from the spectrometric signal obtained when the deproteinized sample was aspirated into the flame.

The four acids were directly compared for their applicability to the determination of cadmium in whole blood (Table 1). It was observed that use of nitric acid gave the largest volume of supernatant liquid from blood, and also from serum or plasma. The nitric acid treatment gave a product with essentially the same uptake rate as the aqueous calibration

Table 1. Comparative performance of acids as protein precipitants

Acid	Cadmium signal, <i>cps</i>	Volume of supernatant liquid, ml	Uptake rate, ml/min
HCl (2.0 <i>M</i>)	119	—	9.0
CA (1.5%)	101	1.6	2.9
TCA (1.0%)	94	1.6	2.9
HNO ₃ (2.0 <i>M</i>)	340	2.0	9.0

standards, whereas CA and TCA gave products with markedly higher viscosity, necessitating use of an uptake-rate correction. The uptake rate for the nitric acid products was practically the same (9.0 ml/min) for all samples tested.

Hydrochloric acid proved unsuitable as a protein precipitant because it caused excessive frothing and gave variable volumes of supernatant liquid. The optimum concentration of nitric acid for sample preparation was found to be 2.0M, as shown in Fig. 1.

Analytical recoveries

The efficiency of nitric acid in releasing metals from blood, for analysis, was assessed by adding known amounts of inorganic analytes to untreated blood samples, deproteinating them, and determining the recoveries of the analytes. The recoveries (Table 2) for cadmium and zinc, in whole blood and serum respectively, were all acceptable.

Good recoveries and accuracy were also obtained for iron in serum, but the recovery for iron in whole blood was very poor. It appears from this that protein precipitation does not facilitate the release of iron from red-cell protein and this may be attributed to the strong covalent bonding of iron in the haemoglobin molecule.

The concentration levels found for the deproteinated serum and plasma samples were generally higher than those for aqueous dilutions of the same samples (Table 3) and this is consistent with the acid denaturing of plasma proteins, which quantitatively releases metal ions by proton exchange.²⁰ The 60% increase in the calcium concentration found for plasma and serum by the deproteination method,

Table 2. Analytical recoveries for Cd and Zn from whole blood and serum

Cd (in whole blood)			Zn (in serum)		
Added, $\mu\text{g/l.}$	Found, $\mu\text{g/l.}$	Apparent recovery, %	Added, mg/l.	Found, mg/l.	Apparent recovery, %
0	1.16	—	0	0.82	—
2	3.14	99	0.100	0.93	101
4	5.56	110	0.400	1.22	99
6	7.67	108	0.800	1.63	100
8	9.80	108	1.000	1.82	100
10	11.40	102	2.000	2.83	100

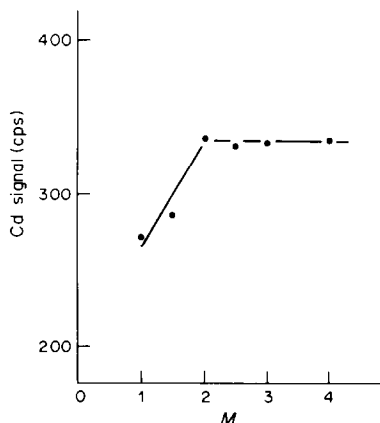


Fig. 1. Optimization of the nitric acid concentration for protein precipitation.

compared to the aqueous dilution results, indicates the more efficient release of this metal by the acid medium. The same trend was observed, though to a lesser extent, for other essential elements, e.g., iron, sodium and potassium.

When the protein precipitation method was compared with previous work⁸ a threefold improvement in blood cadmium detection limits was observed. The use of deproteination with nitric acid in the determination of cadmium in whole blood was further tested by comparison with the routine CFAAS procedure employed at Glasgow Royal Infirmary. The deproteinated samples were analysed for cadmium by use of a Perkin-Elmer 2280 spectrometer with an HGA-500 atomizer. The results, presented in Fig. 2, are in good agreement.

The presence of particulate matter in the flame, which is a characteristic of aspirated blood samples, contributes significantly to the spectroscopic noise. Since in atomic-fluorescence spectrometry it is the flame noise levels that ultimately determine the attainable detection limit, it is essential to minimize all such noise. When the particles in the flame are of atomic or molecular size, Rayleigh scatter predominates as the normal limiting factor in fluorescence measurements,²² but for particles which have a diameter significantly greater than the wavelength of the incident radiation the noise-limiting factor will be governed by Mie scatter.²³ Mie scatter is a major problem when diluted blood is aspirated into the flame, because of the size of the particles and the high particulate content of the nebulized sample.

Table 3. Comparison of results obtained for samples treated by deproteination and by aqueous dilution

Element	Matrix	Concentration found, mg/ml		Increase, † %
		Deproteination	Aq. dilution	
Ca	Plasma	0.113	0.069	65
Ca	Serum*	0.104	0.064	62
Na	Serum	3.04	2.93	4

*The lower calcium values for serum are expected because of the involvement of Ca in coagulation.

†Increase = 100 (Deprotn. signal - Dilution signal)/(Dilution signal).

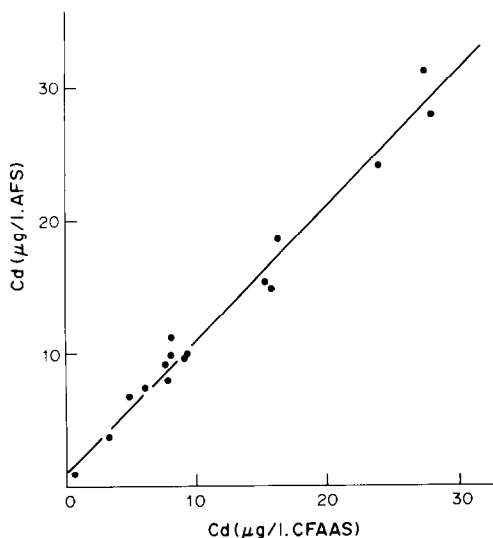


Fig. 2. Correlation diagram for the analysis of blood for cadmium by AFS (F) and CFAAS (A). Regression equation: $F = mA + C = 1.02A + 0.91$. The standard deviation of the scatter²¹ of the F values about the line = $1.33 \mu\text{g/l}$.

The absence of particulate matter in the deproteinated sample reduces the high scatter signal associated with blood analyses by flame AFS. Furthermore, the deproteinated sample does not clog the nebulizer (clogging is a problem when the haemolysis/dilution procedure is used). The particulate content of the sample presented to the flame by the acid-deproteination and Triton X-100/hydrochloric acid procedure was evaluated by making cadmium measurements on the treated blood samples, both with and without scatter correction. The correction for scatter⁸ involved nebulization of a highly scattering matrix [e.g., calcium phosphate (in hydrochloric acid) or 2% aluminium solution], irradiation of the flame with both the EDL and a continuum source, and balancing of the two signals

by adjustment of the continuum source intensity (measured at the cadmium wavelength). This provides automatic compensation for scatter, but any variation in the balance between the two irradiation intensities will result in a corresponding variation in the scatter-correction. This sets a noise limit on the lowest level of detection of the cadmium signal and was one reason for modifying the temperature-control system for the EDL. It is clear from the results (Table 4) that the deproteinated matrix gives virtually scatter-free signals.

The techniques used to assess the analyte content of the deproteinated samples are listed in Table 5. Their analytical figures of merit are described in terms of detection limits and precision. The deproteination method gives lower detection limits than the other matrix-modification procedures.

CONCLUSIONS

The results obtained by flame spectrometric techniques for the determination of metals in blood are highly dependent on the viscosity of the matrix. The use of protein precipitation with dilute nitric acid has been shown to give good results. This technique gives a detection limit of $0.05 \mu\text{g/l}$ for cadmium in blood and provides a scatter-free matrix which closely resembles the aqueous calibration standards. The high accuracy and precision afforded, together with the efficient release of metal ions, make this procedure eminently suitable for use with the techniques of flame atomic spectrometry.

The instrument used in this assessment of protein precipitation was an atomic-fluorescence spectrometer. It is very versatile in that it can function in a line-source mode for single-element analyses, where maximum sensitivity is important, or in a continuum-source mode for the more abundant metals. It may also be operated as a flame atomic-emission spectrometer. Each of these configurations incorporates

Table 4. Scatter signals from matrices used in blood analyses

Pretreatment method*	Matrix†	Scatter signal, cps	Equivalent cadmium concentration, $\mu\text{g/l}$.
A	W.B. 1	0	0.0
B	W.B. 1	301	2.6
A	W.B. 2	2	0.0
B	W.B. 2	266	2.3
A	W.B. 3	0	0.0
B	W.B. 3	230	2.0
A	Plasma 4	0	0.0
B	Plasma 4	11	0.1
A	Plasma 5	0	0.0
B	Plasma 5	13	0.1
None	2% Al solution	18617	163
None	2% $\text{Ca}_3(\text{PO}_4)_2$ solution (in hydrochloric acid)	19099	168

*A = Deproteination with an equal volume of 2M nitric acid.

B = Treatment⁸ with hydrochloric acid and Triton X-100 and dilution.

†W.B. = whole blood.

Table 5. Figures of merit for the flame spectrometric techniques used for blood analysis

Analyte	Technique	Wavelength, <i>nm</i>	Concn. tested, <i>µg/l.</i>	Relative std. devn.,* %	Detection limit, <i>µg/l.</i>
Cd	LSAFS	228.8	8	1.9 (10)	0.05
Zn	CSAFS	213.9	500	1.6 (15)	74
Mg	CSAFS	285.2	40	2.3 (15)	2
Ca	CSAFS	422.7	500	0.8 (15)	10
Fe‡	CSAFS	248.3	500	0.9 (15)	4
Ca	FAES	422.7	1000	0.5 (15)	26
Na	FAES	589.0	1000	0.9 (15)	1
K	FAES	404.4	10000	2.2 (15)	213

*Number of replicates given in brackets.

†As defined in text.

‡Serum iron.

automatic background correction. The instrument can thus offer an analytical service with rapid sample throughput and high standards of accuracy and precision and obviously has considerable potential for the determination of most metals of interest in the clinical laboratory.

Acknowledgements—The authors wish to thank the Scottish Home and Health Department for the award of a Post-doctoral Fellowship (to C.L.R.B.). They also wish to acknowledge the continued support of the Eastern District, Greater Glasgow Health Board.

REFERENCES

1. A. A. Cernik, *At. Absorpt. Newsl.*, 1973, **12**, 163.
2. T. T. Gorsuch, *The Destruction of Organic Matter*, Pergamon Press, Oxford, 1970.
3. G. F. Carter and W. B. Yeoman, *Analyst*, 1980, **105**, 295.
4. G. Kaiser, P. Tschöpel and G. Tölg, *Z. Anal. Chem.*, 1978, **291**, 278.
5. G. Kaiser, D. Godtz, G. Tölg, G. Knapp, B. Maichin and H. Spitzky, *ibid.*, 1978, **291**, 278.
6. L. Kotz, G. Heinze, G. Kaiser, S. Pahlke, M. Veber and G. Tölg, *Talanta*, 1979, **26**, 681.
7. G. E. Batley and Y. J. Farrar, *Anal. Chim. Acta*, 1978, **99**, 283.
8. R. G. Michel, M. L. Hall, J. M. Ottaway and G. S. Fell, *Analyst*, 1979, **104**, 491.
9. P. R. Sthapit, J. M. Ottaway and G. S. Fell, *ibid.*, 1983, **108**, 235.
10. R. G. Michel, J. Sneddon, J. K. Hunter, J. M. Ottaway and G. S. Fell, *ibid.*, 1981, **106**, 288.
11. R. J. Henry and C. P. Szustkiewicz, in *Clinical Chemistry*, R. J. Henry, C. P. Szustkiewicz, D. C. Cannon and J. W. Winkelmann (eds.), 2nd Ed., p. 389. Harper & Row, New York, 1974.
12. E. Cohn, *Blood Cells and Plasma Proteins*, p. 30. Academic Press, New York, 1953.
13. C. V. J. van Oss, *Prog. Sep. Purif.*, 1968, **1**, 187.
14. O. Einarsson and S. Lindstedt, *Scand. J. Clin. Lab. Invest.*, 1969, **23**, 367.
15. P. Baily and T. A. Kilroe-Smith, *Anal. Chim. Acta*, 1975, **77**, 29.
16. I. Andersen and H. Zachariassen, *Proc. Intern. Symp. Clin. Chem. Chem. Toxicol. Metals*, Monte Carlo, March 1977.
17. M. Stoeppler, K. Brandt and T. C. Rains, *Analyst*, 1978, **103**, 714.
18. M. Stoeppler and K. Brandt, *Z. Anal. Chem.*, 1980, **300**, 372.
19. G. S. Fell, J. M. Ottaway and F. E. R. Hussein, *Br. J. Ind. Med.*, 1977, **34**, 106.
20. M. H. Saier and C. D. Stiles, *Molecular Dynamics in Biological Membranes*, Springer-Verlag, New York, 1975.
21. O. L. Davies, *Statistical Methods in Research and Production*, 3rd Ed., p. 150. Oliver & Boyd, London, 1967.
22. N. Kerker, *The Scattering of Light*, Academic Press, New York, 1969.
23. H. C. Van de Hulst, *Light Scattering by Small Particles*, Chapman & Hall, London, 1957.

Dedication—Dedicated to Dr. R. A. Chalmers.

DETERMINATION OF TRACE LEVELS OF CALCIUM IN STEELS BY CARBON-FURNACE ATOMIC-ABSORPTION AND ATOMIC-EMISSION SPECTROMETRY

JOSE ALVARADO and FRANCISCO CAMPOS

Chemistry Department, Simon Bolivar University, Apartado 80659, Caracas 1080, Venezuela

JOHN M. OTTAWAY

Department of Pure and Applied Chemistry, University of Strathclyde, Cathedral Street, Glasgow, Scotland

(Received 14 May 1985. Accepted 23 August 1985)

Summary—Methods are described for the determination of trace levels of calcium in steels by atomic-absorption and atomic-emission spectrometry with a carbon furnace for atomization and excitation. In both cases, a commercial electrothermal atomic-absorption instrument was used. Samples were analysed after dissolution in a mixture of nitric, hydrochloric, and hydrofluoric acids.

Although calcium compounds play a major role in the reduction of impurity levels during the production of iron, the final levels of calcium in finished steels are low and generally in the $\mu\text{g/g}$ range. In the past, calcium alloy additions during steelmaking have been recommended for the deoxidation and desulphurization of steels^{1–3} and have also been used in the control of the type and distribution of non-metallic inclusions.^{4,5} Calcium determination in steel samples is not a common requirement in steelworks analysis, but does occasionally appear important.⁶ It is then useful to have available a simple procedure using readily available instrumentation with a sensitivity of approximately $1 \mu\text{g/g}$ and offering acceptable precision and accuracy. The traditional approach to this problem has been to use flame atomic-absorption spectrometry with a nitrous oxide-acetylene flame,^{5,7–10} but such methods generally lack the sensitivity required and may give unacceptable precision at the levels of calcium found in most steel samples. Headridge and Richardson⁹ did provide a flame AAS method for the determination of 2–60 $\mu\text{g/g}$ calcium levels in steels, but this required a solvent-extraction preconcentration procedure. Although a convenient means of increasing the sensitivity of the measurement, and of separating the analyte from the major components of the sample, such procedures increase the analysis time, and complicate unnecessarily the essential simplicity of atomic-absorption procedures. They may also increase the possibility of errors due to contamination.

Atomic-absorption spectrometry with electrothermal atomization (ETA-AAS) should provide the sensitivity required for the determination of trace levels of calcium in steel samples. In fact, application of ETA-AAS to calcium determinations in general is rare,¹¹ and limited to materials such as snow¹² and high-purity water.¹³ The reasons for the lack of

interest in applying ETA-AAS to calcium determinations may be several. Many types of sample certainly contain calcium levels amenable to determination by use of flame atomization, but in any case the determination of calcium by ETA-AAS with commercial instrumentation has suffered from four readily defined problems. In some early instruments, excessive radiation from the wall or surface of the atomizer was able to enter the monochromator, causing severe noise in the atomic-absorption signal. Until recently, background-correction procedures did not adequately cover the wavelength of the most sensitive calcium line. Although instruments incorporating the use of visible-range continuum sources, the Zeeman effect, and the Smith-Hieftje method for background-correction are now available, the majority of instruments in current use still suffer from this limitation. Finally, the graphite used for fabrication of the atomizer usually contains significant levels of calcium, which must be removed or controlled, and as calcium is a ubiquitous element, there are often contamination problems when low levels are being determined. In our experience the last two factors often lead to unacceptable precision unless rigorously controlled.

In a recent paper, Fu *et al.*¹⁴ described an electrothermal atomic-emission spectrometry method for the determination of calcium in steel samples. Although this procedure gave acceptable sensitivity, accuracy and precision for the trace levels of calcium found in steels, it made use of an instrument which was purpose-built for carbon-furnace atomic-emission measurements.¹⁵ Thus the instrument was based on a high-resolution echelle monochromator, and incorporated a square-wave wavelength-modulation system, which gives accurate and automatic background correction at all wavelengths, including that of the calcium line of interest (422.7 nm).

Table 1. Instrumental parameters for calcium determination

	Perkin-Elmer 306/HGA-500	Perkin-Elmer 503/HGA-2100
Wavelength, <i>nm</i>	422.7	422.7
Lamp current, <i>mA</i> *	14	20
Spectral bandwidth, <i>nm</i>	0.7	0.2
Volume of sample, $\mu\text{l}\dagger$	10	10
Argon flow-rate, <i>ml/min</i>	300	104
Temperature, °C: hold time, <i>sec</i>		
Drying	140–30§	100–25
Ashing	1300–40§	1100–20
Atomization	2700–5¶	2800–6

*For the absorption measurements only.

†Solutions were applied to the furnace with Eppendorf micropipettes fitted with disposable plastic tips.

§A heating rate of 10 was used.

¶At maximum heating power.

Carbon-furnace atomic-emission signals can readily be sensitively measured with commercial electrothermal atomic-absorption instruments,¹⁶ but automatic background correction is not then available, and it is necessary to measure the background separately and subtract it from the total signal obtained in the presence of the analyte, to obtain the net atomic-emission intensity. Whilst this procedure is more tedious, it allows the sensitivity of the emission technique to be utilized by any laboratory possessing a commercial ETA-AAS system, and such a procedure was earlier adopted for the determination of a number of elements in steels.¹⁷ Calcium was not one of the elements included in that study, and the only other report of calcium determination by electrothermal atomic-emission spectrometry was based on the use of a molybdenum micro-tube atomizer.¹⁸ It is, however, interesting that some of the earliest observations made with the King furnace were of calcium atomic emission and absorption spectra.¹⁹

Since electrothermal atomic-absorption instruments are now widely available, it seemed worthwhile to investigate the practical difficulties involved in the determination of calcium in steels with typical commercial instruments. In the event, it proved possible to develop and test procedures for this determination by both carbon-furnace atomic-absorption and carbon-furnace atomic-emission spectrometry with commercial ETA-AAS instruments, and the results of these studies are reported in this communication.

After this work was completed, we became aware of a report of the development of another carbon-furnace atomic-absorption procedure for the determination of calcium in steels.²⁰ The method is similar to our procedure, but uses laboratory-coated pyrolytic-graphite tubes, and significantly different results were obtained. Some of the difficulties investigated in the present work do not appear to have been considered and may be the cause of anomalous results.

EXPERIMENTAL

Instrumentation

Two different atomic-absorption/emission spectrometer/graphite furnace systems were used.

(a) A standard Perkin-Elmer model 306 atomic-absorption spectrometer equipped with an HGA-500 graphite-furnace atomizer in conjunction with a Servoscribe 1s strip-chart recorder.

(b) A standard Perkin-Elmer model 503 atomic-absorption spectrometer equipped with an HGA-2100 graphite-furnace atomizer and coupled to a Perkin-Elmer model 056 strip-chart recorder.

Both spectrometers were provided with a deuterium-arc background-correction system. A Varian-Techtron calcium lamp and a Perkin-Elmer multi-element lamp (calcium, magnesium, zinc) were used as sources for the atomic-absorption measurements. Standard and pyrolytically-coated graphite tubes were used as atomizers. The instruments were operated under the conditions listed in Table 1.

Reagents

Reagents of the highest purity available were used throughout. To avoid calcium losses due to diffusion into the glassware walls, and to be able to use hydrofluoric acid, plastic vessels were employed during the preparation of standards and samples. Distilled demineralized water was used for dilution.

Stock calcium solution, 500 $\mu\text{g/ml}$. Dissolve 1.249 g of previously dried primary standard calcium carbonate in water containing sufficient "AristaR" nitric acid to complete dissolution. Transfer the solution to a 1-litre standard flask, add more nitric acid to make the final nitric acid concentration 1% v/v and dilute to the mark with water.

Stock iron solution, 10.0 mg/ml . Dissolve 0.50 g of high-purity iron granules (BCS 149/3) in a slight excess of "AristaR" nitric acid (1 + 1), transfer the solution to a 50-ml standard flask and dilute to the mark with water and enough nitric acid to give a 1% v/v final concentration.

Stock nickel solution, 1000 $\mu\text{g/ml}$. Dissolve 1.000 g of nickel metal in a minimum volume of "AristaR" nitric acid (1 + 1). Transfer the solution to a 1-litre standard flask, add enough acid to make its final concentration 1% v/v and dilute to the mark with water.

Stock chromium solution, 1000 $\mu\text{g/ml}$. Dissolve 3.735 g of potassium chromate in water and dilute to 1 litre.

Stock strontium solution, 10.0 mg/ml . Dissolve 2.415 g of strontium nitrate dihydrate in water, add enough "AristaR" nitric acid to give a final 1% v/v concentration, transfer the solution to a 100-ml standard flask and dilute to the mark with water.

Standard calcium solutions, 0.025–0.2 $\mu\text{g/ml}$. Prepare immediately before use by appropriate dilution of the stock calcium solution with water.

Sample treatment

Weigh 0.5 g of steel sample into a 100-ml polytetrafluoroethylene beaker and dissolve it in a minimum volume of a mixture of "AristaR" nitric and hydrochloric

acids (3 + 1), then add 40 μ l of concentrated hydrofluoric acid. When the reaction has subsided, heat gently until the solution is fully oxidized. Transfer the solution to a 100-ml plastic standard flask and dilute to the mark with water.

RESULTS AND DISCUSSION

Presence of calcium in the graphite atomizer

Calcium is present as an impurity in most graphites used for fabrication of electrothermal atomizer tubes, and presents a problem in any calcium determination. This problem usually manifests itself as a poor precision of measurement (>20% RSD). Before any analysis is attempted, the calcium present in the atomizer must be removed, which can be done effectively by repeated heating at high temperatures (~2800°). The number of heating cycles needed for cleaning the tube sufficiently to bring the blank signal to an insignificant level could be taken as an indication of the amount of calcium present in the graphite and the relative difficulty of removing it. Approximately 10–15 firings were required for standard electrographite and pyrolytic-graphite coated tubes, the electrographite tubes being rather worse than the coated tubes. The repeated high-temperature firing of the tube, necessary before analysis can start, causes a deterioration in tube lifetime and performance. The electrographite tubes rapidly became dusty and more porous and exhibited poorer reproducibility and sensitivity, owing to increased soaking of the analyte solution into the graphite. Pyrolytic-graphite coated tubes deteriorated much less significantly and gave much better performance after cleaning and were used throughout this study. After initial removal of the calcium impurity, a single cleaning stage is perfectly adequate between atomization cycles.

Reproducibility and sensitivity

Calibration graphs for absorption and emission determinations were plotted from peak-height mea-

surements for aqueous calcium standards containing 1% v/v nitric acid. Background measurements in the atomic-emission work were made sequentially with the sample measurements, and the background signal corresponding to the maximum peak-height for the analyte emission plus background signal was recorded and subtracted to give the net analyte atomic-emission signal.

No background signal was observed for atomic-absorption signals from aqueous solutions, but the atomization of steel solutions gave rise to significant background signals caused by the steel matrix. This was first observed with a Perkin-Elmer HGA 72 atomizer, which has an open-ended furnace arrangement, and is mainly due to matrix condensation with air to give a "smoke" which is formed in the optical beam and gives rise to a background signal due to scatter. In the HGA 500/2100 series this problem is minimized, as condensation with air takes place out of the optical beam of the spectrometer. Since neither of the instruments used in this work was provided with background-absorption correction facilities for measurements at 422.7 nm, the background signal was made negligible by appropriate choice of ashing conditions, and the use of high gas flow-rates during the atomization stage. An attempt was made to operate with the deuterium-arc background system, but use of the hollow-cathode lamp at low currents led to unacceptable signal-to-noise ratios. At the matrix levels investigated and with the atomization programme adopted, no matrix-induced background was observed in atomic-emission measurements.

The reproducibility of the instrumental measurement of calcium was routinely tested with a 10- μ l injection of a 0.05 μ g/ml solution of calcium in 1% v/v nitric acid medium. Typical results are shown in Table 2. A similar experiment performed with a solution of BCS 261/1 steel standard containing 17 μ g of calcium per g (0.085 μ g/ml in the sample solution) gave slightly higher RSD values for all three systems used. The RSD values are a little higher than

Table 2. Figures of merit for the analysis of trace levels of calcium in steels by electrothermal atomization

	Atomic-absorption		Atomic-emission
	PE306/HGA-500	PE503/HGA-2100	PE503/HGA-2100
Reproducibility, RSD (for 10 readings) for:			
Ca aqueous standard (0.05 μ g/ml), %	3.2	3.4	4.7
BCS 261/1, %	5.4	5.0	6.5
Reproducibility, RSD (for 10 complete determinations) for:			
BCS 261/1, %	8.8	7.5	8.3
BCS 333, %	11.3	9.7	12.2
Detection limit, μ g/ml	0.003*	0.008*	0.009†
Linear calibration range (orders of magnitude)	2	2	2

*Detection limit expressed as twice the standard deviation for a calcium solution of concentration slightly greater than the detection limit.

†Detection limit (DL) calculated from $DL = 2 C_0 RSD_b / (S/B)$ where $C_0 = Ca$ concentration of test solution, RSD_b = relative standard deviation of 10 blank measurements, S/B = signal-to-background ratio.

Table 3. Determination of trace levels of calcium in steels by electrothermal atomization

Sample	Calcium content* found by AAS, $\mu\text{g/g}$		Calcium content* found by AES, $\mu\text{g/g}$
	PE306/HGA500	PE503/HGA2100	PE503/HGA2100
BCS 261/1	15.5	14.7	17.0
BCS 325	4.2	5.6	5.0
BCS 330	2.5	5.8	4.5
BCS 331	3.0	4.2	3.5
BCS 333	4.5	4.0	3.8
BCS 334	3.5	4.7	5.2
BCS 335	4.0	4.5	3.0
BCS 401	6.7	5.9	5.6
BCS 403	6.0	5.1	5.9
BCS 405	17.0	19.1	24.7
BCS 409	12.0	13.8	12.5
BCS SS 31	9.8	—	—
BCS SS 32	2.2	—	—
BCS SS 35	20.0	—	—
BCS SS 67	6.5	—	—
BCS SS 69	6.7	—	—
NBS 32e	—	3.3	2.9
NBS 72f	—	2.7	2.2
NBS 160b	—	3.2	3.3
NBS 344	—	4.2	3.0
NBS 339	—	3.5	3.2

*Corrected for blank solutions.

would be expected for most elements in determinations with modern instrumentation, even allowing for the manual injection procedure, and may be due to residual small amounts of calcium impurity. The reproducibility for atomic-emission measurements is slightly poorer than that for atomic-absorption, which may be a result of the subtraction procedure used for emission background correction. In all cases, the precision is undoubtedly adequate for the determination of trace amounts of calcium in steel samples.

Interference studies

The effects of the presence of some of the major components of steels (iron, chromium and nickel) on the absorption/emission signals of a $0.05 \mu\text{g/ml}$ calcium solution were examined. Concentrations equivalent to those found in the standard steels BCS 334 and 219/3 were the highest levels tested. Very small enhancements were observed, and these were traced to calcium impurities in the iron and nickel metals and chromium salt used to prepare the standard solutions. BCS standard 261/1 was analysed by the standard-additions method and this procedure gave exactly the same result as that obtained by using a calibration graph prepared from aqueous calcium standards. Finally, to test for the possibility of potential interferences due to excessive ionization of calcium during atomization, strontium in the range $500\text{--}1000 \mu\text{g/ml}$ was added to a typical calcium solution. No appreciable difference of either the absorption or net emission signal was observed for calcium with and without the strontium addition.

Determination of calcium in steels

The results of the interference studies indicated the validity of analysing steel for calcium by either

atomic-absorption or atomic-emission by use of the commercial instrumentation without background-correction facilities, and simple aqueous (1% v/v nitric acid) calcium standards. Two steel samples were analysed (ten separate samples of each) to test the reproducibility of the whole procedure. The results are shown in Table 2. The calcium content of BCS 261/1 is approximately $17 \mu\text{g/g}$ ($0.085 \mu\text{g/ml}$ in the injected solution) and of BCS 333 approximately $4 \mu\text{g/g}$ ($0.02 \mu\text{g/ml}$ in the solution). The RSD values obtained reflected the levels of calcium in these samples, and gave detection limits of 0.6 and $1.6 \mu\text{g/g}$ by atomic-absorption and $1.8 \mu\text{g/g}$ by atomic-emission spectrometry. The performance of all three instrumental methods appears adequate. Until recently, no standard steel samples had been assigned a certified calcium content, but a value of $17 \mu\text{g/g}$ has now been assigned to BCS 261/1. The results obtained agree satisfactorily in this case (Table 3). Results obtained for other samples show acceptable agreement between the different measurement techniques (absorption or emission) and in different laboratories carried out at significantly different times (in Scotland and Venezuela). Whilst these results do not allow a total confirmation of analytical accuracy, for which a wider range of certified materials or more different analytical procedures would have been preferable, the good agreement represents useful supporting evidence.

CONCLUSIONS

The results presented in this paper suggest that typical commercially available electrothermal atomic-absorption instruments may be used successfully for the determination of calcium in steel samples. Either atomic-absorption or atomic-emission

measurements can be used although the latter are slower owing to the need to use sequential background-signal measurement. The calcium levels in typical steel samples can be determined with adequate precision without the need for preconcentration or extraction procedures. As long as care is taken to remove the effect of calcium impurities in the graphite tube, either method can be used by laboratories with ETA-AAS equipment. Simpler procedures or better performance might be possible with spectrometric systems incorporating automatic background-correction facilities at the calcium wavelength, and an automatic sample-dispenser, but the present method is probably acceptable for most of the routine requirements of the steel industry.

Acknowledgements—The authors are grateful for the provision of pyrolytic-graphite coated tubes for the HGA 500 by Dr. B. Lersmacher of Phillips Research Laboratories, Aachen, German Federal Republic, and would like to thank B. Welz of Perkin-Elmer, Bodenseewerk, West Germany for the loan of the HGA 500 electrothermal atomizer.

REFERENCES

1. C. E. Nelson and B. L. Otis, *U.S. Patent*, No. 2221263, 1940.
2. E. C. Smith and G. T. Motock, *U.S. Patent*, No. 2255016, 1941.
3. D. R. Moore, *U.S. Patent*, No. 2026243, 1935.
4. R. A. Grange, F. J. Shortsleeve, D. C. Hitty, W. O. Binder, G. T. Motock and C. M. Offenbauer, *Boron, Calcium, Columbium and Zirconium in Iron and Steel*, Wiley, New York, 1957.
5. M. L. Taylor and C. B. Belcher, *Anal. Chim. Acta*, 1969, **45**, 219.
6. H. G. Engell, M. Köhler, H. G. Fleischer, R. Thielmann and E. Schürmann, *Stahl und Eisen*, 1984, **104**, 443.
7. G. L. Vassilaros and J. P. McKaveney, *Talanta*, 1966, **13**, 15.
8. P. H. Scholes, *Analyst*, 1968, **93**, 197.
9. J. B. Headridge and J. Richardson, *ibid.*, 1969, **94**, 968.
10. *Euronorm 177*, European Standardization Committee, 1983.
11. C. W. Fuller, *Electrothermal Atomisation for Atomic Absorption Spectrometry*, The Chemical Society, London, 1977.
12. J. H. Cragin and M. M. Herron, *At. Abs. Newsl.*, 1973, **12**, 37.
13. A. R. Knott, *ibid.*, 1975, **14**, 126.
14. B. Fu, J. M. Ottaway, J. Marshall and D. Littlejohn, *Anal. Chim. Acta*, 1984, **161**, 265.
15. J. M. Ottaway, L. Bezur and J. Marshall, *Analyst*, 1980, **105**, 1130.
16. J. M. Ottaway, R. C. Hutton, D. Littlejohn and F. Shaw, *Wiss. Z. Karl-Marx-Univ. Leipzig, Math.-Naturwiss. R.*, 1979, **28**, 357.
17. J. M. Ottaway and F. Shaw, *Anal. Chim. Acta*, 1978, **99**, 217.
18. M. Suzuki and K. Ohta, *Talanta*, 1981, **28**, 177.
19. A. S. King, *Astrophysics J.*, 1905, **21**, 236.
20. T. Glenc and J. Jurezyk, *Hutnik*, 1981, **48**, 147.

Dedication—Dedicated to Dr. R. A. Chalmers in celebration and recognition of his 20 years of dedicated service as Editor of *Talanta*. On his retirement from a distinguished career at the University of Aberdeen, the authors and all our colleagues at the University of Strathclyde join in sending our good wishes, and trust he will continue to serve the Journal in his efficient and friendly manner for many years to some.

John Ottaway

SAMPLE PRETREATMENT IN THE TRACE DETERMINATION OF DRUGS IN BIOLOGICAL FLUIDS

ANIL C. MEHTA

Department of Pharmacy, The General Infirmary, Leeds, Yorkshire, England

(Received 12 July 1985. Accepted 21 August 1985)

Summary—Because of their complex nature, biological samples are often subjected to a pretreatment step before instrumental analysis. This paper outlines the methods available for sample preparation prior to gas or high-pressure liquid chromatography. Practical aspects are emphasized.

Analysis of biological fluids for drugs and their metabolites requires detailed consideration of the methods for collection, storage, and preparation of samples before the analysis. The drug is usually present at trace levels (mg/l. or below) in a complex biological matrix, and the potentially interfering endogenous substances (which are usually present at higher concentrations than the drug) need to be removed before the analysis.¹⁻⁴ The amount of sample preparation required depends on the chemical nature and concentration of the drug or metabolite, the sample type, and the nature of any interfering substances. It also depends on instrumental factors such as the sensitivity of the high-pressure liquid chromatographic (HPLC) detectors, or the tolerance of specific gas-chromatographic (GC) detectors to contamination.⁵ The sample preparation step should therefore be capable of concentrating the sample and at the same time reducing the amount of interfering material so as to prolong column and/or detector life. No sample pretreatment is required for immunoassays (*e.g.*, Syva EMIT or Abbott TD₅₀ assays) which are increasingly used in hospitals for diagnostic tests and routine monitoring of certain drugs such as antiepileptics. However, most of the routine and research drug assays in hospitals are done by chromatographic techniques, for which sample preparation is necessary. In general, the sample clean-up procedure is simpler for HPLC than for GC. Prechromatographic sample treatment for plasma, serum and urine will be considered here.

In drug analysis the most commonly sampled body fluid is plasma or serum, because a good correlation between drug concentration and therapeutic effect is usually found. Urine is useful when a drug or a rapidly formed metabolite is extensively excreted in it. Drugs can usually be detected as metabolites in urine for some time after they have become undetectable in blood. Urine analysis for drugs is used in connection with urinary excretion and bio-availability studies. Saliva and cerebrospinal fluid (CSF) are also analysed for drugs, but less frequently. Drug concentrations in saliva are sometimes assumed

to represent free plasma levels, but this is found to be true for only a few drugs (*e.g.*, carbamazepine, phenytoin). For others, the correlations are less satisfactory or apparently non-existent.⁶⁻⁸ It is not practical to analyse CSF samples routinely, but occasionally CSF levels may be required if damage to the blood-brain barrier is suspected.

SAMPLING AND STORAGE

Collection of an uncontaminated specimen at the correct time in relation to the dose is vital in any projects involving drug analysis. If insufficient care is taken in collection and handling of biological specimens, data generated by using even the most sophisticated techniques may be invalidated. If plasma or serum is analysed, the expressions "blood samples" or "blood levels" should not be used in description of the analytical procedure unless whole-blood samples are also to be analysed for some reason (for example, for drugs with high affinity for red cells, such as chlorthalidone or cyclosporin). Specimen collection tubes containing anticoagulants (for blood) or preservatives (for urine) are commercially available. The choice of anticoagulant may affect assay results, as may some plasticizers released from blood collection tubes made of plastic. The sample should be accompanied by a request form containing adequate information about the patient and therapy, including co-administered drug(s). The latter may be useful in the prediction of interferences and for development of an appropriate strategy for sample clean-up.

On no account must the blood sample be frozen without treatment, because it would be haemolysed. It is essential to avoid this, since haemolysis prevents subsequent separation of plasma or serum. After collection of blood (5–10 ml) a clot can be allowed to form and the supernatant liquid (serum) collected after centrifugation. Coagulation is complete in about 30 min at room temperature. Alternatively the blood can be collected in a tube containing an anticoagulant (*e.g.*, heparin, EDTA) and the super-

natant liquid (plasma) collected after centrifugation. Since the anticoagulation effect is temporary, collected specimens must be centrifuged quickly to prevent eventual clotting. Plasma is more frequently used than serum in drug analysis. Although assay results for plasma or serum are usually identical, plasma is preferred to serum since the anticoagulated blood can be centrifuged immediately, whereas serum cannot be sampled until coagulation is complete. Moreover, it is relatively easy to centrifuge blood that has been treated with anticoagulant, since the plasma separates quickly and the maximal volume can be recovered if required.

Drug may be lost to the container or be degraded during storage. Thus, the stability of a drug in biological fluid at various storage temperatures should be studied, so that any effect of storage on the ultimate analysis can be predicted. This is especially important if samples arrive irregularly and assays are done on a batch basis. Fresh plasma or serum samples can usually be kept for 6 hr at room temperature, or for 1–2 days in a refrigerator at 4° (this slows down enzymatic and bacteriological processes). For longer-term storage, samples should be frozen at –20°C. Recently, the Council of the Pharmaceutical Society has issued guidelines for a pharmacy-based pharmacokinetic service which includes instructions on sampling and storage of blood.⁹

Urine drug analysis is done either on a single or a 24-hr specimen. Both pH and volume are important factors in urine drug analysis, and must be recorded immediately on collection. If urine is allowed to stand at room temperature, bacterial action causes the decomposition of urea into ammonium carbonate and subsequently to ammonia, with a resulting increase in pH. Urine can be preserved by freezing at –20° or by addition of a preservative. Freezing is to be preferred, since the preservative may interfere with the drug analysis. Toluene, boric acid, and concentrated hydrochloric acid are commonly used as urine preservatives.

Frozen samples of plasma/serum or urine should be brought to room temperature and subjected to vortex-mixing for 10 sec to ensure homogeneity before analysis.

DIRECT INJECTION

After centrifugation to remove particulate matter, and suitable dilution (preferably with mobile phase), urine can be injected directly into a liquid chromatograph. For example, antibiotics¹⁰ and other drugs¹¹ can be determined in urine by HPLC with on-column injection. To protect the analytical column from irreversible adsorption or blockage a precolumn should be used when the direct injection method is employed. Similarly, blood can be analysed for alcohols or anaesthetic gases by direct injection into a gas chromatograph.^{12,13} However, such direct on-column injection of samples is possible in only a

few cases, since biological samples contain material such as lipids or proteins which deposit in the chromatographic column and impair its performance, and such substances can also contaminate GC detectors. To avoid these problems, sample clean-up is necessary. The most widely used procedures are protein precipitation, and solvent and solid-phase extractions. These procedures improve the sensitivity and selectivity of the assay, and the performance of the chromatographic equipment, relative to those for direct introduction of samples.

PROTEIN PRECIPITATION

In this method, one volume of plasma or serum is mixed with three volumes of acid (6% w/v perchloric acid) or organic solvent (ethanol, methanol, acetonitrile). This precipitates the proteins and releases the drug from protein-binding sites. After vortex-mixing and centrifugation, an aliquot of the clear supernatant liquid is injected into the HPLC column. Some protein precipitants, such as trichloroacetic acid (10% w/v) or acetone, absorb in the ultraviolet region and should be used in conjunction with an ultraviolet detector only if the solvent front does not interfere with the peaks of interest. This method of sample preparation is simple, rapid, accurate and is increasingly used in analysis of drugs by HPLC.

The protein precipitation method serves to protect columns against deposits of proteins. The reagents mentioned above will remove 99% of the proteins if three volumes are added to one volume of sample.¹⁴ Dilution of the sample effectively decreases the sensitivity, but this drawback can be counteracted to some extent by increasing the sample injection volume say up to 100 μ l. It should be remembered that the supernatant liquid contains many constituents other than proteins, and often the drug peak is accompanied by extraneous peaks in the chromatogram. It may, therefore, still be necessary to make a judicious choice of HPLC conditions in order to obtain adequate separation of the drug peak.

The deproteination procedure can sometimes give low recoveries for drugs that are strongly bound to proteins. Also, certain protein precipitants may coprecipitate or degrade the drug or its metabolites. For acid-labile or easily oxidizable drugs, it is advisable to use organic solvents instead of perchloric acid for deproteination. On the other hand, certain drugs require a strong reagent, such as perchloric acid, for quantitative recovery. For these reasons, when a new method is being developed, several precipitation reagents, in various proportions, should be investigated, to test their efficiency in removing proteins and producing a relatively interference-free supernatant liquid with good recovery of the drug. Although methanol is slightly less effective as a protein precipitant than other organic solvents,¹⁴ it should be used whenever feasible, because of its relatively low cost and low toxicity.

The protein-precipitation method is particularly useful for highly polar (*e.g.*, antibiotics) or amphoteric (*e.g.*, sulphonamides) drugs, which are difficult to extract from plasma with organic solvents. Since the method is straightforward, it should be considered first whenever possible. Analyses with good reproducibilities are often possible, without the use of internal standards.¹⁵

Proteins can also be removed by ultrafiltration of plasma or serum, but the ultrafiltrate contains only the free (*i.e.*, unbound) fraction of the drug. Modern ultrafiltration membranes provide nearly complete removal of proteins, so ultrafiltration is becoming a useful tool in the monitoring of free drug levels in plasma or serum.¹⁶

SOLVENT EXTRACTION

Liquid-liquid solvent extraction is by far the most widely used method for the preparation of biological samples for subsequent analysis, owing to its versatility.¹⁷⁻²⁰ Samples treated by solvent extraction are chromatographically cleaner than protein-precipitation samples, in that they contain lower amounts of interfering substances. Also, since the sample can be concentrated in the process, the limit of detection is improved. The choice of sample size depends on the amount of specimen which can be obtained conveniently from the patient, and on the sensitivity of the assay. Generally a single extraction step involving 1 ml of sample (pH adjusted if necessary) and 5 ml of organic solvent, which may give over 80% recovery, is adequate for the routine assay of a large number of samples. The addition of a large amount of the extractant is intended to prevent or minimize emulsion formation. Glassware used in extractions must be scrupulously clean and free from any residual detergents.

Extraction by shaking on a roller mixer is time-consuming but more effective than other methods because the mixing of the two phases is more uniform. Shaking by vortex mixer is quicker, provided that equilibrium is reached rapidly. With a vortex mixer, 1 min of gentle shaking is recommended, since vigorous shaking favours emulsion formation. If emulsions occur, they can be broken by centrifugation.

The polarity of the extractant and pH of the aqueous phase (sample) are major factors to be considered in the design of a suitable solvent extraction scheme. Trial extractions should be performed and the solvent/pH combination which gives a high recovery of the drug and minimal extraction of interfering material should be chosen. As the polarity of the solvent increases, the range of compounds extracted also increases. Drugs of high polarity are difficult to extract and require strongly polar, and hence non-selective, solvents. Chin and Fastlich²¹ have listed a number of drugs that are extractable in the presence of sodium dihydrogen phosphate with

diethyl ether but not with hexane. Bailey and Kelner²² have investigated the extraction recoveries of 28 acidic drugs from water and plasma, with hexane, diethyl ether, toluene, *n*-butyl chloride and chloroform. As classes, the barbiturates, sulphonamides, and diuretics were optimally extracted with diethyl ether from both water and plasma, but considerable variation in recovery was noted between solvents for the other drugs.

It is possible to select a mixture of solvents which, although it does not completely extract the drug, does give cleaner extracts. For example, barbiturates can be extracted from blood with a mixture of equal volumes of hexane and ether at pH 7.5. The use of a more polar solvent or a low extraction pH increases the co-extraction of interfering material considerably.²³

As well as having the correct polarity, the solvent should be of highest purity, non-toxic, not highly flammable, and have a suitable volatility. It should be redistilled if the preservative or a trace impurity is found to react with the drug or produce an interfering peak on the chromatogram. The most popular solvents for extraction are diethyl ether and chloroform. Although ether is flammable, it has the advantages that it is reasonably selective, and can be readily evaporated for recovery of the drug. Its low density facilitates phase transfer after extraction and minimizes contamination of the organic extract with the aqueous phase during the transfer step. Moreover, ether emulsions are easier to break. Solvents such as benzene or carbon tetrachloride should be avoided because of their toxicity. Toluene, chloroform or dichloromethane should be used instead.

The effect of pH is important in solvent extraction, particularly for the ionizable drugs. It is the uncharged (*i.e.*, non-ionized) form of the drug which is extracted into the organic solvent. Thus, acidic drugs are extracted under acidic conditions and basic drugs under alkaline conditions. The optimum pH for extraction of acidic drugs usually lies 1-2 pH units below the pK_a value and for basic drugs 1-2 pH units above the pK_a value. Amphoteric drugs also show an optimum pH for extraction. The extraction of neutral drugs is independent of pH; they are extractable over a wide pH range. Hence, they can be co-extracted with acidic or basic drugs, but they remain in the organic phase on back-extraction of the other drug into an alkaline or acidic (as appropriate) aqueous phase. However, consideration of pH is important even when assaying neutral drugs. A higher pH is often desirable to ensure cleaner extracts, since many endogenous compounds are acidic and hence are not extracted from alkali. Several methods involving extraction of drugs at a single pH have been reported, particularly in the context of toxicological monitoring.²⁴

Another useful method is pre-extraction of interfering substances into an organic phase which is then discarded. Urine contains large amounts of endo-

genous compounds, and a preliminary extraction from acidic urine improves the purity of the subsequent basic extract. Urine can also be cleaned up by extraction with diethyl ether or n-hexane before HPLC.⁵ Sometimes the drug may be extracted into a very small volume of organic solvent (100 μ l or less). After centrifugation, an aliquot of organic solvent is injected directly into a GC.^{25,26} The avoidance of a solvent evaporation step minimizes the possibility of losing drugs by adsorption onto glassware, and prevents the volatilization of certain drugs such as amphetamine. This approach is quick, simple, and particularly suitable for rapid screening of drugs of abuse.

Extraction can be problematic when the drug is water-soluble at all pH values (water-soluble amphoteric and neutral drugs, zwitterions), since pH adjustment does not help in this situation. In some cases, a salting-out procedure (addition of an excess of salt to the sample before extraction) can shift the partition equilibrium in favour of extraction, and result in a better extraction yield for the drug in question. Such an approach has been used by Horning *et al.*²⁷ in the screening of plasma and urine for acidic, basic and neutral drugs and their metabolites. By using ammonium carbonate as the salt and ethyl acetate as the solvent, they were able to extract drugs with recoveries better than 80%. The identification and determination were done by GC or GC-MS. An advantage of salt-solvent extraction is that emulsion formation is minimized. Polar water-miscible solvents (*e.g.*, n-propanol, acetonitrile) can also be used as extractants in this technique, because the presence of an excess of inorganic salt results in a phase separation in which the upper layer consists mainly of the organic solvent.²⁸

Back-extraction

Gas chromatographic analysis usually requires further purification of extracts, for example by back-extraction, to prevent extraneous substances present in the initial extract from contaminating the GC detectors, particularly the nitrogen/phosphorus detector and the electron-capture detector.^{5,13,29} The drug present in the first extract is back-extracted into an aqueous phase of appropriate pH. This should reduce the amount of neutral material contaminating the drug, since neutral molecules remain in the organic solvent. For back-extraction of basic drugs into an acidic aqueous phase, sulphuric and phosphoric acid are preferred to hydrochloric acid, because many hydrochlorides are soluble in organic solvents. After the back-extraction, the pH of the aqueous phase is readjusted to that of the first extraction, and the drug is re-extracted into an organic solvent. The solvent is then evaporated and the residue is either converted into a derivative²⁹⁻³² prior to GC or redissolved in an appropriate medium, an aliquot of the solution being injected into the GC.

Extraction of metabolites

Metabolites of a drug are usually more polar than the drug itself, and if the metabolites are of interest, then the solvent chosen should be capable of extracting all the compounds of interest, so that they can subsequently be separated and determined by GC or HPLC. However, if desired, extraction with solvents of increasing polarity and/or at different pH values can achieve selective separation of a drug from its major metabolites. Another approach to extracting the more polar metabolites is to extract the drug, then add a high concentration of a salt such as sodium chloride to the aqueous phase, and re-extract. This forces the desired compounds into the organic phase. The salting-out procedure does not always work, but it has been used in the extraction of hydroxy metabolites of barbiturates from urine.²⁰ Occasionally the metabolites are similar in polarity to the parent drug, and both the metabolites and the drug are extracted by the same solvent. Partition of the extracted compounds between solvent and a buffer of appropriate pH can sometimes separate the individual components sufficiently to permit analytical determination, as in the case of chlorpromazine and imipramine metabolites.³³ A review by Martin and Reid³⁴ and a book edited by Reid and Leppard³⁵ deal with solvent extraction and other approaches to isolating metabolites.

It should be emphasized that absolute specificity is difficult to achieve by selective extraction alone, and co-extraction of metabolites is inevitable (except where very different molecular structures are involved). Thus, the separation usually must include a chromatographic step. HPLC is generally the method of choice,^{35,36} since the drug and its metabolites can usually be analysed without conversion into derivatives or use of extensive clean-up procedures. After evaporation of the extraction solvent, the residue can be dissolved in the mobile phase and an aliquot of the solution injected into the HPLC.

Silanization of glassware or the inclusion of 1–2% of alcohol (ethanol or 3-methylbutan-1-ol) in a non-polar extractant such as hexane or heptane usually prevents adsorption of the drug onto glassware during the solvent evaporation step. Adsorption is much more noticeable when a drug is present at low concentrations. The measures described are not always effective, and others may have to be devised.

Hydrolysis of conjugates

Many drugs and metabolites are present in urine as conjugates such as glucuronides or sulphates, which are very polar and essentially not extractable into organic solvents. It is often necessary to hydrolyse these conjugates so as to release the parent molecules for extraction. This is done chemically with hydrochloric acid or sodium hydroxide, or enzymatically with enzymes such as β -glucuronidase. Chemical hydrolysis decreases the yield of drugs that are heat-

labile (*e.g.*, certain benzodiazepines) and sensitive to aggressive reagents. Enzymatic methods, on the other hand, are slow but the mild conditions required are less likely to cause degradation of the compounds to be determined. After hydrolysis, the products can be extracted after pH adjustment. If necessary, the extract can be cleaned up further by back-extraction. Generally a urine sample is divided into two subsamples. One is hydrolysed to give the total (*i.e.*, conjugated and unconjugated) concentration of the drug, and the other is extracted without hydrolysis to give the free (*i.e.*, unconjugated or directly extractable) concentration of the drug. The concentration of the bound (*i.e.*, conjugated) form is obtained by subtraction. This is done, for example, in the determination of oxmetidine and its sulphoxide metabolite.³⁷

Ion-pair extraction

A useful approach to dealing with a highly polar ionic drug is to convert it into a neutral ion-association complex by addition of an excess of suitable ions of opposite charge, and extract it into an organic solvent such as chloroform. The counter-ions used may be inorganic (halide, perchlorate, thiocyanate) or polar organic (benzoate, sulphonate, tri- or tetra-alkylammonium). Formation of the complex depends on factors such as the pH of the aqueous phase, the polarity of the extracting phase, and the nature and concentration of the counter-ion. The ion-association complex technique can be used for all kinds of ionizable drugs, but it offers particular advantage for compounds that are difficult to extract in unchanged form (penicillins, amino-acids, conjugated metabolites). This is the only method that allows extraction of quaternary ammonium compounds.^{24,38} For example, tubocurarine can be extracted from an alkaline plasma or tissue solution into dichloromethane after ion-pair formation with potassium iodide. The use of this approach to achieve selective extractions has been discussed by Schill³⁹ and Tomlinson.⁴⁰

A further variation of the technique is extractive alkylation. In this procedure the drug is extracted as an ion-pair into an organic solvent where it immediately reacts with an alkyl halide to form a derivative suitable for analysis by GC. Usually tetra-alkylammonium salts are used as ion-pairing reagents and alkyl halides as alkylating agents. This approach is quicker than other derivative-formation methods and has proved useful for GC analysis of several classes of drugs,³⁰ such as barbiturates⁴¹ and sulphonamides.^{42,43}

LIQUID-SOLID EXTRACTION

In liquid-solid extraction the sample is poured directly onto a column packed with solid adsorbent, and compounds of interest are eluted with organic

solvent for subsequent analysis. Among the many adsorbent materials that have been used are Celite, alumina, silica, chemically bonded silica, Florisil, and non-ionic and ion-exchange resins. These materials fall into two broad categories, according to whether they retain all the sample, or only the drugs and related compounds. In the first group, a hydrophilic packing materials such as inert particles of diatomaceous earth (kieselguhr) is used to adsorb sample (including water) over a large surface area. The second group is more selective, and requires either hydrophobic (*e.g.*, by bonded silica) or ion-exchange retention of the drug and metabolites.

In the case of the first group, the sample (a complex aqueous solution) is adsorbed by the support so that a thin aqueous film is formed on the surface of each particle. A small volume of a water-immiscible organic solvent such as chloroform is then passed through the column and this effectively extracts the drug from the aqueous film of sample. Water and endogenous material such as pigments, particulates and polar compounds are retained in the matrix. This type of extraction is essentially a liquid-liquid extraction, so drugs can be selectively eluted by approaches similar to those used in liquid-liquid extraction.

The second type of liquid-solid extraction works on chromatographic principles. Compounds of interest are retained on the adsorbent surface when the sample is passed through. Certain undesirable compounds which are adsorbed at this stage may be removed by washing with a specific solvent or buffer. Drugs and related compounds are then eluted by passing an appropriate solvent through the column. The elution solvent may be miscible or immiscible with water, because little sample water remains on the column. The eluate is processed further as required or injected directly into the HPLC. Such chromatographic systems can be tailored to requirements by choosing adsorbents with suitable properties (polar, non-polar, or ionic).

Liquid-solid extraction can be done with homemade columns, for example a Pasteur pipette packed with adsorbent. However, disposable columns of various sizes (up to 20 ml), and covering a wide range of adsorbents, are available commercially (*e.g.*, from Waters Associates, Analytichem International). These columns have a high sample-loading capacity but are for single use only, since components left in the column matrix by a previous sample could affect the performance on subsequent use. In spite of this, some workers^{44,45} have shown that C₁₈ bonded-phase disposable columns can be regenerated and used again without any loss of performance. Vacuum manifold devices are available from the companies listed above, to allow simultaneous extraction of up to 10 samples in a few minutes under gentle vacuum.

The liquid-solid extraction technique is becoming a serious challenger to conventional solvent extraction (liquid-liquid partition). It is simple and time- and labour-saving (though prepacked disposable

columns are by no means cheap). There are no losses due to emulsion formation and the extraction results in cleaner samples, which extend the life of the analytical column. The efficiency and reproducibility are as good as, or better than, those of liquid-liquid extraction. The technique is well suited to automation and is particularly useful for highly polar or amphoteric compounds which are difficult to extract from samples at any pH (e.g., antibiotics). The columns can also be used for sample storage during transportation.

Adsorbents such as charcoal⁴⁶ and XAD-2 resins⁴⁷ are popular in screening for drugs of abuse in urine, whereas columns containing purified diatomaceous earth, reversed-phase or ion-exchange material are increasingly used for extraction of drugs as individuals or groups. For example, serum can be extracted with diatomaceous earth for the HPLC determination of prednisone and prednisolone.⁴⁸ Sample concentrates for GC determination of tricyclic antidepressants⁴⁵ and HPLC determination of anti-convulsants⁴⁹ and benzodiazepines and metabolites⁵⁰ can be obtained by extraction of samples with reversed-phase disposable columns. Ion-exchange resin columns are particularly valuable for the extraction of ionic compounds such as aminoglycosides.⁵¹

Suppliers of prepacked extraction columns do "in house" development work to expand the applications and the range of their products. It is sometimes beneficial to contact them for advice on specific problems.

INTERNAL STANDARDS

During sample preparation, it is usual to add a fixed amount of an internal standard to each sample at the earliest possible stage, to permit correction for losses during sample treatment and to minimize errors due to variation in instrument response (column, detector, etc.), injection volume, or yield of a derivative. Most internal standards are compounds chemically similar to the drug to be assayed. An internal standard should be well separated on the chromatogram, not only from the drug but also from other peaks. The ratio of the detector response (peak height or area) for the drug and the internal standard is then used in calibration and assay.

Fike⁵² has investigated a number of organic compounds, mostly aromatic hydrocarbons, for use as internal standards in GC analysis of drugs. Retention times at various temperatures on five commonly used columns have been determined. McAllister⁵³ has recommended prazepam, a structural analogue of diazepam, as a possible internal standard for the GC determination of diazepam. Prazepam can also be used as internal standard for the HPLC determination of diazepam or other benzodiazepines, for example clobazam.⁵⁴

FUTURE DEVELOPMENTS

Since sample pretreatment is an important but labour-intensive step in GC and HPLC analysis, it seems likely that use of microprocessor-controlled automated systems for this task will increase greatly in the future. This is a new area and at present only a few systems exist. Such equipment is of value when large numbers of samples are to be analysed routinely. The Technicon FAST-LC unit provides on-line solvent extraction of drugs from serum, including solvent evaporation, redissolution of drug in the mobile phase and injection into the HPLC column. The Du Pont Prep 1 system is based on solid-phase extraction, and incorporates an XAD-2 resin cartridge. The drugs and metabolites are isolated on the column and eluted with a selected solvent. The extract, after solvent evaporation, is presented in dry form for subsequent analysis by GC, HPLC, or GC-MS. Procedures are described for the isolation of anti-epileptic drugs⁵⁵ from biological samples with the FAST-LC system and of barbiturates and other drugs⁵⁶ with the Prep 1 system. Recently, the Zymark Corporation has introduced a robotic system⁵⁷ to automate sample-handling procedures, including liquid- and solid-phase extractions. The system is programmed by the user to meet the requirements of a particular procedure. Clarke and Robinson have surveyed different approaches to the automation of sample preparation prior to HPLC.⁵⁸

Apart from automation, the current trend towards liquid-solid extraction seems likely to continue, and new or modified adsorbents will appear, offering more selectivity in solid-phase extraction.

Another relatively recent development which has been engaging attention is on-line sample preparation/concentration by direct injection of plasma/serum or urine into the HPLC.^{59, 61} On-line concentration and clean-up is done with a small precolumn. Chromatography takes place, after column-switching, in an analytical column. If two pre-columns are used, they can be alternately switched to avoid loss of time in the sample washing step. At present there are practical problems, especially during unattended operation, e.g., clogging of the autoinjector needle, baseline shift, and increase in back-pressure. However, the principle of on-line sample handling may well be widely applicable once the practical problems are overcome. The technique has the following advantages: (1) possible sources of error during extraction, including adsorption losses during solvent evaporation, are avoided; (2) unstable samples can be processed immediately; (3) analytical time is reduced. Tamai *et al.*⁶² have used a protein-coated HPLC column for the direct injection of plasma samples containing propranolol and its hydroxy metabolite. Before sample injection, the reversed-phase C₁₈ column is saturated with protein by repeated injection of bovine serum albumin. The protein-coated column shows no affinity for protein but does have an affinity

for drug molecules. Although the results with propranolol are encouraging, more work needs to be done before this approach is routinely applied to other drugs.

REFERENCES

1. E. Reid, *Analyst*, 1976, **101**, 1.
2. E. Reid (ed.), *Blood Drugs and Other Analytical Challenges*, Horwood, Chichester, 1978.
3. E. Reid (ed.), *Trace Organic Sample Handling*, Horwood, Chichester, 1981.
4. J. L. Valentine, in *Drug Fate and Metabolism, Methods and Techniques*, E. R. Garrett and J. L. Hirtz (eds.), Vol. 4, p. 151. Dekker, New York, 1983.
5. J. A. F. de Silva, *J. Chromatog.*, 1983, **273**, 19.
6. R. A. de Zeeuw, in *Trace Organic Sample Handling*, E. Reid (ed.), p. 176. Horwood, Chichester, 1981.
7. J. C. Mucklow, *Ther. Drug Monit.*, 1982, **4**, 229.
8. C. Knott and F. Reynolds, *ibid.*, 1984, **6**, 35.
9. Guidelines for a Pharmacy-based Pharmacokinetic Service, *Pharm. J.*, 1985, **234**, 626.
10. L. O. White and D. S. Reeves, in *Biological/Biomedical Applications of Liquid Chromatography*, G. L. Hawk (ed.), Vol. 4, p. 185. Dekker, New York, 1982.
11. P. Lagerström, *J. Chromatog.*, 1981, **225**, 476.
12. A. S. Curry, G. W. Walker and G. S. Simpson, *Analyst*, 1966, **91**, 742.
13. B. Scales, *Intern. Lab.*, 1978, **8** (November/December), 37.
14. J. Blanchard, *J. Chromatog.*, 1981, **226**, 455.
15. P. J. Meffin and J. O. Miners, in *Progress in Drug Metabolism*, J. W. Bridges and L. F. Chasseaud (eds.), Vol. 4, p. 261. Wiley, New York, 1980.
16. A. Mehta, *Lab. Pract.*, 1984, **33**, 80.
17. E. G. C. Clarke (ed.), *Isolation and Identification of Drugs*, Pharmaceutical Press, London, 1969.
18. H. Varley, A. H. Gowenlock and M. Bell, *Practical Clinical Biochemistry*, Vol. 2, p. 260. Heinemann, London, 1976.
19. K. A. Connors, *A Textbook of Pharmaceutical Analysis*, 3rd Ed., p. 343. Wiley, New York, 1982.
20. R. Gill and A. C. Moffat, *Anal. Proc.*, 1982, **19**, 170.
21. D. Chin and E. Fastlich, *Clin. Chem.*, 1974, **20**, 1382.
22. D. N. Bailey and M. Kelner, *J. Anal. Toxicol.*, 1984, **8**, 26.
23. R. Gill, A. A. T. Lopes and A. C. Moffat, *J. Chromatog.*, 1981, **226**, 117.
24. J. V. Jackson, in *Isolation and Identification of Drugs*, E. G. C. Clarke (ed.), Vol. 2, p. 914. Pharmaceutical Press, London, 1975.
25. J. Ramsey and D. B. Campbell, *J. Chromatog.*, 1971, **63**, 303.
26. V. Aggarwal, R. Bath and I. Sunshine, *Clin. Chem.*, 1974, **20**, 307.
27. M. G. Horning, P. Gregory, J. Nowlin, M. Stafford, K. Lertratanakoon, C. Butler, W. G. Stillwell and R. M. Hill, *ibid.*, 1974, **20**, 282.
28. J. C. Mathies and M. A. Austin, *ibid.*, 1980, **26**, 1760.
29. J. A. F. de Silva and C. V. Puglisi, in *Drug Fate and Metabolism, Methods and Techniques*, E. R. Garrett and J. L. Hirtz (eds.), Vol. 4, p. 245. Dekker, New York, 1983.
30. C. M. Kaye, in *Progress in Drug Metabolism*, J. W. Bridges and L. F. Chasseaud (eds.), Vol. 4, p. 165. Wiley, New York, 1980.
31. W. Sadee and G. C. M. Beelen (eds.), *Drug Level Monitoring—Analytical Techniques, Metabolism and Pharmacokinetics*, p. 33. Wiley, New York, 1980.
32. J. D. Nicholson, *Analyst*, 1978, **103**, 1, 193.
33. E. O. Titus, in *Fundamentals of Drug Metabolism and Drug Disposition*, B. L. Ladu, H. G. Mandel and E. L. Way (eds.), p. 419. Williams and Wilkins, Baltimore, 1971.
34. L. E. Martin and E. Reid, in *Progress in Drug Metabolism*, J. W. Bridges and L. F. Chasseaud (eds.), Vol. 6, p. 197. Wiley, New York, 1981.
35. E. Reid and J. P. Leppard (eds.), *Drug Metabolite Isolation and Determination*, Plenum Press, New York, 1983.
36. G. G. Skellern, *Analyst*, 1981, **106**, 1071.
37. G. S. Murkitt, R. M. Lee and R. D. McDowall, *Anal. Proc.*, 1984, **21**, 246.
38. H. M. Stevens and A. C. Moffat, *J. Forensic Sci. Soc.*, 1974, **14**, 141.
39. G. Schill, in *Assay of Drugs and Other Trace Compounds in Biological Fluids*, E. Reid (ed.), p. 87. North-Holland, Amsterdam, 1976.
40. E. Tomlinson, *J. Pharm. Biomed. Analysis*, 1983, **1**, 11.
41. M. Garle and I. Petters, *J. Chromatog.*, 1977, **140**, 165.
42. O. Gyllenhaal, U. Tjärnlund, H. Ehrsson and P. Hartvig, *ibid.*, 1978, **156**, 275.
43. O. Gyllenhaal, B. Näslund and P. Hartvig, *ibid.*, 1978, **156**, 330.
44. R. J. Allan, H. T. Goodman and T. R. Watson, *ibid.*, 1980, **183**, 311.
45. T. C. Kwong, R. Martinez and J. M. Keller, *Clin. Chim. Acta*, 1982, **126**, 203.
46. J. M. Meola and M. Vanko, *Clin. Chem.*, 1974, **20**, 184.
47. M. P. Kullberg and C. W. Gorodetzky, *ibid.*, 1974, **20**, 177.
48. J. T. Stewart, I. L. Honigberg, B. M. Turner and D. A. Davenport, *ibid.*, 1982, **28**, 2326.
49. R. C. George, *ibid.*, 1981, **27**, 198.
50. T. J. Good and J. S. Andrews, *J. Chromatog. Sci.*, 1981, **19**, 562.
51. J. P. Anhalt and S. D. Brown, *Clin. Chem.*, 1978, **24**, 1940.
52. W. W. Fike, *J. Chromatog. Sci.*, 1973, **11**, 25.
53. C. B. McAllister, *J. Chromatog.*, 1978, **151**, 62.
54. N. Ratnaraj, V. Goldberg and P. T. Lascelles, *Analyst*, 1984, **109**, 813.
55. S. van der Wal, S. J. Bannister and L. R. Snyder, *J. Chromatog. Sci.*, 1982, **20**, 260.
56. J. Balkon, B. Donnelly and D. Prendes, *J. Forensic Sci.*, 1982, **27**, 23.
57. J. E. H. Stafford, *Lab. Pract.*, 1985, **34**, 19.
58. G. S. Clarke and M. L. Robinson, *Anal. Proc.*, 1985, **22**, 137.
59. R. W. Giese, *Clin. Chem.*, 1983, **29**, 1331.
60. B. L. Karger, R. W. Giese and L. R. Snyder, *Trends Anal. Chem.*, 1983, **2**, 106.
61. U. Juergens, *J. Chromatog.*, 1984, **310**, 97.
62. G. Tamai, I. Morita, T. Masujima, H. Yoshida and H. Imai, *J. Pharm. Sci.*, 1984, **73**, 1825.

Dedication—Dedicated to Dr. R. A. Chalmers, with congratulations on his 20 years as Editor of *Talanta*.

ANALYSIS OF SWEEPS

THE CUPROUS SULPHIDE COLLECTING SYSTEM

SILVE KALLMANN

Ledoux & Co., 359 Alfred Avenue, Teaneck, NJ 07666, U.S.A.

(Received 20 March 1985. Accepted 2 August 1985)

Summary—A new method for collection of precious metals in analysis of "sweeps" is presented. It is based on use of copper sulphide as collecting agent. The oxidation state of the copper has been carefully investigated and the chemistry of the system is discussed. The method gives good accuracy and reproducibility and can be combined with a wide variety of methods of determination.

Because of their substantial intrinsic value, precious metals are commonly recycled after use. Because of the wide variations in composition, it is desirable to reduce precious-metal "scrap" to a form which can be sampled effectively. If in powdered form, this scrap is generally referred to as "sweeps".

Sweeps may contain from 0.01 to 50% of total precious metals and a variety of base-metal compounds. Analytical requirements for sweeps depend on the net weight of the lot being evaluated and the value of the precious metals in it.

In a previous paper¹ the collection of precious metals from sweeps by means of nickel sulphide, first proposed by analysts at the National Institute of Metallurgy, in South Africa,^{2,3} was discussed. In this procedure the sample is fused with a flux consisting of nickel powder or a nickel salt, sulphur, alkali-metal carbonate, silica and alkali-metal borate. On cooling, the heavier nickel sulphide phase separates readily from the lighter phase consisting of a glass-like slag containing the non-sulphide-forming constituents of the sample. The precious-metal sulphides accompany the nickel sulphide. The latter is readily soluble in hydrochloric acid, whereas the precious-metal sulphides remain insoluble. We expressed our disappointment that gold could not be recovered quantitatively by this method and conjectured that gold, unlike the other precious metals, does not readily form a sulphide and therefore appears to pass partially as free gold into the slag or to become embedded in the walls of the assay crucible.

In our study¹ we observed that in the presence of increasing amounts of copper the collection of gold by nickel sulphide markedly improved, presumably by a mechanism involving the formation of "copper metal which alloys with gold during the fusion step, before it and the gold are converted into their sulphides".

The realization of the beneficial effect of copper on the collection of gold by nickel sulphide eventually motivated us to investigate the copper-precious-

metal sulphide system, concerning which there appears to be no analytical literature.

EXPERIMENTAL

Opening up of samples

Thoroughly mix 1-25 g of finely ground sample (finer than 100-mesh) with a flux consisting of 20 g of silica (or an amount equal to the sample weight, whichever is the larger), 100 g of sodium carbonate, 60 g of boric acid, 35 g of cupric oxide and 15 g of sulphur. For alumina-based catalysts add an extra 10 g of silica. Transfer the charge to a "40-g" assay crucible, place in a furnace at about 850°, and close the furnace. After the initial reaction, which involves the release and expulsion of CO₂ and H₂O, increase the temperature gradually to 1200°, and maintain at this temperature for about 30 min.

Remove the crucible from the furnace and pour the molten mass into an iron mould. Cover with the inverted assay crucible to avoid loss of slag during cooling. When the copper sulphide button is sufficiently cool to be handled comfortably (50-60°), remove it from the mould and gently separate any adhering slag with a hammer or some other tool, but exercise care, since the button is somewhat brittle.

To recover traces of precious metals retained by the slag, return the latter to the assay crucible and add a mixture of 50 g of sodium carbonate, 30 g of boric acid, 15 g of cupric oxide and 8 g of sulphur. Cover the charge with a little borax to avoid oxidation of sulphur during the initial heating. Place the crucible in a furnace at 800°, close the furnace, heat again gradually to about 1200°, and maintain at this temperature for about 10 min. Pour the molten mass into an iron mould, cool and separate the copper sulphide button (which will usually weigh a little less than half as much as the first button).

Weigh the two buttons together (total weight usually 60-63 g) and grind them in appropriate equipment to about 100-mesh particle size. Reweigh to establish any grinding loss, which will be taken into consideration during the final calculations. Analyse for one or more of the precious metals by one of the methods given below.

Treatment of the copper sulphide

Since the copper sulphides, particularly Cu₂S, are only slightly soluble in hydrochloric acid, dissolution procedures suitable for nickel sulphide are obviously not applicable. The following approaches have been thoroughly investigated.

Decomposition with aqua regia. This technique is applicable to the determination of one or more of the precious

metals (except osmium, but see discussion) in amounts greater than 4 mg. This minimum of 4 mg is due to the fact that the method does not involve removal of copper.

Decomposition with sulphuric acid, formic acid and thio-sulphate. This approach is applicable to the determination of silver, gold, platinum and palladium, each in amounts greater than 1 mg. Ruthenium and osmium are largely lost during the heating with sulphuric acid. Rhodium and iridium are only partially dissolved and are incompletely recovered. If rhodium and iridium are to be determined, Method III (below) should be used (but see discussion for a modification allowing determination of rhodium).

Decomposition with hydrobromic acid. This more recent approach is applicable to determination of all the precious metals (osmium requires some modification) in amounts greater than 0.2 mg. Results obtained during the last year indicate that this approach may be preferable in most instances to the other dissolution techniques. A slightly modified version of this method allows the determination of osmium (Method IIIA).

Method I, aqua regia method for Ag, Au, Pt, Pd, Ir, Ru and/or Rh

Transfer the ground copper sulphide to a 1-litre beaker. Cover the beaker and add 500 ml of concentrated hydrochloric acid and from time to time 10–15 ml portions of concentrated nitric acid to give rapid but not too violent decomposition of the copper sulphide. Add up to 150 ml of the nitric acid over a period of about 1.5–2 hr until there is apparently no more reaction. Warm on a hot-plate until the renewed reaction slows down, then boil down the solution to about 300 ml. Dilute to 500 ml with water, cool, add 2 ml of concentrated hydrofluoric acid and filter through a medium-porosity paper into an 800-ml beaker. Wash about 5 times with 2% v/v nitric acid. Wipe the beaker with a piece of filter paper and add this to the funnel. Evaporate the filtrate to a convenient volume.

Ignite the filter paper and contents in a zirconium crucible at low temperature until all organic matter and sulphur have been oxidized. Mix the residue with an appropriate amount of sodium peroxide and heat until a clear melt is obtained. Cool, transfer the crucible to a 600-ml beaker, leach the melt with water, then remove the crucible and rinse it with hot water. Clean the crucible with concentrated hydrochloric acid and add the solution to the 600-ml beaker. Acidify the solution with concentrated hydrochloric acid and heat until clear. If necessary, evaporate the solution to an appropriate volume. Combine this solution with the *aqua regia* solution containing the bulk of the copper, and dilute to volume in a 1-litre standard flask, adding sufficient hydrochloric acid to give a final 30% v/v concentration of the acid to prevent precipitation of silver chloride. Determine all the elements except silver by d.c. plasma spectrometry,¹ using aliquots diluted by at least a factor of 4. Determine silver by atomic-absorption spectrometry (AAS).¹ See discussion for an alternative procedure involving separate handling of the soluble and insoluble fractions.

Method II, sulphuric acid/formic acid/thiosulphate method for Ag, Au, Pt and/or Pd

Transfer the ground copper sulphide to a 1-litre beaker. Add 250 ml of concentrated sulphuric acid. Heat first at a temperature of about 250°. When the reaction subsides, increase the temperature to the boiling point of sulphuric acid and maintain at this temperature for a minimum of 3 hr. Should the solution become too viscous, indicating the removal of too much acid, add more acid to ensure complete decomposition of the sample. Cool, wash down the sides of the beaker with water, add about 100 ml of water and 20 ml of formic acid and stir. When the reaction slows down, heat at low temperature for about 30 min. Dilute with hot water to about 800 ml. If a silver determination is required, add sufficient hydrochloric acid to precipitate the silver.

Heat the solution just to the boil then remove from the heat. After 1 min, add 1 g of sodium thiosulphate. Heat again and boil for about 5 min. Remove from the heat, again add 1 g of sodium thiosulphate and boil for 5 min. Maintain the volume of the solution at 800 ml. Allow to stand for at least 3 hr, preferably overnight.

If some copper sulphate crystallizes out during the cooling, dissolve it by gently heating or, after the filtration, by washing with warm water. Filter off the residue on a medium porosity paper and wash a few times with warm water. Discard the filtrate.

Wash the precipitate into the original 1-litre beaker. Dilute to about 150 ml, add 15 ml of concentrated nitric acid and 7 ml of concentrated hydrochloric acid. Boil the solution for about 5 min to dissolve the maximum amount of sulphides (mostly copper sulphide), cool, and filter with the same paper, washing the paper 5 times with 2% v/v nitric acid and wiping the beaker with a piece of filter paper, adding this to the funnel. Evaporate the filtrate on a steam-bath.

Ignite the paper and residue in a zirconium crucible and fuse with sodium peroxide as in Method I. Add the acidified solution of the cooled melt to the main solution. Since in this case silver accompanies the other precious metals, maintain a 20% v/v hydrochloric acid concentration, which will keep up to 50 mg of silver in solution in a volume of 250 ml. Make up the combined solution to volume and complete the analysis as in Method I.

Method III, hydrobromic acid method for Ag, Au, Pt, Pd, Rh, Ru and Ir

Transfer the ground copper sulphide to an 800-ml or 1-litre beaker. Add 500 ml of concentrated hydrobromic acid and heat for at least 3 hr on a steam-bath or at low heat on a hot-plate. Then heat to the boiling point and let simmer for about 2 hr or until the volume has been reduced to 400 ml. Dilute with 200 ml of water and cool to room temperature.

Add 2 ml of concentrated hydrofluoric acid and mix. Filter through a 15-cm hardened paper containing a generous amount of filter-paper pulp. Wash the paper a few times with 30% v/v hydrochloric acid. (Determine HBr-soluble silver in the filtrate by AAS or evaporate the filtrate to dryness and convert the copper bromide into copper sulphate by heating to fuming with about 200 ml of concentrated sulphuric acid. After cooling and dilution, precipitate the silver as chloride. The copper bromide solution may also contain a amount of gold, which can easily be determined by AAS as described below or recovered with thiosulphate from the copper sulphate solution in conjunction with the silver determination.)

Wash the precious-metal sulphide precipitate into the original beaker, and treat it with concentrated nitric and hydrochloric acids as described in Method II, third and fourth paragraphs. Determine Au, Pt, Pd, Rh, Ru, Ir by d.c. plasma spectrometry¹ or, if preferred, by inductively-coupled plasma spectrometry (ICP spectrometry). HBr-insoluble silver is best determined by AAS. If present at suitable concentrations, some of the precious metals other than silver can also be determined by AAS.¹

Determination of traces of gold in the hydrobromic acid filtrate. Transfer the solution to a 1-litre standard flask. Transfer a 25–100 ml aliquot to a 250-ml separatory funnel. Add a measured volume of butyl acetate (10–25 ml), shake for 1 min, allow the phases to separate, draw off the lower phase into a second separatory funnel and extract it with an additional 10 ml of butyl acetate. Draw off the lower layer and discard. Combine the two butyl acetate extracts in a standard flask of appropriate size, dilute to volume with butyl acetate and mix. Measure the gold by AAS directly in the butyl acetate solution.¹ The sensitivity is about 0.1 µg/ml. If preferred, evaporate the butyl acetate extract to

dryness and after treatment of the residue with a nitric/perchloric acid mixture, determine the gold, in cyanide medium, by AAS or d.c. plasma spectrometry.¹

Method IIA, determination of osmium after hydrobromic acid treatment of the copper sulphide

Treat the ground copper sulphide, which should contain at least 50 mg of any other platinum metal, with hydrobromic acid as described in Method III, and filter under suction, with a Gooch crucible containing a fibre-glass filter, finally transferring the precious-metal sulphides into the crucible. Wash a few times with 30% v/v hydrochloric acid to remove copper bromide, then wash in succession with ethanol, diethyl ether and carbon disulphide. Maintain the suction for a few minutes to remove residual CS₂. Transfer the precipitate and filter pad to a zirconium crucible and remove any adhering particles by wiping with a fibre-glass filter pad. Dry the pads and residue, add an appropriate amount of sodium peroxide and fuse until a clear melt is obtained. Cool, transfer the crucible to a 400- or 600-ml beaker, leach with water, wash the crucible and keep it for further cleaning. Boil the contents of the beaker for a few minutes to remove excess of peroxide, add 25 ml of saturated sulphur dioxide solution and acidify the solution with hydrochloric acid. Clean the zirconium crucible with concentrated hydrochloric acid and add the washings to the beaker. Warm until the solution clears, adding, if necessary, a few drops of concentrated hydrofluoric acid to dissolve any precipitated silica.

Cool the solution, transfer it to a standard flask of appropriate size and determine osmium and other precious metals by d.c. plasma spectrometry (DCP)¹ or, if preferred, by inductively-coupled plasma spectrometry (ICP).

DISCUSSION

The composition of the copper sulphide button

As will be demonstrated later, the stoichiometry of the copper sulphide affects the quantitative collection of gold but not that of the other precious metals. Though there is a considerable literature on the composition of copper sulphides produced by heating copper or copper compounds with sulphur, there are no literature reports on analytical applications of the copper sulphide system.

The composition of copper sulphides may range from orthorhombic or pseudohexagonal Cu₂S (as the mineral chalcocite), through orthorhombic Cu_{1.96}S (as the mineral djurleite), isometric Cu₆S₅ (as the mineral digenite), orthorhombic Cu₇S₄ (as the mineral anilite), to hexagonal CuS (as the mineral covellite).^{4,5}

Because of the complex parameters of our fusion scheme, which has to accommodate samples of widely varying compositions and weights, little help was expected from the published literature in

elucidating the composition of the copper sulphide generated in our procedure.

Since CuS (covellite) is unstable at temperatures above 450°C, it was not expected to be formed even in the presence of an excess of sulphur. The expectation was that the fusion temperature of our procedure, which reaches 1250°, would favour the formation of Cu₂S, which has a melting point of 1127°. Our operation, however, involves a cooling period for the separation of the matte (synthetic sulphide) phase from the slag phase. It must therefore be assumed that during the cooling period the Cu₂S will, at least in part, react with excess of sulphur to form, depending on the quantity of sulphur available, digenite (Cu_{1.8}S) or anilite (Cu_{1.75}S). Since some of the non-precious metal components of the sample may also form sulphides and the fusion charge may be subject to some oxidation during heating and cooling, the precise composition of the copper sulphide formed will vary from sample to sample and also, but to a lesser extent, depend on the position of the assay crucible in the furnace.

Although X-ray diffraction studies performed for us at several establishments⁶⁻⁹ do not fully agree, the general conclusion can be drawn that the composition of the copper sulphide will vary between Cu₂S and Cu_{1.75}S as long as the fusion process is based on a ratio of 35 g of cupric oxide to 15 g of sulphur, a ratio which was experimentally shown to yield optimum gold recoveries (Table 1). While the amount of sulphur specified in our procedure (15 g) is theoretically in excess of that required for the formation of any of the copper sulphides listed above, this excess of sulphur is partially consumed in formation of the sulphides of the precious and certain base metals and is partially oxidized in some of the reactions taking place during various stages of the fusion.

Using only 10 or even 12 g of sulphur, instead of the 15 g specified in our procedure, caused the formation of a copper sulphide button of poor appearance and frequently resulted in a blueish coloured slag which indicated incomplete formation of copper sulphide and presumably of the precious-metal sulphides. Using more than 18 g of sulphur yielded a good looking copper sulphide button, but gold collection was incomplete (Table 1).

Experiments done in the early stages of this investigation indicated that the collection of silver and the platinum group elements is quantitative, irre-

Table 1. Chemical analysis of copper sulphides obtained with various CuO/S ratios

CuO used, g	S used, g	Copper found, %	Sulphur found, %	Atomic ratio Cu/S	Na ₂ O found, %	Gold recovery, %
35	15	78.00	21.05	1.866	0.65	100
35	15	75.15	23.36	1.620	1.05	100
35	15	78.25	20.65	1.908	0.80	100
35	20	72.47	26.20	1.388	1.14	95
35	25	70.64	28.23	1.260	1.15	91
36	30	68.00	30.87	1.109	1.26	87

spective of whether 15, 20, 25 or even 30 g of sulphur are used to react with 35 g of cupric oxide. This was not entirely surprising, since these elements form, under varying experimental conditions, stable sulphides such as Ag_2S , PtS and PtS_2 , Rh_2S_3 , and Rh_9S_8 , RuS_2 , IrS_2 , and OsS_2 . In contrast, the existence of stable gold sulphides appears to be uncertain, with only Au_2S being listed in Gmelin¹⁰ as a verified but unstable compound. In connection with our work on the nickel sulphide system,¹ we established that gold is largely reduced by the sulphur to the free metal during the fusion process, passing partially into the slag and partially being retained by the walls of the assay crucible. Since gold can be collected by copper sulphide, it must be assumed that this involves the formation of a gold sulphide, presumably Au_2S , in solid solution with Cu_2S . This is borne out by our tests incorporating ¹⁹⁵Au into our fusion charge. The results indicate that the slag and the assay-crucible walls retain less than 0.1% of the total gold, provided that (a) the 35/15 CuO/S ratio is applied, and (b) the total amount of gold in the sample charge does not exceed 0.75 g. This assumption is indirectly confirmed by X-ray diffraction studies, which indicate the presence of free gold only when there is more than 1 g of gold in 60 g of copper sulphide. It was noted by one observer that the powder diffraction analyser indicated no free elemental gold in the original sample, but samples which had been exposed to the air for several days showed a progressive increase in the elemental gold peak and the appearance of copper sulphate compounds.⁶

That, unlike nickel sulphide, copper sulphide (presumably as Cu_2S) forms solid solutions with gold sulphide (presumably as Au_2S) or is isomorphous with it is not altogether surprising, since nickel belongs to group VIII of the periodic table, and copper, silver and gold belong to group IB. (As a corollary, preliminary tests with silver sulphide, Ag_2S , as the matrix showed that it quantitatively collects copper and gold.)

Increasing S/CuO ratios favour the formation of copper sulphides approaching the composition of CuS , instead of Cu_2S (see Table 1). This leads to the assumption that gold sulphide does not form solid solutions with CuS for the simple reason that AuS does not exist. Excess of sulphur apparently leads to the formation of metallic gold, with attendant gold losses to the slag and crucible.

All copper sulphide buttons produced in our laboratory contained a small amount of sodium (see Table 1). About half of the sodium is water-soluble and unexpectedly was found to be in the form of sodium sulphite and/or sodium thiosulphate. Although the source of the sodium is undoubtedly the sodium carbonate used as a flux component, no other species contained in the flux could be detected in the cleaned copper sulphide by emission spectrographic analysis. The data in Table 1 indicate that the sodium content of the copper sulphide increases with the percentage

of sulphur in the flux. It is assumed that the formation of Na_2SO_3 and $\text{Na}_2\text{S}_2\text{O}_3$ is part of a complex overall reaction during the fusion process and the cooling of the resulting Cu_2S underneath the slag. The water insoluble sodium fraction was found to be a part of the copper sulphide structure. $\text{Cu}_4\text{Na}_3\text{S}_4$ is the only such compound listed in X-ray diffraction tables. (It should be noted that in calculating the stoichiometry of the copper sulphide, Table 1, the sulphur results were not corrected for the amount of sulphur contained in any Na_2SO_3 , $\text{Na}_2\text{S}_2\text{O}_3$ or $\text{Cu}_4\text{Na}_3\text{S}_4$.)

Individual features of the copper sulphide method

Fusion of the sample. It is essential that the furnace door be kept closed during the entire fusion process, to avoid losses of sulphur by oxidation.

On the assumption that the slag cannot be entirely removed from the sulphide button, sodium carbonate is used instead of potassium carbonate (which is used in the nickel sulphide procedure flux) to prevent formation of K_2PtCl_6 in the *aqua regia* dissolution procedure.

Dissolution of the residue insoluble in aqua regia. Fusion of the residue with sodium peroxide, though quite effective, imposes limitations on the final volumes used for AAS and/or DCP measurements. For dealing with small quantities of precious metals, the alternative acid treatments described should be considered.

The aqua regia dissolution procedure. To counteract the effect of silica introduced into the system by incomplete removal of the slag, a small amount of hydrofluoric acid is added to the cold diluted solution to form silicofluoride and thus act as a filtering aid. (For the same reason, hydrofluoric acid is also used in Method III.)

The solubility of individual precious-metal sulphides (which may partly be in solid solution with copper sulphide) in *aqua regia* varies from virtually zero for ruthenium and iridium, and very slight for rhodium, to almost 100% for gold (Table 2). Most unexpectedly, 80–90% of the osmium sulphide remains insoluble if the sample contains at least 50 mg of any other "insoluble" precious-metal sulphide, and more than 70% of it is insoluble if osmium is the only precious metal present. The insolubility of the sulphides of Ru, Ir and Os, the slight solubility of rhodium sulphide, and the relative solubility of platinum and palladium sulphides in *aqua regia* depends to a large extent on their relative concentration and also on their ratio to the sum of all precious-metal sulphides present. (The limited solubility, in *aqua regia*, of the precious-metal sulphides collected by copper sulphide is in sharp contrast to the high solubility of precious-metal sulphides prepared by passing hydrogen sulphide into their chloride solutions.)

The fraction insoluble in *aqua regia* contains virtually all of the ruthenium and iridium and only traces

Table 2. Solubility of precious-metal sulphides in *aqua regia*

	Ag	Au	Pt	Pd	Rh	Ru	Ir	Os
Present, mg	—	50	30	25	25	50	10	25
Insoluble, %	—	2	85	60	98	101*	101*	85
Present, mg	75	120	150	120	75	75	75	50
Insoluble, %	15	24	83	75	100	99	99	85
Present, mg	100	120	150	120	—	—	—	—
Insoluble, %	13	6	72	57	—	—	—	—
Present, mg	25	30	12	10	25	25	25	—
Insoluble, %	6	2	80	55	98	98	99	—
Present, mg	50	50	50	50	—	—	—	—
Insoluble, %	10	7	30	45	—	—	—	—
Present, mg	—	—	—	—	50	100	100	—
Insoluble, %	—	—	—	—	99	101*	99	—
Present, mg	—	25	25	25	20	—	—	—
Insoluble, %	—	3	72	77	98	—	—	—

*The apparent manufacture of an element is an artefact due to experimental error.

of rhodium, even in the presence of an *aqua regia*-soluble, copper-rich, fraction containing almost all of the gold and significant amounts of platinum and palladium. Hence, the sensitivity of Method I for the determination of Ir, Ru, and Rh can be much improved by fusing the insoluble residue (from the *aqua regia* treatment) with a minimum amount of sodium peroxide and measuring the concentration of the precious metal by DCP in the virtual absence of copper, in volumes of 250 ml or less. The *aqua regia*-soluble fraction containing the copper can be examined with adequate sensitivity for possible traces of Rh and major quantities of gold, platinum and palladium (Table 2). In individual determinations,

however, the effect of copper and sulphuric acid (formed by oxidation of the sulphide) on measurements of trace amounts of precious metals cannot be entirely disregarded.

Figure 1, for instance, shows the effect of various concentrations of copper (as sulphate) on DCP measurements of 1- $\mu\text{g}/\text{ml}$ palladium at 3242.703 Å. It is apparent that the final sample solution should not contain more than 10 mg of copper per ml for measurements of 1- $\mu\text{g}/\text{ml}$ palladium to be meaningful. Examination of the spectra of other precious metals at the 1- $\mu\text{g}/\text{ml}$ level in the presence of various amounts of copper (as sulphate) showed similar effects of copper (Table 3). Table 3 clearly demonstrates the necessity of adding copper to DCP standards when the concentration of the precious metal is less than 5 $\mu\text{g}/\text{ml}$ and that of copper is 10 mg/ml.

As can be seen from Table 3, the effects of copper are negligible in the case of gold and most pronounced in the case of palladium. The copper interference is usually positive, but for ruthenium is slightly negative. The extent of interference depends to a large extent on variations in the photomultiplier settings and gains used to compensate for substantial differences in the sensitivities of the signals from the precious metals at the interference-free wavelengths chosen.

Extensive tests made in our laboratory indicate that there are only minor effects from copper when its concentration is less than 10 mg/ml or the concentration of the precious metal is more than 5 $\mu\text{g}/\text{ml}$.

The sulphuric acid dissolution method. Formic acid is used to precipitate any palladium and platinum which may have been partially solubilized by the strong fuming with sulphuric acid. The additional precipitation of a small amount of copper sulphide with sodium thiosulphate ensures complete precipitation of trace amounts of gold, silver, platinum and palladium. The mechanism of this reaction will be explained in a separate paper.

It was mentioned earlier that rhodium is not quantitatively collected in Method II. This is due to

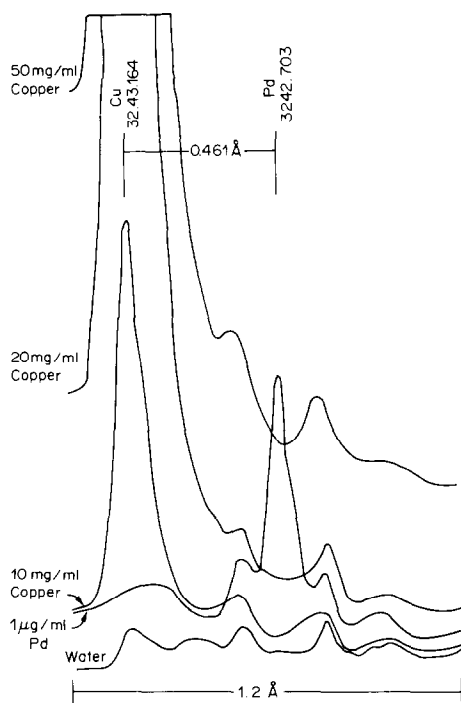


Fig. 1. Effect of copper on DCP measurements of 1- $\mu\text{g}/\text{ml}$ Pd.

Table 3. Effect of copper on DCP measurements of the precious metals (all solutions contained 1% NaCl and 1.6% LaCl_3)

Precious metal, $\mu\text{g/ml}$	Copper added, mg/ml	Precious metal found,* $\mu\text{g/ml}$		Wavelength, \AA
Au	1	0	0.963	2675.95
	1	10	0.985	
	5	0	4.86	
	5	10	4.94	
	0	0	0.045	
	0	10	0.057	
Pt	1	0	1.12	2659.45
	1	10	1.03	
	5	0	5.10	
	5	10	5.02	
	0	0	0.202	
	0	10	0.125	
Pd	1	0	1.23	3242.70
	1	10	1.23	
	5	0	4.80	
	5	10	5.00	
	0	0	0.229	
	0	10	0.281	
Rh	1.34	0	1.30	3434.89
	1	10	0.924	
	2.68	0	2.59	
	5	10	5.05	
	0	0	0.065	
	0	10	-0.044	
Ir	1	0	1.14	2639.71
	1	10	1.02	
	5	0	4.61	
	5	10	4.92	
	0	0	0.260	
	0	10	0.211	
Ru	0.973	0	1.06	3728.03
	1	10	0.867	
	5.83	0	5.76	
	5	10	4.63	
	0	0	0.018	
	0	10	-0.246	

*Non-zero values obtained when no precious metal is present are artefacts of the experimental system.

the formation of a stable rhodium sulphate complex which prevents quantitative collection of the rhodium as sulphide. In line with earlier observations¹¹ it was expected that rhodium sulphate would be converted into cationic rhodium chloride by prolonged treatment with concentrated hydrochloric acid. Subsequently, the following modified procedure was developed, which ensures quantitative collection of the rhodium as sulphide.

Heat the sample strongly with sulphuric acid as described in Method II. Omit the treatment with formic acid. Raise the cover of the beaker and evaporate to dryness or until fumes of SO_3 cease to escape. Cool, add 300 ml of water, mix, add 150 ml of concentrated hydrochloric acid and boil for 1 hr with the beaker covered. Raise the cover and evaporate the solution to 300 ml. Dilute to 700 ml with hot water and precipitate the precious metals with four ~1-g additions of sodium thiosulphate, boiling for 2-3 min between additions. Allow to settle. Filter and continue as described in Method II. Since silver

chloride is considerably soluble in the hydrochloric acid medium used for the precipitation of the precious metals, do not discard the filtrate. Transfer it to a 1-litre standard flask, dilute to volume and measure the silver concentration by AAS.

The hydrobromic acid dissolution method. The dissolution of Cu_2S in hydrobromic acid (Method III) was derived from the classical use of this acid in the evolution procedure for determining sulphur in brasses or bronzes.¹² It will be recalled that owing to the greater stability of CuBr , copper can reduce the protons from concentrated hydrobromic acid, though it cannot reduce those from concentrated hydrochloric acid. It was therefore conjectured that hydrobromic acid would be an equally efficient solvent for Cu_2S . Method III is the best proof that this reasoning is correct. (It should be mentioned that hydrobromic acid is quite expensive if bought in small quantities; buying the technical grade, which is quite satisfactory, in a 50-gallon drum, results in a 75-80% saving over the single 1-gallon bottle price.)

The most attractive feature of the technique is that, with the exception of silver and possibly small amounts of gold, the other precious metals are not dissolved during the dissolution of the copper sulphide. (However, even gram amounts of silver pass almost quantitatively into the filtrate, from which the silver can be readily recovered or in which it can be easily determined by AAS. Provisions have been made to determine any soluble gold by easy AAS measurements. It is assumed that the small amount of gold dissolved arises from the decomposition of the Au_2S in solid solution with Cu_2S .) The remaining precious metals and small amounts of silver are collected together, virtually uncontaminated by copper. Base-metal sulphides collected by the Cu_2S (e.g., those of Pb, Bi, Ni, Fe, Co, Sn) are all soluble in hydrobromic acid and are quantitatively removed. Of particular interest is the tolerance of the method for substantial amounts of lead. It is assumed that a small amount of gold may be dissolved by the action of cupric bromide formed by aerial oxidation of cuprous bromide. This dissolution can be prevented by adding a small amount of zinc metal to the solution and/or the filter paper before the filtration.

Unless an osmium determination is required (OsO_4 would be lost during ignition and requires the modification outlined in Method IIIA) fusion of the HBr-insoluble residue with sodium peroxide after ignition in a zirconium crucible therefore represents the most rapid approach for determining all the precious metals instrumentally in one master solution. Starting with the dissolution of the Cu_2S in hydrobromic acid, a master solution can be prepared for instrumental measurements in less than 5 hr.

If the concentration of the precious metals (particularly platinum and palladium) is greater than may be desirable for instrumental analysis, determination of one or more of the precious metals by gravimetric methods may be preferred. One approach successfully

used in our laboratory consists of: (1) treatment of the HBr-insoluble material with dilute *aqua regia*, followed by filtration to remove all but traces of the copper, most of the gold and small amounts of platinum and/or palladium (Solution A); (2) ignition of the *aqua regia*-insoluble residue to convert the precious metals in the combined Solutions A and C (Ag by AAS); (5) gravimetric determination of the *regia* followed by filtration (Solution B) and fusion of the ignited residue from (3) with sodium peroxide and acidification of the leached melt with hydrochloric acid (Solution C); (4) DCP measurement of the precious metals in the combined Solutions A and C (Ag by AAS); (5) gravimetric determination of the major concentration of platinum and/or palladium in Solution B.

This method represents a good example of a recent trend in analytical chemistry, demonstrating the interdependence of classical chemical and instrumental techniques.

Interferences

In the collection of the precious metals with copper sulphide. Base metals which do not form sulphides do not interfere, since they will aggregate in the slag. Thus there is no interference from Al_2O_3 , MgO , CaO , TiO_2 , BaO , Ta_2O_5 , Nb_2O_5 , ZrO_2 , V_2O_5 and even from Cr_2O_3 (which seriously interferes in lead collection schemes).

Sulphide-forming elements are collected together with the Cu_2S ; these include Ni, Co, Fe, Pb, Sn, Bi, but up to 2 g of these elements (the amount tested) will not interfere individually or as a group with the collection of the precious metals by copper sulphide.

Up to 7 g of combined precious metals, with a limit of 0.75 g for gold, can be quantitatively collected by copper sulphide, but for determination of less than 10 mg of precious metals it is advisable to add to the

sample charge 20–25 mg of a precious metal which is not to be determined, to avoid physical losses of the precious metals during the treatment of the copper sulphide.

Interferences in the measurements. The effect of copper and sulphuric acid on DCP measurements when Method I is used has already been discussed. A fourfold dilution (to yield 10 mg/ml Cu) allows the measurements of all the precious metals at the 1- $\mu\text{g}/\text{ml}$ level. Sodium salts introduced as a result of fusing the acid-insoluble residue with sodium peroxide do not interfere if the final concentration of sodium chloride is not greater than 1%. Measurements by ICP may require additional dilution.

All sulphide-forming elements collected by the copper sulphide will be found in the *aqua regia* solution, but do not interfere in the DCP measurements provided their individual concentrations in the final solution are below the test limit, namely 1 mg/ml.

In Methods II, III and IIIA virtually all the copper is removed. Residual amounts of copper (< 1 mg/ml) and sulphuric acid (< 0.1 mg/ml) have no effect on DCP measurements of any of the precious metals at levels of 0.5 $\mu\text{g}/\text{ml}$ or more. All sulphide-forming base elements have been removed and therefore do not interfere. The sodium chloride introduced as a result of the sodium peroxide fusion and acidification of the melt presents no difficulties so long as its concentration in the final solution is kept at 1%, the preferred level for all DCP measurements.

Flame AAS measurements of Au, Pd, and Rh match in precision those by DCP. AAS measurements of Pt, however, are significantly affected by sodium chloride. Ru and Ir determinations by DCP are much superior to those by AAS. It is assumed that ICP is equal to DCP in its ability to measure the precious metals. XRF and flameless AAS measurements of the precious metals appear feasible in

Table 4. Cu_2S collection method applied to synthetic standards made by additions to blank sweep sample No. 1.; all measurements by DCP except for Ag (AAS)

Element	<i>Aqua regia</i> decomposition		H_2SO_4 decomposition		HBr decomposition	
	Added, mg	Found, mg	Added, mg	Found, mg	Added, mg	Found, mg
Au	25.2	24.9	50.3	49.6	18.2	18.4
	85.3	86.2	125.7	123.3	34.5	35.2
Ag	125.4	126.2	130.3	132.8	25.7	24.0
	65.3	63.4	75.6	75.7	250.8	253.7
Pt	68.7	69.4	25.2	25.4	17.2	17.9
	257.5	259.0	120.6	122.0	34.3	33.0
Pd	175.4	173.8	63.1	62.2	15.0	15.2
	60.5	61.6	68.4	67.5	38.5	37.8
Rh	15.2	15.2	24.7	—	4.8	4.8
	63.7	63.0	18.5	—	28.5	29.7
Ru	7.5	7.3	15.5	—	38.5	39.6
	18.4	18.9	30.3	—	3.9	3.5
Ir	16.8	17.2	60.2	—	40.7	41.4
	12.0	12.3	75.4	—	5.4	5.4

Table 5. Analysis of sweep sample 27303

Collection method	Isolation method	Final measurement	Contents, %						
			Ru	Rh	Ir	Pt	Pd	Au	Ag
Cu ₂ S	HBr	DCP	40.5	15.10	4.94	0.728	0.460	0.425	—
Cu ₂ S	HBr	DCP	40.3	15.20	4.90	0.709	0.463	0.427	—
Cu ₂ S	HBr	AAS	—	15.05	—	—	—	0.420	1.56
Cu ₂ S	HBr	AAS	—	15.14	—	—	—	0.433	1.60
Cu ₂ S	<i>Aqua regia</i>	DCP	40.4	15.22	4.96	0.730	0.483	0.395	—
Cu ₂ S	<i>Aqua regia</i>	DCP	40.3	15.07	4.96	0.735	0.474	0.407	—
Cu ₂ S	<i>Aqua regia</i>	AAS	—	15.05	—	—	—	—	1.50
Cu ₂ S	<i>Aqua regia</i>	AAS	—	15.20	—	—	—	—	1.62
*NiS	HCl	DCP, AAS	40.2	15.07	4.93	0.711	0.475	0.393	1.50
*Na ₂ O ₂	Direct fusion	DCP, AAS	39.8	14.9	4.63	0.70	0.46	0.42	—
	measurements	AAS	—	14.8	—	—	—	—	1.46

*From previous work.

Table 6. Analysis of sweep sample 92822-224

Collection method	Isolation method	Final measurement	Contents, %						
			Au	Ag	Pt	Pd	Rh	Ru	Ir
Cu ₂ S	HBr	DCP	0.695	—	0.278	0.172	1.79	0.060	0.108
Cu ₂ S	HBr	DCP	0.692	—	0.280	0.170	1.76	0.058	0.104
Cu ₂ S	HBr	AAS	0.690	6.90	—	0.162	1.75	—	—
Cu ₂ S	HBr	AAS	0.700	6.92	—	0.168	1.80	—	—
†Cu ₂ S	H ₂ SO ₄	DCP	0.689	—	0.270	0.168	1.78	—	—
†Cu ₂ S	H ₂ SO ₄	DCP	0.701	—	0.282	0.180	1.75	—	—
†Cu ₂ S	H ₂ SO ₄	AAS	0.695	6.90	—	0.175	1.78	—	—
*NiS	HCl	DCP	0.659	—	0.274	0.162	1.77	0.055	0.106
*NiS	HCL	AAS	0.650	6.85	0.277	0.167	1.77	—	—
*Na ₂ O ₂	Direct measurement	DCP	0.69	—	0.275	0.185	1.76	0.066	0.10
*Na ₂ O ₂	Direct measurement	AAS	—	6.87	—	—	1.74	—	—
*Ag bead	Parting	DCP	0.694	—	0.273	0.164	1.78	—	0.108
*Ag bead	Parting	AAS	0.686	—	0.274	0.160	1.76	—	—
*Outside									
Lab. No. 1			0.706	6.87§	0.294	0.171§	1.78	0.064§	0.110
*Outside									
Lab. No. 2			0.630	7.16§	0.250	0.160§	1.75	0.052§	0.100

†Modified procedure.

*From previous work.

§No referee analysis required.

Table 7. Analysis of sweep sample 92822-424

Collection method	Isolation method	Final measurement	Contents, %						
			Au	Ag	Pt	Pd	Rh	Ru	Ir
Cu ₂ S	HBr	DCP	0.282	—	0.770	0.945	0.412	0.042	0.070
Cu ₂ S	HBr	AAS	0.284	1.15	—	—	—	—	—
†Cu ₂ S	H ₂ SO ₄	DCP	0.286	—	0.775	0.928	0.402	—	—
†Cu ₂ S	H ₂ SO ₄	AAS	0.289	1.15	0.764	0.943	—	—	—
Cu ₂ S	<i>Aqua regia</i>	DCP	0.288	—	0.770	0.928	0.402	0.060	0.065
Cu ₂ S	<i>Aqua regia</i>	AAS	—	1.17	—	—	—	—	—
*NiS	HCl	DCP	0.266	—	0.772	0.940	0.387	0.071	0.068
*NiS	HCl	AAS	0.260	1.13	0.773	0.932	0.400	—	—
*Na ₂ O ₂	Direct measurement	DCP	0.28	—	0.76	0.94	0.41	0.05	0.076
*Ag Bead	Parting	DCP	0.282	—	0.763	0.932	0.383	—	0.070
*Ag Bead	Parting	AAS	0.280	—	0.764	0.935	0.391	—	—
*Outside									
Lab. No. 1			0.294	1.17	0.835	0.966	0.388	0.082§	0.081
*Outside									
Lab. No. 2			0.280	1.04	0.770	0.930	0.380	§	0.069

†Modified procedure.

*From previous work.

§No referee analysis required.

Table 8. Determination of osmium, iridium, ruthenium and rhodium

	Iridium, %	Osmium, %	Ruthenium, %	Rhodium, %
Method IIIA, HBr decomposition	12.10	14.15	4.35	2.80
Method I, <i>aqua regia</i> decomposition	11.96	14.29	4.27	2.80
Method I, <i>aqua regia</i> decomposition	11.80	14.45	4.28	2.83
Outside Lab. No. 1 (unknown methods)	12.27	14.06	4.18	2.75
Outside Lab. No. 2 (unknown methods)	11.85	14.00	4.05	2.78

some instances, but were not included in this investigation.

Mutual interference of precious metals. No measurable interference was noted in DCP measurements of any one precious metal at the 1- $\mu\text{g/ml}$ level in the presence of 200 $\mu\text{g/ml}$ of any other individual precious metal or 1000 $\mu\text{g/ml}$ total concentration in a mixture of precious metals.

Recommended methods

For general purposes we prefer the hydrobromic acid method, reserving the others for quality control or cross-checking. However, if only Au, Pt and Pd are to be determined, Method II is recommended, and the *aqua regia* technique (Method I) is perhaps preferable for comparatively large amounts of all the precious metals or for trace amounts of Ir or Ru in the presence of larger amounts of the other precious metals.

Validation of the method

No standard samples were available, but comparison with results obtained by other techniques or made available to Ledoux & Co. by co-operating clients after the conclusion of referee analyses demonstrates the validity of the proposed procedure. As in our earlier publication,¹ synthetic standards were also used for verification. Tables 4–8 give the results.

Acknowledgement—The generous and valuable assistance of Paul Blumberg and Charles Maul, senior members of Ledoux & Co.'s analytical staff, in various phases of this investigation is gratefully acknowledged.

REFERENCES

1. S. Kallmann and C. Maul, *Talanta*, 1983, **30**, 21.
2. M. M. Kruger and R. V. D. Robert, *Natl. Inst. Met. Rep. S. Afr. Rept.* No. 1432, 1972.
3. R. V. D. Robert, E. van Wyk and R. R. Palmer, *ibid.*, No. 1371, 1971.
4. K. Frye (ed.), *The Encyclopedia of Mineralogy*, Hutchinson Ross Publishing Co., Stroudsburg, 1981.
5. *Gmelins Handbuch der Anorganischen Chemie*, 8th Ed., Copper, Part B, System 60, Sec. 1. Verlag Chemie, Weinheim, 1958.
6. P. L. Burneside, Freeport Minerals Co., Private communication, 22 September 1983.
7. F. Coyle, Cabot Corp., Private communication, 4 August 1984.
8. J. Dann, GTE-Sylvania, Private communication, 4 December 1984.
9. D. K. Smith, Pennsylvania State University, Private Communication, 23 September 1983.
10. *Gmelins Handbuch der Anorganischen Chemie*, 8th Ed., Gold, System 62. Verlag Chemie Weinheim, 1954.
11. F. E. Beamish, *The Analytical Chemistry of Noble Metals*, pp. 270–271. Pergamon Press, Oxford, 1966.
12. F. J. Welcher (ed.), *Standard Methods of Chemical Analysis*, 6th Ed. Vol. IIA, p. 842. Van Nostrand, Princeton, 1963.

Dedication—Undoubtedly other contributors to *Talanta* will point out the depth of Dr. Chalmers' knowledge in the field of Analytical Chemistry. Others will emphasize his substantial editorial skills. I wish to add as his prime asset his modesty and humanity. A couple of examples will suffice:

(1) In reviewing for Dr. Chalmers a paper involving the extraction of gold, I mentioned that the author stated that equilibrium was established in half a minute, but that he specified a ten minute shaking period. Dr. Chalmers' reply: "I agree, however when you and I were young, half a minute meant half a minute. For the new generation you have to specify ten minutes to get the equivalent of half a minute shaking period."

(2) After his visit to our laboratory in Teaneck, I sent Dr. Chalmers a note remarking that "we all enjoyed his brief stay at our laboratory." What I actually wanted to say is that his visit was too brief. Dr. Chalmers' answer: "This reminds me of the time I read in New Delhi, on a cinema marquee in splashy letters, the announcement: 'At Popular Request, Last Performance'."

(3) This last example really reveals his magnanimity as an editor and human being: I had given a paper at the Eastern Analytical Symposium entitled "Interdependence of Chemical and Instrumental Methods in the Analysis of Precious Metals." I had given Dr. Chalmers a copy of the talk just for information purposes. After reading the material, he actually considered publication in *Talanta*. I was therefore a little embarrassed when I was approached by the editors of *Analytical Chemistry* to prepare a report on a related subject. I naturally contacted Dr. Chalmers for his advice. He immediately replied that I should submit the paper to *Analytical Chemistry* because it would have there a much larger readership. Not only this, he offered to help me in the preparation of the manuscript.

ETUDE ANALYTIQUE DU GOODRITE 3114, ANTIOXYDANT DES POLYOLEFINES

COMPORTEMENT VIS A VIS DES AGENTS DE STERILISATION

F. PELLERIN, C. MAJCHERCZYK et D. BAYLOQC

Laboratoire de Chimie Analytique, Centre d'études Pharmaceutiques, Université de Paris XI,
rue J. B. Clément; F 92290 Chatenay Malabry, France

(Reçu le 18 janvier 1985. Accepté le 20 mars 1985)

Résumé—Un procédé d'identification et de dosage par HPLC, du Goodrite 3114 et des produits formés sous l'action d'agents de stérilisation, est décrit. La structure du produit de dégradation résultant de l'irradiation γ a été établie. Une méthode de recherche des migrations est proposée.

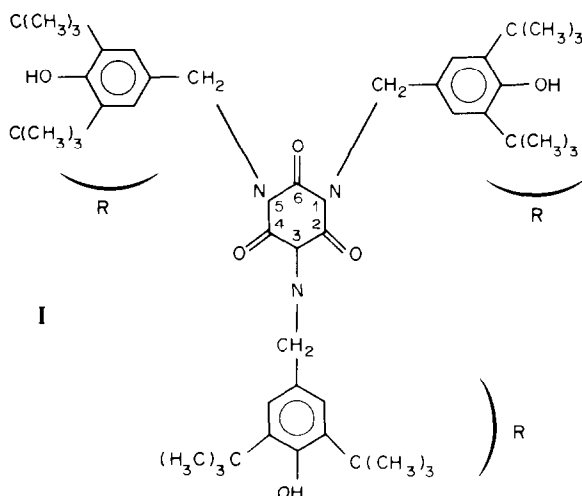
De nombreux antioxydants phénoliques sont introduits dans les polyoléfines haute et basse densité, et les polypropylènes, en vue de protéger le polymère au cours des traitements de conservation et également au cours de sa transformation. De très nombreux travaux ont été consacrés à leur mise en évidence et à leur dosage, au moyen des techniques spectrophotométriques, et chromatographiques.¹⁻⁴ Les antioxydants phénoliques, en nombre limité, sont utilisés pour la stabilisation des polyoléfines, à usage alimentaire, pharmaceutique, ou médico chirurgical.

Le Goodrite 3114, tris(di-tert butyl 3,5 hydroxybenzyl 4-S-triazine-2,4,6 (1H,3H,5H) trione, ou tris(di-tert butyl 3,5 hydroxybenzyl-4) isocyanurate (I), est utilisé comme antioxydant à usage alimentaire dans de nombreux pays.

stérilisation ainsi que les risques de migration dans les médicaments.

De nombreux travaux et brevets ont été consacrés à l'étude du rôle et des transformations des antioxydants au cours de la radiostérilisation des matières plastiques;⁵⁻⁸ en règle générale, les produits de dégradation n'ont pas été isolés.

Le présent mémoire décrit une méthode de chromatographie liquide permettant l'identification et le dosage du Goodrite 3114, avant et après traitement à l'oxyde d'éthylène et aux rayonnements γ . Les produits de dégradation ont été mis en évidence et la structure du produit formé après irradiation a été établie. Une étude d'interactions en vue de révéler d'éventuelles migrations d'antioxydants a été effectuée.



PARTIE EXPERIMENTALE

Réactifs

Plaques de polypropylène ne renfermant pas d'antioxydant. Plaques de polypropylène renfermant 0,2% de Goodrite 3114. Plaques de polypropylène renfermant 0,2% de Goodrite 3114, irradiées par rayonnements (2,5 et 10 Mrad). Goodrite 3114 pur. Goodrite 3114 irradié à 2,5 et 10 Mrad.

Appareillage

Chaîne de chromatographie liquide comprenant: une pompe Chromatem 320 équipée d'un Programmateur 420; une vanne d'injection (Rhéodyne) munie d'une boucle de 20 μ l; un détecteur ultraviolet visible (Spectroflow) à longueurs d'ondes variables, dont l'échelle des sensibilités, exprimées en densités optiques varie de 0,001 à 2,999. Une colonne de silice greffée à polarité de phase inversée C₁₈ (7 μ m): 25 cm de longueur.

Mode opératoire

Extraction. Le mode d'extraction peut être direct, en utilisant un solvant spécifique de l'antioxydant, ou indirect, par dissolution du matériau par un solvant approprié et précipitation du polymère par le méthanol. Ce deuxième procédé permet d'obtenir en solution l'ensemble des additifs contenus dans le matériau.

L'emploi de cet antioxydant dans les polyoléfines à usage pharmaceutique ou médico-chirurgical, implique sa mise en évidence et son dosage dans les matériaux. Pour cette application, il convient de considérer son comportement vis à vis des agents de

Chromatographie. Phase mobile; acétonitrile/eau (95/5), débit: 1,5 ml/min. Longueur d'onde: 280 nm. Atténuation: 0,002. Solution de référence: Goodrite 3114 dilué dans le tétrahydrofurane (0,005 à 0,050%).

RESULTATS ET DISCUSSION

Conditions d'extraction

La chromatographie réalisée sur l'extrait obtenu à partir des plaques de polypropylène témoins ne renfermant pas de Goodrite 3114 ne révèle aucun additif. Le procédé permet de déterminer les teneurs en Goodrite 3114 des plaques de polypropylène par comparaison avec le chromatogramme d'une solution témoin de cet antioxydant. Les résultats montrent que l'extraction est complète (trouvé 0,205%; théorie 0,200%).

Action de l'époxyéthane (oxyde d'éthylène)

Les plaques ont été exposées à l'oxyde d'éthylène dans des conditions plus agressives que celles généralement retenues pour la stérilisation du matériel médico-chirurgical. Ces plaques ont subi dix stérilisations successives. L'examen du chromatogramme obtenu à partir de la solution extractive (dichlorométhane) montre l'absence du pic correspondant au Goodrite 3114, ainsi que celle d'un éventuel produit de dégradation. Les plaques traitées à l'oxyde d'éthylène ont été extraites par dissolution-précipitation; le chromatogramme obtenu, examiné comparativement à celui correspondant à l'analyse d'une solution témoin de Goodrite 3114, montre la disparition de l'antioxydant et l'apparition d'un pic différent de celui du Goodrite 3114 et de l'extrait des plaques de polypropylène n'ayant pas été exposées à l'oxyde d'éthylène. Le temps de rétention est accru et quelques essais nous conduisent à formuler l'hypothèse de la formation d'un dérivé d'oxydation dont la structure en cours d'étude n'a pas été actuellement précisée.

Action des rayonnements γ

L'irradiation à 10 Mrad du Goodrite 3114 fait apparaître une intense coloration bleue. Après irradiation, les plaques de polypropylène ne révèlent aucune coloration, alors que celles renfermant 0,2% d'antioxydant présentent une coloration jaune.

La chromatographie en phase liquide, effectuée dans les conditions décrites ci-dessus, d'une solution de Goodrite 3114 irradiée à 2, 5 et 10 Mrad, révèle la présence d'un composé non décélé dans l'échantillon témoin non irradié. Ce composé est caractérisé par un temps très réduit par rapport à celui du Goodrite 3114 (Fig. 1, E, F) qui permet d'émettre l'hypothèse de la formation d'un produit de dégradation résultant de la coupure de la molécule I.

L'examen des chromatogrammes obtenus à partir des plaques irradiées et non irradiées, renfermant l'antioxydant (Fig. 1, B, C, D), met en évidence la diminution importante du Goodrite 3114; celui-ci n'est plus extractible par le dichlorométhane.

Le produit de dégradation a été obtenu par dissolution-précipitation du matériau; l'examen des solutions obtenues dans ces conditions, à partir des plaques de polypropylène irradiées, montre la présence d'un pic dont le temps de rétention est identique à celui obtenu dans l'examen de la solution effectuée directement à partir du Goodrite 3114.

Spectrométrie de masse du Goodrite irradié

Les produits de dégradation formés par irradiation du Goodrite 3114 et des plaques de polypropylène qui le contiennent se sont révélés identiques, après les analyses en chromatographie liquide dans les conditions décrites ci-dessus.

L'étude de la structure du produit de dégradation formé par irradiation du Goodrite a été effectuée directement sur l'antioxydant ayant subi une irradiation de 10 Mrad.

L'analyse a été effectuée par couplage GLC/MS, à partir d'une solution de Goodrite 3114 irradiée; la GLC/MS a été conduite dans les conditions suivantes.

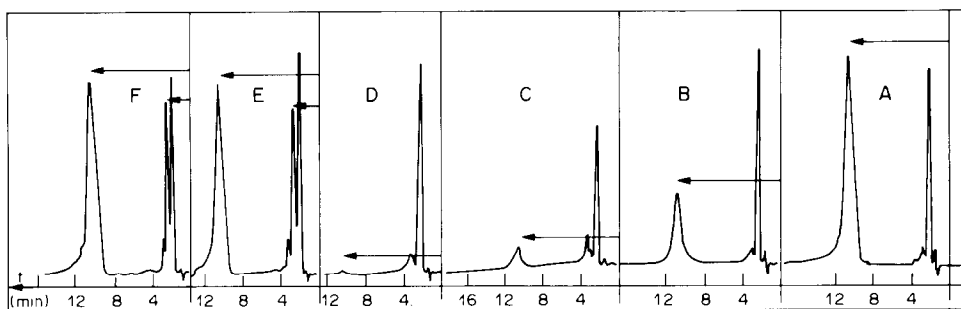


Fig. 1. A, Solution de Goodrite 3114 dans le tétrahydrofurane. B, Goodrite 3114 extrait d'un polypropylène non stérilisé. C, Goodrite 3114 extrait du polypropylène stérilisé à 2,5 Mrad. D, Goodrite 3114 extrait du polypropylène irradié à 10 Mrad. E, Goodrite 3114 pur, irradié à 2,5 Mrad: (1) produit de dégradation du 3114; (2) Goodrite 3114 résiduel. F, Goodrite 3114, irradié à 10 Mrad: (1) produit de dégradation du 3114; (2) Goodrite 3114 résiduel.

Chromatographie

Colonne: OV1; 25 m × 0,3 mm.
 Gaz porteur: hélium, à 0,35 bar.
 Température de l'injecteur: 260°
 Température du four: 280°.
 Programmation: 40° à 160° (40°/min)
 160° à 260° (10°/min).
 Système d'injection: splitless.

Spectrométrie de masse

Spectromètre: NERMAG 10-10c.
 Traitement de données: Ordinateur P.D.-P 11.
 Ionisations: impact électronique à 20 eV et ionisation chimique par le méthane.

Résultats

Quel que soit le procédé d'ionisation appliqué, il n'a pas été possible de mettre en évidence le pic de masse du Goodrite 3114 ($m/z = 784$), irradié ou non, du fait de sa segmentation au cours du stade chromatographique. En effet, la séparation par GLC révèle dans le cas du Goodrite 3114 non irradié un composant dont le pic de masse correspond à $m/z = 218$ (II); l'analyse fragmentaire confirme la structure du radical R constitutif de la molécule initiale.

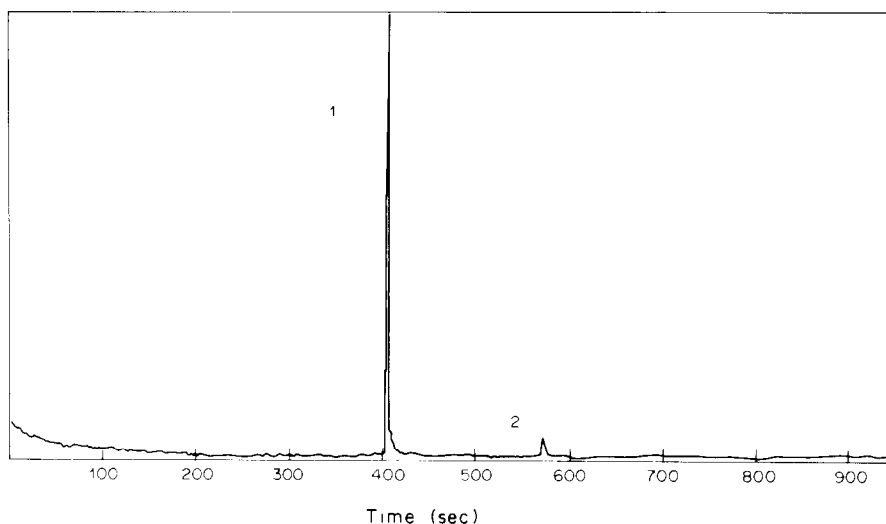
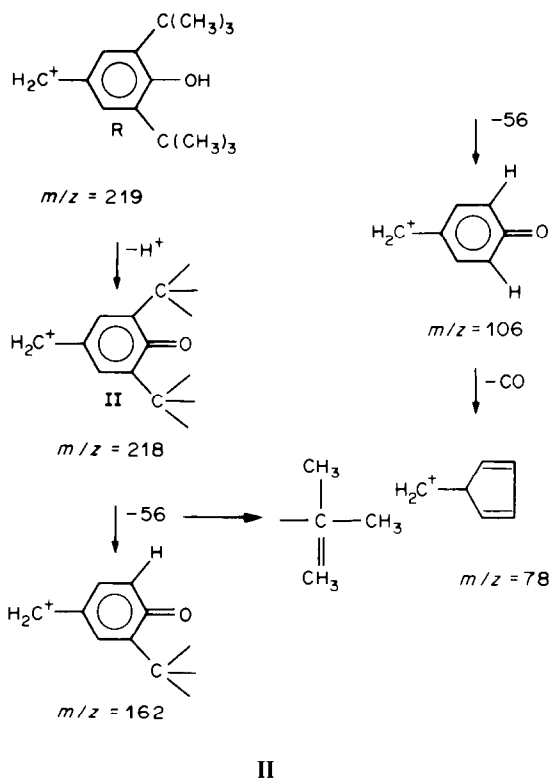
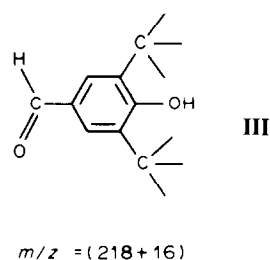


Fig. 2. GLC du Goodrite 3114 irradié à 10 Mrad: (1) produit de dégradation; (2) Goodrite 3114 résiduel. Colonne OV1; solvant H_2CCl_2 ; injection 1,5 μ l; température de l'injecteur 260°; programmation: 40 à 160° (40°/min), 160 à 260° (10°/min).

Dans le cas de l'échantillon irradié, la séparation chromatographique (Fig. 2), fait apparaître un produit dérivé du Goodrite 3114 absent dans l'analyse du témoin non irradié.

Le spectre de masse obtenu par le procédé d'impact électronique (20 eV) à partir du composé dérivé du Goodrite 3114 irradié et séparé par GLC, révèle un pic de masse $m/z = 234$. Celui-ci correspond à une structure oxydée du radical R en position para, soit le di-tert butyl-3,5 hydroxy 4-benzaldéhyde (III).

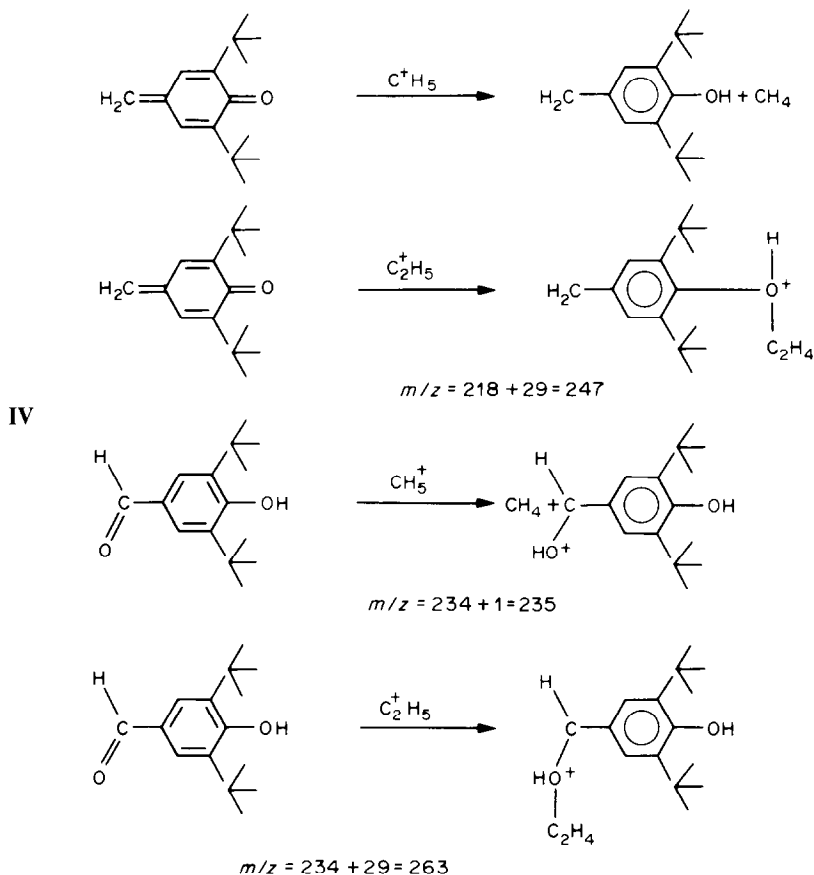


L'application du procédé d'ionisation chimique, après la séparation chromatographique, confirme les résultats.

Les spectres de masse obtenus à partir des composés séparés par GLC, révèlent les pics de masse suivants.

	(M + 1) ⁺	(M + 29) ⁺
Composant 1	218 + 1 = 219	218 + 29 = 247
Composant 2	234 + 1 = 235	234 + 29 = 263

Les structures des formes ionisées correspondent aux configurations suivantes:



En conclusion, l'analyse par spectrométrie de masse, couplée à GLC, permet de conclure à la présence d'un produit d'oxydation de structure monomérique, dans l'échantillon soumis aux irradiations (10 Mrad). Le résultat est obtenu par les deux procédés d'impact électronique (20 eV), et d'ionisation chimique par le méthane.

La structure de ce dérivé correspond au di-tert butyl 3,5 hydroxy 4-benzaldéhyde.

MIGRATION DU GOODRITE ET DE SES PRODUITS DE DÉGRADATION DANS LES MÉDICAMENTS

Divers polyoléfines sont utilisées pour la fabrication des excipients à usage pharmaceutique, ou de matériel médico-chirurgical, tel que les seringues pour

l'injection parentérale. L'emploi de ces matériaux est subordonné à une étude d'interactions "contenant-contenu", et notamment à la recherche de décharges des additifs dans les solutés. Une telle étude doit être entreprise dans chaque cas particulier. Toutefois, des résultats antérieurs^{9,10} ont montré que certains solvants hydro organiques des médicaments injectables ont un pouvoir extractif important vis à vis des polyoléfines; tel est le cas en particulier des solutions de polysorbate qui se sont révélées d'excellents liquides de simulation, et qui sont présentes dans de nombreuses formules médicamenteuses.

Ce dernier procédé a été appliqué au polypropylène renfermant 0,2% de Goodrite 3114, directement, après irradiation à 10 Mrad, et stérilisation à l'oxyde d'éthylène (5 stérilisations successives).

Mode opératoire

Le polypropylène irradié, et non irradié, a été mis en contact avec une solution de polysorbate 40 à 2% dans un tampon phosphate pH = 4,5 durant 48 heures à la température ambiante et à 45°; la solution a été examinée par HPLC, selon la technique décrite ci-dessus, qui permet de révéler la présence du Goodrite 3114 et de ses produits de dégradation engendrés

par les traitements de stérilisation (rayons γ et oxyde d'éthylène).

L'examen du chromatogramme obtenu après l'analyse des solutions de simulation, montre qu'aucune décharge n'est décelable après leur contact avec les plaques de polypropylène non stérilisées aux rayons γ , à l'oxyde d'éthylène.

Ces résultats ne permettent pas d'extrapoler l'absence de décharges observées dans un cas particulier à tous les solutés, et il convient pour chaque type, d'envisager une étude spécifique; néanmoins ce procédé peut être proposé comme schéma d'études d'interactions entre un matériau plastique et divers solutés.

LITTÉRATURE

1. F. Pellerin, D. Baylocq, D. André, C. Majcherczyk et El Alham, *Ann. Pharm. Franc.*, 1984 **42**, 15.
2. T. R. Crompton, *Eur. Polym. J.*, 1968, **4**, 473.
3. J. Denning et J. A. Marshall, *Analyst*, 1972, **97**, 710.
4. C. Majcherczyk, *Thèse de Doctorat de 3eme Cycle*, Université de Paris XI, à paraître.
5. M. Kasai, T. Tchikawa et K. Kosegaki, *Brevet Belg.*, 896275 AI, 1983.
6. K. Kogaki, R. Takeshita et K. Kabayashi, *Brevet Belg.*, 894434 AI, 1981.
7. G. V. Reed, *Brevet FR*, 822892 AI, 1982.
8. Y. Arnaud, *Pharm. Hosp. Franc.*, 1973, **24**, 24.
9. F. Pellerin, D. Dimitrescu et D. André, *Sc. Techn. Pharm.*, 1981, **3**, 10.

Summary—An HPLC method for the identification and determination of Goodrite 3114 and of the product derived from it by γ -ray irradiation is described. The chemical structure of the by-product obtained by the γ -irradiation has been established. A technique for research on migration phenomena is proposed.

Dédicace—Le présent article est dédié au Dr. R. A. Chalmers, qui anime avec compétence et enthousiasme le développement international de *Talanta*; comme rédacteur en chef, il a porté et maintient la revue à son haut niveau international et contribué à l'évolution de la chimie analytique.

Comme Président de la Division de Chimie Analytique de l'IUPAC (1981-85) et Membre de l'Advisory Board de *Talanta*, j'éprouve un très grand plaisir à rendre hommage à l'action continué de R. A. Chalmers, la justesse de ses jugements aussi bien qu'aux qualités humaines qui font rédacteur en chef le pivot de la qualité d'une revue scientifique.

F. Pellerin

DETERMINATION OF SILVER, BISMUTH, CADMIUM, COPPER, IRON, NICKEL AND ZINC IN LEAD- AND TIN-BASE SOLDERS AND WHITE-METAL BEARING ALLOYS BY ATOMIC-ABSORPTION SPECTROPHOTOMETRY

CHOW CHONG

Geological Survey Laboratory, Scrivenor Road, P.O. Box 1015, Ipoh, Perak, Malaysia

(Received 5 March 1985. Accepted 22 August 1985)

Summary—A simple atomic-absorption spectrophotometry method is described for the determination of silver, bismuth, cadmium, copper, iron, nickel and zinc in lead- and tin-base solders and white-metal bearing alloys, with use of a single sample solution. The sample is dissolved in a mixture of hydrobromic acid and bromine, then fumed with sulphuric acid. The lead sulphate is dissolved in concentrated hydrochloric acid. The method is particularly suitable for the determination of silver and bismuth, which are co-precipitated with lead sulphate. The other elements can also be determined after removal of the lead sulphate by filtration.

Lead- and tin-base solders and white-metal bearing alloys differ widely in composition. The major elements range in concentration from 0.1 to 99% for Pb, 0.5 to 95% for Sn and 0.02 to 20% for Sb. The alloys also contain various amounts of trace elements such as silver, bismuth, copper, zinc, nickel, cadmium and iron. Spectrophotometric,¹⁻⁵ spectrographic⁶ and polarographic⁷ methods have been used in the determination of the trace elements. The lead can be separated as lead sulphate^{2,3,6} or chloride,⁷ or complexed with tartrate⁴ or EDTA.⁵ Atomic-absorption spectrophotometry (AAS) has also been proposed for the determination of these trace elements after the sample has been dissolved with various acid mixtures and reagents. Farrar⁸ used a mixture of hydrobromic acid and bromine to dissolve lead-base bearing alloys and type metal for determination of copper and zinc by AAS. Hwang and Sandomato⁹ used a special mixture of nitric acid, fluoroboric acid and water in the ratio 3:2:5 v/v to dissolve tin-lead solders. They claimed that the resulting solutions remained stable for up to 48 hr. Carleer *et al.*¹⁰ used *aqua regia* to dissolve lead- and tin-base solder for the determination of several major, minor and trace elements by AAS. Mixtures of fluoroboric, nitric and tartaric acids,¹¹ and of fluoroboric acid and hydrogen peroxide¹² have been used to dissolve type metal and lead alloys, respectively, for the determination of tin and antimony by AAS. In general, the greatest problem in the dissolution is the stability of the solution, because precipitation of lead and some of the trace elements can occur on dilution or after standing for some time.

A mixture of hydrobromic acid and bromine is effective in dissolving lead- and tin-base solders and

white-metal bearing alloys and has the advantage that tin, antimony and arsenic may be removed by volatilization on fuming with sulphuric acid. However, there have been many reports^{4,13} of the partial co-precipitation of some elements with the lead sulphate produced. In this study it was found that the co-precipitation of silver and bismuth with lead sulphate was substantial, rendering invalid any attempt to remove the precipitate and determine silver and bismuth in the solution. However, if the lead sulphate is dissolved in concentrated hydrochloric acid, the solution, after dilution, is stable for some weeks and silver and bismuth can easily be determined by AAS. Other trace elements such as nickel, cadmium, zinc, copper and iron can also be determined in the same solution or, since they are not co-precipitated with lead sulphate, they can also be determined after the lead sulphate has been filtered off.

EXPERIMENTAL

Instrumentation

A Varian Techtron model AA875 atomic-absorption spectrophotometer, equipped with a 10-cm air-acetylene burner was used in all measurements. Standard single-element hollow-cathode lamps were used as line sources. The air and acetylene flows were set at 28 and 9, respectively, the aspiration rate was 6 ml/min and the absorbance read-out integration time was 3 sec. Other conditions used were as indicated in Table 1.

Reagents

Standard copper, iron, cadmium and nickel solutions (1000 µg/ml). Dissolve 0.25 g of the metal in 12.5 ml of concentrated hydrochloric acid. Add 3 drops of concentrated nitric acid in the case of nickel and copper. Make up accurately to 250 ml with distilled water. Dilute to the desired concentration.

Table 1. AAS conditions

Element	Wavelength, nm	Band width, nm	Lamp current, mA	Absorbance expansion factor
Ag	328.1	0.5	3.5	1
Bi	223.1	0.2	10	1
Cd	228.8	0.5	3.5	1
Cu	324.8	0.5	3.5	1
Fe	248.3	0.2	5	1, 10*
Ni	232.0	0.2	3.5	2
Zn	213.9	1.0	5	5

*For very low iron values.

Standard silver solution (1000 µg/ml). Dissolve 0.25 g of silver metal in 25 ml of 50% nitric acid. Make up accurately to 250 ml with distilled water. Dilute to the desired concentration. Keep in a dark place.

Standard zinc solution (1000 µg/ml). Dissolve 0.3112 g of zinc oxide, previously dried for 1 hr at 105°, in 12.5 ml of concentrated hydrochloric acid. Make up accurately to 250 ml with distilled water. Dilute to the desired concentration.

Standard bismuth solution (1000 µg/ml). Dissolve 0.2787 g of bismuth oxide, previously dried for 1 hr at 105°, in 12.5 ml of concentrated hydrochloric acid. Make up accurately to 250 ml with distilled water. Dilute to the desired concentration but maintain the acid concentration at 2% to prevent hydrolysis of bismuth.

Procedures

Method involving the dissolution of lead sulphate. Weigh accurately 0.4 g of lead-base bearing metal or 1.0 g of tin-base bearing metal or 0.5 g of solder into a 150-ml beaker. Add 10 ml of concentrated hydrobromic acid, followed by 2 ml of saturated bromine water. Cover with a watch-glass and heat on a hot-plate with occasional swirling until the sample is completely dissolved. It may be necessary to add a little more hydrobromic acid or a few extra drops of bromine for complete dissolution, depending on the type of sample. Wash down the glass cover and sides of the beaker and add 4 ml of 50% sulphuric acid and heat to strong fuming on top of a thin asbestos sheet on a hot-plate, then until the lead sulphate is white. Direct heating on a hot-plate before this stage may lead to spattering. Heat the beaker directly on the hot-plate until the lead sulphate becomes crystalline and about 0.5 ml of sulphuric acid remains. Allow to cool, add 40 ml of concentrated hydrochloric acid and stir until all the lead sulphate has dissolved. Dilute with distilled water and transfer the solution to a 200-ml standard flask. Cool to room temperature and make up to the mark. Transfer 50.0 ml of the solution as soon as possible into a 100-ml standard flask and dilute to the mark with distilled water; this step must be done quickly because solutions containing large amounts of lead may yield a small amount of lead sulphate precipitate on standing. However, the diluted 50-ml aliquot is stable for some weeks. The final solution is now suitable for aspiration and AAS deter-

mination of the various elements but may be further diluted where necessary, as in the case of the determination of copper in tin-base bearing metal.

Preparation of calibration graph. Prepare a blank and mixed standards of silver, bismuth, cadmium, copper, iron, nickel and zinc by pipetting aliquots (as indicated in Table 2) into a series of 150-ml beakers. Add 10 ml of concentrated hydrobromic acid and 2 ml of saturated bromine water and proceed as for samples.

Method involving the separation of lead sulphate. Weigh accurately 0.25–1.0 g of sample into a 150-ml beaker and proceed as above, up to the point at which about 0.5 ml of sulphuric acid remains. Then cool, add 10 ml of 1% v/v sulphuric acid and filter off the precipitate on a 9-cm Schleicher and Schüll No. 589³ paper (or equivalent, e.g., Whatman No. 40), collecting the filtrate in a 100-ml standard flask. Wash the precipitate with 40 ml of 1% sulphuric acid. Make the solution up to the mark with distilled water. The solution is now ready for aspiration and the determination of the various elements. It may be diluted with 1% sulphuric acid when necessary to bring the absorbance within the calibration range.

Preparation of calibration graph. Prepare a blank and mixed standards of copper, zinc, cadmium, nickel and iron by pipetting aliquots (as indicated in Table 3) into a series of 150-ml beakers. Add 10 ml of concentrated hydrobromic acid, 2 ml of saturated bromine water and 4 ml of 50% sulphuric acid. Heat to fuming until about 0.5 ml of sulphuric acid remains. Allow to cool and transfer to a 100-ml standard flask with 50 ml of 1% sulphuric acid, and dilute to the mark with distilled water.

RESULTS AND DISCUSSION

Co-precipitation of some elements with lead sulphate

Lead sulphate has been reported¹³ to co-precipitate a number of elements such as silver, bismuth, copper, antimony, calcium and strontium under certain conditions. However, there is some disagreement on the co-precipitation of certain elements by lead sulphate.

Table 2. Concentration range of standard solutions used in procedure involving dissolution of lead sulphate

Element	Stock solution, ppm	Aliquot,* ml	Concentration† in 100 ml, ppm
Ag	10	4.0, 8.0, 12.0	0.1, 0.2, 0.3
Bi	100	2.0, 4.0, 6.0	0.5, 1.0, 1.5
Cd	10	4.0, 8.0, 12.0	0.1, 0.2, 0.3
Cu	100	0.4, 1.2, 2.4	0.1, 0.3, 0.6
Fe	100	0.4, 1.2, 2.4	0.1, 0.3, 0.6
Ni	10	2.0, 4.0, 6.0	0.05, 0.10, 0.15
Zn	10	0.8, 1.6, 2.4	0.02, 0.04, 0.06

*For making up to a volume of 200 ml.

†After dilution of 50 ml of the 200-ml standard solution to 100 ml.

Table 3. Concentration range of standard solutions used in procedure involving separation of lead sulphate

Element	Stock solution, ppm	Aliquot, ml	Concentration in 100 ml, ppm
Cd	10	1.0, 2.0, 3.0	0.1, 0.2, 0.3
Cu	100	0.5, 1.0, 2.0	0.5, 1.0, 2.0
Fe	10	1.0, 3.0, 6.0	0.1, 0.3, 0.6
Ni	10	1.0, 1.5, 2.0	0.1, 0.15, 0.20
Zn	1	2.0, 4.0, 6.0	0.02, 0.04, 0.06

Karabash *et al.*⁶ reported that there was no co-precipitation of some twenty metals, including nickel, zinc, cadmium, copper, bismuth, iron and silver at concentrations of 10^{-6} – 10^{-10} % of that of the lead. Zhenpu Wang and Cheng⁴ reported serious co-precipitation of aluminium, bismuth and iron with lead sulphate, but Luke² and Ota³ determined aluminium and iron, respectively, in tin and lead alloys without considering co-precipitation with lead sulphate. In this study it was found that cadmium, copper, iron, nickel and zinc were co-precipitated to a negligible extent with lead sulphate, as shown in Table 4.

The degree of co-precipitation of silver and bismuth seems to depend on the conditions used. If a lead nitrate solution is used and hydrobromic acid and bromine are not added, the degree of co-precipitation of bismuth and silver with lead sulphate is about 19 and 27%, respectively. If hydrobromic acid and bromine are added, however, the degree of

co-precipitation increases to 75 and almost 100%, respectively.

Solubility of lead sulphate and the stability of its solution

The solubility of lead sulphate in hydrochloric acid was studied at room temperature. It was found that to dissolve lead sulphate completely and keep it in solution after dilution to 200 ml with water, at least 13 ml of concentrated hydrochloric acid per 100 mg of lead will be required for the initial dissolution, for 200–500 mg of lead. The 200 ml of solution obtained in this way can be diluted fourfold without reprecipitation of lead sulphate.

Determination of silver, bismuth, cadmium, copper, iron, nickel and zinc

From Table 4, it is clear that silver and bismuth are considerably co-precipitated with lead sulphate whereas the other elements are not. The results given

Table 4. Co-precipitation of bismuth, silver, copper, nickel, cadmium, zinc and iron with lead sulphate*

Element	Amount added, mg		Co-precipitated, %
	mg	mg	
Bi	0.100	0.020	–80
	0.500	0.155	–69
Ag	0.100	0.001	–99
	0.500	0.001	–100
Cu	0.100	0.100	0
	0.500	0.500	0
Ni	0.100	0.101	+1
	0.500	0.495	–1
Cd	0.010	0.010	0
	0.050	0.046	–8
Zn	0.0100	0.0104	+4
	0.0500	0.0510	+2
Fe	0.100	0.101	+1
	0.500	0.500	0

*The amount of lead was 1 g, added as lead nitrate solution.

Table 5. Determination of silver, bismuth, cadmium, copper, iron, nickel and zinc (%) in NBS samples by the lead sulphate dissolution method

Element	NBS 53e lead-base bearing metal		NBS 54d tin-base bearing metal		NBS 127b solder (Sn 40, Pb 60)	
	NBS value	Value found	NBS value	Value found	NBS value	Value found
Ag	—	0.024	0.003	0.004	0.01	0.016
Bi	0.052	0.052	0.044	0.048	0.06	0.070
Cd	—	0.003	—	0.005	—	<0.001
Fe	<0.001	<0.001	0.027	0.028	—	0.002
Ni	0.003	0.004	0.002	0.003	0.012	0.012
Cu	0.054	0.053	3.62	3.64	0.011	0.011
Zn	—	0.0005	—	0.0005	—	<0.0001

Table 6. Determination of silver, bismuth, cadmium, copper, iron, nickel and zinc (%) in NBS samples by the lead sulphate separation method

Element	NBS 53e lead-base bearing metal		NBS 54d tin-base bearing metal		NBS 127b solder (Sn 40, Pb 60)	
	NBS value	Value found	NBS value	Value found	NBS value	Value found
Ag	—	<0.001	0.003	0.001	0.01	<0.001
Bi	0.052	0.011	0.044	0.020	0.06	<0.01
Cd	—	0.003	—	0.005	—	<0.001
Fe	<0.001	<0.001	0.027	0.028	—	0.001
Ni	0.003	0.003	0.002	0.003	0.012	0.011
Cu	0.054	0.052	3.62	3.60	0.011	0.011
Zn	—	0.0006	—	0.0006	—	<0.0001

Table 7. Recovery of silver, bismuth, cadmium, copper, iron, nickel and zinc in a solder sample (Sn 60, Pb 40)*

Element	Amount added, μg	Amount obtained, μg	Recovery, %
Ag	25	25.2	101
Bi	250	240	96
Cd	25	26	104
Cu	150	149	99
Fe	100	96	96
Ni	25	24	96
Zn	10	10	100

*0.5 g of solder sample was analysed by the lead sulphate dissolution method.

in Tables 5 and 6 show that good agreement has been obtained with NBS values for nickel, iron and copper by both the proposed methods, whereas for silver and bismuth the lead sulphate separation method gives exceedingly low results as a result of co-precipitation. Thus the lead sulphate dissolution method is recommended for determination of silver and bismuth. As the silver value in NBS 127(b) is given to only two decimal places, it is not possible to compare the third decimal place. Consequently this sample was analysed for silver seven times by the lead sulphate dissolution method. The silver value was found to range from 0.0158% to 0.0160% with a coefficient of variation of 0.6%. Although the lead sulphate dissolution method can be used to determine a wider range of elements, the lead sulphate separation method has the advantage that a larger sample size can be used and is thus useful for elements that are present in very small amounts and are not co-precipitated with lead sulphate.

Recovery test

To test the validity of the lead sulphate dissolution method, known amounts of silver, bismuth, cadmium, copper, iron, nickel and zinc were added to a solder sample (Sn 60, Pb 40), the mixture was analysed and the recovery (total concentration obtained for the element minus concentration of element present in the sample) was calculated. The results are given in Table 7 and the good recovery obtained shows that the lead sulphate dissolution method is reliable.

Conclusion

The lead sulphate dissolution method avoids those

analytical problems associated with the co-precipitation of other elements and the insolubility of lead sulphate. The only limitation is that it cannot be used for large samples having high lead contents, because reprecipitation of lead sulphate occurs on dilution.

Acknowledgements—Grateful acknowledgement is made to the Director-General, Geological Survey, Malaysia, for his permission to publish this paper and to the Assistant Director-General and the Director of Geochemistry for their encouragement.

REFERENCES

1. *Chemical Analysis of Metals and Metal Bearing Ores*, ASTM, Part 12, 1980, E42 and E57.
2. C. L. Luke, *Anal. Chem.*, 1952, **24**, 1122.
3. K. Ota, *Bunseki Kagaku*, 1956, **5**, 3; *Anal. Abstr.*, 1956, **3**, 2731.
4. Zhenpu Wang and K. L. Cheng, *Talanta*, 1982, **29**, 551.
5. K. L. Cheng, R. H. Bray and S. W. Melsted, *Anal. Chem.*, 1955, **27**, 24.
6. A. G. Karabash, L. S. Bondarenko, G. G. Morozova and Sh. I. Peizulayev, *Zh. Analit. Khim.*, 1960, **15**, 623; *Anal. Abstr.*, 1961, **8**, 1895.
7. J. R. Bishop and H. Leibmann, *Analyst*, 1953, **78**, 117.
8. B. Farrar, *At. Absorpt. Newsl.*, 1965, **4**, 325.
9. J. Y. Hwang and L. M. Sandomato, *Anal. Chem.*, 1970, **42**, 744.
10. R. Carleer, J. P. François and L. C. Van Poucke, *Bull. Soc. Chim. Belg.*, 1981, **90**, 357.
11. J. U. Gouin, J. L. Holt and R. E. Miller, *Anal. Chem.*, 1972, **44**, 1042.
12. T. M. Quarrell, R. J. W. Powell and H. J. Cluley, *Analyst*, 1973, **98**, 443.
13. I. M. Kolthoff and P. J. Elving, *Treatise on Analytical Chemistry*, Part II, Vol. 6, p. 111. Interscience, New York, 1964.

SHORT COMMUNICATIONS

SEPARATION OF NITROIMIDAZOLES BY REVERSED-PHASE HIGH-PRESSURE LIQUID CHROMATOGRAPHY

BISHOP B. SITHOLE* and ROBERT D. GUY

Trace Analysis Research Centre, Chemistry Department, Dalhousie University, Halifax, Nova Scotia, Canada

(Received 30 April 1985. Revised 22 August 1985. Accepted 13 September 1985)

Summary—A mixture of eight *N*-substituted and unsubstituted nitroimidazoles has been separated by high-pressure liquid chromatography with 5% ethanol as the eluent. Compounds with the same capacity ratios were selectively detected electrochemically by differential pulse polarography with a hanging mercury drop electrode. The HMDE detector had higher detection limits than the photometric detector set at 315 nm.

Nitroimidazoles are microbial agents used mainly as feed additives to treat histomoniasis in poultry, swine dysentery and bovine venereal disease.¹ They are also used as radio-sensitizing agents on hypoxic tumour cells.² Lately concern has been expressed that many of the compounds have mutagenic or carcinogenic activity.¹ They have been determined by various procedures, including ultraviolet spectrophotometry,³ thin-layer chromatography,⁴ polarography,⁵ and high-pressure liquid chromatography (HPLC).⁶ Most of the reports in the literature deal with simple mixtures which can be resolved by changing the wavelength used for photometric detection, or the pH or strength of the eluent.

This report describes the separation of eight nitroimidazoles by reversed-phase HPLC on a C-18 bonded-phase column. Most of the compounds could be resolved by use of photometric detection, and electrochemical detection by differential pulse polarography enabled pairs of compounds with the same capacity ratios but different reduction potentials to be distinguished.

EXPERIMENTAL

Chemicals

All chemicals were of analytical reagent grade. The nitroimidazoles used were 2-nitroimidazole (Aldrich), metronidazole (Sigma), 2-methyl-5-nitroimidazole (Pfaltz & Bauer), 4-nitroimidazole, 1-methyl-4-nitroimidazole, 1-methyl-5-nitroimidazole and 1,2-dimethyl-5-nitroimidazole (all synthesized⁷⁻¹⁰ from imidazole and 1-methylimidazole).

Apparatus

HPLC separations were done by use of a Constametric III

pump (Laboratory Data Control, Riviera Beach, Florida), a home-made pulse-damper, and a Rheodyne sample-injection valve Model 7125 with a 100- μ l loop. The column was a Bio-Rad ODS-10 (25 cm \times 4.6 mm bore; 10 μ m particle size) with C-18 bonded-phase packing, and the spectrophotometric detector was a Bio-Rad Model 1305 variable wavelength instrument with a deuterium lamp set at a wavelength of 315 nm. The electrochemical detector was a PAR Model 303 static mercury drop electrode coupled to a Model 174A polarographic analyser (PARC, Princeton, N.J.). The electrode was operated in the hanging-drop mode.

For photometric detection the eluent was 5% ethanol and for electrochemical detection the eluent was 5% ethanol in 0.1M sodium acetate buffer (pH 4.5). The flow-rate was 1.0 ml/min. The retentions of the compounds were expressed as capacity ratios k' , which were determined from the formula:

$$k' = \frac{t_R - t_0}{t_0}$$

where t_R and t_0 are the retention times of a sample component and of a non-retained compound (represented by 25 μ l of 0.1M nitric acid), respectively. The eluent was degassed thoroughly under vacuum and the polarographic cell was kept under a blanket of high-purity nitrogen.

Pretreatment of animal samples

Samples from poultry, such as turkey tissue or eggs, were macerated with aqueous borax solution (2 g in 8 ml of water) and extracted with benzene (25 ml). The organic phase was separated by centrifugation and decantation, then stripped with 0.2M hydrochloric acid (5.0 ml). The aqueous phase was then neutralized with 2M potassium hydroxide, ethanol was added, the pH was adjusted with acetate buffer, and the HPLC separation performed.

RESULTS AND DISCUSSION

Figure 1 shows a typical chromatogram (photometric detection) and Table 1 displays the capacity ratios and detection limits of the compounds studied. The chromatographic conditions give satisfactory separation of most components in the mixture. However, problems arise if both 2-nitroimidazole and

*Monitoring and Criteria Division, Environmental Health Centre, Health and Welfare Canada, Tunney's Pasture, Ottawa, Ontario, Canada.

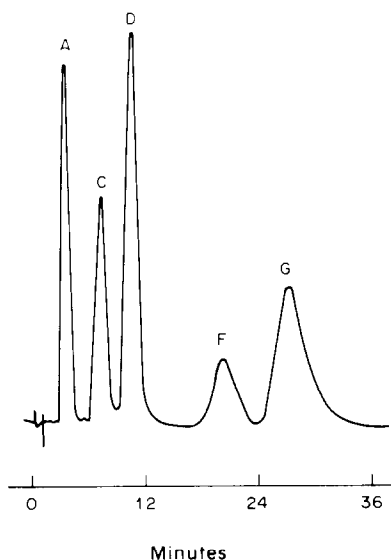


Fig. 1. HPLC chromatogram of nitroimidazoles with photometric detection: peaks for A, 2-nitroimidazole; C, 2-methyl-5-nitroimidazole; D, 1-methyl-4-nitroimidazole; F, metronidazole; G, 1-methyl-5-nitroimidazole.

4-nitroimidazole, or both metronidazole and 1,2-dimethyl-4-nitroimidazole are present, since the first pair give completely overlapping signals, and metronidazole gives a shoulder on the trailing edge of the 1,2-dimethyl-4-nitroimidazole peak. The polarographic reduction potentials of the nitroimidazoles in 0.1M acetate buffer (pH 4.5) are shown in Table

2, and show that polarography would permit analysis of a two-component mixture but not of a more complex system. A solution to this problem lies in combining selective polarographic determination with the HPLC separation.

Several methods of polarographic detection are possible, including direct current polarography and the pulse polarographic techniques, in which a rectangular polarization-voltage waveform is used. Differential pulse polarography acts as a selective detector since the applied (ramp) potential can be set for the peak of the desired compound, and other compounds with different peak potentials will not be detected. This may be used for the selective detection of compounds which have the same capacity ratios but different reduction potentials. We have used this technique for the detection of those nitroimidazoles which could not be resolved by photometric detection.

A hanging mercury drop electrode (HMDE) was used in the electrochemical detector to eliminate noise from varying drop size. A check of the polarographic curves of the nitroimidazoles in the eluent indicated cathodic shifts of 15–25 mV. The reduction potentials of the compounds in the eluent are shown in Table 2. This table suggests that two potentials may be useful for these compounds—a potential of -400 mV *vs.* Ag/AgCl would be suitable for 2-nitroimidazole, 1-methyl-5-nitroimidazole, metronidazole and dimetridazole, and a potential of -514 mV *vs.* Ag/AgCl would be suitable for the other four compounds. Figure 2 illustrates the select-

Table 1. HPLC characteristics of nitroimidazoles in 5% v/v aqueous ethanol.

Compound	k'	Sensitivity*	Detection limit, ng
A 2-nitroimidazole	2.09	0.141	1
B 4-nitroimidazole	2.09	0.096	2
C 2-methyl-5-nitroimidazole	5.18	0.054	3
D 1-methyl-4-nitroimidazole	6.46	0.032	4
E 1,2-dimethyl-4-nitroimidazole	9.50	0.021	7
F metronidazole	10.00	0.021	7
G 1-methyl-5-nitroimidazole	12.36	0.032	4
H dimetridazole	19.72	0.042	4

*Absorbance per μg .

Table 2. Polarographic characteristics of nitroimidazoles

Compound	Peak potential, mV	
	in water	in 5% ethanol
A 2-nitroimidazole	-372	-392
B 4-nitroimidazole	-491	-511
C 2-methyl-5-nitroimidazole	-544	-564
D 1-methyl-4-nitroimidazole	-552	-575
E 1,2-dimethyl-4-nitroimidazole	-498	-518
F metronidazole	-420	-435
G 1-methyl-5-nitroimidazole	-408	-438
H dimetridazole	-380	-399

All solutions were 0.1M in acetate buffer (pH 4.5). Potentials were measured against an Ag/AgCl electrode. Conditions: differential pulse polarography; dropping mercury electrode; 50-mV pulse; 1 drop/sec; medium drop size; scan-rate 2 mV/sec.

Table 3. HPLC electrochemical detection of nitroimidazoles in pH 4.5 0.1M acetate buffer containing 5% ethanol

Compound	Applied potential, mV	Detection limit, ng
A 2-nitroimidazole	-400	300
B 4-nitroimidazole	-514	320
E 1,2-dimethyl-4-nitroimidazole	-514	325
F metronidazole	-400	320
H dimetridazole	-400	600

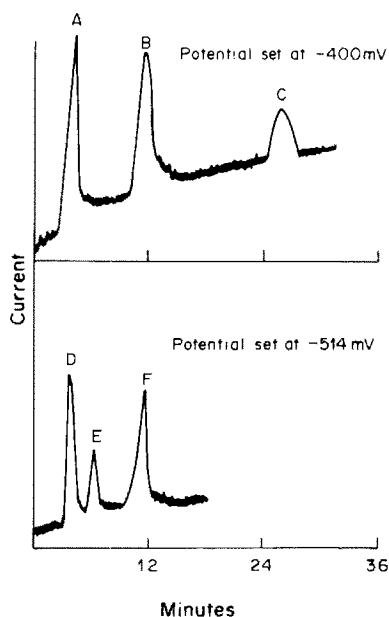


Fig. 2. HPLC chromatograms of nitroimidazoles with electrochemical detection: 5% ethanol in 0.1M pH-4.5 acetate buffer. A, Polarograph potential set at -400 mV; peaks for A, 2-nitroimidazole; F, metronidazole; H, dimetridazole. B, Polarograph potential set at -514 mV; peaks for B, 4-nitroimidazole; C, 2-methyl-5-nitroimidazole; E, 1,2-dimethyl-4-nitroimidazole.

ivity of the HMDE detection for 2- and 4-nitroimidazole, metronidazole and 1,2-dimethyl-4-nitroimidazole. The calibration curves were linear in

the 0.01–2.0 $\mu\text{g/ml}$ range studied. Table 3 gives the applied potentials and detection limits for HPLC and electrochemical detection of these compounds. The sensitivity of the electrochemical detector was about two orders of magnitude poorer than that of photometric detection. This is partly due to difficulties from oxygen in the electrolyte and to pump pulsations. Most electrochemical work reported in the literature is for the oxidative mode, where dissolved oxygen is not a problem.

Acknowledgement—This work was supported by a grant from the Natural Sciences and Engineering Research Council of Canada.

REFERENCES

1. R. E. Bambury, in *Burger's Medicinal Chemistry*, M. E. Wolff (ed.), Part II, p. 41. Wiley, New York, 1979.
2. G. E. Adams, *Brit. Med. Bull.*, 1973, **28**, 48.
3. D. W. Fink and A. Fox, *Anal. Chim. Acta*, 1979, **106**, 389.
4. E. Gattavecchia and D. Tonelli, *J. Chromatog.*, 1980, **193**, 340.
5. D. Dumanović, S. Perkućin and J. Volke, *Talanta*, 1971, **18**, 675.
6. E. Gattavecchia, in *Radiosensitisers of Hypoxic Cells*, A. Breccia, C. Rimondi and G. E. Adams (eds.), p. 187. Elsevier, Amsterdam, 1979.
7. F. L. Pyman, *J. Chem. Soc.*, 1922, **121**, 2615.
8. C. E. Hezeldine, F. L. Pyman and J. Winchester, *ibid.*, 1924, **125**, 1431.
9. V. K. Bhagwat and F. L. Pyman, *ibid.*, 1925, **127**, 1832.
10. L. F. Story, W. E. Allsebrook and J. M. Gulland, *ibid.*, 1942, 232.

Dedication—This paper is dedicated to Dr. R. A. Chalmers on the occasion of his 20th year as Editor-in-Chief of *Talanta*.

B. Bruce Sithole

DETERMINATION OF TOTAL PHOSPHORUS IN WATER BY PHOTOCHEMICAL DECOMPOSITION WITH ULTRAVIOLET IRRADIATION

LIU ZAIYOU and WU LIMIN

Department of Chemistry, Northeast Normal University, Chang Chun, People's Republic of China

(Received 20 March 1985. Revised 19 May 1985. Accepted 29 August 1985)

Summary—A simple and convenient photochemical decomposition method has been developed for the determination of total phosphorus in natural and sewage water. Organic phosphorus compounds and inorganic polyphosphates may be completely converted into orthophosphate in the presence of 0.3M sulphuric acid and 0.12% potassium persulphate with 50 min irradiation. The relative standard deviations found for analysis of natural water (P 35 $\mu\text{g/l.}$) and sewage (P 2.4 mg/l.) were 5.7% and 1.0% respectively. The method gives results comparable to those obtained by digestion with persulphate.

Armstrong *et al.*¹ first used a high-pressure mercury-arc lamp to decompose organic phosphorus compounds in sea-water for determination of organic phosphorus. They showed that phosphorus may be liberated as orthophosphate from organic matter by irradiation for 2 hr in the presence of hydrogen peroxide, and that inorganic polyphosphates were not hydrolysed by the same procedure. Their apparatus handled 12 samples at a time. Later, Henriksen² combined thermal hydrolysis with photo-decomposition to decompose polyphosphates in order to determine total phosphorus in water, and designed equipment for simultaneous treatment of up to 24 samples. Goossen and Kloosterboer³ used a 75-W Zn–Cd–Hg medium-pressure lamp to convert organic and hydrolysable phosphates completely into orthophosphate in only 30 min. In their reactor, however, only one water sample (50 ml) could be irradiated at a time.

The method of photo-decomposition is particularly attractive, but the earlier procedures had the disadvantage of either long irradiation times or restriction to one sample at a time. We have chosen potassium persulphate as a photochemical oxidant, and have found it more effective than hydrogen peroxide, which is commonly used. In 0.3M sulphuric acid containing 0.12% potassium persulphate, the photo-decomposition of organic phosphorus compounds and the thermal hydrolysis of polyphosphates may be completed in 50 min by irradiation. In our reactor, 12 water samples can be decomposed simultaneously.

EXPERIMENTAL

Apparatus

The reactor (Fig. 1) consists of a 1000-W high-pressure mercury-arc lamp (1st Lamp Factory, Shanghai, China), a reactor body (65 cm long, 24 cm diameter) and a cooling fan. The guard tube used by Henriksen is unnecessary. The reactor holds twelve sample tubes, each with a capacity of 50 ml. The sample tubes are made of fused quartz and a

stopper with a capillary hole is needed to relieve the pressure generated during the irradiation.

The standard flasks and sample tubes are filled with concentrated sulphuric acid, stood overnight, then emptied and thoroughly rinsed. They are kept filled with distilled water when not in use. The treatment with sulphuric acid is required only occasionally.

Reagents

Potassium dihydrogen phosphate (99.8% pure, 0.1098 g) was dissolved in redistilled water and made up to 500 ml (P 50 mg/l.), and diluted 500-fold before use. All organic and inorganic phosphorus-containing solutions were prepared with a phosphorus concentration of 1000 $\mu\text{g/l.}$ and stored in dark brown bottles. Potassium persulphate (7.5 g), previously recrystallized and dried in a desiccator, was dissolved in 250 ml of redistilled water. This solution may be stored for two weeks in the dark at room temperature.

Procedure

A calibration graph is prepared by the method described by Shoji *et al.*⁴ The same slope is obtained with or without photo-decomposition applied to the standards. For photo-decomposition, pipette the phosphorus-containing solutions (10–30 ml) into sample tubes. To each, add 2.0 ml of 3.0% potassium persulphate and 1.0 ml of 7.5M sulphuric acid and make up to 50 ml with redistilled water. Put the sample tubes into the reactor and switch the lamp on. After 10 min

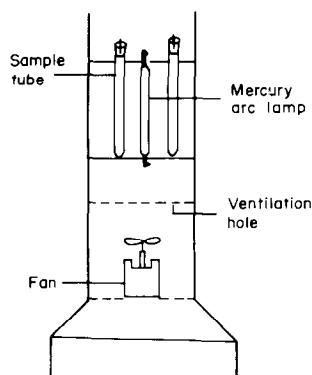


Fig. 1. Diagram of photo-decomposition reactor.

Table 1. Effect of acidity on the hydrolysis of polyphosphates

[H ₂ SO ₄], M	Na ₄ P ₂ O ₇ ·10H ₂ O			(NaPO ₃) ₆		
	0.1	0.2	0.3	0.1	0.2	0.3
Hydrolysis, %	21.6	37.2	44.9	18.6	35.4	51.2

irradiation, turn on the cooling fan and continue to irradiate for a predetermined time. After cooling, pipette a suitable volume for determination of orthophosphate. In water analysis, use the same procedure but with an overall irradiation time of 50 min.

RESULTS AND DISCUSSION

Acidity

Initial experiments showed that even if the irradiation time was prolonged to 2 hr, the polyphosphates may not be hydrolysed to orthophosphate in neutral medium.⁵ According to our experiments, the major factors for hydrolysis of inorganic polyphosphates are the acidity and temperature of the solution. Solutions of sodium pyrophosphate and hexametaphosphate (both containing 400 μg of phosphorus per l.) were adjusted to different acid concentrations, and irradiated for 20 min. The results (calculated as orthophosphate) given in Table 1 show that the hydrolysis depends on the acid concentration, and the results are not affected by the presence of potassium persulphate. According to Table 1, it seems that a still higher acidity might give higher yields of orthophosphate. We have tested acidities up to 0.5M, and the rate of hydrolysis was not much increased when the acidity was higher than 0.3M sulphuric acid. To avoid the tedious adjustment of

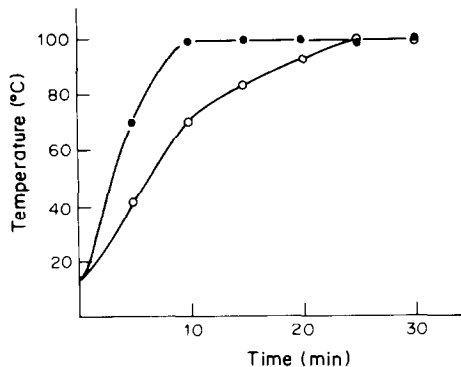


Fig. 2. Relationship between temperature and irradiation time. ○—○ The cooling fan was turned on after 10 min irradiation. ●—● The lamp and the cooling fan were turned on at the same time.

Table 2. Effect of irradiation time on the hydrolysis of polyphosphates (400 μg of P per l.)

Irradiation time, min	20	25	30	35	40	50	60	120
Hydrolysis, P ₂ O ₄ ⁴⁻	44.9	56.8	73.7	97.8	98.2	99.4	98.1	100
% (PO ₃) ₆	51.2	58.9	80.3	96.4	98.3	99.2	100	98.6

Table 3. Results of interference test

P added, μg/l.				Recovery, %
PO ₄ ³⁻	(PO ₃) ₆	organic P	P found, μg/l.	
250	250	250	764	102
250	0	500	755	101
200	200	400	790	98

Table 4. Water analysis for total P

Sample	Phosphorus found			
	Natural water, μg/l.		Sewage, mg/l.	
	(a)	(b)	(a)	(b)
1	28	24	11.70	11.70
2	26	29	3.87	3.69
3	22	24	3.15	3.21
4	42	41	1.48	1.39
5	324	321		

(a) Proposed method. (b) Wet chemical digestion with potassium persulphate in an autoclave.⁶

pH for the irradiation and again for the final determination, 0.3M sulphuric acid was used in further work.

Temperature and irradiation time

The rate of hydrolysis of inorganic polyphosphates is dependent on temperature. In our reactor, the heat needed for hydrolysis is supplied by the high-pressure mercury-arc lamp. It has been found that the sample

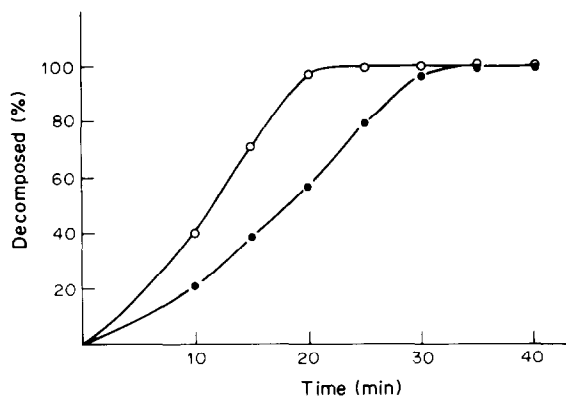


Fig. 3. Photo-decomposition of organically bonded phosphorus in 0.3M H₂SO₄ containing 0.12% K₂S₂O₈. ○—○ P 400 μg/l. in *O,O*-dimethyl-(2,2,2-trichloro-1-hydroxyethyl) phosphonate solution. ●—● P 400 μg/l. in triethylphosphate solution.

Table 5. Recoveries of total phosphorus spikes

Water sample	1	2	3	4	5	6	7	8
Original P, $\mu\text{g/l.}$	16	23	19	37	293	185	484	393
Added P, $\mu\text{g/l.}$	63	63	63	63	625	625	625	625
P found, $\mu\text{g/l.}$	77	81	90	88	907	823	1100	1010
Recovery, %	97.5	94.2	110	88.0	98.8	102	99.2	99.1

solutions may be brought to their boiling point much faster by the proposed system with controlled cooling than by the commonly used cooling methods.^{1,2} The relationship between temperature and irradiation time for different cooling methods is shown in Fig. 2. For 0.3M sulphuric acid and controlled cooling, the results given in Table 2 show that irradiation for longer than 40 min does not increase the concentration of orthophosphate in solution. To ensure complete photo-decomposition, water samples are irradiated for 50 min, and then analysed for their orthophosphate contents.

Photo-decomposition of organically bonded phosphorus

The most favourable acidity for photo-decomposition of organic phosphorus compounds was found to be pH 2–4, and most of these compounds may be completely decomposed by irradiation for 10 min in the presence of potassium persulphate. Phosphorus may also be liberated from organically bonded materials by irradiation in 0.3M sulphuric acid containing potassium persulphate. In this case, however, at least 35 min are required for completing the reaction (Fig. 3).

Glycerol-2-phosphate, *O,O*-dimethyl-2,2-dichlorovinyl phosphate, *O,O*-dimethyl-*O*-(1-chloro-1-*N,N*-diethylcarbamoyl) phosphate, tributylphosphine oxide, *O,O*-dimethyl-*S*-(*N*-methylcarbamoyl)methyl phosphorodithioate, and *O,O*-dimethyl-*S*-(1,2-dicarbethoxyethyl) dithiophosphate are all decomposed quantitatively. In view of the quantitative decomposition of these compounds, it seemed pointless to test others.

Interferences

Mixtures of phosphorus compounds in different ratios were added to water. The results given in Table 3 show that there was no mutual interference between the different phosphorus compounds in the photo-decomposition and determination process.

Analysis of water samples

Various water samples, including natural and sewage water, were analysed by the proposed method and commonly used methods. The results are shown in Table 4.

Precision and accuracy

The precision for total phosphorus determination was measured as the relative standard deviation of *n* replicate analyses of natural water (mean P 35 $\mu\text{g/l.}$, r.s.d. 5.7%, *n* = 10) and sewage (mean P 2.38 mg/l., r.s.d. 1.0%, *n* = 8). The accuracy was assessed by measuring the recovery of known amounts of phosphorus added to water samples. The results are shown in Table 5.

Acknowledgements—We are very grateful to Professor Xu Shushen and Mr. Wang Zongxiao for their enthusiastic help in finishing this work.

REFERENCES

1. F. A. J. Armstrong, P. M. Williams and J. D. H. Strickland, *Nature*, 1966, **211**, 481.
2. A. Henriksen, *Analyst*, 1970, **95**, 601.
3. J. T. H. Goossen and J. G. Kloosterboer, *Anal. Chem.*, 1978, **50**, 707.
4. S. Motomizu, T. Wakimoto and K. Tōei, *Analyst*, 1983, **108**, 361.
5. F. A. J. Armstrong, *J. Mar. Biol. Assoc. U.K.*, 1968, **48**, 143.
6. J. C. Valderrama, *Marine Chemistry*, 1981, **10**, 109.

NAFRONYL ION-SELECTIVE MEMBRANE ELECTRODES AND THEIR USE IN PHARMACEUTICAL ANALYSIS

MARIANA S. IONESCU, VERONICA BADEA, G. E. BAIULESCU*
and V. V. COȘOFREȚ†

Institute of Chemical and Pharmaceutical Research Bucharest, 74351-Sos.Vitan 112, Bucharest-3,
Romania

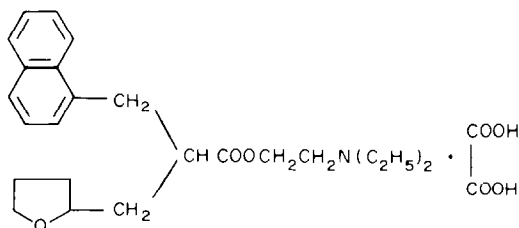
(Received 21 December 1984. Accepted 17 April 1985)

Summary—A simple potentiometric method is described for the rapid determination of nafronyl-drugs in pharmaceutical preparations such as tablets. Nafronyl ion-selective membrane electrodes with either the nafronyl-dipicrylamine ion-pair complex in 1,2-dichloroethane or the nafronyl-dinonylnaphthalenesulphonic acid ion-pair complex in a PVC matrix as electroactive materials were used. Both electrodes exhibit near-Nernstian responses to protonated-nafronyl activity from 10^{-2} to about $10^{-5}M$, in pH ranges that depend on the nature of the electroactive material used in the membrane. Nafronyl in the mg-range can be determined by potentiometric titration with sodium tetraphenylborate solution, with a relative standard deviation of less than 2.0%. No interference from any excipients in the tablets was observed.

Ion-selective membrane electrodes are used extensively for quality control of various drugs and have become a useful tool for solving analytical problems connected with complex pharmaceutical formulations.¹⁻⁵ Some of these sensors are responsive to a large number of compounds, whereas others are specially designed to be highly selective for a particular substance, and are often not commercially available. Not all such sensors provide acceptable sensitivity and selectivity for the drug of interest.

In this paper, two types of nafronyl-selective membrane electrodes are described, one based on the nafronyl-dipicrylamine ion-pair complex dissolved in 1,2-dichloroethane, and the other on the nafronyl dinonylnaphthalenesulphonic acid (DNNS) ion-pair complex embedded in a PVC matrix. These electrodes exhibit useful analytical characteristics for the determination of nafronyl-drugs either as the pure substances or in complex pharmaceutical preparations.

Nafronyl oxalate [2-(1-naphthyl)methyl-3-(2-furyl)propanoic acid 2-(diethylamino)ethyl ester oxalate, I] is a well-known vasodilator used (as "Praxilene") in therapeutical practice since 1972.⁶



*Department of Analytical Chemistry, National Institute of Chemistry, 77208-Spl.Independenței 202, Bucharest-6, Romania.

†Author for correspondence.

EXPERIMENTAL

Reagents

All reagents, except nafronyl oxalate (which was synthesized and purified by us) were of analytical-reagent grade. Pharmaceutical preparations were purchased from a local drugstore.

Standard 0.01M nafronyl oxalate solution was prepared by dissolving the appropriate amount in acetate buffer solution (pH 4.5). Working solutions were prepared by serial dilutions with pH-4.5 acetate buffer. Standard 0.05M sodium tetraphenylborate was prepared and standardized as previously described.⁷

Apparatus

Potentiometric measurements were made with a Prætitronic type MV 870 pH/mV meter and potentiometric titrations were performed with an automatic Radiometer assembly composed of a TTT2 titrator, ABU 12 autoburette and SBR 2C titrigraph recorder. The pH measurements were made with a Radiometer G 202C glass electrode and a saturated calomel electrode. For all measurements a Radiometer K 401 saturated calomel electrode was used in conjunction with the indicator electrode.

Nafronyl-dipicrylamine liquid ion-exchanger

The nafronyl-dipicrylamine complex was precipitated by mixing 10 ml of 0.01M nafronyl oxalate with 10 ml of 0.01M dipicrylamine solution (made by dissolving the reagent in 5% sodium carbonate solution by heating) in a separatory funnel, and dissolved in 25 ml of 1,2-dichloroethane by shaking the mixture for about 15 min. The organic phase was separated, dried by passage through a folded filter paper containing anhydrous sodium sulphate, transferred to a 50-ml standard flask and made up to volume with 1,2-dichloroethane. This solution ($5 \times 10^{-3}M$ concentration) was the electroactive material for electrode A.

Construction of electrodes

Electrode A was made by impregnating the support material (a graphite rod 15 mm long and 6.5 mm in diameter, made water-repellent and with a stainless-steel wire inserted in it to serve as reference) with the electroactive material obtained as described above. The electrode was stored in the electroactive material solution between measurements.

The construction of electrode B, based on the nafronyl-DNNS ion-pair, has been described elsewhere.^{8,10} The membrane composition was 4.0% DNNS, 64.0% plasticizer (*o*-nitrophenyloctyl ether) and 32.0% PVC. The electrode body was filled with $10^{-3}M$ nafronyl oxalate solution at pH 4.5 (acetate buffer). The electrode was preconditioned by soaking it for 24 hr in $0.01M$ nafronyl oxalate and was stored in the same solution when not in use.

Potentiometric titration of nafronyl oxalate

A 25.0-ml aliquot of the sample solution (adjusted to pH 4.5 with acetate buffer) was pipetted into the reaction-cell and titrated with $0.05M$ sodium tetraphenylborate. The inflection point of the titration curve was taken as the end-point.

Potentiometric assay of nafronyl oxalate in tablets

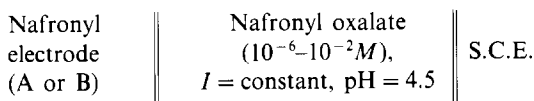
Five tablets were finely powdered and a portion of the powder equivalent to about 50 mg of nafronyl oxalate was weighed into a 50-ml beaker, dissolved in about 30 ml of pH-4.5 acetate buffer and potentiometrically titrated as above.

RESULTS AND DISCUSSION

Characteristics of the electrodes

Typical calibration curves for the electrodes at constant ionic strength and pH (both adjusted with pH-4.5 acetate buffer) are shown in Fig. 1.

The e.m.f. measurements were made with an electrochemical cell of the type:



The e.m.f. is given by:

$$E_{(A)} = E'_{0(A)} + 0.051 \log [\text{nafronyl}^+] \quad (\text{for electrode A}) \quad (1)$$

and

$$E_{(B)} = E'_{0(B)} + 0.052 \log [\text{nafronyl}^+] \quad (\text{for electrode B}) \quad (2)$$

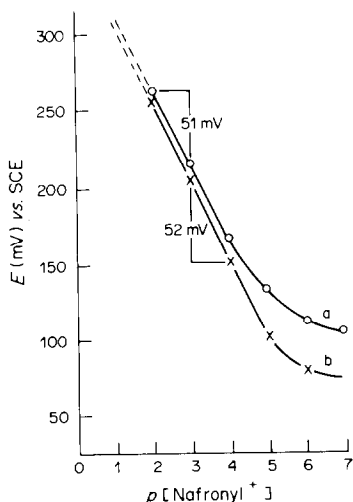


Fig. 1. Electrode functions for (a) electrode A, (b) electrode B (constant ionic strength and pH maintained with pH 4.5 acetate buffer).

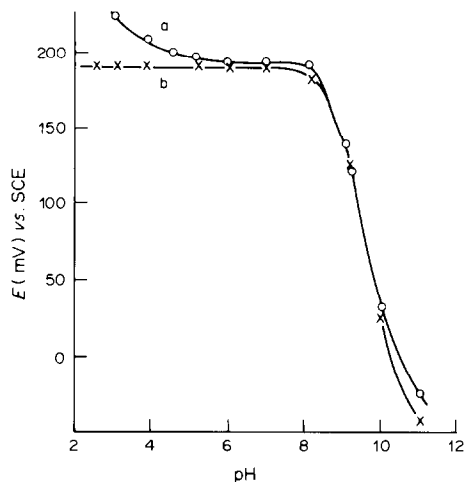


Fig. 2. Effect of pH on the response of (a) electrode A, (b) electrode B to $10^{-4}M$ nafronyl oxalate.

where the E'_0 values are the conditional standard potentials for electrodes A and B, under the conditions for use of the cell. The electrode responses are linear over the range from 10^{-2} to about $10^{-5}M$, with sub-Nernstian slopes. Electrode B reached stable potential readings (± 0.2 mV) within 30–60 sec, depending on the nafronyl concentration; the response time of electrode A was a bit longer, but still less than 1 min for 10^{-2} and $10^{-3}M$ solutions. The detection limits were $1.0 \times 10^{-5}M$ for electrode A and $3.2 \times 10^{-6}M$ for electrode B.

The influence of pH on the electrode responses to $10^{-4}M$ nafronyl oxalate is shown in Fig. 2. The working pH range depends on the nature of the electrode. In acidic medium the nafronyl-DNNS complex is stable, but the nafronyl-dipicrylamine complex is not, the dipicrylamine becoming protonated. Electrode A is H^+ -sensitive outside the pH range from about 5 to 7. At $pH > 7$ free base precipitates in the aqueous test solution, the concentration of unprotonated nafronyl species increases, and lower e.m.f. readings are recorded for both electrodes.

Potentiometric selectivity coefficients for both electrodes were measured by the mixed solution method and calculated as previously described.¹⁰ Both electrodes show high selectivity with respect to most inorganic and organic cations tested. The selectivity coefficients, $K_{Nafr^+ J^+}^{pot}$ with respect to glycine, L-histidine, methionine, nicotinamide, atropine, scopolamine, diethanolamine, K^+ , Na^+ , Ca^{2+} and Mg^{2+} were all less than 10^{-3} . Most excipients in pharmaceutical tablets (usually lactose or glucose as diluent and corn starch or gelatin as binder) do not interfere.

Analytical applications

For the determination of nafronyl in aqueous solutions either the standard-addition method or

potentiometric titration can be used. We found titration to be advantageous, especially for assay of complex pharmaceuticals. When 0.05M sodium tetraphenylborate is used as titrant, the potential jumps around the equivalence point are high enough for accurate evaluation of the equivalence volumes.

The average recovery in analysis of six pure nafronyl oxalate samples, each in duplicate and weighing between 40 and 70 mg was 100.6%, standard deviation 1.9%. For nafronyl oxalate assay in three pharmaceutical products a relative standard deviation of 1.0–1.5% was obtained.

The potentiometric method requires no prior separation steps and may be applied directly to coloured or turbid solutions. The accuracy of the method is typical of most ion-selective electrode potentiometric titrations of pharmaceuticals.

REFERENCES

1. V. V. Coşofreţ, *Ion Selective Electrode Rev.*, 1980, **2**, 159.
2. *Idem*, *Membrane Electrodes in Drug-Substances Analysis*, Pergamon Press, Oxford, 1982.
3. T. C. Pinkerton and B. L. Lawson, *Clin. Chem.*, 1982, **28**, 1946.
4. E. Pungor, Z. Fehér, G. Nagy and K. Tóth, *Anal. Proc.*, 1982, **19**, 79.
5. V. V. Coşofreţ and R. P. Buck, *Ion-Selective Electrode Rev.*, 1984, **6**, 59.
6. M. Sittig, *Pharmaceutical Manufacturing Encyclopedia*, p. 437. NDC, Park Ridge, N.J., 1979.
7. D. Negoiu, M. S. Ionescu and V. V. Coşofreţ, *Talanta*, 1981, **28**, 377.
8. G. J. Moody, R. B. Oke and J. D. R. Thomas, *Analyst*, 1970, **95**, 910.
9. C. R. Martin and H. Freiser, *Anal. Chem.*, 1980, **52**, 562.
10. V. V. Coşofreţ and R. P. Buck, *Anal. Chim. Acta*, 1984, **162**, 357.

Dedication—Dedicated to Bob Chalmers, with congratulations and greetings from the Black Sea.

ANALYTICAL DATA

CORRECTION FACTORS FOR THE GLASS ELECTRODE IN AQUEOUS *N,N*-DIMETHYLFORMAMIDE SOLUTIONS

GUSTAVO GONZALEZ, DANIEL ROSALES, JOSE L. GOMEZ ARIZA and ALFONSO GUIRAUM PEREZ
 Department of Analytical Chemistry, Faculty of Chemistry, University of Seville, 41012 Seville, Spain

(Received 24 July 1985. Accepted 13 September 1985)

It is well known that titrations are often done in aqueous organic solvent media in order to determine pK_a values for sparingly soluble compounds, with measurement of so-called pH-values obtained by use of a pH-electrode and a pH-meter, generally calibrated with aqueous buffers. The bias due to neglecting the medium effects and the liquid-junction potentials leads to a non-thermodynamic or "apparent" pK_a value.

It has been known for some time that there are several aprotic polar solvents in which 1:1 electrolytes are dissociated at low concentrations. We have chosen *N,N*-dimethylformamide (DMF) as such a solvent to study the pK_a variations of a set of acidic systems because its dielectric constant is relatively high, but lower than that of water, and because of its frequent use as a polar solvent. By means of the Van Uitert and Haas¹ method, and using the relations reported by Reynaud² for ionic activity coefficients in DMF-water mixtures, we have obtained the corrections to be made to glass-electrode readings for 0-90% v/v mixtures of DMF with water.

When a pH-meter is calibrated with aqueous buffers, and the pH-measurement is made in mixed solvent solutions, the absolute error in the pH is given by

$${}_s\text{pH} - B = \log U_H^0 = \log {}_m\gamma_H + ({}^sE_j - {}^*E_j)F/2.303RT$$

where ${}_s\text{pH}$ is $-\log a_H$ in the mixed solvent, B is the reading of the pH-meter and sE_j and *E_j are the liquid-junction potentials between the saturated aqueous solution of potassium chloride and the aqueous or the mixed-solvent solution respectively. The term $\log U_H^0$ is usually called the "correction factor" for the glass electrode,^{1,3,4} and ${}_m\gamma_H$ is the hydrogen-ionic activity coefficient in the medium used.

If the stoichiometric concentration, C_H , of a strong acid (e.g., hydrochloric acid), in a mixed-solvent solution is known, the ${}_s\text{pH}$ value can be evaluated by means of the expression

$${}_s\text{pH} = -\log {}_s a_H = -\log C_H - \log \gamma_H$$

The ionic activities can be evaluated as reported by Reynaud.² By comparison of the ${}_s\text{pH}$ value with the

Table 1. Evaluation of $\log U_H^0$ at 25°C

DMF, % v/v	DMF mole fraction	$\log U_H^0 \pm s^*$	Density, $d_4^{25}, g/ml$	Dielectric [†] constant
0	0	0.001 ± 0.005	0.997 ₁	78.54
5	0.012	-0.055 ± 0.003	0.996 ₅	77.93
10	0.025	-0.088 ± 0.009	0.996 ₄	77.32
15	0.039	-0.091 ± 0.004	0.996 ₂	76.10
20	0.052	-0.093 ± 0.006	0.996 ₁	74.86
25	0.071	-0.129 ± 0.004	0.996 ₀	73.63
30	0.089	-0.182 ± 0.018	0.995 ₉	72.40
35	0.109	-0.247 ± 0.013	0.995 ₈	70.96
40	0.131	-0.309 ± 0.005	0.995 ₆	69.52
45	0.155	-0.344 ± 0.019	0.995 ₅	67.73
50	0.182	-0.386 ± 0.010	0.995 ₀	65.95
55	0.212	-0.468 ± 0.003	0.994 ₁	63.84
60	0.247	-0.476 ± 0.011	0.992 ₈	61.74
65	0.286	-0.490 ± 0.020	0.991 ₁	59.27
70	0.332	-0.536 ± 0.007	0.987 ₈	56.73
75	0.387	-0.560 ± 0.015	0.983 ₈	53.88
80	0.454	-0.491 ± 0.009	0.978 ₉	51.04
85	0.537	-0.422 ± 0.006	0.972 ₇	48.20
90	0.647	-0.176 ± 0.009	0.964 ₁	45.35

*The values of $\log U_H^0$ (s = standard deviation) were the averages from three independent experiments on solutions of the same solvent composition at different ionic strength and hydrogen concentration.

†From Bougard and Jadot.⁵

apparent pH. B , the electrode correction is obtained by:

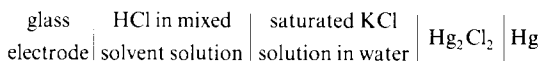
$$\log U_{\text{H}}^{\circ} = -\log C_{\text{H}} - \log \gamma_{\text{H}} - B = {}_s\text{pH} - B$$

With $\log U_{\text{H}}^{\circ}$ known, the corrections to the apparent $\text{p}K_{\text{a}}$ can be obtained by means of the expression:

$${}_s\text{p}K_{\text{a}} = \text{apparent } \text{p}K_{\text{a}} + \log U_{\text{H}}^{\circ}$$

where ${}_s\text{p}K_{\text{a}}$ is the $\text{p}K_{\text{a}}$ value in the standard state in the mixed solvent.

We have used a typical cell



The pH-meter was calibrated at $25^{\circ}\text{C} \pm 0.1^{\circ}$ with aqueous buffers. The correction factors, $\log U_{\text{H}}^{\circ}$, for the glass electrode in aqueous mixtures of DMF were evaluated by comparing the apparent pH values with the stoichiometric hydrogen-ion concentrations in 0.01–0.002M hydrochloric acid, corrected by means of the corresponding activity coefficient. The results obtained are given in Table 1.

The small standard deviation of $\log U_{\text{H}}^{\circ}$ indicates that the liquid-junction potentials are virtually constant for a given solvent composition. Furthermore,

single $\log U_{\text{H}}^{\circ}$ evaluations in basic media (pH 8–9) showed negligible variation compared with those obtained in acid media.

A minimum value for $\log U_{\text{H}}^{\circ}$ can be observed at a DMF mole fraction of 0.4. This behaviour is in good agreement with that reported by other authors for ion–solvent interactions in aqueous DMF media, showing that in such mixtures $\Delta G_{\text{H}}^{\circ}$ and other properties show an extremum at around that composition.^{5,7}

Further experiments in order to evaluate other ${}_s\text{p}K_{\text{a}}$ changes in water–DMF mixtures will be the subject of a future paper.

REFERENCES

1. L. G. Van Uitert and C. G. Haas, *J. Am. Chem. Soc.*, 1953, **75**, 451.
2. R. Reynaud, *Bull. Soc. Chim. France*, 1967, 4597.
3. H. M. N. H. Irving and U. S. Mahnot, *J. Inorg. Nucl. Chem.*, 1968, **30**, 1215.
4. Y. K. Agrawal, *Talanta*, 1979, **26**, 599.
5. J. Bougard and R. Jadot, *J. Chem. Thermodyn.*, 1975, **7**, 1185.
6. R. Smits, D. L. Massart, J. Juillard and J. P. Morel, *Electrochim. Acta*, 1976, **21**, 431.
7. K. Das, K. Bose and K. K. Kundu, *ibid.*, 1981, **26**, 479.

Dedication—The authors would like to dedicate this paper to Dr. R. A. Chalmers on his 20th anniversary as Editor of *Talanta* as a mark of their appreciation of his valued assistance over the years.

A FORTH PACKAGE FOR COMPUTER-CONTROLLED FLOW-INJECTION ANALYSIS

F. T. M. DOHMEN and P. C. THUISSEN*

Department of Analytical Chemistry, University of Nijmegen, Toernooiveld,
6525ED Nijmegen, The Netherlands

(Received 24 July 1985. Accepted 18 October 1985)

Summary—An automated flow-injection system with a computer-controlled sample changer, injection device and digital photometer is described, for use with an Apple II. The software is understandable, flexible and easily adaptable to different computers provided with the programming language FORTH.

FORTH is a relatively new computer language and quite unknown to most analytical chemists. It comprises an operating system, assembler, interpreter, compiler, editor and so on. Since FORTH is all these things at once, it can be described as a programming environment. The language is easy to learn and makes otherwise complex programming straightforward and simple. In contrast to the standard languages, it is not restricted by a finite set of instructions and data structures. The user can create his own extensions for the required application. All the programming work consists of adding new words to a rather limited dictionary already known to the machine. The programs operate very rapidly and efficiently, retaining the advantages of an interpreter and the speed of a compiler, and can still be more compact than assembler.¹⁻³

For analytical instrumentation FORTH provides an environment for on-line control, data-acquisition, data-processing and report-generation. Some introductory papers on FORTH are already available in the analytical literature.⁴⁻⁷ A software package in BASIC for automated flow-injection analysis by use of a professional computer was described earlier.⁸ As an exercise a similar program has been written in FYSFORTH 0.3 for the same instrumental arrangement, with an Apple II computer.⁹

Flow-injection analysis is a widely used, reliable and versatile routine method for the determination of various chemical constituents.¹⁰ It is based on the injection of a small volume of sample into a continuously flowing stream. The moving bolus may be treated with reagents, diluted, incubated, dialysed, extracted *etc.*, and the final product is led to a detector to generate a peak-shaped signal. Calibration is done with standards similarly treated, with use of the height, width or area of the peaks. Operation of the system is easy to automate with a computer. This paper describes a program for control of the sample changer, switching of the injection

valve and registration of the signal. Additionally the flow-rates, the sample-size and the lengths of the reaction coils may be placed under computer control. In automated flow-injection analysis the application of on-line optimization as well as on-line calibration are real possibilities that have recently been developed.^{11,12}

Hardware

The entire system comprises:

- (1) an Apple II equipped with minimal one-disk drive and the parallel interface U-DT (two 16-bit 6522 I/O) in slot 4;
- (2) a Gilson Minipuls II pump and a Skalar Sampler 1000 sample-changer;
- (3) a BIFOK FIA 05 flow-injection device with an L100-1 injection valve and an FIA 06 photometer.

To demonstrate the approach an arbitrarily chosen routine method serves as an example. The complete system for the determination of chloride in aqueous samples in the ppm-range¹⁰ is depicted in Fig. 1. Figure 2 shows the most important connecting lines between the computer and the instrumental arrangement. The sample-changer is interfaced so that all its functions are directed by the computer. The switches

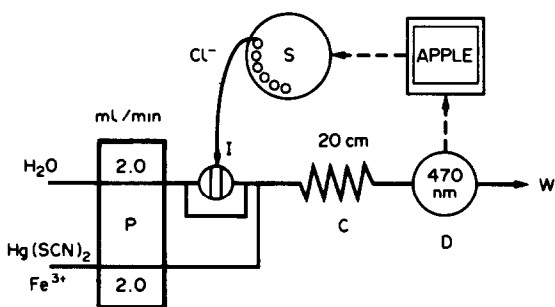


Fig. 1. Scheme of the flow-injection system for the determination of Cl^- with $\text{Hg}(\text{SCN})_2$ and Fe^{3+} in water.¹⁰ The hardware consists of a peristaltic pump P, a sample changer S, an injection valve I, the waste W, a reaction coil C, a photometric detector D and an Apple II computer.

*Author for correspondence.

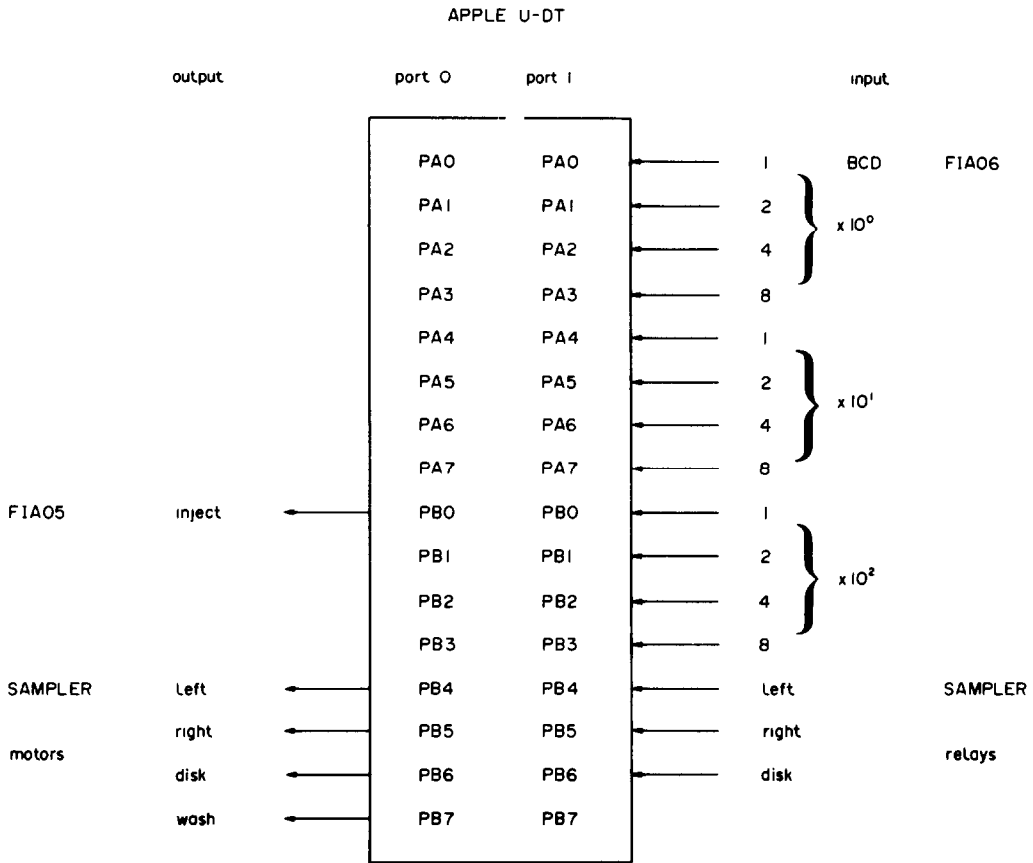


Fig. 2. Scheme of the most important lines connecting the computer to the sample changer, injection device and photometer. The different functions are explained in the text.

of the wash, sample turntable disk, and left and right sampler-arm motors are controlled by parallel output. The status of the micro-relays indicating the position of the disk and sampler arm is read in by parallel input. In a similar way the rotation of the injection valve is controlled by the computer. The BCD-output of the digital photometer is connected to the parallel input of the computer (0-1 V, 12 bits for 3 digits).

Software

The programming in FORTH starts from the original dictionary. After some initial definitions it moves to user-understandable words such as **Check.system**, **Injection**, **Move.disk**, **Move.sampler**, **Read.bcd** and **Measure**. Then these themselves are used to make up the main program, called **Fia**. A short description of the most important words in the program listing follows (see below). Communication between different words is provided by a data stack, in addition to constants, variables, strings or user-defined data-structures. Usually single-length numbers in the range from -32,768 to 32,767 are employed on the data stack. The data required by a

word are shown between brackets, with the top of the stack to the right separated by an arrow (→) from the data returned after execution:

Numbers: denote the number of data points to be measured.

Disk.position: is the current position of the turntable disk.

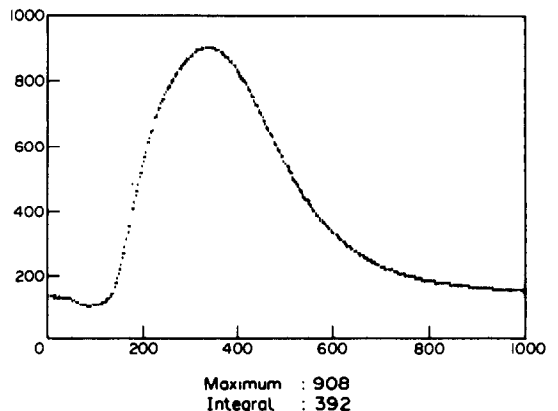


Fig. 3. Example of a digitized flow-injection peak as displayed by the graphics of the Apple II.

Target: is the direction in which the sampler arm has to be moved.

Maximum: denotes the height of the measured peak.

Integral: denotes the area of the measured peak.

Inject, Left, Right, Disk and Wash: define the required I/O-lines towards the injection valve and sample changer.

Port.0B, Port.0A, Port.1B and Port.1A: are the memory locations in the computer of the two 16-bit parallel I/O-ports.

Port.set0 and Port.set1: are the memory locations of the initial port settings for each line to be either input or output.

Input (n → n): returns the status of the required input lines.

Output (n →): switches and masks the desired output lines.

Check.system: examines for a proper start for the status of the interface card, **Check.interface**, for the position of the turntable disk **Check.disk**, and of the

FORGET-ALL
LOAD GRAPHICS.COMD

```

REVISION FIA.REV "---- FIA-SYSTEM VSN 0.1 ----" CR

: INJECTION
  INJECT OUTPUT
  INJECT OUTPUT ;

: WASH.MOTOR
  WASH OUTPUT ;

: MOVE.DISK
  DISK INPUT 0> IF
  DUP DUP 0> IF DISK OUTPUT
  DISK.POSITION + 40 MOD TO DISK.POSITION
  0 DO
    BEGIN DISK INPUT 0= UNTIL
    BEGIN DISK INPUT 0> UNTIL
  LOOP
  DISK OUTPUT THEN
  ELSE DROP BELL CR ." DISK ERROR "
  THEN ;

: MOVE.SAMPLER
  0 TO TARGET
  LEFT INPUT 0> IF RIGHT TO TARGET THEN
  RIGHT INPUT 0> IF LEFT TO TARGET THEN
  TARGET 0> IF TARGET OUTPUT
  BEGIN TARGET INPUT 0> UNTIL
  TARGET OUTPUT
  ELSE BELL CR ." SAMPLER ERROR "
  THEN ;

: WAIT
  0 DO 10000 0 DO LOOP LOOP ;

: READ.BCD
  PORT.1A C@ PORT.1B C@
  16 MOD 100 * SWAP 16 /MOD 10 * + + ;

: CALCULATE
  DUP MAXIMUM MAX TO MAXIMUM
  DUP S->D INTEGRAL D@ D+ INTEGRAL D! ;

: MEASURE
  TO NUMBERS
  0 1000 Y SIZE
  0 NUMBERS X SIZE
  PAGE BOX AXES NOMIX
  0 0 INTEGRAL D! 0 TO MAXIMUM
  NUMBERS 0 DO
    READ.BCD
    CALCULATE
    I SWAP SCALE PLOT
  LOOP
  HOME 22 VTAB
  ." Maximum      : " MAXIMUM , CR
  ." Integral     : " INTEGRAL D@
  NUMBERS M/ . DROP ;

: FIA
  GRAPHICS 3 COLOR NOMIX
  CHECK-SYSTEM
  BEGIN
  PAGE 10 HTAB ." Flow Injection Analysis " CR
  10 VTAB 0 HTAB ." Give number of samples : "
  QUERY-WORD NUMBER
  1 = IF
  0 DO
    MOVE.SAMPLER
    12 WAIT
    INJECTION
    MOVE.SAMPLER
    1000 MEASURE
    1 MOVE.DISK
  LOOP
  THEN CR
  ." Do you want to quit (Y/N) "
  KEY &Y = UNTIL CR ;

: INPUT
  PORT.1B @ AND ;

: OUTPUT
  PORT.0B @ XDR PORT.0B ! ;

: CHECK.INTERFACE
  FFFF PORT.SET0 !
  FFFE PORT.0B !
  0000 PORT.SET1 !
  PORT.SET0 @ FFFF XDR
  PORT.SET1 @ 0000 XDR
  OR IF BELL CR ." INTERFACE ERROR "
  THEN ;

DECIMAL

: CHECK.DISK
  DISK INPUT 0= IF
  BELL CR ." Press return to start disk "
  KEY CR DROP
  DISK OUTPUT
  BEGIN DISK INPUT 0> UNTIL
  DISK OUTPUT THEN ;

: CHECK.SAMPLER
  RIGHT INPUT 0= IF
  BELL CR ." Press return to suck sample "
  KEY CR DROP
  RIGHT OUTPUT
  BEGIN RIGHT INPUT 0> UNTIL
  RIGHT OUTPUT THEN ;

: CHECK.SYSTEM
  CHECK.INTERFACE
  CHECK.SAMPLER
  CHECK.DISK ;

```

Fig. 4. The program.

sampler arm **Check.sampler**. If not correct these words will signal and ask for action.

Injection: rotates the valve that introduces the sample into the system.

Wash.motor: switches the wash motor either on or off.

Move.disk ($n \rightarrow$): steps the turntable disk a given number of places.

Move.sampler: the sampler arm is moved to the right-hand position from the left-hand, and *vice versa*.

Read.bcd ($\rightarrow n$): reads a signal from the digital voltmeter and converts the BCD code into a 3 decimal value.

Measure ($n \rightarrow$): performs the general layout for the graphics, reads and plots the measurements. The height and area of the peak-shaped signal are computed on-line by **Calculate**. These values are displayed afterwards.

Fia: the main program to perform flow-injection analysis checks first the status of the system and asks for the number of samples. Therafter, the samples are repeatedly taken, injected and measured, and the results are processed and plotted. The photometer signal is read 1000 times during 24 sec, including plotting and processing of the measurements. One complete manipulation of the turntable disk and the sampler arm takes about 4 sec. For taking the sample into the injection loop (100 μ l) a pause of about 12 sec is provided by **Wait** ($n \rightarrow$). Thus for each sample a total period of about 40 secs is required.

Each word can be used independently for testing or other applications. Some examples:

10 Wait /wait about 10 secs
Check.system /test for a proper start

Read.bcd /read the signal and display it
Injection /rotate the valve
5 Move.disk /move the disk five steps ahead
Move-sampler /switch the sampler arm
Fia /start the main program

An example of a flow-injection peak measured and displayed by the graphics of the Apple II is shown in Fig. 3. The time scheduling of the delay in the different words should be found by experimentation, since no real-time provisions are employed. The software (Fig. 4) is flexible and can easily be extended if other advanced implementations are required.

REFERENCES

1. L. Brodie, *Starting FORTH*, Prentice-Hall, Englewood Cliffs, NJ, 1981.
2. A. Winfield, *The Complete FORTH*, Sigma Technical Press, Wilmslow, Cheshire, UK, 1983.
3. W. P. Salman, O. Tisserand and B. Toulout, *FORTH*, Camelot Press, Southampton, 1984.
4. F. Macintyre, *Intern. Lab.*, 1985, **15**, No. 2, 12; 1985, **15**, No. 3, 14.
5. D. P. Zollinger and M. Bos, *Trends Anal. Chem.*, 1985, **4**, 60, 112.
6. F. T. M. Dohmen and P. C. Thijssen, *ibid.*, 1985, **4**, 167.
7. P. C. Thijssen and F. T. M. Dohmen, *ibid.*, 1985, **4**, 218.
8. L. T. M. Prop, P. C. Thijssen and L. G. G. van Dongen, *Talanta*, 1985, **32**, 230.
9. Mountain View Press Inc., PO Box 4656, Mountain View, CA94040, U.S.A.
10. J. Růžička and E. H. Hansen, *Flow Injection Analysis*, Wiley, New York, 1981.
11. D. Betteridge, T. J. Sly, A. P. Wade and D. G. Porter, *Anal. Chem.*, 1985.
12. P. C. Thijssen, L. T. M. Prop, G. Kateman and H. C. Smit, *Anal. Chim. Acta*, 1985, **174**, 27.

DETERMINATION OF PHENOTHIAZINES BY CHARGE-TRANSFER COMPLEX FORMATION WITH CHLORANILIC ACID

N. A. ZAKHARI,* M. RIZK, F. IBRAHIM and M. I. WALASH

Department of Analytical Chemistry, Faculty of Pharmacy, Mansoura University, Mansoura, Egypt

(Received 1 March 1985. Revised 9 August 1985. Accepted 5 October 1985)

Summary—A rapid and sensitive spectrophotometric method has been developed for the micro-determination of some phenothiazine derivatives as the pure substances and in different dosage forms. The method depends on the formation of stable donor-acceptor complexes between phenothiazines and chloranilic acid in an acetonitrile-2-propanol solvent mixture. The resulting intensely purple chloranilic acid radical anion possesses a characteristic absorption maximum at 515 nm. Beer's law is obeyed over the concentration ranges 1-6, 1-10 and 5-30 $\mu\text{g/ml}$ for prochlorperazine dimaleate, trifluoperazine dihydrochloride and thiethylperazine dihydrochloride, with apparent molar absorptivities of 7.76×10^4 , 1.95×10^4 and $6.64 \times 10^3 \text{ l. mole}^{-1} \text{ cm}^{-1}$, respectively. Statistical comparison of the results with those of an official method shows excellent agreement and indicates no significant difference in precision.

Numerous procedures are available for determining phenothiazine derivatives, *e.g.*, titrimetric,^{1,3} spectrophotometric,^{4,6} polarographic,⁷ gas chromatography⁸ and high-pressure liquid chromatography⁹ methods. Chloranilic acid, 2,5-dichloro-3,6-dihydroxy-1,4-benzoquinone, has been used for determination of certain metal ions,^{10,11} and recently has found application to the microdetermination of basic compounds by charge-transfer complex formation in various solvent systems. Several amino-acids have been determined in water,¹² some alkaloids in dioxan,^{13,14} and piperazine and a number of its salts in chloroform-2-propanol mixture.¹⁵

Phenothiazine derivatives are known to be powerful electron donors, and hence to form charge-transfer complexes with many π -acceptors.¹⁶ The donated electrons may originate either from the conjugated portion of the *N*-substituted phenothiazine, producing a π - π complex or from the terminal nitrogen atom of the substituent, as in the case of free phenothiazine bases, forming *n*- π complexes.¹⁷

Although various workers^{16,18} have reported the formation of charge-transfer complexes of phenothiazines with a large number of π -acceptors (not including chloranilic acid), their major interest was to throw light on a proposed relation between physiological action and electron-donating power.¹⁹ No attempt was made to utilize this sensitive reaction for the determination of phenothiazine drugs.

The purposes of the present investigation were (a) to study the changes in the absorption spectrum of chloranilic acid on addition of phenothiazine free

bases, and (b) to develop a simple assay procedure for phenothiazine drugs as the pure substances as well as in various dosage forms.

EXPERIMENTAL

Apparatus

Spectra were recorded on a Perkin-Elmer 550-S double-beam spectrophotometer, with 1-cm cells.

Materials

Prochlorperazine dimaleate, trifluoperazine dihydrochloride and thiethylperazine dihydrochloride were obtained from commercial sources and their purity was determined by the BP and USP methods.^{20,21}

Reagents

All the chemicals used were of analytical-reagent grade and the solvents were of spectroscopic grade. A 0.1% chloranilic acid solution in acetonitrile, and 2% aqueous tartaric acid and 6*M* ammonia solutions were used.

Preparation of sample solutions

An accurately weighed 100-mg portion of the phenothiazine salt was transferred into a 250-ml separating funnel with a little distilled water and alkalinized to litmus paper with ammonia solution, 1 ml being added in excess. The liberated phenothiazine base was then extracted with five 15-ml portions of chloroform with shaking for 3 min each time. The extract was dried by shaking with anhydrous sodium sulphate for 5 min, then filtered into a 100-ml standard flask, and finally made up to volume with anhydrous chloroform, which was also used to wash the sodium sulphate and filter.

For preparation of working solutions in acetonitrile, an accurately measured volume (not less than 1.0 ml) of this solution was evaporated to dryness by means of a stream of dry nitrogen and the residue obtained was dissolved in acetonitrile and made up to volume in a standard flask of suitable size with the same solvent.

General procedure

Accurately measured volumes of the acetonitrile solutions of the phenothiazine free bases, equivalent to 25-150, 25-250 and 125-750 μg of prochlorperazine dimaleate,

*To whom enquiries should be directed.

trifluoperazine dihydrochloride and thiethylperazine dihydrochloride respectively, were transferred into a series of 25-ml flasks, to give final concentrations of 1–6, 1–10 and 5–30 $\mu\text{g/ml}$. Then 5 ml of chloranilic acid solution were added to each followed by 5 ml of 2-propanol. The solutions were mixed well and made up to volume with acetonitrile, and the absorbance was measured at 515 nm against a reagent blank. A calibration graph was drawn or a regression equation calculated.

Procedure for tablets

Twenty tablets were weighed and finely powdered. An accurately weighed portion of the powder, equivalent to about 50 mg of the phenothiazine salt, was treated in the same way as the pure drugs in the calibration procedure, and an accurately measured volume of the acetonitrile solution thus obtained, containing about 0.08, 0.13 or 0.5 mg of prochlorperazine dimaleate, trifluoperazine dihydrochloride or thiethylperazine dihydrochloride, respectively, was transferred into a 25-ml standard flask and treated in the same way as the standards.

Procedure for injections

An accurately measured volume of the mixed contents of ten ampoules, equivalent to 50 mg of the drug, was analysed as just described for tablets.

Procedure for suppositories

Ten suppositories were accurately weighed, broken up into small pieces, melted and mixed well. An accurately weighed portion equivalent to 50 mg of phenothiazine drug was transferred into a 250-ml separating funnel and dissolved in 50 ml of tartaric acid solution. The solution was shaken for 5 min with 50 ml of diethyl ether. The acid layer was then transferred into a second separating funnel and extracted with another 50 ml of ether, this operation being repeated once more. The combined ether extracts were then shaken for 5 min with 10 ml of tartaric acid solution, and the ether layer was discarded. The acid solution was then alkalinized with ammonia and the analysis completed as already described.

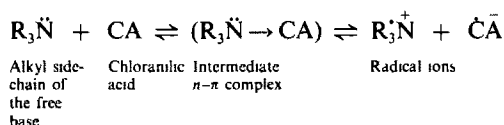
RESULTS AND DISCUSSION

A chloranilic acid solution in acetonitrile is faint purple. The spectrum of $0.5 \times 10^{-4} M$ chloranilic acid in acetonitrile possesses a major band at 315 nm with an absorbance of 0.86 (un-ionized form) and a broad very weak band at about 525 nm (chloranilic acid anion), Fig. 1. Addition of phenothiazine bases to this solution causes an immediate change in the absorption spectrum, with a new characteristic band at 515 nm, believed to be due to chloranilic acid radical anions.

Reactions involved

Chloranilic acid in organic solvents exists in the un-ionized form and acts as a π -acceptor in a similar manner to quinones.¹² Therefore, the addition of compounds possessing a lone pair of electrons, such as phenothiazine free base, results in formation of a charge-transfer complex of the $n-\pi$ type. This complex is believed to be an intermediate molecular association compound, for which, in appreciably polar solvents, complete transfer of the charge takes place, producing the corresponding radical ion,

which is responsible for the production of the intense absorption band at 515 nm, Fig. 2.



This type of reaction was first reported by Buckley *et al.*²² Fulton and Lyons¹⁸ have described a similar pathway for the reaction of a number of phenothiazine bases, which contain either tertiary or secondary amino groups, with chloranil in acetonitrile medium. According to these authors, the chloranil radical anion band was measured at 540 nm. Further reaction between the radical ions results in formation of an aminoquinone derivative, which absorbs at 590 nm, and the liberation of a chloride ion. This interpretation is supported by the experimental finding that a trimethylamine-chloranil mixture in acetonitrile also has two bands, at 540 and 590 nm, corresponding to the chloranil radical anion and the aminoquinone derivative, respectively.

Optimization of variables

To develop a quantitative method based on this reaction, a search was conducted for the most effective π -acceptor.

Chloranil, bromanil, tetracyanoethylene and dichlorodicyanobenzoquinone in various concen-

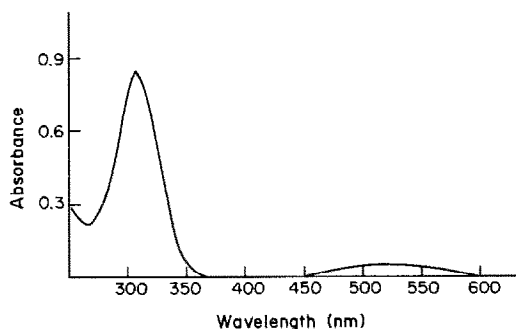


Fig. 1. Absorption spectrum of $0.5 \times 10^{-4} M$ chloranilic acid solution in acetonitrile.

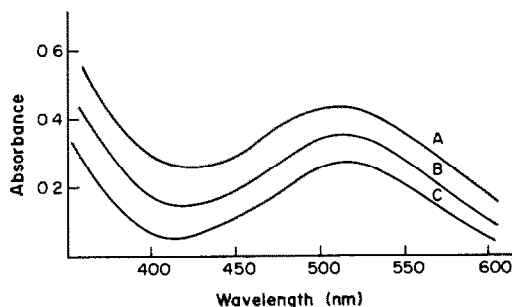


Fig. 2. Absorption spectrum of phenothiazine bases with chloranilic acid. A, 10 $\mu\text{g/ml}$ trifluoperazine dihydrochloride; B, 3 $\mu\text{g/ml}$ prochlorperazine dimaleate; C, 20 $\mu\text{g/ml}$ thiethylperazine dihydrochloride.

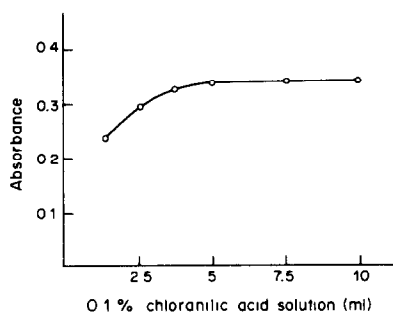


Fig. 3. Effect of chloranilic acid concentration on formation of trifluoperazine dihydrochloride-chloranilic acid charge-transfer complex.

trations failed to give quantitative results although many solvents were tried. In contrast, chloranilic acid in acetonitrile readily reacts stoichiometrically with all three phenothiazine derivatives investigated, forming a stable purple chloranilic acid radical anion. Acetonitrile proved to be the most suitable solvent. Chloroform, 2-propanol, dichloroethane and chloroform-2-propanol mixture were not suitable, because the complex formed in these solvents either had low absorbance or was precipitated on dilution.

Pure acetonitrile as solvent was found to cause opalescence only with high phenothiazine concentrations, and this difficulty was overcome by adding small amounts of 2-propanol. A 5:1 v/v acetonitrile-2-propanol mixture was used successfully for all the drugs investigated, over the concentration ranges examined. The reaction was instantaneous and the product remained stable for at least 1 hr.

The most effective chloranilic acid concentration was found to be given by use of 5 ml of 0.1% solution. Figure 3 shows the relationship between absorbance and concentration of chloranilic acid at fixed phenothiazine salt concentration.

Performance characteristics

Under the proposed experimental conditions, there was linear correlation between absorbance and final concentration over the ranges 1-6, 1-10 and 5-30 $\mu\text{g/ml}$, with corresponding molar absorptivities of 7.76×10^4 , 1.95×10^4 and $6.64 \times 10^3 \text{ l. mole}^{-1} \text{ cm}^{-1}$ for prochlorperazine dimaleate, trifluoperazine dihydrochloride and thiethylperazine dihydrochloride, respectively.

Table 1. Determination of phenothiazine derivatives*

Prochlorperazine dimaleate		Trifluoperazine dihydrochloride		Thiethylperazine dihydrochloride	
Taken, $\mu\text{g/ml}$	Mean recovery \pm S.D., %	Taken, $\mu\text{g/ml}$	Mean recovery \pm S.D., %	Taken, $\mu\text{g/ml}$	Mean recovery \pm S.D., %
1	99.5 \pm 0.5	1	100.4 \pm 0.6	5	100.0 \pm 0.5
2	100.3 \pm 0.4	2	99.8 \pm 0.4	10	100.9 \pm 0.6
3	100.2 \pm 0.5	3	100.0 \pm 0.4	15	99.7 \pm 0.6
4	101.0 \pm 0.4	5	100.7 \pm 0.8	20	99.8 \pm 0.5
5	100.7 \pm 0.8	7	99.4 \pm 0.4	25	100.6 \pm 0.4
6	101.1 \pm 0.6	10	99.8 \pm 0.3	30	99.5 \pm 0.5

*Five determinations at each level.

Table 2. Assay of phenothiazine derivatives in some pharmaceutical preparations by the chloranilic acid and official methods

Drug	Mean recovery \pm S.D.*, %	
	Chloranilic acid method	Official method†
Prochlorperazine dimaleate	100.5 \pm 0.7	99.9 \pm 0.4
Stemetil tablets, 5 mg§	98.7 \pm 0.5	100.3 \pm 0.9
Trifluoperazine dihydrochloride	100.0 \pm 0.6	100.4 \pm 0.6
Stelazine tablets, 5 mg‡	101.2 \pm 0.8	101.7 \pm 0.3
Stelazine tablets, 15 mg	100.2 \pm 1.0	102.0 \pm 0.5
Thiethylperazine dihydrochloride	100.1 \pm 0.7	99.6 \pm 0.5
Torican tablets, 6.5 mg‡‡ (Thiethylperazine)	99.2 \pm 0.6	100.5 \pm 0.4
Torican ampoules, 6.5 mg	101.1 \pm 0.9	100.2 \pm 0.6
Torican suppositories, 6.5 mg	100.2 \pm 0.7	98.8 \pm 0.4

*Average of at least five determinations, calculated relative to nominal content.

†According to BP 1980, except for thiethylperazine dihydrochloride (USP XX, NF XV).

§May and Baker, England.

‡Smith Kline and French, England.

‡‡Swiss Pharma, Egypt, under licence from Sandoz, Switzerland.

Regression analysis indicated a very small intercept on the ordinate. The reproducibility of the method was determined by analysis of six samples covering the recommended concentration range for each of the phenothiazines investigated. As shown by the recoveries and standard deviations, Table 1, the method is reproducible, accurate and precise.

Application to dosage forms

Results for determination of the three drugs in different dosage forms by the proposed method are presented in Table 2, and show good agreement with those of the official procedures.

This conclusion was confirmed by statistical analysis, the *t*-test and *F*-test showing no significant difference in accuracy and precision between the official methods and the proposed chloranilic acid method.

REFERENCES

1. S. A. Soliman, H. Abdine and N. A. Zakhari, *J. Pharm. Sci.*, 1975, **64**, 129.
2. M. Gajewska, M. Ciszewska and A. Goldnik, *Chem. Anal. (Warsaw)*, 1978, **23**, 503.
3. N. V. Pathak, I. C. Shukla and S. R. Shukla, *Talanta*, 1982, **29**, 58.
4. A. G. Davidson, *J. Pharm. Pharmacol.*, 1976, **28**, 795.
5. B. Kure and M. D. Morris, *Talanta*, 1976, **23**, 398.
6. A. S. Issa, Y. A. Beltagy and M. S. Mahreous, *ibid.*, 1979, **25**, 710.
7. F. W. Teare and R. N. Yadav, *Can. J. Pharm. Sci.*, 1978, **13**, 69.
8. T. J. Gillespie and I. G. Sipes, *J. Chromatog.*, 1981, **223**, 1.
9. A. G. Butterfield and R. W. Sears, *J. Pharm. Sci.*, 1977, **66**, 1117.
10. D. D. Perrin, *Organic Complexing Reagents*, p. 189. Interscience, New York, 1964.
11. J. F. Verchere, *J. Chem. Res.*, 1978, **5**, 178.
12. M. A. Slifkin, B. M. Smith and R. H. Walmsley, *Spectrochim. Acta*, 1969, **25A**, 1479.
13. M. A. El-Sayed and S. P. Agarwal, *Talanta*, 1982, **29**, 535.
14. S. P. Agarwal and M. A. El-Sayed, *Analyst*, 1981, **106**, 1157.
15. M. Rizk, M. I. Walash and F. Ibrahim, *Spectrosc. Lett.*, 1984, **17**, 423.
16. R. Foster and P. Hanson, *Biochem. Biophys. Acta*, 1966, **112**, 482.
17. M. A. Slifkin, *Charge-Transfer Interaction of Biomolecules*, Academic Press, London, 1971.
18. A. Fulton and L. E. Lyons, *Aust. J. Chem.*, 1968, **21**, 873.
19. A. Szent-Györgyi, *Introduction to a Submolecular Biology*, p. 107. Academic Press, New York, 1960.
20. *The British Pharmacopoeia*, HM Stationery Office, London, 1980.
21. *The United States Pharmacopoeia XX-National Formulary XV*, USP, Rockville, Md., 1980.
22. D. Buckley, H. B. Henbest and P. Slade, *J. Chem. Soc.*, 1957, 4894.

EXTRACTION AND SPECTROPHOTOMETRIC DETERMINATION OF TITANIUM(IV) WITH MALACHITE GREEN AND *p*-CHLOROMANDELIC ACID, WITH APPLICATION TO MILD STEELS

SHIGEYA SATO and SUMIO UCHIKAWA

Faculty of Education, Kumamoto University, 2-40-1, Kurokami, Kumamoto 860, Japan

(Received 30 April 1985. Accepted 30 September 1985)

Summary—A very sensitive, selective and simple method for extraction and spectrophotometric determination of titanium(IV) with an α -hydroxy acid has been developed. *p*-Chloromandelic acid reacts with titanium in weakly acidic aqueous solution at room temperature to form a complex anion extractable into chlorobenzene with Malachite Green as counter-ion. Titanium is determined indirectly by measuring the absorbance of Malachite Green in the extract at 630 nm. The calibration graph is linear for titanium(IV) over the range 0.25–7.5 μM (0.05–1.44 μg); the apparent molar absorptivity is $1.31 \times 10^5 \text{ l. mole}^{-1} \text{ cm}^{-1}$. The method has been successfully applied to the determination of titanium in mild steels.

Most spectrophotometric methods for titanium(IV) have been based on its reactions with suitable colour-producing reagents such as hydrogen peroxide,^{1,2} diantipyrylmethane^{3,4} and tiron^{5,6} and measurement in aqueous solution. Trioctylphosphine oxide,⁷ *N*-benzoyl-*N*-phenylhydroxylamine⁸⁻¹⁰ and *N*-phenyl-laurohydroxamic acid¹¹ have been used as reagents for extraction and spectrophotometric determination of titanium. Some of these reagents have disadvantages such as low sensitivity and selectivity, slow reaction, or the need for strongly acidic media for complete colour development. Mori *et al.*¹² have reported a sensitive method based on the colour reaction between *o*-hydroxyhydroquinonephthalein and titanium(IV) in the presence of a surfactant (Tween 20). This method is very simple, but time-consuming because of the heating step used. It is difficult to obtain high sensitivity by using flame atomic-absorption spectrometry, owing to the formation of a highly stable oxide species in the flame.

In our laboratory, several α -hydroxy acids have been investigated as complexing agents for the extraction and spectrophotometric determination of boron and antimony, and highly sensitive and selective determination methods have been reported.¹³⁻¹⁷ In further work on these systems, it was found that the titanium-*p*-chloromandelic acid complex can be extracted into chlorobenzene with Malachite Green as counter-ion and that the colour of the resulting organic phase is very stable. A method for determination of titanium has been based on this and applied to analysis of mild steel. The proposed method is sensitive, selective, convenient and rapid. Interference from boron and antimony(III) can be eliminated by the use of tartrate buffer, and iron(III) can be masked with ethyleneglycol-bis(2-aminoethyl ether)tetra-acetic acid (EGTA).

EXPERIMENTAL

Apparatus

Hitachi model 181 and 624 digital spectrophotometers were used, with 10-mm glass cells. The pH-values were measured with a Hitachi-Horiba M-8 pH-meter.

Reagents

Standard titanium(IV) solution. A commercially available titanium standard solution (1000 ppm TiOSO_4 in $\sim 1N$ sulphuric acid) was used and working solutions were made by suitable dilution as required.

Malachite Green (MG) solution, $1 \times 10^{-3}M$. Prepared from guaranteed MG (oxalate).

***p*-Chloromandelic acid (*p*-MACl) solution,** $5.0 \times 10^{-3}M$.

Sodium acetate buffer (pH 3.0). Prepared from 0.1M sodium acetate and 0.5M sulphuric acid.

Tartrate solution, $5.2 \times 10^{-3}M$. Prepared from 0.01M tartaric acid and adjusted to pH 3.0 with sodium hydroxide solution.

Ethyleneglycol-bis(2-aminoethyl ether)tetra-acetic acid (EGTA) solution 0.2M. Adjusted to pH 9 with sodium hydroxide solution.

Use demineralized water throughout.

Standard procedure

Take an aliquot of standard titanium(IV) solution containing up to 1.44 μg of titanium, in a 10-ml test-tube equipped with a stopper. Add 1.0 ml of sodium acetate buffer, 0.2 ml of *p*-MACl solution and 0.5 ml of MG solution. Dilute to 4.0 ml with water and shake the solution with 4.0 ml of chlorobenzene for 5 min. Separate the phases and measure the absorbance of the organic phase at 630 nm, using a 10-mm glass cell, with chlorobenzene as reference.

Analysis of steel samples

Weigh the steel sample (up to 0.2 g) into a 100-ml fused silica beaker, and dissolve it in 20 ml of sulphuric acid (1 + 6) by heating, and then gradually add 5 ml of 35% hydrogen peroxide solution. When the sample has dissolved, boil the solution on the hot-plate for about 10 min to completely remove the hydrogen peroxide. Adjust the solution to pH 1.8–2.0 with 8M sodium hydroxide, transfer the solution to a 100-ml standard flask and make up to volume with water.

Table 1. The reagent blank and the apparent molar absorptivity (ϵ , $l.mole^{-1}.cm^{-1}$) for titanium complexes with α -hydroxy acids and dyes, extracted into chlorobenzene

Complexing reagent	Ethyl Violet		Crystal Violet		Methyl Violet		Brilliant Green		Malachite Green	
	blank	ϵ	blank	ϵ	blank	ϵ	blank	ϵ	blank	ϵ
2-Hydroxy-2-methylbutyric acid	0.44	2.7×10^4	0.29	2.8×10^4	0.34	4.0×10^3	0.10	2.5×10^4	0.13	7.8×10^4
2-Hydroxyisocaproic acid	0.22	9.0×10^4	0.15	1.17×10^5	0.23	1.17×10^5	0.18	7.3×10^4	0.07	1.23×10^5
Mandelic acid	0.38	—*	0.28	9.4×10^4	0.35	3.1×10^4	0.34	4.3×10^4	0.12	9.1×10^4
<i>p</i> -Chloromandelic acid	0.16	8.0×10^3	0.41	1.3×10^4	0.17	2.2×10^4	0.22	1.24×10^5	0.08	1.31×10^5
<i>p</i> -Bromomandelic acid	0.17	2.0×10^3	0.33	1.6×10^4	0.08	2.0×10^4	0.24	1.10×10^5	0.07	1.17×10^5

*No extraction of complex.

Transfer 0.3 ml of this solution into a stoppered 10-ml test-tube. Add 0.2 ml of EGTA solution, 1.0 ml of tartrate solution, 0.2 ml of *p*-MACl solution and 0.5 ml of MG solution, then extract and measure as in the standard procedure. The apparent molar absorptivity obtained by this procedure is $1.17 \times 10^5 l.mole^{-1}.cm^{-1}$, about 11% less than that obtained by the standard procedure.

RESULTS AND DISCUSSION

Selection of complexing agent, cationic dye and extraction solvent

We have found that α -hydroxy acids are useful complexing agents, especially for metals which form oxo-ions in solution.

We have now examined the reactions between titanium and glycolic acid, lactic acid, 2-hydroxy-2-methylbutyric acid, 2-hydroxyisocaproic acid, mandelic acid, *p*-chloromandelic acid and *p*-bromomandelic acid, along with extraction of the products into 4-methyl-2-pentanone, 1,2-dichloroethane, dichloromethane, chloroform, chlorobenzene, benzene, toluene, carbon tetrachloride and cyclohexane with the dyes Ethyl Violet, Methyl Violet, Crystal Violet, Brilliant Green, Malachite Green and Methylene Blue as counter-ions. With each acid, different combinations of solvents and dyes were examined. The titanium complexes with glycolic or lactic acid cannot be extracted into any of the solvents listed, and none of the ion-association species formed between a

titanium complex anion and a dye can be extracted into carbon tetrachloride or cyclohexane. 4-Methyl-2-pentanone, 1,2-dichloroethane, dichloromethane and chloroform cannot be used as the solvent (except with Methylene Blue) because of the high extractability of the cationic dyes themselves. Of the other solvents, chlorobenzene was preferred. Table 1 lists the apparent molar absorptivities of the complexes and the absorbances of the reagent blanks obtained with chlorobenzene as solvent. It is clear that the MG-*p*-MACl-chlorobenzene system should be the most suitable for the determination of micro amounts of titanium(IV). For Methylene Blue, the best combination was with 2-hydroxyisocaproic acid and chloroform, the apparent molar absorptivity and the reagent blank being $4.5 \times 10^4 l.mole^{-1}.cm^{-1}$ and 0.095, respectively.

Absorption spectra

The absorption spectra of the reagent blank and of the ion-association species formed between the titanium-*p*-MACl complex and MG in chlorobenzene are shown in Fig. 1. MG is not extracted in the absence of *p*-MACl, whether titanium is present or not. The maximum absorption occurs at 630 nm.

Experimental variables

Extraction at various pH values resulted in maximum and constant absorbance of the organic phase

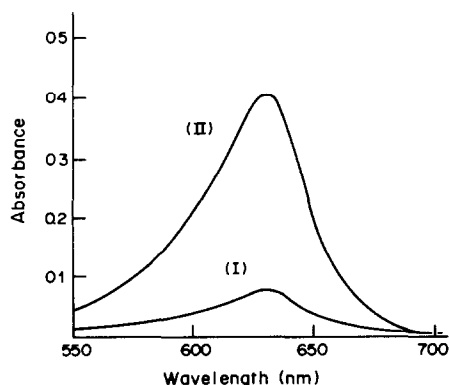


Fig. 1. Absorption spectra: (I) reagent blank; (II) $2.5 \times 10^{-6}M$ Ti(IV) (0.48 μg). Malachite Green, $1.3 \times 10^{-4}M$; pH, 3.0; *p*-chloromandelic acid, $2.5 \times 10^{-4}M$; reference, chlorobenzene.

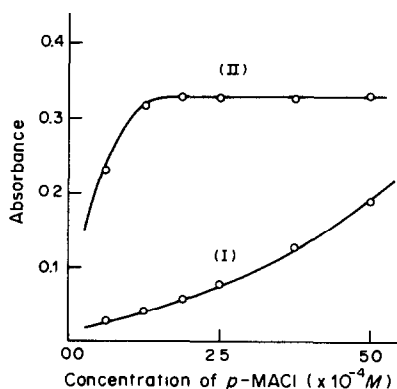


Fig. 2. Effect of *p*-chloromandelic acid concentration: (I) reagent blank; (II) net absorbance (Ti = $2.5 \times 10^{-6}M$). Malachite Green, $1.3 \times 10^{-4}M$; pH, 3.0.

Table 2. Effect of other ions on the determination of 0.48 μg of titanium in 4 ml

Ion	Added as	Amounts added,* μg	Recovery, %	Ion	Added as	Amounts added,* μg	Recovery, %
Cl^-	KCl	360	103	As(III)	As_2O_3	300	105
Br^-	NaBr	80	102	As(V)	Na_2HAsO_4	400	103
I^-	NaI	4.8	105	Sb(III)	SbCl_3	0.2	107
ClO_4^-	KClO_4	0.4	106			1.0†	104
SCN^-	KSCN	0.1	105	Sb(V)	$\text{K}[\text{Sb}(\text{OH})_6]$	200	101
NO_3^-	NaNO_3	8.2	107	Se(IV)	H_2SeO_3	400	103
SO_4^{2-}	Na_2SO_4	1000	103	B(III)	H_3BO_3	1.6	106
H_2PO_4^-	KH_2PO_4	300	94			4.0†	103
Be^{2+}	BeSO_4	45	99	Cr^{3+}	$\text{KCr}(\text{SO}_4)_2$	260	102
Mg^{2+}	MgCl_2	150	103	Mn^{2+}	MnCl_2	300	99
Ca^{2+}	CaCl_2	200	101	Fe^{2+}	Mohr's salt	60	104
Sr^{2+}	SrCl_2	450	103	Fe^{3+}	Ferric alum	6.7	105
Ba^{2+}	BaCl_2	700	97			670§	103
Al^{3+}	Potassium alum	150	97	Co^{2+}	CoCl_2	300	97
In^{3+}	InCl_3	550	96	Ni^{2+}	NiCl_2	300	99
Pb^{2+}	PbCl_2	1000	95	Cu^{2+}	CuSO_4	300	97
				Zn^{2+}	ZnSO_4	330	100

*Amounts added per 4 ml.

†In the presence of $1.3 \times 10^{-3} M$ tartrate.

§In the presence of EGTA ($5 \times 10^{-3} M$).

over the pH range 2.0–3.5, and pH 3.0 was chosen as optimal. The absorbance of the reagent blank increased with increase in MG concentration, but the net absorbance for the extracted complex was constant for MG concentrations $> 1.0 \times 10^{-4} M$ in the aqueous solution extracted. The concentration of MG was fixed at $1.25 \times 10^{-4} M$ for convenience. The effect of *p*-MACl concentration was examined, with the results shown in Fig. 2. Maximal and constant net absorbance was obtained with $> 1.5 \times 10^{-4} M$ *p*-MACl in the aqueous phase extracted. The concentration of *p*-MACl was therefore fixed at $2.5 \times 10^{-4} M$.

An extraction time of about 2.5 min was necessary to attain constant absorbance, but for routine work 5 min is recommended for safety.

Composition of the complex

The apparent molar absorptivity for titanium in the extract is about twice the molar absorptivity (*ca.* $6.8 \times 10^4 \text{ l. mole}^{-1} \text{ cm}^{-1}$) for MG itself in aqueous solution, suggesting that the mole ratio of MG and Ti in the extracted species is 2:1. The composition of the extracted species could not be determined by the continuous-variation or the mole-ratio methods, because of the large excess of *p*-MACl and MG required for its formation. However, it is suggested that either $[\text{TiO}(\text{p-MACl})_2]^{2-}$ or $[\text{Ti}(\text{p-MACl})_2]^{2-}$ is formed and extracted as its ion-association complex with Malachite Green.

Calibration graph

The calibration graph obtained by the standard procedure was linear over the range 0.25–7.5 μM titanium in the aqueous phase (0.05–1.44 μg of Ti). The apparent molar absorptivity calculated from the slope of the graph was $1.31 \times 10^5 \text{ l. mole}^{-1} \text{ cm}^{-1}$, and the absorbance of the reagent blank was 0.078. These

figures were independent of temperature in the range 7–30°. The coefficient of variation of the absorbance for 2.5 μM titanium was 2.4% (10 replicates). The absorbance of the organic phase remained constant for at least 60 min.

Effect of other ions

Table 2 shows the apparent recovery in determination of 0.48 μg of titanium in presence of various other ions. Iodide, perchlorate, thiocyanate and nitrate, which are bulky and of low surface-charge density, caused positive errors even at low levels. Boron and antimony(III) gave positive errors because they react with *p*-MACl to form extractable complex anions, whereas antimony(V) did not interfere, owing to its slow reaction rate at room temperature. Phosphate gave negative errors, because at relatively high concentration it forms a precipitate with titanium, but chloride and sulphate did not interfere. Most cations tested did not interfere when present in 600-fold ratio to the amount of titanium, but iron(III) gave rise to positive errors when present in 14-fold ratio. The interference of boron (up to 4.0 μg) and antimony(III) (up to 1.0 μg) could be eliminated by the addition of tartrate ($1.3 \times 10^{-3} M$). Iron(III) (up to 670 μg) could be masked by addition of EGTA at the $5.0 \times 10^{-3} M$ level, but the slope of the calibration graph was decreased by about 11%.

Determination of titanium in steel samples

The proposed method was applied to the determination of titanium in carbon steels.¹⁸ Any residue from the sulphuric acid–hydrogen peroxide treatment was collected on filter paper, dried at 110° and ignited in a platinum crucible at 600°; silica in the product was removed by treatment with sulphuric acid and hydrofluoric acids and the residue was fused with potassium pyrosulphate. The cooled melt was dis-

Table 3. Determination of titanium in steel

Sample* (certified value, %)	Sample solution,† g/100 ml	Titanium added,§ µg	Titanium found,† µg	Ti content found, %	Recovery, %	
NBS 362 (0.084)	0.0532	0	0.134	0.0841		
		0.240	0.376		101	
		0.479	0.599		97	
	0.1001	0	0.251	0.0837		
		0.479	0.725		99	
	0.1004	0	0.248	0.0823		
	0.1504	0	0.375	0.0832		
	0.1983	0	0.502 #	0.0844		
	0.2007	0	0.504	0.0837		
		0.240	0.751		103	
		0.479	0.973		98	
	JSS 171-3 (0.036)	0.0824	0	0.090	0.0366	
0.479			0.555		97	
0.1124		0	0.119	0.0354		
0.1509		0	0.167	0.0369		
0.1973		0	0.207	0.0349		
0.2031		0	0.221	0.0362		
	0.479	0.710		102		

*Other components. NBS 362: C, 0.16; Mn, 1.04; Si, 0.39; V, 0.04; Mo, 0.068; W, 0.20; Sn, 0.016; Al, 0.09; Zr, 0.19; Sb, 0.013; Cu, 0.50; Ni, 0.59; Cr, 0.30; Co, 0.30; As, 0.09%. JSS171-3: C, 0.042; Mo, 0.035; As, 0.045; Sn, 0.034; Cr, 0.067; Al, 0.040; Ca, 0.0013; Ni, 0.11%.

†0.3 ml of sample solution was analysed.

§The titanium solution was added to the sample solution in the test-tube.

‡Mean of eight determinations.

Standard deviation 0.015 µg.

solved in dilute sulphuric acid, then the solution was filtered if necessary, adjusted to pH 1.8–2.0 with 8M sodium hydroxide, diluted to 50 ml, and analysed for titanium by the procedure for steel analysis. No significant amounts were found to be present, so any residue from the dissolution step can safely be discarded.

The iron(III) and any boron and antimony(III) present could be dealt with by adding EGTA and tartrate. Table 3 shows that the values obtained are in good agreement with the certified values. Results of recovery tests for titanium by the standard addition method are also shown in Table 3. The standard deviation for the determination of titanium in the NBS 362 steel was reasonably good (see footnote to Table 3). The method is suitable for routine work, because the time for analysis of steel samples is also satisfactory, being less than 100 min (60 min for dissolution of steel sample, 20 min for preparation of sample solution and 20 min for determination of titanium).

Acknowledgements—The authors express their thanks to Dr. E. Iwamoto of Hiroshima University for helpful dis-

cussions. They are also grateful to Miss F. Nakamura and Miss M. Araki for their assistance in the work.

REFERENCES

1. A. Weller, *Chem. Ber.*, 1882, **15**, 2592.
2. A. Weissler, *Ind. Eng. Chem., Anal. Ed.*, 1945, **17**, 695.
3. P. G. Jeffery and G. R. E. C. Gregory, *Analyst*, 1965, **90**, 177.
4. H. Ishii, *Bunseki Kagaku*, 1967, **16**, 110.
5. J. H. Yoe and A. R. Armstrong, *Anal. Chem.*, 1947, **19**, 100.
6. D. N. R. Nichols, *Analyst*, 1960, **85**, 452.
7. J. P. Young and J. C. White, *Anal. Chem.*, 1959, **31**, 393.
8. S. C. Shome, *Analyst*, 1950, **75**, 27.
9. K. Tanaka and N. Takagi, *Bunseki Kagaku*, 1963, **12**, 1175.
10. H. Ishii and H. Einaga, *ibid.*, 1968, **17**, 976.
11. H. D. Gunawardhana, *Analyst*, 1983, **108**, 952.
12. I. Mori, Y. Fujita and K. Sakaguchi, *Bull. Chem. Soc. Japan*, 1982, **55**, 3649.
13. S. Sato, *Anal. Chim. Acta*, 1983, **151**, 465.
14. S. Sato and S. Uchikawa, *Bunseki Kagaku*, 1984, **33**, E87.
15. S. Sato, S. Uchikawa, E. Iwamoto and Y. Yamamoto, *Anal. Lett.*, 1983, **16**, 827.
16. S. Sato, *Talanta*, 1985, **32**, 341.
17. *Idem*, *ibid.*, 1985, **32**, 447.
18. *Japan Industrial Standards*, G 1223, 1981.

MEASUREMENT OF ACIDITY CONSTANTS OF BENZOTHIADIAZINES BY SOLVENT EXTRACTION WITH USE OF A MEMBRANE PHASE-SEPARATOR

ANJUM S. KHAN and FREDERICK F. CANTWELL*

Department of Chemistry, University of Alberta, Edmonton, Alberta, Canada

(Received 6 August 1985. Accepted 25 September 1985)

Summary—For extraction studies a “filter-probe” porous Teflon membrane phase-separator is used in conjunction with a spectrophotometer fitted with a small-volume flow-cell and a peristaltic pump to measure absorbance of the organic phase as a function of aqueous phase pH. Acidity constants of monoprotic (HA) and diprotic (H₂A) acid benzothiadiazines have been measured with the apparatus. Accurate pK_a values for these compounds are difficult to measure by other techniques. Mixtures of n-octanol and chloroform in various proportions can be used as the organic phase in order to adjust the distribution coefficient of the neutral species to give optimum precision and accuracy in measurement of the pK_a values.

Solvent extraction possesses several advantages over other techniques which are used to measure ionization constants of acids and bases. It is applicable to compounds which have low solubility in water, or similar or even identical electronic absorption spectra for the conjugate acid-base species, or an especially high or low ionization constant, or, in the case of diprotic acids and bases, have very similar values for the two ionization constants.¹⁻⁶ Solvent extraction can also be adapted to measure ionization constants of several compounds simultaneously in the same solution.⁷ Greater precision and accuracy are achieved with this technique when the concentrations of the solute are measured directly in both phases rather than just in one phase. The use of continuous segmented solvent flow to achieve phase-distribution equilibrium and of porous membranes to achieve phase-separation greatly facilitates simultaneous measurements in both phases.¹

Nevertheless, for the sake of simplicity of experimental apparatus and because pK_a values precise to 0.1–0.2 are quite adequate for many purposes such as toxicological and pharmacological predictions and the design of analytical separations, it is still most common to measure the solute concentration in only one phase in a batch equilibration experiment. It should be possible to make such measurements of phase-distribution equilibria more conveniently by using a “filter-probe” porous membrane phase-separator rather than by the traditional separatory funnel technique.^{8, 10}

In designing an analytical separation scheme involving the benzothiadiazine compound polythiazide¹¹ it became necessary to measure the pK_a value of this compound. A literature survey revealed

that the state of knowledge about the pK_a values of both monoprotic and diprotic benzothiadiazines is uncertain, largely because these compounds exhibit the properties listed above which make pK_a measurements difficult—low solubility in water, small spectral shifts on ionization, high pK_a values and overlapping ionization in the case of the diprotic compounds.^{12–14} Therefore, in addition to polythiazide several other benzothiadiazines were included in a study designed to demonstrate simultaneously the use of the “filter-probe” membrane phase-separator for pK_a measurements by solvent extraction and to obtain reasonably accurate pK_a values for typical members of this traditionally difficult to measure class of compounds.

EXPERIMENTAL

Apparatus

The extraction vessel was a glass beaker with a Teflon lid, similar in design to that described previously for continuous solvent-extraction measurements.¹⁰ The pH of the aqueous phase was raised incrementally by addition of concentrated sodium hydroxide solution from a microburette, as described earlier.¹⁵ Since the concentration of sodium hydroxide solution was high enough for the total volume delivered never to be more than about 1% of the initial volume of the aqueous phase, dilution effects in the aqueous phase during a run were ignored. A Fisher Accumet Model 520 meter with a combination glass/silver-silver chloride electrode was used for pH measurements. The absorbance at the wavelength of maximum absorption by the sample compound was measured as the organic phase was circulated through an 80- μ l flow-cell in a Cary 118 spectrophotometer. To pump the organic phase selectively through the flow-cell, a porous Teflon membrane (Zitex Filter Membrane, 10–20 μ m pore size, triple layer 4 mils thick, No. E249-122, Chemplast Inc., Wayne, N.J.) was stretched over the end of the “filter-probe”,¹⁶ and pumping was accomplished with a Gilson “Minipuls-2” peristaltic pump and Technicon “Acidflex” pump tubing. The extraction mixture was stirred by magnetic stirrer, and its temperature was kept at 25 \pm 1.

*Author to whom reprint requests should be directed.

Reagents

Water was demineralized, distilled and finally distilled from alkaline permanganate. All organic solvents were of reagent grade. Cyclohexane was further purified by passage through a silica gel column. Chloroform was washed three times with an equal volume of water and filtered through dry paper before use. Drug compounds obtained from the Faculty of Pharmacy, University of Alberta, were used without further purification. Primary suppliers for the various drug compounds were: polythiazide (Pfizer), methylothiazide (Abbot), althiazide (Pfizer), cyclothiazide (Lilly), flumethiazide (Squibb) and 8-chlorotheophylline (G. D. Searle). All other chemicals were of analytical-reagent grade.

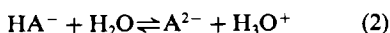
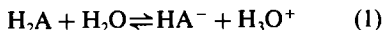
Solvent extraction procedure

The aqueous phase was 0.010M sodium chloride. Both phases, aqueous and organic, were pre-equilibrated with one another before use. Stock solutions of the compounds to be studied were prepared in water-saturated organic solvent. An accurately measured volume of presaturated organic solvent was first pipetted into the extraction vessel containing the magnetic stirring bar. The Teflon lid with the "filter-probe", return line, pH-electrode and vortex spoiler was clamped in place; the pump was started and the spectrophotometer was set at 100% transmittance with the organic phase circulating through the flow-cell. Next an accurately measured 10 or 20 ml aliquot of stock solution of the sample compound in organic solvent was pipetted into the beaker and the absorbance was allowed to come to a steady value, A_{in} . The concentration of the compound in the organic phase was in the range from $1 \times 10^{-5}M$ to $1 \times 10^{-4}M$ at this point. The pump was stopped, an accurately measured volume of aqueous phase was added, and the magnetic stirrer and the pump were started. The total organic phase volume was in the range 50–80 ml and the aqueous phase volume was 25–50 ml. The absorbance of the circulating organic phase was noted after about 2 min, when it had become constant at its new value, A . The aqueous-phase pH was measured after the stirrer had been switched off. With stirrer on again, a few μ l of sodium hydroxide solution were added and the sequence of measurements of equilibrium absorbance and pH was repeated. Addition of further increments of alkali and measurements of A and pH were repeated until the desired pH range had been covered.

RESULTS AND DISCUSSION

Dependence of distribution on pH

For a diprotic acid H_2A the ionization steps in the aqueous phase are:



and the extraction equilibrium for the neutral species between organic solvent and the aqueous phase is:



The subscript o indicates a species in the organic phase and lack of a subscript indicates a species in the aqueous phase. In this treatment "side-reactions" such as aggregation (*e.g.*, dimerization) of H_2A in the organic phase,⁹ dissociation of H_2A in the organic phase,^{4,5} and extraction of HA^- or A^{2-} as ion-pairs with cations in the system (*e.g.*, $NaHA$)¹⁷ are all assumed to be absent. The only one of these side-reactions that is potentially liable to occur at the low

sample concentrations employed is dissociation of H_2A in the organic phase. While this may be of some concern in polar organic solvents such as *n*-octanol, it is not likely to be significant in the less polar solvents employed in the present work.^{4,5}

In the experiment, the absorbance of the organic phase is measured before addition of aqueous phase (A_{in}) and at various times after incremental increases in the aqueous-phase pH (A). The *distribution ratio* of the sample component between organic and aqueous phases is defined as

$$D \equiv \frac{[H_2A]_o}{C} \quad (4)$$

where C is the total concentration (mole/l.) of all sample component species in the aqueous phase at any pH. The value of D is pH-dependent. Assuming that Beer's law applies, the organic phase sample concentration is related to absorbance by:

$$[H_2A]_o = \frac{TA}{V_o A_{in}} \quad (5)$$

where T is the total number of moles of sample component added to the system and V_o is the volume (litres) of organic phase. The aqueous phase concentration, C , can be calculated as follows:

$$C = \frac{T}{V} \left(\frac{A_{in} - A}{A_{in}} \right) \quad (6)$$

where V is the volume (litres) of aqueous phase. Combining equations (4)–(6) gives:

$$D = \frac{V}{V_o} \left(\frac{A}{A_{in} - A} \right) \quad (7)$$

Plots of D vs. pH for a hypothetical family of acids for which $pK_{a1} = 9$ and pK_{a2} has various values are presented in Fig. 1. When $pK_{a2} = \infty$ (*i.e.*, $K_{a2} = 0$) the acid is monoprotic. For a monoprotic acid the typical sigmoidal relationship between D and pH, with the inflection point occurring at pK_{a1} , is seen.^{1,18} For $pK_{a2} < \infty$ (*i.e.*, $K_{a2} > 0$) the plot drops more sharply as pK_{a2} approaches pK_{a1} , although in the mid-region of the curve significant differences from the mono-

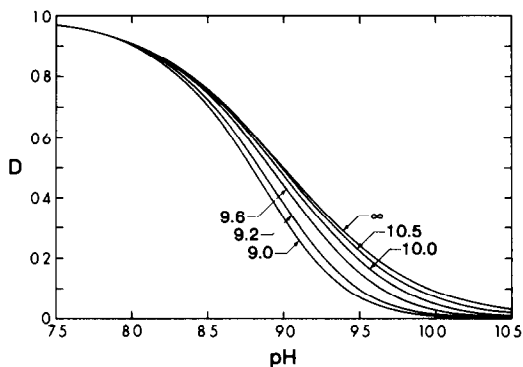


Fig. 1. Plot of D vs. pH for hypothetical diprotic acids with $pK_{a1} = 9.0$ and $\kappa = 1$. Numbers by the curves are the values of pK_{a2} . (When $pK_{a2} = \infty$ the acid is monoprotic.)

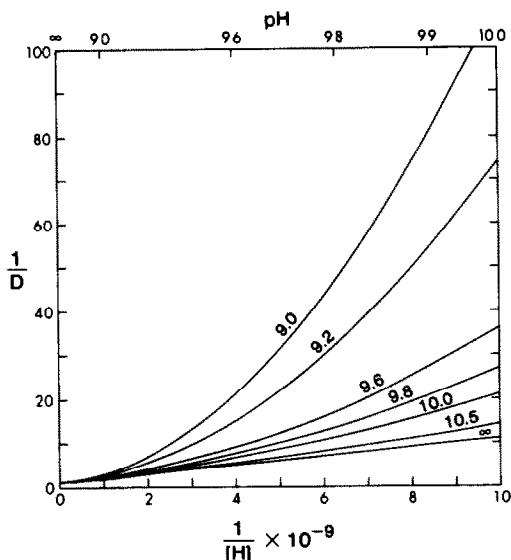


Fig. 2. Plots of $1/D$ vs. $1/[H]$ for the same hypothetical diprotic acids as in Fig. 1.

protic case begin to appear only when pK_{a2} is less than about $(pK_{a1} + 1.5)$.

The dependence of D on aqueous phase acidity can alternatively be represented as a plot of $1/D$ vs. $1/[H]$. For a diprotic acid H_2A the following relationship can be derived:

$$\frac{1}{D} = \frac{1}{\kappa} + \frac{K_{a1}}{\kappa[H]} \left(1 + \frac{K_{a2}}{[H]} \right) \quad (8)$$

where κ is the distribution coefficient for the neutral species corresponding to the equilibrium in equation (3):

$$\kappa = \frac{[H_2A]_o}{[H_2A]} \quad (9)$$

and the quantities K_{a1} and K_{a2} are the first and second acid ionization constants corresponding to the equilibria given in equations (1) and (2).⁴ From equation (8) it is seen that a plot of $1/D$ vs. $1/[H]$ is a parabola.^{4,5} Non-linear parabolic least-squares fitting of the data yields the values of κ , K_{a1} and K_{a2} .

For a monoprotic acid HA (neutral species) the second term in the parentheses in equation (8) is equal to zero and a plot of $1/D$ vs. $1/[H]$ is a straight line. From its slope and intercept, obtained by linear regression, κ and K_{a1} can be obtained.¹⁸ The linear dependence of $1/D$ on $1/[H]$ for a monoprotic acid with $pK_{a1} = 9$ is exhibited by the curve labelled ∞ in Fig. 2. For $pK_{a2} < \infty$ a deviation (parabolic) appears and becomes more marked as pK_{a2} gets closer to pK_{a1} . For pH values in the vicinity of pK_{a1} , significant deviations from the straight line for the monoprotic case begin to appear only when pK_{a2} is less than about $(pK_{a1} + 1.5)$. pK_{a2} can be evaluated experimentally only when a significant deviation from linearity is present. If measurements are performed at $pH \gg pK_{a1}$ then significant deviations from the mono-

protic acid curve occur even when $pK_{a2} \gg pK_{a1}$. However, such measurements cannot usually be made with acceptable experimental accuracy, because the fraction extracted into the aqueous phase is so high that the organic phase concentrations and hence absorbances are too small to be accurately measured [*i.e.*, there is an uncertain value of A in equation (7)].

Another approach to the calculations has been used to measure acidity constants from solvent extraction data, in which the dependence of D on $[H]$ is linearized for a diprotic acid,³ but it was not employed in the present study.

In the solvent extraction technique the most accurate measure of pK_{a2} is obtained when the value of pK_{a2} is close to the value of pK_{a1} .³⁻⁵ In this sense it is complementary to the potentiometric and spectrophotometric techniques, which are more reliable when pK_{a1} and pK_{a2} are farther apart. It can be shown from statistical reasoning that pK_{a2} for a diprotic acid should not normally be lower than $pK_{a1} + 0.6$.¹⁹ This condition corresponds to the curves labelled 9.6 in Figs. 1 and 2. However, if conformational changes occur in the HA^- species it is possible that this rule will be violated and pK_{a2} may be less than 0.6 higher than pK_{a1} or even be below it.

In Figs. 1 and 2 the distribution coefficient of the neutral species, κ , was taken as 1. If a different value is used, the resulting plots will be identical to the ones shown except that the vertical axis values (D or $1/D$) will be changed proportionately.

pK_a values

Acidity constants were measured by the solvent extraction technique, with a "filter-probe" membrane phase-separator, for seven compounds—five of which were benzothiadiazines. Four of the compounds were monoprotic acids and three diprotic. The pK_a values are presented in Table 1. Because previous work had produced accurate values which could be used for comparison purposes, the monoprotic acid 3,5-dimethylphenol was also investigated. Two different solvents were used as the organic phase, cyclohexane and chloroform. Within experimental error, the pK_a values measured in both solvent systems agreed with the literature values. A second monoprotic non-benzothiadiazine, 8-chlorotheophylline, was also included in the study because its pK_a value has recently been measured by using solvent extraction/flow-injection analysis.^{18,26} The value reported here agrees within experimental error with the previously reported value. The agreement with literature values for the two compounds, 3,5-dimethylphenol and 8-chlorotheophylline, is consistent with earlier observations that distribution ratios can be measured accurately with the "filter-probe" system.^{9,10,16}

The structures of the five benzothiadiazines are shown in Fig. 3. The acidic proton of the monoprotic compounds is on the nitrogen atom of the sulphamyl group attached to the 7-position. The additional

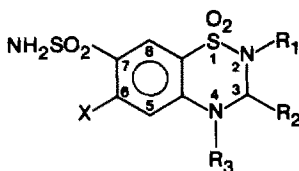


Fig. 3. Structures of benzothiadiazines.

	X	R ₁	R ₂	R ₃
Methylclothiazide	Cl	CH ₃	CH ₂ Cl	H
Polythiazide	Cl	CH ₃	CH ₂ SCH ₂ CF ₃	H
Althiazide	Cl	H	CH ₂ SCH ₂ CHCH ₂	H
Flumethiazide	CF ₃	H	—	—
Cyclothiazide	Cl	H	bornyl	H

acidic proton present in the diprotic benzothiadiazines is on the other nitrogen atom at the 2-position. The literature values reported in Table 1, with the exception of those from references 22, 23 and 24 (marked in the table with superscripts *i, j, k*), have been converted into "mixed-constants" at an ionic strength of 0.01 in order to allow comparison with the "found" values measured in the present study. Activity coefficients were estimated with the Davies equation.²⁵

No pK_{a2} value has previously been reported for althiazide. Significant discrepancies between the val-

ues measured in the present study and those in the literature exist for the monoprotic acid polythiazide and for pK_{a1} of the diprotic acid cyclothiazide. For polythiazide a very small spectral shift occurs on deprotonation, so 9.65 and 9.12, both measured spectrophotometrically, are probably less accurate than the value of 9.82 reported here.¹² The value 9.1 comes from extrapolation, to 100% water medium, of the values obtained by potentiometric titration in aqueous-acetone mixed solvent—a technique which cannot be relied on for accuracy.²⁷ Finally, the literature value >11 for polythiazide is clearly in error. The pK_a values for the second discrepant compound cyclothiazide were measured in the present work by using three organic phases consisting of various mixtures of *n*-octanol and chloroform. The grand-mean value of 9.35 ± 0.04 is significantly higher than the value of 8.8 measured in two spectrophotometric studies reported in the literature. This compound shows only small spectral shifts on loss of its protons.¹² This, along with the closeness of its pK_{a1} and pK_{a2} values to one another, makes the spectrophotometric method likely to be less accurate than the solvent extraction method, for which overlapping constants cause no problems in data evaluation. The literature value of 9.1 for cyclothiazide was obtained for aqueous ethanol medium (30% v/v ethanol) and

Table 1. Values found in the present study and in the literature

Compound	Solvent	κ	pK_{a1}		pK_{a2}	
			found ^a	literature ^f	found ^a	literature
3,5-Dimethylphenol	Cyclohexane	1.52	10.16 ± 0.16	10.16 ^b 10.15 ^c	(monoprotic)	
	Chloroform	16	10.4 ± 0.2	10.16 ± 0.01^d	(monoprotic)	
8-Chlorotheophylline	Chloroform	1.46	5.44 ± 0.05	5.44 ± 0.06^e	(monoprotic)	
	Chloroform	0.95	9.47 ± 0.01	9.4 ± 0.2^f 9.5 ^g	(monoprotic)	
Polythiazide	Chloroform	3.32	9.82 ± 0.04	9.65^h	(monoprotic)	
				9.1 ± 0.1^i 9.1 ^g $>11^i$		
Althiazide	Methylene chloride	3.12	8.52 ± 0.06	8.4 ± 0.3^j	10.00 ± 0.007	N.V.R. ^o
Flumethiazide	Octanol/chloroform (20/80)	0.148	6.43 ± 0.09	6.3 ^g	?"	N.V.R. ^o
				6.0 ± 0.2^j 6.44 ^j		
Cyclothiazide	Octanol/chloroform (5/95)	2.76	9.29 ± 0.07	8.8 ^h	10.65 ± 0.1	11.0 ^h
	Octanol/chloroform (10/90)	5.64	9.37 ± 0.05	(9.1) ^{k,m}	10.66 ± 0.1	
	Octanol/chloroform (15/85)	10.6	9.38 ± 0.1	8.8 ^g	10.88 ± 0.1	(10.5) ^{k,m}

^aMeasured at ionic strength 0.01. The \pm value represents the standard deviation of at least triplicate runs for the "found" values, and represents reported or estimated uncertainties for literature values.

^bReference 20.

^cReference 21.

^dReference 1.

^eReference 26.

^fReference 12.

^gReference 13.

^hReference 14.

ⁱReference 22.

^jReference 23.

^kReference 24.

^lLiterature values have been converted into "mixed constants" at ionic strength of 0.01 by using the Davies equation²⁵ to estimate activity coefficients, except for those with superscripts *i, j* and *k*.

^mLiterature value measured in 30:70 v/v ethanol-water mixture.

ⁿReliable values could not be obtained for pK_{a2} .

^oN.V.R., no value reported in the literature.

can therefore be expected to differ from the value for aqueous medium.²⁷

The present method did not yield a reliable value for pK_{a2} of flumethiazide. This is most likely to be due to the fact that $pK_{a2} \gg pK_{a1}$. The first proton lost from this compound ($pK_{a1} = 6.43$) is probably the one attached to the nitrogen atom in the 2-position, which is adjacent to the electron-delocalizing $-\text{N}=\text{C}-$ group in the 3,4-position. The second deprotonation step would therefore be from the sulphamyl group in the 7-position which, in comparison with the monoprotic compounds, probably has a pK_{a2} of 9–10. As discussed earlier, if $pK_{a2} \gg pK_{a1}$, the solvent extraction technique cannot be used to measure pK_{a2} .

Choice of solvent

The most accurate pK_a measurements are obtained when κ has a value near 1. In general, values of κ between 0.1 and 10 can be used. If κ is very small then the absorbance A in equation (7) experiences a large uncertainty due to photometric error, so D in equation (8) is also uncertain. On the other hand if κ is large then in the vicinity of $\text{pH} \approx pK_a$, which is the region where data must be collected because it is where D is changing most markedly with pH (Fig. 1), the change in A with pH is small, so the term $(A_m - A)$ in equation (7) will involve a small difference, and hence D will again be uncertain.¹⁸

The use of mixed organic solvents as the organic phase provides a convenient means of bringing the value of κ into the desired range. As shown by the data for cyclothiazide, mixtures of n-octanol and chloroform are convenient for this purpose. The compound flumethiazide has such a low solubility in chloroform that it was necessary to use a 20:80 v/v mixture of n-octanol/chloroform to raise κ above 0.1.

The uncertainties shown for the "found" pK_a values in Table 1 represent the standard deviation of at least triplicate runs. Although for several of the entries the uncertainties are small, this high precision should not be taken as general. The technique of solvent extraction in which absorbance is measured in only one of the phases is capable, in general, of precisions and accuracies of only 0.1–0.2 pK_a units. For more reliable values, the absorbances of both phases should be measured.¹

The present study has demonstrated that, by the use of a "filter-probe" membrane phase-separator, pK_a values can conveniently be measured with a precision and accuracy satisfactory for routine applications. The apparatus required is simple and all

measurements, over a range of pH , are made on one solution in a single beaker. It is hoped that such a device will contribute to the more widespread routine use of solvent extraction in the measurement of pK_a values.

Acknowledgements—This work was supported by an Alberta Heritage Foundation for Medical Research Post-doctoral Fellowship to A.S.K., by the Natural Sciences and Engineering Research Council of Canada and by the University of Alberta.

REFERENCES

1. L. F. Fossey and F. F. Cantwell, *Anal. Chem.*, 1985, **57**, 922.
2. T. Sekine, Y. Hasegawa and N. Ihara, *J. Inorg. Nucl. Chem.*, 1973, **35**, 3968.
3. G. Schill, *Acta Pharm. Suecica*, 1965, **2**, 99.
4. K. Ezumi and T. Kubota, *Chem. Pharm. Bull.*, 1980, **28**, 85.
5. T. Kubota and K. Ezumi, *ibid.*, 1980, **28**, 3673.
6. J. Hanamura, K. Kobayashi, K. Kano and T. Kubota, *ibid.*, 1983, **31**, 1357.
7. T. M. Xie and D. Dyrssen, *Anal. Chim. Acta*, 1984, **160**, 21.
8. F. F. Cantwell and H. Y. Mohammed, *Anal. Chem.*, 1979, **51**, 218.
9. M. Carmichael and F. F. Cantwell, *Can. J. Chem.*, 1982, **60**, 1286.
10. F. F. Cantwell and M. Carmichael, *Anal. Chem.*, 1982, **54**, 697.
11. A. S. Khan and F. F. Cantwell, *Talanta*, 1985, **32**, 901.
12. U. G. Hennig, *M.Sc. Thesis*, University of Alberta, 1979.
13. U. G. Hennig, R. E. Moskalyk, L. G. Chatten and S. F. Chan, *J. Pharm. Sci.*, 1981, **70**, 317.
14. M. Yamazaki, T. Suzuka, Y. Ito, S. Itoh, M. Kitamura, K. Ohashi, Y. Takeda, A. Kamada, Y. Orita and H. Nakahama, *Chem. Pharm. Bull.*, 1984, **32**, 2380.
15. R. A. Hux, S. Puon and F. F. Cantwell, *Anal. Chem.*, 1980, **52**, 2388.
16. H. Y. Mohammed and F. F. Cantwell, *ibid.*, 1980, **52**, 553.
17. G. Schill, in *Ion Exchange and Solvent Extraction*, Vol. 6, J. A. Marinsky and Y. Marcus (eds.), Chapter 1. Dekker, New York, 1974.
18. L. Fossey and F. F. Cantwell, *Anal. Chem.*, 1983, **55**, 1882.
19. E. Q. Adams, *J. Am. Chem. Soc.*, 1916, **38**, 1503.
20. D. T. Chen and K. A. Laidler, *Trans. Faraday Soc.*, 1962, **58**, 480.
21. E. F. G. Herrington and W. Kynaston, *ibid.*, 1957, **53**, 138.
22. A. Scriabine, E. C. Schreiber, M. Yu and E. H. Wiseman, *P.S.E.B.M.* 1962, **110**, 872.
23. E. Essig, *Am. J. Physiol.* 1961, **201**, 303.
24. F. C. Novello and J. M. Sprague, *Ind. Chem. Belge*, 1967, **32** (Special no.), 222.
25. C. W. Davies, *J. Chem. Soc.*, 1938, 2093.
26. L. Fossey, *Ph.D. Thesis*, University of Alberta, 1985.
27. A. Albert and E. P. Sergeant, *Ionization Constants of Acids and Bases*, Chapman & Hall, London, 1971.

POLYCRYSTALLINE AND MONOCRYSTALLINE ANTIMONY, IRIDIUM AND PALLADIUM AS ELECTRODE MATERIAL FOR pH-SENSING ELECTRODES

EITA KINOSHITA, FOLKE INGMAN, GUNNAR EDWALL* and SIGVARD THULIN*
Departments of Analytical Chemistry and Applied Physics*, The Royal Institute of Technology,
S-100 44 Stockholm, Sweden

STANISŁAW GŁĄB
Department of Chemistry, Warsaw University, Warsaw, Poland

(Received 4 July 1985. Accepted 25 September 1985)

Summary—Different ways of making pH-sensing electrodes from monocrystalline or polycrystalline antimony, iridium and palladium have been investigated. Monocrystalline antimony and iridium are superior to the polycrystalline elements with respect to reproducibility between electrodes and stability of the electrode potential over long periods of time. No good palladium/palladium oxide electrode could be obtained by electrochemical oxidation and the thermal preparation method could not take advantage of the properties of the monocrystalline palladium. Therefore, only polycrystalline palladium was used to study this type of electrodes. The different electrodes were compared with respect to the manner of preparation, the pH-response (reproducibility and time response) and the effect that different complexing ligands present in the measuring solutions may have on the electrode response. Also, the redox-response of the electrodes and the effect of different oxygen pressures on the electrode potentials were studied. The monocrystalline antimony electrodes have the best reproducibility and long-term stability but also respond to complexing ligands and to variations in the oxygen pressure. Monocrystalline iridium electrodes can be obtained by continuously cycling the potential between -0.25 and $+1.25$ V (SCE) in $0.5M$ sulphuric acid. They do not respond to the complexing ligands tested, and have fairly good long-term stability, but the reproducibility between electrodes is inferior to that of the monocrystalline antimony electrodes. Polycrystalline antimony and iridium electrodes were inferior to the monocrystalline ones. The properties of the palladium electrodes were similar to those of the iridium ones.

The determination of pH in special situations, for example *in vivo* applications where the fragility of the glass electrode is a drawback, requires pH-sensors that can easily be miniaturized and built into physically rugged sleeves. Furthermore, the electrodes should have a good pH-response and little or no response to the complex-forming ligands that are present in most biological fluids. One class of potentially suitable micro-electrodes is that of metal/metal oxide electrodes.

Recently, electrodes based upon antimony, iridium and palladium have mainly been the subject of scientific interest. The present group of authors has previously studied antimony/antimony oxide¹ and palladium/palladium oxide electrodes² as pH-sensors. Monocrystalline antimony electrodes were introduced by Edwall.³ The effect of complex-forming ligands in solution on the calibration of electrodes was studied by Głab *et al.*,¹ who recommended procedures for the calibration of the antimony electrode.

Various kinds of iridium electrodes are described in the literature. Perley and Godshalk⁴ were the first to use iridium for measuring pH. De Rooij and Bergveld⁵ used electrodes made by cycling the potential of the iridium electrode continuously between

-0.25 and $+1.25$ V (SCE) for around 200 cycles. Thermal methods of preparation were used by Papeschi *et al.*⁶ and by Ardizzone *et al.*⁷ The first group used the electrode to monitor pH in biological fluids, and the second made a closer study of the electrode mechanism. Iridium dioxide electrodes were studied by Fog and Buck,⁸ who used iridium dioxide on an inert electrode of the Růžicka Selectrode type (Radiometer, Copenhagen). Data on the reproducibility, pH range and some interfering ions were given. A similar mechanism was utilized by Katsube *et al.*,⁹ who used a sputtered film of iridium oxide on a support of steel or tantalum.

Electrodes for pH-determination, based on the palladium/palladium oxide couple, have been studied by many workers. Grubb and King¹⁰ devised a method for preparing electrodes by coating palladium wires with sodium hydroxide and oxidizing them at 800° for 20 min. Chung-Chiun Liu *et al.*¹¹ used electrochemical oxidation in a mixed melt of sodium nitrate and lithium chloride. The present group studied the utility of monocrystalline palladium as a material for palladium/palladium oxide electrodes² but concluded that no advantage was offered by this material since the electrochemically deposited oxide layer did not function well for pH-

sensing purposes, and the thermally prepared oxide had no defined crystal structure.

The aim of the present work was to study different ways of making pH-sensing electrodes from monocrystalline or polycrystalline antimony, iridium or palladium. Also, it was desired to study the reproducibility between electrodes and the stability of the electrode potential over long periods of time. The different electrodes were to be compared with respect to the manner of preparation, the pH-response (reproducibility and time response) and the effect that different complexing ligands present in the solutions may have on the electrode response. Further, the redox-response of the electrodes and the effect of different oxygen pressures on the electrode potentials were to be investigated.

EXPERIMENTAL

Monocrystalline antimony and iridium electrodes were made by the following method.

The pieces of antimony or iridium, which were 0.6 mm in diameter and 2 mm long, were degreased in trichloroethylene. An electrical contact lead was attached with conductive epoxy resin (MRC 4912, Materials Research).

The electrode was then cast in epoxy resin (Araldite, Ciba-Geigy) to form a plastic cylinder approximately 3 mm in diameter and with the exposed metal surface at the bottom end. The electrodes were ground and polished, with 1- μ m diamond paste in the final step.

The same procedure was used to make polycrystalline iridium electrodes. However, the polycrystalline iridium wire was 0.25 mm in diameter, and 12 pieces, each 3 mm long, were connected in a bundle, connected by silver-epoxy resin, and cast in one piece of epoxy resin to make an electrode.

The palladium electrodes were made as follows. Polycrystalline palladium wire (99.9% pure, 1 mm diameter and 10 mm long) was ground to remove any oxide present, and cleaned with acetone, ethanol and concentrated nitric acid. The clean wire was then immersed in a 50% aqueous solution of sodium hydroxide and subsequently dried in a flow of nitrogen. The coated wire was placed in an electrically heated oven at 750°. After 20 min, the oxidized wire was rinsed with distilled water. One end of the wire was cleaned from oxide and used for the electrical connection. This part of the wire was covered by silicone rubber sealant (Dow Corning Silastic 734 RTV) and tubing to prevent it from coming into contact with the test solution.

Reagent-grade chemicals and doubly distilled water were used for the solutions. All measurements were made at 25° (thermostatic bath). Magnetic stirring was employed. In order to keep the partial pressure of oxygen constant, air

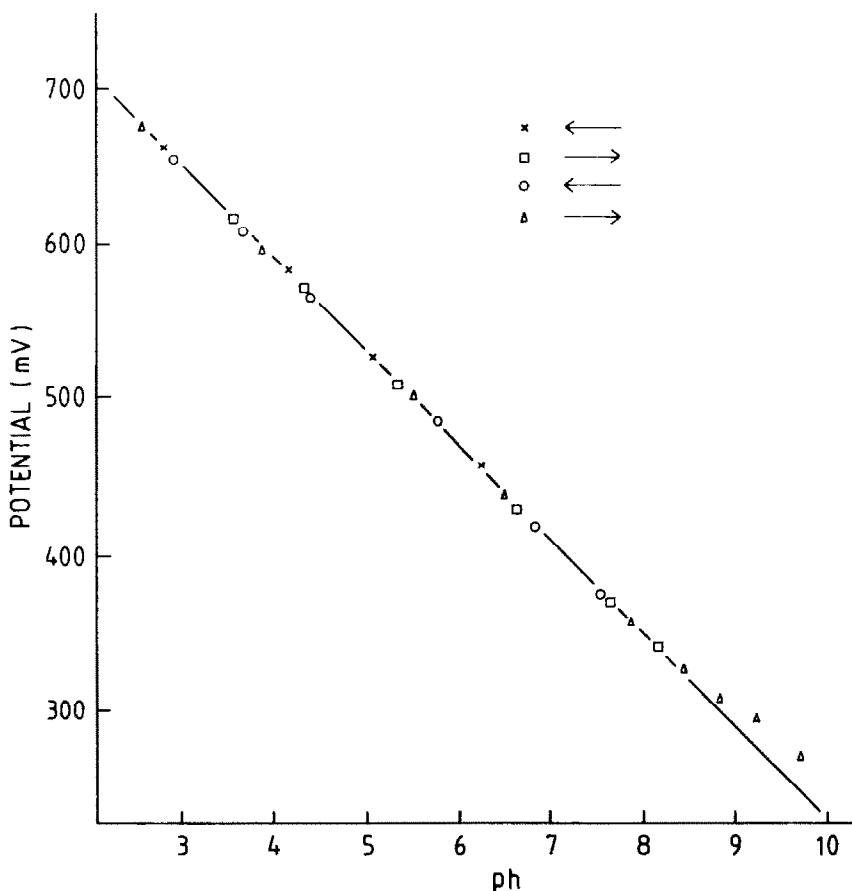


Fig. 1. Titration of 0.02M TRIS/0.14M NaNO₃ (to keep the ionic strength at 0.16). A palladium electrode made by thermal oxidation was used for measuring the potentials. The arrows indicate the direction of titration. The following equations were obtained by regression. For the pH-range 2.5–10, $E = 821 - 58.6 \text{ pH}$, $r^2 = 0.9982$; for the pH-range 2.5–8.3, $E = 821.6 - 59.6 \text{ pH}$, $r^2 = 0.9993$. The number of points was 39 in the first case, 34 in the second.

was bubbled through the test solutions before and during the measurements. The oxygen response measurements utilized mixtures of oxygen and nitrogen obtained from AGA Specialgas AB, Stockholm. Their oxygen partial pressures were 2.1 ± 0.1 , 2.3 ± 0.1 , 3.8 ± 0.1 , 7.4 ± 0.1 , 13.4 ± 0.1 and 20.7 ± 0.1 kPa ($100 \text{ kPa} \equiv 1 \text{ bar}$).

The equipment used for the titrations has been described previously. All potential values given in this paper are referred to the standard hydrogen electrode unless stated otherwise.

Throughout this paper, the electrodes have been calibrated to measure hydrogen-ion concentration (denoted by ph) at the given ionic strength instead of hydrogen-ion activity (denoted by pH). The technique has been described elsewhere.¹

RESULTS

The ph-response of the various types of electrode

The monocrystalline antimony electrodes exhibit a very good ph -response in the absence of complexing agents, for example in unbuffered solution or when TRIS [tris(hydroxymethyl)aminomethane] is used to buffer the ph of the solution.¹ For six electrodes studied, the E -value measured at $\text{ph} = 7.4$ was -174.7 mV, S.D. 0.3 mV and the slope was -52.0 mV/ ph , S.D. 0.1 mV/ ph . The commercially available polycrystalline antimony electrodes showed a less reproducible dependence of potential on ph , and the standard deviation for six electrodes was higher than for the monocrystalline electrodes. Electrodes made by Ingold, Tacussel and Radiometer were tested (two of each make) and the results were: E -value at $\text{ph} = 7.4$ was -171.8 mV, S.D. 2.7 mV and slope -52.6 mV/ ph , S.D. = 0.1 mV/ ph . The polycrystalline

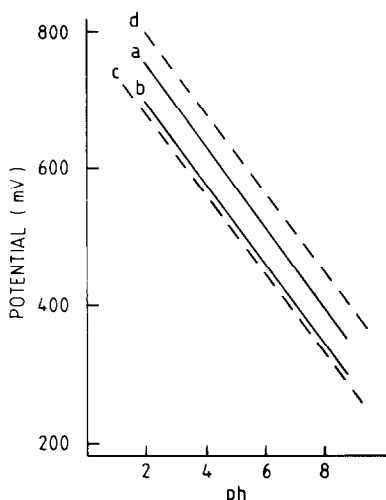
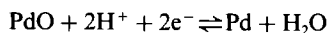


Fig. 2. The dependence of the potential of palladium electrodes, made by thermal oxidation, on ph in $0.02M$ TRIS/ $0.14M$ NaNO_3 , the ph was varied by adding either $0.05M$ HNO_3 / $0.11M$ NaNO_3 or $0.05M$ NaOH / $0.11M$ NaNO_3 , a and b , lines valid for the data obtained with the thermally oxidized palladium electrodes having the highest and the lowest E° value, respectively; c and d , lines calculated from literature data for the reaction $\text{PdO} + 2\text{H}^+ + 2\text{e}^- \rightleftharpoons \text{Pd} + \text{H}_2\text{O}$. Two different E° values were used: line c — 790 mV;¹² line d — 917 mV.¹³

electrodes also had inferior long-term stability in comparison with the monocrystalline antimony electrodes, and were sensitive to the speed of stirring of the solution. The potential is a linear function of ph over the ph range 2–10.

For palladium/palladium oxide electrodes made by thermal oxidation for 20 min at 750° , the ph -response was linear over the ph range 2.5–8 as shown in Fig. 1. The E° -value for these electrodes decreased by ~ 20 mV during the first two days after preparation, but then remained unchanged for a few months. The E° -values differed between individual electrodes. In our study, fifteen electrodes were tested. Figure 2 shows the range within which all the results lay. The greatest difference in E° between two samples was about 50 mV. The potential values for the thermally prepared palladium/palladium oxide electrodes fell between the values that could be calculated for the reaction



from an E° -value of 0.79 V (determined experimentally by Hoare¹²), and an E° -value of 0.917 V (calculated from thermodynamic data¹³). Most of the electrodes in the group tested had potentials which were closer to the value calculated from Hoare's value than to the thermodynamic value.

Iridium/iridium oxide electrodes obtained by continuously cycling the potential of the iridium electrode between -0.25 and $+1.25$ V (SCE) in $0.5M$ sulphuric acid, so-called AIROF-electrodes (Anodic Iridium Oxide Film electrodes), exhibited a linear response over the ph -range 2.5–8.7, as can be seen in Fig. 3. At ph -values higher than 8.7, the potential of the electrode drifted away in a positive direction from the straight line. The correlation coefficients for the linear part of the E vs. ph plots were slightly better for monocrystalline (0.9990–0.9997) than for polycrystalline electrodes (< 0.999). No clear trend could be observed in E° or slope when electrodes were prepared by cycling voltammetrically for 100, 200 or 400 cycles, other experimental parameters being equal. The slope differed within the group of electrodes and consequently the different electrodes also had different E° -values. In general, the slopes of the E vs. ph plots obtained with polycrystalline AIROF-electrodes were lower (62–68 mV/ ph) than the slopes obtained by using monocrystalline AIROF-electrodes (69–74 mV/ ph).

Response-rates of the electrodes

From a practical point of view, the speed with which the electrode will respond to a change in ph -value of the solution is important. Our experimental set-up permitted us to make only a relative comparison of the response times of the glass electrode and the metal/metal oxide electrodes. The potential values of the electrodes were recorded for $0.02M$ orthophosphate/ $0.14M$ sodium nitrate medium subsequent to very fast addition of either strong

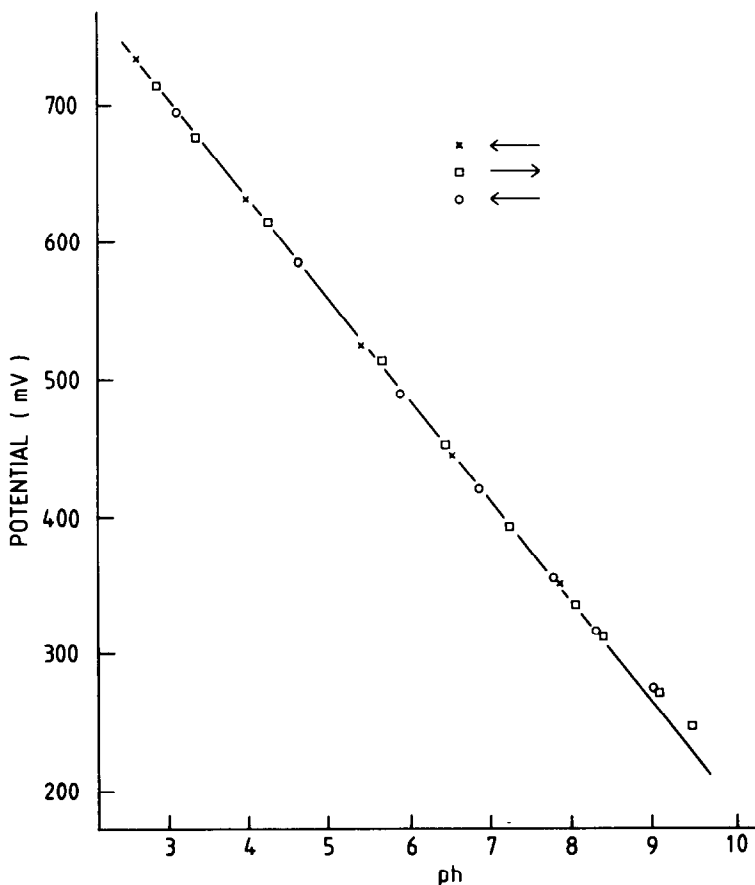


Fig. 3. Titration of 0.02M phosphate/0.14M NaNO₃. The electrode was a monocrystalline AIROF electrode obtained by cycling the potential between -0.25 and $+1.25$ V (SCE) for 200 cycles, at a scan-rate of 100 mV/sec. The data can be described by the regression line E (mV) = $714 - 71.2$ ph, $r^2 = 0.9990$. The number of experimental points was 32 and the pH range 2.5–9.5.

acid (0.05M nitric acid/0.11M sodium nitrate) or strong base (0.05M sodium hydroxide/0.11M sodium nitrate). The pH was changed in steps: from pH 6 to pH 2.5, from pH 2.5 back to pH 6, from pH 6 to pH 8.3 and from pH 8.3 back to pH 6. The response rates were evaluated from the time required for the electrodes to reach 95% of the new steady-state value after change in the composition of the solution.

Monocrystalline antimony electrodes have response times that are similar to the response time of the glass electrode used (Ingold, type HA-401 M5, Ingold, Switzerland) over the entire pH-range.

Thermally prepared palladium/palladium oxide electrodes have response times similar to the glass electrode in acidic or neutral solution. In the alkaline range, the response times are 6–10 times those for the glass electrode for increase in pH and 2–4 times longer than for the glass electrode for decrease to pH 6.

AIROF-electrodes exhibit response times similar to or slightly longer than those for the glass electrode in alkaline solution. Monocrystalline AIROF-electrodes have 3–10 times longer response times than the glass electrode in acidic solution. The number of

cycles used in preparation of the electrode had no clear effect on the response time. Polycrystalline AIROF-electrodes responded more slowly than the monocrystalline ones.

The effect of complexing agents on the electrode response

A comparison of the effects of some complex-forming ligands on the potential of the various electrode types studied can be based on the results summarized in Fig. 4. The potential of the antimony electrode is non-linear for pH < 8 in the presence of all ligands tested except TRIS. Among the ligands affecting the antimony electrode is orthophosphate, so certain standard buffer solutions cannot be used to calibrate this type of electrode. Orthophosphate had no effect on the potential of the thermally oxidized palladium electrodes, nor on the potential of the AIROF-electrodes. However, oxalate, being a strong reducing agent, will affect the potential of these electrodes. For palladium, a potential shift of between +1 and +5 mV was observed for 0.02M sodium oxalate (0.14M in sodium nitrate) relative to the response for TRIS of the same concentration.

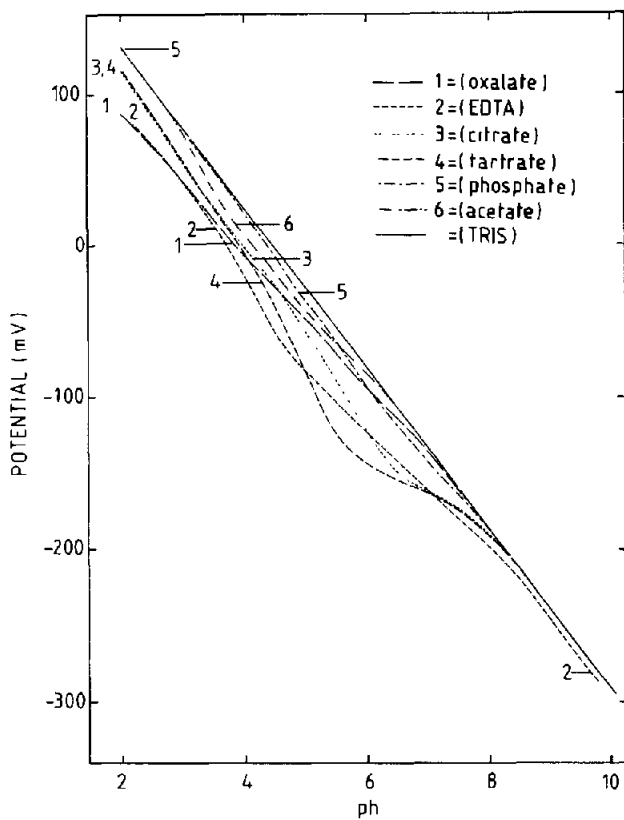


Fig. 4(a).

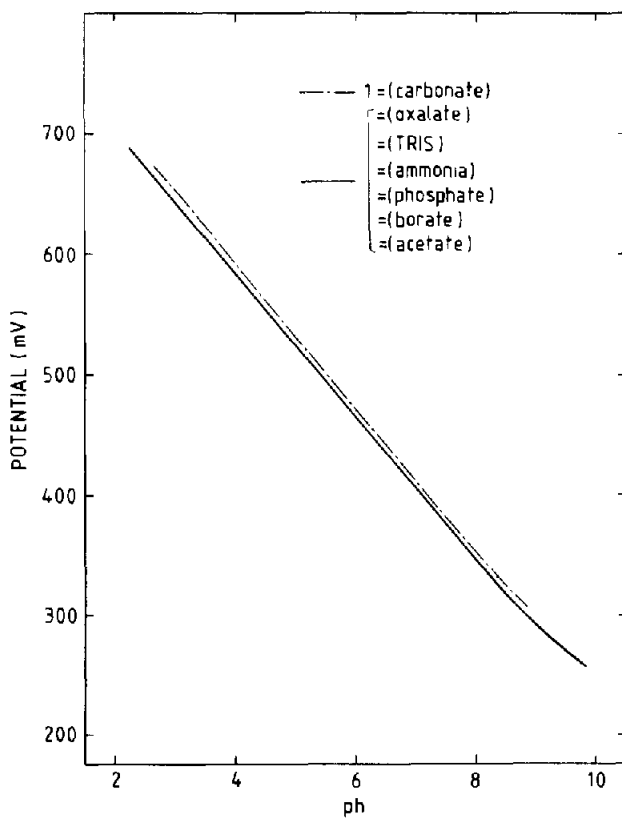


Fig. 4(b).

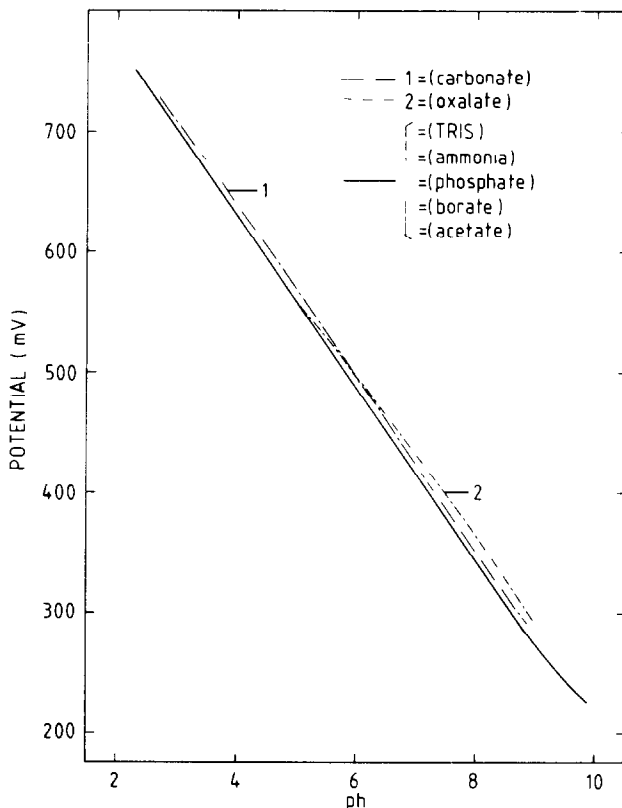


Fig. 4(c).

Fig. 4. The dependence of potential on pH for *a*, antimony/antimony oxide, *b*, palladium/palladium oxide and *c*, AIROF electrodes, in 0.14M NaNO₃/0.02M ligand medium.

Also, the response times of the palladium electrodes were longer in the presence of oxalate than in its absence. The potential of neither the monocrystalline nor polycrystalline AIROF electrode was affected by the same concentration of oxalate in the pH range 2.5–4.5, but shifts of about +10 mV were observed for neutral solution.

The HCO₃⁻/CO₂ system does not affect the pH-response of the antimony electrode but preliminary results indicate that calibration plots of the palladium electrode and the AIROF-electrode are shifted by between +5 and +8 mV in the presence of this system.

The effect of redox systems in the solution

Non-linear calibration plots were obtained for all metal/metal oxide electrodes in the presence of a redox buffer (Fig. 5). However, the effect of ferrocyanide on the antimony electrode is different from that on the palladium and AIROF electrodes. The potentials are shifted towards higher values and there is a "bump" in the curve at around pH 5. The potential *vs.* pH plots for the latter two electrode types are the same as for a platinum wire in the solution, indicating that the response is due to slight variations in the redox potential and not to the change in pH. Only at very low ferrocyanide/ferrocyanide concen-

trations did the potential of the palladium electrode differ from the potential of the platinum wire.

The palladium electrode retained its pH-response after being used in the ferricyanide/ferrocyanide buffer, but lost it after being used in a bromine/bromide redox buffer. Dissolution of the oxide phase by formation of palladium bromide complexes is the most probable explanation.

The effect of oxygen pressure on the electrode response

Various mixtures of oxygen and nitrogen [oxygen content 2, 8 and approx. 20% (air)] were bubbled through a 0.02M orthophosphate/0.14M sodium nitrate solution at pH 6.5. In this way, the oxygen response of the thermally prepared palladium electrode or the AIROF electrodes could be tested. The results are summarized in Fig. 6. The potential change 2 hr after switching from air to the mixture of 8% oxygen in nitrogen was only 3 mV for the palladium electrode and the monocrystalline AIROF electrode. Consequently, oxygen is probably not directly involved in reactions with the electrode material, or if it is, the reactions proceed very slowly. Thus in practice these electrodes are not sensitive to oxygen.

The polycrystalline AIROF electrodes behaved differently. Their oxygen response was both greater and faster. Switching from air to 8% oxygen resulted

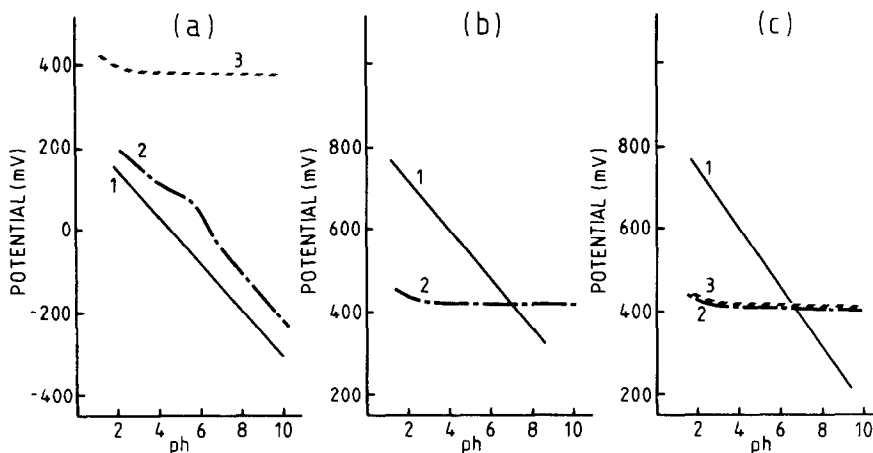


Fig. 5. The redox sensitivity of the metal/metal oxide electrodes recorded for curves 1, 0.02M TRIS/0.14M NaNO₃; curves 2, the same solution, containing also (a) 0.009M Fe(CN)₆⁴⁻ + 0.001M Fe(CN)₆³⁻ for the Sb-electrode, (b) 0.01M Fe(CN)₆⁴⁻ + 0.01M Fe(CN)₆³⁻ for the Pd-electrode, and (c) 0.001M Fe(CN)₆⁴⁻ + 0.001M Fe(CN)₆³⁻ for the AIROF electrode. A platinum-wire electrode was used as a check of the redox response (curves 3; for Pd, curves 2 and 3 coincided).

in a potential change of around 10 mV after 1 hr and switching from 2% oxygen to air again gave rise to a sharp change in the potential.

The difference between the monocrystalline and polycrystalline AIROF electrodes could be attributed

to structural differences. The oxidized electrodes displayed obvious differences under an optical microscope (Fig. 7). The monocrystalline electrode appeared uniform, with no visible colour differences, whereas the polycrystalline electrode showed a regu-

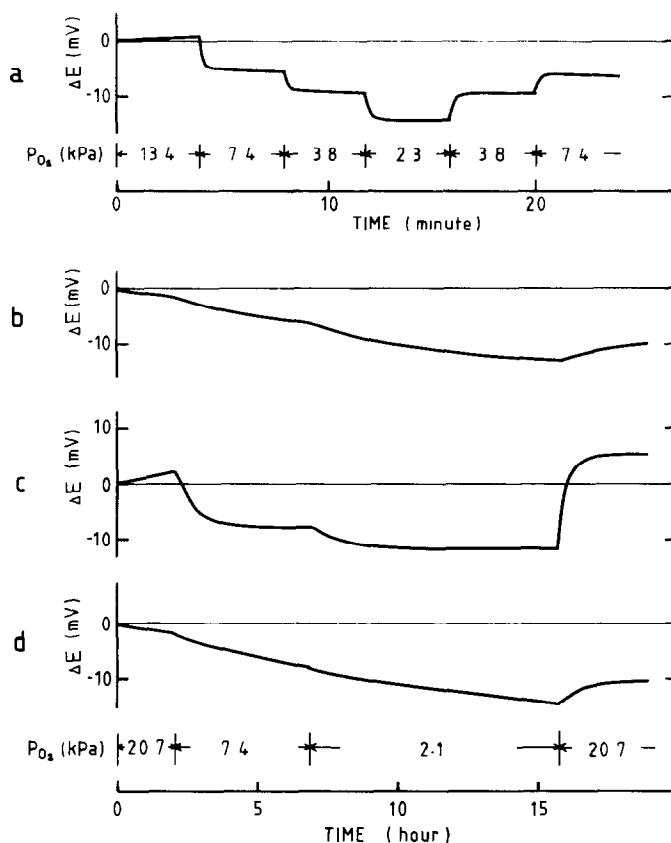


Fig. 6. The change in the electrode potential of the various types of electrode, on changing the partial pressure of oxygen above the test solution, as a function of time. The oxygen pressures used are indicated. (a) The antimony electrode, (b) the palladium electrode, (c) the polycrystalline and (d) the monocrystalline AIROF electrode.

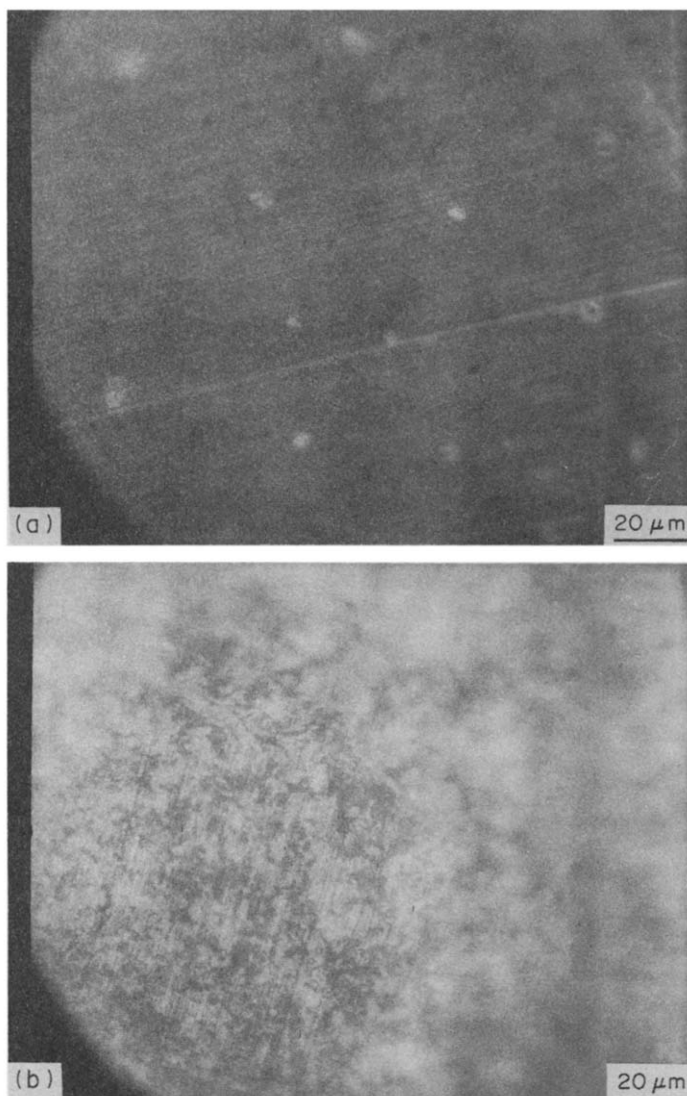


Fig. 7. Photomicrographs showing the surfaces of (a) monocrystalline and (b) polycrystalline AIROF electrodes after oxidation for 200 cycles between -0.25 and $+1.25$ V.

lar pattern of two colours (blue and yellow). It is tempting to attribute this pattern to the grain structure of the polycrystalline electrode. However, attempts to use a scanning electron microscope to analyse different parts of the electrode surfaces showed no difference between the two types of electrode.

Antimony electrodes have a definite oxygen response.¹⁴ For the monocrystalline electrodes it is comparatively fast, of the order of 15 sec, and reproducible, as seen in Fig. 6. The antimony electrodes were tested in distilled and demineralized water in order to avoid the influence of complex-forming ligands (such as orthophosphate). The gas mixtures consisted of carbon dioxide at 5.4 ± 0.1 kPa partial pressure to keep the pH constant, various partial pressures of oxygen, and nitrogen to make up the balance.

The potential response was linearly related to the logarithm of the oxygen partial pressure. For ten electrodes of 6N (*i.e.*, 99.9999%) purity, the slope of the response graph was 15.5 ± 0.7 mV per unit change in $\log p_{O_2}$ and the correlation coefficient was typically 0.99. The purity of the antimony affected the stability of the E^0 -value and also the slope of the oxygen-response curve. Electrodes of only 4N purity showed a potential drift of some mV per hr and a response slope of 13.6 ± 1.1 mV/ $\log p_{O_2}$. For polycrystalline electrodes, the oxygen response was more sluggish and irreproducible, both between electrodes and with time.

When the monocrystalline electrodes were inspected with a scanning electron microscope the 6N purity electrodes were evenly corroded, whereas impurity inclusions, mainly of lead and copper, could be found in the surface of the 4N purity electrodes. The

inclusions were standing up like towers in the otherwise generally corroded surface. The inclusions could have acted as cathodic sites for the reduction of oxygen in the corrosion reaction. The inferior stability of less pure electrodes can thus be understood, as the inclusions will in due time be undermined by selective corrosion and thereby the cathodic area will be changed.

DISCUSSION

The results presented in the previous section make it possible to compare the different types of pH-sensing electrodes on the basis of the differences in their properties.

Preparation. The monocrystalline antimony electrodes are simple to make. Antimony monocrystals are readily chipped into pieces and easily machined and ground. Orienting the monocrystals with a tightly packed crystal plane towards the solution requires some skill. The palladium and iridium electrodes are not as simple to make. The crystals are hard and difficult to machine. The observation about orientation applies to monocrystalline iridium as well as to antimony.

The ph-response. Monocrystalline antimony electrodes have a good response over the pH range 2–10. The response slope is typically 52 mV/pH. The thermally oxidized palladium/palladium oxide electrodes have a good response in the pH range 2.5–8.2 with a slope which is typically 59.6 mV/pH. AIROF electrodes can be used in the pH range 2.5–8.5. Monocrystalline AIROF electrodes give typical response slopes in the range 69–74 mV/pH, whereas the slopes for the polycrystalline electrodes are 62–68 mV/pH.

Reproducibility of the E° -values between electrodes. Within a group of monocrystalline antimony electrodes, the differences in E° values are very low. A typical standard deviation for six electrodes was 0.3 mV. The differences between electrode samples are substantially greater for the thermally oxidized palladium/palladium electrodes than for the antimony electrodes. However, the E° -value for a particular electrode is quite stable during its life-time. The E° -values of the AIROF electrodes differ, too, because the slope is different for different samples.

The response time. Monocrystalline antimony electrodes respond as fast as the glass electrode. The palladium electrode has a fast response in acidic and neutral solution, but slower in alkaline medium (pH > 8.2). Monocrystalline AIROF electrodes have response similar to or slightly slower than that of the glass electrode in alkaline solution but substantially slower response in the acidic range. Polycrystalline AIROF electrodes respond more slowly than do the monocrystalline ones.

The effect of complexing ligands. Antimony electrodes are very sensitive to several ligands, some of them components of standard buffers. None of the

common ligands except bicarbonate affects the palladium/palladium oxide electrode. The same is true for the AIROF electrode, but it is also slightly affected by oxalate in neutral and alkaline media.

The effect of redox systems present in the solution. All three types of electrode are affected by redox systems to an extent that makes their practical use difficult under such circumstances.

The effect of oxygen pressure. Palladium and monocrystalline AIROF electrodes display the same kind of slow response towards a change in the oxygen pressure. The polycrystalline AIROF electrodes show a faster and more definite oxygen response. The fastest and also most stable and reproducible oxygen response was, however, found for pure monocrystalline antimony electrodes. These can in fact be used as oxygen electrodes if the pH of the measuring solution can be kept constant. The oxygen response was not significantly different from that for a four-electron oxygen reduction process.

CONCLUSIONS

The type of metal/metal oxide pH-sensing electrode to choose in a particular case depends on the relative importance of the various properties of the electrodes. Monocrystalline antimony electrodes are the choice when fast response, good reproducibility between electrodes and stability are important. Their potential is, however, sensitive to several ligands that may be present in the solutions tested, and particular care is required in the choice of buffers for the calibration.

Thermally oxidized palladium/palladium oxide electrodes are insensitive to most common complexing agents. The slope of the calibration curve varies very little from one electrode to another, which simplifies their calibration. The preparation requires access to a furnace capable of maintaining a temperature of 750°. Monocrystalline palladium does not offer any advantage over the polycrystalline material.

Monocrystalline AIROF electrodes are also insensitive to most complexing agents. They are simple to make and to regenerate after polishing off the oxide layer. Both the slopes and the E° values differ between electrodes, which makes calibration difficult. The response time is comparatively long, particularly in acidic medium. The monocrystalline AIROF electrodes are preferable to the polycrystalline ones.

The potential of all the electrode types discussed is affected by variations in the oxygen partial pressure, reproducibly for the monocrystalline antimony electrode. Also, all types are affected by the presence of redox buffers in the solution.

Acknowledgements—Thanks are due to Professor Adam Hulanicki, University of Warsaw, Poland, for fruitful discussions during the course of this work. Financial support from the Swedish Board for Technical Development is gratefully acknowledged.

REFERENCES

1. S. Gląb, G. Edwall, P.-A. Jångren and F. Ingman, *Talanta*, 1981, **28**, 301.
2. E. Kinoshita, S. Gląb, F. Ingman and G. Edwall, *Electrochim. Acta*, in press.
3. G. Edwall, *Med. Biol. Eng.*, 1978, **16**, 661.
4. G. A. Perley and J. B. Godshalk, *U.S. Patent* No. 2,416,949, *British Patent* No. 567,722, June 10, 1942.
5. N. F. de Rooij and P. Bergveld, *Proc. Int. Conf. Nijmegen 1980*, pp. 156-165. Karger, Basel, 1981.
6. G. Papeschi, S. Bordi, M. Carlà, L. Criscione and F. Ledda, *J. Med. Eng. Tech.*, 1981, **5**, 86.
7. S. Ardizzone, A. Carugati and S. Trassatti, *J. Electroanal. Chem.*, 1981, **126**, 287.
8. A. Fog and R. P. Buck, *Sensors and Actuators*, 1984, **5**, 137.
9. T. Katsube, I. Lauks and J. N. Zemel, *ibid.*, 1982, **2**, 399.
10. W. T. Grubb and H. L. King, *Anal. Chem.*, 1980, **52**, 270.
11. C.-C. Liu, B. C. Bocchicchio, P. A. Overmyer and M. R. Neuman, *Science*, 1980, **207**, 188.
12. J. P. Hoare, *J. Electrochem. Soc.*, 1964, **111**, 611.
13. W. M. Latimer, *Oxidation Potentials*, 2nd Ed., Prentice-Hall, New York, 1952.
14. P. A. Jångren and G. Edwall, *Electrochim. Acta*, 1980, **25**, 1585.

KINETIC DETERMINATION OF TRACES OF MANGANESE IN DIFFERENT MATERIALS BY ITS CATALYTIC EFFECT ON THE METHYLENE GREEN-PERIODATE REACTION

M. HERNANDEZ CORDOBA, P. VIÑAS and C. SANCHEZ-PEDREÑO*

Department of Analytical Chemistry, Faculty of Chemistry, University of Murcia, Murcia, Spain

(Received 14 May 1985. Accepted 25 September 1985)

Summary—The oxidation of Methylene Green by sodium periodate is a slow process. A kinetic method based on the catalytic effect of manganese(II) on this reaction in the presence of 1,10-phenanthroline as activator is described. The reaction is followed spectrophotometrically by measuring the decrease in the absorbance of the dye at 620 nm. Under the optimal experimental conditions [$4 \times 10^{-3}M$ Methylene Green, $0.2M$ acetate buffer (pH 4), $2 \times 10^{-3}M$ 1,10-phenanthroline, $2.5 \times 10^{-3}M$ sodium periodate, 35°], manganese(II) between 0.2 and 30 ng/ml is determined by the tangent method. The accuracy of the method and the influence of 44 foreign ions have been studied and an equation for the kinetics of the catalysed reaction is proposed. The procedure has been applied to the determination of manganese in water, milk and beer with excellent results.

The importance of being able to determine manganese at the nanogram level is widely recognized. Recently, several catalysed reactions for this purpose have been described.¹⁻¹⁴ Although catalytic reactions offer good sensitivity, several attempts have been made to decrease the detection limit for manganese(II) by using activator ligands. The activators most widely used have been 1,10-phenanthroline,¹⁵⁻¹⁹ 2,2'-bipyridyl,¹⁹ ethylenediamine²⁰ and nitrilotriacetic acid.²¹⁻²³ The oxidation of numerous organic compounds by periodate is catalysed by Mn(II), but no report concerning the catalytic oxidation of thiazine dyes has been found.

In the present study, the manganese-catalysed Methylene Green-periodate reaction in the presence of 1,10-phenanthroline as activator is described. A new and sensitive method for the determination of manganese with a detection limit of 0.2 ng/ml is reported. The procedure has been applied to the analysis of beer, milk and tap water with excellent results.

EXPERIMENTAL

Reagents

All chemicals used were of analytical reagent grade and the solutions were prepared with doubly distilled water.

Methylene Green solution, $4 \times 10^{-4}M$. Prepared from the commercial product (Fluka, C.I. 52020) without further purification, by dissolving 0.0365 g in 250 ml of water.

Manganese(II) standard solution, $0.01M$. Prepared from the sulphate (Merck) and standardized with EDTA. Working solutions were prepared by dilution just before use.

Other reagent stock solutions were $1M$ acetate buffer (pH 4), $0.01M$ 1,10-phenanthroline and $0.05M$ sodium periodate.

Apparatus

A Pye Unicam SP8-100 double-beam spectrophotometer with 1-cm cells and constant-temperature cell-holder was used for recording spectra and absorbance-time curves.

General procedure

In a 10-ml standard flask place 1 ml of $4 \times 10^{-4}M$ Methylene Green, 2 ml of $1M$ acetate buffer (pH 4), 2 ml of $0.01M$ 1,10-phenanthroline and an appropriate volume of diluted manganese(II) solution to keep the final concentration of the cation between 0.2 and 30 ng/ml. Keep the flask in a thermostat at $35.0 \pm 0.5^\circ$ for 15 min, then add 0.5 ml of $0.05M$ sodium periodate and dilute to volume with water. Turn on the recorder, mix the solution by vigorous shaking, transfer it to the spectrophotometer cell (kept at $35.0 \pm 0.5^\circ$) and record the absorbance-time curve at 620 nm. Prepare a calibration graph by using the same procedure and obtaining $\tan \alpha = \Delta A / \Delta t$ for the initial straight-line portions of the absorbance vs. time plots.

Determination of manganese in samples

Milk. Add 10 ml of concentrated nitric acid to 10 ml of milk in a 100-ml Erlenmeyer flask and heat to near dryness. Repeat the addition of nitric acid. Cool, add 5 ml of $2M$ sulphuric acid and heat until the nitric acid is evaporated and white fumes begin to appear. To complete the destruction of the organic matter, add 2 ml of concentrated hydrogen peroxide and heat. Cool, adjust to pH 4 with sodium hydroxide, dilute to volume in a 50-ml standard flask, and analyse a suitable aliquot.

Beer. Heat 10 ml of beer in a 100-ml Erlenmeyer flask to near dryness. Then proceed as for milk, finally dilute to volume in a 15-ml standard flask, and analyse a suitable portion of this solution.

RESULTS AND DISCUSSION

Preliminary experiments showed that the oxidation of Methylene Green (MG) by periodate is a slow process which is catalysed by Mn(II), and that 1,10-phenanthroline has an activating effect on the

*To whom correspondence should be addressed.

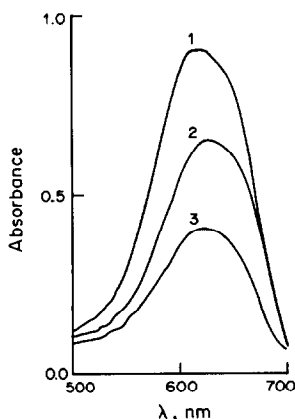


Fig. 1. Catalytic effect of manganese(II) (activation by 1,10-phenanthroline) on the Methylene Green-periodate reaction: $4 \times 10^{-5}M$ MG, $0.2M$ acetate buffer (pH 4), $2.5 \times 10^{-3}M$ $NaIO_4$, 35° . (1) Uncatalysed reaction. (2) Catalysed reaction: 20 ng/ml Mn(II). (3) Activated reaction: 20 ng/ml Mn(II), $2 \times 10^{-3}M$ 1,10-phenanthroline.

reaction. Figure 1 shows both the catalytic and activating effects at pH 4. All spectra were recorded 5 min after the start of the reaction.

The reaction was followed spectrophotometrically by measuring the decrease in the absorbance of the Methylene Green at 620 nm. The slope of the absorbance *vs.* time graph was used as a measure of the reaction rate.

Effects of reaction variables

The variation of the reaction rate with pH was studied over the range 2–11, with different Britton–Robinson buffer solutions. Figure 2 shows the results obtained in the presence and absence of manganese (20 ng/ml). The catalysed reaction rate

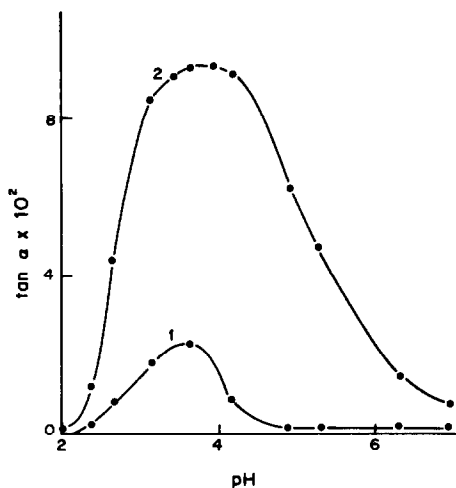


Fig. 2. Variation of the reaction rate with pH: $4 \times 10^{-5}M$ MG, $0.04M$ Britton–Robinson buffer, $2 \times 10^{-3}M$ 1,10-phenanthroline, $2.5 \times 10^{-3}M$ $NaIO_4$, 25° . (1) Uncatalysed reaction, (2) 20 ng/ml Mn(II).

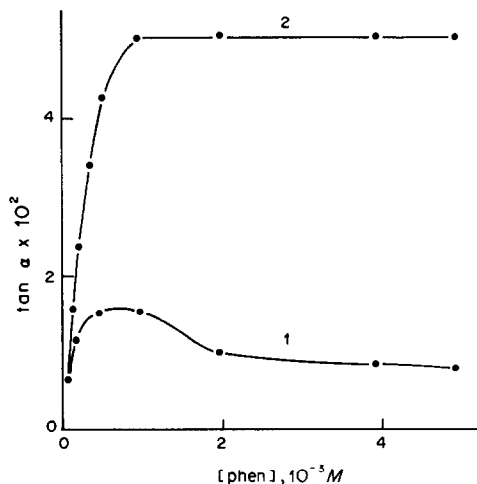


Fig. 3. Dependence of the reaction rate on the activator concentration: $4 \times 10^{-5}M$ MG, $0.2M$ acetate buffer (pH 4), $2.5 \times 10^{-3}M$ $NaIO_4$, 25° . (1) Uncatalysed reaction, (2) 20 ng/ml Mn(II).

does not depend on pH in the range 3.5–4.2. A pH of 4 was chosen because it leads to the maximum difference between the catalysed and uncatalysed reaction rates. As pointed out elsewhere,¹⁸ activation is due to the formation of catalytically active complexes of manganese with phenanthroline. The theoretical formation curves for these complexes indicate that at pH 4 the 1:1 complex predominates.

The influence of several buffer solutions at pH 4 was tested. The best results were obtained with 0.05–0.4M acetate buffer. A 0.2M acetate buffer concentration was chosen.

As can be seen in Fig. 3, the reaction rate increases linearly with 1,10-phenanthroline concentration up to $10^{-3}M$ for both the catalysed and uncatalysed reactions. Increasing the activator concentration above $10^{-3}M$ does not affect the rate of the catalysed

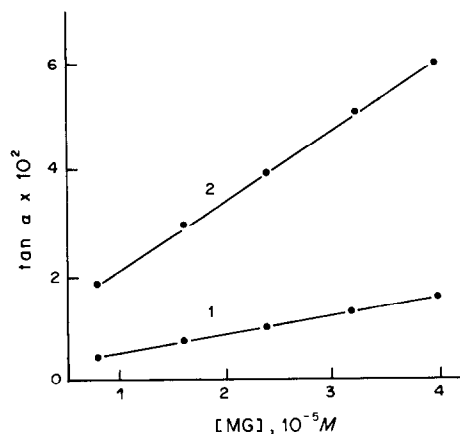


Fig. 4. Dependence of the reaction rate on the MG concentration: $0.2M$ acetate buffer (pH 4), $2 \times 10^{-3}M$ 1,10-phenanthroline, $2.5 \times 10^{-3}M$ $NaIO_4$, 25° . (1) Uncatalysed reaction, (2) 20 ng/ml Mn(II).

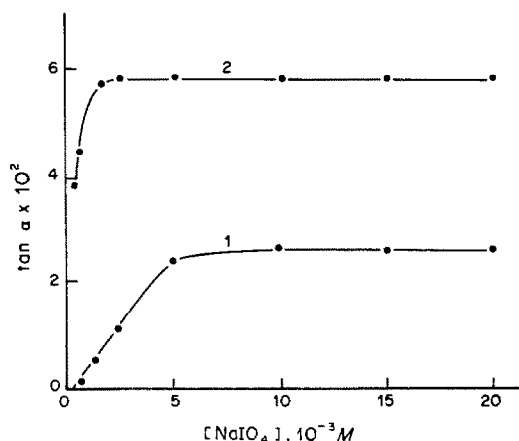


Fig. 5. Variation of the reaction rate with periodate concentration: $4 \times 10^{-5}M$ MG, $0.2M$ acetate buffer (pH 4), $2 \times 10^{-3}M$ 1,10-phenanthroline, 25° . (1) Uncatalysed reaction, (2) 20 ng/ml Mn(II).

reaction. The maximum difference between the two rates is obtained with $2 \times 10^{-3}M$ 1,10-phenanthroline, so this was the concentration chosen as optimal. The theoretical curves for formation of the Mn(II)-phenanthroline complexes show that the catalyst is completely complexed with a $2 \times 10^{-3}M$ ligand concentration at pH 4, which strongly suggests that the activator complex is the catalytic agent.

The variation of the reaction rate with MG concentration is shown in Fig. 4. Both the catalysed and uncatalysed reactions increase their rate with dye concentration in the range studied (8×10^{-6} – $4 \times 10^{-5}M$). A $4 \times 10^{-5}M$ MG concentration, which provides an adequate absorbance at 620 nm, was chosen.

Figure 5 shows the effect of sodium periodate concentration in the range 2×10^{-4} – $2 \times 10^{-2}M$. The rate of the catalysed reaction increases with periodate concentration up to $2.5 \times 10^{-3}M$ and then becomes constant. A $2.5 \times 10^{-3}M$ concentration was chosen because it gave maximum rate of the catalysed reaction and a low value for the blank reaction.

The dependence of the reaction rate on temperature was studied between 20 and 40° for the uncatalysed reaction and in the presence of Mn(II) (10 ng/ml). In the absence of catalyst, the reaction

Table 1. Dependence of the reaction rate on temperature

Temperature, $^\circ C$	$K^* \times 10^2, \text{min}^{-1}$	
	Uncatalysed reaction	Catalysed reaction
19.7	0.352	0.97 ₈
23.4	0.375	1.27 ₃
26.9	0.413	1.75 ₀
31.9	0.451	2.39 ₅
35.0	0.498	2.71 ₁
38.6	0.531	3.11 ₂

Conditions: $4 \times 10^{-5}M$ Methylene Green, $0.2M$ acetate buffer (pH 4), $2 \times 10^{-3}M$ 1,10-phenanthroline, $2.5 \times 10^{-3}M$ NaIO₄, 10 ng/ml Mn(II). $K^* = [\log(A_1/A_2)]/(t_2 - t_1)$.

rate increases slightly with temperature. The temperature effect is more pronounced for the catalysed reaction. Table 1 shows the overall pseudo first-order constants, K^* , calculated as slopes of first-order plots at different temperatures. A temperature of 35° was selected for further studies. The calculated activation energy is 12.9 ± 0.2 kcal/mole for the catalysed reaction.

Rate equation

The kinetic data obtained for the reaction variables are summarized in Table 2.

The following kinetic equation is proposed for the manganese(II)-catalysed Methylene Green-periodate reaction in the presence of 1,10-phenanthroline as activator:

$$-\frac{d[\text{MG}]}{dt} = K[\text{MG}][\text{Mn}^{2+}]$$

This equation is useful for the proposed experimental conditions; K is the rate constant for the catalysed reaction.

Calibration graph and effect of foreign ions

The absorbance-time curves at different manganese concentrations are shown in Fig. 6. Such curves were treated by different kinetic methods and the highest reproducibility was found for use of the tangent method. Under the optimal experimental conditions (see Fig. 6) a linear calibration graph was obtained for manganese between 0.2 and 30 ng/ml.

Table 2. Kinetic data for the Mn(II)-catalysed Methylene Green-periodate reaction

Variable	Uncatalysed reaction		Catalysed reaction	
	Concentration range, M	Kinetic order	Concentration range, M	Kinetic order
H ⁺	10^{-11} – 10^{-4}	+1	10^{-11} – 10^{-4}	+3/2
	10^{-4} – 3×10^{-4}	–3/2	10^{-4} – 3×10^{-4}	0
	3×10^{-4} – 10^{-2}	–1/4	3×10^{-4} – 10^{-2}	–1/3
1,10-Phenanthroline	2×10^{-4} – 10^{-1}	0	2×10^{-4} – 10^{-1}	+1/2
	10^{-1} – 5×10^{-1}	–1/2	10^{-1} – 5×10^{-1}	0
Methylene Green	8×10^{-6} – 4×10^{-5}	+1	8×10^{-6} – 4×10^{-5}	+1
Periodate	5×10^{-4} – 5×10^{-3}	+1	2.5×10^{-4} – 1.5×10^{-1}	+1/4
	5×10^{-3} – 2×10^{-2}	0	1.5×10^{-1} – 2×10^{-2}	0

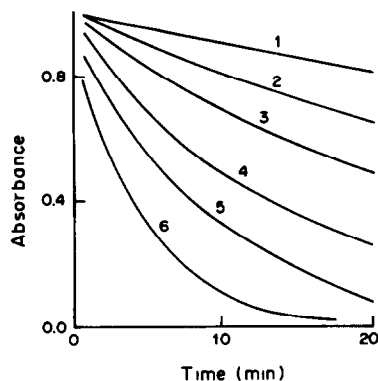


Fig. 6. Absorbance-time curves: $4 \times 10^{-3}M$ MG, $0.2M$ acetate buffer (pH 4), $2 \times 10^{-3}M$ 1,10-phenanthroline, $2.5 \times 10^{-3}M$ $NaIO_4$, 35° . $[Mn(II)]$, ng/ml: (1) 0.0, (2) 2.5, (3) 5.1, (4) 10.2, (5) 15.2, (6) 25.4.

The standard deviation of the method for 10-ng/ml manganese (10 determinations) was ± 0.5 ng/ml, with a mean relative error of $\pm 3.8\%$.

Interference by foreign ions in the system was studied with $1.5 \times 10^{-7}M$ manganese solution containing the foreign ion. The results are summarized in

Table 4. Determination of manganese in milk and beer

Sample	Manganese, ng/ml	
	Kinetic method*	AAS
Milk 1	290	278
2	237	222
3	155	166
4	340	306
Beer 1	210	225
2	191	180

*In the presence of $0.02M$ $H_2P_2O_7^{2-}$ to avoid the interference of Fe(III).

Table 3. The proposed method is quite selective. No ion interferes when present at less than 10-fold molar ratio to Mn(II). The strongest interference is caused by Fe(III), which also catalyses the MG-periodate-phenanthroline reaction. However, the tolerance for Fe(III) can be improved by using dihydrogen pyrophosphate as masking agent. In $0.02M$ $H_2P_2O_7^{2-}$ medium, a 20-fold molar ratio of Fe(III) to Mn(II) is tolerated, but it is necessary to make a new calibration graph for Mn(II) in the presence of the masking agent. Fe(III) is only tolerated in molar ratio

Table 3. Interference of foreign ions in the determination of $1.5 \times 10^{-7}M$ manganese(II)

Limiting molar ratio, $[Ion]/[Mn(II)]$	Foreign ion
2000*	ClO_4^- , NO_3^- , SO_4^{2-} , HPO_4^{2-} , $H_2P_2O_7^{2-}$, CO_3^{2-} , Cl^- , F^- , IO_3^- , ClO_2^- , BrO_3^- , VO_3^- , citrate, tartrate, As(V), Ce(IV), Cd(II), Ca(II), Sr(II), Ba(II), Mg(II), In(III), Al(III), Tl(I)
1000	As(III)†, Cr(III), Th(IV), Zn(II)
500	Br ⁻ †, MoO_4^{2-} †, WO_4^{2-} †, oxalate†, Cu(II), Ni(II)
200	$Cr_2O_7^{2-}$ †, Pb(II), Co(II), Bi(III)
100	Ce(III), Hg(II)
50	SCN^-
20	EDTA, Fe(III)§
10	I^-

*Maximum ratio tested.

†Ions which increase the reaction rate.

§In the presence of $0.02M$ $H_2P_2O_7^{2-}$.

Table 5. Determination of manganese in water, and recovery determined by the standard addition method

Sample	Mn, ng/ml	Mn taken, ng/ml	Mn added, ng/ml	Total Mn found, ng/ml	Recovery, %
Water 1	6.7	2.0	—	2.1	—
			2.0	4.2	105
			4.0	5.8	93
			6.0	8.0	98
Water 2	5.7	1.7	—	1.7	—
			2.0	3.5	90
			4.0	5.9	105
			6.0	7.8	102
Water 3	3.3	1.0	—	1.0	—
			2.0	3.1	105
			4.0	4.9	98
			6.0	6.8	97

$[\text{Fe(III)}]/[\text{Mn(II)}] = 0.2$ in the absence of $\text{H}_2\text{P}_2\text{O}_7^{2-}$. Most of the ions tested decrease the reaction rate. The ions which increase the reaction rate are indicated in Table 3.

Applications

The proposed method has been applied to the determination of manganese in milk and beer. The results obtained for 3 determinations of each sample are given in Table 4 and shown to be in good agreement with those obtained by AAS.

The method has also been applied to the determination of manganese in tap water and the results obtained by the standard addition method are summarized in Table 5.

REFERENCES

1. H. Weisz and K. Rothmaier, *Anal. Chim. Acta*, 1975, **75**, 119.
2. *Idem*, *ibid.*, 1976, **82**, 155.
3. P. N. Linnik and B. I. Nabivanets, *Zh. Analit. Khim.*, 1976, **31**, 2444.
4. C. E. Efstathiou and T. P. Hadjiioannou, *Anal. Chem.*, 1977, **49**, 414.
5. *Idem*, *Talanta*, 1977, **24**, 270.
6. T. Yamane and T. Fukasawa, *Bunseki Kagaku*, 1977, **26**, 300.
7. D. Pérez-Bendito, M. Valcárcel, M. Ternero and F. Pino Pérez, *Anal. Chim. Acta*, 1977, **94**, 405.
8. M. A. Sekheta, G. A. Milovanović and T. J. Janjić, *Mikrochim. Acta*, 1978 **I**, 297.
9. A. Ya. Sychev, V. G. Isak and U. Pfannmeller, *Zh. Analit. Khim.*, 1978, **33**, 1351.
10. I. F. Dolmanova, G. A. Zolotova and M. A. Ratina, *ibid.*, 1978, **33**, 1356.
11. J. L. Burguera and A. Townshend, *Talanta*, 1981, **28**, 731.
12. A. Moreno, M. Silva, D. Pérez-Bendito and M. Valcárcel, *ibid.*, 1983, **30**, 107.
13. A. A. Alexiev and K. L. Mutaftchiev, *Anal. Lett.*, 1983, **16**, 769.
14. S. Rubio, A. Gómez-Hens and M. Valcárcel, *Analyst*, 1984, **109**, 717.
15. A. Ya. Sychev and Ya. D. Tiginyanu, *Zh. Analit. Khim.*, 1969, **24**, 1842.
16. Ya. D. Tiginyanu and V. I. Oprya, *ibid.*, 1973, **28**, 2206.
17. R. P. Pantaler, L. D. Alfimova and A. M. Bulgakova, *ibid.*, 1975, **30**, 1584.
18. A. A. Alexiev and K. L. Mutaftchiev, *Mikrochim. Acta*, 1982 **I**, 441.
19. M. Otto, J. Rentsch and G. Werner, *Anal. Chim. Acta*, 1983, **147**, 267.
20. S. U. Kreingol'd, V. K. Komarova, V. I. Martsokha and E. M. Yutal', *Zh. Analit. Khim.*, 1974, **29**, 2324.
21. H. A. Mottola and C. R. Harrison, *Talanta*, 1971, **18**, 683.
22. D. P. Nikolelis and T. P. Hadjiioannou, *Analyst*, 1977, **102**, 591.
23. *Idem*, *Anal. Chem.*, 1978, **50**, 205.

SOLVENT EXTRACTION OF *N*-CYCLOHEXYL-*N*-NITROSOHYDROXYLAMINE (cnha) INTO SOME ORGANIC SOLVENTS AND OF THE Cu(II)-cnha COMPLEX INTO METHYL ISOBUTYL KETONE

G. RAURET, L. PINEDA, M. VENTURA and R. COMPAÑO

Department of Analytical Chemistry, University of Barcelona, Barcelona, Spain

(Received 18 March 1985. Revised 9 September 1985. Accepted 25 September 1985)

Summary—The distribution equilibria of *N*-cyclohexyl-*N*-nitrosohydroxylamine (cnha) in the water–chloroform, water–hexane, water–methyl isobutyl ketone (MIBK) and water–isopentyl alcohol systems, and of the Cu(II)-cnha complex in the water–MIBK system have been studied. From the distribution data the dissociation and distribution constants of the reagent have been calculated; their values are $pK_a = 5.55 \pm 0.10$; $\log K_{DR} = 2.46 \pm 0.05$ (chloroform), 1.76 ± 0.11 (MIBK), 1.06 ± 0.07 (hexane) and 1.48 ± 0.06 (isopentyl alcohol). In the same way the values of the distribution and stability constants of the Cu(II) complex have been obtained; $\log K_{DC} = 3.51$; $\log \beta_1 = 7.23 \pm 0.10$ and $\log \beta_2 = 12.00 \pm 0.08$. For the determination of cnha in the aqueous phase saturated with MIBK, a spectrophotometric method based on the coloured complex formed by the reagent with Fe(III) has been established. Finally, an analytical method for Cu(II) by atomic-absorption spectrometry after its extraction with cnha into MIBK, is proposed. Its detection limit is $4.6 \mu\text{g/l}$, its precision $\pm 2.1\%$ and its accuracy 97.5%. This method has been applied to the determination of the copper content in the surface water of the Congost River of Catalonia (Spain).

N-Aryl-*N*-nitrosohydroxylamines, especially cupferron and neocupferron, have been widely applied to the separation and preconcentration of inorganic ions.¹ These reagents are very good extractants but are not very stable^{2,3} so only a few authors³⁻⁸ have studied the equilibria involved in the extraction.

Buscarons and Canela^{9,10} reported that *N*-cycloalkyl-*N*-nitrosohydroxylamines behave similarly to cupferron as analytical reagents but they have the advantage of greater stability. They also studied¹¹ the extraction of several metals with *N*-cyclohexyl-*N*-nitrosohydroxylamine (cnha) and chloroform, and calculated the extraction constants for Cu(II), Pb(II) and Al(III) in the water–chloroform system. Later, Petrukhin and Kolycheva¹² gave values for the distribution constants of cnha in several water–organic solvent systems and reported qualitative data on the extraction behaviour of some metal ions with the same reagent in chloroform, using a paper chromatography method. They paid special attention to the extraction of Cu(II), determining the stoichiometry of the extracted species and the equilibrium constants involved in the extraction.

The first part of the present paper deals with the distribution of cnha in some organic solvent–aqueous buffer systems. Because of the high absorbance of methyl isobutyl ketone (MIBK) in the ultraviolet region, where cnha has its maximum absorption, a new spectrophotometric method based on the coloured complex formed by the reagent and Fe(III) has been established to determine the cnha concentration in aqueous phases saturated with MIBK.

In the second part, the extraction of Cu(II) with cnha into MIBK, which is the best solvent medium for use in atomic-absorption analysis, is reported; the distribution constant and the stability constants (in water) of the Cu(II)-cnha complexes are given. A method for the determination of Cu(II) by atomic-absorption spectrometry has been based on these results and applied to the analysis of a river water. The copper values found have been compared with those found by a standard method¹³ and by cupferron as the extractant, the experimental conditions for which in the water–MIBK system have also been established.

EXPERIMENTAL

Apparatus

A Beckman Acta MVII spectrophotometer, with 1-cm quartz cells, and a double-beam Perkin-Elmer 4000 atomic-absorption spectrophotometer, with a copper hollow-cathode lamp and an air-acetylene flame, were used. A Radiometer PHM64 pH-meter, equipped with a glass-calomel electrode pair, standardized with buffer solutions at pH 4.008 and 6.865 (25°) prepared from Merck salts according to DIN 19266, was also used.

Reagents

The sodium salt of *N*-cyclohexyl-*N*-nitrosohydroxylamine was obtained from the potassium salt (BASF) by acidification, extraction of cnha with diethyl ether, and back-extraction with aqueous sodium hydroxide solution. Addition of dioxan to the aqueous solution precipitated the white sodium salt of cnha, which was used as the reagent because perchloric acid and sodium perchlorate were to be used for acidification and ionic strength adjustment.

The copper salt of cnha was obtained by precipitation at pH 7 from aqueous solutions of the sodium salt of cnha and

copper nitrate. The copper content was determined by atomic-absorption spectrometry after dissolution of the solid in nitric acid.

A stock solution of copper (1 g/l.) was prepared by dissolving the pure metal in perchloric acid, and standardized gravimetrically.¹⁴

Chloroform, hexane, MIBK and isopentyl alcohol were purified by distillation. All other chemicals were of analytical grade and used without further purification.

Procedures

Distribution measurements of cnha. Ten ml of an aqueous buffer solution containing the sodium salt of cnha (9×10^{-5} – $10^{-2}M$), with an ionic strength of 0.1 and saturated with the organic solvent, and 10 ml of organic solvent saturated with water, were shaken together at $25.0 \pm 0.1^\circ$ in 30-ml glass-stoppered vials, long enough for equilibrium to be attained. After phase separation the cnha concentration in the aqueous phase was determined by one of the following methods.

Method A (for chloroform, hexane and isopentyl alcohol). An aliquot of the aqueous phase was adjusted to pH 10 with sodium hydroxide solution and diluted to 25 ml. The absorbance was measured at 246 nm against a blank and compared with that of a standard.

Method B (for MIBK). Into a 25-ml standard flask, an appropriate volume of the aqueous phase to give a final cnha concentration between 10^{-2} and $10^{-4}M$, enough 1M perchloric acid to make the final solution 0.1M in acid, 5 ml of butyl glycol and 2.5 ml of a 1-g/l. solution of Fe(III) were introduced and diluted to the mark with water saturated with MIBK. An analogous solution without cnha was prepared as a blank. The absorbance was measured at 418 nm after 15 min.

Distribution of Cu(II) complex. Ten ml of aqueous phase saturated with the organic solvent and containing appropriate concentrations of copper and the sodium salt of cnha, were shaken with either 1 or 10 ml of MIBK saturated with water for 10 min in a thermostatic bath at $25.0 \pm 0.1^\circ$. The pH of the aqueous phase was adjusted with perchloric acid, and sodium perchlorate was added to give a constant ionic strength of 0.1. A phase-volume ratio, V_w/V_o , of 1 was used in the experiments at pH 1–2, and of 10 for the pH range from 2 to 9. After phase separation, the equilibrium concentrations of copper in the organic and aqueous phases were determined by atomic-absorption spectrometry at 324.8 nm. It had been checked previously that the pH of the aqueous

phase had no influence on the absorption readings. Solutions of the copper salt of cnha in MIBK were used to obtain a calibration graph for the metal determination in the organic phase.

Determination of copper in water. A 100-ml sample of water, 2 ml of 1M acetic acid–sodium acetate buffer (pH 5) 1 ml of 0.1M aqueous cnha or cupferron solution and 10 ml of MIBK saturated with water were transferred into a separatory funnel. After 1 min of shaking, the aqueous phase was discarded and the organic phase was aspirated into the flame of the atomic-absorption spectrophotometer. Reference solutions prepared by extracting aqueous phases containing between 10 and 500 $\mu\text{g/l. Cu(II)}$ were used for the calibration. Measurements were made at 324.8 nm.

RESULTS AND DISCUSSION

Spectrophotometric determination of cnha with Fe(III)

Iron(III) forms a yellow complex with cnha which is soluble in water in presence of 20% v/v butyl glycol. Its absorption spectrum shows a maximum between 414 and 420 nm. The acidity of the solution influences the colour intensity, 0.1M acid being optimum. In order to avoid high blank absorbances, a final Fe(III) concentration of 100 mg/l. is used. In these conditions the absorbance remains stable for more than 1 hr and Beer's law is obeyed for cnha up to 150 mg/l. ($\log \epsilon = 2.84$). The precision of the method is $\pm 0.3\%$.

Several ions, particularly phosphate and acetate, interfere in the proposed method, so no buffer solutions containing these substances were used in the distribution equilibria studies of cnha in the MIBK–water system.

Distribution of cnha in water–organic solvent systems

Effect of shaking time. The absorbance of the aqueous phase after equilibration with the organic solvent does not depend on the shaking time, so equilibrium is attained almost immediately when the phases are shaken.

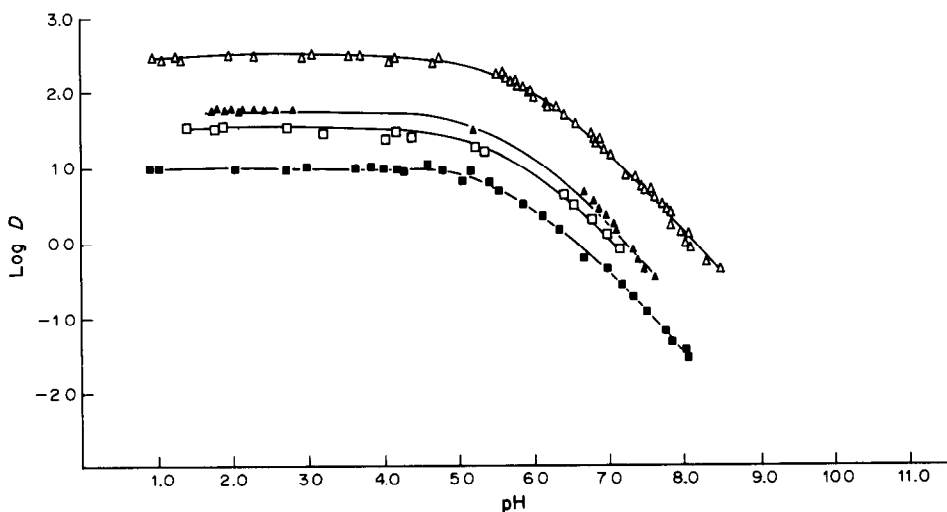


Fig. 1. Distribution of cnha between aqueous solutions and organic solvents: \triangle chloroform; \blacktriangle MIBK; \square isopentyl alcohol; \blacksquare n-hexane.

Table 1. Distribution and dissociation constants of cnha

Solvent	ϵ	log K_{DR}			pK_a	
		Graphical calcn.	Numerical calcn.	Other values	Graphical calcn.	Numerical calcn.
Chloroform	4.9	2.50	2.46 ± 0.05	$1.98 \pm 0.03^*$ 2.18† 2.14§	5.70	5.67 ± 0.06
MIBK	13.1	1.76	1.76 ± 0.11	1.92†	5.62	5.44 ± 0.16
n-Hexane	1.9	1.02	1.06 ± 0.07	$0.9 \pm 0.1^*$	5.62	5.55 ± 0.10
Isopentyl alcohol	14.8	1.59	1.48 ± 0.06		5.60	5.73 ± 0.08

ϵ = Dielectric constant.

*Petrakhin and Kolycheva.¹²

†Value for cupferron.¹⁵

§Value for cupferron.²

Influence of the reagent concentration. The distribution ratios of cnha in the chloroform, hexane and MIBK systems with water are not affected by variation in reagent concentration in the range 10^{-4} – $10^{-2}M$, so molecular association in the organic phase seems negligible.

The pH-dependence of the distribution equilibria. Assuming that there is no reagent polymerization in the organic phase, then for a monobasic acid such as cnha the distribution ratio is related to the pH of the aqueous phase according to $D = K_{DR}/(1 + K_a/[H^+])$, where K_{DR} is the distribution constant and K_a is the dissociation constant of the reagent. Figure 1 shows the plots of log D vs. pH for the n-hexane, chloroform, MIBK and isopentyl alcohol systems. When $[H^+] \gg K_a$, the distribution ratio is independent of the pH and $D = K_{DR}$; in this region the molecular species is dominant in both phases. When $[H^+] \ll K_a$ the slope of the linear segment is -1 , and corresponds to the region where the anionic species is dominant in the aqueous phase.

Distribution and ionization constants of cnha. Table 1 gives the log K_{DR} values determined in this work, together with those found in the literature for the same reagent¹² and for cupferron.^{2,15} The results were obtained by means of Sillén's graphic method¹⁶ and the LETAGROP-DISTRIBUTION program.¹⁷ Our value for the n-hexane system agrees with the one found by Petrakhin and Kolycheva¹² but the values for the chloroform system differ. According to these authors this difference may be attributed to different mixtures of cnha tautomers co-existing in the solutions, which may affect the distribution ratio.¹⁸

K_{DR} for cnha in the chloroform system is higher than the values for the other solvent systems, and also than the reported K_{DR} values^{2,15} for cupferron. In the MIBK system the K_{DR} value of cupferron is higher than that of cnha. This behaviour can be attributed to specific solvent-solute interactions. If we consider that cnha has a more basic nitrogen atom and a less acidic proton than cupferron, and that the solvent donorities and solvent-acceptor numbers¹⁹ of chloroform and acetone (which should give specific interactions similar to those of MIBK) are 17.0 and <1 , and 12.5 and 23.1 respectively, we can conclude that

the interactions of cnha with chloroform are stronger than those of cupferron. The reverse is valid for MIBK, which agrees with the experimental values found in this work for the distribution constants.

The ionization constant of cnha is also obtained by the methods applied for the determination of K_{DR} . The values are given in Table 1 and agree with the values found by Buscarons and Canela¹¹ except for the isopentyl alcohol system, a fact which can be attributed to the high solubility of this solvent in water.

Distribution of the copper complex in the water-MIBK system

In the ranges of pH and metal concentration studied in this work, the presence of hydroxo-complexes of Cu(II) can be neglected.²⁰ Assuming that only mononuclear species are formed, the distribution ratio will be given by

$$D = \frac{[M]_{o,tot}}{[M]_{w,tot}} = \frac{\sum_n \sum_m [ML_n(HL)_m]_o}{\sum_n [ML_n]_w} \quad (1)$$

where M represents the metal, HL the extracting agent and the subscripts o and w denote the organic and aqueous phases respectively. If only one species is extracted and the metal is present in the aqueous phase predominantly as the cation M^{n+} , equation (1) can be written as

$$D = \frac{[ML_n(HL)_m]_o}{[M^{n+}]_w} = \frac{K_m K_{DC} \beta_n K_a^n [HL]_o^{(m+n)}}{K_{DR}^n [H^+]_w^n} = \frac{K_{ex} [HL]_o^{(m+n)}}{[H^+]_w^n} \quad (2)$$

where β_n is the formation constant of ML_n in the aqueous phase, K_{DC} its distribution constant, K_m the adduct formation constant in the organic phase, K_a and K_{DR} the dissociation and distribution constants of the reagent, respectively, and K_{ex} the extraction constant of $ML_n(HL)_m$. Taking logarithms in equation (2) gives

$$\log D = \log K_{ex} + (m+n) \log [HL]_o + n \text{ pH} \quad (3)$$

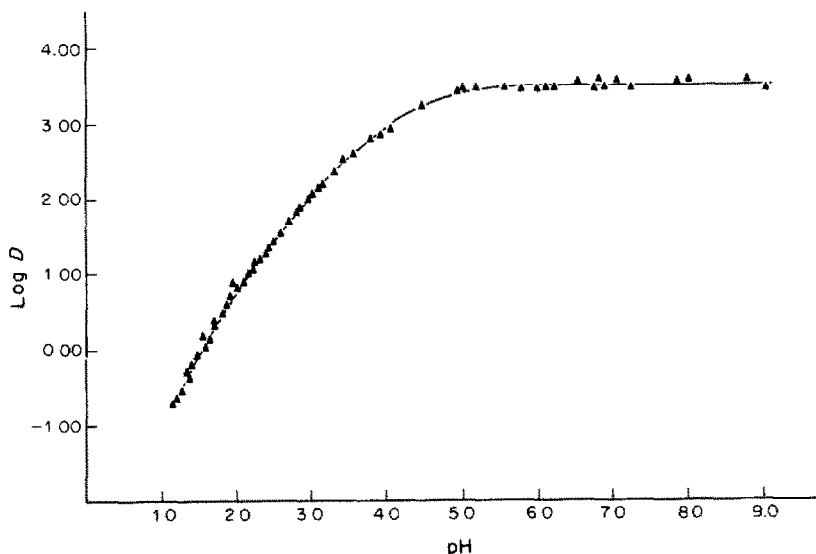


Fig. 2. Influence of pH on the distribution ratio. Initial [cnha] in the aqueous phase: $1.0 \times 10^{-2}M$ between pH 1 and 2 (where $V_w/V_o = 1$) and $1.0 \times 10^{-3}M$ at pH > 2 (where $V_w/V_o = 10$). Initial [copper]: $1.28 \times 10^{-4}M$.

If $\log D$ is plotted *vs.* pH at constant $[HL]_o$, or *vs.* $\log[HL]_o$ at constant pH, straight lines with slopes n and $(m+n)$, respectively, are obtained. When the pH is increased, the complexes with the extracting agent become the predominant species in the aqueous phase, and the distribution ratio is given by

$$D = \frac{K_{ex}[HL]_o^{(m+n)}}{[H^+]_w^n \left(1 + \sum_n \beta_n [L^-]^n \right)} \quad (4)$$

When species other than ML_n can be neglected in the aqueous phase, a plot of $\log D$ *vs.* pH will give a straight line with a slope of zero, in this case

$$\log D = \log K_{DC} \quad (5)$$

Influence of shaking time. The $\log D$ values obtained at pH 1.10, with the shaking time varied between 1 and 20 min, show that distribution equilibrium is attained after 1 min of shaking. In subsequent experiments an extraction time of 10 min was adopted.

Composition of extractable complexes. To determine the composition of the extractable complexes, experiments were done in which the pH of the aqueous phase and the initial concentrations of Cu(II) and cnha were successively varied. Varying the copper concentration had no effect on the distribution ratio, suggesting that only mononuclear species were extracted in the range of metal concentrations studied (2.46×10^{-6} – $6.15 \times 10^{-5}M$).

In Fig. 2 $\log D$ is plotted *vs.* pH. The curve shows three segments, which differ in slope. At pH 1–2 a straight line with slope of 1.92 points to the validity of equation (3) and indicates that $n = 2$. Between pH 2 and 4 the distribution curve tends towards a slope of 1. Finally, at pH > 5, the distribution ratio becomes independent of the pH.

To determine the value of m in equation (3), a

series of extractions with cnha concentrations between 10^{-3} and $3 \times 10^{-2}M$, at a pH value near to 1, was performed. Despite the fact that the initial pH was the same for all the samples, small differences were found in the equilibrium pH values. For this reason $\log D - 2 \text{ pH}$ is plotted *vs.* $\log[HL]_o$ in Fig. 3. From the values of pH, initial concentration ($[HL]_{o,in}$) of cnha and equilibrium copper concentration in the organic phase, the $[HL]_{o,eq}$ values were calculated by means of the equation

$$[HL]_{o,eq} = \frac{[HL]_{o,in} - 2[Cu]_{o,eq}}{1 + (1 + K_a/[H^+])/K_{DR}} \quad (6)$$

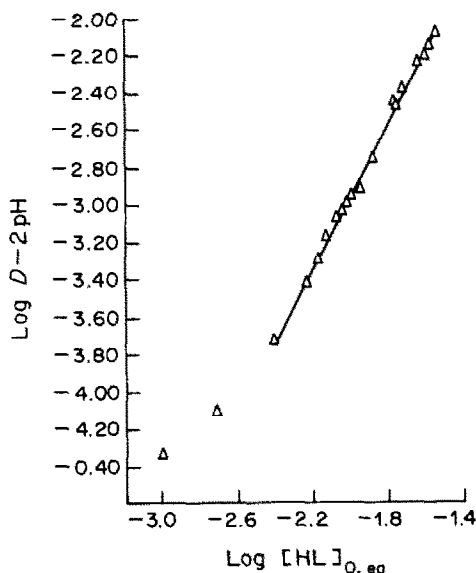


Fig. 3. Distribution of Cu(II) as a function of the equilibrium [cnha] in the organic phase. Initial pH = 1.10. Initial [copper]: $1.28 \times 10^{-4}M$.

Table 2. Survey of the equilibrium constants for the extraction of Cu(II) with cnha into MIBK

Method	$\log K_{\text{ex}}$	$\log K_{\text{DC}}$	$\log \beta_1$	$\log \beta_2$
Graphical	1.05	3.50	7.13	11.90
LETAGROP	1.11 ± 0.06	3.51	$7.7 \pm 0.6^*$	$14.9 \pm 0.3^*$
			7.23 ± 0.10	12.00 ± 0.08

*Petrukhin and Kolycheva.¹²

A phase-volume ratio of 1 was used in this series of experiments. The values of K_{DR} and K_a are given in Table 1. The points in Fig. 3 fall on a straight line with slope 1.92, indicating $m + n = 2$ and accordingly $m = 0$. Hence no adducts with the extracting agent are formed and the stoichiometry of the extracted complex is CuL_2 .

Influence of the ionic strength. The values of $\log D$ obtained at constant pH and cnha concentration were independent of the ionic strength of the aqueous phase, varied between 0.05 and 1.0M by addition of sodium perchlorate, also showing that the perchlorate does not take part in the distribution equilibrium.

Calculation of the equilibrium constants. From the distribution data the extraction (K_{ex}) and the distribution (K_{DC}) constants, as well as the stability constants of the species CuL_2 and CuL^+ in the aqueous phase, were obtained by graphical and numerical methods. According to equation (3) the K_{ex} value can be calculated from the intercept of the straight line obtained by plotting $\log D$ vs. pH when the predominant species in the aqueous phase is Cu^{2+} . From the segment of slope 2 in Fig. 2 a value of 1.05 for $\log K_{\text{ex}}$ is obtained.

The Sillén curve-fitting method¹⁶ was used to obtain the values of K_{DC} , β_1 and β_2 shown in Table 2. In Fig. 4, $\log D$ vs. $\log [L^-]$ is plotted, superimposed on the normalized curves of $\log D^*$ vs. $\log u$, at different values of the parameter p , in the conditions of best fit. The normalized variables and p are defined by $D^* = D/K_{\text{DC}}$; $u = \beta_2^{1/2} [L^-]$; $p = \beta_1 / \sqrt{\beta_2}$.

The values of the constants obtained graphically were refined by means of the program LETAGROP-DISTRIBUTION;¹⁷ the final values and their standard deviations are given in Table 2. There is good agreement between the constants obtained by the two methods. Figure 5 shows the difference $\log D_{\text{calc}} - \log D_{\text{exp}}$.

The value of the distribution constant of the species CuL_2 in the system studied is higher than that obtained when chloroform is used as organic solvent.¹² As can be seen in Table 2, the value of β_1 calculated in this work agrees with that obtained by Petrukhin and Kolycheva¹² but the values of β_2 differ. However, the number of experimental points treated in this paper to obtain the β_2 value is much greater than that used in the Russian work, and mainly at ligand concentrations in which CuL_2 predominates in the aqueous phase.

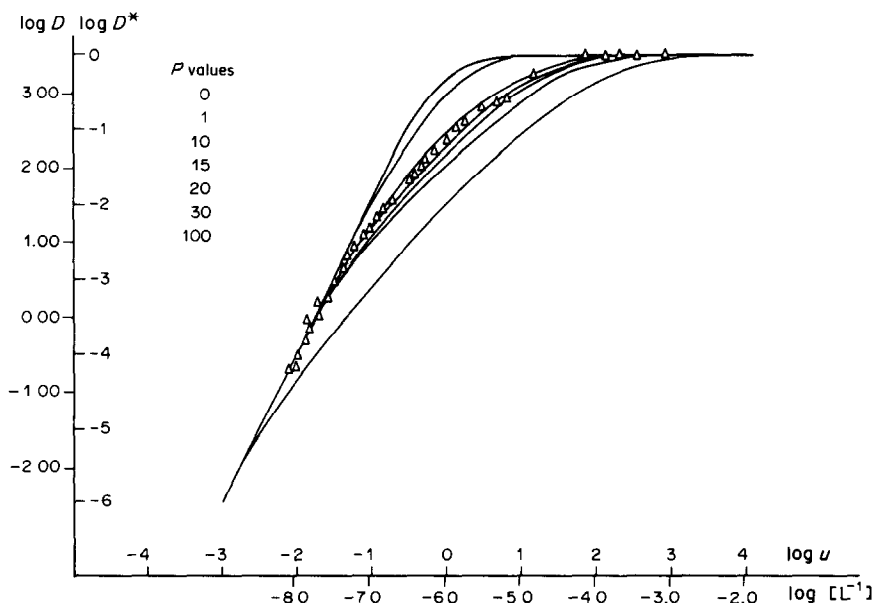


Fig. 4. The experimental curve of $\log D$ vs. $\log [L^-]$ superimposed on the normalized curves $\log D^*$ vs. $\log u$, at different values of the parameter p , in the conditions of best fit. $D^* = 1/(1 + p/u + 1/u^2)$.

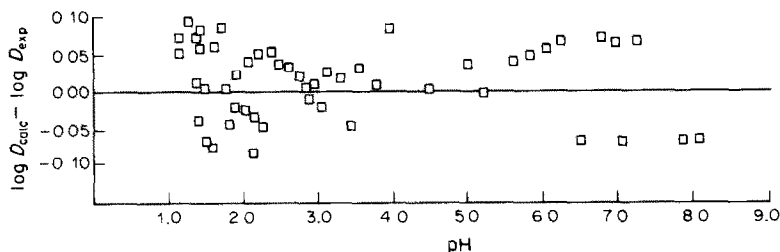


Fig. 5. The differences between the measured values of the distribution ratio of Cu(II) and those calculated by the program LETAGROP, as a function of pH.

Determination of copper by atomic-absorption spectrometry

The high values of the recovery factor (>99.9%) in the copper extraction with cnha in MIBK at pH > 4, suggested use of the system for determination of this element in natural waters.

Because of the lack of stability of cupferron in acid medium, especially in presence of MIBK, which accelerates decomposition of the reagent, it was not possible to make a complete study of the distribution equilibria of the copper-cupferron complex. However, to compare the extractions with cnha and cupferron, the recovery factor with the latter was determined at several pH values between 2.7 and 6.7; it ranged between 99.3 and 103.7% and showed that extraction is quantitative under these conditions, even though partial decomposition of the reagent takes place.

The accuracy, precision and detection limit for the determination of copper in water by atomic-absorption spectrometry after extraction with cnha or cupferron into MIBK were compared with the values for a standard method with ammonium pyrrolidinedithiocarbamate (apdc) as extracting agent.¹³ The accuracy was evaluated by known-addition recovery experiments with 5, 10 and 15 μg of copper

added to 100 ml of water containing 5 μg of the metal. The precision (relative standard deviation) was determined by extracting ten identical samples with a copper content of 244 $\mu\text{g}/\text{l}$. and making three absorbance readings for each sample. The detection limit was calculated according to IUPAC²¹ as three times the standard deviation of the blank (determined from triplicate measurement of each of ten blanks). The results are summarized in Table 3. It can be concluded that the determination of Cu(II) in natural waters by atomic-absorption spectrometry after extraction with cnha or cupferron in MIBK is a good method, with accuracy and precision better than those of the APHA standard method and detection limits of the same order of magnitude as for that method.

Determination of copper in the Congost River surface water

The Congost River is a long tributary of the Besos River. Both cross a highly industrialized area in the east of Catalonia (Spain), and their waters are very polluted. The samples were taken at five points along the river, every month from July to December of 1982, as described in a previous paper.²² Figure 6 shows the copper content of the river water, ex-

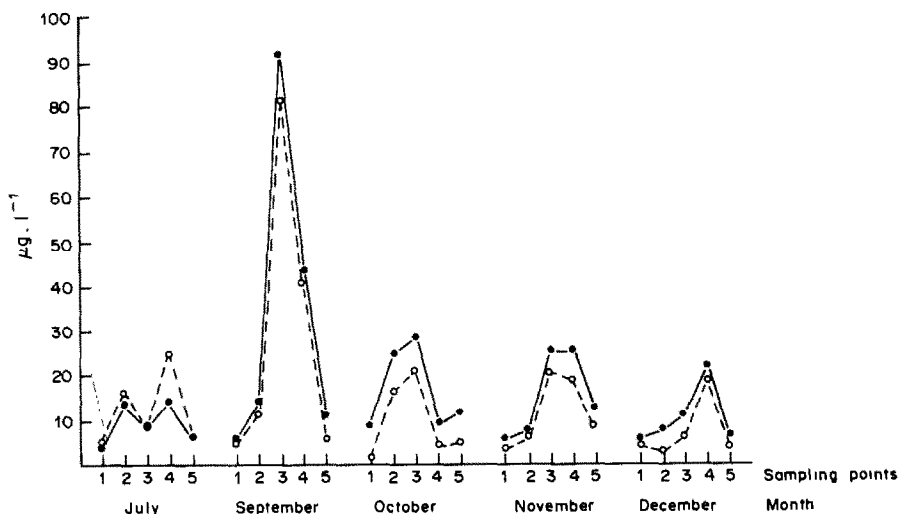


Fig. 6. Copper content in the Congost River, determined by atomic-absorption spectrometry after extraction with cnha (●) or apdc (□) into MIBK.

Table 3. Characteristics of the methods for determination of copper with cnha, cupferron or apdc

	cnha	cupferron	apdc
Detection limit, $\mu\text{g/l.}$	4.6	2.9	0.8
Precision,* %	2.1	1.7	3.2
Accuracy,†	97.5	98.2	86.3

*Expressed as the relative standard deviation.

†Expressed as the recovery determined by the known-addition method.

pressed in $\mu\text{g/l.}$, obtained with cnha and apdc as extracting agents. It can be concluded that there are no significant differences between the results obtained with the two reagents. All the values in Fig. 6 are below the maximum level permitted by the Spanish standards for the quality of river waters.

REFERENCES

1. T. Sekine and Y. Hasegawa, *Solvent Extraction Chemistry*, pp. 437–440. Dekker, New York, 1977.
2. D. M. Kemp, *Anal. Chim. Acta*, 1962, **27**, 480.
3. S. J. Lyle and A. D. Shendrikar, *ibid.*, 1966, **36**, 286.
4. N. H. Furman, W. B. Mason and J. S. Pecola, *Anal. Chem.*, 1949, **21**, 1329.
5. J. Starý and J. Smižanská, *Anal. Chim. Acta*, 1963, **29**, 545.
6. G. K. Schweitzer and L. H. Howe, *ibid.*, 1967, **37**, 316.
7. A. T. Pilipenko, E. A. Shpak and A. I. Samchuk, *Ukr. Khim. Zh.*, 1972, **38**, 1052.
8. A. A. Nadezhoda, K. P. Ivanova and F. P. Gorbenko, *ibid.*, 1980, **46**, 1315.
9. F. Buscarons and J. Canela, *Anal. Chim. Acta*, 1973, **67**, 349.
10. *Idem, ibid.*, 1974, **71**, 468.
11. *Idem, ibid.*, 1974, **70**, 113.
12. O. M. Petrukhin and N. V. Kolycheva, *Zh. Analit. Khim.*, 1980, **35**, 1478.
13. APHA-AWWA-WPCF, *Standard Methods for the Examination of Water and Waste-water*, 15th Ed., American Public Health Association, Washington, 1980.
14. A. I. Vogel, *Textbook of Quantitative Inorganic Analysis*, 4th Ed., p. 424. Longmans, London, 1978.
15. D. Dyrssen, *Svensk Kem. Tid.*, 1952, **64**, 213.
16. L. G. Sillén, *Acta Chem. Scand.*, 1976, **10**, 186.
17. D. Hay Liem, *ibid.*, 1971, **25**, 1521.
18. O. M. Petrukhin and N. V. Kolycheva, personal communication.
19. V. Gutmann, *The Donor–Acceptor Approach to Molecular Interactions*, Plenum Press, New York, 1978.
20. C. F. Baes and R. E. Mesmer, Jr., *The Hydrolysis of Cations*, p. 267. Wiley, New York, 1976.
21. IUPAC, *Compendium of Analytical Nomenclature*, p. 117. Pergamon Press, Oxford, 1978.
22. R. Rubio, J. Hugué and G. Rauret, *Water Res.*, 1984, **18**, 423.

SELECTIVE SEPARATION OF METAL IONS BY USE OF CHELATE-FORMING RESINS PREPARED BY MODIFICATION OF CONVENTIONAL ANION-EXCHANGERS WITH SPADNS AND ORANGE II

KRYSTYNA BRAJTER and EWA DĄBEK-ZŁOTORZYŃSKA

Department of Chemistry, University of Warsaw, Pasteura 1, 02-093 Warsaw, Poland

(Received 30 January 1985. Revised 27 August 1985. Accepted 25 September 1985)

Summary—Anion-exchangers loaded with SPADNS or Orange II or SPADNS + Nitroso-R salt are used for selective separation of bismuth and cadmium, which are then determined by AAS.

Extensive investigations have been made¹⁻¹⁰ of chelate-forming resins prepared by modification of the common anion-exchange resins with sulphonated aromatic compounds which display high affinity for anion-exchangers. When immobilized on an exchange resin these reagents transform it into a selective exchanger which prefers some metal ions much more than others, according to the complexing ability of the immobilized agent. Ferron, Nitroso-R salt, Alizarin S, chromotropic acid, Bromopyrogallol Red, Tiron and Xylenol Orange have been used in this way in our laboratory. The usefulness of this technique has been confirmed by others.¹¹⁻¹⁹

This paper describes the properties of the chelating resin obtained by modification of the macroporous anion-exchanger Amberlyst A-26 with SPADNS [2-(*p*-sulphonylazo)-1,8-dihydroxy-3,6-naphthalenedisulphonic acid] and of the anion-exchanger Varion AT-400 with Orange II [*p*-(2-hydroxy-1-naphthylazo)benzenesulphonic acid]. Both reagents contain oxygen and nitrogen atoms as electron-donors. The complexation ability of SPADNS and Orange II depends strongly on pH. In acid medium they react with only a limited number of metal ions. As a result, the SPADNS resin reacts with very few metal ions in acid medium, for instance Bi(III), as we show in this paper.

We also describe the usefulness of the resin obtained by the modification with two complexing reagents, SPADNS and Nitroso-R salt for the separation of metal ions. Such a procedure enables retention of a great number of metal ions on the resin bed and if a "reverse separation method" is used (only one metal ion passing into the effluent, the others being retained) selective separation of some metal ions is possible. We have shown that selective

separation of Cd(II) from other metal ions is thus possible.

EXPERIMENTAL

Reagents

SPADNS, Orange II and Nitroso R-salt (NRS) were recrystallized from ethanol.

The solutions of metal ions were prepared by dissolving appropriate weights of the analytical grade sulphates or nitrates, and standardized by EDTA titration or atomic-absorption spectrometry (AAS).

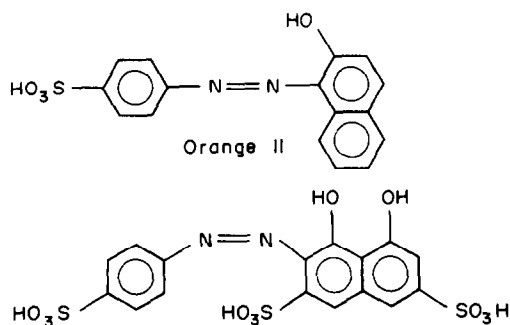
Amberlyst A-26 (Rohm and Haas) macroporous strongly basic anion-exchanger in chloride form (0.45-0.55 and 0.1-0.2 mm particle size, 3.46 meq/g capacity) and the strongly basic anion-exchanger Varion AT-400 (Nitro-Kemia, Hungary) in chloride form (0.4-0.5 mm particle size, 3.45 meq/g capacity) were used for preparation of the chelating resins.

Preparation of chelating resin

A mixture of chelating agent and anion-exchanger was shaken at room temperature until the supernatant liquid became colourless. The resin was then filtered off, washed with water and methanol, air-dried and stored in the refrigerator.

Determination of exchange capacity for complexing agents

In the batch method a 200-mg portion of anion-exchanger was stirred with 20 ml of a 0.02M solution of the chelating



Scheme 1.

*This paper was presented at Euroanalysis V, Cracow, 26-31 August 1984.

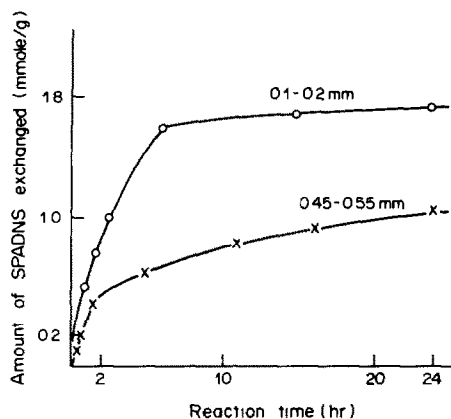


Fig. 1. Adsorption of SPADNS on the anion-exchange resin.

agent, and the concentration of the latter in the liquid phase was measured at regular intervals by spectrophotometry (Fig. 1). In the dynamic method 1000 ml of 0.002M solution of the chelating agent was passed through a bed of 1.0 g of ion-exchanger, and 100-ml fractions of the effluent were analysed by spectrophotometry (Table 1).

Stability of the modified resin in mineral acid and sodium chloride media

The resin (500 mg) loaded with the complexing agent (0.2 mmole per g of resin) was packed in a column (8 mm bore tube fitted with a stopcock), and 100 ml of mineral acid or sodium chloride solution of known concentration were passed through it at a flow-rate of 1.0 ± 0.1 ml/min. The amount of complexing agent appearing in the effluent was determined spectrophotometrically (Table 2).

Determination of exchange capacity of SPADNS resin for bismuth (III)

Portions of SPADNS-Amberlyst resin (200 mg) loaded with 0.10, 0.20 and 0.40 mmole of SPADNS per g of resin were shaken for about 12 hr with Bi(III) in 3:1 molar ratio to SPADNS, at pH = 1.5. The amount of Bi(III) left in solution was determined 12 hr later.

Determination of retention of metal ions on modified resins

A portion of loaded resin corresponding to 200 mg of the original chloride-form resin was shaken for 12 hr with 20 ml of the metal ion solution, the concentration of which corresponded to a 1:10 molar ratio of metal ion to ligand immobilized in the resin phase. The concentration of metal ion left in solution was determined 12 hr later by AAS. This period was found to be adequate for reaching equilibrium.

Table 1. Total amount of chelating agent loaded on anion-exchanger (chloride form)

Chelating agent	Total amount loaded, mmole/g	
	Batch method	Elution method
Orange II*	0.8 ± 0.1	0.6 ± 0.1
SPADNS†	$1.0 \pm 0.1§$	—
	$1.7 \pm 0.1‡$	$1.8 \pm 0.1‡$
NRS	$1.8 \pm 0.1§$	—

*The total capacity of Varion AT-400 (0.4–0.5 mm) is 3.45 meq/g.

†The total capacity of Amberlyst A-26 is 3.46 meq/g.

§Resin beads 0.45–0.55 mm diameter.

‡Resin beads 0.1–0.2 mm diameter.

Table 2. Resistance of the loaded resins to mineral acids and sodium chloride (0.5 g of resin; capacity of chelating agent 0.2 mmole/g; 100 ml of eluent)

Eluent	Concentration, M	Release, %		
		Orange II	SPADNS	NRS
HCl	0.1	0.1	0.1	0.1
	0.5	—	0.1	7.0
	1.0	—	1.0	28
HNO ₃	0.1	0.5	0.1	4.0
	0.5	1.0	4.0	52
	1.0	3.0	16	80
HClO ₄	0.1	1.0	26	94
	0.5	—	80	—
	1.0	—	99	—
NaCl	0.1	—	0.1	1.0
	0.5	—	0.5	6.0
	1.0	—	2.0	22

Determination of Bi(III) in Pb(NO₃)₂

A 0.5-g sample of lead nitrate was dissolved in 50 ml of doubly distilled water, and 5 ml of this solution (pH = 1.3–1.5) were introduced into a column of 0.1 g of resin loaded with 0.025 mmole of SPADNS. The lead was eluted with 50 ml of 0.001M nitric acid, followed by bismuth with 20 ml of 1.0M nitric acid.

RESULTS AND DISCUSSION

Table 1 gives the exchange capacities determined by the batch method. It can be seen that the capacity is higher for the smaller particle-size beads of Amberlyst A-26. As the apparent capacity of the Amberlyst A-26 for SPADNS is about 50% greater than the exchange capacity of the resin, other sorption effects besides simple ion-exchange must be involved. The resistance of the SPADNS and Orange II chelate-forming resins to mineral acids depends on the affinity of the acid anions for the anion-exchanger; the affinity sequence is $\text{ClO}_4^- > \text{NO}_3^- > \text{Cl}^-$, and perchloric acid therefore displaces the reagents more effectively than nitric or hydrochloric acid does (Table 2).

The retention of metal ions on SPADNS and Orange II chelate-forming resins was investigated as a function of pH. The results are presented in Figs. 2 and 3. It is seen that varying the pH gives good differentiation of the selectivity of the SPADNS or Orange II resins for metal ions, especially in the acid range. These two resins more strongly retain metal ions that have higher preference for oxygen as a donor atom. The SPADNS resin in acid medium is selective for Bi(III) and Zr(IV); Co(II), Ni(II) and other metal ions preferring nitrogen as a donor atom are practically not bound to the resin in acid medium. Our investigations show that the binding capacity for bismuth(III) increases linearly with increase in the amount of SPADNS loaded, and the binding ratio of Bi(III) to SPADNS on the resin is about 1:1.

Experiments performed in dynamic conditions confirmed that in the pH range 1.3–1.5 Bi(III) can be

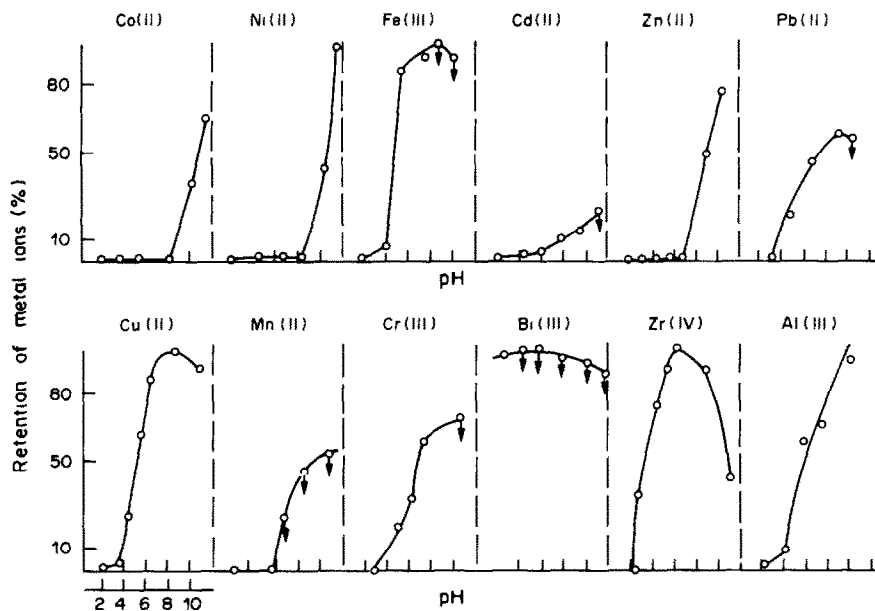


Fig. 2. Retention of metal ions on SPADNS resin as a function of pH.

quantitatively separated from Ni(II), Co(II), Cu(II), Cd(II), Cr(III), Mn(II), Pb(II), Fe(III) and Zn(II) when these ions are present in 2500-fold ratio to the bismuth (Table 3). Especially important from a practical point of view is the separation from lead. This method of separation was therefore adopted for the determination of Bi(III) in *p.a.* lead nitrate. The Bi(III) content found by flameless atomic-absorption spectrometry (AAS) without separation was $1.0 \times 10^{-3}\%$, but that found when separation was

used was $3.7 \pm 0.2 \times 10^{-3}\%$. Considerable attention has been paid to ion-exchange separation of Bi(III) from other metal ions.²⁰

The batch method results show (Fig. 2), that the SPADNS resin has the least affinity for cadmium, because of the very weak complexes formed by Cd(II) with SPADNS. If the "reverse separation method" is used, cadmium(II) should be separable from several metal ions. As cadmium is one of the most poisonous metals present in the environment, its determination

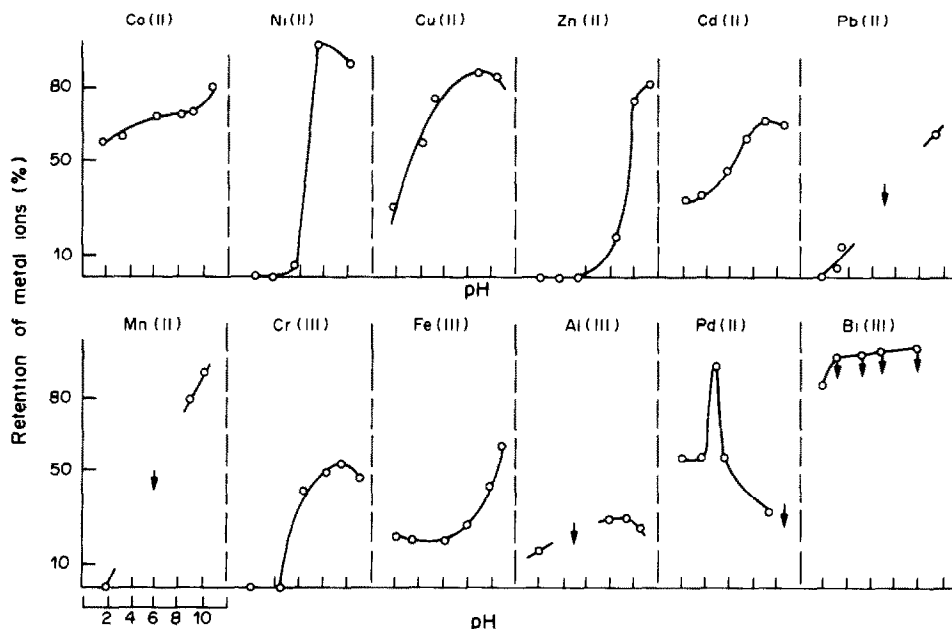


Fig. 3. Retention of metal ions on the Orange II resin as a function of pH.

Table 3. Separation of Bi(III) from various ions on SPADNS resin (column diameter 5.8 mm; 0.1 g of 0.1–0.2 mm resin beads; 0.25 mmole of SPADNS per g of resin, 10 ml of solution at pH 1.3–1.5; loading at 0.5 ml/min, elution at 1.0 ml/min; all foreign metals eluted with 30 ml of $10^{-3}M$ HNO_3 , Bi eluted with $1.0M$ HNO_3 ; averages of 10 determinations)

Amount of Bi			Metal ions in mixture	Amount of Me		
Added, mg	Found,§ mg	Error, %		Added, mg	Found,§ mg	Error, %
1.00*	0.997	0.3	Ni	1.00	1.00	—
			Mn	1.00	1.00	—
			Cr	1.00	1.00	—
			Cd	1.00	1.01	+1
			Zn	1.00	1.01	+1
			Co	1.00	1.01	+1
			Cu	1.00	0.99	-1
			Fe	1.00	0.98	-2
			Pb	1.00	1.00	—
			0.004†	0.0041	2.5	Ni
Mn	1.00	1.00				—
Cr	1.00	1.00				—
Cd	1.00	1.01				+1
Zn	1.00	1.02				+2
Cu	1.00	0.98				-2
Co	1.00	1.00				—
Fe	1.00	0.98				-2
Pb	1.00	1.00				—
0.004†	0.0043	7.5				Pb

*50 ml of eluent.

†20 ml of eluent.

§For determination by AAS, standards were prepared in the same way as the sample solutions.

as a pollutant is very important from a practical point of view. Most methods described in the literature use AAS for cadmium determination, especially in analysis of natural waters. Our investigations (Fig. 4) showed that several interferences were observed in the determination of cadmium by flameless AAS in the presence of other metal ions. If precise determination of cadmium is necessary, the influence of the other metal ions should be taken into consideration. The best method of avoiding such interferences is to separate the cadmium from the other metals.

Preliminary investigations showed that the SPADNS resin allowed the separation of Cd(II) from Pb(II), Cu(II) and Fe(III), but not from Co(II) or Ni(II), which partly pass into the effluent along with cadmium. Thus, we decided to use a resin bed modified with two reagents, SPADNS and NRS, to make it possible to retain Co(II) and Ni(II); NRS was used in our earlier work⁴ and shown to have high preference for Ni(II), Cu(II), Fe(III) and especially Co(II), but not for Pb(II) (Fig. 5). The results presented in Table 4 show that quantitative separation of Cd(II) from Pb(II), Cu(II), Co(II), Fe(III)

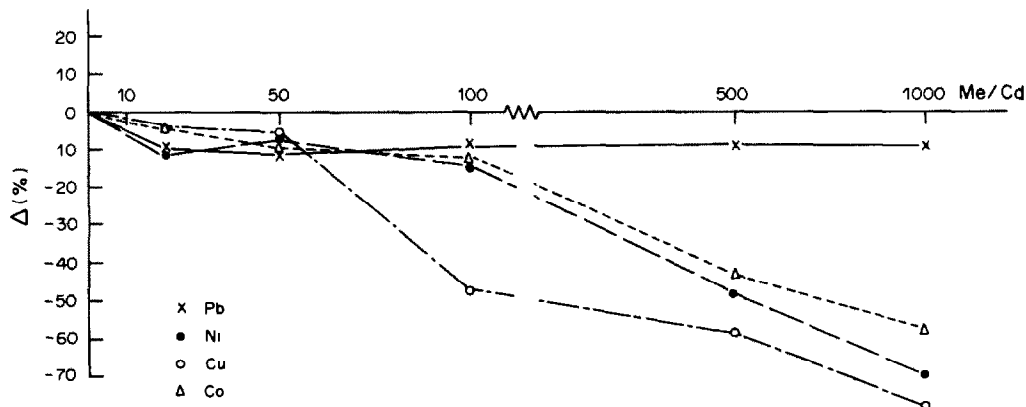


Fig. 4. Effect of Pb, Co, Cu and Ni on the AAS signal of Cd, expressed as relative change in signal.

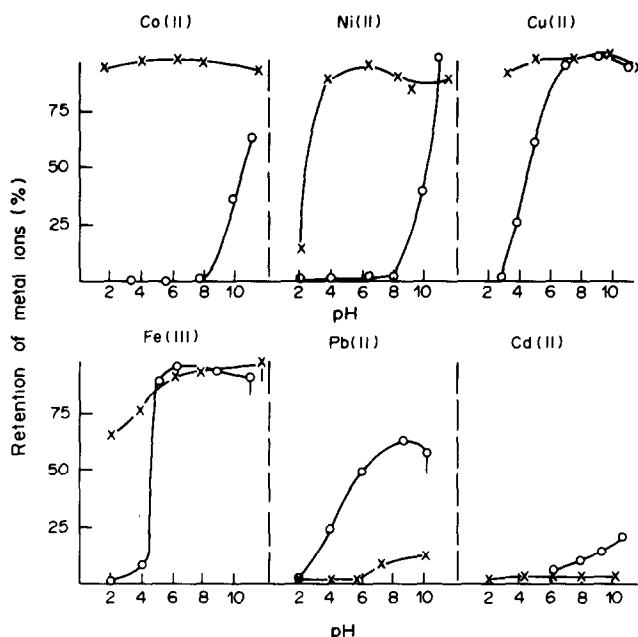


Fig. 5. Retention of metal ions on —○— SPADNS resin, —×— NRS resin, as a function of pH.

and Ni(II) is possible on the SPADNS + NRS resin by the reverse separation method. It should be noted that concentrations of Cd(II) lower than 0.01 ppm could not be determined.

The retention curves for the Orange II resin are shifted to slightly higher pH than those for the SPADNS resin, probably because the metal-

Orange II complexes are weaker than the SPADNS complexes.

The experiments with the Orange II resin (Fig. 3) show that separations of the following pairs of metal ions are possible at suitably chosen pH values: Al-Ni; Pb-Mn(II); Al,Pb,Zn-Ni; Al,Pb,Zn-Mn(II). Results for analysis of such mixtures are given in Table 5.

Table 4. Separation of Cd from other metals on mixed NRS/SPADNS resins diameter of column 5.8 mm; 0.2 g of 0.1–0.2 mm resin beads; 0.1 g of NRS resin (NRS 0.5 mmol/g) + 0.1 g of SPADNS resin (SPADNS 0.1 mmole/g; 50 ml of solution at pH = 6.3–7.0, loading and elution at 1 ml/min, other metals all eluted with 10 ml of 2M HClO₄; average of 10 determinations)

Amount of Cd*			Metal ions in mixture	Amount of Me		
Added, μg	Found,† μg	Error, %		Added, μg	Found,† μg	Error, %
20	20	—	Cu	20	20	—
			Fe	20	19.4	-3.0
			Pb	20	19.2	-4.0
			Ni	20	19.6	-2.0
			Co	20	20.1	+0.5
0.5 (corresponds to 0.01 ppm)	0.48	-4.0	Cu	20	20	—
			Fe	20	19.5	-2.5
			Pb	20	19.4	-3.0
			Ni	20	19.8	-1.0
			Co	20	19.9	-0.5

*Cd passes through the resin bed without being retained if its concentration is ≥ 0.01 ppm.

†For determination by AAS, standards were prepared in the same way as the sample solutions.

Table 5. Separation of the synthetic mixtures of metal ions on Orange II resin (0.5 g of resin 0.2-mmole/g Orange II; 15 ml of mixture of metal ions + Orange II, [Me]:[Orange II] = 1:1, at pH = 11.5; loading and elution at 1 ml/min; average of 4 determinations)

Metal ion	Elution agent	Amount of metal, mg		
		Added	Found*	Error, %
Al	} 60 ml of 0.25M NaOH 50 ml of 0.2M HCl	20.0	20.0	—
Ni		0.20	0.199	-0.5
Al	} 60 ml of 0.25M NaOH 50 ml of 0.2M HCl	6.00	6.05	+0.8
Mn		0.04	0.039	-2.5
Pb	} 50 ml of 0.25M NaOH 50 ml of 0.2M HCl	5.00	4.98	-0.4
Mn		0.04	0.038	-5.0
Al	} 60 ml of 0.25M NaOH 50 ml of 0.2M HCl	6.00	6.01	-0.2
Pb		5.00	4.99	-0.2
Zn		4.94	4.95	+0.2
Ni		0.20	0.199	-0.5
Al	} 60 ml of 0.25M NaOH 50 ml of 0.2M HCl	6.00	6.02	0.3
Pb		5.00	4.98	0.4
Zn		4.94	4.95	0.2
Mn		0.04	0.039	-2.5

*For determination by AAS, standards were prepared in the same way as the sample solutions.

REFERENCES

1. W. Kemula and K. Brajter, *Chem. Anal. Warsaw*, 1968, **13**, 305.
2. *Idem, ibid.*, 1968, **13**, 503.
3. *Idem, ibid.* 1970, **15**, 351.
4. K. Brajter, *ibid.*, 1973, **18**, 125.
5. *Idem, J. Chromatog.*, 1974, **102**, 385.
6. *Idem, Proc. 3rd Symposium Ion-Exchange, Balatonfüred, Hungary*, 28-31 May 1974.
7. *Idem, Chem. Anal. Warsaw*, 1976, **21**, 1195.
8. K. Brajter and E. Dąbek-Złotorzyńska, *Talanta*, 1980, **27**, 19.
9. K. Brajter and E. Olbrych-Sleszyńska, *ibid.*, 1983, **30**, 355.
10. K. Brajter and E. Dąbek-Złotorzyńska, paper presented at Euroanalysis V, Cracow, Poland, 26-31 August 1984.
11. H. Tanaka, M. Chikuma, A. Harada, A. Ueda and S. Yube, *Talanta*, 1976, **23**, 489.
12. J. E. Going, G. Wesenberg and G. Andrejat, *Anal. Chim. Acta*, 1976, **81**, 349.
13. H. Akaiwa, H. Kawamoto, N. Nakata and Y. Ozeki, *Chem. Lett.*, 1975, **10**, 1049.
14. K. S. Lee, W. Lee and D. W. Lee, *Anal. Chem.*, 1978, **50**, 255.
15. M. Chikuma, M. Nakayawa, T. Itoh, H. Tanaka and K. Itoh, *Talanta*, 1980, **27**, 807.
16. H. Akaiwa, H. Kawamoto and K. Ogura, *ibid.*, 1981, **28**, 337.
17. H.-E. Chao and N. Suzuki, *Anal. Chim. Acta*, 1981, **125**, 139.
18. M. Nakayama, M. Chikuma, H. Tanaka and K. Tanaka, *Talanta*, 1982, **29**, 503.
19. *Idem, ibid.*, 1983, **30**, 455.
20. F. W. Strelow and T. N. van der Walt, *Anal. Chem.*, 1981, **53**, 1632.

APPLICATION OF PLATINUM GAUZE ACTIVATED BY HYDROGEN TO THE ADSORPTION SEPARATION OF SILVER TRACES AND THEIR DETERMINATION BY AAS OR SPECTROPHOTOMETRY

ZOFIA BOGUSZEWSKA, MARIA KRASIEJKO and BOGNA PALMOWSKA-KUŚ
Department of Analytical Chemistry, Technical University of Warsaw,
00-664 Warsaw, ul. Noakowskiego 3, Poland

(Received 26 October 1983. Revised 18 June 1985. Accepted 23 August 1985)

Summary—A method ("electrosorption") has been developed for separation of silver from copper by its deposition through internal electrolysis with hydrogen adsorbed on a platinum surface. The silver can then be stripped and determined by atomic-absorption spectrometry or the dithizone method. The activation of the platinum surface with adsorbed hydrogen can be achieved either electrolytically or by passing hydrogen gas through the solution in which the platinum is immersed. The method of electrosorption has been successfully applied to determination of trace levels of silver in copper metal.

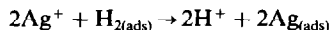
Electrolysis with an electrode of small surface area, maintained at very negative potential, is well known as a technique for the separation of traces of heavy metals from matrices such as water, biological materials and possibly salts of alkali or alkaline-earth metals.

It is also known that a metal monolayer can be formed on the surface of an inert electrode (such as a platinum electrode) at a potential considerably more positive ("underpotential") than that required for deposition of macroscopic quantities of the metal.¹⁻⁸ However, no analytical use seems to have been made of this fact.

In a previous paper⁹ we presented the results of studies on the separation of silver traces from various media by controlled potential electrolysis. We showed that deposition of silver traces on a platinum gauze electrode under "underpotential" conditions (formation of a monolayer) was just as effective as deposition under "Nernst" conditions (formation of a bulk phase). Deposition in the underpotential range also makes it possible to separate trace quantities of silver from metal matrices. As an analytical application we examined the electrolytic separation of silver traces from copper and other materials from the copper industry,⁹ since the "normal" potential for copper is higher than that of other base metals. The results obtained led us to expect that the method should be useful for separation of silver traces from various metallic matrices.

In the present work, we make use of another under-exploited facet of redox chemistry, namely that silver can be deposited as a monolayer on an inert (platinum) electrode through an adsorption mechanism. The reaction is based on adsorption of hydrogen on a platinum surface, and its redox reaction with

silver ions, involving "internal electrolysis," to give an adsorbed layer of silver metal.¹⁰



This process has not hitherto been applied in analytical practice.

It was first necessary to investigate the conditions for the electrosorption (internal electrolysis and adsorption) separation of silver traces on a platinum gauze of large surface area. It was found that hydrogen adsorbed on the platinum gauze surface lowers the electrode potential, making it possible for silver traces to be deposited.

EXPERIMENTAL

Reagents

Silver nitrate. Aqueous 1-mg/ml stock solution, suitably diluted to give working solutions.

Dithizone. A 0.002% solution in carbon tetrachloride, prepared by dilution of 0.01% solution.¹¹

EDTA solution, 0.25 M.

Water. Triply distilled in glass apparatus.

Radioactive silver (¹¹⁰Ag), as AgNO₃ in 0.1 M HNO₃. Radioactivity 1 mCi/ml, specific activity 1.2 mCi/mg of Ag; working solution (solution A; Ag⁺ about 0.8 μg/ml) prepared by 1000-fold dilution of the initial solution with water.

Apparatus

Platinum gauzes. A 4 × 14 cm piece of gauze (containing 2% Ir), ~140 mesh/cm², permanently attached to the inside wall of a 60-ml Teflon beaker. A 2.5 × 1.5 cm 320 mesh/cm² pure platinum gauze, folded double. A 2.5 × 2.0 cm piece of platinum foil.

Deposition of silver by electrolysis at controlled potential

The working electrode (platinum gauze, 320 mesh, 2.5 × 1.5 cm, folded double) was set at the desired potential vs. an SCE (with a potentiostat) and the working and auxiliary (platinum foil, 2.5 × 2 cm) electrodes were inserted

into a magnetically stirred solution in a Teflon beaker, the reference electrode (SCE) connected to a potentiostat being used only as reference.

Before and during experiments with ^{110}Ag , the activity of 1 ml of the solution was measured with a scintillation probe, in a polyethylene ampoule.

The silver deposited was removed from the electrode by rinsing the surface with 5 ml of hot nitric acid (1 + 1) (added from a pipette rinsed with the same acid), then water. The solution was made up accurately to 10 ml with water, and the silver content was determined by measuring its activity.

In the work with non-radioactive silver, the metal deposited was stripped with acid in the same way, and determined by AAS, the 328.07 nm line being used.

Deposition of silver by electrosorption reaction with adsorbed hydrogen

Before insertion into the test solution the platinum gauze was connected to the millivoltmeter (pH-meter), and the SCE reference electrode was connected to the test solution by a salt bridge. The change in silver concentration during the reaction and amount of silver deposited were determined in a way similar to that used in the electro-deposition studies

Determination of silver in copper

The copper sample was dissolved in concentrated nitric acid in a covered Teflon beaker, and the solution was heated to remove nitrogen oxides and then evaporated until copper nitrate began to crystallize. It was then diluted accurately to known volume with water and its acidity determined. The solution was stored in a Teflon bottle.

The platinum gauze (140 mesh, 4×14 cm, permanently fixed in the Teflon beaker), rinsed in hot nitric acid (1 + 1) and then in water, was cathodically polarized in the supporting electrolyte (0.1M $\text{KNO}_3 + 0.1\text{M HNO}_3$) for 20–40 sec by use of a 4.5-V battery. The platinum gauze potential was controlled by means of a millivoltmeter (pH-meter), with an SCE as reference, connected by a salt bridge to the solution into which the platinum gauze was dipped. The electrolysis was stopped just as liberation of oxygen on the anode (platinum foil) was seen to begin. The potential of the gauze was then about -250 mV.

The gauze thus prepared was removed and immersed in 50 ml of copper solution (in 0.3–0.6M nitric acid) containing $< 15 \mu\text{g}$ of silver. The solution was stirred for 10 min; the gauze potential was about $+500$ mV. After deposition of the silver by electrosorption the solution was removed, and the deposited silver was stripped from the gauze with 5 ml of boiling nitric acid (1 + 1) (from a pipette, initially rinsed with the hot acid), with a final rinsing with water.

The silver solution thus obtained was made up to volume in a 10-ml standard flask with water, and analysed for silver by atomic-absorption spectrometry (AAS). Alternatively, the solution containing the stripped silver was evaporated to about 0.5 ml, cooled, transferred to a separatory funnel, and diluted to about 10 ml, then 1 ml of 5M sulphuric acid was added and the solution was extracted with successive 2-ml portions of dithizone solution until the last portion contained only copper dithizonate (violet tint). The combined extracts were then washed with 0.5M sulphuric acid and the silver was stripped with two portions of 1M hydrochloric acid (10 and 5 ml). The organic phase was discarded and 2 ml of EDTA solution were added to the aqueous phase, with enough ammonia to give pH 4.5–5. Silver was again extracted with excess of dithizone, the surplus dithizone was removed from the organic phase with dilute ammonia solution, and the organic phase was transferred to a standard flask of suitable capacity, made up to the mark with the solvent, and mixed. Then the absorbance was measured at 460 nm against a blank, and the silver content read from a calibration graph.

RESULTS AND DISCUSSION

Influence of hydrogen on electrolytic deposition of silver traces

We investigated the electrolytic separation of $0.8 \mu\text{g}$ of ^{110}Ag on a 2.5×1.5 cm platinum gauze (320 mesh) after preliminary electrolysis ($E = -0.4$ V, volume 50 ml, time 10 min) to enrich the test solution in hydrogen. From the dependence of silver recovery on applied potential (Fig. 1a) we can conclude that set potentials of between $+0.8$ and $+0.9$ V are relatively useful for the separation of silver traces. This is at variance with our previous recommendation.⁹ Recoveries up to 100% can be obtained at set potentials of 0.8–1.2 V if a larger piece of gauze is used. The influence of the preliminary electrolysis on the electrolytic deposition of silver traces can be explained from measurements of the working electrode potential. The differences between the set potential and the actual potential are shown in Fig. 1b. In solutions that had not been preliminarily electrolysed, the electrode worked at the set potential values (curve 1, Fig. 1b). The higher silver recovery from solutions that had been preliminarily electrolysed (*i.e.*, before introduction of the silver) in the range of high set potentials is due to the adsorption of hydrogen. An electrode thus activated with hydrogen at-

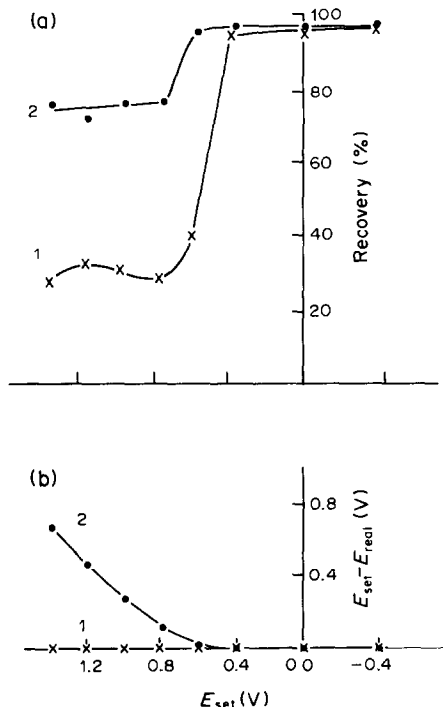


Fig. 1. (a) Influence of the electrode potential on the silver recovery. (b) Differences between the set (E_{set}) and actual (E_{real}) electrode potentials (0.1M $\text{HNO}_3 + 0.1\text{M KNO}_3$; $0.8 \mu\text{g}$ of ^{110}Ag ; $V = 50$ ml; $t = 10$ min; working electrode platinum gauze). Curve 1—solutions without preliminary electrolysis; curve 2—solutions after preliminary electrolysis (-0.4 V, 10 min).

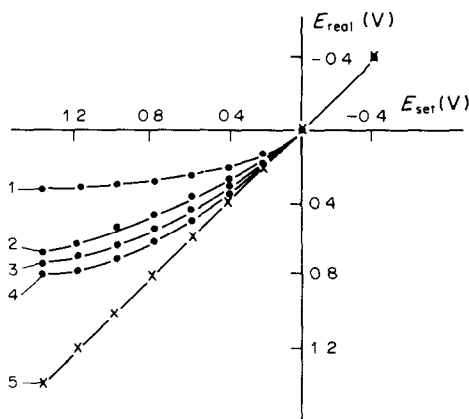


Fig. 2. Relation of the real working electrode potential to the set value at different times of electro-deposition (0.1M HNO₃ + 0.1M KNO₃; 0.8 μg of ¹¹⁰Ag; V = 50 ml; working electrode platinum gauze). Solutions after preliminary electrolysis, subsequent electro-deposition time: 1—0 min; 2—2 min; 3—5 min; 4—10 min. Curve 5 shows the values for solutions without preliminary electrolysis, for 0–10 min of subsequent electro-deposition.

tained potential values favourable for deposition of a silver monolayer.

It has been found that after preliminary electrolysis has been applied the initial value of the real electrode potential in the subsequent electro-deposition is not identical with the set voltage applied (Fig. 2, curve 1), but slowly approaches the set value as electro-deposition proceeds (curves 2–4, in Fig. 2). Curve 5 shows that the real and set potentials are identical if no preliminary electrolysis is applied.

Similar effects were obtained in other experiments, examples of which are illustrated in Figs. 3 and 4. During the first stage, the electrode was cathodically polarized (–0.4 V vs. SCE), and its surface and the solution were saturated with hydrogen. During the second stage the electrode was held at +0.8 V vs. SCE; the adsorbed hydrogen was anodically oxidized and the electrode surface was covered with platinum oxide. The time needed for the electrode to attain the set potential was ~10 min (Fig. 3).

Alternatively the sequence of platinum electrode potentials was reversed. During the first stage (electrode at 0.8 V vs. SCE) the electrode was covered with a layer of platinum oxide; during the second stage (–0.4 V vs. SCE) this layer was reduced and the surface of the working electrode was covered with hydrogen (Fig. 4). The working electrode needed about 20 min to attain the set potential. In both experiments, application of a potential lower than 0.55 V vs. SCE to the working electrode made it possible to deposit silver (Figs. 3 and 4).

The set potential for deposition of half the silver on the platinum surface without preliminary electrolysis was about +0.55 V (Fig. 1, curve 1).

At real potentials ≥ +0.8 V deposition of silver is negligible. Instead, silver already deposited at lower

electrode potential is transferred into solution (Figs. 3 and 4).

In the second stage of the experiments represented in Figs. 3 and 4 the auxiliary electrode also reached potentials at which silver traces were deposited. The amounts of silver deposited on the working and auxiliary electrodes were measured and are shown in Figs. 3 and 4.

It can be stated that the durability of the silver monolayer on the gauze electrode depends to some degree on the previous treatment given to the electrode. Preliminary electrolysis at +0.8 V (Fig. 4) makes the transition of silver into the solution in the second stage easier than in the experiment represented in Fig. 3. During the whole experiment represented in Fig. 4 the auxiliary electrode potential was favourable for silver deposition on the electrode. The large fraction of total silver found on the electrode is in agreement with this.

Influence of hydrogen on adsorption of silver traces on a platinum gauze

The electrosorption of silver traces on platinum gauze activated with hydrogen is represented in Fig. 5. Curve 1 shows the process of adsorption in a solution without hydrogen introduced. Silver was not completely deposited, because the potential attained by the gauze (+0.6 V) was not sufficient for deposition of a silver monolayer. It has been estimated that the “capacity” of the gauze used was ~8 μg (~7 × 10⁻⁸ mole) of silver monolayer. Curve 2 shows the effect of introducing hydrogen by preliminary electrolysis. The gauze attained lower potentials but silver was completely deposited. Curve 3 shows that

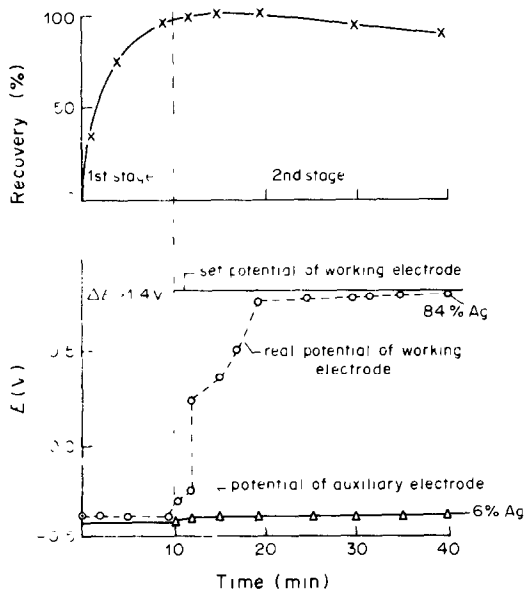


Fig. 3. Investigation of the processes of electro-deposition of trace amounts of silver. Gauze working electrode, foil auxiliary electrode. (1 ml of solution A; V = 50 ml; 0.1M KNO₃, 0.1M HNO₃).

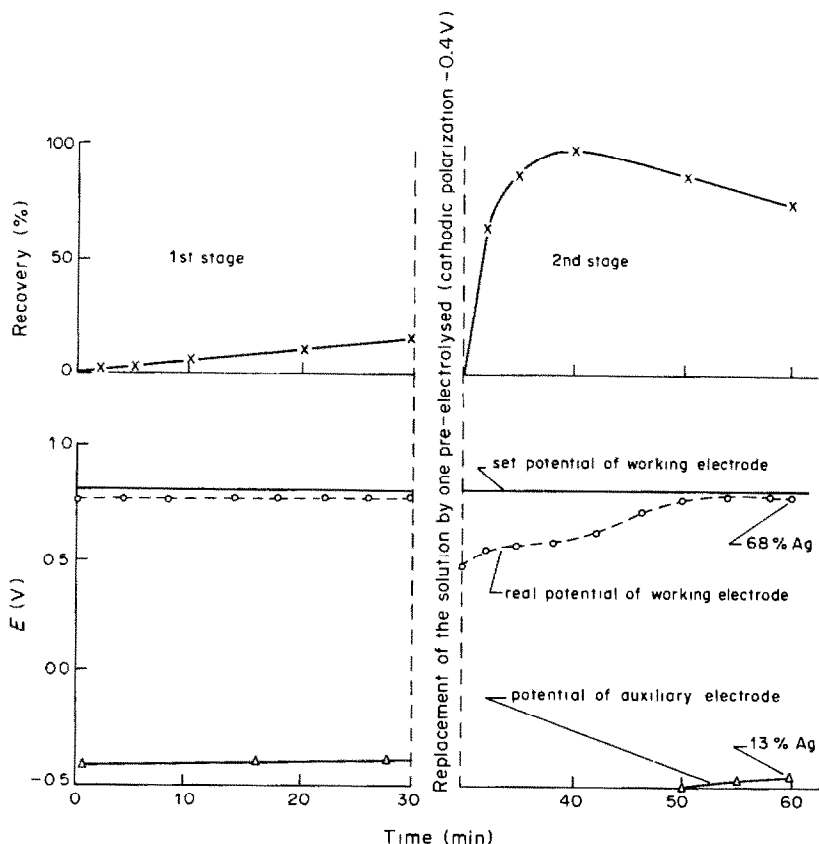


Fig. 4. Investigation of the process of electro-deposition of trace amounts of silver, with a fresh electrolyte solution of the same composition introduced for the second stage. Electrodes and solutions as for Fig. 3.

the adsorption process still takes place even if the hydrogen is introduced into the solution by bubbling from a gas cylinder; because of deoxygenation of the solution and its saturation with hydrogen the platinum gauze reached very low potential values and silver was deposited completely.

The gauze potential appears to be dependent on the degree of O_2 and H_2 adsorption on the gauze but is independent of the adsorption of silver if the solution contains only trace amounts of that element.

Development of the method of platinum-gauze activation with hydrogen

The gauze used had a silver monolayer capacity of less than $15 \mu\text{g}$. The gauze was initially washed with boiling nitric acid (1 + 1) and water, then $10 \mu\text{g}$ of silver were deposited on it. The results obtained were similar to those for adsorption of the smaller amounts of radioactive silver, reported above. It was advisable to pre-electrolyse the solution to introduce hydrogen into it before the traces of silver were added and the gauze was placed in it (Fig. 6a). The gauze potential was considerably diminished in this way (Fig. 6b).

Activation of the gauze by this method or by continuous passage of a stream of hydrogen is inconvenient in analytical practice, so we attempted to

devise a method of activation by cathodic polarization of the platinum gauze in a solution of supporting electrolyte free from silver. If the oxygen liberation zone is not separated from the remainder of the solution only a short electrolysis should be applied. If the preliminary electrolysis is stopped just as liberation of oxygen on the anode is seen to begin (*i.e.*, within 10–20 sec), then when transferred to the test solution the gauze acquires a potential suitable for silver monolayer formation (Fig. 7).⁹ Recovery of $10 \mu\text{g}$ of silver was 93% complete and was the same as in the controlled-potential electrolysis with underpotential conditions (+0.4 V).⁹ The gauze potential was independent of the electrolyte composition (Fig. 7). If the preliminary electrolysis was not stopped just as liberation of oxygen was seen to begin, oxygen was adsorbed on the platinum gauze, the gauze potential attained values $> +0.6 \text{ V}$, and silver was not completely deposited.

Determination of silver in copper

The results for determination of silver in spectrally pure copper are given in Table 1. The accuracy was checked by the standard-addition method. These results for AAS determination of silver after adsorption deposition on a hydrogen-activated gauze are in agreement with those obtained earlier⁹ for

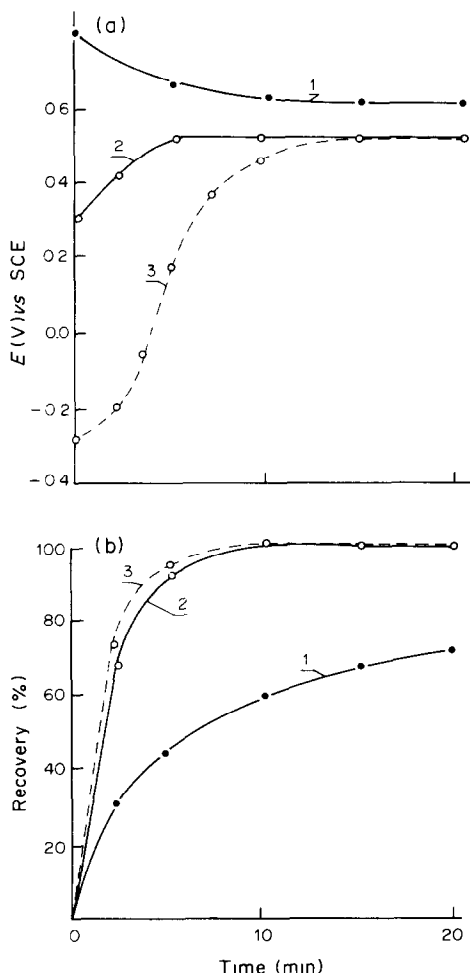


Fig. 5. Investigation of the adsorption of trace amounts of silver on platinum gauze: 1—solutions without preliminary electrolysis; 2—solution after preliminary electrolysis for 10 min at -0.4 V cathode potential; 3—solution saturated with hydrogen passed from a gas cylinder for 5 min (1 ml of solution A; $V = 50$ ml; $0.1M$ $KNO_3 + 0.1M$ HNO_3).

its determination after underpotential electrolytic separation (at $+0.4$ V vs. SCE), viz. $3.6 \times 10^{-4} \pm 0.17 \times 10^{-4}\%$. The silver content determined without preliminary separation was $4.8 \times 10^{-4}\%$.⁹

Table 1. Results of silver determination in the spectrally pure copper by AAS

Copper, g	Ag added, μg	Ag found, μg	Ag found in sample,* $10^{-4}\%$
1.05		4.0	3.8
1.05		3.3	3.2
1.05		3.6	3.4
2.10		7.6	3.6
2.10		7.7	3.7
1.05	2	5.7	3.7
1.05	2	5.5	3.5
1.05	10	13.4	3.4
1.05	10	13.3	3.3

*Mean $3.5 \times 10^{-4}\%$; standard deviation $0.2 \times 10^{-4}\%$.

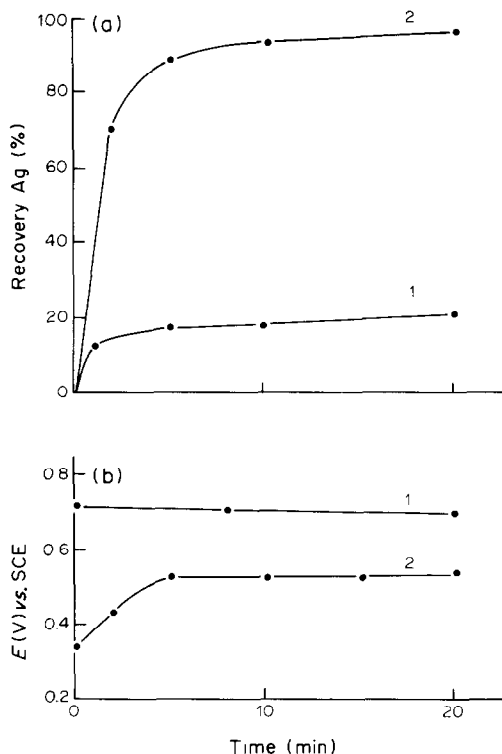


Fig. 6. Investigation of trace silver adsorption on a platinum gauze ($10 \mu g$ of Ag; V 50 ml; $0.1M$ $HNO_3 + 0.1M$ KNO_3), Curve 1—supporting electrolyte without preliminary electrolysis. Curve 2—supporting electrolyte after preliminary electrolysis (-0.4 V, 10 min).

The results of dithizone determination of silver in an electrolytic copper are given in Table 2. Silver was separated from the matrix by adsorption or by underpotential electrolysis at $+0.4$ V vs. SCE; the results were in good agreement. They also agreed with the results of AAS determination after underpotential electrolytic separation.

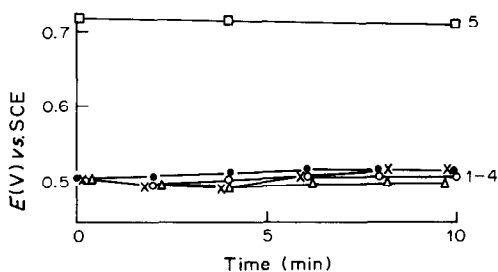


Fig. 7. Investigation of the adsorption of trace amounts of silver on a platinum gauze preliminarily cathodically polarized for 20–40 sec (4.5 V; $i = 1.7$ A) in $0.1M$ $KNO_3 / 0.1M$ HNO_3 ($V = 50$ ml). 1—Supporting electrolyte ($0.1M$ $KNO_3 / 0.1M$ HNO_3 , without preliminary electrolysis); 2—supporting electrolyte + $10 \mu g$ of Ag; 3—supporting electrolyte + $10 \mu g$ of Ag + 1 g of Cu; 4—supporting electrolyte + 1 g of Cu; 5—supporting electrolyte; gauze without preliminary cathodic polarization.

Table 2. Results of silver determination in electrolytic copper

Method		Weight of sample, g	Silver content found,		Average, 10 ⁻³ %	Standard deviation, 10 ⁻³ %
Separation	Determination		μg	10 ⁻³ %		
Adsorption	Spectrophotometry	1.0	10.9	1.09	1.03	0.05
			9.9	0.99		
			10.5	1.05		
			9.7	0.97		
			10.3	1.03		
Electrolysis	Spectrophotometry	1.0	11.0	1.10	1.04	0.04
			10.2	1.02		
Electrolysis	Spectrophotometry	0.5	5.05	1.01	1.01	—
			5.15	1.03		
Electrolysis	AAS	1.0	10.1	1.01	1.01	—
			10.1	1.01		

After the matrix separation as little as 1 μg of silver could be determined with dithizone, because no other reagents were introduced into the solution.

As reported previously,⁹ stripping the deposited silver from the platinum gauze is vital for the accuracy of the determination.

CONCLUSIONS

Introduction of hydrogen has an important influence on the potential of a platinum gauze with large surface area. In this way it affects deposition of silver traces both by electrolysis at controlled potential and by electrosorption. During the electrolysis the gauze potential (in the range of its positive values) lags behind the set potential value. This is not observed for electrodes of very small surface area. These results demonstrate the importance of the method of preparation of both the electrode and the solution. It is common practice to clean electrodes by electrolysis, but the consequences are rarely taken into consideration.

When they are given proper consideration, however, it is seen that it can be deduced that production of an adsorbed film of hydrogen on a platinum surface of large area, whether by electrolysis or

simple passage of the gas through the solution in which the surface is immersed, gives quantitative deposition of a layer of adsorbed silver by internal electrolysis through interaction with the adsorbed hydrogen. The technique can be used for separation of trace amounts of silver from matrix metals, and for purification of reagents containing traces of silver.

REFERENCES

1. L. B. Rogers, D. P. Krause, J. C. Griess, Jr. and D. B. Ehrlinger, *J. Electrochem. Soc.*, 1949, **95**, 33.
2. J. C. Griess, Jr., J. T. Byrne and L. B. Rogers, *ibid.*, 1951, **98**, 447.
3. J. T. Byrne, L. B. Rogers and J. C. Griess, Jr., *ibid.*, 1951, **98**, 452.
4. D. P. Sandoz, R. M. Peekema, H. Freund and C. F. Morrison, Jr., *J. Electroanal. Chem.*, 1970, **24**, 165.
5. G. W. Tindall and S. Bruckenstein, *Electrochim. Acta*, 1971, **16**, 245.
6. D. M. Kolb, M. Przasnyski and H. Gerischer, *J. Electroanal. Chem.*, 1974, **54**, 25.
7. S. Stucki, *ibid.*, 1977, **80**, 375.
8. S. H. Cadle and S. Bruckenstein, *Anal. Chem.*, 1971, **43**, 1858.
9. Z. Boguszevska, M. Krzyżanowska and Z. Trybula, *Chem. Anal. Warsaw*, 1984, **29**, 147.
10. S. Szabó and F. Nagy, *J. Electroanal. Chem.*, 1976, **70**, 357.
11. Z. Marczenko, *Spectrophotometric Determination of Elements*, p. 492, Horwood, Chichester, 1976.

SHORT COMMUNICATIONS

PRECONCENTRATION OF COBALT WITH *N*-(DITHIOCARBOXY)SARCOSINE AND AMBERLITE XAD-4 RESIN

YUKIO SAKAI and NAOKO MORI

Faculty of Education, Miyazaki University, Funatsuka, Miyazaki 880, Japan

(Received 29 July 1985. Accepted 18 October 1985)

Summary—Cobalt reacts with *N*-(dithiocarboxy)sarcosine (DTCS) to form a 1:3 Co:DTCS complex which is so stable that after its formation no decomposition occurs even in 4*M* hydrochloric acid. The complex is sorbed on a column of Amberlite XAD-4 copolymer from an acidic solution and eluted with 10 ml of a 1:1:3 v/v mixture of 1.0*M* ammonia solution (pH = 9), 0.1*M* EDTA and methanol. The absorbance of the eluted chelate is measured at 320 nm against water ($\epsilon = 2.15 \times 10^4$ l. mole⁻¹. cm⁻¹). The recovery of cobalt from 1 litre of tap-water or sea-water is quantitative. The effect of diverse ions can be eliminated by the addition of EDTA after chelation of the cobalt. The copper complex with DTCS is partly sorbed on the column because of its slow rate of decomposition by EDTA, but most of the copper chelate sorbed can be eluted with hydrochloric acid and any co-eluted with the cobalt chelate can be completely decomposed by heating the eluate. Cobalt enrichment factors of at least 100 are obtained, so the method is applicable to the determination of cobalt at the ng/ml level.

Several techniques are available for concentrating traces of metal ions from natural waters. Solvent extraction is one of the most widely used, but is sometimes tedious, and the concentration factor obtained can be limited by mutual solubility of the phases. Chromatography is useful for obtaining high concentration factors, and Amberlite XAD copolymers, which have porous structure and large specific surface area, have been used to sorb various water-soluble organic substances^{1,2} and metal chelates.³⁻⁵

In an earlier paper,⁶ we reported the photometric determination of copper after preconcentration by sorption of its *N*-(dithiocarboxy)sarcosine (DTCS) chelate on Amberlite XAD-2 resin and elution with an ammonia solution in 60% methanol. Concentration factors of 20 were achieved by the method.

In the present investigation, the work has been extended to cobalt, with the XAD-4 resin, which is superior to XAD-2 in sorption capacity.⁷⁻⁹

EXPERIMENTAL

Reagents

DTCS was synthesized as the diammonium salt by the following procedure.¹⁰ To 20 ml of carbon disulphide, a solution of 25 g of sarcosine in 60 ml of 10*M* ammonia solution was added. The reaction flask was stoppered and the mixture was stirred for 10 hr at room temperature. After the unreacted carbon disulphide had been removed from the reaction flask, ethanol was added dropwise until white crystals appeared. The flask was then allowed to stand overnight in a refrigerator. The white product obtained was filtered off, washed with ethanol, and dried in a vacuum desiccator. The yield was about 60%. The reagent is now available from Dojindo Labs. Inc., 2861 Kengun, Kumamoto-shi, 862 Japan. A 0.02*M* aqueous solution of DTCS was used. All other solutions used were prepared from analytical-reagent grade chemicals.

Buffer solutions were purified by adding DTCS solution and passing the mixture through a column of Amberlite XAD-4 copolymer.

Column preparation

Amberlite XAD-4 copolymer (Rohm and Hass, 20-60 mesh) was cleaned prior to use by extraction for 8 hr with methanol in a Soxhlet extractor. The resin was packed into a glass tube (20 cm long, 9 mm bore) to give a resin bed about 8 cm in height. The column was washed with 100 ml of 1.0*M* hydrochloric acid in 50% methanol and then 100 ml of 0.2*M* ammonia solution in 10% methanol. Finally, the column was washed with a large volume of distilled water to remove methanol from the column.

Standard procedure for preconcentration

An aliquot of standard cobalt solution was placed in a 100-ml standard flask, 2 ml of 0.2*M* sodium triphosphate (TPP), 1 ml of 0.02*M* DTCS and 1 ml of 0.1*M* EDTA were added successively, and after the cobalt chelation with DTCS was complete, 1 ml of 6.0*M* hydrochloric acid was added and the whole was diluted to volume with distilled water. This solution was loaded onto the column at a flow-rate of 5.0 ml/min by means of a peristaltic pump, then the column was washed with 20 ml of 1.0*M* hydrochloric acid at the same flow-rate. The cobalt chelate sorbed on the column was eluted with 10 ml of a 1:1:3 v/v mixture of 1.0*M* ammonia (pH = 9), 0.1*M* EDTA and methanol at a flow-rate of 0.7 ml/min. The eluate was then heated for 10 min to decompose any co-eluted copper-DTCS chelate. Finally, the absorbance of the eluate was measured at 320 nm in a 10-mm quartz cell.

RESULTS AND DISCUSSION

Formation of cobalt chelate with DTCS

The cobalt chelate with DTCS shows two absorption maxima, at 320 and 630 nm. As the molar absorptivities at these wavelengths are 2.24×10^4 and 500 l. mole⁻¹. cm⁻¹ respectively, the absorbance measurements are made at 320 nm. The cobalt chelation

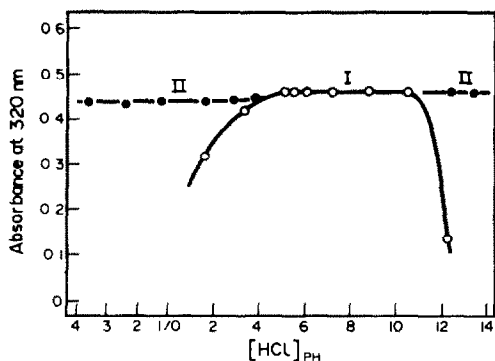


Fig. 1. Effect of pH on the formation of cobalt chelate with DTCS. Co(II) taken 29 $\mu\text{g}/25\text{ ml}$; reference reagent blank. I, pH adjusted prior to cobalt chelation (○), II, pH adjusted after cobalt chelation (●).

with DTCS is strongly dependent on pH (Fig. 1). When the pH is adjusted before the addition of DTCS, the absorbance is maximal and constant for the pH range 5–10 (curve I). The decrease in absorbance at pH < 5 is due to decomposition of the DTCS, and that at pH > 10 is due to hydrolysis of the cobalt ion. In contrast, once formed, the cobalt chelate is stable in the range from 3.6*M* hydrochloric acid to 0.3*M* sodium hydroxide (curve II), and the absorbance does not change for at least 3 days even in 3.6*M* hydrochloric acid medium. The extreme stability of cobalt (III) complexes in acid solution is well known, and the cobalt in the DTCS chelate is presumably in the tervalent state. The molar ratio method indicates that the cobalt chelate has a composition of 1:3 cobalt:DTCS, which would agree with this.

A small decrease of the absorbance in the acidic solution is probably due to decomposition of the DTCS chelates of other metal ions, introduced into the solution as contaminants from the water and reagent solutions used.

Optimum conditions for sorption, washing and stripping

The sorption of the cobalt chelate is considerably affected by the ionic strength and acidity of the solution. Recovery is quantitative when the ionic strength of the solution loaded onto the column is > 0.05. However, when the ionic strength is adjusted to 0.05 with potassium phosphate buffer (pH = 7), the recovery decreases with increasing volume of the solution, *viz.*, 90% from 250 ml of solution and 65% from 500 ml.

The effect of the acidity on the sorption is shown in Fig. 2. The acidity was adjusted with hydrochloric acid, and at pH > 4.0 the ionic strength was kept at 0.02 with potassium chloride. As shown in Fig. 2, sorption of the cobalt chelate increased linearly with the acidity and recovery was quantitative at pH < 4.0. The quantitative sorption from an acidic solution can be interpreted as due to strong inter-

action between the undissociated carboxyl group in the cobalt-DTCS chelate and XAD-4 copolymer, by analogy with the retention of amino-acids by XAD copolymers, including XAD-4.² In the present study, the solution was acidified to pH 1.2 with hydrochloric acid.

At this acidity all the other metal-DTCS chelates are decomposed, but the rate of decomposition of the copper chelate is slow under these conditions, and the residual chelate is sorbed on the XAD-4 column along with the cobalt chelate.

Washing the column with hydrochloric acid decomposes the sorbed copper chelate; more than 90% of the copper chelate on the column can be washed away with 20 ml of 1.0*M* hydrochloric acid.

The stripping solution adopted was similar to that reported previously [pH 9 ammonia solution (0.2*M*) in 60% methanol],¹⁰ but with EDTA added to decompose any residual copper chelate in the eluate.

Calibration graph

The calibration graph is linear over the cobalt concentration range 0.18–2.52 $\mu\text{g}/\text{ml}$ in the eluate. The precision was $\pm 0.3\ \mu\text{g}$ (95% confidence limits) for determination of 12.6 μg of cobalt in 100 ml of solution. As the molar absorptivity obtained is $2.15 \times 10^4\ \text{l. mole}^{-1}\cdot\text{cm}^{-1}$, recovery from the column with 10 ml of stripping solution is estimated to be about 96% complete. The absorbance of a blank was < 0.010.

Effect of foreign ions

Investigation of masking of foreign ions revealed that the combined use of TPP and EDTA was effective. TPP prevents the chelation of iron(III), manganese(II) and chromium(III) with DTCS. The EDTA must be added after formation of the cobalt chelate, because otherwise it masks cobalt from chelation with DTCS. The DTCS chelates of cadmium, lead, nickel and copper are decomposed by EDTA.

The decomposition of the copper chelate largely depends on the concentration of EDTA, because the

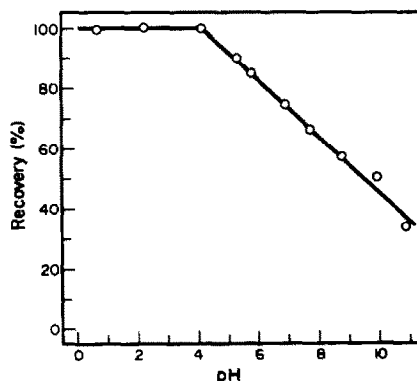


Fig. 2. Effect of pH on the recovery of cobalt. At pH > 4.0 the ionic strength was kept at 0.02 with potassium chloride. Co(II) taken 8.80 μg .

Table 1. Effect of foreign ions on recovery of cobalt (8.80 μg)

Ion	Added, mg	Co found, μg	Recovery, %
Al(III)	2.0	8.59	98
Cr(III)	1.0	8.78	100
Mn(II)	1.2	8.69	99
Fe(III)	1.1	8.89	101
Ni(II)	1.2	10.30	118
Cu(II)	0.65	8.75	99
	1.3	4.42	50
Zn(II)	1.4	8.89	101
Cd(II)	1.1	8.98	102
Hg(II)	0.94	9.24	105
Pb(II)	2.0	9.05	103

Table 2. Recovery of cobalt from 1000 ml of water samples (five replicates)

Sample	Co added, μg	Co found, μg	Recovery (C.V.), %
Distilled water	8.80	8.85	100 (1.6)
Tap-water	8.80	8.59	98 (4.5)
Sea-water	3.52	3.54	101 (7.3)
	8.80	9.19	104 (2.5)

degree of dissociation of the Cu-DTCS chelate is comparable to that of the Cu-EDTA chelate in the medium. At pH 7 the conditional stability constant for $\text{Cu}(\text{DTCS})_2$ is $10^{19.2}$, while that for CuEDTA is $10^{15.4}$.¹² From these conditional stability constants and the concentrations of DTCS and EDTA used, the molar ratio of $\text{Cu}(\text{DTCS})_2$ to CuEDTA in the medium is calculated to be 0.25. This suggests high dependence of the decomposition on the EDTA concentration. In addition, the rate of decomposition of the copper-DTCS chelate was slow. Hence, the copper chelate is eliminated in three stages: (1) decomposition with EDTA in the sample solution; (2) decomposition of the chelate sorbed onto the XAD-4 resin, by washing with 20 ml of 1.0M hydrochloric acid after the sorption; (3) decomposition with EDTA by heating the cobalt eluate for 10 min.

The effect of foreign ions on the determination of 8.8 μg of cobalt is summarized in Table 1. It is seen that the presence of about 1 mg of each foreign ion except for nickel and copper does not cause a significant error. The presence of a few mg of alkali and alkaline-earth metals does not interfere. The positive error apparently caused by nickel was found to be due to cobalt contained as an impurity in the nickel solution used; this was confirmed by atomic-absorption analysis. The negative error from larger amounts of copper is due to its consumption of some of the DTCS added, so a larger amount of DTCS reagent should be added to deal with this.

Recoveries from tap-water and sea-water

Recoveries of cobalt from 1000-ml water samples were examined. The samples, filtered through a 0.45- μm Millipore membrane, were spiked with 3.52

or 8.80 μg of cobalt and analysed by the standard procedure. The volume of DTCS solution added was increased to 10 ml to compensate for the dilution effect on the reaction with cobalt.

The average values of five determinations are summarized in Table 2, from which it is seen that quantitative recoveries were obtained. The results also indicate that the method can be applied to the determination of cobalt at ng/ml concentrations. Sample volumes up to 2 litres can probably be handled by the procedure given.

Conclusions

The method is fairly simple and highly selective. A feature of the method is that cobalt in highly saline water can be concentrated in a small volume of eluate. Almost all other metal ions except copper can be masked with TPP and EDTA. The resulting complexes appear not to be sorbed on the XAD-4 resin,⁶ so the selective separation of cobalt is possible by the method.

The method can be useful for preconcentration prior to cobalt determination by other methods such as atomic-absorption spectrometry. In addition, the cobalt chelate with DTCS can easily be decomposed by the addition of hydrogen peroxide to the cobalt eluate, followed by heating.¹³ Hence, the method can also be used for preconcentration of cobalt before photometric determination with more sensitive reagents such as 4-(5-bromo-2-pyridylazo)-1,3-diaminobenzene and its derivatives.^{13, 15}

Like the XAD-2 column,⁶ the XAD-4 column is easily regenerated by washing with a large volume of water after the elution and can be used repeatedly.

REFERENCES

- G. A. Junk, J. J. Richard, M. D. Greaser, D. Witiak, J. L. Witiak, M. D. Arguello, R. Vick, H. J. Fritz and G. V. Calder, *J. Chromatog.*, 1974, **99**, 745.
- E. P. Kroeff and D. J. Pietrzyk, *Anal. Chem.*, 1978, **50**, 502.
- R. B. Willis and D. Sangster, *ibid.*, 1976, **48**, 59.
- Y. Sugiura, Y. Suzuki and Y. Miyake, *Proc. Third NEA Seminar on Marine Radioecology, Tokyo, Japan, October, 1979*.
- J. L. Lundgren and A. A. Schilt, *Anal. Chem.*, 1977, **49**, 974.
- Y. Sakai, *Talanta*, 1980, **27**, 1073.
- D. J. Pietrzyk and Chi-Hung Chu, *Anal. Chem.*, 1977, **49**, 757.
- G. R. Aiken, E. M. Thurman, R. L. Malcolm and H. F. Walton, *ibid.*, 1979, **51**, 1799.
- D. J. Pietrzyk and J. D. Stodola, *ibid.*, 1981, **53**, 1822.
- Y. Sakai and K. Kurogi, *Bunseki Kagaku*, 1979, **28**, 429.
- A. Hulanicki, *Talanta*, 1967, **14**, 1371.
- A. Ringbom, *Complexation in Analytical Chemistry*, Wiley, New York, 1963.
- Y. Sakai, *Anal. Sci.*, 1985, **1**, 373.
- S. Shibata, M. Furukawa and K. Goto, *Anal. Chim. Acta*, 1974, **71**, 85.
- S. Shibata and M. Furukawa, *Bunseki Kagaku*, 1974, **23**, 1412.

INDIRECT SPECTROPHOTOMETRIC METHODS FOR THE DETERMINATION OF ANTIBIOTICS WITH IODINE OR PERIODATE, AND METOL AND SULPHANILAMIDE

C. S. P. SASTRY, T. E. DIVAKAR and U. VIPLAVA PRASAD

Food and Drug Laboratories, School of Chemistry Andhra University, Waltair 530 003, India

(Received 12 June 1985. Revised 30 August 1985. Accepted 18 October 1985)

Summary—Two spectrophotometric methods are described for the determination of antibiotics. In the first method, penicillins, cephalosporins, streptomycin and griseofulvin are estimated by oxidizing them under neutral or slightly acidic conditions, after alkaline hydrolysis, by means of a known and excessive quantity of iodine solution. The excess of iodine is determined at pH 3.0 with metol and sulphanilamide. In the second method, dihydrostreptomycin, framycetin and the acid hydrolysis product of chloramphenicol are determined by a method involving oxidation with sodium metaperiodate, masking the excess of periodate with sodium molybdate, and using metol and sulphanilamide at pH 3.0 to determine the iodate formed. In both methods the absorbance of the resulting *p*-*N*-methylbenzoquinoneminoimine sulphanilamide charge-transfer complex is measured at 520 nm.

Several spectrophotometric methods for assay of penicillins,¹ cephalosporins,² griseofulvin,³ streptomycin,⁴ dihydrostreptomycin⁵ and chloramphenicol⁶ are cited in the literature. The reported titrimetric procedures for estimation of these antibiotics with oxidants such as iodine⁷⁻⁹ and sodium metaperiodate^{5,10} are not satisfactory for microgram quantities. Metol and iodine¹¹ or potassium iodate¹² have been found to be valuable reagents for the determination of primary aromatic amines. This paper describes the use of metol and sulphanilamide for the indirect spectrophotometric determination of the amounts of iodine and sodium metaperiodate consumed during oxidation of the antibiotics. In the first method, penicillins (potassium penicillin G, potassium phenoxymethyl penicillin, methicillin, sodium amoxicillin, sodium cloxacillin and sodium ampicillin), cephalosporins (cephaloxin monohydrate, cephalothin and cephaloridine), streptomycin and griseofulvin are hydrolysed initially with alkali, then oxidized with standard iodine solution in excess under neutral or slightly acidic conditions. The iodine consumed is measured by estimating the excess of iodine spectrophotometrically at pH 3.0. In the second method, dihydrostreptomycin, framycetin and the acid hydrolysis product of chloramphenicol¹³ are determined by a method involving oxidation with periodate, masking the excess of periodate with sodium molybdate,¹⁴ and using metol and sulphanilamide at pH 3.0 to determine the iodate formed. In both cases metol is oxidized to *p*-*N*-methylbenzoquinoneminoimine which then forms a charge-transfer complex with the sulphanilamide present, and the absorbance of the complex is measured at 520 nm. The procedures have been applied

to a wide variety of pharmaceutical preparations of the antibiotics mentioned.

EXPERIMENTAL

Apparatus

A Shimadzu UV-140 double-beam spectrophotometer with matched 1.0-cm quartz cells was used for absorbance measurements.

Reagents

Aqueous solutions of iodine (0.0037*M* I₂ in 0.05*M* potassium iodide), sodium metaperiodate (0.2%), metol (0.2%), sulphanilamide (0.2%), sodium molybdate (1.0%), hydrochloric acid (0.1, 1, 3 and 4*M*), sodium hydroxide (0.1, 1, 3 and 4*M*) and potassium hydrogen phthalate-hydrochloric acid buffer (pH 3.0)¹⁵ were prepared.

Antibiotic solutions

Aqueous solutions (200 µg/ml) of penicillins, cephalosporins, streptomycin, dihydrostreptomycin and framycetin, and a methanolic solution (200 µg/ml) of griseofulvin were prepared. The hydrolysis product of chloramphenicol [2-amino-3-(*p*-nitrophenyl)propane-1,3-diol] was obtained by heating chloramphenicol (50 mg) with 3*M* hydrochloric acid (5 ml) under reflux on a steam-bath for 2 hr, followed by neutralization with sodium hydroxide solution (3*M*), and the solution was then diluted accurately to 250 ml.

All chemicals and reagents used were of analytical or pharmaceutical grade. Distilled water was used throughout.

Procedures

A. For estimating the iodine consumed. Transfer 0.2–2.0 ml (accurately measured) of antibiotic solution into a 25-ml standard flask. Add 1.0 ml of sodium hydroxide solution (1*M* for penicillins, 0.1*M* for streptomycin and 4*M* for cephalosporins and griseofulvin) and set the mixture aside for 20 min at 30° (in the case of streptomycin and griseofulvin heat on a boiling water-bath for 4 min and 15 min respectively).

Add 1.0 ml of hydrochloric acid (1*M* for penicillins, 0.1*M* for streptomycin and 4*M* for cephalosporins and griseofulvin) and 2.00 ml of 0.0037*M* iodine solution and keep the

Table 1. Concentration ranges and regression equations

Compound	Concentration range (C), $\mu\text{g/ml}$	Regression equation*
Potassium penicillin G	2-14	$A = 0.587 - 0.0399C$
Sodium amoxycillin	2-14	$A = 0.525 - 0.0355C$
Sodium cloxacillin	2-14	$A = 0.529 - 0.0339C$
Potassium penicillin V	2-14	$A = 0.527 - 0.0342C$
Methicillin	2-14	$A = 0.534 - 0.0332C$
Sodium ampicillin	2-14	$A = 0.519 - 0.0345C$
Cephalexin monohydrate	2-14	$A = 0.540 - 0.0327C$
Cephaloridine	2-14	$A = 0.557 - 0.0279C$
Cephalothin	2-14	$A = 0.541 - 0.0272C$
Griseofulvin	2-14	$A = 0.521 - 0.0252C$
Streptomycin sulphate	2-16	$A = 0.520 - 0.0251C$
Chloramphenicol	4-28	$A = -0.004 + 0.0214C$
Dihydrostreptomycin sulphate	4-24	$A = -0.001 + 0.0180C$
Framycetin sulphate	4-24	$A = 0.001 + 0.0125C$

*Found in this work; must be determined independently by users of the method.

solution in the dark for 15 min. Then add 15 ml of pH 3.0 buffer and 1.5 ml of metal solution. After 2 min, add 1.5 ml of sulphanilamide solution and make up to the mark with distilled water. After 10 min measure the absorbance at

520 nm with distilled water as reference. In the same way prepare a corresponding reference solution simultaneously, containing the sample, but with 1.0 ml of distilled water instead of the 1.0 ml of sodium hydroxide solution. Subtract

Table 2. Analysis of dosage forms by proposed and reference methods

Drug	Recovery* \pm s.d., %	
	Proposed method	Reference method†
Potassium penicillin G powder	99.1 \pm 0.5	97.3 \pm 1.1
Pentids tablet (Sarabhai)	98.9 \pm 0.7	96.9 \pm 1.2
Pentids syrup (Sarabhai)	98.6 \pm 0.6	97.8 \pm 0.9
Sodicillin injection (HAL)	98.8 \pm 0.7	97.2 \pm 1.3
Sodium amoxycillin powder	100.6 \pm 0.6	99.2 \pm 0.9
Amoxylin capsule (Biddle Sawyer)	100.1 \pm 0.4	99.9 \pm 1.0
Cemoxin (suspension) (Cevoe pharma)	99.8 \pm 0.6	99.3 \pm 1.2
Sodium cloxacillin powder	101.2 \pm 0.4	98.1 \pm 0.9
Cloxacillin capsule (Biochem)	100.9 \pm 0.5	98.9 \pm 1.0
Cloxacillin injection (Biochem)	100.7 \pm 0.5	99.0 \pm 0.9
Potassium penicillin V powder	102.0 \pm 0.7	98.7 \pm 1.3
Crystapen V tablet (Glaxo)	101.9 \pm 0.6	99.6 \pm 1.0
Crystapen V syrup (Glaxo)	102.7 \pm 0.9	98.1 \pm 1.4
Methicillin powder	100.1 \pm 0.3	—
Sodium ampicillin powder	100.9 \pm 0.4	98.9 \pm 1.3
Ampisyn capsule (Cipla)	101.3 \pm 0.7	99.1 \pm 0.9
Olinkid tablets (Cufic)	101.0 \pm 0.6	98.6 \pm 1.0
Biocillin drops (Biochem)	102.1 \pm 0.9	101.3 \pm 1.4
Ampisyn syrup (Cipla)	98.1 \pm 0.4	96.7 \pm 0.9
Ampisyn injection (Cipla)	98.4 \pm 0.5	97.6 \pm 0.8
Cephalexin monohydrate powder	99.1 \pm 0.3	98.1 \pm 1.0
Cephaxin capsule (Biochem)	100.7 \pm 0.4	98.0 \pm 0.9
Cephacillin tablets (Biddle Sawyer)	101.3 \pm 0.5	103.4 \pm 0.6
Cephaxin dry syrup (Biochem)	100.9 \pm 0.6	102.1 \pm 0.7
Cephaloridine powder	97.1 \pm 0.3	96.7 \pm 0.9
Cephodine injection (IDPL)	96.9 \pm 0.5	98.1 \pm 0.8
Sodium cephalothin powder	98.1 \pm 0.6	96.1 \pm 1.1
Griseofulvin powder	100.1 \pm 0.3	101.3 \pm 0.4
Grisovin-FP tablet (Glaxo)	101.0 \pm 0.4	101.1 \pm 0.6
Streptomycin sulphate powder	102.0 \pm 0.2	101.0 \pm 0.9
Sugacin injection (HAL)	101.2 \pm 0.4	98.3 \pm 0.8
Clorstrep capsule (Parke Davis)	99.2 \pm 0.3	98.1 \pm 0.7
Chloramphenicol powder	97.1 \pm 0.9	96.3 \pm 1.4
Halctin capsule (HAL)	98.8 \pm 1.0	97.2 \pm 1.0
Chloromycetin injection (Parke Davis)	102.1 \pm 0.7	101.9 \pm 0.8
Dihydrostreptomycin sulphate powder	99.3 \pm 0.3	—
Framycetin sulphate powder	100.7 \pm 0.4	—

*Average of 6 determinations, value based on nominal content.

†Penicillins, cephalorins and streptomycin determined by the BP methods,⁷ griseofulvin by the Bhatkar and Madkauer method,¹ and chloramphenicol by the method of Anupa *et al.*⁶

the absorbance of the sample solution from that of the reference. Prepare a calibration graph similarly. The difference in absorbance corresponds to the iodine consumed in oxidizing the antibiotic.

B. For estimating periodate consumed. To a 25-ml standard flask containing 0.2–2.0 ml of antibiotic solution (accurately measured), add 1.0 ml of sodium metaperiodate solution and set the mixture aside for a suitable period (framycetin, acid hydrolysis product of chloramphenicol, 10 min; dihydrostreptomycin 40 min), maintaining the pH in the range 7.0–7.5. Then add 1.5 ml of sodium molybdate solution and after 10 min add 15 ml of pH 3.0 buffer and 1.5 ml of metol solution. After 2 min, add 1.5 ml of sulphanilamide solution and heat for 2 min at 70°. Cool, make up to the mark with distilled water, and measure the absorbance at 520 nm against a reagent blank. Prepare the calibration graph similarly.

Analysis of pharmaceutical preparations

Take a known quantity of sample equivalent to 100 mg of the antibiotic, dissolve it in 100 ml of water (methanol in the case of griseofulvin), filter if necessary, and dilute accurately to 250 ml. Dilute the solution as necessary and determine the antibiotic content by procedure A or B, as appropriate.

RESULTS AND DISCUSSION

In procedure A, the iodine consumed during the oxidation of antibiotic is indirectly determined spectrophotometrically with metol and sulphanilamide. In procedure B, the iodate formed during the oxidation of the antibiotic with periodate is also estimated spectrophotometrically with metol and sulphanilamide. The experimental conditions in both procedures have been established through control experiments. Beer's law is valid over the concentration ranges presented in Table 1. The unknown drug concentration in different pharmaceutical preparations can be calculated from calibration graphs or their corresponding regression equations.

The results of the assay of the pharmaceutical preparations (tablets, capsules, injection and syrups) presented in Table 2 compare favourably with those obtained by other methods.

The proposed methods can be applied to the determination of penicillins, cephalosporins, streptomycin, griseofulvin, and chloramphenicol in various pharmaceutical preparations even when they are present in microgram quantities. Other ingredients such as glucose, lactose, starch, vitamins, sulpha drugs and sodium phosphate usually present in pharmaceutical preparations do not interfere.

The basis of the methods is as follows. Although penicillins, cephalosporins, streptomycin and griseofulvin do not themselves consume iodine, the prod-

ucts resulting from their treatment with alkali (which produces a free imine group through hydrolytic cleavage of the β -lactam ring in penicillins and cephalosporins, maltol from streptomycin and griseofulvin acid from griseofulvin)^{7,9} do. Sodium metaperiodate has a rather selective oxidizing action on 1,2-diols, cleaving a carbon-carbon bond and producing two aldehydes.^{5,10} Framycetin and dihydrostreptomycin react directly with periodate owing to the presence of a 1,2-diol system. Although chloramphenicol does not react with periodate, its acid hydrolysis product (containing an amino group at position 2, vicinal to both hydroxyl groups of the propyl side chain) does.

The potential interference of glucose and lactose in the determination of the antibiotics mentioned, except framycetin and dihydrostreptomycin, is avoided by subtracting the amount of oxidant consumed by the antibiotic from that consumed by the hydrolysed product.

The purple-red charge-transfer complex may be presumed to arise by electron transfer from the highest π molecular orbital of sulphanilamide to the lowest empty orbitals (π^*) of two adjacent *p-N*-methylbenzoquinonemonoimine molecules (formed *in situ* on treating metol with iodine or iodate).¹¹

REFERENCES

1. N. A. Nayak, P. G. Ramappa, H. S. Yathirajan and S. Manuappa, *Anal. Chim. Acta*, 1982, **134**, 411.
2. M. M. Abdel-Khalek and M. S. Mahrous, *Talanta*, 1984, **31**, 635.
3. R. G. Bhatkar and D. C. Madkauer, *Indian J. Pharm. Sci.*, 1980, **42**, 139.
4. Y. Fujita, I. Mori and S. Kitano, *Chem. Pharm. Bull.*, 1983, **31**, 1289; *Chem. Abstr.*, 1983, **99**, 98676s.
5. W. A. Vail and C. E. Bricker, *Anal. Chem.*, 1952, **24**, 975.
6. D. Anupa, S. Medhekar and K. S. Boparai, *Indian J. Pharm. Sci.*, 1982, **44**, No. 6, 149.
7. *British Pharmacopoeia*, H.M. Stationery Office, London, 1980.
8. A. Sauciuc and L. Ionescu, *Rev. Chim.*, 1966, **17**, 47; *Chem. Abstr.*, 1966, **64**, 19319c.
9. H. W. Unterman, *Pharm. Zentralhalle*, 1965, **104**, 245; *Chem. Abstr.* 1965, **63**, 2853e.
10. A. Valseth and A. Wickstrom, *Medd. Norsk. Farm. Selsk.*, 1955, **17**, 345; *Chem. Abstr.*, 1956, **50**, 5979a.
11. C. S. P. Sastry, T. M. K. Reddy and B. G. Rao, *Indian Drugs*, 1984, **21**, No. 4, 145.
12. R. Ramakrishna, P. Siraj and C. S. P. Sastry, *Acta Ciencia Indica*, 1980, **6**, 140.
13. U. Chandra and P. N. Pandey, *Labdev*, 1967, **5**, 333, *Chem. Abstr.*, 1968, **68**, 16191c.
14. G. Nishi and A. Townshend, *Talanta*, 1968, **15**, 1377.
15. Yu. Lurie, *Handbook of Analytical Chemistry*, p. 253. Mir, Moscow, 1975.

THERMOMETRIC TITRATION OF THE DODECYL SULPHATE ION WITH METAL-PHENANTHROLINE COMPLEXES

TOSHIAKI HATTORI and HITOSHI YOSHIDA*

Department of Chemistry, Faculty of Science, University of Hokkaido, 060 Sapporo, Japan

(Received 13 June 1985. Accepted 17 October 1985)

Summary—Dodecyl sulphate forms precipitates with certain metal-1,10-phenanthroline complexes. This is the basis of a simple and direct thermometric titration of dodecyl sulphate with $\text{Cd}(\text{phen})_3^{2+}$

In recent years sodium dodecylsulphate has been recommended as a reference standard in determination of anionic surfactants. However, sodium dodecyl sulphate itself needs standardization by acid-base titration after hydrolysis with acid. The hydrolysis is time-consuming and the mixture is apt to bump on heating, and a large sample is required. A simple and direct method for standardization of dodecyl sulphate (DS^-) solutions is therefore highly desirable.

Some metals form precipitates with large anions in the presence of 1,10-phenanthroline (phen). These systems have been used for gravimetric determination of cadmium,¹ conductometric titration of nitrate,² perchlorate,³ cadmium,⁴ and so on.⁵ Anionic surfactants also form insoluble ternary ion-association compounds with certain metal-phenanthroline complexes, and these can be extracted into organic solvents.⁶⁻⁸ If such compounds can readily be quantitatively formed with DS^- , they might be useful in a titrimetric determination of DS^- .

Thermometric titration is a widely applicable and rapid analytical method and we have found it to be one of the best methods for the study of the interaction between anionic and cationic surfactants to produce precipitates.⁹ We have also found that poly(vinyl alcohol) (PVA) prevents aggregation of the precipitate formed. The purpose of this paper is to demonstrate the usefulness of the metal-phen complex system as the titrant for thermometric titration of DS^- in aqueous PVA medium.

EXPERIMENTAL

Apparatus

The differential thermometric titration apparatus used has already been described in detail.¹⁰

Reagents

Sodium dodecyl sulphate (minimum assay 98.0%) was standardized by acid-base titration after acid hydrolysis.¹¹ A 0.1M $\text{Cd}(\text{phen})_3^{2+}$ solution was prepared by dissolving 0.08 mole of 1,10-phenanthroline monohydrate in 25 ml of

1M cadmium acetate stock solution and diluting to 250 ml with distilled water. The cadmium acetate stock solution was standardized by EDTA titration, with Eriochrome Black T as indicator, at pH 10. The $\text{Cd}(\text{phen})_3^{2+}$ solution is stable for at least a few months, but the free phenanthroline in the solution tends to decompose in light, so it is preferable to store the solution in the dark. Other metal-phen complexes were prepared analogously, except for $\text{Fe}(\text{II})$ -phen, which was prepared from ferrous chloride.

Procedure

One of the twin burettes is filled with 0.1M $\text{Cd}(\text{phen})_3^{2+}$ solution, and the other with distilled water as a reference. The sample solution, containing 20–200 μmoles of DS^- , is placed in a 100-ml Dewar flask. Five ml of 0.5M acetate buffer (pH 5) and 5 ml of 2.5% PVA solution are added, and the mixture is diluted to 50 ml with distilled water. In the reference flask 50 ml of distilled water are placed. When their temperatures are the same, the solutions in the two flasks are simultaneously titrated with the twin burette system, the rate of addition being 0.1 ml/min, and the difference in temperature is recorded as a function of titrant volume added.

RESULTS AND DISCUSSION

Reaction of some metal-phen complexes with DS^-

Some relatively stable metal-phen complexes were thermometrically titrated with DS^- ; they were the $\text{Ni}(\text{II})$, $\text{Fe}(\text{II})$, $\text{Cu}(\text{II})$, $\text{Hg}(\text{II})$, $\text{Zn}(\text{II})$, $\text{Cd}(\text{II})$, and $\text{Pb}(\text{II})$ complexes. The last four gave large apparent enthalpy changes for the reaction, and the titration curves showed a clear end-point at a 2:1 molar ratio of DS^- to phenanthroline complex. The heats of formation of the precipitates are shown in Table I. The other metal-phen complexes gave smaller enthalpy changes in reaction with DS^- .

Hg -phen complex should be the best titrant for DS^- , but unfortunately is somewhat unstable on

Table I Heat of precipitation of $\text{M}(\text{phen})_3\text{DS}_2$

Complex	$-\Delta H, \text{kJ/mole}$
$\text{Hg}(\text{phen})_3\text{DS}_2$	80.6
$\text{Cd}(\text{phen})_3\text{DS}_2$	74.4
$\text{Zn}(\text{phen})_3\text{DS}_2$	50.6
$\text{Pb}(\text{phen})_3\text{DS}_2$	42.6

*Author for correspondence.

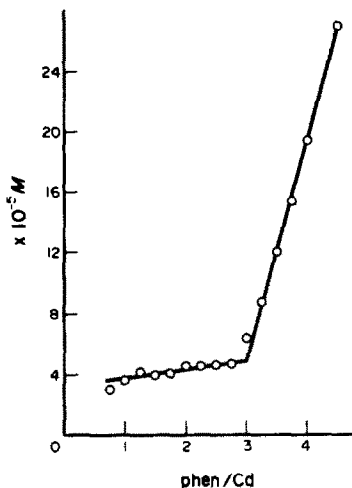


Fig. 1. Concentration of phen in the filtrate vs. initial phen:Cd molar ratio.

storage. The Cd-phen complex, which gives the next largest enthalpy change, is stable and the cadmium acetate stock solution keeps without decomposition. Therefore Cd-phen complex was selected as the titrant for DS^- .

Composition of Cd-phen-DS precipitate

The molar ratio of phen to cadmium in the precipitate was examined by a spectrophotometric method with iron(II) as described earlier.² A series of solutions containing a constant amount of cadmium, the required amount of DS^- and various amounts of phen in 0-4.0 molar ratio to cadmium, was adjusted to pH 5. After a few hours, these solutions were centrifuged. Part of each supernatant liquid was filtered and the phenanthroline in the filtrates was measured by the iron(II) method, at 510 nm. The results are shown in Fig. 1, and it is clear that the molar ratio of phen to cadmium is 3.0. From this result and the end-point of the titration of $Cd(phen)_3^{2+}$ with DS^- , it may be concluded that the composition of the precipitate is $Cd^{2+}:phen:DS^- = 1:3:2$. This is different from that for the iodide complex $Cd(phen)_2I_2$.¹

Titration of dodecyl sulphate ion

The end-point of the titration is influenced by the pH of the titrand solution, and the type and quantity of the buffer solution. Of the buffer solutions tried,

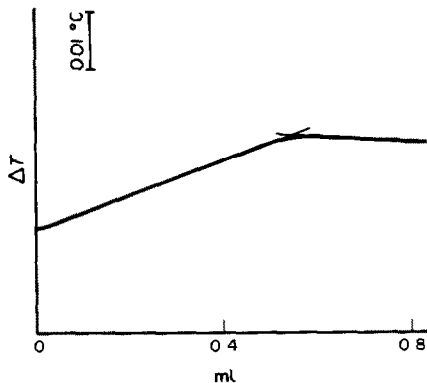


Fig. 2. Typical titration curve of 2.2 mM sodium dodecylsulphate (110 μ moles) with 0.1M $Cd(phen)_3^{2+}$.

Table 2. Determination of dodecyl sulphate (10 determinations)

Taken, μ moles	Mean Found, μ moles	r.s.d., %
21.2	21.2	2.4
106.0	106.8	0.9
212.0	212.9	0.4

0.05M acetate buffer of pH 4.0-6.0 gave the best results.

PVA was found useful for inhibiting aggregation of the precipitate, as in the earlier work.⁹ The presence of 0.1-2.0% PVA gives good results but at high concentrations PVA tends to be precipitated in presence of electrolytes. A typical titration curve is shown in Fig. 2 and the analytical results are given in Table 2.

The effect of various anions on the determination was also investigated. The results are summarized in Table 3. Some anions with low charge density, such as perchlorate, iodide and nitrate, interfere since they also react with $Cd(phen)_3^{2+}$. Perchlorate ion gives serious positive error, but the anions listed in Table 3 cause $\leq 1\%$ error when present at the concentration ratios shown.

REFERENCES

- H. Yoshida, K. Mizuno, M. Taga and S. Hikime, *Bunseki Kagaku*, 1976, **25**, 12.
- I. Hayashida, M. Taga and H. Yoshida, *Talanta*, 1981, **28**, 349.
- I. Hayashida, H. Yoshida, M. Taga and S. Hikime, *Bunseki Kagaku*, 1980, **29**, 304.

Table 3. Effect of various anions on triplicate determination of 103.3 μ moles of DS^-

Anion	Added as	Ion/ DS^-	Found, μ moles	r.s.d., %
none	—	—	103.8	
I^-	KI	0.1	103.8	0.8
NO_3^-	$NaNO_3$	1	104.3	1.0
Br^-	KBr	5	104.0	0.8
Cl^-	NaCl	10	103.9	0.4
SO_4^{2-}	Na_2SO_4	10	103.9	0.7
$\Phi-SO_3^-$ *	$\Phi-SO_3Na$	10	103.9	0.6
$H_2PO_4^-$	NaH_2PO_4	10	103.8	0.6

*Benzenesulphonate ion.

4. H. Yoshida, I. Hayashida, M. Taga and S. Hikime, *ibid.*, 1977, **26**, 461.
5. I. Hayashida, H. Yoshida, M. Taga and S. Hikime, *ibid.*, 1979, **28**, 748.
6. C. G. Taylor and B. Fryer, *Analyst*, 1969, **94**, 1106.
7. C. G. Taylor and J. Waters, *ibid.*, 1972, **97**, 533.
8. A. Le Bihan and J. Courtot-Coupez, *Bull. Soc. Chim. France*, 1970, **1**, 406; *Anal. Lett.* 1977, **10**, 759.
9. T. Hattori, H. Yoshida and M. Taga, *1985 Winter Meeting of the Hokkaido Branch of Japan. Soc. Anal. Chem.* Abstract 1A20.
10. H. Yoshida, T. Hattori, H. Arai and M. Taga, *Anal. Chim. Acta*, 1983, **152**, 257.
11. *Japanese Industrial Standard: Testing Method for Industrial Water*, JIS K0102, 30.1, 1981.

SPECTROPHOTOMETRIC DETERMINATION OF BENZOTHIADIAZINES IN DOSAGE FORMS

F. BELAL, M. RIZK, F. IBRAHIEM and M. SHARAF EL-DIN
Department of Analytical Chemistry, Faculty of Pharmacy,
University of Mansoura, Mansoura, Egypt

(Received 5 June 1985. Accepted 3 October 1985)

Summary—The analytical utility of ethyl acetoacetate for the spectrophotometric determination of benzothiadiazine diuretics has been studied. The procedure developed is based on coupling of the diazotized drugs with the reagent, which possesses an active methylene group. The stoichiometry of the reaction is presented. The nominal recovery of the drugs from pharmaceutical preparations ranges from 97.6 ± 0.7 to $102.3 \pm 0.3\%$. The suggested method is simple, sensitive and applicable to unit dose analysis.

Benzothiadiazines are widely used as potent diuretics of low toxicity, and several methods have been developed for their determination. These include non-aqueous titration,^{1,2} direct ultraviolet spectrophotometry,¹ colorimetry,^{1,2} polarography¹ and complexometric,^{3,4} amperometric,⁵ thermometric⁶ and bromometric titrations.^{7,8} Differential spectrophotometry and the orthogonal function method¹¹ have also been used. Benzothiadiazines are determined colorimetrically after hydrolysis, diazotization, and coupling with amines and phenols.^{1,2,12,13} GLC,¹⁴ HPLC^{15,16} and LC-MS¹⁷ are the methods of choice for the determination of benzothiadiazines in biological fluids.

The coupling reaction of the diazo derivative, being an electrophilic substitution, can take place not only with phenols and amines, but also with carbanions associated with an active hydrogen atom.¹⁸ A colorimetric method for the determination of such a carbanionic compound, namely ethyl acetoacetate, has been based on its reaction with the diazo-derivative of 4-nitroaniline, to give a coloured product.¹⁹ The use of compounds with an active methylene groups as reagents for the determination of primary aromatic amines was first reported by Belal and co-workers, who employed ethyl acetoacetate²⁰ and barbituric acid²¹ as coupling reagents to determine some pharmaceutical primary aromatic amines.

This paper presents a simple and sensitive procedure for the estimation of six benzothiadiazines (Table 1), by coupling of the diazotized hydrolysed amines with the reagent. The method is simple, sensitive and readily adaptable to unit dose analysis.

EXPERIMENTAL

Reagents

- Ethyl acetoacetate, 5% ethanolic solution.
- Sodium nitrite, 0.5% aqueous solution.
- Urea, 2% aqueous solution.
- Sodium hydroxide, 20% and 50% aqueous solutions.

Pure drug samples were kindly provided by various manufacturers, and used as such. Pharmaceutical preparations containing the compounds studied were obtained from the Egyptian market or were laboratory-made.

Procedures

Calibration graph. Dissolve 50 mg of the pure compound in 10 ml of 20% sodium hydroxide solution by boiling under reflux for 30 min, and cool. Add 15 ml of concentrated hydrochloric acid, and dilute accurately to 100 ml with water. Dilute this solution tenfold with 1M hydrochloric acid for analysis. Transfer to 25-ml standard flasks suitable volumes of this solution to cover the working range (Table 1). Add 1 ml of sodium nitrite solution to each, cool the flasks in an ice-bath for 3 min, add 2 ml of urea solution and after 3 min add 1 ml of ethyl acetoacetate solution followed by 6 ml of 50% sodium hydroxide solution. Measure the absorbances against a reagent blank at λ_{\max} (Table 1). Use the same procedure for analysis of nominally pure drug samples.

Analysis of tablets. Weigh 20 tablets and pulverize them. Extract a known weight of the powder, equivalent to 50 mg of the pure drug, by shaking it with three successive 25-ml portions of 0.8% sodium hydroxide solution; filter the extract into a 100-ml standard flask, and wash the filter and dilute to volume with water. Boil 10 ml of this solution with 10 ml of 20% sodium hydroxide solution under reflux for 30 min and cool. Add 15 ml of concentrated hydrochloric acid, and dilute accurately to 100 ml with water. Dilute this solution tenfold with 1M hydrochloric acid for analysis. Proceed as described above, starting from the words "Transfer to 25-ml standard flasks suitable volumes"

Table 1. Data for the reaction of benzothiadiazines and ethyl acetoacetate

Compound	λ_{\max} , nm	Molar	Working
		absorptivity,* $l \cdot \text{mole}^{-1} \cdot \text{cm}^{-1}$	range, $\mu\text{g/ml}$
Chlorothiazide	425	3.46×10^4	2-15
Hydrochlorothiazide	425	3.16×10^4	2-20
Trichlormethiazide	425	3.23×10^4	2-24
Benzthiazide	425	3.02×10^4	2-24
Bendroflumethiazide	430	2.32×10^4	2-30
Methylclothiazide	430	1.26×10^4	4-48

*Mean of 12 determinations.

RESULTS AND DISCUSSION

Benzothiadiazines are hydrolysed completely to yield 2,4-disulphamoylanilines, and these can be coupled with ethyl acetoacetate in strongly alkaline medium to produce yellow compounds. This reaction can be used for spectrophotometric determination of some benzothiadiazine diuretics. Scheme I represents a possible reaction pathway for the formation of the azo compounds, with hydrochlorothiazide as the model.

The coupling reaction is instantaneous, and the colour remains stable for more than 24 hr. The optimum concentrations of the reagents were determined, and are those used in the procedure.

The molar absorptivities of the products from chlorothiazide, hydrochlorothiazide, benzthiazide and trichloromethiazide (Table 1) are nearly the same because hydrolysis of all four compounds yields the same product, 5-chloro-2,4-disulphamoylaniline. Bendroflumethiazide, on the other hand, yields 5-trifluoromethyl-2,4-disulphamoylaniline, and methylclothiazide yields 5-chloro-2-(*N*-methylsulphamoyl) 4-sulphamoylaniline.

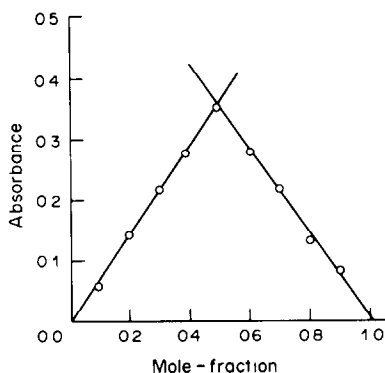
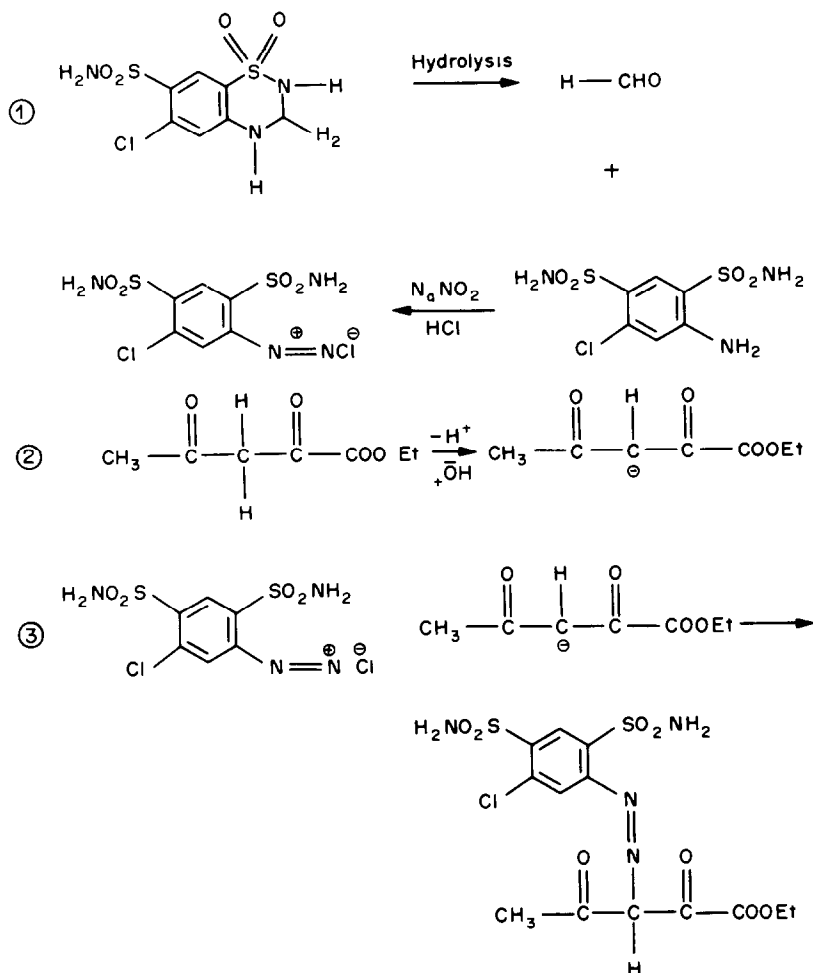


Fig. 1. Continuous variations plot for reaction of methylclothiazide and ethyl acetoacetate (total concentration of reactants $2 \times 10^{-3}M$).

Figure 1 shows the continuous variations graph for methylclothiazide as a model.²² Complementary volumes of $2 \times 10^{-3}M$ solutions of the hydrolysed and diazotized drug, and of ethyl acetoacetate (0:10, 1:9, 2:8...9:1, 10:0) were mixed in 25-ml standard flasks with 6 ml of 50% sodium hydroxide solution



Scheme I.

Table 2. Analysis of commercial and laboratory-made tablets by the proposed and official methods

Preparation	Recovery, %	
	Proposed method	Official method
Hydrochlorothiazide tablets† (24 mg/tablet)	101.8 ± 0.5	102.3 ± 0.4
Chlorothiazide tablets§ (25 mg/tablet)	98.7 ± 0.4	99.5 ± 0.2
Trichlormethiazide tablets§ (25 mg/tablet)	97.8 ± 0.7	98.5 ± 0.5
Methylclothiazide tablets§ (25 mg/tablet)	102.4 ± 0.5	101.9 ± 0.3
Bendroflumethiazide tablets† (25 mg/tablet)	102.3 ± 0.3	101.8 ± 0.5
Benzthiazide tablets§ (25 mg/tablet)	99.5 ± 0.4	98.8 ± 0.5

*Means and coefficients of variation for 6 determinations.

†Commercially available tablets.

§Laboratory-made tablets.

and the solutions made up to the mark with water. The absorbances were measured and plotted against the mole fraction of the drug.

The systems all obeyed Beer's law over the concentration ranges shown in Table 1. The method was applied to analysis of commercial and laboratory-made tablets containing the benzothiadiazines, with the results shown in Table 2. Lactose, starch, magnesium stearate and talc, which are commonly used as excipients, were found not to interfere in the analysis. Hydralazine hydrochloride and reserpine, which are co-formulated with hydrochlorothiazide, also had no effect. Statistical analysis²³ (*F*-test and *t*-test) of the results obtained by the suggested method and by the standard colorimetric methods^{1,2} showed no significant difference between the performance of the two methods.

The method suggested has the advantages of being simple and sensitive. It may be considered as a general method for the spectrophotometric determination of benzothiadiazines. The method has the additional advantage that the coloured products are soluble in alkali, so they do not precipitate and do not need extraction.

REFERENCES

1. *The United States Pharmacopeia*, XX, pp. 67, 77, 138, 378, 514, Mack Publishing, Easton, Pa, 1980.
2. *The British Pharmacopeia*, pp. 48, 104, 138, 224, 738, 747, 816, HM Stationary Office, London, 1980.
3. L. Przyborowski and G. Pionka, *Farm. Pol.*, 1976, **32**, 399; *Chem. Abstr.*, 1976, **85**, 149190z.
4. N. Teodorescu, L. Petroniu and Gh. Ciogolea, *Farmacia*, 1967, **15**, 13; *Chem. Abstr.*, 1967, **66**, 98546.
5. M. Madgearu, H. Beral and E. Cuciureanu, *ibid.*, 1968, **16**, 471; *Chem. Abstr.* 1969, **70**, 6558e.
6. A. B. DeLo and M. J. Stern, *J. Pharm. Sci.*, 1966, **55**, 173.
7. P. Kertész, *Acta. Pharm. Hung.*, 1969, **33**, 150; *Chem. Abstr.*, 1964, **60**, 1540b.
8. *Idem*, *ibid.*, 1969, **39**, 127; *Chem. Abstr.*, 1969, **71**, 33474b.
9. T. D. Doyle and F. R. Fazzari, *J. Pharm. Sci.*, 1974, **63**, 1921.
10. H. Abdine, M. A. El-Sayed and Y. M. El-Sayed, *J. Assoc. Off. Anal. Chem.*, 1978, **61**, 695.
11. *Idem*, *Analyst*, 1980, **105**, 222.
12. J. P. Hunt, V. P. Shah, V. K. Prasad and B. E. Cabana, *Anal. Lett.*, 1980, **13**, 135.
13. D. Suria, *Clin. Biochem.*, 1978, **11**, 222.
14. E. Redalisu, V. V. Tipins and W. E. Wagnen, Jr., *J. Pharm. Sci.*, 1978, **67**, 726.
15. P. A. Tisdall, T. P. Moyer and P. J. Anhalt, *Clin. Chem.*, 1980, **26**, 702.
16. V. P. Shah, J. Lee and V. K. Prasad, *Anal. Lett.*, 1982, **15**, 529.
17. C. Eckers, D. S. Skrabalak and J. D. Henion, *Clin. Chem.*, 1982, **28**, 1882.
18. A. K. Connors, *Reaction Mechanisms in Organic Chemistry*, p. 244. Wiley-Interscience, New York, 1973.
19. M. S. Rosenthal, *J. Biol. Chem.*, 1949, **179**, 1235.
20. S. Belal, E. A. El-Neaeny and S. Soliman, *Talanta*, 1978, **25**, 290.
21. S. Belal, S. Soliman and M. M. Bedair, *J. Drug Res. Egypt*, 1983, **14**, 195.
22. P. Job, *Ann. Chim. (Paris)*, 1928, **9**, 113.
23. R. Caucutt and R. Boddy, *Statistics for Analytical Chemists*, Chapman & Hall, London, 1983.

A RAPID METHOD FOR THE DETERMINATION OF SOME ANTIHYPERTENSIVE AND ANTIPYRETIC DRUGS BY THERMOMETRIC TITRIMETRY

U. M. ABBASI and FATEH CHAND

Department of Analytical Chemistry, Institute of Chemistry University of Sind, Jamshoro, Sind, Pakistan

M. I. BHANGER and S. A. MEMON

National Centre of Excellence in Analytical Chemistry, University of Sind, Jamshoro, Sind, Pakistan

(Received 6 September 1983. Revised 27 August 1985. Accepted 25 September 1985)

Summary—A simple and rapid method is described for the direct thermometric determination of milligram amounts of methyl dopa, propranolol hydrochloride, 1-phenyl-3-methylpyrazolone (MPP) and 2,3-dimethyl-1-phenylpyrazol-5-one (phenazone) in the presence of excipients. The compounds are reacted with *N*-bromosuccinimide and the heat of reaction is used to determine the end-point of the titration. The time required is approximately 2 min, and the accuracy is analytically acceptable.

N-Bromosuccinimide (NBS) is a valuable reagent for the determination of many organic compounds.¹ Its use as a titrant for the determination of ascorbic acid was first introduced by Barakat *et al.*² Pathak *et al.*³ have reported the titration of methyl dopa and propranolol hydrochloride with NBS, with Methyl Red as indicator. Potentiometric titration of pharmaceuticals with NBS is also reported in the literature.^{4,5} The usefulness of NBS results from its high oxidation potential and applicability in oxidation, substitution and addition reactions.^{2,6}

In analysis of pharmaceuticals problems sometimes arise if the matrix is coloured or the components of the formulation are not all readily soluble in the reaction medium. The classical methods of analysis therefore often involve a filtration or solvent extraction step before the active ingredient is in a suitable medium for determination. Thermometric titrimetry overcomes this problem provided the reaction chosen is selective for the active ingredient, the heat of reaction is large enough, and the excipients are thermally neutral. By taking advantage of the rapid bromination reaction of NBS with organic compounds, we have developed a simple, fast and selective thermometric method which is quantitative and accurate for the determination of milligram amounts of some antihypertensive and antipyretic drugs.

EXPERIMENTAL

Instrumentation and procedure

The instrument was as described earlier,⁷ with certain modifications. The basic electrical circuit had a simple d.c. Wheatstone bridge, incorporating a thermistor of nominal resistance 10 k Ω at 25 $^{\circ}$ (Standard Telephone and Cables Ltd., model F-14). The off-balance voltage was fed into an operational amplifier and the output recorded (2-mV full-scale deflection) at a chart-speed of 6 cm/min.

For accurate and precise delivery of the titrant and titrand a Mettler automatic titrator model DV 11 or 13 was coupled with the instrument. The delivery rate was found gravimetrically to be 4.47 ml/min. The titrant was maintained at a constant temperature of 24.00 \pm 0.01 $^{\circ}$ by passage through a thermostat before entering the titration vessel. The titration vessel was a thick-walled polythene bottle of nominal capacity 15 ml, and was thermally insulated in a polystyrene block so that heat losses during titration were not significant. A known amount of sample was placed in the titration vessel and stirred mechanically at constant speed until thermal stability was achieved. It was then titrated with NBS and the amount of sample estimated from the enthalpogram.

Reagents

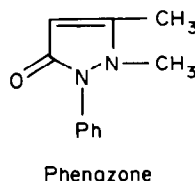
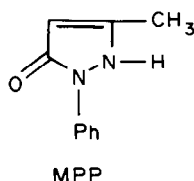
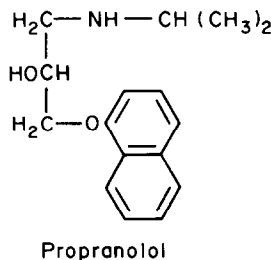
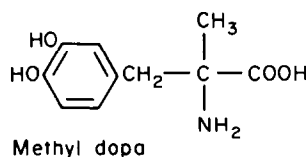
The methyl dopa (Merck, Sharp and Dohme) and propranolol hydrochloride (Ciba-Geigy) used were of pure pharmaceutical grade. The phenazone and MPP were prepared by a standard procedure.⁸ The identity and purity of all these reagents were checked by taking melting points and mixed melting points, followed by ultraviolet spectroscopy,^{9,10} thin-layer chromatography, and analysis by a standard method.¹¹ Standard solutions (100 ml) were prepared by dissolving accurately weighed amounts in doubly distilled water. The NBS was standardized iodometrically.¹²

RESULTS AND DISCUSSION

Methyl dopa, propranolol hydrochloride, phenazone and MPP were thermometrically titrated with standard NBS solution. The results obtained (Table 1) were precise and accurate with relative standard deviations in the range 0.3–0.6%. The chemical structures of these compounds are given below. Various matrix ingredients such as starch, lactose and magnesium stearate, frequently used in pharmaceutical preparations, were found to have no effect on the determinations. Hence single-dosage forms can be analysed. All these data suggest that the test compounds are brominated readily and quantitatively.

Table I. Summary of results for NBS determination of the test compounds (11 different sample weights)

Compound	Range taken, mg	Recovery, %	Mean, %	Standard deviation, %
Methyl dopa	5-55	98.7-99.8	99.6	0.3
Propranolol hydrochloride	10-60	98.6-100.0	99.6	0.5
MPP	5-55	98.3-100.0	99.3	0.5
Phenazone	5-55	98.4-100.0	99.4	0.6



As seen from the structures, methyl dopa and propranolol contain many reactive sites for bromination. According to the literature,¹²⁻¹⁵ amino, methylene, phenyl and carboxylic groups undergo bromination by substitution.

In the pyrazolone derivatives, MPP and phenazone, substitution by an electrophile can take place at the 4-position.¹⁶ Bromine is the most likely electrophilic reagent under the conditions used, so it is assumed that the reaction product is the 4-bromo derivative. This derivative can easily be prepared by treatment of the parent compound with NBS in carbon tetrachloride or aqueous acetic acid.⁵ The molar reacting ratio for MPP and phenazone shows that one mole of the former consumes two moles of NBS. The secondary amino-group in MPP is labile to attack by a bromine atom, so the second mole of NBS is consumed to give the 2,4-dibromo derivative. Furthermore, bromine atoms at low concentration give an *N*-bromo rather than a *C*-bromo-derivative.¹⁷ It has been reported that *N*-halocompounds are easily converted into halogen and amines, whereas *C*-halogenation is non-reversible.¹⁸ Accordingly a bromine atom substituted on the nitrogen atom at the 2-position of MPP would be labile, and liberate iodine from potassium iodide under back-titration conditions.¹⁹ There is no such replaceable hydrogen atom in phenazone, however, so only one mole of NBS is consumed per mole of phenazone. The reaction ratios for methyl dopa and propranolol hydro-

chloride with NBS are 4 and 5 moles of NBS respectively per mole of pharmaceutical, and the bromination pattern is complicated.¹⁹ However, the mechanism of interaction between NBS and these compounds is not fully understood. We only suggest that most of the bromination occurs at the sites mentioned here.

CONCLUSION

In previously reported methods³ for the determination of methyl dopa and propranolol hydrochloride the concentration of sulphuric acid was critical. In the assay of phenazone and MPP a concentration of acetic acid less than 9*M* at the end-point causes the change in colour of the indicator to be less sharp, leading to difficulties in end-point detection. Moreover, titration of MPP and phenazone in more dilute acetic acid is always accompanied by precipitation of the bromo-derivative. The proposed thermometric method for the determination of these pharmaceutical compounds is more precise, accurate, selective and rapid in aqueous media in the presence of manufacturing impurities, than the classical and potentiometric techniques. It provides analytically acceptable results for routine analysis.

Acknowledgements—The authors are grateful to Merck, Sharp and Dohme (Karachi) for a valuable gift of pure methyl dopa.

REFERENCES

1. N. K. Mathur and C. K. Narang, *The Determination of Organic Compounds with N-Bromosuccinimide and Allied Reagents*, Academic Press, New York, 1975.
2. M. Z. Barakat, M. F. Abdul Wahab and M. M. El-Sadr, *Anal. Chem.*, 1955, **27**, 538.
3. V. N. Pathak, S. R. Shukla and I. C. Shukla, *Analyst*, 1982, **107**, 1086.
4. M. M. Amer, A. M. Taha, B. A. El-Zeany and O. A. El-Sawy, *ibid.*, 1982, **107**, 908.
5. *Idem*, *ibid.*, 1982, **107**, 1054.
6. I. Haroun and F. Khattab, *Indian J. Pharm.*, 1978, **40**, 12.
7. U. M. Abassi and L. S. Bark, *4th International SAC Conference*, 1977.
8. A. I. Vogel, *Textbook of Practical Organic Chemistry*, 4th Ed., p. 882. Longmans, London, 1978.
9. E. G. C. Clarke, *Isolation and Identification of Drugs in Pharmaceutical, Body Fluids and Post-mortem Materials*, Pharmaceutical Press, London, 1974.
10. R. C. V. Weast, *Handbook of Chemistry and Physics*, 58th Ed., CRC Press, Cleveland, 1978.
11. *The Pharmacopoeia of Japan*, 9th Ed., p. 595. Society of Japanese Pharmacopoeia, Yakuji Nippo Ltd., Tokyo, 1976.
12. M. Z. Barakat and M. F. A. El-Wahab, *Anal. Chem.*, 1954, **26**, 1973.
13. R. D. Tiwari, J. P. Sharma and I. C. Shukla, *Talanta*, 1967, **14**, 853.
14. M. Z. Barakat and M. Shaker, *Analyst*, 1964, **89**, 216.
15. C. A. Grobe and R. J. Schmidt, *Experimentia*, 1979, **5**, 199.
16. J. Ledrut and G. Combes, *Compt. Rend.*, 1950, **231**, 1513.
17. P. S. Skell, D. N. Tuleen and P. D. Readio, *J. Am. Chem. Soc.*, 1963, **85**, 2850.
18. S. Patai, *The Chemistry of Functional Groups*, Interscience, New York, 1968.
19. A. M. Taha, O. A. El-Sawy, A. M. Amer and B. A. El-Zeany, *Analyst*, 1982, **107**, 1272.

NUCLEAR MAGNETIC RESONANCE SPECTROMETRY OF CHEMICALLY AND PHYSICALLY ALTERED POROUS SILICA SURFACES UNDER GAS CHROMATOGRAPHIC CONDITIONS

R. K. GILPIN* and M. E. GANGODA†

Department of Chemistry, Kent State University, Kent, Ohio 44242, U.S.A.

(Received 20 August 1984. Revised 21 May 1985. Accepted 25 September 1985)

Summary—Conventional nuclear magnetic resonance spectrometry in solution, in combination with ^{13}C labelling, has been utilized to investigate differences in freedom of motion of similar chemically altered and physically modified porous silica sorbents under dry conditions, and the results have been correlated with previously reported results for chemically altered solvated surfaces. Spin-lattice relaxation time of the labelled terminal methyl groups decreases in the order chemically modified solvated ligands, chemically bonded unsolvated ligands, and physically sorbed unsolvated molecules.

Various techniques have been used in preparing chromatographic sorbents, including thermal treatment, salt modification, physical coating, and chemical reactions, alone or in combination, *e.g.*, reaction of a chlorosilane with the sorbent followed by physical coating with liquid phase. The physical coating and chemical reaction procedures have been the most widely accepted methods of achieving selectivity in gas and liquid chromatography respectively. Characterization of such modified materials has been important in the development of reproducible materials with known selectivities, and many methods have been used for the purpose.

Most recently, spectral probing of the surface has emerged as a technique for investigation of the properties of sorbents. The methods used include fluorescence,^{1,2} infrared^{3,4} and photoacoustic^{4,5} spectroscopy as well as nuclear magnetic resonance (NMR) spectrometry.⁶⁻²¹ Key questions which have only partially been answered are concerned with the steric and motional aspects of the molecules immobilized on the surface.

NMR spectrometry, especially of ^{13}C , has been widely applied to study various aspects of modified surfaces. Information thus gained falls into several classes: (1) characterization of attached ligands;^{4,6-10} (2) determination of degree of surface modification;¹³ (3) elucidation of bonding chemistry;¹⁴ (4) measurement of molecular dynamics.¹⁵⁻¹⁷ Most of these studies have been made by using magic-angle spinning and proton cross-polarization, especially for chemically attached ligands, for which line-broadening occurs owing to restricted molecular mobility.

In the past, conventional NMR has been used to investigate adsorbed molecules,¹⁸⁻²⁰ but until recently its application to chromatographic-type, bonded-phase surfaces has been limited owing to problems of signal intensity and multiple-line coalescence arising from the broad resonances of similarly shifted signals.^{7,16,21} These problems have been minimized by ^{13}C enrichment of a chosen carbon atom in the attached ligand.²²⁻²⁴ Using such chemically modified materials, we have examined various aspects of the surface, including surface-backbone structure,^{7,21} preferential surface solvation in binary aqueous-organic systems (corresponding to liquid chromatography),²¹ and changes in spin-lattice relaxation as a function of position of labelling, surface-attachment chemistry, and degree of coverage.¹⁶ As a follow-up this report presents a comparison of data for chemically modified and physically coated porous silica under dry conditions (*i.e.*, corresponding to gas chromatography). Further, it correlates these dry-state (*i.e.*, unsolvated surface) data with the previously reported liquid-state (*i.e.*, solvated surface) data.¹⁶

EXPERIMENTAL

Materials

The synthesis of the labelled chlorosilanes used has been described previously,²⁴ but for convenience is summarized below. Two labelled compounds were made, one with a ^{13}C -enriched terminal carbon atom in the alkyl chain and the other with the labelled carbon atom attached to the silicon atom. For the first, 1-bromoundecene was reacted with magnesium to produce the corresponding Grignard reagent, ^{13}C -labelled carbon dioxide was bubbled through the solution to yield dodecenoic acid which was then reduced to the corresponding alcohol with lithium aluminium hydride, and the alcohol was treated with tosyl chloride in the presence of pyridine to give the tosylate. The tosylate was reacted with sodium iodide in acetone to yield the iodoalkene, which was reduced with lithium aluminium hydride to form terminally labelled dodecene. This was

*Author to whom correspondence should be addressed.

†Present address: Department of Chemistry, University of Oklahoma.

finally coupled with dimethylchlorosilane to produce $^{13}\text{C}_{12}$ -labelled n-dodecyltrimethylchlorosilane. For the second, octylmagnesium bromide was prepared and reacted with labelled carbon dioxide; the resulting acid was reduced with lithium aluminium hydride and the alcohol formed was treated with phosphorus tribromide to yield ^{13}C -labelled 1-bromononane. From this compound nonylmagnesium bromide was prepared and reacted with excess of silicon tetrachloride to yield $^{13}\text{C}_1$ -labelled n-nonyltrichlorosilane.

Both compounds were purified by distillation under reduced pressure and their structures verified by infrared spectroscopy, and proton and carbon NMR spectrometry.

From these products the corresponding labelled alkyltrimethylsilanes were prepared by treatment with excess of methylmagnesium iodide in diethyl ether followed by addition of dilute hydrochloric acid and shaking. The organic layer was separated and dried over anhydrous sodium sulphate, the ether was removed by gentle heating, and the remaining liquid was distilled under reduced pressure to yield the pure product. The identity of these materials was verified by infrared analysis.

The chemically modified surfaces were prepared by reacting²¹ excess of the labelled chlorosilane with 10- μm particle-size chromatographic-grade LiChrosorb SI-60 porous silica with a reported surface area of approximately 550 m^2/g .

The physically coated sorbents were prepared by mixing 1 g of the same lot of silica with an appropriate amount (*i.e.*, enough to give the desired loading) of the n-nonyltrimethylsilane or n-dodecyltrimethylsilane in about 20 ml of dry diethyl ether, mixing thoroughly with a vortex shaker, letting stand overnight and then drying for 1 hr at 105°.

NMR studies

Approximately 1 g of each material was placed in a 10-mm NMR tube and spin-lattice measurements were made with a Varian model FT-80 NMR spectrometer at ambient temperature in the absence of solvent, with C_6D_6 as the external reference compound. An inversion recovery pulse sequence was employed.

RESULTS AND DISCUSSION

The observed spin-lattice relaxation times (T_1) and the widths of the resonances at half intensity ($\nu_{1/2}$) are summarized in Table 1. In all cases a series of at least seven different pulse delays was employed. The resulting fit for each inversion recovery experiment was linear with a regression coefficient of at least 0.99. The standard deviation of the mean for multiple determinations of individual T_1 values ranged between 0.03 and 0.06 sec.

Physically coated materials

The spin-lattice relaxation time increased with increasing amount of sorbed material. As shown in Table 1, this corresponded to approximate doubling of T_1 with tripling of surface coverage. On the basis of the surface area listed by the manufacturer (550 m^2/g), such an increase in T_1 seems unreasonable. For example, for nonyltrimethylsilane, assuming uniform coverage of the total area available, the surface concentration of the silane should have been approximately 0.6 molecules/ nm^2 for the 11.6% coverage and 1.9 molecules/ nm^2 for the 34.7% coverage.

It has been suggested by several investigators²⁵⁻²⁸ that significant molecular exclusion may occur with similar porous silica materials. For adsorbents with porosity and structure close to those used in the current investigation, even under vigorous reaction conditions only about 30-40% of the surface area determined by BET may be available.²⁷

In our studies, if a similar reduction in available surface area is assumed (*e.g.*, $0.35 \times 550 \text{ m}^2/\text{g}$) an effective coverage of 2 and 6 molecules/ nm^2 area for the 12-35% loading range is not unreasonable. If this is accepted, arguments for self-association of the sorbed molecules, resulting in a quasi-liquid state, seem reasonable, and the observed increase in spin-lattice relaxation time with increasing surface concentration of the sorbed material is in agreement with expected liquid behaviour.²⁹⁻³¹ These data are also indicative of increasing motional freedom with increasing surface coverage and support the ideas of those investigators²⁵⁻²⁸ who have suggested that the available area is considerably smaller than the BET area.

Chemically bonded materials

The T_1 and $\nu_{1/2}$ values, which were also determined under unsolvated conditions, were greater than the corresponding values for the physically coated sorbents. The T_1 values demonstrate an overall significantly different degree of motional freedom for the sorbed molecules than for the chemically attached ligands. The spin-lattice relaxation time for the C_1 carbon atom of the n-nonyltrichlorosilane

Table 1. Spin-lattice relaxation and band-width data for physically coated and chemically altered surfaces under unsolvated conditions

Modification reagent	Carbon, † %	T_1 , sec	$\nu_{1/2}$, Hz
$(\text{CH}_3)_3\text{Si}^*\text{CH}_2(\text{CH}_2)_7\text{CH}_3$ (PC)§	11.6	0.75	70
	23.1	1.21	66
	34.1	1.41	62
$(\text{CH}_3)_3\text{Si}(\text{CH}_2)_{11}^*\text{CH}_3$ (PC)	11.5	0.77	76
	34.0	1.90	66
$\text{Cl}_3\text{Si}(\text{CH}_2)_{11}^*\text{CH}_3$ (CB)	13.7	2.25	125
$\text{Cl}(\text{CH}_3)_2\text{Si}(\text{CH}_2)_{11}^*\text{CH}_3$ (CB)	9.5	2.64	110
$\text{Cl}_3\text{Si}^*\text{CH}_2(\text{CH}_2)_7\text{CH}_3$ (CB)	8.0	—	720

*Denotes position of ^{13}C enrichment.

†Indicates surface loading.

§Mode of attachment: (PC) physically coated; (CB) chemically bonded.

Table 2. Spin-lattice relaxation data for chemically altered surfaces under solvated conditions

Modification reagent	Carbon,† %	T_1 , sec
$\text{Cl}(\text{CH}_3)_2\text{Si}(\text{CH}_2)_{11}^*\text{CH}_3$	9.5	3.50
$\text{Cl}_2\text{Si}(\text{CH}_2)_{11}^*\text{CH}_3$	10.8	3.25
$\text{Cl}_3\text{Si}(\text{CH}_2)_{11}^*\text{CH}_3$	13.7	2.66

*Denotes position of ^{13}C enrichment.

†Indicates surface loading.

chemically-modified surface has not been reported, owing to the extremely broad resonance (720 Hz) and resulting unfavourable signal-to-noise ratio.

For the physically coated samples with similar coverages, $v_{1/2}$ and T_1 were nearly independent of the position of labelling. However, in the case of the chemically bonded groups the decrease in line-width for the free end of the chain shows the effect of anchoring by chemical attachment. For similar chemically attached ligands studied under dry conditions by magic-angle spinning and cross-polarization techniques, Sindorf and Maciel¹⁵ suggested that rotation is the dominant factor in the overall mobility of the terminal methyl carbon atom.

Similarly, we have demonstrated¹⁶ that the same applies for chemically attached solvated ligands. In that earlier work a rather sharp drop in T_1 at increased surface coverage was interpreted as suggesting that an overall decrease in end-group mobility occurs once a certain critical surface concentration is attained. Data from those studies are summarized in Table 2. The overall higher values of T_1 for the solvated bonded state (Table 2) compared to data for the physically sorbed molecules (Table 1) suggest a relatively greater degree of motion for the end carbon atom in the chemically bonded solvated material than for that in the physically sorbed material, owing to the fact that the dominant means of relaxation is by rotation of the end methyl group in the terminal unit of such bonded ligands.

CONCLUSION

The results reported demonstrate considerable differences between physically coated and chemically modified surfaces in terms of motional freedom. Such differences should result in differences in chromatographic behaviour (e.g., in experimentally measured thermodynamic values). Work on this is

now in progress. The data further show a significant degree of exclusion of the sorbed material as well as sorption in self-associated micro-clusters.

REFERENCES

1. C. H. Lochmuller, D. B. Marshall and J. M. Harris, *Anal. Chim. Acta*, 1981, **131**, 263.
2. C. H. Lochmuller, D. B. Marshall and D. R. Wilder, *ibid.*, 1981, **130**, 31.
3. L. C. Sander, J. B. Callis and L. R. Field, *Anal. Chem.*, 1983, **55**, 1068.
4. D. E. Leyden, D. S. Kendall, L. W. Burggraf, F. J. Pern and M. DeBello, *ibid.*, 1982, **54**, 101.
5. C. H. Lochmuller, S. F. Marshall and D. R. Wilder, *ibid.*, 1980, **52**, 19.
6. G. E. Maciel, D. W. Sindorf and V. J. Bartuska, *J. Chromatog.*, 1981, **205**, 438.
7. M. E. Gangoda and R. K. Gilpin, *J. Mag. Res.*, 1983, **53**, 140.
8. E. Bayer, K. Albert, J. Reiners, M. Nieder and D. Muller, *J. Chromatog.*, 1983, **264**, 197.
9. K. Tanaka, S. Shinda and Y. Saito, *Chem. Lett.*, 1979, **179**.
10. G. R. Hays, A. D. H. Clague, R. Huis and G. V. D. Velden, *Appl. Surf. Sci.*, 1982, **10**, 247.
11. W. H. Dawson, S. W. Kaiser, P. D. Ellis and R. R. Inners, *J. Am. Chem. Soc.*, 1981, **103**, 6780.
12. I. D. Gay, *J. Phys. Chem.*, 1974, **78**, 38.
13. D. W. Sindorf and G. E. Maciel, *ibid.*, 1982, **86**, 5208.
14. *Idem*, *J. Am. Chem. Soc.*, 1983, **105**, 3767.
15. *Idem*, *ibid.*, 1983, **105**, 1848.
16. R. K. Gilpin and M. E. Gangoda, *Anal. Chem.*, 1984, **56**, 1470.
17. D. Slotfeldt-Ellingsen and H. A. Resing, *J. Phys. Chem.*, 1980, **84**, 2204.
18. D. Michel, *Surf. Sci.*, 1974, **42**, 453.
19. D. Michel, H. Pfeifer and J. Delmau, *J. Mag. Res.*, 1981, **45**, 30.
20. I. D. Gay and S. Liang, *J. Catal.*, 1976, **44**, 306.
21. R. K. Gilpin and M. E. Gangoda, *J. Chromatog. Sci.*, 1983, **21**, 352.
22. M. E. Gangoda and R. K. Gilpin, *J. Labelled Compd. Radiopharm.*, 1982, **XIX**, 283.
23. *Idem*, *ibid.*, 1982, **XIX**, 1081.
24. R. K. Gilpin and M. E. Gangoda, *ibid.*, 1984, **XXI**, 299.
25. M. F. Burke, A. K. Moreland and L. B. Rogers, *Sepr. Sci.*, 1968, **3**, 107.
26. M. F. Burke and D. G. Ackerman, Jr., *Anal. Chem.*, 1971, **43**, 573.
27. R. K. Gilpin and M. F. Burke, *ibid.*, 1973, **45**, 1383.
28. K. K. Unger, N. Becker and P. Roumeliotis, *J. Chromatog.*, 1976, **125**, 115.
29. G. E. Maciel, J. F. Haw, I-Ssuer Chuang, B. L. Hawkins, T. A. Early, D. R. McKay and L. Petrakis, *J. Am. Chem. Soc.*, 1983, **105**, 5529.
30. J. R. Lyster, Jr., H. M. McIntyre and D. A. Torchia, *Macromolecules*, 1974, **7**, 11.
31. J. E. Anderson, Kang-Jen Liu and R. Ullman, *Discuss. Faraday Soc.*, 1970, **49**, 257.

COLORIMETRIC DETERMINATION OF PIPERAZINE WITH *p*-BENZOQUINONE

ABDEL-AZIZ M. WAHBI, MOHAMMAD A. ABOUNASSIF and E. A. GAD-KARIEM

Pharmaceutical Chemistry Department, College of Pharmacy, King Saud University, P.O. Box 2457,
Riyadh-11451, Saudi Arabia

(Received 17 December 1984. Revised 15 August 1985. Accepted 13 September 1985)

Summary—Piperazine and its salts are reacted with aqueous alcoholic *p*-benzoquinone, buffered at pH 5.4, to give a coloured product with maximum absorption at 516 nm. The piperazine base has a molar absorptivity of $0.96 \times 10^4 \text{ l. mole}^{-1} \cdot \text{cm}^{-1}$ and Beer's law is obeyed over the range 2–10 $\mu\text{g/ml}$. When applied to three commercial preparations, the proposed method gave mean recoveries within 1% of those obtained by the official gravimetric method. The relative standard deviation was less than 1%.

Piperazine and its salts have been determined by gravimetric, spectrophotometric and complexometric methods.¹ The colour reaction with *p*-benzoquinone was first reported by Foucry,² and later developed into a quantitative method,³⁻⁵ based on heating the reaction mixture at 80°. This reaction with *p*-benzoquinone seems to be general for amines and Benson and Spillane⁶ have described its use for determination of a wide range of amines (aliphatic, primary and secondary, alicyclic and heterocyclic amines), again by conducting the reaction at elevated temperature.

This paper presents a simpler direct method for the determination of piperazine by reaction with *p*-benzoquinone at room temperature, without prior separation of the free base. The method is very suitable for routine analysis and can replace the official gravimetric method,⁷ which is based on precipitating the dipicrate salt.

EXPERIMENTAL

Reagents

p-Benzoquinone solution, 1%. Freshly prepared, in 95% ethanol.

Buffer solution.⁸ Prepared by mixing 44.7 ml of 0.1 *M* citric acid and 55.3 ml of 0.2 *M* disodium hydrogen orthophosphate to give 100 ml of buffer (pH 5.4).

Piperazine solution, 0.004%. Prepared in water by accurate dilution of a concentrated solution of piperazine with distilled water.

Piperazine dihydrochloride solution, 0.008%. Prepared by accurate dilution of a concentrated piperazine dihydrochloride monohydrate solution.

Piperazine citrate solution, 0.010%. Prepared by accurate dilution of a concentrated solution of piperazine citrate $3\text{C}_4\text{H}_{10}\text{N}_2 \cdot 2\text{C}_6\text{H}_8\text{O}_7 \cdot 5\frac{1}{2}\text{H}_2\text{O}$.

Piperazine phosphate solution, 0.008%. Prepared by accurate dilution of a concentrated solution of piperazine phosphate monohydrate $\text{C}_4\text{H}_{10}\text{N}_2 \cdot \text{H}_3\text{PO}_4 \cdot \text{H}_2\text{O}$

Procedure for calibration graph

Pipette 1–5 ml volumes of standard piperazine or piperazine salt solution into 20-ml standard flasks. Add 2 ml of buffer solution (pH 5.4) and 2 ml of *p*-benzoquinone

solution to each. Allow to stand for 30 min, then dilute to volume with distilled water. Prepare a reagent blank by diluting 2 ml of the buffer and 2 ml of *p*-benzoquinone solution to 20 ml with distilled water. Measure the absorbance of the standards against the reagent blank in 1-cm cells at 516 nm.

Assay of pharmaceutical preparations

Transfer an accurately weighed amount of granules or an accurately measured volume of piperazine solution equivalent to 40 mg of piperazine base ($\text{C}_4\text{H}_{10}\text{N}_2$) or 80 mg of piperazine hydrate ($\text{C}_4\text{H}_{10}\text{N}_2 \cdot 6\text{H}_2\text{O}$) or piperazine salts into a 250-ml standard flask. For granules add 100 ml of water to dissolve them, and wait till effervescence ceases. Make the solution up to volume with water. Pipette 25 ml of the clear solution into a 100-ml standard flask and complete to volume with water. Pipette 3 ml of the final solution into a 20-ml standard flask and proceed as described for the calibration graph.

RESULTS AND DISCUSSION

Ethanollic *p*-benzoquinone solution reacts with piperazine to give a red colour with maximum absorption at 516 nm (Fig. 1). The absorbance of the yellow reagent blank solution at 516 nm is only about 0.04.

The effect of the pH of the buffer used has been examined (Fig. 2) and the optimum pH for high sensitivity, minimal blank reading and high stability found to be 5.4. The colour reaches maximum intensity in 30 min and remains stable for 2½ hr (Fig. 3).

Beer's law was found to be obeyed over the concentration range 2–10 $\mu\text{g/ml}$ for piperazine base and 4–20 $\mu\text{g/ml}$ for its salts (Table 1). The apparent molar absorptivities (referred to the parent compound) were found to be $0.96 \times 10^4 \text{ l. mole}^{-1} \cdot \text{cm}^{-1}$ for piperazine dihydrochloride and piperazine phosphate, and $2.97 \times 10^4 \text{ l. mole}^{-1} \cdot \text{cm}^{-1}$ for piperazine citrate.

The method was applied to the determination of piperazine in three commercial preparations. The results obtained were compared with those obtained by the official gravimetric method based on weighing the dipicrate salt. Thus for "Uvilon Solution" la-

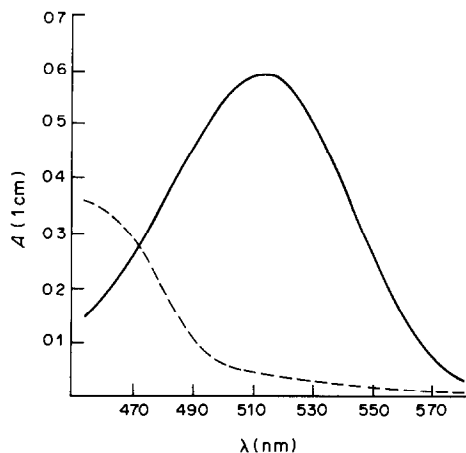


Fig. 1. Absorption spectra of piperazine citrate·5½H₂O (15 µg/ml)-*p*-benzoquinone complex (—) and reagent blank (---), pH 5.4.

belled to contain 1000 mg of piperazine hydrate (C₄H₁₀N₂·6H₂O) neutralized with citric acid per 5 ml of solution, the recoveries (relative to nominal content) found were 94.4 ± 0.6 and 94.2 ± 0.5% (mean and standard deviation) for the *p*-benzoquinone and the official method, respectively. "Urosolvin" effervescent granules, labelled to contain 1.8 g of piperazine hydrate, C₄H₁₀N₂·6H₂O, 4.2 mg of colchicine, 1.8 mg of atropine sulphate and 9.6 g of sodium citrate per 70 g, have been assayed by the two methods and the recoveries were 103.0 ± 0.6 and 103.4 ± 0.4%, respectively. "Piperazine Midy" effervescent granules labelled to contain 3.50% of piperazine hydrate gave recoveries of 102.2 ± 0.8 and 101.5 ± 0.6%, respectively (Table 2). Application of the *t*- and *F*-tests⁸ showed that there was no significant difference in precision and accuracy between the proposed and the official methods. The official gravimetric method⁷ was also applied to ascertain the purity of the piperazine, piperazine dihydrochloride monohydrate, piperazine phosphate monohydrate and piperazine citrate [(C₄H₁₀N₂)₃·2C₆H₈O₇·5½H₂O] used in the work. The values obtained were 97.8 ± 0.2, 99.6 ± 0.2, 99.8 ± 0.1 and 101.4 ± 0.1%, respectively, based on 4 replicates of each. The relatively low purity of the piperazine base (97.8%) is attributed to the presence of water of deliquescence, but this was taken into

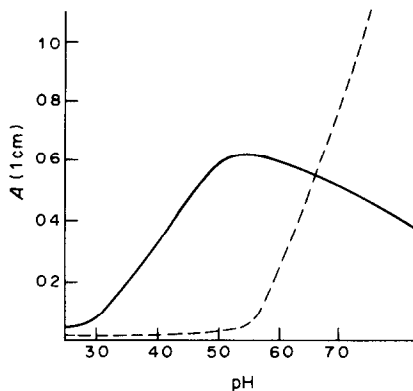


Fig. 2. Effect of pH on absorbance of the colour produced on reaction of *p*-benzoquinone with piperazine.

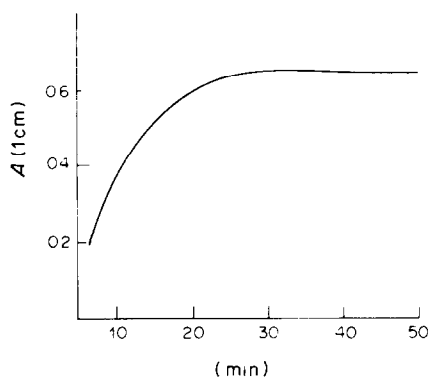


Fig. 3. Effect of time on absorbance of the colour developed on reaction of *p*-benzoquinone with piperazine.

account in constructing the calibration graph. The calibration graphs for piperazine base and piperazine hexahydrate are practically identical.

The method has the advantage over the previous methods⁴⁻⁶ that no heating is required. Since *p*-benzoquinone reacts with primary, secondary, alicyclic and heterocyclic amines,⁶ any of these compounds, if present, might interfere with the determination. Piperazine degradation products containing primary or secondary amine groups might also give a positive reaction. However, this is also the case with the official gravimetric method, which is thus no more specific than the proposed method.

Benson and Spillane⁶ reported that condensation may take place between an amine and *p*-benzoquinone at position 2 or positions 2 and 5 when the

Table 1. Beer's law linearity ranges and regression equations

Compound	Linearity range, µg/ml	Regression equation*
Piperazine	2-10	$A = 0.002 + 0.0998C$
Piperazine dihydrochloride·H ₂ O	4-10	$A = 0.004 + 0.0483C$
Piperazine·H ₃ PO ₄ ·H ₂ O	4-20	$A = 0.001 + 0.0423C$
Piperazine citrate·5½H ₂ O	5-25	$A = 0.006 + 0.0332C$

*C = concentration in µg/ml.

Table 2. Comparison of the recommended procedure with the official BP (1980) method

Sample	Recovery \pm S.D., %			
	Official method	<i>p</i> -Benzoquinone method	<i>F</i> *	<i>t</i> *
Uvilon solution	94.2 \pm 0.5 (<i>n</i> = 4)	94.4 \pm 0.6 (<i>n</i> = 5)	1.70 (9.12)	0.47 (2.365)
Urosolvin eff. granules	103.4 \pm 0.4 (<i>n</i> = 4)	103.0 \pm 0.6 (<i>n</i> = 5)	2.21 (9.12)	1.18 (2.365)
Piperazine Midy eff. granules	101.5 \pm 0.6 (<i>n</i> = 4)	102.2 \pm 0.8 (<i>n</i> = 5)	1.70 (9.12)	0.49 (2.365)

n = number of replicates.

*Results in parentheses indicate tabulated levels at *P* = 0.05.

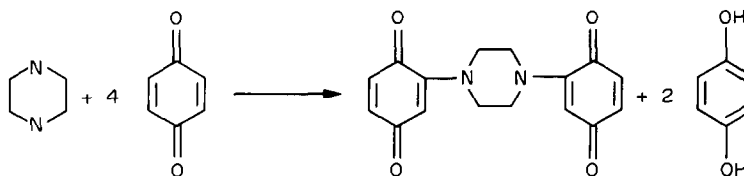


Fig. 4. Proposed reaction mechanism.

reaction is done at 80° in chloroform. However, application of the molar-ratio and continuous-variations methods under the conditions given in this paper showed the reacting ratio of *p*-benzoquinone to piperazine to be 4:1. This can be explained as due to an oxidation-reduction reaction as shown in Fig. 4.

REFERENCES

1. M. S. Rizk, M. I. Walsh and F. A. Ibrahim, *Analyst*, 1981, **106**, 1163.
2. M. Foucry, *J. Pharm. Chim.*, 1934, **20**, 116.
3. J. W. Cavett and J. P. Heotis, *J. Assoc. Off. Agric. Chem.*, 1955, **41**, 323.
4. H. F. Beckmann and L. Feldman, *J. Agri. Food Chem.*, 1960, **8**, 227.
5. M. F. Loucks and L. Nauer Jr., *J. Assoc. Offic. Anal. Chem.*, 1967, **50**, 268.
6. G. A. Benson and W. J. Spillane, *Anal. Chem.*, 1976, **48**, 2149.
7. *British Pharmacopoeia*, pp. 352-353. Her Majesty's Stationery Office, London, 1980.
8. *Documenta Geigy, Scientific Tables*, 6th Ed., p. 314. Geigy, Manchester, 1962.

SORPTION OF SILVER, GOLD AND PALLADIUM WITH A POLYTHIOETHER FOAM

A. S. KHAN and A. CHOW

Department of Chemistry, University of Manitoba, Winnipeg, Manitoba, Canada

(Received 22 March 1985. Revised 23 July 1985. Accepted 10 September 1985)

Summary—Silver, gold and palladium can be sorbed by a thiopolymer of the type $[\text{HO}(\text{CH}_2\text{CH}_2\text{OCH}_2\text{SS})_n\text{CH}_2\text{CH}_2\text{OH}]$. The distribution coefficient for palladium increases with halide concentration, with iodide having the largest effect. Silver can be extracted from chloride, nitrate or picrate media. The different distribution coefficients for gold in hydrochloric acid and in sodium chloride suggest that different sorption mechanisms predominate.

In 1970 Bowen reported the use of polyether-based polyurethane foam for the sorption of several substances from aqueous media.¹ Since then, polyurethane foam has been widely used for the sorption and concentration of both inorganic and organic species.² The sorption of platinum metals by polyether foam from thiocyanate media,³ of gold(III) from chloride media⁴ and as a thiourea complex from perchlorate solution,⁵ and of silver from picrate solution⁶ have been reported.

The hard and soft acid-base theory⁷ predicts that a polythioether foam should give greater sorption and selectivity than a similar polyether foam for soft metal ions such as gold(III), palladium(II), silver(I), mercury(I) and copper(I). In fact, the use of organic sulphur compounds as solvents for extraction of several of these metals has been reported. Palladium(II) has been extracted from chloride solution by neutral organic sulphur compounds such as alkylsulphides⁸ and petroleum sulphides⁹ and solvents of this type have also been used to recover gold(III), from both nitric and hydrochloric acid solutions.¹⁰ The extraction of silver from nitric acid by diesel oil¹¹ and of silver(I) and mercury(I) with a macrocyclic polythioether¹² has also been recorded. Although polyether foam is a more efficient extraction agent than its monomeric analogue, diethyl ether, there has been little analytical use of polymeric thioethers. The synthesis and use of SH-polyurethane foam for the concentration of mercury(II) was reported earlier.¹³ While the present work was in progress, the synthesis and use of a polymeric thioether of the type $(\text{CH}_2\text{-S})_n$ for the sorption of platinum metals appeared.¹⁴

The present work uses a thiopolymer (Thiokol) for the sorption of noble metals from halide and other media.

EXPERIMENTAL

Apparatus

A model 306 Perkin-Elmer atomic-absorption spectrometer was used for the determination of metal ions

except for one study where ^{110m}Ag tracer was used and the samples were analysed with a Baird Atomic 530A gamma-spectrometer with a 2-in. well-type (NaI(Tl)) detector.

Reagents

Stock solutions of Pd(II) and Au(III) (1000 $\mu\text{g/ml}$) were prepared from palladium chloride and sodium tetrachloroaurate(III) dihydrate in 0.2M hydrochloric acid. A silver solution (1000 $\mu\text{g/ml}$) was prepared from analytical grade silver nitrate and ^{110m}Ag was obtained from NEN (Canada) Ltd. The Thiokol polymer was a gift from Dunlop (Canada) Ltd. and had been prepared by reacting polymer ZL574 (from Morton Thiokol, Trenton, NJ, U.S.A.) with diphenylmethane di-isocyanate. ZL574 is a hydroxy-terminated polymer of general formula $[\text{HO}(\text{CH}_2\text{-CH}_2\text{-OCH}_2\text{-CH}_2\text{-S-S})_n\text{CH}_2\text{-CH}_2\text{OH}]$ with molecular weight ~ 4000 and sulphur content 36–38%. Before use the polymer was soaked in 0.1M nitric acid for 24 hr, washed with water until free from acid, then washed with acetone and finally air-dried. All other chemicals used were analytical-reagent grade. The water was doubly distilled and demineralized.

Procedure

The sample solutions and polymer were placed in Erlenmeyer flasks and equilibrated by mechanical shaking for at least 2 hr. The degree of sorption was determined by measuring the concentration of metal ion in the aqueous phase before and after equilibration with polymer. The distribution coefficient (D in l./kg) was calculated from the degree of extraction (% E) according to the equation

$$\frac{\% E}{100 - \% E} \times \frac{V}{W} = D \text{ (l./kg)}$$

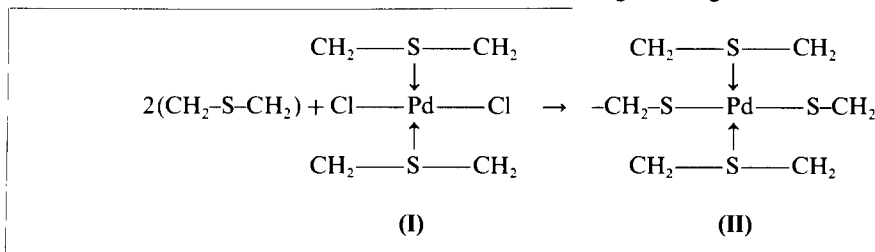
where V is the volume of sample solution (ml) and W is the weight of polymer (g).

RESULTS AND DISCUSSION

The results of preliminary studies showed that Pd(II) and Au(III) are effectively sorbed by the thiopolymer from chloride solutions, whereas Pt(II) is recovered to a lesser extent and Pt(IV) sorbs poorly. Ag(I) was efficiently sorbed even from nitrate media. The results of detailed studies of the sorption behaviour of Pd(II), Ag(I) and Au(III) by the polymer from different solutions are given below.

Palladium

Results for the sorption of Pd(II) from the halide solutions are shown in Fig. 1. The sorption increases according to halide in the order $\text{Cl}^- < \text{Br}^- < \text{I}^-$, as expected from the change in hydrophobicity. It can also be seen that in all three systems the sorption increases with the increase in initial concentration of halide, reaches a plateau and then declines with further increases, with this effect more prominent for iodide. Solutions up to $0.08M$ in iodide become turbid after addition of Pd(II), but a further increase in iodide concentration gives clear solutions. It is



likely that PdI_2 is formed at lower concentrations of iodide and dissolves as PdI_3^- or PdI_4^{2-} in presence of excess of iodide.

Another important feature of Fig. 1 is that the sorption profiles of Pd(II) from hydrochloric acid and sodium chloride solutions are identical, which suggests that Pd(II) is not sorbed by the thiopolymer as an acidic species of the type H_2PdCl_4 . Although the extraction of H_xMX_y type species has been established¹⁵ for the extraction of several metal ions from halide solutions by oxygen-containing organic solvents, it has been reported by several workers¹⁶ that Pd(II) is extracted by sulphur-containing organic solvents as a solvated species of the type $\text{PdX}_2 \cdot 2\text{RS}$. Assuming that PdX_2 is also the species sorbed in the present system, the decrease in sorption of palladium at higher concentrations of halide ion can be attributed to the increased concentration of the less sor-

bable species of the type PdX_3^- and PdX_4^{2-} . The log D vs. log $[\text{X}]$ curves in Fig. 1 indicate that the palladium complexes with lower and higher halide content are less extractable than those with intermediate metal-halide ratios. A low ratio limit of 0.4:1 (Cl:Pd) has been observed¹⁴ for the extraction of Pd from chloride media at high temperature by polymeric $(\text{CH}_2\text{S})_n$. These authors have suggested that the co-ordinately solvated species (I) extracted at room temperature is converted at higher temperature into a polymeric mercaptide (II) which also forms donor-acceptor bonds with the sulphur atoms in the neighbouring molecules.

It is not clear from our results whether the sorbed Pd species is solvated or co-ordinated in the thiopolymer. However, it is certain that Pd is not sorbed as an acidic complex by the thiopolymer.

Silver

The sorption profiles of silver from nitrate, chloride and picrate solutions are shown in Fig. 2. The sorption of silver by the thiopolymer increases with increase in the initial concentration of nitrate over the entire concentration range studied, whereas the sorption from chloride solution becomes almost constant from $>1M$ hydrochloric acid. The sorption of silver from picrate media shows a levelling off at $>2 \times 10^{-4}M$ initial picrate concentration. Silver has been extracted from nitrate solutions by several sulphur-containing organic solvents.¹⁷ In addition, the extraction of silver from nitric acid solutions by

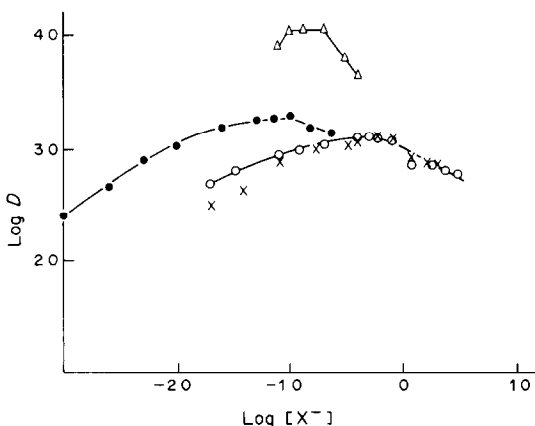


Fig. 1. Sorption of palladium from halide solutions; 45 ml of 10 ppm palladium solution; 0.05 g of polythioether foam; 2 hr equilibration. \times : Cl^- (NaCl); \circ : Cl^- (HCl); \bullet : Br^- (HBr); Δ : I^- (HI).

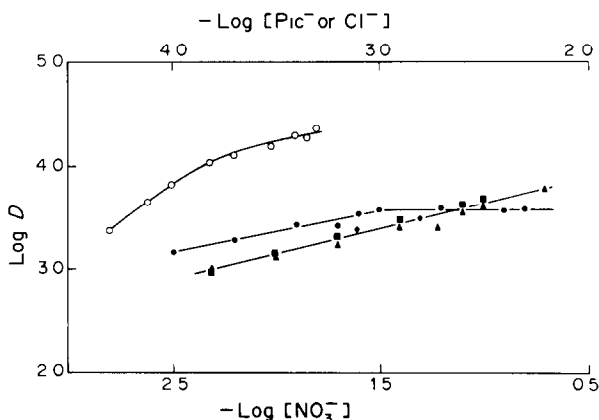


Fig. 2. Sorption of silver; 95 ml of 1 ppm silver solution; 0.10 g of polythioether foam; 3 hr equilibration. \circ : Pic^- ; \bullet : Cl^- ; \blacktriangle : NO_3^- (HNO_3); \blacksquare : NO_3^- (KNO_3); \blacklozenge : NO_3^- (NaNO_3).

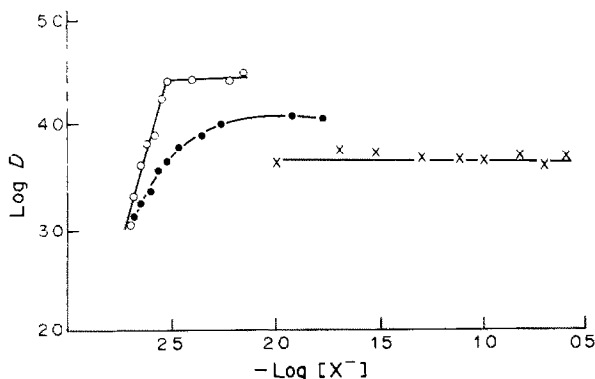


Fig. 3. Sorption of gold; 90 ml of 10 ppm gold solution; 0.10 g of polythioether foam; 3 hr equilibration. O: Cl^- (HCl); ●: Cl^- (NaCl); x: NO_3^- (HNO_3).

diesel oil has also been attributed¹¹ to the presence of sulphur compounds. A polythio-crown ether has been used¹² to extract silver from chloride, picrate and perchlorate solutions. By comparing the sorption behaviour of silver from nitric acid with that from a potassium or sodium nitrate system (Fig. 2), it is clear that, as with palladium, the sorption of silver from nitrate solution by the thiopolymer does not involve any acidic species of the type HAgX_2 , which has been reported¹⁸ to be the silver species extracted from chloride solutions by triphenylphosphine oxide. On the other hand, a solvated species of $\text{AgX} \cdot 2\text{R}_2\text{S}$ type has been established¹⁷ as the silver species extracted by sulphur-containing solvents.

The value of unity for the slope of the $\log D$ vs. $\log [\text{Pic}]$ plot is consistent with the sorption of an $[\text{AgPic}]$ species, which would agree with previous work on extraction of solvated species. On the other hand the smaller slopes for the chloride and nitrate systems suggest that sorption of silver from these solutions more likely involves a co-ordinated species.

Gold

Figure 3 shows the results of Au(III) sorption by the thiopolymer from hydrochloric acid, nitric acid and sodium chloride solutions. The most striking feature is that unlike silver and palladium, gold is sorbed to different extents from hydrochloric acid and sodium chloride solutions. Since the thiopolymer contains both oxygen and sulphur atoms in the polymeric chains, the increase of the sorption of Au(III) from hydrochloric acid solutions can be attributed to the sorption of HAuCl_4 type species by the oxygen-containing portions of the polymer. The extraction of gold from acidic chloride solutions by oxygen-containing solvents is well documented.¹⁵ On the other hand, the sulphur content of the thiopolymer has a dominant role in the sorption of Au(III) from sodium chloride solutions, but whether

Au(III) is sorbed as a solvated species of the type $\text{AuCl}_3 \cdot \text{XRS}$ or as a co-ordinated species is not apparent.

The sorption of gold(III) from nitric acid (Fig. 3) is practically constant over the entire range of nitric acid concentration studied and is similar to results reported¹⁷ for the extraction of gold and some other noble metals from nitric acid by organic sulphides.

These results clearly show that the thiopolymer is very effective for the sorption of silver, gold and palladium. In addition to these metals, it is likely that other soft metal ions, e.g., Cu(I), Hg(I), can be sorbed by the thiopolymer and that it should be possible to select suitable conditions for the separation of some of the noble metals. Further studies are required to establish the composition of the species sorbed.

Acknowledgement—This work was supported by the Natural Science and Engineering Research Council of Canada and the University of Manitoba Research Grants Committee.

REFERENCES

1. H. J. M. Bowen, *J. Chem. Soc. A*, 1970, 1082.
2. G. J. Moody and J. D. R. Thomas, *Chromatographic Separation and Extraction with Foam Plastics and Rubbers*, Dekker, New York, 1982.
3. S. J. Al-Bazi, *Ph.D. Thesis*, University of Manitoba, 1983.
4. P. Schiller and G. B. Cook, *Anal. Chim. Acta*, 1971, **54**, 364.
5. T. Braun and A. B. Farag, *ibid.*, 1973, **66**, 419.
6. A. S. Khan, W. G. Baldwin and A. Chow, *ibid.*, 1983, **146**, 201.
7. R. G. Pearson, *J. Am. Chem. Soc.*, 1963, **85**, 3533.
8. V. G. Torgov, V. N. Andrievskii, E. N. Gilbert, I. L. Kotlyarevskii, V. A. Mikhailov, A. V. Nikolaev, V. N. Pronin and D. D. Trostsenko, *Izv. Sib. Otd. Akad. Nauk SSSR, Ser. Khim. Nauk*, 1969, 148; *Chem. Abstr.*, 1970, **72**, 93804.
9. V. T. Athavale, M. N. Karnik, R. M. Sathe, V. Venkatasubramanian and Ch. Venkateswarlu, *Indian J. Chem.*, 1967, **5**, 585.
10. V. A. Pronin, M. V. Usol'tseva, Z. N. Shastina, N. K. Gusarova, E. P. Vyalkh, S. V. Amosova and B. A. Trofimov, *Russ. J. Inorg. Chem.*, 1973, **18**, 1016.
11. G. N. Shvirin, B. N. Laskorin, E. M. Shvirina and G. V. Kuzmichev, *Tsvet. Metal.*, 1966, **39**, 11; *Chem. Abstr.*, 1966, **65**, 18214.
12. D. Sevdic and H. Meider, *J. Inorg. Nucl. Chem.*, 1977 **39**, 1403, 1409.
13. M. A. J. Mazurski, A. Chow and H. D. Gesser, *Anal. Chim. Acta*, 1973, **65**, 99.
14. Yu. A. Zolotov, O. M. Petrukhin, G. I. Malofeeva, E. V. Marcheva, O. A. Shiryayeva, V. A. Shestakov, V. G. Miskar'yants, V. I. Nefedov, Yu. I. Murinov and Yu. E. Nikitin, *ibid.*, 1983, **148**, 135.
15. Y. Marcus and A. S. Kertes, *Ion Exchange and Solvent Extraction of Metal Complexes*, Chapter 9, Wiley-Interscience, New York, 1969.
16. M. Mojski, *Talanta*, 1978, **25**, 163.
17. *Idem*, *Chem. Analit. (Warsaw)*, 1979, **24**, 207.
18. V. I. Levin and M. D. Kozlova, *Radiokhimiya*, 1965, **7**, 534; *Chem. Abstr.*, **64**, 18494.

USE OF *p*-CHLORANILIC ACID FOR THE COLORIMETRIC DETERMINATION OF SOME ANTIMALARIALS

M. S. MAHROUS, M. ABDEL SALAM, A. S. ISSA
and M. ABDEL-HAMID

Department of Pharmaceutical Chemistry, Faculty of Pharmacy, University of Alexandria,
Alexandria, Egypt

(Received 1 March 1985 Revised 8 May 1985. Accepted 29 August 1985)

Summary—A simple and sensitive colorimetric method for the assay of quinine sulphate, primaquine diphosphate, amodiaquine hydrochloride and pyrimethamine is described. The method is based on the interaction of the drugs and *p*-chloranilic acid to give a stable product with an intense colour which can be used for the determination of these antimalarials in their pharmaceutical preparations.

The aminoquinoline antimalarials have been determined colorimetrically with ammonium reineckate¹ and *trans*-aconitic acid,² or by the acid dye technique³ or formation of a ternary complex with cobalt thiocyanate.⁴ Primaquine has been determined by the diazotization method⁵ and with diazo-*p*-nitroaniline,⁶ 2,6-dichloroquinone chlorimide and 1,2-naphthoquinone-4-sulphonic acid.⁷ Spectrophotometric,⁸ gravimetric⁹ and titrimetric¹⁰ methods have been used for determination of amodiaquine. Pyrimethamine (a pyrimidine derivative) has been determined by an extractive colorimetric method using Methyl Orange, Bromophenol Blue or Cresol Purple,¹¹ and by conductimetric titration.¹²

p-Chloranilic acid has recently been used for the spectrophotometric determination of some alkaloids in dioxan medium,¹³ and the aim of the present work was to use this reagent in acetonitrile medium for spectrophotometric determination of some antimalarials. The method developed has been applied to the determination of quinine sulphate, primaquine diphosphate, amodiaquine hydrochloride and pyrimethamine in pure form and in pharmaceutical preparations. The colour produced in the reaction is attributed to ion-pair formation.¹⁴

EXPERIMENTAL

Reagents

Pharmaceutical grade quinine sulphate, primaquine phosphate, amodiaquine hydrochloride and pyrimethamine. *p*-Chloranilic acid solution, 0.2% in acetonitrile. All the reagents were analytical grade and the solvents spectroscopic grade.

Standard solutions

An accurately weighed amount of the drug or its salt equivalent to 0.1 g of the free base was dissolved in about 20 ml of water. The solution was quantitatively transferred to a separatory funnel, made alkaline with ammonia solution and shaken with four 20-ml portions of chloroform,

for 2 min each time. The extracts were pooled in a 100-ml standard flask after passage through a filter paper containing anhydrous sodium sulphate, the paper being washed and the solution made up to volume with chloroform.

Calibration graphs

Volumes of the standard solution ranging from 0.2 to 1.0 ml were transferred into a series of 5-ml standard flasks and the solvent was removed by immersing the flasks in a water-bath kept at 70°. The residue was dissolved in 2 ml of acetonitrile, then 1 ml of *p*-chloranilic acid solution was added. The volume was made up to 5 ml with acetonitrile and the absorbance measured at 522 nm against a reagent blank prepared simultaneously.

Analysis of tablets

Ten tablets were finely powdered and the powder thoroughly mixed. An accurately weighed quantity of the powder equivalent to 0.1 g of the free base was transferred to a separatory funnel containing about 20 ml of water. The mixture was shaken for 15 min, then made alkaline with ammonia solution and the base was extracted and determined by the procedures above.

RESULTS AND DISCUSSION

Quinine, primaquine, amodiaquine and pyrimethamine react instantaneously with *p*-chloranilic acid in acetonitrile medium to give a purple product which has a broad absorption peak with a maximum at 522 nm. The reagent has a broad peak with a maximum at 435 nm (Fig. 1).

p-Chloranilic acid (*p*-CA) exists as the orange undissociated species H₂A at very low pH, the dark purple HA⁻ at intermediate pH, and the pale violet A²⁻ at high pH.

Since the reaction product in acetonitrile is purple, we consider that HA⁻ is the form in which the *p*-CA is involved in the reaction with the chosen antimalarials, and hence that there is proton transfer from *p*-CA to the basic centre of the antimalarials (Scheme 1). The ion-pair salt obtained dissociates to

Table 1 Results for assay of dosage forms of antimalarial drugs with *p*-chloranilic acid

Preparation*	Mean \pm SD, %	
	Proposed method	Official BP method
Quinine sulphate tablets (150 mg/tab.) ^M	101.3 \pm 0.7	98.2 \pm 0.8
Primaquine diphosphate tablets (Primaquine 15 mg/tab.) ^M	100.5 \pm 0.5	98.8 \pm 1.8
Amodiaquine hydrochloride tablets (Camoquine 260 mg/tab.) ^{P^D}	99.7 \pm 0.4	97.8 \pm 0.7
Pyrimethamine tablets (Daraprim 25 mg/tab.) ^{B^W}	99.9 \pm 0.6	98.5 \pm 0.3

*M, Misr Co.; B, Bayer Co.; P.D., Park Davis; B.W., Burroughs Wellcome.

†Six separate determinations

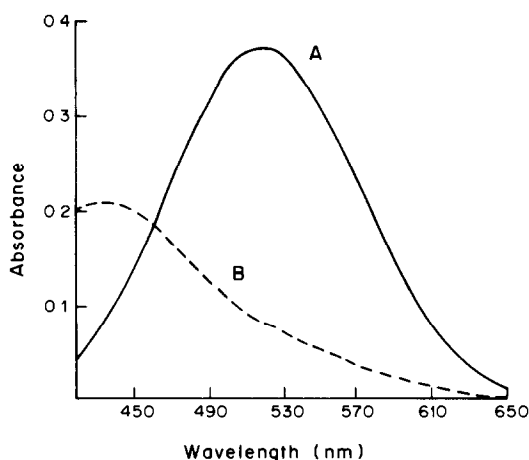
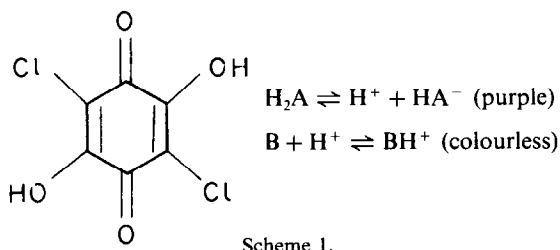


Fig. 1. Absorption spectra of A, primaquine-*p*-chloranilic acid reaction product measured against reagent blank; B, reagent blank measured against acetonitrile. Primaquine concentration = 120 μ g/ml; *p*-CA concentration = 2×10^3 μ g/ml.

give the purple HA^- anion.¹⁴ This dissociation is promoted by a solvent with high dielectric constant.



We reject the alternative mechanism involving a radical anion CA^- , since we have found no ESR signal suggesting its presence.¹⁴

p-Chloranilic acid gives an immediate colour reaction with the drug bases at room temperature. For quantitative purposes a volume of 1 ml of 0.2% *p*-CA in acetonitrile for a final volume of 5 ml is the optimal quantity for maximal colour formation. The colour is stable for at least 5 hr.

Beer's law is valid over the concentration range 0.04–0.20 mg/ml for amodiaquine, primaquine and pyrimethamine and 0.04–0.12 mg/ml for quinine.

Application of official methods and the proposed method for assay of the test compounds in their dosage forms gave the results presented in Table 1. Student's *t*-test showed that the proposed and official methods are equally accurate (95% confidence level). The proposed method is simpler, faster and more sensitive than the official procedures. These advantages suggest its application in the analysis and quality control of these antimalarials in their pharmaceutical preparations. Substances having no basic centre are not expected to interfere, since extraction of the antimalarial base precedes the colour reaction. Although the method will not differentiate between the antimalarials investigated it is useful for routine analysis and quality control.

REFERENCES

- S. K. Sheng, C. I. Hsieh and S. H. Peng, *Yao Hsueh Pao*, 1965, **12**, 622; *Chem. Abstr.*, 1966, **64**, 7967c.
- R. Strufe, *Clin. Chim. Acta*, 1960, **5**, 753.
- P. D. Shirsat, *Indian J. Pharm.*, 1976, **38**, 77.
- S. M. Hassan, M. E.-S. Metwally and A. A. Abou-Ouf, *Analyst*, 1982, **107**, 1235.
- British Pharmacopoeia 1980*, Vol. 1, p. 365. H.M. Stationery Office, London, 1973.
- S. M. Hassan, M. E.-S. Metwally and A. A. Abou-Ouf, *Anal. Lett.*, 1982, **15**, 213.
- A. A. Abou-Ouf, S. M. Hassan and M. E.-S. Metwally, *Analyst*, 1980, **105**, 1113.
- United States Pharmacopoeia*, XXth Revision, p. 41. Mack, PA, 1980.
- British Pharmacopoeia 1980*, Vol. 1, p. 31. H.M. Stationery Office, London, 1973.
- T. S. Wu, C.-C. Sun and T. H. Teng, *Yao Hsueh Hsueh Pao*, 1958, **6**, 353; *Chem. Abstr.*, 1959, **53**, 20691d.
- R. T. Sane and A. Y. Dhamanker, *Indian Drugs*, 1981, **19**, 80.
- K. N. Kolic, P. Popovic and M. Bodiroga, *Arch. Farm.*, 1982, **32**, 9.
- M. A. El-Sayed and P. S. Agarwal, *Talanta*, 1982, **29**, 535.
- M. A. El-Sayed, M. Abdel-Hamid, M. A. Korany, M. Abdel-Hady and S. M. Galal, *Spectrosc. Lett.*, 1984, **17**, 803.

SIMULTANEOUS POLAROGRAPHIC DETERMINATION OF CADMIUM AND TELLURIUM IN ELECTRO-DEPOSITED CADMIUM TELLURIDE THIN FILMS

ANDRZEJ DARKOWSKI† and MICHAEL COCIVERA*

Guelph-Waterloo Centre for Graduate Work in Chemistry, University of Guelph, Guelph,
Ontario, Canada

(Received 29 March 1985. Accepted 6 August 1985)

Summary—A polarographic method has been developed for the simultaneous determination of cadmium and tellurium in thin-film cadmium telluride. The procedure involves dissolution of the film with concentrated nitric acid, which is subsequently removed by evaporation. The Cd(II) and Te(IV) waves are well separated at pH 10, but sufficient ammonia must be present to prevent the precipitation of cadmium hydroxide.

The cathodic electro-deposition of thin-film cadmium telluride has been reported by a number of workers.¹⁻⁷ The interest in this material arises because it has an energy band-gap well suited to the solar spectrum, has a direct transition and absorbs strongly, and can be deposited as either *n*- or *p*-type. This last property is related to the composition of the film. An excess of cadmium results in *n*-type and an excess of tellurium in *p*-type CdTe.⁸ In a number of studies of electro-deposition from solutions containing Cd(II) and Te(IV), X-ray diffraction and electron microprobe analysis were used to determine the composition of the film in relation to its type of conductivity.³⁻⁶ Since these techniques cover small surface areas, polarography can act as an effective complement to them because it can provide the average composition of the whole film as well as the total amount of material deposited. In addition, polarography has the advantages of speed and cheapness. It has been very helpful in our studies of new electrochemical processes for the preparation of thin-film cadmium telluride,⁷ with special regard to correlation of composition with deposition conditions. We have found that the non-aqueous cathodic electro-deposition of CdTe from solutions containing Cd(II) and tri-*n*-butylphosphine telluride results in a *p*-type film which contains a slight excess of cadmium.⁷ Consequently, since an excess of cadmium usually produces *n*-type CdTe, it would appear that the excess is not uniformly distributed throughout the films and may occur in small pockets and hence not affect the type of conductivity.

EXPERIMENTAL

The calibration procedure made use of standard solutions of Cd(II) and Te(IV), which were mixed to provide solu-

tions containing various Cd/Te concentrations and ratios. The cadmium solutions were prepared from cadmium perchlorate, and the tellurium(IV) solutions by dissolving elemental tellurium in concentrated nitric acid, which was then removed by evaporation after addition of few ml of sulphuric acid. The pH of the mixed solution was raised to 10 by addition of ammonia solution, and 0.1M ammonium sulphate was used as the supporting electrolyte. The total volume of the solution was brought to 25 ml. At equimolar cadmium and tellurium concentrations of $5 \times 10^{-4}M$ or lower, the tellurium wave was not distorted, and the diffusion current for the tellurium was exactly twice that for the cadmium (Table 1).

Cadmium telluride films for analysis were dissolved in a few drops of concentrated nitric acid, after which a few ml of sulphuric acid were added and the excess of nitric acid was removed by evaporation. The solution was diluted to 20 ml. After addition of 0.125 g of ammonium sulphate and adjustment of the pH to 10 with ammonia solution, sufficient distilled water was added to adjust the cadmium and tellurium concentrations to close to $10^{-4}M$. As a check of this procedure, authentic samples of 99.99% pure CdTe were dissolved in the same manner and analysed.

The polarographic analysis was performed with a PAR 174A polarographic analyser operating in the normal mode. A drop-time of 1 sec and a potential scan of 5 mV/sec were employed. These conditions provided two clean waves that were well separated, with $E_{1/2}$ at -600 ± 20 mV for Cd(II) and -800 ± 10 mV for Te(IV), vs. Ag/AgCl. A pool of mercury was used as the counter-electrode.

RESULTS AND DISCUSSION

Figure 1 shows the polarogram of a solution containing Cd(II) and Te(IV), both at $1 \times 10^{-4}M$ concentration. Since the cadmium reduction involves two electrons, the fact that the tellurium reduction current is twice that of the cadmium indicates a four-electron reduction for the tellurium. Table 1 indicates that this current ratio holds for concentrations up to $5 \times 10^{-4}M$. Consequently it appears that Te(IV) is reduced to elemental tellurium under these conditions. The diffusion current was linearly proportional to concentration for both elements, the slopes of the calibration graphs

*Author to whom correspondence should be addressed.

†On leave from Department of Chemistry, Warsaw Technical University.

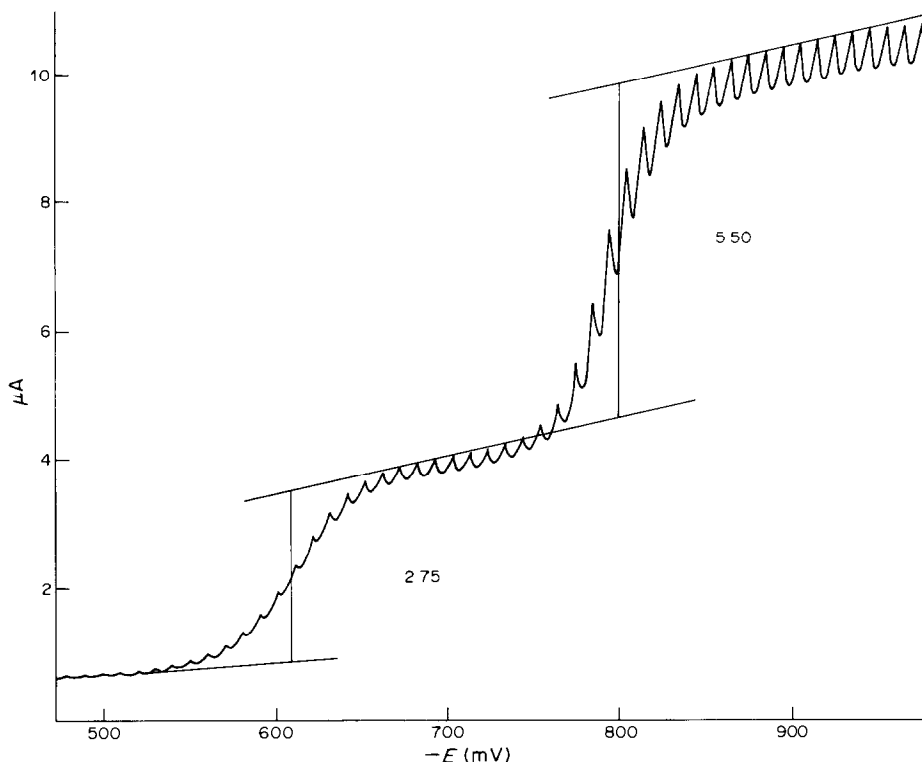


Fig. 1. Polarographic waves due to Cd(II) and Te(IV), both $10^{-4}M$, with $E_{1/2}$ at -610 and -800 mV vs. Ag/AgCl, respectively. Supporting electrolyte was $0.1M$ ammonium sulphate.

Table 1. Polarography of standard solutions containing Cd(II) and Te(IV)

[Cd(II)], $10^{-4}M$	[Te(IV)], $10^{-4}M$	Diffusion current, μA		Current ratio, i_{Te}/i_{Cd}
		Cadmium	Tellurium	
5.0	5.0	1.32	2.64	2.0
2.0	2.0	0.52	1.06	2.0 ₄
1.0	1.0	0.275	0.55	2.00
0.50	0.50	0.132	0.270	2.05
0.50	1.0	0.134	0.563	4.20
2.0	1.0	0.50	0.52	1.0 ₄

being 26 and 52 $\text{mA} \cdot \text{l} \cdot \text{mole}^{-1}$ for cadmium and tellurium respectively. Cadmium concentrations larger than $5 \times 10^{-4}M$ are not practical because the increased ammonia concentration that is required to prevent precipitation of cadmium hydroxide results in poor separation between the Cd(II) and Te(IV) reduction waves. Below $5 \times 10^{-5}M$ concentration the ratio of the diffusion currents for the two waves deviates from 2 and calibration curves must be employed. A CdTe film electro-deposited on a titanium plate was dissolved and the procedure applied to the solution; two waves were obtained, which were similar to those in Fig. 1. We have found no wave for Te(VI), for which $E_{1/2}$ is quoted⁹ as -1.34 V at pH 9.2 in the presence of ammonium chloride. As a control, the dissolution procedure was repeated with a bare titanium plate; no waves were observed over the scan range employed for the CdTe analysis. Table

2 lists some results of analyses of authentic samples of 99.99% pure CdTe. For ten replicate analyses the

Table 2. Polarographic analysis of 99.99% pure CdTe and electro-deposited thin-film CdTe

[CdTe], $10^{-4}M$	Measured concentrations, $10^{-4}M$		Atomic ratio, Te/Cd
	[Cd(II)]	[Te(IV)]	
1.50*	1.5 ₆	1.5 ₃	0.98
1.00*	1.0 ₃	1.0 ₃	1.0 ₀
0.75*	0.77 ₅	0.78 ₇	1.0 ₁
0.50*	0.52 ₂	0.52 ₇	1.0 ₁
Film†	0.51	0.58	1.1 ₁
Film†	0.91 ₅	0.98	0.99 ₄

*Prepared by dissolution of 99.99% pure CdTe according to the procedure in text.

†Dissolution of thin-film CdTe that had been electro-deposited on titanium.

average Te/Cd ratio was 0.99₆ with a standard deviation of 0.01₂ and 95% confidence limits of ± 0.01 . The close agreement between the measured concentration and that based on the mass of material dissolved indicates that the dissolution procedure causes little loss of tellurium by evolution of hydrogen telluride. For comparison, the results⁷ for two electro-deposited CdTe thin films are also listed.

The advantage of this analytical procedure is that it is relatively quick because cadmium and tellurium are determined simultaneously with a minimum of handling. The polarographic analysis for tellurium in the presence of 0.1 M sodium hydroxide⁹ is less attractive because cadmium is precipitated under these conditions and, therefore, cannot be determined simultaneously with the tellurium. Likewise, polarographic analysis in dilute nitric acid is less attractive because two pre-waves occur before the tellurium

wave,¹⁰ and we have found that the tellurium wave is sometimes distorted by hydrogen evolution.

REFERENCES

1. M. P. R. Panicker, M. Knaster and F. A. Kroger, *J. Electrochem. Soc.*, 1978, **125**, 566.
2. G. Fulop, M. Doty, P. Meyers and C. H. Liu, *Appl. Phys. Lett.*, 1982, **40**, 327.
3. R. N. Bhattacharya, K. Rajeshwar and R. N. Noufi, *J. Electrochem. Soc.*, 1984, **131**, 939.
4. J. Llabres, *ibid.*, 1984, **131**, 464.
5. M. Takahashi, K. Uosaki and H. Kita, *ibid.*, 1984, **131**, 2304.
6. K. Uosaki, M. Takahashi and H. Kita, *Electrochim. Acta*, 1984, **29**, 279.
7. A. Darkowski and M. Cocivera, unpublished work.
8. D. de Nobel, *Philips Res. Rep.*, 1959, **14**, 361.
9. M. Heyrovský and P. Zuman, *Practical Polarography*, p. 198. Academic Press, New York, 1968.
10. D. C. Whitnack, T. M. Donovan and M. H. Ritchie, *Electroanal. Chem. Interfacial Chem.*, 1967, **14**, 205.

ANALYTICAL DATA

ADSORPTION OF UNIVALENT AND BIVALENT METAL NITRATES ON HYDROUS LEAD DIOXIDE

ADSORPTION BEHAVIOUR OF POTASSIUM, CUPRIC, ZINC, CADMIUM AND NITRATE IONS

HIROAKI KAWANO

Osaka Municipal Technical Research Institute, Osaka, Japan

YOSHIKAZU NAKAI, TOSHIO MATSUDA and TOYOSHI NAGAI

Department of Chemistry, Ritsumeikan University, Kyoto, Japan

(Received 31 January 1985. Revised 22 April 1985. Accepted 20 August 1985)

Summary—The individual adsorption behaviour of potassium, cupric, zinc, cadmium and nitrate ions on hydrous lead dioxide (HLD) was investigated. HLD was found to be an amphoteric ion-exchanger with an equi-adsorption point in the vicinity of pH 4.6. For bivalent metal ions, the amount of adsorption increased with pH (at pH > 3) and there was almost 100% adsorption at pH > 6. Both the adsorption capacity and the adsorption affinity on HLD were in the order copper(II) > zinc(II) > cadmium(II).

Hydroxides and hydrous oxides of various metals have been used as co-precipitation¹ or adsorption^{2,3} reagents for separation or concentration of trace amount of materials from matrices. For example, the oxides and hydrous oxides of multivalent metals, such as zirconium, titanium and thorium, have been applied as synthetic ion-exchangers.⁴ It has also been found that the hydrous oxide of manganese(IV) (HMO) behaves as a cation-exchanger, and that a surface redox reaction on the HMO is correlated to the adsorption behaviour.⁵ However, the adsorption properties of the corresponding compound of lead(IV) have been little explored.

Recently, hydrous lead dioxide (HLD), freshly prepared by hydrolysis of lead tetra-acetate, has been studied in our laboratory. We have already reported that HLD is a superior adsorbent for bismuth ions in acidic medium and that traces of bismuth in a copper metal standard (about 10⁻⁵%) can be quantitatively collected on HLD.⁶ In another investigation the adsorption of bismuth on HLD from bismuth-EDTA solution was examined and it was found that HLD oxidizes EDTA over the pH range from 1 to 12.⁷

In the present work, the adsorption behaviour of potassium, cupric, zinc, cadmium and nitrate ions on HLD was investigated, to elucidate the fundamental adsorptive properties of HLD.

EXPERIMENTAL

Reagents

A 0.05M solution of lead tetra-acetate in glacial acetic acid was standardized by potentiometric titration with

sodium oxalate⁷ and the concentration of lead(IV) in the lead dioxide suspension was measured simply by visual titration with sodium oxalate.⁸ A 1M potassium nitrate standard solution was prepared from potassium nitrate that had been crystallized twice from water and then dried for 5 hr at 110°. Bivalent metal ion solutions were prepared from the analytical-reagent grade nitrates. A 0.065M sodium tetraphenylborate (Na-TPB) solution and a 0.025M zephiramine (tetradecyldimethylbenzylammonium chloride) solution, used for the determination of potassium, were prepared and standardized with 0.1000M potassium chloride standard solution as described previously.^{9,10}

A 10% nitron solution in 0.1M acetic acid, used for the determination of nitrate, was prepared. The other reagents were of analytical-reagent grade, and the water used was made by distilling demineralized water containing a little potassium permanganate and sodium hydroxide

Adsorption of potassium and nitrate

The HLD was prepared as reported previously.⁷ HLD (4 mmoles) and 5 ml of 1M potassium nitrate adjusted to a selected pH value with 1M nitric acid or potassium hydroxide solution were placed in a 50-ml standard flask, diluted to 50 ml with distilled water, brought to a temperature of 30°, and stirred for 5 hr. The HLD was then filtered off with a 0.45- μ m pore-size membrane filter, and the potassium and nitrate in the filtrate were determined as described below. The pH of the solution was also measured, immediately after filtration, under a nitrogen atmosphere because of the low buffering capacity of the solution. The amount of each ion adsorbed was calculated from the difference in its concentration before and after adsorption.

For determination of potassium, 10 ml of filtrate, 3 ml of 3M sodium hydroxide (potassium-free) and 20 ml of 0.065M Na-TPB solution were added to a 100-ml standard flask, and the mixture was diluted to 100 ml with distilled water, allowed to stand for 20 min at 30°, and then filtered off with a 1- μ m pore-size membrane. The excess of tetraphenylborate in a 25-ml portion of the filtrate was titrated

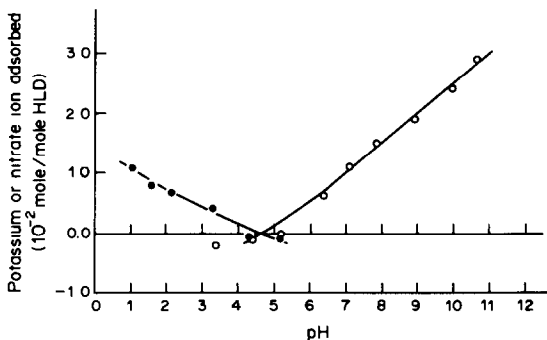


Fig. 1. Effect of pH on the adsorption of potassium (○) and nitrate (●) ions on hydrous lead dioxide (HLD). HLD 4×10^{-3} mole; potassium or nitrate ion 5×10^{-3} mole; solution volume 50 ml; shaking time 5 hr, temperature 30° .

with 0.025M zephiramine solution, with Clayton Yellow as indicator.⁹⁻¹²

Nitrate was determined in a 10-ml aliquot with nitron.¹³

Adsorption test for bivalent metal ions

HLD (5×10^{-4} mole; about 0.14 g of $PbO_2 \cdot 2H_2O$), a known amount of metal ion solution, 10 ml of 0.1M potassium nitrate and 20 ml of buffer solution (0.2M acetic acid/sodium acetate or 0.1M nitric acid/borax) were placed in a 200-ml Erlenmeyer flask and diluted to 100 ml with distilled water. The suspension was shaken for 1 hr, at $30^\circ C$. The HLD was then filtered off with a 0.45- μm membrane and the concentration of the metal ion in the filtrate was determined by differential pulse polarography, at the appropriate pH.¹⁴ The amount of metal ion adsorbed was found by difference.

RESULTS AND DISCUSSION

Adsorption behaviour of potassium and nitrate

In a preliminary test of accuracy, for six analyses of 10 ml of 0.1000M potassium nitrate, the recoveries of potassium and nitrate were 100.0 ± 0.2 and $98.6 \pm 0.1\%$ respectively.

The effect of pH on the adsorption of potassium and nitrate ions on HLD is shown in Fig. 1. For 2-6 replicates at each pH value the mean deviations were ± 0.032 and ± 0.013 mole per mole of HLD for potassium and nitrate ions, respectively. Equal amounts of potassium and nitrate ions were adsorbed at about pH 4.6, and HLD preferentially adsorbed the cation at higher pH, the anion at lower pH.

Adsorption behaviour of copper(II), zinc(II) and cadmium(II)

Effect of pH. Figure 2 shows that the effect of pH on the adsorption behaviour is very similar for all three ions.

Effect of metal ion concentration. This was investigated at about pH 6 with 5×10^{-4} mole of HLD. The results are summarized in Fig. 3. The limiting adsorption capacities were about 0.13, 0.08 and 0.04 mole per mole of HLD for copper(II), zinc(II) and cadmium(II), respectively.

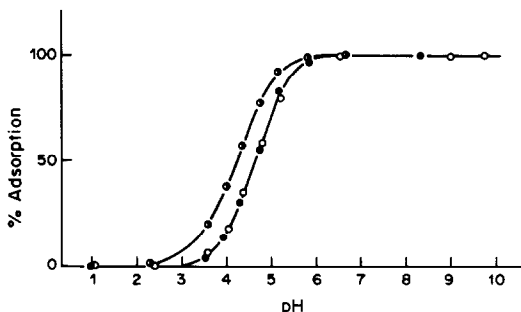


Fig. 2. Effect of pH on the adsorption of copper(II) (●), zinc(II) (●) and cadmium(II) (○) on HLD. HLD 5×10^{-4} mole; metal ion 2×10^{-6} mole; solution volume 100 ml; shaking time 1 hr; temperature 30° .

One hour of shaking was adequate for equilibrium to be reached. The adsorption values of pH 4 were practically constant over the temperature range from 30 to 70° .

From the results, the adsorption capacities for these metal ions on HLD is in the order copper(II) > zinc(II) > cadmium(II), which is in accord with the sequence of decreasing ionic crystal radius (Cu^{2+} 0.72 Å, Zn^{2+} 0.74 Å, Cd^{2+} 0.97 Å)¹⁵ and increasing negative logarithm of solubility product for the hydroxides, [pK_{sp} 18.2 for $Cu(OH)_2$, 15.3 for $Zn(OH)_2$ and 13.2 for $Cd(OH)_2$, all at 0.1 ionic strength].¹⁶

Effect of competing ions. The effect of the presence of another metal ion on adsorption of the three metal ions was studied at pH 6, as follows. After 2×10^{-4} mole of metal ion (adsorbate ion) had been

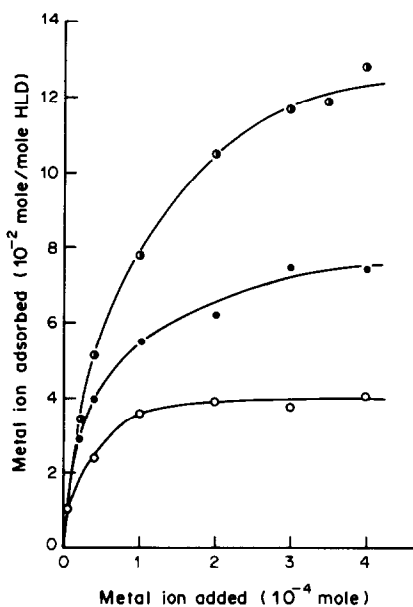


Fig. 3. Relation between the concentration of metal ion added and the amount of metal ion adsorbed on HLD at pH 6. HLD 5×10^{-4} mole; solution volume 100 ml; shaking time 1 hr; temperature 30° ; ● copper(II); ● zinc(II); ○ cadmium(II).

Table I. Competitive adsorption of metal ions on the hydrous lead dioxide

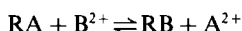
Adsorbed ion	Competing ion	Adsorption of adsorbed ion			Amount of adsorption of competing ion*, 10 ⁻² mole/mole HLD
		Without competing ion present,* 10 ⁻² mole/mole HLD	With competing ion present,* 10 ⁻² mole/mole HLD	Residual adsorbed ion, %	
Cu(II)	Zn(II)	9.5 ± 1.4	8.4 ± 0.6	88	1.8 ± 0.5
	Cd(II)		9.4 ± 0.5	99	1.0 ± 0.3
Zn(II)	Cu(II)	5.9 ± 0.5	3.1 ± 0.3	53	7.7 ± 0.2
	Cd(II)		5.2 ± 0.3	88	1.5 ± 0.3
Cd(II)	Cu(II)	3.2 ± 0.7	1.8 ± 0.2	57	7.9 ± 0.6
	Zn(II)		1.9 ± 0.3	58	4.6 ± 0.5

*Average and standard deviation are based on five or nine replicates.

shaken for 1 hr with 5×10^{-4} mole of HLD as described above, the same amount of another metal ion (competing ion) was added, and the mixture was shaken again for 1 hr. The individual amounts of the two metal ions adsorbed were then determined as above.

The results in Table 1 clearly show that the adsorption equilibrium between metal ion and HLD was mainly controlled by an ion-exchange reaction, the degree of exchange being dependent on the nature of the competing ion. There was little desorption of copper(II) by addition of zinc(II) or cadmium(II), but both copper and zinc caused considerable desorption of cadmium. Copper had more effect than cadmium on the desorption of zinc.

The ion-exchange reaction for bivalent metal ions can be simply written^{17,18} as



in which R represents the ion-exchanger. The selectivity coefficient, S_A^B , of the reaction can be calculated from

$$S_A^B = \frac{X_A \bar{X}_B}{\bar{X}_A X_B}$$

where \bar{X}_A and \bar{X}_B are the mole fractions of the metal ions A^{2+} and B^{2+} in the exchanger and X_A and X_B the corresponding mole fractions in the solution, A^{2+} and B^{2+} being the adsorbed ion and competing ion, respectively. The values of S_{Cu}^{Zn} and S_{Cu}^{Cd} were calculated to be 0.18 and 0.08, respectively, from the data in Table 1.

Conclusions

From the results for the individual adsorption of potassium, copper, zinc, cadmium and nitrate ions

and the effects of competing ions, it is concluded that hydrous lead dioxide (HLD), freshly prepared by hydrolysis of lead tetra-acetate, behaves as an amphoteric ion-exchanger, which acts as a cation adsorbent at $pH > \sim 4.6$ and an anion adsorbent at $pH < \sim 4.6$.

Acknowledgement—The present work was partially supported by a Grant-in-Aid for Scientific Research from the Ministry of Education.

REFERENCES

1. T. Shigematsu, *Bunseki Kagaku*, 1973, **22**, 618.
2. M. Abe, *ibid.*, 1974, **23**, 1254.
3. K. Terada, *Bunseki*, 1980, 539.
4. A. Ruvarac, in *Inorganic Ion Exchange Materials*, A. Clearfield (ed.), p. 141. CRC Press, Boca Raton, 1982.
5. R. R. Gadde and H. A. Laitinen, *Anal. Chem.*, 1974, **46**, 2022.
6. S. Ito, T. Matsuda and T. Nagai, *Bunseki Kagaku*, 1980, **29**, 655.
7. *Idem*, *Talanta*, 1984, **31**, 292.
8. *Idem*, *Bunseki Kagaku*, 1977, **26**, 687.
9. T. Iwachido, *Talanta*, 1966, **13**, 341, 1697.
10. K. Ueno, M. Saito and K. Tamaoku, *Bunseki Kagaku*, 1969, **18**, 81.
11. E. D. Schall, *Anal. Chem.*, 1957, **29**, 1044.
12. E. M. Epps and J. C. Burden, *ibid.*, 1958, **30**, 1882.
13. F. J. Welcher, *Organic Analytical Reagents*, Vol III, p. 138, Van Nostrand, New York, 1949.
14. G. W. C. Milner, *The Principles and Applications of Polarography and other Electroanalytical Processes*, pp. 204, 214, 283. Longmans, London, 1962.
15. H. L. Friedman and C. V. Krishnan, in *Water*, F. Franks (ed.), Vol. 3, p. 55. Plenum Press, New York, 1973.
16. A. Ringbom, *Complexation in Analytical Chemistry*, p. 339. Interscience, New York, 1963.
17. D. Britz and G. H. Nancollas, *J. Inorg. Nucl. Chem.*, 1969, **31**, 3861.
18. M. Abe, in *Inorganic Ion Exchange Materials*, A. Clearfield (ed.), p. 161, CRC Press, Boca Raton, 1982.

ANNOTATION

SPECTROPHOTOMETRIC METHODS FOR THE EVALUATION OF ACIDITY CONSTANTS—I

NUMERICAL METHODS FOR SINGLE EQUILIBRIA

A. G. ASUERO, M. J. NAVAS and J. L. JIMENEZ-TRILLO

Department of Bromatology, Toxicology and Applied Chemical Analysis, Faculty of Pharmacy,
The University of Seville, 41012 Seville, Spain

(Received 31 March 1985. Accepted 25 September 1985)

Summary—The spectrophotometric methods applicable to the numerical evaluation of acidity constants of monobasic acids are briefly reviewed. The equations are presented in a form suitable for easy calculation with a programmable pocket calculator. The aim of this paper is to cover a gap in the education analytical literature.

Among the physico-chemical properties of molecules, the acidity constants are of vital importance both in the analysis of drugs as well as in the interpretation of their mechanism of action.¹⁻⁴ Evaluation of the acidity constants of organic reagents is also of great value in planning analytical work,⁵ e.g., the acidity constants can be employed in the design of titration procedures and examining the possibility of separation of mixtures of compounds by extraction. The complexing properties of a molecule depend on the number and steric disposition of its donor centres as well as on its acid-base properties. The evaluation of acidity constants from spectrophotometric measurements has been treated by several authors.⁶⁻¹⁰ In the present paper attention is focused on the numerical methods for estimating acidity constants from spectrophotometric data. An attempt has been made to review the literature on the use of measurements in the ultraviolet and visible regions for determining acidity constants, but no attention will be paid to the experimental details of the methods. The original methods have been modified in order to obtain expressions more convenient for use with a programmable pocket calculator.

THE BASIC ALGEBRA

The ionization equilibrium of a monobasic acid, $HR \rightleftharpoons H + R$, is characterized by the acidity constant,

$$K_a = \frac{[H][R]}{[HR]} \quad (1)$$

The ionic strength and temperature of the solution are assumed to be kept constant, so that mixed¹¹ or conditional¹² constants are used in the calculations. Charges are omitted for simplicity.

If A is the measured absorbance (for 1-cm path-length) of a solution containing a total concentration

$C_R = ([R] + [HR])$ of the acid, then assuming that Beer's law holds, we have:

$$A = \frac{A_0 + A_1[H]/K_a}{1 + [H]/K_a} \quad (2)$$

where A_0 and A_1 are the absorbances of the pure forms of the reagent, R and HR, respectively. Equation (2) can be rearranged to give:

$$K_a = [H] \left(\frac{A - A_1}{A_0 - A} \right) \quad (3)$$

The slope of the graph of A vs. pH is given by:

$$\frac{dA}{d(\text{pH})} = -2.303 (A_1 - A_0) f_0 f_1 \quad (4)$$

where f_0 and f_1 are the molar fractions⁹ of R and HR, respectively. Stationary points are given by the condition $dA/d(\text{pH}) = 0$, and correspond to the limiting values $f_0 = 0$ and $f_1 = 0$, to which the graph tends asymptotically. The expression on the right-hand side of (4) will also be zero if $A_1 = A_0$, and then A will not change as the pH is varied. Differentiation of equation (4) gives

$$\frac{d^2A}{d(\text{pH})^2} = -2.303 (f_0 - f_1) \frac{dA}{d(\text{pH})} \quad (5)$$

and the condition $d^2A/d(\text{pH})^2 = 0$ will locate the point of inflexion in the graph of A vs. pH. At this point, $f_0 = f_1 = 0.5$, and $[H] = K_a$. Rewriting equation (2) for this point (A'' , pH'') gives

$$A'' = (A_1 + A_0)/2 \quad (6)$$

Thus, at the midpoint of the break in the curve, $\text{pH} = \text{p}K_a$, and the value of $dA/d(\text{pH})$ at this point is

$$\left[\frac{dA}{d(\text{pH})} \right]_{\text{pH}''} = -2.303 (A_1 - A_0) \times 0.5^2 = -0.576 \Delta A \quad (7)$$

where $\Delta A = A_1 - A_0$. Equation (7) was reported by Buděšinský¹³ in a paper dealing with the spectrophotometric evaluation of acidity constants of several azo-derivatives of chromotropic acid.

NUMERICAL METHODS

Equation (3) contains three unknowns: A_1 , A_0 and K_a , so, by measurement of the absorbances at three different pH values (with the concentration of acid, C_R , kept constant) it is possible to evaluate the acidity constant. Four different experimental situations¹⁰ can be envisaged, depending on whether the molar absorptivities of the pure forms R and HR are available ($\epsilon_i = A_i/C_R$). The appearance of an isosbestic point in a series of spectra for different acidities (at constant temperature and ionic strength constants) establishes the validity of application of the method.

Case I: A_0 and A_1 known

In the first instance, the measurement of the ratio $[R]/[HR]$ at a given pH value is sufficient for a value of K_a to be obtained. This implies the obtention of the absorption spectra of the pure forms HR and R and a mixture of HR and R at a pH close to pK_a . It is usually assumed that A_0 and A_1 can be obtained directly by measurement of solutions of sufficiently high and low pH, respectively, and application of equation (3).¹⁴

As pointed out by Rossotti and Rossotti,¹⁵ measurements of this type were first applied in the study of ionic equilibria in solution in the period 1912–1916. In 1926, Stenström and Goldsmith¹⁴ evaluated the acidity constants of phenol and tyrosine by absorbance measurements in the ultraviolet region. Prior to 1945, rather inaccurate photographic methods for determining the molar absorptivity were usually employed, although in 1924 von Halban and Ebert¹⁶ reported the evaluation of the acidity constant of picric acid by use of a photoelectric colorimeter.¹⁷

An alternative procedure¹⁸ is to determine graphically the pH value at which $A = A''$ [equation (6)]. In this case, a complete absorbance *vs.* pH plot must be obtained in order to draw a smoothed curve through the experimental data. So far as we know, Bjerrum,¹⁹ in 1915, was the first investigator to make use of this relation.

Case II: A_0 known; A_1 and K_a unknown

An example of this situation occurs when sparing solubility of a compound in water makes difficult the determination of the molar absorptivity of the acid form, or if the pK_a value is too low.

From equation (2) or (3) we have:

$$(A_0 - A)K_a + [H]A_1 = [H]A \quad (8)$$

The required unknowns can be obtained by solving pairs of simultaneous equations derived from (8) (*e.g.*, by Cramer's rule), for two solutions *a* and *b*:

$$K_a = \frac{[H]_a[H]_b(A_b - A_a)}{[H]_b(A_b - A_0) - [H]_a(A_b - A_0)} \quad (9)$$

$$A_1 = \frac{[H]_b A_b (A_b - A_0) - (A_b - A_0)[H]_a A_a}{[H]_b (A_a - A_0) - (A_b - A_0)[H]_a} \quad (10)$$

Equation (9) was described by Lunn and Morton²⁰ in a paper dealing with the absorption spectra of pyridoxine and related compounds, in 1952. By dividing the numerator and denominator of expressions (9) and (10) by $[H]_b(A_b - A_a)$, and as in Ingman's paper,²¹ writing

$$\frac{A_a - A_0}{A_b - A_0} = r \quad \text{and} \quad \frac{[H]_a}{[H]_b} = q \quad (11)$$

we get

$$K_a = [H]_a \left(\frac{1-r}{r-q} \right) \quad (12)$$

$$A_1 = \frac{A_b r - q A_a}{r - q} \quad (13)$$

Equation (12) was given by Ingman²¹ in 1973, as a variant of a method of indirect colorimetry described by Sacconi²² in 1950 and termed "single incomplete colour change."

The route described by Ingman is shown below with slight modifications. For a monobasic acid we have:

$$A = A_0 f_0 + A_1 f_1 \quad (14)$$

and since $f_0 + f_1 = 1$, we obtain

$$f_1 = \frac{A - A_0}{A_1 - A_0} \quad (15)$$

For two different solutions *a* and *b*, it follows that

$$\frac{[HR]_a}{[HR]_b} = \frac{f_{1a}}{f_{1b}} = \frac{A_a - A_0}{A_b - A_0} = r \quad (16)$$

Thus $f_{1a} = r f_{1b}$. On the other hand,

$$\begin{aligned} K_a &= [H]_a \left(\frac{1-f_{1a}}{f_{1a}} \right) = [H]_b \left(\frac{1-f_{1b}}{f_{1b}} \right) \\ &= [H]_b \left(\frac{1-f_{1a}/r}{f_{1a}/r} \right) \end{aligned} \quad (17)$$

which leads to

$$f_{1a} = \frac{r-q}{1-q} \quad (18)$$

Introduction of this expression for f_{1a} into $K_a = [H]_a(1-f_{1a})/f_{1a}$ gives equation (12).

Case III: A_1 known; A_0 and K_a unknown

An example of this situation occurs when a compound rapidly hydrolyses in basic medium, or the pK_a is very high, since it is then not possible to evaluate

accurately the molar absorptivity of the species R. Equation (2) or (3) can be rearranged to give:

$$\frac{[H](A - A_1)}{K_a} - A_0 = -A \quad (19)$$

Arranging pairs of observations (A , pH) to eliminate A_1 , we get²⁰

$$K_a = \frac{[H]_b(A_b - A_1) - [H]_a(A_a - A_1)}{A_a - A_b} \quad (20)$$

and by dividing the numerator and denominator of this expression by $[H]_b(A_b - A_1)$ we obtain

$$K_a = [H]_a \left(\frac{r' - q'}{1 - r'} \right) \quad (21)$$

where

$$r' = \frac{A_a - A_1}{A_b - A_1} \quad \text{and} \quad q' = \frac{[H]_b}{[H]_a} \quad (22)$$

Equation (21) was reported by Ingman.²¹

Likewise for A_1 we get

$$A_1 = \frac{q' A_a - r' A_b}{q' - r'} \quad (23)$$

Case IV: A_1 , A_0 and K_a unknowns

Equation (19) can be rearranged to give:

$$\frac{A[H]}{K_a} - \frac{A_1[H]}{K_a} - A_0 = -A \quad (24)$$

Rosenblatt²³ in 1954 pointed out that a set of equations (24) can be solved for values of K_a . As we have recently demonstrated,²⁴ the resolution of any three solutions a , b and c , gives the following expressions for K_a , A_1 and A_0 :

$$K_a = [H]_b \frac{q_{11} r'' (q_1 - 1) + q_1 (1 - q_{11})}{r'' (1 - q_1) + (q_{11} - 1)} \quad (25)$$

$$A_1 = \frac{A_c (q_{11} - 1) + A_a r'' (1 - q_1)}{r'' (1 - q_1) + (q_{11} - 1)} \quad (26)$$

$$A_0 = \frac{q_{11} r'' (A_a - A_b q_1) + q_1 (A_b q_{11} - A_c)}{q_{11} r'' (1 - q_1) + q_1 (q_{11} - 1)} \quad (27)$$

where

$$\frac{A_c - A_b}{A_a - A_b} = r''; \quad \frac{[H]_a}{[H]_b} = q_1; \quad \frac{[H]_c}{[H]_b} = q_{11} \quad (28)$$

Expression (25) was also described by Ingman,²¹ again on the basis of the paper by Sacconi, who called case IV "double incomplete colour change". In a forthcoming paper²⁵ equilibrium data will be presented.

An expression equivalent to (25) was deduced by Romain and Colleter²⁶ in 1958, as we can see in the following. From equation (15) we have

$$A = (A_1 - A_0) f_1 + A_0 \quad (29)$$

and for three different solutions a , b and c , it follows that

$$\frac{A_c - A_b}{A_a - A_b} = \frac{f_{1c} - f_{1b}}{f_{1a} - f_{1b}} = \left(\frac{[H]_b - [H]_c}{[H]_b - [H]_a} \right) \left(\frac{K_a + [H]_a}{K_a + [H]_c} \right) \quad (30)$$

since

$$f_{1r} = \frac{[H]_r}{[H]_r + K_a} \quad (31)$$

Expression (30) can be rearranged to

$$\left(\frac{A_c - A_b}{A_a - A_b} \right) \left(\frac{[H]_a - [H]_b}{[H]_c - [H]_b} \right) = Y = \frac{K_a + [H]_a}{K_a + [H]_c} \quad (32)$$

which gives finally,

$$K_a = \frac{[H]_a - Y[H]_c}{Y - 1} \quad (33)$$

an expression reported by Romain and Colleter²⁶ and applied to the evaluation of pK_a for substances of therapeutic interest: acetylsalicylic acid, vitamin B₆, antipyrine and 1-phenyl-3-methyl-pyrazolone.

According to equations (28) and (32)

$$Y = r'' \left(\frac{q_1 - 1}{q_{11} - 1} \right) \quad (34)$$

By introducing this value for Y into (33) and rearranging, we obtain (25).

An interesting method for the evaluation of the acidity constant of Thymol Blue was reported by Lai and Burkhart²⁷ in 1975. The method is applicable to the "double incomplete colour change" if the following conditions are satisfied. Two wavelengths are selected so that the absorbance due to the form HR at the first wavelength (λ) and the absorbance due to the form R at the second wavelength (λ') are negligible. If A and A' are the absorbances at λ and λ' ; then

$$A = \epsilon_0 [R] \quad (35)$$

$$A' = \epsilon_1 [HR] \quad (36)$$

If the concentration of reagent is kept constant but the pH is changed then $\Delta[R] = -\Delta[HR]$ and

$$\frac{\epsilon_1}{\epsilon_0} = -\frac{\Delta A'}{\Delta A} \quad (37)$$

so

$$\frac{[R]}{[HR]} = -\frac{A \Delta A'}{A' \Delta A} \quad (38)$$

Once the concentration quotient is known, the acidity constant is easily evaluated from (1).

CONCLUSION

Although the principles of spectrophotometric evaluation of acidity constants of monoprotic acids are described in some detail in almost every modern textbook of analytical chemistry for cases in which

the limiting absorbances of HR and R species are known, little attention is paid to the treatment of raw absorbance vs. pH data for more complicated cases. A complete coverage of this topic from the point of view of numerical evaluation is given in this paper.

A collection of programs for use with a Texas Instruments TI 58/59 pocket calculator and based on the equations developed in this paper has been devised and is available from the authors on request.

REFERENCES

1. M. van Damme, *Ph.D. Thesis*, Université libre de Bruxelles, Faculté de Médecine & Pharmacie, 1978.
2. C. Crevoisier and P. Buri, *Pharm. Acta Helv.*, 1971, **51**, 193.
3. F. Fontani and I. Setnikar, *Il Farmaco*, 1973, **28**, 547.
4. D. W. Newton and R. B. Kluza, *Drug. Intell. Clin. Pharm.*, 1978, **12**, 546.
5. H. Irving, H. S. Rossotti and G. Harris, *Analyst*, 1955, **80**, 83.
6. J. Bres, F. Bressolle and M. T. Huguet, *Trav. Soc. Pharm. Montpellier*, 1976, **36**, 331.
7. R. F. Cookson, *Chem. Revs.*, 1974, **74**, 5.
8. J. H. Magill, *Res. Develop. Ind.*, 1963, **27**, 18.
9. W. A. E. McBryde, *Talanta*, 1974, **21**, 987.
10. R. W. Ramette, *J. Chem. Educ.*, 1967, **44**, 647.
11. J. N. Brønsted, *Chem. Revs.*, 1928, **5**, 231.
12. A. Ringbom, *Complexation in Analytical Chemistry*, Interscience, New York, 1963.
13. B. W. Buděšínský, *Talanta*, 1969, **16**, 1277.
14. W. Stenström and N. Goldsmith, *J. Phys. Chem.*, 1926, **30**, 1683.
15. F. J. C. Rossotti and H. Rossotti, *The Determination of Stability Constants*, McGraw-Hill, New York, 1961.
16. H. von Halban and L. Ebert, *Z. Physik. Chem.*, 1924, **112**, 359.
17. R. W. Ramette, *Chemical Equilibrium and Analysis*, Addison-Wesley, Reading, Massachusetts, 1981.
18. J. P. Phillips and L. L. Merritt, *J. Am. Chem. Soc.*, 1948, **70**, 410.
19. N. Bjerrum, *Samm. Chem. Chemische-Tech., Vorträge*, 1915, **21**, 1.
20. A. K. Lunn and R. A. Morton, *Analyst*, 1952, **77**, 718.
21. F. Ingman, *Talanta*, 1973, **20**, 993.
22. L. Sacconi, *J. Phys. Coll. Chem.*, 1950, **54**, 829.
23. D. H. Rosenblatt, *J. Phys. Chem.*, 1954, **58**, 40.
24. A. G. Asuero, M. J. Navas and D. Rosales, *Talanta*, 1984, **31**, 233.
25. A. M. Jimenez, M. A. Herrador, M. J. Navas, J. L. Jimenez-Trillo and A. G. Asuero, unpublished work.
26. P. Romain and J. C. Colleter, *Compt. Rend.*, 1958, **247**, 1456.
27. S. T. F. Lai and R. D. Burkhart, *J. Chem. Educ.*, 1976, **53**, 500.
28. M. J. Navas, *Ph.D. Thesis*, Faculty of Pharmacy, University of Seville, 1985.

FLOW-INJECTION ANALYSIS WITH MULTIDETECTION AS A USEFUL TECHNIQUE FOR METAL SPECIATION

J. RUZ, A. RIOS, M. D. LUQUE DE CASTRO and M. VALCARCEL

Department of Analytical Chemistry, Faculty of Sciences, University of Córdoba, Córdoba, Spain

(Received 21 May 1985. Accepted 15 November 1985)

Summary—The analytical potential of a closed flow-injection system with multidetection by a single detector (for calculation of rate constants, reaction rate, dilution and amplification methods, etc.) is extended to simultaneous determinations for chromium speciation, with injection of the reagent(s) into the sample solution (which acts as the carrier).

The analytical information obtained by flow-injection analysis, FIA, can be extended by use of a multidetection system to obtain sequential or simultaneous values of the analytical signal, measured at different times or with different values of the instrumental variable. This can be done in three different ways.

(a) By use of several detectors (of the same¹ or different² nature) arranged in series³ or in parallel.⁴ In some cases the use of a double-beam spectrophotometer also permits this form of measurement.⁵ In every case, more than one signal peak is obtained per sample injected.

(b) By use of fast-scan detectors (e.g., a diode-array detector) which simultaneously measure the analytical signal at several values of the instrumental variable⁶ (e.g., with the diode-array detector, the wavelength).

(c) By use of a single conventional detector in a closed-flow system.⁷ Detection for each sample is performed as a function of time, with as many peaks as the number of times, n , that the sample plug passes through the detector, until equilibrium is attained.

The last procedure has the advantage of simplicity. The envelope of the maxima or minima of the n peaks obtained defines typical kinetic profiles which provide analytical information and are the basis of the different types of determinations which can be done with this multidetection system.

In this paper we consider the use of this method for the simultaneous determination of species in a system in which, in contrast to the one described earlier,⁷ the sample acts as carrier and circulates continuously in a closed loop into which the reagents are injected. The reaction system chosen was Cr(VI)–1,5 diphenylcarbazide,⁸ which in acidic medium yields a coloured product that is photometrically monitored at 540 nm. This reaction has been used for chromium speciation by FIA determination of first Cr(VI) and then total chromium after oxidation of Cr(III) to Cr(VI).⁹⁻¹² In the new method Cr(VI) and Cr(III) are determined separately.

EXPERIMENTAL

Reagents

Aqueous solution of 1,5-diphenylcarbazide (DPC): 0.425 g of DPC dissolved in 100 ml of ethanol and diluted to 250 ml with water. Aqueous solution of Ce(NH₄)₂(NO₃)₆: 0.489 g dissolved in 250 ml of 0.1M nitric acid. Stock aqueous solutions of Cr(VI) and Cr(III) (100 µg/ml) in 0.1M nitric acid.

Apparatus

A Pye Unicam SP6-500 single-beam spectrophotometer equipped with a Hellma 178.12 QS flow-cell (inner volume 18 µl), a Gilson Minipuls-2 peristaltic pump, a Tecator L100-1 and home-made dual injection valves were used.

Manifold

In the configuration used, shown in Fig. 1, the chromium sample circulates continuously through the system. When the selecting valve is switched to channel 2, the sample remains confined in the closed circuit, while the reagents [DPC and Ce(IV)] are injected simultaneously by means of the valves V_A and V_B, respectively. When the sample contains only Cr(VI) the recording obtained shows as many peaks as the number of times that the reacting plug (DPC + sample) passes through the detector before the solution held in the closed system is homogenized. The splitting of the first peak is due to the large volume of reagent injected (Fig. 2a). If the sample contains only Cr(III) the indicator reaction takes place when the reagent plugs meet after dispersing throughout the closed system (Fig. 2b). When the sample contains both oxidation states of chromium, there is superimposition of the indicator reaction signals corresponding to both species (Fig. 2c).

RESULTS AND DISCUSSION

The variables influencing the system were optimized separately for Cr(VI) and Cr(III), the following results being obtained.

Increasing L_1 from 50 to 550 cm results in an increase in A_λ for Cr(III), with splitting of the first peak, and in a decrease in A_λ for Cr(VI). As a compromise, $L_1 = 100$ cm was chosen. The oxidation reaction for Cr(III) is slow; hence L_2 was fixed at 300 cm. The optimum flow-rate is 3.1 ml/min, and the values of V_A and V_B are 130 and 230 µl, respectively. Larger volumes result in unwanted splitting of the

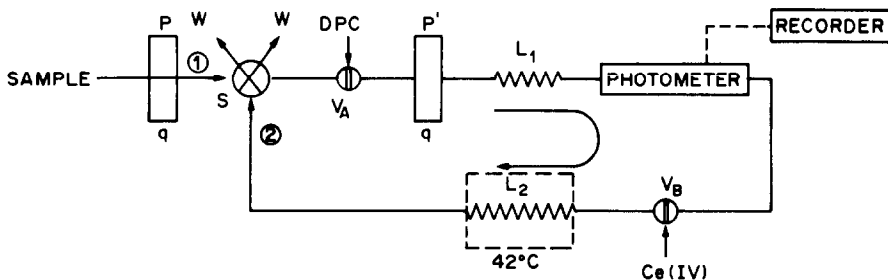


Fig. 1. Closed system with continuous sample flow. When valve S is switched to position 2, the sample is confined in the closed system, where oxidant and reagent are injected simultaneously.

peaks. The acidic medium (optimum for developing the indicator reaction) is provided by dilute nitric acid since the presence of sulphuric acid in the system gives rise to the formation of complex species with Cr(III) and inhibits or slows down the indicator reaction.¹³ The optimum concentrations of oxidant and DPC are 0.5 g/l. and 0.17%, respectively.

The relations of the concentration of the analytes in the sample to the parameters inferred from the recording are listed in Table 1, and are linear for A_∞ (absorbance at equilibrium), A_1 (absorbance of the first peak), B_1 and B_2 (absorbances of the first and second minima, respectively) and $V_{2,1}$ (increase in absorbance between the first and second peaks).

The base-line and the peak height for each recording change with time (dispersion) in such a way that the envelope of the minima defines a kinetic curve. The increase between two consecutive minima is representative of the reaction rate of the system and is proportional to the analyte concentration in the sample. The rate constant, k , is given by the expression $\log(A_\infty - A_i) = mt + n$ where $m = -k/2.303$ and A_i is the absorbance of the minimum. The values

of k thus found for different analyte concentrations are also shown in Table 1.

This configuration also allows the direct analysis of a very concentrated or very dilute sample of the analyte, the analytical measurement being taken as the absorbance of the minimum between peaks or the sum of the absorbances of the first n peaks of the recording, respectively. Figure 3 is illustrative of the application of the technique for analysis of dilute solutions by the amplification method ($\Sigma_1^2 A$, $\Sigma_1^3 A$ are the sums of the absorbances of the first two and three peaks, respectively), and of concentrated samples by the dilution method, which uses the absorbances of the minima (B_2 and B_3 are the absorbances of the second and third minima, respectively). The straight lines shown in Fig. 3 are indicative of the potential of these methods.

The equations corresponding to the Cr(VI) and Cr(III) calibration curves, correlation coefficients and determination ranges for different measurements which can be performed on a recording of the type obtained with this configuration are shown in Table 2.

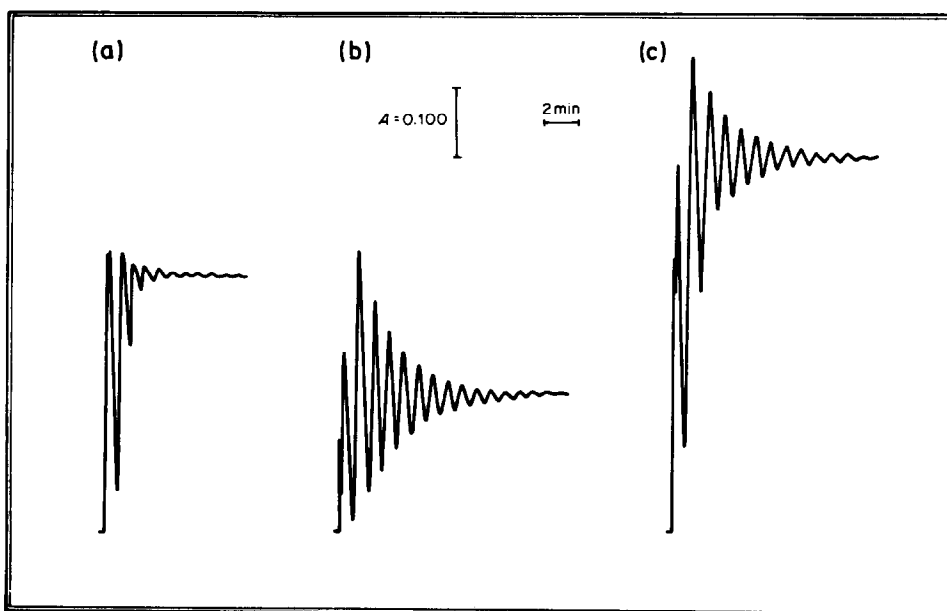


Fig. 2. Recordings obtained with the configuration in Fig. 1 for samples containing; (a) Cr(VI); (b) Cr(III); (c) a mixture of Cr(III) and Cr(VI).

Table 1. Influence of the analyte concentration on the signals from the system

	A_{∞}	A_1	A'_1	B_1	B_2	$V_{2,1}$	k, min^{-1}
[Cr(VI)], $\mu\text{g/ml}$							
0.0	0.008	0.110	0.060	-0.028	-0.020	0.004	—
0.1	0.076	0.136	0.118	0.031	0.060	0.029	0.530
0.2	0.133	0.209	0.164	0.035	0.124	0.089	1.319
0.4	0.258	0.325	0.290	0.056	0.216	0.160	1.320
0.6	0.370	0.398	0.408	0.065	0.272	0.207	1.313
0.8	0.479	0.474	0.526	0.066	0.338	0.272	1.336
1.0	0.590	0.563	0.613	0.106	0.452	0.346	1.267
1.2	0.693	0.658	0.705	0.183	0.597	0.414	1.301
1.4	0.772	0.720	0.805	0.141	0.595	0.454	1.255
1.6	0.862	0.815	0.888	0.199	0.700	0.501	1.232
[Cr(III)], $\mu\text{g/ml}$							
0.5	0.073	*	0.142	-0.007	0.009	0.016	0.239
1.0	0.125		0.168	0.003	0.028	0.025	0.276
2.0	0.172		0.233	-0.005	0.032	0.037	0.290
3.0	0.290		0.350	0.021	0.075	0.054	0.313
4.0	0.355		0.455	0.018	0.090	0.072	0.325
5.0	0.440		0.688	0.034	0.119	0.085	0.318
6.0	0.505		0.770	0.036	0.138	0.102	0.329

*For Cr(III) A_1 is equal to the signal given by the blank.

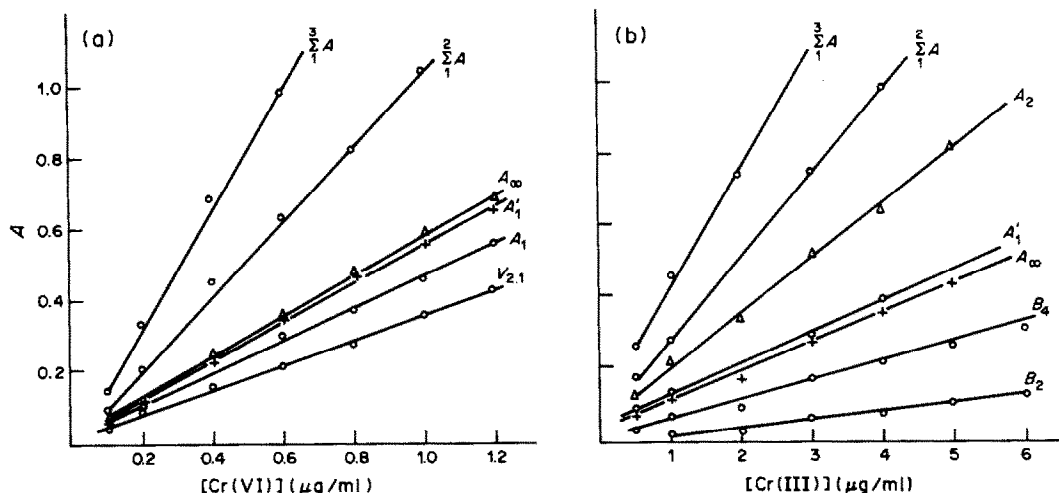


Fig. 3. Calibration curves obtained by use of different points on the recordings from closed-flow systems.

Table 2. Determination of Cr(VI) and Cr(III) (normal, amplification and dilution methods)

Species	Method	Equations*	Correlation coefficient
Cr(VI)	Normal	$A_1 = 0.435[\text{Cr(VI)}] + 0.015$	0.9940
		$A_1 = 0.534[\text{Cr(VI)}] + 0.013$	0.9965
		$A_2 = 0.547[\text{Cr(VI)}] + 0.009$	0.9976
		$A_{\infty} = 0.538[\text{Cr(VI)}] + 0.029$	0.9971
	Amplification	$V_{2,1} = 0.300[\text{Cr(VI)}] + 0.031$	0.9963
		$\Sigma_2^1 A = 0.954[\text{Cr(VI)}] + 0.048$	0.9891
		$\Sigma_1^3 A = 1.562[\text{Cr(VI)}] + 0.032$	0.9969
Dilution	$B_2 = 0.417[\text{Cr(VI)}] + 0.048$	0.9965	
	$B_3 = 0.535[\text{Cr(VI)}] + 0.036$	0.9980	
Cr(III)	Normal	$A'_1 = 0.091[\text{Cr(III)}] + 0.019$	0.9820
		$A_2 = 0.154[\text{Cr(III)}] + 0.050$	0.9964
		$A_3 = 0.124[\text{Cr(III)}] + 0.049$	0.9955
		$A_{\infty} = 0.080[\text{Cr(III)}] + 0.028$	0.9939
	Amplification	$V_{2,1} = 0.016[\text{Cr(III)}] + 0.004$	0.9987
		$\Sigma_2^1 A = 0.159[\text{Cr(III)}] + 0.059$	0.9962
	Dilution	$\Sigma_1^3 A = 0.287[\text{Cr(III)}] + 0.101$	0.9959
		$B_2 = 0.026[\text{Cr(III)}] + 0.008$	0.9938
		$B_3 = 0.039[\text{Cr(III)}] + 0.022$	0.9967

*Concentrations in $\mu\text{g/ml}$.

Table 3. Resolution of mixtures of chromium(VI) and chromium(III)

Added, $\mu\text{g/ml}$		Found, $\mu\text{g/ml}$		Relative error, %	
[Cr(VI)]	[Cr(III)]	[Cr(VI)]	[Cr(III)]	[Cr(VI)]	Cr(III)]
1.20	3.00	1.21	3.12	+ 0.8	+ 4.0
1.00	4.00	1.01	3.84	+ 1.0	- 4.0
1.00	1.00	0.97	1.05	- 3.0	+ 5.0
0.60	2.00	0.59	2.09	- 1.7	+ 4.5
0.80	1.00	0.77	0.95	- 3.7	- 5.0

The simultaneous determination of Cr(VI) and Cr(III) is another possibility offered by this configuration. The concentration of Cr(VI) in the mixture is proportional to the height of the first peak, since in its first passage through the detector the DPC plug has not yet met the oxidant and therefore the contribution of Cr(III) is nil. The Cr(III) concentration is obtained from $V_{2,1}$, because at the first minimum Cr(VI) has already reacted and the difference in absorbance between the first and the second minima is due to the contribution of the reaction of Cr(III). Table 3 lists the results obtained in the resolution of the mixture of both oxidation states of chromium together with the errors corresponding to each determination.

REFERENCES

1. D. J. Hooley and R. E. Dessy, *Anal. Chem.*, 1983, **55**, 313.
2. E. A. G. Zagatto, A. O. Jacinthe, L. C. R. Pessenda, F. J. Krug, B. F. Reis and F. H. Bergamin, *Anal. Chim. Acta*, 1981, **125**, 37.
3. R. Virtanen, *Anal. Chem. Symp. Ser.*, 1981, **8**, 375.
4. W. D. Basson and J. F. Van Staden, *Z. Anal. Chem.*, 1980, **302**, 370.
5. A. Fernández, M. D. Luque de Castro and M. Valcárcel, *Anal. Chem.*, 1984, **56**, 1146.
6. F. Lázaro, A. Ríos, M. D. Luque de Castro and M. Valcárcel, *Flow Analysis III*, Birmingham, 1985.
7. A. Ríos, M. D. Luque de Castro and M. Valcárcel, *Anal. Chem.*, 1985, **57**, 1803.
8. American Public Health Association, American Water Works Association and Water Pollution Control Federation, *Standard Methods for the Examination of Water and Wastewater*, 14th Ed., pp. 192. New York, 1975.
9. B. P. Bubnis, M. R. Straka and G. E. Pacey, *Talanta*, 1983, **30**, 841.
10. T. P. Lynch, N. J. Kernoghan and J. N. Wilson, *Analyst*, 1984, **109**, 839.
11. J. C. Andrade, J. C. Rocha and N. Baccan, *ibid.*, 1985, **110**, 197.
12. J. Ruz, A. Ríos, M. D. Luque de Castro and M. Valcárcel, *Anal. Chim. Acta*, in the press.
13. N. Fogel, J. M. Tai and J. Yarbrough, *J. Am. Chem. Soc.*, 1962, **84**, 1145.

EFFECT OF TEMPERATURE ON GENERATION AND DECOMPOSITION OF THE GROUP Vb ELEMENT HYDRIDES AND ESTIMATION OF THE KINETIC STABILITY OF GASEOUS BISMUTH HYDRIDE BY ATOMIC-ABSORPTION SPECTROMETRY

KATSUYUKI FUJITA and TAKEO TAKADA*

Department of Chemistry, College of Science, Rikkyo (St Paul's) University, Nishi-Ikebukuro, Toshima-ku, Tokyo 171, Japan

(Received 20 May 1985. Revised 8 November 1985. Accepted 15 November 1985)

Summary—During work on atomic-absorption determination of arsenic, antimony and bismuth by the hydride-generation method with sodium tetrahydroborate, the thermal and kinetic stabilities of the hydrides at various generation temperatures were studied. The arsenic and antimony hydrides are very stable even at 40° but bismuth hydride is very unstable both thermally and kinetically, even at 25°. The approximate rate constants for the decomposition of gaseous bismuth hydride at 0, 10, 25 and 40° were found to be 0.05, 0.10, 0.24 and 0.29 min⁻¹ respectively.

The group Vb elements form gaseous trihydrides such as NH₃, PH₃, AsH₃, SbH₃ and BiH₃, and the stability of these hydrides falls rapidly along the series.¹ The dissociation energies of the M-H bonds of the first four are in accord with this trend in stabilities: 391, 321, 297 and 257 kJ/mole.² However, BiH₃ is extremely unstable thermally, so the chemical and physical properties of this compound have been rarely studied.^{3,4}

Although the hydride generation technique in atomic-absorption spectrometry (AAS) has been widely exploited and many investigations have been made of the optimal generation conditions, interferences *etc.*, the thermal instability of the gaseous hydrides of certain elements has not been taken into account and the effect of temperature on the generation and decomposition of the hydrides has not been thoroughly studied.

Two methods are generally utilized to transfer the generated gaseous hydride to the atomizer for AAS. In one the hydride is collected in a balloon or suitable vessel and after a specified time, transferred to the atomizer (collection mode).^{5,8} In the other mode, the hydride is directly transferred to the atomizer without collection (direct-transfer mode).^{9,15} Fernandez⁵ examined the collection mode for seven hydride-forming elements (Ge, Sn, As, Sb, Bi, Se, Te) and reported that bismuth hydride was very unstable, and that prolonging the collection time resulted in a much poorer detection limit, on account of decomposition of the hydride, and the optimal collection time was found to be 30 sec. Chapman and Dale¹⁶ compared the collection mode with the direct-transfer mode for seven hydride-forming elements (Sn, Pb, As, Sb, Bi,

Se, Te), and investigated the stabilities and the kinetics of generation of these hydrides. They reported that bismuth hydride was generated more slowly than SnH₄, PbH₄ and H₂Te. Lee¹⁷ reported that the cold-trap method was unsuitable for bismuth, because bismuth hydride was so unstable that thermal decomposition occurred during the warming period needed to volatilize the trapped hydride and stated that only 5-15% of the trapped hydride was volatilized by this method.

The work described in this paper was done to estimate the thermal and kinetic stability of the gaseous hydrides of arsenic, antimony and bismuth, by means of a flame-heated T-shaped tube atomizer with simple hydride generation and collection systems. In particular, the effects of temperature on the generation and decomposition of the hydrides are reported for the first time.

EXPERIMENTAL

Apparatus

A Nippon Jarrell-Ash model AA8500 atomic-absorption spectrometer with a 10-cm single-slot burner was used. The hydride generation and atomization system was similar to that previously described¹⁸ except that the exterior of the pipe between the reaction vessel and the atomizer was wrapped with insulating tape. A Yamato model CTE-22W "Coolnics" was used to control the temperature of the water-bath in which the reaction vessel was immersed.

The absorbance was recorded with a Rika Denki model 361 recorder. The atomization tube was heated with an air-acetylene flame; the temperature at the centre of the tube was measured with a chromel-alumel thermocouple.

Reagents

All reagents except for sodium tetrahydroborate were of analytical-reagent grade. All water used was redistilled.

Sodium tetrahydroborate solution. Sodium tetrahydroborate (98% assay, Nisso-Ventron) was dissolved in

*To whom correspondence should be directed.

0.1% sodium hydroxide solution and filtered through paper. This solution could be used for a few days.

Arsenic(III) stock solution, 1000 ppm. Arsenious oxide (0.1320 g) was dissolved in a small amount of water containing 0.40 g of sodium hydroxide, and then diluted to 100 ml with water.

Antimony stock solution, 1000 ppm. Antimony potassium tartrate (0.2740 g) was dissolved in 100 ml of water.

Bismuth(III) stock solution, 1000 ppm. High-purity bismuth (0.1000 g) was dissolved in 5 ml of 2M nitric acid and the solution evaporated to dryness. The residue was taken up with a small amount of 1M hydrochloric acid and the solution diluted to 100 ml with 1M hydrochloric acid.

RESULTS AND DISCUSSION

Conditions for atomization

The most critical variables in the atomization process are the carrier gas flow-rate and the atomization temperature. The dependence of the absorbance on the nitrogen flow was investigated in the range 0.6–2.2 l./min and found to be independent of it between 0.6 and 1.0 l./min, for all three elements.

The influence of the atomization temperature is shown in Fig. 1. The temperature was changed by changing the acetylene/air flow-ratio. Since the temperature also depends on the carrier gas flow-rate, the nitrogen flow-rate was maintained at 1.0 l./min.

In contrast to bismuth, which gave the same absorbance at atomization temperatures between 800 and 920°, arsenic and antimony gave absorbances which first increased with temperature (up to 860°) and then remained almost constant. This indicates that the thermal stability of arsenic and antimony hydride is considerably higher than that of bismuth hydride. The conditions shown in Table 1 are recommended as optimal.

Conditions for hydride volatilization

The effect of sodium tetrahydroborate concentration on the efficiency of generation of the hydrides from 40 ng of arsenic, antimony and bismuth was investigated. One ml of tetrahydroborate solution was injected into 10 ml of sample solution, and the absorbance was measured as a function of tetrahydroborate concentration. It increased with tetrahydroborate concentration up to 0.5% for antimony and bismuth, and 1.0% for arsenic, a constant value being obtained with 1.0–1.5% tetrahydroborate for all three elements. It was also found that varying the hydrochloric acid concentration between 1.0 and 1.5M had little or no effect on the absorbance. Hence 1.0 ml of 1% sodium tetrahydroborate solution, a

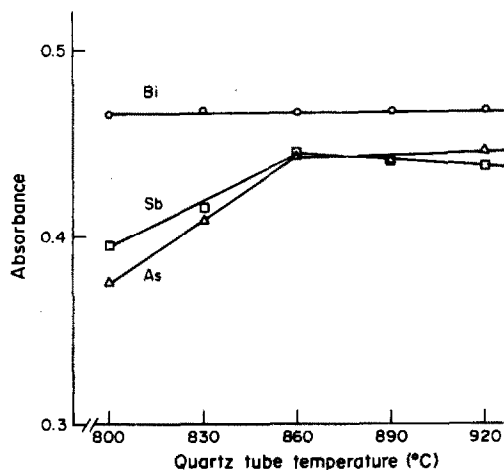


Fig. 1. Effects of atomization temperature on the peak absorbance of 40 ng of As(III), 40 ng of Sb(III) and 50 ng of Bi(III). The collection time was kept at 60 sec.

reaction medium of 1M hydrochloric acid, and a total volume of 10.0 ml of sample solution were chosen as optimal for hydride generation from all three elements.

Thermal and kinetic stabilities of the gaseous hydrides

Figure 2 shows the effect of sample temperature on the signal of the hydrides of arsenic, antimony and bismuth for a fixed collection time of 60 sec. In contrast to arsenic and antimony, bismuth gives a narrow plateau of practically constant and maximal

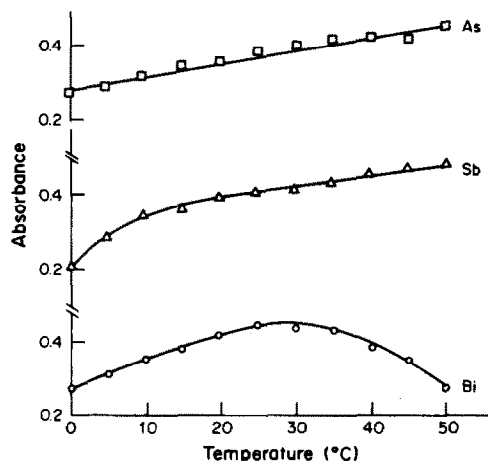


Fig. 2. Effects of temperature on the peak absorbance of 40 ng of As(III), 40 ng of Sb(III) and 50 ng of Bi(III). The collection time was kept at 60 sec.

Table 1. Conditions for AAS measurement

Parameter	As(III)	Sb(III)	Bi(III)
Wavelength, nm	193.7	217.6	223.1
Lamp current, mA	10	16	10
Temperature of quartz tube, °C	920	920	830
Flow-rate of carrier-gas (N ₂), l./min	1.0	1.0	1.0

response over the range 25–35. Since (as shown below) no further reduction of the three elements took place at 25 when the collection time was increased, the increase in absorbance is attributed to decrease in the solubility of the gaseous hydrides in the solution. For bismuth, however, if the temperature is too high there is thermal decomposition of the hydride generated, resulting in lower absorbance. At the optimum generation temperature there will be a short-lived steady-state balance between generation and decomposition. The arsenic and antimony hydrides are more stable.

The effect of collection time (period between adding the reductant and sweeping the volatilized gases into the atomizer) on the absorbance is shown in Figs. 3 and 4. In the cases of arsenic and antimony hydride (Fig. 3), no loss by decomposition was observed for storage periods up to 4 min, even at 40°. The lower absorbances at shorter collection times are a measure of the generation reaction-rate.

On the other hand, for bismuth hydride, the maximum absorbance value was obtained for collection periods ranging from 60 to 130 sec at 25° (Fig. 4, curve 1). At 40° the maximum absorbance value was obtained in the collection period range from 25 to 45 sec. At both temperatures the hydride generation was relatively rapid but the hydride was thermally unstable.

Since a closed system is used for the generation reaction and hydride collection, a greater amount of hydride remains in solution. To confirm this thermal decomposition, after the first measurement a further 1.0 ml of sodium tetrahydroborate solution was added to the sample solution and after 60 sec the absorption signal was measured as before. Curve 2 in Fig. 4 shows the result. The longer the collection times in the first measurement, the greater the absorbance obtained in the second measurements. This indicates that a fraction of the hydride will dissolve in the solution and is also unstable. It decomposes slowly at a temperature of 25°. Presumably, it reacts with protons to give hydrogen gas and bismuth(III)

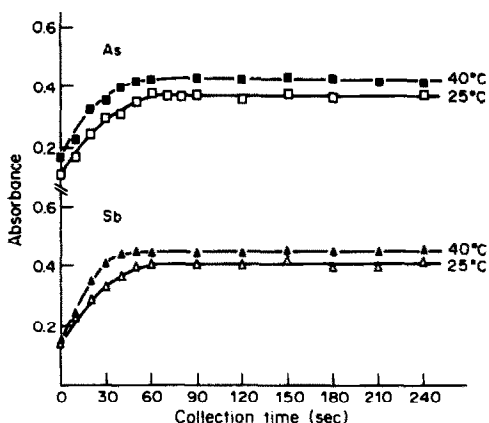


Fig. 3. Effects of collection time on the peak absorbance of 40 ng of As(III) and 40 ng of Sb(III) at 25° and 40°.

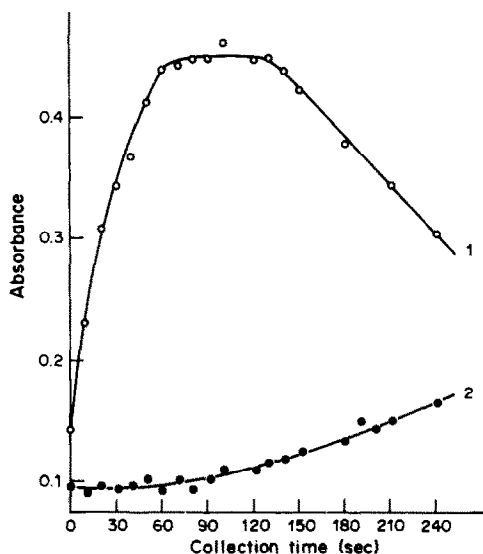


Fig. 4. Effects of collection time on the peak absorbance of 50 ng of Bi(III) at 25°. 1, First measurement; 2, after the first measurement a further 1.0 ml of NaBH₄ solution was added to the sample solution and after 60 sec the absorbance was measured.

ions which can be reduced by sodium tetrahydroborate again.

It is thought that the stability of bismuth hydride in solution is dependent upon the temperature and the pH. The decomposition reaction will be accelerated by increasing the temperature and lowering the pH.

At temperatures of 0 and 10°, the maximum absorbances were obtained for collection times in the ranges 140–390 and 90–300 sec respectively. Although bismuth hydride is more stable at these temperatures, the hydride generation becomes very slow, and longer collection times are required. Figure 5 shows that for bismuth hydride there is a critical optimum combination of generation temperature and collection time. Because a closed system is used for the reduction reaction and hydride collection the resulting increase in gas pressure (from the hydrogen generated) causes a greater amount of hydride to remain in solution, and this makes it difficult to determine the kinetics of the hydride reactions. However, if the absorbance after the peak in Fig. 5 is due only to the bismuth hydride in the gas phase in the reaction vessel, this section of the plot should give information about the kinetics of the decomposition process.

Figure 6 shows that a linear plot of log absorbance vs. time was obtained for each temperature, which suggests a first-order reaction, and the decomposition process is postulated as $\text{BiH}_3 \rightarrow \text{Bi} + \frac{3}{2} \text{H}_2$. If this assumption is correct, a rate constant (k) can be determined. The values obtained are listed in Table 2 together with the half-life (τ) of the decomposition. In view of the experimental results, we conclude that bismuth hydride in the gas phase is extremely unsta-

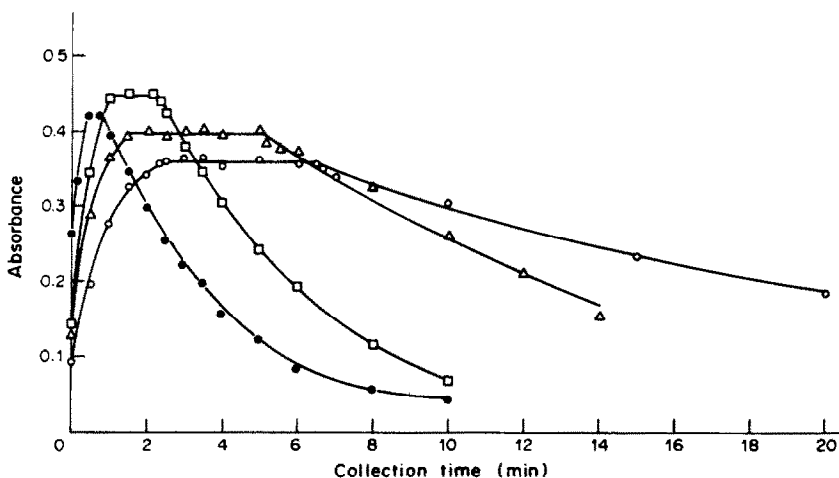


Fig. 5. Effects of collection time on the peak absorbance of 50 ng of Bi(III) at various temperatures (○) 0°; (△) 10°; (□) 25°; (●) 40°.

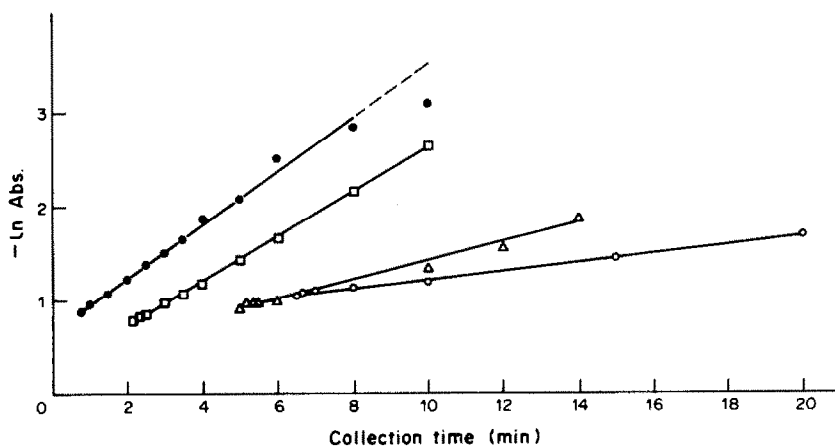


Fig. 6. Plots of $-\ln$ absorbance vs. collection time for the decomposition of bismuth hydride at various temperatures. (○) 0°; (△) 10°; (□) 25° (●) 40°

Table 2. Kinetic parameters of the decomposition of BiH_3

Temperature, °C	k^* , min^{-1}	τ^\dagger , min
0	0.05	14.7
10	0.10	6.9
25	0.24	2.9
40	0.29	2.4

*Rate constant.

†Half life.

ble, and readily undergoes thermal decomposition to bismuth, which is deposited on the inside of the reaction vessel as a mirror,³ or settles into the solution.

Conclusions

In the hydride-generation technique in atomic-absorption spectrometry, the stability of the gaseous hydride generated can affect the signal and hence the sensitivity obtained. Arsenic and antimony hydrides are thermally and kinetically stable, and their thermal

stabilities are similar, but bismuth hydride is very unstable even at room temperature, and care must be taken in designing methods based on its use in AAS.

REFERENCES

1. J. D. Lee, *A New Concise Inorganic Chemistry*, 3rd Ed., Van Nostrand Reinhold, New York, 1977.
2. D. A. Johnson, *Some Thermodynamic Aspects of Inorganic Chemistry*, 2nd Ed., pp. 202–203. Cambridge Univ. Press, Cambridge, 1982.
3. R. T. Sanderson, *Inorganic Chemistry*, Reinhold, New York, 1967.
4. F. A. Cotton and G. Wilkinson, *Advanced Inorganic Chemistry*, 4th Ed., Interscience, New York, 1980.
5. F. J. Fernandez, *At. Absorpt. Newsl.*, 1973, **12**, 93.
6. F. J. Schmidt and J. L. Royer, *Anal. Lett.*, 1973, **6**, 17.
7. M. Bédard and J. D. Kerbyson, *Anal. Chem.*, 1975, **47**, 1441.
8. S. Kobayashi, T. Nakahara and S. Musha, *Talanta*, 1979, **26**, 951.
9. K. C. Thompson and D. R. Thomerson, *Analyst*, 1974, **99**, 595.
10. J. E. Drinkwater, *ibid.*, 1976, **101**, 672.
11. R. C. Rooney, *ibid.*, 1976, **101**, 749.

12. H. D. Fleming and R. G. Ide, *Anal. Chim. Acta*, 1976, **83**, 67.
13. P. K. Hon, O. W. Lau, W. C. Cheung and M. C. Wong, *ibid.*, 1980, **115**, 355.
14. B. Weltz and M. Melcher, *Spectrochim. Acta*, 1981, **36B**, 439.
15. B. Vanloo, R. Dams and J. Hoste, *Anal. Chim. Acta*, 1983, **151**, 391.
16. J. C. Chapman and L. S. Dale, *ibid.*, 1979, **111**, 137.
17. D. S. Lee, *Anal. Chem.*, 1982, **54**, 1682.
18. T. Takada and K. Fujita, *Talanta*, 1985, **32**, 571.

SYNTHESIS AND CHARACTERIZATION OF 1,2-CYCLOHEXANEDIONE BIS-BENZOYL- HYDRAZONE AND ITS APPLICATION TO THE DETERMINATION OF Ti IN MINERALS AND ROCKS

M. GARCIA-VARGAS, S. TREVILLA and M. MILLA

Department of Analytical Chemistry, Faculty of Sciences, University of Cádiz, Puerto Real, Cádiz, Spain

(Received 13 March 1984. Revised 26 September 1985. Accepted 15 November 1985)

Summary—The synthesis, spectroscopic characteristics and analytical applications of 1,2-cyclohexanedione bis-benzoylhydrazone are reported. The reaction of this new compound with titanium(IV) has been studied spectrophotometrically. An orange 1:2 metal/ligand complex ($\lambda_{\max} = 477$ nm, $\epsilon = 1.05 \times 10^4$ l. mole⁻¹. cm⁻¹) is formed at pH 1.75–3.0 in 3:2 v/v ethanol–water medium. The method is simple and selective and has been satisfactorily applied to the determination of titanium in bauxite, Portland cement, amphibolites and granites.

Aroylhydrazones have been mainly used as chromogenic reagents for the determination of metal ions.¹⁻⁶ Bis-aroylhydrazones have also been used as analytical reagents, particularly those derived from oxalyldihydrazone.¹ Lever⁷ has reported the spectrophotometric and fluorimetric properties of the bis-(4-hydroxybenzoylhydrazone) derivatives of glyoxal, methylglyoxal and dimethylglyoxal, the glyoxal derivative being used for the colorimetric determination of calcium and cadmium. Zinc has been determined gravimetrically with the bis(2-hydroxybenzoylhydrazone) and bis-(5-bromo-2-hydroxybenzoylhydrazone) of dimethylglyoxal.⁸ The analytical properties of diphenylglyoxal and dipyridylglyoxal bis(2-hydroxybenzoylhydrazone)⁹⁻¹² and bis-benzoylhydrazone¹³ have also been investigated. Less attention has been paid to the use of bis-aroylhydrazones derived from cyclic ketones.

In the present paper, the synthesis, properties and analytical applications of 1,2-cyclohexanedione bis-benzoylhydrazone (CHBBH) are reported. A rapid and simple method for the colorimetric determination of titanium has been developed and applied to the determination of this element in mineral and siliceous materials.

EXPERIMENTAL

Reagents

Salts and solvents of analytical-reagent grade purity or better were used throughout and all solutions were prepared with distilled demineralized water.

CHBBH solutions, 0.2, 0.1, 0.05 and 0.0375% in ethanol, 0.1 and 0.05% in dimethylformamide and 0.05% in chloroform, were prepared.

A stock titanium(IV) solution (Ti 1.046 g/l.) was prepared by dissolving titanium metal in 4M hydrochloric acid and oxidizing with concentrated nitric acid, and standardized gravimetrically with cupferron.¹⁴ Working solutions of the required concentration were prepared daily from this solution.

Buffer solution of pH 2.4 was made by dissolving 94.5 g of monochloroacetic acid and 16.2 g of sodium hydroxide in water and diluting to 1 litre. Other buffer solutions (phthalate, acetate and ammonia) were prepared by conventional methods.

Preparation of the reagent

The reagent was synthesized by the general procedure for related compounds.^{5,6} Benzoylhydrazide, 1 g in 14 ml of ethanol, was mixed with 0.41 g of cyclohexanedione in 15 ml of ethanol, several drops of concentrated hydrochloric acid were added and the mixture was refluxed for 30 min.

The white crystals (tetragonal symmetry, $a = b = 15.78$ Å, $c = 19.82$ Å) produced were filtered off, washed, recrystallized from ethanol and dried at 100°. Yield 60%; melting point 209°.

Elemental analysis gave C 68.7%, H 5.8%, N 16.3%. C₂₀H₂₀N₂O₂ requires C 68.98%, H 5.74%, N 16.09%.

The reagent is thermally stable in air up to the melting point, as deduced from data obtained by thermogravimetry and differential thermal analysis.

Spectrophotometric procedures

Ionization constant. Determined by the Stenström and Goldsmith¹⁵ and Phillips and Merritt¹⁶ methods by measuring the absorbance at 325 and 360 nm against water, for solutions adjusted to various pH values.

Determination of titanium. In a 25-ml standard flask, place a suitable volume of sample solution containing up to 100 µg of Ti(IV), 15 ml of 0.05% CHBBH solution in ethanol, 5 ml of monochloroacetate buffer and dilute with water to the mark. After 5–10 min measure the absorbance at 477 nm against water.

Prepare a calibration graph by using standard titanium solutions treated in the same way.

Decomposition of samples

Amphibolites and granite. Dry the sample at 110°, weigh accurately 0.5–1 g in a platinum crucible, add a 6-fold weight of lithium metaborate and fuse at 1000° for 2 hr. Cool, extract the melt with 2M hydrochloric acid and remove the silica precipitate, collecting the filtrate in a 500-ml standard flask and making up to volume with dilute hydrochloric acid. Use a 1–4 ml portion for the determination of titanium.

Portland cement. Weigh accurately ca. 1 g of sample (dried at 110°) into a beaker and dissolve it in hydrochloric

Table 1. Ultraviolet spectra of CHBBH in some common solvents

Solvent	D^*	$\lambda_{\max}, \text{nm}$	ϵ_s $l. \text{mole}^{-1}. \text{cm}^{-1}$	$\lambda_{\max}, \text{nm}$	ϵ_s $l. \text{mole}^{-1}. \text{cm}^{-1}$
Dimethylformamide	37.6	335	1.06×10^4	277	8.69×10^3
Methanol	32.63	329	1.13×10^4	266	1.20×10^4
Ethanol	24.3	328	1.13×10^4	265	1.14×10^4
Acetone	20.7	335	1.02×10^4	—	—
3-Methylbutan-1-ol	14.7	335	1.13×10^4	—	—
n-Pentanol	13.9	334	1.14×10^4	273	1.14×10^4
Isobutyl methyl ketone	13.11	340	1.02×10^4	—	—

* D = dielectric constant at 25°.

acid, evaporate to dryness, digest with 6*M* hydrochloric acid and filter off the silica precipitate. Dilute the filtrate to volume with water in a 500-ml standard flask. Use a 3 or 4 ml portion for the determination.

Bauxite. Weigh about 1 g of sample into a Kjeldahl flask, heat for 60 min with a mixture of concentrated sulphuric, nitric and hydrochloric acids (1:1:1 v/v), evaporate to fumes of sulphuric acid, leach with dilute hydrochloric acid and filter. Fuse the residue with potassium pyrosulphate and extract the cooled melt with dilute hydrochloric acid and filter. Combine the filtrates in a 500-ml standard flask and make up to the mark with water. Take a 1 or 2 ml portion for the determination.

In all instances, add 0.2 ml of thioglycollic acid to avoid possible interferences.

RESULTS AND DISCUSSION

Analytical properties of the reagent

The wavenumber of the C=O band of aroylhydrazones in the infrared spectrum has already been reported.¹⁷⁻²⁰ The absorption bands associated with the imine group are also well known.^{21,22} The bands at 3220 and 3170 cm^{-1} can be attributed to the N—H stretching vibration for associated secondary amines.²³ Amide I (1655 cm^{-1} , very strong), amide II (1510 cm^{-1} , medium) and amide III (1270 cm^{-1} , strong) bands are assigned in agreement with the

observations made by Domiano *et al.*¹⁸ and Pelizzi and co-workers.^{19,20}

Table 1 shows the spectral characteristics of the reagent (1.15×10^{-4} *M* solution) in some common organic solvents. The reagent shows two maxima (at 265–280 and 335–340 nm), except in acetone, 3-methylbutan-1-ol and isobutyl methyl ketone. The absorption spectrum shows a slight red-shift as the polarity of the solvent decreases. The main absorption band is probably due to an $n \rightarrow \pi^*$ transition.¹⁸

In 4% ethanol–water medium CHBBH is pale yellow in acidic or neutral media, and bright yellow in alkaline solution. The spectra are shown in Fig. 1. The red shift from 330 to 345 nm in basic media (curves 4 and 5) is due to formation of anionic species of the type $>C=N-N-C<O^-$. The blue shift from 265 to 245 nm in acid medium (curve 1) is attributed to protonation of a nitrogen atom in the hydrazide group and to hydrolysis of the reagent to yield its parent species. The dissociation constant for the proton of the —CONH— group, was evaluated by the Phillips and Merritt¹⁶ and Stenström and Goldsmith¹⁵ methods. The value found was 10.4 ± 0.1 , in agreement with those obtained for related aroylhydrazones.^{13,24} Solutions of the reagent in ethanol, dimethylformamide, methanol, acetone

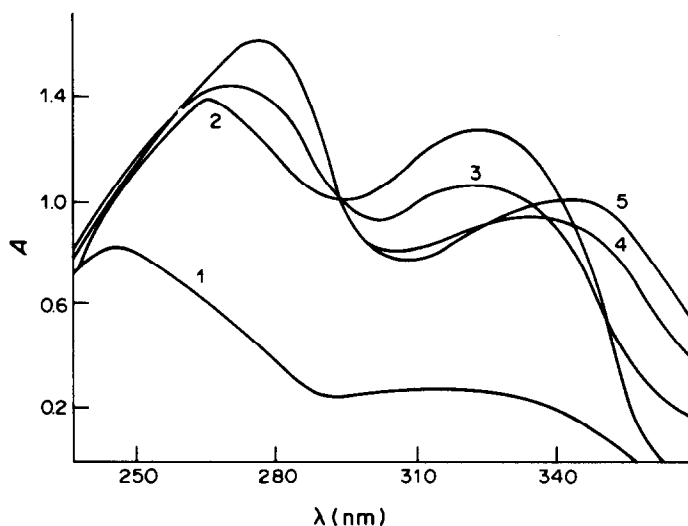


Fig. 1. Absorption spectra of CHBBH (1.15×10^{-4} *M*) in 4% aqueous ethanol medium at different pH values: 1, pH = 2.34; 2, pH = 4.23; 3, pH = 9.88; 4, pH = 11.30; and 5, pH = 12.83.

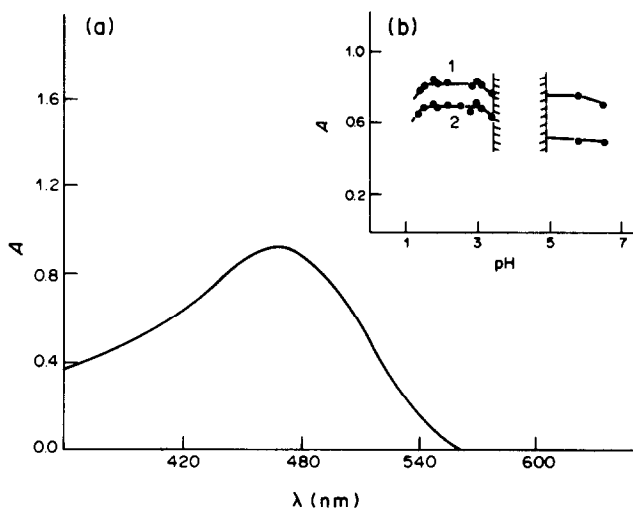


Fig. 2. (a) Absorption spectrum of the Ti(IV)-CHBBH chelate in 60% aqueous ethanol at pH 2.4 (titanium concentration 4.18 $\mu\text{g/ml}$). (b) pH-absorbance graph of the chelate at (1) 477 nm, and (2) 500 nm (the pH values between parallel segments correspond to a region where precipitation occurs).

and n-pentanol are stable for at least a month, whereas the reagent decomposes in 3-methylbutan-1-ol and isobutyl methyl ketone. In acid aqueous solution, CHBBH is rapidly hydrolysed, but in moderately strong basic media no hydrolysis takes place. However, the hydrolysis is less severe in aqueous ethanol as the proportion of ethanol is increased.

Reducing substances, such as thiosulphate, ascorbic acid and hydroxylamine, do not affect the rate of hydrolysis of the reagent in aqueous ethanol solution, but sulphite appears to stabilize the reagent in moderately strong acid medium. Persulphate and hydrogen peroxide have no effect on the reagent at low pH, but hydrogen peroxide decomposes it in basic media.

A systematic study of the reaction of CHBBH with 40 different ions showed that the most interesting metal complexes were formed in chloroacetate buffer (pH 2.4), acetate buffer (pH 4.5) or ammonia buffer

(pH 9.5) with Fe(III), Fe(II), Ti(IV), Pd(II), V(V), Sb(III), W(VI), Mo(VI), Cu(II) and Bi(III). The presence of at least 40% v/v ethanol is necessary to prevent the precipitation of the metal chelate or excess of reagent. Once formed, the chelates are all readily extracted into chloroform but when the metal ion solutions are shaken with a chloroform solution of the reagent only the Cu(II), Mo(VI), Bi(III) and Sb(III) complexes are extracted.

Spectrophotometric study of the Ti(IV)-CHBBH system

Formation of the Ti(IV) chelate. An aqueous Ti(IV) solution reacts with an ethanolic solution of CHBBH in acidic medium (optimum pH value 1.8-3.0) to form an orange chelate that shows excellent analytical properties. The spectrum shows an absorption maximum at 477 nm, where the reagent does not absorb (Fig. 2). The titanium chelate is completely

Table 2. Tolerance limits in the determination of 45 $\mu\text{g}/25\text{ ml}$ of Ti(IV) with CHBBH

Ion*	Tolerance limit, mg/25 ml
Ba ²⁺ , Na ⁺ , Ti(I), Hg(I), ascorbic acid, H ₃ BO ₃ , Cl ⁻ , NO ₃ ⁻ , Ni ²⁺	50
Mg ²⁺ , Sr ²⁺ †, Cs ⁺ †, Br ⁻ , ClO ₃ ⁻ , S ₂ O ₃ ²⁻ , acetate	40
Benzoate	30
Ca(II), Ag(I), Rb(I)†, SCN ⁻ , B ₄ O ₇ ²⁻	25
La(III), Li(I), Zn(II), Hg(II), Pb(II), As(III), ClO ₄ ⁻	20
S ²⁻	10
Al(III), Fe(CN) ₆ ³⁻ , tartrate	5
Th(IV), Cr ₂ O ₇ ²⁻ , BrO ₃ ⁻ , NO ₂ ⁻ , CrO ₄ ²⁻ , CO ₃ ²⁻ , SO ₂ ²⁻ , citrate	2.5
Co(II), Cd(II), SiO ₃ ²⁻ , NH ₄ ⁺ , MnO ₄ ⁻	1.5
Cu(II)	0.5
H ₂ O ₂ , AsO ₄ ³⁻ , In(III)	0.3
Sb(III)	0.2

*Cations were added in the form of chlorides or nitrates; anions were added in the form of sodium or potassium salts.

†Maximum concentration tested. The mean value for eleven samples with 2 $\mu\text{g/ml}$ Ti gave a relative error of 0.3% for a probability level of 95% ($P = 0.05$).

Table 3. Tolerance limits of foreign ions in the presence of masking agents

Ion	Tolerance limit* $\mu\text{g/ml}$	Masking agent†
Al(III)	600	Tiron (1000 $\mu\text{g/ml}$)
Al(III)	600	
Mo(VI)	20	
Ce(III)	10	
Sb(III)	6	
Fe(III), Pd(II)	2	Tartaric acid (200 $\mu\text{g/ml}$)
Ag(I), Hg(II)	1200	
Cu(II)	100	
Ag(I), Zn(II), Hg(II)	1000	
W(VI)	10	
Ag(I), Hg(II)	1200	Thiourea (4000 $\mu\text{g/ml}$)
As(III)	800	
Cu(II)	80	
Bi(III)	60	
Sb(III)	12	
Cu(II), Hg(II), Pb(II)	1600	Thiocyanate (1000 $\mu\text{g/ml}$)
Bi(III)	100	
Sn(IV)	80	
Sn(II), Fe(III)	60	
Pb(II)	1000	
Co(II)	120	Sulphide (400 $\mu\text{g/ml}$)
Cu(II)	100	
Fe(II)	30	
Bi(III), Fe(III), Pd(II)	10	
Fe(CN) $_6^{4-}$	200	
F $^-$	80	Thioglycolic acid (4000 $\mu\text{g/ml}$)
F $^-$	10	
SO $_4^{2-}$, PO $_4^{3-}$, SO $_3^{2-}$, CO $_3^{2-}$	2000	
Mn(II)	20	
Pd(II)	100	
Zr(IV)	100	Thiosulphate (1000 $\mu\text{g/ml}$)
		Zn(II) (800 $\mu\text{g/ml}$)
		La(III) (800 $\mu\text{g/ml}$)
		H $_3$ BO $_3$ (5000 $\mu\text{g/ml}$)
		Ba(II)
		Peroxydisulphate (crystals) + Ag(I)
		DMG§ (1000 $\mu\text{g/ml}$)
		Periodate (0.5 g)

*If a precipitate is formed, filter or centrifuge before measuring absorbance.

†The amount added is shown in parenthesis.

§DMG: dimethylglyoxime.

Table 4. Comparative determination of Ti in rocks and siliceous materials by the CHBBH and AAS methods

Sample	Ti, %		
	CHBBH method		
	Present procedure*	SAM†	AAS§
Amphibolite (A-63)	0.81 ± 0.01	0.80 ± 0.03	0.75
Amphibolite (A1512)	0.94 ± 0.02	1.01 ± 0.05	0.98
Amphibolite (A-1618)	0.264 ± 0.04	0.30 ± 0.01	0.25
Granite (G-3)	0.12 ± 0.01	0.11 ± 0.02	0.10
Granite (G-8)	0.44 ± 0.01	0.50 ± 0.03	0.46
Portland cement (BCS, No. 372)	0.34 ± 0.02‡	0.32 ± 0.03‡	0.33
Bauxite (BAS, No. 87)	2.24 ± 0.03‡	2.28 ± 0.04‡	2.25

*Mean value and range of duplicate analyses corresponding to two different weights of every sample, with two aliquots of different volume from each sample solution.

†SAM: standard addition method.

§Quadruplicate determinations by atomic-absorption spectroscopy.

Since the sensitivity is lower than that of the CHBBH-based method, a larger sample is needed.

‡Given as percentage of TiO $_2$.

||Certified value as percentage of TiO $_2$.

Table 5. Comparison between the spectrophotometric determination of titanium by the CHBBH method and other methods

Reagent	Optimal acidity	λ_{\max} , nm	ϵ , $l \cdot \text{mole}^{-1} \cdot \text{cm}^{-1}$	Interfering ions ^a	Ref.
Hydrogen peroxide	H ₂ SO ₄	410	0.7×10^3	Fe ³⁺ , F ⁻ , C ₂ O ₄ ²⁻ , Mo(VI), V(V), U(VI), citrate	26
Benzohydroxamic acid	5M HCl	370	2.4×10^3	Ce(IV), V(V), Mo(VI), W(VI), Fe ³⁺	27, 28
Chromotropic acid	pH 2.7-4.6	410	1.15×10^4	Fe ³⁺ , Zr(IV), F ⁻ , oxidants	29
Tiron	pH 4.3-9.6	390	1.59×10^4	Fe ³⁺ , U(VI), Mo(VI), Zr(IV), Al ³⁺ , Cu ²⁺ , V(V), rare earths	30
Aesculatin	pH 5.5	420	—	Be ²⁺ , Ni ²⁺ , Th(IV), Cu ²⁺ , Ce(IV), Zr(IV), Mo(VI), Fe ³⁺ , Fe ²⁺	31
<i>N</i> -Benzoyl- <i>N</i> -phenylhydroxylamine	pH 1.7-1.85	340	5.0×10^3	Fe ³⁺ , V(V), Mo(VI)	32
Phenylfluorone	pH 9-10	460	—	Fe ²⁺ , Zr(IV), V(V), Cr(VI), W(VI), Mo(VI), Nb(V), Ta(V)	33
Calcichrome	pH 4.2	565	1.15×10^4	Fe ³⁺ , Al ³⁺ , Cu ²⁺ , Ni ²⁺ , V(V), Zr(IV)	34
Chrome Azurol S	pH 3.2	570	—	Al ³⁺ , Fe ³⁺ , Cu ²⁺ , W(VI), Cr(VI)	35
Kaempferol	—	425	5.4×10^3	Zr(IV), U(VI), Mo(VI), Th(IV), Sc ³⁺ , Be ²⁺ , Al ³⁺ , Fe ³⁺ , lanthanides	36
Sulphosalicylic acid	pH 3.2-4.9	445	8×10^3	Al ³⁺ , Ni ²⁺ , Mo(VI), Fe ³⁺ , Zr(IV)	37
Fast Grey R.A.	0.002M HNO ₃	554	1.2×10^4	Fe ³⁺ , V(V), Zr(IV), Cu ²⁺ , Ga ³⁺ , F ⁻ , Cd ²⁺ , W(VI)	38
Catechol Violet	pH 3.3-3.5	690	5.5×10^4	Zr(IV), Sb ³⁺ , Ga ³⁺ , In ³⁺ , Al ³⁺ , Pb ²⁺ , Ce(IV), W(VI)	39
Adrenaline	Conc. H ₂ SO ₄	500	1.7×10^3	Ta(V), Nb(V), W(VI), Mo(VI), Al ³⁺ , Fe ³⁺ , Ni ²⁺ , Co ²⁺ , V(V)	40
Pyridoxal salicyloylhydrazone	pH 0.9-2.5	390	5.5×10^3	Mo(VI), W(VI), Cr ³⁺ , F ⁻ (at 390 nm)	3
		440	3.9×10^3		
Diphenylglyoxal bisbenzoylhydrazone	pH 4.7	520	810	Not studied	13
Dipyridylglyoxal bisbenzoylhydrazone	pH 4.7	395	8.9×10^3	Not studied	13
Salicylaldehyde 2-methylisonicotinoylhydrazone	pH 1.8-3.8	425	4.44×10^4		41
1,2-Cyclohexanedione bisbenzoylhydrazone	pH 1.8-3.0	477	1.05×10^4	See Tables 2 and 3	This work

*Ions interfering when present at the same concentration level as titanium.

formed within 5 min of mixing the reagents and remains stable for at least 2 hr.

To find the conditions needed (a) to avoid precipitation of the metal chelate and reagent excess, (b) to decrease the rate of hydrolysis of the reagent, and (c) to increase the sensitivity of the reaction, the influence of the organic solvent/water ratio (ethanol/water and DMF/water from 1:4 to 3:2 v/v, and ethanol/DMF/water 2:1:2 v/v), the choice of buffer solution (phthalate and chloroacetate) and the amount of reagent solution (1–14 ml of 0.2% solution in ethanol) was examined. The optimal conditions found were a medium containing 60% v/v ethanol, 2–12 ml of 0.2% reagent solution, and chloroacetate buffer. The ionic strength of the solution and the order of addition of the reagents are immaterial.

The continuous-variations method showed the formation of two complexes, with metal/ligand ratios of 1:1 and 1:2. The 1:1 complex is not observed when the absorbance measurements are made more than 2 hr after preparation of the samples. The Asmus method²⁵ also gave the 1:1 ratio and a new ratio of 2:3, possibly from averaging of the 1:1 and 1:2 ratios. The charge on the Ti(IV) complex and the reagent was investigated by anion-exchange, and it was concluded that the complex is positively charged, but the reagent is neutral.

Spectrophotometric determination of titanium

Under the optimum conditions for formation of the titanium complex, the absorbances at 477, 490 and 500 nm are all linearly related to the titanium concentration over the range 0.25–8.25 $\mu\text{g/ml}$.

A systematic study of interferences in the determination of 1.8 $\mu\text{g/ml}$ Ti(IV) (Table 2) showed that Bi(III), Fe(III), Mo(VI), Sn(II), V(V) and Zr(IV) interfere when present at the same concentration level as Ti(IV), but Fe(II), Mn(II), Pd(II), Sn(IV), U(VI), W(VI), $\text{Fe}(\text{CN})_6^{4-}$, F^- and PO_4^{3-} interfere at greater concentration. The tolerance limits for most interfering species can be increased by addition of masking agents (Table 3) and this enlarges the scope of the CHBBH system for practical determination of titanium.

Determination of titanium in bauxite and siliceous materials

The proposed method was satisfactorily applied to the determination of titanium in two standard samples (bauxite and Portland cement) and several rocks (amphibolites and granites). Table 4 summarizes the results obtained. Those for the rock analysis are compared with those obtained by atomic-absorption spectrometry. The method of standard additions was also used for validation.

CONCLUSION

The proposed procedure compares satisfactorily with other methods proposed for the spectrophotometric determination of titanium(IV) (Table 5). The method is relatively free from interferences

because most metal chelates of CHBBH are not completely formed in moderately strongly acidic media, and their absorption maxima occur at wavelengths shorter than 435 nm; the selectivity is increased by the addition of suitable masking agents.

REFERENCES

1. M. Katyal and Y. Dutt, *Talanta*, 1975, **22**, 151.
2. M. Gallego, M. Valcárcel and M. Garcia-Vargas, *Analyst*, 1983, **108**, 965.
3. *Idem*, *Mikrochim. Acta*, 1983, **1**, 289.
4. *Idem*, *Microchem. J.*, 1982, **27**, 328.
5. M. Garcia-Vargas, J. M. Bautista Rodriguez, S. Avila Navas and R. Coy-Yll, *ibid.*, 1982, **27**, 519.
6. M. Gallego, M. Valcárcel and M. Garcia-Vargas, *Anal. Chim. Acta*, 1982, **138**, 311.
7. E. Lever, *ibid.*, 1973, **65**, 311.
8. W. Schwartz and V. Dieckmann, *Wiss. Z. Tech. Hochsch. Otto von Guericke, Magdeburg*, 1969, **13**, 173.
9. M. Silva and M. Valcárcel, *Analyst*, 1980, **105**, 193.
10. *Idem*, *Ann. Quim.*, 1980, **76**, 129.
11. *Idem*, *Microchem. J.*, 1980, **25**, 117.
12. *Idem*, *ibid.*, 1980, **25**, 289.
13. M. Silva, M. Gallego and M. Valcárcel, *Talanta*, 1980, **27**, 615.
14. L. Erdey, *Gravimetric Analysis*, Part II, p. 461. Pergamon Press, London, 1965.
15. W. Stenström and N. Goldsmith, *J. Phys. Chem.*, 1926, **30**, 1683.
16. J. P. Phillips and L. L. Merritt, *J. Am. Chem. Soc.*, 1948, **70**, 410.
17. M. Garcia Vargas, M. Gallego and M. de la Guardia, *Analyst*, 1979, **104**, 613.
18. P. Domiano, A. Musatti, M. Nardelli and C. Pelizzi, *J. Chem. Soc. Dalton Trans.*, 1975, 295.
19. C. Pelizzi and G. Pelizzi, *ibid.*, 1980, 1970.
20. C. Pelizzi, G. Pellizi, G. Predieri and S. Resola, *ibid.*, 1982, 1349.
21. D. Prevoršek, *Compt. Rend.*, 1957, **245**, 2041.
22. J. Fabian, M. Legrand and P. Poirier, *Bull. Soc. Chim. France*, 1956, 1461.
23. E. Pretsch, T. Clerc, J. Seibl and W. Simon, *Tablas para la elucidación estructural de compuestos orgánicos por métodos espectroscópicos*, p. 197. Alhambra, Madrid, 1980.
24. M. Garcia-Vargas, J. M. Bautista and P. de Toro, *Microchem. J.*, 1981, **26**, 557.
25. E. Asmus, *Z. Anal. Chem.*, 1960, **178**, 104.
26. G. Charlot, *Chim. Anal.*, 1953, **35**, 51.
27. Y. K. Agrawal, *Chem. Era*, 1975, **11**, 21.
28. Y. K. Agrawal, S. Patke, T. P. Sharma, P. C. Verna and P. C. Maru, *Z. Anal. Chem.*, 1976, **280**, 30.
29. W. W. Brandt and A. E. Preiser, *Anal. Chem.*, 1953, **25**, 567.
30. A. E. Harvey and D. L. Manning, *J. Am. Chem. Soc.*, 1952, **74**, 4744.
31. B. D. Jain and H. B. Singh, *J. Indian Chem. Soc.*, 1964, **41**, 29.
32. J. E. Schwarberg and R. W. Moshier, *Anal. Chem.*, 1962, **34**, 525.
33. O. P. Singh and T. C. Sharma, *Indian J. Appl. Chem.*, 1970, **33**, 300.
34. H. Ishii and H. Einaga, *Bunseki Kagaku*, 1966, **15**, 821.
35. Y. Horiuchi and H. Nishida, *ibid.*, 1966, **15**, 913.
36. B. S. Garg and R. P. Singh, *J. Indian Chem. Soc.*, 1968, **45**, 1047.
37. M. Ziegler and O. Glemser, *Z. Anal. Chem.*, 1953, **139**, 92.
38. H. Khalifa and A. A. El-Sirafy, *ibid.*, 1967, **230**, 429.
39. M. Malát, *ibid.*, 1964, **201**, 262.
40. L. Jerman and F. Poláček, *Anal. Chim. Acta*, 1966, **36**, 240.
41. A. V. Dolgorev, *Zh. Analit. Khim.*, 1973, **28**, 1093.

EVALUATION OF FILTER PAPERS AS SUBSTRATES FOR SOLID-SURFACE ROOM-TEMPERATURE FLUORIMETRY AND PHOTOCHEMICAL FLUORIMETRY

JOËLLE FIDANZA

Département de Chimie, Faculté des Sciences, Université de Dakar, Dakar, Senegal

JEAN-JACQUES AARON*

44, Elysée-2, 78170—La Celle-St. Cloud, France

(Received 4 July 1985. Accepted 8 November 1985)

Summary—Filter papers (Whatman Nos. 1 and 41, S & S 904) and anion-exchange filter paper (Whatman DE-81) have been evaluated for their use as substrates in solid-surface room-temperature fluorescence (RTF) and photochemical fluorescence (RTPF). Several chemical treatments of filter papers are found not to reduce significantly their background fluorescence signal. Analyte fluorescence signals are 2–4 times higher on filter papers than on silica-gel TLC plates. Absolute limits of detection range between 0.6 and 40 ng on the Whatman filter papers, depending on the test compound. Filter papers are proposed as convenient, inexpensive, and easy-to-handle substrates for RTF and RTPF measurements.

In recent years, solid-surface room-temperature fluorescence (SS-RTF) has become an important technique for the analysis of a variety of organic compounds, such as polycyclic aromatic hydrocarbons, nitrogen heterocycles, pesticides and drugs, because of the small amount of sample needed, and simplicity, sensitivity, and relatively low cost.¹ In some cases, SS-RTF has also been shown to be useful in combination with room-temperature phosphorescence.^{2–5} Several solid substrates, such as silica gel,^{4,5} aluminium oxide,⁶ filter paper^{3,4,7} and acetylated cellulose⁵ have been used in RTF. Recent work in our laboratory has involved the use of silica gel thin-layer chromatoplates for room-temperature photochemical fluorescence (RTPF) analysis of several aminoquinoline derivatives.^{11–14} In this latter method, ultraviolet irradiation of samples adsorbed on silica gel induced a photochemical reaction which led to strongly fluorescent photoproducts.¹⁴ However, until now, no attempt has been made to study the analytical performance and possible drawbacks, such as background fluorescence, of filter papers, in comparison with other supports currently used in SS-RTF and RTPF.

The goal of the present study was to test several types of filter papers and compare them with other solid substrates, in order to evaluate their background fluorescence and analytical usefulness for quantitative SS-RTF and/or RTPF determination of selected organic compounds.

EXPERIMENTAL

Apparatus

All SS-RTF and RTPF measurements were performed with a Turner model 111 filter fluorimeter fitted with a 110–850 or 110–851 ultraviolet lamp, 7–60 or 7–54 emission and 2–A excitation filters, and 10% or 1% neutral density filters. For the photolysis, a 200-W Osram mercury arc lamp was used, with an Oriol model 8500 power supply.

A new aluminium single-sample holder was constructed (Fig. 1), and positioned in the standard Turner fluorescence sample compartment. It was used to hold 0.6-cm diameter filter paper discs or 0.5-cm² squares of plastic-backed silica gel and aluminium oxide thin layers. The discs were obtained by punching filter paper with a standard office paper punch. The plastic-backed silica-gel and aluminium oxide squares were cut with scissors. The samples were placed under the cover plate of the sample holder and held in place by two screws.

Reagents

Chloroquine and primaquine diphosphate salts and dantrolene (Sigma), 6-methoxyquinoline (Aldrich) and quinine sulphate (Prolabo) were used as received. Solvents used were analytical grade acetone, phosphoric acid, ethanol, propan-2-ol, triethanolamine, and distilled water. The triethanolamine spray was a 1:9 v/v mixture of triethanolamine and propan-2-ol.

The S & S 904 and Whatman Nos. 1 and 41 filter papers were obtained commercially and the Whatman DE-81 anion-exchange filter paper was donated by Prof. J. D. Winefordner. Precoated 5 × 20 cm silica gel and aluminium oxide N plastic sheets (Polygram, Macherey-Nagel) were used.

Procedures

Fluorimetric and photochemical fluorimetric measurements. Once the paper, plastic-backed silica gel or aluminium oxide was put in the sample holder, portions (5 μ l) of solvent or solution were spotted onto it with a Hamilton 10- μ l microsyringe. The samples were dried for 10 min with a hot-air current. For the photochemical fluorimetric measurements,

*Author to whom all correspondence should be addressed.

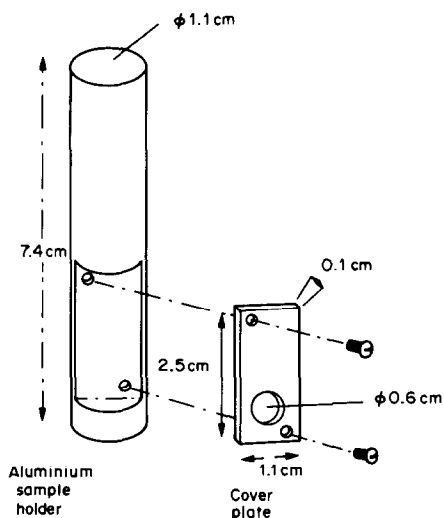


Fig. 1. The new RTF and RTPF sample holder.

the sample holder was placed about 60 cm from the mercury arc lamp and irradiated for a fixed time, then immediately transferred to the fluorimeter sample compartment, and the fluorescence intensity of the spots was measured.

Treatment of the papers. To try to reduce the fluorescence background of the papers, several treatments were tested. Filter paper discs were washed with 20 ml of demineralized water, 0.5M sodium hydroxide, 0.7M phosphoric acid, 0.5M potassium chloride, ethanol, or acetone, for periods between 1 and 60 hr, then dried in an oven at 100° for various periods between 30 min and 24 hr. On removal from the oven, the discs were placed in the sample holder and allowed to cool for about 10 min, after which the background fluorescence measurements were performed. After heating for 1 hr, the discs soaked in phosphoric acid had begun to char, and those treated with sodium hydroxide solution had turned yellow. In another test, the filter paper discs were irradiated for 2 hr with the mercury arc lamp, and removed at 10-min intervals during this period, for their fluorescence signals to be measured, but no change in the fluorescence background was noted.

RESULTS AND DISCUSSION

Background fluorescence

Table 1 gives the results for the background fluorescence of different kinds of plain and treated filter papers, compared with that of silica gel and aluminium oxide as substrates. It can be seen that Whatman No. 1 filter paper gives significantly lower background fluorescence signals than the other papers, for the same excitation. The Whatman No. 1 paper background fluorescence is also practically equal to that of the aluminium oxide TLC plate, and slightly lower than that of the silica gel thin-layers. For all papers studied, no significant decrease of the background fluorescence was found to be caused by the washing and heating treatments. In fact, soaking in 0.5M sodium hydroxide even increased the background signal. The background fluorescence signals were lower in all cases when the 110–851 ultraviolet lamp was used instead of the 110–850 visible-region lamp. This indicates that the background emitting

species has a more intense absorption band at around 370 nm, the main excitation region of the 110–850 lamp.

Analyte fluorescence signal

We have compared the fluorescence signals of several selected compounds adsorbed on the different papers under study, and on silica gel and aluminium oxide thin layers (Table 2). It is interesting to note that the analyte fluorescence signals are 2–4 times higher on filter papers than on silica gel thin layers, except for primaquine which gives approximately the same signal on all substrates. On aluminium oxide thin layers, the fluorescence intensity of the analytes is significantly lower than on other substrates, except that of dansyl chloride. Whatman No. 41 and S & S 904 papers give only a slight improvement of the analyte signals, compared to DE-81 anion-exchange filter paper. However, for dansyl chloride, the largest fluorescence signal is obtained on DE-81.

Ultraviolet irradiation has a significant effect on the fluorescence signal of the photoactive analytes adsorbed on filter papers. A 2–3 min irradiation of

Table 1. Effect of the treatment of filter papers on the background fluorescence signal

Substrate	Solvent ^a	Blank fluorescence		
		Relative intensity ^b		
		Visible region lamp ^c	UV lamp ^d	
S & S 904 filter paper	None	2.1	1.3	
	Water	2.1	1.3	
	0.5M NaOH	6.2	1.8	
	0.5M KCl	2.5	1.45	
	Acetone	2.5	1.05	
	Ethanol	2.8	1.3	
DE-81 anion-exchange paper	None	1.7	1.1	
	Water	1.7	1.1	
	0.5M NaOH	3.2	1.8	
	0.5M KCl	2.0	1.3	
	Acetone	2.3	1.05	
	Ethanol	3.7	2.3	
Whatman No. 1 filter paper	None	1.3	0.9	
	Water	1.3	1.0	
	Whatman No. 41 filter paper	None	1.4	1.1
		Water	1.5	1.1
		0.5M NaOH	3.4	1.6
		0.5M KCl	1.5	1.1
Acetone		1.6	0.95	
Ethanol		1.5	0.9	
Silica gel	None	1.6	1.0	
TLC plate				
Aluminium oxide	None	1.3	1.0	
TLC plate				

^aSolvent or solution used for soaking filter papers; "none" means that the blank fluorescence signal of untreated plain filter paper or other substrate was measured.

^bBlank fluorescence relative intensity was normalized to the blank fluorescence intensity (1.0) of silica gel substrate (UV lamp).

^c110–850 lamp with emission maximum at 370 nm.

^d110–851 far-UV lamp with major emission (about 95%) at 254 nm.

Table 2. Comparison of the analyte fluorescence signals determined on several substrates

Substrate	Relative fluorescence signal ^a			
	Chloroquine ^b	6-Methoxy quinaldine ^c	Primaquine ^d	Dansyl chloride ^e
S & S 904 filter paper	4.3	12.1	3.9	12.2
DE-81 anion-exchange filter paper	4.1	10.5	2.1	14.0
Whatman No. 41 filter paper	3.4	12.9	3.4	12.0
Silica gel TLC plate	1.8	5.0	3.2	7.5
Aluminium oxide TLC plate	1.2	3.8	NF	15.8

^aAll fluorescence relative intensities were normalized to the blank fluorescence intensity (1.0) of aluminium oxide substrate.

^bAqueous solution of 1000- $\mu\text{g/ml}$ chloroquine (after a 4-min irradiation time).

^c1.75M H_3PO_4 solution of 6-methoxyquinaldine (50 $\mu\text{g/ml}$).

^d3.0M H_3PO_4 solution of primaquine (1000 $\mu\text{g/ml}$) (after a 4-min irradiation time).

^eAcetone solution of dansyl chloride (200 $\mu\text{g/ml}$) (after spraying with triethanolamine solution).

^fNF = not fluorescent.

chloroquine and primaquine adsorbed on Whatman No. 41 paper produces a 2–4-fold increase of the signal (Fig. 2). This behaviour is very similar to that previously noted by us for the photolysis of the same compounds adsorbed on silica gel thin layers.^{12,13} It shows that filter papers are convenient solid substrates for use in the photochemical-fluorimetric method.

Analytical figures of merit

Table 3 gives RTF and RTPF calibration data and limits of detection for the selected compounds adsorbed on Whatman No. 41 or No. 1 filter papers. The linear dynamic ranges are relatively large, between 20 and 250 times the LOD. Slopes of the log–log calibration curves are close to unity for most

of the compounds, and the correlation coefficients indicate that the precision of the plots is reasonably satisfactory, except for chloroquine. The absolute limits of detection (LOD) are relatively low for measurements on filter papers, ranging from 0.6 to 40 ng, and are generally lower than those obtained on aluminium oxide or silica gel chromatoplates, with the same sample holder and optical system. For example, the LOD of quinine sulphate is about thirty times higher on a silica gel TLC plate than on filter paper.

CONCLUSION

We can conclude from this study that filter papers constitute satisfactory substrates for RTF and RTPF

Table 3. RTF and RTPF analytical data for selected compounds adsorbed on filter papers

Compound ^a	Substrate ^b	LDR, ^c ($\mu\text{g/ml}$)	Slope ^d	Correlation coefficient ^d	Absolute LOD, ^e ng
Chloroquine ^f	W-41	100	0.70	0.951	40
Dansyl chloride ^g	W-41	50	0.80	0.987	7
	AL-O	250	0.87	0.995	8
6-Methoxyquinaldine	W-41	100	0.94	0.994	0.6
Quinine sulphate	W-1	50	1.02	0.995	2.5
	SIL	75	0.80	0.985	75
Primaquine ^f	W-41	20	0.53	0.997	5

^aChloroquine solutions were prepared in water. Dansyl chloride solutions were prepared in acetone. 6-Methoxyquinaldine and quinine sulphate solutions were prepared in 1.75M and 3.5M phosphoric acid respectively.

^bW-41 and W-1 mean Whatman No. 41 and No. 1 filters; AL-O means an aluminium oxide TLC plate; SIL means a silica gel TLC plate.

^cLinear dynamic ranges, expressed as the ratio of the upper concentration of linearity (within 5%) and the limit of detection.

^dSlopes and correlation coefficients calculated from the log–log calibration plots by a microcomputer program.

^eAbsolute limit of detection, defined as the amount of compound (in 5 μl of sample solution) giving a signal-to-noise ratio of 3.

^fFluorescence intensities determined after an irradiation time of 4 min (for chloroquine) and 2 min (for primaquine).

^gA triethanolamine solution is sprayed on the substrate before measurements.

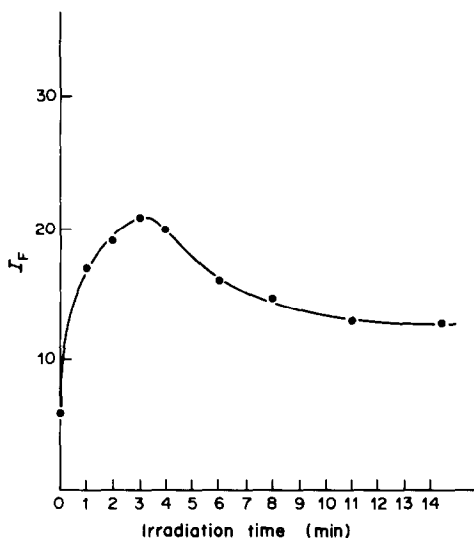


Fig. 2. Effect of irradiation time on the relative fluorescence intensity of chloroquine (concentration $1 \times 10^3 \mu\text{g/ml}$) adsorbed on Whatman No. 41 filter paper.

measurements. Although the fluorescence background of filter papers is not reduced by chemical or photochemical means, it does not seem to be much higher than that of silica gel or aluminium oxide thin layers, when our new sampling device is used. There-

fore, filter papers can be used in place of silica gel or aluminium oxide thin layers with comparable sensitivity, linear dynamic range, and precision for room-temperature fluorimetry and photochemical fluorimetry. The sampling procedure used with filter papers is also more convenient for the operator, and less expensive than the conventional glass-backed silica gel chromatoplates.

REFERENCES

1. R. J. Hurtubise, *Solid Surface Luminescence Analysis*, Dekker, New York, 1981.
2. C. D. Ford and R. J. Hurtubise, *Anal. Lett.*, 1980, **13**, 485.
3. R. A. Dalterio and R. J. Hurtubise, *Anal. Chem.*, 1984, **56**, 819.
4. *Idem, ibid.*, 1984, **56**, 1183.
5. R. J. Hurtubise, *Talanta*, 1981, **28**, 165.
6. J. C. Young, *J. Chromatog.*, 1976, **124**, 17.
7. P. G. Seybold, D. A. Hinckley and T. A. Heinrichs, *Anal. Chem.*, 1983, **55**, 1996.
8. E. Lue Yen-Bower, J. L. Ward, G. Walden and J. D. Winefordner, *Talanta*, 1980, **27**, 380.
9. J. L. Ward, E. Lue Yen-Bower and J. D. Winefordner, *ibid.*, 1981, **28**, 119.
10. R. P. Bateh and J. D. Winefordner, *ibid.*, 1982, **29**, 713.
11. J. Fidanza and J. J. Aaron, *Analisis*, 1981, **9**, 118.
12. J. J. Aaron and J. Fidanza, *Talanta*, 1982, **29**, 383.
13. J. J. Aaron, S. A. Ndiaye and J. Fidanza, *Analisis*, 1982, **10**, 433.
14. J. J. Aaron, J. Fidanza and M. D. Gaye, *Talanta*, 1983, **30**, 649.

THE DISTRIBUTION OF ELEMENTS BETWEEN POLYETHER-TYPE POLYURETHANE FOAM, CYCLIC POLYETHERS AND HYDROFLUORIC ACID SOLUTION

R. CALETKA*, R. HAUSBECK and V. KRIVAN

Sektion Analytik und Höchstreinigung, Universität Ulm, Oberer Eselsberg N 26, D-7900 Ulm/Donau,
F.R.G.

(Received 23 May 1985. Revised 21 October 1985. Accepted 1 November 1985)

Summary—The extraction of fifteen elements in the systems consisting of polyurethane foam (polyether type)/HF-alkali-metal fluoride and cyclic polyether/HF-alkali-metal fluoride has been investigated. Little or no extraction was found for Co, Zn, Fe, Zr, Hf, Sn(IV), Nb, Pa, As(V), Mo, and W. Only Ta, Sb, Re, and Tc are well extracted with either polyurethane foam or dicyclohexano-18-crown-6 in dichloroethane under the conditions investigated. The mechanism of the extraction is discussed. The most interesting separation possibilities have been tested.

In our previous work,¹ we used polyurethane foam pretreated with extractants, for the separation of tantalum from hydrofluoric acid media, and observed that tantalum was also separated by unloaded polyurethane foam. In recent reviews on the use of polyurethane foam materials for separations,^{2,3} it was shown that "soft" anions, such as thiocyanate, heavy halides, picrate, *etc.* are the most readily extracted anionic species. From this point of view, the distribution behaviour of complex fluorides is rather surprising.

The purpose of the present work was to study the retention of certain elements forming stable anionic fluoro-complexes in hydrofluoric acid media by polyether-based polyurethane foam. Since rhenium and technetium exhibited similar retention behaviour, they were also included in this study. For comparison, the extraction with cyclic polyethers was also studied.

EXPERIMENTAL

Chemicals

Polyurethane foam, a polyether of PWE/40 open-cell type, was obtained from Greiner GmbH, Kremsmünster, Austria. It had a bulk density of 0.042 g/cm³. The foam was cut with a cork-borer, treated with acetone and 2M hydrochloric acid for several hours, thoroughly rinsed with demineralized water, and then washed in a plastic syringe with acetone as described before,¹ and dried.

The cyclic polyethers dibenzo-18-crown-6 (DB-18,6), dicyclohexano-18-crown-6 (DC-18,6), 18-crown-6 (C-18,6) (obtained from Ventron GmbH, Karlsruhe, F.R.G.) and 12-crown-4 (C-18,4) (Aldrich Chemical Co. Inc., Steinheim/Albuch, F.R.G.) were of *p.a.* purity.

Dichloroethane, used as a solvent in the extraction experiments, was purified by washing with dilute sulphuric acid and water, followed by distillation.

Estimation of the distribution ratios

The distribution data were obtained under static conditions (batch method) by use of radiotracer techniques. The radiotracers were prepared by irradiation of high-purity metals or their compounds in a nuclear reactor. The radionuclide purity of the tracers was checked by high-resolution gamma-ray spectrometry. Except where otherwise mentioned, the solutions contained 5–10 µg of the labelled element per ml; the concentrations of niobium and tin were about 50 µg/ml and in the case of technetium no carrier was present.

The distribution ratio, D_f , defined as the ratio of the total analytical amount of the given element per gram of dry foam to the total amount of the element in 1 ml of the external solution, was determined at $21 \pm 1^\circ$. The volume-weight ratio of solution to foam was 58 ml/g. The foam and aqueous solution were shaken in plastic vials for 24 hr.

The extraction experiments with crown ethers were done by mixing (in polypropylene vials) 2 ml of the organic phase with 2 ml of aqueous solution containing the element under investigation, and shaking the mixture for 10 min, at 21° . The phases were separated and the distribution of the element was determined by measuring the radioactivity of an aliquot of each of the two phases. The distribution ratio D_1 is defined as the ratio of the total concentration of the element in the organic phase to the concentration of the element in the aqueous phase.

Separation procedures

For the batch separations, 5 ml each of the aqueous and organic phases were mixed for 15 min in a polypropylene syringe. The phases were then separated and measured. For column separations, beds 45 mm long and 9 mm in diameter were made with two polyurethane foam cylinders (0.270 g of foam). Other conditions were the same as described earlier.¹

RESULTS

Retention on the polyurethane foam

Figure 1 shows experimental distribution ratios plotted as a function of hydrofluoric acid concentration. The uptake of tantalum on the polyurethane

*Author for correspondence.

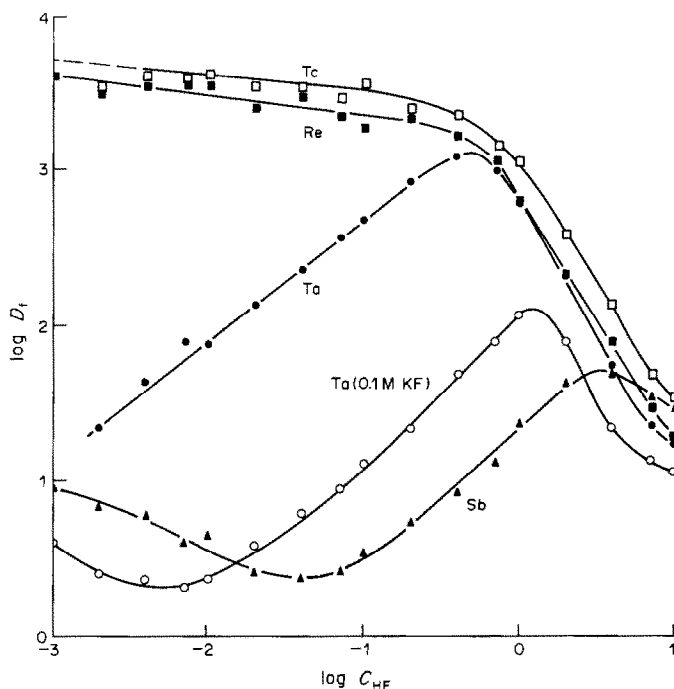


Fig. 1. Dependence of the distribution ratio on the hydrofluoric acid concentration for Ta, Re, Tc, and Sb in the system polyurethane foam/HF: D_f = distribution ratio; C_{HF} = hydrofluoric acid molar concentration.

foam increases with hydrofluoric acid concentration to a maximum at about $0.8M$ acid. Making the aqueous phase $0.1M$ in potassium fluoride leads to a considerable decrease in the distribution ratios, but the general character of the tantalum plot shown in Fig. 1 remains. The slopes of the plots for the linear part of the curves before the maximum are 0.71 and 1.03 for pure hydrofluoric acid solutions and those also containing potassium fluoride, respectively.

The influence of ammonium, sodium or potassium fluoride concentration on the tantalum distribution was also investigated, the concentration of hydrofluoric acid being kept constant at $0.4M$. From the data given in Fig. 2 it can be seen that, at concentrations $\geq 0.1M$, potassium fluoride decreases the retention of tantalum somewhat more effectively than the other two fluorides do.

The dependence of the distribution ratio for antimony(V) (see Fig. 1) on the hydrofluoric acid concentration shows a similar character to that for tantalum, but the maximum value of D_f is lower and occurs at a higher hydrofluoric acid concentration than for tantalum. The elements Zr, Hf, Sn(IV), Nb, Pa, As(V), Mo, and W are only slightly retained on polyurethane foam from hydrofluoric acid in the concentration range 10^{-3} – $10M$ (the D_f -values are ≤ 10). For Co, Zn and Fe(III), no retention from 1 – $2M$ hydrofluoric acid was observed. The distribution of Tc(VII) and Re(VII) is also shown in Fig. 1. These elements are well retained from 10^{-3} – $0.5M$ hydrofluoric acid. For this acid range the distribution ratio remains almost constant, but at higher acid

concentrations the fraction retained decreases sharply in the same manner as in the case of tantalum. Technetium is retained a little more strongly than rhenium.

Extraction with cyclic polyethers

The distribution of tantalum as a function of hydrofluoric acid concentration is shown in Fig. 3 for

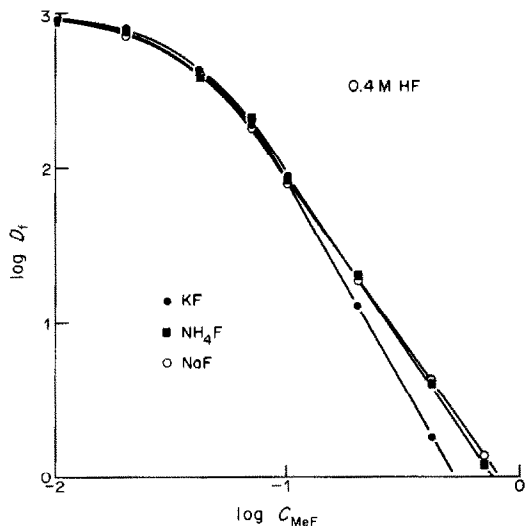


Fig. 2. The effect of KF, NaF and NH_4F on the retention of tantalum on polyurethane foam from $0.4M$ HF: D_f = distribution ratio; C_{MeF} = metal fluoride molar concentration.

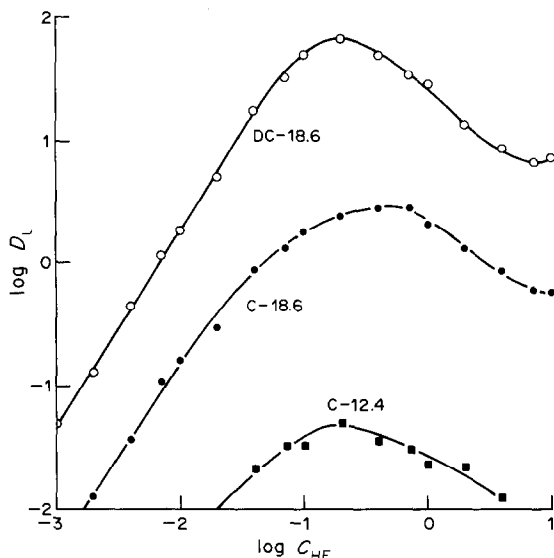


Fig. 3. Dependence of the distribution ratio on the HF-concentration in the extraction of tantalum with 0.01M cyclic polyether solutions in dichloroethane from hydrofluoric acid solutions: D_1 = distribution ratio; C_{HF} = hydrofluoric acid molar concentration.

various crown ethers. These results show that the best extraction of tantalum can be achieved with dicyclohexano-18-crown-6 in dichloroethane. Chloroform and benzene proved to be unsuitable for this purpose.

For all the extractants studied, the distribution ratio of tantalum increases with increasing acid concentration, passing through a maximum for 0.2–0.5M acid.

Figure 4 shows the influence of potassium fluoride on the extraction of tantalum, in two types of experi-

ment. In the first (open symbols), the hydrofluoric acid concentration was kept constant at 1M while the concentration of potassium fluoride was varied from 10^{-4} to 1M, and in the second (filled symbols), the solutions were 0.1M in potassium fluoride and the concentration of hydrofluoric acid was varied from 10^{-3} to 10M. It can be seen that the general character of all the plots is similar. However, the various cyclic polyethers differ substantially in their extraction efficiency for tantalum. For dicyclohexano-18-crown-6 (the most effective), maximum extraction is obtained from solutions 0.01–0.2M in potassium fluoride and 0.1–1M in acid.

Particular attention was paid to the influence of various fluorides on the extraction of tantalum with dicyclohexano-18-crown-6. In the series of experiments the concentration of hydrofluoric acid was kept constant at 0.2M. In the absence of the fluoride salts, $\log D_1$ was found to be 1.81. The results summarized in Fig. 5 show that the distribution ratio for tantalum decreases according to the fluoride used, in the order $KF > NH_4F > NaF$, with sodium fluoride significantly reducing the extraction efficiency.

The plot of $\log D_1$ vs. \log [dicyclohexano-18-crown-6], at a constant aqueous phase composition (0.2M acid), gave a straight line for which the equation $\log D_1 = 0.807 \log [DC-18,6] + 3.35$ holds over the range 10^{-5} – 10^{-1} M DC-18,6. The slope and point of intersection for a solution 1M in hydrofluoric acid and 0.1M in potassium fluoride were 0.775 and 3.33, respectively.

With the cyclic polyethers, as with the foams, all other elements studied showed only negligible extraction, with distribution ratios below 10^{-2} , except for technetium and rhenium. Figure 6 shows the results for the extraction of these two elements with

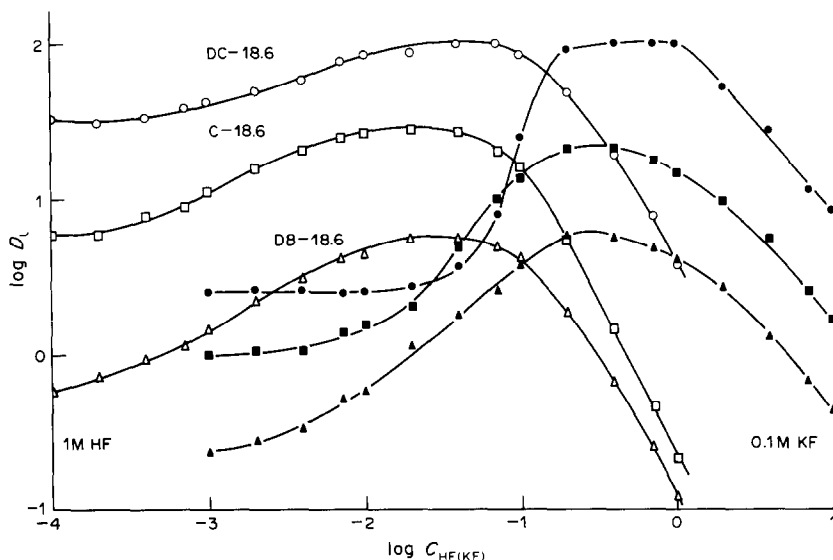


Fig. 4. Distribution ratios for the extraction of tantalum with cyclic polyethers from hydrofluoric acid-potassium fluoride solutions: D_1 = distribution coefficient; $C_{HF(KF)}$ = molar concentration of varied component of system.

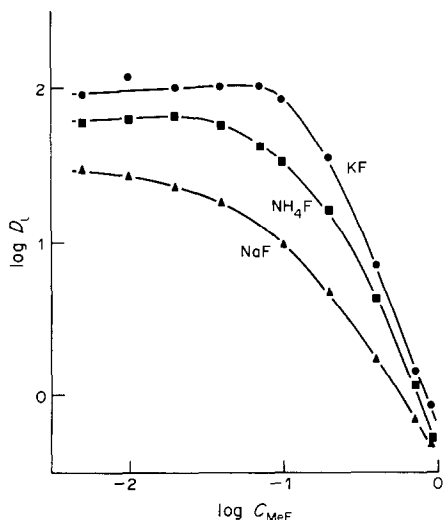


Fig. 5. The effect of KF, NaF and NH_4F on the extraction of tantalum with $0.01M$ dicyclohexano-18-crown-6 in dichloroethane from $0.2M$ HF: notation as in Fig. 3.

dicyclohexano-18-crown-6 from solutions of hydrofluoric acid alone and in mixtures with potassium fluoride.

In the absence of potassium fluoride, the extraction is moderate and the plot of $\log D_1$ vs. $\log C_{\text{HF}}$ shows a broad maximum at 0.1 – $0.2M$ hydrofluoric acid. The addition of potassium fluoride leads to a significant increase in the D_1 -value, whereas addition of hydrofluoric acid to a solution that is $0.1M$ in potassium fluoride has the opposite effect. Under all conditions used, technetium is slightly better extrac-

ted than rhenium, but the plots have the same shape for both elements.

Applications

The results obtained in the distribution study indicate that polyurethane foam or a cyclic polyether can be used to provide new and effective procedures for the separation of Ta, Tc and Re from a number of other elements, and in particular from refractory metals such as Nb, Mo and W. Some examples are given below.

Extraction with $0.01M$ dicyclohexano-18-crown-6 in dichloroethane can be used for the batch separation of traces of tantalum from niobium at concentrations up to 30 mg/ml in $1M$ hydrofluoric acid medium. At least 99.9% of the tantalum is found in the organic phase after repeated extraction, with niobium left quantitatively in the aqueous phase. Similar results are obtained for the separation of technetium from molybdenum, and of rhenium from molybdenum and tungsten, the aqueous phase being $1M$ in ammonium fluoride and $0.1M$ in hydrofluoric acid.

The possibilities for column separation are demonstrated in Fig. 7. Tantalum is strongly sorbed from $1M$ hydrofluoric acid onto the polyurethane foam column, but niobium is not retained at all. The tantalum can be eluted with $1M$ nitric acid/ 0.3% hydrogen peroxide mixture (recovery 95 – 97%) or with acetone (recovery $>99\%$).

In another experiment, a column of polyurethane foam was coupled with a column of the same size loaded with Dowex 1×8 . A 100 -mg sample of

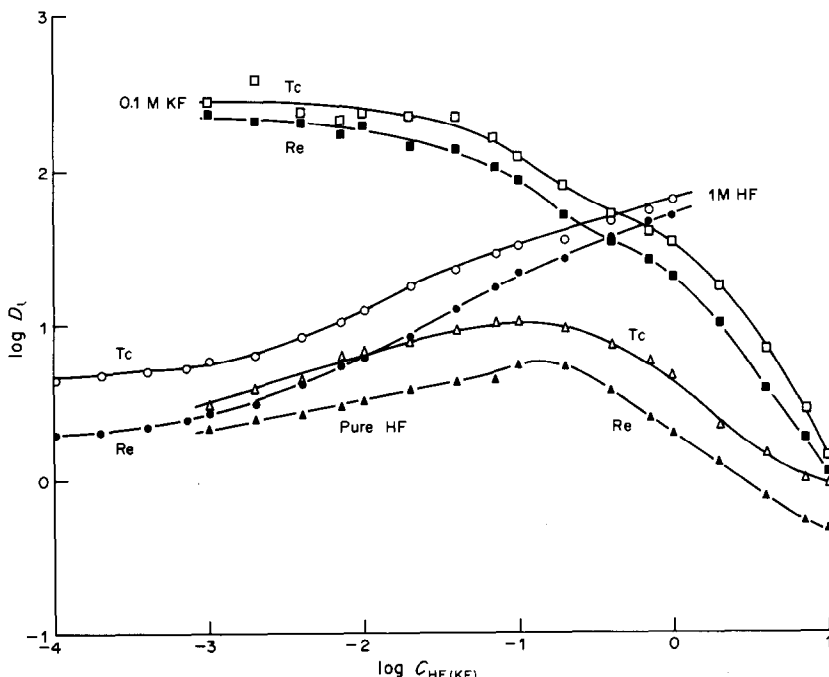


Fig. 6. Distribution ratios for the extraction of technetium and rhenium with $0.01M$ dicyclohexano-18-crown-6 in dichloroethane from hydrofluoric acid (Δ , \blacktriangle) and from HF-KF mixtures (\square , \blacksquare , $0.1M$ KF, xM HF; \circ , \bullet , $1M$ HF, xM KF). Notation as in Fig. 4.

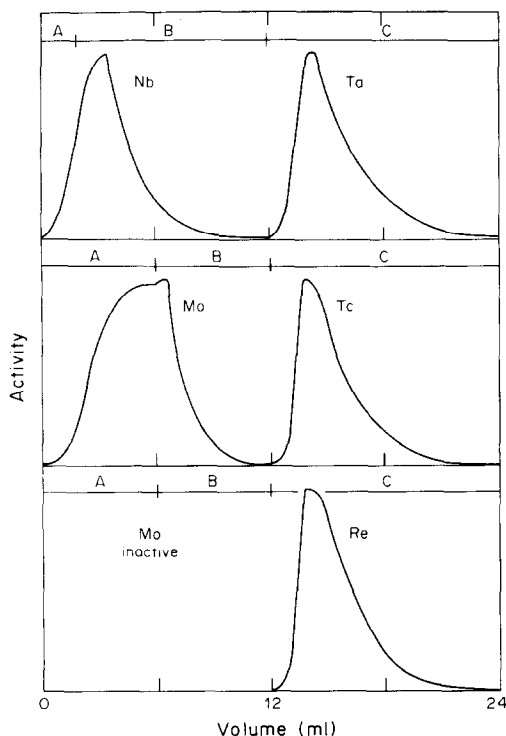


Fig. 7. Separations of Nb-Ta, Mo-Tc, and Mo-Re on polyether-type polyurethane foam under dynamic conditions. Polyurethane-foam column 45 × 9 mm, flow-rate: 0.5–0.7 ml/min. Top: A, 100 mg of Nb in 1M HF; B, 1M HF; C, 1M HNO₃ + 0.3% H₂O₂. Middle: A, 100 mg of Mo in 0.1M HF + 1M NH₄F; B, 0.1M HF + 1M NH₄F; C, 1M HNO₃. Bottom: A, 100 mg of Mo in 0.1M HF + 1M NH₄F; B, 0.1M HF + 1M NH₄F; C, 1M HNO₃.

irradiated niobium pentoxide containing 1500 ppm of tantalum was dissolved in ~0.5 ml of concentrated hydrofluoric acid and the solution was diluted to 5 ml to give a 1M hydrofluoric acid medium. This solution was passed through the column system, followed by 15 ml of 1M hydrofluoric acid. The effluent contained most of the trace impurities, including the alkali-metal and transition elements, but not tantalum activity (the decontamination factor was $\geq 10^8$), and the anion-exchanger column contained 0.2% of the tantalum activity. This Dowex column can be further washed with 40% hydrofluoric acid for elution of such elements as Hf, Zr, Mo, Pa, leaving the niobium and traces of tantalum sorbed on the column.

For separation of molybdenum from technetium or of rhenium from molybdenum or tungsten, the aqueous solution was made 1M in ammonium fluoride and 0.1M in hydrofluoric acid (see Fig. 7). The technetium or rhenium could be eluted with a recovery of 98–99% with 1M nitric acid. Elution with 1M hydrochloric acid was not satisfactory. If a 1M hydrofluoric acid medium was used without the addition of ammonium fluoride, about 2–6% of the technetium or the rhenium was found in the initial effluent. From the mechanisms discussed below for the distribution of rhenium and technetium, it can be

assumed that these two elements can also be retained on polyurethane foam from other media such as chloride, nitrate *etc.*, at lower acidity of the solution.

DISCUSSION

Bowen,⁴ who first studied the retention of anionic complexes on polyurethane foam, assumed that polyether-type polyurethane foam has anion-exchange sites of various strengths as a result of the tendency of the ether oxygen atoms and/or the nitrogen atoms of the urethane linkage to accept protons. It is known that anionic fluoro-complexes of tantalum are efficiently extracted by many extractants, such as ketones, amines, phosphates, *etc.* The strong anion-exchange of tantalum from hydrofluoric acid media with anion-exchangers containing amine groups has also been described. In both cases, the extraction and anion-exchange can take place from concentrated solutions of the acid, where the complexation of tantalum as well as protonation of the extractants (or the exchanger amine groups) is complete. However, from Figs. 1 and 3 it can be seen that the distribution ratio of tantalum decreases when the hydrofluoric acid concentration is above a certain level, for both types of material, the acyclic polyurethane foam and the cyclic polyethers. Tantalum, in general, shows great similarity between its retention on the foam and its extraction with crown ethers, which implies that the anion-exchange mechanism is improbable.

The mechanism of the retention of metal ions by polyurethanes has been systematically studied by Hamon *et al.*,⁵ who have discussed all possible retention processes, *viz.* surface adsorption, solvent extraction, ligand addition or exchange, base anion-exchange and cation-chelation. They concluded that the foam acts predominantly as a long acyclic polyether chain, and the extraction of anions is due to the complexation of counter-cations in the cavities formed by the polyether chain; the efficiency of the extraction depends on how well the cation fits.

The cations participating in the complexation include those of the alkali metals and hydronium ions.⁵ The ionic diameter of the hydronium ion is close to that of K⁺ and NH₄⁺ and matches closely the cavity size of both the foam and the 18-crown-6 type compounds. Complexation of the hydronium ion by crown ethers and cryptates has already been reported.^{6,7} Al-Bazi and Chow⁸ supposed that H₃O⁺ ions are held in the cavities of polyurethane by both ion-dipole interaction and hydrogen-bonding whereas K⁺ ions are held only by ion-dipole interaction.

The retention of tantalum on polyurethane foam as well as the extraction of polycyclic crown ethers can then be described as a distribution of anionic complexes of the type TaF_n⁵⁻ⁿ⁻ ($n \geq 6$). The sorption by foam materials is caused by complexation of hydronium ions in the cavities formed by the polyethylene oxide chain of the polymer. According to Tadokoro

et al.,⁹ the polyethylene oxide has a helical structure which contains seven chemical units and two turns in the repeat unit of length 19.3 Å. In the extraction with a cyclic polyether, the anionic tantalum complexes are the counter-ions to the H_3O^+ or K^+ ions held in the cavities of the polyether ring.

Technetium and rhenium are present in aqueous solution as the weakly hydrated soft anions TcO_4^- and ReO_4^- . Accordingly, the extraction of these two elements with crown ethers can be explained as due to formation and extraction of the ion-association complexes $[\text{K}(\text{H}_3\text{O}), \text{crown}]^+ \cdot \text{MeO}_4^-$ (where $\text{Me} = \text{Tc}$ or Re). The counter-ion in the organic cavity is either K^+ or H_3O^+ . In view of the greater effect of potassium fluoride on the extraction of these two elements with dicyclohexano-18-crown-8 (see Fig. 6), it might be concluded that K^+ is more efficient than H_3O^+ as the counter-ion.

With the polyurethane foam, the anions MeO_4^- are the counter-ions to the H_3O^+ -ions held in the cavities of the polyethylene oxide chain of the polymer.

This conclusion agrees well with the results obtained by infrared spectroscopy for a synthetic tantalum fluoride-polyether complex.¹⁰ On the basis of these experimental results, we assume that the extraction of tantalum can be explained by the formation of the complex $[\text{H}_3\text{O}, (\text{DC}-18,6)]^+ \cdot \text{TaF}_6^-$.

The increase in the D_f and D_1 values for tantalum (Figs. 1 and 3) with increasing acid concentration (up to the acidity for D_{max}) can be attributed to the conversion of oxofluorotantalates into fluorotantalates. The acids HTcO_4 and HReO_4 are very strong and stable over a wide pH-range in aqueous solution, so the extraction of Tc and Re with both the polyurethane foam and the crown ether takes place even at low acidity.

The decrease in D_f and D_1 for tantalum at acidities higher than that for D_{max} can be connected with either the formation of highly co-ordinated and non-extractable complexes such as TaF_8^{3-} *etc.*¹¹ or an increase in the concentration of HF_2^- ions, which can be regarded as competing with the fluorotantalate complexes for ion-association. The latter possibility seems to be the more important, as the behaviour of rhenium and technetium, which do not form fluoro-complexes and are present as MeO_4^- -type oxoanions even at higher hydrofluoric acid concentrations, is comparable with that of tantalum.

The equilibrium constant for $\text{HF} + \text{F}^- \rightleftharpoons \text{HF}_2^-$ is reported¹² to be $\sim 10^{0.6}$ and as the concentration of hydrofluoric acid is increased there will consequently be a shift to the right in its dissociation into H^+ and F^- . Although hydrofluoric acid is a weak acid in dilute aqueous solutions ($\text{p}K \cong 3.1$), its acidity increases with concentration, and this has been attributed to extensive dissociation, coupled with hydrogen-bonded ion-pair formation ($\text{H}_3\text{O}^+ \dots \text{F}^-$), a consequence of which is a decrease in free fluoride concentration.¹³

This could explain why alkali-metal fluoride con-

centrations $\geq 0.1M$ cause a rapid decrease in the D_f and D_1 values in the extraction of tantalum with both the cyclic polyether and the polyurethane foam.

In the media considered in this work, niobium, molybdenum and tungsten are assumed to exist predominantly as anionic oxofluoro-complexes, which are stable even at high acid concentrations. From this point of view it is not surprising that practically no detectable retention and extraction of these elements is observed. On the other hand, hafnium and protactinium form only simple fluoro-complexes,¹⁴ and are neither retained on polyurethane foam nor extracted with cyclic ethers. A possible explanation of these apparent discrepancies is the formation of the species HfF_6^{2-} and PaF_7^{2-} , which are not extracted. The effect of alkali-metal fluoride on the distribution of tantalum at $C_{\text{MeF}} \geq 0.1M$ (Figs. 2 and 5) could also be explained by the formation of higher fluoro-complexes such as TaF_7^{2-} and TaF_8^{3-} .

Retention on polyurethane foam was also observed for the fluoro-complexes of antimony(V), and the behaviour of tantalum and antimony with polyurethane foam in hydrofluoric acid solution is similar to that in their extraction as ion-association complexes into solvents such as ketones, amines and TBP, as well as to that in anion-exchange, and is probably due to the formation of complexes of the same type and having similar properties, presumably TaF_6^- and SbF_6^- . However, the formation of the antimony species takes place at slightly higher concentrations of hydrofluoric acid than that of the tantalum species.

Acknowledgements—Financial assistance for this work was provided by the Bundesministerium für Forschung und Technologie, Bonn, F.R.G. The authors would like to thank the FRM Reaktorstation Garching, TU München, F.R.G., for making available free of charge the irradiation facilities. Thanks are also due to Greiner GmbH, Kremsmünster, Austria, for providing the polyurethane foam material.

REFERENCES

1. R. Caletka and V. Krivan, *Z. Anal. Chem.*, 1985, **321**, 61.
2. G. J. Moody and J. D. R. Thomas, *Analyst*, 1979, **104**, 1.
3. T. Braun, *Z. Anal. Chem.*, 1983, **314**, 652.
4. H. J. M. Bowen, *J. Chem. Soc.*, 1970, 1082.
5. R. F. Hamon, A. S. Khan and A. Chow, *Talanta*, 1982, **29**, 313.
6. R. M. Izatt, B. L. Haymore and J. J. Christensen, *J. Chem. Soc., Chem. Commun.*, 1972, 1308.
7. J. Cheney and J. M. Lahn, *ibid.*, 1972, 487.
8. S. J. Al-Bazi and A. Chow, *Talanta*, 1982, **29**, 507.
9. H. Tadokoro, Y. Chatani, T. Yoshihara, S. Tahara and S. Murahashi, *Makromol. Chem.*, 1964, **73**, 109.
10. R. Caletka, R. Hausbeck and V. Krivan, unpublished work.
11. L. P. Verga and H. Freund, *J. Phys. Chem.*, 1962, **66**, 21.
12. L. G. Sillén and A. E. Martell, *Stability Constants of Metal-Ion Complexes*, Suppl. No. 1, Chemical Society, London, 1971.
13. P. A. Giguère, *J. Chem. Educ.*, 1979, **56**, 571.
14. M. N. Bukhsh, J. Flegenheimer, F. M. Hall, A. G. Maddock and C. Ferreira de Miranda, *J. Inorg. Nucl. Chem.*, 1966, **28**, 421.

A FURTHER INSIGHT INTO THE MECHANISM OF BIOSORPTION OF METALS, BY EXAMINING CHITIN EPR SPECTRA

M. TSEZOS

Department of Chemical Engineering, McMaster University, Hamilton, Ontario, Canada

S. MATTAR

Department of Chemistry, University of Toronto, Toronto, Ontario, Canada

(Received 11 June 1985. Revised 17 September 1985. Accepted 26 October 1985)

Summary—Experimental chitin–uranium–copper EPR spectra have been simulated by computer. The simulation suggests that the chitin–copper–uranium EPR spectra are primarily due to a chitin–copper interaction, with insignificant contribution from other paramagnetic species. The simulation suggests two possible complex configurations, both involving one ligand nitrogen atom.

One of the recent developments in biotechnology is the identification of a new type of adsorbents of biological origin which have high sequestering capacity for organic or inorganic pollutants. One of these adsorbents is the inactive biomass of *Rhizopus arrhizus* that has been demonstrated to give selective sequestration of radionuclides, such as uranium, thorium or radium, from aqueous solution.^{1,2} A detailed investigation of the uranium and thorium uptake by *R. arrhizus* has led to the identification of the cellular components mainly responsible for the observed uptake and has allowed hypothesis of a mechanism for the process of radionuclide biosorption.^{3,4}

Biosorption of uranium by *R. arrhizus* is concentrated at the cell wall of the dead mycelium. Chitin, a crystalline aminopolysaccharide and a basic building block of the *R. arrhizus* cell wall, has been identified as the active constituent of the mycelial cell wall responsible for the biosorptive behaviour. In order to improve the understanding of the mechanism of uranium uptake by dead cells of *R. arrhizus* the competitive uptake of uranium by chitin in the presence of copper was investigated. Equilibrium data for competitive uranium adsorption, along with the result of other spectral investigation techniques, have already been reported.⁵ The information accumulated thus far has provided concrete evidence that the chitin amine nitrogen and a free radical associated with the chitin macromolecule are responsible for the co-ordination and sequestering of uranium as well as of other cations by the cell wall chitin.³

Equilibrium and spectral data on the competitive uranium uptake by chitin have shown that the uranium uptake capacity can be reduced by transition metal ions, such as copper (II), which compete with uranium for the chitin amine sites.⁵ In an effort to acquire evidence for the three dimensional arrangement of the metal chitin complex, it was decided to examine the electron paramagnetic resonance (EPR)

spectra of the chitin–uranium–copper system. The present work is not intended to be an exercise in theoretical EPR spectroscopy but rather an application of this type of spectroscopy in the area of biosorption, aiming at providing information on the mechanism of biosorption.

EXPERIMENTAL

The EPR spectra were determined by using a Varian E3 EPR spectrometer. The magnetic field sweep and the magnitude of the spin Hamiltonian tensor components were calibrated by means of a solid sample of diphenylpicrylhydrazyl free radical. All the sample tubes were checked and found to be free of any spurious and extraneous resonances in the temperature range 77–298 K. Special care was taken to ensure that the resonance line-shapes were not distorted by excessive amplitude modulation or microwave power. The experimental procedure and conditions used in the preparation of the chitin samples have been described previously.⁵

RESULTS AND DISCUSSION

Natural chitin has a naturally occurring organic free radical in its crystalline structure, Fig. 1.⁵ Since radicals are usually short-lived, the stable EPR spectrum of the free radical suggests that the radical is trapped and stabilized in the rigid crystalline chitin matrix. Upon introduction of uranium ions alone into chitin, the free radical EPR spectrum changes, suggesting an interaction with uranium, Fig. 2.⁵ When copper(II)–ions are also introduced, the EPR spectrum of chitin changes further, mainly because of the copper–chitin interaction. The chitin–uranium–copper spectrum (Fig. 3) appears to be primarily the result of chitin–copper interaction. The contribution of the uranium interaction does not appear to be significant. It was decided to focus the investigation on the copper–chitin interaction since it produces a better defined EPR spectrum and is representative of the metal–chitin interaction system. The recorded

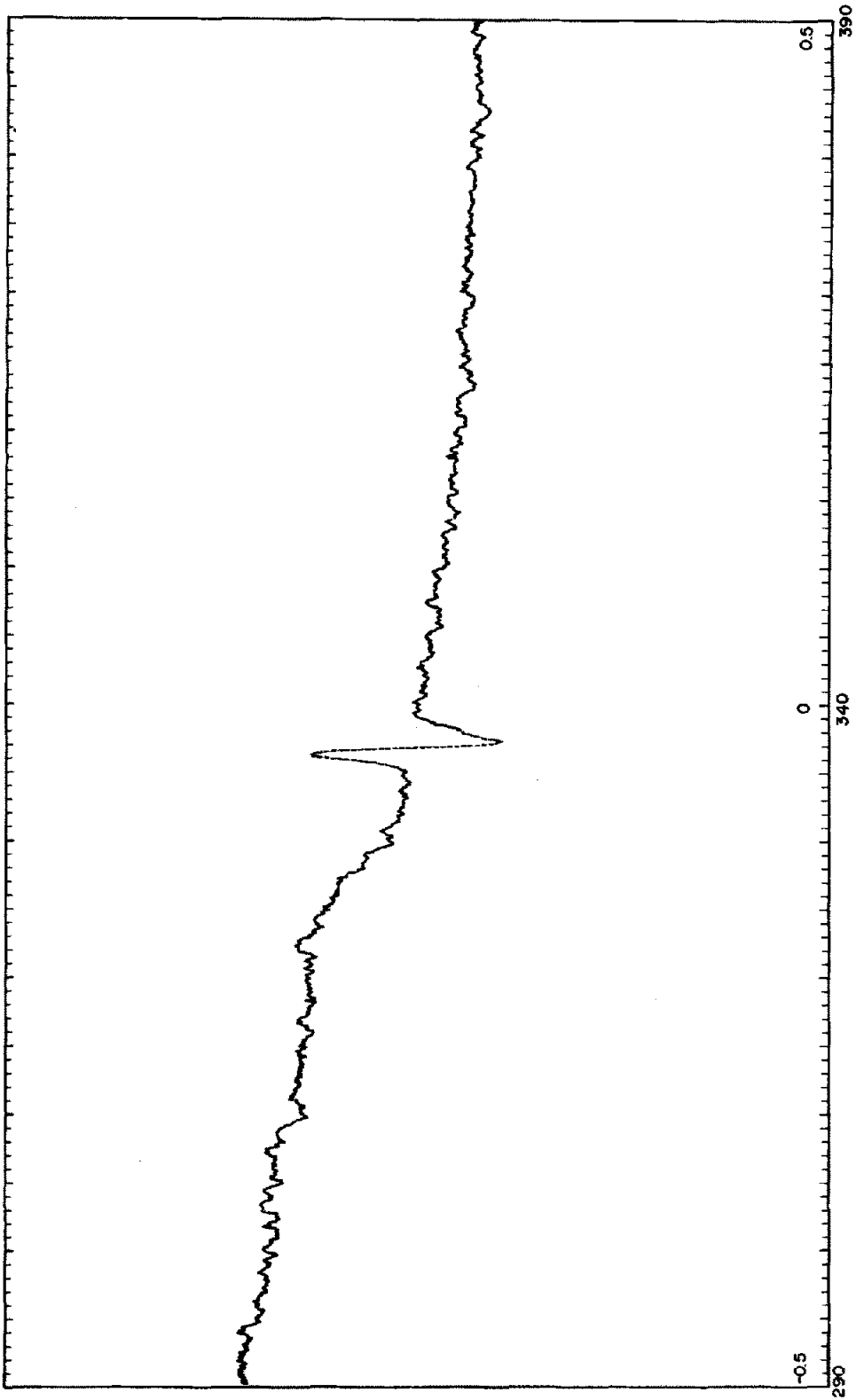


Fig. 1. Experimental EPR spectrum of natural chitin. Total scan range 100 mT, centred around 340 mT.

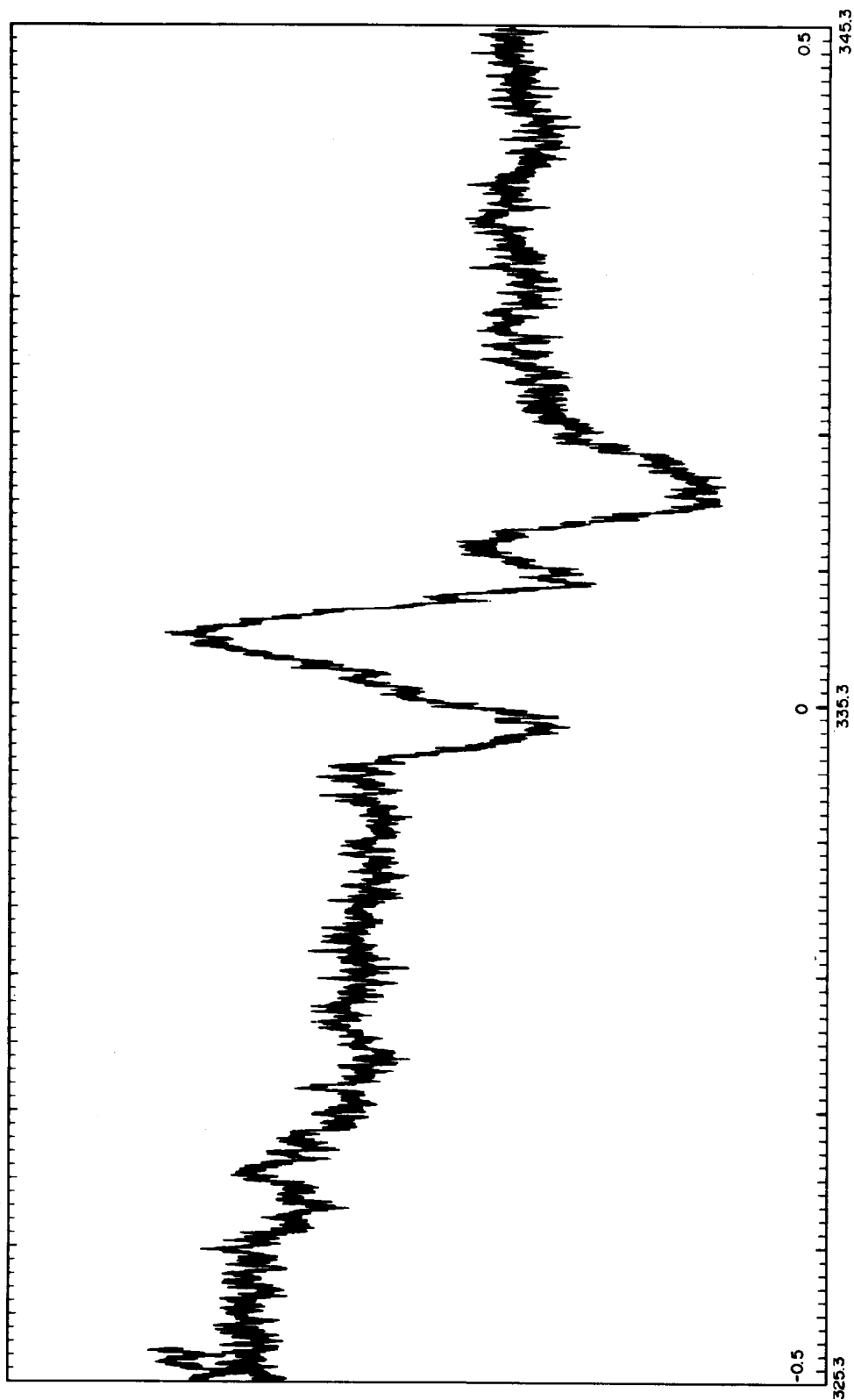


Fig. 2. Experimental EPR spectrum of chitin equilibrated with uranium. Total scan range 20 mT, centred around 335.3 mT.

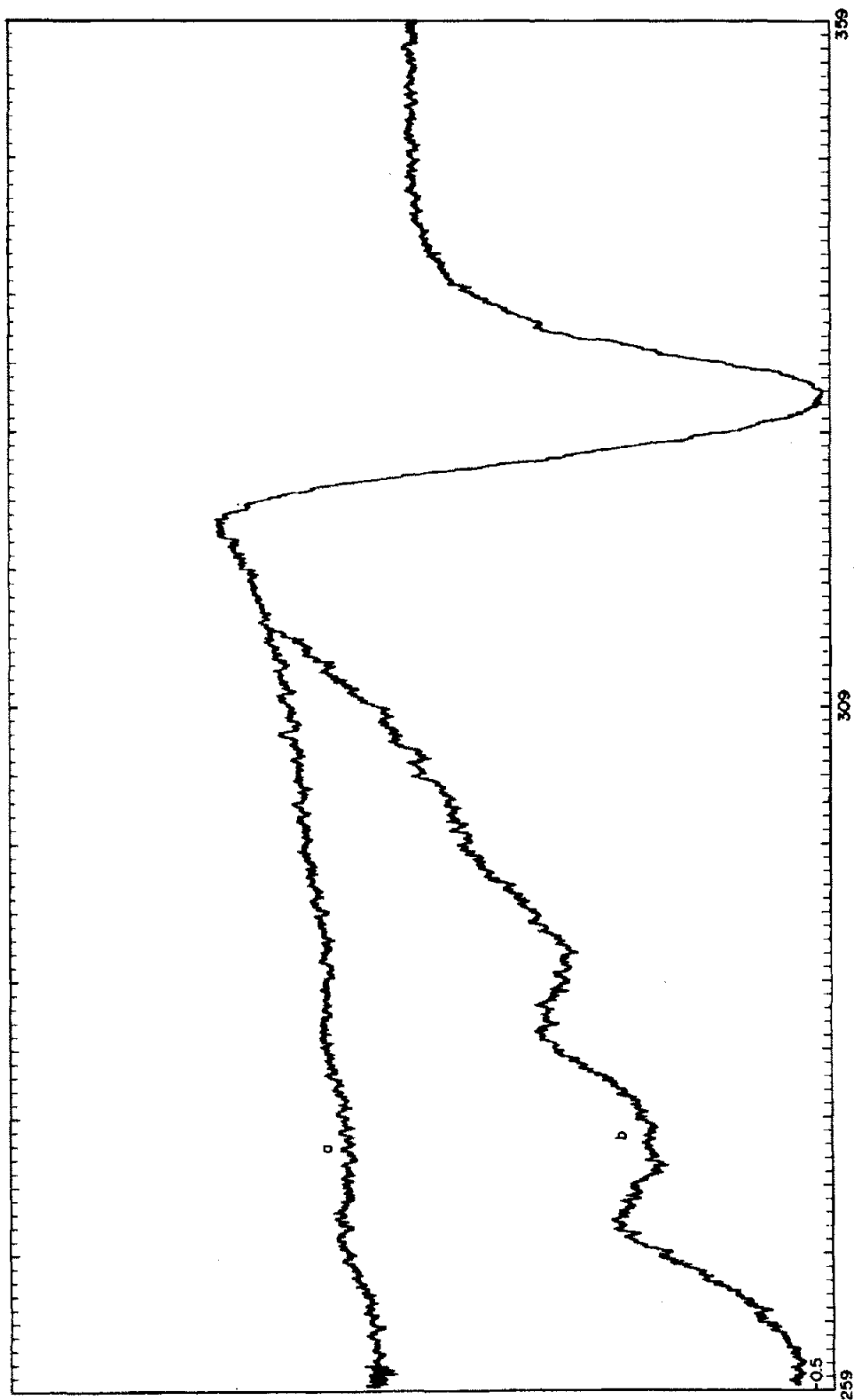


Fig. 3. Experimental EPR spectrum of chitin equilibrated with a copper-uranium solution (pH = 4.0). For the parallel components, receiver gain was increased 1.25 times. Total scan range 100 mT, centred around 309 mT.

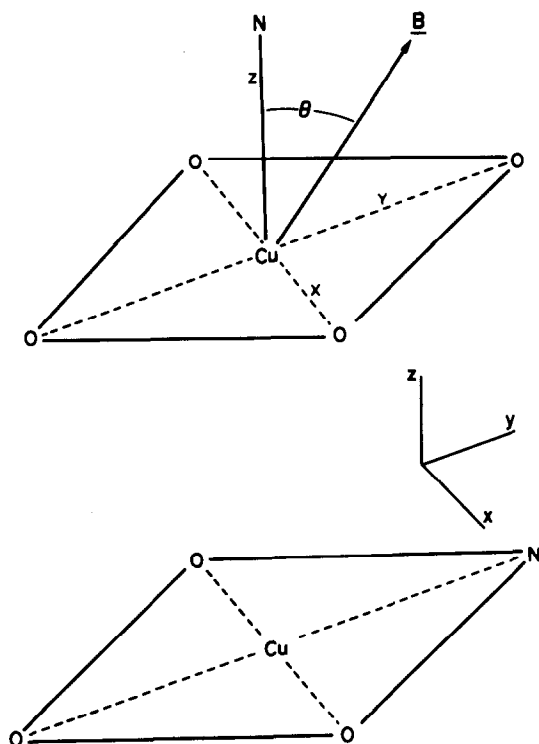


Fig. 4. Suggested environments of Cu moieties in the chitin network.

copper–chitin spectrum corresponded well with the ones reported in the literature.⁶ Chemical equilibrium data for the chitin–uranium–copper system have confirmed that the affinity of chitin is greater for copper than for uranium.⁵

Figure 3 is a typical example of the experimental EPR spectrum of chitin following uptake of copper and uranium from solution at pH 4.0. Although the resonance components in the z -direction (Fig. 4) are weak, under conditions of higher spectrometer sensitivity they become more discernible, as shown on line b in Fig. 3. This EPR spectrum indicates that there exist two main sites for the Cu–chitin interaction in the solid chitin matrix. The major site is denoted as I and the minor site is called site II. The suggestion of two sites is in agreement with the fact that solid chitin exists mainly as a mixture of two isomorphous phases, namely α - and β -chitin. Thus when copper ions interact with chitin, two different major complexes may be formed, depending on whether the chitin involved in complexation is of the α - or β -form.

Owing to the large line-widths of the EPR resonances the spectra are difficult to analyse, and computer simulation was tried as it is a technique that can assist in the resolution of spectral features. Such simulation enables the determination of most of the effective spin Hamiltonian tensor components. The estimated tensor components for the spectrum in Fig. 3 are listed in Table 1. Chitin is an aminopolysaccharide and there is extensive experimental evidence in the literature indicating that the amino nitrogen atom is the site for the co-ordination of metal ions.³⁷⁻⁹ Because of the three-dimensional arrangement of the chitin monomer units, it is possible that when a metal ion is complexed it may interact with more than one nitrogen ligand atom. The possibility that the environment of the co-ordinated copper contains at least open nitrogen atom was thus investigated. The spectrum was simulated by means of a Fortran IV program which makes provisions for superhyperfine splittings, assuming that potentially one, two, three, or four nitrogen atoms participate in a copper–chitin complex.¹⁰

In simulating the line-shapes the best results were achieved when it was assumed that the Cu(II) moiety was associated with one nitrogen atom, resulting in a three-fold splitting of the resonances, with equal relative intensities. Owing to the unresolved nature of the superhyperfine splittings, it could not be unequivocally determined whether the ligand nitrogen atom was axially or equatorially attached. Such unresolved superhyperfine splittings are not uncommon, and occur in the EPR spectra of most Cu(II)–amine complexes such as bis(ethylenediamine) copper (II).¹¹

Figure 5 shows the simulated resonance field positions of the ^{65}Cu isotope of the copper complex situated at site I, *vs.* $\cos \theta$, where θ is the angle between the external applied magnetic field, B , and the principal molecular axis of symmetry of the molecule (Fig. 4). From this figure it can be seen that the electronic magnetogyric and nuclear hyperfine tensor components, g_{zz} and A_{zz} , at an angle of $\theta = 0$, are greater than the corresponding components g_{xx} , g_{yy} , A_{xx} and A_{yy} at an angle of $\theta = 90^\circ$. The EPR spectrum generated by these resonance field positions is shown in Fig. 6. This spectrum, which includes the contributions of the superhyperfine interactions from one nitrogen nucleus, is separated into its four copper hyperfine components. These lines are labelled 1, 2, 3 and 4 respectively and the overall spectrum is labelled 5.

Table 1. Effective spin-Hamiltonian parameters for Cu(II)-chitin

Chitin site	ν , GHz	g_{xx}	g_{yy}	g_{zz}	A_{xx}^*	A_{yy}^*	A_{zz}^*	$A_{xx}(\text{N})^\dagger$	$A_{yy}(\text{N})^\dagger$	$A_{zz}(\text{N})^\dagger$
I	9.45	2.062	2.062	2.311	20.00	20.00	154.47	2.5	2.5	1.9
II	9.45	2.060	2.060	2.321	18.00	18.00	145.80	2.5	2.5	1.7

* 10^{-4} cm^{-1} .

†Nitrogen superhyperfine tensor components (mT).

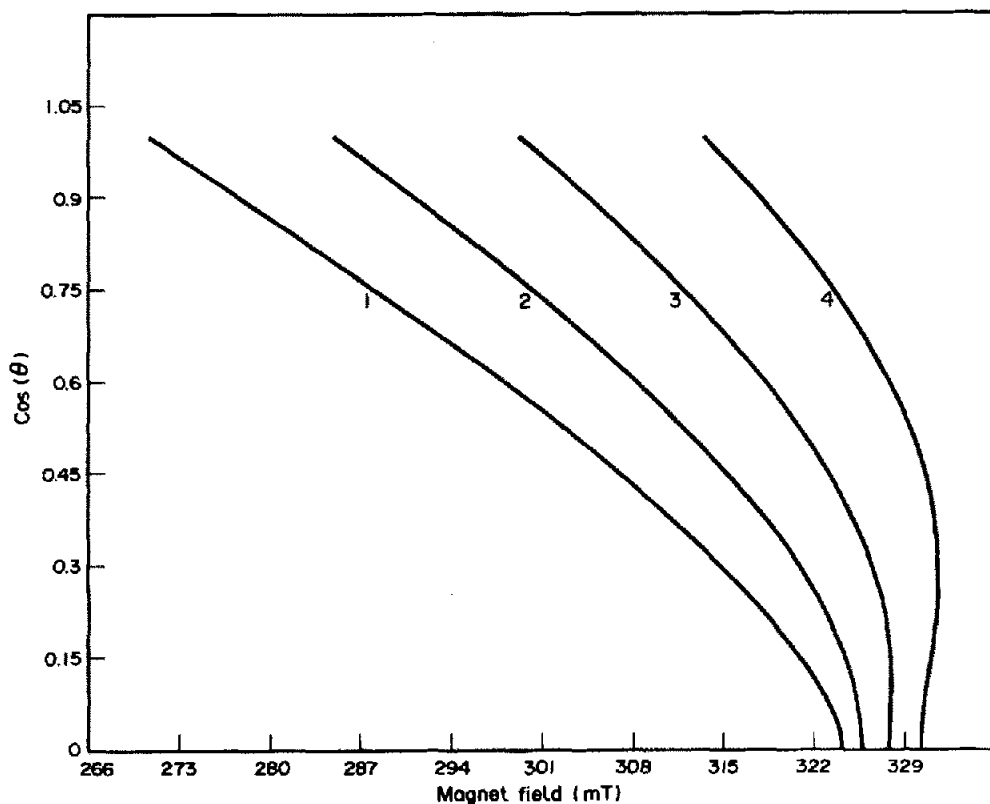


Fig. 5. Simulated resonance field positions as a function of $\cos \theta$. The four copper hyperfine fields are labelled 1, 2, 3 and 4.

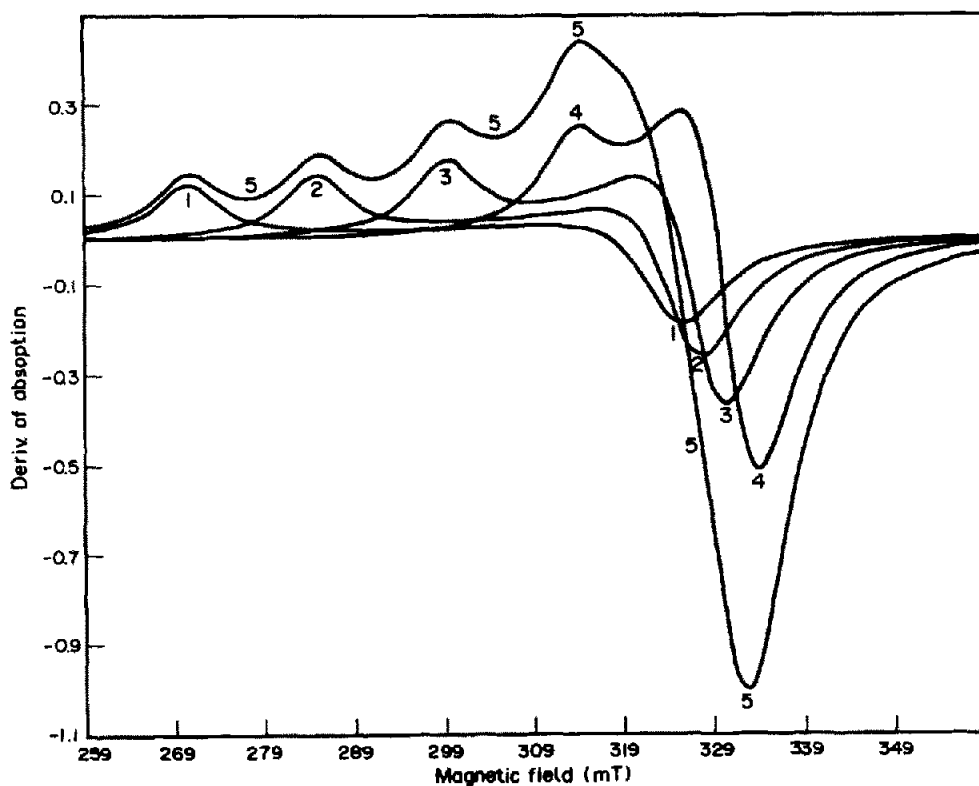


Fig. 6. The simulated EPR spectrum of site I for the Cu(II)-chitin complex. The four copper hyperfine splittings are labelled 1, 2, 3 and 4 and the overall spectrum is 5.

The spectra presented in Figs. 5 and 6 also assist in understanding the sloping of the overall spectrum 5 in the region 260–310 mT. This sloping appears to be the result of the large line-widths of the resonances along the z -axis, which in turn results in the overlap of their wings, thus producing the apparently sloping base-line. The spectra in Figs. 5 and 6 also indicate that the four perpendicular hyperfine lines along the x and y axes lie close to one another, in contrast to the parallel components that are some distance apart. This is interpreted as the result of the larger copper hyperfine tensor component A_{zz} as compared to A_{xx} and A_{yy} . Consequently the corresponding EPR spectrum (Fig. 6) is unresolved and more intense along the perpendicular components A_{xx} and A_{yy} .

The simulated spectra for ^{63}Cu and ^{65}Cu , as well as their resultant effect for site I, taking into account their natural abundance isotopic ratio, are shown in Fig. 7. Although the spectral line shapes of the parallel components are better resolved in the simulated than in the experimental spectrum (Fig. 3), when the spectrum of the minor site II is also taken into account the experimental spectrum is well reproduced by our simulation (Fig. 6). The best simulated spectrum is obtained when the abundance of the two sites is in the ratio 1:0.13, implying 13% of β -chitin in the sample. This ratio is not unreasonable and agrees well with the ratios reported in the literature.⁷

Relation of the spin Hamiltonian components to the nature of the Cu–chitin complex

Assuming that the unpaired electron for the Cu(II)–chitin complex resides in a molecular orbital that is mainly $d_{x^2-y^2}$ (Cu) $>$ in character, then the g tensor components may be approximately expressed as

$$g_{\parallel} = g_{zz} \approx 2.0023 - \frac{8\lambda}{\Delta E_0}$$

and

$$g_{\perp} = g_{xx} = g_{yy} \approx 2.0023 - \frac{2\lambda}{\Delta E_1},$$

where λ is the spin–orbit coupling constant for the copper atom, ΔE_0 is the energy separation between the $|d_{x^2-y^2}(\text{Cu})>$ and $|d_{xy}(\text{Cu})>$ states, and ΔE_1 is the energy difference between the $|d_{x^2-y^2}(\text{Cu})>$ and either the $|d_{yz}(\text{Cu})>$ or $|d_{xz}(\text{Cu})>$ orbitals.¹² Since the spin–orbit coupling constant is negative (using a hole formalism for the Cu $3d^9$ system) and ΔE_0 is usually smaller than ΔE_1 , it is expected that all the diagonal g tensor components will be greater than the corresponding value for the free electron, g_e . In addition, the g_{xx} and g_{yy} components are expected to be smaller than the g_{zz} component, which is in accordance with the experimental and simulated spectra. Generally the spin–orbit coupling constant, λ , for CuN_4 is less than that for CuO_4 complexes,

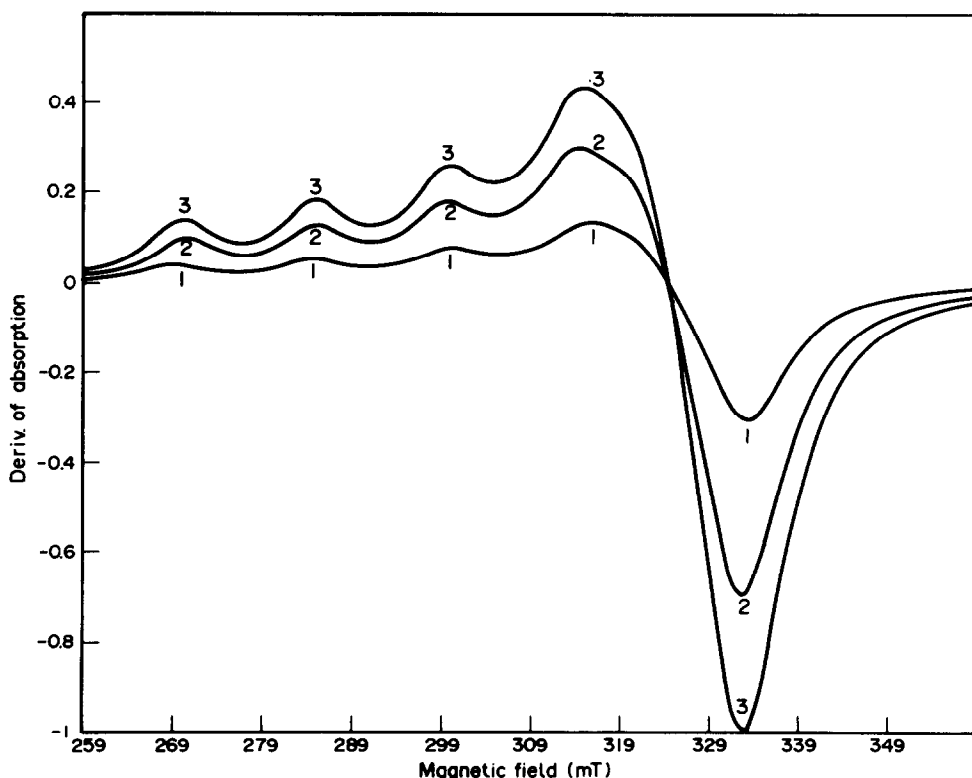


Fig. 7. Simulated EPR spectra from ^{63}Cu and ^{65}Cu chitin complexes. Resultant spectrum is labelled 3.

whereas the ligand-field energies, ΔE_1 and ΔE_0 , are of the same order of magnitude. Consequently it is expected that the g tensor components should be larger for CuO_4 complexes than for the respective components of CuN_4 complexes. The values of $g_{zz} = 2.311$ and $g_{xx} = g_{yy} = 2.062$, determined by the simulation, suggest the existence of two most likely local copper moieties. The first includes three oxygen and one nitrogen atoms in the equatorial plane and the second has four oxygen atoms in its equatorial plane and an additional nitrogen atom along the z -axis. Both of these moieties are schematically presented in Fig. 4. Two-dimensional arrangements for the complex of copper with chitin have been proposed in the literature, and agree reasonably well with the proposed three-dimensional models.^{12,13}

The absolute values of the copper hyperfine tensor components for site I were estimated to be $A_{zz} = 154.47 \times 10^{-4} \text{ cm}^{-1}$ and $A_{xx} = A_{yy} \approx 20.0 \times 10^{-4} \text{ cm}^{-1}$. The theoretical expressions for these tensor components are given approximately by¹³

$$A_{zz} \approx \frac{g_e g_N \beta \beta_N}{\langle r^3 \rangle} \left\{ -K - \frac{4}{7} + \frac{3}{7}(g_{\perp} - 2) + (g_{\parallel} - 2) \right\}$$

$$A_{xx} = A_{yy} \approx \frac{g_e g_N \beta \beta_N}{\langle r^3 \rangle} \left\{ -K + \frac{2}{7} - \frac{11}{7} \frac{\lambda}{\Delta E_1} \right\}$$

Spin-orbit coupling and the unquenching of orbital angular momentum contribute the factors $(g_{\parallel} - 2)$, $\frac{3}{7}(g_{\perp} - 2)$ and $\frac{11}{7}(g_{\perp} - 2)$. On the other hand the dipolar interactions result in values of $-\frac{4}{7}$ and $\frac{2}{7}$ for A_{zz} , and for A_{xx} and A_{yy} respectively. Although the dipolar and spin-orbit coupling contributions oppose one another for A_{zz} and reinforce each other in A_{xx} and A_{yy} , the value of A_{zz} is found, from the simulation of the experimental spectrum, to be much larger than A_{xx} and A_{yy} . This is due to the isotropic Fermi contact interaction (K) resulting from the existence of electronic charge density at the copper nucleus. In the case of Cu(II) , the Fermi term arises from the core s electrons that are spin-polarized. It is very difficult to estimate in advance the contribution to the Fermi term arising from core polarization. However, from the values of the copper hyperfine tensor components that were estimated by the simulation, the value of K was found to be 0.312. This value is close to values that have been reported for other Cu(II) complexes.¹⁵ The value found for K indicates that A_{zz} is negative, whereas both A_{xx} and A_{yy} are estimated to be positive, equal and approximately $20.0 \times 10^{-4} \text{ cm}^{-1}$. The g and A tensors for the Cu(II) complex suggest that the unpaired electron of

the Cu(II) -chitin complex sites lies in a molecular orbital that is mainly $|d_{x^2-y^2}(\text{Cu})\rangle$ in character.

CONCLUSIONS

The experimental and simulated EPR spectra of the chitin-uranium-copper system suggest the following conclusions.

Copper appears to form two separate complexes with chitin at two possible sites, designated as sites I and II, which are probably related to the existence of the two main crystalline forms of chitin (α and β).

From the present simulation and previous experimental work, both copper complexes are thought to involve one nitrogen ligand atom, with the remaining ligands oxygen atoms. The proposed possible configurations of the copper environment for sites I and II are presented schematically in Fig. 4.

The estimated g tensor components ($g_{zz} > g_{yy} \approx g_{xx}$) indicate that the copper complex has its unpaired electron lying in the copper $|d_{x^2-y^2}\rangle$ orbital.

The chitin-uranium-copper EPR spectrum appears to be primarily the result of the chitin-copper interaction. Any contributions to the spectrum by uranium or a free radical do not appear to be significant.

Acknowledgements—This work was supported by the NSERC Operating Grant of the first author.

REFERENCES

1. M. Tsezos and B. Volesky, *Biotechnol. Bioeng.*, 1981, **23**, 583.
2. M. Tsezos and D. Keller, *ibid.*, 1983, **25**, 201.
3. M. Tsezos and B. Volesky, *ibid.*, 1982, **24**, 381.
4. *Idem*, *ibid.*, 1982, **24**, 955.
5. M. Tsezos, *ibid.*, 1983, **25**, 2025.
6. L. D. Hall and M. Yalpani, *Carbohydr. Res.*, 1980, **83**.
7. R. A. A. Muzzarelli, *Chitin*, Pergamon Press, New York, 1977.
8. V. Sabramanian, T. Yoshinari and B. D'Anglejan, *Marine Sciences Centre Report*, No. 27, McGill University, Montreal, 1974.
9. R. A. A. Muzzarelli and O. Tubertini, *Talanta*, 1969, **16**, 1571.
10. S. M. Mattar, *Ph.D. Thesis*, McGill University, 1981.
11. W. B. Lewis, M. Alei, Jr. and L. O. Morgan, *J. Chem. Phys.*, 1966, **45**, 4003.
12. Z. Tamura and M. Miyazaki, *Chem. Pharm. Bull.*, 1965, **13**, 33.
13. F. Yaku and T. Koshijima, *Proc. First International Symposium on Chitin*, p. 401. Department of Nuclear Engineering, M.I.T., 1978.
14. A. Abragam and M. H. L. Pryce, *Proc. Roy. Soc., A*, 1951, **206**, 164.
15. K. E. Falk, E. Ivanova, B. Roos and T. Vanngard, *Inorg. Chem.*, 1970, **9**, 556.

DETERMINATION OF SILVER, ANTIMONY, BISMUTH, COPPER, CADMIUM AND INDIUM IN ORES, CONCENTRATES AND RELATED MATERIALS BY ATOMIC-ABSORPTION SPECTROPHOTOMETRY AFTER METHYL ISOBUTYL KETONE EXTRACTION AS IODIDES

ELSIE M. DONALDSON

Mineral Sciences Laboratories, Canada Centre for Mineral and Energy Technology,
Department of Energy, Mines and Resources, Ottawa, Canada

MOHUI WANG

Chengdu Geological College, Chengdu, People's Republic of China

(Received 17 September 1985. Accepted 24 October 1985)

Summary—Methods for determining $\sim 0.2 \mu\text{g/g}$ or more of silver and cadmium, $\sim 0.5 \mu\text{g/g}$ or more of copper and $\sim 5 \mu\text{g/g}$ or more of antimony, bismuth and indium in ores, concentrates and related materials are described. After sample decomposition and recovery of antimony and bismuth retained by lead and calcium sulphates, by co-precipitation with hydrous ferric oxide at $\text{pH } 6.20 \pm 0.05$, iron(III) is reduced to iron(II) with ascorbic acid, and antimony, bismuth, copper, cadmium and indium are separated from the remaining matrix elements by a single methyl isobutyl ketone extraction of their iodides from $\sim 2M$ sulphuric acid– $0.1M$ potassium iodide. The extract is washed with a sulphuric acid–potassium iodide solution of the same composition to remove residual iron and co-extracted zinc, and the extracted elements are stripped from the extract with 20% v/v nitric acid–20% v/v hydrogen peroxide. Alternatively, after the removal of lead sulphate by filtration, silver, copper, cadmium and indium can be extracted under the same conditions and stripped with 40% v/v nitric acid–25% v/v hydrochloric acid. The strip solutions are treated with sulphuric and perchloric acids and ultimately evaporated to dryness. The individual elements are determined in a 24% v/v hydrochloric acid medium containing $1000 \mu\text{g}$ of potassium per ml by atomic-absorption spectrophotometry with an air–acetylene flame. Tin, arsenic and molybdenum are not co-extracted under the conditions above. Results obtained for silver, antimony, bismuth and indium in some Canadian certified reference materials by these methods are compared with those obtained earlier by previously published methods.

Recently, we published a study of the methyl isobutyl ketone (MIBK) extraction of 15 elements as iodides from $0.1\text{--}5M$ sulphuric acid/ $0.01\text{--}0.5M$ potassium iodide solutions.¹ This study showed that silver, antimony, bismuth, copper, cadmium, indium, tellurium(IV) and thallium(III) can all be quantitatively extracted into MIBK in one extraction from $2M$ sulphuric acid/ $0.05\text{--}0.5M$ potassium iodide when the volume ratio of the organic to aqueous phase is 1:2. Furthermore, at the 500-mg level, $\leq 1.5\%$ of any zinc present is extracted from solutions that are up to $\sim 0.1M$ in potassium iodide and up to $\sim 2M$ in sulphuric acid. The back-extraction of these elements was also investigated. In recent years, individual atomic-absorption spectrophotometric (AAS) and light-absorption spectrophotometric methods have been developed in this laboratory for the determination of some of the elements above, *viz.* silver,²⁻⁴ antimony,⁵ bismuth^{6,7} and indium⁸ in zinc sulphide

ores and concentrates, zinc processing products and other diverse sulphide ores and related materials. However, the results of the extraction study suggested that the group extraction of these elements, plus copper and cadmium, from $\sim 2M$ sulphuric acid– $0.1M$ potassium iodide might provide an alternative and relatively rapid flame AAS method for the determination of all six elements in the materials listed. Because these materials usually contain only trace amounts of thallium and tellurium, determination of these two elements by flame AAS was not considered feasible.

AAS methods⁹⁻²⁰ based on extraction of the iodides of one or more of the elements above, and other elements including zinc and lead, into MIBK [or MIBK containing compounds such as tri-*n*-octylamine,¹⁷ trioctylphosphine oxide¹² and tricaprylmethylammonium chloride (Aliquat 336)^{9,10}] from hydrochloric,^{9-12,18-20} sulphuric,^{14,17} perchloric¹³ and phosphoric acid^{15,16} media have been reported for various types of materials. However, none of these

methods is directly applicable to samples containing relatively large amounts of lead, because in hydrochloric acid media lead is co-extracted as the iodide,^{9,10,12,18} whereas in sulphuric, perchloric and phosphoric acid media, the lead sulphate produced by reaction with sulphuric acid and/or by the oxidative decomposition of sulphide ores must be filtered off before the extraction step. This results in the loss of appreciable amounts of antimony, bismuth and silver, which are retained by the precipitate.¹ The occluded silver can be readily recovered by washing the precipitate with $\sim 4M$ ammonia solution.^{2,3} However, the development of a suitable group iodide extraction/AAS method, which would be applicable to the determination of both antimony and bismuth in ores of moderate and high lead content, and which would involve extraction from sulphuric acid media, would require that provision be made for the recovery of these occluded elements from the lead sulphate precipitate. This, as well as the group back-extraction of the elements under consideration, was investigated in this work. Although the extracted elements can be determined directly in the MIBK extract by AAS,^{9-12,14-20} an aqueous medium was chosen because of the wide variation in the contents of some of these elements in sulphide ores and related materials. This simplifies the dilutions needed, and results in sample and calibration solutions that are usually more stable than MIBK extracts.^{10,18}

The proposed method *A* involves the separation of antimony, bismuth, copper, cadmium and indium from the matrix elements by a single MIBK extraction of their iodides from $\sim 2M$ sulphuric acid/0.1M potassium iodide, after the recovery of antimony and bismuth from lead and calcium sulphates by coprecipitation with hydrous ferric oxide at pH 6.20 \pm 0.05. The extracted elements are stripped from the extract with 20% v/v nitric acid containing 20% v/v hydrogen peroxide and ultimately determined in 24% v/v hydrochloric acid medium containing 1000 μ g of potassium per ml by AAS with an air-acetylene flame. Method *B* involves the extraction of silver, copper, cadmium and indium under the same conditions, after the removal of lead sulphate by filtration and recovery of the occluded silver from the precipitate by washing with dilute ammonia solution. The extracted elements are stripped with 40% v/v nitric acid containing 25% v/v hydrochloric acid to keep silver iodide in solution, and determined as described above. Results obtained for silver, antimony, bismuth and indium in some Canadian certified reference materials by these methods are compared with those obtained earlier by previously published methods.

EXPERIMENTAL

Apparatus

A Perkin-Elmer model 5000 spectrophotometer, equipped with a single-slot 10-cm air-acetylene burner, was used for all atomic-absorption measurements. Operating conditions were those recommended by the manufacturers,

and the burner position and flame parameters for each element were optimized for maximum absorbance while aspirating standard solutions. Hollow-cathode lamps, the impact bead and the most sensitive resonance lines were used for all the elements determined, and background correction was employed for antimony and bismuth. Each element was determined by using the direct read-out device after calibration of the instrument with two or three calibration solutions of different concentrations. Under these conditions and depending on the concentrations of the calibration solutions, the instrumentally computed scale expansions ranged from ~ 1 up to ~ 7 , 11, 7, 10, 3 and 13 for silver, antimony, bismuth, copper, cadmium and indium, respectively. Depending on the volume of sample solution, 2 or 3 sec integration times were used in conjunction with an aspiration rate of ~ 6 ml/min.

Reagents

Standard silver solution, 100 μ g/ml. Dissolve 0.1000 g of pure silver foil in ~ 25 ml of 25% v/v nitric acid, add ~ 10 ml of 50% v/v sulphuric acid and evaporate the solution to fumes of sulphur trioxide. Cool the solution, dissolve the salts by heating gently with ~ 100 ml of concentrated hydrochloric acid, then dilute to volume with water in a 1-litre standard flask containing ~ 300 ml of concentrated hydrochloric acid. This solution is stable for at least 2 months.

Standard antimony(III) solution, 1000 μ g/ml. Dissolve 0.5338 g of pure potassium antimony tartrate (dried at 105° for 1 hr) in water and dilute to 200 ml.

Bismuth, indium, copper and cadmium solutions, 1000 μ g/ml. Dissolve 0.5000 g of each of the pure metals by heating gently with ~ 40 ml of 25% v/v nitric acid. Cool and dilute each solution to 500 ml with water.

Copper plus cadmium solution, 100 μ g/ml. Transfer 25 ml of each stock solution to a 250-ml standard flask and dilute the resulting mixed solution to volume with water.

Indium solution, 100 μ g/ml. Dilute a 25-ml aliquot of the stock solution to 250 ml with water as described above.

Antimony plus bismuth solution, 100 μ g/ml. Dilute 25 ml of each stock solution plus 50 ml of concentrated hydrochloric acid to 250 ml as described above.

Iron(III) solution, 5 mg of iron/ml. Dissolve 12.5 g of ferric sulphate nonahydrate in ~ 300 ml of hot water containing ~ 10 ml of concentrated hydrochloric acid. Cool and dilute to 500 ml with water.

Potassium solution, 10.0 mg/ml. Dissolve 19.0 g of potassium chloride in water and dilute to 1 litre.

Bromine, 20% v/v solution in carbon tetrachloride.

Sulphurous acid. Water saturated with sulphur dioxide.

Tartaric acid, 5% solution.

Ammonium chloride, 15% solution.

Potassium iodide, 2M solution.

Sulphuric acid (2M)-potassium iodide (0.1M) wash solution. Prepare a sufficient volume of solution just before use, containing 22 ml of 50% v/v sulphuric acid and 5 ml of 2M potassium iodide solution per 100 ml.

Nitric acid (20% v/v)-hydrogen peroxide (20% v/v) solution. Prepare a sufficient volume of solution just before use, by appropriate dilution of concentrated nitric acid and 30% w/v hydrogen peroxide.

Nitric acid (40% v/v)-hydrochloric acid (25% v/v) solution. Prepare a sufficient volume of solution just before use, and cool to room temperature.

Aqua regia. Mix 3 parts of concentrated hydrochloric acid with 1 part of concentrated nitric acid. Prepare fresh as required.

Sulphuric acid, 50% v/v.

Sulphuric acid, 1% and 5% v/v. Store in a plastic squeeze-type wash bottle and a glass wash-bottle, respectively.

Ammonia, 25% v/v solution. Store in a plastic squeeze-type wash-bottle.

Ammonia, 10% v/v solution. Store in a dropping bottle.
Hydrochloric acid, 10% v/v. Store in a dropping bottle.
MIBK. Analytical-reagent grade.

Calibration solutions

Prepare 0.5-, 1-, 1.5-, 2-, 2.5- and 3- $\mu\text{g/ml}$ silver solutions by adding the corresponding volumes of 100- $\mu\text{g/ml}$ standard silver solution to 100-ml standard flasks (Note 1). Add 10 ml of 10.0-mg/ml potassium solution to each flask, followed by sufficient concentrated hydrochloric acid for the final solutions to be 24% v/v hydrochloric acid, then dilute each solution to volume with water. Using the 100- $\mu\text{g/ml}$ standard antimony plus bismuth solution and the 100- $\mu\text{g/ml}$ indium solution, prepare, in a similar manner, one series of calibration solutions containing 0.5, 1, 2, 3, 5, 10, 15 and 20 $\mu\text{g/ml}$ each of antimony and bismuth and a second series containing the same concentrations of indium (Note 2). In the same way, prepare solutions containing 0.5, 1, 1.5, 2, 2.5, 3 and 4 $\mu\text{g/ml}$ each of copper plus cadmium, then prepare a zero calibration solution by diluting 25 ml of 10.0-mg/ml potassium solution and 60 ml of concentrated hydrochloric acid to 250 ml with water.

Procedures

A—Determination of antimony, bismuth, copper, cadmium and indium. Transfer up to 1 g of powdered sample, containing up to $\sim 500 \mu\text{g}$ each of antimony, bismuth, cadmium and indium and not more than $\sim 150 \text{ mg}$ each of calcium and lead and 20 mg of copper, to a 400-ml Teflon beaker. Cover the beaker and add 5 ml of 20% bromine solution in carbon tetrachloride and 15 ml of concentrated nitric acid. Mix and allow the solution to stand for ~ 15 min, then heat gently to remove the bromine and carbon tetrachloride. Add 25 ml of 50% v/v sulphuric acid, heat until the evolution of oxides of nitrogen ceases, then remove the cover and wash down the sides of the beaker with water. Add 10 ml of concentrated hydrofluoric acid and carefully evaporate the solution until copious fumes of sulphur trioxide are evolved. Cool, cover the beaker with a Teflon cover (Note 3), add 5 ml of *aqua regia* (Note 4) and heat until the evolution of oxides of nitrogen ceases, then remove the cover and evaporate the solution to fumes of sulphur trioxide. Cool, wash down the sides of the beaker with water and evaporate to fumes again to ensure the complete removal of hydrofluoric and nitric acids. Cool, add 10 ml of 5% tartaric acid solution and 50 ml of water and heat gently to dissolve the salts. Cool the solution to room temperature and, if necessary, filter it (Whatman 11-cm No. 40 paper) into a 400-ml Pyrex beaker. Wash the beaker and paper each three times with ~ 5 –10-ml portions of 1% v/v sulphuric acid, then once each with water. Reserve the filtrate. If the antimony, bismuth and copper contents of the sample are expected to be $\leq 200 \mu\text{g}$, run a blank through the whole procedure.

Using a jet of water, wash the residue into the original Teflon beaker, then place the beaker under the funnel and add, in succession, three 25-ml portions of hot 15% ammonium chloride solution to the funnel to dissolve any residual lead and calcium sulphates. Wash the paper once with water, then reserve it. Add 3 ml of concentrated hydrochloric acid, 1 ml of concentrated nitric acid (Note 5) and 5 ml of 5 mg/ml iron(III) solution to the resulting solution, cover, and boil vigorously for ~ 30 min to ensure the complete dissolution of lead sulphate. Cool the solution to room temperature, then adjust the pH to 6.20 ± 0.05 with concentrated and 10% v/v ammonia solution, and with 10% v/v hydrochloric acid if required. Cover the beaker and boil the solution for ~ 1 min to coagulate the precipitate; allow it to settle, then filter the solution through the original filter paper and wash the beaker and the paper plus precipitate each thoroughly three or four times with water to remove chloride. Discard the filtrate and place the beaker containing the initial filtrate under the funnel. Wash down the sides of

the precipitation beaker with ~ 10 ml of hot 5% v/v sulphuric acid and add the solution to the funnel containing the precipitate. Wash the beaker once more with the hot acid solution, followed by water, then wash the paper three times with ~ 5 ml portions of the acid solution to dissolve any remaining precipitate. Discard the paper. Place a glass rod in the solution to prevent bumping, cover the beaker, evaporate the solution to ~ 60 ml, then cool it to room temperature.

Transfer the solution to a 250-ml separatory funnel marked at 100 ml, add 3 g of ascorbic acid, then stopper the funnel and shake until most of the acid has dissolved. Add 5 ml of 2M potassium iodide solution, dilute the solution to the mark with water and allow it to stand for 30 min to ensure complete complex formation. Add 50 ml of MIBK, stopper the funnel and shake it for 2 min. Allow several min for the layers to separate, then drain off and discard the aqueous layer. Wash the extract by shaking it for ~ 30 sec with 20 ml of freshly prepared 2M sulphuric acid–0.1M potassium iodide. Discard the wash solution. Add 25 ml of freshly prepared 20% v/v nitric acid–20% v/v hydrogen peroxide solution to the extract and shake for 2 min (Note 6). Allow the layers to separate, then drain the lower (aqueous) layer into a 150-ml beaker and wash the stem of the funnel with water. Strip the MIBK phase twice more by shaking it for ~ 1 min with 10 ml of the strip solution and then for ~ 30 sec with 5 ml. Collect these solutions in the beaker containing the initial strip solution and wash the stem of the funnel with water each time (Note 7).

Add 1 ml of 10.0-mg/ml potassium solution, 2 ml of 50% v/v sulphuric acid and 1 ml of concentrated perchloric acid to the combined strip solution. Place a thin glass rod in the solution to prevent bumping, then cover the beaker and evaporate the solution to fumes of perchloric acid. Continue to heat the solution for ~ 10 min to destroy organic material, then cool to room temperature, add 2 ml of *aqua regia* and heat until the evolution of oxides of nitrogen ceases. Cool, remove the cover and evaporate the solution to dryness. Wash down the sides of the beaker with water and evaporate the solution to dryness again to remove all the sulphuric acid. Add 2.4 ml of concentrated hydrochloric acid and 3 ml of sulphurous acid to the beaker containing the blank. Depending on the lowest expected content of any of the elements to be determined, add sufficient concentrated hydrochloric acid to the beaker containing the sample for the final solution to be 24% v/v in hydrochloric acid (Note 8), then add sufficient 10.0-mg/ml potassium solution for 1 ml to be present for each 10 ml of final solution in excess of 10 ml (Note 9). Add 5 ml of sulphurous acid followed by sufficient water for the hydrochloric acid concentration to be $\sim 50\%$ v/v (Note 10). Cover both beakers and boil the solutions gently for ~ 5 –7 min to remove sulphur dioxide (Note 11), then cool to room temperature. Transfer the blank solution to a 10-ml standard flask and the sample solution to a flask of appropriate size (25–100 ml). Dilute each solution to volume with water and mix.

Using the conditions described under *Apparatus*, determine the concentrations of antimony, bismuth, copper, cadmium and indium at 217.6, 223.1, 324.8, 228.8 and 303.9 nm, respectively, spraying the sample solution into an appropriately adjusted air-acetylene flame. If dilution of the solution is necessary, add sufficient concentrated hydrochloric acid and 10.0-mg/ml potassium solution to the aliquot taken, for the final concentrations of acid and potassium to be 24% v/v and 1.0 mg/ml respectively (Note 12). Calculate the contents of each element (in μg), then, if necessary, correct the results obtained for antimony, bismuth and copper by subtracting those obtained for the blank.

B—Determination of silver, copper, cadmium and indium. Treat up to 1 g of powdered sample (Note 1), containing up to $\sim 500 \mu\text{g}$ each of silver, cadmium and

indium and not more than ~10 mg of calcium, 350 mg of lead (Note 13) and 20 mg of copper, with bromine in carbon tetrachloride solution and nitric acid as described above, then add 10 ml of concentrated hydrochloric acid, 5 ml of concentrated perchloric acid and 15 ml of 50% v/v sulphuric acid. Heat until the evolution of oxides of nitrogen ceases, then cool the solution and remove the cover. Add 10 ml of concentrated hydrofluoric acid and carefully evaporate the solution to fumes of perchloric acid (Note 14). Cool, wash down the sides of the beaker with water and evaporate the solution to ~5 ml. Cool, add 20 ml of 50% v/v sulphuric acid and ~35 ml of water and heat to dissolve the salts. Cool the solution to room temperature and, if necessary, filter it as described above into a 250-ml separatory funnel marked at 100 ml. Wash the beaker once with water, then twice with ~10-ml portions of 25% v/v ammonia solution to dissolve any insoluble silver compounds adhering to the sides. Wash the paper and residue thoroughly (Note 15) three times with ~7-ml portions of 25% v/v ammonia solution to recover the silver retained by the lead sulphate, then wash the beaker and paper each once with 5% v/v sulphuric acid. Discard the paper.

After the addition of ascorbic acid and potassium iodide solution dilute the solution to 100 ml with water, allow it to stand for 30 min, then proceed with the MIBK extraction and washing step as described in Procedure A. Strip the solution as described, using 40% v/v nitric acid–25% v/v hydrochloric acid solution instead of the nitric acid–hydrogen peroxide solution. After the addition of the recommended volumes of potassium solution, 50% v/v sulphuric acid and concentrated perchloric acid, treat the sample and blank solutions as described in Procedure A but omit the additions of *aqua regia* and sulphurous acid and the final boiling step. If necessary, warm the solutions very gently (Note 16) to dissolve the residue, then dilute them to suitable volumes and determine silver (at 328.1 nm), copper, cadmium and indium as described above.

Notes

1. For silver determinations, all glassware and Teflon-ware should be washed with ~25% v/v ammonia solution, followed by water.

2. As mentioned subsequently under *Calibration solutions*, relatively exact additions (graduated pipette) of concentrated hydrochloric acid are necessary for indium calibration solutions. If desired, calibration solutions containing copper, cadmium and indium can be prepared.

3. A watch-glass should not be used, because if the hydrofluoric acid has not all been removed in the preceding step it will etch the glass and result in the contamination of the solution by antimony and other elements from the glass. If antimony is not of interest and a relatively large amount is present, it can be removed at this stage by volatilization as the bromide by adding ~10 ml of concentrated hydrobromic acid and evaporating the solution to fumes of sulphur trioxide again. In this case the subsequent additions of *aqua regia* and sulphurous acid can be omitted.

4. *Aqua regia* is added to ensure that all the antimony is present as antimony(V).⁵

5. Nitric acid is added to prevent possible loss of antimony by volatilization as the chloride during the subsequent boiling step.⁵

6. The MIBK phase should be colourless after shaking for 2 min. If it is not, add more strip solution and continue shaking until the extract becomes colourless.

7. **Warning.** After the stripping step shake the MIBK phase with ~100 ml of water to remove some of the co-extracted acid before draining the solvent into a waste bottle. If this is not done, a potentially dangerous exothermic reaction can occur if the combined stripped extracts are allowed to stand for some time, particularly in a tightly closed bottle, before disposal.

8. If indium is to be determined, the exact volume of

concentrated hydrochloric acid required must be added (Note 2) and the subsequent boiling step to remove sulphur dioxide must not be prolonged, or hydrochloric acid will be lost by evaporation. This causes a high result for indium because the hydrochloric acid concentration in the sample solution will be lower than that in the calibration solutions and cause less depression of the indium signal.

9. Additional 10.0-mg/ml potassium solution is not required for the blank solution, which is ultimately diluted to 10 ml, because 1 ml was added to the strip solutions before the evaporation step. For final sample solution volumes of 25, 50 and 100 ml, add 1.5, 4 and 9 ml, respectively.

10. An approximately 6M hydrochloric acid medium is required for the rapid reduction of antimony(V) to antimony(III) with sulphurous acid.⁵

11. The boiling step should not be prolonged because antimony will be lost by volatilization if the solution is evaporated to low volume or to dryness.

12. The additional 10.0-mg/ml potassium solution and concentrated hydrochloric acid required for some dilutions are as follows: 2 ml of sample solution diluted to 25 ml requires 2.3 ml of potassium solution and 5.6 ml of concentrated hydrochloric acid; 2 ml/50 ml requires 4.8 and 11.6 ml; 5 ml/25 ml requires 2.0 and 4.8 ml; 5 ml/50 ml requires 4.5 and 10.8 ml; and 4 ml/100 ml requires 9.6 and 23.0 ml, respectively. For dilutions of 2 ml/100 ml, or more dilute solutions, which may be required for the determination of copper, the small amounts of potassium and hydrochloric acid in the aliquots taken do not need to be considered.

13. If silver is not of interest, up to ~50 mg of calcium and ~600 mg of lead can be present.

14. If much antimony is present, it can be removed as described in Note 3.

15. For the residue to be washed effectively, any that adheres to the sides of the paper should be gently loosened with a glass rod. If silver is not of interest, the beaker and residue can be washed with 1% v/v sulphuric acid.

16. Gentle warming minimizes loss of hydrochloric acid (Note 8) during the dissolution step.

RESULTS AND DISCUSSION

Calibration solutions

Calibration solutions containing 24% v/v hydrochloric acid were chosen, to keep silver in solution without the addition of diethylenetriamine as recommended previously,² and 1 mg of potassium per ml (as the chloride) was added to both the sample and calibration solutions as an ionization suppressant, particularly for cadmium and indium. Silver solutions prepared in this way and containing $\leq 1 \mu\text{g}$ of silver per ml are stable for at least one week. Solutions of higher concentration should be prepared fresh every 2 or 3 days because their absorbance may decrease on standing. Calibration solutions containing both antimony and bismuth should be prepared fresh every 2 weeks. Those containing indium, copper and cadmium are stable for at least one month. Except for indium solutions, it is not necessary to add the exact required volume of concentrated hydrochloric acid; 24 ± 1 ml per 100 ml is adequate. However, for indium calibration solutions rather more accurate additions are necessary because of the severe depressive effect of hydrochloric acid on indium absorption in an air–acetylene flame.²¹ In this work, it was found that, at the 10- $\mu\text{g}/\text{ml}$ level, indium absorbance was depressed ~27 and 32% in the

presence of 20 and 25% v/v hydrochloric acid, respectively. For convenience, the hydrochloric acid concentration of the calibration solutions was kept the same for both Procedures *A* and *B*. However, if only Procedure *A* is used, the acid concentration can be reduced to ~15% v/v. A lower concentration is not recommended, because bismuth may then hydrolyse in the solutions.

Separation of silver, antimony, bismuth, copper, cadmium and indium by extraction as iodides and back-extraction of the complexes

Previous¹ and later work showed that, in the presence of 500 mg of zinc, 50 mg of iron and ascorbic acid as a reductant for iron(III), up to at least 500 μg each of silver, bismuth, cadmium and indium, and up to at least 20 mg of copper can be simultaneously and quantitatively extracted into 50 ml of MIBK from ~100 ml of 2M sulphuric acid–0.1M potassium iodide solution and subsequently stripped from the extract with 40% v/v nitric acid containing 20–25% v/v hydrochloric acid to keep silver iodide in solution. However, although antimony, in the presence of tartaric acid to prevent hydrolysis,¹ is also quantitatively extracted under these conditions, it is not stripped with solutions containing hydrochloric acid, probably because of the formation of SbCl_5 , which remains in the MIBK phase. Similar behaviour was observed previously for tin¹ and was attributed to the formation of SnCl_4 or possibly negatively charged chloro-complexes. Subsequent tests with pure antimony and silver solutions showed that antimony can be stripped from the extract first with 5–20% v/v nitric acid, followed by stripping of the silver with nitric–hydrochloric acid solution as described above. However, low and erratic results were consistently obtained for silver when this double stripping technique was applied to some Canadian Certified Reference Materials Project (CCRMP) ores and concentrates in which the lead sulphate formed during decomposition was first washed with 25% v/v ammonia solution to remove occluded silver, followed by dissolution of the precipitate with ammonium chloride and recovery of the occluded antimony and/or bismuth by co-precipitation with hydrous ferric oxide as described in Procedure *A*. In these tests the beaker containing the combined solution, after the dissolution of the hydrous ferric oxide precipitate, was washed with 25% v/v ammonia solution before the extraction step,² to ensure the recovery of any insoluble silver compounds adhering to the sides of the beaker after concentration of the solution by evaporation. Ultimately, because subsequent tests suggested that silver in the sample extracts is not completely stripped by this double stripping technique, a separate method was developed for the determination of antimony, as well as for bismuth, copper, cadmium and indium, in which these elements are stripped from the extract with 20% v/v nitric acid containing 20% v/v hydro-

gen peroxide.¹ Silver is not stripped under these conditions.

Treatment of the strip solutions

In Procedure *A*, involving the determination of antimony, *aqua regia* is added before the evaporation of the strip solution to dryness, to convert all the antimony present into antimony(V). This prevents or inhibits the formation of a mixed antimony(III and V) species which is not readily reduced to antimony(III).⁵ Because the atomic-absorption of antimony depends on its oxidation state, this treatment ensures that ultimately all the antimony present in the final solution will be in the same, antimony(III), state as in the calibration solutions after reduction of the resultant antimony(V) with sulphurous acid in ~6M hydrochloric acid.^{1,5} High results will be obtained if antimony(V) is present in the final solution. The additions of *aqua regia* and sulphurous acid are not necessary for Procedure *B*. However, in both Procedures *A* and *B*, ~10 mg of potassium is added as the chloride to the strip solutions to prevent or inhibit the formation of insoluble antimony⁵ and silver³ compounds on evaporation of the solutions to dryness in the presence of sulphuric and perchloric acids.

Recovery of antimony and bismuth retained by lead and calcium sulphates, by co-precipitation with hydrous ferric oxide

Previous work showed that if lead sulphate is removed by filtration before the extraction step, it retains appreciable amounts of bismuth and antimony,¹ and subsequent work showed that calcium sulphate behaves similarly. Consequently, a simple and reasonably rapid method was required for the recovery of these occluded elements. Because it has been reported recently²² that trace amounts of antimony(V), bismuth and tin(IV) can be separated from up to 10 g of lead by co-precipitation with hydrous ferric oxide at pH 4.0–4.5, with ammonia solution for pH adjustment, the applicability of this separation procedure was investigated in this work. However, this method yielded low results for both bismuth and antimony(V) [prepared by oxidation of antimony(III) with *aqua regia*] in the absence of lead, because of the low pH used for co-precipitation. Subsequent work showed that essentially complete co-precipitation of both elements can be obtained at ~pH 6–7. Because lead would be expected to be co-precipitated as the hydrous oxide at pH values approaching 7, a pH of 6.20 ± 0.05 was chosen for further work, and tests showed that, under these conditions, bismuth and antimony can be quantitatively recovered from precipitates containing up to ~150 mg each of calcium and lead. With larger amounts of lead some co-precipitation of lead may occur and cause low results for antimony and bismuth.

Effect of diverse ions

At the sulphuric acid and potassium iodide concen-

Table 1. Determination of antimony, bismuth, copper, cadmium and indium in CCRMP reference materials and zinc concentrates by Procedure A

Sample*	Nominal composition, %	Sb		Bi		Cu		Cd		In	
		Certified value, %	Found, $\mu\text{g/g}$	Certified value, %	Found, $\mu\text{g/g}$	Certified value, %	Found, $\mu\text{g/g}$	Certified value, %	Found, $\mu\text{g/g}$	Certified value, %	Found, $\mu\text{g/g}$
PR-1-Molybdenum ore	39.2 Si, 2.4 Al, 1.4 Ca, 1.2 Fe, 0.8 S, 0.6 Mo			0.111 \pm 0.004	1073 1084	0.01†	74.8 77.2				
CPB-1-Lead concentrate	0.7 SiO ₂ , 64.7 Pb, 8.4 Fe, 17.8 S, 4.4 Zn	0.36 \pm 0.03	3697 3740	0.023 \pm 0.002	227 225	0.254 \pm 0.004	2511 2556	0.0143 \pm 0.0005	151 157		
CZN-1-Zinc concentrate	10.9 Fe, 30.2 S, 44.7 Zn, 7.5 Pb	0.052 \pm 0.003	529 541	27 \pm 3 $\mu\text{g/g}$ ‡	22.8 22.6	0.144 \pm 0.003	1437 1446	0.132 \pm 0.002	1384 1380	86 \pm 17 $\mu\text{E/g}$ §	87.0 85.6
MP-1-Zinc-tin-copper-lead ore	19.4 Si, 3.6 Al, 3.4 Ca, 5.7 Fe, 11.8 S, 15.9 Zn, 2.4 Sn, 1.9 Pb, 0.8 As			0.024 \pm 0.002	237 240	2.09 \pm 0.03	2.05, % 2.08, %	0.07†	547 556	0.069 \pm 0.003	661 656
MP-1a-Zinc-tin-copper-lead ore	41.8 SiO ₂ , 1.5 Ca, 6.2 Fe, 12.7 S, 19.0 Zn, 1.3 Sn, 0.8 As			0.032 \pm 0.002	325 320	1.44 \pm 0.01	1.43, % 1.42, %			0.033 \pm 0.001	337 328
MP-2-Tungsten-molybdenum ore	76.1 SiO ₂ , 5.4 Al, 2.7 Ca, 3.7 Fe, 0.7 S, 0.7 W, 0.3 Mo	7.8¶	7.8	0.246 \pm 0.006	2500 2503						
Zinc concentrate-731	55.7 Zn, 8.7 Fe, 32.0 S		7.6 8.8								
Zinc concentrate-732	49.8 Zn, 11.0 Fe, 32.6 S	9.2¶	8.8								

*The first six samples are CCRMP reference ores and concentrates. The subsamples taken were 1, 0.25, 1, 0.3, 0.5, 0.5, 1 and 1 g, respectively.

†Approximate value obtained during preliminary CCRMP work.

‡Recent certified value.²⁵

§CCRMP value given for information only (not certified)

¶Result obtained previously by a spectrophotometric iodide method.

trations used for the extraction of silver, antimony, bismuth, copper, cadmium and indium, germanium, arsenic and molybdenum are not extracted into MIBK, and tin is not significantly extracted. Thallium(III) and tellurium(IV) are completely extracted and palladium is almost completely extracted, but the amounts of these elements present in ores and concentrates—relative to silver and the other elements—would not be expected to interfere in their extraction or to cause error in their determination by flame AAS. Selenium is reduced to the elemental state by ascorbic acid before the extraction step. Zinc is partly extracted—~6 mg at the 500-mg level—but can be readily removed from the extract by washing it once with ~20 ml of 2M sulphuric acid—0.1M potassium iodide solution. Residual iron is also removed under these conditions.¹

As found previously, silver occluded by lead sulphate,² but not by calcium sulphate,³ can be recovered by washing the precipitate with 25% v/v ammonia solution. Up to ~10 mg of calcium and ~350 mg of lead can be present in the sample without producing appreciable error in the silver result.³ As mentioned earlier, up to at least 20 mg of copper—which is usually present in much larger amounts in ores and related materials than are the other elements of interest—can be present during the extraction step, and up to 1 mg of copper per ml will not cause significant error in the AAS determinations of silver, antimony, bismuth, cadmium and indium.

Applications

Tables 1 and 2 show that the results obtained for antimony, silver and copper in six diverse CCRMP ores and concentrates are in excellent agreement with either the values obtained during the preliminary CCRMP work or the certified values, or are within, or almost within, the 95% confidence limits. The

results obtained for cadmium in MP-1 also agree reasonably well with the approximate value obtained during the preliminary CCRMP work, but those obtained for CPB-1 and CZN-1 are slightly higher than, but still in good agreement with, the certified values. Except for bismuth in CZN-1 (Table 1) and indium in MP-1 (Tables 1 and 2), the results obtained for indium and bismuth are also in good agreement with the certified values or those given for information only. Although that obtained for bismuth in CZN-1 is slightly lower than the recently certified value,²³ it is in excellent agreement with the mean results (Table 3) obtained previously in this laboratory by three different methods involving both spectrophotometric⁶ and AAS finishes⁷ after separation of bismuth from matrix elements by various extraction and co-precipitation procedures. Similarly, the result obtained for indium in MP-1 is lower than the certified value but in good agreement with previous results (Table 3) obtained by extraction/flame atomic-emission, extraction/AAS and iron collection/AAS methods.⁸ From the results of this work and that shown in Table 3, it is considered highly probable that the certified values for bismuth in CZN-1 and for indium in MP-1 are slightly high. The results (Table 1) obtained for antimony in the industrial zinc concentrates agree well with previous results obtained by a spectrophotometric iodide method after separation of antimony by co-precipitation with hydrous ferric and lanthanum oxides followed by chloroform extraction as the xanthate.⁵ Those obtained for silver (Table 2) agree with the mean result obtained by an acid-decomposition/AAS method involving no separations.⁴ Table 3 shows that the mean results obtained for antimony and bismuth in various CCRMP reference materials by Procedure A, for silver by Procedure B and for indium by both procedures are all in excellent agreement with the mean values

Table 2. Determination of silver, copper, cadmium and indium in CCRMP reference materials and zinc concentrates by Procedure B

Sample*	Ag		Cu		Cd		In	
	Certified value, $\mu\text{g/g}$	Found, $\mu\text{g/g}$	Certified value, %	Found, $\mu\text{g/g}$	Certified value, %	Found, $\mu\text{g/g}$	Certified value, %	Found, $\mu\text{g/g}$
CBP-1	626 \pm 6	627	0.254 \pm 0.004	2511	0.0143 \pm 0.0005	154		
		620		2524		152		
CZN-1	93 \pm 3	94.3	0.144 \pm 0.003	1448	0.132 \pm 0.002	1395	86 \pm 17 $\mu\text{g/g}\dagger$	86.0
		95.0		1433		1385		86.2
MP-1	57.9 \pm 2.2	59.0	2.09 \pm 0.03	2.04 ₂ %	0.07 \ddagger	540	0.069 \pm 0.003	645
		59.0		2.06 ₂ %		540		649
MP-1a	69.7 \pm 2.2	69.6	1.44 \pm 0.01	1.41 ₆ %			0.033 \pm 0.001	323
		71.2		1.41 ₄ %				332
MP-2	4.9 \pm 0.3	5.2						
		5.4						
Zinc concentrate-731	51.1 \ddagger	52.0						
		51.6						
Zinc concentrate-732	51.1 \ddagger	51.1						
		51.4						

*Subsamples taken are given in footnote to Table 1.

\ddagger See pertinent footnote to Table 1.

\ddagger Mean of two results by an acid-decomposition/AAS method.⁴

Table 3. Comparison of the mean results obtained for silver, bismuth, antimony and indium in CCRMP reference materials by the proposed method with those obtained by previously published methods

Element	Method*	Samples and mean values, $\mu\text{g/g}$ (or %)†					
		PR-1	CPB-1	CZN-1	MP-1	MP-1a	MP-2
Ag ($\mu\text{g/g}$)	TBA-chloroform extraction/AAS finish ²		623 (2)	94.7 (2)	59.3 (2)	67.5 (5)	5.5 (5)‡
	TBA-MIBK extraction/AAS finish ³			94.2 (2)	60.5 (5)	70.4 (2)	
	Acid-decomposition/AAS finish ⁴ Proposed method <i>B</i>		629 (2) 624 (2)	94.9 (2) 93.2 (5)	60.5 (3) 58.9 (5)	70.2 (5) 70.4 (2)	
Bi (%)	DDTC and xanthate extractions/ spectrophotometric iodide finish ⁶	0.107 (6)	0.0215 (10)‡	0.0023 (10)‡	0.022 (6)		5.3 (2)
	DDTC extraction/AAS finish ⁷	0.113 (1)	0.023 (1)	0.0023 (1)	0.023 (1)		
	Fe collection/AAS finish ⁷ Proposed method <i>A</i>	0.109 (1) 0.108 (2)	0.021 (1) 0.0226 (2)	0.0022 (1) 0.0023 (5)	0.022 (1) 0.0231 (5)	0.0319 (45)‡ 0.0323 (2)	0.249 (5)‡ 0.250 (2)
Sb (%)	Fe-La collection—xanthate extraction/spectrophotometric iodide finish ⁵		0.370 (10)‡	0.0541 (10)‡			
	Fe-La collection/AAS finish ⁵ Proposed method <i>A</i>		0.367 (1) 0.372 (2)	0.054 (1) 0.0534 (5)			
In ($\mu\text{g/g}$)	<i>N</i> -butyl acetate—HBr extraction/ FAES finish ⁶			86.6 (5)	659 (3)	328 (3)	
	<i>N</i> -butyl acetate—HBr extraction/ AAS finish ⁸			87.3 (5)	652 (1)	328 (1)	
	Fe collection/AAS finish ⁸ Proposed methods <i>A</i> and <i>B</i>		85.9 (1) 88.0 (10)		665 (1) 655 (10)	340 (1) 330 (4)	

*TBA = tribenzylamine; DDTC = diethyldithiocarbamate; FAES = flame atomic-emission spectroscopy.

†Results shown are the means of the number of determinations shown in parentheses and, except for the results of this work (calculated from results in Tables 1, 2 and 4) and those indicated by the following footnote, are taken from previously published papers (references given in second column).

‡Mean result obtained during the interlaboratory certification programme.

Table 4. Precision for silver, antimony, bismuth, copper, cadmium and indium in a CCRMP concentrate, ore and soil sample

Sample	Element found by Procedure <i>A</i> and/or <i>B</i> , $\mu\text{g/g}^*$											
	Ag		Sb		Bi		Cu		Cd		In	
	<i>B</i>	<i>A</i>	<i>A</i>	<i>A</i>	<i>A</i>	<i>B</i>	<i>A</i>	<i>B</i>	<i>A</i>	<i>B</i>		
<i>CZN-1</i>												
Mean	93.2	534	22.5	1445	1451	1383	1396	88.1	87.9			
SD	1.47	4.34	0.24	6.66	13.10	5.08	6.27	1.88	1.73			
RSD, %	1.6	0.8	1.1	0.5	0.9	0.4	0.4	2.1	2.0			
<i>MP-1</i>												
Mean	58.9		231	2.082%	2.054%	555	540	659	651			
SD	0.41		7.65	0.023%	0.014%	4.83	2.70	4.55	8.01			
RSD, %	0.7		3.3	1.1	0.7	0.9	0.5	0.7	1.2			
<i>SO-2†</i>												
Mean	10.1	10.5	10.3	3.80		10.4		11.4				
SD	0.12	0.45	0.10	0.25		0.12		0.27				
RSD, %	1.2	4.3	1.0	6.6		1.2		2.4				

*Results reported in $\mu\text{g/g}$ unless otherwise indicated. Except for Cu in SO-2 (7 determinations) the means reported are those for 5 determinations.

†The approximate percentage chemical composition of SO-2 is 25.0 Si, 8.1 Al, 2.0 Ca, 5.6 Fe and 0.9 Ti. Except for Cu (no additions), the respective mean values given for SO-2 include the amount of each element present in a 1-g subsample plus that added (10 μg). The approximate means of duplicate determinations of Ag, Sb, Bi, Cd and In in SO-2 by the proposed method were 0.3, 0.5, 0.9, 0.2 and 1.2 $\mu\text{g/g}$, respectively.

obtained previously by other methods. The results shown in Tables 1 and 2 are the means of four or five AAS measurements. For convenience, all the results by the proposed methods, except for copper in MP-1 and MP-1a, are given in $\mu\text{g/g}$. This was not possible for all cases in Table 3 because many of the earlier results used for comparison purposes were reported in weight per cent to three decimal places only.

Table 4 shows that the precision for all six elements in CZN-1, and for five elements in MP-1, by the proposed methods is good and that Procedures *A* and *B* yield approximately similarly precise results for copper, cadmium and indium. Ore samples containing microgram quantities of all six elements were not available to determine the precision at low levels. Consequently, except for copper, which is present in microgram quantities, 10 μg each of antimony, bismuth, cadmium and indium were added to five 1-g subsamples of SO-2, a CCRMP podzolic soil sample, and the resulting synthetic samples were analysed for these elements and copper by Procedure *A*. Silver, added to five separate subsamples, was determined by Procedure *B*. The results (Table 4) show that the precision for silver, antimony, bismuth, cadmium and indium, at about the 10- $\mu\text{g/g}$ level, is reasonably good, and that for copper, at about the 4- $\mu\text{g/g}$ level, is moderately good. In these tests, each result obtained for the six elements is the mean of 4–6 AAS measurements at, except for copper, about the 0.4- $\mu\text{g/ml}$ level; copper was measured at about the 0.2- $\mu\text{g/ml}$ level. The relative standard deviations for these measurements were 1.5, 16.3, 3.8, 8.6, 1.6 and 11.0% for silver, antimony, bismuth, copper, cadmium and indium, respectively. This indicates that, at these levels, sufficient AAS measurements must be taken, particularly for antimony, bismuth, copper

and indium, if a reasonably accurate result is desired. Compared with the other elements, which required little or no correction for reagent blanks, as indicated below, the poorer precision for copper (Table 4), which at the resonance line used is relatively sensitive by flame AAS, may be caused by a variable blank effect because a relatively high copper blank (2.5 μg) was obtained in these tests. The mean value obtained for copper is also somewhat lower than, but still in reasonably good agreement with, the recommended value of $7 \pm 1 \mu\text{g/g}$ which is the mean of ~ 200 results ranging from 3 to 14 $\mu\text{g/g}$. The mean values for the other five elements include the amount of each present in the sample.

The proposed methods are suitable for samples containing $\sim 0.2 \mu\text{g/g}$ or more of silver and cadmium, $\sim 0.5 \mu\text{g/g}$ or more of copper and $\sim 5 \mu\text{g/g}$ or more of antimony, bismuth and indium. Smaller amounts can also be determined if the final sample solution is diluted to 10 ml instead of 25 ml. However, this volume of solution may not be sufficient for the determination of all the elements desired, particularly if dilutions are necessary. Procedure *B* is better than Procedure *A* for the determination of indium because the final hydrochloric acid concentration can be controlled more readily. If antimony is not of interest in Procedure *A*, nor silver in Procedure *B*, a dilute nitric acid–potassium nitrate medium would probably be more advantageous for the determination of indium and the other elements. In this case, corresponding calibration solutions would have to be prepared and any silver chloride present in the final sample solution would have to be removed by filtration. In this work, in which doubly demineralized water was used, the reagent blanks for copper, antimony and bismuth were ≤ 2.5 , ≤ 1.4 and $\leq 0.7 \mu\text{g}$,

respectively. No blanks were obtained for silver, cadmium and indium. The proposed methods are not applicable to samples containing a large amount of copper.

REFERENCES

1. E. M. Donaldson and M. Wang, *Talanta*, 1986, **33**, 35.
2. E. M. Donaldson, *ibid.*, 1982, **29**, 1069.
3. *Idem*, *ibid.*, 1984, **31**, 443.
4. E. M. Donaldson, E. Mark and M. E. Leaver, *ibid.*, 1984, **31**, 89.
5. E. M. Donaldson, *ibid.*, 1979, **26**, 999.
6. *Idem*, *ibid.*, 1978, **25**, 131.
7. *Idem*, *ibid.*, 1979, **26**, 1119.
8. *Idem*, *CANMET Report 83-4E*, Energy, Mines and Resources Canada, Ottawa, 1983.
9. J. G. Viets, *Anal. Chem.*, 1978, **50**, 1097.
10. J. G. Viets, R. M. O'Leary and J. R. Clark, *Analyst*, 1984, **109**, 1589.
11. J. B. Headridge and J. Richardson, *ibid.*, 1970, **95**, 930.
12. K. E. Burke, *ibid.*, 1972, **97**, 19.
13. J. S. Kane, *Anal. Chim. Acta*, 1979, **106**, 325.
14. T. Kono and S. Kobayashi, *Bunseki Kagaku*, 1970, **19**, 1491; *Chem. Abstr.*, 1971, **74**, 94017p.
15. C. Tsutsami, H. Koizumi and S. Yoshikawa, *ibid.*, 1976, **25**, 150; *Chem. Abstr.*, 1976, **85**, 19144b.
16. T. Kono and A. Nemori, *ibid.*, 1975, **24**, 419; *Chem. Abstr.*, 1976, **84**, 25372v.
17. B. Ya. Spivakov, V. I. Lebedev, V. M. Shkinev, N. P. Krivenkova, T. S. Plotnikova, I. P. Kharlamov and Yu. A. Zolotov, *J. Anal. Chem. USSR*, 1976, **31**, 621.
18. A. M. Aziz-Alrahman, M. A. Al-Hajjaji and I. Z. Al-Zamil, *Intern. J. Environ. Anal. Chem.*, 1983, **15**, 9.
19. H. Suzuki, Y. Nakayama and K. Ishikawa, *New Mater. New Processes*, 1983, **2**, 19.
20. M. Jawaid, B. Lind and C. G. Elinder, *Talanta*, 1983, **30**, 509.
21. H. Haraguchi and K. Fuwa, *Bull. Chem. Soc. Japan*, 1975, **48**, 3056.
22. Y. Harada, N. Kurata and Y. Goto, *Bunseki Kagaku*, 1984, **33**, 71; *Anal. Abstr.*, 1984, **46**, 10B88.
23. H. F. Steger and W. S. Bowman, *CANMET Report 84-10E*, Energy, Mines and Resources Canada, Ottawa, 1984.

TRACE-METAL DETERMINATION BY SECOND-HARMONIC ALTERNATING-CURRENT ANODIC STRIPPING VOLTAMMETRY

CLINIO LOCATELLI*, FRANCESCO FAGIOLI and CORRADO BIGHI

Department of Chemistry, University of Ferrara, Via L. Borsari 46, 44100 Ferrara, Italy

TIBOR GARAI

Research Laboratory for Inorganic Chemistry, Hungarian Academy of Sciences, Budaörsi Ut 45, H-1112 Budapest, Hungary

(Received 4 July 1985. Accepted 24 October 1985)

Summary—Second-harmonic alternating-current voltammetry can be used for the sequential determination of two electroactive species having very similar half-wave potentials ($\Delta E_{1/2} < 50$ mV). Since the concentrations of such metals in samples of special interest are often at trace levels, for their determination second-harmonic a.c. voltammetry (extremely selective but not sufficiently sensitive) can usefully be combined with the anodic stripping method, which has a very high analytical sensitivity. The determination of tin and lead as well as of indium and cadmium in 1M hydrochloric acid is described. The half-wave potentials are only 35 and 45 mV apart, respectively, for these systems. A three-electrode cell was used with a long-lasting sessile-drop mercury electrode as the working electrode, with a drop-time of 240–300 sec. The detection limit was found to be 10^{-8} M for all four elements studied. The precision expressed as the relative standard deviation was 2–3% and the relative error was 1–2%.

Anodic stripping voltammetry is at present the most powerful electroanalytical method for the determination of trace metals.^{1,2} Modern voltammetric techniques have increased the sensitivity and selectivity of the method.³ The hanging mercury drop electrode (HMDE) has been partly superseded by the mercury film electrode (MFE),^{4,5} which gives better resolution,⁶ though the HMDE gives more reproducible results at higher concentrations. Recently Andruzzi and Trazza⁷ introduced the long-lasting sessile-drop mercury electrode (LLSDME), which compares favourably with the HMDE.⁸ It has been used for the determination of metals in water⁹ and plant materials.¹⁰

Second-harmonic a.c. voltammetry has been found to offer the best resolution in ASV with the MFE as the working electrode⁶ and the resolution is found to depend on the substrate.⁵ The resolutions attainable by a.c. anodic stripping voltammetry techniques with the semi-stationary electrodes do not necessarily follow the relationships valid for a.c. polarography, however, since the fundamental and second-harmonic a.c. functions are distorted in the case of anodic oxidations of amalgams.^{11,12}

In the present work the simultaneous determination of certain pairs of metals with a small difference in half-wave potential ($\Delta E_{1/2} < 50$ mV) by a.c. anodic stripping voltammetry (ACASV) at the LLSDME was investigated.

EXPERIMENTAL

The apparatus and reagents were as described previously.⁸ The procedures are fairly standard and are indicated in the text.

RESULTS AND DISCUSSION

The difference in half-wave potential ΔE is 35 mV for tin(II) and lead(II), and 45 mV for indium(III) and cadmium(II) in 1M hydrochloric acid medium. Various organic complexing agents have been used to increase these ΔE values and facilitate determination of these pairs of ions.^{13–15} These additions can be avoided if second-harmonic a.c. voltammetry is used.^{16,17}

Since the concentrations of these ions are often at trace levels, combination of the selectivity of second-harmonic a.c. voltammetry with the sensitivity of anodic stripping is useful for their determination.

Tin(II) and lead(II)

Calibration graphs. The experimental conditions for the determination of these ions by first and second-harmonic a.c. anodic stripping voltammetry are reported in Table 1. The demodulation phase angle ϕ was carefully set, to minimize the capacitive current.

The calibration graphs obtained for the two species by first and second-harmonic ACASV are summarized in Table 2. In the second-harmonic method the peak current was calculated for the cathodic peak of tin and the anodic peak of lead.¹² The peak-width

*To whom correspondence should be addressed.

Table 1. Experimental conditions for first and second-harmonic ACASV*

Parameter†	Sn(II)	Pb(II)	Cd(II)	In(III)
E_d , V vs. SCE	-0.700	-0.700	-0.800	-0.800
$\phi_{\text{first harmonic}}$, degrees	270 + 80	270 + 89	0 + 0.5	0 + 0
$\phi_{\text{second harmonic}}$, degrees	270 + 67	270 + 72§	270 + 65	270 + 64§

*Electrolysis time 180 sec; rest time between deposition and start of recording 30 sec; scan rate 10 mV/sec; frequency 100 Hz; amplitude of a.c. voltage 10 mV; stirring rate 800 rpm.

† E_d = electrodeposition potential.

§Phase angle used in the simultaneous determination.

Table 2. Calibration curves for tin(II) and lead(II)*

Method	Sn(II)	Pb(II)
First harmonic	$i_p = (1.665 \pm 0.003) \times 10^6 c$ $r = 0.9999$; $s_r = 1.0\%$; D.L. = $1.2 \times 10^{-8} M$	$i_p = (3.77 \pm 0.02) \times 10^6 c$ $r = 0.9999$; $s_r = 3.2\%$; D.L. = $5.3 \times 10^{-9} M$
Second harmonic	$i_p = (2.025 \pm 0.019) \times 10^5 c$ $r = 0.9997$; $s_r = 2.4\%$; D.L. = $9.9 \times 10^{-8} M$	$i_p = (4.69 \pm 0.09) \times 10^5 c$ $r = 0.9989$; $s_r = 3.0\%$; D.L. = $4.3 \times 10^{-8} M$
Range of concentrations	$0-5 \times 10^{-7} M$	$0-2 \times 10^{-7} M$

*The limit of detection, D.L., is expressed according to the IUPAC recommendation¹⁸ (99% probability). The units are A for peak current, i_p , and M for c. The uncertainties reported correspond to a probability of 95%.

measured at half-height ($W_{1/2}$) for the first-harmonic a.c. voltamperograms and the peak-to-peak separation of potentials ($p-p$) for the second-harmonic a.c. voltamperograms are given in Table 3. The theoretical values for the reversible electrode process, i.e., $W_{1/2} = 90/n$ and $p-p = 68/n$ mV (where n is the

number of electrons involved in the electrode process²), are indicated in brackets.

Simultaneous determination. The simultaneous determination of tin and lead has been examined. Examples of first and second-harmonic a.c. anodic stripping voltamperograms of the mixture are shown

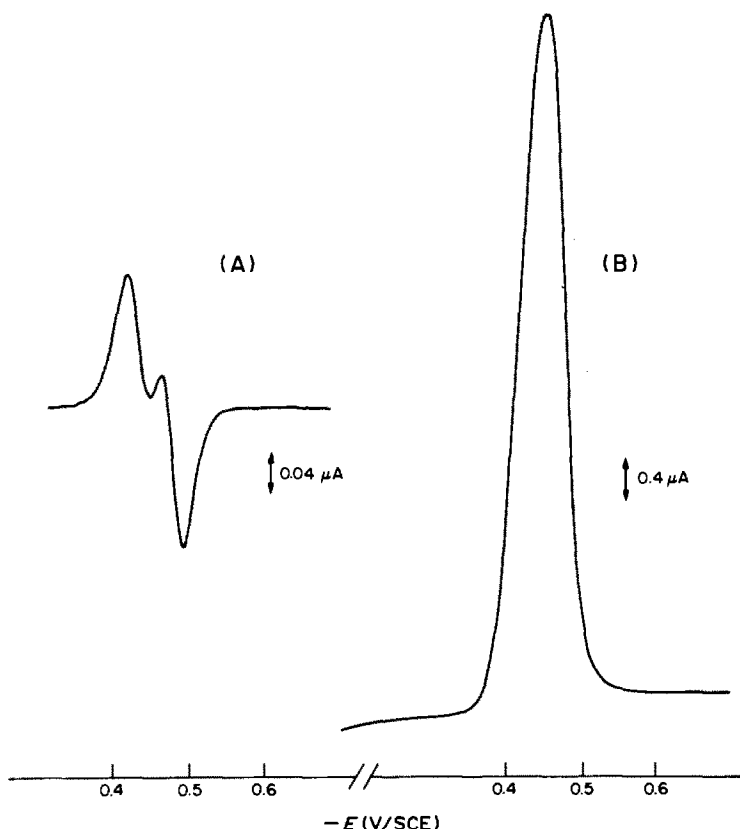


Fig. 1. Alternating-current anodic stripping voltamperograms of a tin and lead mixture: $c_{\text{Pb}} = 2.99 \times 10^{-7} M$; $c_{\text{Sn}} = 7.90 \times 10^{-7} M$. Curve A: second-harmonic. Curve B: first-harmonic. Experimental conditions as in Table 1.

Table 3. Polarographic wave parameters in 1M hydrochloric acid*

Parameter	Sn(II)	Pb(II)	Cd(II)	In(III)
E_p first harmonic, V vs. SCE	-0.480 ± 0.005 (-0.470)	-0.445 ± 0.005 (-0.435)	-0.640 ± 0.005 (-0.642)	-0.590 ± 0.005 (-0.597)
E_p second harmonic, V vs. SCE	-0.480 ± 0.005 (-0.470)	-0.435 ± 0.005 (-0.435)	-0.645 ± 0.005 (-0.642)	-0.595 ± 0.005 (-0.597)
$W_{1/2}$, mV	48 ± 5 (45)	48 ± 5 (45)	45 ± 5 (45)	35 ± 5 (30)
$p-p$, mV	35 ± 5 (34)	38 ± 5 (34)	38 ± 5 (34)	28 ± 5 (23)

*Errors reported correspond to a probability of 95%.

Table 4. Simultaneous determination of tin and lead in mixtures by second-harmonic ACASV*

	Determination of Sn(II) in the presence of Pb(II)	Determination of Pb(II) in the presence of Sn(II)
Univariate analysis	$i_p = (2.054 \pm 0.014) \times 10^3 c$ $r = 0.9996$; $s_r = 2.2\%$; $e = +1.4\%$ D.L. = $9.8 \times 10^{-8} M$	$i_p = (4.65 \pm 0.01) \times 10^3 c$ $r = 0.9991$; $s_r = 1.8\%$; $e = -0.8\%$ D.L. = $4.3 \times 10^{-8} M$
Bivariate analysis	$i_p = -0.00045 + (2.052 \pm 0.008) \times 10^3 c_{Sn}$ $+ (6 \pm 15) \times 10^2 c_{Pb}$ $r = 0.9997$; $s_r = 1.5\%$; $e = +1.3\%$ D.L. = $9.7 \times 10^{-8} M$	$i_p = -0.00027 + (4.651 \pm 0.009) \times 10^3 c_{Pb}$ $+ (3.6 \pm 5.0) \times 10^2 c_{Sn}$ $r = 0.9999$; $s_r = 1.9\%$; $e = -0.7\%$ D.L. = $4.3 \times 10^{-8} M$

*D.L., units and errors are defined in footnotes to Table 2.

Table 5. Calibration curves for indium(III) and cadmium(II)*

	In(III)	Cd(II)
First harmonic	$i_p = (1.72 \pm 0.02) \times 10^3 c$ $r = 0.9990$; $s_r = 2.9\%$; D.L. = $1.1 \times 10^{-9} M$	$i_p = (2.36 \pm 0.05) \times 10^3 c$ $r = 0.9987$; $s_r = 2.2\%$; D.L. = $8.5 \times 10^{-10} M$
Second harmonic	$i_p = (1.46 \pm 0.01) \times 10^6 c$ $r = 0.9997$; $s_r = 2.5\%$; D.L. = $1.4 \times 10^{-8} M$	$i_p = (1.48 \pm 0.01) \times 10^6 c$ $r = 0.9998$; $s_r = 2.3\%$; D.L. = $1.0 \times 10^{-8} M$
Range of concentrations	$0.2 \times 10^{-7} M$	$0.1 \times 10^{-7} M$

*D.L., units and errors are defined in footnotes to Table 2.

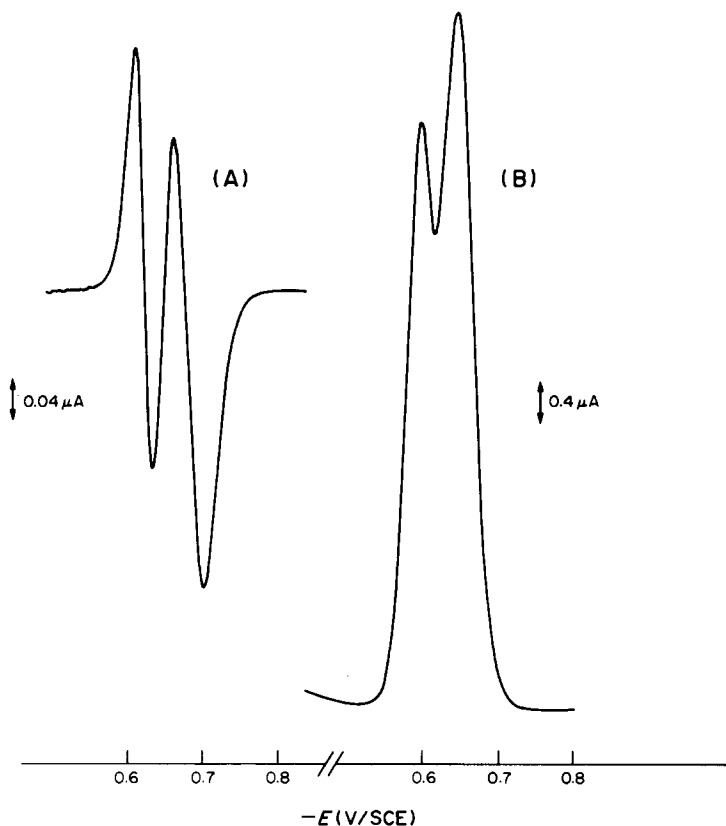


Fig. 2. Alternating-current anodic stripping voltamperograms of an indium and cadmium mixture: $c_{\text{In}} = 3.49 \times 10^{-7} M$; $c_{\text{Cd}} = 3.05 \times 10^{-7} M$. Curve A: second-harmonic. Curve B: first-harmonic. Experimental conditions as in Table 1.

in Fig. 1. In the second-harmonic voltamperogram (curve A), the peaks due to the two electroactive species were well separated, whereas only an increase in the half-peak width was observed (70 mV) in the first harmonic voltamperogram (curve B). The simultaneous determination of tin and lead in mixtures by second-harmonic ACASV is possible only in the range of concentration ratios $1:2 \leq c_{\text{Pb}}:c_{\text{Sn}} \leq 1:20$ under the experimental conditions given in Table 1. If the concentration ratio is unfavourable, the determination can be made possible by adjusting the concentration ratio to within the stated range by addition of a suitable amount of the appropriate standard metal solution.

The regression functions calculated on the basis of the respective peak current values for mixtures of tin

and lead are shown in Table 4. The univariate analysis neglects the presence of the second element, whereas the bivariate analysis takes it into account. For either element the slopes of the univariate and bivariate regression equations and of the individual calibration curves are practically identical, showing that there is negligible mutual interference in the range of concentration ratios considered. The precision expressed as the relative standard deviation, s_r , is 2–3% and the relative error, e , is 1–2%. The detection limits are very low, but the concentration range is narrow.

Indium(III) and cadmium(II)

Calibration graphs. Table 1 gives the experimental conditions for the determination of indium and cad-

Table 6. Simultaneous determination of indium and cadmium in mixtures by second-harmonic ACASV*

	Determination of In(III) in the presence of Cd(II)	Determination of Cd(II) in the presence of In(III)
Univariate analysis	$i_p = (1.474 \pm 0.004) \times 10^6 c$ $r = 0.9999$; $s_r = 1.4\%$; $e = +0.6\%$ D.L. = $1.4 \times 10^{-8} M$	$i_p = (1.502 \pm 0.005) \times 10^6 c$ $r = 0.9999$; $s_r = 1.4\%$; $e = +1.2\%$ D.L. = $1.2 \times 10^{-8} M$
Bivariate analysis	$i_p = -0.0004 + (1.474 \pm 0.003) \times 10^6 c_{\text{In}}$ $+ (7.3 \pm 2.3) \times 10^3 c_{\text{Cd}}$ $r = 0.9999$; $s_r = 1.7\%$; $e = +0.6\%$ D.L. = $1.4 \times 10^{-8} M$	$i_p = 0.0002 + (1.507 \pm 0.003) \times 10^6 c_{\text{Cd}}$ $+ (2.1 \pm 3.7) \times 10^3 c_{\text{In}}$ $r = 0.9999$; $s_r = 1.8\%$; $e = +1.5\%$ D.L. = $1.2 \times 10^{-8} M$

*D.L., Units and errors are defined in the footnotes to Table 2.

mium by first and second-harmonic ACASV, and Table 5 the calibration data.

For the second-harmonic method the cathodic peak current of cadmium and the anodic peak current of indium were used. The wave parameters are shown in Table 3 together with the theoretical values (in brackets).

Simultaneous determinations. Indium(III) and cadmium(II) were simultaneously determined in the concentration ranges covered by the individual calibration curves. Examples of the first and second-harmonic a.c. anodic stripping voltamperograms are shown in Fig. 2. Only the second-harmonic method (curve A), gives separation of the two peaks. Indium and cadmium can be determined by second-harmonic ACASV in the range of concentration ratios $15:1 \leq c_{\text{In}}:c_{\text{Cd}} \leq 1:15$ under the experimental conditions listed in Table 1. If the concentration ratio is unfavourable, again it can be adjusted to within the required range by addition of the appropriate standard solution. The regression functions relating to indium and cadmium mixtures are summarized in Table 6. The mutual interferences are again negligible.

The relative standard deviation and relative error are both 2–3%.

Conclusion

It can be concluded that the combination of second-harmonic a.c. voltammetry and the anodic stripping technique gives very high sensitivity in the

trace level determination of metals which have very similar half-wave potentials.

REFERENCES

1. F. Vydra, K. Štulík and E. Juláková, *Electrochemical Stripping Analysis*, Horwood, Chichester, 1976.
2. A. M. Bond, *Modern Polarographic Methods in Analytical Chemistry*, Dekker, New York, 1980.
3. W. Kemula and Z. Kublik, *J. Electroanal. Chem.*, 1959, **1**, 92.
4. T. M. Florence, *ibid.*, 1970, **26**, 293.
5. *Idem*, *ibid.*, 1970, **27**, 273.
6. G. E. Batley and T. M. Florence, *ibid.*, 1974, **55**, 23.
7. R. Andruzzi and A. Trazza, *Talanta* 1982, **29**, 751.
8. C. Locatelli, F. Fagioli, C. Bighi and T. Garai, *Anal. Lett.*, 1984, **17**, 623.
9. R. Andruzzi, A. Trazza and G. Marrosu, *Talanta*, 1982, **29**, 751.
10. C. Locatelli, F. Fagioli, C. Bighi, S. Landi and T. Garai, *Ann. Chim. Rome*, 1984, **74**, 521.
11. T. Garai and J. Dévay, *Hung. Sci. Instrum.*, 1972, **25**, 27.
12. F. Fagioli, T. Garai and J. Dévay, *Ann. Chim. Rome*, 1974, **64**, 633.
13. E. Jacobsen and G. Tandberg, *Anal. Chim. Acta*, 1969, **47**, 285.
14. E. Desimoni, F. Palmisano and L. Sabbatini, *Anal. Chem.*, 1980, **52**, 1889.
15. K. Wikiel and Z. Kublik, *J. Electroanal. Chem.*, 1984, **165**, 71.
16. A. Cinquantini, T. Garai and J. Dévay, *Hung. Sci. Instrum.*, 1975, **34**, 7.
17. F. Fagioli, F. Dondi and C. Bighi, *Ann. Chim. Rome*, 1978, **68**, 111.
18. IUPAC, Anal. Chem. Division, *Spectrochim. Acta*, 1978, **33B**, 219.

COMPARISON OF FOUR DIGESTION METHODS FOR THE DETERMINATION OF SELENIUM IN BOVINE LIVER BY HYDRIDE GENERATION AND ATOMIC-ABSORPTION SPECTROMETRY IN A FLOW SYSTEM

JEAN PETTERSSON, LENA HANSSON and ÅKE OLIN

University of Uppsala, Department of Analytical Chemistry, P.O. Box 531, S-751 21 Uppsala, Sweden

(Received 3 September 1985. Accepted 18 October 1985)

Summary—A flow system for hydride generation and atomic-absorption spectrometry is described, and the results from the optimization of the equipment for selenium determination are reported. For a sample volume of 0.6 ml the limit of detection for selenium was 0.1 $\mu\text{g/l}$. and the imprecision less than 1% RSD at the 10- $\mu\text{g/l}$. level. Four digestion procedures for selenium in bovine liver have been tested. All procedures gave concordant results, provided that the standard-additions method was used. The accuracies of the overall analytical procedures were estimated by comparison with results from neutron-activation analysis and analysis of NBS Bovine Liver, No. 1577. These comparisons proved that the accuracies of the procedures described in this paper are good.

Soils and crops in Scandinavia are low in selenium (about 0.2 $\mu\text{g/g}$ in soil and 0.02 $\mu\text{g/g}$ in crops). Cattle may therefore suffer from selenium deficiency, which can cause a number of diseases such as muscle dystrophia.¹ In some countries (including Sweden) selenium is added to fodder in order to balance the natural deficiency of the element. On the other hand, high selenium levels are poisonous.² The span between beneficial and detrimental concentrations is small, so accurate analytical procedures are required for monitoring the selenium status. For cattle and wild animals analysis of liver specimens may be adequate for this purpose.^{3,4}

The hydride-generation technique combined with atomic-absorption spectrometry (HG-AAS) is a sensitive and convenient method for the determination of selenium. Use of a flow system for sample handling and hydride generation further simplifies the procedure, increases sample throughput and reduces the indeterminate error.

The assay of selenium in biological materials by HG-AAS requires destruction of the organic matter. This is often done with strong acids at elevated temperatures and can lead to losses of volatile selenium compounds such as SeCl_4 and SeO_2 if not properly conducted.^{5,7} The choice of digestion method is highly dependent on sample type. A procedure suitable for water samples⁸ may, for instance, prove inadequate for body fluids⁹ or marine biological samples.¹⁰ Thus each sample type requires the destruction step to be checked and optimized before use.

We describe four digestion procedures suitable for the determination of selenium in bovine liver by HG-AAS. An apparatus utilizing a flow system for HG-AAS is also presented. The limit of deter-

mination (10% RSD) for selenium was 0.25 $\mu\text{g/l}$. The quality of the analytical procedures was evaluated by comparison of the results with those from neutron-activation analysis (NAA) and analysis of NBS SRM 1577, Bovine Liver.

EXPERIMENTAL

Apparatus

The HG-AAS apparatus is outlined in Fig. 1. A Varian AA5 atomic-absorption spectrophotometer equipped with an EDL (Westinghouse) operated at 7.5 W was used together with a commercial flow-injection system (FIA-05, BIFOK, Sweden) and a peristaltic pump (FIA-08). All tubing in the manifold was made of Teflon, with an inner diameter of 0.7 mm. The sample was injected into the carrier stream by a valve (Rheodyne) with a 0.6-ml loop. As purging and carrier gas a stream of nitrogen was used at a flow-rate of 250 ml/min. The gas-liquid mixture was parted in a gas-liquid separator. The gases were passed on to a heated quartz tube (length 180 mm, inner diameter 12 mm), where the hydrogen selenide was atomized at 850°. The quartz tube was electrically heated and the temperature regulated by control of the voltage applied. To prevent the hydrogen produced from igniting at the tube ends, which leads to noisy signals, the ends were left unheated and uninsulated. The absorbance signals, measured at 196.0 nm with a slit-width of 1 mm, were recorded on an x-t recorder (W + W 1100, W + W Electronic Inc., Switzerland) and peak heights evaluated from the recorder tracings. A total time constant of about 2 sec was used for the AAS and recorder.

The digestion vessels were heated in temperature-programmed aluminium blocks, either commercially available (Tecator, Sweden) or laboratory-built. The laboratory-built unit consisted of an aluminium block, one for each type of digestion vessel, placed on a hot-plate. The temperature programme was controlled by a calculator (HP 41-CV) interfaced with a temperature regulator (MDV, Ero Electronics, Italy).

Chemicals

All chemicals used were of analytical grade.

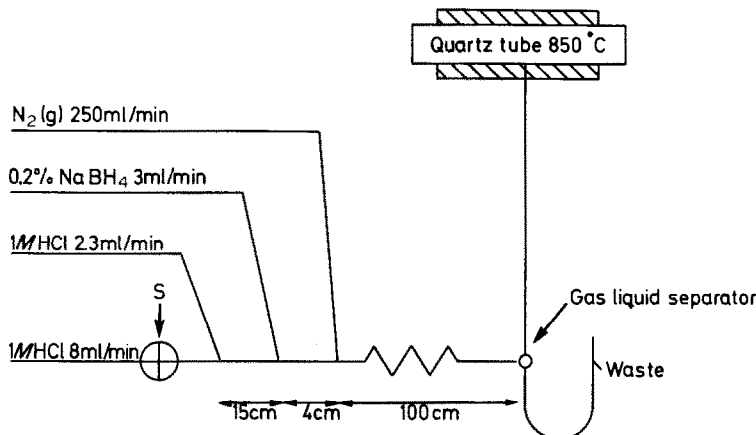


Fig. 1. Flow system used for selenium HG-AAS.

A standard solution of selenium(IV), 1 g/l., was prepared from an ampoule of selenium dioxide in dilute nitric acid (Merck). Its concentration was checked by amperometric titration with thiosulphate after addition of a large excess of iodide and found to be 1.008 g/l. (T. A. Bengtsson, unpublished method). Further standards were prepared from this solution by dilution.

Distilled and Milli-Q-filtered water was used in preparing solutions and in the final washings of the acid-cleaned utensils.

Sample pretreatment

Liver from two calves, one of which had been given selenium-enriched fodder, was analysed.

The liver specimen was freed from visible fat and sinews, homogenized in a Turmix mill and subsequently frozen. The material was then freeze-dried (Hetosicc, CD 52, Heto, Denmark) and again homogenized in the Turmix mill. The freeze-dried specimen was stored in acid-washed plastic boxes at room temperature. The water content of the livers was about 70%.

Digestion procedures

Four different digestion procedures were applied to samples of the dried material weighing 0.1–0.2 g. After digestion any selenate present was reduced to selenite by boiling the digest for 30 min in the presence of 6M hydrochloric acid.^{5,11} The HG-AAS finish was performed within two days after the reduction step.

A. Nitric acid-bomb digestion. The pressure vessel described by Uhrberg is used.¹²

To the quartz tube add the sample and 3 ml of concentrated nitric acid. Place the tube in the pressure vessel and cover it with the Teflon lid acting as a seal. Close the pressure vessel and put it into an aluminium block. Raise the temperature steadily and keep it at 125° for 20 min and at 175° for 90 min. Cool to room temperature and transfer to a Kjeldahl flask with the aid of 9 ml of 6M hydrochloric acid. Boil under reflux for 30 min. Cool, and finally transfer to a 50-ml standard flask and dilute to volume with water.

B. Nitric-perchloric-sulphuric acid digestion. The digestions are done with the concentrated acids in the proportions nitric:perchloric:sulphuric 20:5:2 v/v.¹³

Transfer the sample to a 50-ml Kjeldahl flask and add 20 ml of the mixture of acids. Boil in a heating stand until the sulphuric acid starts to distil. Cool, add 3 ml of water and 6 ml of concentrated hydrochloric acid. Boil the digest for 30 min, transfer it to a 50-ml standard flask and dilute to volume with water.

C. Nitric acid-magnesium nitrate digestion. The digestion agent contains 0.5 g of magnesium nitrate hexahydrate per ml of 100% nitric acid.¹⁴

Put the sample and 5 ml of the digestion agent into a graduated 50-ml glass tube (150 × 14 mm). Insert the tube into an aluminium block and apply the following temperature programme; 85° for 1 hr, 175° for 2 hr and 225° until the tube contents are dry and have stopped climbing up the tube wall. Place the tube in a muffle furnace and dry-ash at 520° for 4 hr. After cooling, add 6 ml of 6M hydrochloric acid and 3 ml of concentrated hydrochloric acid. Boil the digest for 30 min, cool and dilute to the mark with water.

D. Nitric-perchloric acid digestion. The digestion procedure developed by Frank¹⁵ utilizes a mixture of concentrated nitric and perchloric acids (7:3 v/v).

Place the sample and 10 ml of the mixture of acids in a glass tube (24 mm bore). Raise the temperature to 225° according to the nine-step programme described by Frank.¹⁵ Reduce the volume of perchloric acid to about 1 ml by gently blowing filtered air into the tube. Add 3 ml of water and 6 ml of concentrated hydrochloric acid and boil the digest for 30 min. Cool, transfer to a 50-ml standard flask and dilute to volume with water.

RESULTS AND DISCUSSION

Hydride generation

Several types of equipment have been described for the generation of hydrides in a flow system and the subsequent determination of the hydride-forming elements by AAS after thermal atomization of the hydrides.^{16–21} The equipment used here is adapted from that of Åström²² and modified to suit the requirements for the determination of selenium. A supporting hydrochloric acid stream has been added to ensure complete acidification of neutral and slightly basic samples (see Fig. 1).

The absorbance registered by the spectrophotometer will depend on the design and operating conditions of the hydride-generating unit in a manner that is not well understood. Empirical optimization of the various parameters involved is therefore necessary. These include (i) flow-rate and concentration of the hydrochloric acid in the carrier and support streams, (ii) flow-rate and concentration of the sodium tetrahydroborate solution used as reducing agent, (iii) flow-rate of the nitrogen carrier gas, and (iv) atomization temperature.

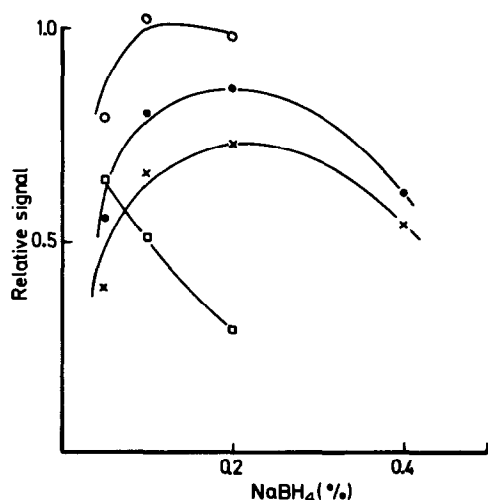


Fig. 2. The relative signal from 10 $\mu\text{g/l.}$ selenium as a function of the concentration of sodium tetrahydroborate at different concentrations of hydrochloric acid: \square 0.2M, \circ 0.5M, \bullet 1M, \times 2M.

Figure 2 shows the peak height of the selenium signal as a function of the concentration of tetrahydroborate at different constant concentrations of hydrochloric acid. Under standard conditions the flow system was run with solutions of 1M hydrochloric acid and 0.2% sodium tetrahydroborate in 0.2% sodium hydroxide. The flow-rate of the reducing agent is not critical and a broad maximum is observed between 2.5 and 5.5 ml/min. As expected, the selenium signal increases with the flow-rate of the hydrochloric acid until back-pressure causes leakages. The flow-rates chosen for trouble-free performance are given in Fig. 1. The influence of the flow-rate of the stream of nitrogen gas used for purging and transport of the selenium hydride is shown in Fig. 3. A working flow-rate of 250 ml/min was used. The selenium signal as a function of the

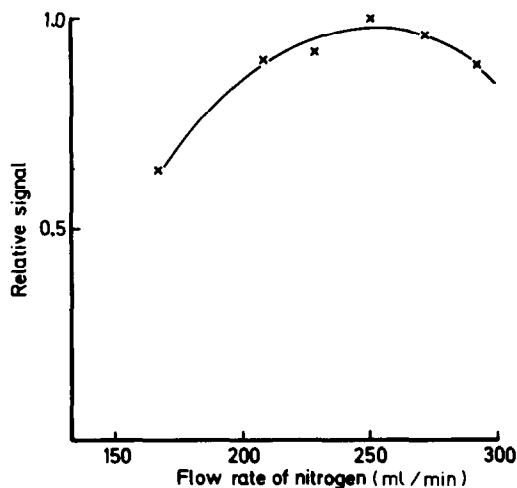


Fig. 3. The relative signal from 10 $\mu\text{g/l.}$ selenium as a function of the flow-rate of nitrogen.

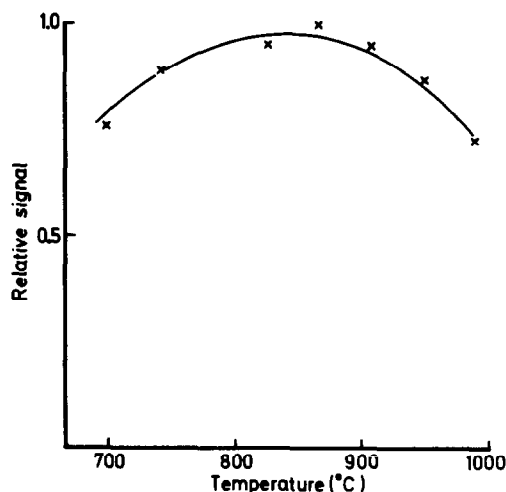


Fig. 4. The relative signal from 10 $\mu\text{g/l.}$ selenium as a function of the temperature of the quartz tube.

temperature in the quartz tube is depicted in Fig. 4. The optimum at around 850° has also been reported by others.^{17,23}

The lengths of the coils and tubings were found to have only a minor influence on sensitivity. On the other hand, the condition of the tubings may affect the signals significantly. For instance, after repeated injection of solutions containing considerable amounts of copper ($\approx 1 \mu\text{g/ml}$), memory effects occur in the form of decreased signals.

The shape of the absorption peak as registered by a transient-recorder is shown in Fig. 5. The peak area is linearly dependent on sample volume up to at least 2 ml. For speed and convenience a sample volume of 0.6 ml was chosen, leading to a cycle time of about 45 sec. Peak height was used as the measure of the analytical signal. The detection limit (3σ) for selenium with the equipment was 0.1 $\mu\text{g/l.}$ and the calibration graph was linear up to about 15 $\mu\text{g/l.}$ under standard working conditions. The characteristic concentration of selenium (for 1% absorption)

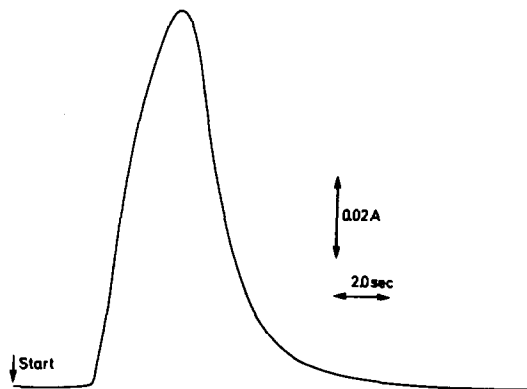


Fig. 5. Absorbance vs. time for 10 $\mu\text{g/l.}$ selenium, as registered by a transient-recorder.

Table 1. Results from the test of the evaluation methods; duplicate digests were prepared for each destruction method and each digest was subjected to all three evaluation methods

Digestion method	Se concentration, $\mu\text{g/g}$ (dry weight)					
	Pure standards		Matched standards		Standard-additions	
	1	2	1	2	1	2
A	1.03	1.02	1.22	1.21	1.45	1.43
B	0.86	0.79	1.32	1.21	1.47	1.43
C	1.32	1.35	1.28	1.31	1.43	1.46
D	1.10	1.10	1.12	1.12	1.39	1.48
Mean ($n = 8$)	1.07		1.22		1.44	
RSD, % ($n = 8$)	18.3		6.3		2.0	

was $0.39 \mu\text{g/l}$. The imprecision was less than 1% RSD at the $10\text{-}\mu\text{g/l}$. selenium level. Figure 6 shows some recorder tracings for different concentration levels of selenium.

Evaluation methods

Three methods were tested for the evaluation of the selenium concentration from the absorbance signal, *viz.* selenite standards in hydrochloric acid, matched selenite standards, and standard-addition. The matched standards, in addition to hydrochloric acid, contained the estimated amounts of the digestion agents remaining after the decomposition step. In the standard-addition method three aliquots were taken from the digest. Standard additions were made to two of them and all samples were made up to the same volume with water to ensure that the concentrations of non-selenium components were equal. The tests

were performed on the specimen from the calf that had been given selenite as an additive. The results are presented in Table 1.

The discrepancies between the results obtained by these evaluation methods (Table 1) are due to interferences. When pure standards are used for calibration, interferences from both the matrix and the acids used in the digestion step will show up. From experiments with selenite solutions, nitrate, sulphate and perchlorate were all found to suppress the selenium signal when present in large concentrations. This effect is not present in digestion method C, since nitrate is removed. The perchlorate interference is virtually absent in method D when the perchlorate concentration in the final solution is below $0.3M$. Hence an evaporation step was included in this digestion method. The acids used in procedure B have been used in different proportions by various

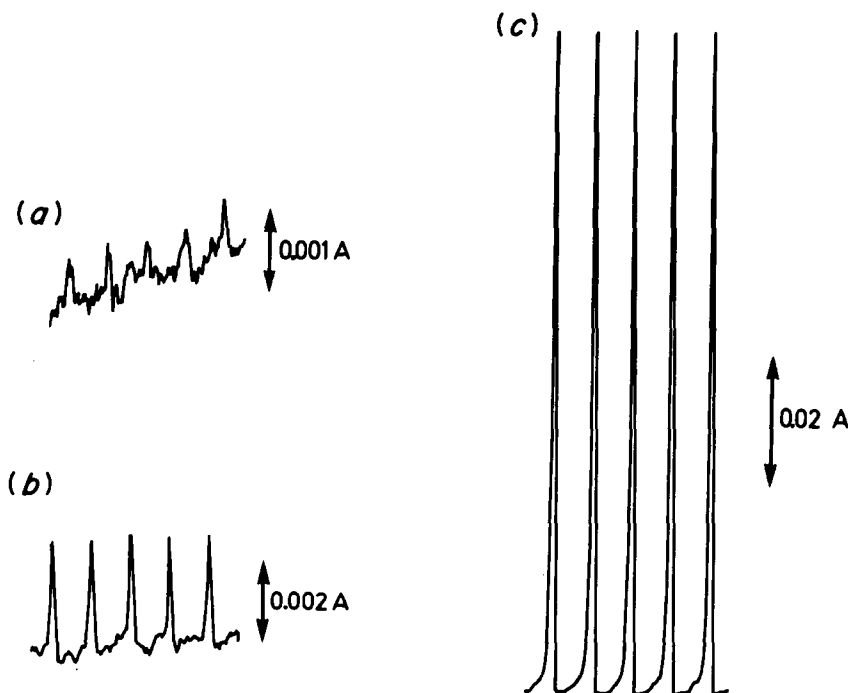


Fig. 6. Recorder traces of selenium signals at different concentration levels; (a) $0.05 \mu\text{g/l}$., (b) $0.25 \mu\text{g/l}$., (c) $10 \mu\text{g/l}$.

Table 2. Selenium concentration (dry weight) in bovine livers

Digestion method	Liver from calf, normally fed				Liver from calf, given Se as additive				NBS Bovine Liver 1577			
	Mean, $\mu\text{g/g}$	RSD, %	CI*, $\mu\text{g/g}$	<i>n</i>	Mean, $\mu\text{g/g}$	RSD, %	CI*, $\mu\text{g/g}$	<i>n</i>	Mean, $\mu\text{g/g}$	RSD, %	CI*, $\mu\text{g/g}$	<i>n</i>
A	1.13	0.5	1.11–1.14	3	1.45	2.2	1.41–1.48	6	1.12	2.8	1.07–1.17	4
B	1.12	1.8	1.10–1.15	5	1.44	2.1	1.40–1.48	6	1.11	1.5	1.08–1.14	4
C	1.08	3.0	1.03–1.13	4	1.42	3.0	1.37–1.48	5	1.12	2.9	1.07–1.17	4
D	1.02	5.5	0.93–1.11	4	1.39	3.7	1.33–1.44	6	1.04	3.4	0.98–1.10	4
All	1.09†	5.1	1.05–1.12	16	1.42§	3.1	1.40–1.45	23	1.10‡	3.9	1.07–1.12	16

*Confidence interval (95%).

†NAA (Studsvik) ^{76}Se : $1.088 \pm 0.137 \mu\text{g/g}$; ^{81}Se : $1.044 \pm 0.124 \mu\text{g/g}$; NAA (Isotopcentralen): $1.071 (\pm <10\%) \mu\text{g/g}$.

§NAA (Studsvik) ^{76}Se : $1.557 \pm 0.122 \mu\text{g/g}$; ^{81}Se : $1.363 \pm 0.110 \mu\text{g/g}$; NAA (Isotopcentralen): $1.451 (\pm <10\%) \mu\text{g/g}$.

‡Certified value $1.1 \pm 0.1 \mu\text{g/g}$.

workers. A method with little sulphuric acid has been chosen here to minimize the interference from sulphate.

The difference between the results obtained by use of matched standards and by the standard-additions method is most certainly caused by interference from copper.⁵ In the samples injected the concentration of copper was about 0.5 mg/l. (as determined by AAS). Figure 7 shows the variation of the analytical signal caused by copper at 0–10 mg/l. levels with different concentrations of hydrochloric acid in the carrier and support flows. Although a somewhat smaller disturbance from copper is experienced with increasing concentration of hydrochloric acid, this advantage is partly offset by a general decrease of the analytical signal with increasing concentration of acid and by corrosion problems. Hence, 1M hydrochloric acid, which is optimal for interference-free work, was adhered to as carrier medium.

The results from the evaluation with standard additions are concordant and indicate that this evaluation method must be used to obtain reliable results.

Accuracy and precision

The precision and accuracy of the procedures were determined from replicate determinations on the two specimens of calf liver and on NBS Bovine Liver (No. 1577). The results obtained by the standard-addition method are given in Table 2. The imprecision of procedures A–C is 3% RSD or less and no significant difference appears between the results from these digestion methods. Procedure D tends to yield a somewhat larger RSD and a lower result than the other methods. The lower value might be due to losses of SeO_2 in the evaporation step.²⁴ This step is probably unnecessary when the standard-additions method is used for evaluation, but this point has not been tested.

The accuracy is very satisfactory as can be inferred from the results obtained with the NBS reference material. The calf livers were also analysed by NAA (Studsvik Energiteknik AB, Studsvik, Sweden and Isotopcentralen, Copenhagen, Denmark).

As shown in Table 2, the NAA results agree, within

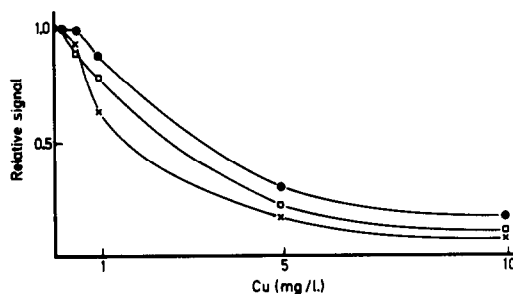


Fig. 7. The relative signal from 10 $\mu\text{g/l}$. selenium as a function of copper concentration. The concentrations of hydrochloric acid in the flow system were: \times 1M, \square 2M, \bullet 4M.

the limits of error reported, with the HG–AAS results.

Conclusions

In conjunction with HG–AAS the digestion procedures will allow an accurate determination of selenium in liver provided the result is evaluated by the standard-additions method, but it would be desirable to find a means of eliminating copper during the sample preparation. It might then be possible to use matched standards for evaluation and to avoid fouling of the tubings. The fouling can only be partly overcome by rinsing, so the tubings have to be replaced occasionally.

Acknowledgement—Thanks are due to Dr. A. Frank for preparing and putting the liver samples at our disposal, and for doing the nitric–perchloric acid digestions.

REFERENCES

- H. E. Ganther, in *Selenium*, R. A. Zingaro and W. C. Cooper (eds.), pp. 548–549. Van Nostrand-Reinhold, New York, 1974.
- W. C. Cooper and J. R. Glover, in *Selenium*, R. A. Zingaro and W. C. Cooper (eds.), Chapter 11. Van Nostrand-Reinhold, New York, 1974.
- A. Frøslie, *Foderjournalen*, 1980, No. 1–2, 26.
- W. C. Cooper and J. R. Glover, in *Selenium*, R. A. Zingaro and W. C. Cooper (eds.), p. 659. Van Nostrand-Reinhold, New York, 1974.

5. S. E. Raptis, G. Kaiser and G. Tölg, *Z. Anal. Chem.*, 1983, **316**, 105.
6. R. Bock and D. Jacob, *ibid.*, 1964, **200**, 6.
7. K. S. Subramanian and J. C. Méranger, *Analyst*, 1982, **107**, 157.
8. D. D. Nygaard and J. H. Lowry, *Anal. Chem.*, 1982, **54**, 803.
9. B. Welz and M. Melcher, *Anal. Chim. Acta*, 1984, **165**, 131.
10. *Idem.* *Anal. Chem.*, 1985, **57**, 427.
11. F. A. Gooch and P. S. Evans Jr., *Z. Anorg. Chem.*, 1895, **10**, 253.
12. R. Uhrberg, *Anal. Chem.*, 1982, **54**, 1906.
13. *Kungl. Lantbruksstyrelsens kungörelser m.m.*, 1950, No. 9.
14. K. W. M. Siu and S. S. Berman, *Talanta*, 1984, **31**, 1010.
15. A. Frank, *Z. Anal. Chem.*, 1976, **279**, 101.
16. J. A. Fiorino, J. W. Jones and S. G. Capar, *Anal. Chem.*, 1976, **48**, 120.
17. F. D. Pierce, T. C. Lamoreaux, H. R. Brown and R. S. Fraser, *Appl. Spectrosc.*, 1976, **30**, 38.
18. P. N. Vijan and G. R. Wood, *Talanta*, 1976, **23**, 89.
19. H. Narasaki and M. Ikeda, *Anal. Chem.*, 1984, **56**, 2059.
20. M. Yamamoto, M. Yasuda and Y. Yamamoto, *ibid.*, 1985, **57**, 1382.
21. C. C. Y. Chan, *ibid.*, 1985, **57**, 1482.
22. O. Åström, *ibid.*, 1982, **54**, 190.
23. B. Lloyd, P. Holt and H. T. Delves, *Analyst*, 1982, **107**, 927.
24. J. Piwonka, G. Kaiser and G. Tölg, *Z. Anal. Chem.*, 1985, **321**, 225.

DYE-SURFACTANT INTERACTIONS: A REVIEW

M. E. DIAZ GARCIA and A. SANZ-MEDEL*

Analytical Chemistry Department, Chemistry Faculty, University of Oviedo, Oviedo, Spain

(Received 5 March 1985. Accepted 10 October 1985)

Summary—The present state of knowledge of the mechanisms of dye-surfactant interactions for "normal" aqueous micelles is surveyed. The nature of the forces which lead to the binding of dye molecules in micelles, the influence of the cationic, anionic or non-ionic character of a surfactant on the absorption and/or fluorescence behaviour (below and above the critical micelle concentration), ion-association processes and the influence of additives on these processes are discussed. Some discussion along these lines on related systems (reverse micelles, vesicles, polyelectrolytes) is included.

In analytical chemistry the main use of surfactants is in spectrophotometry and fluorimetry, particularly in the development of new methods of metal-ion determination.¹⁻⁸ The addition of cationic surfactants to a negatively-charged coloured binary complex may result in the formation of new analytical systems (sensitized reactions). In such sensitized systems, the addition of a surfactant may lead to lowering of the pH at which the complex is formed, red-shifts in absorption bands, and increases in molar absorptivity or fluorescence intensity. Usually, the metal-chelate complexes formed in the micellar systems are more stable than those formed in the absence of micelles.⁶ Micelles are responsible for many of the practical applications of detergents such as: (i) enhancement of the solubility of organic compounds in water,⁹⁻¹¹ owing to their incorporation in the micelle, where they experience an altered micro-environment; (ii) catalysis of many reactions,¹² usually explained in terms of a "concentration effect" in the micellar pseudophase; (iii) alteration of reaction pathways, rates and equilibria.¹³⁻¹⁶ Additionally, micelle systems are convenient to use because they are optically transparent, stable and relatively non-toxic.^{16,17}

These beneficial effects show the advantage of such surfactant systems in the development of new spectrophotometric and fluorimetric methods for determining micro amounts of metal ions, anions, biological compounds, drugs and pesticides.

Typical chromophoric reagents which have been used to determine metal ions by use of surfactants as a third component include derivatives of the triphenylmethane series,¹ azo-compounds,¹⁸⁻²⁰ anthraquinone dyes,²¹ phenoxazone,^{22,23} and oxine derivatives.^{24,25} Although considerable attention has been paid to the analytical applications, the nature and mechanism of these types of reaction are still not clearly understood. The electrostatic interactions between oppositely-charged surfactants and dyes are well understood (Hartley rules),²⁶ but do not in

themselves explain the spectral changes observed. It seems probable^{25,27} that once the electrostatic forces have brought together the oppositely-charged molecules, hydrophobic interactions take place, dramatically changing the micro-environment experienced by the chromophore²⁵ or lumophore.²⁷ Knowledge of dye-surfactant interaction should be of great value in understanding the chemical equilibria, mechanisms and kinetics of surfactant-sensitized colour and/or fluorescence reactions. In this review, data scattered throughout the literature on dye-surfactant interactions are discussed in the light of our own experience.

NORMAL MICELLE FORMATION

A surfactant (*surface active agent*) is a molecule or ion that possesses both polar (or ionic) and non-polar moieties, *i.e.*, it is amphiphilic. Large variations in structure are possible; the polar group can have varied charge and nature (*e.g.*, alkylsulphate, alkylphosphate or alkylammonium) and be attached to alkyl groups of varying lengths (8-18 carbon atoms) or to other hydrophobic moieties (Table 1).

In very dilute solutions, surfactants dissolve and exist as monomers, but when their concentration exceeds a certain minimum, the so-called critical micelle concentration (c.m.c.), they associate spontaneously to form aggregates. The term "micelle" is used for an entity of colloidal dimensions, in dynamic equilibrium with the monomer from which it is formed. As the surfactant concentration increases above the c.m.c., the addition of fresh monomer results in the formation of new micelles, so the monomer concentration remains essentially constant and approximately equal to the c.m.c. Micelle formation is a result of the dual nature of the surfactant molecule, the hydrophobic part trying to escape from the bulk water, and the hydrophilic part interacting strongly with the water. Water has an open structure because of three-dimensional hydrogen-bonding, which permits the existence of clusters of water

*Author for correspondence.

Table I. Micelle-forming amphiphilic molecules

Cationic surfactants	
$\text{CH}_3-(\text{CH}_2)_n-\overset{\oplus}{\text{N}}-(\text{CH}_2)_3 \text{X}^\ominus$	
$\text{CH}_3-(\text{CH}_2)_n-\overset{\oplus}{\text{N}} \begin{array}{c} \diagup \\ \text{C}_6\text{H}_5 \\ \diagdown \end{array} \text{X}^\ominus$	$\text{X}^\ominus = \text{F}^-, \text{Cl}^-, \text{Br}^-, \text{I}^-, \text{NO}_3^-$
$\text{CH}_3-(\text{CH}_2)_n-\overset{\oplus}{\text{N}}\text{H}_3 \text{X}^\ominus$	
Anionic surfactants	
$\text{CH}_3-(\text{CH}_2)_n-\text{OSO}_3^\ominus \text{M}^\oplus$	
$\text{CH}_3-(\text{CH}_2)_n-\text{OPO}_3^{2-} \text{M}^\oplus$	$\text{M}^\oplus = \text{Li}^+, \text{Na}^+, \text{K}^+, \text{Ca}^{2+}, \text{Mg}^{2+}$
$\text{CH}_3-(\text{CH}_2)_n-\text{SO}_3^\ominus \text{M}^\oplus$	
Non-ionic surfactants	
$\text{CH}_3-(\text{CH}_2)_n-\text{C}_6\text{H}_5-\text{O}-(\text{CH}_2-\text{CH}_2-\text{O})_m-\text{H}$	
$\text{CH}_3-(\text{CH}_2)_n-\text{N} \begin{array}{c} \diagup \\ \text{C}_6\text{H}_5 \\ \diagdown \end{array} \text{N}-\text{R}$	
Zwitterionic surfactants	
$\text{CH}_3-(\text{CH}_2)_n-\overset{\oplus}{\text{N}}(\text{CH}_3)_2-\text{CH}_2-\text{SO}_3^\ominus$	

molecules containing cavities of specific sizes, which can accommodate non-polar chains.²⁸ The "flickering cluster" model of water structure²⁹ postulates that the formation of hydrogen bonds is predominantly a co-operative phenomenon; formation of a hydrogen bond between any two given atoms results in the binding of each atom by hydrogen bonds to neighbouring molecules. In this way, cavities of different volumes (Fig. 1), surrounded by hydrogen-bonded water molecules, are formed.²⁹

For a given surfactant, at a given temperature, only a certain amount of monomer can be accommodated in the cavities and any further addition of surfactant will result in the formation of micelles. In other words, the further addition of surfactant provides a driving force to minimize contact of the monomer hydrocarbon chains with water. Therefore, according to Langmuir's principle of differential solubility, the hydrocarbon chains cluster to form a core (micellar core), while the polar groups interact with the water.³⁰

Molecular conformation of micelles

Each micelle consists of a certain number of monomer molecules (aggregation number, N), which determines its general size and shape. The exact size and shape of micelles is still uncertain but it is assumed that an ionic micelle in dilute aqueous solution is roughly spherical (Fig. 2). The charged (or polar)

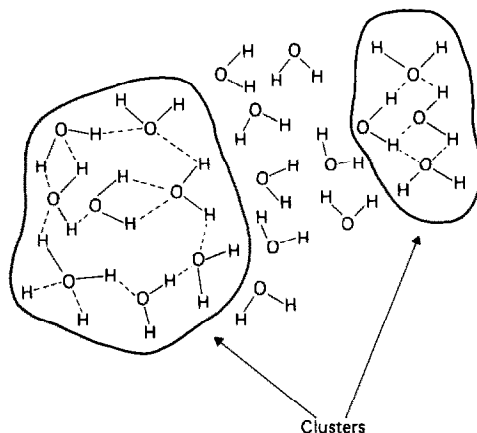


Fig. 1. Schematic representation of hydrogen-bonded water molecules in liquid water.

hydrophilic groups are directed towards the aqueous phase (Stern layer), while the hydrocarbon chains are directed away from the water (forming the hydrophobic central core). The region adjacent to the Stern layer contains a high density of counter-ions of the polar heads (Gouy-Chapman double layer) and separates the hydrophobic interior from the bulk aqueous phase.¹⁶ This model visualizes a micelle as "an oil drop with an ionic or polar coat".³¹ On the macroscopic scale, a micellar medium could be described as a mixed aqueous-organic solvent.³²

It is interesting to note that although it is usually assumed that there is a fairly well-defined water layer around the micellar surface, there is no agreement on the composition of the micellar core, *i.e.*, whether it consists of pure hydrocarbon or of hydrocarbon chains mixed with water. Water penetration of the micellar core is still a matter of controversy. Experimental evidence has been produced supporting the view that water cannot rigorously be excluded from

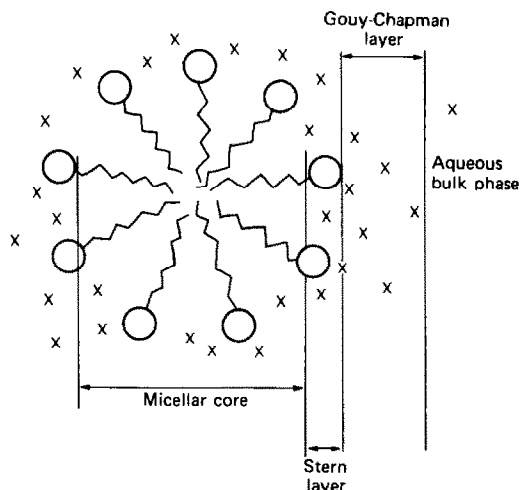


Fig. 2. Two dimensional representation of a model spherical ionic micelle. \times : counter-ions, \bigcirc : ionic head-groups, \sim : hydrocarbon tails.

the micellar core. This conclusion is supported not only by early NMR studies^{32,33} but also from the more recent ¹³C-NMR investigations.³⁴ Many spectroscopic studies indicate that there is significant penetration of water into micelles.³⁵ Recent fluorescence studies on the hydrogen-bonding in micellar aggregates^{36,37} indicate that the distinction between polar and non-polar sites in the micelles is inaccurate; in fact, it has been proposed that micelles are loose and porous structures in which water and hydrophobic regions are constantly in contact.^{38,39}

Current thought on this controversial "water exposure of micelles" is founded mainly on low-angle neutron-scattering experiments which allow the study of unperturbed micelles.⁴⁰ This modern concept discusses the main characteristics of the molecular conformation in micelles in terms of the predictions of the "interphase model".⁴¹ Interphase theory predictions are in agreement with experimental data and are particularly consistent with some principal features of micellar structure:⁴⁰

(1) the micellar core is virtually devoid of water, according to Langmuir's original principle of differential solubility;

(2) micellar chains are randomly distributed and steric forces determine the final structure;

(3) contact of the hydrophobic sections of the micelle with water results from a disordered structure in which the terminal groups or chain ends are near the micellar surface and thus exposed to bulk water.⁴⁰

Although the "water penetration" concept of the hydrophobic sections of micelles is now less acceptable than the "water exposure" concept, this controversial topic is still under debate.^{42,43}

Surfactant-induced spectral changes

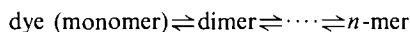
In aqueous solution, micelle formation is usually detected by some change in the physical properties of the solution, such as surface tension, conductivity, viscosity, and emf,⁴⁴⁻⁴⁶ or some optical or spectroscopic property of the solution (*e.g.*, light-scattering behaviour or spectral changes accompanying solubilization of dyes in surfactant micelles).⁴⁷⁻⁵⁰ Since this latter spectral method is based on dye-surfactant interactions, it deserves further elaboration.

Hartley²⁶ first noticed that the colour of sulfonaphthalein indicators changed on the addition of detergents, and this effect occurred only when the charge on the detergent aggregate was opposite in sign to that on the dissociated indicator molecule. This behaviour proved to be quite general, as azo,⁵¹ triphenylmethane⁵²⁻⁵⁴ and merocyanine dyes⁵⁵ all exhibited the same effect.

At concentrations below the c.m.c., addition of a surfactant to a dye solution may bring about the formation of colloidal dye-surfactant submicellar aggregates (mixed micelles) or insoluble dye-

surfactant salts. The actual species formed depends mainly on the nature of the dye: Bromophenol Blue and Bromocresol Green solutions at low concentrations of 1-carbethoxypentadecyltrimethylammonium bromide, in acid and alkaline solution, show turbidity;⁵⁴ Bromopyrogallol Red in solution at cetylpyridinium bromide concentrations below the c.m.c. and at pH 2-3 precipitates as a dye-surfactant salt.⁵⁶ Formation of an insoluble salt between ionic dyes and oppositely-charged detergents is most common, but is not a completely general phenomenon. In fact, some dyes, such as Phenol Red⁵⁴ or 8-hydroxyquinoline-5-sulphonic acid produce neither turbidity nor precipitation²⁵ along with the spectral change induced by addition of the cationic surfactant.

The nature of the dyes and their own tendency to aggregate⁵⁷⁻⁵⁹ have to be considered to explain such phenomena. Dyes are also amphiphiles, in the sense that bulky non-ionic moieties are attached to the ionic or analytical groups, but as they lack long-chain alkyl groups they have weak surface activity and do not form micelles in water. Depending on the balance between the hydrophobic and hydrophilic tendencies of any particular dye, increases in dye concentration can lead to stepwise aggregation, *i.e.*, the formation of dimers, trimers, polymers and finally colloids:⁶⁰



If a surfactant is added to such a dye solution at submicellar concentrations, both the surfactant monomer and the dye aggregates can interact to form a special kind of micelle (mixed micelle)⁶¹ at concentrations far below the normal c.m.c. characteristic of the surfactant. This dye-surfactant interaction accounts for the often observed fact that the so-called "spectral change dye method"⁴⁷ does not provide a true c.m.c. value. In fact, in such cases, the change in absorbance or fluorescence intensity of a dye solution in the presence of increasing surfactant concentrations may not reflect the formation of micelles of the surfactant (homomicelles) but that of mixed micelles or dye-surfactant salts. A comparison of some c.m.c. values of cetylpyridinium bromide, as determined in our laboratory by different methods under different conditions, is presented in Table 2 and clearly illustrates this point. As can be seen, not only the nature and concentration of the dye, but also the reaction medium can markedly influence the surfactant c.m.c. values.

Once the surfactant concentration has reached a value close to or above the c.m.c. neither turbidity nor precipitation is observed. Solubilization of the dye-surfactant "salt-like" ion-pairs in the micellar phase and/or the final incorporation of the dye into the micelles (homomicelles) is taking place.

Many of the features observed in the spectral behaviour of dye-surfactant systems carrying opposite charge can often be extended to general sensitized reactions in micellar media.

Table 2. Comparison of critical micelle concentrations of cetylpyridinium bromide, obtained by different methods

Method	Additive	c.m.c., $10^{-4}M$	pH	Reference
Conductivity	none	6.39	5	25
Surface tension	none	6.86	5	50
	KCl, 0.01M	3.76	5	56
	HCl, 1M	4.96	—	56
	Buffer HAc/NaAc 0.2M	2.58	4.5	50
	8-Hydroxyquinoline-5-sulphonic acid	3.76	6	25
	Dimethylformamide	2.39	0 (HCl, 1M)	57
Spectral dye-change	Eosin	0.04	6	58
	Pyrogallol Red	2.80	2.8	59
	Bromopyrogallol Red	0.99	0 (HCl, 1M)	56
	Bromopyrogallol Red	ppte.	2	50
	Thorin	ppte.	9	56
	Eriochrome Black T	depends on dye concn.	9	60

Mukerjee and Mysels,⁴⁸ using spectrophotometric and electrical conductivity measurements of the pynacyanol-sodium dodecylsulphate system identified the presence of two types of dye-surfactant aggregates: (i) below the c.m.c. a dye-surfactant salt which formed a coarse (visible suspension) stable slurry in the presence of more than a stoichiometric amount of surfactant, and (ii) dye-rich micelles, at below and around the c.m.c., which solubilized the water-insoluble dye-detergent salt. Malik *et al.*⁶⁷⁻⁶⁹ reported that spectral changes for several dyes are due to electrostatic forces involving interactions between the anionic (or cationic) surfactant and the basic (or acidic) dye. They claimed, however, that chemical interaction giving a stoichiometric dye-surfactant complex was very improbable. Guha *et al.*⁷⁰ attributed the changes in the absorption spectra and the decrease in fluorescence intensity of thionine to the formation of a dye-surfactant complex at sodium dodecylsulphate concentrations below the c.m.c.; at concentrations above the c.m.c. the appearance of the dye absorption spectrum, with a small red-shift and increased extinction coefficient, was interpreted as due to the incorporation of the dye into the micelles.

Nature of the dye-surfactant interaction

The existence of true ion-association complexes formed at below the c.m.c. between ionic surfactants and dyes with opposite charge is supported by most of the published data.^{54,71-74} These complexes are electrically neutral, and often poorly soluble in water but readily extractable by low-polarity solvents. They have stoichiometric surfactant/dye ratios. At surfactant concentrations at the c.m.c. value and above, the solubilizing effect of the micelles begins to be important and the ion-association complexes are incorporated into the micelles.

Electrostatic interaction of anionic dyes with the surface of cationic surfactant micelles takes place through the negatively charged groups of the dye

($-\text{SO}_3^-$, $-\text{COO}^-$). However, this kind of electrostatic interaction could not explain by itself the spectral changes observed during the interaction. In fact, bulky non-micelle forming species such as the diphenylguanidinium or tetraethylammonium ion, have no effect *per se*. Moreover, simple ion-pairing between a negative group such as $-\text{SO}_3^-$ or $-\text{COO}^-$ of the dye and a quaternary ammonium ion does not perturb the chromophore.⁷⁵ In the presence of cationic surfactants, aromatic compounds with sulphonic⁷⁶ or carboxylic acid groups⁷⁷ do not act simply as counter-ions, but are incorporated into the water-rich Stern layer of the micelle in a sandwich arrangement. This permits not only the hydration of the hydrophilic $-\text{SO}_3^-$ (or $-\text{COO}^-$) group, but also the solvation of the aromatic ring of the dye by the $-\text{N}(\text{CH}_3)_3$ group and the participation of van der Waals interactions between adjacent surfactant chains and the dye organic moiety (hydrophobic forces). In this situation, the micro-environment of the chromophore has clearly changed, from that existing in the bulk aqueous phase, and this change is the cause of the spectral shifts observed. Since dyes based on aromatic rings are widely used in spectrophotometry and fluorimetry, this picture can be considered general (and is probably operative in most analytical dye-surfactant systems at concentrations above the c.m.c.). In this context, it is worth mentioning the importance of the presence of an $-\text{SO}_3^-$ group in the dye. The electronic parameters for aromatic substituents⁷⁸ indicate that an $-\text{SO}_3^-$ group gives less resonance interaction with the aromatic system than does a $-\text{COO}^-$ group. In the latter case, the negative charge is delocalized and distributed over the terminal $-\text{COO}^-$ group and the aromatic ring; thus the cationic end of the surfactant will tend to interact electrostatically less with the $-\text{COO}^-$ group than with an $-\text{SO}_3^-$ group, on which the charge is localized. The $-\text{COO}^-$ group will therefore be buried deeper in the micelle Stern layer than will the $-\text{SO}_3^-$ group, leading to diminished electrostatic

interaction between the —COO^- groups and the charged head-groups of the surfactant.

It has been reported⁷⁹ that the ionic association of charged micelles with an aromatic dye through the —SO_3^- group promotes electron-withdrawal from the aromatic rings along the conjugated π -system, so leading to the ionization of easily dissociated groups in the dye (—OH groups). The resulting ionized group may further associate with another surfactant molecule. The spectral shifts then observed may be due to the deprotonation of an —OH group on the dye, with the incorporation of the chromophore into a single conjugation plane.⁷⁹ In this case, maximum delocalization of the π -electronic system of the dye can occur.

Russian authors claim^{51,80,81} that the sulphonic acid group in the triphenylmethane dye series is isolated and that its electrons are not able to interact with the aromatic π -electron system. However, it has been demonstrated⁸² that the electrons on the sulphonic acid group may participate in the π -system through the empty d -orbitals of the sulphur atom. Association of the —SO_3^- group with the surfactant reduces the fraction of total charge on it, so promoting electron-withdrawal from the entire π -electron system of the dye and causing energetic dissymmetry, with consequent dissociation of ionizable hydroxyl groups. In this way, micelles affect not only the electronic structure of the dyes but also their basicity and hence the $\text{p}K_a$ of indicators.¹⁶ Micelles can either stabilize or destabilize charged dye species, depending on the sign of their surface charge, as shown in Table 3.

The proton-release occurring during the reaction between an anionic dye and a cationic surfactant produces a change in the spectrum which is similar to that observed on increasing the pH of the dye solution. Such $\text{p}K_a$ shifts for solubilized indicators have been attributed to the influence of the surface potential of micelles.^{85, 87} The $\text{p}K_a$ changes also appear to be related to the reduction of the difference in free energy between the acidic form of the dye and its anion in the micelle.^{77,88, 90} Extensive incorporation of an anionic dye into a cationic micelle implies that the

free energy of the anionic form decreases more than that of the un-ionized form, as the anion is more polarizable and firmly attached to the positive end-groups of neighbouring surfactant molecules.⁹¹

There is multiple binding in these associated micellar species: evidence has been produced indicating that hydrophobic interaction, not charge compensation, plays the main role in binding between dyes and surfactants. The exact nature of this interaction, however, has not yet been satisfactorily explained. Chiang and Lukton⁹² report that their results on the interaction between 2-*p*-toluidinylnaphthalene-6-sulphonate and sodium dodecylsulphate (NaDDS) micelles suggest that the binding force is hydrophobic. Analogously, Birdi *et al.*⁹⁰ claim that the interaction of NaDDS micelles with 1-anilino-naphthalene-8-sulphonate is hydrophobic in nature. The interaction between some mono-azo dyes with a series of non-ionic surfactants has been shown⁹³ to be hydrophobic in nature and occurs between dyes and the ethylene oxide chains of the non-ionic surfactant. Minch⁵⁵ showed, from spectral changes of merocyanine dyes in cationic and anionic micelles, that in all cases the spectra were red-shifted when the dye was incorporated into micelles and that the magnitude of the shift increased with more hydrophobic dyes. Biedermann and Datyner⁹⁴ also suggested that the interactions of some azo dyestuffs with NaDDS micelles increased with increasing lipophilicity of the dyes.

According to current thought,⁴⁰ the inclusion of a dye molecule within a micelle is not strictly akin to placing it in a hydrophobic region in the micellar core, but is more like placing it in a hydrophobic environment where it is exposed to water. A consideration of hydrocarbon chains in micelles as disordered structures could explain why the nature of the dye may determine its binding site within the micelle assembly.⁹⁴ In other instances, the factors responsible for the spectral changes have been ascribed to the *deaggregation of the dye* molecules by association with micelles,⁹⁵ to the joint effect of deaggregation and the *change in the molecular environment*,^{96,97} or to

Table 3. $\text{p}K_a$ shifts of various species, as a function of surfactant charge-type

Species	Alone	Cationic surfactant	Anionic surfactant	Non-ionic surfactant	Reference
Phenol Red, $\text{p}K_{a_2}$	7.68	7.66*			54
Bromophenol Blue, $\text{p}K_{a_2}$	3.89	3.02*			54
Bromocresol Green, $\text{p}K_{a_2}$	4.58	4.08*			54
8-Quinolinol, $\text{p}K_{a_1}$	5.02	4.26†	5.72§	5.02‡	83, 84
$\text{p}K_{a_2}$	9.67	9.35†	10.29§	9.76‡	83, 84
Quinine, $\text{p}K_{a_1}$	4.13	4.20†	5.35§		83
$\text{p}K_{a_2}$	8.52	7.57†	9.79§		
Umbelliferone, $\text{p}K_{a_1}$	7.75	6.75	8.25§		85
Methyl Red, $\text{p}K_{a_1}$	4.95	3.67	6.63§	5.20‡	85
4-Nitrophenol, $\text{p}K_{a_1}$	7.15			7.11‡	84

*Carboxypentadecyltrimethylammonium bromide.

†Dodecyltrimethylammonium chloride.

‡Triton X-100

§Sodium dodecylsulphate.

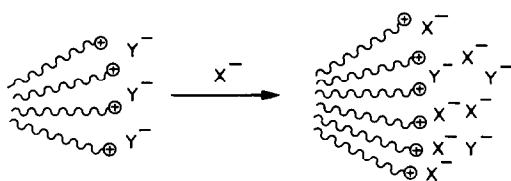
||Dodecyltrimethylammonium bromide.

the localization of the chromophore within the hydrophobic micellar interior.⁹⁸

INFLUENCE OF ADDITIVES

Strong electrolytes

Micelles are sensitive to small changes in the ionic strength of the aqueous solution. The change in the c.m.c. of cetylpyridinium bromide in aqueous solution with electrolyte concentration⁶² reveals two trends, one occurring at low and the other at high concentrations of the added salt (see Table 4). Addition of salts to ionic micelle solutions reduces the mutual electrostatic repulsions of charged head-groups.⁹⁹



Thus, addition of a salt anion, X^- , to cationic micelle solutions results in an increase of counter-ion dissociation (α). The degree of displacement of the Y^- counter-ion will depend on the nature of the X^- anion, and usually follows the order in the lyotropic series.¹⁰⁰

On the other hand, electrolyte addition leads to an increased aggregation number and micellar diameter^{99,101} because if the electrical surface potential is reduced, more polar heads, and hence more monomers, can constitute a given micelle (increase in N and size).

Regarding the usual decrease observed in the c.m.c. values after salt addition (Table 4) some authors speculate that it is related to the ability of the salt to "melt" Frank-Evans "icebergs"; micelle formation is an entropy-directed process and is influenced by changes in the water structure surrounding surfactant ions.^{102,103} If structure-breaking ions are present in solution, the water icebergs²⁸ will "thaw" to a more random state. Destruction of icebergs around the monomeric surfactant ions would result in easier

micelle formation at a lower surfactant level.¹⁰⁴ However, Schick¹⁰² claims from the iceberg picture that a structure-breaking ion should reduce micelle formation. Whatever the theoretical approach to this effect, it has to be borne in mind that c.m.c. decreases with electrolyte addition and that the c.m.c. is a measure of the ease of micelle formation: the lower the value of the c.m.c. the higher the tendency to micelle formation.

If the strong electrolyte concentration becomes sufficiently high, not only the size of the micelle changes but also its shape, e.g., spherical sodium dodecylsulphate micelles become rod-like at high salt (NaCl) concentrations¹⁰⁵ and cetylpyridinium bromide micelles grow steadily to form elongated semiflexible rods, with increasing sodium bromide concentration.¹⁰⁶ In the case of non-ionic surfactants, the c.m.c. is only slightly dependent on salt concentration.¹⁰⁷

As the magnitude of the ionic strength has a negligible effect on the spectral behaviour of dyes alone,^{55,74,108} the main role in the spectral changes observed when the salt concentration is increased in a dye-surfactant solution should be played by the surfactant-electrolyte interactions. The absorption spectrum of Bromopyrogallol Red at pH 4 and ionic strength 0.2M (fixed by the acetate buffer used) shows a maximum at 580 nm when cetylpyridinium bromide micelles are present.⁶² The addition of sodium chloride releases the dye from the micelles and the absorption spectrum changes to resemble that of Bromopyrogallol Red in the absence of cetylpyridinium micelles. The band at 580 nm decreases in intensity with sodium chloride concentrations ranging from 0.2 to 0.6M. At the higher salt concentrations the absorbance decrease is much less pronounced and a break-point is observed (at $[NaCl] \approx 0.48M$), which may correspond to the change in shape and size of the micelles.

The fact that the absorption spectrum of the free Bromopyrogallol Red reappears on addition of sodium chloride suggests that electrostatic forces play a fundamental role in dye-micelle binding, maintaining the dye in or near to the micelle.

The saturation of the micelle surface (Stern layer) by strong electrolytes should dissociate the dye-micelle associate, restoring the properties of the aqueous dye. This would also account for the observed increases in pK_a of the dye-surfactant association complex when the electrolyte concentration is increased.^{54,91} It has to be stressed, however, that other authors have indicated that addition of strong electrolytes may cause, conversely, an acceleration of the rate of dye penetration into micelles¹⁰⁹ or even a more effective inclusion of the dye into the micelle.⁷⁰ This is another example of how the studies and basic knowledge on micellar interactions available so far may be contradictory and insufficient to permit a clear choice between different possible interpretations of micellar reactions.

Table 4. Effect of added electrolytes on the c.m.c. of cetylpyridinium bromide⁶²

Added electrolyte	c.m.c., $10^{-4}M^*$
Aqueous solution	6.86
KCl, 0.01M	3.76
KCl, 0.1M	4.20
KCl, 1M	7.14
HCl, 0.2M	3.50
HCl, 1M	4.96
NaCl, 0.1M	3.40
NaCl, 1M	4.96
NaCl, 1.5M	4.56

*Surface tension measurements at 20 C.

Hydrophobic additives

Ionic micelles contain binding sites for both hydrophobic and hydrophilic solutes. For instance, addition of alcohols to aqueous solutions of surfactant aggregates is known to influence the properties of micelles. Alcohols penetrate the interior of the micelle without appreciably changing its volume, forming mixed micelles.¹¹⁰ The alcohol hydroxyl group is hydrogen-bonded to the surfactant head-groups, increasing the distance and hence decreasing the repulsion between them.¹¹¹ The effect of added alcohols on the c.m.c. of surfactant solutions is dependent on the nature of the alcohol, e.g., 1-propanol (or 2-propanol) decreases the c.m.c. of n-dodecyltrimethylammonium bromide and sodium dodecylsulphate more effectively than does ethanol¹¹² owing to some stabilization of the mixed micelles through direct hydrophobic interactions. 1-Propanol is more soluble than ethanol in the micellar phase, thereby promoting micelle formation.

In general, organic molecules (or ions) tend to reduce the c.m.c. of surfactants, the reduction increasing with the size of the alkyl group. The c.m.c. for n-dodecyltrimethylammonium bromide micelles is decreased by a factor of 40 as n changes from 0 to 5 in the series $\text{CH}_3-(\text{CH}_2)_n-\text{COO}^-$.¹¹³ The alkyl chain length of the additive also has an appreciable effect on the total number of monomers which form a micelle; it has been shown that if a longer hydrocarbon chain is used, in order to enhance the hydrophobic interaction with micelles, the aggregation number¹¹³ of the micelles is reduced.

The effect of some hydrophobic solutes has been considered in a number of studies¹¹²⁻¹¹⁴ but very little attention has been directed^{115,116} towards the measurement of the effect of added hydrophobic molecules on the properties of solutes already incorporated in micelles.

THE NATURE OF THE SURFACTANT

The spectral changes observed for different anionic dyes in the presence of surfactant micelles show that cationic surfactants affect the spectral characteristics of such dyes more strongly and over wider acidity ranges than other types of surfactant do. This means that charge-type effects are operative.

Changes in the nature of the cationic head-group of the surfactant, however, apparently play only a minor role, and it is the length of the hydrocarbon tail which is the predominant factor in determining the appearance of new peaks and/or band-shifts in the spectra.⁷⁵ Solubilization of a dye in micellar solutions can be attributed to hydrophobic interactions and it seems clear that the same kind of interactions are responsible for the dye spectral changes observed in micelles. In the light of solubilization experiments Lianos *et al.*¹¹⁷ concluded that there is a limiting chain length (more than 10 carbon atoms) for the solu-

bilization of arenes and that such solubilization does not seem to be sensitive to probe size, as pyrene and naphthalene showed similar behaviour.¹¹⁷ In a similar way, the spectral changes are first observed when the hydrocarbon chain length of the surfactant rises to 11 or 12 carbon atoms, which coincides with the appearance of surface-active properties in the molecule.⁷⁵ In other words, the length of the hydrocarbon chain in the surfactant is primarily responsible for the hydrophobic properties and could represent its degree of hydrophobicity. If the chains of the surfactants are very short, the corresponding micelles are extremely labile, with very short lifetimes. This would explain why such "small" micelles are unable to solubilize the arenes.¹¹⁸

Owing to electrostatic repulsion, the interaction between anionic dye ions and the head-groups of anionic surfactants should produce neither new spectral bands nor changes in absorbance or fluorescence intensity. However, as mentioned earlier, lipophilicity may often be the driving force for interaction, rather than the electrostatic interaction^{55,90,92,94} and some spectral changes can be explained in this way. A similar explanation can also be given for non-ionic surfactant effects on the spectral behaviour of dyes: Coomassie Brilliant Blue G-250 does not show any spectral shift with anionic detergents such as sodium dodecylsulphate or sodium deoxycholate, but does with non-ionic surfactants, probably owing to transfer of the dye from a hydrophilic to a hydrophobic micellar environment.¹¹⁹

If a charge-type effect can combine with the classical hydrophobic interactions then both kinds of interactions, electrostatic and hydrophobic, seem to act concurrently, bringing about the largest spectral changes, as shown for anionic dye-cationic surfactant complexes by Savvin *et al.*⁷⁵ or for metal chelate-cationic surfactant species by Sanz-Medel *et al.*^{25,27}

In any case, it seems clear that the surfactant character has the decisive role in determining the observed spectral changes, since bulky ions, which are non-micelle-forming (e.g., tetraethylammonium) do not give rise to effects similar to those observed in the presence of micelle-forming agents.^{56,75}

SOME RELATED SYSTEMS

The implications of a model for the interactions in micelles are significant not only for micelles in water but also for related assemblies, since the principles of organization are thought to be quite general.³⁰ For this reason the following related assemblies are reviewed.

Reverse micelles

The surfactant interactions in non-aqueous media have been investigated less¹²⁰ than those in aqueous surfactant systems. The surfactant aggregates in organic solvents are described as having a "reverse

micellar structure", in which the hydrocarbon tails are in contact with the solvent and the polar head-groups form the micellar core.

The aggregation number in such reverse micelles is relatively small, *e.g.*, less than 10 for alkylammonium carboxylates, compared with up to 100 for aqueous micelles,¹⁶ but it is supposed that these systems would exhibit an experimentally determinable c.m.c. Although many of the common methods for c.m.c. determination in aqueous solution are not applicable to reverse micellar systems, because of the low degree of aggregation and because ionic surfactants do not ionize in organic media, the "spectral change method" has been proposed for determination of the c.m.c. of Aerosol-OT [sodium di-(2-ethylhexyl)sulphosuccinate]¹²¹ with the dye 7,7,8,8-tetracyanoquinodimethane. Breaks in the plots of absorbance against surfactant concentration were interpreted as corresponding to the surfactant c.m.c. However, the concept of c.m.c. as explained for normal micelles is no longer applicable in these systems and is still subject to controversy. Reverse micelles alter the micro-environment of solubilized reactants and thus affect their stereochemistry, dissociation constants, redox potentials and reactivities.¹²²

In analytical chemistry scant use has been made of reverse micelles. Many organic reactions have been studied in reverse micelle systems but few studies have been made on inorganic reactions.¹²³⁻¹²⁵ In view of this situation, the study of analytical systems in reverse micelles is an unexploited research field.

Synthetic bilayer membranes (vesicles and lamellae)

Vesicles are the simplest membrane-mimetic colloidal systems and their use as membrane models has been recently reviewed.^{126,127} Although they are usually made of biomaterials such as lecithin, vesicles have recently been made from synthetic surfactants.¹²⁸ The main difference between vesicles and micelles is geometric: single-chain surfactants, *e.g.*, cetyltrimethylammonium bromide, form micelles, while double-chain surfactants, such as dioctadecyltrimethylammonium bromide, form vesicles. A

typical diagram of a vesicle and a bilayer membrane is shown in Fig. 3. The hydrophobic sections are in contact and separated from the inner and outer water phases by the polar head-groups.

Single-compartment vesicles (and bilayer membranes) are able to encapsulate and retain a number of substrates: 8-azaguanine is successfully incorporated (34% entrapment) in positively charged dioctadecyltrimethylammonium chloride vesicles, while in cationic single-compartment liposomes (phospholipid membranes) the uptake of this molecule is only 1.8%.¹²⁹

Some cyanine and merocyanine dyes show unusual spectral behaviour when bound to synthetic membranes,¹³⁰ the spectral variation is highly specific to the chemical structure of the membrane-forming amphiphile. The fluorescence of a probe molecule is drastically increased when the probe is added to a suspension of bilayer aggregates. This enhancement is caused by the entrance of probe molecules into the bilayer. The lower polarity of the environment and the restriction of the twisting of the excited probe molecule result in a pronounced increase in the quantum yield.^{131,132} These phenomena provide a way to achieve control of the spectra of dye molecules in the bilayer membranes, useful not only in model studies of biological chromophores (membrane-bound chlorophyll)^{133,134} but also from an analytical point of view.

As with micelles, it is difficult to define the nature of the spectral changes after the addition of a probe to a bilayer membrane solution and even to determine clearly whether it is hydrophobic or hydrophilic in character.

Polyelectrolytes

The phenomenon called "metachromasia" results from the interaction between a cationic dye and a polyelectrolyte in aqueous solution. Metachromatic changes of colour have been studied for a number of dyes such as Crystal Violet,^{135,136} Triplafavine¹³⁷ and Methylene Blue^{138,139} with simple polyelectrolytes (sodium polyphosphate, polymethacrylic acid).

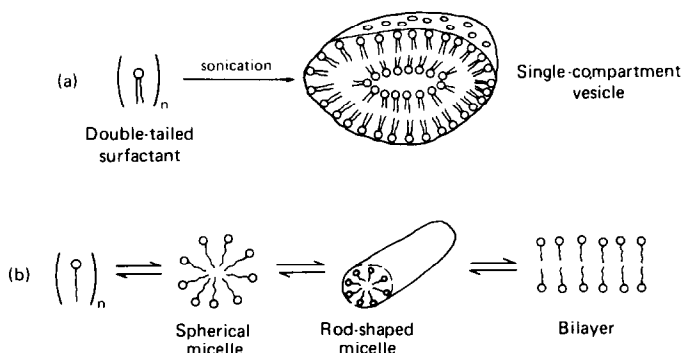


Fig. 3. Schematic representation of: (a) single-compartment vesicle, (b) conversion of detergents into spherical micelles, rod-like micelles and bilayers.

The exact nature of these changes is again not known, but it has been shown¹⁴⁰ that hydrophobic attractive forces between a dye and a poly-ion may in some instances predominate over electrostatic forces. The binding of Eosin-Y to poly-L-lysine has been found to be purely electrostatic in nature, in contrast to its binding to poly(*p*-xylylviologen), which has both an electrostatic and a hydrophobic component.¹⁴¹ Changes in apparent acidity constants of indicators in polyelectrolyte solutions have been attributed mainly to the large charge density of polyions and also to non-electrostatic interactions.¹⁴²

The optical behaviour of a metachromatic dye bound to polyelectrolytes depends on the chemical structure of the dye, on the nature of the polyelectrolyte and on the binding equilibrium.^{136,143} It can be related, in some aspects, to the behaviour of micellar systems.

Acknowledgement—Thanks are due to Professor W. L. Hinze (Wake Forest University, North Carolina, U.S.A.) for his thoughtful and critical reading of this manuscript.

REFERENCES

- V. N. Tikhonov, *Zh. Analit. Khim.*, 1977, **32**, 1435.
- R. K. Chernova, *ibid.*, 1977, **32**, 1477.
- N. Ishibashi and K. Kina, *Anal. Lett.*, 1972, **5**, 637.
- Idem*, *Microchem. J.* 1974, **19**, 26.
- K. Kina, K. Tamura and N. Ishibashi, *Bunseki Kagaku*, 1974, **23**, 1406.
- W. L. Hinze, *Solution Chemistry of Surfactants*, K. L. Mittal (ed.), Vol. 1, pp. 79–127. Plenum Press, New York, 1979.
- L. J. Cline Love, J. G. Habarta and J. G. Dorsey, *Anal. Chem.*, 1984, **56**, 1132A.
- W. L. Hinze, H. N. Singh, Y. Baba and N. G. Harvey, *Trends Anal. Chem.*, 1984, **3**, 193.
- Y. Jean and H. J. Ache, *J. Am. Chem. Soc.*, 1977, **99**, 7504.
- S. Tagashira, *Anal. Chem.*, 1983, **55**, 1918.
- H. Hoshino, T. Saitoh, H. Taketomi and T. Yotsuyanagi, *Anal. Chim. Acta*, 1983, **147**, 339.
- A. D. James and B. H. Robinson, *J. Chem. Soc. Faraday Trans. 1*, 1978, **74**, 10.
- S. Dieckmann and J. Frahim, *ibid.*, 1979, **75**, 2199.
- E. Pramauro and E. Pelizzetti, *Anal. Chim. Acta*, 1981, **126**, 253.
- P. D. I. Fletcher and B. H. Robinson, *J. Chem. Soc. Faraday Trans. 1*, 1984, **80**, 2417.
- J. H. Fendler and E. J. Fendler, *Catalysis in Micellar and Macromolecular Systems*, Academic Press, New York, 1975.
- W. L. Hinze, T. E. Riehl, H. N. Singh and Y. Baba, *Anal. Chem.*, 1984, **56**, 2180.
- J. Ibrail and L. Sommer, *Z. Anal. Chem.*, 1981, **306**, 129.
- Liu Shao-pu, *Analyst*, 1982, **107**, 428.
- M. H. Abernethy and R. T. Fowler, *Clin. Chem.*, 1982, **43**, 3D21.
- Liu Shao-pu, *Fenxi Hsi Hua Hsueh*, 1977, **5**, 366.
- N. T. Son, J. Lasovský, E. Ružička, J. Šimek and J. Sztokowska, *Collection Czech. Chem. Commun.*, 1979, **44**, 1568.
- N. T. Son, E. Ružička and J. Lasovský, *ibid.*, 1979, **44**, 3264.
- K. Goto, H. Tamura, M. Onodera and M. Nagayama, *Talanta*, 1973, **21**, 183.
- J. I. García Alonso, M. E. Díaz García and A. Sanz-Medel, *ibid.*, 1984, **31**, 361.
- G. S. Hartley, *Trans. Faraday Soc.*, 1934, **30**, 44.
- A. Sanz-Medel, J. I. García Alonso and E. Blanco González, *Anal. Chem.*, 1985, **57**, 1681.
- H. S. Frank and M. W. Evans, *J. Phys. Chem.*, 1945, **13**, 507.
- J. L. Kavanau, *Water and Solute-Water Interactions*, Holden-Day, New York, 1964.
- C. Tandford, *The Hydrophobic Effect*, 2nd Ed., Wiley-Interscience, New York, 1980.
- G. S. Hartley, *Quart. Revs.*, 1948, **2**, 152.
- N. Muller and R. H. Birkhahn, *J. Phys. Chem.*, 1967, **71**, 957.
- J. Clifford, *Trans. Faraday Soc.*, 1965, **61**, 1276.
- F. M. Menger, J. M. Jerkunica and J. C. Johnston, *J. Am. Chem. Soc.*, 1978, **100**, 4676.
- F. M. Menger, H. Yoshinaga, K. S. Venkatesubban and A. R. Das, *J. Org. Chem.*, 1981, **46**, 415.
- M. A. J. Rodgers, *Chem. Phys. Lett.*, 1981, **78**, 509.
- Idem*, *J. Phys. Chem.*, 1981, **85**, 3372.
- P. Fromjertz, *Chem. Phys. Lett.*, 1981, **77**, 460.
- F. M. Menger and D. W. Doll, *J. Am. Chem. Soc.*, 1984, **106**, 1109.
- K. A. Dill, D. E. Koppel, R. S. Cantor, J. D. Dill, D. Bendedouch and S. H. Chen, *Nature*, 1984, **309**, 42.
- K. A. Dill and P. J. Flory, *Proc. Natl. Acad. Sci. U.S.A.*, 1980, **77**, 3115; 1981, **78**, 676.
- F. M. Menger, *Nature*, 1985, **313**, 603.
- B. Cabane, *ibid.*, 1985, **314**, 385.
- K. M. Kale, E. L. Cussier and D. F. Evans, *J. Phys. Chem.*, 1980, **84**, 593.
- H. Sato, M. Kawasaki and K. Kasatani, *ibid.*, 1983, **87**, 3759.
- M. Abe, M. Ohsato, N. Suzuki and K. Ogino, *Bull. Chem. Soc. Japan*, 1984, **57**, 831.
- M. L. Corrin and W. D. Harkins, *J. Am. Chem. Soc.*, 1974, **96**, 679.
- P. Mukerjee and K. J. Mysels, *ibid.*, 1955, **77**, 2937.
- de E. Vendittis, G. Palumbo, G. Parlato and V. Bocchini, *Anal. Biochem.*, 1981, **115**, 278.
- M. Rujimethabahas and P. Wilairat, *J. Chem. Educ.*, 1979, **56**, 342.
- S. B. Savvin, R. K. Chernova and S. N. Shtykov, *Zh. Analit. Khim.*, 1978, **33**, 865.
- E. Colichman, *J. Am. Chem. Soc.*, 1951, **73**, 3385.
- V. Svodoba and V. Chromý, *Talanta*, 1965, **12**, 431.
- J. Rosendorfova and L. Čermáková, *ibid.*, 1980, **27**, 705.
- M. J. Minch and S. Sadiq-Shah, *J. Org. Chem.*, 1979, **44**, 3253.
- M. E. Díaz García, E. Blanco González and A. Sanz-Medel, *Microchem. J.*, 1984, **30**, 211.
- P. Mukerjee and A. K. Ghosh, *J. Am. Chem. Soc.*, 1970, **92**, 6403.
- B. H. Robinson, A. Löffler and G. Schwarz, *J. Chem. Soc. Faraday Trans. 1*, 1973, **69**, 56.
- E. H. Braswell, *J. Phys. Chem.*, 1984, **88**, 3653.
- R. L. Reeves, M. S. Maggio and S. A. Harkaway, *ibid.*, 1979, **83**, 2359.
- K. M. Kali, E. L. Cussler and D. F. Evans, *ibid.*, 1980, **84**, 593.
- M. E. Díaz García and A. Sanz-Medel, unpublished results.
- Idem*, *Talanta*, 1985, **32**, 189.
- A. Sanz-Medel, C. Cámara Rica and J. A. Pérez Bustamante, *Anal. Chem.*, 1980, **52**, 1035.
- E. Blanco González, M. E. Díaz García and A. Sanz-Medel, submitted for publication to *Quim. Anal.*
- J. I. García Alonso and A. Sanz-Medel, unpublished results.
- W. V. Malik and S. P. Verma, *J. Phys. Chem.*, 1966, **70**, 26.

68. W. V. Malik and R. Haque, *J. Am. Chem. Soc.*, 1963, **67**, 2082.
69. W. V. Malik and O. P. Jhamb, *J. Electroanal. Chem.*, 1970, **27**, 151.
70. S. N. Guha, P. N. Moorthy and K. N. Rao, *Proc. Indian Acad. Sci.*, 1982, **91**, 73.
71. R. R. Hautala, N. E. Schore and J. N. Turro, *J. Am. Chem. Soc.*, 1973, **95**, 5508.
72. S. P. Moulik, S. Ghosh and A. R. Das, *Colloid Polym. Sci.*, 1979, **257**, 645.
73. V. Buresová, L. Kubáň and L. Sommer, *Collection Czech. Chem. Commun.*, 1981, **46**, 1090.
74. V. Skarydová and L. Čermáková, *ibid.*, 1982, **47**, 776.
75. S. B. Savvin, I. N. Marov, R. K. Chernova, S. N. Shtykov and A. B. Sokolov, *Zh. Analit. Khim.*, 1981, **36**, 850.
76. C. A. Bunton, M. J. Minch, J. Hidalgo and L. Sepúlveda, *J. Am. Chem. Soc.*, 1973, **95**, 3262.
77. C. A. Bunton and M. J. Minch, *J. Phys. Chem.*, 1974, **78**, 1490.
78. M. S. Tute, *Adv. Drug Res.*, 1979, **6**.
79. B. W. Bailey, J. E. Chester, R. M. Dagnall and T. S. West, *Talanta*, 1968, **15**, 1359.
80. R. K. Chernova, L. N. Kharlamova, V. V. Belousova, E. G. Kulapina and E. G. Iumina, *Zh. Analit. Khim.*, 1978, **33**, 858.
81. S. B. Savvin, R. K. Chernova, V. V. Belousova, L. K. Sukhova and S. N. Shtykov, *ibid.*, 1978, **33**, 1473.
82. G. J. Yakatan and S. G. Schulman, *J. Phys. Chem.*, 1972, **76**, 508.
83. A. L. Underwood, *Anal. Chim. Acta*, 1982, **140**, 89.
84. H. Hoshino, T. Saitoh, H. Taketomi and T. Yotsuyanagi, *ibid.*, 1983, **147**, 339.
85. M. Montal and C. Gitler, *Bioenergetics*, 1973, **4**, 363.
86. M. S. Fernández and P. Fromjertz, *J. Phys. Chem.*, 1977, **81**, 1755.
87. N. Funasaki, *ibid.*, 1979, **83**, 1998.
88. C. F. Hiskey and T. A. Downey, *ibid.*, 1954, **58**, 835.
89. M. T. A. Behme and E. H. Cordes, *J. Am. Chem. Soc.*, 1965, **87**, 260.
90. K. S. Birdi, H. N. Singh and S. V. Dolsager, *J. Phys. Chem.*, 1979, **83**, 2733.
91. M. J. Minch, M. Giaccio and R. Wolff, *J. Am. Chem. Soc.*, 1975, **97**, 3766.
92. H-C. Chiang and A. Lukton, *J. Phys. Chem.*, 1975, **79**, 1935.
93. D. M. Stevenson, D. G. Duff and D. J. Kirkwood, *J. Soc. Dyers Colour.*, 1981, **97**, 13.
94. W. Biedermann and A. Datyner, *J. Colloid Interface Sci.*, 1981, **82**, 276.
95. R. C. Kapoor and V. N. Mishra, *J. Indian Chem. Soc.*, 1976, **53**, 965.
96. H. Sato, M. Kawasaki, Y. Kasatani, N. Kusumoto, N. Nakashima and K. Yoshihara, *Chem. Lett.*, 1980, 1529.
97. R. Humphry-Baker, M. Grätzel and R. Steiger, *J. Am. Chem. Soc.*, 1980, **102**, 847.
98. T. Wolff, *Ber. Bunsenges. Phys. Chem.*, 1981, **85**, 145.
99. C. Tandford, *J. Phys. Chem.*, 1974, **78**, 2469.
100. J. W. Larsen and L. J. Magid, *J. Am. Chem. Soc.*, 1974, **96**, 5774.
101. J. N. Phillips and K. J. Mysels, *J. Phys. Chem.*, 1955, **59**, 325.
102. M. J. Schick, *ibid.*, 1964, **68**, 3585.
103. K. W. Hermann, *ibid.*, 1962, **66**, 295.
104. J. Steigman and N. Shane, *ibid.*, 1965, **69**, 968.
105. S. Hayashi and S. Ikeda, *ibid.*, 1980, **84**, 744.
106. G. Porte, J. Appell and Y. Poggi, *ibid.*, 1980, **84**, 3105.
107. A. Ray and G. Nemethy, *J. Am. Chem. Soc.*, 1971, **93**, 6787.
108. A. K. Ghosh and P. Mukerjee, *ibid.*, 1970, **92**, 6408.
109. Y. Miyashita and S. Hayane, *J. Colloid Interface Sci.*, 1982, **86**, 344.
110. W. D. Harkins, R. W. Mattoon and R. Mittelman, *J. Chem. Phys.*, 1947, **15**, 763.
111. R. Zana, S. Yiv, C. Strazielle and P. Lianos, *J. Colloid Interface Sci.*, 1981, **80**, 208.
112. M. F. Emerson and A. Holtzer, *J. Phys. Chem.*, 1967, **71**, 3320.
113. E. W. Anacker and A. L. Underwood, *ibid.*, 1981, **85**, 2436.
114. M. Abu-Hamdiyyah and L. Al-Monsour, *ibid.*, 1979, **83**, 2236.
115. M. Shinitzky, A. C. Dianoux, C. Gitler and G. Weber, *Biochemistry*, 1971, **10**, 2106.
116. J. N. Turro and Y. Tanimoto, *Photochem. Photobiol.*, 1981, **34**, 157.
117. P. Lianos, M-L. Viriot and R. Zana, *J. Phys. Chem.*, 1984, **88**, 1098.
118. E. Aniansson, S. Wall, M. Almgren, H. Hoffmann, I. Kielman, W. Ullbricht, R. Zana, J. Lang and C. Tondre, *ibid.*, 1976, **80**, 905.
119. K. S. Rosenthal and F. Koussali, *Anal. Chem.*, 1983, **55**, 1115.
120. J. H. Fendler, *Acc. Chem. Res.*, 1976, **9**, 153.
121. S. Muto and K. Meguro, *Bull. Chem. Soc. Japan*, 1973, **46**, 1316.
122. C. J. O'Connor, T. D. Lomax and R. E. Ramage, *Adv. Colloid Interface Sci.*, 1984, **20**, 21.
123. K. V. Krishnamurty and G. M. Harris, *J. Phys. Chem.*, 1960, **64**, 346.
124. T. Masui, F. Watanabe and A. Yamagishi, *ibid.*, 1977, **81**, 494.
125. *Idem*, *ibid.*, 1980, **84**, 34.
126. J. H. Fendler, *Acc. Chem. Res.*, 1980, **13**, 7.
127. *Idem*, *Chem. Brit.*, 1984, 1098.
128. J. H. Fendler and P. Tundo, *Acc. Chem. Res.*, 1984, **17**, 3.
129. J. H. Fendler and A. Romero, *Life Sci.*, 1976, **18**, 1453.
130. N. Nakashima, H. Fukushima and T. Kunitake, *J. Chem. Soc., Chem. Commun.*, 1982, 707.
131. N. Nakashima and T. Kunitake, *J. Am. Chem. Soc.*, 1982, **104**, 4261.
132. J. T. D'Agostino, *ibid.*, 1972, **94**, 6445.
133. K. Kurihara, Y. Toyoshima and M. Sukigara, *J. Phys. Chem.*, 1977, **81**, 1833.
134. A. Warshel, *J. Am. Chem. Soc.*, 1979, **101**, 744.
135. K. Yamaoka, M. Takatsuki, K. Yaguchi and M. Miura, *Bull. Chem. Soc. Japan*, 1974, **47**, 611.
136. W. H. J. Stork, P. L. de Hasseth, W. B. Schippers, C. M. Kormeling and M. Mandel, *J. Phys. Chem.*, 1973, **77**, 1772.
137. K. Yamaoka, M. Takatsuki and M. Miura, *Bull. Chem. Soc. Japan*, 1975, **48**, 2739.
138. M. K. Pal and M. Schubert, *J. Phys. Chem.*, 1961, **65**, 872.
139. G. R. Seely and R. R. Knotts, *Carbohydr. Polym.*, 1983, **3**, 109.
140. T. Okubo and N. Ise, *J. Am. Chem. Soc.*, 1973, **95**, 2293.
141. G. R. Jones, R. B. Cundall, D. Murray and D. A. Duddell, *J. Chem. Soc. Faraday Trans. II*, 1984, **80**, 1201.
142. E. Baumgartner, R. Fernández-Prini and D. Turyn, *J. Chem. Soc. Faraday Trans. I*, 1974, **70**, 1518.
143. O. Ortono, V. Vitagliano, R. Sartorio and L. Constantino, *J. Phys. Chem.*, 1984, **88**, 3244.

DETERMINATION OF TRACE AMOUNTS OF MOLYBDENUM IN PLANT TISSUE BY SOLVENT EXTRACTION-ATOMIC-ABSORPTION AND DIRECT-CURRENT PLASMA EMISSION SPECTROMETRY

LAURI H. J. LAJUNEN* and AARO KUBIN

Department of Chemistry, University of Oulu, SF-90570 Oulu, Finland

(Received 3 July 1984. Revised 17 September 1985. Accepted 3 October 1985)

Summary—Methods are presented for determination of molybdenum in plant tissue by flame and graphite-furnace atomic-absorption spectrometry and direct-current argon-plasma emission spectrometry. The samples are digested in $\text{HNO}_3\text{-H}_2\text{SO}_4\text{-HClO}_4$ mixture, and Mo is separated and concentrated by chelation and extraction. Three organic solvents (methyl isobutyl ketone, di-isobutyl ketone and isoamyl alcohol) and two ligands (8-hydroxyquinoline and toluene-3,4-dithiol) were studied. The procedure were tested on pine needle and birch leaf samples.

The determination of molybdenum in botanical material and natural water has received considerable attention.¹⁻⁵ There are several papers on the use of spectrometric methods. The most commonly used colorimetric method for molybdenum at trace level is based on formation of the coloured thiocyanato complex, $\text{MoO}(\text{SCN})_2^{2-}$, and its extraction into an organic phase.⁶⁻¹² The detection limit (about 0.5 mg/l. in aqueous solutions) attained by flame atomic-absorption spectrometry is not low enough for determination of molybdenum in plant materials (less than 1–10 $\mu\text{g/g}$), and several elements interfere.⁵ By means of liquid-liquid extraction molybdenum can be simultaneously concentrated and separated from most interfering cations. Atomic-absorption spectrometric methods based on the separation and preconcentration of molybdenum by extraction of its thiocyanate, 8-hydroxyquinolate, diethyldithiocarbamate, pyrrolidinedithiocarbamate and α -benzoinoximate complexes into methyl isobutyl ketone (MIBK) have been reported.¹³⁻¹⁶ Usually, methods involving stripping of the molybdenum into an aqueous phase were preferred. Many authors have reported on various aspects of the use of graphite-furnace atomic-absorption spectrometry for molybdenum determination. The method is often used in conjunction with a separation, although molybdenum can be determined directly in very complex matrices without separation or even background correction.¹⁷⁻²¹ The use of argon-plasma emission spectrometry for determination of molybdenum in mixed fertilizer has also been reported.²²

The aim of the present study was to make a comprehensive investigation of different liquid-liquid

extraction procedures, followed by flame atomic-absorption, graphite-furnace atomic-absorption and direct-current plasma atomic-emission spectrometric determination of molybdenum. The methods were applied to determination of molybdenum in birch leaves and conifer needles after solvent extraction.

EXPERIMENTAL

Reagents

All reagents and solvents were analytical-reagent grade, and distilled demineralized water was used.

A standard molybdenum solution (1000 mg/l.) was prepared by dissolving 1.500 g of MoO_3 in the minimum of 0.1M sodium hydroxide, adding some water, making slightly acidic (pH 3–4) with 0.1M hydrochloric acid and diluting to 1.0 litre with water. Working solutions were prepared from this stock solution by appropriate dilution.

8-Hydroxyquinoline solutions, 1%, in MIBK, di-isobutyl ketone (DIBK) and isoamyl alcohol were used.

Toluene-3,4-dithiol solution was prepared by adding 2 ml of ethanol to 0.3 g of zinc-dithiol complex followed by 4 ml of water and 2 g of sodium hydroxide. The solution was mixed well and diluted to 100 ml with water.

Instrumentation

A Pye Unicam SP-9 800 atomic-absorption spectrometer equipped with an SP 9 computer, an SP 9 graphite furnace (normal graphite tubes were used), a nitrous oxide-acetylene 6-cm single-slot burner head (N_2O flow-rate 6 l./min, C_2H_2 flow-rate 4 l./min), a molybdenum hollow-cathode lamp, and a deuterium lamp for background correction, were used. The line 313.3 nm was used, with 0.5 nm spectral band-pass. The absorbances due to reagent blanks (carried through all steps) were subtracted from absorbances of standards and samples to yield net absorbances.

For determining Mo as its toluene-3,4-dithiol chelate in MIBK, the following instrumental settings for the graphite-furnace atomic-absorption measurements are recommended: wavelength 313.3 nm, band-pass 0.5 nm, sample volume 15 μl , drying temperature/time 140°/30 sec, ashing temperature/time 700°/30 sec, atomization temperature/

*Author for correspondence.

time $2500^{\circ}/3.0$ sec, and cleaning temperature/time $2700^{\circ}/2.5$ sec.

A Spectra Span IIB single-channel direct-current argon-plasma emission spectrometer equipped with an HP 85 computer was used for the plasma measurements. The instrumental settings were the following: wavelength 281.615 nm, entrance slit $100 \times 300 \mu\text{m}$, exit slit $100 \times 300 \mu\text{m}$, and plasma position "0", which is the middle one of the three available measurement points in the excitation region of the d.c. plasma.

Extraction procedures

Three organic solvents, MIBK, DIBK and isoamyl alcohol, and two ligands, 8-hydroxyquinoline (oxine) and toluene-3,4-dithiol, were examined. For each extraction system, the optimum pH for extraction, linear range of calibration, sensitivity, characteristic concentration, precision, optimum ligand/metal ratio, aqueous phase/organic phase ratio, and optimum shaking time were examined. For these experiments known amounts of Mo stock solution were taken, adjusted to the desired pH values with sodium hydroxide and hydrochloric acid, and diluted to 25 ml with water. Then 5 ml of 1% oxine solution dissolved in MIBK or DIBK, or 5 ml of aqueous dithiol solution, were added, and the mixtures were shaken with 0–20 ml of one of the organic solvents for 15 min. The layers were separated and the organic phase was introduced into the flame atomic-absorption spectrometer for measurement of the Mo signal.

Sample preparation by wet digestion

A 2–4 g sample of needles or leaves (dried at 70° for 24 hr

and then ground) was weighed into a 300-ml Kjeldahl flask and 10–40 ml of a mixture of concentrated nitric, sulphuric and perchloric acids (3:1:1 v/v) were added. The mixture was left overnight and then heated at 105° for 2 hr, 160° for 3 hr and 205° for about 1 hr (after which the mixture was clear). After cooling, the contents of the flasks were transferred quantitatively into 100-ml standard flasks and diluted to volume with water; then 25-ml portions were transferred to 100-ml separatory funnels. For the flame and graphite-furnace AAS measurements Mo was extracted as its dithiol complex into MIBK, and for the DCP-AES measurements it was extracted as its dithiol complex into isoamyl alcohol as described above. The tubing for sample-introduction in the DCP-AES apparatus was not resistant to MIBK or DIBK, which was why only the isoamyl alcohol system was used.

Sample preparation by dry ashing

A dried (24 hr at 70°) and ground sample (2–4 g) was weighed into a ceramic crucible and heated at 500° for 24 hr. The ash was then dissolved in 3 ml of concentrated hydrochloric acid, by heating on a hot-plate until the solution was clear. The sample was then transferred into a 25-ml standard flask and diluted to volume with water. A corresponding amount of hydrochloric acid was added to each standard solution. Then 2 ml of dithiol solution were added to the 25 ml of sample solution and the molybdenum complex was extracted with 5 ml of organic solvent (giving approximately fivefold concentration).

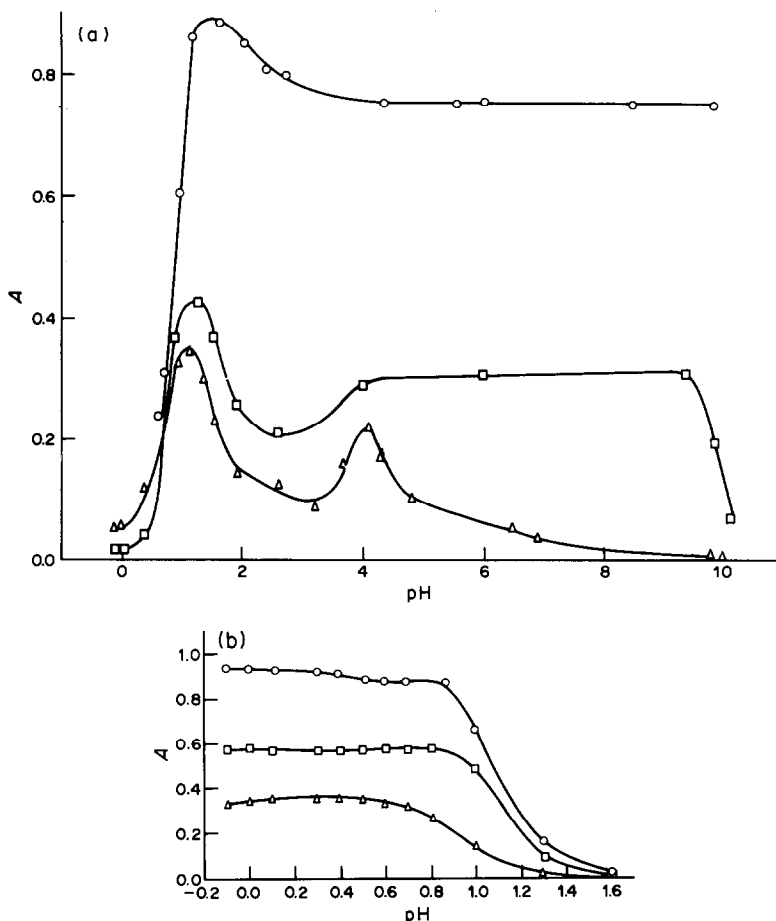


Fig. 1. Extraction of molybdenum as a function of pH. (a) the Mo-oxine equilibrium system; (b) the Mo-dithiol system: \circ MIBK; \square DIBK; \triangle isoamyl alcohol.

RESULTS AND DISCUSSION

Flame atomic-absorption spectrometry

Figure 1 shows the effect of pH on the various extraction systems studied. For both ligands (oxine and dithiol) the most useful solvent is MIBK, and the least useful is isoamyl alcohol. The oxine-MIBK extraction can be done at either pH 1.5 or 4-10. For the dithiol-MIBK system the extraction should be done in the pH range 0 ± 0.1 , or 0.6-0.8.

On the basis of the calibration curves presented in Fig. 2 the relative sensitivities and linear dynamic ranges can be evaluated. The sensitivity is greatest with MIBK as solvent and least with isoamyl alcohol. The upper limits of the linear dynamic ranges are 30, 30 and 25 mg/l. for the oxine system with MIBK, DIBK, and isoamyl alcohol as solvents, respectively,

and 30, 25 and 25 mg/l. for the corresponding dithiol systems. The oxine-isoamyl alcohol system is not recommended, because of the maximum in the calibration graph.

Table 1 gives the characteristic concentrations (M_0 concentration for 1% absorption), detection limits (background + three times its standard deviation), and relative standard deviations (five replicates for 15-mg/l. Mo). The lowest values are again obtained with the MIBK systems. The precision (RSD) for the DIBK systems is significantly poorer than that for the MIBK and isoamyl alcohol systems.

Figure 3 records the absorbances for various ligand/metal molar ratios. According to these plots, the minimum $C_L:C_{M_0}$ ratios required to give an almost constant degree of extraction of molybdenum into the different organic solvents are 7, 25 and 8 for

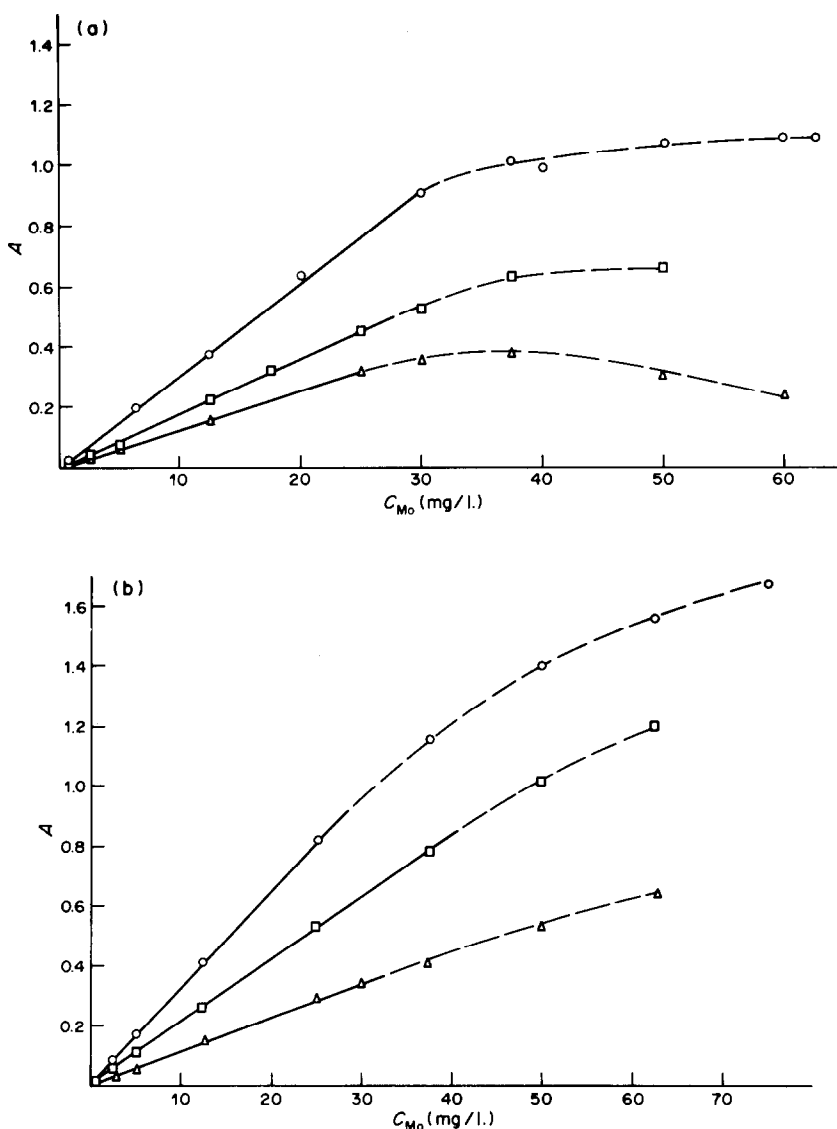


Fig. 2. Calibration curves. (a) the Mo-oxine equilibrium system; (b) the Mo-dithiol system: ○ MIBK; □ DIBK; △ isoamyl alcohol.

Table 1. Characteristic concentrations, instrumental detection limits (DL) and relative standard deviations (RSD) for five replicates in the ideal concentration region for various Mo extraction systems in determination of Mo by flame AAS

Ligand	Solvent	Characteristic concentration, mg/l.	DL, mg/l.	RSD, %
Oxine	MIBK	0.14	0.053	0.7
	DIBK	0.27	0.073	7.0
	Isoamyl alcohol	0.35	0.14	1.8
Dithiol	MIBK	0.13	0.045	0.8
	DIBK	0.21	0.074	3.9
	Isoamyl alcohol	0.37	0.15	0.7

MIBK, DIBK and isoamyl alcohol, respectively, for the oxine system, and 8, 10 and 7 for MIBK, DIBK and isoamyl alcohol for the dithiol system.

In the next step the effect of the volume ratio of the aqueous and organic phases was studied (Fig. 4). For these experiments the volume of the organic phase (V_{org}) was kept constant and the volume of the aqueous phase (V_{aq}) was varied. The amount of molybdenum present was the same in each case, and after extraction the molybdenum concentration in the organic phase should have been 10 mg/l. In the

absorbance *vs.* V_{aq}/V_{org} plots, maxima were obtained for the three dithiol systems, whereas for the oxine systems the absorbance either increased or remained constant with increasing V_{aq}/V_{org} ratio. Because the aqueous phase and organic solvents were not mutually saturated before use, the phenomena presented in Fig. 4 can be interpreted in terms of the change of volume and dielectric constant in the organic phase. The solubilities of water in MIBK, DIBK and isoamyl alcohol are 2.4, 0.75 and 9.7 g/100 g, respectively, and the solubilities (g/100 g) of these solvents in water are 2.04 (MIBK), 0.04 (DIBK) and 2.85 (isoamyl alcohol). The dielectric constants decrease in the following order: MIBK > isoamyl alcohol >> DIBK. When the water content in the organic phase increases, the reciprocal value of the permittivity also increases and raises the solubility of polar compounds. According to the differences of the electronegativities between molybdenum and oxygen, nitrogen or sulphur (O 3.5, N 3.0, S 2.5), the metal-ligand bonds in the Mo-oxine complex (Mo-O and Mo-N bonds) can be assumed to be more polar than those in the Mo-dithiol complex (Mo-S bond). Thus, the solubility of Mo-oxinate should be higher than that of the Mo-dithiol complex in solvents with high dielectric constant. In the case of DIBK there would be practically no volume change as the aq/org ratio increases from 1 to 20, but

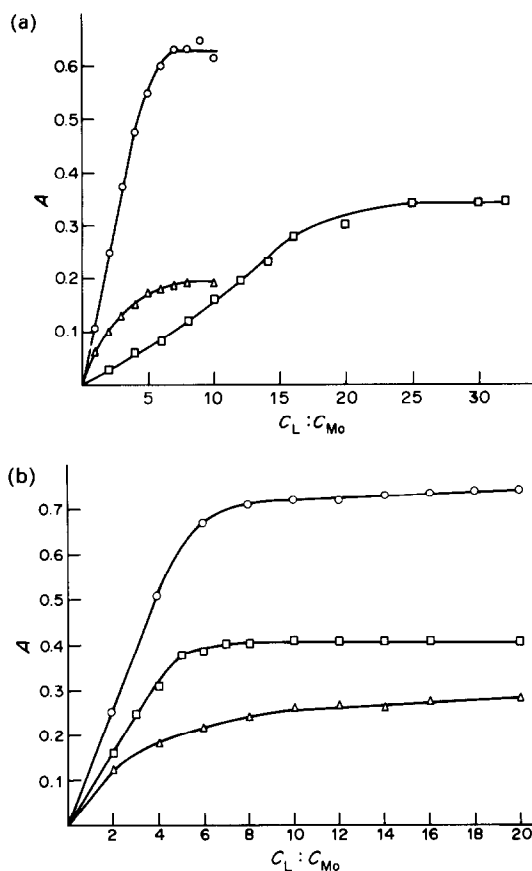


Fig. 3. The dependence of the degree of the extraction on the ligand/molybdenum molar ratio for each extraction system. (a) Mo-oxine system; (b) Mo-dithiol system: ○ MIBK; □ DIBK; △ isoamyl alcohol.

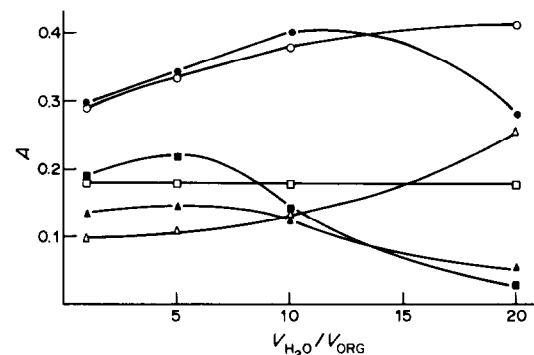


Fig. 4. The effect of the volume ratio of the aqueous and organic phases on the extraction. Open symbols, Mo-oxine system; filled symbols, Mo-dithiol system; ○/● MIBK; □/■ DIBK; △/▲ isoamyl alcohol.

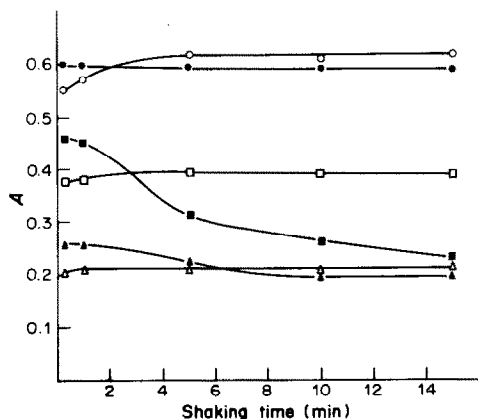


Fig. 5. The effect of shaking time on the extraction. Symbols are the same as in Fig. 4.

for both MIBK and isoamyl alcohol there would be an appreciable decrease in volume of the organic phase (about 50% for the isoamyl alcohol and 40% for the MIBK). In the case of the Mo-oxine system the increase of the absorbance with increasing V_{aq}/V_{org} ratio with MIBK and isoamyl alcohol can be attributed mainly to the volume change in the organic phase. For the Mo-dithiol system, however, the dielectric constant change with high V_{aq}/V_{org} ratios must be more important than the volume change in the organic phase.

The effect of the shaking time on the absorbance measurements is shown in Fig. 5. The volumes of the aqueous and organic phases were both 5 ml in each experiment, the molybdenum concentration of the aqueous phase before the extraction was 20 mg/l., and shaking times between 15 sec and 15 min were applied. The extraction is at its maximum and the absorbances are constant with increasing shaking time for all the dithiol systems after about 2 min. For the oxine-MIBK system the degree of extraction is the same between 15 sec and 15 min, whereas for the other two oxine systems the absorbance decreases

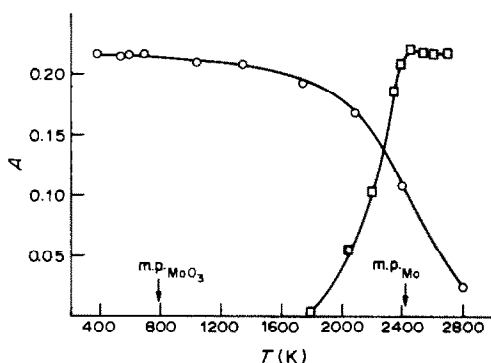


Fig. 6. The ashing/atomization plot for the Mo-dithiol-MIBK system: \circ the ashing temperature is varied and the atomization temperature kept constant (2600°); \square the atomization temperature is varied and the ashing temperature kept constant (700°).

Table 2. Determination of molybdenum ($\mu\text{g/g}$) in pine needles and birch leaves by different sample preparation (A = wet digestion, B = dry ashing) and detection methods

Sample	Flame AAS		Graphite furnace AAS	DCP-AES	
	A	B	B	A	B
Pine needles	< 0.2	< 0.2	0.16	0.22	0.18
Birch leaves	< 0.2	< 0.2	0.22	—	0.23

with increasing shaking time, especially for the oxine-DIBK system.

Graphite-furnace atomization

According to the results of the extraction experiments described above, the most suitable extraction system for the determination of molybdenum is the dithiol-MIBK system, which was therefore selected for further study by graphite-furnace atomic-absorption. Figure 6 shows the ashing/atomization plots for the molybdenum-dithiol-MIBK system, and the optimum ashing and atomization temperatures are seen to be 700° and 2600° , respectively. The calibration graph is linear up to about 0.25 mg/l. The precision obtained by peak-area measurement was found to be better than that by peak-height measurement, the RSD varying between 1.1 and 3.7%, and 3.7 and 7.3%, respectively.

DCP emission spectrometry

Because the usual aspiration tubing cannot withstand MIBK and DIBK solutions, the organic phase selected for the plasma experiments was isoamyl alcohol. The emission lines 202.030, 281.615 and 379.825 nm can be used for the determination of molybdenum in aqueous solutions. Owing to the large background noise caused by isoamyl alcohol, the lines at about 202 and 380 nm are not suitable for the determination of molybdenum in isoamyl alcohol. Thus, the line at 281 nm used in the plasma measurements. The calibration graphs were linear up to 20 and 15 mg/l. and the detection limits were 0.15 and 0.5 mg/l. for the oxine and dithiol systems, respectively. The slope of the dithiol calibration graph was about 1.3 times that of the oxine graph.

Testing the methods

The results obtained by the various methods are collected in Table 2. Owing to the low molybdenum content in plant samples, it is not possible to determine it by flame atomic-absorption spectrometry. However, the results obtained by the graphite furnace and DCP-AES methods are in fair agreement with each other, but the concentrations in the samples tested were near the detection limit of the plasma method.

REFERENCES

1. S. U. Khan, R. O. Cloutier and M. Hidiroglou, *J. Assoc. Off. Anal. Chem.*, 1979, **62**, 1062.

2. D. O. Wilson, *Commun. Soil. Sci. Plant Anal.*, 1979, **10**, 1319.
3. A. B. Carel and J. W. Wimberley, *Anal. Lett.*, 1982, **15**, 493.
4. Y. K. Chau and K. Lum-Shue-Chan, *Anal. Chim. Acta*, 1969, **48**, 205.
5. M. Ternero and I. Gracia, *Analyst*, 1983, **108**, 310.
6. P. R. Haddad, P. W. Alexander and L. E. Smythe, *Talanta*, 1975, **22**, 61.
7. K. S. Patel, H. Khatri and R. K. Mishra, *Anal. Chem.*, 1983, **55**, 1823.
8. B. Tamhina, M. J. Herak and V. Jagodic, *Anal. Chim. Acta*, 1975, **76**, 417.
9. T. J. Koralewski and G. A. Parker, *ibid.*, 1980, **113**, 389.
10. K. S. Patel, R. M. Verma and R. K. Mishra, *Anal. Chem.*, 1982, **54**, 52.
11. M. Mitra and B. K. Mitra, *Talanta*, 1977, **24**, 698.
12. R. R. Rao and M. Khopkar, *Analyst*, 1983, **108**, 346.
13. C. H. Kim, P. N. Alexander and L. E. Smythe, *Talanta*, 1976, **23**, 229.
14. L. R. P. Butler and P. M. Mathews, *Anal. Chim. Acta*, 1966, **36**, 319.
15. J. R. Castillo, M. A. Bellarra and J. Aznarez, *At. Spectrosc.*, 1982, **3**, 58.
16. C. A. Helsby, *Talanta*, 1973, **20**, 779.
17. V. B. Scheizer, *At. Abs. Newsl.*, 1975, **14**, 137.
18. J. Sneddon, J. M. Ottaway and W. B. Rowston, *Analyst*, 1978, **103**, 776.
19. T. Nakahara and C. I. Chakrabarti, *Anal. Chim. Acta*, 1979, **104**, 99.
20. M. M. Barbooti and F. Jasim, *Talanta*, 1981, **28**, 359.
21. D. R. Neuman and F. F. Munshower, *Anal. Chim. Acta*, 1981, **123**, 325.
22. T. C. Woodis, Jr., J. H. Holmes, Jr., J. D. Ardis and F. J. Johnson, *J. Assoc. Off. Anal. Chem.*, 1980, **63**, 1245.

SHORT COMMUNICATIONS

SIMPLE SAMPLE-CELL POSITIONER FOR REDUCING THE IMPRECISION DUE TO PLACEMENT OF TEST-TUBE TYPE SAMPLE CELLS

J. D. INGLE, JR

Department of Chemistry, Oregon State University, Corvallis, Oregon 97331, U.S.A.

(Received 2 October 1985. Accepted 15 November 1985)

Summary—The construction and evaluation of a sample-cell positioner for test-tube type cells in simple single-beam spectrophotometers are described. Use of the sample-cell positioner reduces the uncertainty due to cell-positioning, by about an order of magnitude.

Noise, read-out resolution, and sample-cell positioning can affect the measurement precision of solution spectrophotometric measurements, as shown in recent studies.¹⁻⁴ These studies provide a more fundamental understanding of the measurement process and a framework for optimization of experimental conditions, pinpointing the dominant sources of imprecision in absorbance measurements, and indicating the ways in which instrumental improvements can be made. The importance of reproducibility in sample-cell positioning is not always fully appreciated, and the effect of sample-cell position on precision is not even mentioned in many recent textbooks. The usual specification of spectrophotometer baseline noise is based on repeated measurement with the cell left in position and therefore does not account for random errors due to changes in sample-cell positioning in analytical practice.

This imprecision can be characterized by a sample-cell positioning flicker-factor ξ_2 ,^{3,4} which is the contribution of sample-cell positioning to the overall relative standard deviation (RSD) of the reference (100% transmission signal). It is calculated as the square root of the difference between the square of the RSD of the reference signal when the sample-cell is moved between each measurement and the square of the RSD of the reference signal obtained by repetitive measurements with the cell left in position. A value of 0.1% for ξ_2 is equivalent to a standard deviation (σ_A) of 4.3×10^4 for absorbances near zero (e.g., at the detection limit).

Cell-transmission flicker noise is caused by spatial inhomogeneities in the transmission characteristics of the sample cell. Every time the sample cell is repositioned in the cell holder, the beam of light may pass through a slightly different part of the cell. Spatial differences in the refractive index, absorptivity, thickness, and surface flatness of the cell walls, or microscopic bubbles, can cause scattering, absorp-

tion or reflective losses and hence the cell transmission can vary according to the position where the light-beam strikes the cell walls. These spatial inhomogeneities in the optical properties of the cell wall can also cause the image of the light-beam on the photocathode of the detector to be changed or displaced by slight differences in sample-cell position. This can cause variation in the measured signal because the radiance-response or quantum efficiency of the cathode varies spatially across its surface. The condition of the cell wall surfaces is also critical, because scratches, dust particles, or lint from cleaning can result in the transmission varying with cell position.

Clearly ξ_2 depends upon the type, age, and quality of the sample cell, the type of sample holder, and the spectrophotometer, the position and width of the incident beam, the type and characteristics of the reference solution (e.g., its refractive index) and the technique of the operator. Imprecision due to cell positioning is automatically practically eliminated by use of dual-wavelength spectrophotometers.⁵

Two basic types of sample cell are used for most spectrophotometric measurements; they are rectangular and circular in cross-section. Generally ξ_2 is lower for rectangular cells because a higher quality of glass or quartz is used, the cell walls are flat instead of curved, and positioning is less subject to variation because rotation is strongly restricted by the cell-carrier, in contrast to the case for cells with circular cross-section. With square cells, ξ_2 has been found to be 0.04% with a Cary 118C⁶ and 0.7% with a McPherson EU-701A spectrophotometer.⁵ With circular-type sample cells, ξ_2 was found to be 0.3% with a Turner 330 and 0.7% with a Spectronic 20 instrument.⁴

This paper is concerned with the construction and evaluation of a simple sample-cell positioner for test-tube shaped sample cells used in simple single-beam spectrophotometers. It was previously shown

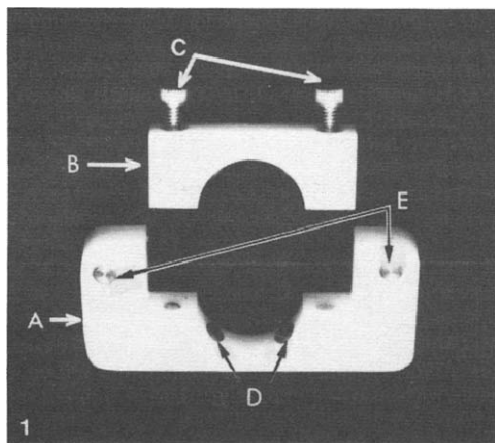


Fig. 1. Photograph of sample-cell positioner. A, Section A. B, Section B. C, Allen screws. D, Rubber pads. E, Alignment pins.

that the measurement precision of this type of spectrophotometer could be greatly improved merely by adding a high-resolution digital read-out so that measurements were limited by noise and not by read-out resolution.⁴ With high-resolution read-out, cell-transmission flicker noise limits the precision at low absorbances. The sample-cell positioner significantly reduces the magnitude of cell-transmission flicker noise, simplifies cell positioning, and reduces the operator skill required.

EXPERIMENTAL

A Turner 330 spectrophotometer (G. K. Turner Associates, Palo Alto, CA) was used for all measurements. A Heath Model EU-805 Universal Digital Instrument (Heath Co., Benton Harbor, MI) in the digital voltmeter (DVM) mode was connected to the 1-V output terminals of the spectrophotometer to form the high-resolution read-out system. The DVM was used on the 1-V range with a 1-sec integration time (10 μ V resolution). All measurements were made at 420 nm with the room lights out to minimize stray light problems.

The sample-cell positioner is shown in Figs. 1 and 2. It consists of two sections (A and B in Fig. 1), made out of 3/16-in. thick natural Delrin. The sample cell is inserted into the hole (0.52-in. diameter) formed by sections A and B, and then B is secured to A with two 2-56 Allen screws (Fig. 2). Four 3/32-in. diameter rubber pads (made from buna-N O-ring rope) (Fig. 1) are inserted into holes around the inside circumference of the positioner (two in each section) to extend about 0.02 in. beyond the Delrin surface. These pads prevent breakage of the cell when the securing screws are tightened. Two 1/8-in. brass pins (Fig. 1) are inserted through holes drilled in section A. Two holes are drilled in the plastic sample-cell holder of the spectrometer to accept these pins (Fig. 2) and to provide reproducible positioning. The sample-cell positioner is secured so that its top surface is about 3 mm below the top of the cell, to ensure that the vertical position of the cell is determined by the cell positioner and not by the metal strip at the bottom of the cell holder.

RESULTS AND DISCUSSION

The precision of measurements made with use of the sample-cell positioner was compared with the precision obtained without it. The sample cell was

filled with distilled water for all measurements and carefully wiped with lens tissue. The reference voltage varies by typically $\pm 5\%$ on rotation or vertical movement of the sample cell, which indicates the importance of cell positioning. First, 6 sets of 6 measurements were made without use of the cell positioner, the sample cell being totally removed from the cell holder and then replaced between each measurement. About 5 sec were spent in lining up the vertical white line on the cell with the raised plastic mark on the cell holder in the conventional manner. Next, 6 sets of 6 measurements were made with the same cell secured in the sample-cell positioner and the cell positioner assembly totally removed between measurements. When the assembly was inserted into the cell holder, two fingers were used on section B of the positioner to push the positioner firmly down and back. The average RSD values of the 6 sets of measurements with and without use of the sample-cell positioner were calculated.

The average value of ξ_2 or the RSD of the reference voltage was 0.5% without use of the cell positioner and 0.03% with it. The value of ξ_2 depends upon the particular spectrophotometer, cell holder, and sample cell. The experiment was repeated with a different but equivalent combination of spectrophotometer, sample cell, cell holder, and cell positioner and ξ_2 was found to be 0.2% and 0.03% without and with the



Fig. 2. Photograph of sample-cell positioner secured to sample cell and placed in sample-cell holder.

positioner, respectively. Thus the cell positioner improves the measurement precision by a factor of 7–17 by ensuring that the cell is more reproducibly positioned from run to run. The RSD of the reference signal when the cell is not moved at all is <0.01%, so cell-transmission flicker noise limits the precision even when the positioner is used.

The cell positioner provides other advantages. It is faster to use and requires less effort by the operator in cell-positioning and hence reduces operator error. If several sample cells are to be used in an analysis scheme, a sample-cell positioner for each would allow the cells to be calibrated against each other and for the cell corrections to remain essentially constant. For simple inexpensive spectrophotometers with analogue meter readout, the addition of the cell positioner, plus a $3\frac{1}{2}$ digit voltmeter (available for less than \$100), would allow measurements at low absorbances to be made with an RSD of 0.1% provided

other sources of random error were not the limiting factor.

Acknowledgements—I appreciate partial support of this work by the National Science Foundation (Grant CHE-8401784). I wish to thank John Archibald for construction of the device.

REFERENCES

1. J. D. Ingle, Jr. and S. R. Crouch, *Anal. Chem.*, 1972, **44**, 1375.
2. J. D. Ingle, Jr., *ibid.*, 1973, **45**, 861.
3. L. D. Rothman, S. R. Crouch and J. D. Ingle, Jr., *ibid.*, 1975, **47**, 1226.
4. J. D. Ingle, Jr., *Anal. Chim. Acta*, 1977, **88**, 131.
5. K. L. Ratzlaff and H. bin Darus, *Anal. Chem.*, 1979, **51**, 256.
6. J. D. Ingle, Jr., *Similarities and Differences in Precision Characteristics of Molecular Absorption and Atomic Absorption Measurements*, Fisher Award Symposium, 1976 National ACS Meeting, New York.

DEVELOPMENT AND APPLICATION OF ORGANIC REAGENTS FOR ANALYSIS—VII*

EXTRACTION AND FLUORIMETRIC DETERMINATION OF PERCHLORATE IONS WITH 2,6-DI-*p*-TOLYL-4-PHENYLPYRYLIUM CHLORIDE

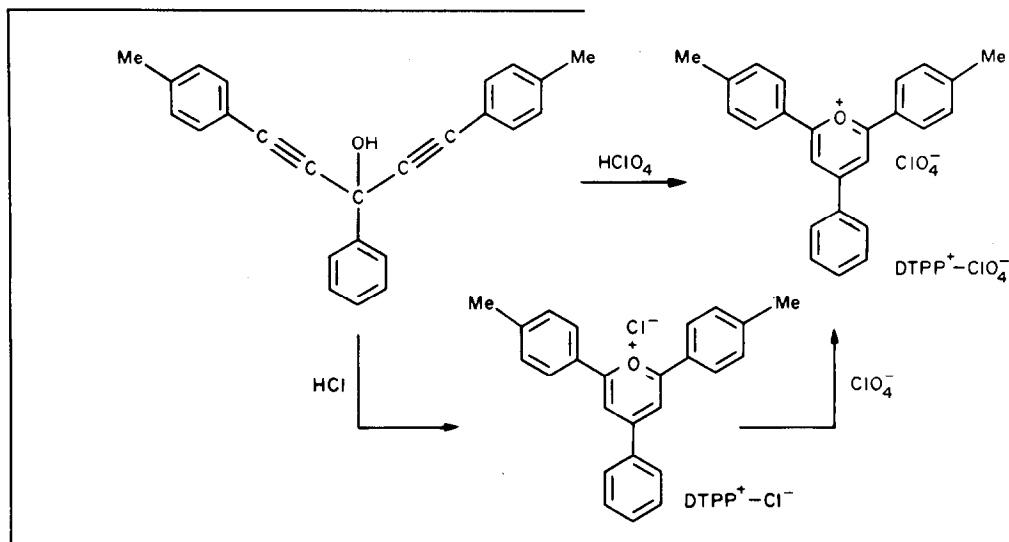
KENICHIRO NAKASHIMA, SHOKO TOMIYOSHI, SHIN'ICHI NAKATSUJI and SHUZO AKIYAMA
Faculty of Pharmaceutical Sciences, Nagasaki University, 1-14, Bunkyo-machi, Nagasaki 852, Japan

(Received 15 August 1985. Revised 5 November 1985. Accepted 15 November 1985)

Summary—An extraction-fluorimetric method for the determination of micro quantities of perchlorate ions, based on their extraction into chlorobenzene with 2,6-di-*p*-tolyl-4-phenylpyrylium chloride (DTPP⁺-Cl⁻) has been developed. DTPP⁺-Cl⁻, a newly synthesized reagent, reacts with perchlorate ions to form 1:1 ion-pairs, which can be extracted into chlorobenzene. The ion-pair (DTPP⁺-ClO₄⁻) has very strong yellowish-green fluorescence in chlorobenzene, with an emission maximum at 376 nm. The relationship between perchlorate ion concentration and relative fluorescence intensity is linear over the range 0.01–1.0 ppm. Several inorganic perchlorates have been determined satisfactorily by the method.

Several methods based on ion-pair extraction with dyes have been reported for the spectrophotometric determination of perchlorate ions.¹⁻⁵ Recently, we have developed the ethyne analogues of triphenylmethane dyes and demonstrated that the introduction of an acetylene bond into a triphenylmethane

fluorogenic reagent, 2,6-di-*p*-tolyl-4-phenylpyrylium chloride (DTPP⁺-Cl⁻), which was developed from a study of the synthesis of pyrylium salts from substituted 1,4-pentadiyn-3-ols with perchloric acid (Scheme 1),⁸ and on an extraction-fluorimetric determination of perchlorate ion with this reagent.



dye system causes a large red shift in the longest wavelength absorption maximum.⁶ One of these compounds, derived from Malachite Green, *viz.* 1,1-bis(*p*-dimethylaminophenyl)-3-phenyl-2-propynyl chloride, has been successfully used for the determination of micro amounts of perchlorate ion.⁷ In this paper, we wish to report on a very sensitive

RESULTS AND DISCUSSION

Fluorescence spectra and solvents for extraction

The extraction of the ion-pair (DTPP perchlorate) into chloroform, chlorobenzene, dichloromethane, dichloroethane, benzene and toluene was examined. Dichloromethane and dichloroethane were found not to be suitable solvents because DTPP⁺-Cl⁻ was also extracted. Figure 1 shows the fluorescence spectra of DTPP perchlorate in chlorobenzene, which is the

*Part VI: S. Akiyama, H. Akimoto, S. Nakatsuji and K. Nakashima, *Bull. Chem. Soc. Japan*, 1985, **58**, 2192.

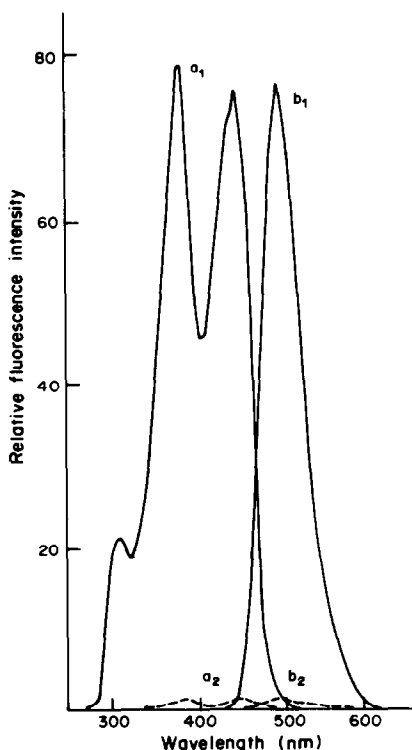


Fig. 1. Excitation and emission spectra of $\text{DTPP}^+\text{-ClO}_4^-$ in chlorobenzene: a, excitation spectra; b, emission spectra; a₁ and b₁: $\text{DTPP}^+\text{-ClO}_4^-$; a₂ and b₂: reagent blank.

preferred solvent because it gives a smaller reagent blank than chloroform does. The excitation maxima of the ion-pair are at 310, 376 and 455 nm, and the emission maximum is at 495 nm. The best wavelength to use for excitation is 376 nm.

Effect of pH on extraction

The relative fluorescence intensity (RFI) is constant for extraction of a fixed amount of perchlorate in the pH range 0.2–1.8, into chlorobenzene (Fig. 2), and pH 1.0 is chosen as optimum.

Effect of reagent concentration, reaction time, mixing time and stability of the ion-pair

It was found that at least a tenfold molar excess of

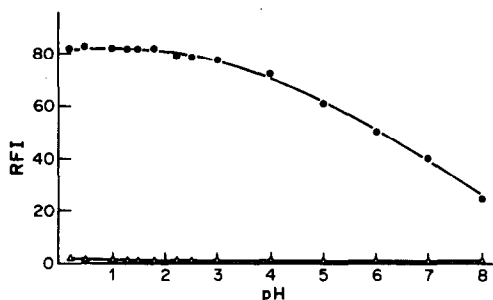


Fig. 2. Effect of pH on the extraction of the ion-pair into chlorobenzene. —●—: $5 \times 10^{-3} \text{ M NaClO}_4$; —△—: reagent blank.

Table 1. Tolerance limits ($< \pm 5\%$ error) of diverse ions in the determination of $5 \times 10^{-6} \text{ M}$ perchlorate

Tolerance limit, M	Ion added
1×10^{-3}	NO_2^- , NO_3^- , BO_3^-
5×10^{-4}	Br^- , CH_3CO_2^- , $\text{C}_2\text{O}_4^{2-}$, PO_4^{3-}
2.5×10^{-4}	BrO_3^- , IO_3^- , CrO_4^{2-}
5×10^{-5}	Cl^- , ClO_3^-
1×10^{-5}	SCN^-
$< 5 \times 10^{-6}$	I^- , IO_4^- , MnO_4^-

the reagent is necessary for complete association with the perchlorate ion. The reaction is complete within 3 min at room temperature. Thus, a reaction time of 5 min was selected as the optimum. The minimum vortex-mixing time for complete extraction of the ion-pair with chlorobenzene was found to be 10 sec at room temperature. The RFI at 495 nm was constant for 24 hr when the solution was kept in the dark, but for only *ca.* 20 min if it was kept in room lighting.

Composition of the ion-pair

The composition of the ion-pair was studied by the continuous variations method and found to be 1:1 ($\text{DTPP}^+\text{-ClO}_4^-$). The excitation and emission spectra of the ion-pair were in accord with those of DTPP perchlorate prepared by the reaction of 1,5-bis-*p*-tolyl-3-phenyl-1,4-pentadiyn-3-ol with perchloric acid.⁸

Calibration graph

The calibration graph obtained by the procedure showed good linearity over the perchlorate concentration range 0.01–1 ppm in the final solution. Reproducibility experiments level showed coefficients of variation of 2.3 and 1.6% for 10 results at the 0.05 and 0.5 ppm perchlorate levels, respectively.

Effect of diverse ions

For the determination of 0.5 ppm ($5 \times 10^{-6} \text{ M}$) perchlorate by the method, various anions can be tolerated at the levels given in Table 1, the tolerance limit being taken as the amount required to cause an error of less than $\pm 5\%$ in the relative fluorescence intensity. A small amount of permanganate gives a fairly large negative error, presumably because of its oxidizing action. Otherwise only iodide and thiocyanate interfere. There is no interference from

Table 2. Determination of perchlorates*

Sample	Content, † %	Coefficient of variation, %
HClO_4 (60%)	90.4	3.1
NaClO_4	100.5	2.3
LiClO_4	99.6	2.2
NH_4ClO_4	102.2	3.1

*By the standard addition method with KClO_4 as standard.

†Expressed as the ratio of perchlorate found to perchlorate expected to be present, mean of five results.

cations in molar ratios to perchlorate up to 500 or more.

Analysis of inorganic perchlorates

As an example of the applicability of the method proposed, representative inorganic perchlorates were analysed. Table 2 shows the results obtained from the standard addition graphs, which all had parallel slopes. These results are considered to be satisfactory.

This method is quite simple, rapid and more sensitive than the conventional methods.^{1-5,7}

EXPERIMENTAL

Apparatus

Fluorescence spectra and intensities were measured with a Hitachi Model 650-10S spectrofluorimeter and 10 × 10 mm quartz cells. A Toa HM 5A pH-meter was used for pH measurements.

Reagents

2,6-Di-p-tolyl-4-phenylpyrylium chloride. The reagent was prepared as follows. To a solution of 1,5-bis-*p*-tolyl-3-phenyl-1,4-pentadiyn-3-ol⁸ (0.845 g, 2.51 mmoles) in 10 ml of dioxan, 0.5 ml of concentrated hydrochloric acid was added with stirring. After 1 hr, the crystals deposited were collected, washed with diethyl ether, and recrystallized from acetone-diethyl ether (1:1, v/v) to afford hygroscopic orange crystals of DTTPP⁺-Cl⁻ (0.636 g, 64%) m.p. ca. 190°; found C, 75.1%; H, 6.0%; C₂₃H₂₁OCl· $\frac{3}{2}$ H₂O requires C, 74.95%; H, 5.71%. The molar absorptivity was 2.77×10^4 l. mole⁻¹. cm⁻¹ at 365 nm (ethanol solution).

DTTPP⁺-Cl⁻ solution. A $3.0 \times 10^{-4}M$ solution of DTTPP⁺-Cl⁻ in 0.1M sulphuric acid was prepared.

Standard perchlorate solution. A stock solution ($1.0 \times 10^{-2}M$) was prepared by dissolving 0.1386 g of potassium perchlorate (analytical reagent grade, dried at 105°) in 100 ml of demineralized and redistilled water. The working solution was prepared by diluting the stock solution as required.

Adjustment of pH. Sulphuric acid (0.1M) and 0.1M citric acid-0.2M disodium hydrogen phosphate were used for adjustment of pH in the ranges 0.2-1.8 and 2.2-8.0 respectively.

Analytical-reagent grade chemicals were used whenever possible, without further purification.

Procedure

Transfer 1 ml of the sample solution containing up to 5.0 µg of perchlorate into a 25-ml glass-stoppered test-tube. Add 3 ml of dilute sulphuric acid (pH 1) and 1 ml of DTTPP⁺-Cl⁻ solution. Mix for 10 sec with a vortex mixer and let stand for 5 min. Add 5 ml of chlorobenzene and mix for 10 sec with the vortex mixer. Discard the aqueous layer and centrifuge the organic layer for 5 min at 3000 rpm. Measure the relative fluorescence intensity at 495 nm with excitation at 376 nm.

Acknowledgement—The authors wish to express their gratitude to the Ministry of Education, Science and Culture of Japan for a Grant-in-Aid for Scientific Research.

REFERENCES

1. S. Uchikawa, *Bull. Chem. Soc. Japan*, 1967, **40**, 798.
2. S. Motomizu, S. Fujiwara and K. Tōei, *Anal. Chim. Acta*, 1981, **128**, 185.
3. I. Iwasaki, S. Utsumi and C. Kang, *Bull. Chem. Soc. Japan*, 1963, **36**, 325.
4. S. Yamasaki, H. Ohura, K. Yano and I. Nakamori, *Bunseki Kagaku*, 1979, **28**, 566.
5. M. Tsubouchi and Y. Yamamoto, *ibid.*, 1970, **19**, 966.
6. S. Akiyama, K. Yoshida, M. Hayashida, K. Nakashima, S. Nakatsuji and M. Iyoda, *Chem. Lett.*, 1981, 311.
7. S. Akiyama, K. Nakashima, S. Nakatsuji, M. Hamada and Y. Izaki, *Bull. Chem. Soc. Japan*, 1983, **56**, 947.
8. S. Nakatsuji, K. Nakashima, K. Yamamura and S. Akiyama, *Tetrahedron Lett.*, 1984, **25**, 5143.

DETERMINATION OF TUNGSTEN IN ROCKS AND MINERALS BY CHELATE EXTRACTION AND ATOMIC-ABSORPTION SPECTROMETRY

N. K. ROY and A. K. DAS*

Geological Survey of India, 27 J. L. Nehru Road, Calcutta 700016, India

(Received 22 May 1985. Accepted 8 November 1985)

Summary—An atomic-absorption method for determination of tungsten in rocks and minerals is proposed. The method involves sample decomposition by acid digestion or by pyrosulphate fusion, followed by chelate extraction of tungsten by *N*-benzoylphenylhydroxylamine in toluene. Atomic-absorption measurements are made on the organic phase aspirated into a nitrous oxide-acetylene flame. Quantitative extraction with efficient separation from other elements is achieved in a single extraction from strong acid media. The method is rapid and reliable in terms of precision and accuracy and is applicable to rocks and minerals containing tungsten in the range from 100 ppm to 15%.

Flame atomic-absorption methods for determination of tungsten find only limited application in geochemical analysis because of the poor atomic-absorption sensitivity for tungsten¹ and the susceptibility to interference from other elements.² Musil and Doležal³ have proposed an atomic-absorption method for determination of tungsten in ferrous alloys, employing double extraction from fairly concentrated hydrochloric acid media with thiocyanate and methyl isobutyl ketone.

The superiority of *N*-benzoylphenylhydroxylamine (BPHA) as an extracting agent for metal ions is well established⁴ and there are reports of quantitative extraction of tungsten by this reagent under suitable conditions. The purpose of the present work was to develop an atomic-absorption method for determination of low levels of tungsten in rocks and minerals by employing BPHA-toluene extraction and flame AAS measurements on the organic phase.

EXPERIMENTAL

Apparatus

A Perkin-Elmer 303 instrument fitted with a 50-mm nitrous oxide-acetylene burner head was used for atomic-absorption measurements at 400.9 nm, with a Fisher tungsten hollow-cathode lamp as source. The more sensitive lines (255.1 and 294.7 nm) were not used, because of an unfavourable signal-to-noise ratio.

Reagents and standards

Standard tungsten solution (1000 µg/ml) was prepared by dissolving the calculated amount of tungstic acid in dilute sodium hydroxide solution and diluting with water to the necessary volume. Further dilutions were made as necessary before use.

N-Benzoylphenylhydroxylamine (BPHA) solution (0.2%) was prepared in toluene.

All chemicals used were of analytical-reagent quality.

Preliminary studies

Preliminary studies indicated that tungsten is quantitatively extracted by BPHA in toluene from 8–10*N* sulphuric or hydrochloric acid medium. It was also found that the extraction of iron can be suppressed if sulphuric acid is used instead of hydrochloric acid. No other elements except Ti, Sn, Mo, Nb and Ta are likely to be extracted under these conditions, but their presence up to certain limits does not cause any interference in the AAS determination of tungsten. The extraction is also not affected by the presence of anions such as citrate, tartrate or borate. Results of determination of tungsten in some synthetic mixtures are shown in Table 1.

Recommended procedures

Sample decomposition (acid digestion method). The powdered sample (0.5 g) is mixed with concentrated hydrofluoric acid (10 ml) and perchloric acid (5 ml) in a Teflon beaker and the mixture is slowly heated to dryness. The residue is warmed with hydrofluoric acid (2 ml) for a few minutes and then treated with a saturated solution of boric acid (5 ml)

Table 1. Determination of tungsten in synthetic mixtures containing metal ions extracted under the experimental conditions; W taken 500 µg

Interferent	Tungsten absorbance*	RSD, %
Ti(IV), 50 mg†	0.215	7.5
Mo(VI), 100 mg	0.218	6.8
Sn(IV), 100 mg	0.217	6.2
Nb(V), 50 mg	0.219	6.3
Ta(V), 50 mg	0.218	6.7
V(V), 50 mg	0.216	6.1
None	0.216	5.5

*Average of five determinations.

†With higher amounts there is precipitation of titanium and difficulty in phase separation.

*Present address: Geological Survey of India, Chemical Laboratory, Shillong 793003, India.

and water (10 ml). The solution is stirred well and filtered into a 50-ml standard flask and diluted to volume.

Sample decomposition (pyrosulphate fusion). The powdered sample (0.5 g) is mixed with approximately 4 g of potassium pyrosulphate in a hard-glass test-tube. The mixture is fused with a Bunsen burner flame and kept molten for about 10 min. The fused mass, after cooling, is heated with 0.1M tartaric acid solution (10 ml) on a hot water-bath for about 30 min. The mass is stirred occasionally in order to disintegrate the lumps. The solution is filtered into a 50-ml standard flask and diluted to volume.

Extraction of tungsten. An aliquot of sample solution containing 100–500 µg of tungsten is transferred to a separatory funnel, 30 ml of sulphuric acid (1 + 1) are added and the mixture is diluted to about 60 ml with water. The mixture is then shaken vigorously with BPHA–toluene reagent (5 ml) and for 1 min. The layers are allowed to separate and the aqueous phase is rejected. The organic phase is collected in a dry test-tube containing about 1 g of anhydrous sodium sulphate and allowed to stand for 10 min. The clear supernatant liquid is aspirated into the flame for AAS measurement.

Calibration. For calibration, 0, 1, 2, 4, 6, 8 and 10 ml volumes of standard tungsten solution (100 µg/ml) are taken in a series of separatory funnels, and the tungsten is extracted and its atomic absorption measured as just described.

RESULTS AND DISCUSSION

The proposed method has been applied to analysis of a number of tungsten-bearing rocks and minerals and the results are shown in Table 2. They agree well with those obtained by the X-ray fluorescence method. Two CANMET reference materials (MP-1a and MP-2) and one IGS sample (IGS-26) have also been analysed by this method and the results compared with the recommended values. The relative standard deviation (RSD) for MP-2 was found to be 5.6%.

The method is practically free from interferences and is very easy to apply. Both decomposition methods are equally efficient for silicate rocks, scheelite and wolframite samples, but for tungsten-bearing

Table 2. Determination of tungsten in rocks and minerals

Sample	W found, %	
	Present method	Other values
Granite	0.22	0.25*
Scheelite-bearing rock	1.05	1.10*
Scheelite-bearing rock	1.20	1.18*
Scheelite-bearing rock	2.24	2.30*
CANMET MP-2	0.67	0.65†
CANMET MP-1a	0.04	0.04†
IGS-26	13.37	13.58§

*XRF values.

†Recommended values from CANMET report.

§Recommended value from IGS report.

cassiterite samples the acid digestion method gives low values, probably because of incomplete decomposition of the cassiterite. There is no difficulty, however, in the pyrosulphate decomposition method. Both decomposition methods are applicable for samples containing tungsten from 100 ppm up to 15%.

The aspiration rate and burning characteristics of toluene in the nitrous oxide–acetylene flame are also quite favourable and as good as those for MIBK. AAS measurement of the toluene phase also has the benefit of sensitivity enhancement by a factor of 3.8 (compared to that for aqueous solutions).

Acknowledgements—The authors are thankful to Sri C. K. Ganguli, Director (Geochemistry), for his kind interest and encouragement in this work. Thanks are also due to the Director General, Geological Survey of India, for his kind permission to publish the paper.

REFERENCES

1. M. Pinta, *Atomic Absorption Spectrometry*, Hilger, London, 1975.
2. R. C. Rooney and C. G. Pratt, *Analyst*, 1972, **27**, 400.
3. J. Musil and J. Doležal, *Anal. Chim. Acta*, 1977, **92**, 301.
4. A. K. De, S. M. Khopkar and R. A. Chalmers, *Solvent Extraction of Metals*, Van Nostrand-Reinhold, 1970.

ANALYTICAL APPLICATION OF EMULSIONS

DETERMINATION OF LEAD IN GASOLINE BY ATOMIC-ABSORPTION SPECTROPHOTOMETRY

E. CARDARELLI, M. CIFANI, M. MECOZZI and G. SECHI
Department of Chemistry, University "La Sapienza" of Rome, Rome, Italy

(Received 21 March 1985. Revised 5 September 1985. Accepted 18 October 1985)

Summary—A simple rapid method of determining lead in gasoline by AAS with use of stable emulsions has been developed. The emulsions were stabilized with propan-2-ol or a mixture of ethanol and a surface-active agent. The results obtained showed good reproducibility and accuracy and the method is suitable for routine analysis.

Determination of lead in gasoline by AAS with use of water-gasoline emulsions stabilized by surfactants is rapid and precise but suitable experimental conditions must be chosen. The amount of organic phase must be kept below 2% or the emulsion become too viscous to be easily aspirated.^{1,2} In addition, a surfactant with a suitable HLB (hydrophilic-lipophilic balance) for stabilizing the emulsion must be selected.^{1,2} The need for such a method arises because of the comparative slowness of the titrimetric determinations.^{3,4} Some AAS methods have already been developed, in which the gasoline sample is diluted with a suitable solvent. Robinson⁵ used iso-octane, and Sebor and Lang proposed xylene because of its ability to dissolve polycyclic hydrocarbons.⁶ A further problem is the variation in response of alkyl-lead compounds with a change in the size of the alkyl group, necessitating a separate calibration curve for each compound.⁷ To overcome this problem, iodine has been added to the samples.^{7,8} This also gives an increase in instrumental response because iodine combines with the lead to produce less flame-refractory compounds.^{6,9} In the present work we determine lead in gasoline by using mixtures emulsified by addition of a surfactant, and/or a water-miscible organic solvent such as ethanol and propan-2-ol. The resulting method is rapid, easy to use and gives increased sensitivity.

EXPERIMENTAL

Procedures

For each solvent tested five emulsions were prepared with the following volume composition: 1% gasoline, 2% surfactant (for emulsions containing ethanol), 10-50% alcohol, remainder distilled water. Each sample was emulsified for 4 min by application of an ultrasonic probe and then aspirated directly into the flame of the spectrophotometer. The absorbance was measured at a wavelength of 217.0 nm. For analysis of gasoline the propan-2-ol method is recommended: 1 ml of gasoline and 50 ml of propan-2-ol are mixed and diluted accurately to 100 ml with water; the mixture is emulsified and aspirated into the flame, and the lead signal at 217.0 nm is measured. Calibration is done by

making standard solutions with a lead-free gasoline and lead nitrate or organolead standards (Conostan or cyclohexyl-lead butyrate dissolved in xylene), or by the standard-addition method.

RESULTS AND DISCUSSION

Both kinds of emulsion were stable for 40 min, as shown by constancy of the absorbance signal and confirmed by turbidimetric measurements. When ethanol was incorporated it was also necessary to add a surfactant to stabilize the emulsion. Both surfactants tested gave practically identical results. The best results were obtained with 50% ethanol, the absorbance being 0.300 and relative standard deviation (rsd) 2.7% for the comparative test. Much better results were obtained with propan-2-ol, which gave a stable emulsion without addition of a surfactant. The 50% propan-2-ol system gave an absorbance of 0.360 (rsd 2.5%) for the comparative test, and a linear calibration graph for emulsions prepared with 1% v/v gasoline and known amounts of a standard lead nitrate solution. The parameters of the graph were practically the same as those for a graph prepared by use of similar emulsions made with 1% gasoline and various volumes of organolead standards (Conostan and cyclohexyl-lead butyrate, diluted with xylene) (see Table 1).

The limit of detection for lead was 0.07 mg/l. in the emulsion. The absorbance at 217.0 nm was measured because at this wavelength it was possible to analyse emulsions containing only 1% of gasoline, which increased the stability of the emulsions. The use of

Table 1. Parameters of calibration curves for determination of lead

Standard	Slope, l./mg	Correlation coefficient
Lead nitrate	0.063	0.997
Cyclohexyl-lead butyrate	0.065	0.996
Conostan	0.061	0.997

Table 2. Results for gasoline samples

Lead found, mg/l.,	
Standard method	Emulsion method
485	478
463	450
496	501
430	440
468	475
476	463
490	499

large amounts of organic solvents confers two main benefits. The polar character of the solvent increases the stability of the emulsions, slowing down separation into two phases,¹¹ and there is an increase in sensitivity, due to a more rapid nebulization and evaporation of the solution.¹² The latter benefit is demonstrated by the limit of detection (about 0.07 mg/l.) which is better than that obtained (at the same wavelength) for aqueous solutions of lead.¹³ For high concentrations of lead a smaller gasoline volume can be used, or the measurement can be made at the less sensitive 283.3 nm line. Table 2 shows there is good agreement between the results obtained by the emulsion method and a standard method.

CONCLUSIONS

A rapid accurate routine method for the determination of lead in gasoline has been developed, based on use of water-gasoline emulsions supported by ethanol or propan-2-ol. An emulsion with 50% propan-2-ol gives a sensitivity greater than that achieved by using ethanol and a surfactant.

REFERENCES

1. J. Hernandez-Mendez, L. Polo-Diez and A. Bernal-Melchor, *Anal. Chim. Acta*, 1979, **108**, 39.
2. J. Hernandez-Mendez, L. Polo-Diez and F. Pedraz-Penalva, *Analyst*, 1980, **105**, 37.
3. *Year Book, Am. Soc. Test. Mater.*, 1980, **25**, D3341.
4. *Ibid.*, 1980, **25**, D2547.
5. J. W. Robinson, *Anal. Chim. Acta*, 1961, **24**, 451.
6. G. Sebor and I. Lang, *ibid.*, 1977, **89**, 221.
7. M. Kashiki, S. Yamazoe and S. Oshima, *ibid.*, 1971, **53**, 95.
8. *Year Book, Am. Soc. Test. Mater.*, 1980, **25**, D3237.
9. A. Tonca, B. Bianchi, M. Mecozzi and G. Sechi, *Rassegna Chim.*, 1985, **1**, 9.
10. *Year Book, Am. Soc. Test. Mater.*, 1980, **25**, D3602.
11. H. Zuidema, *Performance of Lubricating Oils*, pp. 141-145. Reinhold, New York, 1956.
12. *Note sulla spettroscopia di assorbimento atomico*, Instrumentation Laboratory, Wilmington, MA.
13. *Atomic Absorption Methods Manual*, Vol. 1, *Standard Conditions for Flame Operations*. Instrumentation Laboratory, Wilmington, MA, 1976.

ULTRAMICRO FLOW-CELL FOR SEMICONDUCTOR LASER FLUORIMETRY

YUJI KAWABATA, TOTARO IMASAKA and NOBUHIKO ISHIBASHI*
Faculty of Engineering, Kyushu University, Hakozaki, Fukuoka 812, Japan

(Received 2 September 1985. Accepted 30 September 1985)

Summary—A small flow-cell, consisting of a fused silica capillary (200 μm diameter), was constructed for use in fluorimetry. A near-infrared semiconductor laser was used as an excitation source, and an optical fibre (core diameter 50 μm) inserted into the capillary tube was used as a waveguide for light introduction or fluorescence collection. The volume of the flow-cell was 3–60 nl. A polymethine dye could be detected in the range 12–90 fg, and the absolute amount of the sample in the detection volume was 140–370 ag.

In high-pressure liquid chromatography (HPLC), a small detector is essential to maintain good separation resolution. A laser is an excellent light-source for such a highly sensitive HPLC detector because of its good beam coherence and large photon flux. However, background emission is a serious problem for ultratrace analysis in laser fluorimetry. Various types of flow-cells have been designed to reject background emission from the cell windows.¹⁻³

Sepaniak and Yeung have proposed the use of an optical fibre for fluorescence collection.⁴ The high transmittance and well-defined acceptance angle for light collection associated with the optical fibre promise efficient rejection of unwanted emission from the cell walls. In addition, Todoriki and Hirakawa have used the optical fibre as a waveguide for light introduction.⁵ These prototypes were applied for the determination of biochemical samples. However, their flow-cells had volumes of 17–20 μl and are not suitable for the recently developed micro HPLC. At present, no study has been carried out concerning a nanoliter flow-cell using a capillary combined with an optical fibre for laser fluorescence detection. In this study, we constructed such an ultramicro flow-cell for fluorimetry, using a semiconductor laser as an excitation source and an optical fibre as a waveguide for light introduction or fluorescence collection. The sensitivity and detection power of the system are discussed.

EXPERIMENTAL

Apparatus

The apparatus is shown in Fig. 1. Solvent was pumped by a microfeeder (Azuma, MF-2) at a flow-rate of 2 $\mu\text{l}/\text{min}$. The sample was injected into the stream by a micro-loop injector (Jasco, ML422), the capacity of which had been modified to 60 nl. The excitation source of the semiconductor laser (Hitachi, HL7801E, $\lambda = 780 \text{ nm}$, 3 mW) was modulated to square waves (duty cycle 50%) at 100 Hz by a pulse generator (Hewlett Packard, 8013B). Fluorescence from the sample, after passing through an interference filter (Ditric, transmission maximum 850 nm), was detected by a

photomultiplier (Hamamatsu, R636). The output signal was fed through a lock-in amplifier (NF Circuit Design Block, LI-570) to a chart-recorder (Rikadenki, R-50).

A flow-cell was constructed from a fused silica capillary (Shimadzu, bore 200 μm), into which a quartz optical fibre (Fujikura, G50/125.3005, core diameter 50 μm , cladding diameter 125 μm) was inserted. Two optical arrangements were considered: (1) the semiconductor laser was focused onto the side surface of the optical fibre by a ball lens (Moritex, diameter 3 mm) and the sample was irradiated from the end of the fibre, fluorescence being detected through the capillary wall [Fig. 1(1)]; (2) the semiconductor laser was focused into the fused silica capillary perpendicularly and fluorescence was measured through the optical fibre [Fig. 1(2)].

Reagents

A near-infrared fluorophor, 3,3'-diethyl-2,2'-(4,5,4',5'-dibenzo)thiatricbocyanine iodide (NK427), was purchased from Nippon Kanko-Shikiso Kenkyusho. The organic solvent, 2-butanol, was obtained from Kishida Chemical Co. and was used after ultrasonic agitation (Yamato, Bransonic 12) to remove dissolved air. All chemicals were used without further purification.

RESULTS AND DISCUSSION

Sensitivity

The signal intensities and the detection limits for the two optical arrangements are listed in Table 1. For sample excitation through the optical fibre [method (1)], the peak height of the fluorescence signal was 14 μV when a $1 \times 10^{-8} \text{ M}$ sample solution was injected, so the sensitivity was 1400 V.l.mole⁻¹. For fluorescence detection through the optical fibre [method (2)] the fluorescence signal was 3.3 μV when a $7 \times 10^{-8} \text{ M}$ solution was injected and the sensitivity was 50 V.l.mole⁻¹. The difference in sensitivity (a factor of 28) for the two optical arrangements may be attributed to the difference in cell volume (a factor of 20).

Detectability

It was shown previously that a polymethine dye can be detected down to $5 \times 10^{-12} \text{ M}$ by semiconductor laser fluorimetry.⁶ The detection limits for NK427 were 12 and 90 fg for methods (1) and (2),

*Author to whom correspondence should be addressed.

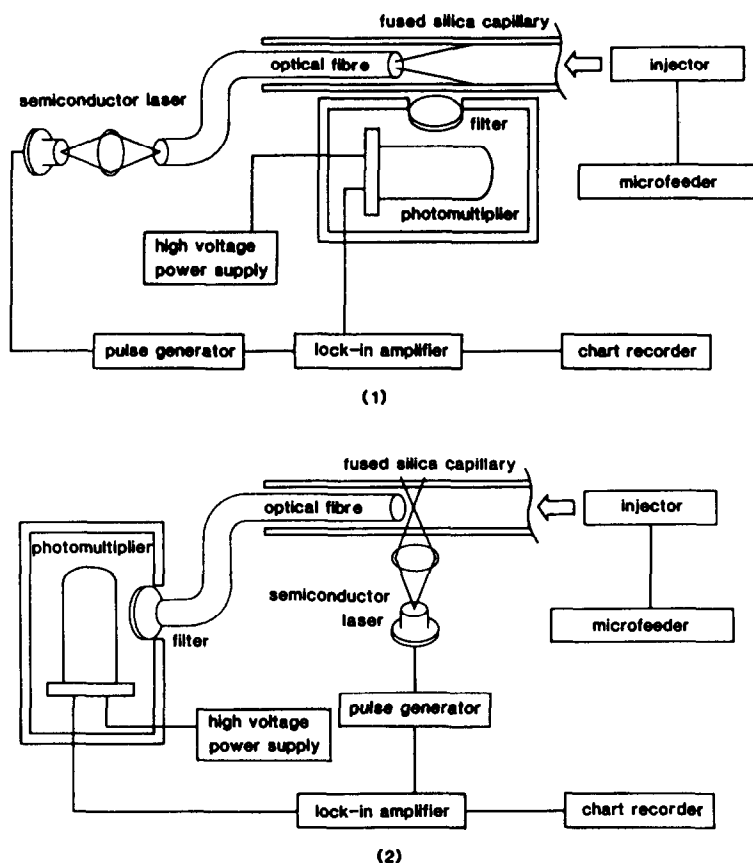


Fig. 1. Schematic diagram of experimental apparatus; (1) sample excited through the optical fibre, (2) fluorescence detected through the optical fibre.

respectively. In method (1) the background signal was due to scattering from the cell wall, and the noise level was $0.6 \mu V$. The background signal was negligibly small in method (2), since scattering from the cell wall was rejected by use of the optical fibre. The noise level decreased to $0.2 \mu V$, which was solely due to the dark current drift of the photomultiplier. The detection limit in method (1) was 7.5 times better than that in method (2), which is consistent with the ratio of the sensitivities and noise levels (9.3). The optical fibre has a numerical aperture of 0.2 which corresponds to an f -number of 2.4 for a fluorescence collection lens in method (2). Thus the collection efficiency of the optical fibre is comparable to that obtained by using an ordinary condensing lens. It is emphasized that the absolute amount of the sample

in the detection volume was 140 ag in method (2), since the detection region was severely restricted by the focused laser beam and the optical fibre.

A further improvement of the detection limit may be possible. A semiconductor laser with an output power of 100 mW is already commercially available, and a laser with an output of 2.6 W has been reported.⁷ Although a laser with an increased output power will give a larger fluorescence signal, the background noise will also increase for method (1). In this case, stabilization of the laser output power is essential to permit cancellation of the background signal. It is claimed that feedback control of the output power with a specially designed integrated circuit (Sharp Co.) can reduce variation in the output power to less than 0.002%. On the other hand the

Table 1. Comparison of the optical-fibre fluorescence-detectors

Item	Excitation through the optical fibre [method (1)]	Detection through the optical fibre [method (2)]
Cell volume, nl	60	3
Background signal, μV	8.5	negligible
Noise level, μV	0.6	0.2
Detection limit for NK427, fg	12	90

background signal is negligible in method (2), and therefore the sensitivity is readily improved by increasing the output power of the exciting source. Cooling of the photomultiplier reduces the noise from the dark current, and gives an improvement in detection sensitivity by more than an order of magnitude.

The emission wavelengths of semiconductor lasers have been significantly shortened over the past few years. A continuous laser at 671 nm⁸ and a pulsed laser at 579 nm⁹ have been reported. The application of semiconductor laser fluorimetry is limited to polymethine dyes at present, but will be widely used in many practical applications using various fluorescent reagents in the near future.

Acknowledgement—This research is supported by a Grant-

in-Aid for Scientific Research from the Ministry of Education of Japan.

REFERENCES

1. G. J. Diebold and R. N. Zare, *Science*, 1977, **196**, 1439.
2. L. W. Hershberger, J. B. Callis and G. D. Christian, *Anal. Chem.*, 1979, **51**, 1444.
3. N. J. Dovichi, J. C. Martin, J. H. Jett, M. Trkula and R. A. Keller, *ibid.*, 1984, **56**, 348.
4. M. J. Sepaniak and E. S. Yeung, *J. Chromatog.*, 1980, **190**, 377.
5. H. Todoriki and A. Y. Hirakawa, *Chem. Pharm. Bull.*, 1984, **32**, 193.
6. T. Imasaka, A. Yoshitake and N. Ishibashi, *Anal. Chem.*, 1984, **56**, 1077.
7. W. Streifer, R. D. Burnhan, T. L. Paoli and D. R. Scifres, *Laser Focus*, 1984, **20**, 100.
8. A. Usui, T. Matsumoto, M. Inai, I. Mito, K. Kobayashi and H. Watanabe, *Jpn. J. Appl. Phys.*, 1985, **24**, L163.
9. M. Ikeda, M. Honda, Y. Mori, K. Kaneko and N. Watanabe, *Appl. Phys. Lett.*, 1984, **45**, 964.

ANALYTICAL DATA

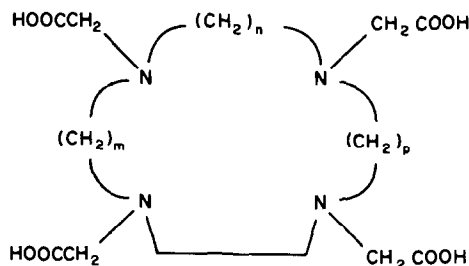
COPPER(II) COMPLEXES OF CYCLIC TETRA-AZATETRA-ACETIC ACIDS—UNUSUAL FEATURES AND POSSIBLE ANALYTICAL APPLICATIONS

RITA DELGADO, J. J. R. FRAÚSTO DA SILVA and M. CÂNDIDA T. A. VAZ
 Centro de Química Estrutural-Complexo I, Instituto Superior Técnico, Lisbon, Portugal

(Received 6 September 1985. Accepted 8 November 1985)

Summary—An examination of the copper(II) complexes of some cyclic tetra-azatetra-acetic acids has shown that the 1,4,7,10-tetra-azacyclotridecane-*N,N',N'',N'''*-tetra-acetic acid complex has an unusually high molar absorptivity and other favourable characteristics which make this ligand a convenient reagent for the fast and easy spectrophotometric determination of moderately small quantities of copper.

In previous works^{1,2} we reported the synthesis and the results of a study of the complexation properties in aqueous solution of a family of cyclic tetra-azatetra-acetic acids with 12–15-membered rings (I). Stability constants of the alkaline-earth and first-series transition-metal ion complexes were determined,¹ and also the thermodynamic parameters of the corresponding formation reactions.²



Scheme 1.

I

General formula of the cyclic tetra-azatetra-acetic acids

a. $m = n = p = 2$:

1,4,7,10-tetra-azacyclododecane-*N,N',N'',N'''*-tetra-acetic acid; cDOTA

b. $m = 3$; $n = p = 2$:

1,4,7,10-tetra-azacyclotridecane-*N,N',N'',N'''*-tetra-acetic acid; cTRITA

c. $m = p = 3$; $n = 2$:

1,4,8,11-tetra-azacyclotetradecane-*N,N',N'',N'''*-tetra-acetic acid; cTETA

d. $m = n = p = 3$:

1,4,8,12-tetra-azacyclopentadecane-*N,N',N'',N'''*-tetra-acetic acid; cPENTA

This note summarizes the results of a study of the electronic spectra in the visible region and of an EPR study of the copper(II) complexes of these ligands. In one case there are some curious features that might lead to analytical applications. A more detailed anal-

ysis of the electronic spectra of the nickel and cobalt complexes will be reported elsewhere.³

In Fig. 1, the visible-region electronic spectra of the copper(II) complexes of cDOTA, cTRITA, cTETA, cPENTA and EDDA are presented and Table 1 summarizes the results in terms of absorption maxima and molar absorptivities, and also gives the corresponding EPR data.

The most striking observation is the high energy of the absorption band of the Cu-cTRITA complex and the abnormally high molar absorptivity of this complex, due to a *d-d* transition.

The EPR spectra of the aqueous solution of the complexes at 77 K are typical of elongated tetragonal copper species, with $g_{\parallel} > g_{\perp} > 2.04$ and $(g_{\parallel} - 2)/(g_{\perp} - 2) \approx 4$ and hyperfine splitting in the g_{\parallel} region. The g_{\parallel} values vary between 2.2 and 2.3—Table 1.

The stability constants of the complexes of the four ligands with this metal ion are similar¹ and analysis of the thermodynamic parameters suggests that only 2 or 3 nitrogen atoms and 2 or 3 carboxylate groups are involved in the co-ordination.²

However, the results obtained in the present work point to a predominant nitrogen-donor environment for copper in the cTRITA complexes and to a predominant oxygen-donor environment in the cDOTA complex; the cTETA complex and, particularly, the cPENTA complex have an intermediate character, *i.e.*, a 2O + 2N environment. Cu-cDOTA has properties close to those of Cu-cEDTA, and Cu-cPENTA is very similar to Cu-EDDA, Table 1, but the values of g_{\parallel} and A_{\parallel} for Cu-cTRITA approach those of the copper-amine complexes.^{4,5} The structure of Cu-cDOTA has been determined in the solid state;⁶ two nitrogen atoms and two carboxylate groups are co-ordinated in the equatorial plane and the two further nitrogen atoms are almost axial (the N-Cu-N angle is 152.6°); however, the EPR spectrum of a solution at pH 9 is more in agreement

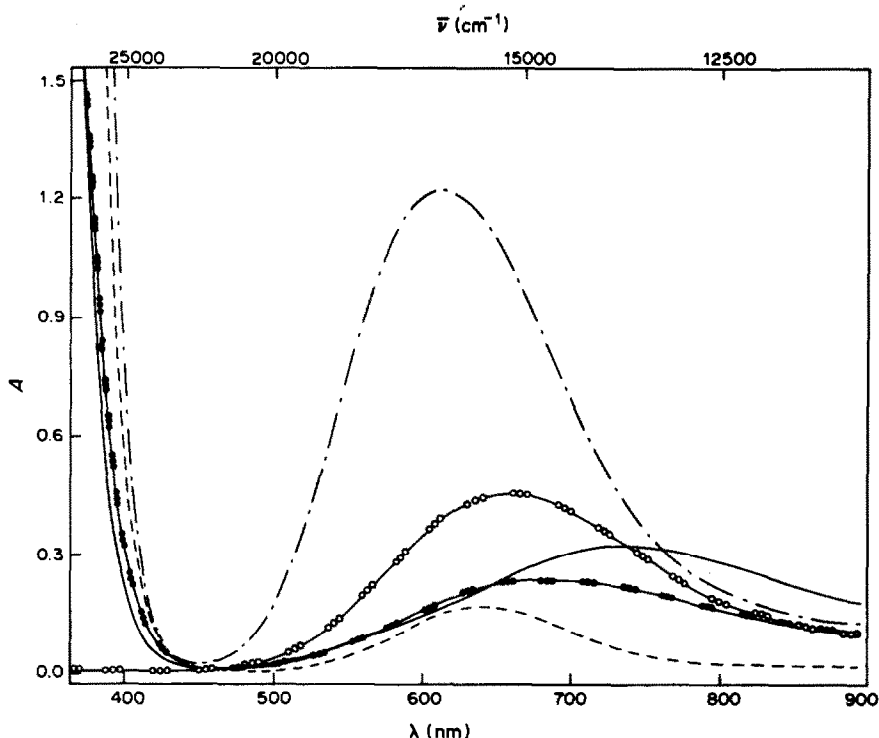


Fig. 1. Visible spectra of the copper(II) complexes of cDOTA (—), cTRITA (---), cTETA (— · —), cPENTA (—●●●—), EDDA (—○ ○ ○—).

with a set of 1N + 3O donor atoms at closer distances to the copper(II) ion.⁴ The same can be said for the EDTA-copper complex, which in aqueous solution (pH > 3) gives a curious EPR spectrum that indicates an equilibrium between two forms.⁷ The g and A values quoted were calculated by assuming that the complex has tetragonal symmetry, and for one of the forms are close to those reported for single crystals of CuH_2EDTA ⁸ which does indeed have 1N + 3O donor atoms at closer distances.

The similarity of Cu-cTETA and specially Cu-cPENTA to the copper complex of ethyl-

enediamine- N,N' -diacetic acid (EDDA) is not surprising, given the higher degree of flexibility and lesser stereochemical constraints in the two larger macrocyclic ligands. Accordingly, two nitrogen atoms and two carboxylate groups must be the closest donors in the co-ordination sphere of copper, as occurs in the EDDA complex.

The structure of Cu-cTRITA cannot be predicted from these observations. It is clear that the introduction of just one methylene group in one of the ethane chains of cDOTA leads to significant changes in the conformation of the ligand and in the orien-

Table 1. Characteristics of the visible-region electronic spectra, and EPR parameters of some copper cyclic tetra-azatetra-acetate and other polyaminocarboxylate complexes in aqueous solution

Ligand	Electronic spectra†		EPR spectra§		
	$\bar{\nu}$, cm^{-1}	ϵ , $\text{mole} \cdot \text{l}^{-1} \cdot \text{cm}^{-1}$	g_{\perp}	g_{\parallel}	A_{\parallel} 10^4 cm^{-1}
cDOTA	13620	100	2.062	2.300	150.3
cTRITA	16390	370	2.047	2.202	190.6
cTETA	15480	70	2.050	2.249	168.0
cPENTA	14300	70	2.050	2.249	178.0
EDDA*	14900	118	2.049	2.237	187.0
EDTA*	13600	99	2.071	2.343	155.9
(two forms)			2.071	2.295	166.0
NH_3 (various)			~2.05	~2.20	—

*Values calculated for tetragonal symmetry.

†Experimental conditions: $T = 25.0^\circ\text{C}$; ligand to metal ratio 1:1; $C_M = 4 \times 10^{-3} \text{ M}$; pH ≈ 9 .

§Experimental conditions: $T = 77 \text{ K}$; microwave power 2 mW; modulation amplitude 1 mT; microwave frequency 9.280 GHz; scan-time 200 sec; ligand to metal ratio 25:1; pH ≈ 9 .

tation of its donor groups. Hence a complex of low symmetry is obtained; this accounts for its high molar absorptivity in the visible region (*cf.* the results obtained by other authors for some deliberately designed non-symmetrical copper complexes in which transitions other than $d-d$ are not expected⁹).

The absorption band is also shifted to higher energies and the value of g_1 , close to that found for various amine complexes of this metal, suggests that at least three nitrogen atoms are closer in the co-ordination sphere of the complex, but this is all that can be inferred from the spectra. On the other hand, the thermodynamic data suggest that two carboxylate groups are also co-ordinated, probably at greater distances.

The molar absorptivities of the complexes of cTRITA with Ni, Co and other metals commonly present in metal alloys are substantially lower than that of the Cu complex in the wavelength range of its maximum absorption. This fact, the high molar absorptivity of the complex, the stability of the colour and the wide range of pH at which complex-formation is complete, make cTRITA a convenient reagent for the fast and easy spectrophotometric determination of moderately small quantities of copper in metal alloys, down to a level lower than that possible with ethylenediamine- N,N' -di- α -

propionic acid, which we have previously proposed for the purpose.¹⁰

Acknowledgements—The authors thank Drs J. J. G. Moura and I. Moura for helpful discussions, and the INIC, Ministry of Education, Portugal, for financial assistance.

REFERENCES

1. R. Delgado and J. J. R. Fraústo da Silva, *Talanta*, 1982, **29**, 815.
2. R. Delgado, J. J. R., Fraústo da Silva and M. Cândida T. A. Vaz, *Inorg. Chim. Acta*, 1984, **90**, 185.
3. *Idem*, *Rev. Port. Química*, to be published.
4. J. Peisach and W. E. Blumberg, *Arch. Biochem. Biophys.*, 1974, **165**, 691.
5. E. I. Solomon, K. W. Penfield and D. E. Wilcox, *Struct. and Bonding*, 1983, **53**, 1.
6. A. Riesen, *Ph.D. Thesis*, Basel, 1984.
7. D. L. Williams-Smith, R. C. Bray, M. J. Barber, A. D. Tsopanakis and S. P. Vincent, *Biochem. J.*, 1977, **167**, 593.
8. B. J. Hathaway, M. J. Baw, D. E. Billing, R. J. Dudley and P. Nicholls, *J. Chem. Soc. (A)*, 1969, 2312; B. J. Hathaway and D. E. Billing, *Coord. Chem. Rev.*, 1970, **5**, 143.
9. R. L. Belford and W. A. Yeranous, *Mol. Phys.*, 1963, **6**, 121.
10. J. J. R. Fraústo da Silva, J. G. Calado and M. Legrand de Moura, *Talanta*, 1965, **12**, 467.

STUDIES ON EXTRACTION OF MANGANESE(II) WITH 1-PHENYL-3-METHYL-4-ACYL-5-PYRAZOLONE

Y. AKAMA, H. YOKOTA, K. SATO and T. NAKAI

Department of Chemistry, Meisei University, Hodokubo, Hino, Tokyo 191, Japan

(Received 7 June 1984. Revised 17 October 1985. Accepted 30 October 1985)

Summary—The extraction of Mn(II) with 1-phenyl-3-methyl-4-acyl-5-pyrazolone (HA) in MIBK has been studied. Mn(II) is extracted as MnA_2 . The extraction constant for each 4-acyl compound was calculated. The effect of temperature on the extraction of Mn(II) has also been investigated.

Since the introduction of the synthesis of 1-phenyl-3-methyl-4-acyl-5-pyrazolone derivatives by Jensen,¹ numerous studies on metal extraction with these reagents have been reported. Of the various reagents in this series, 1-phenyl-3-methyl-4-benzoyl-5-pyrazolone (HPMBP) is the most popular. It is easily prepared by benzylation of 1-phenyl-3-methyl-5-pyrazolone, and is characterized by good chemical stability and its ability to extract metal ions at relatively low pH. HPMBP has been extensively employed for the efficient extraction of actinides,^{2,3} lanthanides,⁴ and other ions.⁵⁻⁸ Recently, we have systematically synthesized 1-phenyl-3-methyl-4-acyl-5-pyrazolone derivatives of the type $(C_{10}H_9N_2O)(C_nH_{2n+1}CO)$ ($n = 2-11$) and studied the extraction of Cu(II) with these reagents.⁹ These 4-acyl derivatives have pK_a values lower than those of other β -diketones, such as thenoyltrifluoroacetone and acetylacetone. Therefore, it was hoped that these derivatives might prove to be more attractive as ligands for the extraction of metals.

As part of this study on the properties of the 4-acyl derivatives in the extraction of metal ions, attention has been paid to the extraction of Mn(II). The extraction constants have been calculated, and the relative effectiveness of the 4-acyl derivatives as extractants compared. The effect of temperature on the extraction of Mn(II) has also been investigated.

EXPERIMENTAL

Reagents

The manganese stock solution was prepared by dissolving the pure metal in perchloric acid, and diluted to 1 ppm Mn(II) concentration for the extraction studies. The 4-acyl derivatives were synthesized as previously described¹ and used in MIBK solution. They were purified by several recrystallizations from methanol, and the analytical data are given in Table I. The reagents are denoted by C_N , in which N is the number of carbon atoms in the acyl chain. All other reagents were of analytical grade.

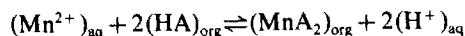
Extraction and analytical procedure

Equal volumes (8 ml) of the aqueous (1 ppm Mn) and organic (0.01M reagent in MIBK) phases were shaken together mechanically for 30 min in a 50-ml glass-stoppered

centrifuge tube at 25°. After centrifugation the two phases were separated and the pH of the aqueous phase was measured. The concentration of Mn(II) in the aqueous phase was determined by atomic-absorption spectrophotometry. The amount of Mn(II) extracted into the organic phase was obtained by difference. Except for the interference studies all experiments were done with the aqueous phase adjusted to ionic strength 0.1M with sodium perchlorate. The pH of the aqueous phase was adjusted with 0.1M acetic acid-sodium acetate buffer solution.

RESULTS AND DISCUSSION

The liquid-liquid extraction was done in the conventional manner with the reagent dissolved in the organic phase and the metal ion in the aqueous phase. The extraction of Mn(II) with 0.01M 4-acyl derivative solutions in benzene is negligible over the pH range studied (3.5-5.5). However, when MIBK is used as the organic solvent the extraction is considerably enhanced, as shown in Fig. 1. We consider that the enhancement must be related to a synergistic effect by MIBK, as indicated by Fig. 2. Plots of $\log D$ vs. pH for extraction of Mn(II) with HPMBP or the 4-acyl derivatives into MIBK all had a slope of 2, indicating the release of two protons per metal ion extracted. Log-log plots of D vs. ligand concentration also gave straight lines of slope 2, for HPMBP, C_3 , C_8 and C_{12} , indicating a 2:1 ligand-Mn(II) ratio in the extracted species. Thus, the extraction can be represented by



$$K_{ex} = [MnA_2]_{org} [H^+]_{aq}^2 / [Mn^{2+}]_{aq} [HA]_{org}^2$$

where HA represents the ligand and A its anion, K_{ex} is the extraction constant for the manganese complex, and org and aq denote the organic and aqueous phases respectively. The values of $\log K_{ex}$ have been calculated for all the systems and are summarized in Table 1. The results indicate that HPMBP gives a much higher $\log K_{ex}$ value than those for the other 4-acyl derivatives, which do not differ significantly from C_3 to C_{12} . To see whether this difference in K_{ex} is due to differences in the acid dissociation constants

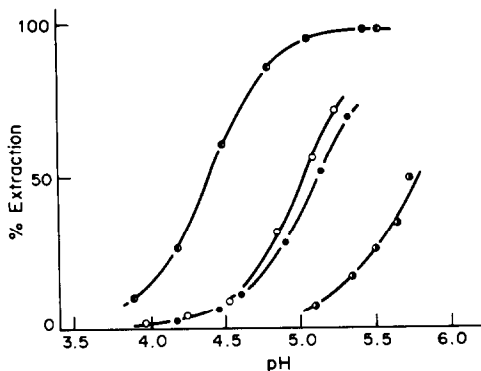


Fig. 1. Effect of pH on the extraction of Mn(II). —●—, 0.01M HPMBP in MIBK; —○—, 0.01M C₁₂ in MIBK; —●—, 0.01M C₃ in MIBK; —○—, 0.03M HPMBP in benzene.

(pK_a) of the ligands, the pK_a values were measured spectrophotometrically in 10% v/v dioxan-water medium at 25°. The ionic strength was maintained at 0.1M with (Na,H)ClO₄. The changes in the absorp-

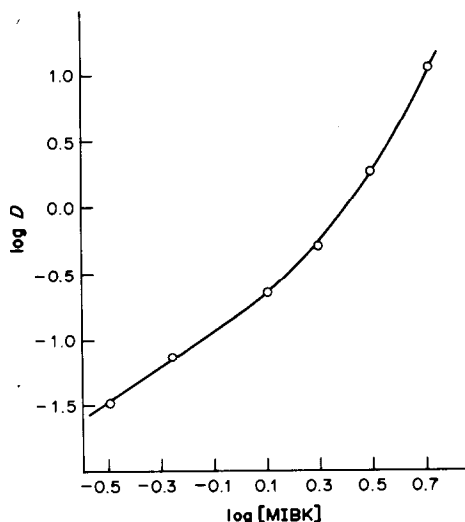


Fig. 2. Variation of $\log D$ with $\log [MIBK]$, for constant [HPMBP], with benzene as diluent.

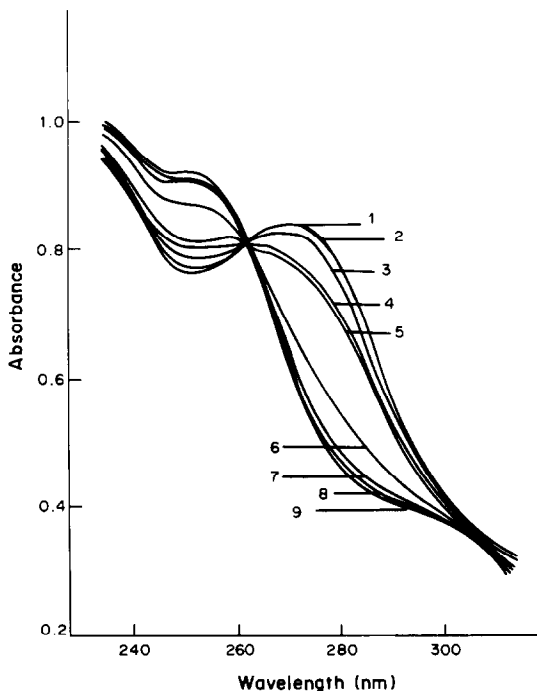


Fig. 3. Absorption spectra of HPMBP in 10% v/v dioxan-water at various pH values. HPMBP $5 \times 10^{-5}M$; pH (1) 10.30; (2) 5.84; (3) 4.80; (4) 4.31; (5) 4.15; (6) 3.39; (7) 2.83; (8) 2.45; (9) 2.30.

tion spectra of HPMBP and C₆ with pH are shown in Figs. 3 and 4. The pK_a values, which are summarized in Table 1, were calculated from

$$pK_a = pH - \log (A - A_{\min}) / (A_{\max} - A)$$

where A_{\min} is the asymptotic absorbance at low pH, A_{\max} is the asymptotic absorbance at high pH and A is the absorbance at any intermediate pH. It is evident that increasing the number of CH₂-groups in the acyl moiety does not influence the pK_a value and there is not much difference in pK_a between HPMBP and the other compounds. The extraction of Mn(II) into MIBK, as a function of temperature (5–40°), for the HPMBP, C₃, C₈ and C₁₂ systems was also studied.

Table 1. Analytical data for the extractants and their Mn(II) complexes

Reagent*	M.p., °C	pK_a in 10% v/v dioxan at 25°C	Solubility at 25 ± 2°C, M		$\log K_{ex}$ for Mn at 25°C	Elemental analysis of reagent†		
			in water	in MIBK		C, %	H, %	N, %
C ₃	61–62	4.1 ₇	2.2×10^{-3}	0.726	-6.2 ₃	68.2 (67.81)	6.2 (6.13)	11.9 (12.17)
C ₄	77–78	4.0 ₆			-6.1 ₃	68.6 (68.83)	6.6 (6.60)	11.5 (11.47)
C ₅	60–61	4.0 ₅	7.7×10^{-5}	0.342	-6.1 ₁	69.6 (69.74)	7.2 (7.02)	11.0 (10.84)
C ₆	59–60	4.1 ₅			-6.0 ₇	70.9 (70.56)	7.5 (7.40)	10.5 (10.29)
C ₇	77–78	4.1 ₀			-6.0 ₈	71.2 (71.30)	7.7 (7.74)	9.9 (9.78)
C ₈	77–78	4.1 ₀	1.5×10^{-5}	0.124	-6.1 ₀	72.9 (71.97)	8.0 (8.05)	9.4 (9.33)
C ₉	29–30	4.1 ₇			-6.0 ₇	72.6 (72.58)	8.3 (8.34)	9.0 (8.91)
C ₁₀	43–44				-6.0 ₃	73.7 (73.14)	8.7 (8.59)	8.6 (8.53)
C ₁₁	46–47				-6.0 ₁	73.6 (73.65)	8.6 (8.83)	8.1 (8.18)
C ₁₂	64–65				-6.0 ₂	74.1 (74.12)	9.0 (9.05)	7.9 (7.86)
HPMBP	117–118	3.8 ₀	7.6×10^{-5}	0.163	-4.7 ₈	73.3 (73.37)	4.9 (5.07)	10.0 (10.07)

*C₃ = C₁₃H₁₄N₂O₂... C₁₂ = C₂₂H₃₂N₂O₂; HPMBP = C₁₇H₁₄N₂O₂.

†Theoretical values are given in parentheses.

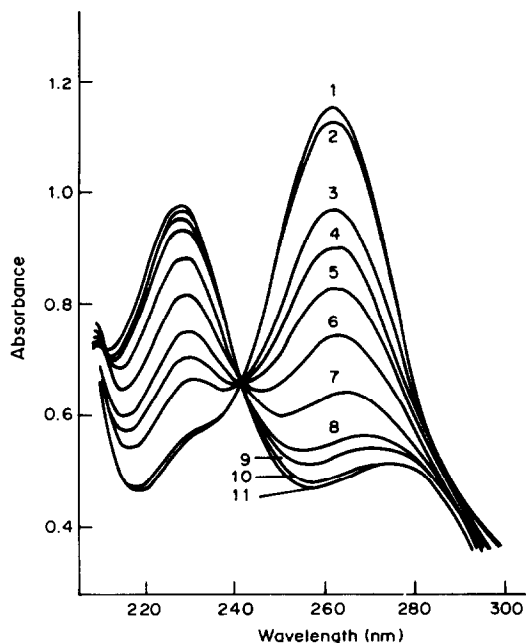


Fig. 4. Absorption spectra of C_6 in 10% v/v dioxan-water at various pH values. C_6 $5 \times 10^{-5}M$; pH (1) 6.51; (2) 5.55; (3) 4.55; (4) 4.35; (5) 4.18; (6) 3.90; (7) 3.60; (8) 3.25; (9) 3.05; (10) 2.65; (11) 2.30.

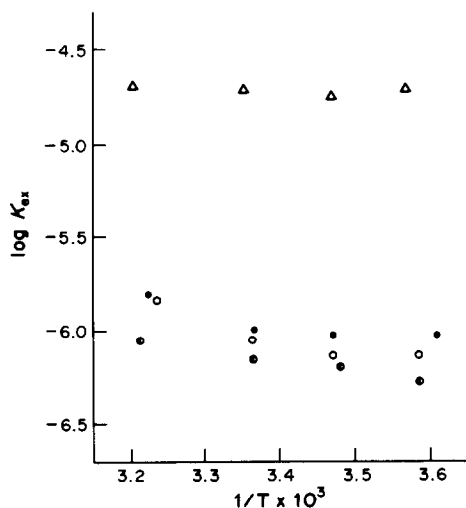


Fig. 5. Variation of extraction constant for Mn(II) as a function of temperature. \triangle , HPMBP; \bullet , C_6 ; \circ , C_{12} ; \ominus , C_3 .

Figure 5 represents the variation of $\log K_{ex}$ as a function of the inverse of the absolute temperature and indicates that the extraction reaction is endothermic.

Table 2. Effect of diverse ions on extraction of $4 \mu g$ of Mn(II): all results are mean values of 3 determinations

Ion	Amount of ion added, mg	Manganese found, μg	Recovery, %
Na	1.6	4.0	100
Mg	0.16	4.0	100
	1.6	3.6	90
Ca	1.6	3.9	98
V(V)	0.16	3.5	88
Fe(III)	0.16	4.0	100
	1.6	4.0	100
Co(II)	0.16	4.0	100
Ni	0.16	4.0	100
Cu	0.16	4.0	100
Zn	0.16	4.0	100
Cd	0.16	4.0	100

Interferences

A solution containing $25 \mu g$ of Mn(II) was placed in a 100-ml beaker, and 5 ml of 5% ammonium citrate solution and 1 or 10 mg of foreign ion were added. The pH was adjusted to *ca.* 8 with ammonia solution, the mixture was diluted to 50 ml with water, and an 8-ml portion was shaken for about 30 min (at 25°) with 8 ml of 0.01M HPMBP solution in MIBK, in a centrifuge tube. After separation of the phases the concentration of Mn in the MIBK was determined directly by an atomic-absorption method. The pH of the equilibrated aqueous solution was *ca.* 6.7.

The effect of foreign ions on the determination of Mn(II) is listed in Table 2. Most of the cations tested do not interfere at the 20-ppm level, but at higher concentrations some can cause incomplete extraction because of competitive complexation with HPMBP.

Acknowledgements—The authors thank Dr M. Kajitani for the elemental analysis of the reagents. The work was partly supported by a Grant-in-Aid for Scientific Research from the Ministry of Education, Science and Culture.

REFERENCES

1. B. S. Jensen, *Acta Chem. Scand.*, 1959, **13**, 1668.
2. M. K. Chmutova, G. A. Pribylova and B. F. Myasoedov, *J. Anal. Chem. USSR*, 1973, **28**, 2076.
3. F. T. Coronel, St. Mareva and N. Yordanov, *Talanta*, 1982, **29**, 119.
4. A. Roy and K. Nag, *J. Inorg. Nucl. Chem.*, 1978, **40**, 331.
5. M. K. Chmutova and N. E. Kochetkova, *J. Anal. Chem. USSR*, 1969, **24**, 112.
6. Yu. A. Zolotov, N. T. Sizonenko, E. S. Zolotvitskaya and E. I. Yakovenko, *ibid.*, 1969, **24**, 15.
7. M. Y. Mirza and F. I. Nwabue, *Talanta*, 1981, **28**, 49.
8. Y. Akama, T. Nakai and F. Kawamura, *Analyst*, 1981, **106**, 250.
9. Y. Akama, K. Sato, M. Ukaji, T. Kawata and M. Kajitani, *Polyhedron*, 1985, **4**, 59.

RAPID ACCURATE ISOTOPIC MEASUREMENTS ON BORON IN BORIC ACID AND BORON CARBIDE

NICOLAS L. DUCHATEAU,* A. VERBRUGGEN, F. HENDRICKX and P. DE BIÈVRE
Central Bureau for Nuclear Measurements, Commission of the European Communities,
Joint Research Centre, B-2440 Geel, Belgium

(Received 25 July 1985. Accepted 6 December 1985)

Summary—A procedure is described whereby rapid and accurate isotopic measurements can be performed on boron in boric acid and boron carbide after fusion of these compounds with calcium carbonate. It allows the determination of the isotopic composition of boron in boric acid and boron carbide and the direct assay of boron or the ^{10}B isotope in boron carbide by isotope-dilution mass spectrometry.

Owing to its high neutron-absorption cross-section, the ^{10}B isotope abundance in boron compounds and the ^{10}B or boron content of materials used in the nuclear industry (e.g., boric acid, boron carbide) are of great interest. Boron can be isotopically analysed by thermal-ionization mass spectrometry of the $\text{Na}_2\text{BO}_2^+ \text{ion}^{1-4}$ or by gas mass spectrometry of the gaseous BCl_2^+ and BF_2^+ ions.^{5,6} These methods tend to be slow because the sample preparation is time-consuming and very critical. Normally boron carbide is dissolved by fusion with alkali followed by a cation-exchange column purification,⁷⁻⁹ or the boron is separated as methyl borate after pyrohydrolysis of the compound under investigation.^{10,11} The boron is then converted into borax for mass spectrometric isotope-ratio measurements.⁴

This paper describes a fast procedure for preparing samples and use of BO_2^- ions for isotopic measurements¹² without further separation.

EXPERIMENTAL

Thermal-ionization mass spectrometry

A mass spectrometer with a 68° magnetic-field sector and 30.5-cm radius of curvature was used for this work. The sample is thermally ionized from a single filament. Ion currents, typically 10^{-11} – 10^{-9} A, are collected in a deep Faraday bucket connected to a 10^9 – 10^{11} ohm input resistor and measured by a vibrating reed electrometer (Cary 401). After analogue-digital conversion, the ion-current intensities are read on a digital voltmeter.

A rhenium filament (0.7 mm wide, 0.025 mm thick) is outgassed under vacuum by passing a current of 3.5 A through it for 100 min. Then $2 \mu\text{l}$ of the sample solution (boron $2 \mu\text{g}/\mu\text{l}$) is deposited on the filament and dried with a current of 0.7–1.0 A. The filament current is then increased until incipient red heat is observed (1.7–1.9 A).

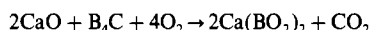
The sample is then mounted in the ion-source, and heated at 800° until the pressure reaches 1×10^{-4} Pa. This temperature is just below the 850° required for BO_2^- ion emission.

With an accelerating potential of -3833 V, the sample is heated to 1000° , and after an ion-beam focusing period of 30 min, 4 runs, each consisting of 10 isotope ratio

measurements, are recorded. Peak-height measurements are made at masses 42 ($^{10}\text{B}^{16}\text{O}^{16}\text{O}^-$) and 43 ($^{11}\text{B}^{16}\text{O}^{16}\text{O}^-$). The baseline is monitored at masses $41\frac{3}{4}$, $42\frac{1}{2}$, $43\frac{1}{4}$, and measured before and after the peak height determinations. A correction is made for $^{10}\text{B}^{16}\text{O}^{17}\text{O}$ interference at mass 43.⁴ No other (isobaric) interferences are observed.

Chemical preparation of the samples for boron isotope-ratio measurements

Modylevskaya *et al.*¹³ have proposed the use of calcium oxide or barium carbonate for sintering boron carbide. We have tested five different calcium/barium compound combinations for their melt-formation properties and subsequent mass-spectrometric behaviour. The reaction (with calcium oxide) is



It is observed that a Ca/B weight ratio of 10 (Ca/B mole ratio 2.7) does not disturb BO_2^- ion emission. However, a Ba/B mole ratio of 2.7 would give too large a weight of barium salt to work with. The weight and mole ratios tested are given in Table 1.

The following procedure is found to work satisfactorily: ca. 0.01 g of finely ground boron carbide is carefully mixed with the calcium or barium compound in a platinum crucible. The crucible is heated in a muffle furnace at 1000° for 150 min. After cooling, the melt is poured into a Teflon beaker and dissolved in 5M hydrochloric acid. This solution is evaporated to dryness and dissolved in water to obtain a $2\text{-}\mu\text{g}/\mu\text{l}$ boron solution. Further experimental observations are summarized in Table 2.

When loaded on the rhenium filament of the mass spectrometer, a drop of sample solution made from the barium hydroxide/boron carbide melt does not attach readily to the surface. Barium borates emit higher ion beams for the same sample size, but ion emission stability is better with calcium borates. Moreover, the dissolution of calcium melts is easier than is that of barium melts. Since calcium carbonate is the purest calcium salt commercially available, this was selected for our method.

Table 1. Ca/B and Ba/B ratios tested

	Stoichiometric		Experimental	
	Weight ratio	Mole ratio	Weight ratio	Mole ratio
Ca	1.85	1	10	5.4
B	1	2	1	2
Ba	6.35	1	15	2.4
B	1	2	1	2

*EC Fellow from Antwerp University.

Table 2. Chemical properties and mass spectrometric behaviour of calcium or barium salt/boron carbide melts

Compound	CaCO ₃	Ca(OH) ₂	CaO	BaCO ₃	BaCO ₃	Ba(OH) ₂ ·8H ₂ O
Origin	Merck 2059 suprapur	Merck 2047 pro analysi	Merck 2112 LAB/DAB 6	Merck 1714 pro analysi	Merck 1714 pro analysi	Merck 1737 pro analysi
Purity, %	>99	>96	≈ 95	>99	>99	>98
Nature	crystalline	powder	—	powder	powder	—
Experimental Ca/B or Ba/B molar ratio	5.02/2	5.26/2	5.17/2	2.23/2	2.32/2	2.33/2
Homogenization	normally no problem, but must be done carefully (boron carbide must be finely ground)					
Fusion temperature, °C	1000 ± 50					
Fusion time, min	120–180					
Dissolution of the product in 5M HCl	easy			difficult		
Melt on the filament	powdery			crystalline		
Vacuum during preheating	gets worse			does not change		
Ion current, A	10 ⁻¹⁰ –10 ⁻⁹			10 ⁻⁹ –10 ⁻⁸		
Ion-current stability	stable (<0.1% imprecision on each run)			less stable (0.1–1% imprecision on each run)		

Boron isotope ratio measurements and ¹⁰B abundance determination

To determine how accurately boron isotope ratios can be measured, a set of 12 melts, 6 made with calcium carbonate and “natural” boric acid (CBNM Isotopic Reference Material 011) and 6 made with calcium carbonate and boron carbide B₄C(t) (Franco-Belge de Fabrication de Combustibles, Dessel, Belgium) was prepared. Each preparation consisted of 184.3 ± 3.2 mg of calcium carbonate and 42.9 ± 1.4 mg of boric acid or 10.3 ± 0.5 mg of boron carbide. Each mixture was analysed three times. The measured ion currents were in the 10⁻¹¹–10⁻¹⁰ A range. The relative standard deviations (for the 3 measurements on an individual sample and for all 6 samples) were better than 0.3%. No difference in precision between boric acid and boron carbide samples was observed (Table 3).

The measurement of CBNM-IRM 011 allowed the correction for isotope fractionation to be made, so that “absolute” determinations became possible by use of the isotope fractionation correction factor *K*:

$$K = \frac{{}^{10}\text{B}/{}^{11}\text{B}_{\text{certified}}}{{}^{10}\text{B}/{}^{11}\text{B}_{\text{observed}}}$$

$$= \frac{0.247\ 26 \pm 0.000\ 32}{0.248\ 58 \pm 0.000\ 64}$$

$$= 0.994\ 69 \pm 0.002\ 86\ (2s\ \text{uncertainty}).$$

This *K*-factor could then be used to correct the observed ¹⁰B/¹¹B ratio in the three boron carbide and four boric acid batches from different origins which were analysed for isotopic composition. Two samples were taken from each batch, converted into calcium borate as described above and measured for boron isotope ratio. When the two isotope ratios of the two samples (from one batch) agreed within 0.3% (the experimentally determined relative standard deviation for boron isotope ratio measurements, Table 3) the mean boron isotope ratio was taken and a 2*s* uncertainty of 0.3% accepted (Table 4). Orthodox uncertainty propagation then yielded 0.3% relative uncertainty for the ¹⁰B atom abundance.¹⁴ The results differ by 1% for the ¹⁰B/¹¹B ratio (Table 4), a phenomenon which is well known, for boron materials of different isotopic composition circulate on the market.¹⁵

The method described does not require a chemical purification and yet does not influence the isotope ratio, as opposed to the method described by Lerner,⁹ where purification is necessary. When the B₄C(F) sample was prepared by both methods and the isotope ratios are measured, the results agreed within experimental error:

present method: ¹⁰B/¹¹B ratio = 0.249 54 ± 0.000 96
Lerner's method: ¹⁰B/¹¹B ratio = 0.249 01 ± 0.001 37

Assay of boron in boron carbide by isotope dilution mass spectrometry (IDMS)

In IDMS, the amount of an element *N_x* in a sample is calculated from the change induced in the isotope ratio *R_x* of two isotopes of that element, if a known amount *N_y* of that element (spike) with another isotope ratio *R_y* is added to the sample, the isotope ratio of the spiked sample being *R_B*:

$$N_x = N_y \left(\frac{R_y - R_B}{R_B - R_x} \right) \left(\frac{1 + R_x}{1 + R_y} \right)$$

In our case *R* = ¹⁰B/¹¹B. A boric acid material isotopically enriched to 95% ¹⁰B (NBS-SRM 952) was used as the spike. The amount of ¹⁰B (most important in the nuclear industry) was directly calculated by using a modified equation:

$$N_x^{10} = N_y \left(\frac{R_y - R_B}{R_B - R_x} \right) \left(\frac{R_x}{1 + R_y} \right)$$

The accuracy of the determination is defined by the accuracy of the measured isotope ratios.¹⁶ A fundamental advantage of IDMS is that the absolute isotope ratios can be measured with high precision and accuracy by calibration with reference isotopic materials or synthetic mixtures of isotopes. Additional advantages are that it is not necessary to separate the spiked element quantitatively from the sample, and that the method is insensitive to chemical interference.

The ¹⁰B/¹¹B isotope ratios *R_B* of the spiked samples ranged between that for natural boron (*R_x* ~ 20/80) and that of the spike (*R_y* ~ 95/5). By use of “natural” boric acid (CBNM-IRM 011) and “¹⁰B-enriched” boric acid (NBS-SRM 952), an isotope fractionation correction factor *K* = 0.9947 ± 0.0028 was determined. The true isotope ratio could then be calculated from *R* = *K**R'* where *R* = the true isotope ratio, *K* = isotope fractionation correction factor and *R'* = the measured isotope ratio (see Table 5).

In an attempt to use amounts of spike and sample materials as small as possible, but still retain the possibility of direct weighing of the original solid materials (no solutions) to within 0.1% uncertainty, the amounts of material were reduced to 45 mg of calcium carbonate, 2.5 mg of boron carbide and 20 mg of ¹⁰B-enriched boric acid (spike). Amounts lower than 2.5 mg could not be weighed directly to within 0.1%.

In the determinations described here, the boron carbide B₄C(t) samples were weighed-spiked, converted into calcium borate and measured for their boron content. The ion-currents were in the 10⁻¹¹–10⁻¹⁰ A range. One g of the boron carbide contains 778 ± 11 mg of elemental boron or 144.0 ± 2.0 mg of ¹⁰B (details and results in Table 6). The B/C atom ratio is 3.9 ± 0.2. Since the chemical blank is less than 3 μg (Table 6) and the uncertainty in the

Table 3. Standard deviations on $^{10}\text{B}/^{11}\text{B}$ isotope ratio measurements of boric acid and boron carbide (all uncertainties are $2s$)*

Sample	Measurement No.	$^{10}\text{B}/^{11}\text{B}$ isotope ratio measurement		
B_4C	1-1	0.251 41		
	1-2	0 98	0.251 18 \pm 0.000 44	RISD (0.18%)
	1-3	1 16		
	2-1	1 94		
	2-2	1 60	0.251 51 \pm 0.000 96	RISD (0.38%)
	2-3	1 00		
	3-1	1 01		
	3-2	0 62	0.250 91 \pm 0.000 50	RISD (0.20%)
	3-3	1 09		
	4-1	1 80		
	4-2	0 93	0.251 30 \pm 0.000 90	RISD (0.36%)
	4-3	1 17		
	5-1	1 03		
	5-2	1 05	0.251 02 \pm 0.000 08	RISD (0.03%)
	5-3	0 97		
6-1	1 18			
6-2	0 98	0.251 07 \pm 0.000 20	RISD (0.08%)	
6-3	1 05			
			0.251 17 \pm 0.000 65	RESD (0.26%)
H_3BO_3	1-1	0.248 36		
	1-2	8 47	0.248 61 \pm 0.000 70	RISD (0.28%)
	1-3	9 01		
	2-1	8 30		
	2-2	8 58	0.248 33 \pm 0.000 48	RISD (0.19%)
	2-3	8 11		
	3-1	8 54		
	3-2	8 41	0.248 61 \pm 0.000 48	RISD (0.19%)
	3-3	8 87		
	4-1	8 65		
	4-2	8 32	0.248 60 \pm 0.000 52	RISD (0.21%)
	4-3	8 83		
	5-1	9 35		
	5-2	8 52	0.248 96 \pm 0.000 84	RISD (0.34%)
	5-3	9 01		
6-1	8 20			
6-2	8 38	0.248 37 \pm 0.000 34	RISD (0.14%)	
6-3	8 53			
			0.248 58 \pm 0.000 64	RESD (0.26%)

*RISD = relative internal standard deviation (3 measurements for a given sample);
RESD = relative external standard deviation (all 6 samples).

Table 4. ^{10}B isotope abundances measured on some boric acid and boron carbide batches

	Measured isotope ratio ($2s = 0.000\ 65$)	K -corrected isotope ratio ($2s = 0.000\ 96$)	^{10}B atom abundance ($\pm 2s$)	^{10}B mass abundance ($\pm 2s$)	Atomic weight of the boron ($\pm 2s$)	Ion current, A
$\text{B}_4\text{C}(t)$	0.251 17	0.249 84	19.99 \pm 0.06	18.52 \pm 0.06	10.810 1 \pm 0.000 6	8.0×10^{-11}
$\text{H}_3\text{BO}_3(\text{T})$	0.251 67	0.250 33	20.02 \pm 0.06	18.55 \pm 0.06	10.809 8 \pm 0.000 6	9.9×10^{-11}
$\text{H}_3\text{BO}_3(\text{N})$	0.248 64	0.247 32	19.83 \pm 0.06	18.36 \pm 0.06	10.811 7 \pm 0.000 6	8.8×10^{-11}
$\text{H}_3\text{BO}_3(\text{D})$	0.249 98	0.248 65	19.91 \pm 0.06	18.44 \pm 0.06	10.810 9 \pm 0.000 6	4.3×10^{-11}
$\text{H}_3\text{BO}_3(\text{M})$	0.248 03	0.246 71	19.79 \pm 0.06	18.33 \pm 0.06	10.812 1 \pm 0.000 6	3.7×10^{-11}
$\text{B}_4\text{C}(\text{N})$	0.251 54	0.250 20	20.01 \pm 0.06	18.54 \pm 0.06	10.809 9 \pm 0.000 6	11.2×10^{-11}
$\text{B}_4\text{C}(\text{F})$	0.250 87	0.249 54	19.97 \pm 0.06	18.50 \pm 0.06	10.810 3 \pm 0.000 6	8.6×10^{-11}

Table 5. Isotope fractionation correction factor K (uncertainties are $2s$)

Isotope reference material	Certified $^{10}\text{B}/^{11}\text{B}$ isotope ratio	Observed $^{10}\text{B}/^{11}\text{B}$ isotope ratio	Isotope fractionation correction factor K
CBNM-IRM 011 natural boric acid	0.247 26 \pm 0.000 32	0.248 58 \pm 0.000 64	0.994 7 \pm 0.002 8
NBS-SRM 952 ^{10}B -enriched boric acid	18.80 \pm 0.02	18.902 \pm 0.050	0.994 6 \pm 0.002 8
			0.994 7 \pm 0.002 8

Table 6. Boron assay of boron carbide ($2s$ uncertainty on each sample) and blank determinations (BI) of the procedure

No.	Amount of CaCO_3 mg	Amount of $\text{H}_3^{10}\text{BO}_3$, (spike) mg	$^{10}\text{B}/^{11}\text{B}$ isotope ratio of the blend	Experimental amount of elemental boron, mg	Experimental amount of ^{10}B , mg	Weighted amount of boron carbide, mg	Weight % boron in boron carbide, ($\pm 2s$ uncertainty)	Weight % ^{10}B in boron carbide, ($\pm 2s$ uncertainty)
1	44.9 \pm 0.4	20.57 \pm 0.02	2.183 7 \pm 0.001 6	1.988 \pm 0.014	0.368 \pm 0.002	2.531 \pm 0.002	78.6 \pm 0.6	14.54 \pm 0.08
2	45.6 \pm 0.4	19.96 \pm 0.02	2.168 4 \pm 0.001 4	1.946 \pm 0.014	0.360 \pm 0.002	2.512 \pm 0.002	77.5 \pm 0.6	14.34 \pm 0.08
3	45.6 \pm 0.4	19.88 \pm 0.02	2.193 7 \pm 0.000 6	1.910 \pm 0.013	0.354 \pm 0.002	2.468 \pm 0.002	77.4 \pm 0.6	14.33 \pm 0.08
4	45.0 \pm 0.4	19.70 \pm 0.02	2.177 7 \pm 0.000 8	1.910 \pm 0.013	0.354 \pm 0.002	2.472 \pm 0.002	77.3 \pm 0.6	14.31 \pm 0.08
5	45.8 \pm 0.4	19.71 \pm 0.02	2.192 1 \pm 0.001 2	1.895 \pm 0.013	0.351 \pm 0.002	2.427 \pm 0.002	78.1 \pm 0.6	14.46 \pm 0.08
BI 1	45.2 \pm 0.4	20.24 \pm 0.02	18.779 \pm 0.068	0.001 5 \pm 0.001 0			77.8 \pm 1.1	14.40 \pm 0.20
BI 2	45.7 \pm 0.4	20.39 \pm 0.02	18.802 \pm 0.022	0.001 2 \pm 0.000 7				

experimentally determined amount of boron is 13 μg , the contribution from this source to the total uncertainty is practically negligible.

An estimate of boron losses during the analysis was made as follows: one sample was spiked normally, another was spiked after the fusion and a third after evaporation of the acid solution. Starting with about 2.2 mg of boron (as boron carbide), about 0.2 mg of boron is lost during the fusion and < 0.1 mg during evaporation of the acid solution to dryness.

Acknowledgements—The authors express their gratitude to all members of the Mass Spectrometry Group at the Central Bureau for Nuclear Measurements for their technical support and to Dr K. Rosman for his stimulating advice. Further, they wish to thank Mrs H. Nagel-Kerslake for editing and typing assistance. Their thanks also go to the Société Franco-Belge de Fabrication de Combustibles, Dessel, Belgium, for making boron carbide available, and to the Directorate General for Science, Research and Development of the Commission of the European Communities (D. Prüss) for a fellowship.

REFERENCES

- H. O. Finley, A. R. Eberle and C. J. Rodden, *Geochim. Cosmochim. Acta*, 1962, **26**, 911.
- M. Shima, *ibid.*, 1963, **27**, 911.
- E. K. Ageyi and C. C. McMullen, *Can. J. Earth Sci.*, 1968, **5**, 921.
- P. De Bièvre and G. H. Debus, *Int. J. Mass Spectrom. Ion Phys.*, 1969, **2**, 15.
- H. G. Thode, J. Macnamara, F. P. Lossing and C. B. Collins, *J. Am. Chem. Soc.*, 1948, **70**, 3008.
- V. Shiuttse, *Sov. Phys. JETP*, 1956, **2**, 402.
- H. Blumenthal, *Anal. Chem.*, 1951, **23**, 992.
- A. R. Eberle and M. W. Lerner, *USAEC Report NBL 216*, 1961, New Brunswick Laboratory, Argonne National Laboratory, Argonne, Ill., U.S.A.
- M. W. Lerner, *The Analysis of Elemental Boron*, 1970, USAEC Division of Technical Information TID-25190, New Brunswick Laboratory, Argonne National Laboratory, Argonne, Ill., U.S.A.
- L. Morgan, *Analyst*, 1964, **89**, 621.
- V. R. Wiederkehr and G. W. Goward, *Anal. Chem.*, 1969, **31**, 2102.
- N. L. Duchateau and P. De Bièvre, *Int. J. Mass Spectrom. Ion Phys.*, 1983, **54**, 289.
- K. D. Modylevskaya, M. D. Lyutaya and T. N. Nazarchuk, *Zavodsk. Lab.*, 1961, **27**, 1345.
- R. Werz, *CBNM Internal Report*, MS-R-23-83, 1983.
- G. H. Debus, P. De Bièvre and J. Spaepen, *J. Nucl. Energ. Parts A/B*, 1963, **17**, 349.
- P. De Bièvre, *Nukleare Analysenverfahren bei der Erzeugung und Industriellen Nutzung von Edelmetallen* (Symposium, Brussels, Nov. 1971, Report No. 71), *Eurisotop*, 1973, p. 519, Commission of the European Communities, Brussels.

MICROSPECTROMETRIE RAMAN MULTICANALE: APPLICATION A L'IDENTIFICATION DU TRIMETHYLACETATE ET DU CAPROATE DE FLUOCORTOLONE ISOLES D'UNE FORME GALENIQUE

A. P. GAMOT,* G. VERGOTEN†, M. SAUDEMON et G. FLEURY‡

Laboratoire de Chimie Analytique* et de Physique† U279 INSERM, Faculté de Pharmacie, Université de Lille II, rue du Professeur Laguesse, 59045 Lille, France et Centre de Technologie Biomédicale INSERM, 13-17, rue C. Guérin-59000 Lille, France

J. BARBILLAT§

Société Dilor§, 244 ter, rue des bois blancs 59000 Lille, France

(Reçu le 18 juillet 1983. Révisé le 18 novembre 1985. Accepté le 6 décembre 1985)

Résumé—Ce travail est une application des résultats obtenus en spectroscopie Raman classique par notre équipe à propos de la fluocortolone et deux de ses esters: le triméthylacétate et le caproate. Afin de s'affranchir des différents problèmes inhérents aux excipients (fluorescence) une extraction par solvant suivie d'une séparation par HPLC a été nécessaire. Le but de ce travail était d'identifier par spectrométrie Raman les deux corticostéroïdes sur la base de leur structure moléculaire à partir des éluats provenant de l'HPLC. Après différents essais réalisés avec les produits en solution (méthanol/eau) nous avons été contraints de revenir à une forme cristalline et de ce fait d'utiliser une microsonde Raman multicanale, ce qui nous a permis d'identifier de façon certaine la structure $\Delta^{1,4}$ 3-one sur des quantités de l'ordre du picogramme.

Dans un précédent travail¹ concernant l'étude par spectrométrie Raman d'esters dérivés de la fluocortolone nous avons montré qu'il était possible d'une part de caractériser ces corticostéroïdes par leur structure $\Delta^{1,4}$ 3-one et d'autre part de différencier la fluocortolone de ses deux esters et chacun des esters entre eux.

Maintenant nous avons appliqué les résultats obtenus à l'identification du triméthylacétate (TMAF) et du caproate (CAF) de fluocortolone contenus en association dans une préparation pharmaceutique à partir d'éluats de chromatographie liquide-liquide (HPLC).

Bien qu'il ne s'agisse pas dans notre étude d'un couplage chromatographie-spectrométrie Raman il est nécessaire de rappeler quelques essais réalisés dans ce domaine.

Les travaux de Chapput *et al.*^{2,3} font état de l'utilisation d'un spectromètre Raman comme détecteur sélectif de la chromatographie en phase liquide afin d'identifier des espèces chimiques à faibles concentrations dans différents solvants. Le couplage des deux techniques est fait par l'intermédiaire d'une microcellule à circulation placée en fin de colonne. Le détecteur du spectromètre Raman monocanal est un photomultiplicateur R.C.A.C. 31034 A.³ Le laser fournit une puissance de 500 mW au niveau de l'échantillon.

Pour accroître l'intensité de la faible lumière diffusée par les solutés deux méthodes sont utilisées conjointement en multipliant le nombre de passage du faisceau laser dans l'échantillon et en collectant

davantage de lumière par l'intermédiaire d'un objectif de transfert à grande ouverture et fort grossissement.

Il est de plus précisé que parmi les trois techniques de détection utilisées² c'est celle du balayage spectral en écoulement continu qui a donné le meilleur résultat.

Pour analyser les effluents provenant de l'HPLC, Saito *et al.*⁴ proposent un nouveau système de détection basé sur la spectrométrie Raman de résonance. Leur étude décrit le couplage d'une microcellule en quartz, à écoulement continu avec le spectromètre. Le pouvoir de détection est considérablement augmenté dans ce cas si la fréquence du rayonnement laser coïncide avec une bande d'absorption électronique du composé analysé. Le laser utilisé fournit 200 mW au niveau de l'échantillon. La mesure de l'intensité de la diffusion en Raman de résonance permet d'obtenir des chromatogrammes similaires à ceux donnés par détection ultraviolette.

Signalons enfin les travaux de King *et al.*⁵ en chromatographie en phase gazeuse où les fractions éluées sont congelées (12 K) sous forme de tâches de 1 mm de diamètre. Ces tâches sont ensuite analysées séquentiellement par spectrométrie Raman.

L'étude présentée dans cette publication a été réalisée à partir d'éluats (HPLC) qui sont analysés séparément. Les premiers essais effectués en solution par spectrométrie Raman n'ont pas été concluants ce qui nous a conduit à éliminer le solvant. Les échantillons polycristallins obtenus ont ensuite été analysés par microspectrométrie Raman à détection

multicanales. Cette technique permet d'une part une irradiation ponctuelle (le volume irradié est de l'ordre de quelques μm^3) de l'échantillon par le laser et d'autre part certaines innovations ont permis d'améliorer considérablement la détection de l'information spectrale. Parmi elles, il faut citer les détecteurs quantiques à rendement élevé (détecteurs multicanaux à barettes de photodiodes) qui associés à l'informatique ont conduit à une nouvelle génération de microanalyseurs Raman multicanaux.⁶ Ces nouveaux appareils permettent d'obtenir un spectre en un temps très court avec moins de perte d'information, un meilleur rapport signal sur bruit tout en conservant la possibilité de suivre l'évolution des phénomènes variant rapidement au cours du temps. Enfin grâce à la sensibilité de la détection les substances sont analysées en utilisant une irradiation laser très faible (80 mW dans cette étude) ce qui évite la destruction de l'échantillon.

Nous décrivons dans un premier temps la méthode utilisée pour extraire et séparer les deux esters (TMAF et CAF), puis les problèmes posés par l'identification en solution (méthanol/eau) de ces composés par spectrométrie Raman classique (mono-canal) et enfin les résultats obtenus en micro-spectrométrie Raman multicanale.

Ce travail a aussi pour but de montrer que si l'HPLC reste un excellent moyen pour séparer, identifier et doser les composés étudiés, elle ne donne en fait que peu de renseignements exploitables instantanément sur la structure des molécules ainsi séparées. C'est pourquoi nous avons voulu associer cette technique à la spectrométrie Raman afin de caractériser avec certitude, sur des bases structurales, les substances isolées (éluates à faible concentration) de leur forme galénique.

PARTIE EXPERIMENTALE

Appareillage

L'équipement HPLC utilisé est constitué d'un chromatographe 5020 Varian, d'un injecteur à boucle de 20 μl et d'une colonne de 250 \times 4 mm conditionnée avec une silice greffée C 18, Lichrosorb RP 18 (Merck) de granulométrie 10 μm . Le détecteur Varian UV 5 est équipé d'un filtre de 240 nm. Il est couplé à un enregistreur intégrateur Hewlett-Packard 3390 A. La phase mobile utilisée est un mélange de méthanol désaéré par passage aux ultrasons et d'eau pour préparations injectables.

La microsonde Raman utilisée est de type Microdil 28 (Société "Dilor"). Les éléments qui la constituent, présentent les caractéristiques suivantes:

- la source est un laser à argon ionisé 514,5 nm (Spectra Physics);
- le microscope conventionnel est muni des objectifs 10 \times , 50 \times , 100 \times ;
- le prémonochromateur consiste en un monochromateur double soustractif de bande passante 800 cm^{-1} ;
- le spectrographe stigmatique est spécialement adapté

pour le détecteur linéaire à photodiode; il comporte deux réseaux (montés dos à dos) de dispersion respective 42 cm^{-1}/mm soit 1 cm^{-1} par diode et 160 cm^{-1}/mm soit 45 cm^{-1} par diode;

—le détecteur comporte une barette de diodes intensifiées refroidies à -25°C .

L'ensemble est couplé à un intégrateur Hewlett-Packard 1000 L, permettant des temps d'intégration de 10 msec à 99 secs.

Méthode et conditions expérimentales

Extraction. Les deux esters de la fluocortolone ont été extraits à chaud par le méthanol afin d'éliminer la plupart des 9 excipients* présents dans la préparation pharmaceutique (crème). La procédure suivante a été retenue:

- extraction pendant 30 mn de 4 g de crème sur plaque chauffante magnétique à l'aide de 70 ml de méthanol à la limite de l'ébullition ($55-60^\circ$);
- refroidissement dans la glace;
- filtration dans une fiole jaugée de 100 ml à l'aide d'un filtre plissé;
- rinçage de l'erlenmeyer et du filtre avec méthanol refroidi;
- ajustage au trait de jauge.

Séparation des deux esters par HPLC. L'échantillon recueilli, prêt pour l'injection possède donc une concentration connue voisine de 10 mg de chaque ester dans 100 ml de méthanol.

Une solution étalon aux mêmes concentrations est également préparée par dissolution directe des deux dérivés dans le méthanol.

Après plusieurs essais, les paramètres permettant une séparation optimale étaient fixés:

- solvant: méthanol/eau, 3:1 v/v;
- débit: 1,5 ml/mn;
- température: 29° .

La reproductibilité des chromatogrammes a été vérifiée après 6 injections d'une solution étalon et 25 injections de la solution méthanolique résultant de l'extraction. Grâce à l'intégrateur couplé au détecteur, il a été aisé de calculer la concentration moyenne des éluats correspondant au triméthylacétate de fluocortolone ($2,56 \pm 0,13$ g/kg de crème) et au caproate de fluocortolone ($2,43 \pm 0,11$ g/kg de crème).

Ce calcul des concentrations n'avait pour but que de vérifier l'absence de pertes au cours de l'extraction. Les valeurs obtenues concordent avec celles indiquées par le fabricant (2,50 g/kg de crème).

Récupération des fractions. A la sortie du détecteur, 25 fractions de chaque ester ont été collectées. Elles proviennent chacune de l'élution de 20 μl d'échantillon à une concentration voisine de 100 $\mu\text{g}/\text{ml}$. Les deux solutions ainsi recueillies, diluées par la phase mobile (méthanol/eau, 3:1 v/v) ont été concentrées au bain-marie à 40° et sous vide jusqu'à obtention d'une solution titrant environ 25 $\mu\text{g}/\text{l}$. Ces échantillons ont ensuite été placés dans des tubes capillaires et conservés à des fins d'analyses ultérieures en spectrométrie Raman classique et microscopique.

Analyse spectrométrique. Dans un premier temps une étude en spectrométrie Raman classique a été faite sur les composés en solution dans le mélange méthanol/eau provenant des éluats. Cependant différents problèmes sont apparus lors des premiers essais. Si les spectres des solvants présentaient des zones sans bandes intenses dans l'intervalle de fréquences caractéristiques des stéroïdes étudiés $1500-1800$ cm^{-1} ,¹ la trop faible concentration des solutés n'a pas permis de mener à bien cette étude. En effet, même les essais effectués sur des solutions étalons saturées n'ont pas donné les résultats escomptés, à une exception près, la fluocortolone base qui est le plus soluble des trois stéroïdes. Pour ce composé une raie caractéristique a pu être enregistrée entre 1500 et 1800 cm^{-1} après 10 accumulations de spectre grâce au système APPLE II couplé au spec-

*Excipients: tétracémate disodique, stéarate de polyoxyéthylène glycol 40, vaseline blanche, huile de vaseline épaisse, alcool stérilique, polymère carboxyvinyle, hydroxyde de sodium, parfum, eau déminéralisée.

tromètre Raman. Un dernier essai en spectrométrie Raman classique a été tenté en utilisant des échantillons de stéroïdes préparés par évaporation du contenu d'un tube capillaire (*cf.* récupération des fractions) sur la paroi d'un support constitué d'une fine baguette de verre de 3 mm de diamètre vers laquelle le rayonnement laser a été dirigé.

Bien que le spectromètre utilisé permette d'obtenir des spectres bien résolus caractérisant les substances étudiées à l'état polycristallin comme cela a déjà été cité dans un travail préliminaire,¹ il s'est avéré qu'il n'était pas approprié à l'étude d'échantillon à faible concentration. Il fallait donc s'adresser à une technique plus fine pour enregistrer des spectres à partir d'échantillons de quelques μm^2 par l'intermédiaire d'un microscope. C'est pourquoi une microsonde Raman multicanale a été utilisée. Elle permet d'accéder à un volume d'échantillon de l'ordre du μm^3 , c'est à dire d'analyser quelques pg de substance de manière non destructive.⁷ Dans ce but les échantillons provenant des éluats d'HPLC ont été préparés par évaporation du contenu d'un capillaire au centre d'une lame de verre sur la surface la plus réduite possible. Les lames sont placées sur la platine du microscope du spectromètre. Elles sont ensuite irradiées, grâce à une optique spéciale, par un faisceau laser de faible puissance (80 mW). Des témoins de substances étalons obtenus dans les mêmes conditions et à des concentrations voisines ont également été préparés.

RESULTATS ET DISCUSSION

Les essais ont d'abord porté sur les préparations concernant les substances étalons et ensuite sur les échantillons provenant des éluats chromatographiques. Les quantités analysées sont de l'ordre du picogramme.

Préparations étalons

Dans un premier temps nous voulions vérifier s'il était possible de caractériser la classe des stéroïdes étudiés, c'est-à-dire la structure $\Delta^{1,4}$ -one (1580–1690 cm^{-1})¹ et ensuite explorer l'intervalle 1690–1750 cm^{-1} pour mettre en évidence les fonctions estérifiées et cétoniques des chaînes latérales respectivement en C_{20} [$\nu(\text{C}=\text{O})$ de la fonction ester] et C_{21} [$\nu(\text{C}=\text{O})$ de la

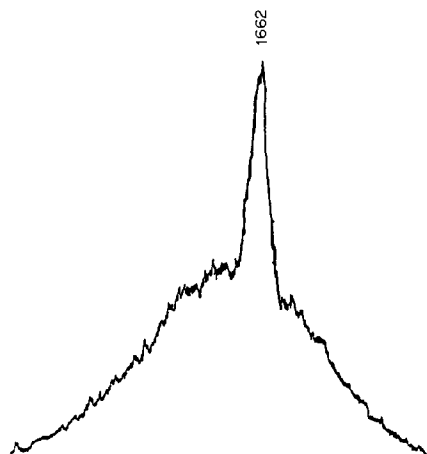


Fig. 1. Triméthylacétate (TMAF) étalon. Centre de la bande passante, 1661 cm^{-1} ; accumulation, 31 \times 2 sec; fente de 300 μm ; puissance du laser 80 mW.

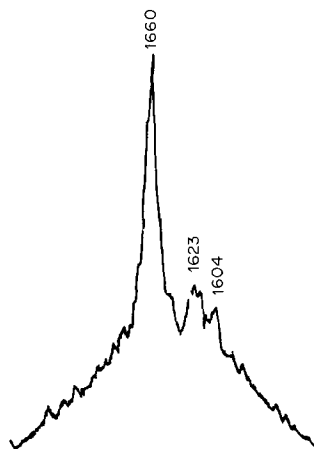


Fig. 2. Caproate (CAF) étalon. Centre de la bande passante, 1661 cm^{-1} ; accumulations, 26 \times 3 sec; fente de 300 μm ; puissance du laser 80 mW.

fonction cétonique]:

- le TMAF étalon a montré sur l'enregistrement une raie intense à 1662 cm^{-1} (Fig. 1) émergeant d'un massif dont le profil ne permet pas d'observer de façon certaine les raies situées de part et d'autre de la raie principale alors que ce composé donnait un spectre bien résolu lors de l'étude préliminaire en spectrométrie Raman monocanale classique,¹
- le CAF étalon a montré les trois raies attendues (Fig. 2), c'est-à-dire une raie intense avec deux raies de plus faible intensité situées vers les fréquences plus basses (répertoriées respectivement à 1660, 1623 et 1604 cm^{-1} ; structure $\Delta^{1,4}$ 3-one).¹

Remarques

Les raies étant plus intenses que lors de l'étude effectuée avec le TMAF (problème de préparation de la lame, choix du microcristal sur lequel la mise au point est faite) nous avons décidé d'explorer à partir de la raie à 1660 cm^{-1} la zone voisine (vers les fréquences plus élevées). Alors que le centre de la bande passante définie par le monochromateur avait été fixé à 1661 cm^{-1} dans le cas de l'enregistrement du spectre de la figure 2 celui-ci a été fixé à 1741 cm^{-1} pour l'enregistrement du spectre de la figure 3. Ce spectre permet de supposer l'existence des deux raies caractéristiques répertoriées à 1745 et 1723 cm^{-1} sans permettre toutefois de les distinguer du fond continu.

Dans un deuxième temps nous avons envisagé selon les mêmes modalités, l'étude d'autres zones spectrales représentatives des chaînes latérales estérifiées¹ fixées sur le carbone 21. En effet les raies situées à 350, 595, 796 cm^{-1} et 1352 cm^{-1} permettant de distinguer respectivement le TMAF du CAF¹ n'ont pu être mises en évidence malgré 23 accumulations de 4 sec chacune. Ce problème semble lié à la faible quantité de substance analysée ainsi qu'à l'intensité des raies qui est plus faible que celle des raies caractérisant la structure $\Delta^{1,4}$ 3-one. De plus la

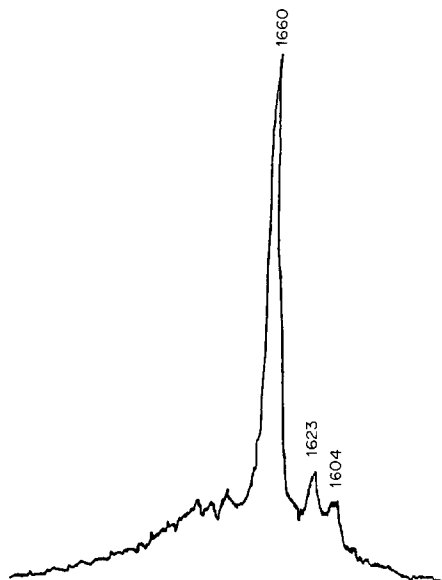


Fig. 3. Caproate étalon; centre de la bande passante 1741 cm^{-1} ; autres conditions voir Fig. 2.

réponse intrinsèque du détecteur fait que les raies sont superposées au fond continu.

Préparation provenant des éluats

Puisque seule la structure $\Delta^{1,4}$ 3-one peut être mise en évidence nous avons testé la préparation sur lame de verre concernant le CAF. Nous avons obtenu le spectre de la figure 4 avec les 3 raies caractéristiques situées à 1660, 1623 et 1604 cm^{-1} .

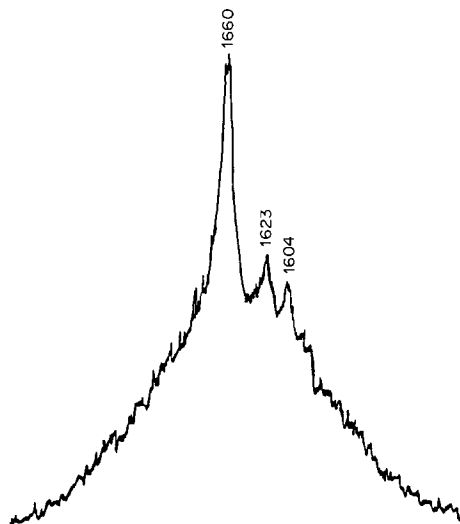


Fig. 4. Caproate échantillon évaporé à sec sur lame de verre; accumulations 27×3 sec; autres conditions voir Fig. 2.

Conclusion

Malgré les faibles quantités de produits présents dans les éluats de chromatographie, nous avons pu montrer dans ce travail qu'il était possible d'allier séparation par HPLC et identification par spectrométrie Raman.

Le problème qui se posait dans la juxtaposition de ces deux techniques résidait dans leur sensibilité respective; la première s'adressant à la séparation et au dosage de quelques ng, la seconde à l'identification sur plusieurs mg de substance en spectrométrie Raman classique. L'utilisation d'une technique récente, représentée par la microsonde Raman capable de tracer un spectre représentatif d'une structure moléculaire à l'aide de quelques pg de substance, a rendu notre étude possible, sur des échantillons polycristallins microscopiques.

En effet, grâce à ce type d'appareillage, nous sommes arrivés à établir l'appartenance d'un des esters de la fluocortolone à la classe des $\Delta^{1,4}$ 3-one stéroïdes. Il a même été possible d'envisager les raies caractéristiques des fonctions ester et cétone. Bien que la totalité de la structure moléculaire n'ait pu être identifiée, de grands espoirs restent permis avec l'arrivée des spectromètres multicanaux de la nouvelle génération.

L'apport de ces modifications dans la technique utilisée pourrait laisser présager des résultats encore plus satisfaisants: l'HPLC servant à séparer et recueillir des fractions pures, de substances totalement identifiables à l'aide des nouvelles microsondes Raman, pour des quantités de l'ordre du picogramme.

Remerciements—Nous remercions les laboratoires Schering qui ont fourni les corticostéroïdes étalons et les préparations pharmaceutiques. Nous tenons également à remercier la société Dilor qui a mis à notre disposition pour cette étude la microsonde "Microdil 28".

LITTÉRATURE

1. A. P. Gamot, G. Vergoten, M. Saudemon et G. Fleury, *Talanta*, 1985, **32**, 373.
2. A. Chapput, B. Roussel et J. Montastier, *J. Raman Spectrosc.*, 1980, **9**, 193.
3. *Idem*, *Compt. Rend.*, 1979, **289C**, 293.
4. S. Saito, N. Teramae et S. Tanaka, *Nippon Kagaku Kaishi*, 1980, **9**, 1363.
5. D. S. King et J. C. Stephenson, *Opt. Laser Technol.*, 1980, **12**, 97.
6. M. Delhayé, M. Bridoux et E. Da Silva, *Spectra 2000*, 1982, **10**, No. 77.
7. M. Delhayé, M. Bridoux et F. Wallart, *Courrier du C.N.R.S.*, 1981, **39**, 23.

Summary—This work is an application of the results obtained by classical Raman spectroscopy for fluocortolone and its trimethylacetate and caproate esters. These drugs are used together in a pharmaceutical preparation. To avoid fluorescence problems with excipients a solvent extraction was first applied, followed by an HPLC separation. The aim was to identify two corticosteroids through their molecular structure by applying Raman spectroscopy to HPLC eluates. Tests with the drugs in aqueous methanol solution proved unsatisfactory so recourse was made to use of the crystalline state and a Raman multichannel microprobe. This allowed the identification, with accuracy, of $\Delta^{1,4}$ -3-one structure with sample quantities as small as 10^{-12} g.

ANALYSE DE MELANGES COMPLEXES SUR LE COUPLAGE CHROMATOGRAPHIE EN PHASE GAZEUSE/SPECTROMETRIE INFRAROUGE PAR TRANSFORMEE DE FOURIER EQUIPE DE COLONNES CAPILLAIRES

G. MERLOT, B. LACROIX, M. T. ROMON, J. P. HUVENNE* et G. FLEURY
Centre Universitaire de Mesure et d'Analyse, Université de Lille II, rue du Professeur Laguesse,
59045 Lille, France

(Reçu le 12 juillet 1985. Accepté le 23 novembre 1985)

Résumé—Afin d'accroître le potentiel analytique du couplage chromatographie en phase gazeuse/spectrométrie infrarouge par transformée de Fourier nous avons adapté notre système à l'utilisation de colonnes capillaires et automatisé les procédures d'acquisition et de traitement des données. Après ces modifications, les performances sont testées au cours de l'analyse de mélanges complexes tels que les huiles essentielles de menthe et de lavande. Une perte en sensibilité et en résolution est constatée par rapport aux détecteurs classiques de chromatographie en phase gazeuse mais les spectres acquis en temps réel sont d'un grand intérêt pour la connaissance des structures moléculaires.

Face aux problèmes de plus en plus complexes posés par l'analyse des milieux biologiques, les techniques de séparation telles que les chromatographies en phase liquide ou en phase gazeuse ont connu, ces dernières années, des progrès technologiques rapides dans plusieurs domaines.

Cette évolution concerne essentiellement la qualité de la colonne, organe responsable de la séparation des constituants du mélange, ainsi que la capacité du système à détecter et identifier les composés séparés.

En ce qui concerne plus spécialement la chromatographie en phase gazeuse (CPG), il faut d'abord signaler la mise au point suivie du développement commercial de colonnes capillaires dont le premier avantage est d'accroître la résolution du chromatogramme. Parallèlement, l'informatisation de techniques physiques a permis d'obtenir d'un composé, un enregistrement spectrométrique caractéristique dans un temps de plus en plus court et sur des quantités de matière de plus en plus faibles. Ceci conduisit à envisager des couplages capables de donner des informations précises en vue d'identifier avec certitude les fractions séparées par CPG. La spectrométrie de masse fut la première technique utilisée¹ mais l'application de la transformée de Fourier a conféré à la spectrométrie infrarouge (IRTF) les critères de rapidité et de sensibilité nécessaires à la réalisation d'un couplage (CPG/IRTF).^{2,3}

Dans un premier temps ce type de couplage n'a fonctionné qu'avec des colonnes remplies et ce n'est

que plus récemment que des systèmes CPG/IRTF ont été transformés en vue de recevoir des colonnes capillaires.

L'objet de cet article est d'exposer les problèmes d'ordre pneumatique, optique, informatique qui se sont posés quand nous avons réalisé cette transformation sur notre système NICOLET 7199 B, ainsi que les solutions que nous y avons apportées. Enfin, nous présenterons des résultats d'analyse attestant du bon fonctionnement de l'installation après modification.

THEORIE

Intérêt des colonnes capillaires

Les premiers résultats expérimentaux obtenus avec des colonnes capillaires annoncées dès 1957⁴ datent de 1959. Depuis cette date, le nombre de publications et d'ouvrages généraux faisant état de travaux analytiques utilisant ces colonnes est devenu considérable. Nous ne citerons que le livre de Tranchant⁵ dont la bibliographie est très complète. Les avantages qui justifient une telle expansion sont essentiellement de trois ordres.

(1) Exprimée par:

$$P = \frac{r^2}{8}$$

où r (cm) est le rayon de la colonne, la perméabilité (P , cm²) est plusieurs centaines de fois supérieure à celle des colonnes remplies. Cela permet d'augmenter la longueur des colonnes sans créer de perte de charge trop importante. La vitesse du gaz vecteur demeure

*Auteur pour correspondance.

presque constante et optimale tout au long de la colonne.

(2) Le rapport (β) volume de phase mobile/volume de phase stationnaire est donné par

$$\beta = \frac{r}{2E_f}$$

ce qui donne pour une colonne capillaire classique de rayon $r = 0,16$ mm, d'épaisseur de film $E_f = 0,2$ μm , une valeur de β égale à 400, soit 20 fois supérieure à la valeur moyenne des colonnes remplies. Dans ce cas, l'avantage est une réduction des temps de rétention conduisant à une plus grande rapidité de l'analyse.

(3) On démontre que pour des composés très retenus dont le facteur de capacité est supérieur à 10, la HEPT est voisine du diamètre interne de la colonne soit pour une colonne de rayon 0,16 mm, un nombre de plateaux théoriques d'environ 3000 plateaux au mètre. Cela se traduit par une augmentation de la résolution et de l'efficacité de la colonne qui sera mieux adaptée à l'analyse de mélanges complexes.

Intérêt du couplage CPG/IRTF

Depuis sa mise au point, le principe de cette méthodologie a été développé dans de nombreux ouvrages, revues ou publications.⁶⁻⁹ Puisque nous en détaillerons ultérieurement les différentes étapes du point de vue de la mise en oeuvre du logiciel, nous rappelons brièvement ici que la mesure permanente de l'absorbance dans le domaine de l'infrarouge d'une cuve à gaz et de son contenu permet de suivre en temps réel l'élution chromatographique. Les composés séparés par la colonne, amenés à l'intérieur de

la cuve par une "interface" absorbent sélectivement le rayonnement infrarouge émis par la source de l'interféromètre. Après l'opération mathématique de transformée de Fourier, l'absorbance calculée établit en temps réel la présence dans la cuve d'un composé élué (Fig. 1). Le spectre infrarouge acquis au moment où le composé est présent avec une concentration maximum dans la cuve donne au spectroscopiste des informations quant à la structure du composé inconnu.

Pour le non-spécialiste, l'informatisation des données permet une comparaison rapide du spectre (exemple: adresse 60) avec une bibliothèque¹⁰ établissant ainsi avec le meilleur accord (Fig. 2) la présence de l'ester méthylique de l'acide myristique. Complémentaire à la mesure habituelle des temps de rétention, cette recherche reproduite à propos de chaque pic chromatographique, permet d'interpréter sans ambiguïté le chromatogramme. De plus, l'examen des spectres consécutifs acquis pendant la sortie d'un pic chromatographique permet de s'assurer si l'élution correspond à un seul composé ou si des molécules de structures voisines se trouvent mal séparées, ce qui se traduirait par une évolution, pendant le pic, du spectre de vibration très spécifique de la configuration de la molécule.

Néanmoins, la mise en oeuvre de ce couplage, bien que justifiée par les 2 avantages précédemment établis peut être différée par l'apparente complexité de son utilisation. Un effort doit donc être accompli en vue d'élargir le domaine d'applications tout en simplifiant le protocole d'utilisation. Le travail que nous avons réalisé va dans ce sens; l'équipement en colonnes capillaires doit permettre d'envisager de nouvelles

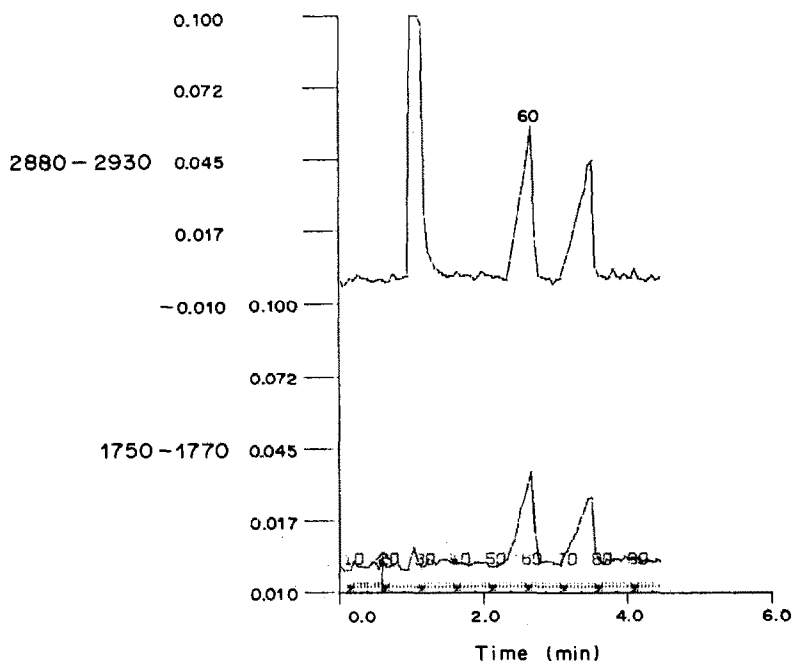


Fig. 1. Chromatogramme en temps réel.

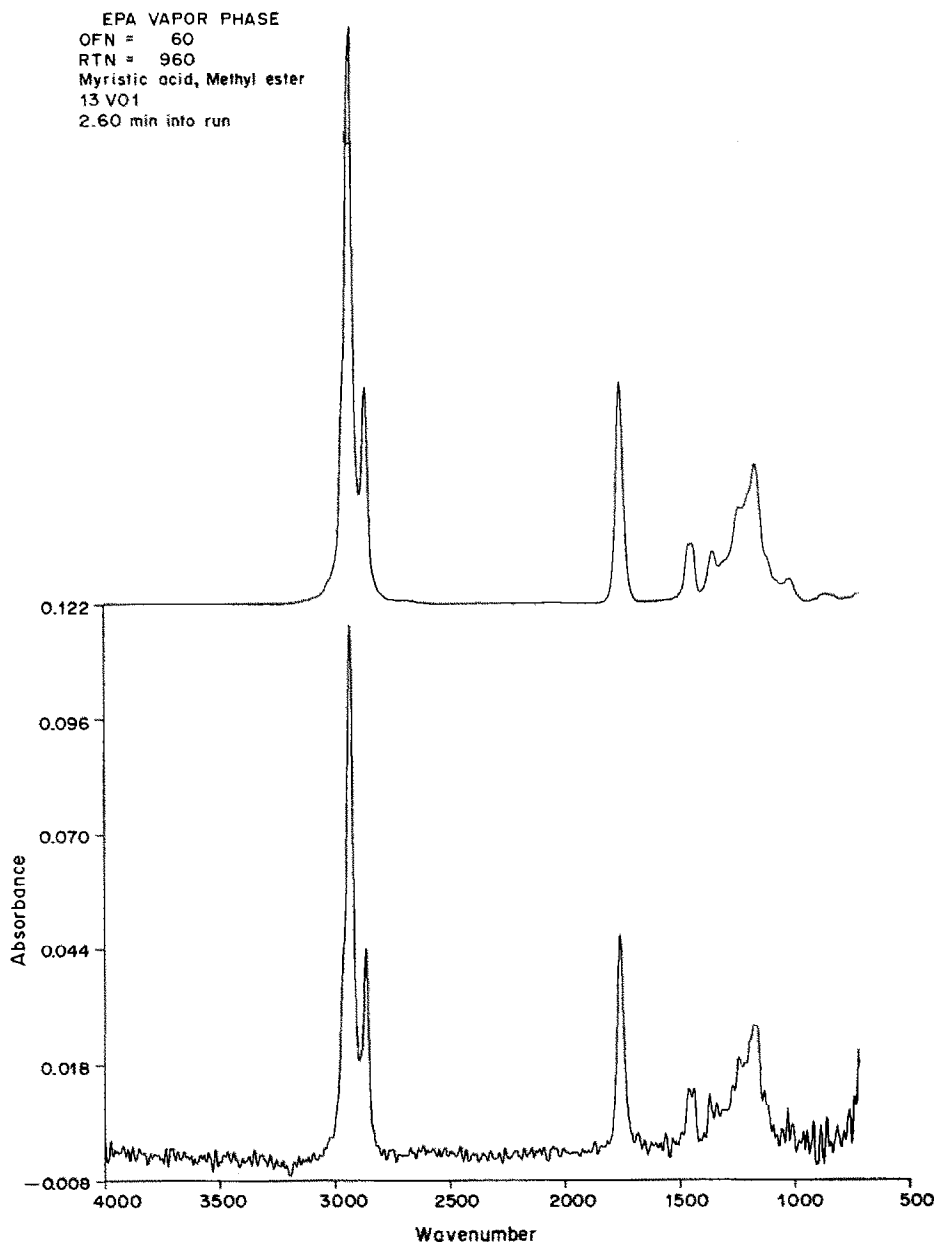


Fig. 2. Identification du fichier "60".

analyses tandis que la mise en oeuvre de nouveaux logiciels a pour but de rendre le système de plus en plus "transparent" pour l'utilisateur dont les préoccupations demeurent essentiellement d'ordre analytique.

REALISATION TECHNIQUE

Adaptation du circuit pneumatique

L'utilisation de colonnes capillaires impose de nouvelles contraintes pour le circuit gazeux que constituent le chromatographe, le spectromètre et leur liaison appelée interface.

Modification du chromatographe. Sur notre appar-

eil Varian 3700 équipé initialement d'un double circuit pneumatique destiné à recevoir les colonnes remplies, le gaz vecteur est régulé en débit pour obtenir la meilleure qualité de séparation chromatographique avec ce type de colonnes.

Sur les colonnes capillaires, on ne peut intervenir sur ce paramètre puisque leur diamètre intérieur faible fixe le débit à ses valeurs de l'ordre de quelques ml/mn. Dans ce cas, c'est sur la pression de gaz à l'entrée de la colonne que l'expérimentateur intervient pour affiner les conditions de l'analyse. La première modification a donc consisté en l'installation d'un régulateur de pression sur l'un des circuits du chromatographe, l'autre circuit gazeux étant conservé en

vue de continuer à recevoir les colonnes classiques. Le régulateur de pression choisi permet de fixer la pression entre 0 et 4 bars.

La seconde modification concerne l'injecteur. Cela consiste en l'adjonction d'une évacuation contrôlée des gaz produits par évaporation dans l'injecteur. Seule une fraction du mélange injecté sera envoyée sur la colonne, le reste étant éliminé vers l'atmosphère.

Du point de vue pratique, la "fuite" se compose d'une vanne-aiguille permettant de régler avec précision le débit de fuite et d'une électro-vanne capable d'ouvrir ou de fermer cette fuite.

Ce dispositif est rendu nécessaire par la limitation de la quantité de matière que peut recevoir la colonne et notamment pour diminuer le signal dû à l'éluion du solvant. Cela est possible, d'autre part, par la régulation en pression du gaz qui rend ce paramètre indépendant du débit de fuite.

Afin d'améliorer la sensibilité du système, un tube de pyrex appelé "insert" est introduit dans l'injecteur. De longueur 9,8 cm, de diamètre intérieur 2 mm, extérieur 4 mm, cet "insert" évite les interactions (adsorption, oxydation...), entre le métal de l'injecteur et les vapeurs produites à des températures souvent élevées.

Modification du spectromètre. Cela concerne la cuve à gaz dont le volume mort ne doit pas diminuer la résolution chromatographique apportée par la colonne capillaire. Même si les colonnes de très faible diamètre intérieur (0,1 mm) ne paraissent pas, pour l'instant, adaptées pour le couplage CPG/IRTF¹¹ les colonnes utilisables ne dépassent pas des diamètres de 0,5 mm.

Un compromis est donc à établir dans le choix d'une cuve dont le diamètre intérieur doit être suffisamment petit pour ne pas remélanger les composés séparés par la colonne, mais qui doit aussi permettre le passage d'une énergie lumineuse suffisante afin de mesurer un spectre dont le rapport signal/bruit soit satisfaisant.

Un tube de diamètre intérieur de 1 mm a été installé. Ses autres caractéristiques telles que la longueur (42 cm), le revêtement intérieur inerte en or, *etc.*, sont conformes à la description donnée par Coffey *et al.*⁸ pour les systèmes à colonnes remplies.

La section du tube, voisine de 0,78 mm², nécessite une focalisation précise du faisceau infrarouge sur la fenêtre d'entrée du tube. La lumière progresse dans le tube par réflexions multiples augmentant ainsi le trajet optique à l'intérieur du gaz absorbant. Pour des températures de la cuve ne dépassant pas 250°, le coefficient de réflexion de l'or est élevé et l'interférogramme transmis est de bonne qualité. Au delà de cette température, les performances optiques du revêtement diminuent et dégradent le rapport signal/bruit. Il sera important de thermostatier la cuve à la température minimum compatible avec l'éluion chromatographique.

Du point de vue du volume mort, environ 330 μ l,

on peut facilement calculer le temps de présence dans la cuve compte tenu du débit de gaz vecteur permis par la colonne.

Dans le cas d'un débit de 2 ml/mn, il faut 10 sec pour parcourir la cellule. On ne peut donc pas exclure la présence simultanée de deux constituants dont les temps de rétention différent de moins de 10 sec.

Pour remédier à ce fait, il faut utiliser un débit additionnel de gaz vecteur en sortie de colonne, c'est-à-dire à l'entrée de l'interface chromatographe-spectromètre.

Modification de l'interface. L'interface est un tube thermostaté dans lequel les constituants gazeux séparés par la colonne sont conduits vers la cellule infrarouge en vue d'être détectés et identifiés. Afin d'éviter toute recombinaison dans l'interface elle-même ou dans la cuve et de favoriser la sensibilité en éliminant les réactions parasites entre les composés et le métal chauffé, nous avons choisi un double conduit. A l'intérieur, un tube de silice fondue de diamètre intérieur 0,32 mm est relié à la sortie de colonne et conduit les constituants séparés jusqu'à l'entrée de la cuve. Autour de ce premier tube, un autre en acier inox de 1,6 mm de diamètre extérieur et de 1 mm de diamètre intérieur conduit le débit additionnel de gaz. L'arrivée de ce "Make-Up" se fait par l'intermédiaire d'un T dans le four du chromatographe. Le mélange "Eluant + Make Up" est réalisé à l'extrémité de l'interface, c'est-à-dire à l'entrée de la cuve.

Adaptation du logiciel

Le couplage CPG/IRTF étant essentiellement un outil pour l'analyste, il ne faut pas que cet utilisateur dont l'intérêt et les compétences peuvent être surtout orientés vers la chromatographie soit handicapé par l'aspect spectroscopique de la méthode ou par son approche informatique.

Notre effort s'est donc porté vers une automatisation des étapes qui vont de l'acquisition des données jusqu'à l'interprétation.

Acquisition des données. En ce qui concerne l'acquisition, le logiciel disponible sur le système Nicolet permet le contrôle permanent du contenu de la cuve à gaz en saisissant des interférogrammes pouvant conduire à des spectres dont la résolution est de 8 cm⁻¹. Pour chaque spectre, plusieurs interférogrammes sont accumulés afin d'améliorer le rapport signal/bruit. Pendant la manipulation, une transformée de Fourier basse résolution (32 cm⁻¹) est calculée, et le spectre est rapporté au spectre de référence acquis avant l'analyse. Le rapport est converti en absorbance et intégré dans les fenêtres spectrales choisies préalablement par l'utilisateur. La mesure de cette absorbance intégrée est tracée en fonction du temps. Le choix des fenêtres spectrales représente à ce stade l'intervention la plus significative de l'opérateur, mais cela ne constitue nullement un obstacle. En effet, pour la plupart des mélanges de molécules organiques, il existe au moins

un domaine de nombres d'onde non spécifique (région de vibration des liaisons C—H: 2950–2980 cm^{-1}) où il est en général possible de mettre en évidence l'élution de nombreux composés. Les étapes suivantes apporteront les renseignements spectroscopiques nécessaires au choix de fenêtres spectrales permettant le tracé d'un chromatogramme plus spécifique des fonctions chimiques des composés séparés appelé ChemigramTM.

Exploitation des données. Dans l'étape précédente ce sont les interférogrammes qui ont été mémorisés par le système. Toutes les informations expérimentales demeurent donc disponibles notamment la résolution de 8 cm^{-1} des spectres malgré le calcul en temps réel qui, par souci de rapidité, avait été limité à la résolution 32 cm^{-1} .

Ces interférogrammes sont utilisés dans un premier temps pour reconstruire le chromatogramme. Deux modes sont proposés à l'utilisateur.

L'algorithme de Gram Schmidt (GSR). Ce protocole mathématique estime les perturbations observées sur les interférogrammes au moment de l'élution des composés par rapport à des interférogrammes de référence acquis avant l'injection.¹² Puisque les inter-

férogrammes contiennent simultanément toutes les informations spectroscopiques, on obtient un tracé chromatographique non spécifique des fonctions chimiques (Fig. 3a).

Le calcul de l'absorbance intégrée (RCN). Utilisant les spectres de basse résolution calculés à partir des interférogrammes, on trace dans chaque fenêtre spectrale souhaitée par l'utilisateur, un chromatogramme qui est à rapprocher du ChemigramTM mais dont la présentation a été améliorée.

Ce résultat est spécifique du composé. Sur la figure 3b, la même analyse conduit à deux reconstructions:

- entre 2880 et 2930 cm^{-1} , on met en évidence un grand pic de solvant (hexane) et deux petits pics correspondant aux esters méthyliques d'acides myristique et pentadecanoïque;
- entre 1750 et 1770 cm^{-1} , seuls les esters sont observés avec des pics plus intenses ce qui permet d'envisager dans cette fenêtre une meilleure sensibilité pour l'analyse.

Durant cette étape, l'utilisateur peut à nouveau faire le choix de procédures tout à fait générales telles que GSR ou RCN dans le domaine de vibration des

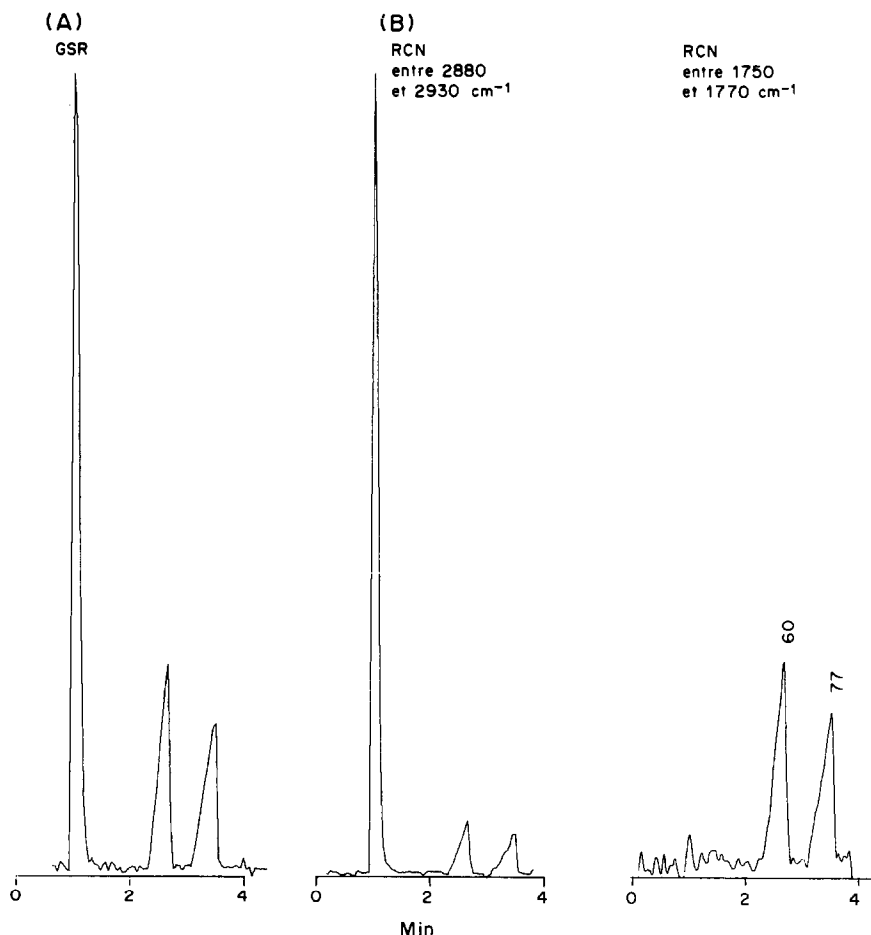


Fig. 3. Chromatogrammes reconstruits.

CH aliphatiques pour obtenir rapidement du mélange inconnu analysé, un bon nombre d'informations. Une exploitation plus performante dans des fenêtres spectrales caractéristiques pourra toujours être menée après examen des spectres. Sur la base du tracé chromatographique, un logiciel de pointé de pics établit l'adresse du fichier enregistré au maximum de concentration d'éluant dans la cuve du spectromètre (Fig. 3b).

Interprétation des résultats. Le programme d'interprétation utilise comme données les interférogrammes et les adresses des fichiers déterminées précédemment. Pour chacun de ces fichiers, correspondant du point de vue analytique à l'éluion d'un

composé, le spectre est calculé à la résolution de 8 cm^{-1} ; le rapport de transmission est obtenu par comparaison au spectre de référence acquis avant l'injection puis transformé en absorbance. Ce résultat expérimental est tracé (Figs. 2 et 4). L'utilisateur peut alors éventuellement reconsidérer les choix antérieurs afin d'utiliser des paramètres spectroscopiques mieux adaptés aux composés analysés. Dans le même temps, une procédure de recherche en bibliothèque est mise en oeuvre afin d'établir quel est le nom du produit dont le spectre est le plus ressemblant au spectre enregistré. Différents modes de recherche¹⁰ sont utilisés par le système afin de proposer à l'utilisateur un certain nombre de choix. Le spectre de la biblio-

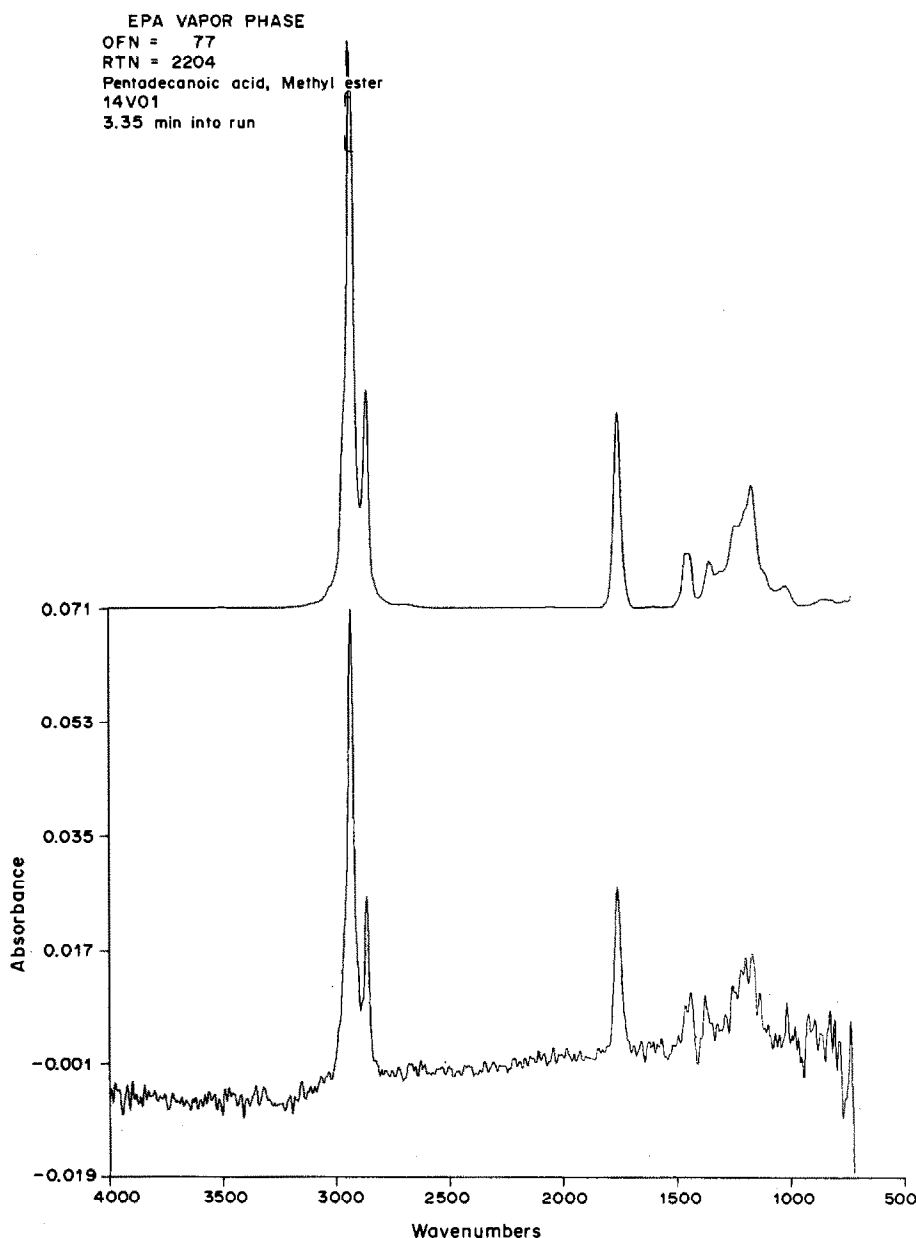


Fig. 4. Identification de l'ester méthylique de l'acide pentadécanoïque.

thèque correspondant au meilleur choix est tracé au dessus de l'enregistrement afin d'en apprécier la concordance. Divers renseignements telles que l'adresse d'origine du fichier expérimental (ici 60 et 77), l'adresse du fichier sélectionné dans la bibliothèque, le nom du composé, le temps de rétention, *etc.*, sont listés.

Le programme travaille selon une procédure itérative considérant séquentiellement chaque pic du chromatogramme.

Analyse quantitative. Le programme de pointé de pics établit également les adresses de début et de fin du pic que nous avons utilisées en concevant un programme où les absorbances sont intégrées dans une région spectrale caractéristique du composé à doser. Cette mesure est cumulée pour chaque spectre pendant toute la durée d'élution du composé. Nous avons vérifié à propos de plusieurs étalonnages la linéarité du résultat et appliqué cette méthode au dosage du tétrahydrocannabinol dans des échantillons de haschisch.¹³

En résumé de cette présentation du logiciel, nous insisterons sur l'automatisation de chaque routine.

L'intervention de l'utilisateur est minimisée grâce à un système qui utilise les résultats des étapes antérieures pour poursuivre l'analyse et l'identification. Le choix primordial de l'opérateur reste cependant celui des fenêtres spectrales où l'élution est contrôlée mais il existe des paramètres moyens qui pourront être affinés sur la base des premiers résultats.

Après l'adaptation des colonnes capillaires et la réalisation à partir des programmes existants d'un logiciel réduisant l'initiative de l'expérimentateur, nous avons testé cette nouvelle configuration du système par l'analyse de mélanges complexes. Par leur nombre élevé de composants et aussi par les grandes différences entre les concentrations relatives de ceux-ci, les huiles essentielles constituent souvent un exemple de choix pour estimer la résolution et la sensibilité d'un système analytique.¹⁴

PARTIE EXPERIMENTALE

Huile essentielle de menthe

Sur le système précédemment décrit, nous avons installé une colonne capillaire en silice fondue CP Wax 57 CB¹⁵ de

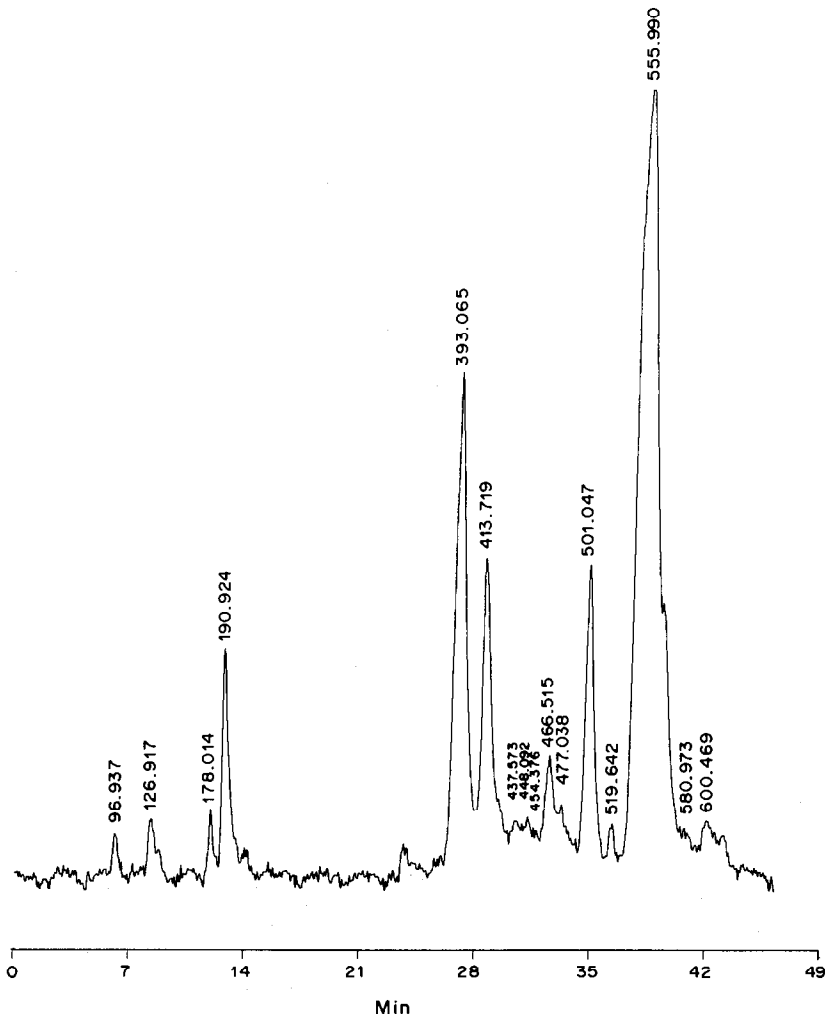


Fig. 5. Chromatogramme reconstruit d'une huile essentielle de menthe.

longueur 25 m et de 0,32 mm de diamètre intérieur. Les conditions expérimentales sont les suivantes:

- injecteur: 200° fuite 75/1
- four: 30° puis 2°/mn jusqu'à 140°
- interface: 150°
- cellule: 150°
- pression hélium: 0,4 bar
- débit de "Make-Up": 3 ml/mn
- volume injecté: 0,1 μ l

Quatre interférogrammes sont accumulés dans chaque fichier, la transformée de Fourier des 1024 premiers points acquis conduit à un spectre de résolution 32 cm^{-1} , l'absorbance intégrée dans les fenêtres 2950–2980 cm^{-1} et 1710–1730 cm^{-1} établit le chromatogramme en temps réel. La reconstruction présentée sur la figure 5 est de type RCN dans la région 2930–2980 cm^{-1} . Le spectre correspondant au

sommet de chaque pic est calculé à la résolution de 8 cm^{-1} et comparé à la bibliothèque "EPA Vapor Phase".

Huile essentielle de lavande

Avec la même colonne CP Wax 57 CB¹⁵ les conditions expérimentales de chromatographie sont cette fois:

- injecteur: 160° fuite 50/1
- four: 60° puis 2°/mn jusqu'à 160°
- interface: 170°
- cuve: 160°
- pression azote: 0,3 bar
- volume injecté: 0,1 μ l
- débit "Make-Up": 3 ml/mn

Les paramètres du spectromètre sont identiques à ceux décrits pour l'expérience précédente sauf les fenêtres spectrales qui sont: 2900–3000, 1730–1770 et 1230–1270 cm^{-1} .

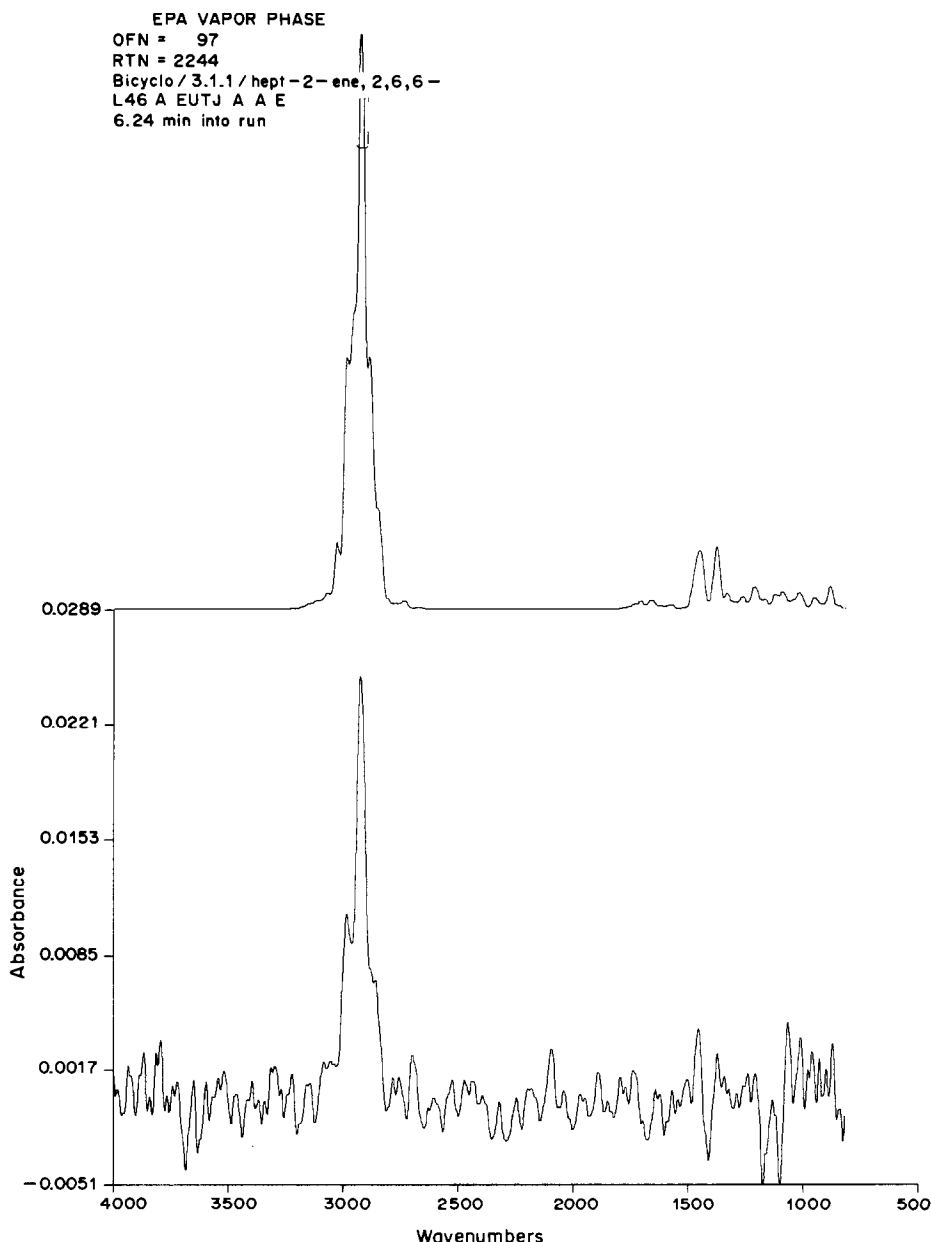


Fig. 6. Identification de l' α -pinène.

RESULTATS ET DISCUSSION

Huile essentielle de menthe

Le système dénombre, sur le chromatogramme de la figure 5, 13 pics ce qui établit une limitation par rapport aux 28 pics qui apparaissent en général sur le chromatogramme détecté par ionisation de flamme. Ceci est dû à la fois à une limite en sensibilité et en résolution.

Ainsi, le myrcène dont le pic FID ne représente que 0,3% de la surface totale n'est pas détecté, mais en même temps des composés tels que le β -caryophyllène ou le pulegone dont les surfaces de pic valent respectivement 3% et 3,8% ne sont pas séparés du menthol, composé le plus abondant (31,3%).

La limite de concentration pour détecter et identifier un composé est obtenue sur cet exemple pour l' α -pinène (1,5%) (Fig. 6). En quantité absolue, cela représente 20 ng de ce composé présent dans la cuve à gaz. Outre l' α -pinène, nous avons identifié le β -pinène, le limonène, l'eucalyptol, etc. Il est aussi intéressant de noter qu'une limitation dans les possibilités du système réside dans l'état actuel de la bibliothèque de spectres. Certains composés, même abondants, n'ont pu être identifiés parce qu'on ne disposait pas du spectre de référence. Néanmoins, dans certains cas, les renseignements fournis peuvent apporter des informations intéressantes à propos de la structure du composé élué. Ainsi le menthol, dont le temps de rétention est environ de 39 mn, est

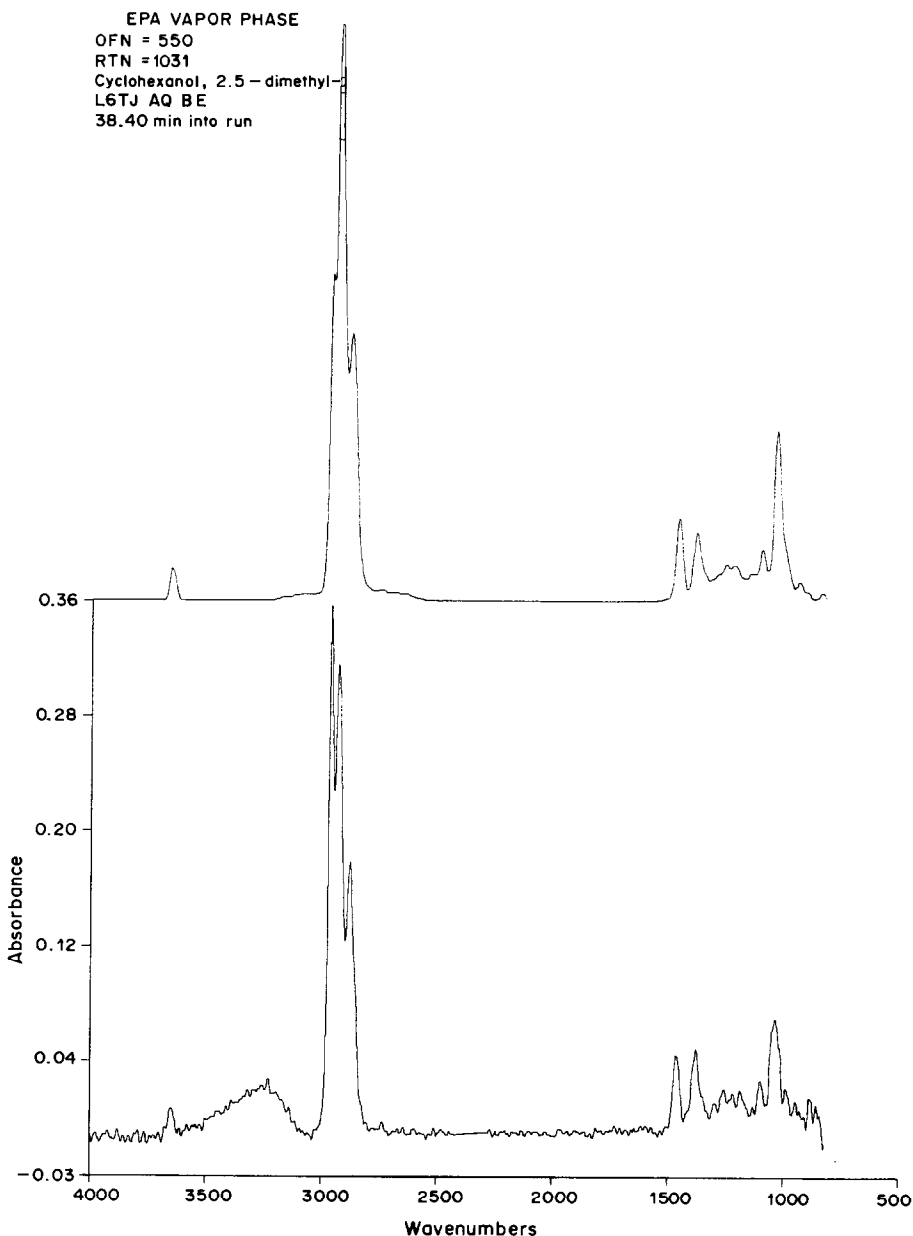


Fig. 7. Interprétation du pic du menthol.

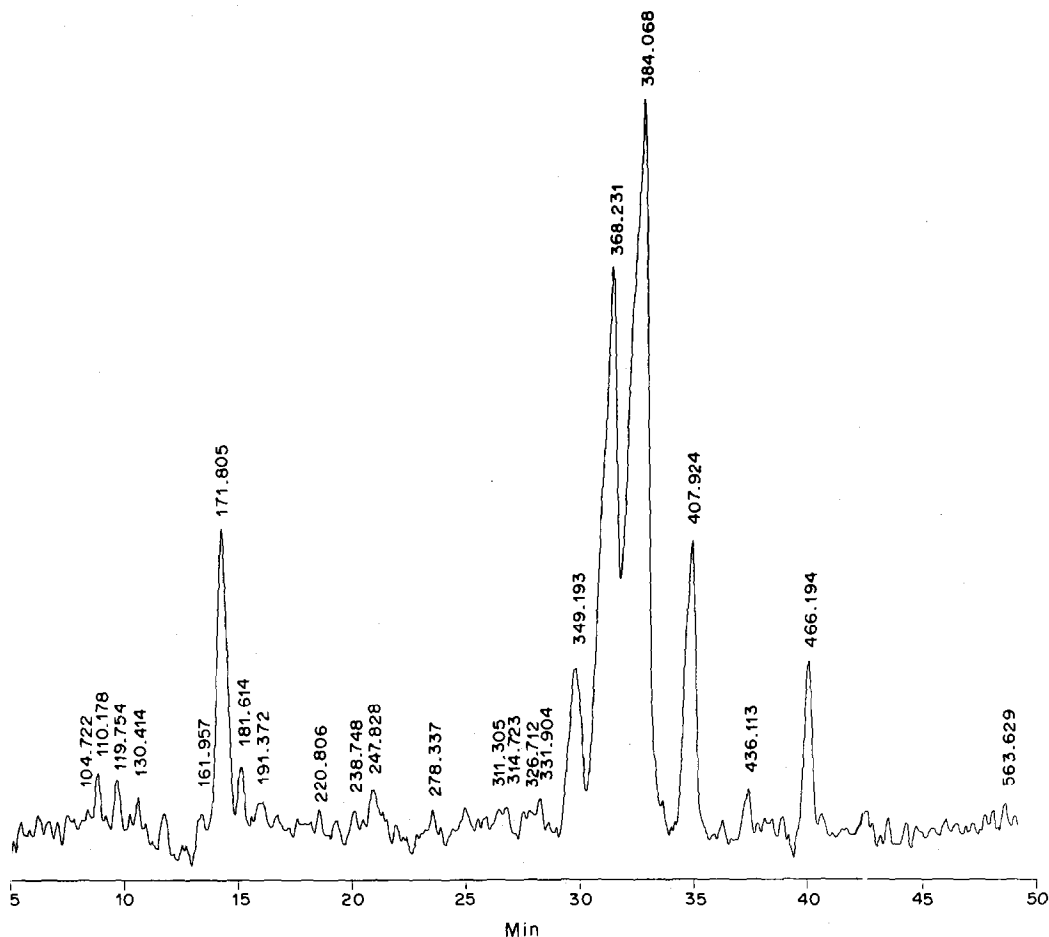


Fig. 8. Chromatogramme reconstruit d'une huile essentielle de lavande.

interprété comme étant le 2,5 diméthyl cyclohexanol ce qui n'est pas très éloigné de sa véritable structure (isopropyl-2, méthyl-5 cyclohexanol) dont le spectre n'existe pas en bibliothèque (Fig. 7).

Huile essentielle de lavande

Vingt-trois pics ont pu être détectés de façon reproductible ce qui permet de les distinguer du bruit de fond du tracé chromatographique (Fig. 8). L'eucalyptol, le linalool, l'acétate de géranyl, le bornéol ont été identifiés grâce à la bibliothèque dont nous disposons. Sur la figure 9, il convient de remarquer que l'amplitude verticale du spectre permettant d'établir la présence de bornéol est de l'ordre de 0,03 unité d'absorbance. Cela se justifie par la faible quantité de produit dans la cuve et se traduit par un rapport signal/bruit faible. Néanmoins, la comparaison aux 3300 spectres de la bibliothèque conduit de manière reproductible à l'identification.

A nouveau dans cet exemple, certains composés bien que concentrés n'ont pu être identifiés à cause de l'absence de référence. Ainsi la recherche menée sur le pic le plus intense à l'adresse 384 établit parmi les diagnostics la présence d'une fonction ester et en

même temps l'existence d'un squelette diméthyl-3,7 octadiène. Or, il s'agit de l'acétate de linalyl (ou bergamol) c'est-à-dire le (diméthyl-3,7 octadiène-1,6)yl-3 acétate. Bien qu'approximatif, ce résultat peut apporter au chimiste des informations intéressantes qui permettront d'élucider une structure si elles sont associées à des renseignements complémentaires obtenus à partir d'autres techniques dont il ne faut pas sous-estimer l'intérêt.

CONCLUSION

Nous avons réalisé la transformation de notre couplage CPG/IRTF Nicolet 7199 B afin qu'il puisse être utilisé avec des colonnes capillaires. Les modifications décrites concernent à la fois le chromatographe, le spectromètre et l'interface qui les relie. Un effort a été fait afin d'automatiser le logiciel d'acquisition et de traitement de données afin que le système soit véritablement un outil d'analyse où l'initiative de l'utilisateur est au maximum limitée des points de vue spectrométrie et informatique.

L'analyse de mélanges complexes tels que les huiles essentielles de menthe et de lavande démontre les

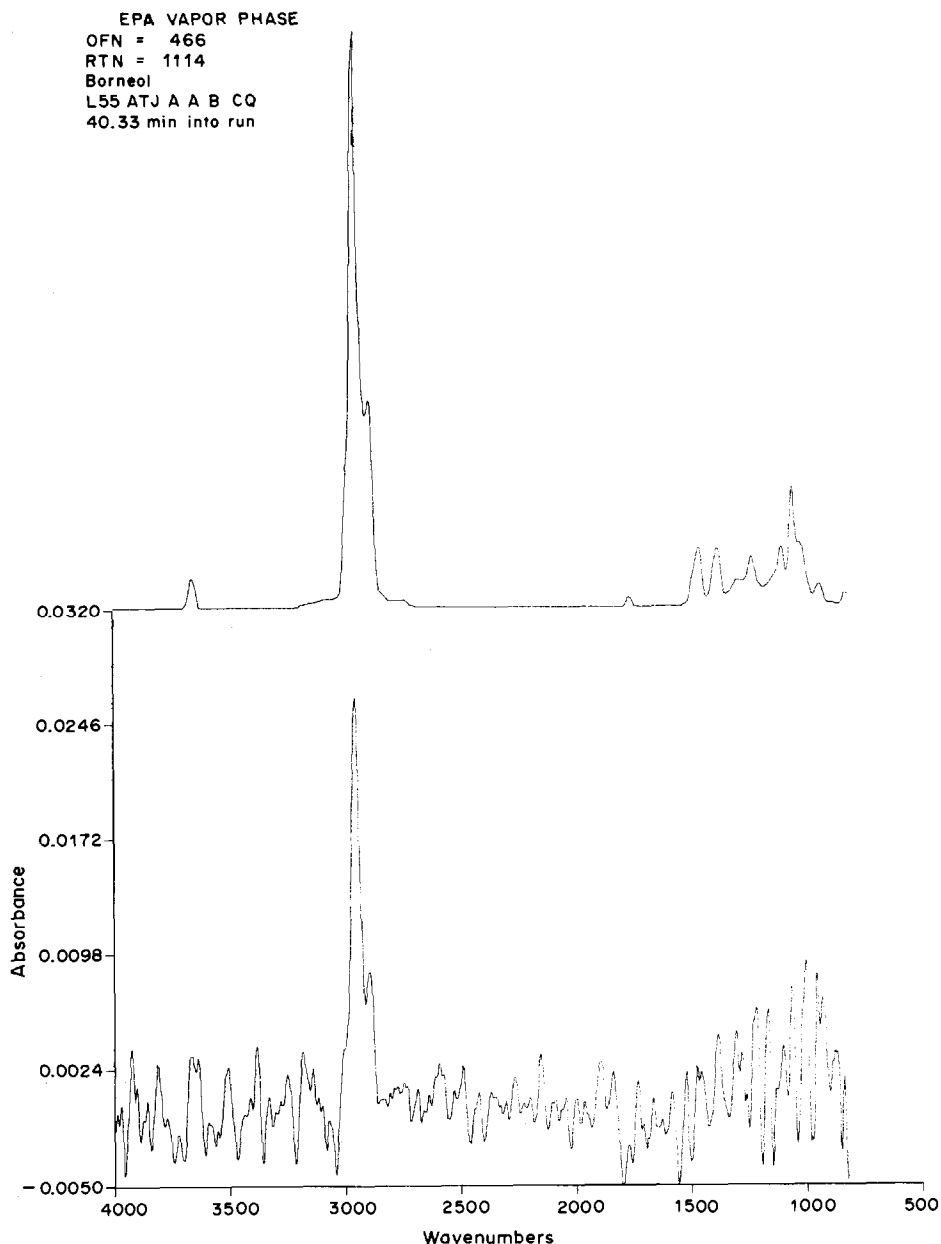


Fig. 9. Identification du bornéol.

possibilités de l'installation. Des limitations en sensibilité et en résolution sont observées à propos de ces mélanges. L'identification dans des conditions extrêmes est obtenue pour 20 ng d'un composé. D'autre part, chaque composé pour lequel le spectre de référence est disponible en bibliothèque est identifié. Dans d'autres cas, un résultat imparfait est obtenu mais utilisé conjointement à d'autres techniques, il peut permettre d'élucider les structures inconnues.

En définitive, nous constatons que la perte de performances purement chromatographiques est largement compensée par l'intérêt du point de vue structural de l'enregistrement des spectres infrarouges en temps réel.

LITTÉRATURE

1. W. H. McFadden, *Techniques of Combined Gas Chromatography/Mass Spectrometry: Applications in Organic Analysis*, Wiley-Interscience, New York, 1973.
2. M. J. D. Low, *Chem. Commun.*, 1966, 371.
3. M. J. D. Low et S. K. Freeman, *Anal. Chem.*, 1967, **39**, 194.
4. M. J. E. Golay, V. J. Coates, H. J. Noebels et I. S. Fagerson, *Theory and Practice of Gas Liquid Partition Chromatography with Coated Capillaries: Gas Chromatography*, Academic Press, New York, 1958.
5. J. Tranchant, *Manuel pratique de chromatographie en phase gazeuse*, 3rd Ed., Masson, Paris, 1982.
6. P. R. Griffiths, *Chemical Infrared Fourier Transform Spectroscopy*, Wiley-Interscience, New York, 1975.
7. M. D. Erickson, *Appl. Spectrosc. Revs.*, 1979, **15**, 261.

8. P. Coffey, D. R. Mattson et J. C. Wright, *Am. Lab.*, 1978, **10**, No. 5, 126.
9. M. T. Romon, B. Lacroix, J. P. Huvenne et G. Fleury, *Innov. Technol. Biol. Med.*, 1982, **3**, 704.
10. S. R. Lowry et D. A. Huppler, *Anal. Chem.*, 1981, **53**, 889.
11. P. R. Griffiths, J. A. de Haseth et L. V. Azarraga, *ibid.*, 1983, **55**, 1361.
12. J. A. de Haseth et T. L. Isenhour, *ibid.*, 1977, **49**, 1977.
13. M. M. Idilbi, J. P. Huvenne, G. Fleury, P. Tran Van Ky, P. Muller et Y. Moschetto, *Analisis*, 1985, **13**, 111.
14. C. L. Wilkins, G. N. Giss, R. L. White, G. M. Brissey et E. C. Onyiriuka, *Anal. Chem.*, 1982, **54**, 2260.
15. R. C. M. de Nijs et J. de Zeeuw, *J. High Resolut. Chromatog. Chromatog. Commun.*, 1982, **5**, 501.

Summary—To increase the analytical potential of the combination of gas chromatography and Fourier-transform infrared spectrometry, we have adapted our system to use of capillary columns, and automated the acquisition and treatment of the data. The performance of the method was tested by analysis of complex mixtures such as the essential oils of peppermint and lavender. The sensitivity and resolution are poorer than those obtained with classical GC detectors but the spectra are very useful for determining molecular structure.

CONTINUED INVESTIGATION OF THE DIAZOTIZATION AND COUPLING SPECTROPHOTOMETRIC TECHNIQUE FOR THE DETERMINATION OF AROMATIC AMINES WITH 8-AMINO-1-HYDROXYNAPHTHALENE-3,6-DISULPHONIC ACID AND *N*-(1-NAPHTHYL)ETHYLENEDIAMINE AS COUPLING AGENTS

GEORGE NORWITZ and PETER N. KELIHER*

Chemistry Department, Villanova University, Villanova, PA 19085, U.S.A.

(Received 1 November 1985. Accepted 21 November 1985)

Summary—Twenty more aromatic amines are determined by the diazotization and coupling spectrophotometric technique, with 8-amino-1-hydroxynaphthalene-3,6-disulphonic acid (H-acid) and *N*-(1-naphthyl)ethylenediamine (N-na) as coupling agents. The following are determined by both methods: 2,4-diaminotoluene, 2-aminobenzotrifluoride, 4-benzoxylaniline, 2,4-dimethyl-6-nitroaniline, 4,5-dimethyl-2-nitroaniline, 2-amino-9-fluorenone, naphthionic acid (sodium salt), 3-aminonaphthalene-2,7-disulphonic acid (monosodium salt), 2-aminonaphthalene-1-sulphonic acid, 4-aminonaphthalene-1-sulphonic acid and 2,4-dibromoaniline. The following are determined only by the N-na method: 5-aminosalicylic acid, 2-amino-4-nitrophenol, 4-amino-2,6-dichlorophenol hydrochloride, 2,5-dimethoxyaniline, 4-aminothiophenol, 4,4'-diaminodiphenylmethane, 1-naphthylamine, 4,4'-diaminobiphenyl-2,2'-disulphonic acid and 4,4'-diaminostilbene-2,2'-disulphonic acid. The optimum acidities for the different aromatic amines for the N-na method vary considerably. A number of aromatic amines cannot be determined by either method.

We have determined many aromatic amines of importance in industry (especially the dye industry), toxicology and pharmacology by use of the diazotization and coupling spectrophotometric technique, using 8-amino-1-hydroxynaphthalene-3,6-disulphonic acid (H-acid) and *N*-(1-naphthyl)ethylenediamine (N-na) (also known as NED) as the coupling agents.¹⁻³ In the present paper, we describe continuation of this work.

EXPERIMENTAL

Apparatus

A Bausch and Lomb model 70 spectrophotometer and a Cary model 219 recording spectrophotometer were used.

Reagents

H-acid reagent (0.75% in water). Prepare from purified technical grade H-acid monosodium salt.³ Store in a brown bottle in a refrigerator.

N-na reagent (0.75% in water). Store in a brown bottle in a refrigerator.

Standard aromatic amine solution A (2.50 mg/ml). Weigh out 0.2500 g of the aromatic amine. For 2,4-diaminotoluene, 2-aminobenzotrifluoride†, 2,4-dimethyl-6-nitroaniline, 4,5-dimethyl-2-nitroaniline, 2-amino-9-fluorenone, 2,4-dibromoaniline, 2-amino-4-nitrophenol, 4-amino-2,6-dichlorophenol hydrochloride, 2,5-dimethoxyaniline, 4-aminothiophenol, 4,4'-diaminodiphenylmethane and 1-naphthylamine, dissolve the amine in methanol and dilute to volume in a 100-ml standard flask with methanol. For 4-benzoxylaniline and 5-aminosalicylic acid, dissolve the amine in a mixture of

2 ml of sulphuric acid (1 + 1) and methanol and dilute to 100 ml with methanol. Dissolve naphthionic acid (sodium salt) and 3-aminonaphthalene-2,7-disulphonic acid (monosodium salt) in water and dilute to 100 ml with water. Dissolve 2-aminonaphthalene-1-sulphonic acid and 4-aminonaphthalene-1-sulphonic acid in 10 ml of 0.5% sodium hydroxide solution and dilute to 100 ml with water.

Standard aromatic amine solution B (25 µg/ml). Prepare fresh daily by diluting a 5-ml aliquot of standard aromatic amine solution A to volume in a 500-ml standard flask with water, but for 2,4-dimethyl-6-nitroaniline, 4,5-dimethyl-6-nitroaniline and 4-benzoxylaniline, add 10 ml of sulphuric acid (1 + 1) before the dilution.

Standard aromatic amine solution C (2.00 mg/ml). For 4,4'-diaminobiphenyl-2,2'-disulphonic acid and 4,4'-diaminostilbene-2,2'-disulphonic acid, dissolve 0.1000 g of the amine in concentrated sulphuric acid and dilute to volume in a 50-ml standard flask with concentrated sulphuric acid.

Standard aromatic amine solution D (20 µg/ml). Transfer a 5-ml aliquot of standard aromatic amine solution C to a 500-ml standard flask, add 10 ml of sulphuric acid (1 + 1) and dilute to volume with water.

Procedures

The following can be determined by both methods: 2,4-diaminotoluene, 2-aminobenzotrifluoride, 4-benzoxylaniline, 2,4-dimethyl-6-nitroaniline, 4,5-dimethyl-2-nitroaniline, 2-amino-9-fluorenone, naphthionic acid (sodium salt), 3-aminonaphthalene-2,7-disulphonic acid (monosodium salt), 2-aminonaphthalene-1-sulphonic acid, 4-amino-1-naphthalene sulphonic acid and 2,4-dibromoaniline. The following can be determined only by the N-na method: 5-aminosalicylic acid, 2-amino-4-nitrophenol, 4-amino-2,6-dichlorophenol hydrochloride, 2,5-dimethoxyaniline, 4-aminothiophenol, 4,4'-diaminodiphenylmethane, 1-naphthylamine, 4,4'-diaminobiphenyl-2,2'-disulphonic acid and 4,4'-diaminostilbene-2,2'-disulphonic acid.

*Author to whom correspondence should be addressed.

†2-Trifluoromethylaniline.

Table 1. Spectrophotometric determination of aromatic amines by the H-acid and N-na methods

Aromatic amine	H-acid				N-na				
	Colour	λ_{\max} , nm	Absorbance*	Acid,† ml	Reagent, ml	Colour	λ_{\max} , nm	Time	Absorbance‡
2,4-Diaminotoluene	rose	532	0.34	3 (HCl)	2.5	reddish	546	90 min	0.35
2-Aminobenzotrifluoride	pink	525	0.53	10 (H ₂ SO ₄)	2.5	cherry	522	90 min	0.35
	red								
4-Benzoxylaniline	purplish	548	0.57	5 (HCl)	10	red	580	16-24 hr	0.21
	red								
2,4-Dimethyl-6-nitroaniline	cherry	530	0.30	5 (H ₂ SO ₄)	2.5	cherry	522	60 min	0.25
	red								
4,5-Dimethyl-2-nitroaniline	reddish	546	0.39	2 (H ₂ SO ₄)	2.5	red	560	30 min	0.29
	violet								
2-Amino-9-fluorenone	purplish	538	0.34	2 (HCl)	2.5	reddish	545	90 min	0.21
	red								
Naphthionic acid (sodium salt) (H ₂ NC ₁₀ H ₆ SO ₃ Na·½H ₂ O)	purplish	552	0.29	5 (H ₂ SO ₄)	2.5	purple	552	45 min	0.33
	red								
3-Aminonaphthalene-2,7-disulphonic acid (monosodium salt)	cherry	534	0.22	20 (H ₂ SO ₄)	10	reddish	557	16-24 hr	0.13
	red								
2-Aminonaphthalene-1-sulphonic acid (Tobias acid)	cherry	536	0.22	5 (H ₂ SO ₄)	10	reddish	553	16-24 hr	0.19
	red								
4-Aminonaphthalene-1-sulphonic acid	reddish	548	0.35	5 (H ₂ SO ₄)	10	reddish	553	16-24 hr	0.23
	violet								
2,4-Dibromoaniline	cherry	536	0.31	5 (HCl)	2.5	purplish	567	90 min	0.24
	red								
5-Aminosalicylic acid	NR-IC	NR-IC	NR-IC	5 (HCl)	10	violet	555	16-24 hr	0.25
	red								
2-Amino-4-nitrophenol	NR-IC	NR-IC	NR-IC	2.5 (H ₂ SO ₄)	2.5	purplish	552	2 hr	0.23
	red								
4-Amino-2,6-dichlorophenol hydrochloride	NR-IC	NR-IC	NR-IC	5 (H ₂ SO ₄)	10	purple	555	2 hr	0.17
	red								
2,5-Dimethoxyaniline	NR-LS†	NR-LS	NR-LS	7 (HCl)	10	violet	574	16-24 hr	0.17
	red								
4-Aminothiophenol	NR-LS	NR-LS	NR-LS	5 (H ₂ SO ₄)	2.5	reddish	542	60 min	0.21
	red								
4,4'-Diaminodiphenylmethane	NR-LS	NR-LS	NR-LS	3 (HCl)	2.5	purple	555	30 min	0.23
	red								
1-Naphthylamine	NR-LS	NR-LS	NR-LS	3 (HCl)	10	violet	565	16-24 hr	0.46
	red								
4,4'-Diaminobiphenyl-2,2'-sulphonic acid	NR-LS	NR-LS	NR-LS	5 (H ₂ SO ₄)	2.5	reddish	567	60 min	0.13
	red								
4,4'-Diaminostilbene-2,2'-disulphonic acid	NR-LS	NR-LS	NR-LS	10 (H ₂ SO ₄)	2.5	violet	565	60 min	0.13
	red								

*For 2 µg/ml concentration.

†NR-IC = not recommended because of insufficient colour.

‡1M HCl, 1 + 1 v/v H₂SO₄.

§For 1 µg/ml concentration.

H-acid method. Prepare a calibration curve by transferring suitable portions of standard aromatic solution B to 100-ml standard flasks. The volumes should be chosen in accordance with the sensitivities indicated in Table 1, to cover the absorbance range up to 0.6. Dilute to about 75 ml with water, add 2.0 ml of 0.3M hydrochloric acid and 2.0 ml of 1% sodium nitrite solution, swirl and allow to stand for 5 min. Add 2.0 ml of 3% sulphamic acid solution, swirl, wash down the neck of the flask and allow to stand for 5 min. Add 10 ml of 6% sodium bicarbonate solution, swirl, add 2.0 ml of H-acid reagent, swirl again, dilute to the mark and allow to stand for 15–45 min. Measure the absorbances against water at the wavelength indicated in Table 1. Deduct the blank and plot the absorbances against mg of aromatic amine per 100 ml. For the analysis of samples, transfer an appropriate aliquot to a 100-ml standard flask and proceed as for the calibration curve.

N-na method. Prepare a calibration curve by transferring portions of standard aromatic amine solution B or D to 50-ml standard flasks, the volumes being chosen (Table 1) to cover the absorbance range up to 0.6. Add the amount of 1M hydrochloric acid or sulphuric acid (1 + 1) indicated in Table 1 and dilute to 30–35 ml with water. Add 1.0 ml of 1% sodium nitrite solution, swirl and allow to stand for 5 min. Add 1.0 ml of 3% sulphamic acid solution, swirl, wash down the neck of the flask and allow to stand for 5 min. Add the amount of N-na reagent indicated in Table 1, dilute to the mark and mix. Measure the absorbances against water at the wavelength and time indicated in Table 1. Deduct the blank and plot absorbances against mg of aromatic amine per 50 ml. For the analysis of samples, transfer an appropriate aliquot to a standard flask and proceed as for the calibration curve.

RESULTS AND DISCUSSION

The aromatic amines investigated in this paper had surprisingly varied solubility characteristics. The stock solutions were prepared with the following five solvents: methanol, methanol containing sulphuric acid, water, dilute sodium hydroxide solution and concentrated sulphuric acid. In preparing the dilute standard solutions, some sulphuric acid had to be added in some instances to keep the aromatic amine in solution.

The spectral characteristics of the dyes are shown in Table 1. Beer's law is obeyed for all the systems tested.

The conditions used for the H-acid method are those previously recommended.³ The optimum conditions for the N-na method, with respect to acidity, amount of reagent and time for colour development are shown in Table 1. The results obtained in the study of the effect of acidity, by addition of various amounts of 1M hydrochloric acid or sulphuric acid (1 + 1), are shown in Table 2. It is seen that the acidity is more critical for some aromatic amines than for others.

The H-acid method is not recommended for 5-aminosalicylic acid, 2-amino-4-nitrophenol and 2-amino-2,6-dichlorophenol hydrochloride because the molar absorptivities are too low. It is not

Table 2. Effect of acid concentration on N-na colours

Aromatic amine	Absorbances for different amounts of acid (per 50 ml)												
	1M HCl, ml				H ₂ SO ₄ (1 + 1), ml								
	2.0	3.0	5.0	10.0	1.0	2.0	3.0	5.0	7.5	10.0	15.0	20.0	25.0
2,4-Diaminotoluene	0.34	0.35	0.34	0.32				0.32					0.25
2-Aminobenzotrifluoride		0.27			0.35					0.35	0.35	0.30	0.15
4-Benzoxylaniline	0.17	0.20	0.21	0.19		0.13		0.10			0.10		
2,4-Dimethyl-6-nitroaniline	*	*	*	*	0.24	0.24		0.25		0.24	0.19		
4,5-Dimethyl-2-nitroaniline	*	*	*	*	0.27	0.29		0.27		0.26	0.14		
2-Amino-9-fluorenone	0.21	0.20			0.09			0.07		0.02			
Naphthionic acid (sodium salt)	0.00			0.00	0.13	0.31		0.33	0.30	0.27	0.23		
3-Aminonaphthalene-2,7-disulphonic acid (monosodium salt)		0.08			0.08			0.09		0.12		0.13	0.13
2-Aminonaphthalene-1-sulphonic acid		0.19			0.19			0.19		0.19			
4-Aminonaphthalene-1-sulphonic acid			0.20		0.20		0.21	0.23		0.22			
2,4-Dibromoaniline	0.23		0.24	0.24						0.21		0.16	0.02
5-Aminosalicylic acid	0.24	0.24	0.25	0.25				0.21	0.18				
2-Amino-4-nitrophenol	0.17		0.19		0.19	0.23	0.23	0.19					
4-Amino-2,6-dichlorophenol hydrochloride		0.11		0.11			0.16	0.17		0.16		0.16	0.03
2,5-Dimethoxyaniline		0.16	0.17	0.17	0.12			0.03					
4-Aminothiophenol		0.15		0.17	0.18			0.21		0.18			
4,4'-Diaminodiphenylmethane		0.23			0.22	0.12				0.13		0.08	
1-Naphthylamine		0.46		0.45				0.42		0.23			
4,4'-Diaminobiphenyl-2,2'-disulphonic acid		0.10				0.12		0.13		0.13	0.11	0.08	
4,4'-Diaminostilbene-2,2'-disulphonic acid		0.09				0.11		0.12		0.13	0.12	0.08	

*Turbidity (no colour).

recommended for 2,5-dimethoxyaniline, 4-aminothiophenol, 4,4'-diaminodiphenylmethane, 1-naphthylamine, 4,4'-diaminobiphenyl-2,2'-disulphonic acid and 4,4'-diaminostilbene-2,2'-disulphonic acid because of the high sensitivity of the dyes to light. All these aromatic amines can be determined by the N-na method.

The accuracy (average relative error about 5%) and precision of the recommended methods is about the same as that obtained previously in the determination of aromatic amines by the H-acid and N-na methods.¹⁻³

Some aromatic amines cannot be determined by either method. They include 2,4-diaminophenol, 2,4-diaminobenzoic acid, 3,3'-diaminobenzidine, *o*-anisidine dihydrochloride and aminonaphthols (5-amino-1-naphthol, 1-amino-2-naphthol hydrochloride, 4-amino-1-naphthol hydrochloride,

1-amino-2-naphthol-4-sulphonic acid and H-acid), all of which produce little or no colour. Diaminotoluenes with two adjacent NH₂ groups (for example, 1,2-diaminotoluene and 3,4-diaminotoluene) do not produce a colour because of internal diazotization and coupling of these NH₂ groups to form a heterocyclic compound (as noted previously for *o*-phenylenediamine²). 1-Aminoanthraquinone produces a purplish-red dye in the N-na method, but the dye starts to precipitate almost immediately even at very high acidity.

REFERENCES

1. G. Norwitz and P. N. Keliher, *Anal. Chem.*, 1982, **54**, 807.
2. *Idem, ibid.*, 1983, **55**, 1226.
3. *Idem, Talanta*, 1984, **31**, 295.

EXTRACTION OF Mo, W AND Tc WITH POLYURETHANE FOAM AND WITH CYCLIC POLYETHER FROM SCN⁻/HCl MEDIUM

R. CALETKA, R. HAUSBECK and V. KRIVAN

Sektion Analytik und Höchstreinigung, Universität Ulm, Oberer Eselsberg N 26,
D-7900 Ulm/Donau, F.R.G.

(Received 25 July 1985. Revised 8 November 1985. Accepted 15 November 1985)

Summary—The extraction of molybdenum, tungsten and technetium by polyether-based polyurethane foam and by a cyclic polyether from aqueous thiocyanate solutions is described. The influence of the reductants stannous chloride and ascorbic acid has also been studied. The possibilities of the polyurethane foam for preconcentration and determination of molybdenum are discussed.

The use of thiocyanate has become of increasing interest for separation and determination of molybdenum and tungsten. Braun¹ showed in 1863 that the coloured thiocyanate complexes of reduced molybdic acid are extracted by diethyl ether. A number of techniques for spectrophotometric determination of molybdenum have been proposed on this basis.²⁻⁵ The reported methods differ mainly with regard to the reducing agents and the solvents used. In most cases, the orange-red thiocyanate complex of quinquevalent molybdenum, obtained after reduction of Mo(VI) with stannous chloride or ascorbic acid in the presence of thiocyanate, is extracted with oxygen-containing solvents such as alcohols, ethers or ketones. For the complexes formed, an Mo:SCN⁻ ratio of 1:3 and 1:5 has been estimated.⁶ The organic phase can be used directly for sensitive determination of molybdenum.

The quantitative extraction of the yellow-green tungsten(V)—thiocyanate complex as well as the complexes of unreduced Mo(VI) and W(VI) has also been determined.⁷⁻¹⁰ These elements are also very strongly retained on anion-exchangers from thiocyanate medium.¹¹⁻¹³

In 1970 Bowen observed that most of the inorganic and organic substances that are extractable with diethyl ether are also well retained on polyurethane foam.¹⁴ In later studies, it was found that the complexes of soft anions are retained on polyether-type polyurethane foam.^{5,16} Recently, the mechanism and application of the retention of thiocyanate complexes of many elements, such as Co, Fe, platinum metals, Zn, was intensively studied by Chow and co-workers.¹⁷⁻¹⁹

In the present work, the extraction of molybdenum and tungsten as thiocyanate complexes from aqueous solutions with polyurethane foam was studied by means of the radiotracer technique. For comparison, the extraction with a cyclic polyether was included in

the study. The behaviour of technetium was also investigated by counting the ^{99m}Tc activity originating from ⁹⁹Mo.

EXPERIMENTAL

Chemicals

Polyurethane foam, a polyether of open cell type, was obtained from Greiner GmbH, Kremsmünster, Austria. The foam was cut with a cork-borer into pieces 9 mm in diameter and 20 mm in length. These were pretreated with acetone and 2M hydrochloric acid for several hours, extensively rinsed with demineralized water, and then washed with acetone and dried. For some experiments, the fine particle form was prepared by crushing the moist foam in a mixer after freezing it with liquid nitrogen. For the extraction of the coloured quinquevalent molybdenum-thiocyanate complex, a sheet of pure white polyurethane foam of unknown origin, 3 mm thick, was cut into discs, 13 mm in diameter.

A 0.01M solution of dicyclohexano-18-crown-6 (p.a. purity obtained from Ventron GmbH, Karlsruhe, F.R.G.) in 1,2-dichloroethane was used in the extraction experiments.

All other chemicals were of analytical grade. The stock solution of stannous chloride (1% in 1M hydrochloric acid) was prepared directly before use, and filtered through a Millipore filter.

The radiotracers ⁹⁹Mo and ¹⁸⁵W were prepared by irradiation of ammonium heptamolybdate and tungsten trioxide in a nuclear reactor. The molybdate was dissolved in bromine water for the oxidation of reduced molybdenum, then the bromine was removed by a stream of air. The tungsten trioxide was dissolved in dilute ammonia solution.

Estimation of the distribution ratios

The distribution data were obtained under static conditions (batch method) by the radiotracer technique. For each element studied, the solution contained about 1-5 µg of inactive carrier per ml.

For the extraction experiments, the phase-volume ratio $V_{org}:V_{aq}$ was 1:1 and the mixing time was 10 min. The distribution ratio D_1 is defined as the ratio of the total concentrations of the element in the organic and the aqueous phase.

In the experiments with polyurethane foam, the volume-weight ratio of the solute to the foam was 52 ml/g and the extraction time was 5-6 hr. The foam was period-

ically squeezed during this time (at about half-hour intervals) by means of a plastic plunger in order to bring fresh solution into contact with the foam. The distribution ratio, D_f , is defined as the ratio of the total analytical amount of the given element per gram of dry foam to the total amount of the element per ml of the external solution.

In the extraction of molybdenum, a mixture of ^{99}Mo ($t_{1/2} = 66$ hr) and ^{99m}Tc ($t_{1/2} = 6.02$ hr) in equilibrium was used for labelling. After the distribution, the activity of ^{99m}Tc (140 keV) was counted immediately after the separation of the phases and again after three days. This method allows the distribution of both elements to be studied simultaneously. From the first and second countings, results for technetium and for molybdenum, respectively, can be obtained. The technetium radioactivity was corrected by means of the equation:

$$A_{\text{Tc}} = \frac{(A_1 - B_1)}{t_1} - \frac{K_1(A_2 - B_2) \exp[K_2 \Delta T]}{t_2}$$

where A_1 and A_2 , B_1 and B_2 , t_1 and t_2 are the activities, backgrounds and counting times (in min) of the first and second measurement, respectively; ΔT is the time difference between the first and second measurements (in hr) and the constants are $K_1 = 0.002586$, $K_2 = 0.01047$.²⁰

Apparatus

The radiochemical purity of the tracers was checked with a high-resolution gamma-spectrometer. The radioactivity of the organic and aqueous phase was measured with a single-channel gamma-ray spectrometer consisting of a 3×3 -in. well-type NaI/Tl crystal and an automatic sample-changer.

RESULTS AND DISCUSSION

The kinetics of the extraction

The time necessary to achieve extraction equilibrium was tested with $1M$ hydrochloric acid and $0.2M$ ammonium thiocyanate.

The extraction with the crown ether solution proved to be very fast; equilibrium was reached in about 3 min.

The results obtained with the foam are shown in Fig. 1. It can be seen that the main part of the activity is retained in the first few minutes after the phases come into contact. After this fast phase, a slow extraction follows and the equilibrium state is reached in about 2–3 hr. An extraction time of 4–5 hr is sufficient for quantitative yield. A longer extraction time should be avoided because of the instability of acidified thiocyanate solutions. On standing overnight, a yellow precipitate of elementary sulphur appeared, accompanied by the development of gaseous H_2S , when the acidity was $\geq 2M$.

Influence of the phase ratio

The distribution ratios of molybdenum and tungsten as a function of volume-weight ratio for extraction with foam from solutions of $1M$ hydrochloric acid and $0.2M$ ammonium thiocyanate are given in Fig. 1. It can be seen that the D_f values remain constant over a wide range of V/m [$\log D_f$ (Mo) ~ 4.9 – 5.0 ; $\log D_f$ (W) ~ 4.1]. In these experiments, a fine-particle form of the foam was used. If larger pieces of the foam were used under the same

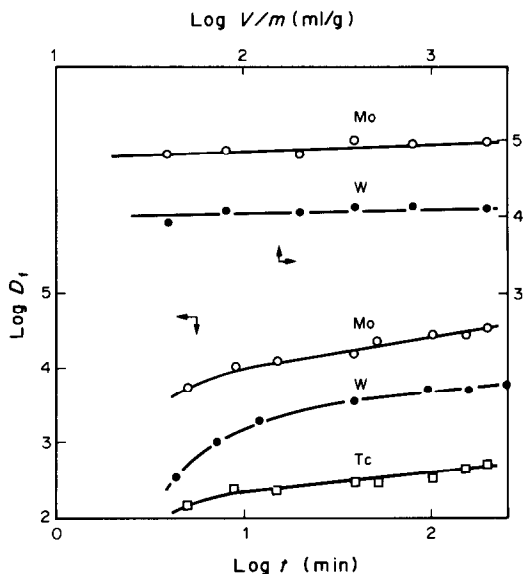


Fig. 1. The kinetics of the extraction with polyurethane foam, and the influence of the phase ratio. D_f —distribution ratio; t —extraction time; V/m —phase ratio. Composition of the aqueous phase: $1M$ HCl and $0.2M$ NH_4SCN .

conditions (see Fig. 2), distribution ratios lower by a factor of 2–3 were obtained. In both cases, equilibrium was reached. This example shows that the foam particle size may be an important factor for the extraction efficiency, presumably because of change in the specific surface area and surface properties resulting from mechanical crushing of the foam.

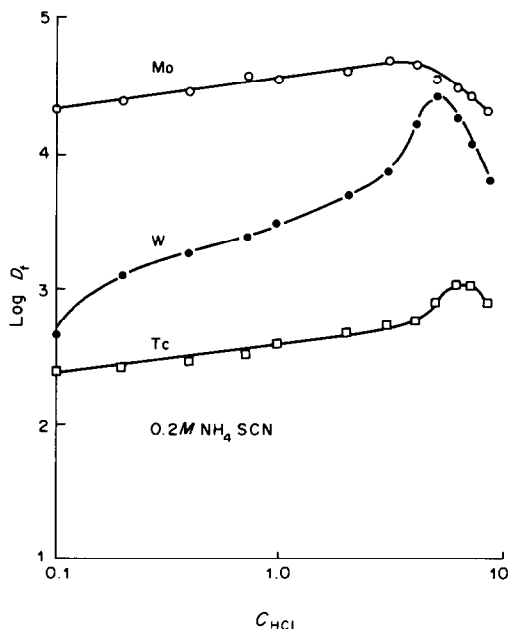


Fig. 2. Extraction of Mo, W and Tc with polyurethane foam. D_f —distribution ratio; C_{HCl} —molar concentration of hydrochloric acid.

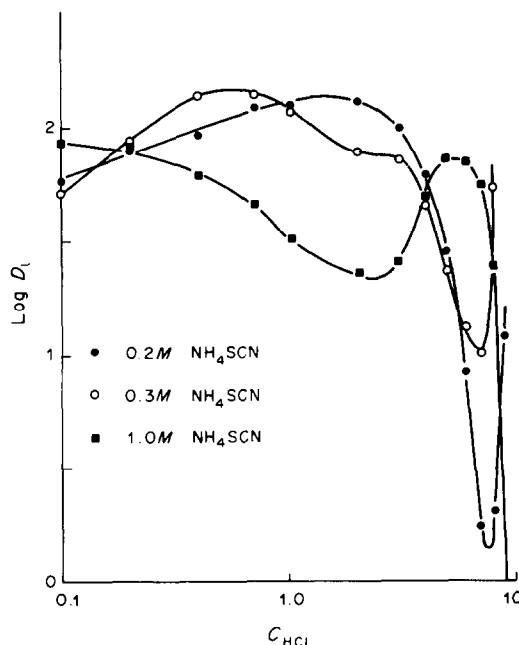


Fig. 3. Extraction of Mo with 0.01M dicyclohexano-18-crown-6 in dichloroethane. D_1 —distribution ratio; C_{HCl} —molar concentration of hydrochloric acid.

Effect of the hydrochloric acid concentration

Figure 2 shows the influence of hydrochloric acid concentration on the extraction of Mo, Tc and W with the foam. The concentration of ammonium thiocyanate was kept constant at 0.2M in these experiments. Molybdenum is well retained on the foam even from solutions of relatively low acidity; the distribution ratio increases slowly with C_{HCl} , reaching a flat maximum at 3–4M acid concentration. A similar behaviour was observed for technetium up to 4M hydrochloric acid, but its extractability is lower by a factor of about 100. The extractability of tungsten is low in more dilute hydrochloric acid. With increasing acid concentration, the distribution ratio D_f (W) increases and passes through a maximum at 5M hydrochloric acid. Further increase of the acid concentration causes a rapid decrease of the D_f value. At $C_{\text{HCl}} \geq 5M$ destruction of the polyurethane foam was observed.

The extraction of molybdenum with cyclic crown ether as a function of hydrochloric acid concentration is given in Fig. 3 for three different ammonium thiocyanate concentrations. With 0.2M thiocyanate, the maximum extraction is achieved with 1–2M acid; at higher acidity, the D_1 value decreases sharply and reaches a minimum at about 7.5M acid concentration. As the concentration of thiocyanates is increased, the minimum shifts to lower acidity and becomes flatter and broader.

Figure 4 shows the plot of $\log D_1$ vs. $\log C_{\text{HCl}}$ for tungsten and technetium at a constant concentration of thiocyanate (0.2M). The extraction of tungsten increases with acidity up to 4M hydrochloric acid but

with higher C_{HCl} , it decreases sharply. A similar behaviour can be observed also for technetium, but the increase of D_1 (Tc) is negligible and the maximum is very flat.

In the case of tungsten, Pfeifer¹⁰ supposed there is formation of the species $\text{WO}_2(\text{SCN})_n^{2-n}$ and $\text{WO}(\text{SCN})_n^{4-n}$. It can be assumed that the increase of the distribution ratio with hydrochloric acid concentration (Figs. 2 and 4) is connected with the conversion of the oxo-cation WO_2^{2+} into WO^{4+} . For molybdenum, the complexes derived from the cation MoO_4^{4+} seem to be the most probable. The decrease of the extractability in concentrated solutions of hydrochloric acid can be caused by the displacement of the SCN^- ligands in the co-ordination sphere by Cl^- ions. In the molybdenum–crown ether system, at $C_{\text{HCl}} \geq 8M$ the extraction of pure chloride complexes is also possible. This follows from an experiment in which molybdenum was extracted with crown ether from hydrochloric acid solution without thiocyanate (Fig. 5). The extraction of molybdenum with polyurethane foam and of tungsten with both the cyclic ether and the foam from 0.1–10M hydrochloric acid is also shown in Fig. 5. It is to be remembered here that chemical destruction of polyurethane foam takes place at acidities $> 5M$.

Effect of thiocyanate concentration

The distribution ratios for extraction with the foam as a function of the ammonium thiocyanate concentration are shown in Fig. 6. The acid concentration was kept constant at 1M. The extractability of molybdenum and tungsten increases with increasing concentration of thiocyanate. The retention of tech-

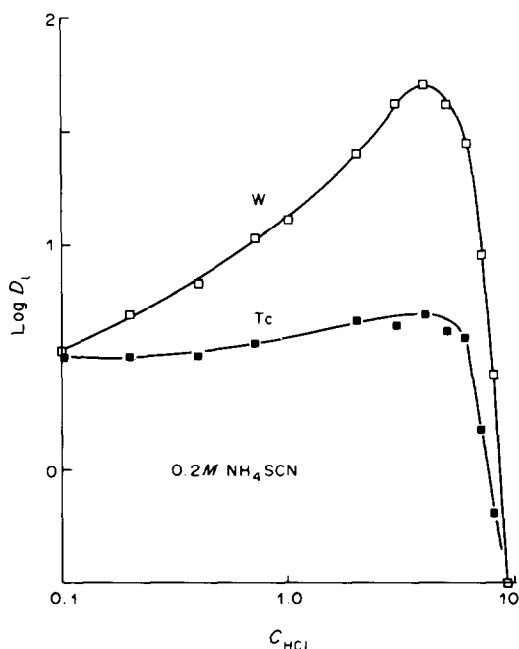


Fig. 4. Extraction of W and Tc with 0.01M dicyclohexano-18-crown-6 in dichloroethane. For notation see Fig. 3.

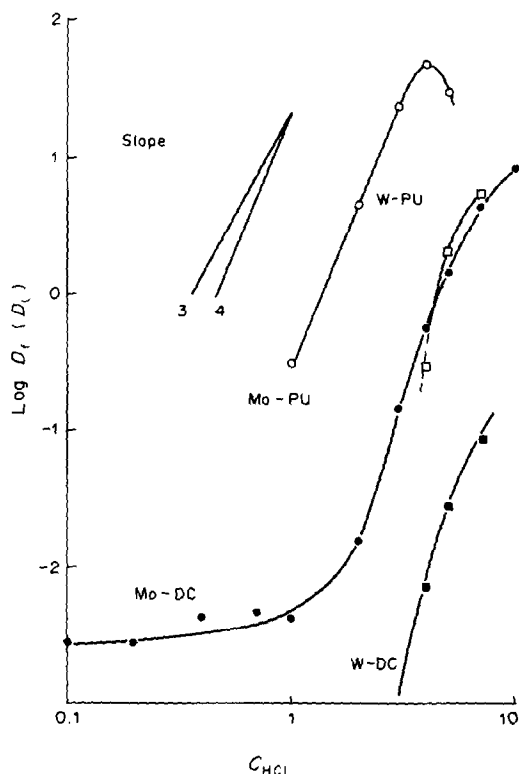


Fig. 5. Extraction of Mo and W from hydrochloric acid solutions. PU—polyurethane; DC—crown ether.

netium remains almost constant over the whole range.

Figures 7 and 8 show the same dependence for the extraction with crown ether. In the case of molyb-

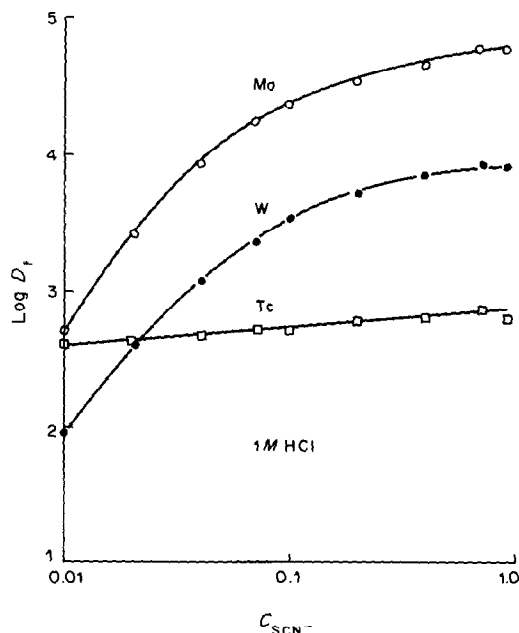


Fig. 6. Extraction of Mo, W and Tc with polyurethane foam from 1M HCl in the presence of thiocyanates. C_{SCN^-} —molar concentration of the thiocyanate.

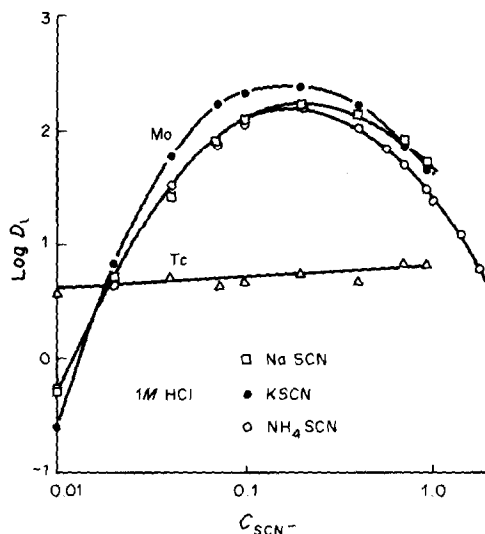


Fig. 7. Extraction of Mo and Tc with 0.01M dicyclohexano-18-crown-6 in dichloroethane from 1M HCl in the presence of thiocyanates.

denum and tungsten, the influence of different thiocyanates was also studied.

The extractability of molybdenum increases steeply with the thiocyanate concentration, reaching a maximum at a concentration of 0.2M and then it decreases to a similar extent. There are only relatively small differences between the three thiocyanates tested; the potassium salt provides the best extractability.

For tungsten, D_r increases with C_{SCN^-} in the concentration region investigated with a small maximum

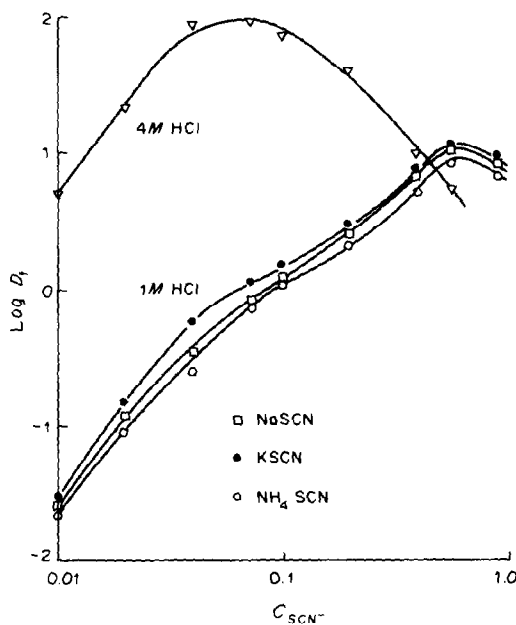


Fig. 8. Extraction of W with 0.01M dicyclohexano-18-crown-6 in dichloroethane from 1M and 4M HCl in the presence of thiocyanates.

at $C_{\text{SCN}^-} = 0.7M$. The different thiocyanates again give similar effects.

It was shown above that the maximum extractability of tungsten is reached at somewhat higher hydrochloric acid concentration than is that of molybdenum, *i.e.*, at $4M$ acidity (see Fig. 4). The influence of the concentration of ammonium thiocyanate on the extractability of tungsten at this acidity was also tested. As can be seen in Fig. 8, the results are of similar character to those for molybdenum at $1M$ hydrochloric acid concentration, but with a shift of the maximum to slightly lower thiocyanate concentration.

This behaviour supports the hypothesis mentioned above that the WO_2^{2+} species is converted into WO^{4+} at higher acidity. On the basis of these results, we conclude that the elements are extracted predominantly as their anionic complexes $\text{MoO}(\text{SNC})_5^-$, $\text{WO}_2(\text{SCN})_3^-$, and $\text{WO}(\text{SCN})_5^-$. These are the counter-ions to the hydronium ion bound in the cavities of the cyclic crown ether or in the cavities formed by the poly(ethylene oxide) chain of the foam polymer.^{17,18} The hydronium ion can also be replaced by alkali-metal or ammonium ions. Al-Bazi and Chow¹⁸ proposed that H_3O^+ ions are held in the cavities of polyurethane by both ion-dipole interaction and hydrogen-bonding, whereas K^+ ions are held only by ion-dipole interaction.

In Figs. 2, 4, 6, and 7 it can be seen that the extraction of technetium is practically independent of the hydrochloric acid and thiocyanate concentrations in the range of 0.1 – $6M$ for C_{HCl} and 0.01 – $1M$ for C_{SCN^-} . This is not surprising, as extraction of the TcO_4^- species can be expected under the given conditions.²¹ Their stabilization is not influenced by the concentration of hydrochloric acid or thiocyanate, except for higher concentrations of acid, from which competitive extraction of hydrogen chloride can be expected. The reduction of Tc(VII) to lower oxidation states in concentrated hydrochloric acid in the presence of SCN^- ions must also be taken into account.

The effect of reduction

Special attention was paid to the extraction of molybdenum and tungsten thiocyanates under reductive conditions. The influence of stannous chloride and ascorbic acid on the extraction with both the foam and the crown ether was examined. The results summarized in Fig. 9 show that increasing the stannous chloride concentration causes in all cases a decrease in the distribution ratio. It is evident that the extraction with crown ether is more strongly affected by the presence of stannous chloride than is the extraction with polyurethane foam. The levels of the respective $\log D$ values in the absence of stannous chloride are indicated with arrows. Ascorbic acid has no influence on the extractability of these elements even if present in concentration up to 8% w/v (the results are not shown).

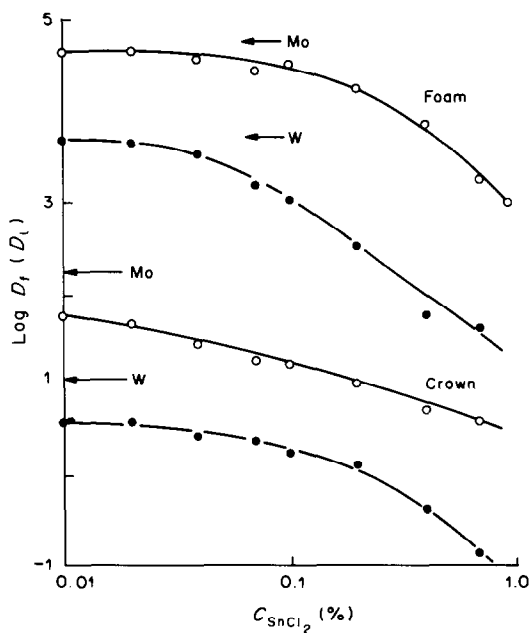


Fig. 9. Extraction of W and Mo with $0.01M$ dicyclohexano-18-crown-6 and polyurethane foam from $1M$ hydrochloric acid- $0.2M$ NH_4SCN medium in presence of stannous chloride.

A possible explanation for the effect of stannous chloride might be formation of colloidal metastannic acid in the oxidation and adsorption of the elements of interest. It can be assumed that the reduced quinquevalent forms of molybdenum and tungsten are as well extracted as the sexivalent species. The reddish complex of molybdenum(V) was quickly and quantitatively extracted with either crown ether solution or the foam.

It was observed that molybdenum(VI) can also be reduced by thiocyanate ions. At higher concentrations of hydrochloric acid and ammonium thiocyanate, the polyurethane foam was reddish owing to the extracted $\text{Mo(V)}-\text{SCN}^-$ complexes.

Preconcentration of molybdenum

It has recently been shown²²⁻²⁵ that extraction with open cell polyurethane foam of polyether type can successfully be used in conjunction with XRF spectrometry for the determination of trace elements. The results for the extraction of molybdenum with polyurethane foam given above show that the efficiency of the extraction is sufficiently high for the preconcentration of traces of molybdenum from large volumes of liquid samples such as sea-water *etc.*

The preconcentration of molybdenum was studied with water samples made $1M$ in hydrochloric acid and $0.2M$ in potassium thiocyanate. The influence of ascorbic acid was also tested. The results are given in Table 1. It can be seen that an effective preconcentration can be achieved even at V/m ratios of about 3000 ml/g. The salinity of the water has only a slight positive influence if any at all.

Table 1. Preconcentration of molybdenum on polyurethane foam

Volume of aqueous phase, ml	Weight of foam, mg	V/m ratio, ml/g	$\log D_f$	Molybdenum retained, %	Notes
50	25†	2000	5.01	98.01	
50*	50†	1000	5.24	99.4	
50*	25†	2000	5.17	98.6	
90*	50†	1800	5.14 ± 0.08	98.7	$n = 3$
40*	14§	2860	4.99 ± 0.03	97.2	$n = 3$
40*	14§	2860	5.03 ± 0.04	97.2	$n = 5$
					0.25 g of ascorbic acid

Aqueous phase: 1M HCl and 0.02M KSCN.

*Sea-water.

†Powder form of the foam.

§Discs of the white foam, 13 mm diameter, 3 mm thickness.

When the pure white foam is used, the extraction of a coloured complex of quinquevalent molybdenum in the presence of ascorbic acid can be visually observed. Fe^{3+} -ions (up to a concentration of 50 $\mu\text{g}/\text{ml}$) do not interfere in this colour reaction. This preconcentration can be used for the semiquantitative colorimetric determination of molybdenum down to about 0.2 μg . Both the Mo(V)- and Mo(VI)-thiocyanate complexes can easily be eluted from polyurethane with acetone (yield >98%).

CONCLUSIONS

Thiocyanate complexes of molybdenum and tungsten are well extracted with solutions of dicyclohexano-18-crown-6 in dichloroethane and with polyether-type polyurethane foam. The complexes of either Mo(VI) or Mo(V) are extracted. Optimum extraction for Mo(VI) is achieved from 1M hydrochloric acid and 0.2M thiocyanate, and for W(VI) from 4M acid and 0.2M thiocyanate. Potassium thiocyanate provides the highest extractability, but which thiocyanate is used is of no great significance. The extraction can be explained by the cation-chelation mechanism, based on the complexation of the hydronium ion and/or alkali-metal cation in the cavities, formed by the crown ether and by the acyclic poly(ethylene oxide) chain of the polyurethane foam. The thiocyanato complex ions form the counter-anions to the included cations.

The system of thiocyanate complex and polyurethane foam offers some attractive possibilities for the preconcentration and determination of traces of molybdenum and tungsten in various matrices.

Acknowledgements—Financial assistance for this work was provided by the Bundesministerium für Forschung und Technologie, Bonn. The authors would like to thank the FRM Reaktorstation Garching, TU München, for making available free of charge the irradiation facilities. Thanks are

also due to Greiner GmbH, Kremsmünster, Austria, for providing the polyurethane foam material.

REFERENCES

- C. D. Braun, *Z. Anal. Chem.*, 1863, **2**, 36.
- C. F. Hiskey and V. W. Meloche, *J. Chem. Soc.*, 1940, 1565.
- A. I. Busev and T. V. Rodionova, *Zh. Analit. Khim.*, 1971, **26**, 578.
- Z. Kh. Sultanova, L. K. Chuchalin, B. Z. Ioffa and Yu. A. Zolotov, *ibid.*, 1973, **28**, 413.
- G. A. Parker, *Analytical Chemistry of Molybdenum*, p. 48. Springer, Berlin, 1983.
- R. G. James and W. Wardlaw, *J. Chem. Soc.*, 1928, 2726.
- V. M. Ivanov, A. I. Busev and T. A. Sokolova, *Zh. Analit. Khim.*, 1975, **30**, 1784.
- R. Prosad and V. Yatirajam, *Indian J. Chem.*, 1964, **2**, 250.
- M. A. Mubayadzhan, *Nauch. Tr. Nauch.-Issled. Gornomet. In-ta (Erevan)*, 1967, **6**, 295.
- V. Pfeifer, *Mikrochim. Acta*, 1960, 518.
- K. Kawabuchi and R. Kuroda, *Anal. Chim. Acta*, 1969, **46**, 23.
- T. Kiriya and R. Kuroda, *ibid.*, 1978, **101**, 207.
- J. Korkisch, L. Gödl and H. Gross, *Talanta*, 1975, **22**, 669.
- H. J. M. Bowen, *J. Chem. Soc.*, 1970, 1082.
- G. J. Moody and J. D. R. Thomas, *Analyst*, 1979, **104**, 1.
- T. Braun, *Z. Anal. Chem.*, 1983, **314**, 652.
- R. F. Hamon, A. S. Khan and A. Chow, *Talanta*, 1982, **29**, 313.
- S. J. Al-Bazi and A. Chow, *ibid.*, 1982, **29**, 507.
- R. F. Hamon and A. Chow, *Talanta*, 1984, **31**, 963.
- A. Simonits, L. Moens, F. de Corte, A. de Wisperlare and J. Hoste, *J. Radioanal. Chem.*, 1981, **67**, 61.
- R. Caletka, R. Hausbeck and V. Krivan, *Talanta*, 1986, **33**, 219.
- A. Chow, G. T. Yamashita and R. F. Hamon, *ibid.*, 1981, **28**, 437.
- A. Chow and S. L. Ginsberg, *ibid.*, 1983, **30**, 620.
- A. S. Khan and A. Chow, *ibid.*, 1984, **31**, 304.
- T. Braun, M. N. Abbas, S. Török and S. Szökefalvi-Nag, *Anal. Chim. Acta*, 1984, **160**, 277.

TRACE DETERMINATION OF YTTRIUM AND SOME HEAVY RARE-EARTHS BY ADSORPTIVE STRIPPING VOLTAMMETRY

JOSEPH WANG* and JAVAD M. ZADEH

Department of Chemistry, New Mexico State University, Las Cruces, NM 88003, U.S.A.

(Received 25 September 1985. Accepted 14 November 1985)

Summary—The interfacial and redox behaviour of rare-earth chelates with Solochrome Violet RS are exploited for developing a sensitive adsorptive stripping procedure. Yttrium and heavy rare earths such as dysprosium, holmium and ytterbium can thus be measured at ng/ml levels and below, by controlled adsorptive accumulation of the metal chelate at the hanging mercury drop electrode, followed by voltammetric measurement of the surface species. With a 3-min preconcentration time, the detection limit ranges from 5×10^{-10} to $1.4 \times 10^{-9}M$. The relative standard deviation at the 7 ng/ml level ranges from 4 to 7%. A separation method is required to differentiate between the individual rare-earth metals.

Several analytical techniques have been applied for the trace measurement of rare-earth elements. These include neutron activation, isotope dilution mass-spectroscopy, X-ray fluorescence spectrometry, atomic-absorption spectrometry and inductivity-coupled plasma spectrometry.¹ Most of these techniques require costly and specialized instrumentation which may not be available in many laboratories. Stripping voltammetry, the most sensitive electro-analytical technique,² may provide an effective and economical alternative. Though lanthanide cations can be reduced to the metals, which are to a certain extent soluble in mercury, conventional anodic stripping measurements are not feasible because of the poorly defined redox reactions, that occur at extremely negative potentials.³ Only a stripping determination of cerium by use of solid electrodes and an indirect determination of several rare-earth elements by displacement reactions with a zinc complex, have been reported.³ Recently we described a sensitive adsorptive stripping method for trace determination of light rare-earth metals, based on the controlled interfacial accumulation of their complexes with *o*-cresolphthalexone on the hanging mercury drop electrode, followed by reduction of the adsorbed complexes.⁴ As a result of such adsorptive accumulation, nanomolar levels of lanthanum, cerium, and praseodymium ions can easily be determined. However, because the potential difference between the peaks of the complex and of the free ligand decreases with increasing atomic number of the rare-earth element, heavy rare-earth metals cannot be determined.

The present paper describes a very sensitive adsorptive stripping procedure for determining yttrium and heavy rare-earth metals by adsorptive accumu-

lation and reduction of their Solochrome Violet RS (SVRS) chelates at the hanging mercury drop electrode. The polarographic behaviour of rare-earth metal chelates with SVRS has been described by Florence and Aylward.⁵ These chelates produce discrete reduction steps which are well separated from that of the free dye. As illustrated in the present study, the interfacial accumulation at the hanging mercury drop electrode permits substantial lowering of the detection limits below those of polarographic measurements at the dropping mercury electrode. Conditions for enhancing the surface concentration of the chelates have been carefully optimized. Applications of adsorptive stripping voltammetry for other trace determinations have been reviewed recently.⁶

EXPERIMENTAL

Apparatus

The equipment used to obtain the voltamperograms, a PAR 264A voltammetric analyser with a PAR 303 static mercury drop electrode, has already been described in detail.^{4,7}

Reagents

All solutions were prepared from doubly distilled water. Stock solutions, 1000 ppm, of yttrium and the rare-earth ions were prepared by dissolving appropriate amounts of the corresponding oxides in acid. The ytterbium stock solution (1000 ppm) was obtained from Aldrich. SVRS was purchased from Aldrich and a $1 \times 10^{-4}M$ stock solution was prepared daily. The supporting electrolyte was 0.02M PIPES (piperazine-1,4-bis(2-ethanesulphonic acid, disodium salt monohydrate, Aldrich), adjusted to pH 11 with sodium hydroxide.

Procedure

Ten ml of $2 \times 10^{-6}M$ SVRS solution in supporting electrolyte were pipetted into the cell, and deaerated by passage of nitrogen for 8 min. The preconcentration potential (usually -0.75 V) was applied to a fresh mercury drop while the solution was stirred (400 rpm). Following the preconcentration step, the stirring was stopped, and after 15 sec the voltamperogram was recorded by applying a linear scan terminating at -1.40 V. After the background stripping

*Author for correspondence.

voltamperogram had been obtained, aliquots of the rare-earth standards were introduced. Nitrogen was passed over the solution surface throughout. All data were obtained at ambient temperature.

RESULTS AND DISCUSSION

Figure 1 shows linear scan voltamperograms for $2.9 \times 10^{-8} M$ (5 ng/ml) ytterbium, in the presence of $2 \times 10^{-6} M$ SVRS after different preconcentration periods. The Yb-SVRS complex yields a well-defined reduction peak at -1.0 V. The peak height increases rapidly with increasing preconcentration time, indicating enhancement of the chelate concentration on the mercury surface. For example, 1- and 3-min preconcentration periods yielded 21- and 56-fold enhancement of the peak current, respectively, relative to that attained without preconcentration (compare curves a, c and e). As a result, ytterbium can easily be determined at levels below 1 ng/ml; in contrast, the detection limit of conventional voltammetric measurements is ~ 5 ng/ml (curve a). Similar

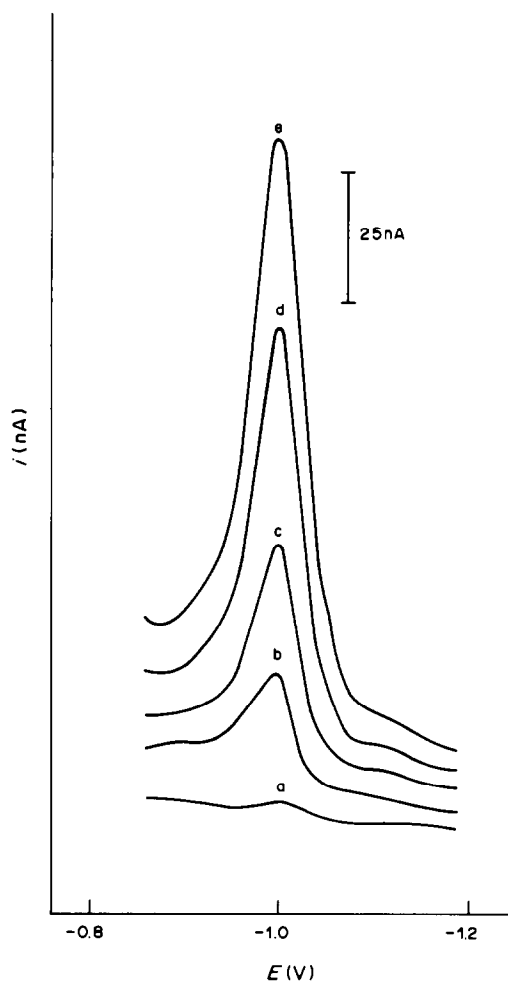


Fig. 1. Linear scan voltamperograms for 5-ng/ml ytterbium in 0.02M PIPES (pH 11) solution, containing $2 \times 10^{-6} M$ SVRS after different preconcentration times: (a) 0; (b) 30; (c) 60; (d) 120; (e) 180 sec. Preconcentration at -0.75 V with 400 rpm stirring. Scan-rate, 50 mV/sec.

behaviour was observed with other rare-earth metals, as described below.

According to Florence and Aylward,⁵ the rare-earth metals combine with SVRS in 1:2 ratio, and there is a four-electron reaction in the discrete reduction step of the chelate. The redox and interfacial behaviour of chelates of SVRS with rare-earth metals can be evaluated by using cyclic voltammetry. Figure 2 shows cyclic voltamperograms for 40 ng/ml ytterbium in $2 \times 10^{-6} M$ SVRS solution in 0.02M PIPES buffer (pH 11). Stirring the solution for 3 min at -0.50 V before starting the first scan (voltamperogram A1), resulted in two distinct cathodic peaks due to the reduction of the adsorbed dye (at -0.79 V) and of the adsorbed chelate (at -1.0 V). No peaks were observed in the anodic branch. Subsequent repetitive scans yielded significantly smaller (but stable) cathodic peaks corresponding to the reduction of dissolved species. Such behaviour indicates that the dye and chelate are being rapidly desorbed from the surface. When the same experiment was repeated after stirring for 3 min at -0.80 V (voltamperogram B1), only a single cathodic peak, due to the reduction of the adsorbed chelate, was observed (at -1.0 V). The adsorption of the SVRS-chelates of yttrium and the heavy rare-earth metals was maximal with stirring for 3 min. The quantity of charge consumed (during the cyclic voltammetry experiment) by the surface process, can be used to calculate the surface coverage, Γ . This, and additional cyclic voltammetry data, are summarized in Table 1. These results indicate that the SVRS chelates of yttrium and the heavy rare-earth metals exhibit similar redox and interfacial behaviour, except for ytterbium, which yields larger and sharper cyclic voltammetric peaks. No simple explanation is available for the different behaviour of ytterbium, as all the chelates are expected to exhibit similar orientation at the surface.

The adsorptive stripping response of rare-earth metals is strongly dependent on the solution and preconcentration conditions. For example, increasing the solution pH from 6 to 10.5 results in a gradual increase of the peak; a sharp decrease in the response is observed at $\text{pH} > 11$ (Fig. 3A). The dependence of the stripping peak current on the preconcentration potential was examined over the range from -0.2 to -0.8 V (Fig. 3B). Potentials ranging from -0.2 to -0.7 V yielded similar peak heights; at potentials more negative than -0.7 V, the peak current increased rapidly. A preconcentration potential of -0.75 V and a pH of 11 offered the best signal-to-

Table 1. Cyclic voltammetry data for the interfacial accumulation of SVRS chelates of yttrium and heavy rare earths (conditions as in Figure 2B)

Element	$E_{p,c}, V$	$b_{1/2}, mV$	$Q, \mu C$	$\Gamma, \text{mole}/\text{cm}^2$
Dy	-0.98	94	0.21	3.7×10^{-11}
Ho	-1.00	94	0.23	4.1×10^{-11}
Y	-0.98	94	0.29	5.1×10^{-11}
Yb	-1.00	77	0.60	1.0×10^{-10}

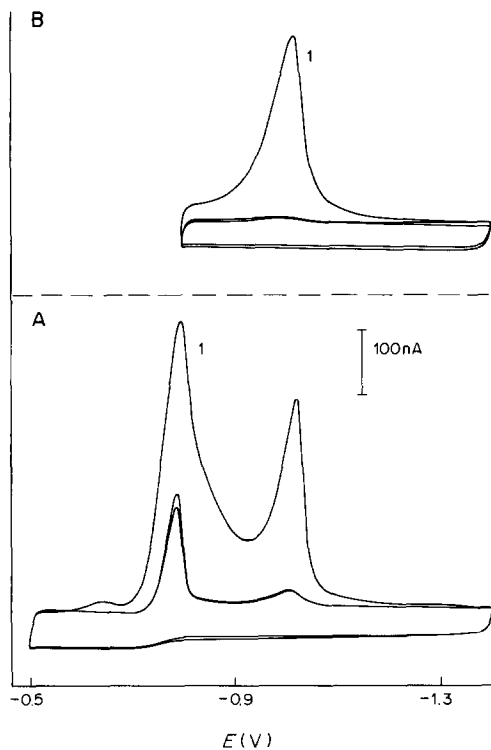


Fig. 2. Repetitive cyclic voltamperograms for 40-ng/ml ytterbium in a 0.02M PIPES (pH 11) solution, containing 2×10^{-6} M SVRS, after 3-min stirring at -0.50 V (A) and -0.80 V (B). Scan-rate, 50 mV/sec.

background characteristics and were used in all subsequent work. Adsorption also takes place under open-circuit conditions, but the response is lower than that achieved at -0.80 V.

The extent of preconcentration depends on the length of time over which the adsorption is allowed to proceed. Figure 4 shows the dependence of the adsorptive stripping peak current on the preconcentration time for yttrium and three rare-earth metals present at the 5-ng/ml level. The peak current increases non-linearly with preconcentration time, as expected for an adsorption-controlled process. Over the 0–240 sec time range examined, only the yttrium peak current levels off (at times longer than 180 sec). With a 240-sec preconcentration, the peak current is about 65 times that obtained without preconcentration for yttrium and the three rare-earth elements evaluated in this study. Obviously, a compromise between increase in sensitivity and in speed would be required when optimizing the preconcentration time.

Quantitative evaluation is based on the dependence of the peak current on the rare-earth metal concentration. Figure 5 illustrates the response for successive 5-ng/ml increases in holmium concentration, with analysis after preconcentration for 60 sec. Well-defined peaks are observed at the ng/ml level. The corresponding direct response (dotted lines) allows convenient determination only at concentrations

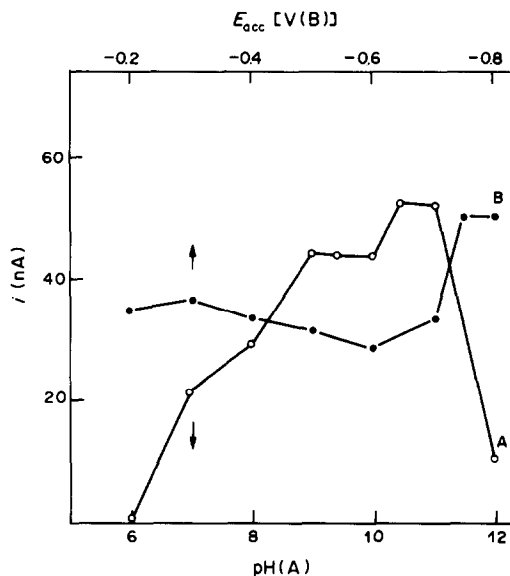


Fig. 3. Effect of solution pH (A) and preconcentration potential (B) on the stripping peak current. Preconcentration for 60 sec in the presence of 10-ng/ml ytterbium. Other conditions as for Fig 1.

>15 ng/ml. The three peaks shown came from measurements for a series of eight successive concentration increments, the results of which are shown as an inset in Fig. 5. The response is linear up to 30 ng/ml, then falls off as full surface coverage is approached (slope of linear portion, $4.25 \text{ nA} \cdot \text{ml} \cdot \text{ng}^{-1}$; correlation coefficient, 0.999). Similar calibration experiments with the other elements tested yielded a linear response over the ranges 0–40 ng/ml for Dy and Yb and 0–30 ng/ml for Y, with slopes ($\text{nA} \cdot \text{ml} \cdot \text{ng}^{-1}$) of 3.32 (Dy), 5.09 (Y) and 5.93 (Yb) and correlation coefficients 0.999 (Dy), 0.998 (Yb) and 0.996 (Y).

The linear range is particularly important when the standard-addition method is used. It is stressed here that the linear range is a function of the precon-

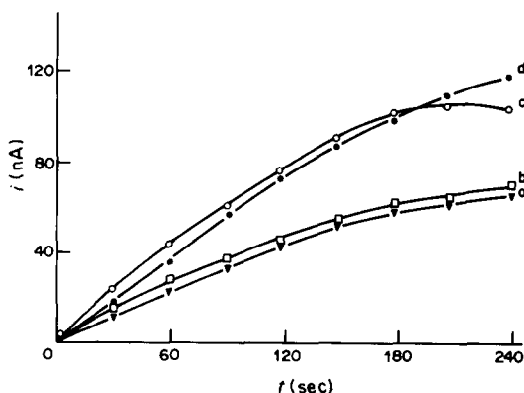


Fig. 4. Dependence of the stripping peak current on the preconcentration time for dysprosium (a), holmium (b), yttrium (c) and ytterbium (d). Other conditions as for Fig. 1.

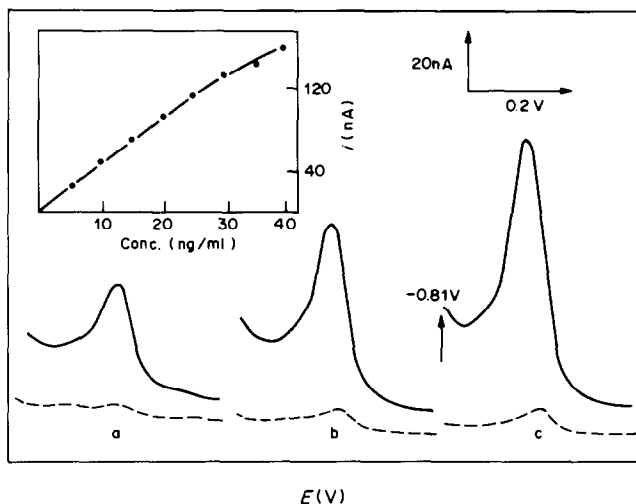


Fig. 5. Stripping voltamperograms obtained for solutions of increasing holmium concentration, 5–15 ng/ml (a–c). Preconcentration for 60 sec. Other conditions as for Fig. 1. Dotted lines represent the response without preconcentration. Also shown is the resulting calibration plot, over the 5–40 ng/ml range, with 60-sec preconcentration.

centration conditions and so can be extended by using shorter preconcentration times or unstirred solutions.

The effective preconcentration associated with the adsorption process lowers the detection limits by 2–3 orders of magnitude compared to those for the corresponding direct measurements. Detection limits were estimated based on the signal-to-noise characteristics ($S/N = 3$) of the 5-ng/ml solutions (180-sec preconcentration, other conditions as for Fig. 1). For dysprosium, holmium, yttrium and ytterbium the limits (ng/ml) found were 0.18 ($1.1 \times 10^{-9}M$), 0.17 ($1.0 \times 10^{-9}M$), 0.13 ($1.4 \times 10^{-9}M$), and 0.09 ($5 \times 10^{-10}M$), respectively. The lower detection limit for ytterbium is in agreement with the larger degree of adsorption of its chelate (as indicated by the cyclic voltammetric data). Such detection limits are comparable to those obtained by other techniques currently used for trace rare-earth metal determination (e.g., neutron activation, atomic absorption), as well as to those obtained by conventional stripping measurements of metals plated electrolytically.

The absorptive preconcentration of the SVRS chelates of yttrium and rare-earth metals results in reproducible stripping peak currents. For eight successive measurements of 7-ng/ml metal concentrations the relative standard deviations were 5% (Dy, Ho) 7% (Y) and 4% (Yb) (60-sec preconcentration, other conditions as for Fig. 1).

The method described provides a simple approach to trace analysis for yttrium and heavy rare-earth metals. These elements can be determined at the ng/ml level with short preconcentration times, but differentiation between the individual species would require a prior separation step, although use of a suitable supporting electrolyte⁵ should permit analysis of mixtures of some of the lanthanides. Such steps would be essential in the presence of lighter rare earth-metals.

Acknowledgement—This work was supported in part by the National Institute of Health, Grant No. GM 30913-02.

REFERENCES

1. I. Roelandts, *Anal. Chem.*, 1981, **53**, 676.
2. J. Wang, *Stripping Analysis: Principles, Instrumentation and Applications*, VCH Publishers, Deerfield Beach, FL 1985.
3. F. Vydra, K. Štulík and E. Juláková, *Electrochemical Stripping Analysis*, p. 247. Ellis Horwood, Chichester, 1976.
4. J. Wang, P. A. M. Farias and J. S. Mahmoud, *Anal. Chim. Acta*, 1985, **171**, 215.
5. T. M. Florence and G. H. Aylward, *Aust. J. Chem.*, 1962, **15**, 65.
6. J. Wang, *Am. Lab.*, 1985, **17**, No. 5, 41.
7. J. Wang, D. B. Luo, P. A. M. Farias and J. S. Mahmoud, *Anal. Chem.*, 1985, **57**, 158.

SAMPLE-PRETREATMENT PROCEDURE FOR ROUTINE LIQUID CHROMATOGRAPHIC ASSAY OF SERUM CORTISOL

ALDO LAGANÀ,* MAURO ROTATORI and GIULIANA VINCI
Dipartimento di Chimica, Università degli Studi di Roma, Roma, Italy

M. PERLA COLOMBINI
Istituto di Chimica Analitica ed Elettrochimica, Università degli Studi di Pisa, Pisa, Italy

ROBERTA CURINI
Dipartimento di Scienze Chimiche, Università degli Studi di Camerino, Camerino, Italy

(Received 27 May 1985. Revised 4 November 1985. Accepted 13 November 1985)

Summary—A specific method for measuring concentrations of cortisol in serum, by preliminary isolation on a "minicolumn" followed by elution and determination by liquid chromatography, is described. This assay requires only 500 μ l of serum. The limit of determination of cortisol was found to be 5 μ g/l. The analytical recovery of cortisol added to serum ranged from 98 to 102%. The coefficients of variation ranged from 2.4 to 3.4% (within-day) and from 3.6 to 8.8% (day-to-day), depending on the cortisol concentration. The method compares well with a commonly used radioimmunological method.

Cortisol (hydrocortisone, 11,17,21-trihydroxy-4-pregnene-3,20-dione) is the main primary glucocorticoid secreted by the human adrenal gland and is a good indicator for cortisol adrenal activity. Moreover, determination of its concentration is very important in diagnosis and treatment of many diseases, such as Cushing's syndrome, adrenal insufficiency and Addison's disease.

Though many analytical methods are currently available for the determination of serum cortisol, the techniques used for its measurement are not entirely specific. The fluorometric assays are influenced by corticosterone, deoxycorticosterone and various pharmaceuticals.¹ Assays based on competitive protein-binding techniques lack specificity, since prednisolone and several other endogenous steroids are also bound.^{2,3}

Recently, many of these methods have been replaced by the simple and more sensitive radioimmunoassay (RIA) techniques. However, the specificity of RIA is limited because anticortisol antibodies may cross-react to varying degrees with other steroids such as cortisone, 11-deoxycortisol, 17-hydroxyprogesterone, corticosterone and deoxycorticosterone.^{2,4,5} Under normal conditions this is not a serious problem, because cortisol is the only steroid hormone present at significant concentration in serum. However, in a number of metabolic and endocrine disorders, the concentrations of the steroids that cross-react with cortisol-antibodies are significant. Therefore, a more specific and sensitive assay for cortisol determination is highly desirable.

High-pressure liquid chromatography (HPLC)—as shown by several authors⁶⁻¹³—is the best technique for obtaining the specificity and simplicity necessary for serum cortisol determination, provided that extraction from the sample is not too slow (there is an increased demand from routine laboratories for improving the speed and reliability of the classical manual extraction).

For the clean-up of biological fluids, a considerable advance was made with the introduction of the "minicolumn" technique, which is based on the extraction of solutes by a solid matrix and their subsequent elution. In this way, it is possible to obtain enrichment of the analyte and elimination of the major contaminants from the biological fluid, enhancing the sensitivity of determination.

This paper describes a simple and specific liquid-chromatography procedure for isolation and determination of serum or plasma cortisol, which employs a particular type of "minicolumn". The method is sensitive enough to determine cortisol at the 5 ng/ml level in only 500 μ l of serum, and can easily be adapted for paediatric samples (200 μ l of serum).

EXPERIMENTAL

Apparatus

A Perkin-Elmer series 3B liquid chromatograph equipped with a Model LC-75 variable-wavelength detector was used. Samples were injected through a Rheodyne Model 7125 injector into a 25 cm \times 4.6 mm "ERBASIL" C₁₈ (10 μ m) column (Farmitalia Carlo Erba) equipped with a Waters Associates C₁₈ "Guard-Pak" Cartridge as guard-tube at the top. The absorbance of the effluent was monitored at 254 nm (sensitivity 0.005 absorbance for full-scale deflection).

*To whom correspondence should be addressed.

Mobile phase and eluents

The water used was purified by passage through Millipore "Norganic" Cartridges. Chromatography-grade methanol and chloroform were obtained from Farmitalia Carlo Erba.

Reagents and standards

All chemicals used were of reagent grade. All steroids tested were purchased from Sigma Chemical Co. Stock cortisol standard solution (1 mg/ml) was made in methanol and diluted with methanol/water (50:50 v/v) to give 0.1, 0.01, 0.005 and 0.001 mg/ml working standards. The stock and working cortisol solutions were stable for at least three months if stored at -20° .

Carbopack B was kindly supplied by Supelco Inc.

Procedure

A "minicolumn" of Carbopack B (80-100 mesh) was prepared by adding 0.5 g of the adsorbent to water, decanting any floating particles, and introducing the suspension into a 15×0.6 cm glass tube with a small pledget of glass wool in the bottom.

A 500- μ l sample of serum was added to 4.5 ml of methanol/water mixture (34:66 v/v) in a vial, and the mixture was passed through the Carbopack B column, the vial being rinsed with two 5-ml portions of water and the rinsings passed through the column. The column was washed with 3 ml of methanol, then the cortisol was eluted with 5 ml of methanol/chloroform (50:50 v/v). The eluate was collected in a conical glass vial. The procedure took about 6 min. The eluate was placed in a water-bath at 40° and evaporated with a stream of nitrogen. The dried extract was dissolved in 50 μ l of methanol/water (50:50 v/v) and 10-20 μ l of the solution were injected into the Erbasil column and eluted with methanol/water (50:50 v/v).

Paediatric serum samples (200 μ l) were processed as above but with injection of 40 μ l into the column.

The cortisol concentrations were calculated by comparing the peak heights with those for the working standards.

The cortisol concentration were also determined with a Beckman RIA kit.

RESULTS AND DISCUSSION

Optimization of the method

To optimize the chromatographic conditions, several mobile phases were tested. Of these, acetonitrile/phosphate buffer,⁸ contrary to literature reports, produced overlapping peaks for cortisone and cortisol. Although in the adult the amount of cortisone in the serum is much less than that of cortisol, the reverse is the case for the human placenta, foetal plasma and amniotic fluid.

Some other eluents, *e.g.*, tetrahydrofuran/methanol/water,¹⁴ gave a retention time of about 20 min for cortisol, which was too long. To obtain a shorter retention time for cortisol and good resolution from the interferent peaks, methanol/water (50:50 v/v) was chosen as the mobile phase; it gave a retention time of about 9.4 min for cortisol. Figure 1 shows the chromatographic behaviour of three different concentrations of cortisol in serum.

Analytical variables

Varying the flow-rate of the wash-liquid and the mobile phase through the minicolumn from 0.5 to 4 ml/min caused no significant variation in the recovery of cortisol. Under the experimental conditions

used, the flow-rate was about 3 ml/min. The effect of repeated use of the minicolumn was examined. After each extraction, the column was cleaned by washing it sequentially with 5 ml of chloroform, 5 ml of methanol and 5 ml of water. After five successive cycles, the cortisol concentration found was correct within the precision of the method, but the flow-rate through the column had decreased to 1 ml/min.

The effect of varying the composition of the mixture used to dilute the biological specimens was assessed. As shown in Fig. 2, we found that cortisol was quantitatively removed by the Carbopack B from serum solution in aqueous methanol containing 30-35% v/v of the organic solvent.

The lower recovery of cortisol at lower methanol content can be presumed to be due to protein binding. An alternative method of displacing substances bound to protein is to add urea,¹⁵ but we found that this procedure gave not more than 75% recovery of cortisol.

Performance characteristics

Recovery. Analytical recoveries (Table 1) were examined by adding known amounts of cortisol to a pooled serum, and subtracting the amount of endogenous cortisol in the serum from the total found. The average recovery in the concentration range considered was 99.9%.

Precision. The reproducibility of the assay was assessed by use of a pooled serum containing added cortisol, as shown in Table 2. The coefficient of variation for these samples ranged from 2.4 to 3.4% for within-day precision, and from 3.6 to 8.8% for day-to-day precision. These data together with those for the recoveries indicate that the proposed method is suitable for operation without an internal standard, which avoids the risk of the sample extraction causing bias in the cortisol/internal standard ratio.

Linearity. Cortisol was added to a pooled serum to give concentrations ranging from 10 to 750 μ g/l., and these were assayed. The calibration graph was linear over this range.

Sensitivity. The lower limit of determination for a 500 μ l sample of serum was found to be 5 μ g/l.

Interferences. The effects of possible interferents, *viz.* about 30 steroids secreted by the adrenal glands and gonads or used in the treatment of various medical disorders, and the metabolites of these endogenous or exogenous compounds,^{8,11} were considered. Only those which showed retention times on the "Erbasil" column near that of cortisol were examined. Aldosterone, 19-hydroxyandrostenedione, prednisone, cortisone, fludrocortisone, and prednisolone were therefore added to serum samples, which were then processed by the proposed procedure. In Table 3 the relative retention times are reported.

Of the steroids chromatographed, only prednisolone is not resolved from cortisol, and hence must be absent from the sample injected. In this case, as

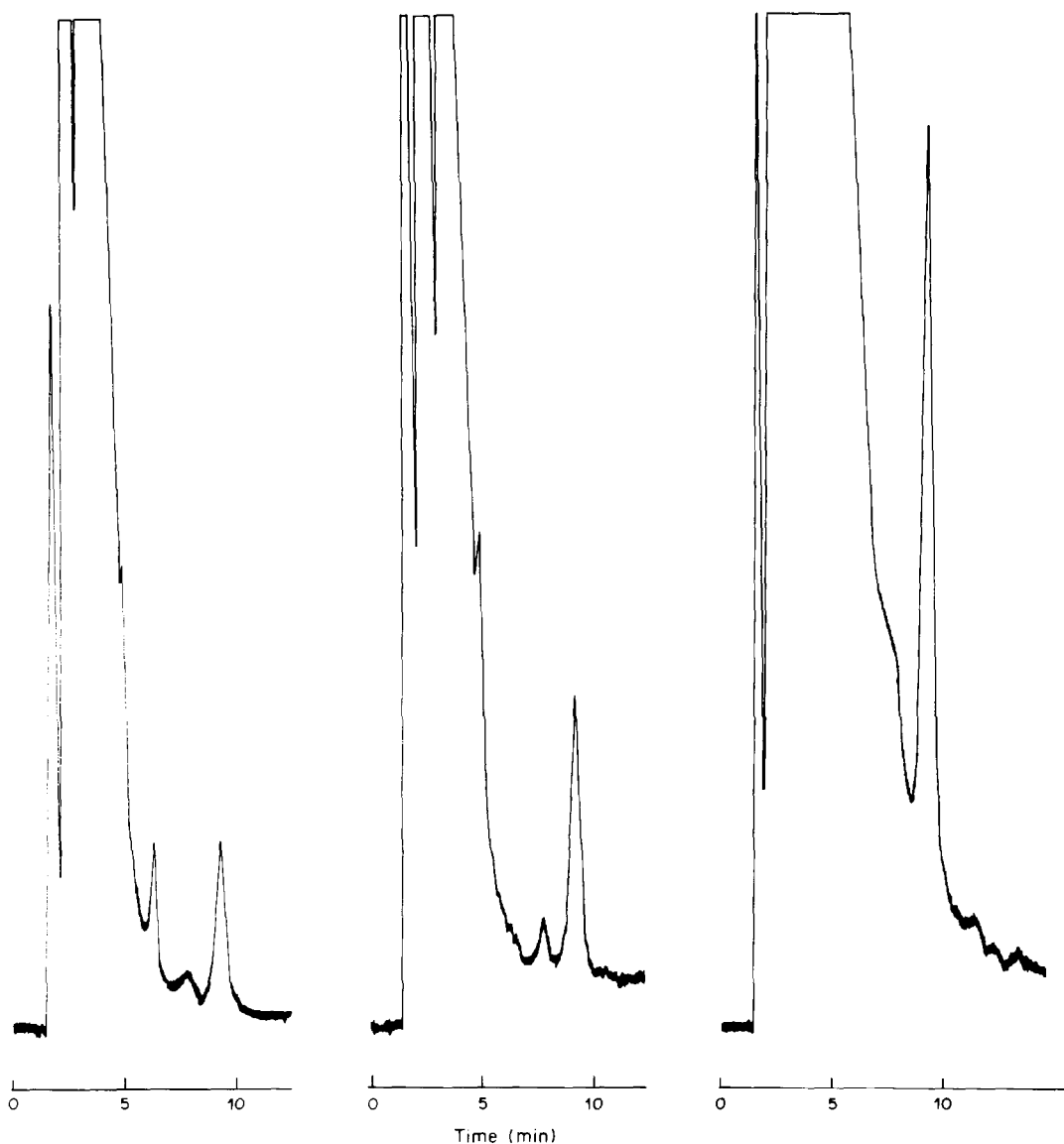


Fig. 1. Chromatograms of serum containing (left) 75, (centre) 123, and (right) 318 μg of cortisol per litre.

Caldarella *et al.* have suggested, the cortisol is separated from any prednisolone present by use of a different solvent system (silica column, mobile phase

methylene chloride/tetrahydrofuran or methanol/glacial acetic acid).^{7,16,17}

Comparison with radioimmunoassay. Analysis of 25 serum samples for cortisol in the range 10–640 $\mu\text{g}/\text{l}$. by RIA and the HPLC procedure gave the regression equation (HPLC value) = $0.81 \times (\text{RIA value}) + 4.6$, with a correlation coefficient of 0.97, almost identical to that reported by other authors.^{10,12}

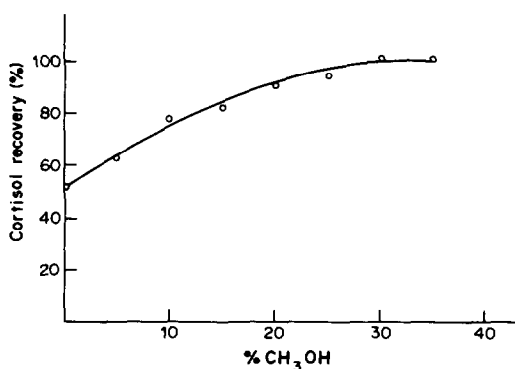


Fig. 2. Effect of methanol content on recovery of cortisol (100 $\mu\text{g}/\text{l}$.) added to serum samples.

Table 1. Analytical recovery of cortisol added to serum*

Added, $\mu\text{g}/\text{l}$.	Found, $\mu\text{g}/\text{l}$.	S.D., $\mu\text{g}/\text{l}$.	CV, %	Recovery, %	Range, $\mu\text{g}/\text{l}$.
25	24.4	1.0	4.1	97.5	23.2–25.5
50	50.6	1.3	2.6	101.3	49.1–51.3
100	99.1	1.9	1.9	99.1	96.6–104.7
250	255	5.1	2.0	102.0	250–260
500	499	11.2	2.2	99.8	484–512

*Six determinations; the serum pool had a cortisol concentration of 105 $\mu\text{g}/\text{l}$.

Table 2. Precision of assays (ten at each concentration) for cortisol in serum

Mean, $\mu\text{g/l.}$	S.D., $\mu\text{g/l.}$	CV, %
<i>Within day</i>		
61.5	2.1	3.4
200	6.9	3.4
400	10.5	2.7
573	13.4	2.4
<i>Day to day</i>		
65.5	5.8	8.8
199	7.2	3.6
370	15.1	4.1
581	23.4	4.0

Table 3. Retention times (50:50 v/v methanol-water eluent) for certain steroids

Steroid	Retention time, min
Aldosterone	6.9
19-Hydroxyandrostenedione	7.3
Prednisone	7.4
Cortisone	8.0
Fludrocortisone	8.8
Cortisol	9.4
Prednisolone	9.5

Conclusion

This study confirms that the isolation of serum cortisol by a particular type of "minicolumn" is useful in the accurate HPLC measurement of cortisol in the diagnosis and management of various clinical disorders of the adrenal and pituitary glands. Our procedure offers the advantages of specificity and simplicity; furthermore, more than one steroid can be measured in each assay, which increases the ver-

satility, efficiency and clinical applications of the method.

Acknowledgement—This work was supported by the Italian Board of Education and by the National Research Council of Italy.

REFERENCES

1. J. W. Goldzieher and P. K. Besch, *Anal. Chem.*, 1958, **30**, 962.
2. H. N. Antoniades, *Hormones in Human Blood*, pp. 727-729. Harvard University Press, Cambridge, MA, 1976.
3. B. E. P. Murphy, *J. Clin. Endocrinol. Metab.*, 1967, **27**, 973.
4. P. Vecsei, B. Penki and R. Kalty, *Experientia*, 1972, **28**, 1104.
5. J. Chakraborty, J. English, V. Marks, M. C. Dumasca and D. J. Chapman, *Br. Clin. Pharmacol.*, 1976, **3**, 903.
6. G. E. Reardon, A. M. Caldarella and E. Canalis, *Clin. Chem.*, 1979, **25**, 122.
7. F. J. Frey, B. M. Frey and L. Z. Benet, *ibid.*, 1979, **25**, 1944.
8. P. M. Kabra, L. L. Tsai and L. J. Marton, *ibid.*, 1979, **25**, 1293.
9. E. Canalis, A. M. Caldarella and G. E. Reardon, *ibid.*, 1979, **25**, 1700.
10. N. R. Scott and P. F. Dixon, *J. Chromatog. Biomed. Appl.*, 1979, **164**, 29.
11. A. M. Caldarella, G. E. Reardon and E. Canalis, *Clin. Chem.*, 1982, **28**, 538.
12. B. T. Hofreiter, A. C. Mizera, J. P. Allen, A. M. Masi and W. C. Hicok, *ibid.*, 1983, **29**, 1808.
13. K. Oka, K. Minagawa, S. Hara, M. Noguchi, Y. Matsuoka, M. Kono and S. Irimajiri, *Anal. Chem.*, 1984, **56**, 24.
14. E. Canalis, G. E. Reardon and A. M. Caldarella, *Clin. Chem.*, 1982, **28**, 2418.
15. P. R. Bach and the Clinical Investigation of Duchenne Dystrophy Group, *ibid.*, 1983, **29**, 1344.
16. J. C. K. Loo, A. G. Butterfield, J. Moffat and N. Jordan, *J. Chromatog.*, 1977, **143**, 275.
17. J. Q. Rose and J. Jusko, *ibid.*, 1979, **162**, 273.

SPECTROPHOTOMETRIC AND SECOND-DERIVATIVE SPECTROPHOTOMETRIC DETERMINATION OF MERCURY IN ORGANOMERCURIALS BY MEANS OF BENZYL 2-PYRIDYL KETONE 2-QUINOLYLHYDRAZONE

J. MEDINILLA,* F. ALES and F. GARCIA SANCHEZ

Department of Analytical Chemistry, Faculty of Sciences, The University, 29071-Málaga, Spain

(Received 6 November 1984. Revised 10 October 1985. Accepted 8 November 1985)

Summary—Mercury(II) reacts with benzyl 2-pyridylketone 2-quinolyldihydrazone (BPKQH) in the pH range 9.0–10.4, to form a stable 1:2 (metal:ligand) complex which has a sharp absorption maximum at 475 nm and molar absorptivity 5.01×10^4 l.mole⁻¹.cm⁻¹. It is proposed for use in spectrophotometric determination of mercury at µg/ml levels and analysis for organomercurials. The sensitivity of the method can be increased significantly by employing derivative spectrophotometry, making mercury determination at ng/ml levels feasible.

Hydrazones have been widely used as reagents for the spectrophotometric determination of various transition metal ions,¹⁻³ mainly Fe, Co, Ni and Pd, but few give colour reactions with mercury ions, an exception being benzyl 2-pyridyl ketone 2-quinolyldihydrazone (BPKQH), the use of which is described here.

Mercury compounds are used in agriculture to control fungus diseases of feeds, bulbs, plants, fruits and vegetation,⁴ and the resulting ecological dangers have been of considerable concern, particularly since organomercury compounds, especially methylmercury,^{5,6} are more toxic to man than inorganic mercury salts. Consequently many highly sensitive analytical methods for mercury have been developed. Spectrophotometry can be made sufficiently sensitive for environmental trace analysis by use of the derivative technique, which is based on the observation⁷ that for Gaussian and Lorentzian bands the amplitude, D_n , of the n th derivative of the absorbance with respect to wavelength ($D_n = d^n A / d\lambda^n$) is inversely related to the original bandwidth, W :

$$D_n \propto 1/W^n$$

Advantage can be taken of this fact to enhance sensitivity in the determination of compounds characterized by a narrow absorption spectrum, such as that of the BPKQH-Hg complex.

EXPERIMENTAL

Reagents

Benzyl 2-pyridyl ketone 2-quinolyldihydrazone (BPKQH) was synthesized as described previously,⁸ and a 1×10^{-3} M solution in absolute ethanol was prepared weekly.

Mercury standard solutions were prepared by suitable dilutions of 1000-ppm commercial stock solution (Merck).

All the standards were prepared with 3% v/v sulphuric acid medium to act as a preservative.

Phenylmercury acetate, methylmercury chloride, ethylmercury chloride and mercuric chloride (Merck) were used as received.

A pH 8.0 buffer solution was prepared from 0.1 M sodium tetraborate and 0.1 M hydrochloric acid.

All the reagents and solvents were of analytical-reagent grade. Distilled demineralized water was used throughout.

Apparatus

A Beckman Acta-III instrument was used for recording spectra and for measurements at fixed wavelength. Derivative spectra were recorded with a Perkin-Elmer Lambda 5 spectrophotometer. Both instruments had matched 1.00-cm quartz cells.

Procedures

Spectrophotometric determination of mercury. Into a 25-ml standard flask transfer 2 ml of 10^{-3} M BPKQH solution and 13 ml of absolute ethanol to ensure a final ethanol content of 60% v/v. Add 5 ml of pH 8.0 buffer solution and a suitable volume of sample solution containing 2.5–75 µg of mercury. Dilute to volume with distilled water and measure the absorbance of the solution at 475 nm against a reagent blank.

Second derivative spectrophotometry. Operate as described above, but use a volume of sample solution containing only 0.75–2.50 µg of mercury. Record the second derivative spectrum at 10-nm wavelength intervals on a chart recorder against a reagent blank, with a response time of 2 sec and a scan-speed of 120 nm/min. Measure the second derivative peak-height amplitude from a trough to a straight line drawn between its neighbouring peaks. Use a suitable calibration blank or empirical equation to convert amplitude (in cm) into concentration.

Procedure for organomercurials. Weigh a suitable amount of sample, containing between 50 µg and 7.5 mg of mercury, and transfer it to a 50-ml beaker. Heat the sample with 3 ml of concentrated sulphuric acid at $65 \pm 5^\circ$ in a water-bath. After 2 hr, add 1 ml of 30% hydrogen peroxide and continue the digestion for 45 min. If necessary, repeat the addition of hydrogen peroxide. Cool, dilute to 50 ml and neutralize. Finally, dilute to 100 ml with demineralized water. Apply the photometric procedure to a suitable volume (1–4 ml) of this solution. If the second-derivative method is used, take a sample weight containing 20–250 µg of mercury.

*Hygiene and Work Safety Centre, Granada, Spain.

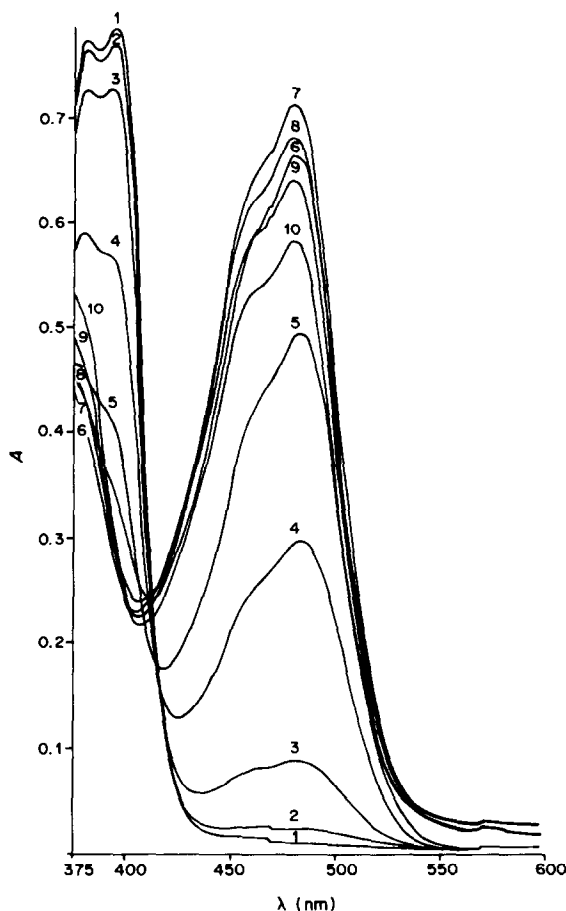


Fig. 1. Absorption spectra of BPKQH-Hg complex at different pH values. [BPKQH] = $1 \times 10^{-4} M$; [Hg] = $2 \times 10^{-5} M$; pH: 1, 3.5; 2, 4.3; 3, 5.5; 4, 6.6; 5, 7.3; 6, 8.2; 7, 9.2; 8, 10.8; 9, 11.3; 10, 12.

RESULTS AND DISCUSSION

BPKQH-Hg complex

The absorption spectra of the orange complex formed between mercury(II) and BPKQH in aqueous ethanolic medium at various pH values are shown in Fig. 1. The spectra have a relatively narrow absorption peak with maximum at 475 nm and a shoulder near 455 nm. From the shape of the absorbance *vs.* pH graph (Fig. 2) it can be seen that the absorbance is constant and maximal at an apparent pH of 9.0–10.4. The pH can be adequately adjusted to an apparent pH of 10.0 by addition of 5 ml of pH 8.0 borate buffer solution.

For complete complexation a tenfold excess of BPKQH is sufficient. The complex is quickly formed and the colour remains stable for at least 2 hr. Slight variations in absorbance are caused by changing the concentration of ethanol in the medium, but ethanol contents below 50% are impractical because of the poor solubility of the complex. Optimum results are obtained in 60% v/v ethanol–water mixture. The order of addition of the reagents has no effect on the absorbance. The metal to ligand ratio in the complex was studied under the selected working conditions by

the continuous variations method, and found to be 1:2.

Derivative spectrophotometry

The shape of the spectrum, characterized by a narrow band at 475 nm, favours improvement of the sensitivity by the derivative approach.⁹

The main instrumental parameters affecting the shape of the derivative spectra are the wavelength-scanning speed (v_{scan}), wavelength range over which the derivative is averaged ($\Delta\lambda$), response time (t_r) and the derivative order. These parameters can be adjusted to optimize the method.

First, the derivative order should be considered. For qualitative work or better discrimination from interference peaks, higher derivative orders are advisable because differentiation discriminates against broad bands to an extent that increases with derivative order; the signal-to-noise ratio (SNR) decreases, however. Resolution is thus improved by the sharpening of the signals through use of successively higher derivative orders. In general, the peak width at half maximum height for the second derivative is about a third of that of the primary function, but the noise is 10 times as great.¹⁰

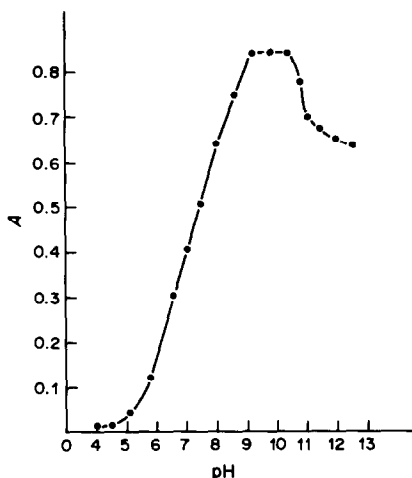


Fig. 2. Effect of pH on the formation of the BPKQH-Hg chelate. $[BPKQH] = 1 \times 10^{-4} M$; $[Hg] = 2 \times 10^{-5} M$; $\lambda = 475 \text{ nm}$.

For quantitative work, if the main goal is to achieve the greatest possible SNR, the derivative order should be the lowest needed to achieve the analytical objective. When the band features are clearly separated, the second derivative provides a good compromise between resolution and SNR.

The extent to which the SNR decreases with derivative order strongly depends on the smoothing ratio,

which is connected with both v_{scan} and t_r . Smoothing reduces both the noise and the signal.¹¹ However, the scan-rate must be compatible with the response time and experimentally it is not possible to increase the scan-speed above a certain critical value, the optimal conditions being determined by the structure of the spectra. For a spectrum with transmission bands having a peak width at half maximum height $\geq \delta\lambda_b$, where $\delta\lambda_b$ is the peak width at half maximum height of the narrowest spectral feature, the scan-speed and response time must satisfy the condition $v_{scan(max)} = \delta\lambda_b/t_r$, where t_r is 4.6 times the time constant of the instrumental system.¹² It must be pointed out that with long response times (low electrical band-widths) noise error can be reduced but drift errors then predominate.

Because the derivative signal is, in practice, obtained with respect to time rather than wavelength, the scan-rate significantly affects both the amplitude of the derivative spectrum and also the effect of background noise. Thus, increasing the scanning speed will present a more rapidly changing absorption signal to the derivative circuit, with a significant improvement in the SNR.

The size of the wavelength increment over which the derivative is taken, $\Delta\lambda$, is another important instrumental parameter. Small wavelength increments give better resolution, but decreased SNR. In practice, the best wavelength increment for a

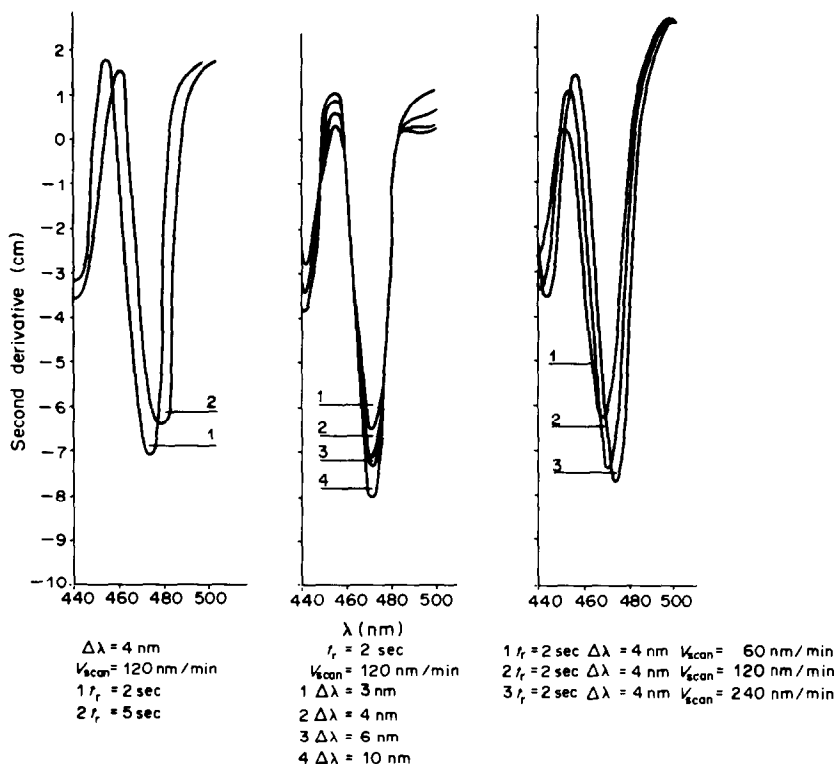


Fig. 3. Influence of instrumental parameters on the derivative spectra. $[BPKQH] = 1.5 \times 10^{-4} M$; $[Hg] = 100 \text{ ng/ml}$.

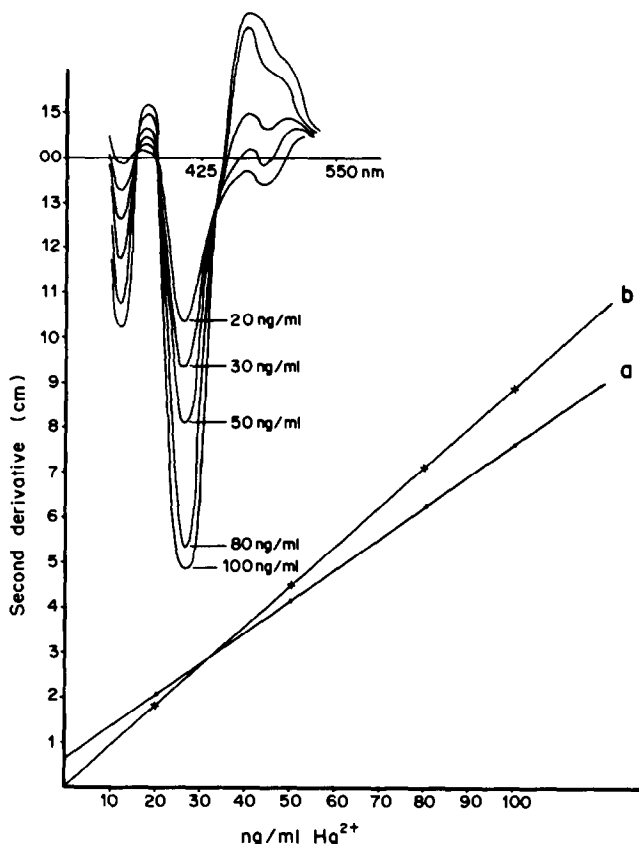


Fig. 4. Second-derivative calibration graphs.

specific sample and instrument parameters is generally found by trial and error.

Various second-order derivative spectra recorded with different $\Delta\lambda$, t_r and v_{scan} values are shown in Fig. 3, and $\Delta\lambda = 10$ nm, $t_r = 2$ sec and $v_{scan} = 120$ nm/min are seen to be the optimal parameters for the determination of mercury.

Characteristics of the analytical methods

In the normal photometric method, Beer's law was obeyed in the mercury concentration range 0–3.0 $\mu\text{g/ml}$, and the graph passed through the origin. The molar absorptivity at $\lambda_{max} = 475$ nm was 5.01×10^4 l.mole⁻¹.cm⁻¹. A Ringbom plot showed that the optimum mercury range for accurate determination was 0.6–3.0 $\mu\text{g/ml}$.

The calibration graph for the second derivative method was linear for 0–100 ng/ml mercury concen-

tration. Two methods of measurement were used. In one the vertical distance from the base-line to a trough was taken; in the other, the vertical distance from a trough to a straight line drawn between its neighbouring peaks.¹³ Figure 4 shows both calibration graphs, together with the second derivative spectra from which they were obtained. The base-line amplitude plot has a positive intercept on the ordinate, whereas the other passes through the origin, and is thus recommended.

The sensitivities of the methods can be reported as calibration sensitivity,¹⁴ $S_C = m$, *i.e.*, the slope of the calibration curve, or as analytical sensitivity¹⁵ $S_A = m/s_s$, where s_s is the standard deviation of the analytical signals at a particular concentration. As deduced from the equation of definition, S_A is related inversely to the ability to distinguish a concentration difference, therefore the inverse relationship $1/S_A$ is

Table 1. Characteristics of the analytical methods

Method	s_b	s_s	S_C	$1/S_A$, ng/ml	$C_L(k=3)$ ng/ml	$C_Q(k=10)$ ng/ml	Linear dynamic range, ng/ml	n	RSD, %
Photometric	2×10^{-3}	2.8×10^{-3}	0.24*	12	25	83	83–3000	11	0.6
Second derivative	6.2×10^{-2} cm	8.2×10^{-2} cm	0.088†	0.93	2	7	7–100	11	1.1

*ml/ μg .

†cm.ml.ng⁻¹.

Table 2. Tolerance for foreign ions

Ion added		Tolerance ratio, Ion/Hg, w/w
Photometric method	Second derivative	
Cl ⁻ , SO ₄ ²⁻		2500
V ⁵⁺		45
Mo ⁶⁺		40
Ca ²⁺ , Ba ²⁺		15
Ag ⁺ , Mg ²⁺ , Al ³⁺ , Cr ³⁺		5
Fe ³⁺	Pb ²⁺	1
	Cd ²⁺ , Fe ³⁺ , Ni ²⁺	0.8
	Cu ²⁺	0.4
Mn ²⁺ , Zn ²⁺		0.1
Pb ²⁺		< 0.1
Pd ²⁺ , Cd ²⁺ , Zn ²⁺ , Co ²⁺		< 0.1
Ni ²⁺ , Cu ²⁺		< 0.1

also given. The limits of detection, C_L , are reported as defined by IUPAC.¹⁶ The limit of quantification, C_Q ,¹⁷ is reported, to establish the lower limit of the linear dynamic range. Table 1 presents the results obtained, together with other details about the precision of the methods.

Interference study

The effect of potentially interfering ions on the determination of mercury at the 1- μ g/ml level was examined over a wide range of concentrations, by the ordinary photometric method. Those species which interfered seriously in the ordinary photometric method were also examined by the second derivative approach for solutions containing 50 ng/ml mercury.

The tolerance criterion was a deviation of the absorbance values or derivative amplitude by more than $\pm 3\%$ from the value expected for mercury alone. The most important interferences are given in Table 2. Use of the second-derivative methods improves the tolerance for certain ions.

Determination of mercury in organomercurials

The recommended procedure for the determination of mercury was applied to several organomercurial compounds to evaluate its effectiveness. The results obtained are shown in Table 3.

Although contamination is the most severe problem affecting mercury determination by any technique, and possibilities for contamination must be scrupulously identified so that blanks and precision statistics are maintained within a tolerable level, losses during manipulation and treatment of the samples may attain significant proportions without appropriate care, especially when mercurial halides are analysed.

Analysis of environmental samples

Grain seeds are still treated with organomercurial fungicides such as Ceresan[®] (methoxyethylmercury chloride), and the risks to workers from exposure to these compounds can be high, especially near the mill-hopper.

Samples were collected in a grain silo near the mill-hopper used to distribute the organomercurial Ceresan[®] to the grain on a conveyor belt. The NIOSH method¹⁸ for sampling mercurial particulate matter was used.

A 37-mm three-body filter cassette with a cellulose membrane (0.45- μ m pore size, MSA) mounted in a back-up pad, was used as the retention element. Calibrated battery-powered personal sampling pumps (model G, MSA) were used at flow-rates between 1 and 2 l/min. Duplicate samples were taken at each of five sites near the mill-hoppers, referred to as A-E in Table 4.

Each sample was treated in the filter as described in the procedure for organomercurials, but with 1 ml

Table 3. Determination of mercury in organomercurials

Samples	Hg taken, μ g/ml	Hg found, [†] μ g/ml	Recovery, %
Phenylmercury acetate	10.0 ₄ \pm 0.08	10.0 ₁ \pm 0.07	99.7
Methylmercury chloride	13.5 ₄ \pm 0.05	13.2 ₆ \pm 0.06	97.9
Ethylmercury chloride	14.5 ₅ \pm 0.07	14.5 ₃ \pm 0.05	99.9
Mercury chloride	12.8 ₁ \pm 0.08	12.3 ₄ \pm 0.08	96.3

*Determined by AAS cold-vapour technique.

[†]Mean of six determinations.

Table 4. Determination of mercury in environmental air samples

Sample	Flow-rate, l/min	Volume of samples, l.	Hg found, ng/ml	Hg in air sample, μ g/m ³
Blank [†]	—	—	28.0 \pm 2.0	—
A	1.82	436.8	7.5 \pm 0.7	2.15
B	1.74	417.6	21.3 \pm 1.9	6.4
C	1.76	422.4	50.5 \pm 2.5	29.9
D	1.81	434.4	49.0 \pm 2.4	28.2
E	1.80	432.0	48.3 \pm 1.6	28.0

*In the 25 ml of final solution measured. Blank subtracted from total found for samples.

[†]Mineralized filter subjected to the procedure.

of concentrated sulphuric acid instead 3 ml, and final dilution to 25 ml. Aliquots of 5 or 2.5 ml were then put through the derivative photometric procedure. The values obtained were corrected for the blank, which was obtained by treating a filter in the same way and then subjected to the procedure.

The conversion of Hg concentration in the solution measured (in mg/ml) into Hg in the air sample (in $\mu\text{g}/\text{m}^3$), was made by dividing the total amount of Hg found in the mineralized filter, by the volume of air sampled.

The results obtained for mercury in environmental samples obtained at different distances from the mill-hoppers show (Table 4) that workers in sites C, D and E were exposed to mercury doses above the upper TLV in air ($0.01 \text{ mg}/\text{m}^3$).

REFERENCES

1. V. Zatka, J. Abraham, J. Holzbecher and D. E. Ryan, *Anal. Chim. Acta*, 1971, **54**, 65.
2. M. Katyal and Y. Dutt, *Talanta*, 1975, **22**, 151.
3. R. B. Singh, P. Jain and R. P. Singh, *ibid.*, 1982, **29**, 77.
4. N. A. Smart, *Residue Rev.*, 1968, **23**, 1.
5. L. J. Goldwater, *Sci. Am.*, 1971, **224**, 15.
6. J. G. Saha and K. S. McKinlay, in *Analytical Aspects of Mercury and Other Heavy Metals in the Environment*, R. W. Frei and O. Hutzinger (eds.), Gordon and Breach, London, 1975.
7. A. F. Fell, *Trends Anal. Chem.*, 1983, **2**, 63.
8. M. Santiago, A. Navas, J. J. Laserna and F. García Sánchez, *Mikrochim. Acta*, 1983 **II**, 197.
9. C. Cruces and F. García Sánchez, *Anal. Chem.*, 1984, **56**, 2035.
10. G. Talsky, L. Mayring and H. Kreuzer, *Angew. Chem. Int. Ed.*, 1978, **17**, 785.
11. T. C. O'Haver and T. Begley, *Anal. Chem.*, 1981, **53**, 1876.
12. T. Vo Dinh and R. B. Gammage, *Anal. Chim. Acta*, 1979, **107**, 261.
13. A. F. Fell, *Proc. Anal. Div. Chem. Soc.*, 1978, **15**, 261.
14. *Spectrochim. Acta*, 1978, **33B**, 242.
15. J. Mandel and R. D. Stiehler, *J. Res. Natl. Bur. Stand.*, 1954, **53**, 155.
16. G. L. Long and J. D. Winefordner, *Anal. Chem.*, 1983, **55**, 712A.
17. *Ibid.*, 1980, **52**, 2242.
18. National Institute of Safety and Hygiene, *Manual of Sampling Data Sheets*, Cincinnati, Ohio, 1976.

AGGREGATION OF *meso*-TETRA- (*p*-SULPHONATOPHENYL)PORPHINE AND ITS Cu(II) AND Zn(II) COMPLEXES IN AQUEOUS SOLUTION

A. CORSINI and O. HERRMANN*

Department of Chemistry, McMaster University, Hamilton, Ontario, Canada

(Received 17 September 1985. Accepted 1 November 1985)

Summary—The aggregation of *meso*-tetra(*p*-sulphonatophenyl)porphine, an analytical reagent for the determination of metals at low concentration, has been studied over a wide concentration range by both spectrophotometric and ¹H NMR methods. Up to a concentration of about $3 \times 10^{-4}M$, the experimental data were satisfactorily accounted for by a monomer-dimer equilibrium. At higher concentrations, the best fit of the chemical shift data required postulation of a tetramer. Analysis of the experimental data for the Zn(II) complex indicated the occurrence of dimerization at higher concentrations.

Synthetic cationic and anionic porphines have been frequently used recently as analytical reagents for the spectrophotometric determination of metal ions at trace concentrations.¹⁻¹³ The intense absorption of the Soret band in metalloporphyrins allows measurement of the metal ions at ng/ml concentrations. Although measurement is usually made directly in the aqueous phase, an ion-association solvent-extraction step is sometimes included in the procedure to enrich the analyte.^{1,12,13}

A general property of porphines and their metal complexes is their tendency to aggregate in aqueous solution. Because of the biological importance of natural porphyrins, the aggregation of model synthetic porphyrins has been extensively studied,¹⁴⁻¹⁶ but an understanding of aggregation behaviour is also of importance for knowledgeable application of synthetic porphines to chemical analysis. For example, aggregation of the ligand affects the concentration of its monomeric form and could prevent quantitative complexation. Similarly, aggregation of metalloporphyrins could cause deviation from linearity in spectrophotometric determinations and also affect values of distribution ratios in separation processes.

Of the several porphines that have been exploited as analytical reagents, *meso*-tetra(*p*-sulphonatophenyl)porphine (TPPS₄) has been particularly useful.^{1,5,7,8,9,11} In the present study, aggregation of this water-soluble anionic porphine has been investigated by spectrophotometric and ¹H NMR methods over a wide concentration range ($\sim 10^{-7}$ – $10^{-1}M$) in the presence of various electrolytes. Solutions of the Cu(II) and Zn(II) complexes have also been examined over the range $\sim 10^{-7}$ – $10^{-3}M$. The experimental data are readily

interpreted in terms of monomer-dimer equilibria. At very high concentrations of the free ligand, the data are consistent with the formation of a tetramer. The results are of interest because they indicate upper concentration levels beyond which simple analytical relationships may no longer obtain.

EXPERIMENTAL

Reagents

The anhydrous salts Na₄TPPS₄ and (NH₄)₄TPPS₄ were prepared as described previously.¹ The salts are strongly hygroscopic and must be weighed with care. The Cu(II) and Zn(II) complexes of TPPS₄ were prepared as described by Herrmann *et al.*¹⁷ Distilled demineralized water (DDW) and analytical-grade reagents were used throughout. Reagents used as electrolytes were recrystallized from DDW and dried prior to use.

Spectrophotometric studies

Spectra in the ultraviolet-visible region were recorded on a Cary 14 double-beam instrument. Measurements at a fixed wavelength were made with a single-beam Hitachi Perkin-Elmer 139 spectrophotometer, with the cell compartment kept at $25.0 \pm 0.2^\circ$. Quartz cells with path-lengths ranging from 100 to 0.1 mm were used. The degree of aggregation was determined from the extent of deviation from the Beer-Lambert law. Electrolyte solutions used [ionic strength (μ) = 0.100] were: 0.100M potassium nitrate, adjusted to pH 6.4; 0.017M potassium dihydrogen phosphate, 0.011M disodium hydrogen phosphate and 0.0500M potassium nitrate, adjusted to pH 7.0; 0.100M sodium acetate, adjusted to pH 9.0. Test solutions of Na₄TPPS₄ were prepared by dispensing appropriate volumes of a $10^{-3}M$ stock solution (in an appropriate electrolyte solution) with a calibrated Gilmont microburette into 10- and 50-ml standard flasks and diluting with the appropriate electrolyte solution. Ten test solutions were prepared within each decade of concentration, ranging from $\sim 10^{-7}$ to $10^{-4}M$ Na₄TPPS₄. These solutions were stored in the dark and used within 24 hr after preparation. The absorbance of the Soret band (412 nm) was measured. For each electrolyte medium, 2-5 runs were made, fresh stock solutions of Na₄TPPS₄ being prepared each time. Absorbance measurements of the Cu(II) (412 nm) and Zn(II) (422, 556 and 596 nm) complexes were made in the phosphate medium only. As the metalloporphyrin solutions appeared to be more photosensitive than solutions of

*Present address: Ontario Hydro Research, Toronto, Canada.

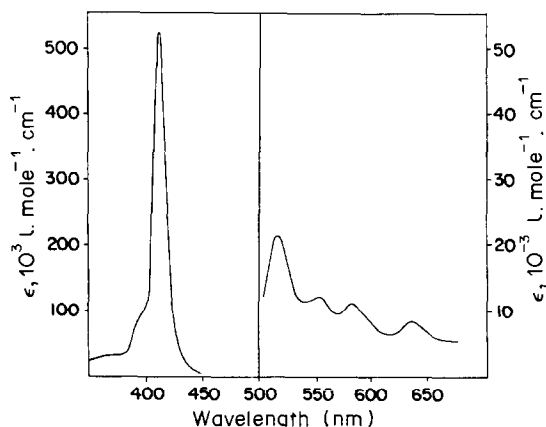


Fig. 1. Absorption spectrum of monomeric Na_4TPPS_4 ($1.8 \times 10^{-6} M$), in phosphate buffer (pH 7.0).

free TPPS_4 , the stock-solution containers were wrapped in aluminium foil and stored in the dark. The concentration ranges of the test solutions were $\sim 10^{-7}$ – 10^{-4} and 10^{-5} – $10^{-3} M$ for the Cu(II) and Zn(II) complexes, respectively. The solutions were used within 2 hr.

^1H NMR studies

Spectra were recorded either on a Varian HA-100 or a Bruker WH-90 Fourier-transform spectrometer. Paramagnetic impurities were removed from the thin-walled NMR tubes by soaking in an alkaline EDTA solution and rinsing with DDW. Because shifts were found for internal references in D_2O solutions of $(\text{NH}_4)_4\text{TPPS}_4$, an external reference was used, consisting of a saturated solution of sodium 2,2,-dimethyl-2-silapentane-5-sulphonate (DSS) in D_2O . Assignment of the NMR signals to the phenyl-ring protons *ortho* and *meta* to the porphine ring was established by use of $(\text{NH}_4)_4\text{TPPS}_4$ in which the *ortho*-positions were 60% deuterated. The deuterated compound was synthesized as before,¹ but from benzaldehyde obtained by oxidation of 60%-*ortho*-deuterated toluene. Experiments which qualitatively showed the dependence of the NMR spectra on $(\text{NH}_4)_4\text{TPPS}_4$ concentration were made over the range 5×10^{-3} – $0.1 M$. For quantitative experiments, individual test solutions of Na_4TPPS_4 ranging in concentration from 1.0×10^{-5} to $0.1 M$, in a phosphate buffer, were used. The phosphate solution was prepared by adjusting the pD of a 0.0295 M disodium hydrogen phosphate solution to pH 7 with DCl. The extent of aggregation was indicated by changes in the *difference* between the chemical shifts of the signals of the *ortho* and *meta* phenyl-ring protons.

RESULTS AND DISCUSSION

Spectrophotometric study of TPPS_4 aggregation

In very dilute solutions, in the pH range 6.4–9.0

TPPS_4 exists in the free-base form and does not form dimers or higher aggregates. The electronic absorption spectrum of monomeric TPPS_4 ($1.8 \times 10^{-6} M$) is shown in Fig. 1. When the concentration is increased 100-fold to $1.8 \times 10^{-4} M$, spectral changes occur which qualitatively suggest intermolecular interactions. The intensity of the Soret band (412 nm) is lowered and the band is broadened, and the band at 635 nm is red-shifted by 14 nm. All other bands are shifted to a lesser extent. These observations are in agreement with findings on the spectral characteristics of co-facial porphyrins,¹⁸ which are dimers held in rigid configuration by bridging alkyl groups.

Additional evidence for aggregation was provided by deviations from the Beer–Lambert law in the nitrate, phosphate and acetate media (pH 6.4–9.0). Deviations became apparent at $\sim 2 \times 10^{-5} M$ concentration and were very significant at $\sim 3 \times 10^{-4} M$. For other anionic porphines, such behaviour has been attributed to aggregation.¹⁴ In view of the low concentrations used, it was assumed that the only species in appreciable concentration were the monomer and dimer. On this basis, equation (1) was readily derived, following Pasternack.¹⁴

$$A = \epsilon_2 C_T / 2 + (2\epsilon_1 - \epsilon_2)(\sqrt{8K_D C_T + 1} - 1) / 8K_D \quad (1)$$

where A = measured absorbance at 412 nm, C_T = analytical concentration of Na_4TPPS_4 , ϵ_1 and ϵ_2 are the molar absorptivities of monomer and dimer, respectively and K_D is the equilibrium constant for formation of the dimer. A non-linear least-squares curve-fitting program (NLWOOD)¹⁹ was used to fit experimental values of A and C_T to equation (1), to obtain values of ϵ_1 , ϵ_2 and K_D . An improved value of ϵ_1 and more precise values of ϵ_2 and K_D were obtained by separate determination of ϵ_1 through a linear least-squares analysis of data obtained at low concentration ($< 2.1 \times 10^{-6} M$), and substitution of this value directly into equation (1). Values obtained by this procedure are given in Table 1.

Inspection of the data in Table 1, including the precision, shows that the values of ϵ_1 , ϵ_2 and K_D are not significantly dependent on the nature of the electrolyte at constant ionic strength; however, as demonstrated by the ^1H NMR studies discussed below, the extent of aggregation is dependent on ionic strength. The ϵ_1 , ϵ_2 and K_D values are independent of pH in the range 6.4–9.0; significant protonation of

Table 1. Spectrophotometric study of dimerization of TPPS_4 in various electrolyte media at 412 nm and 25°

	Nitrate	Phosphate	Acetate
pH	6.4	7.0	9.0
ϵ_1 ,* $l.mole^{-1}.cm^{-1}$	$(491 \pm 1) \times 10^3$	$(510 \pm 3) \times 10^3$	$(473 \pm 3) \times 10^3$
ϵ_2 ,† $l.mole^{-1}.cm^{-1}$	$(422 \pm 14) \times 10^3$	$(394 \pm 7) \times 10^3$	$(399 \pm 27) \times 10^3$
K_D †	$(22.3 \pm 3.5) \times 10^3$	$(15.4 \pm 1.3) \times 10^3$	$(16.4 \pm 3.0) \times 10^3$

* ϵ_1 values obtained by linear regression for at least 36 data points at $\leq 2.1 \times 10^{-6} M$ concentration; precision values are for 95% confidence level.

† ϵ_2 and K_D values obtained by non-linear regression for at least 38 data points between 2.1×10^{-6} and $3.4 \times 10^{-4} M$ concentration.

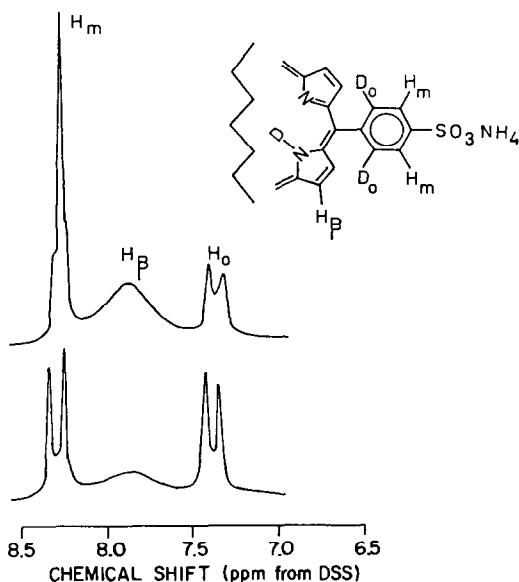


Fig. 2. ^1H NMR spectrum of $(\text{NH}_4)_4\text{TPPS}_4$ (0.077M, bottom) and of its partially deuterated analogue (0.076M, top) in D_2O at 35° . Amplification for top figure was twice that for bottom figure.

the central free-base nitrogen atom occurs only in more acidic solution.^{20,21} As noted by Fleischer *et al.*,²⁰ protonation of TPPS_4 to the dibasic acid form leads to behaviour considerably more complicated than that in neutral and alkaline solution. Our studies confirm this observation and indicate that protonation gives rise to micelle formation rather than simple aggregation; these results will be reported separately.

It is of interest to note that previous reports on aggregation of TPPS_4 in neutral solution are not in agreement. In one report,²⁰ TPPS_4 was found to obey the Beer-Lambert law from 10^{-9} to 10^{-4}M and dimerization was not noted. In the other, TPPS_4 was found to dimerize, with $K_D = 9.6 \times 10^4$.²² The observation of dimerization is in accord with the present study but the value of K_D is about 5 times greater than the average of the values in Table 1. This may be due to the use of HEPES [4-(2-hydroxyethyl)-piperazine-1-ethanesulphonic acid] as buffer. Specific interactions are known to occur between TPPS_4 and large molecules. For example, in our NMR measurements, it was necessary to use DSS as an external reference because when it was used internally, co-aggregation with TPPS_4 occurred, which caused upfield shifts of the signals. Similar effects have been noted previously.²³

^1H NMR study of TPPS_4 aggregation

At TPPS_4 concentrations greater than $\sim 5 \times 10^{-4}\text{M}$, the Soret band is too intense for accurate measurement of absorbance, even with 0.1-mm cells. The use of either the less intense bands at longer wavelengths or of ^1H NMR is more convenient. The results of aggregation studies up to $\sim 0.1\text{M}$ TPPS_4

concentration are reported here. A number of reports have appeared in which aggregation of porphyrins has been investigated by NMR.²⁴⁻²⁶

The ^1H NMR spectrum of TPPS_4 in D_2O is extremely dependent on experimental conditions such as concentration, temperature and electrolyte concentration. In Fig. 2 (bottom), the spectrum of $(\text{NH}_4)_4\text{TPPS}_4$ at high concentration (0.077M) in the absence of inert electrolyte is shown. The spectrum consists of two doublets arising from the phenyl-ring protons, separated by a broad band due to the β -pyrrole protons. Comparison of this spectrum with that (top) of $(\text{NH}_4)_4\text{TPPS}_4$ which had been partially deuterated (60%) in the phenyl position *ortho* to the porphyrin ring allowed unambiguous assignment of the phenyl signals as shown.

The concentration dependence is illustrated in Fig. 3. All the signals are shifted upfield with increasing concentration, but to different extents, resulting in increasing separation between the H_o and H_m doublets. This observation can be satisfactorily accounted for by aggregation in solution, in which the molecules are stacked vertically with their planes approximately parallel. In this orientation, intermolecular interactions due to the ring current result in a greater upfield shift for H_o than for H_m protons. This kind of orientation in other porphyrins has been discussed.^{24,26,27}

The effect of inert electrolytes such as ammonium nitrate or sodium chloride can also be explained by aggregation. At constant concentration of TPPS_4 , increasing amounts of these salts caused upfield shifts

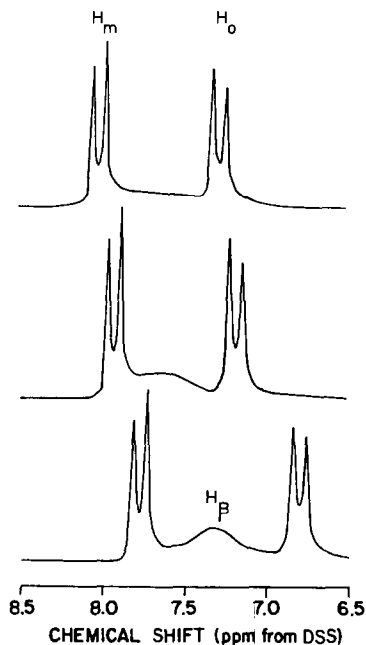


Fig. 3. ^1H NMR spectra of $(\text{NH}_4)_4\text{TPPS}_4$ in D_2O with increasing concentration (35°); top, 0.035M; centre, 0.052M; bottom, 0.102M. Amplification was adjusted appropriately with concentration.

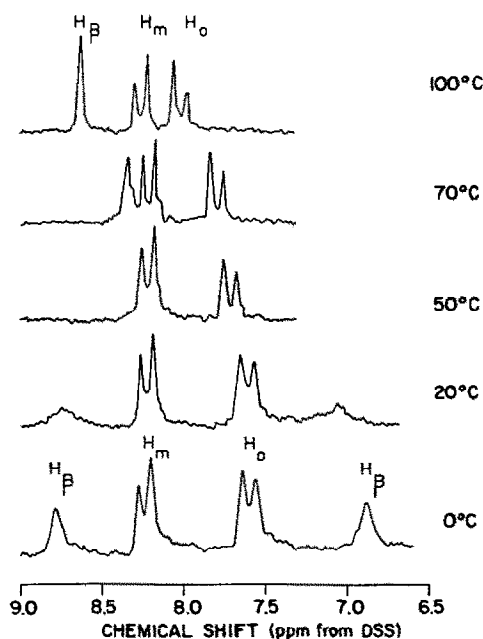


Fig. 4. The effect of temperature on the ^1H NMR spectrum of $(\text{NH}_4)_4\text{TPPS}_4$ (0.014M) in D_2O .

in the same manner as increasing concentrations of the porphine itself. These electrolytes promote aggregation by the salting-out effect.

In the absence of electrolyte and at a fixed concentration of TPPS_4 , shifts to lower field occurred with increasing temperature, resulting in decreasing separation of the H_α and H_β doublets (Fig. 4). This observation is explained by a reduction of aggregation at the higher temperatures. In fact, although not shown in Fig. 4, dilute solutions of TPPS_4 at 100° showed coalescence of the H_α and H_β signals (at $5.0 \times 10^{-3}M$) and even crossover of the signals (at $<1.0 \times 10^{-3}M$). This reversal was also observed in a concentrated solution (0.044M) of the deuterated TPPS_4 in $\text{DMSO}-d_6$, in which the extent of aggregation is minimal. Figure 4 also demonstrates the effect of tautomeric exchange of the central protons between the pyrrole nitrogen atoms. At low temperatures (between -80 and $+20^\circ$, depending on the porphyrin and the solvent), this exchange can be frozen out and two signals observed for the β -pyrrole protons.^{28,29} In D_2O solutions, the central hydrogen atoms are replaced by deuterium, thereby decreasing the rate of tautomerism, so freezing out of the exchange occurs at a relatively high temperature ($<20^\circ$), as observed in the present work. The broad signal observed for moderately concentrated TPPS_4 solutions at ambient temperature (Figs. 2 and 3) indicates moderately slow tautomerism. The signal is too broad to observe at low concentrations.

In the present study, significant interactions were found to occur between TPPS_4 and various compounds selected as internal references. The interaction was especially strong with DSS and it was necessary to use it as an external reference. A further

difficulty was the need to estimate the contribution of the diamagnetic anisotropy of the porphine ring system to chemical shift changes. Because of this problem, the absolute shifts of the phenyl-ring protons were not used to monitor aggregation; rather, the difference in chemical shift between the H_α and H_β protons was used to provide a direct measure of the extent of aggregation.

Following the procedure of Abraham *et al.*,²⁴ equation (2) was derived:

$$\Delta\delta = (\Delta\delta_M[\text{monomer}] + 2\Delta\delta_D[\text{dimer}] + 4\Delta\delta_T[\text{tetramer}])/C_T \quad (2)$$

where $\Delta\delta$ = observed difference in chemical shifts ($\delta\text{H}_\beta - \delta\text{H}_\alpha$); $\Delta\delta_M = (\delta\text{H}_\beta - \delta\text{H}_\alpha)$ for the monomer; $\Delta\delta_D = (\delta\text{H}_\beta - \delta\text{H}_\alpha)$ for the dimer; $\Delta\delta_T = (\delta\text{H}_\beta - \delta\text{H}_\alpha)$ for the tetramer; C_T = molar analytical concentration of TPPS_4 . This equation was varied by the deletion or addition of terms, depending on whether only the monomer and dimer, or the trimer and tetramer as well, were being considered. This equation resembles those generally used in aggregation studies except that the chemical shift of a given proton has been replaced by the difference in chemical shifts. The concentrations of the various species were obtained by solution of the appropriate equilibrium and mass-balance equations. Thus, for the monomer, dimer, tetramer model the mass-balance equation is:

$$C_T = 4[\text{tetramer}] + 2[\text{dimer}] + [\text{monomer}] \\ = 4K_T K_D^2 [\text{monomer}]^4 + 2K_D [\text{monomer}]^2 + [\text{monomer}] \quad (3)$$

where K_T and K_D are the relevant equilibrium constants. The Newton-Raphson iterative method³⁰ was used to solve equation (3). An initial approximation, $[\text{monomer}]_0$, was obtained by assuming the presence of only monomer and dimer species at the lower concentrations and solving the equation

$$[\text{monomer}]_0 = (-2 + 2\sqrt{8K_D C_T + 1}) / 8K_D \quad (4)$$

The value $K_D = 15.4 \times 10^3$ (phosphate buffer) obtained from the spectrophotometric studies was used, together with the program NLWOOD. An estimate of K_T was then calculated and values for the concentrations of monomer, dimer and tetramer could be

Table 2. ^1H NMR study* of aggregation of TPPS_4 in phosphate buffer at pH 7.0 and 25°

$\Delta\delta_M$, ppm	$-0.14 \pm 0.03^\dagger$
$\Delta\delta_D$, ppm	0.56 ± 0.02
$\Delta\delta_T$, ppm	1.91 ± 0.62
K_T	7 ± 6

*17 data points, precision at 95% confidence level.

†The negative value indicates that the H_α signal has crossed to downfield of the H_β signal.

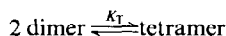
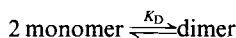
Table 3. Spectrophotometric study of dimerization of Cu(II)- and Zn(II)-TPPS₄ complexes at pH 7.0 and 25°, $\mu = 0.100M$

Complex	No. of data points	Conc. range, M	$\epsilon_{1\lambda}^*$ l. mole ⁻¹ .cm ⁻¹	$\epsilon_{2\lambda}^\dagger$ l. mole ⁻¹ .cm ⁻¹	K_D^\ddagger
Cu(II)	69	1.0×10^{-6} – 5.5×10^{-4}	$(41 \pm 5) \times 10^3$	$(219 \pm 5) \times 10^3$	$(41 \pm 4) \times 10^3$
Zn(II)	41	2.0×10^{-4} – 6.2×10^{-3}	$(20.6 \pm 0.1) \times 10^3$	$(27 \pm 2) \times 10^3$	221 ± 81

* $\epsilon_{1\lambda}$ values obtained by linear regression for at least 16 data points over the range 7×10^{-8} – $6 \times 10^{-7}M$ and 1×10^{-5} – $2 \times 10^{-4}M$ for Cu(II) and Zn(II) complexes, respectively. Precision at 95% confidence levels.

† $\epsilon_{2\lambda}$ and K_D values obtained by non-linear regression; precision at 95% confidence levels.

readily obtained from equilibrium relationships. The iterations were continued until the changes in successive approximations were negligible. The final values for $\Delta\delta_M$, $\Delta\delta_D$, $\Delta\delta_T$ and K_T were obtained by non-linear least-squares fitting of equation (2) to the observed NMR data. Similar procedures were used for the other models. The model which best accounted for the experimental data involves the two main equilibria



Although a mathematically good fit does not necessarily reflect physical reality, it does indicate which model among several is the most reasonable. The data obtained by using this model are given in Table 2. K_T is not a true equilibrium constant because the ionic strength could not be maintained constant at the high concentration levels of TPPS₄.

Aggregation of Cu(II) and Zn(II) complexes

Because the Cu(II) and Zn(II) complexes are stable from pH 3 to pH 10,¹ it was assumed that aggregation would not be appreciably sensitive to pH changes in this range. Therefore, studies were made at pH 7 only and the results are summarized in Table 3. Equation (1) can be extended to include other species such as trimers and tetramers, but a monomer–dimer model allowed the best fit of the data for both the Cu(II) and Zn(II) complexes. Although dimerization of the Cu(II) complex has been previously reported ($K_D = 6.7 \times 10^4$), the Zn(II) complex is stated not to dimerize.²² In the present study, dimerization was indeed found not to occur up to $\sim 2 \times 10^{-4}M$; however, at concentrations above $\sim 3 \times 10^{-4}M$ dimerization was evident. These higher concentrations necessitated the use of the less intense band at 556 nm, which in turn resulted in decreased precision because of the small difference between ϵ_1 and ϵ_2 .

CONCLUSION

The absorbance of TPPS₄, a useful analytical reagent for trace-metal determinations, has been shown to deviate from the Beer–Lambert law in the concentration range $\sim 2 \times 10^{-5}$ – $3 \times 10^{-4}M$. A monomer–dimer equilibrium provided a good fit to the experimental data. At high concentrations, up to 0.1M, the ¹H NMR chemical shift data were best

explained by inclusion of a tetrameric species in the calculations. Evidence has also been obtained for the dimerization of the Zn(II) complex at higher concentrations.

Acknowledgement—The authors gratefully acknowledge financial support for this study from the Natural Sciences and Engineering Council of Canada.

REFERENCES

1. A. Corsini, R. DiFruscia and O. Herrmann, *Talanta*, 1985, **32**, 791.
2. S. Igarishi, M. Nakano and T. Yotsuyanagi, *Bunseki Kagaku*, 1983, **32**, 67.
3. H. Ishii, H. Koh and K. Satoh, *Analyst*, 1982, **107**, 647.
4. *Idem*, *Anal. Chim. Acta*, 1982, **136**, 347.
5. *Idem*, *Nippon Kagaku Kaishi*, 1980, 1919.
6. H. Ishii, K. Satoh, Y. Satoh and H. Koh, *Talanta*, 1982, **29**, 545.
7. M. Tabata and M. Tanaka, *Mikrochim. Acta*, 1982 **II**, 149.
8. *Idem*, *Anal. Lett.*, 1980, **13**, 427.
9. H. Ishii and H. Koh, *Nippon Kagaku Kaishi*, 1978, 390.
10. *Idem*, *Talanta*, 1977, **24**, 417.
11. *Idem*, *Mikrochim. Acta*, 1983 **I**, 279.
12. H. Watanabe, H. Tachikawa and H. Ohemori, *Bunseki Kagaku*, 1982, **31**, 471.
13. H. Ishii, H. Koh and K. Satoh, *ibid.*, 1982, **31**, 389.
14. R. F. Pasternack, *Ann. N.Y. Acad. Sci.*, 1973, **206**, 614.
15. K. M. Smith (ed.), *Porphyrins and Metalloporphyrins*, Elsevier, Amsterdam, 1975.
16. W. I. White, in *The Porphyrins*, D. Dolphin (ed.), Vol. 5, Part 6, Chap. 7. Academic Press, New York, 1978.
17. O. Herrmann, H. Mehdi and A. Corsini, *Can. J. Chem.*, 1978, **56**, 1084.
18. C. K. Chang, *J. Heterocyclic Chem.*, 1977, **14**, 1285.
19. C. Daniel and F. S. Wood, *Fitting Equations to Data*, Wiley–Interscience, New York, 1971.
20. E. B. Fleischer, J. M. Palmer, T. S. Srivastava and A. Chatterjee, *J. Am. Chem. Soc.*, 1971, **93**, 3162.
21. N. Johnson, R. Khosropour and P. Hambright, *Inorg. Nucl. Chem. Lett.*, 1972, **8**, 1063.
22. M. Krishnamurthy, I. R. Sutter and P. Hambright, *J. Chem. Soc., Chem. Commun.*, 1975, 13.
23. E. S. Hand and T. Cohen, *J. Am. Chem. Soc.*, 1965, **87**, 133.
24. R. J. Abraham, P. A. Burbidge, A. H. Jackson and D. B. MacDonald, *J. Chem. Soc. (B)*, 1966, 620.
25. M. Momenteau, J. Mispelter, B. Loock and J. M. Lhoste, *Can. J. Chem.*, 1978, **56**, 2598.
26. T. R. Janson and J. J. Katz, *J. Magn. Reson.*, 1972, **6**, 209.
27. D. A. Doughty and C. W. Dwiggin, Jr., *J. Phys. Chem.*, 1969, **73**, 423.
28. R. J. Abraham, G. E. Kawkes and K. M. Smith, *J. Chem. Soc., Perkin Trans. II*, 1974, 627.
29. C. B. Storm and Y. Teklu, *J. Am. Chem. Soc.*, 1972, **94**, 1745.
30. W. E. Grove, *Brief Numerical Methods*, Prentice-Hall, Englewood Cliffs, New Jersey, 1966.

SIMULTANEOUS SPECTROPHOTOMETRIC DETERMINATION OF *o*-CRESOL RED, SEMI-XYLENOL ORANGE AND XYLENOL ORANGE

S. KICIAK* and H. GONTARZ

Department of Physical Chemistry, Institute of Fundamental Chemistry, Technical University,
Poznań, Poland

(Received 14 June 1985. Accepted 10 September 1985)

Summary—A direct simultaneous spectrophotometric method for the determination of *o*-Cresol Red (CR), Semi-Xylenol Orange (SXO) and Xylenol Orange (XO) in mixtures in the presence of other components usually found in commercial SXO and XO reagents is presented. The method of selecting the most advantageous conditions for the spectrophotometric determination of the three dyes in different mixtures is given.

The mixtures obtained in the syntheses¹⁻⁴ of Xylenol Orange (XO) and Semi-Xylenol Orange (SXO) usually contain *o*-Cresol Red⁵ (CR) and colourless substances such as iminodiacetic acid^{4,5} (IDAA). The last-named does not interfere in the spectrophotometric determination of the other three dyes. A method for determination of XO, SXO and CR is needed for control of the synthesis of XO and SXO, and the separation of XO, SXO and CR, and for monitoring the aging of XO and SXO reagents.

The analysis of two-component mixtures of XO and SXO by spectrophotometry, reported by Murakami *et al.*,⁴ gives good results. The method is based on the equations

$$A_{435} = 26.2 \times 10^3 C_{XO} + 25.2 \times 10^3 C_{SXO} \quad (1)$$

$$A_{510} = 4.72 \times 10^3 C_{XO} + 32.1 \times 10^3 C_{SXO} \quad (2)$$

where A_{435} is the absorbance of a 1-cm layer of a solution containing XO and SXO (in buffer solution at pH 3.11) and A_{510} is that of a 1-cm layer of a solution containing XO and SXO in 1.44M sulphuric acid at the same concentrations as in the buffer. However, this method does not take into consideration the presence of CR in mixtures of XO and SXO. Such mixtures containing CR are often met in analytical practice. Simple chromatographic investigations^{4,5} show that commercial XO reagents may contain up to a few per cent of CR.

The molar absorptivity (ϵ) of CR at 435 nm in buffer solution at pH 3.11 is 20.8×10^3 l. mole⁻¹. cm⁻¹ and that at 510 nm in 1.44M sulphuric acid is 59.0×10^3 . Small amounts of CR in the presence of large amounts of XO caused only small changes in A_{435} because $\epsilon_{CR}/\epsilon_{XO} = 0.79$, but for A_{510}

($\epsilon_{CR}/\epsilon_{XO} = 12.5$) the change can be considerable and the change in the ratio A_{435}/A_{510} is also appreciable.

Combining equations (1) and (2) gives

$$\frac{A_{435}}{A_{510}} = \frac{25.2 + x_{XO}}{32.1 - 27.38x_{XO}} \quad (3)$$

where x_{XO} is the molar fraction of XO in admixture with SXO.

Similar equations can be written to take account of the presence of CR:

$$A_{435} = 26.2 \times 10^3 C_{XO} + 25.2 \times 10^3 C_{SXO} + 20.8 \times 10^3 C_{CR} \quad (4)$$

$$A_{510} = 4.72 \times 10^3 C_{XO} + 32.1 \times 10^3 C_{SXO} + 59.0 \times 10^3 C_{CR} \quad (5)$$

and the relationship between the two absorbances is then

$$\frac{A_{435}}{A_{510}} = \frac{25.2 + x_{XO} - 4.4x_{CR}}{32.1 - 27.38x_{XO} + 26.9x_{CR}} \quad (6)$$

where x_{CR} is the molar fraction of CR. Equation (6) allows prediction of the differences in the x_{XO} and x_{SXO} values found if the presence of CR is neglected (Fig. 1). It can be seen that for a mixture defined by $x_{XO} = 0.80$, $x_{SXO} = 0.16$ and $x_{CR} = 0.04$, $A_{435}/A_{510} = 2.28$ (Fig. 1, curve 3). Neglecting the presence of CR would result in this value of A_{435}/A_{510} (Fig. 1, curve 1) giving $x_{XO} = 0.756$ and $x_{SXO} = 0.244$ in accordance with earlier reports. Therefore even small quantities of CR cannot be ignored in the spectrophotometric determination of XO and SXO by use of simultaneous equations.

Literature data⁴⁻¹⁰ and the initial results of spectrophotometric experiments with CR, SXO and XO in dilute sulphuric acid suggest that the corresponding determination of CR, SXO and XO is possible.

*To whom correspondence should be addressed.

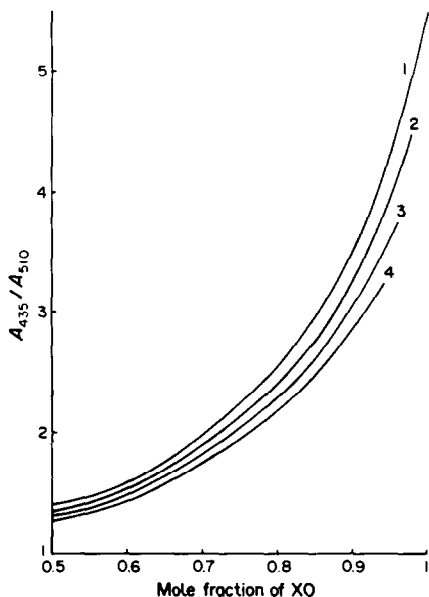


Fig. 1. Absorbance ratio A_{435}/A_{510} vs. mole fraction of Xylenol Orange for mixtures of XO, SXO and CR. Mole fraction of *o*-Cresol Red (x_{CR}): 0.0 (curve 1), 0.02 (2), 0.04 (3), 0.06 (4). A_{435} = absorbance at 435 nm and pH 3.0, A_{510} = absorbance at 510 nm and 1.44M H_2SO_4 .

EXPERIMENTAL

Apparatus

All absorption measurements were made with Zeiss-Jena spectrophotometers with 1-cm cells, the initial measurements with the Specord UV-Vis, and those given in this paper with a Specord 40. The latter model automatically gives the values to four decimal places from 99 absorption measurements, with the standard deviations for 9 chosen points on the absorption curve.

Reagents

SXO and XO were obtained from M. Łożyński of the Organic Chemistry Department, Technical University, Poznań, and were separated and purified as described previously.⁴ The purified samples were free from CR, and any other impurities present did not absorb in the visible region of the spectrum (their content did not exceed 1%).

The commercial sample of CR was recrystallized from ethanol. All other reagents were of analytical grade. A mixture of 0.1M formic acid and 0.1M sodium hydroxide was used as the buffer solution.

All mean values and standard deviations were calculated from 5 independent experiments.

RESULTS AND DISCUSSION

Molar absorptivities of CR, SXO and XO in sulphuric acid

The absorption spectra of XO (Fig. 2) and SXO (Fig. 3) in dilute sulphuric acid are similar to those reported by Murakami *et al.*⁴ but differ from those given more recently by Pantaler and Pulajewa.⁵

The absorption spectra of CR in sulphuric acid solution are shown in Fig. 4. The concentrations of sulphuric acid were so chosen that it was possible to compare the absorption spectra of the different dyes at the same acid concentration as well as the effect of

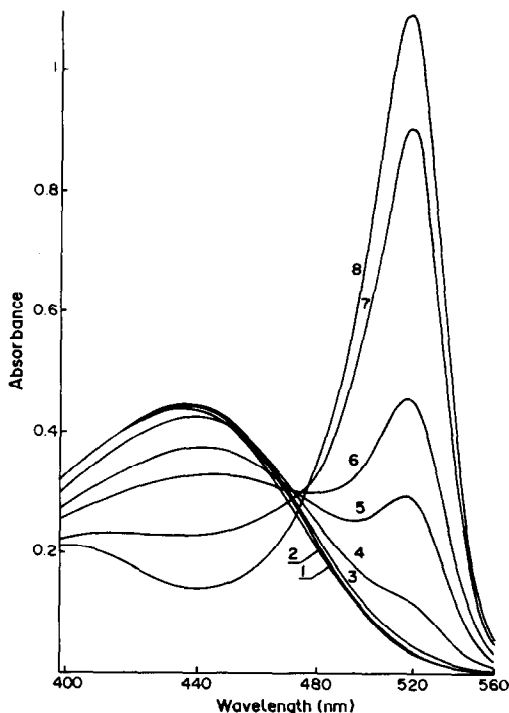


Fig. 2. Absorption spectra of $16 \times 10^{-6}M$ Xylenol Orange in buffer solution at pH 3.0 (curve 1) and for different sulphuric acid concentrations: 0.20M (2), 0.50M (3), 2.00M (4), 3.50M (5), 4.0M (6), 5.0M (7), 6.0M (8).

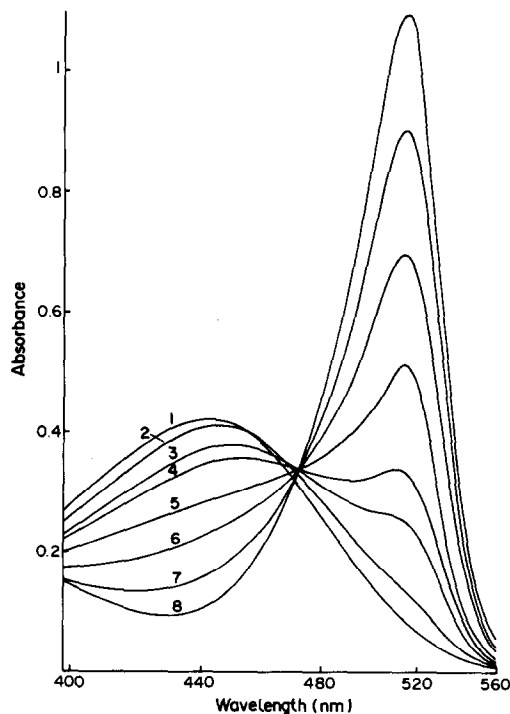


Fig. 3. Absorption spectra of $16 \times 10^{-6}M$ Semi-Xylenol Orange in buffer solution at pH 3.0 (curve 1) and for different sulphuric acid concentrations: 0.015M (2), 0.20M (3), 0.50M (4), 1.0M (5), 2.0M (6), 3.5M (7), 6.0M (8).

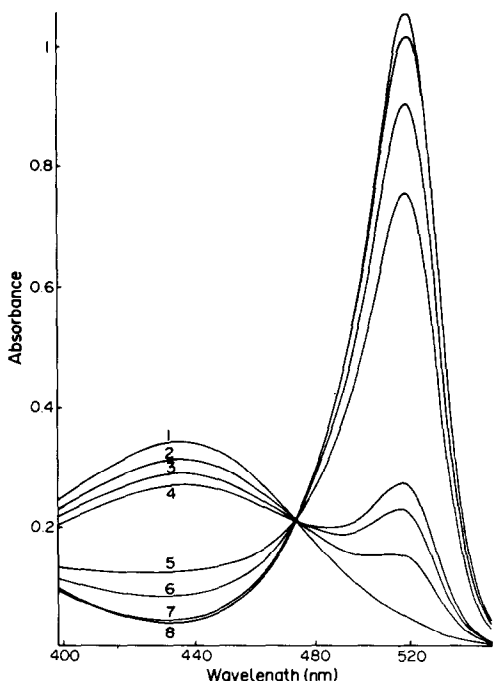


Fig. 4. Absorption spectra of $16 \times 10^{-6}M$ *o*-Cresol Red in buffer solution at pH 3.0 (curve 1) and in solutions of different sulphuric acid concentration: 0.005*M* (2), 0.010*M* (3), 0.015*M* (4), 0.20*M* (5), 0.50*M* (6), 2.0*M* (7), 6.0*M* (8).

varied acidity on the absorption spectra. The spectra obtained at pH 3 in buffer solution are also shown.

At low acidity all three dyes have an absorption maximum near 435 nm, with similar molar absorptivities, whereas at higher acidity (6*M* sulphuric acid) the absorption maxima are at 517 nm and the molar absorptivities are between 2 and 3 times as great as those at 435 nm and pH 3.

The ranges of sulphuric acid concentration in which the greatest changes in absorption spectrum take place are 0.005–0.50*M* for CR, 0.2–4.0*M* for SXO and 3–6*M* for XO. These ranges may be identified by plotting molar absorptivity against sulphuric acid concentration for the maxima at 435 nm (Fig. 5) and 517 nm (Fig. 6) but the ranges overlap and their limits are not sharply defined.

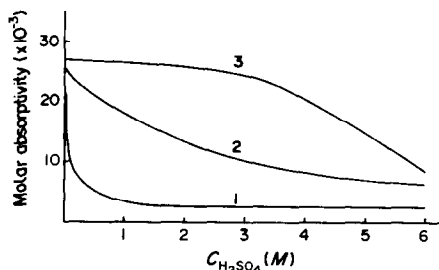


Fig. 5. Molar absorptivities of *o*-Cresol Red (curve 1), Semi-Xylenol Orange (2) and Xylenol Orange (3) vs. sulphuric acid concentration at 435 nm.

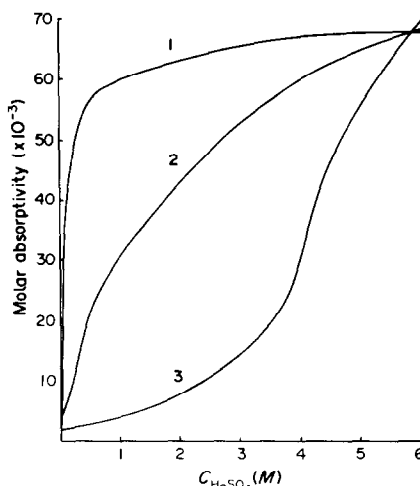


Fig. 6. Molar absorptivities of *o*-Cresol Red (curve 1), Semi-Xylenol Orange (2) and Xylenol Orange (3) vs. sulphuric acid concentration at 517 nm.

Two-component systems

System CR–SXO. As shown in Figs. 5 and 6 the greatest changes in molar absorptivities for CR and SXO take place in 0.2–0.5*M* sulphuric acid media. To select the optimum concentration of sulphuric acid for the simultaneous determination of CR and SXO the molar absorptivities at the absorption maxima (435 and 517 nm) were determined precisely and their difference plotted against sulphuric acid concentration (Fig. 7). It can be seen that the optimum acid concentration is *ca.* 0.4*M*.

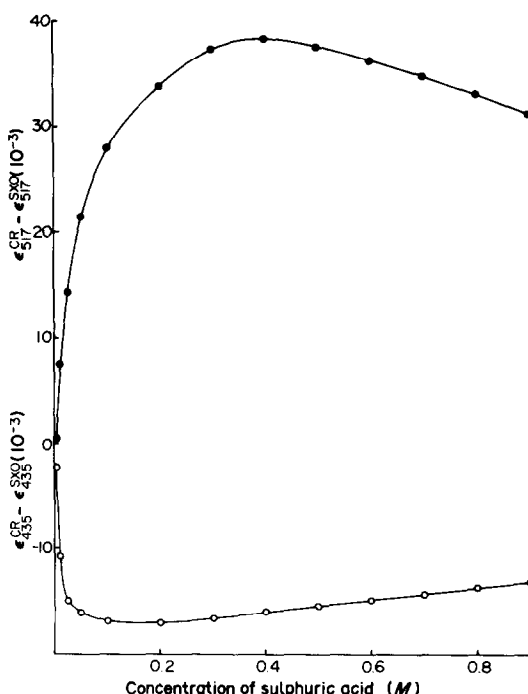


Fig. 7. Difference between molar absorptivities of *o*-Cresol Red and Semi-Xylenol Orange vs. sulphuric acid concentration at 435 nm (○) and at 517 nm (●).

Table 1. Results for the simultaneous spectrophotometric determination* of CR and SXO

Taken†, μM		Found‡, μM	
CR	SXO	CR	SXO
2.0	18.0	$2.0_8 \pm 0.1_6$	$17.8_9 \pm 0.2_4$
5.0	15.0	$4.9_3 \pm 0.1_1$	$15.2_3 \pm 0.1_8$
10.0	10.0	$9.7_3 \pm 0.1_8$	$10.2_4 \pm 0.1_6$
15.0	5.0	$15.1_5 \pm 0.1_7$	$4.7_6 \pm 0.2_0$
18.0	2.0	$18.2_1 \pm 0.1_3$	$2.2_7 \pm 0.1_9$

*In 0.4M sulphuric acid.

†With accuracy $\pm 0.05\mu M$.

‡Mean and standard deviation for 5 measurements

The molar absorptivities of CR and SXO in 0.4M sulphuric acid solution are $\epsilon_{435}^{CR} = 5.5 \times 10^3$, $\epsilon_{517}^{CR} = 57.0 \times 10^3$, $\epsilon_{435}^{SXO} = 22.0 \times 10^3$ and $\epsilon_{517}^{SXO} = 18.5 \times 10^3$ l.mole⁻¹.cm⁻¹. Beer's law is obeyed and the absorbances of CR and SXO are additive over the concentration range $0.5-25 \times 10^{-6}M$, so for a path-length of 1 cm

$$A_{435} = 5.5 \times 10^3 C_{CR} + 22.0 \times 10^3 C_{SXO} \quad (7)$$

$$A_{517} = 57.0 \times 10^3 C_{CR} + 18.5 \times 10^3 C_{SXO} \quad (8)$$

Rearranging gives

$$C_{CR} = (19.09A_{517} - 16.06A_{435}) \times 10^{-6}M \quad (9)$$

$$C_{SXO} = (49.47A_{435} - 4.77A_{517}) \times 10^{-6}M \quad (10)$$

Table 1 shows the results obtained experimentally for given CR and SXO concentrations.

System SXO-XO. It is similarly shown (Fig. 8) that 3M sulphuric acid is the optimum concentration

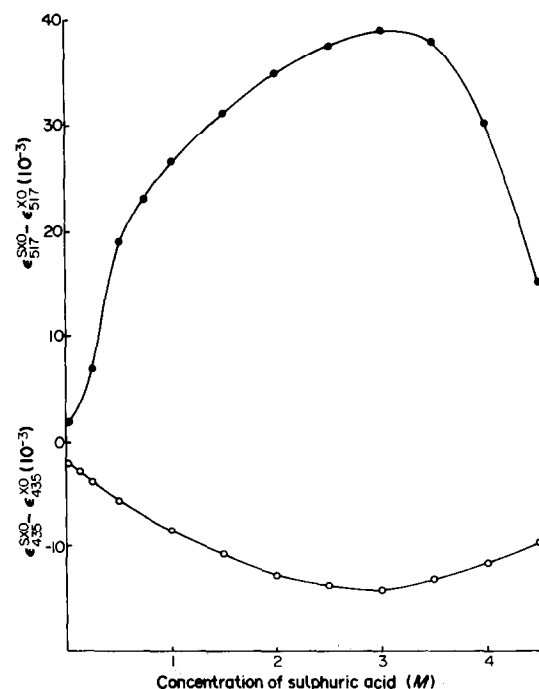


Fig. 8. Difference between molar absorptivities of Semi-Xylenol Orange and Xylenol Orange vs. sulphuric acid concentration for 435 nm (○) and at 517 nm (●).

Table 2. Results for the simultaneous spectrophotometric determination* of SXO and XO

Taken†, μM		Found‡, μM	
SXO	XO	SXO	XO
2.0	18.0	$2.2_0 \pm 0.0_6$	$18.0_8 \pm 0.2_1$
5.0	15.0	$5.1_0 \pm 0.1_3$	$14.8_0 \pm 0.2_2$
10.0	10.0	$10.1_2 \pm 0.1_2$	$10.2_7 \pm 0.1_3$
15.0	5.0	$15.2_6 \pm 0.1_4$	$4.7_6 \pm 0.1_7$
18.0	2.0	$17.9_2 \pm 0.1_6$	$2.2_6 \pm 0.1_9$

*In 3.0M sulphuric acid.

†With accuracy $\pm 0.05\mu M$.

‡Mean and standard deviation for 5 measurements.

for the simultaneous determination of SXO and XO. In this case the molar absorptivities are $\epsilon_{435}^{SXO} = 10.2 \times 10^3$, $\epsilon_{517}^{SXO} = 52.9 \times 10^3$, $\epsilon_{435}^{XO} = 24.3 \times 10^3$ and $\epsilon_{517}^{XO} = 14.1 \times 10^3$ l.mole⁻¹.cm⁻¹. Beer's law is obeyed and the absorbances are additive in the same range of dye concentration $0.5-25.0 \times 10^{-6}M$ as that for the system CR-SXO, so

$$C_{SXO} = (21.28A_{517} - 12.35A_{435}) \times 10^{-6}M \quad (11)$$

and

$$C_{XO} = (46.32A_{435} - 8.93A_{517}) \times 10^{-6}M \quad (12)$$

Values found for C_{SXO} and C_{XO} are given in Table 2.

System CR-XO. Figure 9 shows that 1M sulphuric acid medium is optimal for this system, and the molar absorptivities in it are $\epsilon_{435}^{CR} = 2.70 \times 10^3$, $\epsilon_{517}^{CR} = 59.8 \times 10^3$, $\epsilon_{435}^{XO} = 26.5 \times 10^3$ and $\epsilon_{517}^{XO} = 4.0 \times 10^3$ l.mole⁻¹.cm⁻¹, so

$$C_{CR} = (16.84A_{517} - 2.54A_{435}) \times 10^{-6}M \quad (13)$$

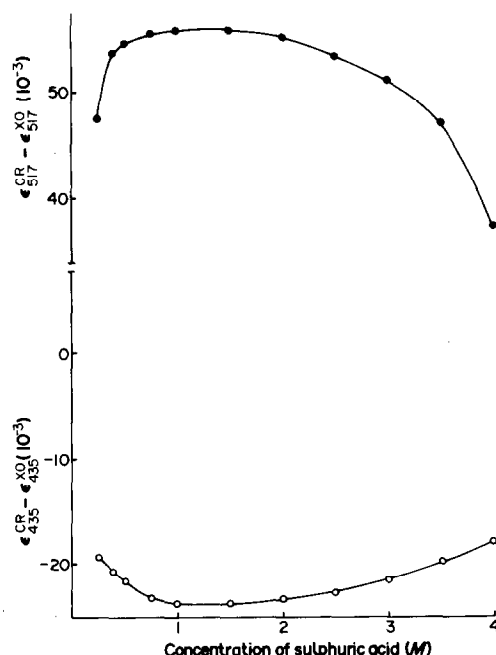


Fig. 9. Difference between molar absorptivities of *o*-Cresol Red and Xylenol Orange vs. sulphuric acid concentration for 435 nm (○) and 517 nm (●).

Table 3. Results for the simultaneous spectrophotometric determination of CR and XO*

Taken†, μM		Found‡, μM	
CR	XO	CR	XO
2.0	18.0	$2.0_4 \pm 0.1_4$	$18.0_1 \pm 0.2_3$
5.0	15.0	$5.0_3 \pm 0.1_2$	$14.8_4 \pm 0.1_7$
10.0	10.0	$9.9_2 \pm 0.1_2$	$9.7_4 \pm 0.1_8$
15.0	5.0	$14.9_6 \pm 0.1_6$	$5.1_2 \pm 0.0_8$
18.0	2.0	$17.8_4 \pm 0.1_7$	$2.1_4 \pm 0.1_1$

*In 1.0M sulphuric acid.

†With accuracy $\pm 0.05\mu M$.

‡Mean and standard deviation for 5 measurements.

and

$$C_{XO} = (37.95A_{435} - 1.7A_{517}) \times 10^{-6}M. \quad (14)$$

Results obtained by using equations (13) and (14) are collected in Table 3.

Three-component system (CR, SXO, XO)

Selection of the conditions for the simultaneous determination of CR, SXO and XO is more complicated than for the two-component systems.

The simultaneous determination of the three dyes in a single solution involves measurements at three wavelengths, where there are significant differences in molar absorptivities. Figures 2–4 show that there are only two narrow ranges of wavelength where such conditions are met. Selection of the third wavelength is difficult but the problem may be overcome in three ways: (A) determination of the total concentration of the three dyes under conditions in which their molar absorptivities are the same and then calculation of the concentrations of two of the three dyes from the absorbances at two other wavelengths; (B) selection of conditions under which the molar absorptivities of one dye are the same at three different wavelengths; (C) use of two or three solutions with different acid concentrations in which CR, SXO and XO have different molar absorptivities.

Method A. The molar absorptivities of CR, SXO and XO at 517 nm in 5.8M sulphuric acid are all in the range $65.0\text{--}70.0 \times 10^3 \text{ l. mole}^{-1} \cdot \text{cm}^{-1}$ (Fig. 6) and the approximate total dye concentration may be calculated from

$$\Sigma C = 14.8 \times 10^{-6} A_{517(5.8M H_2SO_4)}. \quad (15)$$

The conditions for the simultaneous determination of CR and SXO in a two-component system can also be used for determination of CR and SXO in the presence of XO, because of the low molar absorptivity of XO at 517 nm in 0.4M sulphuric acid; $\epsilon_{517(0.4M H_2SO_4)}^{XO} = 3.1 \times 10^3 \text{ l. mole}^{-1} \cdot \text{cm}^{-1}$. Since

$$C_{XO} = \Sigma C - C_{SXO} + C_{CR} \quad (16)$$

substituting into the equations for the absorbances at 435 and 517 nm, and rearrangement, gives the molarities of SXO and CR as

$$C_{SXO} = (682A_{435} + 266A_{517}) \times 10^{-6} - 18.8\Sigma C \quad (17)$$

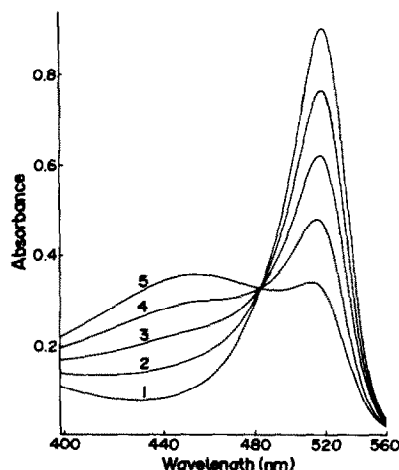


Fig. 10. Absorption spectra for solutions of Semi-Xylenol Orange and of *o*-Cresol Red taken in 0.5M H_2SO_4 ($l = 1$ cm). $16 \times 10^{-6}M$ CR (curve 1), $4 \times 10^{-6}M$ SXO + $12 \times 10^{-6}M$ CR (2), $8 \times 10^{-6}M$ SXO + $8 \times 10^{-6}M$ CR (3), $12 \times 10^{-6}M$ SXO + $4 \times 10^{-6}M$ CR (4), $16 \times 10^{-6}M$ SXO (5).

$$C_{CR} = 5.74\Sigma C - (210A_{435} - 63A_{517}) \times 10^{-6} \quad (18)$$

C_{XO} may then be calculated from equation (16).

The variation in the absorptivities of the three species at 517 nm in 5.8M sulphuric acid, particularly when relatively large amounts of XO are present, results in an uncertainty in the total concentration ΣC . Therefore results obtained by method A were not as accurate and precise as those obtained by methods B and C, the standard deviations being twice as great.

Method B. The concentration of sulphuric acid is chosen so that the molar absorptivities of one of the three dyes has the same value at three wavelengths:

$$\epsilon_{i,\lambda_1} = \epsilon_{i,\lambda_2} = \epsilon_{i,\lambda_3} \quad (19)$$

This condition permits the use of two equations with two unknown concentrations (C_1 and C_2).

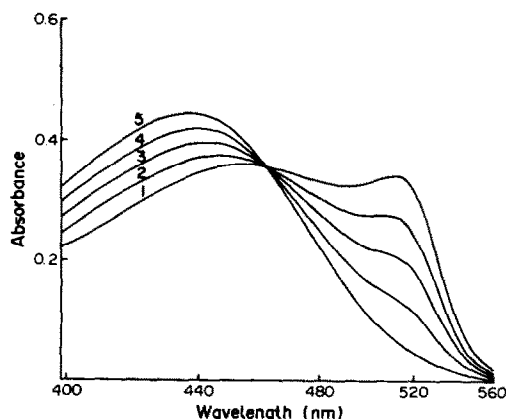


Fig. 11. Absorption spectra for solutions of Semi-Xylenol Orange and Xylenol Orange taken in 0.5M H_2SO_4 ($l = 1$ cm). $16 \times 10^{-6}M$ SXO (curve 1), $4 \times 10^{-6}M$ XO + $12 \times 10^{-6}M$ SXO (2), $8 \times 10^{-6}M$ XO + $8 \times 10^{-6}M$ SXO (3), $12 \times 10^{-6}M$ XO + $4 \times 10^{-6}M$ SXO (4), $16 \times 10^{-6}M$ XO (5).

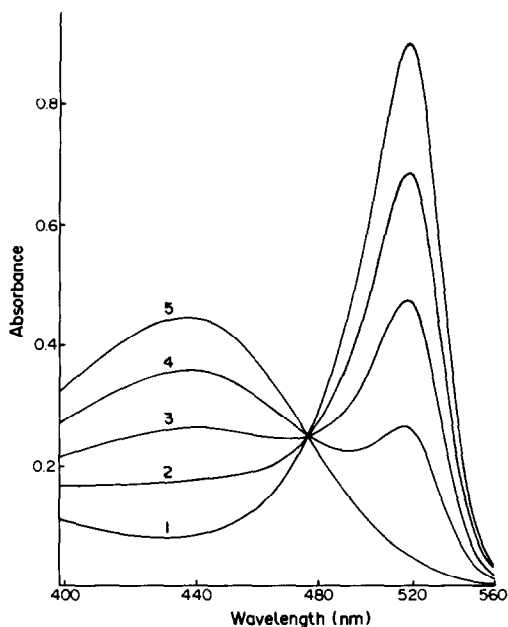


Fig. 12. Absorption spectra for solutions of Xylenol Orange and *o*-Cresol Red in $0.5M$ H_2SO_4 ($l = 1$ cm). $16 \times 10^{-6}M$ CR (curve 1), $12 \times 10^{-6}M$ CR + $4 \times 10^{-6}M$ XO (2), $8 \times 10^{-6}M$ CR + $8 \times 10^{-6}M$ XO (3), $4 \times 10^{-6}M$ CR + $12 \times 10^{-6}M$ XO (4), $16 \times 10^{-6}M$ XO (5).

$$A_{\lambda_1} - A_{\lambda_3} = (\epsilon_{1,\lambda_1} - \epsilon_{1,\lambda_3})C_1 + (\epsilon_{2,\lambda_1} - \epsilon_{2,\lambda_3})C_2 \quad (20)$$

$$A_{\lambda_2} - A_{\lambda_3} = (\epsilon_{1,\lambda_2} - \epsilon_{1,\lambda_3})C_1 + (\epsilon_{2,\lambda_2} - \epsilon_{2,\lambda_3})C_2 \quad (21)$$

It can be seen from Figs. 2-4 that the concentrations of sulphuric acid at which equation (19) is satisfied are $0.015M$ for CR, $0.50M$ for SXO and $3.50M$ for XO. Of these three possibilities the best results were obtained by the simultaneous deter-

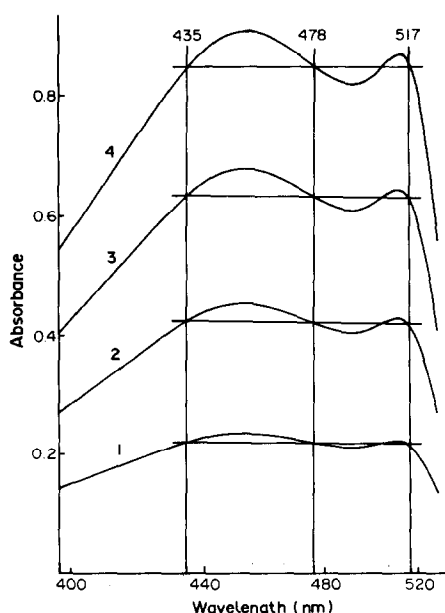


Fig. 13. Absorption spectra for solutions of Semi-Xylenol Orange in $0.5M$ H_2SO_4 . $10 \times 10^{-6}M$ (curve 1), $20 \times 10^{-6}M$ (2), $30 \times 10^{-6}M$ (3), $40 \times 10^{-6}M$ (4).

mination of CR and XO in the presence of SXO in $0.5M$ sulphuric acid. The absorption spectra of the three two-component mixtures at this concentration of sulphuric acid are shown in Figs. 10-12 and those of different concentrations of SXO in Fig. 13. The molar absorptivity of SXO in $0.5M$ sulphuric acid at the chosen wavelengths (435, 478 and 517 nm) is 21.5×10^3 l.mole $^{-1}$.cm $^{-1}$. The corresponding molar absorptivities for the other two dyes are: $\epsilon_{435}^{CR} = 5.05 \times 10^3$, $\epsilon_{478}^{CR} = 16.0 \times 10^3$, $\epsilon_{517}^{CR} = 56.5 \times 10^3$, $\epsilon_{435}^{XO} = 27.4 \times 10^3$, $\epsilon_{478}^{XO} = 15.4 \times 10^3$ and $\epsilon_{517}^{XO} = 3.35 \times 10^3$ l.mole $^{-1}$.cm $^{-1}$. Substitution of these values into equations (20) and (21), and rearrangement, gives:

$$C_{CR} = [34.0 (A_{435} - A_{478}) + 33.9 (A_{517} - A_{478})] \times 10^{-6}M \quad (22)$$

$$C_{XO} = [114.4 (A_{435} - A_{478}) + 30.9 (A_{517} - A_{478})] \times 10^{-6}M \quad (23)$$

or

$$C_{CR} = (34.0 A_{435} + 33.9 A_{517} - 67.9 A_{478}) \times 10^{-6}M \quad (24)$$

$$C_{XO} = (114.4 A_{435} + 30.9 A_{517} - 145.3 A_{478}) \times 10^{-6}M. \quad (25)$$

Substitution of the C_{CR} and C_{XO} values thus obtained, into

$$A_{435} = 5.05 \times 10^3 C_{CR} + 21.5 \times 10^3 C_{SXO} + 27.4 \times 10^3 C_{XO} \quad (26)$$

gives

$$C_{SXO} = (201.1 A_{478} - 107.2 A_{435} - 47.3 A_{517}) \times 10^{-6}M \quad (27)$$

The results thus obtained for mixtures of CR, SXO and XO are collected in Table 4.

Method C. Several systems of two and three solutions with different concentrations of sulphuric acid were tested.

System	Concentration of sulphuric acid, M		
1	0.015	1.50	—
2	0.50	2.00	—
3	0.50	3.50	—
4	0.015	0.40	3.50
5	0.020	0.50	2.00
6	0.050	0.50	3.50

The best results for simultaneous determination of CR, SXO and XO were obtained by using the second system. The measured absorbances are designated as $A_{i(j)}$, where i is the wavelength and j the sulphuric acid concentration.

With the previously given values of the molar absorptivities for CR, SXO and XO in $0.5M$ sulphuric acid and $\epsilon_{517(2.0)}^{CR} = 62.5 \times 10^3$, $\epsilon_{517(2.0)}^{SXO} = 44.0$

Table 4. Results for the simultaneous spectrophotometric determination of CR, SXO and XO in 0.5M H₂SO₄ (method B)*

Taken†, μM			Found‡, μM		
CR	SXO	XO	CR	SXO	XO
1.0	3.0	16.0	0.9 ₁ ± 0.1 ₉	2.7 ₀ ± 0.2 ₅	16.2 ₂ ± 0.2 ₉
2.0	6.0	12.0	1.9 ₈ ± 0.2 ₁	6.1 ₇ ± 0.2 ₉	11.7 ₆ ± 0.3 ₁
2.0	8.0	10.0	2.0 ₉ ± 0.2 ₆	8.1 ₁ ± 0.2 ₃	10.0 ₈ ± 0.1 ₉
3.0	15.0	2.0	2.8 ₉ ± 0.1 ₉	15.4 ₄ ± 0.3 ₉	1.8 ₇ ± 0.2 ₁
5.0	5.0	5.0	4.8 ₈ ± 0.2 ₃	5.1 ₈ ± 0.2 ₆	4.8 ₉ ± 0.2 ₅
5.0	10.0	5.0	5.0 ₆ ± 0.1 ₈	9.8 ₈ ± 0.3 ₀	5.1 ₉ ± 0.2 ₈
8.0	10.0	2.0	7.8 ₆ ± 0.2 ₃	10.1 ₆ ± 0.2 ₇	1.8 ₅ ± 0.1 ₈
8.0	2.0	10.0	8.1 ₃ ± 0.2 ₁	1.8 ₇ ± 0.2 ₄	10.1 ₂ ± 0.2 ₂
10.0	5.0	5.0	9.8 ₄ ± 0.2 ₉	5.2 ₈ ± 0.2 ₉	4.8 ₄ ± 0.2 ₃
16.0	3.0	1.0	16.1 ₉ ± 0.3 ₁	2.8 ₂ ± 0.2 ₀	1.1 ₄ ± 0.2 ₆

*Absorbances measured at 435, 478 and 517 nm.

†With accuracy ± 0.05μM.

‡Mean and standard deviation for 5 measurements.

Table 5. Results for the simultaneous spectrophotometric determination of CR, SXO and XO (method C)*

Taken†, μM			Found‡, μM		
CR	SXO	XO	CR	SXO	XO
1.0	3.0	16.0	1.0 ₇ ± 0.1 ₂	2.8 ₉ ± 0.2 ₁	16.1 ₂ ± 0.2 ₄
2.0	6.0	12.0	2.1 ₀ ± 0.1 ₉	5.8 ₄ ± 0.2 ₃	12.2 ₅ ± 0.1 ₈
2.0	8.0	10.0	2.0 ₇ ± 0.2 ₀	7.9 ₄ ± 0.1 ₉	10.1 ₅ ± 0.2 ₁
3.0	15.0	2.0	3.1 ₂ ± 0.1 ₈	14.8 ₅ ± 0.2 ₆	2.1 ₃ ± 0.1 ₉
5.0	5.0	5.0	4.9 ₁ ± 0.2 ₁	5.0 ₄ ± 0.2 ₃	5.0 ₇ ± 0.1 ₈
5.0	10.0	5.0	4.8 ₄ ± 0.2 ₃	10.1 ₆ ± 0.2 ₉	4.8 ₅ ± 0.2 ₆
8.0	10.0	2.0	8.1 ₆ ± 0.2 ₄	10.0 ₄ ± 0.2 ₆	2.1 ₁ ± 0.2 ₃
8.0	2.0	10.0	7.9 ₀ ± 0.2 ₆	2.1 ₄ ± 0.2 ₁	10.0 ₁ ± 0.2 ₇
10.0	5.0	5.0	10.0 ₈ ± 0.2 ₁	4.8 ₅ ± 0.2 ₇	5.0 ₀ ± 0.2 ₆
16.0	3.0	1.0	16.1 ₃ ± 0.2 ₈	2.8 ₈ ± 0.2 ₀	1.1 ₁ ± 0.1 ₉

*Absorbances measured at 435 and 517 nm in 0.5M sulphuric acid and at 517 nm in 2.0M sulphuric acid.

†With accuracy ± 0.05μM.

‡Mean and standard deviations for 5 measurements.

Table 6. Results for the simultaneous spectrophotometric determination of CR, SXO and XO in commercial XO*

Sample	Year of production	Taken†, mg/l.	Found‡, μM				
			(Method C)			(Marakami method [§])	
			CR	SXO	XO	SXO	XO
1	1971	30.65	3.2	6.9	2.5	10.7	1.9
2	1973	30.25	2.3	8.9	9.8	14.3	7.4
3	1974	29.85	1.3	11.5	14.9	15.9	12.4
4	1978	30.70	1.1	8.3	16.5	11.6	15.1
5	1982	30.70	0.9	10.0	15.5	13.4	14.0
6	1984	30.35	1.3	4.6	21.2	9.0	18.2

*Products obtained from POCh, Poland.

†Mean average concentration 40μM (recalculated as 100% XO).

‡Mean values for 3 determinations.

§Method B gave similar results.

× 10³ and ε_{517(2.0)}^{XO} = 8.30 × 10³ l.mole⁻¹.cm⁻¹, the following equations can be derived:

$$A_{435(0.5)} = 5.15 \times 10^3 C_{CR} + 21.5 \times 10^3 C_{SXO} + 27.4 \times 10^3 C_{XO} \quad (28)$$

$$A_{517(0.5)} = 56.5 \times 10^3 C_{CR} + 21.5 \times 10^3 C_{SXO} + 3.35 \times 10^3 C_{XO} \quad (29)$$

$$A_{517(2.0)} = 62.5 \times 10^3 C_{CR} + 44.0 \times 10^3 C_{SXO} + 8.30 \times 10^3 C_{XO} \quad (30)$$

Solution of these three equations leads to

$$C_{CR} = [1.20A_{435(0.5)} + 39.70A_{517(0.5)} - 20.00A_{517(2.0)}] \times 10^{-6} M \quad (31)$$

$$C_{\text{SXO}} = [59.15A_{517(2.0)} - 10.05A_{435(0.5)} - 64.50A_{517(0.5)}] \times 10^{-6}M \quad (32)$$

$$C_{\text{XO}} = [44.15A_{435(0.5)} - 43.35A_{517(0.5)} - 42.75A_{517(2.0)}] \times 10^{-6}M \quad (33)$$

The results thus obtained for 10 mixtures of CR, SXO and XO are collected in Table 5.

Though the relative errors in the analysis of ternary mixtures (Tables 4 and 5) can be rather large for the minor components, they are much smaller than those obtained by other methods.

The last system of equations, (31)–(33), gave the best results for the analysis of synthetic mixtures of the three dyes and so was used for the simultaneous determination of CR, SXO and XO in some commercial samples of XO. The results of these investigations are collected in Table 6.

CONCLUSIONS

The proposed method for simultaneous determination of *o*-Cresol Red, Semi-Xylenol Orange and

Xylenol Orange is fast, sensitive and sufficiently selective for many possible applications. The accuracy attained for two-component mixtures is similar and that for three-component mixtures superior to that obtained in other spectrophotometric measurements.

REFERENCES

1. J. Körbl and R. Přibil, *Chem. Ind. London*, 1957, 233.
2. E. M. Urinovich, *USSR Patent* 132234, 5 Oct. 1960; *Chem. Abstr.*, 1960, **55**, 11370.
3. D. C. Olson and D. W. Margerum, *Anal. Chem.*, 1962, **34**, 1299.
4. M. Murakami, T. Yoshino and S. Harasawa, *Talanta*, 1967, **14**, 1293.
5. R. P. Pantaler and I. V. Pulayeva, *Zh. Analit. Khim.*, 1977, **32**, 2450.
6. N. F. Kosenko and T. V. Mal'kova, *Izv. Vyssh. Uchebn. Zaved., Khim. Khim. Tekhnol.*, 1981, **24**, 54.
7. N. F. Kosenko, *Zh. Analit. Khim.*, 1982, **37**, 1297.
8. N. M. Dyatlova, V. Ya. Temkina and I. D. Kolpakova, *Kompleksn. Khim. Moscow*, 1970, 192.
9. T. Yoshino, H. Imada, T. Kuwano and K. Iwasa, *Talanta*, 1969, **16**, 151.
10. B. L. Gupta, *ibid.*, 1974, **21**, 683.

SHORT COMMUNICATIONS

DETERMINING GOLD IN WATER BY ANION-EXCHANGE BATCH EXTRACTION

J. B. McHUGH

U.S. Geological Survey, Box 25046, MS 955, Federal Center, Denver, Colorado 80225, U.S.A.

(Received 9 August 1985. Accepted 6 December 1985)

Summary—This paper describes a batch procedure for determining gold in natural waters. It is completely adaptable to field operations. The water samples are filtered and acidified before they are equilibrated with an anion-exchange resin by shaking. The gold is then eluted with acetone-nitric acid solution, and the eluate evaporated to dryness. The residue is taken up in hydrobromic acid-bromine solution and the gold is extracted with methyl isobutyl ketone. The extract is electrothermally atomized in an atomic-absorption spectrophotometer. The limit of determination is 1 ng/l.

Gold is found in natural waters as complex ions or as particulates of colloidal size.¹ The average concentration of gold is 2 ng/l. in river water² and 4 ng/l. in sea-water.³ Gosling⁴ reported the gold content of natural waters in Colorado to range from <1 to 150 ng/l. The gold concentration of surface waters taken from five gold fields in Australia was found⁵ to range from <1 to 130 ng/l. Gold in such ultratrace amounts in natural waters is difficult to determine. To use the gold content of water for hydrogeochemical prospecting, it is necessary to be able to determine gold down to the background level of 2 ng/l.

Previous methods for determining gold in water used rather slow methods to concentrate the gold from the sample, either by evaporation⁶ or by use of an anion-exchange column.⁷

This paper reports the development of a faster method for determining gold in water. Briefly, the gold is concentrated by shaking a filtered and acidified 1-litre sample with an anion-exchange resin for 30 min, eluting the gold from the resin, extracting the gold bromide and chloride complexes into methyl isobutyl ketone (MIBK), then determining the amount of gold by electrothermal atomization in an atomic-absorption spectrophotometer. The limit of detection is 1 ng/l.

EXPERIMENTAL

Instrumentation

A Perkin-Elmer Model 703* atomic-absorption spectrophotometer, equipped with a deuterium background-corrector and an HGA-2000 graphite furnace was used to determine gold. Pyrolytically coated graphite tubes were used. Instrument parameters for gold determination are given in Table 1.

Reagents and standards

AG 1-X8 anion-exchange resin, 100-200 mesh, chloride form (Bio-Rad Laboratories, Catalogue no. 140-1441).

Gold standard solutions. A certified gold solution of 1000 µg/ml was used to prepare gold standards of 10, 1.0, and 0.10 µg/ml by serial dilution. These standards were made up in 1M hydrochloric acid containing 0.05% v/v bromine, and stored in amber glass bottles.

Acetone-nitric acid solution. Acetone-concentrated nitric acid-water (100:5:5 v/v).

Bromine (5% v/v) in concentrated hydrochloric acid.

Bromine (0.5% v/v) concentrated hydrobromic acid.

Hydrobromic acid, 0.1M. Add 24 ml of concentrated hydrobromic acid to 2 litres of demineralized water equilibrate this solution by shaking for 3 min with 100 ml MIBK, and discard the organic layer.

Procedure

Collect a 1-litre water sample in a polyethylene bottle. Filter it through a Millipore HAWP (diameter 47 mm; pore size, 0.45 µm) filter; tests show no loss of gold with this size of filter. Add 10 ml of the 5% bromine-hydrochloric acid solution to the filtered sample. The filtering and acidification can be done in the field or on arrival in the laboratory. The addition of the acid-bromine solution prevents adsorption of gold on the container walls.⁸ It will also convert the gold into AuCl_4^- and AuBr_4^- .

Add 3 g of AG-1-X8 anion-exchange resin to the filtered and acidified sample, and shake the mixture for 30 min on a mechanical shaker. Pour the sample into a 19 × 300 mm chromatographic column fitted with a glass disc. Elute the gold from the resin with 100 ml of acetone-nitric acid solution at a flow-rate of 100 ml/hr into a 250-ml beaker. Use only glass or Teflon apparatus in the elution, to avoid contamination. Evaporate the acetone solution on a hot

Table 1. Instrument parameters

Wavelength	242.8 nm
Spectral band-width	0.7 nm
Calibration mode	Absorbance, peak height
Integration time	6 sec
Background correction	Deuterium arc lamp
Drying	120°, 30 sec
Charring	800°, 15 sec
Atomization	2700°, 6 sec
Purge gas	Argon, interrupted
Sample volume	20 µl

*The use of trade names in this report is for descriptive purposes only and does not constitute endorsement by the U.S. Geological Survey.

Table 2. Gold concentrations in the MIBK phase, and the corresponding absorbance values

Au, ng/ml	Absorbance
0	0.000
1.0	0.007
5.0	0.035
10.0	0.070
25.0	0.175
50.0	0.350

water-bath ($\sim 80^\circ$) to dryness. Add 8 ml of the 0.5% bromine-hydrobromic acid solution to the residue and let stand for 30 min. Warm the solution slightly for 15 min. Cool the solution, transfer it to a 16×150 -mm screw-cap culture tube, rinsing with 8 ml of water. Add 2 ml of MIBK, then cap the tube and shake it for 3 min. Use Teflon liners in the caps. Centrifuge the solution and transfer 1 ml of the MIBK extract into another screw-cap culture tube (16×100 mm) containing 8 ml of 0.1M hydrobromic acid. Cap the tube, shake it for 30 sec, and centrifuge. Place a 20- μ l aliquot of the MIBK extract into the graphite furnace. Atomize the gold electrothermally in an atomic-absorption spectrophotometer for determination.

To prepare the calibration graph, add 0, 0.2, 1.0 and 2.0 ml of the 0.100- μ g/ml gold standard and 0.5 and 1.0 ml

of the 1.00- μ g/ml gold standard to six 25×150 -mm screw-cap culture tubes containing 20 ml of 0.1M hydrobromic acid and 20 ml of MIBK. Cap the tubes and shake them for 30 sec. Atomize 20- μ l aliquots of these standards.

RESULTS AND DISCUSSION

To find whether the 30-min batch extraction technique would transfer all the gold from solution onto the resin, several gold standard solutions (2, 10, 20, 50 and 100 ng/l) were extracted a second time for 30 min with fresh resin. After exchange the solutions were analysed for gold, but none was found.

Three 50-ml aliquots of the acetone-nitric acid solution, at an elution rate of 100 ml/hr, were used to test the efficiency of elution. The first aliquot eluted all the gold added to the resin. No gold was detected in the second and third aliquots. For safety, however, 100 ml of eluent are used in the procedure.

Six test solutions were prepared (each in duplicate) by adding 0, 2, 10, 20, 50 and 100 ng of gold to 1-litre portions of laboratory tap water. The solutions were acidified with 10 ml of 5% bromine-hydrochloric acid solution, and analysed for gold. The absorb-

Table 3. Gold recovery as a function of storage time

Sample set (storage time)	Gold added, ng/l.	Recovery (average of duplicate determinants)	
		ng/l.	%
Set 1 (1 day)			
Sample 1	2.0	2.1	95
Sample 2	2.0	1.7	95
Sample 3	10.0	10.0	99
Sample 4	10.0	9.7	99
Sample 5	20.0	20.0	110
Sample 6	20.0	24.0	110
Set 2 (1 week)			
Sample 1A	2.0	2.4	105
Sample 2A	2.0	1.7	105
Sample 3A	10.0	8.6	88
Sample 4A	10.0	9.0	88
Sample 5A	20.0	16.0	89
Sample 6A	20.0	19.5	89
Set 3 (2 weeks)			
Sample 1B	2.0	1.7	95
Sample 2B	2.0	2.1	95
Sample 3B	10.0	10.0	99
Sample 4B	10.0	9.8	99
Sample 5B	20.0	20.0	100
Sample 6B	20.0	23.0	100
Set 4 (1 month)			
Sample 1C	2.0	1.5	95
Sample 2C	2.0	2.3	95
Sample 3C	10.0	12.0	110
Sample 4C	10.0	10.0	110
Sample 5C	20.0	18.0	95
Sample 6C	20.0	20.0	95
Set 5 (2 months)			
Sample 1D	2.0	2.8	130
Sample 2D	2.0	2.4	130
Sample 3D	10.0	11.5	113
Sample 4D	10.0	11.0	113
Sample 5D	20.0	17.0	92
Sample 6D	20.0	19.5	92

ances obtained compared favourably with those obtained for the gold standard solutions used in calibrating the instrument (Table 2). To test the procedure over a period of time, five sets of six simulated water samples were run through the procedure. The six samples in each set were prepared by adding (in duplicate) 2, 10 and 20 ng of gold to 1-litre volumes of laboratory tap water. Ten ml of 5% bromine-hydrochloric acid solution were added to each sample. After periods of time ranging from 1 day to 2 months, the five sets were analysed for gold. Table 3 shows the storage time, the concentrations of gold added and found, and per cent recovery. Considering the low levels of gold determined, the recovery is extremely good.

This procedure is interference-free. The anion-exchange resin eliminates all cations which may cause interferences.⁷ Gold can be determined in MIBK

medium by atomic-absorption spectrophotometry without interference.⁶

Acknowledgements—The author is grateful to T. T. Chao and R. M. O'Leary for critically reviewing the manuscript.

REFERENCES

1. H. W. Lakin, G. C. Curtin and A. E. Hubert, *U.S. Geol. Survey Bull.* **1330**, p. 80, 1974.
2. A. A. Levinson, *Introduction to Exploration Geochemistry*, p. 612. Applied Publishing, Calgary, Canada, 1974.
3. J. Green, *Geol. Soc. Am. Bull.*, 1959, **70**, 1127.
4. A. W. Gosling, E. A. Jenne and T. T. Chao, *Econ. Geol.*, 1971, **66**, 309.
5. T. W. Hamilton, J. Ellis, T. M. Florence and J. J. Fardy, *Econ. Geol.*, 1983, **78**, 1335.
6. J. B. McHugh, *J. Geochem. Explor.*, 1984, **20**, 203.
7. T. T. Chao, *Econ. Geol.*, 1969, **64**, 287.
8. T. T. Chao, E. A. Jenne and L. M. Heppting, *U.S. Geol. Survey Prof. Paper*, **600-D**, p. 16, 1968.

INTERACTION OF PHENOTHIAZINES WITH NITROSO-R SALT AND EXTRACTIVE SPECTROPHOTOMETRIC DETERMINATION OF PHENOTHIAZINE DRUGS

JAYARAMA, M. VIOLET D'SOUZA, H. S. YATHIRAJAN and RANGASWAMY*

Department of Post-graduate Studies and Research in Chemistry, University of Mysore, Manasagangothri,
Mysore 570 006, India

(Received 13 June 1985. Revised 9 November 1985. Accepted 23 November 1985)

Summary—A selective and sensitive method is based on the interaction of phenothiazines with nitroso-R salt to form 1:1 complexes which are extracted into chloroform and measured spectrophotometrically.

Many methods have been proposed for the estimation of phenothiazines.^{1,2} The low ionization potentials and excellent electron-donor abilities of phenothiazines make them good co-ordinating agents.³⁻⁶ Phenothiazines also form charge-transfer (CT) complexes with organic acceptors.⁷ The donor activity of phenothiazines is so high that even in the ground-state there is practically total transfer of an electron to the acceptor to form CT complexes.

Nitroso-R salt (NRS) (disodium 1-nitroso-2-naphthol-3,6-disulphonate) has been found to form CT complexes with phenothiazines, and this paper describes the reactions of promazine hydrochloride (PMH), chlorpromazine hydrochloride (CPH), triflupromazine hydrochloride (TPH), promethazine hydrochloride (PH), diethazine hydrochloride (DH), fluphenazine hydrochloride (FPH) and perazine (PZ) with NRS and their determination in pure and pharmaceutical forms.

EXPERIMENTAL

A 0.2% NRS solution was prepared in doubly distilled water. Stock solutions of phenothiazines were prepared by dissolving appropriate amounts in doubly distilled water, standardized,⁸ and stored in amber bottles. Absorbance measurements were made on a Beckman DB spectrophotometer. Infrared spectra were recorded with a Perkin Elmer 399 spectrophotometer. All other reagents used were of analytical-reagent grade.

Standard procedures

Pure phenothiazines. Transfer an aliquot of the sample solution containing 1-45, 0.5-60, 2-57, 1.5-65, 0.8-39, 0.2-38 or 0.8-68 ppm of PMH, CPH, TPH, PH, DH, FPH or PZ respectively, to a 100-ml separating funnel containing 15 ml of water. Add 3 ml of 0.2% NRS solution and mix well. Extract the complex with two 5-ml portions of chloroform, shaking for 2 min each time, and dilute the extract to volume in a 25-ml standard flask with chloroform. Measure the absorbance at 382, 380, 365, 390, 380, 395 or 385 nm

respectively, for the compounds listed above, against a reagent blank.

Pharmaceutical preparations. Dissolve a known amount of the sample in doubly distilled water, filter through a Whatman No. 542 filter paper and wash. Dilute the combined filtrate and washings to an appropriate volume and determine the drug content by the standard procedure.

For coloured syrups take a known volume of sample, make it alkaline to litmus with 4M ammonia solution, extract with two 20-ml portions of chloroform and evaporate the extract to dryness. Dissolve the residue with a few drops of 0.1M hydrochloric acid and dilute accurately to 100 ml with water. Analyse an aliquot.

RESULTS AND DISCUSSION

All the phenothiazines tested form bright yellow solid charge-transfer complexes with NRS in aqueous solutions. In acidic media, the phenothiazines undergo oxidation when mixed with NRS, whereas in basic media the phenothiazines precipitate. From aqueous solutions these complexes are easily and quantitatively extracted into chloroform, but NRS is not extracted. Chloroform extracts of the complexes of NRS with PMH, CPH, TPH, PH, DH, FPH and PZ show maximum absorption at 382, 380, 365, 390, 380, 395 and 385 nm respectively and obey Beer's law over the concentration ranges 1-45, 0.5-60, 2-57, 1.5-65, 0.8-39, 0.2-38 and 0.8-68 ppm (in the final solution) respectively. The molar absorptivities are 5.09, 4.98, 3.99, 4.21, 4.01, 5.22 and 3.99×10^3 l.mole⁻¹.cm⁻¹ respectively for the phenothiazines in the order given above. Six determinations at the 20-ppm phenothiazine level gave a relative standard deviation of 0.9, 0.7, 1.8, 1.3, 0.6, 1.4 and 0.6% for the seven compounds (order as before). Extraction constants for the systems studied were obtained by the modified method of isomolar shift.⁹ Mean values of log K_E for the PMH, CPH, TPH, PH, DH, FPH and PZ systems were found to be 7.71, 8.21, 7.89, 6.23, 6.78, 7.91 and 8.01 ± 0.05 re-

*Author for correspondence.

Table 1. Determination of phenothiazines in pure and pharmaceutical products

	Drug present	Nominal amount, mg	Amount found, mg	
			Official method	Proposed method* (rsd, %)
<i>Pure powders</i>				
	PMH	20	BP 1980	19.9 ₇ (0.9)
	CPH	20	BP 1980	19.9 ₈ (0.7)
	TPH	20		20.0 ₂ (1.8)
	PH	20	BP 1973	19.2 ₈ (1.3)
			USP XX	19.9 ₄
	DH	20	BP 1973	20.1 ₀
	FPH	20	USP XX	20.0 ₁
	PZ	20	BP 1980	19.9 ₉
				20.0 ₁ (0.6)
<i>Tablets</i>				
	Sparine	PMH	50	BP 1980 49.8
	Largactil	CPH	25	BP 1973 24.8
	Neurazine	CPH	25	USP XX 25.1
	Siquil	TPH	10	— — 9.8 ₉ (1.8)
	Phenergan	PH	25	BP 1973 24.5
				24.7 ₇ (1.3)
<i>Injections</i>				
	Siquil	TPH	10	— — 9.9 ₁ (1.8)
	Phenergan	PH	25	BP 1973 24.8 ₂
	Largactil	CPH	25	BP 1973 24.9 ₂
				24.9 ₂ (0.7)
<i>Syrups</i>				
	Largactil	CPH	5	— — 4.87 (0.7)
	Promentine	PH	5	USP XX 4.8 ₉
				4.92 (1.3)
<i>Elixir</i>				
	Phenergan	PH	1	BP 1973 0.97
				0.98 (1.3)

*Average of six determinations.

spectively, and the species extracted were stable for 2, 2.5, 2.5, 3, 3, 3 and 2.5 hr. Variation of the shaking time showed that a single extraction for 1 min with 10 ml of chloroform will give complete extraction, but double extraction with 5-ml portions of chloroform is preferred. Prolonged shaking with chloroform has no adverse effect on the extraction.

Many substances associated with pharmaceutical preparations, such as starch, alcohol, magnesium stearate, gum acacia, gelatin, honey, carboxylic acids and esters, yeast extracts and sugars, do not interfere. However, dextrose (1.5 g/ml), talc (0.27 g/ml) and sodium alginate (990 μ g/ml) interfere in the determination of 30 ppm of the phenothiazines in pharmaceutical formulations. The results of the assay of tablets, injections and syrups (Table 1) compare favourably with the official methods^{10,11} of BP 1973, and USP XX 1980. Usually the dyestuffs in coloured tablets do not interfere, but those used in syrups may be co-extracted with the complex and cause difficulty. A preliminary extraction of the phenothiazine from alkaline solution will generally solve the problem, or a sample could be run without addition of NRS, to serve as a comparison blank.

Nature of the solid complexes

The complexes were prepared by mixing equal volumes of equimolar (0.05M) aqueous solutions of the phenothiazine and NRS, extracting into chloroform, evaporating the solvent, then recrystallizing the product from methanol.

TLC tests revealed that there is only a single component present in these complexes. The spots on the TLC plates were representative of neither phenothiazines nor NRS. Chemical analyses and molecular weight determination on the complexes corresponded to 1:1 molar ratio of phenothiazine to NRS. ESR and magnetic moment measurements showed that the complexes were neutral.

The electronic spectra of the reactants do not resemble the spectrum of their complex in methanol solution. NRS shows bands at 218, 263 and 369 nm and the phenothiazines exhibit a sharp band at around 254 and a broad band at around 306 nm. The sharp bands of the phenothiazines are attributed to $\pi-\pi^*$, and the broad bands to $n-\pi^*$ transitions. The bands of NRS at 218 and 263 and the band of phenothiazines at around 306 nm are completely masked in the spectrum of the complexes. All the complexes show a new band in the region 380–390 nm. This band is considered to be of charge-transfer nature and assigned to $n-\pi^*$ type, where the charge is transferred from the highest filled molecular orbital of the donor phenothiazine to the lowest unfilled molecular orbital of the acceptor NRS.

The infrared spectrum of NRS gives bands at 1610 and 3350 cm^{-1} corresponding to the $-\text{N}=\text{O}$ and $-\text{OH}$ groups. The characteristic band of the $-\text{R}_3\text{NH}^+$ group in phenothiazines appears at around 2300–2420 cm^{-1} . These bands are completely absent from the spectra of the complexes. The $-\text{OH}$ band of NRS is considerably shifted and broadened in the

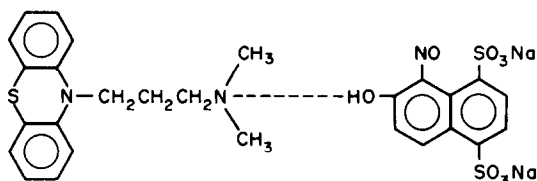


Fig. 1. Possible structure of PMH-NRS complex.

spectrum of the complex, indicating the presence of intermolecular hydrogen bonding in the complexes. Hence the phenothiazines play a dual role in their interactions with NRS, acting both as electron donor in the charge-transfer interaction and as a hydrogen-bonding site through the tertiary amino nitrogen atom in the side-chain. A possible structure for the complex of one of the typical phenothiazines (PMH) with NRS is given in Fig. 1.

Acknowledgement—One of us (RS) gratefully acknowledges financial assistance from the University of Mysore, Mysore.

REFERENCES

1. J. Blažek, *Pharmazie*, 1967, **22**, 129.
2. J. E. Fairbrother, *Pharm. J.*, 1979, **222**, 271.
3. H. S. Gowda and Jayarama, *J. Less-Common Metals*, 1980, **72**, 37.
4. *Idem*, *J. Inorg. Nucl. Chem.*, 1981, **43**, 2329.
5. *Idem*, *Curr. Sci.*, 1981, **50**, 569.
6. Jayarama, K. N. Thimmaiah and M. V. D'Souza, *J. Indian Chem. Soc.*, in the press.
7. R. Foster and C. A. Fyfe, *Biochim. Biophys. Acta*, 1966, **112**, 490.
8. J. Blažek and V. Mareš, *Cesk. Farm.*, 1966, **15**, 349.
9. W. Likussar and D. F. Boltz, *Anal. Chem.*, 1971, **43**, 1265.
10. *British Pharmacopoeia*, H.M. Stationery Office, London, 1980.
11. *United States Pharmacopoeia XX*, U.S. Pharmacopoeia Convention, Rockville, Md, 1980.

AN EXPLORATORY STUDY OF THE INDIRECT FLUORIMETRIC DETERMINATION OF URANIUM(VI) BY ENERGY TRANSFER AND MEASUREMENT OF FLUORESCENT EMISSION BY EUROPIUM(III)

SAMUEL J. LYLE and NIDAL A. ZA'TAR

The Chemical Laboratory, University of Kent at Canterbury, Canterbury, Kent, England

(Received 4 June 1985. Revised 12 November 1985. Accepted 21 November 1985)

Summary—A fluorimetric determination of uranium(VI) is described. It is based on the emission from europium(III) at 594 nm, following its indirect excitation by uranium.

When the uranyl ion in aqueous solution is electronically excited by irradiation in the near ultraviolet, the energy absorbed can be dissipated in several ways by direct or indirect radiative emission or non-radiative thermal degradation. When europium(III) is also present the energy can be non-radiatively transferred to it from the uranium(VI), and then emitted as light. It has been shown¹ that for a fixed concentration of uranyl ion the degree of quenching of the uranium fluorescence produced by irradiation is a linear function of the europium(III) concentration. For the same solution, the fluorescence intensity at the emission wavelength for europium(III) is also a linear function of europium concentration. Tanner and Vargenas² have shown that energy transfer between the uranyl ion and europium(III) is a sensitive function of pH. In 0.1M acid no transfer was observed but at pH 3.87 the transfer was about 100 times that at pH 2.84 for excitation at 347 nm and emission measurement at 590 nm. Thus the nature of the uranium(VI) species is important; it is thought that the energy transfer is not from UO_2^{2+} but rather from some hydrolysed species such as $(\text{UO}_2)_2(\text{OH})_2^{2+}$. It was suggested² that UO_2^{2+} -Eu³⁺ complexes are involved and that the process is intramolecular in nature. We have re-examined the system and studied the europium(III) emission as a function of pH, europium(III) concentration and various excitation and emission wavelengths. We have established conditions under which the intensity of europium emission is linearly related to uranium(VI) concentration, and examined the effects of various ions.

EXPERIMENTAL

All chemicals were of reagent grade. A $1.00 \times 10^{-3}M$ aqueous solution of uranium(VI) was prepared from the acetate and 0.2M europium perchlorate solution was made from europium(III) oxide and perchloric acid. Fluorimetric measurements were made with a Perkin-Elmer MPF3 spectrophotofluorimeter and pH-measurements with a Radiometer PHM62 pH-meter.

Procedure

A volume of solution containing between 0.1 and 2.0 mg of uranium was transferred to a 10-ml beaker, 2.5 ml of 0.2M europium(III) solution were added and the pH was adjusted to 5.5 ± 0.1 by addition of dilute sodium hydroxide solution or perchloric acid. The solution was transferred to a 10-ml standard flask and made up to volume with water. The relative fluorescence intensity (RFI) was measured after 5 min, with excitation and emission wavelengths of 290 and 594 nm respectively, unless otherwise specified.

RESULTS AND DISCUSSION

Excitation and emission spectra in the wavelength ranges 200–500 and 450–650 nm respectively, were obtained from (a) 0.04M europium(III) perchlorate, (b) $4 \times 10^{-4}M$ uranyl acetate, and (c) a mixture 0.08M in europium(III) and $4 \times 10^{-4}M$ in uranium(VI). Figure 1 shows that the main europium emission occurs at 594 nm, and the excitation spectrum for (c) recorded with this as the emission wavelength is very similar to that for (b) except for the sharp peak at 392 nm which is due to direct excitation of europium(III). The emission spectrum resulting from excitation of (c) at 392 nm is similar to that obtained for europium(III) alone, except for the broad peak (centred at 520 nm) due to direct emission from uranium(VI). The emission spectrum obtained on excitation at 290 nm consists of a much more intense direct emission from uranium(VI) with some overlap with that at 594 nm from europium(III), which derives its excitation energy indirectly from the uranium(VI). Figure 2 shows the effect of pH on a typical uranium(VI)–europium(III) system.

The effect of other metal ions and common anions on the emission from the uranyl ion in aqueous solution has been studied by several workers.^{3,4} Recently, Korte and Chessmore⁵ used the SCINTREX UA-3 (Scintrex Ltd., Ontario, Canada) Uranium Analyser, an instrument which has a pulsed nitrogen laser as light-source, to investigate the quenching of uranium(VI) fluorescence by various ions. Figure 3

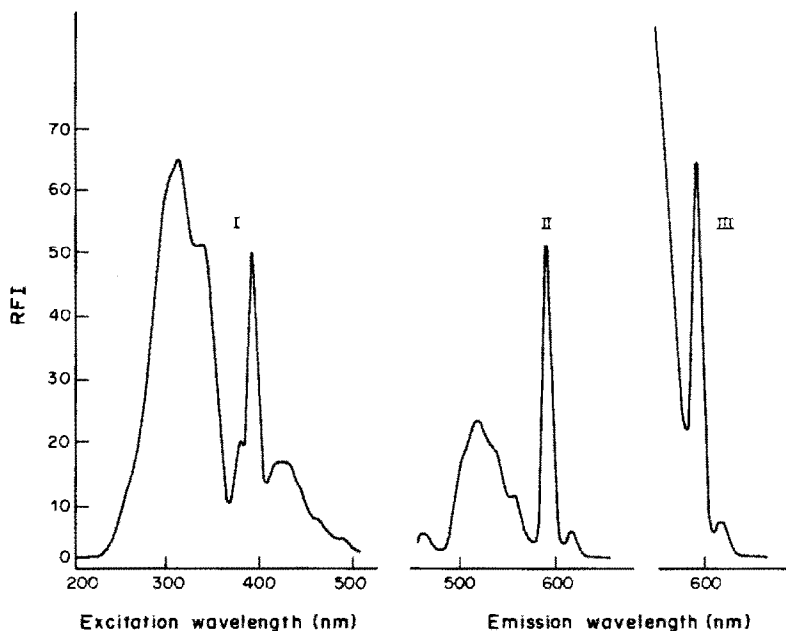


Fig. 1. Excitation and emission spectra obtained from a $4 \times 10^{-4}M$ uranyl acetate and $0.08M$ europium(III) perchlorate solution: I, excitation spectrum with emission wavelength set at 594 nm; II, emission spectrum with excitation at 392 nm; III, emission spectrum with excitation at 290 nm.

compares the interference of some commonly encountered cations in the present method (B) with those from studies (A) with the UA-3 analyser. However, the uranium concentrations used to obtain the results in Fig. 3B were greater than those used by Korte and Chessmore (the UA-3 analyser has a much more intense light-source), so the validity of any conclusions drawn about relative interferences would depend on whether the complex formation and intra-

molecular energy transfer mechanisms function identically at the two uranium concentrations.

The fluorescence intensity (with excitation at 290 nm) is maximal and constant when the solution is

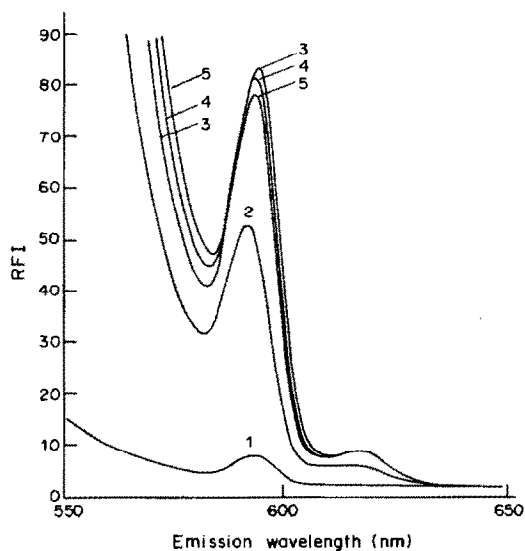


Fig. 2. The effect of pH on the fluorescence intensity at 594 nm from a $4 \times 10^{-4}M$ uranyl acetate and $0.04M$ europium(III) perchlorate solution excited at 290 nm. Curves 1-5 were obtained at pH 4.48, 5.09, 5.54, 5.74 and 5.88, in that order.

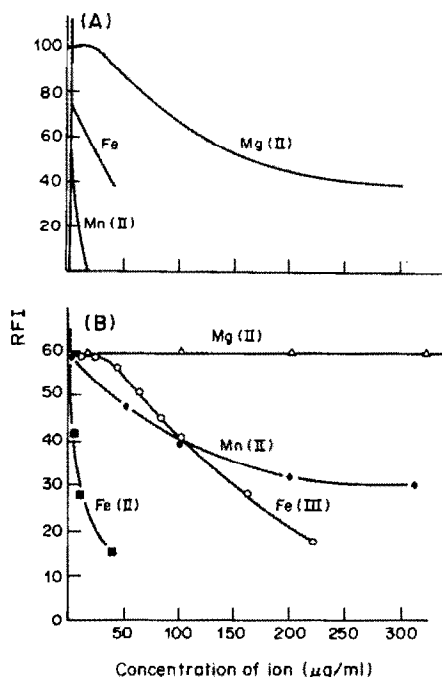


Fig. 3. Effect of other metal ions on uranium(VI) fluorescence emission: A, results⁵ obtained by using the UA-3 uranium analyser (precise U concentration not quoted); B, results obtained by the procedure given in this paper for $112\text{-}\mu\text{g/ml}$ uranium. Mg was added as the acetate, Mn as the chloride, Fe(III) as the chloride and Fe(II) as ferrous ammonium sulphate.

measured at any time between 5 and 300 min after mixing and is not affected by up to 10 min of continuous irradiation. The fluorescence intensity at 594 nm is a linear function of uranium concentration in the range 10–230 $\mu\text{g/ml}$ in the solution measured. The relative standard deviation for 100 $\mu\text{g/ml}$ uranium was 3% for 10 measurements. Use of a more intense source, such as a nitrogen laser, would probably allow use of a much lower uranium concentration, but its effect on interfering ions would need investigation. However, it may be argued that energy transfer from uranium to an interfering ion would be roughly proportional to the concentration of the latter. Consequently, if the europium(III) concen-

tration is made much higher than that of the interfering ion, energy transfer to the former should predominate.

REFERENCES

1. L. Kropp, *J. Chem. Phys.*, 1967, **46**, 843.
2. S. P. Tanner and A. R. Vargenas, *Inorg. Chem.*, 1981, **20**, 4384.
3. R. Matsushima, H. Fujimori and S. Sakuraba, *J. Chem. Soc. Faraday I*, 1974, **70**, 1702.
4. H. D. Burrows, S. J. Formosinho, M. da G. Miguel and C. F. Pinto, *ibid.*, 1976, **72**, 163.
5. N. E. Korte and R. B. Chessmore, *U.S. Dept. Energy Rept.*, GJBX-109 (80), 1980.

A NEW METHOD FOR THE ATOMIC-ABSORPTION DETERMINATION OF LEAD BLENDED AS LEAD ALKYL IN MOTOR SPIRIT

SAMARESH BANERJEE

Research & Control Laboratory, Durgapur Steel Plant, Durgapur-713203, West Bengal, India

(Received 2 May 1984. Revised 31 October 1985. Accepted 15 November 1985)

Summary—The total lead present as tetraethyl-lead (TEL) and tetramethyl-lead (TML) in motor spirit is determined by atomic-absorption spectrometry after decomposition by extraction with a mixture of mercaptoacetic acid and nitrous acid in the presence of hydrochloric acid.

The usual standard methods for the determination of lead in gasoline and aviation spirit are based on EDTA titration,¹ X-ray spectrometry,² spectrophotometry with dithizone,³ and (after extraction with iodine monochloride) atomic-absorption.⁴ The major difficulty in the last method arises because tetraethyl-lead (TEL) and tetramethyl-lead (TML) give calibration graphs of different slope, which makes analysis of a mixture of alkyls difficult; the two alkyls have first to be separated by fractional distillation with a toluene/xylene mixture as chaser,⁵ before aspiration into the flame. Moreover, suitable organometallic standards of known lead content are necessary for standardization.

We have used mercaptoacetate to extract lead from lead naphthenate additives in lubricating oils⁶ but the method gives very poor recovery of lead from lead alkyls. Table 1 shows that iodine monochloride and the method described here give comparable degrees of extraction of lead.

Mercaptoacetic acid has been used for the colorimetric determination of nitrites.^{7,8} It has been reported, however, that the reaction of thiols and nitrite⁹ gives RSNO, which is readily decomposed by metal ions such as Cu(II), Ag(I) and Hg(II). It has been observed that a mixture of mercaptoacetic acid and nitrous acid in presence of hydrochloric acid can readily react with the lead alkyls and convert the alkyl-lead into water-soluble ionic species, and thus the lead can easily be brought into the aqueous phase. The lead content can then be determined conveniently by atomic-absorption with an air/acetylene fuel-lean flame.

EXPERIMENTAL

Apparatus

A Pye Unicam model SP 2900 double-beam atomic-absorption spectrophotometer was used, with a Philips lead hollow-cathode lamp. The instrumental conditions were: wavelength 217 nm, monochromator band-pass 0.4 nm, air flow 5 l./min, acetylene flow 1 l./min, integration period 4 sec.

Reagents

Mercaptoacetic acid solution, 80%.
Sodium nitrite solution, 5%.

Preparation of test solution

From a burette, transfer a suitable volume of the sample of motor spirit, depending on the lead content (see Table 2) into a 100-ml standard flask. Make up to the mark with iso-octane. Shake well to homogenize the sample.

Procedure

Pipette 20 ml of the prepared sample into a 100-ml glass-stoppered separating funnel. Add 10–12 ml of sodium nitrite solution and 0.5 ml of mercaptoacetic acid solution. The aqueous layer turns bright red. Add 5 ml of concentrated hydrochloric acid slowly with occasional shaking, releasing the pressure in the separating funnel through the stopcock. Shake the funnel vigorously for 2–3 min, cooling it under running tap water. The petrol layer turns olive green. Drain the aqueous layer into a 250-ml beaker. Add 10 ml of distilled water to the funnel, shake again and transfer to aqueous layer into the beaker. Repeat the washing, collecting the aqueous phase in the same beaker and heat the aqueous solution to boiling. The red colour is discharged, which shows that the mercaptoacetic acid–nitrous acid complex has been decomposed. Cool the solution, transfer it into a 100-ml standard flask and make up to volume with distilled water. Determine the lead content by atomic-absorption spectrometry, using the appropriate conditions for the instrument used.

Prepare a standard 1-mg/ml lead solution from analytical reagent grade lead nitrate and dilute it tenfold to obtain a 0.1 mg/ml working standard solution. Use this to prepare a calibration graph covering the 25–50 ppm lead range.

RESULTS AND DISCUSSION

The decomposition of the Pb–SR complex takes place in the presence of nitrous acid and hydrochloric acid and the lead is converted into an ionic species after the formation of the alkyl sulphides (R_2S), indicated by their peculiarly disagreeable odour. On prolonged boiling, as the solution becomes syrupy, a vigorous reaction takes place owing to the sudden drastic oxidation of the alkyl sulphides to oxides of sulphur and nitrogen. The excess of RSNO is readily decomposed by heating the solution just to boiling.

Alternatively the RSNO can be destroyed according to Saville,⁹ by use of Hg(II), Ag(I), or Cu(II) as

Table 1. Extraction of lead

Extractant	Lead found, mg
Iodine monochloride	3.10
Mercaptoacetic acid and hydrochloric acid	0.25
Sodium nitrite and hydrochloric acid	2.90
Sodium nitrite, mercaptoacetic acid and hydrochloric acid	3.12 3.10

Table 2. Volume of sample for test solution

Pb content, ppm	Volume of motor spirit, ml
200–300	50
300–500	30
500–1000	15
1000–1500	10

Table 3

Sample*	Pb, ppm	
	Standard method	This method
1	325	328
		326
2	320	324
		322
3	300	305
		302
4	256	256
		258
5	262	260
		262
6	270	272
		274

*Samples 4–6 are motor spirit blended with "mobile compound".

catalyst for decomposition of the RSNO; although Saville makes no mention of lead, presumably the mechanism is the same. To use the Saville method, add 5% copper sulphate solution dropwise to the cold mixture until the red colour of the reaction mixture is just discharged. Avoid excess of copper since a yellow precipitate of copper mercaptide might be formed, which would require an additional filtration step. Typical results are shown in Table 3 and compared with those obtained by the standard iodine monochloride extraction method followed by atomic-absorption spectrometry.

The mobile compounds are essentially higher boiling lubricating oils. The lubricants are mixed with

motor spirit in the ratio of 4 oz per litre of motor spirit for motor cycles and scooters while the engines are new. For old engines the ratio is changed to 1–2 oz/litre according to choice.

Determination of lead in these blended motor spirits is comparatively difficult by the standard method of iodination. The large amount of iodine liberated makes the junction of the aqueous and oily layers indistinct. The present method is free from this problem.

The volumes of mercaptoacetic acid and sodium nitrite solutions given in the method should be adhered to as far as practicable, because excess of the reagent is troublesome to destroy, the decomposition of the nitroso compound taking place violently with the liberation of sulphur trioxide and nitrogen oxide gases.

Although the 283.3 nm line is often preferred for routine determinations because of the better signal-to-noise ratio and lower background interference, we have chosen the 217 nm line which is 2.5 times as sensitive and seems free from interference effects.

Synthetic sample solutions with known lead content were prepared by mixing pure TML and TEL with motor spirit (free from lead) in different proportions. The recovery of lead was found to be 99.8–100.2%. The lower limit of detection of lead was found to be 2.5 ppm but this can be improved by using an electrodeless discharge lamp as light source.

Acknowledgements—Thanks are due to Sri S. Bhattacharjee, Chief Superintendent and Sri J. Banerjee, Chief Chemist, Research & Control Laboratory, for their interest and encouragement. Thanks are also due to the General Manager (Works), Durgapur Steel Plant for according permission to publish the paper.

REFERENCES

1. *Book of ASTM Standards*, 1976, Part 25, p. 223. ASTM, Philadelphia, 1976.
2. *Book of ASTM Standards*, 1975, Part 24, p. 546. ASTM, Philadelphia, 1975.
3. *IP Standards for Petroleum and its Products*, Vol. I, p. 224. Institute of Petroleum, London, 1977.
4. *Book of ASTM Standards*, 1978, Part 24, p. 720. ASTM, Philadelphia, 1978.
5. *Book of ASTM Standards*, 1975, Part 24, p. 136. ASTM, Philadelphia, 1975.
6. S. Banerjee and R. K. Dutta, *Talanta*, 1973, **20**, 181.
7. F. N. Woodward, *Analyst*, 1948, **74**, 179.
8. F. D. Snell and C. Snell, *Colorimetric Methods of Analysis*, Vol. IIIA, p. 318, Van Nostrand, Princeton, 1961.
9. B. Saville, *Analyst*, 1958, **83**, 670.

SPECTROPHOTOMETRIC DETERMINATION OF TITANIUM WITH TANNIN AND THIOGLYCOLLIC ACID AND ITS APPLICATION TO TITANIUM-TREATED STEELS AND FERROUS AND NON-FERROUS ALLOYS

SAMARESH BANERJEE

Research & Control Laboratory, Durgapur Steel Plant, Durgapur-713203, West Bengal, India

(Received 28 March 1985. Revised 4 November 1985. Accepted 21 November 1985)

Summary—A sensitive spectrophotometric method for the determination of titanium by formation of its complex with tannin and thioglycollic acid at pH 4 has been developed. The intense yellow colour is measured at 400 nm and the system obeys Beer's law over the range 0.2–5 ppm titanium in the solution measured. The method is applicable to titanium-treated steels, stainless steels, permanent magnet alloys and duralumin alloys. The interference of Co, Ni, Cr, Mn, V, Mo and W can be eliminated by prior separation of titanium by controlled addition of cupferron in the presence of thioglycollic acid (TGA). Copper can be quantitatively separated by precipitation with TGA and determined complexometrically with EDTA, with PAN as indicator. Niobium interferes even in traces.

Titanium is added to various ferrous and non-ferrous metals because it confers high tensile strength and anticorrosion properties on them. The common reagents for its colorimetric determination are hydrogen peroxide, Tiron,¹ chromotropic acid,² and diantipyrylmethane,³ the last of which gives high sensitivity. The sensitivity of the hydrogen peroxide method is very low (molar absorptivity $\epsilon = 740 \text{ l. mole}^{-1} \text{ cm}^{-1}$) in comparison to the Tiron ($\epsilon = 1.5 \times 10^4$) and chromotropic acid ($\epsilon = 1.70 \times 10^4$) methods. The chromotropic acid method is most sensitive at pH > 4 but many metals, particularly Fe, Mn, V, Cr, Zr, Mo, U and Ni, also give coloured solutions or otherwise interfere. The interference of Ni, Mo, Nb, Ta and Fe can be minimized by addition of ascorbic acid at pH 2–3, but V and W still interfere. Several other reagents, e.g., sulphosalicylic acid,⁴ gallic acid,⁵ catechol⁶ and salicylic acid,⁷ have been suggested. In almost all the methods, the interfering elements are removed by prior electrolysis with a mercury cathode. Atomic-absorption spectrometry has limited application because titanium is not easily atomized in the flame. A method using differential pulse polarography⁸ has been suggested but prior mercury-cathode electrolysis is again needed and the method is time-consuming.

We have used a mixture of tannin and thioglycollic acid (TGA) for the spectrophotometric determination of niobium in niobium-stabilized stainless steels⁹ and also of vanadium in gas-turbine fuel oils.¹⁰ We have now observed that the same reagent can be used for the spectrophotometric determination of titanium. Prior separation of titanium with cupferron in the presence of TGA eliminates the interferences due to Ni, Cr, Mo, Co, V, Mn and W. If copper is present, it can be quantitatively precipitated as its

thioglycollate and estimated complexometrically with EDTA with PAN as indicator.¹¹ This is an added advantage of the method. Only Nb interferes.

EXPERIMENTAL

Reagents

Standard titanium solution (1 mg/ml). Fuse 0.1668 g of pure TiO_2 (dried) with 2 g of potassium pyrosulphate in a silica crucible. Cool, then take up the cake with 50 ml of 30% v/v sulphuric acid by warming. Cool, transfer the solution into a 100-ml standard flask and make up to the mark with distilled water. Dilute this solution 20-fold and 40-fold to obtain 0.05 and 0.025 mg/ml standard solutions.

Tannin-TGA mixture. Mix equal volume of 5% tannic acid solution and 10% v/v thioglycollic acid solution, filter, and store the solution in an amber glass bottle. Prepare fresh every week.

Acetate buffer, pH 4. Dissolve 25 g of sodium acetate trihydrate and 575 ml of glacial acetic acid in 1 litre of distilled water.

Cupferron wash solution. Dissolve 1 g of cupferron in 1 litre of distilled water and add 10 ml of TGA. Prepare daily and filter before use.

Preparation of calibration graph

Pipette 1–10 ml portions (at 1-ml intervals) of standard titanium solution (0.025 mg/ml) into 50-ml standard flasks. To each add 5 ml of tannin-TGA mixture and 20–25 ml of acetate buffer and mix well. Dilute to volume with distilled water. After 15 min measure the absorbances against a reagent blank at 400 nm, using 1-cm glass cells, and draw the calibration curve.

Analysis of samples

Dissolve a suitable weight of sample (according to Table 1) in 60–70 ml of dilute sulphuric acid (1 + 3) with warming. Oxidize with a few drops of concentrated nitric acid and evaporate to fumes. Cool and take up the residue with 50 ml of hydrochloric acid (1 + 2) by warming. Filter off and wash the silica and ignite it in a platinum crucible. Remove the silica as usual with hydrofluoric acid, fuse the residue with a

Table 1. Weights of samples for analysis

Sample	Titanium, %	Weight of sample, g	Standard flask capacity, ml
Haematite, iron and mild steel	0.02-0.07	5	100
Duralumin alloys, stainless steels	0.1-0.15 0.2-0.3	2.5 5	250 500
Permanent magnet alloy	0.6-0.8	1	500

little potassium pyrosulphate, and after cooling take up the cake with 10-15 ml of warm hydrochloric acid (1 + 2) and add it to the main solution. When the sample contains copper, as in case of stainless steels, permanent magnet alloys and duralumin alloys, adjust the hydrochloric acid concentration to about 5% v/v, cool to room temperature and add thioglycolic acid dropwise with constant stirring. In the presence of copper a dirty bluish white precipitate appears, which gradually turns yellow, indicating that the precipitation of copper is complete. Add 0.5 ml of TGA in excess and a little paper pulp, filter off and wash. If desired, use the precipitate for the determination of copper.¹¹

After removal of copper adjust the volume of the solution to 100 ml and add 10 ml of concentrated hydrochloric acid and 20 ml of TGA, cool the solution to below 15° and add freshly prepared 3% cupferron solution dropwise with constant stirring until the precipitation of titanium is complete and a brown precipitate of iron begins to appear. Add 1 ml of cupferron solution in excess and some filter paper pulp. Stir for 2 min, and filter off on a Whatman No. 41 paper and wash the precipitate several times with cupferron wash solution. Carefully ignite the precipitate in a silica crucible and fuse the residue with potassium pyrosulphate, cool and take up the cake with 20 ml of sulphuric acid (1 + 4) with warming. Transfer the solution quantitatively into a standard flask (capacity according to Table 1) and make up to the mark with distilled water.

Pipette a suitable aliquot into a 50-ml standard flask and add 5 ml of tannin-TGA mixture. Add ammonia solution (1 + 1) dropwise until the pH is around 3-3.5 (use a pH-meter or a narrow-range indicator paper). Add 20-25 ml of acetate buffer, mix, dilute to volume with distilled water and after 15 min measure the absorbance of the solution against a reagent blank prepared with same volume of tannin-TGA mixture.

RESULTS AND DISCUSSION

The absorption spectrum of the titanium complex exhibits an absorbance maxima at 400 nm, so this wavelength was chosen for all measurements. The reagent itself has slight absorbance at this wavelength, so measurement against a reagent blank is necessary.

The absorbance is pH-dependent and is maximal at pH 4.0-4.5 but at pH 4.5 the characteristic pink colour of iron with TGA begins to appear. At higher pH tannin reacts with both titanium and iron(III) to form a voluminous precipitate. Although TGA alone does not react with titanium, the tannin-TGA mixture produces a stable yellow colloidal solution with titanium. The coagulation of the colloidal suspension of titanium with tannin-TGA starts at pH 4.5 and becomes rapid above this pH. At pH 4 the colour of the Ti-complex with tannin-TGA mixture suffers no interference due to iron, so all measurements are

made at pH 4. Tannin solution gradually darkens in colour in presence of light and this is retarded by addition of TGA; tannin-TGA mixture keeps well. In stainless steel samples the percentage of copper is much lower than in duralumin alloys. When the determination of copper is not necessary, the amount of sample for analysis may be reduced to 2 g instead of 5 g. The colour of the titanium complex takes about 15 min to reach maximum intensity and is then stable for at least 2 hr. Hence measurements should be made not less than 15 min after the colour starts to form.

Effect of diverse ions

Niobium produces a similar colour under the same conditions and interferes even at 0.5 ppm level. Tantalum up to 10 ppm can be tolerated. Mo, Co, Ni, Cr, Mn, V, W and Cu interfere but this interference can be eliminated by a prior separation of the titanium with cupferron after complexation of the other elements with thioglycolic acid. Iron does not interfere at pH 4. About 5-fold excess of iron is helpful for the separation of low concentrations of titanium with cupferron, since the iron cupferronate acts as a collector.

Complexing anions such as fluoride, oxalate, citrate, tartrate and EDTA depress the colour intensity and should be absent. Excess of chloride, sulphate or nitrate has no effect, but nitrite interferes even in traces. Hydrogen peroxide completely destroys the colour.

Analysis of standard samples

Some typical results for the determination of titanium in standard BCS samples are shown in Table 2.

Table 2. Determination of titanium in standard samples

Sample	Ti, %	
	Certified value	Found
Haematite	0.052	0.050
BCS No. 236/3		0.052
Haematite	0.070	0.070
BCS No. 236/2		0.070
Permanent magnet alloy	0.79	0.80
BCS No. 233		0.78
18/9 Stainless steel	0.32	0.30
BCS No. 235/2		0.32
Duralumin alloy	0.10	0.12
BCS No. 216/1		0.11

Determination of titanium in simulated samples containing 0.5–5.0 mg of Ti gave recoveries of 99.4–100.2%. The molar absorptivity of the titanium species is about 10 times that of the hydrogen peroxide system, and is $0.75 \times 10^4 \text{ l. mole}^{-1} \text{ cm}^{-1}$. In the absence of copper, the sample solution (after the removal of silica) can be directly treated for the precipitation of titanium with cupferron after complexation of interfering elements with TGA.

Acknowledgements—Thanks are due to Sri S. Bhattacharjee, Chief Superintendent (RC & RD) and Sri J. Banerjee, Chief Chemist, Research & Control Laboratory, for their interest and encouragement and also to Sri C. K. Ganguly, Deputy Director (Chemicals), Central Chemical Laboratory, Geological Survey of India, Calcutta for use of the spectrophotometer employed in this work. Thanks are also

due to the General Manager (Works), Durgapur Steel Plant for according permission to publish the paper.

REFERENCES

1. J. H. Yoe and A. R. Armstrong, *Anal. Chem.*, 1947, **19**, 100.
2. W. W. Brandt and A. E. Preiser, *ibid.*, 1953, **25**, 567.
3. A. A. Minon, *Uch. Zap. Permsk. Univ.*, 1955, **9**, 177.
4. M. Ziegler and O. Glemser, *Z. Anal. Chem.*, 1953, **139**, 92.
5. P. N. Dasgupta, *J. Indian Chem. Soc.*, 1929, **6**, 855.
6. J. Piccard, *Chem. Ber.*, 1909, **42**, 434.
7. J. H. Muller, *J. Am. Chem. Soc.*, 1911, **33**, 1506.
8. Y. Yamamoto, K. Hasebe and I. Kambara, *Anal. Chem.*, 1983, **55**, 1942.
9. S. Banerjee and R. K. Dutta, *Talanta*, 1974, **21**, 1091.
10. S. Banerjee, B. P. Sinha and R. K. Dutta, *ibid.*, 1975, **22**, 689.
11. S. Banerjee and R. K. Dutta, *Indian J. Technol. (CSIR)*, 1978, **16**, 42.

ANALYTICAL INVESTIGATIONS ON CEPHALOSPORINS—I SPECTROPHOTOMETRIC DETERMINATION OF CEFTRIAXONE

F. İNCİ ŞENGÜN and KÖKSAL ULAŞ

Department of Analytical Chemistry, Faculty of Pharmacy, University of Istanbul, Istanbul, Turkey

(Received 7 September 1984. Revised 26 September 1985. Accepted 31 October 1985)

Summary—The hydroxylamine–nickel and imidazole–mercury(II) methods for the determination of penicillins and cephalosporins have been adapted to the determination of ceftriaxone both in bulk form and in pharmaceutical formulations.

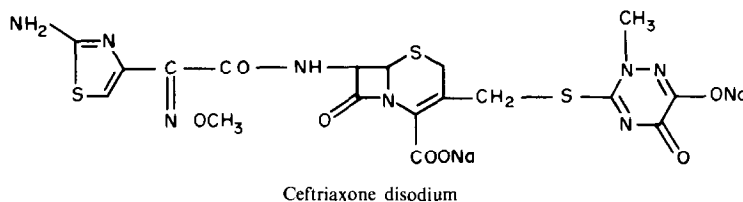
Two well-established spectrophotometric methods have been extensively used for the spectrophotometric determination of penicillins and cephalosporins.¹⁻¹³ The first is based on the reaction reported by Bamberger¹⁴ in 1899, in which hydroxylamine is reacted with a carboxylic acid derivative to form a hydroxamic acid which is then treated with iron(III) to give a coloured complex. Nickel(II) salts have been recommended as a catalyst for formation of the hydroxamic acid¹⁵⁻¹⁷ and have been utilized in cephalosporin analyses.⁴ The other method is based on use of the imidazole–mercury(II) reagent,^{7-11,13} which was previously used in the determination of penicillins by Bundgaard.⁷ We have now examined use of the two spectrophotometric methods for the determination of ceftriaxone.

Procedure for hydroxylamine method

Standard 1 mg/ml stock solution of ceftriaxone was prepared in 1% sodium bicarbonate solution. Then 0.5, 1.0, 1.5, 2.0, 2.5 and 3.0 ml of this solution were pipetted into test-tubes and made up to 3 ml with 1% sodium bicarbonate solution. Hydroxylamine–nickel reagent (2 ml) was added to each test solution and allowed to react at room temperature for 40 min. At the end of this time 5 ml of iron(III) reagent were added to each tube, and the mixtures were left for 15 min more, then centrifuged. A blank solution containing no ceftriaxone was prepared in the same way. The absorbances were measured at 460 nm against the blank solution and a calibration graph was drawn (Fig. 1).

Procedure for imidazole method

Ceftriaxone (12.0 mg) was dissolved in imidazole stock solution (diluted with 10% of its volume of water) and diluted to volume in a 20-ml standard flask with the same



EXPERIMENTAL

Reagents

Hydroxylamine–nickel reagent. Prepared by dissolving 6.95 g of hydroxylamine hydrochloride and 2.90 g of nickel nitrate hexahydrate in about 30 ml of distilled water, adjusting to pH 6.2 ± 0.05 with 10M sodium hydroxide and diluting to 50 ml with distilled water.

Iron(III) reagent. Prepared by dissolving 30 g of ammonium iron(III) sulphate dodecahydrate in 2.7 ml of concentrated sulphuric acid and diluting to 100 ml with distilled water.

Imidazole–mercury(II) reagent. Imidazole stock solution was prepared by dissolving 3.0 g of imidazole in about 70 ml of distilled water, adjusting to pH 6.8 ± 0.05 and diluting to 100 ml with distilled water. The composite reagent was prepared by adding 10 ml of aqueous 0.27% mercuric chloride solution to 100 ml of imidazole stock solution dropwise with continuous mixing. This solution is stable for only one hour.

solvent. Then 0.2, 0.4, 0.6, 0.8 and 1.0 ml of this solution were pipetted into test-tubes (equipped with stoppers) and made up to 1.0 ml with the diluted imidazole stock solution. Next 5 ml of imidazole–mercury(II) reagent were added to each tube. The tubes were stoppered, allowed to stand in a water-bath at 83° for 20 min, then removed and cooled in an ice-bath for a short time to bring the solutions to room temperature, then centrifuged. A blank solution was prepared by adding 5 ml of imidazole–mercury(II) reagent to 1 ml of diluted imidazole stock solution but was not heated. The absorbances were measured at 370 nm against the blank and a calibration graph was drawn (Fig. 1).

Application of the methods to Rocephin[®] vials

The contents of the vial (ceftriaxone disodium, equivalent to 1.0 g of its acid form) were dissolved in the appropriate solvent to give a concentration of 1 mg/ml for the hydroxylamine method and 0.6 mg/ml for the imidazole method. Then 1.5 ml and 0.5 ml of these sample solutions were pipetted into separate test-tubes for use of the hydroxyl-

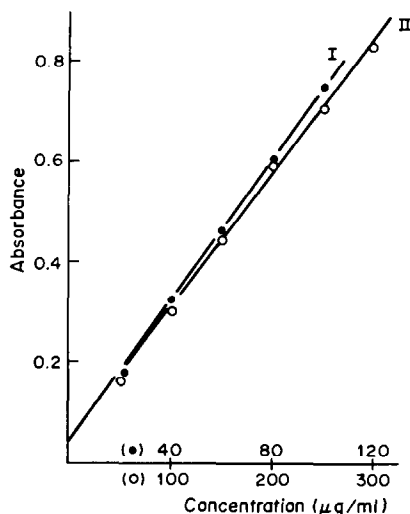


Fig. 1. Calibration curves for ceftriaxone determinations. I, Imidazole method; II, hydroxylamine method.

amine and imidazole methods respectively, and the general procedure used for the preparation of calibration graphs was followed.

RESULTS AND DISCUSSION

The hydroxylamine–nickel method of Mays *et al.*⁴ was examined and the conditions slightly modified to give optimum conditions for ceftriaxone determination. It was found that a reaction period of 30–60 min for the hydroxylamine reaction gave constant and maximal final absorbance, and that 13–25 min was optimal for the iron(III) reaction period.

The optimal conditions for the imidazole method were also established. It was found that the temperature and duration of heating were both important. Heating at 100° was found to give rapid development of an intense colour, but the timing was critical for extended heating. At lower heating temperature the reaction took longer, but the colour produced was more stable, though less intense. Heating at 83° for 18–24 min gave essentially constant absorbance and a 20-min heating period was selected for use. To bring the solutions to room temperature and to avoid subsequent fading if the solution was left at high temperature, the reaction was quenched by brief cooling in ice-water. It was found that there was no absorption maximum in the 370 nm region if the mercury(II) was omitted. It has been reported

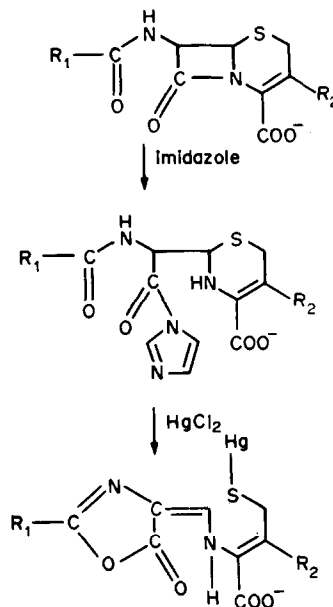


Fig. 2. Mechanism of reaction of ceftriaxone with imidazole–mercury(II) reagent.

that mercury and copper salts decrease the absorbance in the cephalapirin determination,¹² but we find that mercury(II) enhances the absorbance in the ceftriaxone analysis. Increasing the mercury(II) concentration increases the absorbance, but the imidazole–mercury(II) reagent becomes more unstable and a precipitate of mercury salts appears. The 0.27% mercuric chloride concentration used for cefadroxil¹³ proved convenient. The optimum imidazole concentration is 0.4–0.5M, whereas it is reported as 1.2M for penicillins⁷ and cefadroxil¹³ and 0.013M for cephalapirin.¹²

The reaction mechanism of ceftriaxone with imidazole–mercury(II) reagent is possibly similar to those for penicillins.⁷ It depends on the catalytic effect of the imidazole base on the β -lactam bond and on the formation of an oxazolinone ring in the side-chain. Binding of mercury(II) to the thiol group which is freed by the cleavage of the dihydrothiazine ring stabilizes the product (Fig. 2). The methoxyimino group, included in the R₁ substituent, which becomes conjugated to the oxazolinone ring at the end of the reaction, is possibly responsible for the absorption at 370 nm. No absorption maximum at 370 nm was obtained in the determination of

Table 1. Results for analysis of Rocephin* vials (ceftriaxone disodium salt equivalent to 1.0 g of its acid form)

	Imidazole method	Hydroxylamine method
Number of detns. (<i>n</i>)	5	5
Mean value (\bar{x}), mg	1029	1019
Standard deviation (<i>s</i>), mg	7	10
Confidence limits of the mean*, mg	1029 ± 9	1019 ± 12

* $\bar{x} \pm ts/\sqrt{n}$.

cephalosporins which do not contain a methoxyimino group in their structure, the absorption maxima being at 315–345 nm.

Finally, it was observed that in both the hydroxylamine–nickel and imidazole–mercury(II) methods there was no interference by the usual excipients in the ceftriaxone formulations and both methods were applied to assay of Rocephin®. The results are shown in Table 1.

REFERENCES

1. Appendix to *USP XX*, p. 1283.
2. *Code of Federal Regulations 21*, Part 436.205, p. 263, 1978.
3. E. H. Flynn (ed.), *Cephalosporins and Penicillins*, p. 615. Academic Press, New York, 1972.
4. D. L. Mays, F. K. Bangert, W. C. Cantrell and W. G. Evans, *Anal. Chem.*, 1975, **47**, 2229.
5. W. W. Holl, M. O'Brien, J. Filan, T. R. Mazeika, A. Post, D. Pitkin and P. Actor, *J. Pharm. Sci.*, 1975, **64**, 1232.
6. A. E. Kulo, *Farm. Aikak.*, 1976, **85**, 1.
7. H. Bundgaard and K. Ilver, *J. Pharm. Pharmac.*, 1972, **24**, 790.
8. A. Koshiro and T. Fujita, *Kyushu Yakugakkai Kaiho*, 1975, **29**, 17.
9. H. Bundgaard, *Arch. Pharm. Chem. Sci. Ed.*, 1977, **5**, 141.
10. *Idem, ibid.*, 1979, **6**, 81.
11. *Idem, ibid.*, 1979, **7**, 95.
12. J. E. Bodnar, W. G. Evans and D. L. Mays, *J. Pharm. Sci.*, 1977, **66**, 1108.
13. D. Marini and E. Pascucci, *Boll. Chim. Farm.*, 1980, **119**, 52.
14. E. Bamberger, *Ber.*, 1899, **32**, 1805.
15. J. W. Munson and K. A. Connors, *J. Am. Chem. Soc.*, 1972, **94**, 1979.
16. *Idem, J. Pharm. Sci.*, 1972, **61**, 211.
17. K. A. Connors and J. W. Munson, *Anal. Chem.*, 1972, **44**, 336.

ANALYTICAL INVESTIGATIONS ON CEPHALOSPORINS—IV APPLICATION OF ELLMAN'S REAGENT

F. İNCİ ŞENGÜN and İNCİ FEDAI

Department of Analytical Chemistry, Faculty of Pharmacy, University of Istanbul, Istanbul, Turkey

(Received 31 October 1984. Revised 23 October 1985. Accepted 8 November 1985)

Summary—The application of 5,5'-dithiobis(2-nitrobenzoic acid) (Ellman's reagent) for the determination of microgram quantities of various selected cephalosporins in aqueous solution is described. Cephalosporin derivatives (cephalothin sodium, cephacetrile sodium, cefamandole lithium and nafate, cefoperazone sodium and ceftizoxime sodium) have to be treated with 0.5*N* sodium hydroxide before determination with Ellman's reagent, which reacts with free thiol groups. An aliquot of the solution is reacted with Ellman's reagent in pH 7.2 phosphate buffer and the absorbance of the resulting yellow solution is measured at 410 nm. The method, which is simple and precise, has been applied to determination of those cephalosporins in formulations, the results being compared with those obtained by the Ni-hydroxylamine method.

Cephalothin can be determined by iodometry,^{1,2} non-aqueous titrimetry,³⁻⁵ polarography,^{6,7} spectrophotometry,⁸⁻¹⁶ HPLC¹⁷⁻²² or fluorimetry.²³ Some of these methods or others have been used for cephacetrile sodium,^{4,14,18,23-26} cefamandole lithium and nafate,^{17,27-29} cefoperazone sodium³⁰⁻³² and ceftizoxime sodium.^{28,33,34} The aim of the present study was to develop a method generally applicable to cephalosporins and to compare it with the Ni(II)-hydroxylamine method reported by Mays *et al.*⁹ Ellman's reagent was selected for investigation.

EXPERIMENTAL

Reagents

Cephalothin sodium, cephacetrile sodium, cefamandole lithium and nafate, cefoperazone sodium and ceftizoxime sodium standards were kindly provided by Hoechst, Ciba Geigy, Eli Lilly, Pfizer and Boehringer Mannheim respectively. 5,5'-Dithiobis(2-nitrobenzoic acid) (DTNB) was purchased from Janssen Pharmaceutica and hydroxylamine hydrochloride from Merck. All reagents and solvents were of analytical grade. A 0.15*M* phosphate buffer (pH 7.2) and 0.5*M* sodium hydroxide were used. Ellman's reagent was prepared by dissolving 20.0 mg of DTNB in 100 ml of the 0.15*M* phosphate buffer. Demineralized doubly distilled water was used throughout.

Procedure

Aqueous solutions of the cephalosporins were prepared, containing 1.1–2.3 mg/ml cephalosporin. Then 0.2, 0.4, 0.6, 0.8 and 1 ml volumes were pipetted into test-tubes, and made up to 1 ml with distilled water, and 0.5 ml of 0.5*M* sodium hydroxide was added to each. The tubes were then stoppered and kept in a boiling water-bath for 65 min for cephacetrile sodium and 90 min for the other cephalosporins. The tubes were then cooled in an ice-bath for about 1 min, and allowed to come to room temperature. A 50- μ l portion was pipetted into a cuvette containing 3 ml of the Ellman's reagent and the absorbance was measured at 410 nm against a similarly treated blank solution.

Analysis of dosage forms

The contents of the commercial vials were diluted appropriately to give nominally 1-mg/ml solutions, and 1 ml of each solution was analysed by the procedure above.

RESULTS AND DISCUSSION

Ellman's reagent was used for determination of cephradine, cephalothin, cephalixin and cephaloglycine by Kirschbaum¹⁰ but the optimum conditions reported are not generally applicable to cephalosporins. Kirschbaum proposed pH 9.2 as suitable for the assay but the stability of 5,5'-dithiobis(2-nitrobenzoic acid) at this pH was not taken into consideration. Baars *et al.* later investigated the stability of Ellman's reagent and reported that the reagent blank is influenced by pH and temperature.³⁵ It was also observed that at pH 8.0 the absorbance increased significantly with time, whereas only a slight increase was observed at pH 6.5. Vermeij, in the determination of penicillins in urine with the same reagent, has chosen 7.2 as the optimum pH.³⁶ We first studied the degradation of cephalosporins in basic medium. Several degradation studies on cephalosporins had already been done³⁷⁻³⁹ but many questions remained unanswered. Fogg *et al.*, however, have shown that sulphide is a general degradation product of cephalosporins.⁴⁰⁻⁴⁴ The determination with Ellman's reagent is based on cleavage of the S-S bond of the reagent by another thiol compound, producing the yellow anion of 5-thio-2-nitrobenzoic acid (Fig. 1).

We found that the absorbance of the product increased with the pH at which the degradation was done. Various buffers covering the pH range 9.0–11.3 were investigated and finally 0.167*M* sodium hydroxide was chosen as the best degradation agent. The

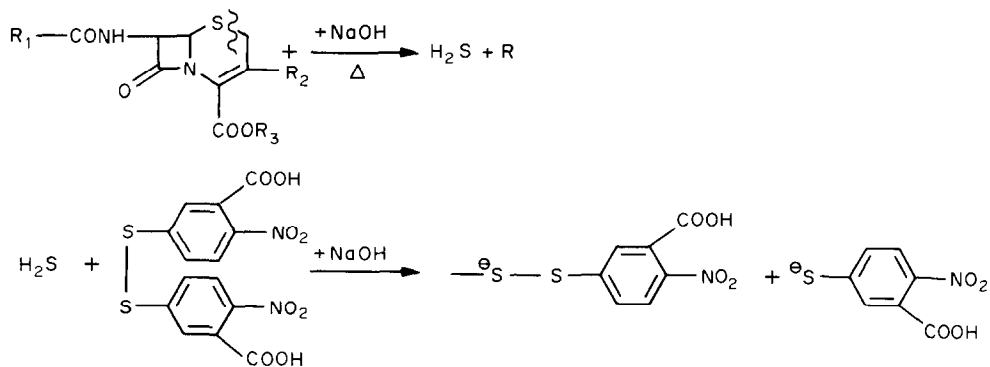


Fig. 1. Mechanism of reaction between cephalosporins and Ellman's reagent.

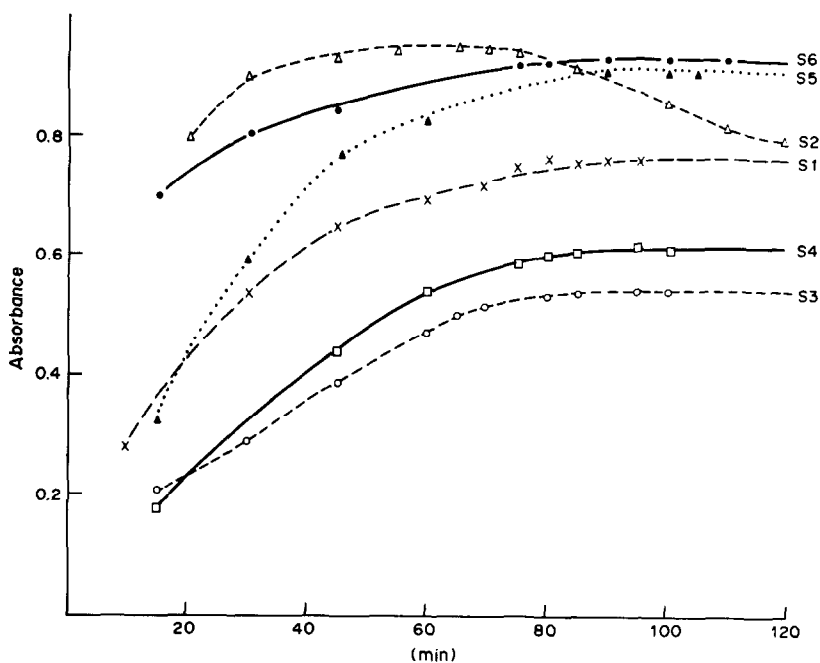


Fig. 2. Rate of formation of 410-nm chromophore as a function of heating time. Initial concentrations (mg/ml): S1, 1.80; S2, 2.02; S3, 1.50; S4, 1.89; S5, 3.45; S6, 1.25 (see Table 1 for identification).

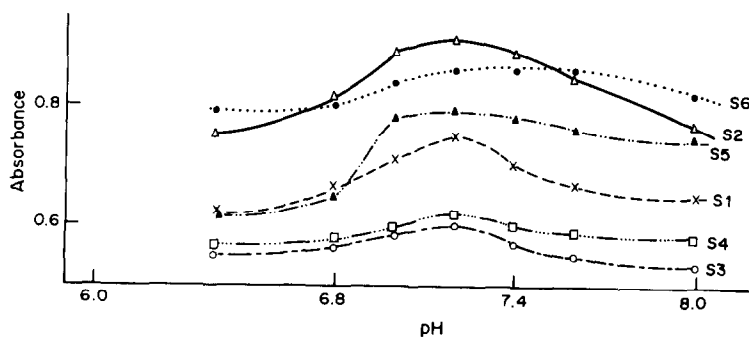


Fig. 3. Extent of formation of 410-nm chromophore as a function of pH. Initial concentrations (mg/ml): S1, 1.80; S2, 1.93; S3, 1.66; S4, 1.92; S5, 2.99; S6, 1.17 (see Table 1 for identification).

Table 1. Linear dynamic range and precision

Compound	Code	Linear dynamic range, $\mu\text{g/ml}$	RSD range, %
Cephalothin sodium	S1	3.6–18	1.5–0.6
Cephacetrile sodium	S2	3.2–16	1.9–0.7
Cefamandole lithium	S3	5.0–25	1.7–0.6
Cefamandole nafate	S4	5.0–25	1.7–0.5
Cefoperazone sodium	S5	6.0–30	1.6–0.6
Ceftizoxime sodium	S6	2.4–12	1.6–0.7

Table 2. Determination of cephalosporins in pharmaceutical formulations

Preparation	Active ingredient	Nominal content, mg	Recovery relative to nominal content*, %			
			Present method		Mays' method	
			Mean	RSD	Mean	RSD
Cepovenin [®] 1.0†	Cephalothin sodium	1000	100.3	0.5	101.4	0.6
Cepovenin [®] 4.0†	Cephalothin sodium	4000	99.5	0.9	100.1	1.9
Keflin [®] 1.0 g§	Cephalothin sodium	1000	100.0	0.5	99.6	1.1
Celospor [®] 1.0 g‡	Cephacetrile sodium	1000	99.5	0.3	99.4	0.5
Celospor [®] 2.0 g‡	Cephacetrile sodium	2000	99.6	0.2	99.5	0.5
Celospor [®] 4.0 g‡	Cephacetrile sodium	4000	100.2	0.5	101.2	1.3
Kefadol [®] ‡	Cefamandole nafate	500	99.6	0.3	99.0	0.6
Cefobis [®] ¶	Cefoperazone sodium	1000	100.2	0.7	100.6	0.9
Cefobis [®] ¶	Cefoperazone sodium	2000	100.7	0.6	100.4	1.3

*Calculated from six measurements of each of nine samples.

†Hoechst AG.

§Mustafa Nevzat İlaç Sanayii A.S. (Turkey),

‡Ciba-Geigy.

#Eli Lilly.

¶Pfizer.

effect of heating time was investigated by heating a mixture of 1 ml of sample solution and 0.5 ml of 0.5M sodium hydroxide in a boiling water-bath for 120 min, withdrawing 50 μl portions at intervals, and analysing them as described in the procedure. The results are shown in Fig. 2. Heating for 65 min for cephalothin sodium and 90 min for the other cephalosporins was selected as optimal.

The effect of pH and the colour development reaction was studied by mixing 50 μl of degraded cephalosporin solution with 3 ml of Ellman's reagent in 0.15M phosphate buffer of various pH values in the range 6.4–8.0 and measuring the absorbance. Figure 3 shows that pH 7.2 is optimal.

The amount of Ellman's reagent needed was determined by measuring the absorbance obtained with increasing amounts of the reagent. It was found that at least a 10:1 molar ratio of DTNB to cephalosporin must be used. A molar ratio of 20 was therefore selected for safety. The colour intensity became maximal almost immediately on addition of the reagent and remained constant for approximately 6 hr.

Precision and sensitivity

The precision was established by six determinations on each of the standard cephalosporin solutions. Relative standard deviations (RSD) between 0.6 and 1.9% were obtained. The lower limit of determination varied from 2.4 to 6.0 $\mu\text{g/ml}$, as listed in Table 1. Small intercepts on the y -axis were found for the calibration graphs.

For the determination of cephalosporins in injectable dosage forms the results in Table 2 were obtained. The method developed yielded good recoveries, with RSD in the range between ± 0.2 and $\pm 0.9\%$ whereas the RSD values for the Mays method varied between ± 0.5 and $\pm 1.9\%$. Our method can confidently be used for the six cephalosporins examined.

REFERENCES

1. S. Okada, K. Hattori and T. Takano, *Bull. Chem. Soc. Japan*, 1965, **38**, 2186.
2. H. Fukuchi, M. Yoshida, M. Kumagai, T. Kitaura, I. Takahashi, T. Shimada and T. Kobayashi, *Hiroshima J. Med. Sci.*, 1978, **27**, 1.
3. A. G. Fogg, M. A. Abdalla and H. P. Henriques, *Analyst*, 1982, **107**, 449.
4. C. Casalini, L. Montecchi, D. Boccali and G. Ceserano, *Boll. Chim. Farm.*, 1975, **114**, 651.
5. J. J. Kaminski and N. Bodor, *Int. J. Pharm.*, 1979, **3**, 151.
6. D. A. Hall, D. M. Berry and C. J. Schneider, *J. Electroanal. Chem.*, 1977, **80**, 155.
7. A. G. Fogg, N. M. Fayad, C. Burgess and A. McGlynn, *Anal. Chim. Acta*, 1979, **108**, 205.
8. P. Papazova, P. R. Bontchev and M. Kacarova, *Pharmazie*, 1977, **32**, 486.
9. D. L. Mays, F. K. Bangert, W. C. Cantrell and W. G. Evans, *Anal. Chem.*, 1975, **47**, 2229.
10. J. Kirschbaum, *J. Pharm. Sci.*, 1974, **63**, 923.
11. M. A. Abdalla, A. G. Fogg and C. Burgess, *Analyst*, 1982, **107**, 213.
12. Y. A. Beltagy, *Zentralbl. Pharm.*, 1977, **116**, 925.
13. A. M. Wahbi and B. Unterhalt, *Z. Anal. Chem.*, 1977, **284**, 128.

14. G. Tortolani and E. Romagoli, *J. Chromatog.*, 1976, **120**, 149.
15. J. Schröder, H. Nöschel and A. Bonow, *Pharmazie*, 1980, **35**, 544.
16. T. Ehle-Nilsson, *Acta Pathol. Microbiol. Scand. Suppl.*, 1977, **259**, 61.
17. V. Quercia, C. De Sena, P. Gambero, G. Pagnozzi, N. Pierini, and M. Terracciano, *Boll. Chim. Farm.*, 1979, **118**, 308.
18. F. Barbato, C. Grieco, C. Silipo and A. Vittoria, *Boll. Soc. Ital. Biol. Sper.*, 1976, **52**, 1746.
19. J. S. Wold and S. A. Turnipseed, *Clin. Chem. Acta*, 1977, **78**, 203.
20. R. P. Buhs, T. E. Maxim, N. Allen, T. A. Jacob and F. J. Wolf, *J. Chromatog.*, 1974, **99**, 609.
21. M. J. Cooper, M. W. Anders and B. L. Mirkin, *Drug Metab. Dispos.*, 1973, **1**, 659.
22. T. F. Rolewicz, B. L. Mirkin, M. J. Cooper and M. W. Anders, *Clin. Pharmacol. Ther.*, 1977, **22**, 928.
23. A. B. C. Yu, C. H. Nightingale and D. R. Flanagan, *J. Pharm. Sci.*, 1977, **66**, 213.
24. C. Casalini, G. Cesarano and G. Mascellani, *Anal. Chem.*, 1977, **49**, 1002.
25. T. Fukogono and K. Maeda, *Chemotherapy (Tokyo)*, 1976, **24**, 78.
26. A. Csiba and H. Graber, *Acta Pharm. Hung.*, 1978, **48**, 10.
27. E. C. Rickard and G. G. Cooke, *J. Pharm. Sci.*, 1977, **66**, 379.
28. M. C. Rován, F. Abadie, A. Leclerc and F. Juge, *J. Chromatog.*, 1983, **275**, 133.
29. A. M. Brisson and J. B. Fourtillan, *ibid.*, 1981, **223**, 393.
30. D. G. Dupont and R. L. DeJager, *J. Liq. Chromatog.*, 1981, **4**, 123.
31. R. R. Muder, W. F. Diven, V. L. Yu and J. Johnson, *Antimicrob. Agents Chemother.*, 1982, **22**, 1076.
32. P. T. R. Hwang and M. C. Meyer, *J. Liq. Chromatog.*, 1983, **6**, 743.
33. C. E. Fasching, L. R. Peterson, K. M. Bettin and D. N. Gerding, *Antimicrob. Agents Chemother.*, 1982, **22**, 336.
34. A. Suzuki, K. Noda and H. Noguchi, *J. Chromatog.*, 1980, **182**, 448.
35. A. J. Baars, E. W. Van Dongen and D. D. Breimer, *Pharm. Weekbl.*, 1977, **112**, 1117.
36. P. Vermeij, *Pharm. Weekbl. Sci. Ed.*, 1979, **1**, 217.
37. A. I. Cohen, P. T. Funke and M. S. Puar, *J. Pharm. Sci.*, 1973, **62**, 1559.
38. T. Yamana and A. Tsuji, *ibid.*, 1976, **65**, 1563.
39. S. M. Berge, N. L. Henderson and H. J. Frank, *ibid.*, 1983, **72**, 59.
40. A. G. Fogg and N. M. Fayad, *Anal. Chim. Acta*, 1979, **110**, 107.
41. A. G. Fogg, N. M. Fayad and R. N. Goyal, *J. Pharm. Pharmacol.*, 1980, **32**, 302.
42. A. G. Fogg and M. J. Martin, *Analyst*, 1981, **106**, 123.
43. M. A. Abdalla and A. G. Fogg, *ibid.*, 1982, **107**, 213.
44. A. G. Fogg, M. A. Abdalla and H. P. Henriques, *ibid.*, 1982, **107**, 449.

USE OF A BISMUTH ION-SELECTIVE ELECTRODE FOR INVESTIGATION OF BISMUTH COMPLEXES OF CITRIC AND MALIC ACIDS

WALENTY SZCZEPANIAK and MARIA REN

Department of Instrumental Analysis, Faculty of Chemistry, A. Mickiewicz University,
 Poznań, Poland

(Received 20 March 1985. Accepted 12 November 1985)

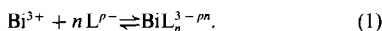
Summary—A bismuth ion-selective electrode has been used to determine the nature and stability of the complexes formed by bismuth with citric acid and malic acid, by measurement of the response of the electrode to different total bismuth concentrations at various combinations of pH and total ligand concentration. The values found were $\beta_2 = 3 \times 10^{13}$ for $\text{Bi}(\text{Cit})_2^{3-}$ and $\beta_3 = 8 \times 10^9$ for $\text{Bi}(\text{Mal})_3^{3-}$.

Citric and malic acids form stable complexes with multivalent cations. These complexes play an important role in biological processes. These two acids are also used for masking such cations.¹⁻³ The bismuth complexes have been investigated polarographically,^{4,5} and the citrate complex potentiometrically.^{4,6} Our bismuth ion-selective electrode⁷ (with reproducibility of ± 0.1 mV) provides an additional means of potentiometric investigations of these complexes.

EXPERIMENTAL

All reagents used were of analytical grade. The potential of the bismuth electrode⁷ was measured with a pH-meter and digital voltmeter system which gave e.m.f. measurements accurate to ± 0.1 mV. A silver/silver chloride electrode was used as reference, with a salt-bridge.³

The complexes are formed according to the equation:



Investigation of the equilibrium resolves itself into: (1) determination of the composition of the complex, (2) determination of the acid form involved, (3) determination of the stability constant.

Composition of the complex

The stability constant is given by

$$\beta_n = \frac{[\text{BiL}_n^{3-\rho n}]}{[\text{Bi}^{3+}][\text{L}^{\rho-}]^n} \quad (2)$$

and by equating the expressions for two solutions of the same pH but different ligand and bismuth concentration, and taking logarithms, we obtain

$$\log \frac{[\text{Bi}^{3+}]_{(1)}}{[\text{Bi}^{3+}]_{(2)}} = n \log \frac{[\text{L}^{\rho-}]_{(2)}}{[\text{L}^{\rho-}]_{(1)}} + \log \frac{[\text{BiL}_n^{3-\rho n}]_{(1)}}{[\text{BiL}_n^{3-\rho n}]_{(2)}} \quad (3)$$

and hence

$$\log \frac{a_{\text{Bi}^{3+}}^{(1)}}{a_{\text{Bi}^{3+}}^{(2)}} = n \log \frac{[\text{L}^{\rho-}]_{(2)}}{[\text{L}^{\rho-}]_{(1)}} + \log \frac{[\text{BiL}_n^{3-\rho n}]_{(1)}}{[\text{BiL}_n^{3-\rho n}]_{(2)}} + \log \frac{f_{\text{Bi}^{3+}}^{(1)}}{f_{\text{Bi}^{3+}}^{(2)}} \quad (4)$$

where $a_{\text{Bi}^{3+}}$ is the activity and $f_{\text{Bi}^{3+}}$ the activity coefficient of the bismuth ion. Plotting $\log a_{\text{Bi}^{3+}}^{(1)}/a_{\text{Bi}^{3+}}^{(2)}$ against $\log [\text{L}^{\rho-}]_{(2)}/[\text{L}^{\rho-}]_{(1)}$ gives a straight line with slope n . To do this requires electrode calibration graphs for Bi(III) solutions (all at the same pH) containing various concentrations of ligand. If the concentration of the ligand is high enough

compared with $[\text{Bi(III)}]$, then the total ligand concentration can be used as the value for the unbound ligand concentration.

The bismuth activity ratio can be calculated from the differences in the electrode potentials (ΔE) for solutions having the same pH and total concentration of Bi(III) but different ligand concentrations:

$$\log \frac{a_{\text{Bi}^{3+}}^{(1)}}{a_{\text{Bi}^{3+}}^{(2)}} = \frac{\Delta E}{S} \quad (5)$$

where S is the slope of the calibration graph of the electrode.

Determination of complexing acid form

The concentration of a particular form of the complexing acid depends on the total concentration of the acid and on the pH. The dependence described by equation (4) refers only to the acid form which plays the main role in complexing the bismuth, provided there is a large excess of ligand.

To identify the acid form involved, the electrode potential is measured for Bi(III) solutions containing the same total concentration of ligand (C_L) but at various pH values. From C_L and the pH the distribution of the various ligand species can be calculated and the dependence of $\log a_{\text{Bi}^{3+}}^{(1)}/a_{\text{Bi}^{3+}}^{(2)}$ on $\log ([\text{L}^{\rho-}]_{(2)}/[\text{L}^{\rho-}]_{(1)})$ determined for each. The ligand form which gives a value of n closest to that obtained in determining the composition of the complex is the one which is principally involved in the complex formation.

Determination of stability constants

In two solutions with different total concentrations of Bi(III), the electrode will show the same potential if the activities of the Bi^{3+} cations are the same, and hence

$$f_1[\text{Bi}^{3+}]_{(1)} = f_2[\text{Bi}^{3+}]_{(2)} \quad (6)$$

With a sufficient excess of ligand present, it may be assumed that:

$$C_{\text{Bi(III)}} = [\text{Bi}^{3+}] + [\text{BiOH}^{2+}] + [\text{BiL}_n^{3-\rho n}] \quad (7)$$

After inserting the expressions resulting from the respective equilibria and transforming, we obtain:

$$[\text{Bi}^{3+}] = \frac{C_{\text{Bi(III)}}}{1 + \frac{[\text{OH}^-]}{K_{\text{BiOH}}} + \beta_n [\text{L}]^n} \quad (8)$$

where K_{BiOH} is the dissociation constant for BiOH^+ .

If we use equation (8) to express equality (6) we obtain the following expression for the stability constant of the

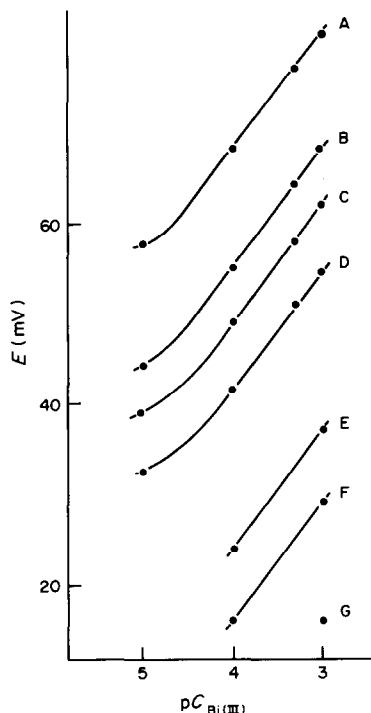


Fig. 1. The dependence of the electrode potential on $pC_{\text{Bi(III)}}$ in solutions containing citric acid at various concentrations.

Curve	A	B	C	D	E	F	G
C_{Cit}, M	0.02	0.06	0.10	0.20	0.20	0.20	0.20
pH	4.0	4.0	4.0	4.0	4.4	4.6	5.0

complex in question:

$$\beta_n = \frac{f_{\text{Bi}^{3+(1)}} C_{\text{Bi(III)(1)}} \left(1 + \frac{[\text{OH}^-]}{K_{\text{BiOH}}(2)}\right) - f_{\text{Bi}^{3+(2)}} C_{\text{Bi(III)(2)}} \left(1 + \frac{[\text{OH}^-]}{K_{\text{BiOH}}(1)}\right)}{f_{\text{Bi}^{3+(2)}} C_{\text{Bi(III)(2)}} [\text{L}^{p-}]_{(1)}^n - f_{\text{Bi}^{3+(1)}} C_{\text{Bi(III)(1)}} [\text{L}^{p-}]_{(2)}^n} \quad (9)$$

RESULTS

Composition of the complexes

To determine the composition of the Bi-Cit and Bi-Mal complexes, the dependence of the electrode potential on $pC_{\text{Bi(III)}}$ was found for solutions having identical pH but varied citric or malic acid concentration.

From the shift of the response curves at fixed pH (as shown in Fig. 1 for the citric acid system) the dependence of $\log a_{\text{Bi}^{3+(1)}}/a_{\text{Bi}^{3+(2)}}$ on $\log [\text{L}^{p-}]_{(2)}/[\text{L}^{p-}]_{(1)}$ was calculated. Corresponding response curves are obtained for the malic acid system. Figure 2 shows that the slopes of the graphs were 2.04 for the citrate system and 2.95 for the malate system, suggesting that the $\text{Bi}(\text{Cit})_2^{3-2p}$ and $\text{Bi}(\text{Mal})_3^{3-3p}$ complexes are formed.

Determination of the acid form in the complex

The electrode potential was measured in bismuth solutions having the same total concentration of citrate or malate but various pH values (as shown in Fig. 1 for the citric acid system; the malic acid system

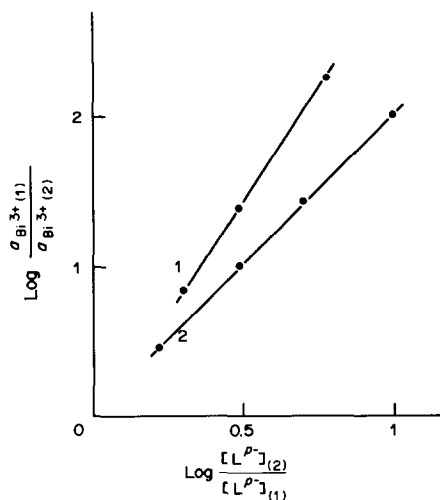


Fig. 2. The dependence of $\log a_{\text{Bi}^{3+(1)}}/a_{\text{Bi}^{3+(2)}}$ on $\log [\text{L}^{p-}]_{(1)}/[\text{L}^{p-}]_{(2)}$ for bismuth complexes with (1) malic acid and (2) citric acid.

behaves analogously). The decrease in electrode potential with increase in pH indicates decrease in Bi^{3+} activity, which must be caused by increase in concentration of the complexing species. Hence the acid forms taking part in the complexation are those which increase in concentration with pH. Therefore H_3Cit , H_2Cit^- , H_2Mal and HMal^- can be excluded because their concentration decreases with increase in pH. For the other acid forms the dependence of

$\log a_{\text{Bi}^{3+(1)}}/a_{\text{Bi}^{3+(2)}}$ on $\log [\text{L}^{p-}]_{(2)}/[\text{L}^{p-}]_{(1)}$ was calculated as before but for the concentrations of the particular acid forms at the pH values used. The slopes were the same as those obtained in determining the composition only for the forms Cit^{3-} ($n = 1.87$) and Mal^{2-} ($n = 2.89$). We conclude that the complexes formed are $[\text{Bi}(\text{Cit}^{3-})_2]^{3-}$ and $[\text{Bi}(\text{Mal}^{2-})_3]^{3-}$.

Stability constants

Stability constant values were calculated from equation (9) and the electrode potential measurements. The activity coefficients were calculated

Table 1. Stability constants found

$\beta_{\text{Bi}(\text{Cit})_2^{3-}}$	$\beta_{\text{Bi}(\text{Mal})_3^{3-}}$
6.3×10^{13}	1.2×10^{10}
3.2×10^{13}	1.2×10^{10}
3.1×10^{13}	0.7×10^{10}
1.4×10^{13}	0.6×10^{10}
1.2×10^{13}	0.5×10^{10}
Mean = 3×10^{13}	Mean = 8×10^9

according to the formula:

$$\log f = -z^2 \left[\frac{0.51\sqrt{I}}{1 + 1.5\sqrt{I}} - 0.2I \right]$$

where I is the ionic strength. The values obtained are presented in Table 1.

Previous workers have presented different views on the composition of these complexes. For the malic acid complex it has been reported⁵ that at pH = 4.5 $[\text{Bi}(\text{HMal})_3]^{2-}$ is formed. For the citric acid complex $\text{Bi}(\text{Cit})_2^-$ has been reported,⁴ whereas Pingarron Carrazon *et al.*⁶ found a 1:1 complex.

REFERENCES

1. K. L. Cheng, *Talanta*, 1961, **8**, 301.
2. K. Majumdar and M. M. Chakrabarty, *Z. Anal. Chem.*, 1957, **154**, 262.
3. F. Umland, A. Jansen, D. Thierig and G. Wünsch, *Theorie und Praktische Anwendung von Komplexbildnern*, Akademische Verlag, Frankfurt/Main 1971.
4. K. B. Yatsimirskii and Yu. A. Zhukov, *Zh. Neorgan. Khim.*, 1962, **7**, 1583.
5. E. G. Chikryzova and I. M. Vataman, *ibid.*, 1970, **12**, 424.
6. J. M. Pingarron Carrazon, R. Gallego Andreu and P. Sanchez Batanero, *Analisis*, 1984, **12**, 358.
7. W. Szczepaniak and M. Ren, *Talanta*, 1983, **12**, 945.
8. K. Ren and W. Szczepaniak, *Chem. Anal. (Warsaw)*, 1976, **21**, 1365.

SPECTROPHOTOMETRIC DETERMINATION OF CADMIUM WITH 2-(5-CHLORO-2-PYRIDYLAZO)- 5-DIMETHYLAMINOPHENOL

M. VILLARREAL, L. PORTA, E. MARCHEVSKY and R. OLSINA

Departamento de Química Analítica, "Dr. Carlos B. Marone", Universidad Nacional de San Luis,
Chacabuco y Pedernera, 5700 San Luis, Argentina

(Received 22 May 1985. Revised 13 December 1985. Accepted 11 January 1986)

Summary—The reaction between cadmium and 2-(5-chloro-2-pyridylazo)-5-dimethylaminophenol (5-CIDMPAP) in aqueous alcohol media at pH 8.8–10.7 results in an intense violet colour which is stable for at least 8 hr. The composition is 2:1 reagent:metal and the formation constant $(5.29 \pm 0.01) \times 10^{18}$. Beer's law is obeyed up to 1.34 ppm of cadmium at 550 nm. The optimal concentration range (Ringbom) is between 0.16 and 0.72 ppm. The apparent molar absorptivity at 550 nm is $(1.20 \pm 0.01) \times 10^5$ l. mole⁻¹. cm⁻¹, making the sensitivity one of the highest known. The interference due to copper(III), iron(III), cobalt(II), nickel(II), gold(III), zinc(II) and manganese(II) can be suppressed.

From the earlier studies of 5-CIDMPAP as a spectrophotometric reagent and metallochromic indicator,¹⁻⁶ it appeared that it would be suitable for determination of cadmium, for which most of the spectrophotometric methods lack selectivity.

EXPERIMENTAL

Instruments

A Varian 634 double-beam spectrophotometer was used for recording spectra and a Beckman DU spectrophotometer for individual absorbance measurements, with 1.0-cm path-length glass or quartz cells.

Reagents

5-CIDMPAP solution. The reagent was prepared by coupling *m*-dimethylaminophenol with 2-chloropyridyl-diazotate, according to Shibata *et al.*,⁶ and used as a solution in 96% ethanol.

Cadmium solution, $1 \times 10^{-3}M$. The 99.99% pure metal (0.1124 g) was dissolved in approximately 30 ml of hydrochloric acid (1 + 1), by gentle heating. After cooling, the solution was quantitatively transferred to a 1000-ml standard flask and diluted to the mark with doubly distilled water. More dilute solutions were made as required.

Sodium tetraborate solution, 0.1M. Prepared with water free from carbon dioxide, and adjusted to pH 9.2 if necessary.

General procedure

A known volume of sample containing not more than 25 µg of cadmium is put into a 25-ml standard flask, then 2 ml of borate buffer (pH 9.2), 1 ml of 0.02% 5-CIDMPAP solution and 11 ml of 96% ethanol are added. The volume is made up to the mark with distilled water and the solution mixed. The absorbance at 550 nm is measured vs. a reagent blank solution. A calibration graph is obtained as usual.

RESULTS AND DISCUSSION

In aqueous solution, cadmium and 5-CIDMPAP form a sparingly soluble reddish complex. In aqueous ethanol, the complex is formed almost instantaneously

after mixing of the reagents and remains stable for at least 8 hr.

Absorption spectra and effect of pH

The spectrum of the complex shows a red shift of 110 nm for the absorption maximum relative to that of the ligand (550 and 440 nm respectively), with an isobestic point at 480 nm (Fig. 1).

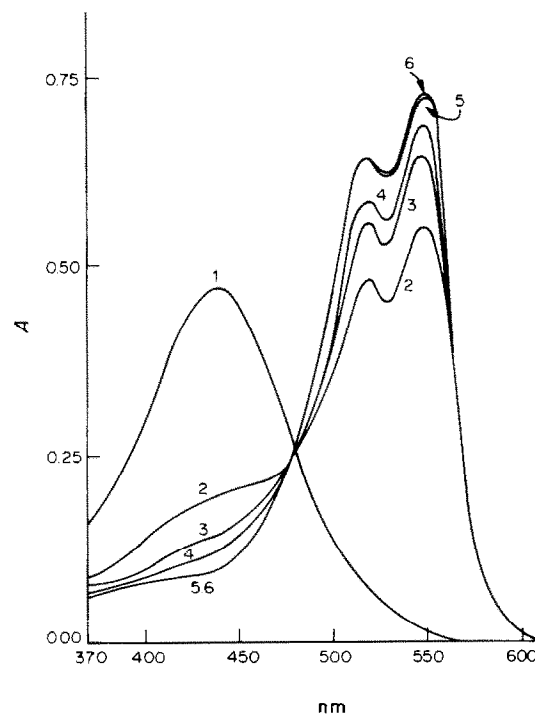


Fig. 1. Absorbance curves of 5-CIDMPAP and its cadmium complex in water-ethanol (50% v/v) solution at pH 9.2. Reagent $1.2 \times 10^{-5}M$; cadmium (1) nil; (2) $4.2 \times 10^{-6}M$; (3) $4.6 \times 10^{-6}M$; (4) $5 \times 10^{-6}M$; (5) $6 \times 10^{-6}M$; (6) $8.4 \times 10^{-6}M$.

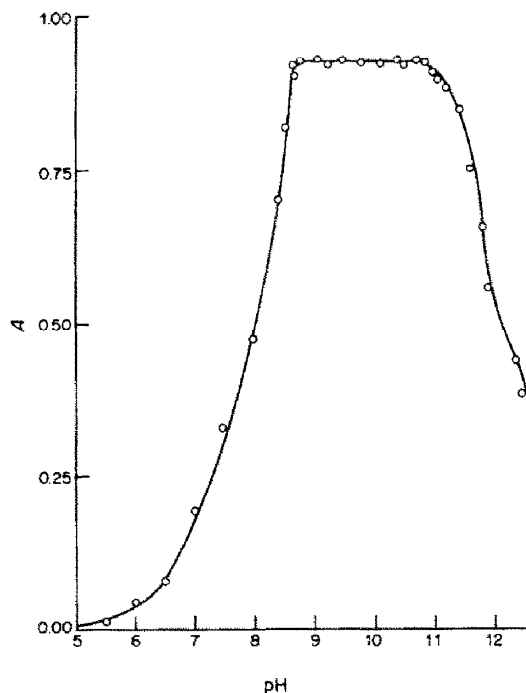


Fig. 2. Effect of pH on the absorbance of the 5-CIDMPAP-cadmium chelate. Reagent $8 \times 10^{-5}M$; cadmium $8 \times 10^{-6}M$ in water-ethanol (50% v/v). Measured vs. reagent blank; 10-mm cells; $\lambda = 550 \text{ nm}$.

The absorption spectrum of the complex in 50% aqueous ethanol was examined at different pH values. Formation of the complex was found to start at pH 5, become maximal at pH between 8.8 and 10.7, and then decrease at higher pH (Fig. 2).

At least 4:1 molar ratio of ligand to cadmium is needed to give practically complete complexation.

Beer's law is obeyed at 550 nm over the cadmium concentration range up to $1.34 \mu\text{g/ml}$ in the final solution measured, the optimum range (Ringbom) being 0.16–0.72 ppm.

Nature of the complex

The continuous-variations⁷ and molar-ratio⁸ methods both showed that a 2:1 ligand-metal complex is

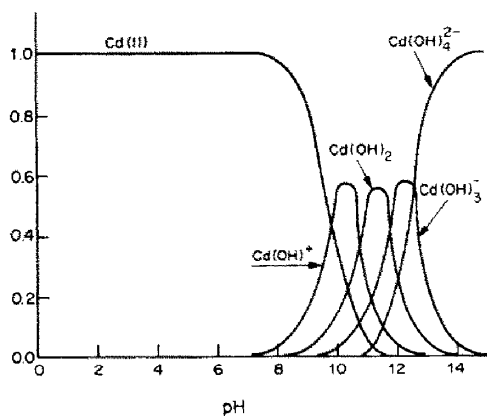


Fig. 3. Normalized cadmium species distribution vs. pH.

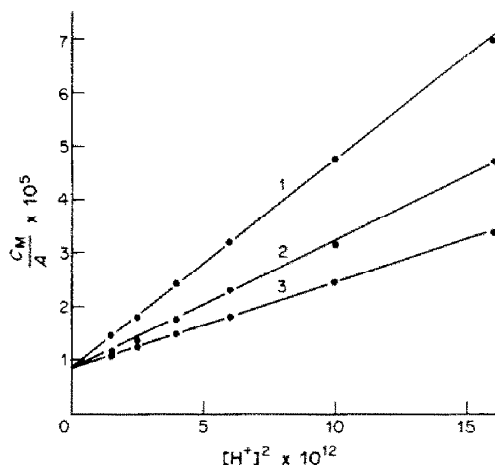
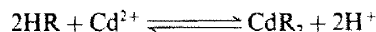


Fig. 4. Betteridge-John plots. C_R/C_{Cd} : (1) 8.3; (2) 10; (3) 13.3; $C_{Cd} = 7.2 \times 10^{-6}M$.

formed. Electrophoretic migration tests showed that the complex is not electrically charged.

Figure 3 shows that Cd^{2+} is the major cadmium species at the pH (9.2) used for the determination, and at that acidity 5-CIDMPAP is present as HR ,⁴ so the chelation reaction should be



To establish the ligand:metal ratio and the number of hydrogen ions involved in the chelation reaction, the Betteridge and John method⁹ was used. Figure 4, used in conjunction with the equation

$$\frac{C_M}{A} = \frac{1}{\epsilon_{ML_2}} + \frac{[\text{H}^+]^2}{K_{ML_2} C_L^2 \epsilon_{ML_2}}$$

shows that the ligand:metal ratio and the number of protons involved were 2:1 and 2, respectively.

Influence of the organic solvent and ionic strength

Because 5-CIDMPAP and its cadmium complex are only sparingly soluble in water, an organic solvent must be added. Methanol, ethanol, acetone and dioxan were tried in different proportions. The molar absorptivities obtained with aqueous methanol or ethanol media do not differ much, and the difference is still less with acetone and dioxan. In all cases, the maximum sensitivity is reached when the organic solvent content is 45–70% v/v. For simplicity and economy 50% v/v aqueous ethanol is recommended.

Change in ionic strength between 0.01 and 0.4 (adjusted with sodium perchlorate) does not affect the absorbance.

Stability constant

The method¹⁰ used to determine the stability constant also allows calculation of the molar absorptivity. The values obtained were $\epsilon = (1.21 \pm 0.01) \times 10^3 \text{ l. mole}^{-1} \cdot \text{cm}^{-1}$ and $K_f = (5.29 \pm 0.01) \times 10^{18}$.

Table 1. Tolerances for some anions in determination of $3.4 \times 10^{-5} M$ Cd

Ion	Molar tolerance ratio (ligand)/(Cd)
Ascorbate acid	10
EDTA	< 1
CH ₃ COO ⁻	1000
Br ⁻	2000
CN ⁻	5
ClO ₃ ⁻	2000
Cl ⁻	2000
F ⁻	1000
PO ₄ ³⁻	< 1
NO ₃ ⁻	2000
C ₂ O ₄ ²⁻	500
SCN ⁻	1000
S ₂ O ₃ ²⁻	5
Tartrate	1000
I ⁻	100

Interferences

These were studied individually, the criterion for interference being a change of $\pm 2\%$ in the absorbance for 20 μg of cadmium, in presence of a 20-fold molar ratio of 5-CIDMPAP.

Table 1 shows the tolerance levels for several anions and masking agents, and Table 2 shows those for cations. EDTA and phosphate interfere at a molar ratio lower than 1:1 with respect to cadmium.

Under the conditions used, gold(III), cobalt(II), nickel(II), copper(II), manganese(II) and zinc(II) not only consume reagent, thus making the cadmium complexation incomplete or even preventing it altogether, but also cause spectral interference.

To increase the tolerances to values compatible with the composition of commonly met samples,

Table 2. Tolerances for some common cations in determination of $7.1 \times 10^{-6} M$ Cd

Ion	Molar tolerance ratio	Error, %
Al(III)	100	+ 1.8*
Mg(II)	200	0
K(I)	10000	0
Na(I)	10000	0
Au(III)	200	+ 1.5†
Mo(VI)	100	+ 1.2
W(IV)	100	0
Li(I)	200	+ 1.6
Ca(II)	3000	0
Sr(II)	2000	0
Ba(II)	2000	0
Pb(II)	10	+ 0.9
Sn(II)	2	+ 2
Sb(III)	1	+ 1.8
Ag(I)	interferes	
Co(II)	1000	+ 0.8*
Ni(II)	1000	+ 1.6*
Cu(II)	1000	+ 1.2*
Fe(III)	1000	+ 1.2*
Mn(II)	1000	+ 1.6*
Zn(II)	50	+ 1.8*

*Prior double extraction from 0.4M HBr with tribenzylamine in dichloroethane.¹¹

†Prior double extraction from 3M HCl with ethyl acetate.¹²

Table 3. Results for Cd in synthetic samples

Sample	Sample composition, %											Cd found %	Std. devn., %	95% Confidence limits, %		
	Co	Ni	Cu	Fe	Mn	Al	Mg	Au	Ca	Sn	Mo				Zn	
1	17.2	6.7	9.2			37.1	21.4					3.2	5.12	5.13	0.02	5.11-5.15
1	37.1	12.8		23.2	13.2	7.0	14.7	75.3	11.8				1.80	1.83	0.02	1.81-1.85
3													2.95	2.94	0.03	2.92-2.96
4		43.3	31.4	11.3					10.2				3.83	3.85	0.02	3.83-3.87
5		62.4				2.7	11.4					21.4	2.07	2.08	0.02	2.06-2.10
6					7.3		16.8	29.3	26.3			19.3	0.95	0.97	0.02	0.95-0.99
7						11.8	73.2			7.6		5.2	1.38	1.40	0.02	1.38-1.42
8	27.6		36.2	17.3	5.2				0.3	11.7			1.64	1.66	0.03	1.63-1.69
9		32.3	16.1	8.3	1.3	39.4							2.61	2.66	0.02	2.64-2.68
10	5.3								79.1	9.2			6.31	6.41	0.05	6.36-6.46

Table 4. Some reagents applied to the spectrophotometric determination of cadmium, and the sensitivities attained

Reagent	λ_{\max} , nm	ϵ , $l. mole^{-1}. cm^{-1}$	Solvent	Ref.
Xylenol Orange	575	2.75×10^4		13
1-(2-Pyridylazo)-2-naphthol	555	4.90×10^4	chloroform	14
Bromobenzothiazolylazocresol	610	4.90×10^4	chloroform	15
Bromobenzothiazole	600	5.76×10^4	xylene	16
5-[Chloro-(2-pyridyl)azo]-2-naphthol	560	7.00×10^4	chloroform	17
4-(2-Pyridylazo) resorcinol	495	8.40×10^4	water	18
Dithizone	520	8.80×10^4	carbon tetrachloride	19
2-[5-Bromo-(2-pyridyl)azo]-5-dimethylaminophenol	555	1.41×10^5	3-Me-1-butanol	20
2-[5-Chloro-(2-pyridyl)azo]-5-dimethylaminophenol	550	1.20×10^5	ethanol-water	this work

several masking agents—cyanide, diethanolamine (DEA), fluoride, oxalate, ascorbic acid, tartaric acid, triethanolamine (TEA)—were tested at their maximum tolerable concentration but were all ineffective. The molar tolerance ratios relative to cadmium are 4000 for DEA and TEA, and 200 for ammonia.

The only recourse seems to be the use of prior separations to remove the interferents.

The interference of gold (III) is partly spectral, but is different in character from that of the other species. Gold(III) is partially reduced by the reagent, a significant proportion of which is thus destroyed, leaving too little to complex all the cadmium. Increasing the 5-CIDMPAP concentration is not the answer, since a number of other difficulties, such as a significant change in the blank, then arise. Fortunately, gold(III), even in relatively high concentrations, can be quantitatively extracted by means of the Yoe and Overholser technique¹² without change in the cadmium concentration. Cobalt(II), nickel, copper (II), iron(III), manganese(II) and zinc can be separated by liquid-liquid extraction according to the method of Vasyutinskii *et al.*,¹¹ with some modifications. The procedure is as follows.

A 20-ml portion of sample solution, containing up to 100 μ g of cadmium, 52 mg of cobalt(II), 52 mg of nickel, 56 mg of copper(II), 49 mg of iron(III), 49 mg of manganese(II) and 29 mg of zinc is mixed with 20 ml of *ca.* 0.8M hydrobromic acid in a 125-ml separatory funnel and shaken for 10 min with 40 ml of 2% tribenzylamine solution in 1,2-dichloroethane. After settling, the phases are separated and 20 ml of the organic phase are shaken with 10 ml of 0.4M hydrobromic acid for 5 min. The organic phase is separated and shaken for 30 min with 20 ml of *ca.* 0.01M sodium tetraborate. The aqueous phase from this final separation is collected and analysed.

APPLICATIONS

The procedure was applied to determination of cadmium in 10 synthetic samples, prepared from analytical grade reagents, and including cations that

could cause interference at the levels used. Table 3 shows the composition of samples and the results obtained.

The method compares favourably in sensitivity with most of the commonly used methods for cadmium except that using the bromo analogue of 5-CIDMPAP, with extraction into 3-methylbutan-1-ol (Table 4).

Acknowledgement—Thanks are due to SUBCYT for financial support, which made it possible to undertake the work.

REFERENCES

1. E. Marchevsky, R. Olsina and C. Marone, *Anal. Asoc. Quim. Argent.*, 1984, **72**, 35.
2. *Idem*, *Anal. Quim. Real Soc. Española de Quimica*, 1984, **80B**, 101.
3. R. Olsina, E. Marchevsky, E. Kamachi and C. Marone, *ibid.*, in the press.
4. R. Olsina, E. Marchevsky and E. Kamachi, *ibid.*, in the press.
5. E. Marchevsky, R. Olsina and C. Marone, *Talanta*, 1985, **32**, 54.
6. S. Shibata, M. Furukawa and K. Toei, *Anal. Chim. Acta*, 1976, **66**, 397.
7. P. Job, *Ann. Chim. Paris*, 1928, **9**, 113.
8. J. H. Yoe and A. L. Jones, *Ind. Eng. Chem., Anal. Ed.*, 1944, **16**, 111.
9. D. Betteridge and D. John, *Analyst*, 1973, **98**, 390.
10. F. Ferretti, R. Olsina and C. Marone, *Anal. Asoc. Quim. Argent.*, 1982, **70**, 501.
11. A. I. Vasyutinskii, N. A. Kisel and E. N. Matveeva, *Zh. Analit. Khim.*, 1968, **23**, 1847.
12. J. H. Yoe and L. G. Overholser, *J. Am. Chem. Soc.*, 1939, **61**, 2058.
13. R. A. Pasechnova and A. Mokhov, *Zh. Analit. Khim.*, 1972, **27**, 2146.
14. S. Shibata, *Anal. Chim. Acta*, 1961, **25**, 348.
15. S. I. Gusev, M. V. Zhakina and I. A. Kozhevnikova, *Zh. Analit. Khim.*, 1971, **26**, 1493.
16. D. A. Drapkina, V. G. Brudz, K. A. Smirnova and N. I. Doroshina, *ibid.*, 1962, **17**, 940.
17. M. Kitano and J. Ubeda, *Nippon Kagaku Zasshi*, 1970, **91**, 760.
18. Z. Marczenko, *Spectrophotometric Determination of Elements*, p. 177. Ellis Horwood, Chichester, 1976.
19. S. Shibata, E. Kamata and R. Nakashima, *Anal. Chim. Acta*, 1976, **82**, 169.

PHOTOMETRIC AND ELECTROCHEMICAL DETECTION OF PURINE AND PYRIMIDINE COMPOUNDS IN REVERSED-PHASE AND ION-EXCHANGE HIGH-PRESSURE LIQUID CHROMATOGRAPHY*

ANNA MARIA GHE†, GIUSEPPE CHIAVARI and JOANIS EVGENIDIS

Istituto Chimico "G. Ciamician" dell'Università, Scuola di Specializzazione in Chimica Analitica,
Via Selmi 2, 40126 Bologna, Italy

(Received 18 February 1985. Revised 10 December 1985. Accepted 11 January 1986)

Summary—An investigation of the optimal conditions for the determination of selected purine and pyrimidine compounds has been made by studying the separation efficiency of reversed-phase columns and ion-exchange columns and comparing the sensitivity of photometric and electrochemical detectors. The combination of ion-exchange HPLC with electrochemical detection proved very good for the separation of electroactive compounds, under the experimental conditions studied. Both types of column allow detection at the picomole level. In general the electrochemical detector appears to be the more sensitive of the two types.

It is well known that various pathological conditions induce in biological fluids (blood, serum, urine) and in cellular extracts, changes of the levels of nucleotides, nucleosides, and the corresponding purine bases,^{1,2} so much so that in recent years such substances have been studied as "biochemical indicators" of various diseases,³ especially those of neoplastic origin.

Many workers have recently tackled the problem of monitoring such substances by means of different techniques, such as HPLC,^{1,3-8} gas chromatography^{9,10} (which requires, however, formation of derivatives of the compounds), and coupled GC-MS.^{11,12}

This study presents an investigation of the HPLC behaviour of 21 purine and pyrimidine compounds (which contain phenol and/or aromatic amino groups, which are potentially liable to electrochemical oxidation),¹³⁻¹⁸ in both reversed-phase chromatography (RPLC) and ion-exchange chromatography (IEC). The feasibility of utilizing the electrochemical detector (ECD) (which has been found useful in determination of uric acid¹⁹) with both types of column has been verified for the whole series of compounds investigated.

EXPERIMENTAL

Apparatus and reagents

A Hewlett-Packard Model 1010A liquid isochromatograph with a Rheodyne 7120 sample injector (20- μ l sample loop), was used.

The detectors were (a) a Hewlett-Packard Model 1032 ultraviolet detector operating at 254 nm, and (b) a Metrohm Model 656 electrochemical detector equipped with a three-

electrode detection cell (Model EA 1096/2) with an internal volume of $\sim 1.3 \mu$ l. The working and auxiliary electrodes were made of glassy carbon; the reference electrode was an Ag/AgCl system. The surface of the working electrode was renewed every day by mechanical polishing with alumina powder (0.3 μ m). A Metrohm VA 641 potentiostat was employed and the detector output was displayed on a Houston Omniscribe recorder and on a C-R, A Shimadzu data processor.

The reversed-phase and anion-exchange columns were: (a) Hibar Merck (Lichrosorb RP₁₈) 10 μ m, 250 \times 4 mm, and (b) Partisil-Whatman (SAX 10), 10 μ m, 250 \times 4.6 mm, respectively.

The following eluents were used: (A) KH₂PO₄ (0.01M) and methanol (95/5 v/v), buffered at pH 4.00 with 2.2M formic acid; and (B) KH₂PO₄ (0.02M) and methanol (80/20 v/v), buffered at pH 5.8 with 0.5M potassium hydroxide, for use with reversed-phase chromatography, and (C) KH₂PO₄ (0.01M) and acetonitrile (90/10 v/v), adjusted to pH 3.3 with 0.5M sulphuric acid, for use with ion-exchange columns.

The pH values desired were obtained by addition of acid or base to the buffer solution, followed by adjustment of the phase-volume ratio by addition of the necessary volume of the organic component. The pH values were measured to ± 0.01 with an Orion Research Model 201 pH-meter.

The solvents (HPLC grade) and other chemicals (RPE grade) used in preparation of the eluents, were obtained from Carlo Erba. The standard purine and pyrimidine compounds were supplied by Sigma Chemical Co., and were of the highest purity available: their standard solutions ($1 \times 10^{-5}M$ and $1 \times 10^{-4}M$) were prepared daily, with the chromatographic eluent as solvent. As a biological model sample a human serum sample pooled from 20 donors was supplied by the "Istituto di Clinica Medica III" of the University of Bologna.

The test sample was prepared¹⁹ by adding 2 ml of 10% trichloroacetic acid solution dropwise to 1 ml of pooled serum with vortex mixing at moderate speed. The vortex mixing was continued for 5 min, then the sample was allowed to stand for 2 hr at 4°. The solution was then centrifuged for 15 min at 700 rpm to separate the cell proteins. The clear supernatant fluid was filtered through a plastic Millipore filter (Swinnex 25) and 10 μ l of filtrate were injected for HPLC analysis.

*Work supported by the National Research Council (Rome, Italy), grant no. 83.00231.03.

†Author to whom correspondence should be addressed.

Table 1. Capacity factors (k')† for purines and nucleosides (20 μ l of $1 \times 10^{-4}M$ solution) on a reversed-phase column (Hibar RP18), with eluents (A) and (B) of different polarity, and on an anion-exchange column (Partisil-Whatman SAX 10) with eluent (C), at flow-rate 2 ml/min

Substance	k'		
	Eluent (A)	Eluent (B)	Eluent (C)
1 Uracil	0.40		0.14
2 Uridine	0.89		0.58
3 *Uric acid	1.05		1.50
4 Hypoxanthine	1.33		0.99
5 *Xanthine	1.44		0.56
6 *Guanine	1.83		3.44
7 Cytosine	1.89		11.3
8 Thymine	1.94		0.06
9 Cytidine	2.11		15.7
10 Inosine	2.33		1.42
11 Allopurinol	2.78		0.14
12 *Guanosine	2.94		2.78
13 Thymidine	4.17		0.14
14 *Xanthosine	4.28		1.11
15 Purine	6.33		0.92
16 Adenosine	—	1.55	2.31
17 *Adenine	15.1	1.75	5.36
18 Theobromine	16.7	2.45	0.14
19 *Theophylline	31.2	3.95	0.06
20 Caffeine	—	10.5	0.03
21 *6-N-Dimethylaminopurine	—	16.8	2.06

† $k' = (T_R - T_{R_0})/T_{R_0}$, where T_R = retention time of the component investigated and T_{R_0} = retention time of a component not retained.

*The asterisk denotes the compounds which can be detected both photometrically and electrochemically.

All experiments were done at room temperature. Each experimental datum used was the mean of at least five consistent measurements.

RESULTS AND DISCUSSION

A series of 21 compounds of the type described was studied by means of both detectors and both types of column, with eluents (A) and (B) for the reversed-phase chromatography and eluent (C) for the ion-exchange chromatography. The choice of eluents resulted from an experimental investigation involving a series of eluents differing in the content and type of organic solvent, and met the criterion of maximum separation among the large number of compounds simultaneously present. The optimal isocratic separation conditions were investigated, since the gradient technique is not applicable when the electrochemical detector is used, because of noise in the signal (see, *e.g.*, Lores *et al.*²⁰).

The capacity factors (k') of the substances, individually determined, are listed in Table 1 along with the experimental conditions. Asterisks mark the compounds which give a response with both detectors.

Reversed-phase chromatography

The data reported in Table 1 are in line with those expected on the basis of the solvophobic theory, the more hydrophobic components showing longer retention times. Several pairs of compounds are not separable, because their k' values are excessively close. In the experimental conditions explored, the

electrochemical detector shows positive responses for oxidation for only eight of the compounds examined.

The purine bases and the nucleosides substituted with easily oxidizable groups (such as $-\text{NH}_2$; $-\text{OH}$; $-\text{NR}_2$) at position 6 of the ring, and with the $\equiv\text{NH}$ group in position 7 unaltered, were found to be electroactive.

Figure 1 presents the separation obtained by reversed-phase HPLC [eluent (A), short retention times], with electrochemical detection, for a mixture of 4 electroactive compounds.

Figures 2 and 3 illustrate the response (current *vs.* applied potential) of the first five electroactive compounds separated by use of eluent (A), and of the remaining three compounds, characterized by higher retention times, separable through the use of eluent (B).

A glance at Fig. 2 shows immediately that uric acid can be determined at a much lower potential than that of the other purines studied. Indeed it is the only compound, under our experimental conditions, which gives a response at the electrochemical detector at potentials lower than +0.75 V and down to +0.55 V (*vs.* Ag/AgCl). This fact singles out its determination as immune from separation problems. When the potential range is extended from +0.75 to +0.95 V, xanthine and guanine become detectable in addition to uric acid.

It is clear that the electrochemical detector results are extremely useful in the case of overlapping elution of pairs of species, one of which is electro-

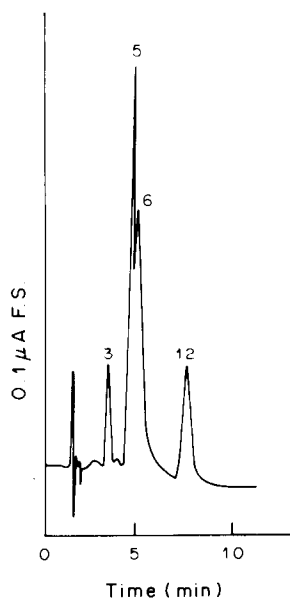


Fig. 1. Separation of bases and nucleosides on Hibar RP18 column: 20 μ l of solution ($1 \times 10^{-5}M$ in each solute, corresponding to 0.2 nmole of each solute); eluent (A); flow-rate 2 ml/min; electrochemical detector (oxidation potential +1.10 V vs. Ag/AgCl); 3 = uric acid; 5 = xanthine; 6 = guanine; 12 = guanosine.

active. Such is the case for the pairs uridine-uric acid*; hypoxanthine-xanthine*; cytosine-guanine*; thymine-guanine*; allopurinol-guanosine*; thymidine-xanthosine*; adenosine-adenine* (see Table 1); the electroactive component is indicated above by an asterisk and is readily detected electrochemically, even at very low concentration, when present in an unresolved composite peak.

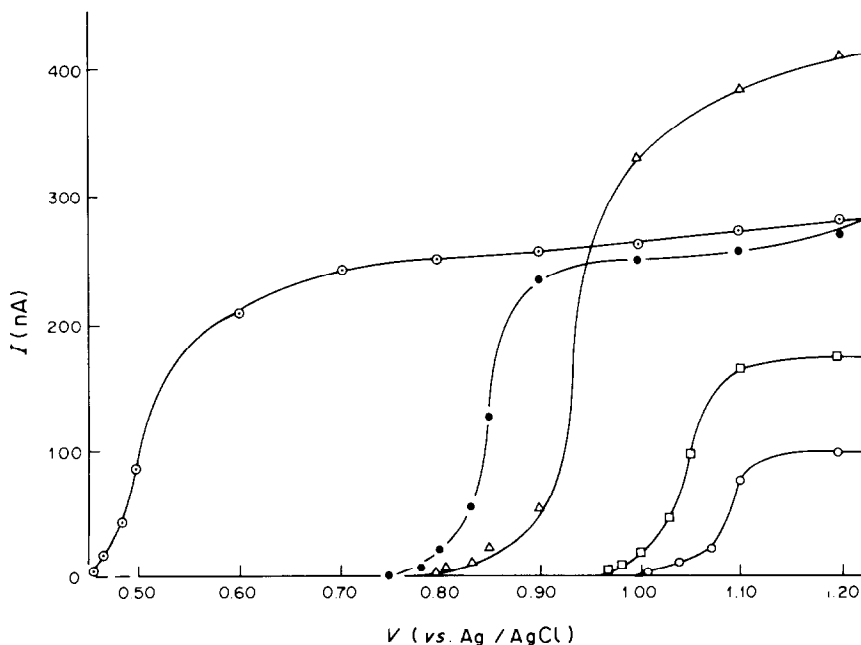


Fig. 2. Dependence of electrochemical detector response on applied potential, for 2 nmoles of substance; Hibar RP18 column; eluent (A); flow-rate 2 ml/min; \odot uric acid; \bullet guanine; \triangle xanthine; \square guanosine; \diamond xanthosine.

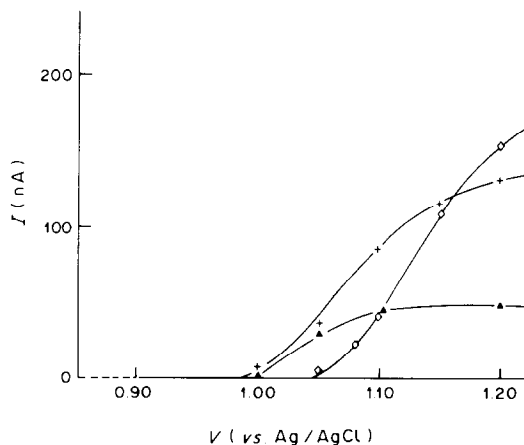


Fig. 3. Relationship between electrochemical detector response and applied potential for 2 nmoles of substance investigated; Hibar RP18 column; eluent (B); flow-rate 2 ml/min; + thiophylline; \blacktriangle 6-N-dimethylaminopurine; \diamond adenine.

Ion-exchange chromatography

The ion-exchange column utilized, in combination with eluent (C), gives the best results, since it allows, in reasonable times, elution of all 21 substances with a single solvent (see Table 1), though theobromine, allopurinol, thymidine and uracil, which have equal k' values, cannot be separated when simultaneously present; not can the purine-hypoxanthine pair be separated.

However, for the thymine-theophylline*, uridine-xanthine* and inosine-uric acid* pairs, the electroactive compound (*) can easily be detected in the unresolved composite peak, by means of the electrochemical detector.

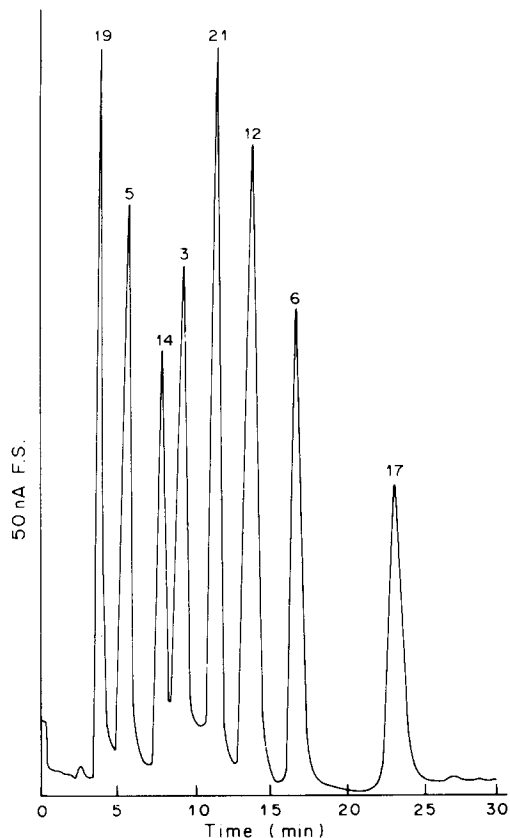


Fig. 4. Ion-exchange HPLC separation of the eight electroactive substances examined, on the SAX 10 column: 20 μ l of solution ($1 \times 10^{-5} M$ in each solute, corresponding to 0.2 nmole of each solute); eluent (C); flow-rate 1 ml/min electrochemical detector (oxidation potential +1.20 V *vs.* Ag/AgCl); 19 = theophylline; 5 = xanthine; 14 = xanthosine; 3 = uric acid; 21 = 6-*N*-dimethylaminopurine; 12 = guanosine; 6 = guanine; 17 = adenine.

Eluent (C) allows the complete separation of all the eight oxidizable substances studied, when they are simultaneously present (Fig. 4).

Figure 5 reports the electrochemical detector responses (current as a function of applied potential) for the eight electroactive substances.

The behaviour closely parallels that observed with the Hibar column, although the characteristic plateau shape is missing, except in the case of uric acid; the difference is reflected in the higher potential values (+1.20 V) necessary for good responses to be obtained.

Lower limits of detection

The detection limits have been determined with both types of column for the eight substances amenable to both types of detector, in order to assess the relative sensitivities. The results are reported in Table 2.

The values were obtained from injection of 20- μ l samples of solutions of decreasing concentration, made from a single standard solution, the criterion for acceptability being a signal/noise ratio of at least 4/1.

The results show that the electrochemical detector is from 2 to 10 times more sensitive than the photometric detector.

Selective determination of uric acid in pooled human serum

The uric acid was determined in 10 μ l of the pooled sample of human serum (deproteinated as described above) with the SAX 10 column [eluent (C), electrochemical detection at +0.70 V *vs.* Ag/AgCl]. The peak obtained had the same retention time as a

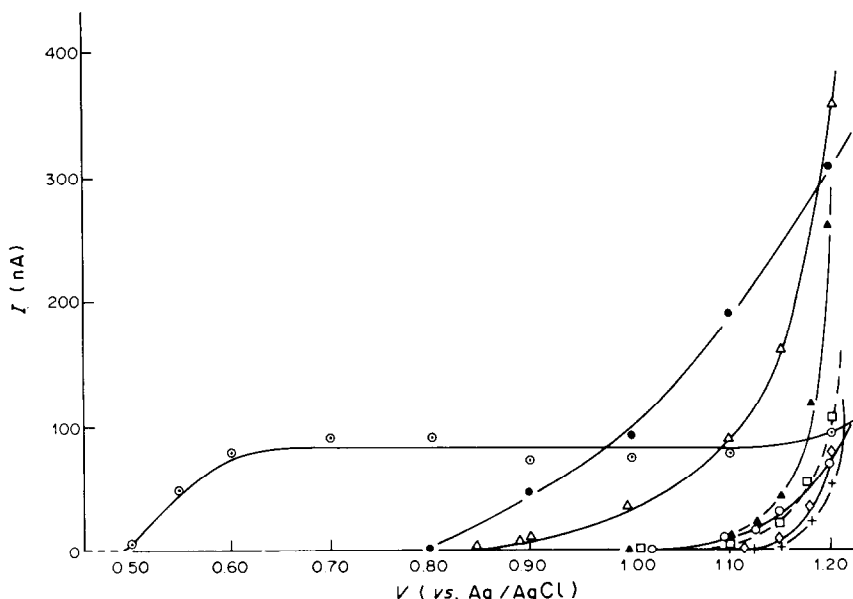


Fig. 5. Dependence of electrochemical detector response on applied potential for 2 nmole of substance investigated: SAX 10 column; eluent (C); flow-rate 1 ml/min; electrochemical detector; \odot uric acid; \bullet guanine; \triangle xanthine; \blacktriangle 6-*N*-dimethylaminopurine; \square guanosine; \circ xanthosine; \diamond adenine; + theophylline.

Table 2. Detection limits on Hibar RP18 and SAX 10 columns, for the eight substances responding to both detection techniques

Substance	Lower limits of determination, <i>pmole</i>			
	Reversed-phase* (Hibar RP18)		Ion exchange† (Sax 10)	
	ECD§	UV‡	ECD§	UV‡
Uric acid	2	10	10	20
Xanthine	2	10	10	20
Guanine	2	10	1	10
Guanosine	10	20	2	10
Xanthosine	10	20	2	10
Adenine	2	10	2	10
Theophylline	10	20	N.R. #	
6- <i>N</i> -Dimethylaminopurine	20	100	10	10

*Flow-rate 2 ml/min; eluents (A) and (B).

†Flow-rate 1 ml/min; eluent (C).

§Oxidation potential = +1.20 V vs. Ag/AgCl.

‡ $\lambda = 254$ nm.

The value is not reported, owing to the excessively low k' value.

standard solution of uric acid under the same experimental conditions.

A further check was made by adding known micro-quantities of uric acid to samples of the same pooled serum, and observing the regular increase of the peak. The addition to a similar sample, in the same experimental conditions, of known quantities of xanthine, guanine and adenine, did not produce any new peak, showing the good selectivity of the method.

The determination of uric acid was done by the method of standard additions.²¹ The results obtained from various portions of the pooled serum (each result being the average of ten determinations) were found to agree within $\pm 2\%$ with the results obtained by the photometric enzymatic uricase method²² for the same samples, and similarly averaged.

CONCLUSIONS

The combination of the ion-exchange column and eluent (C) shows good separation efficiency for the group of substances examined, since it allows, with a single solvent, the isocratic elution of all the compounds, with reasonable retention times, and affords complete separation of the eight electroactive substances.

The electrochemical detector, whenever applicable, gives a higher sensitivity than the photometric detector. It also affords the possibility of a selective response for an electroactive substance giving a peak overlapping those of non-active species.

The separation of electroactive compounds and their determination is satisfactory down to the picomole range.

For determination of uric acid in human serum, the method gives results comparable with those obtained by means of traditional methods. In general, reversed-phase HPLC is most often utilized for separation of purine and pyrimidine compounds because, in combination with photometric detection, it allows

use of a gradient elution system. However, for determination of electroactive purine bases and nucleosides, it appears from the data reported (Figs. 1 and 4; Table 1), that an ion-exchange column and electrochemical detection will give better performance.

Acknowledgements—The authors are grateful to CNR (Roma, Italy) for financial support. They also express thanks to the "Istituto di Clinica Medica III" of the University of Bologna for the samples of human serum kindly supplied.

REFERENCES

1. R. A. Hartwick and R. P. Brown, *J. Chromatog.*, 1976, **126**, 769.
2. P. R. Brown, A. M. Krstulovich and R. A. Hartwick, *J. Clin. Chem. Biochem.*, 1976, **14**, 282.
3. R. A. Hartwick and P. R. Brown, *J. Chromatog.*, 1977, **143**, 383.
4. H. K. Webster and J. M. Whuan, *ibid.*, 1981, **209**, 283.
5. J. C. Kraak, Chu Xuân Ahn and J. Fraanje, *ibid.*, 1981, **209**, 369.
6. M. Ryba and J. Beránek, *ibid.*, 1981, **211**, 337.
7. C. W. Gehrke, K. C. Kuo and R. W. Zumwalt, *ibid.*, 1980, **188**, 129.
8. M. Zakaria, P. R. Brown and E. Grushka, *Anal. Chem.*, 1983, **55**, 457.
9. C. F. Gelijkens, D. L. Smith and J. A. McCloskey, *J. Chromatog.*, 1981, **225**, 291.
10. M. A. Quilliam and J. B. Westmore, *Anal. Chem.*, 1978, **50**, 59.
11. K. Kamei and A. Momose, *Chem. Pharm. Bull.*, 1973, **21**, 1228.
12. H. Miyazaki, Y. Matsunaga, L. Yoshida, S. Arakawa and M. Hashimoto, *J. Chromatog.*, 1983, **274**, 75.
13. D. J. Green and R. L. Perlman, *Clin. Chim.*, 1980, **26**, 797.
14. A. M. Krstulovich, L. M. Bertani-Dziedzic and S. E. Gitlow, *J. Chromatog.*, 1979, **164**, 363.
15. T. Iwamoto, M. Yoshiura and K. Iriyama, *J. Chromatog. Biomed. Appl.*, 1983, **278**, 156.
16. G. Chiavari, V. Concialini and P. Vitali, *J. Chromatog.*, 1982, **249**, 385.
17. V. Concialini, G. Chiavari and P. Vitali, *ibid.*, 1983, **258**, 244.
18. R. J. Henderson Jr. and C. A. Griffin, *ibid.*, 1984, **298**, 231.

19. A. M. Krstulovic, P. R. Brown and D. M. Rosie, *Anal. Chem.*, 1977, **49**, 2237.
20. E. M. Lores, T. R. Edgerton and R. F. Moseman, *J. Chromatog. Sci.*, 1981, **19**, 466.
21. L. A. Pachla, P. T. Kissinger, L. Yu, F. Watson, D. Pragay, M. E. Chilcote, L. M. Weiner and B. R. Romick, *Clin. Chem.*, 1979, **25**, 1847.
22. P. Fossati, L. Prencipe and G. Berti, *ibid.*, 1980, **26**, 227.

COMPORTEMENT ELECTROCHIMIQUE DU TETRAOXYDE DE DIAZOTE DANS LE SULFOLANE

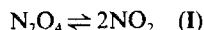
A. BOUGHRIET, M. WARTEL* et J. C. FISCHER

Laboratoire de Chimie Analytique et Marine, Université des Sciences et Techniques de Lille,
Batiment C_x, 59655 Villeneuve d'Ascq, France

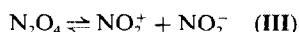
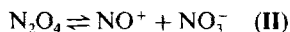
(Reçu le 24 octobre 1985. Accepté le 7 janvier 1986)

Résumé—Les propriétés électrochimiques de N₂O₄ en solution dans le sulfolane anhydre et désoxygéné ont été étudiées à l'aide de la voltammétrie linéaire et cyclique sur électrode de platine poli. L'espèce N₂O₄ s'oxyde selon la réaction $N_2O_4 \rightleftharpoons 2NO_2^+ + 2e^-$, et se réduit en deux étapes: $NO_2 + N_2O_4 + e^- \rightleftharpoons N_2O_3 + NO_2^-$ (1ère étape); $3N_2O_4 + 2e^- \rightleftharpoons 2N_2O_3 + 2NO_2^-$, $N_2O_4 + e^- \rightleftharpoons NO + NO_2^-$, $2N_2O_3 + e^- \rightleftharpoons 3NO + NO_2^-$ (2ème étape). En présence de traces d'eau, l'allure des courbes $i = f(E)$ se complique par l'intervention de deux vagues cathodiques et une vague anodique supplémentaires. Ce phénomène s'explique par la formation des espèces électroactives N₂O₃, HNO₃ et HNO₂ produites lors de la dismutation de N₂O₄ selon $N_2O_4 + H_2O \rightleftharpoons HNO_2 + HNO_3$, suivie de la réaction $HNO_2 + N_2O_4 \rightleftharpoons N_2O_3 + HNO_3$. Les potentiels normaux intervenant au cours de ces processus électrochimiques sont discutés et évalués.

Si en phase gaz,¹ N₂O₄ se dissocie selon



en solution dans un solvant organique, d'autres équilibres hétérolytiques interviennent:



L'équilibre (I) a été étudié par Redmond et Wayland² dans divers solvants organiques par la technique R.M.N; ces auteurs ont remarqué que cette dissociation est faible (dans l'acétonitrile $K_{N_2O_4}^h = 0,30 \cdot 10^{-4}$ à 25°). L'équilibre (II) a été étudié par Cauquis et Serve dans le nitrométhane,^{3,4} et par Bontempelli⁵ dans l'acétonitrile (étude de la réduction des solutions de N₂O₄ sur électrode de platine). La complexité des phénomènes dus à l'eau résiduelle, n'a pas permis à ces auteurs d'atteindre les constantes d'équilibres correspondantes.

Connaissant les valeurs des constantes d'équilibre (I), (II) et (III) dans le sulfolane, que nous avons déterminées à l'aide de techniques électrochimiques et spectroscopique (R.P.E.),^{6,7} nous avons repris l'étude électrochimique de N₂O₄ (sur l'électrode de platine poli) dans ce solvant, où l'impureté "eau" est facilement éliminée. Un mécanisme général des propriétés oxydo-réductrices de N₂O₄ en milieu aprotique sera proposé. Nous évaluerons ensuite l'influence de l'eau sur le comportement électrochimique des solutions de N₂O₄. Les potentiels normaux des couples électrochimiques intervenant lors de la réduction de N₂O₄ seul ou en présence de traces d'eau, seront calculés.

*Auteur pour correspondance.

PARTIE EXPERIMENTALE

La purification du sulfolane a été décrite précédemment⁸ ainsi que la préparation de N₂O₄.⁹ Le perchlorate de tétraéthylammonium (Carlo Erba) est séché à 60° sous pression réduite durant un mois.

Les courbes intensité-potential en régime stationnaire ont été tracés à $30 \pm 1^\circ$ à l'aide d'un ensemble voltampérométrique Tacussel. La vitesse de l'électrode indicatrice de platine (diamètre 0,8 mm) est de 10 tours/sec. La vitesse de balayage des potentiels est de 5 mV/sec. La voltammétrie cyclique a été réalisée à l'aide de la même électrode.

L'électrode de référence est constitué par un fil d'argent plongeant dans une solution de AgClO₄ (0,1M) reliée à la cellule de mesure par un pont rempli d'une solution de (C₂H₅)₄NClO₄ (0,1M). Le potentiel de demi-vague du système ferrocène-ferrocinium est pris comme origine de l'échelle de potentiel.

Toutes les manipulations sont effectuées en boîte à gants. Le dosage de l'eau est effectué par la méthode Karl Fischer (réactif généré par coulométrie¹⁰) après avoir tracé le domaine d'électroactivité du solvant.

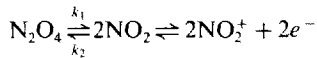
RESULTATS ET DISCUSSION

Etude des propriétés oxydo-réductrices des solutions de N₂O₄ de teneur en eau très faible

L'étude électrochimique de N₂O₄ sur électrode de platine poli a été effectuée dans le sulfolane, en présence de perchlorate de tétraéthylammonium 0,1M à 30°. Pour des teneurs en eau très faibles (de l'ordre de 1 ppm), la courbe $i = f(E)$ (Fig. 1) présente une vague anodique (A) mal résolue, et deux vagues cathodiques très rapprochées: l'une de faible amplitude (B) et l'autre mal définie (C).

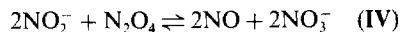
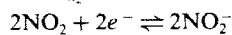
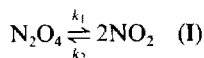
Oxydation des solutions de N₂O₄. La vague anodique (A) apparaît à des potentiels anodiques très élevés $E_{1/2} \approx +1,55$ V par rapport au potentiel de demi-vague du système ferrocène/ferrocinium, et pour une concentration $[N_2O_4] = 5,4 \cdot 10^{-3} M$ à 30°. Une

étude détaillée de cette vague a montré qu'il s'agit de l'oxydation de NO_2 provenant de la dissociation homolytique de N_2O_4 ($K_{\text{N}_2\text{O}_4}^h = [\text{NO}_2]^2/[\text{N}_2\text{O}_4] = 1,43 \cdot 10^{-5}$ à 30°) selon le mécanisme réactionnel:^{7,11}



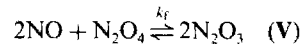
Ce processus électrochimique est contrôlé par la constante cinétique de monomérisation k_1 . L'expression mathématique du courant cinétique nous a permis d'atteindre les constantes cinétiques k_1 et k_2 de la réaction (I).⁷ Le mécanisme de l'oxydation de N_2O_4 dans le sulfolane a ensuite été généralisé à d'autres solvants aprotioniques: nitrométhane, acétonitrile, carbonate de propylène. Les valeurs des potentiels $E_{1/2}$ relevées sur la vague anodique de N_2O_4 en solution dans ces solvants, sont reportées dans le Tableau 1.

Réduction des solutions de N_2O_4 . La vague cathodique (B) (Fig. 1) de faible amplitude et située à $E_{1/2} \simeq +0,58$ V par rapport au potentiel $E_{1/2}$ du système ferrocène/ferricinium, ne dépend pas linéairement de la concentration. Son courant limite n'est pas contrôlé par la diffusion. Une étude en fonction de la température a montré que cette vague présente un caractère cinétique: son coefficient de température est supérieur à 3%. La hauteur de cette vague est légèrement inférieure à celle de l'oxydation de N_2O_4 [vague (A), Fig. 1]. De plus, une voltammétrie cyclique sur cette vague montre que l'oxydation des produits formés lors de ce processus de réduction correspond à celle de N_2O_3 en présence de nitrate. Pour interpréter la vague (B), nous proposons le schéma suivant:

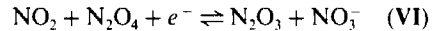


L'oxyde nitrique réagit avec N_2O_4 en excès pour donner le trioxyde de diazote. Comme N_2O_4 est en excès, on peut admettre que la réaction est pratiquement totale. Rappelons que la constante de dissociation moléculaire de N_2O_3 dans le sulfolane est égale à $K_{\text{N}_2\text{O}_3}^m = [\text{NO}]^2[\text{N}_2\text{O}_4]/[\text{N}_2\text{O}_3]^2 = 4,4 \cdot 10^{-5}$ à

30° ,⁶ et la constante cinétique k_1 de formation de N_2O_3 est relativement importante:^{13, 15}



soit globalement:



Cette réaction est en accord avec l'invariance du potentiel de demi-vague avec la concentration. Le système (VI) est limité en partie par la réaction (I) de monomérisation de N_2O_4 [comme dans le cas de l'oxydation de N_2O_4 :⁷ vague (A), Fig. 1], et éventuellement par la réaction d'oxydo-réduction (IV). Nous avons voulu comparer le potentiel théorique de demi-vague avec sa valeur expérimentale obtenue précédemment. Le potentiel normal du couple (VI) s'exprime par la relation:

$$E^\circ(\text{VI}) = \frac{1}{2} [E^\circ(\text{NO} + \text{NO}_3^-/2\text{NO}_2^-) + E^\circ(\text{NO}^+/\text{NO})] + \frac{2,303RT}{F} [\text{p}K_{\text{N}_2\text{O}_3}^i + \frac{1}{2}\text{p}K_{\text{N}_2\text{O}_4}^h - \frac{1}{2}\text{p}K_{\text{N}_2\text{O}_4}^i]$$

où $K_{\text{N}_2\text{O}_3}^i$ et $K_{\text{N}_2\text{O}_4}^i$ représentent les constantes d'équilibres ioniques de N_2O_3 et N_2O_4 selon $\text{N}_2\text{O}_3 \rightleftharpoons \text{NO}^+ + \text{NO}_2^-$ et $\text{N}_2\text{O}_4 \rightleftharpoons \text{NO}^+ + \text{NO}_3^-$. Dans le sulfolane, ces constantes sont égales à $K_{\text{N}_2\text{O}_3}^i = 10^{-11,2}$ et $K_{\text{N}_2\text{O}_4}^i = 10^{-7,2}$ à 30° .^{6,7} $E^\circ(\text{NO} + \text{NO}_3^-/2\text{NO}_2^-)$ et $E^\circ(\text{NO}^+/\text{NO})$ sont les potentiels normaux des systèmes $\text{NO} + \text{NO}_3^- + e^- \rightleftharpoons 2\text{NO}_2^-$ et $\text{NO}^+ + e^- \rightleftharpoons \text{NO}$, respectivement égaux à $+0,07$ V et $+0,72$ V à 30° .^{13, 15} Le calcul du potentiel normal du couple (VI) donne $E^\circ(\text{VI}) = +0,56 \pm 0,04$ V. Dans l'hypothèse où les coefficients de diffusion des espèces mises en jeu dans le système (VI) sont voisins, on peut assimiler le potentiel de demi-vague au potentiel normal. Nous constatons alors que la valeur expérimentale, $E_{1/2} = +0,58$ V, est en bon accord avec le potentiel normal calculé, $E^\circ(\text{VI}) = +0,56 \pm 0,04$ V.

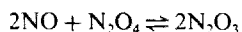
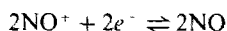
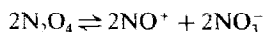
La vague cathodique (C) mal définie et située à un potentiel $E_{1/2}$ moyen $\simeq +0,08$ V pour une concentration $[\text{N}_2\text{O}_4] = 5,4 \cdot 10^{-3}$ M, laisse présager que plusieurs processus électrochimiques interviennent simultanément. De plus, une électrolyse à potentiel imposé ($E_i = -0,47$ V) montre la présence intermédiaire de N_2O_3 (la solution se colore en bleu), puis la formation de NO gazeux, et simultanément la disparition de N_2O_3 . Le nitrate a aussi été caractérisé par la courbe électrochimique réalisée avec cette solution après électrolyse et élimination de NO. Globalement, l'ensemble des deux vagues (B) et (C) correspond à 1 faraday par mole de N_2O_4 . On peut admettre que la réduction de N_2O_4 dans cette étape fait intervenir la dissociation ionique de N_2O_4 en NO^+ et NO_3^- , suivie de la réduction de NO^+ . L'oxyde nitrique NO formé peut ensuite réagir avec N_2O_4 pour conduire à N_2O_3 au moins partiellement. La réduction de N_2O_4 [vague

Tableau 1. Potentiel $E_{1/2}$ de la vague d'oxydation de N_2O_4 dans quelques solvants aprotioniques— $[\text{N}_2\text{O}_4] \simeq 10^{-2}$ M (298 K)

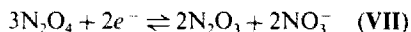
Solvant	$E_{1/2}, V$
Sulfolane	+1,63 +1,56*
Carbonate de propylène	+1,60
Nitrométhane	+2,07
Acétonitrile	+1,82 (Ag ⁺ /Ag 0,01 M) ¹² +1,78 (Ag ⁺ /Ag 0,1 M) +1,74 (Fc ⁺ /Fc)

*Potentiel de demi-vague relevé à 303 K.

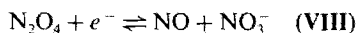
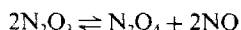
(C)] peut donc s'écrire:



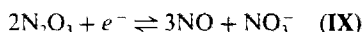
soit globalement:



N₂O₃ étant aussi électroactif, sa réduction intervient à des potentiels un peu plus négatifs. N₂O₃ pouvant être considéré dans notre solvant comme un complexe de NO et N₂O₄, sa réduction peut alors s'écrire:



soit globalement:



Notons qu'en raison de la faible dissociation ionique de N₂O₄ en NO₂⁺ et NO₂⁻ ($K = [\text{NO}_2^+][\text{NO}_2^-]/[\text{N}_2\text{O}_4] = 10^{-22.0}$ à 30° dans le sulfolane⁷), la réaction (III) n'intervient pas lors du processus de réduction de N₂O₄. Cette réduction en plusieurs étapes très proches et mal différenciables expliquerait l'allure de la courbe observée. Afin de confirmer nos hypothèses, nous avons calculé, à l'aide des constantes d'équilibre, les potentiels normaux des couples électrochimiques mis en jeu.

Calcul théorique des potentiels normaux des couples (VII), (VIII) et (IX)

Couple électrochimique (VII): $3\text{N}_2\text{O}_4 + e^- \rightleftharpoons 2\text{N}_2\text{O}_3 + 2\text{NO}_3^-$. On peut facilement exprimer le potentiel normal $E^\circ(\text{VII})$ en fonction de la dissociation

ionique de N₂O₄, $K_{\text{N}_2\text{O}_4}^i$, la constante de dissociation moléculaire de N₂O₃, $K_{\text{N}_2\text{O}_3}^m$, et du potentiel normal du couple NO⁺/NO, $E^\circ(\text{NO}^+/\text{NO})$, selon:

$$E^\circ(\text{VII}) = E^\circ(\text{NO}^+/\text{NO}) + \frac{2,303RT}{F} [\frac{1}{2}pK_{\text{N}_2\text{O}_3}^m - pK_{\text{N}_2\text{O}_4}^i]$$

Le potentiel normal du couple (VII) est donc égal à $+0,42 \pm 0,03$ V.

Couple électrochimique (VIII): $\text{N}_2\text{O}_4 + e^- \rightleftharpoons \text{NO} + \text{NO}_3^-$. Le potentiel normal de la réduction de N₂O₄ s'écrit:

$$E^\circ(\text{VIII}) = E^\circ(\text{NO}^+/\text{NO}) - \frac{2,303RT}{F} pK_{\text{N}_2\text{O}_4}^i = +0,28 \pm 0,02 \text{ V.}$$

Couple électrochimique (IX): $2\text{N}_2\text{O}_3 + e^- \rightleftharpoons 3\text{NO} + \text{NO}_3^-$. Le potentiel normal du système (IX) peut s'exprimer suivant l'équation:

$$E^\circ(\text{IX}) = E^\circ(\text{NO}^+/\text{NO}) + \frac{2,303RT}{F} [pK_{\text{N}_2\text{O}_4}^i - pK_{\text{N}_2\text{O}_3}^m] = +0,01 \pm 0,00 \text{ V.}$$

L'allure de la vague (C) de réduction de N₂O₄ montre qu'à côté des couples (VII) et (IX), il faut aussi tenir compte du couple (VIII). En effet, si seuls (VII) et (IX) interviennent, la vague (C) devrait être divisée en deux vagues distinctes: $E^\circ(\text{VII}) - E^\circ(\text{IX}) = 410$ mV. Au contraire, si le couple (VIII) est envisagé, les différences entre les potentiels normaux sont voisines de 250 mV, et les réactions ne sont plus séparables et donnent donc lieu à

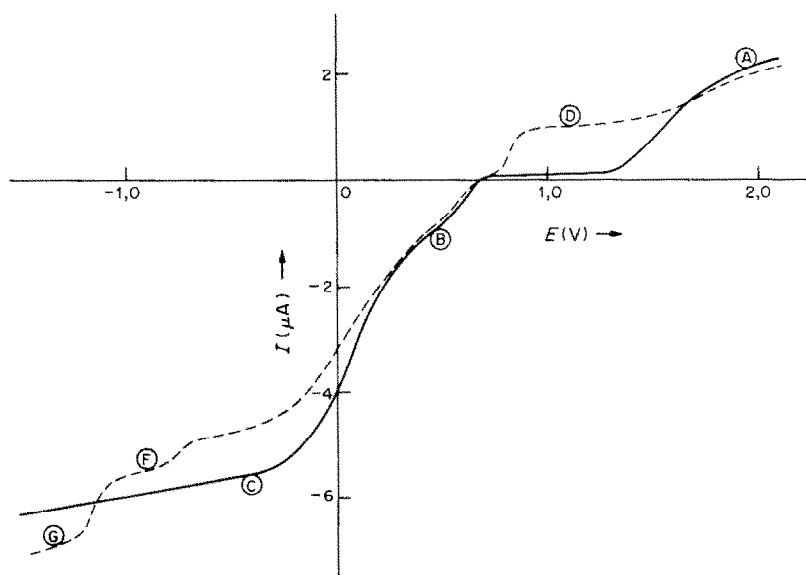


Fig. 1. Courbes intensité-potential relatives aux propriétés oxydo-réductrices de N₂O₄ dans le sulfolane à 30° (électrolyte indifférent: [(C₂H₅)₄NClO₄] = 0,1 M); [N₂O₄] = 5,4 · 10⁻³ M (—); après addition d'eau, [H₂O] = 1,5 · 10⁻³ M (-----).

une vague globale mal définie. Cette intervention du couple (VIII) proviendrait de ce que la réaction (V) entre N_2O_4 et NO n'est pas totale.¹⁴ Un enregistrement de voltammétrie cyclique réalisée avec une solution de N_2O_4 , est en accord avec l'existence de plusieurs systèmes électrochimiques au cours de la réduction de N_2O_4 .

Influence de l'eau dans le processus d'oxydation de N_2O_4

Dans le cas où les solutions de N_2O_4 contiennent des traces d'eau, on observe sur les courbes $i = f(E)$ une vague anodique supplémentaire (D) située à des potentiels moins positifs que l'oxydation de N_2O_4 , $E_{1/2} \approx +0,81$ V (Fig. 1). D'autre part, on constate que cette vague n'est pas contrôlée par la diffusion, sa hauteur augmente cependant avec la concentration d'eau dans le milieu, mais non linéairement, et diminue avec le temps. Un enregistrement de voltammétrie cyclique effectué sur cette vague, est identique à celui obtenu pour une solution de N_2O_3 . Cette formation de N_2O_3 est confirmée par l'apparition d'une coloration bleue lors de l'addition d'eau en quantité voisine de celle de la solution de N_2O_4 . L'apparition de l'espèce N_2O_3 dans le milieu peut s'interpréter selon le schéma:^{7,15}



Un barbotage d'azote décolore cette solution, ce qui confirme la faible stabilité de N_2O_3 et l'élimination de NO de la solution. Cette élimination de NO est responsable de la diminution de la vague d'oxydation au cours du temps (Fig. 2). Remarquons que cette vague n'apparaît pas même après une faible addition d'eau à la solution si on a préalablement ajouté de l'oxygène, le N_2O_3 formé étant alors aussitôt oxydé en N_2O_4 . La formation de N_2O_3 est tributaire des constantes d'équilibres des réactions (X) et (XI). Nous n'avons pas pu déterminer celle correspondante à l'hydrolyse de N_2O_4 en raison du déplacement de l'équilibre au cours du temps, favorisé par l'élimination de NO. Néanmoins, cette constante est modérément déplacée, puisque par addition d'eau, on observe une légère diminution de la vague de réduction de N_2O_4 et apparition simultanée de la vague de réduction de HNO_3 , vague (F) (Fig. 1). La constante d'équilibre de la réaction (XI) a été évaluée:¹⁵

$$K(XI) = 0,25.$$

Influence de l'eau dans le processus de réduction de N_2O_4

En présence d'eau, on constate l'apparition de deux vagues cathodiques supplémentaires (F) et (G) (Fig. 1) situées à des potentiels plus négatifs; nous les avons attribuées à la réduction des deux acides HNO_3 et HNO_2 ¹⁵ (respectivement à $E_{1/2} \approx -0,77$ V et $E_{1/2} \approx -1,15$ V pour un mélange $N_2O_4 + H_2O$ de concentrations $[N_2O_4] = 5,4 \cdot 10^{-3} M$ et $[H_2O] =$

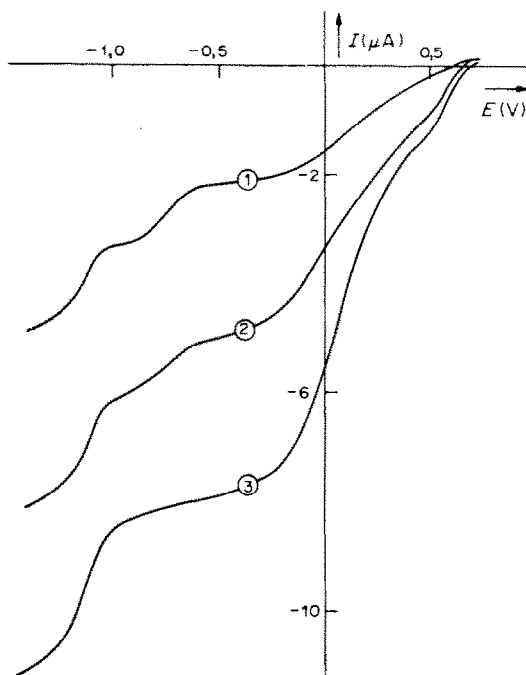
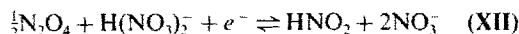


Fig. 2. Faisceau de courbes $i = f(E)$ relatives à la réduction de N_2O_4 en présence d'eau dans le sulfonate à 30° (electrolyte indifférent: $[(C_2H_5)_4NClO_4] = 0,1 M$; $[H_2O] = 1,5 \cdot 10^{-3} M$; (1) $[N_2O_4] = 2,7 \cdot 10^{-3} M$, (2) $5,3 \cdot 10^{-3} M$, (3) $7,9 \cdot 10^{-3} M$).

$1,5 \cdot 10^{-3} M$), ces derniers étant formés en solution par hydrolyse de N_2O_4 suivant la réaction (X). Une électrolyse effectuée sur la vague (C) montre qu'en présence d'eau, cette réduction met en jeu plus d'une mole d'électrons par mole de N_2O_4 (environ 1,1–1,5 e^- par molécule de N_2O_4 selon la teneur en eau dans le milieu), alors que sans eau, nous avons vu que le bilan coulométrique était voisin de 1. D'autre part, la vague (F) attribuée à la réduction de HNO_3 diminue avec une augmentation de la concentration de N_2O_4 , au profit de la vague (G) de réduction de HNO_2 (Fig. 3). Tous ces résultats laissent présager l'intervention dans la deuxième vague d'un autre couple électrochimique (déjà signalé par Serve⁴) en plus des systèmes (VII), (VIII) et (IX):



(le nitrate produit lors des réactions (VI) et (VII) vient complexer l'acide nitrique). Afin de confirmer notre hypothèse, nous avons calculé le potentiel normal E (XII) de ce couple à partir de l'équation:

$$\begin{aligned} E(XII) = & \frac{1}{2}[E(NO^+/NO) \\ & + E'(NO + NO_3^-/2NO_2)] \\ & + \frac{2,303RT}{F} [pK_{HNO_2}^{H^+} - pK_{HNO_3}^{H^+} \\ & - pK_{HNO_3}^{HNO_2} - \frac{1}{2}pK_{N_2O_4}^i] \end{aligned}$$

$K_{HNO_2}^{H^+}$ et $K_{HNO_3}^{H^+}$ représentent les constantes d'acidité de HNO_2 et HNO_3 , respectivement égal à $\sim 20,6$ et

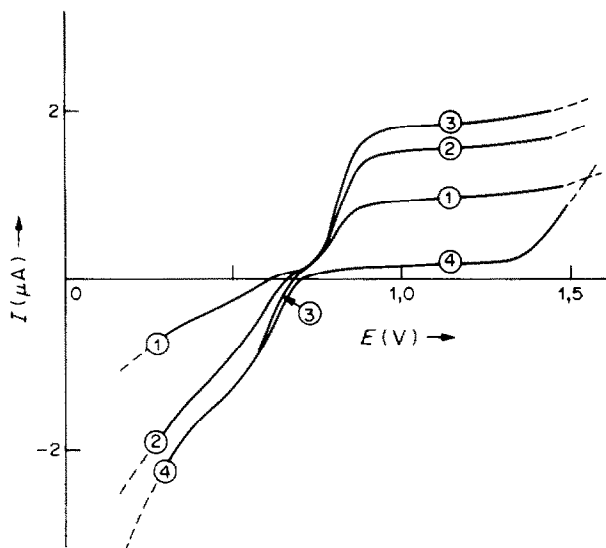
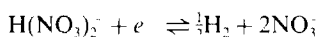
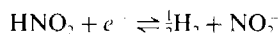


Fig. 3. Courbes intensité-potential de l'oxydation de mélanges N₂O₄ + H₂O dans le sulfolane à 30° (electrolyte indifférent: [(C₂H₅)₄NClO₄] = 0,1M); [H₂O] = 1,5 · 10⁻³M; [N₂O₄] (1) = 2,7 · 10⁻³M; (2) 5,3 · 10⁻³M; (3) 7,9 · 10⁻³M; (4) après 1 hr.

16 à 30°. ^{13,15} $K_{\text{HNO}_3}^{\text{hc}}$ représente la constante d'homoconjugaison de l'acide nitrique selon $\text{H}(\text{NO}_3)_2^- \rightleftharpoons \text{HNO}_3 + \text{NO}_3^-$; $K_{\text{HNO}_3}^{\text{hc}} = [\text{HNO}_3][\text{NO}_3^-] / [\text{H}(\text{NO}_3)_2^-] = 10^{-3}$ à 30°. Le potentiel normal E° (XII) est égal à $+0,27 \pm 0,08$ V. Cette valeur est donc voisine de celle trouvée pour le couple (VIII): $+0,28 \pm 0,02$ V. L'excès de complexe $\text{H}(\text{NO}_3)_2^-$ n'ayant pas réagi dans la vague (C) est responsable de la troisième vague (F):



La quatrième vague (G) est attribuée à la réduction protonique de l'acide nitreux provenant à la fois de l'hydrolyse de N₂O₄ et de la réaction électrochimique (XII):



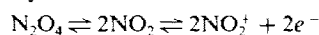
(en faisant l'hypothèse que l'acide nitreux n'est pas complexé par les bases nitrate ou nitrite). Pour des concentrations plus élevées en N₂O₄ (courbes 2 et 3, Fig. 3), la vague de réduction (F) du complexe $\text{H}(\text{NO}_3)_2^-$ disparaît, l'acide nitrique étant totalement consommé par la réaction (XII). Celle correspondant à la réduction de HNO₂ n'augmente plus, étant limitée par la concentration d'eau et par la réaction électrochimique (XII).

Ainsi l'addition d'eau à la solution de N₂O₄ ne modifie pas l'allure de la courbe de réduction de N₂O₄ [vague (C)], puisque le nouveau couple (XII) intervient à un potentiel normal voisin de ceux des couples (VII), (VIII) et (IX) relatifs à la réduction de N₂O₄ seul. Seule la hauteur de la vague est affectée. Nous avons entrepris la même étude dans les solvants aprotiques: acétonitrile, nitrométhane et carbonate de propylène.¹³ Les résultats obtenus dans le sulfolane restent valables dans ces solvants.

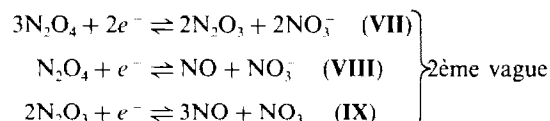
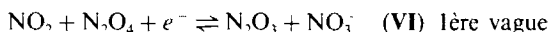
CONCLUSIONS

A l'aide des techniques voltampérométriques, nous avons proposé un mécanisme rendant compte des propriétés oxydo-réductrices du tétraoxyde de diazote, en milieu aprotique, mécanisme complexe que nous avons pu élucider grâce à la connaissance des constantes de dissociations hétérolytiques et homolytiques de N₂O₄, et à l'obtention de solvants de teneurs en eau faibles (de l'ordre du ppm). En absence d'eau, les propriétés oxydo-réductrices peuvent se schématiser:

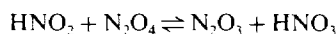
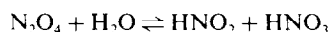
—en oxydation



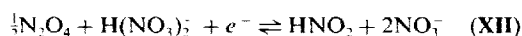
—en réduction



En présence de traces d'eau, ce mécanisme se complique en raison des propriétés électroactives des espèces HNO₃, HNO₂ et N₂O₃ formées par les réactions:



Dans la deuxième vague de réduction de N₂O₄ intervient, en plus des couples (VII), (VIII) et (IX) cités précédemment, une réaction électrochimique supplémentaire:



Les potentiels normaux théoriques des systèmes mis en jeu au cours de la réduction de N₂O₄, ont été

calculés par rapport au potentiel de demi-vague du système ferrocène/ferricinium:

$$E^\circ(\text{VI}) = +0,56 \pm 0,04 \text{ V};$$

$$E^\circ(\text{VII}) = +0,42 \pm 0,03 \text{ V};$$

$$E^\circ(\text{VIII}) = +0,28 \pm 0,02 \text{ V};$$

$$E^\circ(\text{IX}) = +0,01 \pm 0,00 \text{ V};$$

$$E^\circ(\text{XII}) = +0,27 \pm 0,08 \text{ V}.$$

La principale application de ces résultats a été d'expliquer l'effet catalytique apporté par un transfert électronique dans la nitration du naphthalène par une solution de N_2O_4 ou d'un mélange $\text{N}_2\text{O}_4\text{-H}_2\text{O}$.¹⁶

Remerciements—Nous remercions M. B. Trémillon (Professeur à l'Ecole Nationale Supérieure de Chimie de Paris V), ainsi que M. C. P. Andrieux (Directeur de Recherches CNRS à l'Université de Paris VII) pour leurs discussions fructueuses et leurs encouragements.

LITTÉRATURE

1. P. Pascal, *Nouveau Traité de Chimie Minérale*, Tome 10, p. 366, Masson, Paris, 1956.
2. T. F. Redmond et B. B. Wayland, *J. Phys. Chem.*, 1968, **72**, 1626.
3. G. Cauquis et D. Serve, *Compt. Rend.*, 1968, **267C**, 460.
4. D. Serve, *Thèse*, Grenoble, AO 7174, 1972.
5. G. Bontempelli, G. A. Mazzochin et F. Magno, *J. Electroanal. Chem.*, 1974, **55**, 91.
6. A. Boughriet, M. Wartel, J. C. Fischer et Y. Auger, *ibid.*, 1985, **186**, 201.
7. A. Boughriet, M. Wartel, C. Bremard et J. C. Fischer, *ibid.*, 1985, **190**, 103.
8. P. Pierens, Y. Auger, J. C. Fischer et M. Wartel, *Can. J. Chem.*, 1975, **53**, 2989.
9. M. Wartel, A. Boughriet et J. C. Fischer, *Anal. Chim. Acta*, 1979, **110**, 211.
10. J. Bizot, *Bull. Soc. Chim. France*, 1967, **1**, 151.
11. J. C. Fischer, A. Boughriet et M. Wartel, *Talanta*, 1981, **28**, 233.
12. C. L. Perrin, *J. Am. Chem. Soc.*, 1977, **99**, 5516.
13. A. Boughriet, *Thèse*, Lille, 1984.
14. A. Boughriet, A. Coumare, J. C. Fischer et M. Wartel, *J. Electroanal. Chem.*, accepté pour publication.
15. A. Boughriet, J. C. Fischer, G. Leman et M. Wartel, *Bull. Soc. Chim. France*, 1985, **1**, 8.
16. A. Boughriet, C. Bremard, J. C. Fischer et M. Wartel, *Now. J. Chim.*, 1985, **9**, 651.

Summary—Knowing the values of the equilibrium constants corresponding to the reactions $\text{N}_2\text{O}_4 \rightleftharpoons 2\text{NO}_2$ and $\text{N}_2\text{O}_4 \rightleftharpoons \text{NO}^+ + \text{NO}_3^-$ in sulpholane, we have undertaken the electrochemical study of N_2O_4 by means of linear and cyclic voltammetry at the platinum electrode. The N_2O_4 species undergoes one oxidation step $\text{N}_2\text{O}_4 \rightleftharpoons 2\text{NO}_2 \rightleftharpoons 2\text{NO}_2^+ + 2e^-$ and two reduction steps $\text{NO}_2 + \text{N}_2\text{O}_4 + e^- \rightleftharpoons \text{N}_2\text{O}_3 + \text{NO}_3^-$ (1st wave), followed by $3\text{N}_2\text{O}_4 + 2e^- \rightleftharpoons 2\text{N}_2\text{O}_3 + 2\text{NO}_3^-$, $\text{N}_2\text{O}_4 + e^- \rightleftharpoons \text{NO} + \text{NO}_3^-$, $2\text{N}_2\text{O}_3 + e^- \rightleftharpoons 3\text{NO} + \text{NO}_3^-$ (2nd wave). The redox properties of N_2O_4 are complicated by trace quantities of water because of the formation of the electroactive species N_2O_3 , HNO_3 and HNO_2 according to $\text{N}_2\text{O}_4 + \text{H}_2\text{O} \rightleftharpoons \text{HNO}_2 + \text{HNO}_3$ and $\text{N}_2\text{O}_4 + \text{HNO}_2 \rightleftharpoons \text{N}_2\text{O}_3 + \text{HNO}_3$. The standard potentials of the couples concerned have been evaluated and are discussed.

ADSORPTION OF METAL IONS ON ACTIVATED CARBON FROM AQUEOUS SOLUTIONS AT pH 1-13*

HIDEKO KOSHIMA and HIROSHI ONISHI†

University of Tsukuba, Sakura-mura, Ibaraki-ken 305, Japan

(Received 30 September 1985. Revised 21 November 1985. Accepted 7 January 1986)

Summary—Adsorption of microgram amounts of 20 metal species on activated carbon powder from aqueous solutions of pH 1-13 was investigated. The species examined were Cs(I), Y(III), Ce(III), Ti(IV), Zr(IV), Cr(III), Cr(VI), Mn(II), Fe(III), Co(II), Ni(II), Ru(III), Cu(II), Ag(I), Zn(II), Cd(II), Al(III), Pb(II), Sb(III) and Bi(III).

Adsorption of metal chelates on activated carbon has been used for separation and concentration of metal ions.¹ Such separations involve formation (or precipitation) of the chelates and their subsequent adsorption (or filtration) with activated carbon. After studies on the adsorption (collection) of mercury,^{2,3} and silver, gold and platinum⁴ on activated carbon from mineral acid solutions, it was thought worth while to study the adsorption behaviour of a wide variety of metal species on activated carbon from aqueous solutions over a wide pH range and in the absence of chelating agents. Such data should help in planning preconcentration of metals from environmental samples. The adsorption behaviour of many metals in the absence of chelating agents has been described by Sigworth and Smith⁵ and Jackwerth *et al.*,¹ but the scope of the information was limited. Adsorption of individual metal species, *viz.* magnesium(II),⁶ chromium(III, VI),^{7,8} arsenic(III, V),⁹ molybdenum(VI),¹⁰ tungsten(VI)¹¹ and indium(III), tin(IV), antimony(V) and tellurium(IV)¹² has also been reported.

In the present work, the adsorption of 20 metal species by activated carbon from aqueous solutions of pH 1-13 was studied. Experiments without activated carbon were also done for comparison. The metals were determined radiochemically, spectrophotometrically and by atomic-absorption spectrometry (AAS).

EXPERIMENTAL

Materials

Activated carbon powder (Merck, No. 2186) was used after drying at 105° for 2 hr. It was purified by stirring in 1M hydrochloric acid for 3 hr, washing with water, and drying at 105°; it was used only for the adsorption of iron (determination by spectrophotometry and AAS), aluminium, copper and bismuth. This treatment reduced its

iron, aluminium and copper contents from 0.29, 0.22 and 0.018 to 0.15, 0.09 and 0.008 mg/g, respectively.

The membrane filters (0.45- μ m pore size and 25-mm diameter) were cellulose nitrate (Millipore) for tracer experiments and cellulose acetate (Sartorius and Toyo Roshi) for ashing work.

Reagents

The buffer solutions were 0.1M sodium acetate-acetic acid (pH 4-6) and 0.1M borax-hydrochloric acid or sodium hydroxide (pH 7-11).

Stock solutions (1000 mg/l.) of the test species were made by dilution with water after preparation of a more concentrated solution: Cr(III), Co(II) and Zn(II) solutions by dissolving the metals in hydrochloric acid (1 + 1); Cd(II) and Bi(III) solutions by dissolving the metals in nitric acid (1 + 1); Mn(II) solution by dissolving the metal in sulphuric acid (1 + 5); Ni(II) solution by dissolving the metal in *aqua regia*; Al(III) solution by dissolving the metal in a mixture of hydrochloric acid (1 + 1) and nitric acid (1 + 1); Ti(IV) solution by dissolving the metal in a mixture of sulphuric acid (1 + 1) and hydrochloric acid (1 + 1), and oxidizing with nitric acid. Cs(I) and Cr(VI) solutions were prepared by dissolving caesium chloride and potassium dichromate in water. Y(III) solution was prepared by dissolving the oxide in hydrochloric acid (1 + 1). Ce(III) solution was prepared by dissolving ceric oxide in a mixture of perchloric acid (1 + 1) and 30% hydrogen peroxide, adding more hydrogen peroxide, and boiling to reduce Ce(IV). Zr(IV) solution was prepared by dissolving ZrOCl₂·8H₂O in 2M hydrochloric acid and standardized by EDTA titration with Xylenol Orange as indicator. Fe(III), Cu(II) and Sb(III) solutions were prepared by dissolving ferric alum, cupric sulphate and potassium antimonyl tartrate in 0.1M hydrochloric acid. Ag(I) solution was prepared by dissolving silver nitrate in 0.1M ammonia solution. Pb(II) solution was prepared by dissolving lead nitrate in 0.1M nitric acid. Ru(III) solution in dilute hydrochloric acid was purchased from Nippon Engelhard.

The following tracers (Japan Radioisotope Association) were used: ⁵¹Cr (Na₂CrO₄ in 0.1M HCl), ⁵⁴Mn (MnCl₂ in 0.1M HCl), ⁵⁷Co (CoCl₂ in 0.1M HCl), ⁵⁹Fe (FeCl₃ in 0.1M HCl), ⁶⁵Zn (ZnCl₂ in 0.1M HCl), ⁸⁸Y (YCl₃ in 0.1M HCl), ¹⁰⁶Ru (RuCl₃ in 0.1M HCl), ^{110m}Ag [Ag(NH₃)₂NO₃ in 0.1M NH₃], ¹²⁵Sb (SbCl₃ in 0.5M HCl-1 mg/g tartaric acid), ¹³⁴Cs (CsCl in 0.1M HCl) and ¹⁴⁴Ce (CeCl₃ in 0.1M HCl). ⁵¹Cr(III) was prepared by reducing the above-mentioned ⁵¹Cr(VI) with hydroxylammonium chloride.

Apparatus

A Millipore vacuum filtration unit with a glass funnel and fritted-glass base, pH-meters (Corning 130 and Horiba F-7),

*Partly presented at the 33rd Annual Meeting of the Japan Society for Analytical Chemistry, Nagoya, October, 1984.

†Author for reprint requests.

a well-type NaI(Tl) scintillation counter, a spectrophotometer (Shimadzu UV-120-02, 1-cm cells), and an atomic-absorption spectrophotometer equipped with a 10-cm slit burner (Nippon Jarrel-Ash AA-782) were used.

Procedure

The following solutions were prepared: 0.1M HCl (pH 1.1), 0.01–0.001M HCl–0.1M NaClO₄ (pH 2–3), 0.01M CH₃COONa–CH₃COOH–0.1M NaClO₄ (pH 4–6), 0.01M Na₂B₄O₇–(HCl or NaOH)–0.1M NaClO₄ (pH 7–11) and 0.1M NaOH (pH 12.6). When silver, lead and bismuth were examined, nitric acid was used instead of hydrochloric acid. Ten-ml portions of each buffer were transferred into 20-ml Erlenmeyer flasks (borosilicate glass) fitted with ground-glass stoppers. Then 10- μ g quantities of the metal species tested (having adequate activity for tracer experiments) were added to the flasks, followed immediately by 10 mg of activated carbon, and the mixtures were shaken mechanically at room temperature for about 20 hr. Experiments without activated carbon were performed at the same time. In each case the carbon was filtered off on a membrane filter by suction and the vessel and carbon were washed with two 0.5-ml portions of the buffer solution used. The pH of the filtrate plus washings was measured with a pH-meter, then the mixture was made about 1M in hydrochloric acid (or nitric acid for silver, lead and bismuth). Any metal species adsorbed on the surface of the vessel was dissolved off with 1M hydrochloric or nitric acid, as appropriate.

For tracer experiments (Cs, Y, Ce, Cr, Mn, Fe, Co, Ru, Ag, Zn and Sb), the carbon plus filter (or the filter alone, for the comparison tests), the filtrate plus washings, and the acid washings of the vessel were transferred to screw-cap glass vials (25 mm diameter, 70 mm tall), and the volumes were adjusted (if necessary) to 11 ml with 1M hydrochloric or nitric acid, and the activities were measured.

For determinations by spectrophotometry (Ti, Zr, Fe, Al and Bi) and AAS (Fe, Ni, Cu, Cd and Pb), the carbon plus filter (or the filter alone) was ashed in a porcelain crucible at 550° for 1 hr [in the presence of 10–20 mg of Mg(NO₃)₂·6H₂O for Cd and Pb]. A platinum crucible was used for aluminium to avoid contamination from a porcelain crucible. The ash was dissolved in hydrochloric acid (1 + 1) for the determination of Fe, Ni, Cu and Al, and in nitric acid (1 + 1) for the determination of Cd, Pb and Bi. For the determination of Ti and Zr, the ash was fused with potassium hydrogen sulphate and the cooled melt was dissolved in hydrochloric acid (1 + 1). These solutions, the filtrate plus washings and the acid washings of the vessel were then analysed. Titanium(IV) was determined spectrophotometrically with thiocyanate,¹³ zirconium(IV) with Arsenazo III,¹⁴ iron(III) with 1,10-phenanthroline,¹⁵ aluminium(III) with 8-hydroxyquinoline¹⁶ and bismuth(III) with dithizone.¹⁷

RESULTS AND DISCUSSION

Study of experimental conditions

The specific surface area and elemental composition of the activated carbon used were reported in a previous paper.³

Iron(III) was chosen as a model for establishing the conditions for adsorption of the metal species; the experiment was done with ⁵⁹Fe as a radioactive tracer.

The effect of the iron(III) concentration on its adsorption on activated carbon from aqueous solutions of pH 1–13 was studied (Fig. 1). Good recoveries were obtained from 0.1, 1, and 10 mg/l. iron(III) solutions at pH 5–6. Adsorption from aqueous solu-

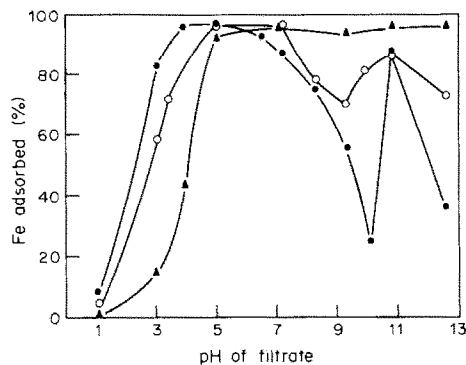


Fig. 1. Effect of iron(III) concentration on adsorption: 1 g of activated carbon per litre of solution; [Fe(III)] (mg/l.): ●, 0.1, ○, 1; ▲, 10.

tions as a function of pH was consequently initially studied with 1 mg/l. concentration of the metal species and the effect of concentration of the metals was then examined at the optimum pH. The effect of contact time on the adsorption of iron(III) (1 mg/l.) at pH 5.0 was studied (Fig. 2). Shaking for any time between about 3 and 20 hr gave practically the same recovery (95–96% with activated carbon and 67–69% with only the filter). Shaking for about 20 hr was chosen.

Varying the ionic strength between 0.01 and 1.0 (with sodium perchlorate) did not affect the degree of adsorption from a 0.1 mg/l. iron(III) solution at pH 5.0. The ionic strength was therefore adjusted to 0.1 with sodium perchlorate for all the systematic tests.

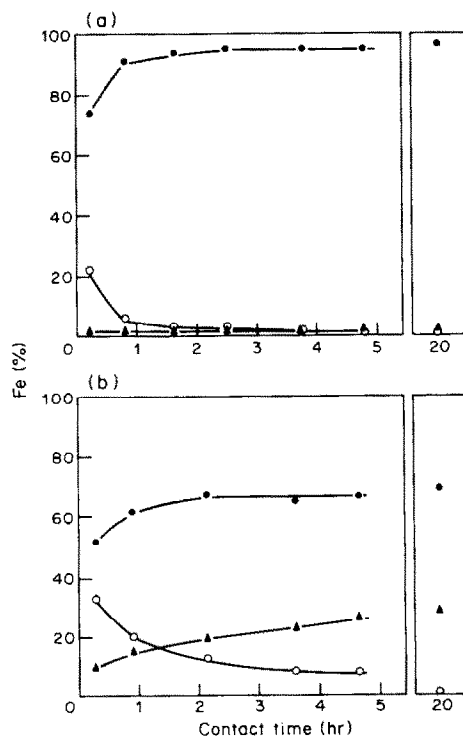


Fig. 2. Effect of contact time on adsorption of iron(III): 1 mg/l. at pH 5.0; (a) with 1 g of activated carbon per litre; (b) without activated carbon; ●, activated carbon plus filter or filter alone; ○, filtrate; ▲, surface of glass vessel.

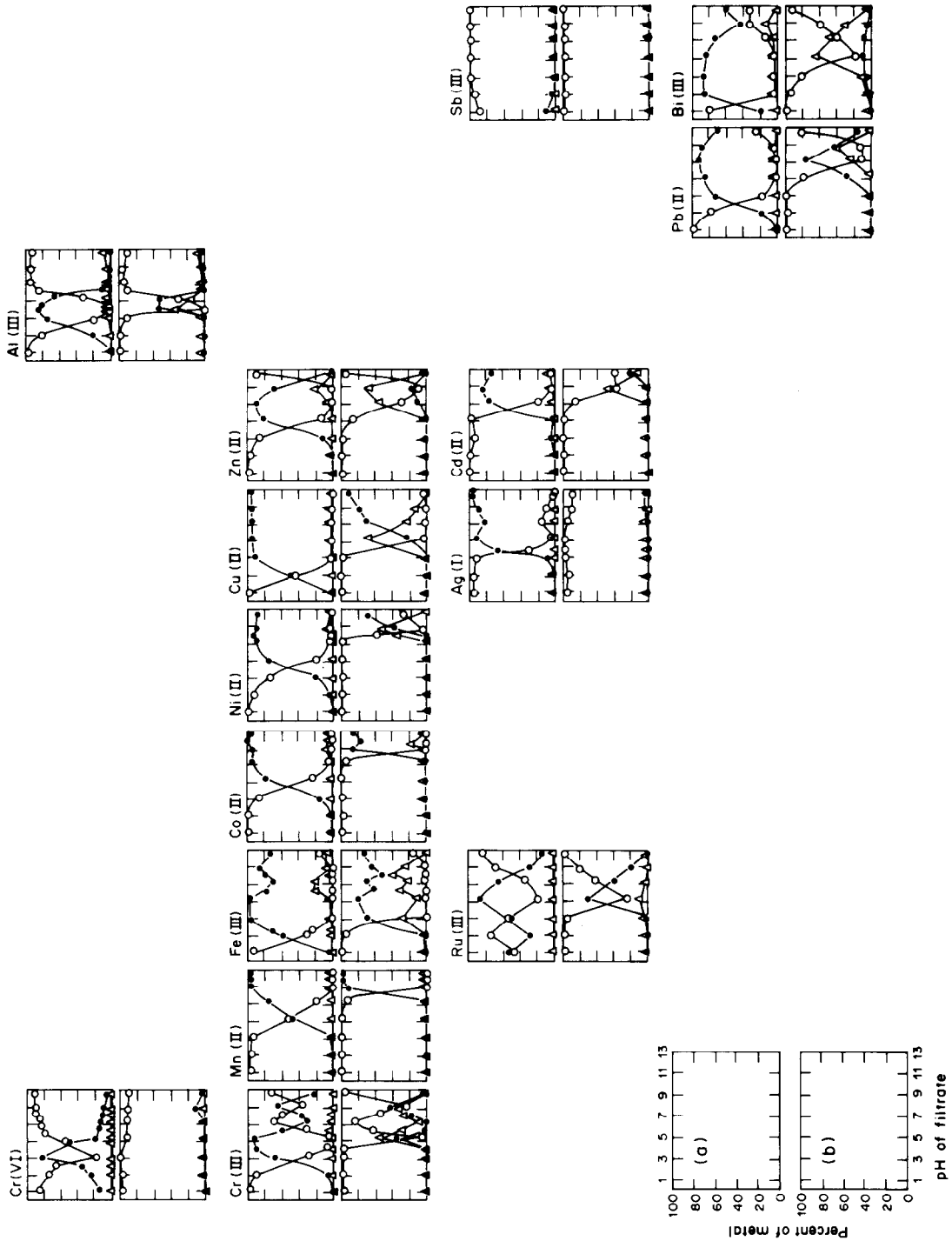


Fig. 3. Adsorption of metals on activated carbon from aqueous solutions as a function of pH: metal 1 mg/l.; (a) with 1 g of activated carbon per litre; (b) without activated carbon; ●, activated carbon plus filter or filtrate alone; ○, filtrate; △, surface of glass vessel.

Table 1. Desorption of iron(III) from activated carbon

Solution for desorption	Fe(III), mg/l.	Overall recovery*, %
1M HCl	0.1†	95
	1.0§	95
	10†	97
6M HCl	0.1†	19
	10†	74
1M HNO ₃	0.1†	93
	10†	94
6M HNO ₃	0.1†	97
	1.0§	96
	10†	97

*Overall recovery (average of two experiments) means the recovery from adsorption at pH 5.0 (20-hr shaking) and desorption (20-hr shaking).

†Unpurified activated carbon, determined radiochemically.

§Purified activated carbon, determined spectrophotometrically.

As shown in Table 1, iron adsorbed on activated carbon at pH 5.0 could be desorbed efficiently by shaking for about 20 hr with 10 ml of 1M hydrochloric acid, 1M nitric acid or 6M nitric acid. However, 6M hydrochloric acid was not effective; iron(III) is adsorbed on activated carbon from $\geq 6M$ hydrochloric acid solutions.^{18,19}

Adsorption of metal species

Figure 3 shows the results obtained for adsorption of 19 metal species (1 mg/l. initial concentration) on activated carbon (1 g/l.) from aqueous solutions as a function of pH. The results are displayed with the elements shown in their positions in the periodic table.

Each graph shows the distribution between the activated carbon plus filter (or filter alone, without carbon), filtrate plus washings and surface of the glass vessel (\equiv acid washings). The total found was always about 100%, but when the aqueous solutions prepared without carbon were filtered after shaking, a few of the elements were sometimes retained on the glass funnel and fritted-glass base of the vacuum filtration unit; in such cases, the former was not used and the latter was washed with acid solution, which was added to the filtrate.

Eighteen of the species tested were adsorbed efficiently on activated carbon; caesium(I) (not shown in Fig. 3) and antimony(III) were not adsorbed. The following pairs showed similar adsorption curves: Y(III) and Ce(III), Ti(IV) and Zr(IV) and Co(II) and Ni(II). The adsorption curves may be grouped into four types: a flat peak for Mn(II), Co(II), Ni(II) and Cu(II); one maximum for Cr(VI), Zn(II), Cd(II), Al(III) and Pb(II); one maximum and one minimum for Y(III), Ce(III), Ti(IV), Zr(IV), Ru(III) and

Table 2. Effect of concentration of metals on adsorption by activated carbon

Metal	pH	Adsorption,* %		
		0.1 mg/l.	1 mg/l.	10 mg/l.
Zr(IV)	4.9	98	97	96
Cr(VI)	5.0	95†	83	41
Fe(III)	5.0	96	96	94
Bi(III)	5.0	91§	87	91
Al(III)	6.2	86§	86	93
Cr(III)	6.4	98†	94	96
Ce(III)	7.2	97	96	92
Ti(IV)	7.2	94	98	99
Y(III)	8.3	101	97	90
Zn(II)	9.3	90	88	75
Pb(II)	9.3	97	93	94
Ni(II)	9.9	98	97	91
Cu(II)	10.8	97	95	97
Cd(II)	10.8	81	86	54
Mn(II)	11.8	96	98	98
Co(II)	11.8	98	98	98
Ag(I)	12.6	95	98	97

*1 g of activated carbon per litre; average of two experiments.

†0.2 mg/l.

§0.5 mg/l.

Bi(III); two maxima and one minimum for Cr(III), Fe(III) and Ag(I).

Two effects of activated carbon can be noted from comparison of the curves obtained with and without carbon present (Fig. 3). First, it reduces the degree of adsorption on the surface of the glass vessel. Secondly, it collects metal hydroxide particles that are small enough to pass through the 0.45- μ m membrane filters.

Activated carbon showed the most remarkable effect on the adsorption of silver(I), which was not retained on the filter alone (Fig. 3). Silver(I) has been reported⁵ to be reduced to the metal on a carbon surface.

Chromium(VI) was considerably adsorbed at pH about 5. This result is consistent with previous work.^{7,8} The adsorption of ruthenium(III) from 0.1M hydrochloric acid (pH 1.1, Fig. 3) may be due to the formation of chloro-complex(es) of ruthenium(III).

The effect of metal concentration on the degree of adsorption on activated carbon at the optimum pH values is shown in Table 2. Recoveries of chromium(VI), zinc(II) and cadmium(II) decreased with increase in metal concentration. The adsorption of the other metals was practically constant over the 0.1–10 mg/l. concentration range.

Figure 3 suggests that activated carbon can be used for non-selective separation or preconcentration of many metals. In addition, separation of iron from manganese can be achieved at pH 5 (Table 3). Fifty ml of aqueous solution of pH 5 (acetate buffer) containing both iron(III) and manganese(II) were shaken for about 20 hr with 50 mg of purified carbon and the carbon was filtered off on a membrane filter with suction.

The carbon and filter were ashed at 550° for 1 hr, the ash was heated with sulphuric acid (1 + 5) plus a

Table 3. Separation of iron(III) from manganese(II) by adsorption on activated carbon at pH 5.0

Fe(III) + Mn(II), mg/l.	Recovery,* %					
	Activated carbon		Filtrate		Surface of vessel	
	Fe	Mn	Fe	Mn	Fe	Mn
1.0 + 1.0	98	2	0	99	1	0
1.0 + 10	99	2	0	97	2	0
10 + 1.0	97	2	0	98	4	0

*Average of two experiments.

few drops of 30% hydrogen peroxide to dissolve manganese, then hydrochloric acid (1 + 1) was added to dissolve iron. The iron and manganese from the ash, the filtrate plus washings, and the surface of the vessel (\equiv acid washings) were then determined by AAS.

Acknowledgement—The authors thank the Radioisotope Centre of this university for permitting the tracer work.

REFERENCES

- For example, E. Jackwerth, J. Lohmar and G. Wittler, *Z. Anal. Chem.*, 1973, **266**, 1; B. M. Vanderborgh and R. E. Van Grieken, *Anal. Chem.*, 1977, **49**, 311; M. Kimura, *Bunseki*, 1981, 297.
- H. Koshima and H. Onishi, *Talanta*, 1980, **27**, 795.
- Idem*, *Bunseki Kagaku*, 1982, **31**, E421.
- Idem*, *ibid.*, 1983, **32**, E149.
- E. A. Sigworth and S. B. Smith, *J. Am. Water Works Assoc.*, 1972, **94**, 386.
- Z. Marczenko, M. Mojski and M. Balcerzak, *Mikrochim. Acta*, 1975 **1**, 539.
- H. Yoshida, K. Kamegawa and S. Arita, *Nippon Kagaku Kaishi*, 1977, 387.
- A. Sai, K. Ohashi, K. Motojima and K. Yamamoto, *Bunseki Kagaku*, 1982, **31**, E361.
- K. Kamegawa, H. Yoshida and S. Arita, *Nippon Kagaku Kaishi*, 1979, 1365.
- A. Sai, A. Onuki, K. Ohashi, K. Motojima and K. Yamamoto, *Bunseki Kagaku*, 1981, **30**, 804.
- K. Ohashi, K. Murakami and K. Yamamoto, *ibid.*, 1983, **32**, E313.
- S. Ambe, *J. Radioanal. Nucl. Chem.*, 1984, **81**, 77.
- J. P. Young and J. C. White, *Anal. Chem.*, 1959, **31**, 393.
- H. Onishi, *Bunseki Kagaku*, 1963, **12**, 1153.
- Y. Toita and H. Onishi, *ibid.*, 1975, **24**, 201.
- H. Onishi and I. Tsukahara, *Kyoko Kodoho: Mukihen*, p. 54. Kyoritsu Shuppan, Tokyo, 1983.
- E. B. Sandell, *Colorimetric Determination of Traces of Metals*, 3rd Ed., p. 348. Wiley-Interscience, New York, 1959.
- H. Koshima, *Anal. Sci.*, 1985, **1**, 195.
- H. Koshima and H. Onishi, *ibid.*, 1985, **1**, 237.

EVALUATION AND IMPROVEMENT OF THE RESOLUTION OF VOLTAMMETRIC MEASUREMENTS

JOSEPH WANG,* DEN BAI LUO and BASSAM FREIHA
 Department of Chemistry, New Mexico State University, Las Cruces, NM 88003, U.S.A.

(Received 1 May 1985. Revised 19 December 1985. Accepted 6 January 1986)

Summary—Two approaches for estimating and improving resolution in chromatography analyses can be applied successfully to voltammetric measurements. It is shown that the resolution of voltammetric procedures yielding symmetric (or nearly symmetric) current peaks can be described by $R = 2\Delta E_p/1.699(b_{1,2,1} + b_{1,2,2})$ where ΔE_p is the difference between the peak potentials of the two analytes, and $b_{1,2,1}$ and $b_{1,2,2}$ are the peak half-widths. The window diagram approach is used to improve the resolution between neighbouring voltammetric peaks by optimization of the supporting electrolyte composition. The applicability of these approaches to differential-pulse anodic-stripping measurements at the mercury film electrode is demonstrated.

Differential-pulse or square-wave polarography and anodic-stripping voltammetry have become commonly used techniques for determining trace levels of electroactive species, and their sensitivity has been discussed several times.¹⁻⁴ On the other hand, many aspects of the resolution of voltammetric peaks have not been evaluated, in spite of selectivity problems associated with analysis of mixtures. The electroactive components of a mixture usually behave independently, so the voltamperogram is simply the summation of the individual peaks or waves. The three techniques mentioned give signals in the form of peaks, and differentiation of the sigmoidal response obtained with techniques such as hydrodynamic modulation voltammetry^{5,6} or normal pulse polarography⁷ will also result in peaks. Clearly, for mixtures the resolution of adjacent voltammetric peaks depends on how far apart and how wide they are. We must decide what criterion for resolution is suitable.

In chromatography, the resolution, R , of two adjacent peaks is defined as the ratio of the peak separation to the mean "base-line width" of the peak (measured as in Fig. 1):

$$R = \frac{(t_2 - t_1)}{0.5(W_1 + W_2)} \quad (1)$$

Alternatively, if the widths are measured halfway between the base-line and the tops of the peaks, the equation becomes

$$R = \frac{2(t_2 - t_1)}{1.699(W_{1,2,1} + W_{1,2,2})} \quad (2)$$

These equations are based on the assumption that both peaks are Gaussian.

The aim of the present work was to establish a similar method for estimating the resolution of two adjacent voltammetric peaks. We have found that for voltammetric techniques yielding symmetric, or nearly symmetric, current peaks, a reliable measure of the extent of overlap can be obtained, and that the window diagram approach^{8,9} is very useful for improving the resolution and optimizing the conditions of voltammetric measurements.

EXPERIMENTAL

The electrochemical cell and the reagents were those described previously¹⁰ unless stated otherwise. Measurements were made with an EG&G PAR model 174 polarographic analyser. The differential-pulse anodic stripping measurements were made at the *in situ* plated mercury electrode, as described previously.¹¹

RESULTS AND DISCUSSION

Quantitative measure of the resolution

Various voltammetric procedures, such as linear-scan voltammetry or stripping measurements at the hanging mercury drop electrode, produce asymmetric

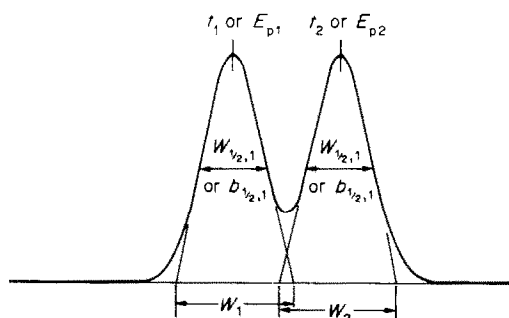


Fig. 1. Definition of parameters used to define resolution.

*Author for correspondence.

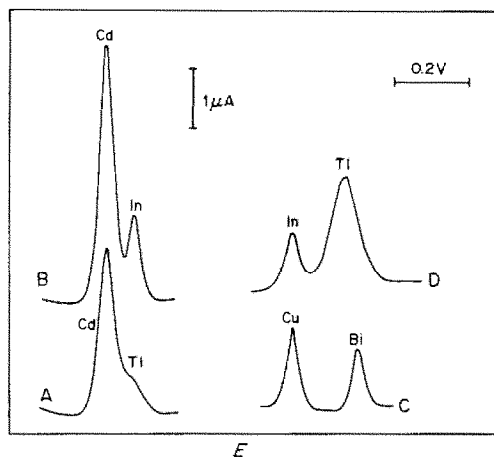


Fig. 2. Differential pulse anodic stripping voltamperograms for various binary mixtures: (A) cadmium ($3 \times 10^{-7}M$)-thallium ($3 \times 10^{-7}M$), (B) indium ($4 \times 10^{-7}M$)-cadmium ($4 \times 10^{-7}M$), (C) copper ($1 \times 10^{-6}M$)-bismuth ($1 \times 10^{-6}M$) and (D) indium ($2 \times 10^{-6}M$)-thallium ($1 \times 10^{-6}M$). Mercury-coated glassy-carbon disk electrode rotated at 1600 rpm for 2 min deposition at -1.1 V. Stripping conditions, scan-rate, 2 mV/sec; amplitude, 25 mV. Supporting electrolytes, 1M HCl (A, B); 1M HCl + 1M ethylenediamine (C, D).

signal peaks even for reversible systems. However, for stripping measurements at the mercury film electrode, differential-pulse, square-wave or a.c. polarography, and various procedures based on differentiation of sigmoidal signals, symmetric (or nearly symmetric) response peaks are obtained. Like those in practical chromatographic measurements these peaks are generally not truly Gaussian in shape. It is almost always a mistake to assume chromatographic peaks are Gaussian in shape,¹²⁻¹⁵ and exponentially modified Gaussian,^{9,16} bi-Gaussian,^{13,17} Gram-Charlier,¹⁸ Poisson¹³ and a combination¹⁹ of Gaussian, exponential and hyperbolic tangent shapes have been employed. The exact mathematical current-potential functions for most voltammetric techniques are not available. Boudreau and Perone²⁰ found that the function which best fitted square-wave voltammetric peaks is a combination of Gaussian and Cauchy functions (with the Gaussian component having the greater effect on the peak shape). Stripping measurements at the mercury film electrode can be described by an approximate Gaussian function.²¹ Hence an analogue of equation (2) can obviously be made the basis for estimating the resolution of symmetric, or nearly symmetric, voltammetric peaks with a relatively flat base-line:

$$R = \frac{2\Delta E_p}{1.699(b_{1/2,1} + b_{1/2,2})} \quad (3)$$

where ΔE_p is the difference between the peak potentials and $b_{1/2}$ is the peak width at half height. As $b_{1/2}$ is commonly used in voltammetric measurements, equation (3) is preferred to the analogue of equation (1), and its utility is illustrated in Fig. 2, which shows

that though for the cadmium-thallium (A) and indium-cadmium (B) mixtures ΔE_p is essentially the same (0.07 V), the extent of overlap of the peaks is very different. The value of R is 0.68 and 0.97 for the cadmium-thallium and indium-cadmium mixtures, respectively. A similar observation applies to the copper-bismuth (C) and indium-thallium (D) systems, which have ΔE_p values of 0.17 and 0.14 V and R values of 2.6 and 1.3 respectively. The value of R clearly provides a reliable estimate of the resolution.

The $b_{1/2}$ value is inversely proportional to the number of electrons (n) participating in the electrode reaction and increases with decreasing rate of electron transfer (once the reaction becomes totally irreversible, the width remains unchanged). For example, the pseudo derivative polarographic techniques (pulse, a.c. and square-wave polarography) show a limiting $b_{1/2}$ value of $90.6/n$ mV.²² For the voltamperograms shown in Fig. 2 the stripping reactions involve transfer of one (Tl), two (Cd, Cu) or three (In, Bi) electrons, and it is clearly the one-electron thallium reaction that creates the most severe overlap problems. Table 1 summarizes the R values obtained for differential-pulse stripping measurements of several binary systems; only the cadmium-indium couple exhibits significant overlap (*cf.* B in Fig. 2).

As $b_{1/2}$ is inversely proportional to the number of electrons transferred, for two reversible systems which both have the same n value, R is proportional to $n\Delta E_p$, which is the estimate frequently used for evaluating the resolution of voltammetric measurements.²⁰ However, this estimate is not useful when the two redox reactions involve different numbers of electrons or different rates of electron transfer. However, in such cases R does provide a reliable measure of the resolution, as it takes into account the different factors (n , reversibility) affecting the peak width.

For truly Gaussian peaks, nearly complete resolution (0.3% overlap) is obtained at $R = 1.5$. For

Table 1. R values and peak-potential separations for different pairs of metals measured by differential pulse anodic stripping voltammetry*

Binary system	ΔE_p , V	R
Cd-Pb	0.21	2.9
Cd-In	0.07	0.97
Cd-Cu	0.39	5.2
Cd-Bi	0.57	9.1
Cu-Pb	0.18	2.3
Cu-In	0.31	4.2
Cu-Bi	0.20	2.9
Pb-In	0.13	1.6
Pb-Bi	0.37	5.9
Bi-In	0.50	8.1

* $5 \times 10^{-7}M$ bismuth, copper and indium; $3 \times 10^{-7}M$ lead and cadmium; supporting electrolyte, 1M HCl. Other conditions as for Fig. 2.

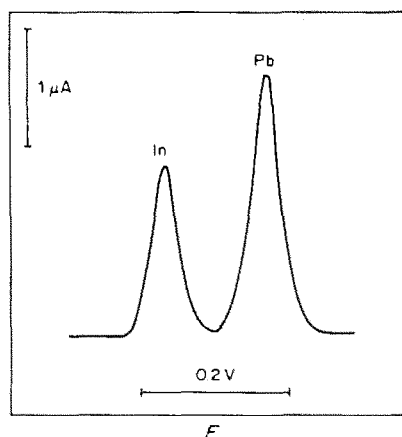


Fig. 3. Differential pulse anodic stripping voltamperogram for $4 \times 10^{-7} M$ indium and lead in $1 M$ HCl. Conditions as for Fig. 2.

differential-pulse stripping measurements (at the mercury film electrode) this would occur at about $R = 1.6$, as calculated from the data in Fig. 3. At $R \leq 0.75$ (i.e., $\geq 50\%$ overlap) the resolution is unsatisfactory for most purposes (e.g., A in Fig. 2). These criteria pertain to approximately equimolar mixtures. Higher resolution may be needed when the concentrations for the two components differ considerably.

Various experimental conditions, e.g., scan-rate, pulse-amplitude or supporting electrolyte, may affect the voltammetric peak potential and peak-width, so to control and improve the resolution the analyst must know how R varies with these conditions. Table 2 shows the effects of the pulse-amplitude and potential scan-rate on the resolution of the peaks of indium and lead, two metals giving rise to overlapping stripping peaks in many media. The best resolution was obtained with 2 mV/sec scan-rate and 50 mV amplitude. These data indicate that the scan-rate has the dominant effect on the resolution; a tenfold increase in scan-rate decreased R by a factor of approximately 3–4, whereas a similar increase in pulse amplitude changed R by only 5–20%. Obviously, changes in the sensitivity or speed associated with these changes in the experimental conditions

Table 2. R values for the lead–indium pair as a function of the differential pulse amplitude (ΔE) and scan-rate (v)^a

$v, \text{ mV/sec}$	$\Delta E, \text{ mV}$			
	10	25	50	100
2	2.0	2.05	2.09	1.95
5	1.56	1.59	1.55	1.46
10	1.05	1.01	0.99	0.96
20	0.72	0.60	0.65	0.55

^a $5 \times 10^{-7} M$ indium and lead; supporting electrolyte, acetate buffer (pH 4.5). Deposition at -1.1 V for 1 min.

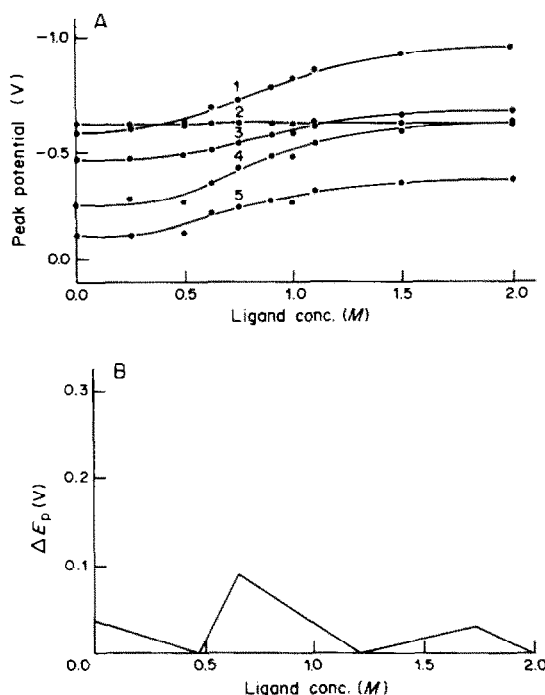


Fig. 4. (A) Dependence of the stripping peak potential on ethylenediamine concentration for indium (1), thallium (2), lead (3), copper (4) and bismuth (5). (B) Window diagram for these metals over the 0–2 M ligand concentration range, in the presence of $1 M$ HCl.

should be taken into account when optimizing the overall performance. Overall, equation (3) provides a reliable measure of the resolution, which can be utilized effectively when various solution or instrumental conditions are changed to improve the separation of neighbouring peaks.

Improved resolution by the window diagram approach

The window diagram approach uses the resolution of all possible pairs of peaks in the sample to obtain the best separation of the worst separated pair of peaks. Most applications of this approach have been in chromatography^{8,9} but it can be exploited in any situation in which optimization of one (or more) of the experimental conditions with respect to one of the dependent variables is required. For example, the method was used successfully with lanthanide-shift nuclear magnetic resonance spectra.²³ Similarly, polarographic measurements can be improved by optimizing the solution pH.²⁴ In this section, we examine the utility of the window diagram approach for optimizing the supporting electrolyte composition to improve the resolution in anodic stripping voltammetry. This possibility results from the fact that most supporting electrolytes have some tendency to complex metal ions, thus affecting the position of the stripping peaks on the potential axis.

Figure 4 shows (A) the effect of ethylenediamine concentration on stripping peak potential for five

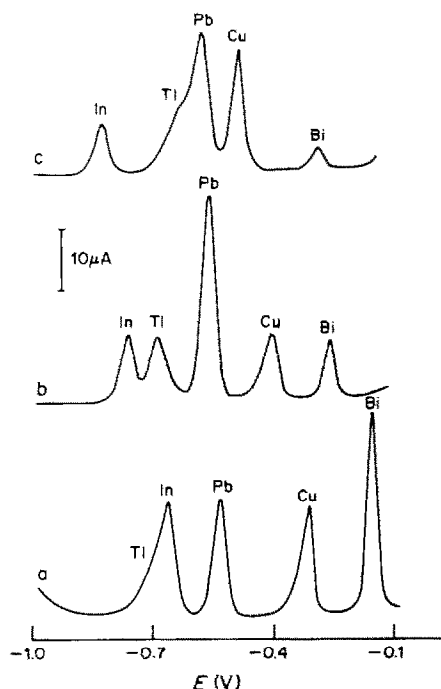


Fig. 5. Differential pulse anodic stripping voltamperograms for $6 \times 10^{-7}M$ thallium, $9 \times 10^{-7}M$ indium, $3 \times 10^{-7}M$ lead, $5 \times 10^{-7}M$ copper and bismuth with (a) 0, (b) 0.65 and (c) 0.90M ethylenediamine and 1M HCl. Deposition for 1-min at -1.1 V. Scan-rate, 1 mV/sec. Rotation speed and amplitude as for Fig. 2.

metals, and (B) the window diagram generated from the data in (A). It is clear that the changes in peak potential differ from metal to metal, as they are dependent on the formation constants of the complexes.³ It should be noted that the plot for the thallium peak potential crosses those for indium, lead and copper over the range of ligand concentration covered. To construct the window diagram, the difference in peak potential of the pair most difficult to resolve is plotted as a function of the ligand concentration. Two "windows" of separation are clearly evident, and define the conditions under which complete separation of the mixture is possible. In practice, the window at a ligand concentration of 0.65M offers the best separation of the peaks of all the metals (under these conditions, ΔE_p for the least separated pair is 92 mV). This is illustrated in Fig. 5, which shows the stripping voltamperograms for these metals at three ligand concentrations. With the optimal ligand concentration, 0.65M, the peaks are well resolved from each other (b); only the indium-thallium pair exhibits some overlap ($R = 1.1$). All five metals present can conveniently be determined. In contrast, severe overlap of the thallium-indium and thallium-lead peaks ($R < 0.4$)

is observed with zero and 0.9M ethylenediamine concentrations, respectively; determination of these metals is not feasible under these conditions. As a result of the optimization obtained by the window diagram approach, the five metals can be measured on the same voltamperogram, within a relatively narrow potential range (from -0.2 to -0.8 V). Additional metals (e.g., zinc, nickel, gallium, antimony) may also be measured within the entire potential range of the mercury working electrode. (The ability to perform such multi-element measurements would also depend on the absence of intermetallic interferences.) The same strategy for improving the resolution in anodic stripping measurements can be achieved by changing other solution or instrumental factors. For example, a change in the mercury film thickness or potential scan-rate alters the peak position to different extents, depending on the number of electrons involved.²⁵ Other approaches for improving the resolution of stripping measurements have been reviewed.³

Acknowledgement—This work was supported in part by the National Institutes of Health, grant No. GM30913-02.

REFERENCES

1. A. M. Bond, *Modern Polarographic Techniques in Analytical Chemistry*, Dekker, New York, 1980.
2. *Anal. Chem.*, 1980, **52**, 229A.
3. J. Wang, *Stripping Analysis: Principles, Instrumentation and Applications*, VCH Publishers, Deerfield-Beach, FL, 1985.
4. G. E. Batley and T. M. Florence, *J. Electroanal. Chem.*, 1974, **55**, 23.
5. J. Wang, *Talanta*, 1982, **29**, 805.
6. B. Miller and J. M. Rosamilla, *Anal. Chem.*, 1983, **55**, 1281.
7. J. E. Anderson and A. M. Bond, *ibid.*, 1981, **53**, 504.
8. R. J. Laub and J. H. Purnell, *ibid.*, 1976, **48**, 799.
9. S. N. Deming and M. L. H. Turoff, *ibid.*, 1978, **50**, 546.
10. J. Wang, *Talanta*, 1982, **29**, 125.
11. J. Wang and D. B. Luo, *ibid.*, 1984, **31**, 703.
12. A. H. Anderson, T. C. Gibb and A. B. Littlewood, *J. Chromatog. Sci.*, 1970, **8**, 640.
13. E. Grushka, M. N. Myers and J. C. Giddings, *Anal. Chem.*, 1970, **42**, 21.
14. J. T. Lundeen and R. S. Juvet, *ibid.*, 1981, **53**, 1369.
15. J. P. Poley and J. G. Dorsey, *ibid.*, 1983, **55**, 730.
16. H. M. Gladney, B. F. Dowden and J. D. Swalen, *ibid.*, 1969, **41**, 883.
17. T. S. Buys and K. de Clark, *ibid.*, 1972, **44**, 1273.
18. O. Grubner, *ibid.*, 1971, **43**, 1934.
19. S. N. Chesler and S. P. Cram, *ibid.*, 1973, **43**, 1354.
20. P. A. Boudreau and S. P. Perone, *ibid.*, 1979, **51**, 811.
21. Z. Stojek and Z. Kublik, *J. Electroanal. Chem.*, 1979, **105**, 247.
22. W. F. Gutknecht and S. P. Perone, *Anal. Chem.*, 1970, **42**, 906.
23. R. L. Laub, A. Pelter and J. H. Purnell, *ibid.*, 1979, **51**, 1878.
24. L. B. Anderson and R. J. Laub, *J. Electroanal. Chem.*, 1981, **122**, 359.
25. K. Wikiel and Z. Kublik, *ibid.*, 1984, **165**, 71.

BEHAVIOUR OF SOME DIALKYL- AND TRIALKYL-LEAD COMPOUNDS IN THE HYDRIDE-GENERATION PROCEDURE USING A NON-DISPERSIVE ATOMIC-FLUORESCENCE DETECTOR

A. D'ULIVO, R. FUOCO and P. PAPOFF

Istituto di Chimica Analitica Strumentale del C.N.R., c/o Dipartimento di Chimica e Chimica Industriale dell'Università di Pisa, Via Risorgimento 35, 56100 Pisa, Italy

(Received 10 September 1985. Accepted 9 November 1985)

Summary—The method of generating covalent hydrides by reduction with sodium tetrahydroborate was applied to aqueous solutions containing traces of R_3Pb^+ and R_2Pb^{2+} compounds ($R = \text{methyl, ethyl}$). For each compound the effects of sample acidity, sodium tetrahydroborate and hydrogen peroxide concentrations, reaction-vessel and transfer-line materials, were measured and the experimental conditions defined for obtaining maximum sensitivity. Experimental evidence indicating the formation of organolead hydrides during the reduction step at room temperature was adduced. The reaction efficiency was found to be 90% for trimethyl-, triethyl- and diethyl-lead and 59% for dimethyl-lead. In the case of inorganic lead the efficiency was only 27%. Without an intermediate preconcentration step, the detection limits obtained for trimethyl-, triethyl-, dimethyl- and diethyl-lead (3 times the standard deviation) were 3–5 ng of lead per litre. A procedure for discriminating between R_3Pb^+ , R_2Pb^{2+} and Pb^{2+} compounds is proposed.

Organolead hydrides are known to be unstable even at low temperatures.^{1,2} Only triethyl- and trimethyl-lead hydrides (not dialkyl-lead dihydrides or plumbane) have so far been isolated.^{3,4} Nevertheless, the stability of plumbane is sufficient to permit determination of Pb^{2+} by atomic-absorption⁵ (AAS) or non-dispersive atomic-fluorescence spectrometry⁶ (NDAFS), by the hydride-generation technique, even at very low concentrations. Recently, Yamauchi *et al.*⁷ extended the tetrahydroborate reduction method to Et_3Pb^+ and Et_2Pb^{2+} determination. The formation of Et_3PbH and Et_2PbH_2 was assumed, but not established.

The aim of the present work was to verify whether methyl-lead compounds react with tetrahydroborate in the same way as the ethyl homologues, and to gain information about the composition of all the volatile hydrides produced. An additional aim was to establish an analytical procedure for the rapid determination of these compounds.

EXPERIMENTAL

Instrumentation

The non-dispersive atomic-fluorescence spectrometer, the hydride reaction vessel and the atomizer were home-made and have been described elsewhere.^{6,8} The experimental parameters are listed in Table I. The gas transfer line was a borosilicate glass tube 30 cm long and 4 mm in bore, joined to the reaction vessel and burner by means of two Teflon joints. A silanated glass-wool filter was inserted into the transfer line to prevent light scattered by droplets from reaching the detector and causing a noisy signal. The reaction vessel and gas transfer line were wrapped in aluminium foil to avoid photodecomposition of the reduction products.

A Gilford Microsample Spectrometer 300 and a PAR model 174 polarographic analyser (EG & G) were used for spectrophotometric and electrochemical measurements, respectively.

Reagents

Hydrochloric acid (30% w/w) and hydrogen peroxide (30% w/w) were Merck Suprapur grade. Sodium tetrahydroborate (BDH reagent for AAS, pellets) was dissolved in 0.1M sodium hydroxide and the solution filtered through a 0.45- μm membrane filter. Lead nitrate (Carlo Erba, analytical reagent grade), trimethyl-lead acetate and triethyl-lead chloride (Ventron reagent) were used to prepare the relevant stock solutions (Pb 1000 $\mu\text{g/ml}$). Triethyl-lead compounds were dissolved in acetic acid/acetate buffer to enhance their solubility. Dialkyl-lead stock solutions were prepared just before use by reaction of the corresponding trialkyl-lead compound with iodine monochloride⁹ by the following procedure: 1 ml of trialkyl-lead stock solution was placed in a 10-ml flask, 0.1 ml of 1M ICI solution was added, and the two were mixed gently; after 5 min 1.5 ml of 0.5M sodium sulphite were added to destroy the excess of ICI and the volume was made up to 10 ml with demineralized water. These solutions were immediately diluted to give 1- $\mu\text{g/ml}$ lead concentration, to improve their stability.¹⁰ A yield of R_2Pb^{2+} better than 95% and a stability of several hours were found by spectrophotometric measurement.¹¹ The $2 \times 10^{-3}M$ 4-(2-pyridylazo)resorcinol sodium salt (PAR), $10^{-2}M$ ethylenediaminetetra-acetic acid (EDTA), ammonia buffer (pH 9) and acetate buffer (pH 5) solutions were made with Carlo Erba analytical-reagent grade compounds. Demineralized doubly distilled water was used in all operations.

Procedure

Five-ml samples of the appropriate acidity were transferred into the reaction vessel. Two micropipettes, one containing 0.5 ml of hydrogen peroxide solution and the other 1 ml of sodium tetrahydroborate solution were placed in the injection ports. Argon was then allowed to flow

Table 1. Experimental parameters

Radio-frequency power for EDL	10 W (expressed as mean power)
Power modulation for EDL	Square-wave, 0–100% amplitude modulation, 0.5 duty cycle
Modulation frequency	7500 Hz
Photomultiplier voltage	750 V
RC time-constant	10 sec
Focusing height	8 mm above the burner top
Burner	Glass tube, 8.5 mm i.d.
Gas flow-rates	Hydrogen 0.3 l./min; argon 1.0 l./min
Sample size	5 ml

through the reaction vessel. Once the base-line was stable, the peroxide, and 40 sec later the tetrahydroborate solution, were injected, but the mixture was not stirred. The gases evolved were conveyed to the argon/hydrogen miniflame atomizer. When hydrogen peroxide was not required the relevant micropipette was removed and the injection port sealed. After reaction, the waste solution was discarded, and the vessel was washed with water, then 0.1M hydrochloric acid, and again with water. A fresh sample could then be placed in the vessel.

RESULTS AND DISCUSSION

Reaction vessel and transfer-line effects

The transfer of the volatile lead compounds, generated during the reduction step, from the reaction vessel to the atomizer, met with some difficulties. It was found that most of the materials generally used for flexible transfer lines, such as Teflon, PVC and silicone rubber, interact to different extents with the organolead hydride flowing through them.

Depending on the lead compound reduced and the transfer-line material, a broadening and tailing of the signal, together with a decrease in peak height, was observed. This effect decreases for the lead compounds in the order $\text{Et}_3\text{Pb}^+ > \text{Et}_2\text{Pb}^{2+} > \text{Me}_3\text{Pb}^+ > \text{Me}_2\text{Pb}^{2+}$. No effect was found for Pb^{2+} .

In the case of Et_3Pb^+ , silicone rubber caused a 90% decrease in peak height, PVC 49%, and Teflon 14%, with respect to the signal obtained by use of borosilicate glass, the material adopted in the present procedure. From the signal-height depressions reported in Table 2 for all the compounds it appears that the ethyl-lead compounds had an interaction with the transfer-line materials about 2.6 times that of the methyl homologues.

The reproducibility of the results was improved by rinsing the transfer line and the reaction vessel, after the daily sets of measurements, with 2M hydrochloric acid for a few hours, then washing with water and drying at 120°. For the reaction products of $\text{Me}_2\text{Pb}^{2+}$ with tetrahydroborate, highly irreproducible results (variation $\pm 100\%$) were obtained when the reaction vessel and transfer line were not protected from light by being wrapped in aluminium foil. None of the other alkyl-lead compounds showed significant photosensitivity.

Tetrahydroborate effect

The effect of tetrahydroborate concentration was studied by using 1 ml of solution and varying its concentration from 4 to 12% w/v. The optimal concentration was found to be 10–12% for all alkyl-lead compounds tested. Lowering the concentration to 4% depressed the signal by about 30% for all the alkyl-lead compounds.

Hydrogen peroxide effect

The effect of hydrogen peroxide concentration was measured in the range 3–10M, the volume added to the reaction vessel being kept constant. No effect was observed for Me_3Pb^+ and Et_3Pb^+ . In the case of $\text{Et}_2\text{Pb}^{2+}$ and $\text{Me}_2\text{Pb}^{2+}$ (Fig. 1), there was a large enhancement of the signals. The relative maximal peak increase was 32-fold for $\text{Et}_2\text{Pb}^{2+}$ with 6M H_2O_2 and 24-fold for $\text{Me}_2\text{Pb}^{2+}$ with 10M H_2O_2 .

Acidity effect

The effect of acidity on peak height for Et_3Pb^+ , Me_3Pb^+ , $\text{Et}_2\text{Pb}^{2+}$ and $\text{Me}_2\text{Pb}^{2+}$, measured in the absence of hydrogen peroxide, is shown in Fig. 2. In

Table 2. Effect of silicone tubing on signal depression for lead compounds

Type of lead compound reduced	Lead concentration, ng/ml	Signal depression†, %		Notes
		Height	Area	
Et_3Pb^+	10	86	78	Broadening and tailing
$\text{Et}_2\text{Pb}^{2+}$	16.5	67	22	Broadening and tailing
Me_3Pb^+	10	34	21	Slight broadening and slight tailing
$\text{Me}_2\text{Pb}^{2+}$	20	24	18	No broadening and no tailing
Pb^{2+}	10	0	0	No broadening and no tailing

*Reduction performed under conditions reported in Table 3 for each lead compound.

†Depression of signals was measured by comparison with those obtained by using glass tube transfer lines. The silicone and glass tubes were 30 cm long and 4 mm in bore.

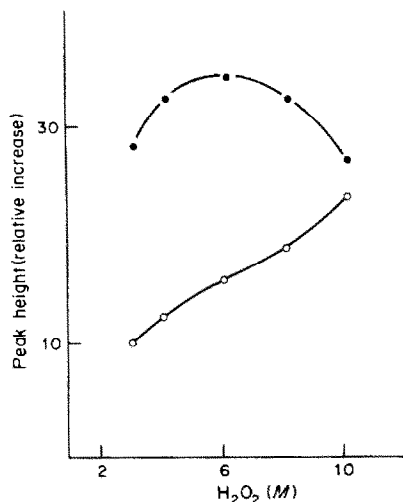


Fig. 1. Effect of hydrogen peroxide concentration on signal of Et₂Pb²⁺ (●) and Me₂Pb²⁺ (○). (Increase relative to that obtained in absence of hydrogen peroxide). Analyte concentration 10 ng (Pb)/ml. Volume of hydrogen peroxide 0.5 ml, other conditions see Table 3.

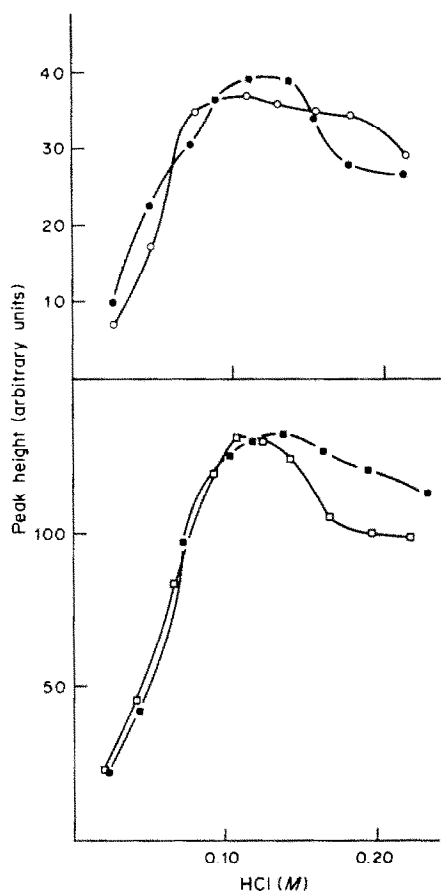


Fig. 2. Effect of sample acidity on signal of Et₃Pb⁺ (■), Me₃Pb⁺ (□), Et₂Pb²⁺ (●) and Me₂Pb²⁺ (○), in absence of hydrogen peroxide. Analyte concentration 10 ng(Pb)/ml for trialkyl- and 100 ng(Pb)/ml for dialkyl-lead compounds.

the range 0.10–0.14M hydrochloric acid the percentage signal amplitude variation is almost the same irrespective of which alkyl group is present. The effect of acidity on peak height for Me₂Pb²⁺ and Et₂Pb²⁺, measured in the presence of hydrogen peroxide, is shown in Fig. 3.

Yamauchi *et al.*⁷ in their studies on the determination of Et₂Pb²⁺ by hydride generation, used 0.004M perchloric acid and 0.75M hydrogen peroxide medium. At a concentration of acid similar to that used in the present procedure, they observed a great improvement in sensitivity, which was associated with degradation of Et₂Pb²⁺. We consider that this degradation cannot be attributed to a direct effect of hydrogen peroxide on R₂Pb²⁺, since we found (by spectrophotometric measurements with the Piloni and Plazzogna method¹¹) no significant variation in R₂Pb²⁺ concentration at the μg/ml lead level, in a 0.10M hydrochloric acid and 0.5M hydrogen peroxide medium, with the same reaction-time as that used in the present hydride generation procedure. Furthermore, if hydrogen peroxide degrades R₂Pb²⁺ to Pb²⁺, after the addition of tetrahydroborate it would be expected that R₂Pb²⁺ would give the same molar response as Pb²⁺, but as shown in Table 3, at constant lead content, the peak heights for Me₂Pb²⁺ and Et₂Pb²⁺ were respectively 3.5 and 5.3 times that for Pb²⁺.

In addition, with the silicone rubber instead of a glass transfer line, a significant effect was observed both in the peak shape and height for R₂Pb²⁺, confirming that the main product of reaction between R₂Pb²⁺ and borohydride is a volatile organolead hydride and not PbH₄, the signal for which is unaffected by the use of silicone rubber tubing. From these results, it may be assumed that the role of hydrogen peroxide is to stabilize the lead in oxidation

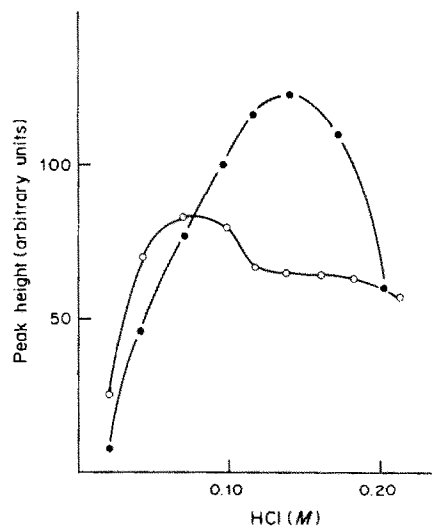


Fig. 3. Effect of sample acidity on signal of Et₂Pb²⁺ (●) and Me₂Pb²⁺ (○) in presence of hydrogen peroxide. Analyte concentration 10 ng(Pb)/ml, other conditions, see Table 2.

Table 3. Analytical figures of merit for lead compounds

Lead compound	Sensitivity*		Apparent blank Pb concentration, ng/l.	Lead detection limit, ng/l.	RSD†, %	Individual optimal conditions
	With H ₂ O ₂	Without H ₂ O ₂				
Me ₃ Pb ⁺	390	390	7§	3§	3.7§	HCl 0.12M, EDTA 10 ⁻⁴ M, 1 ml NaBH ₄ 10%, 0.5 ml H ₂ O ₂ 6M
Et ₃ Pb ⁺	390	390	7§	3§	3.3§	HCl 0.12M, EDTA 10 ⁻⁴ M, 1 ml NaBH ₄ 10%; 0.5 ml H ₂ O ₂ 6M
Me ₂ Pb ²⁺	257	11	10‡	5‡	6.2‡	HCl 0.09M, EDTA 10 ⁻⁴ M, 1 ml NaBH ₄ 10%, 0.5 ml H ₂ O ₂ 10M
Et ₂ Pb ²⁺	390	12	8‡	3‡	4.8‡	HCl 0.12M, EDTA 10 ⁻⁴ M, 1 ml NaBH ₄ 10%, 0.5 ml H ₂ O ₂ 6M
Pb ²⁺	74	1	350‡	60‡	6.0‡	HCl 0.12M, 1 ml NaBH ₄ 10%, 0.5 ml H ₂ O ₂ 3.5M

* (Arbitrary units). ml. ng⁻¹.

† RSD Percentage relative standard deviation at 1 ng(Pb)/ml level, 10 replicate measurements.

§ With or without hydrogen peroxide.

‡ With hydrogen peroxide.

state IV and promote the formation of volatile hydrides. In the case of inorganic lead, the peroxide promotes the formation of Pb(IV), dramatically increasing plumbane formation. The efficiency of generation of plumbane and trialkyl-lead hydrides was calculated by measuring the amount of lead(II) and trialkyl-lead in the residual solutions, after tetrahydroborate reaction, by differential pulse polarography. Standard solutions of 100–150 ng/ml lead concentration were used and each sample was reduced under the optimized experimental conditions. For this purpose, after each injection 0.2 ml of 10M hydrochloric acid was added to the residual solution to destroy the excess of tetrahydroborate. Differential pulse polarography was used because of its ability to discriminate between Pb²⁺, Et₃Pb⁺ and Me₃Pb⁺.¹²

Loss of analyte during the acid addition (assumed to be negligible owing to the final low acidity of the solution) was checked by NDAFS. No production of volatile lead compounds was found to occur. After acidification, the sample was transferred into the polarographic cell, the solution was buffered at pH 5 with acetate buffer, and measurements of residual Pb²⁺ and R₃Pb⁺ were made. From these results the efficiency of analyte volatilization was found to be 27% for Pb²⁺ and 90% for Et₃Pb⁺ and Me₃Pb⁺. This 3.3-fold ratio of efficiencies is comparable to that of 3.5 obtained in the NDAFS measurements of the ratio of peak areas due to R₃Pb⁺ and Pb²⁺. It is therefore assumed that practically all the hydrides formed in solution reach the atomizer and are decomposed to elemental lead. Measurement of residual R₂Pb²⁺ was not possible by polarography owing to presence of the iodide produced during compound preparation. The efficiency of volatilization was determined from the NDAFS signal areas.

Analytical results

The most important analytical figures of merit are presented in Table 3. The optimal experimental conditions found in the present work for each compound

and those found earlier⁶ for Pb²⁺ are also reported. In the determination of all the analytes (except Pb²⁺) the blank was measured in the presence of EDTA, since it was observed that though EDTA suppresses the signal of lead,⁶ up to 10⁴ molar ratio it does not affect the signals for the alkyl-lead compounds tested. The detection limit (3 times the standard deviation of the blank) was found to be practically the same for dialkyl and trialkyl-lead compounds and equal to 3–5 ng of lead per litre. These detection limits, in the case of Et₃Pb⁺ and Et₂Pb²⁺, are lower by a factor of 2.5–3 than those obtained by Yamauchi *et al.*⁷ after a preconcentration step. The linear dynamic range was 3.5 orders of magnitude for Me₂Pb²⁺ and 3.9 for the other alkyl lead compounds.

By using information collected under different chemical conditions, a method for discriminating between R₃Pb⁺, R₂Pb²⁺ and Pb²⁺ was achieved. Table 4 gives the experimental conditions and related sensitivities used in the determination of the different classes of alkyl lead compounds. New conditions were needed because, under the conditions listed in Table 3, dialkyl-lead compounds did not exhibit the same sensitivity, invalidating the correct calculation of the trialkyl-lead concentration.

Under the conditions listed in Table 4 the following four equations relating measured signals to concentration were found valid:

$$S_1 = 210(C_{\text{TML}} + C_{\text{TEL}}) + 202(C_{\text{DML}} + C_{\text{DEL}}) \quad \text{conditions I}$$

$$S_2 = 210(C_{\text{TML}} + C_{\text{TEL}}) + 8(C_{\text{DML}} + C_{\text{DEL}}) \quad \text{conditions II}$$

$$S_3 = 390(C_{\text{TML}} + C_{\text{TEL}}) + 102C_{\text{DML}} + 343C_{\text{DEL}} + 74C_{\text{Pb}} \quad \text{conditions III}$$

$$S_4 = 390(C_{\text{TML}} + C_{\text{TEL}}) + 102C_{\text{DML}} + 343C_{\text{DEL}} \quad \text{conditions IV}$$

where S₁, S₂, S₃ and S₄ are the experimental signals obtained under the relevant conditions and C_{TML},

Table 4. Sensitivities under optimized conditions for the separation of R_3Pb^+ , R_2Pb^{2+} and Pb^{2+}

Sensitivity*					Chemical conditions
Me_3Pb^+	Et_3Pb^+	Me_2Pb^{2+}	Et_2Pb^{2+}	Pb^{2+}	
218	202	201	205	—	I 0.06M HCl, 8M H_2O_2 , $10^{-4}M$ EDTA
218	202	8	8	—	II 0.06M HCl, $10^{-4}M$ EDTA
390	390	102	343	74	III 0.12M HCl, 3.5M H_2O_2
390	390	102	343	—	IV 0.12M HCl, 3.5M H_2O_2 , $10^{-4}M$ EDTA

*Slope of calibration curves in (arbitrary units)·ml·ng⁻¹.

C_{TEL} , C_{DML} , C_{DEL} and C_{Pb} are the concentrations of trimethyl-lead, triethyl-lead, dimethyl-lead, diethyl-lead and inorganic lead, respectively, expressed as ng of lead per ml.

The content of lead was obtained from the S_3 and S_4 signals (at the highest sensitivity for lead) recorded in the presence and absence of EDTA (conditions III and IV). The concentrations of dialkyl-lead compounds were calculated from the S_1 and S_2 signals obtained in the presence and absence of hydrogen peroxide (conditions I and II) and the concentrations of trialkyl-lead compounds were calculated from the S_1 and S_2 signals after subtracting the contribution due to the dialkyl-lead compounds. The relevant equations were

$$C_{Pb} = (S_3 - S_4)/74$$

$$C_{R_2Pb^{2+}} = (S_1 - S_2)/194$$

$$C_{R_3Pb^+} = (S_2 - 8C_{R_2Pb^{2+}})/210$$

The main limitations of the procedure are the impossibility of individual determination of any of the components except lead, the need for calculations by difference, and a decrease in sensitivity for all the alkyl-lead compounds by a factor of 2 when compared with the results obtained under the conditions given in Table 3.

The fact that the sensitivity for R_3Pb^+ compounds averaged 210 and that for R_2Pb^{2+} compounds 202, implies maximum theoretical errors of 4% and 1%, respectively, which is quite acceptable in this kind of analysis.

The accuracy of analysis of mixtures depends, for each group of analytes, on their relative contribution to the total signal and on the standard deviation of the signals involved in the differences.

Owing to the rapidity with which the analyses can be done, reliable average S_i values can be obtained by replication and the overall accuracy greatly increased.

CONCLUSIONS

By changing the chemical conditions for the reaction with sodium tetrahydroborate and the type of

material used for the transport of the volatile products to the atomic-fluorescence spectrometric detector, sound evidence was gained that Me_3Pb^+ , Et_3Pb^+ , Et_2Pb^{2+} and Me_2Pb^{2+} form the corresponding alkyl-lead hydrides at room temperature. The life-time of these alkyl-lead hydrides in the gas phase is sufficiently high to permit their transport to the cell, where they are detected as lead by NDAFS. Only Me_2PbH_2 has been shown to be light-sensitive.

The detection limits under individual optimal conditions (referred to the lead content) are 3–5 ng of lead per litre for trialkyl- and dialkyl-lead compounds.

By use of different chemical conditions the total concentration of trialkyl- and dialkyl-lead compounds and the concentration of inorganic lead can be separately measured.

Whenever more detailed information is required on individual species at the ng/l. lead level, the more time-consuming gas chromatographic/atomic spectrometry methods^{13,14} must be used.

REFERENCES

1. R. Duffy, J. Feeney and H. K. Holliday, *J. Chem. Soc.*, 1962, 1144.
2. R. Duffy and K. Holliday, *ibid.*, 1961, 1679.
3. W. E. Becker and S. E. Cook, *J. Am. Chem. Soc.*, 1960, **82**, 6264.
4. E. Amberger, *Angew. Chem.*, 1960, **72**, 494.
5. K. Jin and M. Taga, *Anal. Chim. Acta*, 1982, **143**, 229.
6. A. D'Ulivo and P. Papoff, *Talanta*, 1985, **32**, 383.
7. H. Yamauchi, F. Arai and Y. Yamamura, *Ind. Health*, 1981, **19**, 115.
8. A. D'Ulivo, C. Festa and P. Papoff, *Talanta*, 1983, **30**, 907.
9. R. Moss and E. V. Browett, *Analyst*, 1966, **91**, 428.
10. H. J. Haupt, F. Huber and J. Gmehling, *Z. Anorg. Allgem. Chem.*, 1972, **390**, 31.
11. G. Pilloni and G. Plazzogna, *Anal. Chim. Acta*, 1966, **35**, 325.
12. M. P. Colombini, R. Fuoco and P. Papoff, *Ann. Chim. Rome*, 1981, **146**, 211.
13. Y. K. Chau, P. T. S. Wong and O. Kramar, *Anal. Chim. Acta*, 1983, **146**, 211.
14. D. Chakraborti, W. R. A. De Jonghe, W. E. Van Mol, R. J. A. Van Cleuvenbergen and F. C. Adams, *Anal. Chem.*, 1984, **56**, 2692.

EXTRACTION AND PHOTOMETRIC DETERMINATION OF LEAD WITH DIAZACROWN ETHER DYE

YUKIO SAKAI and NAKO KAWANO

Faculty of Education, Miyazaki University, Funatsuka, Miyazaki 880, Japan

HIROSHI NAKAMURA and MAKOTO TAKAGI

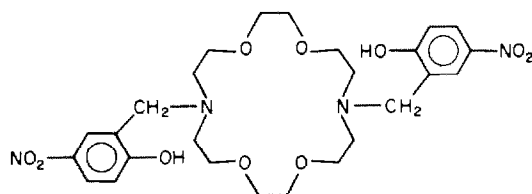
Department of Organic Synthesis, Faculty of Engineering, Kyushu University, Hakozaki, Higashi-ku,
Fukuoka 812, Japan

(Received 2 August 1985. Revised 17 October 1985. Accepted 23 December 1985)

Summary—*N,N'*-Bis(2-hydroxy-5-nitrobenzyl)cryptand-22 (22-Koshland) forms yellow complexes with bivalent metal ions, and these are extractable into 1,2-dichloroethane. The overall extraction constants have been estimated for lead ($10^{-5.4}$), copper ($10^{-5.6}$), mercury ($10^{-5.8}$) and cadmium ($10^{-8.4}$). The result obtained has been applied to extraction and photometric determination of lead. The molar absorptivity at the absorption maximum (406 nm) is 4.47×10^4 l. mole⁻¹. cm⁻¹. The interferences from copper and mercury can be eliminated by the addition of sodium thiosulphate and the interference from cadmium can be eliminated by calculation from the absorbances at 406 and 391 nm (the cadmium complex with 22-Koshland has its absorption maximum at 391 nm). The method has been successfully applied to the determination of lead in zinc powder.

An investigation on complex formation between macrocyclic compounds and metal ions has revealed that the 18-membered crown ether and related compounds form extremely stable cationic complexes with lead.¹⁻⁶ The cationic complexes formed are readily extractable into suitable organic solvents, along with hydrophobic anions. Strongly coloured or fluorescent anions such as picrate and eosinate have frequently been employed as counter-ions for the photometric or fluorimetric determination of trace amounts of lead.⁷⁻⁹

On the basis of the idea that binding of an acidic dye and a crown ether compound would give a new series of extraction and photometric or fluorimetric reagents, we have synthesized such reagents and applied them especially to the determination of alkali-metal and alkaline-earth metal ions.¹⁰⁻¹⁶ Among the reagents synthesized, *N,N'*-bis(2-hydroxy-5-nitrobenzyl)cryptand-22 (22-Koshland)



was found to be a sensitive and selective reagent for calcium among the alkaline-earth metal ions and was successfully applied to its determination in blood serum.¹³ It was also found that this reagent forms a much more stable complex with lead than with calcium,¹⁴ which is compatible with the fact that the lead complex of cryptand-22 is more stable than the corresponding calcium complex.⁴⁻⁶ This immediately

suggests that 22-Koshland would be a selective extraction and photometric reagent for lead.

In this paper, the extraction behaviour of various bivalent heavy metal ions with 22-Koshland was studied with the aim of establishing a selective extraction and photometric method for lead.

EXPERIMENTAL

Reagents

22-Koshland was synthesized from cryptand-22 (Merck, Kryptofix 22) and Koshland-I reagent (2-bromo-methyl-4-nitrophenol, Dojindo Chem. Lab.).¹⁴ The reagent was dissolved in 1,2-dichloroethane to give a $10^{-3}M$ solution, which was stored in a Pyrex flask to minimize contamination by alkali-metal and alkaline-earth metal ions from the container wall. Although the solution becomes contaminated on prolonged (more than a month) storage, it can be regenerated by washing it with a tenth of its volume of 0.02M boric acid, followed by washing twice with distilled water (volume of each wash is the same as that of the boric acid wash).

1,2-Dichloroethane (Wako Pure Chemicals, analytical-reagent grade) and sodium thiosulphate (Merck, "Suprapur" grade) were used without further purification. All other chemicals used were of analytical-reagent grade.

Procedure

An aliquot of sample or standard solution of metal ion was transferred into a 20-ml standard flask, and 2 ml of 0.1M tartaric acid and 1 ml of 0.05M sodium thiosulphate were added. The pH was then adjusted to 6.3 by adding 1 ml of 0.5M hexamine solution previously adjusted to pH 6.3 with acetic acid. Finally the solution was mixed and diluted to 20 ml with water.

A 10-ml portion of this solution was shaken with 10 ml of 1,2-dichloroethane solution of 22-Koshland ($10^{-4}M$) for 30 min, and then centrifuged for 15 min at 3000 rpm. Next 7 ml of the organic phase were accurately measured and transferred to another centrifuge tube. To this was added an equal volume of pH 6.3 buffer solution and the tube was

shaken to remove the bulk of the cadmium complex from the organic phase. After centrifuging, the phases were separated and the absorbances of the organic phase at 391 and 406 nm were measured, for a 10-mm path-length (quartz cell). The absorbance of the lead complex was calculated from both absorbances, by equation (2) below.

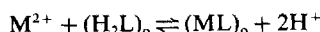
When the concentration of cadmium is less than $4 \times 10^{-6} M$, the washing of the organic phase with pH 6.3 buffer solution can be omitted and the concentration of lead determined from the absorbance at 406 nm.

RESULTS AND DISCUSSION

Extraction equilibrium

As 22-Koshland is a dibasic acid, it is a selective extractant for bivalent cations. Hence, the extraction behaviour of bivalent heavy metal ions, including manganese, iron, cobalt, nickel, copper, zinc, cadmium, mercury and lead, was investigated. Among these metal ions, lead, copper, mercury and cadmium were considerably different in extractability from the others, being quantitatively extracted even at pH 7.0, whereas the other metal ions were not extracted.

The extraction constants (K_{ex}) for bivalent metal ions (M^{2+}) with 22-Koshland (H_2L) were estimated from the pH-dependence of the distribution ratio (D) of the metal ions. The extraction equilibrium may be represented by the equation:



where the subscript "o" indicates the organic phase. The extraction constant can be defined as

$$K_{ex} = \frac{[(ML)_o][H^+]^2}{[M^{2+}][(H_2L)_o]}$$

and thus,

$$\log K_{ex} = \log D - 2pH - \log[(H_2L)_o] \quad (1)$$

Since the complexed metal ion is quantitatively extracted, the distribution ratio of metal ion can easily be determined spectrophotometrically. In addition, as the free 22-Koshland remains in the organic phase, $[(H_2L)_o]$ can be calculated by difference. Consequently, the overall extraction constant can be determined from the pH-dependence of $\log D$, according to equation (1).

Figure 1 shows the plots of $\log D$ against pH. As expected, a linear relationship with a slope of 2 was obtained in every case, indicating the validity of the proposed extraction equilibrium. The extraction constants obtained for the four metal ions are summarized in Table 1 together with those for alkaline-earth metal ions.¹⁴ Although the extraction constants for the other heavy metal ions tested were not determined, they seem to be less than the extraction constant for calcium. It is clearly seen that 22-Koshland is a selective extractant for lead, copper, cadmium and mercury. K_{ex} increases in the order $Cd^{2+} \ll Hg^{2+} < Cu^{2+} < Pb^{2+}$, which is approximately compatible with that of the stability constants for the complexes of these metals with cryptand-22 in aqueous medium,^{4,6} but it is noteworthy that mercury,

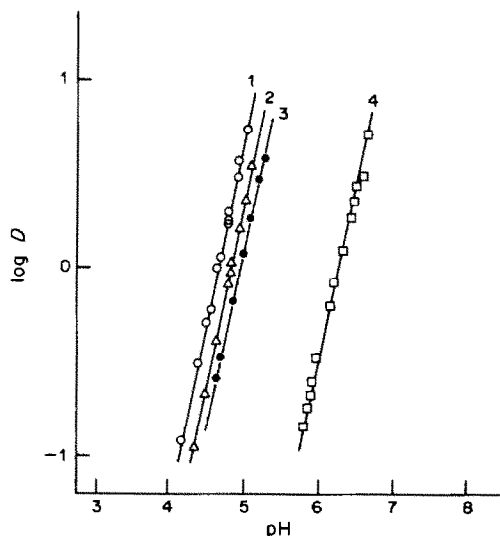


Fig. 1. Effect of pH on the distribution ratios for bivalent metals extracted with 22-Koshland reagent. $[(22\text{-Koshland})_o] = 1.0 \times 10^{-4} M$ (in 1,2-dichloroethane): 1, $1.58 \times 10^{-5} M$ Pb(II) (○); 2, $1.73 \times 10^{-5} M$ Cu(II) (△); 3, $1.96 \times 10^{-5} M$ Hg(II) (●); 4, $1.60 \times 10^{-5} M$ Cd(II) (□).

which forms a very stable complex with cryptand-22 ($\log \beta = 17.85$),⁵ is less extractable than lead and copper. The high stability of the lead complex is accountable for from the match in size between the ionic radius of lead and the cavity size of the cryptand-22 ring of 22-Koshland. Moreover, the lead ion encircled by the cryptand-22 ring of 22-Koshland is probably axially sandwiched between the two nitrophenolate groups of the reagent, either by coordination interaction or ion-ion interaction.⁵

To clarify the selectivity of 22-Koshland for lead, the ratio of K_{ex} of lead to that of the other metal ions is also shown in Table 1, as a separation factor.

Effect of buffer

When the pH of the aqueous phase is adjusted with a small amount of tetramethylammonium hydroxide and/or hydrochloric acid, plots of absorbance of the organic phase against pH show a maximum at around pH 5.5 (curve 1 in Fig. 2), the molar absorptivity being about 3.8×10^4 l.mole⁻¹.cm⁻¹. As the pH is raised above 7, the absorbance gradually

Table 1. Extraction constants (K_{ex}) for bivalent metal ions with 22-Koshland reagent (25°C)

Metal ion	$-\log K_{ex}$	Separation factor for Pb(II)†
Pb(II)	5.4	—
Cu(II)	5.6	1.6
Hg(II)	5.8	2.5
Cd(II)	8.4	10^3
Ca(II)	12.5*	1.3×10^7
Sr(II)	13.5*	1.3×10^8
Ba(II)	15.1*	5×10^9

*Values from reference 4.

† $K_{ex}(\text{Pb})/K_{ex}(\text{M})$.

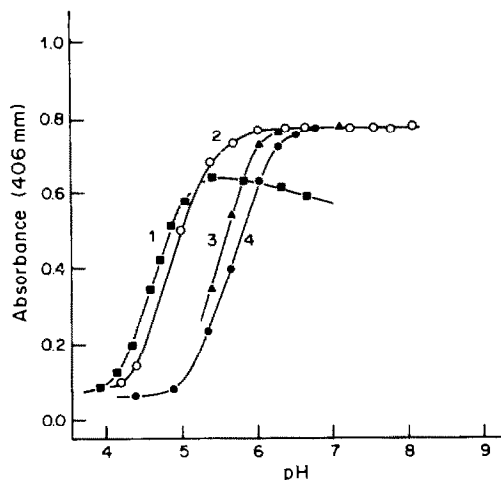


Fig. 2. Effect of complexing agents on the extraction of lead ($1.58 \times 10^{-5} M$) with 22-Koshland reagent: 1, in the absence of complexing agent (■); 2, 0.025M hexamine + 0.01M acetic acid (○); 3, 0.0025M sodium thiosulphate (▲); 4, 0.01M triethanolamine (●).

decreases. A similar trend was observed for the extraction of copper. The decrease at higher pH is probably caused by hydrolysis of the metal ions. It is possible that even at the maximum at around pH 5.5 the extraction of lead is not quantitative. Combined use of triethanolamine or hexamine with acetic acid as the buffer was found to be effective not only in preventing the decrease in extractability at higher pH, but also in making the extraction of lead quantitative, as shown in Fig. 2. When hexamine buffer is used, lead is extracted quantitatively from the aqueous phase at $\text{pH} \geq 6.3$ (Fig. 2). The lower the pH of the aqueous phase, the less is the interference from other metal ions, so the aqueous phase is buffered to pH 6.3 with hexamine and acetic acid. In this case, the concentrations of hexamine and acetic acid must be higher than 0.01M to prevent the hydrolysis of lead. Although the effect of ionic strength on the extraction has not been investigated, it has no noticeable effect up to 0.06.

Effect of foreign ions

The presence of heavy metal ions, except for copper, cadmium, mercury(II) and bismuth, did not interfere in concentrations up to about 0.001M. However, it is necessary to add tartaric acid to prevent hydrolysis. In particular, the precipitation of hydrous iron(III) oxide leads to low analytical results, probably owing to the adsorption of lead.⁹ The addition of tartaric acid is also effective in preventing the hydrolysis of lead at high pH.

As the separation factors for copper and mercury are small (Table 1), it is necessary to eliminate the interference from both ions in determination of lead. Thiosulphate was found to mask both ions. The masking agent itself, at concentrations up to 0.0025M, did not disturb the extraction of lead.

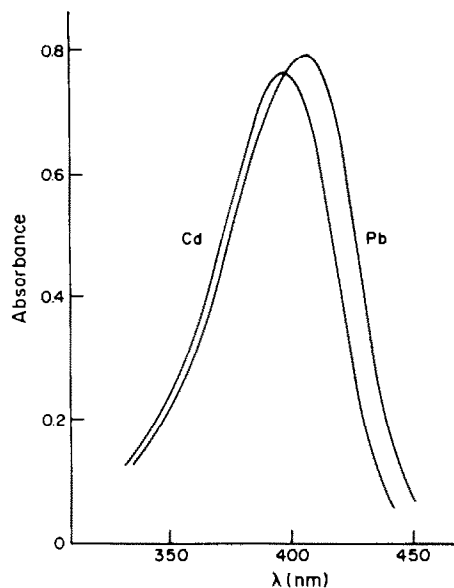


Fig. 3. Absorption spectra of lead and cadmium complexes with 22-Koshland reagent. Concentration of complex = $1.70 \times 10^{-5} M$.

Although the separation factor from cadmium is relatively large (Table 1), this metal can seriously interfere in the determination of lead because it is partly also extracted at pH 6.3. The masking of cadmium by sodium thiosulphate is very poor, but there are two methods to eliminate the interference due to cadmium; one is to wash the organic phase with pH 6.3 buffer solution, and the other is to calculate the net absorbance of the lead complex from measurements at two wavelengths. As shown in Fig. 3, the absorption maximum of the lead complex is at 406 nm, and that of cadmium is at 391 nm. Hence, if the ratios of the molar absorptivities (ϵ) at the two wavelengths are known for both complexes, the absorbance of the lead complex at 406 nm can be calculated by means of the equation¹⁷

$$\text{Abs}_{\text{Pb}}(406 \text{ nm}) = \frac{k_{\text{Cd}} \times \text{Abs}(406 \text{ nm}) - \text{Abs}(391 \text{ nm})}{k_{\text{Cd}} - k_{\text{Pb}}} \quad (2)$$

Table 2. Effect of foreign ions in the determination of $1.52 \times 10^{-5} M$ lead

Foreign ion	Concentration, M	Recovery of lead, %
Fe(III)	2.1×10^{-3}	99.4
Mn(II)	1.1×10^{-3}	98.7
Co(II)	9.2×10^{-4}	98.7
Ni(II)	1.1×10^{-3}	104.0
Cu(II)	2.4×10^{-4}	100.0
Zn(II)	1.4×10^{-3}	99.4
Cd(II)	1.2×10^{-4}	163.7
	1.2×10^{-4}	95.6*
Hg(II)	5.5×10^{-4}	97.1
Bi(III)	3.9×10^{-4}	105.1
Ca(II)	1.5×10^{-3}	102.4
Mg(II)	1.5×10^{-3}	97.1
SO_4^{2-}	0.01	98.8

*Absorbance corrected according to equation (2).

Table 3. Determination of lead in zinc powder

No.	Pb(II) added, M	Pb(II) found, M	Pb in Zn powder, %	C.V., %
1	0	5.9×10^{-6}	0.139	3.7
2	7.9×10^{-6}	1.39×10^{-5}	0.141	1.1

where k represents the ratio $\epsilon_{391}/\epsilon_{406}$ for the metal complex indicated by suffix, and "Abs(406 nm)" and "Abs(391 nm)" represent the absorbances measured at 406 and 391 nm, respectively. The values of k obtained by us were 0.863 for the lead complex and 1.014 for the cadmium complex, but should always be determined with the spectrophotometer used for the analysis. In the present method, the combined use of washing the organic phase with buffer and absorbance correction according to equation (2), is recommended.

The effect of foreign ions was examined, and the tolerance limits are summarized in Table 2. It is seen that for the determination of $1.52 \times 10^{-5}M$ lead, little interference was observed from these ions present in concentrations up to 10–100 times that of lead. Although cadmium interferes seriously, the presence of up to $1.2 \times 10^{-4}M$ cadmium is permissible if absorbance correction is used.

The calibration graph for lead was linear, and the molar absorptivity calculated from the slope was 4.47×10^4 l.mole⁻¹.cm⁻¹, which is approximately equal to that for the calcium complex,¹⁴ though only about half that for the cryptand (2.2.2)–eosin system.⁸

Determination of lead in zinc powder

To examine the applicability of the proposed method, lead in zinc powder was determined. A sample solution was prepared by dissolving 0.3521 g of zinc powder in a small volume of hydrochloric acid and diluting the solution accurately to 100 ml with water. Five-ml portions of the sample solution were analysed with and without spiking with $7.9 \times 10^{-6}M$ lead. The results of five determinations are shown in Table 3, together with the coefficient of variation (C.V.). The values are in good agreement and similar to the result obtained by atomic-absorption spectrometry ($6.0 \times 10^{-6}M$ Pb). The cadmium concentration in the sample solution was found to be $4.0 \times 10^{-6}M$, by atomic-absorption spectrometry, and was below the interference level.

It has been proved that lead is quantitatively

extracted at pH > 6 and photometrically determined with 22-Koshland. The relatively serious interferences from copper, mercury and cadmium can be prevented by using a masking agent and a compensating absorbance measurement.

Compared with the similar method using eosin and cryptand (2.2.2)⁸ or 18-crown-6,⁹ the present method is superior in the pH range for extraction but inferior in sensitivity to the fluorimetric determination with eosin. To improve the sensitivity and selectivity, various chromogenic and fluorogenic crown ether reagents have been synthesized¹⁶ and investigation on their extraction behaviour with metal ions is in progress.

REFERENCES

1. Y. Takeda and H. Kato, *Bull. Chem. Soc. Japan*, 1979, **52**, 1027.
2. R. M. Izatt, R. E. Terry, B. L. Haymore, L. D. Hansen, N. K. Dalley, A. G. Avondet and J. J. Christensen, *J. Am. Chem. Soc.*, 1976, **98**, 7620.
3. F. Arnaud-Neu, B. Spiess and M. J. Schwing-Weill, *Helv. Chim. Acta*, 1977, **60**, 2633.
4. *Idem*, *J. Am. Chem. Soc.* 1982, **104**, 5641.
5. G. Anderegg, *Helv. Chim. Acta*, 1975, **58**, 1218.
6. *Idem*, *ibid.*, 1981, **64**, 1790.
7. T. Sekine, K. Shioda and Y. Hasegawa, *J. Inorg. Nucl. Chem.*, 1979, **41**, 571.
8. W. Szczepaniak and B. Juskowiak, *Anal. Chim. Acta*, 1982, **140**, 261.
9. A. Sanz-Medcl, D. Blanco Gomis, E. Fuente and S. Arribas Jimeno, *Talanta*, 1984, **31**, 515.
10. M. Takagi, H. Nakamura and K. Ueno, *Anal. Lett.*, 1977, **10**, 1115.
11. H. Nakamura, M. Takagi and K. Ueno, *Talanta*, 1979, **26**, 921.
12. *Idem*, *Anal. Chem.*, 1980, **52**, 1668.
13. H. Nishida, M. Tazaki, M. Takagi and K. Ueno, *Mikrochim. Acta*, 1981 **I**, 281.
14. M. Shiga, N. Nishida, H. Nakamura, M. Takagi and K. Ueno, *Bunseki Kagaku*, 1983, **32**, E293.
15. H. Nishida, Y. Katayama, H. Katsuki, H. Nakamura, M. Takagi and K. Ueno, *Chem. Lett.*, **1982**, 1853.
16. M. Takagi and K. Ueno, in "Host Guest Complex Chemistry III", in "Topics in Current Chemistry", Vol. 121, F. L. Boschke (ed.), pp. 39–65. Springer, Berlin, 1984.
17. H. Watanabe, *Talanta*, 1974, **21**, 295.

DETERMINATION OF PALLADIUM WITH THIOCYANATE AND RHODAMINE B BY A SOLVENT-EXTRACTION METHOD

I. LOPEZ GARCIA*, J. MARTINEZ AVILES and M. HERNANDEZ CORDOBA
Department of Analytical Chemistry, Faculty of Chemistry, University of Murcia, Murcia, Spain

(Received 19 February 1985. Revised 3 December 1985. Accepted 9 December 1985)

Summary—Sensitive spectrophotometric and spectrofluorimetric procedures for the determination of palladium have been developed, based on solvent-extraction of the ion-pair formed between Rhodamine B and the anionic complex of Pd(II) with thiocyanate. With an organic to aqueous phase-volume ratio of 1:5, the molar absorptivity is $9.0 \times 10^4 \text{ l. mole}^{-1} \text{ cm}^{-1}$ and the absorbance of the reagent blank is 0.026. Spectrophotometrically, palladium can be determined in the range 0.1–8.8 μg . Spectrofluorimetrically, it can be determined over the range 0.04–1.5 μg . The spectrophotometric procedure has been applied to the determination of palladium in dental alloys, organopalladium compounds and hydrogenation catalysts.

Most of the spectrophotometric methods for palladium determination are based on the formation of chelates with organic reagents.¹⁻³ Conversely, few methods based on the formation of ion-pairs with basic dyes have been developed, e.g., the ion-association compounds of palladium with azide and Methylene Blue,⁹ iodide and pyronine G,¹⁰ and with thiocyanate and Crystal Violet.¹¹ Some ion-association compounds precipitate at the phase boundary or on the walls of the separatory funnel when the aqueous solution is shaken with an organic solvent (flotation methods), and Rhodamine 6G and Methylene Blue have been used for palladium determination in this way.^{12,13}

The purpose of the present work was to find a suitable colour system for the determination of palladium after solvent extraction. We chose Rhodamine B as counter-ion for the anionic thiocyanate-palladium complex. The proposed method is sensitive, has a low reagent blank, and is easy to use.

EXPERIMENTAL

Apparatus

A Pye Unicam SP8-200 spectrophotometer was used for the absorbance measurements. Fluorescence intensity measurements were made with a Perkin-Elmer 3000 spectrofluorimeter; 5-nm band-widths were used in both the excitation and emission systems.

Reagents

All inorganic chemicals used were of analytical reagent grade and doubly distilled water was used throughout. Rhodamine B solution ($10^{-3}M$) was prepared from the commercial product (Merck) without further purification. Standard palladium solution ($5 \times 10^{-3}M$) was prepared from palladium(II) chloride and standardized gravimetri-

cally.¹⁴ Working solutions (1 $\mu\text{g}/\text{ml}$) were prepared from the standard solution on the day of use.

Procedures

Spectrophotometric method. To a volume of sample solution, in a separatory funnel, containing between 0.1 and 8.8 μg of palladium(II), add 5 ml of 4.5M sulphuric acid, 1 ml of 0.025M potassium thiocyanate solution, 2.5 ml of Rhodamine B solution and dilute to 25 ml with water. Extract the mixture with 5 ml of butyl acetate (exactly measured) by shaking the funnel vigorously for 1 min, allow the phases to separate and discard the aqueous phase. Wash the organic layer with two 10-ml portions of 0.9M sulphuric acid, transfer it into a centrifuge tube and centrifuge it. Measure the absorbance of the organic layer at 555 nm against a reagent blank similarly prepared. Prepare a calibration graph, using different volumes of standard palladium(II) solution.

Spectrofluorimetric method. In a separatory funnel place the sample solution (0.04–1.5 μg of palladium), add 5 ml of 4.5M sulphuric acid, 1 ml of 0.015M potassium thiocyanate solution and 1.5 ml of Rhodamine B solution, dilute to 25 ml with water and extract the mixture with 8 ml of butyl acetate (accurately measured). Discard the aqueous phase and wash the organic layer as in the spectrophotometric method. Centrifuge the organic layer, take exactly 5 ml of it and add exactly 2 ml of ethanol. Measure the fluorescence at 573 nm with excitation at 550 nm. Prepare a calibration graph by the procedure described. Run a reagent blank in the same way and subtract its fluorescence from that of the sample.

Procedure for dental alloys

Dissolve 10 mg of sample in 10 ml of *aqua regia* and evaporate to near dryness. Add about 10 ml of water and heat again. Cool, transfer to a separatory funnel and dilute to about 50 ml. Add 10 ml of 1% sodium dimethylglyoximate solution and mix. After 15 min, extract with two 5-ml portions of chloroform (shaking time 30 sec). Evaporate the combined extracts to dryness on a water-bath. Mineralize the residue by evaporation with a mixture of 3 ml of concentrated hydrochloric acid and 2 ml of concentrated nitric acid. Dissolve the residue in 1M hydrochloric acid and make up to volume with water in a 500-ml standard flask. Take an aliquot and determine palladium according to the methods given above.

*Author to whom correspondence should be addressed.

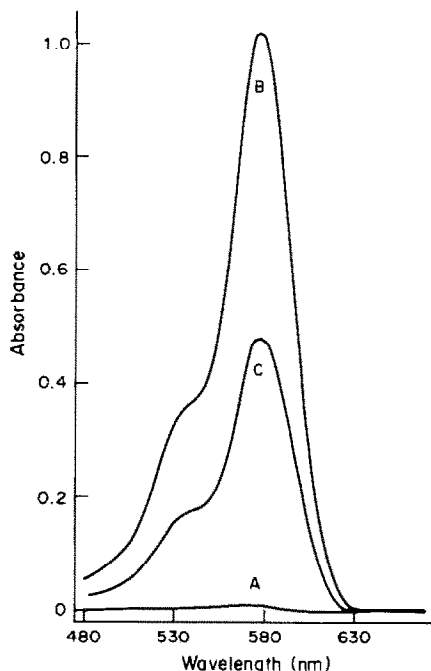


Fig. 1. Absorption spectra. (A) reagent blank (reference, extracting solvent); (B) and (C) with 5.87 and 2.68 μg of palladium, respectively (reference extracting solvent); aqueous phase, 25 ml, organic phase, 5 ml.

Procedure for organopalladium compounds and hydrogenation catalysts

Dissolve the sample as above, filter if necessary and dilute to known volume. Take an aliquot containing 0.04–8.8 μg of palladium and apply one of the recommended procedures.

RESULTS AND DISCUSSION

In a preliminary study we found that palladium forms an ion-association complex with Rhodamine B in the presence of an excess of thiocyanate. This compound is extractable into organic solvents. The use of very polar solvents leads to high values for the reagent blank whereas if the polarity is too low the colourless form of the dye predominates in the organic layer. The best results are obtained with butyl acetate as solvent. The complex extracted is very stable and washing with two 10-ml portions of 0.9M sulphuric acid gives a reagent blank absorbance of about 0.026 at 555 nm.

Figure 1 shows the absorption spectra of the complex in butyl acetate and of the reagent blank obtained as described in the procedure. The absorption spectrum of the extracted ion-association compound is almost identical in shape to the spectrum of an aqueous solution of Rhodamine B, with a slight red-shift of the absorption maximum. The excitation and emission spectra are shown in Fig. 2. As can be seen, maximum fluorescence intensity is obtained at 573 nm, with excitation at 550 nm. Addition of ethanol to the organic phase greatly increases the

fluorescence intensity of the palladium complex. Figure 3 shows the effect of dilution with ethanol. Although the dilution process decreases the final concentration of palladium, the fluorescence intensity is maximal in a 65:35 v/v mixture of butyl acetate and ethanol. Therefore, a dilution of 5 ml of extract with 2 ml of ethanol was used (equivalent to $\sim 70:30$ v/v ratio).

Effect of acidity and reagent concentrations

Sulphuric acid concentration. With fixed concentrations of the other reagents, the absorbance and fluorescence for palladium samples measured against the reagent blank were maximal and constant for the acidity range 0.1–1.8M. The value of the reagent blank decreases gradually with increase in sulphuric acid concentration, but almost constant in the acid range stated. A sulphuric acid concentration of about 0.9M was therefore selected as optimal.

Rhodamine B concentration. As can be seen in Fig. 4 the absorbance for palladium (measured against the reagent blank) is maximal and constant with a dyestuff concentration $> 6 \times 10^{-5}M$. A $10^{-4}M$ Rhodamine B concentration was chosen for the spectrophotometric method. When the spectrofluorimetric procedure is used, a $4 \times 10^{-5}M$ Rhodamine B concentration is recommended because the lower the amount of Rhodamine B used, the lower the reagent blank.

Thiocyanate concentration. Figure 5 shows the effect of thiocyanate concentration on the fluorescence. Similar results were found for the spectrophotometric technique. Consequently, 6×10^{-4} and $10^{-3}M$ concentrations were chosen for the fluorimetric and spectrophotometric procedures, respectively.

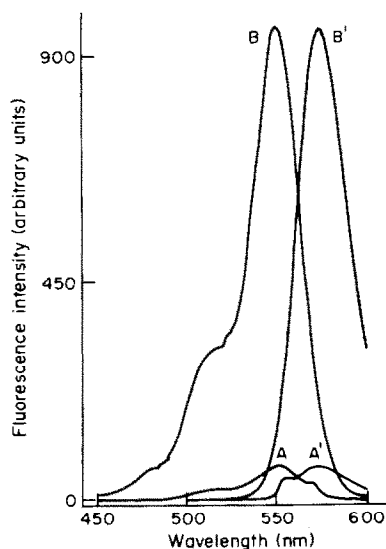


Fig. 2. Excitation and emission ($'$) spectra of reagent blank (A) and the ion-association compound (B) in 5:2 v/v butyl acetate-ethanol mixture; aqueous phase, 1.17 μg of palladium.

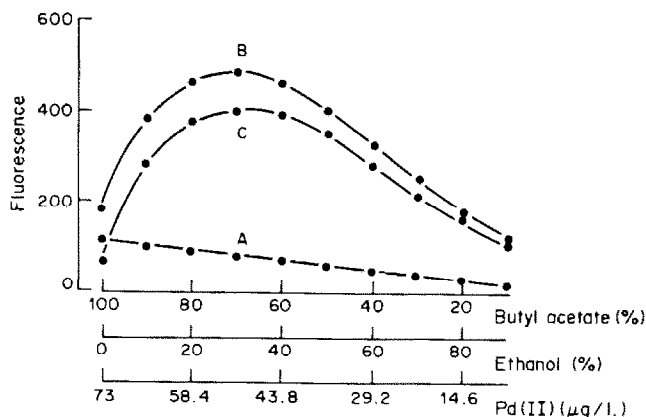


Fig. 3. Effect of dilution with ethanol on fluorescence. (A) reagent blank; (B) and (C) with palladium; (B) reference solvent mixture, (C) reference reagent blank.

Characteristics of the compound extracted

The extraction efficiency under the selected conditions was calculated from the results for two successive extractions of the same sample. A value of about 99% was obtained.

The palladium:Rhodamine B and palladium:thiocyanate molar ratios were calculated by the continuous-variations method, 1:2 and 1:4 ratios respectively being found. Therefore, the extracted compound is [Rhodamine B]₂ [Pd(SCN)₂]⁻.

The rate of extraction is high. Shaking times ranging from 40 sec to 3 min did not produce any change in absorbance, so a 1-min shaking time was selected. Both the absorbance and fluorescence values of the butyl acetate extract remain constant for at least 8 hr.

Calibration graph

Under the recommended conditions, the spectrophotometric calibration graph is linear over the

range 0.1–8.8 μg of palladium. The molar absorptivity at 555 nm calculated from the slope of the graph is 9.0×10^4 l.mole⁻¹.cm⁻¹. The precision is shown in Table 1. The standard deviation for the absorbance of the reagent blank was 0.0011.

The spectrofluorimetric calibration graph was linear over the range 0.04–1.5 μg of palladium. The relative standard deviation of the fluorescence intensity for 10 determinations of 0.5 μg of palladium was 1.3%.

Effect of other ions

The effect of foreign ions on the spectrophotometric determination of 3 μg of palladium is presented in Table 2. An error of ±2% in the absorbance value was considered tolerable. The most serious interferents were Pt(IV), Ag(I), Au(III), Rh(III) and Hg(II). The interference of silver can be avoided by adding bromide and filtering. If Pt(IV), Au(III), Rh(III) or Hg(II) is present a preliminary

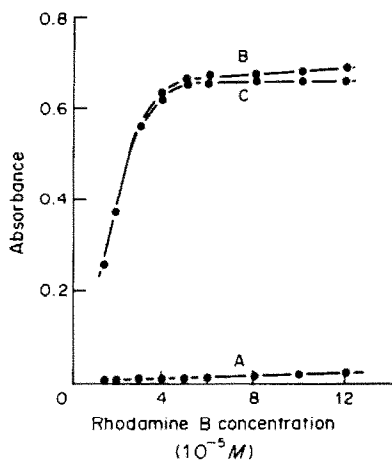


Fig. 4. Effect of concentration of Rhodamine B. (A) reagent blank (reference extracting solvent); (B) and (C) with 4.5 μg of palladium, (B) reference extracting solvent and (C) reference reagent blank.

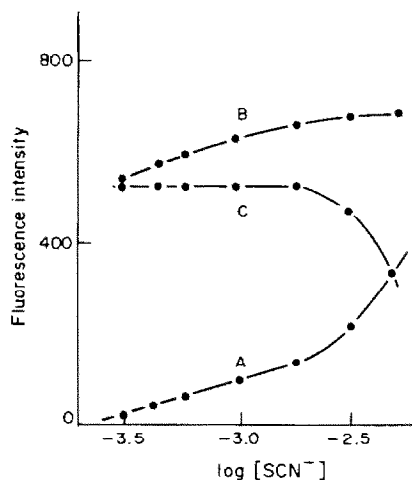


Fig. 5. Effect of the concentration of thiocyanate. (A) reagent blank (reference solvent mixture); (B) and (C) with 0.7 μg of palladium; (B) reference solvent mixture and (C) reference reagent blank.

Table 1. Precision of the spectrophotometric determination of palladium with thiocyanate and Rhodamine B (10 replicates)

Palladium added, μg	Palladium found, μg	Std. devn., μg	Confidence limits (probability level 0.95), μg
1.25	1.25	0.012	1.25 \pm 0.09
3.75	3.74	0.029	3.74 \pm 0.02
6.25	6.26	0.034	6.26 \pm 0.02

Table 2. Effect of foreign ions on the spectrophotometric determination of 3 μg of palladium

Ion	Limiting molar ratio [Ion]/[Pd(II)]
F ⁻ , Cl ⁻ , phosphate, Co(II)	10000*
Zn(II), Ru(III)	5000
Br ⁻ , nitrate, Cu(II), Ni(II), Al(III), Mn(II), Fe(III)§	2000
Cr(VI), Bi(III), Fe(III)	500
Perchlorate, V(V), Ag(I)†	100
Mo(VI), W(VI)	50
Ir(III)	20
I ⁻ , Os(VIII)	1
Pt(IV), Ag(I), Au(III), Hg(II), Rh(III)	<1

*Maximum molar ratio tested.

§In the presence of 0.01M fluoride.

†With pretreatment.

Table 3. Palladium determination in samples

Sample	Pd content, %	Pd found, %*
Dental alloy 1	30†	29.8
Dental alloy 2	22§	22.1
Catalyst (Al ₂ O ₃)	5†	5.0
Catalyst (BaSO ₄)	5†	5.1
Organopalladium compound 1	15.7§	15.6
Organopalladium compound 2	18.4§	18.8

*Average of three determinations.

†Nominal content.

§Palladium found spectrophotometrically by solvent extraction with dimethylglyoxime and chloroform.

separation of palladium from the matrix is necessary. Extraction of palladium dimethylglyoximate with chloroform can be used for this purpose.

Applications

The method was applied to the determination of palladium in dental alloys, catalysts and organopalladium compounds. Samples were analysed according to the recommended spectrophotometric procedure. Table 3 gives the results compared with those obtained by another recommended solvent-extraction method.¹⁵

Conclusion

The methods proposed are simple, rapid and sensitive. Both compare very favourably with most published methods for the determination of palladium by use of ion-association compounds, and they can certainly be classed amongst the most sensitive.

Acknowledgement—The authors thank Dr. G. López (Inorganic Chemistry Department, University of Murcia) for the kind gift of organopalladium samples.

REFERENCES

1. R. Borisova, M. Koeva and E. Topalova, *Talanta*, 1975, **22**, 791.
2. T. Kotsuyanagi, H. Hoshino and K. Aomura, *Anal. Chim. Acta*, 1974, **71**, 349.
3. S. Banerjee and R. K. Dutta, *Zh. Analit. Khim.*, 1975, **277**, 379.
4. B. Morelli, *Analyst*, 1984, **109**, 47.
5. E. L. Kothny, *Mikrochim. Acta*, 1978 **I**, 425.
6. F. Corigliano, S. Di Pascuale and A. Rainieri, *Analyst*, 1977, **102**, 25.
7. A. E. Mahgoub, N. A. Darwish and M. M. Shoukry, *ibid.*, 1978, **103**, 879.
8. P. W. Beaupré and W. J. Holland, *Mikrochim. Acta*, 1978 **II**, 327.
9. R. Kuroda, N. Yoshikuni and Y. Kamimura, *Anal. Chim. Acta*, 1972, **60**, 71.
10. S. Jaya, T. Rao and T. V. Ramakrishna, *J. Less-Common Met.*, 1983, **91**, 261.
11. Z. M. Khvatkova and U. U. Golovina, *Zh. Analit. Khim.*, 1979, **34**, 2035.
12. Z. Marzenko and M. Jarosz, *Talanta*, 1981, **28**, 561.
13. *Idem*, *Analyst*, 1981, **106**, 751.
14. I. M. Kolthoff and P. J. Elving (eds.) *Treatise on Analytical Chemistry*, Part II, Vol. 8, p. 453. Interscience, New York, 1963.
15. R. S. Young, *Analyst*, 1951, **76**, 49.

SIMULTANEOUS TWO- AND THREE-COMPONENT DETERMINATIONS IN MULTICOMPONENT MIXTURES BY EXTRACTION-SPECTROPHOTOMETRY AND THERMOCHROMISM OF ION-ASSOCIATION COMPLEXES

TADAO SAKAI and NORIKO OHNO

Department of Chemistry, Asahi University, 1851 Hozumi, Hozumi-cho, Gifu 501-02, Japan

(Received 29 May 1985. Revised 21 November 1985. Accepted 6 December 1985)

Summary—A selective method of determination of amines and quaternary ammonium salts by solvent extraction and thermochromism of ion-association complexes has been established. The method is based on the formation of ion-association species with tetrabromophenolphthalein ethyl ester and the thermochromism effect in the organic phase at low temperature. The absorbance of the red amine charge-transfer complexes decreases quantitatively (ΔA) with increase in temperature (ΔT), and $\Delta A/\Delta T$ is characteristic of a particular species. This characteristic has been applied for the sensitive and selective determination of amines. The absorbance of the blue quaternary ammonium ion-association complexes does not vary with temperature, however, and the quaternary ammonium compounds can be determined without interference by amines because of the disappearance of the red species at 60°. Methylephedrine, diphenhydramine, ephedrine (amines), benzethonium and/or berberine (quaternary ammonium compounds) in two- and three-component mixtures can be determined by using the thermochromism effect. The method is highly selective, sensitive and reproducible.

Some acid dyes, such as Bromophenol Blue,¹ Bromocresol Green,² Bromothymol Blue³ (diprotic acid dyes), picric acid,⁴ 2,6-dibromophenolindophenol⁵ and tetrabromophenolphthalein ethyl ester⁶ (monoprotic acid dyes) have been used for extractive spectrophotometric determination of amines, alkaloids and quaternary ammonium compounds (R_4N^+). Although the narrow optimum pH range for use with Bromophenol Blue, Bromocresol Green and Bromothymol Blue is of advantage in selective extraction of onium compounds, the extractability of ion-association complexes with these dyes is poor. Of the dyes tested above, tetrabromophenolphthalein ethyl ester (TBPE) has the highest sensitivity and best extractability for secondary and tertiary aromatic amines and quaternary ammonium salts, but the absorption spectra and optimum pH ranges for extraction of various compounds overlap. As a result, TBPE is not suitable for selective determination of quaternary ammonium compounds and amines in multicomponent mixtures.

However, we have found that the red amine-TBPE complexes show regular and reversible thermochromism in the organic phase, whereas almost no absorbance change is observed with the blue R_4N^+ -TBPE complexes.⁷ The absorbance of the red species decreases with increase in temperature. Moreover, we have found that the temperature dependence of the absorbance is specific for each red complex.^{7,8} This thermochromic effect can be applied to remove the interference of amines in the determination of quaternary ammonium compounds.

This paper describes the simultaneous and highly sensitive determination of ephedrine, diphenhydramine, methylephedrine, chlorpheniramine, benzethonium and/or berberine in multicomponent mixtures by use of solvent extraction and thermochromism.

Official methods for these onium compounds are titrimetry⁹ and spectrophotometry.¹⁰

EXPERIMENTAL

Apparatus

A Hitachi model 556 double-beam spectrophotometer equipped with a controlled-temperature cell-holder, and a Hitachi model 057 X-Y recorder were used for absorbance measurements and recording spectra. Stopped quartz cells of 10-mm path-length were used for the measurements. The temperature in the cell was raised from 25° to 50° or 60° by a Komatsu-Yamato CTE-240 circulator.

Reagents

A standard methylephedrine solution ($1 \times 10^{-3} M$) was prepared by dissolving 0.1257 g of "10% methylephedrine hydrochloride powder" in 100 ml of distilled water and the concentration was determined by the official titrimetric method.⁹

A standard diphenhydramine solution ($1 \times 10^{-2} M$) was prepared by dissolving 0.2981 g of diphenhydramine hydrochloride in 100 ml of distilled water.

A standard ephedrine solution ($1 \times 10^{-2} M$) was prepared by dissolving 0.2017 g of ephedrine hydrochloride in 100 ml of distilled water.

A standard chlorpheniramine solution ($1 \times 10^{-2} M$) was prepared by dissolving 0.3909 g of chlorpheniramine maleate in 100 ml of distilled water.

A standard benzethonium solution ($5 \times 10^{-3} M$) was prepared by dissolving 0.2240 g of benzethonium chloride in 100 ml of distilled water.

A standard berberine solution ($1 \times 10^{-3}M$) was prepared by dissolving 0.4078 g of berberine hydrochloride in hot distilled water, cooling and diluting to 1 litre. The concentration was determined by the official method.¹⁰

Working solutions were prepared by accurate dilution. Buffer solution, pH 9.0, was made from equal volumes of 0.3M potassium dihydrogen phosphate and 0.1M sodium borate and the pH was adjusted with 1M sodium hydroxide or 0.5M sulphuric acid.

Tetrabromophenolphthalein ethyl ester solution ($4 \times 10^{-3}M$) was prepared by dissolving 0.7001 g of the potassium salt in 250 ml of ethanol, by heating on an electrical heater, then cooling.

Standard procedure

Pipette 1 ml of sample solution containing two amines (total concentration about 10–50 $\mu\text{g/ml}$), 2 ml of TBPE solution ($4 \times 10^{-3}M$) and 10 ml of buffer solution (pH 9.0) into a 100-ml separating funnel and dilute the mixture with distilled water to 50 ml. Shake the solution mechanically with 10 ml of 1,2-dichloroethane for 5 min. Transfer the organic layer into a test-tube fitted with a stopper and centrifuge it to remove water droplets. Measure the absorbances at the appropriate wavelengths after adjusting the temperature in the cell.

RESULTS AND DISCUSSION

Absorption maxima of ion-association complexes with TBPE

The absorption spectra of the TBPE ion-association species formed with diphenhydramine, methylephedrine, ephedrine and berberine are shown in Fig. 1. The absorption maxima of the three red species are at 573, 550 and 555 nm, respectively; and at 575 nm for chlorpheniramine. The absorption maxima of all the blue species are at 610 nm. It is assumed that secondary and tertiary amines form charge-transfer complexes by hydrogen bonding with the TBPE molecule, and quaternary ammonium salts form ion-pairs which have the colour of the TBPE dye anion when extracted into 1,2-dichloroethane.

Effects of experimental variables

Addition of 2 ml of $4 \times 10^{-3}M$ TBPE (about 40-fold molar ratio to the amines) was found to be sufficient for extraction to be complete. However, the volume of ethanolic TBPE solution added was kept

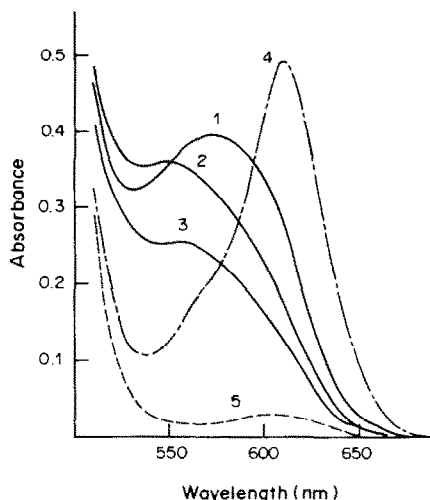


Fig. 1. Absorption spectra of ion-association complexes formed with TBPE: (1) $2 \times 10^{-6}M$ diphenhydramine; (2) $2 \times 10^{-6}M$ methylephedrine; (3) $3 \times 10^{-6}M$ ephedrine; (4) $1 \times 10^{-6}M$ berberine (R_4N); (5) reagent blank: TBPE $1.6 \times 10^{-4}M$; solvent 1,2-dichloroethane; reference water.

at less than 2 ml because the presence of too much ethanol caused an increase in absorbance. The shaking time was fixed at 5 min and the absorbance of the extract was stable for at least 2 hr at room temperature. The molar ratio of TBPE to either amine or quaternary ammonium ion was found to be 1:1 by the continuous-variations method under the recommended conditions. The extraction efficiency was more than 95%, and a single extraction is recommended.

Spectral characteristics

Table 1 shows the molar absorptivities of the red complexes at 25, 50 or 60°, the wavelengths of maximum absorption, and the optimum pH ranges for extraction. The molar absorptivities all decrease with increase in temperature, but the decrease for the red species is much greater than that for the blue complexes, and can be assumed to be caused by dissociation of the complex into protonated TBPE and the free amine, as shown in our previous paper.⁷ The slight decrease in the molar absorptivity of the

Table 1. Optimum pH ranges and molar absorptivities of ion-association compounds with TBPE

Amine	λ_{max} , nm	Molar absorptivity,* $l. \text{mole}^{-1}. \text{cm}^{-1}$		pH range
		25°	50°	
Berberine	610	$9.80 \pm 0.037 \times 10^4$	$9.24 \pm 0.035 \times 10^4$ †	5.5–11.0
Benzethonium	610	$9.00 \pm 0.036 \times 10^4$	$8.23 \pm 0.032 \times 10^4$ †	7.0–11.0
Chlorpheniramine	575	$3.81 \pm 0.020 \times 10^4$	$2.61 \pm 0.015 \times 10^4$	7.5–9.5
Diphenhydramine	573	$3.74 \pm 0.015 \times 10^4$	$2.09 \pm 0.009 \times 10^4$	7.0–9.0
Ephedrine	555	$1.56 \pm 0.012 \times 10^4$	$7.70 \pm 0.05 \times 10^3$	9.0–11.0
Methylephedrine	550	$3.40 \pm 0.014 \times 10^4$	$2.13 \pm 0.017 \times 10^4$	9.0–9.8

*Average and standard deviation of 10 determinations.

†Measured at 60°.

Table 2. Molar absorptivities and their differences ($\Delta\epsilon$) of ion-association compounds with TBPE

Amine	λ , nm	Molar absorptivity,* $10^4 \text{ l. mole}^{-1} \text{ cm}^{-1}$		$\Delta\epsilon$,* $10^4 \text{ l. mole}^{-1} \text{ cm}^{-1}$
		25°	50°	
Diphenhydramine	550	3.37 ± 0.016	1.96 ± 0.012	1.41 ± 0.011
	555	3.49 ± 0.016	2.02 ± 0.013	1.47 ± 0.012
	573	3.74 ± 0.015	2.09 ± 0.009	1.65 ± 0.010
Methylephedrine	550	3.40 ± 0.014	2.13 ± 0.017	1.27 ± 0.011
	573	3.02 ± 0.022	1.90 ± 0.015	1.12 ± 0.010
Ephedrine†	555	1.56 ± 0.012	0.77 ± 0.005	0.79 ± 0.008
	573	1.38 ± 0.009	0.685 ± 0.005	0.695 ± 0.007
Chlorpheniramine	550	3.24 ± 0.023	2.36 ± 0.020	0.88 ± 0.010
	575	3.81 ± 0.020	2.61 ± 0.015	1.20 ± 0.016

*Average and standard deviation of 10 measurements.

†These values refer to extraction at pH 9.0 (where extraction is incomplete) and are apparent molar absorptivities (calculated as if extraction were complete).

blue species can be assumed to be caused by expansion of the 1,2-dichloroethane. The temperature for benzethonium and berberine determination is adjusted to 60° because the colour of the red species apparently disappears at 60°. The temperature for the absorbance measurements was controlled to within $\pm 1^\circ$.

Table 2 shows the molar absorptivities of the TBPE-amine complexes at different wavelengths and temperatures. For any pair of amines which differ sufficiently in these spectral characteristics the following equations can be used to determine both amine concentrations in the organic phase.*

$$C_I = \frac{\Delta A_B \times \Delta \epsilon_{II,A} - \Delta A_A \times \Delta \epsilon_{II,B}}{\Delta \epsilon_{I,B} \times \Delta \epsilon_{II,A} - \Delta \epsilon_{I,A} \times \Delta \epsilon_{II,B}} \quad (1)$$

$$C_{II} = \frac{\Delta A_A \times \Delta \epsilon_{I,B} - \Delta A_B \times \Delta \epsilon_{I,A}}{\Delta \epsilon_{II,A} \times \Delta \epsilon_{I,B} - \Delta \epsilon_{I,A} \times \Delta \epsilon_{II,B}} \quad (2)$$

where $\Delta\epsilon$ is the difference between the molar absorptivities of a given species at 25 and 50°, subscripts I and II indicate amines I and II, subscripts A and B are the wavelengths of maximum absorption of the complexes, and ΔA_A and ΔA_B are defined as

$$\Delta A_A = A_{25, A, nm} - A_{50, A, nm} \quad (3)$$

$$\Delta A_B = A_{25, B, nm} - A_{50, B, nm} \quad (4)$$

Consequently, each amine concentration, C_I and C_{II} , can be experimentally determined by measurements of the absorbance differences (ΔA_A and ΔA_B) as shown in Fig. 2. In this work, as the extraction was done with 50 ml of aqueous phase and 10 ml of 1,2-dichloroethane, the initial concentrations in the aqueous solution will be a fifth of those found in the organic phase. The slightly incomplete extraction is automatically compensated for by using a single extraction in determining the spectral characteristics.

Analysis of commercial drugs

For determination of ephedrine, diphenhydramine, methylephedrine and chlorpheniramine in commercial drugs, a sample solution containing no more than a total amine concentration of 60 $\mu\text{g/ml}$ was treated by the standard procedure. The temperature of the extract in the cell was adjusted to 50° after the absorbance measurement at 25°, and ΔA at two wavelengths was measured. For ephedrine and diphenhydramine mixtures, the wavelengths used were 555 and 573 nm, and for methylephedrine and chlorpheniramine mixtures, 550 and 573 nm. The results obtained are shown in Tables 3 and 4. Values found for ephedrine, diphenhydramine, chlorpheniramine and methylephedrine in the commercial sample solu-

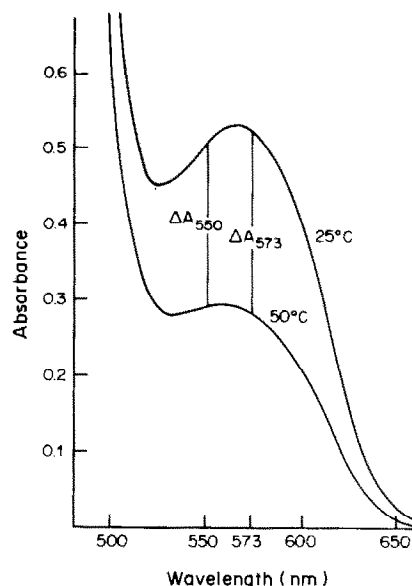


Fig. 2. Absorption spectra of methylephedrine and diphenhydramine mixture with TBPE in 1,2-dichloroethane at 25° and 50°C: methylephedrine, $1 \times 10^{-6} M$; diphenhydramine, $2 \times 10^{-6} M$; TBPE, $1.6 \times 10^{-4} M$; buffer pH 9.0: ΔA_{550} and ΔA_{573} are the differences in absorbance at each wavelength.

*These equations are the correct forms of equations (9) and (10) in an earlier paper (T. Sakai, *Analyst*, 1982, **107**, 640), in which a printing error escaped detection and correction.

Table 3. Determination of methylephedrine and chlorpheniramine in commercial drugs*

Sample	Nominal amount, mg		Methylephedrine		Chlorpheniramine	
	Methylephedrine	Chlorpheniramine	Found, † mg	Range of recovery, %	Found, † mg	Range of recovery, %
1	12.5	3.0	12.32	97.4–99.7	2.93	96.7–98.7
2	10.0	4.0	9.80	97.1–98.9	3.92	95.8–100.3
3	5.0	3.0	5.20	102.8–105.2	2.98	96.3–102.3
4	1.3	1.3	1.31	100.0–101.5	1.30	99.2–100.8

*Other contents: sample 1, pyridoxine hydrochloride 5 mg; sample 2, riboflavin 1.2 mg, pyridoxine hydrochloride 1.6 mg, methionine 40 mg, calcium pantothenate 20 mg, calcium hydrogen phosphate 80 mg, dehydrocholic acid 8 mg, hesperidin 40 mg; sample 3, aminopyrine 2 mg, sulpyrine 20 mg; sample 4, aminopyrine 10 mg, phenacetin 33.3 mg, caffeine 6.7 mg.

†Mean values of three determinations (range of recovery calculated with reference to nominal content in sample).

tions were in good agreement with nominal values obtained from the suppliers. Common inorganic salts, such as sodium chloride, magnesium chloride, sodium carbonate, and organic salts, such as sodium citrate and acetate, did not interfere at levels of 1 mg/ml. However, when the total amount of the two amines was more than 70 $\mu\text{g}/\text{ml}$, the recovery became worse. Substances likely to be present as preservatives or buffering agents exhibited no interference. This method is reasonably precise for the simultaneous and sensitive determinations of amines in complex samples.

Analysis of three-component mixtures

A 1 ml portion of a sample solution containing two amines (total amount, about 15 μg) and about 20 μg of a quaternary ammonium salt was pipetted into a 100-ml separating funnel and the other reagents were added and the mixture was treated as described above. Synthetic sample solutions containing methylephedrine, diphenhydramine, benzethonium and/or berberine were prepared in order to assess the performance of the method. The absorbances at 25° were measured at two wavelengths, 550 and 573 nm, and after the temperature in the cell had been adjusted to 60°, the absorption differences at 550 and 573 nm (ΔA_{550} and ΔA_{573}) were measured. The $\Delta\epsilon$ values previously measured at 550 and 573 nm for methylephedrine were 1.78×10^4 and 1.57×10^4 , and for diphenhydramine 1.97×10^4 and 2.31×10^4 . The concentrations of methylephedrine and diph-

enhydramine were estimated by substituting $\Delta A_{550\text{nm}}$ and $\Delta A_{573\text{nm}}$ in equations (1) and (2). On the other hand, the absorbance of the blue species at 610 nm was measured and the concentration of the quaternary ammonium compound determined from the molar absorptivity at 60°. The results obtained are shown in Table 5. When the total amount of two amines was less than about 10 μg , the recoveries were good. However, more than about 15 μg of amine gave some interference in the determination of a quaternary ammonium salt because dissociation of the red species was depressed and the disappearance of the red colour was not complete. Consequently, a three-component mixture consisting of small amounts of two amines and quaternary ammonium compound can be analysed by applying the thermochromism method, but within a small error. Inspection of equations (1)–(4) and the standard deviations for $\Delta\epsilon$ (Table 2), combined with calculation of the propagated error, shows that an overall uncertainty of about 4% is to be expected.

Conclusion

Thermochromism can be applied for the determination of amines and quaternary ammonium compounds in multicomponent mixtures. Each amine in two-component mixtures or each amine and a quaternary ammonium compound in a three-component mixture can be determined with an error not exceeding ~4%, without separation, but the procedure is somewhat tedious.

Table 4. Determination of ephedrine and diphenhydramine in commercial pharmaceuticals*

Sample	Nominal amount, mg		Ephedrine		Diphenhydramine	
	Ephedrine	Diphenhydramine	Found, † mg	Range of recovery, %	Found, † mg	Range of recovery, %
1	200	100	204.8	101.9–103.0	100.3	97.4–103.2
2	150	100	147.2	96.2–100.1	98.9	97.5–100.3
3	10	10	10.4	103.0–105.0	10.0	99.0–101.0

*Other contents: sample 1, atropine sulphate 1 mg; sample 2, aminopyrine 100 mg, magnesium sulphate 500 mg; sample 3, papaverine hydrochloride 10 mg, noscapine hydrochloride 5 mg, diprophylline 100 mg.

†Mean values of three determinations (range of recovery calculated with reference to nominal content in sample).

Acknowledgement—This research was supported by a Grant-in-Aid for Scientific Research from the Ministry of Education of Japan.

REFERENCES

1. M. E. Auerbach, *Ind. Eng. Chem., Anal. Ed.*, 1943, **15**, 492.
2. H. M. N. H. Irving and J. J. Markham, *Anal. Chim. Acta*, 1967, **39**, 7.
3. G. Schill, *Acta Pharm. Suecica*, 1965, **2**, 13.
4. T. Sakai, *Bunseki Kagaku*, 1978, **27**, 444.
5. S. Tsurubo, N., Ohno and T. Sakai, *Nippon Kagaku Kaishi*, 1980, 828.
6. M. Tsubouchi, T. Sakai, T. Watake, K. Kanazawa and M. Tanaka, *Talanta*, 1973, **20**, 222.
7. T. Sakai, *J. Pharm. Sci.*, 1979, **68**, 875.
8. T. Sakai and N. Ishida, *Chem. Pharm. Bull.*, 1979, **27**, 2846.
9. *The Japanese Pharmacopoeia, IX*, Hirokawa Publishing, Tokyo, 1976, pp. C-320, -354, -391, -492, -1286.
10. *Idem*, p. C-312.

Table 5. Simultaneous determination of three compounds in artificial mixtures

	Taken, $\mu\text{g/ml}$			Found		
	R_4N Benzethonium	R_3N Methylephedrine	R_3N Diphenhydramine	R_4N Benzethonium, $\mu\text{g/ml}$	R_3N Methylephedrine, $\mu\text{g/ml}$	R_3N Diphenhydramine, $\mu\text{g/ml}$
R_4N Benzethonium	22.4	5.4	7.3	24.2	5.50	7.44
	22.4	5.4	4.4	23.5	5.18	4.52
R_4N Berberine	18.6	5.4	4.4	19.3	5.61	4.52
	18.6	10.8	4.4	20.0	10.89	4.52
				Recovery, %	Recovery, %	Recovery, %
				108	102	102
				105	96	103

*Mean values of three determinations.

ELECTROLYTIC PRECONCENTRATION IN INSTRUMENTAL ANALYSIS

ROMAN E. SIODA*

Industrial Chemistry Research Institute, ul. Rydygiera 8, 01-793 Warsaw, Poland

GRAEME E. BATLEY

CSIRO Division of Energy Chemistry, Sutherland, N.S.W. 2232, Australia

WALTER LUND

Department of Chemistry, University of Oslo, Blindern, Oslo 3, P.O. Box 1033, Norway

JOSEPH WANG

Department of Chemistry, New Mexico State University, Box 30, Las Cruces, New Mexico 88003, U.S.A.

STEVEN C. LEACH

Materials Research Laboratory, SRI International, 333 Ravenswood Ave., Menlo Park, California 94025, U.S.A.

(Received 18 September 1984. Revised 20 July 1985. Accepted 6 December 1985)

Summary—The use of electrolytic deposition as a separation and preconcentration step in trace metal analysis is reviewed. Both the principles and applications of the technique are dealt with in some detail. Electrolytic preconcentration can be combined with a variety of instrumental techniques. Special attention is given to stripping voltammetry, potentiometric stripping analysis, different combinations with atomic-absorption spectrometry, and the use of flow-through porous electrodes. It is pointed out that the electrolytic preconcentration technique deserves more extensive use as well as fundamental investigation.

Preconcentration techniques are important in trace and ultratrace analysis, especially for metal species. Many analytical applications are connected with the determination of trace components in pure reagents, high-technology materials, natural waters, soils, air and ores.^{1,2} They have become more important with the increased attention paid to environmental pollution, the search for new mineral resources, *e.g.*, from sea-water, and the arrival of industries requiring ultrapure reagents and materials, such as the electronics and nuclear power industries.

It frequently happens that the trace components of environmental and industrial matrices cannot be directly determined by existing instrumental techniques. This can happen if the trace concentration is below the limit of detection (LOD) for the analytical method applied or the main components of the sample matrix interfere in the determination. In either case, the application of a separation and preconcentration procedure before the instrumental determination may remove the difficulty.

Various separation procedures, such as evaporation, precipitation, extraction, ion-exchange, chromatography and electrolysis, can be considered for the preconcentration of the trace component. For certain types of analytical problem, electrolysis is the

procedure of choice, especially when the interfering matrix components are electrochemically inactive but the trace component can be electro-deposited. Thus, separation is achieved, and simultaneously the trace component is concentrated on a conveniently small electrode area from a highly dilute state in the test solution. The trace component is usually deposited in the elemental state on the cathode, but in certain applications it is anodically oxidized and deposited on the anode, *e.g.*, PbO_2 or MnO_2 .³⁻⁵ Metals may also be deposited in the form of intermetallic compounds, *e.g.*, as amalgams at mercury electrodes, or by formation through *in situ* co-deposition of a second element at an inert electrode, *e.g.*, the co-deposition of arsenic with copper or gold.⁶

After deposition on the electrode, the micro-components are determined by a suitable instrumental method. These methods can be divided into two main groups: (1) methods such as X-ray photoelectron spectroscopy, X-ray fluorescence spectrometry, stripping voltammetry and potentiometric stripping analysis, which can determine the amount of deposit *in situ* on the electrode surface, and (2) optical methods, such as atomic-absorption spectrometry, emission spectrometry, inductively-coupled plasma emission-spectrometry and atomic-fluorescence spectrometry, which all require atomization of the deposit for the determination. Neutron-activation analysis can also be used, applied either directly to the deposit on the electrode surface, or to

*Present address: c/o Professor D. J. Curran, Department of Chemistry, University of Massachusetts, Amherst, MA 01003, U.S.A.

a solution obtained by dissolving the deposit in a trace-free acid.

The direct measurement of heavy metals at ng/l concentrations, in natural waters or digests of environmental samples, is a task beyond the scope of most instrumental methods, unless preconcentration is used. At ultratrace levels of the microcomponent, sample contamination becomes a major problem, precluding the use of such separation procedures as co-precipitation or ion-exchange. Electrolytic preconcentration has the advantage that frequently little or no reagent addition is required, thus minimizing contamination.

The technique also has wide scope, being applicable to more than twenty metals.

THEORY

For proper application of electrolytic preconcentration coupled with an instrumental determination, it is important to understand the theory of electrolysis, as applied to solutions of low concentrations of electroactive species.

For high and moderate concentrations of electroactive species the deposition kinetics will be first-order with respect to the concentration of metal ions in solution:⁷

$$\frac{dc}{dt} = -k_1 c \quad (1)$$

which on integration yields

$$c = c_0 \exp[-k_1 t] \quad (2)$$

where c and c_0 are the concentrations at time t and zero respectively, and k_1 is the rate-coefficient of deposition; k_1 is a function of the experimental parameters which govern the mass transfer to the electrode:

$$k_1 = kDA/\delta V \quad (3)$$

where D is the diffusion coefficient of the electroactive species, δ is the thickness of the diffusion layer, which depends on the rate of stirring of the solution, A is the electrode area and V the solution volume. The simple form of equations (1) and (2) is due to the implicit condition that the applied electrode potential is highly negative (in the case of reduction of metal ions), so that the electrochemical reaction proceeds almost to completion.

As the concentration decreases, the equilibrium potential of the metal ion in solution becomes more negative, according to the Nernst equation:

$$E_{\text{eq}} = E^0 + \frac{0.059}{n} \log \frac{a_{\text{Me}^{n+}}}{a_{\text{Me}}} \quad (4)$$

where E^0 is the standard electrode potential, n is the number of electrons involved in the half-cell, $a_{\text{Me}^{n+}}$ is the activity of Me^{n+} in solution, and a_{Me} is the activity of the reduced metal at the electrode surface.

From equation (4) it can be seen that when an insufficient reduction potential is used, the electrolysis

will terminate before the solution is fully depleted of the metal ions in question. If 99.99% completion is required for a 2-electron reaction, the potential should be chosen at least 0.12 V more negative than E^0 . However, for practical applications equation (4) is of limited value, because slow reaction kinetics at non-ideal electrode surfaces are not taken into consideration. Also, a_{Me} may never reach unity, when the initial concentration of metal ions is very low.

Sioda^{8,9} has pointed out that in certain cases the rate of dissolution of metal deposited on the electrode may become significant if there is an insufficient applied overpotential, or chemical oxidation of the deposit can occur.¹⁰ The chemical oxidation is independent of the overpotential, but depends on the chemical composition and pH of the solution. Such "anomalous metal dissolution"¹¹ has been observed for a number of metals. For this reason Sioda has modified equation (1) to include a dissolution term:

$$\frac{dc}{dt} = -k_1 c + k_2 S/V \quad (5)$$

where S is the surface area of the deposit, and k_2 is the specific rate of dissolution. The surface area of the deposit depend on the geometrical area of the electrode, its surface roughness, and the morphology of the deposit. It also depends on the deposition time, the initial concentration of metal ions in solution, and the rate of mass transport to the electrode. Equation (5) can be integrated after adoption of proper assumptions.^{8,9}

A consequence of equation (5) is that for long deposition times an equilibrium should eventually be reached, which would leave an equilibrium concentration of the metal ions in solution.¹²

PRACTICE

Electrolytic preconcentration has been coupled with a range of instrumental methods of determination, usually being used either to concentrate metals to bring them within the calibration range of the method, or to isolate them from an otherwise interfering matrix. In AAS, for example, high salt and low metal concentrations preclude the determination of many heavy metals at trace levels. Here, electrolytic preconcentration has been widely explored, with electrodes ranging from the mercury drop¹³ and iridium and tungsten wires and loops,¹⁴ to graphite tubes,¹⁵ with either controlled-potential deposition¹⁵ or, in the simplest case, a constant applied voltage.¹⁴ Adsorptive preconcentration, and autodeposition (internal electrolysis, cementation, deposition without applied voltage), on wire electrodes, also show considerable promise for selected matrices. Cementation has also been done with metal reductor columns.¹⁶ An interesting but little used variant is internal electrolysis by means of hydrogen absorbed on an electrode.¹⁷

Electrolysis efficiency is an important factor, and electro-deposition from a recirculated solution onto

mercury-coated pyrolytic-graphite tubes is particularly sensitive. This technique has been applied to metals such as chromium, cobalt, lead and nickel.^{15,18}

An extension of this procedure, using mercury-precoated tubes in a submersible probe as shown in Fig. 1, allows the *in situ* deposition of labile metals from sea-water, with determination of the deposited metals by AAS performed later in the laboratory.¹⁹

A problem common to all electrolytic preconcentrations is the requirement that the metal in solution should be in a form which is electrochemically labile or active. Metals bound in non-labile complexed forms, or adsorbed on colloidal species, may not be deposited unless released by some dissociative treatment, e.g., ultraviolet irradiation or acid digestion. Many new methods overlook this aspect, and are tested only on labile metal salt solutions. The ability of electrochemical techniques to discriminate between certain species, can, however, be an advantage if information on speciation (chemical form) is sought.²⁰

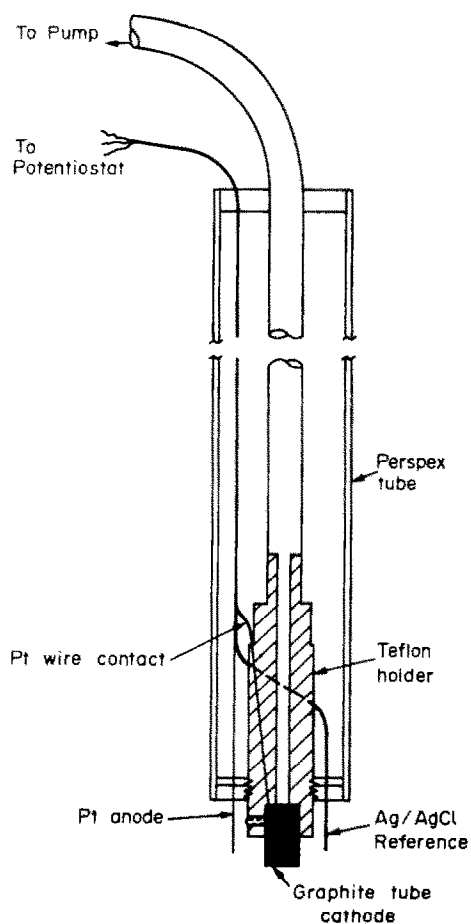


Fig. 1. Electrode probe for *in situ* graphite-tube electro-deposition for AAS determination of Cd and Pb present at ng levels in sea-water. (Reprinted from G. E. Batley, *Anal. Chim. Acta*, 1981, **124**, 121, by permission of the copyright holders, Elsevier Scientific Publishers, Amsterdam.)

APPLICATIONS

Stripping voltammetry

The reversible electro-deposition of metal ions forms the basis of anodic stripping voltammetry (ASV), in which metals are preconcentrated by deposition on a mercury film or mercury drop electrode, or a bare glassy-carbon or gold electrode, and then oxidatively stripped by an anodic voltage scan. The elements amenable to ASV determination are listed in Table 1. The absolute limits of detection (LODs) depend largely on electrode and instrument optimization; concentrations as low as 10–30 ng/l. are detectable for copper, lead, cadmium and zinc in sea-water with common commercial instrumentation.⁶ LODs are somewhat higher for elements such as arsenic, selenium and tellurium, the co-deposition of which with either gold or copper is less reversible.

Anodic stripping voltammetry (ASV) is probably the best known instrumental method which incorporates an electrolytic preconcentration step.^{21–23} It is applied in several different instrumental modifications, one of the most sensitive of which is differential pulse anodic stripping. A typical differential pulse stripping curve is shown in Fig. 2. The peak heights are proportional to the initial concentration of metal ions in solution.

The choice of working electrode and the mode of voltammetric scanning have been the subject of many studies. Mercury films deposited on glassy carbon

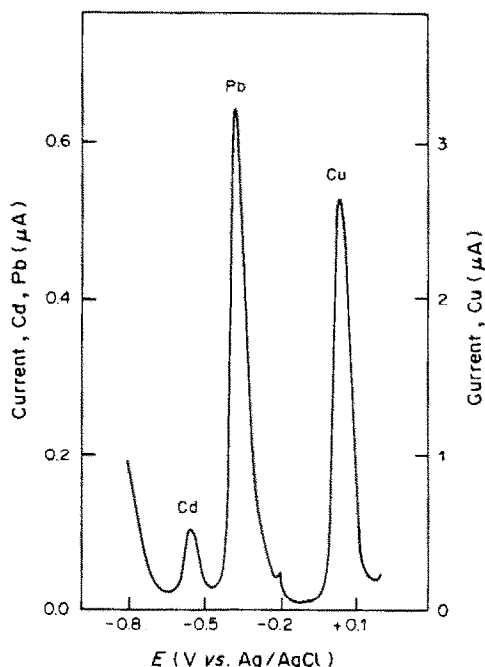


Fig. 2. Differential-pulse anodic stripping voltamperogram of a digested urine sample. The peaks correspond to 3.3 nM Cd, 26 nM Pb and 164 nM Cu. (Reprinted from W. Lund and R. Eriksen, *Anal. Chim. Acta*, 1979, **107**, 37, by permission of the copyright holders, Elsevier Scientific Publishers, Amsterdam.)

Table 1. Trace metals amenable to electrolytic preconcentration from natural waters by the ASV method

Metal	Solution conditions	Deposition potentials, <i>V</i> vs. <i>SCE</i>
Mn	pH 7	-1.7*†
Co, Cr, Ni	pH 4-6	-1.6*†
Zn	pH 3-6	-1.3*
Cd, Cu, Pb, Tl	dilute acid or pH 3-6	-0.9*
Bi, In,§ Sb,§ Sn	2 <i>M</i> HCl	-0.8*
Ag, Au, Hg	dilute acid or pH 3-6	-0.4‡
As, Se, Te	dilute acid	-0.3‡

*Hanging mercury drop or mercury film electrode.

†Poor sensitivity.

§Hanging mercury drop electrode.

‡Glassy-carbon or gold electrode.

offer the best sensitivity, but the hanging mercury drop electrode is probably more versatile and reliable. For the stripping step, differential pulse scanning seems to be the technique of choice, although alternating-current and even direct-current stripping may be used to advantage in certain cases.²⁴

ASV has been widely used for the determination of Cu, Pb, Cd and Zn in environmental samples, owing to the extremely low LODs it offers. The absence of interference effects from a high concentration of alkali-metal salts—which in fact play the necessary role of a supporting electrolyte—makes the method particularly well suited for the determination of trace metals in sea-water. ASV is also used to distinguish between labile and bound metal ions in natural waters; the most comprehensive speciation scheme so far developed is based on this method.²⁵ For biological samples ASV normally necessitates a complete digestion of all organic material, or interfering peaks may be observed on the voltamperogram.²⁶ However, in some cases, *e.g.*, in the analysis of urine, a direct analysis without pretreatment of the sample is possible.²⁷

The main disadvantage of ASV is that for most practical applications it is limited to metals which form soluble amalgams; besides the four mentioned above, these include Sb, Bi, In, Tl and Ga. However,

the determination of the latter elements is less straightforward, owing to irreversibility, inter-metallic-compound formation and peak overlapping. Also, in environmental samples, the concentration of the last four elements may be too low for a direct determination by ASV.

For ions that form insoluble compounds on the surface of a mercury electrode, cathodic stripping voltammetry (CSV) may be used. Although its practical application is restricted, compared to ASV, it has been used for the determination of halide ions as well as selenium.²⁸ Adsorptive electrolytic accumulation can serve as a preconcentration method for many species that cannot be electrolytically plated.²⁹

Potentiometric stripping analysis (PSA)

PSA was introduced by Jagner and Granéli in 1976.³⁰ It is similar to ASV in that the metals to be determined are preconcentrated as amalgams at a mercury electrode but stripping is done by chemical oxidation, *e.g.*, with mercuric ions or oxygen present in the solution, without application of an external potential. During the oxidation process, the variation of potential of the working electrode is recorded as a function of time, and a stripping curve like the one shown in Fig. 3 is obtained. Because the rate of oxidation is constant, and controlled by the transport

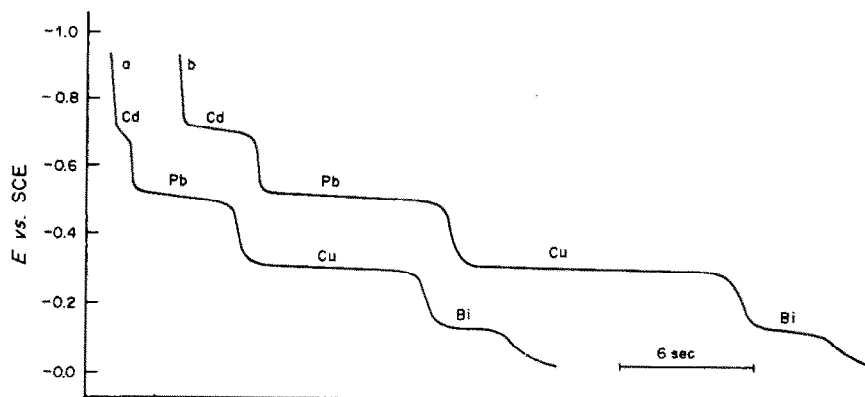


Fig. 3. Potentiometric stripping curve for cadmium, lead, copper and bismuth, with use of mercuric ions for oxidation. (Reprinted from D. Jagner, *Anal. Chem.*, 1978, **50**, 1924, by permission. Copyright 1978, American Chemical Society.)

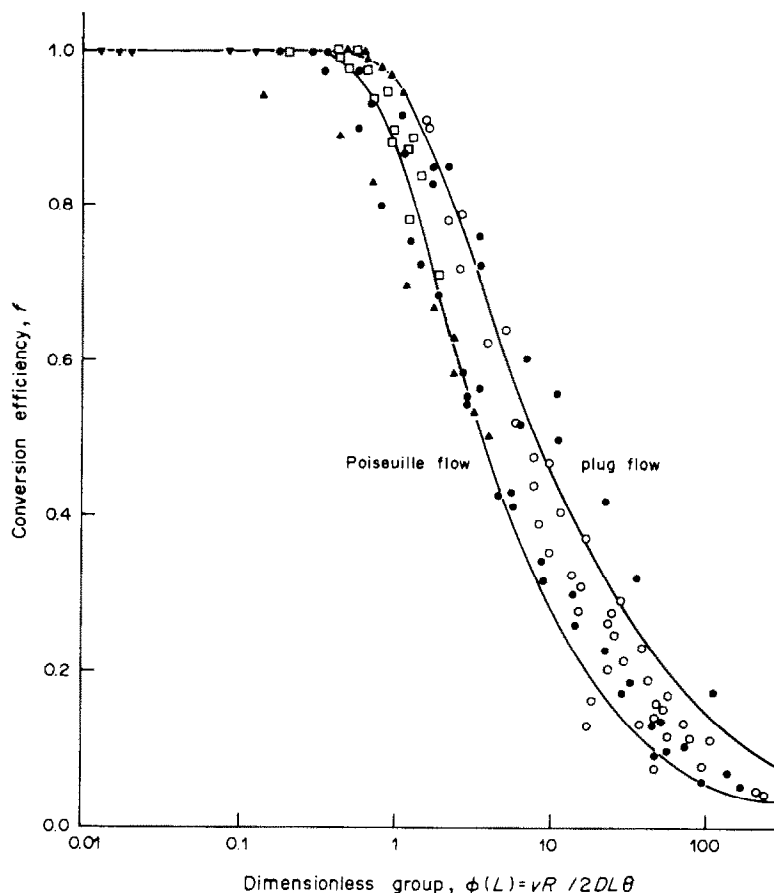


Fig. 4. Theoretical model predicted—region between the curves—and experimental conversion efficiencies of several flow-through porous electrode systems (symbols as in text). (Reprinted from B. G. Ateya, *J. Appl. Electrochem.*, 1980, 10, 627, by permission of the copyright holders.)

of the oxidant to the electrode surface, the time needed for the stripping of each metal is proportional to the concentration of the corresponding metal in solution. PSA is applicable to most metals that can be determined by ASV.⁶

In PSA a mercury film electrode is normally employed. A mercury film deposited *in situ* on glassy carbon is particularly advantageous, because of its high sensitivity, and also because the mercury(II) ions added are used both for film formation and the subsequent potentiometric stripping. Furthermore this electrode can easily be rotated at high speed, which improves the reproducibility, particularly for short stripping times.

In the first version of PSA very long deposition times had to be used, to obtain stripping times of the order of seconds. However, when the concentration of metals is low or the concentration of oxidant is high the stripping may take place so fast (in the course of milliseconds) that an ordinary strip-chart recorder cannot be used. This problem has been overcome by incorporating a microcomputer in the PSA system; the signal can then be displayed at a suitable rate when desired.³¹ In addition, background

subtraction and other manipulations of the signal are easily performed with computerized PSA.

Hence for sub-ppm concentrations of metals PSA requires somewhat more sophisticated instrumentation than does ASV. Also, the necessity to use a mercury film electrode may sometimes be a disadvantage, as with urine samples, which attack the mercury film.³² On the other hand, the removal of oxygen is not needed, and PSA is also relatively insensitive to other electroactive species present in the samples, because—unlike ASV—no current is drawn through the working electrode during the stripping process. This represents an obvious advantage, because it allows a simplified sample pretreatment to be used. Thus, cadmium and lead have been determined in whole blood after simple dilution of the sample with 0.5M hydrochloric acid containing 50 mg of mercury(II) nitrate per litre. However, interferences from electroactive species present in high concentrations may be encountered.³⁴

Like ASV, PSA has mainly been applied to the determination of metals which form soluble amalgams. However, like CSV, the PSA method can be used to determine species such as halides and sele-

nium which form insoluble compounds at the mercury surface. The stripping is then done with a suitable reducing agent, such as amalgamated sodium or zinc.³⁵

Electro-deposition and atomic-absorption spectrometry

Electro-deposition of trace metals, followed by AAS determination, offers several advantages, as already discussed. Consequently, various metals of environmental significance which cannot be measured directly by electrothermal AAS—owing to interference and their low levels in the environment—have thus been measured after electrolytic preconcentration.¹⁸ LODs down to 10 ng/l. have been obtained, but the main advantage over use of AAS alone is the minimization of matrix interferences; for example, Pb, Co and Ni have been determined in sea-water with no interference from the high sodium chloride content.¹⁸ A further potential advantage of this approach is the ability to determine Pb, Co and Ni speciation by selective deposition. Also, speciation of chromium—Cr(VI) and Cr(III)—in natural waters has been studied by carefully controlling the deposition potential and pH.¹⁵ It seems possible that by study of electro-deposition from natural waters of suitably adjusted pH, information can be obtained on the state of complexation of the metal ions present.

The electro-deposition/AAS approach has been successfully applied to the determination of metals such as Cr, Co and Ni, for which ASV measurements are not sensitive enough, owing to irreversible electro-deposition. Other elements, such as Se or Hg, determination of which by ASV or direct AAS suffers from various difficulties, have been measured successfully by the electro-deposition/AAS approach with LODs of 0.1 and 0.08 $\mu\text{g/l.}$, respectively.^{36,37} In a paper by Newton and Davis, LODs for AAS determination of 19 elements have been reported.³⁸

In this technique electrolytic preconcentration is achieved by plating the metals on metal wires of high melting point, *e.g.*, tungsten or iridium,³⁹ or on various graphite surfaces.⁴⁰ The electrode is then transferred to the AAS instrument, where the metal is determined by either flame or electrothermal atomization. The use of a thin metal-wire filament has the advantage that electrothermal atomization can be achieved by simply passing a low current through the wire, or alternatively the filament can be heated in a flame. A combination of both approaches can also be used.³⁶ If the more costly graphite-furnace equipment is available, the graphite tube used as the cathode for electro-deposition can serve as the furnace in the subsequent electrochemical atomization.^{15,18,41} Effective and reproducible electro-deposition is achieved by using a flow system with the graphite tube as working electrode (Fig. 1). Such an arrangement also permits *in situ* electro-deposition, which minimizes errors, *e.g.*, those arising from contamination and adsorption. The flow systems are

designed so as to allow convenient removal and transfer of the graphite tube. Only low plating efficiency, 1–5%, is usually obtained, as expected for open tubular electrodes. Higher efficiency, *i.e.*, lower LODs, may be achieved by recycling the solution or utilizing a thin-layer flow cell.^{19,37}

Flow-through porous electrolytic preconcentration

The use of flow-through porous electrodes (FPEs) for the recovery of metal ions from aqueous solutions has been advocated by several authors, including Bennion and Newman,⁴² and Sioda and Piotrowska.⁴³ However, the present analytical use of these high surface-area electrodes has been mainly limited to controlled-potential coulometry.⁴⁴ The purpose of this section is to indicate the advantages of using flow-through porous electrodes for preconcentrating metal ions from solutions. Some useful theoretical and semi-empirical equations which govern the operation of this are presented, to allow the reader to evaluate this method for future use.

Some of the advantages of the electrolytic flow-through porous preconcentrators include the ability to preconcentrate a single ion selectively from a mixture of ionic species, reuse of the electrode, and use of relatively inexpensive equipment.

The materials that have been used for making FPEs range from a series of fine metal screens (*e.g.*, nickel, platinum or gold), graphite cloth, reticulated vitreous carbon and confined granular carbon. Each of these materials has been studied to determine the mass transport characteristics, and several correlations have been presented which provide a good overall understanding of the mass transport of the species being preconcentrated at the electrode surface. Sioda has given a correlation which can be used to relate the efficiency of preconcentration to the parameters of the electrode and solution.⁴⁵ This correlation has the form:

$$\log \{ \log [1/(1-f)] \} = A + B \log u \quad (7)$$

where f is a conversion efficiency, *i.e.*, preconcentration efficiency from a continuous stream of trace solution, A is a function of the electrode parameters, such as specific surface, length, porosity and cross-sectional area, u is the average linear solution flow velocity, and B is an empirical parameter of hydrodynamic nature.

Ateya has developed a somewhat different theoretical correlation which is useful for many types of FPEs.⁴⁶ Figure 4 presents the fit of Ateya's correlation to the data obtained by several authors, using many kinds of FPEs, and shows that the parameters which control the conversion efficiency are those in the function

$$\Phi(L) = vR^2/2DL0 \quad (8)$$

where v is the volumetric flow-rate of the solution, R is the average pore diameter, D is the diffusion

coefficient of the electroactive species, L is the length of the electrode, and θ is the electrode porosity.

In both cases above, the correlations are good only for FPEs which are completely filled with solution, and assume that the total surface area of the FPE is accessible to the ionic species being preconcentrated from a continuous solution stream.

The following two examples of use of FPEs to remove metal ions from solutions show the attractive features of the flow electrolytic method, which is very effective in the preconcentration of metal ions. Chu *et al.*⁴⁷ used a bed of graphite particles to deposit copper nearly completely from acidic 0.1 mM copper sulphate. Subsequent electrochemical dissolution of the metal gave enrichment by a factor of 1000. Blaedel and Wang⁴⁸ used discs of reticulated vitreous carbon in a flow-through electrolytic cell to detect the presence of 0.1 μ M potassium ferrocyanide in a phosphate buffer solution. Recently, Wang and Dewald^{49,50} have described the deposition of several metals, such as Cd, Cu, Pb and Zn, at a flow-through reticulated vitreous-carbon electrode, and their subsequent stripping. These studies suggested that with FPEs it would be possible to determine these metals at about nM concentrations.

Another approach to electrolytic preconcentration is to use several FPEs in series to concentrate different ionic species from the same solution by controlling the potential of each FPE. After deposition, the metals are anodically dissolved into solution at different times, thus allowing each ion to be detected separately. With the vast array of buffers used in polarography, no new buffering systems are required. In addition, the potentials at which the FPEs are to be maintained are already known in most cases, and consequently only a small amount of experimentation is required to determine the feasibility of using the FPEs for specific preconcentration problems.

Miscellaneous methods

Other instrumental methods used to determine the electro-deposited metals include photometric analysis,⁵¹ emission spectrophotometry,^{52,53} and X-ray fluorescence,^{54,55} although they appear of limited value for ultratrace concentrations in waters. It is more promising to couple electrolytic preconcentration with inductively-coupled plasma emission-spectrometry,^{56,57} spark-source mass spectrometry (SSMS),^{16,58} and atomic-fluorescence spectrometry,⁵⁹ all of which have lower LODs.

Jørstad and Salbu have applied neutron-activation analysis to the determination of 14 elements electro-deposited from "synthetic" sea-water onto mercury and graphite.⁶⁰ LODs of the order of 1–100 ng/l. were obtained. In this multielement procedure, it was necessary to calibrate for every element, because the rates of deposition differed according to the pH, applied voltage and type of electrode used.

Electro-deposition has also been used as an auxiliary preconcentration technique applied, after an initial ion-exchange preconcentration of copper, to obtain the analyte in a form suitable for electron microprobe analysis.⁶¹

CONCLUSIONS

Electrolytic preconcentration has been widely used in conjunction with a variety of highly sensitive determination techniques, for trace and ultratrace analysis.^{62–65} Its advantages and limitations are not as widely known as they should be, a situation which this review is intended to improve. The technique deserves more extensive use and fundamental investigation.

Acknowledgements—S.C.L. thanks Kim Kinoshita of Lawrence Berkeley Laboratories for discussions and help connected with writing for this review. R.E.S. thanks many authors who have kindly sent copies of their research papers as a contribution to this review.

REFERENCES

1. D. E. Leyden and W. Wegscheider, *Anal. Chem.*, 1981, **53**, 1059A.
2. V. Z. Krasilshchik, N. M. Kuzmin and E. Ya. Neiman, *Zh. Analit. Khim.*, 1979, **34**, 2045.
3. L. B. Rogers, *Rec. Chem. Prog.*, 1955, **16**, 197; *Chem. Abstr.*, 1956, **50**, 1495b.
4. M. Haissinsky, *Nuclear Chemistry and Its Applications*, Chapter 20. Addison-Wesley, New York, 1964.
5. N. Tanaka, in *Treatise on Analytical Chemistry*, Part I, Vol. 4, I. M. Kolthoff, P. J. Elving and E. B. Sandell (eds.), pp. 2417ff. Interscience, New York, 1963.
6. G. E. Batley, *Mar. Chem.*, 1983, **12**, 107.
7. J. J. Lingane, *Anal. Chim. Acta*, 1948, **2**, 584.
8. R. E. Sioda, *Anal. Lett.*, 1983, **16**, 739.
9. J. L. Anderson and R. E. Sioda, *Talanta*, 1983, **30**, 627.
10. A. V. Vvedenski and I. K. Marshakov, *Zashchita Metallov*, 1983, **19**, 282.
11. Ya. M. Kolotyrykin and G. M. Florianovitch, *ibid.*, 1984, **20**, 14.
12. *Idem*, *Talanta*, 1985, **32**, 1083.
13. F. O. Jensen, J. Doležal and F. J. Langmyhr, *Anal. Chim. Acta*, 1974, **72**, 245.
14. E. J. Czobiec and J. P. Matousek, *Spectrochim. Acta*, 1980, **35B**, 741.
15. G. E. Batley and J. P. Matousek, *Anal. Chem.*, 1980, **52**, 1570.
16. K. H. Welch and A. M. Ure, *Anal. Proc.*, 1980, **17**, 8.
17. Z. Boguszewska, M. Krasiejko and B. Palmowska-Kús, *Talanta*, 1986, **33**, 155.
18. G. E. Batley and J. P. Matousek, *Anal. Chem.*, 1977, **49**, 2031.
19. G. E. Batley, *Anal. Chim. Acta*, 1981, **124**, 121.
20. T. M. Florence, *Trends Anal. Chem.*, 1983, **2**, 162.
21. T. R. Copeland and R. K. Skogerboe, *Anal. Chem.*, 1974, **46**, 1257A.
22. J. Wang, *J. Environ. Sci. Technol.*, 1982, **16**, 104.
23. *Idem*, *Stripping Analysis: Principles, Instrumentation and Applications*, VCH Publishers, Deerfield Beach, FL, 1985.
24. G. E. Batley and T. M. Florence, *J. Electroanal. Chem.*, 1974, **55**, 23.
25. *Idem*, *Mar. Chem.*, 1976, **4**, 347.
26. M. Oehme and W. Lund, *Z. Anal. Chem.*, 1979, **298**, 260.

27. W. Lund and R. Eriksen, *Anal. Chim. Acta*, 1979, **107**, 37.
28. G. Jarzabek and Z. Kublik, *ibid.*, 1982, **143**, 121.
29. J. Wang, *Am. Lab.*, 1985, **17**, No. 5, 41.
30. D. Jagner and A. Granéli, *Anal. Chim. Acta*, 1976, **83**, 19.
31. A. Granéli, D. Jagner and M. Josefson, *Anal. Chem.*, 1980, **52**, 2220.
32. D. Jagner, M. Josefson and S. Westerlund, *Anal. Chim. Acta*, 1981, **128**, 155.
33. D. Jagner, M. Josefson, S. Westerlund and K. Årén, *Anal. Chem.*, 1981, **53**, 1406.
34. J. K. Christensen, L. Kryger and N. Pind, *Anal. Chim. Acta*, 1982, **136**, 39.
35. J. K. Christensen, L. Kryger, J. Mortensen and J. Rasmussen, *ibid.*, 1980, **121**, 71.
36. B. Holen, R. Bye and W. Lund, *ibid.*, 1981, **130**, 257.
37. D. A. Frick and D. E. Tallman, *Anal. Chem.*, 1982, **54**, 1217.
38. M. P. Newton and D. G. Davis, *ibid.*, 1975, **47**, 2003.
39. H. Brandenberger, *Chimia*, 1968, **22**, 449.
40. C. Fairless and A. J. Bard, *Anal. Lett.*, 1972, **5**, 433.
41. E. Desimoni, F. Palmisano, L. Sabbatini and G. Torsi, *Ann. Chim. (Rome)*, 1979, **69**, 381.
42. D. N. Bennion and J. Newman, *J. Appl. Electrochem.*, 1972, **2**, 113.
43. R. E. Sioda and H. Piotrowska, *Electrochim. Acta*, 1980, **25**, 331.
44. A. N. Strohl and D. J. Curran, *Anal. Chem.*, 1979, **51**, 353.
45. R. E. Sioda, *J. Appl. Electrochem.*, 1978, **8**, 297.
46. B. G. Ateya, *ibid.*, 1980, **10**, 627.
47. A. K. P. Chu, M. Fleischmann and G. J. Hills, *ibid.*, 1974, **4**, 323.
48. W. J. Blaedel and J. Wang, *Anal. Chem.*, 1979, **51**, 799.
49. J. Wang and H. D. Dewald, *J. Electrochem. Soc.*, 1983, **130**, 1814.
50. *Idem*, *Anal. Chem.*, 1983, **55**, 933.
51. A. Mizuike and N. Mitsuya, *Bunseki Kagaku*, 1968, **17**, 1259; *Chem. Abstr.*, 1969, **70**, 63768x.
52. V. Z. Krasilshchik, N. I. Kuznetsova and T. G. Manova, *Zh. Analit. Khim.*, 1977, **32**, 837.
53. G. Volland, P. Tschöpel and G. Tölg, *Spectrochim. Acta*, 1981, **36B**, 901.
54. B. H. Vassos, R. F. Hirsch and H. Letterman, *Anal. Chem.*, 1973, **45**, 792.
55. H. Marshall and J. A. Page, *Spectrochim. Acta*, 1978, **33B**, 795.
56. D. A. Ogaram and R. D. Snook, *Analyst*, 1984, **109**, 1597.
57. E. D. Salim and M. M. Habib, *Anal. Chem.*, 1984, **56**, 1186.
58. P. Paulsen, R. Alvarez and W. Mueller, *ibid.*, 1970, **42**, 673.
59. V. I. Rigin and I. V. Rigina, *Zh. Analit. Khim.*, 1979, **34**, 1121.
60. K. Jørstad and B. Salbu, *Anal. Chem.*, 1980, **52**, 672.
61. H. Malissa and I. L. Marr, *Mikrochim. Acta*, 1971, 741.
62. J. Minczewski, J. Chwastowska and R. Dybczyński, *Separation and Preconcentration Methods in Inorganic Trace Analysis*, pp. 56–59, Horwood, Chichester, 1982.
63. G. Tölg, *Talanta*, 1974, **21**, 327.
64. G. Volland, P. Tschöpel and G. Tölg, *Anal. Chim. Acta*, 1977, **90**, 15.
65. G. Tölg, *Z. Anal. Chem.*, 1979, **294**, 1.

AQUAMETRIC MICRODETERMINATION OF HYDRATION OF ION-EXCHANGE RESINS

F. B. SHERMAN*

N. D. Zelinsky Institute of Organic Chemistry, USSR Academy of Sciences, 47 Leninsky Prospect, Moscow, 117334, USSR

B. M. KATZ and G. N. EVENKO

I. I. Mechnikov Odessa State University, Physics Research Institute, 27 Pasteur St., Odessa, 270059, USSR

(Received 31 May 1984. Revised 1 September 1985. Accepted 18 October 1985)

Summary—An aquametric microtechnique is proposed for measuring the pre-adsorbed (residual) moisture (ΔW) and equilibrium moisture content (H) in macroporous weakly basic anion-exchangers and their gel analogues, during the derivation of water-vapour sorption isotherms by use of a modified McBain balance in a vacuum system. The absolute values of ΔW and H are determined by direct Karl Fischer titration of weighed samples of the anion-exchanger after equilibrium hydration has been achieved at various relative water-vapour pressures (P/P_s). The relationship between ΔW and the sample pretreatment conditions, characteristics of the polymer matrix (basicity and porosity), and the nature of the ionogenic groups in the ion-exchanger has been established. It has been shown that the hydration parameters, in terms of the BET theory and specific anion-exchanger surface area depend largely on ΔW . For instance, in the case of the strongly basic anion-exchangers AB-171 and AB-17-8, which contain quaternary ammonium groups, the degree of hydration in the BET region may be well in excess of the apparent effective capacity (h) of the BET monolayer. It has been shown that the specific surface area for water (S_{H_2O}), calculated from aquametric isotherms by using the BET equation, corresponds to the hydrophilic anion-exchanger surface area, as compared to the S_{H_2O} value calculated from gravimetric isotherms.

A wealth of experimental data on water-vapour sorption (hydration isotherms) by ion-exchange resins has been accumulated by using sorption, spectral, and other techniques.¹ Hydration isotherms are usually interpreted on the assumption that the initial resin samples are predried in vacuum at a temperature that keeps their structure intact when the water is removed. It is common knowledge that thermolabile anion-exchangers dried under such conditions still retain 2–4% w/w of firmly bound residual water.² Conditions for obtaining absolutely dry anion-exchangers without structural change, deamination or degradation remain to be established and that is why some aspects of the determination of pre-adsorbed (residual) moisture (ΔW) require systematic investigation. There is also a lack of data on the relationship between ΔW and sample pretreatment conditions, characteristics of the polymer matrix, and the nature of the ionogenic groups in the ion-exchange resins.

The present paper proposes an aquametric microtechnique for determining ΔW and the equilibrium moisture content H directly, during derivation of water-vapour sorption isotherms in a vacuum system with a modified McBain balance.^{1,3} The absolute ΔW and H values are determined by direct Karl Fischer titration of anion-exchanger samples⁴ brought to

hydration equilibrium at various relative water-vapour pressures (P/P_s). Results are also given which illustrate the effect of drying conditions for a number of ion-exchange resins of different porosity and basicity on the ΔW value and the parameters of the Brunauer, Emmet and Teller (BET)⁵ equation, which is used for interpreting the hydration isotherms.

EXPERIMENTAL

Characteristics of the anion-exchangers examined

Synthetic macroporous anion-exchangers based on a copolymer of styrene with divinylbenzene and di-isopropenylbenzene, synthesized in the presence of an inert solvent,⁶ and some of their chemical gel-like analogues were used. Anion-exchangers in the hydroxide and free base forms, conditioned by a known technique,⁷ were investigated. The samples, their physicochemical properties and compositions are listed in Table I.

Determination of the water content of air-dried samples

Three methods³ were used to determine the water content. The first involved suspension of the resin sample (5–10 mg) for 20 min in methanol (2 ml) directly in the titration cell, the extracted water being titrated with Karl Fischer reagent.⁸ The second method involved drying 0.2 g of sample at 50° and a pressure of 0.1 Pa, to constant weight. The third method involved heating 1 g of resin, with 25 ml of dry (<0.01% water) methanol, in a flask fitted with a reflux condenser, at 50° for an hour and titrating the water with Karl Fischer reagent; extending the extraction time had no tangible effect on the results. A parallel blank experiment was also conducted. The results are summarized in Table 2.

*Author for correspondence.

Table 1. Physicochemical properties of the anion-exchangers examined

Resin	Aminating agent*	Mean pore radius, nm	Total pore volume, cm ³ /g	Bulk density, g/cm ³	Specific surface area with respect to nitrogen, m ² /g	SEC† meq/g	C, %	H, %	N, %
AB-171-4/100	TMA	26.3	0.14	0.654	7.5	2.6	—	—	—
AB-17-8	TMA	0	0	0.750	0.1	3.6	—	—	—
AH-221-12/100	ED	15.3	0.41	0.456	57.0	5.9	78.0	8.3	7.3
AH-221-12/80	ED	23.0	0.46	0.464	90.0	5.1	58.2	9.9	7.3
AH-221D-15/100	ED	0	0	0.610	2.9	6.0	73.5	8.2	9.5
AH-221D-15/80	ED	0	0	0.691	3.4	6.2	72.8	8.2	9.1
AH-221D-15/60	ED	0	0	0.711	0.1	5.5	72.7	8.4	9.4
AH-22-8	ED	0	0	0.496	0.1	5.2	—	—	—
AH-531-12/80	PEI	5.0	0.27	0.649	57.0	4.5	77.8	8.4	8.3
AH-521-12/80	TET	7.0	0.22	0.665	63.0	5.5	75.2	8.2	8.5
AH-511-12/80	DET	9.1	0.36	0.654	78.0	5.8	75.0	8.1	9.2

*TMA = trimethylene, ED = ethylenediamine, PEI = polyethyleneimine, TET = triethylenetetramine, DET = diethylenetriamine.

†SEC = statistical exchange capacity.

Table 2. Water content of the anion-exchangers, found by the various methods, %

Resin	Fischer method, \bar{x}	S_r , (n = 5-7)	Methanol extraction at 50°, \bar{x}	S_r , (n = 4-6)	Vacuum drying at 50°, \bar{x}	S_r , (n = 3-4)
AH-221-12/100	7.68	0.06	7.66	0.1	6.63	0.6
AH-221-12/80	6.03	0.04	—	—	5.56	0.9
AH-221D-15/100	3.75	0.03	—	—	3.74	0.7
AH-221D-15/80	2.77	0.05	—	—	2.58	0.4
AH-221D-15/60	1.50	0.23	—	—	1.45	0.8
AH-531-12/80	2.68	0.14	2.68	0.1	2.48	0.9
AH-421-12/80	2.47	0.07	—	—	2.36	0.5
AH-511-12/80	2.36	0.03	—	—	1.53	0.5

Derivation of hydration isotherms by use of a McBain balance

Water-vapour sorption isotherms were obtained at 25° on a vacuum adsorption apparatus⁹ with a quartz spring balance (Fig. 1). The anion-exchanger samples (~0.2 g) were placed in the preweighed cups of the quartz balance, and the system was heated to 50° and evacuated to a residual pressure of 1.33 Pa. Water vapour was then fed into the system at various pressures and kept there until hydration equilibrium was reached, in 17–20 hr. At a relative water vapour pressure $P/P_s = 0.9$, the maximal amount of bound water (H_s) was determined. Then, the water-vapour pressure was reduced stepwise in the system, and desorption isotherms were derived. The water-vapour pressure was measured with a U-shaped mercury gauge, the difference in levels being measured with a katharometer to within $\pm 0.5\%$. The vacuum adsorption apparatus was kept at $25 \pm 0.1^\circ$ in an air-thermostat.

It is possible in this way to obtain adsorption and desorption isotherms for several anion-exchangers simultaneously within 8–10 days, with a reproducibility within $\pm 5\%$.

Aquametric microdetermination of ΔW and H

Earlier,¹⁰ we described the procedure for obtaining isotherms for water vapour sorption by anion-exchangers by a microtechnique that permits determination, by direct titration with Karl Fischer reagent, of equilibrium hydration, taking due account of the value of ΔW , which is usually not determined when isotherms are derived by other methods. To determine ΔW and absolute moisture content H aquametrically at different equilibrium values of P/P_s , ampoules (50 mm long, diameter 3 mm) containing microsamples

(2–6 mg) of anion-exchangers, as well as control ampoules, were connected to the columns of the McBain balance system by capillaries (Fig. 1). After hydration equilibrium at a specific P/P_s value had been reached, two test ampoules and two control ampoules were detached, wiped clean and opened, and their contents were titrated with Karl Fischer reagent.^{4,11} It was necessary to titrate the control ampoules to determine the water adsorbed on their surface and present in the gas phase in them. The H values were calculated for each water-vapour pressure tested, from the difference between the results for titration of the sample and control ampoules and the formula:

$$H = \frac{0.555 a (\text{WE})}{S (100 - W)}$$

where H is the absolute moisture content in the anion-exchanger (mmole/g); a is the net volume of Karl Fischer reagent used to titrate the sample (ml); (WE) is the water equivalent of the Karl Fischer reagent (mg/ml); S is the exchanger sample weight (mg); W is the initial moisture content of the air-dry sample (% w/w); 0.555 is the conversion factor from % w/w into mmole/g for water.

The value of a is the difference between the titration volume for the sample and for a control ampoule; W is determined by direct titration with the Karl Fischer reagent. ΔW is defined as the equilibrium amount H of exchanger-bound water at a residual water-vapour pressure of 1.33 Pa, and a preselected temperature, when the initial samples have been dried under static conditions. The relationship between H and P/P_s was used to derive the aquametric isotherms¹⁰ (Fig. 2).

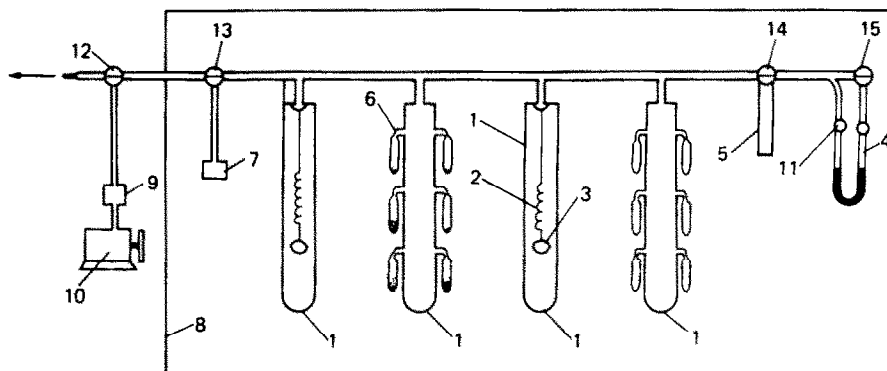


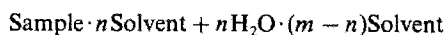
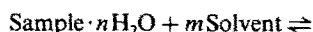
Fig. 1. McBain balance modified for aquametric and gravimetric microdetermination of the anion-exchanger water content at different water-vapour pressures. 1—sorption column; 2—quartz spring; 3—cup containing the adsorbent; 4—mercury gauge; 5—water-vapour supply system; 6—sample and control microampoules; 7—thermocouple; 8—air thermostat; 9—trap; 10—roughing-down pump; 11–15—cocks.

RESULTS AND DISCUSSION

Moisture content of anion-exchangers

Determination of water by Karl Fischer titration of samples in any state of aggregation may be represented primarily as a two-stage process.

1. Dilution of the water-containing sample with a suitable solvent (or solvent mixture), or quantitative extraction of water from the sample with a suitable solvent or solvent mixture:



2. Titration of the water.¹²

Consequently, only water in molecular form^{13,14} and exchangeable with the solvent is determined when the moisture content in solid-phase samples is measured

by Karl Fischer titration. The water is usually extracted with the solvents used to make the standard Karl Fischer reagent or its modifications,^{8,12,15} namely methanol, ethanol, dimethylformamide, pyridine, methylcellosolve, *etc.* The exchange-rate depends on how strongly the water is bound to the sample surface, as well as on the physicochemical properties of the sample, of which the most important are the specific surface area, total volume, and mean pore radius, as well as the nature of the active groups (Table 1).

As expected, the results of determination of the moisture content by various methods (Table 2) are in good agreement for all AH-221D resin samples that do not have true porosity. The results obtained for water in the macroporous exchangers AH-221, AH-511, AH-521, AH-531 by drying were all lower, which can obviously be explained as due to the difficulty of removing the water present in the resin micropores.

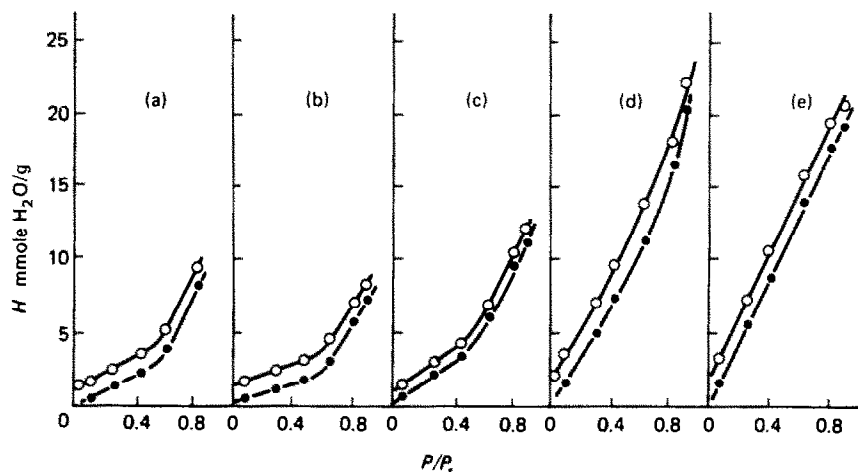


Fig. 2. Aquametric (O) and gravimetric (●) hydration isotherms of (a) AH-511, (b) AH-221, (c) AH-22, (d) AB-17-8 and (e) AB-171.

The reliability of the Karl Fischer method for determining the moisture content of anion-exchangers was verified by the method of standard additions. Microsamples of dried AH-221-12/80 resin in Teflon cups 12 mm long, 6 mm in diameter, with ground-in stoppers, were weighed on a microbalance before and after addition of various amounts of water. The initial moisture content of the resin and the total moisture contents of the treated samples were determined by Karl Fischer titration (Table 3). For AH-221-12/80, containing about 11% of water, the absolute standard deviation was 0.01% (7 replicates).

Among the factors most significantly affecting the titration results is the duration of contact of the sample with the Karl Fischer reagent (or the extraction solvent). The time necessary for a quantitative analysis of the exchangers tested (depending on the nature of the sample) is 10–20 min.

The results obtained (Tables 2 and 3) show that the water content of the resins based on the copolymers of styrene with divinylbenzene and di-isopropenylbenzene may be determined quickly and efficiently by direct Karl Fischer titration. For titrating samples of unknown structures, however, it is necessary to determine experimentally the minimum contact time needed for the determination to be quantitative.

Exchange hydration isotherms

The hydration isotherms of the macroporous weakly basic AH-511, AH-221, AB-171 and their gel analogues were derived by aquametric and gravimetric methods (Fig. 2). According to Brunauer's classification⁵ they are isotherms of the second type, are easily linearly approximated in the region of $P/P_s = 0-0.4$, and may, therefore, be quantitatively

described in terms of the BET equation for poly-molecular adsorption:

$$\frac{P/P_s}{H(1 - P/P_s)} = \frac{1}{hC} + \frac{(C - 1)P}{hCP_s}$$

where H is the amount of sorbed water (mmole/g); h is the monomolecular layer capacity (mmole/g); P/P_s is the relative water-vapour pressure; C is a constant associated with the sorption energy during establishment of the first monolayer.

As can be seen from Fig. 2, the aquametric isotherms (H_A) are higher than the gravimetric (H_G) ones, and $\Delta H = H_A - H_G$, at P/P_s ranging from 0.2 to 0.9, virtually coincides with ΔW , *i.e.*, with the pre-adsorption level of hydration (Table 4). The previously described isotherms for water-vapour sorption by the AB-17^{16,17} and AH-221¹⁸ anion-exchangers predried at 100° and 80°, respectively, with a residual pressure of 0.013 Pa, lie between the aquametric and gravimetric isotherms for these resins. The gravimetric isotherms of water-vapour sorption by ion-exchange resins are therefore relative, their shape and position in the initial region depending strongly on the amount of pre-adsorbed moisture (ΔW) which, in turn, depends on the sample pre-treatment conditions (temperature, residual water-vapour pressure) and some physicochemical properties of the resins (basicity, porosity). For ΔW values for the anion-exchanger samples dried at various residual pressures (0.133–13.3 Pa) and temperatures (25–50°), see Table 4. As expected, the ΔW values depended to a large extent on the residual water-vapour pressure and the drying temperature.

It is therefore evident that the experiment involves only partial dehydration of the exchanger, and the non-removable bound water is probably associated

Table 3. Determination of the moisture content of the AH-221-12/80 resin with Karl Fischer reagent

Amount of water added, %	Mean amount of water found*,		No. of determinations
	%		
2.17	2.15		2
4.50	4.57		4
7.36	7.41		4
11.04	11.10		7

*Corrected for initial moisture content.

Table 4. Relationship of pre-adsorbed moisture ΔW with temperature T and residual pressure P

P, Pa	$T, ^\circ C$	$W, mmole/g$				
		AH-511-12/80	AH-221-12/80	AH-22-8	AB-171-4/100	AB-17-8
13.30	25	1.98	1.48	0.30	2.35	1.36
	50	1.95	1.30	—	—	—
1.33	25	1.75	1.26	0.25	2.27	1.27
	30	1.46	1.24	—	—	—
	40	1.44	1.23	—	—	—
	50	1.38	1.23	—	—	—
0.133	25	1.34	1.22	0.23	1.92	1.22
	50	1.32	1.22	0.23	1.88	1.20

with polar surface groups, namely the amino groups of the respective aminating agents (Table 1). Further dehydration by increasing the drying temperature is limited owing to the low thermal stability of the exchangers and the resulting deamination of the surface amino groups.¹ Thus, the aquametrically determined absolute moisture content (H) consists of two components: pre-absorbed moisture (ΔW) and equilibrium sorption (a) at a given gravimetrically determined P/P_s value. The aquametric isotherms may be regarded as hypothetical sorption isotherms for completely dehydrated samples ($\Delta W = 0$).

The amount ΔW of pre-absorbed moisture, as seen from Table 5, also depends on the matrix structure and the nature of the active groups. As expected, the ΔW values for macroporous samples (AH-221, AB-171) and other chemical gel analogues (AH-22, AB-17) vary, whereas the ΔW value for the gel exchangers is considerably lower than that for the macroporous analogues. The basicity of the anion-exchanger also has a considerable influence on ΔW , especially in gel samples, ΔW increasing with basicity. Such a change can be explained as due to an increase in the polarity of the hydration sites in transition from weakly to strongly basic anion-exchangers. In the weakly basic AH-511, AH-221, AH-22 exchangers, the primary and secondary amino groups of the residues of the respective aminating agents, diethylenetriamine and ethylenediamine, act as potential hydration sites, whereas the strongly basic AB-171 and AB-17 exchangers contain quaternary ammonium groups and hydroxide counter-ions capable of being solvated.

Relationship of the BET parameters and specific surface to the ΔW value

Table 5 presents the statistical exchange capacity (SEC), ΔW , the BET hydration parameters, and the specific surface calculated from the nitrogen and water sorption data. It is evident that the hydration parameters (h , C , H_s and S) determined from the aquametric isotherms are considerably higher than those from the gravimetric isotherms. Such differences, naturally, are first of all explained by the contribution of ΔW to the measured values and, secondly, are limited by the accuracy (reproducibility and correctness) of measurement of the H values by the aquametric (mean $S_r = 0.08$) and gravimetric (mean $S_r = 0.64$) methods (see Table 2). It should also be noted that the h and ΔW values depend on the

basicity and porosity of the exchanger. For instance, the value of h is considerably greater for the weakly basic gel exchanger AH-22 than for the macroporous chemical analogue AH-221, whereas this difference virtually disappears in the case of the strongly basic AB-17 and AB-171 (Table 5).

If the SEC corresponds to the overall number of polar groups available for hydration in the exchanger, then the effective capacity of the BET monolayer (h) in turn determines the number of accessible primary hydration sites on the molecule surface. Comparative analysis of the SEC and h values for each exchanger in Table 5 shows that only 30–60% of the total number of polar sites in the weakly basic AH-511, AH-521 and AH-22 is available for hydration in the BET-monolayer formation area. The presence of strongly basic polar sites (quaternary ammonium ions) in AB-171 and AB-17 provides for a hydration level well above the effective monolayer capacity in the BET region, and the h value is erroneous in this case. Evidently, this has to do with the presence, within the structure of the strongly basic exchangers, of ion-pairs capable of hydration in the monolayer formation region. This being the case, the h value is 1.5–2 times greater than the SEC, regardless of porosity. The aquametric h value for the weakly basic AH-22 resin gel sample (3.43 mmole/g) is considerably higher than that for the macroporous AH-22 (1.61 mmole/g) and AH-511 (2.24 mmole/g). The relative swelling capacity of these resins changes in the same order, being, at the monolayer formation point, 13.5, 5.6 and 11.0% for AH-22, AH-221 and AH-511¹⁹ respectively.

The polymer matrix structure and exchanger basicity have the same effect on the relative values of maximum hydration H (at $P/P_s = 0.9$) and specific surface S_{H_2O} for water as they do on the relationship involving the h values. The S_{H_2O} values determined from the gravimetric and aquametric isotherms are considerably higher for all the exchangers examined than the respective S_{N_2} values determined by the method of thermal desorption of nitrogen. In the latter method the sample is first thoroughly purged of possible impurities by boiling in acetone, followed by vacuum drying, and in the course of the low-temperature nitrogen sorption the sample structure is assumed to be invariable.¹ On the other hand, in the water-vapour method the sample swells and its surface expands, and the calculations with respect to

Table 5. Water vapour sorption capacity and BET equation parameters of anion-exchangers

Resin	SEC, meq/g	W , mmole/g	h , mmole/g		H_s , mmole/g		C		S_{N_2} , m ² /g	S_{H_2O} , m ² /g	
			G	A	G	A	G	A			
AH-511-12/80	5.8	1.32	1.89	2.24	12.26	13.58	12.4	19.4	78	121	143
AH-211-12/80	5.1	1.22	1.08	1.61	7.43	8.97	4.1	9.0	90	70	103
AH-22-8	5.2	0.23	3.38	3.43	11.96	12.38	6.4	8.3	0.1	216	219
AB-171-4/100	2.6	1.88	4.73	5.45	20.82	22.80	10.5	26.8	7.5	302	348
AB-17-8	3.6	1.20	4.76	5.47	19.21	20.40	21.0	26.3	0.1	304	349

G—determined gravimetrically.
A—determined aquametrically.

water refer to the swollen sample, particularly for gels, which have relatively high swelling capacity in the monolayer formation region.¹⁹

Comparative analysis of the data in Table 5 shows that the S_{H_2O} values of weakly basic gel samples are considerably higher than the S_{N_2} values, whereas the difference is insignificant for macroporous samples. The sorption properties of gel samples are nevertheless similar to those of macroporous samples (Table 5), which can be explained as due to the different mechanisms of hydration.

The macroporous anion-exchangers are phase-disperse systems with pores 5–25 nm in size, containing water in two forms: water bound to the polar centres of the polymer network, and water sorbed interstitially in the pores. The reversible hydration of these exchangers points to the absence of capillary condensation, and the steep upward slope of the isotherm as $P/P_s \rightarrow 1$ is explained by the formation of a "lamellar" structure typical of this kind of hydration.²⁰ In the case of the gel exchangers, which lack porosity when dried, hydration occurs mainly by saturation of the polymer matrix with water and is accompanied by considerable swelling of the resin. Moreover, the gel sample starts to swell with the sorption of the first water molecules on the monolayer area, which creates a porous structure even in the initial stage of the sorption process, which is why the isotherms of water-vapour sorption by the macroporous AH-511, AH-221, AB-171 and gel-like AH-22 and AB-17 are identical in shape (Fig. 2).

The data in Table 5 also show that S_{H_2O} calculated from the aquametric isotherms is much higher than that calculated from the gravimetric isotherms. Thus, the specific surface of the exchangers examined, calculated from the aquametric data by the BET equation, seems to correspond to the actual hydrophilic surface.

In conclusion, it is of interest to examine the experimental S_{H_2O} values from a physical point of view. According to existing concepts,²¹ the applicability of the adsorption methods for determining the specific surfaces of porous bodies, particularly adsorbents, depends on the character of their porosity. Since anion-exchangers are polymers with labile structure, it is recommended, for the purpose of obtaining the true parameters of their porous structure, to select for each polymer a suitable sorbate, which would not lead to swelling (the effect of the sorbate on the polymer sorbent should not exceed that on an inorganic sorbent).

On the other hand, the existence of a real interphase in polyelectrolyte proteins swollen by water-vapour sorption has been corroborated by various physical methods, and no room is left for doubt.^{23,24} It is our belief that in the course of water-vapour sorption by anion-exchangers in the monolayer filling region, the polymer skeleton remains unchanged, and a continuous hydration shell fails to form on the surface, because of localization of the polar sites on

the large hydrophobic surface. In this case, the S_{H_2O} values calculated from the BET equation possess a physical meaning, and correspond to that part of the total geometric polymer surface that is covered with water molecules. That the S_{H_2O} values are higher than the corresponding S_{N_2} values, as described above, is explained by the development of the initial surface due to swelling of the polymer matrix, as well as infiltration of water molecules into the structural cavities of the resin, which are inaccessible to inert nitrogen molecules. Therefore, although they have the same physical meaning of specific surface, the S_{H_2O} and S_{N_2} values for a particular sample are nevertheless associated with different states of a polymer with labile structure, and naturally are different.

REFERENCES

1. N. G. Polyansky, G. V. Gorbunov and N. A. Polyanskaya, *Methods of Anion-Exchange Research*, Khimiya, Moscow, 1976.
2. B. M. Kats and E. K. Malinovskii, *Zh. Prikl. Khim.*, 1977, **50**, 1980.
3. G. N. Evenko, B. M. Kats and F. B. Sherman, *Zh. Analit. Khim.*, 1978, **33**, 314.
4. F. B. Sherman, G. N. Evenko and B. M. Kats, *ibid.*, 1982, **37**, 757.
5. S. Brunauer, *Adsorption of Gases and Vapours*, Vol. I, p. 138. Inostrannaya Literatura, Moscow, 1948.
6. G. A. Artyushin, E. I. Lyustgarten, A. B. Pashkov, A. K. Valkov, T. K. Brutzkus, E. V. Zaitsev, V. V. Goler, A. V. Tchistyakova, S. Ya. Kreinina and M. V. Lyubomilova, in *Khimiya i Tekhnologiya polikondensatsionnykh polimerov*, p. 99. Khimiya, Moscow, 1977.
7. F. Helfferich, *Ion-Exchange* (Russ. trans.), p. 490. Inostrannaya Literature, Moscow, 1962.
8. V. A. Klimova, *Major Micromethods of Analysis of Organic Compounds* (English Transl.), p. 162. Mir, Moscow, 1977.
9. G. N. Evenko, B. M. Kats and E. K. Malinovskii, *Izv. Vyssh. Uchebn. Zaved., Khim. i Khim. Tekhnol.*, 1977, **20**, 454.
10. F. B. Sherman, G. N. Evenko and B. M. Kats, *Zh. Fiz. Khim.*, 1983, **57**, 377.
11. M. V. Fateeva, T. I. Nikitina and F. B. Sherman, *Izv. AN SSSR, Biol. Ser.* 1976, 611.
12. F. B. Sherman, *Talanta*, 1980, **27**, 1067.
13. F. B. Sherman and V. A. Klimova, *Izv. AN SSSR, Chem. Ser.*, 1971, 1122.
14. F. B. Sherman, V. A. Klimova, Yu. S. Khodakov, V. S. Nakhshunov, P. I. Yakovlev and Kh. M. Minatchev, *ibid.*, 1972, 764.
15. J. Mitchell and D. Smith, *Aquametry*, 2nd Ed., Vol. 3. Wiley, New York, 1980.
16. A. N. Kirgintsev and A. V. Lukyanov, *Zh. Fiz. Khim.*, 1963, **37**, 233.
17. L. S. Yurkova, A. F. Kolosova and K. M. Olshanova, *ibid.*, 1974, **48**, 1496.
18. L. D. Belyakova, A. V. Kiselev, E. I. Lyustgarten, G. G. Muttik and T. I. Shevchenko, *Kolloidn. Zh.*, 1975, **37**, 540.
19. B. M. Kats and E. K. Malinovskii, in *Sorbtsiya i khromatografiya*, p. 168. Nauka, Moscow, 1979.
20. G. Dickel and K. Bunzl, *Z. Phys. Chem. Frankfurt*, 1963, **39**, 198.
21. M. M. Dubinin, *Usp. Khim.*, 1982, **51**, 1065.
22. A. A. Tager and M. V. Tsilipotkina, *ibid.*, 1978, **47**, 152.
23. J. M. Seehof, B. Kellin and S. W. Benson, *J. Am. Chem. Soc.*, 1953, **75**, 2427.
24. Yu. I. Khurgin, *Zh. Vses. Khim. Obshchest. D. I. Mendeleeva*, 1976, **21**, 684.

MULTIPARAMETRIC CURVE FITTING—IX*

SIMULTANEOUS REGRESSION ESTIMATION OF STOICHIOMETRY AND STABILITY CONSTANTS OF COMPLEXES

JOSEF HAVEL

Department of Analytical Chemistry, College of Science, J. E. Purkyně University, 611 37 Brno,
Czechoslovakia

MILAN MELOUNT†

Department of Analytical Chemistry, College of Chemical Technology, 532 10 Pardubice, Czechoslovakia

(Received 22 January 1985. Accepted 30 September 1985)

Summary—A chemical model (*i.e.*, the number of complexes, their stoichiometry and stability constants with molar absorptivities) in solution equilibria may be established by (*i*) the trial-and-error method in which stability constants are estimated for an assumed set of complexes in the mixture and a fitness test is used to resolve a choice of plausible models to find the true one; (*ii*) the simultaneous estimation of the stoichiometry and stability constants for species divided into "certain" species for which the parameters β_{pur} , (p, q, r) are known and held constant, and "uncertain" species with unknown parameters which are determined by regression analysis. The interdependence of stability constants and particular sets of stoichiometric indices requires that the computational strategy should be chosen carefully for each particular case. The benefits and limitations of both approaches are compared by means of examples of potentiometric titration data analysis by the POLET(84) program and of spectrophotometric data analysis by the SQUAD(84) program. A strategy for efficient computation is suggested.

Potentiometry and spectrophotometry are often used to study solution equilibria. The chemical model of an equilibrium system consists of (*i*) the number of species in equilibrium, (*ii*) their stoichiometry, and (*iii*) their stability constants or molar absorptivities, respectively. The program MESAK¹ determines the average composition of species from potentiometric data. The program PRCEK^{2,3} evaluates the stoichiometric indices p, q, r of an $M_pL_qH_r$ complex from the slopes of linearly transformed relationships, by linear regression. Under simplifying conditions PRCEK may be used to analyse absorbance–pH or absorbance–concentration data for equilibrium systems of even polynuclear complexes⁴ but a preliminary data-treatment of the absorbance–concentration curves should be made,⁵ as the mathematical model used in PRCEK is limited to two complexes only.^{6,7} The program MRLET⁸ algorithmically determines the stoichiometric coefficient q of a complex ML_q by regression analysis of an absorbance *vs.* mole–ratio curve, provided this is the predominant complex in the equilibrium mixture.

Other programs use the operator-controlled "trial-and-error" (heuristic) method of stoichiometry determination^{9,12} in which the stoichiometric coefficients are part of the hypothesis tested, and are either confirmed by regression analysis or are rejected

and replaced by those for a new model. The process is continued until a satisfactory fit of the model and regression analysis is obtained. The initial choice of species stoichiometry is usually based on experience, but automatic selection from a list of possible species and subsequent hypothesis testing has been developed, *e.g.*, the STYRE species-selector introduced by Sillén in LETAGROP^{11,12} and the species selector in PSEQUAD,¹³ which tests several species hypotheses step by step so that the species from a list are included in or excluded from a model quite automatically.

Even with computer assistance, it is rather difficult to test all possible combinations of stoichiometric coefficients. For example, if p, q and r for a ternary complex $M_pL_qH_r$ are restricted to the ranges 0–3, 0–3, and 0–5, respectively, then, excluding proton–metal species and cases where two or all three coefficients are zero, 68 different species can be obtained by combination of the components M, L and H, 2278 combinations of two different species, and so on. Use of chemical experience can radically lower the number of possible combinations to be tested but it is still difficult to test them all. Usually, only a few tens of combinations are tested,¹⁴ though Varga *et al.*¹⁵ investigated up to 128 different models in a solvent extraction experiment. The problems involved have been discussed in a review.¹⁶

The present paper describes a direct algorithmic estimation of stoichiometric indices (the ESI approach) based on simultaneous regression deter-

*Part VIII: *Talanta*, 1985, **32**, 973.

†Author for correspondence.

mination of stoichiometric indices and stability constants. The novelty of the proposed approach is that the stoichiometric indices are estimated as *real numbers* simultaneously with the stability constants. The method has been applied to potentiometric data analysis by the program POLET(84)¹⁷ and to spectrophotometric data analysis by the program SQUAD(84),¹⁸ and some preliminary results have been reported.¹⁹

THEORY

An equilibrium system consisting of metal (M), ligand (L) and proton(s) (H) as basic components combined in a species of general formula $M_pL_qH_r$, may be described by the mass-balance equations (charges omitted for simplicity):

$$c_M = [M] + p \sum_{j=1}^{n_c} (\beta_{pqr} [M]^p [L]^q [H]^r)_j \quad (1)$$

$$c_L = [L] + q \sum_{j=1}^{n_c} (\beta_{pqr} [M]^p [L]^q [H]^r)_j \quad (2)$$

$$c_H = [H] + r \sum_{j=1}^{n_c} (\beta_{pqr} [M]^p [L]^q [H]^r)_j \quad (3)$$

and the overall stability constant

$$\beta_{pqr} = [M_pL_qH_r] / ([M]^p [L]^q [H]^r) \quad (4)$$

Solution equilibria are usually studied by potentiometry, spectrophotometry, extraction, *etc.*, the total analytical concentrations of the basic components c_M , c_L and c_H being known and experimentally adjustable, and representing the independent variable in the regression analysis. The dependent variable y_{exp} is represented in potentiometry by the free concentration of a basic component, indicated by an ion-selective electrode (*e.g.*, pH by a glass electrode), and in spectrophotometry by the absorbance. The functional relationship between y_{exp} , an experimentally adjustable vector of the independent variable, $\mathbf{x}_{\text{exp}} = \{c_M, c_L, c_H, \text{pH}, \text{etc.}\}$ and a vector of the unknown parameters $\boldsymbol{\beta} = \{\beta_{pqr,j}, \epsilon_{pqr,j}, (p, q, r)_j\}$, $j = 1, \dots, n_c$, is a mathematical model formulated in the form $\mathbf{y} = f(\mathbf{x}; \boldsymbol{\beta})$. Here $\beta_{pqr,j}$ and $\epsilon_{pqr,j}$ represent the stability constant and molar absorptivity of the j th species with integers p, q, r as stoichiometric coefficients. The equilibrium mixture contains n_c species.

The general problem is to find estimates for the unknown parameters which will minimize the residual-square sum function U :

$$U = \sum_{i=1}^n w_i [y_{\text{exp},i} - f(x_i; \boldsymbol{\beta})]^2 \approx \text{minimum} \quad (5)$$

where w_i is a statistical weight, usually taken as unity.

The minimization may be done algorithmically or heuristically. The algorithmic process (*e.g.*, SQUAD¹⁸) usually finds a global minimum whereas the heuristic process depends more on human con-

trol. POLET(84)¹⁷ offers a choice of algorithmic or heuristic processing. The user must decide whether a local or global minimum is required. In computational strategy, restrictions and initial guesses for the parameters and minimization steps for particular parameters should be supplied, and special care paid to parameters that are interdependent in the model.

Some difficulty in a non-linear estimation of β_{pqr} and p, q, r may arise when there is an adverse mutual influence of the estimates of one of the stoichiometric coefficients and of β_{pqr} , *i.e.*, if the one parameter is incorrectly estimated, the other is also incorrectly estimated (biased), but the combined effect of the incorrectly estimated parameters, when introduced into the model, may yield quite reasonable predictions. It is worthwhile calculating the correlation coefficients to obtain information about the interactions of parameters.

The ESI approach is based on treating the stoichiometric indices as real numbers instead of integers and varying them simultaneously with the stability constants in the regression process. Though non-integer coefficients of chemical reaction have no physical meaning, treating the coefficients as real numbers leads to estimates which are close to integers for a true chemical model.

The following approaches may be used to estimate the separable parameters: (i) the ESI method, in which the model species are divided into the "certain" species, for which β_{pqr} and p, q, r are held constant, and the "uncertain" species, for which these parameters are directly estimated by regression; (ii) the trial-and-error method, in which p, q and r for all species are fixed integers based on a hypothetical chemical model, and only the stability constants β_{pqr} are estimated by regression.

Other possibilities are based on a combination of the two methods in various computational steps, each of which refines only some of the parameters; for example, known stability constants and stoichiometric indices are kept unchanged during a partial regression refinement of other parameters, and in the last step all the parameters, stability constants and stoichiometric indices are refined to confirm the chemical model found. Simultaneous estimation of the stability constant and of all stoichiometric indices of a particular species seems to be a rare case because the interdependence of parameters, indices and stability constant in equations (1)–(4) does not enable an estimation.

Which computational strategy will prove optimal depends on the number of complexes, previous knowledge of some species in the chemical model, and the experimental design for changing the basic components in the equilibrium system, and therefore an *ad hoc* choice is necessary. The experimental strategies possible for estimation of one stoichiometric coefficient by varying the total concentration of the corresponding basic component are surveyed in Table 1.

Table 1. A survey of experimental possibilities of simultaneous estimation of stability constants and stoichiometric indices of $M_pL_qH_r$ species from various spectrophotometric data according to change of the basic components in the experiment: β'_{pqr} denotes the conditional stability constant

Equilibrium	Dependence	Condition	Estimated parameters	
			Suitable	Not suitable
(1) Protonation of monomer: $L + rH = LH_r$	$A = f(\text{pH})$	$c_L = \text{const.}$	β_{01r}, r	—
(2) Protonation of oligomer: $qL + rH = L_qH_r$	$A = f(\text{pH})$	$c_L = \text{const.}$ $c_L \neq \text{const.}$	β'_{0qr}, r β'_{0qr}, q, r	β_{0qr}, q —
(3) Complex-forming equilibria: $pM + qL + rH = M_pL_qH_r$				
(i) Mole-ratio plots	$A = f(c_M/c_L)$ or $A = f(c_L/c_M)$	pH const. $c_L \neq \text{const.}$ $c_M \neq \text{const.}$	β'_{pqr}, p, q	r
(ii) A -pH plots for an excess of c_L :	$A = f(\text{pH})$	$c_L \gg c_M$ $c_L = \text{const.}$ $c_M = \text{const.}$	β'_{pqr}, p, r	β_{pqr}, q
(iii) A -pH plots for an excess of c_M :	$A = f(\text{pH})$	$c_L \ll c_M$ $c_L = \text{const.}$ $c_M = \text{const.}$	β'_{pqr}, q, r	β_{pqr}, p
(iv) A -pH plots for varied c_M and c_L :	$A = f(\text{pH})$	$c_L \neq \text{const.}$ $c_M \neq \text{const.}$	β_{pqr}, p, q, r	—

EXPERIMENTAL

Computational strategy

Determination of number of species. A set of potentiometric titration curves is transformed into $\{Z, \text{pH}\}$ normalized co-ordinates and the resulting Z matrix is analysed by the factor-analysis algorithm SPECIES.²⁰ For various integers of matrix rank k , the standard deviation of Z , $s_k(Z)$ is calculated and the intersection of two linear parts of the $s_k(Z) = f(k)$ graph indicates the matrix rank k^* which is equal to the number of species in the equilibrium.

The factor-analysis algorithm FA608²¹ is analogously used to analyse the absorbance matrix and the rank is estimated as above. The intersection of two linear parts of the $s_k(A) = f(k)$ graph indicates the matrix rank k^* equal to the number of light-absorbing species, n_c , in the equilibrium mixture.

Stability constants of "certain" species. The graph of n_c complexes is divided into n_{cert} "certain" species, and n_{uncert} "uncertain" species. The stoichiometry of the "certain" species is known either from previous experimentation or the literature. The stability constants $\beta_{pqr,j}, j = 1, \dots, n_{\text{cert}}$ (or corresponding molar absorptivities in spectrophotometric data analysis), are estimated from separate experimental data by the trial-and-error method. A goodness-of-fit test²² establishes the reliability of the parametric estimates found.

Stoichiometry and stability constant of "uncertain" species. Realistic values for the stability constants and stoichiometric coefficients are supplied as initial guesses of the unknown parameters $\{(\beta_{pqr}^{(0)}, p^{(0)}, q^{(0)}, r^{(0)}), j = 1, \dots, n_{\text{uncert}}\}$, and the regression algorithm is applied. Chemical experience, tables of stability constants and knowledge of coordination chemistry should assist in making the initial guesses and choosing the computational strategy for simultaneous estimation of the stoichiometry and stability constants. This estimation sometimes fails if there is a strong interdependence of the indices and the stability constants, resulting in divergence of the minimization algorithm. Care should be taken to choose a minimization routine that will also work for interdependent parameters. The fitness test²² is again used as a criterion for the reliability of the regression estimation.

Final confirmation of chemical model found. The real-number values of the stoichiometric indices of "uncertain"

species are rounded to integers and kept constant in a final refinement of the stability constants (or molar absorptivities) of all the "certain" and "uncertain" species by the trial-and-error method. Before the final refinement, the real-number estimates of the stoichiometric indices should be as close as possible to integers and have low standard deviations. U_{min} should not change much in the final refinement from the value found with the real-number indices.

Computation

The estimation of stoichiometric indices (the ESI method) has been introduced into the programs POLET^{5,10} and SQUAD²⁴ to give two regression programs: POLET(84) for potentiometric data analysis¹⁷ and SQUAD(84) for spectrophotometric data analysis.¹⁸ Our computations were done with the EC 1033 (500 K) computer in the Department of Computing Technique, J. E. Purkyně University, 611 37 Brno and the Computing Centre, College of Chemical Technology, 532 10 Pardubice Czechoslovakia.

DISCUSSION

The ESI method has been applied to potentiometric and spectrophotometric data analysis, and some examples, benefits and limitations of the method are discussed below.

The first example is concerned with the overlapping protonation equilibrium of a weak acid,¹⁰ the simulated data in normalized co-ordinates $\{Z, \text{pH}\}$ were calculated for the two stability constants, $\log \beta_{011} = 3.50$ and $\log \beta_{012} = 8.00$ and also loaded by random errors calculated on the basis of an arbitrary value of $s_{\text{inst}}(Z) = 0.005$. Application of POLET(84) in two runs with different initial guesses for the stability constants and stoichiometric indices, and of the LETAG minimization algorithm²³ in POLET(84), led to the true values of the parameters, and the goodness-of-fit test showed an excellent fit and hence a reliable parametric estimation (Table 2).

Table 2. Simultaneous estimation of stability constants and stoichiometric indices from potentiometric data analysis by POLET(1984)

Example 1. Determination of two overlapping protonation constants of a weak acid from simulated $Z = f(\text{pH})$ data.¹⁰ Selected values $s_{\text{inst}}(Z) = 0.005$, $\log \beta_{011} = 3.50$ and $\log \beta_{012} = 8.00$

Run		Initial guess		Estimated parameters		Degree of fit test	
		$\log \beta_{01r}^{(0)}$	$r^{(0)}$	$\log \beta_{01r}$	r	$s(Z)$	$R \times 10^2$
1	LH	2.5	1	3.473 ± 0.024	0.993 ± 0.005	0.0060	0.316
	LH ₂	7.0	2	7.985 ± 0.020	1.997 ± 0.003		
2	LH	3.5	0	3.502 ± 0.020	1.000 ± 0.005	0.0070	0.368
	LH ₂	8.5	0	8.006 ± 0.005	2.000 ± 0.000		

Example 2. Determination of Bi(III) hydrolysis constants and species stoichiometry from simulated $Z = f(\text{pH})$ data.¹⁰ Selected values $s_{\text{inst}}(Z) = 0.010$, $\log \beta_{1,0,-1} = -1.58$, $\log \beta_{6,0,-12} = 0.33$

Run	Species	Initial guess			Estimated parameters		
		$\log \beta_{pqr}^{(0)}$	$p^{(0)}$	$r^{(0)}$	$\log \beta_{pqr}$	p	r
1	Bi(OH)	-2.0	1	-2	-1.562 ± 0.002	1	-0.988 ± 0.001
2	Bi ₆ (OH) ₁₂	0.33	6	-10	0.319 ± 0.018	6	-11.999 ± 0.013
3	Bi ₆ (OH) ₁₂	0.33	6	-8	0.320 ± 0.002	6	-12.001 ± 0.000
4	Bi ₆ (OH) ₁₂	-1.5	6	-8	0.318 ± 0.016	6	-11.999 ± 0.013
5	Bi ₆ (OH) ₁₂	-2.0	2	-3	0.392 ± 0.017	6.116 ± 0.012	-12.225 ± 0.026
6	Bi ₆ (OH) ₁₂	-2.0	2	-4	0.356 ± 0.044	6.035 ± 0.089	-12.062 ± 0.089

The second example shows that the composition of the complexes might also be determined by the ESI method even when a bad initial guess for the stoichiometric indices is used. For a model consisting of two hydrolytic species, Bi(OH) and Bi₆(OH)₁₂, described by the stability constants¹⁰ $\log \beta_{1,0,-1} = -1.58$ and $\log \beta_{6,0,-12} = 0.33$ and an arbitrary value of $s_{\text{inst}}(Z) = 0.010$, the normalized data $\{Z, \text{pH}\}$ were simulated. Six runs of the ESI approach in POLET(84) computations starting with different initial guesses of the stoichiometric indices were performed. In the first run, the parameters $\log \beta_{6,0,-12} = 0.33$ and $q_1^{(0)} = 0$, $p_2^{(0)} = 6$, $q_2^{(0)} = 0$, and $r_2^{(0)} = -12$ were kept constant while $\log \beta_{pqr,1}$, p_1 and r_1 were estimated for the first species. In the following five runs, the parameters $\log \beta_{1,0,-1} = -1.58$ and $p^{(0)} = 1$, $q^{(0)} = 0$, $r^{(0)} = -2$ and $q_2^{(0)} = 0$ were held constant and $\log \beta_{pqr,2}$, p_2 and r_2 for the second species were estimated. Minimization terminated in all runs with the estimated real-number stoichiometric indices quite close to the true integer coefficients, so they could easily be rounded off to integers and the final refinement of the stability constants performed.

The third example involves regression analysis of spectrophotometric data by SQUAD(84). Simulated spectra as described by Leggett and McBryde²⁴ were calculated for the species LH, LH₂, M(OH), ML, ML₂ and MLH and loaded with a spread of random errors generated for an arbitrary value of the instrumental error, $s_{\text{inst}}(A) = 0.0074$. In the first step, a chemical model was set up with LH, LH₂ and M(OH) as the "certain" species, and ML, ML₂ and MLH as the "uncertain" species. The trial-and-error method was then applied for determination of β_{110} , β_{120} and β_{111} and the corresponding U_{min} value. The statistical

characteristics of the fit achieved serve here as reference values for comparison with those achieved in the subsequent ESI minimization process. As a rather high value of $s_{\text{inst}}(A)$ was chosen in the data simulation, the stability constants found, 9.990, 17.813 and 14.071, should be considered in good agreement with the values used for data simulation, *viz.* 10.00, 17.80, 14.10 (Table 3).

Simultaneous estimation of p , q , r and the corresponding stability constants fails if there is a strong interdependence of the indices. The first three model hypotheses shown for this method in Table 3 differ in the choice of which of p , q , and r is to be varied, the other two being kept constant. This method led to true values for the stability constants and stoichiometry and also degree of fit values the same as those for the reference trial-and-error method. The real-number values of p , q and r are close to integers and may therefore easily be rounded off for refinement of the stability constants.

The last four model hypotheses (Table 3) are all false and demonstrate the ability of the ESI method to distinguish between a true and a false chemical model. For a false model the real-number values found for p , q , r are far from being integers and have no physical meaning, the degree of fit is bad, and the models hypothesized should be rejected.

The protonation equilibrium of 2-(2-thiazolylazo)-4-methoxyphenol (TAMP)⁹ is the last example used here for demonstration of the benefits and limitations of simultaneous estimation of stoichiometry and stability constants. Dissociation of r protons from the acid LH_{*r*}, which has an overall protonation (stability) constant $\beta_{01r} = [\text{LH}_r]/([\text{L}][\text{H}]^r)$, may be indicated by plots of absorbance *vs.* pH. For n_w wavelengths and

Table 3. Determination of stability constants and stoichiometric indices of three uncertain complexes by simulated absorbance matrix analysis with use of the ESI approach in SQUAD(1984); experimental conditions: absorbance matrix generated²⁰ for the absorbance error $s_{\text{inst}}(A) = 0.007404$ and selected model: $\log \beta_{011} = 9.70$, $\log \beta_{012} = 13.30$, $\log \beta_{10-1} = -3.90$, $\log \beta_{110} = 10.00$, $\log \beta_{120} = 17.80$, $\log \beta_{111} = 14.10$; in the regression analysis, the stability constants, stoichiometry and molar absorptivities of "certain" species [LH, LH₂ and M(OH)] were held constant while those of "uncertain" complexes were estimated

Hypothetic chemical model	Species assumed	$\log \beta_{pqr}$	Estimated parameters			Fitness test		Hypothesis of model may be
			p	q	r	$s(A) \times 10^3$	$R \times 10^2$	
A. The trial-and-error method								
1st	ML	9.990 ± 0.028	1	1	0	7.31	0.995	Accepted
	ML ₂	17.813 ± 0.029	1	2	0			
	MLH	14.071 ± 0.018	1	1	1			
B. The method of simultaneous estimation of stoichiometry and stability constants								
2nd	ML	9.727 ± 0.113	0.975 ± 0.015	1	0	7.20	0.974	Accepted
	ML ₂	17.389 ± 0.143	0.951 ± 0.017	2	0			
	MLH	14.267 ± 0.086	1.065 ± 0.027	1	1			
3rd	ML	9.654 ± 0.113	1	0.955 ± 0.015	0	7.35	0.994	Accepted
	ML ₂	18.254 ± 0.139	1	2.062 ± 0.019	0			
	MLH	14.265 ± 0.073	1	1.014 ± 0.006	1			
4th	ML	9.945 ± 0.106	1	1	0.009 ± 0.015	7.35	0.994	Accepted
	ML ₂	17.710 ± 0.194	1	2	0.017 ± 0.30			
	MLH	14.066 ± 0.041	1	1	0.999 ± 0.019			
5th	ML	15.973 ± 0.245	2.254 ± 0.056	1	0	32.85	4.707	Rejected
	ML ₂	17.204 ± 0.268	0.948 ± 0.046	2	0			
6th	ML	5.010 ± 0.137	1	0.448 ± 0.014	0	29.75	4.262	Rejected
	ML ₂	17.759 ± 0.607	1	2.065 ± 0.079	0			
7th	ML	12.837 ± 0.116	1	1	0.627 ± 0.031	40.72	5.835	Rejected
	ML ₂	19.434 ± 0.519	1	2	0.308 ± 0.095			
8th	MLH	12.837 ± 0.116	1	1	0.627 ± 0.031	40.73	5.835	Rejected
	ML ₂	19.434 ± 0.519	1	2	0.308 ± 0.095			

n_s solutions differing in pH, the absorbance matrix, of size ($n_w \times n_s$) represents the input data for SQUAD(84). Separation of the data into individual A -pH curves, and subsequent graphical analysis, may be performed and $\log \beta_{01r}$ and r estimated from the intercept and slope of dependence of $\log(A - \epsilon_{01r}c_L)/(\epsilon_{010}c_L - A) = r \text{ pH} + \log \beta_{01r}$ (for absorbance measurements in 1-cm cells). However, various linear transformation methods are rather sensitive to the choice of segment of the A -pH curve to be analysed and the parametric estimates are always loaded by systematic error. Therefore the rigorous non-linear regression approach of SQUAD(84)¹⁸ is preferred for examining the possibilities and limitations of the ESI method.

Both computational strategies of SQUAD(84), the classical trial-and-error method and the method of simultaneous stoichiometry estimation were applied and the results are compared in Table 4. The trial-and-error method searches for the best degree of fit for various initial guesses of both $\log \beta_{01r}^{(0)}$ and $r^{(0)}$, with the option of keeping r constant and refining $\log \beta_{01r}$, or keeping $\log \beta_{01r}^{(0)}$ at a realistic guessed value and estimating r . The degree of fit is again here a sensitive resolution tool. For a false initial guess of the stoichiometric indices or for quite unrealistic stability constants, the minimization process fails because of a divergence of the minimization algo-

rithm or because of a poorly developed minimum, and also there is a poor fit.

The shape of the residual-square sum function U for the spectrophotometric data of the TAMP A -pH curve at a single wavelength is interpreted by contours computed by the program MINUIT.²⁶ It is evident from Fig. 1 that the minimum is a rather skew and very narrow pit which looks like a cleft. Such a minimum is difficult to reach by most minimizing routines when a bad initial guess of parameters is used. Sillén²⁷ proved that the convergence of a minimization can be speeded up by varying the parameters along the main axis of the skew pit. Therefore POLET(84), which uses this twisting matrix technique, converges better than SQUAD(84), even from bad initial guesses.

Simultaneous estimation of stoichiometry and stability constants is also handicapped if there is a strong interdependence of $\log \beta_{01r}$ and r . The total correlation coefficient for the two parameters $\rho(\log \beta_{01r}, r) = 0.998$ indicates a strong correlation between them and their interdependence may be expressed by the equation $(\log \beta_{01r})_{\text{found}} = (r)_{\text{given}} \times \log \beta_{01r}$. The U response surface may be visualized by means of a three-dimensional graph of U as a function of both parameters, $(10 - U) = f(\log \beta_{01r}, r)$, and the minimum U_{min} is interpreted as the maximum value of $(10 - U_{\text{min}})$. As SQUAD(84) is not able to

Table 4. Simultaneous estimation of protonation constant and one stoichiometric index r of LH, species by SQUAD(1984) analysis of absorbance matrix¹⁰ of TAMP: experimental conditions: $5.0 \times 10^{-5} M$ TAMP, $I = 0.1$ (KNO₃), 1-cm cell, 25°C

Part 1. Absorbance matrix of dimensions $n_w = 7$, $n_s = 15$

pH	Absorbance at						
	440 nm	470 nm	510 nm	540 nm	560 nm	580 nm	610 nm
6.05	0.356	0.373	0.230	0.094	0.052	0.035	0.028
6.42	0.354	0.370	0.240	0.106	0.067	0.050	0.035
6.69	0.343	0.368	0.250	0.128	0.091	0.073	0.051
6.91	0.335	0.357	0.257	0.155	0.124	0.102	0.071
7.11	0.325	0.348	0.270	0.188	0.160	0.135	0.095
7.35	0.302	0.333	0.291	0.241	0.223	0.194	0.132
7.57	0.281	0.315	0.312	0.296	0.278	0.245	0.171
7.87	0.245	0.286	0.350	0.391	0.395	0.355	0.237
8.11	0.215	0.263	0.382	0.465	0.484	0.438	0.290
8.29	0.184	0.248	0.410	0.529	0.557	0.502	0.328
8.53	0.170	0.233	0.436	0.583	0.615	0.556	0.362
8.85	0.154	0.221	0.456	0.630	0.669	0.605	0.393
9.28	0.144	0.218	0.470	0.660	0.710	0.635	0.410
9.90	0.136	0.212	0.480	0.680	0.730	0.660	0.415
11.63	0.134	0.210	0.489	0.700	0.744	0.670	0.423

Part 2. Results of the trial-and-error method and the simultaneous estimation of stability constants with stoichiometric index r : XXX means that too big a number was estimated

Parameters varied	Initial guess		Estimated parameters		Degree of fit test			Hypothesis testing
	$\log \beta_{01r}^{(0)}$	$r^{(0)}$	$\log \beta_{01r}$	r	$U \times 10^2$	$s(A)$	$R \times 10^2$	
A. The trial-and-error method								
β_{01r} only	7.846	1	7.846 ± 0.005	—	0.2288	0.0050	1.18	Accepted
		2	15.790 ± 0.044	—	9.1319	0.0318	5.56	Rejected
		3	23.741 ± 0.074	—	17.9159	0.0446	10.89	Rejected
r only	1.95	1	—	0.2943 ± 0.0068	0.0426	0.0426	10.02	Rejected
	3.90	1	—	0.5136 ± 0.0035	6.3287	0.0045	3.85	Rejected
	7.846	1	—	0.9999 ± 0.0007	0.2287	0.0050	1.18	Accepted
B. The method of simultaneous estimation of stoichiometry and stability constants								
β_{01r}, r	7.846	1	7.464 ± 0.082	0.9520 ± 0.0103	0.1834	0.0045	1.06	Accepted
	7.85	1	7.461 ± 0.079	0.9516 ± 0.0099	0.1834	0.0045	1.06	Accepted
	7.5	1	$6.500 \pm XXX$	0.6158 ± 0.2817	126.8170	0.1187	27.77	Rejected
	1.95	1	0.950 ± 6.121	0.2184 ± 0.1247	22.1310	0.0496	11.60	Rejected

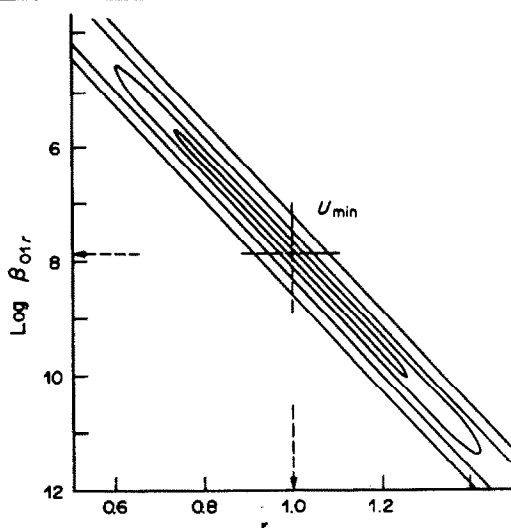


Fig. 1. The contours of residual-squares sum function U on the plot of $\log \beta_{01r}$, vs. r demonstrate a skew and narrow pit and the determination of the co-ordinates of U_{\min} is rather difficult for many minimization routines. Example of A -pH curve of TAMP from Table 4 at 560 nm, computed by MINUIT program.

map a fine structure and reach a skew cleft-like minimum, the fine structure of the maximum was not calculated and plotted (Fig. 2). The position of the crease for the maximum proves strong covariation of the two parameters, since its main axis is situated at an angle to both co-ordinate axes.

The interdependence of $\log \beta_{01r}$ and r should be kept in mind when choosing a realistic value in the initial guess for both parameters. Either a reasonable initial guess of the stability constant should be used, in which case the pit-mapping algorithm²³ in POLET(84)¹⁷ can minimize both parameters simultaneously with good convergence, or one parameter is kept constant at the value of the initial guess and only the other is refined.

The ESI method can be used to confirm an experimentally determined chemical model. When the stoichiometric indices are varied together with the corresponding stability constants, the estimates found for the stoichiometric indices should *not* differ significantly from the tested integer values. When the chemical model is false, the estimated stoichiometric indices are far from being integers and can sometimes

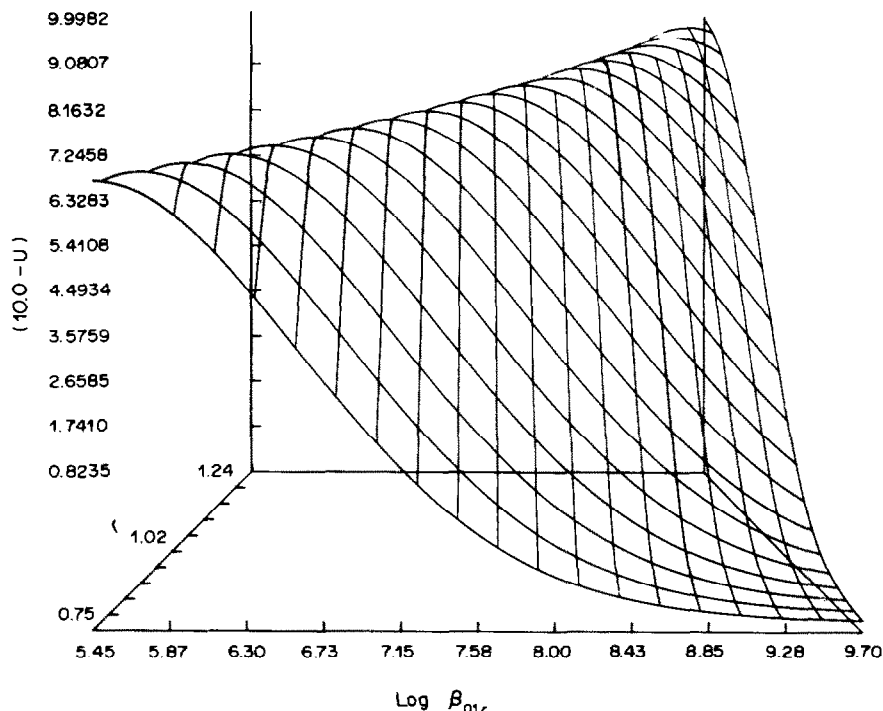


Fig. 2. Three-dimensional graph of $(10.0 - U)$ response-surface for data of Table 4 indicates that both parameters, $\log \beta_{01r}$ and r , are interdependent in a model.

reach quite unrealistic values. When the chemical model tested is incomplete with some species missing, the degree of fit test reliably indicates a very bad fit is achieved.

CONCLUSIONS

It has been demonstrated that stoichiometric indices can be estimated as real numbers simultaneously with stability constants. The proposed method (ESI) can be applied (i) for the direct determination of the stoichiometry of "uncertain" species as one step in finding the correct chemical model, and (ii) for final confirmation of the species composition. The ESI method is also useful in searching for a chemical model and as a diagnostic tool for judging whether a suggested chemical model is true or false. A reliable minimizing subroutine able to estimate covariant parameters is required. Application of the ESI method is under further development.

REFERENCES

1. L. G. Sillén, *Acta Chem. Scand.*, 1961, **15**, 1981.
2. J. Havel and V. Kubáň, *Scripta Fac. Sci. Nat. UJEP Brun.*, *Chemia* 2, 1971, **1**, 87.
3. V. Kubáň, L. Sommer and J. Havel, *Collection Czech. Chem. Commun.*, 1975, **40**, 604.
4. L. Sommer, V. Kubáň and J. Havel, *Spectrophotometric Studies of Complexation in Solution*, *Folia Fac. Sci. Nat. Univ. Purk. Brunensis*, Vol. XI, *Chemia* 7, Op. 1 (1970).
5. J. Havel and M. Meloun, in *Computational Methods for the Determination of Formation Constants*, D. J. Leggett (ed.), Plenum Press, New York, 1985.
6. M. Šucmanová-Vondrová, J. Havel and L. Sommer, *Collection Czech. Chem. Commun.*, 1977, **42**, 1812.
7. J. Vošta and J. Havel, *ibid.*, 1977, **42**, 2871.
8. M. Meloun and M. Javůrek, *Talanta*, 1984, **31**, 1083; V. Řiha, M. Meloun, M. Franz and J. Čermák, *Sb. Věd. Pr., Vys. Šk. Chemickotechnol., Pardubice*, 1975, **33**, 39.
9. M. Meloun and J. Havel, *Computation of Solution Equilibria, Part 1, Spectrophotometry*, *Folia Fac. Sci. Nat. Univ. Purk. Brunensis*, 1986.
10. M. Meloun and J. Havel, *Computation of Solution Equilibria, Part 2, Potentiometry*, *Folia Fac. Sci. Univ. Purk. Brunensis*, in the press.
11. L. G. Sillén and B. Warnqvist, *Arkiv Kemi*, 1969, **31**, 341.
12. N. Ingri and L. G. Sillén, *Acta Chem. Scand.*, 1962, **16**, 173.
13. I. Nagypál and L. Zékány, in *Computational Methods for the Determination of Formation Constants*, D. J. Leggett (ed.), Plenum Press, New York, 1985.
14. J. Havel, in *Coordination Chemistry in Solution*, E. Högföldt (ed.), *Kungl. Tek. Hög. Hand., Trans. Royal Inst. Technol.*, 1972, 277, 371.
15. L. P. Varga, W. D. Wakley, L. S. Nicolson, M. L. Madden and J. Patterson, *Anal. Chem.*, 1965, **37**, 1003.
16. A. Vacca, A. Sabatini and M. A. Gristina, *Coord. Chem. Rev.*, 1972, **8**, 45.
17. J. Havel and M. Meloun, *Talanta*, 1986, in press.
18. M. Meloun, M. Javůrek and J. Havel, *ibid.*, 1986, in press.
19. J. Havel and M. Vrchlabský, *Euroanalysis V, Cracow (Poland)*, 26–31 August 1984, Paper XVIII-20, 465.
20. J. Havel and M. Meloun, *Talanta*, 1985, **32**, 171.
21. J. J. Kankare, *Anal. Chem.*, 1970, **42**, 1322.
22. A. Sabatini, A. Vacca and P. Gans, *Talanta*, 1974, **21**, 53.
23. M. Meloun and J. Čermák, *ibid.*, 1984, **31**, 947.
24. D. J. Leggett and W. A. E. McBryde, *Anal. Chem.*, 1975, **47**, 1065.
25. M. Meloun and M. Javůrek, *Talanta*, 1985, **32**, 973.
26. F. James, *Comp. Phys. Commun.*, 1975, **10**, 343.
27. L. G. Sillén, *Acta Chem. Scand.*, 1964, **18**, 1085.

SHORT COMMUNICATIONS

A NEW REAGENT FOR DETERMINING TRACE SELENIUM BY GAS CHROMATOGRAPHY: 1,4-DIBROMO-2,3-DIAMINONAPHTHALENE

OUYANG ZHENG, XU PEI-YI, XIONG GUAN-LAN and LIU YUE

Department of Chemistry, Jinan University, Guangzhou, People's Republic of China

(Received 14 November 1984. Revised 10 November 1985. Accepted 11 January 1986)

Summary—1,4-Dibromo-2,3-diaminonaphthalene is proposed as a reagent for conversion of selenium into a piaszelenol, for determination by gas chromatography. The limit of detection is 0.03 ng of selenium.

Because selenium plays an important role in human life, the determination of trace selenium is becoming of more and more interest. The use of 2,3-diaminonaphthalene (DAN, I) as a reagent for determining trace selenium by gas chromatography was proposed by Young and Christian.¹ There are also several other reagents for Se,² including the 3,5-dibromo- and 4-nitro-derivatives of 1,2-diaminobenzene (II, III),^{3,4} both of which are more sensitive than I.⁵ In this paper we recommend 1,4-dibromo-2,3-diaminonaphthalene (Br₂-DAN) as a new reagent instead of I since its sensitivity for Se approaches that of II and III.

EXPERIMENTAL

Reagents

Synthesis of Br₂-DAN. Weigh 1.0 g of DAN into a 50-ml three-necked flask. Add a mixture of 0.7 ml of bromine and 6 ml of glacial acetic acid dropwise from a funnel, with vigorous stirring, and maintain the temperature at about 5°. After 10 min, filter off the precipitate on a Buchner funnel and wash it with 10 ml of glacial acetic acid and then 100 ml of 2% sodium carbonate solution. Recrystallize the product from petroleum ether (b.p. 60–90°) four times, and then dry it in a vacuum desiccator. The final product is brown needle-like crystals, m.p. 142°.

Br₂-DAN solution. Weigh out 5 mg of Br₂-DAN, add 2.5 ml of concentrated hydrochloric acid (spectroscopically pure grade), and let stand overnight. When dissolution is complete, dilute with 250 ml of distilled water to make 20 µg/ml Br₂-DAN solution in 0.1M hydrochloric acid.

Preparation of 4,7-dibromo-5,6-benzo-piazselenol (selenium complex). Transfer 1 ml of 20 µg/ml selenium solution (or 1 ml of 0.2 µg/ml solution) into a separatory funnel. Adjust the pH to ~3 with concentrated ammonia solution, and add 2 ml of Br₂-DAN solution. Heat the mixture at 60° in a water-bath for 30 min. Cool, then extract the piaszelenol with 2 ml (or 0.2 ml) of toluene. The toluene extract is stable for at least 4 hr if kept at room temperature in darkness and for one month if stored at 4° in darkness, but is unstable when exposed to bright light. Inject a 0.2-µl portion of the extract into the chromatographic column.

Apparatus

A model SP-2308 gas chromatograph (Beijing, China) equipped with an ECD (⁶³Ni) was used. The column was a glass tube, 1 m long and 2 mm bore, packed with 3% SE-30 on 60–80 mesh Chromosorb G. The carrier gas was 99.999% pure nitrogen, flowing at 40 ml/min. The column

temperature was 210° and the injection port and detector temperatures were both 280°.

RESULTS AND DISCUSSION

Identification of the piaszelenol peak

The chromatogram of the blank and the piaszelenol solution are shown in Fig. 1.

There are two peaks for the blank, and three for the piaszelenol solution, and peak C is evidently due to the Se complex, the retention time for which is about 3 min.

A reagent acidity of 0.1M hydrochloric acid is optimal for formation of the Se complex. The reaction itself is relatively slow. There are two ways of performing the reaction; one is to let the solution stand for 2 hr at room temperature, and the other is to keep it at 60° for 30 min. If the temperature rises above 60°, the height of the Se peak is decreased, and some minor peaks appear in the chromatogram; we attribute this to decomposition of the Se complex.

The detector response was linear over the range 1–10 ng of selenium, and the limit of detection was 0.03 ng of selenium.

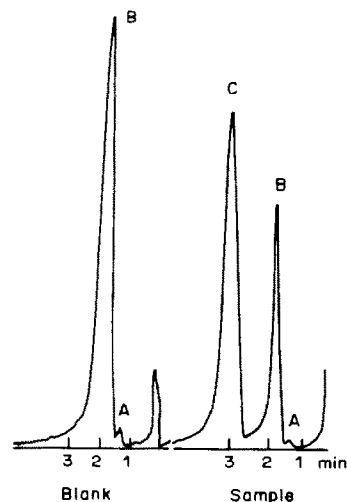


Fig. 1. Amount of Se injected: 2 ng.

Since the interference of a large number of ions with the formation of the DAN complex had already been investigated by Lott *et al.*,⁶ and the characteristics of DAN are similar to those of Br₂-DAN, we restricted our investigation of interferences to testing iron(III) as a model interferent in confirming the reference by Lott *et al.* to the efficiency of 0.1M EDTA as a masking agent. We found that the interference of a 1000-fold amount of iron(III), relative to Se, can be suppressed by adding 1 ml of 0.1M EDTA, but too much EDTA results in decrease in the peak height for selenium.

This method has been used for determining trace selenium in Chinese medicinal herbs, down to the 10 ng/g level.

REFERENCES

1. J. W. Young and G. D. Christian, *Anal. Chim. Acta*, 1973, **65**, 127.
2. S. Dilli and I. Sutikno, *J. Chromatog.*, 1984, **300**, 265.
3. D. C. Reamer and C. Vellion, *Anal. Chem.*, 1981, **53**, 2166.
4. K. Toei and Y. Shimoishi, *Talanta*, 1981, **38**, 967.
5. Y. Shimoishi, *J. Chromatog.*, 1977, **136**, 85.
6. P. F. Lott, P. Cukor, G. Moriber and J. Solga, 1963, **35**, 1159.

THE DETERMINATION OF SAMARIUM, EUROPIUM, GADOLINIUM AND DYSPROSIUM IN URANIUM PRODUCTS BY DIRECT-CURRENT PLASMA EMISSION SPECTROMETRY

FRANCES FLAVELLE and ALAN D. WESTLAND

Ottawa-Carleton Chemistry Institute, Department of Chemistry, University of Ottawa, Ottawa, Canada

(Received 5 August 1985. Accepted 7 January 1985)

Summary—Samarium, europium, gadolinium and dysprosium were separated from uranium-containing materials by means of solvent extraction with Alamine 336, followed by cation-exchange. The elements were determined in the sub-ppm range by means of direct-current plasma atomic-emission spectrometry.

To determine the lanthanide elements, the analyst must decide whether to isolate the individual elements or to rely simply on an element-selective method of determination. Neutron activation,¹⁻³ isotopic-dilution mass spectrometry^{4,5} and X-ray fluorescence are used, but suffer from one or more disadvantages such as interelement interferences, poor sensitivity or cumbersome methodology.

It is possible to determine small amounts of the lanthanides with comparatively little sample preparation by means of plasma atomic-emission spectrometry. Crock and Lichte⁶ have shown that the interelement spectral interferences are not very large if the lanthanides are present in relative amounts that are typical of geological samples. Satisfactory analyses of rocks were obtained by use of a double ion-exchange procedure that isolated the group of lanthanides but did not separate its individual members.

However, Yoshida and Haraguchi⁷ argued that in other types of samples the relative amounts of the lanthanides may be such as to make it advisable to separate the individual members of the group, and used high-pressure liquid chromatography (HPLC) for this purpose. Cassidy⁸ has studied various column materials for HPLC separation of the individual lanthanides and determined the elements in the column effluent by means of a microphotometer cell. Procedures that avoid the necessity for complete separation will probably continue to be attractive for certain purposes.

Crock and Lichte⁶ separated the anionic species with a small anion-exchange column. If a large quantity of such species is present, the need to use a large column would require a subsequent concentration step, such as evaporation, in work with trace amounts. We decided to use a liquid anion-exchange extraction instead of anion-exchange on a column. As the extractant we used Alamine 336. The extraction characteristics of high molecular-weight amines

have been summarized by Furman.⁹ Alamine 336 is a mixed tertiary octyl-decyl amine used primarily in large-scale refining processes.¹⁰ Its use in separation of tracer quantities in fission-product mixtures has been reported by Ahmad *et al.*¹¹ With a view to the analysis of nuclear material, we separated a selection of lanthanide elements at sub-ppm levels from large quantities of uranium, by solvent extraction of the latter, and then from most other cations by use of a strong acid cation-exchanger. Most ions, except those of titanium, zirconium, hafnium, thorium and the lanthanides, are not retained by the resin in hydrochloric or nitric acid.

EXPERIMENTAL

Standard solutions

Atomic-absorption standard solutions (1000 µg/ml) of Sm, Eu, Gd and Dy were obtained from Aldrich Chemical Co., Milwaukee, U.S.A., and were diluted as required, with 2M perchloric or nitric acid, to give the working solutions, which were prepared at frequent intervals and stored in plastic bottles.

Direct-current plasma emission spectrometry (DCP-ES)

A Beckman Spectroscan V combined with a high-energy dc plasma excitation source and a high-resolution echelle grating was used for the determinations. The following wavelengths were chosen: Sm, 442.26; Eu, 381.97; Gd, 335.02; Dy, 353.17 nm. The signal was integrated for 5 sec and the integration repeated once. The spectrometer was calibrated with a series of standards, as the response was not quite linear at low concentrations. The plasma was operated with argon (99.5% pure) as support gas at a flow-rate of 7 l./min.

Solvent extraction

The extractant solution was made by mixing Alamine 336, *o*-xylene and petroleum ether (b.p. 80–100°) in 65:50:100 v/v ratio.

Ion-exchanger

Bio-Rad AG50W-X8 cation-exchange resin, 200–400 mesh, slurried in 2M hydrochloric acid, was packed into tubes of either 0.7 or 1.0 cm inside diameter to a depth of 6.0 cm. Solutions were passed through the columns at about 1 ml/min.

Table 1. Recovery of lanthanides from pure solution by cation-exchange

No.	Element	Wt. taken, μg	Resin mesh size	Acid medium	Recovery, %
1	Eu	3.0	200-400	HNO ₃	98
2	Eu	3.0	200-400	HNO ₃	95
3	Eu	3.0	100-200	HNO ₃	97
4	Eu	3.0	100-200	HNO ₃	95
5	DY	2.0	200-400	HNO ₃	97
6	Dy	2.0	200-400	HNO ₃	104
7	Dy	2.0	100-200	HNO ₃	100
8	Dy	2.0	100-200	HNO ₃	97
9	Eu	3.0	200-400	HCl	93
	Dy	5.0	200-400	HCl	99
10	Eu	3.0	200-400	HCl	92
	Dy	5.0	200-400	HCl	97
11	Dy	5.0	100-200	HCl	87
12	Dy	5.0	100-200	HCl	78
13	Sm	2.0	200-400	HCl	95
	Eu	3.0	200-400	HCl	98
	Gd	2.0	200-400	HCl	94
	Dy	2.0	200-400	HCl	97
14	Sm	2.0	200-400	HCl	100
	Eu	3.0	200-400	HCl	97
	Gd	2.0	200-400	HCl	103
	Dy	2.0	200-400	HCl	75

Analysis of UO₃ and UO₂ samples

Dissolve 10 g of UO₃ sample in 20 ml of 6*M* hydrochloric acid and 5 ml of water; transfer the solution to a 250-ml separatory funnel. For UO₂ samples dissolve 10 g of the oxide in a mixture of 20 ml of 6*M* hydrochloric acid and 5 ml of concentrated nitric acid; after the reaction has subsided, transfer the solution to a 250-ml separatory funnel.

Extract uranium and other extractable anionic species by shaking for 1 min with 100 ml of Alamine 336 solution and discard the extract. Transfer the aqueous phase to a second separatory funnel. Add 10 ml of concentrated hydrochloric acid and extract with a further 100 ml of Alamine 336 solution.

Separate the aqueous phase and bring its acid concentration to $\leq 2M$ by adding an equal volume of water. Pass this solution through a moistened 7.0-cm Whatman No 40 filter paper into the ion-exchange column, conditioned with 2*M* hydrochloric acid. After the sample solution has passed through, wash the column with 50 ml of 2*M* hydrochloric acid. Test the last few ml of effluent for complete removal of uranium by adding 1 ml of 0.05% aqueous Arsenazo III solution; if a blue tint appears, continue the washing with acid until the effluent is free from uranium. Elute the lanthanides with 25 ml of 7.5*M* hydrochloric acid, reduce the volume of eluate by evaporation, and make it up to volume in a 10- or 25-ml standard flask with water. Analyse this solution for the lanthanides by DCP-ES. Regenerate the column for the next sample by passing 2*M* hydrochloric acid through it.

RESULTS AND DISCUSSION

Extraction of uranium

The conditions of extraction are rather critical if uranium is to be removed efficiently in two or three extractions. The same conditions should also be effective for common elements such as iron, copper and zinc, as well as certain actinides. It is reported that a hydrochloric acid medium is suitable in such cases.⁹ A residue of a few mg of uranium can be

tolerated, as there is a final clean-up in the ion-exchange step. If a sample initially contains several grams of uranium it is necessary to adjust the acid concentration and extraction volumes carefully.

A stock solution of uranium nitrates was purified by passing it through a column of Dowex 50-X8, and served as a supply of low-lanthanide uranium that could be salted with known quantities of lanthanides. A quantity of U₃O₈ was prepared by heating uranyl nitrate at 800° for 1.5 hr and reduced to UO₂ by heating for 1 hr at 900° in a stream of hydrogen. The trioxide was prepared by precipitating the peroxide with hydrogen peroxide, collecting the precipitate, drying it at 80°, then heating for 5 hr at 350° and 1 hr at 400° in a stream of oxygen.

For the determination of lanthanides at the lowest levels that are encountered in refined uranium products, it is necessary to use a 10-g sample. This quantity of uranium will load the extractant nearly to capacity, so careful attention has to be given to volumes and acid concentrations. The procedure described above was found suitable for uranium oxide samples.

Ion-exchange of the lanthanides

The larger column (see above) had twice the volume of the smaller one, but no great difference was found in the minimum volumes of liquid required for washing either column and eluting the lanthanides. This suggested that the rate of ion-exchange was more important than the volume of liquid passed.

Bivalent ions, including UO₂²⁺, but not Sr²⁺ and Ba²⁺, pass through the cation-exchange column when it is washed with 2*M* hydrochloric acid. Tervalent iron is largely removed in the solvent extraction. Aluminium and trivalent cobalt pass through the resin. Titanium, zirconium and thorium are extracted by Alamine 336 from hydrochloric acid, but any unextracted Zr and Th will be held rather strongly by the cation-exchanger and partly eluted with the lanthanides. Build-up, especially of Th, on the resin may therefore occur, so fresh resin may be needed for each sample. In our work with purified uranium, the resin was not regularly replaced. If a large quantity of titanium, zirconium or thorium is present, it may be necessary to determine it and make a correction in the spectroscopic determination of the lanthanides. We return to this question later.

When aliquots of standard lanthanide solutions were diluted to 70 ml with 2*M* hydrochloric acid, the solutions were passed through the ion-exchanger and the resin was washed with 50 ml of 2*M* hydrochloric acid, no lanthanides were detected in either the effluent or the washings. The lanthanides were then eluted with 25 ml of 7.5*M* hydrochloric acid, the volume of eluate was reduced by evaporation, and made up to 10 or 25 ml with water for determination of the lanthanides. The resin column was regenerated for the next sample by passing 2*M* hydrochloric acid through it. The results in Table 1 show the recoveries.

Table 2. Recovery of lanthanides from uranium

Sample	Element	Taken, ppm	Found, ppm	Recovery, %
1	Eu	0.30	0.31(5)	105
	Gd	0.20	0.21	103
	Dy	0.20	0.19	95
2	Eu	0.30	0.30(5)	102
	Gd	0.20	0.19	95
	Dy	0.20	0.20	100
3	Sm	0.20	0.19(5)	97
	Eu	0.30	0.29(5)	98
	Gd	0.20	0.21	105
	Dy	0.20	0.21(5)	107
4	Sm	0.040	0.035	88
	Eu	0.060	0.063	105
5	Sm	0.040	0.038	95
	Eu	0.060	0.066	110
	Gd	0.040	0.045	112
	Dy	0.040	0.040	100
6	Sm	0.040	0.038	95
	Eu	0.060	0.063	105
	Gd	0.040	0.037	93
	Dy	0.040	0.017	43

*Amount, in μg of lanthanide per g of UO_3 (a 10-g portion of UO_3 was used for making the sample).

In three cases, the recovery of dysprosium was less than 90%. We do not believe that this element was lost to the initial effluent from the ion-exchange column, as the heavier lanthanides are the most strongly held, and no dysprosium was found in the initial effluent or washings, nor was any found in the eluate obtained with a second portion of eluent. Crock and Lichte⁶ reported good recoveries of the heavier lanthanides, so we attribute the discrepant results to instrumental error. At the wavelengths employed, the response for dysprosium is the poorest of those for the elements used in this study.

When samples were submitted to solvent extraction, the aqueous layer was found to contain traces of the amine used. To avoid fouling of the ion-exchange resin, the sample solutions were passed through a moistened 7.0-cm Whatman No. 40 filter paper placed in a funnel in the top of the column. The rather viscous amine remained on the paper. Tests of recoveries after this filtration revealed no losses by adsorption on the paper.

Test of procedure

The complete procedure was applied to unsalted uranium solutions to obtain the blank values. Samples were salted with known amounts of lanthanides

and analysed by the complete procedure. The results are given in Table 2. The solutions were all prepared from 10-g samples of UO_3 .

A comment about the blank values is in order. If two successive 25-ml portions of the 7.5M hydrochloric acid used as eluent were passed through a resin column that had received an unsalted uranium sample, the two eluates gave approximately the same blank values. This is suggestive of the behaviour of thorium, which is eluted slowly.

If the blank is small, it can be determined by passing a second 25-ml portion of eluent through the column after elution of the lanthanides. A correction for thorium interference can be made by measuring the second eluate at the various wavelengths used for the lanthanides. This method of blank correction was used for samples 4–6 in Table 2.

The mean error for samples 1–3 was 3.8%. With the exclusion of the final dysprosium results, which we regard as an obvious outlier, the mean error for samples 4–6 was 6.8%. The aliquots taken for analysis of these latter samples were only one-fifth as large as those for samples 1–3.

The levels at which these determinations were made were about an order of magnitude below the limits of detection by atomic-absorption spectrometry.

Acknowledgement—This work was supported by Eldorado Resources Ltd., Ottawa, Canada.

REFERENCES

1. S. F. Marsh, *Anal. Chem.*, 1967, **39**, 641.
2. R. A. Schmitt, R. H. Smith, J. E. Lasch, A. W. Mosen, D. A. Olehy and J. Vaselevskis, *Geochim. Cosmochim. Acta*, 1963, **27**, 577.
3. J. J. McCown and R. P. Larsen, *Anal. Chem.*, 1961, **33**, 1003.
4. J. H. Jolly, *Rare Earth Elements and Yttrium, Mineral Facts and Problems*, Bureau of Mines, U.S. Department of the Interior, Washington, D.C., 1975.
5. A. Masuda, N. Nakamura and T. Tanaka, *Geochim. Cosmochim. Acta*, 1973, **37**, 239.
6. J. G. Crock and F. E. Lichte, *Anal. Chem.*, 1982, **54**, 1329.
7. K. Yoshida and H. Haraguchi, *ibid.*, 1984, **56**, 2580.
8. S. Elchuk and R. M. Cassidy, *ibid.*, 1979, **51**, 1434.
9. N. H. Furman (ed.), *Standard Methods of Chemical Analysis*, 6th Ed., Vol. IIA, p. 190. Van Nostrand Reinhold, New York, 1963.
10. See for example, N. Sezginer, *Turkish J. Nuclear Sciences*, 1984, **11**, 65; B. Floh, *Report Inst. Energ. At., Saõ Paulo, Brazil*, 1976.
11. S. Ahmad, A. Thoren and G. Skarnemark, *J. Radioanal. Nucl. Chem.*, 1984, **86**, 247.

FLOW INJECTION DETERMINATION OF ERGONOVINE MALEATE WITH AMPEROMETRIC DETECTION AT THE KEL-F-GRAPHITE COMPOSITE ELECTRODE

F. BELAL* and J. L. ANDERSON

Department of Chemistry, University of Georgia, Athens, Georgia 30602, U.S.A.

(Received 2 September 1985. Accepted 6 January 1986)

Summary—The Kel-F-graphite electrode was used for the electrochemical detection of ergonovine maleate in a flowing stream. It was found useful in the analyte concentration range 0.5–20 $\mu\text{g/ml}$, with a detection limit of 50 ng/ml ($1.1 \times 10^{-7} M$). A procedure was developed for assay of ergonovine maleate in tablets, and the results obtained agreed with those given by the official U.S. Pharmacopeia method.

Ergonovine maleate is a naturally occurring, water-soluble, amino ergot alkaloid, used as an orally active oxytocic drug. Ergonovine maleate may be determined by several analytical techniques, including spectrophotometry,¹ colorimetry,² titrimetry,³ fluorimetry,⁴ thin-layer chromatography,⁵ paper chromatography,⁶ gas chromatography,⁷ high-pressure liquid chromatography⁸ and radio-immunoassay.⁹

Recently much attention has been given to methods for rapid, repetitive determination of components in samples injected into flowing streams,¹⁰ and electrochemical detectors have been used for an ever-increasing range of samples processed in this manner.^{11–13} For many species, electrochemical detectors can surpass refractive index, ultraviolet absorption or fluorescence detectors in selectivity, detection limit, simplicity and cost. Carbon-based electrodes are often preferred for amperometric detection in the oxidative mode. The earlier literature on carbon electrodes has been summarized.^{14,15} The Kel-F-graphite (Kelgraf) composite electrode has been evaluated for general voltammetric applications, and found to be useful for a wide range of species in a variety of solvents.^{15–17}

This report describes the use of the Kelgraf composite electrode as an amperometric detector in the flow-injection determination of ergonovine maleate. A procedure for assay of ergonovine in tablets has been developed and shown to give results in agreement with those given by the official U.S. Pharmacopeia method. The suggested procedure is characterized by simplicity, high sensitivity and rapidity.

EXPERIMENTAL

Reagents

Ergonovine maleate was kindly provided by Eli Lilly, Indiana, USA. Other chemicals were reagent grade, and

used without further purification. Distilled water was passed through activated charcoal and two stages of mixed-bed ion-exchangers in a Barnstead Nanopure system before use. The mobile phase was a 1:4 v/v mixture of methanol and an aqueous buffer (pH 7) consisting of 0.010M phosphate buffer and 2% sodium acetate, prepared as described earlier.¹⁷

Apparatus

Cyclic voltamperograms were obtained with a conventional three-electrode system, consisting of the Kelgraf working electrode, a platinum auxiliary electrode, and a silver/silver chloride/3.5M potassium chloride reference electrode, used in conjunction with a Bioanalytical Systems model CV-1A potentiostat with output monitored by a digital oscilloscope (Nicolet Instrument Corporation model 200), then transferred from the oscilloscope to an X-Y recorder (Houston Omnigraphic model 200). The flow-injection analyses were performed with a FIAStar model 5001 system (Tecator, Denmark). The mobile phase was pumped through the cell at ambient temperature, at a fixed flow-rate of 0.45 ml/min under a nitrogen gauge-pressure of 0.4 bar. Samples were injected manually by means of a microsyringe (1-ml tuberculin syringe, Becton Dickinson and Co.) into the sample injector (loop volume 25 μl). Potentials were controlled and the current monitored by means of an EG&G Princeton Applied Research model 174A potentiostat. Cell currents were displayed on a strip chart recorder.

Working electrode

The electrode was fabricated as previously reported¹⁵ and consisted of 15% graphite by weight. After manual sanding with progressively finer-grit sandpaper, the electrode was polished to a smooth, shiny finish with 1- μm alumina (Buehler Micropolish).

Sample preparation

A stock solution (1.00 mg/ml) of ergonovine maleate was prepared in the mobile phase solution, and diluted with mobile phase solution to provide working standards in the 1–20 $\mu\text{g/ml}$ range.

Procedures

Calibration graph. Working standards were injected, and the current was measured at an applied potential of +0.85 V vs. the Ag/AgCl reference electrode.

Analysis of tablets. Tablets containing ergonovine maleate were ground, and a weighed portion of the powder was mixed with a known volume of mobile phase solution and

*Permanent address: Department of Chemistry, College of Pharmacy, University of Mansoura, Mansoura, Egypt.

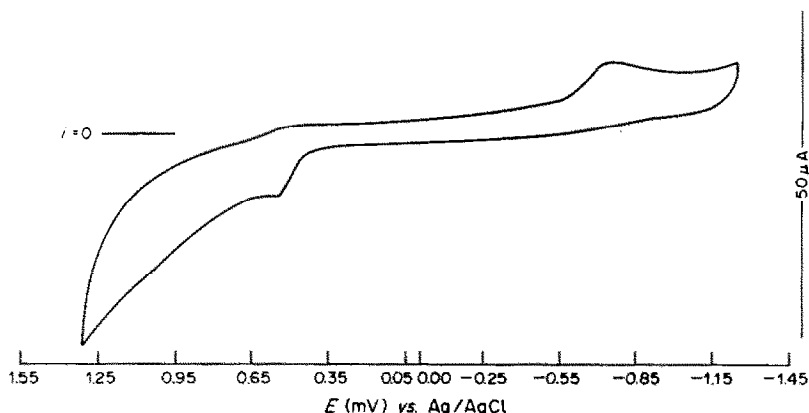


Fig. 1. Cyclic voltamperogram of ergonovine maleate ($1 \times 10^{-3}M$) in phosphate buffer (pH 7)–methanol (4:1 v/v) at the Kel-F–graphite electrode. Scan-rate 500 mV/sec.

exposed to ultrasonic radiation. The solution was filtered and a known volume was suitably diluted with mobile phase to bring the analyte concentration within the calibration range, and assayed in the same way as the standards.

RESULTS AND DISCUSSION

Ergonovine is an amino ergot alkaloid, and can be oxidized at positive potentials, as can many other amines.¹⁸ Figure 1 shows the cyclic voltamperogram of ergonovine maleate in the mobile phase solution; it exhibits an oxidative wave ($E_p = +0.56$ V) and a reductive wave ($E_p = -0.76$ V). The electrode process is completely irreversible on the time-scale of these measurements, because the two waves are separated by 1.32 V, whereas a fully-reversible one-electron transfer reaction would result in a separation of only 57 mV.¹⁹ The oxidative wave was chosen for the analysis. Figure 2 shows the voltamperogram obtained for ergonovine maleate in the FIA system with electrochemical oxidation at the Kelgraf electrode. A potential of +0.85 V was selected for the

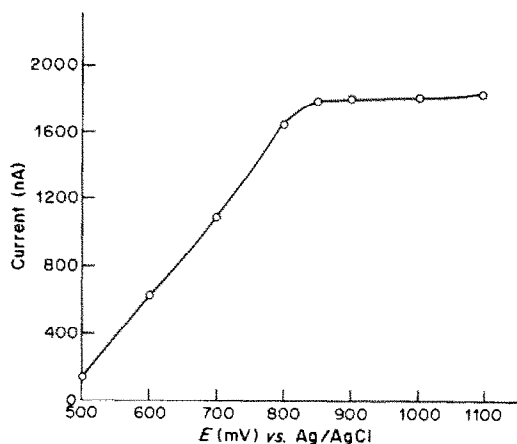


Fig. 2. Hydrodynamic voltamperogram of 0.1 g/l. ergonovine maleate at the Kel-F–graphite electrode, in phosphate buffer (pH 7)–methanol (4:1 v/v). Flow-rate 0.45 ml/min.

amperometric determination, since it represented the lowest potential on the plateau at which maximum drug sensitivity could be obtained.

At a potential of +0.85 V vs. the Ag/AgCl/3.5M KCl reference electrode, the current–concentration curve was linear over the 1–20 $\mu\text{g/ml}$ concentration range investigated, the slope, intercept and correlation coefficient being typically 17.0 nA. μg^{-1} , 1.07 nA and 0.9999 respectively. The reproducibility of the electrode was tested by running four replicate injections of ergonovine maleate concentrations of 1, 2, 5 and 10 $\mu\text{g/ml}$. Mean peak currents of 16.8, 33.8, 84.0 and 170.0 nA respectively were obtained, with relative standard deviations of 0.4, 0.2, 0.1 and 0.1% respectively. The detection limit was 50 ng/ml ($1.1 \times 10^{-7}M$), estimated as the concentration giving a signal equal to twice the peak-to-peak noise level of the background signal. It appears to be better than that observed for most reported methods of determination of ergonovine maleate.

The procedure was used for the determination of ergonovine maleate in tablets: the results in Table 1 indicate that the drug can be determined conveniently by this method with good accuracy and precision. Also, there is good agreement between the results given by the suggested method and those given by an official method.² Statistical analysis of the results by the *F*- and *t*-tests²⁰ showed no significant difference between the performance of the two methods.

The amperometric method described here has several advantages which should make it useful in

Table 1. Determination of ergonovine maleate in synthetic and commercial tablets

Nominal content	Recovery,* %	
	Present method	Official method ²
2.0 mg/tablet	100.2 \pm (0.4)	99.8 \pm (0.3)
2.5 mg/tablet	100.0 \pm (0.4)	99.7 \pm (0.3)
3.0 mg/tablet	100.1 \pm (0.5)	99.7 \pm (0.3)
4.0 mg/tablet	100.1 \pm (0.4)	99.9 \pm (0.2)

*Mean \pm standard deviation, based on 6 separate determinations and calculated on basis of nominal content.

meeting the need for a fast and reliable procedure for ergonovine maleate assay. The high sensitivity, simplicity, good reproducibility and inexpensive equipment, help to make it ideal for routine analysis of ergonovine maleate and its tablets.

The major advantage of the flow-injection analysis used is its speed. The calculated residence time in the tubing and electrode is 5 sec. Allowing a time of 20 sec between injections, a rate of determination of up to 150 samples/hr appears feasible, the limiting factor being sample-preparation time.

REFERENCES

1. J. Bayer, *Acta. Pharm. Hung.*, 1958, **28**, 35; *Chem. Abstr.*, 1959, **53**, 2541a.
2. *United States Pharmacopeia*, XXth Revision, p. 284. Mack, Easton, Pa., 1980.
3. V. P. Georgievskii, *Probl. Analit. Khim.*, 1970, **1**, 94; *Chem. Abstr.*, 1971, **74**, 146428V.
4. R. D. Kirchhoefer, *J. Assoc. Off. Anal. Chem.*, 1978, **61**, 1433.
5. G. E. Ferraro, S. L. Debenedetti and J. D. Coussio, *J. Pharm. Pharmacol.*, 1976, **28**, 729.
6. T. G. Alexander and D. Banes, *J. Pharm. Sci.*, 1961, **50**, 201.
7. D. L. Sondack, *ibid.*, 1974, **63**, 584.
8. G. Szepesi, M. Gazdag and L. Terdy, *J. Chromatog.*, 1980, **191**, 101.
9. G. Koch, M. Johansson and E. Arvidsson, *J. Clin. Chem. Clin. Biochem.*, 1980, **18**, 367.
10. J. Růžička and E. H. Hansen, *Anal. Chim. Acta*, 1980, **114**, 19.
11. A. N. Strohl and D. J. Curran, *Anal. Chem.*, 1979, **51**, 1050.
12. P. W. Alexander and M. H. Shah, *Talanta*, 1979, **26**, 97.
13. H. K. Chan and A. G. Fogg, *Anal. Chim. Acta*, 1979, **111**, 281.
14. E. Pungor and É. Szepesváry, *ibid.*, 1968, **43**, 289.
15. J. E. Anderson, D. E. Tallman, D. J. Chesney and J. L. Anderson, *Anal. Chem.*, 1978, **50**, 1051.
16. D. J. Chesney, J. L. Anderson, D. E. Weisshaar and D. E. Tallman, *Anal. Chim. Acta*, 1981, **124**, 321.
17. J. L. Anderson, K. K. Whiten, J. D. Brewster, T. Y. Ou and W. K. Nonidez, *Anal. Chem.*, 1985, **57**, 1366.
18. R. N. Adams, *Electrochemistry at Solid Electrodes*, Dekker, New York, 1968.
19. A. J. Bard and L. R. Faulkner, *Electrochemical Methods*, p. 219. Wiley, New York, 1980.
20. D. H. Sanders, A. F. Murph and R. J. Eng, *Statistics*, McGraw-Hill, New York, 1976.

THE OXIDATION OF IODIDE TO IODATE FOR THE POLAROGRAPHIC DETERMINATION OF TOTAL IODINE IN NATURAL WATERS

KAZUFUMI TAKAYANAGI

Centre Champlain des Sciences de la Mer, Ministère des Pêches et des Océans, C.P. 15500, 901 Cap
Diamant, Quebec, G1K 7Y7, Canada

GEORGE T. F. WONG

Department of Oceanography, Old Dominion University, Norfolk, Virginia 23508, U.S.A.

(Received 22 October 1984. Revised 20 December 1985. Accepted 30 December 1985)

Summary—A simple method has been designed for the oxidation of iodide to iodate in natural waters and subsequent determination of the iodate by differential pulse polarography. Iodide is oxidized to iodate with sodium hypochlorite and the excess of oxidizing agent is destroyed with sodium sulphite. The concentration of iodide is calculated as the difference between the concentrations of iodate in a sample before and after the oxidation.

Several methods have been proposed for the oxidation of iodide in sea-water to iodate for subsequent polarographic analysis. Herring and Liss¹ used photo-oxidation by irradiation with ultraviolet light. Smith and Butler used chlorine water as the oxidizing agent² and later³ suggested that a combination of this and the irradiation method might give the best results. In practice, these methods have serious limitations. During ultraviolet irradiation of sea-water, hydrogen peroxide is formed, and interferes with the current peak of iodate since it also has a half-wave potential at around -1.1 V.⁴ A current peak which may interfere by overlap with that of iodate has also been reported in the polarogram of chlorinated sea-water.⁵ The ideal oxidizing agent should oxidize iodide to iodate quantitatively, and any other oxidation products and the excess of oxidant itself should either not interfere with the current peak of iodate or be easily destroyed.

We have found that sodium hypochlorite is such an oxidant, its excess being easily destroyed with sulphite. The concentration of total dissolved iodine species in the original solution may thus be determined as iodate by differential pulse polarography as described by Herring and Liss.¹ This method is simple, free of interference and reliable. Our results are reported in this paper.

EXPERIMENTAL

Reagents and apparatus

Standard solutions of potassium iodate and iodide were prepared. With the exception of the sodium hypochlorite, all the chemicals used were of ACS reagent-grade. A Princeton Applied Research Model 174 polarographic analyser equipped with a Houston Omnigraphic recorder, a dropping mercury electrode controlled by a drop-timer, a standard calomel electrode and a platinum wire counter-electrode, was used.

Procedures

Pipette 25 ml of sea-water into a 50-ml beaker. Add 0.2 ml of 0.2% sodium hypochlorite solution and leave the mixture for 30 min at room temperature. Then add 0.1 ml of 0.4M sodium sulphite and 0.1 ml of 0.1M EDTA and transfer the sample to a polarographic cell. Remove oxygen from the sample by bubbling oxygen-free nitrogen through it. Scan the differential pulse polarogram from -0.5 to -2.0 V, with a drop-time of 1 sec, a scan-rate of 5 mV/sec and a modulation amplitude of 25–50 mV.

Construct a calibration graph for each sample by measurement of the peak current after consecutive additions of known volumes of a standard potassium iodate solution. For determination of the iodate originally present in the sample, analyse another aliquot of sample without addition of sodium hypochlorite and sodium sulphite.

RESULTS AND DISCUSSION

The possible interference of sulphite was examined by polarography of a standard iodate solution in 0.5M sodium chloride–4 mM sodium bicarbonate solution and in a sample of sea-water, with and without added sulphite. Sulphite does not have a current peak that may interfere with that of iodate. It also does not react with iodate in any manner that may alter the iodate peak height.

The concentration of iodide in natural waters rarely exceeds $0.4 \mu\text{M}$.^{2,6,9} Stoichiometrically, for 25 ml of $1 \mu\text{M}$ iodide, only $0.075 \mu\text{mole}$ of sodium hypochlorite, or $2.8 \mu\text{l}$ of 0.2% solution, is needed for the complete oxidation to iodate. Various volumes of 0.2% sodium hypochlorite solution were added to 25-ml aliquots of a $0.4 \mu\text{M}$ solution of iodide in an estuarine water sample (2.64% salinity). The excess of hypochlorite was destroyed with sodium sulphite, and the iodate determined. Oxidation of iodide was quantitative when more than 0.03 ml of sodium hypochlorite solution was added (Table 1). In our procedure, 0.2 ml of 0.2% sodium hypochlorite solu-

Table 1. The amount of hypochlorite needed for complete oxidation of added iodide to an estuarine water sample

NaOCl solution added, ml	$\Sigma I, \mu M$			Recovery of added iodide, %
	Initial	Added*	Found	
0.01	0.31	0.40	0.65	85
0.02	0.31	0.40	0.67	88
0.03	0.31	0.40	0.70	98
0.05	0.31	0.40	0.70	98
0.10	0.31	0.40	0.71	100
0.20	0.31	0.40	0.71	100

*As potassium iodide.

tion is used, which ensures that a large excess of hypochlorite is present and the reaction will reach completion readily.

The reaction time needed for complete oxidation was also examined. A $0.25 \mu M$ iodide solution was made in $0.5 M$ sodium chloride– $4 mM$ sodium bicarbonate medium, and $0.2 ml$ of 0.2% sodium hypochlorite solution was added to each of a series of 25-ml aliquots of the iodide solution. These solutions were allowed to stand for various periods of time, the oxidation then being stopped with sodium sulphite and the iodate concentration determined. A reaction time of 20 min or more gave $>92\%$ complete oxidation (Fig. 1). Similar results were obtained (Fig. 1) for $0.5 \mu M$ iodide solution in a medium ($0.5 M NaCl$ – $0.8 mM KBr$ – $4 mM NaHCO_3$) similar to sea-water (which is about $0.5 M$ in sodium chloride, $0.8 mM$ in bromide and $2 mM$ in bicarbonate) and in the estuarine water (2.64% salinity). We chose oxidation for 30 min as optimal.

Since the reaction between sulphite and hypochlorite to form sulphate and chloride has $1:1$ stoichiometry, $6 \mu moles$ of sulphite or only $0.015 ml$ of $0.4 M$ sulphite solution will be needed to destroy all the hypochlorite added ($0.2 ml$ of 0.2% solution). To $25 ml$ of the estuarine water, $0.2 ml$ of 0.2% sodium hypochlorite solution was added, followed by sequential addition of known amounts of $0.04 M$ sodium sulphite, the polarogram of the mixture being

recorded after each sulphite addition. The results are presented in Table 2. Without the addition of hypochlorite, the iodate in the original sample yielded a current peak at $-1.15 V$ applied potential. Addition of hypochlorite caused a uniformly high current at applied potentials from -0.7 to $-1.7 V$ and the current peak for iodate was completely hidden. With less than $0.2 ml$ of $0.04 M$ sulphite added, the polarogram was erratic and spurious current peaks were found. With more than $0.3 ml$ of $0.04 M$ sulphite, a well defined iodate current peak of constant height was observed, but the peak appeared at slightly lower applied potential when less than $0.6 ml$ of sulphite was added. With more than $0.6 ml$ of sulphite added, the current peak appeared at the same applied potential as that for iodate in the untreated sample. We therefore chose use of $0.1 ml$ of $0.4 M$ sodium sulphite solution ($\equiv 1.0 ml$ of $0.04 M$ solution) for destroying the excess of hypochlorite. This ensures a sufficiently large excess of sulphite and minimizes the volume change in the sample.

The determination of iodide in an artificial sea-water solution,¹⁰ the $0.5 M$ sodium chloride– $4 mM$ bicarbonate solution, and the samples of estuarine water and sea-water was examined. Various known amounts of standard potassium iodide solution were added to samples of each medium and the concentrations of total iodine species were determined. The recovery of iodide and of total iodine was $98 \pm 3\%$ and is considered quantitative within experimental

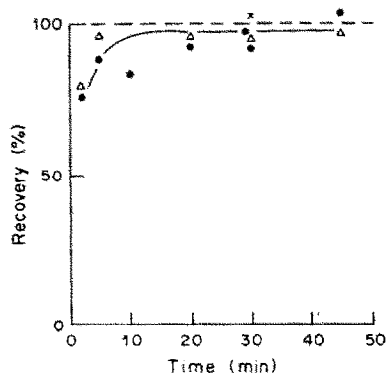


Fig. 1. The effect of reaction time with hypochlorite on recovery of iodide. ●: $0.5 M NaCl$ – $4 mM NaHCO_3$; ×: $0.5 M NaCl$ – $0.8 mM KBr$ – $4 mM NaHCO_3$; △: estuarine water.

Table 2. The amount of sulphite needed to destroy excess of hypochlorite

Na_2SO_3 solution added, ml	Position of the peak (applied potential), V	Peak height,* μA
†	-1.15	0.0160
0	—§	—
0.1	—	—
0.2	—	—
0.3	-1.28	0.0185
0.4	-1.25	0.0183
0.6	-1.15	0.0190
0.8	-1.15	0.0183

*The difference between the peak heights before and after the oxidation step is due to the iodide in the sample.

†A sample of estuarine water without added hypochlorite or sodium sulphite.

§See text.

Table 3. Recovery of iodide in various water media

Sample	$\Sigma I, \mu M$			Recovery of added iodide, %
	Initial	Added*	Found	
ASW†	0	0.24	0.23, 0.24	98 ± 3
ASW	0	0.48	0.45, 0.44	93 ± 1
DMW§	0	0.50	0.48, 0.47	95 ± 1
DMW	0	0.39	0.39	100
NaCl-NaHCO ₃ ‡	0	0.40	0.39, 0.39, 0.40, 0.40	99 ± 1
Estuarine water # (2.64% salinity)	0.31	0.40	0.69, 0.72, 0.72	100 ± 5
Sea-water # (3.28% salinity)	0.33	0.25	0.57, 0.58, 0.56	96 ± 4
			Average	98 ± 3 (1σ)

*As potassium iodide.

†Artificial sea-water.

§Demineralized water, pure potassium iodide solution added.

‡0.5M NaCl-4 mM NaHCO₃.

Estuarine water and sea-water were collected from the St. Lawrence Estuary.

error (Table 3). The analytical precision was estimated¹¹ from six sets of duplicate measurements on natural waters and laboratory-prepared samples and found to be 0.01 μM (Table 4). Since the recovery of iodide added to the samples of estuarine water and sea-water is quantitative (Table 3) and these samples represent typical river water and sea-water, it suggests that in most natural waters other oxidizable constituents, such as organic species, are not present in large enough quantities to impede the effective oxidation of iodide to iodate. For waters with atypically high concentrations of dissolved organic matter such as sewerage, empirical recovery tests should be made to ensure that sufficient chlorine is available to satisfy the chlorine demand of the organic materials as well as the oxidation of iodide to iodate.

Concentrations of iodide and iodate in coastal sea-water collected from the St. Lawrence Estuary were determined. The results from the samples collected at 48°58'N and 67°54'W are shown in Fig. 2. The shapes of the profiles and the concentration ranges of iodide and iodate are consistent with the known geochemical behavior of iodine in the ocean.⁶⁻⁹

Herring and Liss¹ have shown that the polarographic current of iodate is sensitive to changes in

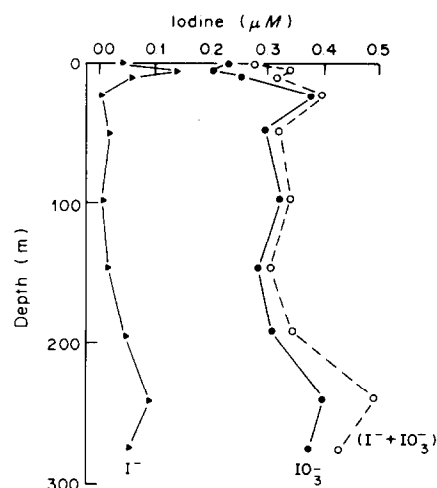


Fig. 2. Vertical profiles of total iodine, iodate and iodide in the St. Lawrence Estuary at 48°58'N and 67°54'W.

Table 4. Duplicate measurements of total iodine (ΣI) in natural waters and artificial media

Sample	ΣI found, μM
ASW*	0.23, 0.24
NaCl-NaHCO ₃ †	0.23, 0.24
Sea-water§ (salinity 3.22%)	0.36, 0.37
Sea-water§ (salinity 3.46%)	0.44, 0.45
Sea-water§ (salinity 3.41%)	0.40, 0.42
Estuarine water‡ (salinity 0.97%)	0.11, 0.11

*0.25 μM I⁻ in artificial sea-water.

†0.25 μM I⁻ in 0.5M NaCl-4 mM NaHCO₃.

§Sea-waters collected from various depths in the Gulf of St. Lawrence.

‡Estuarine water collected from the St. Lawrence Estuary.

ionic strength (salinity) and pH. Thus, this method cannot be applied directly to brackish and fresh waters such as estuarine, river and ground waters, where considerable variations in salinity and pH may occur. However, these problems can be circumvented by adding a combined ionic strength adjuster and buffer (ISA-buffer) to the samples. By adding 2 ml of the ISA-buffer, (3.75M sodium chloride-50 mM sodium bicarbonate) to 25-ml aliquots of 0.5 and 0.39 μM iodide, we obtained a quantitative recovery of iodide (as iodate) from pure potassium iodide solution (Table 3). The peak height to iodate concentration ratio was 0.09 $\mu A \cdot l \cdot \mu mole^{-1}$ at a modulation amplitude of 50 mV. This value is similar to that observed for sea-water medium. For natural river and estuarine waters, 1 ml of the ISA-buffer was added to samples having salinity between 0.8 and 1.8‰, and 2 ml were added to samples having salinity <0.8‰, and the peak height to iodate concentration ratio was again about 0.09 $\mu A \cdot l \cdot \mu mole^{-1}$ at the same modulation amplitude.

Acknowledgements—We wish to thank the chief scientist, Dr. Daniel Cossa, and the officers and crew of "Navimar Un" for their helpful co-operation and assistance in the collection of the coastal sea-water samples. We also thank Y. Clermont for his laboratory assistance. One of us (K.T.) was supported by the Natural Sciences and Engineering Research Council of Canada during the latter stage of this research.

REFERENCES

1. J. R. Herring and P. S. Liss, *Deep-Sea Res.*, 1974, **21**, 777.
2. J. D. Smith and E. C. V. Butler, *Nature*, 1979, **277**, 468.
3. E. C. V. Butler and J. D. Smith, *Deep-Sea Res.*, 1980, **27A**, 489.
4. J. Heyrovský and P. Zuman, *Practical Polarography*, p. 237. Academic Press, New York, 1968.
5. G. T. F. Wong, *Environ. Sci. Technol.*, 1982, **16**, 785.
6. S. Tsunogai, *Deep-Sea Res.*, 1971, **18**, 913.
7. S. Tsunogai and T. Henmi, *J. Oceanog. Soc. Japan*, 1971, **27**, 67.
8. G. T. F. Wong and P. G. Brewer, *Geochim. Cosmochim. Acta*, 1977, **41**, 151.
9. H. Elderfield and V. W. Truesdale, *Earth Plan. Sci. Lett.*, 1980, **50**, 105.
10. J. Lyman and R. H. Fleming, *J. Mar. Res.*, 1940, **3**, 134.
11. W. J. Youden, *Statistical Methods for Chemists*, pp. 12–17. Wiley, New York, 1964.

SIMULTANEOUS DETERMINATION OF LIGHT RARE EARTHS IN MONAZITE SAND BY DENSITOMETRY ON THIN-LAYER CHROMATOGRAMS

HSU ZHANG-FA, JIA XI-PIN and HU CHAO-SHENG

Department of Chemistry, East China Normal University, 3663 Chung Shan Road (N), Shanghai,
People's Republic of China

(Received 27 June 1985. Revised 28 September 1985. Accepted 23 December 1985)

Summary—The determination of individual light rare-earth metals in monazite sand is described, based on TLC with a mixture of di-isopropyl ether, diethyl ether, di(2-ethylhexyl)phosphate and nitric acid (8:8:0.4:0.07 v/v) as eluent. Linear densitometric calibration graphs are obtained for individual light rare-earths in the range 0.015–0.60 μg . The minimum detectable quantities of La, Ce, Pr, Nd and Sm are 9, 10, 20, 13 and 12 ng, respectively. The relative standard deviations for the determination of La, Ce, Pr, Nd and Sm in monazite sand were 1.8, 1.1, 5.9, 1.9 and 6.5%, respectively. Results were in good agreement with those obtained by spectrophotometry.

The increased applications of the rare-earth elements in the metallurgical and optical glass industries and their utilization in ever increasing amount makes it worthwhile to develop a rapid, sensitive and accurate technique for their determination, but few such methods have so far been proposed.

The high efficiency of thin-layer chromatography (TLC) has resulted in its wide application in the analysis of organic and inorganic materials, but difficulties have been encountered in the separation of the rare-earth elements because of their similar chemical properties.

Specker and co-workers^{1,4} and Chen *et al.*⁵ have described the separation and determination of rare earths by TLC. In some cases, silanated silica gel has also been used as adsorbent,⁶ but the procedures proposed were time-consuming and no results for the analysis of monazite sand were given.

In the present work, the TLC behaviour of the complexes of rare-earth metals with di(2-ethylhexyl)phosphate (HDEHP) is investigated. For the determination of La, Ce, Pr, Nd and Sm in monazite sand, prior extraction and back-extraction are necessary.

With a mixture of HDEHP, di-isopropyl ether, diethyl ether and nitric acid (0.4:8:8:0.07 v/v) as eluent, a TLC-densitometric method for the determination of La, Ce, Pr, Nd and Sm in monazite sand has been developed.

EXPERIMENTAL

Apparatus

A double-beam densitometer equipped with a TLC scanner, an integrator and a microcomputer was used for all measurements.

Reagents

Di(2-ethylhexyl)phosphate (HDEHP). A chemically pure grade was used in the eluent.

Chromogenic reagent, analytical grade. Chlorophosphonazo-*m*-NO₂ (CPAmN)⁷ (100 mg) was dissolved in 95% ethanol in a 500-ml standard flask, 1.3 ml of concentrated hydrochloric acid was added and the mixture was diluted to the mark with 95% ethanol.

Rare-earth metal stock solutions (5 mg/ml). The appropriate amount of ignited rare-earth oxide ("Specpure", Johnson-Matthey)⁷ was dissolved in dilute hydrochloric acid, and the solution diluted to the required volume.

Mixed rare-earth metal stock solution (0.15 mg/ml). Made by mixing 1.5 ml each of the individual light rare-earth stock solutions and of a similar yttrium solution in a 50-ml standard flask and making up to the mark with 10% v/v hydrochloric acid.

1-Phenyl-3-methyl-4-benzoyl-5-pyrazolone (PMBP). A 0.1M solution in chloroform.

Analysis of monazite sand⁸

Dissolve a sample containing up to 12 mg of rare-earth metals in 3 ml of concentrated sulphuric acid, by heating gently for about 30 min. Cool, add 10 drops of hydrogen peroxide to reduce cerium(IV) and evaporate nearly to dryness, until the residue appears white. Cool, add water, transfer to a 25-ml standard flask and make up to the mark with water. Filter through a dry paper, discarding the first portion of the filtrate, and collect the rest in a 25-ml polyethylene bottle. Take an aliquot (containing ~5 mg of rare-earth metals) in a 60-ml separatory funnel. Add 2 ml of 10% sodium potassium tartrate (Rochelle salt) solution, one drop of Methyl Orange indicator and sufficient concentrated ammonia solution (or 20% sodium hydroxide solution) to change the colour of the solution to orange. Add 4 ml of buffer solution, pH 5.5 (0.2M sodium acetate-acetic acid), adjust the volume to 15 ml, add an equal volume of 0.1M chloroform solution of PMBP, shake for 2 min and allow the layers to separate. Repeat the extraction with fresh PMBP solution twice more and strip each organic extract with three 15-ml portions of formic acid (pH 1.9). Combine the aqueous extracts in a 250-ml beaker, add several drops of concentrated hydrochloric acid, evaporate almost to dryness, cool and moisten the residue with concentrated hydrochloric acid. Add a little water, transfer to a 10-ml standard flask and make up to the mark with 0.5% v/v hydrochloric acid. Filter through a dry paper, discarding the first few drops of the filtrate, and collect the remainder in a 10-ml polyethylene bottle.

Table 1. R_f values of rare-earth metals with different eluents

HNO ₃ , ml	HDEHP, ml	iPr ₂ O/Et ₂ O, ml	$R_f \times 100^*$					
			La	Ce	Pr	Nd	Sm	Y
0.05			12 ± 1	32 ± 5	55 ± 2	66 ± 2	88 ± 1	98 ± 2
0.07	0.40	8/8	11 ± 1	35 ± 4	51 ± 1	63 ± 1	86 ± 1	98 ± 2
0.09			7 ± 2	30 ± 4	49 ± 1	61 ± 1	78 ± 3	98 ± 2
0.11			0	21 ± 2	47 ± 1	50 ± 2	68 ± 5	98 ± 2
	0.25		5 ± 3	27 ± 3	42 ± 2	52 ± 3	75 ± 4	98 ± 2
	0.30		7 ± 1	29 ± 3	45 ± 1	55 ± 1	78 ± 1	98 ± 2
0.07	0.50	8/8	13 ± 2	39 ± 2	55 ± 1	69 ± 1	90 ± 3	98 ± 2
		15/0	3 ± 1	11 ± 2	17 ± 1	26 ± 2	60 ± 1	98 ± 2
		8/7	4 ± 1	16 ± 2	30 ± 1	46 ± 1	60 ± 1	98 ± 2
		7/8	9 ± 1	28 ± 1	47 ± 2	56 ± 2	60 ± 1	98 ± 2
0.07	0.40	5/10	13 ± 1	35 ± 2	54 ± 3	67 ± 3	98 ± 2	98 ± 2
		0/15	20 ± 4	46 ± 5	58 ± 3	68 ± 3	98 ± 2	98 ± 2

*Mean and range of 3 runs.

Coat TLC plates (20 × 20 cm) with a 0.25 mm thickness of silica gel H slurried in 4% ammonium nitrate solution containing 1% sodium carboxymethylcellulose (CMC). Dry the plates at 120° for 90 min and store in a desiccator.

Apply 0.2–4.0 μl of mixed standard rare-earth metal solution at one end of the start line on the plate for reference purposes, and 1.0–2.0 μl of the sample solution at the other, keeping the spot diameter at ≤ 4 mm by drying under an infrared lamp and controlling the spotting. Develop in a solvent-saturated atmosphere in a conventional tank by the ascending front technique until the solvent front has travelled at least 10 cm. Dry the plate at 70° for 15 min and spray it with 0.02% CPAmN solution while it is still hot. Dry for a further 10 min at 70° to develop the spots (which begin to fade after 12 hr).

Scan the plate with a densitometer in the double-beam (sample at 665 nm, background at 430 nm) and reflectance modes. Two ways of scanning are possible, linear or zigzag (9.9 × 1.0 mm and 1.25 × 1.25 mm, respectively). Scan each spot on the same plate in the direction of development at a rate of 20 cm/min (for both scanning modes). The linear scatter parameter (SX) chosen is 3.⁹

RESULTS AND DISCUSSION

Effect of foreign ions

The effect, on the TLC separation of the rare earths, of common ions normally present in a solution of monazite sand was examined, and it was found that phosphate present in the sample interfered by precipitating some of the rare-earth content. The extraction and stripping procedures were necessary for the removal of phosphate in the analysis of monazite sand. For other samples, such as cerium-based alloys or fission products, these steps may not be necessary.

Choice of eluent

The R_f values obtained for La, Ce, Pr, Nd, Sm and Y with different eluents are listed in Table 1. The HDEHP–di-isopropyl ether–diethyl ether–nitric acid (0.4:8:8:0.07 v/v) eluent, was found best in terms of spot size, intensity and R_f values of light and heavy rare-earth metals. Alteration in the concentration of HDEHP or nitric acid affects the separation of light and heavy rare-earth metals, the R_f values increasing with decreasing acidity and increasing volume of HDEHP. With the selected eluent, the heavy rare-

earth metals (represented by yttrium) migrated with the solvent front. Either di-isopropyl ether or diethyl ether can be used as diluent for the HDEHP, but though use of diethyl ether alone shortens the time of development, the spot-size is unsatisfactory, and when di-isopropyl ether alone is used, the R_f values of Sm and the Y sub-group are nearly equal to 1.0 and although the spots are sharp, the development time is lengthened and the difference in R_f values for adjacent elements is insufficient for scanning purposes (especially for Pr and Nd). For these reasons, a 1:1 v/v ratio of the two ethers is used. Pr and Nd, which have proved very difficult to separate by TLC, are separated satisfactorily with this eluent.

The TLC plate

Since CPAmN is also a chromogenic agent for calcium, calcium sulphate cannot be used as binder or substrate, so silica gel H is used with 1% CMC solution as binder. To improve the shape and size of the spots, 4% ammonium nitrate is also present in the 1% CMC solution.

If the spot is not dried before development, the water present has a considerable effect on the R_f values. For successful separation, this water is removed by drying at 70° for 15 min. An alternative is to put the samples on an unactivated TLC plate and then dry it at 120° for 90 min before development; the composition of the sample does not undergo any chemical change and any errors are insignificant.

Choice of scanning linear scatter parameter

In the analysis of the TLC plate with a densitometer, there is no linear relationship between absorbance and concentration, owing to scattering of the monochromatic light beam by the adsorbent on the plate. Errors can arise from heterogeneity of the coloured spot and use of too large a light-beam area, so a small beam was used (1.25 × 1.25 mm for zigzag scanning and 0.9 × 1.0 mm for linear scanning) to minimize determination errors. The non-linear relation between absorbance and concentration was processed by microcomputer according to the

Table 2. Results for determination of individual light rare-earth metal oxides (%) in monazite sand

Sample	Element	Present method*	Spectrophotometric method (I)†	Spectrophotometric method (II)§
1	La(III)	14.4 ± 0.3	14.3	
	Ce(IV)	21.5 ± 0.2	20.9	
	Pr(III)	3.4 ± 0.2	3.5	
	Nd(III)	12.0 ± 0.2	11.8	
	Sm(III)	2.1 ± 0.1	2.2	
	Total	53.4	52.7	53.0
2	La(III)	10.1 ± 0.2	10.2	
	Ce(IV)	18.5 ± 0.2	18.3	
	Pr(III)	4.0 ± 0.2	4.0	
	Nd(III)	10.9 ± 0.2	10.7	
	Sm(III)	1.9 ± 0.1	2.0	
	Total	45.4	45.2	45.2

*Mean (± standard deviation) of 6 determinations.

†TLC plate developed as described, spots scraped off, rare-earth complex eluted and determined by spectrophotometry.

§Sample solution determined by spectrophotometry⁸ to give total rare-earth content.

Kubelka–Munk theory of light scattering⁹. A linear scatter parameter (SX) of 3 was chosen for calibration purposes.

Calibration curves, reproducibility and limits of detection

The integrated intensity of the spots was found to be a linear function of the rare-earth metal concentration (over the range 0.015–0.60 µg). All the light rare-earth metals gave similar calibration graphs. The results for samples can easily be obtained by scanning the spots for mixed rare-earth metal standards, and for the samples, processed on the same plate, and analysing the integrator output by microcomputer. The reproducibility was established by measurement of 6 spots each containing 0.3 µg of each light rare-earth metal, processed on the same plate. The relative standard deviations were 1.8, 1.2, 5.1, 1.6 and 4.8% for La, Ce, Pr, Nd and Sm, respectively. When the experiment was repeated on three different plates (total of 18 spots), the corresponding values were 2.3, 1.5, 5.9, 2.5 and 5.7%. The minimum detectable quantity, defined as that quantity of individual light rare-earth metal giving a signal equal to twice the fluctuation of the blank value, and located on the linear portion of the calibration graphs was 9, 10, 20, 13 and 12 ng for La, Ce, Pr, Nd and Sm, respectively.

Determination of individual light rare-earth metals in monazite sand

To demonstrate the effectiveness of the method, two 1-µl samples of solution prepared from monazite sand were spiked with 1 µl of mixed standard rare-earth metal solution and analysed. The recoveries for duplicate samples were 93–108% and the results shown in Table 2 are in reasonable agreement with those obtained by gravimetry and spectrophotometry.

REFERENCES

1. K. Jung and H. Specker, *Z. Anal. Chem.*, 1977, **288**, 28.
2. K. Jung, J. Maurer, J. Urlichs and H. Specker, *ibid.*, 1978, **291**, 328.
3. H. Specker and A. Hufnagel, *ibid.*, 1984, **318**, 198.
4. K. Jung and H. Specker, *ibid.*, 1980, **300**, 15.
5. Y. Chen, K. Zheng, H. Luo and J. Cheng, *Fenxi Huaxue*, 1983, **11**, 101; *Chem. Abstr.*, 1983, **99**, 47201a.
6. H. Specker and W. Herrmann, *Chem. Lab. Beitr.*, 1981, **32**, 519.
7. C. G. Hsu, C. S. Huo, X. P. Jia and J. M. Pan, *Anal. Chim. Acta*, 1981, **124**, 177.
8. G. F. Cheng, H. X. Huang, Z. S. Hu and X. P. Jia, *J. East China Normal University (Nat. Sci. Ed.)*, 1983, **2**, 73.
9. H. Yamamoto, T. Kurita, J. Suzuki, R. Hira, K. Nakano, H. Makabe and K. Shibata, *J. Chromatog.*, 1976, **116**, 29.

ATOMIC-ABSORPTION SPECTROPHOTOMETRIC DETERMINATION OF TIN BY HYDRIDE GENERATION IN NON-AQUEOUS MEDIUM AFTER EXTRACTION

JOSE AZNAREZ, JOSE M. RABADAN, ANGEL FERRER and PILAR CIPRES

Department of Analytical Chemistry, Faculty of Sciences, University of Zaragoza, Zaragoza, Spain

(Received 19 April 1985. Revised 29 September 1985. Accepted 1 November 1985)

Summary—Tin at the microgram level was extracted into chloroform with *N*-nitrosophenylhydroxamic acid (ammonium salt) from 0.5–1.5*M* hydrochloric acid medium. Tin hydride was generated from 1 ml of the chloroform extract mixed with 3 ml of 1% sulphuric acid solution in *N,N*-dimethylformamide, by injection of 3 ml of 2% sodium tetrahydroborate solution in *N,N*-dimethylformamide through the septum of the hydride generator. Tin was then determined by AAS at 224.6 nm with an acetylene–air flame, and nitrogen as carrier gas. The peak-height of the signal was linearly related to amount of tin up to 20 µg. The sensitivity of the determination was improved by the extraction. The method was applied to determination of tin in tinned foods and aluminium-base alloys with good accuracy and precision.

The determination of As, Sb, Bi, Ge, Pb, Sn, Se and Te by atomic-absorption spectrophotometry (AAS) through volatile hydride generation with sodium tetrahydroborate is a well-known analytical method.¹ Attempts have recently been made to determine In and Tl in the same way.² In our previous papers^{3,4} the generation of antimony and lead hydrides with tetrahydroborate reduction in non-aqueous extracts, followed by AAS determination, was studied. This method improved the sensitivity and selectivity and suppressed several interferences. Moreover, many organic solvents have reduction potentials lower than that for water, so with these solvents it is possible to perform reductions that would be impracticable in water.

This paper describes determination of tin by AAS through solvent extraction followed by hydride generation from the extract.

The sensitivity of determination of tin by flame AAS is poor, the limit being about 0.5 µg/ml at 224.6 nm. The sensitivity can be improved by using hydride generation, the limit being 15 ng/ml at 224.6 nm in a hydrogen–air flame with argon as carrier gas,⁵ and even 7 ng/ml has been reported.⁶ With an electrically heated quartz tube and argon as carrier gas the limit of detection was 0.45 ng/ml at 286.3 nm with 6% relative standard deviation.⁷ Evans and Jackson⁸ have determined tin in tinned foods by hydride generation and AAS at 224.6 nm with an electrically heated quartz tube and nitrogen as carrier gas, with 7% relative standard deviation for tin at 10–40 ng/ml concentrations.

In our method, the tin is extracted into chloroform with *N*-nitrosophenylhydroxamic acid (ammonium salt) from 0.5–1.5*M* hydrochloric acid solutions. An aliquot of the extract is mixed with an *N,N*-dimethylformamide (DMF) solution of sulphuric acid in a

hydride generator and tin hydride is generated by injection of sodium tetrahydroborate solution in DMF. Nitrogen is used as carrier gas to introduce the hydride into the acetylene–air flame. The AAS signal at 224.6 nm is measured.

EXPERIMENTAL

Apparatus

A Pye Unicam SP-90 Series 2 atomic-absorption spectrophotometer with a three-slot burner was used, with a Westinghouse tin hollow-cathode lamp, and our own design of volatile-hydride generator.⁹

Reagents and solutions

All solutions were prepared with analytical-reagent grade chemicals and doubly distilled water.

Stock solution of tin, 1000 µg/ml. Prepared by dissolving 1.000 g of tin in 200 ml of concentrated hydrochloric acid and diluting to volume with water in a 1000-ml standard flask. Working solutions were prepared fresh daily by appropriate dilution of the stock solution with 1*M* hydrochloric acid, after addition of 25 ml of 2.5% ascorbic acid solution to improve stability.

Ammonium *N*-nitrosophenylhydroxamate solution, 1.5%. Prepared fresh daily in doubly distilled water.

Sodium diethyldithiocarbamate (NaDDTC) solution, 1.0%. Prepared fresh daily.

Ammonium pyrrolidinedithiocarbamate (APCD) solution, 1.0%. Prepared fresh daily.

Ammonium *N*-benzoyl-*N*-phenylhydroxamate solution, 1.0%. Prepared fresh daily.

Sodium tetrahydroborate solution (2%) in DMF. This solution can be used for two weeks.

Sulphuric acid solution (1% v/v) in DMF. This solution can be used for at least two weeks.

DMF was purified by distillation, the fraction distilling between 148 and 150° being used.

Procedure

Take a known volume of solution containing up to 100 µg of tin, in a 100-ml separatory funnel, add 3 ml of *N*-nitrosophenylhydroxamate solution and enough concentrated hydrochloric acid to bring the final solution to

0.5–1.5M hydrochloric acid concentration. Add 10 ml of chloroform and shake the mixture mechanically for 5 min. Let the phases separate. Place 1 ml of the chloroform extract and 3 ml of 1% sulphuric acid solution in DMF in the hydride generator. Inject 3 ml of the tetrahydroborate solution in DMF through the septum of the generator. Measure the peak height of the atomic-absorption signal for tin at 224.6 nm, using an acetylene-air flame and nitrogen as carrier gas (at a flow-rate of 400 ml/min). Prepare a calibration graph by applying the same procedure to standard working solutions. Run blank determinations on the reagents used, by the same procedure.

RESULTS AND DISCUSSION

Extraction of tin

Tin was extracted into chloroform with NaDDTC, APDC, ammonium *N*-benzoyl-*N*-phenylhydroxamate, and ammonium *N*-nitrosophenylhydroxamate, under the conditions (pH, reagent concentration and shaking time) reported in the literature. It was found that the yield of hydride, measured as the peak height of the atomic-absorption signal, did not depend on the extraction reagent used, provided the extraction was practically 100% complete, but ammonium *N*-nitrosophenylhydroxamate was preferred because it could be used over a greater range of acidity. The extraction yield obtained for 25 µg of tin from 0.5–1.5M hydrochloric acid was $97.0 \pm 0.5\%$, in agreement with the literature.¹⁰

Concentration of sodium tetrahydroborate

The solubility of sodium tetrahydroborate in DMF at room temperature is about 5–6%, depending on the water content of the DMF. For generation of tin hydride by the procedure given above, the optimum concentration of the tetrahydroborate solution in DMF was found to be 2%. This solution was slightly turbid and filtration through a 0.45-µm glass-fibre filter resulted in lower blank signals, indicating slight contamination of the sodium tetrahydroborate by tin, as reported by Smith.⁵ This solution remained stable for two weeks.

Acids for tin hydride generation

In aqueous solution tin hydride is generated from 0.1–0.2M hydrochloric or sulphuric acid media. The yield of hydride decreases with increasing acid concentration, making the sensitivity for tin poorer. A solvent-miscible acid is also needed for hydride generation from non-aqueous solution.^{3,4} Acetic, hydrochloric and sulphuric acid solutions in DMF

have been tried and a 1–1.2% sulphuric acid solution is preferred because it gives faster generation and evolution of tin hydride, and it is easier to make the solution water-free. This solution remains stable for at least two weeks at room temperature. The generation of tin hydride is practically instantaneous and is completed in 30 sec. The signal peak is sharp and easy to measure.

Optimization of atomic absorption of tin

The best signals were obtained with acetylene flow-rate 1.0 l./min, air flow-rate 5.5 l./min, nitrogen flow-rate 400 ml/min, observation height above the burner 5 mm, slit-width 0.1 mm, lamp current 12 mA and wavelength 224.6 nm.

Calibration graph, sensitivity, detection limit and precision

The peak-height of the atomic-absorption signal for tin was linear from 0.1 to 20 µg of tin in 1 ml of chloroform extract, with a correlation coefficient of 0.999. The characteristic concentration (for 1% absorption) and detection limit (twice the standard deviation of the blank) were 0.014 and 0.006 µg/ml respectively. Ten repetitive determinations of 5 µg of tin gave a relative standard deviation of 4.1%.

Blank solutions gave a small but measurable tin signal, proportional to the amount of sodium tetrahydroborate injected, indicating tin-contamination of the reagent, as already reported.⁵ Filtration of the tetrahydroborate solution or passage of nitrogen through it for 40 min¹¹ decreased the blank signal but did not eliminate it. The tin content of the sodium tetrahydroborate used was about 1–2 µg/g.

Interferences

The maximum concentrations tested or the tolerance limits in the determination of 100 µg of tin (10 µg/ml in the chloroform extract) are shown in Table 1.

Applications

The method has been applied to determination of tin in canned foods such as vegetables and fruit-juices, and in aluminium-based alloys.

The samples of foods were dissolved by the method proposed by the Analytical Methods Committee.¹² The recovery was tested by the standard-addition method and found to be 97.4% (r.s.d. 3.6%), for 10 µg of added tin. The results are shown in Table 2.

Table 1. Interferences in the determination of 100 µg of tin

Species	Tolerance limit, mg
Li ⁺ , Na ⁺ , K ⁺ , Mg ²⁺ , Ca ²⁺ , Sr ²⁺ , Ba ²⁺ , NO ₃ ⁻ , SO ₄ ²⁻	60*
Mn ²⁺ , Pb ²⁺ , Al ³⁺ , Ge ⁴⁺ , phosphate, tartrate	30*
Zn ²⁺ , Cu ²⁺ , Fe ²⁺ , Fe ³⁺ , Sb ³⁺ , Ti ⁴⁺	20†

*Maximum amount tested.

†Amount causing an error not exceeding 4% in the peak height for tin.

Table 2. Determination of tin in canned foods

Sample	Tin found, $\mu\text{g/g}$	r.s.d.* , %
Orange juice	102	2.5
Pineapple juice	82	4.6
Tomato juice	112	3.1
Asparagus	135	3.6

*Ten replicates.

Table 3. Determination of tin in aluminium-base alloys

Sample*	Sn, %		r.s.d.†, %
	Certified	Found	
A	0.622	0.63	2.8
B	0.510	0.52	2.6

*A: 0.62% Mn; 0.38% Cu; 0.40% Ni; 0.30% Fe; 0.87% Mg; 0.30% Zn; 0.15% Pb. B: 0.63% Mn; 0.52% Cu; 0.50% Ni; 0.38% Fe; 0.63% Mg; 0.38% Zn; 0.29% Pb.

†Ten replicates.

Aluminium-base alloys were also analysed for tin. The samples were dissolved in concentrated hydrochloric acid and diluted to known volume with 1M hydrochloric acid, and aliquots were analysed.

The results are shown in Table 3. The recovery of 10 μg of added tin was 97.6%, with 3.9% r.s.d. (5 determinations).

REFERENCES

1. R. G. Godden and D. R. Thomerson, *Analyst*, 1980, **105**, 1137.
2. Y. Du and Y. Zhang, *Talanta*, 1984, **31**, 133.
3. J. Aznárez, F. Palacios and J. C. Vidal, *Analyst*, 1984, **109**, 123.
4. J. Aznárez, F. Palacios, J. C. Vidal and J. Galban, *ibid.*, 1984, **109**, 713.
5. A. E. Smith, *ibid.*, 1975, **100**, 300.
6. F. J. Fernandez, *At. Abs. Newsl.*, 1973, **12**, 93.
7. P. N. Vijan and C. V. Chan, *Anal. Chem.*, 1976, **48**, 1788.
8. W. H. Evans, F. J. Jackson and D. Dellar, *Analyst*, 1979, **104**, 16.
9. J. R. Castillo, J. Lanaja, M. C. Martinez and J. Aznárez, *ibid.*, 1982, **107**, 1488.
10. S. J. Lyle and A. D. Shendrikar, *Anal. Chim. Acta*, 1966, **36**, 286.
11. R. S. Braman and M. A. Tompkins, *Anal. Chem.*, 1979, **51**, 12.
12. Analytical Methods Committee, *Analyst*, 1983, **108**, 109.

ANALYTICAL DATA

DISSOCIATION OF 5-FLUORO- AND 3,5-DINITROSALICYLIC ACIDS IN WATER-METHANOL MIXTURES AT 25°

G. POULIAS, N. PAPADOPOULOS and D. JANNAKOUDAKIS

Laboratory of Physical Chemistry, Department of Chemistry, Aristotelian University of Thessaloniki,
Greece

(Received 25 April 1985. Revised 1 December 1985. Accepted 23 December 1985)

Summary—The association constants and molar conductivities, extrapolated to zero concentration, have been determined for 3,5-dinitrosalicylic and 5-fluorosalicylic acids in water-methanol mixtures at 25°.

Although reproducible "pH" readings may be obtained in many mixed solvents, the pH-meters used are usually calibrated in aqueous buffers. Unfortunately the asymmetry potential may shift on transfer of the glass electrode from such a buffer to a mixed solvent, and "pH" values obtained under such conditions have no quantitative significance.¹

Studies of the electrolytic conductance of acids in the entire range of methanol-water mixtures provide a convenient and accurate means for determining the acid ionization constants. The determination of the dissociation constant of an acid in a binary mixed solvent provides useful data for the theoretical understanding of the ionization process in systems where two dipoles, methanol and water in our case, as well as the anion, can compete for the proton. In addition it serves the practical purpose of providing buffers for the calibration of pH-meters in these systems.

In this paper we examine the conductance behaviour of 5-fluoro- and 3,5-dinitrosalicylic acids in methanol-water mixtures at 25°.

EXPERIMENTAL

3,5-Dinitrosalicylic acid (Carlo Erbo R.S. for chromatography) was recrystallized from 2-propanol and dried under vacuum over phosphorus pentoxide. 5-Fluorosalicylic acid (Aldrich Co., 99% purity) was recrystallized twice from water and dried under vacuum over phosphorus pentoxide. The acids were titrated potentiometrically by weight with standard sodium hydroxide solution and found to be $\geq 99.8\%$ pure. The purification of the solvents and details of the experimental procedure have been reported elsewhere.²

RESULTS AND DISCUSSION

The experimental data were treated by the method proposed by Pethybridge and Taba,³ which uses the Lee and Wheaton conductance equation.^{4,5} The equivalent conductances at infinite dilution, association constants and standard deviations calculated from the experimental data for 3,5-dinitro- and 5-fluorosalicylic acids in methanol-water mixtures are listed in Table 1.

Salicylic acids form an intramolecular hydrogen bond which lowers the potential energy and enhances the acid strength. Because of the *ortho*-effect of the —OH group the dissociation constants of these acids are considerably higher than that of benzoic acid. In addition to the *ortho*-effect, the inductive and resonance effects of the other substituents affect the ionization of the acid. *Meta* substituents cannot conjugate directly with the carboxylic group. Their resonance interaction with the aromatic ring produces changes in the electron density at the *ortho* and *para* positions and these affect the acid strength by induction. However, *meta* substituents in salicylic acid can influence the dissociation of the carboxylic group indirectly through the hydrogen bond. For 5-fluorosalicylic acid the inductive and resonance effects oppose each other, whereas for 3,5-dinitrosalicylic acid the resonance has a further strengthening effect. This compound behaves as a strong electrolyte in the mixed solvent up to 60% w/w in methanol; at higher methanol content association occurs, to an extent which increases dramatically, until in pure methanol this acid behaves as a weak electrolyte. It is noteworthy that 3,5-dinitrobenzoic

Table 1. Conductance parameters

[MeOH], % w/w	Λ_0	σ_A , %	K_A
3,5-dinitrosalicylic acid			
0	375.4	0.04	<4
20	245.8	0.07	<4
40	169.3	0.04	<4
60	123.0	0.06	4.1
80	97.3	0.04	25.4
90	95.6	0.04	1.16×10^2
95	101.3	0.06	4.23×10^2
98	112.1	0.11	1.520×10^3
100	186.9	0.03	1.353×10^4
5-fluorosalicylic acid			
0	381.0	0.04	4.97×10^2
20	250.6	0.08	8.30×10^2
40	170.4	0.08	1.667×10^3
60	126.8	0.09	4.78×10^3
80	106.6	0.11	3.00×10^4

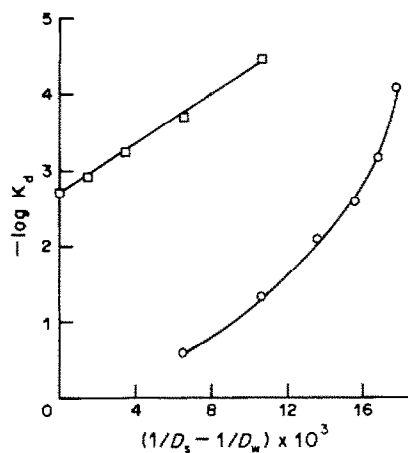


Fig. 1. Dependence of $-\log K_d$ on $(1/D_s - 1/D_w)$ for 5-fluoro- (□) and 3,5-dinitrosalicylic (○) acids in water-methanol mixtures.

acid is a rather weak electrolyte in water, whereas 3,5-dinitrosalicylic acid is completely dissociated in this solvent.

The free energy of dissociation contains an electrostatic and a non-electrostatic term,⁶ the first being given by the Born equation. When there is no change in the solvation of an acid and its anion in a binary mixed solvent, a plot of pK vs. $(1/D_s - 1/D_w)$ should give a straight line (D_s, D_w are the dielectric constants of the solvent and of water, respectively). Figure 1 shows that for 5-fluorosalicic acid the plot is a straight line, whereas for 3,5-dinitrosalicylic acid the plot is a curve, indicating a specific solute-solvent interaction, in accordance with its dissociation behaviour in the methanol-water system.

The dependence of Λ_0 on the methanol percentage is shown in Fig. 2: Λ_0 decreases as the solvent is enriched in methanol and displays a minimum near 95% w/w methanol. At this point the proton-jump mechanism of conduction is replaced by normal

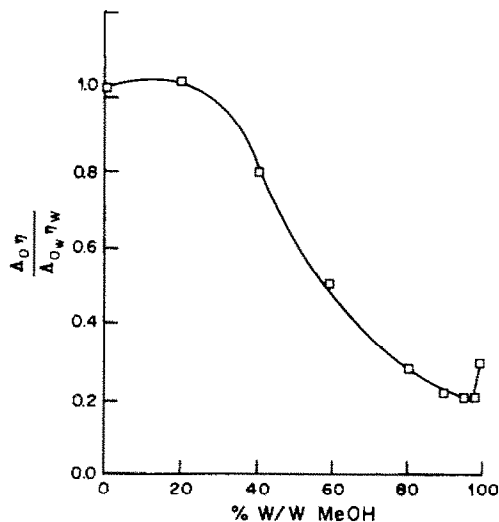


Fig. 2. Dependence of the normalized Walden product on the methanol contents, for 3,5-dinitrosalicylic acid.

migration of hydronium ions solvated by methanol molecules. At still higher methanol concentration the conductivity rises again because the jump mechanism is restored in part.

REFERENCES

1. R. G. Bates, *Determination of pH*, 2nd Ed., Wiley, New York, 1973.
2. G. Ritzoulis, N. Papadopoulos, V. Galiatsatos, D. Christodoulou and D. Jannakoudakis, *Z. Naturforsch.*, 1983, **38A**, 579.
3. A. D. Pethybridge and S. S. Taba, *J. Chem. Soc. Faraday Trans. I*, 1980, **76**, 368.
4. W. H. Lee and R. J. Wheaton, *J. Chem. Soc. Faraday Trans. II*, 1978, **74**, 743, 1456.
5. G. Ritzoulis, N. Papadopoulos, A. Hatzikytiakous and D. Jannakoudakis, *Electrochim. Acta*, 1984, **29**, 817.
6. R. G. Bates, in *Hydrogen-Bonded Solvent Systems*, A. K. Covington and P. Jones (eds.), p. 49, Taylor & Francis, London, 1968.
7. B. E. Conway, J. O'M. Bockris and H. Linton, *J. Chem. Phys.*, 1956, **24**, 834.

SOLVENT EXTRACTION OF ZINC WITH 5,7-DICHLORO-2-METHYL-8-HYDROXYQUINOLINE INTO CHLOROFORM

A. IZQUIERDO, R. COMPAÑO and E. BARS

Department of Analytical Chemistry, University of Barcelona, Barcelona, Spain

(Received 25 September 1985. Accepted 6 December 1985)

Summary—The distribution equilibria of the zinc complex with 5,7-dichloro-2-methyl-8-hydroxyquinoline in the water–chloroform system have been studied at 25°. The influence of pH, reagent and metal concentrations, and the presence of sodium perchlorate in the aqueous phase has been determined. From quantitative evaluation of the extraction equilibrium data, it has been deduced that the complex extracted is the simple 1:2 chelate, ZnR_2 , although at ligand concentrations higher than 0.3M, the self-adduct complex seems to begin to form. The extraction constant of the ZnR_2 species, refined by means of the program Letagrop-Distribution, has the value $\log K_{ex} = -6.15 \pm 0.07$.

The extraction of zinc with 8-hydroxyquinoline (oxine) and its derivatives has been extensively studied. Most of the work deals with the equilibria involved in the extraction process¹⁻¹⁷ and only a few workers have dealt with determination of the metal by colorimetry^{18,19} or fluorimetry.^{20,21} A survey of the literature reveals important differences in the proposed composition of the species extracted.

Several authors^{4,5,7-9} deduce that the complex extracted is the self-adduct $ZnR_2(RH)$, where R represents the oxinate anion and RH the oxine molecule. On the other hand, the formula $ZnR_2(RH)_2$ has also been proposed.^{3,10} Although sodium or potassium perchlorate was used in most cases to adjust the ionic strength, the influence on the distribution equilibria was not investigated. Oki and Terada,¹³ Rakovskii *et al.*¹⁴ and Sekido *et al.*¹⁷ have pointed out that perchlorate, as well as other fairly hydrophobic anions, can participate in the extraction equilibrium and have reported that the complex extracted into chloroform^{13,17} is the ion-pair $Zn_2R_3(RH)_3^+ \cdot ClO_4^-$ whereas that extracted into dichloroethane¹⁴ is $Zn(RH)_2^+ \cdot R^- \cdot ClO_4^-$.

In previous papers^{22,23} the extraction of 5,7-dichloro-2-methyl-8-hydroxyquinoline (Cl_2MeOxH) into some organic solvents and of its complexes with Co(II) and Ni(II) into chloroform was reported. The present paper is devoted to the distribution equilibria of the zinc complex of Cl_2MeOxH in the water–chloroform system, which have been studied in order to ascertain the influence of the two chlorine atoms and the methyl group on the composition of the extracted species. The fluorescence exhibited by the complex extracted into chloroform could serve for the determination of small quantities of zinc, although it is seriously interfered with by several metal ions.

EXPERIMENTAL

Reagents

5,7-Dichloro-2-methyl-8-hydroxyquinoline ("Supro", Troponwerke, Köln) was purified as described earlier.²²

Chloroform, containing 0.5% of ethanol as stabilizer, was shaken with several portions of distilled water, dried with anhydrous sodium sulphate and distilled, the fraction boiling at 60–61° being collected.

Stock solution of zinc (1 g/l.), prepared from analytical-reagent grade $Zn(NO_3)_2 \cdot 4H_2O$ (Merck), was standardized gravimetrically.²⁴

All other chemicals were of analytical grade and used without further purification.

Apparatus

A double-beam Perkin–Elmer 4000 atomic-absorption spectrophotometer with a zinc hollow-cathode lamp, a Beckman Acta MVII ultraviolet–visible spectrophotometer with 10-mm quartz cells, and an Aminco SPF 500 spectrophotofluorimeter equipped with a 250-W xenon arc lamp and connected to a Hewlett-Packard 7225 graphics plotter were used. All the fluorescence measurements were obtained with 10 × 10-mm quartz cells and with the instrument operating in the ratio mode.

A Radiometer PHM 64 pH-meter, equipped with a glass–calomel electrode pair, standardized with buffer solutions at pH 4.008 and 6.865 (25°) prepared from Merck salts according to DIN 19266, was used.

Procedure

Ten ml of buffered zinc solution with an ionic strength of 0.1 (adjusted with sodium sulphate) and saturated with chloroform, and 10 ml of Cl_2MeOxH solution in chloroform saturated with water, were shaken at $25.0 \pm 0.2^\circ$ in 30-ml glass-stoppered vials, long enough for equilibrium to be attained. After phase separation the metal was determined either in the aqueous phase by atomic-absorption spectrophotometry or in the organic phase by a previously established²⁵ spectrophotometric method. The main characteristics of this method are given in Table 1.

The pH of the aqueous phase was adjusted with sodium acetate or borate. Experiments done with different concentrations of these substances showed that at concentrations below 0.05M they do not alter the distribution of zinc. The pH of the aqueous phase after extraction, measured at $25.0 \pm 0.2^\circ$, was taken as the equilibrium pH value.

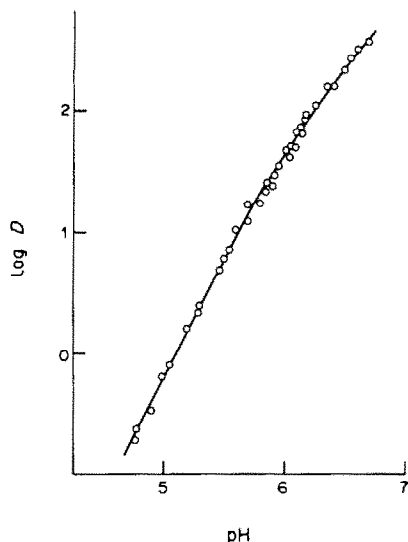


Fig. 1. The pH-dependence of the distribution ratio. $(\text{Cl}_2\text{MeOxH})_{(o)} = 10^{-2}M$; $(\text{Zn}^{2+})_{(w)} = 5.4 \times 10^{-5}M$.

RESULTS AND DISCUSSION

Influence of the shaking time

The effect of the shaking time on the degree of extraction was studied at two pH values, 7.0 and 8.6, and with two reagent concentrations, 2×10^{-3} and $10^{-2}M$. In all cases equilibrium was attained in less than 10 min. A shaking period of 15 min was therefore chosen for safety. The precipitation of the complex reported to take place during the shaking with oxine in the absence of perchlorate,¹⁶ did not appear to occur with Cl_2MeOxH .

Extraction as a function of pH

With $10^{-2}M$ Cl_2MeOxH in chloroform, the extraction begins at pH 4.5, becomes quantitative (>99.9%) between pH 6.0 and 9.5, and then decreases. The pH-dependence of the distribution ratio is shown in Fig. 1; the plot is linear up to pH 5.7, with a slope of 2.00, and at higher pH values the slope decreases, indicating that species other than the cation Zn^{2+} become predominant in the aqueous phase.

Influence of zinc concentration

To find whether polynuclear species are extracted, the influence of the metal concentration on the distribution ratio was studied at pH 5.0. Despite the fact that the initial pH was the same for all the samples, small differences in the equilibrium pH values were found. For this reason $\log D - 2 \text{pH}$ vs. $\log (\text{Zn}^{2+})_{w, \text{initial}}$ was plotted, and gave a straight line with zero slope. The fact that the distribution ratio is independent of the zinc concentration shows that only mononuclear species are extracted.

Effect of perchlorate

According to Oki and Terada¹³ the presence of sodium chlorate in the aqueous phase at a concen-

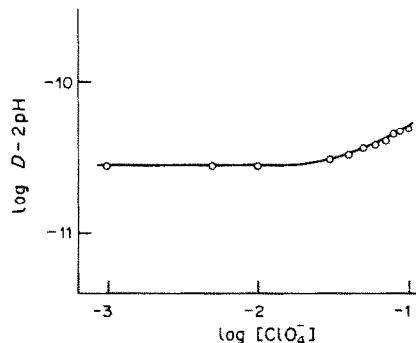


Fig. 2. Effect of NaClO_4 on the extraction. $(\text{Cl}_2\text{MeOxH})_{(o)} = 10^{-2}M$; $(\text{Zn}^{2+})_{(w)} = 1.9 \times 10^{-5}M$; $\text{pH} = 5.15 \pm 0.02$.

tration of $10^{-2}M$ or higher, is necessary for extraction of the Zn-oxine complex; on the contrary, zinc is quantitatively extracted by Cl_2MeOxH , over a wide pH range, in presence of either sodium perchlorate or sodium sulphate. To ascertain whether the perchlorate anion participates in the distribution equilibrium, a series of extractions was done with the perchlorate concentration varied between 10^{-3} and $10^{-1}M$, and the ionic strength adjusted to 0.15 with sodium sulphate. In Fig. 2, $\log D - 2 \text{pH}$ vs. the initial concentration of perchlorate in the aqueous phase is plotted; below $0.05M$, the perchlorate does not affect the distribution equilibrium, but at higher concentrations the slope of the curve increases to 0.45, suggesting that a mixture of species, some containing perchlorate and some not, is extracted.

Effect of ligand concentration

The influence of Cl_2MeOxH concentration was studied in the range 10^{-2} – $5 \times 10^{-1}M$. Two series of extractions were performed, at pH 4.88 and 3.70, respectively. Because of the high value of the Cl_2MeOxH distribution ratio at these pH values²² the initial reagent concentration in the organic phase was taken as the equilibrium concentration; in the same way, because of the excess of Cl_2MeOxH present, the amount of reagent used in the complex formation was also neglected. The two straight lines in Fig. 3 (a and b) have slopes of 1.95 and 2.11, respectively.

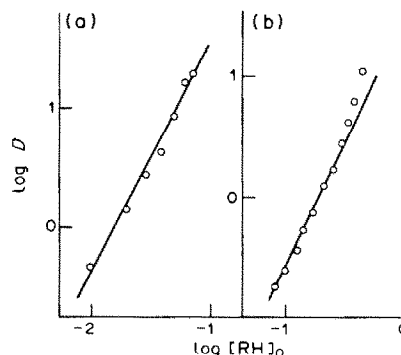
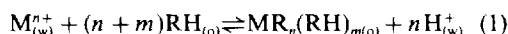


Fig. 3. Distribution of zinc as a function of Cl_2MeOxH concentration. $(\text{Zn}^{2+})_{(w)} = 2.7 \times 10^{-5}M$; (a) $\text{pH} = 4.88$; (b) $\text{pH} = 3.70 \pm 0.01$.

Composition of the extracted species

If only mononuclear species are extracted, under the conditions in which perchlorate does not take part in the distribution equilibrium, the extraction process may be represented by the equation



where M^{n+} represents the metal ion, RH the extractant reagent and the subscripts (w) and (o) denote the aqueous and organic phases respectively. The extraction constant of the species $MR_n(RH)_m$ is given by

$$k_{ex} = \frac{(MR_n(RH)_m)_{(o)}(H^+)_{(w)}^n}{(M^{n+})_{(w)}(RH)_{(o)}^{(n+m)}} \quad (2)$$

When $MR_n(RH)_m$ is the only extractable species and the metal is present in the aqueous phase predominantly as the cation M^{n+} , the metal distribution ratio (D) and the extraction constant are related by

$$\log D = \log K_{ex} + n \text{pH} + (n + m) \log (RH)_{(o)} \quad (3)$$

The slope of the plots of $\log D$ vs. pH, at constant $(RH)_{(o)}$, and of $\log D$ vs. $\log (RH)_{(o)}$, at constant pH, will give the values of the coefficients n and $(n + m)$, respectively.

From the slope analysis of the curves shown in Figs. 1 and 3, the values $n = 2$ and $n + m = 2$, and hence $m = 0$, are deduced. This leads to the conclusion that the composition of the extracted complex, when $(ClO_4^-) < 0.05M$, $(Zn^{2+})_{(w),init}$ ranges from 10^{-5} to $10^{-3}M$ and $(Cl_2MeOxH)_{(o)}$ varies between 0.01 and 0.3M, is the simple 1:2 chelate, ZnR_2 . When the ligand concentration is higher than 0.3M, the slope of the experimental plot tends towards a value of 3, suggesting the extraction of the self-adduct complex $ZnR_2(RH)$. On the other hand, the solubility of Cl_2MeOxH in chloroform does not allow obtention of $\log D$ values at higher reagent concentrations than those already studied.

Although it has not been possible to confirm the formation of this adduct complex with a large number of experimental points, its extraction would represent a behaviour similar to that found in the extraction²³ of Co and Ni with Cl_2MeOxH , and would contrast with the inability of 2-methyl-8-hydroxyquinoline to form the self-adduct, which has been attributed to steric hindrance by the methyl group.⁹

The behaviour of Cl_2MeOxH , as well as that of the 5-iodo⁹ and 5,7-dibromo⁶ derivatives of oxine (both of which form a simple chelate, ZnR_2 with zinc) indicates that, in order to explain the ability of oxine derivatives to form adduct complexes, other factors besides steric hindrance must be taken into account.

Calculation of the extraction constant

According to equation (3) a plot of $\log D$ vs. $2 \text{pH} + 2 \log (RH)_{(o)}$ will give a straight line of slope 1 and intercept $\log K_{ex}$; hence, from such a graph the extraction constant can be obtained. In Fig. 4, the

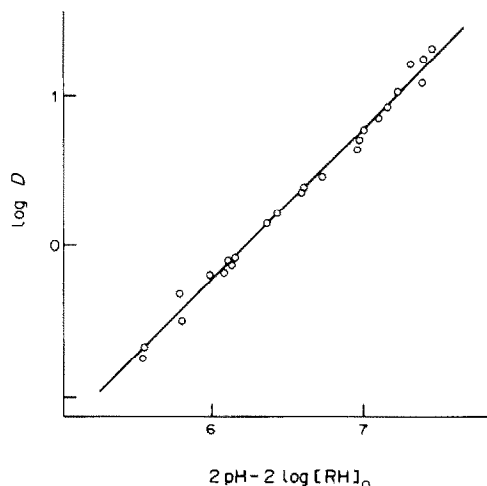


Fig. 4. Graphical calculation of the extraction constant. The equation of the straight line is $\log D = -6.25 + 1.01 [2 \text{pH} + 2 \log (RH)_{(o)}]$.

$\log D$ values corresponding to the species ZnR_2 have been plotted and $\log K_{ex} = -6.25$ is obtained. This value, obtained graphically, has been refined by means of the program Letagrop-Distribution;²⁷ the final result is $\log K_{ex} = -6.15 \pm 0.07$.

Fluorescence of the extracted complex

Because of the fluorescence exhibited by the complex extracted into chloroform, the possibility of developing a fluorimetric method for zinc has been examined. The band maxima of the excitation and emission spectra are found at 399 and 544 nm, respectively. With a $10^{-3}M$ solution of Cl_2MeOxH in chloroform, the maximum fluorescence intensity is attained in the pH range 7.0–9.2; likewise the emission intensity remains constant for concentration ratios $(Cl_2MeOxH)_{(o)}/(Zn^{2+})_{(w)} > 6$. The calibration curve is linear up to 1.2 $\mu\text{g/ml}$ Zn(II) concentration but with $Zn(II) < 0.03 \mu\text{g/ml}$ the fluorescence of the reagent blank and that of the sample are very similar. A 0.5 $\mu\text{g/ml}$ Zn(II) solution gives a fluorescence reading of 61.8% of that corresponding to a 0.08 $\mu\text{g/ml}$ quinine sulphate solution in 0.05M sulphuric acid.

However, the presence of several other metals interferes seriously with the determination of zinc, so the method is of limited value.

REFERENCES

1. F. Umland and W. Hoffman, *Z. Anal. Chem.*, 1959, **168**, 268.
2. F. Umland, *ibid.*, 1962, **190**, 186.
3. J. Starý, *Anal. Chim. Acta*, 1963, **28**, 132.
4. G. K. Schweitzer and W. van Willis, *ibid.*, 1964, **30**, 114.
5. G. K. Schweitzer, R. B. Neel and F. R. Clifford, *ibid.*, 1965, **33**, 514.
6. O. Navrátil and J. Kotas, *Collection Czech. Chem. Commun.*, 1965, **30**, 1824.
7. Fa-Chun Chou, Q. Fernando and H. Freiser, *Anal. Chem.*, 1965, **37**, 361.

8. N. P. Rudenko and A. I. Sevastyanov, *Zh. Neorgan. Khim.*, 1968, **13**, 184.
9. Fa-Chun Chou and H. Freiser, *Anal. Chem.*, 1968, **40**, 34.
10. S. Oki, *Bunseki Kagaku*, 1969, **18**, 822.
11. T. Lengyel, *Proc. Symp. Coord. Chem. 3rd*, 1970, **1**, 157.
12. J. Kubala and D. Mazonska-Wydrzynska, *Zesz. Nauk. Politech. Slask. Chem.*, 1972, **60**, 65.
13. S. Oki and I. Terada, *Anal. Chim. Acta*, 1972, **61**, 49.
14. E. E. Rakovskii, B. L. Serebryanyi and N. D. Klyueva, *Zh. Analit. Khim.*, 1974, **19**, 1086.
15. *Idem*, *ibid.*, 1974, **29**, 1710.
16. E. Sekido, Y. Yoshimura and L. Masuda, *J. Inorg. Nucl. Chem.*, 1976, **38**, 1183.
17. E. Sekido and Y. Yoshimura, *ibid.*, 1976, **38**, 1187.
18. W. L. Medlin, *Anal. Chem.*, 1960, **32**, 632.
19. H. Koshimura, *Bunseki Kagaku*, 1976, **25**, 269.
20. K. Watanabe and K. Kawagaki, *Bull. Chem. Soc. Japan*, 1975, **48**, 1945.
21. D. Yamamoto, M. Tsukada and S. S. Lynn, *Meiji Daigaku Nogakubu Kenkyu Hokoku*, 1978, **44**, 25.
22. A. Izquierdo and R. Campañó, *Mikrochim. Acta*, 1983 **I**, 371.
23. A. Izquierdo, R. Campañó and E. Bars, *ibid.*, 1984 **II**, 343.
24. A. I. Vogel, *Quantitative Inorganic Analysis*, 3rd Ed., p. 532. Longmans, London, 1968.
25. R. Campañó, *Doctoral Thesis*, University of Barcelona, 1982.
26. IUPAC, *Compendium of Analytical Nomenclature*, Pergamon Press, Oxford, 1978.
27. D. Hay Liem, *Acta Chem. Scand.*, 1971, **25**, 1521.

DETERMINATION OF CHLORPROMAZINE AND THIORIDAZINE BY DIFFERENTIAL PULSE VOLTAMMETRY IN ACETONITRILE MEDIUM

N. ZIMOVÁ and I. NĚMEC

Department of Analytical Chemistry, Faculty of Natural Sciences, Charles University, 12840 Prague, Czechoslovakia

J. ZIMA

Czechoslovak Academy of Sciences, Institute of Microbiology, 14220 Prague, Czechoslovakia

(Received 24 February 1984. Revised 4 February 1986. Accepted 14 February 1986)

Summary—This work describes optimal conditions for the determination of chlorpromazine and thioridazine by DPV, with a detection limit of $4.0 \times 10^{-7} M$ (0.16 $\mu g/ml$). The well-defined peaks indicate that direct measurement in a medium of 0.03M perchloric acid in acetonitrile is possible and the use of DPV is advantageous when small amounts are to be determined. The sample procedure for pharmaceutical tablets is simple and fast. The method is useful for control of the quality and purity of phenothiazine drugs. The possibility of using numerical analysis to resolve composite signals of the compounds studied has also been demonstrated.

Chlorpromazine and thioridazine are among the most important tranquilizers. Because of their frequent use, their metabolism, pharmacokinetics and relationship between concentration level in the plasma and the clinical response, have been studied in detail. Of paramount importance to such studies is the development of analytical methods suitable for determining the concentrations of the parent drugs.

Titrimetric,^{1,2} spectrophotometric,³⁻⁵ fluorescence,⁶ radioimmunoassay,^{7,8} and chromatographic⁹⁻¹³ methods are used in bioanalytical research and pharmaceutical practice for determination of chlorpromazine and thioridazine. Amperometric methods have also been used for their detection in HPLC,¹¹⁻¹³ and pulse polarographic methods for direct determination.^{14,15}

This work deals with the use of differential pulse voltammetry for determination of phenothiazine drugs.

EXPERIMENTAL

Apparatus

Differential pulse voltammetry (DPV) was performed with a PA 3 polarographic analyser (Laboratorní přístroje, Prague) with clock-time of 0.2 sec, pulse-width 100 msec, sampling window 20 msec, scan-rate 1-5 mV/sec and modulation amplitude 12.5, 20 and 50 mV.

The indicator electrode was a platinum disk [electrode area (*A*) 0.16 or 0.11 cm²], the reference electrode a silver sheet dipping into 0.01M silver nitrate/1.0M sodium perchlorate solution in acetonitrile, and the auxiliary electrode a platinum wire spiral.

The electrolytic cell has already been described.¹⁶ Its working compartment was filled with 0.1M sodium perchlorate in acetonitrile, to which was added the substance under investigation. Nitrogen was continuously passed over the surface of the solution during the electrochemical measurement (done at 20°).

Computation

Hardware. An HP 9845B, option 250, desk-top computer with total read/write memory of 187 kbyte was used for the data treatment. The following additional read-only memories (ROMs) were installed to improve the programming capabilities of the mainframe—an input/output ROM, an enhanced graphics ROM, an advanced programming ROM, and a structured programming ROM. A keyboard or an HP9874A digitizer was used for data input. For interaction with the CRT—zooming, input of the parameter values, searching for points *etc.*—a light pen was used. An HP7470A plotter was used as the graphics output device.

Software. An easy-to-use interactive program was written in BASIC—about 2000 lines, making full use of enhanced HP BASIC.

The optimization was done in two steps. First, the base electrolyte curve was digitized and approximated by polynomial regression (an HP utility library routine), and the DPV curve was digitized (approximately 100 points were taken within a potential range of 0.5 V). Second, the sum of Gaussian exponentials was fitted to the DPV peaks, together with a polynomial function obtained by using the classical Gauss-Newton method. The initial values of the parameters must be estimated for a non-linear optimization problem. For the polynomial function, the parameters obtained in the first step were used, while for the Gaussian function, approximate peak-maximum co-ordinates and approximate peak half-widths were digitized for each peak. The results of the iterative computation were displayed on the CRT and terminated by user intervention.

Reagents

Acetonitrile (AN), reagent grade, was purified by the method proposed by Walter and Ramaley;¹⁷ its purity was checked by spectrophotometry. Its water content was below 0.003% (found by gas chromatography).

Thioridazine hydrochloride (Sandoz, Switzerland), chlorpromazine hydrochloride (Léčiva, Prague), thioridazine hydrochloride 25-mg pills (Léčiva, Prague), and Plegomazine 25-mg pills (Egyt, Budapest) were obtained commercially. The other reagents were as described previously.¹⁸

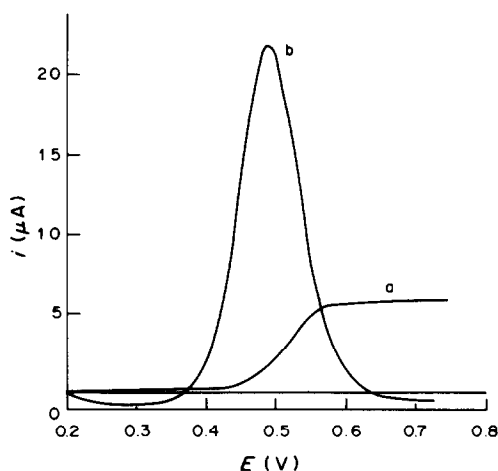


Fig. 1. Diffusion current recordings of the anodic oxidation of chlorpromazine ($7 \times 10^{-5}M$) in $0.1M$ $NaClO_4$ in an AN medium, c_{HClO_4} $0.03M$, scan-rate 2 mV/sec, electrode area 0.11 cm^2 ; (a) d.c. voltamperogram, 1226 rpm; (b) DP voltamperogram, clock time 0.2 sec, pulse amplitude 50 mV.

Sample preparation

Standard solutions of the substances studied were prepared by dissolving 25 mg (precisely weighed) in AN in a 10 -ml standard flask.

For tablet analysis, one tablet was weighed, crushed to powder and dissolved in 2 ml of AN, then the solution was quantitatively transferred to a centrifuge tube and centrifuged at 4000 rpm; the solution was transferred quantitatively to a 10 -ml standard flask and diluted to the mark with AN. Alternatively the centrifugation was omitted and an aliquot of the supernatant solution in the flask was used, after the insoluble material had settled out.

RESULTS AND DISCUSSION

Direct current and cyclic voltammetry were used to determine the optimal conditions for the determination of chlorpromazine and thioridazine, taken as models of the phenothiazine drugs.¹⁸ On the basis of the results, the DPV determination was done by oxidation of the derivatives to the radical cation in AN medium with a perchloric acid concentration of $0.03M$.

The higher sensitivity of the DPV method under the conditions described above is apparent from comparison of the d.c. and DP voltammetry (Fig. 1).

The maximum peak current and peak symmetry were optimized by systematic variation of the modulation amplitude, ΔE , and scan rate, v . Optimum conditions for maximum sensitivity were: scan-rate 2 mV/sec, modulation amplitude 50 mV, clock-time 40 sec. The peak-width at half-height, $W_{1/2}$, approached the theoretical value for small E values.¹⁹

Calibration graphs for the standard solutions (Table 1) were linear over the concentration range 7×10^{-7} – $1.4 \times 10^{-5}M$ (i.e., 0.25 – 6.2 $\mu g/ml$) with a detection limit of $4.0 \times 10^{-7}M$ (0.16 $\mu g/ml$).

The method described above can be applied for determination of relatively low concentrations of chlorpromazine and thioridazine in tablet forms (Table 2). The relative standard deviations of the peak currents were $\leq 5\%$ for both chlorpromazine and thioridazine. The average recovery from tablet samples was $94 \pm 3\%$ for chlorpromazine and $97 \pm 3\%$ for thioridazine. As both sample preparation procedures yielded similar results, the second is recommended because it is simpler.

Table 1. Calibration graphs of chlorpromazine in an acetonitrile solution of $0.1M$ $NaClO_4$ ($c_{HClO_4} = 0.03M$; pulse amplitude 50 mV, scan-rate 2 mV/sec, electrode area 0.16 cm^2 , temperature 20°)

[Chlorpromazine], [μM]	i_p , μA	E_p , V	$W_{1/2}$, V	$i_p/[chlorpromazine]$, $A.l.mole^{-1}$
0.70	0.46	0.50	0.100	0.66
1.40	0.90	0.51	0.100	0.64
2.10	1.38	0.51	0.100	0.66
2.80	1.96	0.51	0.100	0.66
3.50	2.30	0.50	0.100	0.66
4.90	3.10	0.51	0.100	0.63
7.00	4.48	0.50	0.100	0.64
9.10	5.60	0.50	0.095	0.62
10.50	6.60	0.50	0.095	0.63
14.00	8.80	0.50	0.095	0.63

Table 2. Analysis of tablet forms of the drugs (conditions as for Table 1)

Concentration, $\mu g/ml$	Chlorpromazine		Thioridazine	
	Found, $\mu g/ml$	Recovery, %	Found, $\mu g/ml$	Recovery, %
0.25	0.21	92.8	0.25	100.0
0.75	0.70	93.3	0.74	98.9
1.25	1.12	90.3	1.17	94.4
1.75	1.71	98.3	1.62	93.1
2.50	2.40	96.8	2.39	96.4

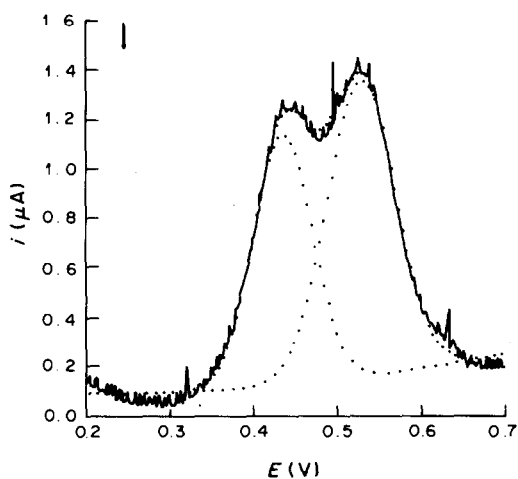


Fig. 2. DP voltamperogram for anodic oxidation of 1:1 w/w mixture of thioridazine and chlorpromazine (each 1.3 $\mu\text{g/ml}$), conditions as for Table 3; (—) experimental curves; (.....) theoretical curves.

The DPV curves were analysed by numerical methods. The classical Gauss–Newton method for non-linear function-fitting was used. A good agreement of the experimental data for an individual peak and the Gaussian function $i = \Delta i_p \exp\{-[(E - E_p)/W_{1/2}]^2\}$ was obtained (the relative standard deviation of the current was less than 1%). As the background current (which has no relation to the redox reaction studied) had to be compensated for, a polynomial expansion of a certain degree was added to the sum of the exponentials and all the parameters were optimized together. The best results were obtained for a quadratic polynomial, whereas cubic and linear functions exhibited significant deviations from the experimental baseline.

The fact that the Gaussian function reasonably approximates the experimental data suggests the possibility of separating overlapping bands by numerical methods. The determining factor in assays of a mixture of substances with similar half-wave potentials is the peak half-width. As the minimum peak-width for one-electron oxidation is 90.4 mV,¹⁹ it is apparent that the peaks of the two substances (the difference between the half-wave potentials of chlor-

promazine and thioridazine is 110 mV) cannot be completely separated by a derivative pulse technique. In the simple case of close to 1:1 ratio of the concentrations it is possible to determine them approximately, directly from the DPV recording (Table 3, Fig. 2) and calibration graphs made with equimolar mixtures. It is more correct, however, to compare the areas (A_1 and A_2) under the curves, which in this case is only possible by using numerical treatment.

Numerical resolution of the two peaks is possible over the concentration range from 2×10^{-6} to $1 \times 10^{-3} M$. The concentrations of the substances can be calculated from the peak areas thus obtained (Fig. 3), by using linear calibration graphs measured for each of the substances separately, as it has been found that the points on the calibration graphs change by less than 1% when both substances are present in the solution, provided that their concentration ratio lies in the range from 0.35 to 3.5. Some typical results are shown in Table 4.

The DPV data were treated by an off-line technique, *i.e.*, the plotter analogic traces were manually digitized. This kind of evaluation increases the overall

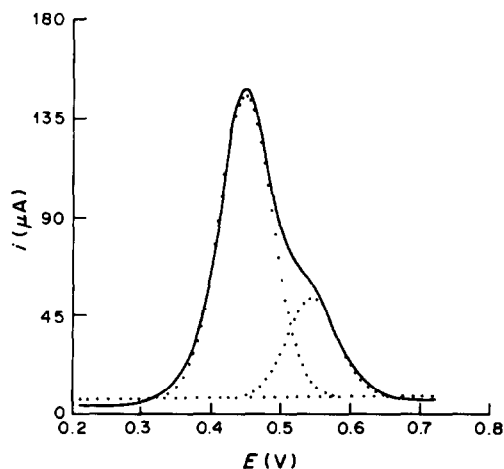


Fig. 3. DPV recordings for a mixture of thioridazine ($4.4 \times 10^{-4} M$) and chlorpromazine ($1.3 \times 10^{-4} M$) in AN solution of 0.1M NaClO₄, (c_{HClO_4} 0.03M; scan-rate 5 mV/sec; pulse amplitude 20 mV; electrode area 0.11 cm²; temperature 20°); (.....) theoretical curves; (—) experimental curves.

Table 3. Calibration data for a 1:1 w/w mixture of thioridazine (1) and chlorpromazine (2), (pulse amplitude 12.5 mV, scan-rate 1 mV/sec, other conditions as for Table 1)

Concentration,* $\mu\text{g/ml}$	$i_p(1)$, μA	$i_p(2)$, μA	$E_p(1)$, V	$E_p(2)$, V	$i_p(1)/i_p(2)$	Slope, $A.l.mole^{-1}$	
						(1)	(2)
0.75	0.27	0.30	0.44	0.54	0.90	0.15	0.14
1.25	0.53	0.60	0.45	0.54	0.88	0.17	0.17
1.99	0.96	1.02	0.44	0.53	0.94	0.20	0.18
2.48	1.15	1.26	0.44	0.54	0.91	0.19	0.18
Aver. value			0.44	0.54	0.91	0.18	0.17
Std. devn.	0.03	0.05					

*Of each component.

Table 4. Determination of a mixture of thioridazine and chlorpromazine in various concentration ratios, in AN solution of 0.1M NaClO₄, c_{HClO₄} = 0.03M

Sample	[Thioridazine], μM	Found, μM	Recovery, %	[Chlorpromazine], μM	Found, μM	Recovery, %
1	3.01	2.87	95.4	3.50	3.46	98.9
2	380	356	93.7	1096	1067	97.4
3	399	366	91.7	805	797	99.0
4	413	412	99.8	595	556	93.4
5	423	406	96.0	484	456	94.2
6	174	167	96.0	134	127	94.8
7	443	429	96.8	128	125	97.7

error by introduction of an operator-dependent error; however, various kinds of on-line data-acquisition systems are commercially available,^{20,21} and their use can be recommended.

When solid electrodes are used, the history of the electrode plays an important role and careful cleaning is imperative. We therefore recommend back-polarization of the electrode to the initial potential value.

REFERENCES

1. M. Gajewska, M. Ciszewska and A. Goldnik, *Chem. Anal.*, (Warsaw), 1978, **23**, 503.
2. J. Blažek and M. Pinkasová, *Česk. Farm.*, 1980, **28**, 367.
3. A. S. Issa, Y. A. Beltagy and M. S. Mahrous, *Talanta*, 1978, **25**, 710.
4. P. G. Ramappa, H. S. Gowda and A. N. Nayak, *Analyst*, 1980, **105**, 663.
5. A. N. Nayak, P. G. Ramappa and H. S. Yathirajan, *Ann. Quim.*, 1982, **78**, 86.
6. I. S. Forrest, S. D. Rose, L. G. Brookes, B. Halpern, A. V. Bacon and L. A. Silberg, *Agressologie*, 1970, **12**, 127.
7. D. H. Efron, S. R. Harris, A. A. Manian and L. E. Gaudette, *Psychopharmacologia*, 1971, **19**, 207.
8. K. K. Midha, J. C. K. Loo, J. W. Hubbard, M. L. Rowe and I. J. McGilveray, *Clin. Chem.*, 1979, **25**, 166.
9. A. C. Mehta, *Analyst*, 1981, **106**, 1119.
10. S. Stevenson and E. Reid, *Anal. Lett.*, 1981, **14**, 1785.
11. G. McKay, K. Hall, J. K. Cooper, E. M. Hawes and K. K. Midha, *J. Chromatog.*, 1982, **232**, 275.
12. K. Murakami, K. Murakami, T. Ueno, J. Hijakata, K. Shirasawa and T. Muto, *ibid.*, 1982, **227**, 103.
13. J. E. Wallace, E. L. Shimek, S. Stavchansky and S. C. Harris, *Anal. Chem.*, 1981, **53**, 960.
14. T. B. Jarbawi, W. R. Heineman and G. J. Patriarche, *Anal. Chim. Acta*, 1981, **126**, 57.
15. J. Wang and B. A. Freiha, *Talanta*, 1983, **30**, 837.
16. I. Němec, H. L. Kies and I. Němcová, *Anal. Chim. Acta*, 1970, **49**, 541.
17. M. Walter and L. Ramaley, *Anal. Chem.*, 1973, **45**, 165.
18. N. Zimová-Šulcová, I. Němec, K. Waisser and H. L. Kies, *Microchem. J.*, 1985, **32**, 33.
19. E. P. Parry and R. A. Osteryoung, *Anal. Chem.*, 1965, **37**, 1634.
20. K. J. Stutts, M. A. Dayton, R. M. Wightman, *ibid.*, 1982, **54**, 995.
21. J. F. Price, S. L. Cooke and R. P. Baldwin, *ibid.*, 1982, **54**, 1011.

ANALYSIS OF VARIANCE IN DETERMINATIONS OF EQUIVALENCE VOLUME AND OF THE IONIC PRODUCT OF WATER IN POTENTIOMETRIC TITRATIONS

ANTONIO BRAIBANTI†, CLAUDIO BRUSCHI, EMILIA FISICARO and MARZIA PASQUALI
 Istituto di Chimica Farmaceutica/Sezione di Chimica Fisica, Università di Parma, Parma, Italy

(Received 29 May 1985. Revised 20 January 1986. Accepted 4 February 1986)

Summary—Homogeneous sets of data from strong acid–strong base potentiometric titrations in aqueous solution at various constant ionic strengths have been analysed by statistical criteria. The aim is to see whether the error distribution matches that for the equilibrium constants determined by competitive potentiometric methods using the glass electrode. The titration curve can be defined when the estimated equivalence volume VEM, with standard deviation (s.d.) $\sigma(\text{VEM})$, the standard potential E_0 , with s.d. $\sigma(E_0)$, and the operational ionic product of water K_w^* (or E_w^* in mV), with s.d. $\sigma(K_w^*)$ [or $\sigma(E_w^*)$] are known. A special computer program, BEATRIX, has been written which optimizes the values of VEM, E_0 and K_w^* by linearization of the titration curve as a Gran plot. Analysis of variance applied to a set of 11 titrations in 1.0M sodium chloride medium at 298 K has demonstrated that the values of VEM belong to a normal population of points corresponding to individual potential/volume data-pairs ($E_i; v_i$) of any titration, whereas the values of $\text{p}K_w^*$ (or of E_w^*) belong to a normal population with members corresponding to individual titrations, which is also the case for the equilibrium constants. The intertitration variation is attributable to the electrochemical component of the system and appears as signal noise distributed over the titrations. The correction for junction-potentials, introduced in a further stage of the program by optimization in a Nernst equation, increases the noise, i.e., $\sigma(\text{p}K_w^*)$. This correction should therefore be avoided whenever it causes an increase of $\sigma(\text{p}K_w^*)$. The influence of the ionic medium has been examined by processing data from acid–base titrations in 0.1M potassium chloride and 0.5M potassium nitrate media. The titrations in potassium chloride medium showed the same behaviour as those in sodium chloride medium, but with an s.d. for $\text{p}K_w^*$ that was smaller and close to the expected instrumental noise, whereas the titrations in nitrate medium had a high noise level and even the determination of VEM was less certain. Procedures are also proposed for obtaining reference sets of data and checking the conformity of the solutions and apparatus to the chosen reference.

GLOSSARY OF THE MOST IMPORTANT SYMBOLS

N = normality of the titrant solution (meq/ml)
 E_0 = standard chain potential (mV)
 V_0 = initial volume of the solution (ml)
 E_i = e.m.f. at the i th point of a potentiometric titration (mV)
 v_i = added volume of titrant at the i th point (ml)
 w_i = statistical weight of the i th point
 $V_i = V_0 + v_i$ = total volume in the cell at the i th point (ml)
 V_e = equivalence volume (ml)
 $\text{pH} = -\log[\text{H}^+]$
 $\text{pOH} = -\log[\text{OH}^-]$
 $K_w = [\text{H}^+][\text{OH}^-]$ = ionic product of water
 K_w^* = operational ionic product of water
 $\beta = 2.302 RT/F$ = Nernst coefficient (59.157 mV at 298 K)
 $E_w^* = \beta \log K_w^* = -\beta \text{p}K_w^*$
 EJ1 = junction potential in acidic range (mV)
 EJ2 = junction potential in alkaline range (mV)
 VE1 = equivalence volume from acidic branch of Gran plot (ml)

VE2 = equivalence volume from alkaline branch of Gran plot (ml)
 $\text{VEM} = (\text{VE1} + \text{VE2})/2$ = estimated equivalence volume (ml)
 $(\Delta/2) = 100 (\Delta/2)/\text{VEM}$ = per cent deviation of VEM
 $\sigma(x)$ = standard deviation of any variable x
 k_T = total number of titrations
 $k = 1, 2, \dots, k_T$ = index of a given titration
 i_T = total number of points in all titrations
 \bar{i}_T = mean number of points per titration
 i_k = total number of points in the k th titration
 $i_{k(ac)}$ = total number of points in acid region in the k th titration
 $i_{k(alk)}$ = total number of points in alkaline region in the k th titration
 Φ = degrees of freedom
 Y_{ac}, Y_{alk} = ordinates of Gran plots in the acidic and alkaline ranges, respectively.

INTRODUCTION

In our studies on the assessment of models for the investigation of metal–proton–ligand equilibria in aqueous solution,^{1,2} we have shown that the formation constant, $\beta_{pqr} = [\text{M}_p\text{H}_q\text{L}_r]/[\text{M}]^p[\text{H}]^q[\text{L}]^r$, of a

†To whom correspondence should be addressed.

given species $M_pH_qL_r$, is affected by an error which is randomly distributed between the titrations performed rather than between individual points of the titrations. In fact the intra-titration (or point-to-point) standard deviation σ_i , the inter-titration (or titration-to-titration) standard deviation σ_{it} and the intra-laboratory standard deviation are related to the standard deviation σ_{pqr} or $\log \beta_{pqr}$ by

$$\sigma_{pqr}^2 = \sigma_i^2 + \sigma_{it}^2 + \sigma_{lab}^2 \quad (1)$$

Analysis of variance (ANOVA) applied to the results of homogeneous sets of data has shown that $\sigma_{pqr}^2 \cong \sigma_{it}^2$.

Though the formation constants are usually refined by computer program, the standard electrode potential, E_0 , and the operational ionic product of water, K_w^* (or E_w^* in mV), used to calculate them are generally obtained from the Nernst equation by direct calculation without refinement. K_w^* is a conditional constant dependent on the apparatus and electrodes used. It does not correspond exactly to the ionic product of water, K_w .

To investigate whether E_0 , K_w^* , and the equivalence volume, VEM, from the strong acid-strong base potentiometric titrations used to standardize the electrochemical apparatus are also affected by an error distribution analogous to that for the formation constants, we have applied ANOVA to sets of standardization data. However, since none of the several programs proposed for treating potentiometric titrations³⁻⁸ performs ANOVA on sets of titrations, we have developed a FORTRAN program, BEATRIX, which converts the points of several individual homogeneous titrations into both Gran⁹ and Nernst plots and performs ANOVA on these to analyse the distributions of errors.

The purpose of the present treatment is not to show that this model is the best for the purpose, but rather to show how a proper analysis of the distribution of errors between points or between titrations is made possible by assuming any well-defined model.

LINEARIZATION OF A TITRATION PLOT

The relation between e.m.f. and volume of titrant is given by the well-known sigmoidal curve (Fig. 1) which is the main reference model of the system. For solutions of strong monobasic acids and monoacidic bases, such a curve is exactly symmetrical around the

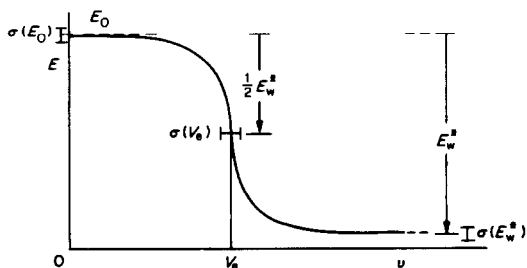


Fig. 1. Titration curve, defined by points E_0 , V_e , E_w^* with errors (e.s.d.) $\sigma(E_0)$, $\sigma(V_e)$, $\sigma(E_w^*)$ respectively.

midpoint $[V_e; (E_0 + E_w^*)/2]$ unless there is a dilution effect.

The vertical displacement of the whole curve depends on the value of E_0 , and the position of the inflexion point and the amplitude of the curve are determined by the values of V_e and E_w^* , respectively. Therefore fitting the model to the experimental points consists in the determination of the parameters V_e , E_0 and E_w^* with standard deviations $\sigma(V_e)$, $\sigma(E_0)$ and $\sigma(E_w^*)$ respectively. A titration curve can be linearized in two ways: (i) by using the Nernst equation $f(E, \text{pH}) = 0$ or (ii) by using the Gran plot $f(10^{(E-E_0)/\beta}, v) = 0$.

In a strong acid-strong base titration, the relationship between the pH of the solution and the e.m.f. E , is given by the Nernst equation:

$$E = E_0 + \beta \log[H^+] = E_0 - \beta \text{pH} \quad (2)$$

where $\beta = 2.302 RT/F$. This relation can be transformed by expressing $[H^+]$ as a function of the added volume of titrant, v :

$$E = E_0 + \beta \log \left\{ \frac{N}{2} \left(\frac{V_e - v}{V_0 + v} \right) + \sqrt{\left[\frac{N}{2} \left(\frac{V_e - v}{V_0 + v} \right) \right]^2 + K_w} \right\} \quad (3)$$

where V_0 is the initial volume of acid titrated, K_w is the ionic product of water, N is the normality of the titrant (the base), and V_e is the equivalence volume.

In the acidic region ($v < V_e$), this equation can be approximated to

$$E = E_0 + \beta \log(V_e - v)N/V_T \quad (4)$$

At neutralization ($v = V_e$)

$$E = E_0 + \beta \log \sqrt{K_w^*} = E_0 + \frac{1}{2} E_w^* \quad (5)$$

In the alkaline region ($v > V_e$), equation (2) gives:

$$E = E_0 + \beta \log \frac{K_w^*}{[\text{OH}^-]} = E_0 + E_w^* - \beta \text{pOH} \quad (6)$$

and, to a good approximation,

$$E = E_0 + E_w^* - \beta \log(v - V_e)N/V_T \quad (7)$$

E_0 and E_w^* are the e.m.f. values obtained at points $[H^+] = 1M$ and $[\text{OH}^-] = 1M$, respectively. Since the experimental points usually do not cover the whole sigmoidal curve, E_0 and E_w^* generally lie outside the experimental range and must be determined by extrapolation. In the acidic range, dE/dv for equation (4) is continuous for any point not too close to the equivalence point, and its limit is zero for $v \rightarrow \infty$. In the alkaline range dE/dv for equation (7) leads to an analogous conclusion. Thus the curve tends asymptotically to a horizontal straight line on either side of the potential "break" in the equivalence region, and cannot suddenly change even outside the range covered by the titration.

From equation (4), $E = E_0$ only for

$$v = \frac{N(V_e - V_0)}{N + 1} = V^* \quad (8)$$

and therefore for

$$V_T = V_0 + V^* = \frac{N(V_e + V_0)}{N+1} = V_T^* \quad (9)$$

Under these conditions [see equations (2) and (4)], $[H^+] = 1M$, implying that: (i) V^* is the volume of titrant which must be added to give a 1M solution of hydrogen ions, (ii) E_0 is the resulting e.m.f. V^* is negative for $V_0 > NV_e$, which is the situation of interest, and can be considered either as a "virtual" volume of as attainable by removal of water by evaporation from the acid in the cell until the concentration of hydrogen ions in the cell is 1M. On the contrary, if V^* is positive, it means that $V_T^* = V_0 + V^* > V_0$ and in this case V_T^* would be reached during the titration. Thus E_0 would not be an extrapolated value, but it would be associated with a specific titration point.

The Gran method linearizes equation (3) by means of the expression

$$Y_{ac} = V_T[H^+] = V_T 10^{(E-E_0)/\beta} \quad (10)$$

for the acidic range, and

$$Y_{alk} = V_T[OH^-] = V_T \frac{K_w^*}{[H^+]} = V_T K_w^* 10^{(E_0-E)/\beta} \quad (11)$$

in the alkaline range.

Both (10) and (11) are functions of the added volume of titrant, v . In this way, equation (4) becomes (acidic range):

$$V_T 10^{E/\beta} = N(V_e - v) 10^{E_0/\beta} \quad (12)$$

and equation (6) becomes (alkaline range)

$$V_T 10^{-E/\beta} = \frac{N}{K_w^*} (v - V_e) 10^{-E_0/\beta} \quad (13)$$

Plotting the left-hand side of equation (12) vs. v gives a straight line with slope = $-N 10^{E_0/\beta}$. For any value of this slope, the dependent variable vanishes only for a single value of v , namely V_e . Therefore it is possible

to determine V_e if N and E_0 are unknown. On the other hand, if N is known, E_0 may be calculated.

In the alkaline region [equation (13)], the plot of $V_T 10^{-E/\beta}$ vs. v is a straight line with slope = $N 10^{-E_0/\beta}/K_w^*$. Since N and E_0 have been determined from calculations in the acidic region, it is thus possible to determine the operational value for the ionic product of water, K_w^* .

In a perfect model the two branches of the curve and therefore the two lines of the Gran plot will converge to a single point on the abscissa. However their intersections with that axis, VE1 and VE2, calculated from the experimental points do not necessarily coincide (Fig. 2).

It is thus convenient to assume $VEM = (VE1 + VE2)/2$ is a reasonable estimate of the equivalence point, V_e . In particular,¹⁰ its variance is equal to that of $\Delta/2 = (VE1 - VE2)/2$:

$$\text{Var}(\Delta/2) = \frac{1}{4}[\text{Var}(VE1) + \text{Var}(VE2)] = \text{Var}(VEM) \quad (14)$$

since $\text{Var}(A \pm B) = \text{Var}(A) + \text{Var}(B)$.

Hence¹⁰ the coefficient of variation is obtained from

$$\begin{aligned} \text{Var}\left[\left(\frac{\Delta}{2}\right)\%\right] &= \text{Var}\left(\frac{\Delta/2}{VEM} \times 100\right) \\ &= 10^4 \text{Var}\left(\frac{\Delta/2}{VEM}\right) \\ &= 10^4 \left[\frac{\text{Var}(\Delta/2)}{(VEM)^2} + \frac{(\Delta/2)^2 \text{Var}(VEM)}{(VEM)^4} \right] \\ &= 10^4 \left[\frac{1}{(VEM)^2} + \frac{(\Delta/2)^2}{(VEM)^4} \right] \text{Var}(\Delta/2) \end{aligned} \quad (15)$$

The second term of the sum inside the square brackets may be neglected, and

$$\text{Var}\left[\left(\frac{\Delta}{2}\right)\%\right] \sim \frac{10^4 \text{Var}(\Delta/2)}{(VEM)^2} \quad (16)$$

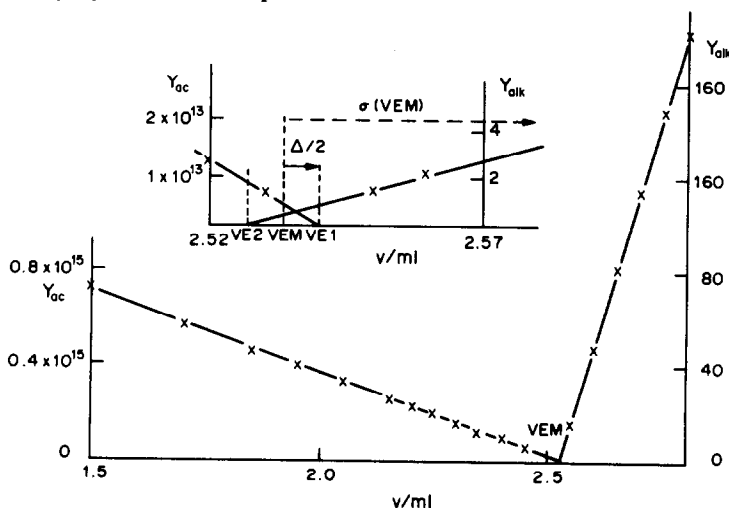


Fig. 2. Gran plot. The ordinates Y_{ac} and Y_{alk} are defined by equations (10) and (11); the abscissa is the volume of titrant. The insert in the upper part is an enlargement of the section around VEM. Note that in this example (data from Table 1) $\sigma(VEM) > \Delta/2$, and that $\sigma(VEM)$ is approximately the same as the precision (~ 0.005 ml) of the burette.

DESCRIPTION OF THE PROGRAM

BEATRIX fits the titration points first to the Gran equations with optional weighting. It calculates the weights, when requested, according to the criterion¹¹ of Avdeef *et al.*:

$$W_i = \frac{1}{\text{Var}(N) + \left[\frac{dE}{dv} \sigma(v) \right]^2} \quad (17)$$

E_0 , VEM and E_w^* are determined, together with their variances, from the Gran fit. $(\Delta/2)\%$ and its variance are also calculated and tested for significance. VEM, E_0 and E_w^* from the Gran plot are then used to fit the same titration to the Nernst equation. Junction potentials are introduced according to the modified Nernst equation:

$$E = E_0 - \beta \text{pH} + (\text{EJ1})[\text{H}^+] + (\text{EJ2})[\text{OH}^-] \quad (18)$$

in order to correct deviations from linearity, if any. Equation (18) is a simplified form of the Henderson equation and assumes constant ionic strength across the liquid junction, a situation which should be maintained by using the same ionic medium in the titrant and in the solution. The Nernst fitting may be performed by assuming the Nernst coefficient β to be fixed or adjustable or both.

If there are two or more titrations to be treated, the program also performs ANOVA among all of them. This may be performed on the weighted or unweighted Gran fits.

It is possible, with the appropriate option, to use the values of E_0 and $\text{p}K_w^*$ obtained from Nernst plots of individual titrations as input data in order to back-calculate the titrant concentration from the results of the Gran fit. If the concentration has been previously measured by independent methods, this approach provides feed-back control of other results from the Gran procedures. In this case, the ANOVA is extended to the corresponding results of all titrations. In fact, since it is assumed that E_0 may vary from one titration to another, its variance among all titrations becomes meaningless: this makes the variance of the titrant concentration useful, providing some information about the variance of the set of titrations. Needless to say, the titrant solution used for each titration must be the same.

The current version of the program was developed for batch use, and is run on the CDC Cyber 7600 computer of C.I.N.E.C.A., (Casalecchio, Bologna, Italy). It uses mathematical and statistical sub-routines from the CERN and IMSL libraries.

EXPERIMENTAL

Materials

Solutions in 0.1M potassium chloride medium. Freshly boiled doubly distilled water was used throughout. Hydrochloric acid (*ca.* 0.15M) and potassium hydroxide (*ca.* 0.35M) solutions were prepared by diluting the contents of BDH Analar CVS ampoules and standardized against tris(hydroxymethyl)aminomethane (Schuchart, dried at 104°), and potassium hydrogen phthalate (C. Erba, dried at

120°), respectively. Appropriate weights of potassium chloride (C. Erba, CGS, dried at 130°) were added to the acid solutions (*ca.* 100 ml) to be titrated, to give an ionic strength of 0.1M at the start of the titration.

Solutions in 1.0M sodium chloride medium. The materials and conditions were the same as for the potassium chloride medium except that sodium hydroxide and chloride were used.

Solutions in 0.5M potassium nitrate medium. Nitric acid (*ca.* 0.1M) and potassium hydroxide (*ca.* 0.2M) solutions were prepared by diluting the contents of Merck Titrisol ampoules and standardized in the same way as the other acid and base solutions. Potassium nitrate from C. Erba was used.

Measurements

Potassium chloride medium. The potentiometric measurements were made with a Radiometer PHM 52 digital voltmeter equipped with a Radiometer G225B glass electrode and a K401 saturated KCl/calomel electrode with porous diaphragm.

A Metrohm E415-5 motor burette was employed. The titration vessel was kept at $25 \pm 0.1^\circ$ and a stream of nitrogen pre-equilibrated with potassium chloride flowed over the test solution. Room temperature was maintained at $25 \pm 0.5^\circ$. The potentiometer had an accredited precision of better than 0.1 mV.

Sodium chloride and potassium nitrate media. The potentiometric measurements were made with an automatic apparatus assembled in our laboratory and described elsewhere.¹² The titrations were the same as those used in the nickel-glycine project.¹³

DISCUSSION

The application of the program and the information provided can be best illustrated with reference to specific examples.

Intra-titration error

The fitting of a set of experimental data (ionic medium 1.0M sodium chloride) to the linear Gran plot is reported in Table 1. The input data are V_0 (the initial volume of the solution), β (the Nernst coefficient), N (the normality of the titrant solution), v_i (the volume of titrant added), E_i (the e.m.f. measured after equilibration at the i th point). The program counts the total number of points, i_k , and the number in the acidic ($i_{k(\text{ac})}$) and alkaline ($i_{k(\text{alk})}$) ranges.

The output data are the slope and intercept of the straight lines in the Gran plot $Y = A + BX$, equations (12) and (13):

<i>Acidic range</i>	<i>Alkaline range</i>
$B = -N 10^{E_0/\beta}$	$B = (N \times 10^{-E_0/\beta})/K_w$
$A = NV_e 10^{E_0/\beta}$	$A = -(NV_e 10^{-E_0/\beta})/K_w^*$
$X = v_i$	$X = v_i$
$Y = V_T 10^{E_i/\beta}$	$Y = V_T 10^{-E_i/\beta}$

Certain values in Table 1 are useful for judging the reliability of the experiment. The value of E_0 can be compared with other values of the standard potential obtained with the same electrochemical cell. Moreover, the estimated standard deviation (E_0), which should not be very different from the instrumental precision, is 0.13 mV, close to that assumed for the instrumental precision (0.1 mV). The pH range in this titration was 1.6–11.6.

Table 1. Example of INPUT-OUTPUT for a single titration

INPUT DATA†											
$V = 99.62$ ml, $N = 0.9656M$, Nernst coefficient = 59.157 mV, $\sigma(v) = 0.005$ ml											
EJ1, EJ2 adjustable. Points: $i_k = 33$, $i_{k(ac)} = 18$, $i_{k(alk)} = 15$											
i	v, ml	E, mV	i	v, ml	E, mV	i	v, ml	E, mV	i	v, ml	E, mV
1	0.00	783.3	9	1.95	745.4	17	2.45	696.1	25	2.85	217.1
2	0.05	782.8	10	2.05	740.6	18	2.50	673.9	26	2.90	213.4
3	0.55	777.0	11	2.15	734.7	19	2.55	309.8	27	2.95	210.2
4	0.95	771.2	12	2.20	731.1	20	2.60	259.7	28	3.00	207.3
5	1.25	765.8	13	2.25	726.9	21	2.65	243.5	29	3.05	204.8
6	1.50	760.2	14	2.30	722.0	22	2.70	233.9	30	3.15	200.4
7	1.70	754.6	15	2.35	715.9	23	2.75	226.9	31	3.25	196.9
8	1.85	749.5	16	2.40	707.9	24	2.80	221.5	32	3.35	193.8
									33	3.50	189.9

OUTPUT DATA§ ($\pm \sigma$)(a) without junction potentials: $Y = A + BX$ (Gran straight lines).

acidic range

$$A = (1741 \pm 3) \times 10^{12}$$

$$B = -(685 \pm 8) \times 10^{12}$$

$$VE1 = 2.54 \pm 0.01 \text{ ml}$$

$$E = 878.5 \pm 0.1 \text{ mV}$$

alkaline range

$$A = -(1686 \pm 6) \times 10^{-4}$$

$$B = (667 \pm 2) \times 10^{-4}$$

$$VE2 = 2.53 \pm 0.09 \text{ ml}$$

$$E_w^* = -809.9 \pm 0.9 \text{ mV}$$

$$pK_w^* = 13.69 \pm 0.02$$

mean‡

$$VEM = 2.53 \pm 0.04 \text{ ml}$$

$$\Delta/2 = 0.006 \pm 0.042 \text{ ml}$$

$$\sigma(\text{VEM}\%) = 1.65\%$$

$$\sigma[(\Delta/2)\%] = 1.65\%; t = 0.15; P = 11.8\%$$

(b) with junction potentials:

acidic range

$$E = (\text{EJ1})[\text{H}^+] + E_0 - \beta \text{pH}$$

$$E_0 = 879 \text{ mV}; \text{EJ1} = 20 \text{ mV}$$

alkaline range

$$E = (\text{EJ2})[\text{OH}^-] + E_0 + E_w + \beta \text{pOH}$$

$$pK_w^* = 13.65; \text{EJ2} = 580 \text{ mV}; \sigma(E_w^*) = 4.0 \text{ mV}$$

† N = base concentration.

§Unweighted cycle.

‡ $t = [(\Delta/2)\%]/\sigma[(\Delta/2)\%]$.

The value of pK_w^* (13.690), which depends on the ionic strength of the solution, falls within the range of values obtained in similar titrations by different laboratories.¹³ The standard deviation pK_w^* is more meaningful when expressed as $\sigma(E_w^*) = 0.91$ mV, and is poorer than the instrumental precision. This value is significantly reduced by statistical weighting of the data points, but in any case confirms the generally accepted view that the glass electrode should be used with caution in the very alkaline region.

The values of VEM together with those for $\Delta/2$ and $(\Delta/2)\%$, deserve special comment. VEM and $\Delta/2$ have the same variance, so $\sigma[(\Delta/2)\%]$ is an estimate of the relative error in VEM, equation (16); in the titration reported in Table 1, $\sigma[(\Delta/2)\%] = 1.65\%$. This rather high value is probably due to errors in measuring accurately the small increments of titrant added. $\Delta/2$ can be considered as reflecting some type of systematic error. Therefore the ratio of $\Delta/2$ to its own standard deviation, and hence to $\sigma(\text{VEM})$, i.e.,

the value $t = (\Delta/2)/\sigma(\Delta/2)$, offers an estimate of the significance and relevance of the systematic error within one titration. In this example $t = 0.15$, corresponding to a probability $P = 11.8\%$, which is not significant. Significant values of t would indicate that the experiment should be rejected.

The calculation of junction potentials gives values of $\text{EJ1} = -20.4$ mV and $\text{EJ2} = -580.2$ mV, which are unacceptable. On the other hand the value of $\sigma(pK_w^*)$ [or of $\sigma(E_w^*) = 4.01$ mV] indicates that the correction for junction potentials does not improve the model and should therefore be rejected.

The introduction of weights according to equation (17) improves the results, as shown by the smaller standard deviations (Table 2).

Inter-titration error

The output of the analysis of variance applied to a set of eleven ($K_T = 11$) titrations is reported in Table 3. The example in the preceding tables is the 11th

Table 2. Results of weighted (w) and unweighted (uw) cycles for titration in 1.0M NaCl

	VEM (σ), ml	$\Delta/2$ (σ), ml	$(\Delta/2)\%$ (σ)
w	2.54 (0.04)	-0.001 (0.037)	-0.04 (1.44)
uw	2.53 (0.04)	+0.006 (0.042)	+0.25 (1.65)
	E_0 (σ), mV	pK _w [*] (σ)	E_w^* (σ), mV
w	878.6 (0.1)	13.71 (0.01)	-810.9 (0.8)
uw	878.5 (0.1)	13.69 (0.01)	-810.9 (0.9)

titration ($k = 11$) of the set. The comparison of the values from different experiments is an important way of analysing the reliability of both the equipment and the titration system.

The mean value of $(\Delta/2)\%$ is 0.10, which means that there is a 0.1% systematic error. This is a small and insignificant value, as shown by the value of 1.40 for t ; the tabular value of $t_{0.95}$ is 2.23 for 10 degrees of freedom. Particularly relevant information is given by comparison of the variance $\text{Var}(\bar{x})$ of the mean values, with the estimated inter-point average variance Var_0 , [calculated as the mean for the total ($i_T = 374$) data for the error squares]. For a normal population of points (H_0 hypothesis) the relation $\text{Var}(\bar{x}) \sim \text{Var}_0/\bar{i}_T$ should hold. If $F = \text{Var}(\bar{x})\bar{i}_T/\text{Var}_0$ is > 1 , then the H_0 hypothesis must be rejected and the H_1 hypothesis accepted at a certain significance level. If the H_0 hypothesis is accepted, then we can conclude that the points of each titration belong to the same normal population. The F -test applied to the equivalence volume VEM shows that the H_0 hypothesis can be accepted, *i.e.*, the hypothesis that

$(\Delta/2)\% = 0.10$ is a significant systematic error is rejected.

On the other hand the F -test applied to the mean values of E_0 and pK_w^{*} (or E_w^*) indicates that the H_0 hypothesis must be rejected and H_1 accepted, and therefore that for these quantities the inter-titration or (titration-to-titration) errors are much larger than the inter-point (or point-to-point) errors. Thus the precision of the standard electrode potential and of the operational ionic product of water can be calculated only from the inter-titration variability. This result is in keeping with the conclusion drawn from an analysis of the results of the nickel-glycine project.¹³ Both the standard deviation of E_0 [$\sigma(E_0) = 0.85$ mV] and E_w^* [$\sigma(E_w^*) = 0.66$ mV] are larger than the instrumental error.

The influence of weighting and junction potential corrections is examined in Table 4.

The introduction of possible junction potentials increases $\sigma(E_w^*)$ considerably; also the analysis of the inter-titration error confirms that the correction for junction potentials should be avoided, unless this correction results in a lower value of $\sigma(E_w^*)$.

The introduction of weights according to equation (17) improves the values of the whole set, as shown by the general decrease in the standard deviations, and in particular $\sigma(\text{VEM})$ and $\sigma(E_w^*)$. The latter value [$\sigma(E_w^*) = 0.3$ mV] is not very different from the experimental error that can be evaluated ($\sigma = 0.2$ mV) in the alkaline region by taking into account that E_w^* (see Fig. 1) depends on two independent measurements of e.m.f.

Table 3. Analysis of variance for titrations in 1.0M NaCl; $k_T = 11$; $i_T = 374$; $\bar{i}_T = 34$; $\bar{i}_{T(ac)} = 18$; $\bar{i}_{T(alk)} = 15$

k	$(\Delta/2)\% \pm \sigma$	$E_0 \pm \sigma$, mV	pK _w [*] $\pm \sigma$	$E_w^* \pm \sigma$, mV
1	0.1 \pm 0.6	881.0 \pm 0.2	13.724 \pm 0.002	-811.8 \pm 0.2
2	0.0 \pm 0.4	881.0 \pm 0.1	13.736 \pm 0.003	-812.6 \pm 0.2
3	0.1 \pm 1.1	879.6 \pm 0.1	13.703 \pm 0.010	-810.6 \pm 0.6
4	0.0 \pm 0.7	880.1 \pm 0.1	13.716 \pm 0.006	-811.4 \pm 0.4
5	0.1 \pm 0.8	879.3 \pm 0.2	13.708 \pm 0.006	-810.9 \pm 0.4
6	0.1 \pm 0.7	879.8 \pm 0.1	13.713 \pm 0.006	-811.2 \pm 0.3
7	0.1 \pm 0.8	879.8 \pm 0.2	13.711 \pm 0.006	-811.1 \pm 0.4
8	0.1 \pm 0.8	881.2 \pm 0.2	13.712 \pm 0.006	-811.2 \pm 0.4
9	0.1 \pm 1.0	878.7 \pm 0.2	13.702 \pm 0.008	-810.6 \pm 0.5
10	0.0 \pm 1.6	879.1 \pm 0.1	13.715 \pm 0.015	-811.3 \pm 0.9
11	0.2 \pm 1.7	878.5 \pm 0.1	13.690 \pm 0.015	-809.9 \pm 0.9
Mean values:				
\bar{x}	$(\Delta/2)\%$	E_0 , mV	pK _w [*]	E_w^* , mV
$\sigma(\bar{x})$	0.10	879.8	13.71	-811.2
σ_0	0.07	0.9	0.01	0.7
F	0.99	0.16	0.009	0.5
\bar{i}	1	532.2	25.7	25.7
$\phi_i = k - 1$	34($\bar{i}_{T(ac)}$)	18($\bar{i}_{T(ac)}$)	15($\bar{i}_{T(alk)}$)	15($\bar{i}_{T(alk)}$)
m	10	10	10	10
$\phi_2 = k(i - m)$	4	2	2	2
$F_{0.01}(\phi_1, \phi_2)$	330	176	143	143
	2.32	2.32	2.32	2.32

Notes:

k_T = total number of titrations; \bar{i}_T = mean number of points in each titration; $\bar{i}_{T(ac)}$ = mean number of acidic points; $\bar{i}_{T(alk)}$ = mean number of alkaline points; $\sigma_0 = (\sigma_{\bar{x}}^2)^{1/2}$ = estimated interpoint average standard deviation; m = number of parameters refined by linear least-squares method; $F = \bar{i}\sigma^2(\bar{x})/\sigma_0^2$; $F_{0.01}(\phi_1, \phi_2)$ = tabulated F -value at $P = 0.01$ level.

Table 4. Titrations in 1.0M NaCl; results of ANOVA for weighted (w) and unweighted (uw) cycles (wJ, uwJ, with correction for junction potentials)

		E_0	pK_w^*	E_w^*
w	$\bar{x}(\sigma)$	879.9(0.9) mV	13.720(0.008)	-811.6(0.5) mV
	σ_0/\sqrt{n}	0.04 mV	0.002	0.12 mV
	F		15.8	15.8
uw	$\bar{x}(\sigma)$	879.8(0.9) mV	13.712(0.011)	-811.2(0.7) mV
	σ_0/\sqrt{n}	0.04 mV	0.002	0.13 mV
	F		25.8	25.8
wJ	$\bar{x}(\sigma)$	879.9(0.9) mV	13.695(0.027)	-810.2(1.6) mV
	σ_0/\sqrt{n}	0.03 mV	0.011	0.66 mV
	F		5.9	5.9
uwJ	$\bar{x}(\sigma)$	880.0(0.8) mV	13.680(0.053)	-809.3(3.1) mV
	σ_0/\sqrt{n}	0.03 mV	0.018	1.1 mV
	F		7.9	7.9
		$(\Delta/2)\%$	EJ1	EJ2
w	$\bar{x}(\sigma)$	-0.06(0.04)	—	—
	σ_0/\sqrt{n}	0.23	—	—
	F	~ 0	—	—
uw	$\bar{x}(\sigma)$	0.10(0.07)	—	—
	σ_0/\sqrt{n}	0.24	—	—
	F	~ 0	—	—
wJ	$\bar{x}(\sigma)$	-0.06(0.04)	0.2(6.4) mV.l.mole ⁻¹	-215(221) mV.l.mole ⁻¹
	σ_0/\sqrt{n}	0.24	—	—
	F	~ 0	—	—
uwJ	$\bar{x}(\sigma)$	0.10(0.07)	-5.4(7.3) mV.l.mole ⁻¹	-363(484) mV.l.mole ⁻¹
	σ_0/\sqrt{n}	0.24	—	—
	F	~ 0	—	—
	t	1.4	<1	<1
	t	1.4	<1	<1

It is generally accepted that the value of E_0 can change from one titration to another, because systematic errors will be absorbed by E_0 . Therefore the program, in a further step, assumes that each E_0 is correct for each titration and calculates, as noted above, the titrant concentration. If the same titrant is used throughout the whole set of titrations, then the error of the titrant normality should give an estimate of the inter-titration error in terms of titrant concentration (Table 5).

The relative error of the titre, $\sigma = 0.4\%$, is smaller than the relative error in VEM and therefore acceptable. In every case the conclusion is that the inter-titration errors for values inherent or dependent upon the e.m.f. are those that determine the precision of the values. Thus pK_w^* can be assigned $\sigma(pK_w^*) = 0.01$ [or $\sigma(E_w^*) = 0.59$ mV].

Effect of the ionic medium

To examine the effect of the ionic medium, other sets of data from acid-base titrations in 0.1M potassium chloride and 0.5M potassium nitrate media were analysed. The result of the application of ANOVA to the first set of data is reported in Table 6.

The values show the same trends as for titrations in 1M sodium chloride media. The distribution of σ (VEM) represents a normal population composed of the individual points of any titration. The introduction of weighting improves the results.

The distribution of $\sigma(pK_w^*)$ or $\sigma(E_w^*)$ is mainly affected by inter-titration errors, as observed in the equilibrium constants of the nickel-glycine system¹³ and in the acid-base titrations in 1M sodium chloride medium. The value $\sigma(E_w^*) = 0.29$ mV is even better than that for the sodium chloride system. The intro-

Table 5. Influence of inter-titration error on titrant concentration C (M)

k	$C(\sigma)$	k	$C(\sigma)$	k	$C(\sigma)$
1	0.964(0.009)	5	0.965(0.009)	9	0.967(0.006)
2	0.969(0.003)	6	0.960(0.005)	10	0.972(0.004)
3	0.974(0.004)	5	0.971(0.008)	11	0.967(0.005)
4	0.972(0.005)	8	0.966(0.009)		

Mean value

$$\bar{x}(\sigma) = 0.968(0.004); \sigma_0 = 0.006; \bar{i} = 16.5; F = 6.77; \phi_1 (=k_T - 1) = 10; \phi_2 [=k_T(i - m)] = 160; F(\phi_1, \phi_2) = 2.32$$

Table 6. Titrations in 1.0M KCl; results of ANOVA for weighted (w) and unweighted (uw) cycles (wJ, uwJ, with correction for junction potentials)

		E	pK_w^*	E_w^*
w	$\bar{x}(\sigma)$	368.7(0.6) mV	13.787(0.005)	815.6(0.3) mV
	σ_0/\sqrt{n}	0.074 mV	0.003	0.148 mV
	F		3.99	3.99
uw	$\bar{x}(\sigma)$	368.6(0.6) mV	13.785(0.006)	815.5(0.4) mV
	σ_0/\sqrt{n}	0.089 mV	0.0032	0.187 mV
	F		3.59	3.59
wJ	$\bar{x}(\sigma)$	368.7(0.5) mV	13.771(0.017)	814.7(1.0) mV
	σ_0/\sqrt{n}	0.046 mV	0.005	0.275 mV
	F		13.40	13.40
uwJ	$\bar{x}(\sigma)$	368.8(0.5) mV	13.781(0.013)	815.2(0.8) mV
	σ_0/\sqrt{n}	0.047 mV	0.003	0.203 mV
	F		14.30	14.30
		$(\Delta/2)\%$	EJ1	EJ2
w	$\bar{x}(\sigma)$	-0.11(0.08)	—	—
	σ_0/\sqrt{n}	0.194	—	—
	F	0.17	—	—
	t	1.34	—	—
uw	$\bar{x}(\sigma)$	-0.01(0.13)	—	—
	σ_0/\sqrt{n}	0.242	—	—
	F	0.28	—	—
	t	0.11	—	—
wJ	$\bar{x}(\sigma)$	-0.11(0.08)	-24(22) mV.l.mole ⁻¹	-302(302) mV.l.mole ⁻¹
	σ_0/\sqrt{n}	0.194	—	—
	F	0.17	—	—
	t	1.34	1.11	1.00
uwJ	$\bar{x}(\sigma)$	-0.01(0.13)	-17(23) mV.l.mole ⁻¹	-116(209) mV.l.mole ⁻¹
	σ_0/\sqrt{n}	0.242	—	—
	F	0.28	—	—
	t	0.11	<1	<1

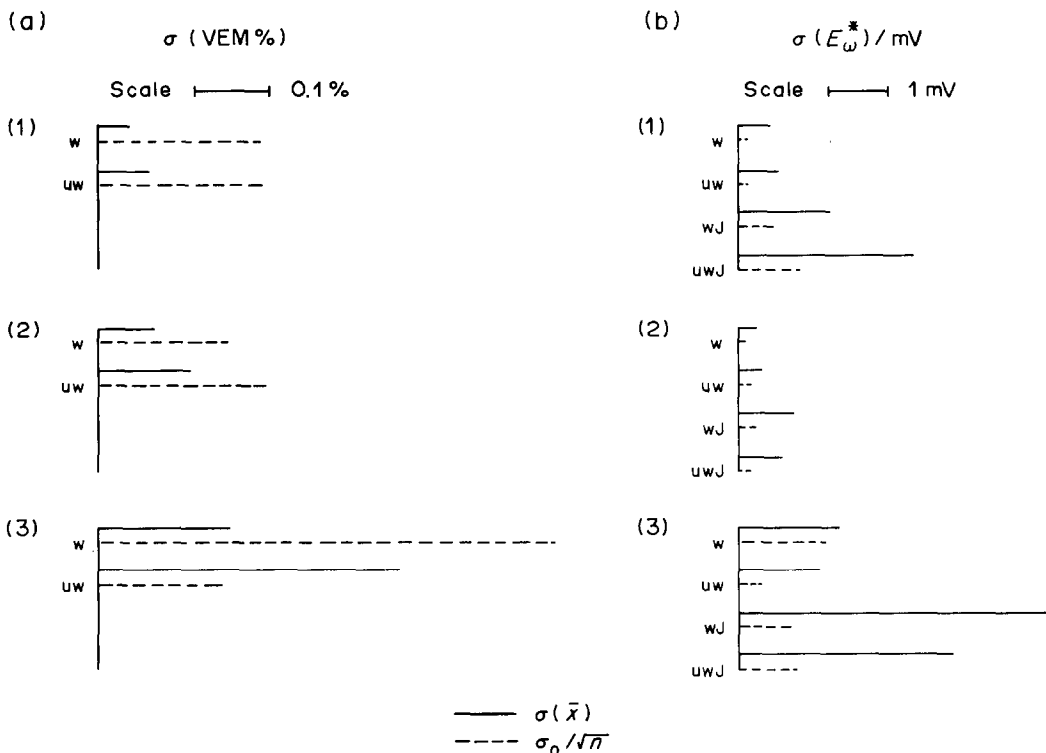


Fig. 3. Inter-titration, $\sigma(\bar{x})$, and intra-titration, σ_0 errors in different ionic media: (1) 1M NaCl; (2) 0.1M KCl; (3) 0.5M KNO₃. Weighted (w) and unweighted (uw) refinements; wJ and uwJ, refinements with introduction of junction-potential correction. Note that for $x = \text{VEM}$, $\sigma(\bar{x}) > \sigma_0(x)/\sqrt{n}$ (normal population of titrations).

Table 7. Titrations in 0.5M KNO₃; results of ANOVA for weighted (w) and unweighted (uw) cycles (wJ, uwJ, with correction for junction potentials)

		E_0	pK_w^*	E_w^*
w	$\bar{x}(\sigma)$	891.1(2.7) mV	13.721(0.031)	-811.7(1.8) mV
	σ_0/\sqrt{n}	0.048 mV	0.027	1.6 mV
	F		1.3	1.3
uw	$\bar{x}(\sigma)$	891.2(2.6) mV	13.727(0.025)	-812.1(1.5) mV
	σ_0/\sqrt{n}	0.041 mV	0.006	0.38 mV
	F		15.4	15.4
wJ	$\bar{x}(\sigma)$	890.8(2.5) mV	13.642(0.110)	-807.0(6.5) mV
	σ_0/\sqrt{n}	0.001 mV	0.016	0.93 mV
	F		49.3	49.3
uwJ	$\bar{x}(\sigma)$	890.7(2.4) mV	13.649(0.065)	-807.4(3.9) mV
	σ_0/\sqrt{n}	0.011 mV	0.017	1.03mV
	F		14.0	14.0
		$(\Delta/2)\%$	EJ1	EJ2
w	$\bar{x}(\sigma)$	-0.46(0.19)	—	—
	σ_0/\sqrt{n}	0.681	—	—
	F	0.1	—	—
uw	t	2.4	—	—
	$\bar{x}(\sigma)$	-0.58(0.43)	—	—
	σ_0/\sqrt{n}	0.181	—	—
wJ	F	5.9	—	—
	t	1.3	—	—
	$\bar{x}(\sigma)$	-0.46(0.19)	68(139) mV.l.mole ⁻¹	-1355(821) mV.l.mole ⁻¹
uwJ	σ_0/\sqrt{n}	0.681	—	—
	F	0.1	—	—
	t	2.4	<<1	1.65
uwJ	$\bar{x}(\sigma)$	-0.58(0.43)	77(122) mV.l.mole ⁻¹	-2206(1715) mV.l.mole ⁻¹
	σ_0/\sqrt{n}	0.181	—	—
	F	5.9	—	—
	t	1.3	<1	1.29

duction of the corrections for junction potentials increases the value of $\sigma(E_w^*)$. This inter-titration error confirms the results of the analysis of the intra-titration error, and appears to be a sort of noise, probably due to junction potentials. We cannot say whether this sort of noise is dependent on the model adopted. Other possible models will be examined, particularly suited to organic or mixed solvents, such as that proposed by Rossotti and Rossotti.¹⁴ These results will also be analysed by the statistical procedures adopted here.

The analysis of the data for the titrations in 0.5M potassium nitrate medium (Table 7) indicates that the choice of electrolyte is critical.

All the results, as shown either by $\sigma(\text{VEM})$ or by $\sigma(pK_w^*)$ are much worse than in the other two systems. The inter-titration noise reaches values so high that even the determination of VEM becomes uncertain. Any effects due to impurities in the materials have been excluded by repeated purity tests.

The general trends of the three systems examined are compared in Fig. 3. The comparison shows that the most reliable results are obtained with 0.1M potassium chloride as background electrolyte.

CONCLUSIONS

The application of classical statistical tests to the analysis of the results of potentiometric strong

acid-strong base titration sets has shown that some procedures ought to be followed in order to obtain reliable results.

(1) To obtain a reference set of data representative of the system, several titrations should be performed under the same experimental conditions with measurements at relatively few points. Single titrations, even with many points, are not recommended. The values of VEM and pK_w^* are first refined by processing separately each titration and averaging the results. Only if the ANOVA is satisfactory may all the single points of every titration be refined together.

(2) The equivalence volumes, VEM, very often form a normal population, the members of which are the values corresponding to the individual points of any titration. The value of $\sigma(\text{VEM})$ represents an assessment of the reliability of the concentrations found. Once the behaviour of a system has been assessed by establishing a reference value, $\sigma(\text{VEM})^{REF}$, only a single titration is needed to test the conformity of a new solution to the standard.

(3) The error in the operational ionic product of water, $\sigma(pK_w^*)$ or $\sigma(E_w^*)$, may be employed to test the reliability of the electrochemical part of the system. Application of ANOVA to pK_w^* (or E_w^*) has shown that the main part of the error reveals itself from one titration to another. The individual points (E_i, v_i) do not represent in this respect a normal population; rather, the titrations form a normal population, the

standard deviation of which, $\sigma(\text{p}K_w^*)$ or $\sigma(E_w^*)$, measures the precision of the determinations. The source of this error seems to be noise due to instability of the junction potentials. When the electrochemical apparatus has been assessed by establishing $\sigma(\text{p}K_w)^{REF} = \sigma(\text{p}K_w^*)$ or $\sigma(E_w^*)$, at least three acid-base titrations are needed to test the conformity of a given electrochemical chain to the standard.

(4) Changing the electrolyte added to keep the ionic strength constant affects the precision of both VEM and $\text{p}K_w^*$. Particularly good results have been obtained in our laboratory with 1M sodium chloride as ionic medium, and even better with 0.1M potassium chloride, which both keep the noise at low level. With the latter ionic medium we have obtained results [$\sigma(E_w^*) \sim 0.26$ mV] very close to the expected effect ($\sigma = 0.2$ mV) of the instrumental error on E_w^* . The use of 0.5M potassium nitrate medium increases the error in both VEM and $\text{p}K_w^*$.

Acknowledgements—This work was supported by a research program M.P.I. 1982, "Termodinamica dei sistemi metallo-legante e proteina-legante". Dr. David J. Leggett and Professor Luigi Dodi are thanked for help in revising the English text.

REFERENCES

1. A. Braibanti, F. Dallavalle, G. Mori and B. Veroni, *Talanta*, 1982, **29**, 725.
2. A. Braibanti, F. Dallavalle, G. Mori and M. Pasquali, *Gazz. Chim. Ital.*, 1983, **113**, 407.
3. R. J. Motekaitis and A. E. Martell, *Can. J. Chem.*, 1982, **60**, 2403.
4. F. Ingman, A. Johansson, S. Johansson and R. Carlsson, *Anal. Chim. Acta*, 1973, **64**, 113.
5. D. M. Barry and L. Meites, *ibid.*, 1974, **68**, 435.
6. G. Arena, E. Rizzarelli, S. Sammartano and C. Rigano, *Talanta*, 1979, **26**, 1.
7. A. Avdeef and J. J. Bucher, *Anal. Chem.*, 1978, **50**, 2317.
8. P. M. May, D. R. Williams, P. W. Linder and R. G. Torrington, *Talanta*, 1982, **29**, 249.
9. G. Gran, *Analyst*, 1952, **77**, 661.
10. A. Braibanti and C. Bruschi, *Ann. Chim. (Rome)*, 1977, **67**, 471.
11. A. Avdeef, S. R. Sofen, T. L. Bregante and K. N. Raymond, *J. Am. Chem. Soc.*, 1978, **100**, 5362.
12. F. Dallavalle and G. Mori, *Ann. Chim. (Rome)*, 1976, **66**, 753.
13. E. Bottari, A. Braibanti, L. Ciavatta, A. M. Corrie, P. G. Daniele, F. Dallavalle, M. Grimaldi, A. Mastroianni, G. Mori, E. Rizzarelli, S. Sammartano, C. Severini, A. Vacca and D. R. Williams, *ibid.*, 1978, **68**, 813.
14. F. J. C. Rossotti and H. Rossotti, *J. Phys. Chem.*, 1964, **68**, 3773.

THE INFLUENCE OF THIOUREA ON THE CATION-EXCHANGE BEHAVIOUR OF VARIOUS ELEMENTS IN DILUTE NITRIC AND HYDROCHLORIC ACIDS*

C. H.-SIEGFRIED W. WEINERT and FRANZ W. E. STRELOW

National Chemical Research Laboratory, Council for Scientific and Industrial Research, P.O. Box 395, Pretoria 0001, Republic of South Africa

REINHARD G. BÖHMER

Department of Chemistry, University of Pretoria, Hillcrest, Pretoria 0083, Republic of South Africa

(Received 18 November 1985. Accepted 23 January 1986)

Summary—Cation-exchange distribution coefficients for 21 elements between the cation-exchange resin AG50W-X4 and dilute nitric and hydrochloric acid containing up to 2.0M concentration of thiourea are presented. The ion-exchange behaviour of the elements and some possible separations are discussed. Four multi-element elution curves are presented, demonstrating the separation of the combinations Ga(Ag, Cu)-Zn(Cd, Pb, In, Sn(IV)), Co-Pb-Sb-Te, Zn-Cd-Bi-Hg, and Ag-Cd-In-Au.

In previous papers^{1,2} we reported the cation-exchange behaviour of several transition and post-transition elements in hydrochloric and hydrobromic acid media containing 0.1 or 0.2M concentration of thiourea (Tu). This work has now been extended to a wider range of thiourea concentrations, and nitric acid as a weakly complexing acid.

EXPERIMENTAL

Reagents

The sulfonated polystyrene cation-exchange resin AG50W-X4 in H⁺-form, (Bio-Rad Laboratories), was used. The particle sizes used for batch and column work were 100-200 and 200-400 mesh, respectively.

The water used was distilled, then passed through an Elgastat demineralizer for further purification.

Stock solutions of the various metals were prepared from analytical reagent grade salts, and standardized by suitable analytical methods.

Hydrochloric and nitric acid were of analytical grade (Merck), and standardized against guaranteed 0.1000M sodium hydroxide ("Titriplex", Merck).

The thiourea was "chemically pure" reagent grade and used without further purification; freshly prepared solutions were used throughout. A standard-addition test with ferric chloride indicated that the original thiourea contained 0.08% thiocyanate. A similar test with lead nitrate indicated the absence (<0.001%) of sulphide. Fresh solutions were clear, but became turbid on standing, owing to the liberation of sulphur, presumably as a result of oxidation by atmospheric oxygen. Detectable amounts of hydrogen sulphide formed in solutions of the thiourea in >0.5M hydrochloric or nitric acid, as a result of acid-catalysed hydrolysis of the thiourea.

Nitric acid concentrations greater than 2.0M could not be used because they resulted in the precipitation of

thiouonium nitrate, and an exothermic evolution of nitric oxide.

The composition of the eluents containing acetone refers to the volume of acetone added, without allowance for any volume changes in mixing.²

Apparatus

Borosilicate glass columns of 20 mm inner diameter containing a resin bed of 43 ml volume (10 g) were used for the elution experiments. All metal determinations were done with a Varian Techtron AA-5 atomic-absorption spectrophotometer; matrix-matched standards were used.

Distribution coefficients

The resin used was dried at 80° in a ventilated oven, and stored in a desiccator over anhydrous silica gel. Residual water was determined by drying at 120°, and the weights of resin were corrected accordingly.

A 2.500-g portion of the dry (80°) resin was shaken mechanically at 20° with 250 ml of a solution containing 0.50 mmole of an element, for 24 hr. The phases were then separated, and the amount of the element in each was determined. The distribution coefficients were calculated¹ and are presented in Tables 1 and 2.

Elution curves

Elution curves for multi-element mixtures were prepared in order to explore more fully the possibilities for separations with the AG50W-X4 resin and dilute acid solutions of thiourea. Flow-rates of 3.0 ± 0.3 ml/min were used throughout.

Separation of Ga, Ag and Cu from Zn, Cd, Pb, In and Sn(IV)

Since Sn(IV) tended to hydrolyse irreversibly at low acid and Tu concentrations, 50 ml of 0.50M nitric acid-0.50M Tu solution was allowed to drain through the column as the first step. A solution containing 0.05 mmole each of Ga³⁺, Cu⁺, Ag⁺, Zn²⁺, Pb²⁺, In³⁺, Sn(IV) and Cd²⁺ in 50 ml of 0.50M nitric acid-0.50M Tu was then passed through the column, followed by 50 ml of the acid/Tu mixture and elution with 1250 ml of 1.5M nitric acid-1.0M Tu. The eluate was collected in 25-ml fractions (25 from the beginning of the elution step), and analysed for each element. The elution curves are shown in Fig. 1.

*Part of this paper is an extract from a D.Sc. Thesis by C.H.-S.W. Weinert, submitted to the University of Pretoria, Republic of South Africa.

Table 1. Distribution coefficients in solutions containing various amounts of thiourea and nitric acid

Element	[Tu], <i>M</i>	[HNO ₃], <i>M</i>				
		0.1	0.2	0.5	1.0	2.0
Ag ⁺	0.1	80	44	18.5	9.3	4.1
	0.01	> 10 ⁴	> 10 ⁴	9000	4300	2300
	0.1	3500	1800	730	350	180
	0.2	1600	820	330	160	83
	0.5	750	370	160	74	39
	1.0	470	230	99	46	24.5
Hg ²⁺	nil	1700	510	91	20.6	7.3
	0.01	> 10 ⁴	> 10 ⁴	1700	760	140
	0.1	> 10 ⁴	> 10 ⁴	2600	820	170
	0.2	> 10 ⁴	ca. 10 ⁴	2400	690	150
	0.5	ca. 10 ⁴	5200	1400	430	110
	1.0	5000	2100	820	270	75
Bi ³⁺	nil	> 10 ⁴	4200	210	34.5	4.5
	0.01	> 10 ⁴	> 10 ⁴	800	131	17.3
	0.1	> 10 ⁴	> 10 ⁴	> 10 ⁴	> 10 ⁴	2000
	0.2	> 10 ⁴	> 10 ⁴	> 10 ⁴	> 10 ⁴	3700
	0.5	> 10 ⁴	> 10 ⁴	> 10 ⁴	> 10 ⁴	2900
	1.0	> 10 ⁴	> 10 ⁴	> 10 ⁴	ca. 10 ⁴	1400
Pb ²⁺	nil	2300	690	86	20.0	5.0
	0.1	2500	860	140	26.5	5.7
	0.5	> 10 ⁴	> 10 ⁴	1530	260	44.6
	1.0	> 10 ⁴	8500	1640		
Sn(IV)	nil	†	†	†	17.5	7.5
	0.1	†	†	†	37.4	11.8
	0.5	†	†	700	185	67.5
	1.0	†	ca. 10 ⁴	2300	490	110
In ³⁺	nil	> 10 ⁴	2600	230	41.3	10.7
	0.1	> 10 ⁴	5200	430	75	15.4
	0.5	> 10 ⁴	ca. 10 ⁴	1190	180	34.8
	1.0	> 10 ⁴	> 10 ⁴	1670	240	45.0
Cd ²⁺	nil	1670	390	75	21.9	7.7
	0.1	4200	1900	310	83	23.1
	0.5	ca. 10 ⁴	8500	1200	270	61
	1.0	ca. 10 ⁴	8400	1000	230	53
Zn ²⁺	nil	1600	400	74	19.5	7.7
	0.1	1700	410	78	21.1	8.5
	0.5	3300	810	140	42.6	16.4
	1.0	ca. 10 ⁴	3200	550	160	46.0
Co ²⁺	nil	1700	440	74	23.7	7.0
	0.1	1600	390	70	21.3	6.5
	0.5	1400	340	61	18.7	6.1
	1.0	1200	310	54	17.5	5.9
Tl ⁺ *	nil	200	93	31.9	13.2	4.4
	0.1	195	92	31.5	12.1	3.2
	0.5	†	†	†	†	†
	1.0	†	†	†	†	†

*0.05 mmole.

†Precipitate.

Table 2. Distribution coefficients in solutions containing various amounts of thiourea and hydrochloric acid

Element	[Tu], <i>M</i>	[HCl], <i>M</i>					
		0.1	0.2	0.5	1.0	2.0	3.0
Pd ²⁺	nil	—	—	—	1.7	—	—
	0.01	—	—	—	1200	—	—
	0.1	10 ⁴	8500	3200	1100	440	350
	0.2	—	—	—	1010	—	—
	0.5	—	—	—	780	—	—
	1.0	—	—	—	520	—	—
	2.0	—	—	—	310	—	—
Au(III)*	0.01§	—	—	—	480	—	—
	0.1	6800	3700	1100	450	180	90
	0.2	—	—	—	410	—	—
	0.5	—	—	—	320	—	—
	1.0	—	—	—	220	—	—
	2.0	—	—	—	120	—	—

Table 2 (Continued)

Element	[Tu], M	[HCl], M					
		0.1	0.2	0.5	1.0	2.0	3.0
Sb ³⁺	nil	†	†	†	†	1.8	1.9
	0.1	610	540	130	32.4	5.4	2.5
	0.5	ca. 10 ⁴	8300	3900	624	62.4	16.6
	1.0	8300	9000	5400	1100	110	25.7
	2.0	6360	6360	4000	710	78	27.2
Bi ³⁺	nil	†	†	0.6	<0.5	<0.5	<0.5
	0.1	ca. 10 ⁴	ca. 10 ⁴	300	18.0	2.3	1.2
	0.5	> 10 ⁴	> 10 ⁴	3300	280	21.7	4.7
	1.0	> 10 ⁴	> 10 ⁴	4800	470	40.2	10.1
	2.0	ca. 10 ⁴	ca. 10 ⁴	3600	400	53	15.2
Cd ²⁺	nil	240	55	4.2	1.1	<0.5	<0.5
	0.1	830	220	28.0	6.9	3.5	2.2
	0.5	4100	1500	210	42.4	12.0	5.0
	1.0	3500	1700	260	60	14.6	7.8
	2.0	2500	1400	230	56	12.6	6.9
Zn ²⁺	nil	660	220	42	10.8	2.4	1.1
	0.1	960	280	42	11.3	1.7	1.1
	0.5	1700	530	90	23.4	7.4	3.9
	1.0	3500	1200	150	39.1	11.3	6.8
	2.0	5200	1700	220	57.1	15.6	9.1
Sn(IV)	nil	†	64	4.1	1.1	<0.5	<0.5
	0.1	†	†	1.4	<0.5	<0.5	<0.5
	0.5	†	300	46	12.1	5.0	3.8
	1.0	3300	1300	120	27.2	11.0	7.1
	2.0	2900	1800	260	55	18.0	11.2
Pb ²⁺	nil	†	†	40	3.8	0.9	<0.5
	0.1	2100	380	27.2	4.6	1.5	1.4
	0.5	ca. 10 ⁴	2400	180	†	†	†
	1.0	ca. 10 ⁴	3200	270	47.4	†	†
	2.0	ca. 10 ⁴	2300	180	46.2	9.7	4.4
In ³⁺	nil	700	84.3	5.9	1.8	1.0	1.0
	1.0	5600	1100	48.3	6.2	2.0	1.4
Ga ³⁺	nil	—	5900	330	44.6	8.5	—
	1.0	—	3800	220	35.0	6.2	—
Tl ⁺ ‡	nil	180	82	26.4	9.1	3.5	2.1
	0.1	190	86	24.9	10.3	4.2	2.3
	0.5	250	112	29.5	10.2	3.9	2.4
	1.0	†	†	†	†	†	†
Co ²⁺	nil	1700	440	64	16.1	5.1	2.9
	1.0	1200	280	49	13.0	4.2	2.6
U(VI)	nil	1300	300	47	12.0	2.3	2.1
	1.0	850	220	41	11.5	1.7	1.6
V(IV)	nil	740	190	36.7	10.4	3.3	2.3
	1.0	320	84	23.0	9.7	3.1	2.1
Mo(VI)*	nil	31.3	19.3	7.5	3.2	1.5	1.1
	0.1	—	120	31	6.7	2.3	—
	1.0	3600	580	320	143	94	58
Ru(III)	0.1	—	—	150	180	200	—
	1.0	—	504	470	440	190	98
Os(IV)*	0.1	—	13	15	14	—	—
	1.0	—	330	320	340	340	320
Ir(IV)*	0.1	3.5	3.2	2.7	3.6	5.2	—
	1.0	—	14	10	7.5	5.0	4.0
Rh(III)	nil	2.7	1.3	0.9	0.6	0.5	0.5
	0.1	67	—	54	51	—	—
	1.0	—	2500	670	450	360	160
Ge(IV), As(III), Re(VII)	nil	<1.0	<1.0	<1.0	<1.0	<1.0	<1.0
	1.0	<1.0	<1.0	<1.0	<1.0	<1.0	<1.0

*Oxidation state prior to reduction by Tu.

†Precipitate.

‡0.05 mmole.

§[Tu] corrected for amount consumed by reduction of element.

||Precipitation as sulphides for As(III) and Re(VII).

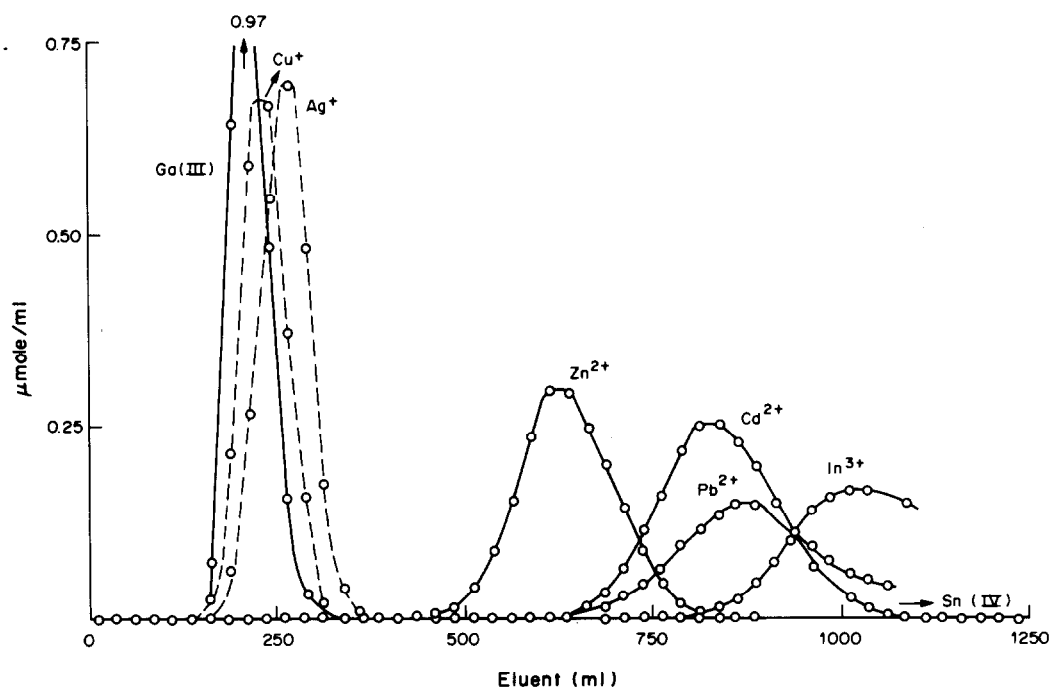


Fig. 1. Elution curve for a mixture of 0.05 mmole each of Ga^{3+} , Cu^+ , Ag^+ , Zn^{2+} , Cd^{2+} , Pb^{2+} , In^{3+} and Sn(IV) with $1.50M \text{HNO}_3$ - $1.0M \text{Tu}$ as eluent. Column: 10 g (43 ml) of AG50W-X4, 200-400 mesh, H^+ -form; internal diameter 2.0 cm; flow-rate 3.0 ± 0.3 ml/min.

Separation of Zn-Cd-Bi-Hg

Figure 2 shows an elution curve for mixture of 0.1 mmole each of Zn^{2+} , Cd^{2+} , Bi^{3+} and Hg^{2+} . The column dimensions, flow-rate, and conditions for sorption were the same as for Fig. 1, except that the initial equilibration of the columns was left out. The eluents used are shown in the figure.

Separation of Co-Pb-Sb-Te

The conditions were similar to those for Fig. 2. The elution sequence and eluents are shown in Fig. 3. A dense plug formed in the upper part of the column on contact with the eluent used for Co^{2+} , as a result of precipitation of most of the lead as the nitrate of a lead-Tu complex, presumably $\text{PbTu}_6(\text{NO}_3)_2$. This plug tended to separate from the bulk of

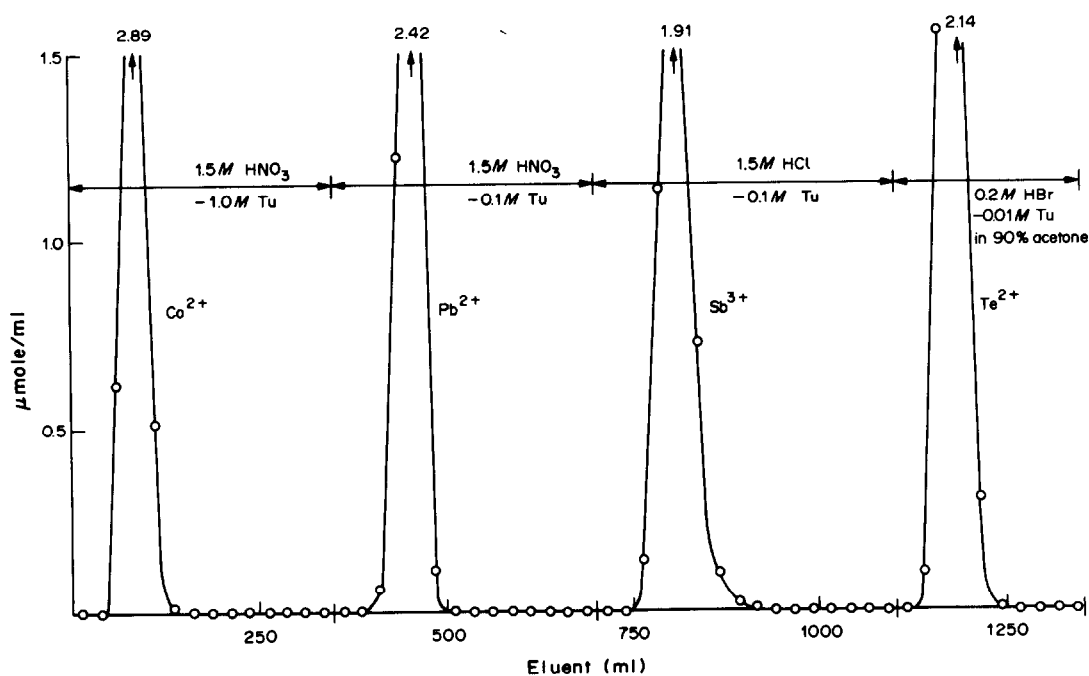


Fig. 2. Elution curve for Co^{2+} , Pb^{2+} , Sb^{3+} and Te^{2+} . Column and flow-rate as for Fig. 1.

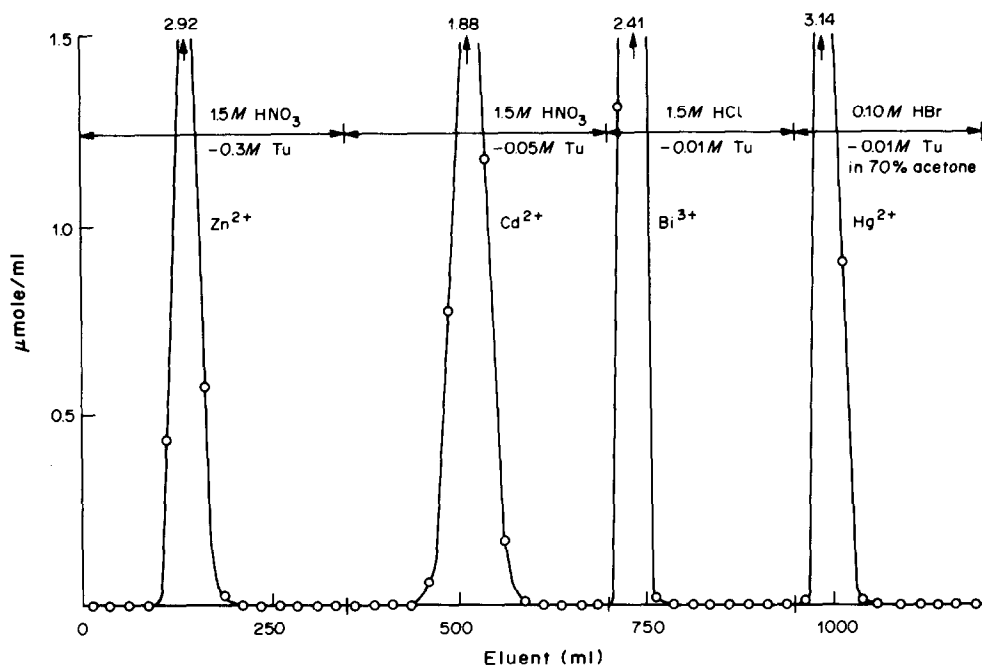


Fig. 3. Elution curve for Zn^{2+} , Cd^{2+} , Bi^{3+} and Hg^{2+} . Column and flow-rate as for Fig. 1.

the resin column because of the contraction caused by the increased nitric acid concentration during the first elution step. The subsequent elution of lead was then associated with channelling and serious tailing. This could be avoided by carefully breaking up the plug into fine particles with a long stirring rod, immediately after it had formed.

Separation of Ag–Cd–In–Au

The conditions were again similar to those for Fig. 2, and the eluent system and elution system and elution curve are shown in Fig. 4.

DISCUSSION

Thiourea is a neutral ligand as well as a reducing agent. It forms complexes with only a relatively small number of elements in aqueous solution. The fully co-ordinated complexes are cationic, and in several cases the central atom is present in an oxidation state lower than that normally encountered in solution. The formation of the complexes is generally associ-

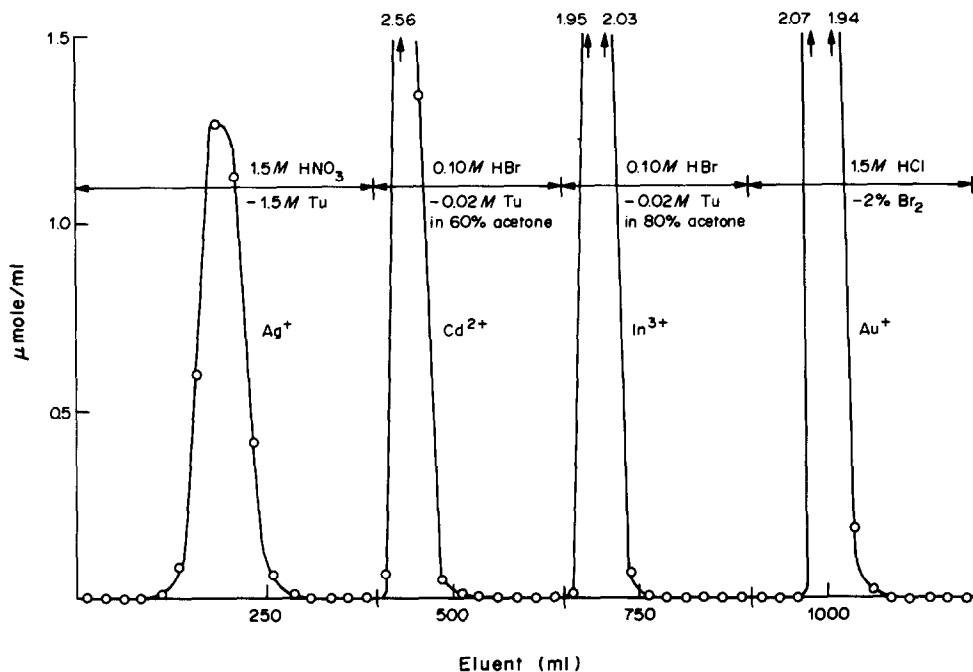


Fig. 4. Elution curve for Ag^+ , Cd^{2+} , In^{3+} and Au^+ . Column and flow-rate as for Fig. 1.

ated with an increase in the distribution coefficient. This increase may occur over different ranges of thiourea concentration, depending on the thermodynamic stability of the complexes. Those of Ag^+ , Au^+ , Pd^{2+} and Hg^{2+} , and, from evidence presented elsewhere,^{1,2} Cu^+ , Pt^{2+} and Te^{2+} , are formed essentially quantitatively at $0.01M$ Tu or lower concentration, provided Tu remains in excess. Zn^{2+} , Pb^{2+} , In^{3+} and Sn(IV) require $1.0M$ Tu or more, and the complexes of Cd^{2+} , Bi^{3+} and Sb^{3+} are formed over an intermediate range of Tu concentrations, 0.01 – $0.1M$. For a few additional elements, *viz.* Mo(VI) , Ru(III) , Os(IV) , Rh(III) and Ir(III) , the distribution coefficients in the presence of Tu are kinetically controlled,^{1,2} and are not included in the present discussion. No other elements except technetium and polonium are known to form significantly stable complexes with Tu in aqueous solution. Thallium(I) precipitates in the presence of relatively small amounts of Tu, as the complex salt TlTu_2X , where X is nitrate, chloride, *etc.* Elution experiments with sub-mg amounts of Tl^+ showed an increase of not more than 10% in the distribution coefficient in up to $1.0M$ Tu. This may indicate that Tl^+ forms a weak complex with Tu.

Selenates and selenites were reduced to red selenium under all conditions investigated. Arsenic(III) and rhenium(VII) show no enhanced sorption in the presence of Tu, but the acid-insoluble sulphides are partially precipitated within 24 hr in solutions containing more than $0.5M$ hydrochloric or nitric acid, apparently by hydrogen sulphide formed as a product of the acid-catalysed hydrolysis of Tu.

Effect of thiourea concentration

The distribution coefficients for most elements show a decrease with increasing Tu concentration. In the case of Co^{2+} and other ions which do not form stable complexes with Tu in aqueous solution, this decrease is quite small, and not associated with an initial increase such as is observed with ions forming more stable thiourea complexes. The slight decrease in the D -values of Co^{2+} , *etc.*, can probably be explained by the fact that thiourea is a strong dipole, which competes for exchange sites in the resin. In other cases, the decrease occurs after the D -values have reached a maximum, and may then be quite significant. This is most noticeable for elements which show markedly enhanced sorption from $0.01M$ Tu media. For Hg^{2+} , Pd^{2+} and Au^+ the decrease becomes apparent at $[\text{Tu}] > 0.1M$, but the values remain relatively high. Therefore, these elements cannot be effectively eluted with aqueous mixtures of Tu and hydrochloric or nitric acid within the concentration limits imposed by the solubility of Tu and its resistance to oxidation and hydrolysis. Previous evidence,^{1,2} together with preliminary elution experiments using, *e.g.*, $1.5M$ hydrochloric acid– $1.0M$ Tu, suggested that the behaviour of Pt^{2+} and Te^{2+} was similar to that of Pd^{2+} . For Ag^+ , the decrease in

D -values with increasing Tu concentration begins at well below $0.1M$ Tu concentration, and continues in such a way that elution is satisfactorily obtained with a sufficiently high Tu concentration ($\geq 1.0M$), in $1.5M$ nitric acid (Figs. 1 and 4). The abnormal maximum in the sorption of Ag^+ as a function of Tu concentration has already been reported by Maes and Cremer.⁴ They arrived at the tentative conclusion that Ag^+ is sorbed as a bi- or poly-nuclear complex in the presence of an insufficient excess of Tu, and as a mononuclear and less strongly sorbed complex when the concentration of Tu is increased. Previous evidence,^{1,2} together with the data in Fig. 1, indicate that the behaviour of Cu^+ in the presence of Tu closely resembles that of Ag^+ .

In general, the Tu concentrations used to effect a particular separation were made as low as possible. In certain instances, other considerations posed restrictions on the lowest Tu concentration that could be used. For example, a minimum of about $0.1M$ Tu was required during all steps preceding the elution of Te^{2+} (Fig. 2), in order to prevent its partial conversion into the metal on the column. Once certain elements which form acid-insoluble sulphides, *e.g.*, Hg^{2+} , have been sorbed as their Tu complexes, they cannot be eluted quantitatively with thiourea-free acids, because of the precipitation of small amounts of their sulphides on the column.

Effect of different acids and their concentration

In general, the distribution coefficients and separation factors, $D_{\text{Me}}/D_{\text{Me}'}$, for two cations Me and Me' for which $D_{\text{Me}} > D_{\text{Me}'}$, decrease with increasing acid concentration at constant Tu concentration. It is therefore important to optimize the acid concentration in order to obtain the best separation factor for a particular pair of elements, and elute Me' with the minimum volume of eluent.

The distribution coefficients tend to be lower in hydrochloric acid than in nitric acid. This difference varies from element to element, and can be correlated with the competitive effect of the chloride ion as a ligand relative to that of the nitrate ion. Since this effect tends to reinforce the effect of thiourea, the best separations for the metals which form relatively weak complexes with Tu are obtained in nitric acid rather than hydrochloric acid. Bi^{3+} and Sb^{3+} are best eluted with hydrochloric or hydrobromic acid, and Pd^{2+} , Au^+ , *etc.* are best eluted with hydrobromic acid–acetone or bromine–hydrohalic acid mixtures.²

Summary of possible separations

Zn^{2+} , Pb^{2+} , Cd^{2+} , In^{3+} , Sn(IV) , Ga^{3+} . Figure 1 shows the separation of Ga^{3+} from Zn^{2+} , Pb^{2+} , *etc.*, with $1.5M$ nitric acid– $1.0M$ Tu. From previous work,³ gallium is known to be more strongly sorbed on AG50W resins than most other elements except thorium, zirconium, hafnium, chromium, scandium, yttrium, and the lanthanides, in up to $3.0M$ nitric acid. It should therefore be relatively easy to separate

Zn^{2+} , Pb^{2+} , *etc.* from most elements which, under comparable conditions, do not form complexes with Tu. Figure 1 thus illustrates a useful separation of Zn^{2+} , Pb^{2+} , *etc.* as a group from practically all elements normally regarded as major elements. Of the ions which form stable complexes with Tu, most will be retained together with Zn^{2+} , Pb^{2+} , *etc.*, the only exceptions among the ions tested being Ag^+ and Cu^+ , which are co-eluted with Ga^{3+} as indicated in Fig. 1.

The distribution coefficients in nitric acid media (Table 1) indicate that it should be possible to separate Zn^{2+} from Pb^{2+} , and Pb^{2+} from Cd^{2+} with separation factors of about 5, by using 0.5M Tu and 0.2M Tu respectively. This was confirmed by elution experiments. $Sn(IV)$ and In^{3+} tend to accompany Pb^{2+} at low, and Cd^{2+} at high Tu concentrations, and to separate these, alternative eluting agents have to be found for the separation of In^{3+} and Cd^{2+} , *e.g.*, 0.1M hydrobromic acid in 60% acetone,⁵ with or without a small amount of Tu, depending on the elements remaining on the column.

The amount of Pb^{2+} that can be tolerated in these separations is subject to rather severe limitations because its solubility decreases markedly with increasing concentration of both Tu and the acid. In hydrochloric acid media, the limited solubility of lead chloride causes further complications.

Bi^{3+} , Sb^{3+} . These elements can be separated easily from the previous group with dilute nitric acid containing 0.1M Tu (Figs. 2 and 3). The thiourea systems do not seem to offer a possibility for separating Sb^{3+} from Bi^{3+} with a separation factor larger than 2.

Au^+ , Hg^{2+} , Pt^{2+} , Pd^{2+} , Te^{2+} . These elements can be separated from either of the above groups by use of a very low Tu concentration, *e.g.*, 0.01M Tu (Figs 2 and 3). For the effective elution of Bi^{3+} and Sb^{3+} , and their separation from Au^+ *etc.*, it is preferable to use hydrochloric acid medium. The separation of Au^+ , Hg^{2+} , *etc.* from each other by using hydrobromic acid-Tu-acetone mixtures has been described in a previous paper.² For the quantitative elution of Au^+ , the use of bromine-hydrochloric acid mixture

is recommended on the basis of other observations reported earlier.²

Ag^+ , Cu^+ . The separation of Ag^+ and Cu^+ from Au^+ , Hg^{2+} , *etc.* by using hydrobromic acid-Tu-acetone mixtures has been described previously.² The present data show that aqueous acids containing a relatively high concentration of Tu, *e.g.*, 1.0M (Fig. 4), can be used for the same purpose. Their use is recommended for the elution of large amounts of Ag^+ or Cu^+ because large amounts of these elements tend to precipitate on the column on elution with, *e.g.*, 0.1M hydrobromic acid-0.01M Tu in 60% acetone.² At a high Tu concentration ($\geq 1.0M$), Ag^+ and Cu^+ can be eluted before Zn^{2+} , *etc.* (Figs. 1 and 4), but at low Tu concentrations ($\leq 0.1M$), the reverse is true, and at 0.01M Tu it should be possible to elute even Bi^{3+} and Sb^{3+} well ahead of Ag^+ and Cu^+ . A separation of Ag^+ and Cu^+ from each other does not appear to be possible in the presence of Tu.

As(III), *Re(VII)*. These species tend to form the corresponding sulphides in Tu-containing acids. Since they are also present initially as anions, they can be eluted well ahead of most other elements by using very dilute Tu solutions in acids, *i.e.*, under conditions in which the rate of hydrolysis of Tu is negligible.

Acknowledgements—The authors thank Mr R. Verheij for assistance in the determination of the distribution coefficients, and Mr H. Lachmann for the microanalysis of some of the precipitates obtained in the course of the present work.

REFERENCES

1. C. H.-S. W. Weinert, F. W. E. Strelow and R. G. Böhmer, *Talanta*, 1983, **30**, 413.
2. C. H.-S. W. Weinert and F. W. E. Strelow, *ibid*, 1983, **30**, 766.
3. F. W. E. Strelow, R. Rethemeyer and C. J. C. Bothma, *Anal. Chem.*, 1965, **37**, 106.
4. A. Maes and A. Cremer, *J. Chem. Soc., Faraday Trans. I*, 1975, **71**, 256.
5. F. W. E. Strelow, M. D. Hanekom, A. H. Victor and C. Eloff, *Anal. Chim. Acta*, 1975, **76**, 377.

A NEW METHOD FOR THE VOLTAMMETRIC DETERMINATION OF NITRITE

KURT KALCHER

Institut für Analytische Chemie, Karl-Franzens Universität, Universitätsplatz 1, A-8010 Graz, Austria

(Received 7 November 1985. Accepted 23 January 1986)

Summary—A voltammetric method is presented for the determination of nitrite by use of a carbon-paste electrode chemically modified with an anion-exchanger. Because it is possible to accumulate nitrite on the electrode surface, trace nitrite concentrations down to 1 ng/ml can be determined.

Prior to their determination electroactive ions can be preconcentrated on an electrode surface by means of ion-exchangers. When carbon-paste electrodes are used, the exchanger can be added to them as finely ground resins or as liquids. Copper,¹ iodide,² gold,³ iridium⁴ and hexacyanoferrate(II,III)⁵ have been determined in this way. Nitrite produces a voltammetric current at carbon-paste electrodes⁶ and therefore offers scope for determination by this method. This paper deals with the experimental conditions required and attempts to define the fundamental relations between parameters such as the preconcentration time, concentration and voltammetric current.

EXPERIMENTAL

Apparatus

A polarographic analyser PAR 264A (Princeton Applied Research) was used throughout, with an automatically controlled electrode assembly⁷ built in our laboratory, and consisting of a "Plexiglas" compartment and a 20-ml titration vessel (EA 880-20 from Metrohm). The reference electrode was a saturated calomel electrode (SCE) connected to the test solution with a 1M potassium chloride salt bridge. A platinum wire was used as counter-electrode. The current was either registered on an x,y-recorder or transferred to an HP 1000 minicomputer after analogue-to-digital conversion by an appropriate interface.⁸

For the preconcentration 50-ml beakers were used, equipped with PTFE-coated stirring bars (30 mm long, 7 mm diameter) driven by a variable-speed magnetic stirrer. A special holder for the electrode allowed its surface to come into contact with the test solution in the beakers.

Reagents

Demineralized water was doubly distilled in a quartz still and finally passed through a Barnstead "Nanopure" cartridge for final purification. All chemicals were of analytical grade (p.a., Merck) except potassium chloride and sodium hydroxide, which were of higher quality (*Suprapur*, Merck). Nitrite standards (concentration 1000 ppm) were prepared by dissolving 37.00 mg of potassium nitrite and 0.02 ml of 30% sodium hydroxide solution (for stabilization) and making up to volume in a 20-ml standard flask with water which had been deaerated with nitrogen (99.999% pure). Nitrogen was also passed through the solution during the dissolution in order to avoid oxidation of nitrite to nitrate. When stored under nitrogen in the dark this stock solution was usable for at least one day. Solutions of lower concen-

trations were prepared immediately before use. The water used for dilution, preconcentration and measurement was also deaerated.

Working electrode

The electrode was a commercially available Monien type carbon-paste electrode⁹ (EA 267 from Metrohm) with a glass tube as filling reservoir and a feed nut for expelling new paste. This type provided the highest degree of reproducibility of the effective surface area.

The paste was prepared from 5 g of spectroscopic grade carbon powder (RWB, Ringsdorf-Werke, Bonn-Bad Godesberg, West Germany), 1.8 ml of liquid paraffin ("Uvasol" from Merck) and 0.235 ml of the liquid anion-exchanger tricaprylmethylammonium chloride (Aliquat 336, Fluka) by mixing them thoroughly to form a homogeneous paste. Commercially available carbon paste (EA 267 C from Metrohm) to which 0.05 ml of ion-exchanger per gram had been added, could also be used.

Renewing the electrode surface

A length of about 3 mm of paste was extended and wiped off, then the surface was smoothed over with a PTFE spatula. The surface was prepared as reproducibly as possible with respect to smoothness and area in order to obtain coherent results. The electrode was then conditioned in a well-stirred mixture of 20 ml of water and 0.04 ml of saturated potassium chloride solution for 30 sec, to obtain reproducible quality of the surface. It was then rinsed briefly with water.

Preconcentration

The conditioned electrode was exposed for the required time to the deaerated, well-stirred (300 rpm) nitrite-containing test solution, removed, and rinsed with water for about half a second. A stream of nitrogen was bubbled through the solution during this step to avoid oxidation processes; this is adequate protection in this procedure and avoids the trouble of working with nitrogen-flushed boxes.

Finally, the electrode was placed in the voltammetric cell and connected to the polarograph.

Voltammetry

The voltammetric measurements were made in aqueous medium with 20 ml of water containing 0.04 ml of saturated potassium chloride solution as supporting electrolyte. Deaeration with nitrogen for 2 min at the beginning of a series of measurements ensured sufficient removal of oxygen from the solution. The voltammetric sweep was started immediately after installation of the electrode in the voltammetric cell. Cyclic voltammetric curves (CV) were recorded from +0.4 to +1.05 V vs. SCE, at a scan-rate of 50 mV/sec, starting in the anodic direction. For quantitative analyses as

well as for investigations of quantitative relations the anodic differential-pulse mode (ADPV) was used owing to its high sensitivity. The initial potential was +0.4 V and the final +1.0 V vs. SCE, and the pulse height 50 mV. A scan-rate of 10 mV/sec and a drop time of 0.5 sec were selected. The current range was set according to the expected peak current.

Evaluation of peak heights

High peaks resulting from large concentrations were analysed with relative ease by the tangent fit method, which was applied to the recorder output, but this method resulted in a very high degree of error for small peaks because of their location on a rising slope of the background current. Therefore, the baseline was synthesized and subtracted digitally from the curve.⁸ The method of subtracting a recorded blank yields similar results if its baseline is of the same shape as that for the test measurement.

Quantitative determinations

The complete procedure—renewal and conditioning of the electrode, recording the background (blank), preconcentration, and measurement of the accumulated nitrite—was applied to the test solution, and repeated after addition of two separate specific amounts of nitrite (standard addition method). The concentration was calculated from the increase in the peak height. The precision could be increased by repeating each cycle and taking the arithmetic means of the peaks.

On average, the time required for a complete analysis with two additions of standard is about 30–40 min.

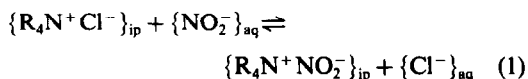
RESULTS AND DISCUSSION

Choice of the ion-exchanger

It is well known that nitrite is very labile when exposed to acid, as it decomposes rapidly into nitrogen oxides and nitric acid. This implies that a weakly basic ion-exchanger, which has its optimum working range at pH < 7, would not be applicable for modification of the electrode. In addition, secondary amine functional groups (as, for example, in the liquid ion-exchanger Amberlite LA2) would react chemically with nitrite to form *N*-nitroso compounds. Hence only a strongly basic ion-exchanger with permanent ammonium groups, even in alkaline medium, should be suitable for ion-pair association with nitrite.

As shown elsewhere,³ liquid ion-exchangers are preferable to resins for electrode modification as the liquid phase exposes many more functional groups to the solution than do particles in a matrix, resulting in a substantial increase in sensitivity. Additionally, the method presented here requires a very high degree of homogeneity of the carbon paste, which can be obtained only by use of a liquid. For these reasons Aliquat 336 is a suitable ion-exchanger for the accumulation of nitrite at the electrode surface.

Sorption of nitrite



Equation (1) describes the ion-exchange process at the carbon paste–solution interface. The subscript ip

indicates the ion-pair on the surface of the electrode, and aq the solvated ion in solution. This reaction involves no electron transfer but is purely physicochemical, so no potential needs to be applied during the preconcentration step.

The electrochemical behaviour of the accumulated nitrite can be monitored by cyclic voltammetry (Fig. 1). The maximum in the first cycle at +0.81 V vs. SCE results from the oxidation to nitrate. The curve obtained represents a typical irreversible process, as the resulting nitrate is also sorbed as an ion-pair but is not re-reduced to nitrite, since no reduction current can be observed within the recorded potential region. This is in agreement with the fact that reduction of nitrate takes place only at very negative potentials even with catalysts such as cadmium, uranium, *etc.*¹⁰ Thus, in the ensuing cycles the maximum is hardly visible, as almost all the sorbed nitrite has already been oxidized. Further cycles show only the current obtained when monitoring the plain, unloaded electrode.

Scans in the differential-pulse mode are shown in Fig. 2. The peak potential is about +0.78 V vs. SCE and is only slightly dependent on the peak current.

Regeneration and stability of the electrode

After the voltammetric measurement the surface of the electrode must be returned to its initial state to provide identical conditions for quantitative evaluation. For this purpose the reproducibility of the surface was investigated (Fig. 3). As the amount of nitrite remaining in the carbon paste is very small (see also Fig. 1) it does not interfere seriously with ensuing measurements as a result of a “memory” effect. The initial state cannot be successfully re-established by treating the electrode with a saturated sodium chloride solution, the anion of which should replace all other sorbed anions, especially nitrate [curve (b) of Fig. 3]; the decrease in the peak current with repeated use is drastic. It is not possible to determine whether nitrate still blocks a large number of exchanging groups or the surface itself changes during the procedure because exchanger dissolves from the surface into the solution. Other attempts to restore the functional groups, *e.g.*, by acid or alkaline treatment, also fail. Only mechanical renewal of the surface gives satisfactory reproducibility [curve (a) of Fig. 3]. If the procedure is applied carefully the deviations are usually below 3.5% for nitrite concentrations > 100 ng/ml. Generating a new surface is the only one of the methods investigated that at all yields congruent results.

An ensuing conditioning step with dilute potassium chloride solution improves the homogeneity of the electrode; the uniformity of the surface is apparently increased.

Time dependence of the accumulation process

According to equation (1) the ion-exchange reaction is a purely physicochemical one and therefore

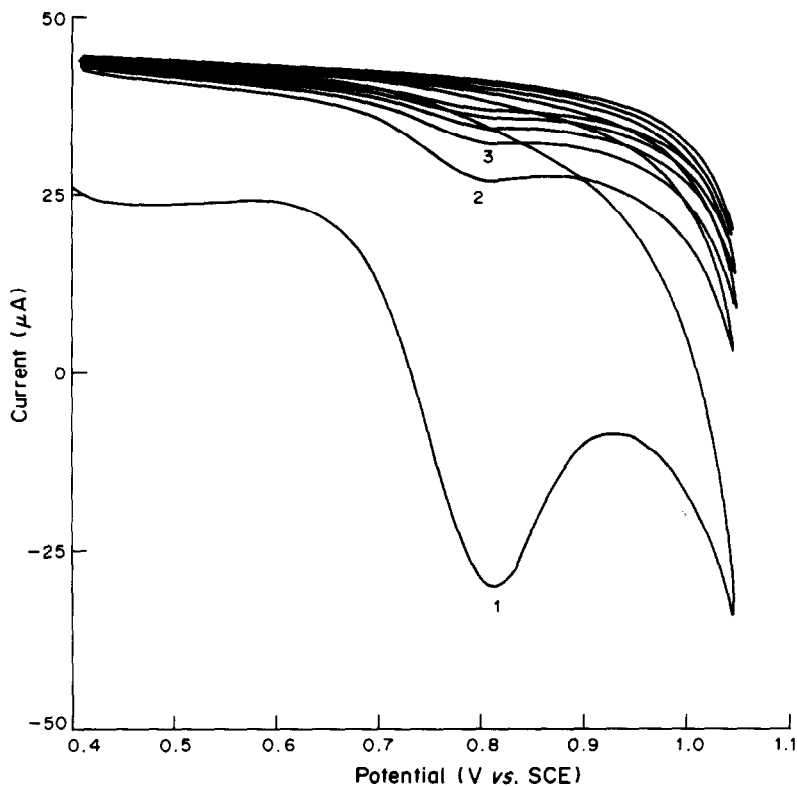


Fig. 1. Cyclic voltamperogram of nitrite accumulated at a modified carbon-paste electrode; accumulation time 1 min; NO_2^- concentration, 5 $\mu\text{g/ml}$.

governed by the law of mass action. This implies the existence of a dynamic equilibrium characterized by equality of the rates of sorption and desorption. As the reaction proceeds slowly, the dependence of the signal on the accumulation time can be observed. Figure 4 shows the relation between differential-pulse voltammetric peak current and the time used for preconcentrating the nitrite, for two different nitrite

concentrations. The linear section at the beginning of the curve soon becomes hyperbolic, approaching as limiting value. This is, of course, due to the fact that the maximum amount that can be preconcentrated is determined by the equilibrium constant for equation (1). Thus for each concentration there is a definite amount which can actually be accumulated and

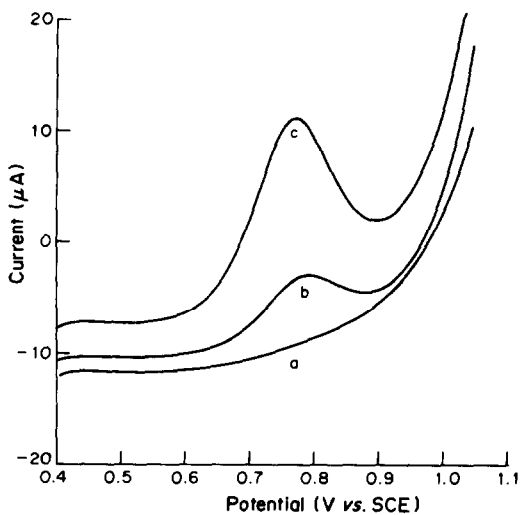


Fig. 2. Differential pulse voltamperograms of nitrite sorbed with an accumulation period of 30 sec; (a) background; (b) NO_2^- 200 ng/ml; (c) NO_2^- 400 ng/ml.

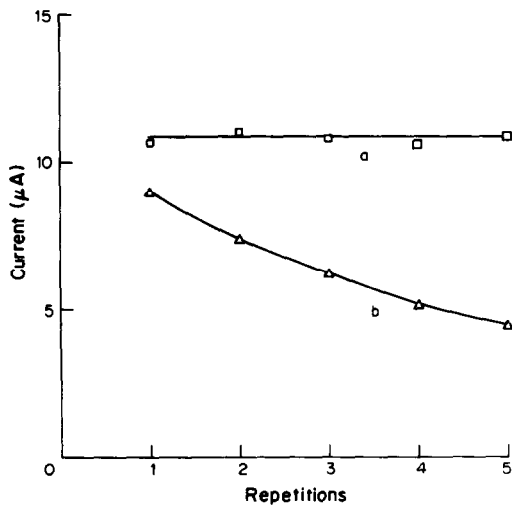


Fig. 3. Reproducibility of performance of the electrode surface on repeated use in ADPV; NO_2^- concentration 500 ng/ml with accumulation for 30 sec; (a) mechanical renewal of the surface; (b) regeneration by exposure to saturated sodium chloride solution for 1 min.

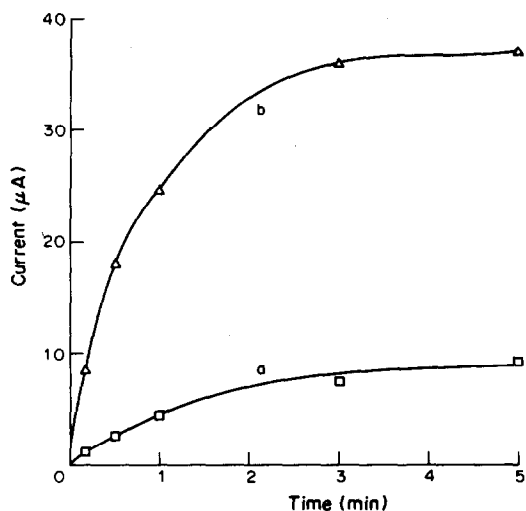


Fig. 4. Dependence of the peak current in ADPV on the accumulation time; (a) NO_2^- 100 ng/ml; (b) NO_2^- 1 $\mu\text{g}/\text{ml}$.

which depends primarily on the affinity for the ion-exchanger. Therefore, the curves shown here are not directly comparable with the time-dependences of stripping methods (anodic or cathodic stripping voltammetry, ASV, CSV) where the signals are often directly proportional to the pre-electrolysis time over a wide range. It is evident that the speed of stirring during the accumulation influences the shape of the curve. If the solution is not agitated, diffusion controls the rate of ion-exchange; the faster the stirring the sooner the maximum sorbable amount of nitrite will be reached. The position of the equilibrium itself, of course, is not affected by the stirring.

When only small amounts of nitrite (far from the equilibrium level) have been accumulated, the sorption should be linearly dependent on the nitrite

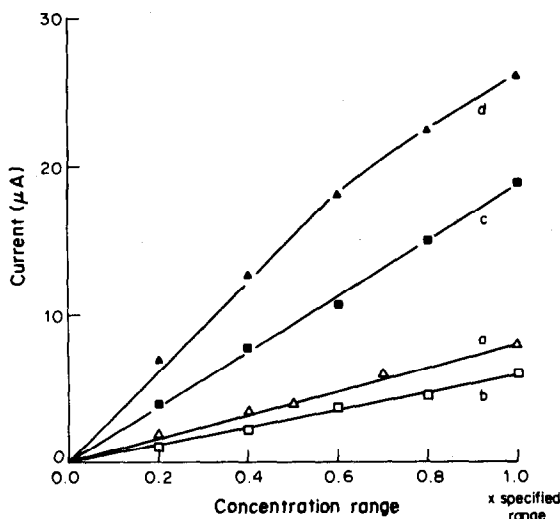


Fig. 5. Relation between concentration and peak current in ADPV; accumulation times and concentration ranges: (a) 3 min, NO_2^- 0–10 ng/ml, 10 \times expansion of current scale; (b) 2 min, NO_2^- 0–100 ng/ml; (c) 30 sec, NO_2^- 0–1 $\mu\text{g}/\text{ml}$; (d) 5 sec, NO_2^- 0–10 $\mu\text{g}/\text{ml}$.

concentration, as explained in the following. If the solution is well stirred, the nitrite concentration in the solution is homogeneous. Further, if only small amounts of nitrite have been exchanged, the large number of chloride-loaded R_4NCl groups is quasi-constant ($d[\text{R}_4\text{NCl}]/dt$ is almost zero), which implies linear proportionality between the amount of nitrite transferred ($d[\text{R}_4\text{NNO}_2]/dt$) and the nitrite concentration in the solution if the kinetic dependence on the latter is pseudo first-order. Thus, to obtain a linear relationship between nitrite concentration and peak current, short deposition times must be selected to avoid saturation effects.

Dependence of the signal on the nitrite concentration

For determinations with internal standards (standard addition method) it is essential that there is a linear relation between concentration and peak current. Otherwise, external standards (calibration curves) have to be used, and problems are then often caused by matrix effects, in which case, the calibration must be performed with matrix-matched standards. The relation between nitrite concentration and peak current in the ADPV, for selected accumulation times, is displayed in Fig. 5. Linear proportionality exists over the range from 1 ng/ml to 6 $\mu\text{g}/\text{ml}$, with appropriate preconcentration. Therefore, the standard addition procedure is the most valid method for evaluating concentrations within this range. Otherwise the solution must be appropriately diluted before analysis.

Accuracy and detection limit

Table 1 lists the recovery of nitrite with different methods. For comparison, a determination of 500 ng/ml nitrite by a standard photometric procedure [using sulphanilamide and *N*-(1-naphthyl)-ethylenediamine].¹¹ Low concentrations have a higher relative deviation than high ones. With an increasing number of either replications or standard additions the accuracy is increased. For the methods under consideration duplicate measurements with addition of two standards yield the best results. The estimated maxima of relative errors of a single determination with calibration curves are about 3% for 500 ng/ml, 7% for 50 ng/ml and 15–20% for 5 ng/ml nitrite.

The detection limit lies at about 1 ng/ml nitrite for all methods. This corresponds to 0.3 ng/ml ($2.2 \times 10^{-8} M$) nitrite-nitrogen content. Lower concentrations are hardly detectable since the ratio of peak height to background current falls below the resolution ability of the apparatus. As stated above, excessive deposition times do not improve the sensitivity, as the maximum amount which can be exchanged is limited by the equilibrium constant. Compared with other methods of determining nitrite, for example, spectrophotometry of the coupled diazo-compound, the method is very sensitive and shows a wide range of linearity between concentration and signal. Ion chromatography in its stan-

Table 1. Recovery of nitrite with different methods [a—calibration graphs; b—standard-addition method; c—spectrophotometry with sulphanilamide and *N*-(1-naphthyl)-ethylenediamine]; each standard increment was half the amount of nitrite in the solution

Concentration, ng/ml	Method	Determinations	No. of standard increments	Found, ng/ml	Relative error, %
500	a	1	0	492	-1.6
50	a	1	0	48.3	-3.4
5	a	1	0	5.4	+8.0
500	a	3	0	496	-0.8 (2.0)†
50	a	3	0	48.9	-2.2 (2.8)†
5	a	3	0	5.3	+6.0 (15.4)†
500	b	1	1	478.6	-4.3
50	b	1	1	52.9	+5.9
5	b	1	1	6.0	+20.0
500	b	1	2	496.0	-0.8
50	b	1	2	51.0	+2.0
5	b	1	2	5.8	+16.0
500	b	2	2	498.0	-0.4
50	b	2	2	50.5	+1.0
5	b	2	2	5.6	+12.0
500	c	2	0	495.0	-1.0

†The values in brackets denote the coefficient of variation.

dard mode has a higher detection limit (30–50 ng/ml) but is faster than the present method and matches it in sensitivity if more sophisticated arrangements, such as use of ion-exchange precolumns¹² or phosphorescence-quenching detection¹³ are used. Other voltammetric procedures, such as polarographic reduction of nitrite in acidic medium,¹⁴ polarography with sulphanilic or orthanilic acid¹⁵ or 2,6-xyleneol,¹⁶ as well as sensing with a platinum electrode modified by chemisorption of iodine^{17,18} and sealed with polyvinylpyridine, are less sensitive.

Interferences

All anionic species in the solution interfere with the accumulation process of nitrite in that they compete for the active sites of the ion-exchanger, but if they are present at low concentrations and have low affinity for the exchanger they cause no notable changes in the nitrite signal responses. Table 2 dis-

plays the alterations in peak current when the test solution contains other ionic species at various concentrations. The interference of almost all ions which were examined is remarkably high, but this is not as disappointing as it might look. In many cases the linear relation between peak current and concentration is maintained and interference is confined to a mere decrease in sensitivity, as a function of interferent concentration; in such cases the standard additions method can be used. Of course, this must be checked in each case, depending on the problem. Only when higher concentrations of bromide, iodide and cyanide are present does the determination of nitrite become impossible, mainly on account of a large overlapping peak from the interfering species. For media containing large amounts of these ions other methods for determining nitrite must be applied.

The method could be extended to determination of nitrate, by means of its prior reduction to nitrite.

Table 2. Interferences in the determination of 100 ng/ml NO₂⁻ (corresponding to 2.2 × 10⁻⁶M) accumulated for 1 min at an interfering ion concentration of 10 μg/ml

Interferent	Salt added	Interferent concentration, 10 ⁻⁴ M	Change in peak current, %
Cl ⁻	KCl	2.8	-58
Br ⁻	KBr	1.2	-92
I ⁻	KI	0.8	*
SO ₄ ²⁻	K ₂ SO ₄	1.0	-20
NO ₃ ⁻	KNO ₃	1.6	-66
ClO ₄ ⁻	NaClO ₄	1.0	-50
H ₂ PO ₄ ⁻	KH ₂ PO ₄	1.0	-50
CN ⁻	KCN	3.8	*
[Fe(CN) ₆] ⁴⁻	K ₄ [Fe(CN) ₆]	0.4	-68
CH ₃ COO ⁻	CH ₃ COOK	1.7	-40

The decrease in current was due to ion-exchange selectivity; ions marked with an asterisk gave voltammetric oxidation reactions overlapping that of nitrite.

REFERENCES

1. J. Wang, B. Greene and C. Morgan, *Anal. Chim. Acta*, 1984, **158**, 15.
2. K. Kalcher, *Z. Anal. Chem.*, 1985, **321**, 666.
3. *Idem*, *Anal. Chim. Acta*, 1985, **177**, 175.
4. *Idem*, submitted for publication in *Z. Anal. Chem.*
5. *Idem*, submitted for publication in *Analyst*.
6. C. Olson and R. N. Adams, *Anal. Chim. Acta*, 1960, **22**, 582.
7. K. Kalcher, *Z. Anal. Chem.*, 1986, **323**, 238.
8. K. Kalcher and C. Jorde, *Computers & Chemistry*, in press.
9. H. Monien, H. Specker and K. Zinke, *Z. Anal. Chem.*, 1967, **225**, 342.
10. M. E. Bodini and D. T. Sawyer, *Anal. Chem.*, 1977, **49**, 485.
11. *Deutsche Einheitsverfahren zur Wasser-, Abwasser- und Schlamm-Untersuchung*, 3rd Ed., p. D10. Verlag Chemie, Weinheim, 1982.

12. P. R. Haddad and A. L. Heckenberg, *J. Chromatog.*, 1985, **318**, 279.
13. C. Goojer, P. R. Markies, J. J. Donherbroek, N. H. Velthorst and R. W. Frei, *ibid.*, 1984, **289**, 347.
14. R. Annino and J. E. McDonald, *Anal. Chem.*, 1961, **33**, 475.
15. S. T. Sulaiman, *ibid.*, 1984, **56**, 2405.
16. A. M. Hartley and R. M. Bly, *ibid.*, 1963, **35**, 2094.
17. J. A. Cox and P. J. Kulesza, *J. Electroanal. Chem. Interfacial Electrochem.*, 1984, **175**, 105.
18. *Idem*, *Anal. Chim. Acta*, 1984, **159**, 349.

DETERMINATION OF AMMONIUM IN A BUDDINGTONITE SAMPLE BY ION-CHROMATOGRAPHY

PAUL R. KLOCK* and PAUL J. LAMOTHE
U.S. Geological Survey, Menlo Park, CA 94025, U.S.A.

(Received 16 September 1985. Revised 4 December 1985. Accepted 23 January 1986)

Summary—An ion-chromatographic method for the direct determination of ammonium, potassium, and sodium in geologic materials is described. Samples are decomposed with a mixture of hydrofluoric and hydrochloric acids in a sealed polycarbonate bottle heated in a microwave oven. The ion-chromatograph separates the cations and determines them by conductivity measurement. The ammonium concentrations thus determined have been verified by use of an ammonia-specific electrode. A total of 32 analyses of ammonium salts by both techniques showed an average error of -4% , with a relative standard deviation (RSD) of 6% . The ammonium concentrations found in a buddingtonite sample had an RSD of 2.2% and their mean agreed with that obtained by the Kjeldahl method. By use of the prescribed dilution of the sample, detection limits of 0.1% can be achieved for all three cations.

Cenozoic basalt and andesite samples that have been hydrothermally altered by ammonia-containing hot-spring waters generally have an ammonium ion content of a few per cent. Ammonium minerals are now postulated as pathfinders for gold in hydrothermal deposits.¹ The study reported here resulted from an increasing need for analytical data to test current theories regarding gold deposits. The ammonium ion, which has a radius of 1.43 \AA , substitutes for sodium (0.97 \AA) and potassium (1.33 \AA) ions in alkali feldspars.²⁻⁴ An ammonium aluminosilicate mineral, $(\text{NH}_4)\text{AlSi}_3\text{O}_8 \cdot 0.5\text{H}_2\text{O}$, known as buddingtonite, was first found near a hot-spring mercury-ore deposit at Sulfur Bank, Lake County, California.^{5,6} Originally, the ammonium in buddingtonite was determined by the Kjeldahl procedure for total nitrogen.⁶ Other methods used for determination of total nitrogen or ammonia in rocks and silicate minerals have included decomposition with hot pyrophosphoric acid,⁷ sulphuric acid in sealed glass tubes,⁸ sodium hydroxide fusion in a closed system,⁹ combustion and gas chromatography,¹⁰ and thermal-neutron activation.^{11,12} These methods are time-consuming and usually require several hours just for sample decomposition. One of them,⁹ which differentiates the forms of nitrogen present, used decomposition in a closed polyethylene bottle, followed by neutralization, distillation, reduction, and finally colorimetric determination of ammonia by the Nessler method. However, the total nitrogen content in unaltered rocks ranges from 10 to $30 \mu\text{g/g}$ and is apparently independent of rock type, and these trace analysis methods are less suitable for the ammonium levels found in buddingtonite *etc.*

To obtain a rapid, accurate, and direct measurement of ammonium in geological samples, we have developed a method which reduces sample decomposition time to a few minutes and eliminates all sample-pretreatment steps. The method also determines potassium and sodium in the sample. Polycarbonate bottles and a microwave oven are used for sample dissolution, and ion-chromatography (IC) for cation separation and detection. Microwave ovens are currently being used routinely in fast and efficient dissolution of various samples, including silicates.¹³⁻¹⁶ IC determination of ammonium has been well documented,¹⁷⁻²⁰ but its application to the analysis of rocks and minerals has been limited to the determination of anions²¹⁻²⁶ and of anions and cations in fluid inclusions.²⁷ We have also investigated an ammonia-specific electrode as an alternative detection device for the determination of ammonium.

EXPERIMENTAL

Apparatus

Samples were decomposed in 250-ml polycarbonate bottles fitted with polypropylene screw caps (Nalge† No. 3122-0250). The screw threads were double-wrapped with Teflon tape to ensure a tight seal.

Heating was by means of a 650-W, 0.04-m^3 capacity microwave oven equipped with a removable revolving carousel. To purge the oven with compressed air during and after the heating cycle, approximately 14 lengths of 3-mm outer diameter plastic tubing were inserted through the existing ventilation holes in the side of the microwave-oven cavity. These small tubes were brought out of the oven through the rear ventilation slots and inserted into two lengths of 9-mm bore tubing. All exposed metal parts inside the oven were covered with plastic tape to prevent corrosion. The oven was placed in a fume hood to provide for adequate ventilation.

A polyethylene food container (Tupperware No. 1257-6 cake carrier), the top of which can be sealed to prevent the release of any fumes escaping from the polycarbonate bottles, was used to construct a bottle rack. The rack accommodated 12 bottles arranged in an annular pattern.

*Author for correspondence.

†Any use of tradenames and trade marks in this report is for descriptive purposes only and does not constitute endorsement by the U.S. Geological Survey.

Because the microwave energy inside the oven cavity was inhomogeneously distributed, no sample bottles were placed in the centre of the rack. This arrangement ensured that all samples were subjected to the same microwave flux.

IC measurements were made with a Dionex model 16 IC with conductivity detection, equipped with two cation-separator columns (6 × 250 and 9 × 250 mm) and a 9 × 250 mm suppressor column. All three columns were supplied by Dionex (part nos. 30014, 30192 and 30015, respectively); the resin of the separator column was comparable to that in their CS-1 column. The eluent was 0.008M nitric acid at a flow-rate of 3.07 ml/min. Other conditions were: 100- μ l sample loop, applied pressure 1.4–2.8 MPa, a 1-V full-scale recorder input, and a recorder chart speed of 1.0 cm/min. A conductivity-detector scale of 10 μ S was used along with the strip-chart recorder for peak height measurement.

Potentiometric measurements were made with an Orion ammonia electrode, model 95-10, and a Corning pH-meter. The pH of all sample and standard solutions was adjusted to above 11 with sodium hydroxide.

Reagents

Stock solutions (1000 μ g/ml) of ammonium, potassium and sodium ions were prepared from the chlorides and demineralized water. More dilute standard solutions were prepared just before use. Analytical grade reagents were used throughout.

Procedure

Place a 0.100-g sample, ground to pass 200 mesh, in a 250-ml polycarbonate bottle. Add 1 ml of 3M hydrochloric acid and 4 ml of 40% hydrofluoric acid. Tightly cap the bottles and place them in the bottle rack. Place the covered rack (containing 12 samples) on the carousel in the microwave oven. Turn on the compressed air and heat the samples at a high oven setting (650 W) for 30 sec. Remove the bottles, retighten the caps, and return them to the oven. Heat once more at the 650-W setting for 2 min. Allow the compressed air to purge the oven cavity for another 2 min before removing the sample rack. Remove the bottles from the rack and allow to cool.

For subsequent IC analysis, dilute the sample solutions with 245 ml of water. Mix thoroughly and inject the solutions directly into the IC.

For potentiometric analysis, just before measuring add 15 ml of 10M sodium hydroxide to each of the cooled sample bottles removed from the microwave oven, and then 230 ml of water. Mix thoroughly, cool, and measure directly with the ammonia-specific electrode. Care should be exercised because, if left to stand overnight, the alkaline solution will crack the bottom of the polycarbonate bottle.

Caution. During the dissolution, some acid fumes may leak from around the bottle caps. This leakage will create a health hazard unless the microwave oven is properly vented to a fume hood. The melting point of polycarbonate is 135°. Care must be taken to ensure that the bottle contents remain below this temperature, especially if the heating time is increased or the volume of solution in the microwave cavity is reduced. Therefore, if fewer than 12 samples need to be decomposed, bottles containing water or reagent blanks must be included to maintain a constant volume of solution in the oven during each run.

RESULTS AND DISCUSSION

Sample decomposition

Use of sealed polycarbonate bottles for decomposition eliminates losses of nitrogen, such as could occur through bumping during a Kjeldahl digestion, and prevents ammonia contamination from the laboratory air. It also improves the efficiency of decom-

position and helps retain the volatile species. The sample is in an acidic medium throughout the decomposition procedure. Transfer of sample contents from the polycarbonate bottles to volumetric glassware should be avoided because of the hydrofluoric acid present; etching of the glassware prevents accurate determination of the alkali-metals. The samples are diluted to final volume (250 ml) directly in the polycarbonate bottle or after transfer to plastic containers.

Validation of the procedure

We investigated the effectiveness of the decomposition procedure by determining the amount of ammonium recovered from known weights of reagent grade ammonium chloride. The results are listed in Table 1. Although the values were somewhat scattered, the mean recovery was 98.1%, with a relative standard deviation (RSD) of 2.9%.

Sample weights and operating conditions for the IC were optimized by assuming an abundance of 5% ammonium in the solid sample. After the decomposition step, dilution to 250 ml was required for the ammonium to give a 10- μ S signal and to be within the working range of the calibration graph (prepared from pure standard solution covering the range 1–15 μ g/g).

To determine whether ammonium is quantitatively released from a geological material, we analysed a buddingtonite sample of known ammonium content. This sample, from San Mateo County, Calif., was previously analysed in the mid-1960s for ammonium (3.8% by the Kjeldahl method) and potassium and sodium (2.16% K⁺ and 0.08% Na⁺, by a wet-chemical technique).²⁸ Recently, the potassium and sodium were determined by a flame-photometric method²⁹ to verify the wet-chemical and IC results. The IC results for sodium, ammonium and potassium

Table 1. Ammonium chloride determination by ion chromatography

Ammonium, μ g/g		Recovery, %
Found	Taken	
4.80	5.15	93.2
5.33	5.27	101.1
5.67	5.46	103.8
5.67	5.83	97.3
5.60	5.95	94.1
6.74	6.76	99.7
7.71	7.68	100.4
8.88	9.08	97.8
9.19	9.64	95.3
9.62	10.1	95.2
10.7	10.7	100.0
11.6	11.7	99.2
14.0	13.8	101.4
14.8	15.0	98.7
14.8	15.2	97.4
15.4	15.8	97.5
15.5	16.3	95.1
Average		98.1
RSD		2.9

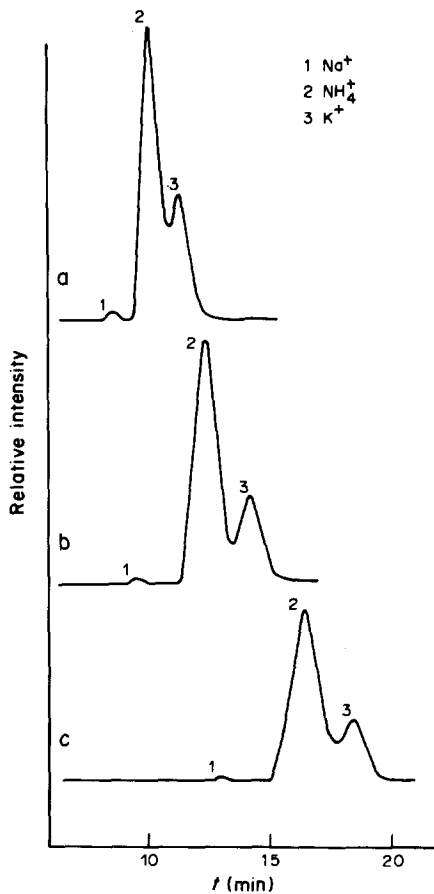


Fig. 1. Chromatograms for the buddingtonite sample, using Dionex separator columns: (a) 9×250 mm, (b) 6×250 and 9×250 mm, and (c) CS-1 and precolumn. Flow-rate 3.1 ml/min for a and b, and 1.2 ml/min for c. Concentrations (in ppm): (a, b) <0.4 Na^+ , 15.2 NH_4^+ , 8.4 K^+ ; (c) <0.4 Na^+ , 5.1 NH_4^+ , 2.8 K^+ (at 1:2 dilution of sample).

in the buddingtonite sample show typical IC cation signals (Fig. 1). However, in the buddingtonite sample the ammonium concentration generally exceeded the potassium concentration. Therefore, two cation-separator columns were required to resolve the two peaks adequately (Fig. 1b). To resolve these two peaks by use of the CS-1 column with precolumn, the sample was further diluted (by a factor of 3) and the flow-rate reduced to 1.2 ml/min (Fig. 1c).

Ammonium was quantitatively detected, and the results (Table 2) showed an RSD of 2.2% for the buddingtonite sample. Potassium was also quantitatively detected, with an RSD of 0.6%, whereas sodium was below the IC detection limit of 0.1%. With the recommended sample weight and dilution volume, a detection limit (taken as twice the standard deviation) of 0.1% in the rock was achievable for all three cations, although with different NH_4^+/K^+ and $\text{NH}_4^+/\text{Na}^+$ ratios, dilution and optimization were required for low-level quantification (Fig. 2). Sodium was well resolved and not affected by the ammonium concentration. After further dilution of the sample by

Table 2. Ammonium, potassium and sodium determination in buddingtonite-rich sample

Species	Present, %	Found, %	n §	RSD, %
NH_4^+	3.8*	3.8	10	2.2
K^+	2.16*, 2.19†	2.1	5	0.6
Na^+	0.08*, 0.04†	<0.1	5	—

*Kjeldahl for NH_4^+ ; wet-chemical for K^+ and Na^+ .²⁸

†Flame photometry.²⁹

§Number of determinations.

a factor of two, 0.1% ammonium was still detectable with as much as 4% potassium present in the sample (Fig. 2c). The hydrothermally altered basaltic-tuff samples used to obtain Fig. 2 contained (%): (2a) 0.3 Na^+ , 1.8 NH_4^+ , 5.0 K^+ ; (2b) 0.9 Na^+ , 0.4 NH_4^+ , 4.2 K^+ ; and (2c) 1.5 Na^+ , <0.1 NH_4^+ , 4.0 K^+ . By varying the sample dilution and optimizing the IC parameters, a lower detection limit for ammonium can be obtained but was not required for this study.

To verify the IC results, the solutions were also analysed for ammonium with a gas-sensing ammonia electrode. The same standard solutions were used for calibrating the IC and the electrode, except that just before potentiometric measurement the solutions were adjusted to pH 11 and a sufficient amount of

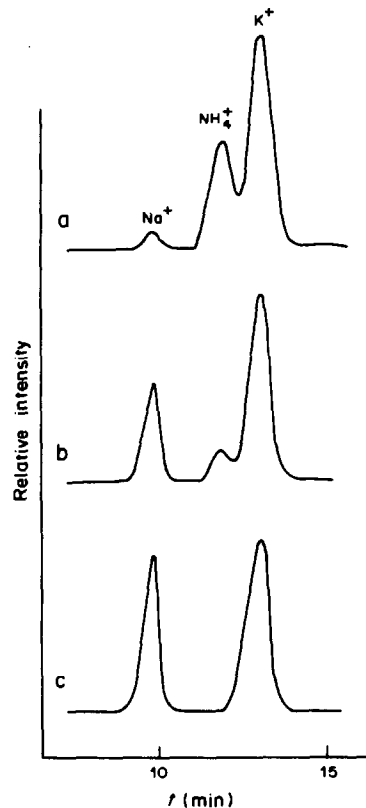


Fig. 2. Chromatograms for samples of hydrothermally altered basaltic-tuffs, showing various NH_4^+/K^+ and $\text{NH}_4^+/\text{Na}^+$ ratios. Samples at 1:1 dilution, following procedure outlined in text. Concentrations (in ppm): (a) 0.5 Na^+ , 3.5 NH_4^+ , 9.9 K^+ ; (b) 1.8 Na^+ , 0.9 NH_4^+ , 8.3 K^+ ; and (c) 3.0 Na^+ , <0.1 NH_4^+ , 8.0 K^+ .

Table 3. Comparison of ammonium recovery by ion-chromatography and ammonia electrode

Sample	NH ₄ ⁺ recovery, %*	
	Ion-chromatography	Ammonia electrode
NH ₄ Cl	98 ± 3 (17)	96 ± 4 (5)
NH ₄ NO ₃	95 ± 7 (5)	93 ± 6 (5)
Buddingtonite	99 ± 2 (10)	103 ± 4 (5)

*Mean and standard deviation of the number of replicates shown in parentheses.

inert electrolyte was added to match the ionic strength of the samples.

The recoveries for known weights of ammonium chloride, ammonium nitrate, and the buddingtonite sample are listed in Table 3. The ammonia-electrode results agree with the IC results, but has the disadvantage of not being able to determine the sodium and potassium.

Interference study

To evaluate possible interference by nitrate in the ammonium analyses, we conducted a study with known weights of ammonium nitrate, but found no evidence for it (Table 3).

Acknowledgements—We thank T. Theodore for valuable discussions and, especially, Richard C. Erd for supplying the buddingtonite sample.

REFERENCES

1. E. I. Bloomstein, *Sympos. Assoc. Explor. Geochem. Abstr.*, 1984, 27.
2. F. J. Stevenson, *Science*, 1959, **130**, 221.
3. *Idem*, *Geochim. Cosmochim. Acta*, 1962, **26**, 797.
4. D. S. Barker, *Am. Mineral.*, 1964, **49**, 851.
5. D. E. White and C. E. Roberson, *Geol. Soc. America, Buddington Volume*, 1962, 397.
6. R. C. Erd, D. E. White, J. J. Fahey and D. E. Lee, *Am. Mineral.*, 1964, **49**, 831.
7. A. P. Vinogradov, K. P. Florenskii and V. F. Volynets, *Geochem.*, 1963, **10**, 905.
8. F. J. Stevenson, *Anal. Chem.*, 1960, **32**, 1704.
9. F. Wlotzka, *Geochim. Cosmochim. Acta*, 1961, **24**, 106.
10. E. K. Gibson, Jr. and C. B. Moore, *Anal. Chem.*, 1970, **42**, 461.
11. T. L. Norris and O. A. Schaeffer, *Geochim. Cosmochim. Acta*, 1982, **46**, 371.
12. P. N. Shulka, B. K. Kothari and P. S. Goel, *Anal. Chim. Acta*, 1978, **96**, 159.
13. S. A. Matthes, R. F. Farrell and A. J. Mackie, *U.S. Bur. Mines Tech. Progr. Rept.*, 1983, **120**, 1.
14. R. A. Nadkarni, *Anal. Chem.*, 1984, **56**, 2233.
15. A. Abu-Samra, J. S. Morris and S. R. Koirtiyohann, *ibid.*, 1975, **47**, 1475.
16. P. Barrett, L. J. Davidowski, Jr, K. W. Penaro and T. R. Copeland, *ibid.*, 1978, **50**, 1021.
17. H. Small, T. S. Stevens and W. C. Bauman, *ibid.*, 1975, **47**, 1801.
18. T. Jupille, D. Burge and D. Togami, *Res. Devel.*, 1984, **26**, 135.
19. K. Harrison, W. C. Beckham Jr., T. Yates and C. D. Carr, *Am. Lab.*, 1985, No. 5, 114.
20. J. R. Benson, *ibid.*, 1985, No. 6, 30.
21. J. M. Baldwin, P. R. Klock and C. Pohl, *Rocky Mountain Conf. 23rd, Abstr.*, 1981, 1.
22. S. A. Wilson and C. A. Gent, *Anal. Lett.*, 1982, **15**, 851.
23. *Idem*, *Anal. Chim. Acta*, 1983, **148**, 299.
24. K. L. Evans and C. B. Moore, *Anal. Chem.*, 1980, **52**, 1908.
25. K. L. Evans, *Thesis*, Arizona State University, 1981.
26. S. Maketon and J. G. Tarter, *Anal. Lett.*, 1985, **18**, 181.
27. J. M. Thompson, S. S. Howe and W. E. Hall, *Rocky Mountain Conf. 25th, Abstr.*, 1983, 108.
28. R. C. Erd, *U.S. Geol. Surv.*, personal communication, 1984.
29. M. J. Cremer, P. R. Klock, S. T. Neil and J. M. Riviello, *U.S. Geol. Surv. O.F.*, 84-565, 1984, 139.

ETUDE DE LA FORMATION DES COMPLEXES EN SOLUTION AQUEUSE—I

METHODE PROTOMETRIQUE INFORMATISEE DE DETERMINATION DES CONCENTRATIONS DES IONS LIBRES EN SOLUTION (METHODE CILS) ET D'ESTIMATION DES CONSTANTES DE STABILITE DES COMPLEXES: CHOIX CRITIQUE DES MODALITES D'APPLICATION A PARTIR D'UN EXEMPLE SIMULE

ROBERT FOURNAISE et CHRISTIAN PETITFAUX

Laboratoire de Chimie de Coordination, Université de Reims Champagne-Ardenne, B.P. 347, 51062
Reims, France

(Reçu le 12 juillet 1985. Révisé le 11 novembre 1985. Accepté le 23 janvier 1986)

Résumé—Lors de l'étude protométrique de la formation des complexes en solution aqueuse, il est très utile de connaître les concentrations des ions libres afin d'en déduire la composition de chaque espèce, puis de calculer des valeurs approchées de leurs constantes de stabilité. A partir de la seule mesure du pH, les concentrations des ions libres peuvent être calculées par une méthode qui comporte un minimum d'étapes d'intégration et de dérivation. Ce procédé, appelé méthode CILS, a été entièrement informatisé et ses modalités d'application sont définies à l'aide d'un exemple simulé.

Alors que l'étude en solution des complexes simples du type MA_n a fait l'objet de nombreux travaux, par contre, celle des systèmes chimiques où interviennent d'autres espèces ne s'est que relativement peu développée. Selon les auteurs, différents cas particuliers ont été envisagés: complexes mixtes, majoritaires ou non, protonés ou hydroxylés, mononucléaires ou polynucléaires. Si l'examen d'une ou deux de ces hypothèses conduit à des études relativement faciles, la prise en compte de toutes ces possibilités nécessite à la fois une étude expérimentale très précise et une automatisation de l'exploitation des mesures.

Afin de déterminer, sans aucune hypothèse initiale, la composition des complexes formés dans des systèmes chimiques compliqués, il est nécessaire de connaître les concentrations des ions libres. Or, généralement, seule la concentration en protons libres est directement mesurable. Deux méthodes pour accéder aux autres concentrations libres à partir de la seule mesure du pH ont alors été élaborées. Elles font appel à l'exploitation judicieuse de plusieurs titrages acido-basiques relatifs à différentes compositions en ion métallique et en complexant et le traitement mathématique résultant contient toujours plusieurs étapes d'intégration et de dérivation.

Les premiers travaux sur les modes d'accès aux concentrations libres non directement mesurables sont dus à Hedström^{1,2} et à Lefèvre.³⁻⁶ Différentes dans leur présentation et dans le procédé d'exploitation des mesures, ces deux méthodes se sont développées inégalement.

Celle de Hedström a été généralisée par Sillén⁷⁻⁹ et Österberg,¹⁰⁻¹³ puis informatisée par Sarkar et Kruck.¹⁴⁻¹⁸ Ses conditions pratiques d'application ont été discutées par McBryde^{19,20} et surtout Wozniak et Nowogrocki.²¹ Ultérieurement, Guevremont et Rabenstein^{22,23} qui ont introduit le nom de méthode FICS (Free Ions Concentrations in Solution), puis Avdeef *et al.*²⁴⁻²⁷ ont repris des études en partie similaires sans mentionner, d'ailleurs, la mise au point précédente.²¹

Par contre, la méthode de la surface potentiométrique de Lefèvre a été utilisée par un nombre plus restreint d'auteurs.²⁸⁻³⁶ De plus, elle n'a jamais été informatisée.

Lorsque l'on compare ces deux procédés d'exploitation des données protométriques, on constate que celui de Lefèvre est nettement le plus simple puisqu'il nécessite beaucoup moins d'étapes d'intégration et de dérivation. Nous nous sommes donc proposé de développer une méthode voisine, appelée méthode CILS (Concentrations des Ions Libres en Solution), en recherchant une informatisation totale de l'exploitation des mesures. Ses modalités d'application seront ensuite précisées sur un exemple simulé, recouvrant une large gamme de pH, alors que les études des autres méthodes étaient limitées presque exclusivement au milieu acide. Outre la composition moyenne des complexes, la méthode CILS fournit également des valeurs approchées des constantes de stabilité des complexes du modèle le plus plausible. Ces valeurs approximatives pourront

alors servir d'estimations initiales lors d'un affinement ultérieur par diverses méthodes, en particulier la méthode des moindres carrés.

SYMBOLISME

- M Ion métallique
 AH_N Forme neutre du complexant
 A Forme basique du complexant
 C_M, C_A Concentrations analytiques en ion métallique et en complexant
 C_H Concentration analytique en protons
 C_H = C_A(N + x_H - x_{OH}) avec x_H et x_{OH} les nombres de moles H⁺ et OH⁻ ajoutés par mole de complexant
 [X] Concentration de l'espèce X
 pH pH = -log [H]
 M_mA_aH_h Espèce formée suivant l'équilibre
 mM + aA + hH ⇌ M_mA_aH_h
 β_{m,a,h} Constante de stabilité d'une espèce

$$\beta_{m,a,h} = \frac{[M_m A_a H_h]}{[M]^m [A]^a [H]^h}$$
 avec m + a ≠ 0
 Pour les espèces hydroxylées, h est négatif
 β̄_{m,a,h} Estimateur d'une constante de stabilité

$$b_{m,a,h} \quad b_{m,a,h} = [M]^m [A]^a [H]^h = \frac{[M_m A_a H_h]}{\beta_{m,a,h}}$$

 K_e Produit ionique de l'eau: K_e = [H][OH]
 C_E Somme des concentrations des espèces participant aux équilibres
 F Fonction auxiliaire:
 F = C_E - C_M ln[M] - C_A ln[A]
 R "Somme des complexes":

$$R = \sum_{m \neq 0, a \neq 0, h} [M_m A_a H_h]$$

 m̄, ā, h̄ Coefficients stoechiométriques moyens
 S Somme des carrés des résidus
 X₀ Valeur initiale ou constante d'intégration.

Dans un souci de simplification, toutes les charges sont volontairement omises.

ELEMENTS THEORIQUES

Relations fondamentales

Chaque point de la courbe de titrage acido-basique d'un mélange ion métallique-complexant est défini par trois équations conditionnelles, chacune d'elles correspondant au bilan d'un constituant:

$$C_M = [M] + \sum_{m,a,h} m \beta_{m,a,h} [M]^m [A]^a [H]^h \quad (1)$$

$$C_A = [A] + \sum_{m,a,h} a \beta_{m,a,h} [M]^m [A]^a [H]^h \quad (2)$$

$$C_H = [H] - \frac{K_e}{[H]} + \sum_{m,a,h} h \beta_{m,a,h} [M]^m [A]^a [H]^h \quad (3)$$

En chaque point, les concentrations analytiques C_M, C_A et C_H sont connues expérimentalement. La somme des concentrations de toutes les espèces participant aux équilibres en solution, C_E, s'écrit:

$$C_E = [H] + \frac{K_e}{[H]} + [M] + [A] + \sum_{m,a,h} \beta_{m,a,h} [M]^m [A]^a [H]^h \quad (4)$$

En employant les différentielles logarithmiques, la différentielle totale de C_E a pour expression:

$$\begin{aligned} dC_E = & ([M] + \sum_{m,a,h} m \beta_{m,a,h} [M]^m [A]^a [H]^h) d \ln[M] \\ & + ([A] + \sum_{m,a,h} a \beta_{m,a,h} [M]^m [A]^a [H]^h) d \ln[A] \\ & + ([H] - \frac{K_e}{[H]} + \sum_{m,a,h} h \beta_{m,a,h} [M]^m [A]^a [H]^h) d \ln[H] \end{aligned}$$

Si l'on introduit les équations (1), (2) et (3), on obtient:

$$dC_E = C_M d \ln[M] + C_A d \ln[A] + C_H d \ln[H] \quad (5)$$

De cette expression fondamentale dérivent les méthodes de détermination des concentrations des espèces libres en solution. Cependant, elle ne peut être exploitée sous cette forme car parmi les trois variables [M], [A] et [H], le plus souvent seule la concentration [H] est effectivement mesurée, l'accès direct aux concentrations [M] et [A] n'étant qu'un cas particulier. Il est alors nécessaire de procéder à des changements de variables, c'est à dire d'avoir recours à une fonction auxiliaire adéquate privilégiant certaines variables.

Soit donc la fonction auxiliaire F, telle que:

$$F = C_E - C_M \ln[M] - C_A \ln[A] \quad (6)$$

En introduisant la relation (5), sa différentielle totale s'écrit:

$$dF = C_H d \ln[H] - \ln[M] dC_M - \ln[A] dC_A \quad (7)$$

Cette différentielle privilégie les variables facilement accessibles expérimentalement que sont C_M, C_A, C_H et [H] et permet d'éliminer les éléments différentiels dln[M] et dln[A]. Elle est l'équation de référence qui permettra le calcul ultérieur des concentrations libres [M] et [A].

Tout d'abord, il est nécessaire de déterminer la fonction auxiliaire F par intégration. Or, la relation (7) conduit à:

$$\left(\frac{\partial F}{\partial \ln[H]} \right)_{C_M, C_A} = C_H \quad (8)$$

D'où

$$F_i = F_0 - (\ln 10) \left[\int_{pH_0}^{pH_i} C_H dpH \right]_{C_M, C_A} \quad (9)$$

La valeur de la fonction auxiliaire F en chaque point i d'un titrage sera donc déterminée en intégrant la fonction C_H = f(pH)_{C_M, C_A} à condition de connaître la constante d'intégration F₀ au pH initial pH₀ et de

maintenir les concentrations C_M et C_A constantes au cours de l'expérience.

Puis, toujours d'après la relation (7), on a:

$$\ln[M] = - \left(\frac{\partial F}{\partial C_M} \right)_{C_A, [H]} \quad (10)$$

$$\ln[A] = - \left(\frac{\partial F}{\partial C_A} \right)_{C_M, [H]} \quad (11)$$

et $\ln[M]$ sera donc déterminé en calculant la dérivée de la fonction $F = f(C_M)_{C_A, [H]}$ au point i , C_A et $[H]$ étant maintenus constants. Afin de connaître la variation de F en fonction de C_M pour un pH fixé, il faudra utiliser les résultats de plusieurs titrages relatifs à des concentrations C_A identiques et C_M différentes.

Pour $\ln[A]$ on procédera de manière analogue, mais en utilisant la fonction $F = f(C_A)_{C_M, [H]}$ à C_M et $[H]$ constants, correspondant maintenant à des concentrations C_M identiques et C_A différentes.

Coefficients stoechiométriques moyens

La connaissance des différentes concentrations libres permet alors d'accéder aux coefficients stoechiométriques moyens. En effet, appelons R la somme des concentrations des espèces complexes où interviennent à la fois le métal et le complexant:

$$R = \sum_{m \neq 0, a \neq 0, h} \beta_{m,a,h} [M]^m [A]^a [H]^h \quad (12)$$

En combinant cette relation avec les équations (4) et (6), on obtient:

$$R = F - [H] - \frac{K_c}{[H]} + C_M \ln[M] + C_A \ln[A] - [M] - [A] - \sum_{m,h} \beta_{m,0,h} [M]^m [H]^h - \sum_h \beta_{0,1,h} [A] [H]^h \quad (13)$$

Si les constantes de stabilité des espèces hydroxylées du métal $\beta_{m,0,h}$ et celles des formes protonées du complexant $\beta_{0,1,h}$ ont été préalablement déterminées par des expériences spécifiques, la connaissance de F , $[M]$, $[A]$ et $[H]$ permet de calculer la "somme des complexes" R . Il est à noter que récemment Avdeef²⁵ a abouti à un résultat analogue, mais en employant une voie nettement plus compliquée.

A partir de la valeur de R , il est alors possible de calculer les coefficients stoechiométriques moyens, exprimés par les formules:

$$\bar{m} = \frac{C_M - [M] - \sum_{m,h} m \beta_{m,0,h} [M]^m [H]^h}{R} \quad (14)$$

$$\bar{a} = \frac{C_A - [A] - \sum_h \beta_{0,1,h} [A] [H]^h}{R} \quad (15)$$

$$\bar{h} = \frac{C_H - [H] + \frac{K_c}{[H]} - \sum_{m,h} h \beta_{m,0,h} [M]^m [H]^h - \sum_h h \beta_{0,1,h} [A] [H]^h}{R} \quad (16)$$

Ces coefficients stoechiométriques moyens permettent soit de connaître la formule d'une espèce si elle est très nettement majoritaire, soit d'envisager les formules plausibles les plus probables lorsque plusieurs complexes coexistent.

Estimation des constantes de stabilité

En chaque point i , la "somme des complexes" est:

$$R_i = \sum_{m \neq 0, a \neq 0, h} \beta_{m,a,h} [M]_i^m [A]_i^a [H]_i^h$$

$$= \sum_{m \neq 0, a \neq 0, h} \beta_{m,a,h} b_{m,a,h,i}$$

soit, sous forme condensée:

$$R_i = \sum_{j=1}^{j=k} \beta_j b_{j,i} \quad (17)$$

k étant le nombre total de complexes intervenant dans R .

Pour déterminer les meilleurs estimateurs β_j des constantes de stabilité, on peut employer la méthode des moindres carrés qui consiste à minimiser la somme:

$$S = \sum_{i=1}^{i=n} \left(R_i - \sum_{j=1}^{j=k} \beta_j b_{j,i} \right)^2 \quad (18)$$

avec n le nombre de points utilisés, et $n > k$.

On en déduit ainsi les équations normales:

$$\sum_i R_i b_{l,i} = \sum_j \left(\beta_j \sum_i b_{j,i} b_{l,i} \right) \text{ avec } l = 1, 2, \dots, k$$

En adoptant une écriture matricielle, ce système s'écrit:

$$V = M \beta$$

avec

$$v_l = \sum_i R_i b_{l,i} \text{ et } m_{l,j} = \sum_i b_{l,i} b_{j,i}$$

Les estimateurs β_j sont alors déduits de la relation:

$$M^{-1} V = \beta \quad (19)$$

ETAT INITIAL

L'application de la méthode CILS implique de connaître pour l'état initial la constante d'intégration

F_0 qui ne peut être déterminée que par l'intermédiaire des concentrations libres $[M]_0$ et $[A]_0$ dans la solution au début du titrage. Si les conditions expérimentales le permettent, le plus simple est de choisir un pH initial pH_0 assez acide afin qu'il n'y ait pas formation de complexes. Dans ce cas particulier, la concentration $[M]_0$ est égale à la concentration analytique C_M . Quant à la concentration $[A]_0$, elle peut être calculée de manière triviale à partir des constantes de protonation du complexant.

Les relations (4) et (6) conduisent alors à:

$$F_0 = [H]_0 + \frac{K_c}{[H]_0} + C_M (1 - \ln[M]_0) + C_A (1 - \ln[A]_0) \quad (20)$$

Par contre, si expérimentalement il est impossible d'atteindre un pH assez faible pour détruire tous les complexes, il est alors nécessaire de procéder par itérations successives. Tout d'abord, on suppose qu'il n'y a pas formation de complexes et les concentrations $[M]_0$ et $[A]_0$ ainsi que F_0 sont calculées de manière approximative selon le principe précédent. Puis l'emploi de la méthode CILS fournit des valeurs grossières des constantes de stabilité. Il est alors possible, en utilisant ces premières valeurs, d'appliquer la méthode de Newton-Raphson aux équations:

$$C_M = [M]_0 + \sum_{m,a,h} m \beta_{m,a,h} [M]_0^m [A]_0^a [H]_0^h$$

$$C_A = [A]_0 + \sum_{m,a,h} a \beta_{m,a,h} [M]_0^m [A]_0^a [H]_0^h$$

On obtient ainsi de meilleures valeurs de $[M]_0$, $[A]_0$ et F_0 qui permettent d'améliorer les valeurs approchées des constantes de stabilité. Ce processus doit être répété jusqu'à convergence.

TECHNIQUES DE CALCUL

Toutes les étapes de calcul ont été automatisées en utilisant des techniques appropriées à l'interpolation, l'intégration et la dérivation. Pour chacune de ces trois opérations, on dispose d'un ensemble de points d'une fonction $y = f(x)$ analytiquement inconnue qui sera assimilée en première approximation à un polynôme $P(x)$.

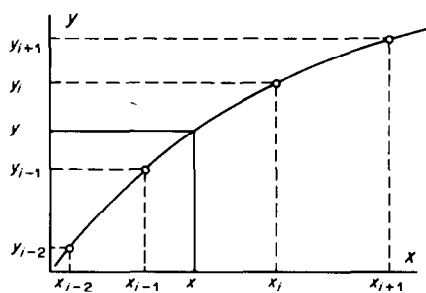
Interpolation (Fig. 1a)

Dans ce cas, à partir de couples quelconques (x, y) connus, on cherche à déterminer d'autres valeurs de la fonction $y = f(x)$ de manière à ce que ces nouvelles valeurs soient régulièrement espacées en abscisse, c'est à dire séparées par une distance constante appelée le "pas".

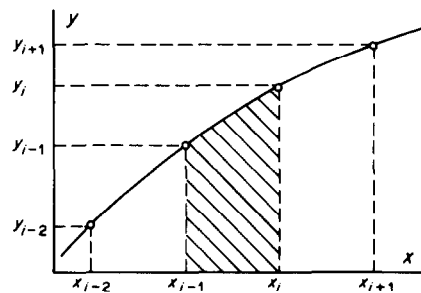
L'interpolation peut être menée en calculant le polynôme $P(x)$ passant par un nombre pair de points (soit quatre, soit six), ceux-ci étant répartis également de chaque côté du point à interpoler. Le polynôme d'interpolation est calculé par la méthode matricielle. Par exemple, si l'on utilise les quatre points d'abscisse x_{i-2} , x_{i-1} , x_i et x_{i+1} , il faut déterminer le polynôme de degré trois:

$$P(x) = a_0 + a_1x + a_2x^2 + a_3x^3$$

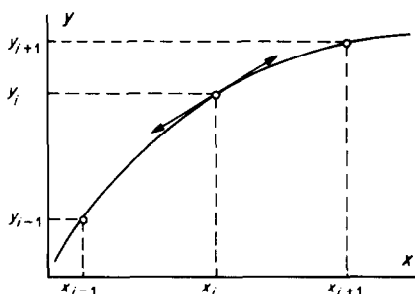
satisfaisant les coordonnées de ces quatre points.



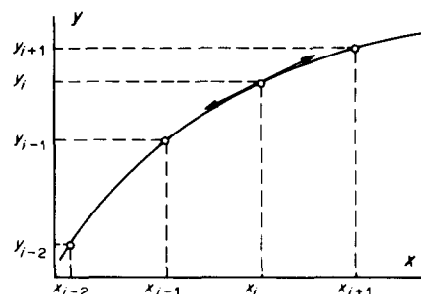
(a) Interpolation



(b) Intégration



(c) Dérivation: degré 2



(d) Dérivation: degré 3

Fig. 1. Techniques de calcul.

On dispose alors d'un système de quatre équations à quatre inconnues qui s'écrit, sous forme matricielle:

$$\begin{pmatrix} y_{i-2} \\ y_{i-1} \\ y_i \\ y_{i+1} \end{pmatrix} = \begin{pmatrix} 1 & x_{i-2} & x_{i-2}^2 & x_{i-2}^3 \\ 1 & x_{i-1} & x_{i-1}^2 & x_{i-1}^3 \\ 1 & x_i & x_i^2 & x_i^3 \\ 1 & x_{i+1} & x_{i+1}^2 & x_{i+1}^3 \end{pmatrix} \times \begin{pmatrix} a_0 \\ a_1 \\ a_2 \\ a_3 \end{pmatrix}$$

c'est à dire de manière condensée:

$$Y = MA$$

Les coefficients du polynôme sont calculés à l'aide de la relation:

$$M^{-1} Y = A$$

puis l'on en déduit la valeur interpolée au point d'abscisse x .

Intégration (Fig. 1b)

Pour calculer l'intégrale définie de la fonction $y = f(x)$ entre x_{i-1} et x_i , on interpole tout d'abord cette fonction par un polynôme de degré trois (quatre points) ou de degré cinq (six points), comme précédemment. Puis, par exemple si l'on utilise quatre points, l'intégrale définie est alors estimée par:

$$\int_{x_{i-1}}^{x_i} P(x) dx = \left[a_0 x + a_1 \frac{x^2}{2} + a_2 \frac{x^3}{3} + a_3 \frac{x^4}{4} \right]_{x_{i-1}}^{x_i}$$

Dérivation

A cause de contraintes expérimentales, le nombre de points disponibles est souvent faible lors de cette étape. Suivant les cas, l'interpolation polynomiale peut s'effectuer soit avec un nombre impair de points (trois ou cinq), soit avec un nombre pair (quatre).

Nombre impair (Fig. 1c). La fonction est alors interpolée par un polynôme de degré deux ou quatre. Par exemple, pour le degré deux, on détermine le polynôme $P(x) = a_0 + a_1 x + a_2 x^2$ passant par les points d'abscisse x_{i-1} , x_i et x_{i+1} .

La dérivée de la fonction $y = f(x)$ au point x_i est alors assimilée à:

$$P'(x_i) = a_1 + 2a_2 x_i$$

Sauf aux extrémités, il existe une certaine symétrie puisque le point x_i pour lequel on détermine la dérivée est encadré par un nombre égal de points.

Nombre pair (Fig. 1d). Le polynôme est de degré trois puisqu'on utilise quatre points. Contrairement au cas précédent, il y a alors une dissymétrie puisque le point x_i est entouré de deux points d'un côté et un de l'autre.

ETUDE DE LA METHODE CILS SUR UN EXEMPLE SIMULE

Afin de situer au mieux le potentiel de cette méthode, le système chimique simulé se doit d'être assez

compliqué et de faire intervenir, à côté des complexes simples du type MA_n , des espèces protonées ou hydroxylées, condensées ou non en ion métallique. Ce choix conduit à utiliser une très large zone de pH, y compris le milieu basique, contrairement à la plupart des auteurs précédents qui ont généralement limité leur étude au milieu acide.

Ces différentes conditions nous ont amenés à choisir comme exemple le système Cu^{2+} -1,3-propanediamine étudié en particulier par Näsänen *et al.*³⁷ à l'aide de méthodes protométriques classiques. Selon ces auteurs, à 25° et force ionique nulle, les constantes de protonation du complexant sont $\log \beta_{0,1,1} = 10,51$ et $\log \beta_{0,1,2} = 18,99$. Celles des différents complexes sont rassemblées dans le tableau 7. Le produit ionique de l'eau a été fixé à $pK_e = 14$ et les constantes de stabilité des formes hydroxylées du cuivre, déduites de la littérature, ont été choisies égales à $\log \beta_{1,0,-1} = -7,60$ et $\log \beta_{2,0,-2} = -10,80$.

Procédé expérimental

La méthode CILS impose de maintenir constantes les concentrations analytiques en ion métallique C_M et en complexant C_A tout au long de chaque titrage conformément à l'équation (9). Cette condition est satisfaite si pour chaque addition de réactif titrant, en général une base forte, on ajoute un volume égal d'une solution contenant à la fois l'ion métallique et le complexant à des concentrations doubles de celles du mélange initial étudié.

Deux procédés expérimentaux peuvent alors être envisagés. L'un consiste à réaliser deux séries d'au moins trois titrages chacune, un de ces titrages étant commun aux deux séries. La première série correspond à des mélanges de même concentration totale en complexant C_A , mais de concentrations analytiques en métal C_M différentes, et permet de calculer la concentration libre $[M]$ aux différents pH de chacune de ces expériences en exploitant l'équation (10). La seconde série relative cette fois à des concentrations C_M identiques et C_A différentes fournit, pour chaque pH de ces courbes de neutralisation, la concentration libre $[A]$ par application de la formule (11). On ne dispose donc finalement à la fois des concentrations libres $[M]$ et $[A]$ que pour le seul titrage commun aux deux séries.

Ce premier procédé expérimental est celui qui a été employé par la plupart des auteurs car le plus simple puisque nécessitant le moins de mesures. Cependant, il présente un inconvénient. En effet, dans ce cas, il n'est possible de connaître la composition moyenne des complexes et calculer leurs constantes de stabilité que pour le seul rapport commun. Or, comme l'ont d'ailleurs remarqué Avdeef et Brown,²⁷ pour ce rapport certaines espèces peuvent se révéler très minoritaires et donc ne pas être détectées, alors qu'elles auraient pu exister de manière non négligeable dans d'autres rapports. Cette critique est également valable pour les auteurs^{22,24} qui préconisent d'utiliser des solutions pour lesquelles $C_A \gg C_M$.

Tableau 1. Composition initiale des différents mélanges: dans un souci de simplification, les rapports C_A/C_M sont ramenés à un rapport de nombres entiers

C_M, M	C_A/C_M		
	$C_A = 0,07 M^*$	$C_A = 0,08 M^\dagger$	$C_A = 0,09 M^\S$
0,03	7/3 (2,33/1)	8/3 (2,67/1)	9/3 (3/1)
0,04	7/4 (1,75/1)	8/4 (2/1)	9/4 (2,25/1)
0,05	7/5 (1,4/1)	8/5 (1,6/1)	9/5 (1,8/1)
0,06	7/6 (1,17/1)	8/6 (1,33/1)	9/6 (1,5/1)
0,07	7/7 (1/1)	8/7 (1,14/1)	9/7 (1,29/1)

* $C_{H_0} = 0,15M$. † $C_{H_0} = 0,17M$. § $C_{H_0} = 0,19M$.

L'autre procédé consiste à réaliser une "matrice" d'expériences composée de plusieurs séries de dosages afin de tenter de remédier à l'inconvénient précédent (Tableau 1). Pour tous les titrages d'une même "colonne", la concentration analytique en complexant C_A est la même, alors que celle en ion métallique C_M est différente. Inversement, chaque "ligne" correspond à des concentrations C_M identiques et C_A différentes. Par conséquent, on dispose dans ce cas des concentrations libres $[M]$ et $[A]$ pour tous les pH de tous les titrages acido-basiques.

Ce procédé expérimental nécessite évidemment beaucoup plus d'expériences que le précédent, ce qui explique qu'il n'ait été que très peu employé. Il est pourtant le plus judicieux car il permet une analyse globale de tous les complexes et c'est pourquoi nous avons été amenés à le choisir lors de l'étude de la méthode CILS.

Titrages simulés

Les différents titrages ont été simulés en respectant les contraintes expérimentales exposées précédemment. La composition des différents mélanges initiaux est donnée dans le Tableau 1, les valeurs de la concentration initiale en protons C_{H_0} ayant été choisies afin que le pH de départ soit toujours égal à 2. Tous les volumes initiaux sont fixés à 50 ml et la concentration de la base forte ajoutée est égale à 1,25M quel soit le titrage envisagé. Afin de maintenir constantes les concentrations totales C_M et C_A , le mélange ajouté simultanément et en volume égal à celui de la base a la composition suivante:

- concentration analytique en ion métallique = $2C_M$
- concentration analytique en complexant = $2C_A$
- concentration analytique en protons = $4C_A$

Une première simulation est effectuée pour chaque courbe de titrage grâce à un programme spécial SIMPH³⁸ qui permet de calculer les grandeurs théoriques C_H , F , $[M]$, $[A]$, R , \bar{m} , \bar{a} et \bar{h} pour des pH variant de 2 à 13 et régulièrement espacés d'un pas égal à 0,5. Ces valeurs théoriques serviront ultérieurement de référence afin de les comparer à celles fournies par la méthode CILS.

Une seconde simulation est ensuite réalisée à l'aide d'un programme spécifique SIMV.³⁸ Pour chaque volume de base ajouté, ce programme calcule le pH de la solution ainsi que la concentration analytique

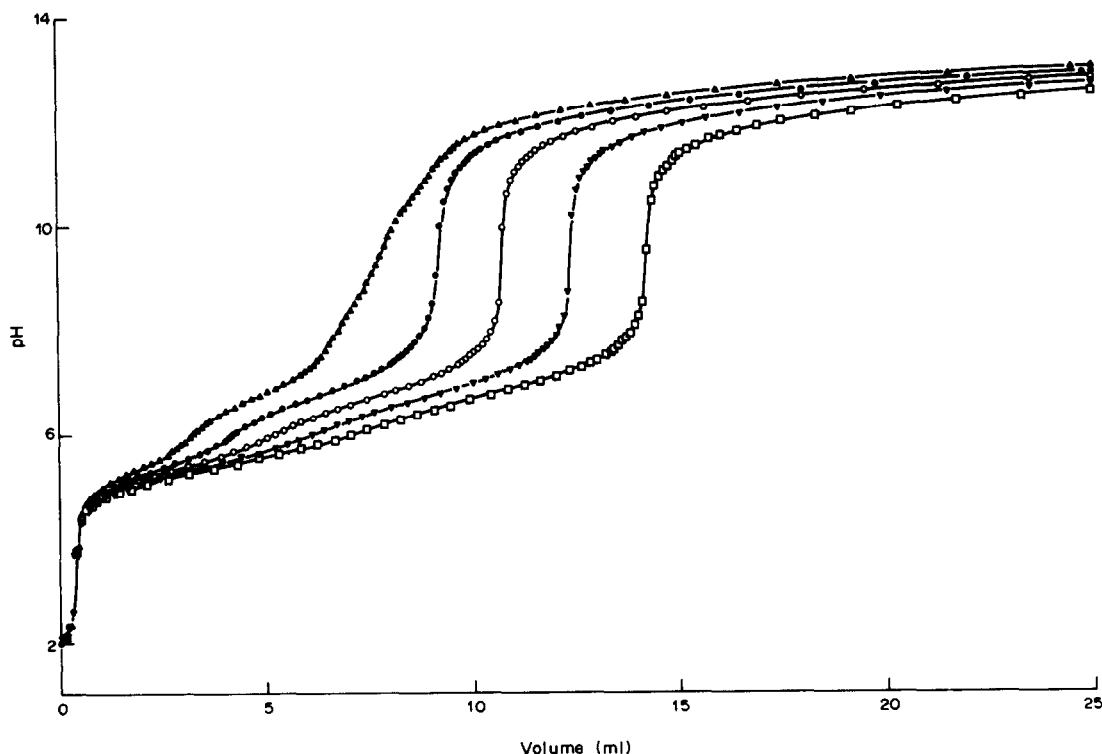


Fig. 2. Courbes de neutralisation à C_M variable. $C_A = 8 \cdot 10^{-2} M$; $C_M = 3 \cdot 10^{-2} M$ (▲), $4 \cdot 10^{-2} M$ (●), $5 \cdot 10^{-2} M$ (○), $6 \cdot 10^{-2} M$ (▼), $7 \cdot 10^{-2} M$ (□).

C_H qui seront les couples de mesures utilisés ultérieurement. Les pH sont arrondis à 0,001, précision obtenue avec les pH-mètres modernes.

A titre d'exemple, les courbes de neutralisation simulées ainsi obtenues pour la "colonne" où la concentration analytique C_A est fixée à $8 \times 10^{-2} M$ sont représentées sur la figure 2, celles de la "ligne" pour laquelle $C_M = 5 \times 10^{-2} M$ étant tracées sur la figure 3.

Calcul de la fonction auxiliaire F

Disposant des différents titrages, on peut alors aborder l'exploitation des mesures. Comme le pH initial des dosages est suffisamment acide pour que tous les complexes soient détruits, les différentes constantes d'intégration F_0 sont ici obtenues par l'intermédiaire de l'équation (20).

Les fonctions $C_H = f(\text{pH})_{C_M, C_A}$ correspondant à chaque titrage sont interpolées à partir de $\text{pH} = 2$ avec un pas égal à 0,1. Ces valeurs de la concentration C_H permettent ensuite de calculer par intégration la fonction F pour des pH régulièrement espacés, en exploitant la formule (9). Ces deux opérations sont menées simultanément par le programme INTEGR³⁸ en utilisant à chaque fois un polynôme d'interpolation de degré trois ou cinq (voir techniques de calcul, au dessus).

A titre d'exemple, pour le rapport 8/5, le tableau 2 permet de comparer les résultats obtenus pour la

concentration analytique en protons C_H suivant le type d'interpolation. Dans l'ensemble, cette étape n'introduit que des erreurs relatives faibles, souvent inférieures à 0,1%, dues à deux causes. D'une part, dans les zones tamponnées ($\text{pH} = 5$ à 8 et $\text{pH} \geq 11$ sur les figures 2 et 3) les erreurs sont à imputer principalement au fait que les pH sont arrondis à 0,001. En effet, l'interpolation menée avec les pH non arrondis afin de disposer de valeurs de référence, montre que dans ces zones l'erreur relative est en général au moins dix fois plus faible. D'autre part, près des points d'équivalence ($\text{pH} = 3$ à 4 et $\text{pH} = 9$ à 10), l'erreur relative pour un même type d'interpolation reste pratiquement identique que les pH soient arrondis à 0,001 ou non. L'incertitude sur les valeurs interpolées est alors principalement due à l'approximation de la fonction $C_H = f(\text{pH})$ par un polynôme.

En outre, si pour les zones tamponnées les erreurs relatives sont d'un ordre de grandeur comparable quel que soit le type d'interpolation choisi avec les pH arrondis à 0,001, par contre au voisinage des points d'équivalence les résultats sont meilleurs lorsque le polynôme d'interpolation est de degré cinq. Ces différentes constatations nous ont donc amenés à retenir finalement les techniques d'interpolation et d'intégration utilisant six points.

Dans le tableau 3 sont rassemblées les valeurs ainsi obtenues pour la fonction auxiliaire F ainsi que les erreurs relatives correspondantes. L'incertitude rela-

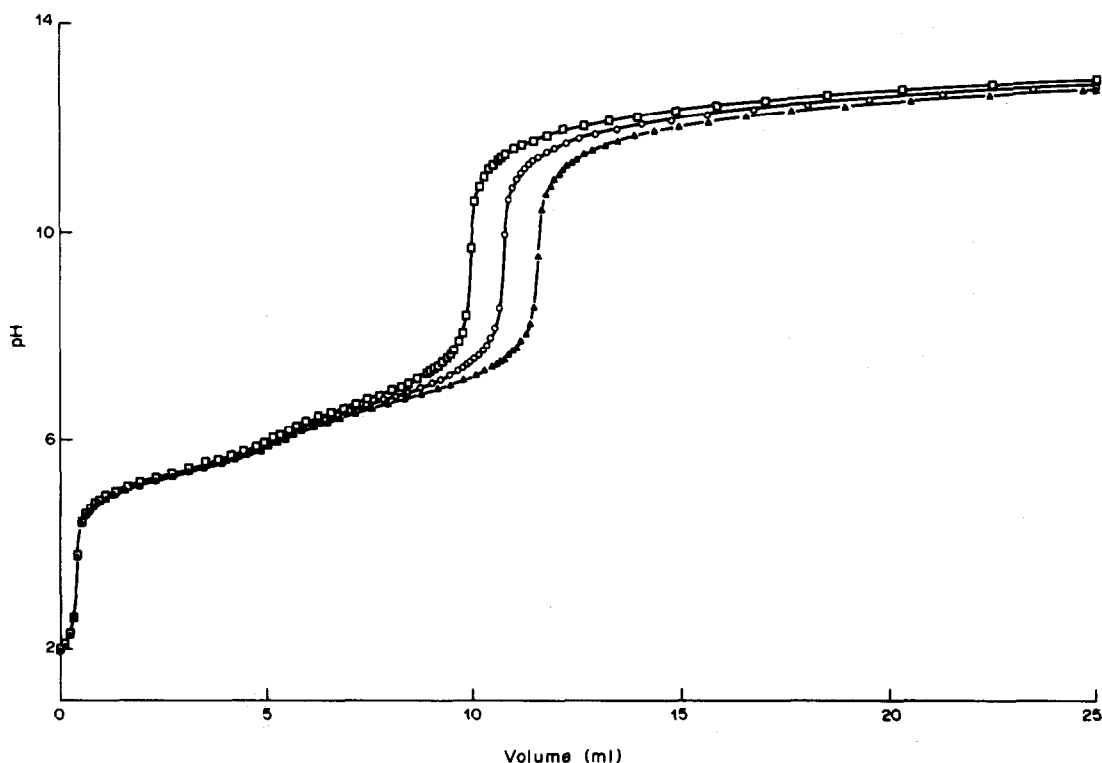


Fig. 3. Courbes de neutralisation à C_A variable. $C_M = 5.10^{-2} M$; $C_A = 7.10^{-2} M$ (\square), $8.10^{-2} M$ (\circ), $9.10^{-2} M$ (\blacktriangle).

Tableau 2. Rapport 8/5: comparaison des valeurs théoriques et interpolées de la concentration analytique en protons C_H

pH	C_H théorique	$\Delta C_H/C_H$			
		pH arrondis à 10^{-3} unité près		Réfèrece: pH non arrondis	
		degré 3	degré 5	degré 3	degré 5
2	$1,699998.10^{-1}$	$1,18.10^{-6}$	$1,18.10^{-6}$	0	0
3	$1,609949.10^{-1}$	$-6,14.10^{-4}$	$-6,16.10^{-4}$	$-6,26.10^{-4}$	$-6,80.10^{-4}$
4	$1,597297.10^{-1}$	$2,47.10^{-3}$	$-6,13.10^{-4}$	$2,45.10^{-3}$	$-6,45.10^{-4}$
5	$1,365186.10^{-1}$	$1,47.10^{-4}$	$1,82.10^{-4}$	$-1,83.10^{-5}$	$-1,46.10^{-6}$
6	$6,108746.10^{-2}$	$3,30.10^{-4}$	$3,33.10^{-4}$	$1,47.10^{-6}$	$3,27.10^{-7}$
7	$6,685458.10^{-3}$	$1,78.10^{-3}$	$1,92.10^{-3}$	$5,91.10^{-5}$	$2,99.10^{-6}$
8	$-1,675382.10^{-2}$	$2,44.10^{-4}$	$1,89.10^{-4}$	$5,55.10^{-5}$	$-1,19.10^{-6}$
9	$-1,970728.10^{-2}$	$4,85.10^{-3}$	$-9,44.10^{-4}$	$4,88.10^{-3}$	$-9,87.10^{-4}$
10	$-2,035902.10^{-2}$	$-7,24.10^{-4}$	$1,60.10^{-4}$	$-7,19.10^{-4}$	$1,51.10^{-4}$
11	$-2,384940.10^{-2}$	$-2,10.10^{-6}$	$2,81.10^{-5}$	$-1,89.10^{-5}$	$4,19.10^{-7}$
12	$-5,347808.10^{-2}$	$-2,14.10^{-4}$	$-2,16.10^{-4}$	$5,24.10^{-6}$	$-2,06.10^{-6}$

tive sur F est toujours minime, ne dépassant que rarement 0,02%.

Détermination de la concentration libre [A]

Connaissant pour chaque titrage les valeurs de la fonction auxiliaire F pour des pH identiques régulièrement espacés d'un pas égal à 0,1, on peut alors porter pour chaque pH de chaque "ligne" les valeurs de F en fonction de la concentration analytique en complexant C_A . On dispose ainsi, à C_M et pH constants, de trois points de la fonction $F = f(C_A)_{C_M, [H]}$ pour lesquels on peut calculer la concentration libre en complexant [A] à l'aide de l'équation (11). Cette étape est réalisée à l'aide du programme CONMCL.³⁸

Un exemple des courbes obtenues pour la "ligne" où la concentration analytique en ion métallique C_M est fixée à $5 \times 10^{-2} M$ est donné sur la figure 4 tandis que le tableau 4 rassemble pour les trois rapports correspondants les erreurs relatives commises sur la concentration libre [A] à partir de pH = 5 où débute la formation des complexes. On constate que l'estimation des dérivées, et par conséquent de la concentration [A], est nettement meilleure pour le rapport 8/5 ce qui est logique puisqu'il correspond au point central.

Tableau 3. Rapport 8/5: comparaison entre les valeurs théoriques de la fonction auxiliaire F et les valeurs calculées à l'aide d'un polynôme d'interpolation de degré 5

pH	F théorique	F calculé	$\Delta F/F$
2	3,253105	3,253105	0
3	2,875695	2,875732	$1,29.10^{-5}$
4	2,506571	2,506888	$1,26.10^{-4}$
5	2,152273	2,152632	$1,67.10^{-4}$
6	1,934051	1,934441	$2,02.10^{-4}$
7	1,853235	1,853613	$2,04.10^{-4}$
8	1,872789	1,873168	$2,02.10^{-4}$
9	1,915919	1,916286	$1,92.10^{-4}$
10	1,962025	1,962368	$1,75.10^{-4}$
11	2,011545	2,011897	$1,75.10^{-4}$
12	2,089820	2,090159	$1,62.10^{-4}$

Détermination de la concentration libre [M]

Pour chaque pH de chaque "colonne", cinq points de la fonction $F = f(C_M)_{C_A, [H]}$ sont connus et, en exploitant l'équation (10), on peut calculer pour chacun d'eux la concentration libre [M].

Deux voies pour calculer les dérivées de la fonction F ont été envisagées. La première consiste à utiliser globalement tous les points, c'est à dire à assimiler la fonction F à un polynôme de degré quatre, puis à en déduire les dérivées en chaque point. La seconde utilise les points par groupe de trois points consécutifs, la dérivée n'étant alors calculée que pour le point central à l'aide d'un polynôme de degré deux

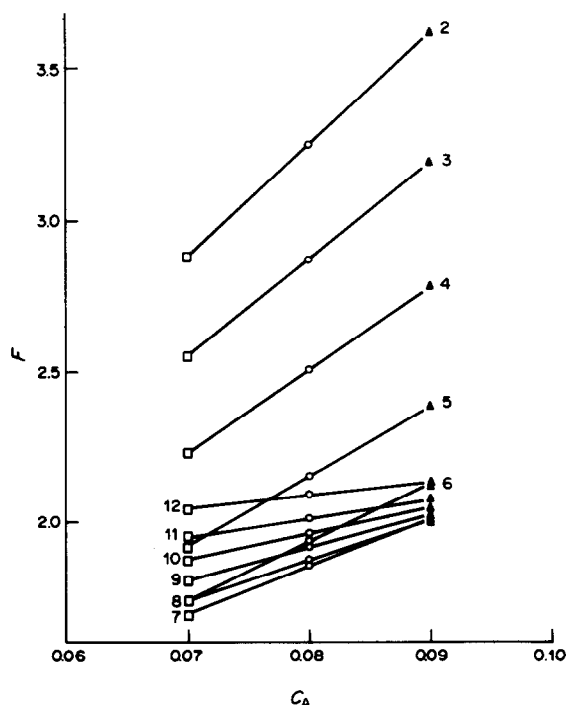


Fig. 4. Variation de F en fonction de C_A de pH = 2 à pH = 12. $C_M = 5.10^{-2} M$; $C_A = 7.10^{-2} M$ (□), $8.10^{-2} M$ (○), $9.10^{-2} M$ (▲).

Tableau 4. Erreur relative $\Delta[A]/[A]$ en % en fonction du pH; interpolation polynômiale de degré 2

pH	Rapport 7/5	Rapport 8/5	Rapport 9/5
5	0,62	-0,17	0,64
5,5	0,67	-0,29	0,91
6	1,73	-0,90	2,40
6,5	3,81	-1,69	3,41
7	4,46	-1,77	3,59
7,5	3,52	-1,24	2,51
8	2,03	-0,38	0,33
8,5	1,14	0,20	-1,38
9	0,66	0,35	-2,17
9,5	0,50	0,31	-2,49
10	0,79	0,23	-2,51
10,5	1,26	0,05	-1,72
11	2,22	-0,53	-0,06
11,5	3,81	-1,36	1,97
12	4,92	-1,88	3,05

passant par ces trois points, sauf évidemment aux extrémités pour lesquelles il n'est plus possible d'encadrer le point considéré.

Pour juger ces deux types de calcul des dérivées, les erreurs relatives sur la concentration en métal libre [M] selon le pH sont rassemblées dans le tableau 5. Les variations observées dépendent de la conjugaison de plusieurs facteurs.

Influence du pH. Quel que soit le rapport indiqué dans le tableau 5, il apparaît que les erreurs relatives $\Delta[M]/[M]$ dépendent largement du pH. On peut faire apparaître une zone comprise entre $\text{pH} = 8$ et $\text{pH} = 11$ pour laquelle les erreurs relatives sont les plus fortes. Si l'on se reporte à la figure 2 représentant les titrages initiaux, cette région correspond à une variation rapide du pH (zone d'équivalence). En outre, l'examen de la représentation graphique de l'évolution de la fonction auxiliaire F à différents pH (figure 5) montre que pour de telles valeurs du pH la courbure de la fonction F s'accroît nettement, l'assimilation de cette fonction à un polynôme devenant alors assez approximative.

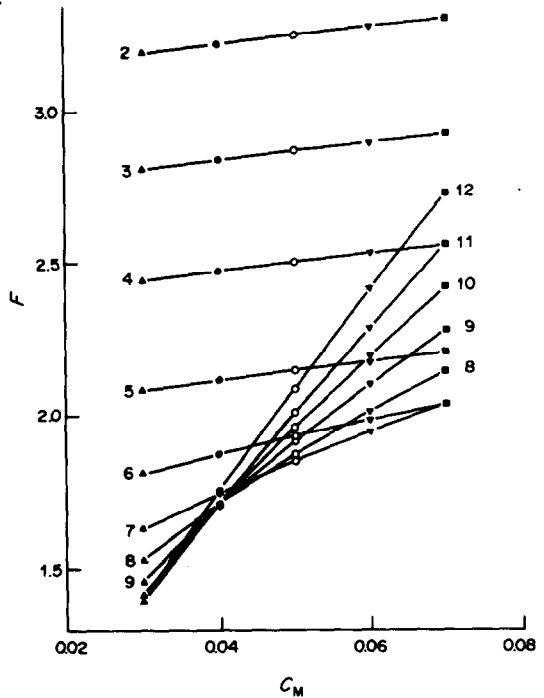


Fig. 5. Variation de F en fonction de C_M de $\text{pH} = 2$ à $\text{pH} = 12$. $C_A = 8 \cdot 10^{-2} M$; $C_M = 3 \cdot 10^{-2} M$ (\blacktriangle), $4 \cdot 10^{-2} M$ (\bullet), $5 \cdot 10^{-2} M$ (\circ), $6 \cdot 10^{-2} M$ (\blacktriangledown), $7 \cdot 10^{-2} M$ (\blacksquare).

Cette grande influence des variations de courbure est le critère prépondérant qui doit être conservé lors de l'examen des autres facteurs.

Importance des valeurs des rapports utilisés. Avec un polynôme d'interpolation de degré quatre, l'incertitude sur la concentration libre [M] est logiquement maximale pour les positions extrêmes et minimale pour le rapport central symétriquement encadré par les quatre autres rapports utilisés. Si l'on compare maintenant entre eux les rapports placés de manière symétrique vis à vis du rapport central, soit les rapports 8/4 et 8/6 d'une part et les rapports 8/3 et 8/7 d'autre part, il apparaît qu'à pH constant

Tableau 5. Erreurs relatives $\Delta[M]/[M]$ en % en fonction du pH; interpolation polynômiale de degré 2 et de degré 4

pH	Rapport 8/3		Rapport 8/4		Rapport 8/5		Rapport 8/6		Rapport 8/7	
	dégré 2	dégré 4	dégré 2	dégré 4	dégré 2	dégré 4	dégré 2	dégré 4	dégré 2	dégré 4
5	1,88	-0,70	-1,27	-0,11	-0,77	-0,05	-0,49	-0,21	1,14	0,80
5,5	1,94	-0,23	-1,41	-0,40	-0,80	0,04	-0,72	-0,06	0,50	-0,73
6	0,92	0,08	-0,99	-0,58	-0,35	0,00	-0,36	-0,07	0,44	-0,12
6,5	0,25	-1,11	-0,54	-0,15	0,58	-0,17	1,79	-0,13	-4,05	0,24
7	2,04	-2,84	-1,62	0,35	-0,59	-0,45	2,21	0,48	-7,09	-2,96
7,5	5,87	-14,05	-6,66	2,41	-5,53	-1,01	0,84	0,91	-5,95	-3,91
8	-1,53	-44,23	-15,80	8,34	-12,29	-0,72	-0,15	-0,59	-4,84	2,36
8,5	-20,50	-70,35	-23,89	17,56	-17,30	1,12	-0,54	-3,73	-4,36	14,73
9	-33,31	-81,10	-28,06	25,21	-19,72	2,92	-0,70	-6,24	-4,14	25,30
9,5	-37,11	-83,69	-29,17	28,09	-20,33	3,59	-0,79	-7,25	-3,99	29,55
10	-33,33	-81,21	-28,02	25,53	-19,65	2,98	-0,82	-6,60	-4,09	26,14
10,5	-20,31	-70,43	-23,94	17,71	-17,17	1,22	-0,66	-4,13	-4,36	15,57
11	-1,14	-44,59	-16,03	8,51	-12,12	-0,55	-0,23	-1,12	-4,92	3,43
11,5	6,54	-15,01	-6,96	2,82	-5,49	-0,89	0,82	0,34	-6,29	-2,87
12	2,12	-4,69	-1,72	1,06	-0,63	-0,46	2,50	0,03	-8,61	-2,77

l'erreur relative $\Delta[M]/[M]$ est dans l'ensemble plus importante pour le rapport le plus grand. Pour un même pH, cette variation des incertitudes sur la concentration libre $[M]$ en fonction du rapport résulte de l'augmentation de la courbure de la fonction auxiliaire F lorsque le rapport C_A/C_M croît, comme le montre la figure 5. Par conséquent, la détermination des dérivées sera sensiblement moins précise pour les rapports élevés.

Influence du degré du polynôme. Il est alors nécessaire de différencier les zones de pH.

—Dans les zones tamponnées (pH compris entre 5 et 8 et pH égal ou supérieur à 11), l'interpolation de degré quatre fournit en général de meilleures valeurs de la concentration libre $[M]$. Seul le rapport 8/3 fait exception puisque le degré deux conduit à des valeurs de meilleure précision. Cette exception est à nouveau liée aux variations de courbure en fonction du rapport. L'exploitation simultanée des cinq points combine des régions de courbures assez différentes. Dans la zone de courbure la plus élevée, elle rend donc l'approximation de la fonction F par un polynôme plus imprécise que si l'on exploite uniquement les trois plus forts rapports pour lesquels la courbure varie relativement moins.

—Dans la zone d'équivalence (pH compris entre 8 et 11), l'effet précédent est encore plus marqué. Ce sont alors généralement les résultats obtenus pour le degré deux qui sont relativement les moins imprécis, tout en étant beaucoup moins bons que ceux relatifs aux zones tamponnées. L'examen de la figure 5 est en accord avec cette constatation, les modifications de courbure en fonction du rapport étant beaucoup plus marquées dans cette zone de pH.

Une comparaison plus fine des valeurs de $\Delta[M]/[M]$ indique que l'écart entre les deux types d'interpolation s'atténue pour les rapports C_A/C_M centraux. Ainsi, les résultats sont voisins pour le rapport 8/4 alors que pour le rapport 8/5 l'interpolation de degré quatre devient même plus précise. En effet, pour ce dernier rapport, symétriquement encadré, la plus grande précision obtenue lors des étapes de dérivation à l'aide d'un polynôme de degré quatre comme dans les zones tamponnées l'emporte sur l'effet néfaste de l'importante variation de courbure entre les cinq points observé dans cette région.

Comparaison de la précision sur les concentrations libres $[M]$ et $[A]$. En comparant le seul rapport 8/5 à degré de polynôme égal, la concentration libre en métal $[M]$ est obtenue d'une manière moins précise que la concentration en complexant $[A]$ (Tableaux 4 et 5). Par contre, lorsqu'on utilise simultanément les cinq points, l'incertitude relative sur la concentration $[M]$ est alors du même ordre de grandeur que celle sur $[A]$.

Cas particulier du rapport globalement 1/1. En plus de sa position extrême défavorable, ce rapport est nettement plus sensible que les autres à la valeur du pH. Si pour les pH inférieurs à 8, les concentrations $[M]$

et $[A]$ sont relativement correctes, par contre en milieu plus alcalin elle sont totalement erronées. Cette anomalie ne peut s'expliquer que par un brusque changement de comportement de la fonction auxiliaire exactement pour ce rapport. Afin de vérifier cette hypothèse, il est nécessaire d'étudier le comportement de cette fonction de part et d'autre du rapport 1/1.

La variation des fonctions $F = f(C_A)_{C_M, [H]}$ et $F = f(C_M)_{C_A, [H]}$ sont représentées respectivement sur les figures 6 et 7. Comme supposé, une espèce de point anguleux apparaît progressivement à partir de pH = 8 exactement pour le rapport 1/1. Il devient ensuite très net après pH = 10, expliquant ainsi les valeurs aberrantes des concentrations libres $[M]$ et $[A]$ obtenues au delà de pH = 8.

Si cette étude du comportement de la fonction auxiliaire F reste purement formelle pour les rapports C_A/C_M inférieurs à 1/1 puisque pour ceux-ci l'hydroxyde $\text{Cu}(\text{OH})_2$ devrait précipiter en milieu neutre et basique, par contre elle montre que même si les complexes formés dans le rapport 1/1 se révèlent assez stables pour éviter cette précipitation, la méthode CILS conduira cependant à des résultats nettement erronés.

Composition moyenne des complexes

Compte tenu des observations précédentes, les concentrations libres en ion métallique $[M]$ employées

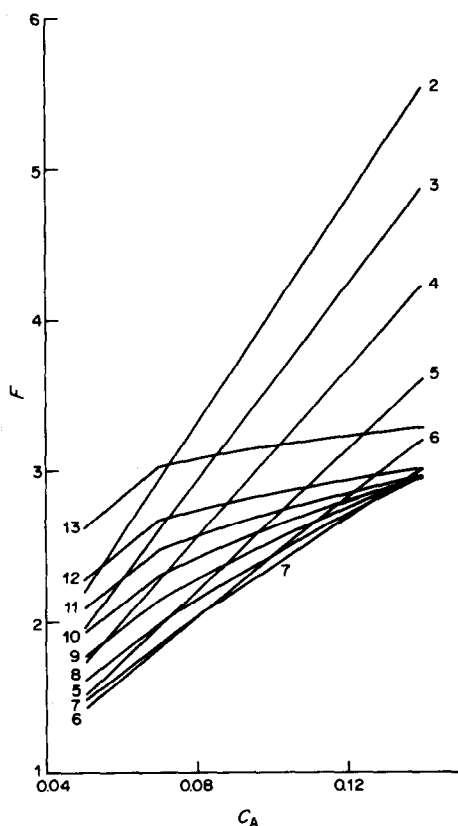


Fig. 6. Variation de F en fonction de C_A de pH = 2 à pH = 13. $C_M = 7 \cdot 10^{-2} M$; C_A varie de $5 \cdot 10^{-2}$ à $1,4 \cdot 10^{-1} M$

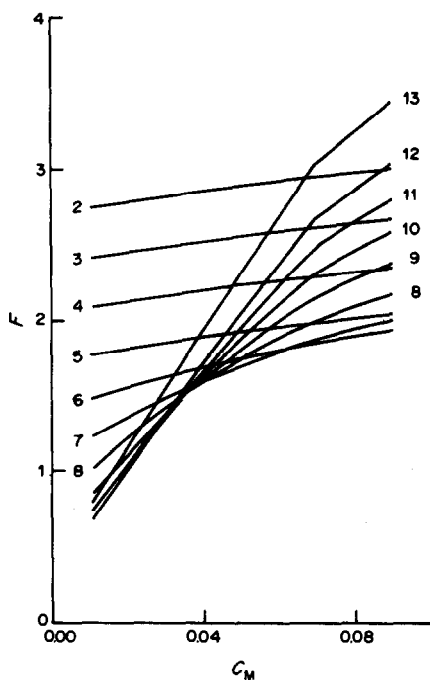


Fig. 7. Variation de F en fonction de C_M de pH = 2 à pH = 13. $C_A = 7.10^{-2}M$; C_M varie de 10^{-2} à $9.10^{-2}M$.

sont celles fournies grâce à l'interpolation polynômiale de degré quatre. La connaissance des concentrations $[M]$ et $[A]$ permet alors de déterminer la "somme des complexes" R puis les différents coefficients stoechiométriques moyens \bar{m} , \bar{a} et \bar{h} par l'intermédiaire du programme MAHBAR³⁸ qui exploite les équations (13) à (16). A titre d'exemple, les résultats obtenus pour deux rapports caractéristiques sont regroupés dans le tableau 6.

Pour le rapport 8/6 et des pH variant de 5 à 8, on constate que \bar{m} augmente régulièrement d'environ 1 à 1,4 alors que \bar{h} qui était initialement à peu près nul diminue jusqu'à $-0,9$. De plus, \bar{a} atteint au maximum environ 1,8 alors que le rapport C_A/C_M n'est que de 1,33/1. Par conséquent, au moins une espèce condensée en cuivre et hydroxylée, probablement $Cu_2A_2(OH)_2$, coexiste avec les complexes simples CuA et CuA_2 . A partir de pH = 11, \bar{m} et \bar{a} diminuent tous deux pour tendre vers 1 alors que \bar{h} évolue vers la valeur entière -2 . Ces variations sont l'indice d'une disparition progressive de l'espèce condensée en cuivre au profit d'un complexe mononucléaire, certainement $CuA(OH)_2$, l'existence simultanée du complexe $CuA_2(OH)_2$ ne pouvant cependant pas être totalement exclue.

Pour le rapport 8/4, de pH = 5 à pH = 8, \bar{m} reste sensiblement égal à 1 alors que \bar{h} diminue jusqu'à environ $-0,2$, indiquant alors la présence d'au moins un complexe hydroxylé mononucléaire au côté de l'espèce majoritaire CuA_2 . La formule la plus plausible est $CuA(OH)$ de composition brute identique à celle du dimère $Cu_2A_2(OH)_2$ précédemment

Tableau 6. Evolution de la composition moyenne des complexes en fonction du pH

pH	Rapport 8/4			Rapport 8/6		
	$\bar{m}_{\text{théorique}}$	$\bar{m}_{\text{calculé}}$	$\bar{h}_{\text{calculé}}$	$\bar{m}_{\text{théorique}}$	$\bar{m}_{\text{calculé}}$	$\bar{h}_{\text{calculé}}$
5	1,000	0,971	0,050	1,000	0,985	0,028
5,5	1,001	0,999	0,006	1,001	0,996	-0,006
6	1,007	1,014	-0,028	1,010	1,015	-0,045
6,5	1,036	1,045	-0,132	1,064	1,099	-0,207
7	1,062	1,072	-0,218	1,176	1,235	-0,519
7,5	1,049	1,037	-0,184	1,268	1,334	-0,766
8	1,029	0,944	-0,120	1,312	1,410	-0,899
11	1,031	0,938	-0,149	1,319	1,432	-0,943
11,5	1,054	1,031	-0,322	1,288	1,369	-1,103
12	1,075	1,072	-0,729	1,212	1,287	-1,351
12,5	1,051	1,047	-1,397	1,093	1,151	-1,733

envisagé. Ensuite, à partir de $\text{pH} = 11$, on retrouve l'apparition très probable de l'espèce $\text{CuA}(\text{OH})_2$.

L'examen des résultats afférents aux autres rapports conduit à des conclusions analogues. En résumé, les formules les plus plausibles des complexes formés correspondent à: $m = 1$ ou 2 , $a = 1$ ou 2 et $h = -1$ ou -2 . Parmi toutes les formules possibles, les plus probables semblent être CuA , CuA_2 , $\text{CuA}(\text{OH})$, $\text{Cu}_2\text{A}_2(\text{OH})_2$ et $\text{CuA}(\text{OH})_2$. L'existence d'autres complexes tels, par exemple, $\text{Cu}_3\text{A}_2(\text{OH})_4$ selon la théorie du "core + links" de Sillén^{39,40} ou bien $\text{CuA}_2(\text{OH})$ ne peut être totalement exclue puisqu'aucun des complexes hydroxylés n'est très nettement majoritaire. Seule l'étude de la variation de la somme minimum [équation (18)] en fonction des différentes combinaisons de complexes envisagées permettra de déterminer celle qui semble la plus probable.

Estimation des constantes de stabilité

Selon les remarques effectuées à la section précédente (détermination de $[M]$), seules les valeurs de R , $[M]$, $[A]$ et $[H]$ obtenues de $\text{pH} = 5$ à $\text{pH} = 8$ d'une part et de $\text{pH} = 11$ à $\text{pH} = 12,4$ d'autre part, ont été exploitées pour déterminer les constantes de stabilité des complexes, les rapports $7/3$, $8/3$ et $9/3$ ainsi que le rapport $7/7$ ayant été exclus des calculs. Le tableau 7 rassemble les résultats obtenus à l'aide du programme ESTCGF,³⁸ qui exploite l'équation (19), pour quelques uns des modèles envisagés.

Pour les modèles I et II qui font intervenir soit le monomère $\text{CuA}(\text{OH})$ soit le dimère $\text{Cu}_2\text{A}_2(\text{OH})_2$ à côté des complexes simples CuA et CuA_2 , les sommes S diffèrent assez peu l'une de l'autre, montrant ainsi que ces deux complexes hydroxylés doivent coexister en solution. Si l'on adjoint à chacun d'eux le complexe $\text{CuA}(\text{OH})_2$ qui semble apparaître en milieu basique (modèles III et IV) à nouveau les valeurs de la somme S sont proches, mais par contre d'un ordre de grandeur dix fois plus faible que pour les combinaisons I et II, indiquant ainsi la présence indéniable de l'espèce $\text{CuA}(\text{OH})_2$. La supposition consistant alors à faire coexister le monomère et le dimère, comme le suggèrent les résultats antérieurs, est confirmée par le modèle V pour lequel la valeur de la somme S est nettement plus faible que les précédentes.

Si à ce système on ajoute l'espèce $\text{Cu}_3\text{A}_2(\text{OH})_4$ précédemment citée, la somme minimum (modèle VI) reste inchangée et l'écart-type de $\log \beta_{3,2,-4}$ est anormalement élevé. Cette hypothèse est donc à rejeter. Enfin, si à la combinaison V on ajoute successivement les espèces $\text{CuA}_2(\text{OH})$ et $\text{CuA}_2(\text{OH})_2$, la somme S ne diminue que très peu alors que les écarts-types relatifs aux $\log \beta_{m,a,h}$ correspondants sont importants (modèles VII et VIII). Ces deux espèces sont donc fort improbables et le meilleur système est certainement le modèle V, c'est à dire qu'il existe essentiellement les espèces CuA , CuA_2 , $\text{CuA}(\text{OH})$, $\text{Cu}_2\text{A}_2(\text{OH})_2$ et $\text{CuA}(\text{OH})_2$.

Cette conclusion est d'ailleurs confirmée *a posteriori* par le tracé, sur les figures 2 et 3, des courbes de neutralisation effectué par l'intermédiaire d'un programme original de simulation graphique de fonctions³⁸ et à l'aide des estimations des constantes de stabilité obtenues pour le modèle retenu. Dans tous les cas, la concordance entre les points expérimentaux et les courbes recalculées est satisfaisante.

CONCLUSIONS

A partir de la seule mesure du pH , la méthode CILS permet de déterminer les formules des complexes les plus probables, sans aucune hypothèse initiale quant à leurs compositions. Elle est donc particulièrement utile pour l'étude des solutions où coexistent de nombreuses espèces puisqu'elle conduit à sélectionner le modèle le plus plausible parmi tous ceux envisageables. Elle est également l'une des rares méthodes qui puisse permettre l'étude de systèmes chimiques où interviennent des complexes à haut degré de nucléarité. Comme il semble irréaliste de tenter de sélectionner le modèle le plus plausible en procédant à un examen exhaustif de l'ensemble des modèles possibles par comparaison des résultats des différents affinements,⁴¹ cette méthode représente donc une étape de grand intérêt puisqu'elle permet de limiter très sensiblement le nombre de modèles raisonnablement envisageables avant un affinement final.

Contrairement aux travaux de Sarkar *et al.*¹⁴⁻¹⁶ ou Avdeef et Kearney,²⁶ la méthode CILS fournit directement les valeurs des constantes de stabilité des complexes du modèle sélectionné, sans avoir recours à des estimations initiales. Cependant, elle ne conduit qu'à des valeurs approximatives des constantes de stabilité au moins pour les espèces minoritaires comme le montre le tableau 7. Par conséquent, il nous semble impératif d'affiner ces valeurs, contrairement à plusieurs auteurs dont Sarkar *et al.*¹⁵⁻¹⁸ ainsi que Guevremont et Rabenstein²³ qui considèrent comme définitives les constantes de stabilité obtenues par des méthodes utilisant les techniques d'intégration et de dérivation. En fournissant de bonnes approximations des constantes de stabilité, la méthode CILS constitue un apport précieux aux techniques d'affinement dont on connaît le risque de divergence lorsque les estimations initiales sont trop éloignées des valeurs finales.

Par rapport à la méthode FICS, celle que nous proposons est plus simple et plus rapide puisqu'elle évite deux étapes supplémentaires d'intégration. Son étude sur un exemple simulé montre que les techniques mathématiques utilisées entraînent toutefois un certain nombre d'incertitudes malgré un traitement entièrement informatisé. Pour tenter de les minimiser, on a intérêt à respecter les conditions suivantes:

—Il est préférable d'utiliser un polynôme de degré cinq pour l'étape d'intégration.

Tableau 7. Log $\beta_{m,n,k}$ obtenus pour différentes combinaisons de complexes; les valeurs entre parenthèses correspondent aux écarts-types σ

No du modèle	S	CuA	CuA ₂	CuA(OH)	Cu ₂ A ₂ (OH) ₂	Cu ₃ A ₂ (OH) ₄	CuA(OH) ₂	CuA ₂ (OH)	CuA ₂ (OH) ₂	CuA ₂ (OH) ₂
I	2,097.10 ⁻²	9,581 (0,006)	16,585 (0,013)	2,738 (0,010)						
II	3,092.10 ⁻²	9,637 (0,006)	16,719 (0,009)		6,819 (0,013)					
III	1,704.10 ⁻³	9,611 (0,002)	16,610 (0,003)	2,620 (0,004)						
IV	2,775.10 ⁻³	9,652 (0,002)	16,700 (0,003)		6,704 (0,005)					
V	8,585.10 ⁻⁴	9,626 (0,001)	16,642 (0,003)	2,411 (0,013)	6,323 (0,020)					
VI	8,585.10 ⁻⁴	9,626 (0,001)	16,642 (0,003)	2,411 (0,013)	6,322 (0,023)	-6,360 (3,898)				
VII	8,468.10 ⁻⁴	9,626 (0,001)	16,638 (0,003)	2,414 (0,013)	6,324 (0,019)					
VIII	8,360.10 ⁻⁴	9,626 (0,001)	16,640 (0,003)	2,412 (0,013)	6,331 (0,019)					
Constantes de référence		9,63	16,65	2,21	6,59					

—Lors de la dérivation, les meilleurs résultats sont obtenus avec un polynôme de degré quatre, les points au voisinage des équivalences devant toutefois être éliminés.

—Les concentrations libres $[M]$ étant plus sensibles aux erreurs que les concentrations $[A]$, il est préférable d'utiliser un nombre supérieur d'expériences à concentration C_M variable que l'inverse.

—Lors de l'étape finale d'estimation des constantes de stabilité, il vaut mieux éliminer les titrages de la "ligne" relative aux rapports C_A/C_M les plus élevés, ainsi qu'éventuellement celui de rapport 1/1.

LITTÉRATURE

1. B. O. A. Hedström, *Arkiv Kemi*, 1953, **6**, 1.
2. *Idem*, *Acta Chem. Scand.*, 1955, **9**, 613.
3. J. Lefevre, *J. Chim. Phys.*, 1957, **54**, 553.
4. *Idem*, *ibid.*, 1957, **54**, 567.
5. *Idem*, *ibid.*, 1957, **54**, 581.
6. *Idem*, *ibid.*, 1957, **54**, 601.
7. N. Ingri, G. Lagerström, M. Frydman et L. G. Sillén, *Acta Chem. Scand.*, 1957, **11**, 1034.
8. N. Ingri et F. Brito, *ibid.*, 1959, **13**, 1971.
9. L. G. Sillén, *ibid.*, 1961, **15**, 1981.
10. R. Österberg, *ibid.*, 1960, **14**, 471.
11. *Idem*, *ibid.*, 1962, **16**, 2434.
12. *Idem*, *ibid.*, 1965, **19**, 1445.
13. *Idem*, *Arkiv Kemi*, 1966, **25**, 177.
14. B. Sarkar et T. P. A. Kruck, *Can. J. Chem.*, 1973, **51**, 3541.
15. T. P. A. Kruck et B. Sarkar, *ibid.*, 1973, **51**, 3549.
16. *Idem*, *ibid.*, 1973, **51**, 3555.
17. B. Sarkar, *J. Indian Chem. Soc.*, 1977, **54**, 117.
18. S. J. Lau et B. Sarkar, *Biochem. J.*, 1981, **199**, 649.
19. W. A. E. McBryde, *Can. J. Chem.*, 1973, **51**, 3572.
20. T. B. Field et W. A. E. McBryde, *ibid.*, 1978, **56**, 1202.
21. M. Wozniak et G. Nowogrocki, *Bull. Soc. Chim. France*, 1974, **3-4**, 435.
22. R. Guevremont et D. L. Rabenstein, *Can. J. Chem.*, 1977, **55**, 4211.
23. *Idem*, *ibid.*, 1979, **57**, 466.
24. A. Avdeef et K. N. Raymond, *Inorg. Chem.*, 1979, **18**, 1605.
25. A. Avdeef, *ibid.*, 1980, **19**, 3081.
26. A. Avdeef et D. L. Kearney, *J. Am. Chem. Soc.*, 1982, **104**, 7212.
27. A. Avdeef et J. A. Brown, *Inorg. Chim. Acta*, 1984, **91**, 67.
28. J. Gandeboeuf et P. Souchay, *J. Chim. Phys.*, 1959, **56**, 358.
29. R. P. Martin et R. A. Pâris, *Bull. Soc. Chim. France*, 1963, **3**, 570.
30. M. Cadot-Smith, *J. Chim. Phys.*, 1963, **60**, 957.
31. *Idem*, *ibid.*, 1963, **60**, 976.
32. M. Bonnet, R. P. Martin et R. A. Pâris, *Bull. Soc. Chim. France*, 1965, **1**, 176.
33. F. Bertin, G. Thomas et J. C. Merlin, *ibid.*, 1967, **7**, 2393.
34. F. Bertin et G. Thomas, *ibid.*, 1968, **3**, 1255.
35. *Idem*, *ibid.*, 1972, **4**, 1665.
36. G. Duc, F. Bertin et G. Thomas-David, *ibid.*, 1975, **3-4**, 495.
37. R. Näsänen, M. Koskinen, R. Salonen et A. Kiiski, *Suomen Kem.*, 1965, **B38**, 81.
38. R. Fournaise, programmes non publiés.
39. L. G. Sillén, *Acta Chem. Scand.*, 1954, **8**, 299.
40. *Idem*, *ibid.*, 1954, **8**, 318.
41. P. Gans, *Adv. Mol. Relaxation Interact. Process.*, 1980, **18**, 139.

Summary—In the study of complex formation in aqueous solution by means of pH measurements, it is very useful to know the free ion concentrations in order to find each species composition and then calculate approximate values of their stability constants. From the pH determination alone, the unmeasured free ion concentrations can be calculated by a method in which a minimum number of integration and derivation steps are required. This process, called CILS, has been entirely computerized, and its conditions of application are illustrated with a simulated example.

MULTIPARAMETRIC CURVE FITTING—X

A STRUCTURAL CLASSIFICATION OF PROGRAMS FOR ANALYSING MULTICOMPONENT SPECTRA AND THEIR USE IN EQUILIBRIUM-MODEL DETERMINATION

MILAN MELOUN

Department of Analytical Chemistry, College of Chemical Technology, CS-532 10 Pardubice,
Czechoslovakia

MILAN JAVŮREK

Computing Centre, College of Chemical Technology, CS-532 10 Pardubice, Czechoslovakia

JOSEF HAVEL

Department of Analytical Chemistry, Purkyně University, CS-611 37 Brno, Czechoslovakia

(Received 6 February 1985. Revised 4 January 1986. Accepted 23 January 1986)

Summary—A functional structure-classification of programs for analysis of spectra elucidates their efficiency for determination of the stoichiometric indices, stability constants and molar absorptivities of complex species. SQUAD (84) introduces new functional units for (i) determination of the number of light-absorbing species, (ii) a rigorous fitness test, (iii) plotting three-dimensional graphs of a paraboloid minimum response-surface as a function of two selected parameters, and a graph of the fitted absorbance response-plane, (iv) simultaneous estimation of stoichiometric indices and stability constants, (v) simulation of an absorbance matrix data by loading with random errors related to the instrumental variance of the absorbance. A guide to experimental procedure and computational strategy for chemical model determination is given and nine diagnostic tools useful in finding the number of species present and their stoichiometry and stability constants by regression analysis of spectra are tested, by use of literature data.

The spectrophotometric study of solution equilibria has been greatly advanced by computer-assisted methods of analysing spectra,¹⁻²⁰ but comparatively few programs are yet available. Programs for calculation of stability constants from spectrophotometric data are usually classified according to the algorithm used,^{1,2} but the structural classification introduced earlier in this series³⁻⁵ seems to be useful for comparing the number and efficiency of the logic tools used in a program. Splitting a program structure into logic units helps in elucidation of its anatomy and makes further program implementation and modification easier. It also helps in understanding the *modus operandi* of a rather sophisticated and long program.

This paper is intended to familiarize the reader with the individual logic units of sophisticated programs for analysis of multicomponent spectra, and is illustrated with eight selected programs, LETAGROP-SPEFO,⁶ FA608 + EY608,⁷ SQUAD(75),⁸ SQUAD(78),⁹ DALSFEEK,¹⁰ PSE-QUAD,¹¹ SQUAD(80)^{12,13} and the new SQUAD(84), the last of which incorporates new diagnostic tools.

FA608 + EY608 and LETAGROP-SPEFO have been extended to include a fitness test, printer-plotting of graphs, *etc.* A guide to efficient experimentation and computer evaluation for validating chemical models is given, and use of the recommended diagnostics is illustrated by an example.

THEORY

Study of equilibria by analysis of multicomponent spectra

In absorbance-data analysis the Lambert-Beer law and the law of absorbance additivity are assumed to hold. The published programs can deal with various numbers, n_c , of components, ranging from three (metal M, ligand L and proton H) for LETAGROP-SPEFO⁶ to five (two metals, two ligands and proton or hydroxide) for SQUAD,^{8,12,13} which form a set of species of general formula $M_p L_q H_r$, a particular chemical model being represented by n_c such species and their stoichiometry, $(p, q, r)_j$, $j = 1, \dots, n_c$, the overall stability constants being expressed in the general form

$$\beta_{pqr} = [M_p L_q H_r] / ([M]^p [L]^q [H]^r) = c / (m^p l^q h^r) \quad (1)$$

For the i th solution measured at the k th wavelength, the absorbance A_{ik} is given by

$$A_{ik} = \sum_{j=1}^{n_c} \varepsilon_{k,j} c_j \\ = \sum_{j=1}^{n_c} (\varepsilon_{pqr,k} \beta_{pqr} m^p l^q h^r)_j \quad (2)$$

where $\varepsilon_{pqr,k}$ is the molar absorptivity of species $M_p L_q H_r$ at the k th wavelength. The absorbance A_{ik} is an element of the $(n_w \times n_c)$ absorbance matrix A for n_s solutions with known concentrations c_M , c_L , and c_H and at n_w wavelengths. The Lambert-Beer law can be written in matrix notation as

$$A = \varepsilon C \quad (3)$$

where ε is the $(n_w \times n_c)$ matrix of the molar absorptivities and C is the $(n_c \times n_s)$ matrix of the concentrations of the species concerned. It is assumed that all n_c species absorb light in the chosen spectral range.

The spectrophotometric equilibrium program is set up to adjust β_{pqr} and ε_{pqr} for any absorbance data by minimizing the residual-square sum function U

$$U = \sum_{i=1}^{n_s} \sum_{k=1}^{n_w} (A_{\text{exp},i,k} - A_{\text{calc},i,k})^2 \\ = \sum_{i=1}^{n_s} \sum_{k=1}^{n_w} \left(A_{\text{exp},i,k} - \sum_{j=1}^{n_c} \varepsilon_{k,j} c_j \right)^2 \approx \text{minimum} \quad (4)$$

where the dependent variable A_{ik} is an element of the $(n_s \times n_w)$ absorbance response-plane, and the independent variables are the total concentrations c_M , c_L and c_H , which are varied in the n_s solutions. Parameters to be determined may be divided into three groups according to the approach to be used in the computation as follows.

(1) A hypothetical chemical model is supplied by the user in the input. This includes a guess for the number of light-absorbing complexes, n_c , and a list of species assumed, or proved by means of an automatic species selector (the trial and error method) to be present. Some programs do not require a guess for n_c as input [e.g., FA608+EY608,⁷ SQUAD(78)⁹ and SQUAD(84)]; instead, advanced factor analysis is used to determine the absorbance matrix rank, which should be equal to or less than n_c . In solutions with a limited number of complexes, direct determination of stoichiometric indices (the variable stoichiometric indices method¹⁴) is an alternative to guessing which complexes are present.

(2) The estimates of the stability constants $\beta_{pqr,j}$, $j = 1, \dots, n_c$, are adjusted by the regression algorithm and at the same time a matrix of molar absorptivities $[(\varepsilon_{pqr,k}, k = 1, \dots, n_w)_j, j = 1, \dots, n_c]$ is estimated from the current values of stability constants.

(3) For a set of current values of β_{pqr} the free concentrations of metal m and ligand l , $[H^+]$ is known from pH measurement, for each solution calculated, and then the concentrations of all the

complexes in the equilibrium mixture, $[M_p L_q H_r]_j$, $j = 1, \dots, n_c$, forming for n_s solutions the matrix C .

Structure of the regression program for analysis of spectra

Each logic unit of this advanced regression program represents one functional block, which may contain one or more subroutine(s), and the diagram in Fig. 1 of reference 5 may therefore be extended for new units. Eight programs will be compared in Table 1, and their structures discussed.

The LETAGROP-SPEFO pit-mapping algorithm by Sillén and Warnqvist⁶ was a pioneering program for chemical-model determination by analysis of spectrophotometric data, and some of its features are still unsurpassed. Absorbance and concentration data are treated separately for each wavelength to adjust β_{pqr} and ε_{pqr} , and then the computer calculates the minimum residual-square sums, and finds the lowest value for U for a set of parameters β_{pqr} . The minimization process to find the "best" stability constants β_{pqr} and molar absorptivities is applied at two levels: the β_{pqr} values are varied on the upper level, and for each set of β_{pqr} , the concentrations and molar absorptivities of the complexes are calculated at the lower level. The sum of squared residuals can be set on input to refer to the absolute residuals or the relative residuals. Negative values of ε_{pqr} are eliminated by subroutine MIKO.

Kankare's regression program FA608+EY608 evaluates equilibrium constants and their standard deviations for multicomponent systems, from spectral data.⁷ The factor analysis algorithm, FA608, estimates the number of independently varying light-absorbing species and eliminates any "outlying" spectra points. The hypothetical chemical model defined by the stoichiometric coefficients of the reaction products is tested by searching for optimum values of the equilibrium constants, molar absorptivities and concentrations of all species of interest by algorithm EY608.

PSEQUAD is an advanced program for analysis of spectrophotometric and potentiometric data on equilibria, developed by Nagypál and Zékány.¹¹ The program calculates all unknown free concentrations of components from the mass-balance equations by an original method, along with stability constants and molar absorptivities.

DALSFEK, by Alcock *et al.*,¹⁰ deals with two types of observable variables, absorbance and the potential of an indicator electrode, and both are used in the program as dependent variables. The total concentrations are assumed to be independent variables. The Marquardt method²⁵ is used to fit free concentrations of each species to the mass-balance equations. The same algorithm is used to refine the stability constants.

SQUAD was developed by Leggett and McBryde⁸ in 1975 and is denoted here as SQUAD(75). Jančář and Havel⁹ made some improvements and

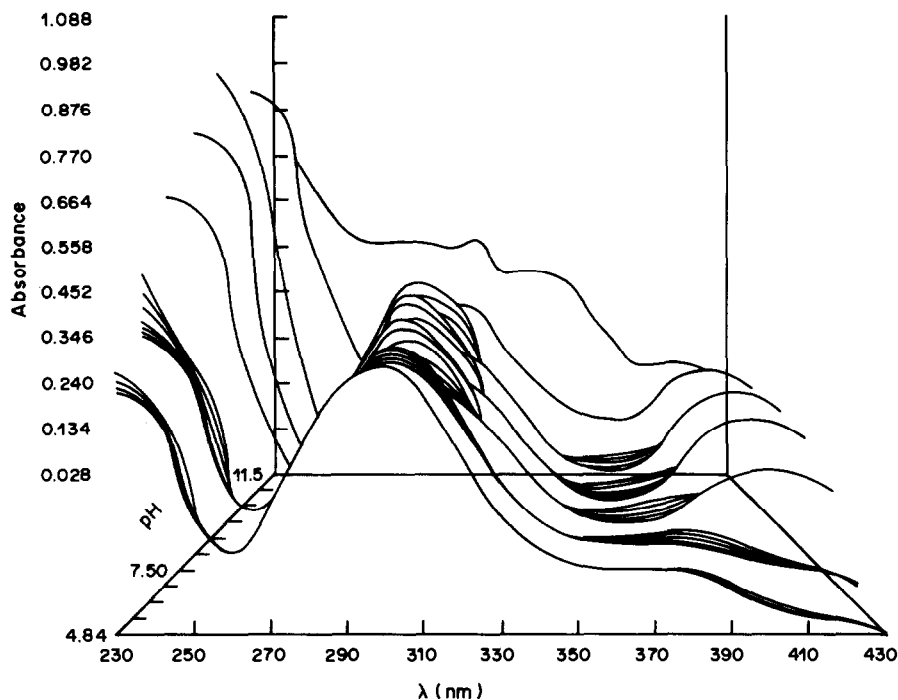


Fig. 1. Three-dimensional graph of the absorbance-response-plane of 37 experimental spectra at 20 wavelengths for various mole-ratios of 2,3-dihydroxynitrobenzene (LH_2) and boric acid (MH), $q_M = c_M/c_L$, vs. pH. Data taken from ref. 47.

produced SQUAD(78), known in the literature as SQUAD-G,^{9,15,16} which can read spectra without a constant wavelength increment. A segmented version of SQUAD(78) can be used with small computers; both versions were extensively tested.⁹ Leggett¹² also revised SQUAD(75) to produce SQUAD(80)¹³ which has "user-friendly" data input to simplify its use. The chemical model hypothesis is changed by addition or removal of one card per species, since all information relevant to a species is collected on one card. The molar absorptivity computation can be done by multiple regression or constrained non-negative linear least-squares. Meloun^{17,18} extended the diagnostic tools in SQUAD(80) for (i) determination of the number of light-absorbing species, (ii) a test for degree-of-fit by statistical analysis of residuals of each spectrum and of the whole absorbance matrix, (iii) a printer-plot of estimated molar absorptivities and their standard deviations vs. wavelength. The result, SQUAD(81), has been tested.^{21,22} The new version SQUAD(84), contains some additional diagnostics, including a three-dimensional graph of the predicted absorbance response-plane through the experimental points, and of the paraboloid response-surface of the U function as a function of two parametric coordinates. SQUAD(84) also generates simulated spectra on the basis of the selected stability constants, molar absorptivities and experimental conditions of the equilibrium system, and produces an absorbance matrix containing elements loaded with random

error. Stoichiometric indices are determined together with the stability constants of the complexes by the stoichiometry estimation method.¹⁴

Logic units

(1) The RESIDUAL-SQUARE SUM unit.

LETAGROP-SPEFO⁶ allows a choice in the formulation of the residual-square-sum, between "absolute" [equation (4)] and "relative" residuals. The other programs in Table I use absolute residuals, and DALSF EK¹⁰ and PSEQUAD¹¹ also allow treatment of potentiometric data. PSEQUAD can minimize a U function composed from volume (or concentration) residuals, potential residuals and absorbance residuals simultaneously, according to the weighting factor for each type of residual selected on input.

(2) The MINIMIZATION unit.

LETAGROP-SPEFO⁶ uses the pit-mapping algorithm²⁴ with "trial-and-error" human-controlled minimization. Kankare⁷ modified Chandler's STEPIT in program EY608. DALSF EK¹⁰ uses Marquardt's method²⁵ and PSEQUAD¹¹ the Gauss-Newton method. The first version of SQUAD was based on SCOGS,²⁶ a Gauss-Newton program. The latest versions of SQUAD use conventional multiple regression (MR) in the SOLVE subroutine for solving a set of over-determined linear equations. The MR technique is interchangeable with the NNLS (the Gauss-Newton non-negative least-squares algo-

Table 1. A survey of advanced spectrophotometric equilibrium programs for chemical model determination

Logic unit	LETAGROP-SPEFO A. Original B. Extended	FA608 + EY608 A. Original B. Extended	A. SQUAD(1975) B. SQUAD(1978)	DALSFEK	PSEQUAD	A. SQUAD(1980) B. SQUAD(1984)
1. RESIDUAL-SQUARE SUM	Absolute and relative absorbance	Absorbance	Absorbance	Absorbance, e.m.f.	Absorbance, e.m.f., volume	Absorbance
2. MINIMIZATION (Process is)	Pit-mapping (Heuristic)	STEPT (Algorithmic)	Gauss-Newton (Algorithmic)	Marquardt (Algorithmic)	Gauss-Newton (Algorithmic)	Multiple regression, NNLS Gauss-Newton method (Algorithmic)
3. ERROR ANALYSIS	$s(A)$ $s(\beta_{ppr}), s(\epsilon_{ppr})$	$s_k(A), s(A)$ $s(\beta_{ppr})$	$s(A)$ $s(\beta_{ppr}), s(\epsilon_{ppr})$ ρ_{ij}	$s(A)$ $s(\beta_{ppr}), s(\epsilon_{ppr})$ ρ_{ij} R -factor	$s(A)$ $s(\beta_{ppr}), s(\epsilon_{ppr})$ r_{ij}, ρ_{ij}, R_i $m_{r,1}, \bar{r} $	$s_k(A), s(A)$ $s(\beta_{ppr}), s(\epsilon_{ppr})$ ρ_{ij}
4. FITNESS TEST	A. Missing B. STATS test	A. $s(r), i = 1, n_s$ B. STATS test	$s(r), i = 1, n_s$	Missing	Random error	A. Missing B. STATS test
5. DATA SIMULATION	Missing	Missing	A. Missing	Missing		A. Missing
6. FREE CONCENTRATION	BDTV routines	STEPT	Newton-Raphson	Gauss-Newton	Newton-Raphson	Constrained Newton-Raphson
7. SPECIES NUMBER	Missing	FA608 Factor analysis	A. Missing B. RANKANAL Triangularization	Separate program	Missing	A. Missing B. FA608
8. ABSORPTIVITY (Process)	Pit-mapping (Heuristic)	STEPT (Algorithmic)	ECOEF routine (Algorithmic)	Marquardt (Algorithmic)	"Third strategy", (Algorithmic)	ECOEF routine (Algorithmic)
9. SPECIES SELECTOR	STYRE block	Missing	Missing	Missing	Species selector	A. Missing B. ESI method
10. VISUALIZATION	Missing	Missing	Missing	Missing	$\epsilon = f(\lambda)$ curves	A. Missing B. A-plane U-plane U contour $\epsilon = f(\lambda)$ curves
11. INPUT (n_s, n_c, n_w, n_t)	3, 20, 25, 50	4, 7, 40, 50	A. 5, 6, 26, 30 B. 5, 10, 50, 70	8, 6, 20, n_s	Dynamic dimensions	5, 14, 40, 40
12. OUTPUT (print of)	(1), (2), (3), (5), (6), (8), (9), (10)	(1), (2), (3), (4), (5), (8), (9), (10)	(1), (2), (3), (4), (5), (6), (8), (9), (10), (11)	(1), (2), (3), (5), (6), (8), (10)	(1), (2), (3), (5), (6), (7), (8), (9), (10)	(1), (2), (3), (4), (5), (6), (7), (8), (9), (10), (11), (12)

ithm) method which computes molar absorptivities, but is protected against the occurrence of negative elements in the solution vector.

(3) The ERROR ANALYSIS unit.

In LETAGROP-SPEFO,⁶ as in LETAGROP in general, there are several statistical measures: the standard deviation of the absorbance, $s(A)$, denoted here as SIGY, is found by dividing U_{\min} by the number of degrees of freedom; the standard deviations of the stability constants, $s(\beta_i)$, are found by defining the "D-boundary" supercurve,²⁷ and taking the standard deviation $s(\beta_i)$ for each β_i parameter as the maximum difference, $s(\beta_i) = [(\beta_D - \beta_{\min})]_{\max}$ between the value (β_D) for β_i at any point on the D boundary and the value (β_{\min}) for β_i at the minimum.

Program EY608⁷ calculates the covariance matrix, and the square roots of its diagonal elements represent the standard deviations of the parameters. The standard deviation of the absorbance, $s(A)$, is calculated from U_{\min} in the same way as in LETAGROP-SPEFO. DALSF⁸ calculates in its final iteration an unbiased estimate of the variance of an observation with unit weighting, and the standard deviations of the parameters, from the variance-covariance matrix. Correlation coefficients are also calculated to allow consideration of the conditioning of the problem, and the precision of the parameter estimates.

PSEQUAD¹¹ evaluates $s(A)$, the standard deviations of the parameters, $s(\beta_i)$, and the partial, multiple and total correlation coefficients. These are calculated from the elements of the matrix $\mathbf{B} = \mathbf{J}^T \mathbf{W} \mathbf{J}$ where \mathbf{J} is the Jacobian matrix, \mathbf{J}^T is its transpose and \mathbf{W} is the diagonal weighting matrix used in the Gauss-Newton method. The partial correlation coefficient gives a measure of the interdependence of two parameters β_i and β_j with the assumption that the other parameters are fixed in value: $r_{ij} = B_{ij}/(B_{ii}B_{jj})^{1/2}$. The total correlation coefficient also give a measure of the interdependence of two parameters, but the other parameters are regarded as adjustable: $\rho_{ij} = C_{ij}/(C_{ii}C_{jj})^{1/2}$. The multiple correlation coefficient gives a measure of the independence of a given stability constant from all the others, $R_i = [1 - 1/B_{ii}C_{ii}]^{1/2}$ where $\mathbf{C} = \mathbf{B}^{-1}$. All these correlation coefficients may have values between -1 and $+1$. Zero means complete independence, and $+1$ or -1 means complete correlation. Two completely correlated species cannot be included in a chemical model simultaneously, because the relevant stability constants are strongly correlated.

SQUAD estimates $s(A)$, the standard deviations of the stability constants, $s(\beta_i)$, and total correlation coefficients.

(4) The FITNESS TEST unit.

This unit contains the criteria for testing the correctness of a hypothetical chemical model. To identify the "best" or true chemical model when several

are possible or proposed, and to establish whether or not the chemical model represents the data adequately, the residuals should be analysed.²⁸ The goodness-of-fit achieved is easily seen by examination of the differences between the experimental and calculated values of the dependent variable, $r_{i,k} = A_{\text{exp},i,k} - A_{\text{calc},i,k}$. One of the most important statistics calculated is the standard deviation of the dependent variable, $s(A)$, calculated from the set of refined parameters at the end of each minimization cycle, and when the minimization is terminated. It is usually compared with the standard deviation of absorbance calculated by a factor analysis, $s_k(A)$, and if $s(A) \leq s_k(A)$, or $s(A) \leq s_{\text{inst}}(A)$, the instrumental error of the spectrophotometer used, the fit is considered to be good. Although statistical analysis of residuals^{4,28-30} gives the most rigorous test of the degree of fit, realistic empirical limits are often used.^{15,16} For example, when $s_{\text{inst}}(A) \leq s(A) \leq 0.005$, the degree of fit is taken as acceptable, whereas $s(A) > 0.010$ indicates that a good fit has still not been obtained. The statistical tools applied to a set of residuals have been described.^{4,29,30}

If $s(A)$ or the mean residual and its standard deviation are too large compared with $s_k(A)$ and $s_{\text{inst}}(A)$, respectively, the postulated stoichiometry of the chemical model tested is incorrect, or the minimization algorithm has found a false minimum. Graphical presentation of the residuals assists the detection of an outlier spectrum point, a trend in the spectrum residuals, or an abrupt shift of level in the spectra. The actual distribution of the spectrum residuals is tested to find out whether it is Gaussian,^{4,29} by means of the residual mean $m_{r,1}$, the mean residual $|\bar{r}|$, and its standard deviation $s(r)$, the skewness $m_{r,3}$ (should be zero), the kurtosis $m_{r,4}$ (should be 3) and the Pearson χ^2 test. If the Hamilton R -factor of relative fit, expressed as a percentage ($R \times 100\%$), is $< 0.5\%$ the fit is excellent, but if it is $> 2\%$ the fit is poor. The R -factor gives a rigorous test of the null hypothesis H_0 (giving R_0) against the alternative H_1 (giving R_1). H_1 can be rejected at the α significance-level if $R_1/R_0 > R_{(m,n-m,\alpha)}$, where n is the number of experimental points, m is the number of unknown parameters, and $(n-m)$ is the number of degrees of freedom. The value of $R_{(m,n-m,\alpha)}$ may be found in statistical tables.³⁰

Most programs calculate only $s(A)$. EY608 and LETAGROP-SPEFO calculate $s(A)$ for each spectrum; we have extended both to allow statistical analysis of residuals by the STATS subroutine.²⁹ PSEQUAD¹¹ calculates $m_{r,1}$ and $|\bar{r}|$ as well. Rigorous residuals analysis by the STATS subroutine²⁹ is included in SQUAD(84).

(5) The DATA SIMULATION unit.

To test the reliability of program function for a particular type of equilibrium, simulated data are often used. For true values of the parameters (stability constants and molar absorptivities) and

given concentrations and pH, "theoretical spectral points" are calculated precisely. Each theoretical point is then transformed into an "experimental" one by the addition of a random error, e , generated by a random-error generator, and related to the instrumental error of absorbance, $s_{\text{inst}}(A)$, set by the user on input. These random errors should have Gaussian distribution, but this must be checked as described earlier.⁴

Loading points with high random errors is likely to cause a decrease in the accuracy and precision of the parametric estimates; the lower the value of $s_{\text{inst}}(A)$, the more accurate and precise are the estimates. When many parameters are to be refined or there are ill-conditioned parameters in a chemical model, spectra of lower precision may result in erroneous and uncertain values of the parametric estimates.

Only PSEQUAD,¹¹ SQUAD(78)⁹ and SQUAD(84) allow such data simulation. SQUAD(84) checks the actual distribution of the errors as well.

(6) The FREE CONCENTRATION unit.

The BDTV procedure³¹ in LETAGROP-SPEFO solves the equilibrium and mass-balance equations for various cases with 2–4 reacting components. Free concentrations are estimated by the same approach as in HALTAFALL.³²

Subroutine SS608 in EY608⁷ calculates the free-concentration matrix C .

DALSF EK¹⁰ includes a routine which uses a Gauss–Newton iteration on some "guessed" concentrations, with the current values of the stability constants and the mass-balance equations, to calculate the concentrations of all species in the system.

In PSEQUAD¹¹ the calculation of the unknown free concentration is done by a standard Newton–Raphson procedure, with Cholesky's algorithm to solve the linear equations. The free concentrations are calculated on a logarithmic scale, so no negative concentration may occur in the course of the iteration.²³

SQUAD contains the subroutine CCSCC which calls COGSNR,²⁶ in which the concentrations of species in the i th solution are calculated for the current set of stability constants by a constrained Newton–Raphson method originated by Sayce.²⁶

A clear insight into complicated ionic equilibria is offered by a distribution diagram of the relative free concentrations of species, for an assumed chemical model under varied reaction conditions. The relative free concentrations $[M_p L_q H_r]/c_M$ or $[M_p L_q H_r]/c_L$ can be expressed by a distribution coefficient, δ_{pqr} and the distribution curves, $\delta_{pqr} = f(\log[L])$ or $f(\text{pH})$ then show the contribution of a particular complex $M_p L_q H_r$, as a function of the free ligand concentration, or pH, respectively.

(7) The SPECIES NUMBER unit.

Since the rank of the absorbance matrix has been proved to be equal to or less than the number of

absorbing species in solution,^{33–41} it is useful to determine this rank (k) at the beginning of the analysis, so that a hypothesis can be made about a chemical model. The program for analysing multicomponent spectra, FA608 + EY608,⁷ contains the factor-analysis method originated by Simmonds³³ and also applied by Wernimont³⁴ to matrix-rank determination. Kankare⁷ states the conditions under which k may be less than n_c and gives a method for deciding when this is probably the case. The factor analysis program FA608⁷ can also be used to smooth the spectra.

In SQUAD(78) Jančár and Havel⁹ used the method of reduced matrix analysis originated by Wallace and Katz^{36,39} and modified by Varga and Veatch.⁴⁰ However, this method has met with some criticism,^{7,41} so factor analysis is preferred for determination of matrix rank. Meloun^{17,18} therefore implemented subroutine FA608 in SQUAD(80) and SQUAD(84).

The programs in Table 1 do not contain any routine for determination of the number of light-absorbing species.

(8) The ABSORPTIVITY unit.

The adjustment of β_{pqr} and ϵ_{pqr} in LETAGROP-SPEFO⁵ is done at two levels. The β_{pqr} values are varied at an upper level, and the free concentrations of the various species in each solution are calculated. Then, for each wavelength, the contribution to U for each of a series of varied values of ϵ_{pqr} is calculated. With the assumption of a second-degree surface the values for ϵ_{pqr} that give the minimum contribution to U from that wavelength are calculated. After one shot for each wavelength, the computer calculates the minimum U obtained. Negative "insignificant" values of ϵ_{pqr} are eliminated by routine MIKO.

EY608⁷ estimates the molar-absorptivities matrix by subroutine SS608 together with the free concentrations of all the species, C .

DALSF EK¹⁰ calculates the molar absorptivities from Beer's law in every iteration in calculation of the stability constants.

PSEQUAD¹¹ determines the molar absorptivities along with the stability constants by a procedure similar to the "third strategy" in LETAGROP.⁴³

All versions of SQUAD employ subroutine ECOEF which calculates molar absorptivities ϵ_{jk} of the j th species for the k th wavelength by an algorithm derived from Nagano and Metzler.¹⁹

(9) The SPECIES SELECTOR unit.

Only LETAGROP-SPEFO and PSEQUAD use a species selector to search for a true chemical model from several proposed ones.

To the initial set of species, STYRE⁴⁴ in LETAGROP-SPEFO can add one after another from a list of species to be tested. A new species is accepted only if it improves U for the given data and its β_{pqr} value satisfies the "rejection factor (F_σ)" criterion that $\beta_{pqr} > F_\sigma s(\beta_{pqr})$. Species from the initial

set may be rejected in the process. The test for the "final" set of species is that no new species are accepted when all the rejected ones are recycled through STYRE. For given data and a tentative list of species, the set of β_{par} values that gives the lowest value of U and satisfies for each species the F_σ condition is accepted. The value to be taken for F_σ is related to the confidence level for significance of the β -value, as tabulated below,

F_σ	0	0.5	1.0	1.5	2.0	2.5	3.0
Confidence level, %	50	69	84	93.3	97.7	99.4	99.9

Rejection of a certain species by the species selector does not necessarily mean that it does not exist, but only that there is no evidence for its existence. Many papers of the Swedish school quote "maximum" possible values for the formation constants of rejected species, for instance, $\log[\beta_{par} + 3s(\beta_{par})]$.

PSEQUAD contains a new species selector based on sequential testing of species. If the change in U is less than 0.005% or the present maximum number of iterations is reached, the program terminates. Selection begins by exclusion of the positively marked species from a list, and when this finishes, it starts to test negatively marked species.

(10) The VISUALIZATION TOOLS unit.

The response-surface plane of the U paraboloid is a graph of U as a function of selected parameters, in the neighborhood of the "pit", U_{min} . It gives a visual representation of the influence of each parameter on U . For two parameters chosen on input, the paraboloid response-surface ($C-U$) in three dimensions is plotted by DIGIGRAPH equipment,⁴⁵ C is a numerical constant, e.g., 1.0 or 10.0. A regular paraboloid shape shows that both parameters are well-conditioned in the model and may lead to accurate and precise results, whereas a "saucer" shape indicates ill-conditioned parameters, which lead to uncertain results.

Another three-dimensional graph, the absorbance response-plane, demonstrates the degree of fit to the spectra, and shows the changes in absorbance on variation of the concentrations of the basic components.

Only SQUAD(84) will draw both response-planes. In all SQUAD versions, a printer plot gives a rapid comparison of experimental and calculated spectra. Calculation of the contributions to the experimental spectrum by the various individual species can improve the experimental design by suggesting which concentration ratios give little information about the equilibria.

A graph of molar absorptivity of all species vs. wavelength is printed by EY608, PSEQUAD and SQUAD(84), and a graph of standard deviation of molar absorptivity vs. wavelength by SQUAD(84) only.

(11) The INPUT unit.

Each program has its own method of organizing data input. This is rather a hindrance to comparative studies of programs.

(12) The OUTPUT unit.

This unit prints the results which should contain: (1) a table of proposed chemical models; (2) the experimental and computational strategy chosen; (3) the experimental (or simulated) absorbance matrix; (4) the rank of the absorbance matrix; (5) intermediate results of the minimization process; (6) the calculated absorbance and residual matrix; (7) a statistical analysis of residuals; (8) an error analysis; (9) distribution diagrams; (10) a table or graph of calculated molar absorptivities and standard deviations; (11) deconvolution of each spectrum to give the absorbance response-plane through the experimental points; (12) a graph of the U response-plane for two selected parameters.

EXPERIMENTAL

Computation

An EC 1033 computer was used. The programs were: extended LETAGROP-SPEFO,⁶ extended FA608 + EY608,⁷ original PSEQUAD,¹¹ SQUAD(78),⁹ SQUAD(80),^{12,13} SQUAD(81), SQUAD(84). SQUAD(84) and its structure are described in this paper; it was compared with other programs and some experiences with its use are discussed.

Guide for determination of chemical model by analysis of spectra

(1) *Instrumental error of absorbance measurement, $s_{inst}(A)$.* The Wernimont procedure³⁴ for examination of spectrophotometer performance should be used with solutions of potassium dichromate to evaluate $s_{inst}(A)$. Then FA608⁷ is used to calculate the residual standard deviation, $s_k(A)$ for matrix ranks $k = 1, 2, \dots$. The graph of $s_k(A) = f(k)$ consists of two straight lines intersecting at $\{s_k^*(A); k^*\}$ where k^* is the matrix rank for the system. Since $k^* = 1$ for $K_2Cr_2O_7$, the value of $s_k(A)$ for $k^* = 1$ is a good estimate of the instrumental error, i.e., $s_{inst}(A) = s_k^*(A)$.

(2) *Experimental design.* Since preparation of a large number of separate solutions is tedious, simultaneous monitoring of absorbance and pH during internal or external titrations is valuable.^{3,46} The total concentrations of the components should be varied between as wide limits as possible, so the continuous-variation and mole-ratio methods are useful. In a titration, the total concentration of one of the components changes incrementally over a relatively wide range, but the total concentrations of the other components change only by dilution, or not at all if they are present at the same concentration in the titrant and titrand. However, the absorbance cannot be varied over a large range without decreasing the precision of its measurement, and is effectively confined to a range of about one order of magnitude, e.g., $0.1 < A < 1.2$, though the range of concentrations measured can be increased by use of different path-lengths, e.g., 5, 1, and 0.1 cm.

A recording spectrophotometer is less likely to yield good results for subsequent computer-assisted evaluation than a good null-type instrument. Complex-forming equilibria are usually studied in the visible and ultraviolet regions, 200–800 nm. The wavelength-range selected should be such that every species makes a significant contribution to the absorbance. Little information is obtained in regions of great spectral overlap or where the molar absorptivities of

two or more species are linearly interdependent (because the change in absorbance with changes in c_M , c_L and c_H then becomes rather small). If only a small number of wavelengths is used, those of maxima or shoulders should be chosen, because small errors in setting the wavelength are then less important. It is best to use wavelengths at which the molar absorptivities of the species differ greatly, or a large number of wavelengths spaced at equal intervals.

(3) *Number of light-absorbing species and elimination of "outliers"*. Kankare's factor analysis algorithm FA608 is used to estimate the number of absorbing species in the equilibrium system. When there are no "outliers" (grossly erroneous points) in the spectra examined, $s_k^*(A) \lesssim s_{\text{init}}(A)$. Outliers are detected by FA608, and these points are corrected, then the $s_k(A) = f(k)$ plot is recalculated. The spectra are then free from gross errors and ready to be analysed by the regression program.

(4) *List of species for "species selector"*. A search should begin with the major species indicated by preliminary data analysis. Suggested species can then be added one at a time.⁴⁴ Model selection is based on finding the lowest U value.

(5) *Choice of computational strategy*. The input data should specify whether β_{par} or $\log \beta_{\text{par}}$ values are to be refined, multiple regression (MR) or non-negative linear least-squares analysis (NNLS) is desired, baseline correction is to be performed, *etc.* In description of the model, it should be indicated whether stability constants are to be refined or held constant and whether molar absorptivities are to be refined, and complexes for the species selector should be listed.

(6) *Simultaneous estimation of stoichiometry and stability constants*. A group of complexes in a given equilibrium system is divided into "certain" complexes of known stoichiometry, with stability constants estimated by the trial-and-error method, and "uncertain" complexes, for which the stoichiometry and stability constants are estimated simultaneously by regression analysis. Chemical experience and tables of stability constants help in making initial guesses of unknown parameters. The ESI method¹⁴ can also be used to confirm the suggested chemical model; it should give estimates of the stoichiometric indices that do not differ significantly from plausible integers.

(7) *Diagnostics indicating a correct chemical model*. When a minimization terminates, some diagnostics are examined to determine whether the results should be accepted. An incorrect chemical model with false stoichiometric indices p , q and r may lead to slow convergence, cyclization or divergence of the minimization. To reach a better chemical model, the following should be considered.

First diagnostic: the physical meaning of the parametric estimates. The physical meaning of the stability constants, molar absorptivities, and stoichiometric indices is examined. β_{par} and ϵ_{par} should not be too high or too low, and ϵ_{par} should not be negative; p , q and r should be real, and close to integers.

Second diagnostic: the physical meaning of the species concentrations. The calculated distribution of the free concentration of the components and the complexes of the chemical model should show molarities down to about 10^{-8} M. Since a species present at about 1% relative concentration or less in an equilibrium behaves as a numerical noise in regression analysis, a distribution diagram makes it easier to judge quickly the contributions of individual species to the total concentration. Since the molar absorptivities will be generally in the range 10^3 – 10^5 l. mole⁻¹. cm⁻¹, species present at less than ca. 0.1% relative concentration will affect the absorbance significantly only if their ϵ is extremely high.

Third diagnostic: standard deviations of parameters. The absolute values of $s(\beta_j)$, $s(\epsilon_j)$, $s(p_j)$, $s(q_j)$, $s(r_j)$ give information about the last U -contour or D -boundary of the hyperparaboloid neighbourhood of the pit, U_{min} . For well-

conditioned parameters, the last U -contour is a regular ellipsoid, and the standard deviations are reasonably low. High s values are found with ill-conditioned parameters and a "saucer"-shaped pit. The F_σ test, $s(\beta_j)F_\sigma < \beta_j$ should be met. The set of standard deviations of ϵ_{par} for various wavelengths, $s(\epsilon_{\text{par}}) = f(\lambda)$, should have a Gaussian distribution; otherwise erroneous estimates of ϵ_{par} are obtained.

Fourth diagnostic: parametric correlation coefficients. Partial correlation coefficients, r_{ij} , indicate the interdependence of two parameters β_j and β_i when the others are fixed in value. Total correlation coefficients, ρ_{ij} , indicate this interdependence when all parameters are refined, and the multiple correlation coefficient, R_i , measures the independence of one parameter from all the others. Correlation coefficients are a guide to the precision of the parameter estimates.

Fifth diagnostic: degree-of-fit test. Examination of the spectra and the graph of the predicted absorbance response-plane through all the experimental points will reveal whether the results calculated are consistent and whether any gross experimental errors were made in measurement of the spectra. Alternatively, the statistical measures $m_{r,1}$, $|F|$, $m_{r,2}$, $m_{r,3}$, $m_{r,4}$, $s(r)$, χ^2 , and the Hamilton R -factor can be calculated.

Sixth diagnostic: stoichiometric indices by the ESI method. The calculated p , q and r values should be close to integers with low standard deviations. Final refinement of β and ϵ and p , q , r values should not change U_{min} much if correct stoichiometric indices have been found.

Seventh diagnostic: deconvolution of the spectra. Resolution of each experimental spectrum into the spectra for the individual species shows whether the experimental design was efficient. If for a particular concentration range the spectrum consists of just a single component, further spectra for that range would be redundant, though they should improve the precision. In ranges where many components contribute significantly to the spectrum, several spectra should be measured.

Eighth diagnostic: response surface of the minimum of (C - U). For two parameters specified on input, the $(C - U)$ paraboloid response-surface is plotted in three dimensions. The shape of the paraboloid is very informative. Only a regular and well-developed paraboloid indicates well-conditioned parameters with quite reliable values.

(8) *Use of simulated data for setting up a computation strategy*. Use of a simulated absorbance matrix allows investigation of the sensitivity of each parameter in the proposed chemical model, examination of the influence of instrumental error on the precision and accuracy of the estimated parameters, and choice of an optimum computational strategy.

Simulated spectra points should be loaded with Gaussian random errors. The resulting distribution is checked by statistical analysis by calculating the error mean, $m_{e,1}$, the mean error $|\bar{e}|$, and its standard deviation $s(e)$, the skewness $m_{e,3}$, and the kurtosis $m_{e,4}$. Pearson's χ^2 test can be applied to test for Gaussian distribution, and the Hamilton R -factor calculated as a reference number for future comparison with the R -factor for experimental data.

DISCUSSION

The reaction of 2,3-dihydroxynitrobenzene (LH₂) and boric acid (MH) was studied by Kankare; the complex MLH₂ was found.⁴⁷ The spectra measured for various mole ratios of the components, $q_M = c_M/c_L$, as a function of pH, are used here to demonstrate the efficiency of the diagnostic tools, and illustrate the procedure for experimental and computational chemical model determination.

Table 2. Stoichiometry and stability constants for 2,3-dihydroxynitrobenzene (LH₂) and boric acid (MH)⁴⁷ [absorbance matrix from Fig. 1; computational conditions: $n_2 = 3$, $n_c = 4$, $r_w = 20$, $n_1 = 37$, $\lambda_{\text{start}} = 230$ nm, $\lambda_{\text{end}} = 420$ nm, estimated matrix rank $k^* = 4$ for $s_1^2(A) = 0.00384$, $\log \beta_{01} = 8.98$ was kept constant for all computations]

Model testing	A. Guessed stoichiometry approach			B. Estimated stoichiometry approach, (ESI)		
	FA608+EY608	PSEQUAD	SQUAD(1984)	SQUAD(1984)	SQUAD(1984)	
Refined	$\beta_{112}, \beta_{011}, \beta_{012}$	$\beta_{112}, \beta_{011}, \beta_{012}$	β_{112}	β_{112}, r_1	$\beta_{112}, p_1, r_1, r_2, r_3$	$\beta_{112}, p_1, q_1, q_2, q_3$
MLH ₂ , log β_{112}	23.639 ± 0.010	23.353 ± 0.029	23.385 ± 0.005	23.177 ± 0.042	22.904 ± 0.087	23.353 ± 0.031
p_1, q_1, r_1	1, 1, 2	1, 1, 2	1, 1, 2	1, 1, 1.976 ± 0.006	0.976 ± 0.008, 1, 1.954 ± 0.008	1.085 ± 0.011, 0.950 ± 0.008, 2
$\lambda_{\text{max}}, \delta_{112}$	300, 6665	300, 6666	300, 6705	300, 6670	300, 6684	300, 6282
LH ₂ , log β_{011}	11.242 ± 0.007	11.172 ± 0.028	11.242	11.195	11.195	11.195
p_2, q_2, r_2	0, 1, 1	0, 1, 1	0, 1, 1	0, 1, 1	0, 1, 1.000 ± 0.002	0, 1.003 ± 0.004, 1
$\lambda_{\text{max}}, \delta_{011}$	310, 4487	310, 4473	310, 4497	310, 4471	310, 4464	310, 4512
$\lambda_{\text{max}}, \delta_{011}$	410, 3425	410, 3449	410, 3410	410, 3449	410, 3458	410, 3427
LH ₂ , log β_{012}	17.842 ± 0.027	17.838 ± 0.029	17.842	17.848	17.848	17.848
p_3, q_3, r_3	0, 1, 2	0, 1, 2	0, 1, 2	0, 1, 2	0, 1, 2.000 ± 0.002	0, 1.000 ± 0.004, 2
$\lambda_{\text{max}}, \delta_{012}$	300, 6482	300, 6461	300, 6482	300, 6472	300, 6472	300, 6484
U_{min}	0.01961	0.01966	0.02137	0.01896	0.01906	0.02010
$s(A)$	0.00563	0.00548	0.00569	0.00536	0.00538	0.00552
Correlation coefficients:	missing	$\rho(1,2) = 0.91$ $\rho(1,3) = 0.92$ $\rho(2,3) = 0.96$	not calculated	$\rho(1, r_1) = 0.98$	$\rho(1, p_1) = 0.89$ $\rho(1, r_1) = -0.90$ $\rho(1, r_2) = 0.27$ $\rho(1, r_3) = 0.21$ $\rho(p_1, r_1) = -0.68$ $\rho(p_1, r_2) = 0.25$ $\rho(p_1, r_3) = 0.22$ $\rho(r_1, r_2) = 0.04$ $\rho(r_1, r_3) = 0.11$ $\rho(r_2, r_3) = 0.90$	$\rho(1, p_1) = 0.39$ $\rho(1, q_1) = -0.10$ $\rho(1, q_2) = -0.13$ $\rho(1, q_3) = 0.09$ $\rho(p_1, q_1) = 0.28$ $\rho(p_1, q_2) = 0.28$ $\rho(p_1, q_3) = 0.79$ $\rho(q_1, q_2) = 0.97$ $\rho(q_1, q_3) = 0.04$ $\rho(q_2, q_3) = 0.04$
R_i	$r(1,2) = -0.27$ $r(1,3) = -0.42$ $r(2,3) = -0.72$	$R_1 = 0.93$ $R_2 = 0.96$ $R_3 = 0.96$				
where for i and j						
1 means β_{112}						
2 means β_{011}						
3 means β_{012}						
Residual mean	4.70E-6	-2.01E-6	-2.44E-6	-2.28E-6	-2.37E-6	-1.63E-6
Mean residual	0.00350	0.00350	0.00350	0.00333	0.00334	0.00349
Std. dev	0.00564	0.00546	0.00569	0.00536	0.00538	0.00552
Skewness	0.642	-0.344	-0.641	-0.625	-0.623	-0.299
Curstosis	8.131	6.516	7.838	8.092	8.022	7.359
R-factor	0.01262	0.01206	0.01258	0.01185	0.01188	0.01220
CPU time, sec	110	105	168	425	1072	619

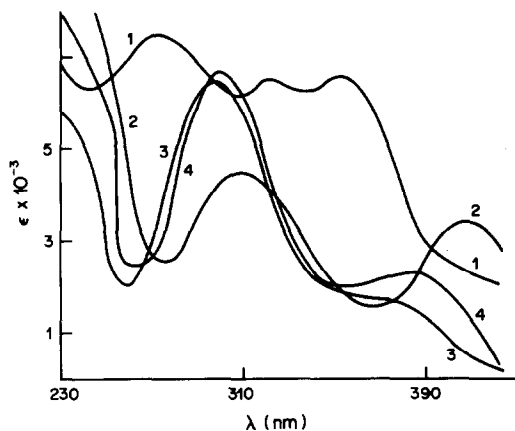


Fig. 2. Curves of estimated molar absorptivities of complex MLH_2 [curve (4)], and of variously protonated forms of ligand, L [curve (1)], LH [curve (2)], LH_2 [curve (3)] calculated by analysis of the spectra in Fig. 1.

The 3 ($=n_c$) components M, L and H were mixed to obtain 37 ($=n_s$) solutions. The spectra were measured at 20 ($=n_w$) wavelengths from 230 ($=\lambda_{start}$) to 420 nm ($=\lambda_{end}$). Figure 1 shows the three-dimensional absorbance response-plane graph. The chemical model proposed has 4 ($=n_c$) species, L, LH, LH_2 and MLH_2 which absorb light in the range used, and one, MH, which does not. The "certain" species proposed,¹⁴ (L, LH, LH_2 and MH) may be studied in an independent experiment and their protonation constants determined. The "uncertain" complex¹⁴

MLH_2 has to be established and its stoichiometry, stability constant and molar absorptivity have to be estimated. The stability constants and molar absorptivities of all the species in the system are finally refined in the last step of the computation. Three regression programs using the trial-and-error method to confirm a suggested model hypothesis, *viz.* an extended version of Kankare's FA608 + EY608 program, PSEQUAD, and SQUAD(84) were used, and their advantages compared. Only SQUAD(84) allowed use of the method of variable stoichiometric indices.¹⁴

After smoothing of the spectra (removal of outliers), the factor analysis program FA608 found the intersection on the $s_k(A) = f(k)$ curve at $s_k^*(A) = 0.00384$ and $k^* = 4$. EY608 found the equilibrium constant ($-\log \kappa$) of the reaction $LH_2 + MH - H^+ = MLH_2 + H_2O$ to be $(-\log \kappa) = 3.456 \pm 0.010$, which leads to $\log \beta_{112} = 23.639 \pm 0.010$. Programs PSEQUAD and SQUAD(1984) estimate the overall stability constants β_{pqr} . Because L, LH, LH_2 are also light-absorbing, Kankare⁴⁷ refined the protonation constants $\log \beta_{011}$ and $\log \beta_{012}$ simultaneously with $\log \beta_{112}$. The results obtained from the various regression programs are compared in Table 2.

For the stoichiometric indices of all the species in the model, the stability constants β_{112} , β_{011} and β_{012} and molar absorptivities at 20 wavelengths were estimated. All three programs found the same values for parameters β_{pqr} and ϵ_{pqr} . The degree-of-fit test showed only small differences between the results from the three programs; the best fit was achieved by

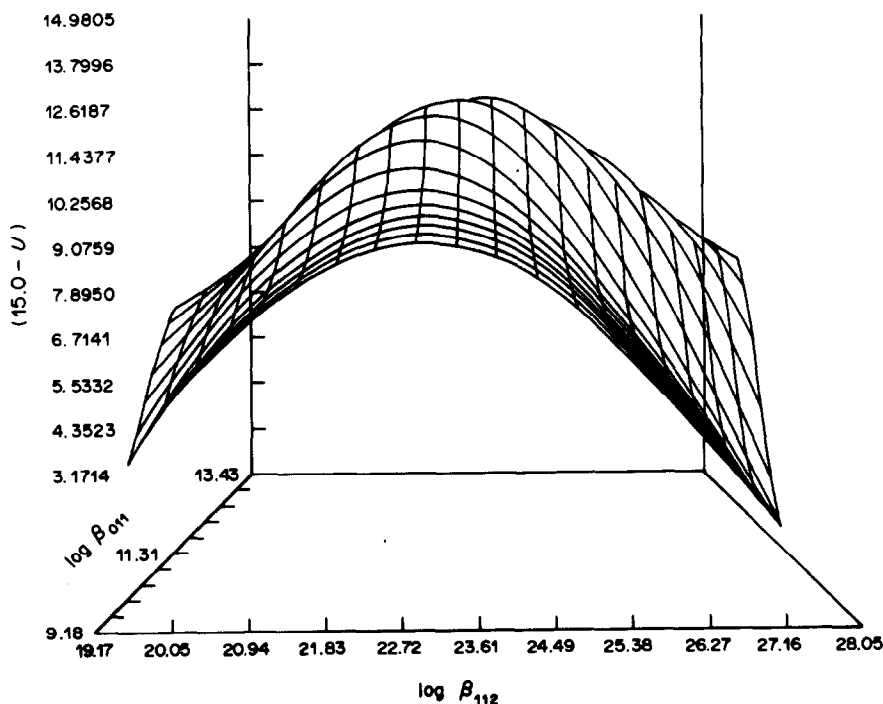


Fig. 3. The three-dimensional graph of a $(10.0 - U)$ response-surface for data in Fig. 1 indicates that $\log \beta_{011}$ and $\log \beta_{112}$ are well-conditioned in the model because the surface exhibits a maximum.

SQUAD(84). The graphs of the estimated ϵ_{112} , ϵ_{011} , ϵ_{012} and ϵ_{010} values vs. λ were also in good agreement (Fig. 2). Good agreement was also found between all the [L], [LH], [LH₂] and [MLH₂] values calculated.

Because SQUAD(84) can determine the stoichiometric indices, the right-hand half of Table 2 ("Estimated stoichiometry approach") shows the results of the simultaneous estimation of the stoichiometric indices with β_{pqr} and ϵ_{pqr} . However, these indices and the corresponding stability constants are interdependent, so special care must be taken with the choice of computational strategy and indices to be estimated. To decrease the number of unknown parameters, the stability constants of "certain" species were held at constant values achieved in previous runs, but the corresponding molar absorptivities were always estimated. The last four columns show the determination of β_{112} values obtained (1) without any stoichiometric indices, (2) with stoichiometric index r_1 , (3) with stoichiometric indices p_1 , r_2 and r_3 , and (4) with stoichiometric indices p_1 , q_1 , q_2 and q_3 .

The left-hand half of Table 2 ("Guessed stoichiometry approach") shows quantities that refer to the sought pit, such as U , $s(A)$, and the degree-of-fit test results. The results of runs where indices are also sought are compared with those in the reference columns (the third and the fourth column of the left-hand half of Table 2) to see whether some other species stoichiometry should be considered in order to achieve a better fit.

For this comparison and to choose the best

strategy in various runs of one program, or for comparison between two programs, examination of the program diagnostics should be useful. The proposed chemical model—MLH₂, L, LH, and MH—may also thus be confirmed.

The 1st diagnostic: the estimates of β_{112} , β_{011} , β_{012} and ϵ_{112} , ϵ_{010} , ϵ_{011} and ϵ_{012} do have physical meaning.

The 2nd diagnostic: the calculated free concentrations do have physical meaning. [MLH₂] ranged from 8×10^{-5} to $10^{-13}M$, [LH] from 9×10^{-5} to $10^{-6}M$, [LH₂] from 10^{-4} to $10^{-10}M$, [L] from 10^{-5} to $10^{-13}M$ and [MH] from 5×10^{-3} to $10^{-12}M$.

The 3rd diagnostic: the low standard deviations indicate that the parametric estimates were quite precise.

The 4th diagnostic: the $\rho(i,j)$ values of 0.90–0.98 indicate the high degree of interdependence of the i th and j th parameters, so these parameters are estimated with some uncertainty. The low correlation coefficients in the last columns show that the choice of these parameters to be refined was good. The stability constants and stoichiometric indices of a particular complex were partly interdependent. It is not convenient to determine them simultaneously in one run, but good results are obtained when stoichiometry of another species is estimated.

The 5th diagnostic: the degree-of-fit test indicates that the mean residual, $|\bar{r}|$, value is $\leq s_t^*(A)$ obtained by factor analysis, so the termination of minimization can be accepted as successful. The Hamilton R -factor is 1%, which indicates a good fit.

The 6th diagnostic: refining only β_{112} and (r_1, r_2, r_3)

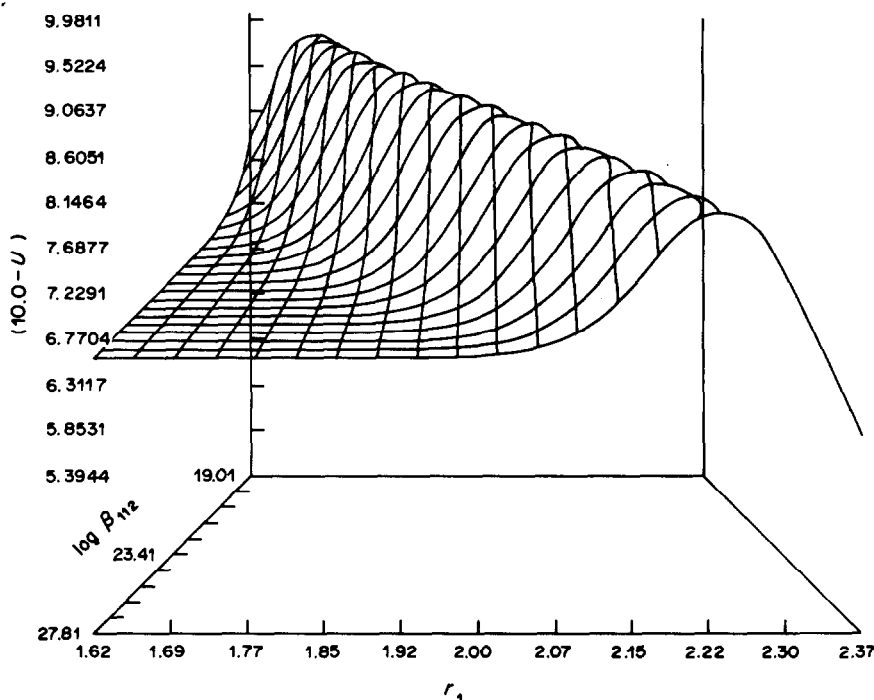


Fig. 4. The three-dimensional graph of another $(10.0 - U)$ response-surface for the data in Fig. 1 indicates that $\log \beta_{011}$ and r_1 are interdependent and badly conditioned in the model, because the surface does not show a definite maximum.

or (p_1, r_1, r_2, r_3) or (p_1, q_1, q_2, q_3) led to real values for the indices, that were quite near to integers, even when bad initial guesses were used. This may be taken as confirmation that true stoichiometric indices were found.

The 7th diagnostic: deconvolution of the spectra into absorbance increments for the individual species helps in planning future efficient experimentation.

The 8th diagnostic: the $(C - U)$ paraboloid response-surface (where $C = 10.0$) clearly indicates the precision of the parameter estimates. The top of the $(10.0 - U) = f(\beta_{112}$ and $\beta_{011})$ or $(10.0 - U) = f(\beta_{011}$ and $r_1)$ surface indicates that two parameters are well-conditioned in the model (Fig. 3), whereas the shape of the maximum surface for parameters in $(10.0 - U) = f(\beta_{112}$ and $r_1)$ indicates that β_{112} and r_1 are interdependent in the model, so their determination is rather uncertain (Fig. 4).

CONCLUSIONS

Structural classification of programs for studying equilibria by analysis of spectral data makes it easier to explain a sophisticated *modus operandi*. SQUAD(84) is a versatile program containing more diagnostic tools than the other programs of similar structure.

The program is available from the authors on request.

REFERENCES

1. D. J. Leggett, *Am. Lab.*, 1982, **14**, No. 1, 29.
2. F. Gaizer, *Coord. Chem. Rev.*, 1979, **27**, 195.
3. M. Meloun and J. Havel, *Computation of Solution Equilibria, Part 1, Spectrophotometry*, Folia Fac. Sci. Nat. Univ. Purk. Brunensis, Brno, 1986.
4. M. Meloun and J. Cermák, *Talanta*, 1984, **31**, 947.
5. M. Meloun and M. Javůrek, *ibid.*, 1985, **32**, 973.
6. L. G. Sillén and B. Warnqvist, *Ark. Kemi*, 1968, **31**, 377.
7. J. J. Kankare, *Anal. Chem.*, 1970, **42**, 1322.
8. D. J. Leggett and W. A. E. McBryde, *Anal. Chem.*, 1975, **47**, 1065; D. J. Leggett, *ibid.*, 1977, **49**, 276.
9. L. Jančář and J. Havel, *Scripta Fac. Sci. Nat., Univ. Purk. Brunensis*, 1984, **14**, 73.
10. R. M. Alcock, F. R. Hartley and D. E. Rogers, *J. Chem. Soc., Dalton*, 1978, 115.
11. I. Nagypál and L. Zékány, in *Computational Methods for the Determination of Formation Constants*, D. J. Leggett (ed.), Plenum Press, New York 1985.
12. D. J. Leggett, Personal communication (1980).
13. D. J. Leggett, S. L. Kelly, L. R. Shine, Y. T. Wu, D. Chang and K. M. Kadish, *Talanta*, 1983, **8**, 579.
14. J. Havel and M. Meloun, *ibid.*, 1986, **33**, 435.
15. L. Jančář, J. Havel, V. Kubáň and L. Sommer, *Collection Czech. Chem. Commun.*, 1982, **47**, 2654.
16. M. Macka and V. Kubáň, *ibid.*, 1982, **47**, 2676.
17. M. Meloun, *Equilibria study by non-linear regression of instrumental curves*, Conference on advances and application of analytical chemistry, Piešťany, 7–10 September 1982.
18. M. Meloun, *Computation of Solution Equilibria*, Conference on optimization in analytical chemistry, Trenčianské Teplice, 19 April 1983.
19. K. Nagano and D. E. Metzler, *J. Am. Chem. Soc.*, 1967, **89**, 2891.
20. T. Kaden and A. Zuberbühler, *Talanta*, 1971, **18**, 61.
21. I. Šamaliková, *Thesis*, College of Chemical Technology, Pardubice 1982.
22. J. Burgerová, *Thesis*, College of Chemical Technology, Pardubice 1983.
23. I. Nagypál, I. Páka and L. Zékány, *Talanta*, 1978, **25**, 549.
24. N. Ingri and L. G. Sillén, *Ark. Kemi*, 1964, **23**, 97.
25. D. W. Marquardt, *J. Soc. Ind. Appl. Maths.*, 1963, **11**, 431.
26. I. G. Sayce, *Talanta*, 1968, **15**, 1397.
27. L. G. Sillén, *Acta Chem. Scand.*, 1962, **16**, 159, 1964, **18**, 1085.
28. D. Himmelblau, *Process Analysis by Statistical Methods*, Wiley, New York 1969.
29. A. Sabatini, A. Vacca and P. Gans, *Talanta*, 1974, **21**, 53.
30. W. C. Hamilton, *Statistics in Physical Science*, Ronald Press, New York 1964.
31. R. Arnek, L. G. Sillén and O. Wahlberg, *Ark. Kemi*, 1968, **31**, 353.
32. N. Ingri, W. Kakolowicz, L. G. Sillén and B. Warnqvist, *Talanta*, 1967, **14**, 1261 (*errata*, 1968, **15**, No. 3, ix).
33. J. L. Simmonds, *J. Opt. Soc. Am.*, 1963, **53**, 968.
34. G. Wernimont, *Anal. Chem.*, 1967, **39**, 554.
35. G. Weber, *Nature*, 1961, **190**, 27.
36. R. M. Wallace and S. K. Katz, *J. Phys. Chem.*, 1964, **68**, 3890.
37. S. Ainsworth, *J. Phys. Chem.*, 1961, **65**, 1968.
38. *Idem*, *ibid.*, 1963, **67**, 1613.
39. R. M. Wallace, *ibid.*, 1964, **64**, 899.
40. L. P. Varga and F. C. Veatch, *Anal. Chem.*, 1967, **39**, 1101.
41. I. J. Bernstein and J. L. Kaminskii, *Spectrophotometric Analysis in Organic Chemistry (in Russian)*, Khimiya, Leningrad, 1975.
42. D. A. Harville, *Technometrics*, 1973, **15**, 509.
43. L. G. Sillén and B. Warnqvist, *Ark. Kemi*, 1968, **31**, 315.
44. *Idem*, *ibid.*, 1968, **31**, 341.
45. M. Javůrek, *Ph.D. Thesis*, College of Chemical Technology, Pardubice 1986.
46. M. Meloun and M. Javůrek, *Talanta*, 1984, **12**, 1083.
47. J. J. Kankare, *Personal Communication of typical data set for program EY608*.

MULTIPARAMETRIC CURVE FITTING—XI

POLET COMPUTER PROGRAM FOR ESTIMATION OF FORMATION CONSTANTS AND STOICHIOMETRIC INDICES FROM NORMALIZED POTENTIOMETRIC DATA

JOSEF HAVEL

Department of Analytical Chemistry, Purkyně University, Kotlářská 2, CS-611 37 Brno, Czechoslovakia

MILAN MELOUN*

Department of Analytical Chemistry, College of Chemical Technology, CS-532 10 Pardubice,
Czechoslovakia

(Received 9 July 1985. Accepted 15 November 1985)

Summary—The FORTRAN computer program POLET(84) analyses a set of normalized potentiometric titration curves to find a chemical model, *i.e.*, the number of species present and their stoichiometry, and to determine the corresponding stability constants $\log \beta_{pqr}$ and unknown stoichiometric indices p , q , r , and s of up to quaternary $M_pL_qY_rH_s$ complexes. The program belongs to the ABLET family, based on the LETAG subroutine, and can use an algorithmic and/or heuristic minimization strategy, or a beneficial combination of both. The data, a set of potentiometric titration curves plotted as volume and potential, are converted into normalized variables (formation function, pH) and then a computer-assisted search for a chemical model by POLET(84) is applied. The procedure for efficient application of POLET(84) in an equilibrium analysis is described and the program is validated by use of literature and simulated data. The reliability of the chemical model and its parameters is established by the degree-of-fit achieved, and the closeness of the stoichiometric indices to integral values.

The formation function Z has traditionally been used in analysis of potentiometric titration data. The algorithms developed by Sillén and co-workers¹⁻³ are still widely accepted as the most accurate method of determining a chemical model, *i.e.*, the number of complexes, and their stability constants and stoichiometry. Since then, many computer programs have been written for the analysis of potentiometric titration data, such as MINQUAD,⁹ SCOGS,¹⁰ ACBA,¹¹ PSEQUAD,¹² TITFIT,¹³ MARFIT,¹⁴ MUCOMP,¹⁵ ESTA,¹⁶ but none of these accommodates a straight determination of the stoichiometric indices p , q , r of $M_pL_qH_r$ complexes. Various programs applied in potentiometric study of solution equilibria have been critically surveyed.¹⁷⁻²¹

All the programs mentioned above search for the most probable chemical model by the trial-and-error method, and the stability constants and compositions of the complexes are estimated by the curve-fitting technique. If a particular fit being examined is considered false, another set of complexes of different stoichiometry is tried and so on, until the best fit to the data is found. Such treatment needs considerable computer time and an examination of all possible combinations of species is sometimes impossible.

When p and q for M_pL_q , for example, each have a limiting value of 10, a large number of individual species is possible.

The program POLET (version 1984) directly determines the stoichiometric coefficients and stability constants of the complexes by means of the recently published ESI method.²² The species are divided into two groups: "certain" species of known stoichiometry for which only the stability constants are to be estimated, and "uncertain" species of completely unknown stoichiometry (or with at least some indices unknown) for which both the stability constants and stoichiometric indices are estimated simultaneously. The program is a member of the ABLET family²³ and can use either an algorithmic or heuristic strategy, or a combination of both. Like MRLET²⁴ and PRCEK,²⁵ the POLET(84) estimates the stoichiometric indices by multiparametric curve fitting and the chemical model selected is then validated by the statistical analysis of residuals.

THEORY

Chemical model

The complex-formation equilibria of n basic components, for example, $n = 4$, may be described by the general reaction and stability constant:

Part X: *Talanta*, 1986, 32, 513.

*Author for correspondence.

$$pM + qL + rY + sH = M_pL_qY_rH_s \quad (1)$$

$$\beta_{pqrs} = [M_pL_qY_rH_s]/[M]^p[L]^q[Y]^r[H]^s$$

$$= c_{pqrs}/m^p l^q y^r h^s \quad (2)$$

with the mass-balance equations

$$c_M = m + pS \quad (3)$$

$$c_L = l + qS \quad (4)$$

$$c_Y = y + rS \quad (5)$$

$$c_H = h + sS \quad (6)$$

where

$$S = \sum_{i=1}^{n_c} \beta_{pqrs,i} m^p l^q y^r h^s \quad (7)$$

and c_M, \dots, c_H are the total analytical concentrations of the four basic components and m, l, y, h are the free equilibrium concentrations.

For the more common ternary ($n = 3$) and binary ($n = 2$) equilibria, the complexes $M_pL_qH_r$ or M_pL_q will be referred to as the (p, q, r) or (p, q) species. When protons are split off, the hydroxo species $M_pL_q(OH)_r$ are treated as protonated species with negative r value, i.e., $M_pL_qH_{-r}$, and the corresponding Z function is then also negative if no other equilibrium occurs.

The formation function Z

The primary data of the potentiometric titration curve, with original variables $(V_H, E_H)_{M,L}$ must be converted into the normalized variables $(Z, pH)_{M,L}$. The free equilibrium concentration of the basic component H is measured potentiometrically:

$$E = E^0 + (RT/nF) \ln h + E_j \quad (8)$$

where E_j is the liquid-junction potential and Z is the average number of component entities H bound per M or L,

$$Z \equiv Z_{H/M} = (c_H - h)/c_M = rS/c_M \quad (9)$$

and

$$Z \equiv Z_{H/L} = (c_H - h)/c_L = rS/c_L \quad (10)$$

for the $M_pL_qH_r$ complexes in the model.

Regression analysis

Regression analysis of (Z, pH) curves consists of the estimation of chosen unknown parameters, i.e., the stability constants β_{pqrs} and stoichiometric indices p, q, r and s of up to quaternary $M_pL_qY_rH_s$ complexes by minimizing the difference between the experimental and calculated values of Z . The dependent variable Z represents the average number of moles of protons bound per mole of M (if the program key $KV = 1$) or of L (if the program key $KV = 2$) and is easily calculated from the original titration data. For NB titration curve points described by data-pairs $\{Z, pH\}$, the sum of the squared residuals

$$U = \sum_{j=1}^{NB} w_j (Z_{exp,i} - Z_{calc,i})^2 = \text{minimum} \quad (11)$$

is minimized; w_j is the statistical weight, usually taken as unity, and $Z_{calc,i}$ is calculated according to equations (9) and (10) for the current estimation of the parameters.

POLET(84) estimates the stability constants of polynuclear and/or mixed complexes of any system with one metal and two ligands or two metals and one ligand. When an ion-selective electrode is used to indicate the free concentration of component X (where X stands for M or L or Y), the basic component H being indicated potentiometrically may be replaced by that component X. The mixed hydroxo-species $M_pL_q(OH)_r$ are treated as protonated species with negative r values, but negative Z values also mean proton-deficient species. It is impossible to distinguish between a bound OH^- group and a proton split off from a water molecule.

The choice of basic ligand component is up to the user. For example, L can stand for any protonated form of a ligand of up to a tetrabasic acid LH_4 , and the four dissociation constants of LH_4 might be supplied in the input if they are already known and there is no request to refine them.

POLET(84) uses the pit-mapping algorithm LETAG, and does the minimization heuristically (steps controlled by the operator) or algorithmically (steps controlled by the program). A combined strategy, heuristic control followed by algorithmic, is beneficial in the first part of the minimization, when the user must decide whether it is sufficient to know the location of some local minimum or whether a global minimum is required. The user has to supply here initial guesses of the parameters to be refined, the minimization steps, and an organizational framework to control the process from iteration to iteration. Final refinement can then be managed algorithmically. Parameters which may reach a negative value must be specified in the input.

POLET(84) consists of three specific units, the INPUT block, the RESIDUAL-SQUARE SUM block and the MAIN block, along with six permanent blocks of ABLET system described previously.²³

The INPUT block reads the input data $\{Z, pH\}$ by format-free reading subroutines, and the dissociation constants pK_{a1}, \dots, pK_{aj} of the j -basic ligand acid (if $j \neq 0$) and the side-reaction coefficients $\alpha_{L(H)}$ are then calculated. These coefficients are used in calculation of the initial estimates of the free equilibrium concentrations of all the complexes in a given equilibrium system, $[M_pL_qY_rH_s]$; $j = 1, \dots, n_c$. The free concentrations m, l, y and h are calculated by the subroutine COGS adapted from Perrin and Sayce²⁶ and modified according to Ginzburg.²⁷

The RESIDUAL-SQUARE-SUM block calculates, in subroutine UBBE, the calculated $Z_{calc,i}$ value for each point, starting from the total concentrations of the basic components and the free concentrations

computed by COGS for the current estimates of the parameters, p , q , r and s , and β_{pqrs} .

The MAIN part contains a function as written in the description of ABLET.²³ The OUTPUT block was extended to include printer-plotting of the distribution diagrams for all complex species in the chemical model.

EXPERIMENTAL

Equilibrium analysis by POLET(84)

(1) *Potentiometric equilibrium titration.* Data collection is performed as a potentiometric "equilibrium titration",⁸ where usually c_M and c_I are kept constant in the equilibrium solution and c_H is varied by addition of acid from a burette; $c_H = (V_H c_{H,T} + V_0 c_{H,0}) / (V_0 + V_H)$ where $c_{H,0}$ and $c_{H,T}$ are the total concentrations of protons in the titrand and titrant, and V_0 is the initial volume of titrand and V_H the volume of titrant added from the burette. Suitable electrodes are used to measure $[H^+]$ to obtain data pairs $(c_H, [H^+])_{M,L}$ over a wide concentration range of M and L; the "inert medium method"²⁸ or the "self medium method"²⁹⁻³² can be used.

(2) *Conversion of primary (V_H, E_H) into normalized (Z, pH) data.* A calibration titration of a strong acid with a strong base is done to determine three parameters: the standard potential E^0 of the electrode cell used, the Nernst coefficient $2.303 (RT/nF)$ and the ionic product of water pK_w , by application of the regression program MAGEC.³³ With these three parameters and the Nernst equation the primary data $(V_H, E_H)_{M,L}$ are converted into normalized quantities $(Z, pH)_{M,L}$. This conversion can be done by computer program TRAVE³⁴ or by pocket-calculator.

(3) *The number of species by factor analysis of (Z, pH) data.* The number of complex species in solution may be determined by a factor analysis with program SPECIES³⁵ from a set of potentiometric titration curves, each containing n_i points and measured for n_x total concentrations of M or L to give finally the $(n_x \times n_x)$ matrix Z by finding the rank of matrix Z . The number of species in equilibrium is equal to the rank of matrix Z . However, for a simple mononuclear system the number of species can be estimated from the number of inflection points on the $Z = f(pH)$ curves.

(4) *MESAK treatment of data.* The MESAK treatment³⁶ is used to limit the number of ternary complexes (p, q, r) from which the final combination giving the "best" fit may be selected. MESAK can give valuable information about the average composition of the complexes, \bar{p} , \bar{q} , and \bar{r} . Such treatment can thus give initial information about the principle species in a solution, and its use is for guidance only.

(5) *Determination of chemical model.* After data conversion and preliminary data analysis by MESAK, the final selection of the true chemical model from several proposed models is performed with POLET. The complex species are divided into the "certain species" of known stoichiometry (usually, but not necessarily the principal species of the equilibrium mixture) for which only the stability constants are to be estimated, and the "uncertain species" of partly known stoichiometry for which both the stability constants and some stoichiometric coefficients are to be estimated simultaneously. Use is made of combined, heuristic, and finally algorithmic strategy in the LETAG minimization process.

Three strategies for chemical model search are possible:

- species are tested by the trial-and-error method and only stability constants are refined;
- for uncertain species with some unknown indices the stability constants are refined simultaneously with selected indices by the ESI approach;
- for the most probable chemical model found a final refinement of stability constants and stoichiometric indices is performed; for a true model the parameters are

not changed significantly by refinement and the refined indices should be close to integer values.

Of course, the indices for the basic components for which the free and/or total concentrations have not been varied during collection of titration data cannot be estimated, e.g., when the pH is kept constant in a titration the number of protons r in $M_p L_q H_r$ cannot be determined.

Computation

Potentiometric data analysis by POLET(84) was done with the EC 1033 (500 K) computer in The Department of Computing Techniques, J. E. Purkyně University, CS-611 37 Brno and in The Computing Centre, College of Chemical Technology, CS-532 10 Pardubice, Czechoslovakia. A listing of POLET(84), specimen data and detailed manual are available on request.

DISCUSSION

The major objective of this project was to provide a computing tool for investigating chemical models on the basis of estimating the stoichiometry of various complexes in a complex-forming system by analysis of potentiometric data. To illustrate the performance of POLET(84) a set of simulated data was used first. Table 1 shows the POLET output in shortened form. Two hydrolysed species, $Bi(OH)$ and $Bi_6(OH)_{12}$, described by the stability constants $\log \beta_{1,-1} = -1.58$ and $\log \beta_{6,-12} = 0.33$, were selected and for six different concentrations of Bi^{3+} ions and 8 values of the different variable pH for each concentration, precise values of the dependent variable Z were calculated. With a selected value of the instrumental standard deviation $s_{inst}(Z)$, random errors were generated and imposed on the precise Z values. With the simulated data in Table 1, statistical analysis of the generated errors proved a Gaussian normal distribution of random errors by statistical values describing this error set.

Before minimization was started, complex $M_1(OH)_1$ was chosen as the "certain species" with known stoichiometry, and complex $M_6(OH)_{12}$ as the "uncertain species" for which the stoichiometry was to be estimated. Minimization was started heuristically from the initial guess of the parameters to be estimated, $(\log \beta_{6,-12})^{(0)} = 2.0$, $p_2^{(0)} = 2.0$ and $r_2^{(0)} = -3.0$, and the other parameters were kept at the values initially guessed, $(\log \beta_{1,-1})^{(0)} = -1.58$, $p_1^{(0)} = 1.0$ and $r_1^{(0)} = -1.0$. The minimization terminated with the estimates $\log \beta_{6,-12} = 0.3643 \pm 0.0456$, $p_2 = 6.051 \pm 0.094$ and $r_2 = -12.094$. Statistical analysis of the residuals proved the parameters found were sufficiently reliable, as all the statistical characteristics describing the residual set had the same values as those of the generated errors. When even incorrect values of both stoichiometric coefficients were used in the initial guess, POLET found the true values of p and r .

POLET(84) was further validated by the use of some literature titration data. Sasaki³⁷ studied the $CrO_4^{2-}-H^+$ equilibria by potentiometric titration with use of the glass electrode, and from a set of (Z, pH) data concluded there were two protonation

Table 1. Validation of POLET(84) by the simulated data set of Bi^{3+} hydrolysis: for two hydrolytic species, $\text{Bi}(\text{OH})$ ("certain complex") and $\text{Bi}_6(\text{OH})_{12}$ ("uncertain complex") the (Z, pH) data were simulated: conditions: $\log \beta_{1,-1} = -1.58$, $\log \beta_{6,-12} = 0.33$ and $s_{\text{inst}}(Z) = 0.01$

Parameter	Numerical values						
	Selected for simulation	Initial guess	Refined estimation				
Kept at a constant value:							
$(\log \beta_{pr})_1$	-1.58	-1.58	-1.58				
p_1	1.0	1.0	1.0				
r_1	-1.0	-1.0	-1.0				
Refined:							
$(\log \beta_{pr})_2$	0.33	-2.0	0.3643 ± 0.0456				
p_2	6.0	2.0	6.0510 ± 0.0944				
r_2	-12.0	-3.0	-12.0940 ± 0.1899				
<i>i</i>	Variables			Simulation		Refinement	
	pH	c_M	Z_{accur}	Error	Z_{exp}	Z_{calc}	Residual
1	0.00	0.0010	-0.025665	-0.009245	-0.0349	-0.0257	-0.0092
2	0.20	0.0010	-0.040080	-0.000098	-0.0402	-0.0401	-0.0001
3	0.40	0.0010	-0.062074	0.021240	-0.0408	-0.0621	0.0212
4	0.60	0.0010	-0.094920	0.000784	-0.0941	-0.0949	0.0008
5	0.80	0.0010	-0.142581	-0.008168	-0.1507	-0.1426	-0.0082
6	1.00	0.0010	-0.214157	0.003395	-0.2108	-0.2138	0.0031
7	1.50	0.0010	-1.456644	0.003001	-1.4536	-1.4535	-0.0001
8	2.00	0.0010	-1.905545	0.005408	-1.9001	-1.9036	0.0034
9	0.00	0.0050	-0.025590	-0.005515	-0.0311	-0.0256	-0.0055
10	0.20	0.0050	-0.040079	-0.007127	-0.0472	-0.0401	-0.0071
11	0.40	0.0050	-0.062877	0.000559	-0.0615	-0.0621	0.0006
12	0.60	0.0050	-0.095591	0.011835	-0.0838	-0.0956	0.0118
13	0.80	0.0050	-0.231336	0.008999	-0.2223	-0.2299	0.0076
14	1.00	0.0050	-0.945959	0.013832	-0.9321	-0.9446	0.0125
15	1.50	0.0050	-1.849614	-0.010417	-1.8600	-1.8481	-0.0120
16	2.00	0.0050	-1.975067	-0.001604	-1.9767	-1.9737	-0.0030
17	0.00	0.0100	-0.025587	0.008234	-0.0174	-0.0256	0.0082
18	0.20	0.0100	-0.040079	0.009674	-0.0304	-0.0401	0.0097
19	0.40	0.0100	-0.062182	0.008625	-0.0536	-0.0622	0.0086
20	0.60	0.0100	-0.115114	0.009703	-0.1054	-0.1147	0.0093
21	0.80	0.0100	-0.665716	0.007558	-0.6582	-0.6654	0.0073
22	1.00	0.0100	-1.363112	0.006533	-1.3566	-1.3625	0.0059
23	1.50	0.0100	-1.914916	0.010549	-1.9044	-1.9136	0.0093
24	2.00	0.0100	-1.985988	-0.000731	-1.9867	-1.9846	-0.0021
25	0.00	0.0250	-0.025590	-0.002978	-0.0286	-0.0256	-0.0030
26	0.20	0.0250	-0.040128	0.005527	-0.0346	-0.0401	0.0055
27	0.40	0.0250	-0.072272	0.000462	-0.0718	-0.0721	0.0003
28	0.60	0.0250	-0.533428	-0.030596	-0.5636	-0.5343	-0.0293
29	0.80	0.0250	-1.290659	-0.011390	-1.3020	-1.2914	-0.0106
30	1.00	0.0250	-1.690188	0.007523	-1.6827	-1.6899	0.0071
31	1.50	0.0250	-1.960133	-0.000719	-1.9609	-1.9588	-0.0020
32	2.00	0.0250	-1.993483	0.002612	-1.9909	-1.9921	0.0013
33	0.00	0.0500	-0.025593	-0.011159	-0.0368	-0.0256	-0.0112
34	0.20	0.0500	-0.041633	-0.000825	-0.0425	-0.0416	-0.0009
35	0.40	0.0500	-0.246769	-0.005953	-0.2527	-0.2481	-0.0046
36	0.60	0.0500	-1.060399	0.004531	-1.0559	-1.0627	0.0069
37	0.80	0.0500	-1.586509	-0.003288	-1.5898	-1.5869	-0.0029
38	1.00	0.0500	-1.823634	0.006896	-1.8167	-1.8230	0.0062
39	1.50	0.0500	-1.977581	-0.003577	-1.9812	-1.9763	-0.0048
40	2.00	0.0500	-1.996346	-0.006328	-2.0027	-1.9950	-0.0077
41	0.00	0.1000	-0.025805	0.010394	-0.0154	-0.0258	0.0104
42	0.20	0.1000	-0.083661	-0.004300	-0.0880	-0.0840	-0.0039
43	0.40	0.1000	-0.769383	0.004190	-0.7652	-0.7735	0.0083
44	0.60	0.1000	-1.442235	-0.000197	-1.4424	-1.4440	0.0015
45	0.80	0.1000	-1.763447	0.000463	-1.7630	-1.7633	0.0003
46	1.00	0.1000	-1.900189	-0.004241	-1.9044	-1.8994	-0.0050
47	1.50	0.1000	-1.987427	-0.011020	-1.9984	-1.9861	-0.0123
48	2.00	0.1000	-1.997958	0.006222	-1.9917	-1.9966	-0.0048
$S_{\text{error}}(Z) = 0.0089$				$S_{\text{resid}}(Z) = 0.0088$			
Error mean = 8.18E-4				Residual mean = 5.48E-4			
Mean error = 0.0066				Mean residual = 0.0066			
Standard deviation = 0.0086				Standard deviation = 0.0085			
Skewness (should be 0) = -0.463				Skewness (should be 0) = -0.445			
Curtosis (should be 3) = 4.808				Curtosis (should be 3) = 4.487			
Hamilton R-factor, % = 0.721				Hamilton R-factor % = 0.712			

Table 2. Comparison of (Z, pH) data analysis of CrO₄²⁻-H⁺ system by POLET(84), projection map method used by Sasaki,³⁷ and LETAGROP-Z + ETA; input data taken from Sasaki³⁷

Parameter	POLET(84)	Projection map	LETAGROP-Z + ETA
log β ₁₁	6.0092 ± 0.0014	5.89 ± 0.02	5.9086 ± 0.0019
log β ₂₂	13.9892 ± 0.0018	13.98 ± 0.04	14.0012 ± 0.0028
q ₁	1.0156 ± 0.0003	1	1
r ₁	1.0054 ± 0.0005	1	1
q ₂	1.9995 ± 0.0004	2	2
r ₂	1.9994 ± 0.0007	2	2
s(Z)	0.00266	0.00719	0.00431
Residual mean	-3.15E-3	5.08E-3	2.64E-4
Mean residual	0.0020	0.0059	0.0034
Standard deviation	0.0026	0.0072	0.0043
Skewness (should be 0)	-0.202	1.411	0.445
Curtosis (should be 3)	4.781	2.494	2.914
Hamilton R-factor, %	0.424	1.161	0.696

constants, log β₁₁ = 5.89 ± 0.02 and log β₂₂ = 13.98 ± 0.04. These data were first analysed by the projection map method with program PROKA and then the resulting normalized data (Z, pH) by the POLET(84) program. Low values of the residuals and the Hamilton R-factor indicated that a good

degree-of-fit was achieved and the parameter estimation was reliable (Table 2).

The complex-forming system of vanadium(V) and tartrate to form M₂LH and M₄L₂H₄ complexes and the aggregates M₃ and M₄ was used to illustrate the determination of stability constants only. Here, M

Table 3. Z = f(pH) data analysis of vanadate(V)-tartrate system by POLET(84) and a comparison of some results with those obtained by LETAGROP-ETITR program: values of log β₀₁₁ = 3.685 and log β₀₁₂ = 6.36 taken from Bartušek and Šustáček,⁴⁰ total concentration in mole/l.

pH	c _M	c _L	Z	pH	c _M	c _L	Z
7.26	0.0199	0.146	0.1375	7.17	0.0199	0.145	0.182
7.08	0.0195	0.144	0.2385	6.99	0.0193	0.142	0.322
6.89	0.0189	0.139	0.438	6.79	0.0185	0.136	0.577
6.69	0.0181	0.133	0.710	6.58	0.0178	0.131	0.812
7.24	0.020	0.0983	0.0959	7.06	0.0198	0.0971	0.168
6.98	0.0196	0.0961	0.226	6.89	0.0193	0.0947	0.311
6.79	0.0189	0.0927	0.438	6.69	0.0184	0.0904	0.588
6.59	0.018	0.0883	0.735	7.04	0.0201	0.0493	0.079
6.955	0.020	0.049	0.111	6.875	0.0198	0.0487	0.1535
6.79	0.0196	0.0481	0.224	6.695	0.0192	0.0472	0.333
6.595	0.0188	0.046	0.477	6.485	0.0183	0.0488	0.646
6.92	0.0051	0.0373	0.107	6.83	0.0051	0.0373	0.145
6.75	0.0051	0.0372	0.200	6.66	0.0050	0.0370	0.288
6.56	0.005	0.0368	0.419	6.46	0.0050	0.0366	0.568
6.355	0.0050	0.0363	0.710	6.26	0.0491	0.0362	0.818
6.80	0.0051	0.0249	0.108	6.72	0.0051	0.0248	0.147
6.64	0.0051	0.0248	0.208	6.55	0.0050	0.0247	0.305
6.45	0.0050	0.0245	0.448	6.35	0.0050	0.0243	0.610
6.245	0.0050	0.0242	0.749	6.605	0.0051	0.0124	0.099
6.525	0.0051	0.0124	0.150	6.44	0.0050	0.0124	0.222
6.345	0.0050	0.0123	0.341	6.245	0.0050	0.0122	0.496
6.14	0.0050	0.0121	0.657				
Species by POLET(84)				Species by LETAGROP-ETITR			
	log β _{par}			log β _{par}		Reference	
M ₃	7.360 ± 0.016			7.20		38	
M ₄	9.67 ± 0.14			10.15		38	
M ₄ L ₂ H ₄	39.80 ± 0.01			39.750 ± 0.008		39	
M ₂ LH	11.805 ± 0.020			11.820 ± 0.020		39	
U × 10 ³ , s(Z) 6.56, 0.01267				8.60, 0.014 39			
Residual mean	2.0E-3						
Mean residual	0.0096						
Standard deviation	0.0124			Not calculated			
Skewness (should be 0)	0.658						
Curtosis (should be 3)	2.520						
Hamilton R-factor, %	2.862						

stands for the vanadate anion. The equilibria are complicated by competitive hydrolysis of vanadium(V). In alkaline medium the species MOH and M_2OH prevail, and in neutral medium M_3 and M_4 ionic aggregates predominate.

Six potentiometric titrations for two total vanadium(V) concentrations (5 and 20mM) and six tartrate concentrations (12.5, 25, 37.5, 50, 100 and 150mM) in the pH range from 6.1 to 7.1 were performed by addition of mineral acid to a mixture of vanadate and tartrate (Table 3). The titration data were converted into ($Z_{H/M}$, pH) variables and analysed by POLET(84). Of the six stability constants, two were kept at constant values, $\log \beta_{011} = 3.685$ and $\log \beta_{012} = 6.360$, while the remaining four were refined, the resulting estimates being $\log \beta_{300} = 7.3604 \pm 0.0164$, $\log \beta_{400} = 9.6735 \pm 0.1430$, $\log \beta_{211} = 11.8049 \pm 0.0196$, $\log \beta_{424} = 39.7951 \pm 0.0196$ with SIGY [i.e., $s(Z)$, cf. Meloun and Čermák²³] = 0.01267. On the assumption that the experimental error of Z , $s_{inst}(Z)$, was 0.01 for the given experimental arrangement, the refined parameters were considered reliable. The degree-of-fit also proved there was sufficient refinement of the parameters. The polyvanadate stability constants found were in satisfactory agreement with those obtained by Brito *et al.*³⁹ from a quite independent data set by using LETAGROP-ETITR.

Other examples of application of POLET(84) can be found^{17,18,42} and the use of direct stoichiometry estimation by the ESI approach has been demonstrated in a comparison of three programs, POLET(84), LETAGROP-ETITR and MINI-QUAD, applied to the complexation systems of molybdate-malic acid, molybdate-citric acid and borate-malic acid.⁴²

REFERENCES

1. L. G. Sillén, *Acta Chem. Scand.*, 1962, **16**, 159.
2. N. Ingri and L. G. Sillén, *ibid.*, 1962, **16**, 173.
3. L. G. Sillén, *ibid.*, 1964, **18**, 1085.
4. N. Ingri and L. G. Sillén, *Arkiv Kemi*, 1964, **23**, 97.
5. L. G. Sillén and B. Warnqvist, *ibid.*, 1968, **31**, 315.
6. *Idem*, *ibid.*, 1968, **31**, 341.
7. R. Arnek, L. G. Sillén and O. Wahlberg, *ibid.*, 1968, **31**, 353.
8. P. Brauner, L. G. Sillén and R. Whiteker, *ibid.*, 1968, **31**, 365.
9. A. Sabatini, A. Vacca and P. Gans, *Talanta*, 1974, **21**, 53.
10. I. G. Sayce, *ibid.*, 1968, **15**, 1397.
11. G. Arena, E. Rizzarelli, S. Sammartano and C. Rigano, *ibid.*, 1979, **26**, 1.
12. I. Nagypál and L. Zékány, in *Computational Methods for the Determination of Formation Constants*, D. J. Leggett (ed.), Plenum Press, New York, 1985.
13. A. D. Zuberbühler and T. A. Kaden, *Talanta*, 1982, **29**, 201.
14. H. Gampp, M. Maeder, A. D. Zuberbühler and T. A. Kaden, *ibid.*, 1980, **27**, 513.
15. M. Wozniak and G. Nowogrocki, *Talanta*, 1978, **25**, 633, 643; 1979, **26**, 381, 1135; *J. Chem. Soc. Dalton*, 1981, 2423.
16. P. M. May, K. Murray and D. R. Williams, *Talanta*, 1985, **32**, 483.
17. J. Havel and M. Meloun, in *Computational Methods for the Determination of Formation Constants*, D. J. Leggett (ed.), Plenum Press, New York, 1985.
18. M. Meloun and J. Havel, *Computation of Solution Equilibria*, Part 2, *Potentiometry*, *Folia Fac. Sci. Nat., Univ. Purkynianae Brunensis*, Bruno, 1986.
19. F. R. Hartley, C. Burgess and R. M. Alcock, *Solution Equilibria*, Ellis Horwood, Chichester, 1980.
20. F. Gaizer, *Coord. Chem. Revs.*, 1979, **27**, 195.
21. P. Gans, *Advan. Mol. Relax. Interact. Proc.*, 1980, **18**, 139.
22. J. Havel and M. Meloun, *Talanta*, 1985, **33**, 435.
23. M. Meloun and J. Čermák, *ibid.*, 1984, **31**, 947.
24. M. Meloun and M. Javůrek, *ibid.*, 1984, **31**, 1083.
25. J. Havel and V. Kubáň, *Scripta Fac. Sci. Nat., Univ. Purkyn. Brunensis, Chemia* 2, 1971, **1**, 87.
26. D. D. Perrin and I. G. Sayce, *Talanta*, 1967, **14**, 883.
27. G. Ginzburg, *ibid.*, 1976, **23**, 149.
28. G. Biedermann and L. G. Sillén, *Arkiv Kemi*, 1953, **5**, 425.
29. G. Biedermann and L. Ciavatta, *Acta Chem. Scand.*, 1962, **16**, 2221.
30. S. Hietanen and L. G. Sillén, *ibid.*, 1959, **13**, 533, 1828.
31. Å. Olin, *ibid.*, 1960, **14**, 814.
32. N. Ingri, *ibid.*, 1963, **17**, 573.
33. P. M. May, D. R. Williams, P. W. Linder and R. G. Torrington, *Talanta*, 1982, **29**, 249.
34. P. Ulmgren and O. Wahlberg, *Univ. Stockholm Chem. Commun.*, 1970, No. IV.
35. J. Havel and M. Meloun, *Talanta*, 1985, **32**, 171.
36. L. G. Sillén, *Acta Chem. Scand.*, 1961, **15**, 1981; N. Ingri, G. Lagerström, M. Frydman and L. G. Sillén, *ibid.*, 1957, **11**, 1034.
37. Y. Sasaki, *ibid.*, 1962, **16**, 719.
38. L. G. Sillén, *ibid.*, 1956, **10**, 803.
39. F. Brito, N. Ingri and L. G. Sillén, *ibid.*, 1964, **18**, 1557.
40. M. Bartušek and V. Šustáček, *Collection Czech. Chem. Commun.*, 1983, **48**, 2785.
41. J. Havel and M. Vrchlabský, *Euroanalysis V*, Cracow, Poland, 26–31 August 1984.
42. M. Bartušek, D. Matula and J. Havel, *Collection Czech. Chem. Commun.*, in press.

SPECTROPHOTOMETRIC METHODS FOR THE EVALUATION OF ACIDITY CONSTANTS—II

NUMERICAL METHODS FOR TWO-STEP OVERLAPPING EQUILIBRIA

A. G. ASUERO, J. L. JIMENEZ-TRILLO and M. J. NAVAS

Department of Bromatology, Toxicology and Applied Chemical Analysis, Faculty of Pharmacy,
 The University of Seville, 41013 Seville, Spain

(Received 6 August 1985. Accepted 11 January 1986)

Summary—A brief review of the numerical methods employed in the evaluation of acidity constants of two step overlapping equilibria is given. A new alternative to the method of three equations developed by Thamer is also proposed in this paper. Taking into account the Gauss-elimination method, several variants to the original method of Thamer are devised.

For a diprotic acid with the equilibria $H_2R \rightleftharpoons HR + H$ and $HR \rightleftharpoons R + H$ the mixed acidity constants¹ are given by

$$K_{a1} = \frac{[HR]\{H\}}{[H_2R]}; \quad K_{a2} = \frac{[R]\{H\}}{[HR]} \quad (1)$$

where square brackets represent concentrations, and braces indicate activities. If the Beer-Lambert law holds, the absorbance of a solution containing a total concentration C_R of ligand is given by

$$A = \frac{A_0 + A_1 \frac{\{H\}}{K_{a2}} + A_2 \frac{\{H\}^2}{K_{a2}K_{a1}}}{1 + \frac{\{H\}}{K_{a2}} + \frac{\{H\}^2}{K_{a2}K_{a1}}} \quad (2)$$

where A_j is the absorbance of a solution of H_jR ($j = 0, 1, 2$) at concentration C_R . Equation (2) may be derived from the simple expressions

$$A = A_0 f_0 + A_1 f_1 + A_2 f_2 \quad (3a)$$

$$C_R = [R] + [HR] + [H_2R] \quad (3b)$$

$$f_j = [H_jR]/C_R \quad (3c)$$

and the equilibrium equation involving K_{a1} and K_{a2} . A detailed treatment of the algebra connected with the absorbance *vs.* pH curves for diprotic acids has been given by Irving *et al.*² The original paper should be consulted for the details, which are too lengthy to include here. The numerical methods applicable to the spectrophotometric evaluation of acidity constants of monoprotic acids³ have been considered in a previous paper. Here, the numerical methods of Thamer and Voigt⁴ and Zsako *et al.*⁵ are reformulated, Thamer's method⁶ is extended in order to evaluate the limiting absorbances of the species R, HR and H_2R (A_0, A_1 and A_2 respectively; $A_j = \epsilon_j[H_jR]$, ϵ_j being the molar absorptivity of the j th species), a new reformulation of the three-equation

method is proposed (A_0 and A_2 known) and two new methods, applicable in cases in which either A_2 or A_0 is unknown are also reported. The calculations are inherently laborious and can only be effected conveniently by minicomputer (a Casio PB 700 was used).

METHODS WHICH REQUIRE THAT THE A -pH GRAPHS HAVE A MAXIMUM OR MINIMUM IN THE REGION IN WHICH THE SPECIES HR PREDOMINATES

A number of authors have reported methods for obtaining pK_{a1} and pK_{a2} values when the molar absorptivity of the species HR is either greater or smaller than that of R and H_2R . Two approaches will be considered here: the methods described by Thamer and Voigt⁴ and by Zsako *et al.*⁵ The numerical formulation of Ang's method⁷ as well as its extension⁸ to equilibria with three overlapping steps will be considered in subsequent papers.

Method of Thamer and Voigt

Rewriting equation (2) for the point (A' , pH') at either a minimum or a maximum on the A *vs.* pH curve, it follows that

$$A_1 = (A' - A_0) \frac{K_{a2}}{\{H'\}} + A' + (A' - A_2) \frac{\{H'\}}{K_{a1}} \quad (4)$$

At the point (A' , pH'), $dA/d(\text{pH}) = dA/d\{H\} = 0$, so, from equation (2) we have

$$(A_1 - A_0)K_{a2}K_{a1} + 2(A_2 - A_0)\{H'\}K_{a2} + (A_2 - A_1)\{H'\}^2 = 0 \quad (5)$$

By introduction of expression (4) into this relation, the equation

$$x^2 + [K_{a1} + (1 - b)\{H'\}]\{H'\}x - b[K_{a1} + \{H'\}]\{H'\}^3 = 0 \quad (6)$$

is obtained, where

$$b = \frac{A' - A_2}{A' - A_0}; \quad x = K_{a1} K_{a2} \quad (7)$$

The real positive root of this equation is $x = \{H'\}^2 b$.

On the other hand, if we introduce expression (4) into equation (2) and take into account that $K_{a1} K_{a2} = \{H'\}^2 b$, we obtain

$$K_{a2} = \frac{\{H\}(A' - A)}{(A - A_0) + (A - A_2)q^2/b - (A' - A_0)q - (A' - A_2)q/b} \quad (8)$$

where $q = \{H\}/\{H'\}$.

The value of K_{a2} can be calculated from experimental values of pH and A provided that values of A' , pH' , A_0 and A_2 are available. Once the values of K_{a2} , K_{a1} [from equations (7) and (8)] and of A_1 [from equation (3)] are known, the theoretical graph of absorbance *vs.* pH at any appropriate wavelength can easily be derived by applying equation (2). Thamer and Voigt⁴ derived the following expression in order to calculate a curve through the experimental points

$$A = A_2 + b \left[\frac{\left(2 + \frac{K_{a1}}{\{H\}}\right)(A' - A_0) + \frac{b}{q}}{\frac{K_{a1}}{\{H\}} + q + \frac{b}{q}} \right] \quad (9)$$

If measurements are made at a wavelength at which the species R and H_2R have identical molar absorptivity, then $A_0 = A_2$, and hence $b = 1$ and equation (8) is reduced to

$$K_{a2} = \frac{\{H\}(A' - A)}{(A - A_0)(1 + q^2) - 2q(A' - A_0)} \quad (10)$$

This method was originally applied to determination of the dissociation constants of isophthalic, terephthalic and chloranilic acids.⁴ Evans *et al.*⁹ have applied it to pyridine monocarboxylic acids. Kiss and Szekely¹⁰ have re-examined Thamer and Voigt's method.

Method of Zsako *et al.*

This approach to estimating K_{a1} and K_{a2} also requires the molar absorptivity of R to be intermediate between those of HR and H_2R or that of H_2R to be between those of R and HR.

From equation (5)

$$K_{a2} = \frac{\{H'\}(A_1 - A_2)}{2(A_2 - A_0) + \frac{K_{a1}}{\{H'\}}(A_1 - A_0)} \quad (11)$$

Introducing this value for K_{a2} into equation (2) results in

$$\frac{1}{\{H\}} K_{a1}^2 - 2QK_{a1} - 2\{H'\} \left(\frac{A_2 - A}{A_1 - A} \right) \alpha = 0 \quad (12)$$

where

$$Q = \frac{1}{2} \left(\frac{A - A_2}{A_1 - A} \right) + q + \frac{q^2 \beta}{2} \left(\frac{A - A_0}{A_1 - A_0} \right) \quad (13)$$

with

$$\alpha = (A_0 - A_2)/(A_1 - A_0)$$

and

$$\beta = (A_1 - A_2)/(A_1 - A_0),$$

and

$$q = \{H\}/\{H'\}$$

as before.

The positive root of equation (12) is

$$K_{a1} = \left(Q + \left[Q^2 + 2q\alpha \left(\frac{A_2 - A}{A_1 - A} \right) \right]^{1/2} \right) \{H\} \quad (14)$$

The computation of A_1 , A_0 (or A_2) and K_{a1} entails a trial and error procedure. The first values adopted for A_1 and A_0 are A' and A at the maximum (or minimum) pH value tested, respectively; then A_1 is gradually increased (decreased) and A_0 decreased (increased), as appropriate, until the best constancy for K_{a1} is reached, *e.g.*, by minimizing the standard deviation of K_{a1} . Once K_{a1} is known, K_{a2} is evaluated by applying equation (11). This method has been applied to evaluation of the acidity constants of the dioximes of 1,2-cycloheptanedione and 1,2-cyclooctanedione.⁵ However, the procedure is tedious because it involves two variables at a time.

METHODS WHICH REQUIRE THAT THE MOLAR ABSORPTIVITY OF HR BE INTERMEDIATE BETWEEN THOSE OF R AND H_2R

The main difficulty of Thamer and Voigt's method in practice is to locate accurately the maximum or minimum in the A -pH graph. In such a treatment it is necessary to obtain a number of results around pH' before the proper curve can be established. No restriction on the shape of the A -pH curve is imposed in the following treatment. Four experimental situations exist depending on whether either or both of the limiting absorbances A_2 and A_0 are known or unknown.

Case I—The absorptivities of both R and H_2R can be directly determined

Equation (2) can be rearranged to give

$$(A - A_0)K_{a2} - A_1\{H\} + (A - A_2)\{H\}^2/K_{a1} = -A\{H\} \quad (15)$$

If A_0 and A_2 can be obtained from measurements at the upper and lower extremes of the pH range, respectively, this equation contains three unknowns: A_1 , K_{a1} and K_{a2} . The required unknowns can be evaluated by solving simultaneous equations derived from equation (17) for three solutions *a*, *b* and *c*.

Robinson and Biggs¹¹ measured absorbances at three different pH values in determining the acidity constants of *p*-aminobenzoic acid and four ester

derivatives, as did Mattoo¹² and Pal'chevskii *et al.*¹³ in the determination of the acidity constants of *p*-hydroxybenzoic acid, although in that case $\Delta pK_a > 5.0$. However no equations relating K_{a1} and K_{a2} with experimental data were given by these authors. This was done by Thamer.⁶ Here we give a reformulation of the three-equation method for diprotic acids which leads to more straightforward expressions than those reported by Thamer⁶ and allows K_{a1} , K_{a2} and A_1 to be evaluated from experimental *A*-pH data for three solutions *a*, *b* and *c*.

Using the properties of determinants, we get for K_{a2}

$$K_{a2} = \frac{\begin{vmatrix} 1 & A_a & X_4\{H\}_a \\ 1 & A_b & X_5\{H\}_b \\ 1 & A_c & X_6\{H\}_c \end{vmatrix}}{\begin{vmatrix} X_4\{H\}_a^2 & X_1 & \{H\}_a \\ X_5\{H\}_b^2 & X_2 & \{H\}_b \\ X_6\{H\}_c^2 & X_3 & \{H\}_c \end{vmatrix}} \quad (16)$$

where

$$\begin{aligned} X_1 &= A_a - A_0 & X_4 &= A_a - A_2 \\ X_2 &= A_b - A_0 & X_5 &= A_b - A_2 \\ X_3 &= A_c - A_0 & X_6 &= A_c - A_2 \end{aligned} \quad (17)$$

Putting

$$\begin{aligned} \{H\}_a/\{H\}_b &= q_1; \\ \{H\}_c/\{H\}_b &= q_{II}; \\ Y_1 &= A_a - A_b; \\ Y_2 &= A_b - A_c; \\ Y_3 &= A_c - A_a \end{aligned} \quad (18)$$

we obtain finally

$$K_{a2} = \{H\}_c q_1 \frac{q_{II} X_4 Y_2 + X_5 Y_3 + q_{II} X_6 Y_1}{X_4 q_1^2 (X_3 - X_2 q_{II}) + X_5 (X_1 q_{II} - X_3 q_1) + X_6 q_{II}^2 (X_2 q_1 - X_1)} \quad (19)$$

In analogous manner we may evaluate K_{a1} and A_1 from

$$K_{a1} = -\{H\}_b \frac{X_4 q_1^2 (X_3 - X_2 q_{II}) + X_5 (X_1 q_{II} - X_3 q_1) + X_6 q_{II}^2 (X_2 q_1 - X_1)}{X_1 Y_2 q_{II} + X_2 Y_3 q_1 q_{II} + X_3 Y_1 q_1} \quad (20)$$

and

$$A_1 = \frac{X_4 q_1^2 (X_3 A_b - X_2 q_{II} A_c) + X_5 (X_1 q_{II} A_c - X_3 q_1 A_a) + X_6 q_{II}^2 (X_2 q_1 A_a - X_1 A_b)}{X_4 q_1^2 (X_3 - X_2 q_{II}) + X_5 (X_1 q_{II} - X_3 q_1) + X_6 q_{II}^2 (X_2 q_1 - X_1)} \quad (21)$$

Equations (19) and (20) are essentially identical with those given by Thamer,⁶ and the same unique values for the constants are obtained by both methods, although there is no simple transformation between this and Thamer's formulation. The absence of any assumption in the derivation makes equations (21)–(23) more attractive than the approximate ones

proposed by several earlier workers,^{14–17} starting from totally different principles.

Case II (Thamer's method)—the absorptivities of H_2R , R and HR are unknown

In this case, the form of the *A*-pH graphs depends on the relative magnitudes of five parameters: A_0 , A_1 , A_2 , K_{a1} and K_{a2} . The resolution of five linear equations of the form (2) in order to evaluate the unknown parameters was first suggested by Rosenblatt,¹⁸ although no attempt was made to do it, because of the inherent difficulty in resolution of fifth-order determinants. An answer to this problem was reported by Thamer, as shown below.

The difference in absorbance between two solutions *i* and *a* is given [according to equation (2)] by

$$A_i - A_a = \frac{A_0 + A_1 \frac{\{H\}_i}{K_{a2}} + A_2 \frac{\{H\}_i^2}{K_{a2} K_{a1}}}{1 + \frac{\{H\}_i}{K_{a2}} + \frac{\{H\}_i^2}{K_{a2} K_{a1}}} - A_a \quad (22)$$

Equation (22) can be rewritten as

$$\begin{aligned} (A_i - A_a) K_{a1} K_{a2} + (A_i - A_a) K_{a1} \{H\}_i + (A_i - A_a) \{H\}_i^2 \\ - (A_0 - A_a) K_{a1} K_{a2} - (A_1 - A_a) K_{a1} \{H\}_i \\ - (A_2 - A_a) \{H\}_i^2 = 0 \end{aligned} \quad (23)$$

When *i* = *a*, it follows that

$$\begin{aligned} -K_{a1} K_{a2} (A_0 - A_a) - \{H\}_a K_{a1} (A_1 - A_a) \\ - \{H\}_a^2 (A_2 - A_a) = 0 \end{aligned} \quad (24)$$

Combination of equations (23) and (24), followed by rearrangement, yields

$$\begin{aligned} \{H\}_i (A_i - A_a) K_{a1} + (A_i - A_a) K_{a1} K_{a2} + (\{H\}_a \\ - \{H\}_i) K_{a1} (A_1 - A_a) + (\{H\}_a^2 - \{H\}_i^2) (A_2 - A_a) \\ = -\{H\}_i^2 (A_i - A_a) \end{aligned} \quad (25)$$

Making *i* = *b*, *c*, *d* and *e* gives a system of four linear equations with five terms and four unknowns.

With the relations

$$\begin{aligned} X_i &= \{H\}_c^4 Z_i \\ p_I &= \{H\}_a / \{H\}_c \\ p_{II} &= \{H\}_b / \{H\}_c \end{aligned}$$

$$\begin{aligned} p_{III} &= \{H\}_d / \{H\}_c \\ p_{IV} &= \{H\}_e / \{H\}_c \end{aligned} \quad (26)$$

the equations given by Thamer⁶ for the first two unknowns may be modified to

$$K_{a1} = \{H\}_c \left[\frac{Z_1(p_{II} + 1) + Z_2(p_{II} + p_{III}) - Z_3(p_{II} + p_{IV}) - Z_4(1 + p_{III}) + Z_5(1 + p_{IV}) + Z_6(p_{III} + p_{IV})}{Z_1 - Z_2 + Z_3 + Z_4 - Z_5 + Z_6} \right] \quad (27)$$

$$K_{a2} = \{H\}_c \left[\frac{Z_1 p_{II} - Z_2 p_{II} p_{III} + Z_3 p_{II} p_{IV} + Z_4 p_{III} - Z_5 p_{IV} + Z_6 p_{III} p_{IV}}{-Z_1(p_{II} + 1) + Z_2(p_{II} + p_{III}) - Z_3(p_{II} + p_{IV}) - Z_4(1 + p_{III}) + Z_5(1 + p_{IV}) + Z_6(p_{III} + p_{IV})} \right] \quad (28)$$

where

$$\begin{aligned} Z_1 &= (A_b - A_a)(A_c - A_a)(p_I - p_{III})(p_I - p_{IV}) \\ &\quad \times (p_{II} - 1)(p_{III} - p_{IV}) \\ Z_2 &= (A_b - A_a)(A_d - A_a)(p_I - 1)(p_I - p_{IV}) \\ &\quad \times (p_{II} - p_{III})(1 - p_{IV}) \\ Z_3 &= (A_b - A_a)(A_e - A_a)(p_I - 1)(p_I - p_{III}) \\ &\quad \times (p_{II} - p_{IV})(1 - p_{III}) \\ Z_4 &= (A_c - A_a)(A_d - A_a)(p_I - p_{II})(p_I - p_{IV}) \\ &\quad \times (1 - p_{III})(p_{II} - p_{IV}) \\ Z_5 &= (A_c - A_a)(A_e - A_a)(p_I - p_{II})(p_I - p_{III}) \\ &\quad \times (1 - p_{IV})(p_{II} - p_{III}) \\ Z_6 &= (A_d - A_a)(A_e - A_a)(p_I - p_{II})(p_I - 1) \\ &\quad \times (p_{III} - p_{IV})(p_{II} - 1) \end{aligned} \quad (29)$$

Once the values of K_{a1} and K_{a2} are known, equation (2) can be rearranged to give

$$A_0 + A_1 \frac{\{H\}}{K_{a2}} + A_2 \frac{\{H\}^2}{K_{a2} K_{a1}} = A \left(1 + \frac{\{H\}}{K_{a2}} + \frac{\{H\}^2}{K_{a2} K_{a1}} \right) \quad (30)$$

Linear equations in four terms and three unknowns of this type [equation (30)] can be used to evaluate the A_0 , A_1 and A_2 values (obtained from any three solutions) by Gaussian elimination.¹⁹ In this way the inherently laborious calculations involved in the resolution of a system of five linear equations of the form (2) in order to evaluate the unknown parameters A_0 , A_1 , A_2 , K_{a1} and K_{a2} are avoided. This was accomplished by Roth and Bunnett²⁰ by computer.

Solving equation (30) for three solutions a , b and c , we obtain

$$A_2 = \frac{(D_c - D_a) - (D_b - D_a) \left(\frac{B_c - B_a}{B_b - B_a} \right)}{(C_c - C_a) - (C_b - C_a) \left(\frac{B_c - B_a}{B_b - B_a} \right)} \quad (31)$$

$$A_1 = \frac{(D_b - D_a) - (C_b - C_a) A_2}{B_b - B_a} \quad (32)$$

$$A_0 = D_a - B_a A_1 - C_a A_2 \quad (33)$$

where

$$\begin{aligned} B_i &= \frac{\{H\}_i}{K_{a2}} \\ C_i &= \frac{\{H\}_i^2}{K_{a2} K_{a1}} \end{aligned}$$

$$D_i = A_i \left(1 + \frac{\{H\}_i}{K_{a2}} + \frac{\{H\}_i^2}{K_{a2} K_{a1}} \right) \quad (34)$$

Case III—Only the absorptivity of H_2R is known

By rearrangement of equation (23) we have

$$\begin{aligned} (\{H\}_a - \{H\}_i)[K_{a1}(A_1 - A_a)] + (A_i - A_a)[K_{a1}K_{a2}] \\ + \{H\}_a(A_i - A_a)[K_{a1}] = -\{H\}_i^2(A_i - A_a) \\ - (\{H\}_a^2 - \{H\}_i^2)(A_2 - A_a) \end{aligned} \quad (35)$$

The three equations of form (35), (with $i = b, c$ and d) may be solved¹⁹ for the three unknowns $K_{a1}(A_1 - A_a)$, $K_{a1}K_{a2}$ and K_{a1} [shown in square brackets in equation (35)] by Gaussian elimination. Finally, A_0 is evaluated by means of equation (2) for any point (A , pH).

Case IV—Only the absorptivity of R is known

Dividing equation (23) by $\{H\}_i^2$ gives

$$\begin{aligned} \left(\frac{A_i - A_a}{\{H\}_i} \right) K_{a1} + \left(\frac{A_i - A_a}{\{H\}_i^2} \right) K_{a1} K_{a2} \\ - K_{a1} K_{a2} \left(\frac{A_0 - A_a}{\{H\}_i^2} \right) - K_{a1} \left(\frac{A_1 - A_a}{\{H\}_i} \right) \\ - (A_2 - A_a) = 0 \end{aligned} \quad (36)$$

When i is equal to a we get

$$\begin{aligned} K_{a1} K_{a2} \left(\frac{A_0 - A_a}{\{H\}_a^2} \right) + K_{a1} \left(\frac{A_1 - A_a}{\{H\}_a} \right) \\ + (A_2 - A_a) = 0 \end{aligned} \quad (37)$$

Combining equations (36) and (37) yields

$$\begin{aligned} \left[\frac{1}{\{H\}_a} - \frac{1}{\{H\}_i} \right] K_{a1}(A_1 - A_a) \\ + \left[\frac{(A_i - A_a)}{\{H\}_i^2} + \frac{(A_0 - A_a)}{\{H\}_a^2} \right] \\ \times K_{a1} K_{a2} + \left[\frac{(A_i - A_a)}{\{H\}_i} \right] K_{a1} = A_a - A_i \end{aligned} \quad (38)$$

The three unknowns $K_{a1}(A_1 - A_a)$, $K_{a1}K_{a2}$, and K_{a1} can again be evaluated by solving three equations of the form (38) by the Gaussian elimination method.¹⁹

The fourth unknown A_2 is then evaluated by applying equation (2):

$$A_2 = A_j + (A_j - A_1) \frac{K_{a1}}{\{H\}_j} + (A_j - A_0) \frac{K_{a2}K_{a1}}{\{H\}_j^2} \quad (39)$$

for (A_j, pH_j) and $j = a, b, c$ or d .

A program¹⁹ for use with a Casio PB 700 mini-computer, and based on the equations developed for Cases I–IV has been devised and is available from the authors on request. Programs for use with a Texas TI 59 pocket calculator and based on the equations developed^{19,21} have also been devised. The use of a pocket calculator to perform the calculations is necessary in order to maintain arithmetic precision.

In a forthcoming paper²² data for the overlapping equilibria of glyoxal bis(4-phenyl-3-thiosemicarbazone) will be presented.

REFERENCES

1. A. Ringbom, *Complexation in Analytical Chemistry*, Interscience, New York, 1963.
2. H. M. Irving, H. S. Rossotti and G. Harris, *Analyst*, 1955, **80**, 83.
3. A. G. Asuero, M. J. Navas and J. L. Jimenez-Trillo, *Talanta*, 1986, **33**, 195.
4. B. J. Thamer and A. F. Voigt, *J. Phys. Chem.*, 1952, **56**, 225.
5. J. Zsako, J. Horak, Z. Finta, C. S. Varhelyi and I. Mitrache, *Mikrochim. Acta*, 1979 **I**, 405.
6. B. J. Thamer, *J. Phys. Chem.*, 1955, **59**, 450.
7. K. P. Ang, *ibid.*, 1958, **62**, 1109.
8. A. G. Asuero, unpublished work.
9. R. F. Evans, E. F. G. Herington and W. Kynaston, *Trans. Faraday Soc.*, 1953, **49**, 1284.
10. G. Kiss and F. Szekely, *Acad. Repub. Pop. Rom., Fil. Cluj, Stud. Cercet. Chim.*, 1961, **12**, 171.
11. R. A. Robinson and A. I. Biggs, *Aust. J. Chem.*, 1957, **10**, 128.
12. B. N. Mattoo, *Trans. Faraday Soc.*, 1956, **52**, 1462.
13. V. V. Pal'chevskii, M. S. Zakhar'evskii and E. A. Malinina, *Vestn. Leningrad. Univ.* 15, No. 16, *Ser. Fiz. i Khim.*, 1960, No. 3, 95.
14. E. B. Hughes, H. G. Jellinek and B. A. Ambrose, *J. Phys. Colloid. Chem.*, 1949, **53**, 414.
15. C. V. Banks and A. B. Carlson, *Anal. Chim. Acta*, 1952, **7**, 291.
16. B. Buděšínský, *Talanta*, 1969, **16**, 1277.
17. F. J. Barragán, J. L. Gomez-Ariza and F. Pino, *ibid.*, 1983, **30**, 555.
18. D. H. Rosenblatt, *J. Phys. Chem.*, 1954, **58**, 40.
19. J. L. Jimenez-Trillo, *Ph.D. Thesis*, University of Seville, 1985.
20. B. Roth and F. Bunnett, *J. Am. Chem. Soc.*, 1965, **87**, 334.
21. M. J. Navas, *Ph.D. Thesis*, University of Seville, 1985.
22. A. M. Jimenez, M. A. Herrador, M. J. Navas, J. L. Jimenez-Trillo and A. G. Asuero, to be submitted.

SHORT COMMUNICATIONS

ENHANCEMENT OF THE FLUORESCENCE OF THE ZINC-MORIN COMPLEX BY A NON-IONIC SURFACTANT

F. HERNANDEZ HERNANDEZ, J. MEDINA ESCRICHE and M. T. GASCO ANDREU
Department of Analytical Chemistry, University College of Castellon, University of Valencia,
12004 Castellon, Spain

(Received 28 August 1985. Revised 29 January 1986. Accepted 4 February 1986)

Summary—A method is described for the fluorimetric determination of zinc, based on formation of a zinc-morin complex in the presence of a non-ionic surfactant. The complex has practically no fluorescence in the absence of surfactant, but the addition of Genapol PF-20 (non-ionic surfactant, ethylene oxide-propylene oxide condensate) makes possible the fluorimetric determination of low concentrations of zinc as it enhances the fluorescence of the complex about 75-fold. Maximum fluorescence is produced at pH 4.7 ± 0.2 (acetic acid-acetate buffer), with 1.5% surfactant and 0.009% morin. The fluorescence is excited at 433 nm and measured at 503 nm. The calibration graph is linear up to 150 ng/ml zinc concentration and the detection limit is 3 ng/ml. The relative standard deviation (11 replicates) is 2.4% for zinc at 20 ng/ml concentration and 1.7% for 100 ng/ml. Of 29 ions studied, Al^{3+} , Be^{2+} , Zr^{4+} and Cd^{2+} strongly increase the fluorescence of the system, and Fe^{3+} , Ni^{2+} , Cu^{2+} , $Ti(IV)$ and Co^{2+} decrease the fluorescence signal.

In recent years, surfactants have become of great interest because they provide a reaction medium in which the sensitivity and selectivity of numerous reactions are improved, and the metal complexes formed in micellar media are generally more stable than those formed in the absence of micelles. Most work has been done on spectrophotometric determinations, but surfactants are now also being applied successfully in fluorimetry,¹ giving even higher sensitivity and lower detection limits. The first of these applications was to the determination of aluminium with lumogallion in the presence of the non-ionic surfactant polyethylene glycol monolauryl ether.² Recently, Sanz Medel and co-workers^{3,4} and Hinze *et al.*⁵ have reviewed the applications of micellar media in fluorimetric analysis.

With morin as fluorimetric reagent, only the complexes of Nb,^{3,4,6} Ta,⁴ Al⁷ and Pb⁸ have been sensitized by the use of surfactants. The fluorescence of the Nb-morin system is strongly enhanced by cationic surfactants (*e.g.*, CTAB gives an 80-fold increase) but anionic and non-ionic surfactants are without effect.³ It has been postulated that cationic surfactants interact electrostatically with the ternary anionic niobium-morin complex formed in sulphate solutions $[NbO(OH)SO_4 \cdot H_4R]^-$, to form an ion-association compound.^{3,6} The micelle-enhanced fluorimetric method³ has a detection limit of 1 ng/ml and is highly selective. Analogously, in sulphuric acid medium, Ta forms with morin a negatively charged ternary complex containing sulphate ions which fluoresces in CTAB micellar solutions owing to the formation of an ion-association complex with the cationic CTAB micelles.⁴

The non-ionic surfactant Genapol PF-20 (ethylene oxide-propylene oxide condensate) strongly increases the fluorescence of the aluminium-morin complex (about 8-10-fold).⁷ Analogously, this surfactant sensitizes the fluorescence of the Pb-morin system about 9-fold,⁸ which makes possible the fluorimetric determination of Pb with morin, as in the absence of surfactant this system has only very weak fluorescence.

From the strong interference of zinc in the Al-morin-Genapol and Pb-morin-Genapol systems (zinc does not interfere in the absence of the surfactant) we deduced that the very weak fluorescence of the Zn-morin system in acid media is significantly enhanced by addition of Genapol, and have therefore studied the effect.

EXPERIMENTAL

Apparatus

Fluorescence intensity (I_f) measurements were made on a Perkin-Elmer 3000 spectrofluorimeter with 10 and 5 nm band-pass in the excitation and emission paths, respectively, and 1-cm quartz cells. The cell temperature was kept constant within $\pm 0.5^\circ$. A Crison Digilab 517 pH-meter (reading to ± 0.001) was used.

Reagents

All reagents used were of analytical grade (Merck).

Zinc stock solution, 1000 $\mu\text{g/ml}$. Prepared by dissolving the contents of an ampoule of Titrisol standard zinc solution in water and diluting accurately to 1 litre. Working solutions were prepared by appropriate dilution with water.

Morin solution, 0.18% in absolute ethanol.

Acetate buffer (pH 4.7). Prepared by mixing 8.04 g of anhydrous sodium acetate with 5.9 ml of glacial acetic acid and diluting with water to 100 ml.

Surfactant solution. Made by dissolving 15 g of Genapol

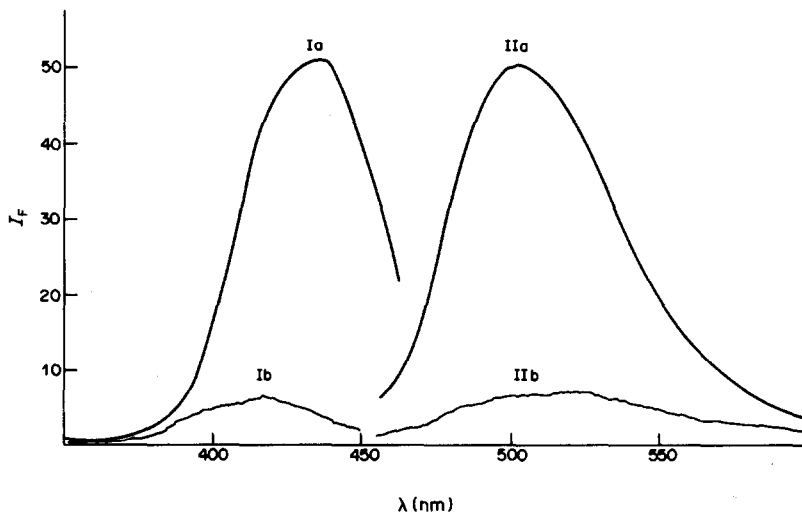


Fig. 1. Excitation (I) and emission (II) spectra: (a) Zn-morin-Genapol (scale $\times 1$); (b) Zn-morin (scale $\times 10$), Zn concentration 100 ng/ml, morin 0.009%, Genapol 1.5%, pH 4.7 (acetic acid-acetate buffer), 25°C.

PF-20 (Hoechst) (propylene oxide-ethylene oxide ratio 1.6) in water and diluting to 100 ml (final concentration $5.2 \times 10^{-2} M$).

Distilled and demineralized water was used throughout.

General procedure

An aliquot of standard zinc solution (up to 15 μg of zinc) was transferred into a 100-ml beaker and 5 ml of morin solution were added. The pH was adjusted to 4.7 with 10 ml of acetate buffer. Then 10 ml of surfactant solution were added, and the solution was diluted with water to 100 ml (the ionic strength, maintained with the acetate buffer, was 0.1M) and mixed well. After 45 min the fluorescence intensity was measured (at 25°C) at 503 nm with excitation at 433 nm.

RESULTS AND DISCUSSION

Figure 1 shows the excitation and emission spectra of the Zn-morin and Zn-morin-Genapol systems (100 ng/ml of Zn and pH 4.7). As can be seen, the presence of 1.5% Genapol PF-20 greatly increases the fluorescence intensity (> 75 -fold) and causes a shift in the excitation maximum from 418 to 433 nm.

Maximum fluorescence occurred at 503 nm in both instances. Though in Fig. 1 the emission maximum of the Zn-morin complex in the absence of surfactant appears to occur at ~ 520 nm, this actually corresponds to the fluorescence of the free morin at pH

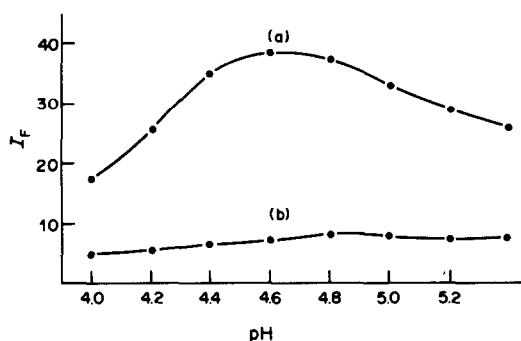


Fig. 2. Effect of pH on the fluorescence over the optimum range (adjusted with acetic acid-acetate buffer): (a) Zn-morin-Genapol; (b) morin-Genapol. Zn concentration 100 ng/ml, morin 0.005%, Genapol 1.5%, 25°C.

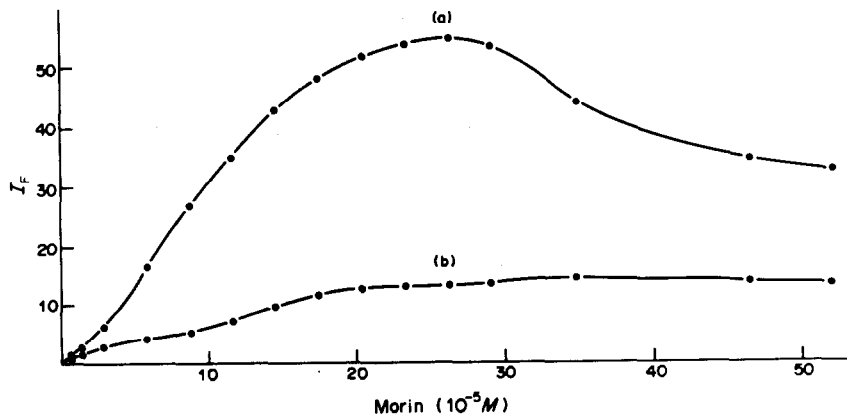


Fig. 3. Effect of morin concentration: (a) Zn-morin-Genapol; (b) morin-Genapol. Zn concentration 100 ng/ml, Genapol 1.5%, pH 4.7 (acetic acid-acetate buffer), 25°C.

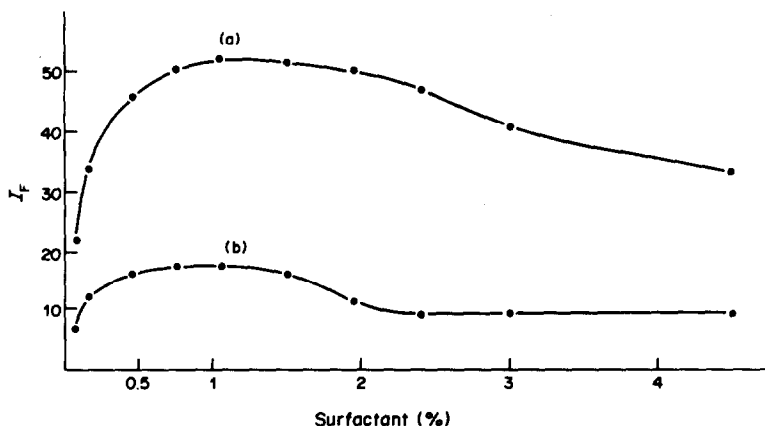


Fig. 4. Effect of Genapol concentration: (a) Zn-morin-Genapol; (b) morin-Genapol. Zn concentration 100 ng/ml, morin 0.009%, pH 4.7 (acetic acid-acetate buffer), 25°C.

4.7, and with zinc concentrations > 500 ng/ml the emission maximum of the zinc complex clearly occurs at 503 nm.

We had previously established⁷ that the surfactant used in this work was the most appropriate (amongst various non-ionic and cationic surfactants tested) for the sensitization of the Al-morin complex.

Reaction conditions

The system was found to give fluorescence only between pH 3 and 6, with maximum intensity at pH 4.5-4.8 (Fig. 2), and with a morin concentration of $2.6 \times 10^{-4} M$ (Fig. 3). Rigid control of pH is essential, and pH 4.7 was selected as optimal.

The optimum surfactant concentration was 1.5%, but variation between 0.8 and 2.0% of surfactant caused a maximum change of only 4% in I_F (Fig. 4).

I_F was maximal and practically constant when the ethanol concentration was lower than 7.5%. Higher concentrations decreased the response (Fig. 5), presumably because the ethanol destroys the micelles. A 5% v/v concentration of ethanol was chosen as optimal; this volume of ethanol is furnished by the morin solution.

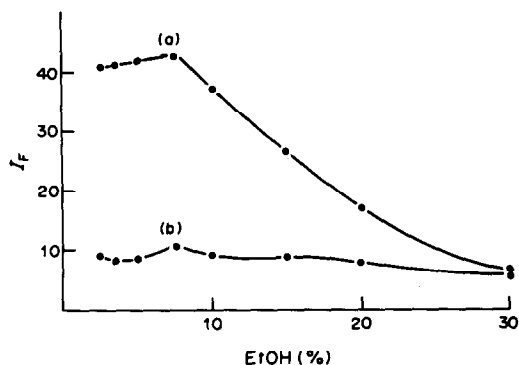


Fig. 5. Effect of ethanol concentration: (a) Zn-morin-Genapol; (b) morin-Genapol. Zn concentration 100 ng/ml, morin 0.009%, Genapol 1.5%, pH 4.7 (acetic acid-acetate buffer), 25°C.

Maximum fluorescence was obtained at 25-30°, but the stability was higher at temperatures $\leq 25^\circ$, with a slight initial decrease of I_F and then constant response for 1 hr. This temperature and a measurement time of 45 min were chosen as optimal.

Analytical characteristics

The calibration graph was linear up to 150 ng/ml zinc concentration, with an intercept on the ordinate, corresponding to the fluorescence of the free reagent.

The relative standard deviation (r.s.d., 11 replicates) for zinc at the 20-ng/ml level was 2.4%, and 1.7% for 100 ng/ml.

The detection limit, estimated as the zinc level giving a net signal three times the standard deviation of the blank, was 3 ng/ml.

Interferences

The effect of 29 ions on the fluorescence of the Zn-morin-Genapol system at the 20-ng/ml zinc level was studied (Table 1). The tolerance level was set at the amount causing less than $\pm 4.8\%$ change (i.e., twice the r.s.d.) in I_F . The main interferences are produced by Al, Be and Zr, which form highly fluorescent complexes with morin. Moreover, Cd and Hg(II), which are in the same periodic group as Zn, also increase the fluorescence.

Table 1. Tolerances for diverse ions [Zn concentration 20 ng/ml, morin 0.009%, Genapol 1.5%, pH 4.7 (acetic acid-acetate buffer), 25°C]

C_{ion}/C_{Zn}	Ion
> 500	Cl^- , HCO_3^- , NO_3^- , HPO_4^{2-} , SiO_3^{2-} , Ba^{2+} , Na^+ , NH_4^+
250	F^- , SO_4^{2-} , K^+
100	Mn^{2+} , Sr^{2+}
50	Ca^{2+} , Cr^{3+} , Mg^{2+}
25	Pb^{2+} , Sn^{2+}
5	Hg^{2+} , V(V)
2	Co^{2+}
1	Cu^{2+} , Ni^{2+} , Ti(IV)
0.5	Fe^{3+} , Cd^{2+}
0.1	Be^{2+} , Zr(IV)
0.02	Al^{3+}

Fe(III), Co(II), Cu(II), Ni(II) and Ti(IV) interfere by decreasing the fluorescence.

REFERENCES

1. W. L. Hinze, in *Solution Chemistry of Surfactants*, K. L. Mittal (ed.), Vol. 1, pp. 79-127. Plenum Press, New York, 1979.
2. N. Ishibashi and K. Kina, *Anal. Lett.*, 1972, **5**, 637.
3. A. Sanz Medel and J. I. Garcia Alonso, *Anal. Chim. Acta*, 1984, **165**, 159.
4. A. Sanz Medel, J. I. Garcia Alonso and E. Blanco Gonzalez, *Anal. Chem.*, 1985, **57**, 1681.
5. W. L. Hinze, H. N. Singh, Y. Baba and N. G. Harvey, *Trends Anal. Chem.*, 1984, **3**, 193.
6. A. T. Pilipenko, T. A. Vasil'chuk and A. I. Volkova, *Zh. Analit. Khim.*, 1983, **38**, 855.
7. J. Medina Escriche, M. de la Guardia Cirugeda and F. Hernández Hernández, *Analyst*, 1983, **108**, 1386.
8. J. Medina Escriche, F. Hernández Hernández, R. Marin and F. J. Lopez, *ibid.*, 1986, **111**, 235.

FLUORIMETRIC DETERMINATION OF BORON AT MICROGRAM LEVEL

J. M. MIR and C. MARTINEZ

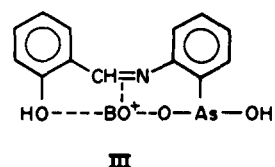
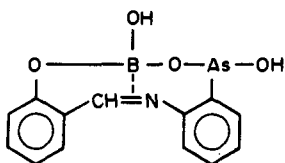
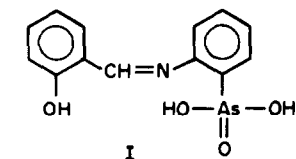
Analytical Chemistry Department, Faculty of Sciences, University of Zaragoza, Zaragoza, Spain

(Received 16 May 1984. Revised 20 January 1986. Accepted 29 January 1986)

Summary—The synthesis, characterization and application of 2-(2-hydroxybenzylideneimine)benzenearsonic acid (HBBA) as a reagent for the fluorimetric determination of boron are described. This reagent reacts with boric acid in 85% w/w sulphuric acid medium to yield a fluorescent compound. The reagent is not fluorescent in those conditions. Heating at 90° for 45 min is needed for the compound to be formed. The linear calibration range is 0.1–8 µg/ml in the solution measured. The detection limit of the method is 0.01 µg/ml. The method has been applied to determine boron in vegetal material.

Benzoin has long been the most widely used reagent for fluorimetric determination of boron,¹ but other reagents have more recently been used for this purpose, including carminic acid,² 2-hydroxy-4-methoxy-4'-chlorobenzophenone³ and dibenzoylmethane.⁴

During a study of new imine derivatives as analytical reagents⁵ we have found that 2-(2-hydroxybenzylideneimine)benzoarsonic acid (HBBA, I) reacts with boric acid in sulphuric acid medium to form a compound which exhibits fluorescence, as expected from its molecular structure and the effect of substituents on fluorescence.⁶ By analogy with hydroxy-anthraquinones, boric acid is expected to react with HBBA at high acidity⁷ and to have structure II.⁸ A strongly acid medium is needed, otherwise a structure like III will be obtained, which has no fluorescence, on account of its low molecular rigidity.⁸



EXPERIMENTAL

Apparatus

Absorbance measurements were made with a Pye Unicam SP8-100 double-beam spectrophotometer with the necessary accessory to convert it into a spectrofluorimeter, a monochromator to isolate the required line from the radiation source (excitation monochromator) and a series of filters to analyse the fluorescence radiation. A 10.2 × 5.47 mm cross-section cell containing quinine sulphate solution was used as reference, and a 10.0 × 10.47 mm cell to contain the sample.

Reagents

HBBA. For the synthesis dissolve 7.2 g of salicylaldehyde in 50 ml of ethanol and 5 ml of concentrated hydrochloric acid. Heat under reflux for 5 hr, and add 12.5 g of *o*-aminobenzenearsonic acid dissolved in 150 ml of ethanol. Let the solution cool, then add 200 ml of distilled water, neutralize to pH 4 with 5M sodium hydroxide and leave in the refrigerator for 12 hr. The product (yield 80%) is a yellow solid, with m.p. 226°, sparingly soluble in water, acetone or acetic acid, but soluble in concentrated sulphuric acid, hot ethanol and in dilute sodium hydroxide solution. It is purified by recrystallization from ethanol, and vacuum sublimation.

The reagent is used as a 0.05M solution in concentrated sulphuric acid (s.g. 1.84).

Standard boron solution, 1000 µg/ml. Dissolve 5.715 g of pure boric acid and dilute to volume with water in a 1000-ml standard flask. Store the solution in a plastic bottle. Prepare working solutions by dilution just before use.

Quinine sulphate solution. Dissolve 0.500 g of quinine sulphate in 100 ml of 0.05M sulphuric acid.

Sulphuric acid, 85% w/w (s.g. 1.78). Dilute (with caution!) 86 ml of concentrated sulphuric acid (s.g. 1.84) to 100 ml with distilled water.

Procedure

To 1 ml of sample solution containing up to 80 µg of boron, add 5 ml of reagent solution and 1 ml of concentrated sulphuric acid (s.g. 1.84), heat at 90° for 45 min, let cool to room temperature and dilute to 10 ml with 85% w/w sulphuric acid. Measure the relative fluorescence intensity (using a Kodak 5 cut-off filter) at 430 nm, with excitation at 403 nm, against a quinine sulphate solution as reference. Prepare a calibration graph with standard boron solutions by the same procedure.

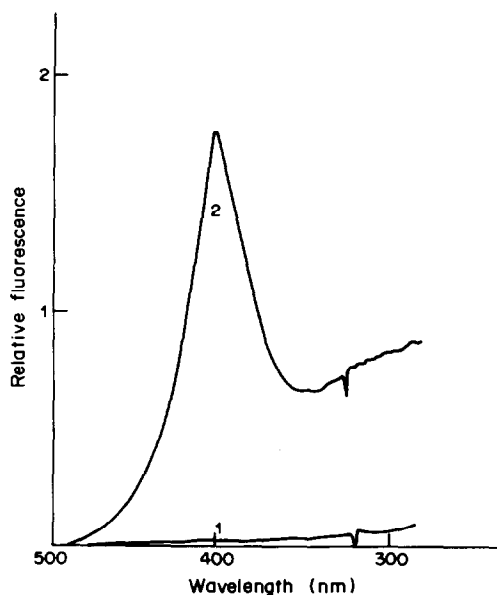


Fig. 1. Fluorescence excitation spectrum, relative to quinine sulphate solution as reference. 1, Reagent blank solution, 0.05M in concentrated sulphuric acid. 2, Boron-HBBA complex, 1 $\mu\text{g}/\text{ml}$ boron, 85% w/w H_2SO_4 , heated for 45 min at 90° .

RESULTS AND DISCUSSION

Figure 1 shows the excitation spectrum of a 0.05M HBBA solution in concentrated sulphuric acid. There is no fluorescence. However the boric acid-reagent product is fluorescent, with an excitation maximum at 403 nm. Since the spectrophotometer used did not have an emission monochromator, various cut-off filters were tried, and a Kodak 5 filter gave the best relative fluorescence intensity.

Sulphuric acid concentration

The reaction between boric acid and HBBA needs both a strong acid and a dehydrating medium. Sulphuric acid is the obvious choice. Maximum relative fluorescence was obtained with a sulphuric acid concentration between 80 and 85% w/w (Table 1).

Time and temperature

Various temperatures and heating times were tested. The relative intensity of the fluorescence was measured after cooling the solutions to room temperature. Results are shown in Fig. 2. Heating at 100°

Table 1. Effect of sulphuric acid concentration on the relative fluorescence intensity of the boron-HBBA complex

Sulphuric acid, % w/w	Relative fluorescence
70	0.81
75	1.60
80	1.70
85	1.99
90	1.17

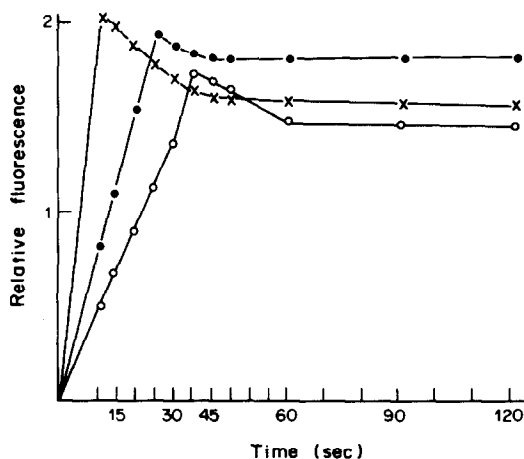


Fig. 2. Influence of temperature and heating time on relative fluorescence intensity. \circ — 80° ; \bullet — 90° ; \times — 100° .

gives maximum fluorescence intensity in 10 min but the fluorescence then decreases, becoming constant after about 45 min of heating. Similar behaviour is observed at lower temperatures but the final constant fluorescence intensity is greatest for heating at 90° . The relative fluorescence intensity of the cooled solution is constant for 5 hr. Therefore heating at 90° for 45 min is optimal.

Reagent excess

It was found that for a fixed amount of boron (1 μg) the relative fluorescence intensity was maximal and constant if the reagent concentration was 0.05–0.2M (Table 2). A reagent concentration of 0.05M was selected for practical use.

Calibration graph

The fluorescence intensity is a linear function of boron concentration in the range 0.1–8 $\mu\text{g}/\text{ml}$ in the solution measured.

Interferences

A variation of 3% in the relative fluorescence intensity from a 1 $\mu\text{g}/\text{ml}$ final boron concentration was considered to indicate interference.⁹

Li^+ , Na^+ , K^+ , NH_4^+ , Ag^+ , Al^{3+} , Ca^{2+} , Mn^{2+} , Pb^{2+} , Sn^{2+} , Ba^{2+} , Sr^{2+} , Cl^- , AsO_2^- and SiO_3^{2-} do not

Table 2. Effect of HBBA concentration fluorescence value for 1 ppm boron

[HBBA], M	Relative fluorescence
0.005	1.62
0.01	1.68
0.02	1.71
0.05	1.83
0.07	1.83
0.10	1.83
0.20	1.83

Table 3. Influence of foreign ions on determination of 1 ppm boron

Element	Interferent, μg	Ratio B/I	Change in I_F value, %
Li^+ , Na^+ , K^+ , NH_4^+ , Ag^+ , As^{3+} , Al^{3+} , Ca^{2+} , Mn^{2+}			
SiO_3^{2-} , Cl^- , SO_4^{2-} , PO_4^{3-} ,	2000	1:2000	0
Pb^{2+} , Sn^{2+} , Ba^{2+} , Sr^{2+}	400	1:400	0
$\text{C}_2\text{O}_4^{2-}$	15	1:15	0
Cu^{2+}	5	1:5	+6
Ni^{2+}	1.2	1:1.2	+47
Co^{2+}	1.2	1:1.2	+21
Fe^{3+}	0.2	1:0.2	-4

Table 4. Analysis of plant samples

Plant	Average* found, $\mu\text{g/g}$	CIIAF value†,		Boron recovered, $\mu\text{g/g}$		Recovery, %‡	
		$\mu\text{g/g}$	Boron added, $\mu\text{g/g}$ §	A	B	A	B
Grape	44.6	44.5	45.0	89.0	89.2	99.3	99.5
Orange	41.0	40.0	40.0	80.6	80.4	95.5	99.2
Olive	15.7	15.0	15.0	31.0	30.4	100.9	99
Peach	32.8	32.5	30.0	62.0	62.5	98.7	99.5
Apple	34.6	34.0	35.0	70.0	69.7	100.6	100.1

*Ten determinations; coefficient of variation 2% in all cases.

†Value certified by CIIAF.

‡A = addition before calcination; B = addition after calcination.

§Two sets of experiments, with boron added before calcination in one and after it in the other.

interfere when present in 400:1 w/w ratio to boron, but Fe^{3+} , Cu^{2+} , Ni^{2+} , Co^{2+} and $\text{C}_2\text{O}_4^{2-}$ interfere strongly. Iron(III) in 1:5 ratio to boron causes a negative error, but copper, nickel and cobalt (in 5:1 ratio to boron) enhance the signal considerably by formation of fluorescent compounds which mask the emission from the boron compound. Nitrate and iodide interfere because they cause precipitation of the reagent.

Application

The method was applied to determine low concentrations of boron in vegetable matter by the following procedure.

Heat a 1-g sample of dried vegetable matter with 0.1 g of calcium oxide for 3 hr at 200° and then for 6 hr at 550°. Dissolve the residue in 1 ml of concentrated sulphuric acid and 3 ml of methanol. Heat at 65° for 15 min to distil the methyl borate formed and collect it. Make up the resulting solution to 5 ml with water, hydrolysing the ester. To 1 ml of this solution, add 5 ml of reagent solution, 1 ml of reagent solution and 1 ml of 96% (w/w) sulphuric acid, heat at 90° for 45 min, let cool to room temperature and dilute to 10 ml with 85% (s.g. = 1.78) sulphuric acid. Measure the fluorescence intensity as already described and

read off the boron content from a calibration graph prepared at the same time.

The values obtained are shown in Table 4 and compared with those given by the Interinstitute Committee on Foliage Analysis (CIIAF) who supplied the samples. The same table shows the recovery achieved for additional boron being added either before or after calcination of the vegetable matter. It can be seen that there are no losses during the determination.

REFERENCES

1. C. A. Parker and W. J. Barnes, *Analyst*, 1960, **85**, 828.
2. G. Ogner, *Commun. Soil Sci. Plant. Anal.*, 1980, **11**, 1209.
3. D. Mounier, C. A. Menzinger and M. Marcantonatos, *Anal. Chim. Acta*, 1972, **60**, 233.
4. J. Aznárez, A. Bonilla and J. M. Mir, *Anales Aula-Dei*, 1979, **14**, 510.
5. J. M. Mir, *Doctoral Thesis*, University of Zaragoza, 1982.
6. J. Robert and C. E. White, *Anal. Chem.*, 1964, **36**, 2141.
7. V. I. Kuznetsov, *Tr. Komisi po Analit. Khim. Akad. Nauk, SSR*, 1960, **11**, 35.
8. A. A. Nemodruk and Z. Karalova, *Analytical Chemistry of Boron*, p. 49. Ann Arbor Publishers, Ann Arbor, 1969.
9. T. S. West, *Analyst*, 1962, **87**, 630.

SELECTIVE COMPLEXOMETRIC DETERMINATION OF PALLADIUM WITH THIOSULPHATE AS MASKING AGENT

SARALA RAOOT and K. N. RAOOT

Defence Metallurgical Research Laboratory, Kanchanbagh, Hyderabad-500 258, India

(Received 21 May 1985. Revised 3 January 1986. Accepted 23 January 1986)

Summary—A selective complexometric method is suggested for the determination of palladium, sodium thiosulphate being used as releasing agent. To a solution containing palladium and other cations, excess of EDTA is added and the surplus is back-titrated with lead nitrate solution at pH 5–5.5 in sodium acetate buffer with Xylenol Orange as indicator. EDTA equivalent to palladium is then released quantitatively with sodium thiosulphate and is titrated with the lead nitrate solution. The interference of various cations has been studied and the method applied for the analysis of alloys.

Existing complexometric methods¹⁻⁶ for palladium deal with its estimation directly or by back-titration only in pure solutions or in presence of platinum group metals, which do not react with EDTA. Alloys of palladium with copper and nickel are widely used as contact materials and those with rare-earth metals as magnetic materials. These alloys cannot be analysed directly by EDTA titration, since the associated metals are also chelated. In order to work out procedures for these alloys, it is necessary to evolve selective masking or releasing agents for palladium. In our earlier papers we reported dimethylglyoxime,⁷ 1,2,3-benzotriazole,⁸ 1,10-phenanthroline,⁹ thiourea,¹⁰ pyridine¹¹ and thiocyanate¹² as selective releasing agents for palladium.

Here we describe a simple method of selective decomposition of the palladium-EDTA complex by addition of sodium thiosulphate at pH 5–5.5 and room temperature. The liberated EDTA is then titrated with lead nitrate solution with Xylenol Orange as indicator. The interference of various cations, including copper, has been investigated and the results are presented in this paper.

EXPERIMENTAL

Reagents

Palladium(II) chloride solution. Prepared by dissolving 1.0 g of the salt (Johnson-Matthey) in minimum amount of hydrochloric acid and making up to 1 litre, and standardized gravimetrically¹⁸ with ascorbic acid as reductant, a 50-ml aliquot being used.

EDTA solution, 0.01M.

Lead nitrate solution, 0.01M.

Buffer solution (pH 5.5). Prepared by mixing 100 ml of 1M acetic acid and 50 ml of 1M sodium hydroxide and making up to 500 ml.

Xylenol Orange, 0.1% aqueous solution.

Sodium thiosulphate, 3% solution. Solutions of various metal ions (concentration 1 mg/ml) were prepared from suitable salts. All chemicals used were of analytical reagent grade.

Estimation of palladium in presence of other cations

To a solution containing 3–30 mg of palladium(II) and various amounts of foreign metal ions, add excess of 0.01M EDTA and dilute to 70–80 ml. Adjust the pH of the solution with 2% sodium hydroxide solution to between 4 and 5 and then to 5–5.5 with sodium acetate-acetic acid buffer. Add a few drops of Xylenol Orange indicator and titrate the excess of EDTA with 0.01M lead nitrate solution to the sharp colour change from yellow to red. Add 1–10 ml of 3% sodium thiosulphate solution (8 mg of the reagent for each mg of palladium), shake, and titrate the liberated EDTA with 0.01M lead nitrate to the same end-point as in the first titration.

Application to alloys

Dissolve 0.1–0.2 g of the sample, accurately weighed, in the minimum amount of *aqua regia* and dilute to volume in a 100-ml standard flask. Transfer a suitable aliquot into a conical flask, add excess of 0.01M EDTA and complete the determination of palladium as described above.

RESULTS AND DISCUSSION

The stability constant of the palladium(II)-EDTA complex is reported¹³ to be 26.4. Although sodium thiosulphate is used for the estimation of palladium¹⁴ in neutral medium at 80°, there is no mention of the stability constant of the palladium-thiosulphate complex in the literature. However, experimental data show that it is more stable than the palladium-EDTA complex and hence thiosulphate is able to displace the EDTA instantaneously. On the other hand, common metal ions (including copper) form weaker complexes with thiosulphate¹⁵ than with EDTA. Thus the EDTA complexes of common metal ions remain unaffected by the thiosulphate added and these metals do not interfere in the present method.

The release of EDTA from its palladium complex by sodium thiosulphate was found to be instantaneous at room temperature and at pH 5–5.5. It was found during the preliminary investigation that 80–100 mg of sodium thiosulphate causes immediate release of the EDTA bound to 12 mg of palladium,

Table 1. Determination of palladium in presence of foreign metal ions and in alloys

Foreign ion added, mg	Palladium, mg			Error, %
	Taken	Found		
Cu(II)	22.0	2.95	2.93	-0.7
	11.0	11.80	11.76	-0.3
Ni(II)	25.0	5.90	5.93	+0.5
	12.5	14.75	14.68	-0.5
Pb(II)	25.0	4.72	4.74	+0.4
	5.0	17.70	17.72	+0.1
Zn(II)	20.0	8.85	8.83	-0.2
	10.0	41.30	41.39	+0.2
Cd(II)	15.5	5.90	5.88	-0.1
	7.2	23.60	23.67	+0.3
Co(II)	12.0	11.80	11.86	+0.5
	5.0	29.50	29.47	-0.1
Mn(II)	5.0	11.80	11.86	+0.5
	3.0	17.70	17.77	+0.4
Fe(III)	10.0	2.95	2.98	+1.0
	20.0	14.75	14.79	+0.3
Al(III)	5.0	29.50	29.58	+0.3
	20.0	4.72	4.71	-0.2
Bi(III)	10.0	35.40	35.32	-0.2
	25.0	5.90	5.93	+0.5
La(III)	26.0	5.90	5.88	-0.3
	6.5	14.75	14.79	+0.3
Y(III)	24.0	11.80	11.81	+0.1
	6.0	11.80	11.76	-0.3
Ce(III)	13.6	2.95	2.93	-0.7
	6.8	17.70	17.77	+0.4
Sm(III)	25.0	4.72	4.74	+0.4
	5.0	14.75	14.79	+0.3
Tb(III)	17.8	5.90	5.93	+0.5
	4.7	29.50	29.58	+0.3
Ti(IV)	10.0	8.85	8.88	+0.3
	15.0	13.60	13.57	-0.2
Zr(IV)	15.0	23.60	23.62	+0.1
	5.0	41.30	41.18	-0.3
Ru(III)	11.5	8.85	8.83	-0.2
	5.7	23.60	23.67	+0.3
Rh(III)	9.8	11.80	11.81	+0.1
	4.9	35.40	35.27	-0.4
Ir(III)	12.4	2.95	2.98	+1.0
	6.2	29.50	29.42	-0.3
Ru(III)	12.4	13.60	13.54	-0.4
	6.2	5.90	5.88	-0.3
Pt(IV)	8.4	14.75	14.68	-0.5
	4.2	23.60	23.67	+0.3

giving a clear solution. Lower quantities result in a turbid solution, but larger quantities have no adverse effect on the titration. There is no change of pH on addition of the releasing agent, so the liberated EDTA can be titrated immediately. It can be seen from Table 1 that many cations can be tolerated. Although thiosulphate is used to mask copper(II) in EDTA titrations, it does so only if added before the EDTA, reducing the copper(II) and forming a stable complex with the copper(I) produced.^{16,17} It cannot reduce copper(II) in the presence of EDTA, since the copper(II)-EDTA complex is so much stronger than the copper(I)-EDTA complex that the conditional redox potential for the copper(II)/copper(I) couple is 0.5 V. Mercury(II), tin(II), tin(IV) and thallium(III) interfere seriously. More than 5 mg of manganese makes the end-point protracted, owing to displacement of EDTA from the manganese-EDTA complex

Table 2. Determination of palladium in synthetic solutions and solid alloy samples

Sample*	Palladium, mg	
	Taken	Found†
40% Cu-Pd	25.38	25.44
		25.32
45% Cu-Pd§	22.41	22.39
		22.35
40% Ni-Pd	25.26	25.22
		25.35
39% Ni-Pd§	27.06	27.11
		27.08
35% Co-Pd	26.16	26.07
		26.10
40% La-Pd	23.98	24.08
		23.95
64% Sm-Pd	28.04	28.17
		28.10

*Synthetic samples unless otherwise mentioned.

†Mean of three estimations by thio-sulphate release; the second value quoted in each case is the mean of three gravimetric estimations with ascorbic acid.¹⁶

§Solid alloy samples.

by the back-titrant lead nitrate, the conditional stability constants of manganese(II)-EDTA and lead(II)-EDTA at pH 5.5 in acetate medium being $\log K = 7.1$ and $\log K = 8.9$ respectively.

Among the masking agents we suggested earlier, dimethylglyoxime and benzotriazole produce precipitates, making handling of more than 15 mg of palladium difficult. Heating is also necessary with these reagents. Though 1,10-phenanthroline yields a soluble complex, many cations interfere and the applications are limited. Thiourea is free from these limitations, but interference due to copper must be prevented by using a temperature of 8° for titration, and a minimal excess of the reagent (which causes problems in analysis of unknown samples). Quantitative release of EDTA with pyridine needs either heating the solution at 60° for 10 min or keeping at room temperature for 1 hr, and the reagent is unpleasant to use because of its smell. Thiosulphate is therefore much superior, since it yields a soluble complex even with large quantities of palladium, releases the EDTA instantaneously in the cold, and tolerates a large number of cations without the need for special conditions.

The relative standard deviations calculated for ten replicates at the 2.95 mg and 14.75 mg levels were 0.9 and 0.2% respectively. Table 1 shows that a maximum error of 1.0% was obtained only for the lowest quantity of palladium studied. For mixtures, solid samples or synthetic solutions containing more than 10 mg of palladium (Table 2), the error did not exceed more than 0.5%. It is seen that the values obtained by using the present releasing agent are in good agreement with those of the gravimetric method with ascorbic acid.¹⁸

Acknowledgement—Grateful thanks are due to Dr. P. Rama Rao, Director, DMRL, for permission to publish this paper.

REFERENCES

1. W. M. McNevin and O. Kriege, *Anal. Chem.*, 1955, **27**, 535.
2. J. Kinnunen and B. Merikanto, *Chemist-Analyst*, 1955, **44**, 11.
3. V. Suk and M. Malát, *ibid.*, 1956, **45**, 30.
4. J. Kinnunen and B. Merikanto, *ibid.*, 1958, **47**, 11.
5. H. Khalifa and M. M. Khater, *Z. Anal. Chem.*, 1962, **191**, 339.
6. I. M. Yurist and Z. V. Tynkova, *Zavodsk. Lab.*, 1962, **28**, 798.
7. K. N. Raoot and S. Raoot, *Indian J. Chem.*, 1974, **12**, 1007.
8. K. N. Raoot, S. Raoot and V. G. Vaidya, *ibid.*, 1979, **18A**, 90.
9. S. Raoot and K. N. Raoot, *Indian J. Technol.*, 1980, **18**, 345.
10. K. N. Raoot and S. Raoot, *Talanta*, 1981, **28**, 327.
11. S. Raoot, K. N. Raoot and V. Lalitakumari, *Analyst*, 1982, **107**, 1382.
12. K. N. Raoot, S. Raoot and V. Lalitakumari, *ibid.*, 1983, **108**, 1148.
13. J. Kragten, *Talanta*, 1981, **28**, 327.
14. D. I. Ryabchikov, *Zh. Analit. Khim.*, 1946, **1**, 47.
15. Yu. Lurie, *Handbook of Analytical Chemistry*, p. 295. Mir, Moscow, 1975.
16. I. I. Kalinichenko, *Zavodsk. Lab.*, 1958, **24**, 266.
17. K. L. Cheng, *Anal. Chem.*, 1958, **30**, 343.
18. R. Ripan and G. Pop, *Rev. Roum. Chim.*, 1967, **12**, 13.

FLOW-INJECTION ANALYSIS WITH THE IRON-INDUCED PERBROMATE-IODIDE REACTION: SPECTROPHOTOMETRIC DETERMINATION OF IRON

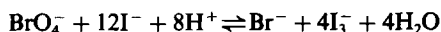
T. D. YERIAN, T. P. HADJIOANNOU* and G. D. CHRISTIAN

Center for Process Analytical Chemistry, University of Washington, Seattle, WA 98195, U.S.A.

(Received 23 April 1985. Revised 21 December 1985. Accepted 23 January 1986)

Summary—Total iron is determined by a flow-injection spectrophotometric technique. The production of I_3^- from the iron(II)- or iron(III)-induced perbromate-iodide reaction is monitored at 353 nm. Calibration graphs are linear from 10 to 100 ng/ml with correlations up to 0.9998 and can be extended up to 10 μ g/ml by appropriate adjustment of conditions. The average sampling rate is 30 samples/hr. Detection limits and relative standard deviations compare well with those of other FIA methods.

The reaction of perbromate and iodide proceeds very slowly in alkaline, neutral or acidic solutions, with the following stoichiometry in acid solution:



Bromide is formed in acidic solutions, bromate in neutral or alkaline solutions. In the presence of iron(II), the oxidation of iodide is accelerated, apparently through perbromate oxidation of iron(II) to iron(IV), which subsequently oxidizes iodide to iodine.¹

With many typical chromogenic reagents for iron, either oxidation of iron(II) to iron(III) or reduction of iron(III) to iron(II) is required before total iron can be determined.²⁻⁴ At high concentrations of iodide, iron(III) is reduced quickly to iron(II), hence in the iodide-perbromate system the two oxidation states of iron cannot be distinguished and a separate oxidation or reduction step is not necessary in such a medium.

Though sensitive, most chromogenic reagents are only somewhat selective. The iron(II)-induced perbromate-iodide reaction has the advantage of being specific for iron and has been used successfully in the spectrophotometric determination of ng/ml levels of iron.⁵

The purpose of this study was to adapt this iron-determination technique to a flow-injection system at a level of sensitivity that would allow analysis of natural water samples.

EXPERIMENTAL

Reagents

Stock iron(II) solution, 100 ppm. Prepared from $Fe(NH_4)_2(SO_4) \cdot 6H_2O$ dissolved in water, plus 2.5 ml of

concentrated sulphuric acid per litre, and standardized against potassium dichromate.

Stock iron(III) solution, 100 ppm. Prepared from $Fe(NH_4)(SO_4)_2 \cdot 12H_2O$ dissolved in water, plus 2.5 ml of concentrated sulphuric acid per litre, and for highest accuracy standardized, e.g., by iodometry.

Stock potassium perbromate solution, 0.01M.

Stock nitric acid, 1.2M.

Stock sodium nitrate solution, 2.5M.

All solutions were prepared with doubly demineralized water; all chemicals used were analytical reagent grade, unless otherwise specified. Standard iron solutions were prepared from stock solutions; stock sodium nitrate solution and nitric acid were added to give final concentrations of 0.5M and 0.125M respectively. The carrier stream consisted of 0.5M sodium nitrate and 0.125M nitric acid, prepared by dilution of the stock solutions. Perbromate solutions were diluted so that the final solutions were 0.5M in sodium nitrate. The 0.5M sodium iodide reagent was prepared as needed. Water samples were diluted to twice their initial volume by addition of enough stock sodium nitrate solution, stock nitric acid and demineralized water to make the final solutions 0.5M in sodium nitrate and 0.125M in nitric acid.

Procedure

Iron(II) standards, samples, and the carrier solutions are prepared daily from the same stock solutions. Standards and samples are analysed on the day of preparation. Reagent solutions and the carrier solution are degassed before use, to minimize microbubbles in the flow-cell. The absorbance is measured at 353 nm, where there is an absorption maximum for I_3^- .

The FIA manifold is shown in Fig. 1. The manifold tubing is 0.5 mm "Teflon" or "Microline". Mixing tees are "Teflon"; standard fittings are used throughout. Solutions are pumped with a 4-line peristaltic pump (Gilson Minpuls II). The detector is a DU-7 Beckman spectrophotometer equipped with a modified 8- μ l Varian flow-cell (model VUV-10).

The sample loop used for analysis has a volume of 100 μ l. The tubing of the sample loop and the manifold tubing past the sample-injection point are knotted, to minimize broadening of the product peak.⁶ A three-line system was chosen for a number of reasons. The confluence design— injection of the sample into solvent, then merging with the reagent line—is an effective way to ensure adequate mixing.⁷ The confluence design also prevents the appearance of negative

*On leave from Laboratory of Analytical Chemistry, University of Athens, 104 Solonos Street, Athens 144, Greece.

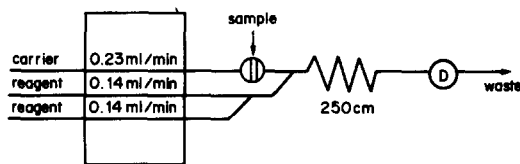


Fig. 1. Manifold design. Carrier stream is $0.5M$ NaNO_3 and $0.125M$ HNO_3 ; reagent 1 is $0.5M$ NaI ; reagent 2 is $2.5 \times 10^{-3}M$ KBrO_4 and $0.15M$ NaNO_3 . Total flow-rate is 0.5 ml/min.

or distorted peaks, which can result when the reagent absorbs significantly at the wavelength used.⁹ The reagents, I^- and BrO_4^- , do react slowly to form I_3^- , so the background I_3^- concentration is minimized when the reagents are not premixed. The manifold is also designed so that there is only a very short length of tubing between the reagent merging point and the carrier-line merging point.

The dispersion D is determined by pumping an I_3^- solution ($2 \times 10^{-5}M$) through all three lines to obtain the signal corresponding to an undispersed plug of I_3^- , C° ; C^{max} is the absorbance corresponding to the maximum signal after injection of $100 \mu\text{l}$ of the I_3^- solution.⁹ To determine $S_{1/2}$ (the sample volume giving 50% of the saturation signal height), the "steady state" signal is obtained by injection of $500 \mu\text{l}$ of the I_3^- solution into the carrier stream; smaller volume injections are then made until a response equivalent to 50% of the $500\text{-}\mu\text{l}$ signal is generated.⁹ Thus, $t_{1/2}/T$ refers to the carrier stream, while C°/C^{max} is determined with respect to all three lines. These factors were found to have the values $T = 79$ sec, $D = C^\circ/C^{\text{max}} = 2.4$, $S_{1/2} = 40 \mu\text{l}$, $t_{1/2} = 19$ sec, $t_{1/2}/T = 0.24$; for definition of the terms see Růžička and Hansen.⁹

RESULTS AND DISCUSSION

Calibration

A calibration graph for the range from 10 to 100 ng/ml was generated by duplicate injections of six iron(II) standard solutions, and had the following characteristics: coefficient of correlation 0.9998, slope 2.48×10^{-3} ml/ng, intercept 8.77×10^{-4} , and standard error 4.6×10^{-3} ng/ml. Similar curves were obtained on each day of analysis. Repetitive injections of 100-ng/ml iron(II) samples yielded a relative standard deviation (rsd) of 0.6% and of 10-ng/ml iron(II) samples an rsd of 3.0%. Injection of 30.0, 60.0 and 80.0 ng/ml iron(II) solutions gave calculated values of 29.8, 60.5 and 80.0 ng/ml. The detection limit, calculated as three times the standard deviation of the background, was 0.4 ng/ml. Analysis of samples with higher concentrations of analyte could best be accommodated by use of a faster flow-rate, increasing system through-put, with a lower concentration of perbromate in order to slow the rate of I_3^- production and allow extension of the linear region. Linear response up to 10 $\mu\text{g}/\text{ml}$ was verified.

The peak obtained by this method is enhanced substantially as the pH is decreased below 2.0. With 100- μl samples of 10 $\mu\text{g}/\text{ml}$ iron(II), a tenfold increase in acid concentration in carrier, reagent, and sample streams resulted in about threefold increase in the response peak. Iron samples (10 $\mu\text{g}/\text{ml}$) that were 0.0125 or 0.125M in perchloric acid gave re-

sponses 2.3 or 3.8 times greater than that of a sample with no perchloric acid. For larger sample volumes, the increase in peak height with increase in acid concentration was less significant.

Analysis for iron(III)

Injection of 100-ng/ml iron(III) solutions gave peaks similar in height to those for 100-ng/ml iron(II), indicating that iron(III) caused catalysis of the reaction at the same rate as iron(II), so total iron can be measured directly.

Interferences

Although this determination is specific for iron, the kinetics of the response can be affected by the sample matrix. When sodium perchlorate and perchloric acid are used as the background electrolyte instead of sodium nitrate and nitric acid the response is unaffected, but use of sodium chloride and hydrochloric acid increases the iron response by 9%. If 100 ppm EDTA is added to the matrix, the response for 100-ng/ml iron(II) is diminished by 68%. Calculations from the conditional formation constants of the iron(II) and iron(III) EDTA chelates at the acidities used indicate that iron(II) would not be appreciably chelated, whereas iron(III) would be strongly chelated, so the effect does not appear to be the result of diminished free iron(II) concentration. The iron(IV)-EDTA complex formation constant is not available, and it may be that the EDTA effectively decreases the activity of the catalytic intermediate. This has been used as a tool to determine ligands such as EDTA, EGTA, and DPTA.¹⁰

Optimization

The major difficulty is the noisy base line. There are many factors contributing to the noisy signal. Perbromate and iodide react slowly in the absence of iron, resulting in a background response. With the carrier stream 0.125M in nitric acid, the absorbance in the absence of sample is increased further. At 0.5 ml/min flow-rate the background absorbance is about 0.46. The sample response increases relative to the background signal as the flow-rate is decreased, but the compromise results in a lower sampling rate. The peak obtained by this method is enhanced substantially as the acidity is increased below pH 2.0. In the design used, the carrier is acidified to the same degree as the sample, so there is no blank response. However, this does increase background (carrier) absorbance and noise level, so there is a trade-off between these factors.

One reagent line is 0.5M sodium iodide. The other two lines are made 0.5M in sodium nitrate to minimize the refractive index and viscosity differences in the lines, another major contributor to the background noise. Although the pump used was not a one-speed pump, major flow-rate changes were made by changing the size of the peristaltic pump tubing. The smaller the internal diameter of the tubing, the

smaller the pulses from the pump, and the steadier the baseline response. A pulseless pump could improve the detection limit, and allow for faster flow-rates (larger tubing), thus increasing the sampling rate.

To conserve the potassium perbromate reagent, a merging zone technique¹¹ or a split-loop injection technique¹² could be used. In both schemes, a plug of reagent is merged with or injected with the sample, instead of use of a continuous stream of reagent. This would make it feasible to use higher concentrations of perbromate than the $2.5 \times 10^{-3} M$ reported, allowing further increase in the sensitivity or in sampling rate, as under existing conditions the response is approximately linearly related to the perbromate concentration.

The relative standard deviations could be improved by using a constant-temperature system; further optimization would depend on the types of sample to be analysed, and could be achieved with a simplex approach. Starch indicator could also be used, with monitoring of the characteristic blue complex with I_3^- , to improve sensitivity. The starch/ I_3^- complex is unaffected by the perbromate matrix.

Water analysis

Tap water, well water, lake water and sea-water were analysed by this technique. All the fresh water samples gave reproducible values in the range 12–30 ng/ml. Standard additions of iron(II) to sea-water samples, to increase the iron concentration by 20 and 40 ng/ml, gave responses that indicate no significant interference from the 1:1 diluted sea-water matrix.

Applications

This system is well suited for analysis of a wide variety of iron-containing samples. Its sensitivity is

sufficient for determination of iron in natural waters. For many iron analyses, it is necessary to use a dissolution procedure with strong acids, e.g., in the case of standard rocks,¹³ and animal¹⁴ or plant digests.¹⁵ These types of samples could easily be analysed by this technique.

Acknowledgements—The authors thank O. Antonsen of Eidgenössisches Institut für Reaktorforschung, Wurelingen, Switzerland, for provision of potassium perbromate, and James Hungerford, University of Washington, for suggestions and technical assistance.

REFERENCES

1. L. A. Lazarou and T. P. Hadjiioannou, *Anal. Lett.*, 1978, **11**, 779.
2. J. Mortatti, F. J. Krug, L. C. R. Pessenda and E. A. G. Zagatto, *Analyst*, 1982, **107**, 659.
3. V. V. S. Eswara Dutt, D. Scheeler and H. A. Mottola, *Anal. Chim. Acta*, 1977, **94**, 289.
4. V. V. S. Eswara Dutt, A. Eskander-Hanna and H. A. Mottola, *Anal. Chem.*, 1976, **48**, 1207.
5. L. A. Lazarou, E. P. Diamandis and T. P. Hadjiioannou, *Chim. Chronika, New Series*, 1982, **11**, 3.
6. H. Engelhard and U. D. Neue, *Chromatographia*, 1982, **15**, 403.
7. J. Růžicka and E. Hansen, *Flow Injection Analysis*, Wiley, New York, 1981.
8. H. Bergamino, B. F. Reis and E. A. G. Zagatto, *Anal. Chim. Acta*, 1978, **97**, 427.
9. J. Růžicka and E. H. Hansen, *ibid.*, 1984, **161**, 1.
10. L. A. Lazarou and T. P. Hadjiioannou, *Anal. Chem.*, 1979, **51**, 790.
11. E. A. G. Zagatto, A. O. Jacintho, L. C. R. Pessenda, F. J. Krug, B. F. Reis and H. Bergamino, *Anal. Chim. Acta*, 1981, **125**, 37.
12. J. Růžicka and E. H. Hansen, *ibid.*, 1985, **173**, 3.
13. R. Kuroda, I. Ida and K. Oguma, *Mikrochim. Acta*, 1984, **1**, 377.
14. D. W. Burns, M. L. Parsons, L. L. Herbaugh and R. T. Staten, *Anal. Chem.*, 1985, **57**, 1048A.
15. J. Mortatti, F. J. Krug, L. C. R. Pessenda, E. A. G. Zagatto and S. Storgaard Jørgensen, *Analyst*, 1982, **107**, 659.

A GRAVIMETRIC PROCEDURE FOR THE DETERMINATION OF WET PRECIPITATED SULPHUR, DISSOLVED SULPHUR, SOLUBLE SULPHIDES AND HYDROGEN SULPHIDE

DODDABALLAPUR K. PADMA

Department of Inorganic and Physical Chemistry, Indian Institute of Science, Bangalore 560 012, India

(Received 18 October 1984. Revised 13 December 1985. Accepted 23 January 1986)

Summary—Elemental sulphur (in wet precipitated form or dissolved in organic solvents) and hydrogen sulphide have been determined gravimetrically at room temperature by conversion into copper sulphide by elemental copper in presence of an organic solvent such as benzene or acetonitrile. Any solvent in which sulphur is soluble can be used. The black copper sulphide formed can be weighed or determined iodometrically. Analysis indicates the black compound to be $Cu_{1.8}S$. This room temperature method is a versatile one-step procedure sensitive to microgram or macro amounts of sulphur. It has been used for determining the solubility of sulphur in tetrahydrofuran and dioxan. The apparent heat of solution indicates that sulphur dissolves in these solvents without any marked solute-solvent interactions.

Several methods are available for detection and determination of elemental sulphur,¹⁻³ and are mainly based on oxidative or reductive decomposition and measurement of the sulphur dioxide, sulphuric acid or hydrogen sulphide produced. Typical methods are oxidation to sulphate and precipitation as barium sulphate⁴ or reduction to hydrogen sulphide by hydrazine hydrate.⁵ Though accurate, these methods are time-consuming. During electrochemical studies with copper-copper fluoride electrodes in acetonitrile/benzene solutions, we observed that in the presence of sulphur, the copper reacted spontaneously to form a black precipitate of copper(I) sulphide. Some metals are known to react with elemental sulphur spontaneously but sluggishly at room temperature. The observation above indicates that the presence of the organic solvent hastens the reaction. Similarly, hydrogen sulphide is known to tarnish metals at room temperature but reacts with them completely only at high temperatures.⁶ In the present study, it was observed that hydrogen sulphide spontaneously reacts quantitatively with copper in acetonitrile medium at room temperature (25°) to form copper(I) sulphide. On the basis of these observations a method has been developed for determination of hydrogen sulphide and elemental sulphur.

EXPERIMENTAL

Reagents

Analytical-grade acetonitrile and benzene were used without purification. Copper, as thin strips (3 × 1 × 0.2 cm), powder, and gauze, was degreased, etched with dilute nitric acid, washed well with water and acetone, well dried in vacuum and stored under nitrogen in a desiccator.

A stock sulphur solution in benzene or acetonitrile was prepared by dissolving 1000 mg of resublimed sulphur in 1 litre of the solvent, and diluted as required to obtain working standards.

Hydrogen sulphide generated in a Kipps apparatus was suitably dried and stored in evacuated glass globes fitted with vacuum stopcocks and ground-glass joints. Known weights were withdrawn for tests.

Procedures

Gravimetric determination of elemental sulphur (10-50 mg). About 400 mg of well-dried copper powder and a small Teflon-coated magnet-follower are placed in a well-stoppered 25-ml flat-bottomed flask, which is then accurately weighed. Ten ml of sample solution containing 5-50 mg of sulphur are added and the solution is gently stirred over a magnetic stirrer for about 1 hr. The copper powder, which now appears black, is allowed to settle, then the flask is connected to a vacuum line (the stopper being stored in a desiccator) by means of a Teflon adaptor sleeve (grease must not be used), and the solvent distilled off under reduced pressure, the last traces being removed under vacuum. The flask is disconnected from the vacuum line, the stopper replaced and the flask reweighed. The increase in weight corresponds to the uptake of sulphur from the solution. Alternatively, the black powder can be filtered off in a previously weighed porosity-3 or porosity-4 sintered-glass crucible, washed with water, acetone and diethyl ether, and dried at 110° for 2 hr. The increase in weight of the copper corresponds to the weight of sulphur in the sample solution.

In experiments with 5.0, 10.0, 25.0 and 50.0 mg of sulphur, the net increases in weight were 5.0, 10.0, 24.9 and 50.0 mg respectively. For higher amounts of sulphur eight times as much copper should be used and stirring continued for 2 hr.

Titrimetric determination of sulphur. The copper/copper sulphide mixture obtained as above can be analysed for its sulphur content by an iodometric method already published.⁵ The black solid, freed from solvent, is placed in the reduction apparatus. About 15 ml of hydriodic acid (~67%) are added drop by drop over a period of 10 min and the contents gently boiled. The hydrogen sulphide liberated is swept out with a current of nitrogen and collected in an alkaline suspension of cadmium acetate. Iodometric determination of the trapped sulphide gives the sulphur content.

Determination of wet precipitated sulphur. Sulphur precipitated from aqueous solutions is suspended in 50 ml of

acetonitrile or benzene and stirred well with approximately 3 g of copper powder. The sulphur dissolves and is precipitated as copper(I) sulphide and determined as described above. The reaction goes to completion even if the solution has a 10% water content, so there is no need to dry the sulphur before the determination.

Determination of hydrogen sulphide. A known volume (~200 ml) of the gas sample is condensed over a suspension of ~500 mg of copper powder in 100 ml of acetonitrile in a reaction tube (~300 ml capacity) provided with ground-glass joints, vacuum stopcocks and a Teflon-coated magnetic follower at the bottom, by standard vacuum techniques, with liquid-nitrogen cooling. The stopcocks are closed, the coolant is removed, and the contents are allowed to come to room temperature. The suspension is stirred for 2 hr for completion of the reaction. The solvent is removed under vacuum and the sulphur content determined titrimetrically.

In a typical experiment with 158.0 mg of H₂S, corresponding to 148.7 mg of sulphur, the amount found experimentally was 148.4 mg. Solutions of ionic sulphides react with copper in a similar manner. Fifty ml of acetonitrile are added to 10 ml of the sulphide solution, followed by about 1 g of copper powder. The mixture is stirred for 1 hr in a closed flask, and the resulting copper(I) sulphide is analysed for sulphur iodometrically, as above.

All experiments were repeated at least three times and the deviation in the values was found to be less than 1%.

RESULTS AND DISCUSSION

Composition of copper sulphide formed

Sulphur (500 mg) was dissolved in 100 ml of benzene, in a 250-ml wide-mouthed bottle. Thin strips of copper were suspended in the solution. The copper sulphide produced detached itself from the strips and fell to the bottom. The mixture was left overnight, long enough for all the sulphur to react. The copper strips were removed, the solvent was distilled off and the black copper sulphide was dried under vacuum. A known weight of this product was analysed for copper content by standard methods⁷ and sulphur content iodometrically as described above.

In a typical experiment with 38.0 mg of copper sulphide taken, the amounts found were 29.6 mg of copper and 8.2 mg of sulphur. Thus, the observed composition is Cu_{1.8}S, a non-stoichiometric copper sulphide. In repeated determinations the composition varied from Cu_{1.75}S to Cu_{1.8}S.

Solubility of sulphur in tetrahydrofuran and dioxan

The solubility of sulphur in these solvents is not given in the literature, and has now been determined at three temperatures.

Tetrahydrofuran was refluxed over lithium aluminium hydride for not less than 4 hr and then distilled, as recommended by King and Pews,⁸ and dioxan was purified by the method described by Vogel.⁹ Saturated solutions of resublimed sulphur in these dry solvents were prepared and equilibrated at three different temperatures. Five ml of the clear solution were added to 15 ml of benzene or acetonitrile and the sulphur content determined iodometrically as described above. The content was also determined by

Table 1. Solubility data for sulphur

Solvent	T, K	Solubility (S), g/kg	
		Present method	Reduction method ¹⁰
Dioxan	288	4.2	4.2
	296	4.8	4.8
	308	5.9	6.0
Tetrahydrofuran	273	5.8	5.8
	295	10.8	10.9
	308	15.5	15.5

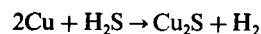
a previously reported reductimetric method.¹⁰ The results are given in Table 1. These data were obtained by repeating each set of experiments at least 4 times, and triplicate samples were taken for each experiment. The deviation between the readings was less than 1%.

The apparent heat of solution was calculated from a graph of log S vs. 1/T. The values for dioxan and tetrahydrofuran are 4.1 and 4.6 kcal/mole respectively. Such comparatively low values indicate that sulphur dissolves in these solvents without significant interaction with them.

Conclusions

The results indicate that copper reacts spontaneously at room temperature with elemental sulphur, sulphides and hydrogen sulphide, in benzene or acetonitrile medium, to form a black precipitate identified as copper(I) sulphide. The observed composition has been found to be Cu_{1.8}S. Reaction between copper and sulphur in benzene was reported over 30 years ago. The present study resulted in a rapid gravimetric procedure applicable to elemental sulphur (dissolved in benzene or other organic solvents, or as wet precipitated sulphur), sulphides and hydrogen sulphide. Procedures for their determination have been standardized. The copper(I) sulphide formed can also be estimated iodometrically after reduction.

Copper is reported to react with hydrogen sulphide at high temperature as follows:¹²



but in the present study, no hydrogen evolution was observed.

N.B. (1) Benzene and acetonitrile are toxic substances so the determination should be done in a fume cupboard or a closed system.

(2) Transfer operations should be carefully done so as not to lose any of the flaky powdery copper sulphide.

REFERENCES

1. T. S. Ma and R. C. Rittner, *Modern Organic Elemental Analysis*, p. 424. Dekker, New York, 1979.
2. T. S. Ma and M. Gutterson, *Anal. Chem.*, 1980, **52**, 42R.
3. T. S. Ma, T. M. Wang and M. Gutterson, *ibid.*, 1982, **54**, 87R.
4. N. H. Furman (ed.), *Standard Methods of Chemical*

- Analysis*, 6th Ed., Vol. I, p. 1004. Van Nostrand, Princeton, 1962.
5. D. K. Padma, S. K. Vijayalakshamma and A. R. V. Murthy, *Res. Ind. (India)*, 1976, **21**, No. 1, 32.
 6. M. C. Sneed, J. L. Maynard and R. C. Brasted, *Comprehensive Inorganic Chemistry*, Vol. 2, p. 72. Van Nostrand, Princeton, 1954.
 7. A. I. Vogel, *Quantitative Inorganic Analysis*, 3rd Ed., p. 496. ELBS, India, 1961.
 8. J. F. King and R. G. Pews, *Can. J. Chem.*, 1964, **42**, 1294.
 9. A. I. Vogel, *A Text-book of Practical Organic Chemistry*, 4th Ed., Longmans, London, 1978.
 10. D. K. Padma, V. S. Bhat and A. R. V. Murthy, *Res. Ind. (India)*, 1979, **24**, No. 3, 34.
 11. T. P. Hoar and A. J. P. Tucker, *J. Inst. Metals*. 1952-1953, **81**, 665.
 12. A. A. Brooks, *J. Am. Chem. Soc.*, 1953, **75**, 2464.

DIFFUSION COEFFICIENTS AND COMPLEX EQUILIBRIA IN SOLUTION—V

LIMITATIONS TO THE VALIDITY OF THE DIFFUSION EQUATIONS

D. R. CROW

School of Applied Sciences, The Polytechnic, Wolverhampton, England

(Received 13 January 1986. Accepted 13 March 1986)

Summary—The ligand-concentration dependence of the limits of applicability of equations involving diffusion parameters and ligand numbers is discussed. Estimation of \bar{n} from preliminary values of formation constants derived from the pseudo-formation curve often provides proof of the direct correlation between \bar{n} and Δi_d for a proportion of the ligand concentration range, but not all of it. The limitation is especially noticeable for systems where full co-ordination is approached well within the range of experimental values of ligand concentration.

Previous papers in this series¹ have shown that changes in diffusion current (Δi_d) of a metal ion, resulting from progressive mononuclear complex formation brought about by the addition of ligand, may be used to calculate formation constants. The validity of the expression $\bar{n} \approx k \Delta i_d$ has been confirmed for a variety of metal-ligand systems; integration of pseudo-formation curves (Δi_d vs. $\log[X]$), combined with a means devised for measuring k , has made it possible to calculate values of the function $F_0[X]$.² This polynomial function of the consecutive overall formation constants and free ligand concentration may be subjected to conventional Leden analysis³ to produce values for the constants.

A more detailed analysis, based on the variation of mean diffusion coefficients as defined by

$$\bar{D} = \frac{\sum_0^N D_j \beta_j [X]^j}{\sum_0^N \beta_j [X]^j} \quad (1)$$

has been shown^{1,4} to be capable of generating realistic sequences of formation constants once preliminary values have been obtained by means of pseudo-formation curves.

The experimental data required can most conveniently be provided by d.c. polarographic measurements; indeed diffusion currents are, from the theoretical point of view, a significant component of the expression for $F_0[X]$ developed by DeFord and Hume⁵ in terms of the shifts of half-wave potential. Many workers have tended to pay less attention to the careful measurement of currents since, so long as current changes are small, the term $\log I_M/I_C$ in equation (2) (applicable at 298 K with the usual values for universal constants included) is of rela-

tively small significance.

$$F_0[X] = \text{antilog} \left[16.915n \Delta E_{1/2} + \log \frac{I_M}{I_C} \right] \quad (2)$$

That being said, however, careful scrutiny of reported analyses reveals that inclusion of erratically varying values of I_M/I_C , caused by insufficient care in measurement of metal ion concentration, can cause extra scatter on derived graphs. This may occur to such an extent that omission of the correction term, when small, is arguably of some advantage, on the principle that no correction is better than a badly made one. On the other hand, for larger values of the current term, its omission or its inclusion as an unreliable quantity can both cause significant problems.

Exploitation of the *independent significance* of varying diffusion currents requires that they be measured particularly carefully. When properly interpreted, they provide *supporting evidence* of complexation and associated equilibrium data for the case of systems showing reversible electrochemical character. For those classed as irreversible, two new approaches to the determination of formation constants have become available.⁴

As with all parameters which are used to indicate quantitatively the stages of a complexation process, it is important that the diffusion currents are available not only in sufficient quantity but in an even distribution over the ligand concentration range in which the stepwise association occurs. There are many instances in the literature where, with hindsight, it is clear that the experimental data have been clustered around some stages of the cumulative process to the detriment of others. After an initial experimental run, provisional values of constants may be used to identify approximately the ranges of

ligand concentration where various species predominate. Measurements should then be repeated to give a suitable representation of the distributions of the various complexes. The present paper will show that methods based upon currents tend to highlight the difficulties associated with such complications and to make it clear that data influenced by processes other than the primary complexation reactions can be misleading. The data used throughout are those reported independently by other authors⁶ for complexation systems involving cadmium and methylthiourea, dimethylthiourea and ethylthiourea as ligands.

The full expression for the relationship between the mean ligand number, \bar{n} , and Δi_d is⁷

$$\bar{n} = k \left[\Delta i_d - \frac{(\Delta i_d)^2}{2i_{d_1}} \right] \quad (3)$$

where i_{d_1} is the diffusion current of the aquo metal ion and k is a constant, determination of which was the subject of previous communications.¹ Equation (3) may be expanded and rewritten in terms of the Ilkovič constant (k') and diffusion coefficients (D), as

$$\bar{n} = k \left[(i_{d_1} - i_{d_2}) - \frac{(i_{d_1} - i_{d_2})^2}{2i_{d_1}} \right]$$

where i_{d_2} is the diffusion current corresponding to a given value of \bar{n} or as

$$\bar{n} = k \left[(k'D_1^{1/2} - k'\bar{D}_2^{1/2}) - \frac{(k'D_1^{1/2} - k'\bar{D}_2^{1/2})^2}{2k'D_1^{1/2}} \right]$$

where \bar{D}_2 is the mean diffusion coefficient of the mixture of diffusing species determined by the prevailing value of \bar{n} . Expansion of the numerator of the second term and rearrangement yields

$$\bar{n} = k \left[(k'D_1^{1/2} - k'\bar{D}_2^{1/2}) - \frac{(k')^2(D_1 - 2D_1^{1/2}\bar{D}_2^{1/2} + \bar{D}_2)}{2k'D_1^{1/2}} \right]$$

$$= k \left[(k'D_1^{1/2} - k'\bar{D}_2^{1/2}) - k' \left(\frac{D_1^{1/2}}{2} - \bar{D}_2^{1/2} + \frac{\bar{D}_2}{2D_1^{1/2}} \right) \right]$$

Therefore

$$\bar{n} = k \left[\frac{k'D_1^{1/2}}{2} - \frac{k'\bar{D}_2}{2D_1^{1/2}} \right]$$

or

$$\frac{\bar{D}_2}{D_1^{1/2}} = D_1^{1/2} - \frac{2}{kk'} \bar{n} \quad (4)$$

Clearly it is only possible to use \bar{D}_2 data in equation (1) within a range of \bar{n} values for which equation (4) holds.

Simpler development of the limiting form of equation (3) [*i.e.*, without the term $(\Delta i_d)^2/2i_{d_1}$] yields

$$\bar{D}_2^{1/2} = D_1^{1/2} - \frac{\bar{n}}{kk'} \quad (5)$$

RESULTS AND DISCUSSION

Plots confirming the validity of the limiting form of equation (3) as well as of equations (4) and (5) for the systems involving cadmium complexes with methylthiourea, dimethylthiourea and ethylthiourea are shown in Figs. 1–3. In each case values of \bar{n} were estimated from values of formation constants obtained from integration of the respective pseudo-formation curves. The relationships are seen to hold up to the region where \bar{n} is of the order of 3.5; data corresponding to this range of ligand concentration may be used to calculate the expected value of Δi_d when maximum co-ordination is developed. This in turn permits calculation of D_{MX_4} . In each of the three systems maximum co-ordination is approached at ligand concentrations in the region of 0.35M. For the methyl and dimethyl substituted ligands the

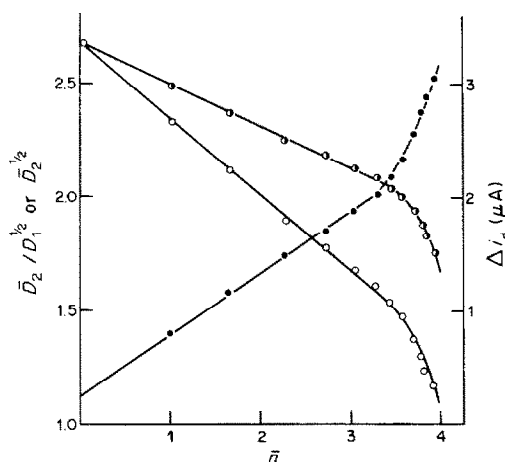


Fig. 1. Plots of $\bar{D}_2/D_1^{1/2}$ (O), $\bar{D}_2^{1/2}$ (●) (both 10^{-3} cm/sec^{1/2}) and Δi_d (●) vs. mean ligand number, \bar{n} , for the system cadmium-methylthiourea. Ratio of slopes of $\bar{D}_2/D_1^{1/2}$ and $\bar{D}_2^{1/2}$ graphs = 1.81; the theoretical value predicted by equations (4) and (5) is 2.0.

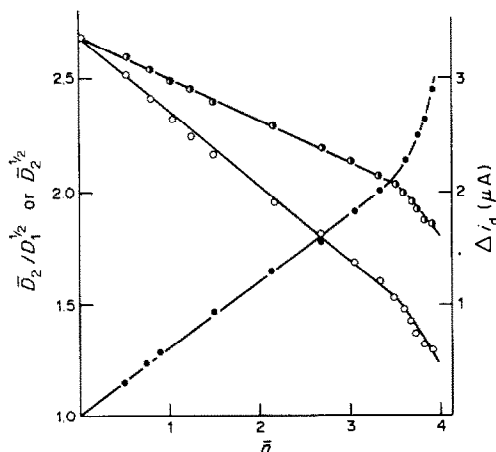


Fig. 2. Plots of $\bar{D}_2/D_1^{1/2}$ (O), $\bar{D}_2^{1/2}$ (●) (both 10^{-3} cm/sec^{1/2}) and Δi_d (●) vs. \bar{n} for the system cadmium-dimethylthiourea. Ratio of slopes of $\bar{D}_2/D_1^{1/2}$ and $\bar{D}_2^{1/2}$ graphs = 1.75; the theoretical value is 2.0.

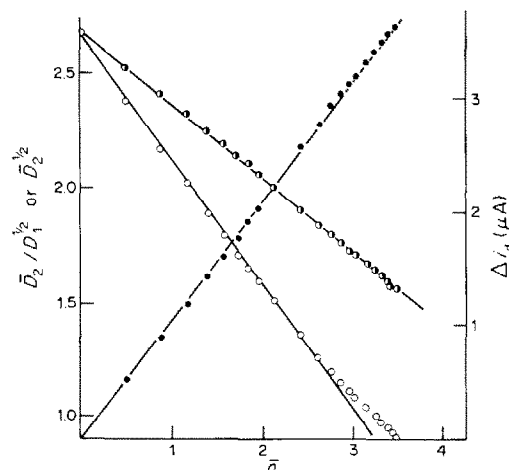


Fig. 3. Plots of $\bar{D}_2/D_1^{1/2}$ (○), $\bar{D}_2^{1/2}$ (●) (both 10^{-3} cm/sec $^{1/2}$) and Δi_d (●) vs. \bar{n} for the system cadmium–ethylthiourea. Ratio of slopes of $\bar{D}_2/D_1^{1/2}$ and $\bar{D}_2^{1/2}$ graphs = 1.72; the theoretical value is 2.0.

theoretical limiting current as \bar{n} approaches 4 is significantly *higher* than the experimental limiting currents approached at the highest ligand concentrations. This suggests that, as the *primary* complexation process nears completion, further processes may occur, the effect of which on observed currents begins to be shown by distortion of the i_d vs. $[X]$ curve. Such distortions are frequently less obvious in aqueous than in mixed aqueous/non-aqueous solvents,⁵ their presence being shown in such media much more clearly by plots of the type shown in Figs. 1–3. So far as construction and integration of pseudo-formation curves are concerned, this may mean that it is not immediately obvious in all cases whether at higher ligand concentrations Δi_d data are in error or

not. In practice this need presents few real problems since (a) if distortion of i_d vs. $[X]$ curves is not obvious, errors are likely to be smaller (though not necessarily insignificant) and (b) since pseudo-formation curves are based on *logarithmic* concentration scales, distortion of these is usually confined to a relatively small range of $\log[X]$. Figures 4–6 show the current data reported by Lane *et al.*⁶ plotted together with interpolated points at rounded and more convenient values of ligand concentration. Pseudo-formation curves based on the latter data are shown inset for each system.

Integration of the respective pseudo-formation curves, as described previously, yields values of $\log F_0[X]$ appropriate to selected values of free ligand concentration. Estimates of the constant k for each system were obtained from the limiting slopes of the graphs of $\log F_0'[X]$ vs. $\log[X]$ by using the condition

$$\left[\frac{d \log F_0'[X]}{d \log[X]} \right]_{\text{lim}} = \frac{n_{\text{max}}}{k} \quad (6)$$

it being assumed that n_{max} was 4 for each case. $F_0[X]$ data, derived from the relation $\log F_0[X] = k \log F_0'[X]$, were used to obtain a set of formation constants for each system. These provisional values were used to estimate values of the mean ligand number for the range of free ligand concentrations. Expected Δi_d values and limiting currents for $\bar{n} = 4$ were estimated from appropriate plots of Figs. 1–3 and these led to a set of diffusion coefficients for each complex species, as described earlier. Formation constant data obtained from pseudo-formation curves and mean diffusion coefficients, together with those reported in the literature, are collected for comparison in Table 1. The measure of agreement between the values reported by Lane *et al.* and those obtained here is quite good (and within the limits

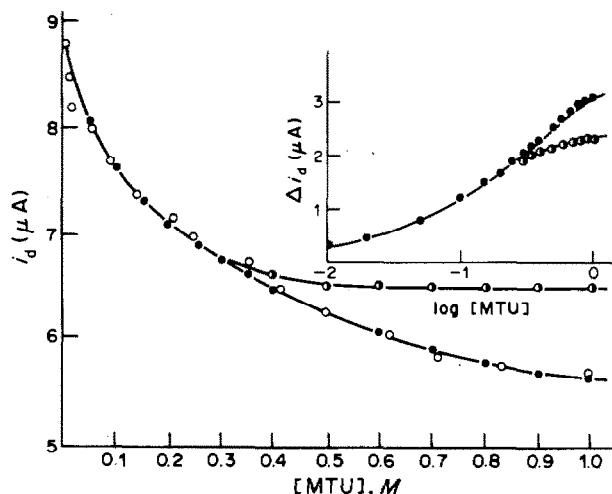


Fig. 4. Variation of diffusion current of $10^{-3}M$ Cd^{2+} in the presence of increasing concentration of methylthiourea, [MTU]: (○) reported experimental points, (●) interpolated points used to construct the inset pseudo-formation curve. In the inset curve, fully shaded circles correspond to interpolated points, half-shaded circles correspond to theoretical Δi_d values at high \bar{n} values derived from Fig. 1.

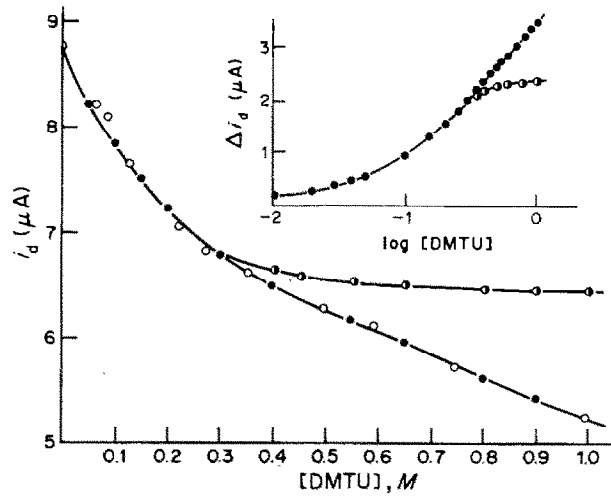


Fig. 5. Variation of diffusion current of $10^{-3}M$ Cd^{2+} in the presence of increasing concentration of dimethylthiourea, [DMTU]; symbols as in Fig. 4.

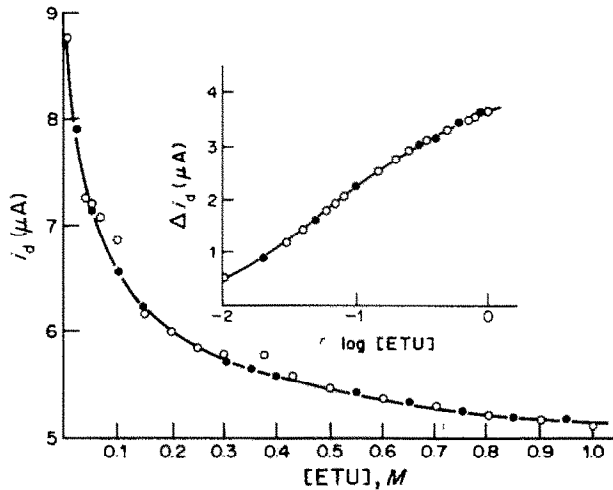


Fig. 6. Variation of diffusion current of $10^{-3}M$ Cd^{2+} ion in the presence of increasing concentration of ethylthiourea [ETU]; (○) reported experimental points, (●) interpolated points. In this case distortion of the curve is minimal and all points correspond closely to those required for the pseudo-formation curve.

Table 1. Comparison of values of overall formation constants derived from three sources for the systems of complexes formed between cadmium and substituted thioureas

Ligand	Data source				
	β_1	β_2	β_3	β_4	
Methylthiourea	a	43	240	575	17000
	b	43	250	600	15000
	c	43 ± 3	$(2.5 \pm 2) \times 10^2$	$(5.8 \pm 0.8) \times 10^2$	$(1.15 \pm 1.5) \times 10^4$
Dimethylthiourea	a	50	50	500	9700
	b	45	100	500	9160
	c	30 ± 3	$(1.87 \pm 0.2) \times 10^2$	$(8.3 \pm 1.0) \times 10^2$	$(6.6 \pm 1.0) \times 10^3$
Ethylthiourea	a	25	100	1000	31000
	b	55	1350	8800	11800
	c	59 ± 5	$(1.28 \pm 0.06) \times 10^3$	$(9.5 \pm 0.8) \times 10^3$	$(1.87 \pm 0.2) \times 10^4$

a—Values reported by Lane *et al.*⁶

b—Values obtained by integration of pseudo-formation curve constructed from interpolated currents derived from data reported by Lane *et al.*⁶

c—Values estimated by application of mean diffusion coefficients.

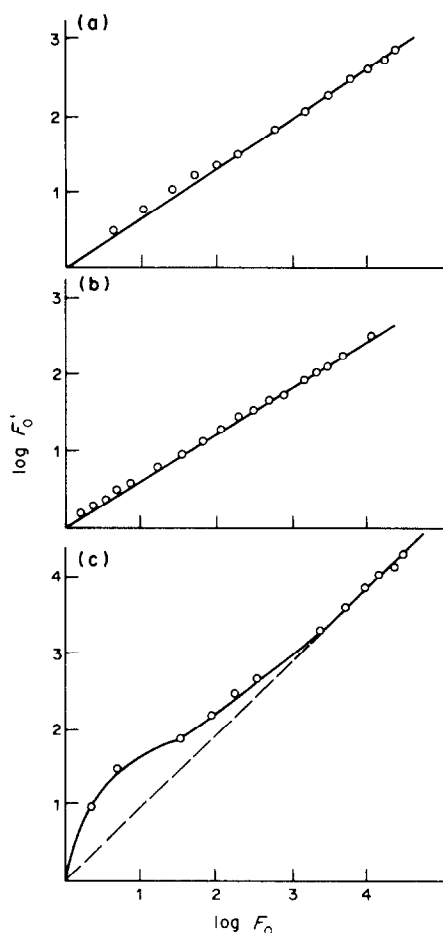


Fig. 7. Graphs of $\log F'_0$ (derived from integration of pseudo-formation curve) vs. $\log F_0$ (derived from reported half-wave potentials): (a) cadmium-methylthiourea; slope = 1.454, compared with 1.412 from $d \log F'_0/d \log [\text{MTU}]$; (b) cadmium-dimethylthiourea; slope = 1.600, compared with 1.630 from $d \log F'_0/d \log [\text{DMTU}]$; (c) cadmium-ethylthiourea; slope = 1.029, compared with 1.025 from $d \log F'_0/d \log [\text{ETU}]$.

expected) for the systems involving the methyl and dimethyl substituted ligands. There is, however, considerable disparity in the case of the system with ethylthiourea. In this connection it is worth comparing the $\log F'_0[\text{X}]$ data calculated on the basis of varying diffusion currents with the values of $\log F_0[\text{X}]$ obtained from half-wave potentials. Plots of $\log F'_0[\text{X}]$ vs. $\log F_0[\text{X}]$ are shown in Fig. 7. Correlation is extremely good for methylthiourea and dimethylthiourea and the slopes agree closely with the values of the constant k determined independently. For the system involving ethylthiourea, the correlation is only good for values of $F_0[\text{X}]$ corresponding to ligand concentrations $> 0.5M$. Clearly the half-wave potentials reported at lower ligand concentrations are in error, as is made plain in Fig. 8 in which observed $E_{1/2}$ values are plotted against the concentration of ethylthiourea. Also included on this graph for comparison are the esti-

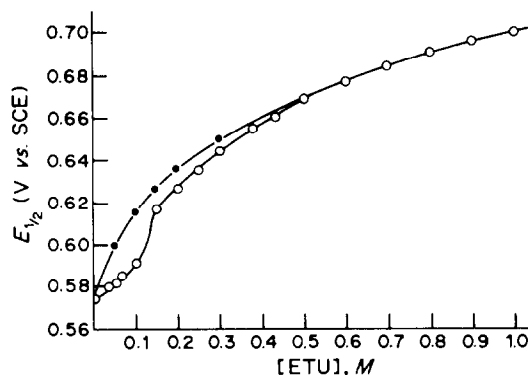


Fig. 8. Plot of reported half-wave potentials of Cd^{2+} vs. concentration of ethylthiourea (open circles). Shaded circles correspond to estimated values of $E_{1/2}$ calculated from interpolated values of $F_0[\text{X}]$ derived from Fig. 7(c).

mated values of half-wave potential based on Fig. 7(c) by using interpolated values of $F_0[\text{X}]$. It is to this range of underestimated half-wave potentials that we must attribute the serious discrepancies in the β_2 and β_3 values listed in Table 1 for the ethylthiourea system. The validity of the data derived from the methods based on currents, reported for this case, is demonstrated in Table 2. From this it is seen that there is much better agreement between the high concentration values of $F_0[\text{X}]$, calculated from current-derived constants, and the experimental values obtained by Lane *et al.*, than there is with those obtained from their calculated formation constants.

The low values of diffusion currents occurring for ligand concentrations in excess of about $0.35M$ for methylthiourea and dimethylthiourea can cause problems in assessing the magnitude of the term $\log I_M/I_C$ in equation (2). The significance of incorrect allowance for this quantity is shown in Tables 3 and 4. In both tables the concentrations calculated by Lane on the basis of his dilution method have been used in the calculation of values of the $F_0[\text{X}]$ functions. While it is evident that there is fair agreement between the reported values (column *a*) and those calculated by using the resultant formation constants (column *b*), this is largely a measure of internal consistency. What is eminently clear is that very

Table 2. Comparison of $F_0[\text{X}]$ data deriving from various sources for the system cadmium-ethylthiourea: (a) values reported by Lane *et al.*; (b) values calculated from the polynomial, with the calculated formation constants reported by Lane *et al.*; (c) values calculated from the polynomial, with Crow's formation constants

[ethylthiourea], <i>M</i>	$F_0[\text{X}]$				
	(a)	(b)	(c)	(b)/(a)	(c)/(a)
0.5	2433	2102	2693	0.864	1.107
0.6	4742	4286	4951	0.904	1.044
0.7	8676	7854	8388	0.905	0.967
0.8	13049	13295	13352	1.019	1.023
0.9	20249	21173	20236	1.046	1.000
1.0	29039	32126	29479	1.106	1.015

Table 3. Comparison of values of $F_0[X]$ functions derived from different sources for the system cadmium–methylthiourea: (a) reported values; (b) values calculated from reported formation constants; (c) values calculated from $E_{1/2}$ data with no current correction; (d) values calculated from $E_{1/2}$ data with modified current correction as revealed by the pseudo-formation curve; (e) values calculated from formation constants generated by the application of methods based on currents

[methylthiourea], M	$F_0[X]$				
	(a)	(b)	(c)	(d)	(e)
0.0498	3.27	3.92	2.98	3.27	3.90
0.2072	51.19	53.67	42.06	51.19	53.63
0.4144	583.8	602.3	435.3	595.7	546.8
0.4973	1221	1192	877	1174	1075
0.6216	2952	2797	2066	2786	2508
0.7104	4203	4688	2823	3804	4193
0.8288	10000	8550	6598	8962	7628
1.0000	17820	17859	11471	15460	15893

serious errors in values of $F_0[X]$ functions may be caused by omission of the current-correcting term in equation (2) (column *c*). Of equal importance, however, can be errors introduced by invalid correction. From Tables 3 and 4 it is seen that up to about $0.5M$ ligand concentration there is less serious discrepancy between values of $F_0[X]$ derived from all sources, whether based on experimental data and including corrections, or calculated from derived constants (although values based on experimental data but which include no current correction are significantly lower). At higher ligand concentrations there are separate closer matches between the data of columns *a* and *b* on the one hand and columns *d* and *e* on the other. The latter are regarded as being of greater significance, deriving as they do from more nearly independent sources.

A further problem that can arise with graphs of i_d vs. $[X]$ of the type found for methylthiourea (Fig. 4) is that it can be tempting to assume that the limiting current reached at the highest ligand concentrations is a reflection of maximum co-ordination of the metal ion by the ligand. This limiting value of current can, in principle, be used to estimate D_{MX_N} and thence all intermediate D_{MX_i} between D_M and D_{MX_N} . Such treat-

ment for the system cadmium–methylthiourea produced ($\bar{D} - D_{MX_i}$) data which proved to be quite useless for generating formation constants. It is necessary first to identify the region of ligand concentration where i_d and \bar{n} are linearly related and then to obtain the maximum value of i_d at n_{max} . Only then is a satisfactory value of D_{MX_N} obtainable.

It is noticeable that while analysis of pseudo-formation curves tends to produce a *high* value for the formation constant of the highest complex, the more elaborate method based on ($\bar{D} - D_{MX_i}$) functions tends to result in the reverse effect. Calculated data from Table 3 tend to support a value of 1.5×10^4 for β_4 , close to the value of 1.7×10^4 reported as obtained by using DeFord–Hume analysis, but rather different from the value of 1.15×10^4 resulting from the use of diffusion coefficients. That the last value is low is supported by the fact that the limiting slope of the graph of $\Delta E_{1/2}$ vs. $\log[X]$ produces 1.2×10^4 for β_4 , with no current correction included. Further, DeFord–Hume analysis of the data in column *c* of Table 3 yields a value of 1.12×10^4 for β_4 . Despite these small inconsistencies, the essential validity of the treatment is endorsed by the curves in Fig. 9, where values of \bar{D} calculated from the data $\beta_1 = 43$;

Table 4. Comparison of values of $F_0[X]$ functions derived from different sources for the system cadmium–dimethylthiourea; columns are labelled as in Table 3

[dimethylthiourea], M	$F_0[X]$				
	(a)	(b)	(c)	(d)	(e)
0.0911	6.02	7.02	5.55	6.02	6.53
0.1290	9.40	12.04	8.18	9.40	11.83
0.2211	52.34	43.08	42.06	52.34	41.97
0.2714	80.15	80.88	62.09	80.15	75.93
0.3512	245.4*	194.0	184.8	191.2	171.9
0.3512	194.5‡	194.0	184.8	191.2	171.9
0.4975	710.6	694.1	508.6	680.3	570.8
0.5970	1360	1387	948	1278	1122
0.7463	3172	3283	2067	2794	2524
1.0000	10420	10301	5690	7727	7662

*When reported half-wave potentials are plotted as a function of ligand concentration, this value is clearly incorrect.

‡Value for $F_0[X]$ calculated from corrected half-wave potential obtained by graphical interpolation.

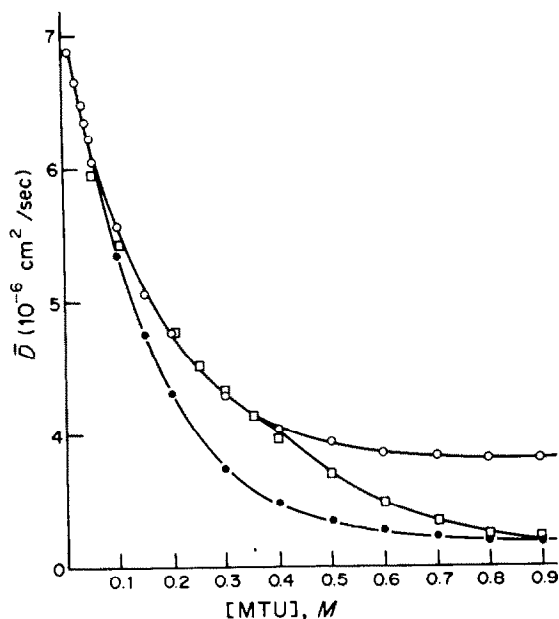


Fig. 9. Plots of experimental and calculated values of mean diffusion coefficients for the system cadmium-methylthiourea. Squares correspond to points interpolated from reported data. Other points are calculated from the values $43, 2.5 \times 10^2, 6.0 \times 10^2, 1.5 \times 10^4$ for $\beta_1, \beta_2, \beta_3, \beta_4$, together with two sequences of values of individual diffusion coefficients $D_M - D_{MX_n}$, viz. 7.200, 6.210, 5.295, 4.452, 3.687 (open circles) and 7.200, 6.003, 4.915, 3.936, 3.070 (shaded circles), (all values $\times 10^{-6} \text{ cm}^2/\text{sec}$).

$\beta_2 = 2.5 \times 10^2$; $\beta_3 = 6.0 \times 10^2$; $\beta_4 = 1.50 \times 10^4$ and two sets of D_{MX_n} data (one set based on $\bar{n} = k \Delta i_d$ and providing $D_{MX_4} = 3.69$, the other obtained by using the lowest observed current and providing $D_{MX_4} = 3.07$) are plotted to complement data derived from experimental diffusion currents.

Such problems with limiting values of currents would seem to arise from the development of almost full co-ordination well within the available range of ligand concentration, at which point secondary processes occur which interfere with the one being monitored. While such interferences are frequently much

larger in mixed solvents, at least they are then much clearer, and large distortions of the i_d vs. $[X]$ curves are observed. In aqueous media the distortions may set in so gradually that they might escape notice.

CONCLUSIONS

Previously proposed expressions, relating parameters deriving from polarographic diffusion currents of metal ions and the extent of their complexation, as reflected in the magnitude of mean ligand number, are seen to be essentially correct. Methods devised for determination of formation constants from current measurements are not only valid in their own right but also complementary to those based on use of half-wave potentials. Current corrections required for the latter determinations can be seriously misjudged and may cause major errors in the values of the plotting functions used in graphical extrapolation procedures. In cases where experimental diffusion currents are too low at higher ligand concentrations, and reflect limitations of the applicability of the simple expression $\bar{n} = k \Delta i_d$ [and of the extended form as expressed in equation (3)], the construction, integration and analysis of pseudo-formation curves may not be seriously impaired. Problems are more likely to be caused in such cases for the calculation of equilibrium data by means of $(\bar{D} - D_{MX_n})$ functions unless particular care is taken to obtain a reliable value of D_{MX_n} .

REFERENCES

1. D. R. Crow, *Talanta*, 1982, **29**, 733; 739; 1983, **30**, 659; 1984, **31**, 421.
2. S. Fronaeus, *Acta Chem. Scand.*, 1950, **4**, 72.
3. I. Leden, *Z. Phys. Chem (Leipzig)*, 1941, **188**, 160.
4. D. R. Crow, *Electrochim. Acta*, 1983, **28**, 1799.
5. D. D. DeFord and D. N. Hume, *J. Am. Chem. Soc.*, 1951, **73**, 5321.
6. T. J. Lane, J. W. Thompson and J. A. Ryan, *ibid.*, 1959, **81**, 3569.
7. D. R. Crow, *J. Electroanal. Chem. Interfacial Electrochem.*, 1968, **16**, 137.

THE ANALYSIS OF FERROALLOYS

R. S. YOUNG

Apt. 605, 1178 Beach Drive, Victoria, B. C. V8X 2M9, Canada

(Received 24 November 1985. Accepted 13 March 1986)

Summary—Procedures are outlined for the determination of the principal elements in ferroalloys.

A ferroalloy is an alloy of iron and one or more other elements. It is used primarily to introduce into a molten ladle of steel certain proportions of the alloy metal to give the finished product definite chemical and physical properties. Ferroalloys are also employed for recarburizing, as cleansing and deoxidizing agents to combine with oxygen, oxides, or other impurities and pass these into the slag. Ferrosilicon is also used in some heavy media separations of ore constituents.

The chemical analysis of ferroalloys is important, not only to producers, but also to the large number of consumers of these materials in the metallurgical industries.

SAMPLING

Most ferroalloys are hard, abrasive, or tough; some components may also be brittle. Crushers, pulverizers, and other sampling equipment must be such that the minimum contamination from iron and other metals is ensured. Manganese steel or properly hardened alloy steel, and hardened and tempered chromium steel are commonly employed. Samples of ferroalloys prepared for chemical analysis are usually comminuted to pass a 100-mesh sieve. Some, like ferromolybdenum, contain veins or bands of material of varying composition and should be pulverized to 200-mesh before thorough mixing. Another reason for great care in sample preparation is that many ferroalloys are high in price. Specifications have been published by authoritative bodies for the sampling of ferroalloys.^{1,2}

DECOMPOSITION

It is well known in analytical chemistry that most materials produced at, or subjected to, high temperatures are not readily dissolved by single acids, and often only slowly by mixed acids. Ferroalloys, now produced almost exclusively in an electric furnace, are no exception to this generalization; they often require for dissolution a sodium peroxide fusion, attack with nitric and hydrofluoric acids in a platinum dish, or some other drastic procedure.

Ferrophosphorus can be brought into solution by hot concentrated sulphuric acid. Ferrocobalt and ferronickel can usually be decomposed by *aqua regia*; if a small residue remains it can be treated with hydrofluoric and sulphuric acid in a platinum crucible, or fused with sodium carbonate, and added to the main portion. Ferromanganese, ferromolybdenum and ferrovandium can generally be dissolved by sulphuric and nitric acids; if the silica content is high, a little hydrofluoric acid may be required. Ferromanganese can also be decomposed by nitric-perchloric acid mixture.

Ferroboron, ferrochromium and ferrosilicon are opened out by a sodium peroxide fusion. This fusion method can also be used for ferrotungsten and ferrozirconium, or these alloys can be brought into solution by hydrofluoric, sulphuric and nitric acids. Ferrotitanium is dissolved in sulphuric, nitric and hydrofluoric acids. Ferroniobium and ferrotantalum are usually decomposed by hydrochloric-hydrofluoric acid mixture, with the final addition of a little nitric acid if necessary.

SEPARATIONS

Iron is not usually separated from the other constituents of ferroalloys, but occasionally this is desirable. The separation can be done by conventional procedures such as precipitation by ammonia, sodium peroxide fusion and dissolution of the melt in water, ether extraction from hydrochloric acid, cupferron-chloroform extraction, electrolysis at a mercury cathode, zinc oxide precipitation, or ion-exchange.³

Other separation methods are often used for certain ferroalloys. Silicon in ferrosilicon is nearly always determined gravimetrically by dehydration of silicic acid, ignition to silica, and final volatilization of silica by treatment with hydrofluoric acid. Nickel is often separated by precipitation with dimethylglyoxime, and zirconium by precipitation as phosphate or with mandelic acid.

DETERMINATIONS

Iron

Strange as it may seem, iron is not often deter-

mined in ferroalloys; if it is required, the outline below should provide sufficient information.

When a double ammonia precipitation is used and the iron in the final precipitate is dissolved in hydrochloric acid, reduced with stannous chloride and titrated with standard potassium dichromate, the only interferences are likely to be caused by molybdenum, tungsten and vanadium. Only traces of molybdenum and tungsten are left in the iron precipitate after two ammonia precipitations, and these have no significant effect on the potassium dichromate titration. If its content is more than 1% of that of iron, vanadium will interfere and must be separated before the reduction and titration. This can be conveniently done by an initial separation of vanadium by treatment with sodium hydroxide, or by an ether separation of iron from 6*M* hydrochloric acid.

Carbon, sulphur, silicon and phosphorus

In ferroalloys, the elements carbon, sulphur, silicon, and phosphorus are very important, and their determination is almost invariably required. The methods used for the various ferroalloys do not differ appreciably, and can conveniently be discussed collectively.

Carbon. Carbon in ferroalloys is usually determined by conventional direct combustion in a stream of oxygen and weighing of the resulting carbon dioxide collected in an absorption bulb. The temperatures employed are: ferroboration, at least 1100°; ferrocobalt, ferromolybdenum, ferronickel and ferrophosphorus, 1100–1200°; ferrovandium, 1150–1200°; the remaining ferroalloys require a temperature of 1200–1350°.

Unless the silicon content is high, ferrovandium usually does not need an accelerator. For the other ferroalloys, the addition of ingot-iron filings and copper oxide as accelerators is routine practice.

Sulphur. The analysis for sulphur in ferroalloys generally follows the conventional barium sulphate gravimetric procedure.^{1,2,4-6} Ferroboration and ferrochromium are opened out by fusion with sodium peroxide. Ferrocobalt, ferromanganese, ferronickel, ferrophosphorus and ferrovandium are decomposed by nitric acid, followed if necessary by a little hydrochloric or perchloric acid. Ferrosilicon is brought into solution with nitric–hydrofluoric–perchloric acid mixture. Ferroniobium, ferrotantalum, ferrotitanium, ferrotungsten and ferrozirconium are dissolved in nitric–hydrofluoric acid mixture.

Sulphur in ferromolybdenum requires a slightly different procedure. After dissolution in nitric acid, removal of any silicon by dehydration in hydrochloric acid, precipitation of sulphate with barium chloride, and filtration. The precipitate is ignited, then fused with sodium carbonate, and the cooled fusion cake is dissolved in water, and the solution filtered. Molybdenum is removed with α -benzoin-oxime, and sulphate is precipitated again from the filtrate with barium chloride.¹

Sulphur in some ferroalloys can be determined by the combustion and iodate titration method. In this, a major part of the sulphur in the sample is converted into sulphur dioxide by combustion in a stream of oxygen; accelerators of copper, iron or tin are used. During the combustion the sulphur dioxide is absorbed in an acidified starch–iodide solution and titrated with potassium iodate solution. The latter is standardized against ferroalloys of known sulphur content to compensate for the characteristics of a given apparatus and for variation in the degree of conversion of sulphur into sulphur dioxide.

Silicon. Silicon is usually determined in ferroalloys by the traditional method of dehydration of silicic acid, filtration, and final volatilization of silica by hydrofluoric acid.^{1,2,4,5,7} Ferrocobalt, ferronickel and ferrophosphorus can be decomposed by nitric–sulphuric acid mixture: dissolution of many ferrovandiums by this means is satisfactory, but if the sample contains more than 4% of silicon, it is not completely soluble and a sodium peroxide fusion is required.

A sodium peroxide fusion must be used for silicon in ferroboration, ferrochromium, ferroniobium, ferrosilicon, ferrotantalum, ferrotitanium, ferrotungsten and ferrozirconium. For ferrotungsten, phosphoric–perchloric acid mixture is used for the dehydration step.

Phosphorus. For most ferroalloys, analysis for phosphorus follows the conventional alkalimetric method with precipitation by ammonium molybdate, filtration, dissolution of the precipitate in an excess of standard sodium hydroxide solution and final titration with standard nitric acid.^{2,4,5,8}

For ferrophosphorus, a cupferron–chloroform extraction is used to separate iron before precipitation of the phosphate with ammonium molybdate. Phosphorus in ferrotungsten, after initial decomposition of the sample with nitric–hydrofluoric acid mixture, is determined by the tartrate–magnesia procedure.^{1,8} Phosphorus is first separated as magnesium ammonium phosphate; this is dissolved in nitric acid and the phosphate is precipitated with ammonium molybdate and determined alkalimetrically as usual.

Dissolution techniques used in analysis for phosphorus are generally as follows: nitric–sulphuric acid mixture for ferrocobalt and ferronickel, hot concentrated sulphuric acid for ferrophosphorus, sodium peroxide fusion for ferroboration, ferrochromium and ferrosilicon, nitric–hydrochloric–sulphuric acid mixture for ferromolybdenum, nitric–hydrofluoric–perchloric acid mixture for ferromanganese, ferroniobium, ferrotantalum, ferrotungsten, ferrovandium and ferrozirconium. For ferrochromium, the removal of chromium by volatilization as chromyl chloride is often advantageous.

Alloying elements

Boron. In analysis of ferroboration, after removal of interfering cations by ion-exchange and of carbon

dioxide under reflux, boron is titrated to pH 6.9 with standard sodium hydroxide solution in the presence of mannitol.^{1,2,4,5,9}

Chromium. After a sodium peroxide fusion of ferrochromium, and dissolution of the cooled melt in dilute sulphuric acid, the dichromate produced is reduced by excess of standard ferrous ammonium sulphate solution, the surplus of which is titrated with standard potassium permanganate solution, with ferroin as indicator.^{1,2,4,5} Potassium dichromate may also be used for the back-titration.

If the ferrochromium contains a significant amount of manganese, the chromium and manganese are oxidized by ammonium persulphate with silver nitrate as catalyst. The permanganate is reduced with hydrochloric acid before titration of the dichromate, and Zimmermann-Reinhardt reagent should be added to avoid chloride interference in the titration.

Cobalt. After separation of cobalt from iron in ferrocobalt by the zinc oxide method, or cupferron-chloroform or ether extraction, the analysis can be completed gravimetrically by the l-nitroso-2-naphthol procedure, or by electrolysis in ammoniacal solution.^{1,2,4,5}

Cobalt can also be determined in ferrocobalt in the presence of iron by potentiometric oxidation titration in ammoniacal solution with potassium ferricyanide, in the presence of ammonium citrate to keep iron in solution.

Manganese. Manganese in ferromanganese is determined by the standard bismuthate titrimetric procedure, or by potentiometric titration of manganese(II) with standard potassium permanganate in a neutral sodium pyrophosphate solution.^{1,2,4,5}

Molybdenum. Molybdenum in ferromolybdenum is usually determined by reduction to molybdenum(III) after treatment in a Jones reductor, followed by titration with potassium permanganate.^{1,2,4,5,10-12} A preliminary separation of iron by precipitation with ammonia will also remove other elements such as antimony, arsenic, chromium, niobium, titanium, uranium and vanadium, which are also reduced by amalgamated zinc to products that can be oxidized by permanganate. If tungsten is present, it can be separated from molybdenum by precipitation with hydrogen sulphide in the presence of tartrate.

Nickel. Nickel in ferronickel can be separated by cupferron-chloroform, ether extraction, or zinc oxide, and determined gravimetrically with dimethylglyoxime, or electrolytically in ammoniacal solution.^{1,2,4,13,14}

Niobium. Niobium in ferroniobium can be isolated by ion-exchange on a Dowex-1 column from hydrochloric-hydrofluoric acid solution, and eluted by ammonium chloride-hydrofluoric acid. Precipitation with cupferron and ignition to niobium pentoxide at 1100° completes the analysis.^{1,2,4,15,16}

Some samples of ferroniobium contain appreciable quantities of tantalum and titanium. The material is dissolved in a hydrochloric-hydrofluoric acid mixture

and transferred to an anion-exchange column. Titanium, iron and other elements are eluted with an ammonium chloride-hydrochloric acid-hydrofluoric acid mixture. This eluate is treated with boric acid and cupferron, and the precipitate, containing the titanium, is ignited, then fused with potassium hydrogen sulphate, and the cooled melt is leached with dilute sulphuric acid. The titanium is converted into its peroxy complex with hydrogen peroxide and determined photometrically at 410 nm. The niobium is eluted with an ammonium chloride-hydrofluoric acid mixture. Tantalum is then eluted with an ammonium chloride-ammonium fluoride solution adjusted to pH 5-6. The eluates are treated with boric acid to demask the fluoride complexes and mask the free fluoride, and the niobium and tantalum are precipitated with cupferron, ignited, and weighed as the pentoxides.

Phosphorus. After a cupferron-chloroform separation of iron, phosphorus in ferrophosphorus is precipitated with ammonium molybdate in nitric acid medium, filtered off, dissolved in an excess of standard sodium hydroxide solution and back-titrated with standard nitric acid.^{1,2,4,8}

Silicon. Ferrosilicon is fused with sodium peroxide, the cooled melt is leached with water and acidified with hydrochloric acid, and the solution is evaporated to dryness for dehydration of the silicic acid, and subsequent determination in the usual way.

Tantalum. Tantalum in ferrotantalum can be isolated by ion-exchange and determined as already described in the section above on niobium.

Titanium. After dissolution of ferrotitanium in sulphuric, nitric and hydrofluoric acid mixture, and separations in acid and alkaline tartrate-hydrogen sulphide medium, titanium is precipitated with cupferron, ignited at 1050-1100° and weighed as the dioxide.

Vanadium and zirconium, if present, are precipitated by cupferron along with titanium, and appropriate corrections must be applied. The mixed oxides are fused with potassium pyrosulphate, the cooled melt is dissolved in sulphuric acid, and zirconium is determined gravimetrically as the phosphate. Vanadium is determined potentiometrically on a separate sample in nitric-sulphuric acid medium with standard ferrous ammonium sulphate.^{1,2,4,5,17,18}

Tungsten. In ferrotungsten, tungsten is determined by the conventional digestion-cinchonine method, with final ignition of tungsten trioxide at a temperature not exceeding 750°.^{1,2,4,5,17,18}

Vanadium. Ferrovandium is dissolved by sulphuric-nitric-hydrofluoric acid mixture, the solution is evaporated to fumes of sulphuric acid and cooled, and vanadium is oxidized at room temperature to the quinquevalent state by potassium permanganate. The excess of permanganate is reduced with sodium nitrite and the excess of nitrite is destroyed by urea. The vanadium is titrated with standard ferrous ammonium sulphate to the quad-

trivalent state, with sodium diphenylamine sulphonate as indicator.^{1,2,4,5,19}

Zirconium. Zirconium in ferrozirconium can be separated from iron by ether extraction or mercury-cathode deposition of the latter, or by addition of phosphoric acid to a 10% sulphuric or hydrochloric acid solution containing hydrogen peroxide.

Alternatively, the zirconium can be precipitated with mandelic acid, the precipitate collected and washed, and ignited at 800–1000° to ZrO₂. This method is specific for zirconium (and hafnium).^{1,2,4,5,20,21}

OTHER ELEMENTS

A few other elements are routinely, or occasionally, determined as minor or trace components in the analysis of ferroalloys: aluminium, antimony, arsenic, copper, lead, manganese and tin.

In addition to the methods briefly outlined below (using gravimetric, volumetric, photometric, and atomic-absorption techniques), X-ray fluorescence can be employed for determining these constituents. The instrument is calibrated against standards of the same material analysed by using reference chemical methods of analysis.

Aluminium

In ferroboration, after preliminary separation of iron and aluminium with ammonia and dissolution of the hydroxide in acid, iron is separated by cupferron–chloroform extraction. The excess of cupferron in the filtrate is destroyed with nitric and perchloric acids, and aluminium is determined photometrically with aurintricarboxylic acid.^{1,2,4,5,22,23}

For ferrotitanium, a cupferron–chloroform extraction will leave aluminium in the aqueous phase, free from titanium, iron, vanadium and zirconium. Aluminium can then be precipitated with ammonia and ignited to the oxide. Phosphorus accompanies the aluminium, and if present in significant quantity must be determined and corrected for.

Aluminium in ferrovandium is determined by precipitating iron and vanadium with cupferron, and finally precipitating aluminium as the phosphate in a nearly neutral solution containing ammonium acetate.¹

The small quantities of aluminium in ferroalloys may also be determined by atomic-absorption spectrometry, with a nitrous oxide–acetylene flame.^{24–29}

Antimony

Antimony in ferrotungsten is determined in the precipitate from the analysis for tin. Antimony sulphide is oxidized with nitric acid, heated to 600°, and finally weighed as the oxide Sb₂O₄.¹

Antimony in ferroalloys can be determined by hydride-generation and atomic-absorption spectrometry.^{25–30}

Arsenic

In ferrochromium, ferromanganese and ferrosilicon, arsenic is first separated by distillation as its trivalent chloride, oxidized to arsenic(V), then converted into arsenomolybdate, which is finally reduced by hydrazine sulphate to molybdenum blue, which is measured photometrically at 850 nm.^{4,23}

For ferrotungsten, arsenic is also separated initially by distillation, but the final determination is usually done by titration with standard iodine solution, with starch as indicator.

Arsenic can also be determined in ferroalloys by hydride-generation and atomic-absorption spectrometry.^{25–29,31–33}

Copper

Copper in ferromolybdenum, after separation by precipitation with sodium thiocyanate, is determined by the iodide⁴ or electrolytic^{4,34,35} method.

For ferrotungsten, copper is precipitated by hydrogen sulphide in the presence of tartaric acid. Any antimony and tin present accompany the copper but their sulphides are dissolved by potassium hydroxide–potassium sulphide solution. Copper is finally determined by the usual iodide or electrolytic methods.

Copper may also be determined in ferroalloys by atomic-absorption spectrometry with an air–acetylene flame.^{25–29}

Lead

Analysis for lead in ferrochromium, ferromanganese and ferromolybdenum is sometimes required. After dissolution of the sample, iron is separated by precipitation with ammonia. Interfering metals in the filtrate are complexed with sodium citrate and sodium cyanide, then the lead–dithizone complex is extracted with chloroform, and measured photometrically at 520 nm.²³

Atomic-absorption spectrometry can also be used for lead in ferroalloys, with an air–acetylene flame and the line at 217.0 nm.^{25–29,36}

Manganese

Manganese in ferrotungsten is determined by the conventional persulphate–arsenite method in which manganese(II) is oxidized to permanganate with ammonium persulphate in the presence of silver nitrate, and the permanganate is titrated with standard sodium arsenite solution.^{4,37}

Lower levels of manganese can also conveniently be determined by atomic-absorption spectrometry, by using an air–acetylene flame and the line at 279.5 nm.^{25–29}

Tin

Determination of tin in ferrotungsten is occasionally required. It is usually isolated, with copper and antimony, by precipitation with hydrogen sul-

phide in the presence of tartaric acid. Tin and antimony are separated from copper by dissolution of their sulphides in potassium hydroxide-potassium sulphide solution, and tin is separated from antimony in a hydrochloric acid-oxalic acid solution, with hydrogen sulphide. Final determination of tin is done in the customary manner by reduction with pure lead, and titration with standard iodine solution, with starch as indicator.^{4,38}

The hydride-generation technique of atomic-absorption is suitable for determination of low contents of tin in various ferroalloys.^{25,29,39}

REFERENCES

1. A.S.T.M., *Chemical Analysis of Metals and Metal Bearing Ores*, Philadelphia, Pa., 1984.
2. T. S. Harrison, *Handbook of Analytical Control of Iron and Steel Production*, Ellis Horwood, Chichester, 1979.
3. R. S. Young, *Separation Procedures in Inorganic Analysis*, Griffin, London, 1980.
4. *Idem*, *Chemical Analysis in Extractive Metallurgy*, Griffin, London, 1971.
5. B. S. Handbook No. 19, *Standard Methods of Analysis of Iron, Steel, and Associated Materials*, British Standards Institution, London, 1970.
6. J. H. Karchner (ed.), *The Analytical Chemistry of Sulphur and its Compounds*, Wiley-Interscience, New York, Part 11, 1970; Part 2, 1972.
7. L. V. Myohlyayeva and V. V. Krasnoshchekov, *Analytical Chemistry of Silicon*, Halsted-Wiley, New York, 1974.
8. A. A. Fedorov, F. V. Chernyakhovskaya, A. S. Veridub *et al.*, *Analytical Chemistry of Phosphorus*, Nauka, Moscow, 1974.
9. A. A. Nemodruk and Z. K. Karalova, *Analytical Chemistry of Boron*, Halsted Press, New York, 1971.
10. W. T. Elwell and D. F. Wood, *Analytical Chemistry of Molybdenum and Tungsten*, Pergamon Press, Oxford, 1971.
11. A. I. Busev, *Analytical Chemistry of Molybdenum*, Halsted Press, New York, 1971.
12. N. M. Pyatiletova, A. D. Yarashenko, I. S. Novikova and T. M. Orlov, *Analysis of Molybdenum and its Alloys*, Metallurgiya, Moscow, 1974.
13. F. A. Lowenheim and R. S. Young, in *Encyclopedia of Industrial Chemical Analysis*, F. D. Snell and L. S. Ettre (eds.), Vol. 16, Interscience, New York, 1972.
14. C. L. Lewis and W. L. Ott, *Analytical Chemistry of Nickel*, Pergamon Press, Oxford, 1970.
15. I. M. Gibalo, *Analytical Chemistry of Niobium and Tantalum*, Halstead Press, New York, 1971.
16. W. T. Elwell and D. F. Wood, *The Analysis of the New Metals Titanium, Zirconium, Hafnium, Niobium, Tantalum, Tungsten and Their Alloys*, Pergamon Press, Oxford, 1966.
17. A. I. Busev, V. M. Ivanov and T. A. Sokolova, *Analytical Chemistry of Tungsten*, Nauka, Moscow, 1976.
18. J. J. Topping, *Talanta*, 1978, **25**, 61.
19. V. N. Muzgin, L. B. Khamazina, V. L. Zolotavin and I. Ya. Bezrukov, *Analytical Chemistry of Vanadium*, Nauka, Moscow, 1981.
20. A. K. Mukherji, *Analytical Chemistry of Zirconium and Hafnium*, Pergamon Press, Oxford, 1970.
21. S. V. Elinson and K. I. Petrov, *Analytical Chemistry of Zirconium and Hafnium*, Halsted Press, New York, 1971.
22. V. N. Tikhonov, *Analytical Chemistry of Aluminium*, Nauka, Moscow, 1971.
23. E. B. Sandell and H. Onishi, *Photometric Determination of Traces of Metals*, 4th Ed., Wiley, New York, 1978.
24. W. D. Cobb and T. S. Harrison, *Analyst*, 1971, **96**, 764.
25. K. C. Thompson and R. J. Reynolds, *Atomic Absorption, Fluorescence and Flame Emission Spectroscopy*, 2nd Ed., Griffin, London, 1978.
26. J. C. Van Loon, *Atomic Absorption Spectroscopy*, Academic Press, New York, 1980.
27. L. Ebdon, *An Introduction to Atomic Absorption Spectroscopy*, Heyden, London, 1982.
28. J. E. Cantle, *Atomic Absorption Spectroscopy*, Elsevier, New York, 1982.
29. A. Varma (ed.), *CRC Handbook of Atomic Absorption Analysis*, Vols. 1 and 2, CRC Press, Boca Raton, Florida, 1984.
30. A. A. Nemodruk, *Analytical Chemistry of Antimony*, Nauka, Moscow, 1978.
31. A. A. Nemodruk, *Analytical Chemistry of Arsenic*, Nauka, Moscow, 1976.
32. P. J. Brooke and W. H. Evans, *Analyst*, 1981, **106**, 514.
33. C. J. Peacock and S. C. Singh, *ibid.*, 1981, **106**, 931.
34. J. A. Plumbeck, *Electroanalytical Chemistry; Basic Principles and Applications*, Wiley, New York, 1982.
35. P. T. Kissinger and W. R. Heineman (eds.), *Laboratory Techniques in Electroanalytical Chemistry*, Dekker, New York, 1984.
36. R. K. Roschnik, *Analyst*, 1973, **98**, 596.
37. A. K. Lavrukhina and L. V. Yukina, *Analytical Chemistry of Manganese*, Nauka, Moscow, 1974.
38. V. B. Spivakovskii, *Analytical Chemistry of Tin*, Nauka, Moscow, 1975.
39. M. O. Andreae and J. T. Byrd, *Anal. Chim. Acta*, 1984, **156**, 147.

SELECTIVE KINETIC FLUORIMETRIC DETERMINATION OF COPPER AT THE ng/ml LEVEL

M. C. GUTIERREZ, A. GOMEZ-HENS and M. VALCARCEL

Department of Analytical Chemistry, Faculty of Sciences, University of Córdoba, Córdoba, Spain

(Received 24 July 1985. Revised 6 February 1986. Accepted 13 March 1986)

Summary—A kinetic fluorimetric method for copper, based on a previously described system with 1,1,3-tricyano-2-amino-1-propene as reagent, has been developed. It has been shown that the determination is based on copper-catalysed oxidation of the reagent rather than on complex formation with it, although complex-formation with imidazole seems needed to stabilize the copper(I) that is thought to be the catalyst. The application of several kinetic methods (tangent, fixed-time and variable-time) allows determination of very low concentrations of copper (1–35 ng/ml) with a sensitivity about 100 times that of an earlier method. Of 47 ions tested, only EDTA interfered when present at the same concentration as copper. The method has been applied to the determination of copper in blood serum samples.

This study aims to show the possibility of transforming an equilibrium method into a kinetic one and improving the sensitivity, selectivity and rapidity of the determination. We have chosen the copper–1,1,3-tricyano-2-amino-1-propene (TRIAP) system described by Ritchie and Harris.¹ This method involves treating copper(II) with TRIAP at about pH 8 and measuring the fluorescence intensity of the product in acidic medium. These authors considered that the reaction involved the formation of a fluorescent complex. However, it is well-known that paramagnetic ions usually quench the fluorescence of organic molecules and their complexes are thus non-fluorescent.² Furthermore, we have shown that when this system is kept out of contact with oxygen it is non-fluorescent, and that treating the reagent with an oxidant such as hydrogen peroxide, in the absence of copper, gives a product with the same fluorescence characteristics as those yielded in the presence of copper. These facts show that it is logical to assume the oxidation of TRIAP by dissolved oxygen in the above-mentioned method, copper possibly acting as a catalyst.

In this paper we describe a simple kinetic fluorimetric method for copper. Its sensitivity is about 100 times that of the Ritchie and Harris method¹ and it is faster because no incubation or sample pH-adjustment is necessary.

EXPERIMENTAL

Reagents

Standard copper solution, 1 mg/ml. Prepared from cupric nitrate and standardized iodometrically. Working solutions were prepared daily by suitable dilution.

1,1,3-Tricyano-2-amino-1-propene (TRIAP) solution, 4×10^{-3} M. Prepared by dissolving 26.4 mg of reagent in 50 ml of distilled water.

Imidazole-hydrochloric acid buffer. Made by dissolving 0.3404 g of imidazole in water and 6 ml of 0.2 M hydrochloric acid, and diluting to 100 ml.

Reagent-grade chemicals and pure solvents were used.

Apparatus

A Perkin-Elmer spectrofluorimeter, model 650-10S, fitted with a device for kinetic measurement and with 1-cm quartz cells was used. The cell compartment was kept at constant temperature by water circulating from a thermostatic tank. The sensitivity was set at 3, and the excitation and emission slits were set to give 6-nm spectral band-pass. A set of fluorescent polymer samples was used daily to adjust the spectrofluorimeter, to compensate for changes in source intensity.

Procedure

To a 10-ml standard flask containing the sample or standard solution (10–300 ng of copper) were added 1 ml of imidazole-hydrochloric acid buffer solution, 0.5 ml of aqueous 7.2×10^{-4} M TRIAP solution and 3 ml of 0.25 M hydrogen peroxide. The mixture was diluted to the mark with distilled water and a portion transferred to a 1-cm fluorescence cell kept at $72 \pm 0.1^\circ$. Measurements were started 2 min after preparation of the samples and the reaction was monitored by means of the rate of change in fluorescence (λ_{ex} 330, λ_{em} 395 nm).

Net fluorescence values were obtained by subtracting the values for a blank solution prepared in a similar way and containing no copper.

Determination of copper in blood serum

A 1-ml sample of serum was heated in a porcelain crucible, either in a sand-bath for 10 min or on a hot-plate for 5 min, to evaporate the liquid, then the residue was heated in a muffle furnace at 700° for 30 min. The residue was dissolved in 5 ml of 1.2 M hydrochloric acid and the clear solution, previously neutralized with sodium hydroxide, was transferred to a 25-ml volumetric flask and treated as above.

RESULTS AND DISCUSSION

Study of the fluorescence reaction

Ritchie and Harris¹ have shown that TRIAP is not fluorescent in acidic medium, whereas under the same conditions the reaction product of copper(II) and TRIAP has an intense yellow fluorescence (λ_{ex} 365, λ_{em} 510 nm). These authors mixed TRIAP and copper at pH about 8 in the presence of imidazole, heated the mixture for 15 min at $37-40^\circ$ and then lowered the

pH with hydrochloric acid. We have repeated this work and obtained the same results. However, we found that when the sample is prepared in the same way but without the copper(II), and an oxidant such as hydrogen peroxide or potassium peroxodisulphate is added, the solution shows the same fluorescence characteristics as those developed in the presence of copper. However, the fluorescence does not develop when the sample is prepared with copper(II) but in an inert atmosphere (*viz.* after removal of dissolved oxygen from the solution by passage of a stream of argon). These facts prove that the fluorescence is not caused by a complex-formation reaction but by oxidation of TRIAP by dissolved oxygen, with copper probably acting as a catalyst.

Imidazole plays a major role in the system, as noted by Ritchie and Harris.¹ These authors tested several buffer systems, including acetate, borate, citrate, imidazole and tris(hydroxymethyl)amino-methane, and chose imidazole, but did not explain why. In this system imidazole probably acts as an activator of the catalytic effect of copper by formation of a complex with this ion,³ which favours the oxidation of TRIAP.

The fluorescence developed varied enormously according to the TRIAP concentration. Figure 1 shows the emission spectra of various mixtures of TRIAP and other components. At $4 \times 10^{-5} M$ (Fig. 1A) TRIAP yields a broad band with a maximum at 390–400 nm (λ_{ex} 330 nm) in the presence of hydrogen peroxide, imidazole and copper. However, at a concentration of $8 \times 10^{-4} M$ it exhibits a very different behaviour (Fig. 1B). A new peak appears at 490–500 nm, both in the presence and absence of imidazole. From curves 2 and 3 it appears that in the absence of imidazole, the presence of copper decreases the fluorescence intensity of the

TRIAP–hydrogen peroxide solution, perhaps by formation of a non-fluorescent complex with the oxidation product of TRIAP. However, in the presence of imidazole, the signal obtained with copper is higher than that in its absence (curves 4 and 5), probably because imidazole, which is in a great excess in the solution, forms a complex with copper and prevents the formation of the complex between copper and the oxidation product of TRIAP. Furthermore, we have verified that under these conditions hydrogen peroxide can act as a reductant for copper, and it is also known that copper(I) forms a complex with imidazole,³⁻⁵ which may be responsible for the acceleration of the oxidation reaction of TRIAP. The role of imidazole would be to stabilize copper(I) in order to raise the Cu(I)/Cu(II) potential high enough for hydrogen peroxide to reduce copper(II). This reaction could take place by means of a free-radical mechanism and the free-radical would be responsible for the oxidation of TRIAP. Also, a copper(II)–TRIAP complex may react with hydrogen peroxide to yield the copper(I)–imidazole complex plus oxygen *in situ* at the TRIAP site, resulting in the oxidation of this last.

The band obtained at 390–400 nm (Fig. 1A) for low concentration of TRIAP (similar to that used in our method) could be attributed to the formation of a condensation product between TRIAP and imidazole. Owing to the reactive ability of TRIAP, which bears a charge-deficient carbon atom, and to the nitrogen in the imidazole ring, which has a lone electron-pair, the formation of this condensation product is perfectly feasible, its oxidation by hydrogen peroxide being favoured by the presence of copper. This is consistent with the fact that the enhancement effect of copper is only observed when

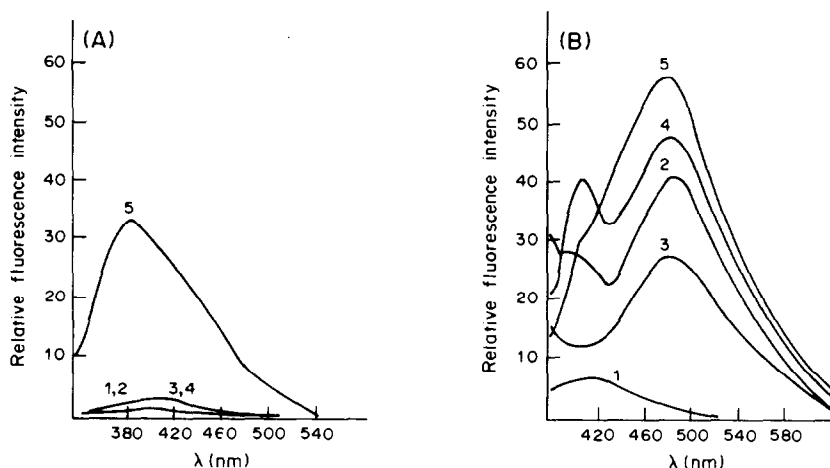


Fig. 1. Emission spectra of TRIAP (1), TRIAP + H₂O₂ (2), TRIAP + H₂O₂ + Cu (3), TRIAP + H₂O₂ + imidazole (4), TRIAP + H₂O₂ + imidazole + Cu (5). (A) [TRIAP] = $4 \times 10^{-5} M$, λ_{ex} = 330 nm; (B) [TRIAP] = $8 \times 10^{-4} M$, λ_{ex} = 370 nm; [imidazole] = $5 \times 10^{-3} M$; [H₂O₂] = $2 \times 10^{-2} M$; [Cu²⁺] = 0.1 $\mu g/ml$; temperature = 60°; reaction time = 30 min.

TRIAP is accompanied by imidazole. This study was done at pH 7.5; if the solution is acidified, as in the Ritchie and Harris¹ work, the maximum at 390–400 nm disappears (possibly owing to the destruction of this condensation product) as the band at 490–500 nm corresponding to the product of oxidation of TRIAP appears.

The product of oxidation of TRIAP with hydrogen peroxide in the presence of a large excess of imidazole shows different fluorescence characteristics (λ_{ex} 330, λ_{em} 400 nm) from those of the product yielded in its absence (λ_{ex} 370, λ_{em} 490 nm). Both have been isolated and analysed, the results being: C 27.7%, N 30.7% and H 4.6% for the first and C 43.2%, N 30.2% and H 2.2% for the second. From these data, it is logical to assume that the product obtained depends on the particular conditions used, but we have not been able to pursue this further, because both products are very insoluble and their NMR spectra cannot be obtained; they are also very involatile and not amenable to mass spectrometry. Furthermore, their infrared spectra show few and uncharacteristic bands.

Effect of the reaction variables

The system was optimized by altering each variable in turn, the others being kept fixed.

Changing the temperature over the range 40–85° (Fig. 2A) gave maximal and constant reaction rate at 70–80°. A temperature of 72° was selected for further studies. From an Arrhenius plot the activation energy was calculated to be 10.8 ± 0.2 kcal/mole.

The reaction rate was found to be maximal and constant over the pH range 7.4–7.8. An imidazole–hydrochloric acid buffer was used to adjust the pH of the samples to 7.5. The reaction rate did not change when the buffer concentration was varied between 2.5×10^{-3} and $7.5 \times 10^{-3} M$ (Fig. 2B). The reaction rate was decreased if the dielectric constant of the solution was lowered by addition of organic solvents such as ethanol or dimethylformamide. The best results were obtained with an aqueous medium.

Variation of ionic strength up to 0.75 (potassium chloride) did not affect the reaction rate. Changing the TRIAP concentration (Fig. 2C) showed that constant and maximal rate is obtained with 4.0×10^{-5} – $1.1 \times 10^{-4} M$ reagent concentration. The hydrogen peroxide concentration also has an optimal range (Fig. 2D), 6.2×10^{-2} – $10^{-1} M$. The order of addition of reagents does not affect the development of the reaction.

The initial slopes of fluorescence *vs.* time curves for solutions containing different amounts of copper(II), recorded against a similar solution containing no copper, indicate a first-order reaction with respect to copper. The various kinetic dependences are summarized in Table 1. On the basis of our kinetic investigations, the following equation is suggested for the oxidation of TRIAP with hydrogen peroxide:

$$d(\text{TRIAP})_{\text{ox}}/dt = k[\text{Cu(II)}]$$

where $(\text{TRIAP})_{\text{ox}}$ is the concentration of oxidized reagent and k is the conditional rate constant.

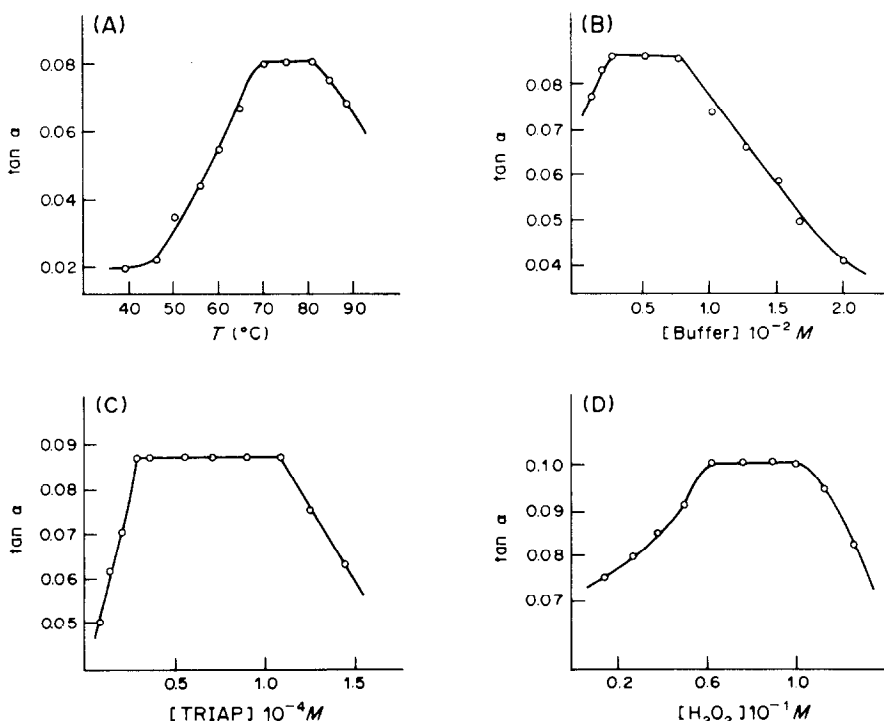


Fig. 2. Effect of the temperature (A), and the buffer solution (B), TRIAP (C) and hydrogen peroxide (D) concentrations on the reaction rate of the TRIAP–H₂O₂–imidazole–Cu system.

Table 1. Summary of kinetic data

Dependence of V_0 on	Concentration range, M
[TRIAP] ^{1/2}	$0.7 \times 10^{-5} - 2.9 \times 10^{-5}$
[TRIAP] ⁰	$2.9 \times 10^{-5} - 1.1 \times 10^{-4}$
[TRIAP] ⁻¹	$1.1 \times 10^{-4} - 2.2 \times 10^{-4}$
[H ₂ O ₂] ^{1/4}	$1.2 \times 10^{-2} - 6.2 \times 10^{-2}$
[H ₂ O ₂] ⁰	$6.2 \times 10^{-2} - 10^{-1}$
[H ₂ O ₂] ^{-3/4}	$10^{-1} - 1.2 \times 10^{-1}$
[H ⁺] ^{1/4}	$3.3 \times 10^{-10} - 1.3 \times 10^{-8}$
[H ⁺] ⁰	$1.3 \times 10^{-8} - 4.5 \times 10^{-8}$
[H ⁺] ^{-2/3}	$4.5 \times 10^{-8} - 3.5 \times 10^{-7}$
[Buffer] ⁰	$10^{-3} - 7.5 \times 10^{-3}$
[Buffer] ⁻¹	$7.5 \times 10^{-3} - 2.0 \times 10^{-2}$

Characteristics of the analytical methods

The fluorescence *vs.* time curves obtained for different amounts of copper(II) under optimum conditions were analysed by the tangent, fixed-time and variable-time methods. For the fixed-time method, measurements were made 2 min after sample

Table 2. Kinetic fluorimetric determination of copper(II)

Method	Cu concentration range, ng/ml	r.s.d., %
Tangent	1-30	± 2.9
Fixed-time	1-35	± 3.0
Variable-time	5-30	± 3.5

*Relative standard deviation.

Table 3. Effect of various ions on the determination of 15 ng/ml of copper

Tolerance ratio, [Ion]/[(Cu(II))]	Ion added
100	Na ⁺ , K ⁺ , Mg ²⁺ , Ca ²⁺ , Sr ²⁺ , Ba ²⁺ , Cr ³⁺ , Mn ²⁺ , Cd ²⁺ , Hg ²⁺ , Pd ²⁺ , Au ³⁺ , F ⁻ , Cl ⁻ , Br ⁻ , I ⁻ , NO ₃ ⁻ , SO ₄ ²⁻ , S ₂ O ₈ ²⁻ , S ₂ O ₃ ²⁻ , ClO ₄ ⁻ , ClO ₃ ⁻ , BrO ₃ ⁻ , IO ₃ ⁻ , IO ₄ ⁻ , B ₄ O ₇ ²⁻ , acetate, tartrate
75	MoO ₄ ²⁻ , SO ₃ ²⁻
50	Be ²⁺ , Pb ²⁺ , Fe ²⁺ , AsO ₂ ⁻
25	Zn ²⁺ , Fe ³⁺ , Hg ₂ ²⁺ , Pt ⁴⁺ , Al ³⁺ , PO ₄ ³⁻ , C ₂ O ₄ ²⁻ , citrate
5	Co ²⁺ , Ag ⁺ , P ₂ O ₇ ⁴⁻ , Sb ³⁺
1	EDTA

Table 4. Determination of copper in blood serum

Sample	Cu ²⁺ found, µg/ml	
	Fluorimetric method*	Atomic-absorption spectrophotometric method
1	1.06 ± 0.02	1.06
2	1.44 ± 0.04	1.44
3	0.75 ± 0.02	0.87
4	1.25 ± 0.05	1.06
5	0.94 ± 0.02	1.00
6	0.94 ± 0.03	1.12
7	0.68 ± 0.01	0.75

*Average of six determinations ± s.d.

preparation. For the variable-time method the reciprocal of the time needed to obtain a relative fluorescence intensity of 10% was plotted against the copper(II) concentration. In all cases the calibration graph was linear over the concentration range indicated in Table 2, which also gives the relative standard deviations ($P = 0.05$, $n = 11$). The precision was similar for all three methods.

The selectivity was tested by studying the effect of 47 foreign ions on the initial rate (Table 3). Of these, 28 do not interfere, at least at concentrations 100 times that of the copper. Only one ion (EDTA) interfered when present at the same concentration as copper, which is indicative of the high selectivity of this method.

Applications

The method has been applied satisfactorily to the determination of copper in blood serum. The results were checked by liquid-liquid extraction followed by atomic-absorption spectrometry.⁶ The results obtained by both techniques are in good agreement (Table 4).

CONCLUSIONS

A review of fluorimetric methods for copper has recently been published.⁷ Although it is well-known that paramagnetic ions such as copper(II) usually do not form fluorescent chelates, the review presented several methods in which the formation of a chelate was the basis of the fluorescence reaction. In fact, the method of Ritchie and Harris¹ was included in this group, but we have now shown that it is based on a redox reaction.

In general, several of the fluorimetric methods for copper present similar sensitivity to that of the method described in this paper, but few have been applied to the determination of copper in practical samples. In the above-mentioned review, the method of Ritchie and Harris was presented as the most selective, although only fifteen ions were tested in their work. Only one of the 47 ions tested in our method interferes at the same concentration level as copper, which makes evident the high selectivity. Furthermore, the sensitivity has been improved about 100-fold by the use of kinetic measurements, and as these are made at the beginning of the reaction and involve no change in the experimental conditions, the determination is very fast.

REFERENCES

1. K. Ritchie and J. Harris, *Anal. Chem.*, 1969, **41**, 163.
2. G. G. Guilbault, *Practical Fluorescence, Theory, Methods and Techniques*, p. 120. Dekker, New York, 1973.
3. G. C. F. Clark, G. J. Moody and J. D. R. Thomas, *Anal. Chim. Acta*, 1978, **98**, 215.
4. B. R. James and R. J. P. Williams, *J. Chem. Soc.*, 1961, 2007.
5. C. J. Hawkins and D. D. Perrin, *ibid.*, 1962, 1351.
6. M. Silva and M. Valcárcel, *Analyst*, 1982, **107**, 511.
7. A. Fernández-Gutiérrez, A. Muñoz de la Peña and M. Román, *Ann. Chim. (Rome)*, 1984, **74**, 1.

THE INFLUENCE OF OPTICAL DESIGN ON THE SIGNAL TO NOISE CHARACTERISTICS OF POLARIMETERS

JOUKO J. KANKARE

Department of Chemistry, University of Turku, SF 20500 Turku 50, Finland

ROGER STEPHENS

Department of Chemistry, Dalhousie University, Halifax, Nova Scotia, Canada

(Received 12 August 1985. Revised 22 January 1986. Accepted 28 February 1986)

Summary—A high-frequency modulation technique is employed to reduce the sensitivity of an instrument to flicker noise. A 5-mW He-Ne laser is used as the source to achieve a high signal to shot-noise ratio. The high-frequency modulator acts as the limiting noise-source in the particular apparatus used, as a result of residual static birefringence in the optical head. An analysis of the origin of the modulator noise is given. The apparatus is tested with L(+)-tartaric acid. A rotation detection limit of 3×10^{-4} degree is achieved (signal to noise ratio of 3:1).

The value of highly sensitive methods for the detection of optical rotation has been shown,¹⁻⁴ for instance in the field of HPLC detection, and interest in the performance of the apparatus needed for these measurements is a natural consequence. A previous communication discussed the signal to noise behaviour of such apparatus at the shot-noise limit, *i.e.*, the condition which is normally encountered at low light levels.⁵

As the available source intensity increases, it becomes more likely that an instrument will be limited by flicker noise rather than by shot noise.⁶ This reduces the potential sensitivity of the instrument below the inherent limit set by shot noise, and prevents the user from taking full advantage of the available source flux. In polarimetry there are two possibilities for dealing with such a situation. The first is to lower the background transmission of the apparatus by the use of optical components of suitably high quality, which lowers the amplitude of the flicker signal accordingly. Alternatively a higher background signal is accepted, in which case the instrument itself must be able to reject flicker noise by some means. The first procedure has been thoroughly explored by Yeung *et al.*¹⁻⁴ Some implications of the second procedure are the subject of the present work.

Use is made here of a linearized response function, which increases the signal magnitude relative to the (approximately) quadratic response of conventional apparatus using crossed polarizers. The benefits of such linearized response functions have been discussed in detail elsewhere.^{5,7}

THEORY

An apparatus which can provide a high degree of discrimination against many sources of flicker noise is shown schematically in Fig. 1. The apparatus will

be described by means of the Jones calculus.⁸ Thus the Jones matrix of the system, **S**, is given by:

$$\mathbf{S} = \mathbf{P}_y \mathbf{R}(\alpha) \mathbf{M} \mathbf{R}(\theta) \mathbf{P}_x \quad (1)$$

where **P_x** and **P_y** are the polarizer matrices, **R(α)** and **R(θ)** are the rotation matrices of an optically active sample, α, and of an offset angle, θ, applied to the polarizer **P_x**; **M** is the matrix of a modulation element, assumed to be a linearly birefringent medium with an oscillating retardance given by $\delta = \delta_0 \sin \omega t$. Thus if all components are assumed to be ideal, then:

$$\mathbf{S} = \begin{pmatrix} 0 & 0 \\ 0 & 1 \end{pmatrix} \begin{pmatrix} \cos \alpha & \sin \alpha \\ -\sin \alpha & \cos \alpha \end{pmatrix} \times \begin{pmatrix} e^{i\delta} & 0 \\ 0 & e^{-i\delta} \end{pmatrix} \begin{pmatrix} \cos \theta & \sin \theta \\ -\sin \theta & \cos \theta \end{pmatrix} \begin{pmatrix} 1 & 0 \\ 0 & 0 \end{pmatrix}$$

Hence

$$\begin{aligned} I_t &= \frac{1}{2} I_0 (\sin^2 \alpha \cos^2 \theta + \cos^2 \alpha \sin^2 \theta \\ &\quad + \frac{1}{2} \sin 2\alpha \sin 2\theta \cos 2\delta) \quad (2) \\ &= \frac{1}{2} I_0 \{ \sin^2 \alpha \cos^2 \theta + \cos^2 \alpha \sin^2 \theta \\ &\quad + \frac{1}{2} \sin 2\alpha \sin 2\theta [J_0(2\delta_0) \\ &\quad + 2 \sum_{K=1}^{\infty} J_{2K}(2\delta_0) \cos 2K\omega t] \} \quad (3) \end{aligned}$$

where I_0 and I_t respectively are the unpolarized source intensity and the intensity transmitted by polarizer **P_y**, and $J_{2K}(2\delta_0)$ is the Bessel function of order 2K.

Equation (3) shows that all the modulated terms contained in I_t are linear in $\sin \alpha$, and therefore vanish in the absence of a sample ($\alpha \rightarrow 0$). An analogous derivation shows that the modulated terms also vanish if α is replaced by a linearly birefringent medium. Thus the optical configuration represented by equation (1) provides a particularly selective arrangement which generates no spurious signals in

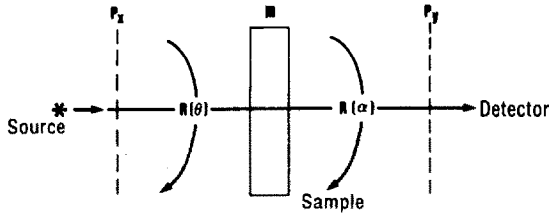


Fig. 1. Schematic apparatus. M is a variable linear retarder; P_x and P_y are the polarizer and analyser. $R(\theta)$ and $R(\alpha)$ are respectively the rotations applied to P_x and to the light-beam by the sample.

the presence of linear birefringence (a real advantage in a highly sensitive system, since the effect of residual window strain, for instance, is otherwise difficult to avoid), and which automatically discriminates against amplitude instability of the modulator as well as flicker noise in the source [as carried by the $\sin^2\theta$ term in equation (2)]. The last property requires that $2K\omega$ be high enough to reach a frequency at which source flicker is not significant. In the present work the values $K=1$, $2\omega=100$ kHz proved to be satisfactory.

In practice, the cancellation of instrumental noise which is implied by this discussion becomes increasingly difficult to achieve as the source intensity is increased and the signal to shot-noise ratio of the equipment improves. The main source of uncorrected noise in the present experiments proved to be the photoelastic modulator (PEM 3, Hinds International, Oregon) which was used for the modulation element, M . The noise parameters of importance for this particular device include the amplitude stability of the a.c. stress axis, the presence of residual static birefringence in the optical head, and the relative orientation of the a.c. and static axes.

The effects of these parameters can be described by rewriting the ideal matrix M in equation (1) as:

$$M = \begin{pmatrix} e^{i(\delta+\rho)} & i\rho \sin 2\phi \operatorname{sinc}(\delta+\rho) \\ i\rho \sin 2\phi \operatorname{sinc}(\delta+\rho) & e^{-i(\delta+\rho)} \end{pmatrix} \quad (4)$$

where 2ρ is the static retardance and ϕ is the angle between the ρ and δ axes, assumed to be small. The derivation of this matrix is given in the appendix. Upon substitution of equation (4) into equation (1), equation (3) becomes:

$$I_t = \frac{1}{2} I_0 \{ \sin^2\theta - \rho \sin 2\theta \sin 2\phi \sin(\delta+\rho) \operatorname{sinc}(\delta+\rho) + \rho^2 \sin^2 2\phi \operatorname{sinc}^2(\delta+\rho) \cos^2\theta \} \quad (5)$$

Equation (5) describes the background noise of the real system at $\alpha=0$. Fourier analysis of this equation shows that the amplitudes of the modulated terms depend on all 3 variables ρ , ϕ and δ_0 . Thus it is evident that, no matter how well the PEM axis is aligned to coincide with the polarizers P_x or P_y , some variation in the amplitude of each harmonic will occur, owing to fluctuations in δ_0 , unless the axes of the static and alternating retardances happen to

coincide exactly. That is, a comparison of equations (2) and (5) shows that the existence of residual static birefringence in the modulator head provides a mechanism whereby amplitude instability of the modulator appears as noise, despite the alignment of the a.c. stress axis with the polarizers; an alignment which would otherwise lead to the total cancellation of such amplitude noise in an ideal instrument.

EXPERIMENTAL

In construction of the practical apparatus a 5-mW He-Ne laser (Saven AB) was used as the source. The sample cell was a quartz flow-through cell of 5-mm optical path-length (Starna Ltd., type 44). The polarizers were either Glan-Taylor prisms (8 mm aperture, schlieren-free calcite; Karl Lambrecht), or plastic dichroic sheets (Edmund Scientific, N.J.). Their respective extinction ratios at 632.8 nm were 3×10^{-6} and 4×10^{-5} . Light from the analyser was transmitted directly onto a 1P 28 photomultiplier through a fibre-optic link. A second optical channel could be added by insertion of a beam-splitter in front of the sample cell, to allow a reference intensity to be measured if required (Fig. 2). Signals were measured on a PAR model 128A lock-in amplifier with the reference set to the 2ω (100 kHz) harmonic. A time-constant of 1 sec was used for all measurements.

Linearized optical rotation apparatus is tolerant towards stray light, and shows good vibrational immunity provided that the vibrational displacements are small compared to the offset angles used. These characteristics were found to be retained even at the sensitivity levels achieved here. Neither the presence of stray light nor sensitivity to vibration presented any particular problem; all components were simply mounted on a 1-m steel optical rail placed directly on a standard laboratory bench under normal fluorescent lighting.

Since the apparatus was intended to work at relatively large values of θ (up to $\sim 20^\circ$), it was necessary that the photomultiplier should transmit frequencies up to 100 kHz at unusually high background-light levels. At the same time the voltage across the dynode chain, and in particular at the first dynode, should be high in order to minimize noise from the tube itself. The method used to meet these requirements was to connect the first 5 dynodes only as amplifying stages. The remaining dynodes and the final anode were strapped to a regenerative parallel LC resonant circuit. Details are given in Fig. 3. The circuit output was initially tested by continuous exposure at about 1 mW for 10 hr, and found

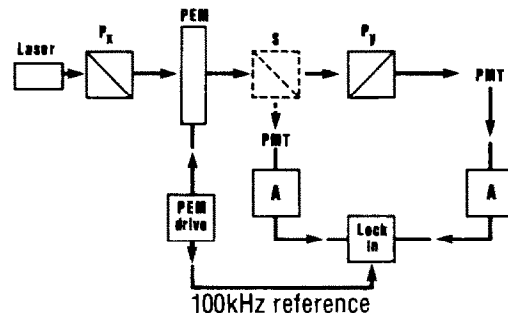


Fig. 2. Apparatus. A, 100-kHz tuned pre-amplifier. PMT, photomultiplier. PEM, photoelastic modulator. P_x , P_y , polarizer and analyser. S, optional beam-splitter, removed from the optical path unless a reference signal is required for double-beam operation. The sample cell is located between S and P_y .

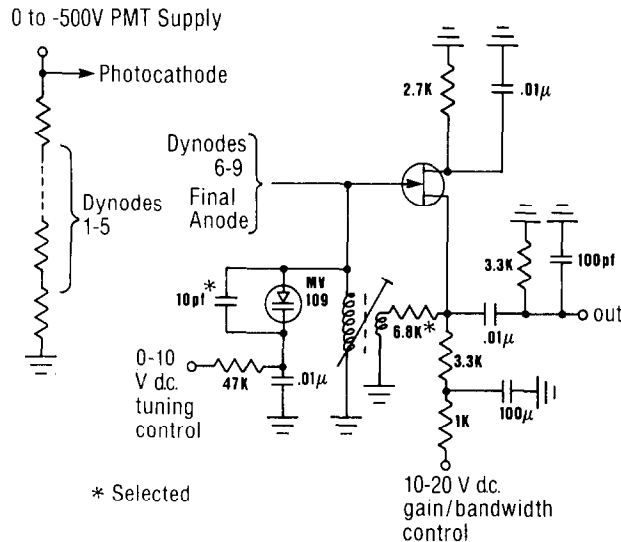


Fig. 3. Circuit diagram of the phototube preamplifier.

to be stable. Linearity was checked by varying the light intensity by means of a known filter system. Measurement of the d.c. cathode current as a function of increasing dynode voltage gave a stable plateau at $2.0 \mu\text{A}$, corresponding to a photoelectron emission rate of $3.2 \times 10^{13}/\text{sec}$, and allowing the source power to be estimated as $\sim 4 \text{ mW}$.⁹ It was concluded from these preliminary measurements that the stability of the detector system was adequate for the intended use, and in particular that photocathode fatigue was unlikely to be of major concern.

Alignment of the apparatus was achieved by crossing the polarizers and adjusting the x,y position and rotational angle of the PEM until the 100-kHz (2ω) signal was minimized. The polarizer angle (θ) was then set to the required value and the sample cell inserted. The sample cell was rotated to remove the 100-kHz signal caused by reflection from the windows. Similar care was needed to align the beam-splitter when the reference optical channel was used. Test solutions of L(+)-tartaric acid (Merck) were introduced into the cell by means of a peristaltic pump. Concentrations of 1.67–16.7 g/l. were used, corresponding to optical rotation angles of 0.001 – 0.01° in the apparatus used.

The amplitude of the PEM was adjusted empirically to give a maximum signal [i.e., $J_2(2\delta_0)$ at a maximum; sensitivity to fluctuations in δ_0 at a minimum].

Switching on the PEM was found to cause an increase in the 100-kHz noise, even when P_x and P_y were fully crossed and when the stress axis of the PEM was aligned with P_x or P_y (i.e., $\alpha = \theta = 0$). This observation arises from the finite value of I_1 in equation (5) when $\theta = 0$. In addition a finite signal could be observed at $\sin 2\omega t$, i.e., a signal showing a 90° phase shift relative to the expected 2ω harmonic. Such signals caused no particular difficulties but did require the phase of the lock-in to be adjusted accurately to ensure their rejection.

RESULTS AND DISCUSSION

The dependences of the output noise and of the signal to noise ratio on the offset angle θ are shown in Figs. 4 and 5. The noise data in Fig. 4 show that source flicker is not significant, since the noise curves with the PEM removed are a linear function of θ . They also show that modulation noise is effectively compensated by a dual-channel measurement. The

increase of the noise level with θ when the PEM is in position is approximately quadratic. This observation means that the second harmonic ($\cos 2\omega t$) terms generated by the last two terms in equation (5) must be of comparable magnitude. This sort of relation clearly depends for its existence on the particular values of ϕ and ρ which a given instrument happens to show; the combination of a low noise level at $\theta = 0$ and the quadratic growth with increasing θ , which are shown in Fig. 4 and which characterize the present device, may not necessarily be reproduced by other types of modulator.

The quadratic increase in noise with θ markedly influences the signal to noise curve in Fig. 5, shifting the optimum from the value of $\sim 3^\circ$ which would be expected for the shot-noise limited case to about 1° ,

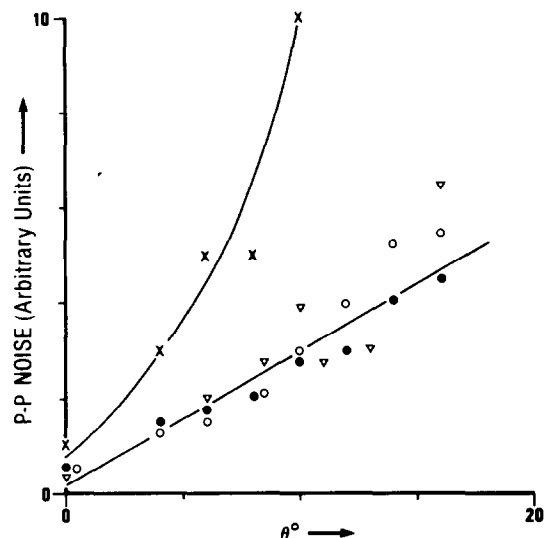


Fig. 4. Output noise levels. Symbols ●, ○ represent respectively single- and dual-channel operation with the PEM switched off. Symbols ×, ▽ are respectively single- and dual-channel results with the PEM in operation.

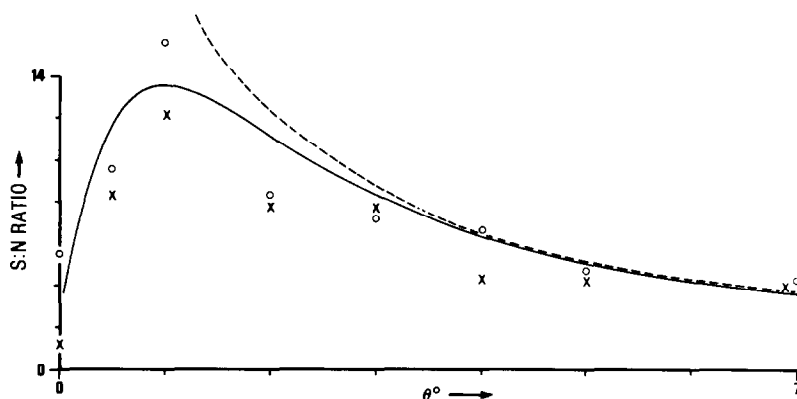


Fig. 5. Output signal to noise ratios. Symbols \times , \circ are results for the prism and polaroid sheet polarizers, respectively. The dashed curve is proportional to $1/\theta$.

and causing the signal to noise curve to decrease in inverse proportion to θ beyond the maximum, instead of giving the rather flat plateau which is characteristic of the shot-noise limited situation.

Experimental signals are shown in Fig. 6 for 1.67 g/l. L(+)-tartaric acid, with an offset angle of $\theta = 1^\circ$. A comparison trace is given, for a linearized system (1° offset again) with the PEM removed and amplitude modulation of the laser intensity. The comparison illustrates the practical utility of the PEM configuration used; its selectivity clearly extends to the provision of efficient discrimination against pumping fluctuations and the passage of bubbles through the sample cell.

It is evident from the results in Figs. 5 and 6 that the signal to noise ratios given by the prism and by the polaroid sheet polarizers are comparable. Detection limits for a signal to noise ratio of 3:1 were estimated as about 3×10^{-4} degree in both cases.

CONCLUSIONS

The origin and magnitude of the flicker noise that is actually observed in an optical polarimeter is governed by the particular instrument design used. The present approach suppresses flicker noise by a selective modulation technique, which adopts a

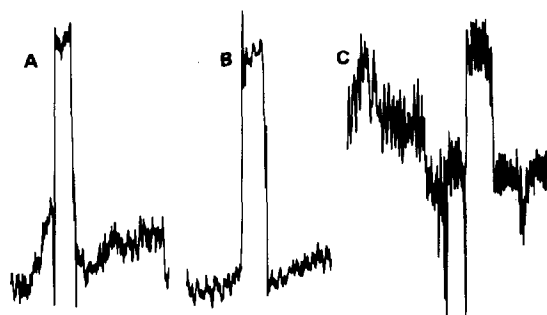


Fig. 6. Recorder traces for (A) $\alpha = 0.001^\circ$ rotation, prism polarizers; (B) $\alpha = 0.003^\circ$, polaroid sheets; (C) a linearized system with the PEM removed; $\alpha = 0.01^\circ$. The offset angle, θ , was 1° in each case.

modulation frequency high enough to avoid source flicker, and an optical design which minimizes the occurrence of direct modulation of background optical transmission. These characteristics permit optical linearization techniques to be employed to advantage. Such techniques are desirable because they allow satisfactory results to be obtained with polarizers of quite ordinary quality, for reasons which have already been discussed.⁵ They also improve the tolerance of the apparatus to vibration and the pick-up of stray light. Therefore a design such as the one described here is felt to be of use, since its application leads to sensitive measurement of optical rotation with apparatus that is robust in operation and of modest cost.

Various procedures were examined as possible methods to eliminate the modulation noise of a single-channel measurement. These included modification of the optical train and the use of electronic correlation procedures (*e.g.*, between the ω and 2ω amplitudes). None succeeded. This is perhaps unsurprising; equation (5) shows that the amplitude coefficients of the various harmonics do not necessarily bear any simple relation to each other, even if ρ and ϕ are truly constant. If ρ and ϕ can also vary in addition to δ_0 , then the noise output of the device becomes still more complicated. Therefore it is concluded that the use of some form of dual-channel measurement probably offers the only way to correct for residual modulator noise in the present type of apparatus.

It should be noted that the modulated signal/translated flicker-noise ratio is constant, and greater than the modulated signal/baseband shot-noise ratio. In the region of the detection limit, the measurement is automatically shot-noise limited if the integration time is short enough. This can be arranged by starting with an arbitrarily short integration time, increasing it until flicker noise appears, and then reducing it again until flicker noise is precluded.

Acknowledgements—The author is indebted to the Finnish Academy of Sciences and to the Natural Sciences and

Engineering Research Council of Canada for support of this work.

REFERENCES

1. E. S. Yeung, L. E. Steenhoek, S. D. Woodruff and J. U. Kuo, *Anal. Chem.*, 1980, **52**, 1399.
2. J. C. Kuo and E. S. Yeung, *J. Chromatog.*, 1981, **223**, 321.
3. *Idem, ibid.*, 1982, **253**, 199.
4. D. R. Bobbitt and E. S. Yeung, *Anal. Chem.*, 1984, **56**, 1577.
5. J. J. Kankare and R. Stephens, *Talanta*, 1984, **31**, 689.
6. H. V. Malmstadt, C. G. Enke and S. R. Crouch, *Electronics and Instrumentation for Scientists*, Benjamin/Cummings, California, 1981.
7. R. Stephens, *Spectrochim. Acta*, 1982, **38B**, 1077.
8. J. J. Kankare and R. Stephens, *ibid.*, 1980, **35B**, 849.
9. *RCA Photomultiplier Handbook*, RCA Solid State Division, Lancaster, PA, 1980.
10. R. M. A. Azzam and N. M. Bashara, *Ellipsometry and Polarized Light*, p. 119. North-Holland, Amsterdam, 1977.

APPENDIX

The PEM is considered to show the usual modulated retardance, $\delta = \delta_0 \sin \omega t$. In addition it will be assumed that there is a static retardance, ρ . Let the optical path in the PEM be divided into infinitesimal slices, denoted alternately by d and p (Fig. 7), with associated Jones matrices \mathbf{D} , \mathbf{P} . If the light is propagated in the positive z -direction, the Jones matrix of a pair of slices, d and p, is \mathbf{PD} . The wave, described by a Jones vector \hat{r} , is modified as a result of its propagation through the incremental path length between x and $x + \Delta x$. Thus

$$\hat{r}(x + \Delta x) - \hat{r}(x) = \mathbf{PD}\hat{r}(x) - \hat{r}(x) = (\mathbf{PD} - \mathbf{I})\hat{r}(x) \quad (1')$$

Dividing both sides of equation (1') by Δx and taking the limit as Δx approaches zero gives the differential equation of propagation for the Jones vector \hat{r} as

$$\frac{d\hat{r}}{dx} = \mathbf{N}(x)\hat{r}(x) \quad (2')$$

where

$$\mathbf{N}(x) = \lim_{\Delta x \rightarrow 0} \frac{\mathbf{PD} - \mathbf{I}}{\Delta x} \quad (3')$$

Now consider the PEM in the form of a thick (non-infinitesimal) slab for which the overall Jones matrix is \mathbf{T} . Then the Jones vector $\hat{r}(x)$ of a light-wave that has travelled a total distance x , starting from an initial Jones vector $\hat{r}(0)$ at $x = 0$, is given by

$$\hat{r}(x) = \mathbf{T}(x)\hat{r}(0) \quad (4')$$

where $\mathbf{T}(x)$ is the Jones matrix characterizing the section between the planes at 0 and x . Differentiating (4') with respect to x , we get

$$\frac{d\hat{r}}{dx} = \frac{d\mathbf{T}}{dx} \hat{r}(0) \quad (5')$$

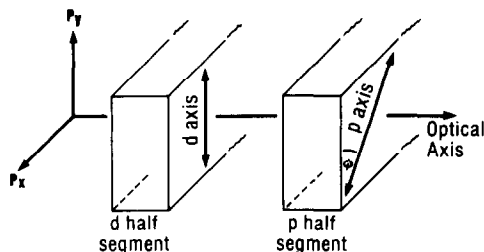


Fig. 7. One segment of a variable retarder comprising alternate modulated and static layers (d and p respectively).

From equations (2'), (4') and (5') we finally get

$$\frac{d\mathbf{T}}{dx} = \mathbf{N}\mathbf{T} \quad (6')$$

In the general case \mathbf{N} is a function of x , and equation (6') can be solved by using, for example, the Volterra product integral or the theory of matricants. In the present case we assume that

$$\mathbf{D} = \begin{pmatrix} e^{i\Delta\delta} & 0 \\ 0 & e^{-i\Delta\delta} \end{pmatrix} \quad (7')$$

where $\Delta\delta$ is the dynamic retardance, at a certain time, of the infinitesimal slab d . Allowing $\Delta x \rightarrow 0$ also means that $\Delta\delta$ tends to zero and we can write

$$\mathbf{D} = \mathbf{I} + i\Delta\delta \begin{pmatrix} 1 & 0 \\ 0 & -1 \end{pmatrix} \quad (8')$$

It is now assumed, for generality, that the optical axis of the static retardance makes an angle ϕ with the axis of dynamic retardance. Hence

$$\begin{aligned} \mathbf{P} &= \begin{pmatrix} \cos \phi & -\sin \phi \\ \sin \phi & \cos \phi \end{pmatrix} \begin{pmatrix} e^{i\Delta\delta} & 0 \\ 0 & e^{-i\Delta\delta} \end{pmatrix} \begin{pmatrix} \cos \phi & \sin \phi \\ -\sin \phi & \cos \phi \end{pmatrix} \\ &= \begin{pmatrix} \cos^2 \phi e^{i\Delta\delta} + \sin^2 \phi e^{-i\Delta\delta} & i \sin 2\phi \sin \Delta\delta \\ i \sin 2\phi \sin \Delta\delta & \sin^2 \phi e^{i\Delta\delta} - \cos^2 \phi e^{-i\Delta\delta} \end{pmatrix} \\ &\rightarrow \mathbf{I} + i\Delta\rho \begin{pmatrix} \cos 2\phi & \sin 2\phi \\ \sin 2\phi & -\cos 2\phi \end{pmatrix} \end{aligned} \quad (9')$$

$\Delta x \rightarrow 0$

Thus

$$\mathbf{PD} = \mathbf{I} + i\Delta\delta \begin{pmatrix} 1 & 0 \\ 0 & -1 \end{pmatrix} + i\Delta\rho \begin{pmatrix} \cos 2\phi & \sin 2\phi \\ \sin 2\phi & -\cos 2\phi \end{pmatrix} \quad (10')$$

(with the cross terms $\Delta\rho\Delta\delta$ neglected) and from (3')

$$\mathbf{N} = i \frac{d\delta}{dx} \begin{pmatrix} 1 & 0 \\ 0 & -1 \end{pmatrix} + i \frac{d\rho}{dx} \begin{pmatrix} \cos 2\phi & \sin 2\phi \\ \sin 2\phi & -\cos 2\phi \end{pmatrix} \quad (11')$$

We assume now that both $d\delta/dx$ and $d\rho/dx$ are independent of position within the PEM element. In that case the solution of (6') satisfying the boundary condition $\mathbf{T}(0) = \mathbf{I}$ is

$$\mathbf{T}(x) = e^{\mathbf{N}x} \quad (12')$$

and especially, if the thickness of the PEM slab is b ,

$$\mathbf{T} = e^{b\mathbf{N}} \quad (13')$$

Now $d\delta/dx$ and $d\rho/dx$ are constant, which gives

$$\frac{d\delta}{dx} b = \delta; \quad \frac{d\rho}{dx} b = \rho \quad (14')$$

and consequently

$$b\mathbf{N} = i\delta \begin{pmatrix} 1 & 0 \\ 0 & -1 \end{pmatrix} + i\rho \begin{pmatrix} \cos 2\phi & \sin 2\phi \\ \sin 2\phi & -\cos 2\phi \end{pmatrix} \quad (15')$$

Calculation of the exponential (13') is considerably simplified by the fact that

$$(b\mathbf{N})^2 = -\gamma^2 \mathbf{I}; \quad \gamma = \sqrt{(\delta^2 + \rho^2 + 2\delta\rho \cos 2\phi)} \quad (16')$$

This gives

$$(b\mathbf{N})^{2k} = (-1)^k \gamma^{2k} \mathbf{I}; \quad (b\mathbf{N})^{2k+1} = (-1)^k \gamma^{2k} b\mathbf{N} \quad (17')$$

Hence

$$\begin{aligned} e^{b\mathbf{N}} &= \mathbf{I} + b\mathbf{N} + \frac{1}{2} (b\mathbf{N})^2 + \frac{1}{3!} (b\mathbf{N})^3 + \frac{1}{4!} (b\mathbf{N})^4 + \dots \\ &= \mathbf{I} + b\mathbf{N} - \frac{1}{2} \gamma^2 \mathbf{I} - \frac{1}{3!} \gamma^2 b\mathbf{N} + \frac{1}{4!} \gamma^4 \mathbf{I} + \dots \\ &= \cos \gamma \mathbf{I} + \frac{1}{\gamma} \sin \gamma b\mathbf{N} \end{aligned} \quad (18')$$

or

$$\mathbf{T} = \begin{pmatrix} \cos \gamma + i \frac{\delta + \rho \cos 2\phi}{\gamma} \sin \gamma & i \frac{\sin \gamma}{\gamma} \rho \sin 2\phi \\ i \frac{\sin \gamma}{\gamma} \rho \sin 2\phi & \cos - i \frac{\delta + \rho \cos 2\phi}{\gamma} \sin \gamma \end{pmatrix}$$

Assuming that ϕ is small, we have $\cos 2\phi \simeq 1$, which gives $\gamma \simeq \delta + \rho$, and hence

$$\mathbf{T} \simeq \begin{pmatrix} e^{i(\delta + \rho)} & i\rho \sin 2\phi \operatorname{sinc}(\delta + \rho) \\ i\rho \sin 2\phi \operatorname{sinc}(\delta + \rho) & e^{-i(\delta + \rho)} \end{pmatrix} = M \quad (20')$$

(19') where $\operatorname{sinc}(\delta + \rho) = \sin(\delta + \rho)/(\delta + \rho)$.

ARSENIC DETERMINATION WITH GRAPHITE-CLOTH RIBBON IN GRAPHITE-FURNACE ATOMIC-ABSORPTION SPECTROMETRY

ETSURO IWAMOTO*, CHAN-HUAN CHUNG, MANABU YAMAMOTO and YUROKU YAMAMOTO
Department of Chemistry, Faculty of Science, Hiroshima University, Hiroshima 730, Japan

(Received 3 May 1985. Revised 3 December 1985. Accepted 28 February 1986)

Summary—The determination of arsenic by atomic-absorption spectrometry with use of a graphite-cloth ribbon placed inside various types of graphite tubes was investigated. It was found that the graphite-cloth ribbon greatly enhances the sensitivity for arsenic and reduces the interferences from various heavy metals, especially when it is placed inside a pyrolytic graphite tube and a nitric acid matrix is used. This is attributed to condensation of arsenic on the ribbon, owing to a temperature lag during the drying and ashing cycles, and to the formation of interlamellar compounds of arsenic with graphite.

Determination of arsenic is very important in biochemistry, environmental chemistry, and the semiconductor industry, and the use of graphite-furnace atomic-absorption spectrometry (GFAAS) for the purpose has been studied by many investigators,¹⁻¹⁰ but is accompanied by difficulty and unreliability which are due to volatilization losses of arsenic during the ashing cycle and to interactions of arsenic with carbon and certain metal salts.^{8,11} Matrix modification techniques¹² using transition metal salts have been empirically demonstrated to be effective for reducing the volatility.³ Some graphite-surface treatments^{6,13} have been developed to reduce the extent of chemical interferences.

Quite recently, we found that the sensitivity for selenium (which is also volatile) is greatly enhanced by using a graphite-cloth ribbon which is placed inside a graphite tube and on which the sample is deposited.¹⁴ Furthermore, it was found that non-pyrolytic graphite (NPG) tubes with a porous surface are more effective than pyrolytic graphite (PG) tubes in enhancing the sensitivity for semi-metallic elements such as As and Se.¹⁵ These results suggest that the volatile arsenic species need to interact with carbon if higher sensitivity is to be attained.

In this study, the determination of arsenic was investigated by using the graphite cloth ribbon and various sample media, and comparing its performance with that of the PG, NPG, and L'vov platform tubes. The effect of various foreign ions was also examined.

EXPERIMENTAL

Apparatus

The experiments were done with a Perkin-Elmer 5000 atomic-absorption spectrophotometer, an HGA-500 graphite furnace and an AS-40 sample-introduction system.

Deuterium-continuum background-correction was used. A Perkin-Elmer Data System 10 and a Watanabe WX4675 plotter were used to record the absorbance signal profiles. A Hamamatsu Photonics hollow-cathode lamp was used as light-source. The analytical wavelength and spectral bandwidth were 193.7 and 0.7 nm, respectively. The graphite furnaces used were of four types: (i) non-pyrolytic graphite tube (PE-NPG, Perkin-Elmer, part no. 070699), (ii) pyrolytic-graphite coated tube (PE-PG, Perkin-Elmer, part no. 4559-4), (iii) pyrolytic-graphite coated tube (G-PG, German Perkin-Elmer, part no. 091054), and (iv) pyrolytic-graphite platform tube (platform-PG, Perkin-Elmer). Graphite cloth made from poly(acrylonitrile) was cut to give pieces 1.5 mm wide, 25 mm long, and 0.3 mm thick, weighing about 5 mg. The position of the graphite cloth ribbon in the graphite tube is given in Fig. 1. The furnace programme is given in Table 1. Maximum-power heating was used for the atomization step. A CHINO recording pyrometer was used to calibrate the temperature settings.

Reagents

All solutions were prepared from analytical-reagent grade chemicals and distilled water, and stored in polyethylene bottles. Standard arsenic solution (1000 $\mu\text{g/ml}$) was prepared by dissolving 1.320 g of arsenious oxide in 10 ml of 10M sodium hydroxide, and diluting accurately to 1000 ml with water.

Extraction of arsenic(III) with ammonium pyrrolidinedithiocarbamate (APDC)

Take an aliquot of aqueous solution, containing 500 ng of arsenic(III), in a separatory funnel. Add 2 ml of acetate buffer solution (pH 5.0, 1M acid + 1M sodium salt = 1 + 1.8) and 1.0 ml of 4% APDC solution. Shake the solution with 10 ml of mixed solvent (carbon tetrachloride-chloroform, 1:1 v/v) for 5 min (extraction of the arsenic is almost complete under these conditions¹⁶). Separate the organic phase and use a 30- μl aliquot for determination of the arsenic.



Fig. 1. Position of the graphite cloth ribbon in the graphite tube: (a) graphite tube; (b) graphite cloth ribbon.

*Author for correspondence.

Table 1. Instrumental parameters for the arsenic determination

	Drying	Ashing	Atomization	Conditioning
Temperature, °C	200	Variable	2450	2700
Ramp time, sec	40	30	0	1
Hold time, sec	10	5	5	2
Flow gas, ml/min	300	300	20	300

RESULTS AND DISCUSSION

Effects of the graphite tube texture

Absorbances were measured for 1.5 ng of arsenic atomized from various types of tubes and sample solutions. The results are given in Table 2. Graphite cloth ribbon of the size given in the experimental section was used throughout the work because increasing the size decreases the sensitivity. The standard deviation (range method) of the absorbance (for 3–5 repetitions) was less than 0.013. As in the case of selenium,¹⁴ higher sensitivity was generally obtained with NPG tubes than with platform-PG tubes, and the graphite cloth ribbon enhanced the sensitivity even further. The nitric acid matrix gives the highest sensitivity for each type of tube. This trend is different from that for selenium, for which hydrochloric acid gives the highest sensitivity, except for the PG tube.

When an element is atomized from the wall of a graphite tube, the graphite surface plays various roles: energy supply for atomization, reduction of metal oxides to metals, and retention of analyte by formation of interlamellar compounds and carbides. It has been pointed out that the porous nature of non-pyrolytic graphite is responsible for penetration (or diffusion) of sample into the tube and for compound formation with carbon, leading to lower sensitivity and interferences by certain metal salts.^{17,18}

It was to overcome this disadvantage that coating the tube surface with a thin layer of pyrolytic graphite was developed;^{19,20} it gave a significant improvement in sensitivity over non-pyrolytic graphite, especially for highly non-volatile elements such as copper, molybdenum, and vanadium.²⁰ Quite recently we found that the effect of the surface texture (PG or NPG) of the tube on sensitivity is related to the nature of the analyte: the more metallic the analyte element, the more its AAS sensitivity is favoured by

use of a PG surface.¹⁵ Analogously, the sensitivities for the semi-metallic elements of groups III, IV, V, and VI in the periodic table are much higher with NPG tubes than PG tubes. The results in Table 2 are consistent with the results obtained previously.¹⁵

The formation of molecules such as As₄ and As₂ has been proposed as one of the reasons for the difficulty in determining arsenic,²¹ but it is likely that the most critical factor is loss by volatilization during the drying and ashing cycles.¹¹ Of the three acids tested as sample media, hydrochloric acid gives the lowest sensitivity, because arsenic trichloride is easily vaporized. Figure 2 shows the effect of ashing tem-

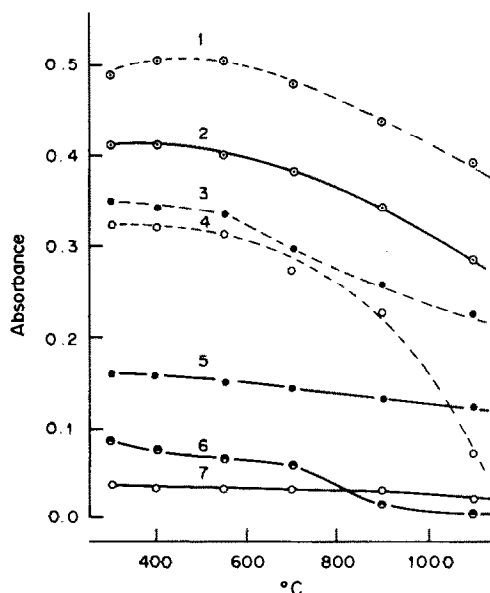


Fig. 2. Effect of ashing temperature on the absorbance for arsenic in hydrochloric acid (—) and nitric acid (----) media. 1 and 2, a G-PG tube with the ribbon; 3, a PE-NPG tube; 4, a G-PG tube; 5, a PE-NPG tube; 6, a platform PG tube; 7, a G-PG tube.

Table 2. Absorbances obtained by using various types of graphite tubes*

Sample medium	With ribbon						
	PE-NPG†	PE-PG§	G-PG§	Platform PG‡	PE-NPG	PE-PG	G-PG
HCl	0.167	0.010	0.040	0.102	0.348	0.348	0.411
HNO ₃	0.352	0.164	0.343	0.243	0.366	0.413	0.519
H ₂ SO ₄	0.270	0.011	0.183	0.128	0.316	0.376	0.464
CHCl ₃ -CCl ₄ (APDC-As)	0.201	—	0.172	0.083	0.360	—	0.456

* The amount of arsenic was 1.5 ng and the concentration of acid 0.05M.

† Non-pyrolytic graphite tube.

§ Pyrolytic-graphite coated tube.

‡ Pyrolytic-graphite platform tube.

perature on the absorbance. For the same medium, the NPG surface gives higher absorbances than the PG surface does, over the temperature range examined, so the increasing sensitivity with non-pyrolytic tubes can be attributed to less volatilization of arsenic during the ashing cycle. Koreckeva *et al.*¹¹ measured the radioactivity of ⁷⁴As left on the surface of an NPG tube after thermal treatment at different temperatures (200–1000°) and showed that the β -radioactivity was lower than the γ -radioactivity, indicating penetration of the arsenic into the graphite or formation of compounds between graphite and arsenic, whereas there was no difference in the relative activity when a glassy-carbon tube was used. They also suggested that when aqueous samples are analysed the surface of an NPG tube should provide conditions or active sites for formation of lamellar compounds containing arsenic, for which the presence of oxygen and hydrogen is needed.²² Nitric acid is known to create more available active sites,¹¹ and as shown in Fig. 2, gives higher absorbances than hydrochloric acid medium does, for both kinds of tube. This supports the hypothesis of chemical interaction between arsenic and graphite in the NPG tube, and it is therefore likely that in nitric acid medium the porous graphite keeps arsenic on its surface “chemically” long enough for much greater conversion into elemental As to occur, than is the case for “physical” retention (*i.e.*, without formation of compounds).

The fact that the porous nature of the furnace texture favours lower loss of arsenic is compatible with the increase in sensitivity obtained by using the graphite cloth ribbon (which has a larger specific surface area). The ribbon is heated primarily by radiation from the tube wall, so the temperature of the ribbon is lower than that of the tube until constant maximum temperature is reached. When the sample solution is deposited on the ribbon, only part remains on the piece of graphite cloth (which is small in size) by capillary action, and the rest comes into contact with the tube wall. The arsenic on the tube wall will be evaporated earlier than that on the ribbon surface during the atomization process, and could be partly condensed on the ribbon, where interlamellar compounds of arsenic with the graphite could be formed, leading to a lower volatilization loss. Such condensation of arsenic on the ribbon surface is also indicated by the fact that the effect of the ribbon on sensitivity is more marked for the PG tube than for the NPG tube, since the volatilization of arsenic will be easier from the PG tube, where there is little or no soaking of the solution into the graphite layers. Thus with the ribbon, the atomization effectively takes place at the maximum ribbon temperature with minimum condensation on the surrounding wall, and the absorption signal is delayed by the ribbon temperature lag. This behaviour is clearly shown in Fig. 3, where the temperature profile is that for the tube wall without the graphite cloth ribbon present. The peak maximum is delayed by 0.2 sec by which time

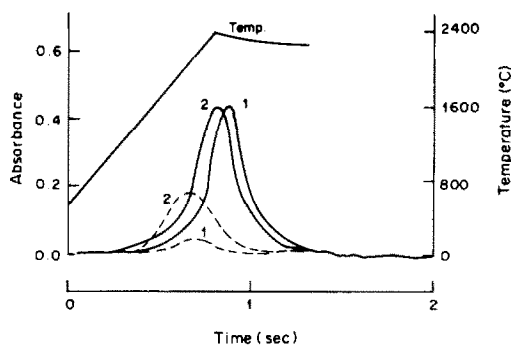


Fig. 3. Atomization-time and temperature-time profiles for arsenic (1.5 ng) with (—) and without (----) the ribbon in the G-PG tube at an ashing temperature of 550°. 1, Hydrochloric acid medium; 2, APDC-As in CHCl_3 - CCl_4 medium.

the maximum temperature has almost been attained. If a larger piece of graphite cloth ribbon is used, the absorbance for a given amount of arsenic is lowered, presumably because it takes longer for the ribbon to reach a high enough temperature for effective atomization.

For the more volatile elements, matrix interferences often arise from gas-phase reactions, because of the limited ashing temperature. Recent studies on lead determination by Woodriff *et al.*^{23,24} indicated that this gas-phase interference can be substantially reduced by sufficiently increasing the temperature and residence time. Such an effect may also be expected from using the graphite cloth ribbon, which causes delayed sample vaporization in the same way as the L'vov platform; this is confirmed by Fig. 2.

In the case of copper, for which PG gives higher sensitivity than NPG does, the sensitivity remains almost unchanged when the graphite cloth ribbon is used (Fig. 4). Since the absorbance signal is delayed, it is likely that a lowering effect of the porous nature of the ribbon on the copper absorbance is compensated by the opposite effect of the temperature lag.

Effect of foreign ions

The effects of copper, nickel, molybdenum and iron on the arsenic absorbance were investigated for

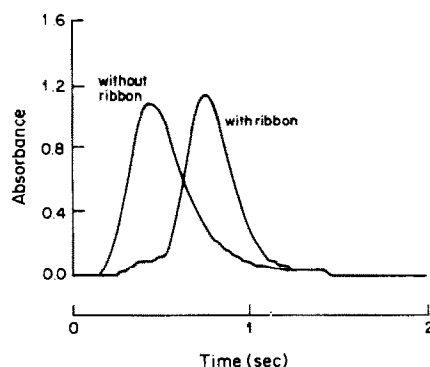


Fig. 4. Atomization-time profiles for copper (0.7 ng) with a G-PG tube and 0.05M nitric acid medium.

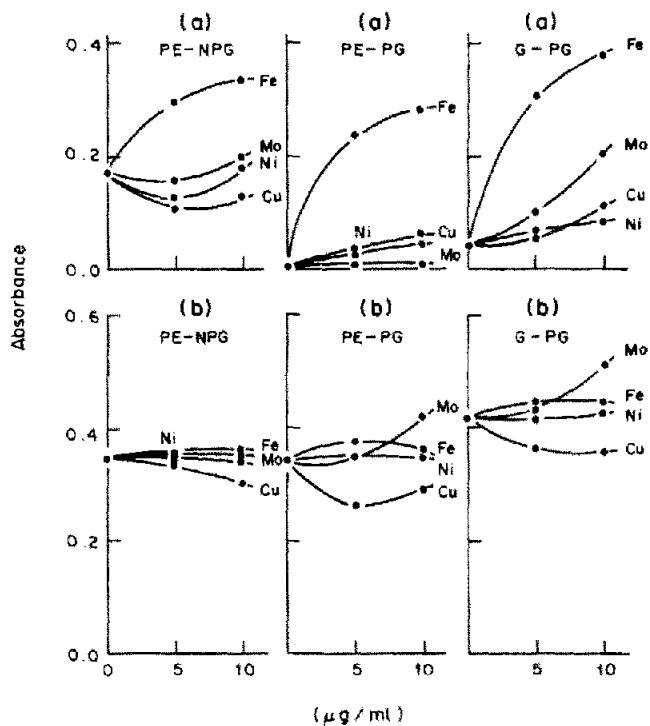


Fig. 5. Effect of foreign ions on sensitivity for arsenic (50 ng/ml) in 0.05M hydrochloric acid medium without (a) and with (b) a graphite cloth ribbon.

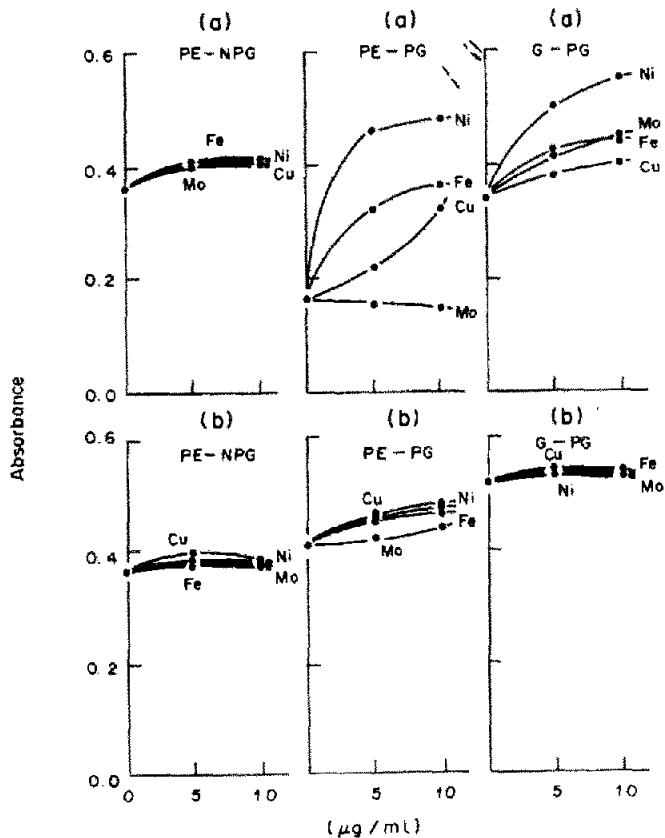


Fig. 6. Effect of foreign ions on sensitivity for arsenic (50 ng/ml) in 0.05M nitric acid medium without (a) and with (b) a graphite cloth ribbon.

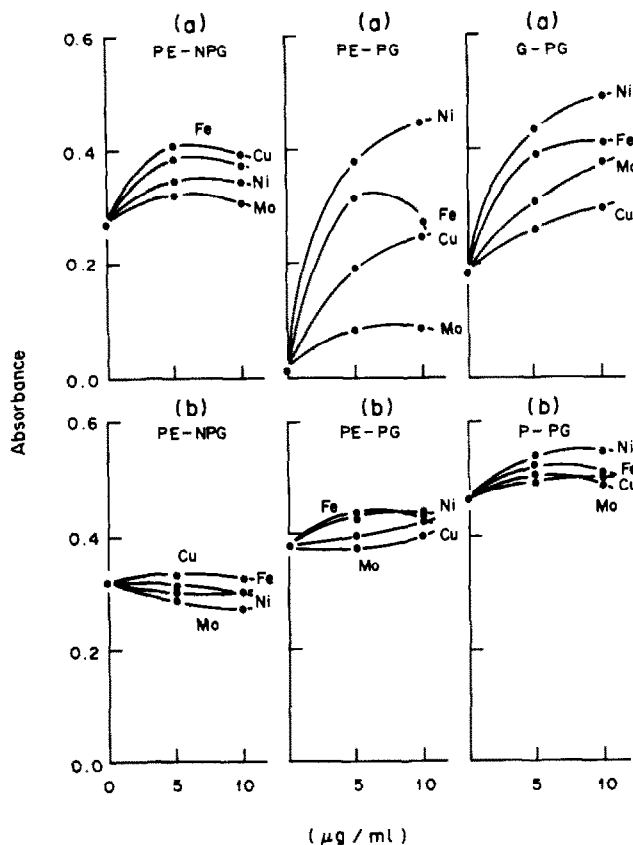


Fig. 7. Effect of foreign ions on sensitivity for arsenic (50 ng/ml) in 0.05M sulphuric acid medium without (a) and with (b) a graphite cloth ribbon.

all the systems. These ions are often used as matrix modifiers to decrease the volatility of arsenic during the ashing cycle. These metals were added in 100- and 200-fold weight ratio to arsenic. The results obtained are shown in Figs. 5-9. As pointed out earlier,^{25,26} even small alterations in the pyrolytic graphite quality cause changes in foreign ion effects. The following trends are observed: (a) without the ribbon, these

metals all give enhancement effects except with the NPG tube and the platform-organic extract combination; (b) the use of the ribbon gives higher sensitivity and almost eliminates the foreign ion effects; (c) no enhancement effects are observed for the APDC-As extract.

Observation (a) is the matrix-modifier effect, which becomes more marked when the sensitivity in the

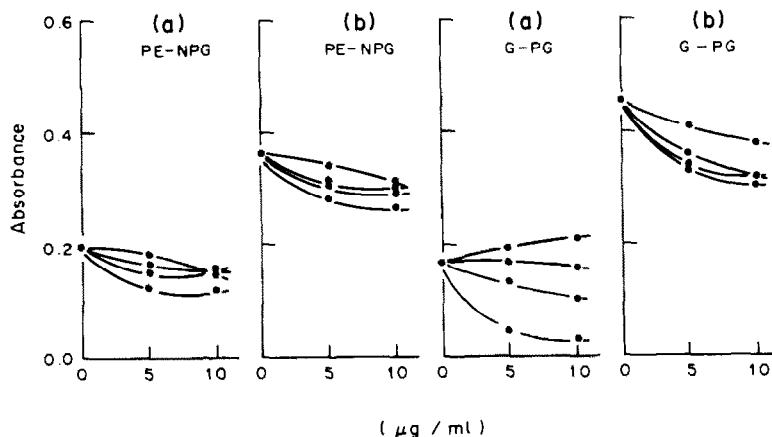


Fig. 8. Effect of foreign ions on sensitivity for APDC-arsenic (50 ng/ml) in CHCl₃-CCl₄ medium without (a) and with (b) a graphite cloth ribbon.

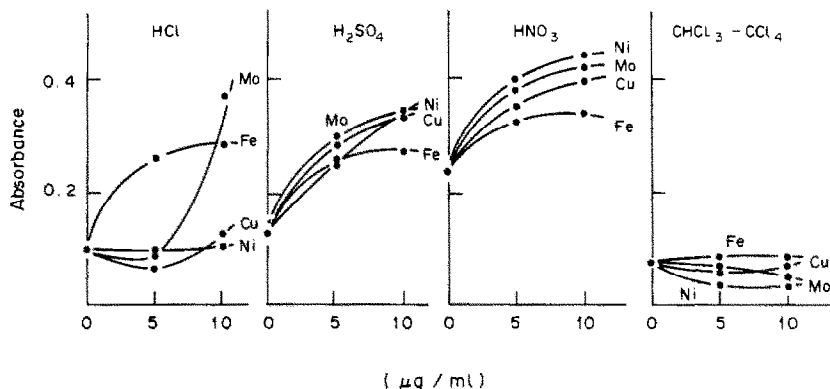


Fig. 9. Effect of foreign ions on sensitivity for arsenic (50 ng/ml) with the platform tube in various media.

absence of foreign ions is low, as seen typically for the PE-PG-sulphuric acid system. The largest enhancement effect is obtained with nickel in sulphuric and nitric acid media, and with iron in hydrochloric acid medium. Korečková *et al.*¹¹ suggested that there are two mechanisms for stabilizing arsenic: one is the formation of intermetallic compounds with arsenic and the other is stabilization of the oxidizing centres on graphite for forming interlamellar compounds. In view of the fact that the modifier effect is not seen for the NPG-nitric acid system, the chemical interaction of arsenic with porous graphite, *i.e.*, interlamellar compound formation, seems more important than intermetallic compound formation for arsenic stabilization. This is further supported by observation (b) which is most marked for nitric acid medium. The graphite cloth ribbon has a contact area large enough to accommodate arsenic as interlamellar compounds even in the presence of foreign ions.

Observation (c) holds even for the PG tube. This is explained by less interaction of arsenic with these metals because of formation of their stable sulphides during the ashing cycle since the metal-sulphur bond already exists in the APDC-complexes of these metals.

It is concluded that loss of arsenic by volatilization in the ashing stage is reduced by condensation and re-evaporation due to a temperature lag effect and by interlamellar compound formation with graphite, and so the interferences from foreign ions are substantially reduced. The best conditions for this are provided by using the graphite cloth ribbon-nitric acid system.

Acknowledgements—The authors thank Dr. M. Ikeda of Nippon Jarrel Ash, Ltd. for providing the graphite cloths and making available the pyrometer used. This research was supported in part by a Grant-in-Aid for Scientific Research (Nos. 57470031, 58540363 and 58030061) from the Ministry of Education, Science and Culture.

REFERENCES

1. Y. Yamamoto and T. Kamada, *Bunseki Kagaku*, 1976, **25**, 567.
2. T. Kamada, *Talanta*, 1976, **23**, 835.
3. P. R. Walsh, J. L. Fasching and R. A. Duce, *Anal. Chem.*, 1976, **48**, 1014.
4. K. C. Tam, *Environ. Sci. Technol.*, 1974, **8**, 734.
5. V. Hudnik and S. Gomišček, *Anal. Chim. Acta*, 1984, **157**, 135.
6. K. Ohta and M. Suzuki, *Talanta*, 1978, **25**, 160.
7. D. Chakraborti, W. De Jonghe and F. Adams, *Anal. Chim. Acta*, 1980, **119**, 331.
8. F. D. Pierce and H. R. Brown, *Anal. Chem.*, 1977, **49**, 1417.
9. A. U. Shaikh and D. E. Tallman, *ibid.*, 1977, **49**, 1093.
10. A. W. Fitchett, E. H. Daughtrey, Jr. and P. Mushak, *Anal. Chim. Acta*, 1975, **79**, 93.
11. J. Korečková, W. Frech, E. Lundberg, J.-Å. Persson and A. Cedergren, *Anal. Chim. Acta*, 1981, **130**, 267.
12. R. D. Ediger, *At. Absorpt. Newsl.*, 1975, **14**, 127.
13. R. B. Baird and S. M. Gabriellian, *Appl. Spectrosc.*, 1974, **28**, 273.
14. C. H. Chung, E. Iwamoto, M. Yamamoto, Y. Yamamoto and M. Ikeda, *Anal. Chem.*, 1984, **56**, 829.
15. E. Iwamoto, C. H. Chung and Y. Yamamoto, to be published.
16. C. H. Chung, E. Iwamoto, M. Yamamoto and Y. Yamamoto, *Spectrochim. Acta*, 1984, **39B**, 459.
17. B. V. L'vov, *ibid.*, 1978, **33B**, 153.
18. B. V. L'vov, *Atomic Absorption Spectrochemical Analysis*, Hilger, London, 1970.
19. S. A. Clyburn, T. Kantor and C. Veillon, *Anal. Chem.*, 1977, **46**, 2213.
20. R. E. Sturgeon and C. L. Chakraborti, *ibid.*, 1977, **49**, 90.
21. J. W. Robinson, R. Garcia, G. Hindman and P. Slevin, *Anal. Chim. Acta*, 1974, **69**, 203.
22. G. R. Henning, in *Progress in Inorganic Chemistry*, F. A. Cotton (ed.), Vol. 1, p. 125. Interscience, New York, 1959.
23. L. R. Hageman, J. A. Nichols, P. Viswanadham and R. Woodriff, *Anal. Chem.*, 1979, **51**, 1406.
24. S. R. Lawson and R. Woodriff, *ibid.* 1982, **54**, 2050.
25. J. R. Montgomery and G. N. Peterson, *Anal. Chim. Acta*, 1980, **117**, 397.
26. W. Slavin, D. C. Manning and G. R. Carrick, *Anal. Chem.*, 1981, **53**, 1504.

KALMAN FILTERING FOR THE EVALUATION OF THE CURRENT-TIME FUNCTION IN d.c. POLAROGRAPHY

M. Bos

Department of Chemical Technology, Technical University Twente, P.O. Box 217, 7500 AE Enschede,
The Netherlands

(Received 4 November 1985. Accepted 21 February 1986)

Summary—Kalman filtering was applied to the current *vs.* time data obtained at the growing mercury drop of a DME under d.c. polarographic conditions, to separate the faradaic and capacitive components of the electrode current. Polarograms consisting of the pure faradaic current *vs.* applied d.c. potential were subjected to a four-parameter curve-fitting procedure to obtain the polarographic characteristics, *viz.* half-wave potential, limiting current and slope of the log plot together with the baseline current. The method was tested with cadmium and zinc in the 10^{-6} – $10^{-5}M$ range. The standard deviations of the half-wave potentials and the limiting current/concentration ratios were found to be 1.0 mV and 0.04 respectively.

In polarography the analytical signal from the faradaic process at the electrode is obscured at low concentrations by the capacitive response caused by the charging of the electrical double-layer capacitance. Many methods have been devised to minimize the contribution of this capacitive component to the compound current signal, mostly by instrumental techniques, *e.g.*, fast and differential pulse polarography. With the advent of powerful on-line computers another approach has become viable in which mathematical processing of the measurements is used to separate the faradaic and capacitive components of the electrode current.

Numerous examples of the use of sophisticated data-processing techniques, such as the fast Fourier transform (FFT) procedure, curve-fitting, pattern recognition and Kalman filtering, combined with elaborate measurement procedures can be found in the literature for the a.c., pulse and stripping polarographic techniques.¹⁻⁷ Direct-current polarography, however, is still a favourite technique for the study of complex-formation equilibria.⁸⁻¹⁰ It has the advantage that the processes at the electrode are well understood and described by relatively simple equations.¹¹ In d.c. polarography the problem of separating the faradaic and capacitive response is mainly solved by mathematical data-processing. If this separation can be successfully achieved, a lower detection limit and better precision for the half-wave potential and limiting current can be obtained, owing to the absence of distortion of the polarographic wave by the capacitive component. This considerably extends the range of application of the polarographic method for determining stability constants. Moreover complicated schemes for baseline correction become superfluous, as the baseline will be a horizontal straight line. The feasibility of this approach has been

demonstrated by Soong and Maloy,¹² who applied a Riemann–Liouville transform (RLT) to the current–time data obtained at the growing mercury drop during normal d.c. polarography, to separate the faradaic and capacitive responses.

This paper describes an alternative route, the Kalman filter technique, to reach this goal. It has the advantage that a more complex model, with more than two parameters, can be accommodated and that it can directly process the incoming *i*–*t* data without the need to gather and store the complete set of measurements which is characteristic for curve-fitting methods. The data-processing algorithm is rather simple and its speed allows real-time processing.

THEORY

The instantaneous current in d.c. polarography

The instantaneous cell current in d.c. polarography consists of a faradaic and a capacitive component:

$$i(t) = i_f(t) + i_c(t) \quad (1)$$

The capacitive part $i_c(t)$ can be described by

$$i_c(t) = k_c t^{-1/3} \quad (2)$$

The constant k_c is potential-dependent, but can be considered constant during the growth of a given mercury drop if the voltage scan-rate is sufficiently low. For the instantaneous faradaic current the time-dependence is generally expressed by a $\frac{1}{6}$ order parabola, as in the Ilkovič equation. However, owing to the spherical shape of the mercury drop there is a difference in the shape and size of the diffusion space inside and outside it. This gives rise to two different situations, depending on whether the product of the electrode reaction forms an amalgam or is transported back into the solution. Kůta and Smoler¹³ give

a complete account of this subject and use the following relationship, derived by Koutecky¹⁴ and Weber,¹⁵ to express the instantaneous faradaic current:

$$i = \frac{0.732nFD^{1/2}cm^{2/3}t^{1/6}\lambda}{(\lambda + \sqrt{D_{ox}/D_{red}})} \times \left[1 + \frac{3.96D_{ox}^{1/2}t^{1/6}(\lambda \pm 1)}{m^{1/3}(\lambda + \sqrt{D_{ox}/D_{red}})} \right] \quad (3)$$

In this equation λ denotes the potential function

$$\lambda = \exp[-(E - E_0)nF/RT] \quad (4)$$

and the other symbols are those normally used in polarography. The two situations arise from the use of either the plus (no amalgam formation) or the minus sign (amalgam formation) in the second term in the brackets of the numerator of equation (3). On the basis of these equations Kůta and Smoler showed that the instantaneous faradaic current can be expressed as

$$i_f(t) = k_f t^\beta \quad (5)$$

where β is given by

$$\beta = \frac{1}{6} + 0.661D^{1/2}m^{-1/3}t^{1/6}\theta \quad (6)$$

with

$$\theta = (\lambda \pm 1)/(\lambda + \sqrt{D_{ox}/D_{red}}) \quad (7)$$

In their work these authors determined β for the faradaic curves for various cases and found that they could use a time-independent mean value that was significantly different from $\frac{1}{6}$ and changed with voltage in the polarographic wave for the case of amalgam formation. For the total cell current, equations (1), (2) and (5) give rise to:

$$i(t) = k_c t^{-1/3} + k_f t^\beta \quad (8)$$

This model equation (8) can be used in the Kalman filter scheme to estimate the parameters k_c , k_f and β . If the k_f data obtained in this way are plotted against d.c. potential the resulting polarograms will show horizontal straight baselines and plateaus because the capacitive current component has been eliminated completely.

Kalman filter theory

The Kalman filter is a mathematical technique that can be used to estimate the state of a process in real-time from noise-corrupted measurements on that process.¹⁶⁻¹⁸ Here only the operational equations for the evaluation of the $i-t$ curves of d.c. polarography by means of equation (8) are given. The state of the process is completely characterized by the parameters k_c , k_f and β and is denoted by the vector x . As these parameters are considered to be time-invariant in the description of the $i-t$ curve for a growing single mercury drop, the state-to-state transition matrix is the unity matrix. The equation for the measurements in which the current is averaged over the interval

from t to $t + \Delta t$ follows from the integration of (8) over this interval:

$$\bar{i}(t \rightarrow t + \Delta t) = x_1[t^{-1/3} + (\Delta t/6)t^{-4/3}] + x_2[t^{x_3} + (\Delta t x_3/2)t^{(x_3-1)}] \quad (9)$$

The elements of the state-to-measurement transition vector C can now be calculated:

$$\begin{aligned} C_1 &= \delta i(t)/\delta x_1 = t^{-1/3} - (\Delta t/6)t^{-4/3} \\ C_2 &= \delta i(t)/\delta x_2 = t^{x_3} + (\Delta t x_3/2)t^{(x_3-1)} \\ C_3 &= \delta i(t)/\delta x_3 = x_2[t^{x_3} \ln(t) \\ &\quad + (\Delta t/2)t^{x_3} + (\Delta t x_3/2)\ln(t)t^{x_3}] \end{aligned} \quad (10)$$

The mathematical model for the current-time relationship at constant potential at a growing mercury drop can be written as

$$\dot{\hat{x}}^* = \hat{x} + F\hat{w} \quad (11)$$

and

$$\hat{y}^* = C\hat{x}^* + n^* \quad (12)$$

in which x denotes the state vector of the process, consisting of the elements $[k_c, k_f, \beta]$; \hat{x} is the estimated current state of the process, and \hat{x}^* stands for the predicted state of the process one step ahead in time. The product $F\hat{w}$ is the process noise contribution. Equation (12) gives the measurement prediction \hat{y}^* which is calculated from the predicted state of the process \hat{x}^* by the state-to-measurement transition matrix C (in this case a vector). Its elements $[C_1, C_2, C_3]$ are given by equation (10); n^* is the noise associated with the measurements. The predicted co-variance of the state \hat{V}^* is given by:

$$\hat{V}^* = \hat{V} + FwF^T \quad (13)$$

where \hat{V} is the estimate of the current co-variance matrix. F and w are defined in equation (11) and F is the transpose of F^T . The prediction of the output signal co-variance V_y^* follows from:

$$\hat{V}_y^* = C\hat{V}^*C^T + N_y \quad (14)$$

in which N_y is the measurement noise variance. With the results of (13) and (14) the Kalman gain matrix K^* can be calculated as:

$$K^* = (\hat{V}^*C^T)/\hat{V}_y^* \quad (15)$$

With this Kalman gain, the calculated prediction of the measurement, and the actual value of the measurement y_m^* , a better estimate of the state vector can be calculated when this actual measurement value becomes available:

$$\hat{x}^* = \hat{x}^* + K^*[y_m^* - y^*] \quad (16)$$

A new estimate of the error co-variance matrix of the state can be found from:

$$\hat{V}^* = (I - K^*C^*)\hat{V}^* \quad (17)$$

I being the identity matrix.

Cycling through equations (11)–(17) for each new

measurement constitutes the Kalman filter procedure and provides improving estimates of the state of the process, *viz.* the wanted values of the capacitive and faradaic contributions to the total cell current, together with the exponent of the time-dependence of the faradaic part. If this exponent [β in equation (8)] is known and not dependent on the d.c. voltage the filter equations reduce to a one-measurement two-state system for which the Kalman gain matrices for the cell current *vs.* time series can be calculated off-line before the experiment is run. The real-time calculations are then reduced to the application of equations (11), (12) and (16) for each new measurement.

EXPERIMENTAL

Chemicals

Potassium chloride, cadmium sulphate (both Merck Suprapur) and zinc sulphate (Merck reagent grade) were used as received. The nitrogen used to remove oxygen from the samples in the polarographic cell was from HoekLoos (very pure grade). All solutions were prepared with demineralized water that had been filtered through Millipore Q2 filters.

Apparatus

A PAR model 174 polarograph was equipped with a Radiometer polarographic stand, type E64, DLT1 drop-life timer, and type 950-116 mercury capillary. The capillary characteristics for a 41-cm mercury head were: natural drop-time 3.7 sec and drop-rate 2.39 mg/sec (in 0.01M KCl with open circuit).

The polarographic instrumentation was interfaced to a PDP11/10 minicomputer (Digital Equipment Corp.) through the analogue-to-digital (A/D) and digital-to-analogue (D/A) converters in a Laboratory Peripheral System (LPS, Digital Equipment Corp.). Both the A/D and D/A converters provided 12-bit resolution and voltage ranges of ± 5 V. Timing was controlled by the LPSKW real-time clock option of the LPS.

For comparison purposes computerized d.c. tast polarography experiments were run on a Metrohm E506 polarograph equipped with an E505 polarographic stand and interfaced to a BASIS 108 microcomputer as described earlier.⁹ The characteristics of the DME used in these experiments were natural drop-time 5.1 sec and drop-rate 1.09 mg/sec (0.01M KCl, open circuit, mercury head 65 cm).

Computer programs

Two computer programs were written in FORTRAN IV. One was based on the one-measurement two-state description, in which the faradaic and capacitive factors k_f and k_c were estimated by the Kalman filter for a given and fixed exponent β for the time-dependence of the faradaic component of the current. In the second program this exponent β was estimated along with k_f and k_c . The data-acquisition routines were written in the assembly language MACRO-11 and linked to the main FORTRAN routine. The current measurements were performed at 80-msec intervals. To eliminate line-frequency noise the current measurements were programmed in such a way that during each 80-msec interval a window of one line-frequency period (20 msec) was used, during which a series of current measurements was performed at a sampling frequency of 20 kHz. This series was then averaged and the result used as y_m^* in the Kalman filter equations [*cf.* equation (16)]. Synchronization of these current measurements with the mercury drop-life was controlled by the electromechanical drop-life timer, which was activated from within the program.

For the one-measurement three-state filter the software is not fast enough to keep up with the 80-msec interval between the measurements. In this case the current *vs.* time data have to be stored and the Kalman filter calculations performed after all measurements on a single mercury drop have been completed. Although this slows down the recording of a polarographic wave considerably, it offers the possibility of reiterating all data through the filter, making the procedure less sensitive to bad initial estimates for the states and the co-variance matrix. Moreover, a fair initial estimate for the states can be calculated by using the assumption that the capacitive component will have decayed completely for the last data-point. This will give a good initial estimate for the faradaic part which, in turn, can be applied to the first data-point to estimate the capacitive contribution. The initial estimate used for β was 0.1667.

The program output the k_f *vs.* d.c. potential data to a chart recorder, which then displayed d.c. polarograms from which the capacitive-current contribution had been eliminated. These data were also stored in a disk file for use by a curve-fitting program that calculated half-wave potential, limiting k_f , slope of the log plot, and baseline current of the polarographic waves, from the k_f *vs.* d.c. potential values. The program used was an extension of a previously published three-parameter procedure,¹⁹ the baseline current being the fourth parameter. This feature is especially useful when baseline extrapolation methods fail owing to the presence of a preceding polarographic wave in the vicinity of the wave of interest.

Procedures

The polarographic experiments were run with solutions that had been deoxygenated by passage of nitrogen for 15 min. During the recording of the polarograms nitrogen was passed over the solution. The current/time data for the growing mercury drops were obtained by sampling the current at 80-msec intervals. For cadmium 20 data-points were acquired from a single drop, whereas for zinc the current was sampled 40 times per drop. The current/time data were normally evaluated with the one-measurement two-state Kalman filter, with a fixed value for β . The value to use for β was determined beforehand with the one-measurement three-state procedure. In the calculation the variance of the measurements was set at one A/D converter unit and the process noise was set to zero. The initial estimates for the diagonal co-variance matrix elements were set at unity, the off-diagonal elements at zero.

RESULTS AND CONCLUSIONS

Table I shows the results obtained with the method for cadmium in the concentration range 10^{-5} – 10^{-6} M. The supporting electrolyte was 0.01M potassium chloride. The corresponding polarograms were calculated from the *i-t* curves for the growing mercury drops at different d.c. potentials. The one-measurement two-state (k_f and k_c) model was used in

Table I. Kalman filter d.c. polarography for Cd(II)/0.01M KCl

[Cd], 10^{-6} M	Limiting k_f , nA	$E_{1/2}$, mV	Limiting $k_f/[Cd]$, 10^6 nA.l.mole ⁻¹
0.99	23.2	-568.7	23.5
1.96	49.9	-568.8	25.5
2.91	68.0	-569.5	23.4
3.85	92.7	-569.4	24.1
5.66	142.1	-568.9	25.1
Mean		-569.0 \pm 0.4	24.3 \pm 0.9

Table 2. Kalman filter d.c. polarography for Zn(II)/0.01M KCl

[Zn], 10 ⁻⁶ M	Limiting k_f , nA	$E_{1/2}$, mV	Limiting $k_f/[Zn]$, 10 ⁶ nA.l.mole ⁻¹
3.98	27.0	-991.0	6.78
9.90	66.8	-991.8	6.75
19.60	130.3	-993.2	6.65
29.10	188.2	-990.7	6.47
38.50	254.8	-991.0	6.62
Mean		-991.5 ± 1.0	6.65 ± 0.12

the Kalman filter procedure. The average value for β was found to be 0.19 from a preliminary experiment in which the one-measurement three-state (k_f , k_c and β) model was used. The same value was calculated by Kúta and Smoler.¹³ The characteristics of the polarographic waves were evaluated with the four-parameter (limiting k_f , $E_{1/2}$, slope and baseline current) curve-fitting procedure described above. From this table it can be concluded that d.c. polarographic characteristics can be obtained for cadmium with good constancy, down to a concentration of 10⁻⁶M. Although more sensitive electroanalytical methods are available, such as anodic-stripping or square-wave polarography,²⁰ the method described here has the advantage that its results can be used directly in well established methods that rely on d.c. polarographic data to calculate physicochemical parameters, e.g., complex-formation constants.

The results also indicate that it is possible to fit the baseline faradaic current as a fourth parameter along with the limiting k_f , $E_{1/2}$ and slope of the log plot. There is then no need for baseline current extrapolation procedures, which means that systems that do not give a distinct baseline section in the polarogram can be evaluated by using only the rising part of the waves. Similar results to those obtained for cadmium were also found for the zinc system (Table 2). For this the average value of β was found to be 0.27. The one-measurement three-state procedure used here to determine the average value of β can also be used for more fundamental studies of the nature of the electrode process.¹³ In the Kalman filter calculations the value of the integral double-layer capacitance is also determined as part of the process. In this work no attention was paid to these values, but clearly this facility makes the method a suitable tool for the study of double-layer phenomena. In particular the potential corresponding to zero charge can be obtained accurately and easily from a plot of the integral double-layer capacitance vs. d.c. potential.

For comparison d.c. tast experiments were run for zinc and cadmium. The lower concentration limit of which the results were of quality similar to those obtained with the Kalman filter technique turned out to be 10⁻⁵M, as can be seen from Table 3. The reason for the breakdown of the d.c. tast method below this

Table 3. Computerized d.c. tast polarography for Zn(II)/0.01M KCl

[Zn], 10 ⁻⁶ M	Limiting current, nA	$E_{1/2}$, mV	$i_d/[Zn]$, nA.l.mole ⁻¹
5.74	11.4	-983.3	1.99
7.15	16.9	-984.6	2.36
8.55	21.6	-985.5	2.52
11.31	33.5	-985.0	2.96
31.7	117.4	-986.5	3.70
49.7	196.6	-986.7	3.96
66.3	269.1	-986.9	4.06
83.3	336.5	-987.0	4.03
97.4	396.7	-986.0	4.07

concentration is mainly the uncertainty introduced by the baseline extrapolation needed. Owing to the substantial contribution of the capacitive component when high sensitivity is used for current measurement, the curvature of the baseline changes with d.c. potential in a complex manner, thus ruling out simple baseline-correction techniques for d.c. tast polarography at high sensitivities.

Acknowledgements—The author wishes to thank Prof. W. E. van der Linden for his general support, Mrs. A. M. W. van Veen Blaauw for doing the d.c. tast experiments, Ir. A. R. van Heusden for his help with Kalman filter theory and Mrs. B. E. M. M. Verbeeten for preparing the manuscript.

REFERENCES

- D. E. Smith, *Anal. Chem.*, 1976, **48**, 517A.
- R. J. O'Halloran, J. C. Schaar and D. E. Smith, *ibid.*, 1978, **50**, 1073.
- P. F. Seelig and R. de Levie, *ibid.*, 1980, **52**, 1506.
- P. F. Seelig and H. N. Blount, *ibid.*, 1976, **48**, 252.
- T. F. Brown, D. M. Caster and S. D. Brown, *ibid.*, 1984, **56**, 1214.
- J. E. Anderson and A. M. Bond, *ibid.*, 1983, **55**, 1934.
- M. Ichise, H. Yamagishi and T. Kojima, *J. Electroanal. Chem. Interfacial Electrochem.*, 1978, **94**, 187.
- A. Laouenan and E. Suet, *Talanta*, 1985, **32**, 245.
- D. Ph. Zollinger, M. Bos, A. M. W. van Veen-Blaauw and W. E. van der Linden, *Anal. Chim. Acta*, 1985, **167**, 89.
- J. A. Santaballa, C. Blanco, F. Arce and J. Casado, *Talanta*, 1985, **32**, 931.
- D. J. Leggett, *ibid.*, 1980, **27**, 787.
- F. Soong and J. T. Maloy, *J. Electroanal. Chem. Interfacial Electrochem.*, 1983, **153**, 29; J. T. Maloy and F. Soong, *Proc. Intern. Symp. LCEC and Voltammetry, Indianapolis*, 1983, pp. 102-106.
- J. Kúta and I. Smoler in *Progress in Polarography*, P. Zuman and I. M. Kolthoff (eds.) Vol. I, p. 43. Interscience, New York, 1962.
- J. Kouřecký, *Czech. J. Phys.*, 1953, **2**, 51.
- J. Weber, *Coll. Czech. Chem. Commun.*, 1959, **24**, 1424.
- R. E. Kalman, *Trans. A.S.M.R., Ser. D, J. Basic Eng.*, 1960, **82**, 35.
- R. E. Kalman and R. S. Bucy, *ibid.*, 1961, **83**, 95.
- A. H. Jazwinski, *Stochastic Processes and Linear Filtering Theory*, Chapters 7, 8, 9. Academic Press, New York, 1970.
- M. Bos, *Anal. Chim. Acta*, 1976, **81**, 21.
- J. J. O'Dea, J. Osteryoung and R. A. Osteryoung, *J. Phys. Chem.*, 1983, **87**, 3911.

EXTRACTION AND SPECTROPHOTOMETRIC DETERMINATION OF TITANIUM(IV) WITH ALIZARIN AND FLUORIDE

R. LOPEZ NUÑEZ, M. CALLEJON MOCHON* and A. GUIRAUM PEREZ

Department of Analytical Chemistry, Faculty of Chemistry, University of Sevilla, 41012 Sevilla, Spain

(Received 1 October 1985. Revised 3 February 1986. Accepted 21 February 1986)

Summary—The characteristics of the mixed-ligand titanium(IV)–fluoride–alizarin complex, including the optimum conditions of formation and extraction into methyl isobutyl ketone, are described. A simple and sensitive procedure for spectrophotometric determination of titanium has been developed. At pH 9.5–10.3 titanium reacts with alizarin in the presence of fluoride to form a red-violet complex that is completely extractable into methyl isobutyl ketone, and has its absorption maximum at 513 nm. The molar absorptivity at 513 nm is $7.0 \times 10^4 \text{ l. mole}^{-1} \text{ cm}^{-1}$. Beer's law is obeyed up to 22 μg of titanium in 30 ml of solution. The method has been used for the determination of titanium in an oxide mixture and aluminium alloy samples.

Mixed-ligand complexes have found increasing use, particularly in spectrophotometric analysis, because of their high sensitivity and selectivity. Recently alizarin was used with other ligands to form mixed-ligand metal complexes¹⁻⁶ and thereby enhance the sensitivity and selectivity of the spectrophotometric determination of the metals. During studies on the sensitizing effects of common ligands (fluoride, cyanide, thiocyanate, ascorbate, oxalate and EDTA) on the reaction of metals with alizarin, fluoride was found to produce a marked increase in the absorptivity of the Ti(IV)–alizarin system, owing to the formation of a Ti(IV)–fluoride–alizarin complex. This paper deals with extraction of this mixed-ligand complex into methyl isobutyl ketone (MIBK) and the subsequent spectrophotometric determination of titanium(IV) in the organic phase.

EXPERIMENTAL

Reagents

All reagents used were analytical grade.

Standard titanium(IV) solution. A stock solution of Ti(IV) was prepared by fusing 1.85 g of high-purity titanium(IV) oxide with 15 g of potassium pyrosulphate in a platinum crucible, cooling, dissolving the fusion cake by boiling with approximately 250 ml of 1M sulphuric acid, cooling, and diluting to volume in a 1-litre standard flask with 1M sulphuric acid. This solution (titanium concentration approximately 1100 ppm) was standardized by an EDTA back-titration procedure with copper as titrant and PAN as indicator.

Alizarin solution ($4.6 \times 10^{-3}\text{M}$). Alizarin (0.1104 g), dissolved in 100 ml of MIBK. This solution was stable for at least two months. It was diluted as required.

Buffer solution. A 1.0M fluoride buffer was prepared by dissolving 37.0 g of ammonium fluoride, and enough ammonia to give pH 10.0, in 1 litre of water. This solution was stored in a polyethylene bottle.

EDTA solution, $2.7 \times 10^{-2}\text{M}$. Prepared by dissolving about 10 g of the disodium salt dihydrate and diluting to 1 litre with water.

Determination of titanium

Transfer x ml of titanium(IV) solution in 1M sulphuric acid and containing not more than 22 μg of titanium into a 100-ml separatory funnel. Add $(1 - x)$ ml of 1M sulphuric acid, 25 ml of buffer solution, 4 ml of distilled water and 10 ml of $4.6 \times 10^{-4}\text{M}$ alizarin solution in MIBK. Shake the mixture gently for 45 min, then let stand for 5 min, discard the aqueous phase, centrifuge the organic phase, and measure its absorbance at 513 nm against a reagent blank similarly prepared. Construct a calibration graph for the range up to 22 μg of titanium.

Analysis of "TON" III oxide mixture

A. Weigh about 0.5 g accurately into a platinum crucible, add 6 g of potassium pyrosulphate, fuse the mixture, then leach the cooled melt with 100 ml of 4M sulphuric acid. Transfer the solution into a 250-ml conical flask and heat on a sand-bath to reduce the volume to approximately 25 ml. Cool, add 100 ml of hydrochloric acid (1 + 1) and heat to boiling. Filter off the silica, collecting the filtrate in a 250-ml standard flask, cool, and dilute the solution to the mark with hydrochloric acid (1 + 1). Transfer a 25-ml aliquot of this solution to a separating funnel and extract the iron with four 25-ml portions of diethyl ether. Evaporate the aqueous solution to dryness, then with 2M sulphuric acid take up the residue, transfer the solution to a 25-ml standard flask and dilute it to the mark. Take a 1-ml aliquot, add 3 ml of $2.7 \times 10^{-2}\text{M}$ EDTA and determine the titanium as described above.

B. Weigh about 0.5 g accurately into a platinum crucible, add 1 ml of distilled water, 0.5 ml of concentrated sulphuric acid and 10 ml of concentrated hydrofluoric acid, and warm gently to remove the excess of hydrofluoric acid. Evaporate to dryness, then with 6M hydrochloric acid take up the residue and dilute the solution to volume in a 250-ml standard flask. Take a 25-ml aliquot of this solution, then remove the iron and determine the titanium as just described.

Analysis of aluminium alloy

To about 2.0 g of sample, weighed accurately, in a 200-ml conical flask, slowly add 75 ml of hydrochloric acid (1 + 1), and when the alloy has dissolved, evaporate almost to

*To whom all correspondence should be addressed.

dryness and then add 50 ml of hydrochloric acid (1 + 1). Transfer the solution to a separating funnel and extract the iron with four 25-ml portions of diethyl ether. Heat the solution to remove the ether dissolved in it, cool, add 5 ml of $2.5 \times 10^{-2} M$ cupferron solution and extract the titanium cupferronate with 10 ml of MIBK. Transfer the organic phase into a 10-ml standard flask and dilute to the mark with MIBK. Take a 2-ml aliquot, add 3 ml of $0.3 M$ potassium cyanide and proceed as above for the determination of titanium, adding 2 ml of MIBK to each of the standards used in constructing the calibration graph.

RESULTS AND DISCUSSION

Absorption spectra

Alizarin solution in MIBK reacts with titanium(IV) in basic media in presence of fluoride to produce a red-violet complex in the organic phase. The absorption spectra of the mixed-ligand complex extracted into MIBK and of a sample prepared in the same way without titanium, both measured against the solvent as reference, are given in Fig. 1. These spectra have maximal difference in absorbance at 513 nm. The spectra similarly obtained for samples containing titanium(IV), alizarin and ammonium chloride, at pH 10.0, and titanium(IV), alizarin and enough $0.1 M$ sodium hydroxide to obtain the necessary pH, are practically the same as the spectrum of the alizarin solution. These facts can only be interpreted as indicating the formation of a mixed-ligand complex.

Effects of experimental conditions

A standard amount of titanium(IV) was allowed to react with $1 M$ ammonium fluoride solution buffered to pH 8.6–10.8 and $4.6 \times 10^{-4} M$ alizarin solution in MIBK, to form the mixed-ligand complex extracted into the organic solvent. A plot of absorbance against pH (Fig. 2) showed that maximal and constant absorbance was obtained at pH 9.5–10.3.

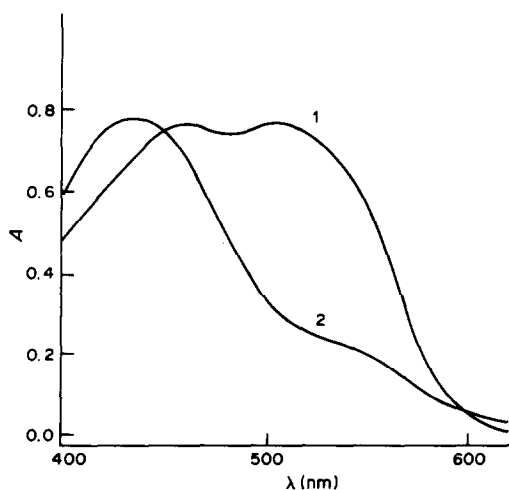


Fig. 1. Absorption spectra measured against MIBK. (1) Ti(IV)-fluoride-alizarin complex, $[Ti]_{aq} = 2.8 \times 10^{-5} M$, $[fluoride]_{aq} = 1.8 \times 10^{-2} M$, $[alizarin]_o = 3.4 \times 10^{-4} M$; (2) reagent blank.

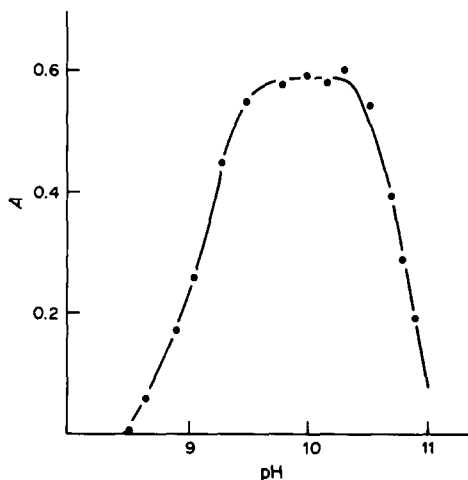


Fig. 2. Effect of pH on the formation and extraction of Ti(IV)-fluoride-alizarin complex (reagent blank subtracted). Fluoride buffer solutions of pH 8.5–10.9 were used for pH adjustment. $[Ti]_{aq} = 1.5 \times 10^{-5} M$, $[alizarin]_o = 4.6 \times 10^{-4} M$, $[fluoride]_{aq} = 0.83 M$.

The effect of the fluoride concentration on the complex formation was investigated for $7.6 \times 10^{-6} M$ titanium(IV) solutions buffered with x ml of $1 M$ ammonium fluoride/ammonia and $(25 - x)$ ml of $1 M$ ammonium chloride/ammonia, both of pH 10.0. Maximum colour formation was found when the fluoride concentration exceeded $0.25 M$ (Fig. 3). It was also found that a "lake" of titanium(IV)-alizarin is precipitated when the fluoride concentration was less than about $2.0 \times 10^{-2} M$.

The effect of the alizarin concentration on the colour formation in the organic phase was then investigated. A maximum and constant absorbance was obtained when the alizarin concentration exceeded 10-fold molar ratio to that of titanium (Fig. 3).

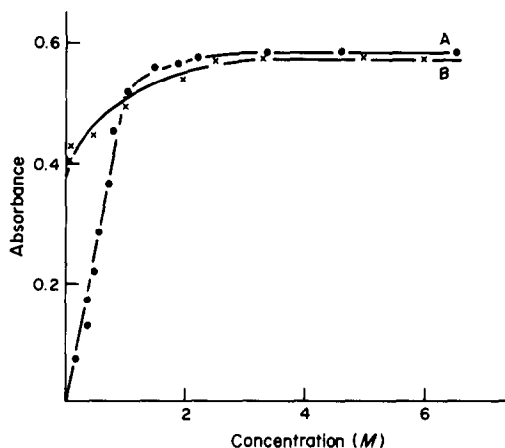


Fig. 3. Effect of alizarin and fluoride concentrations on the formation and extraction of the mixed-ligand complex: (A) molar concentration ($\times 10^4$) of alizarin in the organic phase, $[Ti]_{aq} = 7.6 \times 10^{-6} M$, $[fluoride]_{aq} = 0.83 M$; (B) molar concentration ($\times 10$) of fluoride in the aqueous phase, $[Ti]_{aq} = 7.6 \times 10^{-6} M$, $[alizarin]_o = 4.6 \times 10^{-4} M$.

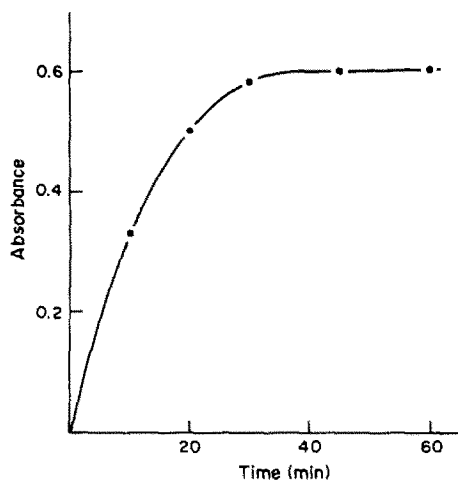


Fig. 4. Effect of shaking-time. $[Ti]_{aq} = 7.6 \times 10^{-6}M$, $[fluoride]_{aq} = 0.83M$, $[alizarin]_o = 4.6 \times 10^{-4}M$.

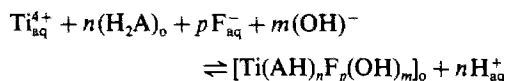
The extraction is maximal after 35–40 min shaking time (Fig. 4), and the absorbance of the red-violet colour produced remains constant for at least 1 hr.

The efficiency of the extraction was determined by destroying the extracted titanium complex and determining the titanium in it; a single extraction was found to be 91% complete.

The effect of the phase-volume ratio was studied, to obtain the optimal conditions. The absorbance of the organic reagent phase was practically constant for the range 3:1–5:1, aqueous phase:organic phase, and decreased for ratios greater than 5:1.

Equilibrium of extraction and nature of the extracted species

Because the extracted species must be uncharged, the charge of the titanium must be neutralized by the dissociated ligand species, fluoride and possibly hydroxide ions. Thus, the equilibrium between an aqueous solution containing titanium and fluoride and an organic solution containing alizarin (H_2A) could be formally expressed as:



If the mixed-ligand complex is denoted by Q, the extraction constant is:

$$K_{ex} = \frac{[Q]_o [H^+]_{aq}^{n+m}}{[Ti^{4+}]_{aq} [H_2A]_o^n k_w^m [F^-]_{aq}^p} \quad (1)$$

As titanium(IV) can form soluble fluoride and hydroxide complexes, these equilibria can compete with that of chelate formation. This can be allowed for by means of a Ringbom α -coefficient,⁷ $[Ti^{4+}] = [Ti^{4+}]^1 / \alpha_{Ti(OH,F)}$. Since the distribution coefficient for the titanium system is $D = [Q]_o / [Ti^{4+}]_{aq}^1 = [Q]_o / [Ti^{4+}]_{aq} \alpha_{Ti(OH,F)}$, substitution, solution for D

and taking logarithms gives

$$\log D = \log K_{ex} + m \log k_w + \log \alpha + (n+m)pH + n \log [H_2A]_o + p \log [F^-]_{aq}$$

Plotting $\log D$ vs. $\log [H_2A]_o$ at constant pH and $[F^-]_{aq}$ yields a slope equal to the ligand:metal ratio in the extracted species. The slope of 2.03 obtained indicates a 1:2 titanium:alizarin ratio. The Asmus method gave the same ratio (Fig. 5).

The distribution coefficient was determined by assuming that the titanium is totally complexed as the chelate when the alizarin concentration is very high, and that $\alpha_{Ti(OH,F)}$ is then practically unity. Hence

$$D = \frac{rA}{A_{max} - A}$$

where r is the phase-volume ratio ($r = V_{aq}/V_o$), V_{aq} being the volume of aqueous phase and V_o the volume of the organic phase, A the absorbance of the extract for a given alizarin concentration and A_{max} the absorbance of the extract for a large excess of alizarin.

To determine the metal:fluoride ratio, the complex in MIBK solution was washed three times with ammonium chloride/ammonia buffer (pH 10.0) and then destroyed with 1M hydrochloric acid. The alizarin remained in the organic phase. The aqueous phase was made up to a standard volume and the titanium in it was determined by the method proposed here, and the fluoride was determined spectrophotometrically by the Ce(III)-alizarin complexan method.⁸ The metal:fluoride ratio was found to be 1:1.

The results obtained show that the molar ratio of Ti(IV):fluoride:alizarin in the complex is 1:1:2. We

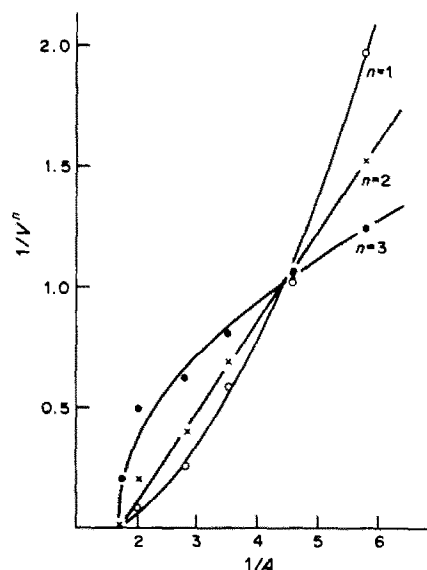


Fig. 5. The Asmus method applied to the Ti-alizarin system. $[Ti]_{aq} = 2.3 \times 10^{-5}M$ in 0.95M fluoride buffer solution, pH 10.0. A = absorbance, V = volume (ml).

assume that the complex must also contain one hydroxide ion if it is to be uncharged.

Calibration graph

Under the optimal conditions above, a linear calibration graph was obtained over the range 0–22 μg of titanium in the aqueous phase. The apparent molar absorptivity was calculated to be $7.0 \times 10^4 \text{ l. mole}^{-1} \cdot \text{cm}^{-1}$ at 513 nm. A Ringbom plot⁹

showed that the optimum range for determination was 5.7–16 μg of titanium. The mean value from eleven determinations of 11 μg titanium gave a relative standard deviation ($P = 0.05$) of 1.4%.

Effect of other ions

The possible interference of various ions was examined by introducing them into a solution containing 11 μg of titanium. The tolerance limit was fixed as the

Table 1. Tolerance ratios of foreign ions on the determination of 11 μg of titanium in 30 ml of aqueous phase

Tolerable foreign ion/Ti(IV) ratio, w/w	Ions
5000	CN ⁻
3500	EDTA
1000	Br ⁻ , I ⁻ , ClO ₃ ⁻ , BrO ₃ ⁻ , IO ₃ ⁻ , ClO ₄ ⁻ , SO ₃ ²⁻ , S ₂ O ₃ ²⁻ , SeO ₃ ²⁻ , NO ₃ ⁻ , HPO ₄ ²⁻ , P ₂ O ₇ ⁴⁻ , C ₂ O ₄ ²⁻ , SCN ⁻ , acetate, citrate, tartrate and phthalate
500	NO ₂ ⁻ , B ₄ O ₇ ²⁻ , ascorbate
100	Mg(II), Be(II), Sr(II)*, Ba(II)*, Al(III)*, Mn(II)*, Co(II)*, Ni(II)*, Ag(I), Zn(II), Cr(VII), AsO ₂ ⁻ , AsO ₄ ³⁻ , Pb(II)*
75	Tl(I), Cd(II), Mo(VI)
50	Hg(I), Hg(II), Bi(III)*, W(VI), V(VI), S ₂ O ₈ ²⁻
10	La(III), Cu(II)*, U(VI)
1	Sn(II)*, Sb(III), Fe(III)†
0.5	Ce(IV), Th(IV)
0.5	Ga(III)*, In(III)*, Zr(IV)*

*In presence of $1.7 \times 10^{-3} M$ EDTA.

†In presence of $4.0 \times 10^{-3} M$ cyanide.

Table 2. Determination of titanium in TON III and aluminium alloy

Sample	General composition, %	TiO ₂ or Ti, %	
		Present method	Certificate value
TON III	SiO ₂ , 50.74; Al ₂ O ₃ , 22.30; TiO ₂ , 1.22; Fe ₂ O ₃ , 14.90; CaO, 0.05; MgO, 0.28; Na ₂ O, 0.15; K ₂ O, 2.40; loss on ignition, 7.96	Procedure A 1.18 ± 0.01	1.22
		Procedure B 1.26 ± 0.02	
Aluminium alloy	Cu, 0.001; Zn, 0.015; Fe, 0.08; Al, 99.85; Mn, 0.001; Si, 0.035; V, 0.004; Ga, 0.009; Ti, 0.002	0.0025 ± 0.0003	0.002

*Mean and standard deviation of six determinations.

Table 3. Sensitivities of methods for the spectrophotometric determination of titanium

Methods	λ_{max} , nm	ϵ , $10^4 \text{ l. mole}^{-1} \cdot \text{cm}^{-1}$	Reference
<i>N</i> -Phenyl-laurohydroxamic acid and phenylfluorone	560	12.3	11
4-(2-Thiazolylazo)catechol	520	7.2	12
Chlorpromazine hydrochloride	417	2.6	13
Bromopyrogallol Red and 1-hexadecylpyridinium	630	2.6	14
Sulphonitrazo E	555	1.6	15
Diantipyrinylmethane	385	1.5	16
Tiron	410	1.4	17
Chromotopic acid	410	1.2	18
Sulphosalicylic acid	445	0.8	19
<i>N</i> -Benzoyl- <i>N</i> -phenylhydroxylamine	340	0.5	20
Fluoride and alizarin	513	7.0	this method

maximum amount of an ion causing an error no greater than 3% in the absorbance of the extract. The results are given in Table I. Some elements interfere at an ion/Ti(IV) ratio of less than one (e.g., Sn, Fe, Co, Cu and Mn) but their interference may be reduced by addition of EDTA and cyanide.

Analysis of samples

The method was satisfactory applied to the determination of titanium in an oxide mixture "TON III" (Hoepfner) and an aluminium alloy (B.C.S. No. 195 g). To separate it from the aluminium alloy, titanium was precipitated with cupferron¹⁰ and separated by extraction with MIBK. Table 2 gives the results.

Comparison with other titanium reagents

As can be seen from Table 3, this is one of the most sensitive methods for titanium. It is simple and relatively free from interferences, in presence of EDTA and cyanide.

REFERENCES

1. V. A. Nazarenko and G. V. Flyantifova, *Zh. Analit. Khim.*, 1972, **27**, 2369.
2. D. I. Zul'fugarly and I. K. Guseinov, *Azerb. Khim. Zh.*, 1972, **2**, 173.
3. E. T. Beschetnova and L. G. Anisimova, *Fiz-Kim. Metody Anal. Kontrolya Proizvod. Mezhvus. Sb.*, 1976, **2**, 40.
4. N. L. Shestidesyatnaya and N. M. Milgaeva, *Koord. Khim.*, 1978, **4**, 1544.
5. *Idem, ibid.*, 1981, **7**, 1380.
6. M. Román Ceba, A. Arrebola Ramírez and J. J. Berzas Nevado, *Talanta*, 1982, **29**, 142.
7. A. Ringbom, *Complexation in Analytical Chemistry*, Interscience, New York, 1973.
8. M. Hanocq and L. Molle, *Anal. Chim. Acta*, 1968, **40**, 13.
9. A. Ringbom, *Z. Anal. Chem.*, 1939, **115**, 332; A. Ringbom and F. Sundman, *ibid.*, 1939, **115**, 402; 1940, **116**, 104.
10. J. Starý and J. Smižanská, *Anal. Chim. Acta*, 1963, **29**, 545.
11. H. D. Gunawardhana, *Analyst*, 1983, **108**, 952.
12. V. M. Ivanov and K. V. Nguyen, *Zh. Analit. Khim.*, 1980, **35**, 903.
13. T. H. Puzanowska and M. Tarasiewicz, *Microchem. J.*, 1984, **29**, 341.
14. L. I. Ganago and L. V. Kovaleva, *Zh. Analit. Khim.*, 1982, **37**, 1209.
15. E. S. Orlova and L. I. Tokhova, *ibid.*, 1983, **38**, 1243.
16. A. A. Minin and S. M. Pashvintseva, *Uch. Zap. Permsk. Gos. Univ.*, 1973, **298**, 154.
17. J. Fries and H. Getrost, *Organic Reagents for Trace Analysis*, Merck, Darmstadt, 1977.
18. W. W. Brandt and A. E. Preiser, *Anal. Chem.*, 1953, **25**, 567.
19. M. Ziegler and O. Glemser, *Z. Anal. Chem.*, 1953, **139**, 92.
20. J. E. Schwarberg and R. W. Moshier, *Anal. Chem.*, 1962, **34**, 525.

THE APPLICATION OF DIRECT CURRENT PLASMA SPECTROMETRY TO THE STUDY OF THE FRACTIONATION OF IRON AND PHOSPHORUS IN SURFACE WATERS

I. T. URASA* and A. M. O'REILLY†

Department of Chemistry, Hampton University, Hampton, Virginia 23668, U.S.A.

(Received 20 December 1984. Revised 6 February 1986. Accepted 13 February 1986)

Summary—By use of a direct-current plasma as the excitation source for atomic-emission measurements, samples containing various amounts of particulate matter can be analysed with precisions of better than $\pm 10\%$ relative standard deviation provided that particle agglomeration is controlled by acidification and/or filtration. Sample acidification and filtration can have profound effects on the determination of elemental fractionation and distribution in surface waters. By application of a controlled acidification and filtration process, the fraction of an element that is particle-bound and that which is soluble in water can be estimated. The magnitudes of the particle-bound and water-soluble fractions are influenced by a number of factors, including the concentration and average size of the solids in the water, the position of the sample in the water column, and the type of sediment underlying the water column.

The identification and determination of the different forms of trace elements in water still require a great deal of study. Though several articles concerning this subject have appeared in the literature,¹⁻¹⁰ it appears that the extent to which factors associated with sample collection, preservation, treatment, and measurement come into play is not well documented.

There are two general approaches to analysis of water samples for trace elements: (1) the sample is introduced directly into the measurement system without any processing; (2) the sample is acidified and/or filtered before introduction into the measurement system. Whether a sample is to be filtered and/or acidified before analysis depends on several things, including the objective of the analysis (whether the information sought is total element content or the content of certain species of the element of interest), sample characteristics, and the analytical technique used. Typically, acidification is used to dissolve large particles and to minimize loss of the analyte by adsorption. Trefry and Metz¹¹ used different sample acidification procedures to achieve selective leaching of elements from sediments and soils. Others¹²⁻¹⁵ have investigated the effect of pH on trace metal determination in sediments. It has been demonstrated through these studies that not only is there a relationship between the amount of element leached and the sample pH, but also that variations exist owing to differences in the properties of the elements measured, sample characteristics, the type

of acid used, and the measurement procedure employed.

On the other hand, sample filtration is used as a means of separating dissolved from undissolved species and to eliminate solid material that might affect adversely the quality of the analytical data obtained. Traditionally, 0.45 μm pore-size filters are used.¹⁶ Several investigators have investigated element speciation on the basis of particle size distribution, using filters with nominal pore sizes ranging from 0.01 to 100 μm .¹⁷⁻²³ Here also, variations were observed, which depended on the elements measured, the type of filters used, and sample characteristics. In some cases, acidification and filtration may be unnecessary and can be omitted; in others, these procedures may be essential. It is therefore important that for a given analysis all the influential factors are well understood.

Though many methods are available for trace element measurements, most of them are not well suited to the analysis of samples with a complex matrix. Many require some form of sample-processing, which may be undesirable for some speciation measurements.

The application of the direct-current plasma (DCP) to trace analysis of solutions appears not to suffer some of the limitations of other techniques, since the DCP is reported²⁴⁻²⁶ to give high sensitivity, wide linear response range, insensitivity to matrix and interference effects, excitation of both metals and non-metals, and signals that are independent of the form of the element being measured.

In research on the distribution of elements between particulate matter and solution, the measurement technique employed must be able to analyse particles of various sizes with essentially equal efficiency.

*Author to whom all correspondence should be addressed.

†Present address: Department of Chemistry, University of Florida, Gainesville, Florida 32611, U.S.A.

Therefore, the purpose of the work reported here was two-fold: (1) to evaluate the application of the DCP to the analysis of samples of varying particle composition, and (2) to study the fractionation and distribution of trace elements in surface waters, with iron and phosphorus as models. Iron was chosen to represent those elements which tend to be adsorbed on particulate matter in solution, and phosphorus to represent non-metals of environmental importance. This research focused on the individual and mutual influence of sample acidification and filtration on the fractionation of these elements.

EXPERIMENTAL

Instrumentation

Atomic-emission measurements were made with a d.c. plasma and echelle spectrometer system (Spectraspan IV). Data acquisition and reduction were done with a built-in microprocessor with output to a data terminal (Texas Instruments, Model 700).

Reagents

Analytical-reagent grade ferric nitrate and phosphoric acid (Mallinckrodt), hydrochloric acid and nitric acid (Baker "Analyzed"), 1000-ppm standard iron solution (Fisher) and distilled and demineralized water (Mill-Q Water Purification System) were used.

Filters

Membrane filters (0.20, 0.45, 0.80 μm) (Nalgene Sterilization Filtration Units Types S) were used.

Samples

Water samples were obtained from several sources in the Hampton Roads area in Virginia (see Table 1). Surface and bottom water samples were obtained from selected sites on the Chickahominy River by means of a metal-free bottle. Sediment samples were also obtained from the Chickahominy River at the same locations as the water samples, with a metal-free grab. Since the objective was to evaluate the effects of acidification and filtration, all samples were filtered and/or acidified in the laboratory within 24 hr after sampling.

Procedure

The atomic emission of iron and phosphorus was determined, with the DCP as excitation source, at 373.4 and 213.6 nm respectively. The DCP was operated as previously described.²⁴

The effects of acidification and filtration were studied first, the acidification being done with various concentrations of hydrochloric and nitric acid. Portions of each solution were filtered through 0.20, 0.45 and 0.80 μm membrane filters and the ratio of analyte found in the filtrate to that found in the unfiltered solution was determined by DCP/atomic emission in each case. The filtration study was later extended by use of sintered-glass crucibles, of various porosities.

To evaluate the influence of position in the water column on the fractionation of iron and phosphorus, surface (taken at a few cm depth) and bottom (taken approximately 10 cm above sediment level) samples of the river water column were acidified, filtered and analysed as above.

Sediments were characterized with respect to colour, texture and water content. Samples of dried sediment were ground to an average particle size of about 100 μm and known amounts were digested with water and with various concentrations of hydrochloric acid, and the residues were analysed for iron and phosphorus.

RESULTS AND DISCUSSION

Effects of acidification on particle size distribution

Acidification and filtration are commonly applied to water samples before analysis, but for certain purposes can be undesirable. In speciation work, it is desirable to preserve the original condition of the sample, and acidification prevents this since it changes the distribution pattern of the particulate matter. Filtration precludes direct determination of the total concentration of the element of interest. Therefore, it is important to know both the effect of acidification and filtration on the analysis, and the implications of omitting these procedures.

Acidification effects were evaluated first, and the results obtained are shown in Fig. 1. As can be seen, less than 20% of the iron in the unacidified solution passed into the filtrate. This is attributed to the tendency of iron to form colloidal material in aqueous medium. As the acid concentration was increased, the iron fraction in the filtrate also increased, levelling off at 3M acid concentration, all the iron then being in the filtrate. It is interesting that essentially the same results were obtained with all three filter pore-sizes. All the phosphorus was present in the filtrate, irrespective of the sample treatment.

Effects of particle agglomeration and settling

The study just discussed suggests that sufficient acidification can produce species with nominal particle size $<0.2 \mu\text{m}$ and dissolve all the particle-bound iron, thus allowing estimation of the total iron content. Total iron can also be determined by direct aspiration of the unfiltered sample into the DCP, which can tolerate fairly large particles without loss of atomization efficiency. However, for unacidified samples, particle agglomeration and settling can be a problem. With the DCP, it can take up to 70 sec to make one measurement. Thus, if successive mea-

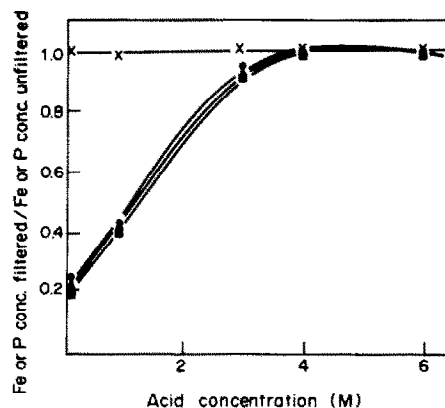


Fig. 1. Effect of acidification on particle size distribution for iron solution filtered with 0.80 μm (●), 0.45 μm (▲), 0.20 μm (■) membranes, and phosphorus solution filtered with 0.45 μm membrane filter (×). The precision of each data point is $\leq 10\%$ RSD.

Table 1. Water samples used in this work

Sample	Source	Characteristics
I	Chickahominy River at Walker's Dam, surface water	Conductivity = 128 μ mho; pH 6.8. Visibly large particulate matter; brownish.
II	Wastewater, Hampton Roads Sanitation district, James River Plant	Conductivity = 400 μ mho; pH 4.60. Greyish, high salt content; high chloride content.
III	Chickahominy River at Holdcroft, surface sample	Conductivity = 3050 μ mho; pH 7.5. No visible particulate matter; slightly cloudy.
IV	Tap water, Analytical Chemistry Laboratory, Hampton University	Conductivity = 200 μ mho; pH 6.25. Clear; colourless.
V	Wastewater, industrial discharge, Hercules, Inc.	Conductivity = 60 μ mho; pH 3.75. Dark brown; large salt content, organic layer present.

*The sites for samples I and III are approximately 10 miles apart, the latter being down the river closer to the mouth of the Chesapeake Bay.

surements are made on the same sample solution, which is common practice, the first result can differ significantly from the last, if changes occur in the sample during the measurement cycles.

This was found to be the case when an unacidified and unfiltered natural water sample (sample I, Table 1) was aspirated into the DCP for determination of iron content. The sample was shaken and then aspirated for 15 min, which represents about 13 separate measurement cycles. Figure 2 shows the iron concentrations found along with the values obtained for similar sample aliquots after filtration through 0.20, 0.45 and 0.80 μ m filters. The iron concentration of the unfiltered sample apparently decreased exponentially with time, but that found for the filtered samples remained constant. Also, the iron contents of the three filtrates were approximately identical, im-

plying that most of the particles were >0.80 μ m in size, and contained more than 90% of the iron.

The apparent decrease in iron content of the unfiltered sample with time can be attributed to several processes, including agglomeration and subsequent gravitational settling of iron-containing particles, settling of iron-containing solids, adsorption on the walls of the container, and loss in the spray chamber where large particles may lose momentum and fail to reach the plasma excitation zone. Particle agglomeration and settling appear to be by far the most influential of these processes. Figure 2 shows that a 0.8 or 0.45 μ m pore-size filter can remove substantial amounts (in this particular case, over 90%) of the measurable iron, which may therefore be regarded as being associated with the "solids" in the sample solution. To check whether or not the apparent decrease in the iron content of the unfiltered sample was due to severe clogging and/or changes in plasma conditions, the sodium contents of the filtrates and the unfiltered sample were also determined. All the fractions gave identical concentration as depicted by the horizontal line. This was confirmed by removing the residue from the filter and analysing it for iron; the results corresponded approximately to the 90% of the concentration measured during the first cycle.

For a given sample, the extent to which this "settling effect" is experienced may depend on the volume of the solution, the position at which the sample tubing is placed in the solution, and the time between the initial mixing and aspiration of the sample. However, the effect can be considerably reduced, if not completely eliminated, if the sample is constantly stirred during aspiration (Fig. 3).

In a later experiment, with a further sample from the same source as sample I, single measurements were made at 15-min intervals, the sample being removed from the DCP instrument and left un-stirred between measurements. The second and third

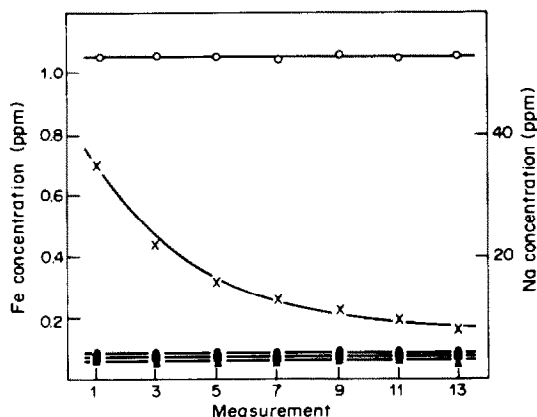


Fig. 2. Concentrations of iron and sodium found in water sample I in measurements at 70-sec intervals. Iron concentrations in samples unfiltered (x) and filtered with 0.80 μ m (●), 0.45 μ m (■), and 0.20 μ m (▲) filters. Sodium concentration in filtered and unfiltered sample (○). Each data point represents the mean of three replicate measurements. The precision of each mean was \leq 10% RSD.

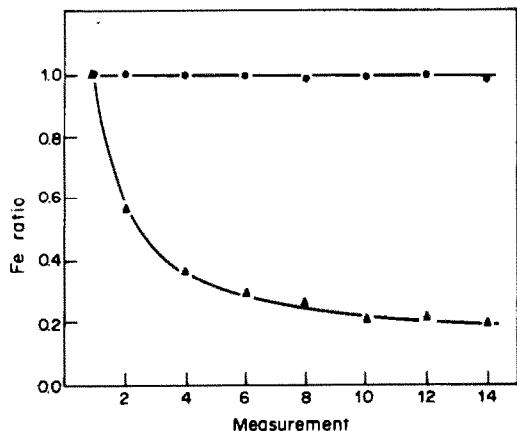


Fig. 3. Effects of stirring on "settling effect" (ratio of Fe found in measurement to Fe found in measurement 1). Measurements done at 70-sec intervals: with sample stirring (●); without sample stirring (▲).

measurements both gave an iron content that was $75 \pm 2\%$ of that found by the initial measurement (mean of three sets of determinations), thus confirming that settling takes place whether the sample is being aspirated or not, and that the effect levels off in about 15 min for the samples used in this work.

Whether there will be a settling effect for a given sample depends upon the concentration of the solids in it. This was demonstrated by examining samples II and III, which have particle distributions quite different from each other and from that of sample I. As shown in Fig. 4, the iron content (as a fraction of the total iron in the sample) in the three filtrates was 15% in the $0.2 \mu\text{m}$ filtrate, 20% in the $0.45 \mu\text{m}$ filtrate and 23% in the $0.80 \mu\text{m}$ filtrate. The settling effect was less pronounced than for sample I, corresponding to the shift towards smaller particle size in the size distribution. Again, phosphorus showed no settling

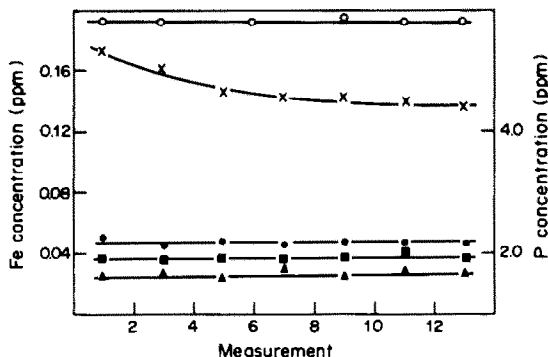


Fig. 4. Concentrations of iron and phosphorus found in water sample II in measurements at 70-sec intervals. Iron concentrations: unfiltered sample (x), filtered $0.80 \mu\text{m}$ (●) $0.45 \mu\text{m}$ (■), $0.20 \mu\text{m}$ filters (▲). Phosphorus concentration in unfiltered sample (○). Each data point represents the mean of three replicate measurements with a precision of $\leq \pm 10\%$ RSD.

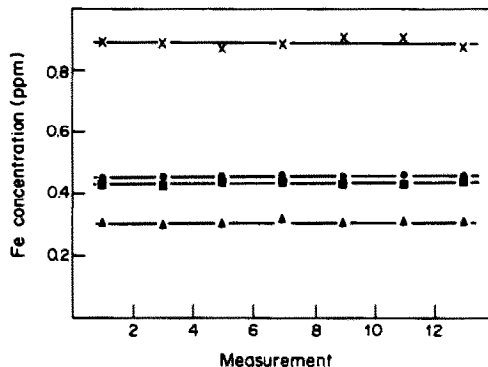


Fig. 5. Concentration of iron found in water sample III in measurements at 70-sec intervals. Unfiltered sample (x), filtered with $0.80 \mu\text{m}$ (●), $0.45 \mu\text{m}$ (■), $0.20 \mu\text{m}$ filters (▲). The precision of each data point is $\leq \pm 10\%$ RSD.

effect, confirming the difference in behaviour between elements. Sample III was described as being clear with very little visible particulate matter. The iron fraction in the filtrates was 35% in the $0.20 \mu\text{m}$ filtrate, 45% in the $0.45 \mu\text{m}$ filtrate and 50% in the $0.80 \mu\text{m}$ filtrate, and no settling effect was observed, as shown in Fig. 5.

From Figs. 2–5, it can be concluded that for elements such as iron, which tend to be adsorbed on particulate matter and/or form colloidal species, the concentration found in the filterable fraction is greatly influenced by the solids in the sample. High concentrations of solids and large sizes of particulate matter will decrease the concentration of such species in the filtrates. There will be poorer precision and reliability of analysis of unfiltered samples if appropriate corrective measures are not taken. However, from the results for the three samples studied, it appears that these adverse effects are negligible if the fraction of the sample that will pass through a $0.45 \mu\text{m}$ filter contains at least 50% of the total analyte concentration. Later, two further samples were examined, separate portions being filtered with media of various porosities, and the iron in the filtrates being determined. Table 2 shows that the bulk of the iron was associated with large particles.

It must be pointed out, however, that the analytical manipulations can affect the degree of the settling effects experienced, especially in direct analysis of samples without filtration and/or acidification. The rate at which the sample is introduced into the DCP can be crucial, for example. If several replicate measurements can be performed within the first few seconds, the settling effect can be reduced considerably, but other factors must also be considered. For example, the very high temperature of the DCP makes this atomization technique better able than the flame and electrothermal systems used in AAS, to tolerate comparatively large particles without deterioration in signal. Therefore, at least with DCP, the

Table 2. Distribution of iron between particles of different size range

Filter	Sample 1			Sample 2		
	Mean Fe, ppm	Fe ratio (Filtered/Unfiltered)	Fe retained by filter, %	Mean Fe, ppm	Fe ratio (Filtered/Unfiltered)	Fe retained by filter, %
Unfiltered	3.24 ± 0.03			1.76 ± 0.02		
Membrane, 0.45 μm	0.13 ± 0.05	0.04	96	0.02 ± 0.005	0.01	99
Sintered glass, fine (4-5.5 μm)	0.17 ± 0.04	0.05	95	0.04 ± 0.003	0.02	98
Sintered glass, medium (10-15 μm)	0.19 ± 0.04	0.06	94	0.06 ± 0.01	0.03	97
Sintered glass, coarse (40-60 μm)	0.37 ± 0.05	0.11	89	0.44 ± 0.01	0.25	75
Sintered glass, extra coarse (170-220 μm)	2.14 ± 0.03	0.66	34	1.19 ± 0.005	0.68	32

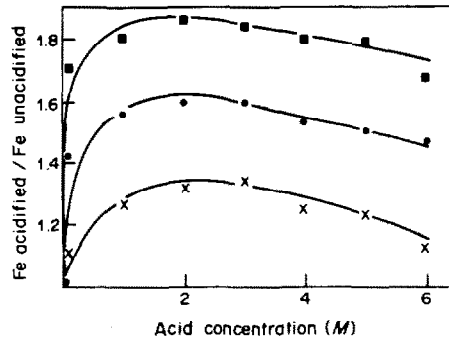


Fig. 6. Effect of acidification on the measured iron concentration in filtered and unfiltered samples: filtered, acidified with HCl (■), filtered, acidified with HNO₃ (●), unfiltered, acidified with HCl (×). The precision of each data point is ≤ ± 10% RSD.

adverse settling effects can be minimized simply by continuous agitation of the sample during aspiration.

The relationship between acidification and particle size distribution was investigated by comparing the iron content of acidified/filtered and acidified/unfiltered portions of sample I, acidification being done first. As shown in Fig. 6, not only did acidification cause an increase in the measured Fe concentration but this increase was more pronounced for the filtered samples. This indicates an increase in the concentration of Fe species with particle size smaller than 0.45 μm. Also, hydrochloric acid is more efficient than nitric acid for acidification, but for both acids the optimum concentration is 1-3M.

Influence of sample characteristics

Five different water samples (see Table 1) were adjusted to 1.0M hydrochloric acid concentration, filtered (0.45 μm membrane filters) and each filtrate was analysed for iron. The results are shown in Table 3.

The tap water had the largest fraction of filterable iron (*i.e.*, passing the filter) in the unacidified sample, so was the least affected by acidification. As might be expected, for all the water samples studied, acidification resulted in an increase in iron concentration in the filtrate to different extents.

Table 3. Fraction of iron in acidified (1.0M HCl) and unacidified water samples [means and standard deviations (range method) of three replicates] with and without filtration

Sample	Unacidified	Acidified
	Ratio: Filtered/Unfiltered	Ratio: Filtered/Unfiltered
I	0.10 ± 0.02	0.69 ± 0.02
II	0.20 ± 0.02	0.60 ± 0.02
III	0.45 ± 0.01	1.00 ± 0.02
IV	0.67 ± 0.01	1.07 ± 0.01
V	0.31 ± 0.02	0.50 ± 0.02

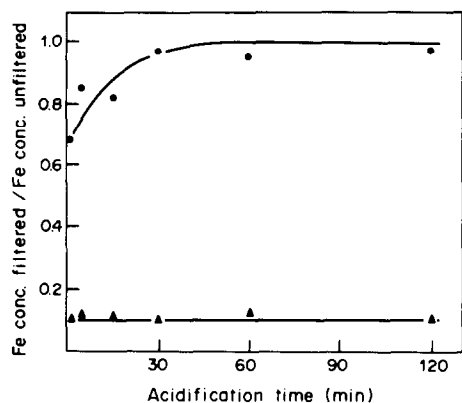


Fig. 7. Effect of duration of acidification: acidified sample (●), unacidified sample (▲). The precision of each data point is $\leq \pm 10\%$ RSD.

Effect of the duration of acidification

The duration of acidification can also influence the particle-size distribution. When equal portions of sample I were acidified (to 1.0M hydrochloric acid concentration), stirred for various periods of time, filtered (0.45 μm membrane), and the filtrates were analysed for iron, the amount of iron in the filtrate increased with stirring time (Fig. 7), becoming constant for ≥ 30 min stirring, practically all the iron then being in the filtrate. The iron content of filtered unacidified samples remained practically unchanged over the same period. These results indicate that a sufficient time must elapse between acidification and filtration, and should preferably be established experimentally for each sample. The alternative is to use a higher concentration of acid, which in certain situations may be undesirable.

Water column effects

Most elements, especially those which tend to form insoluble compounds, tend to increase in concentration with increasing depth in the water column. Table 4 shows the iron concentrations found for surface, bottom, and sediment samples obtained at Walker's Dam (Table 1). Though acidification did not cause much change in the iron content found for the surface and bottom samples, it increased that for the sediment sample by a factor of 10. This means that only about 10% of the iron in this sediment is in some form that can be described as water-bound,

Table 4. Fe content of surface, bottom and sediment samples from Walker's Dam

Position	Fe, ppm	
	Acidified	Unacidified
Surface	0.78 ± 0.04	0.77 ± 0.04
Bottom (7 m)	1.0 ± 0.03	0.87 ± 0.04
Sediment	$2.3 \times 10^4 \pm 100$	$2.3 \times 10^3 \pm 100$

and hence aspirable into the DCP. The term water-bound iron does not necessarily mean water-soluble; indeed the DCP can tolerate the introduction of relatively large particle sizes, some of which can be completely insoluble in water. The processing and preparation of sediment samples is discussed in the next section.

Influence of sediment characteristics on element content and fractionation

Sediments vary considerably in composition. In this study, two types of sediment were analysed for iron and phosphorus. The first was grey to dark grey in colour with a fine, soft texture and a water content of about 70%. The second was light brown; the texture was coarse and sandy, and the water content 30%. The sediments were dried at 80° to constant weight. This temperature was chosen to minimize thermal breakdown of colloidal and/or organic iron species. Samples of the sediments were then ball-milled to an average particle size of 100 μm . Known amounts were heated again at 80° for 2 hr and then digested with hydrochloric acid or distilled and demineralized water.

The acid digestion was done first with 50 ml of concentrated hydrochloric acid for 24 hr with stirring but no heating; then the mixture was heated at 100° with stirring, for another 2 hr. The resulting solution was decanted into a 100-ml standard flask and made up to volume with distilled and demineralized water. The final acid concentration was approximately 6M. The solution was aspirated directly into the DCP. Digestion with water was done similarly.

The results are shown in Table 5. These data indicate that not only did the soft, fine-textured sediment contain more iron than the coarse type, but also most of this iron was in the form of water-insoluble compounds. This is indicated by the fact that 10 times more iron was found in the acid-digested than in the water-digested sample. The dis-

Table 5. Iron and phosphorus content of river sediments

Sediment*	Extraction	Content, $\mu\text{g/g}$	
		Fe	P
Type I	Acid	$2.3 \times 10^4 \pm 0.01 \times 10^4$	928 ± 15
	DDW	$2.3 \times 10^3 \pm 0.1 \times 10^3$	149 ± 15
Type II	Acid	$1.1 \times 10^4 \pm 0.01 \times 10^4$	186 ± 4
	DDW	$2.3 \times 10^3 \pm 0.01 \times 10^3$	108 ± 2

*Type I: Dark grey, soft clay, fine particles.

Type II: Light brown, sandy, coarse particles.

tribution of phosphorus in the two types of sediment followed a similar pattern even though the actual concentrations measured were much smaller than the corresponding iron concentrations. Data such as these may have important implications for the role played by sediments on the bioavailability of elements in a water column.

CONCLUSION

Acidification and filtration of samples can have a profound effect on the determination of elemental fractionation and distribution in surface waters. Use of controlled acidification and filtration allows estimation of the fractions of an element that are particle-bound or soluble in water. The magnitudes of these fractions are influenced by the concentration and average size of solids in the water, the position of the sampling site in the water column, and the nature of the sediment underlying the water column.

Acidification increases the concentration of certain elements in the filtrate, but requires a certain minimum time for giving its full effect. The d.c. plasma is particularly suitable for analysis of complex samples containing large particles. If unacidified/unfiltered samples are used, some elements such as iron appear to undergo a "settling effect" resulting in a decrease in analyte concentration owing to adsorption, agglomeration and settling. Samples containing various concentrations of "solids" and particulate matter can be analysed by DCP with precisions of better than $\pm 10\%$ RSD provided the "settling effect" is avoided by proper acidification of the sample prior to aspiration, and/or by stirring the sample during aspiration.

Acknowledgements—This work was supported by a grant from the U.S. Environmental Protection Agency. Grant Number R808676020. The U.S. Environmental Protection Agency does not necessarily endorse any commercial products used in the study and that the conclusions represent the views of the authors and do not necessarily represent the opinions, policies, or recommendations of the Environmental Protection Agency. Thanks to R. A. Jordan and M. A. Taylor for assisting with sample collection.

REFERENCES

1. A. Siegel, in *Organic Compounds in Aquatic Environment*, S. J. Faust and J. V. Hunter (eds.), Dekker, New York, 1971.
2. *Trace Element Speciation in Surface Waters and Its Ecological Implications*, G. G. Leppard (ed.), Plenum Press, New York, 1983.
3. *Chemical Analysis of Inorganic Constituents of Water*, J. C. Van Loon (ed.), CRC Press, Boca Raton, Florida, 1982.
4. *Metallic Contaminants and Human Health*, D. K. D. Lee (ed.), Academic Press, New York, 1972.
5. P. D. Goulden, *Environmental Pollution Analysis*, Heyden, Philadelphia, 1978.
6. W. Stumm and P. A. Brauner, in *Chemical Oceanography*, 2nd Ed., J. P. Riley and G. Skirrow (eds.), Academic Press, New York, 1974.
7. R. Andrew, K. E. Biesinger and G. E. Glass, *Water Res.*, 1977, **11**, 309.
8. W. Sunder and R. R. L. Guillard, *J. Mar. Res.*, 1976, **34**, 511.
9. T. M. Florence and G. E. Batley, *Talanta*, 1977, **24**, 151.
10. Y. K. Chau and K. Lum-Shue-Chau, *Water Res.*, 1974, **8**, 383.
11. J. H. Trefry and S. Metz, *Anal. Chem.*, 1984, **56**, 754.
12. D. E. Coffin, *Can. J. Soil Sci.*, 1963, **43**, 7.
13. R. P. Gambrell, R. A. Khalid and W. H. Patrick, Jr., *Environ. Sci. Technol.*, 1980, **14**, 431.
14. R. Van Valin and J. W. Morse, *Mar. Chem.*, 1982, **11**, 535.
15. S. A. Sinex, A. Y. Cantillo and G. R. Helz, *Anal. Chem.*, 1980, **52**, 2342.
16. D. P. H. Laxen and M. I. Chandler, *ibid.*, 1983, **54**, 1350.
17. W. Stumm and H. Bilinski, in *Advances In Water Pollution Research*, S. H. Jenkins (ed.), pp. 39–49. Pergamon Press, Oxford, 1973.
18. I. P. H. Laxen and R. M. Harrison, *Sci. Total Environ.*, 1981, **19**, 59.
19. A. J. Bale and A. W. Morris, *Estuarine Coastal Shelf Sci.*, 1981, **13**, 1.
20. E. R. Sholkovitz, E. A. Boyle and N. B. Price, *Earth Planet. Sci. Lett.*, 1978, **40**, 130.
21. G. Figueres, J. M. Martin and M. Meybeck, *Neth. J. Sea Res.* 1978, **12**, 329.
22. I. Ayoyama, I. Sakai and Y. Inove, *Mizu Shori Gijutsu*, 1976, **17**, 913.
23. K. Y. Chen, C. S. Young, T. K. Jan and N. Rohatgi, *J. Water Pollut. Control Fed.*, 1974, **46**, 2663.
24. I. T. Urasa, *Anal. Chem.*, 1984, **56**, 904.
25. *Idem*, *Ph.D. Thesis*, Colorado State University, Fort Collins, CO, 1977.
26. R. K. Skogerboe and I. T. Urasa, *Appl. Spectrosc.*, 1978, **32**, 527.

SEPARATION AND PRECONCENTRATION OF THE RARE-EARTH ELEMENTS AND YTTRIUM FROM GEOLOGICAL MATERIALS BY ION-EXCHANGE AND SEQUENTIAL ACID ELUTION

J. G. CROCK, F. E. LICHTÉ, G. O. RIDDLE and C. L. BEECH

U.S. Geological Survey, Denver Federal Center, MS 928, Denver, Colorado 80225, U.S.A.

(Received 31 July 1985. Revised 17 January 1986. Accepted 4 February 1986)

Summary—The abundance of rare-earth elements (REE) and yttrium in geological materials is generally low, and most samples contain elements that interfere in the determination of the REE and Y, so a separation and/or preconcentration step is often necessary. This is often achieved by ion-exchange chromatography with either nitric or hydrochloric acid. It is advantageous, however, to use both acids sequentially. The final solution thus obtained contains only the REE and Y, with minor amounts of Al, Ba, Ca, Sc, Sr and Ti. Elements that potentially interfere, such as Be, Co, Cr, Fe, Mn, Th, U, V and Zr, are virtually eliminated. Inductively-coupled argon plasma atomic-emission spectroscopy can then be used for a final precise and accurate measurement. The method can also be used with other instrumental methods of analysis.

The rare-earth elements (REE) and yttrium, as a group or separately, have been determined by many instrumental techniques, including colorimetry,^{1,2} isotope-dilution-mass-spectrometry,³ spark-source mass-spectrometry,⁴ neutron-activation analysis,⁵ optical-emission spectrometry,⁶ atomic-absorption spectrometry,⁷ and inductively-coupled argon plasma atomic-emission spectrometry (ICAP-AES).^{8,9} Most of the spectroscopic methods, including ICAP-AES, are affected by spectral interferences, and a separation and preconcentration step is thus necessary when ICAP-AES is used to determine the REE and Y at or near their chondritic abundances. This step should reduce the total salt concentration in the analytical solution (to allow use of a large sample dissolved in a small volume), eliminate potentially interfering non-REE, and completely recover the REE and Y as a group (because the yield cannot be determined by the addition of a tracer). Ion-exchange separation of the REE and Y has already proved useful for the purpose¹⁰ and the procedure has now been improved, by eliminating the need to use anion-exchange following cation-exchange.⁸

EXPERIMENTAL

Sample dissolution

A mixture of hydrochloric, nitric, hydrofluoric and perchloric acids was used to decompose 1.000-g samples of the geological material, as described earlier.¹¹ The chromatographic separation was studied with basalt and granite standards spiked with 1 mg each of As, Be, Ce, Cu, Ho, La, P, Sc, Th, U, V, Y, Zn and Zr, all added individually as solutions before the sample decomposition digestion, to

bring the concentration of these elements above the detection limits of the ICAP-AES procedure.¹² The residue from evaporation of the acids was dissolved in 50 ml of 1M hydrochloric acid.

Baker "Intra Analyzed" hydrochloric and nitric acids, G. F. Smith doubly-distilled perchloric acid, and Baker reagent-grade hydrofluoric acid were used throughout.*

ICAP-AES

A 63-channel Jarrell-Ash ICAP spectrometer model 1160 Atom Comp was used. The operating parameters are given in Table 1. A description of the instrument and a listing of the analytical wavelengths are given elsewhere.^{8,12} Calibration was done with REE and Y standards prepared by serial dilution of solutions made from individual 99.999% pure REE oxides (Spex Industries); new bottles of the oxides were used for the purpose, to avoid error from uptake of atmospheric moisture and carbon dioxide.

Ion-exchange procedure

Fractions of eluate were collected over equal-time (3 min) rather than equal-volume intervals for determination of the elution patterns, the fractions being about 4-5 ml in volume. A modified Technicon auto sampler II was used as the fraction collector. The ion-exchange apparatus consisted of a 30 × 1 cm column fitted with a coarse glass frit and a 250-ml reservoir for the eluent. The column was packed with a 20-cm long bed of 100-200 mesh Bio-Rad AG50-X8 cation-exchange resin equilibrated with 1M hydrochloric acid. In the elution studies, about 50 fractions were collected in each experiment and analysed by ICAP-AES for the elements of interest.

The elution procedure was as follows:

- (1) load 50 ml of sample solution (in 1M hydrochloric acid);
- (2) elute with 50 ml of 2M hydrochloric acid, followed by 50 ml of 2M nitric acid, discarding both eluates;
- (3) elute with 50 ml of 6M nitric acid, followed by 50 ml of 8M nitric acid, combine the eluates and evaporate to dryness for subsequent REE and Y determination;
- (4) regenerate the column by washing with 100 ml of 8M nitric acid; the column can be regenerated at least 20 times before breakdown of the resin is observed.

*Use of trade and company names is for descriptive purposes only and does not imply endorsement by the U.S. Geological Survey.

Table 1. Standard operating conditions for the ICAP system

Power	1150 W
Gas flow	18 l./min (coolant)
	450 ml/min (sample)
Sample uptake	0.7 ml/min
Observation height	14 mm above load coil
Dispersion	0.54 nm/mm
Nebulizer	Modified Babington
Optics	1:3 magnification
Slits	"25 μ ", entrance
	"50 μ ", exit
Internal standard	Lu, 5 μ g/ml, 261.5 nm (elution studies)
	Cd, 10 μ g/ml, 226.5 nm (REE analysis)

RESULTS AND DISCUSSION

The REE and Y chondritic abundances sum to about 5 μ g/g, so the concentration of an individual REE is often below the detection limit of many analytical methods. This problem can be dealt with by preconcentration and separation of the REE and Y, so that, for example, a 1,000-g sample can be dissolved and the REE and Y can be concentrated in a 5-ml final volume instead of the normal 50 or 100 ml obtained in an acid digestion. Separating the REE and Y from the rock matrix removes the bulk of the dissolved salts and also minimizes spectral interferences from non-REE in the ICAP-AES determination. After the cation-exchange separation proposed here, the only important spectral interferences that remain are those from the REE themselves.

This investigation examined the interferences in ICAP-AES, but the information obtained can also be applied to other measurement techniques such as atomic-absorption spectrometry or neutron-activation analysis. The elution study was conducted with representative members of the REE group;

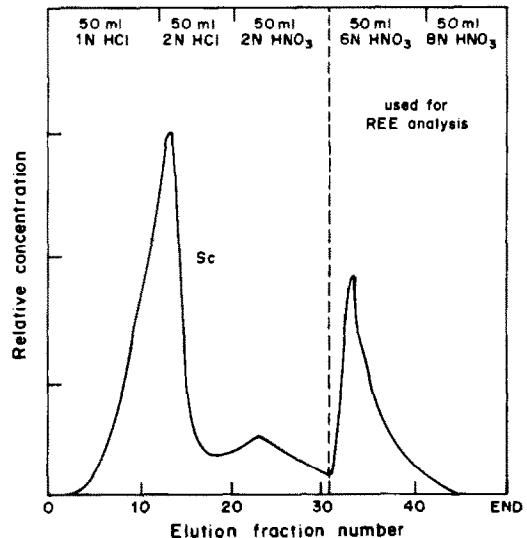
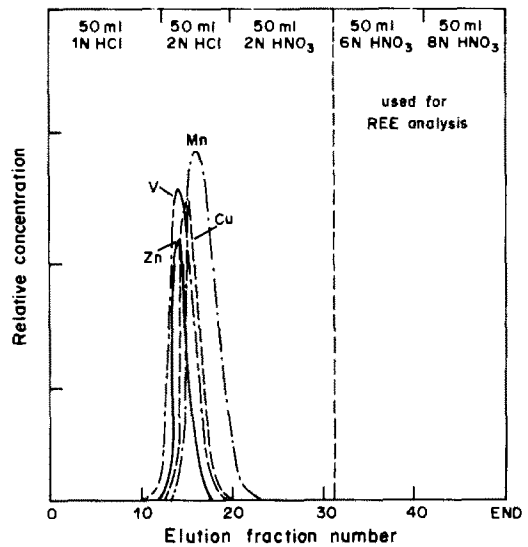
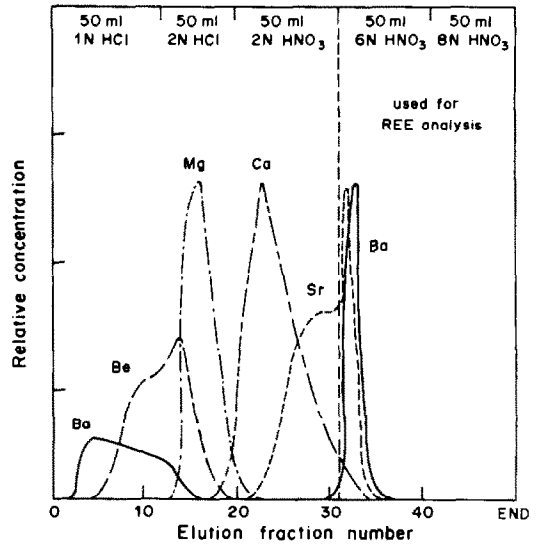
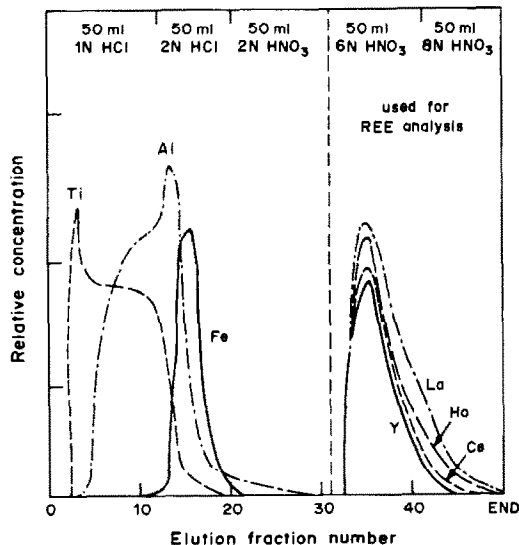


Fig. 1. Separation of selected metals by gradient elution, from a solution obtained by acid decomposition of an in-house basalt standard.

Table 2. Recovery* of non-REE in the elution fractions used for REE analysis

	Granite		Basalt	
	Amount of element in original sample, mg/g	Recovery, %	Amount of element in original sample, mg/g	Recovery, %
Al	75	4.0	95	1.7
Ba	0.63	98	0.97	100
Ca	16	2.5	52	0.8
Fe	28	0.1	66	0.1
K	31	<0.1	28	<0.1
Mg	5.4	<0.01	24	<0.01
Mn	0.72	0.1	15	0.1
Na	20	0.5	20	0.2
P	0.20	<0.01	3.0	<0.01
Sc	0.009	85	0.021	93
Sr	0.22	32	1.29	13
Ti	2.0	0.2	4.5	1.1
V	0.038	0.1	0.19	0.3

$$\text{*Recovery} = \frac{\text{mg present in REE fraction}}{\text{mg present in original sample}} \times 100.$$

Recovery based on non-spiked digestions of the in-house standards.

cerium and lanthanum as lighter REE, holmium as an end-member of both the lighter and heavier REE, and yttrium to characterize the elution of the heavy REE as well as its own behaviour. The bulk of the REE and Y was eluted with 50 ml of 6M nitric acid and the remainder with 50 ml of 8M nitric acid (Fig. 1). In contrast, corresponding elution of the REE and Y with hydrochloric acid requires more than 160 ml of eluent and gives broader peaks.¹¹

The similarity of the ionic charge and radius of scandium to the REE suggest that this element should behave similarly to the REE in the system, but its cation-exchange behaviour is in fact quite different, since it produces several peaks in the chromatogram, most of it being eluted before the REE, but a substantial fraction with the REE (Fig. 1).

The alkali and alkaline-earth metals (except strontium and calcium, which are also split) are removed

Table 3. Comparative concentrations of the REE and Y in U.S. Geological Survey standard basalt BCR-1*

	This study†	ICAP-AES [§]	Neutron-activation analysis average [§]	Isotope-dilution average ³	Usable value ¹⁴
Y	33.3 ± 0.4	35.3 ± 0.3			40
La	24.8 ± 0.3	26.6 ± 0.2	25.3 ± 0.5	25.3 ± 0.9	27
Ce	52.2 ± 1.2	53.8 ± 0.2	54.5 ± 1.1	54.0 ± 0.8	53
Pr	6.7 ± 0.1	7.29 ± 0.06			7
Nd	28.8 ± 0.4	29.7 ± 0.3	29.1 ± 0.6	28.6 ± 0.5	26
Sm	6.6 ± 0.1	6.7 ± 0.3	6.67 ± 0.20	6.7 ± 0.2	6.5
Eu	2.05 ± 0.03	1.98 ± 0.08	1.97 ± 0.04	1.95 ± 0.03	2.0
Gd	7.0 ± 0.1	6.9 ± 0.2	6.64 ± 0.32	6.63 ± 0.08	1.55‡
Tb	1.2 ± 0.1	1.0 ± 0.1			1.0
Dy	6.4 ± 0.2	6.72 ± 0.08	6.47 ± 0.21	6.3 ± 0.1	7
Ho	1.25 ± 0.01	1.40 ± 0.02			1.2
Er	3.59 ± 0.06	3.80 ± 0.03		3.61 ± 0.09	3.5
Tm	0.50 ± 0.01	0.57 ± 0.02	0.57 ± 0.05		0.6
Yb	3.40 ± 0.05	3.70 ± 0.03	3.48 ± 0.14	3.39 ± 0.04	3.4
Lu	0.49 ± 0.01	0.524 ± 0.004	0.55 ± 0.03	0.54 ± 0.03	0.5

*All values given as µg/g.

†The mean and 95% confidence limit of 3 splits, each analysed 3 times (n = 9).

‡Abbey¹⁵ lists Gd as 6.6 µg/g.

§H. T. Millard, U.S. Geological Survey, Denver, CO, private communication, 1981.

Table 4. Comparative concentrations of the REE and Y in U.S. Geological Survey standards basalt BHVO-1*

	This study†	ICAP-AES ⁸	Neutron-activation analysis average ¹⁶	Isotope-dilution average§	Usable value ¹⁶	Usable value ¹⁴
Y	24.2 ± 0.4	25.7 ± 0.3			28 ± 2	27
La	15.2 ± 0.2	16.2 ± 0.1			16.7 ± 0.8	17
Ce	37.5 ± 1.0	38.2 ± 0.7	43.2 ± 3.9	38.4	41 ± 4	39
Pr	5.2 ± 0.3	5.66 ± 0.05			5.6	
Nd	24.8 ± 0.6	25.4 ± 0.2	25.9 ± 6.6	24.5	24 ± 6	24
Sm	6.08 ± 0.09	6.4 ± 0.2	6.84 ± 0.29	6.08	6.1 ± 0.7	6.1
Eu	2.18 ± 0.04	2.18 ± 0.07	2.74 ± 0.6	2.09	2.0 ± 0.4	2.0
Gd	6.8 ± 0.2	7.0 ± 0.3	9.2 ± 0.7	6.09	7 ± 2	6.0
Tb	0.99 ± 0.07	0.86 ± 0.08	1.02 ± 0.07		1.0 ± 0.2	1.0
Dy	5.3 ± 0.1	5.59 ± 0.07		5.26	4.8 ± 0.26	5
Ho	0.90 ± 0.02	1.06 ± 0.04			0.94	
Er	2.47 ± 0.05	2.63 ± 0.03		2.49	2.0 ± 0.3	
Tm	0.29 ± 0.02	0.34 ± 0.02	0.34 ± 0.05		0.31 ± 0.04	0.3
Yb	2.02 ± 0.05	2.19 ± 0.03	2.46 ± 0.23	2.02	2.1 ± 0.5	1.9
Lu	0.26 ± 0.01	0.291 ± 0.003			0.32	

*All values as $\mu\text{g/g}$.

†The mean and the 95% confidence limit of 3 splits, each analysed 3 times ($n = 9$).

§D. Lambert and E. C. Simmons, Colorado School of Mines, Dept. of Geochemistry, Golden, CO, private communication, 1981.

in the loading and first elution (steps 1 and 2), like other major elements, including Al, Cu, Fe, Mn, Ti, U, V, Zn and Zr, which need to be separated to reduce the total salt concentration and eliminate spectral interference. A major advantage of the sequential acid elution is the removal of iron (Fig. 1). Some elements which behave as anionic or molecular species in the sample digest are also eliminated. Arsenic and phosphorus are typical examples and pass through the cation-exchange column very quickly.

The removal of Zr and U is important because they often pose spectral interference problems by ICAP-AES. The appearance of some of the Al, Ba, Ca, Sc, Sr and Ti in the REE fraction does not matter, as they do not interfere at the levels present.

The cation-exchange procedure is very effective for separating and eliminating many common matrix elements, and removing possibly interfering non-REE elements, as shown in Table 2, for typical granite and basalt samples. In contrast to the chromatographic elution study, no spiking was used to enhance the elution behaviour of the minor components in these samples, and the data in Table 2 should represent the behaviour of most common silicate rock samples. These results also suggest that the splitting of Ba, Ca, Sc and Sr may be a column-loading effect.

The results for application of the method to a series of established and recently introduced geological standard reference materials to test its precision and accuracy, compare favourably with the published and accepted values (Tables 3-5).

The means and 95% confidence limits for analysis of four recently introduced U.S. Geological Survey

standards (without accepted published values), based on the triplicate analysis of three splits, are also presented (Table 6).

Conclusions

The elution behaviour of a variety of alkali, alkaline-earth and transition-metal elements commonly found in geological material has been established for a cation-exchange procedure using hydrochloric acid and nitric acid sequentially as eluents. This separation eliminates the need for a separate anion-exchange procedure to eliminate Fe when only nitric acid is used as the eluent.⁸ The method also requires smaller eluent volumes than those needed in schemes using only hydrochloric acid as eluent¹² and is, therefore, more rapid. The total eluent volume is 24% less than that in an earlier method.⁸ A complete separation can be finished in approximately 4 hr, and lower reagent blanks can be expected because less reagent is used.

The results obtained for a variety of geological reference materials demonstrate that the procedure allows precise and accurate analysis of geological samples for their REE and Y content. Also, because the total salt concentration is reduced and potentially interfering elements are eliminated, the procedure can be used in conjunction with other methods for the final determination of the REE and Y.

A possible drawback of the method is that if the sample is not completely soluble in the acid mixture, and a lithium metaborate fusion is used, the fusion cake will not be always completely soluble in the 50 ml of 1M hydrochloric acid used in the procedure (boric acid is precipitated).

Table 5. REE and Y content* of 5 new U.S. Geological Survey standards

	DNC-1 Diabase§		W-2 Centerville Diabase§		BIR-1 Icelandic Basalt§		SDC-1 Mica Schist		STM-1 Nepheline Syenite	
	This study†	Abbey (1983)	This study†	Abbey (1983)	This study†	Abbey (1983)	This study†	Abbey (1983)	This study†	Abbey (1983)
Y	16.1 ± 0.2	18	19.7 ± 0.3	23	14.4 ± 0.2	16	32.3 ± 0.7	42	41.9 ± 0.3	46
La	3.48 ± 0.04	3.6	10.2 ± 0.2	10.5	0.51 ± 0.05	0.65	41.2 ± 0.5	42	144 ± 3.0	150
Ce	7.8 ± 0.1	9.1	22.2 ± 0.4	23	1.9 ± 0.3	1.6	87.6 ± 1.0	92	257 ± 2	260
Pr	0.9 ± 0.1		2.8 ± 0.1		0.2 ± 0.1		10.6 ± 0.1		26.6 ± 0.6	
Nd	4.9 ± 0.1	5.2	12.8 ± 0.2	13.5	2.4 ± 0.1		40.8 ± 0.6	38	80.1 ± 0.9	78
Sm	1.3 ± 0.1	1.4	3.2 ± 0.1	3.3	1.1 ± 0.1	1.0	8.1 ± 0.1	8.3	12.5 ± 0.1	13
Eu	0.61 ± 0.01	0.59	1.14 ± 0.02	1.1	0.53 ± 0.01	0.55	1.65 ± 0.02	1.7	3.58 ± 0.07	3.7
Gd	2.4 ± 0.1		3.9 ± 0.1		2.3 ± 0.1		7.4 ± 0.2	7.2	9.2 ± 0.2	10
Tb	0.4 ± 0.1	0.4	0.7 ± 0.1	0.65	0.4 ± 0.1		1.4 ± 0.4	1.2	1.8 ± 0.1	1.6
Dy	2.67 ± 0.04	3.0	3.82 ± 0.07		2.4 ± 0.1	3.7	6.3 ± 0.2		7.9 ± 0.2	
Ho	0.56 ± 0.02		0.73 ± 0.02		0.51 ± 0.02		1.18 ± 0.03		1.46 ± 0.04	2
Er	1.90 ± 0.04		2.18 ± 0.05		1.69 ± 0.04		3.46 ± 0.09		4.15 ± 0.07	
Tm	0.27 ± 0.01	0.3	0.31 ± 0.01	0.4	0.23 ± 0.02		0.48 ± 0.01	0.7	0.57 ± 0.04	
Yb	1.94 ± 0.02	2.0	2.04 ± 0.04	2.1	1.63 ± 0.03	1.7	3.41 ± 0.10	4.2	4.39 ± 0.03	4.3
Lu	0.28 ± 0.01	0.32	0.18 ± 0.01	0.33	0.23 ± 0.01	0.29	0.47 ± 0.02		0.62 ± 0.01	

*All concentrations are as µg/g.

†The mean and 95% confidence limits of 3 splits, each analysed 3 times (n = 9).

‡This newly issued USGS standard is described elsewhere.¹⁸

Table 6. REE and Y content* of 4 new U.S. Geological Survey standards

	SDO-1 Devonian Ohio shale	TLM-1 Tonalite	AMH-1 Mt. Hood Andesite	GSM-1 Gabbro
Y	35.6 ± 0.6	23.3 ± 0.3	14.4 ± 0.3	8.2 ± 0.3
La	35.2 ± 0.7	12.1 ± 0.5	16.0 ± 0.6	2.0 ± 0.2
Ce	71.8 ± 1.2	27.4 ± 0.5	33.3 ± 0.9	4.8 ± 0.3
Pr	9.2 ± 0.2	3.8 ± 0.4	4.1 ± 0.2	0.7 ± 0.2
Nd	36.3 ± 0.6	16.7 ± 0.4	17.3 ± 0.4	3.4 ± 0.2
Sm	7.6 ± 0.1	4.0 ± 0.1	3.6 ± 0.1	1.1 ± 0.1
Eu	1.65 ± 0.03	1.03 ± 0.02	1.18 ± 0.03	0.56 ± 0.01
Gd	7.8 ± 0.2	4.4 ± 0.1	3.7 ± 0.3	1.6 ± 0.1
Tb	1.4 ± 0.3	0.7 ± 0.1	0.7 ± 0.2	0.3 ± 0.1
Dy	6.1 ± 0.2	4.3 ± 0.1	2.8 ± 0.1	1.7 ± 0.1
Ho	1.14 ± 0.02	0.81 ± 0.02	0.49 ± 0.02	0.31 ± 0.01
Er	3.26 ± 0.06	2.50 ± 0.04	1.46 ± 0.07	1.01 ± 0.03
Tm	0.44 ± 0.01	0.34 ± 0.02	0.20 ± 0.01	0.15 ± 0.01
Yb	3.11 ± 0.05	2.38 ± 0.04	1.37 ± 0.04	0.94 ± 0.01
Lu	0.44 ± 0.01	0.34 ± 0.01	0.19 ± 0.01	0.120 ± 0.005

*All concentrations as $\mu\text{g/g}$. The mean and 95% confidence limits of 3 splits, each analysed 3 times ($n = 9$).

REFERENCES

1. C. V. Banks and D. W. Klingman, *Anal. Chim. Acta*, 1956, **15**, 356.
2. H. Onishi and C. V. Banks, *Talanta*, 1963, **10**, 389.
3. G. N. Hanson, in *Accuracy in Trace Analysis: Sampling, Sample Handling, Analysis*, Vol. II, P. D. LaFleur (ed.), p. 937. U.S. Govt. Printing Office, Washington D.C., 1976.
4. S. R. Taylor and M. P. Gorton, *Geochim. Cosmochim. Acta*, 1977, **41**, 1375.
5. L. A. Haskin, T. R. Wildeman and M. A. Haskin, *J. Radn. Chem.*, 1968, **1**, 337.
6. S. Berman, *Geochim. Cosmochim. Acta*, 1957, **12**, 271.
7. J. G. Sen Gupta, *Talanta*, 1981, **28**, 31.
8. J. G. Crock and F. E. Lichte, *Anal. Chem.*, 1982, **54**, 1329.
9. J. N. Walsh, F. Buckley and J. Barker, *Chem. Geol.*, 1981, **33**, 141.
10. J. G. Crock, F. E. Lichte and T. R. Wildeman, *Chem. Geol.*, 1984, **45**, 149.
11. J. G. Crock and R. C. Severson, *U.S. Geol. Surv. Circular*, 1980, No. 841.
12. J. G. Crock, F. E. Lichte and P. H. Briggs, *Geostds. Newsl.*, 1983, **7**, 335.
13. R. A. Zielinski, *Geochim. Cosmochim. Acta*, 1975, **39**, 713.
14. G. N. Hanson, *Ann. Rev. Earth Planet. Sci.*, 1980, **8**, 371.
15. S. Abbey, *Geol. Surv. Can. Paper*, 1983, No. 83-15.
16. *Idem, ibid.*, 1980, No. 80-14.
17. P. A. Baedecker, J. J. Rowe and E. Steinness, *J. Radn. Chem.*, 1977, **40**, 115.
18. E. S. Gladney and W. E. Goode, *Geostds. Newsl.*, 1981, **5**, 31.
19. C. C. Graham, M. D. Glascock, J. J. Carni, J. R. Spalding and T. G. Spalding, *Anal. Chem.*, 1982, **54**, 1623.
20. F. J. Flanagan, *U.S. Geol. Surv. Bull.*, 1984, No. 1623.

SPECTROPHOTOMETRIC DETERMINATION OF INDIUM IN NICKEL ALLOYS AND ZINC ORES WITH 1-(2-PYRIDYLMETHYLIDENEAMINE)-3- (SALICYLIDENEAMINE)THIOUREA

DANIEL ROSALES, ISABEL MILLAN and JOSE L. GOMEZ ARIZA

Department of Analytical Chemistry, Faculty of Chemistry, University of Sevilla, 41012 Sevilla, Spain

(Received 12 September 1985. Accepted 23 November 1985)

Summary—A sensitive method for the spectrophotometric determination of indium with 1-(2-pyridylmethylideneamine)-3-(salicylideneamine)thiourea is proposed. A yellow complex is formed at pH 4.5 (succinate buffer) in a medium containing 40% dimethylformamide, and the absorbance is measured at 415 nm. The molar absorptivity is $6.2 \times 10^4 \text{ l. mole}^{-1} \text{ cm}^{-1}$. The relative standard deviation of the procedure is 1.5%. The method has been applied to determination of indium in a nickel alloy and three zinc ores, with prior isolation of indium by co-precipitation with ammonia and extraction into *n*-butyl acetate from 5*M* hydrobromic acid.

The content of indium in the earth's crust is about $10^{-5}\%$. In sphalerites, chalcopyrites, sulphostannates and sulphogermanates, which are the principle sources of indium, the content ranges from less than $10^{-4}\%$ to $10^{-1}\%$.¹ Indium is usually recovered as a by-product in the zinc industry, and is responsible, together with lead, cadmium and tin, for the embrittlement of zinc alloys.² Indium is used to protect bearings from corrosion, as a semiconductor, in non-ferrous metallurgy, in electric contacts and reflectors, in the jewellery trade, in fluorescent glass and in the dental profession. Certain indium compounds are also used as colouring matter in the ceramic industry.

The indium content in different materials has been determined by several methods: polarographically in beryllium compounds,³ zinc and zinc alloys^{1,2,4} and pure tin;⁵ by anodic-stripping voltammetry in tin;⁶ by radioactivation methods in feldspars,⁷ cylindrite,⁸ gallium,^{1,9} zinc,^{1,9,10} rocks^{1,11,12} and biological materials;¹³ titrimetrically with EDTA in aluminium¹⁴ and sphalerite;¹ by emission spectroscopy in minerals and rocks,^{1,15} aluminium alloys,¹⁶ cadmium¹⁷ and zinc alloys;¹⁸ by atomic-absorption spectrometry in foodstuffs,¹⁹ sulphides,^{20,21} aluminium,¹⁷ zinc¹⁸ and nickel alloys;²² by infrared spectroscopy in silicon crystals;²³ fluorimetrically with Rhodamine 6Z in gallium,²⁴ with quinolin-8-ol in dusts¹ and with Butylrhodamine B, sulphonazo and Rhodamine 6G or 3B in minerals;^{20,24-26} and spectrophotometrically with dithizone in uranium and thorium salts,²⁵ mineral and zinc compounds^{20,28} and germanium,²⁹ with diphenylcarbazone in germanium,²⁴ with arsenazo,³⁰ morin,³¹ salicylfluorone,³² Rhodamine 6F,³³ Bromopyrogallol Red,³⁴ 5,7-dibromoquinolin-8-ol,^{24,35,36} Methylthymol Blue²⁴ and Rhodamine 6G²⁶ or B²⁷ in

zinc compounds or similar matrices, with 4-(2-pyridylazo)resorcinol in minerals^{31,37} and silver-tin alloys,³⁸ with quinalizarin in organic matter,¹ with phenylfluorone in lead concentrate,²⁴ with quinolin-8-ol in cylindrite,⁸ germanium²⁹ and ores,^{24,26} with trihydroxyfluorones in cassiterite,²⁴ with Malachite Green in gallium²⁶ and with 1-(2-pyridylazo)-2-naphthol in zinc compounds³⁹ and germanium films.⁴⁰

In almost all these methods, a prior separation of indium from associated elements is necessary. Separations have been done by extraction of the bromide or iodide complex into diethyl ether,^{1,3,26,29,41} di-isopropyl ether,^{28,34,41} *n*-butyl acetate,^{15,26} chloroform²⁶ and diantipyrylmethane;²⁶ with dithizone into chloroform,^{1,27,41} with an alkylphosphoric acid into octane,²⁶ with thiosulphate into 15% tributyl phosphate in kerosine;⁴² with diethyldithiocarbamate into isobutyl methyl ketone,^{16,26} with quinolin-8-ol into chloroform;⁸ and with thiothenoyltrifluoroacetone.³² Separations have also been done by precipitation with hydrogen sulphide,⁴¹ ammonia^{1,26,41} or sodium hydroxide;^{1,4} by hydrolysis with potassium cyanate;¹ and by ion-exchange^{1,14,20,41,44} or chromatographic methods.^{1,12,25} Indium can be preconcentrated by co-precipitation with cadmium, aluminium or iron-(III).^{26,34}

During studies on Schiff's bases derived from thiocarbohydrazide,⁴⁵ it was found that the asymmetric compound 1-(2-pyridylmethylideneamine)-3-(salicylideneamine)thiourea (PST) behaves as a sensitive reagent for the spectrophotometric determination of indium. In this paper, development and testing of the method involving the use of PST is described. The method has been applied to the determination of indium in several samples.

EXPERIMENTAL

Apparatus

Perkin-Elmer Model 554 and Coleman Model 55 spectrophotometers and a Beckman Model 70 pH-meter with a combined SCE-glass electrode were used.

Reagents

All chemicals used were of analytical-reagent grade or better. Water that had been glass-distilled and demineralized was used throughout. A 0.1% PST solution in dimethylformamide (DMF) was prepared from PST·H₂O, which was synthesized as described previously.⁴⁵ This solution was stable for 3 months. A standard solution of In(III) (4.742 g/l.) in 1M hydrochloric acid was prepared from indium nitrate pentahydrate and standardized by EDTA titration. Working solutions were prepared by suitable dilution. A succinate buffer of pH 4.5 was prepared by dissolving 12 g of succinic acid and 17 g of potassium hydroxide in distilled water and diluting to 1 litre.

Recommended procedure

Into a 25-ml standard flask, transfer an aliquot of sample solution containing up to 37 µg of indium, 3–5 ml of pH 4.5 succinate buffer, 3 ml of 0.1% PST solution and 7 ml of DMF. Dilute to the mark with water and mix well. Measure the absorbance at 415 nm (1.0-cm cell) against a similarly prepared reagent blank. Use a calibration graph or empirical equation to convert the absorbance into concentration.

Determination of indium in alloys and ores

Weigh accurately about 1 g of sample, transfer it into a beaker, heat it first with 5 ml of concentrated hydrochloric acid and then with 10 ml of concentrated nitric acid and 2 ml of bromine, and evaporate the solution nearly to dryness, on a sand-bath. Then add 2 ml of concentrated sulphuric acid and heat until copious white fumes are evolved. After cooling, take up the residue with approximately 25 ml of 1.5M hydrochloric acid and filter the solution through a Whatman 41 filter paper into a 50-ml standard flask. Wash the beaker and filter paper with 1.5M hydrochloric acid to make up the volume to the mark. Place 25 ml of this solution in a 250-ml beaker and dilute it to ~50 ml with water. Add concentrated ammonia solution dropwise with stirring until the solution is alkaline, then let it stand for 15 min. Filter (Whatman 44 filter paper) and wash the residue with 50 ml of 1% ammonium chloride solution adjusted to pH 9 with ammonia. Discard the filtrate. Dissolve the residue by adding 10–20 ml of 5M hydrobromic acid dropwise and transfer the solution into a 100-ml separating funnel. Reduce iron(III) by addition of several drops of 15% titanium(III) chloride solution and extract the indium by shaking with 10 ml of n-butyl acetate for 3 min. Discard the aqueous layer and wash the extract by shaking it first for 1 min with 3 ml of 5M hydrobromic acid containing 2 or 3 drops of 15% titanium(III) chloride solution and then with 3 ml of 5M hydrobromic acid for 30 sec. Strip the indium from the organic phase with two 20-ml portions of 6M hydrochloric acid containing 2 or 3 drops of 30% hydrogen peroxide. Evaporate the solution to dryness on a sand-bath, dissolve the residue in water and dilute it to volume in a 25-ml standard flask. Determine the indium content by the recommended procedure, using 5 ml of buffer solution.

RESULTS AND DISCUSSION

PST and In(III) in weakly acid media form a yellow complex which has an absorption maximum at 415 nm. The intensity of the colour developed remains constant with at least a 7-fold molar excess of reagent, and a 3-ml volume of 0.1% reagent solution was therefore chosen. The absorbance of the complex

at 415 nm is independent of pH over the range 4.0–5.5. In preliminary studies it was found that large amounts of acetate decrease the absorbance of the complex, so a succinate buffer of pH 4.5 was selected for the analytical procedure. The amount of this buffer added (1–5 ml) has no effect on the absorbance. The absorbance of the reagent blank at 415 nm was 0.037 ± 0.003 (7 samples).

Choice of solvent

The absorption spectra of the In(III)–PST complex at pH 4.5 in various water-soluble solvents were similar. A mixture of water and DMF was chosen because the reagent was more soluble in it. The concentration of DMF affects the absorbance of the complex, but the absorbance is constant over the range 28–48% v/v DMF and a medium containing 40% DMF is recommended. In this medium the complex is stable for more than 1 month. The order in which the reagents are added was found to be immaterial.

Stoichiometry of the complex

The continuous-variation and mole-ratio methods failed because the complex is weak. Therefore, a modified Holme and Langmyhr method⁴⁶ and that of Asmus⁴⁷ were applied to the mole ratio data. Both methods showed that the composition of the complex was 1:1. The conditional formation constant at pH 4.5 was 5.25 ± 0.10 .⁴⁵

Calibration and precision

Beer's law is obeyed over the range 0–1.5 ppm indium. The molar absorptivity is 6.2×10^4 l.mole⁻¹.cm⁻¹, which compares well with the values obtained for other complexes used for spectrophotometric determination of indium. The optimum working range, as evaluated by Ringbom plot, is 0.3–1.5 ppm indium. The relative standard deviation ($P = 0.05$) found was 1.0% for 0.57 ppm of indium (11 samples). For investigation of between-day variation, single determinations were made on eleven different days. All absorbances were within the range 0.301–0.320 (0.57 ppm indium) and the relative standard deviation was 1.5%. This is a better value than the 5% obtained in the extractive spectrophotometric determination of indium with dithizone.⁴⁸

Interferences

Results of the interference studies are given in Table 1. The tolerance criterion was taken as the largest amount of foreign ion causing an error of not more than $\pm 5\%$ in the determination of 0.57 ppm indium. Cations interfered by giving higher absorbance or opalescence, whereas anions gave lower absorbance, except for iodate, periodate and nitrite, which oxidized the reagent, giving a yellow colour. Attempts to eliminate the interferences by addition of masking agents were unsuccessful. It must be noted

Table 1. Tolerance for foreign ions in the determination of 0.57 ppm indium

Tolerance, ppm	Ion or species
>1000	Alkali metals, Be(II), Mg(II), Ca(II), Sr(II), Ba(II), Al(III), Tl(I), NH_4^+ , $\text{B}_4\text{O}_7^{2-}$, NO_3^- , SO_4^{2-} , SO_3^{2-} , SCN^- , F^- , Cl^- , Br^- , I^- , ClO_3^- , ClO_4^- , BrO_3^- , CO_3^{2-} , acetate, trichloroacetate, ascorbate
100	Ga(III), Y(III), La(III), Ce(IV), Th(IV), U(VI), Zr(IV), NO_2^- , AsO_4^{3-} , AsO_2^- , SeO_3^{2-} , IO_3^- , IO_4^- , tartrate
30	Mo(VI), W(VI), Mn(II)
20	Sn(II), Sb(III), Ti(IV), Cr(III)
10	PO_4^{3-} , $\text{P}_2\text{O}_7^{4-}$, $\text{S}_2\text{O}_3^{2-}$
5	$\text{C}_2\text{O}_4^{2-}$, citrate
3	Os(VIII), Ag(I), Au(III)
0.5	Pb(II)
0.1	Bi(III), V(V), Cu(II), Hg(II)
0.05	Fe(II), Fe(III), Co(II), Ni(II), Pd(II), Zn(II), Cd(II)
<0.05	EDTA, S^{2-}

that there were high tolerance levels for Be, Al, Tl(I) and Ga.

Applications

Owing to the fact that the reagent PST is not selective enough for the direct determination of indium in alloys and ores, a prior separation from interfering ions is necessary. Attempts were made to separate indium by extraction into diethyl ether or

n-butyl acetate from hydrobromic acid solution, following the method described by Busev *et al.*²⁶ but were unsuccessful because anodic-stripping voltammetry tests showed that the extracts were contaminated with lead, zinc and nickel (this last only in the case of the nickel alloy), and chemical tests also showed the presence of iron. Therefore, a double separation of indium by co-precipitation with Fe(III) or Al(III) hydroxide, then extraction of HInBr_4 into n-butyl acetate, after reduction of Fe(III) with Ti(III), was chosen. When this method was used, anodic-stripping voltammetry showed only the presence of trace amounts of lead, which could be removed by treating the sample with sulphuric acid.

The procedure was used to determine the indium content of a nickel alloy and three zinc ores. The results obtained are given in Table 2 and are in good agreement with those quoted in the certificates of analysis, and with the results obtained with 1-(2-pyridylazo)-2-naphthol.

Other reagents have been proposed for the spectrophotometric determination of indium (Table 3), but most of them are less sensitive than PST. The disadvantage of the low selectivity of PST, which is common to all reagents for the spectrophotometric determination of indium, may be overcome by co-precipitation with Fe(III) or Al(III) hydroxide and extraction with n-butyl acetate from hydrobromic acid solution. In this manner, indium contents as low as 20 $\mu\text{g/g}$ in alloys and ores can be accurately

Table 2. Determination of indium in a nickel alloy and zinc ores

Sample	Amount taken, g	Indium found,* %	Indium content, %
Zn-Sn-Cu-Pb Ore	1.0120	0.0330 \pm 0.0006	0.033†
Zinc concentrate	1.0147	0.0187 \pm 0.0002	0.019†
Zinc blende	1.0200	0.00288 \pm 0.00011	0.00269§
Nickel alloy	1.3966	0.00228 \pm 0.00008	0.0020† 0.00222§

*Mean and range of three determinations.

†Certificate content.

§By the 1-(2-pyridylazo)-2-naphthol method.⁴⁰ Mean of three determinations.

‡Approximate content given in the BCS certificate.

Table 3. Comparison with other reagents used for the spectrophotometric determination of indium

Reagent	Optimum pH	λ_{max} , nm	ϵ , $10^3 \text{ l. mole}^{-1} \text{ cm}^{-1}$	Remarks	Ref.
Chrome Azurol S and cetrinide	5.2-6.2	630	123	Ga(III), Al(III) interfere	49
Dithizone	6.5-10.5	510	69	Extraction into CHCl_3	48
PST	4.0-5.5	415	62	40% DMF	This work
Bromopyrogallol Red	6.5-9.0	540	42.5	Extraction into benzyl alcohol	34
4-(2-Pyridylazo)resorcinol	3.4-4.5	510	32.7	Ga(III), Al(III) interfere	24
1-(2-Pyridylazo)-2-naphthol	5.0-6.0	545	24.5	24% DMF	40
	5.4-6.7	560	21.2	Extraction into CHCl_3	40
Rhodamine S	HBr	530	23.5	Extraction into benzene	41
5,7-Dibromoquinolin-8-ol	3.0-4.5	415	17.6	Extraction into CHCl_3	36
Quinolin-8-ol	3.2-4.5	400	15.0	Extraction into CHCl_3	41
Xylenol Orange	3.7-6.5	560	15.0	Ga(III), Al(III) interfere	41

determined with a 1-g sample. A further advantage of the method is the high stability of the complex.

Acknowledgement—We thank D. González Arjona and E. Roldán Gonzáles for the anodic-stripping voltammetry tests.

REFERENCES

1. A. I. Busev, *The Analytical Chemistry of Indium*, Pergamon Press, Oxford, 1962.
2. G. F. Reynolds and H. I. Shalgosky, *Anal. Chim. Acta*, 1958, **18**, 345; 1958, **18**, 607; 1958, **18**, 612; 1958, **19**, 190.
3. G. W. C. Milner, *Analyst*, 1951, **76**, 488.
4. G. F. Reynolds and H. I. Shalgosky, *Anal. Chem.*, 1954, **26**, 783.
5. D. J. Ferrett and G. W. C. Milner, *Analyst*, 1955, **80**, 132.
6. R. D. DeMars, *Anal. Chem.*, 1962, **34**, 259.
7. A. A. Smales, J. van R. Smit and H. Irving, *Analyst*, 1957, **82**, 539.
8. H. Irving, J. van R. Smit and L. Salmon, *ibid.*, 1957, **82**, 549.
9. J. Hoste and H. van den Berghe, *Mikrochim. Acta*, 1956, 793.
10. Y. Kusaka, *Nippon Kagaku Zasshi*, 1959, **80**, 1419; 1960, **81**, 1087.
11. A. A. Abdullaev, E. M. Lovanov, A. P. Novikov, M. M. Romanov and A. A. Khaidarov, *Zh. Analit. Khim.*, 1960, **15**, 701.
12. T. B. Pierce and P. F. Peck, *Analyst*, 1961, **86**, 580.
13. K. Kobayashi and K. Kudo, *J. Radioanal. Chem.*, 1979, **54**, 49.
14. J. Korkisch and I. Hazan, *Anal. Chem.*, 1964, **36**, 2308.
15. G. M. Eskenazy and E. I. Mincheva, *Analyst*, 1978, **103**, 1179.
16. A. J. Aller, *Anal. Chim. Acta*, 1982, **134**, 293.
17. *Methods for Emission Spectrochemical Analysis*, pp. 195–198. ASTM, Philadelphia, 1957.
18. A. Gómez Coedo, M. Dorado López and J. M. Sistiaga, *Rev. Metal. (Madrid)*, 1979, **15**, 379.
19. W. H. Evans, P. J. Brooke and B. E. Lucas, *Anal. Chim. Acta*, 1983 **148**, 203.
20. E. A. Jones and A. F. Lee, *Rep. Natl. Inst. Metall. (S. Afr.)*, No. 2022, 1979, p. 38; *Anal. Abstr.*, 1981, **41**, 2B66.
21. A. T. Pilipenko and A. J. Samchuk, *Zh. Analit. Khim.*, 1979, **34**, 2128.
22. A. M. Aziz-Alrahman and J. B. Headridge, *Analyst*, 1979, **104**, 944.
23. D. H. Lemmon and J. C. Swartz, *J. Mol. Struct.*, 1980, **61**, 415.
24. F. D. Snell, *Photometric and Fluorimetric Methods of Analysis*, Part I, pp. 469–496. Wiley, New York, 1978.
25. A. Wo, Sh. Zhong, P. Wang and H. Shen, *Fenxi Huaxue*, 1981, **9**, 347; *Anal. Abstr.*, 1982, **42**, 2B70.
26. A. I. Busev, V. G. Tiptsova and V. M. Ivanov, *Analytical Chemistry of Rare Elements*, pp. 291–310. Mir, Moscow, 1981.
27. V. T. Athavale, T. P. Ramachandran, M. M. Tillu and G. M. Vaidya, *Anal. Chim. Acta*, 1960, **22**, 56.
28. T. A. Collins, Jr. and J. H. Kanzelmeyer, *Anal. Chem.*, 1961, **33**, 245.
29. C. L. Luke and M. E. Campbell, *ibid.*, 1953, **25**, 1588; 1956, **28**, 1340.
30. T. Matsumae, *Bunseki Kagaku*, 1959, **8**, 167.
31. N. L. Olenovich, L. I. Koval'chuk and E. P. Lozitskaya, *Zh. Analit. Khim.*, 1974, **29**, 47.
32. V. A. Nazarenko and R. V. Ravitskaya, *Zavodsk. Lab.*, 1965, **31**, 1301.
33. I. S. Levin and T. G. Azarenko, *Zh. Analit. Khim.*, 1965, **20**, 452.
34. S. G. Jadhav, P. Murugaiyan and Ch. Venkateswarlu, *Anal. Chim. Acta*, 1976, **82**, 391.
35. Z. Gregorowicz and M. Marczak, *Chem. Anal. (Warsaw)*, 1969, **14**, 159.
36. S. Stevanovic, V. Golubonic and J. Misovic, *Hem. Ind.*, 1981, **35**, 108.
37. P. P. Kish and S. T. Orlovskii, *Zh. Analit. Khim.*, 1962, **17**, 1057.
38. L. Huang, W. Sang, S. Lu and H. Wu, *Fenxi Huaxue*, 1984, **12**, 556; *Anal. Abstr.*, 1985, **47**, 2B64.
39. Sh. Shibata, *Anal. Chim. Acta*, 1960, **23**, 434.
40. K. L. Cheng and B. L. Goydish, *ibid.*, 1966, **34**, 154.
41. H. Onoshi, *Treaties on Analytical Chemistry*, I. M. Kolthoff and P. J. Elving (eds.), Part II, Vol. 2, pp. 1–105. Wiley-Interscience, New York, 1962.
42. I. S. El-Yamani and E. I. Shabana, *Talanta*, 1984, **31**, 630.
43. K. R. Salanke and S. M. Khopkar, *Anal. Chim. Acta*, 1973, **66**, 307.
44. F. W. E. Strelow and T. N. van der Walt, *S. Afr. J. Chem.*, 1979, **32**, 13.
45. D. Rosales, G. González and J. L. Gómez Ariza, *Talanta*, 1985, **32**, 467.
46. J. C. Jimenez Sánchez, J. A. Muñoz Leyva and M. Román Cebea, *Anal. Chim. Acta*, 1977, **90**, 223.
47. E. Asmus, *Z. Anal. Chem.*, 1960, **178**, 104.
48. J. Fries and H. Getrost, *Organic Reagents for Trace Analysis*, pp. 179–182. Merck, Darmstadt, 1977.
49. B. Evtimova and D. Nonova, *Anal. Chim. Acta*, 1973, **67**, 107.

SHORT COMMUNICATION

EXTRACTION-SPECTROPHOTOMETRIC DETERMINATION OF VANADIUM WITH *N-m*-TOLYL-*N*-PHENYLHYDROXYLAMINE AND ITS APPLICATION TO COAL AND COAL FLY-ASH

SADANOBU INOUE,* SUWARU HOSHI and MUTSUYA MATSUBARA

Department of Environmental Engineering, Kitami Institute of Technology, Kitami-shi, 090 Japan

(Received 11 February 1986. Accepted 28 February 1986)

Summary—*N-m*-Tolyl-*N*-phenylhydroxylamine is proposed for the spectrophotometric determination of small amounts of vanadium. The reddish-violet complex formed with the reagent in 3 *M* hydrochloric acid after extraction with chloroform shows an absorption maximum at 530 nm, and obeys Beer's law for 0–76.5 μg of vanadium in 10 ml of chloroform. The proposed method has been successfully applied to the determination of vanadium in coal and coal fly-ash.

Many *N*-benzoyl-*N*-phenylhydroxylamine derivatives have been proposed for the spectrophotometric determination of vanadium either in aqueous or non-aqueous solutions,¹ and several are particularly valuable for determination of small amounts of vanadium. Majumdar and Das² reported that *N*-benzoyl-*o*-tolylhydroxylamine behaves as a selective reagent for vanadium under suitable experimental conditions (that is, vanadium can be determined in the presence of a large excess of various metal ions and anions) and also³ that *N*-benzoyl-*m*-tolylhydroxylamine and *N*-benzoyl-*p*-tolylhydroxylamine have similar characteristics to the *o*-tolyl derivative. However, *N*-benzoyl-*o*-tolylhydroxylamine was obtained in only low yield (about 15%),⁴ and it was found that this was caused by excessive formation of reduction products other than tolylhydroxylamine, particularly *o*-toluidine. *N*-Cinnamoyl-*N*-phenylhydroxylamine⁵ has been recommended as a more sensitive reagent than *N*-benzoyl-*N*-phenylhydroxylamine and *N*-benzoyl-*o*-tolylhydroxylamine, but it is not selective for vanadium.

In this paper, the determination of small amounts of vanadium with *N-m*-tolyl-*N*-phenylhydroxylamine is described. This reagent can be obtained in higher yield (49%) than *N*-benzoyl-*o*-tolylhydroxylamine, from *m*-toluoyl chloride and phenylhydroxylamine. The conditions for determination of small amounts of vanadium were studied in detail, and the proposed method was applied successfully to the determination of vanadium in coal and coal fly-ash.

EXPERIMENTAL

Reagents

Standard vanadium(V) solution, 3.75×10^{-2} M. Prepared by dissolving 1.09 g of ammonium metavanadate in 5.0 ml of 50% v/v sulphuric acid and diluting to 250 ml with water.

Potassium permanganate solution, 0.3%.

*Author for correspondence.

N-m-Tolyl-*N*-phenylhydroxylamine solution, 0.1% in chloroform. *N-m*-Tolyl-*N*-phenylhydroxylamine was prepared from *m*-toluoyl chloride and phenylhydroxylamine as described previously (yield 49%).⁶

All other reagents used were of analytical grade.

Apparatus

A Hitachi model 200-10 spectrophotometer with 10-mm quartz cells, and a Hitachi-Horiba F-7AD pH-meter were used.

Procedure

Measure a known volume of sample solution containing up to 76 μg of vanadium into a separating funnel, and dilute to about 35 ml with water; add 0.3% potassium permanganate solution dropwise until the pink colour persists for 5 min, then add 2 ml of saturated sodium fluoride solution, 10 ml of 0.1% *N-m*-tolyl-*N*-phenylhydroxylamine solution in chloroform and 15 ml of concentrated hydrochloric acid. Immediately shake for 1 min, and allow the phases to separate. Dry the organic layer with anhydrous sodium sulphate and measure the absorbance at 530 nm against chloroform.

Analysis of coal

Take 0.5–1.0 g of sample in a silica crucible. Heat gradually in a muffle furnace at 275° for 1 hr, at 550° for 1 hr, and finally at 750° for 2 hr.⁷ Treat the resulting ash with a mixture of 10 ml of concentrated hydrofluoric acid and 10 ml of concentrated nitric acid in a 50-ml Teflon beaker at 150° on a hot-plate and evaporate to dryness. Cool, then add a mixture of 10 ml of concentrated nitric acid and 10 ml of 60% perchloric acid, cover the beaker with a Teflon lid then digest at 250° on a hot-plate for about 4 hr until a pale yellow colour is obtained, then evaporate to dryness at 150°. Cool, then dissolve the residue in about 20 ml of water, with gentle heating. Cool and transfer the solution to a separating funnel. Determine vanadium as described above.

Analysis of coal fly-ash

Weigh about 0.2 g of coal fly-ash into a 50-ml Teflon beaker and treat it in the same way as the ash in the coal analysis above.

RESULTS AND DISCUSSION

Absorption spectra

The absorption spectra of the reagent and the vanadium-*N-m*-tolyl-*N*-phenylhydroxylamine com-

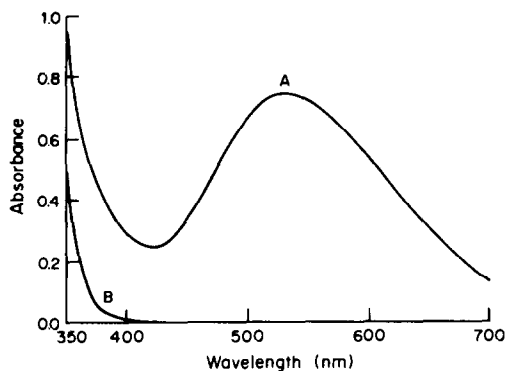


Fig. 1. Absorption spectra of *N-m-tolyl-N-phenylhydroxylamine* and its vanadium complex, in chloroform. A, complex with 76.4 μg of vanadium; B, 0.1% reagent solution; reference, chloroform.

plex in chloroform are shown in Fig. 1. The absorption spectra for the vanadium complex extracted into chloroform from solutions that are 3–6M in hydrochloric acid have maximum absorption at 530 nm and an apparent molar absorptivity of $5.0 \times 10^3 \text{ l. mole}^{-1} \cdot \text{cm}^{-1}$. The reagent solution in chloroform (0.1%) has little absorption at 530 nm, as shown in Fig. 1.

Effect of acidity and reagent concentration on the extraction of vanadium

The effect of acidity on the extraction of vanadium was investigated by changing the hydrochloric acid concentration in aqueous medium; the results are

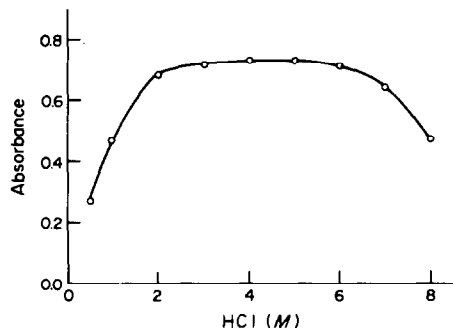


Fig. 2. Effect of hydrochloric acid concentration on absorbance. Vanadium 76.4 μg ; $V_{\text{org}} = V_{\text{aq}} = 10 \text{ ml}$; wavelength 530 nm.

shown in Fig. 2. The maximum absorbance was obtained with hydrochloric acid concentrations between 3 and 6M, and the colour remained unchanged for at least 24 hr at room temperature. A large excess of the reagent can be used even for small amounts of vanadium, because it has no effect on the colour.

Beer's law

The system obeys Beer's law for 0–76 μg of vanadium in 10 ml of chloroform. The method has about the same sensitivity as the *N-benzoyl-N-phenylhydroxylamine* method ($\epsilon = 4.65 \times 10^3 \text{ l. mole}^{-1} \cdot \text{cm}^{-1}$) and *N-benzoyl-o-tolylhydroxylamine* method ($\epsilon = 5.25 \times 10^3$).⁴ The relative standard deviation of the absorbance at 530 nm was 0.3% (12 replicates with 46 μg of vanadium).

Table 1. Effect of other ions on determination of 76.4 μg of V

Ion	Added as	Added, mg	V found, μg	Error, μg
Pb ²⁺	Pb(NO ₃) ₂	25	75.7	-0.7
Hg ²⁺	HgCl ₂	25	76.5	+0.1
Cu ²⁺	CuSO ₄ · 5H ₂ O	5	76.5	+0.1
Fe ³⁺	FeNH ₄ (SO ₄) ₂ · 12H ₂ O	10	76.0	-0.4
Co ²⁺	CoCl ₂ · 6H ₂ O	20	75.6	-0.8
Ni ²⁺	NiCl ₂ · 6H ₂ O	25	75.8	-0.6
Mn ²⁺	MnCl ₂ · 4H ₂ O	2	76.4	0
Zn ²⁺	ZnCl ₂	20	76.5	+0.1
Al ³⁺	AlCl ₃ · 6H ₂ O	30	76.5	+0.1
Cr ³⁺	CrCl ₃ · 6H ₂ O	25	74.9	-1.5
Ti ⁴⁺	Ti(SO ₄) ₂	2	77.8	+1.4
		15*	76.5	+0.1
Cd ²⁺	CdSO ₄ · xH ₂ O	25	76.4	0
Bi ³⁺	Bi(NO ₃) ₃	15	76.6	+0.2
Mg ²⁺	Mg(NO ₃) ₂ · 6H ₂ O	20	77.2	+0.8
Ca ²⁺	CaCl ₂	20	76.4	0
Ba ²⁺	BaCl ₂ · 2H ₂ O	20	76.7	+0.3
W ⁶⁺	Na ₂ WO ₄ · 2H ₂ O	1	76.0	-0.4
Mo ⁶⁺	(NH ₄) ₆ Mo ₇ O ₂₄ · 4H ₂ O	1	75.7	-0.7
Cr ⁶⁺	K ₂ CrO ₄	1	75.3	-1.1
Citrate	(NH ₄) ₂ HC ₆ H ₅ O ₇	0.1	75.5	-0.9
Oxalate	Na ₂ C ₂ O ₄	20	76.0	-0.4
Tartrate	KOOCCH(OH)—			
	CH(OH)COONa · 4H ₂ O	1	75.7	-0.7
EDTA	Na ₂ H ₂ EDTA · 2H ₂ O	25	76.4	0
Phosphate	Na ₂ HPO ₄	20	77.0	+0.6
F ⁻	NaF	25	76.0	-0.4

*After addition of 2 ml of saturated sodium fluoride solution.

Table 2. Analytical results for vanadium in coal and coal fly-ash

Sample	No. of replicates	Mean V found, ppm	Relative std. devn., %
Coal			
NBS SRM 1632a	8	42.6 (44)*	2.1
NBS SRM 1632b	8	14.1 (14)*	2.6
Coal fly-ash			
NBS SRM 1633a	10	292 (300)*	0.9

*NBS provisional value.

Effect of other ions

The effects of various ions on the proposed method are reported in Table 1. No interference was observed from large amounts (2–25 mg) of the following ions: Pb(II), Hg(II), Cu(II), Fe(III), Co(II), Ni(II), Mn(II), Zn(II), Al(III), Cr(III), Cd(II), Bi(III), Mg(II), Ca(II), Ba(II), oxalate, EDTA, phosphate and fluoride. The interference of titanium(IV) could be avoided by adding 2 ml of saturated sodium fluoride solution as masking agent. Molybdenum(VI), tungsten(VI) and chromium(VI) were tolerated in amounts up to 13 times that of vanadium. Iron(III) (10 mg) caused a negative error when the sample solution was allowed to stand for few min after the addition of concentrated hydrochloric acid in the procedure, but this can be avoided by performing the extraction immediately after adding the concentrated hydrochloric acid.

Results for analysis of coal and coal fly-ash

Table 2 shows the precision and accuracy obtained for analysis of standard reference samples of coal (SRM 1632a and 1632b) and coal fly-ash (SRM 1633a), issued by the National Bureau of Standards. The results were in good agreement with the certified or provisional values. The relative standard deviations were ~1–3%. These results confirm the usefulness of the proposed method for determination of vanadium.

REFERENCES

1. U. K. Gupta and S. G. Tandon, *Anal. Chim. Acta*, 1973, **66**, 39.
2. A. K. Majumdar and G. Das, *ibid.*, 1964, **31**, 147.
3. *Idem*, *ibid.*, 1966, **36**, 454.
4. P. G. Jeffery and G. O. Kerr, *Analyst*, 1967, **92**, 763.
5. U. Priyadarshini and S. G. Tandon, *ibid.*, 1961, **86**, 544.
6. S. Inoue, H. Inai, S. Hoshi and M. Matsubara, *Anal. Sciences*, 1985, **1**, 423.
7. R. I. Nadkarni, *Anal. Chem.*, 1980, **52**, 929.

DEGRADATION OF NITRILOTRIACETIC ACID (NTA) BY OXIDATION WITH LEAD DIOXIDE SUSPENSION

TOSHIO MATSUDA and TOYOSHI NAGAI

Department of Chemistry, Ritsumeikan University, Kyoto, Japan

(Received 11 November 1985. Revised 17 February 1986. Accepted 28 February 1986)

Summary—Degradation of nitrilotriacetic acid (NTA) by oxidation with lead dioxide suspension has been studied by differential pulse polarography. The NTA was degraded over the pH range from 4 to 9, with formation of glycine or a mixture of iminodiacetic acid and glycine. After shaking with lead dioxide for 1 hr at 30° and pH ~7, the NTA was almost completely decomposed, the molar reacting ratio of Pb(IV) to NTA being ~17:1; down to $1 \times 10^{-5}M$ NTA was decomposed in a shaking time as short as 15 min and at a temperature as low as 5°. The iron(III)-NTA complex was also degraded under the same conditions, and the iron released was adsorbed on the lead dioxide.

Investigation of oxidative degradation of organic substances, such as detergents and complexing agents, has become important in analytical and environmental chemistry.¹⁻⁵ The use of ozone,^{2,6} persulphate,⁴ and ultraviolet irradiation⁵ in degradation processes has been widely investigated in waste-water treatment. Nitrilotriacetic acid (NTA) was used in synthesis of detergents in certain countries in the late 1960s, and recently the effect of NTA and its metal complexes on the environment and in toxicology has received considerable attention.^{2,7-9}

As described earlier, lead dioxide oxidizes EDTA in sulphuric acid medium,¹⁰ and iminodiacetic acid (IDA) and nitrilotriacetic acid in nitric acid medium¹¹ with moderate speed at room temperature. Hydrous lead dioxide (HLD), prepared by hydrolysis of lead tetra-acetate and then washed with water to remove the acetic acid produced, is an amphoteric ion-exchanger with an equi-adsorption point in the vicinity of pH 4.6,¹² and will isolate bismuth from bismuth-EDTA solution over the pH range from 1 to 12.¹³

In the study reported here, degradation of NTA by oxidation with HLD suspension was examined over the pH range from 4 to 11, with special attention to the reaction of NTA and its iron(III) complex at about pH 7.

EXPERIMENTAL

Reagents

A 0.01M NTA solution and a 0.01M iron(III)-NTA solution were prepared from reagent grade NTA and ammonium ferric sulphate, and accurately diluted as required. A 0.05M lead tetra-acetate solution in glacial acetic acid was prepared and standardized as reported previously.^{12,13}

The water used was obtained by distilling demineralized water containing a little potassium permanganate and sodium hydroxide.

Apparatus

The polarograph, spectrofluorimeter and incubator used were those employed previously.^{11,13} A Shimadzu UV-260

spectrophotometer was used. Unless otherwise stated, all measurements were performed at $25 \pm 0.5^\circ$.

Procedures

Hydrous lead dioxide (HLD) was prepared by adding 10 ml of 0.05M lead tetra-acetate solution dropwise to 100 ml of distilled water, then centrifuging, removing the supernatant liquid, and washing twice with 100-ml portions of distilled water.¹³ A 0.5 mmole portion (about 0.14 g of $PbO_2 \cdot 2H_2O$) was used for each degradation test.

Degradation in buffered solution. The HLD, a known amount of NTA solution, 20 ml of buffer solution and 10 ml of 1M potassium nitrate were placed in a 100-ml Erlenmeyer flask fitted with a rubber stopper, and the mixture was diluted to 100 ml with distilled water. The buffers (0.1M) were CH_3COOH/CH_3COONa (pH 3.5-6.0), $HNO_3/Na_2B_4O_7$ (pH 6.7-9.1) and $Na_2B_4O_7/NaOH$ (pH 9.9-11.0). The mixture was shaken for 1 hr, at 30°. The HLD was then filtered off with a 0.45- μ m pore-size membrane filter. The concentration of NTA in the filtrate was determined by differential pulse polarography of the lead(II)-NTA complex.¹⁴ A mixture of 25 ml of filtrate, 5 ml of 0.01M lead(II), 5 ml of 1M potassium nitrate and 1 ml of 0.25% gelatin solution was adjusted to pH 4.7, and diluted to volume in a 50-ml standard flask. A portion of this solution was deaerated, and the differential pulse polarogram was recorded between -0.4 and -1.2 V vs. SCE at a scan-rate of 5 mV/sec and 100 mV pulse amplitude. The peak current at -0.70 V vs. SCE was measured, and the concentration of NTA was calculated from a calibration graph.

Degradation in unbuffered solution. The pH of the suspension was adjusted with a little 0.1M nitric acid or 0.1M sodium hydroxide solution. The rest of the procedure was the same as for tests in buffered solution.

Degradation of iron(III)-NTA. HLD and an appropriate amount of iron(III)-NTA in buffered solution at about pH 7 were shaken for 1 hr at 30°, and the HLD was filtered off. The concentration of iron(III) in the filtrate was determined spectrophotometrically with 1,10-phenanthroline,¹⁵ and the concentration of NTA was determined polarographically after reduction of iron(III) with ascorbic acid.

Other analyses of the filtrate

The amount of lead(II) in the filtrate was determined directly by polarography, after acidification to 0.2M in nitric acid.

Glycine was determined fluorimetrically by the standard-addition method with fluoescamine¹⁶ by mixing 3 ml of the

filtrate, 0–3 ml of $1 \times 10^{-4} M$ standard glycine solution, 10 ml of 0.1M borate buffer (pH 9.0) and 10 ml of 0.03% fluorescamine solution in a 50-ml standard flask, diluting to volume, and after 10 min standing time at room temperature measuring the fluorescence at 480 nm, with an excitation wavelength of 400 nm.

RESULTS AND DISCUSSION

Degradation of NTA in buffered solution

The effect of pH on the decrease in NTA concentration (initial value $1 \times 10^{-4} M$) is shown in Fig. 1. There was almost 100% decrease over the pH range 4–9, with shaking for 1 hr at 30° . The amount of lead(II) in the supernatant solution increased with decrease of pH below about 6.

The relation between initial concentration of NTA and the amount destroyed by a constant amount of HLD at pH 7 is shown in Fig. 2. There was practically complete decomposition of NTA in 1 hr at 30° when the molar ratio of NTA to Pb(IV) was below about 0.06.

Degradation in unbuffered solution

To examine the possible utility of HLD for degradation of NTA in environmental samples, the reaction in unbuffered solution at about pH 7 was investigated.

Table 1 shows that degradation was 100% complete over the NTA concentration range from 1×10^{-5} to $1 \times 10^{-4} M$. It was also found that a shaking time as short as 15 min, at a temperature as low as 5° , would give >99% decomposition of the NTA.

Degradation of iron(III)-NTA

Table 2 shows there was almost 100% decomposition of NTA over the concentration range from 1×10^{-5} to $1 \times 10^{-4} M$ iron(III)-NTA. Further, when $1 \times 10^{-4} M$ iron(III)-NTA was shaken with HLD for 15 or 30 min at a temperature of 5° , there was almost 100% decrease in the concentrations of NTA and iron. In addition, the iron liberated was found to be completely adsorbed by the HLD.

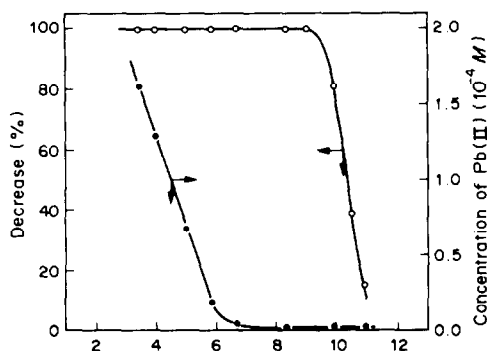


Fig. 1. Decrease in NTA added, and change in concentration of lead(II) in solution, as a function of pH. HLD 5×10^{-4} mole, NTA $1 \times 10^{-4} M$, solution volume 100 ml, shaking time 1 hr, temperature 30° .

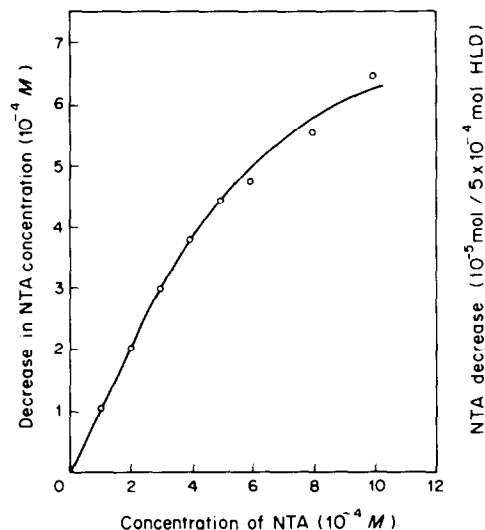


Fig. 2. Relation between the decrease in amount of NTA and the concentration of NTA added. HLD 5×10^{-4} mole, solution volume 100 ml, shaking time 1 hr, temperature 30° , pH 7.

The degradation process

The amounts of glycine and lead(II) produced were measured, for separate experiments at about pH 4 and 7.

The effect of the other substances present (lead nitrate, formaldehyde and IDA) on the fluorometric determination of glycine was studied beforehand with standard glycine solution, and the error was found to be $\pm 2.2\%$. In the supernatant solution from shaking $1 \times 10^{-4} M$ NTA with HLD, the molar ratio of glycine produced to NTA added was found to be 0.9 at about pH 4 and 0.4 at about pH 7.

From Fig. 1 it is seen that at pH around 4, about two moles of lead(II) were produced per mole of NTA. In the pH ~ 7 experiment the ratio of lead(II) obtained in the supernatant solution to the NTA taken was only about 0.02, so the amount of lead(II) adsorbed on the HLD was determined. The HLD separated from the suspension at about pH 7 was shaken with 0.02M NTA at pH 12 for 1 hr, and the amount of lead(II)-NTA complex extracted was determined by polarography, after acidification to 0.2M in nitric acid, and slightly more than a 1:1 molar ratio of lead(II) to NTA was found to have been collected on the HLD.

Table 1. Relation between the decrease in amount of NTA and the initial concentration of NTA in unbuffered solution at about pH 7 (HLD 5×10^{-4} mole, solution volume 100 ml, shaking time 1 hr, temperature 30°)

Initial concentration of NTA, M	Decrease in NTA, %
1×10^{-5}	>99
5×10^{-5}	>99
1×10^{-4}	>99
6×10^{-4}	85 ± 1
1×10^{-3}	71 ± 1

Table 2. Relation between the decrease in amount of NTA and of iron(III) and the concentration of iron(III)-NTA complex added in unbuffered solutions at about pH 7 (HLD 5×10^{-4} mole, solution volume 100 ml, shaking time 1 hr, temperature 30°)

Initial concentration of iron(III)-NTA, M	Decrease in NTA, %	Decrease in iron(III), %
1×10^{-5}	>99	>99
5×10^{-5}	>99	>99
1×10^{-4}	>99	>99
5×10^{-4}	61 ± 3	63 ± 2

From these results, it is evident that NTA is degraded by HLD at moderate speed at about pH 7, by a surface redox process. The reaction in feebly acidic media results mainly in glycine, and according to previous work¹¹ IDA is produced in the first step in the oxidation of NTA by HLD, so the products at about pH 7 can be considered to be IDA and glycine.

It seems probable that the lead(II) produced at about pH 7 is retained on the HLD, as a compound such as the hydroxide.

The NTA in the iron(III) complex is similarly degraded, and the iron(III) released is also retained on the HLD, again probably as the hydroxide.

Conclusions

It appears that HLD would be applicable to the degradation of NTA and its metal complexes in environmental samples, without producing too much contamination with lead(II).

Acknowledgements—The authors thank Mr. Yoshikazu Nakai for assistance with the experimental measurements. This work was partially supported by a Grant-in-Aid for Scientific Research from the Ministry of Education, Science and Culture.

REFERENCES

1. T. M. Florence, *Talanta*, 1982, **29**, 345.
2. J. L. Means, T. Kucak and D. A. Crerar, *Envir. Pollut. (Ser. B)*, 1980, **1**, 45.
3. R. G. Clem and A. T. Hodgson, *Anal. Chem.*, 1978, **50**, 102.
4. P. D. Goulden and D. H. J. Anthony, *ibid.*, 1978, **50**, 953.
5. G. E. Batley and Y. J. Farrar, *Anal. Chim. Acta*, 1978, **99**, 283.
6. S. D. Razumovskii and G. E. Zaikov, *Ozone and its Reactions with Organic Compounds*, Elsevier, Amsterdam, 1984.
7. A. C. Rossin, R. Perry and J. N. Lester, *Envir. Pollut. (Ser. A)*, 1982, **29**, 271.
8. R. Perry, P. W. W. Kirk, T. Stephenson and J. N. Lester, *Water Res.*, 1984, **18**, 255.
9. N. S. Thom, *ibid.*, 1971, **5**, 391.
10. S. Ito, T. Matsuda and T. Nagai, *Talanta*, 1980, **27**, 25.
11. T. Matsuda and T. Nagai, *ibid.*, 1983, **30**, 951.
12. H. Kawano, Y. Nakai, T. Matsuda and T. Nagai, *ibid.*, 1986, **33**, 191.
13. S. Ito, T. Matsuda and T. Nagai, *ibid.*, 1984, **31**, 292.
14. R. Pribil, *Analytical Applications of EDTA and Related Compounds*, p. 35. Pergamon Press, Oxford, 1972.
15. F. D. Snell and C. T. Snell, *Colorimetric Methods of Analysis*, 3rd Ed., Vol. II, p. 314, Van Nostrand-Reinhold, New York, 1949.
16. S. De Bernardo, M. Weigele, V. Toome, K. Manhart, W. Leimgruber, P. Böhlen, S. Stein and S. Udenfriend, *Arch. Biochem. Biophys.*, 1974, **163**, 390.

SEQUENTIAL EXTRACTION AND DETERMINATION OF COPPER AND NICKEL WITH 2,4-DIHYDROXYACETOPHENONE THIOSEMICARBAZONE

A. VARADA REDDY and Y. KRISHNA REDDY

Department of Chemistry, Sri Venkateswara University, Tirupati 517 502, India

(Received 3 June 1985. Revised 20 December 1985. Accepted 28 February 1986)

Summary—2,4-Dihydroxyacetophenone thiosemicarbazone (DAPT) forms a 1:1 complex with copper(II) which can be extracted into n-butanol or ethyl acetate from acetic acid–sodium acetate (pH 5.0) buffer, and a 1:1 nickel(II) complex which can be extracted into n-butanol from ammonium chloride–ammonia (pH 7.5) buffer. The difference between the $pH_{1/2}$ values for extraction of the two complexes is 3.4 and this has been exploited for their sequential extraction and determination. The molar absorptivities for the copper and nickel complexes are 1.5×10^4 l.mole⁻¹.cm⁻¹ at 390 nm and 8.2×10^3 l.mole⁻¹.cm⁻¹ at 385 nm respectively. The procedure has been applied to the analysis of cupronickel.

2,4-Dihydroxyacetophenone thiosemicarbazone (DAPT) has been used as a reagent for spectrophotometric determination of copper(II) and cobalt(II),¹ and for extraction and determination of cobalt(II),² silver(I)³ and palladium(II).⁴ Here we report its use for sequential extraction and determination of copper(II) and nickel(II).

EXPERIMENTAL

Reagents

All the chemicals used were of analytical grade, and the solutions were doubly distilled before use.

Copper sulphate solution, 0.025M. Standardized by iodimetry,⁵ and diluted as required.

Ammonium nickel sulphate hexahydrate solution, 0.025M. Standardized gravimetrically by the dimethylglyoxime method,⁵ and diluted as required.

2,4-Dihydroxyacetophenone thiosemicarbazone solution. The reagent was prepared according to the procedure described by Aydin and Baykut,¹ and used as its n-butanol and ethyl acetate solutions.

Determination of copper(II)

Transfer an accurately measured aliquot of sample solution (not more than 5 ml) containing 15–120 μ g of copper(II) into a 50-ml separating funnel, add 5.0 ml of acetic acid–sodium acetate buffer (pH 5.0) and dilute to 10 ml. Extract the copper with two 10-ml portions of $7.85 \times 10^{-3}M$ DAPT in ethyl acetate, with shaking for 30 sec. Dry the combined extracts with anhydrous sodium sulphate and decant into a 25-ml standard flask, washing the drying agent and diluting to the mark with the same solvent. Measure the absorbance at 390 nm against a reagent blank prepared in the same way.

Determination of nickel(II)

Transfer an exactly measured aliquot of solution (not more than 5 ml) containing 40–200 μ g of nickel into a 50-ml separating funnel, add 5 ml of ammonium chloride–ammonia buffer (pH 7.5) and dilute to 10 ml. Extract the nickel with 10 ml of $3.41 \times 10^{-3}M$ DAPT in n-butanol with shaking for 30 sec. Separate the extract, dry it with anhydrous sodium sulphate and decant it into a 25-ml standard flask, washing the drying agent and diluting to the mark with the same solvent. Measure the absorbance at 385 nm against a reagent blank similarly prepared.

Analysis of cupronickel

Weigh about 100 mg of sample into a 100-ml beaker and dissolve it in nitric acid (1 + 1). Add 5 ml of concentrated hydrochloric acid and evaporate the solution nearly to dryness on a water-bath, then repeat this treatment, to remove the bulk of the nitric acid. Take up the residue in water and dilute to volume in a 100-ml standard flask. Dilute this stock solution in an appropriate size of standard flask and transfer a suitable portion into a separating funnel, add 10 ml of acetate–acetic acid buffer (pH 3.8) and extract with three 5.0-ml portions of 0.08% DAPT solution in n-butanol, shaking for 1 min each time. Dry the combined extracts with anhydrous sodium sulphate, and decant into a 25-ml standard flask, using n-butanol to wash the drying agent and dilute to the mark.

Increase the pH of the aqueous phase to 7.5 with 1.0M sodium hydroxide. Extract with two 5.0-ml portions of the 0.08% DAPT solution, shaking for 1 min each time. Combine, dry, and transfer the extracts to a 20-ml standard flask, rinsing the drying agent and diluting to the mark with n-butanol.

Measure the absorbance of the copper and nickel complexes at 390 and 385 nm respectively.

RESULTS AND DISCUSSION

The Cu–DAPT complex in n-butanol has maximal absorption at 390 nm (λ_{max}) whereas that of the reagent is at 270 nm and that of the nickel complex in n-butanol is at 385 nm (Fig. 1). The effect of pH on the extraction is shown in Fig. 2. Copper is extracted completely at pH 3.6–10.0 and nickel at pH 7.0–8.0. At least a 25-fold molar excess of reagent is needed for maximal extraction of copper and at least 12-fold molar excess for nickel. The systems obey Beer's law in the range 0.8–5.5 ppm for copper and 1.0–8.0 ppm for nickel, the molar absorptivities of the complexes being 1.5×10^4 and 8.2×10^3 l.mole⁻¹.cm⁻¹ at λ_{max} for copper and nickel respectively. The colour is stable for more than 48 hr. Ethyl acetate can be used instead of n-butanol for extraction of copper and gives a much higher distribution coefficient ($D = 16.0$) than that with n-

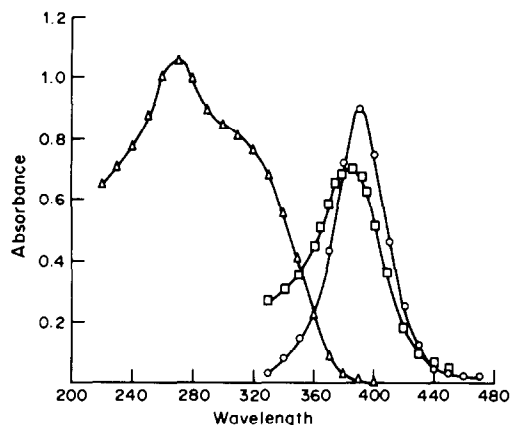
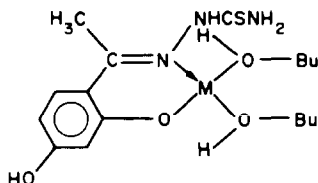


Fig. 1. Spectra of DAPT (Δ), Cu-DAPT (\circ) and Ni-DAPT (\square).

butanol ($D = 9.0$). Three extractions are necessary with the latter but only two with the former, for complete removal of the copper. The distribution coefficient for nickel between *n*-butanol and the aqueous phase is very high (>100) and a single extraction suffices.

The composition of the copper complex was studied by the continuous-variations,⁶ molar ratio⁷ and slope analysis⁸ methods. In all cases the composition of the copper complex was found to be 1:1, and it is possible that the extracted complex is solvated with *n*-butanol:



Scheme 1.

The composition of the nickel complex was studied by the slope analysis method.⁸ The plot of $\log D$ vs. $\log[\text{reagent}]$ has two linear regions with slopes of 1 and 2 respectively (Fig. 3), but there is no shift in λ_{max} of the complex at higher concentrations of the re-

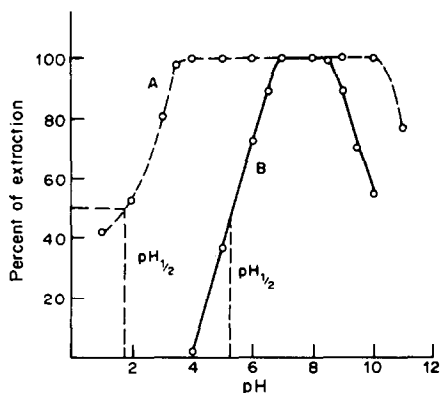


Fig. 2. Extraction of Cu-DAPT (A) and Ni-DAPT (B) as a function of pH.

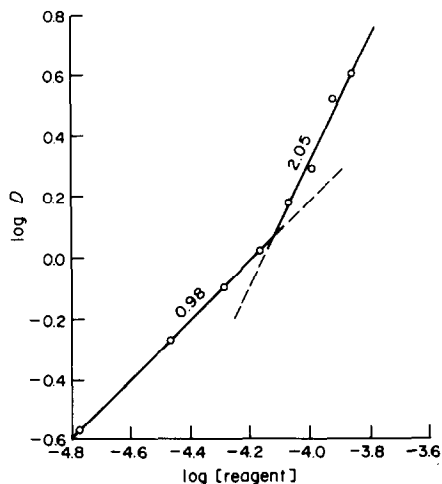
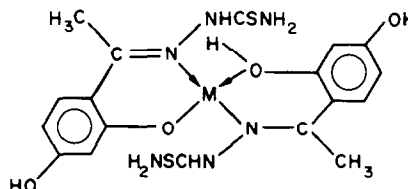


Fig. 3. Composition of nickel complex by slope analysis.

agent. Hence, self-adduct formation is thought to take place in the organic phase. This has been confirmed by plotting $\log D[\text{H}^+]/[\text{reagent}]$ vs. $\log[\text{reagent}]$ (Fig. 4). The two linear regions obtained, with slopes of 0 and 1, confirm self-adduct formation. The proposed structure of the adduct is:



Scheme 2.

Interferences

The tolerance limits for interfering ions were set at the amounts required to cause not more than $\pm 1\%$ change in the absorbance for a fixed amount of metal, and are reported in Table 1. Silver(I), mercury(II), palladium(II), vanadium(V), EDTA, thiosulphate and cyanide interfere seriously in the copper deter-

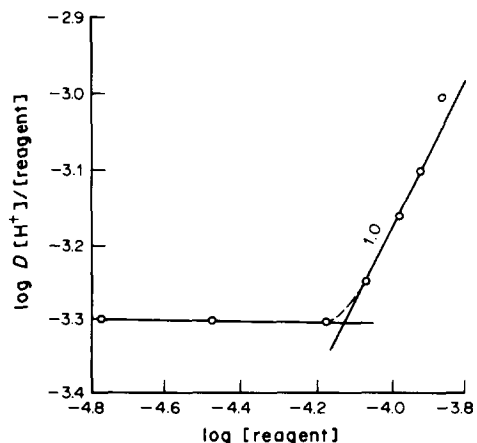


Fig. 4. Confirmation of adduct formation for nickel complex.

Table 1. Effect of foreign ions on the extraction of copper(II) and nickel(II)

Ion added	Tolerance limit, mg		Ion added	Tolerance limit, mg	
	Cu(II)	Ni(II)		Cu(II)	Ni(II)
Ag(I)	Nil	Nil	V(V)	0.2	Nil
Al(III)	5.0	—	W(VI)	2.5	2.5
As(V)	—	1.0	Zn(II)	5.0	5.0
Bi(III)	2.5	1.0	Fluoride	5.0	5.0
Cd(II)	5.0	5.0	Chloride	5.0	5.0
Co(II)	2.5	Nil	Bromide	5.0	5.0
Cu(II)	—	Nil	Nitrate	—	5.0
Fe(III)	0.5	Nil	Oxalate	5.0	Nil
Hg(II)	Nil	1.0	Citrate	5.0	Nil
Mn(II)	2.5	2.5	Ascorbate	5.0	5.0
Mo(VI)	2.5	1.0	Tartrate	5.0	3.0
Ni(II)	0.5	—	EDTA	Nil	Nil
Pb(II)	2.5	1.0	Phosphate	3.0	Nil
Pd(II)	Nil	Nil	Pyrophosphate	2.5	Nil
Sn(II)	1.0	—	Thiocyanate	3.0	3.0
Ti(IV)	2.5	—	Thiosulphate	Nil	Nil
U(VI)	2.5	2.5	Cyanide	Nil	Nil

Table 2. Determination of copper in brass, bronze, copper concentrate and chalcopyrites

Sample	Reported composition	Copper found,* %
Brass	Cu 67.4, Zn 28.6, Sn 1.09, Pb 2.23, Fe 0.30, Ni 0.33 and P 0.01	67.2 ± 0.4
Bronze	Cu 88.4, Sn 10.1, Pb 0.02, Fe 0.01, P 1.31 and Sb 0.07	88.0 ± 0.5
Copper concentrate	Cu 33.0 ± 0.2†	32.6 ± 0.2
Chalcopyrites	Cu 2.5 ₇ ± 0.2 ₃ †	2.5 ₄ ± 0.1

*Mean and standard deviation of five determinations.

†As determined iodometrically. The sample also contains iron, lead, zinc and aluminium.

mination even when present only in traces. The interference of iron(III) can be avoided by using fluoride or ascorbate as masking agent. Citrate can be used to mask higher amounts of nickel(II) and tin(II). Silver(I), cobalt(II), copper(II), iron(III), palladium(II), vanadium(V), oxalate, citrate, EDTA, phosphate, pyrophosphate and cyanide interfere seriously in the nickel determination. Fluoride can be used for masking iron(III).

Sequential determination of copper and nickel in cupronickel

Copper and nickel can be determined sequentially by exploiting the difference between the $pH_{1/2}$ values (Fig. 2). It is clear from the figure that nickel is not extracted at all at $pH < 4.0$, whereas copper is extracted completely at $pH > 3.8$. Hence after the extraction of copper at $pH > 3.8$ the pH is raised to 7.5 and nickel extracted. This has been successfully applied for the analysis of cupronickel.

Applications

Standard brass and bronze samples (British Chemical standards) and chalcopyrites and copper concentrate supplied by Andhra Pradesh Mining Corporation, Mylaram, India, were analysed for

copper by the standard procedures^{5,9} and by the proposed procedure. The results are reported in Table 2. The composition of a cupronickel sample, found by the proposed procedure (Cu 74.6 ± 0.2%; Ni 24.4 ± 0.2%), agreed reasonably well with that found by a standard method⁹ (Cu 75.0%; Ni 25.0%).

Acknowledgement—The authors thank the University Grants Commission, New Delhi, for financial assistance to one of them (A.V.R.).

REFERENCES

1. A. Aydin and F. Baykut, *Chim. Acta. Turc.*, 1975, **3**, 51.
2. A. V. Reddy, M. L. P. Reddy and Y. K. Reddy, *J. Radiochem. Nucl. Chem. Lett.*, 1984, **86**, 391.
3. A. V. Reddy, G. S. Reddy and Y. K. Reddy, *ibid.*, 1985, **93**, 275.
4. A. V. Reddy and Y. K. Reddy, *J. Indian Inst. Sci.*, in press.
5. A. I. Vogel, *A Text Book of Quantitative Inorganic Analysis*, 3rd Ed., Longmans, London, 1961.
6. P. Job, *Ann. Chem. Paris*, 1928, **9**, 113.
7. J. H. Yoe and A. L. Jones, *Ind. Eng. Chem., Anal. Ed.*, 1944, **16**, 111.
8. H. R. Bent and C. L. French, *J. Am. Chem. Soc.*, 1941, **63**, 568.
9. W. W. Scott and N. H. Furman, *Standard Methods of Chemical Analysis*, 6th Ed., Vol. I, pp. 404, 411. Van Nostrand, Princeton, 1963.

BINDING PROPERTIES OF AMINOPOLYCARBOXYLATO LIGANDS BOUND TO CELLULOSE

M. C. GENNARO, E. MENTASTI and C. SARZANINI

Department of Analytical Chemistry, University of Torino, Via Giuria 5, 10125 Torino, Italy

(Received 25 September 1985. Revised 28 January 1986. Accepted 21 February 1986)

Summary—The uptake of metal ions by EDTA bound to cellulose filters has been examined and compared with the corresponding uptake by iminodiacetic acid and *N*-methyliminodiacetic acid bound to cellulose. The results are interpreted in terms of steric hindrance, geometric factors, electrostatic interactions and thermodynamics.

In our previous studies on preconcentration techniques, chelating materials were prepared by binding iminodiacetic acid (IDA) and *N*-methyliminodiacetic acid (MIDA) groups on cellulose filter discs.¹⁻³ Both materials were very efficient in fixing metal cations from very dilute solutions and the co-ordination properties of both ligands were enhanced when bound to cellulose, relative to those in aqueous solution. This behaviour was tentatively explained by assuming that a pair of iminodiacetic groups bound on cellulose may assume a geometrical structure resembling that of ethylenediaminetetra-acetic acid (EDTA). It therefore seemed of interest to prepare and characterize a new material with EDTA groups as the chelating agents.

EXPERIMENTAL

The filters were prepared by a procedure similar to that already described.¹ Whatman 41 cellulose filters were chlorinated by reaction at 90° with POCl₃ in anhydrous dimethylformamide (DMF) as solvent, and then reacted with a saturated solution of EDTA (disodium salt) in DMF/water mixture (~3:1 v/v) at about 105° for about 150 min. This reaction proceeds through nucleophilic substitution. It cannot be predicted whether the ligand attack on the chlorinated cellulose will involve both the nitrogen atoms of EDTA, but the uptake of EDTA allows hypotheses to be made concerning the mechanism of ligand bonding.

The preconcentration technique and instrumentation employed were as described in previous papers.¹⁻³

The experimental data obtained for retention were compared with the data calculated for complexation by the ligand in aqueous solution. An SEL 32/27 computer, connected to a Teleray 100 terminal and an OKI-84 printer, was used for this with the program BASECO,⁴ which can perform equilibria calculations for up to 50 possible components. The original program was partially modified in order to obtain plots of the distribution of each complex species as a function of pH.

RESULTS AND DISCUSSION

Figure 1 (dashed lines) shows the experimentally found uptake in the pH range between 1.0 and 9.0 from 100.0 ml of 1 ppm solutions of Cu(II), Pb(II),

Zn(II), Ni(II), Co(II), Cd(II), Ca(II), Mg(II), Hg(II) and Fe(III). The particular pH ranges examined were chosen so that there should be no formation of insoluble species, according to reported data.

Table 1 lists the capacity values (expressed as μ mole/g of filter) for the metal ions studied. These values are the maximum amounts of each metal fixed by 1.00 g of EDTA filter during passage of a 100.0 ppm metal-ion solution (flow-rate about 11 ml/min) at the pH for maximum uptake. The capacity values previously found for the IDA- and MIDA-filters,¹⁻² are also given for comparison.

Even though the complexes formed with the immobilized ligand might show stoichiometries and stabilities different from those found for the same metal and ligand systems in aqueous solution, there is likely to be a correlation between the two systems, so the experimental uptake data were compared with the calculated distribution of the complex species in aqueous medium as a function of pH.

To assign a molar concentration to the bound EDTA, it was assumed that the number of μ moles of EDTA bound on a filter would be the same as the maximum number of μ moles of Cu(II) retainable by the filter (since this is the metal for which the capacity value is highest). This amount is then regarded as present in the volume of solution passed through the filter.

The formation constants used for the calculation were corrected for ionic strength.⁵⁻⁷

It is reasonable to accept that the fixation of metal ions on the filter is due partly to ion-exchange equilibria likely to take place, and partly to the formation of complexes between the metal and the ligand, at a given pH. The continuous lines in Fig. 1 show the distributions of the complexes. In contrast to the results obtained with the IDA- and MIDA-filters, the experimental uptakes are greater than the calculated values only for certain metals and at low pH. In particular, this is the case for Ca(II) and Mg(II), for which the calculated degree of complex formation is very low, whereas experimental uptake

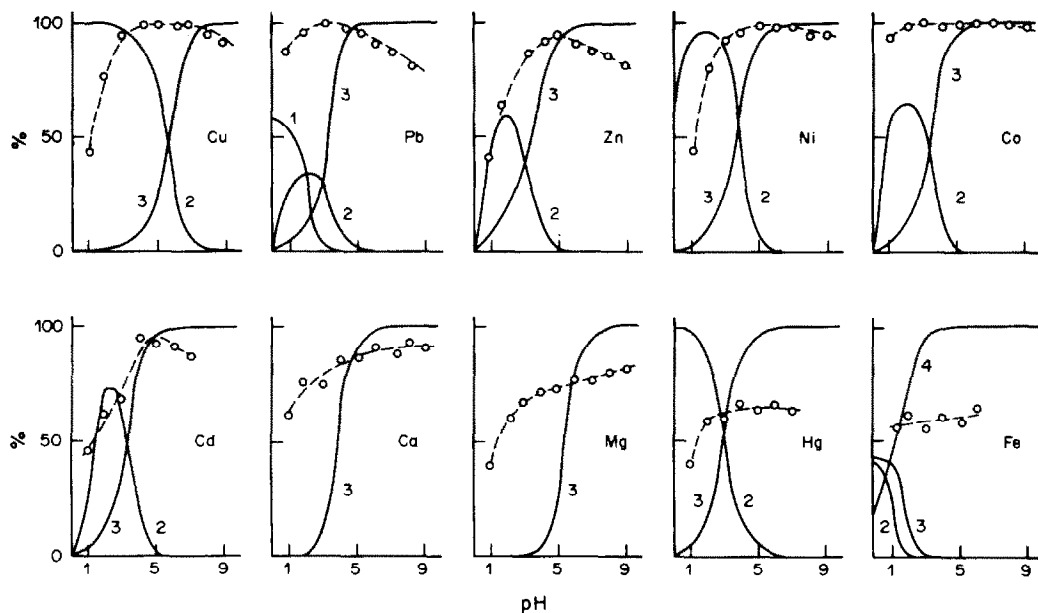


Fig. 1. Experimental uptake on an EDTA-filter (dashed lines) and relative species distribution, as a function of pH, for solutions with $C_{\text{metal}} = 1.00 \text{ mg/l.}$ and $C_{\text{EDTA}} = 5.38 \times 10^{-4} M$. 1, $\text{MeH}_2(\text{EDTA})$; 2, $\text{MeH}(\text{EDTA})$; 3, $\text{Me}(\text{EDTA})$; 4, $\text{Me}(\text{OH})_2(\text{EDTA})$.

is quite high at pH 2.0 (70%) and pH 3.0 (63%). Cd(II) and Pb(II) are also more strongly retained at low pH than expected from the distribution calculations.

Good agreement between the calculated and experimental results is observed only for Ni(II), Co(II) and Cu(II). For the other metals considered, though the experimental and calculated values are similar,

Table 1. Maximum capacity for uptake of the metals investigated on an EDTA-filter (for comparison the data for an IDA-filter and MIDA-filter are also reported)

Cation	Amount fixed on an EDTA-filter,		Amount fixed on an IDA-filter, $\mu\text{mole/g}$	Amount fixed on an MIDA-filter, $\mu\text{mole/g}$
	mg/filter	$\mu\text{mole/g}$		
Cu(II)	3.42	336	202	106
Pb(II)	5.30	160	218	127
Zn(II)	2.19	209	157	69
Co(II)	1.86	197	171	53
Cd(II)	3.56	198	172	111
Ca(II)	2.09	325	109	109
Mg(II)	0.66	169	182	131
Hg(II)	3.21	100	88	85
Fe(III)	1.07	160	109	109

Table 2. Percentage uptake on an EDTA-filter from 100.0 ml of multicomponent solution at different pH values and containing $100 \mu\text{g}$ of each cation (mean and standard deviation of three replicates)

Cation	pH 2.01	pH 3.02	pH 4.02	pH 5.00
Cu(II)	96.0 ± 0.5	94.9 ± 0.6	60.8 ± 0.4	84.3 ± 0.5
Pb(II)	89.5 ± 0.6	95.5 ± 0.4	67.9 ± 0.4	70.0 ± 0.4
Cd(II)	60.6 ± 0.3	94.2 ± 0.2	74.5 ± 0.2	77.9 ± 0.3
Ca(II)	67.0 ± 0.3	88.0 ± 0.2	74.9 ± 0.1	87.2 ± 0.1
Mg(II)	49.9 ± 0.1	79.6 ± 0.1	54.5 ± 0.2	62.3 ± 0.1
Hg(II)	58.2 ± 0.9	47.4 ± 0.8	47.5 ± 1.0	36.5 ± 0.9
Fe(III)	82.3 ± 1.0	92.8 ± 0.9	64.8 ± 0.8	44.0 ± 0.9
Co(II)			56.4 ± 0.9	68.3 ± 0.5
Ni(II)			43.6 ± 0.5	72.4 ± 0.4
Zn(II)			71.5 ± 0.3	71.6 ± 0.3

Table 3. Computed distribution of principal Me-EDTA species in the 10-component mixture (Table 2) at pH 4.02 and 5.00

Metal	Species	Distribution, %	
		pH 4.02	pH 5.00
Cu	CuEDTA	2.5	20.1
	CuHEDTA	97.5	79.9
Pb	PbEDTA	97.0	99.8
	PbHEDTA	3.0	0.2
Cd	CdEDTA	99.9	99.9
	CoEDTA	99.9	99.0
Ni	CoHEDTA	0.1	1.0
	NiEDTA	86.3	98.5
Zn	NiHEDTA	13.7	1.5
	ZnEDTA	92.6	99.3
Ca	ZnHEDTA	7.4	0.7
	CaEDTA	7.6	88.0
Mg	CaHEDTA	0.5	0.6
	MgEDTA	0.1	10.8
Hg	MgHEDTA	0.1	0.5
	HgEDTA	92.6	99.2
Fe	HgHEDTA	7.4	0.8
	Fe(OH) ₂ EDTA	100.0	100.0

the latter are generally greater than the former, particularly for Hg(II) and Fe(III). To find an explanation for this unexpected behaviour, various parameters that could affect the fixation mechanism may be considered. The capacity values and complex formation constants certainly have to play a role. The ionic radii may also be considered, even though they are so similar for the cations investigated that they seem unlikely to affect the mechanism.

On this basis, the quantitative uptake of Ni(II) and Cu(II) might be regarded as due to the high stability constants of their EDTA complexes, except that Co(II) also has a high uptake but lower stability constants, and Fe(III), Hg(II) and Pb(II) are poorly retained, even though their complexes have high stability constants. However, Pb(II) and Hg(II) have the largest ionic radii and it may be asked whether this disadvantages the chelation mechanism on the cellulose-EDTA.

With regards to Fe(III), it may be useful to remember the reaction by which the filters are prepared, *viz.* by nucleophilic substitution. This reaction results in the formation of positive charges on the nitrogen atoms of the EDTA molecules that are bound to the cellulose. By electrostatic repulsion these charges might inhibit the fixation of cations, particularly Fe(III), which is the only trivalent ion among those examined.

In general, in the formation of metal complexes on the treated filter, co-ordination to nitrogen is precluded, because of the positive charge already mentioned, and co-ordination with the carboxylic groups is predominant. This might explain the similar behaviour of the transition and alkaline-earth metal ions.

The species distribution as a function of pH was

also calculated for solutions containing EDTA and up to ten cations, and experimentally tested (Table 2).

Comparison shows that the calculated behaviour differs considerably from that obtained experimentally (Table 3). This is a consequence of the large difference in the affinities of the metal ions for the EDTA-filter and for EDTA in aqueous solution.

When the composition of the mixture is varied, the relative uptakes also vary, depending more on the properties of the components than on their number.

Some ions always behave the same irrespective of the composition of the mixture. For instance, Fe(III) and Hg(II) are always less strongly retained than expected, whereas Ca(II) and Mg(II) show uptake yields greater than their complex formation constants would suggest.

The conclusion is inescapable that when bound to a substrate such as cellulose, a ligand such as EDTA exhibits properties different from those it displays in solution.

The unique features of EDTA bound to cellulose are mainly due to steric hindrance effects, geometric factors and electrostatic interactions, involving not only the carboxylate groups but also the quaternary nitrogen atoms formed after linkage to cellulose.

In this respect it should be pointed out that two opposing effects on metal chelation arise from the binding of EDTA to cellulose: on the one hand the bonding of EDTA through nitrogen atom(s) to the cellulose reduces its co-ordinating ability, and on the other the loss of rotational entropy by the ligand, as a result of rigidity induced by anchoring to the cellulose, should lead to a smaller rotational entropy loss in the complexation reaction (*cf.* the entropy effect on the stability constants of DCTA and EDTA complexes). These effects, in conjunction with those of the ionic radii, charges, configurations and co-ordination properties of the metal ions concerned, may well account, at least in part, for the disparity between the theoretical and experimental uptake values. These effects will also depend on the structure of the ligand itself, which may account for the uptake of certain metal ions being greater with bound IDA than with bound EDTA.

REFERENCES

1. M. C. Gennaro, C. Baiocchi, E. Campi, E. Mentasti and R. Aruga, *Anal. Chim. Acta*, 1983, **151**, 339.
2. M. C. Gennaro, C. Sarzanini, E. Mentasti and C. Baiocchi, *Talanta*, 1985, **32**, 961.
3. M. C. Gennaro, E. Mentasti, C. Sarzanini and C. Baiocchi, *Anal. Chim. Acta*, 1985, **174**, 259.
4. S. Sammartano and C. Rigano, personal communication.
5. A. E. Martell and R. M. Smith, *Critical Stability Constants*, Vol. 1, Plenum Press, New York, 1971.
6. D. D. Perrin, *Stability Constants of Metal Ion Complexes*, Part B, Pergamon Press, London, 1979.
7. L. G. Sillén and A. E. Martell, *Stability Constants of Metal Ion Complexes*, The Chemical Society, Special Publications 17 and 25, London, 1964 and 1971.

POLAROGRAPHIC DETERMINATION OF TRACE AMOUNTS OF THORIUM

ZAOFAN ZHAO, XIAOHUA CAI, PEIBIAO LI and HANDONG YANG

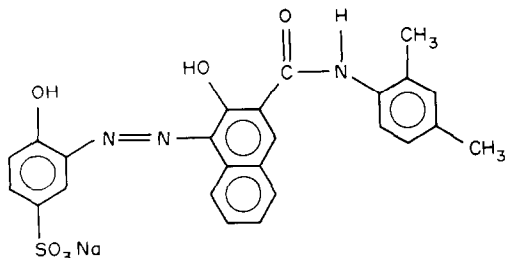
Department of Chemistry, University of Wuhan, Wuhan, People's Republic of China

(Received 10 June 1985. Revised 30 November 1985. Accepted 21 February 1986)

Summary—A sensitive linear-sweep polarographic method for the determination of thorium is described. It is based on the thorium complex with Xylidyl Blue I (XBI) in a medium containing ethylenediamine, 1,10-phenanthroline, oxalic acid and ninhydrin, at pH 10.5–11.5. The complex has been proved to be $\text{Th}(\text{XBI})_2$, with $\log \beta' = 9.6$. The method can be used to determine trace amounts of thorium over the range 3.5×10^{-8} – $3 \times 10^{-6} M$. The detection limit is $1 \times 10^{-8} M$. A solvent extraction procedure is necessary to eliminate interference from several cations. The method has been applied to determination of traces of thorium in minerals, with good results.

The direct polarographic determination of thorium is possible in non-aqueous solvents.¹ Some indirect methods have been developed, based on precipitation² or a displacement reaction between Th(IV) and Pb(II)–EDTA³ or Bi(III)–EDTA⁴ *etc.* The catalytic polarographic wave of thorium in the presence of lithium nitrate has been used for the determination of microgram amounts of thorium.⁵ However, none of these systems is sensitive enough for practical use. An alternative is to complex thorium with a polarographically active organic ligand, and determine the thorium indirectly by linear-sweep polarography (LSP). Among the ligands used are cupferron⁶ and Alizarin S.⁷ The sensitivity is quite good.

We have found Xylidyl Blue I (XBI) to be a very good ligand for the determination of thorium by LSP. XBI—sodium 1-azo-2-hydroxy-3-(2,4-dimethyl-carboxanilido)-naphthalene-1'-(2-hydroxybenzene-5-sulphonate)—has the structure:



It is used as an acid–base indicator and a spectrophotometric reagent for the determination of magnesium.⁸ We have found that it can also be used for determining uranium by LSP with excellent results.⁹ The reaction of thorium with XBI has not pre-

viously been reported. Our experimental results show that thorium reacts with XBI to form a polarographically active complex. The molar ratio of Th:XBI in the complex is 1:2, and the conditional formation constant $\log \beta'$ is 9.6. In LSP, the cathodic peak potential of the complex wave is -0.8 V vs. SCE . Under the selected conditions, the detection limit is $1 \times 10^{-8} M$, and the peak current is a linear function of thorium concentration over the range 3.5×10^{-8} – $3 \times 10^{-6} M$. A solvent extraction procedure is proposed for removing some interfering ions. The procedure has been used for the determination of thorium in ores.

EXPERIMENTAL

Reagents

The Xylidyl Blue I was used, without further purification, as a $10^{-3} M$ solution in water. A $10^{-2} M$ stock solution of thorium in $0.1 M$ hydrochloric acid was prepared from the oxide and diluted to $10^{-4} M$ and $10^{-3} M$ with $0.1 M$ hydrochloric acid to give the working solutions. All chemicals used were of analytical reagent grade.

Apparatus

A JP-1A oscillopolarograph (Chengdu Instrumental Factory, China) and PO4 Polariter (Radiometer, Denmark) were used. For derivative polarography with the JP-1A oscillopolarograph the conditions were: drop-time 7 sec, scan-rate 250 mV/sec, scan from -0.5 to 1.0 V , mercury head 50 cm, and mercury flow-rate 2.0 mg/sec. The three-electrode system comprised a dropping mercury electrode (DME), platinum counter-electrode, and saturated calomel electrode (SCE) as reference. All potentials were referred to the SCE. The electrolytic cell was a 10-ml beaker.

Procedures

Calibration graph. Mix standard thorium solution (to cover the concentration range 3.5×10^{-8} – $3 \times 10^{-6} M$) with 0.3 ml of $10^{-3} M$ XBI, 2.5 ml of 10% v/v ethylenediamine (en) solution, 0.1 ml of $10^{-3} M$ 1,10-phenanthroline (phen), 0.4 ml of $10^{-2} M$ ninhydrin and 0.25 ml of $0.1 M$ oxalic acid.

Adjust the pH to 10.5–11.5 with 0.1M hydrochloric acid, dilute the sample to 10 ml, then let it stand for about 10 min. Record the derivative linear-sweep polarogram from -0.5 to -1.0 V (*vs.* SCE). Measure the peak heights of the polarogram at -0.8 V (*vs.* SCE) in the usual way. Usually the oxygen dissolved in the solutions need not be removed. Draw the calibration graph.

Analysis of ore samples. To 0.2 g of ore sample in a 150-ml beaker add 4–5 g of a 1:1:1 mixture of ammonium chloride, nitrate and fluoride. Heat gently until vapour is no longer evolved. Cool, add 5 ml of *aqua regia* and continue heating until most of the acid has evaporated, then add 1 ml of hydrochloric acid (1 + 1) and evaporate to dryness. Cool, add a further 5 ml of hydrochloric acid (1 + 1) and heat to dissolve the residue. Cool and transfer to a 150-ml separating funnel. Add 5 ml of 20% sulphosalicylic acid solution. Add 50% sodium hydroxide solution until the solution is yellow, then hydrochloric acid (1 + 1) until the colour is brown-red; the pH will now be in the range 1.5–2. Reduce Fe^{3+} to Fe^{2+} and decolorize the solution by adding ascorbic acid solution. Add 15 ml of 0.01M PMBP (1-phenyl-3-methyl-4-benzamidopyrazolone) solution in benzene and shake the mixture for 30 sec. Wash the organic phase three times with 3% v/v hydrochloric acid. Add 15 ml of 4M hydrochloric acid and shake, then collect the aqueous phase in a 50-ml beaker, cover with a watch-glass and evaporate the solution to dryness. Add 3 or 4 drops of hydrochloric acid (1 + 1) and 2 ml of distilled water, and heat. Determine the thorium by the procedure used for the calibration.

RESULTS AND DISCUSSION

Polarographic wave of thorium–XBI complex

XBI gives three well-defined reduction peaks in LSP, which are attributed to reduction of the azo- and amido-groups.¹⁰ In the presence of small amounts of thorium, a new peak P appears at almost the same reduction potential as the third wave of XBI, and the reagent peaks P1 and P2 decrease

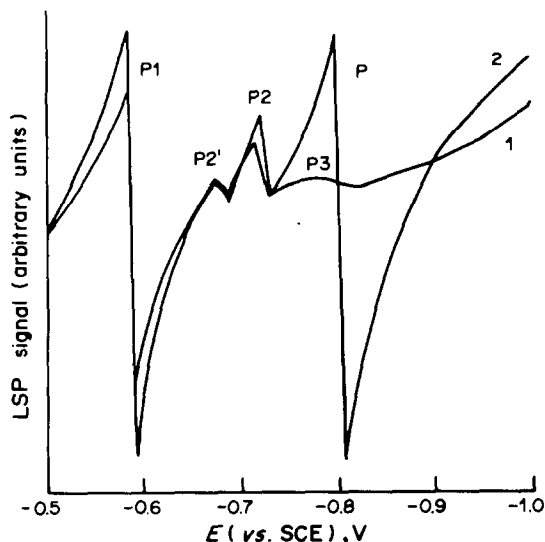


Fig. 1. Derivative linear-sweep polarograms. 1, 2.5% v/v ethylenediamine, $10^{-4}M$ phenanthroline, $2.5 \times 10^{-3}M$ oxalic acid and $4 \times 10^{-4}M$ ninhydrin (pH 11.0); 2, as for 1, plus $10^{-6}M$ thorium.

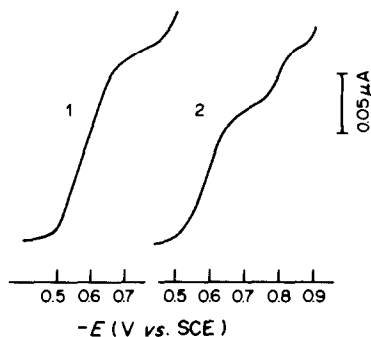


Fig. 2. Direct current polarograms. 1, XBI alone, supporting electrolyte as for Fig. 1; 2, as for 1, plus $10^{-5}M$ thorium.

(Fig. 1). The height of this new peak is directly proportional to the thorium concentration over the range 3.5×10^{-8} – $3 \times 10^{-6}M$. Furthermore, as seen from Fig. 2, there is a d.c. polarographic wave for the thorium–XBI complex, at a more negative potential than that of XBI itself. There is no doubt that the new wave is due to the complex. This behaviour is very similar to that of the aluminium–Mordant Violet complex.¹¹ Other evidence for formation of a thorium–XBI complex was obtained from spectrophotometry, λ_{max} for XBI being 590 nm whereas that for the thorium complex is 515 nm.

The ratio of thorium to XBI in the complex and hence the conditional formation constant for the complex were found by using the equation¹²

$$\log[h/(h_{max} - h)] = a \log[R] + \log \beta'$$

where h is the peak height, h_{max} is the maximum peak height, $[R]$ is the concentration of XBI, β' is the conditional formation constant of the complex, and a is the molar ratio of thorium to XBI. We found that Th:XBI = 1:2 and $\log \beta' = 9.6$.

It is well known that thorium(IV) is not reduced at the DME in aqueous solution. Therefore, the only possible explanation for the polarographic behaviour of the thorium–XBI complex is reduction of XBI in the complex,¹⁰ which takes place at more negative potentials than that of free XBI.

Optimum conditions for the determination of thorium

For practical purposes, various supporting electrolytes, such as en–HCl and NH_3 – NH_4Cl buffer solutions have been tested, and of these the ethylenediamine system was found to be the best, because the polarogram of the complex is then well-defined and the sensitivity is reasonably high. We have also found that the sensitivity is considerably increased by the addition of organic compounds such as acetylacetone, oxalic acid, glycine or ninhydrin to the medium used. Oxalic acid and ninhydrin are preferred because they give better defined peaks than do glycine and acetylacetone. Furthermore, we have found that the background is decreased nearly to zero by the presence of small amounts of 1,10-phenanthroline ($10^{-4}M$), so this is another im-

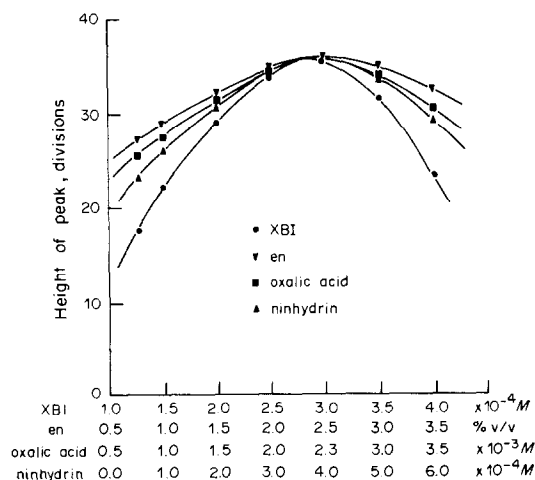


Fig. 3. Effect of concentration of various supporting electrolyte components on the wave height; $10^{-6}M$ thorium.

portant component in the supporting electrolyte. The optimum concentrations of ethylenediamine, oxalic acid, ninhydrin and XBI were found to be 2.5% v/v, $2.5 \times 10^{-3}M$, $4 \times 10^{-4}M$ and $3 \times 10^{-5}M$, respectively, as can be seen from Fig. 3. The mechanism for the enhancement effect of these organic reagents is not clear.

At low pH the peak height is low because of the insolubility of XBI. However, if the pH is too high, the peak height is again low, but because of hydrolysis of the thorium ion. The optimum pH range for the solution is from 10.5 to 11.5 (see Fig. 4).

The effect of common ions

More than forty anions and cations were examined for possible interference in the determination of thorium by LSP. The results for cations are shown in Table 1. Most of the common metal ions have little effect. Only uranium and the lanthanides interfere seriously, because they behave in the same way as thorium in the system used. A prior separation is needed to eliminate their interference.

Less than 1000-fold amounts of S^{2-} , F^{-} , Cl^{-} , Br^{-} , I^{-} , NO_3^{-} , SO_3^{2-} , SO_4^{2-} , PO_4^{3-} , SiO_3^{2-} , 500-fold

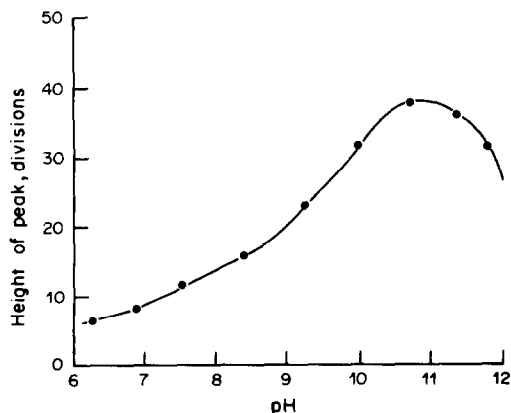


Fig. 4. Effect of pH on the wave height. Conditions as for Fig. 1.

Table 1. Study of cationic interference

Ion, X	Maximum concentration ratios tolerated, [X]/[Th]
Fe^{3+} , Ag^{+} , Ni^{2+} , Pd^{2+}	1000
Zn^{2+}	800
Be^{2+} , Cu^{2+} , Cr^{3+} , Mn^{2+}	200
Sn^{2+}	100
Pb^{2+} , Cd^{2+} , Bi^{3+} , In^{3+} , La^{3+} , Ce^{4+}	50
UO_2^{2+}	20
RE	0-5

Table 2. Determination of thorium in ores

Sample	Found, %	Reference value, %
1*	0.0068 ± 0.0006	0.0075
2*	0.0030 ± 0.0002	0.0028
3†	0.0010 ± 0.0001	0.00099
4†	0.00096 ± 0.0002	0.00081

* From Yichang Institute of Geology and Mineral Resources.

† From the Central Laboratory of Geological Bureau of Hubei.

amounts of $S_2O_3^{2-}$ and 100-fold amounts of NO_2^{-} do not interfere in the determination of thorium.

Determination of thorium in ores

Four mineral samples were analysed by this method. These samples contained large amounts of Sn, Fe, Bi, Cu, Pb, Sb and small amounts of Th, U, lanthanides, etc. Owing to the possible interference from uranium and rare-earth elements in the samples, a solvent extraction separation (with PMBP in benzene)¹³ was used. The results are listed in Table 2. It is obvious that the proposed procedure is good enough for practical use.

Acknowledgement—This project was supported by the science fund of the Chinese Academy of Sciences.

REFERENCES

- G. Gritzner and V. Gutman, *Z. Anal. Chem.*, 1969, **224**, 245.
- C. W. C. Milner, *The Principles and Applications of Polarography*, p. 236. Longmans, London, 1962.
- H. Flaschka, S. Khalafalla and F. Sadek, *Z. Anal. Chem.*, 1957, **156**, 321.
- M. Sugawara, Y. Murayama and T. Kambara, *ibid.*, 1978, **293**, 104.
- P. Szefer, *ibid.*, 1977, **287**, 46.
- S. R. Yao, J. X. Chen and C. F. Li, *Fenxi Huaxue*, 1985, **12**, 671.
- J. N. Li and Z. F. Zhao, *ibid.*, 1985, **12**, 347.
- C. K. Mann and J. H. Yoe, *Anal. Chem.*, 1956, **28**, 202.
- X. H. Cai, P. B. Li and Z. F. Zhao, *Proceedings of the Third National Electroanalytical Chemistry Meeting*, Changchun, July, 1984, p. 44.
- Z. F. Zhao, X. H. Cai and P. B. Li, unpublished work.
- H. H. Willard and J. A. Dean, *Anal. Chem.*, 1950, **22**, 1264.
- Z. M. Luo, *Ternary Complexes and Their Applications in Analytical Chemistry*, p. 90, People's Educational Press, Beijing, 1981.
- Analytical Division of Chemistry Department of Zhejiang University, *A Handbook of Analytical Chemistry*, Book 2, p. 174. Chemical Industry Press, Beijing, 1982.

ANALYTICAL DATA

SALICYLALDEHYDE-1-PHTHALAZINOHYDRAZONE AS AN ANALYTICAL REAGENT

M. CALLEJON MOCHON, M. CENTENO GALLEGO and A. GUIRAUM PEREZ

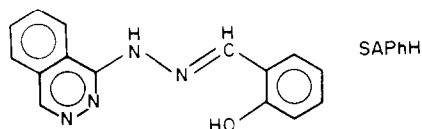
Department of Analytical Chemistry, Faculty of Chemistry, University of Sevilla, 41012 Sevilla, Spain

(Received 5 August 1985. Revised 17 December 1985. Accepted 3 March 1986)

Summary—The synthesis, characteristics and analytical properties of salicylaldehyde-1-phthalazino-hydrazone are described. Spectral characteristics, pK values, the effect of oxidizing and reducing agents, resistance to hydrolysis, and reactions with common cations are reported.

Hydrazones have attracted much attention as analytical reagents and their applications have been reviewed by Katyál *et al.*^{1,2} and recently by Singh *et al.*³ Many nitrogen-heterocycle hydrazones derived from 2-hydrazinopyridine and 2-hydrazinoquinoline have been prepared and explored for their potential as analytical reagents. The introduction of a quinoline ring into the hydrazide molecule increases the sensitivity of the reagent. However, few heterocyclic hydrazones derived from 1-hydrazinophthalazine have been prepared and studied. Otomo and Nakayama⁴ have described synthesis of the 2-pyridyl (PaPhH), 2-quinolyl (QAPhH) and 2-benzothiazolyl (BAPhH) phthalazinohydrazones and applied these compounds to extractive spectrophotometric determination of palladium in the presence of chloride. Ishii *et al.*⁵ have described the synthesis of furfural-1-phthalazinohydrazone (FPH) and 5-methylfurfural-1-phthalazinohydrazone (MFPH), and proposed MFPH for spectrophotometric determination of nickel. These compounds have an =N—CH—NH—N= group which is capable of forming a five-membered chelate ring.⁶⁻⁸ The secondary amine proton in this grouping has been shown to be quite labile when the ligand undergoes coordination with a metal ion. The complexes formed on elimination of this proton are intensely coloured and are amenable to analytical application.

This paper describes the synthesis, properties and analytical study of the 1-phthalazinohydrazone derivative of salicylaldehyde (SAPhH):



EXPERIMENTAL

Reagent

Synthesis of SAPhH. To 1.48 g of 1-hydrazinophthalazine hydrochloride (0.0075 mole) dissolved in 20 ml of boiling distilled water and 1.5 ml of hydrochloric acid, a hot

solution containing 0.92 g of salicylaldehyde in 10 ml of ethanol was slowly added, and the mixture was heated until a precipitate appeared. After cooling to room temperature the yellow product was filtered off and recrystallized from ethanol containing 5% v/v concentrated hydrochloric acid. The product was the monohydrochloride and was scarcely soluble in water, appreciably soluble in ethanol and very soluble in dioxan.

The purity of the reagent (m.p. 247–248°) was checked by thin-layer chromatography on silica gel. Microanalysis gave C 59.7%, H 4.6%, N 18.4%, Cl 12.0%; $C_{15}H_{12}N_4O \cdot HCl$ requires C 59.93%, H 4.37%, N 18.63%, Cl 11.79%.

Other reagents. Salts and solvents were of analytical grade. All metal ion solutions were standardized. Distilled water was used throughout.

Procedures

Determination of acid-dissociation constants. A 1-ml aliquot of a solution of SAPhH ($7.5 \times 10^{-4} M$) in ethanol was placed in a 25-ml standard flask, and enough ethanol to make its final concentration 24% v/v was added. The ionic strength was fixed at 0.1 with potassium chloride and the pH adjusted with potassium hydroxide solution and hydrochloric acid. The solution was then diluted to the mark with distilled water and mixed, and the absorbances at three different wavelengths were measured. Absorbance vs. pH curves were plotted, and the pK_a values were evaluated by the Maroni and Calmon⁹ (parallel straight-lines and concurrent straight-lines methods), and by the Sommer¹⁰ and Agren¹¹ methods.

Spectrophotometric and spectrofluorimetric study. The absorption and fluorescence spectra were recorded for samples with 1 or 2 ppm of cation and the reagent in excess (between 10- and 100-fold). The general procedure was to mix 5 ml of 0.1% ethanolic reagent solution, 10 ml of ethanol, various amounts of metal ion and 5 ml of buffer solution (acetic acid-acetate, pH 4.3, and ammonium chloride-ammonia, pH 9.2) and dilute with water to 25 ml.

RESULTS AND DISCUSSION

Infrared spectrum

Bands in the infrared spectrum (potassium bromide disc) were assigned to the stretching vibrations (in cm^{-1}) of NH (3250m, 3190m) and C=N (1610s), (m = medium, s = strong). The aromatic portions of the molecule cause numerous bands and their overlap makes detailed assignments difficult. The principal bands and their assignments are given in Table 1.

Table 1. Infrared spectra

Frequency, cm^{-1}	Assignment
3250 m	N—H stretch
3190 m	N—H stretch
1610 s	C=N stretch
1595 s	Aromatic ring
1355 s	$\nu_{in-plane}^{CH}$
1255 s	C—O stretch
915 s	$\delta_{out-of-plane}^{OH}$
750 s and 675 w	<i>o</i> -substitution $\delta_{out-of-plane}^{CH}$

Table 2. Ultraviolet spectra of the reagent in common solvents

Solvent	λ_{max} , nm	ϵ , $10^3 l. mole^{-1}. cm^{-1}$
Water	356	14.4
Dimethylformamide	380	23.2
Methanol	370	26.8
Ethanol	368	22.9
Benzyl alcohol	359	20.5
Acetone	362	23.3
Chloroform	376	15.0

Ultraviolet spectrum

The ultraviolet absorption spectra of $2 \times 10^{-5} M$ SAPHH in 28% ethanol solution at various pH values are plotted in Fig. 1; the absorption maximum in acid medium undergoes a red-shift in both neutral and alkaline media. The spectral characteristics of the reagent in several solvents are given in Table 2.

Acid-base equilibria

The spectra of aqueous solutions of the reagent are pH-dependent. The changes can be attributed to protonation of one nitrogen of the phthalazine nucleus in acid medium¹² and the dissociation of the phenol group in alkaline medium.

The dissociation constants of the reagent were measured by spectrophotometric methods.⁹⁻¹¹ Figure 2 shows the absorbance *vs.* pH graph, and the pK_a values shown in Table 3 are the arithmetic means of the values obtained from measurements at three different wavelengths.

Stability

Dilute ethanolic solutions of the reagent ($1.3 \times 10^{-4} M$) are very stable and $3.3 \times 10^{-3} M$ solutions are stable for longer than a week. Acid and basic solutions are also very stable.

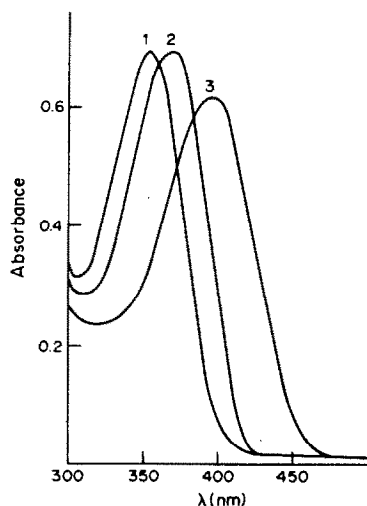


Fig. 1. Absorption spectra of SAPHH in 28% v/v ethanol solution at (1), pH 2.8; (2), pH 7.8; (3), pH 11.5; $C_R = 2.6 \times 10^{-5} M$.

Table 3. pK_a values of the reagent*

Method	pK_{a1}	pK_{a2}
Parallel straight lines ⁹	4.53 ± 0.01	10.03 ± 0.03
Concurrent straight lines ⁹	4.52 ± 0.02	10.03 ± 0.07
Agree-Sommer ^{10,11}	4.53 ± 0.01	10.03 ± 0.06
Mean value	4.53 ± 0.01	10.03 ± 0.06

*Mean of three evaluations.

Influence of oxidizing and reducing agents

Ammonium per sulphate slightly alters the absorption spectra of the reagent, especially in ammonium chloride-ammonia buffer and basic medium, but hydrogen peroxide and reducing agents (ascorbic acid, sodium sulphite) are without effect at any pH. No catalytic effect on treatment with hydrogen peroxide at pH 4.3 and 9.2 is exerted by Ni(II), Pd(II), Cu(II), Ag(I), Zn(II), Cd(II), Hg(II), Mn(II), Co(II) and Fe(III) at the $0.5 \mu g/ml$ level.

Spectrophotometric study of reactions with cations

The chromogenic properties of SAPHH, on reaction with different cations in acetic acid-sodium acetate (pH 4.7) and ammonium chloride-ammonia (pH 9.2) media, were tested. The most sensitive reactions are those of Co(II), Cu(II), Mn(II), Cr(III), Zn(II), Pd(II), Ce(IV), In(III) and Ga(III) (Table 4),

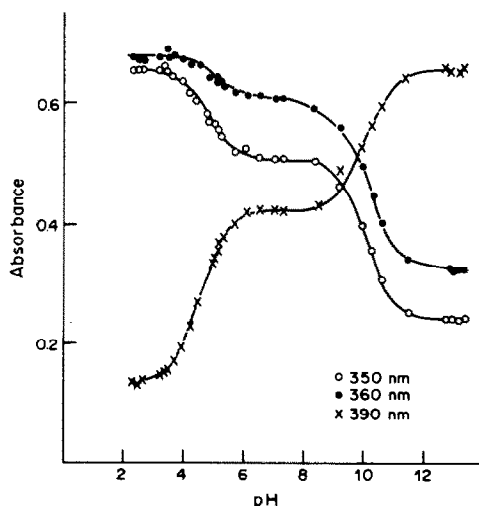


Fig. 2. Influence of pH on the absorption of the reagent; $C_R = 3.0 \times 10^{-5} M$.

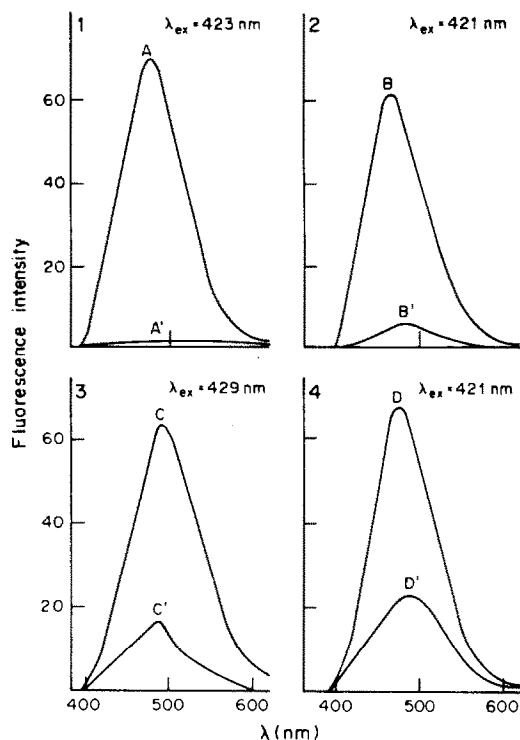


Fig. 3. Fluorescence spectra of 1A, Ga(III); 2B, Al(III); 3C, Zn(II); 4D, In(III) chelates with SAPHH in 80% v/v ethanol solution at pH 2.8, 2.5, 4.8, 6.6, respectively and of the reagent in the same conditions (1A', 2B', 3C', 4D'). $C_R = 2.6 \times 10^{-5} M$ and $C_M = 80 \text{ ng/ml}$.

but are not particularly useful. A similar study was made with 3-hydroxybenzaldehyde-1-phthalazino-hydrazone but it also was not of much analytical use.

Fluorescence studies

The fluorescence spectra of the chelates were stud-

ied, and it was verified that Ga(III), Al(III), In(III) and Zn(II) (Fig. 3) show the greatest sensitivity, especially gallium (Table 5). To evaluate the effect of pH, solutions containing 1 ppm of Ga(III), Al(III), In(III) or Zn(II) and a 40:1 molar ratio of reagent, were prepared in 80% ethanol at room temperature. The pH was changed by addition of 4 ml of appropriate buffer solutions. In all instances, the fluorescent complexes are formed in acid media (Table 5).

At the optimum pH, with $2.6 \times 10^{-5} M$ reagent and total ethanol content 80%, linear calibration graphs were obtained for the ranges 1–10 ng/ml gallium, 10–60 ng/ml indium and 10–100 ng/ml zinc.

The stoichiometry of the complexes was determined by Job's method with spectrophotometric and fluorimetric measurement. In all instances, the results indicated a 2:1 molar ratio reagent:cation.

CONCLUSIONS

Salicylaldehyde-1-phthalzinohydrazone is easily obtained and shows high stability in ethanol solution. Its reactions with metal ions exhibit reasonable spectrophotometric sensitivity for Co, Cu, Mn, Cr, Zn, Pd, In and Ga. In addition, SAPHH is a promising fluorimetric reagent for Ga, Al, In and Zn.

REFERENCES

1. M. Katyal and Y. Dutt, *Talanta*, 1975, **22**, 51.
2. M. Katyal and W. A. E. McBryde, *Tech. News. Service Sarabhai Chemicals, Barola (India)*, 1978, **X**, Nos. 1 and 2.
3. R. B. Singh, P. Jain and R. P. Singh, *Talanta*, 1982, **29**, 77.
4. M. Otomo and I. Nakayama, *Microchem. J.*, 1980, **25**, 75.

Table 4. Spectrophotometric characteristics of complexes in solution

Metal ion	Buffer solution, pH 4.3			Buffer solution, pH 9.2		
	λ_{max} , nm	ϵ , $10^3 \text{ l. mole}^{-1} \text{ cm}^{-1}$	Colour of complex	λ_{max} , nm	ϵ , $10^3 \text{ l. mole}^{-1} \text{ cm}^{-1}$	Colour of complex
Co(II)	422	27.4*	yellow	419	17.7	yellow
Cu(II)	420	10.0	yellow	418	21.1	yellow
Mn(II)	—	—	—	426	16.3	yellow
Cr(III)	438	9.7	yellow-green	—	—	—
Zn(II)	418	20.0*	yellow	418	21.6	yellow
Pd(II)	442	6.5	yellow-green	450	21.1	yellow-green
Ce(IV)	—	—	—	418	23.8	yellow
In(III)	415	36.0*	yellow	420	30.5	yellow
Ga(III)	425	42.0*	yellow	—	—	—

*In acetic acid-potassium acetate buffer, pH 5.7.

Table 5. Fluorimetric characteristics of ML_2 complexes in solution

Metal ion	λ_{max} , nm		Optimum pH (apparent)	Linear fluorescence range, ng/ml
	Excitation	Emission		
Ga(III)	423	486	2.6–3.0	1–10
Al(III)	421	470	2.0–2.7	10–60
In(III)	421	485	4.5–5.0	10–60
Zn(II)	429	493	6.3–6.8	10–100

5. H. Ishii, T. Odashima and T. Imamura, *Analyst*, 1982, **107**, 885.
6. A. A. Schilt, J. F. Wu and F. H. Case, *Talanta*, 1975, **22**, 388.
7. H. Alexaki-Tzivanidou, *Anal. Chim. Acta*, 1975, **75**, 231.
8. Idem, *Microchem. J.*, 1977, **22**, 388.
9. P. Maroni and J. P. Calmon, *Bull. Soc. Chim. France*, 1964, 519.
10. L. Sommer, *Folia Fac. Sci. Nat. Univ. Purkyn. Brno*, 1964, **5**, 1.
11. A. Agreen, *Acta. Chem. Scand.*, 1955, **9**, 49.
12. M. H. Palmer, *The Structure and Reactions of Heterocyclic Compounds*, Vol. VII, Arnold, London, 1967.

X-RAY DIFFRACTION DATA FOR SIX ANALGESICS

J. E. KOUNTOURELLIS and F. A. UNDERWOOD*

School of Physics, University of Bath, Bath, England

P. P. GEORGAKOPOULOS and A. RAPTOULI

School of Pharmacy, Aristotelian University of Thessaloniki, Thessaloniki, 540 06, Greece

(Received 9 December 1985. Accepted 10 February 1986)

Summary—X-Ray diffraction data for six analgesics have been obtained by the powder diffractometer technique. The data are tabulated in terms of the lattice spacings and the relative intensities of the lines. The results have been confirmed by the Debye-Scherrer method.

X-Ray diffraction data have been used to characterize six analgesics in terms of d values (in Å), the interplanar spacings, and the relative intensities of the lines, with the intensity of strongest line taken as 100, according to the system of Hanawalt.

These data are not included in the 1984 Powder Diffraction File,¹ so the new information may be useful for the identification of the crystalline organic compounds investigated. Generally, in pharmaceuticals the characterization of a medical compound and its polymorphic forms is important because they may exhibit differences in bio-availability, shelf-life, suspendibility and rheology.

EXPERIMENTAL

Reagents

The drugs, kindly supplied by the manufacturers, were furbiprofen, ketoprofen, ibuprofen, naproxen, salicylamide and salicin.^{3,4} The proton and ¹³C nmr spectra were in agreement with the molecular structures.

Apparatus

A Philips diffractometer goniometer PW 1050 was used for recording the diffractometer traces. The instrument was calibrated with silicon as a standard.

Determination

The X-ray powder diffractometer patterns were recorded by mounting ca. 1 g of ground sample in a window in an aluminium specimen-holder and then exposing it to the X-ray beam for 40 min, copper $K\alpha$ radiation being used. It was essential, for the most satisfactory results, that the number of crystallites contributing to each reflection was sufficiently large to generate signals of reproducible intensity, and that the preferred orientation of the crystallites was held to a minimum. Since there is a close correlation between the method of packing and the preferred orientation, we checked that the two basic methods of preparing the samples (the McCreery and Byström-Asklund methods) gave identical results.⁵⁻⁷ The samples were scanned over $2\theta = 5-45^\circ$, and the lines occurring at 2θ above 45° were

omitted, being small and numerous and, typically of organic compounds, falling sharply in intensity. The results were in agreement with film data obtained with a 114.83-mm diameter powder camera and cobalt $K\alpha$ radiation (Debye-Scherrer method).

RESULTS AND DISCUSSION

Table 1 shows the data obtained. The d values of the interplanar spacing together with the relative intensities of the lines are in good agreement for both methods of sample preparation. Although the d values and the relative intensities for ibuprofen have been reported previously¹ it was observed that preparation of the sample can suffer from preferred orientation, as shown by the intense line at a low Bragg angle ($d = 14.60$ Å). For identification purposes this line should not be taken into account, as it is not truly one of the three most intense. In this research, by employing specific methods of sample loading, preferred orientation was reduced to a minimum, so the results are valid and reproducible.

Acknowledgement—The authors would like to thank Mr. Chapman for his technical assistance.

REFERENCES

1. *Powder Diffraction File*, Joint Committee on Powder Diffraction Standards, Swarthmore, PA 19081, 1984.
2. A. G. Gilman, L. S. Goodman and A. Gilman, *The Pharmacological Basis of Therapeutics*, 6th Ed., Macmillan, New York, 1980.
3. Martindale, *The Extra Pharmacopoeia*, 28th Ed., The Pharmaceutical Press, London, 1982.
4. American Medical Association, *Drug Evaluation*, Saunders, Philadelphia, PA 19105, 1984.
5. H. P. Klug and L. E. Alexander, *X-Ray Diffraction Procedures for Polycrystalline and Amorphous Materials*, 2nd Ed., pp. 364-374. Wiley, New York, 1974.
6. A. M. Byström-Asklund, *Am. Mineral.*, 1966, **51**, 1233.
7. J. T. R. Owen, J. E. Kountourellis and F. A. Underwood, *J. Assoc. Off. Anal. Chem.*, 1981, **64**, 1164.

*Author for correspondence.

Table 1. The lattice spacings and relative intensities of lines for six analgesics

Flurbiprofen		Ketoprofen		Ibuprofen		Naproxen		Salicylamide		Salicin	
<i>d</i> , Å	<i>I</i> / <i>I</i> ₁	<i>d</i> , Å	<i>I</i> / <i>I</i> ₁	<i>d</i> , Å	<i>I</i> / <i>I</i> ₁	<i>d</i> , Å	<i>I</i> / <i>I</i> ₁	<i>d</i> , Å	<i>I</i> / <i>I</i> ₁	<i>d</i> , Å	<i>I</i> / <i>I</i> ₁
<u>12.30</u>	<u>100</u>	<u>13.80</u>	<u>58</u>	<u>14.60</u>	<u>50</u>	<u>13.40</u>	<u>40</u>	<u>10.50</u>	<u>93</u>	<u>10.70</u>	<u>20</u>
8.60	6	6.76	18	7.31	14	<u>7.02</u>	26	<u>6.46</u>	17	7.76	39
8.17	26	<u>6.19</u>	<u>64</u>	6.97	5	6.66	11	5.57	17	<u>7.21</u>	<u>93</u>
6.28	5	5.47	4	6.37	15	5.31	20	5.44	31	6.24	12
5.79	12 sh	5.25	9	6.07	12	4.93	10	<u>5.26</u>	<u>100</u>	5.64	12
<u>5.57</u>	<u>50</u>	5.13	21	<u>5.37</u>	<u>100</u>	<u>4.70</u>	<u>100</u>	4.87	11	5.44	43
						4.46	24 sh				
5.40	35	<u>4.85</u>	<u>100</u>	5.05	45	4.37	28	4.67	3	5.31 sh	8
		<u>4.62</u>	4								
5.16	4	4.44	14	4.75	18 sh	3.99	<u>50</u>	4.25	9	5.22	8
4.98	4	4.04	11	4.67	27 sh	3.95	<u>48 sh</u>	4.13	3	4.98	13
4.53	20	3.90	<u>98</u>	4.58	46	3.76	28	3.87	3	4.48	47
4.44	8	<u>3.74</u>	28	<u>4.42</u>	<u>95</u>	3.53	4	<u>3.51</u>	24	<u>4.08</u>	<u>98</u>
								3.41	6 sh		
4.31	<u>48</u>	3.43	9	4.08	18 sh	3.27	19	3.22	14	3.88	9
4.13	42	3.29	17	3.99	<u>65</u>	3.21	16	3.05	2	3.66	100
3.97	18	3.23	16	3.91	8 sh	3.15	15	2.780	8	3.46	66
										3.39 sh	12
										3.26	8
3.83	16	3.19	12	3.83	4	2.998	5	2.690	4	3.12	16
3.75	30	3.14	7	3.68	8	2.858	5	2.622	6	2.998	6
3.51	14	3.04	13	3.63	9	2.763	3	2.404	4	2.849	8
3.34	6 sh	2.747	4	3.56	19	2.667	2			2.730	4
3.30	8	2.600	4	3.48	10	2.543	4			2.652	4
3.15	3	2.481	3	3.29	11 sh	2.332	3				
3.06	14 sh	2.455	3	3.23	23	2.265	3				
3.02	18	2.350	3	3.18	10						
2.979	14	2.321	2	3.13	7						
2.885	6	2.281	3								
2.780	3										
2.644	10										
2.495	5										
2.423	5										

The three most intense lines are underlined.

sh = shoulder attached to strong line.

ANALYTICAL APPLICATIONS OF SYNCHRONOUS FLUORESCENCE SPECTROSCOPY

S. RUBIO, A. GOMEZ-HENS and M. VALCARCEL

Department of Analytical Chemistry, Faculty of Sciences, University of Córdoba, Córdoba, Spain

(Received 13 September 1985. Accepted 29 March 1986)

Summary—A review is presented of the fundamental principles and analytical applications of synchronous excitation fluorescence spectroscopy, constant-energy synchronous fluorescence spectroscopy and variable-separation synchronous excitation fluorescence spectroscopy.

Conventional fluorescence involves generating an emission spectrum by scanning the emission wavelength, λ_{em} , as the sample is irradiated at a single excitation wavelength, λ_{ex} . Similarly, an excitation spectrum is obtained by scanning the excitation wavelength while recording the emission signal at a single wavelength. Another possibility is to vary λ_{ex} and λ_{em} simultaneously. This technique has several variants, depending on the scan-rates of the two monochromators.

(1) If the scan-rate is constant for both monochromators, and therefore a constant wavelength interval, $\Delta\lambda$, is kept between λ_{em} and λ_{ex} , the technique is known as *synchronous excitation fluorescence spectroscopy*. This technique is very simple and is the most frequently used of all synchronous modes.

(2) The excitation and emission wavelengths may be varied simultaneously in such a manner that a constant frequency difference, $\Delta\nu$, is maintained between them. This technique, *constant-energy synchronous fluorescence spectroscopy*, has scarcely been used to date.

(3) The excitation and emission wavelengths may be varied simultaneously but at different rates. These different rates allow the construction of planes at angles between 45° and 90° to the excitation x -axis throughout the whole spectrum. Known as *variable-separation synchronous excitation fluorimetry*, this technique has also had only limited use.

SYNCHRONOUS FLUORESCENCE SPECTROSCOPY

The technique was introduced by Lloyd,¹ who applied it to a mixture of C₂₀ polynuclear hydrocarbons from the pyrolysis and combustion of organic materials: benzo(*k*)fluoranthene, benzo(*a*)-pyrene and perylene. The emission spectra obtained at the optimum fixed excitation wavelengths were contrasted with those obtained with synchronous scanning, with a wavelength interval of 23 nm. The better resolution of synchronous spectra was evident with this example. Synchronous spectra are simpler,

with narrower peaks and hence more characteristic than conventional ones.² A schematic representation of the principles of the technique is shown in Fig. 1.

Originally, the technique was employed empirically, especially in forensic research,³⁻⁵ but there was a lack of detailed information and methodology, which made it difficult for non-specialists to understand and exploit the possibilities offered by this simple approach. Vo-Dinh⁶ attempted to remedy this by presenting the basic theory, and suggesting experimental procedures to allow measurement of spectral signatures from complex samples, and other specific information of analytical interest.

The synchronous fluorescence intensity, I_s , depends on the character of the normal excitation and emission spectra as well as on the wavelength difference, $\Delta\lambda$, between the excitation, λ_{ex} , and emission, λ_{em} , wavelengths. This intensity can be expressed as:

$$I_s = KcdE_x(\lambda_{ex})E_m(\lambda_{ex} + \Delta\lambda)$$

or, alternatively

$$I_s = KcdE_x(\lambda_{em} - \Delta\lambda)E_m(\lambda_{em})$$

where E_x is the excitation function at a given excitation wavelength ($\lambda_{ex} = \lambda_{em} - \Delta\lambda$), E_m is the normal emission intensity at the corresponding emission wavelength ($\lambda_{em} = \lambda_{ex} + \Delta\lambda$), c is the analyte concentration, d is the thickness of the sample and K is a characteristic luminescence constant comprising the "instrumental geometry factor" and related parameters. The synchronous signal can be considered either as an emission or excitation spectrum, with a synchronously scanned excitation or emission wavelength, respectively. The spectral distribution is a function of the difference between the excitation and emission wavelengths, $\Delta\lambda$. The maximum fluorescence intensity for a particular component occurs when $\Delta\lambda$ corresponds to the difference between the wavelengths of the absorption and emission maxima.⁷

According to Vo-Dinh,⁶ the main characteristics of synchronous fluorescence spectroscopy are as follows.

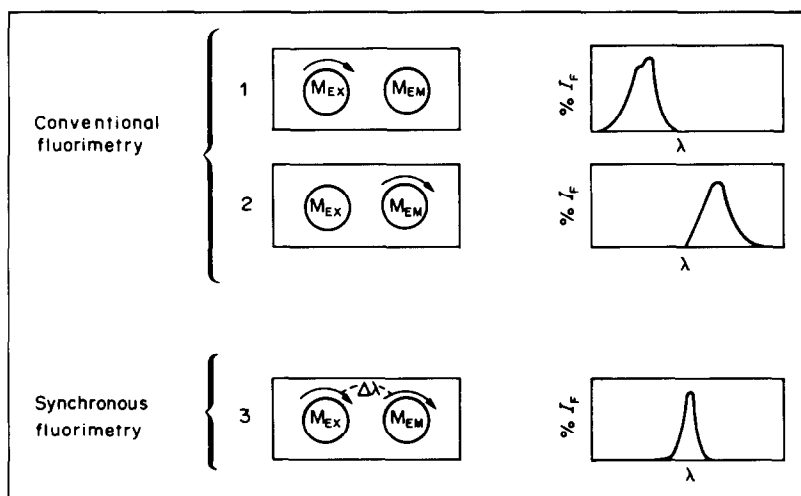


Fig. 1. Schematic comparison between conventional [excitation (1) and emission (2) spectra] and synchronous fluorimetry (3). (M_{ex} = excitation monochromator, M_{em} = emission monochromator).

(a) Narrowing of spectral bands. This effect is essentially a result of the multiplication of two simultaneously increasing and/or decreasing functions.

(b) Simplification of emission spectra. Whereas in conventional spectrofluorimetry at a fixed λ_{ex} , it is only possible to increase the intensity of all the emission bands at the same time, the synchronous technique allows the stronger peaks to be increased selectively by use of a suitable $\Delta\lambda$.

(c) Contraction of the spectral range. From an analytical viewpoint, the whole spectrum might not be of much interest, and many of the details may not generally be considered; their presence results only in confusing the total spectrum because of overlap with the emission of other components in the sample.

It is experimentally possible to modify the spectral bandwidth of the synchronous signal by changing $\Delta\lambda$ or the Stokes shift (which can be varied by modifying the solvent environment). However, synchronous spectrometry does still suffer from the limitations inherent in the luminescence technique, namely: spectral distortions caused by intermolecular interactions, and by static, as well as dynamic, quenching processes. The characteristics and applications of this technique have been the subject of a recent report.⁸

Lloyd and Evett⁹ have developed a theory for predicting peak wavelengths and intensities in synchronous fluorescence spectra. By assuming that the excitation and emission peak maxima can be represented as Gaussian peaks, they were able to predict the peak maxima in the synchronous spectrum with a reasonable degree of accuracy. The mean difference between calculated and observed maxima in the synchronous spectra of 33 compounds was 1.95 nm.

When the fluorescence of a compound is perturbed by Rayleigh and Raman scatter, the synchronous excitation technique allows an improvement in the measurement over conventional techniques, if appropriate $\Delta\lambda$ values are selected.¹⁰ This has been observed

experimentally in the determination of phenol in aqueous solution.

The main difficulty encountered in the application of the synchronous scan technique is that the best $\Delta\lambda$ value must be known beforehand for optimum results and, in some multicomponent systems, several different $\Delta\lambda$ values might be necessary to achieve complete identification. The best $\Delta\lambda$ values can readily be determined from a three-dimensional plot. The three-dimensional spectra¹¹ in which one axis represents the excitation wavelength, a second the emission wavelength and the third the intensity, give a complete description of the fluorescence behaviour of a compound. These spectra are also known as excitation-emission matrix spectra, contour spectra and total luminescence spectra. They can be measured with a videofluorimeter, which is a computer-controlled instrument capable of automatically acquiring total luminescence spectra spanning up to 240 nm in emission and excitation wavelengths at a spatial resolution of 1 nm per point in as short a time as 16.7 msec.¹² The rationale of synchronous scanning is readily visualized on three-dimensional spectra, because the synchronous spectrum represents the intensity profile of a 45° section through the three-dimensional plot. Talmi *et al.*,¹³ using a silicon-intensified target vidicon as parallel detector, have shown that diagonal scans across the spectral matrix provide spectral information identical with that obtained by synchronous luminescence systems, but without mechanical scanning and with simultaneous data acquisition. The wavelength difference between the emission and excitation monochromators, $\Delta\lambda$, can be selected in the software after data acquisition. Weiner¹⁴ has also shown the equivalence of simultaneous scanning and three-dimensional plotting of fluorescence spectra.

Although the synchronous spectrum of a mixture is more ambiguous than the total luminescence spec-

trum, the former can readily be recorded on a simple fluorimeter capable of simultaneously scanning the excitation and emission monochromators. A video-fluorimeter is rather expensive and not as sensitive as a conventional fluorimeter, whereas one of the most attractive features of the synchronous excitation technique is its instrumental simplicity. Any commercial or laboratory-constructed luminescence spectrometer can be employed for synchronous measurements. The synchronous luminescence-scanning method discards the total luminescence information outside the scanning line, but is a very simple and effective means of obtaining data for several compounds in a single measurement.¹⁵

White¹⁶ has achieved a thirty-fold increase in the sensitivity of a fluorescence spectrophotometer by rotating the monochromator slit-images by 90° to permit the sample to be viewed along the length of the excitation slit image, and adding concave retro-mirrors behind the sample in each beam. With this design, and using the synchronous excitation technique, this author determined an analytical calibration for rhodamine from 10⁻⁶ down to 10⁻¹² g/ml.

APPLICATIONS

Determination of polynuclear aromatic hydrocarbons

The interest in monitoring polynuclear aromatic compounds has increased in recent years because of their potential as carcinogens and their frequent occurrence in the environment. Synchronous fluorescence spectroscopy has been applied to the identification and determination of these compounds, since their synchronous spectra give considerably more structural information than the conventional spectra.

Futoma *et al.*¹⁷ have given a comprehensive review of the application of spectroscopic techniques to analysis for these compounds in the aqueous environment. They presented synchronous fluorescence spectroscopy as an important technique which can satisfactorily solve many of the problems of such analyses.

Qualitative analysis

Lloyd's first application of synchronous fluorescence spectroscopy was in the field of forensic science. In a first study,³ conventional and synchronous fluorescence spectra of anthracene, benzo(*a*)pyrene, perylene and benzo(*k*)fluoranthene mixtures, and of a used automobile engine oil were compared. Later, various other similar materials likely to be encountered in the scientific investigation of crime⁴ were also examined qualitatively. Also, synchronous fluorescence spectroscopy in association with gradient-elution liquid chromatography has been used in qualitative and quantitative analysis for polynuclear hydrocarbons in engine oils, petrols and exhaust deposits.⁵ Materials such as soots, tars, petroleum residues, oil spots, creosotes and rubber have been characterized for forensic purposes.^{18,19}

The synchronous excitation technique as a means of characterizing crude oil samples has been evaluated by John and Soutar.⁷ They used samples from a number of different locations and studied the factors related to the identification of crude oils, such as solvent, wavelength increment, concentration, temperature and frequency band-pass. Although unambiguous identification is not always possible, this rapid technique, used in conjunction with other analytical methods, reduces the effort required to identify a source of oil pollution.²⁰ Lloyd²¹ has also reviewed the experimental variables affecting the fluorescence of the compounds present in petroleum. Synchronous spectra are highly sensitive to quenching by oxygen or halogenated compounds, but they are no more or less sensitive than conventional spectra to quenching effects.

Eastwood *et al.*²² have applied several luminescence techniques at both room and lower temperatures to the qualitative analysis of oil spill. The combination of low-temperature luminescence and synchronous scanning results in a valuable technique which often yields greater spectral structural information for heavy oils than either technique separately. The increased resolution achieved by the synchronous technique has been demonstrated by Wakeham²³ in comparing conventional and synchronous fluorescence spectra of indigenous and petroleum-derived hydrocarbons in sediments from Lake Washington.

The fate of crude oil spilled on sea-water has been studied in outdoor tanks by monitoring the concentrations of oil in the surface film, water column and sediments by synchronous fluorescence spectroscopy, for as long as three months.²⁴ This study was centred on the possible levels and forms of oil pollution that can be expected to occur in sea-water and possible affect marine organisms.

Lloyd²⁵ has used partly quenched synchronous fluorescent spectra in the characterization of complex mixtures. Quenching effects in conjunction with synchronous excitation significantly increase the number of distinctive features available for identification of different compounds with similar but unquenched spectra.

Synchronous fluorimetry has been used to identify the number of condensed rings in aromatic molecules.²⁶ The components of the sample, a coal-derived liquid, were initially separated by HPLC into fractions with different numbers of aromatic rings. Each fraction was further separated into secondary fractions according to numbers of carbon atoms, by reversed-phase HPLC, such fractions being monitored by synchronous fluorescence spectrometry. The results obtained indicate the potential usefulness of the technique as a method for analysis of complex mixtures, despite the limitation that some molecules yield only weak peaks.

Several studies^{27,28} have indicated that synchronous excitation spectra may exhibit greater changes be-

tween unweathered and weathered samples than conventional emission spectra do; this observation should be further investigated before the technique is utilized with weathered oils.

Vo-Dinh *et al.*²⁹ found a selectivity enhancement with the synchronous technique applied to the characterization of naphthalene derivatives in synthane gasifier waste-water. It was necessary to use dilute solutions (less than 10^{-2} $\mu\text{l/l}$.) for quantitative analysis. Non-linearity in the analytical curves and decrease in the intensity of some emission bands are observed at high concentrations.

Synchronous fluorescence spectroscopy has been used in analysis of coal-gasifier waste-water for its cresol and phenol content since it can discriminate between the three isomers of cresol.³⁰⁻³²

The fluorescence associated with benzo(*a*)pyrene (BP) moieties covalently attached to the nucleic acid (DNA plus RNA) isolated from the epidermis of BP-treated mice has been examined at 77 K in frozen aqueous solutions by use of a photon-counting fluorimeter operating in the synchronous scanning mode.³³ A $\Delta\lambda$ of 28 nm, which coincides with the difference in wavelength between the excitation and emission maxima for the fluorescence of bound BP, was chosen.

Quantitative analysis

Synchronous-fluorescence and room-temperature phosphorescence techniques have been used to determine selected polynuclear hydrocarbons in a coal liquid (solvent-refined coal) product without a prior separation step.³⁴ Ten polynuclear aromatic compounds, including anthracene, 2,3-benzofluorene, benzo(*a*)pyrene, benzo(*e*)pyrene, carbazole, dibenzothiophene, fluoranthene, fluorene, perylene and pyrene, were identified. Relative standard deviations for replicate determinations ranged from 10 to 30% for concentrations in the range 0.1–6 mg/g (compared with 5–10% for HPLC or GC-MS analysis of the round-robin sample used).

The analysis of an environmental sample (an air particulate extract from an industrial site) by synchronous fluorescence and room-temperature phosphorescence has been reported by Vo-Dinh *et al.*³⁵ Several polynuclear aromatic compounds, including anthracene, benzo(*a*)pyrene, benzo(*e*)pyrene, 2,3-benzofluorene, chrysene, 1,2,5,6-dibenzanthracene, dibenzothiophene, fluoranthene, fluorene, phenanthrene, perylene, pyrene and tetracene were determined qualitatively and quantitatively. The quantitative results obtained by both techniques were compared, and the relative standard deviation was 5–15% for synchronous fluorescence and 10–30% for room-temperature phosphorescence. The techniques are complementary; thus, perylene and tetracene can be detected only by synchronous fluorescence, whereas synchronous room-temperature phosphorescence is very suitable for differentiating between isomeric benzopyrenes and dibenzanthracenes.³⁶

A silicon-intensified target vidicon has been evaluated as a detector for synchronous fluorescence spectroscopy.³⁷ Synchronous spectra were obtained as diagonals through the data matrix corresponding to fixed wavelength differences between excitation and emission wavelengths. Single- and two-component mixtures of anthracene, 9,10-diphenylanthracene, perylene, and tetracene were studied. Relative pooled standard deviations were around 1% for single-component samples and 4–8% for two-component samples. Detection limits at the 95% confidence level were between 0.005 mg/l. (perylene) and 0.17 mg/l. (anthracene).

Synchronous luminescence has been used in several applications of biological and environmental interest, such as the identification and determination of the carcinogenic polycyclic aromatic hydrocarbon dibenz(*a,h*)anthracene in extracts from cigarette smoke.³⁸ The efficiency of the technique has been demonstrated in the direct determination of anthracene and 2-methylanthracene in a raw coal liquid.^{39,40} Tachibana and Furusawa⁴¹ have determined ppm levels of carbazole and anthracene in zone-refined dibenzofuran.

Latz *et al.*^{42,43} have cautioned against using only synchronous spectroscopy for quantitative measurements on multicomponent samples. They suggested that the loss of spectral information resulting from the use of the synchronous technique increases the risk of error. Lloyd⁴⁴ has refuted this statement, attributing the errors found by Latz to inner-filter effects.

Other applications

Synchronous fluorimetry has been used for trace concentration measurements in hydrology.⁴⁵ Fluorescein, eosin, Sulphorhodamine G, Rhodamine B and Rhodamine WT were determined.

In contrast to fixed-excitation spectra, no peaks due to Rayleigh scattering are found in synchronous fluorimetry, and the relative sensitivities of the wavelength of Raman and fluorescent peaks to changes in the synchronous excitation interval are different. This fact allows the use of Raman peaks as a reference for checking the purity of fluorescence-grade solvents.⁴⁶

Miller,⁴⁷ in a survey of recent advances in molecular luminescence analysis included synchronous-scanning spectroscopy as a technique for increasing selectivity, and applied it to the resolution of tyrosine and tryptophan. At small $\Delta\lambda$ values the synchronous fluorescence of a tyrosine-tryptophan mixture is characteristic of tyrosine, but at large $\Delta\lambda$ values, the spectra observed are similar to that of tryptophan.

André *et al.*,⁴⁸ who called the technique the "constant step" method, used it for drug analysis. It is possible to detect morphine in the presence of quinine only for morphine-to-quinine ratios ≥ 10 ; this problem cannot be solved by conventional fluorimetry. In the case of LSD-quinine mixtures, the maxima are too close to permit separation. However, provided

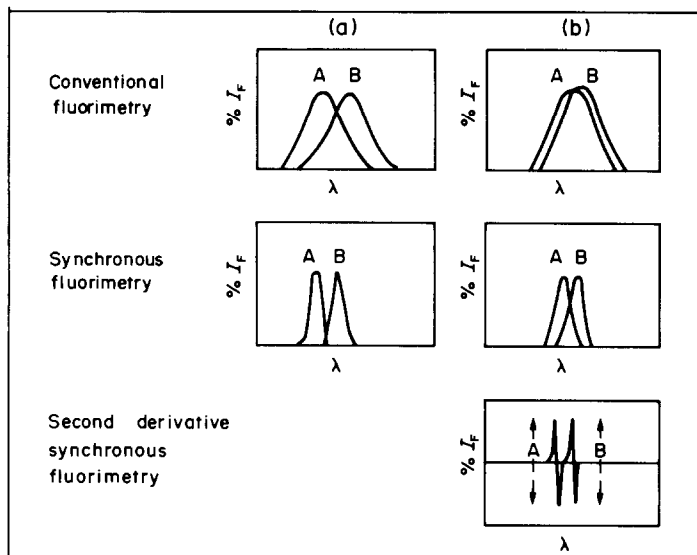


Fig. 2. Schematic comparison between conventional, synchronous and derivative synchronous spectra of two hypothetical compounds, A and B, with slight (a) and strong (b) overlap of the emission spectra.

that the LSD–quinine concentration ratio is ≥ 1 , the presence of quinine poses no problem in the determination of LSD. The technique has also been used to determine trace amounts of fluorescent dyes.⁴⁹

A quantitative determination of LSD in methanol has been described.⁵⁰ In 4 mM hydrochloric acid and with $\Delta\lambda = 110$ nm, the detection limit was 0.1 ng/ml. In 1 M sodium hydroxide and with $\Delta\lambda = 180$ nm, the detection limit was reduced by a factor of 50. The presence of other hallucinogens caused interference, even at high concentrations of LSD. The interference due to high concentrations of quinine and harmine was overcome by doing the analysis in two different media.

A low-cost differential fluorimeter for detection and determination of LSD in illicit preparations has been described.⁵¹ There was good agreement between the results obtained by this method and those found by direct synchronous spectrofluorimetry.

Derivative synchronous fluorescence spectroscopy

The combination of synchronous and derivative fluorimetry was first suggested by John and Soutar,⁷ to enhance minor spectral features and allow more reliable identification of oil "fingerprint" spectra. The application of derivative techniques to luminescence spectroscopy has been reported by Green and O'Haver,⁵² but to date, there have been few reports on its application to synchronous fluorescence spectroscopy. Although direct synchronous spectra are often sufficiently resolved for analytical purposes, the second derivative of the synchronous spectrum could prove helpful in some cases in differentiating closely spaced bands. The main advantages of this technique are selectivity, sensitivity, rapidity, simplicity and low cost. A schematic representation of the spectra obtained by conventional, synchronous and derivative

synchronous fluorimetry is shown in Fig. 2. For two hypothetical compounds, A and B, when the overlap of the conventional spectra is not very great, the synchronous technique avoids such overlap (case a). However, when the conventional spectra overlap strongly, the synchronous technique reduces the extent of the overlap, but still does not allow the mixture to be resolved. Resolution is possible if the derivative synchronous spectrum is measured (case b).

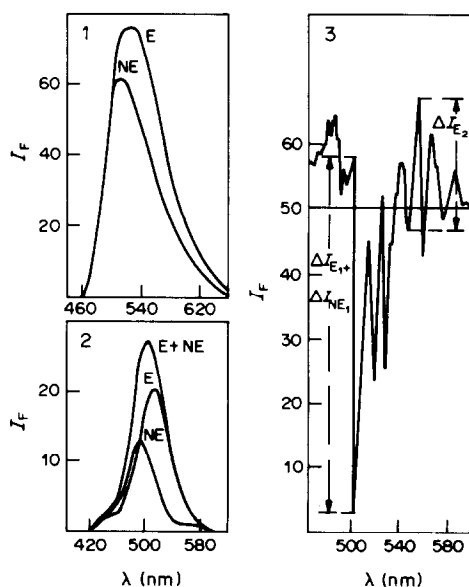


Fig. 3. Simultaneous determination of epinephrine (E) and norepinephrine (NE) at the ng/ml level by derivative synchronous fluorimetry. (1) Conventional fluorescence spectra ($\lambda_{\text{ex E}} 415$, $\lambda_{\text{ex NE}} 400$ nm); (2) Synchronous fluorescence spectra ($\Delta\lambda = 100$ nm); (3) Second-derivative synchronous fluorescence spectrum.

The experimental approaches used to obtain derivative spectra may be divided into two general classes: those operating on the output signal of the spectrometer (electronic differentiation, mechanical tachometer, numerical differentiation) and those operating on the light-beam in the optical part of the spectrometer (dual-wavelength spectrometry, wavelength modulation). Of these, electronic differentiation is the simplest, the least expensive, and the easiest to incorporate into any existing spectrometer.⁵³

The enhancement of relatively minor spectral features by second-derivative synchronous fluorimetry has been made evident by Lloyd,²¹ who compared the results obtained for a motor oil by direct and derivative synchronous fluorimetry.

The derivative technique was also used to analyse a synthetic mixture of several aromatic compounds.⁵⁴ Later, it was applied to an extract from an atmospheric sample (collected in a workplace environment)³⁹ which had previously been analysed by direct synchronous fluorimetry.³⁵ The second-derivative peaks are narrower than those found by direct synchronous scanning.

Miller *et al.*⁵⁵ have described some applications in analytical biochemistry. It was possible to resolve three-component mixtures (phenylalanine, tyrosine and tryptophan), and proteins were also studied.

The suitability of second-derivative synchronous fluorimetry for simultaneous determination of epinephrine and norepinephrine in urine has recently been shown⁵⁶ (Fig. 3). These catecholamines were separated from the matrix by cation-exchange and subsequently determined by use of the trihydroxyindole reaction. Analytical recovery was about 94% for epinephrine and 91% for norepinephrine, with a relative standard deviation of approximately 5%. There is great interest in this technique for clinical chemistry, especially since it may be an alternative to HPLC, which is rather time-consuming for routine clinical assays and requires special and expensive instrumentation.

There have been few applications of derivative synchronous fluorimetry in inorganic analysis. First-derivative synchronous fluorimetry has been used for the determination of magnesium,⁵⁷ in a method based on the formation of a fluorescent chelate with salicylaldehyde 2-pyridylhydrazone. This chelate has also been studied by conventional fluorimetry; both the sensitivity and selectivity are improved by use of derivative synchronous scanning. A similar study of the cadmium-benzyl 2-pyridyl ketone 2-quinolylhydrazone chelate⁵⁸ gave similar results. Conventional fluorimetry and first- and second-derivative synchronous fluorimetry were used in this case. The most sensitive response was obtained by the first-derivative technique.

Although there are many individual determinations that benefit from the use of derivative synchronous fluorimetry, the main interest in this

technique lies in its ability to resolve complex mixtures. This has been shown in the analysis of binary and ternary mixtures of titanium, zirconium and hafnium, by formation of fluorescent chelates with biacetylmonoxime nicotinylhydrazone in an acidic medium.⁵⁹ The fluorescence behaviour of these complexes had previously been studied by conventional fluorimetry, and procedures for analysis of binary mixtures had been reported,⁶⁰ but required use of several samples and calibration graphs. With second-derivative synchronous fluorescence, it is possible to analyse binary mixtures in a single scan, and ternary mixtures in two scans.

CONSTANT-ENERGY SYNCHRONOUS FLUORESCENCE SPECTROSCOPY

The evaluation of total luminescence data and relationships between the spectral regions of sample solutions has led to the development of this new technique. The excitation and emission monochromators are scanned simultaneously, synchronized in such a manner that a constant energy difference is maintained between them:

$$10^{-7} (1/\lambda_{\text{ex}} - 1/\lambda_{\text{em}}) = \Delta\bar{\nu} = \text{constant}$$

This technique was developed by Inman and Winefordner,⁶¹ but it has been little used up to the present, mainly owing to the lack of commercially available instruments. The spectra are usually obtained with a laboratory-constructed fluorimeter interfaced to a minicomputer. To maintain the constant energy-difference, the emission monochromator is stepped at a constant speed, and the speed of the excitation monochromator is changed. Total luminescence spectra are obtained by using repetitive emission scans, and stepping the excitation monochromator over the range of interest.⁶²

Constant-energy synchronous fluorescence offers better selectivity than conventional fluorimetry for multicomponent analysis of simple polynuclear aromatic hydrocarbons.⁶¹ The spectra obtained at a constant $\Delta\bar{\nu}$ for mixtures of these compounds are spectrally clearer than those obtained at a constant $\Delta\lambda$.

The technique has been extended to low-temperature conditions by reducing the sample temperature to that of liquid nitrogen (77 K) or helium (4 K).⁶³ Polynuclear aromatic hydrocarbons were determined, with only two scans needed to characterize seven of them: acenaphthene, 2,3-benzofluorene, 3,4-benzopyrene, anthracene, perylene and naphthalene were identified from a 1400-cm⁻¹ scan, and only pyrene required a 2800-cm⁻¹ scan. This technique has also been applied to the spectral resolution of mixtures of polyaromatic hydrocarbon isomers and polyaromatic hydrocarbon alkyl homologues.⁶⁴

Inman and Winefordner⁶⁵ have also shown that constant-energy synchronous fluorimetry reduces solvent interference by Raman scatter similarly to the

way in which constant-wavelength synchronous fluorimetry reduces Rayleigh-scatter interference.

Correlation techniques have been used for the optimization of $\Delta\bar{\nu}$.⁶⁶ Mathematically, the correlation procedure is:

$$C_{1,2}(\tau) = 1/2T \int_{-T}^T f_1(t)f_2(t - \tau) dt \quad (1)$$

where $C_{1,2}(\tau)$ is the cross-correlation between two functions, f_1 and f_2 , t is time, τ is the time delay between the two functions and T is the period of each function.

The luminescence intensity is defined mathematically for the fluorescence of a dilute solution containing a single component as

$$M_{ij} = \alpha x_i y_j \quad (2)$$

where $\alpha = 2.3\phi_f b c$ = product of wavelength-independent terms, ϕ_f = fluorescence quantum efficacy, b = thickness, c = concentration; $x_i = I_0(\lambda_i)\epsilon(\lambda_i)$ = product of excitation-wavelength terms, $I_0(\lambda_i)$ = intensity of radiation incident on the sample, $\epsilon(\lambda_i)$ = molar absorptivity; $y_j = \gamma(\lambda_j)\kappa(\lambda_j)$ = product of emission-wavelength terms, $\gamma(\lambda_j)$ = fraction of the fluorescence emitted at wavelength λ_j ; $\kappa(\lambda_j)$ = detection-system response function.

The difference in wavenumber, $\Delta\bar{\nu}$, corresponding to the energy difference, is $\bar{\nu}_i - \bar{\nu}_j = \Delta\bar{\nu}$, where $\bar{\nu}_i$ and $\bar{\nu}_j$ are the energy counterparts of λ_i and λ_j . Equation (2) can be re-written as:

$$M_{ij} = \alpha x(\bar{\nu}_j + \Delta\bar{\nu})y(\bar{\nu}_j) \quad (3)$$

and equation (1) becomes:

$$C_{1,2}(\Delta\bar{\nu}) = (\alpha/2T) \int x(\bar{\nu}_j + \Delta\bar{\nu})y(\bar{\nu}_j) d\Delta\bar{\nu} \quad (4)$$

A similar treatment has been devised for constant $\Delta\lambda$. The application of correlation techniques to room-temperature fluorescence, low-temperature fluorescence and low-temperature phosphorescence shows the utility of synchronous luminescence spectroscopy.

VARIABLE-SEPARATION SYNCHRONOUS EXCITATION FLUORESCENCE SPECTROSCOPY

In this technique the scan speeds of the emission and excitation monochromators are different. In effect, planes are recorded at angles between 45 and 90° to the excitation x -axis throughout the spectrum. The emission monochromator must be scanned at a higher rate than the excitation monochromator; *i.e.*, the plane measured must be at an angle greater than 45° to the x -axis. The angles of the planes generated by this technique are determined from the following equation:

$$\theta = \tan^{-1}[(\text{emission scan speed}) / (\text{excitation scan speed})] \quad (5)$$

In this case neither $\Delta\lambda$ nor $\Delta\bar{\nu}$ is maintained

constant. The continuous variation of the wavelength separation between the monochromators can be achieved either mechanically, by varying the scan speeds of the two monochromators,² or digitally, in which case the luminescence data are stored for subsequent microcomputer processing.⁶⁷

This technique was proposed by Kubic *et al.*⁶⁸ and applied to the forensic examination of automobile engine lubricants.⁶⁹ The fluorescence behaviour of 61 automobile lubricants has been studied by conventional fluorimetry, synchronous fluorimetry at constant $\Delta\lambda$, and by variable synchronous fluorimetry.⁷⁰ A similar study has been made of 45 used automobile engine oils collected from the dipsticks of the vehicles in a public car park.⁷¹ These studies showed that fluorescence techniques should not be the only tool used for the analysis of multi-component lubricants, but used in conjunction with chromatography, infrared spectroscopy and elemental analysis.

Miller,² who has labelled this technique as variable-wavelength or variable-angle synchronous scanning, has shown that two different but related types of applications are feasible: (a) optimum resolution of overlapping spectra and (b) simultaneous analysis of two compounds from a single spectrum. Thus, the spectra of phenylalanine and tryptophan show some degree of overlap, so two entirely separate experiments would normally be necessary to determine both compounds in a mixture. However, by use of this technique the two compounds can be studied in a single spectrum and can therefore be determined in the presence of each other.

Recently, variable-angle synchronous scanning fluorescence spectroscopy has been applied to two pharmaceutical determinations:⁷² chlorpromazine in the presence of its chief degradation product, chlorpromazine sulphoxide, and oxytetracycline in the presence of the additives vitamin C, thiamine, nicotinamide and riboflavin.

The angle of the scan trajectory can also be varied continuously through the emission-excitation matrix to describe any desired path under computer control. This new technique, known as non-linear variable-angle synchronous scanning, offers several possibilities: (a) in a complex system, the maximum and minimum emission intensities can be explored by traversing the peaks and valleys; (b) a curved trajectory can be followed through the emission-excitation matrix, allowing light-scattering peaks to be avoided; (c) overlapping systems that cannot be resolved by linear scanning can be resolved by this technique.

REFERENCES

1. J. B. F. Lloyd, *Nature*, 1971, **231**, 64.
2. J. N. Miller, *Analyst*, 1984, **109**, 191.
3. J. B. F. Lloyd, *J. Forens. Sci. Soc.*, 1971, **11**, 83.
4. *Idem, ibid.*, 1971, **11**, 153.
5. *Idem, ibid.*, 1971, **11**, 235.

6. T. Vo-Dinh, *Anal. Chem.*, 1978, **50**, 396.
7. P. John and I. Soutar, *ibid.*, 1976, **48**, 520.
8. I. M. Warner and L. B. McGown, *CRC Crit. Rev. Anal. Chem.*, 1982, **13**, 155.
9. J. B. F. Lloyd and I. W. Evett, *Anal. Chem.*, 1977, **49**, 1710.
10. J. C. André, M. Bouchy and M. L. Viriot, *Anal. Chim. Acta*, 1979, **105**, 297.
11. G. D. Christian, J. B. Callis and E. R. Davidson, in *Modern Fluorescence Spectroscopy*, Vol. 4, E. L. Wehry (ed.), pp. 111–165. Plenum Press, New York, 1981.
12. D. W. Johnson, J. B. Callis and G. D. Christian, *Anal. Chem.*, 1977, **49**, 747A.
13. Y. Talmi, D. C. Baker, J. R. Jadamec and W. A. Saner, *ibid.*, 1978, **50**, 936A.
14. E. R. Weiner, *ibid.*, 1978, **50**, 1583.
15. T. Vo-Dinh, *Proc. 6th Annual FACSS Meeting*, Philadelphia, Pennsylvania, 1979.
16. J. U. White, *Anal. Chem.*, 1976, **48**, 2089.
17. D. J. Futoma, S. R. Smith and J. Tanaka, *CRC Crit. Rev. Anal. Chem.*, 1982, **13**, 117.
18. J. B. F. Lloyd, *Chem. Br.*, 1975, **11**, 442.
19. *Idem*, *Analyst*, 1975, **100**, 82.
20. P. John and I. Soutar, *Proc. Anal. Div. Chem. Soc.*, 1976, **13**, 309.
21. J. B. F. Lloyd, *Analyst*, 1980, **105**, 97.
22. D. Eastwood, S. H. Fortier and M. S. Hendrick, *Am. Lab.*, 1978, **10**, No. 3, 45.
23. S. G. Wakeham, *Environ. Sci. Technol.*, 1977, **11**, 272.
24. D. C. Gordon, Jr., P. D. Keizer, W. R. Hardstaff and D. G. Aldous, *ibid.*, 1976, **10**, 580.
25. J. B. F. Lloyd, *Analyst*, 1974, **99**, 729.
26. T. Katoh, S. Yokoyama and Y. Sanada, *Fuel*, 1980, **59**, 845.
27. U. Frank and M. Gruenfield, *Anal. Qual. Control Newsl. (U.S. EPA)*, 1977, 32.
28. J. R. Jadamec, S. Fortier, S. Buchanan and G. L. Hufford, Paper presented to Society of Naval Architects and Marine Engineers, New London, Connecticut, 1978.
29. T. Vo-Dinh, R. B. Gammage, A. R. Hawthorne and J. H. Thorngate, *Environ. Sci. Technol.*, 1978, **12**, 1297.
30. R. B. Gammage, T. Vo-Dinh, A. R. Hawthorne, J. H. Thorngate and W. W. Parkinson, in *Carcinogenesis*, Vol. 3, P. W. Jones and R. I. Freudenthal (eds.), pp. 155. Raven Press, New York, 1978.
31. T. Vo-Dinh, R. B. Gammage and A. R. Hawthorne, in *Polynuclear Aromatic Hydrocarbons*, P. W. Jones and P. Leber (eds.), Ann Arbor Sci. Publ., Ann Arbor, 1979.
32. T. Vo-Dinh, R. B. Gammage, A. R. Hawthorne and J. H. Thorngate, in NBS Special Publication No. 519, p. 679. National Bureau of Standards, Washington, D.C., 1979.
33. R. O. Rahn, S. S. Chang, J. M. Holland, T. J. Stephens and L. H. Smith, *J. Biochem. Biophys. Methods*, 1980, **3**, 285.
34. T. Vo-Dinh and P. R. Martínez, *Anal. Chim. Acta*, 1981, **125**, 13.
35. T. Vo-Dinh, R. B. Gammage and P. R. Martínez, *Anal. Chem.*, 1981, **53**, 253.
36. T. Vo-Dinh and R. G. Gammage, *ibid.*, 1978, **50**, 2054.
37. J. E. Thompson and H. L. Pardue, *Anal. Chim. Acta*, 1983, **152**, 73.
38. D. G. Gillespie, Imperial Tobacco Ltd., Bristol, United Kingdom, personal communication.
39. T. Vo-Dinh, *Appl. Spectrosc.*, 1982, **36**, 576.
40. Analytical characterization Group Review Meeting, National Bureau of Standards, 4 February 1981, Washington, DC.
41. M. Tachibana and M. Furusawa, *Bull. Chem. Soc. Japan*, 1983, **56**, 2254.
42. H. W. Latz, A. H. Ullman and J. D. Winefordner, *Anal. Chem.*, 1978, **50**, 2148.
43. *Idem*, *ibid.*, 1980, **52**, 191.
44. J. B. F. Lloyd, *ibid.*, 1980, **52**, 189.
45. J. C. André, M. Bouchy, M. Niclaude and Ph. Baudot, *Anal. Chim. Acta*, 1977, **92**, 369.
46. J. B. F. Lloyd, *Analyst*, 1977, **102**, 782.
47. J. N. Miller, *Proc. Anal. Div. Chem. Soc.*, 1979, **16**, 203.
48. J. C. André, Ph. Baudot and M. Niclaude, *Clin. Chim. Acta*, 1977, **76**, 55.
49. J. C. André, *Ing. Ind. Chim.*, 1975, **78**, 5.
50. P. Baudot and J. C. André, *Anal. Lett.*, 1982, **15**, 471.
51. *Idem*, *J. Anal. Toxicol.*, 1983, **7**, 69.
52. G. L. Green and T. C. O'Haver, *Anal. Chem.*, 1974, **46**, 2191.
53. T. C. O'Haver, in *Modern Fluorescence Spectroscopy*, Vol. 1, E. L. Wehry (ed.), pp. 65–81. Plenum Press, New York, 1976.
54. T. Vo-Dinh, in *Modern Fluorescence Spectroscopy*, Vol. 4, E. L. Wehry (ed.), pp. 188. Plenum Press, New York, 1981.
55. J. N. Miller, T. A. Ahmad and A. F. Fell, *Anal. Proc.*, 1982, **19**, 37.
56. M. Valcárcel, A. Gómez-Hens and S. Rubio, *Clin. Chem.*, 1985, **31**, 1790.
57. C. Cruces Blanco and F. García Sánchez, *Anal. Chem.*, 1984, **56**, 2035.
58. F. García Sánchez, A. Navas and M. Santiago, *Anal. Chim. Acta*, 1985, **167**, 217.
59. S. Rubio, A. Gómez-Hens and M. Valcárcel, *Anal. Chem.*, 1985, **57**, 1101.
60. M. A. Cejas, A. Gómez-Hens and M. Valcárcel, *Anal. Chim. Acta*, 1984, **158**, 287.
61. E. L. Inman, Jr. and J. D. Winefordner, *Anal. Chem.*, 1982, **54**, 2018.
62. J. H. Rho and J. L. Stuart, *ibid.*, 1978, **50**, 620.
63. E. L. Inman, Jr. and J. D. Winefordner, *Anal. Chim. Acta*, 1982, **141**, 241.
64. M. J. Kerkhoff, L. A. Files and J. D. Winefordner, *Anal. Chem.*, 1985, **57**, 1673.
65. E. L. Inman, Jr. and J. D. Winefordner, *Anal. Chim. Acta*, 1982, **138**, 245.
66. E. L. Inman, Jr., M. J. Kerkhoff and J. D. Winefordner, *Spectrochim. Acta*, 1983, **39**, 245.
67. B. J. Clark, A. F. Fell, I. E. Aitchison, D. M. G. Pattie, M. H. Williams and J. N. Miller, *ibid.*, 1983, **38**, 61.
68. T. A. Kubic, T. Kanabrocki and J. Dwyer, Paper presented at the American Academy of Forensic Sciences 32nd Annual Meeting, 1980.
69. C. M. Kanabrocki, Undergraduate research, C.W. Post College, New York, 1979.
70. T. A. Kubic, C. M. Lasher and J. Dwyer, *J. Forens. Sci.*, 1983, **28**, 186.
71. T. A. Kubic and F. X. Sheehan, *ibid.*, 1983, **28**, 345.
72. B. J. Clark, A. F. Fell, K. T. Milne, D. M. G. Pattie and H. Williams, *Anal. Chim. Acta*, 1985, **170**, 35.

A NEW NUMERICAL METHOD OF FINDING POTENTIOMETRIC TITRATION END-POINTS BY USE OF RATIONAL SPLINE FUNCTIONS

KRZYSZTOF REN

Faculty of Chemistry, A. Mickiewicz University, 60-780 Poznań, Grunwaldzka 6, Poland

ANNA REN-KURC

Institute of Mathematics, A. Mickiewicz University, 60-769 Poznań, Matejki 46/48, Poland

(Received 16 October 1984. Revised 15 October 1985. Accepted 11 April 1986)

Summary—A new numerical method of determining the position of the inflection point of a potentiometric titration curve is presented. It consists of describing the experimental data (emf, volume data-points) by means of a rational spline function. The co-ordinates of the titration end-point are determined by analysis of the first and second derivatives of the spline function formed. The method also allows analysis of distorted titration curves which cannot be interpreted by Gran's or other computational methods.

Potentiometric titration has certain advantages, one of which is the possibility of using all the data points to compute the end-point, though the computation itself can be tedious. Selection of the method of calculation is a major problem, and has a direct influence on the accuracy of the determinations. The many methods proposed may be divided into two basic types: (a) direct graphical interpretation of the titration curve; (b) mathematical interpretation of the co-ordinates of the measurement points.

Graphical methods include Behrend's method,¹ Bröttger's method,² and Tubbs's method.³ Other methods developed⁴⁻⁶ are less convenient and do not increase the accuracy.

The computational methods have developed along three lines. The first assumes that the end-point is at the inflection point of the titration curve, and calculates it from data points in the region of the inflection point.⁷⁻²¹

The second approach assumes that the equation of the titration curve is accurately known, and calculates the end-point from only one or two points on that part of the titration curve corresponding to the ion that is monitored potentiometrically being present in excess.²²⁻²⁹ The main factor influencing the accuracy of these methods is the precision of the values of the various parameters in the equation used to describe the titration curve.

The methods in the third group are based on linearization of the titration curve³⁰ and are probably the best to use in analytical practice. The principles of these methods are derived from Gran's work.^{31,32} Gran suggested plotting the function

$$G(V) = V_e - V = K(V_0 + V) 10^{E/S} \quad (1)$$

where V_e is the volume of titrant added to reach the end-point, V_0 the initial volume of titrand solution, V the volume of titrant added at any stage of titration,

E the potential of the ion-selective electrodes, S the slope of the electrode response, and K a constant containing various parameters, including E° for the electrode.

Gran assumed that $G(V)$ is a linear function and that the titration end-point occurs at V_e , the value of V at which $G(V)$ becomes zero and crosses the V -axis.

The applicability of Gran's method and its various modifications is limited, however.³³ First, linearization methods cannot be used when the titration curve is distorted, which often happens when ion-selective electrodes are used. It has been found, for instance,³⁴⁻³⁶ that ignorance of selectivity coefficients and the real value of S causes serious errors in determining the titration end-point. These parameters may change during a titration. In a precipitation titration, the non-linearity of the Gran function is further increased if the solubility of the precipitate is ignored,³⁷ though the solubility can be allowed for.³⁸ Some of the simplifications used in the linearization methods, as well as distortions in the titrimetric data, can cause deviations of the functions from linearity. The end-point is then determined graphically, which may require rejection of some of the initial and final points of the $G(V)$ function, this being done visually on the basis of some rules of thumb. It is usually impossible, however, to apply this method by numerical processing of the results, because the application of linear regression requires definition of the range from which the measurement points for the calculations are to be taken.³⁷ Moreover, the $G(V)$ function proposed by Gran is based on the assumption that the response slope of the electrode is a constant exponential dependence. The $G(V)$ function is positive for all values of V . The lack of mathematical foundation for the rectilinear approximation of the $G(V)$ function has been clearly pointed out by Gran.

These disadvantages, especially of Gran's method, were the reason for our search for another method having a better mathematical foundation. We have assumed that the titration end-point is defined with sufficient accuracy³⁹ as the inflection point of the curve. Our computational method determines the inflection point of any potentiometric titration curve by analysis of the data-points with rational spline functions. The main advantage of the method is the possibility of evaluating the maximum error and of using computer techniques for the calculations. The program has been written in BASIC in a version suitable for a Sinclair ZX 81 minicomputer, and may constitute a basis for the construction of an automatic titrator.

MATHEMATICAL FOUNDATIONS

The main problem is to find a suitable numerical description of a potentiometric titration curve. As the curve is essentially sigmoid, this is a difficult numerical problem. Most of the classical interpolation methods, such as polynomials, polynomial spline functions and exponential spline functions give decidedly bad results, since they all oscillate strongly.⁴⁰

The impossibility of eliminating these oscillations when applying these methods to description of titration curves led us to examine the use of rational spline functions. The term "spline" in mathematics refers to a differentiable function that between each pair of neighbouring measurement points is defined

in which $t = (V - V_i)/h_i$ where $h_i = V_{i+1} - V_i$, and A_i, B_i, C_i, D_i are coefficients ensuring continuity of the first and second derivatives of $S(V)$, which is tantamount to imposing conditions of interpolation. Thus, if $S(V_i) = E_i$ and $S(V_{i+1}) = E_{i+1}$, then

$$B_i + D_i = E_i; \quad A_i + C_i = E_{i+1}. \quad (3)$$

We can use (3) to eliminate A_i and B_i from (2) to obtain the following form of the spline function:

$$\begin{aligned} S(V) = & E_i(1-t) + E_{i+1}t \\ & + C_i \left[\frac{t^3}{1+p_i(1-t)} - t \right] \\ & + D_i \left[\frac{(1-t)^3}{1+p_i t} - (1-t) \right] \end{aligned} \quad (4)$$

for $V \in \langle V_i, V_{i+1} \rangle$, with $i = 1, \dots, (n-1)$.

To impose the condition of continuity of the first derivative of $S(V)$ we have to calculate $S'(V)$ for $V = V_i$ and $V = V_{i+1}$:

$$\begin{aligned} S'(V_i) &= \frac{E_{i+1} - E_i}{h_i} - \frac{(2+p_i)D_i}{h_i} - \frac{C_i}{h_i} \\ S'(V_{i+1}) &= \frac{E_{i+1} - E_i}{h_i} + \frac{(2+p_i)C_i}{h_i} + \frac{D_i}{h_i} \end{aligned} \quad (5)$$

$[i = 2, \dots, (n-1)]$.

Solving these equations gives

$$\begin{aligned} C_i &= \frac{-(3+p_i)(E_{i+1} - E_i) + h_i S'(V_i) + (2+p_i)h_i S'(V_{i+1})}{(2+p_i)^2 - 1} \\ D_i &= \frac{(3+p_i)(E_{i+1} - E_i) - h_i S'(V_{i+1}) - (2+p_i)h_i S'(V_i)}{(2+p_i)^2 - 1} \end{aligned} \quad (6)$$

by a function of a specific type, e.g., a polynomial. Between neighbouring measurement points, a rational spline function typically takes the form of a polynomial of the 3rd degree divided by the product of a polynomial of the 1st degree and a parameter [p in equation (2) below] which allows removal of curve oscillation and is the essential element distinguishing rational spline functions from the classical interpolation methods mentioned above.

Thus if (V_i, E_i) represents the co-ordinates of the i th point ($i = 1, \dots, n$) then the rational spline function $S(V)$ passes through all the measurement points, which may be denoted by writing $S(V_i) = E_i$. If $V \in \langle V_i, V_{i+1} \rangle$, for $i = 1, \dots, n-1$, then the value of the spline function may be calculated⁴¹ from

$$\begin{aligned} S(V) = & A_i t + B_i(1-t) \\ & + \frac{C_i t^3}{1+p_i(1-t)} + \frac{D_i(1-t)^3}{1+p_i t} \end{aligned} \quad (2)$$

$[i = 1, \dots, (n-1)]$.

To ensure continuity of the second derivative $S''(V)$ we differentiate equation (4) twice, for $V \in (V_{i-1}, V_i)$ and $V \in (V_i, V_{i+1})$, and calculate the value of both functions at the point V_i :

$$\begin{aligned} S''(V_i) &= \frac{2D_i}{h_i^2}(3+3p_i+p_i^2); \quad V \in (V_i, V_{i+1}) \\ S'(V_i) &= \frac{2C_{i-1}}{h_{i-1}^2}(3+3p_{i-1}+p_{i-1}^2); \quad V \in (V_{i-1}, V_i) \end{aligned} \quad (7)$$

$[i = 2, \dots, (n-1)]$.

Continuity of $S''(V)$ requires

$$h_i^2 C_{i-1}(3+3p_{i-1}+p_{i-1}^2) = h_{i-1}^2 D_i(3+3p_i+p_i^2). \quad (8)$$

Inserting C_{i-1} and D_i from (6) into (8) and collecting

terms in $S'(V_{i-1})$, $S'(V_i)$ and $S'(V_{i+1})$ gives

$$\begin{aligned} & \lambda_i Q_{i-1} S'(V_{i-1}) + [\lambda_i Q_{i-1} (2 + p_{i-1}) + (1 - \lambda_i) \\ & \quad \times Q_i (2 + p_i)] S'(V_i) + (1 - \lambda_i) Q_i S'(V_{i+1}) \\ & = \lambda_i Q_{i-1} (3 + p_{i-1}) \frac{(E_i - E_{i-1})}{h_{i-1}} \\ & \quad + (1 - \lambda_i) Q_i (3 + p_i) \frac{(E_{i+1} - E_i)}{h_i} \end{aligned} \quad (9)$$

$[i = 2, \dots, (n - 1)]$, where

$$\begin{aligned} \lambda_i &= h_i / (h_{i-1} + h_i) \quad \text{and} \\ Q_i &= (3 + 3p_i + p_i^2) / [(2 + p_i)^2 - 1]. \end{aligned}$$

This gives a set of $(n - 2)$ linear equations with n unknown quantities $S'(V_i)$; ($i = 1, \dots, n$).

These equations are supplemented by the boundary conditions $S''(V_1) = S''(V_n) = 0$. It is also possible to use other linear boundary conditions.

The matrix of the set (9) is tridiagonal with a predominant diagonal and so is non-singular.

The values $S'(V_i)$ obtained as a solution of the set of equations (9) allow the calculation of the coefficients C_i and D_i from equation (6) and then of coefficients A_i and B_i from equation (3). Inserting these A_i , B_i , C_i and D_i values into (2) gives the rational spline function for every $\langle V_i, V_{i+1} \rangle$ range.

It should be stressed here, that since $S(V)$, $S'(V)$ and $S''(V)$ are continuous functions, and p_i is a parameter controlling the curvature of $S(V)$, small values of p_i may cause oscillation of the spline function for certain data points. This can be seen from equation (2), since

$$\begin{aligned} \lim_{p_i \rightarrow 0} \left(A_i + B_i(1-t) + \frac{C_i t^3}{1 + p_i(1-t)} + \frac{D_i(1-t)^3}{1 + p_i t} \right) \\ = A_i + B_i t + C_i t^3 + D_i(1-t)^3 \end{aligned}$$

which is a classical polynomial spline function of 3rd degree, with tendencies towards oscillation. At the other extreme ($p_i \rightarrow \infty$), we have

$$\begin{aligned} \lim_{p_i \rightarrow \infty} \left(A_i + B_i(1-t) + \frac{C_i t^3}{1 + p_i(1-t)} + \frac{D_i(1-t)^3}{1 + p_i t} \right) \\ = A_i + B_i t \end{aligned}$$

a spline function of the 1st degree, *i.e.*, a continuous broken line, non-differentiable.

Hence if p_i is too large, the approximation and a zero points of $S''(V)$ may have a large error. If, however, p_i is close to zero, the approximation of $S''(V)$ is good but the tendency towards oscillation is disadvantageous for approximation of $S'(V)$. The oscillations disappear when greater p_i values are taken. The value of p_i to be used is thus very important and must result from a compromise between quenching of oscillation and good approximation of the second derivative, which is of special importance. It is known from numerical practice⁴¹ that good results in approximation of functions with large gradients are obtainable with $p_i \gg 10$.

We have connected the value of p_i with the co-ordinates of the data points by

$$p_i = \frac{Q \Delta E_i}{R \Delta V_i} \quad (10)$$

$$R = \max_i \left| \frac{\Delta E_i}{\Delta V_i} \right| \quad (11)$$

where

$$\Delta E_i = E_i - E_{i-1} \quad \text{and}$$

$$\Delta V_i = V_i - V_{i-1},$$

for $i = 2, \dots, n$.

The values of p_i calculated in this way are always lower than Q , and we assume a value of 10 for Q , ($Q = \max p_i$).

As a result we obtain the following set of p values:

$$p = \left(\frac{|\Delta E_1| Q}{\Delta V_1 R}, \frac{|\Delta E_2| Q}{\Delta V_2 R}, \dots \right). \quad (12)$$

This procedure for choosing p_i allows calculation of a rational spline function that is free from oscillation, and the additional inflection points associated with it, and with good approximation for its second derivative. We approximate the inflection points on the titration curve by calculation from the spline equation.

It should be pointed out that all calculated inflection points of the titration curve result directly from the co-ordinates (V_i , E_i) of the measurement points and not from spurious oscillation of the fitted function.

The possibility of arithmetically obtaining more inflection points than would result from the stoichiometry of the titration reaction requires some comment. The emf of the measurement cell during the titration is influenced by a number of factors and may differ from the "theoretical" value resulting from the characteristics of the electrodes and the equilibria which should be established in the solution. Those factors include instrumental errors, instability of indicator electrode readings, fluctuations of the reference electrode potential, errors in measurement of titrant volume, variation in junction potentials and ionic strength, and the possibility of only partial establishment of equilibrium in the solution. These factors may cause the occurrence of fluctuations in the titration curve, especially in its initial and final sections, and these fluctuations will cause additional (but false) inflection points to be calculated as artefacts, and corresponding to meaningful points in the titration. The greater the density of the measurement points (smaller increments of titrant added), and the smaller the emf change between neighbouring points, the greater will be the number of such artefacts. The problem of such inflection points does not arise in direct graphical location of the titration end-point, because the fluctuations responsible are always smoothed out in plotting the curve.

From the calculated inflection points of the titration curve we should then select the one corresponding to the chemical reaction taking place during the titration. This will be the inflection point for which $S'(V)$ is greatest if the approximated curve is increasing, or lowest if the curve is decreasing.

Analysis of the error of the method

The error of interpolation with a rational spline function is taken as the difference between the real but unknown function $E(V)$ of the titration curve, and the spline function $S(V)$ constructed on the basis of the set of data points (V_i, E_i) :

$$\text{Error} = \max_{V \in (V_1, V_n)} |E^{(j)}(V) - S^{(j)}(V)| \quad (13)$$

where $j = 0, 1, 2$ is the order of the derivative of $E(V)$ or $S(V)$. It has been shown^{42,43} that the following evaluations of the error hold:

$$\max_{V \in (V_1, V_n)} |E^{(j)}(V) - S^{(j)}(V)| \leq K \max_i |V_{i+1} - V_i| \quad (14)$$

$$\max_{V \in (V_i, V_{i+1})} |E^{(j)}(V) - S^{(j)}(V)| \leq K_i (V_{i+1} - V_i) \quad (15)$$

where K is a constant ("smoothness module") dependent on $E(V)$.^{42,43} K is constant for every curve; we cannot influence its magnitude. Curves having approximate shapes also have approximate K values. K_i is a constant dependent on the course of $E(V)$ in the section (V_i, V_{i+1}) , just as the constant K depends on the course of $E(V)$ in the section (V_1, V_n) . Because we cannot influence the value of K , we can decrease the error of approximation only by a proper distribution of the experimental points. From (15) it is evident that where there is a large variation of the function (large K_i values), more measurement points should be used in order to minimize the approximation error, as is in fact done in practice for direct graphical location of the end-point (though not for Gran plots). Consequently the approximation of the second derivative of $E(V)$ by $S''(V)$ will be the better, the better we distribute the measurement points V_i , but will also be worse as K increases. Theoretically, the error of approximation of $E''(V)$ and hence of the titration end-point will not exceed $\max_i h_i$.

In practice the error will be far smaller, not exceeding h_e , [$h_e = V_{e+1} - V_e$, and the equivalence point will be in the range (V_e, V_{e+1})]. Thus the maximum error of titration will not exceed the titrant increment within which the equivalence point is transversed.

Instructions for users of the program

The V_i, E_i data are arranged in order of decreasing values of V_i . We have provided for reading-in 100 measurement points. The read-in data and their assigned numbers are projected on the VDU screen. The end of data-collection is indicated by reading-in any negative number instead of V .

After 40 measurement points have been read-in (VDU screen filled), corrections, if any, may be made. For this the program waits for the input of 3 numbers in the following sequence: number of the measurement point (given on the VDU screen); correct value of V_i ; correct value of E_i . The end of the data-correction is signalled by reading-in any negative number instead of the number of the measurement point. As a result of the calculations we obtain the co-ordinates of the titration end-point, and, for checking, recovered the number of measurement points (n) and the parameter Q (usually 10) of the rational spline function. The program may also write out (on application) all calculated inflection points of the interpolation curve and the values of the spline functions $S(V)$ for given values of V in the range (V_0, V_n) .

To explain details of the operation of the program a block diagram is given in Fig. 1.

The program consists of two parts. The first includes instructions corresponding to the block diagram and is sufficient for calculation of the inflection point of the titration curve, and values of the interpolation function at any point V from the range (V_0, V_n) .

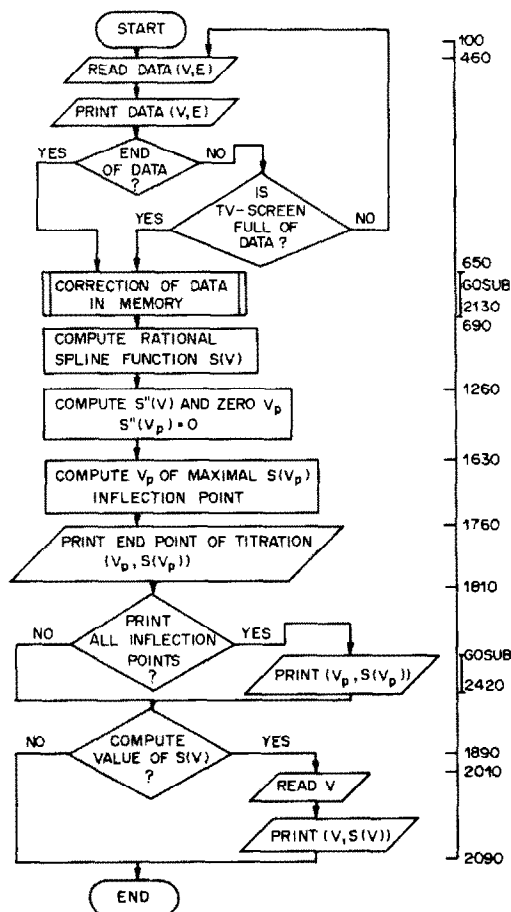


Fig. 1. Flow-diagram of computer program. The numbers on the right refer to the corresponding part of the program and are included for the convenience of those requesting it.

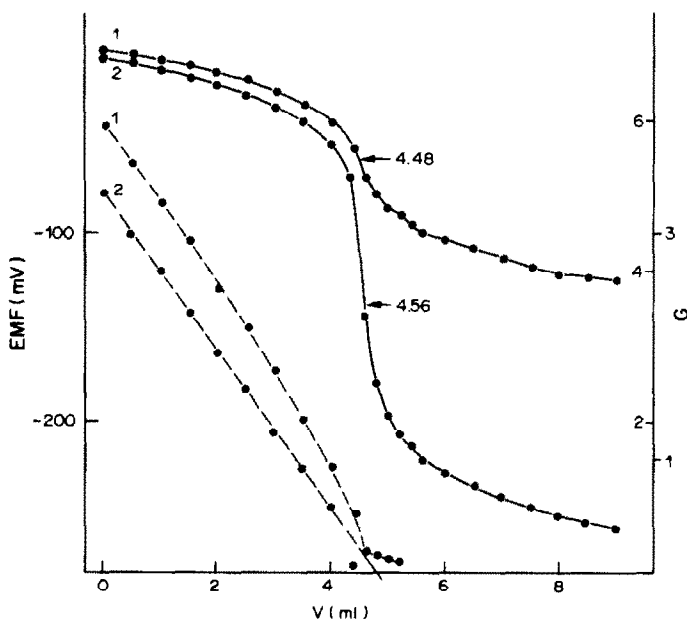


Fig. 2. Curves of the precipitation of Tl^+ with sodium tetraphenylborate. Thallium(I) ion-selective electrode with liquid membrane.⁴⁴ Theoretical end-point 4.50 ml. Composition of sample solutions: 1, $10^{-4}M Tl^+$ in the presence of $10^{-3}M Pb^{2+}$ masked with $10^{-2}M EDTA$, pH 5; 2, $10^{-4}M Tl^+$, pH 9.

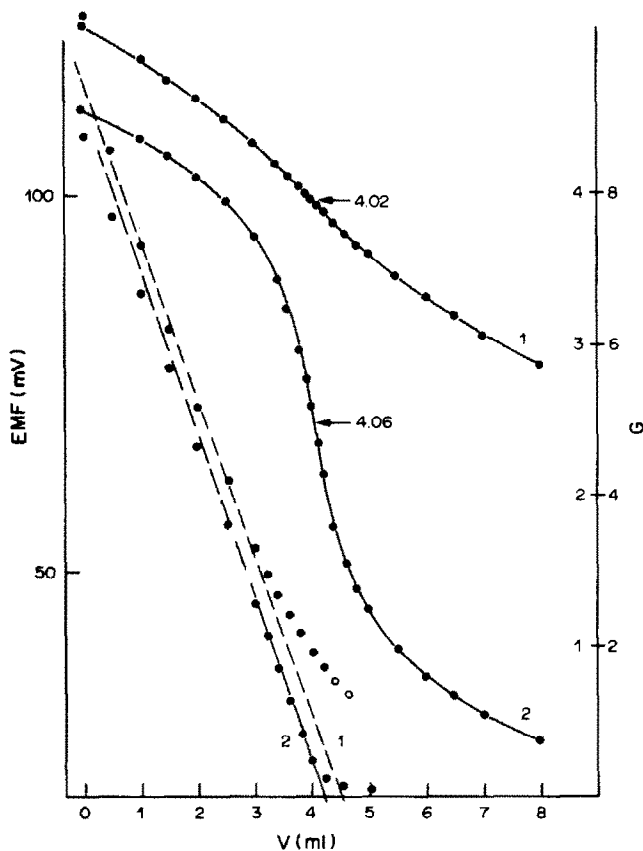


Fig. 3. Curves of the complexometric titration of Cu^{2+} with BADMF.⁴⁵ Crytur 29-17 copper-selective electrode. Theoretical end-point 4.00 ml. Composition of sample solutions: 1, $10^{-10}M Cu^{2+}$ in presence of $10^{-1}M Ni$, pH 6; 2, $10^{-3}M Cu^{2+}$, pH 6.

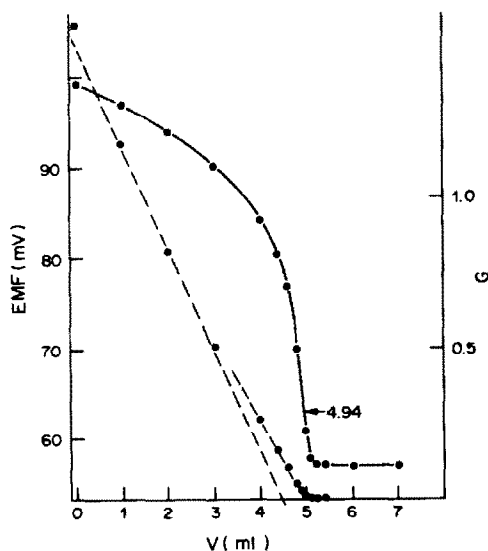


Fig. 4. Curves of complexometric titration of $10^{-3}M$ Bi^{3+} with EDTA in presence of $10^{-3}M$ Al^{3+} at pH 6. Bismuth(III) liquid-membrane ion-selective electrode.⁴⁶ Theoretical end-point 5.00 ml.

The second part is a set of instructions which, added to the basic program (with preservation of the line numeration) allows VDU display of the measurement points, the position of the inflection point of the curve and the graph of the spline function formed. Realization of those graphical possibilities requires the use of an HRG attachment (MEMPAK) with the ZX-81 minicomputer. The program listing is available on request.

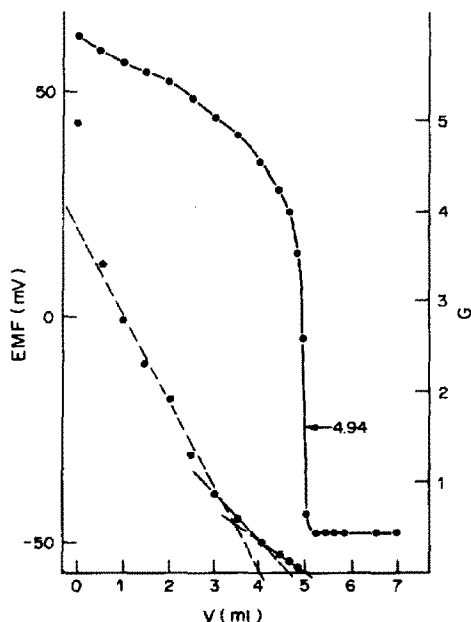


Fig. 5. Curves of the precipitation titration of $10^{-2}M$ Pb^{2+} with potassium chromate at pH 4. Lead liquid-membrane ion-selective electrode ($0.1M$ lead dicycylthiophosphate in trioctyl phosphatate). Theoretical end-point 5.00 ml.

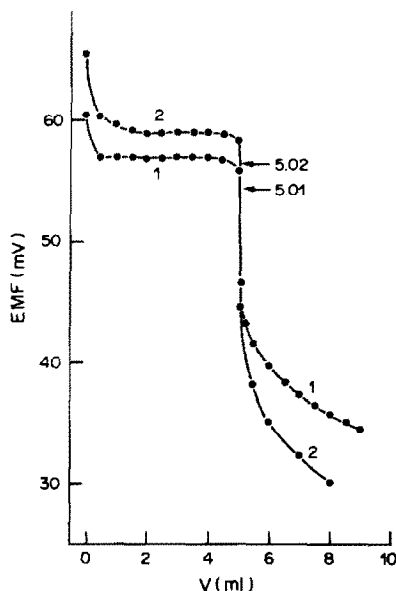


Fig. 6. Curves of potentiometric EDTA titrations of (1) $10^{-3}M$ Al^{3+} , (2) $10^{-3}M$ Fe^{3+} at pH 6 (ammonium acetate buffer) with Bi^{3+} as indicator ion.⁴⁷ Indicator electrode as for Fig. 4. Theoretical end-points 5.00 ml.

Examples of calculations

Figures 2–6 present curves of various potentiometric titrations which have been interpreted by the proposed method. The calculated inflection points are marked by arrows and the corresponding titrant volumes are given on the diagrams. In all cases the titrant was ten times more concentrated than the titrand. The titrations were done under conditions in which, for various reasons, distortion of the titration curves occurred before, and especially after, the end-point. Curves with distortions of that kind cannot be as accurately interpreted by other methods of determining the titration end-point.

In addition to the titration curves, the figures also show titration curves linearized by Gran's method, which obviously does not give satisfactory results for the titrations chosen.

The measurement points used for the calculations are marked as dots on the diagrams.

Acknowledgement—The investigations were financially supported by the Ministry of Science, Higher Education and Technology (Problem No. MRI.32).

REFERENCES

1. R. Behrend, *Z. Phys. Chem. Leipzig*, 1883, **11**, 466.
2. W. Bröttger, *ibid.*, 1897, **24**, 253.
3. C. F. Tubbs, *Anal. Chem.*, 1954, **26**, 1670.
4. F. L. Hahn and G. Weiler, *Z. Anal. Chem.*, 1926, **69**, 417.
5. R. Kohn and V. Zitko, *Chem. Zvesti*, 1958, **12**, 261.
6. S. Ebel, *Z. Anal. Chem.*, 1969, **245**, 108.
7. J. C. Hostetter and H. S. Robert, *J. Am. Chem. Soc.*, 1919, **41**, 1337.
8. S. R. Cohen, *Anal. Chem.*, 1966, **38**, 158.
9. F. Fenwick, *Ind. Eng. Chem., Anal. Ed.*, 1932, **4**, 144.

10. F. L. Hahn and M. Frommer, *Z. Phys. Chem. Leipzig*, 1927, **127**, 1.
11. *Idem, ibid.*, 1928, **133**, 290.
12. F. L. Hahn, *Z. Anal. Chem.*, 1929, **76**, 146.
13. *Idem, Anal. Chim. Acta*, 1954, **11**, 396.
14. *Idem, Mikrochim. Acta*, 1958, 400.
15. *Idem, Z. Anal. Chem.*, 1958, **163**, 169.
16. *Idem, ibid.*, 1960, **177**, 113.
17. *Idem, ibid.*, 1961, **183**, 183.
18. *Idem, Mikrochim. J.*, 1962, **6**, 199.
19. *Idem, Z. Anal. Chem.*, 1969, **244**, 229.
20. F. L. Hahn and G. Weiler, *ibid.*, 1926, **69**, 417.
21. J. M. H. Fortuin, *Anal. Chim. Acta*, 1961, **24**, 175.
22. G. Horvai and E. Pungor, *ibid.*, 1980, **116**, 87.
23. S. Yamaguchi and T. Kusuyama, *Z. Anal. Chem.*, 1979, **295**, 256.
24. G. Johanson and W. Backen, *Anal. Chim. Acta*, 1974, **69**, 415.
25. O. Aström, *ibid.*, 1978, **97**, 259.
26. T. Demokos and J. Hawas, *Hung. Sci. Instrum.*, 1976, **36**, 7.
27. T. Anfält and D. Jagner, *Anal. Chim. Acta*, 1971, **57**, 165.
28. K. Weidmeier and W. Rellstab, *Z. Anal. Chem.*, 1973, **264**, 337.
29. G. Arena, E. Rizzarelli and S. Sammartano, *Talanta*, 1979, **26**, 1.
30. B. Cavanagh, *J. Chem. Sci.*, 1930, 1425.
31. G. Gran, *Acta Chem. Scand.*, 1950, **4**, 559.
32. *Idem, Analyst*, 1952, **77**, 661.
33. D. Dyrssen, J. Jagner and F. Wengelin, *Computer Calculation of Ionic Equilibria and Titration Procedures*, Almquist & Wiksell, Stockholm, 1968.
34. J. Buffle, N. Parthasarathy and D. Monnier, *Anal. Chim. Acta*, 1972, **59**, 427.
35. J. Buffle, *ibid.*, 1972, **59**, 439.
36. A. Ivaska, *Talanta* 1979, **27**, 161.
37. T. Eriksson, *Anal. Chim. Acta*, 1972, **58**, 437.
38. C. McCallum and D. Midgley, *ibid.*, 1973, **65**, 155.
39. W. Lund, *Talanta*, 1976, **23**, 619.
40. Carl de Boor, *A Practical Guide to Splines*, pp. 22-38. Springer, Berlin, 1978.
41. Y. Zavyalov, *Metody spline-funktsii*, Mir, Moscow, 1980.
42. L. Schumaker, *Spline Functions: Basic Theory*, Wiley, New York, 1982.
43. J. Ahlberg, E. Nielson and J. Walsh, *The Theory of Spline Functions*, Academic Press, New York, 1967.
44. W. Szczepaniak and K. Ren, *Anal. Chim. Acta*, 1976, **82**, 37.
45. W. Szczepaniak and K. Kuczyński, *Chem. Anal. Warsaw*, 1978, **23**, 273.
46. W. Szczepaniak and K. Ren, *Talanta*, 1983, **30**, 945.
47. *Idem, ibid.*, 1984, **31**, 212.

FLUOROMETRIC DETERMINATION OF NITRITE

P. DAMIANI and G. BURINI

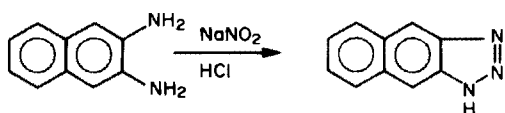
Istituto di Chimica Bromatologica, Facoltà di Farmacia, Università degli Studi, 06100 Perugia, Italy

(Received 20 August 1984. Revised 19 December 1985. Accepted 26 March 1986)

Summary—A sensitive, simple and rapid fluorometric procedure for the determination of nitrite is described. It is based on the reaction of nitrite with 2,3-diaminonaphthalene in acidic solution to form 1-[H]-naphthotriazole, a highly fluorescent compound in alkaline medium. The detection limit is ~0.5 ng/ml in the test sample (1% relative fluorescence intensity). Application of the method to analysis of a milk sample was tested with aliquots spiked with known amounts of nitrite.

Many methods are available for the determination of nitrite in environmental samples. The spectrophotometric methods¹⁻⁹ are subject to various interferences by other ions, oxidants, coloured matter and turbidity, especially in biological samples. Electrometric methods^{10,11} are also available, as well as HPLC of the free ion¹²⁻¹⁶ and GLC or HPLC of its organic derivatives.¹⁷⁻²⁸ However, some of these methods require close control of conditions, some have unsatisfactory detection limits and some, which are too complex and time-consuming, are unsuitable for routine application.

Fluorometric methods have also been described for determination of trace levels of nitrite,²⁹⁻³⁵ and are all based on the reaction of nitrite with various reagents to produce fluorescent compounds. Some of these methods^{29,30,34} use 2,3-diaminonaphthalene (DAN) to form 1-[H]-naphthotriazole with nitrite (or nitrate previously reduced to nitrite³⁰), according to the reaction:



DAN (2,3-diaminonaphthalene) 1-[H]-naphthotriazole

Wiersma²⁹ described a DAN procedure that permitted measurement of nitrite at the 6.5 ng/ml level. The method used a double extraction with carbon tetrachloride but gave only 94% recovery of the naphthotriazole.

Any new procedure for the rapid and accurate determination of nitrite at trace levels is of interest, because of the risk of its reaction with secondary amines to form carcinogenic nitrosamines and cause methaemoglobinaemia in infants.

This paper describes a fluorometric procedure based on use of DAN, but not requiring an extraction step. This procedure is very simple and rapid, and allows measurement of nitrite at levels as low as 0.4 ng/ml.

EXPERIMENTAL

Reagents

All reagents used were of analytical grade and all water used was demineralized and doubly distilled.

Standard sodium nitrite solutions. A 100- μ g/ml nitrite stock solution was made by dissolving 0.150 g of sodium nitrite, previously dried for 2 hr at 110°, in distilled water, and diluting accurately to 1000 ml. A 50-ng/ml working solution was made by diluting 0.5 ml of the stock solution to 1000 ml with distilled water. Both solutions should be prepared fresh daily.

2,3-Diaminonaphthalene (DAN) solution. Made fresh daily, by dissolving 0.10 g of DAN in 1000 ml of 0.25M hydrochloric acid.

Sodium hydroxide solution, 0.58 M. Made by dissolving 23.2 g of sodium hydroxide pellets in distilled water and diluting to 1000 ml.

EDTA solution, 4000 ppm. Made by dissolving 4 g of EDTA disodium salt dihydrate in distilled water and diluting to 1000 ml.

Apparatus

A Perkin-Elmer 203 spectrofluorimeter (Hg lamp) was used, with excitation wavelength 365 nm, emission wavelength 405 nm, sensitivity control 5, range selector $\times 10$.

Procedure

Prepare a set of 5-ml volumes of standard solutions containing 0.0, 10.0, 20.0, 30.0, 40.0, 50.0 ng of nitrite (NO_2^-) per ml by pipetting suitable volumes of working standard solution and distilled water into test-tubes. Add 0.5 ml of DAN solution to each, mix and let stand for 10 min; these solutions have a pH of 1.6. Add to each tube 0.25 ml of 0.58M sodium hydroxide and mix; these solutions have a final pH of 11.6. Measure the relative fluorescence intensities at 405 nm, with excitation at 365 nm, after adjusting the instrument response to range from zero for the blank to 100% for the highest standard. For test samples use 4 ml of sample plus 1 ml of water or 1 ml of 4000-ppm EDTA solution, as appropriate.

RESULTS AND DISCUSSION

The conditions given in the procedure are based on the results given below. In the exploratory work the fluorescence intensities were measured in arbitrary units with fixed instrument settings but no standards.

Effect of DAN concentration

A series of 5-ml aliquots of nitrite solution (50 ng/ml) were treated with DAN solutions (in

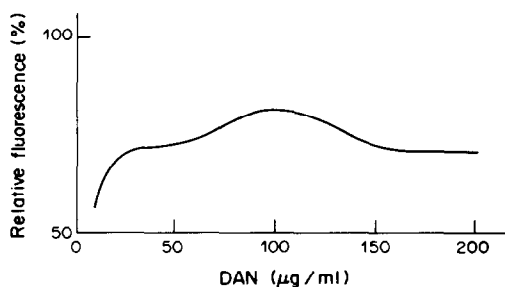


Fig. 1. Effect of DAN concentration.

0.25M hydrochloric acid) varying in concentration from 10 to 200 $\mu\text{g/ml}$ (in increments of 10 $\mu\text{g/ml}$). As shown in Fig. 1, 0.5 ml of the 100- $\mu\text{g/ml}$ DAN solution gave the highest fluorescence intensity. This concentration is optimal but not critical, because use of any concentration in the range 90–110 $\mu\text{g/ml}$ changes the intensity by less than 2% relative to the optimum.

Effect of reaction pH

Five-ml portions of 50-ng/ml nitrite working solution were treated with 0.5 ml of 100- $\mu\text{g/ml}$ DAN solution at pH values between 0.5 and 2.0 (at intervals of 0.1) and the fluorescence intensities were read after adjustment of the pH to 11.65. The results are reported in Fig. 2. The optimum pH is 1.6, the tolerance range being 1.3–1.7.

Effect of final pH

In spectral evaluation of alkaline and acidic naphthotriazole solutions (Fig. 3) it was verified that the ratio of the two molar absorptivities ($\epsilon_{\text{alk}}/\epsilon_{\text{acid}}$) at 365 nm (the excitation wavelength used) is always larger than 1.00. If the fluorescence yield remains the same, the fluorescence intensity of alkaline naphthotriazole solutions should be higher than that of acid solutions. The acid reaction with DAN was performed under the optimum conditions already established, then the pH was adjusted to values between 7.5 and 13.5 (at intervals of 0.1) before the fluorescence intensity was measured. Figure 4 shows that pH 11.6–11.7 is optimal, but use of any pH in the range 11.3–12.0 will result in not more than 2% error relative to the optimum. The higher fluorescence signal in alkaline pH medium may also be explicable by the rule³⁶ according to which all

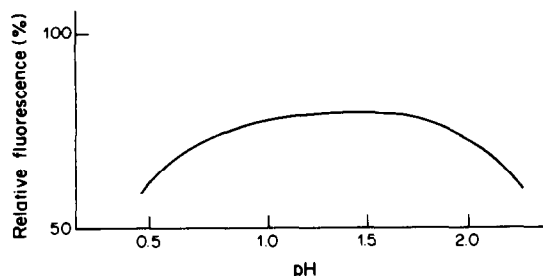


Fig. 2. Effect of reaction pH.

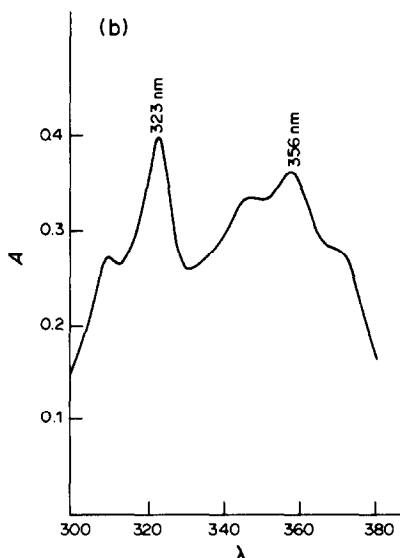
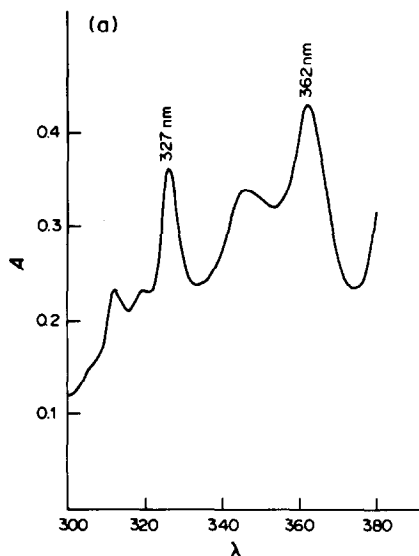


Fig. 3. Ultraviolet spectra of naphthotriazole solution at (a) pH 11.65, (b) pH 1.64.

phenomena that stabilize excited electronic levels (particularly the n, π^* ; note the red-shift in the spectrum for alkaline medium, Fig. 3), influence the intersystem crossing yield. Hence deactivation of the

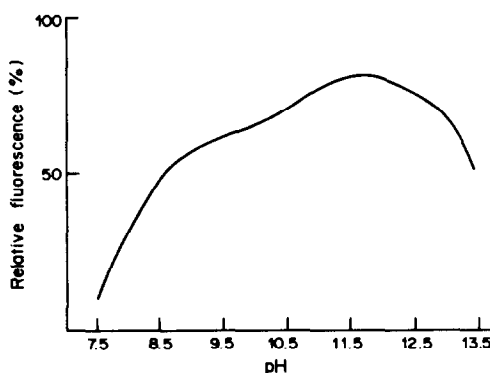


Fig. 4. Effect of final pH.

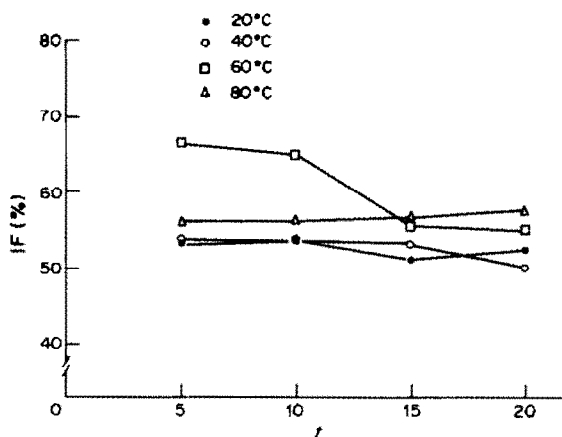


Fig. 5. Effect of time and temperature (● 20°; ○ 40°; □ 60°; △ 80°).

excited state through a triplet state is not allowed, and consequently the fluorescence yield is higher.

Effect of time and temperature

The results obtained with varied times and temperatures but otherwise optimum conditions are summarized in Fig. 5, and show that reaction at 60° for 5–10 min gives the highest fluorescence intensity, but reaction at room temperature for any time between 5 and 20 min is more practical, since the fluorescence is less dependent on variation in the conditions, and the procedure is simpler.

Identification of 1-[H]-naphthotriazole

1-[H]-naphthotriazole was prepared on the macro-scale and recrystallized from aqueous ethanol, and dissolved in hexadeuteroacetone, and its NMR spectrum was obtained with a Perkin-Elmer R-24B NMR spectrometer at 60 MHz (internal standard: 1% tetramethylsilane solution). The spectrum (Fig. 6) showed signals at $\delta = 6.60$ –7.10 ppm (multiplet, 4H) and 7.60 ppm (singlet, 2H), indicative of the naphthalene group, and at 14.00 ppm (wide singlet, 1H), indicative of the $=\text{NH}$ group.

Fluorescence stability

The fluorescence intensity is stable for 10 min, then gradually fades.

Interferences

To investigate applications of the procedure, 4-ml aliquots of 50-ng/ml nitrite solution were added to

Table 1. Effect of various ions on the fluorometric determination of nitrite

Ion*	Allowable concentration†, ppm
Cl ⁻	19000
SO ₄ ²⁻	12000
NO ₃ ⁻	1000
HCO ₃ ⁻	300
SO ₃ ²⁻	50
S ²⁻	0.5
H ₂ EDTA ²⁻	1500
Zn ²⁺ ‡	1000
NH ₄ ⁺	340
Ca ²⁺	300
Fe ²⁺ §	1
Fe ³⁺	1
Mg ²⁺	0.5
Mg ²⁺	60‡

*Anions as sodium salts, cations as chlorides.

†No interference at below suggested concentrations (in 4 ml of sample solution).

‡As sulphate.

§In presence of 1000 ppm EDTA in the 4 ml of test solution.

1-ml portions of solutions containing known and increasing amounts of various ions (examined one at a time), and these solutions were analysed as described, with centrifuging if necessary (to remove any precipitate).

As shown in Table 1, the procedure is more tolerant towards anions (except sulphide) than cations. The interference of zinc, calcium and magnesium, however, can be minimized by adding 1-ml of 4000-ppm EDTA solution to 4 ml of test solution containing the interfering cation (see Table 1 for results for magnesium, the most important interfering metal ion).

Accuracy and precision

The calibration graph is linear over the nitrite concentration range from 2.5 to 40 ng/ml in the 5 ml of sample solution, but concentrations up to 400 ng/ml can be satisfactorily determined. The coefficients of variation found (10 replicates at each level) were 8.8, 2.7, 1.4, 1.1 and 1% at the 2.5, 10, 20, 30 and 40 ng/ml levels respectively, with corresponding relative deviations of -3.0, +1.0, -0.5, +0.2 and +0.1% of the means from the concentration taken.

Table 2. Results of quadruplicate analyses of a whole-milk sample

NO ₂ ⁻ added, ppm	Fluorimetric method			Colorimetric method ³⁷		
	Range found, ppm	Std. devn., ppm	Recovery, %	Range found, ppm	Std. devn., ppm	Recovery, %
0	0.28–0.29	0.005	—	0.34–0.38	0.02	—
0.50	0.78–0.79	0.005	99–101	0.80–0.86	0.03	94–98
1.00	1.23–1.28	0.025	96–100	1.32–1.50	0.09	96–109
2.00	2.15–2.20	0.025	94–96	2.34–2.60	0.13	100–109

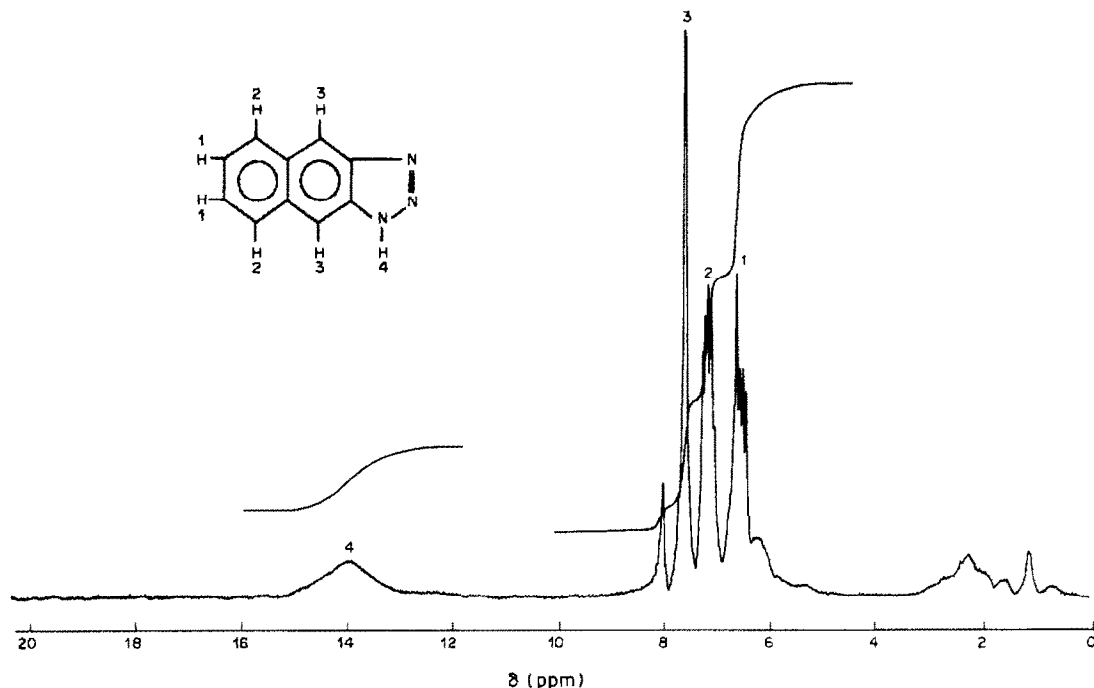


Fig. 6. NMR spectrum of 1-[H]-naptotriazole in d_6 acetone at 60 MHz.

Determination of nitrite in a milk sample

To judge the efficiency of the method for analysis of a food sample, several aliquots of a milk sample were spiked with known amounts of nitrite and analysed. A 20-ml portion of spiked milk sample was pipetted into a 200-ml standard flask and freed from proteins and fat according to a standard method,³⁷ then 5 ml of the filtrate obtained were used for the fluorometric determination. The results are summarized in Table 2, along with those obtained by the standard method.³⁷ The procedure is also suitable for determination of nitrate, after its reduction to nitrite, e.g., with a cadmium column.³⁷

REFERENCES

- P. Griess, *Chem. Ber.*, 1879, **12**, 426.
- L. Ilosvay, *Bull. Soc. Chim. France*, 1889, **3**, 388.
- G. Lunge, *Z. Anal. Chem.*, 1889, **28**, 666.
- A. Adriaanse and J. E. Robbers, *J. Sci. Food Agric.*, 1969, **20**, 321.
- R. Truhaut and P. L. Nguyn, *Ann. Falsif. Expert Chim.*, 1966, **59**, 401.
- A. J. McKay, *Austr. J. Dairy Technol.*, 1974, **29**, 34.
- R. Benassi, *Boll. Lab. Chim. Prov.*, 1964, **15**, 490.
- F. Bernejo-Martinez and M. Zunzunegui-Perez, *Inf. Quim. Anal. Pura Apl. Ind.*, 1972, **23**, 163.
- R. A. Nicholas and J. B. Fox, *J. Assoc. Off. Anal. Chem.*, 1973, **56**, 922.
- J. Davidek and A. Žáčková, *Z. Anal. Chem.*, 1962, **189**, 320.
- F. Henrioul, *Rev. Ferment.*, 1963, **18**, 51.
- R. G. Gerritse, *J. Chromatog.*, 1979, **171**, 527.
- I. Molnar, H. Knauer and D. Wilk, *ibid.*, 1980, **201**, 225.
- U. Leuenberger, R. Gauch, K. Rieder and E. Baumgartner, *ibid.*, 1980, **202**, 461.
- H. J. Cortes, *ibid.*, 1982, **234**, 517.
- J. R. Thayer and R. C. Huffaker, *Anal. Biochem.*, 1980, **102**, 110.
- H. Noda, M. Minemoto, T. Asahara, A. Noda and S. Iguchi, *J. Chromatog.*, 1982, **235**, 187.
- D. J. Glover and C. Hoffsommer, *ibid.*, 1974, **94**, 334.
- W. D. Ross, G. W. Buttler, T. G. Duffy, W. R. Rehg, M. T. Wininger and R. E. Sievers, *ibid.*, 1975, **112**, 719.
- J. W. Tesch, W. R. Rehg and R. E. Sievers, *ibid.*, 1976, **126**, 743.
- Y. L. Tan, *ibid.*, 1977, **140**, 41.
- R. L. Tanner, R. Fayer and J. Gaffney, *Anal. Chem.*, 1979, **51**, 865.
- K. Funazo, M. Tanaka and T. Shono, *ibid.*, 1980, **52**, 1222.
- A. Tanaka and A. Watanare, *J. Chromatog.*, 1980, **194**, 21.
- A. Tanaka, N. Nose, F. Yamada, S. Saito and A. Watanabe, *ibid.*, 1981, **206**, 531.
- A. Tanaka, N. Nose and H. Iwasaki, *ibid.*, 1982, **235**, 173.
- K. Funazo, K. Kusano, A. Tanaka and T. Shono, *Analyst*, 1982, **107**, 82.
- A. Tanaka, N. Nose, S. Saito, H. Masaki and H. Iwasaki, *Bunseki Kagaku*, 1982, **31**, 265.
- J. H. Wiersma, *Anal. Lett.*, 1970, **3**, 123.
- C. R. Sawicki, *ibid.*, 1971, **4**, 761.
- N. K. Podberezskaya, E. A. Shilenko and V. A. Sushkova, *Issled. obl. Khim. Fiz. Metod. Anal. Miner. Syr'ya*, 1971, 90.
- G. Oshima and K. Nagasawa, *Chem. Pharm. Bull.*, 1972, **20**, 1492.
- L. J. Dombrowski and E. J. Pratt, *Anal. Chem.*, 1972, **44**, 2268.
- G. L. Wheeler and P. F. Lott, *Microchem. J.*, 1974, **19**, 390.
- H. D. Axelrod and N. A. Engel, *Anal. Chem.*, 1975, **47**, 922.
- M. A. El-Sayed, *Acc. Chem. Res.*, 1968, **1**, 8.
- International Dairy Federation, FIL-IDF 50 A, 1980/FIL-IDF 95, 1980.

MICELLAR MODIFICATION OF THE SPECTRAL, INTENSITY AND LIFETIME CHARACTERISTICS OF THE FLUORESCENCE OF FLUORESCIN-LABELLED PHENOBARBITAL

TERESA L. KEIMIG and LINDA B. MCGOWN†

Department of Chemistry, Oklahoma State University, Stillwater, OK 74078, U.S.A.

(Received 19 February 1986. Accepted 24 March 1986)

Summary—The effects of association with micelles on the fluorescence properties of fluorescein-labelled phenobarbital were studied as a function of pH (in the range 5.8–7.8) and micelle concentration. The largest changes were observed at pH 5.8, including red-shifts of 10 nm in the emission and excitation maxima, spectral intensity enhancements as great as 500%, and 0.5-nsec increases in fluorescence lifetime. Micelles induced much greater changes than cyclodextrins, which were also studied. These studies indicate the potential usefulness of micelles and cyclodextrins as auxiliary binding reagents for both heterogeneous and homogeneous fluoroimmunoassay techniques.

Micelles have been widely studied in recent years and their ability to change the fluorescence characteristics of some molecules has been recognized as a valuable property and has potential value in immunoassay systems. In heterogeneous fluoroimmunoassays, micelles could be used to increase the fluorescence intensity of the fluorescent labelled antigen (Ag*) after removal of the antibody-bound Ag* fraction to improve detection limits. Micelle-induced spectral shifts could be of value in avoiding spectral interferences due to sample constituents. The micellar modification of fluorescence properties may also be exploited for homogeneous fluoroimmunoassays to improve the discrimination between free and antibody-bound Ag*. For example, the use of sodium dodecyl sulphate, an anionic micellar species, to increase the fluorescence intensity and polarization differences between free and antibody-bound fluorescein-labelled gentamicin has recently been incorporated in a solvent perturbation fluoroimmunoassay technique.¹ Micellar modification of fluorescence lifetimes could be applied to homogeneous techniques based on fluorescence-lifetime differences between free and antibody-bound Ag*, such as the recently described phase-resolved fluoroimmunoassay for phenobarbital by labelling with fluorescein isothiocyanate.²

This paper describes the effects of micelles on the fluorescence intensity, excitation and emission maxima, and fluorescence lifetimes of phenobarbital labelled with fluorescein isothiocyanate (P*) as a function of pH and micelle concentration. Four micellar cationic surfactants, dodecylamine hydrochloride (DAC), dodecyltrimethylammonium chloride (DTAC), hexadecyltrimethylammonium chloride (CTAC), and tetradecyltrimethylammonium bromide

(TTAB) were studied, as well as one non-ionic surfactant, *N,N*-dimethyldodecylamine-*N*-oxide (LDAO). The effects of association of P* with beta- and gamma-cyclodextrins were also studied.

EXPERIMENTAL

Fluorescein-labelled phenobarbital (P*) was prepared *in situ*.¹ The DAC and DTAC were purchased from Eastman, and the CTAC, LDAO and TTAB from Fluka. Beta-cyclodextrin was purchased from Sigma and gamma-cyclodextrin from ICN Biochemicals. All compounds were used without further purification.

Demineralized distilled water was used for all preparations. The P* stock solution was prepared by 100-fold dilution of the chromatographically purified reaction product. The concentration of the stock solution was estimated to be 30 μ M by using a calibration curve generated with fluorescein isothiocyanate (Sigma). Unbuffered solutions of all surfactants were prepared at concentrations above their reported CMC values and mixed by ultrasonic treatment for 30 min. Cyclodextrin solutions were similarly prepared. The concentrations of these solutions are given in Table 1. Buffered solutions of the surfactants were prepared at the same concentrations as the unbuffered solutions, in 0.010M sodium phosphate buffers ranging in pH from 5.8 to 7.8. Constant ionic strength ($\mu = 0.10M$) buffered solutions of TTAB were prepared by addition of the appropriate amount of sodium chloride.

In all studies, the analytical concentration of P* in the cuvette was calculated to be 0.21 μ M from the estimated concentration of the P* stock solution (see above).

All fluorescence measurements, including steady-state intensities and dynamic phase shifts and demodulations, were made with an SLM 4800S Spectrofluorometer in ratiometric modes, with a portion of the excitation beam diverted to a reference photomultiplier to compensate for fluctuations in source output and (for dynamic measurements) excitation modulation. A 450-W xenon arc lamp was used for excitation, Hamamatsu R928 photomultipliers for detection, and an APPLE II+ microcomputer for on-line acquisition of fluorescence spectral and lifetime data and for lifetime calculations.

For dynamic measurements, slits were set at 16 nm and 0.5 nm band-pass for the excitation monochromator entrance and exit, respectively, 0.5 nm for the modulation tank

†Author for correspondence.

Table 1. Effects of micelles and cyclodextrins on the fluorescence properties of fluorescein-labelled phenobarbital (P*)

Added species ^a	$\lambda_{em}, \text{max},^b \text{nm}$	Intensity ratio ^c	$\tau_p,^d \text{nsec}$	$\tau_m,^e \text{nsec}$	pH ^f
none	516	1.00	4.00 ^g	4.00 ^g	n.d.
CTAC (3.0)	526	2.64	4.39	4.45	6.0
DAC (15)	523	1.36	4.07	4.23	4.6
DTAC (22)	526	2.54	4.28	4.30	6.6
LDAO (4.0)	522	1.05	3.68	3.86	7.1
TTAB (7.0)	525	2.72	4.40	4.44	6.0
β -CD ^h (2.0)	516	2.05	4.15	4.12	n.d.
γ -CD ^h (2.0)	517	1.57	4.23	4.07	n.d.

^aConcentration in parentheses, mM.

^bEmission maximum with excitation at 490 nm.

^cRatio of intensity in presence of the added species to that in its absence, each measured at its emission maximum.

^dFluorescence lifetime calculated from phase-delay, determined with the P* solution (τ 4.00 nsec) as reference.

^eFluorescence lifetime calculated from demodulation, determined with the P* solution (τ 4.00 nsec) as reference.

^fpH of the cuvette solution; n.d. indicates pH not determined.

^gFluorescence lifetimes determined with a scattering solution as reference.

exit, and 16 nm for both the entrance and exit of the emission monochromator. All slits were set at 2 nm band-pass for steady-state intensity measurements, except for the excitation entrance slit which was set at 16 nm. An excitation polarizer set at 35° from the vertical axis was used for all measurements.

Temperatures in the fluorometer sample chamber were maintained at $25.0 \pm 0.1^\circ$ with a Haake A81 temperature-control unit. Disposable polyethylene cuvettes (Precision Cells) were used to contain solutions for fluorescence measurements.

Unless otherwise noted, the fluorescence lifetimes of the P* were determined relative to a reference solution of Acridine Orange in absolute ethanol (U.S. Industrial Chemical Co.), which was found (from phase-delay measurements) to have a lifetime of 3.19 ± 0.02 nsec relative to a scattering solution, at the wavelengths used in this work. Equations for these calculations have been described elsewhere.⁶ All fluorescence lifetimes are reported as the average of five measurements taken in the "100 average" mode, in which each measurement is the average of 100 samplings performed internally by the spectrofluorometer.

Absorption spectra were acquired with a Perkin-Elmer Lambda Array 3840 Spectrophotometer.

RESULTS AND DISCUSSION

All the fluorescence lifetimes reported here had standard deviations in the range 5–50 psec. A lifetime of 4.04 nsec had previously been found for P* by using phase-shift measurements.²

Effects of various micelles and cyclodextrins in unbuffered solution

The effects of five micelle-forming species and of beta- and gamma-cyclodextrins are summarized in Table 1. The pH values of each of the unbuffered micellar solutions are also listed. All five micellar species caused red shifts ranging from 5 to 10 nm in the emission maximum of P*. No shifts in the emission maximum were observed with the cyclodextrins. Fluorescence enhancement was observed with all species, and was highest with CTAC, DTAC and TTAB. All species except LDAO, which was the

only non-ionic micelle used, caused increases in the observed lifetime. CTAC and TTAB were chosen for further studies.

Studies of CTAC and TTAB effects in buffered solutions

A shift in the emission maximum of P* to 526 nm was observed with both CTAC and TTAB at all pH values studied, indicating an absence of pH-dependence. Fluorescence enhancements of P* in CTAC and TTAB as a function of pH are shown in Table 2. Enhancements are expressed as peak-to-peak values (*i.e.*, the ratio of the intensity of micelle-P* to that of P*, each measured at its emission maximum). A small trend towards increased enhancement was observed as the pH was decreased, with a dramatic increase at pH 5.8.

Absorption spectra of P* and of TTAB-P* at pH 5.8 are shown in Fig. 1. The spectra show a definite increase in absorptivity in the presence of TTAB, indicating that the so-called fluorescence enhancement is at least partially due to absorption rather than quantum-yield changes. For simplicity, we will continue to refer to the fluorescence intensity increase as enhancement.

Table 2. Ratios of the intensity of P* in the presence of micelles to the intensity in the absence of micelles, as a function of pH, measured at $\lambda_{ex} = 490$ nm and at the appropriate λ_{em} under the same buffer and pH conditions

pH	Intensity ratios (CTAC)	Intensity ratios (TTAB)
5.8	6.24	5.12
6.0	2.29	1.35
6.2	1.39	1.80
6.4	1.17	1.30
6.6	1.41	1.39
6.8	1.03	1.26
7.0	1.16	1.23
7.3	1.05	1.20
7.5	1.01	1.07
7.8	0.91	0.91

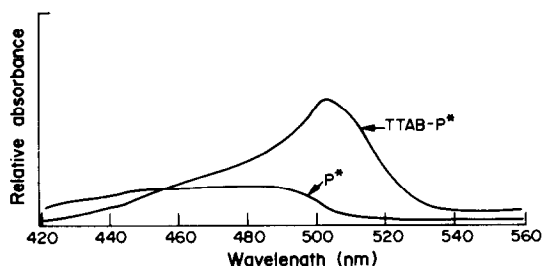


Fig. 1. Absorption spectra of fluorescein-labelled phenobarbital with TTAB (TTAB-P*) and without TTAB (P*) in buffered solution at pH 5.8.

The fluorescence lifetime difference of 0.3 nsec between micelle-P* and P* remained fairly constant over the pH range studied for P* in the presence of both CTAC and TTAB.

Studies of the effects of TTAB in buffered constant ionic strength solutions

The effects of TTAB on P* fluorescence were studied in buffered solutions adjusted to 0.10M ionic strength with sodium chloride. Differences between the fluorescence lifetimes of TTAB-P* and P* as a function of pH are shown in Table 3. The change in lifetime calculated from demodulation remained fairly constant, but the change in lifetime calculated from phase-delay showed a definite increase with decreasing pH.

The effects of pH on the relative intensities of P* and TTAB-P* are shown in Fig. 2, and the ratios of these intensities are listed in Table 3. Smaller relative enhancements were observed for the constant ionic strength solutions than for the buffered solutions without sodium chloride added (Table 2).

Fluorescein is weakly acidic, with pK_{a1} and pK_{a2} values of 4.4 and 6.7, respectively.⁷ The completely dissociated form is highly fluorescent, and the

Table 3. The intensity ratios of TTAB-P* to P* and the differences between the fluorescence lifetimes of the two as a function of pH, in constant ionic strength solutions

pH	Intensity ratio ^a	$\Delta\tau_p^b$, nsec	$\Delta\tau_m^c$, nsec
5.8	1.38	0.37	0.43
6.0	1.30	0.37	0.52
6.2	1.15	0.36	0.46
6.4	1.11	0.29	0.46
6.6	1.19	0.35	0.44
6.8	1.30	0.31	0.45
7.0	1.07	0.29	0.46
7.2	0.98	0.33	0.46
7.4	0.98	0.26	0.46
7.6	0.97	0.27	0.44
7.8	0.88	0.26	0.47

^aIntensities measured at $\lambda_{ex} = 490$ nm, and at the emission maximum of the solution, both at the same pH.

^bFluorescence lifetime of TTAB-P* minus that of P* as calculated from phase-shift lifetimes

^cFluorescence lifetime of TTAB-P* minus that of P* as calculated from demodulation lifetimes.

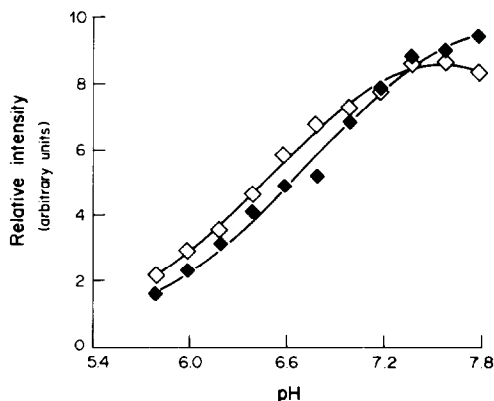


Fig. 2. Fluorescence intensity of P* (◆) and TTAB-P* (◇) as a function of pH in constant ionic strength buffer.

fluorescence intensity of fluorescein solutions increases with increasing pH. As shown in Fig. 2, in the low pH range, the fluorescence of P* is enhanced by association with TTAB, but above pH 7.2 TTAB causes a decrease in intensity relative to that in the absence of the micelle, which is higher because of the increased dissociation of the fluorescein label.

The emission maximum of P* was shifted from 516 to 525 nm and the excitation maximum from 492 to 501 nm on association with TTAB at all pH values studied. The excitation and emission spectra of P* with and without TTAB at pH 7.0 are shown in Fig. 3. The ratio of the intensity of TTAB-P* to that of P*, measured at the wavelength maxima for the latter ($\lambda_{ex} = 501$ nm and $\lambda_{em} = 525$ nm) was found to be 2.7 at pH 5.8 and 1.7 at pH 7.0.

The fluorescence wavelength maxima and lifetimes of P* as a function of TTAB concentration were studied at pH 5.8 (Table 4). Spectral shifts are almost negligible at TTAB concentrations below 0.6mM. Fluorescence lifetimes decrease with increasing TTAB concentration up to around 1mM, when they jump to a higher value that remains constant at higher concentrations. The initial decrease in lifetime indicates quenching of the P* fluorescence at TTAB

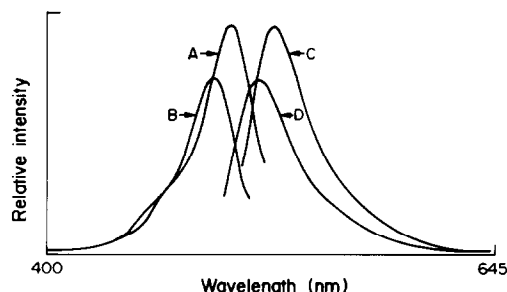


Fig. 3. Excitation and emission spectra of fluorescein-labelled phenobarbital (P*) with and without TTAB in constant ionic strength buffer at pH 7.0. (A) TTAB-P* excitation spectrum, $\lambda_{em} = 525$ nm, (B) P* excitation spectrum, $\lambda_{em} = 517$ nm, (C) TTAB-P* emission spectrum, $\lambda_{ex} = 501$ nm, (D) P* emission spectrum, $\lambda_{ex} = 492$ nm.

Table 4. Fluorescence excitation and emission maxima and the difference between the fluorescence lifetimes of TTAB-P* and P* as a function of total TTAB concentration in pH 5.8 constant ionic strength solutions

$C_{\text{TTAB}}, \text{mM}$	$\lambda_{\text{ex}}, \text{nm}$	$\lambda_{\text{em}}, \text{nm}$	$\Delta\tau_{\text{p}}^{\text{a}}, \text{nsec}$	$\Delta\tau_{\text{m}}^{\text{b}}, \text{nsec}$
0	491	517	—	—
0.46	492	518	0	0.06
0.58	492	518	-0.13	-0.04
0.69	496	525	-0.27	-0.06
1.0	502	525	0.32	0.45
3.1	501	525	0.36	0.48
7.0	501	525	0.36	0.49

^aSee (b), Table 3.

^bSee (c), Table 3.

Table 5. Fluorescence emission maxima, intensity ratios and the difference between the fluorescence lifetimes of TTAB-P* and P* as a function of total TTAB concentration in pH 7.0 constant ionic strength solutions

$C_{\text{TTAB}}, \text{mM}$	$\lambda_{\text{em}}, \text{nm}$	Intensity		
		ratio ^a	$\Delta\tau_{\text{p}}^{\text{b}}, \text{nsec}$	$\Delta\tau_{\text{m}}^{\text{c}}, \text{nsec}$
0	516	—	—	—
0.69	521	0.28	-0.57	-0.17
0.81	525	0.42	-0.12	0.08
0.91	525	0.75	0.24	0.36
1.0	525	0.84	0.30	0.41
3.1	525	—	0.34	0.49
7.0	525	1.07	0.32	0.49

^aRatio of the intensity of TTAB-P* to P*, measured at $\lambda_{\text{ex}} = 490 \text{ nm}$ and at the emission maximum of the solution.

^bSee (b), Table 3.

^cSee (c), Table 3.

concentrations below its CMC. Above the CMC, the lifetimes achieve a maximum value corresponding to that of P* protected by micelle-association. Table 5 shows the results of a similar study at pH 7.0. Similar trends are observed in the emission maxima and lifetimes, but the transitions occur at slightly lower TTAB concentrations. Relative intensities are also shown for both pH values, and indicate that there is

indeed a quenching effect at TTAB concentrations below the apparent CMC.

CONCLUSIONS

Changes observed in P* fluorescence upon association with micelles included pH-independent spectral shifts and pH-dependent fluorescence intensity and lifetime changes. Cyclodextrins did not induce spectral shifts in P* fluorescence, and the induced lifetime changes were not as large as those observed for the micellar systems. However, large intensity enhancements were observed that might prove valuable in certain applications. Future research into the application of auxiliary binding reagents such as micelles and cyclodextrins to immunoassay systems will require studies of the effects of the auxiliary reagents on the antibody-bound as well as the free labelled antigen. Therefore, it is difficult to predict which reagents will prove most valuable for a particular immunoassay technique. The studies described here demonstrate that significant changes in the fluorescence properties of fluorescein-labelled phenobarbital can be achieved by using micelles, and, to a lesser degree, cyclodextrins.

Acknowledgements—The authors are grateful to the National Institute on Drug Abuse for support of this research through Grant No. DA 03674.

REFERENCES

1. C. J. Halfman, F. C. L. Wong and D. W. Jay, *Anal. Chem.*, 1985, **57**, 1928.
2. F. V. Bright and L. B. McGown, *Talanta*, 1985, **32**, 15.
3. F. V. Bright, R. A. Bunce and L. B. McGown, *Org. Prep. Proc. Intl.*, in press.
4. J. H. Fendler and E. J. Fendler, *Catalysis in Micellar and Macromolecular Systems*, Academic Press, New York, 1975.
5. A. Malliaris, J. LeMoigne, J. Sturm and R. Zana, *J. Phys. Chem.*, 1985, **89**, 2709.
6. D. A. Barrow and B. R. Lentz, *J. Biochem. Biophys. Meth.*, 1983, **7**, 217.
7. M. Martin and L. Lindqvist, *J. Lumin.*, 1975, **10**, 381.

ANALYSIS OF ANTHRANILIC ACID BY LIQUID CHROMATOGRAPHY

THOMAS M. SCHMITT*, ROBERT J. ZIEGLER†, EAD S. MUZHER,

ROBERT J. DOYLE‡ and JAMES L. FREERS§

Central Research and Development, BASF Wyandotte Corporation, Wyandotte, MI 48192, U.S.A.

(Received 27 November 1985. Accepted 23 March 1986)

Summary—Analytical methods for the assay of anthranilic acid and for determination of the impurities methyl anthranilate, anthranoylanthranilic acid and 3- and 4-aminobenzoic acid are described. A Microbondapak C18 column is used for both the assay and the impurity determination. The assay is based on isocratic development with a mobile phase of 35:65 v/v methanol/pH-3 phosphate buffer, with benzoic acid as internal standard. The impurities are separated by gradient elution. The standard deviation of the assay method is about 1% and the limit of detection for the impurities is about 0.01%.

Anthranilic acid (AA) is a chemical intermediate widely used in the synthesis of pharmaceuticals, perfumes, dyes, resins and agricultural chemicals. It occurs biologically as a tryptophan metabolite. Depending on the process used in its manufacture, synthetic AA may be contaminated with low levels of methyl anthranilate and anthranoylanthranilic acid. The structures are shown in Fig. 1. *m*-Aminobenzoic acid and *p*-aminobenzoic acid may also be present.

AA may be titrated with base, with nitrous acid, or with bromine.^{1,2} None of these approaches is selective in the presence of the usual impurities. Colorimetric methods are more selective, although other organic amines interfere.^{3,4} More specificity is attained by use of paper chromatography⁵ or thin-layer chromatography.^{6,7} AA has been determined in biological samples by gas chromatography after formation of derivatives^{8,9} or conversion into methyl salicylate.¹⁰ Liquid chromatographic procedures for determining trace levels of AA in biological samples have recently been published.^{11,12} AA was one of a series of substituted benzoic acids studied in the development of a semi-empirical liquid-chromatography optimization strategy.¹³

Methyl anthranilate is a natural product with a strong odour, occurring in materials such as orange blossoms, grapes and jasmine. It has been determined in wine and other grape beverages by spectrophotometry,¹⁴ fluorimetry,¹⁵ gas chromatography^{16,17} and liquid chromatography with fluorimetric detection.¹⁸ The literature is silent on

determination of anthranoylanthranilic acid. Two recent papers show the use of HPLC to separate the three aminobenzoic acid isomers from each other. One is a normal phase method,¹⁹ the second a reversed-phase method with added zinc.²⁰

Because we use AA in the synthesis of specialty products, we have investigated HPLC for the quality control of this compound.

EXPERIMENTAL

Apparatus

The HPLC system consisted of two model 6000A pumps controlled by a model 660 Solvent Programmer, a 3.9 × 300 mm μ Bondapak C18 column, a model U6K injector, a model 440 fixed-wavelength ultraviolet absorbance detector used at 254 nm (all from Waters Associates), and a Honeywell Elektronik 196 2-pen strip-chart recorder. Peak areas were integrated by a Hewlett-Packard model 3354 data system.

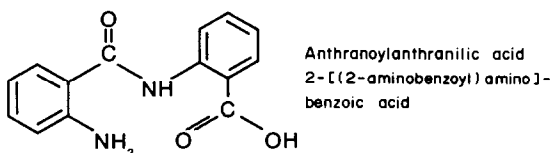
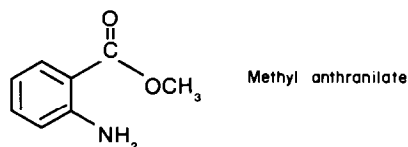
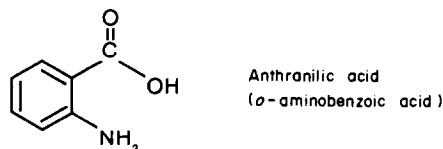


Fig. 1. Structures of the compounds.

*Author to whom correspondence should be sent.

†Present address: Waters Associates, Inc., Milford, MA 01757.

‡Present address: Widger Chemical Corporation, Warren, MI 48090.

§Present address: Ford Motor Company, Allen Park Test Laboratory, Allen Park, MI 48101.

Reagents

Methanol, sodium hydroxide, phosphoric acid and glacial acetic acid were all ACS reagent grade. The sodium acetate trihydrate was Fisher HPLC grade. The benzoic acid was US National Bureau of Standards reference material. The anthranilic acid was prepared by vacuum sublimation of recrystallized AA (Kodak). Methyl anthranilate (Aldrich) was used as received. The anthranoylanthranilic acid was synthesized by BASF AG. Sodium phosphate buffer solutions, 0.02M, pH 3.0 or 6.0, was prepared by diluting 1.35 ml of reagent grade concentrated phosphoric acid to 1 litre with demineralized water, and adjusting the pH by dropwise addition of 50% reagent grade sodium hydroxide solution; these solutions are susceptible to microbial growth, but are stable for one week if refrigerated.

Procedures

For assay, calibration solutions were prepared by weighing about 0.1 g of sublimed AA and 0.3 g of benzoic acid (as internal standard) into a 100-ml standard flask. Methanol was added to dissolve the mixture and make the solution up to volume. A second standard was prepared in the same way, along with duplicate solutions of samples mixed with internal standard. The volume injected was 10 μ l. A typical chromatogram is shown in Fig. 2.

For determination of the aminobenzoic acid isomers, the same procedure was used, but without the internal standard and with only one solution of each sample. To increase the sensitivity, 100- μ l injections were made. A typical chromatogram is shown in Fig. 3.

For determination of methyl anthranilate and anthranoylanthranilic acid, a calibration solution of the two impurities was made by weighing 30 mg of the first and 2 mg of the second into a 50-ml standard flask, adding 2 ml of methanol to dissolve the materials, then diluting to volume with pH-6 buffer. This standard solution was diluted tenfold before use. The sample solution was prepared by

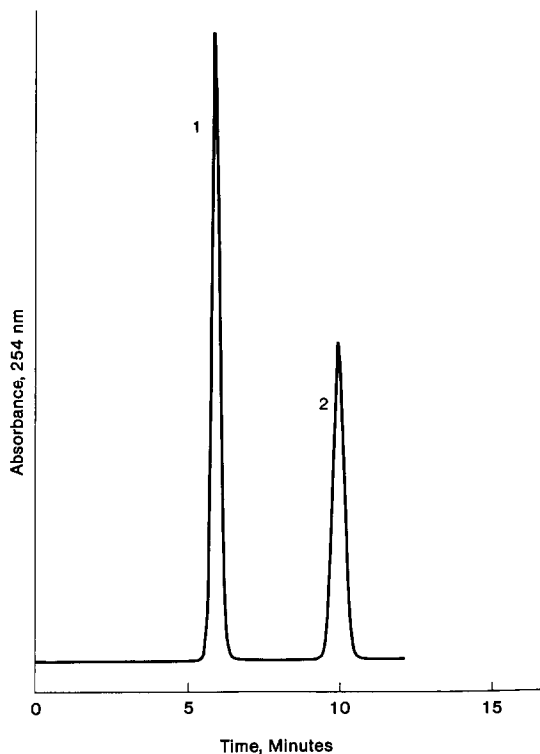


Fig. 2. Assay of anthranilic acid. Peak 1, anthranilic acid; peak 2, benzoic acid (internal standard).

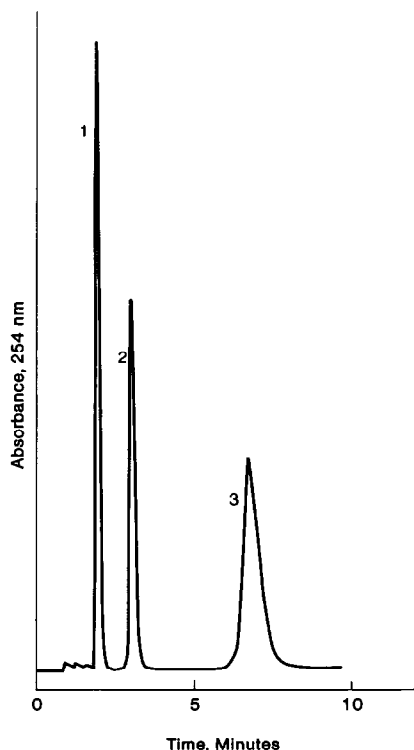


Fig. 3. Aminobenzoic acid isomers. Peak 1, 4-aminobenzoic acid; peak 2, 2-aminobenzoic acid; peak 3, 3-aminobenzoic acid.

dissolving 0.3 g in 15 ml of methanol in a 100-ml standard flask, and diluting to volume with pH-6 buffer. Injections of 25 μ l were made. Figure 4 shows a chromatogram.

Chromatographic conditions

For assay of anthranilic acid, the mobile phase was a 35:65 v/v mixture of methanol and aqueous pH-3.0 sodium phosphate buffer, at a flow-rate of 1.5 ml/min. For determination of methyl anthranilate and anthranoylanthranilic acid gradient elution was used: solvent A was aqueous pH-6.0 sodium acetate buffer, solvent B was methanol. The gradient was linear from 0 to 60% B in 35 min, then from 60 to 100% B in 4 min (to cleanse the column of impurities from the aqueous buffer), then linear from 100 back to 0% B in 10 min (to prepare for the next injection). For determination of the aminobenzoic acid isomers, the mobile phase was a 1:1 v/v mixture of methanol and 0.02M aqueous acetic acid, and the separation was done on a Waters Radial PAK C18 cartridge at a flow-rate of 2.5 ml/min.

The eluents were filtered (0.45- μ m membrane) and degassed before use. To avoid the corrosive effects of stagnant buffer solutions, demineralized water and then pure methanol were pumped through the entire system at the end of each day's analysis.

RESULTS AND DISCUSSION

Since the aminobenzoic acid isomers, anthranoylanthranilic acid and the internal standard, benzoic acid, are organic acids, their polarity can be controlled by adjusting the pH of the eluent. We thus have two means of controlling retention on the column: acid strength and solvent polarity.

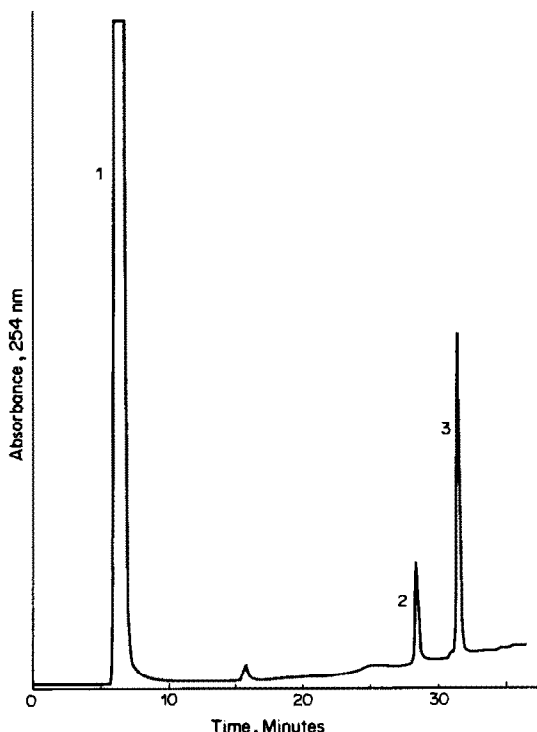


Fig. 4. Determination of anthranoylanthranilic acid (peak 2) and methyl anthranilate (peak 3) in anthranilic acid (peak 1).

We chose to make the assay by an internal standard procedure. Benzoic acid was an excellent choice because it is eluted as a symmetrical peak under the same conditions as anthranilic acid. In addition, it is available in high purity (our NBS standard was certified as 99.958% pure).

The injection size for the impurity determination was deliberately made large enough for the main component, AA, to cause saturation of the recorder trace. This permits more accurate quantification of the low-level impurities.

The precision of the instrumentation for assay was determined by making multiple injections of the same solution. The relative standard deviation was 0.4%. The precision of the entire procedure was determined by making single injections of ten separate calibration solutions. The relative standard deviation was 2.8%. The absolute accuracy of the method is, as with all chromatographic methods, at the mercy of the stan-

dard chosen for calibration. If the standard chosen is, for example, only 99% pure, then the results of the HPLC assay will be high by 1% (relative). The HPLC method is at a disadvantage to the acidimetric or diazotization titration procedures in this regard, since these titrants can be independently standardized. However, various impurities cause positive interference in the titration methods, but will not affect the HPLC result.

The precision of the determination of anthranoylanthranilic acid and methyl anthranilate was measured by making single injections of five separate solutions of an AA sample fortified with the two impurities at the 0.2% level for the former and 0.6% for the latter, the relative standard deviations found being 3.1 and 1.2% respectively. This is quite acceptable for impurity measurement. To estimate the accuracy of the procedure, a recovery study was conducted; the results are shown in Table 1. The accuracy is acceptable, but does not approach 100%. We believe the problem is the long retention times of the two impurities. In a gradient-programming method like this one, impurities from the aqueous solvent begin to be eluted from the column toward the end of the chromatogram, making integration of the peaks of interest more difficult. Modifications aimed at shortening the retention times for the impurities would be expected to give improved accuracy.

Because of the synthesis route, 3- and 4-amino-benzoic acid are not typical impurities in commercial AA. We did, however, modify our system to separate these compounds also. The required baseline resolution is obtained by using a lower pH and higher methanol concentration than for the assay. Interestingly, the order of elution differs from that reported in the literature.^{19,20} This shows the power of being able to modify elution behaviour by means of both solvent polarity and acid strength.

These methods have been used in our laboratory for more than eight years, without serious difficulty.

CONCLUSION

HPLC is a powerful and convenient tool for the analysis of AA. It is equally effective for assay and for impurity determination. HPLC is superior to the other techniques in that it is much less subject to interference than the classical analytical techniques.

Table 1. Recovery study

Run	Anthranoylanthranilic acid			Methyl anthranilate		
	Added, %	Found, %	Recovery, %	Added, %	Found, %	Recovery, %
1	0.0	0.025	—	0.0	0.0	—
2	0.042	0.070	104	0.16	0.14	88
3	0.082	0.11	103	0.31	0.28	90
4	0.13	0.16	103	0.50	0.48	96
5	0.17	0.17	87	0.66	0.61	92
6	0.24	0.32	120	0.90	0.84	93

Benzoic acid is a suitable internal standard for the assay procedure.

REFERENCES

1. L. G. Hargis and D. F. Boltz, *Talanta*, 1964, **11**, 57.
2. M. Z. Barakat, A. S. Fayzalla and S. El-Aassar, *Microchem. J.*, 1973, **18**, 308.
3. D. Kupfer and D. E. Atkinson, *Anal. Biochem.*, 1964, **8**, 82.
4. V. I. Korotkova, V. N. Noskov and V. P. Chistota, *Zh. Analit. Khim.*, 1975, **30**, 1607; *Anal. Abstr.*, 1976, **31**, 1030.
5. M. Y. Kamel and R. A. Hahmed, *J. Chromatog.*, 1978, **157**, 440.
6. M. P. Walsh, *Clin. Chim. Acta*, 1965, **11**, 263.
7. R. Humbel and C. Marsault, *J. Chromatog.*, 1973, **79**, 347.
8. K. Hirano, K. Mori, N. Tsuboi, S. Kawai and T. Ohno, *Chem. Pharm. Bull.*, 1972, **20**, 1412; *Anal. Abstr.*, 1973, **24**, 1036.
9. J. F. Douglas and Y. Philopoulous, *J. Pharm. Sci.*, 1977, **66**, 1645.
10. K. Hirano, M. Naruse, S. Kawai and T. Ohno, *J. Chromatog.*, 1972, **70**, 53.
11. C. Escande, B. Bousquet and C. Dreux, *Feuill. Biol.*, 1979, **20**, 121; *Anal. Abstr.*, 1980, **39**, 2D208.
12. H. H. Schott, D. Langenback-Schmidt and K. Zinke, *J. Chromatog.*, 1982, **245**, 85.
13. S. L. Deming and M. L. H. Turoff, *Anal. Chem.*, 1978, **50**, 547.
14. R. L. Brunelle, G. E. Martin and V. G. Ohanesian, *J. Assoc. Off. Agric. Chem.*, 1965, **48**, 341.
15. D. J. Casimir, J. C. Moyer and L. R. Mattick, *J. Assoc. Off. Anal. Chem.*, 1976, **59**, 269.
16. A. Zlatkis, G. R. Shoemaker and P. G. Simmonds, *J. Gas Chromatog.*, 1967, **5**, No. 3, 19A.
17. R. R. Nelson, T. E. Acree, C. Y. Lee and R. M. Butts, *J. Assoc. Off. Anal. Chem.*, 1976, **59**, 1387.
18. A. T. Rhys-Williams and W. Slavin, *J. Agric. Food Chem.*, 1977, **25**, 756.
19. U. Streule and A. V. Wattenwyl, *Chromatographia*, 1979, **12**, 25.
20. V. Walters and N. V. Raghavan, *J. Chromatog.*, 1979, **176**, 470.

THE EFFECT OF HYDROLYSED ALUMINIUM SPECIES IN FLUORIDE ION DETERMINATIONS

W. F. PICKERING

Chemistry Department, University of Newcastle, N.S.W. 2308, Australia

(Received 27 January 1986. Accepted 13 March 1986)

Summary—The limited ability of added ligands to mask the interference of Al(III) in fluoride determination by means of ion-selective electrode measurements has been re-examined, and an explanation based on competing equilibria developed. When the Al(III) level exceeds the fluoride content, the excess of Al(III) forms colloidal hydrous oxide particles in the pH range 4-9, and this solid strongly sorbs fluoride. Under these conditions, masking ligands have to promote both decomposition of AlF_x soluble complexes and release of sorbed fluoride by substrate dissolution. The latter is a slow process, particularly with an "aged" gel, and long equilibration periods can be required for total fluoride release. Ion-chromatography studies have shown that the amount of fluoride lost through sorption on the hydrous oxide particles (isolated during the membrane filtration/degassing step) can be quite high. By analogy, preliminary phase separation of natural water samples must also separate sorbed fluoride and soluble fluoride complexes. In the presence of Al(III), accurate analysis for fluoride requires removal of the aluminium, or isolation of fluoride from the matrix, or very careful pretesting of masking efficiencies.

The interference of aluminium in fluoride ion determinations is usually attributed to the formation of soluble aluminium fluoro-species, and the influence of this reaction can be minimized by (i) isolating the fluoride as a volatile product (e.g., a microdistillation step is included in some automated fluoride analysers), (ii) chemical removal of the aluminium (e.g., solvent extraction with 10% 8-quinolinol solution in can result¹ in nearly complete fluoride recoveries, with initial aluminium levels up to 500 mg/l., (iii) decomposition of the AlF_x complexes.

The last approach has been widely adopted in conjunction with fluoride ion-selective electrode measurements, since competing ligand species can be conveniently added with the total ionic strength adjustment buffer (TISAB). The ability of various masking agents to release fluoride has been examined by several groups; citrate,²⁻⁶ DCTA (*trans*-1,2-diaminocyclohexane-*N,N,N',N'*-tetra-acetic acid)⁷ and Tiron⁸ are said to offer the best recoveries of fluoride. The different views expressed arise in part from the fact that the degree of release varies with buffer pH, reagent concentration, and relative amounts of aluminium and fluoride present.

The optimum pH for low-level fluoride determinations has been given as around 5, and at this pH citrate has been demonstrated³ to be the most efficient masking agent for relatively low levels of aluminium. In another study,⁴ involving ten different formulations, 1M triammonium citrate (plus DCTA) was found to be the most effective reagent. It was noted that the sensitivity range could be extended by using more dilute buffers, but the penalty was some interference from magnesium and aluminium. However, if the citrate level is kept constant during successive dilution, the aluminium interference effects decline,

and in 0.5M citrate buffer (pH 6) the permissible aluminium concentration increases markedly with decreasing fluoride concentration.⁶

At low fluoride levels, the ion-selective electrode response at pH > 8 can be in error (because of interference by hydroxide ions), but use of higher pH reduces aluminium interference. At pH ~ 8, recommended masking agents include 0.25M sodium citrate,⁵ 1M sodium citrate² and tris(hydroxymethyl)aminomethane.³ At pH 12, formation of the tetrahydroxo-aluminate ion tends to eliminate aluminium interference.²

The formulations proposed by electrode manufacturers are usually based on acetate buffer systems with added citrate or DCTA, and these cope adequately with low levels of aluminium, iron and magnesium. With higher aluminium contents modified reagents are needed, and this aspect is not always recognized by novice analysts. It has been shown,² for example, that in the presence of 500 mg/l. aluminium the interference effect is most marked when the Al:F ratio exceeds 10:1.

For the analysis of aluminium fluoride compounds (such as cryolite) or determination of fluoride in aluminium compounds, the materials are usually fused (or dissolved) in alkaline media. Aluminium interference has then been minimized by making measurements at pH 12, or at pH 8 in presence of 1M sodium citrate,² by extensive dilution,⁹ by complexation with DCTA,¹⁰ or by masking with sulphosalicylate and EDTA (pH ~ 9.5).¹¹

An important aspect, rarely mentioned by authors, is the time required for the masking of aluminium to become complete. In their detailed study, Nicholson and Duff⁴ noted, for example, that a minimum time of 20 min was desirable but 24 hr was preferable. The

validity of this statement has been confirmed in a recent study of fluoride sorption on hydroxo-aluminium species.¹² This investigation also provided an insight into the competing equilibria involved, and the analytical aspects are described in this communication.

The study described here also included some measurements by ion chromatography (IC), a technique being promoted as an alternative to ion-selective electrode potentiometry. A recent paper¹³ describes successful application of IC to the simultaneous determination of inorganic anions in Bayer and aluminium process liquors, but another investigator¹⁴ found it necessary to remove aluminium beforehand (by passage through a cation-exchange column in H^+ -form).

EXPERIMENTAL

Measurement techniques

For the specific ion-selective electrode measurements a Philips® fluoride electrode and meter (model PW 9409) were utilized. Calibration was based on dilution of $10^{-2}M$ sodium fluoride stock solution, and if TISAB was present Nernstian response was observed at concentrations $> 10^{-4}M$ (in presence of $> 0.5M$ masking agent) or $> 10^{-5}M$ (with dilute TISAB). Three TISAB solutions were tested: TISAB-A (1M acetic acid, 1M NaCl, 1mM sodium citrate, pH 5-5.5), TISAB-B (1M acetic acid, 1M NaCl, 4 g/l. DCTA, pH 5-5.5) and TISAB-C (0.5M KCl, 0.5M potassium acetate, 1M sodium citrate, pH ~ 7.5). The onset of deviation from linearity is commonly explained in terms of the solubility of the LaF_3 crystal¹⁵⁻¹⁷ but a later study³ has indicated that other factors, including fluoride impurity in reagents, can be involved. Comparison tests demonstrated, for example, that the linearity limit varies with both the chemical composition of the buffer/complexing system and pH, the optimum pH for sub-mg/l. fluoride measurements being around 5.

The equipment used for anion determination by liquid chromatography consisted of a Kortec pumping unit, a Hamilton PRP-X1000 column, a 500- μ l sample loop, and an Erma ERC-751 refractive-index detector unit. The eluent (0.003M benzoic acid, pH 6.3) was delivered at 2 ml/min, the fluoride elution time was approximately 2 min, and the calibration graph (based on peak height) was linear for fluoride down to 0.2 mg/l.

Aluminium interference studies

Into clean acid-washed plastic vials were added standard sodium fluoride solution, various volumes of 0.0023M aluminium nitrate (pH 2) and enough distilled water and 0.1M nitric acid (when required) to yield 25.0 ml of test solution having a pH of 5-5.5; fluoride levels of 1, 6, or $10 \times 10^{-4}M$, and aluminium contents ranging from 0 to 25 mg/l, were examined.

The vials were sealed and their contents mixed overnight in an end-over-end stirrer unit immersed in a water-bath held at 25°. Next day the vials were centrifuged before aliquots of the solution were mixed with an equal volume of one of the TISAB solutions. The response of the fluoride electrode was then noted. In a later series of studies, the TISAB/test solution mixture was allowed to stand overnight before the potentials were measured. Potential measurements were also made on the original test solutions (*i.e.*, with no TISAB) in order to assess the decrease in fluoride signal as a result of the aluminium present, and to confirm that the system pH was within the range 5-6.

Before introduction of test aliquots into the chromatography unit, the vial contents were filtered (by suction)

through a 0.45- μ m membrane disc. This step degassed the liquid and removed any particulate solids. Fluoride measurements were also made on test samples at various time between 15 min and 4 hr after the aluminium and fluoride solutions were mixed.

RESULTS AND DISCUSSION

The results obtained are typified by the curves shown in Fig. 1. With TISAB/complexing solutions and the fluoride electrode, nearly complete fluoride recovery was obtained only in the presence of a high concentration of ligand, with prolonged contact between masking and test solutions.

In many respects these curves complement the results reported by Kauranen,³ who observed that the recovery of fluoride by use of TISAB formulations declined with increasing aluminium concentration. The effect was most marked with reagents having low ligand concentrations and low system pH (*e.g.*, 4.6). With 1 mg/l. fluoride and 2-20 mg/l. aluminium (*i.e.*,

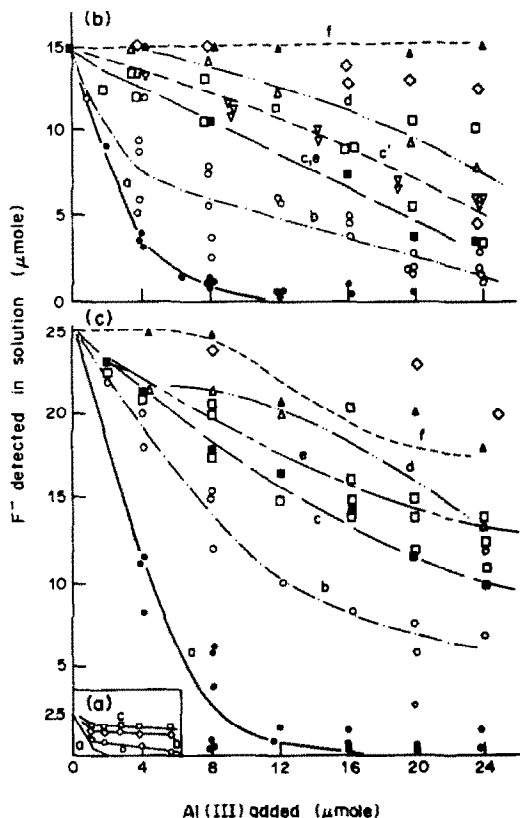


Fig. 1. The effect of added Al(III) on the amount of F^- detected in solution. Initial NaF concentrations were: a, $1 \times 10^{-4}M$ (*i.e.*, 2.5 μ mole/25 ml); b, $6 \times 10^{-4}M$; c, $1 \times 10^{-3}M$. a (●) Free F^- by ISE without TISAB. b (○) Apparent F^- by ISE with TISAB-A. c (■) Total F^- in solution by IC with 15-180 min delay before filtration. c' (▽) Total F^- in solution by IC with no delay before filtration. d (△) Apparent F^- by ISE with TISAB-C. e (□) Apparent F^- by ISE with TISAB-B. f (▲) Apparent F^- by ISE after overnight treatment with TISAB-C. (◇) Apparent F^- by ISE after overnight treatment with TISAB-B.

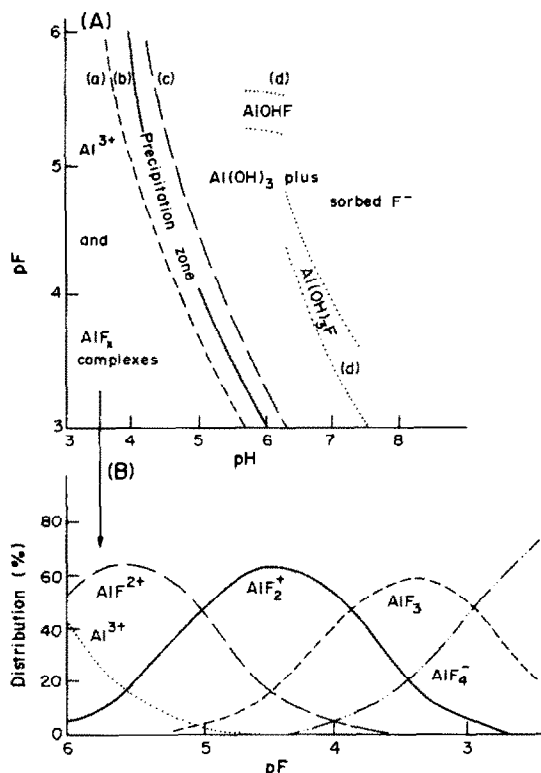


Fig. 2. Effect of pH and pF on the distribution of Al(III). (A) Zones of Al(OH)₃ and AlF_x complex domination. Onset of precipitation is calculated for initial Al(III) levels of (a) 10⁻²M, (b) 10⁻³M, (c) 10⁻⁴M. The fluoro-hydroxo complex zones reported by Dyrsen¹⁹ are shown by (d). (B) Dependence of AlF_x speciation on equilibrium F⁻ level.

mole ratio of Al:F > 1.4), nearly total release of fluoride (after ~ 15 min interaction) was observed only with 0.4M citrate (pH 5 or 7.7) or Tris-buffer (pH 8.4). With Al:F ~ 1 or less, >90% recovery was achieved with buffers containing 0.1M sodium citrate (pH 4.6 and 5), 0.4M sodium tartrate (pH 5), 0.006–0.1M DCTA (pH 5) and 0.1M Tiron (pH 5). In our studies, using "aged" mixtures, recovery levels were much lower (Fig. 1A).

Calculations based on the relative stability of the soluble complexes formed by aluminium with fluoride and other ligands, indicate that fluoride recovery should be nearly complete with most of the buffer/ligand mixtures tested. Such calculations, however, ignore the limited lability of aluminium complexes, the limited solubility of hydrous aluminium oxide, and sorption of fluoride by colloids.

Figure 2A shows the pF–pH regions associated with a transition from predominance of AlF_x to that of Al(OH)₃ (as calculated from stability constant and solubility product data), and it will be noted that at pH 5 or above the dominant aluminium species is the hydrous oxide. The presence of ligands can slow the hydrolysis and coagulation of colloidal particles, so the contribution of this phase (which strongly sorbs fluoride from solution^{12,18}) can be time-dependent. The sorption capacity is maximal at around pH 6,

declining rapidly to nearly zero in the region pH 7–9 because of dissolution of the solid to form Al(OH)₄⁻.¹²

Curves *a* in Fig. 1 show how the amount of free fluoride in solution decreased with increasing addition of aluminium ions. When the molar ratio of F⁻:Al(III) exceeded ~2, the dominant reaction was formation of AlF_x species, with the relative distribution of AlF₂⁺, AlF₂⁺ and AlF₃ being predictable from the equilibrium fluoride level by use of a diagram such as Fig. 2B. At lower F⁻:Al ratios, hydrolysis of aluminium was not totally suppressed, and the diminution in free fluoride was attributed to a combination of complex formation and sorption of fluoride by hydrous aluminium oxide.

In the absence of a solid phase, the release of fluoride on addition of TISAB solutions is determined by the efficiency of the ligand-exchange process, a step which can be measurably slow, owing to the limited lability of aluminium complexes. When a hydrous aluminium oxide phase is present, total retrieval of fluoride requires either dissolution of this solid phase or complete desorption of sorbed fluoride, both potentially much slower processes.

The prefiltration step used in ion-chromatography removed most of any solid phase present, hence the IC curves (*c'* and *c*) indicate the amount of fluoride sorbed by the aluminium gel. It was found that the fraction "lost" was smaller when the vial contents were filtered shortly after mixing of the aluminium and fluoride (at pH 5–6), as in curve *c'*, than when there was a delay of 15–180 min (curve *c*). This difference in behaviour can be attributed to the rates of the hydrolysis reaction and the sorption process.

Centrifuging the vials before removing aliquots for ion-selective electrode measurements settled little of the colloidal hydroxide, as demonstrated by the fact that overnight contact with some ligand mixtures yielded almost complete fluoride recoveries.

The relative positions of the chromatographic results (curves *c*) and TISAB–B release values (curves *e*) in Fig. 1 imply that DCTA (4 g/l.) reacts primarily with AlF_x, with sorbed fluoride only being released on prolonged contact (points ◇). TISAB–A containing 0.1M sodium citrate (curves *b*) appears to displace fluoride only partially from AlF_x, whereas 1M citrate (curves *d*) seems to retrieve about half the sorbed fluoride, this proportion increasing with contact time (curves *f*). With the mixed phase systems, the behaviour was sensitive to change in experimental parameters (*e.g.*, aging and reaction times) and this led to scatter in the results (*e.g.*, curves *b*). As expected, with lower initial fluoride level the position of curve *a* moved to the left, that is, onset of hydrous oxide formation occurred at lower total aluminium contents (*cf.* Fig. 1A, B and C).

The thermodynamic data associated with the formation of hydroxo and fluoro complexes have recently been re-evaluated.¹⁹ The predominance diagram in Fig. 2 clearly outlines how pH and pF control the nature of the major aluminium species

present under different conditions. In acid media, the major species are AlF_x (where x varies from 1 to 3, depending on pH); at $\text{pH} > 7$, the dominant species in solution is $\text{Al}(\text{OH})_4^-$. The formation of $\text{Al}(\text{OH})_4^-$ is a masking process, so the high fluoride recoveries obtained by using complexing solutions of $\text{pH} > 8$ probably reflect a combination of this reaction and dissolution of residual traces of hydrous aluminium oxide by added ligands.

Analytical considerations

The analytical significance of this study depends on the nature of the sample being examined. For example, the pH of natural waters tends to lie in the pH range 4–8, so any aluminium present should be in the form of a soluble complex (e.g., aluminium fulvate) or an aged hydroxy species. The amount of the latter may be minimal owing to sorption on other colloidal matter or coagulation, with subsequent gravitational settling into the sediment phase. Any residual solid (plus sorbed fluoride) would normally be removed during the membrane filtration step that usually precedes analysis. The aluminium complexes in solution should react smoothly with added TISAB/ligand mixtures (provided sufficient time is allowed), leading to almost total recovery of soluble fluoride content.

When the original fluoride-bearing samples are solids, their total dissolution may require treatment with strong acid or strong base, or alkaline fusion followed by acidification. The resulting sample solutions, of very low or very high pH may not be adjusted to the desired analytical pH range (5–6) until just before addition of TISAB (for ion-selective electrode measurement) or degassing membrane-filtration (for ion chromatography). Under these circumstances the amount of hydroxo-aluminium species formed (when $[\text{Al}(\text{III})] > [\text{F}^-]$) will then vary with the experimental procedure, and loss of fluoride through sorption on colloids could be quite variable.

Although the difficulties associated with aluminium interference in measurements with fluoride-selective electrodes have been studied in some detail before, time-variable effects have not usually received sufficient emphasis.

For determinations based on anion chromatography, much remains to be learned about

aluminium interference effects. With excess of aluminium present, low values seem inevitable unless the aluminium is removed (e.g., by extraction or ion-exchange) before the pH is brought into the range for precipitation of the hydrous oxide. Even with $[\text{F}^-] > [\text{Al}(\text{III})]$, the presence of AlF_x complexes has been observed to influence the shape and position of the fluoride elution peak, signifying only partial break-up of the complexes on migration through the column. Some investigators have apparently overcome such problems,¹³ but caution is advised whenever experimental conditions are changed, e.g., use of a different eluent, column, or detector.

In any study, the analyst must carefully define exactly what is being determined (e.g., free or total fluoride), and must then ensure that the procedure adopted provides a good estimate of it.

Acknowledgements—This project was supported by the Australian Research Grant Scheme, and this help is gratefully acknowledged. The experimental studies were conducted by Helen Farrah and Janece Slavek, and the author is greatly indebted to these conscientious and capable research assistants.

REFERENCES

1. K. Nicholson and E. J. Duff, *Analyst*, 1981, **106**, 904.
2. R. T. Oliver and A. G. Clayton, *Anal. Chim. Acta*, 1970, **51**, 409.
3. P. Kauranen, *Anal. Lett.*, 1977, **10**, 451.
4. K. Nicholson and E. Duff, *ibid.*, 1981, **14**, 493.
5. B. Vickery and M. L. Vickery, *Analyst*, 1976, **101**, 445.
6. N. Shiraishi, Y. Murata, G. Nakagawa and K. Kodama, *Anal. Lett.* 1973, **6**, 893.
7. J. E. Harwood, *Water Res.*, 1969, **3**, 273.
8. S. Tanikawa, H. Kirhari, N. Shiraishi, G. Nakagawa and K. Kodama, *Anal. Lett.*, 1975, **8**, 879.
9. J. C. Van Loon, *ibid.*, 1968, **1**, 393.
10. M.A. Peters and D. M. Ladd, *Talanta*, 1971, **18**, 655.
11. T. A. Palmer, *ibid.*, 1972, **19**, 1141.
12. H. Farrah, J. Slavek and W. F. Pickering, submitted to *Aust. J. Soil Sci.*
13. Kwat The and R. Roussel, *Light Met.*, 1984, 115.
14. B. E. Andrew, private communication.
15. M. S. Frant and J. W. Ross, *Science*, 1966, **154**, 1553.
16. P. A. Evans, G. J. Moody and J. D. R. Thomas, *Lab. Pract.*, 1971, **20**, 644.
17. E. W. Baumann, *Anal. Chim. Acta*, 1971, **54**, 189.
18. C. A. Bower and J. J. Hatcher, *Soil Sci.*, 1967, **103**, 151.
19. D. Dyrrsen, *Vatten*, 1984, **40**, 30.
20. V. Zutic and W. Stumm, *Geochim. Cosmochim. Acta*, 1984, **48**, 1493.

ACID-BASE AND CHELATOMETRIC PHOTO-TITRATIONS WITH PHOTSENSORS AND MEMBRANE PHOTSENSORS

TSUTOMU MATSUO

Kobe Technical College, Maikodai, Tarumi-ku, Kobe-shi 655, Japan

YOSHITAKA MASUDA and EIICHI SEKIDO

Department of Chemistry, Faculty of Science, Kobe University, Nada-ku, Kobe-shi 657, Japan

(Received 13 December 1984. Revised 25 February 1986. Accepted 12 March 1986)

Summary—Photosensors (PS) and membrane photosensors (MPS), which can be immersed in the test solution and facilitate the measurement of concentration, have been developed by miniaturizing an optical system consisting of a light source and a photocell. For use in acid-base or complexometric titrations a poly(vinyl chloride) membrane containing an acid-base or metallochromic indicator can be applied as a coating to the photocell. Spectrophotometric determination of copper(II), and photometric acid-base and chelatometric titrations have been performed with the PS and MPS systems.

The absorbance of solutions is normally measured with a spectrophotometer and this instrument can therefore be employed to follow the course of spectrophotometric titrations. Modifications have been made to the spectrophotometer cell to give flow-through operation^{1,2} and facilitate titration.³ A photodiode-array has also been used in a titrator.⁴

In the work described here, the spectrophotometer is replaced by a photosensor (PS) system consisting of a miniaturized and integrated light-source and photocell which can be directly immersed in the test solution. Furthermore, if the photocell surface is coated with a poly(vinyl chloride) (PVC) membrane⁵ incorporating an acid-base or metallochromic indicator, the sensor can be converted into a membrane photosensor (MPS) for use as the end-point detector in titrations.

EXPERIMENTAL

Reagents

All the chemicals used were of analytical grade. In the preparation of the membrane, low molecular-weight PVC and tetrahydrofuran (THF), dioctyl phthalate (DOP) and Eriochrome Black T (EBT) were used. Solutions (0.1M) of sodium hydroxide and hydrochloric acid were standardized by use of 0.1M potassium phthalate. Methyl Orange was dissolved in distilled water to give a 0.1% solution. Stock solutions of 0.2M copper sulphate, 0.2M magnesium chloride, 0.2M ferric chloride and 0.05M zinc sulphate were standardized by complexometric titration⁶ with 0.01M EDTA. An ammonia-ammonium chloride buffer solution (pH 10) was used to adjust the pH of the test solution. A methanolic solution of EBT (0.5%) was used as indicator.

Apparatus

A digital multimeter (SOAR ME-530) was used to display the resistance (R) of the CdS photocell and the illuminance of the photo-IC (i.e., photo-diode with an integral amplifier). Light-emitting diodes (LED) having a peak wavelength of 555 or 660 nm were used. Hamamatsu CdS photocells and a Siemens TFA 1001W photo-IC were used.

A stabilized d.c. power supply (Kikusui Model 7326) was used for the light sources, the voltage (1.5–2.5 V) being varied to give the appropriate light output.

RESULTS AND DISCUSSION

Construction of the photosensor and membrane photosensor

Two types of photosensor were constructed. The membrane versions are shown in Fig. 1. The optical system of type A consists of an LED and a CdS photocell, and that of type B of a small lamp with a lens and a photo-IC. When the polycarbonate tubes are removed, both types may be employed as immersion-type sensors.

The absorbance is measured as a function of the resistance (R) of the CdS photocell in type A by means of a digital multimeter. The light-emitting diode, which has a high light output and a hemispherical top is suitable as a source of illumination. In order to maximize sensitivity, the wavelength of the LED is varied to give a colour (red, green or yellow) to match the absorption profile of the test solution. This can be done by using a multicolour LED with a simple additional circuit.

An amplifier is included in the photo-IC used in the type B sensor and the circuit shown in Fig. 1 is used for measuring the illuminance. If a digital multimeter is connected to the circuit, the illuminance is transduced into a voltage signal (1 mV \equiv 1 lux). Then from the illuminances observed with the PS or MPS immersed in the test solution and in water, the absorbance of the test solution can be calculated. A suitable wavelength range is selected by means of a coloured cellophane filter affixed to the lens. The lamp, filter and photo-IC are all sealed in epoxy resin to prevent contact with the test solution.

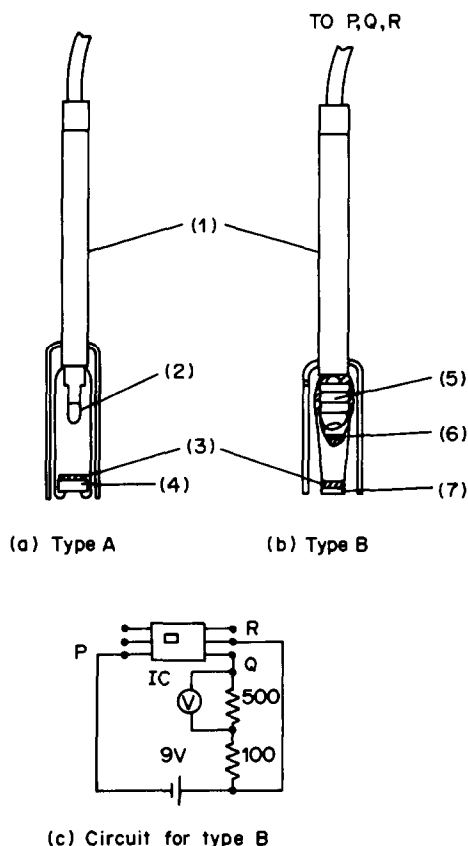


Fig. 1. Construction of photosensor and photomembrane sensor. (1) Polycarbonate tube, (2) LED, (3) photomembrane, (4) CdS photocell, (5) lamp, (6) filter, (7) photo-IC.

Type A photosensors are suitable for measuring a continuous change of absorbance such as that observed in the course of a photo-titration; those of type B may conveniently be used to measure concentrations. Since both types measure absorbance, the test solution must be coloured. Colourless solutions must have an appropriate indicator reagent added, but an alternative MPS has been constructed. This sensor has a membrane coated onto the CdS photocell or photo-IC. The membrane is prepared by dissolving 1 g of PVC, 1 g of DOP and 0.15 g of EBT (or other indicator) in 30 ml of THF, spreading the solution on a glass plate to a thickness of 1 mm and letting it dry for one day. A piece of the resulting film is then attached to the photo-IC or the CdS photocell at the point on which the incident radiation falls.

Spectrophotometric determinations and complexometric photo-titrations

A calibration graph for copper(II) was obtained with a PS (type A) with a red-emitting LED. Copper(II) solutions covering a range of concentrations were placed in 10-ml sample tubes. The PS was immersed in each solution in turn and the R values of the CdS photocell were measured. The absorbance was a linear function of copper(II) concentration

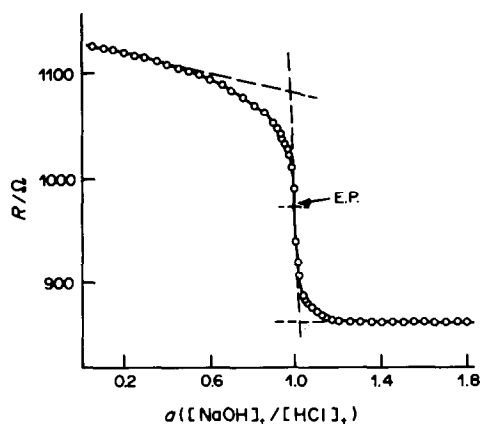


Fig. 2. Acid-base photo-titration curve for 0.1M HCl with 0.1M NaOH, with a type A PS (with green-emitting LED).

between 4.0 and 18mM with a sensitivity (slope) of 48 l./mole. The same graph was obtained with a type B photosensor. An acid-base titration was done, with a PS (type A with a green-emitting LED) as detector and Methyl Orange as indicator. The titration curve is shown in Fig. 2. As the titration proceeds the value of R decreases gradually until the end-point is reached, when there is a sharp drop. The end-point is given by the inflection point of the graph, taken as the mid-point between the intersections of extrapolations of the three linear sections of the graph.

A mixture of 5 ml of 0.01M zinc sulphate, a few drops of EBT solution and 1 ml of $\text{NH}_3\text{-NH}_4\text{Cl}$ buffer was titrated with 0.01M EDTA, with a PS (type B with a green-yellow filter) as detector. Since a photo-IC is used in the type B PS the illuminance is plotted against volume of EDTA added (Fig. 3). The end-point can be taken as the mid-point of the sudden decrease in intensity of the illuminance.

Zinc sulphate solution has also been titrated with EDTA with a type A PS (red-emitting LED) as detector. According to Ringbom's theory,⁷ we have calculated the position of the end-point ($\alpha = 1$), and it is consistent with the experimental value. The

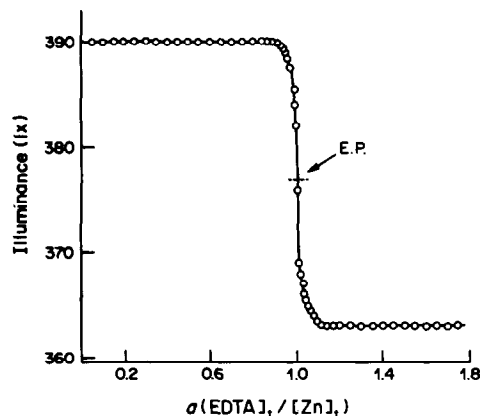


Fig. 3. Chelatometric photo-titration curve (0.01M ZnSO_4 with 0.01M EDTA) obtained by using a type B PS (with green-yellow filter).

Table 1. Titration of zinc with 0.01M EDTA

	[Zinc] found, mM	
	sensor	visual
	9.50	9.60
	9.50	9.50
	9.60	9.60
	9.60	9.70
mean	9.55	9.60
std. devn.	0.06	0.08

results are summarized in Table 1 and compared with those obtained by using a pale blue visual end-point, detectable within one drop of EDTA, without over-titration. The coefficient of variation obtained by the PS method is slightly smaller than that calculated from the results of the visual method. The titration with the instrumental end-point can be done as quickly as that with a visual end-point.

Magnesium chloride solution (0.01M) in $\text{NH}_3\text{-NH}_4\text{Cl}$ buffer was titrated with 0.01M EDTA with a type A PS (with a red-emitting LED) as detector and EBT as indicator (Fig. 4). An iron(III) and copper(II) mixture (each 0.025M) was titrated with 0.05M EDTA, with a type A PS (with a red-emitting LED) as detector. Figure 5 shows that for this mixture the end-points for iron(III) and copper(II) can be found correctly from the intersections of extrapolated linear portions of the curve.

The titration curve obtained by using an MPS (type B) with a green-yellow filter and a membrane containing EBT, for titration of 0.01M zinc sulphate with 0.01M EDTA at pH 10, is shown in Fig. 6. Since a distinct decrease in the illuminance was observed when the stoichiometric amount of EDTA had been added, it is clear that the MPS is useful as a photo-titration indicator. The decrease in the illuminance results from the reaction of the metal ion with EBT dissolved in the membrane. The EBT remains in the

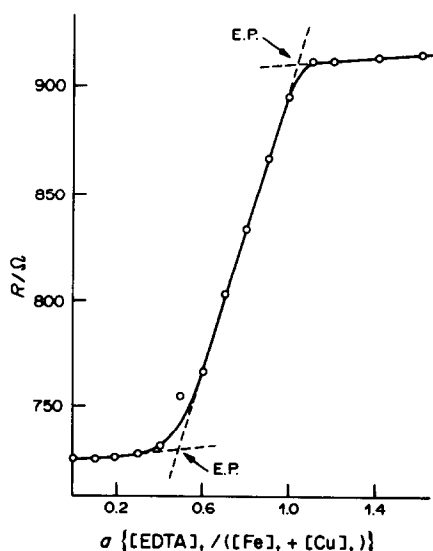


Fig. 4. Chelatometric photo-titration curve (0.01M MgCl_2 with 0.01M EDTA) obtained by using a type A PS (with red-emitting LED).

membrane throughout, and initially the membrane is blue until enough zinc diffuses into it to give a colour change. Hence the change to red should proceed so long as there is free zinc in the solution, though not at constant rate, since the zinc concentration is decreasing throughout the titration. Also, the rate of diffusion within the membrane will be fairly low, and there will be no further reaction until fresh zinc ions have penetrated the layers already converted into the Zn-EBT complex. Therefore, the shape of the titration curve is due to the slow rate of diffusion of metal ion and ligand into the membrane. Similar results are obtained when using Xylenol Orange as indicator. When Type A is used as an MPS both the thickness of the membrane and the concentration of the indicator reagent must be half of those for

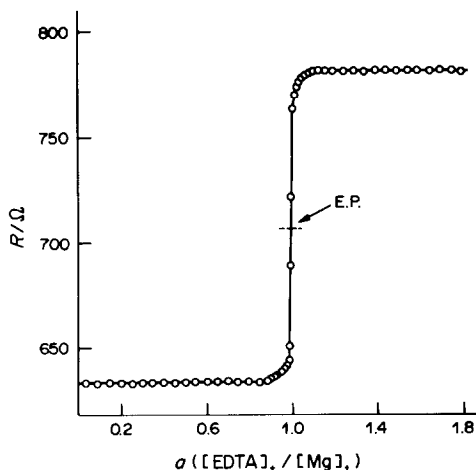


Fig. 5. Photo-titration of mixture of iron(III) and copper(II) with EDTA by using a type A PS (with red-emitting LED) $[\text{Fe}^{3+}] = [\text{Cu}^{2+}] = 0.025\text{M}$, $[\text{EDTA}] = 0.05\text{M}$.

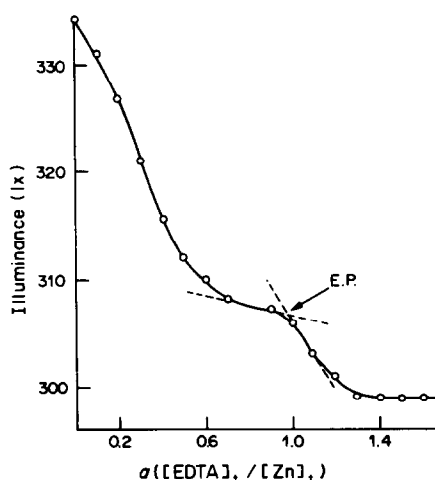


Fig. 6. Photo-titration of 0.01M zinc with 0.01M EDTA, by using a type B MPS (with green-yellow filter).

the type B sensor, because of the low illuminance produced by the type A LED.

The indicator-dye photometric methods employed in this experiment can be used successfully for quantitative work. However, the nature of the metal-dye-ligand interactions at the membrane surface requires further investigation.

CONCLUSION

It has been verified that both the PS and MPS developed here may be used as sensors of absorbance. These sensors are simple and inexpensive, and the measurement can be rapidly performed by immersing them in the test solution. They are also suitable for measuring continuous changes in absorbance such as those observed during the course of a titration

and may have applications as sensors for automatic titrations and in continuous flow analysis.

REFERENCES

1. V. V. Kuznetsov and M. S. Lyauffer, *Zh. Analyt. Khim.*, 1983, **38**, 2210.
2. S. D. Frans and J. M. Harris, *Anal. Chem.*, 1984, **56**, 466.
3. V. I. Martynov, *U.S.S.R. SU983536* (Cl. G01N31/16), 23 Dec. 1982; from *Otkrytiya, Izobret Prom. Obraztsy, Tovarnye Znaki*, No. 47, 168; *Chem. Abstr.*, 1983, **98**, 172223q.
4. A. H. B. Wu, T. Rotunno and H. V. Malmstadt, *Int. Lab.*, 1982, **12**, March, 16.
5. S. H. Hoke and A. G. Collins, *Report 1979, BETC/RI-79/10*; *Chem. Abstr.*, 1980, 93, 19641q.
6. K. Ueno, *Chelatometric Titration*, p. 242. Nankodo, Tokyo, 1972.
7. A. Ringbom, *Complexation in Analytical Chemistry*, pp. 85-86. Wiley, New York, 1963.

THE SPECIATION OF MANGANESE IN FRESHWATERS

BARRY CHISWELL and MAZLIN B. MOKHTAR

Department of Chemistry, University of Queensland, St Lucia, Queensland 4067, Australia

(Received 13 December 1985. Accepted 28 February 1986)

Summary—The extent of current knowledge regarding the speciation of manganese in freshwaters is delineated, and the analytical methods whereby such knowledge is obtained are discussed. Particular attention is paid in the review to the use of electron paramagnetic resonance spectroscopy.

Speciation of an element is the determination of the individual physicochemical forms of that element which together make up its total concentration in a sample. In the aquatic environment trace metals may exist in a number of forms, and the interactions between trace metals and the components of the aquatic system, including the biota, sediments, colloids and water, are largely influenced by specific forms of the metals. Speciation is necessary in order to understand the fate, toxicity, and biological activity of trace metals and their counter-ions in natural waters. It is also a prerequisite for the formulation of water-quality criteria for trace metals.

In natural waters, trace elements may be present in one of the following forms:

- (i) free metal ions surrounded by a layer of water molecules in the first co-ordination sphere;
- (ii) inorganic complexes;
- (iii) organic complexes;
- (iv) in association with colloids and particulate materials such as clays, iron oxides and organisms.

The distribution of a trace element between these forms depends on the nature of the metal and on certain environmental variables. The most important of the latter include pH, E_h (aerobic or anaerobic nature of the water), concentrations of the major anions and cations, and the types and amounts of the organics, colloids and particulate matter present.

Manganese is undoubtedly one of the most ubiquitous metals in the lithosphere, being present, albeit often at trace levels, in most living organisms, and often in large concentration in a wide range of geological materials.¹ The necessity for an adequate supply of manganese for growth of plants and in the nourishment of animals has been well-documented, and supplemental use of trace amounts of the metal has been found necessary in many parts of the world for both plant and animal nutrition. Problems associated with the presence of an excess of the element are far less common than those arising from its absence. Exposure to very high levels of the metal over long periods has been found necessary for chronic manganese poisoning to occur, and such exposure has

been documented only for persons working with manganese ores in situations where proper precautions are not taken.²

However, the presence of manganese in piped water supply systems, such as urban networks and hydroelectric systems, has been shown to create problems of some significance. Difficulties arise when either micro-organisms present in the water metabolise the manganese present in solution, depositing insoluble "manganese dioxide"³ along the growing bacterial stalk of the organism, or the purification of drinking water by chlorination leads to the deposition of brown manganese oxides from solution. The bacterial growths can reduce the bore of the pipe and hence the water flow, which can be a problem in both hydroelectric³ and town water-supply systems,⁴ and both the microbiological "manganese dioxide" and the chlorine-precipitated brown manganese oxides yield unattractive dirty water which can cause stains on washing and in swimming pools.

The removal of manganese during treatment of impounded waters is a problem for many water authorities situated along the eastern Australian seaboard. In this region are concentrated the major urban developments in Australia, and the presence of manganese in the water supply is found, at problem levels, from Cairns in the north to Melbourne in the south.

No one method of water treatment to remove the metal is in general use. Indeed, given that the speciation of the metal has been difficult to elucidate, and will undoubtedly vary (i) from dam to dam; (ii) with seasonal variations; (iii) within any one dam at different levels; it is not surprising that various treatments have been shown to have variable success rates. The key to any successful manganese removal treatment is knowledge of the speciation of the metal; thus speciation studies, as well as being of intrinsic scientific value, have important practical applications. This review discusses the possible range of forms in which manganese is likely to occur in impounded fresh waters and streams, and presents the methods that have been used to elucidate the speciation of the metal.

POSSIBLE MANGANESE SPECIES IN NATURAL WATERS

In the natural environment manganese can occur in three common oxidation states, +II, +III and +IV. Mixed oxidation-state systems can also occur.

Manganese(II) species

The stable form in acidic media is Mn(II). In dilute solution, the manganese salts of strong acid anions, in the absence of complexing ligands, yield the hexa-aquo Mn^{2+} cation. There is evidence⁵ that loss of a proton from one of the six water molecules commences at a pH as low as 3.5. If this is so, at neutral pH these solutions will have both water molecules and hydroxide ion attached to the Mn^{2+} cation. The description $Mn^{2+}(aq)$ will be used throughout this review to describe the species obtained in these solutions at pH values below 7.

Under certain conditions $Mn^{2+}(aq)$ will form complexes with either inorganic or organic ligands. Two types of complex are usually distinguished:

(i) outer sphere in which the hydration shell of the metal ion remains intact and bonding of the complexing ligand is by weak charge effects;

(ii) inner sphere in which ligands (H_2O or OH^-) originally attached to the metal are replaced, and strong new metal–ligand bonds are formed.

Turekian⁶ has calculated, using Gibbs free-energy data, the relative importance of manganese complexes in streams and surface waters, and shown that for a potential of +500 mV, pH 7, and an $Mn^{2+}(aq)$ concentration of $5 \mu g/l.$, the concentration of the most likely inorganic inner sphere complexes, $[Mn(HCO_3)]^+(aq)$ and $[Mn(SO_4)](aq)$, will only be important when the concentrations of bicarbonate and sulphate exceed their average concentrations in natural waters by factors of 10 and 30, respectively, and $[MnCl]^+(aq)$ is only likely to form when the chloride concentration is over 1000 times that normally found in water. However, a manganese concentration of $5 \mu g/l.$ would be low for many stream waters in Eastern Australia,⁷ and indeed manganese concentrations in impounded water supplies in this area are invariably much higher. North Pine Water Supply Dam in Brisbane regularly has epilimnion (warm upper layer of water) concentrations of manganese of $10\text{--}200 \mu g/l.$ and hypolimnion (cold lower layer) concentrations of up to $4000 \mu g/l.$ A survey of dam waters in Queensland indicates that these levels are not uncommon. Of course dam “turnover” can lead to much greater concentrations of manganese in the epilimnion than the $200 \mu g/l.$ quoted above.

At manganese concentrations of $50\text{--}200 \mu g/l.$, calculations similar to those of Turekian would suggest that $[Mn(HCO_3)]^+(aq)$ and perhaps $[Mn(SO_4)](aq)$ would start to form in natural waters. Experimental results⁸ indicate, however, that at a manganese concentration of $100 \mu g/l.$ an increase in sulphate

concentration from a “normal” value of $2.5 \mu g/l.$ to a value of $250 \mu g/l.$ leads to negligible $[Mn(SO_4)](aq)$ formation. At the much higher levels of manganese found in the hypolimnion of lakes, Turekian’s approach suggests that inorganic manganese complexes would be present. However, Carpenter⁹ has claimed that, even in sea-water, with chloride concentrations of some $200 mg/l.$ and manganese concentrations up to $15 mg/l.$, only about 15% of the manganese is present as $[MnCl]^+(aq)$, some 10% as $[Mn(SO_4)](aq)$ and less than 5% complexed by carbonate, bicarbonate and organic ligands. Such results are in stark contrast to calculations based on the equilibrium constants reported by Morris and Short,¹⁰ but it must be remembered that in the natural environment where many metal ions and ligands will be present, in proportions that can vary from sample to sample, it is not realistic to consider only parts of the whole system as though they occur in isolation.

Callender and Bowser¹¹ agree with Turekian that the likely soluble inorganic complexes in freshwaters will be $[Mn(HCO_3)]^+(aq)$ and $[Mn(SO_4)](aq)$, but also propose that $[MnCl]^+(aq)$ will form. Our experimental results⁸ indicate that such a species is unlikely in dam water; at a manganese concentration of $1 mg/l.$, a chloride concentration of some $5 g/l.$ is required for 10% of the Mn^{2+} to be complexed. Other possible soluble inorganic species, such as $[Mn(OH)]^+(aq)$, $[MnF]^+(aq)$, $[MnCl_2](aq)$, $[MnCl_3]^- (aq)$ and $[Mn(OH)_3]^- (aq)$ all appear to be less likely to form than the chloride, sulphate and bicarbonate complexes mentioned above.⁶ Thus, most experimental work indicates that in both the epilimnion and hypolimnion of freshwater lakes and dams, very little soluble manganese will be present in the form of inorganic complexes.

There is, of course, enormous potential for complexation of manganese by naturally occurring organic ligands. Stumm and Morgan¹² have summarized the properties of fulvic and humic acids; these are claimed to be the strongest complexing agents that are likely to be found in natural waters. Both types of acid are complicated mixtures of products obtained by the natural breakdown of dead organic matter. Whereas humic acids are precipitated in acid solution, fulvic acids are soluble at all pH values, which suggests that they possess more available phenolic and carboxylic acid oxygen-donor sites for binding of metal atoms than humic acids do.

Although there is much evidence¹¹ of the complexation of iron by both humic and fulvic acids, there is, as yet, little evidence regarding their complexation of manganese. Gamble *et al.*¹³ used proton NMR line-broadening studies to show that $Fe^{3+}(aq)$ appears to form inner-sphere complexes with fulvic acid, but that complexation of $Mn^{2+}(aq)$ is at most outer-sphere in nature. However, as the manganese concentration used in the work was much greater ($100 mg/l.$) than that normally associated with natural waters, it is uncertain how reliably the results can be extrapo-

lated to speciation studies of naturally occurring freshwaters. The foregoing evidence indicates that soluble Mn(II) species in streams and impounded waters will be present, almost exclusively as $\text{Mn}^{2+}(\text{aq})$, unless the concentration of bicarbonate and/or sulphate is abnormally high, or where (and little is known of this) organic ligand complexation occurs.⁹

The most likely form of insoluble Mn(II) would appear to be MnCO_3 , MnO or its hydrate $\text{Mn}(\text{OH})_2$, only precipitates at $\text{pH} > 11$, and then only when the p_e of the solution is negative. On the other hand, MnCO_3 will precipitate at about $\text{pH} 7.5$ over a range of p_e values* from roughly -22 to $+7$. However, MnCO_3 has a solubility of about 65 mg/l. in natural water and will thus only be precipitated when very large concentrations of carbonate and/or manganese are present.¹¹

All that can be said with certainty is that insoluble inorganic forms of Mn(II) in natural waters occur by adsorption of $\text{Mn}^{2+}(\text{aq})$ on other insoluble materials.

Likely examples of such materials are iron hydroxides, clays and manganese dioxide. The possibility that insoluble Mn(II) species can be formed by either organic ligand complexation leading to precipitation, or adsorption of $\text{Mn}^{2+}(\text{aq})$ on insoluble organic material, cannot be reliably commented upon from our present state of knowledge.

Manganese(III) species

The speciation of this oxidation state in natural waters is basically unknown.^{14,15} The cation $[\text{Mn}(\text{H}_2\text{O})_6]^{3+}$ is known, but is unstable in acid solution with respect to disproportionation into Mn(II) and MnO_2 , and in alkaline solution the Mn(III) oxohydroxide, $\text{MnO}(\text{OH})$, is thermodynamically unstable with respect to both Mn(II) and Mn(IV) oxides. At least in its simple salts, Mn(III) does not appear to be stable in aqueous solution unless the insoluble mixed oxidation-state Mn_3O_4 is produced.

The possibility of obtaining both soluble and insoluble Mn(III) complexes of naturally occurring organic ligands cannot realistically be commented upon; our lack of knowledge of the basic chemistry of Mn(III) is still monumental. Only in the last few years has any research in this area been undertaken, and results are few and far between.¹⁶

Manganese(IV) species

Little is known of the speciation of this oxidation state in freshwaters. It has often been assumed that the insoluble form of manganese in such waters is manganese dioxide, but as will be shown, this assumption is not necessarily always true.

Nothing is known of the speciation of soluble Mn(IV) in natural waters. As pointed out elsewhere,¹⁶ the basic chemistry of both the Mn(III) and Mn(IV) oxidation states has received scant attention from inorganic chemists, who are only now commencing the work necessary to an understanding of the environmental chemistry of manganese. The species $[\text{Mn}(\text{H}_2\text{O})_6]^{4+}$ would be, even if obtained, most transient, yielding Mn^{2+} in acid solution, and precipitating as $\text{MnO}_2 \cdot x\text{H}_2\text{O}$ in alkaline solution. Simple Mn(IV) salts such as $\text{Mn}(\text{SO}_4)_2$ have been prepared, but are, as predicted by thermodynamic considerations, most unstable in the natural environment. The only binary Mn(IV) compound known to be stable in nature is manganese dioxide. Mn(IV) may be stabilized in nature through complexation with organic ligands; there appears to be no evidence either for or against such complexation. However, there seems little doubt that neither soluble nor insoluble inorganic complexes of Mn(IV) are likely in natural waters.

Speciation of manganese dioxide is not a simple matter. The compound exists in many different forms,^{17,18} some of which are non-stoichiometric and thus not easily amenable to techniques used to study chemical solids. Nevertheless, at $\text{pH} > 8$, insoluble manganese dioxide is a stable form of manganese in natural waters. However, whether it is the main form of insoluble manganese, as postulated by many workers, is very much open to question.

Analysis of manganese-containing deposits obtained by filtration of natural waters normally indicates the presence of insoluble forms of other metal ions, such as iron, aluminium, calcium and magnesium. Insoluble compounds, particularly of iron and aluminium, are likely to form agglomerates with particles of MnO_2 , as well as adsorbing soluble forms of manganese, to yield essentially insoluble manganese; clays and insoluble organic matter can operate in a similar manner.

OXIDATION OF SOLUBLE MANGANESE

The foregoing can be summarized by stating that at our present level of knowledge, we can say only that in natural waters manganese occurs either as the main soluble form of $\text{Mn}^{2+}(\text{aq})$, or in insoluble form, of which MnO_2 is often at least a component. "Insolubility" is, of course, only definable in terms of a working definition, which for water studies is most usually based on whether a given species will pass through a $0.45\text{-}\mu\text{m}$ pore-size filter.

In practical terms the water chemist attempts to remove troublesome soluble manganese by oxidizing it to the insoluble form. The oxidation of $\text{Mn}^{2+}(\text{aq})$ in the absence of any catalytic effect is slow. Hem¹⁹ claims that more than 5% of $\text{Mn}^{2+}(\text{aq})$ is unchanged after two years in aqueous solution open to the air at $\text{pH} 8$. He points out that such materials as quartzose and feldspathic sand grains can increase oxidation rates by a factor of 10.

*For a definition of p_e and examples of its use, see, for instance, S. Kotrlý and L. Sůcha, *Handbook of Chemical Equilibria in Analytical Chemistry*, Horwood, Chichester, 1985, p. 37 and Chapter 13.

Crerar *et al.*²⁰ have developed a model for ferromanganese nodule growth which postulates that MnO₂ precipitation in natural water requires a catalytic process. They suggest that the reaction:



requires adsorbing substrates to lower the activation energy of the oxidation by about 50 kJ/mole. Other workers^{21,22} have shown that the autocatalytic oxidation of Mn(II) on colloidal particles of MnO₂ proceeds rapidly only at pH > 8.5. Dubinina²³ pointed out that this is a high pH for natural waters, and that the presence of bicarbonate and sulphate would perhaps reduce this rate substantially, and claimed that the oxidation of Mn(II) in natural waters "is due to the activity of metabolically-liberated hydrogen peroxide", which indicates the importance of the participation of catalase in this reaction, because in the absence of catalase the normal chemical behaviour of peroxide is to reduce Mn(IV) to Mn(II)



When it is remembered that the presence of an iron metallo-enzyme is required for the catalase decomposition of organically produced hydrogen peroxide to water and oxygen, it can be seen that the metabolically mediated oxidation of Mn(II) will only occur in the presence of iron.

METHODS OF MANGANESE SPECIATION

Measurement of the chemical forms of a metal requires a highly selective analytical technique. In addition, the preliminary separation steps and the analytical measurement itself must be chosen to avoid, as far as possible, disturbing the equilibria between the chemical species in the sample. In natural waters the sampling process itself may lead to some disruption of the chemical equilibria, but this can be minimized by using rapid separation procedures and avoiding pretreatment of samples as far as possible.

Ion-selective electrodes

Very few analytical techniques can respond to only one particular species of an element in solution, *i.e.*, be "species-specific". Some of the most sensitive analytical instruments, such as the atomic-absorption spectrometer, cannot be used in speciation work because they measure only the total metal concentration.

However, one good example of a species-specific technique is ion-selective electrode potentiometry. Metal ion-selective electrodes (ISEs) respond only to the activity (or concentration) of the free hydrated metal ion, with response related to potential by the Nernst equation.²⁴⁻²⁷ Applications of ISE are regularly reviewed.²⁸⁻³¹

The measurement of the concentration of a particular ion in complex mixtures of chemical substances

can take from a few seconds to several minutes, depending on conditions. However, interference from other ions is a major drawback, as is the fact that the concentrations of most metal ions in natural waters are too low to be measured by an ISE.⁷ For example, Hirata and Higashiyama³² have described an ion-selective chalcogenide electrode which is responsive to Mn²⁺(aq), but the response is non-linear and extends only down to 10⁻⁵M, a concentration which is relatively high for natural waters, and the electrode, which suffers from interference problems from other cations, does not appear to be of use for Mn²⁺(aq) concentrations below 0.5 mg/l. Midgley and Mulcahy³³ have prepared a manganese(IV) oxide electrode by impregnation of a PTFE-graphite substrate, and tested this as a manganese(II) sensor. It has a Nernstian response down to 5 × 10⁻⁵M (2.8 mg/l.). The main disadvantages with this electrode are its long response time (about 20 min) and the pH-control requirement. Lead, iron(III) and iron(II) interfere, but other bivalent transition metal ions have little effect.

Anodic-stripping voltammetry

The most commonly used technique for speciation of heavy metals in waters is anodic-stripping voltammetry (ASV). This technique can be used to distinguish between "labile" and "bound" metal species.³⁴ The former species take part in the electrode reaction, while the latter do not. The bound metal is thus determined as the difference between total (determined, for example, by atomic-absorption spectrometry) and labile metal. It is proposed that the labile metal species should be defined as uncomplexed or weakly complexed ions, whereas the bound metal species comprise soluble metal-organic complexes, metal bound to high molecular-weight organic ligands, and metal adsorbed on colloids.³⁵ From this point of view the technique is not particularly species-specific, as all electrochemically active species, including free metal ions and labile inorganic and organic complexes, are determined simultaneously.

A major problem with the use of ASV in speciation studies of natural waters is the presence of organic compounds. These can be adsorbed on the electrode and markedly change the pattern of metal deposition and stripping.³⁵ Similar, but rarely serious, problems can arise from the presence of some inorganic anions in the sample.³⁶ A further experimental problem with ASV is the need to add a total ionic strength adjustment buffer (TISAB) to prevent any changes in ionic strength or pH during the course of the analysis. This will almost certainly alter the equilibria in the natural water sample, *e.g.*, acetate buffer has been reported to form complexes with many metals,³⁶ though practically all of them are weak.

ASV determinations of manganese in natural waters have been performed by several workers.³⁷⁻³⁹ Rapid determination of Mn(II) at concentrations down to 0.01 µg/l. by differential pulse anodic-

stripping voltammetry (DPASV) at a mercury film electrode (MFE) has been reported,³⁷ but the calibration graph was non-linear at concentrations above 10 $\mu\text{g/l}$. The most serious interference in DPASV analysis for Mn(II) is caused by the hydrogen wave, which completely masks the Mn(II) peak. Addition of sodium tetraborate buffer can eliminate the hydrogen wave, but probably alters the equilibrium. The very negative potential required for Mn(II) (-1.70 V vs. SCE) means that practically all other amalgam-forming species in solution will be co-deposited at the MFE. The most serious interferences are caused by Cr, Co, Ni and Cu.

Both flow and batch potentiometric stripping analysis (PSA) have been used³⁸ to determine Mn(II) concentrations in natural waters. The former is faster and easily automated and gives a detection limit of 1.8 nM (0.10 $\mu\text{g/l}$.) Mn (defined as three times the standard deviation of the blank signal). However, it involves pH adjustment of the sample and suffers interference from formation of an intermetallic compound with copper in the amalgam. Large volumes of sample are required at low concentrations, and long deposition times are then necessary. The negative potential for Mn(II) deposition can cause concurrent reduction of protons and other dissolved species, and the oxidation of amalgamated Mn to Mn(II) is not fully reversible.

Polarography

Several workers have used differential pulse polarography (DPP) to determine manganese in natural waters. Manganese at $\mu\text{g/l}$. levels has been determined by DPP⁴⁰ in fresh, estuarine and sea-waters buffered at pH 9.5 with a citrate-borate solution. Polarographic determination of manganese in unbuffered natural waters always experiences strong interference from the chromium and iron signals which overlap the manganese signal.

Polarographic determination of Mn(II) has a number of drawbacks. The reproducibility is very poor and the calibration graph non-linear.⁴¹ The method is slow, requiring about 15 min for one analysis. Over the manganese concentration range from $2 \times 10^{-6}\text{ M}$ (0.11 mg/l .) to 10^{-4} M (5.5 mg/l .) d.c. polarography is recommended instead of DPP.^{42,43}

Physical separation techniques

Physical separation techniques are used to separate "soluble" from "insoluble" forms of the metal, and to separate these two fractions into various subgroups. The specificity of these physical separations is, of course, directly related to the nature and complexity of the sample. Some of the separation methods used in speciation studies are as follows.

Filtration. Various standard pore-size filters have been used to separate soluble and insoluble fractions. Probably the most commonly used nominal pore-size is 0.45 μm . There is no intrinsic reason for using such

a pore-size, but a recent paper⁴⁴ indicates that for manganese in the particle-size range from 10^{-3} to $10^2\ \mu\text{m}$ in three out of four lakes studied, virtually all of the metal-carrying particulate matter would be retained by the 0.45- μm filter.

Liquid-liquid extraction. Solvent extraction with chloroform or carbon tetrachloride has been used in an attempt to determine organically-associated copper in sea-water,³⁴ but the method gave low results. Attempts to undertake a similar separation of manganese in natural waters have not been reported, but studies¹³ on the complexing power of natural ligands for the metal suggest that the technique may be unsuitable.

Ultrafiltration, dialysis, centrifugation and electrophoresis. These techniques can separate metal species associated with colloidal particles from ionic metal species. In ultrafiltration and dialysis, the pore-size of the membrane used must be specified because the diameters of the metal species that are retained or passed are defined accordingly.

Ultrafiltration membrane filters have pore diameters of 1–15 nm. Advantages of the ultrafiltration technique are its simplicity and the selectively variable pore-size of the filters. Small pore-size filters are expensive, however, and the long filtration time may result in metal-ion adsorption on the collected solids. Ultrafiltration separates two metal fractions in natural waters. The filtrate (ultrafilterable metal fraction) contains free metal ions and inorganic and organic complexes which have diameters less than the pore-size of the filter membrane used. The retained fraction contains metal species of size greater than the pore-size of the filter. Ultrafiltration, ion-exchange filtration and centrifugation, together with spectrophotometric methods and activation analysis, have been used to study the interactions between humus and trace elements in freshwater.⁴⁵

Dialysis is not widely used in speciation studies of trace metals because of the long equilibration time of at least 24 hr,⁴⁶ and consequent risk of adsorption losses. The major advantage of this technique is the very small membrane pore-size of 1–5 nm, which allows only the free metal ions and the smallest complexed species to diffuse through the membrane. Serious problems associated with the use of the technique have been summarized;^{34,35} in general these are associated with the fact that the membrane can affect the equilibria in the sample being dialysed.

Centrifugation is less susceptible to the adsorption effects that create problems in dialysis, but generally fails to collect a range of smaller particles.

The interactions of Cu(II), Pb(II), Cd(II), Zn(II) and Mn(II) with humic and tannic acids have been studied by using a combination of dialysis, ultrafiltration and atomic-absorption spectroscopy, and the stability constants of these complexes have been calculated.⁴⁷ A combination of centrifugation, dialysis, ion-exchange filtration and electrophoresis has been used in studying the effect of storage of river

water on the physicochemical forms of trace elements.⁴⁶

Ion-exchange. Cation and anion-exchange resins divide dissolved metal into anionic, cationic or neutral (not sorbed by either resin) species. The most commonly used ion-exchange resin is Chelex-100 which contains iminodiacetic acid units attached to a polystyrene matrix, and binds free metal ions and metal ions from complexes which have stabilities lower than that of the metal-Chelex complex.⁷ Chelex-100 has been used for collection of various metals from natural waters.^{13,35} $Mn^{2+}(aq)$ is quantitatively retained at neutral pH, as are $Fe^{3+}(aq)$, $Pb^{2+}(aq)$ and $Zn^{2+}(aq)$, but such retention is often pH-dependent. Adjustment of pH to obtain quantitative retention will undoubtedly change the speciation.

Nuclear magnetic resonance spectrometry (NMR)

The direct study of speciation of trace elements in natural waters by means of NMR is virtually unknown. This is because most metals of interest have a nuclear spin (I) greater than 1, leading to a nucleus with an uneven and non-spherical distribution of charge. This gives rise to an electric quadrupole moment (besides the magnetic moment), which interacts strongly with many types of bonding electrons and can obscure or greatly complicate the nuclear magnetic effect; ⁵⁵Mn is a good example of a nucleus subject to such obscuration.

However, the technique is of use in speciation studies if the NMR spectra of the ligands associated with the metal are examined instead of the NMR spectrum of the metal itself. Gamble *et al.*¹³ studied the interactions between Mn^{2+} and a well-characterized fulvic acid by observing the changes of the proton NMR spectrum of the water present. This method was also used by Frankel *et al.*,⁴⁶ who determined the structure of the $MnSO_4$ inner-sphere complex by proton NMR; the sulphate ion was found to act as a bidentate ligand.

The width of the NMR signal in an aqueous solution of Mn^{2+} is proportional to the number of water molecules co-ordinated to the metal, any decrease in line-width being indicative of the number of co-ordinated water molecules replaced by sulphate ions. A combination of NMR and electron paramagnetic resonance spectroscopy (EPR) has been applied in studying the effects of physical and chemical treatments of chloroplast manganese.⁴⁹

Electron paramagnetic/spin resonance spectroscopy (EPR/ESR)

A most important technique for Mn(II) speciation studies is that of EPR. EPR signals are usually obtained from paramagnetic species with an odd number of unpaired electrons. Speciation studies are based on observing the changes in the EPR spectra of the paramagnetic species that take place as a result of formation of complexes between the ligands (in-

cluding solvent molecules) and the metal ion. Because Mn(II) gives such good EPR spectra, the technique has been widely used for qualitative work, and to a somewhat lesser extent in quantitative analysis. The latter application appears to have been first made by Guilbault and Lubrano,⁵⁰ using the principle that the EPR signal intensity is proportional to the concentration of the paramagnetic electrons, and hence to the $Mn^{2+}(aq)$ concentration.

$Mn^{2+}(aq)$ gives a very strong six-peak EPR signal in aqueous solutions or in mixtures of water and some organic solvents. Complexation (either inner or outer sphere) causes changes in signal intensity and peak shape.

Guilbault and Lubrano⁵⁰ found a linear relationship between the amplitude of the fourth peak from the low-field side of the first derivative absorption curve, and the concentration of $Mn^{2+}(aq)$ in the range from $10^{-3}M$ (55 mg/l.) to $10^{-6}M$ (55 μ g/l.). We⁸ have obtained similar results over the $Mn^{2+}(aq)$ range from 100 mg/l. down to 30 μ g/l., with reproducibility of $\pm 3\%$. For $Mn^{2+}(aq)$ the EPR method of quantitative analysis is superb. It is rapid, non-destructive, and can be used over a very wide range of sensitivities without the need for dilution or preconcentration. Furthermore, it is highly selective, operates over virtually the whole pH range, requires no sample pretreatment (*e.g.*, buffering), and needs only a very small sample (0.2 ml). The major drawback of the technique is, of course, the cost of the EPR spectrometer. It would seem likely that the suitability and accuracy of other (cheaper) methods for speciation of Mn(II) in solution will be established by EPR studies; such a programme is now being undertaken in our laboratories.

The six-peak spectrum is created by the nuclear hyperfine splitting of the five equivalent electronic spins by the ⁵⁵Mn, 100% abundant, $I = \frac{5}{2}$ nuclear spin. Owing to second-order quantum mechanical effects, the average spacing between the six lines is not equal.⁵¹ From the low-field side of the spectrum, the peak widths range from 22.8 G for the first peak to 19.1 G for the fourth peak (the tallest and narrowest of the peaks). As the fourth peak is the one least affected by the second-order effects, it is the most useful for quantitative measurements.

For solutions of $Mn^{2+}(aq)$ of concentrations less than 0.1M (5.5 g/l.) contributions to line-widths by interactions between neighbouring $Mn^{2+}(aq)$ ions are negligible.^{52,53} Thus in the concentration ranges of interest to the natural-water chemist, the line-width of the EPR spectrum is determined only by the Mn(II)-ligand relaxation processes. Ligand interaction with $Mn^{2+}(aq)$ to form an outer-sphere complex causes a small distortion of the symmetry of the field about the $Mn^{2+}(aq)$ ion. This produces a spectrum with broader and shorter peaks than those obtained for the unassociated $Mn^{2+}(aq)$; the area under the fourth peak, however, remains constant. The formation of an inner-sphere complex reduces

the symmetry of the $\text{Mn}^{2+}(\text{aq})$ ion markedly below cubic and causes very rapid relaxation; the EPR spectrum of the new species has very broad, often unmeasurable, peaks.⁵⁴

Three different types of measurement have been applied to the fourth EPR peak to assess the speciation of the manganese in a given solution, *viz.* the peak height, width and area for a given solution are compared with those for a known standard containing only $\text{Mn}^{2+}(\text{aq})$.

The peak-height is related to the concentration of the cubic-symmetry $[\text{Mn}(\text{H}_2\text{O})_6]^{2+}(\text{aq})$; as this species is decreased either by reduction in total Mn(II) in solution, or by removal of $\text{Mn}^{2+}(\text{aq})$ by complexation, a concomitant reduction in peak-height would be expected. Carpenter⁶⁰ claims that outer-sphere complexation does not reduce the concentration of $\text{Mn}^{2+}(\text{aq})$ in solution, but the charge effect is strong enough to reduce the peak-height and broaden the peak-width, the peak-area remaining constant. On the other hand, Carpenter claims that if only inner-sphere complexation occurs, the peak area is reduced, as the peak-width remains constant, but the peak-height is reduced by the reduction in concentration of $\text{Mn}^{2+}(\text{aq})$. Thus interaction of chloride ions with a known concentration of $\text{Mn}^{2+}(\text{aq})$ would yield peak-height reduction and peak-broadening but constant peak-area if the complexation were outer-sphere, but reduced peak-height and peak-area but no peak-broadening if the complexation were inner-sphere.

Carpenter's interpretation is based on the work of Burlamacchi *et al.*,^{52,53} Hayes and Myers⁵¹ (who claim that inner-sphere complexation will yield peak-broadening only at temperatures above 80°) and Pearson and Buch.⁵⁵ McBride⁵⁶ has also used peak-broadening as a measure of outer-sphere complexation, while Vishnevskaya *et al.*⁵⁷ have used peak-area decrease to indicate formation of inner-sphere complexes of low symmetry.

As a standard system in which it is claimed there is no anion-association with the $\text{Mn}^{2+}(\text{aq})$ ion, a number of workers have used aqueous solutions of manganese(II) perchlorate. For instance Burlamacchi *et al.*^{52,53} report insignificant changes in peak-width in solutions of $\text{Mn}(\text{ClO}_4)_2$ up to 0.5M concentration. Carpenter,⁵⁴ and Hayes and Myers,⁵¹ have reported similar results and interpreted them to indicate no complexation of any type between the manganese cation and the perchlorate anion. Broadening of the Mn(II) EPR peak-width at much higher concentrations of $\text{Mn}(\text{ClO}_4)_2$, *viz.* 1–3.2M, has been studied by Hinckley and Morgan.⁵⁸ Dipole–dipole interaction was proposed as the predominant intermolecular relaxation process at these higher concentrations. Above a concentration of 2.3M, the hyperfine structure of the absorption is not resolved, and the spectrum appears as a single broad absorption peak.

To investigate the nature of the interaction between various anionic groups with $\text{Mn}^{2+}(\text{aq})$ in solu-

tion, different groups have studied the EPR spectral changes of aqueous $\text{Mn}(\text{ClO}_4)_2$ solutions on addition of such groups. Thus Hayes and Myers⁵¹ studied the effect of chloride and sulphate on EPR peak-width of $\text{Mn}(\text{ClO}_4)_2$ solutions over the temperature range 20–200°. In the range 20–80°, no change in peak-width of a 0.05M $\text{Mn}(\text{ClO}_4)_2$ solution was observed on increasing the chloride concentration of the solution from 0.025 to 0.100M. On the other hand, the addition of sulphate appeared to alter the EPR peak-width at all temperatures, such alterations not being simply related to concentration changes. Reference to the known formation constants for $[\text{MnCl}]^+(\text{aq})$ and $[\text{MnSO}_4](\text{aq})$ was used to explain complexation by the sulphate ion, but lack of binding of chloride.

Carpenter⁵⁴ has studied the speciation of Mn(II) in sea-water by EPR spectroscopy. Using a chloride concentration range of 0.3–1.0M, he found a linear decrease in Mn(II) peak-height with increasing chloride concentration up to at least 0.7M. Like Hayes and Myers,⁵¹ he found no increase in peak-width on increasing the chloride concentration; he therefore proposed that the interaction is of the inner-sphere type. He used his results to calculate a thermodynamic equilibrium constant of 1.37 at 20°. When studying the effect of sulphate, Carpenter found that both the width and area of the EPR signal varied, suggesting the formation of both inner- and outer-sphere complexes. Depending on the choice of activity coefficients for $\text{Mn}^{2+}(\text{aq})$ and $\text{SO}_4^{2-}(\text{aq})$, the equilibrium constant for the association of the ions in aqueous solution was found to be between 93 and 145.

Guilbault and Meisel⁵⁰ have studied the effects of chloride, sulphate, acetate and other anions on the $\text{Mn}^{2+}(\text{aq})$ peak, and have reported the maximum concentration of these substances that can be added before measurable effects can be seen in the EPR peaks.

Mn(II) solutions of different pH values, saturated with N_2 , CO_2 or O_2 were all found to give rise to initial EPR signals very similar to those obtained for the untreated Mn(II) solutions.⁵⁹ This work used MnSO_4 solutions ranging from $10^{-5}M$ to 0.1M in concentration, and the results were claimed to show that the major species in solution from pH 2.0 to 6.3 is $[\text{Mn}(\text{H}_2\text{O})_6]^{2+}(\text{aq})$, with $[\text{MnOH}]^+(\text{aq})$ only forming above pH 9.0. The solubility in solutions saturated with CO_2 is controlled by the solubility product of MnCO_3 , although at pH 6, $[\text{Mn}(\text{H}_2\text{O})_6]^{2+}(\text{aq})$ is still claimed to be the major species of manganese present.

The forms of the major constituents of some eighty ferromanganese nodules from marine and freshwater environments were determined by Wakeham and Carpenter⁶⁰ by EPR methods, and Blanchard and Chasteen determined Mn(II) in powdered barnacles.⁶¹

Carpenter⁵⁴ used EPR work to show that certain marine waters had 72–77% of their manganese

present as $Mn^{2+}(aq)$, 14–16% as complexes with chloride, and 10–12% as complexes with sulphate. The results showed that less than 5% of the total manganese was associated with CO_3^{2-} , HCO_3^- or organic ligands. He proposed that the lack of organic complexation may well be due to a preference of natural organic ligands for other metals common in the lithosphere, *viz.* Ca, Mg and Fe.

Gamble *et al.*⁶² have used EPR spectroscopy to investigate the interaction of $Mn^{2+}(aq)$ with fulvic acid. They proposed that manganese binds to this ligand in nature by simultaneous electrostatic interaction between the metal ion and negative ligand groups, and hydrogen-bonding of metal-co-ordinated water molecules to oxygen atoms on the fulvic acid groups; the result is essentially outer-sphere complexation. McBride⁵⁶ proposed, on the basis of EPR work, a similar type of binding of $Mn^{2+}(aq)$ to humic acid extracted from mineral soil.

In this context it is interesting to note that Farmer and Popov,⁶³ in using EPR spectroscopy to calculate the thermodynamic constants and stabilities of manganese(II) complexes with phosphonoformic acid, phosphonoacetic acid, phosphonopropionic acid, citric acid, some crown ethers and a cryptand, from the decrease in signal intensity, found that the crown ethers did not complex with Mn(II).

CONCLUSION

The foregoing analysis of available data indicates that the most likely form of soluble manganese in freshwater is $Mn^{2+}(aq)$, although the possibility of complexation, particularly of the outer-sphere type, with naturally occurring organic ligands cannot be ruled out in our present state of knowledge. If such complexation does occur, it may stabilize both soluble Mn(III) and Mn(IV) species.

The speciation of insoluble manganese in freshwater is, as yet, little understood. There seems little doubt that in many cases one form of insoluble manganese will be hydrated manganese(IV) oxide. However, it is experimentally difficult to deal with speciation of non-stoichiometric systems. These insolubles may contain one or more of the following:

- (1) one or many of the forms of MnO_2 ;
- (2) Mn(II), Mn(III) or Mn(IV) oxides adsorbed on either insoluble organic or inorganic material;
- (3) insoluble Mn(II), Mn(III) or Mn(IV) complexes.

The difficulty of oxidizing Mn(II) in freshwater is well-established, but the reasons are, as yet, by no means understood. Current evidence points to the mediation of biological species as being essential to such oxidation.

Although the problems of identifying the speciation of insoluble forms of manganese in freshwater still largely await the attention of the water chemist, work on electrochemical methods, in particular

anodic-stripping voltammetry, and use of ion-exchange resins and electron paramagnetic spectroscopy have been useful in partially determining soluble manganese speciation. In particular, EPR spectroscopy has been used to establish the amount of $Mn^{2+}(aq)$ present in solution, and to predict the likelihood of formation of soluble complexes of this ion by naturally occurring inorganic and organic ligands.

In speciation work it must always be remembered that kinetic factors may overrule thermodynamic predictions. A discussion of this in connection with manganese is given by Kragten.⁶⁴

REFERENCES

1. G. C. Cotzias, *Mineral Metabolism*, Vol. II, *The Elements*, Part B, C. L. Comar and F. Bromar (eds.), p. 403. Academic Press, New York, 1982.
2. B. L. Vallee and R. J. P. Williams, *Chem. Brit.*, 1968, **4**, 397.
3. P. A. Tyler and K. C. Marshall, *Arch. Mikrobiol.*, 1967, **56**, 344.
4. S. D. Faust and O. M. Aly, *Chemistry of Water Treatment*, p. 51. Butterworths, Boston, 1983.
5. C. F. Wells and M. A. Salam, *J. Inorg. Nucl. Chem.*, 1969, **31**, 1083.
6. K. K. Turekian, *Handbook of Geochemistry*, Vol. 1, K. H. Wedepohl (ed.), p. 297. Springer-Verlag, Berlin, 1978.
7. B. T. Hart, *Chem. Aust.*, 1982, **49**, 260.
8. B. Chiswell and M. B. Mokhtar, unpublished results.
9. R. Carpenter, *Geochim. Cosmochim. Acta*, 1983, **47**, 875.
10. D. F. C. Morris and E. L. Short, *J. Chem. Soc.*, 1961, 5148.
11. E. Callender and C. J. Bowser, *Freshwater Ferromanganese Deposits*, in *Handbook of Strata-bound and Stratiform Ore Deposits*, K. H. Wolf (ed.), p. 371. Elsevier, Amsterdam, 1976.
12. W. Stumm and J. J. Morgan, *Aquatic Chemistry*, pp. 514–516. Wiley, New York, 1981.
13. D. S. Gamble, C. H. Langford and J. P. K. Tong, *Can. J. Chem.*, 1976, **54**, 1239.
14. E. V. Grill, *Geochim. Cosmochim. Acta*, 1982, **46**, 2435.
15. G. P. Klinkhammer and M. L. Bender, *Earth Planet. Sci. Lett.*, 1980, **46**, 361.
16. B. Chiswell, L. Lindoy and E. D. McKenzie, *Manganese*, in *Comprehensive Coordination Chemistry*, Vol. 3, G. Wilkinson (ed.), Pergamon Press, Oxford, in press.
17. Gmelin, *Handbuch der Anorganischen Chemie*, Springer-Verlag, Berlin, 1973, **C1**, 1; 1973, **C2**, 1.
18. Gmelin, *Handbuch der Anorganischen Chemie*, Springer-Verlag, Berlin, 1975, **C3**, 1.
19. J. D. Hem, *U.S. Geol. Survey Water-Supply Paper*, 1964, 1667(B), 1.
20. D. A. Crerar, R. K. Cormick and H. L. Barnes, *Acta Mineral. Petrogr.*, 1972, **20**, 217.
21. J. D. Hem, *U.S. Geol. Survey Water-Supply Paper*, 1963, 1667(A), 97.
22. J. J. Morgan and W. Stumm, *J. Colloid Sci.*, 1964, **19**, 347.
23. G. A. Dubinina, in *International Symposium on Geology and Geochemistry of Manganese*, I. M. Varentsov and Gy. Grasselly (eds.), p. 309. Schweizerbart Verlag, Stuttgart; Akadémiai Kiadó, Budapest, 1980.
24. R. A. Durst, *Ion-Selective Electrodes*, U.S. Dept. of Commerce, Washington, D.C., 1969.

25. H. Freiser (ed.), *Ion-Selective Electrodes in Analytical Chemistry*, Vol. 2, Plenum Press, New York, 1980.
26. J. Veselý, D. Weiss and K. Štulík, *Analysis with Ion-Selective Electrodes*, Horwood, Chichester, 1978.
27. J. Koryta, *Ion Selective Electrodes*, 2nd Ed., Cambridge University Press, Cambridge, 1983.
28. G. H. Fricke, *Anal. Chem.*, 1980, **52**, 259R.
29. M. E. Meyerhoff and Y. M. Fraticelli, *ibid.*, 1982, **54**, 27R.
30. M. A. Arnold and M. E. Meyerhoff, *ibid.*, 1984, **56**, 20R.
31. J. Koryta, *Anal. Chim. Acta*, 1972, **61**, 329; 1977, **91**, 1; 1979, **111**, 1; 1982, **139**, 1; 1984, **159**, 1.
32. H. Hirata and K. Higashiyama, *Talanta*, 1972, **19**, 391.
33. D. Midgley and D. E. Mulcahy, *ibid.*, 1985, **32**, 7.
34. T. M. Florence and G. E. Batley, *CRC Crit. Rev. Anal. Chem.*, 1980, **9**, 219.
35. B. T. Hart and S. H. R. Davies, *A Study of the Physico-chemical Forms of Trace Metals in Natural Waters and Wastewaters*, Aust. Water Resources Council, Canberra, *Tech. Paper*, 1978, No. 35.
36. Y. K. Chau and K. Lum-Shue-Chan, *Water Res.*, 1974, **8**, 383.
37. R. J. O'Halloran, *Anal. Chim. Acta*, 1982, **140**, 51.
38. H. Eskilsson and D. R. Turner, *ibid.*, 1984, **161**, 293.
39. D. P. H. Laxen, W. Davison and C. Woof, *Geochim. Cosmochim. Acta*, 1984, **48**, 2107.
40. M. P. Colombini and R. Fuoco, *Talanta*, 1983, **30**, 901.
41. S. Knox and D. R. Turner, *Estuarine Coastal Mar. Sci.*, 1980, **10**, 317.
42. W. Davison, *Limnol. Oceanog.*, 1977, **22**, 746.
43. W. Davison, *J. Electroanal. Chem.*, 1976, **72**, 229.
44. D. P. H. Laxen and I. M. Chandler, *Geochim. Cosmochim. Acta*, 1983, **47**, 731.
45. P. Benes, E. T. Gjessing and E. Steinnes, *Water Res.*, 1976, **10**, 711.
46. P. Benes and E. Steinnes, *ibid.*, 1975, **9**, 741.
47. R. D. Guy and C. L. Chakrabarti, *Can. J. Chem.*, 1976, **54**, 2600.
48. L. S. Frankel, T. R. Stengle and C. H. Langford, *J. Inorg. Nucl. Chem.*, 1966, **29**, 243.
49. R. Khanna, S. Rajan, Govindjee and H. S. Gutowsky, *Biochim. Biophys. Acta*, 1983, **725**, 10.
50. G. G. Guilbault and G. J. Lubrano, *Anal. Lett.*, 1968, **1**, 725.
51. R. G. Hayes and R. J. Myers, *J. Chem. Phys.*, 1964, **40**, 877.
52. L. Burlamacchi and E. Tiezzi, *J. Mol. Struct.*, 1968, **2**, 270.
53. L. Burlamacchi, G. Martini and E. Tiezzi, *J. Phys. Chem.*, 1970, **74**, 3980.
54. R. Carpenter, *Geochim. Cosmochim. Acta*, 1983, **47**, 875.
55. R. G. Pearson and T. J. Buch, *J. Chem. Phys.*, 1962, **36**, 1277.
56. M. B. McBride, *Soil Sci.*, 1978, **126**, 200.
57. G. P. Vishnevskaya, F. M. Gumerov and A. F. Grigor'evn, *J. Struct. Chem.*, 1980, **21**, 498.
58. C. C. Hinkley and L. O. Morgan, *J. Chem. Phys.*, 1966, **44**, 898.
59. E. E. Angino, L. R. Hathaway and T. Worman, *Adv. Chem. Ser.*, 1971, **106**, 299.
60. S. Wakeham and R. Carpenter, *Chem. Geol.*, 1974, **13**, 39.
61. S. C. Blanchard and N. D. Chasteen, *Anal. Chim. Acta*, 1976, **82**, 113.
62. D. S. Gamble, M. Schnitzer and D. S. Skinner, *Can. J. Soil Sci.*, 1977, **57**, 47.
63. R. M. Farmer and A. I. Popov, *Inorg. Chim. Acta*, 1982, **59**, 87.
64. J. Kragten, *Atlas of Metal-Ligand Equilibria in Aqueous Solution*, p. 27. Horwood, Chichester, 1977.

A NEW LIQUID-MEMBRANE ELECTRODE FOR SELECTIVE DETERMINATION OF PERCHLORATE

SAAD S. M. HASSAN* and M. M. ELSAIED

Department of Chemistry, Faculty of Science, Ain Shams University, Cairo, Egypt

(Received 30 November 1985. Revised 15 January 1986. Accepted 28 February 1986)

Summary—A new liquid-membrane electrode which responds to perchlorate ion is described. It incorporates a $10^{-2}M$ solution of the nitron-perchlorate ion-pair complex, in nitrobenzene, as a liquid membrane. The electrode exhibits near-Nernstian response for 10^{-2} – $2 \times 10^{-5}M$ perchlorate with an anionic slope of 56 mV/pClO₄. The response time is 20–90 sec, the working pH 2.5–8.5, the lower limit of detection $8 \times 10^{-6}M$ perchlorate and the selectivity for perchlorate relative to 27 inorganic and organic anions of different nature is reasonably high. Periodate, permanganate and thiocyanate, however, interfere. Determination of 2–1000 µg/ml perchlorate in aqueous solutions shows an average recovery of 98.8% and a mean relative standard deviation of 1.9%. The electrode has been successfully used for direct potentiometric determination of the purity of perchlorate propellants and the solubility products of some sparingly soluble perchlorates.

Since the introduction of the first perchlorate ion-selective electrode in 1968 by Ross,^{1,2} many perchlorate membrane-electrode systems have been developed. These incorporate the perchlorate ion-association complexes of some metal chelates, long-chain quaternary ammonium ions and organic dyes, as electroactive species, dispersed in lipophilic solvents, polymeric membranes and hydrophobic porous matrices. The perchlorate complexes of tris-(phenanthroline)iron(II),¹⁻⁷ tricaprylylmethylamine (Aliquat 336S),⁸⁻¹¹ tridodecylhexadecylamine,¹² triheptylhexadecylamine,¹³ tetrapropylamine,¹⁴ tetrabutylamine,¹⁴ benzylhexadecyldimethylamine,¹⁵ *N*-ethylbenzothiazole-2,2'-azine,¹⁶ the dimethyltetradecylamine derivative of Amberlite XAD-2 resin,¹⁷ the trioctylamine derivative of styrene-divinylbenzene copolymer,¹⁸ Ethyl Violet,¹⁹ Gentian Violet,²⁰ Brilliant Green,²¹ and Methylene Blue,²² have all been utilized as the electroactive materials. These complexes are either dissolved in organic solvents such as 1,2-dichloromethane,¹⁴ 1-decanol,^{8,9} nitrobenzene,^{4,18,22} tetrachloroethane,²⁰ chlorobenzene,²¹ and nitro-*p*-cymene,^{1,2} or dispersed in poly(vinyl chloride) matrix.^{5-7,10,12,13} Hydrophobic porous graphite rods,¹⁵ and fritted glass discs,^{4,20} have also been used to support the electroactive materials.

Many of these electrodes, however, are not sensitive enough to permit measurement of low levels of perchlorate, and/or display poor selectivity in the presence of various common contaminants. For most of these electrodes, selectivity data have been reported for only a few ions. The present work describes the preparation, characterization and some possible applications of a new perchlorate ion-

selective electrode based on the use of the nitron-perchlorate ion-pair complex, in nitrobenzene as solvent. The sensitivity and stability offered by this simple electrode configuration are high enough to allow accurate determination of low levels of perchlorate. The selectivity coefficients measured for many inorganic and organic anions of different nature are negligibly small.

EXPERIMENTAL

Apparatus

All emf measurements were made at $25 \pm 1^\circ$ (unless otherwise stated) with an Orion microprocessor "Ionalyzer" (Model 901), the nitron-perchlorate liquid-membrane electrode and an Orion double-junction Ag/AgCl electrode (Model 90-02), with its outer chamber filled with 10% sodium nitrate solution, as the reference electrode. An Orion glass-calomel combination electrode (Model 91-02) was used in pH adjustment.

Reagent

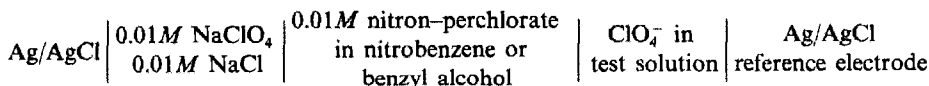
All solutions were prepared with demineralized doubly distilled water and all chemicals were of analytical reagent grade unless otherwise stated. A 0.1M stock perchloric acid solution was prepared in 0.1M sodium chloride and standardized by potentiometric titration with standard sodium carbonate solution (glass-calomel electrode system). A 0.1M stock sodium perchlorate solution was also prepared in demineralized doubly distilled water. Standard perchlorate solutions (10^{-2} – $10^{-6}M$) were freshly prepared by accurate dilutions of the stock perchloric acid and sodium perchlorate solutions with 0.1M sodium chloride and demineralized doubly distilled water, respectively.

Procedures

Membrane preparation. Nitron-perchlorate was prepared by mixing 30 ml of aqueous 0.01M perchloric acid with 30 ml of 0.01M nitron solution in 10% acetic acid. The mixture was cooled in ice-water and the precipitate was filtered off by suction, washed with demineralized doubly distilled water, dried at about 110° for 20 min and ground. The liquid ion-exchanger was prepared by making a 0.01M solution of nitron-perchlorate in nitrobenzene.

*Author for correspondence; current address: Department of Chemistry, Qatar University, Doha, Qatar.

Electrode preparation. An Orion liquid-membrane electrode barrel (Model 92) was used for electrode assembly with a porous membrane (Orion 92-06-04). The internal reference solution was 0.01M sodium chloride/0.01M sodium perchlorate. After assembly of the electrode, the internal reference solution and the liquid ion-exchanger were injected into the appropriate ports. The electrode was conditioned by soaking in 0.01M sodium perchlorate for 2 days. When not in use, the electrode was kept immersed in the same solution.



Electrode calibration. Portions (25 ml) of 10⁻²–10⁻⁶M perchloric acid or sodium perchlorate standard solutions were transferred to 50-ml beakers, and adjusted to pH 3–7 by addition of dilute sodium hydroxide solution. The nitron-perchlorate liquid-membrane electrode, in conjunction with a double-junction Ag/AgCl reference electrode, was immersed in the stirred solutions. The potentials were displayed on a chart recorder and the stable values were plotted as functions of pClO₄, to give a calibration graph.

Electrode selectivity. The selectivity coefficients were evaluated by the mixed solution method of Srinivasan and Rechnitz²³ from potential measurements on solutions containing 10⁻³M sodium perchlorate and various concentrations (10⁻²–10⁻³M) of the interfering anion. Equation (1) was used for the calculation, where Δ*E* is the change in potential in the presence of a second anion, *j*^{z-}, *S* is the slope of the calibration graph for perchlorate and *a*₁ and *a*₂ are the concentrations of perchlorate and the second anion, respectively.

$$K_{ij}^{\text{pot}} = (10^{\Delta E/S} - 1)a_1/(a_2)^{1/z} \quad (1)$$

Determination of perchlorate in propellants. A quantity of the powder equivalent to 0.2–10 mg of perchlorate ion was weighed out, transferred to a 50-ml beaker and dissolved in 25 ml of 0.1M sodium chloride. The pH was adjusted to 3–7 and the potential was recorded as for the calibration standards and the perchlorate concentration read off the calibration graph.

Solubility of sparingly soluble perchlorates. A 1-g portion of the sparingly soluble perchlorate was suspended in 50 ml of demineralized doubly distilled water in an airtight Erlenmeyer flask. The mixture was shaken vigorously for 3 hr in a thermostat adjusted to 35 ± 1° and allowed to stand for an hour at the same temperature before potential measurement as previously described. The perchlorate concentration was read from the calibration graph prepared with aqueous standard sodium perchlorate solutions. The solubility (*M*) and solubility product (*K_{sp}*) were then calculated.

RESULTS AND DISCUSSION

Nature and composition of the membrane

The strong organic base 4,5-dihydro-1,4-diphenyl-3,5-phenylimino-1,2,4-triazole (nitron) forms a fairly insoluble crystalline nitrate and perchlorate.²⁴ In this study a nitron-perchlorate precipitate was prepared and examined as a novel electroactive material in a liquid-membrane responsive to the perchlorate ion. Elemental analysis of the product agreed with the composition C₂₀H₁₆N₄·HClO₄. The most significant absorption bands in the infrared spectrum of the precipitate, at 3320 and 1100 cm⁻¹, are assigned to stretching vibrations of the secondary amino and perchlorate groups, respectively.

The solubility of nitron-perchlorate in some lipophilic solvents such as nitrobenzene, 1-octanol, 1-decanol and benzyl alcohol was tested. Nitron-perchlorate has high solubility in both nitrobenzene and benzyl alcohol. Hence, solutions of nitron-perchlorate in both solvents were prepared and examined as liquid-membranes for potentiometric determination of perchlorate by use of the electrochemical cell.

The emf may be expressed as a function of perchlorate activity according to the equation

$$E = E_0 - S \log[a_1 + K_{ij}^{\text{pot}}(a_2)^{1/z}] \quad (2)$$

where *E*₀ is the conditional standard potential of the electrode under the conditions used in the cell, *S* is the slope of the calibration graph, *K*_{*ij*}^{pot} is the selectivity coefficient, *a*₁ and *a*₂ are the activities of the perchlorate ion and of a foreign ion of charge *z*, in the test solution, respectively. A similar equation can be used to relate the emf to concentration.

Performance characteristics of the membrane

The response characteristics of an electrode incorporating 0.01M nitron-perchlorate in nitrobenzene were evaluated at 25 ± 1°. The potential-response to perchlorate was linear for aqueous solutions over at least 3 orders of magnitude of activity or concentration, with near-Nernstian slope (Fig. 1). The activity coefficient for perchlorate in 0.1M sodium chlo-

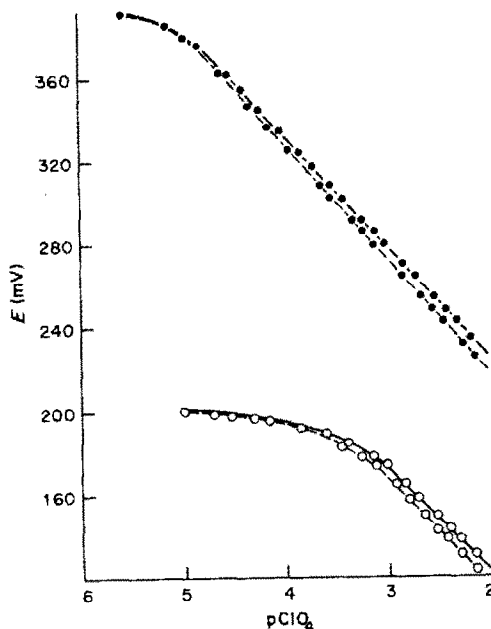


Fig. 1. Potential-response curves for nitron-perchlorate liquid-membrane electrodes with nitrobenzene (●) and benzyl alcohol (○) as membrane solvent as functions of activity (—) and concentration (---).

ride, as calculated from an extended Debye-Hückel relation, is 0.76.

Least-squares analysis of the data showed that the calibration plot was linear from 10^{-2} to $2 \times 10^{-5} M$ with a slope of 56 mV/pClO_4 . The standard deviation of a measurement was 0.8 mV . The lower limit of detection, defined as the concentration of perchlorate corresponding to the intersection of the extrapolated linear segments of the calibration graph, was $8 \times 10^{-6} M$. This limit is lower than those obtained with many other previously described electrodes.^{5,8,10,25} With benzyl alcohol as the solvent, however, the electrode response was poor, probably because benzyl alcohol is more viscous and more soluble in water, and has a lower dielectric constant than nitrobenzene.

Potential stability and response time

The results obtained from 5 different perchlorate electrodes, all with nitrobenzene as the membrane solvent but prepared over a period of 6 months, showed that the reproducibility of the potential readings on the same day for the same perchlorate solutions was within $\pm 1.2 \text{ mV}$. The variation in potential reading for a given pClO_4 during 6 weeks of normal use was within $\pm 3 \text{ mV}$. Electrode age up to 6 weeks had no significant effect on the slope of the calibration plot, which remained within 1.8 mV/pClO_4 of its original value. The liquid membrane was usable for 6 weeks before renewal.

The average response time, defined as the time required for the electrode to reach a potential within $\pm 1 \text{ mV}$ of the final equilibrium value after transfer between perchlorate solutions differing in concentration by a factor of 10, or after rapid 10-fold increase in concentration by addition of sodium perchlorate, was 20 sec for concentrations $\geq 10^{-3} M$ and 90 sec for concentrations $\leq 10^{-4} M$.

Effect of pH on the membrane response

Figure 2 shows that the electrode potential is independent of pH in the range 2.5–8.5 (the electrode

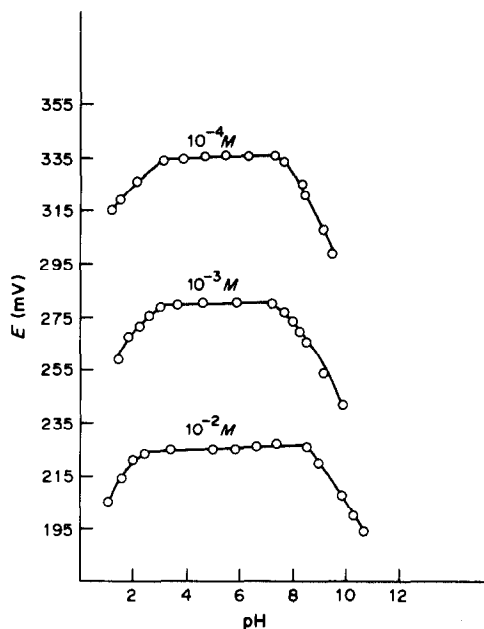


Fig. 2. Effect of pH on the potential response of nitron-perchlorate liquid-membrane electrode at different concentrations of ClO_4^- .

potential did not vary by more than $\pm 2 \text{ mV}$ for any perchlorate concentration in the range of 10^{-2} – $10^{-4} M$). Above pH 9, however, there was a substantial decrease in the electrode potential, probably owing to gradual dissociation or decomposition of nitron-perchlorate at the membrane surface.

Effect of other anions

The performance of the electrode in the presence of 30 different inorganic and organic anions was assessed by measuring the selectivity coefficient values ($K_{i,j}^{\text{pot}}$) by the mixed solution method.^{23,26} The results obtained (Table 1) show that the electrode displays high selectivity for perchlorate.

Table 1. Selectivity coefficients for some common anions with the nitron-perchlorate liquid-membrane electrode

Interfering ion (j)	$K_{i,j}^{\text{pot}}$	Interfering ion (j)	$K_{i,j}^{\text{pot}}$
F^-	4.1×10^{-3}	$\text{Fe}(\text{CN})_2^{2-}$	1.3×10^{-4}
Cl^-	7.2×10^{-4}	$\text{Fe}(\text{CN})_6^{4-}$	8.2×10^{-5}
ClO_3^-	4.3×10^{-3}	MnO_4^-	2.6
Br^-	2.7×10^{-3}	CrO_4^{2-}	6.2×10^{-4}
BrO_3^-	1.3×10^{-3}	H_2PO_4^-	5.3×10^{-3}
I^-	8.3×10^{-2}	CO_3^{2-}	2.7×10^{-4}
IO_3^-	1.1×10^{-3}	VO_3^-	1.3×10^{-4}
IO_4^-	3.6	MoO_4^{2-}	3.1×10^{-4}
NO_2^-	3.2×10^{-3}	WO_4^{2-}	3.5×10^{-4}
NO_3^-	1.1×10^{-3}	Acetate ⁻	4.2×10^{-3}
SO_3^{2-}	3.2×10^{-4}	Oxalate ²⁻	3.0×10^{-4}
SO_4^{2-}	3.8×10^{-4}	Tartrate ²⁻	3.2×10^{-4}
$\text{S}_2\text{O}_3^{2-}$	2.8×10^{-4}	Succinate ²⁻	2.8×10^{-4}
$\text{S}_2\text{O}_8^{2-}$	7.7×10^{-4}	Citrate ³⁻	1.2×10^{-4}
CNS^-	1.8	Benzoate ⁻	4.3×10^{-3}

Surprisingly, the electrode displays only a weak response to nitrate ($K_{ij}^{pot} = 1.1 \times 10^{-3}$) although nitron reacts quantitatively with both perchlorate and nitrate under the same conditions. To understand this phenomenon, the partition of perchlorate and nitrate between water and a solution of $10^{-2}M$ nitron in nitrobenzene was tested by measuring the concentrations of both ions in the aqueous phase after the extraction. The results showed that nitrobenzene extracted the perchlorate and retained the nitron-perchlorate almost quantitatively. The degree of extraction of nitrate was only about a hundredth of that of perchlorate, probably owing to the difference in the hydration energies of the two ions. It is known that the perchlorate ion is more hydrophobic and larger than the nitrate ion. The hydration enthalpies (ΔH_{aq}°) are -57.1 and -74.5 kcal/mol and the ionic radii are 2.45 and 1.96 Å for the perchlorate and nitrate ions, respectively.²⁷ The larger, more hydrophobic, anion has the smaller hydration enthalpy.²⁷ Competition between the perchlorate ion and the smaller and more strongly hydrated nitrate ion thus favours preferential extraction of the former by the membrane phase, causing the higher selectivity of the electrode for perchlorate. The effect of relative anion hydration energies has similarly been used to explain the solvent extraction behaviour of some anions^{28,29} and the selectivity of some anion-exchange resins.³⁰

Compared with some of the commercially available perchlorate ion-selective electrodes,^{31,32} the nitron-perchlorate liquid-membrane electrode is notably tolerant of Br^- , NO_2^- , NO_3^- , ClO_3^- and carboxylate anions and is less affected by many other inorganic anions (Table 1). It has been reported that NO_3^- , NO_2^- , Br^- , ClO_3^- , CN^- and I^- ions cause serious errors with some perchlorate membrane electrodes, as evidenced by the 5–25% error produced when there are equal quantities of these ions and perchlorate.^{31,32} The use of the nitron-perchlorate liquid-membrane electrode for the determination of perchlorate in the presence of these ions, however, is without complications. Mixtures containing 10–100 $\mu\text{g/ml}$ perchlorate and ten times that concentration of any of these ions can be determined with the present electrode by the calibration graph method, with an average recovery of 97–102% and mean standard deviation of 2.3%.

The nitron-perchlorate liquid-membrane electrode responds, however, to CNS^- , IO_4^- and MnO_4^- ions. Most of the commercially available perchlorate ion-selective electrodes are also known to respond to MnO_4^- , IO_4^- and $Cr_2O_7^{2-}$ ions.³² Fortunately, the interference of a 10-fold ratio of IO_4^- or MnO_4^- to ClO_4^- is completely circumvented by prior heating of the test solution at 60–80° for 10 min with glycerol and oxalic acid, respectively. On the other hand, the responses of the electrode to CNS^- , IO_4^- and MnO_4^- were linear over the concentration range 10^{-2} – $10^{-4}M$ with slopes of 40, 52 and 65 mV/decade, respectively.

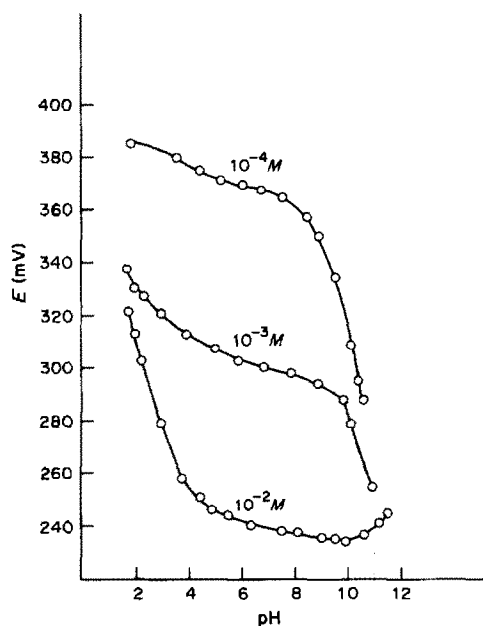


Fig. 3. Effect of pH on the potential response of the nitron-perchlorate liquid-membrane electrode at different concentrations of MnO_4^- .

This suggests possible use of the electrode as a potentiometric sensor for determination of these ions. Direct potentiometric determination of 50–1000 $\mu\text{g/ml}$ CNS^- , IO_4^- and MnO_4^- concentrations at pH 6–7 by use of calibration graphs prepared with standard solutions of these ions showed an average recovery of 97% and a mean standard deviation of 3.1%. The effect of pH on the electrode responses for CNS^- and IO_4^- was rather similar to that for ClO_4^- itself, with a working range of pH 3–7, but the MnO_4^- response was more seriously affected, as shown by Fig. 3.

Table 2. Direct potentiometric determination of the perchlorate ion with the nitron-perchlorate liquid-membrane electrode

[ClO_4^-]		Relative standard deviation, † %
Taken, $\mu\text{g/ml}$	Recovery, * %	
2.0	97.1	2.8
5.0	98.4	2.5
10.0	99.5	1.8
19.9	98.9	1.9
29.8	99.1	1.7
39.8	98.9	2.0
79.6	99.4	1.8
99.5	100.0	1.7
199.0	98.5	2.1
298.5	98.0	1.8
398	99.3	1.8
597	97.9	1.7
796	98.5	1.5
995	99.5	1.3

*Average of 3 measurements.

†Range method.

Table 3. Direct potentiometric determination of perchlorate in propellants

Compound*	[ClO ₄ ⁻], %		Relative standard deviation, %
	Theory	Recovery†	
Ammonium perchlorate	84.68	98.2	1.7
Urea perchlorate	61.99	99.1	1.9
Hydrazine perchlorate	75.09	98.5	2.1
Ethylamine perchlorate	68.38	97.9	1.8
Ethylenediamine perchlorate	61.99	99.2	1.7

*Concentration used 10–200 µg/ml.

†Average of 5 measurements.

Table 4. Direct potentiometric determination of the solubility products of some sparingly soluble perchlorates

Compound	K _{sp}		
	Present method at 35°	Potentiometric method ²⁵ at 35°	Gravimetric method at 25°
Potassium perchlorate	1.6 × 10 ⁻²	1.6 × 10 ⁻²	8.9 × 10 ^{-2*}
Hexa-amminecobalt(III) perchlorate	9.2 × 10 ⁻⁶	9.4 × 10 ⁻⁶	6.3 × 10 ^{-6†}
Tetrakis(pyridine)copper(II) perchlorate	5.2 × 10 ⁻⁵	5.4 × 10 ⁻⁵	—
Nitron perchlorate	2.9 × 10 ⁻⁸	—	3.8 × 10 ^{-8§}

*Nordmann.³³†Taylor *et al.*³⁴§Vogel.²⁴

Determination of perchlorates

The use of the nitron–perchlorate liquid-membrane electrode for direct potentiometric determination of perchlorate was first examined with 2.5–1225 µg/ml sodium perchlorate (equivalent to approximately 2–1000 µg/ml perchlorate), in triplicate. The average recovery was 98.8% and mean standard deviation 1.9% (Table 2). The purity of some perchlorate compounds commonly used as propellants was also determined by preparing the sample solution in 0.1M sodium chloride (to control the ionic strength), adjusting the pH to 3–7 if necessary, and measuring the potential; a sodium perchlorate calibration graph was used. The average recovery was 98.6% and mean standard deviation 1.8% (Table 3).

The solubilities of some sparingly soluble perchlorates were also determined. The equilibrium potentials of saturated solutions of potassium, hexa-amminecobalt(III), tetrakis(pyridine)copper(II) and nitron perchlorates were directly measured at 35 ± 1°. The solubility products computed and given in Table 4 compare favourably with values previously recorded by other measurement techniques.^{24,25,33,34}

REFERENCES

- J. W. Ross, in *Ion Selective Electrodes*, R. A. Durst (ed.), p. 57. U.S. Govt. Printing Office, Washington, D.C., 1969.
- Orion Research Inc., *British Patent*, 1197264 (1968).
- N. Ishibashi and H. Kohara, *Anal. Lett.*, 1971, **4**, 785.
- E. Hopirtean, E. Veress and V. Muresan, *Rev. Roum. Chim.*, 1977, **22**, 1243.
- T. J. Rohm and G. G. Guilbault, *Anal. Chem.*, 1974, **46**, 590.
- M. Čakrt, J. Berčik and Z. Hladký, *Z. Anal. Chem.*, 1976, **281**, 295.
- A. Hulanicki and R. Lewandowski, *Chem. Anal. (Warsaw)*, 1974, **19**, 53.
- C. J. Coetzee and H. Freiser, *Anal. Chem.*, 1968, **40**, 2071.
- Idem, ibid.*, 1969, **41**, 1128.
- H. J. James, G. P. Carmack and H. Freiser, *ibid.*, 1972, **44**, 856.
- K. Suzuki, H. Ishiwada, T. Shirai and S. Yanagisawa, *Bunseki Kagaku*, 1981, **30**, 751.
- F. Jasim, *Iraq. J. Sci.*, 1979, **20**, 430.
- P. Ni, X. Du and G. Wu, *Fenxi Huaxue*, 1982, **10**, 750.
- S. Back, *Anal. Chem.*, 1972, **44**, 1696.
- C. Luca, G. Semencescu and C. Nedea, *Rev. Chim. (Bucharest)*, 1974, **25**, 1015.
- M. Sharp, *Anal. Chim. Acta*, 1972, **62**, 385.
- A. Jyo, T. Imato, K. Fukamachi and N. Ishibashi, *Chem. Lett.*, 1977, 815.
- T. Imato, A. Jyo and N. Ishibashi, *Anal. Chem.*, 1980, **52**, 1893.
- J. Pan and Y. Liu, *Fenxi Huaxue*, 1981, **9**, 593.
- E. Hopirtean and E. Stefaniga, *Rev. Roum. Chim.*, 1978, **23**, 137.
- A. G. Fogg, A. S. Pathan and D. T. Burns, *Anal. Chim. Acta*, 1974, **73**, 220.
- M. Kataoka and T. Kambara, *J. Electroanal. Chem.*, 1976, **73**, 279.
- K. Srinivasan and G. A. Rechnitz, *Anal. Chem.*, 1969, **41**, 1203.
- A. I. Vogel, *A Text Book of Quantitative Inorganic Analysis*, 3rd Ed., p. 131. Longmans, London, 1975.
- T. M. Hseu and G. A. Rechnitz, *Anal. Lett.*, 1968, **1**, 629.
- T. S. Ma and S. S. M. Hassan, *Organic Analysis Using Ion Selective Electrodes*, Academic Press, London, 1982.
- R. E. Reinsfelder and F. A. Schultz, *Anal. Chim. Acta*, 1973, **65**, 425.
- R. M. Diamond and D. G. Tuck, *Progr. Inorg. Chem.*, 1960, **2**, 109.
- N. A. Gibson and D. C. Weatherburn, *Anal. Chim. Acta*, 1972, **58**, 159.
- B. Chu, D. C. Whitney and R. M. Diamond, *J. Inorg. Nucl. Chem.*, 1962, **24**, 1405.

31. Orion Research Instruction Manual of Perchlorate Ion Selective Electrode (Model 93-81), 1979.
32. R. J. Baczuk and R. J. DuBois, *Anal. Chem.*, 1968, **40**, 685.
33. J. Nordmann, *Qualitative Testing and Inorganic Chemistry*, p. 325. Wiley, New York, 1957.
34. M. A. Taylor, J. A. Baur and C. E. Bricker, *Anal. Chem.*, 1968, **40**, 436.

SHORT COMMUNICATIONS

DETERMINATION OF LEVAMISOLE HYDROCHLORIDE WITH HgI_4^{2-} BY A TURBIDIMETRIC METHOD AND FLOW-INJECTION ANALYSIS

J. MARTINEZ CALATAYUD* and CAMPINS FALCO

Departamento de Química Analítica, Facultad de Química, Universidad de Valencia, Burjassot (Valencia), Spain

(Received 30 October 1985. Revised 25 March 1986. Accepted 11 April 1986)

Summary—This paper is concerned with the use of ion-association compounds in the analysis of pharmaceutical samples by FIA. The usual extraction into an organic phase is avoided by using turbidimetric detection. Determination of levamisole with HgI_4^{2-} has been developed as a practical example: the experimental variables were optimized by the modified simplex method. The calibration graph is linear over the levamisole concentration range 7–32 $\mu\text{g/ml}$. The reproducibility (rsd) and injection sample rate are 0.9% and 80/hr, respectively.

Few papers on flow-injection analysis (FIA) are concerned with turbidimetric detection, and so far only ammonia and sulphate ions have been determined in this way.

Krug *et al.*¹ proposed using Nessler's reagent for turbidimetric detection of ammonia (in the 0.5–6 $\mu\text{g/ml}$ range) in natural water samples. A protective agent was required in order to prevent gradual deposition of precipitate on the walls of the FIA system. Good precision and accuracy were achieved with a sampling rate of 120/hr.

Sulphate has been turbidimetrically determined²⁻⁷ with barium, at sampling-rates from 60/hr,⁶ to 250/hr.⁵ The widest application range⁶ was for sulphate concentrations from 5.0 to 200 $\mu\text{g/ml}$. Hemmings and Macdonald⁸ reported a procedure with 2-aminopyrimidine hydrochloride as reagent, using the merging-zones technique to save sample and reagent; 95 μl of both species are consumed in each determination, in the 0–10 $\mu\text{g/ml}$ sulphate range, and the sampling-rate is up to 60/hr.

Liquid-liquid distribution of ion-association compounds and their photometric detection is a broadly used procedure in drug analysis: it is a sensitive and precise technique for the determination of basic drugs.⁹⁻¹¹ Since the initial work of Karlberg and Thelander¹² on determination of caffeine in acetylsalicylic acid preparations, with sodium laurylsulphate interference eliminated by addition of tetraphenylammonium ion (which forms an ion-pair with the laurylsulphate and transfers it to the organic phase, where it does not contribute to the analyte absorbance at 275 nm), some applications of FIA automated solvent extraction and ion-association complex formation to drug evaluation have appeared in the literature. They include determination of codeine

with picrate,¹³ procyclidine hydrochloride, also with picrate,¹⁴ and anionic^{15,16} and cationic¹⁷ surfactants in pharmaceutical formulations. Steroid and bile acid sulphates have been determined in clinical analysis with lucigenin.¹⁸

This paper is concerned with turbidimetric detection in FIA procedures based on ion-association compounds, and deals with evaluation of levamisole with tetraiodomercurate(II) as precipitating reagent. The procedure was optimized by the modified simplex method (MSM), the parameters concerned being sample volume, reaction coil-length, flow-rate, pH and reagent concentration.

Levamisole hydrochloride is the laevo-isomer of tetramisole hydrochloride; both are anthelmintic drugs, but the former has fewer side-effects. Holbrook and Scales¹⁹ have determined tetramisole in animal tissue extract polarographically, and Mourot *et al.*²⁰ have evaluated it by HPLC in the routine analysis of veterinary anthelmintics, but both methods require mg quantities of the drug. Some liquid extraction-colorimetry methods have been proposed for evaluation of tetramisole in μg amounts, with various dyestuffs.²¹ Sodium nitroprusside²² and cobalt thiocyanate²³ have also been proposed as reagents.

No pharmacopoeial method is given in the BP or USP for determination of the two drugs.

EXPERIMENTAL

Reagents

Aqueous solutions of levamisole hydrochloride. The solid (donated by Química Farmacéutica Bayer) was found, by non-aqueous potentiometric titration with perchloric acid in acetic acid medium, to be $100.7 \pm 0.3\%$ pure (5 replicates).

Channing's solution. Mercuric iodide (1.00 g) and potassium iodide (0.80 g) were dissolved, mixed and diluted to 100 ml with demineralized water.

Buffer solutions. Made with citric acid and disodium hydrogen phosphate, at 0.5M ionic strength and adjusted to the desired pH.

*Author for correspondence.

Carrier stream. A mixture of 10 ml of buffer solution and V ml of Channing's solution was made up to 50 ml with demineralized water.

Other reagents were of analytical grade.

FIA assembly and procedure

The sample solution was injected into the carrier stream and the turbidity measured spectrophotometrically with a Coleman 55 (Perkin-Elmer) instrument provided with an 18- μ l flow-cell (Hellma) and a Unicam 45 A-R (Pye Unicam) recorder. The Tecator 5020 apparatus, sample injector and pumps were used and the reaction-coil was a 0.5-mm bore Teflon tube.

RESULTS AND DISCUSSION

A qualitative study of formation of ion-association compounds of levamisole was done by mixing 1 ml of $4.2 \times 10^{-4} M$ levamisole solution, 1 ml of $1.20 \times 10^{-3} M$ dyestuff or $2.64 \times 10^{-5} M$ inorganic anion and 1 ml of buffer. No precipitate was formed with Bromocresol Purple or Green, Thymol Blue, Bromophenol Blue, Methylthymol Blue, Phenol Red and Arsenazo B, but HgI_4^{2-} , CdI_4^{2-} and BiI_4^- gave yellow, white and orange precipitates respectively.

Spectra from 400 to 750 nm for suspensions obtained from $5.3 \times 10^{-5} M$ levamisole plus $2.64 \times 10^{-3} M$ HgI_4^{2-} or BiI_4^- solutions were recorded in order to choose the most suitable counter-ion for levamisole determination (no precipitate was obtained with levamisole and CdI_4^{2-} at these concentrations). The influence of levamisole concentration was also tested.

Figure 1a shows the spectra measured against demineralized water immediately after production of the turbidities. The absorption peak at 430 nm for the levamisole- HgI_4^{2-} system is due to the ion-association compound, since no absorption is observed with the clear solution. For the levamisole- BiI_4^- system no absorption peak was observed, so absorbance measurements were made at 700 nm, where the reagent does not absorb.

The calibration graph is steeper for the HgI_4^{2-} system (Fig. 1b) so this is preferred for practical use, although the limit of detection is lower for the BiI_4^- system.

Spectra over the range 400–500 nm recorded at 30-sec intervals show a decrease in absorbance with time; the stability is not improved by addition of protective colloids, such as sucrose, glucose and starch, and this prevents use of this reaction in a batch procedure.

The influence of pH was tested by adding hydrochloric acid or sodium hydroxide solution to a $5.6 \times 10^{-5} M$ levamisole/ $2.11 \times 10^{-3} M$ HgI_4^{2-} mixture and recording the absorbance at 430 nm; the best pH range was found to be 3.30–7.65. Various buffer solutions were tested and the citric acid/phosphate system was selected.

The stoichiometry of the product was established by conductometric titration of 55 ml of $8.1 \times 10^{-4} M$ HgI_4^{2-} or $3.20 \times 10^{-4} M$ levamisole with $2.00 \times 10^{-2} M$

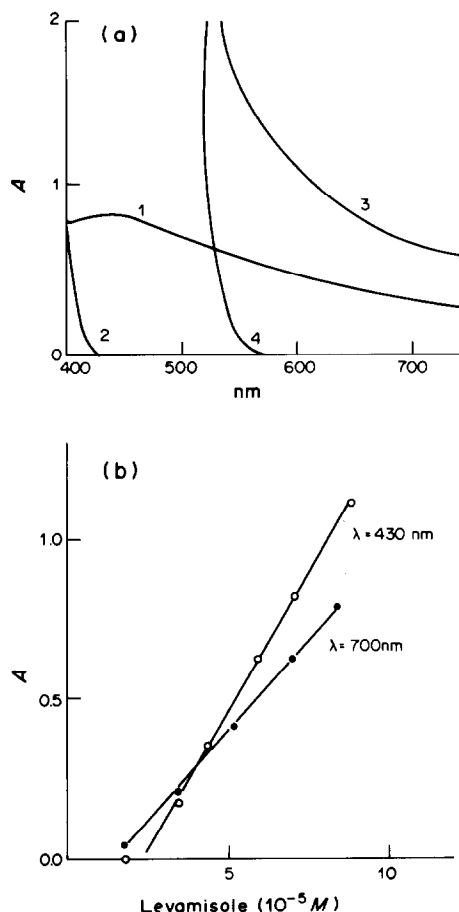


Fig. 1. (a) Spectra of $7.0 \times 10^{-5} M$ levamisole solutions: 1, with $2.6 \times 10^{-3} M$ HgI_4^{2-} ; 2, blank solution for 1; 3, with $2.64 \times 10^{-3} M$ BiI_4^- ; 4, blank solution for 3. (b) Calibration curve: \circ $2.64 \times 10^{-3} M$ HgI_4^{2-} , pH 5.60; \bullet $2.64 \times 10^{-3} M$ BiI_4^- , pH 2.00.

levamisole or $2.20 \times 10^{-3} M$ HgI_4^{2-} respectively (see Fig. 2) and found to be 2:1 levamisole: HgI_4^{2-} . It is a relatively weak compound, because precipitation is not clearly observed until there is a 20-fold molar ratio of HgI_4^{2-} to levamisole and the maximum

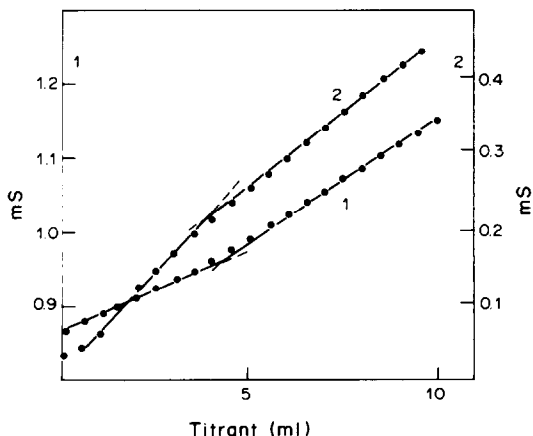


Fig. 2. Conductometric titrations: 1, titrant levamisole; 2, titrant HgI_4^{2-} .

Table 1. Range of variables examined

Reaction coil length	55–315 cm
Flow-rate	1.27–3.33 ml/min
pH	5.00–7.00
HgI ₄ ²⁻ concentration	2.2×10^{-3} – $2.20 \times 10^{-2} M$
Sample size	30–200 μ l

absorbance is obtained at > 50-fold molar concentration ratio.

MSM of optimization

The range of FIA variables to be studied was provided by the results of the preliminary spectrophotometric work. The peak-height was the parameter to be optimized. The range of variables is shown in Table 1.

Once a stable chart-recorder base-line had been obtained, a sample was injected, the reaction took place and the resulting peak was collected and the absorbance value at 430 nm read. This was repeated until an $\text{rsd} \leq 1\%$ was obtained for the peak-height (four or five repetitions usually sufficed).

The program of the MSM for this work was operated with six vertices, and was written on the basis of references 24–26. The initial simplex was chosen according to Yarbrow and Deming²⁴ with a side-length of 1 and the vertex at the origin of the co-ordinates. The region of the variables was normalized by the modification proposed by Morgan and Deming.²⁵ The optimal conditions obtained for $1.0 \times 10^{-4} M$ levamisole are: pH 5.00, flow-rate 3.14 ml/min, reaction-coil length 77 cm, sample size 200 μ l and reagent concentration $5.8 \times 10^{-3} M$.

The influence of ionic strength on the peak-height is constant over the range 0.07–0.12 M (Fig. 3).

The calibration graph was linear for 7–32 μ g/ml levamisole, with $8.55 \times 10^{-3} M$ HgI₄²⁻ as carrier (57-fold molar ratio to the maximum concentration of levamisole).

The linear range is wider than those for the methods³ using Solochrome Dark Blue or Black T, Bromothymol Blue, Bromophenol Blue and Bromocresol Green (which lie between 2.0–2.5 μ g/ml as the lower limit and 10–20 μ g/ml as the upper), but narrower than that obtained with Bromocresol Purple (5–50 μ g/ml).

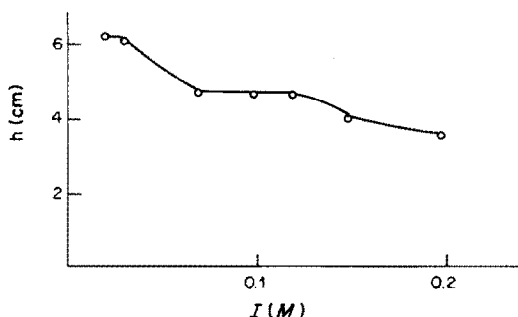


Fig. 3. Influence of ionic strength: levamisole concentration $7.1 \times 10^{-5} M$, HgI₄²⁻ concentration $4.03 \times 10^{-3} M$ in carrier stream (pH 5.00, buffer citric acid/Na₂HPO₄).

The reproducibility of the analysis was tested by injecting into the reagent stream 40 samples of $9.1 \times 10^{-5} M$ levamisole; the rsd was 0.9% (similar to that of the method of Sane *et al.*³). The sample injection rate obtainable was 80/hr.

No cleaning solution was used for the manifold tubing, but of those tested 6M hydrochloric acid gave good results.

The levamisole content of Nemanthel was determined (veterinary drug, declared formulation: 10 g of levamisole, 0.1 g of clorferinamine maleate, and excipient to give 100 g total weight of sample). A 0.5-g portion of previously powdered sample was dissolved and diluted accurately to 250 ml with demineralized water, and further diluted ten-fold (5 ml to 50 ml) and 200 μ l were directly injected into the carrier; the result obtained was $11.8 \pm 0.2\%$ (average value of three replicates). This sample was checked by the method of Sane *et al.*³ with Bromocresol Purple, the average of 3 replicates being $12.0 \pm 0.2\%$.

REFERENCES

1. F. J. Krug, J. Růžička and E. H. Hansen, *Analyst*, 1979, **104**, 47.
2. H. Bergamin F^o, B. F. Reis and E. A. G. Zagatto, *Anal. Chim. Acta*, 1978, **97**, 427.
3. F. J. Krug, H. Bergamin F^o, E. A. G. Zagatto and S. S. Jorgensen, *Analyst*, 1977, **102**, 503.
4. S. Baban, D. Beetlestone, D. Betteridge and P. Sweet, *Anal. Chim. Acta*, 1980, **114**, 319.
5. W. D. Basson and J. F. van Staden, *Water Research*, 1981, **15**, 333.
6. J. F. van Staden, *Z. Anal. Chem.*, 1982, **310**, 239.
7. F. J. Krug, E. A. G. Zagatto, B. F. Reis, F. D. Bahia, A. O. Jacintho and S. S. Jorgensen, *Anal. Chim. Acta*, 1983, **145**, 179.
8. P. Hemmings and A. M. G. Macdonald, *Flow Analysis II*, Lund, Sweden, June 1982.
9. H. Mohammed and F. F. Cantwell, *Anal. Chem.*, 1979, **51**, 1006.
10. *Idem, ibid.*, 1980, **52**, 553.
11. F. F. Cantwell and M. Carmichael, *ibid.*, 1982, **54**, 697.
12. B. Karlberg and S. Thelander, *Anal. Chim. Acta*, 1978, **98**, 1.
13. B. Karlberg, P. A. Johansson and S. Thelander, *ibid.*, 1979, **104**, 21.
14. L. Fossey and F. F. Cantwell, *Anal. Chem.*, 1982, **54**, 1693.
15. J. Kawase, A. Nakae and M. Yamanaka, *ibid.*, 1979, **51**, 1640.
16. K. Kine, *Dojin*, 1979, **14**, 9.
17. J. Kawase, *Anal. Chem.*, 1980, **52**, 2124.
18. M. Maeda and A. Tsuji, *Analyst*, 1985, **110**, 665.
19. A. Holbrook and B. Scales, *Anal. Biochem.*, 1967, **18**, 46.
20. D. Mourout, B. Delepine, J. Boisseau and G. Gayot, *J. Pharm. Sci.*, 1979, **68**, 796.
21. R. T. Sane, D. S. Sapre and V. G. Nayak, *Talanta*, 1985, **32**, 148.
22. D. M. Shingbal and S. V. Joshi, *Indian Drugs*, 1984, **21**, 396.
23. R. T. Sane, B. R. Shinde, A. K. Parikh and S. P. Tikekar, *ibid.*, 1984, **21**, 257.
24. L. A. Yarbrow and S. N. Deming, *Anal. Chim. Acta*, 1973, **73**, 391.
25. S. L. Morgan and S. M. Deming, *Anal. Chem.*, 1974, **46**, 1170.
26. J. A. Nelder and R. Mead, *Computer J.*, 1965, **7**, 308.

THE ELECTROCHEMICAL GENERATION OF SMALL AMOUNTS OF HYDROGEN CYANIDE

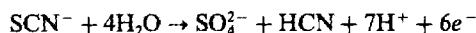
ZUZANA TOCKSTEINOVÁ and FRANTIŠEK OPEKAR*

UNESCO Laboratory of Environmental Electrochemistry, J. Heyrovský Institute of Physical Chemistry and Electrochemistry, Czechoslovak Academy of Sciences, Jilská 16, 110 00 Prague 1, Czechoslovakia

(Received 24 February 1986. Accepted 8 April 1986)

Summary—Hydrogen cyanide was generated by constant-current oxidation of an aqueous solution of potassium thiocyanate at a platinum wire anode. In a solution of 0.1M potassium thiocyanate and 0.01M potassium sulphate at a nitrogen flow-rate of 3.5–5.0 ml/sec, the rate of production of HCN was a linear function of the generation current I from 10 to 200 μ A. The relative standard deviation for an HCN production rate of 6.07 ng/sec ($I = 130 \mu$ A) was 1.8% and that for 0.92 ng/sec ($I = 20 \mu$ A) was 5.9%. The time required to establish steady-state production after a change in the generation current was 10 min.

Electrolytic generation of gases for standardization of gas analysers has been used for some time.^{1–4} We have constructed a simple apparatus for calibrating hydrogen cyanide detectors, which generates the gas by controlled-current oxidation of thiocyanate in aqueous solution according to the overall reaction⁵



The advantages of electrochemical generation over the use of permeation systems^{6,7} lie in the possibility of rapidly changing the rate of production of hydrogen cyanide and thus also its concentration in the carrier gas by more than an order of magnitude, and in avoidance of use of the highly toxic liquid HCN or alkali-metal cyanide solutions. Although the mechanism for the electro-oxidation of thiocyanate is very complicated⁸ and hydrogen cyanide is very soluble in water, under certain experimental conditions 100% yield can be attained according to the equation above, as well as 100% transfer of the HCN into the gas phase.

EXPERIMENTAL

The apparatus is depicted schematically in Fig. 1. The carrier gas—nitrogen—was first saturated with water vapour by passage through water in two bubblers (A) and then passed into the generator (B). Because hydrogen cyanide is very soluble in water, the nitrogen was bubbled directly through the frit (2) to the cell compartment (1) containing the working electrode (the anode). This compartment had an internal diameter of 10 mm and was charged with 1.0 ml of electrolyte, consisting of 0.1M potassium thiocyanate and 0.01M potassium sulphate at pH 6.5. The anode was a spiral of 50 mm of platinum wire (diameter 0.4 mm) sealed into a glass tube (3) with polyethylene rings (4) fitted on it to limit carry-over of the electrolyte into the outlet tube. The auxiliary platinum cathode was placed in

a separate chamber (5) containing 0.01M potassium sulphate, to minimize contamination of the generated HCN by hydrogen sulphide formed in the reduction of thiocyanate. The controlled electrolysis current from the galvanostat (C) could be varied in the range 10–200 μ A. The nitrogen enriched in hydrogen cyanide, and flowing at 1–5 ml/sec, was dried by passage over concentrated sulphuric acid (vessel D, Fig. 1).

The dynamic behaviour of the generator was monitored by measuring the response of a porous Teflon membrane electrode gold-coated on one surface (AuPME). The gas from the generator was introduced on the uncoated side of the membrane, the other side being immersed in 0.01M sodium hydroxide and held at 0.1 V vs. an Ag/AgCl electrode.⁹

The amount of hydrogen cyanide produced was checked by absorbing it from the nitrogen stream in 12 ml of 0.1M sodium hydroxide in an absorber with a frit, for a defined period of time, and determining it spectrophotometrically¹⁰ after neutralization with acetic acid, chlorination by chloramine-B and reaction with dimedone-pyridine reagent.

All the chemicals were of analytical-reagent grade and the measurements were made at laboratory temperature, $24 \pm 2^\circ$.

RESULTS AND DISCUSSION

The time required to establish a steady-state production after switch-on, or after changing the generating current, was determined from the response of the AuPME (Fig. 2). It was found that 10 min sufficed for a new output rate to be established, whether the generating current was increased or decreased.

A certain minimum flow-rate of nitrogen was necessary to ensure complete transfer of hydrogen cyanide from the solution into the gas phase. It is apparent from Fig. 3 that the flow-rate must be greater than 3 ml/sec for this particular design of cell. Acidifying the electrolyte to facilitate transfer of the hydrogen cyanide into the gaseous phase is not possible in this system since it also gives rise to

*Author for correspondence.

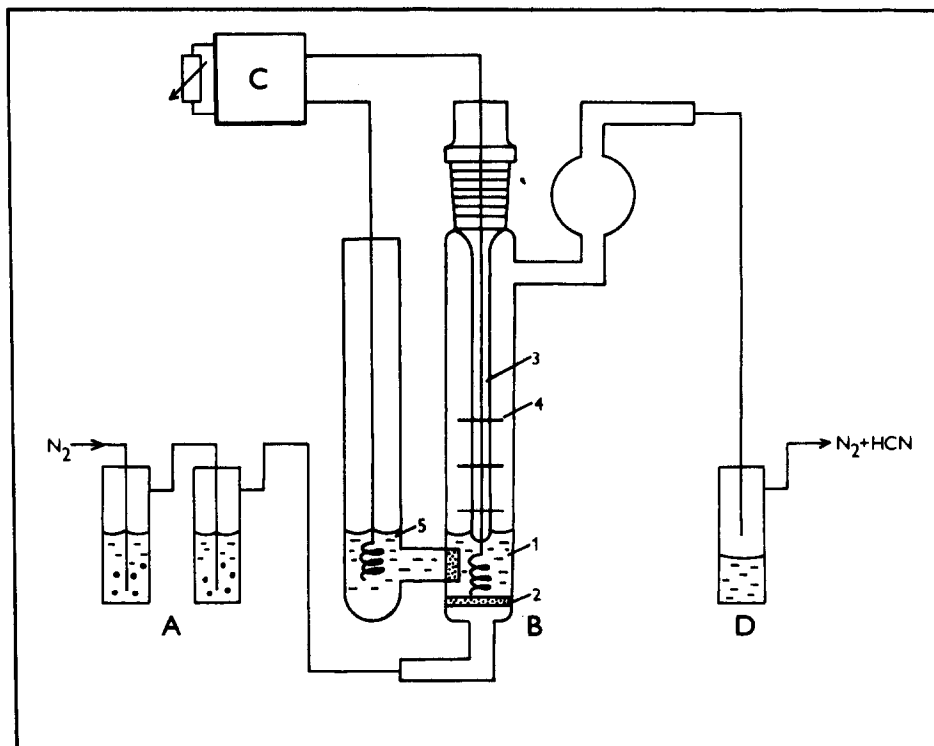


Fig. 1. The electrochemical HCN generator (description in the text).

decomposition of the thiocyanate to yield cyanide without any electrolysis—even in 0.01M sulphuric acid. We assume that at lower nitrogen flow-rates the HCN generated accumulates in the solution as a

result of less efficient contact between the gas and the liquid.

The dependence of the rate of production, R , of hydrogen cyanide (in ng/sec) on the generating current I (in the range 10–200 μA) for a nitrogen flow of 3.5–5.0 ml/sec was found, from 10 measurements, to obey the linear relationship $R = aI + b$, where a is

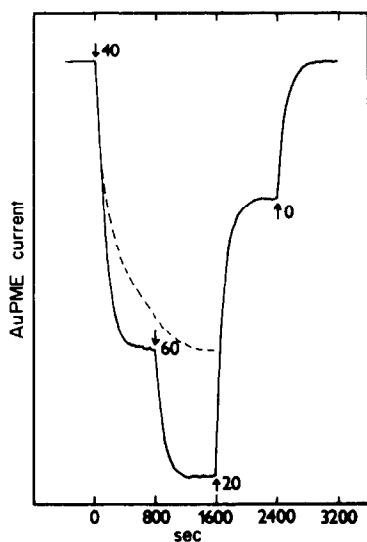


Fig. 2. The dynamic behaviour of the generator, depicted as the dependence of the AuPME current on the generation time at the given generation currents (μA). Generation in 0.1M KSCN + 0.01M K_2SO_4 , nitrogen flow-rate 4 ml/sec. Dashed line—generation current 40 μA in a solution of 0.5M KSCN + 0.01M K_2SO_4 . AuPME current sensitivity 1.6 μA full scale.

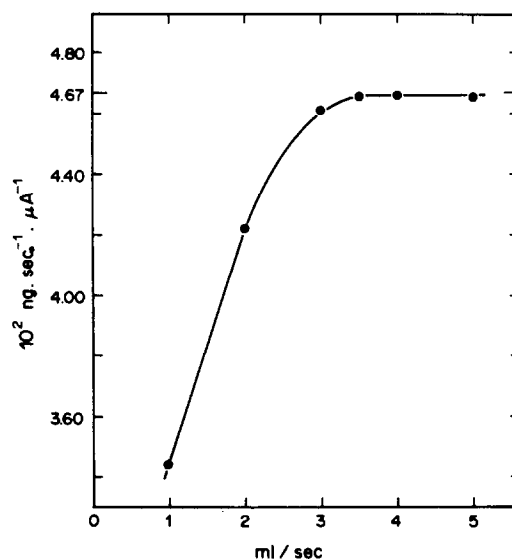


Fig. 3. Dependence of the rate of production of HCN in the gas phase on the nitrogen flow-rate. Generation in 0.1M KSCN + 0.01M K_2SO_4 .

$(4.65 \pm 0.09) \times 10^{-2} \text{ ng} \cdot \text{sec}^{-1} \cdot \mu\text{A}^{-1}$, and b is $0.02 \pm 0.10 \text{ ng/sec}$, with a standard deviation of $6.5 \times 10^{-2} \text{ ng/sec}$ and a correlation coefficient of 0.9997. The mean slope corresponds to $(99.5 \pm 1.9)\%$ of the theoretical value. Relative standard deviations of 1.8 and 5.9% were found from 10 measurements over 5 hr at a nitrogen flow-rate of 4 ml/sec for generation currents of $130 \mu\text{A}$ (HCN production rate 6.07 ng/sec) and $20 \mu\text{A}$ (0.92 ng/sec), respectively.

No effect was observed ascribable to acidification of the electrolyte solution by the hydrogen-ions formed during production of HCN, but when the electrolyte was buffered to pH 6.5 by addition of a phosphate buffer the generation efficiency dropped by about 14%. Such buffering of the solution apparently affects the reaction mechanism of thiocyanate oxidation.

Increasing the potassium thiocyanate concentration above 0.3M caused a marked increase in the time required to attain a steady-state production rate (see Fig. 2). The concentration of thiocyanate must therefore not exceed 0.3M if the speed of generation response is to be acceptable. A decrease in the thiocyanate concentration, on the other hand, simply reduces the length of time for which the generator can be run on a single filling of electrolyte.

The constancy of the production rate (without exchange of the electrolyte) in 0.1M potassium thiocyanate was studied over a period of 5 hr (see above). The actual lifetime of the electrolyte is actually much longer, as theoretically the thiocyanate content in the solution should decrease by only 10% in 8 hr at a generation current of $200 \mu\text{A}$.

REFERENCES

1. P. Hersch, C. J. Sambucetti and R. Deuringer, *Chim. Anal. (Paris)*, 1964, **46**, 31, and references therein.
2. M. Přebyl, *Z. Anal. Chem.*, 1966, **217**, 7.
3. L. Walendziak and M. Wroński, *Chem. Anal. (Warsaw)*, 1977, **22**, 55.
4. T. Yoshimori, H. Kawahara, T. Hara and A. Ikeeda, *Anal. Chim. Acta*, 1978, **98**, 171.
5. M. M. Nicholson, *Anal. Chem.*, 1959, **31**, 129.
6. A. W. Barendsz and G. van der Linden-Tak, *Z. Anal. Chem.*, 1975, **274**, 207.
7. F. Opekar, *Chem. Listy*, 1983, **77**, 884.
8. A. Rius and S. Terol, *An. Real. Soc. Esp. Fiz. Quim.*, 1949, **45B**, 359.
9. F. Opekar and S. Bruckenstein, *Anal. Chim. Acta*, 1985, **169**, 407.
10. V. Kratochvíl, *Collect. Czech. Chem. Commun.*, 1960, **25**, 299.

RAPID TECHNIQUE FOR DISTILLATION OF METHYL BORATE FOR ICP ATOMIC-EMISSION SPECTROMETRIC DETERMINATION OF BORON IN STEEL

MINORU HOSOYA, KŌICHI TOZAWA and KUNIO TAKADA

The Research Institute for Iron, Steel and Other Metals, Tohoku University, Sendai 980, Japan

(Received 22 January 1986. Accepted 5 April 1986)

Summary—The analysis time for determination of boron in steel can be remarkably shortened by simultaneous distillation of methyl borate and evaporation of the distillate for analysis by ICP atomic-emission spectrometry. Methyl borate, distilled with a large quantity of methanol, is collected in 4% sodium hydroxide solution heated in a water-bath at 90°. As the boiling point of the mixture of absorption solution and methanol is lower than 90°, the solvent mixture is easily evaporated. The limit of detection corresponds to 35 ng of boron in 0.5 g of steel.

As even micro amounts of boron in steel affect its physical properties such as toughness and hardness, it is important to determine the boron at such levels. This is generally done by spectrophotometry with curcumin,¹⁻⁶ Methylene Blue,^{1,7,8} carmine⁹ and 1-(sali-cylideneamino)-8-hydroxynaphthalene-3,6-disulphonic acid (azomethin H),¹⁰ and by atomic-emission spectrometry with an inductively-coupled argon plasma (ICP)¹¹⁻¹³ or argon plasma torch.¹⁴ However, because of interference by other components of steels, the boron (with few exceptions^{6,13}) is separated before its determination. The separation methods used include distillation of methyl borate,^{1,2,9,11,14} extraction of borate^{3,4,11} or a boron complex,^{1,7,8} removal of iron by extraction⁵ or precipitation,¹⁰ and isolation of boron as boric acid by pyrohydrolysis.^{12,15} Because of its simplicity, distillation of methyl borate is generally used.^{11,16-19} However, the distillation and the evaporation of the distillate to dryness take a long time. Here we introduce a comparatively small and simple apparatus for the distillation, and a means of simultaneously evaporating the distillate, for subsequent determination of boron by ICP atomic-emission spectrometry (ICP-AES). The analysis time is thus remarkably shortened.

Procedure

High-purity iron (0.5 g) was weighed out and transferred into the fused silica distillation flask. One ml of standard boron solution, 5 ml of sulphuric acid (1 + 1) and 15 ml of phosphoric acid (1 + 1) were added, the iron was dissolved by gentle heating, and oxidized to iron(III) by addition of 2 ml of concentrated nitric acid. The solution was heated until fumes of sulphuric acid appeared, and then cooled. The stirrer bar was added and the flask attached to the distillation unit as shown in Fig. 1. The solution was stirred at about 400 rpm and heated with the stirrer hot-plate set at about 160°. Argon, as carrier-gas, was passed at 50 ml/min through the Tygon tube (1) into the flask but was not bubbled through the solution. Methanol (35 ml) was added from the polypropylene separatory funnel (2) at about 10 ml/min. The methyl borate formed was distilled along with methanol and collected in 4 ml of absorption solution (4% sodium hydroxide) kept at 90° by the water-bath. Distillation was continued for 20 min, then the distillation flask was replaced by an empty glass flask and the argon flow-rate was increased to 300 ml/min for evaporation of the absorption solution (for a period of 5 min). The residue in the test-tube was dissolved with a little distilled water, the guide tube was detached, and the inner and outer walls of its tip were rinsed with a little distilled water. The combined solution and washings were diluted to exactly 10 ml with distilled water, and the boron was determined by ICP-AES under the conditions in Table 1.

Boron in iron and steels was determined in a similar manner, with 0.5-g samples.

EXPERIMENTAL

Apparatus

The apparatus is shown in Fig. 1. The solution in the distillation flask is simultaneously stirred and heated with a combined hot-plate and magnetic stirrer (Iwaki Glass PC-351). The ICP-AES equipment is listed in Table 1.

Reagent

A standard solution of boron (5.00 µg/ml), made with boric acid, and a 4% sodium hydroxide solution were both prepared in distilled water and stored in polyethylene bottles. High-purity iron (99.99%, Mitsuwa Chemical Co. Ltd.) and special grade reagents (Wako Pure Chemical Co. Ltd.) were used.

RESULTS

Volume of methanol

The results in Table 2 show that when distillation was continued until most of the methanol was removed from the distillation flask, all the boron was recovered when more than 30 ml of methanol was used. Hence 35 ml was chosen for the volume of methanol to be added.

Distillation time

Table 3 shows that with use of 35 ml of methanol all the boron was recovered when the distillation

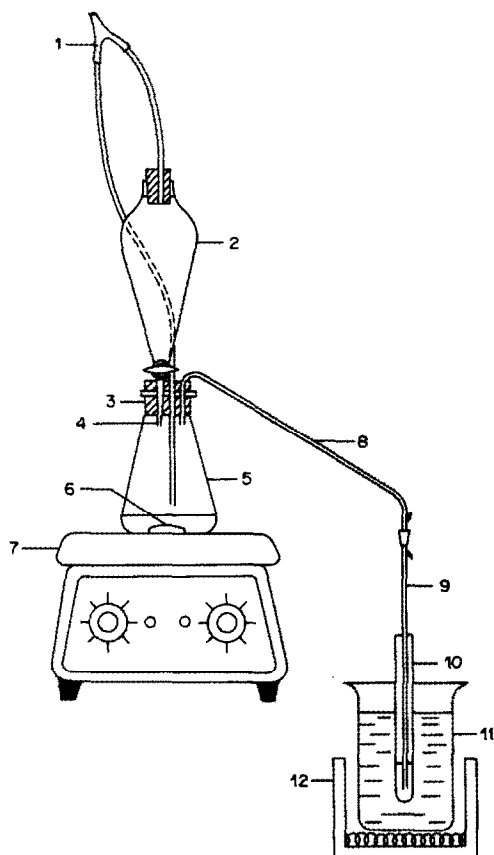


Fig. 1. Schematic diagram of the distillation apparatus. 1, Tygon tube; 2, polypropylene separatory funnel (100 ml); 3, silicone rubber plug; 4, polypropylene tube; 5, fused silica distillation flask (200 ml); 6, stirrer bar; 7, magnetic stirrer and hot-plate; 8, 9, fused silica tubes (~200 mm long, 4 mm bore); 10, fused silica test-tube (180 mm long, 16 mm bore); 11, water-bath; 12, heater.

time was more than 10 min. In view of the rapid evaporation of the absorption solution and the volume of methanol distilled with the methyl borate, a distillation time of 20 min was chosen.

Volume of absorption solution

Table 4 shows that all the boron taken was absorbed if more than 3 ml of absorption solution was

Table 1. Instruments and operating conditions

ICP generator	Shimadzu ICPS-2H, rf power 1.6 kW
Argon flow-rate	
outer gas	10.5 l./min
intermediate gas	1.5 l./min
carrier gas	1.0 l./min
Observation height above coil	16.0 ± 2.5 mm
Monochromator	Shimadzu GE-340, Entrance slit 30 μm
Detector	Hamamatsu Photonics R955 photomultiplier
Recorder	Rikadenki R-10
Analytical line	B(I) 249.773 nm

Table 2. The correlation between the volume of methanol and recovery of boron (5 μg)

Methanol, ml	Distillation time*, min	Recovery, %
10	5	25.2
15	10	80.8
20	15	90.9
25	20	96.9
30	25	99.3
35	30	99.9
40	35	100.3

*Distillation was continued until most of the methanol was removed.

Table 3. The correlation between the distillation time and recovery of boron (5 μg of B, 35 ml of methanol)

Distillation time, min	Recovery, %
5	84.6
7	97.2
10	99.2
15	100.0
20	99.8
25	100.1
30	100.1

used, so the volume selected was 4 ml. In the Japanese Industrial Standard (JIS) method for determination of boron¹ in iron and steel, the concentration of sodium hydroxide solution used for the absorption was 0.8, 4 or 8%, according to the boron content of the sample, and a 5-ml volume was used. We chose to use a 4% solution.

ICP-AES of boron

The ICP-AES signal obtained under the conditions in Table 1 was linearly related to boron concentration up to 1 μg/ml, both for standard solutions analysed directly, and for standard solutions treated according to the procedure given, and the two calibration graphs then obtained had the same slope, indicating that distillation and recovery of boron was complete.

Determination of boron

Analysis of standard and practical samples, by use of a calibration graph obtained with high-purity iron

Table 4. The correlation between the volume of absorbing solution (4% NaOH) and recovery of boron (5 μg)

Volume, ml	Recovery, %
2	96.1
3	99.2
4	99.8
6	99.7
8	100.1

Table 5. Determination of boron in iron and steel

Sample	Proposed method, %	Certified value, %
JSS 002-1 (high purity iron)	0.00005 0.00008	0.00007
JSS 159-3*	0.0013 0.0013	0.0013
JSS 165-4*	0.0009 0.0009	0.0009
JSS 172-4*	0.0011 0.0011	0.0012
NBS 1162*	0.0006 0.0005	0.0005
Iron	0.0002 0.0002	0.0002†
Fe-3%Ni-0.5%P	0.0005 0.0005	0.0005†

*Low-alloy steel.

†Methylene Blue spectrophotometry (JIS G 1227).¹

and standard boron solution, gave the results shown in Table 5. The results agreed with the certified values or those obtained by the Methylene Blue method.¹ When JSS 361-1 low-alloy steel (certified boron value 0.0009%) was analysed, the average boron content found (9 determinations) was 0.0008₈%, relative standard deviation (rsd) 4%. These values indicate that the method gives good precision and accuracy for determination of boron at this level.

The detection limit, defined as the concentration of boron giving a signal equal to three times the standard deviation of the background ICP-AES signal, is 0.0036 µg/ml, which corresponds to 36 ng of boron in a 0.5-g sample. However, boron is a common contaminant of reagents and appropriate correction must be made for it. In the work described here, commercial special grade reagents were used, and the reagent blank for the procedure was found to be 2 µg of boron. The boron content of the 0.5-g samples tested ranged from 1 to 6.5 µg, so in some cases the boron content of the reagents was greater than that of the sample. From the results for JSS 361-1 it is evident that the absolute standard deviation of the determination of a net boron content of 4.4 µg was ~0.18 µg, which is about the same as the average absolute deviation from the mean boron content found in the high-purity iron, so a limit of determination of 0.5 µg of boron would seem realistic.

Analysis time

The JIS method for boron¹ requires 100–140 min for the distillation and evaporation steps in the isolation of boron, whereas the present method re-

quires only 25 min, which shortens the analysis time considerably.

DISCUSSION

In the conventional method^{1,9,18,19} for distillation of methyl borate, methanol condensed by the water-cooled condenser continuously dilutes the sodium hydroxide absorption solution, and this greatly lengthens the subsequent evaporation of the absorption solution to dryness. In the present system, the initial formation of methyl borate is accelerated, and the methyl borate and methanol distilled are absorbed as a mixture of gas and liquid phase. As the absorption solution is kept at 90° and is purged by a flow of carrier gas at 50 ml/min, there is continuous removal of water and methanol from it. The volume of the solution therefore decreases and consequently all the methyl borate is trapped and saponified.

In determination of boron by ICP-AES the emission intensity of the BI 249.773 nm line varies with the volume of methanol in the test solution. Therefore, the absorption solution has to be evaporated completely to dryness to remove all the methanol.

Acknowledgement—The authors would like to acknowledge the continuing guidance of Prof. Kichinosuke Hirokawa.

REFERENCES

- JIS G 1227—1980, *Japanese Industrial Standard Method for Determination of Boron in Iron and Steel*.
- 1956 *Book of ASTM Methods for Chemical Analysis of Metals*, p. 132. American Society for Testing Materials, 1956.
- E. M. Donaldson, *Talanta*, 1981, **28**, 825.
- J. Aznarez and J. M. Mir, *Analyst*, 1984, **109**, 183.
- H. Goto, Y. Kakita and K. Takada, *Bunseki Kagaku*, 1969, **18**, 52.
- T. S. Harrison and W. D. Cobb, *Analyst*, 1966, **91**, 576.
- L. Pasztor and J. D. Bode, *Anal. Chem.*, 1960, **32**, 277.
- O. P. Bhargava and W. G. Hines, *Talanta*, 1970, **17**, 61.
- S. Wakamatsu, *Bunseki Kagaku*, 1958, **7**, 372.
- M. Takeuchi and S. Takeyama, *ibid.*, 1983, **32**, T66.
- G. Mezger, E. Grallath, U. Stix and G. Tölg, *Z. Anal. Chem.*, 1984, **317**, 765.
- R. M. Hamner and L. A. De'Aeth, *Talanta*, 1980, **27**, 535.
- Y. Endo, T. Hata and N. Sakao, *Bunseki Kagaku*, 1983, **32**, T50.
- T. Akiyoshi and T. Tsukamoto, *ibid.*, 1978, **27**, 85.
- T. Yoshimori, T. Miwa and T. Takeuchi, *Talanta*, 1964, **11**, 993.
- C. L. Luke, *Anal. Chem.*, 1955, **27**, 1150.
- C. L. Luke and S. S. Flaschen, *ibid.*, 1958, **30**, 1406.
- T. Takeuchi and T. Yoshimori, *Bunseki Kagaku*, 1960, **9**, 780.
- M. Suzuki and T. Takeuchi, *ibid.*, 1960, **9**, 592.
- M. Miyamoto, *ibid.*, 1963, **12**, 120.

SPECTROPHOTOMETRIC DETERMINATION OF CHROMIUM IN WASTE WATER AND SOIL

WEN-BIN QI and LI-ZHONG ZHU

Department of Chemistry, Hangzhou University, Zhejiang, People's Republic of China

(Received 29 July 1985. Revised 15 March 1986. Accepted 5 April 1986)

Summary—The reaction of Cr(VI) with *o*-nitrophenylfluorone (NPF) in presence of cetyltrimethylammonium bromide (CTMAB) to form a purplish red complex at pH 4.7–6.6 by heating at 50° for 10 min has been investigated. The composition of the complex is 1:2:2 [Cr(VI):NPF:CTMAB], the wavelength of maximum absorbance is 582 nm. The molar absorptivity is $1.11 \times 10^5 \text{ l. mole}^{-1} \text{ cm}^{-1}$. Beer's law is obeyed up to 0.2 $\mu\text{g/ml}$ Cr(VI) concentration. The interference of several ions, including Cu^{2+} , Fe^{3+} and Al^{3+} , is eliminated by addition of a masking mixture containing KF, DCTA and tartrate. A new sensitive method for determination of chromium in waste water and soil is presented.

The determination of trace amounts of chromium(VI) has received considerable attention owing to concern with environmental pollution. At present, the most commonly used reagent for spectrophotometric determination of chromium(VI) is diphenylcarbazone (DPC),^{1,2} but the sensitivity of the method is not high and the complex is unstable. Recently, phenylfluorones have been applied to determination of chromium(VI).^{3,4} In this paper, a new and highly sensitive method for determination of chromium(VI) is described. It is based on the reaction of Cr(VI) with *o*-nitrophenylfluorone (NPF) in presence of cetyltrimethylammonium bromide to form a purplish red complex at pH 4.7–6.6 on heating at 50° for 10 min. The proposed method is more sensitive than the diphenylcarbazone method and the coloured product more stable, and it has been used for determination of chromium(VI) in waste water and soil, with satisfactory results.

EXPERIMENTAL

Apparatus

A UV 210 A double-beam ultraviolet spectrophotometer (Shimadzu, Japan) and a model 72 spectrophotometer (Shanghai 2nd Analytical Instrument Factory) were used for absorbance measurements.

Reagents

Standard 1-mg/ml solution of chromium(VI). Dissolve 0.2827 g of $\text{K}_2\text{Cr}_2\text{O}_7$ in 100 ml of water, and dilute this to obtain a 10 $\mu\text{g/ml}$ working solution.

***o*-Nitrophenylfluorone solution,** $5 \times 10^{-4}\text{M}$. Dissolve 0.0457 g of NPF in 250 ml of absolute ethanol.

Cetyltrimethylammonium bromide solution, $5 \times 10^{-3}\text{M}$.

Masking reagents. A 2.0% potassium fluoride, 0.02% *trans*-1,2-diaminocyclohexanetetra-acetic acid (DCTA) and 1.0% potassium sodium tartrate (Tar) solution.

Buffer solutions (pH 2.5–6.9). Prepared by mixing 0.1M acetic and 0.1M sodium acetate in appropriate ratios.

All chemicals used were of analytical-reagent grade.

General procedure

Into a 25-ml standard flask pipette 0.50 ml of standard 10- $\mu\text{g/ml}$ Cr(VI) solution, 2.0 ml of $5 \times 10^{-4}\text{M}$ NPF solu-

tion, 5 ml of buffer solution (pH 5.2), 8.0 ml of $5 \times 10^{-3}\text{M}$ CTMAB, dilute to the mark with water and mix thoroughly. Heat the solution in a water-bath at 50° for 10 min. After cooling, measure the absorbance at 582 nm in a 1-cm cell against a reagent blank.

RESULTS AND DISCUSSION

Absorption spectra

The absorption spectra of the complex and reagent blank were measured against water over the range 440–640 nm. The absorption maximum of the complex is at 582 nm and that of the reagent blank is at 530 nm (Fig. 1). We chose 582 nm as the measurement wavelength. The optimal pH for formation of the complex is 4.7–6.6.

Effect of reagent concentrations

When the general procedure was followed with varied amounts of the reagents, maximum and constant absorbance was obtained with 1.5–2.5 ml of NPF solution and 4.0–15.0 ml of $5 \times 10^{-3}\text{M}$ CTMAB so 2.0 and 8.0 ml respectively of these reagents were selected as optimal volumes.

Effect of temperature

It takes 3.5 hr for the colour to develop at room temperature (18°), but only 8 min at 50°. Once the colour has developed, the absorbance remains constant for at least 52 hr.

Calibration graph and sensitivity

Beer's law is obeyed up to 0.2 $\mu\text{g/ml}$ Cr(VI) concentration and the apparent molar absorptivity of the product is $1.11 \times 10^5 \text{ l. mole}^{-1} \text{ cm}^{-1}$.

Composition of the complex

The molar ratio of chromium to NPF in the complex was determined by the continuous-variations and molar-ratio methods and found to be 1:2. The molar ratio of chromium to CTMAB in the

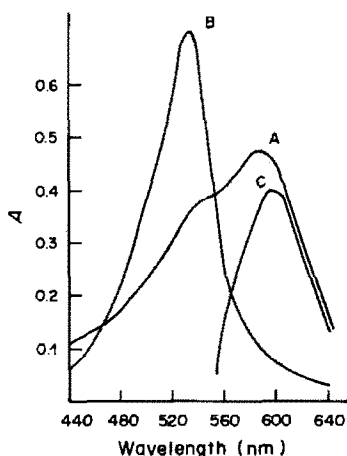


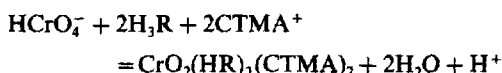
Fig. 1. Absorption spectra of (A) Cr(VI)-NPF-CTMAB complex vs. water; (B) reagent blank vs. water; (C) the complex vs. reagent blank. $[Cr] = 3.8 \times 10^{-6}M$, $[NPF] = 4 \times 10^{-5}M$, $[CTMAB] = 1.6 \times 10^{-3}M$.

complex was established as 1:2 by the Asmus and molar-ratio methods.

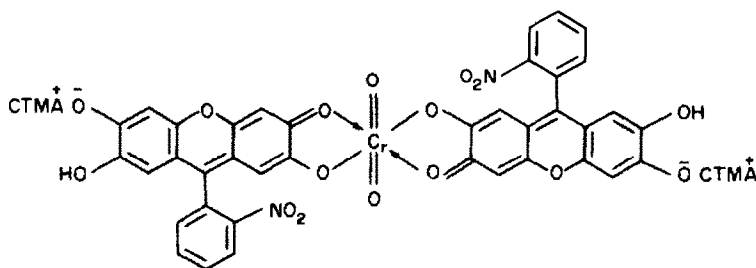
Nature of the reaction

In the absence of CTMAB, chromium(VI) gives only a very weak complex with NPF, but in the presence of appropriate amounts of CTMAB, a much more stable complex is formed.

From the behaviour of NPF, NPF + CTMAB, Cr(VI) + NPF and Cr(VI) + NPF + CTMAB in extraction with chloroform, determination of the number of protons released in the reaction and examination of the infrared spectra of NPF, Cr(VI) + NPF, NPF + CTMAB and Cr(VI) + NPF + CTMAB, it has been deduced that the reaction between Cr(VI), NPF (H_3R) and CTMAB may be represented by:



There is no oxidation or reduction involved.⁵ At pH 5-6, the predominant form of Cr(VI) at a concentration of $4 \times 10^{-6}M$ is $HCrO_4^-$.^{6,7} A possible structure for the complex is:



Interferences

The selectivity of the proposed method was investigated by determining $5 \mu g$ of Cr(VI) in the presence of various other ions. The results indicated that Al(III), Fe(III), Cu(II) and Ti(IV) interfere

Table 1. Effect of foreign ions on determination of $5 \mu g$ of Cr(VI)

Ions	Added, μg	Cr(VI) found, μg
Cr ³⁺	15	5.04
Ag ⁺	80	4.88
Ca ²⁺	2000	5.00
Mg ²⁺	2000	5.00
Cd ²⁺	500	5.04
Co ²⁺	200	4.90
Cu ²⁺	40	5.08
Hg ²⁺	500	5.07
Mn ²⁺	50	4.95
Ni ²⁺	500	5.00
Pb ²⁺	300	4.94
Al ³⁺	100	5.04
Fe ³⁺	30	5.04
Zn ²⁺	400	5.06
Sn ⁴⁺	100	5.04
Ti ⁴⁺	5	5.09
SiO ₃ ²⁻	1000	5.09
NO ₃ ⁻	3000	4.88
PO ₄ ³⁻	4000	4.95
AsO ₄ ³⁻	5000	4.97

severely. However, the tolerance level for these ions may be increased by adding a masking mixture (a mixture of 0.5 ml of 2% KF, 0.2 ml of 0.1% DCTA and 0.5 ml of 1.0% Tar). The tolerance limits for diverse ions in the presence of masking mixture are given in Table 1.

Spectrophotometric determination of Cr(VI) and total chromium in waste water

Determination of Cr(VI). Pipette an appropriate amount of waste water into a 25-ml standard flask, add 2.0 ml of NPF solution, 1.2 ml of masking mixture, 5.0 ml of buffer solution (pH 5.2) and 8.0 ml of $5 \times 10^{-3}M$ CTMAB. Dilute to the mark with water and mix. Heat the solution in a water-bath at 50° for 10 min. Cool, then measure the absorbance at 582 nm in a 2-cm cell against a reagent blank. Chromium(VI) may be determined in the presence of at least three times as much chromium(III). The results are satisfactory compared with those obtained by means of diphenylcarbazone (see Table 2).

Determination of total chromium. Pipette 25 ml of waste water into a 100-ml beaker, add 1.0 ml of 9M sulphuric acid and 2 drops of 2% potassium permanganate solution, and boil the mixture for 5 min (if the permanganate colour is discharged, add a little

Table 2. Results for determination of Cr(VI) and total chromium in waste water*

Sample No.	Diphenylcarbazone method				Proposed method				Comparison between the two methods ($p = 0.95$)			
	Chromium, ppm		S_1 , ppm		Chromium, ppm		S_2 , ppm		F		t	
	Cr(VI)	Cr _{tot}	Cr(VI)	Cr _{tot}	Cr(VI)	Cr _{tot}	Cr(VI)	Cr _{tot}	Cr(VI)	Cr _{tot}	Cr(VI)	Cr _{tot}
1	0.575	1.46	0.0036	0.004	0.575	1.46	0.0032	0.004	1.3	1.0	0	0
2	2.62	11.00	0.012	0.034	2.64	10.95	0.024	0.083	2.0	6.0	1.8	1.3
3	0.992	1.76	0.005	0.007	0.994	1.76	0.004	0.006	1.2	1.35	0.04	0.21
4	2.01	6.17	0.008	0.03	2.08	6.20	0.005	0.02	2.7	1.90	1.5	1.7

*In Tables 2 and 3, 5–10 replicates were run for each sample, and F and t are lower than the critical tabular values.

Table 3. Results for determination of chromium in soil

Sample No.	Diphenylcarbazone method				Comparison between the two methods ($p = 0.95$)	
	Cr, ppm		S_1 , ppm		F	
	Cr	S_1	Cr	S_2	F	t
1	183.4	2.94	180.2	1.9	2.3	2.0
2	59.4	0.341	59.4	0.441	2.0	0

more permanganate solution). Cool, add 1.0 ml of 20% urea solution, mix and add 2% sodium nitrite solution dropwise with frequent shaking, until the purplish-red colour is just discharged. Adjust the solution to pH 6 and transfer it into a 50-ml standard flask and dilute to the mark with water. Use the general procedure to analyse this solution for the total Cr(VI) thus produced. Calculate the amount of chromium(III) in the waste water by difference if desired.

Determination of chromium in soil. Extract the soil samples in the usual way, then add 10% sodium hydroxide solution dropwise to the extract until the pH is 7–8. Separate the Fe(III) and Al(III) hydroxides by centrifugation. Decant the supernatant solution and adjust it to pH 3–4 with 6M hydrochloric acid. Transfer the solution into a 100-ml standard flask and dilute to the mark with water. Take appro-

priate amounts of this solution for determination of chromium according to the procedure above.

The results shown in Table 3 are in reasonable agreement with those determined by the diphenylcarbazone method.

REFERENCES

1. M. Bose, *Anal. Chim. Acta*, 1954, **10**, 209.
2. H. Marchart, *ibid.*, 1964, **30**, 11.
3. Fan Zhang, Guo-nan Chen, Yi-qiang Yang and Shao-peng Hung, *Chemical Journal of Chinese Universities*, 1984, **5**, 791.
4. Gan-qing Xi and De-xiu Liang, *Fenxi Xuaxue*, 1984, **12**, 209.
5. Wen-bin Qi and Li-zhong Zhu, *Acta Chim. Sinica*, in press.
6. R. K. Tandon, P. T. Crisp, J. Ellis and R. S. Balser, *Talanta*, 1984, **31**, 227.
7. Shen-yang Tong and Ke-an Li, *ibid.*, 1986, **33**, in press.

SPECTROPHOTOMETRIC DETERMINATION OF MERCURY(II) AND SILVER(I) WITH COPPER(II) AND DIETHYLDITHIOCARBAMATE IN THE PRESENCE OF TRITON X-100

M. C. GARCIA ALVAREZ-COQUE, R. M. VILLANUEVA CAMAÑAS,
M. C. MARTINEZ VAYA, G. RAMIS RAMOS and
C. MONGAY FERNANDEZ

Departamento de Química Analítica, Facultad de Química, Universidad de Valencia,
Burjasot (Valencia), Spain

(Received 22 November 1985. Accepted 29 March 1986)

Summary—Procedures for the determination of mercury and silver by displacement of diethyldithiocarbamate (DDTC) from its copper complex in the presence of 1% Triton X-100, and measurement of the decrease in the Cu(DDTC)_2 absorbance, are described. The use of the surfactant avoids the need for an extraction step. Reproducibility within 1% and detection limits of 0.25 ppm Hg(II) and 0.45 ppm Ag(I) have been obtained, and linear calibration ranges up to 13 ppm Hg(II) and 15 ppm Ag(I). In the presence of 0.1M EDTA very good selectivity is achieved.

Diethyldithiocarbamate (DDTC) is commonly used for spectrophotometric determination of Cu(II) ¹⁻⁵ and of Ni(II) , Mn(II) , Pb(II) and V(V) .³ The complexes are insoluble in water and are extracted for measurement.

Hg(II) and Ag(I) give white insoluble complexes which are more stable than the yellow Cu(II) complex and can be indirectly determined by a displacement reaction. Hg(II) may be determined by shaking with a chloroform solution of the Cu(II) complex and measuring the absorbance decrease of the organic phase⁶ or the amount of Cu(II) which goes into the aqueous phase, by titration with EDTA⁷ or by a catalytic-kinetic method with hydroquinone and peroxide.⁸

(4-Sulphobenzyl)dithiocarbamic acid has been proposed for the determination of Hg(II) and Ag(I)⁹ because the complexes formed are water-soluble and an extraction is avoided. Better reproducibility and shorter analysis time are achieved.

The extraction may also be avoided by using non-ionic surfactants to form micellar solutions of the DDTC complexes in aqueous medium. Cu(II) has been determined with DDTC in the presence of Triton X-100 as the solubilizing agent.¹⁰ Here we describe use of the same medium for the displacement reactions of Hg(II) and Ag(I) with Cu(DDTC)_2 .

EXPERIMENTAL

Reagents

Stock $\text{Hg(NO}_3)_2 \cdot \text{H}_2\text{O}$ and AgNO_3 solutions were standardized with sodium chloride and $\text{CuSO}_4 \cdot 5\text{H}_2\text{O}$ solution

was standardized iodometrically. The Na_2DDTC solutions were freshly prepared in 0.09M NH_4NO_3 -0.06M NH_3 buffer (pH ~ 9).

Determination of mercury and silver

To determine mercury, 10 ml of 0.25M EDTA, 1 ml of 25% Triton X-100 solution, 1 ml of $4.5 \times 10^{-3}\text{M}$ Cu(II) and 5 ml of the sample solution were mixed in a 25-ml standard flask, followed by 5 ml of $9 \times 10^{-4}\text{M}$ DDTC at pH 9 and dilution to the mark. A similar procedure was followed for the determination of silver, but with 0.0225M Cu(II) . The absorbance was measured at 445 nm against a blank prepared with the sample solution but no DDTC. The calibration graphs were linear up to 13 ppm of Hg(II) and 15 ppm of Ag(I) in the final solution.

RESULTS AND DISCUSSION

Optimal conditions

The optimal stability of the Cu(DDTC)_2 micellar solution is attained in an $\text{NH}_4^+/\text{NH}_3$ medium at pH 8-9 in the presence of 1% Triton X-100,¹⁰ and the selectivity of the reaction is high in the presence of EDTA.

To determine small amounts of Hg(II) and Ag(I) by the displacement reaction, an excess of Cu(II) relative to DDTC must be present. The concentration of the residual copper complex then depends only on the DDTC and Hg(II) or Ag(I) concentrations. DDTC concentrations between 1.4×10^{-4} and $3.0 \times 10^{-4}\text{M}$ give parallel calibration curves. A reagent concentration of $1.7 \times 10^{-4}\text{M}$ has been chosen because it gives an absorbance of about 1 in the absence of mercury and silver.

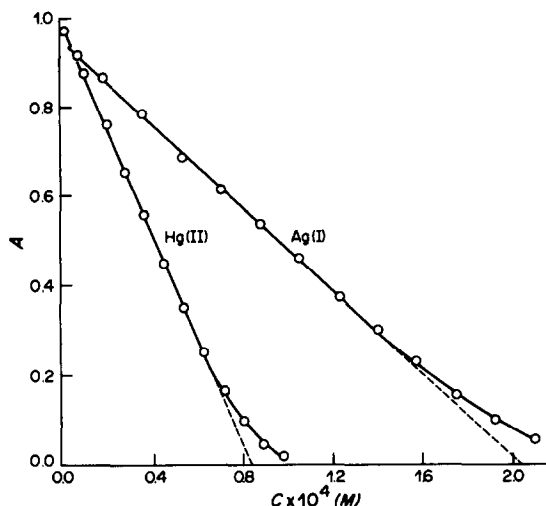


Fig. 1. Calibration curves. Cu(II) $1.73 \times 10^{-4}M$ for Hg(II) and $8.65 \times 10^{-4}M$ for Ag(I). DDTC $1.71 \times 10^{-4}M$ in both cases.

Calibration curves for Hg(II) and Ag(I) obtained with [Cu(II)]/[DDTC] molar ratios in the range 1:2–100:1 show a straight segment followed by curvature at the lower absorbance values (see *e.g.*, Fig. 1). The effect of the excess of Cu(II) on the slope and extent of the straight segment is small for mercury, and larger for silver. [Cu(II)]/[DDTC] molar ratios of about 1:1 and 5:1 are recommended for the determination of mercury and silver, respectively.

The slope of the linear calibration graph for the determination of Hg(II) is the same in absolute value ($1.16 \times 10^4 l. mole^{-1}. cm^{-1}$) as that for Cu(II), but opposite in sign, as expected from the stoichiometry of the DDTC complexes, whereas the slope of the linear calibration graph for silver is slightly less than half this value, in accordance with the 1:1 stoichiometry of the silver complex, the relative stabilities of the complexes and the large excess of copper.

Reproducibility and detection limits

Relative standard deviations $< 1\%$ were obtained for series of five determinations, at three different Hg(II) and Ag(I) concentrations (Table 1). The detection limits were determined by repeatedly measuring the absorbance of the Cu(II)–DDTC solution without Hg(II) or Ag(I) present. From the standard deviations of these absorbances (six replicates, $s = 0.005$), detection limits of 0.25 ppm for

Table 1. Reproducibility

Metal	C, ppm	Mean A	C.V., % ($n = 5$)
Hg(II)	3.6	0.785	0.2
	7.2	0.555	0.4
	10.9	0.239	0.7
Ag(I)	3.8	0.783	0.3
	7.5	0.622	0.6
	11.3	0.462	0.4

Table 2. Interferences in the determination of 7.2 ppm of mercury and 7.5 ppm of silver

Ion	Hg(II)		Ag(I)	
	[Ion], ppm	Error, %	[Ion], ppm	Error, %
Cl ⁻	3000	1.6	5	-13
SO ₄ ²⁻	3000	-2.2	1500	-1.7
PO ₄ ³⁻	1500	-1.8	250	-1.5
Ag ⁺	1	0.5	—	—
	3	29	—	—
Ca ²⁺	3000	-0.5	1000	-1.6
Mg ²⁺	1500	1.1	350	-1.4
Pb ²⁺	3600	2.0	2500	-1.8
Hg ²⁺	—	—	1	7.0
Ni ²⁺	1000	2.4	800	1.0
Co ²⁺	400	1.9	100	1.3
Cd ²⁺	2000	1.1	2000	-2.3
Zn ²⁺	2300	1.5	1500	-2.3
Mn ²⁺	1000	1.1	250	-1.1
Al ³⁺	600	1.2	500	-1.8
Fe ³⁺	350	2.0	550	1.8
Cr ³⁺	150	-2.2	150	-0.5
BiO ⁺	7	1.2	4	-2.0
Sn(IV)	75	2.7	—	—
MoO ₄ ²⁻	2000	-2.0	2000	-1.8
VO ₃ ⁻	50	1.4	200	-1.2

Hg(II) and 0.45 ppm for Ag(I) were calculated (3 σ criterion).

Interferences

As shown by Table 2, large amounts of many foreign ions can be tolerated in both determinations. Interference caused by formation of coloured EDTA complexes is eliminated by using a blank prepared with the sample itself. Precipitation of Sn(IV) is avoided by addition of tartrate. Thus, among the ions

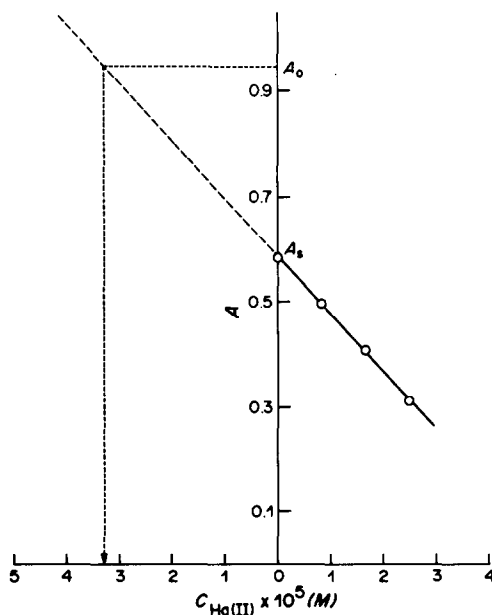


Fig. 2. Standard addition method for Hg(II) (sample 3). DDTC $1.73 \times 10^{-4}M$.

studied, only BiO^+ and Ag(I) interfere seriously in the determination of Hg(II) , and only BiO^+ , Cl^- and Hg(II) interfere in the determination of Ag(I) . The interference of BiO^+ is due to the formation of the stable yellow Bi(DDTC)_3 complex.¹¹

When copper is the major component of the sample, more accurate results are obtained if the concentration of Cu(II) in the sample solutions and standards is similar. In this case a standard addition method may also be applied, as shown in Fig. 2. The value A_0 in the figure would correspond to the absorbance of the sample solution if Hg(II) were not present and is given by

$$A_0 = -\frac{mC_{\text{DDTC}}}{2}$$

where m is the slope of the standard additions plot for mercury and C_{DDTC} is the molar concentration of DDTC. Hence if A_s is the absorbance for the sample with no added mercury,

$$C_{\text{Hg(II)}} = \frac{C_{\text{DDTC}}}{2} + \frac{A_s}{m}$$

The method leads to results as good as those obtained by the direct method for Hg(II) , but low results are obtained in the determination of Ag(I) .

Application of the methods

The proposed methods have been applied to the

Table 3. Analysis of amalgams for mercury

Sample	Composition, %	Mercury found*, %
1	Hg 0.98 ₅ Zn 99.0	0.99 ₁ ± 0.008
2	Hg 0.67 ₀ Cd 99.3	0.67 ₉ ± 0.002
3	Hg 0.60 ₃ Cu 99.4	0.60 ₈ ± 0.002† 0.60 ₈ §
4	Hg 0.19 ₃ Pb 99.8	0.19 ₇ ± 0.001

*Mean ± standard deviation.

†Calibration curve obtained by using a concentration of Cu(II) similar to that of the sample solution.

§Standard addition method.

Table 4. Analysis of alloys for silver

Sample	Composition, %	Silver found*, %
1	Ag 2.95 ₀ Al 97.05	2.95 ± 0.01 ₃
2	Ag 1.01 ₀ Fe 72.6 Cr 18.3 Ni 8.10	1.01 ₄ ± 0.004
3	Ag 0.97 ₆ Cu 58.3 Mn 19.5 Ni 21.2	0.99 ₀ ± 0.004†
4	Ag 0.95 ₀ Ni 99.05	0.96 ₀ ± 0.006
5	Ag 0.30 ₇ Pb 99.7	0.30 ₂ ± 0.002

*Mean ± standard deviation.

†Calibration curve obtained by using a concentration of Cu(II) similar to that of the sample solution.

determination of mercury and silver in various metallic samples. The results obtained from series of five replicates are shown in Tables 3 and 4. Good agreement between expected and found values is achieved.

REFERENCES

1. F. J. Welcher (ed.), *Standard Methods of Chemical Analysis*, 6th Ed., Vol. IIIB, Van Nostrand, Princeton, 1966.
2. F. D. Snell and L. S. Ettre, *Encyclopedia of Industrial Chemical Analysis*, Vol. 10, Interscience, New York, 1970.
3. J. Fries and H. Getrost, *Organic Reagents for Trace Analysis*, Merck, Darmstadt, 1977.
4. H. Koshimura, *Bunseki Kagaku*, 1973, **22**, 97.
5. M. Nabrzyski, *Anal. Chem.*, 1975, **47**, 552.
6. S. Komatsu and S. Kuwano, *Nippon Kagaku Zasshi*, 1962, **83**, 1262.
7. T. Nomura, K. Ito, T. Nakamura and S. Komatsu, *Nippon Kagaku Kaishi*, 1972, No. 1, 44.
8. V. I. Rychkova and I. F. Dolmanova, *Zh. Analit. Khim.*, 1979, **34**, 1414.
9. Y. Tanaka and S. Zenki, *Bunseki Kagaku*, 1974, **23**, 1190.
10. M. C. Garcia Alvarez-Coque, M. C. Martínez Vayá, G. Ramis Ramos, R. M. Villanueva Camaño and C. Mongay Fernández, *Quim. Anal.*, in press.
11. G. Eckert, *Z. Anal. Chem.*, 1957, **155**, 23.

SPECTROPHOTOMETRIC DETERMINATION OF IRON IN PROCESS SAMPLES FROM THE CHEMICAL CLEANING OF COAL

COLIN D. CHRISWELL*, RICHARD G. RICHARDSON and RICHARD MARKUSZEWSKI
Ames Laboratory, USDOE, Iowa State University, Ames, IA 50011, U.S.A.

(Received 15 October 1985. Revised 13 January 1986. Accepted 23 March 1986)

Summary—Iron is removed during the desulphurization and demineralization of coal by a chemical cleaning process utilizing a mixture of molten sodium hydroxide and potassium hydroxide. When 1,10-phenanthroline is used for spectrophotometric determination of the iron in the various caustic, aqueous and acidic process streams, organic materials leached from the coal by the molten caustic interfere with the colour-forming reaction. Pre-oxidation of the samples with potassium persulphate has proved to be an effective means of removing the interfering organic material before the iron determination.

Most of the iron in coal is present as pyrite (FeS_2), although other minerals such as iron sulphates may also be present. During the cleaning of coal with molten caustic,¹⁻⁵ iron is converted into soluble forms which are removed with the spent caustic, with the water washings of the separated coal, and with the acid washings of the water-washed clean coal.

In the present work it was found that spectrophotometric analyses of these process streams for iron (with 1,10-phenanthroline) yielded erratic results, apparently because of interference by the organic matter solubilized during the cleaning or washing steps. Several widely used oxidation procedures were found to be ineffective for removing the interfering organic material. The use of chlorine gas was very effective, but the potential hazards and relatively poor availability of this reagent make its use less convenient. It was finally found that oxidation of acidified samples with potassium persulphate will effectively remove all interferences due to organic material. The procedure is convenient to apply, and the oxidation is accomplished relatively quickly.

EXPERIMENTAL

Apparatus

A Varian DMS-100 spectrometer and 1-cm optical path-length disposable cuvettes were used. Only standard laboratory glassware was employed. Before each use it was rinsed with 30% v/v hydrochloric acid and then with demineralized water to remove any iron contamination.

Reagents

Hydroxylamine hydrochloride solution, 60%.

Buffer solution. To a solution of 250 g of ammonium acetate in 150 ml of distilled water add 700 ml of glacial acetic acid.

1,10-Phenanthroline solution. Dissolve 100 mg of 1,10-phenanthroline monohydrate in 100 ml of distilled water containing two drops of concentrated hydrochloric acid.

Stock iron solution. Dissolve 1.404 g of ferrous ammonium sulphate hexahydrate in approximately 50 ml of 40% v/v sulphuric acid, then dilute the solution to exactly 1 litre to yield a stock 200- $\mu\text{g}/\text{ml}$ iron solution.

Standard iron solution. Dilute a 50.00-ml aliquot of stock iron solution to the mark in a 1-litre standard flask with demineralized water to yield a 10- $\mu\text{g}/\text{ml}$ iron solution.

Procedures

Calibration. Pipette 1.00, 5.00, 10.00, 15.00 and 25.00 ml of the standard iron solution into five 50-ml standard flasks and use a sixth flask for a reagent blank. Then add 5 ml of reductant, 10 ml of buffer, and 2 ml of 1,10-phenanthroline solution to each flask, and dilute to the mark with demineralized water. After 30 min. measure the absorbance of each calibration standard at 510 nm with no cell in the reference beam. Subtract the absorbance of the reagent blank from the absorbances for the standards. Plot the net absorbances against the concentrations.

Oxidation of samples. It is recommended that each sample is analysed in triplicate. For a sample in aqueous solution, pipette 10.00 ml into a 50-ml beaker. If the sample is in the form of solid spent caustic, dissolve approximately 1.5 g, accurately weighed, in demineralized water, make up to volume in a 100-ml standard flask, and pipette 10.00 ml of this solution into a 50-ml beaker. Cautiously add concentrated sulphuric acid to the solution until the pH is ~ 1 . Place the beaker on a hot-plate and bring the solution to the boil. Add a scoopful (approximately 0.5 g) of potassium persulphate and allow the reaction to proceed for a few minutes. Add additional 0.5-g portions of potassium persulphate until the solution is colourless or no further diminution of colour is observed. In all cases, add at least five scoopfuls (2.5 g total) of potassium persulphate. Then allow the solution to cool and add demineralized water to bring the total volume to about 40 ml. Transfer the solution to a 100-ml standard flask and dilute to the mark with demineralized water.

Determination of iron. Pipette a volume of x ml of the oxidized solution, estimated to contain between 50 and 150 μg of iron, into a 50-ml standard flask and develop and measure the colour in the same way as for the calibration

*Author for correspondence.

solutions. Prepare an identical sample, but without addition of phenanthroline, and read the absorbance in the same way as the others. Subtract this absorbance from that of the corresponding solution containing phenanthroline, and use the net absorbance to find the concentration of iron in the solution ($y \mu\text{g/ml}$), from the previously prepared calibration curve.

Calculations. For samples in aqueous solutions:

$$\text{concentration of iron} = 500 y/x \mu\text{g/ml}$$

For solid samples:

concentration of iron =

$$5 \times 10^4 y/x \text{ (weight of sample, g) } \mu\text{g/g}$$

RESULTS AND DISCUSSION

The determination of iron in aqueous solutions by formation of a coloured complex with 1,10-phenanthroline is well established.⁶⁻⁸ Alternative colorimetric procedures exist for the determination of iron in caustic solutions.⁹⁻¹² In our case, however, direct application of any of these methods resulted in significant interferences from the organic matter in the samples, and neutralization of the caustic and prolonged oxidation were required to degrade the organic material. The key to the required modification of this method was the development and demonstration of an effective procedure for the removal of interferences caused by the organic matter.

Previous work at our laboratory had shown that the organic material present in coal-cleaning process streams can be classified as humic acid type material and phenolic material.¹³ Oxidation of this material with perchloric acid would clearly be the method of choice,¹⁴ but owing to the high potassium content of the samples, a voluminous precipitate would form,

making the oxidation potentially hazardous because of the risk of "bumping" during reflux. Oxidation with hydrogen peroxide was found to yield erratic results that were usually lower than those obtained when no oxidation at all was used. Presumably, peroxide oxidation led to the formation of carboxylic acids which competed with the phenanthroline for complexation of the iron. Oxidation of the organic material with hydrogen peroxide also required a reaction time of at least 16 hr, which was unacceptable. The use of chlorine as an oxidant for the organic material was studied briefly. Preliminary results indicated that bubbling chlorine through sample solutions would effectively degrade organic materials, but this procedure was abandoned because of the potential hazards and inconvenience involved.

As shown in Table 1, pre-oxidation of the samples with potassium persulphate considerably increased the values obtained for the concentration of iron.

The lightly coloured spent-caustic samples yielded slightly lower iron values without the pre-oxidation. This was undoubtedly due to competition of humic-type acids in these samples with the 1,10-phenanthroline for complexation of the iron. In contrast, the highly coloured water-wash samples yielded slightly lower results after oxidation of the organic material. The slightly higher values for the unoxidized samples could be due to the background absorbance of the organic matter. Blank determinations could not fully compensate for the highly coloured organic components contained in these samples before oxidation. The essentially colourless acid-wash samples are known to contain organic material exhibiting properties similar to those of phenols, naphthols, thiophenols and thionaphthols.¹³

Table 1. Effects of pre-oxidation by potassium persulphate on the determination of iron in various process samples; the relative standard deviation (rsd, %) is given in brackets, for five replicate determinations

Sample	Description	Concentration of iron found, $\mu\text{g/ml}$	
		Before oxidation	After oxidation
A-1	Spent caustic—lightly coloured	94 (0.9)	104 (1.4)
B-1	Spent caustic—lightly coloured	93 (0.6)	109 (1.5)
A-2	Water wash—intensely coloured	21 (3.8)	19 (7.5)
C-2	Water wash—intensely coloured	17.9 (1.1)	16 (5.1)
D-2	Water wash—intensely coloured	5.6 (3.6)	0 (—)
A-3	Acid wash—colourless	90 (0.3)	165 (1.1)
B-3	Acid wash—colourless	90 (0.25)	129 (0.6)
C-3	Acid wash—colourless	90 (0.0)	374 (0.7)

Table 2. Recovery of standard additions of iron

Sample E-2 (water wash)			Sample F-1 (spent caustic)			Sample G-3 (acid wash)		
Added, $\mu\text{g/ml}$	Found, $\mu\text{g/ml}$	Recovered, %	Added, $\mu\text{g/ml}$	Found, $\mu\text{g/ml}$	Recovered, %	Added, $\mu\text{g/ml}$	Found, $\mu\text{g/ml}$	Recovered, %
0	17	—	0	113	—	0	127	—
47	65	102	47	159	98	47	176	104
95	113	101	95	204	97	95	221	100
189	208	101	189	294	98	189	317	101
284	306	102	284	389	97	284	412	100
378	398	101	328	496	101	328	498	98
473	491	100	473	577	98	473	583	96

Table 3. Comparison of iron determinations by AAS (standard-additions method) and the 1,10-phenanthroline method

Sample	Iron found	
	AAS	Phen
P-1 (spent caustic), $\mu\text{g/ml}$	16.8	17.2
P-1 (precipitate from spent caustic), $\mu\text{g/g}$	154	153
P-2 (water wash), $\mu\text{g/ml}$	10.5	9.2
P-3 (acid wash), $\mu\text{g/ml}$	383	368

It appears that these components can complex a significant fraction of the iron and make it unavailable for complexation with 1,10-phenanthroline.

Reproducibility

Eight separate sets of five determinations each were performed on spent-caustic, acid-wash and water-wash samples from the chemical cleaning of coal. The relative standard deviations for these sets (see Table 1) ranged from 0.6 to 7.5% and were mostly about 1.5%. It is notable that when no oxidation was performed, the precision of the determinations was generally better by a factor of about two. The additional manipulation of samples apparently introduced more random errors into the determination. However, for the purpose of evaluation of coal-cleaning process streams the precision obtained is acceptable.

Validation

The method of standard additions was applied to obtain some assurance that the results obtained with the modified method were accurate. As Table 2 shows, the recoveries were essentially quantitative. However, if a small quantity of a competing ligand were left unoxidized and already complexed with iron, it would not affect the recovery of the added iron, and the standard-additions method would not reveal the error in the original result. For that reason comparison was also made with results obtained by atomic-absorption spectrometry (AAS), and Table 3 shows that comparable results were obtained. These findings imply that the spectrophotometric procedure yielded accurate results.

Since the findings also imply that AAS will yield accurate results for samples of this type, either technique can be used for the determination of iron. However, for samples from the chemical cleaning of coal, we find that the spectrophotometric procedure

is far more convenient. Relatively small numbers of samples are produced at any given time, and it is simpler and faster to calibrate the instrument and perform the determinations by spectrophotometry than by AAS.

Acknowledgement—Ames Laboratory is operated for the U.S. Department of Energy by Iowa State University under Contract No. W-7405-Eng-82. This work was supported by the Assistant Secretary for Fossil Energy, Office of Direct Coal Utilization, through the Pittsburgh Energy Technology Center, Pittsburgh, Pennsylvania. The assistance of Robert Z. Bachman and the Analytical Services Group at the Ames Laboratory in determining iron by atomic-absorption spectrometry is greatly appreciated.

REFERENCES

1. P. X. Masciantonio, *Fuel*, 1965, **44**, 269.
2. R. A. Meyers, *Hydrocarbon Processing*, June 1979, 123.
3. R. Markuszewski, D. Mroch, G. A. Norton and W. E. Straszheim, *Am. Chem. Soc. Div. Fuel Chem. Preprints*, 1985, **30**, No. 2, 41.
4. P. Chiotti and R. Markuszewski, *Ind. Eng. Chem. Proc. Des. Dev.*, 1985, **24**, 1137.
5. R. A. Meyers, *Proc. 1st Annual Pittsburgh Coal Conference, Pittsburgh, PA*, 17–21 Sept. 1984, 381.
6. *Standard Methods for the Examination of Water and Wastewater*, 14th Ed., Am. Publ. Health Assoc., Washington, D.C., 1976.
7. W. B. Fortune and M. G. Mellon, *Ind. Eng. Chem., Anal. Ed.*, 1938, **10**, 60.
8. A. A. Schilt, *Analytical Applications of 1,10-Phenanthroline and Related Compounds*, Pergamon Press, Oxford, 1969.
9. F. Trusell and H. Diehl, *Anal. Chem.*, 1959, **31**, 1978.
10. A. A. Schilt, G. F. Smith and A. Heimbuch, *ibid.*, 1956, **28**, 809.
11. M. N. Hale and M. G. Mellon, *J. Am. Chem. Soc.*, 1950, **72**, 3217.
12. D. P. Poe, A. D. Eppen and S. P. Whoolery, *Talanta*, 1980, **27**, 368.
13. C. D. Chriswell, unpublished data, 1985.
14. A. A. Schilt, *Perchloric Acid and Perchlorates*, G. F. Smith Chemical Co., Columbus, OH, 1979.

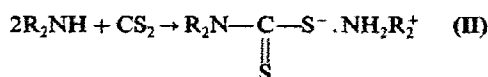
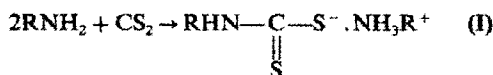
ANALYTICAL APPLICATIONS OF THE AMINE-CARBON DISULPHIDE REACTION IN ACETONITRILE

B. C. VERMA*, S. CHAUHAN, NEELAM SHARMA, USHA SHARMA,
D. K. SHARMA and ANILA SOOD
Chemistry Department, Himachal Pradesh University, Shimla-5, India

(Received 11 April 1985. Revised 13 March 1986. Accepted 29 March 1986)

Summary—The ease with which carbon disulphide transforms primary and secondary amines in acetonitrile medium into the corresponding monoalkylammonium monoalkyldithiocarbamates and dialkylammonium dialkyldithiocarbamates respectively and the simplicity and reliability of potentiometric and spectrophotometric determination of dithiocarbamates with copper(I) perchlorate in the same medium, provide simple, accurate and reliable methods for the determination of primary and secondary amines and of organic isothiocyanates.

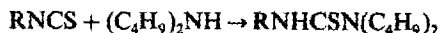
Primary and secondary amines react with carbon disulphide in organic solvents to yield monoalkylammonium monoalkyldithiocarbamates (I) and dialkylammonium dialkyldithiocarbamates (II) respectively,¹ but tertiary amines do not react.



Hence primary or secondary amines can be assayed in the presence of tertiary amines by means of those reactions and any suitable method for determination of the resulting dithiocarbamates. In acetonitrile medium, these reactions are rapid, smooth and quantitative at room temperature and the dithiocarbamates can be determined with copper(II) or copper(I) perchlorate in the same medium at room temperature.² The method has certain advantages over acidimetric determination of the amines. Tertiary amines and other basic compounds do not interfere and a spectrophotometric method can be used for the determination of microamounts of the amines. This application is straightforward and gives results of acceptable precision and accuracy.²

The usefulness of the reaction has been extended by its application to the indirect micro-determination of organic isothiocyanates. The isothiocyanate is reacted with a known and excessive amount of dibutylamine in dimethylformamide to produce the

corresponding substituted thiourea.^{3,4}



The solution is then diluted with acetonitrile, a drop of carbon disulphide is added and the dibutyldithiocarbamate is titrated photometrically with copper(I) perchlorate at 430 nm.²

EXPERIMENTAL

Reagents

Acetonitrile. Distilled twice from phosphorus pentoxide (5 g/l.).

Dimethylformamide. Commercial grade material was purified by storage over analytical-reagent grade anhydrous sodium carbonate for 2 days. The solvent was then decanted and distilled, the fraction distilling at 148.5–149.5° being collected and stored in a brown bottle.

Copper(I) perchlorate standard solution in acetonitrile. Prepared as described earlier.²

Alkyl isothiocyanates. Prepared by known methods.⁵ Phenyl isothiocyanate was distilled before use. Carbon disulphide ("Baker Analyzed") was used as received.

Procedure

An aliquot of dimethylformamide solution of the organic isothiocyanate was mixed with a known excess of standard dibutylamine solution (in dimethylformamide) and the volume made up to 2 ml with the solvent. After 10 min, the solution was diluted to 6 ml with acetonitrile, mixed with a drop of carbon disulphide, and titrated spectrophotometrically at 430 nm with standard copper(I) perchlorate solution at room temperature (~23°). Dilution correction was applied and the titration curve plotted in the usual way. The results are given in Table 1.

RESULTS AND DISCUSSION

Organic isothiocyanates find extensive use as intermediates in the synthesis of polymers and are also of

*Author for correspondence.

Table 1. Determination of organic isothiocyanates

Isothiocyanate*	Amount found†, μg
Methyl	9.89 ± 0.04
n-Propyl	10.09 ± 0.04
Isopropyl	10.09 ± 0.06
n-Butyl	10.07 ± 0.03
Isobutyl	9.93 ± 0.03
Phenyl	9.91 ± 0.03

*Amount taken, 10 μg.

†Mean ± standard deviation (10 determinations).

pesticidal importance. The results in Table 1 show

that the proposed method is useful for their determination.

Acknowledgement—The authors thank the University Grants Commission, New Delhi, for financial support.

REFERENCES

1. E. E. Reid, *Organic Chemistry of Bivalent Sulphur*, Vol. IV, p. 211. Chemical Publishing Co., New York, 1962.
2. B. C. Verma, S. Chauhan, A. Sood, D. K. Sharma and H. S. Sidhu, *Talanta*, 1985, **32**, 139.
3. B. C. Verma and S. Kumar, *Analyst*, 1973, **98**, 900.
4. J. A. Vinson, *Anal. Chem.*, 1969, **41**, 1661.
5. N. L. Drake, *Org. Synth.*, 1941, **21**, 81.

ANNOTATION

INTERFERENCES FROM BIVALENT CATIONS IN THE DETERMINATION OF SELENIUM BY HYDRIDE-GENERATION AND ATOMIC-ABSORPTION SPECTROMETRY

A DISCUSSION OF THE CLAIM THAT THE METAL IONS ARE REDUCED TO THE METALLIC STATE BY SODIUM BOROHYDRIDE

RAGNAR BYE

Department of Chemistry, University of Oslo, Oslo 3, Norway

(Received 25 July 1985. Revised 12 February 1986. Accepted 29 March 1986)

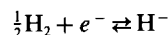
Summary—The cause of interference by bivalent cations in the determination of selenium by hydride-generation and atomic-absorption is still the subject of debate. It is suggested that these ions react with sodium borohydride to produce the metal borides and not, as generally supposed, the elemental metals. The metal borides are known to be highly reactive and could cause decomposition of the selenium hydride before it reaches the detection unit.

Many efforts have been made to minimize the well known interferences from the ions of silver, copper, nickel, cobalt, iron, tin, cadmium and other metals in determination of selenium by hydride-generation and atomic-absorption spectrometry, HGAAS. There are, however, only a few reports on the possible mechanisms involved in the interfering process. Recently, interesting papers by Welz and co-workers have appeared, reporting detailed studies of the interference patterns of bivalent ions.¹⁻³ Most authors have proposed that the interferences are caused by capture of the selenium hydride by the metal precipitate formed immediately by reaction between the metal ion and the added borohydride ions. It is a common assumption that the precipitates formed from the interfering ions consist of the element in the metallic state. However, Brown *et al.* proposed briefly that the precipitates could be borides rather than metals.⁴

The reducing effect of borohydride is probably due to formation of nascent hydrogen which, in acid solutions, reduces selenium(IV) directly to selenium hydride. The term "nascent" describes hydrogen gas in a state (probably as radicals) which is especially active. Another common way to produce nascent hydrogen is by reaction between zinc and hydrochloric acid.

From a thermodynamic point of view there should be no difference in principle between nascent hydrogen and ordinary hydrogen gas as far as the standard electrode potential is concerned (zero volt). This means that hydrogen gas can theoretically reduce all metal ions having a positive standard potential to the metallic state, but not the ions having negative

E^0 -values under standard conditions. Another possibility is that the hydride ion itself is the reducing ion. In that case the standard potential of the half-reaction



—2.23 V,⁵ must be considered. If the hydride ion is the reductant all metal ions having a standard potential more positive than that of magnesium could be reduced to the metals. Water would also be reduced, to give hydroxide ions and hydrogen.

In an attempt to arrive at a better understanding of these important interfering reactions, the present paper reports some theoretical considerations and experimental results to support the assumption that the precipitates formed by some metal ions in the HGAA process are unlikely to be the elemental metals, but rather metal borides. In this context attention is also drawn to earlier papers in which the catalytic power, and hence the preparation, of metal borides is described. Finally, a possible mechanism for the reaction between the interfering metal precipitates and selenium hydride is proposed.

EXPERIMENTAL

The bivalent ions of the following metals were considered: Sn, Ni, Co, Cd, Fe and Zn. All of these have negative E^0 -values.

A series of "beaker" experiments was performed, in which 100 ml of a 0.10M solution of an ion (prepared from the chloride) in 1.0M hydrochloric acid were treated with 5 ml of a 3% solution of sodium borohydride in 1% sodium hydroxide solution. The results observed are given in Table 1.

The precipitate from the nickel solution was immediately filtered off, washed with water, dried at 80° and examined by X-ray analysis.

Table 1

Ion	E^0, V	Observed effect of added NaBH_4
Sn(II)	-0.14	Bright yellow precipitate*
Ni(II)	-0.23	Black precipitate
Co(II)	-0.28	Black precipitate
Cd(II)	-0.40	Black precipitate†
Fe(II)	-0.41	Black precipitate
Zn(II)	-0.76	No precipitate

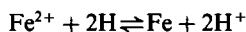
*The bright yellow colour quickly turned greyish black.
 †A very minute amount of precipitate was observed for a short while and was quickly dissolved in the solution.

RESULTS AND DISCUSSION

The precipitate from the nickel solution was found to be amorphous, as reported by others,⁸ and no metallic nickel was detected. A qualitative test showed the presence of boron.

There are some remarkable results in Table 1. First, the bright yellow precipitate formed from the tin solution is not easily explained. If it is metallic tin, its colour should be different. Secondly, the difference in behaviour of cadmium and iron, although both half-cells have almost the same E^0 -value.

If the metals, for instance iron, were formed by reduction with nascent hydrogen the following equilibrium should be forced to the right:



From the E^0 -values, however, the equilibrium constant is 1.3×10^{-14} , so it is very hard to understand how such a reaction, forming a large amount of iron precipitate, could be feasible.

If it is argued that the hydride ion is the reductant, then elementary zinc should also be formed. Also, the colour of the tin precipitate would still not be explained.

Identical experiments with addition of zinc powder (2 g) instead of sodium borohydride resulted in formation of nascent hydrogen, but no precipitate was observed in any of the solutions, as expected.

In the literature there are several reports on metal borides used as catalysts for hydrogenation and organic desulphuration reactions.⁶⁻⁹ Preparation of such borides was described as early as 1953,⁶ and the topic was reviewed in 1976.⁸ It is noteworthy that in the papers cited it is always recommended to synthesize the borides by the reaction between sodium borohydride and the metal ions (mostly by use of the

metal chloride solutions). Moreover, in the case of cobalt,⁶ the precipitate was analysed and found to consist of a metal boride with an apparent stoichiometry of Co_2B .

In one of the papers the desulphuration of peptides (*i.e.*, splitting of C—S bonds) by nickel boride was described.⁷ This suggests a mechanism for the suppression of selenium hydride formation by metal borides: the covalent radii of sulphur and selenium are 1.03 and 1.17 Å, respectively,¹⁰ and the bond energies for H—Se and C—S are 73,¹⁰ and 65 kcal/mole,¹² respectively, and it is tempting to propose that the selenium hydride molecules are cleaved by the metal boride, leaving elemental selenium in the solution.

CONCLUSIONS

The interference caused by certain metal ions in the determination of selenium by the hydride-generation atomic-absorption technique could be due to capture and decomposition of the selenium hydride by the precipitate formed on addition of sodium borohydride. Such precipitates are probably not elemental metals, but rather metal borides.

REFERENCES

1. B. Welz and M. Melcher, *Analyt.*, 1984, **109**, 569.
2. *Idem, ibid.*, 1984, **109**, 577.
3. B. Welz and M. Schubert-Jacobs, *J. Anal. At. Spectrom.*, 1986, **1**, 23.
4. R. M. Brown, R. C. Fry, J. L. Moyers, S. J. Northway, M. Denton and G. S. Wilson, *Anal. Chem.*, 1981, **53**, 1560.
5. *Handbook of Chemistry and Physics*, 51st Ed., CRC, Cleveland, 1970.
6. H. I. Schlesinger, H. C. Brown, A. E. Finholt, J. R. Gilbreath, H. R. Hoekstra and E. K. Hyde, *J. Am. Chem. Soc.*, 1953, **75**, 215.
7. M. A. Paz, A. Bernath, E. Henson, O. Blumenfeld and P. M. Gallop, *Anal. Biochem.*, 1970, **36**, 527.
8. R. C. Wade, D. G. Holah, A. N. Hughes and B. C. Hui, *Catal. Rev. Sci. Eng.*, 1976, **14**, 211.
9. J. M. Pratt and G. Swinden, *Chem. Commun.*, 1969, 1321.
10. F. A. Cotton and G. Wilkinson, *Advanced Inorganic Chemistry*, 3rd Ed., Interscience, New York, 1972.
11. M. Schmidt, W. Siebert and K. W. Bagnall, *The Chemistry of Sulphur, Selenium, Tellurium and Polonium*, Pergamon Press, Oxford, 1975.
12. E. S. Gould, *Mechanism and Structure in Organic Chemistry*, Holt, Rinehart and Winston, New York, 1962.

TRACE MEASUREMENTS OF THE ANTINEOPLASTIC AGENT METHOTREXATE BY ADSORPTIVE STRIPPING VOLTAMMETRY

JOSEPH WANG*, PENG TUZHI, MENG-SHAN LIN and TIM TAPIA

Department of Chemistry, New Mexico State University, Las Cruces, NM 88003, U.S.A.

(Received 18 March 1986. Accepted 16 May 1986)

Summary—An extremely sensitive voltammetric method is presented for trace measurement of the cancer chemotherapy drug methotrexate. The method is based on controlled adsorptive preconcentration of methotrexate on the hanging mercury-drop electrode, followed by voltammetric determination of the surface species. Cyclic voltammetry was used to explore the interfacial behaviour. The adsorptive stripping response was evaluated with respect to preconcentration time and potential, pH, concentration dependence, stripping mode, possible interferences, and other variables. The detection limit found was $2 \times 10^{-9} M$ (5-min preconcentration), the response was linear, and the relative standard deviation (at the $1.6 \times 10^{-7} M$ level) 2.2%. Sensitive adsorptive stripping measurements were also obtained by use of a carbon-paste disk electrode. Applicability to urine analysis is illustrated.

Anticancer drugs have become, during the last decade, increasingly important in the treatment of neoplastic diseases. One of the most widely used is the antifolate methotrexate (4-amino-*N*¹⁰-methylpteroyl-glutamic acid; Amethopterin). High doses of methotrexate are now being used to treat previously unresponsive cancers.¹ In spite of its therapeutic effectiveness, the clinical utility of methotrexate is hampered by its toxicity. Reliable analytical procedures are thus required to optimize therapy and minimize side-effects. Several types of assay are currently used for clinical monitoring of methotrexate. These include radioimmunoassay,² enzyme-multiplied immunoassay,³ fluorimetry⁴ and HPLC with ultraviolet⁵ or amperometric⁶ detection.

The polarographic behaviour of methotrexate has been elucidated by Gurira and Bowers.⁷ The compound exhibits three two-electron/two-proton reduction steps in neutral and acidic media. In a separate study,⁸ the same workers exploited the electrochemical reduction for determination of methotrexate at the mM and μM concentration levels by sampled d.c. polarography and differential pulse polarography, respectively. The present work reports an extremely sensitive voltammetric procedure for trace measurement of methotrexate, based on its adsorptive accumulation at the hanging mercury-drop electrode. Adsorptive stripping voltammetry has been shown to be an important analytical method for a wide range of electroactive compounds that can be adsorbed onto electrode surfaces. The method has been successfully applied for trace measurements of

important pharmaceutical compounds such as digoxin,⁹ diazepam and nitrazepam,¹⁰ adriamycin¹¹ and chlorpromazine.¹² Work to date has recently been summarized.¹³ The characteristics and advantages of an effective adsorptive stripping procedure for methotrexate are elucidated in this paper.

EXPERIMENTAL

Apparatus and reagents

Stripping and cyclic voltamperograms were obtained with an EG & G Princeton Applied Research Corp. (PAR) Model 264A stripping analyser. The working electrode was a PAR Model 303A static mercury-drop electrode. The sample cell (PAR Model 0057) was fitted with an Ag/AgCl (saturated KCl) reference electrode and a platinum wire auxiliary electrode. The cell was covered with aluminium foil. A magnetic stirrer and stirring bar (1 cm long, 2 mm thick) provided mixing during the preconcentration step. A PAR Model 0073 X-Y recorder was used for the collection of experimental data. A 3-mm diameter carbon-paste disk electrode was used for analogous measurements in the anodic potential range, in conjunction with a PAR Model 174 polarographic analyser.

Stock solutions ($2 \times 10^{-4} M$) of methotrexate (Sigma) were prepared daily by dissolving appropriate weights of it in 1 ml of 0.1M sodium hydroxide and making up to volume in a 100-ml standard flask with demineralized water. The solutions were stored in the dark at 4°. All other solutions were prepared with demineralized water and analytical-grade reagents. Urine samples were obtained from healthy volunteers.

Procedure

A known volume (10 ml) of the 0.05M phosphate buffer (pH 2.5) supporting electrolyte solution was added to the cell and deaerated by passage of nitrogen for 8 min (and for 30 sec before each adsorptive stripping cycle). The preconcentration potential (usually $-0.2 V$) was applied to the

*To whom correspondence should be addressed.

electrode for a selected time, while the solution was stirred at 400 rpm. The stirring was then stopped, and after 15 sec the voltamperogram for a negative-going potential scan was recorded. The scan was terminated at -1.5 V, and the adsorptive stripping cycle was repeated with a new mercury drop. After the background stripping voltamperogram had been obtained, aliquots of the drug standards were introduced. The entire procedure was automated, as controlled by the PAR 264A stripping analyser. Throughout this operation, nitrogen was passed over the solution surface. All data were obtained at room temperature.

RESULTS AND DISCUSSION

Figure 1 shows repetitive cyclic voltamperograms for $1 \times 10^{-6}M$ methotrexate in $0.05M$ phosphate buffer (pH 2.5). Stirring the solution for 1 min at -0.10 V prior to the first scan (designated as 1), results in three cathodic peaks at *ca.* -0.51 , -0.87 , and -1.05 V; a small peak is observed (at -0.42 V) on scanning in the positive direction. Subsequent scans yield substantially smaller cathodic peaks that represent the response of solution-phase species (*i.e.*, rapidly desorbed product); the shift in potential of the first peak and disappearance of the second peak should be noted. For analytical purposes, the first (and large) cathodic peak is the most useful; this peak is attributed to reduction of the pyrazine ring.⁷

Hence, all subsequent work was based on measurement of the magnitude of this peak. With the $1 \times 10^{-6}M$ methotrexate solution, full surface coverage was achieved after 60 sec of stirring. Under these conditions the charge transferred in the first reduction step corresponds to $0.37 \mu C$, as calculated by integration of the peak. A surface coverage of 1.28×10^{-10} mole/cm² can be estimated by division of the charge by the conversion factor nFA ($n = 2$).⁷ Each adsorbed methotrexate molecule thus occupies an area of 1.30 nm². The effects of potential scan-rate (v) on the peak current and potential were evaluated for the surface-bound methotrexate (Fig. 2). A $\log i_p$ vs. $\log v$ plot was linear over the 5 – 200 mV/sec range (*a*), with a slope of 0.64 (correlation coefficient 0.998). Slopes of 1.00 and 0.50 are expected for ideal reactions of surface and solution species, respectively. A 52 -mV negative shift in the peak potential was observed upon increasing the scan-rate in the range given. The plot of E_p vs. $\log v$ (*b*) was also linear (correlation coefficient 0.997).

The spontaneous adsorption of methotrexate can be used as an effective preconcentration step prior to the voltammetric measurement. In this way, highly sensitive measurements of the drug can be achieved by means of adsorptive stripping voltammetry. Figure 3 shows linear-scan voltamperograms for

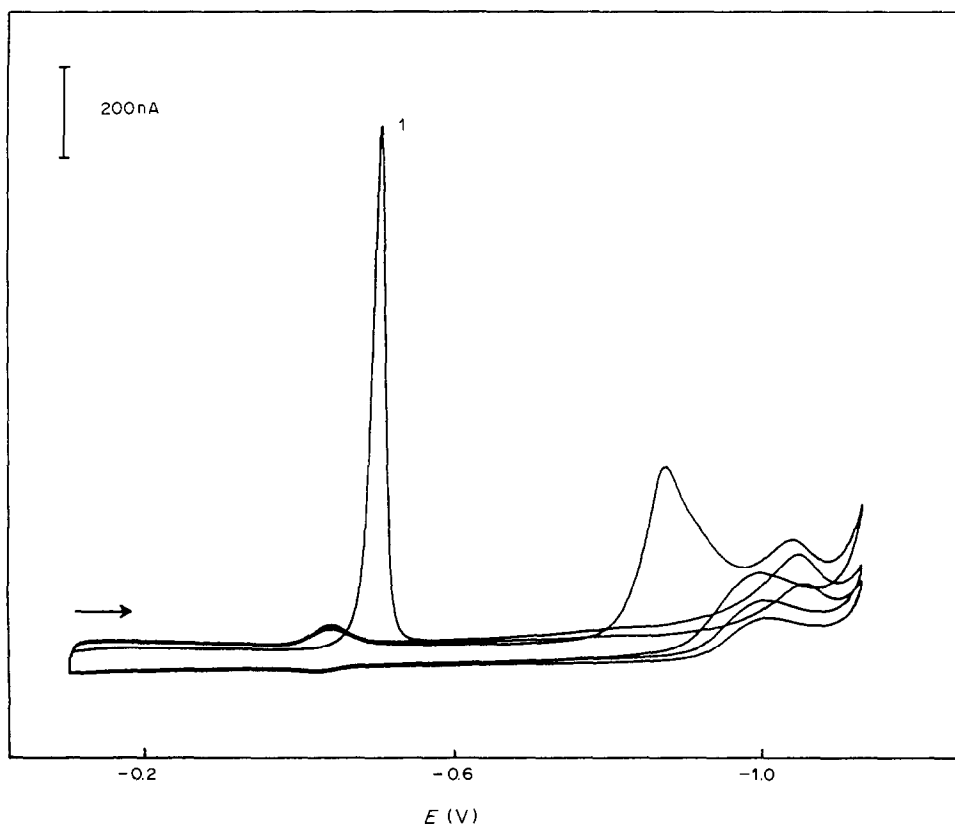


Fig. 1. Repetitive cyclic voltamperograms for $2.5 \times 10^{-6}M$ methotrexate in $0.05M$ phosphate buffer (pH 2.5), after 1 min stirring (400 rpm) at -0.10 V. Scan-rate 50 mV/sec.

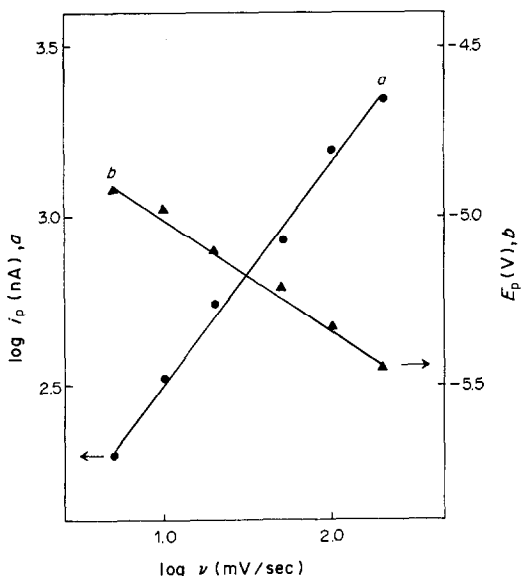


Fig. 2. Dependence of the logarithm of the peak current (a) and of the peak potential (b) on the logarithm of the potential scan-rate. Other conditions as in Fig. 1.

$4 \times 10^{-8} M$ methotrexate after different preconcentration times. While determination at this level is not feasible without preconcentration (a), well-defined peaks are observed following preconcentration (b-d). The longer the preconcentration time, the more methotrexate is adsorbed, and the larger the peak current.

$2 \times 10^{-9} M$ is estimated, based on the signal corresponding to three times the noise of the response following 300-sec preconcentration (d). This detection limit corresponds to 9 ng in the 10 ml of solution used. Also shown in Fig. 3 are peak current vs. preconcentration time plots for $4 \times 10^{-8} M$ and $1 \times 10^{-7} M$ methotrexate solutions. At both levels the peak current increases linearly with preconcentration time [slopes of 0.25 nA/sec ($4 \times 10^{-8} M$) and 0.94 nA/sec ($1 \times 10^{-7} M$)].

Adsorptive stripping measurements of methotrexate can also be performed with various solid electrodes. Such schemes utilize the anodic behaviour of the drug⁶ as well as its interfacial accumulation at carbon surfaces. For example, Fig. 4 shows differential pulse voltamperograms for $2 \times 10^{-7} M$ methotrexate following 0 (a) and 1 (b) min accumulation at the carbon-paste electrode. A single oxidation peak is observed at ca. +0.75 V. The use of a short preconcentration period results in a substantial (6-fold) enhancement of the peak height. A detection limit of around $1 \times 10^{-8} M$ is estimated from the signal-to-noise characteristics of the data. A 1-min "cleaning" period (at +1.3 V) is essential after the voltammetric scan, to desorb the drug from the surface. Though use of carbon electrodes eliminates the need for sample deaeration, the reproducibility and sensitivity are inferior to those of measurements at the static mercury-drop electrode. The latter was therefore used in the final procedure.

The solution pH has a strong effect on the adsorptive stripping response (Fig. 5a). For example,

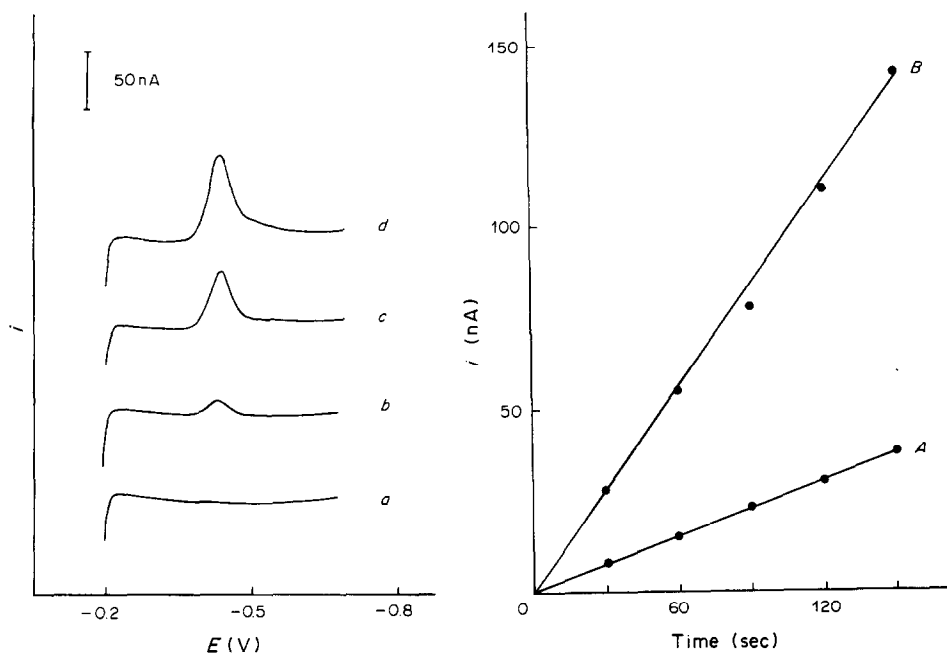


Fig. 3. Effect of preconcentration period on the stripping voltamperogram for $4 \times 10^{-8} M$ methotrexate in 0.05M phosphate buffer (pH 2.5). Preconcentration period: (a) 0, (b) 60, (c) 180, (d) 300 sec. Preconcentration potential $-0.2 V$; scan-rate 50 mV/sec. Also shown are the resulting current-time plots at different concentrations: (A) $4 \times 10^{-8} M$; (B) $1 \times 10^{-7} M$.

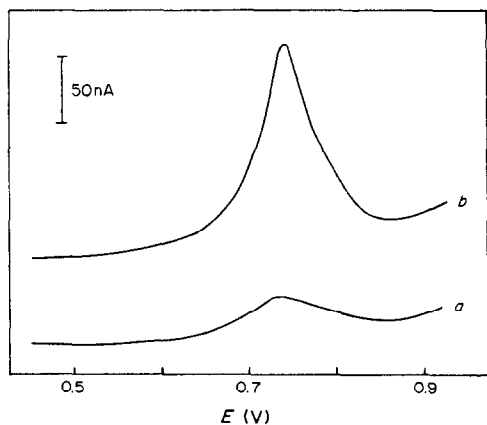


Fig. 4. Differential-pulse voltamperograms for $2 \times 10^{-7} M$ methotrexate following 0 (a) and 1 (b) min pre-concentration at the carbon-paste electrode. Preconcentration potential +0.4 V; stirring-rate, 400 rpm. Differential-pulse amplitude of 50 mV and scan-rate 5 mV/sec. Electrolyte, 0.05M phosphate buffer (pH 4).

increasing the pH from 1.5 to 2.5 results in a sharp increase in the peak; a gradual decrease in the response is observed at pH > 2.5. A similar decrease was observed in polarographic measurements of the drug.⁷ A negative shift in peak potential, from -0.36 to -0.78 V was observed on increasing the pH from 1.5 to 9.0. Such a shift is expected from the involvement of protons in the redox process. The dependence of the stripping peak current on the preconcentration potential was examined over the range from 0 to -0.35 V (Fig. 5b). Methotrexate exhibits strong adsorption over the entire range. A potential of -0.2 V offered the best signal-to-noise characteristics and was chosen as optimal. Figure 6 compares the effects of linear-scan and differential-

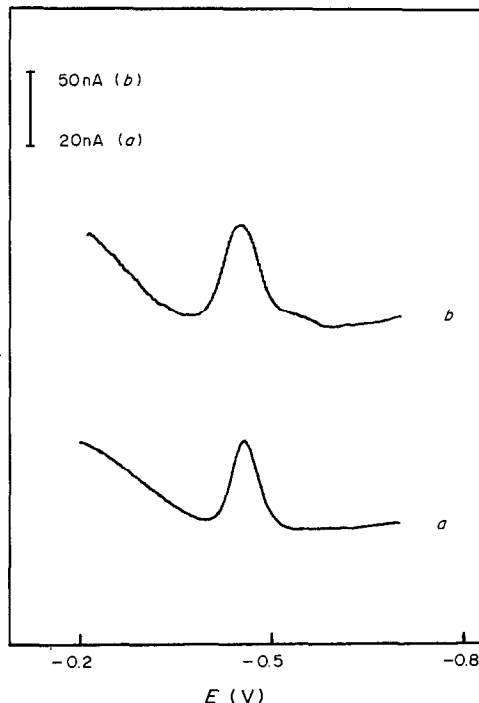


Fig. 6. Linear scan (a) and differential pulse (b) stripping voltamperograms for $1 \times 10^{-7} M$ methotrexate. Preconcentration time 30 sec. Potential-pulse conditions: 50 mV amplitude, 5 mV/sec scan-rate. Other conditions as in Fig. 3.

pulse waveforms on the methotrexate response. Both stripping modes exhibit similar signal-to-background characteristics. The linear-scan mode was selected for use because of its speed (reduction of scan-time by a factor of 10) and sharper peak.

The quantitative evaluation is based on the dependence of the peak current on methotrexate con-

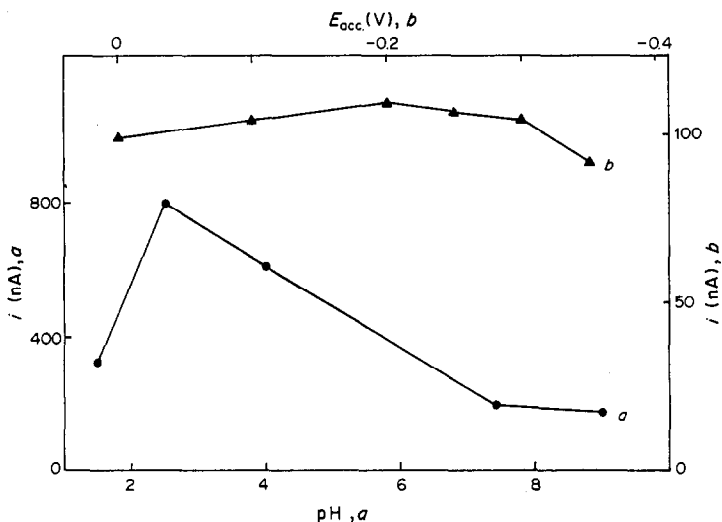


Fig. 5. Effects of the pH (a) and preconcentration potential (b) on the methotrexate peak current. Methotrexate concentration (a) $1 \times 10^{-6} M$; (b) $2 \times 10^{-7} M$. Preconcentration time 1 min. Other conditions as in Fig. 3.

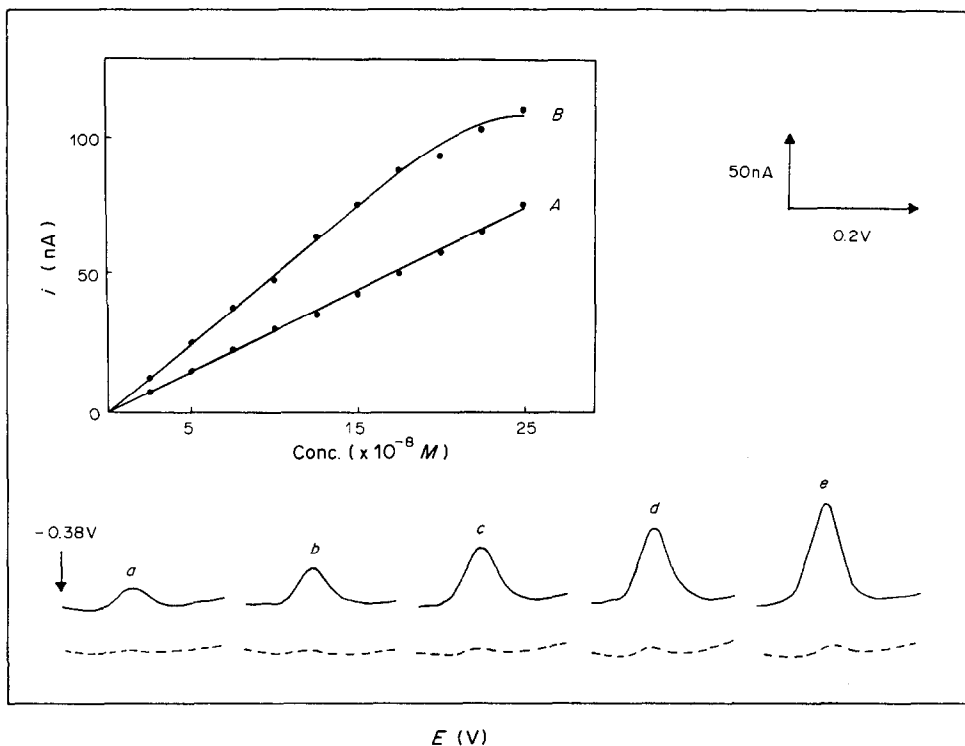


Fig. 7. Stripping voltamperograms obtained for solutions of increasing methotrexate concentration, $2.5\text{--}12.5 \times 10^{-8}M$ (a-e). Preconcentration period 30 sec. Other conditions as in Fig. 3. Dotted lines represent the response without preconcentration. Also shown are the resulting calibration plots after different preconcentration times: (A) 30, (B) 60 sec.

centration. Figure 7 shows voltamperograms for solutions of increasing methotrexate concentration, from 2.5×10^{-8} to $1.25 \times 10^{-7}M$, after 60-sec preconcentration. Well-defined stripping peaks were observed over this concentration range. In contrast, the corresponding solution-phase response (dotted line) is not useful for quantitative work at this level. Also shown in Fig. 7 are the resulting calibration plots for the $2.5\text{--}25 \times 10^{-8}M$ range, obtained at different preconcentration times. For 30-sec preconcentration (A), the response is linear for the entire range (slope $2.9 \text{ nA}/10^{-8}M$; intercept 0.0 nA ; correlation coefficient 0.998). The 60-sec plot (B) exhibits deviation from linearity at concentrations higher than $2 \times 10^{-7}M$, as expected for a process that is limited by adsorption of the analyte (slope of the initial linear portion $5.0 \text{ nA}/10^{-8}M$; intercept -0.3 nA ; correlation coefficient 0.999). The reproducibility was estimated by ten successive measurements on a stirred $1.6 \times 10^{-7}M$ methotrexate solution (90-sec preconcentration); the mean peak current was 128 nA , range $125\text{--}132 \text{ nA}$, and a relative standard deviation of 2.2% .

The presence of other surface-active compounds can affect the adsorptive stripping response, particularly through competitive coverage. The influence of model surfactants, dodecyl sodium sulphate and gelatine, on the methotrexate stripping response was

tested. Successive standard additions of dodecyl sodium sulphate, up to 10 ppm , did not affect the magnitude of the $2 \times 10^{-7}M$ methotrexate peak, but caused a gradual increase of the background current at potentials positive to the peak. Gelatine had a more pronounced effect on the methotrexate stripping peak. Additions of this colloidal protein, up to 6 ppm , caused a gradual increase of the methotrexate peak (by up to 50%); further additions of gelatine, up to 10 ppm , caused a sharp depression of the peak (to 20% of its original magnitude). The effects of other antitumour agents, which may be co-administered with methotrexate, were also investigated. The addition of $3 \times 10^{-7}M$ fluorouracil or chlorambucil did not interfere in the determination of $1 \times 10^{-7}M$ methotrexate.

Figure 8 demonstrates the feasibility of measuring methotrexate in urine samples. No sample preparation was used, other than a $1:4$ dilution with the supporting electrolyte. Urine samples with ascending methotrexate concentrations, $5\text{--}15 \times 10^{-7}M$ (b-d) yielded well-defined peaks, following a very short preconcentration period. The blank urine voltamperogram (a) shows no interfering peaks. A preconcentration potential of -0.3 V was used, as interference was observed following accumulation at -0.2 V . Analysis of more complex body fluids, and/or differentiation between the parent drug and

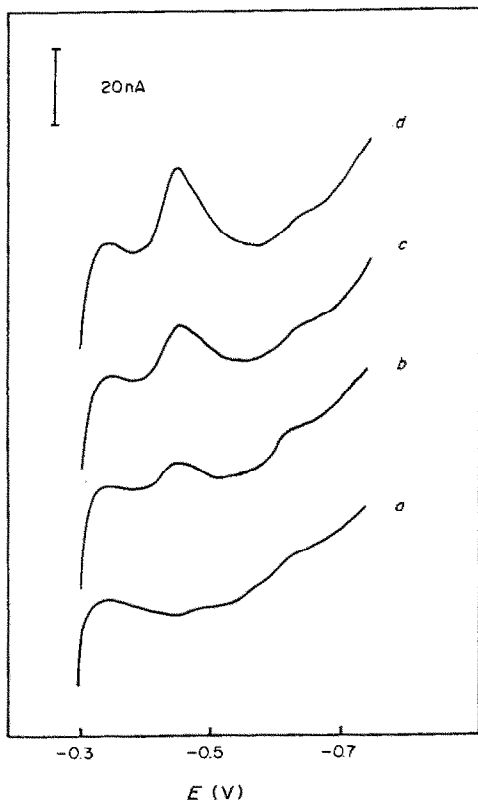


Fig. 8. Voltamperograms for diluted (1 + 4) urine solutions spiked with different levels of methotrexate: (a) 0M; (b) $5 \times 10^{-7}M$; (c) $1 \times 10^{-6}M$; (d) $1.5 \times 10^{-6}M$. Preconcentration for 10 sec at -0.3 V. Phosphate buffer (pH 2.5) was used for dilution. Scan-rate, 50 mV/sec.

its major metabolite (7-hydroxymethotrexate) would require a pretreatment procedure, *e.g.*, selective extraction, commonly used in clinical laboratories. (The increased polarity characterizing the metabolite may minimize its interfacial accumulation, *i.e.*, its interference.) Work is in progress in our laboratory toward the development of highly sensitive adsorptive stripping procedures for other important antineoplastic agents.

Acknowledgement—This work was supported by the National Institutes of Health, grants No. RR08136-12 and GM30913-03.

REFERENCES

1. A. Goldin, *Cancer Treat. Rep.*, 1978, **62**, 307.
2. C. Bohown, F. Dorbey and C. Bonden, *Clin. Chem.*, 1974, **57**, 263.
3. J. B. Gashaw and J. G. Miller, *ibid.*, 1978, **25**, 1032.
4. M. M. Kincade, W. R. Vogler and P. G. Dayton, *Biochem. Med.*, 1974, **10**, 337.
5. E. Watson, J. Cohen and K. Chan, *Cancer Treat. Rep.*, 1978, **62**, 381.
6. F. Palmisano, T. R. I. Cataldi and P. G. Zambonin, *J. Chromatog.*, 1985, **344**, 249.
7. R. C. Gurira and L. D. Bowers, *J. Electroanal. Chem.*, 1983, **146**, 109.
8. R. C. Gurira and L. D. Bowers, *Clin. Chem.*, 1981, **27**, 1088.
9. J. Wang, J. S. Mahmoud and P. A. M. Farias, *Analyst*, 1985, **110**, 855.
10. R. Kalvoda, *Anal. Chim. Acta*, 1983, **148**, 79.
11. E. N. Chaney and P. P. Baldwin, *Anal. Chem.*, 1982, **54**, 2556.
12. J. Wang and B. A. Freiha, *ibid.*, 1983, **55**, 1285.
13. J. Wang, *Am. Lab.*, 1985, **17**, No. 5, 41.

EVALUATION OF COUPLED TRANSPORT ACROSS A LIQUID MEMBRANE AS AN ANALYTICAL PRECONCENTRATION TECHNIQUE

JAMES A. COX*, ATUL BHATNAGAR and ROBERT W. FRANCIS JR.†

Department of Chemistry and Biochemistry, Southern Illinois University at Carbondale, Carbondale,
IL 62901, U.S.A.

(Received 22 January 1986. Accepted 14 May 1986)

Summary—When two aqueous solutions are separated by a liquid membrane that contains a complexing agent which is a conjugate base of a weak acid, a metal ion can be transported from the solution of the higher pH against its concentration gradient into the more acidic solution. With Cu(II) as the analyte and a liquid membrane consisting of a mixture of oximes dissolved in kerosene, enrichment factors for a prescribed dialysis time in a simple experimental apparatus were nearly independent of Cu(II) concentration over the range 10^{-4} – $10^{-7}M$. With 0.1M hydrochloric acid as the receiver, the enrichment factor was independent of ionic strength and of sample pH in the range 4–9. The effect of sample pH on the interference of Fe(III) was examined. With a pH-2.5 formate buffer, the enrichment factor for Cu(II) decreased as the Fe(III) concentration increased, but in a pH-9.3 ammonium buffer, 0.14 mM Fe(III) did not interfere with the transport of Cu(II) from a 16 μM copper sample.

Dialysis has been often used as a sample pretreatment step in analytical chemistry. Although passive systems, which only employ diffusion that is driven by a concentration gradient of an analyte across a membrane, can successfully separate the analyte from complicated sample matrices,¹ they do not enable the analyte to be concentrated. Active systems such as Donnan dialysis and electrodialysis have been demonstrated to concentrate analytes as well as to separate them from the sample matrix. In the former case, an ionic-strength gradient across an ion-exchange membrane establishes a potential that drives an analyte with the appropriate charge sign from the lower ionic-strength solution (the sample) into the more concentrated electrolyte (the receiver). In the latter case, passage of current through the solutions that are separated by an ion-exchange membrane provides the driving force. When the receiver volume is less than that of the sample, the analyte can thereby be concentrated.

Quantification is typically done on the basis of a fixed-time kinetic measurement.²⁻⁴ That is, the dialysis is performed for a prescribed time during which the experimental conditions are controlled so that the quantity of the analyte transported into the receiver during that time is a constant fraction of its initial concentration in the sample. Although electrodialysis has been used in this manner,^{5,6} the description of such conditions for Donnan dialysis is much simpler.^{7,8}

Donnan dialysis has several attractive features as

an analytical preconcentration method. Enrichment factors of over 50 have been attained in 15 min,^{9,10} and the transport rate is independent of the sample composition over a wide range of conditions such as moderate levels of surfactants, pH, and the presence of complexing agents, provided that the receiver electrolyte composition is carefully controlled.¹¹ Perhaps its primary advantage over other common concentration methods for ionic species is that the analyte is enriched into an aqueous receiver in a single step. Thus, it is rapid and compatible with a wide variety of attendant instrumental methods.

The fundamental weakness of Donnan dialysis is that the enrichment factor becomes a function of sample ionic strength when the electrolyte concentration exceeds about 0.01M.¹² For this reason we have pursued the development of pH-driven coupled transport across a liquid membrane as an analytical tool. Our hypothesis is that the pH-driven method should be independent of ionic strength and thus provide a technique complementary to Donnan dialysis in terms of the sample types that can be studied.

Liquid membranes that contain mobile carriers have been used in analytical chemistry primarily in potentiometric ion-selective electrodes. The analytical application of experiments designed to yield significant mass transport across such membranes has not been reported; however, the theory has been described and tested.¹³⁻¹⁵ The most common applications have dealt with the removal of selected ionic species from aqueous systems. For example, Cu(II) was recovered from a stream by coupled transport through a membrane consisting of benzophenoximes, alone or mixed with substituted aliphatic oximes (LIX-64N or LIX-65N) dissolved in hexachloro-1,3-

*To whom correspondence should be addressed.

†Present address, Sigma Chemical Co., St. Louis, Mo., U.S.A.

butadiene and supported in a porous polypropylene film.¹⁶ The general mechanism is that at the sample-membrane interface, Cu(II) forms a neutral complex with the LIX-reagent, a reaction which releases protons into the sample. The neutral complex diffuses to the membrane-receiver interface, where protons from the receiver displace the Cu(II) into that solution. As long as the receiver solution is more acidic than the sample, the pH differential pumps the Cu(II) across the membranes. With didodecylamine as the mobile carrier and a relatively alkaline receiver solution, the nitrate level of aqueous samples was decreased by a comparable mechanism.¹⁷ With an amine as the mobile carrier, UO_2^{2+} was transported into an alkaline receiver; the efficiency was independent of sample pH in the range 1.5–3.5.¹⁸

Because it is the most extensively characterized system, the LIX-containing membrane with Cu(II) as the analyte was selected for the present study, the object of which was to determine whether this coupled transport mechanism could be used for analytical preconcentration, with fixed-time kinetic measurement.

EXPERIMENTAL

Reagents

The complexing agent was LIX-64N (Henkel Corp., Minneapolis, MN), which is a water-insoluble mixture of substituted oximes. Structural information has been reported by others.^{19,20} It was used without purification. Before its introduction into the membrane, the reagent was generally diluted (1 + 9) with kerosene. A Celgard 2400 microporous polypropylene membrane (Celanese Corp.) was used as the support. It had a 38% porosity, an effective pore size of 0.02 μm , and a nominal thickness of 0.025 mm. The membrane was loaded by immersion in the diluted liquid ion-exchange reagent.

The water was purified with a Sybron/Barnstead NANO-pure II system. The hydrochloric acid was purified by storing the concentrated reagent grade acid and distilled water in adjacent Petri dishes in a sealed chamber (a desiccator) for several days. The resulting acidified aqueous solution was standardized and diluted to the desired concentration. The pH 4.7 acetate buffer (0.1M) was purified by solvent extraction with the diluted liquid ion-exchanger. Other chemicals (reagent grade) were used without purification.

Apparatus

The dialysis cells were of a previously reported design,⁸ except that a liquid membrane was used. The design consisted of a Plexiglas cylinder which was closed at one end by the membrane. The closed tube contained the receiver solution. The assembly was dipped into a magnetically stirred sample to start the experiment. The receiver was 5 ml of 0.1M hydrochloric acid and the sample volume was 200 ml. The exposed area of the mounted membrane was 11.3 cm^2 . The dialysis time was 60 min unless otherwise stated. After the dialysis, the receiver contents were diluted with water to 25 ml, and the analyte therein was determined by atomic-absorption spectrometry with a Perkin-Elmer model 2280 instrument. The enrichment factor, EF, was calculated as the ratio of the analyte concentration in the receiver after dialysis to the initial concentration in the sample. Generally flame atomization was used, but for Cu(II) concentrations below 10^{-6}M a Perkin-Elmer HGA-400 graphite furnace was used for the atomization.

RESULTS AND DISCUSSION

In order for coupled transport across a liquid membrane to be a practical analytical tool, the method must yield enrichment factors that are at least comparable to those obtained by Donnan dialysis under identical conditions, and independent of the initial sample concentration over a wide range. The former requirement was tested by performing a series of experiments with a $1.57 \times 10^{-5}\text{M}$ Cu(II) sample in a pH-4.7 acetate buffer. With undiluted LIX 64N as the liquid phase of the membrane and with a 1 + 1 dilution of LIX 64N by kerosene, significant transport did not occur. Instead, a blue-green precipitate formed on the sample-membrane interface. A 30-min dialysis with the 1 + 9 dilution of LIX 64N with kerosene as the liquid phase of the membrane yielded an enrichment factor of 6. Under identical conditions, except that an anion-exchange membrane with a thickness of less than 50 μm was used, Donnan dialysis yielded enrichment factors of about 10–15 for various anions.⁸ Considering that Donnan dialysis has been optimized, the enrichment factor for the present experiment was sufficient to merit further study. All subsequent experiments were performed with the 1 + 9 dilution as the liquid phase of the membrane.

Increasing the dialysis time to 60, 90 and 120 min resulted in enrichment factors of 11, 13 and 15, respectively. The non-linearity may be due to partial loss of the LIX reagent during the dialysis or depletion of the analyte from the sample. Subsequent experiments generally employed 60 min as the dialysis time. As a precaution in this preliminary study, the polypropylene membrane was washed with ethanol and re-impregnated with the liquid phase between experiments.

Under the conditions prescribed above, the enrichment factor was nearly independent of the initial concentration of Cu(II) over about three orders of

Table 1. Effect of the initial sample concentration of Cu(II) on the coupled-transport enrichment factor

[Cu(II)], M	EF*
1.5×10^{-7}	10.2 ± 0.4
1.0×10^{-6}	10.1 ± 0.6
3.0×10^{-6}	10.5 ± 1.0
6.0×10^{-6}	8.9 ± 1.8
1.0×10^{-5}	10.9 ± 0.7
3.0×10^{-5}	11.7 ± 0.7
6.0×10^{-5}	10.3 ± 0.6
1.0×10^{-4}	13.5 ± 1.2
3.0×10^{-4}	7.7 ± 0.4
6.0×10^{-4}	4.0 ± 0.4
1.0×10^{-3}	3.3 ± 0.6

*Standard deviation of six trials in the following conditions: sample, 200 ml in pH-4.7 acetate buffer; receiver, 5 ml of 0.1M HCl; dialysis time, 60 min; membrane area, 11.3 cm^2 .

magnitude. The results are shown in Table 1. At Cu(II) concentrations above 0.1 mM, the enrichment factor decreased as the concentration increased. This was undoubtedly due to saturation of the available exchange sites on the membrane and/or formation of a precipitate at the sample-membrane interface; the latter was not visually apparent, however.

At Cu(II) concentrations below about 0.1 mM the rate of the process is essentially limited by the concentration of Cu(II) in the aqueous phase at the sample-membrane interface rather than by the exchange-site concentration. This is supported by results on the effect of dialysis time on the enrichment factor. Under the conditions given in Table 1 but with a fixed Cu(II) concentration of $5.0 \times 10^{-5} M$ and dialysis times of 0.25, 0.50, 1.0, 1.5, 2.0 and 4.5 hr, the respective enrichment factors were 5.0, 9.4, 12, 20, 26 and 33. The maximum possible value was 40, so after 4.5 hr equilibrium was being approached.

That the enrichment factor in Table 1 is nearly constant means that the linear dynamic range of the resulting analytical method is not significantly shortened by the preconcentration method. The relatively poor precision is probably related to the wide variation in room temperature during the course of this study and to fluctuation in the magnetic stirring efficiency. Donnan dialysis typically shows about 8% relative standard deviation in the enrichment factor when controlled temperature and stirring rate are not employed.¹² Variation in the loading of the microporous membrane may also be important; means of controlling this factor will be the subject of a future study.

Because this coupled transport process is driven by a pH-gradient across the membrane, the acidity of the sample can be expected to influence the transport rate. As shown in Fig. 1, a plot of enrichment factor *vs.* sample pH has a rather broad, flat, maximum. This is indicative of a mass-transport limit to the enrichment rate rather than limitation by the distribution coefficient of Cu(II), since the latter is a

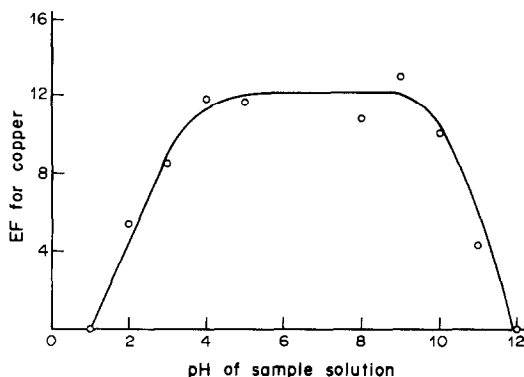


Fig. 1. Effect of sample pH on the enrichment factor for Cu(II). Experimental conditions were the same as for Table 1 except that formate, acetate and ammonium buffers were used in the appropriate pH regions. The copper concentration was $1.6 \times 10^{-5} M$.

Table 2. Effect of ionic strength on the enrichment factor for Cu(II)

[NaCl], M	EF*
1.0×10^{-4}	9.8
1.0×10^{-3}	10.1
1.0×10^{-2}	9.5
1.0×10^{-1}	9.4
1.0	10.1

*For $1.6 \times 10^{-5} M$ Cu(II). The other experimental conditions were the same as for Table 1.

function of sample pH. The existence of a region where the enrichment factor is independent of pH is important for the design of analytical experiments, since buffering the sample may not be necessary. In addition, many samples could be studied without any adjustment of pH.

As previously stated, a major reason to develop coupled transport across a liquid membrane as an analytical technique is to complement Donnan dialysis for the study of high ionic-strength samples. The data summarized in Table 2 demonstrate that, as predicted, the liquid membrane method yields an enrichment factor that is independent of ionic strength. With Donnan dialysis, sodium chloride concentrations above 0.01 M would decrease the enrichment factor, even if 1.0 M hydrochloric acid were used as the receiver electrolyte.¹²

An important characteristic of Donnan dialysis is that the enrichment factor for a given cation is not influenced by the presence of other cations in the sample (assuming that the total ionic strength is moderate to low) as long as the receiver electrolyte cation has the higher affinity for the fixed sulphonate sites on the membrane.^{7,12} To determine whether our present experimental system shares this characteristic, the dialysis of $1.6 \times 10^{-5} M$ Cu(II) was performed in the presence of Fe(III) with sample pH values of 2.5 (formate buffer), 4.7 (acetate buffer), and 9.3 (ammonium buffer). At pH 2.5 and 9.3, transport of Fe(III) was not observed; nevertheless, the enrichment factor for Cu(II) was affected, particularly at pH 2.5 (Table 3). At pH 2.5, Fe(III) may interfere by forming a charged complex with the mobile carrier. Transport of Fe(III) will not occur since a charged complex will not partition into the membrane, but the reaction will decrease the available sites for Cu(II), especially if the Fe(III) complex is non-labile and/or relatively strong. The slight decrease of the enrichment factor for Cu(II) with an increase in Fe(III) concentration at pH 9.3 is undoubtedly due to the formation of an insoluble Fe(III) species (probably the hydrated oxide) which partially blocks the membrane pores; a rust-coloured deposit was observed on the sample-membrane interface at the highest Fe(III) concentrations used at pH 9.3.

Table 3. Effect of Fe(III) on the transport of Cu(II) across the 1,64N-kerosene membrane

[Fe(III)], <i>M</i>	Cu EF*		
	pH 2.5	pH 4.7	pH 9.3
0	6.8	10.7	13.0
3.6×10^{-5}	4.1	11.2	12.9
7.2×10^{-5}	2.9	12.1	13.0
1.1×10^{-4}	1.8	10.5	11.6
1.4×10^{-4}	1.2	9.6	10.2
1.8×10^{-4}	0.8	9.5	9.5

*For $1.6 \times 10^{-5} M$ Cu: other experimental conditions were the same as for Table 1.

At pH 4.7, transport of Fe(III) was observed. With $1.6 \times 10^{-5} M$ Cu(II) and $1.8 \times 10^{-5} M$ Fe(III) in the original sample, the enrichment factors for Cu and Fe were 10.8 and 1.8, respectively. Nevertheless, the effect of Fe(III) concentration on the enrichment factor for Cu(II) was quite small, as shown in Table 3. As at pH 9.3, a precipitate formed at the highest Fe(III) concentrations.

Because of the effect of Fe(III) on the enrichment factor for Cu(II), a calibration curve method is not suited for analysis of samples when the present coupled-transport procedure is used for preconcentration. For the standard-addition method to be used, it must be demonstrated that the enrichment factor for Cu(II) is independent of the concentration of Cu(II) in the presence of an interferent such as Fe(III). This requirement was satisfied in the study of a simulated sample at both pH 2.5 and pH 9.3. The sample contained 1.0 mg/l. Cu(II) and 4.0 mg/l. Fe(III). The usual preconcentration and atomic-absorption analysis procedures were applied to the original sample and to samples dosed with an additional 2, 4, 6, 8 or 10 mg/l. Cu(II). The results were analysed by plotting absorbance *vs.* the change in concentration and extrapolating to obtain the original Cu(II) concentration. At pH 2.5, the results of a linear least-squares analysis were: Cu(II), 0.99 mg/l.; correlation coefficient, 0.9994; slope, 0.011 l./mg. At pH 9.3, the results were: Cu(II), 0.94 mg/l.; slope, 0.067 l./mg; correlation coefficient, 0.9990. The

higher slope for the latter set is in accord with the results reported in Table 3.

This study has demonstrated that coupled transport across a liquid membrane has potential application as an analytical preconcentration and matrix normalization technique. Several problems, including the effect of mixtures of complex-forming cations on the enrichment factor of the analyte, the modest enrichment factors with the present experimental design, and the low precision must be solved for it to be a practical technique.

Acknowledgement—This work was supported by the National Science Foundation under Grant CHE-8215371.

REFERENCES

1. F. R. Nordmeyer and L. D. Hansen, *Anal. Chem.*, 1982, **54**, 2605.
2. G. L. Lundquist, G. Washinger and J. A. Cox, *ibid.*, 1975, **47**, 319.
3. J. E. DiNunzio and M. Jubara, *ibid.*, 1983, **55**, 1013.
4. R. L. Wilson and J. E. DiNunzio, *ibid.*, 1981, **53**, 692.
5. J. A. Cox and R. H. Carlson, *Anal. Chim. Acta*, 1981, **130**, 313.
6. *Idem*, *Clin. Chem.*, 1982, **28**, 1986.
7. J. A. Cox, T. Gray, K. S. Yoon, Y.-T. Kim and Z. Twardowski, *Analyst*, 1984, **109**, 1603.
8. J. A. Cox and N. Tanaka, *Anal. Chem.*, 1985, **57**, 2370.
9. J. A. Cox and G. R. Litwinski, *ibid.*, 1983, **55**, 1640.
10. M. L. Bruce, J. W. Carnahan and J. A. Caruso, *Pittsburgh Conf. Anal. Chem. Appl. Spectrosc.* Atlantic City, NJ, March, 1983, Abstr. No. 268.
11. J. A. Cox and Z. Twardowski, *Anal. Chim. Acta*, 1980, **119**, 39.
12. J. A. Cox and J. E. DiNunzio, *Anal. Chem.*, 1977, **49**, 1272.
13. K. A. Smith, J. H. Meldon and C. K. Cotton, *AIChE J.*, 1973, **19**, 102.
14. E. L. Cussler, *ibid.*, 1971, **17**, 1300.
15. J. D. Goddard, J. S. Schultz and S. K. Suchdeo, *ibid.*, 1974, **20**, 625.
16. K. H. Lee, D. F. Evans and E. L. Cussler, *ibid.*, 1978, **24**, 860.
17. M. M. Kreevoy and C. I. Nitsche, *Environ. Sci. Technol.*, 1982, **16**, 635.
18. W. C. Babcock, R. W. Baker, E. D. Lachapelle and K. L. Smith, *J. Membr. Sci.*, 1980, **7**, 71.
19. R. W. Baker, M. E. Tuttle, D. J. Kelly and H. K. Lonsdale, *ibid.*, 1977, **2**, 213.
20. A. W. Ashbrook, *Hydrometallurgy*, 1975, **1**, 5.

STUDIES WITH AN INORGANIC ION-EXCHANGE MEMBRANE EXHIBITING SELECTIVITY FOR Pb(II) IONS

SURESH K. SRIVASTAVA, SATISH KUMAR, CHAKRESH K. JAIN
and SURENDER KUMAR

Department of Chemistry, University of Roorkee, Roorkee-247667, India

(Received 22 August 1984. Revised 27 February 1986. Accepted 30 April 1986)

Summary—A solid membrane electrode made with titanium arsenate as membrane material and "Araldite" as binder has been used to measure the activity of lead in the concentration range from 0.1M to $5 \times 10^{-6}M$. The electrode is unaffected by many cations, nitrate and acetate. The response time is 40–60 sec over the whole concentration range (in a static system) and the electrode has a working life of at least four months. The electrode can work in the pH range 2–5 and is tolerant of ethanol up to a content of 30% v/v. It has been successfully used for end-point indication in potentiometric titration of lead. A membrane treated with cationic surfactant exhibits better selectivity.

In continuation of our work on the permeability and selectivity of inorganic membranes^{1,2} we report the properties of a titanium arsenate membrane.

EXPERIMENTAL

Reagents

Titanium(IV) chloride, sodium arsenate heptahydrate and lead nitrate were used as received.

Instruments

An expanded scale pH-meter was used for pH measurements. Conductance measurements were performed with a Systronics 302 conductivity meter and emf values were measured with a Phillips potentiometer reading to 0.1 mV.

Preparation of membranes

Titanium arsenate was prepared and characterized as reported by Qureshi *et al.*³ Homogeneous membranes made with the product were not stable, but heterogeneous membranes obtained by binding the titanium arsenate gel with "Araldite" were found to be quite satisfactory.

The 200-mesh powdered exchanger was further ground in a mortar, then mixed homogeneously with "Araldite" and the mixture was spread on a filter paper, and covered with another filter paper. This "sandwich" was pressed gently between two glass plates and left to dry. When the membrane had dried and hardened, a disc, 1.5 cm in diameter, was cut out and the filter papers were detached. A large number of membranes (thickness 1 mm) of different compositions were prepared and examined under the electron microscope for homogeneous distribution of the exchanger in the "Araldite" and for cracks on the surface. Membranes with 40% "Araldite" content showed the best electrochemical performance together with good conductance and stability, and were selected for further studies.

The membranes were equilibrated with 0.1M lead nitrate for a week, the solution being periodically replaced. Shorter equilibration times resulted in membranes that gave unstable response.

Measurements of emf

The electrode assembly was the same as that used before,² the reference solution being 0.1M lead nitrate for all mea-

surements. Saturated calomel electrodes were used as reference electrodes with saturated potassium nitrate solution as external filling solution. All measurements were made at $25 \pm 0.1^\circ$.

Determination of water content

The membrane was immersed in water for several days, then wiped and weighed and dried in a vacuum desiccator at room temperature until constant weight was reached.

Measurement of specific conductance

The method recommended by Lakshminarayanaiah and Subrahmanyam⁴ was used for measuring the membrane conductance at three different concentrations (0.1, 0.01 and 0.001M) of electrolyte solution. The membrane was cemented between two halves of a U-tube, which was then left filled with a solution of the electrolyte (of the desired concentration) for a week. The solution was then replaced by mercury (equilibrated with the same electrolyte) and the conductance was measured by connecting the two mercury columns to the conductivity bridge. The effective area and thickness of the membrane in contact with the equilibrated mercury were 1.29 cm² and 1.6 mm respectively.

RESULTS AND DISCUSSION

Potentials observed with the membrane when interposed between 0.1M lead nitrate reference solution and solutions of lead nitrate of various concentrations (10^{-7} – $5 \times 10^{-1}M$) are shown in Fig. 1 together with a plot for similar solutions adjusted to constant ionic strength (1M) with sodium nitrate. The response is linear over the concentration range 10^{-5} – $10^{-1}M$ with a non-Nernstian slope of 33.3 mV/pPb. The potentials remain almost constant below a lead concentration of $10^{-6}M$. According to the IUPAC recommendations on ion-selective electrodes,⁵ the practical limit of detection may be taken as the concentration corresponding to the point of intersection of the two extrapolated lines shown in Fig. 1. Thus this electrode can be used to measure

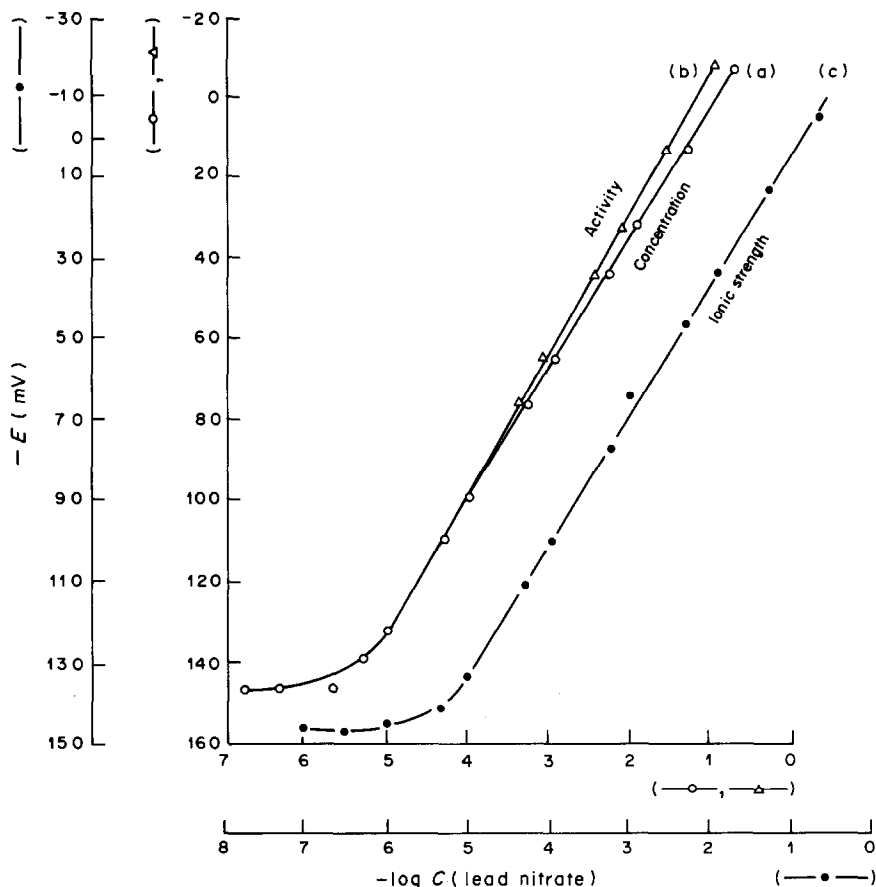


Fig. 1 (a) Potential vs log of concentration of lead nitrate; (b) potential vs. log of activity of lead nitrate; (c) potential vs. log of concentration of lead nitrate at constant ionic strength.

lead ion activity in the concentration range from $10^{-1}M$ down to $5 \times 10^{-6}M$. The plot at constant ionic strength (Fig. 1c) almost corresponds to the concentration plot (Fig. 1a).

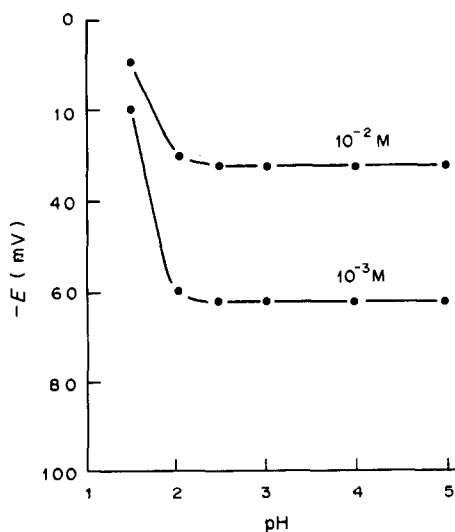


Fig. 2. Effect of pH on membrane potential.

The response time is 40 sec for 10^{-4} – $10^{-1}M$ solutions and ~ 50 – 60 sec for 10^{-6} – $10^{-5}M$ solutions. The potential remains stable for at least 20 min. The working life is usually about 4 months. The standard deviation of the potentials is 0.2 mV. When not in use the membrane is kept immersed in distilled water. If it shows deterioration, regeneration by equilibrating with 0.1M lead nitrate can be tried. If this fails, the membrane is discarded.

The pH-dependence of the response has been investigated at two lead concentrations (10^{-2} , $10^{-3}M$)

Table 1. Specific conductance of the titanium arsenate membrane in presence of different cations

Cation (M)	[M] Specific conductance, $\mu\text{mho/cm}$		
	0.1M	0.01M	0.001M
H ⁺	30.7	12.1	6.1
Li ⁺	10.1	10.0	9.0
Na ⁺	19.6	19.1	18.5
K ⁺	21.3	20.7	20.1
Pb ⁺	36.5	35.1	32.1
Cs ⁺	40.2	38.3	36.9
Ba ²⁺	8.4	8.4	8.0
Ca ²⁺	7.7	7.5	7.3

Table 2. Selectivity coefficients, $k_{A,B}^{pot}$, for titanium arsenate membrane in $10^{-2}M$ and $10^{-3}M$ solutions of interfering ions

Ions	$k_{A,B}^{pot}$		
	Original membrane		Detergent-treated membrane
	0.1M	0.01M	0.01M
Na ⁺	0.11	0.10	0.08
K ⁺	0.33	0.32	0.13
Li ⁺	0.15	0.13	0.11
NH ₄ ⁺	0.24	0.22	0.21
Ag ⁺	0.15	0.14	0.02
Cs ⁺	0.31	0.30	0.11
Tl ⁺	0.32	0.23	0.11
Rb ⁺	0.25	0.25	0.11
Mg ²⁺	0.01	0.01	
Mn ²⁺	0.02	0.02	
Cd ²⁺	0.02	0.01	
Sr ²⁺	0.02	0.02	
Zn ²⁺	0.03	0.04	
Cu ²⁺	0.03	0.02	
Hg ²⁺	0.04	0.03	
Ni ²⁺	0.01	0.01	
Fe ³⁺	0.01	0.00	
Al ³⁺	0.01	0.01	
Cr ³⁺	0.01	0.00	
Th ⁴⁺	0.08	0.01	

(Fig. 2), pH adjustment being made with nitric acid. The response is constant at pH 2–5. The increase in potential at pH < 2 may be attributed to interference by protons.

The water content of the saturated membrane was found to be 8.5% in agreement with the low degree of swelling (18%).

The specific conductances of membranes equilibrated with aqueous solutions of various electrolytes at three different concentrations are given in Table 1, and are almost invariant with changing electrolyte concentration except for H⁺ ions. This indicates that Donnan exclusion is fully effective over this concentration range except for the proton system.

The selectivity for lead was determined by the fixed interference method⁵ and the selectivity coefficients, $k_{A,B}^{pot}$, at two levels of interfering ions are reported in Table 2.

The selectivity is quite good with respect to bivalent and multivalent ions. Univalent ions may interfere. Sodium, unless taken as sodium nitrate, would also interfere.

If the membrane is modified by soaking in $10^{-4}M$ cetylpyridinium chloride for 4 days, the selectivity with respect to univalent cations (except NH₄⁺) is further improved. Surfactant solutions, if present at low concentrations, also do not affect the modified membrane. The electrode is quite tolerant to nitrate and acetate, but chloride, sulphate and sulphide ions interfere.

The slope of the electrode response is the same in ethanol–water and acetone–water mixtures (up to 30% v/v organic component) as in water, but the linear range is shorter (5×10^{-4} – $5 \times 10^{-2}M$ lead) but with higher ethanol or acetone concentration the response time increases and there is a potential drift.

The electrode can be used as an end-point indicator in potentiometric titrations involving lead ions, e.g., titration with molybdate. For the titration of 25 ml of 0.01M lead nitrate with 0.01M sodium molybdate

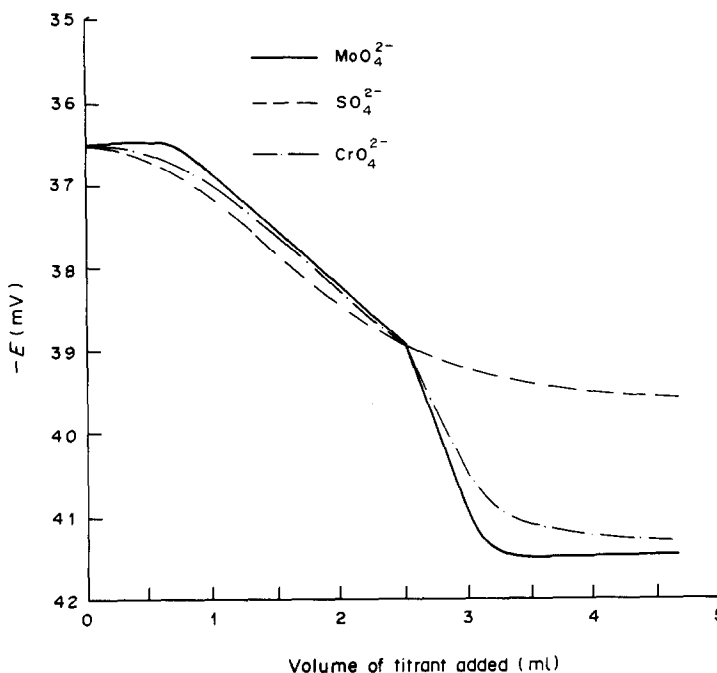


Fig. 3. Curves for titration of 25 ml of 0.01M lead nitrate with 0.1M sodium molybdate (—), sodium chromate (— · —) or sodium sulphate (---).

the standard deviation (10 replicates) found was 0.04 ml, *i.e.*, the relative standard deviation was 1.6%. In the initial stages (Fig. 3), the potential change is insignificant and there is no precipitation of lead molybdate, but after this induction period there is a more rapid change in potential (though much less than would be expected from the calibration graph and the solubility product of lead molybdate) accompanied by precipitation. We can only suggest that there is some interaction between the electrode and molybdate ions, and a test showed that a change in potential of up to 15 mV could be obtained by immersion of the electrode in sodium molybdate solutions. Similar titration plots were obtained for the lead–chromate system, but the lead–sulphate system proved impractical (Fig. 3). The end-point is taken as the intersection of the two steep linear sections of the plot.

Most of the lead-selective electrodes reported⁶ involve a lead salt matrix and suffer interference from copper, mercury, silver *etc.* The assembly proposed in

this paper incorporates an inorganic gel as sensing material, has almost the same working range as that reported in other papers⁶ and is free from interference by the ions mentioned above.

Acknowledgements—Two of the authors (C. K. Jain and Surender Kumar) are grateful to the Council of Scientific and Industrial Research, India for financial support to make these investigations.

REFERENCES

1. S. K. Srivastava, S. Kumar, C. K. Jain and Surender Kumar, *Indian J. Chem.*, 1983, **22A**, 395.
2. W. U. Malik, S. K. Srivastava and A. Bansal, *Anal. Chem.*, 1982, **54**, 1399.
3. M. Qureshi and S. A. Nabi, *J. Inorg. Nucl. Chem.*, 1970, **32**, 2059.
4. N. Lakshminarayanaiah and V. Subrahmanyam, *J. Phys. Chem.*, 1968, **72**, 4314.
5. G. G. Guilbault, *Ion-Selective Electrode Rev.*, 1979, **1**, 139.
6. M. E. Meyerhoff and Y. M. Fraticelli, *Anal. Chem.*, 1982, **54**, 27R.

ETUDE DE L'INTERACTION ION-AMMONIUM TETRAMINES CYCLIQUES PAR POTENTIOMETRIE ET RMN A L'AIDE DU PROGRAMME MICMAC

ELISABETH SUET* et ANDRE LAOUEANAN

Université de Bretagne Occidentale, Département de Chimie, 6, Avenue V. Le Gorgeu,
29287 Brest-Cedex, France

(Reçu le 31 décembre 1985. Accepté le 28 avril 1986)

Résumé—La formation de complexes entre l'ammonium et le 1,4,8,11-tétra-azacyclotétradécane (1), le 1,5,9,13-tétra-azacycloheptadécane (2), le 1,5,10,14-tétra-azacyclo-octadécane (3) et le 1,6,11,16-tétra-azacyclo-eicosane (4) est étudiée par titrages pH-métriques et RMN ¹H. Les résultats indiquent que seuls les ligands 2 et 3 forment des complexes avec NH₄⁺ en milieu basique. Les valeurs des constantes de stabilité des complexes 1:1 et 2:1, libre et protoné, sont données. La relation entre taille de cavité, basicité, complexation ou transprotonation est commentée. Une version améliorée du programme MICMAC permettant l'exploitation simultanée des données pH-métriques et RMN a été mise au point.

Summary—The complex formation of ammonium ion in water with 1,4,8,11-tetra-azacyclotetradecane (1), 1,5,9,13-tetra-azacyclohexadecane (2), 1,5,10,14-tetra-azacyclo-octadecane (3) and 1,6,11,16-tetra-azacyclo-eicosane (4) has been studied by potentiometric titration and ¹H NMR. The results indicate that only ligands 2 and 3 form complexes with NH₄⁺ in basic solutions; the stability constants of complexes (1:1, 2:1, free and protonated) are given. The relationship between the ligand ring size, basicity, and complexation or transprotonation is discussed. An improved version of the program MICMAC allowing simultaneous least-squares adjustment of pH-titration and ¹H NMR data has been created.

Pedersen fut le premier à rapporter que le dibenzo-18 couronne-6 forme des complexes avec les ions NH₄⁺ et R-NH₃⁺ (R = alkyl).¹ Cette découverte a suscité depuis lors de nombreuses études sur l'interaction ions ammonium-macrocycles, la plupart des travaux portant sur les ions ammonium substitués.²⁻¹² Nous sommes intéressés dans ce travail à l'ion NH₄⁺, substrat particulièrement important par son rôle en biologie et en biochimie; bien que Lehn *et al.*¹³ aient trouvé le récepteur idéal de cet ion (log K = 6,1 pour le complexe SC-24, NH₄⁺ dans l'eau), nous avons entrepris d'étudier le comportement d'une série homogène de tétra-azamacrocycles vis-à-vis de NH₄⁺; en effet, les tétra-azamacrocycles ne s'associent ni aux alcalins, ni aux alcalino-terreux; nous pouvons donc espérer une meilleure sélectivité par rapport à ces ions.

Ces composés sont susceptibles de former des complexes par liaison hydrogène N—H—N⁺; lorsque la taille du cycle augmente, la cavité devient de plus en plus labile, et l'examen des modèles moléculaires (Corey-Pauling-Koltin) montre que, à partir d'une certaine taille, les quatre atomes d'azote du cycle peuvent adopter une conformation tétraédrique favorable à une inclusion de l'ion NH₄⁺ dans la cavité intramoléculaire. Cette influence de la taille de la cavité a été largement démontrée lors de nos précédentes études.¹⁴⁻¹⁶

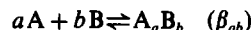
Dans ce travail, les complexes NH₄⁺-tétra-azamacrocycles ont été étudiés en milieu basique (pH > 8) par titrages potentiométriques et par mesure des déplacements chimiques en RMN du proton.

PRINCIPE

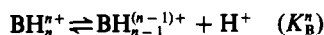
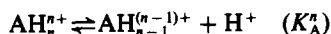
Les différents résultats expérimentaux ont été exploités à l'aide du programme MICMAC¹⁷ qui permet la détermination de constantes d'équilibre à partir de méthodes physico-chimiques variées.

Potentiométrie

Dans le cas général, l'interaction entre deux espèces A et B se traduit par l'équilibre:



Si, par ailleurs, ces espèces possèdent des propriétés acido-basiques, il est nécessaire d'introduire des équilibres d'échanges de proton:



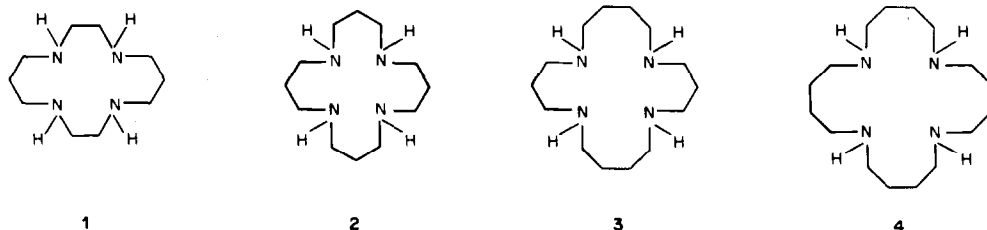
avec

$$K_A^n = \frac{[AH_{n-1}^{(n-1)+}][H^+]}{[AH_n^{n+}]}; \quad K_B^n = \frac{[BH_{n-1}^{(n-1)+}][H^+]}{[BH_n^{n+}]}$$

Les formes protonées des espèces A et B peuvent également interagir et donner lieu à des équilibres du type:



*Auteur pour correspondance. Adresse actuelle: 14, Avenue de Tarente, 29200 Brest, France.



Scheme 1

Dans le cadre de cette étude, les courbes de titrage des ligands, en l'absence puis en présence de NH_3 , par un acide fort (HNO_3) ont été analysées en minimisant sur chacune des courbes de titrage la somme des carrés des résiduels:

$$U = \sum_i (\text{pH}_i^{\text{exp}} - \text{pH}_i^{\text{calc}})^2$$

Résonance magnétique nucléaire

Lorsque l'échange entre les différentes espèces demeure rapide par rapport à l'échelle de temps RMN, seul un signal moyen est observé pour un noyau donné. Le déplacement de ce signal moyen est fonction de la composition de la solution et peut être utilisé pour déterminer les constantes de complexation.¹⁷⁻¹⁹ Le déplacement chimique observé est la moyenne pondérée:

$$\delta_{\text{obs}} = \sum_k X_k \delta_k$$

où X_k = fraction molaire et δ_k = déplacement chimique de l'espèce k .

L'ajustement à l'aide du programme MICMAC porte sur les déplacements chimiques des signaux N—CH₂ des ligands, qui sont les plus influencés par la formation de complexes. La fonction à minimiser est:

$$U = \sum_i (\delta_i^{\text{calc}} - \delta_i^{\text{exp}})^2$$

Les paramètres ajustables peuvent être les constantes d'acidité, de complexation, et les déplacements chimiques des différentes espèces.

Utilisation simultanée des ces deux méthodes

Il est intéressant, lorsque cela est possible, d'associer plusieurs techniques expérimentales lors de l'étude d'équilibres complexes en solution. Dans ce cas, l'ajustement porte sur des paramètres communs aux différentes expériences (constantes d'équilibre) et sur des paramètres propres à chacune d'elles. L'ajustement réalisé sur chaque expérience considérée isolément conduit à autant de jeux de "meilleures" constantes. La question est alors de savoir lequel de ces jeux retenir;²⁰ une solution possible consiste à faire la moyenne de ces différentes valeurs. Ce procédé, qui néglige la propagation des erreurs et les covariances, nous paraît discutable. Nous estimons de loin préférable de traiter simultanément la totalité des données expérimentales. Le bénéfice

d'une telle démarche est analogue à celui obtenu par l'exploitation simultanée des données spectrophotométriques recueillies à plusieurs longueurs d'onde, lors de la détermination d'une constante d'équilibre.²¹

L'utilisation simultanée d'un ensemble de données inhomogènes impose l'emploi d'une pondération. L'expression habituelle du poids est:

$$W_{ij} = \frac{1}{\sigma_{y_{ij}}^2 + \left(\frac{\partial y_{ij}}{\partial x_{ij}}\right)^2 \sigma_{x_{ij}}^2}$$

où i = numéro du point, j = numéro de l'expérience.

Le poids ainsi exprimé dépend de l'unité de la grandeur mesurée, et n'est valable que pour l'expérience j . On utilise généralement des poids normalisés:

$$W_{ij}^* = \frac{W_{ij}}{(\sigma o)_j^2}$$

La variance de poids unité, $(\sigma o)_j^2 = \max(W_{ij})_i$, correspond au maximum de poids sur l'ensemble des points i (à j constant) et dépend également de l'unité de la mesure.

Cette dépendance est inacceptable dans le cas d'un ajustement simultané; le poids ne peut être que sans dimension. D'autre part, il est nécessaire de tenir compte de l'amplitude des variations de la grandeur observée. Ces arguments nous ont conduits à introduire dans l'expression du poids l'écart-type empirique (σe):

$$(\sigma e)_j^2 = \frac{1}{n_j} \sum_i (y_{ij} - \bar{y}_j)^2$$

$$\bar{y}_j = \frac{1}{n_j} \sum_i y_{ij}$$

d'où

$$W_{ij} = \frac{(\sigma e)_j^2}{\sigma_{y_{ij}}^2 + \left(\frac{\partial y_{ij}}{\partial x_{ij}}\right)^2 \sigma_{x_{ij}}^2}; \quad W_{ij}^* = \frac{W_{ij}}{(\sigma o)_j^2}$$

j = numéro de l'expérience; n_j = nombre de mesures dans l'expérience j .

Le poids ainsi exprimé est sans dimension, ainsi que le variance de poids unité $(\sigma o)_j^2 = \max(W_{ij})_{i,j}$. La fonction à minimiser s'écrit alors:

$$U = \sum_j \sum_{i=1}^{n_j} W_{ij}^* (y_{ij}^{\text{exp}} - y_{ij}^{\text{calc}})^2$$

Adaptation du programme MICMAC

Comme nous l'avons amplement démontré dans notre précédent article,¹⁷ le programme MICMAC est à même de traiter différentes expériences. Dans le cadre de cette étude, il a été nécessaire d'étendre cette possibilité à l'exploitation simultanée des résultats. L'architecture du programme a permis de réaliser cette extension sans qu'il soit nécessaire d'en changer la structure; en particulier, les entrées et les sorties sont conservées. Nous avons introduit dans le module spécifique (MOSP) les équations de calcul du pH et du déplacement chimique. Les expressions nécessaires au calcul des concentrations sont communes aux deux expériences et ont pu être codées dans une seule routine. A notre connaissance, cette démarche est originale; aucun programme publié à ce jour n'offre cette possibilité. D'autre part le programme a été amélioré de façon à tester le modèle proposé au cours de l'ajustement. Les espèces non significatives ($\partial y_{\text{calc}}/\partial K \approx 0$) sont rejetées; l'ajustement se poursuit automatiquement sur les autres paramètres. Cette nouvelle version de MICMAC permet à l'expérimentateur de disposer d'une méthode de calcul appropriée quelles que soient les techniques expérimentales utilisées, et de bénéficier pleinement de la complémentarité des expériences. Ainsi, le libre choix des manipulations est assuré, et la priorité reste choix chimique. Ce travail montre que l'on peut traiter des problèmes compliqués sur micro-ordinateur lorsque le programme est judicieusement conçu.

RESULTATS ET DISCUSSION*Résonance magnétique nucléaire du proton*

On procède dans un premier temps à la détermination des déplacements chimiques des formes libres et protonées des différents ligands. Les spectres ^1H des ligands sont enregistrés en présence de quantités croissantes de D_2SO_4 (Fig. 1a). La connaissance des $\text{p}K_a$ permet de déterminer la contribution de chacune des espèces protonées au déplacement chimique du signal moyen observé. Les spectres ^1H du ligand sont à nouveau enregistrés en présence de quantités croissantes de NH_4^+ en solution dans D_2O (Fig. 1c). Les valeurs des déplacements chimiques précédemment déterminés permettent de calculer les courbes obtenues en présence de quantités croissantes de NH_4^+ agissant uniquement en tant qu'acide de $\text{p}K_a$ 9,2 (Fig. 1b) et de les comparer aux courbes expérimentales. Toute différence entre les courbes ne peut s'interpréter qu'en terme de complexation.

Un comportement différent de chacun des ligands vis-à-vis de l'ion NH_4^+ est observé; on peut cependant noter des similitudes entre les ligands 2 and 3 (Scheme 1).

Potentiométrie

Le comportement acido-basique des ligands¹⁵ et de NH_4^+ étant connu, nous avons entrepris d'analyser les courbes de titrage par un acide fort du mélange équimoléculaire L-NH_3 (Fig. 2).

Ici le même type de courbe est observé pour les quatre ligands:

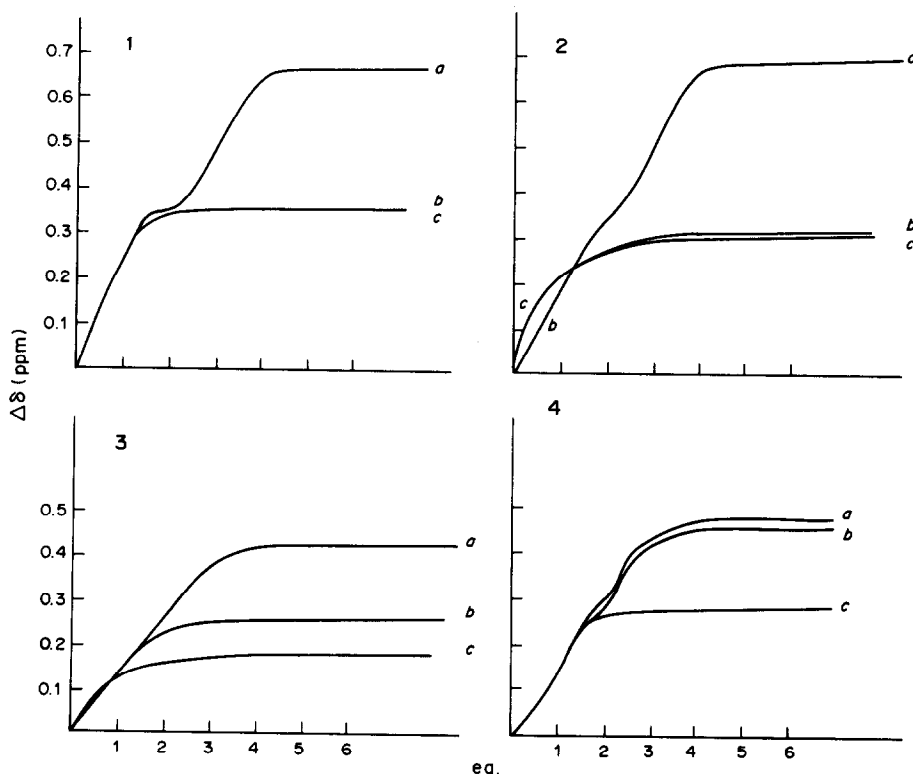


Fig. 1. Déplacements des signaux N-CH_2 : (a) courbe expérimentale obtenue par addition d'acide, (b) courbe calculée pour NH_4^+ agissant en tant qu'acide, (c) courbe expérimentale par addition de NH_4^+ .

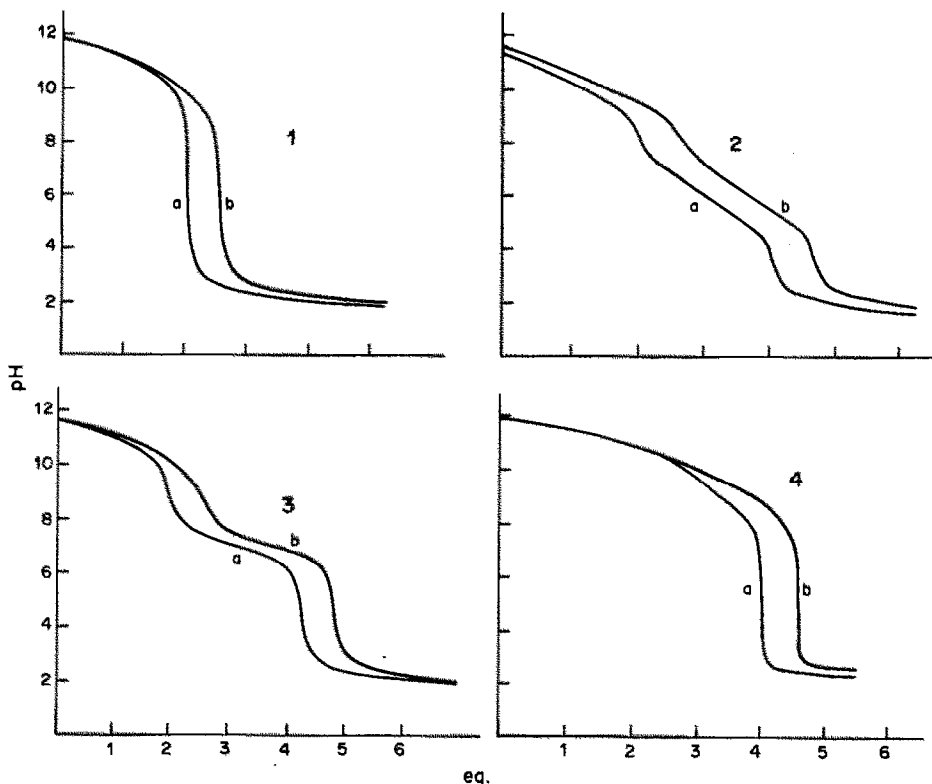


Fig. 2. (a) Courbes de titrage des ligands par HNO_3 , (b) courbes de titrage des mélanges équimoléculaires L-NH_3 par HNO_3 .

- absence de saut de pH pour un équivalent d'acide ajouté,
- l'écart d'un équivalent de proton correspondant au dosage de NH_3 introduit ne se retrouve que pour des valeurs de pH notablement inférieures au pK de l'ammonium.

Ligand 1. Les courbes RMN calculées et expérimentales (b) et (c) coïncident parfaitement sur tout le domaine étudié. NH_4^+ agit donc uniquement en tant qu'acide et ne donne pas lieu à la formation de complexes aux pH considérés. On observe uniquement les réactions de transprotonation:

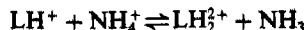


Tableau 1. Valeurs des pK_n [$T = 20^\circ$; $I = 0,1M$ (KNO_3)]

	pK_1	pK_2	pK_3	pK_4
1	11,54	10,35	2,43	1,97
2	10,77	9,63	6,90	5,38
3	11,44	10,51	7,27	6,90
4	11,82	11,38	10,63	8,87

Tableau 2. Tailles de cavité estimations des cavités à l'aide de modèle Corey-Pauling-Koltin, $R(\text{NH}_4^+) = 1,43\text{\AA}$

Ligand	1	2	3	4
$R \text{ \AA}$	0,60 à 75	0,80 à 1,1	1,2 à 1,5	1,8 à 2,4

Ce résultat, compatible avec les valeurs des pK_1 et pK_2 du ligand 1 (tableau 1), était prévisible: en effet, la cavité du ligand est trop petite et trop rigide pour pouvoir s'adapter à l'ion NH_4^+ (tableau 2).

Ligand 4. Les courbes de dosage pH-métrique (a) et (b) sont confondues jusqu'au-delà de 2 équivalents de proton ajoutés. Ceci indique l'absence de complexes stables dans cette région. Ces courbes ne sont pas exploitables quantitativement; les phénomènes (faibles) s'ils existent, sont masqués par la basicité du ligand qui, à cette dilution, se comporte pratiquement comme une base forte. Les courbes (b) et (c) obtenues en RMN (Fig. 1), mettent en évidence l'action de NH_4^+ en tant qu'acide jusqu'à deux équivalents, comme dans le cas du ligand 1. Au-delà de deux équivalents de NH_4^+ , la courbe (b) s'écarte notablement de la courbe (c): il n'y a pas, comme on pouvait s'y attendre au vu des pK_n , fixation d'un troisième proton. Il semble que le ligand diprotoné interagisse avec NH_4^+ , donnant lieu à la formation de complexes. Cependant, la courbe pH-métrique n'apportant aucun renseignement quantitatif, il paraît hasardeux de vouloir chiffrer les phénomènes.

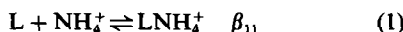
Ligands 2 et 3. Le comportement des ces deux ligands présente de nombreuses analogies. L'écart entre les courbes (a) et (c) obtenues en RMN, et (a) et (b) en pH-métrie indique clairement que ces deux ligands donnent lieu à la formation de complexes suffisamment stables pour permettre une étude quantitative. Nous avons donc entrepris d'ajuster les

Tableau 3. Modèle I

	Ligand 2	Ligand 3
Pot.	$\log \beta_{11} < -1$ $\sigma^2 0,059$	$\log \beta_{11} < -1$ $\sigma^2 0,079$
RMN	$\log \beta_{11} 4,37 \pm 0,39$ $\sigma^2 0,24 \cdot 10^{-3}$	$\log \beta_{11} 6,39 \pm 0,16$ $\sigma^2 0,34 \cdot 10^{-3}$

courbes expérimentales à partir de différentes hypothèses. Les modèles qui suivent tiennent compte des équilibres de protonation du ligand (K_1, K_2, K_3, K_4) et de NH_3 (K_A).

Modèle I: nous nous plaçons ici dans le cas le plus simple qui est la formation d'un complexe 1:1 selon l'équation:



Les résultats obtenus à partir de ce modèle figurent dans le tableau 3.

On observe un total désaccord entre l'ajustement obtenu à partir des mesures potentiométriques et RMN. Dans le premier cas, les valeurs de β_{11} ne sont pas significatives et les résiduels sont très largement supérieurs aux erreurs expérimentales, alors que la RMN conduit à des valeurs de β_{11} correspondant à des complexes stables. Il est clair que ce modèle doit être rejeté.

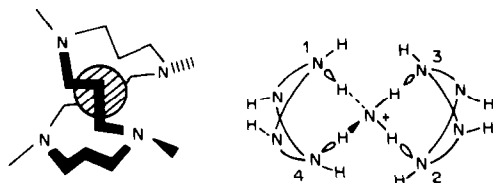
Modèle II: le modèle précédent conduisait notamment à des résiduels importants pour le rapport $\text{NH}_4^+/\text{L} = 0,5$. La cavité des ligands 2 et 3 étant suffisamment labile, l'existence d'un complexe 2:1 de type sandwich respectant la structure tétraédrique de l'ion NH_4^+ peut être envisagée:



Ce modèle fait donc intervenir les équilibres (1) et (2). Les résultats obtenus sont rassemblés dans le tableau 4.

Les valeurs obtenues en potentiométrie et en RMN sont plus proches que précédemment; l'introduction du complexe 2:1 diminue notablement les écarts pour le rapport $\text{NH}_4^+/\text{L} = 0,5$. Cependant, le désaccord reste important et les résiduels demeurent supérieurs aux erreurs expérimentales. Les valeurs de pH calculées diffèrent plus particulièrement des valeurs expérimentales entre 2 et 3 équivalents de proton ajoutés.

Modèle III: Les remarques précédentes nous conduisent à envisager l'existence d'espèces protonées. Alors que l'addition de protons détruit le complexe 1:1 par rupture des liaisons $\text{N}-\text{H}-\text{N}^+$, le complexe sandwich peut fixer des protons puisque deux atomes d'azote par cycle sont disponibles et suffisamment

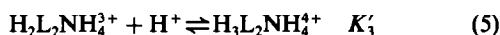


Scheme 2

Tableau 4. Modèle II

	Ligand 2	Ligand 3
Pot.	$\log \beta_{11} 2,72 \pm 1,09$ $\log \beta_{21} 2,88 \pm 12,0$ $\sigma^2 0,055$	$\log \beta_{11} 2,58 \pm 2,21$ $\log \beta_{21} 4,21 \pm 8,21$ $\sigma^2 0,073$
RMN	$\log \beta_{11} 3,28 \pm 0,41$ $\log \beta_{21} 5,96 \pm 0,64$ $\sigma^2 0,20 \cdot 10^{-4}$	$\log \beta_{11} 4,92 \pm 1,10$ $\log \beta_{21} 6,94 \pm 1,37$ $\sigma^2 0,24 \cdot 10^{-4}$

éloignés de la charge positive. Aux équilibres (1) et (2) s'ajoutent les équilibres suivants:



Ce modèle conduit à ajuster six constantes d'équilibre auxquelles s'ajoutent, dans le cas de la RMN, six déplacements chimiques, soit un total de douze paramètres. Du fait de la symétrie du complexe sandwich et de l'éloignement respectif des atomes d'azote, les atomes N_1 et N_2 d'une part, N_3 et N_4 d'autre part sont peu différents et de basicité comparable. Nous avons donc remplacé les paramètres ajustables K'_1, K'_2, K'_3 et K'_4 par $K'_{12} = \sqrt{K'_1 K'_2}$ et $K'_{34} = \sqrt{K'_3 K'_4}$. Les différents résultats sont rassemblés dans le tableau 5.

Ce modèle conduit à une amélioration spectaculaire de l'ajustement des mesures pH-métriques (σ^2 est 200 fois plus faible que dans le modèle II). L'ajustement des courbes RMN est également satisfaisant. Dans les deux cas, les déviations standards sur la grandeur mesurée (σ) sont inférieures aux erreurs expérimentales. Il faut remarquer également qu'un bon accord est obtenu pour l'ensemble des constantes d'équilibre, compte-tenu des incertitudes correspondantes. Au vu ces résultats, il nous paraît légitime de retenir ce modèle qui justifie l'ensemble des résultats expérimentaux. Nous avons donc entrepris dans un calcul final l'ajustement simultané des courbes RMN et pH-métriques afin d'affiner les valeurs des constantes en minimisant la somme pondérée des carrés des résiduels:

$$U = \sum_{i=1}^{n_1} W_{i1}^* (\text{pH}_i^{\text{calc}} - \text{pH}_i^{\text{exp}})^2 + \sum_{i=1}^{n_2} W_{i2}^* (\delta_i^{\text{calc}} - \delta_i^{\text{exp}})^2$$

Tableau 5. Modèle III

	Ligand 2	Ligand 3
Pot.	$\log \beta_{11} 2,88 \pm 0,42$ $\log \beta_{21} 5,66 \pm 0,54$ $\text{p}K'_{12} 10,56 \pm 0,18$ $\text{p}K'_{34} 9,43 \pm 0,13$ $\sigma^2 0,29 \cdot 10^{-4}$	$\log \beta_{11} 3,02 \pm 0,53$ $\log \beta_{21} 5,44 \pm 0,71$ $\text{p}K'_{12} 11,41 \pm 0,45$ $\text{p}K'_{34} 9,67 \pm 0,39$ $\sigma^2 0,82 \cdot 10^{-4}$
RMN	$\log \beta_{11} 2,78 \pm 0,39$ $\log \beta_{21} 5,26 \pm 0,47$ $\text{p}K'_{12} 10,48 \pm 0,25$ $\text{p}K'_{34} 9,11 \pm 0,66$ $\sigma^2 0,23 \cdot 10^{-5}$	$\log \beta_{11} 3,12 \pm 0,41$ $\log \beta_{21} 5,66 \pm 0,39$ $\text{p}K'_{12} 11,29 \pm 0,40$ $\text{p}K'_{34} 9,55 \pm 0,26$ $\sigma^2 0,31 \cdot 10^{-5}$

Tableau 6. Modèle III, ajustement simultané*

Ligand 2	Ligand 3
$\log \beta_{11}$ 2,88 \pm 0,29	$\log \beta_{11}$ 2,93 \pm 0,31
$\log \beta_{21}$ 5,67 \pm 0,27	$\log \beta_{21}$ 5,33 \pm 0,35
pK'_{12} 10,65 \pm 0,11	pK'_{12} 11,35 \pm 0,21
pK'_{34} 9,43 \pm 0,08	pK'_{34} 9,65 \pm 0,14
σ^2 0,14.10 ⁻⁴	σ^2 0,34.10 ⁻⁴

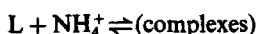
*(a) RMN: $\sigma_y = 0,005$ ppm; $\sigma_x = 0,002$ ml

(b) Pot.: $\sigma_y = 0,01$ pH; $\sigma_x = 0,005$ ml.

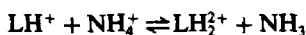
Les valeurs de constantes obtenues lors de l'ajustement simultané (tableau 6) sont compatibles avec les valeurs du tableau 5 et sont assorties d'incertitudes plus faibles. La cohérence de ces résultats confirme la validité du modèle III et sa capacité à expliquer l'ensemble des phénomènes observés sur le domaine étudié. On peut remarquer que les incertitudes sont assez élevées; ce dernier point s'explique par le fort degré de recouvrement des équilibres et la basicité voisine des atomes d'azote des ligands et de l'ammoniac. Notons également que les constantes d'acidité du complexe sandwich sont en bon accord avec la basicité des atomes d'azote concernés.

CONCLUSION

La complexation de l'ammonium par les tétraazamacrocycles fait intervenir deux facteurs prépondérants: la taille de la cavité du ligand et sa basicité. L'accroissement de la taille de la cavité s'accompagne de l'augmentation de la basicité, ce qui s'avère favorable à la complexation des anions.¹⁴ Dans le cas de l'ammonium, ces deux facteurs sont antagonistes et un compromis doit être réalisé, en raison de la compétition entre les réactions de complexation:



et celles de transprotonation:



Au vu des pK_1 et pK_2 (tableau 1), les phénomènes de transprotonation sont à peu près identiques pour les ligands 1, 2 et 3. La différence de comportement s'explique donc essentiellement par la taille de la cavité. Le ligand 1 est trop petit pour inclure l'ion NH_4^+ et trop rigide pour former un complexe 2:1. Les ligands 2 et 3 ont une cavité de taille suffisante pour s'adapter à l'ion NH_4^+ dans un complexe 1:1, et suffisamment labile pour réaliser la coordination tétraédrique de l'ion ammonium dans une structure de type sandwich. La stabilité des complexes formés avec ces deux ligands est quasi-identique. Dans le cas du ligand 4, la cavité est trop grande (tableau 2) pour permettre une interaction efficace par liaison hydrogène. De plus, sa basicité est telle que les réactions de transprotonation inhibent les phénomènes de complexation en milieu basique. Cependant, la RMN met

clairement en évidence l'interaction de ce ligand sous forme diprotonée avec NH_4^+ , ce qui n'est pas sans analogie avec le comportement des ligands 2 et 3.

Ce travail nous a amenés à accroître les possibilités déjà nombreuses du programme MICMAC. L'utilisation simultanée de la pH-métrie et de la RMN, ainsi que l'étude systématique de différents modèles, nous a permis de caractériser les espèces présentes en solution aux pH supérieurs à 8. Nous espérons que des études ultérieures permettront d'élucider l'ensemble des phénomènes d'interaction ammonium-macrocycle.

PARTIE EXPERIMENTALE

Les sels minéraux NH_4X ($\text{X} = \text{NO}_3^-$, ClO_4^-) sont de qualité puriss p.a. (Fluka). La synthèse des ligands 2, 3 et 4 a été décrite précédemment.¹⁴ Le ligand 1 est utilisé sous sa forme commerciale (Ventron). Toutes les mesures (potentiométrie et RMN) sont effectuées à force ionique constante 0,1M (KNO_3).

Potentiométrie

L'eau est purifiée puis déminéralisée (Millipore Milli-RO4, Milli-Q de Millipore). L'acide HNO_3 est obtenu par dilution d'une solution commerciale et titré par une solution Titrisol de KOH (Merck, p.a.). Le mélange ligand 10^{-2}M , NH_3 $9,77 \cdot 10^{-3}\text{M}$ est neutralisé par HNO_3 $0,17\text{M}$. Les réactifs sont additionnés à l'aide d'une microburette à piston multi-Dosimat E415 graduée au 0,01 ml. Les valeurs de pH sont lues sur un pH-mètre millivoltmètre ORION Modèle 811, utilisant une électrode combinée ORION 91-95.

Résonance magnétique nucléaire

Les spectres de RMN ^1H ont été enregistrés sur un appareil JEOL JMN FX 100. Les courbes sont obtenues par addition de quantités croissantes de D_2SO_4 $0,1\text{M}$ ou de NH_4ClO_4 $0,1\text{M}$ dans D_2O , sur une solution du ligand $0,25\text{M}$ (D_2O). Les déplacements chimiques sont donnés par rapport au TSP. Tous les résultats ont été exploités par le programme MICMAC.

Remerciements—La partie expérimentale de ce travail a été réalisée au laboratoire de synthèse organique de la Faculté des Sciences de Brest (Prof. R. Guglielmetti). L'étude RMN a été réalisée au service de RMN de la Faculté des Sciences de Brest (Ing. J. Y. Le Gall).

LITTERATURE

1. C. J. Pedersen, *J. Am. Chem. Soc.*, 1967, **89**, 7017.
2. J.-M. Lehn, *Struct. Bonding (Berlin)*, 1973 **16**, 1.
3. *Idem*, *Pure Appl. Chem.*, 1978, **50**, 871.
4. *Idem*, 1979, **51**, 979.
5. *Idem*, *Acc. Chem. Res.*, 1978, **11**, 49.
6. D. J. Cram et J. M. Cram, *ibid.*, 1978, **11**, 8.
7. J. F. Stoddart, *Chem. Soc. Rev.*, 1979, **8**, 85.
8. J. C. Metcalfe, J. F. Stoddart et G. Jones, *J. Am. Chem. Soc.*, 1977, **99**, 8317.
9. J. C. Metcalfe, J. F. Stoddart, G. Jones et W. E. Hull, *J. Chem. Soc. Chem. Commun.* 1980, 543.
10. R. M. Izatt, J. D. Lamb, C. S. Swain, J. J. Christensen et B. L. Haymore, *J. Am. Chem. Soc.*, 1979, **101**, 6273.
11. *Idem*, *ibid.*, 1980, **102**, 3032.
12. R. A. Schultz, E. Schlegel, D. M. Dishong et G. W. Gokel, *J. Chem. Soc. Chem. Commun.*, 1982, 243.
13. E. Graf, J.-F. Kintzinger, J.-M. Lehn et J. Le Moigne, *J. Am. Chem. Soc.*, 1982, **104**, 1672.
14. E. Suet et H. Handel, *Tetrahedron Lett.*, 1984, **25**, 645.

15. E. Suet, A. Laouenan, H. Handel et R. Guglielmetti, *Helv. Chim. Acta*, 1984, **67**, 441.
16. E. Suet, *Thèse de 3ème cycle*, Brest, 1984.
17. A. Laouenan et E. Suet, *Talanta*, 1985, **32**, 245.
18. H. L. Surprenant, J. E. Sarnesi, R. R. Key, J. T. Byrd et C. N. Reilley, *J. Magn. Reson.*, 1980, **40**, 231.
19. J. F. Desreux, E. Merciny et M. F. Loncin, *Inorg. Chem.*, 1981, **20**, 987.
20. M. Asso, D. Denlian, L. Asso et C. Granier, *Can. J. Chem.*, 1984, **82**, 2379.
21. W. E. Wentworth, W. Hirsch et E. Chen, *J. Phys. Chem.*, 1967, **71**, 218.

FLUOROMETRIC DETERMINATION OF NITRITE IN NATURAL WATERS WITH 3-AMINONAPHTHALENE-1,5-DISULPHONIC ACID BY FLOW-INJECTION ANALYSIS

SHOJI MOTOMIZU, HIROSHI MIKASA and KYOJI TÔEI

Department of Chemistry, Faculty of Science, Okayama University, Tsushima-naka, Okayama-shi 700,
Japan

(Received 28 January 1986. Revised 19 March 1986. Accepted 26 April 1986)

Summary—Nitrite in river and sea-water was determined fluorometrically by flow-injection analysis. In acidic medium, nitrite was reacted with 3-aminonaphthalene-1,5-disulphonic acid (C-acid) to form the diazonium salt, which was converted into the fluorescent azoic acid salt in an alkaline medium. The carrier stream, into which the sample solution was injected, was distilled water. The reagent solution stream, which contained C-acid, EDTA and hydrochloric acid, was mixed with the carrier stream in a 13-m length of Teflon tubing (bore 0.5 mm) maintained at 90° in a thermostatic bath. After passing through the mixing coil, the stream was mixed with an alkaline solution. The fluorescence intensity (excited at 365 nm) was measured at 470 nm. The detection limit ($S/N = 3$) was $1 \times 10^{-9}M$ (14 ng/l. nitrite-nitrogen) and the RSD of 10 injections of $10^{-6}M$ nitrite was 0.4%. Analyses can be done at a rate of up to 45/hr.

Determination of trace amounts of nitrite is of importance, particularly in the fields of environmental chemistry, geochemistry and limnology. Many spectrophotometric methods for nitrite have been reported. Diazotization and coupling reactions have often been used for the spectrophotometric determination of trace amounts of nitrite in river waters, sulphanilamide or sulphanilic acid and *N*-(1-naphthyl)ethylenediamine being the most popular couples.^{1,2} Okada *et al.*³ reported a more sensitive method, using *p*-aminoacetophenone and *m*-phenylenediamine. Such methods have been adapted to flow-injection analysis.⁴⁻⁹

Axelrod *et al.*¹⁰ reported the fluorometric determination of nitrite with 5-aminofluorescein: the method is time-consuming (reaction time about 1 hr) and 5-aminofluorescein is very expensive. We have found that some naphthylamine derivatives, especially sodium 3-aminonaphthalene-1,5-disulphonate are sensitive fluorometric reagents for nitrite, inexpensive, and readily available.

This paper describes a fluorometric method for the determination of nitrite suitable for the determination of low (0.01 µg/l.) levels in natural waters.

EXPERIMENTAL

Reagents

All naphthylamine derivatives were obtained from Tokyo Kasei Kogyo Co. Ltd., and used without further purification. They were dissolved in 0.01M hydrochloric acid.

A stock solution of $1 \times 10^{-3}M$ sodium nitrite was prepared by dissolving the salt (dried at 100–110°) in water. Working solutions were freshly prepared by diluting the stock solution.

The reagent solution stream was made by dissolving 0.035 g of sodium 3-aminonaphthalene-1,5-disulphonate (disodium salt of C-acid) in 100 ml of 0.01M hydrochloric acid, mixing 3 ml of this solution with 3 ml of 0.1M disodium ethylenediaminetetra-acetate (disodium EDTA), 50 ml of concentrated hydrochloric acid and 244 ml of distilled water.

The carrier stream was distilled water. The alkaline solution stream was 20% sodium hydroxide solution.

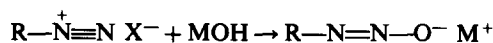
Apparatus

The fluorescence was measured with a Hitachi 650-10S spectrofluorimeter with an 18-µl flow-through cell and recorded with a Toa Dempa FBR-251A recorder. Two double-plunger micro pumps (Sanuki Kogyo Co. Ltd) were used for propelling the reagent, carrier, and sodium hydroxide solutions. The sample (360 µl) was injected by a 6-way injection valve into the carrier stream. The flow lines were made from Teflon tubing. The reaction coil (RT₁) was kept at 90° in a thermostatic bath. A diagram of the flow system is shown in Fig. 1.

RESULTS AND DISCUSSION

Examination of the fluorometric reagents for nitrite

It is well known that aromatic amines react with nitrite in acidic medium to form diazonium salts, which are converted into azoic acid salts in alkaline medium:



where HX is an acid and MOH is a base.

When R is a naphthyl group, the product $R-N=N-O^-$ is fluorescent. Several naphthylamine derivatives were examined for the fluorescence

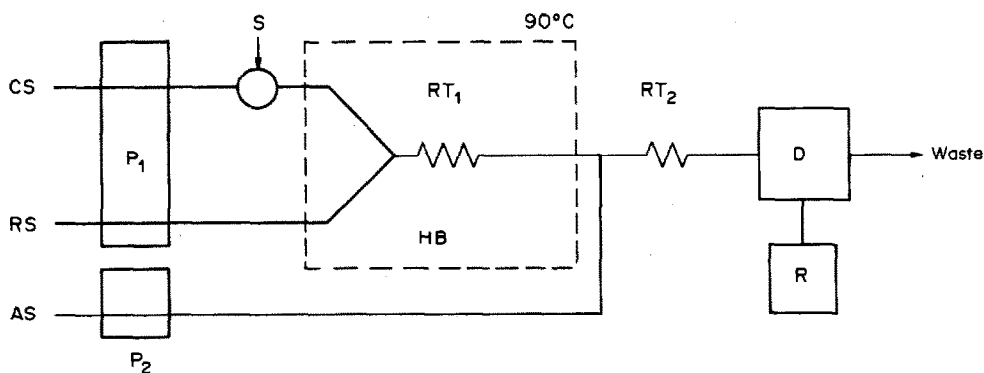
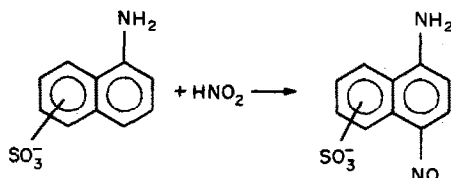


Fig. 1. Schematic diagram of flow system. CS, carrier solution (distilled water); RS, reagent solution (C-acid, EDTA and HCl); AS, alkaline solution (NaOH); S, sample injection valve (sample size $360 \mu\text{l}$); P₁ and P₂, Sanuki double-plunger pumps (flow-rate 0.7 ml/min); RT₁ and RT₂, reaction tubing (1, 13 m ; 2, 1 m); D, detector (Hitachi 650-10S spectrofluorophotometer equipped with $18\text{-}\mu\text{l}$ flow-through cell); R, recorder; HB, heating bath. Tubings: Teflon (bore 0.5 mm).

intensity of their products (Table 1). Of the seven derivatives examined, the products from C-acid and amino G-acid exhibited a stronger fluorescence intensity than the original naphthylamines, while the others showed a quenching effect, *i.e.*, a lower fluorescence intensity than that of the starting materials. This is because 1-naphthylamine and its derivatives (which show the quenching effect) easily yield nitroso compounds, which have lower fluorescence intensities than those of the parent naphthylamines:



J-acid, though it is a derivative of 2-naphthylamine, has a hydroxyl group, and also easily yields the nitroso compound. The products from C-acid and amino G-acid have the same excitation and emission wavelength characteristics, but the fluorescence in-

tensity of the C-acid product is stronger than that of the amino G-acid product. In all further experiments, the C-acid salt was therefore used.

Optimization of the reagent solution stream

The fluorescence intensity was found to increase with concentration of C-acid up to $1 \times 10^{-5} \text{ M}$, and to be constant at higher concentrations. Increasing the C-acid concentration also increased the instability of the base-line, however, so a concentration of $1 \times 10^{-5} \text{ M}$ was chosen. The fluorescence intensity also increased with hydrochloric acid concentration, becoming constant at $[\text{HCl}] > 0.5 \text{ M}$. A concentration of 2 M hydrochloric acid was therefore chosen. Disodium EDTA was added to the reagent solution to give a final concentration of 10^{-3} M in order to prevent the formation of metal hydroxides when the reagent stream was mixed with the sodium hydroxide solution.

Optimization of the flow system

The peak height decreased gradually with increase in flow-rate, and with decrease in length of reaction

Table 1. Fluorescence of naphthylamine derivatives

Naphthylamine	$\lambda_{\text{ex}}, \text{nm}$	$\lambda_{\text{em}}, \text{nm}$	Behaviour*
1-Naphthylamine	365	460	Q
1-Aminonaphthalene-5-sulphonic acid (1,5-Cleve's acid) sodium salt	365	480	Q
1-Aminonaphthalene-6-sulphonic acid (1,6-Cleve's acid) sodium salt	365	480	Q
1-Aminonaphthalene-7-sulphonic acid (1,7-Cleve's acid) sodium salt	365	480	Q
3-Aminonaphthalene-1,5-disulphonic acid (C-acid) disodium salt	365	470	F
7-Aminonaphthalene-1,3-disulphonic acid (amino G-acid) dipotassium salt	365	470	F
2-Amino-5-naphthol-7-sulphonic acid (J-acid)	380	480	Q

*Q: Fluorescence decreased by adding nitrite.

F: Fluorescence increased by adding nitrite.

coil, but the longer the reaction coil, the lower the sampling rate, so as a compromise, a 13-m long reaction tube and a flow-rate of 0.7 ml/min were chosen.

The effects of the length of the reaction coil (RT₂) and of the flow-rate of the sodium hydroxide solution were examined and a tube length of 1 m and flow-rate of 0.7 ml/min were chosen.

The peak height increased with sample volume injected, and 360 μ l was chosen to satisfy the requirements of sensitivity and sampling rate.

The reaction coil (RT₁) was immersed in a thermostatically controlled bath and the peak height was found to increase with reaction temperature, but at above 95° air-bubbles formed in the reaction tubing, so a bath-temperature of 90° was selected.

The fluorescence intensity was maximal with excitation at 365 nm and emission measurement at 470 nm.

Calibration graph, reproducibility and detection limit

Linear calibration graphs for various concentration ranges were obtained by varying the sensitivity of the spectrofluorimeter. The lowest calibration range was $0-3 \times 10^{-7}M$, with a detection limit [corresponding to a signal-to-noise ratio (S/N) = 3] of $1 \times 10^{-9}M$ (14 ng/l. nitrite-nitrogen), and the highest $0-5 \times 10^{-5}M$. The proposed method is therefore one of the most sensitive available for nitrite. The relative standard deviation for 10 injections of $10^{-6}M$ nitrite was 0.4%.

By use of still higher spectrofluorimeter sensitivity, nitrite at concentrations below $1 \times 10^{-9}M$ can be detected, but the base-line is shifted. This is due to contamination by oxides of nitrogen from the ambient air.

Table 2. Effect of co-existing ions and compounds on fluorescence from $1 \times 10^{-6}M$ nitrite

Ion or compound	Concentration, M	Relative peak height
None		100
Na ⁺	10 ⁻¹	99
Cl ⁻	10 ⁻¹	99
K ⁺	10 ⁻²	101
Ca ²⁺	10 ⁻²	101
Mg ²⁺	10 ⁻²	99
Br ⁻	10 ⁻²	101
SO ₄ ²⁻	10 ⁻²	99
NH ₄ ⁺	10 ⁻²	99
Al ³⁺	10 ⁻³	100
Co ²⁺	10 ⁻³	98
Ni ²⁺	10 ⁻³	102
Zn ²⁺	10 ⁻³	103
Cd ²⁺	10 ⁻³	101
NO ₃ ⁻	10 ⁻³	102
HPO ₄ ²⁻	10 ⁻³	100
F ⁻	10 ⁻³	99
HCO ₃ ⁻	10 ⁻³	101
SCN ⁻	10 ⁻³	101
Fe ³⁺	10 ⁻⁴	99
Cu ²⁺	10 ⁻⁴	98
HAsO ₄ ²⁻	10 ⁻⁴	99
I ⁻	10 ⁻⁵	99
Fe ²⁺	10 ⁻⁶	99
Methylamine	10 ⁻⁴	100
Diethylamine	10 ⁻⁴	101
Glycine	10 ⁻⁴	101
Leucine	10 ⁻⁴	99
Lysine	10 ⁻⁴	98
Urea	10 ⁻⁴	101
LBS*	10 ⁻⁵	101
Humic acid	1 μ g/ml	99

*Laurylbenzenesulphonic acid sodium salt.

Interferences

Table 2 summarizes the effect of other ions and some compounds. With the exception of sodium

Table 3. Determination of nitrite in natural waters

Sample†	Nitrite found, 10 ⁻⁷ M	
	Proposed FIA method	Other method‡
River waters		
Asahi R.* ¹	3.3	3.1
Nishi R.* ¹	5.2	5.5
Zasu R. A* ¹	22.7	23.7
B* ²	12.3	13.3
C* ²	17.8	17.6
Sea-waters		
Seto Inland Sea		
at Kogushi* ³	8.4	8.6
at New Okayama Port A* ³	10.0	10.8
B* ⁴	15.6	
at Kuban* ⁴	6.9	
at Desaki* ⁴	0.9	
Lake water		
Kojima L.* ¹	38.8	38.1

†Samples taken on 16 April 1985(*¹), 18 April 1985(*²), 30 April 1985(*³) and 26 February 1985(*⁴).

‡Spectrophotometric method for nitrite with sulphanilic acid and *N*-(1-naphthyl)ethylenediamine.¹

chloride there were no interferences. Sodium chloride added at concentrations above 0.2M lowered the reproducibility, presumably owing to the presence of nitrite impurity in it. To examine the interference of large amounts of sodium chloride, sea-water samples were diluted to the same volume with distilled water and injected. Plots of peak height against volume of sea-water taken for dilution were all linear and passed through the origin. The nitrite contents found by the proposed FIA method for sea-water samples were almost the same as those obtained by the spectrophotometric method with sulphanilic acid and *N*-(1-naphthyl)ethylenediamine (Table 3). From these results, it appears feasible to determine nitrite in river, sea and lake waters by the proposed method.

REFERENCES

1. B. E. Saltzman, *Anal. Chem.*, 1954, **26**, 1949.
2. *APHA-AWWA-WPCF, Standard Methods for Examination of Water and Wastewater*, 14th Ed., p. 434. American Public Health Association, Washington, DC, 1975
3. M. Okada, H. Miyata and K. Tôei, *Analyst*, 1978, **104**, 1195.
4. M. F. Giné, H. Bergamin F^o, E. A. G. Zagatto and B. F. Reis, *Anal. Chim. Acta*, 1980, **114**, 191.
5. E. A. G. Zagatto, A. O. Jacintho, J. Mortatti and H. Bergamin F^o, *ibid.*, 1980, **120**, 399.
6. L. Anderson, *ibid.*, 1979, **110**, 123.
7. J. F. V. Standen, *ibid.*, 1982, **138**, 403.
8. S. Nakashima, M. Yagi, M. Zenki, A. Takahashi and K. Tôei, *Bunseki Kagaku*, 1982, **31**, 732.
9. *Idem*, *Anal. Chim. Acta*, 1983, **155**, 263.
10. H. D. Axelrod and N. A. Engel, *Anal. Chem.*, 1975, **47**, 922.

OXYDATION ELECTROCHIMIQUE DE LA KHELLINE ET DE L'AMIKHELLINE: ETUDE PAR VOLTAMMETRIE CYCLIQUE

J. M. KAUFFMANN, G. J. PATRIARCHE* et M. CHATEAU-GOSSELIN

Institut de Pharmacie, Université Libre de Bruxelles, Campus Plaine 205/6, Boulevard du Triomphe,
B-1050 Bruxelles, Belgium

B. GALLOHERMOSA

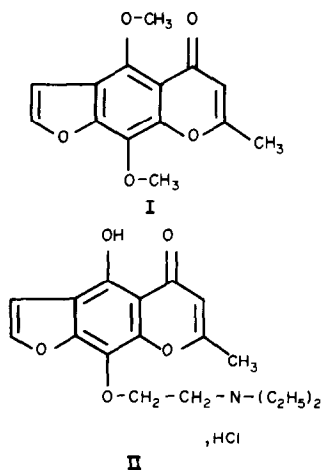
Euskal Herriko Unibertsitatea, Facultad de Ciencias Apdo 644, 48080 Bilbao, Spain

(Reçu le 13 janvier 1986. Accepté le 11 avril 1986)

Résumé—L'étude oxydative de la khelline et de l'amikhelline, molécules à noyau chromone, a été réalisée par voltammétrie cyclique sur une électrode à pâte de carbone et une électrode polymère modifiée. L'interprétation des voltampérogrammes a permis de mettre en évidence les mécanismes d'oxydation de ces deux molécules à différents pH. Une méthode de dosage électrochimique est proposée avec une limite de détection à $8 \times 10^{-7}M$. Après oxydation par chauffage à reflux en milieu sulfurique et en présence de vanadium(V), une coulométrie à intensité constante est proposée en se basant sur un dosage en retour via le fer(II).

Summary—The electrochemical oxidation of khelline and amikhelline (chromone derivatives) has been performed by cyclic voltammetry at carbon-paste and polymeric carbon electrodes. The mechanism of oxidation of the two compounds at various pH values has been deduced. The detection limit is $8 \times 10^{-7}M$. A constant-current coulometric procedure is also described, based on the oxidation of the two chromones with vanadium(V) and backtitration of the excess of oxidant with iron(II).

Les deux molécules khelline (I) (méthyl-2, diméthoxy-5,8 furano-6,7 chromone) et amikhelline (II) (chlorhydrate de β -diéthyl aminoéthyl éther de la méthyl 2 dihydroxy-5,8 furano-6,7 chromone) sont des médicaments d'origine naturelle, préconisés dans le traitement coronarien et l'asthme bronchique.¹



Ces substances ont fait l'objet de diverses études physico-chimiques destinées à réaliser leur détermin-

ation sélective et quantitative.² Plusieurs méthodes analytiques s'appuyant sur leurs propriétés oxydo-réductrices ont été préconisées.^{3,4} Parmi celles-ci, la polarographie constitue une technique idéalement adaptée à l'étude des processus redox de substances pharmacologiquement actives.⁵ Elle permet l'étude quantitative de ces molécules grâce à l'électroréduction du noyau chromone. Toutefois leur différenciation est malaisée en raison de la proximité de leurs potentiels de demi-vague.⁴

Très récemment,⁶ Hila *et al.* ont procédé à l'oxydation vanadique de la khelline de manière quantitative ainsi qu'à l'identification spectroscopique des produits de la réaction. Du point de vue électrochimique, l'avènement des électrodes solides modifiées⁷⁻¹⁰ a permis d'explorer le domaine oxydatif et d'étudier plus amplement le comportement redox des médicaments.^{11,12} Le but du présent travail est de mettre en évidence d'une part le comportement électro-oxydatif de la khelline et de l'amikhelline au niveau d'électrodes solides à l'aide des techniques voltampérométriques et coulométriques. D'autre part, sur la base de travaux antérieurs relatifs au comportement électrochimique de nombreux médicaments et du vanadium(V)¹³ nous avons réalisés le dosage coulométrique de la khelline, à l'aide du fer(II), après oxydation à chaud par le vanadium(V).¹⁴

*A qui toute correspondance doit être adressée.

PARTIE EXPERIMENTALE

Appareillage et réactifs

Les mesures réalisées par voltampérométrie et voltammétrie cyclique ont été effectuées à l'aide d'un ensemble PAR 174 A-175 couplé à un enregistreur PAR RE 0074. Outre l'électrode de travail, la cellule comporte une électrode de référence ECS, isolée de la solution par un pont de type "Purley" renfermant une solution d'électrolyte de support. L'électrode auxiliaire est en platine. Les solutions à analyser sont préalablement désoxygénées par barbotage d'azote extra-pur durant 10 mn.

L'électrode de travail est soit:

—une électrode à pâte de carbone (EPC) (Metrohm EA 207), la pâte étant constituée d'un mélange de carbone spectroscopique et de paraffine liquide Uvasol (Metrohm EA 207 C);

—une électrode de carbone polymère (EPCM) (30% p/p) préparée selon un procédé décrit par nous antérieurement.¹⁵

Les coulométries à potentiel contrôlé ont été effectuées à l'aide d'un potentiostat PAR 173 associé à un coulomètre digital PAR 179. Dans ce cas l'électrode de travail est constituée d'un cylindre de platine (diamètre 3,6 cm, hauteur 2 cm).

Les sels utilisés pour la préparation de l'électrolyte de support sont des réactifs de qualité P.A. et sont dissous dans de l'eau tridistillée. Le pH est contrôlé par des mélanges tampons constitués de mono- et de dihydrogénophosphate (0,1M) ou d'acide acétique et d'acétate de sodium (0,1M).

Les molécules investiguées ainsi que les solvants organiques (P.A.) ont été utilisés sans purification préalable. Les solutions mères, renouvelées chaque jour, sont préparées dans du méthanol tandis que les solutions à analyser renferment 10% de méthanol.

Les coulométries à potentiel contrôlé ont été effectuées en milieu aqueux en utilisant des solutions de dépolarisant à 0,004%. En raison de l'électroactivité du méthanol à l'électrode de platine aux potentiels positifs supérieurs à +1,0 V *vs.* ECS, les solutions mères de khelline destinées aux mesures coulométriques renferment 20% d'acétonitrile dans l'acide sulfurique 0,1M.

Le polymère servant à la fabrication de l'électrode est du polyvinylacétate d'éthylène, copolymère à 9% d'acétate d'éthylène (CIBA-Geigy). Le noir de carbone utilisé pour l'incorporation à chaud dans le polymère est du ketjenblack (AKZO-Chemie, Belgique).

En ce qui concerne la coulométrie à intensité constante réalisée sur ces molécules la réaction a été effectuée en utilisant une solution de pentoxyde de vanadium (V_2O_5) 0,1M dans de l'acide sulfurique 0,72M. Cette solution est préparée suivant un mode déjà décrit,⁶ par dissolution à chaud d'une solution d'hydroxide de sodium 1M qui est ensuite neutralisée puis acidifiée jusqu'à obtention d'une concentration en acide sulfurique de 0,72M. Cette solution est étalonnée par un dosage coulométrique à l'aide de fer(II) électrogénéré.

La khelline est oxydée à chaud dans un bain-marie bouillant dans les conditions décrites par Hila *et al.*⁶ La prise d'essai de khelline est introduite dans un ballon rodé surmonté d'un réfrigérant à reflux. L'excès de solution de V_2O_5 , ajouté sera tel que la concentration en ions soit de 30 à 60 fois supérieure à la concentration en khelline. La concentration finale en acide sulfurique du milieu d'oxydation est amenée à 2,5M. Après 1 hr de chauffage à reflux, la solution est refroidie et amenée à un volume déterminé. Une aliquote de la solution contenant du vanadium(V) en excès est alors dosée coulométriquement à l'aide de fer(II) électrogénéré.

L'électrogénération des ions ferreux a été réalisée selon une méthode préconisée par Furman *et al.*¹⁶ dans une cellule en H à deux compartiments séparés par un disque en verre fritté de porosité G_4 . Le catholyte est constitué par une solution de sulfate ferriammonique 0,05M, dissous dans

de l'acide sulfurique 0,05M. Une solution d'acide sulfurique 2,5M sert d'anolyte.

Un cylindre de platine perforé (surface totale 30 cm²) est utilisé comme électrode génératrice tandis qu'une spirale de platine sert d'électrode auxiliaire.

La détection du point final de la réaction est effectuée à l'aide d'un système biampérométrique: une différence de potentiel de 200 mV est imposée entre deux microélectrodes de platine identiques. L'enregistrement des courbes $I = f(t)$ est réalisé automatiquement grâce à un polarographe Radiometer PO₄ déclenché en synchronisation avec le circuit d'électrogénération. L'intensité du courant d'électrolyse est contrôlée à l'aide d'un électromètre Keithley 610 C fonctionnant en milliampéromètre.

En ce qui concerne la voltampérométrie de la khelline et de l'amikhelline les mesures ont été effectuées au niveau des électrodes EPC et EPCM en utilisant la technique impulsionnelle différentielle. Afin d'éviter le polissage manuel de l'électrode, les enregistrements successifs sur une même surface ont été effectués après agitation magnétique de la solution entre chaque tracé. La détermination quantitative des deux dérivés a été réalisée dans de l'acide sulfurique 0,1M contenant 10% de méthanol en utilisant la méthode des ajouts dosés.

RESULTATS ET DISCUSSION

Khelline

Voltammétrie cyclique. Les mesures ont été réalisées en présence de faibles concentrations en dépolarisant ($2 \times 10^{-4}M$) et de manière comparative en utilisant deux électrodes de travail de nature différente. Comme le montre la figure 1 à l'électrode à pâte de carbone (EPC), entre pH 1,0 et 9,0 et pour des vitesses de balayage comprises entre 10 et 500 mV/sec, les tracés comportent un seul pic d'oxydation (E_{pa}), de nature irréversible situé à des potentiels positifs supérieurs à +1,0 V *vs.* ECS.

La linéarité de l'intensité du pic en fonction de la racine carrée de la vitesse de balayage ($I_{pa}/v^{1/2}$) traduit la présence d'un phénomène électrochimique contrôlé par la diffusion de l'espèce électroactive. Le balayage inverse ne laisse pas apparaître de pic de réduction correspondant, il se développe cependant à des potentiels nettement moins positifs un pic de réduction R_1 auquel correspond lors du second cycle d'enregistrement le pic d'oxydation O_1 (Fig. 1). Nous attribuons l'allure inhabituelle du couple O_1/R_1 au niveau de l'EPC à un intense phénomène de désorption de la forme réduite (Fig. 1, courbe a).

Les enregistrements effectués, de manière comparative, au niveau de l'EPCM et de l'EPC dénotent un comportement électro-oxydatif identique. Toutefois une plus grande étendue de potentiel anodique accessible à l'EPCM permet de distinguer une seconde étape d'oxydation de la khelline (E_{pa_2}) sous la forme d'un épaulement proche de l'oxydation du solvant (Fig. 1, courbe b).

La figure 2 reprenant l'évolution des différents potentiels de pics en fonction du pH illustre le parallélisme du compartement de la khelline au niveau des deux électrodes.

Le potentiel d'oxydation de la khelline E_{pa_1} ne varie pas en fonction du pH, ce qui révèle une absence

de transfert de proton lors du processus anodique. Le caractère irréversible résulterait de la formation rapide d'une structure à caractère redox réversible O_1/R_1 .

Au niveau des deux électrodes envisagées, dans la gamme des pH compris entre 1 et 9, l'intensité du pic anodique diminue légèrement entre pH 1 et 4 puis se stabilise. Quant au couple redox O_1/R_1 , celui-ci voit son intensité diminuer progressivement lorsque le pH augmente pour ne plus apparaître au-delà de pH 8,5.

Coulométries à potentiel contrôlé. Plusieurs déterminations ont été réalisées à des pH inférieurs à 2 à l'aide d'une électrode de platine de grande surface ($E = +1,1$ vs. ECS). Les électrolyses à des pH supérieurs à 2 sont inopérantes en raison des limites restreintes de potentiels accessibles à l'électrode de platine. L'évolution des électrolyses est suivie par voltammétrie cyclique au niveau d'une EPC. Au terme de la réaction et après passage de 2,1 Faradays par mole de khelline on obtient quantitativement le couple redox O_1/R_1 .

Etude spectrale. L'étude spectrale des solutions électrolysées fournit les spectres d'absorption de la forme oxydée O_1 en milieu acide [λ_{\max} (H_2SO_4 0,1M): 240, 340 nm], solution qui vire au violet après alcalinisation [λ_{\max} (pH 10): 245, 300, 340, 540 nm].

Nature du couple O_1/R_1 . L'évolution parallèle des potentiels du couple O_1/R_1 en fonction du pH est de 60 mV par unité pH au niveau de l'EPCM et suggère un transfert de deux électrons et deux protons selon un processus réversible: $E_{pa} - E_{pc} = 40$ mV. Si l'on se réfère à l'oxydation chimique de la khelline, celle-ci aboutit à la formation d'une structure diquinonique en position 5,8 colorée en violet en milieu alcalin ($\lambda_{\max} = 540$ nm).²

Compte tenu des différents résultats obtenus nous pouvons établir un mécanisme d'oxydation électrochimique de la khelline dans une gamme de pH comprise entre 1 et 8,5.

La réaction s'effectuerait au niveau des groupements méthoxylés en une étape biélectronique suivie d'une rapide conversion en khelline-quinone, réduite réversiblement aux potentiels des pics O_1/R_1 :

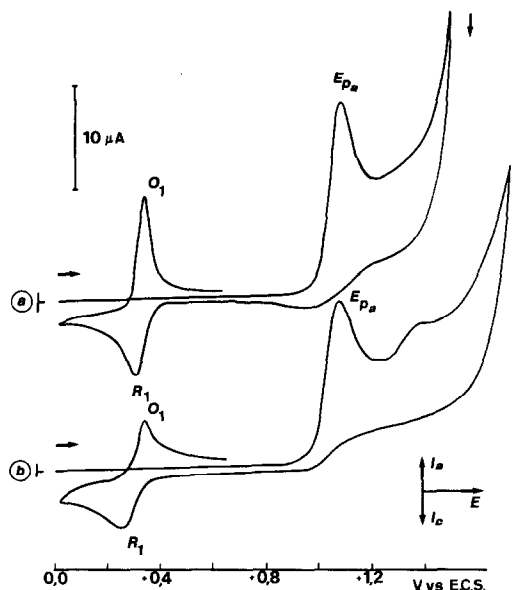
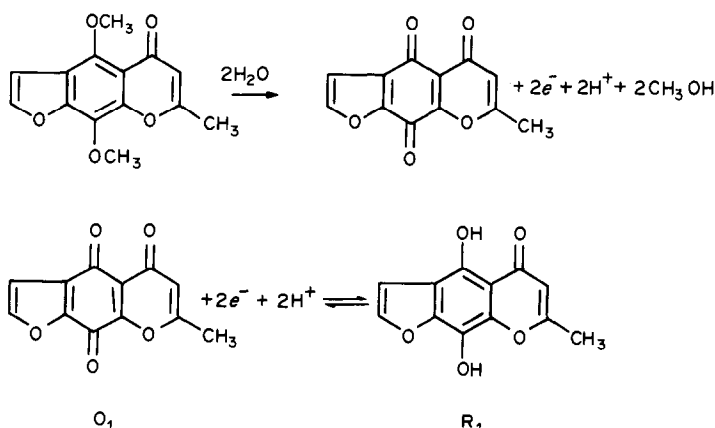


Fig. 1. Voltammétries cycliques d'une solution de $1,7 \times 10^{-4}M$ en khelline; H_2SO_4 (0,1M)–10% CH_3OH ; $v = 20$ mV/sec; (a) EPC; (b) EPCM.

Les résultats légèrement excédentaires obtenus lors des coulométries à potentiel contrôlé (nombre d'électrons supérieurs à 2) peuvent être attribués à une oxydation simultanée du méthanol libéré au cours de la réaction.

Etude en fonction de la concentration. Les droites d'étalonnages ont été établies à l'aide de l'électrode de carbone polymère. A l'EPCM la linéarité de la réponse de l'électrode est parfaitement suivie, les voltampérogrammes présentent une morphologie identique en fonction de la concentration et les droites d'étalonnages établies entre 5×10^{-5} et $3 \times 10^{-6}M$ ont des coefficients de corrélation de l'ordre de 0,9998. La limite de détection se situe vers $8 \times 10^{-7}M$.

Amikhelline

Voltammétrie cyclique. Les mesures ont été

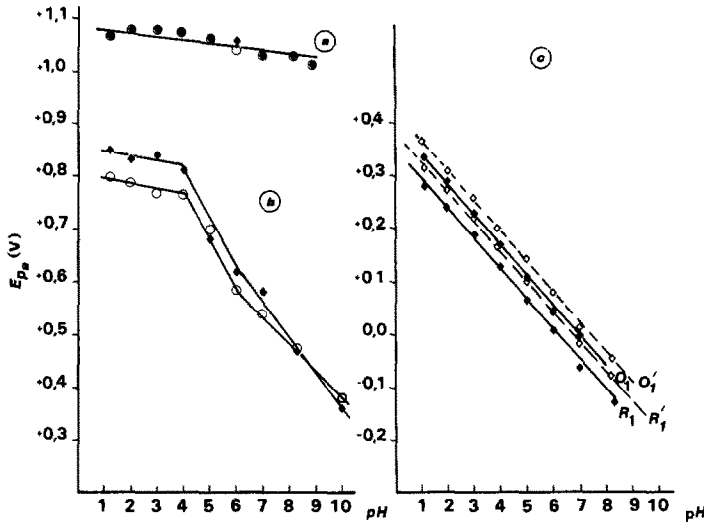


Fig. 2. Evolution du potentiel de pic en fonction du pH. (a) Khelline $10^{-4}M$; (b) amikhelline $10^{-4}M$; (c) électrode à pâte de carbone (EPC); ♦ électrode carbone polymère (EPCM); (d) O_1/R_1 et O_1'/R_1' sur EPC.

effectuées au niveau de l'EPC et de l'EMP entre pH 1,0 et 10,0. Dans toute l'étendue des pH investigués, les tracés comportent un pic d'oxydation E_{pa} à caractère irréversible suivi d'un léger épaulement. A partir de pH 3 apparaît un épaulement supplémentaire proche de l'oxydation du solvant. Un balayage inverse réalisé après le premier pic d'oxydation permet de mettre en évidence un pic de réduction R_1 auquel correspond un pic d'oxydation O_1 (Fig. 3, courbe b).

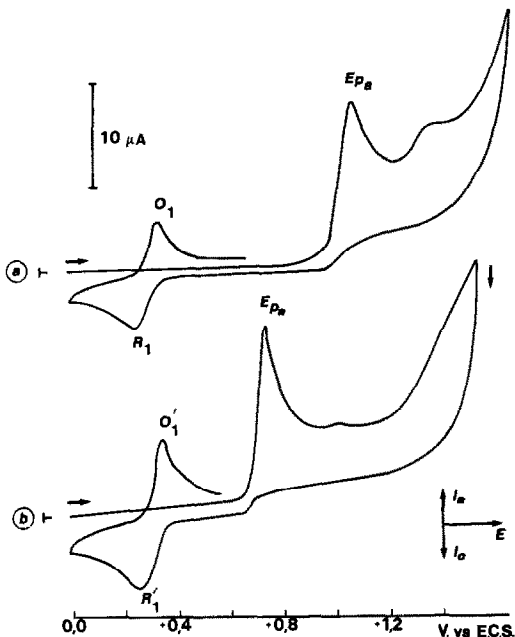


Fig. 3. Voltammétries cycliques sur EPCM; (a) Khelline $1,7 \times 10^{-4}M$; (b) amikhelline $1,7 \times 10^{-4}M$; H_2SO_4 (0,1M)–10% CH_3OH , $v = 20$ mV/sec.

L'allure inhabituelle des pics d'oxydation E_{pa} et O_1 aux pH acides ainsi que l'écart de linéarité de la relation E_{pa} en fonction de $v^{1/2}$ supposent la présence de phénomènes de surface liés à l'adsorption de l'amikhelline et de la forme réduite du couple R_1/O_1 .

L'intensité du pic anodique E_{pa} diminue de moitié entre pH 1 et 4, elle se stabilise ensuite. Entre pH 4 et 6, à de faibles vitesses de balayage (5–20 mV/sec), le pic d'oxydation E_{pa} se déforme donnant naissance à un dédoublement du pic.

Le tracé illustrant l'évolution du potentiel de pic E_{pa} en fonction du pH comporte essentiellement deux segments de droite (Fig. 2). Une portion linéaire entre pH 1 et 4 présente une pente faible de 10 mV par unité pH, la seconde portion entre pH 4 et 10 indique un déplacement régulier vers des potentiels moins positifs avec une pente d'environ 70 mV par unité pH. Le caractère irrégulier de la seconde portion entre pH 4 et 6 résulte de la morphologie complexe du pic à ces valeurs de pH.

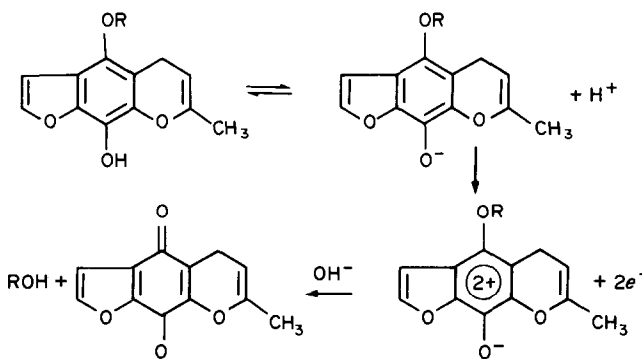
Coulométrie à potentiel contrôlé. Les mesures ont été effectuées en milieu acide et alcalin à un potentiel supérieur au potentiel du pic E_{pa} tout en contrôlant l'évolution de la réaction par voltammétrie cyclique au niveau de l'EPC. En milieu acide, à pH 2 au terme de la réaction on obtient quantitativement le couple R_1'/O_1 après passage de 2,1 Faradays par mole d'amikhelline. En milieu alcalin à pH 9, la fin de l'électrolyse correspond au transfert de 1,6 Faradays par mole d'amikhelline. La voltammétrie cyclique de la solution électrolysée ne présente plus le couple R_1/O_1 , mais à un potentiel positif proche de l'oxydation du solvant un nouveau pic à caractère irréversible apparaît correspondant à une oxydation ultérieure du produit d'électrolyse.

Nature du couple O_1'/R_1' . La position des potentiels des pics O_1 et R_1 , leur évolution parallèle de 60 mV

par unité pH (EPC), ainsi que la disparition du couple O_1/R_1 aux pH supérieurs à 8,5 constituent différents critères suggérant une analogie de comportement entre la khelline et l'amikhelline. L'oxydation de l'amikhelline aboutit également à la formation d'une structure diquinonique. Toutefois l'oxydation aisée de la molécule ainsi que l'influence du pH sur le potentiel du pic E_{pa} correspondent à un comportement spécifique pour l'amikhelline.

La présence d'une fonction phénol au niveau de l'amikhelline exerce un effet marqué sur l'électrooxydation de la molécule.

La réaction s'effectue en une étape biélectronique rapide aux pH inférieurs à 4. Entre pH 4 et 6, l'allure anormale du pic d'oxydation permet de suspecter une oxydation en deux étapes successives très proches. A des pH supérieurs à 6 l'oxydation s'effectue en une étape biélectronique rapide ($E_p - E_{p/2} = 30$ mV). Aux pH supérieurs à 4 le produit est sous la forme phénolate, structure plus facilement oxydable, et le mécanisme peut s'écrire de la façon suivante:



Aux pH inférieurs à 4, le potentiel de pic restant fixe en fonction du pH indique un transfert électronique n'étant pas précédé par un équilibre acido-basique.¹⁷

Aux pH supérieurs à 8,5, différents critères suggèrent un processus oxydatif aboutissant à la formation de structures nouvelles:

(a) disparition du couple R_1/O_1 ;

(b) écart important vis-à-vis de la linéarité de la relation $I_p/v^{1/2}$;

(c) nombre d'électrons inférieur à 2 lié à des phénomènes de surface;

(d) apparition d'un pic supplémentaire à des potentiels positifs.

Dosage coulométrique à intensité constante de la khelline à l'aide du vanadium (V). Hila et al.⁶ ont prouvés que l'oxydation sulfovanadique de la khelline dans un bain-marie bouillant conduisait à la formation d'acide acétique et de dioxyde de carbone. Dans les conditions expérimentales décrites par ces auteurs, cette réaction consomme 16 électrons. Nous avons pu constater qu'une faible augmentation de la température de réaction amenait une oxydation plus poussée de la khelline avec consommation de 18 électrons (tableau 1). Le tableau 2 reprend les

Tableau 1. Oxydation de la khelline par ébullition de la solution

Théorie, mg	Nombre d'électrons (n)
40,0	17,85
35,0	17,25
25,0	17,30
25,0	17,92
12,5	18,30
	n_{moyen} 17,84
	S_M 0,32

résultats obtenus lors de l'oxydation par ébullition à reflux dans un bain marie bouillant pendant une heure. Le contrôle rigoureux des conditions de l'oxydation est bien sûr le facteur limitant la bonne reproductibilité de la méthode. Pour de faibles concentrations de khelline à doser par coulométrie à intensité constante, les résultats obtenus ne sont plus très reproductibles.

Voltammétrie cyclique de la khelline en présence de vanadium(IV) et (V)

Afin d'établir la nature du processus impliquant l'oxydation de la khelline par le vanadium(V), nous avons réalisé l'enregistrement en voltammétrie cyclique d'une solution de khelline en milieu acide

Tableau 2. Oxydation de la khelline à reflux au bain-marie bouillant (n = 16 électrons)

Théorie, mg	Trouvé	
	mg	%
25,15	24,64	98,1
20,00	20,29	101,4
20,00	19,50	98,1
20,00	19,99	99,9
15,15	15,72	103,8
12,50	13,02	104,1
5,90	5,70	96,6
4,72	4,43	93,7
2,50	2,96	118,3
	moyen	101,6
	s_x	6,7

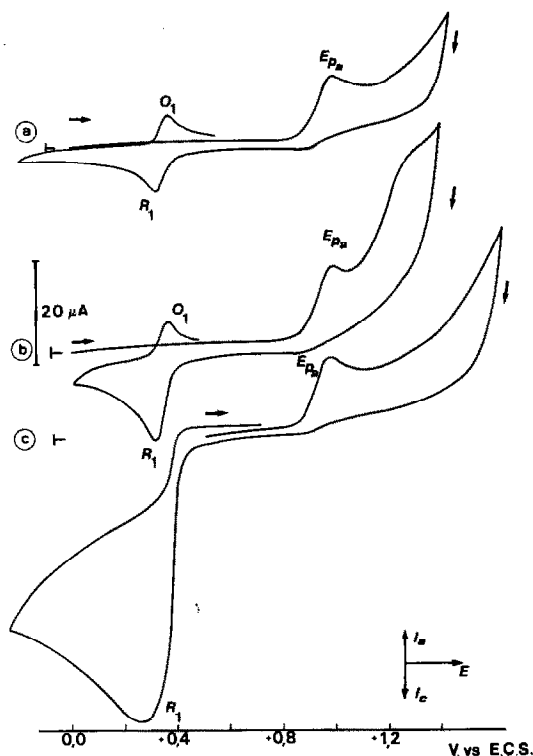
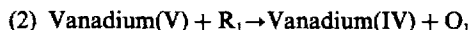
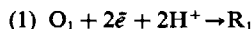


Fig. 4. Voltammétries cycliques sur EPC; H_2SO_4 (2,5M), $v = 20$ mV/sec; (a) Khelline $1,7 \times 10^{-4}M$; (b) khelline $1,7 \times 10^{-4}M$ + vanadium(IV) $5 \times 10^{-4}M$; (c) khelline $1,7 \times 10^{-4}M$ + vanadium(V) $2 \times 10^{-3}M$.

sulfurique 2,5M en présence de vanadium (IV) et (V). Au niveau de l'EPC, le couple vanadium(IV/V) développe une allure irréversible, les tracés comportent un pic d'oxydation à $+1,250$ V vs. ECS. La réduction permet d'observer un pic très étalé dont le potentiel se situe vers $-0,2$ V vs. ECS. La figure 4 illustre le comportement en voltammétrie cyclique de la khelline dans l'acide sulfurique 2,5M en absence (courbe a) et en présence de vanadium(IV) (courbe b). La proximité du potentiel anodique E_{pa} de la khelline et du vanadium(IV) suppose une réaction avec le groupement méthoxylé lors de l'oxydation vanadique de la khelline et formation subséquente de la khelline-quinone correspondante. Le balayage inverse permet de détecter le pic de réduction de la khelline-quinone, toutefois la valeur élevée du courant de réduction $i_{R_1}/i_{O_1} > 1$, suggère la participation d'un processus catalytique lié à la présence de vanadium(V) en solution.

Le tracé de la figure 4 (courbe c), correspondant à l'enregistrement en voltammétrie cyclique de la khelline en présence d'un excès de vanadium(V), permet de mettre davantage le phénomène en évidence. La présence du vanadium(V) provoque

l'apparition d'un intense courant de réduction R_1 , le pic de réoxydation O_1 ayant disparu. Le phénomène observé peut être attribué à un processus de régénération de la khelline-quinone par le vanadium(V), puisque dès sa formation à l'électrode la khelline-hydroquinone (R_1) subirait aussitôt une réoxydation par le vanadium(V) selon le processus global:



Les valeurs des potentiels du pic E_{pa} et du pic correspondant à l'oxydation du vanadium(IV), ainsi que la mise en évidence par voltammétrie cyclique de l'évolution de l'oxydation sulfo-vanadique suggèrent une formation de khelline-quinone. Toutefois la mise en évidence en solution sulfurique et à chaud par Hila *et al.*⁶ de sous-unités oxydées supporte l'hypothèse d'une oxydation ultérieure de la khelline-quinone par le vanadium(V).

Remerciements—Nos remerciements vont au Fonds National de la Recherche Scientifique (FNRS Belgium pour l'aide apportée à l'un d'entre nous (G.J.P.).

LITTÉRATURE

1. G. V. Andrep, G. S. Barsoum et M. R. Kenawi, *J. Pharmacol.*, 1949, 1, 3.
2. M. A. Hassan et M. U. Zubair en *Analytical Profiles of Drug Substances*, K. Florey (ed.), Vol. 9, p. 371. Academic Press, New York, 1980.
3. S. D. Bailey, P. A. Geary et A. E. de Wald, *J. Am. Pharm. Assoc.*, 1951 40, 280.
4. W. C. Ellenbogen, E. S. Rump, P. A. Geary et M. Burke *ibid.*, 1951, 40, 287.
5. G. J. Patriarche, M. Chateau-Gosselin, J. L. Vandenberg et P. Zuman, en *Electroanalytical Chemistry*, A. Bard (ed.), Vol. 11, p. 141 ff. Dekker, New York, 1979.
6. J. E. Hila, M. Tsitini-Souleau, M. Hamon et M. Chastagnier, *Talanta*, 1984, 31, 655.
7. R. N. Adams, *Electrochemistry at Solid Electrodes*, Dekker, New York, 1969.
8. G. J. Patriarche, J. C. Vire et J. M. Kauffmann, *Chim. Nouvelle*, 1984, 2, 91.
9. R. N. Murray en *Electroanalytical Chemistry*, A. Bard (ed.), Vol. 13, p. 191 ff. Dekker, New York, 1984.
10. L. R. Faulkner, *Chem. Eng. News*, 1984, 62, No. 9, 27.
11. J. M. Kauffman, M. P. Prete, J. C. Vire et G. J. Patriarche, *Z. Anal. Chem.*, 1985, 321, 172.
12. J. M. Kauffmann, J. C. Vire et G. J. Patriarche, *Bioelectrochem. Bioenerg.*, 1984 12, 413.
13. J. C. Vire, M. Chateau-Gosselin et G. J. Patriarche, *Mikrochim. Acta*, 1981 1, 227.
14. J. J. Lingane, *Electroanalytical Chemistry*, 2nd Ed., Interscience, New York, 1970.
15. M. P. Prete, J. M. Kauffmann, J. C. Vire, G. J. Patriarche, B. Debye et G. Geuskens. *Anal. Lett.*, 1984, 17, 1391.
16. N. H. Furman, C. N. Reilley et W. D. Cooke, *Anal. Chem.*, 1951, 23, 1665.
17. J. J. M. Holthuis, W. J. Van Oort, F. M. Romkens, J. Renama et P. Zuman, *J. Electroanal. Chem.*, 1985, 184, 317.

SINGLE-POINT TITRATION OF METAL IONS AND LIGANDS BY MEASURING CHANGE IN pH

ANDRZEJ LEWENSTAM,* ARI IVASKA and ERKKI WÄNNINEN†
Department of Analytical Chemistry, Åbo Akademi, 20500 Åbo (Turku), Finland

(Received 7 November 1985. Revised 3 March 1986. Accepted 23 March 1986)

Summary—A single-point titration method is described for the determination of metal ions and ligands. The method is based on deprotonation of a ligand on complexation with a metal. The resultant change in pH is used to calculate the concentration of the analyte. The limits and advantages of the method are discussed. Four selected systems, $\text{Pb}^{2+}\text{-HPO}_4^{2-}$, $\text{Cu}^{2+}\text{-HCO}_3^-$, $\text{Cd}^{2+}\text{-EDTA}$ and $\text{Ni}^{2+}\text{-ethylene-diamine}$ are used to demonstrate the validity of the equations. The method is applied to determination of total carbonate in serum.

Developments in the determination of metal or ligand ions in aqueous samples show tendencies towards automation and reduction of the sample volume. A rather surprising but methodologically important result of this is that some simple and non-specific methods can be used, especially for well defined sample matrices.

A common method of determining non-trace concentrations of metal ions or ligands in a sample is to exploit complexometric or precipitation titrations and nowadays potentiometric sensors are frequently used to monitor the course of a titration. These sensors are becoming more popular because they provide new opportunities to automate and simplify analytical methods. In this work we will present an example of such a development.

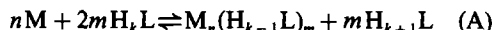
Let us consider the reaction of a metal ion with a protonated ligand (or a protonated anion) in which deprotonation takes place simultaneously with the formation of a metal complex or a slightly soluble salt. If the solution is buffered only by the protonated ligand, and any side-reactions of the metal ion can be disregarded, there will be a change in the pH because of the liberation of hydrogen ions. This change will depend on the concentration of the species involved. The analytical advantages of this phenomenon have long been known and discussed, *e.g.*, by Ringbom¹, and the principle was successfully applied by Schwarzenbach *et al.*² in the determination of water hardness. The same strategy has also been used in metal titrations³ and in the determination of the stability constants of metal chelates.⁴ More recently an empirical approach using the same idea in analytical work has been proposed.⁵ The disadvantages of the method were disclosed by Přebil.⁶ The lack of specificity, and the limited sensitivity and concentration range, seriously restrict the application of the method, which at

best can be used only for samples for which the analytical signal is due practically entirely to the metal-ligand reaction of interest. Attention to the drawbacks rather than the possible advantages of the method has inhibited its further development. Application of automation to chemical analysis has resulted in an increasing interest in simple analytical methods and in our opinion this justifies the revitalization of Ringbom's ideas of 50 years ago.

The aim of this work is to give the theoretical background, the equations which describe the observed change in pH, experimental verification of these equations, and one practical application of the method.

THEORY

When a metal ion M is added to a solution of protonated ligand H_kL the following reaction can be considered (for simplicity all charges are omitted)



It is assumed that the pH of the ligand solution is such that the species H_kL and $H_{k+1}L$ are the main ligand species present, otherwise reaction (A) would be complicated by simultaneous reaction of M with other protonated species of the ligand. In this work we will consider a pH range where the main species are HL and H_2L . Under such conditions reaction (A) reduces to the more specific reaction (B).



In the following presentation the volume of the sample is denoted by V and the concentration of metal ion by C_M . V_0 is the initial volume of the solution of HL , and C_L its total analytical concentration:

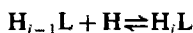
$$C_L = \sum_{i=0}^p [H_iL] \quad (1)$$

where p is the maximum number of protons L can

*On leave from the Department of Chemistry, University of Warsaw, Warsaw, Poland.

†Author for correspondence.

accept in the series of protonation equilibria ($j = 1, 2, \dots, p$)



with constants $K_j = [H_jL]/[H_{j-1}L][H]$.

The side-reaction coefficient $\alpha_{H,L(H)}$ can be calculated in the following way.⁷

$$\alpha_{HL(H)} = \frac{[L] + [HL] + [H_2L]}{[HL]} = \frac{1}{K_1[H]} + 1 + K_2[H] \quad (2)$$

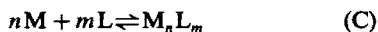
$$\alpha_{H_2L(H)} = \frac{[L] + [HL] + [H_2L]}{[H_2L]} = \frac{1}{K_1K_2[H]^2} + \frac{1}{K_2[H]} + 1 \quad (3)$$

If the species HL and H₂L are not the main ligand^o species, equations (2) and (3) should be modified accordingly.⁷

The equilibrium constant of reaction (B) is

$$K_B = [M_n L_m][H_2L]^m/[M]^n[HL]^{2m} \quad (4)$$

Reaction (B) consists of two protonation reactions, involving HL and H₂L, and reaction (C) with an equilibrium constant given by equation (5)



$$K_{M_n L_m} = [M_n L_m]/[M]^n[L]^m \quad (5)$$

Combination of equations (4) and (5) with the protonation constants gives

$$K_B = K_{M_n L_m} (K_2/K_1)^m \quad (6)$$

Equation (6) can be used to calculate K_B for different systems to predict thermodynamically whether reaction (B) can be used, but it should be remembered that the kinetics may be of over-riding importance. In our case we assume that reaction (B) is fast. The proposed method presupposes that K_B is so large that the equilibrium of reaction (B) lies practically completely to the right, *i.e.*, $K_B > 10^4$. If the metal ion is involved in a hydrolysis reaction $K_{M_n L_m}$ should be converted into a conditional constant by division by $\alpha_{M(OH)}^n$.

The method furthermore presupposes that the ligand should be in excess, *i.e.*, even after addition of the sample the solution should contain both HL and H₂L and therefore continue to behave as a pH-buffer controlling the overall buffer capacity of the system. This requires that the following inequality should be fulfilled:

$$2 \frac{m}{n} V C_M < V_0 C_L \quad (7)$$

It is further assumed that the metal solution is not sufficiently acidic or alkaline to contribute to the observed pH change. Another requirement is that the

total concentration of the ligand should not be lower than $10^{-4}M$, to avoid the effect of dissociation of water. Generally the sample must not contain other metal ions and ligands which could compete with the main reaction (A), which seriously limits the scope of the method,⁶ but this disadvantage might be alleviated by masking of competing ions or if the side-reaction has slow enough kinetics or its extent can be estimated.

According to reaction (B) addition of the metal ions increases the concentration of H₂L and decreases the concentration of HL. Therefore the pH of the ligand solution will decrease to pH₂ from the initial value of pH₁. At pH₁:

$$[HL]_1 = \frac{C_L}{\alpha_{HL(H)_1}} \quad (8)$$

and

$$[H_2L]_1 = \frac{C_L}{\alpha_{H_2L(H)_1}} \quad (9)$$

After addition of the sample to the ligand solution, the concentrations of HL and H₂L will be changed as follows:

$$[HL]_2 = \frac{V_0}{(V_0 + V)} \left([HL]_1 - 2 \frac{m V C_M}{n V_0} \right) \quad (10)$$

$$[H_2L]_2 = \frac{V_0}{(V_0 + V)} \left([H_2L]_1 + \frac{m V C_M}{n V_0} \right) \quad (11)$$

Subscripts 1 and 2 refer to pH₁ and pH₂ respectively. It is obvious from equations (10) and (11) that for the analytical signal to be useful the change in [HL] and [H₂L] must be large enough. This means that the concentration of the metal ion should not be too much smaller than the concentrations of the ligand species. Further, the ratios K_1/K_2 and K_2/K_3 must be such that HL and H₂L are always the main ligand species.

Combinations of equations (8)–(11) with the protonation constants gives the expression for calculation of C_M :

$$C_M = \frac{V_0 C_L}{V} \frac{\left(\frac{[H]_2 K_2}{\alpha_{HL(H)_1} \alpha_{H_2L(H)_1}} - \frac{1}{[H]_2 K_2} \right)}{\left(\frac{m}{n} + \frac{2m}{n} \right)} \quad (12)$$

Equation (12) can be rewritten in the form

$$C_L = \frac{V C_M}{V_0} \frac{\left(\frac{m}{n} + \frac{2m}{n} [H]_2 K_2 \right)}{\left(\frac{[H]_2 K_2}{\alpha_{HL(H)_1} \alpha_{H_2L(H)_1}} - \frac{1}{[H]_2 K_2} \right)} \quad (13)$$

which can be used when the concentration of the ligand is to be determined.

In both cases the approximate concentration of the sample solution should be known beforehand so that

Table 1. Calculation of $\log K_B$ at 25°C and $I = 1.0M$ (KNO_3) by equation (6) for the systems studied

	(a) $Pb^{2+}-HPO_4^{2-}$	(b) $Cu^{2+}-HCO_3^-$	(c) $Cd^{2+}-EDTA$	(d) $Ni^{2+}-en$
n	3	1	1	1
m	2	1	1	1
$\log K_{M,L_m}$	47.85	10.95	16.36	18.44
$\log K_1$	10.79	9.57	9.88	10.20
$\log K_2$	6.50	6.02	6.18	7.60
$\log K_B$	39.3	7.4	12.7	15.8

the amount of reagent added will comply with the restrictions discussed above.

EXPERIMENTAL

Chemicals

All chemicals used were of Merck *pro analysi* grade. Doubly distilled and demineralized water was used. EDTA, phosphate and carbonate solutions were prepared from the sodium salts. Metal ion solutions were made from the nitrates. The "Seronom" artificial serum samples with certified total carbonate concentrations were from Nygaard (Norway); different total carbonate concentrations were obtained by dilution with appropriate sodium bicarbonate solutions.

Apparatus

A Finnpiptette micropipette with a precision of $\pm 2 \mu l$ was used to measure the volume added. In all experiments the temperature was $25.0 \pm 0.1^\circ$. A Metrohm combination electrode and 654 pH-meter with a resolution of ± 0.001 pH were used to measure the pH. Metrohm standard buffers of pH = 4.00, 7.00, and 9.00 were used to calibrate the system.

Procedure

The initial solution was 5.00 ml of 0.05M ligand solution. Metal ion solutions were added in 250- μl increments. All solutions were made up to an ionic strength of 1.0M with potassium nitrate. Before every experiment the pH of the ligand or anion solution was adjusted to $pH_1 \sim pK_{k+1}$ with either sodium hydroxide solution or nitric acid. A stable pH was obtained within 30 sec after every addition in all the cases studied.

RESULTS AND DISCUSSION

The method was tested with four systems: (a) $Pb^{2+}-HPO_4^{2-}$, (b) $Cu^{2+}-HCO_3^-$, (c) $Cd^{2+}-EDTA$ and (d) Ni^{2+} -ethylenediamine (en). In systems (a) and (b) the reaction product is a slightly soluble salt of the metal ion. Complex-forming reactions take place in systems (c) and (d) and the pH of the ligand solution is adjusted so that the main species is the mono-protonated form of the ligand, and metal-ion hydrolysis can be neglected. Equilibrium constants, K_B , for

the four systems were calculated by using equation (6) and are presented in Table 1. Values of the constants used were taken from Martell and Smith.^{8,9} When these values could not be found directly they were corrected to the ionic strength used. In the case of ethylenediamine the value of $\log K_2$ in Table 1 was determined specifically for this work.

As can be seen in Table 1, the constant K_B in all cases is so large that reaction (B) can be assumed to proceed to completion.

Results of the experiments in which the metal ion solutions were added to the protonated anion or ligand solutions are given in Table 2. The pH of the solution was measured after each addition. The value at $V = 0$ ml is pH_1 and the other values are pH_2 . After each addition C_M was calculated from equation (12) and these values are presented in Table 2. Several additions were used to demonstrate that the calculated value of C_M is not dependent on V and that any size of addition may be used as long as the restrictions given in the theoretical section are fulfilled.

As can be seen in Table 2, a fairly constant and accurate value is obtained for the concentration of the metal ion solution for a range of additions of the "sample" solution. Deviation from a constant value of C_M in the Ni^{2+} -en system with increasing addition of nickel solution is due to a change in the stoichiometry of the reaction.

It should be stressed that the accuracy of the method is crucially dependent on the accuracy of the value of $\log K_2$, which should be known to the second decimal place. A variation of ± 0.02 in $\log K_2$ gives an error of approximately $\pm 3\%$ in the calculated values of C_M given in Table 2. The error decreases with decreasing values of pH_2 . Furthermore, if an incorrect value of $\log K_2$ is used, C_M will change with pH_2 . A high ionic strength was chosen in this work to avoid changes in the values of the constants during the experiment.

Table 2. Metal concentrations calculated from the pH of a mixture of V ml of 0.0100M solution of metal ion to 5.00 ml of 0.0500M solution of ligand or anion

V, ml	(a) $Pb^{2+}-HPO_4^{2-}$		(b) $Cu^{2+}-HCO_3^-$		(c) $Cd^{2+}-EDTA$		(d) $Ni^{2+}-en$	
	pH	C_M, M	pH	C_M, M	pH	C_M, M	pH	C_M, M
0.000	7.417		7.430		7.194		8.436	
0.250	7.387	0.00919	7.303	0.01144	7.138	0.00994	8.310	0.01012
0.500	7.356	0.00955	7.222	0.01015	7.086	0.00996	8.200	0.01004
1.000	7.295	0.00994	7.070	0.01019	6.992	0.00997	8.006	0.00990
2.000	7.184	0.01016	6.851	0.01003	6.825	0.01014	7.702	0.00895
4.000	7.013	0.00962	6.487	0.01073	6.542	0.01027	7.221	0.00696

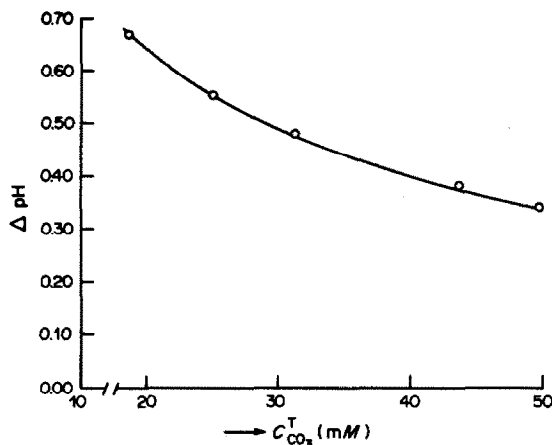


Fig. 1. ΔpH as a function of the concentration of total carbonate, $C_{CO_3}^T$, in serum with a constant addition of cupric nitrate solution. The line is calculated from equation (13) and the points are the measured values.

"Seronorm" artificial serum samples with certified total carbonate concentration were studied. The original carbonate concentration was changed by diluting the sample with a standard solution of sodium bicarbonate. Hydrochloric acid was used to adjust the pH of the serum samples to 7.40 in order to mimic real blood samples. Known volumes of serum samples were mixed with 0.008M cupric nitrate to give $(V/V_0)C_M = 2.0$ and the change in pH was measured. The results are shown in Fig. 1, where the theoretical line is obtained by solving equation (13) for $[H]_2$ and then calculating ΔpH . The observed ΔpH values in serum samples with different total carbonate concentrations fall nicely on the theoretical curve. The difference between the calculated and measured ΔpH values did not exceed ± 0.005 .

CONCLUSIONS

The results in Table 2 confirm the validity of the equations derived, but the determination of metals in unbuffered samples and with no interfering ions is not a realistic application. In most cases the metal-ion samples are themselves rather acidic or alkaline and some kind of sample pretreatment would be needed. This seriously limits the practical application of the

method. In the case of ligand determination, however, the possibilities are much more encouraging, though still rather limited. An appropriate metal ion should be found to give the specific reaction needed, the concentration of the ligand should fall within the applicable concentration range of the method and either the sample should not contain other buffering systems or their buffer capacity should be much lower than that of the ligand to be determined. An almost ideal sample matrix is blood serum, for the determination of total carbonate by the proposed single-point method. As shown in Fig. 1, good agreement between theoretical predictions and empirical results is observed. No competing complexing metal ions are present and the sample is buffered only by the carbonate-bicarbonate system. Substances, *e.g.*, amino-acids, which are present in some samples and can compete with carbonate in the reaction with copper ions, could cause a bias, but under the proposed conditions no side-effects on the analytical signal from the "Seronorm" samples have been found. Problems could arise, however, if the method is used for real serum samples. More detailed studies of the method, including automation, minimization of sample volume, and matrix effects in patients' serum are in progress in our laboratory and will be reported later.

In our opinion the value of the single-point method should be re-assessed, because its simplicity gives it new potential in the context of modern instrumentation, although its scope will still be limited by the lack of specificity.

REFERENCES

1. A. Ringbom, *Doctoral Thesis*, Abo Akademi, 1934.
2. G. Schwarzenbach, W. Biedermann and F. Bangerter, *Helv. Chim. Acta*, 1946, **29**, 811.
3. G. Schwarzenbach and W. Biedermann, *ibid.*, 1948, **31**, 331, 459.
4. G. Schwarzenbach and E. Freitag, *ibid.*, 1951, **34**, 1492.
5. T. Damokos and J. Havas, *Talanta*, 1977, **24**, 335.
6. R. Pfiibil, *Analytical Applications of EDTA and Related Compounds*, p. 110, Pergamon Press, Oxford, 1972.
7. A. Ringbom, *Complexation in Analytical Chemistry*, Wiley, New York, 1963.
8. A. E. Martell and R. M. Smith, *Critical Stability Constants*, Vol. 5, Plenum, New York, 1982.
9. R. M. Smith and A. E. Martell, *Critical Stability Constants*, Vol. 4, Plenum, New York, 1976.

SHORT COMMUNICATIONS

SPECTROPHOTOMETRIC DETERMINATION OF NITRAZEPAM IN TABLETS

SALWA RIZK EL-SHABOURI

Department of Pharmaceutical Chemistry, Faculty of Pharmacy, University of Assiut, Assiut, Egypt

(Received 11 November 1985. Revised 16 March 1986. Accepted 15 May 1986)

Summary—A sensitive spectrophotometric method is reported for the determination of nitrazepam either in pure form or in tablets. The method is based on reduction with zinc dust and calcium chloride followed by reaction with sodium pentacyanoaminoferrate(II) to give a violet product having an absorbance maximum at 560 nm. Beer's law is obeyed over the concentration range 1–20 $\mu\text{g/ml}$ in the final solution. The common excipients in tablets do not interfere. The recovery and precision are similar to those of the official B.P. method.

Methods for the determination of nitrazepam include spectrophotometric,¹ colorimetric,^{2,4} gas chromatographic,^{5,6} TLC,⁷ HPLC,⁸ fluorimetric,⁹ and differential pulse polarographic^{10,11} procedures. The B.P. recommends a non-aqueous titration for the bulk drug and a spectrophotometric method for tablets.¹²

Sodium pentacyanoaminoferrate(II) (SCAF) has been used to detect aromatic nitro compounds.^{13,14} This report describes its use for determining nitrazepam.

EXPERIMENTAL

Reagents

Sodium pentacyanoaminoferrate(II) $\text{Na}_3[\text{Fe}(\text{CN})_5\text{NH}_2]$ (SCAF). Prepared according to Vogel,¹⁵ and used as a 0.1% solution, made fresh daily.

Calcium chloride solution, 10%.

Zinc dust.

Standard nitrazepam solution. Prepared by dissolving 50 mg of nitrazepam (accurately weighed) in 25.0 ml of ethanol. This solution must be freshly prepared daily, and is further diluted with ethanol as required.

All chemicals used were of analytical grade.

Procedures

Calibration graph. Pipette 0.500 ml of the nitrazepam standards (in the range 50–1000 $\mu\text{g/ml}$) into 50-ml conical flasks, containing 100 mg of zinc dust and 5 ml of calcium chloride solution. Let stand for 5 min at room temperature (25°) with occasional shaking. Filter (7-cm Whatman No. 1 papers) into 25-ml standard flasks, washing each residue thoroughly with three 2-ml portions of ethanol. Add 5 ml of SCAF solution to each combined filtrate and washings, mix well, let stand for 10 min at room temperature, and dilute to volume with water. Measure the absorbance at 560 nm against a blank prepared at the same time.

Analysis of tablets. Weigh and powder 20 tablets. Transfer an accurately weighed quantity of the powder, equivalent to about 50 mg of nitrazepam, to a 25-ml standard flask, and dissolve and dilute it to volume with ethanol. Filter (dry paper etc.), and discard the first portion of the filtrate. Dilute an aliquot of the filtrate as required, and determine the nitrazepam content by the procedure above.

RESULTS AND DISCUSSION

Nitrazepam, when reduced with zinc and calcium chloride solution and subsequently reacted with SCAF in aqueous ethanol, produces a violet product having a broad absorption peak with its maximum at 560 nm (Fig. 1) and molar absorptivity $1.15 \times 10^4 \text{ l. mole}^{-1} \text{ cm}^{-1}$. Beer's law is obeyed over the range 1–20 $\mu\text{g/ml}$ in the final solution. The absorbance is stable for 10 hr at room temperature.

Reaction conditions

Any amount of zinc dust in the range 50–300 mg gives the same final absorbance for a fixed amount of nitrazepam, but larger quantities give slightly lower absorbance.

The volume of 10% calcium chloride solution used along with 100 mg of zinc dust can be varied from 1 to 10 ml without altering the completeness of reduction of nitrazepam in the concentration range 1–20 $\mu\text{g/ml}$.

Maximum colour intensity is achieved by reduction for 2 min at room temperature. Further reduction time (up to 20 min) gives no change in the absorbance.

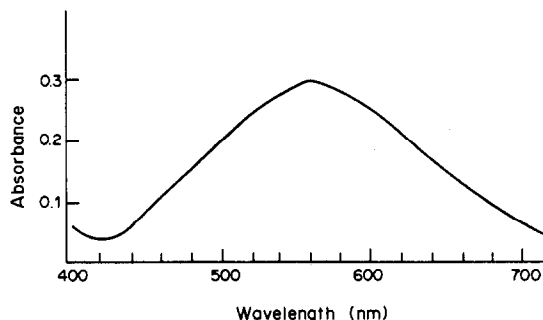


Fig. 1. Absorption spectrum for the coloured reaction product of reduced nitrazepam with SCAF.

Table 1. Determination of nitrazepam in tablets by the proposed method and the B.P. method

Sample	Proposed method			B.P. method Found, *% ± SD
	Found, *% ± SD	Nitrazepam added, mg	Recovery, *% ± SD	
A	98.9 ± 1.1 <i>t</i> = 1.69 <i>F</i> = 2.96	5.00	99.7 ± 0.6	99.3 ± 0.6
B	99.5 ± 1.2 <i>t</i> = 1.36 <i>F</i> = 2.69	10.00	98.7 ± 0.7	99.0 ± 0.8
C	99.2 ± 1.0 <i>t</i> = 1.36 <i>F</i> = 2.89	15.00	99.9 ± 0.8	99.6 ± 0.6

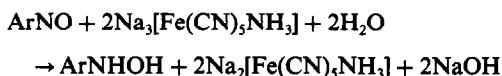
*Average of 10 determinations, calculated on nominal content of 5 mg of nitrazepam. Theoretical values at the 95% confidence level: *t* = 2.26, *F* = 3.18.

Varying the volume of SCAF solution used (from 1 to 10 ml) shows that 3 ml will suffice to give full colour intensity. The colour takes 10 min to reach full intensity.

The final solution can be diluted to volume with water, ethanol, methanol or dioxan with no change in the wavelength of maximum absorption or the molar absorptivity, but use of isopropyl alcohol gives a 25% decrease in the absorbance. Water is preferred. The colour is stable for at least 10 hr.

The method has been successfully applied to the analysis of nitrazepam tablets. Commonly encountered excipients such as starch, talc, lactose, and magnesium stearate do not interfere. The results obtained compare favourably with those of the official method (Table 1).

The chemistry of the colour reaction may be suggested on the basis of a previously reported mechanism.¹⁴ The nitro compound (nitrazepam in this case) is first reduced under the proposed conditions to the corresponding nitroso derivative. Addition of SCAF then causes further reduction to the corresponding hydroxylamine derivative. Subsequent substitution of ammonia in the reagent by the hydroxylamine derivative results in the violet colour.



where ArNO = nitroso derivative of nitrazepam and ArNHOH = hydroxylamine derivative of nitrazepam.

REFERENCES

- O. L. Grom, N. S. Komar and N. S. Ladyzhinshaya, *Farm. Zh. (Kiev)*, 1976, **31**, 82.
- H. Raber and J. Gruber, *Sci. Pharm.*, 1972, **40**, 35.
- N. M. Sanghavi and N. G. Jivani, *Talanta*, 1979, **26**, 63.
- Y. A. Beltagy, A. S. Issa and M. S. Mahrous, *Egypt. J. Pharm. Sci.*, 1978, **19**, 115.
- K. M. Jensen, *J. Chromatog.*, 1975, **111**, 389.
- H. Ehrsson and A. Tilly, *Anal. Lett.*, 1973, **6**, 197.
- P. Haefelfinger, *J. High Resol. Chromatog., Chromatog. Commun.*, 1979, **1**, 39.
- H. B. Hanekamp, W. H. Voogt, P. Bos and R. W. Frei, *J. Liq. Chromatog.*, 1980, **3**, 1205.
- J. Reider, *Arzneimittel-Forsch.*, 1973, **23**, 207.
- P. Van Doorne, *Pharm. Weekblad*, 1975, **110**, 149.
- S. Halvorsen and E. Jacobson, *Anal. Chim. Acta*, 1972, **59**, 127.
- British Pharmacopoeia*, 1980, pp. 305, 793. HMSO, London.
- C. O. Baudisch, *Ber.*, 1921, **54**, 413.
- F. Feigl, *Spot Tests in Organic Analysis*, 7th Ed., pp. 290, 297-299. Elsevier, Amsterdam, 1966.
- A. I. Vogel, *A Text Book of Quantitative Inorganic Analysis*, 3rd Ed., p. 727. Longmans, London, 1975.

SPECTROPHOTOMETRIC DETERMINATION OF PARAQUAT WITH BiI_4^- IN THE PRESENCE OF GUM ARABIC

P. YAÑEZ-SEDEÑO and L. M. POLO DIEZ

Department of Analytical Chemistry, Faculty of Chemistry, University Complutense of Madrid,
28040-Madrid, Spain

(Received 10 October 1985. Revised 16 January 1986. Accepted 15 May 1986)

Summary—A spectrophotometric method for determination of Paraquat, based on its reaction with BiI_4^- ion in the presence of gum arabic, is described. The apparent molar absorptivity of the product is $1.64 \times 10^4 \text{ l. mole}^{-1} \cdot \text{cm}^{-1}$ at 515 nm. Results for the analysis of commercial herbicides are in good agreement with those obtained by the dithionite method.

The 1,1'-dimethyl-4,4'-bipyridylium ion, trade name paraquat, is extensively used as a herbicide and is manufactured as the chloride, sulphate or methylsulphate in different formulations, either as the sole active component or together with 1,1'-ethylene-2,2'-bipyridylium bromide (Diquat). These salts are water-soluble, dissociate completely, and are stable in acid solutions.¹ The toxicity of Paraquat by ingestion is due to the rapid development of pulmonary fibrosis, caused by major lung retention of the ion.

The analytical methods most often used for Paraquat determination are spectrophotometric, based on its reduction to a quite stable blue radical in alkaline dithionite solution;² this method was adopted by the A.O.A.C.³ and has been further modified.¹ Another spectrophotometric method is based on stabilization of a suspension of the precipitate formed by Paraquat and HgI_4^- in the presence of ethanol, acetone or starch,⁴ and measurement of its absorbance at 400–420 nm.

In this work a spectrophotometric method for Paraquat determination, based on its reaction with BiI_4^- in the presence of gum arabic, yielding a pseudo-solution, has been developed.

EXPERIMENTAL

Reagents

A $2.00 \times 10^{-3} \text{ M}$ Paraquat stock solution, prepared by dissolving 0.2572 g of the chloride (Methylviologen, EGA Chemie) in 500 ml of distilled water. Less concentrated solutions were prepared by suitable dilution.

A 0.010 M BiI_4^- stock solution, prepared by dissolving, in the order given, 2.425 g of bismuth nitrate, 75 g of potassium iodide and 1 g of ascorbic acid in 500 ml of distilled water. Less concentrated solutions were prepared by suitable dilution with sulphuric acid to give a final 0.1 M concentration of this acid.

A 2% aqueous solution of gum arabic, filtered before use.

Samples analysed were mixtures of the Paraquat and Diquat herbicides commercially available. The Diquat solution was prepared from Reglone herbicide. All the working solutions were prepared daily.

Paraquat determination in herbicide samples

Transfer the sample (containing 25–250 μg of Paraquat) into a 25-ml standard flask containing 10 ml of $4 \times 10^{-4} \text{ M}$ BiI_4^- solution (0.1 M in sulphuric acid) and 5 ml of 2% gum arabic solution. Dilute to the mark with distilled water and mix thoroughly. Measure the absorbance at 515 nm in a 1-cm glass cell against a reagent blank. Prepare a calibration plot with standard Paraquat solutions to cover the 25–250 μg range.

Paraquat determination in the presence of Diquat in herbicide samples

To a 10-ml test-tube fitted with a screw cap, add the sample (containing less than 0.80 mg of Diquat bromide) and 2 ml of 2 M sodium hydroxide. Dilute accurately to 10 ml with distilled water, cap the tube and leave it for at least 6 hr. Remove the precipitate by centrifugation and pipette 5 ml of the solution. Adjust this solution to pH 1.7 (pH-meter) by adding first 3 M and then 1 M sulphuric acid. Dilute to 25 ml in a standard flask and apply the standard addition method to suitable aliquots, adding 25, 50, 75 and 100 μg of Paraquat (as standard solution) and following the procedure above.

RESULTS AND DISCUSSION

Absorption spectra

When a BiI_4^- solution is added to Paraquat solutions in acid medium, a red precipitate appears which is not soluble in the usual organic solvents. However, in the presence of gum arabic, the precipitation is inhibited and what is apparently a solution, orange in colour, is obtained. The absorption spectrum of this solution (measured with water as reference) shows a band with a maximum at 510 nm (Fig. 1). Under the same conditions a BiI_4^- solution shows an absorption maximum at 435 nm. These results indicate the formation of a compound, probably an ion-association complex. The 75-nm red shift of the BiI_4^- charge-transfer band implies a strong interaction between the donor and acceptor ions.

In the absence of Paraquat, the BiI_4^- solution has a slight absorbance at 510 nm, making it necessary to use it as the spectrophotometric reference solution.

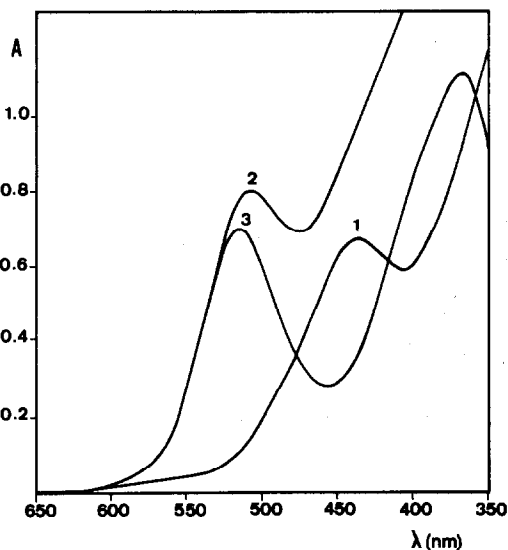


Fig. 1. Absorption spectra; (1) BiI_4^- ; (2) $\text{BiI}_4^- + \text{Paraquat}$; (3) $\text{BiI}_4^- + \text{Paraquat}$ vs. BiI_4^- ; BiI_4^- , $1 \times 10^{-4}M$; Paraquat, $1 \times 10^{-4}M$; pH 1.7 (H_2SO_4); gum arabic, 0.4%.

When the spectra are measured against the blank, the maximum of the absorption band appears close to 515 nm; a second band at 369 nm, though more intense, is less suitable for quantitative purposes, owing to the high blank absorbance and hence lower precision.

Influence of the gum arabic concentration

The concentration of gum arabic necessary to inhibit the precipitation depends on the Paraquat concentration. A low concentration (0.2%) is enough to prevent the precipitation of $10^{-4}M$ Paraquat in the presence of $1 \times 10^{-4}M$ BiI_4^- . However, for stabilization, use of 0.4% gum arabic is recommended. Under those conditions the absorbance does not change appreciably for at least 3 hr, though after 5 hr a slight turbidity appears.

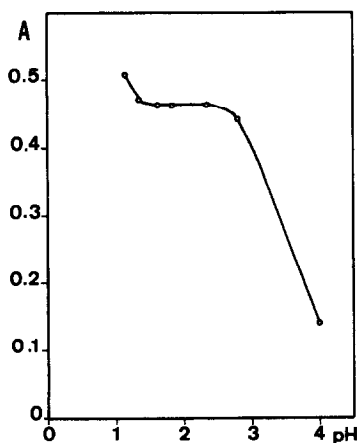


Fig. 2. A/pH plot at 515 nm. Paraquat, $5.23 \mu\text{g/ml}$; BiI_4^- , $1.6 \times 10^{-4}M$.

Effect of pH

As Fig. 2 shows, the absorbance stays practically constant over the pH range 1.5–2.4. At pH 2.4 the absorbance decreases owing to the formation of colourless Bi(III) complexes. At pH < 1.5 the absorbance increases because a slight turbidity appears.

Influence of BiI_4^- concentration; composition of the complex

A mole-ratio plot indicates that the $\text{BiI}_4^-/\text{Paraquat}$ ratio in the complex is 2/1. With higher $\text{BiI}_4^-/\text{Paraquat}$ molar ratios the absorbance stays practically constant for a fixed Paraquat concentration.

Analytical characteristics

Beer's law is obeyed up to $4 \times 10^{-5}M$ Paraquat in the presence of $1.6 \times 10^{-4}M$ BiI_4^- . The apparent molar absorptivity, $1.64 \times 10^4 \text{ l.mole}^{-1}.\text{cm}^{-1}$, is rather higher than that for solutions obtained by reducing Paraquat with dithionite in alkaline medium ($1.18 \times 10^4 \text{ l.mole}^{-1}.\text{cm}^{-1}$).

The optimal Ringbom-Ayres concentration ranges from 1.4 to $8.9 \mu\text{g}$ of Paraquat per ml of final solution. The coefficient of variation obtained from ten replications at the $5.2 \mu\text{g/ml}$ level is 0.4%, which is comparable to that for other spectrometric methods for Paraquat determination. The detection and determination limits, calculated from the standard deviation of the blank are, respectively, 0.05 ($3s_b$) and $0.16 (10s_b) \mu\text{g/ml}$ in the final solution.

Potential interferences from other species found together with Paraquat in its commercial formulations, as well as from some of the usual eluents employed to separate it by ion-exchange¹ were assessed by applying the Kirkbright $\pm 2s$ criterion. It was found that Na^+ , K^+ , NH_4^+ , NO_3^- and SO_4^{2-} do not interfere at up to 3000 times the Paraquat concentration. Bromide and chloride at moderately high levels cause fading of the solution by formation of Bi(III) complexes.

Diquat (1,1'-ethylene-2,2'-bipyridylium) reacts with BiI_4^- in presence of gum arabic at the working pH of the Paraquat determination to form a pseudo-solution having similar analytical properties to that obtained with Paraquat, and also absorbing at 515 nm. However, this interference may be minimized

Table 1. Paraquat recovery in the presence of $40 \mu\text{g}$ of Diquat bromide

Paraquat taken	Paraquat found			
	Calibration plot method		Standard addition method	
	μg	%	μg	%
18.5	20	107	20	108
37.2	37	99	38	101
74.5	76	102	75	101
80.0	80	100	80	100
111.5	109	98	112	101
148.8	146	98	150	101
186.0	177	95	—	—

Table 2. Accuracy of the method

Paraquat, %	Diquat, %	Method				t_{exp}
		Proposed		Reference		
		%	s	%	s	
20	—	23.1	0.1	22.9	0.2	1.58
20	—	23.3	0.1	23.4	0.1	1.58
12	8	12.1	0.2	12.4	0.2	2.15
10	10	10.3	0.3	10.0	0.2	1.97
8	12	8.4	0.2	8.6	0.1	1.50

$t_{5,0.95} = 2.31$.

by removing the Diquat beforehand by precipitation with sodium hydroxide.⁴ The optimum alkali concentration and the time necessary to attain maximum efficiency of Diquat removal were determined experimentally. The absorbance obtained by the Paraquat procedure for solutions originally containing up to 200 $\mu\text{g/ml}$ Diquat bromide is practically constant if the Diquat has been precipitated by treatment with 0.4M sodium hydroxide. The same treatment does not change the absorbance of Paraquat solutions. The maximum tolerable Diquat concentration for the determination of up to 3.20 $\mu\text{g/ml}$ Paraquat was found to be 1.7 $\mu\text{g/ml}$, expressed as concentration in the final solution.

Determination of Paraquat in various samples

The proposed method was applied to some commercial Paraquat and Diquat herbicide mixtures.

Results obtained for Paraquat recoveries in the presence of Diquat are shown in Table 1. With use of calibration plots, Paraquat concentrations higher than 3.20 $\mu\text{g/ml}$ in the final solution give rise to negative errors, probably because of matrix effects produced by the Diquat herbicide used (solution of Reglone). However, as Table 2 shows, these errors may be avoided by applying the standard addition method.

To evaluate the accuracy of the procedures, the results obtained for Paraquat were compared with those obtained by the dithionite method (Table 2). The mixtures studied corresponded to the usual ratios in commercial preparations. The standard addition method was applied for Paraquat-Diquat mixtures. An F -test indicate that the standard deviations for the methods compared do not differ (95% confidence level). The Student- t values show that there are no significant differences between the means, at the same confidence level, testifying to the reliability of the method.

REFERENCES

1. P. F. Lott and J. W. Lott, *J. Chromatog. Sci.*, 1978, **16**, 390.
2. S. H. Yuen, J. E. Bagness and D. Myles, *Analyst*, 1967, **92**, 375.
3. A. A. Carlstrom, *J. Assoc. Off. Anal. Chem.*, 1967, **51**, 1306.
4. M. Ganesan, S. Natesan and V. Ranganathan, *Analyst*, 1979, **104**, 258.

DETERMINATION OF TRACE AMOUNTS OF NICKEL BY ATOMIC-ABSORPTION SPECTROMETRY AFTER CARBONYL GENERATION

J. ALARY, J. VANDAELE and C. ESCRIEUT
INSERM U57, Allée Camille Soula, 31320 Vigoulet Auzil, France

R. HARAN

Laboratoire de Chimie de Coordination du CNRS, 125 route de Narbonne, 31400 Toulouse, France

(Received 25 February 1986. Accepted 14 May 1986)

Summary—A sensitive and reliable method for the atomic-absorption spectrometric determination of micro-amounts of Ni in organic and inorganic samples has been developed, with separation of nickel by carbonyl generation. Foreign anions and cations do not interfere. Only metallic iron hampers the generation of Ni(CO)₄, but this interference can be avoided if the latter is formed in nitric acid medium. In the range 0.02–0.1 µg, Ni can be determined with a precision of about 10%. The detection limit of the proposed method is 10 ng in the aliquot used.

Over the last few years, the determination of nickel has been the subject of numerous investigations as a result of the environmental, toxicological and physiological importance of this element. Under ordinary circumstances the nickel content of various environmental materials ranges from a few µg/g (e.g., in plants) down to 10 ng/ml in biological fluids such as serum¹ and urine² and even less than 1 ng/ml in sea-water.³

The most commonly used method for determination of traces of Ni is graphite-furnace atomic-absorption spectrometry, applied to both environmental analysis⁴ and to body fluids.⁵⁻⁷

The determination of traces of Ni in environmental samples such as atmospheric dust, plants and foods requires use of digestion procedures. However, the determination of ultratraces of Ni, for example in water samples and body fluids, necessitates the absence of reagent contamination. Therefore direct determination methods appear to be the most promising approach. Hence electrothermal atomic-absorption spectrometry in conjunction with Zeeman compensation, or after carbonyl generation, can be expected to improve the determination of traces of Ni.

Recently Vijan⁸ showed the great sensitivity of Ni determination after carbonyl generation and Lee⁹ determined nickel in sea-water by use of the principle. We have undertaken a study to test the validity of the method for the determination of traces and ultratraces of Ni in more complex media.

EXPERIMENTAL

Apparatus

Measurements were performed with a Pye-Unicam SP 9 atomic-absorption spectrophotometer equipped with a

Pye-Unicam SP 9 computer print-out and coupled with a Perkin-Elmer MHS 20 hydride-generator. The following conditions were used.

Spectrophotometer

Wavelength, 232 nm
Spectral band-width, 0.2 nm
Deuterium background correction

MHS 20 Module

Cell temperature, 950°
Gas flow-rates; N₂ 0.5 l./min, CO 0.5 l./min
Calibration volume, 10 ml
Reductant, 3% NaBH₄ + 1% NaOH solution

Reagents

Stock nickel solution (1 mg/ml) was purchased from Merck. More dilute solutions were prepared just before use. Glass-distilled water was used in all operations. All acids used were high-purity products (Merck *suprapur*). The sodium tetrahydroborate (Merck 6371) was used without purification.

The carbon monoxide used was passed through activated charcoal to remove any nickel carbonyl which could be present as an impurity in the gas.

Procedures

Plant and liver tissue. One gram of dry, ground sample, accurately weighed, was placed in a platinum crucible and ashed in a muffle furnace at 500° for 6 hr. After cooling, the residue was transferred into a Teflon beaker and 2 ml of nitric/perchloric acid mixture (4:1 v/v) added. The acid was evaporated to dryness, then 2 ml of concentrated hydrofluoric acid and a few drops of perchloric acid were added. The mixture was again evaporated to dryness, and after cooling the residue was dissolved at room temperature by addition of 20 ml of 5% v/v nitric acid. The precipitate of potassium perchlorate was filtered off. Nickel was then determined in 1 ml of filtrate for plant samples and 5 ml for liver samples.

Steel. A 20-mg sample of steel was placed in a Teflon beaker and 5 ml of a 1:1 mixture of concentrated nitric and hydrochloric acids were added. The mixture was heated until dissolution was complete, and then evaporated to dryness. After cooling, 5 ml of concentrated nitric acid were

added and the solution was made up accurately to 100 ml with distilled water. The aliquots used were in the range 0.5–1 ml.

River water. A 100-ml sample was acidified with 5 ml of 2% v/v nitric acid and evaporated to less than 10 ml; the volume was accurately made up to 10 ml with distilled water and the solution analysed for nickel.

Urine. A 10-ml sample was acidified with 300 μ l of concentrated nitric acid, and three drops of antifoaming agent (Rhodorsil 426) were added prior to direct determination of nickel.

Plasma. A 10-ml portion of plasma from heparinized blood was evaporated to dryness in a platinum crucible and the residue dry-ashed in a muffle furnace at 500° for 6 hr. The residue was taken up with 10 ml of 2% v/v nitric acid.

RESULTS AND DISCUSSION

Sodium borohydride reduces nickel in its compounds to the metal, which then reacts with carbon monoxide to give Ni(CO)₄, which is stripped from the reactor by the carrier gas. Nickel carbonyl is then decomposed by heating to give elemental nickel which is detected by AAS.

Theoretically the rate of formation of nickel carbonyl is determined by the temperature and the partial pressure of CO. However, increasing the CO ratio in the carrier gas is expensive, and a high flow-rate in the silica tube burner decreases the sensitivity of the method.

Thus a carrier gas with a CO content of 50% was chosen, with a flow-rate of 300 ml/min during the reduction step. As the thermal decomposition of Ni(CO)₄ begins at 60°, the temperature of the reactor is of importance if deposition of elemental nickel is not to occur before the carbonyl reaches the quartz heating-cell.

The degree of reduction was found not to differ when the reactor temperature was varied between 4 and 40°, so in all further experiments the reduction was done at room temperature.

Using a reaction time of 10 sec for the reduction step corresponds to an injection of 7.5 ml of borohydride solution, which gives a mean blank value of 5 ng (S.D. 2 ng) of nickel, which gives a detection limit of 10 ng of Ni in the aliquot analysed.

Although the thermal decomposition of Ni(CO)₄ begins at about 60° no nickel peak was recorded when the silica-cell temperature was set lower than 600°. The optimal temperature was found to be 950°; in these experimental conditions, with a flow-rate of 300 ml/min, the carrier gas temperature is about 250°. As shown by the peak shape, complete carbonyl generation requires about 20 sec.

As expected with such a reduction technique, the metallic hydride-forming elements can produce interference.

The effects of Pb, Sb, Bi, Se, As, Sn were investigated; of these elements, only Sn (which has an intense absorption line at 231.7 nm), and to a lesser extent As, show interference. Equal amounts of Ni and Sn give about the same absorbance.

Because of its spectral interference, when tin is present in the samples, it is necessary to use the 341.5 nm line for determination of nickel, at the expense of halving the sensitivity. Of the metal carbonyls, only those of iron and nickel are formed at room temperature and atmospheric pressure.¹⁰ However, in the presence of iron the nickel recovery is strongly decreased. For example, with an Fe/Ni ratio of 100 in hydrochloric or sulphuric acid medium, no nickel absorbance is found. This is caused by the simultaneous reduction of both ions when the borohydride is added, the nickel being entrapped in the iron. As the experimental conditions are not ideal for the formation of iron carbonyl, the presence of the finely divided iron metal prevents the formation of Ni(CO)₄. Isolation and examination (emission spectrography) of the metallic precipitate formed in 2% hydrochloric acid showed the presence of Fe, Ni and

Table I. Determination of Ni (ppm) in standards and unknown samples ($n = 4$)

Samples	Ni present	Ni found	SD	RSD, %	Literature values		
					Range	Method	Reference
Orchard leaves NBS SRM 1571	1.3	1.2	0.1	8.3			
SRM 1570 Spinach	(6)	5.8	0.1	1.7			
SRM 1575 Pine needles	(3.5)	3.1	0.1	3.2			
Steel BCS 320	220	200	10	5			
Steel BCS 324	500	500	20	4			
Atmospheric particles (Urban)	—	80	5	6	50–500	NAA	12
Pooled river waters (rural area)	—	1.2×10^{-3}	2×10^{-4}	17	1.5×10^{-3}	ICP	13, 14
Pooled urine from unexposed subjects	—	3.5×10^{-3}	6×10^{-4}	17	1×10^{-3} -5×10^{-3}	GFAAS	2, 4, 15, 16
Pooled serum from unexposed subjects	—	2×10^{-3}	4×10^{-4}	20	1×10^{-3} -8×10^{-3}	GFAAS	1, 16–19
Bovine liver	—	0.4	0.03	7	<0.4* 0.5*	PIXE ICP	20 21

*Bovine liver NBS 1577.

() uncertified values.

B in agreement with the suggestion made by Bye.¹¹

Investigations conducted in order to avoid this interference showed that if the reduction step takes place in 2% nitric acid medium, Fe³⁺ is reduced only to Fe²⁺ without formation of metallic iron, as shown by the greenish colour of the solution and the absence of a black precipitate.

No significant differences in nickel recovery were found when the reduction was done in 1–5% nitric acid, but there was a negative bias of about 5% for Fe/Ni ratios >200. Therefore use of the standard addition method is required for the accurate determination of nickel in the presence of iron.

No interference was noted from other common anions or cations, even at levels up to 2 g/l.

To test the validity and recovery of the described procedure, assays were performed with standard samples. Nickel was also determined in various environmental samples and biological fluids. Table 1 gives the means of four replicate analyses.

For the analysis of standard samples, Table 1 shows good agreement between the experimental and reference values. The accuracy of the procedure cannot be determined, since biological standards for nickel are not commercially available. However the concentrations found in the environmental and biological samples were of the same order of magnitude as those recently reported in the literature.

The procedure gives a linear calibration over the range 10–100 ng of nickel, with a lower detection limit of 10 ng in the aliquot reduced. Replicate determinations show that the precision is in the range 2–20%, depending on the amount of nickel present.

Although the procedure is less sensitive than that of Lee,⁹ it is simpler and well adapted to routine determination of nickel in a wide range of samples, so it represents a good alternative method for the determination of microamounts.

REFERENCES

1. U. Vollkopf, Z. Grobowski and B. Weitz, *At. Spectrosc.*, 1981, **2**, 68.
2. D. B. Adams, S. S. Brown, F. W. Sunderman and H. Zachariassen, *Clin. Chem.*, 1978, **24**, 862.
3. K. W. Bruland and R. P. Franks, *Anal. Chim. Acta*, 1979, **105**, 233.
4. M. Stoepler, *Nickel in the Environment*, p. 661. Wiley, New York, 1980.
5. K. H. Schafier, M. Stoepler and H. J. Raithei, *Staub Reinhalt Luft*, 1980, **42**, 137.
6. S. S. Brown, S. Nomoto, M. Stoepler and S. W. Sunderman, *Clin. Biochem.*, 1981, **14**, 295.
7. S. W. Sunderman, M. C. Crisostomo, M. Reid, S. M. Hofer and S. Nomoto, *Ann. Clin. Lab. Sci.*, 1984, **14**, 232.
8. P. N. Vijan, *At. Spectrosc.*, 1980, **1**, 143.
9. D. S. Lee, *Anal. Chem.*, 1982, **54**, 1182.
10. F. A. Cotton and G. Wilkinson, *Advanced Inorganic Chemistry*, 3rd Ed., p. 692. Wiley, New York, 1972.
11. R. Bye, *Talanta*, 1986, **33**, 705.
12. J. P. F. Lambert and F. W. Wilshire, *ibid.*, 1979, **51**, 1346.
13. H. Tao, A. Miyazaki, K. Bansho and Y. Umezaki, *Anal. Chim. Acta*, 1984, **156**, 159.
14. P. D. Goulden and D. H. J. Antony, *Anal. Chem.*, 1982, **54**, 1678.
15. F. W. Sunderman, *Pure Appl. Chem.*, 1980, **52**, 527.
16. I. Andersen, W. Torjussen and H. Zachariassen, *ibid.*, 1978, **24**, 1198.
17. H. Zachariassen, J. Andersen, C. Kostel and R. Barton, *Clin. Chem.*, 1975, **21**, 562.
18. C. Camora-Rica and G. F. Kirkbright, *At. Spectrosc.*, 1981, **2**, 172.
19. M. Drazniowsky, I. S. Parkinson, M. K. Ward, S. M. Channon and D. N. S. Kerr, *Clin. Chim. Acta*, 1985, **145**, 219.
20. W. Maenhaut, L. De Reu, H. A. Van Rinsvelt, J. Cafmeyer and P. Van Espen, *Nucl. Instrum. Methods*, 1980, **168**, 557.
21. R. J. Norstrom, R. E. Schweinsberg and B. T. Collins, *Sci. Total Environ.*, 1986, **48**, 195.

EFFECT OF TEMPERATURE ON THE DETERMINATION OF AROMATIC NITRO-COMPOUNDS BY COULOMETRICALLY GENERATED CHROMIUM(II)

ISMAIL M. AL-DAHER

Department of Chemistry, University of Al-Mustansiriyah, Baghdad, Iraq

BYRON KRATOCHVIL

Department of Chemistry, University of Alberta, Edmonton, Alberta, Canada

(Received 25 February 1986; Accepted 14 May 1986)

Summary—The analytical utility of the reaction between aromatic nitro-compounds and electrogenerated chromium(II) can be extended to several previously undeterminable compounds by increasing the temperature of the reaction solution. For some substances the stoichiometry of the reduction is changed; for others the rate of reaction, along with precision and accuracy, is appreciably increased; in at least one instance the reaction becomes less satisfactory as an analytical method. Temperature is thus shown to be an important variable that may explain differences in previously reported stoichiometries.

A number of aromatic nitro-compounds can be determined by reduction with chromium(II). The bivalent chromium required as the reagent is conveniently produced by constant-current coulometric generation from chromium(III) bromide at a mercury cathode in acidic solution.¹⁻⁴ The reduction of the R-NO₂ functional group often consumes 6 electrons, yielding an amine as the product, but 4-electron reduction to a hydroxylamine is also common. A few compounds undergo 5-electron reduction per nitro group, presumably forming coupled hydrazo products.^{2,4}

In evaluation of the scope of the method a number of nitro-compounds were found not to be determinable at room temperature because either the reaction was too slow or the stoichiometry indeterminate. We report here the results of a study of the effect of elevated temperature on these reactions.

EXPERIMENTAL

Apparatus

The coulometer, cell, catholyte, and titration end-point detection procedures were as previously described.² The catholyte in the cell was held at a temperature of 40 or 50 ± 0.5° by an immersion heater dipped into the solution. The heater consisted of a 120-V, 75-W cartridge-type immersion heating element in a glass tube inserted through the cell lid. Power to the heating element was controlled manually with a Variac variable transformer.

Chemicals

Acetonitrile was distilled over calcium hydride and the middle fraction of the distillate retained. For some work, commercially purified acetonitrile (Caledon, ACS Reagent Grade) was used as received. No difference in results was observed. Chromium(III) bromide was washed as described before.²

2,4-Dinitroanisole, 4-nitrophenetole, 2,4-dinitrophenetole, 2,6-dinitrothymol, 2-nitrocinnamic acid and 2-nitrophenol were recrystallized from ethanol until melting points within ± 1° of reported values were obtained. 2-Nitrophenetole and 4-nitroethylbenzene were distilled under vacuum, and the middle fractions retained. 1,8-Dinitronaphthalene was

recrystallized from chloroform. 5-Nitro-1-naphthylamine (Eastman) was used as received.

Titration procedure

The titration procedure was as described before,^{2,4} except that during deaeration the temperature of the catholyte was brought to 40 or 50° with the immersion heater and held at the required temperature during the titrations, by adjustment of the applied voltage. Blanks were run as before,² after which about 1 g of an approximately millimolar solution of a nitro-compound in acetonitrile was injected into the cell with a hypodermic syringe. The amount of sample was determined by weighing the syringe before and after the injection. Chromium(II) was then generated, the time and potential being recorded as for the blank. For some compounds second or third portions of sample solution could be injected and replicate titrations performed in the same catholyte; with others, the products of the first and subsequent titrations interfered with precise selection of the end-points.

RESULTS AND DISCUSSION

Results comparing the reduction of a series of nitro-compounds at 25, 40, and 50° are summarized in Table 1. It can be seen that several of the compounds are determinable with better accuracy at higher temperatures; these include 2-nitrophenetole, 2,4-dinitrophenetole and 5-nitro-1-naphthylamine. For others the precision of the results was improved, and the time of reaction was generally shorter than that at 25°. On the other hand, for some compounds, such as 1,8-dinitronaphthalene, the reaction time was longer and the end-point poorer at 50°, even though the number of electrons taken up per molecule was raised from 10 to 12. For this compound, titration at 25 or 40° is clearly more satisfactory than at 50°. Similar behaviour was observed for 4-nitroethylbenzene, not included in the table, where at 50° the number of electrons, 5, and the time of titration were the same as at 25°, but the end-point was less sharp. Another compound, showing quantitative

Table 1. Effect of temperature on the reduction of aromatic nitro-compounds with coulometrically generated chromium(II)

Compound	Temp., °C	No. of electrons	No. of detns.	Av. error, %	Rel. std. dev., %	No. of titns, per catholyte	Postulated product	Time per titration, min	End-point
4-Nitrophenetole*	25	6	9	-0.3	0.1	5	RNH ₂	7-10	sharp
	40	6	6	-0.4	0.8	3	RNH ₂	6-8	sharp
	50	6	3	-0.4	0.7	3	RNH ₂	6-7	sharp
2,4-Dinitroanisole†	25	10	6	-0.1	0.2	2	H ₂ NRNH ₂ OH	13-16	good
	40	10	4	-0.2	0.8	2	H ₂ NRNH ₂ OH	10-14	good
	50	12	5	-0.5	1.3	2	H ₂ NRNH ₂	7-10	good
2,4-Dinitrophenetole*	25	11	10	0.8	0.9	3-4	(H ₂ NRNH ₂) ₂	10-20	sharp
	40	11	8	0.4	0.6	4	(H ₂ NRNH ₂) ₂	10-15	sharp
	50	12	4	-0.4	0.4	4	H ₂ NRNH ₂	8-10	sharp
2-Nitrophenetole*	25	4	12	8.7	0.2	1	RNHOH	5-10	sharp
	40	4	8	5.4	0.3	2	RNHOH	5-9	sharp
	50	5	5	0.1	0.8	2	(RNH) ₂	5-8	less sharp
5-Nitro-1-naphthylamine†	25	5	7	0.3	0.4	3-4	(H ₂ NRNH ₂) ₂	16-25	fair
	40	5	5	0.1	0.6	3	(H ₂ NRNH ₂) ₂	12-16	good
	50	5	5	0.1	0.9	3	(H ₂ NRNH ₂) ₂	7-10	sharp
1,8-Dinitronaphthalene*	25	10	3	-0.5	0.2	1	H ₂ NRNH ₂ OH	6-8	sharp
	40	10	3	-0.4	0.2	1	H ₂ NRNH ₂ OH	5-8	sharp
	50	12	1	-0.5	—	1	H ₂ NRNH ₂	16	poor
2-Nitrophenol‡	25	5	9	-5.6	2.0	1	(RNH) ₂	slow	poor
2-Nitrophenol††	25	5	2	0.2	1.1	2	(RNH) ₂	13-18	poor
2-Nitrophenol‡	40	5	4	0.2	0.8	2	(RNH) ₂	10-16	poor
2-Nitrophenol††	50	5	4	-0.3	0.6	2	(RNH) ₂	8-10	fair

*Data at 25° from Ref. 4.

†Data at 25° from Ref. 2.

‡Solvent for sample 1:25 EtOH:H₂O.

††Solvent for sample acetonitrile.

11-electron reduction at 25° with a sharp end-point, 2,6-dinitrothymol, was not affected in terms of precision, accuracy or stoichiometry by increasing the temperature from 25 to 50°.

The reduction of 2-nitrocinnamic acid proceeded non-quantitatively at all temperatures studied. The reaction stoichiometry falls somewhere between 3 and 4 electrons at 25° and between 4 and 5 at 50°. Although information on the reactivity at higher temperatures would be valuable, the cell could not be operated at above 50° because of leakage of the agar bridge between the anode and cathode compartments. For 2-nitrophenol the low results for 5-electron stoichiometry when ethanol is present suggest reaction of ethanol with an intermediate in the reduction, leading to incomplete reduction of the nitrophenol to the hydrazo product.

Differences in the temperature of the catholyte solution may explain discrepancies in previously reported results for the reduction of nitro-compounds by chromium(II). Thus, 2-nitrobenzoic acid and 4-nitrobenzoic acid have been reported to undergo 6-electron¹ and 4-electron² reductions, as has 3-nitrophenol.^{2,5} Further measurements on these and related compounds as a function of temperature, along

with isolation and characterization of the reaction products, could clarify the differences.

In summary, the analytical usefulness of electro-generated chromium(II) as a reagent for titration of aromatic nitro-compounds can be extended by performing the reduction at an elevated temperature. Advantages include more rapid achievement of equilibrium and often improved precision and accuracy. For several compounds the stoichiometry of the reaction changes with temperature.

Acknowledgements—Financial support by the Natural Sciences and Engineering Research Council of Canada and by the Universities of Al-Mustansiriyah and Alberta is gratefully acknowledged.

REFERENCES

1. D. A. Aikens and Sr. M. Carlita, *Anal. Chem.*, 1965, **37**, 459.
2. I. M. Al-Daher and B. Kratochvil, *ibid.*, 1979, **51**, 1480.
3. B. Kratochvil and I. M. Al-Daher, *Analyst*, 1981, **106**, 796.
4. I. M. Al-Daher and B. Kratochvil, *Can. J. Chem.*, 1981, **59**, 3346.
5. M. R. Lindbeck and H. Freund, *Anal. Chim. Acta*, 1966, **35**, 74.

DETERMINATION OF ORGANICALLY-ASSOCIATED TRACE METALS IN ESTUARINE SEA-WATER BY SOLVENT EXTRACTION AND ATOMIC- ABSORPTION SPECTROMETRY

KOJI HAYASE, KIMINORI SHITASHIMA and HIROYUKI TSUBOTA

Faculty of Integrated Arts and Sciences, Hiroshima University, Hiroshima 730, Japan

(Received 7 February 1986. Accepted 14 May 1986)

Summary—Chloroform extraction of trace metals (Ni, Cu, Mo, Mn, Cd and Pb) in estuarine sea-water was studied at pH 8 and pH 3, on the basis that the metals would be associated with dissolved organic matter (DOM), which has recently been characterized by reversed-phase liquid chromatography. Ni, Cu, Mo and Mn were extracted more at pH 8 than at pH 3. Cd and Pb were not associated with the DOM at either pH 8 or 3. The percentage of the total dissolved trace metals in sea-water associated with DOM varied from 0 to 14%. The metals extracted into chloroform at pH 8 were assumed to be associated with neutral or weakly basic DOM while at pH 3 they could be associated with either the neutral (or weakly basic) DOM or two types of acidic DOM.

Many trace metals in sea-water are partially associated with dissolved organic matter (DOM) and the nature of the organic compounds involved is of interest in geochemical, biochemical and environmental studies. Some workers¹⁻⁷ have employed reversed-phase liquid chromatography (RPLC) with octadecylsilane for the isolation and characterization of organic complexes of metals in sea-water. Slowey *et al.*⁸ have studied such complexes in sea-water by solvent extraction. They reported^{4-6,8} that 6-70% of the total copper in solution is organically associated Cu. Piotrowicz *et al.*,⁹ using anodic-stripping voltammetry, found that more than 95% of the dissolved copper in surface sea-water is complexed by organic ligands. A large fraction of the organically complexed copper is not isolated by C₁₈-SEP-PAK.¹⁰ Similarly, organic solvents such as chloroform extract only a fraction of the DOM in sea-water.

We have recently investigated the RPLC of DOM extracted into chloroform from estuarine sea-water, using both absorption and fluorescence detectors.¹¹ In our work three kinds of DOM were recognized, one a neutral or weakly basic material that fluoresces and the other two acidic and not fluorescent. It is likely that the three types also differ in their interactions with metal ions. The results for the determination of trace metals associated with the chloroform-extractable DOM in estuarine sea-water is reported in this paper.

EXPERIMENTAL

Reagents

Chloroform of ultrafine grade (Nakarai Co. Ltd.) was used. The stock metal ion solutions, except for Mo, were

made from Johnson-Matthey guaranteed materials by dissolving the metals in nitric acid and were standardized by EDTA titration. For Mo, aqueous ammonium molybdate solution was prepared. The working standard solutions were prepared by diluting the stock solutions with 2M nitric acid. The water used was distilled, demineralized and further purified by the sub-boiling technique.

Sample sea-water

The surface sea-water sample was the same as that reported in our previous paper,¹¹ and was collected on 11 June 1983 from Hiroshima Bay (34°21.1'N, 132°24.2'E) in the Seto Inland Sea by using a specially designed 5-litre surface-water sampler made of polyethylene and cleaned with nitric acid. The surface sea-water was sampled from the bow with the ship moving dead slow ahead to prevent contamination from the ship itself. The sampling station was just beyond a river mouth and the sea-water at the station was rich in both metals and DOM. The salinity of the sample sea-water was 29.1‰. The sample water was filtered through a nitric acid-cleaned 0.4- μ m Nuclepore filter, in a Class 100 clean-room, with use of a nitrogen-pressurized Teflon in-line filtration apparatus. The filtration was done within several hours of sampling. The sample was stored in a nitric acid-cleaned polyethylene bottle.

Apparatus

Atomic-absorption measurements were made with a Perkin-Elmer Model 500 instrument, HGA 5000 graphite furnace and AS 40 auto-sampler.

Procedure

The sea-water sample was used for the extraction of DOM after the filtration. Every step other than evaporation was performed in the clean room. The sample was divided into eight 1-litre aliquots, and each aliquot was extracted with 20 ml of chloroform in a Teflon separating funnel. Four aliquots were extracted at natural pH (8) and the other four at pH 3 (obtained by addition of distilled nitric acid). The four extracts (at each pH) were combined in a quartz dish and gently evaporated to dryness on a hot-plate inside a box flushed with nitrogen. Each residue was treated with

Table 1. Metal concentrations in sea-water

Element	Total dissolved metal concentration, nmole/kg	Extracted by CHCl ₃ at pH 8		Extracted by CHCl ₃ at pH 3,	
		nmole/kg	%*	nmole/kg	%*
Ni	12.0	1.64	14.0	0.07	0.6
Cu	9.1	0.71	7.8	0.60	6.6
Mo	96	0.89	0.9	0.81	0.8
Mn	70	0.25	0.4	0.04	0.06
Cd	0.42	N.D.†	0.0	N.D.	0.0
Pb	0.18	N.D.	0.0	N.D.	0.0

*Percentage of total dissolved metal.

†N.D. = Not detected (< 0.01 nmole/kg).

about 10 ml of 2M nitric acid, followed by evaporation to dryness and heating at 140°. The final residues were each dissolved in 10 ml of 2M nitric acid and stored in Teflon bottles cleaned with hot nitric acid, prior to determination of the metal concentrations by graphite-furnace atomic-absorption spectrometry (GFAAS).

For determination of total dissolved metals in the sample, the following procedure was applied in the clean room. To 1 litre of the filtered sea-water, 5 ml of concentrated nitric acid were added. A few months later, the acidified sample was adjusted to pH 5.3–5.5 with aqueous ammonia and acetic acid and passed through a Chelex 100 column. To elute the major elements, the column was washed with 200 ml of 1M ammonium acetate solution (pH 5.5), followed by 50 ml of water. The trace metals sorbed on the column were eluted with 2M nitric acid. The eluate was evaporated to dryness and then heated at 140° inside a box flushed with nitrogen, the residue finally being dissolved in 10 ml of 2M nitric acid. This solution was analysed by GFAAS.

RESULTS AND DISCUSSION

The concentrations found for the trace metals (total in solution, and extracted by chloroform at pH 8 and 3) are shown in Table 1. In the previous study,¹¹ it was found that chloroform extracted a neutral or weakly basic DOM from the sea-water at pH 8, and two types of acidic DOM in addition to the neutral or weakly basic DOM at pH 3. Although the neutral DOM fluoresced (excitation and emission wavelengths were 320 and 420 nm, respectively), the acidic types of DOM did not.

The trace metals extracted by chloroform at pH 8 are considered to be associated with the neutral or weakly basic DOM (peaks 1-X and 2-X in Figs. 1 and 2 of the previous paper¹¹).

Nickel and copper were obviously associated with the neutral or weakly basic DOM, the fractions being 14 and 8% of the total dissolved nickel and copper, respectively. Kremling *et al.*¹² reported that in Baltic waters about 5% of the total copper was organically associated. The fraction of organically associated copper in sea-waters off Port Hacking in Australia has also been reported as about 5%.⁵ Negishi and Matsunaga¹³ showed that the ratios of organically-bound to total copper ranged from 10 to 70% in lake and river water at Hokkaido in Japan. Mills and Quinn⁶ reported that in the Narragansett Bay estuary the ratio of copper retained by SEP-PAK to total

dissolved copper ranged from 14 to 70%. The corresponding ratio found for Hiroshima Bay water is rather low and is consistent with the values found by Kremling *et al.*¹² and Mackey.⁵ Molybdenum and manganese were little associated with the neutral or weakly basic DOM.

No detectable levels of cadmium and lead were found to be associated with the neutral or weakly basic DOM. Mackey⁵ reported that cadmium was not detected (by atomic fluorescence) in chromatography of material extracted from sea-water by a SEP-PAK cartridge.

The metals extracted with chloroform at pH 3 are associated with both the neutral or weakly basic DOM and the acidic types of DOM. Since cadmium and lead were still not detected in the pH-3 extract, they may not be associated with any type of DOM. For the other four metals examined, the concentrations extracted at pH 3 are lower than those at pH 8. Mills *et al.*⁴ studied the effect of pH on retention of organic copper complexes in sea-water. Their results showed that there was a reduction in the relative amount of organic copper as the pH of the sea-water was decreased, and our result is similar. This effect is attributed to protonation of the functional groups on the DOM when the pH is decreased.

The decrease in the concentration of nickel and manganese extracted when the pH is decreased from 8 to 3 indicates that most of these two metals was associated with the neutral or weakly basic DOM.

Sequential extraction of DOM from sea-water at pH 8 and 3 will be interesting for further investigation of the metals associated with DOM.

Acknowledgements—The authors deeply thank Professor S. Hayano for his valuable suggestions and discussion. They also appreciate the assistance of the captain, officers and crew of the *Toyoshio Maru*, Hiroshima University. This work was financially supported by a grant from the Ministry of Education, Science and Culture, Japan.

REFERENCES

1. J. B. Derenbach, M. Ehrhardt, C. Osterroht and G. Petrick, *Mar. Chem.*, 1978, 6, 351.
2. G. L. Mills and J. G. Quinn, *ibid.*, 1981, 10, 93.

3. J. Lee, *Water Res.*, 1981, **15**, 507.
4. G. L. Mills, A. K. Hanson, J. G. Quinn, W. R. Lammela and N. D. Chasteen, *Mar. Chem.*, 1982, **11**, 355.
5. D. J. Mackey, *ibid.*, 1983, **13**, 169.
6. G. L. Mills and J. G. Quinn, *ibid.*, 1984, **15**, 151.
7. D. J. Mackey, *ibid.*, 1985, **16**, 105.
8. J. F. Slowey, L. M. Jeffrey and D. W. Hood, *Nature*, 1967, **214**, 377.
9. S. R. Piotrowicz, G. R. Harvey, M. Springer-Young, R. A. Courant and D. A. Boran, in *Trace Metals in Sea water*, C. S. Wong, J. D. Burton, E. A. Boyle, K. W. Bruland and E. D. Goldberg (Eds.), pp. 699-717. Plenum Press, New York, 1983.
10. J. R. Donat, P. J. Statham and K. W. Bruland, *Mar. Chem.*, 1986, **18**, 85.
11. K. Hayase, K. Shitashima and H. Tsubota, *J. Chromatog.*, 1985, **322**, 358.
12. K. Kremling, A. Wenck and C. Osterroht, *Mar. Chem.*, 1981, **10**, 209.
13. M. Negishi and K. Matsunaga, *Water Res.*, 1983, **17**, 91.

MINERALIZATION OF SOME ORGANIC SULPHUR COMPOUNDS BY FUSION WITH MOLTEN ALKALI

J. V. GIMENO ADELANTADO and F. BOSCH REIG

Department of Analytical Chemistry, Faculty of Chemistry, University of Valencia, Burjassot, Valencia, Spain

(Received 7 November 1984. Revised 17 March 1986. Accepted 30 April 1986)

Summary—The action of molten alkali-metal hydroxides for the destruction of organic matter containing sulphur has been studied. Various procedures were developed which differed mainly in the initial phase of the process, mainly with respect to homogenization of the reaction mixture, but also with regard to addition of an auxiliary oxidant. The technique is not universally applicable to sulphur compounds, but is useful for decomposition of sulphur compounds with m.p. > 150° and containing sulphonate, thiocarbonyl, phenazothionium and thio groups. The sulphur is converted into sulphate, which is then determined as barium sulphate.

Determination of sulphur in organic compounds normally requires complete destruction of the organic matrix. Numerous methods for this purpose have been described. They include wet oxidation with chloric acid¹ or mixtures of nitric and perchloric acids,²⁻⁴ but the risk of explosion inherent in the use of these acids must be borne in mind. Wet oxidation with potassium permanganate and peroxophosphoric acid⁵ or with sodium peroxychromate⁶ has been proposed but the sulphones are resistant to these methods. The combustion procedures need special conditions for the oxidation and collection of the products.⁷⁻⁹ The Schöniger flask method¹⁰ with slight modifications is often used¹¹ even though the accuracy and precision depend on the nature of the sulphur bond¹² and are unsatisfactory for many organometallic compounds.¹³ The mineralization methods use various pyrolysis conditions,^{14,15} and generally employ catalysts. Hydrogenation procedures have also been developed,^{16,17} but require complicated apparatus. The fusion methods are simpler and often more satisfactory, and can be based on reduction with alkali metals^{18,19} or aluminium dust,²⁰ or oxidation, as described by Bowen,²¹ who used fusion with an equimolar mixture of sodium and potassium nitrates at 390°. However, in the Bowen method some sulphur may be lost by volatilization, and pyrophoric mixtures can be formed, with danger of explosion.

Fusion with sodium hydroxide has been used as a decomposition method in determination of germanium,²² fluorine,²³ and arsenic, antimony and phosphorus.^{24,25}

Here we report on alkaline fusion as a means of decomposing organic sulphur compounds for gravimetric determination of that element, as barium sulphate by the Winkler method.²⁶ As a reference method we used mineralization of the sample with a

mixture of nitric and perchloric acids² and gravimetric determination of barium sulphate by the Hintz and Weber method.²⁷

EXPERIMENTAL

Fusion procedures

In a 50-ml silver or nickel crucible melt 2-4 g (depending on the sample size) of sodium or potassium hydroxide or a eutectic mixture of the two (41:59 w/w). Swirl the crucible so that its bottom and walls are coated with the melt, and let it cool to room temperature. Add a known weight of sample containing about 27 mg of sulphur. Then proceed by one of the following methods.

Methods D and Dox. Warm the crucible gently to melt the alkali, with swirling to mix the melt with the sample. Continue heating until a homogeneous mixture and semi-liquid melt of alkali and organic matter is obtained.

Methods W and Wox. Introduce 0.5-1 ml of water (according to sample size). Wet and mix the sample and the alkali by swirling and gentle heating with a small flame. Continue until a homogeneous mixture is obtained. Evaporate the water by gentle heating and controlled swirling. An alternative to this treatment is to mix the sample with the alkali dissolved in enough water to give a 60-70% solution, and evaporate the water.

Final fusion. Whichever initial treatment was used, continue the heating, with continuous swirling of the melt. For methods Dox and Wox add cautiously, and with quick swirling, small portions of sodium peroxide or sodium nitrate. If necessary, the auxiliary oxidant can be added at the start of the decomposition procedure. Avoid ignition or deflagration of the organic matter, by controlling the heating. If a charred residue is obtained, heat strongly, with swirling, and add oxidant. Continue until a transparent melt is obtained. Let the crucible and contents cool.

An alternative is to use a muffle furnace for the heating, the temperature being raised from 350 to 600° over a period of about 30 min, but the crucible has to be taken out frequently for swirling and inspection.

Dissolve the cooled fusion cake with hot water (up to 50 ml). Transfer the solution to a 250-ml beaker and add 6M hydrochloric acid dropwise with constant stirring to allow the liberated gases to escape. Filter if necessary. Dilute to

about 100 ml and neutralize with 1M hydrochloric acid (Methyl Red indicator) and add 1 ml of acid in excess. Heat to boiling, and to the boiling solution add 10 ml of 5% barium chloride solution slowly and with stirring, then boil for 2–3 min. Keep the beaker covered with a watch-glass and let it cool and stand overnight. Filter off the precipitate on a Whatman No. 42 filter paper, and wash it with water until the washings give no reaction for chloride. Ignite the precipitate with precautions to prevent reduction to barium sulphide,²⁸ and for highest accuracy treat the ignition product with ethanol and sulphuric acid and ignite again to constant weight.²⁹

Acid digestion. Place a known amount of sample (containing around 50 mg of sulphur) in a 100-ml Kjeldahl flask, add 10–15 ml of 1:1 v/v mixture of nitric acid and perchloric acid and stir until the mixture is homogeneous. Heat carefully over several hours until all nitrogen oxides have been expelled, white fumes appear, and the solution is transparent and colourless. Increase the amount of acid mixture and the time or intensity of heating if necessary. Cool, add 10 ml of 6M hydrochloric acid and evaporate almost to dryness. Repeat this treatment with 5-ml portions of concentrated hydrochloric acid (3 or 4 times) until no dense fumes are formed at the end of the evaporation.

Finally precipitate barium sulphate by the procedure described by Hintz and Weber.²⁷

RESULTS AND DISCUSSION

Sulphur mineralization

The mineralization of sulphur in organic compounds by fusion with alkali can be achieved by various procedures, with (method W) or without (method D) addition of water, and with use of auxiliary oxidants (methods Wox and Dox). The presence of water makes it easier to homogenize the alkali-organic matter mixture, and addition of an auxiliary oxidant aids the oxidation of the organic matter. Both additions help in decomposition of substances with low melting point, high volatility, or susceptibility to pyrolysis to yield volatile products which can escape before being attacked by the molten alkali. The proposed method gives quick destruction of the organic matter of the compounds that have

been studied, and easy complete mineralization of the sulphur content.

The compounds tested have various types of sulphur bond (sulpho, thio and epithio groups) and different molecular structures. It has been found that sulphanilic acid responds satisfactorily to all four procedures (D, W, Dox, Wox), whereas thiourea requires use of an auxiliary oxidant from the start of the treatment (methods Dox, Wox). Dithizone can be destroyed by all four methods (D, Dox, W, Wox), but the "dry" methods (D and Dox) produce uncontrolled volatilization during the first phase of the fusion, possibly by pyrolytic decomposition at temperatures lower than that needed for alkaline attack. Methylene Blue is also completely destroyed by all four procedures.

The time required to complete the decomposition depends on the method of heating. With a Bunsen burner, the time required is 10–15 min (depending on the sample and the method used). With a muffle furnace the time required is 30–60 min. It is advisable to keep the heating time as short as possible.

The amount of alkali needed for efficient decomposition is 10–15 times the sample weight. The total amount of auxiliary oxidant should not exceed 0.15 g. The final melt contains the mineralized sulphur in the form of sulphate. The fusion cake is easily soluble, and the solution, after neutralization, is suitable for direct sulphate determination, irrespective of whether a silver or a nickel crucible was used. Silver crucibles are recommended, however, as they are more resistant to alkali, and give less metal contamination of the solution. The efficiency of sulphur mineralization by fusion with alkali has been established by comparison of the results with the theoretical values and those found by the reference method, as shown in Table 1.

CONCLUSIONS

Certain organic sulphur compounds can readily be

Table 1. Determination of sulphur (%) in four organic compounds

Series	Method of destruction of organic matter	Sulphanilic acid (18.47% S)		Thiourea (42.04% S)		Dithizone (12.48% S)		Methylene Blue (10.00% S)	
		\bar{x}	<i>s</i>	\bar{x}	<i>s</i>	\bar{x}	<i>s</i>	\bar{x}	<i>s</i>
I	D	18.42*	0.09	—	—	7.81†	1.29	9.01*	0.09
II	Dox (sodium nitrate)	18.41†	0.13	41.97*	0.11	9.50†	1.07	9.00†	0.09
III	Dox (sodium peroxide)	18.42†	0.14	41.91*	0.10	9.60†	0.98	8.99†	0.08
IV	W	18.42*	0.09	—	—	12.12*	0.09	8.97*	0.08
V	Wox (sodium nitrate)	18.45†	0.09	41.85*	0.10	12.10*	0.08	9.00†	0.09
VI	Wox (sodium peroxide)	18.44†	0.12	41.79*	0.10	12.11*	0.09	9.02†	0.09
VII	Reference acid digestion	18.40*	0.09	41.83*	0.10	12.07*	0.08	8.94*	0.10

*Ten replicates.

†Five replicates.

mineralized by fusion with alkali, without explosion hazard. In some cases an auxiliary oxidant may be needed, and the presence of water in the initial stage may also be beneficial. The method has been tested only with large samples (50–250 mg), however, and is not necessarily applicable on the micro scale. It may also not be applicable to sulphur compounds in general, and should be tested before use for routine analysis of a particular compound.

Acknowledgement—The authors are grateful to Dr. R. A. Chalmers for his comments and review concerning the manuscript.

REFERENCES

1. E. W. McChesney and W. F. Banks, *Anal. Chem.*, 1955, **27**, 987.
2. L. I. Diuguid and N. C. Johnson, *Microchem. J.*, 1967, **12**, 371.
3. A. Wollin, *At. Abs. Newsl.*, 1970, **9**, 43.
4. I. Lemoch, *Ver. Landwirtsch. Chem. Bundesversuchsanst. Linz*, 1975, **10**, 89; *Chem. Abstr.*, 1976, **84**, 40393w.
5. G. D. Tiwari, G. S. Johar and S. R. Trivedi, *Indian J. Appl. Chem.*, 1969, **32**, 191.
6. N. N. Singh, J. V. K. Reddy and K. S. Boparai, *Indian J. Chem.*, 1977, **15B**, 580; *Chem. Abstr.*, 1978, **88**, 31684x.
7. O. Hadžija and Z. Kozarac, *Z. Anal. Chem.*, 1975, **277**, 191.
8. I. Gacs and S. Dombi, *J. Radioanal. Chem.*, 1978, **42**, 375.
9. R. B. Malvankar, S. S. Ramdasi and V. S. Pansare, *Indian J. Chem.*, 1980, **19B**, 722; *Chem. Abstr.*, 1980, **93**, 230324h.
10. W. Schöniger, *Mikrochim. Acta*, 1956, 869.
11. M. Q. Al-Abachi, F. H. Al-Dabbagh and S. T. Sulaiman, *Talanta*, 1980, **27**, 1077.
12. H. Malissa and L. Machherdl, *Mikrochim. Acta*, 1962, 1089.
13. A. D. Campbell, M. J. Brown and D. J. Hannah, *Anal. Chim. Acta*, 1975, **78**, 234.
14. L. Mázor, *Acta Chim. Acad. Sci. Hung.*, 1977, **92**, 105; *Chem. Abstr.*, 1977, **87**, 95064g.
15. M. C. Van Grondelle, P. J. Zeen and R. Van de Craats, *Anal. Chim. Acta*, 1978, **100**, 439.
16. J. W. Frazer and R. K. Stump, *Mikrochim. Acta*, 1968, 1326.
17. M. Wroński, *Talanta*, 1979, **26**, 976.
18. M. A. Chavdari, F. Akhtar and S. P. Shahid, *J. Nat. Sci. Math.*, 1973, **13**, 199; *Chem. Abstr.*, 1976, **85**, 28324n.
19. L. Mázor, *Magy. Kem. Foly.*, 1980, **86**, 153; *Chem. Abstr.*, 1980, **92**, 226168x.
20. A. V. Maklakova and V. D. Osadchii, *Zavodsk. Lab.*, 1975, **41**, 1198; *Chem. Abstr.*, 1976, **84**, 69101k.
21. H. J. M. Bowen, *Anal. Chem.*, 1968, **40**, 969.
22. V. A. Klimova and M. D. Vitalina, *Zh. Analit. Khim.*, 1964, **19**, 1254.
23. R. L. Baker, *Anal. Chem.*, 1972, **44**, 1326.
24. F. Bosch Reig and J. V. Gimeno Adelantado, *Talanta*, 1983, **30**, 437.
25. J. V. Gimeno Adelantado, F. Bosch Reig, A. Pastor García and V. Peris Martínez, *ibid.*, 1983, **30**, 974.
26. L. W. Winkler, *Z. Angew. Chem.*, 1917, **30**, 251; 1920, **33**, 162; L. Erdey, *Gravimetric Analysis*, Part III, p. 86. Pergamon Press, London, 1965.
27. E. Hintz and H. Weber, *Z. Anal. Chem.*, 1906, **45**, 43; L. Erdey, *Gravimetric Analysis*, Part III, p. 84. Pergamon Press, London, 1965.
28. I. M. Kolthoff and E. B. Sandell, *Textbook of Quantitative Inorganic Analysis*, 3rd Ed., p. 333. Macmillan, New York, 1952.
29. A. C. Cumming and S. A. Kay, *Quantitative Chemical Analysis*, 11th Ed., p. 262. Oliver and Boyd, Edinburgh, 1956.

DETERMINATION OF OPTICAL PURITY IN PARTIALLY RACEMIZED SAMPLES OF L-ASPARTIC ACID BY MEANS OF LIQUID CRYSTALS

GIOVANNA BERTOCCHI*

Istituto di Chimica Organica, Università di Bologna, Viale Risorgimento 4, 40136 Bologna, Italy

(Received 4 February 1986. Accepted 25 April 1986)

Summary—A method for the determination of the optical purity of partially racemized samples of L-aspartic acid, based on the measurement of the pitch and handedness of cholesteric mesophases induced in MBBA (*p*-methoxybenzylidene-*p*'-*n*-butylaniline), is described. The minimum quantity of aspartic acid required varies with the optical purity of the sample (from 50 μ g for an enantiomeric purity of 10–20% down to 5 μ g for purities around 90%).

The measurement of the twisting power (β) of an optically active substance in a nematic liquid crystal is an alternative to the classical measurement of optical rotatory power as a way of characterizing the chirality.^{1,2}

One advantage of this technique is the small quantity of substance needed for measurements. Applications of the method to the determination of substances of biological interest in chromatographic fractions have already been described.^{3,4} One of the methods commonly employed for dating samples of archaeological and biological interest, "amino-acid dating,"⁵ consists in measuring the racemization percentage of the natural L-aspartic acid by means of an amino-acid analyser.

The liquid-crystal technique^{3,4} could also be used to solve such analytical problems without recourse to highly sophisticated pieces of apparatus.

In the present note, the method is applied to the determination of the optical purity of partially racemized samples of L-aspartic acid.

EXPERIMENTAL

(With the assistance of Dr. Romano Prati,
Institute of Organic Chemistry, University of Bologna)

Since aspartic acid is not soluble in the nematic solvents investigated, the dimethyl ester of its benzoylamide (DMEBA) was utilized instead, since it is fairly soluble in those liquid crystals. This derivative was synthesized from samples of *ca.* 10 mg of aspartic acid. A similar quantity is usually employed for the formation of the diastereoisomeric L-leucyl-L-aspartic and L-leucyl-D-aspartic acids which are traditionally utilized in the type of analysis involving the amino-acid analyser. The dimethyl ester⁶ was obtained directly from the *N*-benzoyl derivative⁷ without isolation and purification of the amide.

The method of preparation is as follows. To 10.25 mg (7.7×10^{-5} mole) of L-aspartic acid are added 0.05 ml of 2*M* sodium hydroxide. The mixture is cooled in an ice-bath, and 11.55 mg (8.47×10^{-5} mole) of benzoyl chloride and 0.05 ml of 2*M* sodium hydroxide are added with stirring. The solution is kept alkaline by adding more sodium hydroxide if necessary. The reaction mixture is stirred for 15 min at room temperature and then cooled in an ice-bath and acidified (Congo Red indicator) by adding concentrated hydrochloric acid dropwise. The precipitate is washed two or three times with cold water and air-dried for at least a day. The product is dissolved in 2 ml of anhydrous tetrahydrofuran in an ice-bath, then an ethereal solution of diazomethane is added dropwise until its yellow colour persists (the excess of diazomethane is destroyed by the addition of 1 or 2 drops of glacial acetic acid). The reaction mixture is then left in an ice-bath for 2 hr and finally evaporated to dryness.

The product is purified by TLC on silica gel with anhydrous petroleum ether–ethyl acetate mixture (70:30 v/v). The purity is checked by infrared and NMR spectroscopy.

The conversion of L-aspartic acid into the *N*-benzoyl-aspartic diester does not give rise to appreciable racemization. Measurement of the rotatory power before the conversion, and after acid hydrolysis of the product gives practically identical values: $[\alpha]_D^{20} = +25.0^\circ$ ($c = 1.97\%$ in 6*M* hydrochloric acid).⁸ The dimethyl ester of the benzoylamide of D,L-aspartic acid was prepared in the same way.

Pitch values were determined by means of the Grandjean–Cano method based on the observation of discontinuity lines appearing whenever a cholesteric mesophase is inverted in a cell of variable width.^{9–11} A drop of the cholesteric solution (*ca.* 2.5 mg) was placed between a glass plate and a plano-convex lens. The substance was then observed under polarized light in the microscope. Concentric circles corresponding to the Grandjean–Cano discontinuity lines and coloured streamers corresponding to the variation of rotatory power with width were observed.¹²

The pitch value is given by the relation¹¹

$$\frac{r_d^2}{R} = (n - \frac{1}{2})|p| \quad (n = 1, 2, 3 \dots)$$

where R is the radius of curvature of the lens, r_d the radius of the discontinuity circle, and p the pitch (μ m). Measurements were taken with a Zeiss polarized-light microscope and plano-convex lenses of radii from 20 to 40 mm, at a

*Present address: Istituto di Chimica Farmaceutica e Tossicologica, Università di Bologna, via Belmeloro 6, 40126 Bologna, Italy.

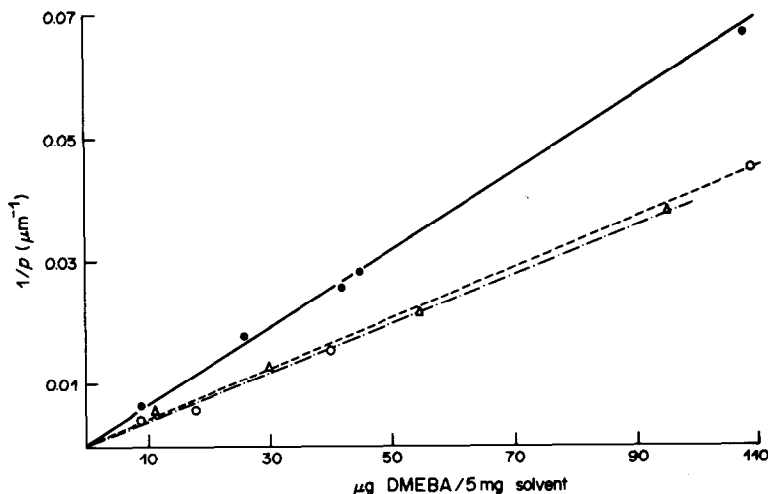


Fig. 1. $1/p$ (μm^{-1}) vs. DMEBA concentration in MBBA (●); Phase IV (○); Nematic Phase 1052 (△).

temperature in the range 18–20°. The twisting power (β , μm^{-1}) of the chiral substance was obtained from the relation^{1,2}

$$\beta_M = 1/pcr$$

where c is the mole fraction and r the enantiomeric purity ($([L] - [D])/([L] + [D])$) of the chiral substance. The nematic solvents were MBBA (*p*-methoxybenzylidene-*p*'-n-butylaniline), Phase IV (a mixture of azoxy compounds) and Nematic Phase 1052 (binary eutectic of aromatic esters).

L-Aspartic acid and D,L-aspartic acid were supplied by Fluka, MBBA by Riedel de Haen, and Phase IV and Nematic Phase 1052 by Merck.

The highest value of β was obtained by use of MBBA. Calibration curves of measured pitch values as a function of the quantity of optically pure DMEBA were drawn. For MBBA the curve of $1/p$ vs. the enantiomeric purity of mixtures of known composition was also drawn.

The total quantity of aspartic esters can be determined with good sensitivity by means of the ultraviolet spectrum (λ_{max} 225 nm, $\epsilon = 1.08 \times 10^4 \text{ l. mole}^{-1} \cdot \text{cm}^{-1}$, ethanol solution).

The solutions used for calibration were obtained from a standard solution of DMEBA in chloroform. Before addition of the liquid crystal, the sample had to be completely freed from chloroform. After addition of the nematic solvent, the solution was mechanically stirred and heated until clear, to allow homogeneous mixing of the solute in the solvent.

The cholesteric handedness was determined from the sign of the rotatory power.³

RESULTS AND DISCUSSION

The twisting power β is positive in all three nematic solvents employed and the average value of β in MBBA is $+3.26 \pm 0.2 \mu\text{m}^{-1}$.

In Fig. 1, $1/p$ is plotted as a function of the concentration of chiral substance, expressed as μg of DMEBA/5 mg of solvent (5 mg of cholesteric mesophase is more than sufficient for two measurements).

The calibration graph is linear in MBBA over a concentration interval ranging from 9 to 100 $\mu\text{g}/5 \text{ mg}$ of solvent. The lower limit represents the lowest concentration value for which a reproducible value of the pitch can be obtained.

Figure 2 shows the variation of $1/p$ with enantiomeric purity, for concentrations from 10 to 40 μg of DMEBA/5 mg of MBBA.

The value of β was found to be practically constant and independent of the enantiomeric purity for concentrations of DMEBA ranging from 10 to 40 $\mu\text{g}/5 \text{ mg}$ of MBBA.

The minimum quantity of aspartic ester required varies with optical purity, from a lowest value of 5 μg to a highest value of 50 μg for an enantiomeric purity around 10–20% (this is the limit of the method⁵ because of racemization during hydrolysis of archaeological samples).

The determination of the optical purity in partially racemized samples of L-aspartic acid by means of the liquid crystal method is thus relatively simple and reproducible and does not require sophisticated apparatus.

The sensitivity is comparable to that afforded by traditional techniques (such as the use of automatic amino-acid analysers).¹⁴

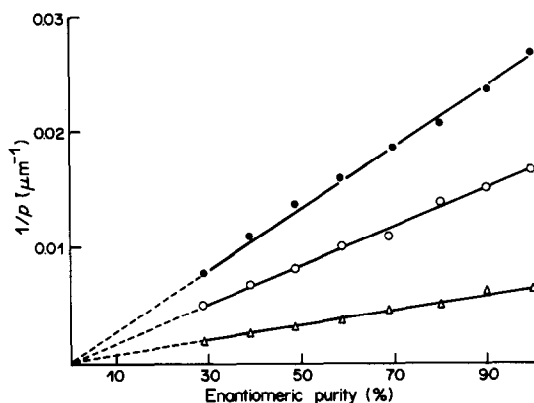


Fig. 2. $1/p$ (μm^{-1}) vs. enantiomeric purity, $([L] - [D])/([L] + [D])$: 10 μg of DMEBA/5 mg of MBBA (△); 25 μg of DMEBA/5 mg of MBBA (○); 40 μg of DMEBA/5 mg of MBBA (●).

Acknowledgements—The author thanks Professors Laura Garuti, Giovanni Gottarelli and Gaetano Maccagnani for discussions.

This work was carried out with the support of C.N.R. (Progetto Finalizzato "Chimica Fine e Secondaria").

REFERENCES

1. E. H. Korte and B. Schrader, in *Advances in Infrared and Raman Spectroscopy*, R. J. H. Clark and R. E. Hester (eds.), Vol. 8, pp. 226–282. Heyden, London, 1981.
2. G. Gottarelli and G. P. Spada, *Mol. Cryst. Liq. Cryst.*, 1985, **123**, 377.
3. G. Bertocchi, G. Gottarelli and R. Prati, *Talanta*, 1984, **31**, 138.
4. G. Bertocchi and R. Prati, *Riv. Ital. Med. Leg.*, 1984, **6**, 108.
5. P. S. Zurer, *Chem. Eng. News*, 1983, **61**, No. 8, 26.
6. H. Pauly and J. Weir, *Chem. Ber.*, 1910, **43**, 661.
7. *Chemistry of the Amino Acids*, J. P. Greenstein and M. Wintz (eds.), Vol. 2, p. 1267. Wiley, New York, 1961.
8. *Merck Index*, 9th Ed., Merck, Rahway, N.Y., 1976.
9. F. Grandjean, *Compt. Rend.*, 1921, **172**, 71.
10. R. Cano, *Bull. Soc. Fr. Miner. Crystallog.*, 1968, **91**, 30.
11. G. Heppke and F. Oestreicher, *Z. Naturforsch.*, 1977, **32A**, 899.
12. J. P. Berthault, J. Billard and J. Jacques, *Compt. Rend.*, 1977, **284C**, 155.
13. F. J. Kahn, *Appl. Phys. Lett.*, 1973, **22**, 8.
14. G. Belluomini and P. Bachin, *Geol. Rom.*, 1980, **19**, 171.

ANALYTICAL DATA

FORMATION AND STABILITY OF ZINC(II) AND CADMIUM(II) CITRATE COMPLEXES IN AQUEOUS SOLUTION AT VARIOUS TEMPERATURES

SANTI CAPONE, ALESSANDRO DE ROBERTIS, CONCETTA DE STEFANO
and SILVIO SAMMARTANO

Istituto di Chimica Analitica dell'Università, via dei Verdi, 98100 Messina, Italy

(Received 16 December 1985. Revised 19 February 1986. Accepted 30 April 1986)

Summary—The citrate complexes of Zn^{2+} and Cd^{2+} have been investigated by pH titration at $I = 0.1M$ (KNO_3) and 10, 25, 35 and 45° . The species found were $[Zn(cit)]^-$, $[Zn(cit)H]$, $[Zn(cit)_2]^{4-}$ and $[Zn_2(cit)_2H_{-2}]^{4-}$, $[Cd(cit)]^-$, $[Cd(cit)H]$, $[Cd(cit)_2]^{4-}$ and $[Cd(cit)H_{-1}]^{2-}$. From the dependence of the formation constants on temperature, ΔH° and ΔS° values were calculated. Speciation in the Zn^{2+} - and Cd^{2+} -citrate systems is discussed with particular attention to formation of polynuclear species. Some comparisons with literature data are made.

Metal(II) citrate complexes are of great interest as models for elucidating the complexation behaviour of natural O-donor ligands (such as humic acids), in the study of polynuclear complex formation, the study of mixed-metal complex-formation and in study of speciation in natural fluids. Although the formation of these complexes has been extensively studied,¹ some problems remain unsolved. In particular, the number and type of species reported by various authors are often in complete disagreement, the studies have been made at a single temperature, and no calorimetric investigations have been reported, so ΔH° and ΔS° for the various species formed are not known, and insufficiently rigorous calculation methods have often been used.

Since we and others are interested in complex formation by citrate²⁻¹³ (binary, mixed-ligand and mixed-metal complexes), it seemed important to start a systematic study on the thermodynamic properties of citrate complexes by using the temperature-dependence of their formation constants and/or by calorimetric measurements. These studies must be accompanied, of course, by rigorous experimental, calculation and statistical methods.

Here, we report a potentiometric study of the Zn^{2+} - and Cd^{2+} -citrate complexes in aqueous solution, with use of the glass pH electrode, at $I = 0.1M$ (KNO_3) and temperatures of 10, 25, 35 and 45° .

EXPERIMENTAL

Materials

The solutions of Zn(II) and Cd(II) nitrates were prepared from analytical reagents (Fluka) and standardized with EDTA.¹⁴ Citric acid (Erba), reagent grade, was used without further purification; its purity, by alkalimetric titration, was >99.7%. Potassium nitrate (Fluka) was recrystallized from ethanol. Potassium hydroxide and nitric acid solutions were prepared from Erba ampoules of concentrates and stan-

dardized against potassium hydrogen phthalate and sodium carbonate, respectively. All solutions were prepared with doubly distilled water, in grade A glassware.

Apparatus

Potentiometric readings were made of the free hydrogen-ion concentration (c_H) by using, randomly, either a Metrohm E 600 potentiometer or a semi-automatic homemade potentiometer (Analog Devices millivoltmeter, Pritel printer and Mostek logic circuits). The two potentiometric systems were connected to Metrohm glass and saturated calomel electrodes. The reproducibility of pH measurement was ± 0.005 . The titrant was delivered by an Amel 882 dispenser, readable to $1 \mu l$. The measurement-cell (50 ml) was kept at a temperature constant within $\pm 0.2^\circ$ and a magnetic stirrer was used. Purified nitrogen was bubbled through the solutions during titrations.

Procedure

The test solution (25 ml) was titrated with $0.1M$ CO_2 -free potassium hydroxide. The electrodes were calibrated, in both the acidic and alkaline regions, by titrating $0.01M$ nitric acid with standard potassium hydroxide under the same experimental conditions. The solutions titrated were as follows: $C_{cit} = 3-10 \times 10^{-3}M$; $C_{Cd, Zn} = 2-5 \times 10^{-3}M$; $C_K = 75-95 \times 10^{-3}M$; $1.2 \leq C_{cit}/C_{Cd, Zn} \leq 3.3$; pH (max) = 8.3-8.8. For each system at each temperature six titrations (~ 35 data points) were done.

Calculations

For the calculations, the non-linear least-squares computer programs ACBA¹⁵ and/or ESAB¹⁶ were used to refine the protonation constants and the ion-product of water, and MINQUAD 76A¹⁷ and SUPERQUAD¹⁸ for the refinement of formation constants. Formation constants are expressed as β_{ppr} according to the equation



where cit^{3-} is the citrate anion.

Negative values of r (for example in the $[Zn_2(cit)_2H_{-2}]^{4-}$ species, see Results and Discussion) indicate both the coordination of an OH^- group and/or the displacement of the proton of the OH^- group of citrate. Since in this work we do not discuss the structure of the complexes, the general notation above (that used in the computer programs) is adopted.

RESULTS AND DISCUSSION

Protonation constants and reference state

The protonation constants of citrate are reported in Table 1, together with the ΔH° and ΔS° values. The agreement with previous findings^{9,11} is satisfactory. It is known that citrate forms weak complexes with alkali-metal ions, so there are two possible methods for investigation of protonation and metal complexes: (i) to use conditional thermodynamic parameters without making allowance for alkali-metal complexes (*i.e.*, in our case, to choose as reference state a 0.1M solution of potassium nitrate); (ii) to take into account in the calculation the formation of the weak alkali-metal complexes (*i.e.*, to choose pure water as reference state). In this work we used the first method. However, it is possible to convert the protonation and metal complex-formation constants as reported previously.¹¹ Moreover, constants at different ionic strengths can be obtained from a general equation for the dependence of formation constants on ionic strength.^{11,19}

Table 1. Thermodynamic parameters for the protonation of citrate at $I = 0.1M$ (KNO_3)*

$T, ^\circ C$		$[(cit)H]^{2-}$	$[(cit)H_2]^-$	$[(cit)H_3]$
10	$\log \beta$	5.73 (3)†	10.17 (4)†	13.15 (4)†
25	$\log \beta$	5.69 (2)	10.03 (2)	12.95 (3)
	$-\Delta G^\circ$	32.5 (1)	57.3 (2)	73.9 (2)
	ΔH°	3 (1)	-2 (1)	-6 (2)
	ΔS°	118 (4)	187 (4)	226 (6)
35	$\log \beta$	5.73 (2)	10.08 (3)	12.97 (4)
45	$\log \beta$	5.83 (3)	10.23 (4)	13.12 (4)

* ΔG° and ΔH° in kJ/mole; ΔS° in J. mole⁻¹.deg⁻¹.

†The figure in brackets is three times the standard deviation and refers to the last digit in the value preceding it.

Zinc(II)-citrate complexes

The species we found are $[Zn(cit)]^-$, $[Zn(cit)H]$, $[Zn(cit)_2]^{4-}$ and $[Zn_2(cit)_2H_{-2}]^{4-}$. These four species are sufficient, on a statistical basis^{17,18,20,21} to fit the experimental data. Many other species, $[Zn(cit)H_2]^+$, $[Zn(cit)_2H]^{3-}$, $[Zn(cit)_2H_2]^{2-}$, $[Zn(cit)_2H_{-1}]^{5-}$ and $[Zn(cit)H_{-1}]^{2-}$ were considered in the calculations, but were rejected in the iterative procedure or gave a negligible improvement in the sum of squares of residuals; to check the significance of the various models, the Hamilton R -test and analysis of variance were used.^{20,21} Calculations with MINQUAD 76A¹⁷ and SUPERQUAD¹⁸ gave the same results. Table 2 lists the formation constants obtained at different temperatures, together with the ΔH° and ΔS° values calculated from the temperature dependence of $\log \beta_{pp}$. Table 3 compares the literature data for this system. The agreement between the literature values and ours is fairly good for species formed in the acidic-neutral range, but for $pH > 7-8$ there is significant disagreement. Some workers have found only the species $[Zn(cit)H_{-1}]^{2-}$ in alkaline solutions.^{23,24} The reported values for the formation constants correspond to a degree of complexation of citrate similar to that calculated from the stability constants for binuclear species (this work and ref. 5). We tested models that included the mononuclear species $[Zn(cit)H_{-1}]^{2-}$ in several calculations for all titration curves and temperatures, but this species was always rejected in favour of the binuclear one. Figure 1 shows the distribution of species in the Zn^{2+} -citrate system.

Cadmium(II)-citrate complexes

The species we found are $[Cd(cit)]^-$, $[Cd(cit)H]$, $[Cd(cit)_2]^{4-}$ and $[Cd(cit)H_{-1}]^{2-}$. Again, many

Table 2. Thermodynamic parameters for the formation of Zn^{2+} -citrate complexes at 25° and $I = 0.1M$ (KNO_3)*

$T, ^\circ C$		$[Zn(cit)]^-$	$[Zn(cit)H]$	$[Zn(cit)_2]^{4-}$	$[Zn_2(cit)_2H_{-2}]^{4-}$
10	$\log \beta$	4.99 (3)†	8.73 (5)†	6.85 (18)†	-3.18 (13)†
25	$\log \beta$	5.02 (3)	8.71 (4)	6.76 (12)	-2.85 (8)
	$-\Delta G^\circ$	28.7 (2)	49.7 (3)	38.6 (7)	-16.3 (5)
	ΔH°	8 (2)	1 (3)	27 (8)	62 (5)
	ΔS°	123 (7)	170 (11)	220 (30)	153 (18)
35	$\log \beta$	5.03 (3)	8.64 (4)	7.13 (9)	-2.44 (7)
45	$\log \beta$	5.23 (3)	8.83 (5)	7.60 (10)	-1.70 (11)

* ΔG° and ΔH° in kJ/mole; ΔS° in J. mole⁻¹.deg⁻¹.

†The figure in brackets is three times the standard deviation and refers to the corresponding final digit(s) in the value preceding it.

Table 3. Literature data for the Zn(II)-citrate system

I, M	$T, ^\circ C$	$\log \beta_{110}$	$\log \beta_{111}$	$\log \beta_{22-2}$	$\log \beta_{11-1}$	$\log \beta_{112}$	$\log \beta_{120}$	Method	Ref.
0.1	25	4.83	8.43	-2.94				pH	5
0.15	25	4.85	8.58					pH	22
0.04-0.4	25				-3.3			polarog.	23
var	23				-2.8			Zn-elec.	24
0.1	20	4.98	8.66			11.28		pH	25
0.5	25	4.27	7.75				5.90	pH	26
0.15	37	5.37			-0.2			pH	27
0.12	25	4.87-4.93	(pH = 3-5)					pH	28

Table 4. Thermodynamic parameters for the formation of Cd^{2+} -citrate complexes at 25° and $I = 0.1M$ (KNO_3)^{*}

$T, ^\circ\text{C}$		$[\text{Cd}(\text{cit})]^-$	$[\text{Cd}(\text{cit})\text{H}]$	$[\text{Cd}(\text{cit})_2]^{4-}$	$[\text{Cd}(\text{cit})\text{H}_{-1}]^{2-}$	$[\text{Cd}_2(\text{cit})_2\text{H}_{-2}]^{4-}$
10	$\log \beta$	3.78 (3)	8.02 (5)	5.79 (12)	-3.98 (7)	—
		3.77 (3)	8.02 (5)	5.81 (11)	-4.19 (8)	-5.86 (10)
25	$\log \beta$	3.71 (3)	7.85 (5)	5.3 (2)	-3.99 (6)	—
		3.71 (3)	7.86 (5)	5.4 (2)	-4.23 (7)	-5.40 (8)
	$-\Delta G^\circ$	21.2 (2)	44.8 (3)	30 (1)	-22.8 (4)	—
		21.2 (2)	44.9 (3)	31 (1)	-24.1 (4)	-30.8 (5)
	ΔH°	8 (2)	1 (3)	20 (10)	18 (4)	—
		8 (2)	2 (3)	1 (15)	9 (5)	53 (5)
	ΔS°	98 (7)	154 (11)	168 (40)	-16 (14)	—
		98 (7)	157 (11)	107 (40)	-51 (18)	74 (19)
35	$\log \beta$	3.85 (4)	7.94 (6)	5.7 (2)	-3.71 (6)	—
		3.82 (5)	7.94 (6)	5.67 (15)	-4.21 (7)	-5.15 (9)
45	$\log \beta$	4.03 (4)	8.19 (6)	5.97 (15)	-3.54 (6)	—
		4.03 (4)	8.20 (6)	6.09 (12)	-3.83 (6)	-4.71 (10)

^{*}See footnotes to Table 2. The first row of values for each parameter is for model (A), the second for model (C); see text.

models were tested, and in this case, there is some doubt about selection of the correct model. The three models: (A) $[\text{Cd}(\text{cit})]^-$, $[\text{Cd}(\text{cit})\text{H}]$, $[\text{Cd}(\text{cit})_2]^{4-}$ and $[\text{Cd}(\text{cit})\text{H}_{-1}]^{2-}$; (B) $[\text{Cd}(\text{cit})]^-$, $[\text{Cd}(\text{cit})\text{H}]$,

$[\text{Cd}(\text{cit})_2]^{4-}$ and $[\text{Cd}_2(\text{cit})_2\text{H}_{-2}]^{4-}$; (C) $[\text{Cd}(\text{cit})]^-$, $[\text{Cd}(\text{cit})\text{H}]$, $[\text{Cd}(\text{cit})_2]^{4-}$, $[\text{Cd}(\text{cit})\text{H}_{-1}]^{2-}$ and $[\text{Cd}_2(\text{cit})_2\text{H}_{-2}]^{4-}$, give a similar fit to the experimental data. Of (A) and (B), (A) gives the best fit and model

Table 5. Literature data for the Cd(II)-citrate system

I, M	$T, ^\circ\text{C}$	$\log \beta_{110}$	$\log \beta_{111}$	$\log \beta_{11-1}$	$\log \beta_{112}$	Method	Ref.
0.1	25	3.65	7.80	-3.81		pH	5
0.15	25	3.98	7.90			pH	22
0.1	20	3.75	7.88		11.00	pH	25
0.04-0.4	25	4.20		-4.5		polarog.	23

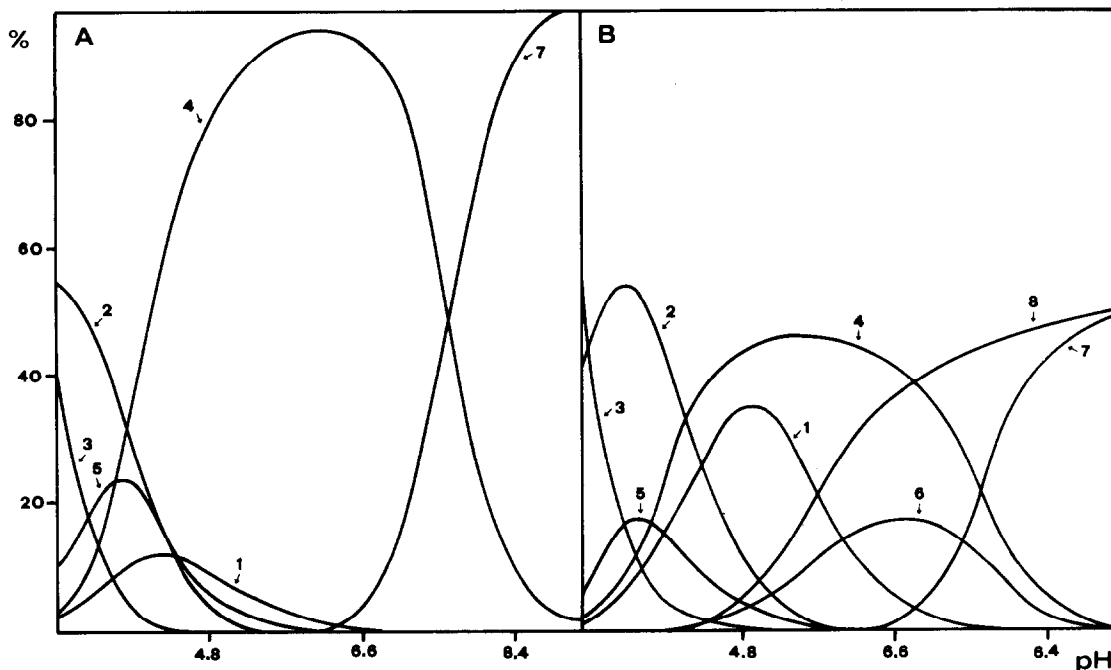


Fig. 1. Species distribution for Zn^{2+} -citrate. A: $C_{\text{Zn}} = 5 \text{ mM}$, $C_{\text{cit}} = 5 \text{ mM}$. B: $C_{\text{Zn}} = 5 \text{ mM}$, $C_{\text{cit}} = 10 \text{ mM}$. Curve 1: $[\text{H}(\text{cit})]^{2-}$; curve 2: $[\text{H}_2(\text{cit})]^-$; curve 3: $[\text{H}_3(\text{cit})]$; curve 4: $[\text{Zn}(\text{cit})]^-$; curve 5: $[\text{Zn}(\text{cit})\text{H}]$; curve 6: $[\text{Zn}(\text{cit})_2]^{4-}$; curve 7: $[\text{Zn}_2(\text{cit})_2\text{H}_{-2}]^{4-}$; curve 8: free cit^{3-} . The percentages are calculated with respect to Zn^{2+} .

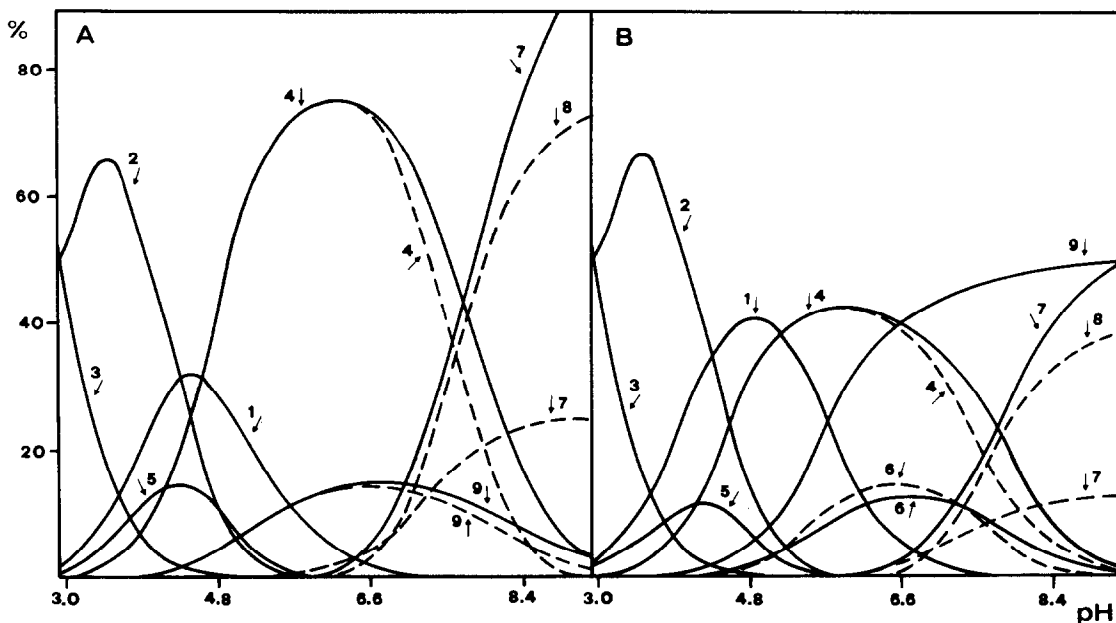


Fig. 2. Species distribution for Cd^{2+} -citrate. A: $C_{\text{Cd}} = 5 \text{ mM}$, $C_{\text{cit}} = 5 \text{ mM}$. B: $C_{\text{Cd}} = 5 \text{ mM}$, $C_{\text{cit}} = 10 \text{ mM}$. Curve 1: $[\text{H}(\text{cit})]^{2-}$; curve 2: $[\text{H}_2(\text{cit})]^-$; curve 3: $[\text{H}_3(\text{cit})]$; curve 4: $[\text{Cd}(\text{cit})]^-$; curve 5: $[\text{Cd}(\text{cit})\text{H}]$; curve 6: $[\text{Cd}(\text{cit})_2]^{4-}$; curve 7: $[\text{Cd}(\text{cit})\text{H}_{-1}]^{2-}$; curve 8: $[\text{Cd}_2(\text{cit})_2\text{H}_{-2}]^{4-}$; curve 9: free cit^{3-} . Full lines: model (A), dashed lines: model (C) (see text). The percentages are calculated with respect to Cd^{2+} .

(C) gives only rather insignificant improvement, so we prefer the four-species model (A).^{*} Table 4 lists the formation constants obtained at different temperatures, together with the ΔH° and ΔS° values calculated from the temperature-dependence of $\log \beta_{\text{pqr}}$. In the same table are reported, for comparison, the thermodynamic parameters calculated from model (C).

Table 5 gives the literature data for this system. It appears that, for the Cd^{2+} -citrate system, there is general agreement both on the species formed and on the values of the formation constants. Two other extensive studies on this system should be mentioned. Grenthe *et al.*²⁹ [25° , $I = 2 \text{ M}$ (NaClO_4), glass and cadmium amalgam electrodes] and Bottari³⁰ (same conditions as used by Grenthe *et al.*) found several minor species, but the experimental conditions were very different from ours. Figure 2 shows the distribution of species for the Cd^{2+} -citrate system.

General comments on the Zn^{2+} - and Cd^{2+} -citrate systems

Citrate is, among low molecular-weight ligands, quite a complicated reagent. The species formed depend strongly on the absolute concentrations of the

components and on the metal/ligand ratio. In the acidic-neutral pH range, the species $[\text{M}(\text{cit})]^-$, $[\text{M}(\text{cit})\text{H}]$ and $[\text{M}(\text{cit})_2]^{4-}$ predominate. When $C_{\text{M}}/C_{\text{L}} \approx 1$ the species $[\text{M}(\text{cit})_2]^{4-}$ is negligible (see Figs. 1 and 2), and when $C_{\text{M}}/C_{\text{L}} < 1$ and $C_{\text{L}} > 0.01 \text{ M}$ ($\text{pH} < 4$) the species $[\text{M}(\text{cit})\text{H}_2]^+$ and $[\text{M}(\text{cit})_2\text{H}]^{3-}$ become significant.^{25,29,30} Binuclear species seem to be absent at acidic-neutral pH values. In alkali the species $[\text{M}(\text{cit})\text{H}_{-1}]^{2-}$ and/or $[\text{M}_2(\text{cit})_2\text{H}_{-2}]^{4-}$ are present, and the species $[\text{Cd}_2(\text{cit})\text{H}_{-1}]$ and $[\text{Cd}_2(\text{cit})_2\text{H}_{-1}]^{3-}$ have also been proposed.^{29†} In our opinion, all these species may form under particular conditions, and the main species (*i.e.*, $[\text{M}(\text{cit})\text{H}_{-1}]^{2-}$ and/or $[\text{M}_2(\text{cit})_2\text{H}_{-2}]^{4-}$) have, for the various transition-metal ions, differing tendencies to form mono- or binuclear complexes.

No values for ΔH° and ΔS° for the metal complexes have been reported previously. The thermodynamic parameters for the protonation are in agreement with our previous findings.^{8,11}

Acknowledgements—We wish to thank C.N.R. and the Ministero della Pubblica Istruzione for financial support.

REFERENCES

1. L. G. Sillén and A. E. Martell, *Stability Constants of Metal Ion Complexes*. Spec. Publns. Nos. 17 and 25. The Chemical Society, London, 1964, 1971; D. D. Perrin, *Stability Constants of Metal Ion Complexes; Organic Ligands*, Pergamon Press, Oxford, 1979; A. E. Martell and R. M. Smith, *Critical Stability Constants*, Vol. 3 and 5, Plenum Press, New York, 1977, 1982.
2. P. G. Daniele, G. Ostacoli and A. Vanni, *Ann. Chim. (Rome)*, 1975, **65**, 465.

^{*}The ratios of the sum of squares of residuals (SUPERQUAD, 25°) are: $U(A)/U(B) = 0.95$ and $U(A)/U(C) = 1.10$. These differences are not statistically significant²⁰ and, therefore, it is best to choose the simpler four-species model with the smaller sum of squares, *i.e.*, model (A).

[†]Similar species were found for the Cu^{2+} -citrate system.^{2,11}

3. *Idem, ibid.*, 1976, **66**, 305.
4. P. G. Daniele and G. Ostacoli, *ibid.*, 1976, **66**, 537.
5. *Idem, ibid.*, 1977, **67**, 37; 1979, **69**, 61.
6. P. Amico, P. G. Daniele, V. Cucinotta, E. Rizzarelli and S. Sammartano, *Inorg. Chim. Acta*, 1979, **36**, 1.
7. P. Amico, P. G. Daniele, G. Ostacoli, G. Arena, E. Rizzarelli and S. Sammartano, *ibid.*, 1980, **44**, L219.
8. G. Arena, R. Cali, M. Grasso, S. Musumeci, S. Sammartano and C. Rigano, *Thermochim. Acta*, 1980, **36**, 329.
9. P. G. Daniele, C. Rigano and S. Sammartano, *Ann. Chim. (Rome)*, 1980, **70**, 119.
10. V. Cucinotta, P. G. Daniele, C. Rigano and S. Sammartano, *Inorg. Chim. Acta*, 1981, **56**, L45.
11. P. G. Daniele, G. Ostacoli, C. Rigano and S. Sammartano, *Transition Met. Chem.*, 1984, **9**, 385; P. G. Daniele, C. Rigano and S. Sammartano, *Talanta*, 1983, **30**, 81; 1985, **32**, 78; S. Capone, A. De Robertis, C. De Stefano, S. Sammartano and R. Scarcella, *Thermochim. Acta*, 1985, **86**, 273.
12. P. Amico, P. G. Daniele, G. Ostacoli, G. Arena, E. Rizzarelli and S. Sammartano, *Transition Met. Chem.*, 1985, **10**, 11.
13. P. Amico, G. Arena, P. G. Daniele, G. Ostacoli, E. Rizzarelli and S. Sammartano, *Mixed Metal Complexes of Biofunctional Ligands: Formation, Stability and Possible Role in Model Systems with Metal Ion Overloads*, in *Environmental Inorganic Chemistry*, K. J. Irgolic and A. E. Martell (eds.), VCH Publ., Deerfield Beech, Florida, 1985.
14. H. A. Flaschka, *EDTA Titrations*, Pergamon Press, London, 1959.
15. G. Arena, E. Rizzarelli, S. Sammartano and C. Rigano, *Talanta*, 1979, **26**, 1.
16. C. Rigano, M. Grasso and S. Sammartano, *Ann. Chim. (Rome)*, 1984, **74**, 537.
17. A. Sabatini, A. Vacca and P. Gans, *Talanta*, 1974, **21**, 53; P. Gans, A. Sabatini and A. Vacca, *Inorg. Chim. Acta*, 1976, **18**, 237; A. Vacca, personal communication, 1977.
18. P. Gans, A. Sabatini and A. Vacca, *J. Chem. Soc. Dalton Trans.*, 1985, 1195.
19. P. G. Daniele, A. De Robertis, C. De Stefano, C. Rigano and S. Sammartano, *J. Chem. Soc. Dalton Trans.*, 1985, 2356; P. G. Daniele, C. Rigano and S. Sammartano, *Anal. Chem.*, 1985, **57**, 2956.
20. W. C. Hamilton, *Statistics in Physical Sciences*, Ronald, New York, 1964; J. Mandel, *The Statistical Analysis of Experimental Data*, Wiley, New York, 1964.
21. A. Vacca, A. Sabatini and M. A. Gristina, *Coord. Chem. Rev.*, 1972, **8**, 45.
22. N. C. Li, A. Lindenbaum and M. J. White, *J. Inorg. Nucl. Chem.*, 1959, **12**, 122.
23. L. Meites, *J. Am. Chem. Soc.*, 1950, **72**, 180; 1951, **73**, 3727.
24. K. N. Kovalenko and L. I. Vistyak, *Russ. J. Inorg. Chem.*, 1959, **4**, 364.
25. E. Campi, G. Ostacoli, M. Meirone and G. Saini, *J. Inorg. Nucl. Chem.*, 1964, **26**, 553.
26. C. Furlani and E. Cervone, *Ann. Chim. (Rome)*, 1962, **52**, 564.
27. J. T. H. Roos and D. R. Williams, *J. Inorg. Nucl. Chem.*, 1977, **39**, 367.
28. K. S. Rajan, S. Mainer and J. M. Davis, *ibid.*, 1978, **40**, 2089.
29. I. Grenthe, P. Wikberg and E. R. Still, *Inorg. Chim. Acta*, 1984, **91**, 25.
30. E. Bottari, *Ann. Chim. (Rome)*, 1975, **65**, 593.

STABILITY CONSTANTS AND MOLAR ABSORPTIVITIES FOR COMPLEXES OF COPPER(II) WITH *N*-METHYLDIETHANOLAMINE, 1,4-BIS(2-HYDROXYPROPYL)-2-METHYLPIPERAZINE, AND 2-AMINO-2-METHYL-1-PROPANOL

JOSEPH R. SIEFKER and RODOLFO V. AROC

Department of Chemistry, Indiana State University, Terre Haute, IN 47809, U.S.A.

(Received 31 March 1986. Accepted 29 April 1986)

Summary—The stability constants and molar absorptivities of complexes of Cu^{2+} with *N*-methyl-diethanolamine, 1,4-bis(2-hydroxypropyl)-2-methylpiperazine, and 2-amino-2-methyl-1-propanol have been determined from spectrophotometric data for very dilute aqueous solutions.

Douheret¹ used potentiometric and polarographic methods to determine equilibrium constants for complexes of Cu^{2+} with some *N*-substituted ethanolamines. We have used spectrophotometric data to determine the stepwise stability constants and the molar absorptivities for the Cu^{2+} complexes of the ligands (L) *N*-methyl-diethanolamine (I), 1,4-bis(2-hydroxypropyl)-2-methylpiperazine (II) and 2-amino-2-methyl-1-propanol (III).

EXPERIMENTAL

Apparatus

A Cary Model 17 spectrophotometer was used to record precise absorbance measurements on solutions at 25°.

Reagents

The *N*-methyl-diethanolamine was obtained from the Aldrich Chemical Company, 1,4-bis(2-hydroxypropyl)-2-methylpiperazine from Wyandotte Chemicals Corporation, and 2-amino-2-methyl-1-propanol from Pennsalt Chemicals Corporation. The copper solutions were prepared from G. Frederick Smith Chemical Company $\text{Cu}(\text{ClO}_4)_2 \cdot 6\text{H}_2\text{O}$. The ligand and copper solutions were standardized by conventional methods.

Procedure

Portions of the ligand and copper solutions were mixed and diluted with water to prepare a series of solutions that were 0.1–0.8 mM in Cu^{2+} and 0.1–2.0 mM in ligand, and the absorption spectra were recorded as soon as possible. No inert electrolyte was added, so the solutions had very low ionic strengths (0.3–2.4 mM). Approximately sixty solutions were prepared and many spectra were obtained.

Calculations

Stability constants and the molar absorptivities at eight wavelengths for the Cu^{2+} complexes were calculated with the computer program developed by Lingane and Hugus.²

RESULTS AND DISCUSSION

The values for the stability constants are given in Table 1 and those for the molar absorptivities in Tables 2–4. The molar absorptivities of the pure metal ion and pure ligand solutions can be taken as zero for all the wavelengths chosen.

Table 1. Values of stability constants for complexes of Cu^{2+} with the ligands

	I	II	III
$\log K_1$	5.22	5.41	5.38
$\log K_2$	2.97	4.70	3.56

Table 2. Values of molar absorptivities (ϵ , $l \cdot \text{mole}^{-1} \cdot \text{cm}^{-1}$) for complexes of Cu^{2+} with *N*-methyl-diethanolamine

λ , nm	250	260	270	280	290	300	310	320
ϵ_{CuL}	1211	1038	829	629	439	298	207	151
ϵ_{CuL_2}	5012	6104	6055	5188	4006	2804	1717	959

Table 3. Values of ϵ ($l \cdot \text{mole}^{-1} \cdot \text{cm}^{-1}$) for complexes of Cu^{2+} with 1,4-bis(2-hydroxypropyl)-2-methylpiperazine

λ , nm	250	260	270	280	290	300	310	320
ϵ_{CuL}	572	384	370	431	436	387	321	263
ϵ_{CuL_2}	2397	2033	1536	1061	719	514	386	298

Table 4. Values of ϵ ($l \cdot \text{mole}^{-1} \cdot \text{cm}^{-1}$) for complexes of Cu^{2+} with 2-amino-2-methyl-1-propanol

λ , nm	260	270	280	290	300	310	320	330
ϵ_{CuL}	842	612	434	307	273	264	248	216
ϵ_{CuL_2}	3197	2485	1775	1198	773	479	301	197

For complexes of Cu^{2+} with *N*-methyl-diethanolamine, Douheret¹ reported $\log K_1 = 4.85$, $\log K_2 = 4.25$, $\log K_3 = 3.35$, and $\log K_4 = 2.0$. We found no evidence for the complexes CuL_3^{2+} and CuL_4^{2+} and therefore have reported only the $\log K_1$ and $\log K_2$ values. The reactions proceed rapidly and with definite fixed reaction stoichiometry, and with the higher molar absorptivities permit the determination of trace concentrations of copper.

REFERENCES

1. G. Douheret, *Bull. Soc. Chim. France*, 1965, 2915.
2. P. J. Lingane and Z. Z. Hugus, Jr., *Inorg. Chem.*, 1970, 9, 757.

THE EXTRACTION OF Zn(II), Cd(II) AND Pb(II) FROM HYDROCHLORIC ACID MEDIA BY AMBERLITE LA-2 HYDROCHLORIDE DISSOLVED IN 1,2-DICHLOROETHANE

WIESŁAWA ZABORSKA and MACIEJ LESZKO

Institute of Chemistry, Jagiellonian University, 30060 Kraków, Poland

(Received 26 February 1985. Revised 13 March 1986. Accepted 29 April 1986)

Summary—The extraction of HCl by the secondary amine (B), known as Amberlite LA-2, dissolved in 1,2-dichloroethane and the aggregation of BHCl have been studied by using a two-phase potentiometric titration technique. The experimental data, treated by a general minimizing program, indicate dimerization: $2 \text{BHCl} \rightleftharpoons (\text{BHCl})_2$. The equilibrium constant of this reaction was calculated. The extraction of ZnCl_2 , CdCl_2 and PbCl_2 , from 0.2, 0.5, 1.0 and 2.0M HCl, and 1M NaCl by Amberlite LA-2 hydrochloride (BHCl), dissolved in 1,2-dichloroethane, has been studied. The complexes $(\text{BHCl})_2\text{ZnCl}_2$, $(\text{BHCl})_2\text{CdCl}_2$ and $(\text{BHCl})_2\text{PbCl}_2$ were found to exist, irrespective of the composition of the aqueous phase. The formation constant of the first was calculated.

Extraction of metals by long-chain amines is greatly influenced by aggregation of amine molecules in the organic phase. Complexes of the type $(\text{R}_3\text{NHX})_n$, formed in solutions of salts of trialkylamines with mineral acid in solvents of low dielectric constant (benzene, heptane, hexane, *o*-xylene, toluene) have been found.¹⁻⁷ In chloroform, which has a higher dielectric constant, the aggregation effects were observed to be weaker; no aggregation,⁸ appearance of only dimers⁹ or of monomers and dimers simultaneously^{10,11} are all possible, depending on the nature of the amine.

In the present study 1,2-dichloroethane ($\epsilon = 10.6$) was the solvent, and the secondary amine Amberlite LA-2 was the extractant. The systems

Amberlite LA-2, 1,2-dichloroethane|HCl

and

(Amberlite LA-2).HCl, 1,2-dichloroethane

| (H, Na)Cl, MeCl_2
| (Me = Zn, Cd, Pb)

were studied.

EXPERIMENTAL

Reagents

The commercial product known as Amberlite LA-2 (Rohm & Haas) a secondary *N*-lauryl (trialkylmethyl)amine, with m.w. 370 was used. 1,2-Dichloroethane (puriss.) was purified by fractional distillation. The other reagents were of analytical grade. All aqueous solutions were prepared with doubly distilled water.

Solutions

Four solutions of free amine, B, in 1,2-dichloroethane with concentrations 0.00837, 0.0218, 0.0440 and 0.0874M, were used to extract the acid. The concentration, $(c_B)_{\text{org}}$, was measured by acid-base titration.

The solutions of the hydrochloride, BHCl, to be used for extraction of metals, were prepared from appropriate amine

solutions (0.00188–0.273M), by shaking them with 2M hydrochloric acid.

The titrant was prepared by mixing equal volumes of 1M hydrochloric acid and 1M sodium chloride.

The solutions of MeCl_2 (Me = Zn, Cd, Pb) in 0.2, 0.5, 1.0 and 2.0M hydrochloric acid in 1M sodium chloride, and in mixtures of the two (H,Na)Cl with $[\text{Cl}^-] = 2M$, were prepared. The initial concentration of metal was 10^{-4} or $5 \times 10^{-4}M$. The concentration of metal ions before and after extraction was determined polarographically.

Methods

Two-phase potentiometric titration. The technique used has been described in detail by Högfeldt.¹ The measuring cell is:

Ag, AgCl, 1M NaCl	aqueous phase: 1M NaCl organic phase: B in 1,2-dichloroethane	glass electrode
----------------------	---	--------------------

The titrant, a mixture of hydrochloric acid and sodium chloride, both at 0.5M concentration, was gradually added to the cell. After equilibration, the potential *E* was measured and the concentration of hydrogen ions in the aqueous phase calculated from

$$E = E_0 + 59.2 \log[\text{H}^+]_{\text{aq}} + j[\text{H}^+]_{\text{aq}} \quad (1)$$

The constants E_0 and *j* were determined in a separate titration without organic phase. The experiments were done at $25 \pm 0.2^\circ$.

The extraction of metals. Equal volumes (20 ml) of the aqueous solution of MeCl_2 (Me = Zn, Cd, Pb) in (H, Na)Cl and of the 1,2-dichloroethane solution of amine hydrochloride were shaken at room temperature ($22 \pm 2^\circ$) for about 20 min. The phases were then separated and the concentration of metal ions in the aqueous phase was determined polarographically.

RESULTS AND DISCUSSION

Extraction of acid

The data obtained from the two-phase titrations are shown in Table 1 and Fig. 1. The values of *Z*,

Table 1. Distribution of hydrochloric acid in the two-phase system: 1.00M (H, Na)Cl Amberlite LA-2 (denoted by B) in 1,2-dichloroethane; the equilibrium concentration of acid in the aqueous phase is given as $-\log[H^+]_{aq}[Cl^-]_{aq}$ (column 1); degree of neutralization $Z = (c_{HCl})_{org}/(c_B)_{org}$ (column 2)

$(c_B)_{org} = 0.0874M$		$(c_B)_{org} = 0.0440M$		$(c_B)_{org} = 0.0218M$		$(c_B)_{org} = 0.0084M$	
$-\log[H^+][Cl^-]$	Z	$-\log[H^+][Cl^-]$	Z	$-\log[H^+][Cl^-]$	Z	$-\log[H^+][Cl^-]$	Z
6.559	0.073	6.521	0.059	6.390	0.058	6.243	0.075
6.489	0.097	6.448	0.077	6.261	0.097	6.129	0.112
6.381	0.146	6.397	0.096	6.141	0.156	6.017	0.168
6.286	0.195	6.288	0.145	6.046	0.214	5.933	0.204
6.195	0.243	6.203	0.193	5.944	0.273	5.857	0.254
6.119	0.292	6.119	0.241	5.853	0.331	5.781	0.305
6.051	0.341	6.051	0.290	5.742	0.390	5.704	0.342
5.966	0.389	5.975	0.338	5.640	0.448	5.628	0.391
5.940	0.437	5.907	0.386	5.565	0.507	5.570	0.425
5.851	0.487	5.823	0.434	5.511	0.565	5.480	0.485
5.782	0.535	5.747	0.483	5.403	0.624	5.411	0.535
5.705	0.584	5.671	0.531	5.305	0.682	5.311	0.605
5.635	0.633	5.578	0.579	5.191	0.741	5.185	0.670
5.551	0.681	5.495	0.627	5.052	0.799	5.105	0.712
5.472	0.730	5.410	0.675	4.855	0.857	5.003	0.762
5.370	0.779	5.345	0.723	4.640	0.915	4.910	0.801
5.262	0.827	5.235	0.772	4.401	0.951	4.795	0.835
5.105	0.876	5.116	0.820	4.083	0.971	4.545	0.903
4.880	0.925	4.990	0.868			4.309	0.940
4.650	0.954	4.785	0.916				
4.403	0.978	4.415	0.964				
4.161	0.987	4.180	0.987				

given by

$$Z = (c_{HCl})_{org}/(c_B)_{org} \quad (2)$$

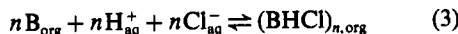
are plotted vs. $-\log[H^+]_{aq}[Cl^-]_{aq}$, where $[Cl^-]_{aq} = 1$.

The total equilibrium concentration of acid in the organic phase, $(c_{HCl})_{org}$, can be calculated from the volume of titrant, the volumes of the phases and the equilibrium concentration of hydrochloric acid in the aqueous phase. The concentration of amine, $(c_B)_{org}$, is known and does not change during extraction.

Generally, multistep equilibria involving monomeric B and BHCl species as well as $(BHCl)_n$ aggregates must be considered.¹⁻¹¹ Unsymmetrical species of the type $B_n(HCl)_n$ are unlikely to be formed.

The finding (Fig. 1) that the four curves corresponding to four amine solutions of increasing concentration are not coincident, indicates clearly the presence of dimers, $(BHCl)_2$, and perhaps of higher aggregates. If aggregates were absent then the constants K_{22}, K_{33}, \dots would be equal to zero, and the value of Z calculated from equations (5) and (6) would not be dependent on b and on the total concentration of amine. One common curve would then be observed.

The stability constant of the aggregate formed in reaction (3)



is given by

$$K_n = [(BHCl)_n]_{org}/[B]^n[H^+]^n[Cl^-]^n \quad (4)$$

The mass balance equations can be written as:

$$(c_{HCl})_{org} = K_{11}b[H^+]_{aq} + 2K_{22}b^2[H^+]_{aq}^2 + \dots \quad (5)$$

$$(c_B)_{org} = b + K_{11}b[H^+]_{aq} + 2K_{22}b^2[H^+]_{aq}^2 + \dots \quad (6)$$

where $b = [B]_{org}$.

With the assumption that two species, BHCl and $(BHCl)_2$, are formed in the organic phase, the values

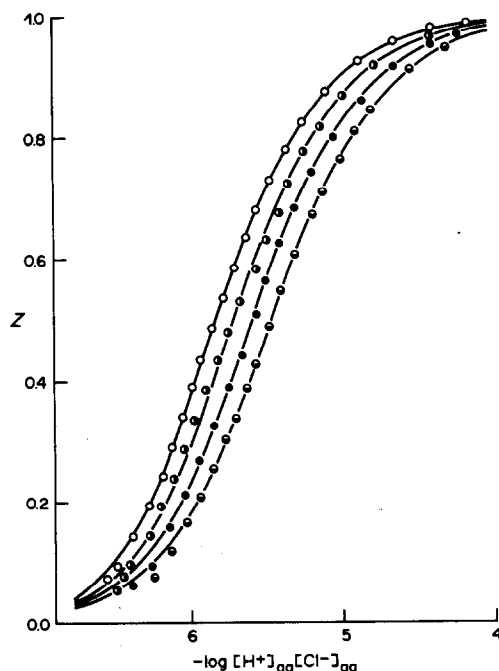


Fig. 1. Experimental degree of neutralization of the amine, $Z = (c_{HCl})_{org}/(c_B)_{org}$ as a function of $-\log[H^+]_{aq}[Cl^-]_{aq}$ for various concentrations of Amberlite LA-2 in 1,2-dichloroethane: 0.0084M (○); 0.0218M (●); 0.0440M (●); 0.0874M (○). Solid lines were calculated from $\log K_{11} = 5.21$ and $\log K_{22} = 12.62$; $[Cl^-] = 1M$.

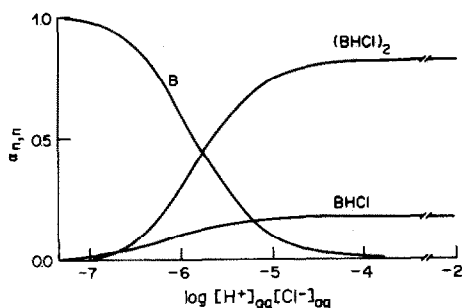


Fig. 2. Fractions of the components B, BHCl and $(\text{BHCl})_2$, in the organic phase as a function of the acidity of aqueous solution at constant amine concentration $(c_B)_{\text{org}} = 0.1M$.

of $\log \bar{K}_{11} = 5.21 \pm 0.07$ and $\log \bar{K}_{22} = 12.62 \pm 0.04$ were computed by minimizing the function U_z , for all the experimental points:

$$U_z = \sum (Z_{\text{calc}} - Z_{\text{exp}})^2 \quad (7)$$

The general program MINUIT from the CERN Library was used. The solid lines in Fig. 1 were calculated from these values; the fit to the experimental points is generally satisfactory. Formation of higher aggregates was also considered, but the correlation was always worse.

Figures 2 and 3 show the distribution of the various species as a function of $[\text{H}^+]$ and amine concentration.

Extraction of ZnCl_2 , CdCl_2 and PbCl_2

The distribution equilibria of MeCl_2 ($\text{Me} = \text{Zn}, \text{Cd}, \text{Pb}$) between the organic phase (Amberlite LA-2 hydrochloride in 1,2-dichloroethane) and aqueous phase (MeCl_2 in 0.2, 0.5, 1.0 and 2.0M HCl and in 1M NaCl) were studied.

Two initial concentrations of MeCl_2 were used and $(c_{\text{BHCl}})_{\text{org}}$ was varied over the range 0.00188–0.273M. The data (Table 2) were plotted (Fig. 4) as $\log D_{\text{Me}}$ vs. $\log(c_{\text{BHCl}})_{\text{org}}$, where

$$D_{\text{Me}} = \frac{[\text{Me(II)}]_{\text{org}}}{[\text{Me(II)}]_{\text{aq}}} \quad (8)$$

For a given hydrochloric acid concentration, the experimental points in Fig. 4 fall on a straight line,

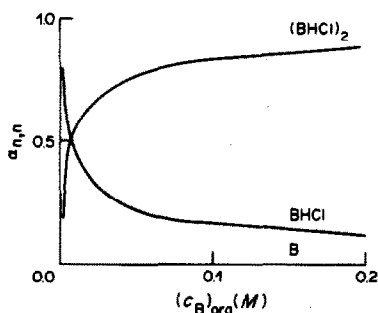
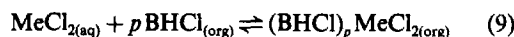


Fig. 3. Fractions of the components B, BHCl and $(\text{BHCl})_2$ in the organic phase as a function of the total amine concentration at constant acidity of the aqueous phase: $-\log[\text{H}^+]_{\text{aq}}[\text{Cl}^-]_{\text{aq}} = 2$. Free amine fraction $\alpha_{00} = 0$ over the whole range.

independent of the initial MeCl_2 concentration. This suggests that MeCl_2 is extracted as mononuclear complexes. The non-integral slopes of the lines indicate however, that the true concentration of amine hydrochloride in the organic phase, $[\text{BHCl}]_{\text{org}}$, differs considerably from its total concentration, $(c_{\text{BHCl}})_{\text{org}}$.

The stoichiometry of an extracted complex and the extraction constant, K_{p1} , were determined as follows.

Equation (9) expresses, generally, several simultaneous reactions ($p = 1, 2, \dots$) and equation (10), their equilibrium constants:



$$K_{p1} = \frac{[(\text{BHCl})_p \text{MeCl}_2]_{\text{org}} \{[\text{BHCl}]_{\text{org}}^p [\text{MeCl}_2]_{\text{aq}}\}}{[\text{MeCl}_2]_{\text{aq}} [\text{BHCl}]_{\text{org}}^p} \quad (10)$$

The total concentration of metal in the organic and the aqueous phases is given by the equations:

$$\begin{aligned} (c_{\text{Me}})_{\text{org}} &= \sum_p [(\text{BHCl})_p \text{MeCl}_2] \\ &= [\text{Me}^{2+}] [\text{Cl}^-]^2 \sum_p K_{p1} [\text{BHCl}]^p \end{aligned} \quad (11)$$

$$(c_{\text{Me}})_{\text{aq}} = \sum_0^N [\text{MeCl}_n^{2-n}] = [\text{Me}^{2+}] \sum_0^N \beta_n [\text{Cl}^-]^n \quad (12)$$

where

$$\beta_n = \frac{[\text{MeCl}_n^{2-n}]}{[\text{Me}^{2+}] [\text{Cl}^-]^n} \quad (13)$$

Since $[\text{Cl}^-] = 1.00M$,

$$D = \sum_p K'_{p1} [\text{BHCl}]_{\text{org}}^p \quad (14)$$

where

$$K'_{p1} = K_{p1} \beta_2 \left/ \sum_0^N \beta_n \right. \quad (15)$$

Equation (14) evaluates an experimental distribution coefficient D as a function of one variable, the equilibrium concentration of the monomeric amine hydrochloride salt, $[\text{BHCl}]_{\text{org}}$.

To find that concentration, dimerization



must be considered. The equilibrium constant of dimerization, calculated from (17),

$$\log \bar{K}_2 = \log \bar{K}_{22} - \log \bar{K}_{11} \quad (17)$$

is $10^{2.20}$. The total concentration of amine salt species is given by

$$\begin{aligned} (c_{\text{BHCl}})_{\text{org}} &= [\text{BHCl}] + 2 \bar{K}_2 [\text{BHCl}]^2 \\ &+ \sum_p p [(\text{BHCl})_p \text{MeCl}_2] \end{aligned} \quad (18)$$

Because of the low concentration of the metals, the presence of metal-containing species can be ignored and the last terms of equation (18) omitted. This simplified equation (18) defines a relationship between the known, total concentration of amine $(c_{\text{BHCl}})_{\text{org}}$ and the unknown concentration of $[\text{BHCl}]_{\text{org}}$. In this way, the experimental points were transformed into a new set of co-ordinates (Fig. 5).

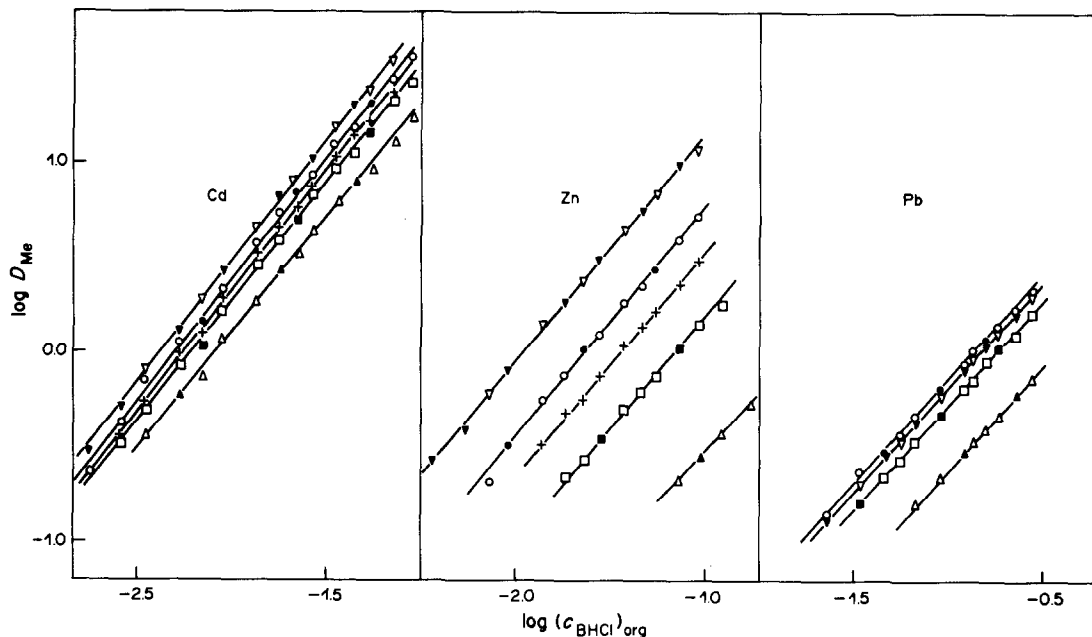


Fig. 4. Distribution ratio $\log D_{Me}$ vs. $\log(c_{BHCl})_{org}$ at four different concentrations of HCl: 2M HCl (∇), 1M HCl (\circ), 0.5M HCl (\square), 0.2M HCl (\triangle) and in 1M NaCl (\times). Open symbols: $[Me] = 5 \times 10^{-4}M$. Filled symbols: $[Me] = 10^{-4}M$. The slopes of the straight lines lie between 1.1 and 1.3.

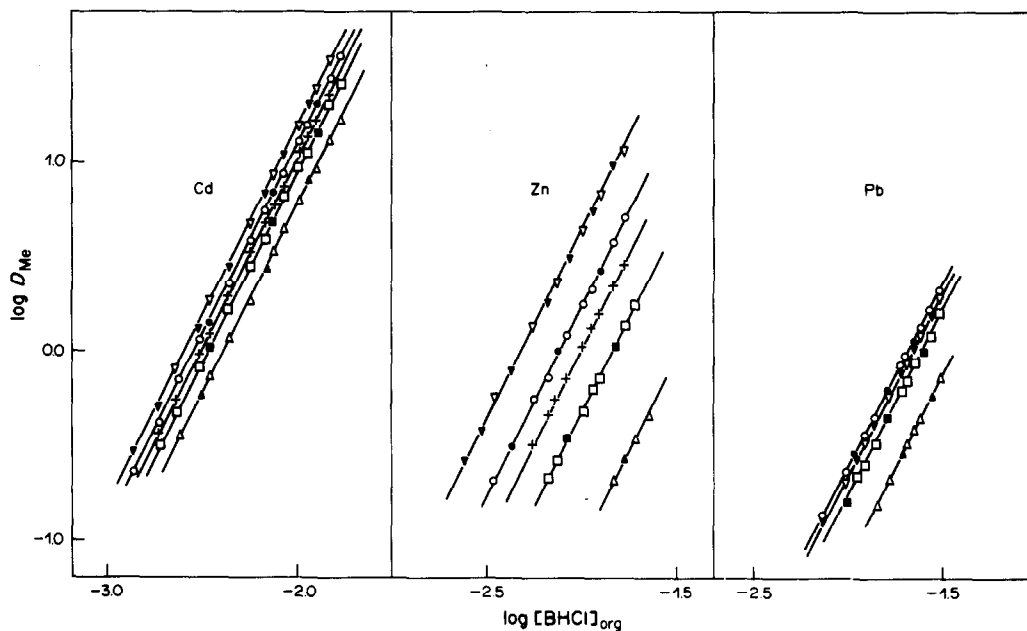


Fig. 5. Distribution ratio $\log D_{Me}$ vs. real concentration of monomeric amine hydrochloride, $\log[BHCl]_{org}$, computed from the dimerization constant $K_2 = 10^{2.20}$ at four different concentrations of HCl: 2M HCl (∇), 1M HCl (\circ), 0.5M HCl (\square), 0.2M HCl (\triangle) and in 1M NaCl (\times). Open symbols: $[Me] = 5 \times 10^{-4}M$. Filled symbols: $[Me] = 10^{-4}M$. Assuming that the slope of the lines is equal to 2, the intercepts ($\log K_2 = 5.25, 4.68$ and 3.85 respectively) were chosen so as to obtain the best fit to the experimental points.

Table 2. Distribution ratios for zinc, cadmium and lead, D , as a function of total concentration of Amberlite LA-2 hydrochloride in 1,2-dichloroethane in four different concentrations of HCl and in 1M NaCl; initial $[Me]_{aq} = 5 \times 10^{-4}M$

$(c_{\text{BHCl}})_{\text{org}}, M$	log D				
	2M HCl	1M HCl	0.5M HCl	0.2M HCl	1M NaCl
zinc chloride					
0.159				-0.330	
0.121			0.250	-0.436	
0.0938	1.057	0.705	0.155	-0.560*	0.470
0.0750	0.990*	0.590	0.0253*	-0.682	0.353
0.0563	0.829	0.430*	-0.131		0.205
0.0469	0.741*	0.342	-0.194		0.124
0.0375	0.638	0.260	-0.300		0.0261
0.0281	0.493*	0.0969	-0.451*		-0.136
0.0234	0.376	0.0200*	-0.565		-0.257
0.0188	0.260*	-0.120	-0.648		-0.322
0.0141	0.140	-0.255			-0.485
0.00938	-0.0985*	-0.489*			
0.00750	-0.237	-0.678			
0.00563	-0.406*				
0.00375	-0.577*				
cadmium chloride					
0.0938		1.560	1.420	1.225	
0.0750	1.535	1.441	1.322	1.112	1.360
0.0563	1.382	1.318*	1.157*	0.975	1.208
0.0469	1.308*	1.192	1.055	0.905*	1.145
0.0375	1.193	1.105	0.977	0.801	1.043
0.0281	1.036*	0.935	0.828	0.645	0.882
0.0234	0.937	0.845*	0.691*	0.520	0.775
0.0188	0.836*	0.742	0.605	0.425*	0.672
0.0141	0.661	0.590	0.464	0.267	0.535
0.00938	0.426*	0.344	0.220	0.0722	0.301
0.00750	0.273	0.170*	0.0370*	-0.131	0.100
0.00563	0.112*	0.0731	-0.0720	-0.235*	-0.0050
0.00375	-0.0937	-0.135	-0.305	-0.435	-0.260
0.00281	-0.286*	-0.375	-0.475		-0.432
0.00188	-0.521*	-0.630			
lead chloride					
0.273	0.290	0.329	0.220	-0.131	
0.227	0.190*	0.231	0.0911	-0.229*	
0.182	0.0962	0.140	0.0131*	-0.340	
0.159	0.0253*	0.0720*	-0.0412	-0.398	
0.136	-0.0443	-0.0111	-0.146	-0.468	
0.121	-0.100*	-0.0696	-0.193	-0.532*	
0.091	-0.229	-0.195*	-0.323*	-0.658	
0.068	-0.370*	-0.330	-0.468	-0.791	
0.0563	-0.483	-0.422	-0.569		
0.0455	-0.569*	-0.522*	-0.650		
0.0340	-0.695	-0.620	-0.795*		
0.0227	-0.896*	-0.851			

*For these points, initial $[Me]_{aq} = 10^{-4}M$.

The slope of the lines, equal to 2, indicates that only one type of complex, $(\text{BHCl})_2\text{MeCl}_2$, is formed in the organic phase, independent of the composition of the aqueous phase.

Plots of $\log D_{\text{Me}}$ vs. $\log[\text{HCl}]$ at constant $[\text{Cl}^-] = 2M$ show that the extraction of the metals increases with increase in the concentration of hydrogen ions (Fig. 6).

Since the values of the stability constants, β_n , of the chloro-complexes, MeCl_n^{2-n} , and the constants K'_{21} known, the equilibrium constant for extraction of a metal, K_{21} , may be calculated from equation (15). The

values of $\log K'_{21}$ are found from the intercepts of the of the lines in Fig. 5. For zinc with $\log \beta_1 = -0.72$, $\log \beta_2 = -0.85$, $\log \beta_3 = -1.50$, $\log \beta_4 = -1.75$,^{12,13} and $\log K'_{21} = 4.68$, the constant $\log K_{21} = 5.11$ was found.

Zinc complexes of the form $(\text{RHCl})_2\text{ZnCl}_2$ have also been found in several other extraction systems¹²⁻¹⁷ with various amines and solvents. A complex with three amine molecules, $(\text{R}_3\text{NHCl})_3\text{ZnCl}_2$, together with one with two, $(\text{R}_3\text{NHCl})_2\text{ZnCl}_2$, was found in benzene and xylene medium by Aguilar *et al.*^{18,19} Diamine complexes of

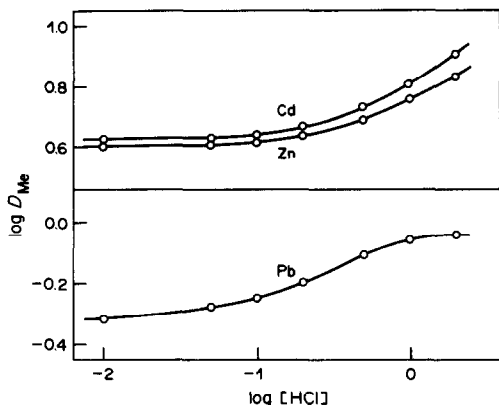


Fig. 6. Distribution ratio $\log D_{Me}$ vs. $\log [HCl]$ at constant $[Cl^-] = 2M$. The concentration of $BHCl$ in the organic phase was constant for each metal and equal to $0.0234M$ for cadmium, $0.0563M$ for zinc and $0.136M$ for lead.

cadmium, $(R_4NCl)_2CdCl_2$, and a monoamine complex of lead, $(R_4NCl)PbCl_2$, have been found previously by one of us.¹⁴

LIST OF SYMBOLS

- B** Amberlite LA-2.
 $[...]_{aq}, [...]_{org}$ free (molar) concentrations of given species in aqueous and organic phase respectively.
c total molar concentration of a given substance.
 D_{Me} distribution ratio for the metal, $D_{Me} = [Me]_{org}/[Me]_{aq}$.
 K_{nn} stability constant of the aggregate $(BHCl)_n$ formed in reaction (3).
 K_2 equilibrium constant of dimerization (16).
 K_{p1} stability constant of the complex $(BHCl)_pMeCl_2$ formed in reaction (9).
 K'_{p1} the constant given by equation (15).
Z degree of neutralization of amine, $Z = (c_{HCl})_{org}/(c_B)_{org}$.
 α_{nn} fraction of amine, B, existing as $(BHCl)_n$; $\alpha_{nn} = n[(BHCl)_n]_{org}/(c_B)_{org}$.

β_n stability constant of chloro-complexes $MeCl_n^{2-n}$ in aqueous HCl solutions.

Acknowledgement—The authors are indebted to Mr. Andrzej Oziebło M.S., for writing the computer program.

REFERENCES

1. E. Högfeldt and F. Fredlund, in *Solvent Extraction Chemistry*, D. Dyrssen, J. O. Liljenzin and J. Rydberg (eds.), p. 383. North-Holland, Amsterdam, 1967.
2. L. Kuča, E. Högfeldt and M. de Jesus Tavares, *Ark. Kemi*, 1970, **32**, 405.
3. L. Kuča and E. Högfeldt, *Acta Chem. Scand.*, 1971, **25**, 1261.
4. M. Aguilar and E. Högfeldt, *Chem. Scripta*, 1972, **2**, 149.
5. O. Budevsky and E. Högfeldt, *ibid.*, 1974, **5**, 107.
6. F. Fredlund, E. Högfeldt, T. A. Korshunova and V. S. Soldatov, *ibid.*, 1977, **11**, 212.
7. M. A. Lodhi and E. Högfeldt, in *Solvent Extraction Chemistry* (ref. 1), p. 421.
8. S. Poturaj and E. Högfeldt, *Acta Chem. Scand.*, 1978, **A32**, 85.
9. B. Warnqvist, in *Solvent Extraction Chemistry* (ref. 1), p. 416.
10. A. T. Casey, R. W. Cattrall and D. E. Davey, *J. Inorg. Nucl. Chem.*, 1971, **33**, 536.
11. F. Fredlund and E. Högfeldt, *Chem. Scripta*, 1977, **11**, 217.
12. D. Dyrssen and M. de Jesus Tavares, in *Solvent Extraction Chemistry* (ref. 1), p. 465.
13. M. Leszko and W. Zaborska, *Polish J. Chem.* 1978, **52**, 1525.
14. W. Zaborska, *Thesis*, Kraków, 1975.
15. K. Inoue, T. Tsuji and I. Nakamori, *J. Chem. Eng. Japan*, 1979, **12**, 353.
16. H. Daud and R. W. Cattrall, *Aust. J. Chem.*, 1982, **35**, 1095.
17. A. K. De, U. S. Ray and N. Parhi, *J. Indian Chem. Soc.* 1982, **59**, 1334.
18. M. Aguilar, *Chem. Scripta*, 1973, **4**, 207; 1974, **5**, 213; 1975, **8**, 37.
19. M. Aguilar and M. Muhammed, *J. Inorg. Nucl. Chem.*, 1976, **38**, 1193.

ANNOTATION

THE DISTRIBUTION OF CHROMIUM(VI) SPECIES
 IN SOLUTION AS A FUNCTION OF pH AND
 CONCENTRATION

TONG SHEN-YANG and LI KE-AN

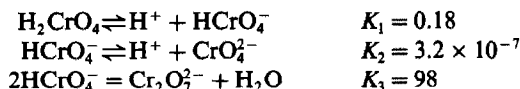
Department of Chemistry, Peking University, Beijing, People's Republic of China

(Received 19 November 1985. Accepted 30 April 1986)

Summary—The distribution of the chromium(VI) species CrO_4^{2-} , $\text{Cr}_2\text{O}_7^{2-}$, HCrO_4^- , and H_2CrO_4 in aqueous solutions with total chromium(VI) concentrations of 10^{-2} – 10^{-6} M at pH 1–8 have been calculated.

Tandon *et al.* have recently calculated the distribution of chromium(VI) species in aqueous solution at various concentrations and pH values,¹ but unfortunately there seem to be one or two mistakes in their presentation of the results.

The equilibrium constants used were:



and the concentration of H_2CrO_4 was calculated by means of the equation:

$$x + \frac{K_1 x}{p} + \frac{K_1 K_2 x}{p^2} + \frac{K_3 K_1^2 x^2}{p^2} - C = 0 \quad (1)$$

where C is the total chromium concentration, x is $[\text{H}_2\text{CrO}_4]$ and p is $[\text{H}^+]$ (but was said in the original paper¹ to be pH). The concentrations of the other three species were calculated from

$$\begin{aligned} [\text{HCrO}_4^-] &= K_1 x / p \\ [\text{CrO}_4^{2-}] &= K_1 K_2 x / p^2 \\ [\text{Cr}_2\text{O}_7^{2-}] &= K_3 K_1^2 x^2 / p^2 \end{aligned}$$

but equation (1) is not correct, since it is based on the equality

$$C = [\text{H}_2\text{CrO}_4] + [\text{HCrO}_4^-] + [\text{CrO}_4^{2-}] + [\text{Cr}_2\text{O}_7^{2-}]$$

which is incorrect, since the material balance in terms of chromium atoms is

$$C = [\text{H}_2\text{CrO}_4] + [\text{HCrO}_4^-] + [\text{CrO}_4^{2-}] + 2[\text{Cr}_2\text{O}_7^{2-}] \quad (2)$$

and the correct equation should be

$$x + \frac{K_1 x}{p} + \frac{K_1 K_2 x}{p^2} + \frac{2K_3 K_1^2 x^2}{p^2} - C = 0 \quad (3)$$

or

$$2K_3 K_1^2 x^2 / p^2 + (1 + K_1 / p + K_1 K_2 / p^2)x - C = 0 \quad (4)$$

from which x can be calculated. To make the results more precise, we have used the corresponding equa-

Table I. Chromium(VI) species (atom%)

pH	C, M	CrO_4^{2-}	$\text{Cr}_2\text{O}_7^{2-}$	HCrO_4^-	H_2CrO_4
1	10^{-2}	0.00	34.62	42.03	23.35
	10^{-3}	0.00	7.00	59.79	33.21
	10^{-4}	0.00	0.80	63.77	35.43
	10^{-5}	0.00	0.08	64.23	35.69
	10^{-6}	0.00	0.01	64.28	35.71
2	10^{-2}	0.00	47.85	49.41	2.74
	10^{-3}	0.00	13.24	82.19	4.57
	10^{-4}	0.00	1.70	93.12	5.17
	10^{-5}	0.00	0.18	94.57	5.25
	10^{-6}	0.00	0.02	94.72	5.26
3	10^{-2}	0.02	49.47	50.24	0.27
	10^{-3}	0.03	14.25	85.25	0.47
	10^{-4}	0.03	1.87	97.56	0.54
	10^{-5}	0.03	0.19	99.22	0.55
	10^{-6}	0.33	0.02	99.40	0.55
4	10^{-2}	0.16	49.54	50.27	0.03
	10^{-3}	0.27	14.29	85.39	0.05
	10^{-4}	0.31	1.87	97.76	0.05
	10^{-5}	0.32	0.19	99.43	0.06
	10^{-6}	0.32	0.02	99.61	0.06
5	10^{-2}	1.59	48.61	49.80	0.00
	10^{-3}	2.68	13.70	83.62	0.00
	10^{-4}	3.05	1.78	95.17	0.00
	10^{-5}	3.09	0.19	96.72	0.00
	10^{-6}	3.10	0.02	96.88	0.01
6	10^{-2}	14.49	40.21	45.29	0.00
	10^{-3}	22.00	9.26	68.74	0.00
	10^{-4}	23.98	1.10	74.92	0.00
	10^{-5}	24.22	0.11	75.67	0.00
	10^{-6}	24.24	0.01	75.75	0.00
7	10^{-2}	69.21	9.17	21.63	0.00
	10^{-3}	75.36	1.09	23.55	0.00
	10^{-4}	76.11	0.11	23.79	0.00
	10^{-5}	76.18	0.01	23.81	0.00
	10^{-6}	76.19	0.00	23.81	0.00
8	10^{-2}	96.80	0.18	3.02	0.00
	10^{-3}	96.95	0.02	3.03	0.00
	10^{-4}	96.97	0.00	3.03	0.00
	10^{-5}	96.97	0.00	3.03	0.00
	10^{-6}	96.97	0.00	3.03	0.00

Table 2. Distribution of Cr(VI) species (atom%); blank entries indicate <0.005 atom%

pH	C, M	CrO ₄ ²⁻				CrO ₅ ³⁻				HCrO ₄ ⁻				H ₂ CrO ₄			
		a	b	c	d	a	b	c	d	a	b	c	d	a	b	c	d
1	10 ⁻²					18.34	19.17	29.59	48.16	52.49	51.96	66.23	50.82	29.16	28.87	4.17	1.02
	10 ⁻³					2.61	2.78	5.35	13.43	62.61	62.50	89.04	84.87	34.78	34.72	5.61	1.67
	10 ⁻⁴					0.27	0.29	0.59	1.73	64.11	64.10	93.52	96.34	35.62	35.61	5.89	1.93
	10 ⁻⁵					0.03	0.03	0.06	0.18	64.27	64.27	94.02	97.86	35.70	35.70	5.92	1.96
	10 ⁻⁶							0.01	0.02	64.29	64.29	94.07	98.02	35.71	35.71	5.92	1.96
2	10 ⁻²				0.01	29.60	30.65	31.37	48.75	66.69	65.70	68.20	51.14	3.70	3.65	0.43	0.10
	10 ⁻³				0.02	5.35	5.67	5.90	13.80	89.66	89.36	93.51	86.02	4.98	4.96	0.59	0.17
	10 ⁻⁴				0.02	0.59	0.63	0.66	1.79	94.18	94.14	98.72	98.00	5.23	5.22	0.62	0.20
	10 ⁻⁵				0.02	0.06	0.06	0.07	0.18	94.68	94.67	98.31	99.60	5.26	5.26	0.63	0.20
	10 ⁻⁶				0.02	0.00	0.01	0.01	0.02	94.73	94.73	99.36	99.76	5.26	5.26	0.63	0.20
3	10 ⁻²				0.09	31.17	32.23	31.55	48.76	68.43	67.37	68.39	51.14	0.38	0.37	0.04	0.01
	10 ⁻³				0.16	5.83	6.18	5.95	13.80	93.61	93.27	93.96	86.03	0.52	0.52	0.06	0.02
	10 ⁻⁴				0.18	0.65	0.69	0.66	1.79	98.77	98.73	99.24	98.01	0.55	0.55	0.06	0.02
	10 ⁻⁵				0.18	0.07	0.07	0.07	0.19	99.35	99.34	99.84	99.61	0.55	0.55	0.06	0.02
	10 ⁻⁶				0.18	0.01	0.01	0.01	0.02	99.41	99.41	99.90	99.78	0.55	0.55	0.06	0.02
4	10 ⁻²				0.92	31.24	32.30	31.47	48.22	68.51	67.45	68.31	50.86	0.04	0.04	0.04	0.04
	10 ⁻³				1.55	5.86	6.20	5.93	13.47	93.79	93.45	93.77	84.99	0.05	0.05	0.06	0.06
	10 ⁻⁴				1.75	0.65	0.70	0.66	1.74	98.98	98.93	99.03	96.51	0.06	0.06	0.06	0.06
	10 ⁻⁵				1.78	0.07	0.07	0.07	0.18	99.56	99.56	99.62	98.04	0.06	0.06	0.06	0.06
	10 ⁻⁶				1.79	0.01	0.01	0.01	0.02	99.62	99.62	99.68	98.19	0.06	0.06	0.06	0.06
5	10 ⁻²				8.75	31.24	31.38	30.58	43.15	68.51	66.48	67.34	48.11				
	10 ⁻³				13.75	5.86	5.90	5.65	10.66	93.79	91.17	91.52	75.60				
	10 ⁻⁴				15.18	0.65	0.66	0.63	1.30	96.30	96.26	96.40	83.51				
	10 ⁻⁵				15.36	0.07	0.07	0.06	0.13	96.83	96.83	96.94	84.50				
	10 ⁻⁶				15.38	0.01	0.00	0.01	0.01	96.89	96.89	97.00	84.60				
6	10 ⁻²				18.72	18.49	18.11	18.11	16.41	58.50	57.79	58.67	29.66				
	10 ⁻³				23.38	23.33	22.72	22.72	2.24	73.07	72.90	73.62	34.69				
	10 ⁻⁴				24.15	24.14	23.49	23.49	0.23	75.47	75.45	76.11	35.40				
	10 ⁻⁵				24.23	24.23	23.58	23.58	0.04	75.73	75.73	76.39	35.48				
	10 ⁻⁶				24.24	24.24	23.58	23.58	0.02	75.75	75.75	76.41	35.48				
7	10 ⁻²				73.51	73.35	72.70	72.70	0.50	22.97	22.92	23.56	5.19				
	10 ⁻³				75.91	75.89	75.23	75.23	0.05	23.72	23.71	24.37	5.21				
	10 ⁻⁴				76.16	76.16	75.53	75.53	0.01	23.80	23.80	24.46	5.21				
	10 ⁻⁵				76.19	76.19	75.53	75.53		23.81	23.81	24.77	5.21				
	10 ⁻⁶				76.19	76.19	75.53	75.53		23.81	23.81	24.47	5.21				

tion written in terms of $y = [\text{HCrO}_4^-]$:

$$2K_3y^2 + (1 + p/K_1 + K_2/p)y - C = 0 \quad (5)$$

It should be stressed that the distribution is calculated in terms of atom%.

RESULTS AND DISCUSSION

The results are listed in Table 1 and plots of the atom% distribution of chromium between the four species as a function of pH and total concentration of chromium(VI) show that the distribution of H_2CrO_4 is that of a dibasic acid. However, as the dichromate ion is a dimer, its distribution depends on both pH and total chromium(VI) concentration. The higher the chromium (VI) concentration, the higher the concentration of dichromate, but at very low Cr(VI) concentrations almost no dichromate is present.

REFERENCE

1. R. K. Tandon, P. T. Crisp, J. Ellis and R. S. Baker, *Talanta*, 1984, **31**, 227.

EDITORIAL NOTE

The Editor-in-Chief and the referee for the original paper¹ apologise for having failed to notice the errors mentioned above. Dr. Tandon has explained that the errors arose during transcription of the equations into the computer program used, and in preparing the final draft of the paper. He has recalculated the distribution with the correct equation and confirms the values reported in Table 1 of *this* paper. An independent HALTAFALL calculation has also given the same values. In the course of checking, the calculations were repeated for the values 33.3, 35.5 and 98 for K_3 . However, it should be pointed out that the values for K_1 , K_2 and K_3 used by Tandon *et al.* and hence by Tong and Li, are rather old, and the following values have since been reported²⁻⁴ for the values at 25°

Ionic strength	K_1	K_2	K_3
0	1.6	3.1×10^{-7}	34
0.1	—	8.1×10^{-7}	—
1.0	5.0	1.8×10^{-6}	94
3.0	12.3 (20°)	1.3×10^{-6}	148

Calculations done with these values at ionic strengths of 0 and 1.0 gave a rather different picture (see Table 2 above) and users of the information should note the remarkable effect of change in ionic strength, and treat all the data with caution.

RAC, MRM

REFERENCES

1. See reference 1 above.
2. R. M. Smith and A. E. Martell, *Critical Stability Constants*, Vol. 4, *Inorganic Complexes*, Plenum Press, New York, 1976.
3. C.F. Baes, Jr. and R. E. Mesmer, *The Hydrolysis of Cations*, Wiley, New York, 1976.
4. O. Lukkari, *Suom. Kemistilehti*, 1970, **B43**, 347.

8	10^{-2}	96.91	96.91	96.80	99.45	0.06	0.07	0.01	0.07	0.01	3.03	3.03	3.03	3.03	3.03	3.14	3.14	3.14	3.14	0.55	0.55
	10^{-3}	96.96	96.96	96.86	99.45	0.01	0.01	0.01	0.01	0.01	3.03	3.03	3.03	3.03	3.03	3.14	3.14	3.14	3.14	0.55	0.55
	10^{-4}	96.97	96.97	96.86	99.45						3.03	3.03	3.03	3.03	3.03	3.14	3.14	3.14	3.14	0.55	0.55
	10^{-5}	96.97	96.97	96.86	99.45						3.03	3.03	3.03	3.03	3.03	3.14	3.14	3.14	3.14	0.55	0.55
	10^{-6}	96.97	96.97	96.86	99.45						3.03	3.03	3.03	3.03	3.03	3.14	3.14	3.14	3.14	0.55	0.55

a K_1 0.18 ($I=0.16$)
 K_2 3.2×10^{-7} ($I=0.33-0.63$)
 K_3 33.5 ($I=0.02$)
 b 35.5 ($I=0$)
 c $I=0$
 0.76
 3.1×10^{-7}
 34.0
 d $I=1$
 0.20
 1.8×10^{-6}
 93.5

KINETIC SPECTROFLUORIMETRIC DETERMINATION OF SILVER, BASED ON ITS CATALYTIC EFFECT ON THE OXIDATION OF PYROCATECHOL-1-ALDEHYDE 2-PYRIDYLHYDRAZONE BY PEROXODISULPHATE IN THE PRESENCE OF 1,10-PHENANTHROLINE AS ACTIVATOR

A. M. AFONSO, J. J. SANTANA and F. GARCIA MONTELONGO

Department of Analytical Chemistry, University of La Laguna, La Laguna, Tenerife, Spain

(Received 24 October 1985. Revised 2 June 1986. Accepted 16 June 1986)

Summary—A kinetic fluorimetric method for the determination of silver is described, based on its catalytic effect on the oxidation of pyrocatechol-1-aldehyde 2-pyridylhydrazone by peroxodisulphate. In aqueous solution silver concentrations of 0.2–0.8 $\mu\text{g/ml}$ can be determined, and 10–80 ng/ml in the presence of 1,10-phenanthroline as activator. The fluorescent species obtained (λ_{ex} 357 nm, λ_{em} 445 nm) results from oxidation of the reagent. The kinetic parameters and the interferences are reported, and the method is applied to the determination of silver in developed panchromatic plates.

Although the sensitivity of catalytic analysis is usually high, it is often far from the maximum attainable and further increase in it is still a serious and real problem.

The lowest concentration of a catalyst M which can be determined by using a so-called indicator reaction ($A + B \rightarrow P$) depends on the sensitivity of detection of the product P, which in turn is closely related to the sensitivity of the monitoring technique used. Thus fluorescence monitoring improves the analytical characteristics of catalytic methods.

At present, the most promising possibility for further increase in the sensitivity of catalytic methods seems to be the use of activators.^{1,2}

As can be seen in Table 1, several kinetic procedures for determination of traces of silver have been based on absorbance measurements but only a few on fluorescence measurements, and only one application of activators in connection with fluorescence monitoring¹⁹ seems to have been made up to the present.²⁰

In this paper, we propose two direct kinetic fluorimetric methods for the determination of silver(I), based on the intense yellow fluorescence which appears when pyrocatechol-1-aldehyde 2-pyridylhydrazone (PCAPH) is oxidized by peroxodisulphate at an appropriate pH, with or without 1,10-phenanthroline as activator, depending on the silver concentration present.

EXPERIMENTAL

Apparatus

All fluorescence measurements were made with a Perkin-

Elmer MPF-44A recording spectrofluorimeter equipped with a 150-W Osram XBO xenon arc, a DSCU-1 corrected-spectra unit (0.5% Rhodamine B in ethylene glycol, as the reference), a UDR-3 digital read-out, a Selecta Frigitherm ultrathermostat, and a 1-cm silica cell. The emission intensity measurement system of the spectrofluorimeter was calibrated daily with a Perkin-Elmer set of fluorescent polymer samples, to compensate for changes in source intensity. All measurements were recorded at a sensitivity of 1.2, with excitation and emission slits giving 6-nm spectral band-pass. The fluorescence intensity was recorded as a function of time at a chart-speed of 1.0 cm/min, with fixed excitation and emission wavelengths.

Solutions

Solutions were made of pyrocatechol-1-aldehyde 2-pyridylhydrazone ($1.0 \times 10^{-3} M$)²¹ in absolute ethanol, standard silver(I) ($1.0 \times 10^{-2} M$ silver nitrate)²², potassium peroxodisulphate (0.2M, prepared daily), and 1,10-phenanthroline ($1.0 \times 10^{-2} M$), and diluted as required.

The ionic strength was maintained constant at 0.21M by adding suitable amounts of 2.5M sodium nitrate. A 0.5M ammonia/ammonium nitrate pH-8.0 buffer solution was used as indicated.

Doubly distilled water and analytical reagent grade chemicals were used.

Determination of silver without activator

In a 25-ml standard flask place 3 ml of the pH-8.0 buffer, 1.5 ml of 2.5M sodium nitrate, a known volume of sample (containing 4.0–16.0 μg of silver), 6 ml of 0.2M potassium peroxodisulphate, and 1.25 ml of ethanolic PCAPH solution, in that order, and make up to volume with distilled water. After 1 min transfer a portion of the reaction mixture to the spectrofluorimeter cell, kept at $55 \pm 0.1^\circ$, and after 2 min, start recording the fluorescence intensity (λ_{ex} 357 nm, λ_{em} 445 nm), and continue the recording for the next 12 min. Correct the measurements by subtracting those for a reagent blank. Calculate the reaction rate from the slope of the fluorescence vs. time curves.

Table 1. Characteristics of the kinetic photometric and fluorimetric methods for silver ($S_2O_8^{2-}$ as the oxidant)

Substrate	pH (buffer)	Activator	λ , nm	Range of applicability $\mu\text{g./ml}$	Reference
Oxine-5-sulphonic acid	2.2 (H_2SO_4)		366,485*	0.006-30	3
Oxine-5-sulphonic acid	1.5-3.5		375,485*	0.012-5	4
Bromopyrogallol Red	2 (HNO_3)	1,10-phenanthroline		0.001-0.013	5
Bromopyrogallol Red	4.62 (acetate)		500†	0.5-1	5
Pyridoxal nicotinyI hydrazone	10.5 (ammonia)		365,450*	0.06-0.72	6
Sulphanilic acid	4.35 (Britton)	2,2'-bipyridyl	535	0.0004-0.003	7
Sulphanilic acid	8.3 (Britton)	ethylenediamine	420	0.001-0.035	8
Sulphanilic acid	4.5 (Britton)		420	1-10	9
Fluorescein	7 (ammonium acetate)		491	0.5-1	10
HCl (0.3M)§	H_2SO_4 [0.22M]		420	0.002-0.008	11
Sodium nitrodiazoaminobenzene disulphonate	4.75		413†	0.0001-0.003	12
Luminol	12 (ammonia)	2,2'-bipyridyl		0.00001-0.00002	13
Direct Green	9.0-9.2	2,2'-bipyridyl	630†	0.0005-0.004	14
Direct Green	9.0-9.2	ethylenediamine	630†	0.0002-0.002	14
Cadion IREA	borate	triethylenetetramine	413	0.0043-0.043	15
Cadion IREA	borate	2-amino-2-methylpyridine	413	0.020-0.150	15
<i>o</i> -Dianisidine	4.5 (acetate)	3-acetylpyridine	450	0.03-2	16
Catechol Violet	7.25 (borate)		508†	0.0002-0.012	17
2-Hydroxybenzaldehyde thiosemicarbazone	ammonia†	2,2'-bipyridyl	365,440*	0.050-0.400	18
Phloxin	5 (acetate)		537	0.003-0.100	19
Phloxin	5 (acetate)		537,553*	0.0005-0.020	19

* λ_{exc} , λ_{em} .

†5-cm cells.

§Ce(IV) as the oxidant.

‡Ag(I) as inhibitor.

Determination of silver with 1,10-phenanthroline as activator

In a 25-ml standard flask place 3 ml of pH-8.0 buffer, 1.5 ml of 2.5M sodium nitrate, a known volume of sample (containing 0.11–2.5 μg of silver), 5 ml of 1,10-phenanthroline solution, 6 ml of 0.2M potassium peroxodisulphate, 1.25 ml of ethanolic PCAPH solution and make up to the mark with distilled water. Make the measurements as described for the method without activator.

Determination of silver in developed panchromatic plates

Treat a known area (about 4 cm^2) of the plate with 3 ml of 3M sodium hydroxide until the gelatinous film separates from the rigid support, which is discarded after washing. Then add 5 ml of concentrated nitric acid and heat until the silver has dissolved completely. Filter and make up to volume in a 100-ml standard flask with 1M nitric acid. Analyse suitable aliquots by using the methods described above, according to the expected silver concentration of the samples.

RESULTS AND DISCUSSION

Pyrocatechol-1-aldehyde 2-pyridylhydrazone (PCAPH) in alkaline media has a weak fluorescence (λ_{ex} 380 nm, λ_{em} 490 nm).²¹ In ammoniacal solution in the presence of oxidizing agents such as periodate, peroxodisulphate or hydrogen peroxide, the oxidation product from the reagent is brown and gives a strong yellow fluorescence (λ_{ex} 357 nm, λ_{em} 445 nm) which is stable for at least 1 hr. The oxidation is very slow in the presence of hydrogen peroxide (> 24 hr needed for completion) and faster with periodate; peroxodisulphate acts at an intermediate rate, Fig. 1.

Several metal ions have been tested as accelerators of the oxidation reactions. Mn(II), Au(III) and Pt(II) catalyse the action of periodate, and Ag(I), Mn(II) and Pt(II) that of peroxodisulphate, Ag(I) showing the highest catalytic action, Fig. 1.

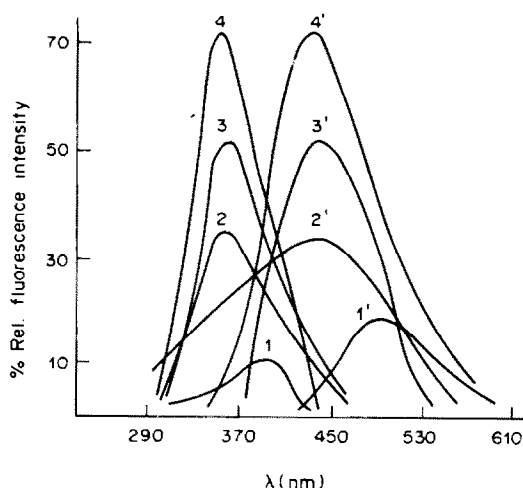


Fig. 1. Excitation and emission (') spectra of the oxidation product of PCAPH ($6.0 \times 10^{-3}M$), pH 8.2, $\lambda_{\text{em}} = 445$ nm, $\lambda_{\text{ex}} = 357$ nm, $t = 2$ hr: (1,1') PCAPH in absence of oxidant, $\lambda_{\text{em}} = 490$ nm, $\lambda_{\text{ex}} = 380$ nm; (2,2') in the presence of $S_2O_8^{2-}$ ($4.8 \times 10^{-2}M$); (3,3') in the presence of IO_4^- ($6.0 \times 10^{-3}M$); (4,4') in the presence of $S_2O_8^{2-}$ ($4.8 \times 10^{-2}M$) and Ag(I) (500 ng/ml).

Table 2. Summary of kinetic data

Concentration range, M	Dependence of the initial rate
$< 3.5 \times 10^{-5}$	$[\text{PCAPH}]^2$
$3.5 \times 10^{-5} - 6.3 \times 10^{-5}$	$[\text{PCAPH}]^0$
$> 6.3 \times 10^{-5}$	$[\text{PCAPH}]^{-1}$
$< 3.4 \times 10^{-2}$	$[\text{S}_2\text{O}_8^{2-}]^{1/2}$
$3.4 \times 10^{-2} - 5.8 \times 10^{-2}$	$[\text{S}_2\text{O}_8^{2-}]^0$
$> 5.8 \times 10^{-2}$	$[\text{S}_2\text{O}_8^{2-}]^{-1/2}$
$< 3.2 \times 10^{-9}$	$[\text{H}^+]^{2/5}$
$3.2 \times 10^{-9} - 4.0 \times 10^{-8}$	$[\text{H}^+]^0$
$> 4.0 \times 10^{-8}$	$[\text{H}^+]^{-1/3}$
< 0.18	$[\text{buffer}]^0$
> 0.18	$[\text{buffer}]^{-6/5}$
0.16–0.31	$[\text{ionic str.}]^0$

As with other substrate/ $S_2O_8^{2-}$ systems the catalytic action of silver(I) in the system PCAPH/ $S_2O_8^{2-}$ seems to involve the Ag(I)/Ag(II) redox cycle with peroxodisulphate as oxidant.⁶ An alternating change of the oxidation state during the reaction may also account for the catalytic effect of Mn(II) and Au(III).

Optimization of the reaction variables

The silver-catalysed oxidation of PCAPH by peroxodisulphate depends on the relative concentrations of buffer, reagent, oxidant, catalyst and ethanol, the pH, ionic strength and temperature. The system was optimized by changing each variable in turn while keeping the others constant. The optimum concentrations were taken as those giving a reaction order as close to zero as possible.³

From the results in Table 2 the conditions selected were $C_{\text{ox}} 4.8 \times 10^{-2}M$, $C_{\text{PCAPH}} 5.0 \times 10^{-5}M$, pH 8.0, and buffer concentration 0.06M.

Maximum and constant catalytic action is observed for pH 7.5–8.5 with ammonium/ammonia buffer, but not with other buffer solutions containing no *N*-donor substances, unless ammonia is added to them. Thus there may be a slight activation effect by ammonia.

Various sodium salts were used to study the influence of ionic strength (*I*) on the reaction rate, sodium nitrate showing the lowest effect. As seen in Fig. 2(A) for values of $I < 0.15M$ the rate of the reaction increases somewhat as theoretically expected,²³ and becomes stable at $I > 0.15M$. Therefore sodium nitrate was chosen to adjust the ionic strength to 0.21M.

The percentage of ethanol in the reaction medium has a strong influence on the reaction rate. Between 2 and 7% v/v the effect is slight, but is maximum for 12% v/v ethanol, Fig. 2(B). A 5% v/v ethanol–water medium was thus chosen for further work.

As this amount of alcohol is too small to affect the refractive index or the dielectric constant of the medium²⁴ and does not alter the absorption spectrum of the oxidation product or of PCAPH, the effect of ethanol on the reaction rate may be due to ethanol solvation of silver(I).

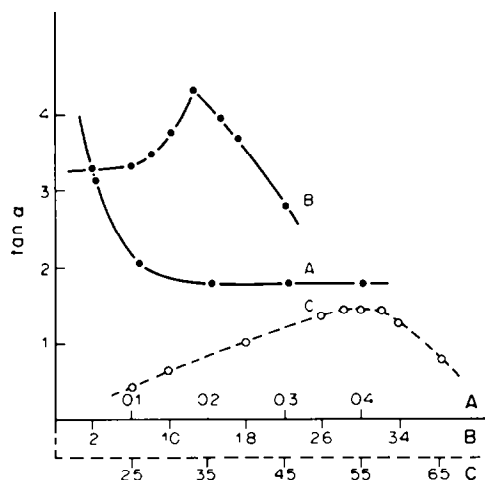


Fig. 2. Influence of (A) total ionic strength (M), (B) % v/v ethanol, and (C) temperature ($^{\circ}C$), on the reaction rate: $[PCAPH] = 6.0 \times 10^{-3} M$, $[S_2O_8^{2-}] = 4.8 \times 10^{-2} M$, $[Ag(I)] = 500$ ng/ml, $pH = 8.2$.

As shown in Fig. 2(C), the reaction rate is maximal over the range 52.5–57.5 $^{\circ}$, so a temperature of 55 $^{\circ}$ was chosen. Application of the Arrhenius equation to the data for the reaction rate at different temperatures gave the activation energy as 8.3 kcal/mole and the frequency factor as 1.16×10^6 sec $^{-1}$ for the catalysed reaction.

The order of addition of the reagents strongly influences the oxidation reaction rate, the order recommended giving the best results.

Activation effect of 1,10-phenanthroline

The effect of some N -donor substances previously employed for activation of $Ag(I)$ -catalysed oxidation reactions was examined, and their efficiency was found to decrease in the order 1,10-phenanthroline > 2,2'-bipyridyl > pyridine > 4-aminopyridine > ammonia. Thus 1,10-phenanthroline was chosen, and it was found that with addition of 5 ml of 0.01 M 1,10-phenanthroline to the reaction mixture, the optimum values for the other variables were the same as for the method without the activator. According to Bontchev and co-workers, activators of 2,2'-

Table 4. Interference levels of foreign ions in the determination of traces of silver by both methods

Tolerance ratio [ion]/[Ag(I)]*	Ion added
100†	Ca, Mg, Li, SO_4^{2-} , SO_3^{2-} , citrate, halides
50	Ba, Sr, Cr(III, VI), $S_2O_3^{2-}$, $B_4O_7^{2-}$, $C_2O_4^{2-}$, SCN^- , tartrate
25	W(VI), U(VI), Al, Ni, Pb, Cu, Co(II), CN^- , S^{2-} , ascorbate
1	Th, Ce(IV), Fe(II, III), Bi, Ga, In, Au(III), As(III), Mn, Be, Zn, Cd, Tl(I), IO_4^- , BrO_3^- , EDTA
< 1	Ti, Os(IV), La, Pd, Pt, Sn(II, IV), Hg(II)

*Ag(I) taken: 496 ng/ml in the method without activator and 50 ng/ml in the method with activator.

†Maximum ratio tested.

bipyridyl type accelerate the rate-determining step of the process, the oxidation of $Ag(I)$ to $Ag(II)$.^{1,25}

Characteristics of the methods

The fluorescence-time curves for different amounts of $Ag(I)$ with and without 1,10-phenanthroline present, were analysed by the tangent, fixed-time and fixed-fluorescence emission methods.²⁶ The fixed time chosen was 10 min; for the fixed emission method, 20% relative fluorescence intensity was selected as reference. The results in Table 3 show that the tangent method gives the highest sensitivity and precision with both methods of determination.

The selectivity of the methods was examined, with and without activator, by using the tangent method. The results are shown in Table 4.

The interferences are mainly chemical, from cations such as Os(IV), Ti(IV), Pd(II) and Pt(II), which have a slight catalytic effect on the oxidation reaction, or anions such as CN^- , $S_2O_3^{2-}$, EDTA, EGTA, *etc.*, which form stable silver complexes. There is also interference by ions such as Fe(II), Zn(II), Ga(II), In(III), *etc.* which form coloured or fluorescent complexes with PCAPH.

As shown in Table 4, use of 1,10-phenanthroline does not improve the selectivity.

Table 3. Characteristics of the kinetic methods

Method	Range of applicability, ng/ml	Ag(I) taken, ng/ml	Ag(I) found (\bar{x}), ng/ml	S^* , ng/ml	G , %
without activator					
tangent	200–800	494	494	9	1.2
fixed time	200–800	496	494	24	3.2
fixed intensity	200–800	496	497	20	2.7
with activator					
tangent	4–100	50	50.3	1.4	1.8
fixed time	20–100	50	48.4	2.2	3.1
fixed intensity	10–84	50	49.2	2.6	3.5

Number of determinations (n) = 10; \bar{x} = mean value; S = standard deviation; G = relative error (= $100tS/\bar{x}\sqrt{n}$; t = Student t for 95% confidence interval).

Table 5. Determination of silver in developed offset pan-chromatic plates

Sample	Silver found*, ng/ml	
	Kinetic-fluorimetric	A.A.S.
	method without activator†	
1	365	364
2	400	404
3	481	488
4	493	496
	method with activator‡	
5	10	10
6	29	30
7	51	50
8	70	71
9	90	91

*Mean values of three determinations; refers to concentration in stripping solution.

†Black zones of the plates.

‡White zones of the plates.

Determination of silver in developed offset pan-chromatic plates

As a practical application the methods were applied to determination of silver in developed pan-chromatic plates used in offset printing. Samples were taken from exposed and unexposed parts of each plate, and suitable aliquots of the solutions (depending on the expected silver concentration) were analysed as described and also by atomic-absorption spectrophotometry. Table 5 shows the agreement between the results.

Acknowledgement—The authors wish to acknowledge support of this work by CAICYT (Spain), grant no. 4133/1979.

REFERENCES

1. P. R. Bontchev, *Talanta*, 1979, **19**, 675.
2. D. P. Nikolalis and T. P. Hadjiioannu, *Rev. Anal. Chem.*, 1979, **4**, 81.
3. R. L. Wilson and J. D. Ingle, *Anal. Chem.*, 1977, **49**, 1066.
4. D. E. Ryan and B. K. Pal, *Anal. Chim. Acta*, 1969, **44**, 385.
5. H. Müller, H. Schurig and G. Werner, *Talanta*, 1974, **21**, 581.
6. M. A. Cejas, A. Gómez Hens and M. Valcárcel, *Mikrochim. Acta*, 1984 **III**, 349.
7. P. R. Bontschev, A. Alexiev and B. Dimitrova, *Talanta*, 1969, **16**, 597.
8. P. R. Bontschev, A. Alexiev and B. Dimitrova, *Mikrochim. Acta*, 1970, 1104.
9. A. Alexiev and P. R. Bontschev, *ibid.*, 1970, 13.
10. C. Sánchez-Pedreño, T. Pérez Ruiz, M. Hernández Córdoba and C. Martínez Lozano, *An. Quim.*, 1983, **79B**, 260.
11. P. R. Bontschev and A. Alexiev, *Mikrochim. Acta*, 1968, 875.
12. E. Yasinskene and E. Yankauskene, *Zh. Analit. Khim.*, 1966, **21**, 940.
13. N. M. Lukovskaya and T. A. Bogoskovskaya, *Ukr. Khim. Zh.*, 1975, **41**, 200.
14. E. Yasinskene and N. Rasevicenka, *Zh. Analit. Khim.*, 1970, **25**, 458.
15. E. Yasinskene and E. Yankauskene, *Lietuvos T.S.R. Moksh. Akad. Darbai, Ser. B*, 1965, 113; *Chem. Abstr.*, 1966, **64**, 13379c.
16. C. Sánchez-Pedreño, M. Hernández Córdoba and P. Viñas, *Microchem. J.*, 1985, **32**, 242.
17. E. Yasinskene and E. Yankauskene, *Trudy Akad. Nauk. Lit. S.S.R.*, 1968, 41; *Anal. Abstr.*, 1970, **18**, 3754.
18. A. Moreno, M. Silva and D. Pérez Bendito, *Anal. Lett.*, 1983, **16**, 747.
19. M. Hernández Córdoba, C. Sánchez-Pedreño and P. Viñas, *Quim. Anal.*, 1985, **4**, 159.
20. M. Valcárcel and F. Grases, *Talanta*, 1983, **30**, 139.
21. A. M. Afonso, J. J. Santana and F. Garcia Montelongo, *Analyst*, 1986, **111**, 327.
22. I. M. Kolthoff, E. B. Sandell, E. J. Meehan and S. Bruckenstein, *Quantitative Chemical Analysis*, 4th Ed., p. 795. Macmillan, London, 1969.
23. M. Kopanica and V. Stará, in Wilson and Wilson's *Comprehensive Analytical Chemistry*, G. Svehla (Ed.), Vol. XVIII, p. 31. Elsevier, Amsterdam, 1983.
24. E. W. Washorn (ed.), *International Critical Tables*, McGraw-Hill, New York, 1933.
25. P. R. Bontchev, A. Alexiev and B. Dimitrova, *Talanta*, 1966, **16**, 597.
26. K. B. Yatsimirskii, *Kinetic Methods of Analysis*, p. 35. Pergamon Press, Oxford, 1966.

TRACE ZINC DETERMINATION BY SYNCHRONOUS DERIVATIVE FLUORIMETRY

F. GARCIA SANCHEZ and M. HERNANDEZ LOPEZ

Department of Analytical Chemistry, Faculty of Sciences, The University, Malaga, Spain

(Received 27 May 1985. Revised 12 May 1986. Accepted 6 June 1986)

Summary—A sensitive and selective synchronous-scanning derivative spectrofluorimetric determination of zinc based on the formation of a fluorescent chelate with 2-furaldehyde 2-pyridylhydrazone (FAPH) is described, and its analytical performance compared with that of the ordinary fluorimetric method. The detection limits lie in the ng/ml range and the coefficient of variation is below 2% in both cases. The methods have been applied to the trace determination of zinc in pig liver tissue and environmental fume samples.

Zinc is essential for growth of micro-organisms, plants and animals, plays an important role in the metabolism of proteins and nucleic acids and is apparently essential for synthesis of DNA and ribosomal RNA.¹

This paper is concerned with the scanning derivative spectrofluorimetric determination of zinc at trace levels. The method, which overcomes sensitivity problems, is based on the specific fluorogenic reaction of zinc with 2-furaldehyde 2-pyridylhydrazone (FAPH).

Several *N*-heterocyclic hydrazones have been used as chromogenic and fluorogenic reagents in the determination of metal ions,² but very few heterocycles with oxygen or sulphur atoms in the aldehyde or hydrazine moieties have been used. The reasons for this are the decreased complexing capacity of the modified ligand structure, and associated instability problems.^{3,4} FAPH gives coloured chelates with several metal ions,⁴ and a specific fluorescence reaction with zinc.

In fluorimetric methods the sensitivities and detection limits are often limited by the nature of the analyte and by the reagent blank signal. However, proper manipulation of the information produced by spectroscopic techniques may lead to a gain in sensitivity. Recently⁵⁻⁸ it has been shown that synchronous scanning combined with derivative fluorescence spectroscopy may be valuable for obtaining better sensitivity and detection limits.

EXPERIMENTAL

Apparatus

A Perkin-Elmer fluorescence spectrophotometer, model MPF-43A, was used, equipped with an Osram XBO 150-W xenon lamp, excitation and emission grating monochromators, 1 × 1-cm fused silica cells, a Hamamatsu R-777 photomultiplier and a Perkin-Elmer 023 recorder. A standard bar of Rhodamine B ($1 \times 10^{-7}M$) gave a fluorescence

signal of 64 units at the following settings: slits 5 nm; sensitivity, coarse 10, fine 7; temperature 25°. It was used to adjust the spectrofluorimeter daily to compensate for changes in source intensity. The fluorescence data are given without spectral correction. To obtain the derivative spectrum, computed numerically, a differential corrected-spectra unit (Perkin-Elmer model DCSU-4) was connected to the spectrofluorimeter. An ultrathermostatic water-bath circulator (Frigitem S-382) was used for temperature control.

Reagents

Fural-2-aldehyde 2-pyridylhydrazone (FAPH) was synthesized in the usual way for hydrazones,⁹ as reported earlier.¹⁰ Solutions ($5 \times 10^{-3}M$) in absolute ethanol were prepared weekly. A 0.1M zinc stock solution was prepared from zinc sulphate heptahydrate in 0.5M sulphuric acid and standardized by EDTA titration. Solutions of lower concentrations were made by dilution with demineralized water. A pH-12.3 buffer solution was prepared from 0.1M glycine and 0.1M sodium hydroxide.

Unless otherwise stated, the reagents were of analytical reagent grade.

Procedures

Normal spectrofluorimetry. Place an aliquot of sample containing 1.25–17.5 µg of zinc and 5 ml of $5 \times 10^{-3}M$ FAPH solution in a 25-ml standard flask. Add 2.5 ml of absolute ethanol followed by 5 ml of pH-12.3 glycine buffer solution. Dilute the mixture to volume with demineralized water and store in the dark until measurement of the fluorescence intensity at 480 nm, with excitation at 426 nm, against a reagent blank.

Synchronous scanning derivative spectrofluorimetry. Place an aliquot of sample (containing 0.25–3.0 µg of zinc) and 5 ml of $5 \times 10^{-3}M$ FAPH solution in a 25-ml standard flask. Add 2.5 ml of absolute ethanol followed by 5 ml of pH-12.3 glycine buffer solution. Dilute to volume with demineralized water and store in the dark until measurement. Record the first or second derivatives ($\Delta\lambda = 10$ nm) of the synchronous spectrum at $\lambda_{em} - \lambda_{ex} = 54$ nm with a time-constant of 0.3 sec and a scan-speed of 120 nm/min. Measure the first derivative peak amplitude from peak to trough, and the second derivative from a trough to the mid-point between its neighbouring peaks.

Analysis of samples

Determination of zinc in environmental fume samples. Fume samples were collected in workshop environments

according to the NIOSH Manual,¹¹ as described previously.¹² An aliquot of the solution obtained was subjected to the synchronous derivative procedure.

Determination of zinc in pig liver tissue. Fresh pig liver (10–15 g) was cut into small portions, care being taken to exclude major blood vessels and connective tissue. The liver was dried at 120° to constant weight, and a 3–4 g sample, accurately weighed, was treated with 10 ml of concentrated nitric acid and 5 ml of concentrated sulphuric acid in a Kjeldahl flask. The mixture was strongly heated until nitrous vapours ceased, and then cooled to room temperature; 3 ml of concentrated perchloric acid were added and the mixture was again strongly heated until nearly dry. After cooling, the residue was taken up and diluted accurately to 50 ml with demineralized water. A clear solution was obtained. Aliquots of this solution were added to different volumes of a standard solution of zinc and then subjected to the standard synchronous-derivative procedure, except that the buffer was introduced before the addition of FAPH.

RESULTS

The FAPH–zinc system; effect of experimental variables

Studies on the reactions of FAPH with metal ions showed that the compound appears to be a fluorogenic reagent for zinc(II).

The excitation and emission spectra of the zinc–FAPH complex in 30% v/v ethanol/water mixture, at an apparent pH of 12.30, are shown in Fig. 1. The presence of Zn(II) produces a considerable increase in the reagent fluorescence intensity. The maximum emission occurs at 480 nm, with excitation at 426 nm.

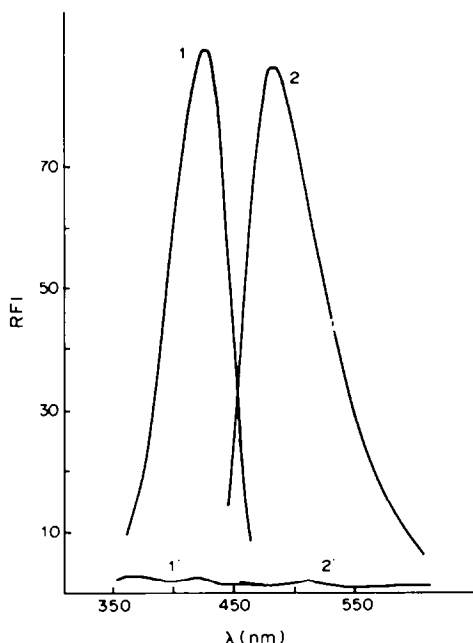


Fig. 1. Excitation (1, 1') and emission (2, 2') spectra of FAPH (1', 2') and its zinc complex (1, 2). $[Zn] = 4 \times 10^{-3}M$; $[FAPH] = 8 \times 10^{-5}M$; apparent pH 12.3; ethanol 30% v/v; sensitivity, coarse 1, fine 7.

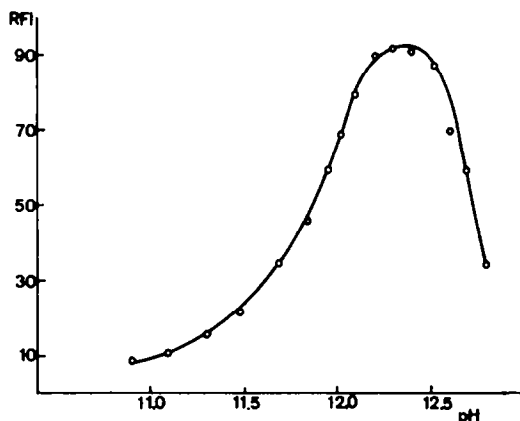


Fig. 2. Effect of pH on the formation of the zinc–FAPH chelate. $[Zn] = 4 \times 10^{-3}M$; $[FAPH] = 8 \times 10^{-5}M$.

Studies on the effect of acidity showed that chelate formation is most complete in alkaline medium. For 30% ethanol solutions, it was found that chelate formation is complete at an apparent pH between 12.2 and 12.4 (Fig. 2). This is expected for this type of ligand, a ferroin-type compound acting as a terdentate planar chelating agent if it is assumed that complexation is accompanied by deprotonation of the imine group of the ligand.

The alkaline medium ensures the formation of a neutral stable 2:1 ligand/metal chelate, given the hexaco-ordinate character of zinc. In the proposed procedure, the pH can be adequately adjusted to the desired range by addition of 5 ml of pH-12.3 0.1M glycine buffer, provided the initial sample pH is in the range 7–12.

The concentration of ethanol in the reaction solution must be precisely controlled, because it causes two opposite effects that counterbalance the effect on the fluorescence intensity and on the stability of the measurements. If the ethanol content is below 10% the solutions are turbid. The fluorescence intensity increases by 55% as the ethanol concentration is increased from 20 to 40%; higher percentages, from 40 to 90%, decrease the fluorescence intensity by 75%. Use of 30% ethanol is satisfactory, giving stable and high fluorescence intensity.

No fluorescence inversion is caused by an excess of reagent up to at least $1.4 \times 10^{-3}M$. Accordingly, 5 ml of $5 \times 10^{-3}M$ FAPH is used in a final volume of 25 ml. The order of addition of the reagents is immaterial. Raising the temperature from 10 to 30° decreases the relative fluorescence intensity from 95 to 25%. The work reported here was done at $15 \pm 0.5^\circ$.

It was observed that exposure of the solutions to light causes fading of the fluorescence (Fig. 3). To ensure better reproducibility, it is important to use a narrow excitation slit and to keep the solutions in darkness until measurement. Under these conditions the chelate formation is instantaneous and the fluorescence stable for at least 1 hr. Mole-ratio and

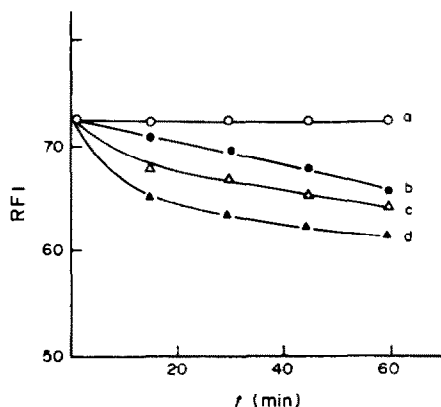


Fig. 3. Effect of light on the fluorescence intensity. (a) Solution stored in darkness. (b) Solution exposed to room light. (c) and (d) Solutions exposed to excitation radiation (band-pass 4 nm and 10 nm respectively).

continuous-variations plots showed that the molar ratio of FAPH to zinc in the complex is 2:1.

FAPH suffers *syn-anti* photochemical transformation, which severely restricts its ability to form co-ordination compounds with metal ions,⁴ but the *syn*-isomer gives an intensely fluorescent chelate with zinc in alkaline medium, whereas the *anti*-isomer does not. Further, this reaction is specific, since no other ion tested gives a fluorogenic reaction with either isomer. The fluorescence emission is highly temperature-dependent.

The difference in reactivity of the *syn*- and *anti*-isomers with zinc can be related to the steric rearrangement caused by the photoisomerization. The *syn*-isomer gives a fluorescent compound because its terdentate character in this form permits the formation of a zinc chelate with extended resonance and induced rigidity. In contrast, the *anti*-isomer gives reduced rigidity and resonance because it is only bidentate.

Support for this hypothesis is provided by the 60% decrease in the fluorescence intensity when the temperature is increased from 10 to 20°. It is not easy to relate this temperature effect to the internal conversion deactivation process but it may be due to a thermal isomerization of the ligand. This hypothesis is reasonable if the thermal barrier is low enough to provide the major route for deactivation of the excited state.¹³

As we have discussed elsewhere,¹⁴ the π -donor character of the furan oxygen atom may be responsible for the selectivity of the zinc reaction.

Synchronously scanned first and second derivative spectrofluorimetry

As discussed above, the band-narrowing effect of the synchronous approach is essential in increasing the derivative amplitudes. Thus, appropriate selection of the constant difference in wavelength between the two monochromators is critical. Although the peak position and half-width ($\lambda_{s,em}$ and $\Delta\lambda_{s,em}$, respectively) can be calculated and predicted,¹⁵ these parameters should be empirically optimized. Application of these calculations gave $\lambda_{s,em} = 480$ nm and $\Delta\lambda_{s,em} = 45.4$ nm.

For empirical selection of the values, various synchronous spectra at different wavelength differences near the Stokes shift were recorded. The best results were obtained for $\lambda_{em} - \lambda_{ex} = 54$ nm. The apparatus used offered three time-constants and four scan-speeds. A combination of a scan-speed of 120 nm/min and a time-constant of 0.3 sec was found to be the best (Fig. 4). For recording either first or second derivative spectra, three different wavelength increments are possible in the DCSU-2 unit (2, 5 and 10 nm). A 10-nm increment was employed; it gave the best signal-to-noise ratio but the lowest resolution (Fig. 4).

Analytical parameters

The calibration graphs were linear over the range 0–120 ng/ml zinc. The ordinary fluorimetry calibration graph is linear over the range 0–700 ng/ml.

The calculated detection and determination limits, together with the sensitivity and the standard deviations of the blank measurements, S_B , and of the analytical signals, S_S , are given in Table I.

Effect of foreign ions

The effect of various species and ions on the determination of zinc at the 0.5 μ g/ml level by normal spectrofluorimetry was examined over a wide range of concentrations. The main interferences in the ordinary fluorimetric method were eliminated by using common masking agents. Those species which interfered in the normal method were investigated by the synchronous derivative approach, with solutions containing 80 ng/ml zinc. The tolerance criterion was

Table I. Characteristics of the analytical methods [A ordinary spectrofluorimetry; B synchronous scanning (first derivative); C synchronous scanning (second derivative)]

Method	S_B	S_S	$C_L (k=3)^*$, ng/ml	$C_Q (k=10)^*$, ng/ml	L.D.R., † ng/ml	Amount taken, ng/ml	Amount found, ng/ml	n	RSD, %
A	0.7 I _F	0.9 I _F	15	50	50–700	500	504	10	1.3
B	0.2 cm	0.2 cm	3	10	10–120	40	41.3	8	2.0
C	0.2 cm	0.2 cm	5	15	15–120	40	40.8	8	1.7

* C_L = limit of detection; C_Q = limit of determination.

†L.D.R. = linear determination range.

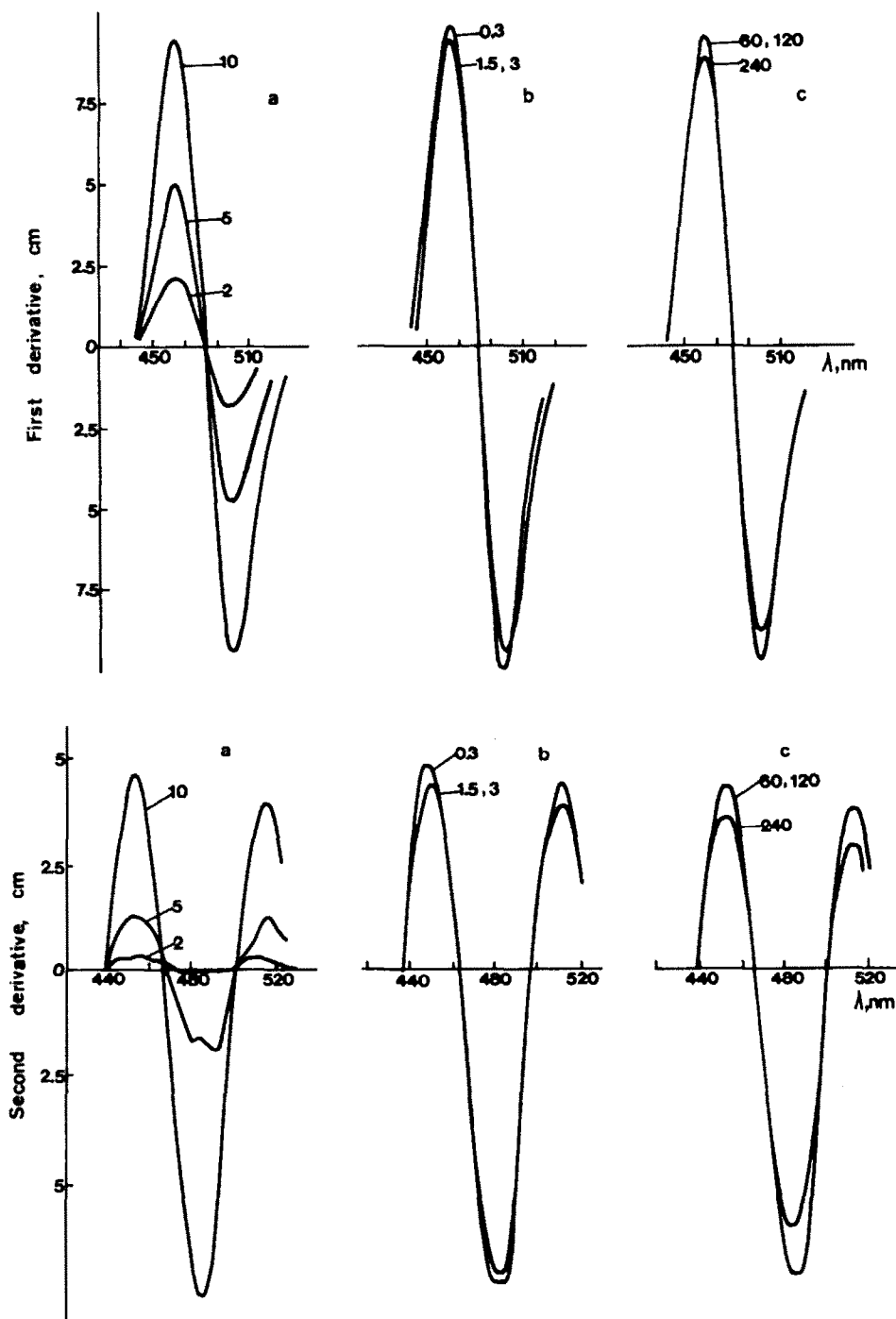


Fig. 4. Influence of instrumental parameters on the first (top) and second (bottom) derivative synchronous spectra: (a) $\Delta\lambda'$ (with scan-speed 120 nm/min and time-constant 0.3 sec); (b) time-constant (with scan-speed 120 nm/min); (c) scan-speed (with time-constant 0.3 sec). $[Zn] = 7.6 \times 10^{-6}M$; $[FAPH] = 1 \times 10^{-3}M$; band-pass, 10 nm.

deviation of the analytical signal by more than two standard deviations from the mean value expected for zinc alone. The results obtained are shown in Table 2, from which it may be deduced that in this case only moderate selectivity is gained in the synchronous derivative approach, and the addition of masking agents is generally more efficient.

Application to real samples

Because the procedures are specially recommended for zinc trace analysis, they were applied to two types of sample: a biological matrix (pig liver tissue) and an inorganic matrix (environmental metallic fume samples). A summary of the results obtained is given in Table 3.

Table 2. Tolerance for foreign ions

Ion added		Tolerance ratio, ion to Zn ²⁺ (w/w)	
Method A (ordinary)		Method B (synchronous)	
without masking	with masking		
urea, acetate, citrate, I ⁻			2.8 × 10 ⁴
F ⁻ , SCN ⁻			1.4 × 10 ⁴
S ₂ O ₃ ²⁻			7 × 10 ³
	^a Al ³⁺		4 × 10 ³
NH ₃ , C ₂ O ₄ ²⁻ , tartrate, PO ₄ ³⁻ , Ca ²⁺			2 × 10 ²
ascorbic acid, thiourea, H ₂ O ₂ , TEA			40
ethylenediamine, Ni ²⁺	^b Fe ³⁺ , ^c Mg ²⁺		20
Al ³⁺	^b Cr ³⁺		10
Ag ⁺ , Tl ³⁺ , Ga ³⁺	^d Cd ²⁺ , ^b Mn ²⁺	Pd ²⁺ , Mn ²⁺ , Co ²⁺	5
EDTA, CN ⁻ , Be ²⁺	^b Co ²⁺	Fe ³⁺	2
NTA, dimethylglyoxime, Cd ²⁺ , Fe ³⁺	^b Cu ²⁺	Cd ²⁺ , Cu ²⁺	1
Mn ²⁺ , Pd ²⁺ , Co ²⁺		Cr ³⁺ , Mg ²⁺	0.5
Cu ²⁺ , Cr ³⁺ , Mg ²⁺			0.1

^aAcetate, 14 mg/ml.

^bCitrate, 14 mg/ml.

^cFluoride, 7 mg/ml.

^dThiocyanate, 7 mg/ml.

Table 3. Determination of zinc in samples of pig liver tissue and in environmental metallic fumes

Samples	Zn present, ^a ng/ml	Zn found, ng/ml		Zn content†	
		1st derivative	2nd derivative	µg/g	mg/m ³
Pig liver	41.2 ^a	42.3 ± 1.2	41.9 ± 1.0	177	
Pig liver	38.4 ^a	40.5 ± 0.9	39.6 ± 0.7	165	
Pig liver	40.4 ^a	41.8 ± 1.0	40.8 ± 0.7	173	
Metallic fumes	60.0 ^b	61.2 ± 1.1	61.0 ± 1.0		1.25
Metallic fumes	58.2 ^b	59.3 ± 0.8	59.2 ± 0.7		1.66
Metallic fumes	82.1 ^b	83.2 ± 1.0	82.6 ± 0.8		1.85

^aIn solution analysed; ^astandard-addition method; ^bby atomic-absorption spectrometry.

†In original sample (dried liver, air).

REFERENCES

- O. S. Chauhan, B. S. Garg, R. P. Singh and I. Singh, *Talanta*, 1981, **28**, 399.
- M. Katyal and Y. Dutt, *ibid.*, 1975, **22**, 151.
- F. Garcia Sánchez and M. Hernández López, *Analyst*, 1985, **110**, 1253.
- Idem*, *Talanta*, 1985, **32**, 967.
- C. Cruces Blanco and F. Garcia Sánchez, *Anal. Chem.*, 1984, **56**, 2035.
- F. Garcia Sánchez, A. Navas and M. Santiago, *Anal. Chim. Acta*, 1985, **167**, 217.
- C. Cruces Blanco and F. Garcia Sánchez, *J. Assoc. Off. Anal. Chem.*, 1986, **69**, 105.
- A. F. Fell, *Trends Anal. Chem.*, 1983, **2**, 63.
- J. S. Geldard and S. Lions, *Inorg. Chem.*, 1963, **2**, 270.
- M. Hernández López and F. Garcia Sánchez, *An. Quim.*, 1981, **77B**, 112.
- National Institute of Safety and Hygiene, *Manual of Sampling Data Sheets*, Cincinnati, Ohio, 1976.
- A. Navas and F. Sanchez Rojas, *Talanta*, 1984, **31**, 437.
- H. Izawa, P. de Mayo and T. Tabata, *Can. J. Chem.*, 1969, **47**, 51.
- M. R. Martinez de la Barrera, J. J. Laserna and F. Garcia Sánchez, *Anal. Chim. Acta*, 1983, **147**, 303.
- J. B. F. Lloyd and I. W. Ewett, *Anal. Chem.*, 1977, **49**, 1710.

ELECTROANALYTICAL DETERMINATION OF VINCA ALKALOIDS USED IN CANCER CHEMOTHERAPY*

AYTEKIN TEMIZER

Department of Analytical Chemistry, Faculty of Pharmacy, Hacettepe University, Ankara, Turkey

(Received 1 April 1985. Revised 28 April 1986. Accepted 6 June 1986)

Summary—A differential pulse polarographic method has been developed for determination of the antineoplastic agents vincristine and vinblastine at ng/ml level, in biological fluids such as plasma and urine. The vincristine and vinblastine are extracted from urine with Amberlite XAD-2. Linear calibration plots are obtained for both over the concentration range 0.005–5 μ g/ml. The relative standard deviations found were 1.7% for analysis of the pure drugs, 7.3% for urine and 8.6% for plasma.

Vincristine (VCR) and vinblastine (VLB) are representative of a class of dimeric alkaloids containing both an indole and a dihydroindole nucleus.¹ These plant alkaloids of the vinca group have been employed for many years as chemotherapeutic agents in the treatment of various neoplastic diseases.^{2,4} The efficacy of VCR or VLB therapy could probably be improved by continuous monitoring of the concentration of the drugs in plasma and urine during treatment, and adjustment of the dose accordingly. VCR or VLB levels are routinely measured by radioimmunoassay.^{5,6} Studies with tritium-labelling in the 4-acetyl position or in the indole aromatic ring of VCR or VLB have proved that these drugs are only slightly metabolized.⁷⁻⁹ HPLC studies have also shown that these drugs are excreted with body fluids nearly unchanged.¹⁰ Procedures developed for detecting VCR or VLB in body fluids include radioimmunoassay,¹¹⁻¹³ microbiological assays,^{14,15} and HPLC.^{10,16} Electrochemical oxidation of vinblastine, catharanthine and vindole at a carbon-paste anode has also been investigated.¹⁷

Alkaloids, in general, produce catalytic waves at the dropping mercury electrode, to an extent that is dependent on the ring system involved. Catalytic hydrogen evolution caused by nitrogen-containing substances or alkaloids has been the subject of several studies.¹⁸⁻²¹ Opium, hydrastic, ipecacuanha, cinchona, tropane and some other alkaloids have been determined by d.c. polarography in the range 10^{-4} – 10^{-3} M in basic buffers.²² Differential pulse polarography (DPP) in conjunction with the extraction of plant material has been used for the determination of pyrrolizidine alkaloids extracted from different *Senecio* species.²³

The purpose of the present work is to describe a sensitive, rapid and easy DPP method for the deter-

mination of VCR and VLB in pure solutions and in biological fluids such as plasma and urine.

EXPERIMENTAL

Material

The water used for solution preparation was distilled in a Barnstead apparatus, then demineralized in a high-capacity mixed-bed resin and finally triply distilled in a Pyrex still to give a product with less than 1 μ mho conductivity. Triply distilled mercury was used throughout. VLB sulphate (lot P87007) and VCR sulphate (lot P66209) (Eli Lilly) were used as received. All chemicals were ACS reagent grade.

Plasma samples were obtained from patients with different kinds of carcinoma who were receiving intermittent chemotherapy, generally by rapid intravenous infusion. None of the patients was receiving other drugs by infusion or antibiotics before venous blood was drawn. It was drawn from the opposite arm 5 min after drug infusion through an indwelling heparin lock. The plasma samples were stored at 4° overnight, then centrifuged at 5000 rpm for 15 min.

Apparatus

An EGG Princeton Applied Research Corp. model 174A polarographic analyser with a Houston Omnigraphic model 2000 X-Y recorder was used. To decrease the IR drop, the reference electrode was located in a salt bridge and connected to the solution by a Luggin capillary with its tip placed close to the tapered dropping-mercury electrode capillary. The capillary used had a mercury flow-rate (m) of 0.232 mg/sec in 0.25M ammonia/0.25M ammonium chloride buffer (pH 9.3) that was 10^{-4} M in tetraethylammonium hydroxide, in open circuit with a mercury height of 80.0 cm. All experiments were performed in a jacketed polarographic cell at a preselected temperature. A Faraday cage and electronic filters were used to eliminate electronic noise. The potentials were taken with Heath Universal Digital Instrument model EU-805.

Polarographic techniques

Polarographic investigations were performed with solutions that had previously been deaerated by passage of oxygen-free nitrogen for 10 min. The purified nitrogen was equilibrated with the supporting electrolyte in a gas-dispersion bottle containing a solution identical to the test solution, to avoid evaporation of the latter in the polarographic cell. This is particularly important here because of the choice of an ammoniacal buffer as supporting electro-

*This work was presented at the 1st International Symposium on Drug Analysis, Brussels, 1983.

lyte. Current *vs.* potential curves were recorded in the d.c., fast, PP and DPP modes. Each solution was scanned over the potential range from -1.2 to -1.7 V *vs.* SCE. A scan-rate of 5 mV/sec, drop-time of 1 sec, modulation amplitude of 50 mV, 90-cm height of the mercury column, and a temperature of $20 \pm 0.01^\circ$ were typically employed.

Extraction procedures

Among the standard techniques used for concentration and clean-up of biological samples are solvent extraction and adsorption on columns of a non-polar adsorbent. Amberlite XAD-2 is particularly suitable for column work because of its inertness at all pH values and its relatively strong adsorbent properties.²⁴⁻²⁶ VCR and VLB were extracted from urine samples by use of this non-ionic resin; 2.1 g of it were packed between pieces of cotton in a commercial polypropylene tube 1.0 cm in diameter and 9.1 cm long. The column was washed with water before use and then the ammoniacal buffer solution (pH 9.3) was passed through it. The urine sample (20 ml) containing VCR or VLB was made

basic with 2M sodium hydroxide and passed through the column, which was then washed with 10 ml of water. The second piece of cotton was taken out, and the VCR or VLB was extracted from the Amberlite XAD-2 by passage of three 5-ml portions of chloroform.²⁵ Plasma samples were adjusted to pH 9.3 with 2M sodium hydroxide and a 10-ml aliquot was extracted with three 10-ml portions of chloroform. The organic fractions thus obtained were evaporated to dryness in the polarographic cell under a stream of nitrogen at room temperature, and 3 ml of the supporting electrolyte mixture were added to the residue. The VCR or VLB was then determined polarographically, the standard-addition technique being used for analysis of biological samples.

RESULTS AND DISCUSSION

Differential pulse polarograms for various concentrations of VCR and VLB in the 0.25M ammoniacal

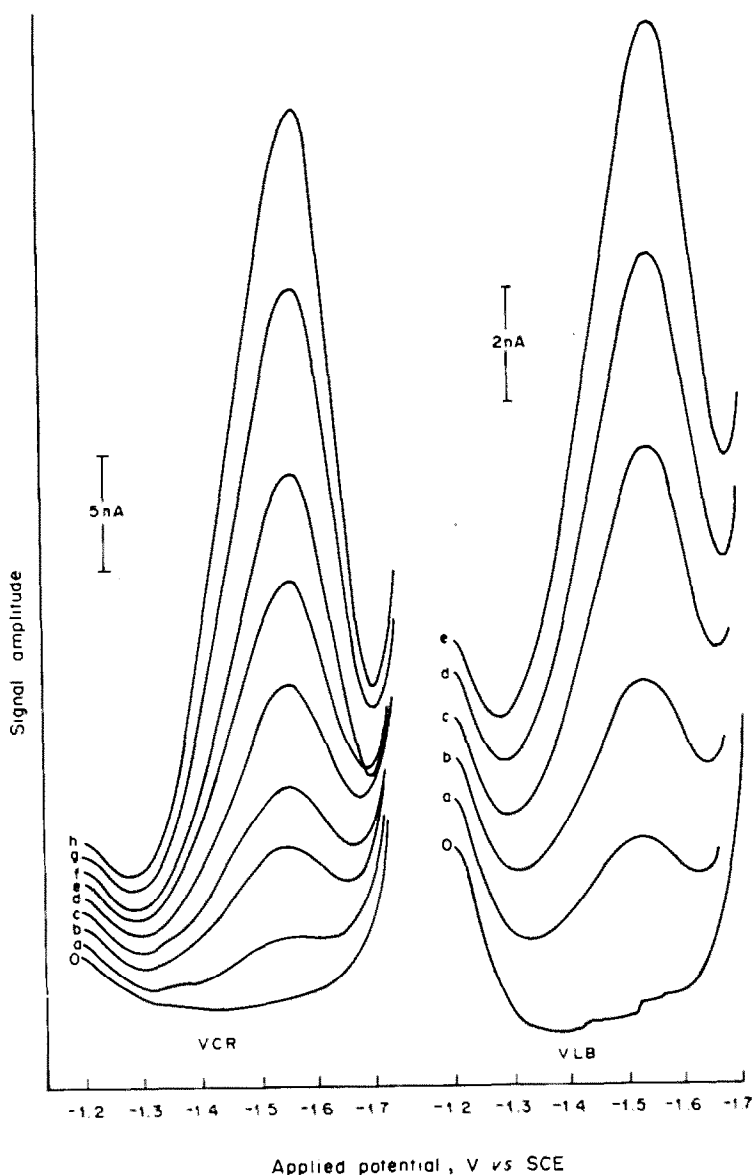


Fig. 1. Differential pulse polarograms of VCR and VLB in 0.25M $\text{NH}_3/0.25\text{M}$ NH_4Cl buffer at pH 9.3 (10^{-4}M Et_4NOH). VCR: o, 0; a, 0.012; b, 0.040; c, 0.062; d, 0.110; e, 0.170; f, 0.234; g, 0.330; h, 0.337 $\mu\text{g/ml}$. VLB: o, 0; a, 0.28; b, 0.56; c, 1.17; d, 1.72; e, 2.33 $\mu\text{g/ml}$.

Table 1. Linear regression characteristics of calibration graphs for VCR and VLB in 0.25M NH₃/0.25M NH₄Cl buffer at pH 9.3 (with 10⁻⁴M Et₄NOH) by DPP (12 data points)

	VCR	VLB
Linear range, $\mu\text{g/ml}$	0.005–5	0.005–5
Slope \pm S.D., $nA.ml.\mu\text{g}^{-1}$	62.1 ± 0.4	3.94 ± 0.06
Intercept, nA	1.2	-0.04

buffer at pH 9.3 and containing tetraethylammonium hydroxide are shown in Fig. 1. Some polarograms, especially those near the lower limit of detection, have been omitted for clarity. The concentration of VCR and VLB is proportional to the signal amplitude over the range 0.005–5 $\mu\text{g/ml}$ (Table 1). Higher concentrations cause curvature of the calibration plot to give a curve similar to a Langmuir adsorption isotherm.

VCR and VLB are large organic molecules used separately in cancer chemotherapy. The most important point in the electroanalysis of these molecules is their adsorption on the electrode surface. After a certain degree of coverage of the electrode surface by the adsorbed molecules, their interaction promotes further adsorption and the surface coverage increases faster than would be expected. An adsorption current was observed at VCR or VLB concentrations above 5 $\mu\text{g/ml}$ as shown by variation of the limiting adsorption current with change in mercury head. Further evidence of adsorption was shown by the dependence of the adsorption wave on temperature, the temperature coefficient being negative. From 5 $\mu\text{g/ml}$ down to 5 ng/ml, the range of calibration, a catalytic current was observed. On account of their complexity, the catalytic peaks for hydrogen evolution have been considered as a special and very interesting branch of polarography. The effect of temperature and height of the mercury head on the peak current proved that the peaks given in Fig. 1 were catalytic in nature; the temperature coefficient was about -4.7%/deg and there was no relationship between the peak current and the height, or square root of the height, of the mercury column. The dependence of the limiting peak current on the VCR or VLB concentration in ammoniacal buffer alone has the form of a Frumkin adsorption isotherm, *viz.* it is S-shaped and calibration cannot be done.²⁷ If a quaternary ammonium salt is added to the buffer, however, the calibration plot has the form of the Langmuir adsorption isotherm, and is linear below 5 $\mu\text{g/ml}$ alkaloid concentration.

The peak potentials of VCR and VLB in the proposed supporting electrolyte are -1.485 and -1.509 V *vs.* SCE respectively. VCR and VLB are never used together in combined chemotherapy, so this similarity in peak potentials is not important. The slope of the calibration graph is higher for VCR than for VLB, as seen in Table 1, presumably owing to the difference in molecular structure, the CHO-

Table 2. Effect of pH on peak current

pH	$i(\text{VCR}), nA$	$i(\text{VLB}), nA$
8.0	58	34
8.2	82	49
8.4	94	66
8.6	110	75
8.8	120	84
9.1	134	98
9.2	138	100
9.3	140	105
9.4	120	90
9.5	100	70

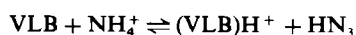
group in VCR being replaced by a CH₃ group in VLB. The lower limits of detection of VCR and VLB by DPP have been found to be lower by a factor of 10³ than those obtainable by anodic oxidation.¹⁷ This is due to the use of DPP in conjunction with a dropping mercury electrode, and the catalytic character of the current.

Compounds containing nitrogen, phosphorus, arsenic or sulphur, that are capable of binding a proton to the free electron-pair of these atoms, are catalytically active.^{21,28,29} The catalytic evolution of hydrogen in the polarography of a large number of different alkaloids shows that the catalytic action is due to the alkaloid accepting an electron from the electrode and transferring it to the hydrogen ion in the solution.¹⁸⁻²³ The catalytic currents due to alkaloids are ascribed to the nitrogen-containing group.

The peak height for VCR and VLB increases when the drop-time increases, because the time available for adsorption is longer. The best drop-time was chosen as 1 sec per drop. The peak heights were found to be proportional to the modulation amplitude. The highest accuracy and precision were obtained with 50-mV modulation amplitude.

The peak potentials and limiting currents of VCR and VLB change with pH. At pH > 10 the peak disappears and at pH < 7 it cannot be observed because of masking by hydrogen evolution from the buffer. The pH is quite critical, and should be controlled to better than ± 0.1 (Table 2).

The catalytic reduction was greatest for an equimolar mixture of the buffer components. Mairanovskii has suggested that for an organic substance to catalyse hydrogen evolution it should be able to exist as a conjugate acid-base pair, which can interact with an acid-base system in the supporting electrolyte,³⁰ *e.g.*,



When the protonated cation is discharged at the electrode, a possible mechanism for hydrogen evolution is

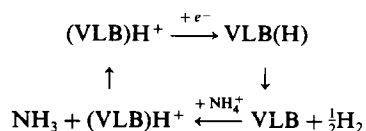


Table 3. Recoveries of VCR and VLB added (ng) to 10 ml of urine or 1 ml of plasma

Alkaloid	Urine		Plasma	
	Added	Found	Added	Found
VCR	40.0	37.0 ± 2.0	4.0	3.6 ± 0.3
VLB	40.0	37.2 ± 2.7	4.0	3.8 ± 0.3

Determination of VCR and VLB in body fluids

The normal concentration of VCR and VLB in biological fluids is $< 0.1 \mu\text{g/ml}$.³¹ The limit of detection in this method is about 1/20 of this value for VCR and 1/5 for VLB. The recovery test results for urine and plasma samples spiked with realistically low levels are shown in Table 3. The relative standard deviation was found to be 1.7% for analysis of pure solutions of the drugs, 7.3% for urine and 8.6% for plasma, and the recoveries were all low, ranging from 90 to 96%.

Acknowledgements—The author wishes to thank Prof. Namik Cevik for supplying biological fluids from the Department of Pediatric Oncology, Faculty of Medicine, Hacettepe University, Ankara.

REFERENCES

1. N. Neuss, M. Gorman, W. Hargrove, N. J. Cone, K. Biemann, G. Büchi and R. E. Manning, *J. Am. Chem. Soc.*, 1964, **86**, 1440.
2. R. L. Noble, C. T. Beer and J. H. Cutts, *Ann. N.Y. Acad. Sci.*, 1958, **76**, 882.
3. I. S. Johnson, J. G. Armstrong, M. Gorman and J. P. Burnett, *Cancer Res.*, 1963, **23**, 1390.
4. G. L. Wantzin, *Scand. J. Haematol.*, 1979, **22**, 375.
5. J. D. Teale, J. M. Clough and V. Marks, *Br. J. Clin. Pharmacol.*, 1977, **4**, 169.
6. J. J. Langone, M. R. D'Onofrio and H. van Vunakis, *Anal. Biochem.*, 1979, **95**, 214.
7. R. J. Owellen and C. A. Hartlee, *Cancer Res.*, 1975, **35**, 975.
8. R. J. Owellen, C. A. Hartlee and F. O. Hains, *ibid.*, 1977, **37**, 2597.
9. R. J. Owellen, M. A. Root and F. O. Hains, *ibid.*, 1977, **37**, 2603.
10. M. C. Castle and J. A. Mead, *Biochem. Pharmacol.*, 1978, **27**, 37.
11. W. A. Creasey, A. I. Scott, C. Wei, J. Kutcher and A. Schwartz, *Cancer Res.*, 1975, **35**, 1116.
12. Y. Hirshaut, G. Weiss and E. Blackham, *Clin. Res.*, 1968, **16**, 360.
13. R. Carmel, *Am. J. Clin. Pathol.*, 1978, **69**, 137.
14. C. G. Smith, L. E. Grady and F. P. Kupiecki, *Cancer Res.*, 1965, **25**, 241.
15. G. J. Dixon, E. A. Dulmage and L. B. Mellet, *ibid.*, 1969, **29**, 1810.
16. R. A. Bender, M. C. Castle, D. A. Mergileth and V. T. Oliverio, *Proc. Am. Assoc. Cancer Res.*, 1977, **18**, 61.
17. J. F. Rusing, B. J. Scheer and I. A. Haque, *Anal. Chim. Acta*, 1984, **158**, 23.
18. H. F. W. Kirkpatrick, *J. Pharm. Pharmacol.*, 1945, **18**, 338.
19. G. Baiulescu and S. Popescu, *Rev. Chim. (Bucharest)*, 1973, **24**, 299.
20. *Idem.*, *ibid.*, 1975, **26**, 253.
21. A. Temizer, *J. Pharm. Belg.*, 1982, **37**, 157.
22. H. F. W. Kirkpatrick, *J. Pharm. Pharmacol.*, 1946, **19**, 8: 1946, **19**, 127; 1946, **19**, 527; 1947, **20**, 87.
23. A. Temizer, A. N. Onar, B. Sener, H. Temizer and A. E. Karakaya, *J. Pharm. Belg.*, 1985, **40**, 75.
24. H. Y. Mohammed and F. F. Cantwell, *Anal. Chem.*, 1978, **50**, 491.
25. R. G. Baum, R. Saetre and F. F. Cantwell, *ibid.*, 1980, **52**, 15.
26. *Amberlite XAD-2*, Technical Bulletin, Rohm & Hass Philadelphia, 1972.
27. S. G. Mairanovskii, L. D. Klukina and A. N. Frumkin, *Dokl. Akad. Nauk. SSSR*, 1960, **141**, 147.
28. M. V. Stackelberg and H. Fassbender, *Z. Electrochem.*, 1958, **62**, 834.
29. M. V. Stackelberg, W. Hans and W. Jensch, *ibid.*, 1958, **62**, 839.
30. S. G. Mairanovskii, *J. Electroanal. Chem.*, 1963, **6**, 77.
31. D. V. Jackson, V. S. Sethi, C. L. Spurr, D. R. White and M. C. Castle, *Proc. Am. Assoc. Cancer Res.*, 1980, **21**, 193.

DIFFERENTIAL PULSE POLAROGRAPHIC DETERMINATION OF THIOL FLOTATION COLLECTORS AND SULPHIDE IN WATERS

JAAKKO LEPPINEN and SUSANNA VAHTILA

Department of Chemistry, Helsinki University of Technology, SF-02150 Espoo, Finland

(Received 21 February 1986. Accepted 6 June 1986)

Summary—Thiol collectors and sulphide can be determined together by differential pulse polarography. Ethyl xanthate, diethyl dithiophosphate, and diphenyl dithiophosphate have been determined in concentrations from 10 μM to 2 mM, and sulphide from 1 μM to 0.5 mM. The method is reliable and rapid; however, the exact behaviour of the thiol collectors must be known since the pattern of current peaks changes as the concentration increases. This method has been used in the study of sulphide mineral flotation and could be utilized at full-scale flotation plants.

So-called thiol collectors are important chemicals in the flotation of sulphide minerals because they greatly improve the floatability of the mineral particles suspended in water. These collectors, of which xanthates (ROCS_2^-) and dithiophosphates ($\text{R}_2\text{O}_2\text{PS}_2^-$) are the most common, usually have two sulphur atoms at their polar ends, enabling them to attach to the surface of mineral particles. The collectors usually occur as the alkali-metal salts, which are soluble in water, and the typical concentrations in flotation processes are between 10^{-5}M and $5 \times 10^{-4}\text{M}$. Furthermore, flotation liquors may contain other sulphur species such as sulphide and thiosulphate. From the point of view of both basic research and flotation plant efficiency, the determination of these different species is of great importance.

Spectrophotometric methods have been widely used in studying the composition of flotation liquors. The main reason is that xanthates are easily determined by ultraviolet spectrophotometry at 301 nm.^{1,2} The determination of diethyl dithiophosphate³ at 227 nm is not as useful because of the presence of interfering species such as sulphide, thiosulphate and carbon disulphide^{1,4} in flotation liquors. On the other hand absorption bands from carbon disulphide, xanthates, and monothiocarbonate⁵ interfere in ultraviolet spectrophotometric determinations of sulphide and thiosulphate.

It is known that xanthates give well-defined waves in normal pulse polarography.⁶⁻⁸ Normal pulse (NPP) and differential pulse polarography (DPP) have both been used successfully in the determination of sulphide and thiosulphate.⁹⁻¹⁰ However, DPP has not previously been used in the determination of xanthates or dithiophosphates.

The determination of ethyl xanthate (EX), diethyl dithiophosphate (DTPEt), and diphenyl dithiophosphate (DTPPh) by DPP is discussed in this paper. Also, the simultaneous determination of sulphide in

solutions containing both sulphide and a collector has been examined. Results for the determination of EX by ultraviolet spectrophotometry and by DPP have been compared and the reliability of the latter method has been assessed.

EXPERIMENTAL

Reagents

Analytical grade chemicals were used throughout the work except for the alkali-metal salts of the thiol collectors, which were synthesised in our laboratory. Sodium sulphide solutions were prepared from $\text{Na}_2\text{S} \cdot x\text{H}_2\text{O}$ and their concentrations checked by potentiometric titration with silver nitrate solution. The sulphide standards were prepared daily by adding 10 ml of SAOB II (sulphur antioxidant buffer) to 90 ml of a standard solution. SAOB II solution was prepared from disodium EDTA, ascorbic acid, and sodium hydroxide according to a standard formulation.¹²

Potassium ethyl xanthate (KEX) was prepared from ethanol, carbon disulphide and potassium hydroxide¹³ and recrystallized from ethanol by addition of n-hexane. Sodium diethyl dithiophosphate (NaDTPEt) was prepared from phosphorus pentasulphide, ethanol and sodium hydroxide.¹⁴ Potassium diphenyl dithiophosphate was prepared from phenol, phosphorus pentasulphide and potassium carbonate by combining two methods.^{15,16} The purities of these reagents were checked by potentiometric titration, ultraviolet spectrophotometry, ¹³C NMR, and infrared spectroscopy.

Polarography

The polarographic measurements were made with a PAR 174 A Polarographic Analyser and PAR 303 A static mercury-drop electrode stand. The polarograms were recorded with a YEW Model 3022 X-Y recorder. The three-electrode assembly consisted of a dropping mercury electrode, a platinum wire auxiliary electrode, and an Ag/AgCl reference electrode against which all the potentials reported in this work were measured. Dissolved oxygen was removed by purging the solution with high-purity nitrogen for 4 min before each potential scan. Typical parameters employed were: drop-time 1 sec, scan-rate 5 mV/sec, modulation amplitude 25 mV, and sensitivity 1 μA .

The volume of the sample to be analysed polarographically was usually about 5 ml and contained 0.06 ml of 2M sodium hydroxide and 0.25 ml of SAOB II. The polarogram of sodium sulphide was recorded in this alkaline

solution, then the solution was acidified with 0.050 ml of glacial acetic acid to a pH of 5.3, and purged for 4 min to remove H_2S , and finally the polarogram of the collector species was recorded.

Ultraviolet spectrophotometry

The spectra for the determination of ethyl xanthate were recorded on a Beckman Acta MVI spectrophotometer, with 10 mm silica cuvettes. The absorption maximum at 301 nm was used for the determination of the concentration of EX, which has a molar absorptivity of approximately 1.75×10^4 l. mole⁻¹. cm⁻¹.³

RESULTS AND DISCUSSION

Ethyl xanthate

The polarographic behaviour of xanthates and of all the other thiol collectors is complex, owing to the adsorption phenomena occurring at the dropping mercury electrode. However, within certain concentration ranges well-defined current peaks are obtained. EX gives a reproducible peak at -0.55 V when the concentration is between $1 \times 10^{-5} M$ and $1.5 \times 10^{-4} M$ as shown in Fig. 1. The current-concentration relationship is not linear over the whole range, however, but only from $7 \times 10^{-5} M$ to $1.5 \times 10^{-4} M$. Thus, the determination of EX must be performed on the basis of a calibration graph (Fig. 2), instead of by the standard addition method, for example.

As the concentration rises above $1.5 \times 10^{-4} M$ a new peak appears at -0.35 V and simultaneously the first peak at -0.55 V decreases slightly. The growth of the peak at -0.35 V continues only up to a concentration of $3 \times 10^{-4} M$ at which point a sharp peak suddenly appears at approximately -0.3 V. As the concentration is further increased the potential of this sharp peak shifts, reaching a final position of -0.4 V at $2 \times 10^{-3} M$. Figure 3 shows the shapes and

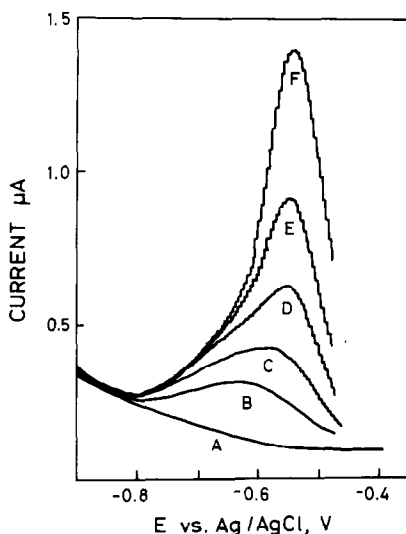


Fig. 1. Differential pulse polarograms of ethyl xanthate. A, 0 M; B, $3.5 \times 10^{-5} M$; C, $5.5 \times 10^{-5} M$; D, $7.3 \times 10^{-5} M$; E, $9.1 \times 10^{-5} M$; F, $1.2 \times 10^{-4} M$.

the positions of the current peaks at the concentrations $2.5 \times 10^{-4} M$ and $7.8 \times 10^{-4} M$. The peak at approximately -0.35 V is analytically interesting and shows a nearly linear current-concentration relationship from $1.5 \times 10^{-4} M$ to $2 \times 10^{-3} M$ (Fig. 4). On more careful examination however, there is a slight deviation from linearity in the range where the change in the shape of the peak occurs. When the concentration of EX is increased above $2 \times 10^{-3} M$ a clear deviation from linearity is observed. However, the calibration graph is still useful up to approximately $4 \times 10^{-3} M$.

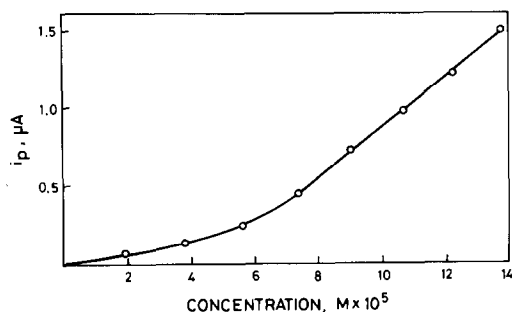


Fig. 2. Calibration curve for ethyl xanthate at -0.55 V.

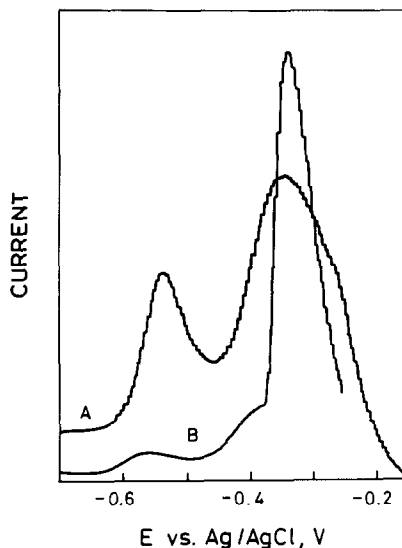


Fig. 3. Differential pulse polarograms of ethyl xanthate. A, $2.5 \times 10^{-4} M$; B, $7.8 \times 10^{-4} M$.

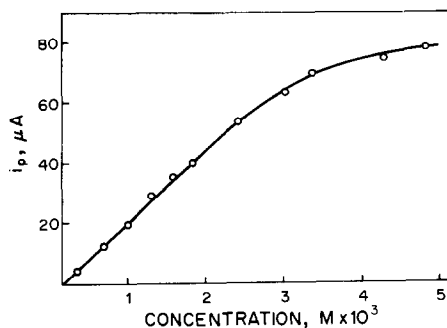
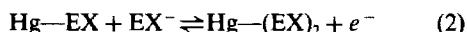


Fig. 4. Calibration curve for ethyl xanthate at -0.35 V.

The existence of several current peaks with increasing concentration of EX has been observed by many authors. Pomianowski¹⁷ has found in his capacitance-potential studies that the surface reactions at DME and HME are very complicated. The first peak at -0.55 V could be due to a single-electron reaction and the formation of a strongly adsorbed layer, *i.e.*,



The second and third peaks at -0.3 and -0.4 V probably originate from another single-electron transfer with the formation of adsorbed dioxanthogen¹⁸ or a mercury-xanthate surface compound,



The formation of mercury(II) xanthate is also possible, with a two-electron transfer, at the higher potentials,¹⁹



With normal pulse polarography, a prewave on the more negative potential side of the main wave has been observed, which remains constant even if the certain concentration is exceeded.^{7,8} This has been explained as originating from a strongly adsorbed film on the electrode. The potential of the first peak observed in DPP is approximately the same as the potential of this prewave.

Comparison of DPP and ultraviolet spectrophotometry

Perhaps the most accurate method for determining xanthate is based on the absorption of ultraviolet radiation at a wavelength of 301 nm.¹⁻³ Therefore results from the differential pulse polarographic method have been compared with those obtained by ultraviolet spectrophotometry over the concentration range from $2 \times 10^{-5}M$ to $1.3 \times 10^{-4}M$, which allows for the direct determination by both methods (Table 1).

The precision of both methods is good at concentrations greater than $5 \times 10^{-5}M$, but there is a rather large error in the values given by DPP at the two lowest concentrations. This is probably because the calibration graph is slightly curved at those concentrations. The relationship of absorbance to concentration is linear over the whole range.

The reproducibility of the DPP method was tested by analysing five replicate samples at five different concentrations (Table 2).

The relative standard deviation was less than 2% except in case A, where it was 3.3%. The R.S.D. for the ultraviolet method is generally better, being as low as 1% at the concentrations examined. Even so, DPP is a reliable method for xanthate determination and clearly has some advantages over the ultraviolet method. For example, the small amount of solid which generally exists in the samples of flotation liquors may disturb the ultraviolet analysis, in which case DPP would give much better results.

Table 1. Comparison of the DPP and ultraviolet spectrophotometry methods

EX concentration, $M \times 10^5$	EX found, $M \times 10^5$	
	DPP	UV
2.00	2.35	2.04
3.50	3.82	3.67
5.00	5.05	5.15
6.00	5.95	6.12
7.00	6.88	7.16
9.00	8.85	9.12
11.0	10.9	11.1
13.0	13.1	13.0

Table 2. A test for the reproducibility of the determination of EX by DPP

Sample	Concentration, $M \times 10^5$				
	A	B	C	D	E
1	5.65	7.12	8.62	10.4	11.9
2	5.50	6.95	8.80	10.2	12.0
3	5.20	6.95	8.50	10.6	11.8
4	5.65	7.12	8.55	10.3	11.6
5	5.35	7.12	8.75	10.2	11.8
Mean	5.47	7.05	8.64	10.3	11.8
R.S.D., %	3.3	1.3	1.5	1.6	1.3

Diethyl dithiophosphate

Iodometric titration¹⁴ and ultraviolet analysis³ can be used to determine the concentration of DTPET. The direct ultraviolet method at 227 nm is seldom successful, owing to the presence of many interfering components in flotation liquors. DPP has not been used for DTPET determination and it is hard to find any information in the literature on the polarographic behaviour of dithiophosphates. We have observed the behaviour of DTPET to be similar to that of EX except that the potentials are more positive. A broad current peak is observed at -0.4 V when the concentration lies between $1 \times 10^{-5}M$ and $1.2 \times 10^{-4}M$ (Fig. 5). There exists a well-defined

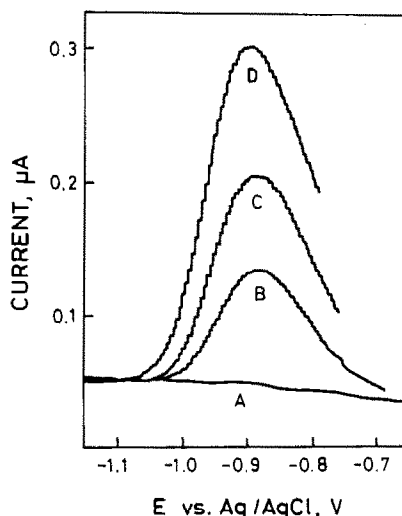


Fig. 5. Differential pulse polarograms of diethyl dithiophosphate. A, $0M$; B, $5.1 \times 10^{-5}M$; C, $8.4 \times 10^{-5}M$; D, $1.2 \times 10^{-4}M$.

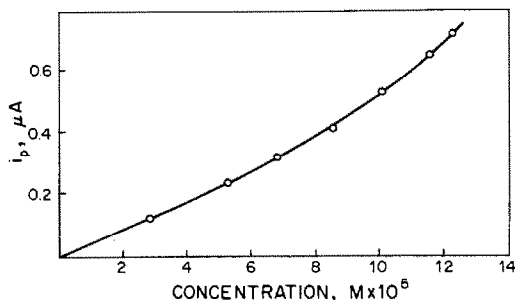


Fig. 6. Calibration curve for diethyl dithiophosphate at -0.4 V.

current-concentration relationship, which is not linear, the height of the peak increasing more rapidly with increasing concentration (Fig. 6).

A new peak appears at -0.15 V when the concentration of DTPEt is 1.4×10^{-4} M. This peak has some analytical importance because the peak height is nearly linearly dependent on concentration up to 1.4×10^{-3} M. Above 1.5×10^{-3} M a new peak appears at -0.2 V, which increases linearly with concentration.

The reproducibility of the determination of DTPEt was good, even better than that for EX, with an R.S.D. of about 0.8% when five replicate samples with a mean concentration of 9.9×10^{-5} M were analysed. There is clearly a complex sequence of reactions at the electrode surface, as in the case of EX, giving rise to several peaks as the concentration increases.

Diphenyl dithiophosphate

Though DTPPh and DTPEt differ only in the hydrocarbon group, a considerable difference is observed in their behaviour at the DME. Because the first peak in the DTPPh polarogram appears at -0.85 V (Fig. 7) SAOB II cannot be used, because it, too, gives rise to a large anodic current as well. The height of the current peak at -0.85 V is not proportional to the concentration (Fig. 8). Even so, this peak can be used to determine the concentration of DTPPh in the range from 1×10^{-5} M to 1×10^{-4} M. When the DTPPh concentration exceeds 2×10^{-4} M a new peak appears at -0.25 V in the polarogram. The current-concentration relationship of this peak gives it analytical importance in the concentration range from 2×10^{-4} M to 3×10^{-3} M.

The relative standard deviation for the determination of DTPPh at 4×10^{-5} M was 2.8% when five replicate samples were analysed.

Collector determination in the presence of sulphide

From a practical point of view it is important that the collector can be determined in the presence of other sulphur-containing anions, such as sulphide. This kind of analysis can be performed if the sulphide is determined first in an alkaline solution and then removed from the solution by acidification to form H_2S , followed by purging. As the determination of

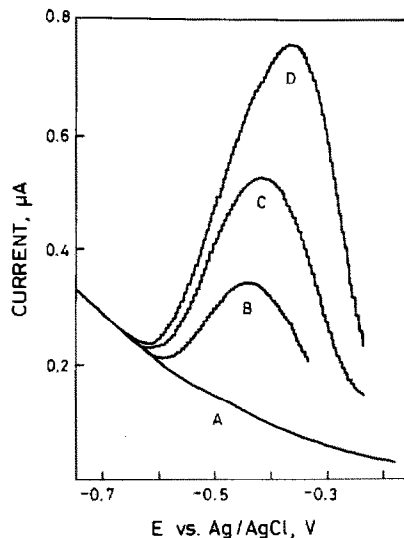


Fig. 7. Differential pulse polarograms of diphenyl dithiophosphate. A, 0M; B, 1.4×10^{-5} M; C, 2.6×10^{-5} M; D, 4.9×10^{-5} M.

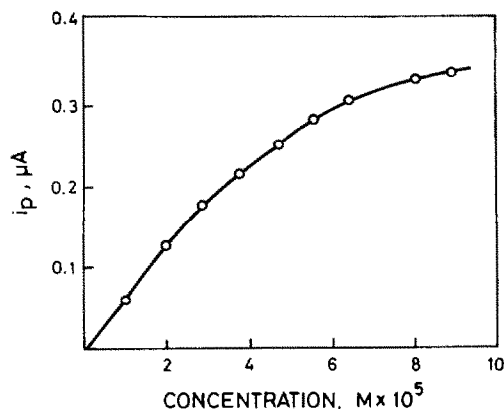


Fig. 8. Calibration curve for diphenyl dithiophosphate at -0.85 V.

sulphide by DPP has been investigated⁹⁻¹¹ it will not be described here in detail. We have found, however, that sulphide can be determined from 1×10^{-6} M to 5×10^{-4} M concentration without any difficulty. The current peak at -0.8 V is linearly dependent on concentration up to 10^{-5} M, above which a slight deviation from linearity is observed. The deviation is contrary to what other authors have reported¹⁰ and may be a result of differences in the experimental systems.

The differential pulse polarograms of sulphide and ethyl xanthate present in the same sample are shown in Fig. 9.

The presence of thiosulphate¹⁰ could also be observed in the same polarogram with EX at a potential of -0.2 V but this will not be discussed here. The removal of sulphide is very important in that the acidification shifts the potential of the sulphide ion to a more positive value. As a result the peaks of EX and sulphide will overlap, making xanthate determinations questionable. Fortunately, sulphide is

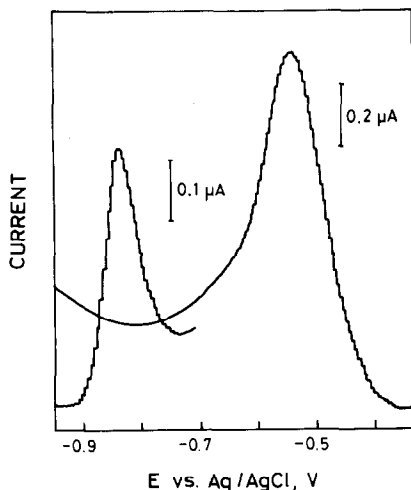


Fig. 9. Simultaneous determination of sulphide and ethyl xanthate. Concentration of EX: $1.1 \times 10^{-4}M$ and of sulphide $7.1 \times 10^{-6}M$.

quite easily removed as H_2S when the pH is below 6. However, too low a pH must be avoided when xanthates are present, because their decomposition rate increases with increasing H^+ concentration.²⁰

Sulphide and DTPEt can also be determined simultaneously by the same procedure. The advantage with thiophosphates is their much better stability in acidic solution, which allows the use of a wider pH range. Slight problems arise, however, in the simultaneous determination of sulphide and DTPPh because in alkaline solution there is only a small difference in the peak potentials of these two components.

Acknowledgement—The financial support provided by the Academy of Finland is gratefully acknowledged.

REFERENCES

1. M. H. Jones and J. T. Woodcock, *Ultraviolet Spectrometry of Flotation Reagents with Special Reference to the Determination of Xanthate in Flotation Liquors*, Institute of Mining Metallurgy, London, 1973.
2. M. J. Maurice and J. L. Mulder, *Microchim. Acta*, 1957, 661.
3. I. Iwasaki and S. R. B. Cooke, *Trans. AIME*, 1957, **208**, 1267.
4. R. N. Tipman and J. Leja, *J. Coll. Interfac. Sci.*, 1969, **29**, 305.
5. P. J. Harris and N. P. Finkelstein, *Int. J. Min. Proc.*, 1975, **2**, 77.
6. Shiou-Chuan Sun and R. T. Holzmann, *Anal. Chem.*, 1957, **29**, 1298.
7. I. Kovács and L. Kékedy, *Z. Anal. Chem.*, 1975, **274**, 27.
8. K. Saraswathi, *Proc. Ind. Acad. Sci.*, 1977, **85**, 514.
9. J. J. Renald, G. Kubes and H. I. Bolker, *Anal. Chem.*, 1975, **47**, 1347.
10. D. L. Noel, *Tappi*, 1978, **61**, 73.
11. E. Blasius, C. Schreier and K. Ziegler, *Arch. Eisenhüttenwes.*, 1974, **45**, 441.
12. M. S. Frant and J. W. Ross, Jr., *Tappi*, 1970, **53**, 1753.
13. E. C. Horning, *Organic Synthesis*, Coll. Vol. 3, Wiley, New York, 1955.
14. H. Bode and W. Arnswald, *Z. Anal. Chem.*, 1962, **185**, 99.
15. J. H. Fletcher, *J. Am. Chem. Soc.*, 1950, **72**, 2461.
16. M. I. Zemlyansky and B. S. Drach, *Zh. Obshch. Khim.*, 1962, **32**, 1962; *Chem. Abstr.*, 1963, **58**, 4450d.
17. A. Pomianowski, *Rocz. Chem.*, 1967, **41**, 1125.
18. J. Leja, *Min. Sci. Engng.*, 1973, **5**, 278.
19. O. Huynh Thi, M. Lamache and D. Bauer, *Electrochim. Acta*, 1981, **26**, 33.
20. I. Iwasaki and S. R. B. Cooke, *J. Am. Chem. Soc.*, 1958, **80**, 285.

DETERMINATION OF TRACE AMOUNTS OF THE FLOTATION COLLECTORS ETHYL XANTHATE AND DIETHYL DITHIOPHOSPHATE IN AQUEOUS SOLUTIONS BY CATHODIC STRIPPING VOLTAMMETRY

ARI IVASKA

Laboratory of Analytical Chemistry, Åbo Akademi, SF-20500 Turku (Åbo), Finland

and

JAAKKO LEPPINEN

Department of Chemistry, Helsinki University of Technology, SF-02150 Espoo, Finland

(Received 21 February 1986. Accepted 24 May 1986)

Summary—A cathodic stripping method has been devised for determination of low concentrations of the flotation collectors ethyl xanthate, diethyl dioxanthogen and diethyl dithiophosphate. The limit of detection for ethyl xanthate was $1 \times 10^{-8} M$ by the differential pulse technique and with deposition for 2 min at $-0.1 V$. Three peaks were observed, each increasing in different concentration ranges of ethyl xanthate. A reaction mechanism is proposed. The detection limit for diethyl dithiophosphate was $1 \times 10^{-7} M$ by the differential pulse technique and with deposition for 3 min at $-0.1 V$. The analytical method was applied to determine ethyl xanthate in a sulphide mineral flotation plant and the amount of adsorbed ethyl xanthate and diethyl dithiophosphate on Cu_2S . It was found that the adsorbed ethyl xanthate forms nearly a monolayer on Cu_2S and that the amount of adsorbed diethyl dithiophosphate corresponds approximately to 0.4 monolayer.

Xanthates have long been used as collectors in sulphide mineral flotation. They are surface-active compounds which are adsorbed on the surface of sulphide minerals and thereby exert their flotation function. In order to obtain the maximum floatability the concentration of xanthate should be kept within certain limits. The concentration in flotation cells is normally 10^{-4} – $10^{-5} M$ and continuous or fairly frequent monitoring of the concentrations is necessary for efficient process control.¹ From the environmental point of view it is also important to measure the concentration of xanthate in the plant effluents. Proper analytical methods are needed to fulfil these requirements. Iodometric titration is one of the oldest methods for determining xanthate.² Spectrophotometric methods are also used³ and a polarographic method has been devised.⁴ The determination of low concentrations of xanthate and similar compounds has so far been a difficult task. The detection limit of the spectrophotometric method is around $10^{-6} M$ which is too high if the method is to be used to monitor xanthate discharges to the environment.

The work we will present in this paper was initiated by the demand to determine flotation collectors at concentrations $< 10^{-6} M$ in aqueous samples from mineral flotation processes. Ethyl xanthate is the most frequently used flotation agent but diethyl dithiophosphate is also sometimes used. In this work we describe a sensitive analytical method for determination of low concentrations of both compounds

by cathodic-stripping voltammetry at a hanging mercury-drop electrode.

EXPERIMENTAL

Chemicals

The compounds studied in this work were potassium ethyl xanthate (EX), diethyl dioxanthogen [(EX)₂], and diethyl dithiophosphate (DTP). The chemical structures of these compounds are shown in Fig. 1. The compounds were synthesized by methods described in the literature.^{5,6} All other chemicals were from Merck and of analytical grade. Doubly distilled water was used in preparing the solutions. The Cu_2S plates were obtained from the Department of Physical Sciences, University of Turku. Samples from the flotation plant were taken in well-washed plastic bottles and assayed the following day.

Instrumentation

A PAR 174A polarograph was used in conjunction with the PAR 303 static mercury-drop stand. The counter-electrode was a platinum wire and the reference electrode a silver-silver chloride electrode in saturated potassium chloride solution. All potentials given are referred to this electrode. A Bryans X-Y plotter was used to record the voltamperograms.

Procedure

Preliminary differential pulse polarographic studies with $10^{-4} M$ solutions of EX and DTP in 0.1M Britton-Robinson buffers between pH 4 and 10 and in 0.1M sodium hydroxide showed that the peak shape and peak potential were almost constant over the whole pH range studied. EX was found to degrade rapidly at pH below 4. DTP is stable even in acidic solutions down to pH = 1.⁷ Therefore 0.1M potassium nitrate was chosen as the supporting electrolyte solution.

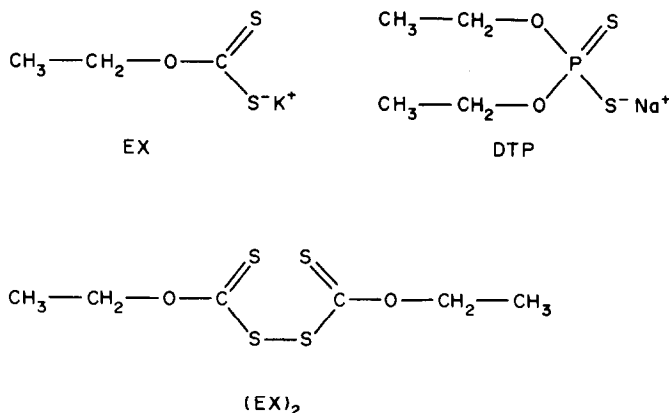


Fig. 1. The compounds studied in this work: EX = potassium ethyl xanthate, DTP = sodium diethyl dithiophosphate and (EX)₂ = diethyl dixanthogen.

The sample solutions, 5 ml, were always purged with pure nitrogen for 8 min before the experiments were started. The mercury drop was first dispensed after the cell was de-aerated. In the stripping experiments the electrode potential was held first at -0.05 or -0.1 V for 60, 120 or 180 sec while the solution was magnetically stirred. After the stirrer was switched off the solution was allowed to become quiescent for 15 sec and the potential was scanned at 20 mV/sec to more negative values. After the scan was completed the cell was removed and the mercury drop was displaced. The used drops were never dislodged into the cell solution. This procedure was followed to minimize the time the drop was in contact with the solution in order to prevent, as much as possible, the chemical reaction which may take place between mercury and the collector chemicals.

In studying the adsorption of EX and DTP on the Cu₂S plate 5 ml of a $4.8 \times 10^{-7} M$ solutions of the compounds were used. The Cu₂S plate was placed in a platinum-wire basket and dipped into the solution for 60 sec. It was then lifted out and 1M potassium nitrate was added to make the solution 0.1M with respect to this salt. This procedure was followed because we wanted to study adsorption in the presence of the collector ions only. The amount of EX and DTP remaining in the cell after the Cu₂S treatment was determined by the standard-addition technique. The amount of EX and DTP adsorbed on the Cu₂S plate was then calculated as the difference between the amounts before and after the Cu₂S treatment. The standard-addition method was found to give more reproducible results than the direct evaluation from the calibration graph. Peak areas rather than peak heights were used.

RESULTS AND DISCUSSION

Cathodic stripping method

Cathodic stripping voltamperograms of solutions of EX and DTP were recorded in the concentration range 1×10^{-8} – $7 \times 10^{-5} M$ and 1×10^{-7} – $1 \times 10^{-5} M$ respectively. Both differential pulse (d.p.) and direct current (d.c.) techniques were used, the former being more sensitive, enabling the EX to be determined at the $10^{-8} M$ level. No attempt was made to find the real detection limit of the method, e.g., by using much longer deposition times. Typical d.p. and d.c. cathodic stripping voltamperograms of EX over the concentration range studied are shown in Fig. 2 (a and

b). As can be seen in Fig. 2b the shape of the d.c. voltamperogram changes with increasing concentration of EX. Two small peaks at -0.55 and -0.65 V can be observed on the d.c. voltamperogram of the $5 \times 10^{-8} M$ solution. As the concentration is increased these two peaks coalesce into a single peak. In the concentration range 2×10^{-7} – $7 \times 10^{-7} M$ the height of this peak at -0.6 V remains constant, and a new and increasing peak appears at -0.45 V. This can clearly be seen in Fig. 2c. Yet a third peak appears in the concentration range 2×10^{-6} – $1 \times 10^{-5} M$. It

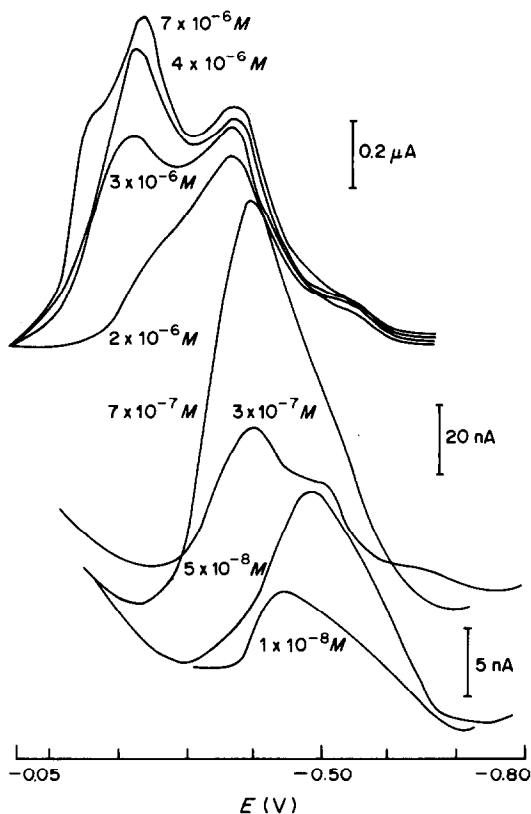


Fig. 2(a).

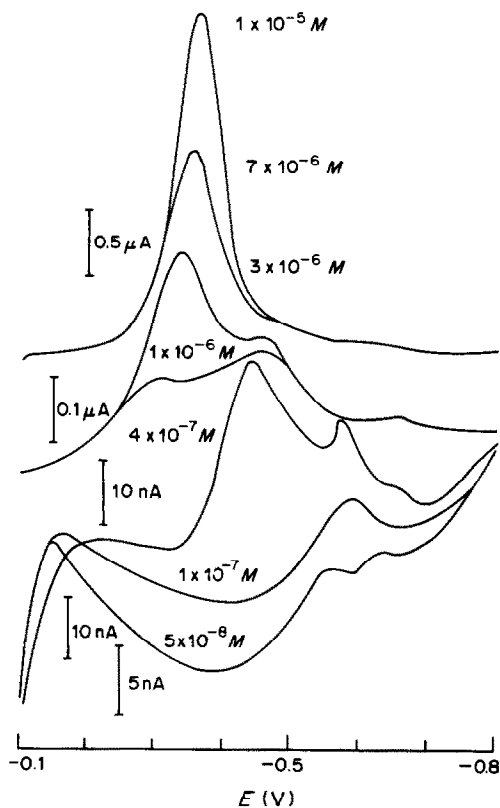


Fig. 2(b).

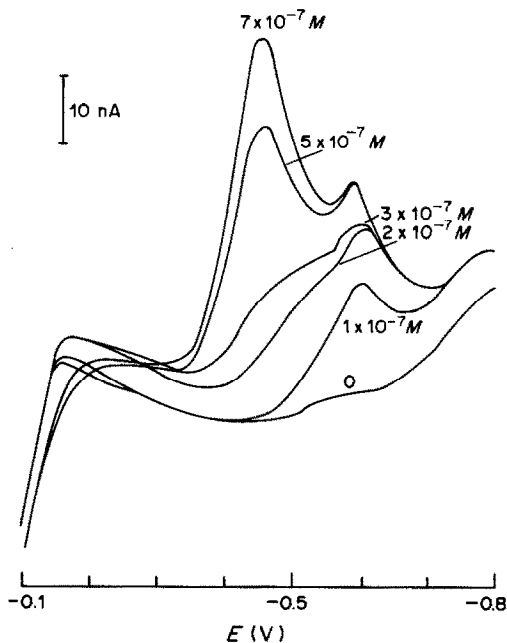


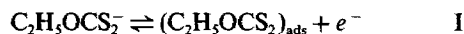
Fig. 2(c).

Fig. 2. Cathodic-stripping voltamperograms of EX in 0.1M KNO_3 , at 25°C, scan-speed 20 mV/sec: (a) d.p. technique, modulation amplitude 25 mV, deposition for 60 sec at -0.05 or -0.1 V, concentration range 1×10^{-8} – 1×10^{-6} M; (b) d.c. technique, deposition for 120 sec at -0.1 V, concentration range 5×10^{-8} – 1×10^{-5} M; (c) expansion of the range 1×10^{-7} – 7×10^{-7} M, d.c. technique.

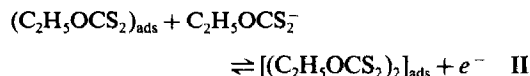
increases with concentration and at the same time the peak potential shifts from -0.30 to -0.34 V. The d.p. voltamperograms also consist of a number of peaks which increase in different concentration ranges. Similar observations have been made in d.p. polarographic studies of EX.⁴ The peak potentials are approximately 0.10 V more positive than those of the corresponding d.c. peaks. Some extra peaks may be found on the d.p. voltamperograms of various compounds forming insoluble mercury salts, making interpretation of such voltamperograms difficult.⁷ Calibration graphs obtained for the different concentration ranges are described in Table 1.

Very little work has been done on the polarography of xanthates in aqueous solution. The products of the electrode reaction are almost insoluble in water, which complicates identification of the reaction mechanism. Strong adsorption phenomena are also involved.⁸ Leja has presented some results of the work of Pomianowski on a.c. polarographic studies of EX in aqueous solution.⁹ Based on the results of Pomianowski we suggest the following charge-transfer reactions take place during the deposition and stripping steps:

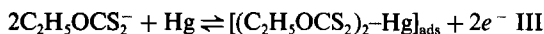
at -0.6 V



at -0.45 V



at -0.30 V



Reactions I and II are obviously restricted by the available surface area, because limits in the corresponding peak heights are observed. The adsorbed product in reaction III is obviously deposited in a thick layer on the electrode surface because the stripping peak increases linearly with concentration over at least the whole range studied in this work, see Table 1.

The d.c. cathodic-stripping voltamperograms of DTP in the concentration range 5×10^{-7} – 1×10^{-5} M are shown in Fig. 3a. Voltamperograms from the narrower concentration range 2×10^{-7} – 5×10^{-7} M are shown in Fig. 3b. As can be seen (Fig. 3) only one peak appears at first, at -0.42 V. When the concentration of DTP increases a second, increasing, peak appears at a more positive potential, -0.28 V, while the height of the peak at -0.42 V remains constant. When the concentration is further increased the height of the peak at -0.28 V remains constant and the peak at -0.42 V starts to grow again and shifts to more negative potentials. When the concentration increases above 5×10^{-6} M the peak height does not change any more. It should be noted that the increase in the height of the more negative peak is less than the increase in the peak heights of EX over the same

Table 1. Calibration graphs of EX, DTP and $(EX)_2$ in 0.1M KNO_3 ; deposition at -0.1 V for 2 min for EX and $(EX)_2$ and 3 min for DTP

Compound	Technique	Concentration range, M^*	E_p, V	r^\dagger	r.s.d., %§
EX	d.c.	1×10^{-7} – 7×10^{-7}	-0.45	0.996	10–5
	d.c.	3×10^{-6} – 1.5×10^{-5}	-0.3	0.999	5–2
	d.p.	1×10^{-8} – 1×10^{-7}	-0.5	0.999	20–10
	d.p.	3×10^{-7} – 1×10^{-6}	-0.4	0.997	5–2
DTP	d.p.	1×10^{-7} – 5×10^{-7}	-0.45	0.999	20–10
	d.p.	5×10^{-7} – 1×10^{-6}	-0.3	0.999	10–10
$(EX)_2$	d.c.	1×10^{-7} – 1×10^{-6}	-0.45	0.962	20–10
	d.c.	1×10^{-7} – 1×10^{-6}	-0.67	0.999	10–10

*Except for the first EX/d.c., where peak area was recorded, the peak height was measured for these calibrations.

†Correlation coefficient.

§Relative standard deviation for 5 determinations at the bottom and top of the range.

concentration range. This may be explained by assuming that the mercury diethyl dithiophosphate compound is electrically non-conducting and is tightly packed on the surface. When the thickness of the layer on the mercury drop increases, the electrode becomes covered by a dense layer of an insulator. At a certain concentration of DTP the layer becomes so thick that it prevents the mercury from diffusing to the surface and hence also prevents the charge-transfer reaction from taking place. Therefore the voltammetric peaks do not increase further with increase in concentration of DTP. The mercury ethyl xanthate compound, on the contrary, seems to be less densely packed, because the peak height still increases with increasing concentration of EX.

The limit of detection for DTP was estimated to be $1 \times 10^{-7} M$. No attempt has been made to elucidate the reaction mechanism, though this obviously has some similarities with that of EX. Calibration data

for DTP in different concentration ranges are given in Table 1. Several d.p. polarographic peaks for DTP have been observed.⁴

Diethyl dixanthogen, $(EX)_2$, has been proposed as a reaction product of the oxidation of ethyl xanthate at solid electrodes.¹⁰ To find whether $(EX)_2$ is involved in the oxidation reactions in flotation liquors the cathodic-stripping voltamperograms of $(EX)_2$ in the concentration range 10^{-7} – $10^{-6} M$ were studied. These curves are shown in Fig. 4. The voltamperograms consist of two peaks at -0.45 and -0.67 V. Both peaks increase with increasing concentration of $(EX)_2$, indicating that reduction of the compound formed during deposition takes place in two steps. The more positive of the peaks appears at approximately the same potential and has approximately the same height as the increasing stripping peak of EX in

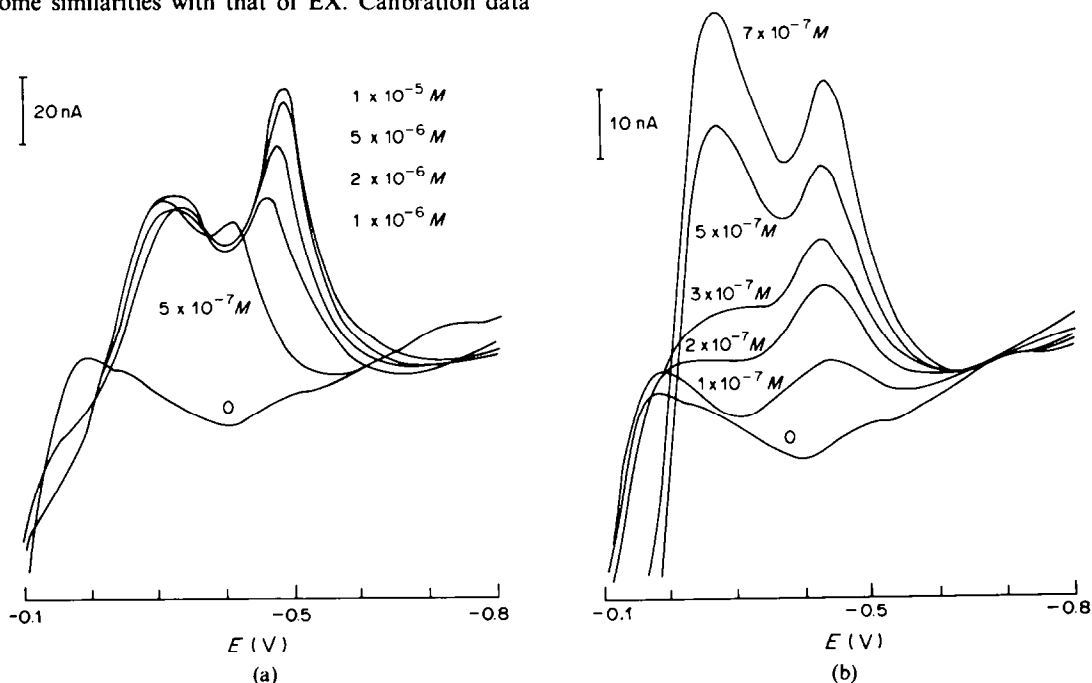


Fig. 3. Cathodic-stripping d.c. voltamperograms of DTP in 0.1M KNO_3 at 25°C, deposition for 180 sec at -0.1 V; scan-speed 20 mV/sec. Concentration range (a) 5×10^{-7} – $1 \times 10^{-5} M$; (b) 1×10^{-7} – $7 \times 10^{-7} M$.

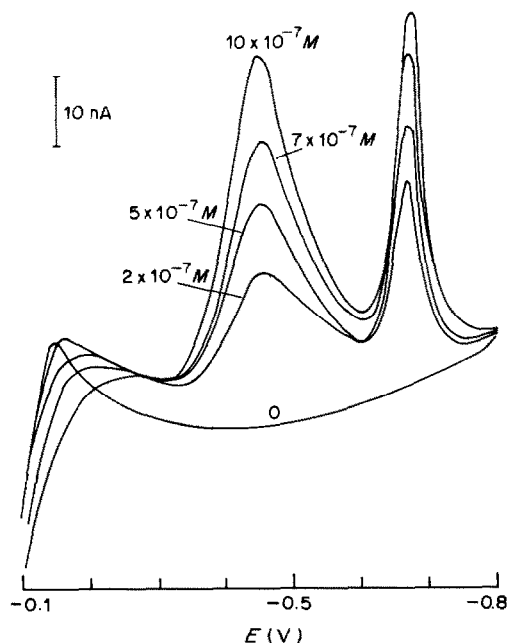


Fig. 4. Cathodic-stripping d.c. voltamperograms of $(EX)_2$ in $0.1M$ KNO_3 . Deposition for 2 min at -0.1 V; scan-speed 20 mV/sec. Concentration range 2×10^{-7} – $10 \times 10^{-7}M$.

the same concentration range. Therefore it is obvious that the stripping peak of $(EX)_2$ at -0.45 V is due to reaction II in the proposed sequence for EX. Because the heights of the two peaks in Fig. 4 are approximately the same it can be concluded that one electron is involved in each reduction step. No attempt was made to clarify the origin of the peak at -0.67 V. Calibration data obtained for both peaks are given in Table 1.

Application to flotation liquors

The analytical method proposed in this work was used to determine EX in the samples taken from different stages of an ore flotation plant: (a) process water, (b) plant effluent and (c) flotation liquor from an Ni–Cu ore concentration plant. The cathodic-stripping determination could not be done immediately on the plant, and the samples were transported to the laboratory and assayed the next day. The main problem in this kind of sampling and assay procedure is aging of the sample, which naturally affects the results. In particular the sample of flotation liquor contained solid particles and EX may have continued to react with them before the sample was assayed. The results of the analyses are given in Table 2. No EX was found in the samples of process water and plant effluent, or at least the concentrations were below the detection limit of $10^{-8}M$ for the d.p. technique used, with 2-min deposition time. The concentrations of EX and $(EX)_2$ in sample (c) were determined from the corresponding calibration

Table 2. Determination of EX and $(EX)_2$ by cathodic-stripping voltammetry in three samples from a flotation plant; the conditions were 2 min deposition at -0.1 V, $0.1M$ KNO_3 medium, at $25^\circ C$

Sample	[EX], M	$[(EX)_2]$, M
Process water	$< 10^{-8}$	$< 10^{-8}$
Plant effluent	$< 10^{-8}$	$< 10^{-8}$
Flotation liquor	3×10^{-7}	1×10^{-7}

graphs. The measurable concentrations of $(EX)_2$ found, indicate that chemical oxidation of EX was taking place in the flotation process. Because of the sampling problems, the results in Table 2 should be interpreted with caution and should rather be taken as guiding values.

Adsorption of EX and DTP on Cu_2S

The reaction between EX and sulphide minerals is a complicated process consisting of several steps, depending on various factors such as the stoichiometry of the sulphide and the concentration of dissolved oxygen. The sulphides themselves are semiconductors and may even have areas of different morphology and electrochemical potential.¹¹

The main purpose of this work was to study how much EX is adsorbed on the surface of copper(I) sulphide. The Cu_2S plate was dipped into 5.25 ml of a solution of $4.8 \times 10^{-7}M$ EX for 1 min, and then the solution was made $0.1M$ in potassium nitrate, the total volume then being 5.75 ml. Standard additions of $1 \times 10^{-5}M$ EX were then made. Following immersion of the Cu_2S plate, the concentration of EX was found to decrease to approximately $2 \times 10^{-7}M$ and the shape of the stripping voltamperogram resembled that for the same concentration in Fig. 2c. However, when standards of EX were added, the peak at -0.60 V started to increase instead of the peak at -0.45 V as had been the case for the experiment in Fig. 2c. Two different Cu_2S plates were used: with the first the concentration of EX changed from $4.4 \times 10^{-7}M$ to $1.6 \times 10^{-7}M$, which means that 16×10^{-10} mole of EX had been adsorbed on the plate. From the physical dimensions of the plate, assumption of a surface roughness of 1.5, and the knowledge¹² that one EX molecule occupies 0.29 nm², it can be calculated that the amount of EX adsorbed corresponds to one monolayer. The same result was observed for the second plate.

The results with DTP were more difficult to explain, mainly because the calibration graph in that concentration range was not linear, making it difficult to apply the standard-addition method. A rough calculation gave an estimate of 0.4 monolayer of adsorbed DTP.

Acknowledgement—A personal grant from Neste Oy Research Foundation to J.L. is gratefully acknowledged.

REFERENCES

1. S. Heimala, S. Jounela, S. Rantapuska and M. Saari, *Proc. XV Int. Min. Proc. Congr.*, Cannes, 1985.
2. E. Rolia, *Trans. Inst. Min. Met., Sect. C*, 1970, **79**, 207.
3. G. Jones and J. T. Woodcock, *Ultraviolet Spectrometry of Flotation Reagents with Special Reference to the Determination of Xanthate in Flotation Liquors*, Institute of Mining Metallurgy, London, 1973.
4. J. Leppinen and S. Vahtila, *Talanta*, 1986, **33**, 795.
5. E. C. Horning, *Organic Synthesis*, Collective Vol. 3, Wiley, New York, 1955.
6. H. Bode and W. Arnsward, *Z. Anal. Chem.*, 1962, **185**, 99.
7. J. E. Andersson and A. M. Bond, *Anal. Chem.*, 1981, **53**, 504.
8. A. M. Bond, A. T. Casey and J. R. Thackery, *J. Electroanal. Chem.*, 1973, **48**, 71.
9. J. Leja, *Miner. Sci. Engng.*, 1973, **5**, 278.
10. O. Huynh Thi, M. Lamache and D. Bauer, *Electrochim. Acta*, 1981, **26**, 33.
11. A. Granville, N. P. Finkelstein and S. A. Allison, *Trans. Inst. Min. Met., Sect. C*, 1972, **81**, 1.
12. A. M. Gaudin and G. S. Preller, *Trans. AIME*, 1946, **169**, 248.

SPECTROPHOTOMETRIC AND SPECTROFLUOROMETRIC DETERMINATION OF ZINC AND CADMIUM WITH 2,2'-PYRIDIL BIS(2-QUINOLYLHYDRAZONE)

KEVIN J. WEST* and RONALD T. PFLAUM†

Department of Chemistry, University of Iowa, Iowa City, Iowa 52242, U.S.A.

(Received 20 August 1985. Revised 22 May 1986. Accepted 4 June 1986)

Summary—The chelating ligand, 2,2'-pyridil bis(2-quinolyldihydrazone), has been used for the spectrophotometric determination of zinc and cadmium in synthetic samples. The molar absorptivities of these metal complexes in 80% ethanol-water solution at pH 8 were found to be 4.60×10^4 and 5.10×10^4 l. mole⁻¹. cm⁻¹ for zinc and cadmium respectively. Beer's law was obeyed for metal-ion concentrations between 1.0×10^{-6} and $2.5 \times 10^{-5} M$. The limits of detection were found to be 52 and 79 ng/ml for zinc and cadmium respectively. The complexes fluoresced in 80% ethanol-water at pH 8 for zinc and at pH 10 for cadmium. The linear range for fluorescence as a function of metal-ion concentration was found to be 5×10^{-7} – $5 \times 10^{-6} M$ for both zinc and cadmium. Transition-metal ions interfere severely with both the spectrophotometric and fluorimetric determinations, and must be removed beforehand. An ion-exchange procedure is suitable for this.

Since the earliest reports of substituted hydrazones,^{1,2} these chelating ligands have been studied as colorimetric reagents for a variety of transition metals. A recent review article³ discusses the various uses of substituted hydrazones. One substituted hydrazone of which only limited use has been made is 2,2'-pyridil bis(2-quinolyldihydrazone), PBQH. The spectrophotometric determination of cobalt⁴ and of palladium⁵ have been reported, but other metal systems have not been evaluated. The ligand reacts with transition-metal ions, including zinc and cadmium, to form intensely coloured complexes in 80% ethanol-water solutions, buffered to pH 8. The molar absorptivities are high, which makes PBQH a sensitive reagent for transition metals. The wavelengths of maximum absorption for the complexes are near one another, making PBQH non-selective for determination of zinc and cadmium. Lack of selectivity is a common characteristic of substituted hydrazone ligands, and necessitates prior separations in analytical use. PBQH also forms fluorescent complexes with zinc and cadmium, the cadmium complex requiring a higher pH for fluorescence to occur. Hence small amounts of cadmium have only a small effect on the fluorescence of the zinc complex, but small amounts of zinc interfere considerably with the fluorescence of the cadmium complex. An anion-exchange procedure⁶ is useful for the preliminary separations.

EXPERIMENTAL

Apparatus

All absorption measurements were made with 1-cm silica cells in a Varian Cary 219 spectrophotometer at room temperature. Fluorescence measurements were made at room temperature with an Aminco-Bowman spectrofluorimeter equipped with a 150-W xenon lamp and a 1P21 photomultiplier tube. A 1-cm fused-silica fluorescence cell was used to hold the sample solutions.

Reagents

PBQH was prepared by the general method of Black *et al.*;⁷ 0.01 mole (2.11 g) of 2,2'-pyridil and 0.02 mole (3.19 g) of 2-hydrazinoquinoline were dissolved in 150 ml of benzene, a trace of *p*-toluenesulphonic acid was added and the solution was refluxed for 17 hr, with a Dean and Stark trap to remove water formed during the reaction. The volume of the reaction solution was reduced to 20 ml and the crude PBQH crystallized upon cooling to room temperature. The product was recrystallized from ethanol; yield 2.65 g (51%) of PBQH, m.p. 149–152°. Elemental analysis gave C 72.5%, H 4.6%, and N 22.4%; C₃₀H₂₂N₈ requires C 72.87%, H 4.45%, and N 22.67%. A $5 \times 10^{-4} M$ solution of PBQH was made by dissolving the reagent in 95% ethanol.

Stock solutions of zinc and cadmium were made by dissolving the metals in concentrated hydrochloric acid and diluting to 1 litre with demineralized water. Aliquots of these solutions were then diluted to give 5×10^{-4} and $2.5 \times 10^{-5} M$ working solutions for the absorption and fluorescence studies respectively.

Appropriate buffer solutions were made by dissolving borax in demineralized water and adjusting the pH to the desired value with hydrochloric acid or sodium hydroxide solution.

Optimization of complexation conditions

The optimum percentage of ethanol in the solvent system and the pH required for complexation were evaluated by mixing aliquots of the ethanolic ligand solution with aliquots of the metal-ion solutions, and adding sufficient ethanol to vary its content from 50 to 90%. The pH was adjusted with 2M sodium hydroxide, and the visible absorp-

*Present address: Indiana University-Purdue University at Fort Wayne, Department of Chemistry, 2101 Coliseum Boulevard East, Fort Wayne, Indiana 46805, U.S.A.
†Author for correspondence.

tion spectrum was recorded for pH values up to 11. The solution was also monitored for evidence of precipitation. The effect of excess of ligand on the complex formation was then evaluated in 80% ethanol at pH 8 by the mole-ratio method.

The optimum complexation conditions found in these absorption studies were used as the starting conditions for the fluorescence studies. The excitation wavelength was set at that for maximum absorption, and the emission was scanned from 350 to 700 nm. The effects of pH and excess of ligand were examined as before.

Preliminary separations

Dissolve the sample containing zinc or cadmium by appropriate means. Prepare a 10-cm long 1-cm bore column of Dowex 1 × 8, 100–200 mesh, anion-exchange resin in chloride form. Place the sample containing zinc and/or cadmium on the column and run it into the resin bed. Rinse the resin bed with 100 ml of 10% sodium chloride solution in 0.12M hydrochloric acid to remove metal ions other than zinc and cadmium. Elute the zinc with 100 ml of 2% sodium chloride solution in 2M sodium hydroxide, and the cadmium with 1M nitric acid. Regenerate the resin bed with the 0.12M hydrochloric acid/10% sodium chloride solution. If only zinc or only cadmium is present with the other metal ions, omit the sodium hydroxide/sodium chloride elution and use 1M nitric acid to elute the zinc or cadmium. Adjust the eluate containing zinc or cadmium to pH 6–7 with dilute hydrochloric acid or sodium hydroxide solution and dilute it accurately to 250 ml with distilled water. Add a 2-ml aliquot of the solution obtained from the preliminary separation (containing 1.6–33 μg of zinc, or 2.8–57 μg of cadmium) to 4 ml of $5 \times 10^{-4}M$ PBQH. Add 2 ml of pH-8 buffer and dilute to volume in a 25-ml standard flask with 95% ethanol. Measure the absorbance at 480 nm for the zinc complex or at 482 nm for the cadmium complex. Calculate the amount of zinc or cadmium present from a previously prepared calibration curve.

Spectrofluorometric determinations

Add a 2-ml aliquot of the solution obtained from the initial separation (containing between 0.8 and 8.3 μg of zinc or 1.4 and 14.1 μg of cadmium) to 1.0 ml of $5 \times 10^{-4}M$ PBQH. Add 2 ml of pH-8 buffer for zinc or pH-10 buffer for cadmium and dilute the solution to volume in a 25-ml standard flask with 95% ethanol. After 10 min, measure the fluorescence at 550 nm, using an excitation wavelength of 480 nm for zinc or 482 nm for cadmium. Calculate the concentration of zinc or cadmium from a previously prepared calibration curve.

Analysis of phosphor bronze

Weigh a 0.5-g sample and dissolve it in 10 ml of nitric acid (1 + 1) with heating. Filter off the metastannic acid and wash it with dilute nitric acid. Evaporate the solution to ~10 ml and dilute it to 25 ml with 2M hydrochloric acid. Separate the zinc by the ion-exchange method already described, and determine it as above.

RESULTS AND DISCUSSION

Studies of the reagent

The reagent, 2,2'-pyridil bis(2-quinolyldihydrazone), Fig. 1, is a bright yellow crystalline solid, insoluble in water, but soluble in dilute acids and common organic solvents. Solutions of PBQH in 95% ethanol are stable for extended periods of time.

PBQH may exist in three isomeric forms, EE, EZ, and ZZ, with respect to the carbon–nitrogen double

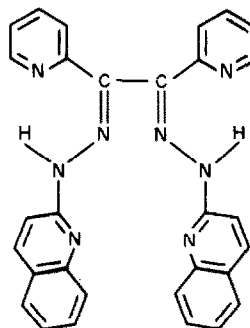


Fig. 1. Structure of the ligand 2,2'-pyridilbis(2-quinolyldihydrazone), PBQH, EE isomer.

bonds. Evidence of all three isomers appears in the deuterochloroform NMR spectrum of the solid isolated from the reaction mixture.

The ultraviolet and visible spectrum of PBQH in an 80% ethanol–water solution shows an absorption maximum at 375 nm. When PBQH reacts with zinc or cadmium in 80% ethanol–water, a new absorption maximum occurs at 480 nm for the zinc complex and 482 nm for the cadmium complex (Fig. 2). Table 1 lists the wavelengths of maximum absorption and the molar absorptivities for the zinc, cadmium, copper, nickel, cobalt, iron, mercury, and palladium complexes of PBQH. Alkaline solutions of PBQH give no colour reaction with lanthanum, actinium, cerium, praseodymium, neodymium, samarium, europium, gadolinium, thorium, and uranium.

Black *et al.*⁷ reported that when solid complexes of zinc and cadmium with a similar ligand, 2,2'-pyridil bis(2'-pyridylhydrazone) are isolated, the EE form of the ligand is present in the complex. Ramirez and Kirby⁸ isolated several isomers of hydrazones and compared the ultraviolet, visible and infrared spectra for differences that could be correlated to isomer structure. They found that the ultraviolet spectrum of the E isomer of a substituted hydrazone exhibits a small bathochromic shift relative to that of the parent hydrazone, whereas the Z isomer exhibits a hypsochromic shift. The ultraviolet spectrum of PBQH exhibits a small bathochromic shift in ethanol solution when the pH is raised from ≤ 7 to ≥ 8 . This suggests that the EE isomer is the predominant form and thus PBQH acts as a quadridentate ligand.

Table 1. Wavelength of maximum absorption and molar absorptivity for selected transition-metal ions

Metal ion	Wavelength, nm	Molar absorptivity, l. mole ⁻¹ . cm ⁻¹
Zn(II)	480	4.60×10^4
Cd(II)	482	5.10×10^4
Cu(II)	465	2.50×10^4
Co(II)	500	1.87×10^4
Fe(II)	475	1.71×10^4
Hg(II)	445	4.10×10^4
Ni(II)	490	2.90×10^4
Pd(II)	A long wing-like response from 450 to 650 nm	

Table 2. Metal-ion concentrations giving 20% change in absorbance of the Zn and Cd complexes ($1.01 \times 10^{-5}M$)

Metal ion	Zinc-PBQH	Cadmium-PBQH
Cd(II)	$2.7 \times 10^{-6}M$ (0.3 ppm)	— (—)
Co(II)	$6.4 \times 10^{-6}M$ (0.4 ppm)	$4.7 \times 10^{-6}M$ (0.3 ppm)
Cu(II)	$4.1 \times 10^{-6}M$ (0.3 ppm)	$4.0 \times 10^{-6}M$ (0.2 ppm)
Fe(II)	$3.0 \times 10^{-5}M$ (1.7 ppm)	$1.8 \times 10^{-5}M$ (1.0 ppm)
Hg(II)	$4.4 \times 10^{-6}M$ (0.9 ppm)	$3.6 \times 10^{-6}M$ (0.7 ppm)
Ni(II)	$4.9 \times 10^{-6}M$ (0.3 ppm)	$4.0 \times 10^{-6}M$ (0.3 ppm)
Pd(II)	$4.2 \times 10^{-6}M$ (0.4 ppm)	$4.8 \times 10^{-6}M$ (0.5 ppm)
Zn(II)	— (—)	$2.3 \times 10^{-6}M$ (0.1 ppm)

Table 3. Spectrophotometric determination of Zn(II) and Cd(II) (3 replicates for each sample) in simulated phosphor-bronzes

Metal	Taken, μg	Found, μg			Error, %
		low	high	mean	
Zn	11.54	11.6	11.9	11.7	+1.4
	19.78	20.4	20.5	20.4	+3.3
	29.65	29.4	29.9	29.6	-0.3
Cd	8.34	8.3	9.0	8.6	+3.0
	19.83	20.2	20.8	20.4	+3.0
	34.00	34.1	35.1	34.6	+1.8
	50.98	50.7	50.8	50.8	-0.4

Complexation conditions

The conditions for maximum colour formation of the zinc and cadmium complexes were found to be very similar. An 80:20 v/v ethanol-water medium was found to be suitable. If the medium contains less than 80% ethanol the complex tends to precipitate after a short time. Between 80 and 90% ethanol is satisfactory, but pH adjustment with an aqueous buffer is difficult when 90% ethanol is used. An apparent pH of ≥ 8 gives maximum complex formation.

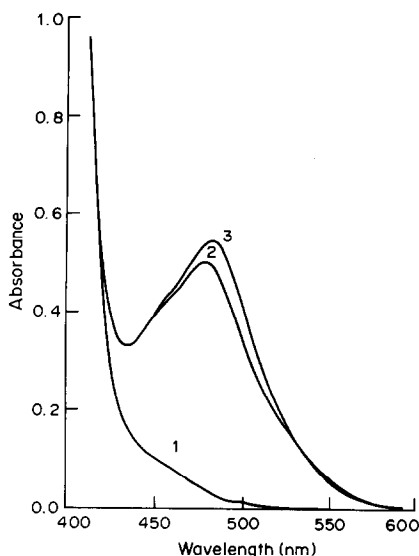


Fig. 2. Absorption spectra of PBQH and its zinc and cadmium complexes. (1) PBQH; (2) zinc complex, $1.01 \times 10^{-5}M$; (3) cadmium complex, $1.01 \times 10^{-5}M$.

A ligand:metal mole ratio of at least 4:1 is required for maximum formation of the complexes, which form rapidly (the reaction is 80% complete in 5 min).

Beer's law is obeyed over the concentration ranges from 1.01×10^{-6} to $2.03 \times 10^{-5}M$ for zinc and from 1.00×10^{-6} to $2.01 \times 10^{-5}M$ for cadmium, the limits of detection being 52 and 79 ng/ml for zinc and cadmium respectively. The molar absorptivities are $4.60 \times 10^4 l. mole^{-1}. cm^{-1}$ for the zinc complex and 5.10×10^4 for the cadmium complex. The zinc and cadmium complexes fluoresce under similar conditions to those used for the spectrophotometric determinations but the fluorescence intensity of the zinc complex is decreased if the ligand:zinc mole ratio exceeds 40:1. The fluorescence intensity is maximal and constant over the pH range 8-10 for zinc and 10-11 for cadmium, but because the zinc complex still fluoresces appreciably at pH 10-11, any zinc must be removed before the cadmium can be determined. The fluorescence reaches a maximum intensity in 10 min and is stable for up to an hour. For both complexes λ_{max} for emission is 550 nm; for excitation λ_{max} is 480 nm for zinc and 482 nm for cadmium. The fluorescence intensity is linear over the concentration range 5.0×10^{-7} - $5.0 \times 10^{-6}M$ for both complexes, and the limit of detection is $3.5 \times 10^{-7}M$ for both.

Effect of diverse ions

Other transition-metal ions interfere considerably in the spectrophotometric determination, as expected from the data in Table 1, and must be removed beforehand. Table 2 lists the concentrations of selected transition-metal ions at which there is a 20% relative change in the absorption spectrum of the zinc and cadmium complexes of PBQH. Alkali-metal, alkaline-earth metal, aluminium, lanthanide and actinide metals do not interfere.

Applications

The zinc in a phosphor-bronze bearing metal was determined by the recommended procedure. Because there was no cadmium in the sample, the zinc was eluted from the ion-exchange column with 100 ml of 1M nitric acid. The determination of zinc and cadmium was validated by application of the whole procedure to simulated samples (Table 3). The zinc content found for NBS 63 phosphor-bronze was

0.484%, (average deviation 0.004%, which is within the limits recommended by the National Bureau of Standards). The certified zinc content is 0.48%.

REFERENCES

1. J. F. Geldard and F. Lions, *J. Am. Chem. Soc.*, 1962, **84**, 2262.
2. C. F. Bell and D. R. Rose, *Talanta*, 1965, **12**, 696.
3. R. B. Singh, P. Jain and R. P. Singh, *ibid.*, 1982, **29**, 77.
4. H. Kulshreshtha, R. B. Singh and R. P. Singh, *Analyst*, 1979, **104**, 572.
5. H. Kulshreshtha, T. B. Singh and R. P. Singh, *Affinidad*, 1980, **37**, 247; *Chem. Abstr.*, 1980, **93**, 230175k.
6. S. Kallmann, C. G. Steele and N. Y. Chu, *Anal. Chem.*, 1956, **28**, 230.
7. D. St. C. Black, A. J. Hartshorn and K. S. Murray, *Aust. J. Chem.*, 1976, **29**, 1153.
8. F. Ramirez and A. F. Kirby, *J. Am. Chem. Soc.*, 1952, **76**, 1037.

VOLTAMMETRIC DETERMINATION OF BENZIDINE AND ITS DERIVATIVES, AT A GLASSY-CARBON ELECTRODE

JIŘÍ BAREK, ANTONÍN BERKA, ZUZANA TOCKSTEINOVÁ and JIŘÍ ZIMA

Department of Analytical Chemistry, Charles University, Albertov 2030, 128 40 Prague 2, Czechoslovakia

(Received 6 January 1986. Revised 7 March 1986. Accepted 24 May 1986)

Summary—Conditions have been found for the determination of benzidine, *o*-tolidine, *o*-dianisidine, 3,3'-diaminobenzidine and 3,3'-dichlorobenzidine by classical and differential pulse voltammetry at a glassy-carbon stationary or rotating electrode, in the concentration range 10^{-5} – $10^{-3}M$. The mechanism of the oxidation is discussed and applications are presented for the determination of these chemical carcinogens and their mixtures either directly, or after preliminary separation by extraction or thin-layer chromatography.

Benzidine and its derivatives are among the proven or suspected carcinogens,¹ which is the cause of the demand for methods for their determination in the industrial and general environment. A survey² has shown that chromatographic methods have been used most often, whereas electrochemical methods have received much less attention. In a study of the oxidation of benzidine and its derivatives at a rotating platinum disk electrode in aqueous solution³⁻⁶ or at a stationary platinum electrode in a mixture of water and acetone,⁷ passivation of the platinum electrode was encountered, which complicated analytical application of the processes studied. The mechanism of the electrochemical oxidation of benzidine and its derivatives has been discussed in some detail in a monograph.⁸ A pyrolytic carbon-film electrode⁹ and a graphite-paste electrode¹⁰ have been used successfully for the determination of some benzidine derivatives: when the differential pulse mode is used the sensitivity of the determination is substantially increased. However, these electrodes are not readily available, whereas glassy-carbon rotating disk electrodes are manufactured by numerous companies. Therefore, the present work deals with the possibilities of voltammetric determination of benzidine and its derivatives by use of this electrode, the surface of which is readily renewed by polishing, which helps to eliminate the problems connected with passivation.

EXPERIMENTAL

Reagents

Stock solutions of benzidine, *o*-tolidine, *o*-dianisidine and 3,3'-diaminobenzidine ($5 \times 10^{-3}M$) and 3,3'-dichlorobenzidine ($1 \times 10^{-3}M$) in 0.1M hydrochloric acid were accurately prepared from the p.a. substances (Merck, Darmstadt). All other chemicals were of p.a. purity (Lachema, Brno). The water was doubly distilled in a fused-silica still. Commercial TLC plates were used (Silufol UV 254, Kavalier, Czechoslovakia).

Apparatus

The voltammetric measurements were made with a PA 2

polarograph, a 4105 XY plotter and an RDE 1 glassy-carbon disk electrode, consisting of a PTFE cylinder 10 mm in diameter with a glassy-carbon rod 3 mm in diameter (all from Laboratorní Přístroje, Prague). A three-electrode circuit was used, with a saturated calomel reference electrode and a platinum-foil counter-electrode; the surface area of the latter was ca. 1 cm². If not stated otherwise, the rotation rate was 2500 rpm, the potential scan-rate 5 mV/sec, the amplitude of the DP voltammetric pulse 12.5 mV, the pulse duration 100 msec and the interval between pulses 1 sec. The spectrophotometric measurements were made with a PU 8800 instrument (Pye Unicam, England) in 1-cm fused-silica cells.

Procedures

The voltammetric measurements were performed in an all-glass vessel with 25 ml of solution. Each measurement was made in triplicate and evaluated statistically. Between measurements, the electrode was rinsed with distilled water, repolished with fine emery paper and velvet, and again rinsed with distilled water.

RESULTS AND DISCUSSION

Direct-current voltammetry

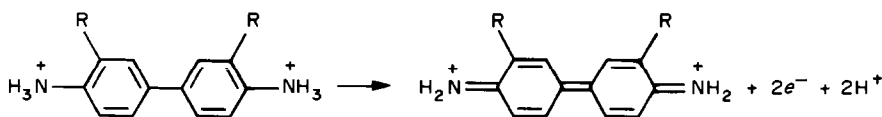
The effect of pH on the shape of the voltamperograms was studied by use of a series of Britton-Robinson buffers with both the stationary and the rotating electrode. The curves are shown in Fig. 1 and their parameters are summarized in Table 1. Except for 3,3'-dichlorobenzidine (see Fig. 1b), the test substances yield a single wave in acidic solution. In alkaline media the wave splits into two, at pH ≥ 6.8 for *o*-dianisidine and at pH > 10 for *o*-tolidine. Electrode passivation increases with increasing pH and causes distortion of the curves.

The order of the experimental half-wave potentials is determined by the properties of the substituents: 3,3'-diaminobenzidine is oxidized most readily because of the strong +M effect of the amino groups; *o*-tolidine and *o*-dianisidine are also oxidized more easily than benzidine, owing to the +M effect of the CH₃ and OCH₃ groups. On the other hand, 3,3'-

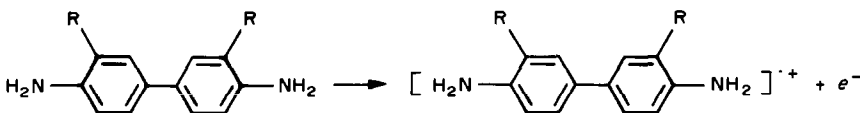
dichlorobenzidine is oxidized with greater difficulty than benzidine because of the $-I$ effect of the chlorine atoms.

The half-wave potentials of all the test substances shift to more positive values with decreasing pH. This can be explained as due to protonation of the amino group, the centre at which the electron transfer occurs. Protonation leads to a decrease of the electron density at the nitrogen atoms, resulting in more difficult electron transfer from the substance to the electrode.

The observed decrease in the limiting currents with increasing pH can be explained by the fact that in acidic media the two-electron oxidation to the quinonedi-imine predominates,⁸



whereas in solutions with a higher pH the one-electron oxidation to the corresponding semiquinone predominates:



This assumption was confirmed by a spectrophotometric study of the oxidation products, in which the rotating electrode was polarized by a constant

potential corresponding to the limiting-current region and samples were taken from time to time and their visible absorption spectra recorded. It was found that the corresponding quinonedi-imines are formed in acidic media, as the shape and position of the absorption maxima at 400–450 nm correspond to the spectra of these substances, described earlier.¹¹ At $\text{pH} > 3$, the formation of the corresponding semiquinones was confirmed analogously; they exhibit absorption maxima at around 600 nm.¹²

It follows from cyclic voltammetry with a stationary electrode at potential scan-rates of 2–10 mV/sec, that in 0.1M hydrochloric acid benzidine, *o*-tolidine and *o*-dianisidine behave almost reversibly, in contrast to the irreversible behaviour of 3,3'-diamino-

benzidine. The cyclic voltamperogram of 3,3'-dichlorobenzidine suggests that the oxidation involves at least partially reversible exchange of two electrons

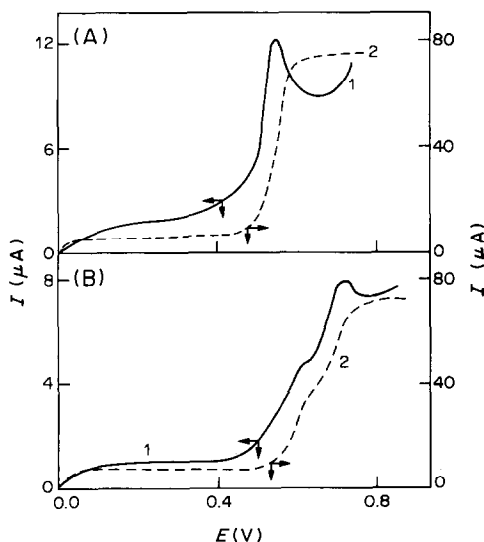


Fig. 1. Typical d.c. voltamperograms of $10^{-3}M$ *o*-tolidine (A) and 3,3'-dichlorobenzidine (B) at the stationary (1) and rotating (2) glassy-carbon disk electrode in 0.1M hydrochloric acid.

(see Fig. 2). The wave of *o*-dianisidine splits into two with increasing pH, while the partially reversible character of the oxidation is retained, whereas the oxidation of *o*-tolidine becomes irreversible with increasing pH.

The curves best suited for analytical purposes were obtained in all cases with the rotating electrode in 0.1M hydrochloric acid; the dependence of the limiting current on the square root of the rotation rate confirmed the convective-diffusional character of the waves. The parameters of the calibration lines, together with the detection limits calculated by the method of Skogerboe and Grant¹³ at a 99% significance level, are listed in Table 2.

Differential pulse voltammetry

The calibration graphs for measurement in 0.1M hydrochloric acid, over a concentration range of 10^{-6} – $10^{-3}M$, and their parameters and the detection limits are given in Table 2. Again, better results were obtained with the rotating electrode (2500 rpm), the currents being about twice those obtained with the stationary electrode. The peak height increased with increasing modulation amplitude, but the reproducibility of the results deteriorated. To attain a low detection limit it is thus necessary to use a small pulse amplitude (12.5 mV) and a low potential scan-rate

Table 1. The effect of pH on the d.c. voltamperograms at a glassy-carbon disk electrode rotating at 2500 rpm

Sample	pH	pH						
		2.2	3.3	4.3	5.3	6.8	8.2	10.0
$10^{-3}M$ Benzidine	$E_{1/2}, mV$	550	530	520	— ^c	—	—	—
	$I_{lim}, \mu A$	69	71	69	—	—	—	—
	α, mV^a	-45	-49	-57	—	—	—	—
$10^{-3}M$ <i>o</i> -Tolidine	$E_{1/2}, mV$	460	460	460	440	400	360	320
	$I_{lim}, \mu A$	73	70	65	63	61	60	54
	α, mV^a	-30	-37	-38	-64	— ^b	—	—
$10^{-3}M$ <i>o</i> -Dianisidine	$E_{1/2}, mV$	475	460	450	425	395	370	275
	$I_{lim}, \mu A$	74	75	75	73	71	59	35
	α, mV^a	-47	-56	-65	-82	— ^b	—	—
$10^{-3}M$ 3,3'-Diaminobenzidine	$E_{1/2}, mV$	390	370	360	340	270	190	125
	$I_{lim}, \mu A$	61	60	59	62	62	35	30
	α, mV^a	-29	-35	-39	-40	— ^b	—	—
$2 \times 10^{-4}M$ 3,3'-Dichlorobenzidine	$E_{1/2}^1, mV^d$	560	560	525	510	— ^c	—	—
	$E_{1/2}^2, mV^d$	675	670	670	650	—	—	—
	$I_{lim}^1, \mu A^d$	8.7	9.1	8.7	6.7	—	—	—
	$I_{lim}^2, \mu A^d$	15.3	15.1	14.8	10.9	—	—	—

^a Slope of logarithmic analysis; ^b logarithmic analysis is impossible because of poorly developed curves; ^c substance precipitates; ^d superscripts 1 and 2 designate the first and second waves, respectively.

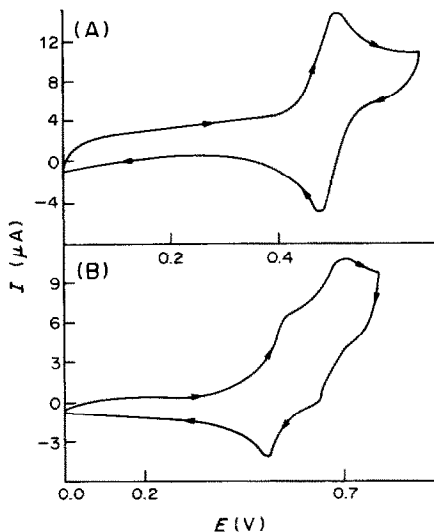


Fig. 2. Typical cyclic voltamperograms of $10^{-3}M$ *o*-tolidine (A) and 3,3'-dichlorobenzidine (B) on the glassy-carbon stationary disk electrode in 0.1M hydrochloric acid at a potential scan-rate of 5 mV/sec.

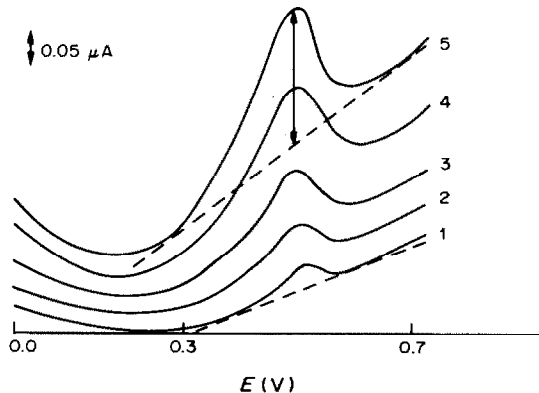


Fig. 3. DP voltamperograms of $2 \mu M$ (1), $4 \mu M$ (2), $6 \mu M$ (3), $8 \mu M$ (4) and $10 \mu M$ (5) *o*-dianisidine. The dashed line represents the baseline from which the peak height was measured. The oscillations on the curves have been smoothed out for clarity.

(5 mV/sec). Higher amplitudes and scan-rates lead to an increase in the transient current, which is apparently caused by slow redox reactions of oxygen-

Table 2. Parameters of the calibration graphs for the substances in the range 10^{-5} - $10^{-3}M$

Substance	Slope, mA.l.mole ⁻¹	Intercept, μA	Corr. coeff.	Detection limit, μM
Direct current voltammetry				
Benzidine	79.7	0.28	0.9985	7
<i>o</i> -Tolidine	67.5	-0.15	0.9990	6
<i>o</i> -Dianisidine	72.2	-0.14	0.9985	8
3,3'-Diaminobenzidine	71.3	0.68	0.9991	9
3,3'-Dichlorobenzidine	69.8	1.06	0.9980	9
DP Voltammetry				
Benzidine	19.1	-0.03	0.9930	2
<i>o</i> -Tolidine	22.9	0.21	0.9938	3
<i>o</i> -Dianisidine	22.3	-0.02	0.9930	1
3,3'-Diaminobenzidine	14.7	0.10	0.9965	3
3,3'-Dichlorobenzidine	20.5	0.02	0.9921	2

containing groups on the glassy-carbon surface.¹⁴ Compared with d.c. voltammetry, the detection limit for the pulse method is lower by a factor of about five. The main advantage of DP voltammetry over d.c. voltammetry, then, lies in the possibility of using the former even for analyses of some mixtures of the test substances (see below). Figure 3 depicts the voltamperograms for the calibration curve for *o*-dianisidine at the lowest concentration range, as well as the method adopted for the determination of the peak height.

Compared with that obtained with carbon-paste electrodes,¹⁰ the sensitivity is lower, but the preparation of a glassy-carbon electrode for measurement is less time-consuming.

APPLICATIONS

Extractive preconcentration

As the carcinogens studied can be reliably determined in aqueous solution only down to a concentration of $10^{-5}M$, the possibility of preconcentration by extraction into benzene was investigated. A 250-ml portion of solution containing benzidine at concentrations in the range 10^{-6} – $10^{-5}M$ was adjusted to pH 7 with sodium hydroxide and extracted with five

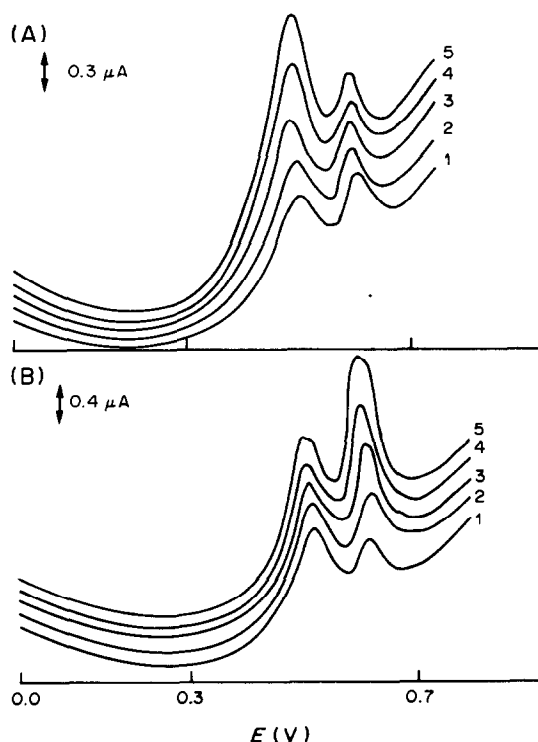


Fig. 4. DP voltamperograms of mixtures of benzidine and *o*-dianisidine. A— $5 \times 10^{-5}M$ benzidine and $2 \times 10^{-5}M$ (1), $4 \times 10^{-5}M$ (2), $6 \times 10^{-5}M$ (3), $8 \times 10^{-5}M$ (4) and $10 \times 10^{-5}M$ (5) *o*-dianisidine. B— $2 \times 10^{-5}M$ (1), $4 \times 10^{-5}M$ (2), $6 \times 10^{-5}M$ (3), $8 \times 10^{-5}M$ (4) and $10 \times 10^{-5}M$ (5) benzidine and $5 \times 10^{-5}M$ *o*-dianisidine. The oscillations have been smoothed out for clarity.

50-ml portions of benzene, which were then combined, and evaporated to dryness in a vacuum rotary evaporator. The residue was dissolved in 25 ml of 0.1M hydrochloric acid and the DP voltamperogram recorded. The measured peak current was a linear function of the concentration, enabling the use of both the calibration curve method and the standard-addition method to evaluate the results. The relative standard deviation for 7 determinations of $4 \times 10^{-6}M$ benzidine was 5.9%.

Direct analysis of mixtures

It became apparent from the peak potentials obtained that many pairs of the test substances were sufficiently separated for a direct determination of one in the presence of another to be possible. This possibility is demonstrated for the pair benzidine–*o*-dianisidine; DP voltamperograms were obtained for a constant concentration of one component and a varying concentration of the other (see Fig. 4). The peak heights for benzidine and *o*-dianisidine were proportional to their concentrations within the range 10^{-5} – $10^{-4}M$ (correlation coefficients > 0.99), the proportionality constant depending on the concentration of the other component of the mixture, because of mutual effects between the two peaks. Hence in an analysis of a binary mixture, the benzidine peak height must be measured first in the test solution (I_p^B), since the relationship $I_p^B = kC_B$ is valid for it (C_B is the benzidine concentration); then the peak height (I_p^{B+S}) is measured after a standard addition of benzidine (C_B^S), for which $I_p^{B+S} = k(C_B + C_B^S)$. In these equations the proportionality constant, k , is the same because the *o*-dianisidine concentration is unchanged (the dilution by the added standard can be neglected). By solving the two equations for the two unknowns, the benzidine concentration in the sample can be calculated.

The procedure for *o*-dianisidine is then analogous, *i.e.*, its concentration is found by a standard addition to the original solution, in which the benzidine concentration now remains the same. The relative standard deviation of the determination of the two substances does not exceed 5%.

Analysis of mixtures after a TLC separation

As the peak potentials in the DP voltamperograms of benzidine and *o*-tolidine are too close together for resolution (a difference of 50 mV), TLC was tested as a separation step before their determination. A sample of 250 μ l of an acetone solution which was 10^{-3} – $10^{-2}M$ in benzidine and 10^{-3} – $10^{-2}M$ in *o*-tolidine was placed on the TLC plate by micropipette, in the form of a band at the start, and dried. The chromatogram was developed by ascending chromatography with a benzene–methanol (4:1) mixture, until the front arrived at 1 cm below the upper edge of the plate. The bands were detected visually under ultraviolet light, the R_F values being 0.54 for benz-

idine and 0.66 for *o*-tolidine. The bands were quite sharply defined.

After development and detection the bands were cut out, with margins of 3 mm along the band and 2 cm at the sides. One side was cut to form a point and the other side was bent so that the strip could be hung in a dish containing acetone as solvent. The carcinogen was thus eluted into a vacuum evaporation vessel, the solvent was evaporated, the residue dissolved in 0.1M hydrochloric acid, diluted to 25 ml, and subjected to voltammetric analysis as above.

Calibration curves were obtained by evaporating 250- μ l portions of individual standard acetone solutions of the substances, in vacuum evaporation vessels, taking up the residues in 0.1M hydrochloric acid and diluting to 25 ml, and recording the voltamperograms. The measured peak currents were proportional to the concentrations of the standards (correlation coefficients >0.995), but the currents obtained by applying the full procedure to the standards were lower by 8%. This systematic error must be eliminated by using the full procedure for constructing the calibration graphs. The relative standard deviation then does not exceed 6% over the concentration range studied.

It can be concluded that both the direct voltammetric procedure and the determination after extractive preconcentration are suitable for checking the efficiency of destruction of these chemical carcinogens in laboratory-waste decontamination.¹⁵ Voltammetric determination after TLC separation

can possibly be applied to the analysis of some dyes derived from these benzidine derivatives.

REFERENCES

1. Anon., *IARC Monographs on the Evaluation of Carcinogenic Risk of Chemicals to Man*, Vol. 4, *Some Aromatic Amines, Hydrazine and Related Substances, N-Nitroso-compounds and Miscellaneous Alkylating Agents*, IARC, Lyon, 1974.
2. H. Egan (ed.), *Environmental Carcinogens—Selected Methods of Analysis*, Vol. 4, *Some Aromatic Amines and Azo Dyes in the General and Industrial Environment*, IARC, Lyon, 1981.
3. L. S. Rajshakrit, *Elektrokimiya*, 1968, **4**, 726.
4. Yu. I. Beilis, *Zh. Obshch. Khim.*, 1970, **40**, 745.
5. Yu. I. Beilis, A. F. Korotkova and A. V. Shikarev, *ibid.*, 1972, **42**, 1597.
6. A. T. Miller, B. Lamb, K. Prater, J. K. Lee and R. N. Adams, *Anal. Chem.*, 1964, **36**, 418.
7. F. T. Eggertsen and F. T. Weiss, *ibid.*, 1956, **28**, 1008.
8. R. N. Adams, *Electrochemistry at Solid Electrodes*, p. 362. Dekker, New York, 1969.
9. K. Lundstrom, *Anal. Chim. Acta*, 1983, **146**, 109.
10. W. M. Chey, R. N. Adams and M. S. Yllo, *J. Electroanal. Chem. Interfacial Electrochem.*, 1977, **75**, 731.
11. J. Barek and A. Berka, *Collect. Czech. Chem. Commun.*, 1976, **41**, 1334.
12. *Idem, ibid.*, 1977, **42**, 1949.
13. R. K. Skogerboe and L. C. Grant, *Spectrosc. Lett.*, 1970, **3**, 215.
14. J. Wang and B. A. Freiha, *Talanta*, 1983, **30**, 317.
15. M. Castegnaro (ed.), *Laboratory Decontamination and Destruction of Carcinogens in Laboratory Wastes: Some Aromatic Amines and 4-Nitrobiphenyl*, IARC Scientific Publications, No. 64, Lyon, 1985.

DETERMINATION OF TRACES OF EDTA, EGTA AND DCTA BY ADSORPTIVE ACCUMULATION OF THEIR COMPLEXES WITH Hg(II) FOLLOWED BY CATHODIC STRIPPING

MAŁGORZATA CISZKOWSKA and ZBIGNIEW STOJEK

Department of Chemistry, Warsaw University, ul. Pasteura 1, 02-093 Warszawa, Poland

(Received 24 November 1985. Revised 12 May 1986. Accepted 24 May 1986)

Summary—The strong adsorption of the Hg(II) complexes of EDTA, DCTA and EGTA on a hanging mercury-drop electrode has been utilized in two procedures for cathodic-stripping determination of these complexing agents in water. The first procedure allows the determination of the free ligands or the total amount of 'available' metal. The second, which requires addition of excess of Hg(II) to the solution, gives the total amount of the ligand. The detection limit is $1 \times 10^{-8} M$ in the final solution at pH 4-6.

There has been extensive discussion of the influence of EDTA on the equilibrium of natural systems¹ and of the biological and medical consequences of chelation of metals in the body.^{2,3}

A need has been shown for new sensitive methods of determination of EDTA and related compounds. Electroanalytical methods are an obvious choice because of their high sensitivity, and the electroactivity of ligands of EDTA type. So far, however, the electroanalytical⁴⁻⁸ and other methods⁹⁻¹¹ developed cannot distinguish between the bound and free forms of these complexones.

It is known that anodic oxidation of a mercury electrode in presence of EDTA leads to formation of HgEDTA complexes, and rigorous examination of the electrode reactions has led to the conclusion that these complexes are strongly adsorbed on the electrode surface.¹²⁻¹⁴ Similar investigation of other complexones [EGTA, ethyleneglycol bis(2-amino-ethylether)-*N,N,N',N'*-tetra-acetic acid and DCTA, 1,2-diaminocyclohexanetetra-acetic acid] has proved the strong adsorption of HgEGTA and HgDCTA.¹⁵ Here we report a cathodic-stripping procedure for the determination of these complexones, based on the strong adsorption of their Hg(II) complexes. The first step in the method is adsorptive accumulation, which has recently gained in importance.¹⁶

EXPERIMENTAL

Cathodic-stripping voltammetry (CSV) was performed by use of a PAR 173 potentiostat and a Unitra GP-02 generator. Cathodic-stripping differential-pulse voltammetric (CSDPV) curves were obtained with a Unitra model PP-04 pulse polarograph. In both cases a Riken Denshi model F-3C X-Y recorder was used. With the PP-04, a pulse amplitude of 40 mV, pulse time of 40 msec, and sampling time (t_s) of 20 msec were applied. Only a fast-scan mode was used, with a delay time equal to the pulse time. The instrument sampled the current before and after pulse application, then the two values were divided by t_s and the

difference between the quotients was sent to the output. This setting produced a square waveform (Fig. 1) and hence gave square-wave voltammetry (SWV) in the Osteryoung mode,¹⁷ and ensured high sensitivity. A Radiometer M-22 rotor with a rotation speed of 1400 rpm was used to stir the solutions during the preconcentration step. A hanging mercury-drop electrode (HMDE) of Kemula and Kublik type served as the indicator electrode. The drop area was 0.024 cm². The counter-electrode consisted of a platinum foil, and an SCE was used as the reference electrode. All potentials are reported vs. SCE.

All solutions were made from guaranteed reagent grade chemicals. The solutions of Hg(II) complexes were prepared

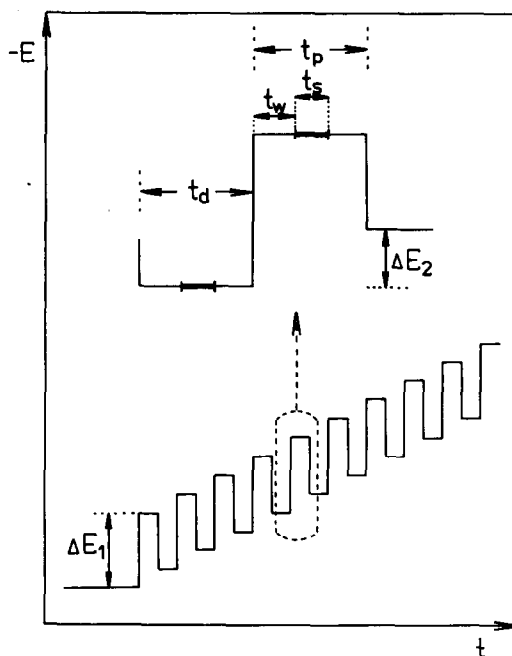


Fig. 1. Schematic diagram of current measurement with the PP-04; t_s —sampling time, t_w —waiting time, t_d —delay time, t_p —pulse time. The settings actually used: $t_s = 40$ msec, $t_w = 40$ msec, $t_d = 100$ msec, $t_p = 100$ msec, $E_1 = 20$ mV, $E_2 = 2$ mV.

by mixing equivalent volumes of Hg(II) and complexone solutions. Solutions were deaerated with argon. The temperature was kept at 19° unless otherwise mentioned.

Procedures

Samples of water were filtered and diluted fivefold with demineralized water before analysis. Acetate buffer was used to keep the pH at 5.8 or 4.8 and to adjust the ionic strength to 0.5M. Samples with a chloride concentration $> 1 \times 10^{-4}M$ (after dilution) were treated to remove the excess of chloride by addition of the necessary (pre-determined) amount of silver nitrate solution, and filtration. Although silver ions do not interfere in the determination, it is recommended not to add an excess of silver, since doing so would increase the background current. Unpurified chlorinated water samples, taken at the city water supply station, were found to need heating with perchloric acid at 60° for 1 hr; the perchloric acid concentration was fixed at 0.001M.

Procedure 1. Transfer 20 ml of sample solution to the electrochemical cell and deaerate it for 10 min with a stream of argon. For preconcentration apply a potential of +0.22 V to a 2.4-mm² hanging mercury drop electrode (HMDE) for 1 min, with stirring, followed by a 30-sec rest period. Scan the potential in a negative direction and record the cathodic stripping voltamperogram in the differential pulse or square-wave mode. Prepare a calibration graph covering the range 10^{-8} – $10^{-6}M$ complexone.

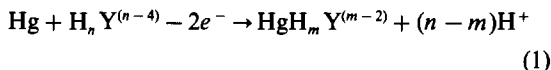
Procedure 2. Add mercury(II) to the sample solution to a level of $2 \times 10^{-5}M$, and then follow procedure 1.

RESULTS AND DISCUSSION

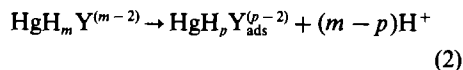
The strong adsorption of the EDTA, DCTA and EGTA complexes of Hg(II) leads at once to the possibility of their preconcentration on mercury electrodes, as shown in Fig. 2, where a few cathodic-stripping curves for each of these chelates are presented. The deposition potential, E_{dep} , should be as positive as possible, but not so positive as to cause excessive oxidation of the electrode material to unbound Hg²⁺.

Stripping was done under linear-scan voltammetric conditions, so that the total charge represented by the area under a stripping curve reflected the amount of the absorbed species. The height of the reduction peak increased with deposition time, t_{dep} . The entire process can be described by the set of reactions:

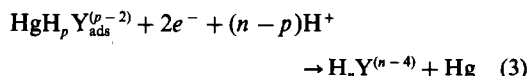
electroformation of the complex:



adsorption of the complex:



reductive stripping of the complex:



The curves in Fig. 2 were obtained at pH 4.8, at which $n = 2$, $m = 0$, and $p = 0$.^{14,15} When the unbound complexones exist in a solution, then electroproduction of the complex [reaction (1)] is necessary before adsorption can take place, and the Hg²⁺ activity is very low both in the bulk solution and at the electrode surface. Since the curves in Fig. 2 were obtained for $1 \times 10^{-5}M$ mercury(II) medium (*i.e.*, with an excess of metal ion), the complexones were already converted into their mercury complexes, and reaction (1) was not needed.

The dependence of the cathodic-stripping peak current on deposition time is presented in Fig. 3. For all the complexones tested the growth of peak current was limited, which is not surprising, as the adsorption will not produce more than a monolayer (more

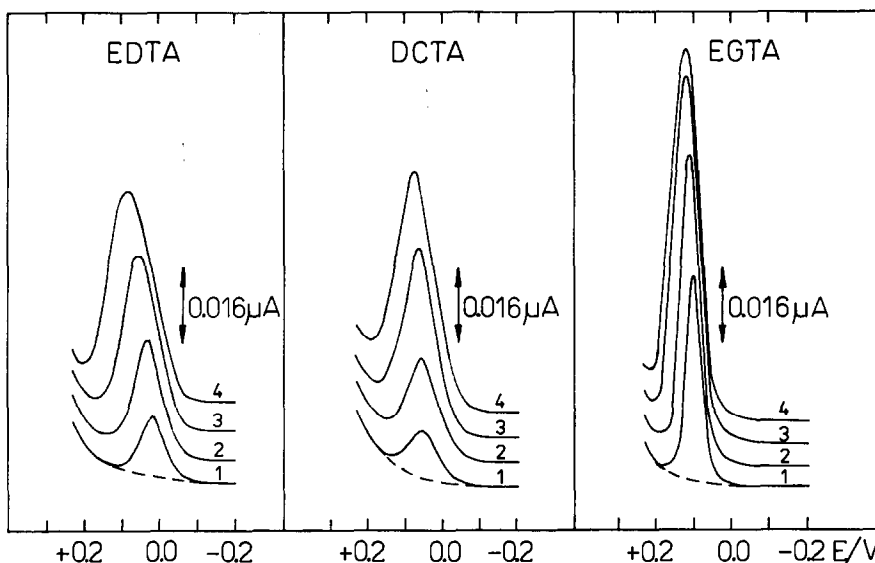


Fig. 2. Cathodic-stripping voltammetric (linear potential scan) curves of $2 \times 10^{-7}M$ EDTA, DCTA and EGTA in 0.05M acetate buffer containing $10^{-5}M$ Hg²⁺ at pH = 4.8. Sweep-rate 20 mV/sec; $E_{\text{dep}} = +0.23$ V; $t_{\text{dep}} = 0.5$ min (1); 1 min (2); 3 min (3); 4 min (4); electrode area 2.4 mm².

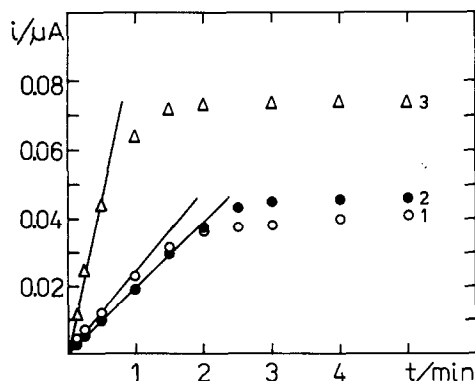


Fig. 3. The dependence of i_p on t_{dep} . Other conditions as for Fig. 2. EDTA (1), DCTA (2), EGTA (3).

precisely, the coverage resulting from the appropriate adsorption isotherm). Under the conditions of Fig. 3 the surface charge densities obtained for a deposition time of 5 min were 13.1, 12.9 and 13.2 $\mu\text{C}/\text{cm}^2$ for EDTA, DCTA and EGTA respectively, less than those expected for a monolayer.^{14,15} The different slopes of i_p vs. t_{dep} plots reflected the fact that the CSV peaks obtained were characterized by different peak widths.

Both the shape and position of the cathodic stripping peaks were pH-dependent. Figure 4 presents some square-wave cathodic-stripping curves obtained at pH 2, 4.8 and 10. The peaks differ in position, height and shape. The worst situation is for pH 2, where the EDTA and DCTA peaks are not only split but also very close to the mercury background current. The peaks are smaller at pH 10, apparently because of limited adsorption at this pH.^{14,15} Table 1 gives some quantitative data on peak width and peak position for these complexes at various pH values. The data refer to square-wave voltammetric experiments. This technique, in our case, gives an analytical signal lower by roughly one order of magnitude and by 30–50% than that obtained by linear-scan voltammetry and regular differential-pulse voltammetry respectively.

We should point out here that both the electro-generated complexes [reaction (1)] and those formed by addition of mercury(II) to the solution are easily accumulated at the mercury electrode. This leads directly to two possibilities in determination of these complexes. In the first, preconcentration and stripping with no mercury(II) added to the solution would reflect the concentration of free ligand. In the second,

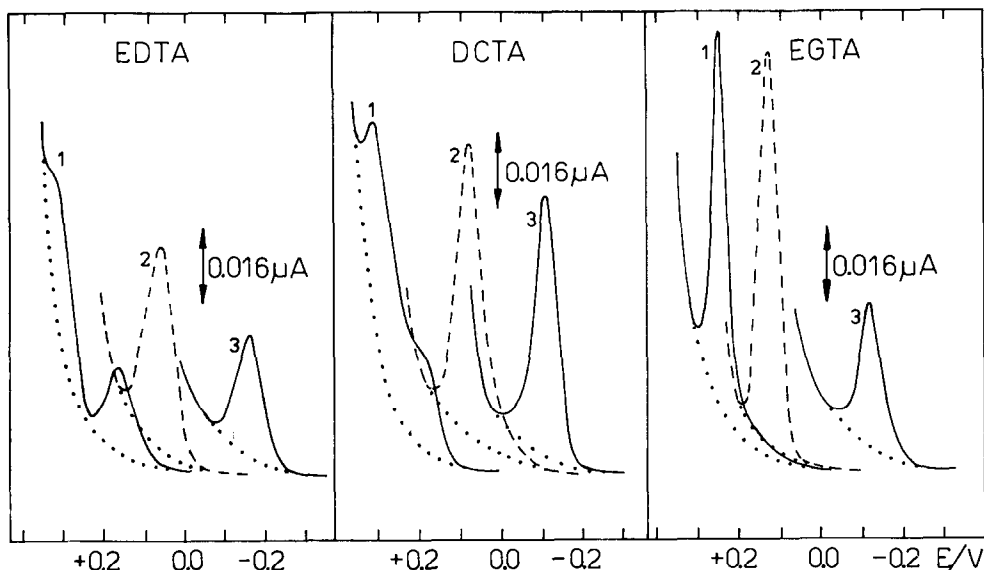


Fig. 4. Cathodic-stripping square-wave voltammetric curves obtained at various pH values. Complexones at $10^{-7}M$; $10^{-5}M$ Hg^{2+} ; $t_{dep} = 100$ sec. Other conditions as for Fig. 1. (1) pH 2; (2) pH 4.8; (3) pH 10.

Table 1. Comparison of the peak potentials and the widths at half-height obtained for EDTA, DCTA and EGTA by cathodic stripping SWV, the solution contained the complexones at $10^{-7}M$ concentration and $10^{-5}M$ Hg^{2+} , $t_{dep} = 100$ sec

	pH 2		pH 4.8		pH 10	
	$b_{1/2}$, <i>mV</i>	E_p , <i>V</i>	$b_{1/2}$, <i>mV</i>	E_p , <i>V</i>	$b_{1/2}$, <i>mV</i>	E_p , <i>V</i>
EDTA	—	+0.32	80	+0.07	80	-0.17
	80	+0.17				
DCTA	—	+0.32	68	+0.08	68	-0.12
	—	+0.21				
EGTA	50	+0.25	50	+0.12	55	-0.11

addition of excess of mercury(II) would allow determination of the total amount of ligand, provided that all metal-complexone species present would undergo a quantitative displacement reaction with mercury(II). From the literature,^{18,19} at pH 4–6 the conditional stability constants of the mercury(II) complexes of EDTA and related compounds are higher than those of most other cations, the most likely interfering species being Fe^{3+} , Bi^{3+} , Sc^{3+} and Sn^{2+} , for which an appropriate (and large) excess of mercury(II) would be necessary. It should also be stressed here that slow dissociation of the metal complexes would have a kinetic effect on the displacement reaction. It would be essential for this reaction to be complete in the bulk solution. At the electrode surface, however, the mercury(II) activity is different and controlled by the electrode potential (this still refers to the second procedure), so the displacement reaction equilibrium may change a little. Since the results can be expected to differ according to the time-scale of the experiment, all plots presented here refer to the same time-scale (t_d , t_s , t_w , t_p all held constant).

Obviously, the best conditions for accumulation and stripping of HgEDTA, HgDCTA and HgEGTA are obtained with moderately acidic or neutral solutions. However, when both peak potential (the more negative the peak potential the better) and efficiency of conversion of metal complexes into Hg(II) complexes are taken into account, the optimal pH range for the determination of complexones seems to be 4.8–5.8 (second procedure). In the case of unbound complexone, to avoid a change in the speciation, the original pH could be kept by adding to a sample the buffer of predetermined pH. However, a pH higher than 7 raises the problem of Ca(II), which will be discussed later. Addition of buffer in both procedures is necessary, since reaction (3) involves protons, and deaeration of a sample usually causes a change in pH.

Analysis of tap water

Various water samples were analysed for complexones. They included water from the city filter station (before and after purification) and tap water. No complexones were detected. Typical calibration graphs for EDTA in fivefold diluted tap water containing pH-5.8 acetate buffer are shown in Fig. 5. Line 1 corresponds to the first procedure [no Hg(II) added] and line 2 to the second. Line 2 passes through the origin, which means that the sample contains neither bound nor free EDTA. Line 1 has two segments, the second being parallel to line 2 but shifted along the concentration axis by the quantity C_2 . In effect, line 1 is a plot of a titration of heavy metal ions (present in the tap water) with the EDTA added, and C_2 is the total concentration of these metals in the solution. Line 1 would also be obtained by the procedure described earlier,¹ in which the complexones are determined by direct oxidation of mercury (and C_2 is the concentration of "available" heavy metals). A different picture is obtained, Fig. 6,

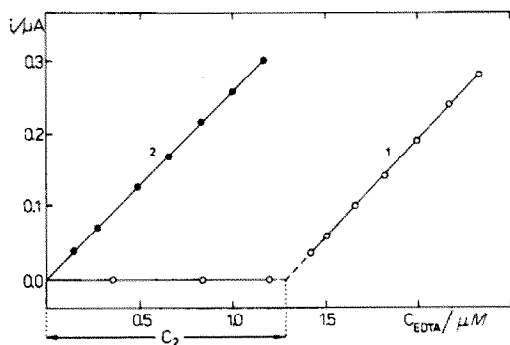


Fig. 5. Calibration curves for added EDTA in 1:4 diluted tap water containing no initial EDTA, $t_{dep} = 1$ min; (1) no Hg^{2+} added; (2) $3.3 \times 10^{-6} M$ Hg^{2+} ; pH = 5.8; temperature 25° . Other conditions as for Fig. 1.

if the dependence of current on EDTA concentration is plotted for tap water already containing EDTA, since line 2 now corresponds to a standard-additions plot, and the intercept on the x-axis gives C_1 , which directly gives the total amount of EDTA (irrespective of form) in the water. However, line 1 indicates that there is still no unbound EDTA, and again C_2 corresponds to the concentration of unbound ("available") heavy-metal ions. Since all the EDTA originally present was in bound form, $C_1 + C_2$ gives the total concentration of heavy-metal ions. Note that C_2 in Fig. 5 is equal to $C_1 + C_2$ in Fig. 6.

For several samples analysed, the available heavy-metal level was in the range 1–6 μM . At the same time the Ca(II) concentration was around $1 \times 10^{-3} M$ and had no influence on the intercept value (see also "Effect of other ions", below). In the pH range 4.8–5.8 the Ca(II)-bound EDTA is sufficiently labile, and the CaEDTA complex sufficiently weak, for the electro-production of the HgEDTA complex (procedure 1) not to be slowed down. At pH 9, the available-metal level would include Ca(II). A detailed discussion on discrimination between Ca(II) and heavy metals was given in the previous paper.¹

DCTA and EGTA give similar plots to those in Figs. 5 and 6, but with EGTA the intercept C_2 for a

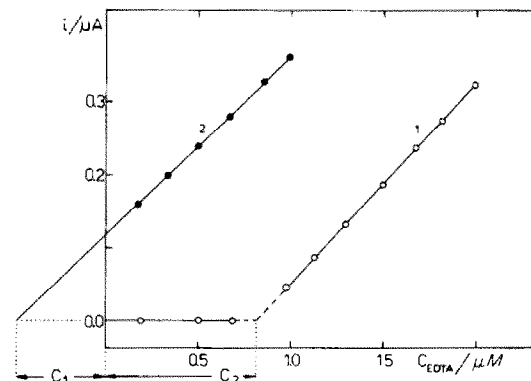


Fig. 6. Calibration curves for EDTA in 1:4 diluted tap water containing EDTA. Other conditions as for Fig. 5.

given metal ion concentration is much smaller than with EDTA, mainly because of the very low conditional stability constants of FeEGTA and ZnEGTA (Fe and Zn are the main heavy-metal impurities in tap water).

The detection limit for complexones was set by the background noise, and corresponded to $1 \times 10^{-8} M$ in the solution in the electrochemical cell, lower than other values published.^{1,4-11} The relative standard deviation calculated for $1 \times 10^{-7} M$ EDTA (five measurements) was 2.9%.

Complexones present together

The simultaneous determination of EDTA and EGTA and of DCTA and EGTA is not straightforward, but is possible, since the differences in peak potentials for both pairs are large enough. To illustrate this possibility, some curves obtained in solutions containing EGTA and EDTA or DCTA at various levels are depicted in Fig. 7. In a limited range of total concentration of complexones, addition of the second compound to a solution with fixed concentration of EGTA and EDTA (in Fig. 7(a) and (b) respectively) gives a second peak rising in proportion to the amount of complexone added. To measure

the height of the second peak, the bottom curves of Fig. 7 should be taken as the background. A mixture of two complexones could be analysed if their total concentration was lower than $10^{-6} M$ and their concentration ratio was between 1:15 and 15:1. However, it is not possible to obtain two separate peaks when EDTA and DCTA are present together, since the difference in their peak potentials is only ca. 6 mV.

Effect of other ions

The influence of several ions on the cathodic-stripping peak height has been examined, including Cl^- , Br^- , I^- , SO_4^{2-} , Ca^{2+} , Zn^{2+} and Fe^{3+} , and is shown in Figs. 8 and 9. Since the peak potentials for both DCTA and EDTA are very close, it is not surprising that the influence of a given ion on their peak is very similar. Chloride up to $1 \times 10^{-4} M$ does not interfere, but at higher concentrations the determination becomes impracticable. Bromide produces an additional peak at more positive potentials, which at bromide concentrations higher than $1 \times 10^{-5} M$ overlaps substantially with the DCTA or EDTA peak. Iodide gives a peak which completely overlaps the complexone peak and makes the method imprac-

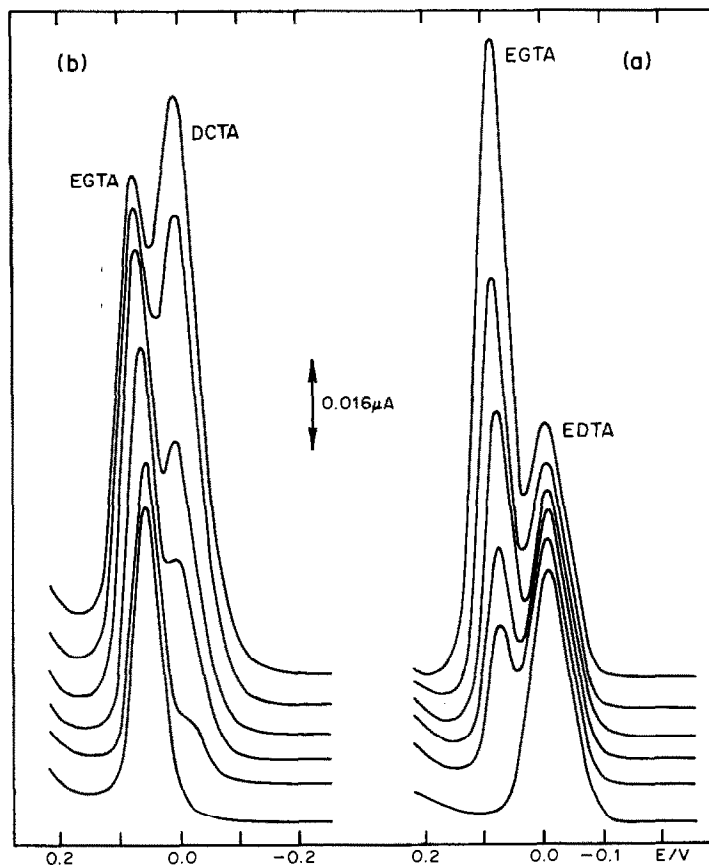


Fig. 7. Cathodic-stripping square-wave voltammetric peaks of EDTA, DCTA and EGTA in 0.05M acetate buffer at pH = 5.8, $10^{-5} M$ Hg^{2+} , $t_{dep} = 1$ min, $E_{dep} = +0.22$ V. (a) $C_{EDTA} = 2 \times 10^{-7} M$, $C_{EGTA} = 0$, 2×10^{-8} , 3×10^{-8} , 5×10^{-8} , 7×10^{-8} , $1 \times 10^{-7} M$ respectively, (b) $C_{EGTA} = 1 \times 10^{-7} M$, $C_{DCTA} = 0$, 4×10^{-8} , 1.4×10^{-7} , 2×10^{-7} , 3.4×10^{-7} , $4 \times 10^{-7} M$ respectively.

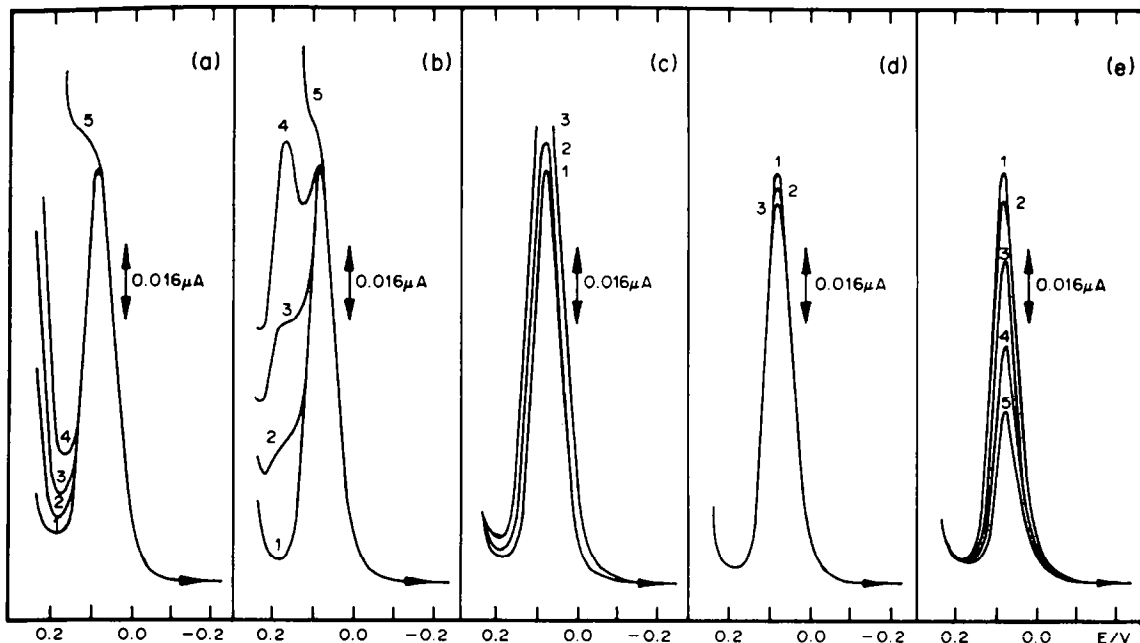


Fig. 8. Influence of various ions on CSSWV peak of DCTA; acetate buffer pH = 4.8 + $2 \times 10^{-7} M$ DCTA + $2 \times 10^{-5} M Hg^{2+}$, $E_{dep} = +0.23 V$, $t_{dep} = 100$ sec, temperature 20° . (a) $C_{Cl^-} = 0$ (1); 2×10^{-5} (2); 5×10^{-5} (3); 1×10^{-4} (4); $1.5 \times 10^{-4} M$ (5), (b) $C_{Br^-} = 0$ (1); 2×10^{-6} (2); 5×10^{-6} (3); 1×10^{-5} (4); $2 \times 10^{-5} M$ (5), (c) $C_{I^-} = 0$ (1); 7×10^{-7} (2); $1 \times 10^{-6} M$ (3), (d) $C_{Ca^{2+}} = 0$ (1); 5×10^{-5} (2); $1 \times 10^{-4} M$ (3), (e) $C_{Zn^{2+}} = 0$ (1); 1×10^{-7} (2); 5×10^{-7} (3); 1×10^{-6} (4); $2 \times 10^{-6} M$ (5).

ticable. These effects are due to competitive adsorption of the mercury halides. Cations usually decrease the height of the cathodic-stripping peaks. Calcium has only a small effect but ions forming

more stable DCTA and EDTA complexes (Cu^{2+} , Zn^{2+} , Fe^{3+}) affect the curves more strongly. This is responsible for the lower slope of the calibration plots for method (2), shown in Figs. 5 and 6, presumably

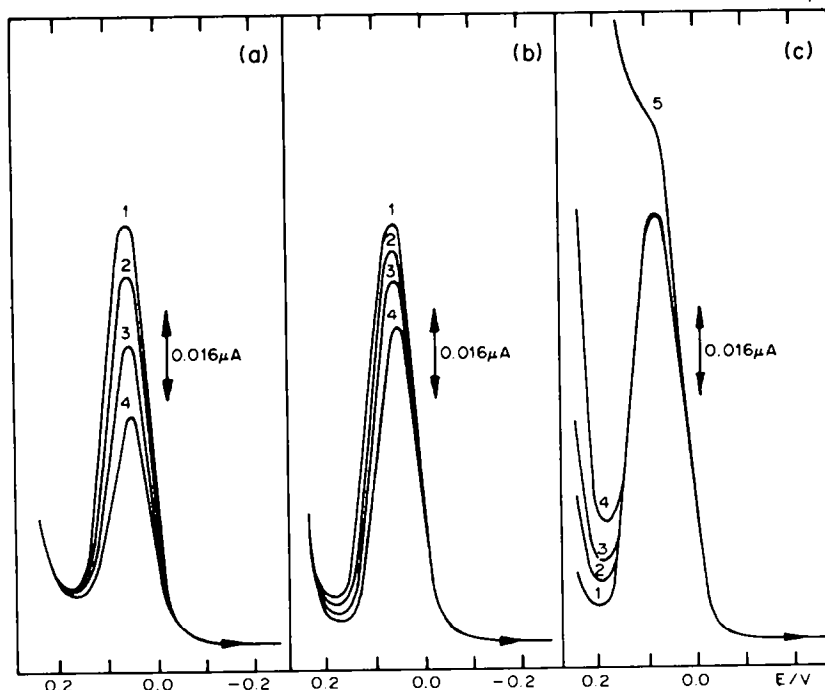


Fig. 9. Influence of various ions on CSSWV peak of EDTA; acetate buffer pH = 4.8 + $2 \times 10^{-7} M$ EDTA + $2 \times 10^{-5} M Hg^{2+}$, $E_{dep} = +0.23 V$, $t_{dep} = 100$ sec, temperature 20° . (a) $C_{Zn^{2+}} = 0$ (1); 1×10^{-7} (2); 5×10^{-7} (3); $1 \times 10^{-6} M$ (4), (b) $C_{Fe^{3+}} = 0$ (1); 1×10^{-7} (2); 5×10^{-7} (3); $1 \times 10^{-6} M$ (4), (c) $C_{Cl^-} = 0$ (1); 2×10^{-5} (2); 5×10^{-5} (3); 1×10^{-4} (4); $1.5 \times 10^{-4} M$ (5).

by a competitive complexation, which may be thermodynamic and/or kinetic in nature. This phenomenon necessitates use of a fixed time-schedule, as indicated earlier. Sulphate does not interfere at concentrations below $1 \times 10^{-3}M$.

The EGTA peak potential is more positive than that for EDTA and DCTA, so the influence of anionic impurities is stronger, but Ca^{2+} , Fe^{3+} and Zn^{2+} affect the EGTA curves less than the EDTA and DCTA plots.

Acknowledgement—This work was supported in part by the Ministry of Science of Poland under grant MR-I-32.

REFERENCES

1. Z. Stojek and J. Osteryoung, *Anal. Chem.*, 1981, **53**, 847.
2. M. R. Quastel, G. B. Segel and M. A. Lichtman, *J. Cell. Physiol.*, 1981, **107**, 165.
3. L. R. Contilene and C. D. Klaassen, *Toxicol. Appl. Pharmacol.*, 1981, **58**, 452.
4. B. K. Afgan, P. D. Goulden and J. F. Ryan, *Anal. Chem.*, 1972, **44**, 354.
5. B. J. A. Haring and W. Delft, *Anal. Chim. Acta*, 1977, **94**, 201.
6. J. P. Haberman, *Anal. Chem.*, 1971, **43**, 63.
7. R. J. Stolzberg, *Anal. Chim. Acta*, 1977, **92**, 139.
8. P. W. Alexander, P. R. Haddad and M. Trojanowicz, *ibid.*, 1985, **177**, 183.
9. T. Nomura and G. Nakagawa, *J. Electroanal. Chem.*, 1981, **111**, 319.
10. D. L. Venezky and W. E. Rudzinski, *Anal. Chem.*, 1984, **56**, 315.
11. T. Raya-Saro and D. Pérez-Bendito, *Analyst*, 1983, **108**, 857.
12. K. Niki, K. Suzuki, G. P. Sato and N. Mori, *J. Electroanal. Chem.*, 1973, **49**, 27.
13. Z. Stojek and J. Osteryoung, *ibid.*, 1981, **127**, 67.
14. Z. Stojek, M. Ciszowska and J. Osteryoung, *ibid.*, 1985, **195**, 405.
15. Z. Stojek and M. Ciszowska, *ibid.*, 1986, **200**, 279; *Polish J. Chem.*, in the press.
16. R. Kalvoda, *Anal. Chim. Acta*, 1982, **138**, 11.
17. J. O'Dea, J. Osteryoung and R. A. Osteryoung, *Anal. Chem.*, 1981, **53**, 693.
18. R. Přibil, *Analytical Applications of EDTA and Related Compounds*, Pergamon Press, Oxford, 1972.
19. A. E. Martell and R. M. Smith, *Critical Stability Constants*, Vol. 1, Plenum Press, New York, 1974.

MULTIPARAMETRIC CURVE FITTING—XII

RESOLUTION CAPABILITY OF TWO PROGRAMS FOR ANALYSING MULTICOMPONENT SPECTRA, SQUAD(84) AND PSEQUAD(83)

MILAN MELOUN

Department of Analytical Chemistry, College of Chemical Technology, CS-532 10 Pardubice,
Czechoslovakia

MILAN JAVŮREK

Computing Centre, College of Chemical Technology, CS-532 10 Pardubice, Czechoslovakia

ALENA HYNKOVÁ

State Veterinary Institute, Rantířovská 93, CS-586 00 Jihlava, Czechoslovakia

(Received 18 October 1985. Revised 3 February 1986. Accepted 24 April 1986)

Summary—The resolving power of multicomponent spectra analysis and the computation reliability of the stability constants and molar absorptivities determined for nine variously protonated anions of three sulphonephthaleins and an impurity, by analysis of data for a mixture by programs SQUAD(84) and PSEQUAD(83), has been examined by use of synthetic and experimentally measured spectra containing severely overlapping spectral bands. The model mixture of Bromocresol Green, Phenol Red, Thymol Blue and azoxine as impurity, with five yellow, three blue and one red species in the pH range from 2 to 10, was used to examine the influence of precision of spectral data and of use of the spectra of the individual components, on the precision and accuracy of the estimated parameters when the chemical model is known. An efficient computation strategy has been found and both programs were shown to lead to the same values and reliability of the parametric estimates. Of the various diagnostics considered, the goodness-of-fit achieved is used as the criterion of whether the parameters found adequately represent the data.

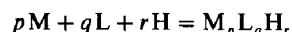
Programs for analysis of multicomponent spectra¹⁻¹⁰ can facilitate the identification and resolution of individual components of a mixture and also determine the stability constants and molar absorptivities of various species in solution equilibria. Multi-wavelength spectrophotometric data in general offer considerably more information than potentiometric data^{8,9} about chemical equilibria. As shown earlier,⁵ SQUAD(84)⁵ and PSEQUAD(83)⁷ are particularly reliable and efficient diagnostic tools. SQUAD(84) provides a systematic method of formulating and testing models of equilibrium systems. The resolving power of these two programs has now been tested by estimation of the very similar protonation constants of four acid/base indicators from spectral measurements on a mixture of all four; it should be noted that the spectral bands of the individual species severely overlap. The reliability of determination of stability constants and molar absorptivity was examined by the use of simulated and experimental data, as a function of the instrumental error of absorbance reading, with and without use of the spectra of the isolated individual components in the absorbance matrix, and with mixtures in which some species involved in the protonation equilibria were of the same colour. The efficiency of both programs has

been verified and a strategy of efficient computation is suggested.

THEORY

Multicomponent spectral analysis

The multicomponent spectral analysis program was described in Part X of this work.⁵ It can adjust $\bar{\beta}_{pqr}$ and $\bar{\epsilon}_{pqr}$ for a given set of spectra by fitting the predicted absorbance-response surface to given spectral data, with one dimension representing the dependent variable (absorbance), and the other two dimensions representing the independent variables, *viz.* the total component concentrations (or pH) of n_c solutions, at n_w wavelengths. The parameters to be determined are (i) the stoichiometric indices, (ii) the stability constants (β_{pqr}) and molar absorptivities (ϵ_{pqr}) and (iii) the free concentrations, of all the species in the chemical model found. The general equations for the complexes are



with

$$\beta_{pqr} = [M_p L_q H_r] / ([M]^p [L]^q [H]^r)$$

where the charges are omitted for simplicity. A chemical model must always be hypothesized for calculation of the stability constants and molar ab-

sorptivities. When the estimated $\bar{\beta}_{pqr}$ and $\bar{\epsilon}_{pqr}$ values for the assumed chemical model have been refined, the agreement between the experimental and predicted data can be examined. If the agreement is not considered satisfactory, new chemical models are tried until a better fit with the experimental data is obtained. The present communication deals with the situation in which the chemical model is known and the reliability of parameter-determination by spectral analysis is examined.

Errors in spectral data

To test the ability of the programs to find true parametric estimates, examination of simulated data is useful, allowing systematic evaluation of the effect of noise levels in the data. Spectral data may be subject to three kinds of error: (i) normally distributed random errors, which cannot be eliminated from the data, (ii) systematic errors, which are sometimes difficult to identify and eliminate, and (iii) gross errors.

When simulated data are used, wavelengths and concentrations are regarded as error-free, and random errors generated in accordance with the selected standard deviation, $s_{\text{inst}}(A)$, are imposed on the calculated absorbances. In experimental work, of course, random and systematic error can arise in both the wavelength settings and the reagent concentrations and cannot usually be distinguished. The sources of systematic error in pH measurement are well known and documented. Coloured impurities in indicators may have acid-base character, in which case the background colour will vary with pH. At low pH some indicators may separate from solution and/or be absorbed on the cuvette walls, and at higher concentrations oligomers and micelles may be formed and changes in ionic strength or reagent concentrations cause a systematic rather than a random error. All statistical tests in the program are based on the assumption that systematic errors are absent from the data.

Spectra modelling with simulated data

Multicomponent spectral analysis programs can also be applied when an adequate chemical model is known and only resolution of the spectra by use of different algorithms is to be investigated. To characterize the program performance, simulated data can be used.¹¹ Model spectra of a mixture of acid/base pairs are simulated as the sum of Gaussian peaks, each generated from three arbitrary constants, the wavelength (λ_{max}), the molar absorptivity (ϵ_{max}) at this wavelength, and the effective band-width (δ) at half-intensity. These constants also describe the degree of overlap of the spectra of the individual species.

This approach allows examination of (i) the effect of the overall spectrophotometric error on the precision and accuracy of parameter estimation, (ii) various regression algorithms, (iii) the sensitivity of

each parameter in the model, and also allows establishment of an optimum computational strategy for efficient data treatment.

The residuals are analysed¹² to test whether the refined parameters adequately represent the data, and should be randomly distributed about the predicted regression curve. To analyse the residuals, the following statistics are compared with those of the generated random errors to find whether both distributions are Gaussian in nature: the error mean $m_{e,1}$ with the residual mean $m_{r,1}$, the mean error $|\bar{e}|$ with the mean residual $|\bar{r}|$, the selected standard deviation $s(e)$ with that of the residuals $s(r)$, the skewness of the error set $m_{e,3}$ with that of the residual set $m_{r,3}$, the curtosis of the error set $m_{e,4}$ with that of the residual set $m_{r,4}$, and finally the Hamilton *R*-factor for relative fit, $R(e)$ with $R(r)$.

EXPERIMENTAL

Reagents

Analytical grade Bromocresol Green (BCG), Phenol Red (PR) and Thymol Blue (TB) were used without purification; chromatography on Whatman No. 2 paper with 1-butanol-acetone-26% ammonia solution (4:3:2 v/v) showed no spots of coloured impurities. Each indicator was dissolved in dilute sodium hydroxide solution and the solution was titrated with 1M perchloric acid. The concentration of each indicator was determined by potentiometric pH-titration with perchloric acid and re-titration with sodium hydroxide. The resulting pH-titration curve was analysed by the regression program ACBA¹³ and the concentrations of the indicator and acid/base impurities, and the ionization constants of the individual indicators, alone or in mixtures, were estimated (Table 1). A goodness of fit test was applied as a criterion of the reliability of refinement. The BCG was found to be 97.8% pure, with a small amount of a coloured impurity; the purities of the other two sulphonephthaleins were 84.7% for PR and 91.3% for TB, and the impurities were inorganic. The 1M sodium hydroxide was found to contain about 6% of carbonate, even though prepared from a 50% solution by dilution in the customary manner. It was standardized with 1M perchloric acid which itself was standardized with mercuric oxide and potassium bicarbonate, with agreement to within 0.1%.

Instruments

A Zeiss Spekol 21 single-beam spectrophotometer was equipped for spectrophotometric titration. The accuracy and precision of the spectrophotometric measurements were checked with standard solutions of potassium chromate and copper(II) sulphate. Reproducibility of absorbance was ± 0.0005 , photometric linearity was better than 0.5% ($0.1 \leq A \leq 1.0$), the wavelength accuracy was better than 1 nm and the spectral band-width was kept at 3 nm. A 10-mm path-length cuvette was used.

The pH was measured with a Radiometer PHM 4d pH-meter with a G202B glass electrode and K410 saturated calomel electrode; calibration was done with Radiometer standard buffers S1500, S1510 and S1316 (p_{aH} 6.865, 7.410 and 4.010 at 25°C).

The titration cell was a jacketed constant-temperature glass vessel of 150 ml volume, closed with a bung carrying the glass and reference electrodes, argon inlet, thermometer, stirrer shaft and polyethylene capillary tip of the micro-burette.

The burette was a home-made micrometer syringe burette of 2500 μl capacity. Its polyethylene capillary tip was immersed in the solution during addition of reagent, but then withdrawn from it to avoid leakage of reagent from the

Table 1. Determination of protonation constant and sulphonephthalein concentration, $c_{L,calc}$, by the regression analysis of the pH-titration curve by the ACBA program

	Bromocresol Green	Phenol Red	Thymol Blue	Mixture of 3 sulphonephthaleins
Initial volume, V_0 , ml	26.00	26.80	25.80	26.15
Ionic strength, M	0.042	0.068	0.039	0.060
BCG: $\log \beta_{11}$	4.84 ± 0.02			4.88 ± 0.01
$c_{L,w}$, M	0.00957			0.00962
$c_{L,calc}$, M	0.00936			
Purity, %	97.8			
PR: $\log \beta_{11}$		7.81 ± 0.00		7.87 ± 0.01
$c_{L,w}$, M		0.00928		0.00958
$c_{L,calc}$, M		0.00786		
Purity, %		84.7		
TB: $\log \beta_{11}$			9.09 ± 0.02	9.12 ± 0.01
$c_{L,w}$, M			0.00973	0.00975
$c_{L,calc}$, M			0.00888	
Purity, %			91.3	
$s(V)_{NaOH}$	0.0019	0.0014	0.0027	0.0042
Residual mean	1.93E-4	-2.04E-4	-1.12E-4	-3.69E-5
Mean residual	0.0015	0.0097	0.0018	0.0031
Standard deviation	0.0017	0.0013	0.0025	0.0040
Hamilton R -factor, %	0.76	0.66	0.97	0.75

tip during the pH and spectral measurements. The burette was calibrated and found precise to $\pm 0.5 \mu\text{l}$.

Spectrophotometric multiple-wavelength pH-titrations

The absorption spectra of the individual sulphonephthaleins and their mixtures, as a function of pH, were measured by means of spectrophotometric multi-wavelength pH-titration as described earlier.¹⁴

Spectra tested

A number of models comprising synthetic data for mixtures of three sulphonephthaleins and an azoxine impurity, that would provide overlapping equilibria and spectral bands, were constructed to test the program performance.

Five protonation constants, one for each of the three sulphonephthaleins and two for the azoxine, were refined. The protonation equilibria involved nine variously protonated and light-absorbing species, over the pH range from 2 to 10, five of the species being yellow, three blue and one red. Figure 1 shows the strong overlap of the various spectra. The relevant pK_a values are 3.05 (azoxine), 4.7 (BCG), 6.9 (PR) and 9.2 (TB). A simplifying factor, however, is that none of the species interact with each other, and there are no-side reactions to consider.

Five sets of spectra were used, as follows:

(A) Synthetic spectra of a BCG + PR + TB + azoxine mixture and of the individual components.

For 37 (n_s) systems containing one or all four ($n_z = 4$) of the basic components (BCG, PR, TB and azoxine) at selected pH values the total absorbances at 32 ($=n_w$) wavelengths ranging from 380 nm ($=\lambda_{start}$) to 690 nm ($=\lambda_{end}$), were calculated and then loaded with random errors. Fourteen of the spectra were for the BCG + PR + TB + azoxine mixture, 8 for the azoxine alone, and 5 for each of the other three indicators.

(B) Synthetic spectra of a BCG + PR + TB + azoxine.

Fourteen of the spectra were the same as those in set (A), and 18 for the BCG + PR + TB mixtures in various concentration ratios and over different pH ranges.

(C) Experimentally measured spectra of a BCG + PR + TB mixture and of the individual components.

The experimental spectra had a higher uncertainty than that with which the synthetic spectra were loaded, so testing was restricted to a mixture of all three sulphonephthaleins ($n_z = 3$) (18 spectra from $\lambda_{start} = 380$ nm to $\lambda_{end} = 690$ nm,

Figs. 2 and 3), and 5 protonation equilibrium spectra for each of the individual components (total $n_z = 33$), with readings at 32 ($=n_w$) wavelengths).

(D) Experimentally measured spectra of a BCG + PR + TB mixture. The 18 spectra for the mixture in set (C) were used.

(E) Experimentally measured spectra of the three individual sulphonephthaleins.

The remaining 15 spectra sets from set (C) were used.

Computation

The protonation constants and molar absorptivities of the sulphonephthaleins were refined with two least-squares programs: SQUAD(84)⁵ and PSEQUAD(83).⁷ The purity of the indicators, the acid-base impurities and the ionization constants were determined with the regression program ACBA.¹³ Computations were performed with the EC 1033 (500 K) computer in the Computing Centre, College of Chemical Technology, Pardubice, Czechoslovakia.

DISCUSSION

Analysis of synthetic data (Tables 2 and 3)

The performance of SQUAD(84)⁵ and PSEQUAD(83)⁷ was first tested with data sets (A) and (B), which allowed systematic variation of the spectral, equilibrium and noise characteristics.

The primary study was to determine the effect of precision of the absorbance data on the precision and accuracy of the estimated parameters. Higher imprecision of the absorbance data would be expected to result in a poorer fit. Estimation of the parameters would be inaccurate because of uncertainty in the pit co-ordinates, as the hyperparaboloid response-surface would have a broad and indefinite minimum. The parametric precision is related to the D -boundary, by the supercurve, $U = U_{min} + s^2(A)$. The standard deviation of each parameter b_i defined by $s(b_i) = \max [(b_D - b_{min})_i]$ can be calculated as the maximum difference between the value for b_i at any

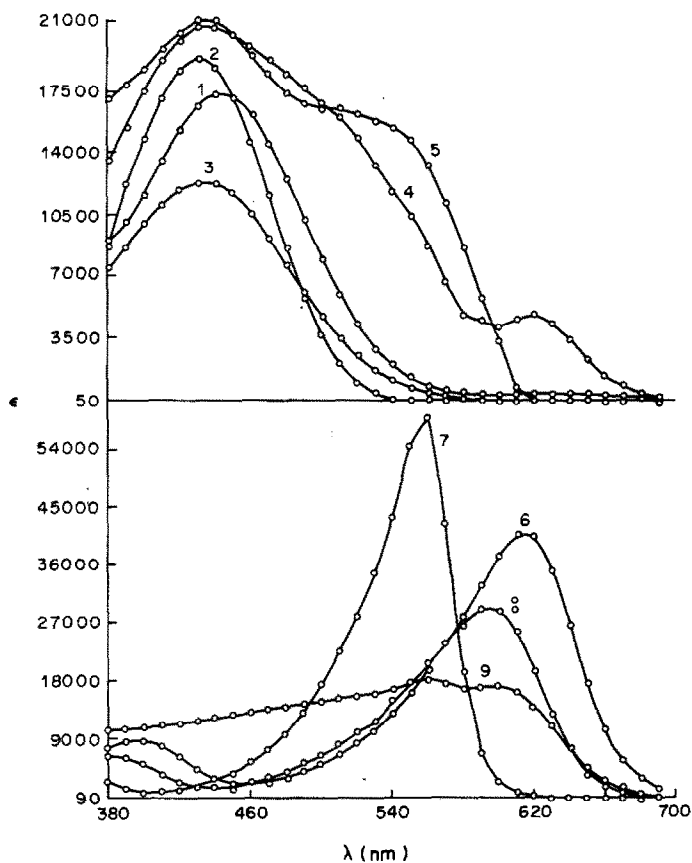


Fig. 1. Absorption spectra (molar absorptivities) of BCG, PR, TB and azoxine impurity in the forms LH_2^- , (1) BCG, (2) PR, (3) TB, (4) azoxine; LH_2^- , (5) azoxine; L^1- , (6) BCG, (7) PR, (8) TB, (9) azoxine, used for simulation of spectral data.

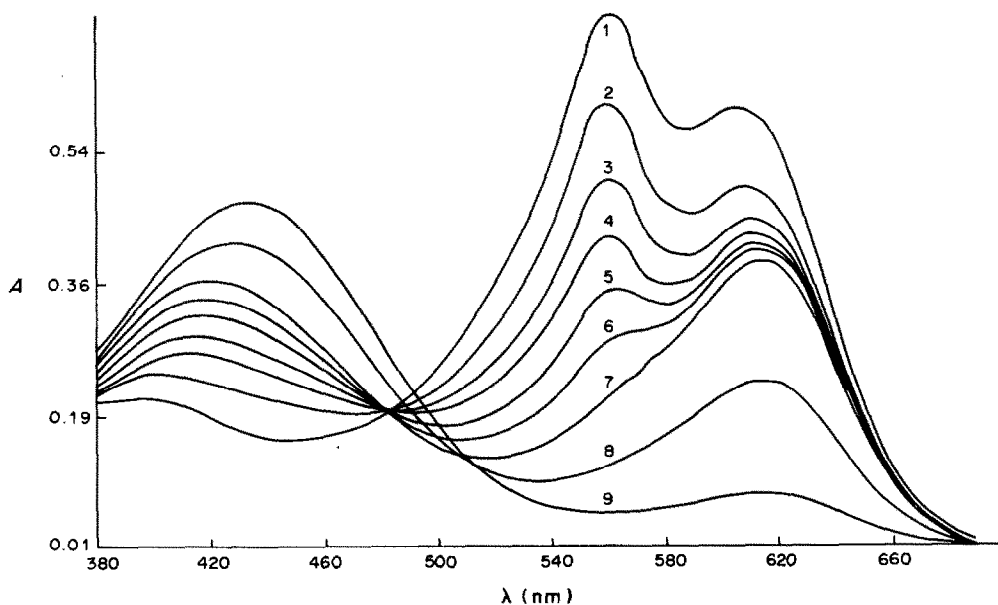


Fig. 2. Absorption spectra of a mixture of BCG + PR + TB for various pH values and a concentration ratio BCG:PR:TB = 0.983:0.578:1.331 where $c_{TB} = 9.89 \times 10^{-6} M$; $d = 1.000$ cm, $l = 0.015$, temperature = 25° . Values of pH: (1) 9.126, (2) 8.608, (3) 8.222, (4) 7.921, (5) 7.640, (6) 7.300, (7) 6.482, (8) 4.873, (9) 4.054.

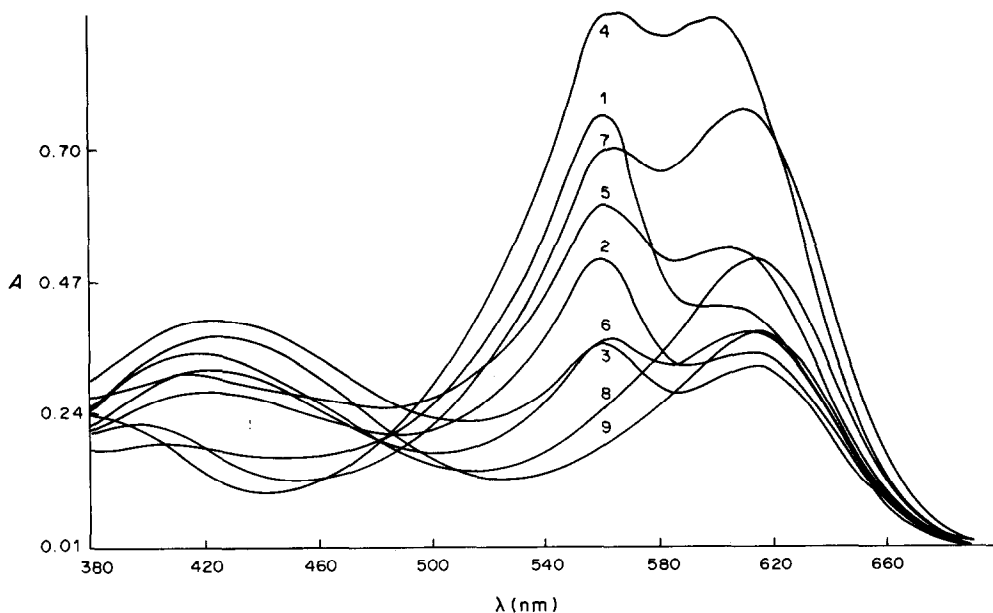


Fig. 3. Absorption spectra of a mixture of BCG + PR + TB for various pH values and a concentration ratio BCG:PR:TB = 0.739:0.827:1.000 for pH: (1) 8.949, (2) 8.023, (3) 7.622 and 0.739:0.414:1.952 with pH (4) 10.019, (5) 8.893, (6) 7.855, and 1.477:0.414:1.000 for pH: (7) 9.190, (8) 5.273, (9) 4.931. $c_{TB} = 9.89 \times 10^{-6} M$, $d = 1.000$ cm, $l = 0.015$, temperature = 25° .

point on the D -boundary, and the value for b_i at the minimum. As the last U contour of the D -boundary is then rather a large ellipse, the parametric standard deviations are larger, and the precision poorer.

SQUAD(84)⁵ starts with data-smoothing of the spectra set, followed by factor analysis FA608.² The position of a break on the $s_k(A) = f(k)$ curve is calculated, and gives $k^* = 9$, with the corresponding co-ordinate $s_9^*(A)$ value (for terminology see Part X⁵ of this series). Five protonation constants and nine molar absorptivities for 32 wavelengths constitute 293 parameters which are refined by the MR algorithm in the first run of the SQUAD program. In the second run, the NNLS algorithm makes the final refinement of all previously found parametric estimates, with all molar absorptivities kept non-negative. The reliability of the parametric estimates may be tested by use of the SQUAD(84) diagnostics.

The first diagnostic indicates whether all parametric estimates have physical meaning and realistic values. The accuracy of these estimates is shown as a systematic error calculated as the deviation from the true values of the parameters. The deviations for the pK_a values and molar absorptivities of set (A) were negligible: even the largest value of $s_{inst}(A)$, 0.015, caused <0.01 deviation in $\log \beta_{11}$ and 1.5% deviation in the molar absorptivities. For set (B), the accuracy for the pK_a estimates was the same as for set (A) for the sulphophthaleins but not for the azoxine. There was a larger effect of $s_{inst}(A)$ for set (B) than for set (A).

The second diagnostic tests whether all calculated free species concentrations have physical meaning, which proved to be the case. The low values of the

standard deviations of all the estimated parameters (the third diagnostic) proved the estimates to be sufficiently precise.

The fourth diagnostic (the correlation coefficients) proved the absence of interdependence for any pair of protonation constants.

The degree-of-fit (the fifth diagnostic) proved that the $s(A)$ value reached at convergence agreed with the absorbance precision $s_{inst}(A)$, chosen for loading the random error, and the Hamilton R -factor confirmed a good degree of fit.

PSEQUAD(83) gave the same results for the parametric estimates and though PSEQUAD does not offer all the diagnostics that SQUAD(84) does, the degree-of-fit achieved proved the sufficient reliability of the estimates and the agreement with SQUAD(84).

The synthetic data were also used for determination of the statistical quantities, $m_{r,1}$, $|F|$, $m_{r,3}$, $m_{r,4}$ and the R -factor, which may be used as reference limits in further analysis of laboratory data. For the selected $s_{inst}(A)$ value of 0.001 the R -factor of the residuals was 0.2%, and for $s_{inst}(A) = 0.003$ it was 0.5–0.6%. This means that when the R -factor for laboratory data with a drift in pH and wavelength is less than 1%, the degree of fit may be considered realistic.

The effect (on the ability to find true parametric estimates) of including the spectra of the pure components in the absorbance matrix for the indicator mixture was estimated by comparing the results of sets (A) and (B). The estimation of well-conditioned protonation constants for the three sulphophthaleins in set (B) seems to be of the same precision and accuracy as for set (A). A slight

Table 2. Determination of protonation constants and molar absorptivities of variously protonated forms of a mixture of three sulphonephthaleins and azoxine impurity by regression analysis of simulated spectra set (A) containing also spectra of basic components, parametric deviations estimated by SQUAD(84) and PSEQUAD(83), $d(\beta) = 10^3[(\log \beta_{11})_{\text{calc}} - (\log \beta_{11})_{\text{true}}]$ and $d(\epsilon) = \epsilon_{\text{calc}} - \epsilon_{\text{true}}$

Program used $s_{\text{best}}(A)$	0.001		0.003		0.008		0.015	
	SQUAD(84)	PSEQUAD(83)	SQUAD(84)	PSEQUAD(83)	SQUAD(84)	PSEQUAD(83)	SQUAD(84)	PSEQUAD(83)
BCG: $\log \beta_{11} = 4.7$	-(0.4 ± 0.6)	-(0.4 ± 0.6)	-(1.4 ± 1.8)	-(1.1 ± 1.8)	-(4.0 ± 4.8)	-(3.7 ± 4.7)	-(7.7 ± 8.9)	-(7.5 ± 8.7)
440 nm, $\epsilon_{11} = 17399$	25	26	77	78	211	210	397	394
610 nm, $\epsilon_{10} = 40858$	-72	-77	-227	-231	-620	-468	1166	-596
PR: $\log \beta_{11} = 7.9$	0.8 ± 0.6	0.7 ± 0.6	2.2 ± 1.9	2.2 ± 1.9	6.0 ± 5.2	6.0 ± 5.1	11.6 ± 9.7	11.7 ± 9.5
430 nm, $\epsilon_{11} = 19401$	-23	-23	-68	-70	-184	-187	-343	-347
560 nm, $\epsilon_{10} = 58702$	9	3	-1	6	13	12	45	32
TB: $\log \beta_{11} = 9.2$	-(0.4 ± 0.6)	-(0.4 ± 0.6)	-(1.3 ± 1.8)	-(1.3 ± 1.8)	-(3 ± 5)	-(3 ± 5)	-(5 ± 9)	-(5 ± 9)
430 nm, $\epsilon_{11} = 12294$	4	5	13	13	35	36	65	66
600 nm, $\epsilon_{10} = 29199$	-6	-6	-28	2	-79	20	-141	-146
Azox.: $\log \beta_{12} = 9.95$	-(0.8 ± 3.2)	0.1 ± 3.4	-(2 ± 90)	-(0.4 ± 90)	-(1 ± 26)	-(2 ± 24)	2 ± 46	8 ± 45
430 nm, $\epsilon_{12} = 21485$	19	18	55	54	-302	-301	273	272
$\log \beta_{11} = 6.9$	0.7 ± 1.0	0.6 ± 1.0	2 ± 3	2 ± 3	5 ± 8	5 ± 8	8 ± 14	10 ± 14
430 nm, $\epsilon_{11} = 21141$	5	6	16	16	491	482	82	78
600 nm, $\epsilon_{10} = 17371$	-15	-19	-58	-59	-157	-159	-305	-292
Factor analysis: $k, s_k(A)$	9, 0.0008		9, 0.0024		9, 0.0060		9, 0.0109	
Fitness test: $s(A)$	0.000915	0.000969	0.00276	0.00274	0.00735	0.00721	0.0137	0.0134
$m_{r,1}$ and $m_{\epsilon,1}$	2.01E-6	2.59E-6	3.23E-7	8.28E-6	-2.69E-5	-8.30E-5	-7.89E-5	-2.52E-4
$ f $ and $ \epsilon $	0.00064	0.00074	0.00191	0.00221	0.00508	0.00383	0.00946	0.01084
$s(r)$ and $s(\epsilon)$	0.00092	0.00106	0.00276	0.00316	0.00735	0.00837	0.01370	0.01562
$m_{r,3}$ and $m_{\epsilon,3}$	0.017	-0.020	-0.022	-0.030	-0.049	-0.045	-0.057	-0.062
$m_{r,4}$ and $m_{\epsilon,4}$	2.150	2.214	2.232	2.240	2.288	2.273	2.308	2.294
$R(r)$ and $R(\epsilon)$, %	0.167	0.193	0.502	0.575	1.337	1.524	2.493	2.842

Table 3. Determination of protonation constants and molar absorptivities of variously protonated forms of a mixture of three sulphonephthaleins and azoxine impurity by regression analysis of simulated spectra set (B) without spectra of basic components; parametric deviations estimated by SQUAD(84) and PSEQUAD(83), $d(\beta) = 10^{10}[(\log \beta_{11})_{\text{calc}} - (\log \beta_{11})_{\text{true}}]$ and $d(\epsilon) = \epsilon_{\text{calc}} - \epsilon_{\text{true}}$

Program used $s_{\text{red}}(A)$	0.001		0.003		0.008		0.015	
	SQUAD(84)	PSEQUAD(83)	SQUAD(84)	PSEQUAD(83)	SQUAD(84)	PSEQUAD(83)	SQUAD(84)	PSEQUAD(83)
BCG: $\log \beta_{11} = 4.7$	$-(0.2 \pm 1.4)$	$-(0.2 \pm 1.5)$	$-(0.5 \pm 4.3)$	$-(0.7 \pm 4.3)$	$-(0.5 \pm 11.4)$	$-(1.3 \pm 11.2)$	4.3 ± 20.5	2 ± 20
440 nm, $\epsilon_{11} = 17399$	-96	-85	-281	-274	-728	-715	-1373	-1500
610 nm, $\epsilon_{10} = 40858$	24	22	111	67	384	176	965	383
PR: $\log \beta_{11} = 7.9$	$-(0.6 \pm 1.6)$	$-(0.6 \pm 1.6)$	$-(2 \pm 5)$	$-(2 \pm 5)$	$-(6 \pm 13)$	$-(7 \pm 13)$	$-(15 \pm 24)$	$-(8 \pm 24)$
430 nm, $\epsilon_{11} = 19401$	173	165	508	508	1366	1359	2713	2740
560 nm, $\epsilon_{10} = 58702$	-39	-26	-103	-103	-318	-351	-986	-41
TB: $\log \beta_{11} = 9.2$	$-(0.2 \pm 1.8)$	(0.1 ± 1.8)	$-(1 \pm 5)$	$-(0.4 \pm 5)$	$-(3 \pm 15)$	$-(4 \pm 14)$	$-(6 \pm 27)$	4 ± 27
430 nm, $\epsilon_{11} = 12294$	17	19	50	53	133	135	251	220
600 nm, $\epsilon_{10} = 29199$	58	56	172	150	473	391	920	853
Azox.: $\log \beta_{12} = 9.95$	1.4 ± 35	12 ± 36	33 ± 98	14 ± 110	81 ± 209	56 ± 250	240 ± 263	162 ± 280
430 nm, $\epsilon_{10} = 21485$	-220	-223	-1671	-659	-1784	-1750	-3500	-3328
$\log \beta_{11} = 6.9$	6.4 ± 9.7	6.8 ± 9.8	19 ± 29	21 ± 29	73 ± 75	82 ± 76	281 ± 113	269 ± 130
430 nm, $\epsilon_{11} = 21141$	-449	-453	-1450	-1354	-3606	-3635	-7275	-7178
600 nm, $\epsilon_{10} = 17371$	-161	-148	-497	-420	-1228	-1023	-1309	-660
Factor analysis: $k, s_k(A)$	9, 0.00074		9, 0.00213		9, 0.00652		9, 0.01199	
Fitness test: $s(A)$	0.00093	0.00094	0.00278	0.00276	0.00745	0.00733	0.0139	0.0137
$m_{r,1}$ and $m_{e,1}$	1.56E-7	-8.83E-6	4.31E-7	-2.65E-5	1.25E-6	-8.21E-5	2.01E-6	-1.91E-4
$ f $ and $ e $	0.00063	0.00075	0.00188	0.00225	0.00502	0.00600	0.00936	0.01213
$s(r)$ and $s(e)$	0.00093	0.00109	0.00278	0.00328	0.00745	0.00876	0.01393	0.01639
$m_{r,3}$ and $m_{e,3}$	-0.047	-0.065	-0.045	-0.066	-0.082	-0.069	-0.079	-0.075
$m_{r,4}$ and $m_{e,4}$	2.129	2.026	2.059	2.039	2.132	2.033	2.133	2.043
$R(r)$ and $R(e)$, %	0.201	0.236	0.600	0.709	1.606	1.888	3.000	3.531

Table 4. Determination of protonation constants and molar absorptivities of variously protonated forms of a mixture of three sulphonephthaleins by regression analysis of experimental spectra sets (C), (D) and (E) by SQUAD(84) (in upper line) and PSEQUAD(83) (in lower line)

	Individual sulphonephthalein				Mixture of sulphonephthaleins			
	BCG	PR	TB	Set (C)	Set (D)	Set (E)	Set (D)	Set (E)
Basic components, n_2	2	2	2	3	3	3	3	3
Colour species, n_c	2	2	2	6	6	6	6	6
Solutions, n_s	5	5	5	33	18	15	18	15
Wavelengths, n_w	32	32	32	32	32	32	32	32
Fitted points, n	165	165	165	1089	594	495	594	495
Refined parameters, m	65	65	65	195	195	195	195	195
Degrees of freedom, $n-m$	100	100	100	894	399	300	399	300
Values of refined parameters								
BCG: $\log \beta_{11}$	4.655 ± 0.004			4.670 ± 0.010	4.730 ± 0.016	4.655 ± 0.007	4.713 ± 0.022	4.655 ± 0.008
440 nm, ϵ_{11}	18248 ± 125			18147 ± 544	16518 ± 1998	18245 ± 279	16518 ± 1998	18245 ± 279
610 nm, ϵ_{10}	18245 ± 176			18144 ± 508	16343 ± 1540	18244 ± 345	16343 ± 1540	18244 ± 345
PR: $\log \beta_{11}$	41673 ± 334	7.862 ± 0.003		41826 ± 569	40716 ± 1185	41675 ± 650	40716 ± 1185	41675 ± 650
	41678 ± 179			41842 ± 416	41206 ± 868	41678 ± 350	41206 ± 868	41678 ± 350
430 nm, ϵ_{11}		7.862 ± 0.003		7.878 ± 0.012	7.863 ± 0.021	7.862 ± 0.008	7.840 ± 0.022	7.862 ± 0.009
560 nm, ϵ_{10}		27002 ± 111		26516 ± 782	21880 ± 2741	27001 ± 432	21880 ± 2741	27001 ± 432
TB: $\log \beta_{11}$		27006 ± 181		26517 ± 732	23004 ± 2000	27005 ± 546	23004 ± 2000	27005 ± 546
430 nm, ϵ_{11}		73705 ± 562		73949 ± 1286	67482 ± 1848	73702 ± 977	67482 ± 1848	73702 ± 977
590 nm, ϵ_{10}		73725 ± 226		73980 ± 879	66796 ± 1720	73722 ± 682	66796 ± 1720	73722 ± 682
			9.180 ± 0.013	9.186 ± 0.011	9.264 ± 0.019	9.180 ± 0.007	9.264 ± 0.019	9.180 ± 0.007
			9.181 ± 0.013	9.187 ± 0.010	9.351 ± 0.025	9.180 ± 0.008	9.351 ± 0.025	9.180 ± 0.008
			13284 ± 312	13677 ± 322	17500 ± 984	13284 ± 188	17500 ± 984	13284 ± 188
			13283 ± 384	13676 ± 301	17300 ± 714	13285 ± 237	17300 ± 714	13285 ± 237
			31219 ± 947	32137 ± 556	38577 ± 1076	31217 ± 564	38577 ± 1076	31217 ± 564
			31227 ± 442	32131 ± 393	39351 ± 895	31217 ± 274	39351 ± 895	31217 ± 274
Factor analysis								
$k, s_k(A)$	2, 0.0018	2, 0.0008	2, 0.0009	6, 0.0010	6, 0.0011	6, 0.0004	6, 0.0011	6, 0.0004
$s(A)$	0.0054	0.0035	0.0173	0.0166	0.0122	0.0106	0.0122	0.0106
Residual mean	0.0053	0.0035	0.0169	0.0164	0.0113	0.0104	0.0113	0.0104
Mean residual	4.17E-7	1.45E-7	2.31E-6	4.14E-5	1.01E-4	5.31E-6	1.01E-4	5.31E-6
Standard deviation	0.0031	0.0017	0.0089	0.0091	0.0079	0.0046	0.0079	0.0046
Skewness (=0)	0.0054	0.0035	0.0173	0.0166	0.0122	0.0106	0.0122	0.0106
Kurtosis (=3)	0.261	-0.264	0.724	-1.617	-0.513	1.048	-0.513	1.048
R-factor (%)	2.576	4.355	3.545	9.141	2.146	8.317	2.146	8.317
	1.24	1.07	4.05	4.80	3.03	2.74	3.03	2.74

difference may be found for the ill-conditioned protonation constants of the azoxine and a significant error appears in the estimated molar absorptivities for set (B). It may be concluded that inclusion of the spectra of the pure basic components increases the accuracy and precision of the estimated parameters.

The programs employ different minimization algorithms, SQUAD(84) using conventional multiple regression for solving a set of overdetermined linear equations, which may be interchanged (during the program execution) with the Gauss–Newton non-negative least-squares algorithm which ensures that computed molar absorptivities are always positive. PSEQUAD(83) is based on the Gauss–Newton method. Both programs gave the same reliability and results, but SQUAD(84) offers more diagnostic tools for assessing the results and for chemical model building.

Analysis of laboratory data (Table 4)

Though both programs were proved satisfactory for analysis of data loaded with a random absorbance error, the experimental data may also suffer from drift in pH and observational wavelength.

The spectra of the isolated, individual sulphonephthaleins were measured first, and analysed, and the protonation constants and molar absorptivities ϵ_{11} and ϵ_{10} were used as reference values for comparison with those found by analysis of the mixture. The precision varied from one sulphonephthalein to another, being highest for Phenol Red and lowest for Thymol Blue. Solutions of Thymol Blue are alkaline and contain carbonate, so some drift of pH may be expected, unless precautions are taken to eliminate the carbonate.

Both programs were tested with data-sets (C), (D) and (E). Sets (C) and (E) gave the same parametric

estimates, which were also in good agreement with those for the individual sulphonephthaleins. There were slight differences for set (D), however, which did not contain the spectra of the individual components.

Processing the laboratory data with SQUAD(84) indicated, through FA608, that $k^* = 6$ and gave the corresponding $s_0^*(A)$ values. This arose because of the very severe overlap of the individual spectra, the factor analysis then not being able to distinguish three of the coloured species from the other six.

The degree-of-fit test showed that the experimental data were less precise than the synthetic data. Nevertheless, both programs were able to find sufficiently true and accurate parameter estimates, with equal reliability.

REFERENCES

1. L. G. Sillén and B. Warnqvist, *Arkiv Kemi*, 1968, **31**, 337.
2. J. J. Kankare, *Anal. Chem.*, 1970, **42**, 1322.
3. D. J. Leggett and W. A. E. McBryde, *ibid.*, 1975, **7**, 1065.
4. D. J. Leggett, *ibid.*, 1977, **49**, 276.
5. M. Meloun, M. Javůrek and J. Havel, *Talanta*, 1986, **33**, 513.
6. D. J. Leggett, S. L. Kelley, L. R. Shine, Y. T. Wu, D. Chang and K. M. Kadish, *ibid.*, 1983, **30**, 579.
7. I. Nagypál and L. Zékány, in *Computational Methods for the Determination of Formation Constants*, D. J. Leggett (ed.), Plenum Press, New York, 1985.
8. H. Gampp, M. Maeder, Ch. J. Meyer and A. D. Zuberbühler, *Talanta*, 1985, **32**, 95.
9. *Idem*, *ibid.*, 1985, **32**, 257.
10. S. D. Frans and J. M. Harris, *Anal. Chem.*, 1984, **56**, 466.
11. M. Meloun and M. Javůrek, *Talanta*, 1985, **32**, 973.
12. M. Meloun and J. Čermák, *ibid.*, 1984, **31**, 947.
13. G. Arena, E. Rizzarelli, S. Sammartano and O. Rigano, *ibid.*, 1979, **26**, 1.
14. M. Meloun and M. Javůrek, *ibid.*, 1984, **31**, 1083.

SHORT COMMUNICATIONS

PRECONCENTRATION AND DETERMINATION OF ULTRATRACES OF LEAD AND BISMUTH

CORRADO SARZANINI, EDOARDO MENTASTI, MARIA CARLA GENNARO and VALERIO PORTA
Dipartimento di Chimica Analitica, Università di Torino, Via P. Giuria 5, 10125 Torino, Italy

PAOLO VOLPE

Istituto di Chimica Generale ed Inorganica, C.so M. d'Azeglio 48, 10125 Torino, Italy

(Received 7 November 1985. Revised 11 June 1986. Accepted 20 June 1986)

Summary—The recovery and preconcentration of Pb(II) and Bi(III) by coupling ion-exchange and precomplexation with 1,2-dihydroxy-3,5-benzenedisulphonic acid and 3,3',4'-trihydroxyfuchstone-2''-sulphonic acid has been investigated. Metal recoveries at 0.1-mg/l. concentrations are better than 99% in the presence of cationic, anionic and non-ionic detergents, or an organic sequestering agent such as NTA, and at high ionic strength. Experiments with radiotracers show total recovery even at 15-ng/l. concentrations. In the light of the results the procedure is proposed as a simple and rapid analytical method to preconcentrate Pb(II) and Bi(III).

Ion-exchange is one of the most useful tools in trace element preconcentration and metal-species distribution studies.¹⁻³ The advantages of ion-exchange for removing interfering components from test solutions⁴⁻⁸ and for preconcentration of metal ions are well known.⁹⁻¹⁴ The use of an anion-exchange resin coupled with precomplexation of metal ions has been investigated¹⁵⁻¹⁸ and this paper presents its application in a rapid procedure for separation and preconcentration of Pb(II) and Bi(III).

The reaction of 1,2-dihydroxy-3,5-benzenedisulphonic acid (Tiron, TI) or 3,3',4'-trihydroxyfuchstone-2''-sulphonic acid (Pyrocatechol Violet, PV) with Pb(II) and/or Bi(III) gives anionic complexes which are retained on an anion-exchange resin owing to the unco-ordinated sulphonate groups and the affinity of the organic moiety for the matrix of the exchanger. Tiron and Pyrocatechol Violet were chosen as complexing agents to compare their efficiency as a function of the difference in number of sulphonate groups and in the aromatic structure.

EXPERIMENTAL

Reagents

Standard metal-ion solutions (Merck "Titrisol") were diluted to a concentration of 1000 mg/l. The isotope stock solutions were obtained from Radiochemical Centre, Amersham, England and diluted to give a specific activity of 1×10^{-5} mCi/ml for ²¹⁰Pb and ²¹⁰Bi, corresponding to 3×10^{-4} mg/l. Pb(II) concentration and carrier-free radiation for Bi(III). Pyrocatechol Violet and the disodium salt of Tiron were reagent grade chemicals.

The macroporous anion-exchange resin Bio-Rad AG-MP 1, 100-200 mesh, chloride form, was used after preliminary purification with 6.0M nitric acid.

All solutions were prepared with demineralized water further purified by a Milli-Q water purification system (Millipore).

All other reagents were reagent grade chemicals. Glassware, polyethylene and polypropylene laboratory vessels were cleaned and washed according to suggested procedures.¹⁹

Apparatus

Metal concentrations were evaluated by d.c. argon-plasma emission spectroscopy (DCP) (Spectraspan). Radioactivity measurements were made with a Packard TRI-CARB Model 2002 (2-channel) liquid scintillator counter. Insta-Gel (Packard) scintillator was added to each sample.

Borosilicate glass tubes (8 mm bore, 30 cm long) were used for making resin columns (by slurry-loading).

A rotary vacuum pump and by-pass flowmeter was used to ensure a constant flow within the range 5-10 ml/min.

Procedures

To a sample volume of 100-1000 ml, 2.0-7.0 ml of 0.05M TI or PV were added, the pH was adjusted to the desired value, and the solution was passed through a column of 0.5-1.0 g of resin dispersed in demineralized distilled water (DDW). After fixation the metal was released by acidic elution with a known volume of eluent. The concentrations of the metal ions in the initial effluent and in the acid eluate were measured in order to evaluate the recovery efficiency. Blanks were periodically run by the same procedure with unspiked solution, and no contamination was found. Each experiment was conducted in triplicate.

Measurements of radioactivity. A 10.0-ml portion of the metal-ion solution recovered from the column was mixed in a 25-ml vial with Insta-Gel scintillator to give a total volume of 20.0 ml and the radioactivity was then measured. This sample/scintillator ratio had previously been established as optimal. To estimate the initial activity, 5.0 ml of ²¹⁰Pb stock solution were mixed with 5.0 ml of scintillator solution. The β -activity of ²¹⁰Pb (0.017 MeV) was obtained with a multi-channel analyser. Since the energy spectrum, Fig. 1, shows a discrete overlap of the ²¹⁰Bi energy with the ²¹⁰Pb window, an additional series of ten experiments was performed with radiotracers to evaluate the ²¹⁰Pb contribution.

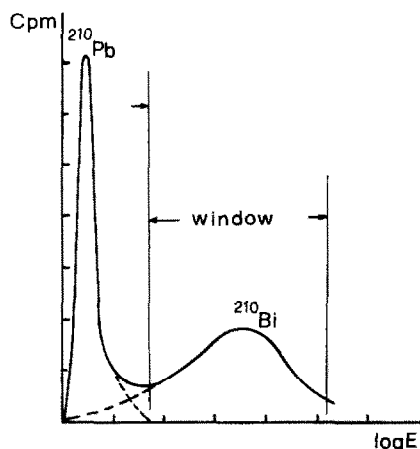


Fig. 1. Spectrum of ^{210}Pb and ^{210}Bi energies; arbitrary units.

RESULTS

Metal recovery as a function of pH

The flow-through uptake was evaluated as a function of pH. Samples (100.0 ml) containing 10.0 μg of Pb(II) or Bi(III) and spiked with radiotracers were added to 2.0 ml of 0.05M chelating agent. Tiron and Pyrocatechol Violet were used alternately and the solutions were brought to the desired pH and passed through the anion-exchange resin preconditioned at the same pH. Various eluents were then tested and 1 and 2M nitric acid were found the most suitable for the recovery of Pb(II) and Bi(III) respectively from the resin. The results showed that all of the lead and bismuth was retained by the resin and 1M nitric acid selectively eluted only the lead, all of which was released by the first 10.0 ml of acid added.

Thus a ^{210}Pb solution, which originally gave a count of 2000 cpm (counting for 50 min), after elution gave a count of only 1689 ± 8 cpm (10 replicate measurements). Since the eluate contained only ^{210}Pb , the composition of the ^{210}Pb solution (which was two years old) was examined and it was found that a considerable amount of ^{210}Bi was present and had given an interference signal (Fig. 1) in the channels used for counting the lead activity of the test solution before the chromatography. A correction factor of 0.844 was therefore applied to the initial activity of the feed solution, and this resulted in satisfactory agreement between the DCP and radioactivity measurements (Tables 1 and 2). Thereafter all experiments were done with use of radiotracers, and blanks were run before and after every experiment.

Preconcentrations

Synthetic samples (1000–2000 ml) containing 10 μg of the metals investigated and spiked with radiotracers, or radiotracers alone (at 15-ng/l. concentration) were prepared. Preconcentrations by the described procedure were performed at pH 9.0, with excellent recovery and enrichment factors of 100–200.

Recoveries of $97.6 \pm 0.4\%$ and $99.8 \pm 0.6\%$ for Pb(II) or $100.0 \pm 0.2\%$ and $100.0 \pm 0.1\%$ for Bi(III) were obtained with Pyrocatechol Violet or Tiron respectively; the mean values and relative standard deviations were estimated from six independent determinations.

Interfering agents

The effectiveness of the method was tested at ionic strengths of the latter 0.1 or 0.5M sodium chloride (similar to that of sea-water) in the presence of a ligand able to compete with TI and PV (nitrilotriacetic acid, NTA, 275–2750 mg/l.) and in the presence of surfactants [cetyltrimethylammonium bromide (CTAB), poly(ethylene glycol) (POLY, M.W. 6000) and sodium dodecyl hydrogen sulphate (SDS)] at 5, 20 and 50 mg/l. concentration. Table 3 shows the results obtained. Varying the flow-rate in the range 5–10 ml/min did not affect the results.

DISCUSSION AND CONCLUSIONS

The results in Tables 1 and 2 show that Bi(III) forms more stable complexes than Pb(II). This is confirmed by the fact that Bi(III) is totally recovered at lower pH than Pb(II). In any case the absence of

Table 1. Recoveries of lead at different pH values; comparison of DCP and radioanalytical measurements [100 ml of solution, Pb(II) 0.1 mg/l.]

pH	Pb(II) recovery, %			
	PV*	PV†	TI*	TI†
1	—	—	—	—
2	—	—	—	—
3	4.8 ± 0.1	4.6 ± 0.5	2.2 ± 0.6	1.9 ± 0.8
4	14.8 ± 0.9	14.3 ± 0.4	9.8 ± 0.7	10.0 ± 2.2
5	38.4 ± 2.3	39.6 ± 1.5	61.2 ± 1.9	59.1 ± 2.0
6	55.3 ± 2.0	56.2 ± 0.3	99.5 ± 0.5	100.4 ± 0.7
7	66.8 ± 1.7	67.7 ± 1.5	100.3 ± 0.5	101.1 ± 0.5
8	89.6 ± 0.5	88.9 ± 0.8	99.8 ± 0.3	99.7 ± 0.5
9	99.8 ± 0.1	99.6 ± 0.7	100.0 ± 0.6	100.1 ± 0.3

Mean and relative standard deviation for three determinations.

*Radioanalytical and †DCP determinations.

Table 2. Recoveries of bismuth ion at different pH values; [100 ml solution, Bi(III): 0.1 mg/l.]

pH	Bi(III) recovery, %*	
	PV	TI
1	89.9 ± 1.6	47.2 ± 1.1
2	91.5 ± 0.9	91.6 ± 1.1
3	98.3 ± 0.5	95.6 ± 0.7
4	100.1 ± 0.8	98.8 ± 0.1
5	99.8 ± 0.4	101.0 ± 0.2
6	100.2 ± 0.3	99.7 ± 0.6
7	100.0 ± 0.4	99.8 ± 0.4
8	99.3 ± 0.1	99.9 ± 0.3
9	100.0 ± 0.2	100.1 ± 0.1

*Mean and relative standard deviation for three determinations.

Table 3. Effect of interfering agents on Pb(II) and Bi(III) recovery [100 ml of solution, pH 9.0, Pb(II) and Bi(III) each 0.1 mg/l.]

Interferent	Concn., mg/l.	Pb(II) recovery, %		Bi(III) recovery %	
		PV	TI	PV	TI
CTAB	5.0	95.7 ± 1.8	99.4 ± 0.1	98.1 ± 0.6	99.5 ± 0.1
	20.0	*	99.3 ± 0.3	*	99.7 ± 0.1
	50.0	*	*	*	*
POLY	5.0	97.3 ± 0.1	100.0 ± 0.1	99.3 ± 0.2	99.9 ± 0.1
	20.0	97.9 ± 0.3	99.6 ± 0.3	99.9 ± 0.1	100.1 ± 0.1
	50.0	98.8 ± 0.3	100.3 ± 0.3	100.2 ± 0.3	100.0 ± 0.3
SDS	5.0	96.4 ± 1.1	99.6 ± 0.4	99.8 ± 0.1	99.6 ± 0.1
	20.0	98.2 ± 0.8	99.7 ± 0.1	99.9 ± 0.1	99.8 ± 0.1
	50.0	99.0 ± 0.4	99.8 ± 0.1	99.8 ± 0.2	99.8 ± 0.1
NTA	275.0	88.7 ± 1.6	98.9 ± 0.4	100.1 ± 0.1	100.0 ± 0.2
	275.0	68.0 ± 1.1	99.9 ± 0.4	99.8 ± 0.2	99.9 ± 0.2
NaCl	0.1 M	97.9 ± 0.1	99.4 ± 0.1	99.5 ± 0.1	100.0 ± 0.2
	0.5 M	98.0 ± 1.0	99.9 ± 0.4	98.7 ± 0.3	98.8 ± 0.1

Mean and relative standard deviations for three determinations.

*In these conditions, separation of insoluble products occurs. Code: CTAB, cetyltrimethylammonium bromide; POLY, poly(ethylene glycol); SDS, sodium dodecyl hydrogen sulphate; NTA, nitrilotriacetic acid.

the ligand in the eluates showed that the decreased recovery of lead at lower pH cannot be attributed to a competition between the sulphonato groups of the ligand and the anion present in solution at these pH values.

The method is an excellent means for separation of Pb(II) from Bi(III) and for its preconcentration [100% recovery of 15-ng/l. Pb(II), preconcentration factor 100–200]. Other methods based on X-ray fluorescence²⁰ or adsorbent²¹ resins show less efficient recovery yields.

The method also appears reliable in the presence of surfactants, whereas similar methods²² do not give quantitative recoveries. It is of interest that SDS may compete in the ion-exchange through its sulphonic group, but the coloured metal complexes show that diffusion is not involved in their retention by the resin.

The applicability of the method to natural systems such as river or sea-water was investigated with synthetic samples. The presence of ligands able to compete with TI or PV in the formation of Pb(II) or Bi(III) complexes was simulated by use of NTA solutions at abnormally high concentrations (275 and 2750 mg/l.) corresponding to a 1:1 and 10:1 molar ratio of NTA to TI or PV.

The yield obtained (100% under optimum conditions) is very satisfactory in comparison with that by a similar method²² which results in only 46% metal recovery at 100-mg/l. NTA concentration. The proposed method is also unaffected by ionic strength, which makes it suitable for preconcentrating trace metal ions in sea-water.

The interaction of the negatively charged sulphonate groups of the complexes with the anion-exchange resin excludes any uptake other than that of metals co-ordinated with TI or PV, resulting in good selectivity and improvement of the accuracy

and precision of metal ion detection after preconcentration.

REFERENCES

1. J. Minczewski, J. Chwastowska and R. Dybczyński, *Separation and Preconcentration Methods in Inorganic Trace Analysis*, Ellis Horwood, Chichester, 1982.
2. T. M. Florence and G. E. Batley, *Talanta*, 1976, **23**, 179.
3. P. Figura and B. McDuffie, *Anal. Chem.*, 1980, **52**, 1433.
4. F. W. E. Strelow, *ibid.*, 1984, **56**, 1053.
5. M. Koide, D. S. Lee and M. O. Strallard, *ibid.*, 1984, **56**, 1956.
6. F. W. E. Strelow, C. R. Van Zyl and C. J. C. Bothma, *Anal. Chim. Acta*, 1969, **45**, 81.
7. J. P. Riley and D. Taylor, *ibid.*, 1968, **40**, 479.
8. J. S. Fritz and G. R. Umbreit, *ibid.*, 1959, **19**, 509.
9. M. I. Abdhullam, O. A. El-Rayis and J. P. Riley, *ibid.*, 1976, **84**, 363.
10. J. F. Pankow and G. E. Janauer, *ibid.*, 1974, **69**, 97.
11. T. Kiriya and R. Kuroda, *Talanta*, 1984, **31**, 472.
12. M. Otha and K. Ohzeki, *Bull. Chem. Soc. Japan*, 1984, **57**, 3571.
13. K. Ohzeki, Y. Satoh, Y. K. Awamura and T. Kambara, *ibid.*, 1983, **56**, 2618.
14. M. Nakayama, K. Itoh, M. Chikuma and H. Tanaka, *Talanta*, 1984, **31**, 269.
15. C. Sarzanini, E. Mentasti, M. C. Gennaro and C. Baiocchi, *Ann. Chim. (Rome)*, 1983, **73**, 385.
16. C. Sarzanini, E. Marengo, M. C. Gennaro, C. Baiocchi and E. Mentasti, *Chemistry for Protection of Environment*, p. 381. Elsevier, New York, 1984.
17. C. Sarzanini, E. Mentasti, M. C. Gennaro and E. Marengo, *Anal. Chem.*, 1985, **57**, 1960.
18. D. P. H. Laxen and M. R. Harrison, *ibid.*, 1981, **53**, 345.
19. C. Sarzanini, E. Mentasti, M. C. Gennaro and V. Porta, *Proc. Ion Exchange: Science and Technology*, NATO School, Troia, 14–26 July 1985, M. Nijhoff (ed.), ASI Series, Netherlands, in the press.
20. R. E. Van Grieken, C. M. Bresseleers and B. M. Vanderborcht, *Anal. Chem.*, 1977, **49**, 1326.
21. J. Chwastowska and E. Mozer, *Talanta*, 1985, **32**, 574.
22. A. Beveridge and W. F. Pickering, *Water Res.*, 1984, **18**, 1119.
23. P. Pakalns and G. E. Batley, *Anal. Chim. Acta*, 1978, **99**, 333.

DETERMINATION OF MOLYBDENUM, CHROMIUM AND VANADIUM BY ION-PAIR HIGH-PRESSURE LIQUID CHROMATOGRAPHY BASED ON PRECOLUMN CHELATION WITH 4-(2-PYRIDYLAZO)RESORCINOL

ZHANG XIAO-SONG, ZHU XIANG-PING and LIN CHANG-SHAN

Department of Applied Chemistry, University of Science and Technology of China, Hefei, Anhui, People's Republic of China

(Received 24 January 1986. Revised 2 April 1986. Accepted 24 May 1986)

Summary—A reversed-phase ion-pair liquid chromatography-spectrophotometric detection system for the separation and simultaneous determination of molybdenum, chromium and vanadium is described. The chelates of the metal ions with 4-(2-pyridylazo)resorcinol are separated on a Zorbax CN column with $1 \times 10^{-3} M$ tetrabutylammonium iodide and $0.01 M$ KH_2PO_4 - Na_2HPO_4 buffer (pH 7.50) in 30:70 v/v methanol-water mixture as the mobile phase, at a flow-rate of 1.0 ml/min. The chelates are detected spectrophotometrically at 540 nm.

Recently, several reports on the application of high-pressure liquid chromatography (HPLC) for separating and determining various metal chelates have been published.¹⁻³ Reversed-phase HPLC with bonded stationary phases has been shown to be one of the most effective separation methods presently available⁴ and this method seems to be convenient for the separation and simultaneous determination of elements that have similar chemical properties, such as molybdenum, chromium and vanadium.

4-(2-Pyridylazo)resorcinol (PAR) is one of the best chelating reagents for precolumn complexation of many metal ions, because of its sensitivity, and solubility in water.⁵ The reagent has been used for separation and determination of iron, cobalt, nickel, copper, zinc,⁶⁻⁸ chromium,⁹ vanadium,¹⁰ platinum and palladium¹¹ by reversed-phase ion-pair liquid chromatography. We have investigated the possibilities of separation and determination of molybdenum, chromium and vanadium with PAR as the chelating reagent in the presence of hydroxylamine and of tetrabutylammonium iodide (TBAI) as the ion-pairing reagent, on a Zorbax CN column. Complexation in the PAR-hydroxylamine system has been studied for molybdenum^{12,13} and vanadium,¹⁴ but apparently not for chromium.

The present study demonstrates that ion-pair reversed-phase liquid chromatographic separation and determination of molybdenum, chromium and vanadium as PAR-chelates are feasible at the ng level.

EXPERIMENTAL

Apparatus

The liquid chromatograph was a Shimadzu system LC-4A equipped with a model SPD-1 spectrophotometric detector and a Chromatopac C-R2A(X). A Shimadzu model UV-240 recording spectrophotometer was used for spectral measure-

ments. A Shanghai model 721 spectrophotometer and a Shanghai model pH S-2 pH-meter were used. A 6- μ m particle-size Zorbax CN column (Du Pont) (250 mm \times 4.6 mm bore) was used for all experiments.

Reagents

Standard solutions of Mo(VI) and Cr(VI) were prepared by dissolving ammonium molybdate, $(NH_4)_6Mo_7O_{24} \cdot 4H_2O$, and potassium chromate, respectively, in water. The stock solution of V(V) was prepared by dissolving ammonium metavanadate, NH_4VO_3 , in 1M sodium hydroxide, then adding sulphuric acid until the solution was slightly acidic. The PAR solution was prepared by dissolving the compound in methanol. The ion-pairing reagent, TBAI, was analytical reagent grade from the Shanghai Chemical Co. The mobile phase consisted of $1 \times 10^{-3} M$ TBAI and $0.01 M$ KH_2PO_4 - Na_2HPO_4 (pH 7.50) in 30:70 v/v methanol-water mixture. All the other reagents were of analytical grade.

Procedure

To a weakly acidic solution containing Mo(VI), Cr(VI) and V(V), 3 ml of 5% hydroxylamine hydrochloride solution, 2.5 ml of $0.1 M$ KH_2PO_4 - Na_2HPO_4 buffer solution (pH 7.50) and 2.5 ml of $2.4 \times 10^{-3} M$ PAR solution were added. The mixture was diluted to about 20 ml with distilled water and heated in boiling water for 80 min. After cooling, the solution was diluted to volume in a 25-ml standard flask. The solution was filtered through a 0.45- μ m membrane filter and a 20- μ l portion was injected into the column. The PAR chelates were eluted with the methanol-water mobile phase at a flow-rate of 1.0 ml/min and detected by the spectrophotometric detector at 540 nm, the sensitivity being set at 0.01 or 0.02 absorbance for full-scale deflection.

RESULTS AND DISCUSSION

Selection of experimental conditions

Effect of hydroxylamine hydrochloride. Preliminary experiments demonstrated that neither Mo(VI) nor Cr(VI) formed a red chelate with PAR at any pH in the absence of hydroxylamine hydrochloride, even at 100°, but in the presence of hydroxylamine hydrochloride, both formed PAR chelates on boiling.

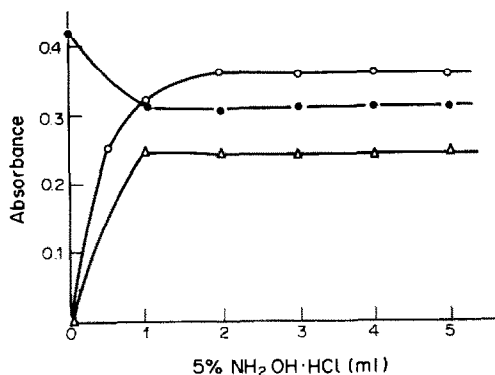


Fig. 1. Effect of the concentration of hydroxylamine hydrochloride. PAR $2.4 \times 10^{-4}M$; Mo(VI) $6.25 \times 10^{-6}M$, \triangle ; Cr(VI) $7.7 \times 10^{-6}M$, \circ ; V(V) $7.8 \times 10^{-6}M$, \bullet ; pH 7.50 KH_2PO_4 - Na_2HPO_4 buffer, 2 cm cell, 540 nm.

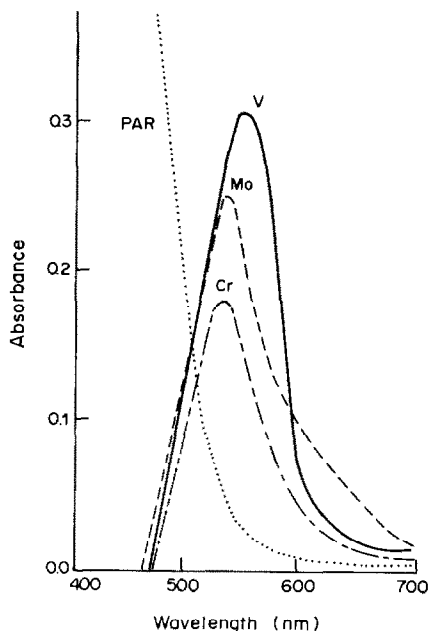


Fig. 2. Absorption spectra of metal-PAR chelates. PAR $2.4 \times 10^{-4}M$; Mo(VI) $1.25 \times 10^{-5}M$; Cr(VI) $7.7 \times 10^{-6}M$; V(V) $1.56 \times 10^{-5}M$; 1 cm cell. Other conditions as for Fig. 1.

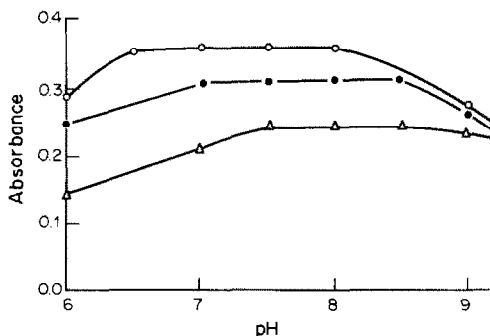


Fig. 3. Effect of pH on the colour development of metal-PAR chelates. Other conditions and symbols as for Fig. 1.

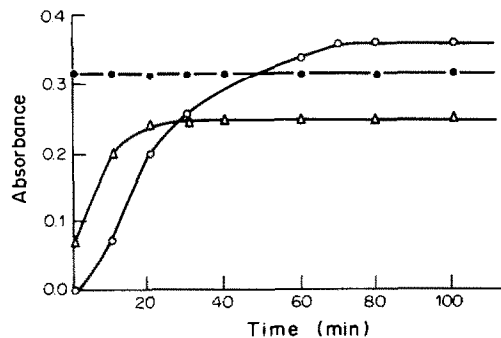


Fig. 4. Colour development time at $100^\circ C$. Other conditions and symbols as for Fig. 1.

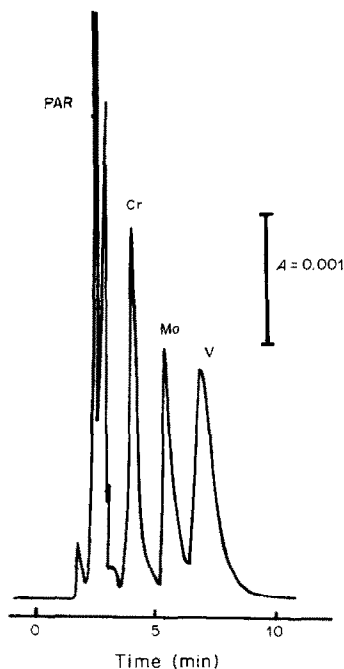


Fig. 5. Separation of metal-PAR chelates on Zorbax CN column; 8 ng each of Mo(VI), Cr(VI) and V(V) injected, other conditions as for Fig. 1.

Hydroxylamine hydrochloride had the dual functions of reducing Cr(VI) to Cr(III) [which reacts with PAR to form the Cr(III)-PAR chelate] and accelerating the colour development of the Mo(VI)-PAR and Cr(III)-PAR chelates. The absorbance of the V(V)-PAR chelate decreased as hydroxylamine hydrochloride was added, but reached a constant value when an excess of hydroxylamine hydrochloride had been added, as shown in Fig. 1.

Selection of detection wavelength. To choose the wavelength for the detection of the eluted PAR chelates of Mo(VI), Cr(III) and V(V), the absorption spectrum of each chelate was measured under the conditions shown for Fig. 2. Mo(VI)-PAR and Cr(III)-PAR exhibited absorption maxima at 530 nm, and V(V)-PAR at 550 nm, and the reagent blank had negligible absorption at 530-550 nm. A wavelength of 540 nm was selected for detection.

Table 1. Coefficients of linear regression lines for calibration of chromatographic detector

Metal ion	Mo(VI)	Cr(VI)	V(V)
Concentration range, mg/l.	0.10–1.0	0.10–1.4	0.10–2.0
Range of amount injected, ng	2–20	2–28	2–40
Slope, absorbance.l.mg ⁻¹	0.0049	0.0023	0.0056
Intercept, absorbance	-0.00008	0.0016	-0.00063
Correlation coefficient	0.9998	0.9991	0.9996

Table 2. Effect of foreign ions on the determination of Mo(VI), Cr(VI) and V(V)

Foreign ion	Added, µg	Found, µg*		
		Mo(VI)	V(V)	Cr(VI)
Al(III)	10	10.1	9.9	9.6
	100	10.2	10.3	3.6
Mg(II)	10	9.5	10.2	10.6
	100	9.9	10.0	13.7
Ni(II)	50	10.5	9.9	9.9
	100	9.5	10.1	4.4
Mn(II)	100	9.9	9.8	12.9
W(VI)	100	9.6	9.7	11.7
Zn(II)	10	10.4	10.1	11.9
Cd(II)	10	10.4	10.2	13.1
Hg(II)	10	9.6	10.0	14.0
Cu(II)	10	10.1	10.4	12.6
Fe(II)	10	10.3	10.2	12.9
Co(II)	5	10.2	10.1	19.6

*10.0 µg each of Mo(VI), V(V) and Cr(VI) originally present

Effect of pH on colour development. The absorption vs. pH curves for the metal-PAR chelates are shown in Fig. 3. A KH_2PO_4 - Na_2HPO_4 solution of pH 7.5 was chosen since it gave maximum development of all three chelates, and was also used in the eluent.

Effect of PAR concentration. It was found that for 15 µg of Mo(VI) and 10 µg of Cr(VI) or V(V), maximal absorbance was obtained by use of not less than 0.3, 1.8 and 0.3 ml of $2.4 \times 10^{-3}M$ PAR respectively. A volume of 2.5 ml of $2.4 \times 10^{-3}M$ PAR was chosen as optimal.

Colour development. The coloured chelate of V(V) with PAR was readily formed at ambient temperature. The colour development of the Mo(VI) complex was incomplete and that of the Cr(VI) complex hardly started at all at ambient temperature. As shown in Fig. 4, the mixture with Mo(VI) should be kept on a steam-bath for at least 30 min and that with Cr(VI) for at least 80 min for constant absorbance to be reached. High temperatures had a negligible effect on the absorbance of the V(V)-PAR chelate.

Chromatogram and calibration graphs

A typical chromatogram is shown in Fig. 5. The retention times of the PAR chelates of chromium, molybdenum and vanadium were 3.97, 5.50 and 6.95 min, respectively, at a flow-rate of 1.0 ml/min.

The slopes and intercepts of the calibration graphs for the simultaneous determination of molybdenum, chromium and vanadium calculated by linear regression analysis of the peak-height (absorbance) vs. metal concentration data are summarized in Table 1. The detection limits (at a signal to noise ratio of 2:1) were 0.82 ng for molybdenum, 1.7 ng for chromium and 0.71 ng for vanadium (full-scale deflection = 0.01 absorbance). Relative standard deviations calculated from five replicate analyses of a solution containing 0.40 mg/l. each of molybdenum, chromium and vanadium were 2.0, 2.0 and 3.3%, respectively.

Effect of foreign ions

The effect of the presence of other ions on the determination of Mo(VI), Cr(VI) and V(V) was examined (Table 2). When present in comparable concentrations to Mo(VI) and V(V), the metal ions examined for interference had no effect on the determination of these ions. All the foreign ions except Al(III), Mg(II) and Ni(II) caused serious interference in the determination of Cr(VI). Before this HPLC method is applied to actual samples, therefore, these interfering ions must be masked or removed by extraction.

REFERENCES

- G. Schwedt, *Chromatographia*, 1979, **12**, 613.
- J. W. O'Laughlin, *J. Liq. Chromatog.*, 1984, **7**, 127.
- T. Yotsuyanagi, *Fenxi Huaxue*, 1984, **12**, 797.
- L. R. Snyder and J. J. Kirkland, *Introduction to Modern Liquid Chromatography*, 2nd Ed., Chapter 7, Wiley, New York, 1979.
- S. Shibata, in *Chelates in Analytical Chemistry*, Vol. 4, H. A. Flaschka and A. J. Barnard (eds.), pp. 116–165. Dekker, New York, 1972.
- H. Hoshino, T. Yotsuyanagi and K. Aomura, *Bunseki Kagaku*, 1978, **27**, 315.
- D. A. Roston, *Anal. Chem.*, 1984, **56**, 241.
- J. E. DiNunzio, R. W. Yost and E. K. Hutchison, *Talanta*, 1985, **32**, 803.
- H. Hoshino and T. Yotsuyanagi, *Anal. Chem.*, 1985, **57**, 625.
- Idem*, *Talanta*, 1984, **31**, 525.
- E. Watanabe, H. Nakajima, T. Ebina, H. Hoshino and T. Yotsuyanagi, *Bunseki Kagaku*, 1983, **32**, 469.
- E. Lassner, R. Püschel, K. Katzengruber and H. Schedle, *Mikrochim. Acta*, 1969, 134.
- E. Lassner, *Talanta*, 1972, **19**, 1121.
- V. V. Lukachina, A. T. Pilipenko and O. I. Karpova, *Zh. Analit. Khim.*, 1973, **28**, 86.

ANALYTICAL DATA

DISSOCIATION CONSTANTS OF ARSENAZO III

IRENA NĚMCOVÁ and BOREK METAL

Department of Analytical Chemistry, Charles University, Albertov 2030, 128 40 Prague 2, Czechoslovakia

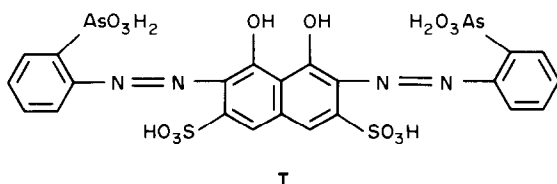
JAROSLAV PODLAHA

Department of Inorganic Chemistry, Charles University, Albertov 2030, 128 40 Prague 2, Czechoslovakia

(Received 28 February 1986. Revised 17 April 1986. Accepted 6 June 1986)

Summary—Commercial samples of Arsenazo III were found to be appreciably impure even after purification as the barium salt. Chromatography on silica gel followed by crystallization yielded a pure sample of the ethanol solvate of the free acid. The dissociation constants of the acid were determined potentiometrically at 25° and $I = 0.1$ (NaClO₄).

Arsenazo III [2,2'-(1,8-dihydroxy-3,6-disulphonaphthalene-2,7-bisazo)bisbenzenearsonic acid, H₈A] (I) is one of the most often used azo-dyes in spectrophotometry, especially for determination of lanthanide and actinide ions. Its dissociation and protonation constants have been determined, but the values reported differ considerably, apparently owing to differing purity of the reagent, which was not specified in the original papers. The character of the synthetic methods used suggests the probable presence of various isomers and of minor impurities in the "purified" samples. The aim of the present work was to purify Arsenazo III and determine its dissociation constants.



EXPERIMENTAL

Apparatus

Potentiometric measurements were made at $25 \pm 0.1^\circ$ in the absence of carbon dioxide. A PHM 64 pH-meter (Radiometer) equipped with a combined glass/saturated calomel electrode, type GK 2401B was used and calibrated⁴ in terms of $-\log\{H^+\}$, with a precision better than ± 0.005 , before each titration.

Chemicals

Sodium hydroxide solution (0.1M, free from carbonate) and 0.1M perchloric acid were dispensed with a precision of better than 0.002 ml from calibrated burettes. The ionic strength was adjusted to 0.1 with a solution of sodium perchlorate which was freed from protolytic impurities by a recommended procedure.⁵ Commercial Arsenazo III (Lachema, Czechoslovakia) was purified⁶ by precipitation as the barium salt, followed by extraction of the free acid from 0.1M hydrochloric acid into butanol/benzene (1:3 v/v). TLC

on silica gel (Silufol plates, Kavalier, Czechoslovakia) with the solvent system, 2-propanol/15% aqueous ammonia solution (1:1 v/v) demonstrated that a few impurities were present, with $R_f = 0.05-0.44$, in addition to the main component with $R_f = 0.59$. For further purification, 100-mg portions of this material were chromatographed on 30 g of 50-120 μ m silica gel in a 2×25 cm column, with the TLC solvent system at a flow-rate of 1.5 ml/min. The combined fractions containing the pure ammonium salt with $R_f = 0.59$ were evaporated to dryness *in vacuo* at 50°, and the residue was dissolved in water and converted into the acid by passage through 100-mesh Dowex 50W 2 (hydrogen form) in a 2×20 cm column at a flow rate of 0.5 ml/min. After evaporation of the eluate to dryness *in vacuo* and dissolution of the residue in 25 ml of ethanol, crystallization was induced by addition of 50 ml of diethyl ether. Filtration, washing with diethyl ether and drying at 25° and a pressure of 0.2 kPa to constant weight yielded 40 mg of purple crystals. The individual portions were finally combined and recrystallized from ethanol/ether. TLC of the product yielded only a single spot with $R_f = 0.59$, and according to the elemental analysis and ¹H NMR, the product was the bis(ethanol) solvate of the free acid of Arsenazo III: found, C 36.0%, H 3.5%, N 6.5%, C₂₆H₃₀As₂N₄O₁₆S₂ (m.w. 866.6) requires C 36.04%, H 3.49%, N 6.52%. ¹H NMR (D₂O, TMS as internal reference): 1.18 ppm t (J = 7.5 Hz), 6H, CH₃; 3.62 q (J = 7.5), 4H, CH₂; 6.9-7.4 m, 10H, aromatics.

RESULTS AND DISCUSSION

Arsenazo III is an octabasic weak acid. The protonation equilibria are described by the protonation constants $\beta_i = [H_iA]/[H]^i[A]$, ($i = 1-8$, charges are omitted). For their determination, an initial volume of 50 ml of a 0.001 or 0.002M solution of the acid was titrated with 0.1M sodium hydroxide until $-\log\{H^+\} = 12$ was attained and then back-titrated with 0.1M perchloric acid to $-\log\{H^+\} = 2$. During the titration, the mean number of protons bound per anion, \bar{n}_H , was calculated for each experimental point; further additions were adjusted so that (i) at least 15 experimental points were accumulated between integral values of \bar{n}_H and (ii) \bar{n}_H reached a limiting value

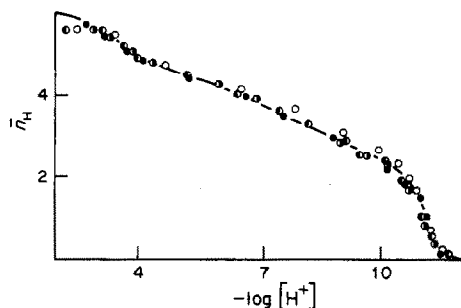


Fig. 1. Formation curve. Experimental points (● for titration of $2 \times 10^{-3}M$ Arsenazo III, ○ for retitration of $2 \times 10^{-3}M$ Arsenazo III, ● for titration of $1 \times 10^{-3}M$ Arsenazo III, ○ for retitration of $1 \times 10^{-3}M$ Arsenazo III) are fitted by the curve calculated from the dissociation constants given in Table 1.

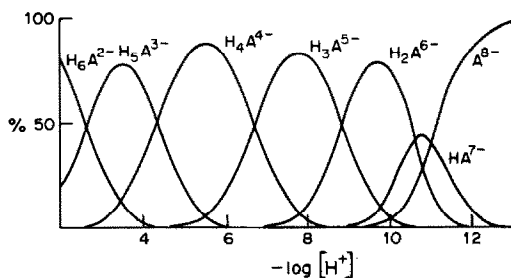


Fig. 2. Distribution diagram of Arsenazo III as a function of $-\log [H^+]$.

at both ends of the titration curve. All the experimental points lay on the same formation curve within experimental error (Fig. 1). The acid-base equilibria were established rapidly and the system was found to be mononuclear with respect to A^{8-} . A trial-and-error fitting of the formation curve yielded preliminary values of the protonation constants β_1 – β_6 , which were then refined by the MINQUAD program.⁷ The final values of $\log \beta_i$ were $\log \beta_1 = 10.99$ (0.05), $\log \beta_2 = 21.57$ (0.02), $\log \beta_3 = 30.36$ (0.06), $\log \beta_4 = 37.06$ (0.09), $\log \beta_5 = 41.45$ (0.13), $\log \beta_6 = 43.95$ (0.14), where the figures in brackets are the standard deviations. As expected, attempted calculation of β_7 and β_8 resulted in their rejection by the program. It can be deduced from the conditions for the rejection

Table 1. Dissociation constants of Arsenazo III

Constant	Value	Dissociation	Previous results (ref. 1; ref. 2)
pK_1	< 1.3	$SO_3H \rightarrow SO_3^-$	1.89; 0.6
pK_2	< 1.3		
pK_3	2.60	$AsO_3H_2 \rightarrow AsO_3H^-$	3.64; 1.6
pK_4	4.29		
pK_5	6.70	$AsO_3H^- \rightarrow AsO_3^{2-}$	6.77; 6.27
pK_6	8.79		
pK_7	10.58	$OH \rightarrow O^-$	9.30; 11.98
pK_8	10.99		

of constants⁸ by MINQUAD that the values of $\log \beta_7$ and $\log \beta_8$ are less than 45.2 and hence inaccessible to standard potentiometry with a glass electrode.

The protonation constants were converted into the pK values (Table 1). As the MINQUAD statistics deal only with β values, no standard deviations of the pK values can be given. Figure 2 shows the distribution of the individual anions. The dissociation is accompanied by colour changes from reddish-purple to deep blue.

On the basis of structural analogy to similar compounds, the pK values can be assigned to individual protonation sites of the molecule. This assignment is identical with that proposed by other authors¹ but, in the absence of additional evidence must be taken as tentative, especially for pK_6 and pK_7 .

REFERENCES

1. P. N. Palei, N. I. Udaltsova and A. A. Nemodruk, *Zh. Analit. Khim.*, 1967, **22**, 1797.
2. B. Buděšinský, *Talanta*, 1969, **16**, 1277.
3. A. Muk, S. B. Savvin and R. F. Propistsova, *Zh. Analit. Khim.*, 1968, **23**, 1277.
4. M. Wozniak and G. Nowogrocki, *Talanta*, 1981, **28**, 575.
5. G. Biedermann and L. G. Sillén, *Arkiv Kemi*, 1953, **5**, 425.
6. V. Radil and P. Grametbauer, *Czech. Pat.*, 212109.
7. A. Sabatini, A. Vacca and P. Gans, *Talanta*, 1974, **21**, 53.
8. A. Sabatini and A. Vacca, *Coord. Chem. Rev.*, 1975, **16**, 161.

FORMATION CONSTANTS OF SOME MERCURY(II) COMPLEXES DETERMINED FROM THEIR ANODIC POLAROGRAPHIC SIGNALS

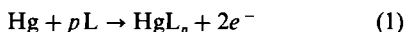
M. ESTEBAN, E. CASASSAS* and L. FERNANDEZ

Departament de Química Analítica, Facultat de Química, Universitat de Barcelona, Av. Diagonal 647,
 08028 Barcelona, Spain

(Received 13 November 1985. Revised 8 April 1986. Accepted 2 June 1986)

Summary—The formation constants of some Hg(II) complexes have been determined from the anodic polarographic signals for the oxidation of mercury in the presence of the following ligands: thiourea and its phenyl- and diphenyl-derivatives, thiocyanate, ethylenediamine, EDTA, methylthioacetic acid, 2,2'-thiobisacetic acid, 3,3'-thiobispropanoic acid, 2,2'-[1,1-methandiylbis(thio)]bisacetic acid and 2,2'-[1,2-ethandiylbis(thio)]bisacetic acid. The use of differential pulse polarography and a.c. polarography instead of d.c. polarography increases the accuracy and precision of the potential measurements and, as a consequence, of the stability constants determined. The results obtained by the different methods are compared.

It is well-known that in the presence of most complexing agents, mercury from the dropping mercury electrode (DME) can be anodically oxidized to the bivalent state,¹ leading to the overall electrode process:



(ionic charges on the ligand and the complex are omitted).

The half-wave potential of the process is related to the ligand concentration, [L], and to the formation constant of the complex, β_p , by the well-known equation^{2,3}

$$E_{1/2} = E_{\text{Hg}^{2+}}^{\circ} + \frac{RT}{2F} \ln \frac{2^{(p-1)} D^{1/2}}{p (D')^{1/2} \beta_p [L]^{(p-1)}} \quad (2)$$

where D and D' are the diffusion coefficients of the ligand and the complex, respectively: the ratio of these is usually taken as unity. The free ligand concentration in equilibrium with the Hg(II)-ions, [L], depends on the total concentration C_L of ligand and the pH, according to the equation

$$[L] = C_L / \alpha_{L(H)} \quad (3)$$

where $\alpha_{L(H)}$ is the proton side-reaction coefficient. Substituting [L] from equation (3) into equation (2) and rearranging, gives:

$$E_{1/2} = E_{\text{Hg}^{2+}}^{\circ} - \frac{RT}{2F} \ln \beta_p - \frac{RT}{2F} \ln C_L^{(p-1)} + \frac{RT}{2F} \ln \frac{2^{(p-1)}}{p} \alpha_{L(H)}^{(p-1)} + \frac{RT}{2F} \ln \frac{D^{1/2}}{(D')^{1/2}} \quad (4)$$

When $p = 1$, i.e., only the HgL complex is formed, $E_{1/2}$ is independent of C_L and is a function of only pH, as has been observed by several authors in the study of the Hg(II) complexes of EDTA, DCTA, EGTA, DTPA⁴⁻⁷ and TTHA.⁸ Equation (4) can also be applied in the less common case of formation of a soluble Hg(I) complex.

From equation (4), β_p values can be determined in two different ways. (a) From the intercept of the linear plot of $E_{1/2}$ vs. $\log C_L$ at constant pH over a C_L range where one particular complex predominates. Low pH values are to be preferred, to minimize complications due to formation of mercury hydroxo-complexes.⁹ If high pH values have to be employed, the theoretical treatment should include the $\alpha_{\text{Hg(OH)}}$ coefficients.⁹ From $E_{1/2}$ vs. $\log C_L$ relationships a great number of β_2 values for Hg(II) complexes have been determined, including those for the thiourea¹⁰⁻¹² and thiocyanate^{1,13} complexes. (b) From the intercept of the linear plot of $E_{1/2}$ vs. $\log \alpha_{L(H)}$ at constant ligand concentration in a pH range where only one complex predominates. The main drawback of this method is that only a restricted pH range can be used if the hydroxo-complexes of mercury are to be neglected. The β_2 value of the Hg(en)₂ complex^{14,15} has been determined by means of this relationship.

In the work reported here, the application of differential pulse polarography (dpp) and alternating current polarography (acp) to the determination of the formation constants of mercury complexes from the data for anodic oxidation of mercury is discussed. The potentials can be measured much more precisely by these techniques than by d.c. polarography (dcp).

The theoretical treatment above starts from the

*Author for correspondence.

basic equations of dcp.² Heath and Hefter,¹⁶ Gómez-Nieto *et al.*¹⁷ and Casassas and Ariño¹⁸ have shown that the DeFord and Hume method,¹⁹ developed from dcp, is also valid when applied to experimental data obtained from dpp and acp. For a reversible diffusion-controlled process, Parry and Osteryoung²⁰ showed that the peak potential of a dpp peak (E_p) and the half-wave potential of the corresponding dcp wave ($E_{1/2}$) are related by the expression $E_p = E_{1/2} - \Delta E/2$, where ΔE is the magnitude of the applied pulse, taken with its sign. Starting from the same assumptions, Smith²¹ and Bond²² have shown that the values of the peak potential or the half-wave potential obtained by fundamental and second-harmonic acp (ac_{1p} and ac_{2p}), respectively, are equal to the $E_{1/2}$ values for the dcp wave. It follows that the shifts in the characteristic potentials in dpp, ac_{1p} and ac_{2p} will be the same as the shifts in the dcp half-wave potential, and that equation (4) can also be applied to dpp and acp data. Casassas and Esteban took this approach further²³ and showed that dpp and acp could be used for the determination of stability constants. In particular, the quality of the dpp and acp signals makes it possible to determine stability constants for systems where the dcp waves are poorly developed.

This paper describes an investigation of mercury complexes with thiourea and its phenyl derivatives, thiocyanate, ethylenediamine, EDTA and the following thioether carboxylic acids: methylthioacetic acid (MTA), 2,2'-thiobisacetic acid (TBA), 3,3'-thiobispropanoic acid (TBP), 2,2'-[1,1-methandiylbis(thio)]bisacetic acid (MDBA) and 2,2'-[1,2-ethandiylbis(thio)]bisacetic acid (EDBA). The formation constants of the predominating Hg(II) complexes have been calculated from the anodic waves.

EXPERIMENTAL

Chemicals and instrumentation

The ligands, all commercial chemicals of high purity, were used without further purification. The other reagents, and the instrumentation were as described previously.²³

All measurements were made at $25 \pm 0.1^\circ$ and an ionic strength of 0.1M (KNO_3) in aqueous medium, except for diphenylthiourea, where the medium was ethanol/water 50% v/v.

Procedure

The $\log \beta_p$ values were determined, by the different polarographic techniques, from the $E_{1/2}$ or E_p vs. $\log C_L$ plots (usually for solutions with $pH < 5$) obtained under conditions chosen so that one soluble complex predominated. $E_{1/2}$ or E_p were determined by standard polarographic procedures. The usual instrumental parameters were: drop-time, 1 sec; mercury height, 50 cm; pulse magnitude, ± 40 mV (dpp) and 10 mV (acp). The formation of mercury hydroxo-complexes was neglected in the calculations.

RESULTS AND DISCUSSION

Table 1 shows the $\log \beta_2$ values for several Hg(II) systems obtained by dcp, dpp and ac_{1p} , compared with some literature values. Good agreement was obtained in all cases, especially by dcp and dpp, the latter usually yielding more precise values than the former. The $\log \beta_2$ values obtained in the study of the thiourea system by ac_{1p} were slightly lower than those obtained by dcp and dpp and those quoted in the literature. Distorted and asymmetrical ac_{1p} peaks were obtained in this case, showing that the ac_{1p} electrode process is not fully reversible. In contrast, the dcp and dpp processes are stated in the literature to be reversible¹⁰⁻¹² and this has been confirmed in the present study. Table 1 also shows the $\log \beta_2$ values for the Hg(II) complexes of phenylthiourea and diphenylthiourea, for which no data could be found in the literature. In both cases the determinations were done by dpp because well-developed and precise peaks were obtained, whereas the dcp waves were poorly developed. Asymmetrical acp peaks were also observed, as a consequence of the acp process being somewhat irreversible.

Table 2 shows the $\log \beta_1$ mean values obtained for the $Hg(EDTA)^{2-}$ complex, compared with those quoted in the literature. Two different sets of $\log \beta_1$ values are shown in the Table, which were determined

Table 1. $\log \beta_2$ values of Hg(II) complexes determined polarographically at 25° in 0.1M potassium nitrate

Ligand	This work		Literature		
	Technique	$\log \beta_2$	$\log \beta_2$	Conditions	Reference
Thiourea	dcp	22.43 (0.24)	22.17 ± 0.6	$25^\circ, 1M$	11
	dpp ^a	21.66 (0.20)	22.47	$25^\circ, 1M$	24
	ac_{1p} ^c	21.06 (0.23)	22.1	$25^\circ, 1M$	25
			21.3	$30^\circ, 0.1M$	26
Phenylthiourea	dpp ^a	20.43 (0.09)			
Diphenylthiourea	dpp ^a	21.34 (0.10)			
Thiocyanate	dcp	16.53 (0.59)	16.43	$25^\circ, 0.2M$	27
	dpp ^a	16.72 (0.17)	16.85	$25^\circ, 1M$	28, 29
	ac_{1p} ^c	17.05 (0.17)	17.46 (17.12)	$25^\circ, Cl^- (Br^-)$	30
			$16.07 + 0.03$	$25^\circ, 1M$	13
			23.17	$25^\circ, 0.1M$	14
Ethylenediamine	dpp ^a	22.92 (0.20)	23.32	$25^\circ, 0.1M$	15
	dpp ^b	23.11 (0.20)	23.24 ± 0.07	$25^\circ, 0.1M$	31

^a: $\Delta E = 40$ mV; ^b: $\Delta E = -40$ mV; ^c: $\Delta E = 10$ mV.

Table 2. Log β_1 values of Hg(EDTA)²⁻ complex determined polarographically at 25° in 0.1M potassium nitrate

Technique	This work		Literature		
	a	b	log β_1	Conditions	Reference
dcp	19.98	22.11	22.15	25°, 0.065M	5
dpp	19.98	22.11	21.64	25°, 0.1M	32
ac ₁ p	20.19	22.25	15.7	20°, 0.1M	4

a: Value determined with the $E_{\text{Hg(II)}}^{\circ}$ value taken from Reference 11.

b: Value determined with the $E_{\text{Hg(II)}}^{\circ}$ value taken from Reference 33.

by using two different published $E_{\text{Hg(II)}}^{\circ}$ values in the calculation. The results show that the differences observed between the values reported here and those quoted in the literature can easily be explained in terms of the $E_{\text{Hg(II)}}^{\circ}$ values taken in the different investigations.

Thioether carboxylic acids

The anodic oxidation of mercury from the DME and the HMDE in the presence of several thioether carboxylic acids has been studied already. Kotek *et al.*³³ studied the anodic dc wave of TBA but reached no conclusion about the nature of the mercury compound formed. Sužnjević *et al.*³⁴ found that EDDBA yielded a reversible anodic polarographic wave corresponding to the formation of a 1:2 Hg(II)-EDDBA complex. The anodic behaviour of MTA, TBA, TBP, MDBA and EDDBA has been investigated systematically by Casassas and co-workers.^{35,36}

MTA, TBA and TBP, all monothiocarboxylate ligands, yield first a reversible diffusion-controlled anodic signal corresponding to the formation of a soluble HgL₂ complex³⁵ and, at more positive potentials (above +0.4 V), a second irreversible signal which seems to be related to a crystallization process. A fuller understanding of this second process for the three thioether acids will require further electrochemical investigation. On the other hand, MDBA and EDDBA, dithiocarboxylate ligands, yield only one reversible diffusion-controlled anodic signal, corresponding to the formation of the soluble HgL₂ complex³⁶ in agreement with the findings of Sužnjević *et al.* for EDDBA.³⁴

Table 3 shows the log β_2 values for the corresponding mercury-thioether complexes. The values obtained by acp are usually higher than those obtained by dcp and dpp, as a consequence of weak adsorption phenomena.^{35,36} The values obtained for EDDBA are in better agreement with the one determined potentiometrically by Napoli³⁷ (18.99 ± 0.07 at 25° and $\mu = 0.5M$) than the one determined polarographically by Sužnjević *et al.*³⁴ (13.82 at 25° and $\mu = 0.1M$). No previous reference to the formation constants of the Hg(II)-MTA, Hg(II)-TBA, Hg(II)-TBP and Hg(II)-MDBA complexes is known.

Table 3. Formation constants of several Hg(II)-thioether-carboxylate complexes determined polarographically at 25° in 0.1M potassium nitrate

Ligand	Technique	log β_2
CH ₃ SCH ₂ COOH (MTA)	dcp	11.93 (0.18)
	dpp ^a	11.81 (0.14)
	ac ₁ p	12.69 (0.20)
S(CH ₂ COOH) ₂ (TBA)	ac ₂ p	13.51 (0.25)
	dcp	13.35 (0.15)
	dpp ^a	14.29 (0.18)
S(CH ₂ CH ₂ COOH) ₂ (TBP)	ac ₁ p	14.65 (0.17)
	ac ₂ p	14.90 (0.20)
	dpp ^a	12.78 (0.15)
(H ₂ CSCH ₂ COOH) ₂ (EDBA)	ac ₁ p	12.57 (0.18)
	ac ₂ p	12.67 (0.20)
	dcp	18.05 (0.20)
H ₂ C(SCH ₂ COOH) ₂ (MDBA)	dpp ^a	17.94 (0.16)
	dpp ^b	18.08 (0.16)
	ac ₁ p	18.35 (0.20)
H ₂ C(SCH ₂ COOH) ₂ (MDBA)	ac ₂ p	18.05 (0.20)
	dpp ^a	10.25 (0.36)
	ac ₁ p	10.20 (0.35)

a: $\Delta E = 40$ mV; b: $\Delta E = -40$ mV.

REFERENCES

1. I. M. Kolthoff and C. S. Miller, *J. Am. Chem. Soc.*, 1941, **63**, 1405.
2. J. Heyrovský and J. Kuta, *Principles of Polarography*, p. 157. Academic Press, New York, 1966.
3. D. R. Crow, *Polarography of Metal Complexes*, p. 173. Academic Press, New York, 1969.
4. B. Matyska and I. Kossler, *Collect. Czech. Chem. Commun.*, 1951, **6**, 221.
5. J. Goffart, G. Michel and G. Duyckaerts, *Anal. Chim. Acta*, 1953, **9**, 184.
6. B. Matyska, J. Doležal and D. Robalová, *Collect. Czech. Chem. Commun.*, 1956, **21**, 107.
7. L. L. Jackson, J. Osteryoung and R. A. Osteryoung, *Anal. Chem.*, 1980, **52**, 66.
8. S. Rubel and M. Wojciechowski, *Anal. Chim. Acta*, 1979, **104**, 215.
9. A. Ringbom, *Complexation in Analytical Chemistry*, p. 356. Academic Press, Wiley, New York, 1963.
10. M. Fedoronko, O. Manousek and P. Zuman, *Chem. Listy*, 1953, **49**, 1494.
11. C. J. Nyman and E. P. Parry, *Anal. Chem.*, 1958, **30**, 1255.
12. M. R. Smyth and J. Osteryoung, *ibid.*, 1977, **49**, 2310.
13. C. J. Nyman and G. S. Alberts, *ibid.*, 1960, **32**, 207.
14. C. J. Nyman, D. K. Roe and D. B. Masson, *J. Am. Chem. Soc.*, 1955, **77**, 4191.
15. J. I. Watters and J. G. Mason, *ibid.*, 1956, **78**, 285.
16. G. A. Heath and G. Hefter, *J. Electroanal. Chem.*, 1977, **84**, 295.
17. M. A. Gómez-Nieto, M. D. Luque de Castro, M. Valcárcel and J. L. Cruz Soto, *Anal. Chim. Acta*, 1984, **156**, 77.
18. E. Casassas and C. Ariño, unpublished work.
19. D. D. DeFord and D. N. Hume, *J. Am. Chem. Soc.*, 1951, **73**, 5321.
20. E. P. Parry and R. A. Osteryoung, *Anal. Chem.*, 1965, **37**, 1634.
21. D. E. Smith in A. J. Bard (Ed), *Electroanalytical Chemistry*, Vol. 1, Chap. 1. Dekker, New York, 1966.
22. A. M. Bond, *J. Electroanal. Chem.*, 1972, **35**, 315.
23. E. Casassas and M. Esteban, *ibid.*, 1985, **194**, 11.
24. H. L. Kiess, *Z. Anal. Chem.*, 1955, **145**, 5.
25. V. F. Toropova, *J. Inorg. Chem. USSR*, 1956, **1**, 52.

26. D. R. Goddard, B. D. Lodam, S. O. Ajayi and M. J. Campbell, *J. Chem. Soc. (A)*, 1969, 506.
27. N. Tanaka, K. Ebata and T. Murayama, *Bull. Chem. Soc. Japan*, 1962, **35**, 124.
28. L. Ciavatta and M. Grimaldi, *Inorg. Chim. Acta*, 1970, **4**, 312.
29. S. Ahrland and L. Kullberg, *Acta Chem. Scand.*, 1971, **25**, 3692.
30. K. B. Yatsimirskii and B. D. Tukhlov, *Zh. Obshch. Khim.*, 1956, **26**, 356.
31. R. E. Smith and A. E. Martell, *Critical Stability Constants*, Vol. 2, p. 36. Plenum Press, New York, 1975.
32. J. I. Watters, J. G. Mason and O. E. Schupp, *J. Am. Chem. Soc.*, 1956, **78**, 5782.
33. J. Kotek, H. Klierová, J. Doležal and M. Kopanica, *J. Electroanal. Chem.*, 1971, **31**, 451.
34. D. Sužnjević, J. Doležal and M. Kopanica, *ibid.*, 1969, **20**, 279.
35. E. Casassas and M. Esteban, *Electrochim. Acta*, 1986, **31**, 327 and unpublished work.
36. E. Casassas, M. Esteban and C. Ariño, *ibid.*, 1986, **31**, in the press, and unpublished work.
37. A. Napoli, *Talanta*, 1980, **27**, 825.

FLUORIMETRIC AND ABSORPTIOMETRIC DETERMINATION OF DISSOCIATION CONSTANTS AND CHROMOGENIC REACTIONS OF BENZYL 2-PYRIDYL KETONE 2-QUINOLYLHYDRAZONE

F. GARCIA SANCHEZ and C. CRUCES BLANCO

Department of Analytical Chemistry, Faculty of Sciences, The University, 29071 Málaga, Spain

J. MEDINILLA

Hygiene and Work Safety Centre, Granada, Spain

(Received 21 March 1986. Accepted 22 May 1986)

Summary—The dissociation constants in the ground state of benzyl 2-pyridyl ketone 2-quinolyldihydrazone (BPKQH) have been determined fluorimetrically and spectrophotometrically in aqueous ethanol medium. The pK_a values of this compound in the excited state have also been established. The analytical properties of the reagent and its chromogenic reactions with some metal ions were studied.

A detailed study of the effects of polarity on the electronic absorption and fluorescence spectra of compounds and the determination of the acidity constants in the ground and excited state can provide information as to the usefulness of the analytical reagents for spectrophotometric and spectrofluorimetric methods.¹⁻³

Spectrophotometry is a simple, clean and accurate method for determination of dissociation constants of organic ligands, but when proton loss or gain results in little rearrangement of the ligand structure, the electronic spectra scarcely change. Generally, the same is true with regard to fluorimetry, but spectral changes may also result if proton gain or loss promotes ligand rigidity, or changes the solvation of the ligand.

Several complications can arise from the dependence of fluorescence emission on the effect of pH changes on both excited-state and ground-state behaviour.^{4,5}

In this paper, we report on the effect of pH on the behaviour of BPKQH in the ground and excited state, studied by spectrophotometry and spectrofluorimetry.

EXPERIMENTAL

Reagents

Benzyl 2-pyridyl ketone 2-quinolyldihydrazone (BPKQH) was synthesized by the procedure of Katiyar and Tandon,⁶ by heating equimolar amounts of benzyl 2-pyridyl ketone and 2-quinolyldihydrazine in ethanol, and recrystallized from 50% aqueous ethanol. The product melted at 140–141°. It was characterized by elemental analysis and its mass and infrared spectra. The elemental analysis gave C 78.0%, H 5.4%, N 16.6%; required: C 78.2%, H 5.2%, N 16.6%.

Instrumentation

A Beckman Acta III spectrophotometer equipped with

1-cm quartz cells was used for spectrophotometric measurements. A Perkin-Elmer MPF-43A spectrofluorimeter equipped with an Osram XBO 150-W xenon lamp was used. An ultrathermostatic Frigiterm S-382 bath was used for temperature control. Crison Digit 501 and Beckman Spandomatic SS pH-meters were used.

Procedures

Reaction with metal ions. In a 14 × 160 mm test-tube, 1 ml of ethanol, 3 drops of 0.1% ethanolic solution of the reagent and 2 drops of a 1-g/l. solution of the metal ion were mixed, diluted to 2 ml with demineralized water, and adjusted to the desired pH by addition of dilute hydrochloric acid or sodium hydroxide solution.

Acidity constants. The pK_a values were determined spectrophotometrically with $2 \times 10^{-5}M$ BPKQH in ethanol-water (60:40 v/v) medium. For spectrofluorimetric measurements, a $1 \times 10^{-4}M$ solution of the reagent in 40:60 v/v ethanol-water was used. In each photometric and fluorimetric titration, the pH was adjusted by adding small amounts of dilute sodium hydroxide and hydrochloric acid. A constant ionic strength medium was ensured by adding 10 ml of 1M potassium nitrate to the solutions. All measurements were made at 25°.

RESULTS AND DISCUSSION

Most sensitive reactions of BPKQH

BPKQH has very little selectivity, giving numerous chromogenic reactions over a wide pH range. Its behaviour is very similar to that of other *N*-heterocyclic hydrazones; it acts as a bi- or terdentate chelating agent, depending on the acidity of the medium. In some cases, chelation is accompanied by elimination of the imine proton of the ligand. (The dissociable imine hydrogen atom of the hydrazone molecule is too far from the co-ordination site to be involved in the chelation.)

However, the loss of a hydrogen atom and the redistribution of the electron-pair leads to a stable

resonant system which is independent of the type of metal ion which forms the chelate. BPKQH can lose its imine proton in strongly alkaline medium ($> \text{pH } 12$) or at lower pH during chelation. Under these conditions, many metal ions form complexes with the anionic form of the ligand, and these are sparingly soluble in water, but soluble when the medium contains a sufficient percentage of ethanol or other solvent of low dielectric constant.

Although BPKQH forms complexes with numerous ions, most of them are yellow or orange-yellow. However, only seven are fluorogenic, those of Zn,⁷ Cd,⁸ Ga, In, Sc, Y, and Zr. Because the polarization capacity of the metal ion contributes little to the general resonance structure, only slight differences in colour are observed between the different fluorescent chelates; all give yellow fluorescence over a wide range of pH.

The most important chromogenic reactions are shown in Fig. 1. The characteristics of these complexes, formed with an excess of reagent ($5 \times 10^{-5} M$) and an ethanol content of 50%, are summarized in Table 1. The high molar absorptivities and the colour contrast of some reactions mean that BPKQH is suitable for use in photometric methods.

Acidity constants in the ground and excited states

Since BPKQH is insoluble in water but soluble in aqueous ethanol, the ground state $\text{p}K_a$ values were determined by absorptiometric and fluorimetric measurements in various aqueous ethanol media.

The effect of activity on the electronic spectra of organic molecules has been widely studied. When the activity of the medium is sufficient to cause protonation of a site in the molecule, another species with different properties and electronic structure is obtained. The protonation of free electron-pairs in a molecule causes the excited state to be stabilised with respect to the ground state, resulting in a red shift in the absorption spectrum.

The ground-state dissociation constants of BPKQH in 60% v/v ethanol-water were determined by the methods of Stenström and Goldsmith⁹ and Sommer.¹⁰ Table 2 shows the results.

From the spectrophotometric measurements, only two protonation constants could be determined. However, three $\text{p}K_a$ values were expected, for the pyridine, quinoline and imine hydrogen atoms. As expected for an *N*-heterocyclic base, protonation of the free base causes a bathochromic shift, attributable to the intramolecular hydrogen bond between the azomethine nitrogen atom and the pyridinium N—H group, which increases electron migration and molecular rigidity.

The problem of determining $\text{p}K_3$ is solved by use of fluorescence spectrometry, which can be applied in the same way as absorption spectrometry for determination of dissociation constant of acids and bases in the ground state, even though fluorimetry is a technique mainly concerned with measurements of energy transfer of molecules in the first excited-singlet state.

In most cases, the method is more accurate than spectrophotometry, because of the better separation between the emission bands of the conjugate acid and base.

The bathochromic shift expected for this kind of molecule is indeed observed in the fluorescence spectra when the acidity of the medium is decreased. A detailed fluorimetric study of a $10^{-4} M$ solution of BPKQH in 40% v/v ethanol-water showed the pH-dependence of the spectra.

To prevent any possibility of proton exchange in the excited state (which could result in wrong $\text{p}K_a$ values) the basic form ($\lambda_{\text{exc}} = 465 \text{ nm}$) was excited selectively. However, the experiments designed to determine $\text{p}K_a^*$ by selective excitation of the acid and basic forms ($\lambda_{\text{exc}} = 305 \text{ nm}$ and $\lambda_{\text{exc}} = 420 \text{ nm}$, respectively) showed that no proton transfer took place during the lifetime of the excited state.

Table 1. Most sensitive reactions of BPKQH

Metal ion	Concentration, M	pH	λ_{max} , nm	$\Delta\lambda^*$, nm	ϵ_{max} , $10^4 \text{ l. mole}^{-1} \cdot \text{cm}^{-1}$	Colour
Co(II)	1×10^{-5}	6.0	512	137	6.1	red
Ni(II)	1×10^{-5}	10.2	480	105	8.2	pink
Hg(II)	8×10^{-6}	9.0	475	100	6.2	yellow-orange
Cu(II)	1.5×10^{-5}	7.3	500	125	5.8	yellow
Cu(II)	1.5×10^{-5}	10.7	475	100	7.0	orange

$$^* \Delta\lambda = \lambda_{\text{max}(\text{complex})} - \lambda_{\text{max}(\text{reagent})}$$

Table 2. $\text{p}K_a$ values of BPKQH by spectrophotometric methods

Method	$\text{p}K_a$	λ , nm					Mean value \pm std. devn.
		315	345	365	375	390	
Stenström and Goldsmith	$\text{p}K_1$	1.43	1.47	1.39	1.52	1.45	1.45 ± 0.04
	$\text{p}K_2$	4.87	4.85	4.83	4.86	4.83	4.85 ± 0.01
Sommer	$\text{p}K_1$	1.43	1.46	1.52	1.62	1.45	1.49 ± 0.07
	$\text{p}K_2$	4.88	4.79	4.83	4.81	4.70	4.80 ± 0.60

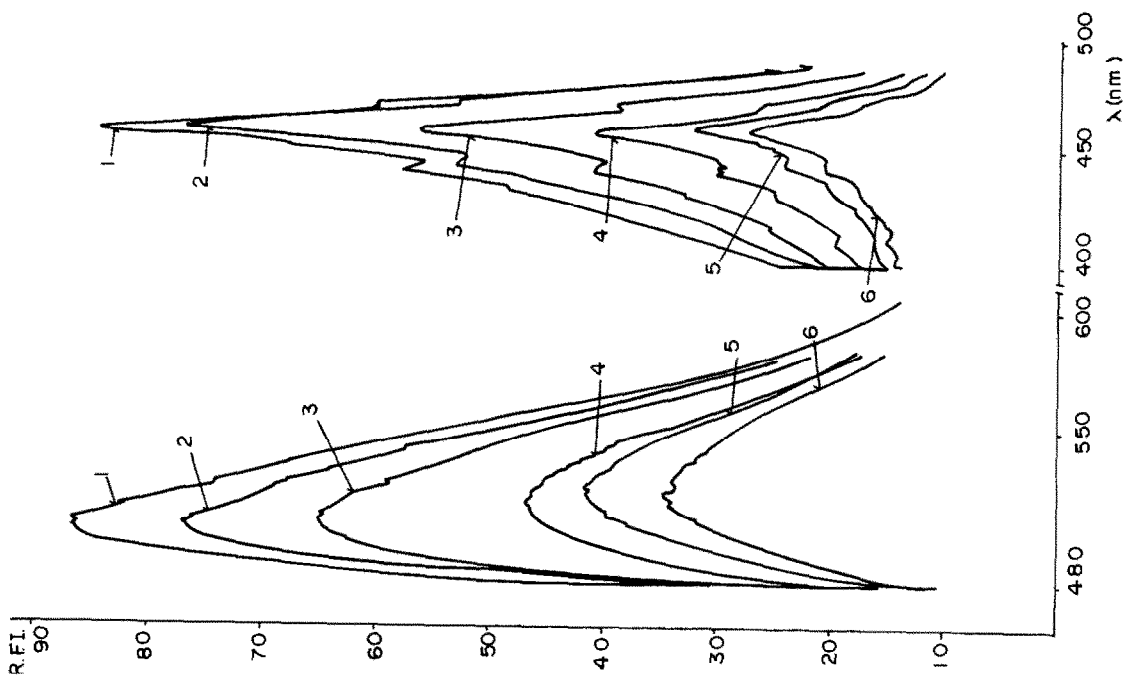


Fig. 2. Fluorescence excitation (B) and emission (A) spectra of BPKQH in 40% ethanol-water ($I = 0.1M$) at 1. pH 7.27; 2. pH 8.30; 3. pH 9.34; 4. pH 10.13; 5. pH 10.71; 6. pH 11.37.

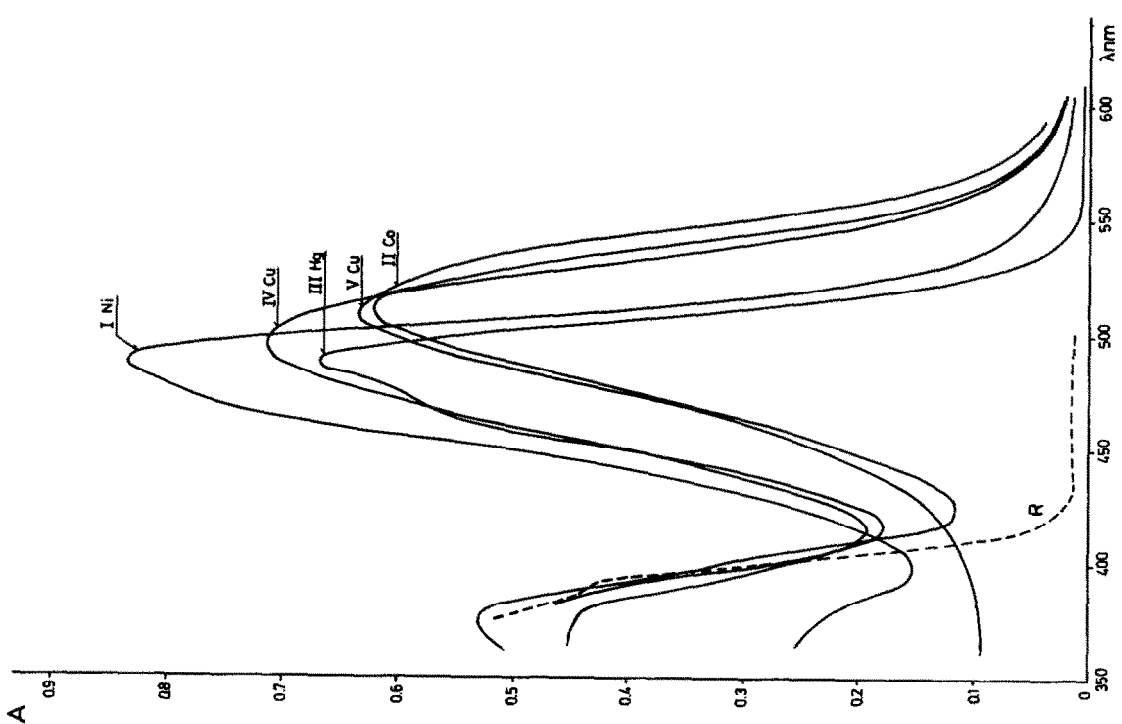


Fig. 1. Absorption spectra of the metal complexes in 50% ethanol-water ($I = 0.1M$), $[BPKQH] = 5 \times 10^{-5}M$; $[Co]$, $[Ni]$, $[Cu] = 1 \times 10^{-5}M$; $[Hg] = 8 \times 10^{-6}M$.

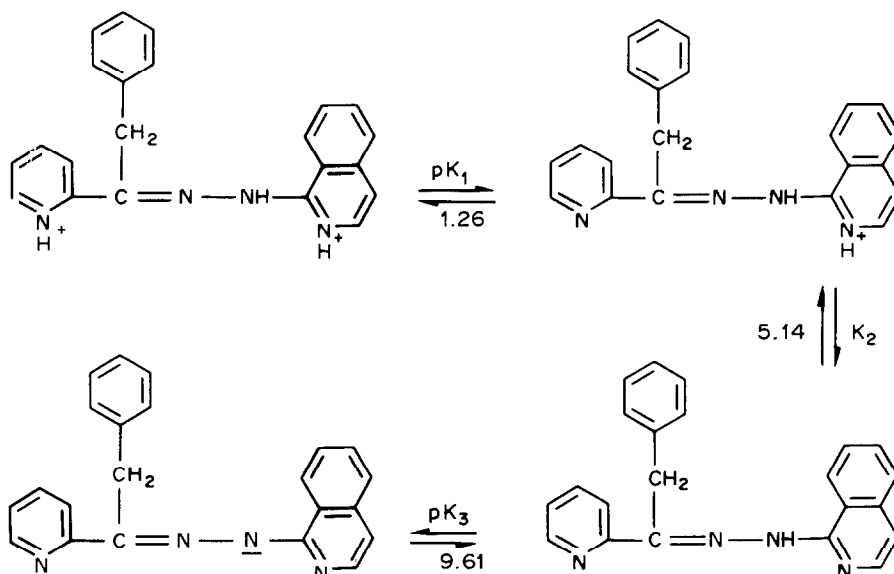


Fig. 3. The dissociation scheme for BPKQH.

The excitation and emission spectra at various pH values in the neighbourhood of pK_3 are shown in Fig. 2.

The fluorescence emission continues to increase as the pH is decreased from 12 to 4, corresponding to protonation of both heterocyclic nitrogen atoms. Also, the expected bathochromic shift of the emission spectrum is observed (~ 10 nm). Below pH 4, the fluorescence is quenched, as the result of protonation of an azomethine nitrogen atom, which is favoured by a medium of low polarity.

The protonation equilibria of BPKQH are given in Fig. 3. Three pK_a values for BPKQH ($pK_1 = 1.26 \pm 0.05$; $pK_2 = 5.14 \pm 0.08$ and $pK_3 = 9.61 \pm 0.17$) were calculated from five points of the fluorimetric titration by application of the equation recommended by Rosenberg *et al.*⁴ The pK_a values determined by the two techniques are in good agreement, and the pK_3 value is as expected.

Thus, fluorimetry appears to be a viable method for the determination of pK_a values of the electronic ground state with an accuracy as good as that of absorption spectrophotometry.

Table 3. pK_a values of BPKQH by Förster-cycle calculations

	Fluorimetry	Absorptiometry
pK_1^*	-0.92	-0.71
pK_2^*	2.96	2.64
pK_3^*	7.43	—

To determine the excited state pK^* values, since no proton transfer occurred during the excited-state lifetime, Förster cycle calculations¹¹ were used. The results are given in Table 3. The values are lower than those for the ground state, which indicates that the compound is a weaker base in the excited state than in the ground state.

It should be stressed however, that the pK_a values reported are all for apparent constants, valid only for the media used for the determinations, no corrections having been applied for the effect of the media on the pH measurements.

REFERENCES

1. M. Román Ceba, C. Cruces Blanco and F. García Sánchez, *J. Photochem.*, 1985, **30**, 353.
2. J. J. Laserna, A. Navas and F. García Sánchez, *J. Luminescence*, 1982, **26**, 427.
3. A. L. Ramos Rubio, C. Cruces Blanco and F. García Sánchez, *Z. Anal. Chem.*, 1986, **323**, 153.
4. L. S. Rosenberg, J. Simons and S. G. Schulman, *Talanta*, 1979, **26**, 867.
5. S. G. Schulman, A. C. Capomacchia and M. S. Rietta, *Anal. Chim. Acta*, 1971, **56**, 91.
6. S. S. Katiyar and S. N. Tandon, *Talanta*, 1964, **11**, 892.
7. M. Santiago, A. Navas, J. J. Laserna and F. García Sánchez, *Mikrochim. Acta*, 1983 **II**, 197.
8. F. García Sánchez, A. Navas and M. Santiago, *Anal. Chim. Acta*, 1985, **167**, 217.
9. W. Stenström and N. Goldsmith, *J. Phys. Chem.*, 1926, **30**, 1683.
10. L. Sommer, *Folia Fac. Sci. Nat. Univ. Purkin. Brno*, 1964, Part 1, 1.
11. T. Förster, *Z. Elektrochem.*, 1950, **54**, 42, 531.

ANNOTATION

DETERMINATION OF STABILITY CONSTANTS OF COMPLEXES FROM THE TITRATION CURVE BY THE MAXIMUM LIKELIHOOD PRINCIPLE

TADEUSZ HOFMAN and MAŁGORZATA KRZYŻANOWSKA

Warsaw Technical University, Faculty of Chemistry, Noakowskiego 3, 00-664 Warsaw, Poland

(Received 25 June 1985. Revised 12 May 1986. Accepted 4 June 1986)

Summary—The numerical methods used to determine stability constants from titration data are analysed. A new method based on the maximum likelihood principle is proposed.

Calculation of stability constants from titration data by a fitting procedure is a widespread technique, and numerous algorithms are available.¹⁻¹⁰ Unfortunately, they use many simplifying assumptions, which although often necessary from the computational point of view, influence the results in an unpredictable way. Since there has been no systematic discussion of these methods, the choice of a particular algorithm is rather arbitrary. The aim of this paper is to review the reported methods, emphasizing both statistical rigour and numerical convenience. It is shown that the conclusions drawn from this analysis can be helpful in creation of new and more accurate algorithms.

Recently, after the first draft of this paper had been prepared, May *et al.*¹¹ published an article discussing the validity of simplifications of models for determination of stability constants. Although their paper takes into consideration more factors than ours does (electrode equation, electrode selectivity and liquid-junction potential), their analysis was only qualitative and totally omitted the statistical aspects of the problem.

DETERMINATION OF STABILITY CONSTANTS

Let an experiment give a set of values of measured parameters designated as the vector \mathbf{r} for each measurement (experimental point). If these parameters are inter-related by a known function (model equation F_m), *i.e.*,

$$F_m(\mathbf{r}, \mathbf{K}) = 0 \quad (1)$$

the vector of unknown model constants \mathbf{K} may be determined by an algorithm usually referred to as the curve-fitting technique. Note that since equation (1) concerns the true values of measured parameters, the sign $\hat{}$ denoting the experimental value is omitted.

In the titrimetric determination of stability constants, vector \mathbf{r} contains the volume of added titrant, initial analytical concentrations of the reactants, free concentration of at least one component (usually the

hydrogen ion), and the initial volume of the system, while \mathbf{K} becomes a vector of the stability constants.

Any fully developed method for finding the model constants \mathbf{K} must specify the following, practically independent, items: (i) definition of the model equation; (ii) form of the objective function, *i.e.*, the function to be minimized to determine the values of the parameters sought, and (iii) the optimization algorithm used to find this minimum. Derivation of the stability constants will be further discussed according to this scheme.

Model equation

The model equation results from the mass balance for each reactant. If it is assumed that a system contains n reactants and m complexes, and the initial analytical concentrations of the reactants (c_i^0) are known, their final analytical concentrations (c_i^*) can be expressed as

$$c_i^* = c_i^0 V^0 / (V^0 + V) = a_i / f_i + \sum_{j=1}^m (v_{ij} / f_j^c) K_j \prod_{k=1}^n a_k^{v_{kj}}; \quad i = 1, 2, \dots, n \quad (2)$$

where a_i , f_i designate the activity and activity coefficient, respectively, for either a reactant or a complex (indicated by superscript c), v_{ij} is the stoichiometric coefficient of component i in complex j ; V^0 and V denote the initial volume of the system and the volume of titrant added, and the stability constant of the j th complex (K_j) is defined as

$$K_j = a_j^c / \prod_{k=1}^n a_k^{v_{kj}} \quad (3)$$

During the titration, the free concentration of at least one component ($c_i = a_i / f_i$) must be monitored. Usually it is the concentration of hydrogen ions which is measured potentiometrically for each experimental point. In that case the analytical concentration of protons (c_{H}^*) may be calculated from

$$c_{\text{H}}^* = (V^0 c_{\text{H}}^0 - V c_{\text{OH}}) / (V^0 + V) + K_w / a_{\text{H}} f_{\text{OH}} \quad (4)$$

For clarity, subscripts H and OH are used to designate protons and hydroxide ions: K_w denotes the ionic product of water and c_{OH} is the concentration of titrant (a strong base). The initial analytical concentration of hydrogen ions (c_H^0) refers to the sum of both free and bound but displaceable protons and is the sum of those connected with the ligand and those supplied by any strong acid added before the titration. Combining equations (2) and (4) for $i = H$ leads to

$$V = \frac{V^0(c_H^0 - c_H^* + K_w/a_H f_{OH})}{(c_{OH} + c_H^* - K_w/a_H f_{OH})} \quad (5)$$

where c_H^* is given by

$$c_H^* = a_H/f_H + \sum_{j=1}^m (v_{Hj}/f_j^c) K_j a_H^{v_j} \prod_{k=2}^n a_k^{v_k} \quad (6)$$

The activities a_k of the remaining reactants may be obtained by solving equation (2) for $k = 2, 3, \dots, n$.

The relations (2), (5) and (6) constitute the full model equation which describes the titration curve. Although the expressions derived are strictly rigorous, some simplifications are necessary to make calculation of the activity coefficients possible. The Debye-Hückel equation is commonly used for this purpose, *i.e.*,

$$-\log_{10} f_i = Az^2 I^{1/2} / (1 + Ba_i' I^{1/2}) \quad (7)$$

where I and z denote the ionic strength and the ionic charge, respectively, and A , B and a_i' are constants dependent on the temperature and the solvent properties. At 25° and for water as the solvent, equation (7) becomes

$$-\log_{10} f_i = 0.512z^2 I^{1/2} / (1 + 1.6I^{1/2}) \quad (8)$$

Objective function

Since the minimum of the objective function determines the values of the desired model constants, it is desirable to define the function in a way which agrees with the principles of statistics. In particular, the optimization should give the most probable values of the unknown constants. According to the maximum likelihood principle (MLP),^{12,13} when the experimental errors are normally distributed and there are no systematic deviations, the objective function which ensures derivation of the most credible constants can be expressed as

$$F(\mathbf{K}) = \sum_i (\hat{\mathbf{f}} - \mathbf{r})_i^T \mathbf{V}_i^{-1} (\hat{\mathbf{f}} - \mathbf{r})_i \quad (9)$$

Summation is performed over all experimental points, $\hat{\mathbf{f}}$ and \mathbf{r} refer to the vectors of the measured and estimated (or calculated) values of the parameters and \mathbf{V}^{-1} is the inverse of the variance-covariance matrix \mathbf{V} , *i.e.*, the matrix which contains the covariances of the measured variables:

$$V_{ij} = \text{cov}(r_i, r_j) \quad (10)$$

When there is no coupling between determinations of

different parameters, the variance-covariance matrix is diagonal.

From the numerical point of view, finding the minimum of function (9) is rather complicated. The model equations are not used directly but are included as the constraints of equation (9), and the estimated values of parameters are treated as additional adjustable values. Therefore a few simplifications which make the calculations less tedious are widely applied. In the first simplification (version A1) measured variables are divided into two groups—dependent (\mathbf{r}) and independent (\mathbf{r}^*). Only the residuals between the former are considered in equation (9). The independent variables are fixed and equal to their measured values, but their experimental errors are taken into account by the additional term in calculating the covariances for the dependent parameters. Since this is done by means of the error-propagation law, the validity of the following first-order approximation must be assumed¹⁴

$$\text{cov}(r_i, r_j) = \sum_k \left(\frac{\partial r_i}{\partial r_k^*} \right) \left(\frac{\partial r_j}{\partial r_k^*} \right) (\delta r_k^*)^2 \quad \text{for } i \neq j \quad (11a)$$

and

$$\text{cov}(r_i, r_i) = (\delta r_i)^2 + \sum_k \left(\frac{\partial r_i}{\partial r_k^*} \right)^2 (\delta r_k^*)^2 \quad (11b)$$

where δr_j denotes the estimated experimental error of parameter r_j and the summation is taken over all independent variables. The main purpose of such a reformulation is to obtain the residuals ($\hat{\mathbf{f}} - \mathbf{r}$) in equation (9) merely as a function of the model constants (\mathbf{K}) and the measured values of the parameters. Thus searching for the minimum of function (9) may be limited to only the determination of the stability constants. The parameters \mathbf{r} do not have to be directly measurable, but they must be functions of the dependent variables. If only one dependent parameter is selected, this version of the MLP is equivalent to the weighted least-squares method with the weights calculated according to the error propagation law as given by equation (11b). The second simplification (version A2), still keeping the division into dependent and independent parameters, considerably eases calculation of the variance-covariance matrix. Either the matrix is estimated from the experimental uncertainties of the dependent variables only or it is assumed to equal the identity matrix. In the latter case the MLP reduces to the unweighted least-squares method.

Optimization technique

Generally, each correctly adopted optimization procedure should give practically the same values of the stability constants if the same objective functions are minimized. This means that the definition of the objective function (with the model equation included) is the only characteristic feature of a well-defined method. Small differences between results obtained by means of various optimization algorithms are

usually caused both by the different convergence criteria used and different ways of approaching the minima. However, when the current values of model parameters converge to the minimum while optimization continues, the residuals between estimates resulting from the different methods gradually disappear. Thus, in the limit, all optimization techniques become equivalent from the point of view of the final results provided. With carefully adjusted values of the convergence parameters the differences between algorithms may be meaningless even for a finite number of iterations. However, for comparison of various methods of determining the stability constants the same optimization procedures should be used if small differences are to be monitored.

The optimization techniques adopted for stability-constant determinations are listed in Table 1. The methods which use the gradient to define the search direction must calculate its values either analytically or numerically. Since the latter procedure assumes certain simplifications which may influence the final result, the accuracy of the gradient estimation will be discussed in the next section of this paper.

ANALYSIS OF EXISTING METHODS

Brief information concerning the methods reported in the literature is collected in Table 1. The validity of each method depends on the simplifications involved. These may be grouped as follows: (i) those accepted during creation of the objective function, (ii) those in the approximations used in the activity coefficient calculation, and (iii) those making possible numerical estimation of the gradient.

It must be emphasized that from the point of view

of the maximum likelihood principle, almost all methods reported may be regarded as oversimplifications. Although a few of them do not exclude the possibility of using weighting, the calculations presented in the original papers follow the unweighted least-squares method. It seems that only Tobias and Yasuda,³ and Perrin and Sayce⁴ used weights calculated according to the error-propagation law, but the relevant information in these papers is rather scanty.

It appears that there is no significant difference between selection of c_{H^+} or V as a dependent variable. Both parameters are inter-related in a simple way through equation (4). Choosing the analytical concentrations of all reactants (LEAST, MINQUAD) as the dependent variables may have some limitations. Since the volume of added titrant (V) is usually very small in comparison with the initial volume of the system (V°), the analytical concentration of a reactant other than hydrogen ions is practically constant and equal to its initial value, as equation (2) clearly states. Despite this, the algorithms mentioned provide estimated (calculated) values of these parameters for each experimental point, which disagrees with the requirement of their constancy. Moreover, the additional computational effort resulting from an increase in the number of adjustable parameters is not negligible.

Generally, the problem of handling the measurable parameters which are fixed for all experimental points (initial concentrations, concentration of titrant and the strong acid, and the initial volume of a system) is rather complicated. Since they are not strictly accurate, owing to experimental errors, they introduce a kind of bias which gives the deviations of the dependent variables a partly systematic character.⁷

Table 1. Comparison of the reported stability-constant derivation methods

Method	Dependent variables	Adjustable parameters	Activity coefficients	Gradient calculation	Optimization technique
Sillén <i>et al.</i> ^{1,2}					
LETAGROP	c_{H^+} or E	K	equal to 1	not used	"pit-mapping"
Tobias and Yasuda ³	c_{H^+}	K	equal to 1	numerical	Gauss-Newton
Perrin and Sayce ⁴					
GAUSS	c_{H^+}	K	fixed for H^+ , otherwise equal to 1	numerical	Gauss-Newton
Sayce ⁵					
SCOGS	V	K	fixed for H^+ , otherwise equal to 1	numerical	Gauss-Newton
Kaden and Zuberbühler ⁶					
VARIAT	V	K	equal to 1	not used	direct-search
Sabatini and Vacca ⁷					
LEAST	c_i^* or $c_i^*/c_i^{*\text{calc}}$ $i = 1, 2, \dots, n$	K , c_i $i = 2, 3, \dots, n$	equal to 1	analytical	Gauss-Newton or Newton-Raphson
Gans and Vacca ⁹	c_{H^+}	K	equal to 1	numerical	Davidon-Fletcher-Powell
Sabatini <i>et al.</i> ⁹	c_i^* $i = 1, 2, \dots, n$	K , c_i $i = 2, 3, \dots, n$	equal to 1	analytical	Gauss-Newton with optimization of the shifts
MINQUAD					
Gampp <i>et al.</i> ¹⁰					
MARFIT	V	K	not defined	not defined	Marquardt

Note: $c_i, c_i^*, c_i^{*\text{calc}}$ —free, analytical, and calculated analytical concentration of component i ; E —potential of electrode; **K**—vector of the stability constants; V —volume of titrant.

Table 2. The absolute mean deviations between calculated and true values of the stability constants pK^*

Set of data	Constant	Simplifications used			Assumed square roots of variances for generated errors (σ)
		Ionic strength constant and equal weights (A)	Equal weights (B)	Proposed algorithm (C)	
1	pK_{LM}	0.11	0.04	0.03	$\sigma_V = 0.005$ ml
	pK_{LMH}	0.19	0.08	0.05	$\sigma_{pH} = 0.01$
2	pK_{LM}	0.15	0.13	0.09	$\sigma_V = 0.015$ ml
	pK_{LMH}	0.31	0.24	0.15	$\sigma_{pH} = 0.03$
3	pK_{LM}	0.14	0.06	0.05	$\sigma_V = 0.005$ ml, $\sigma_{pH} = 0.01$
	pK_{LMH}	0.32	0.15	0.14	$\sigma_V = 0.08$ ml; for all initial concentrations $\sigma_x = 0.5\%x$; ($x = c_L^0, c_M^0, c_{OH}$)

$$* \frac{1}{n} \sum_{i=1}^n |pK_i^{\text{calc}} - pK_i^{\text{true}}|; n = 8 \text{ for the first two sets of data and 3 for the last.}$$

Brauner *et al.*² take into account the possibility of treating them as additional adjustable parameters but there are too many of them to make such a procedure quite safe. It seems therefore that the requirements concerning accuracy of these parameters should be very severe. Another option is to use the MLP in a basic version which guarantees rigorous statistical treatment for this type of variables but also considerably increases the computation time.

No method uses equation (7) to calculate activity coefficients. They are assumed to be unity for all species except hydrogen ions, for which a constant value corresponding to the average ionic strength of the system is sometimes selected. The stability constants derived in this way are related to the thermodynamic constants through multiplication by a coefficient which may be regarded as constant provided that the ionic strength does not change. The ionic strength must always be explicitly specified, for the constants determined to have real physical meaning. The variation of ionic strength during the titration is not usually taken into consideration.

There are at least four methods for calculating the gradient by numerical differentiation. Although it has been suggested that the method may influence the final results,^{7,9} no convincing proof was presented.

NEW ALGORITHM AND ITS APPLICATIONS

A new algorithm has been developed which takes into account the factors neglected up to now. It is based on the following assumptions.

(i) The validity of the error-propagation law is accepted, which makes possible an application of the MLP in version A1. The rigorous use of the MLP is rejected because of its relative numerical complexity.

(ii) The titrant volumes (V) are chosen as a dependent variable with their values calculated by equations (2), (5) and (6).

(iii) The activity coefficients are expressed by equation (7).

Since the program* applied can use either the usual least-squares method or the simpler formulae for the activity coefficients, an attempt was made to estimate the accuracy of the method and compare it with that obtained by means of simpler approaches. For this purpose simulated data were generated which closely corresponded to those for a real system for titration of EDTA and Zn^{2+} with a strong base.¹⁵ The complexes existing in solution were assumed to be LH^{3-} , LH_2^{2-} , LM^{2-} , LMH^{-} (L, H, M denote ligand, proton and metal) with the true values of their stability constants (pK) equal to 10, 16.5, 15 and 18, respectively; the initial analytical concentrations of ligand, metal and hydrogen ions were set at 0.002M, 0.0021M and 0.008M, while the concentration of titrant, initial total volume and ionic strength were 0.2M, 50 ml and 0.1, respectively.

For 50 equispaced pH values between 2 and 5, the corresponding titrant volumes were calculated with the help of equations (2) and (5)–(7). As the last step in creation of the simulated data, the assumed and calculated (true) values of measurable parameters were slightly changed by adding "errors", *i.e.*, randomly generated numbers normally distributed with a mean value of zero and variance corresponding to the expected experimental errors.

Three versions of the method were used (A–C), differing in the extent of the simplifications applied, and based on the following assumptions: (A) constant ionic strength and equality of weighting for all experimental points; (B) only equality of weighting; (C) the weightings were calculated according to the error propagation law, *viz.* by the new algorithm as defined at the beginning of this section. The method was used to determine the stability constants of two complexes, namely LM^{2-} and LMH^{-} , the true values of the protonation constants being assumed to be known. The comparison between the calculated and assumed (*i.e.*, true) values of the stability constants is a reliable measure of the accuracy of the method and the validity of

*Program SCOM written in FORTRAN is available on request from the authors.

the simplifications made. The results are listed in Table 2.

For the first two sets of data the experimental errors were assumed to concern only the titrant volumes and hydrogen-ion activities (pH). In the third, the remaining parameters were also changed in accordance with the expected experimental errors. However, for this last case the assumption (necessary in MLP) that systematic deviations are absent, was violated. The number of data subsets (corresponding to the complete experiments) and stability-constant determinations were 8 for the first two data-sets and 3 for the third.

Discussion

The calculations performed for one simple system (Table 2) indicate the importance of the ionic strength effect. The accuracy obtained in version B may be sufficient, but distinctly better results are obtained if a statistically more rigorous algorithm is used. The errors resulting from use of the proposed method should be attributed to the simplification implying validity of the error propagation law and to the approximate iterative solution of the mass-balance equation (2). The extent of the deviations shown in Table 2 suggests that the actual accuracies of the stability-constant values reported in the literature are considerably lower than those claimed by the authors. Since virtually all commonly used methods of determining the stability constants are equivalent to version A of the method, the accuracies associated with them are expected to be of the same order as those indicated by the first column of Table 2. The calculations performed with the third set of data show a significant influence of the accuracy of the parameters fixed for each experimental point (V° , c_i° , c_{OH}) on the credibility of the final results. In this case method C offers no improvement of accuracy over that given by version B, and we attribute this to the already mentioned violation of the assumptions of the MLP. This result may suggest that adaptation of the full MLP to determine values of the stability constants is desirable.

Two optimization techniques were used to find the minima of the objective function, namely the Marquardt¹⁶ and the Rosenbrock¹⁷ methods. The former utilizes a gradient which may be estimated numerically or calculated from the rigorous analytical expression, while the latter is a direct-search technique. It should be emphasized that even if calculation of the objective function includes solution of the mass-balance equations, the gradient can be derived analytically through solution of a linear

system of equations. Unfortunately, this system is ill-conditioned and special algorithms to improve its solution may be necessary. It was found, however, that the accuracy of the gradient numerical estimation was quite satisfactory. The minima obtained by the Marquardt method were always very close to those obtained by the Rosenbrock algorithm. Nevertheless, it can be recommended to use a fast gradient optimization method first, and after reaching a minimum to employ a direct-search technique, which may eventually slightly improve the optimal value.

CONCLUSIONS

It has been shown that the computational methods used to evaluate stability constants from titration data suffer from the simplifying assumptions imposed. In particular, the assumption that the ionic strength is kept constant is found to be unacceptable. This conclusion agrees with the analysis published recently by May *et al.*¹¹ On the other hand, suggestions that the errors associated with numerical gradient estimation may considerably influence the accuracy of the results, are not confirmed.

A new, more statistically rigorous, algorithm has been defined. Its superiority to the older approaches is shown by calculations performed with simulated data.

REFERENCES

1. N. Ingri and L. G. Sillén, *Acta Chem. Scand.*, 1962, **16**, 173.
2. P. Brauner, L. G. Sillén and K. Whiteker, *Arkiv Kemi*, 1969, **31**, 365.
3. R. S. Tobias and M. Yasuda, *Inorg. Chem.*, 1963, **2**, 1307.
4. D. D. Perrin and I. G. Sayce, *J. Chem. Soc. A*, 1967, 82.
5. I. G. Sayce, *Talanta*, 1968, **15**, 1397.
6. T. Kaden and A. Zuberbühler, *ibid.*, 1971, **18**, 61.
7. A. Sabatini and A. Vacca, *J. Chem. Soc., Dalton Trans.*, 1972, 1693.
8. P. Gans and A. Vacca, *Talanta*, 1974, **21**, 45.
9. A. Sabatini, A. Vacca and P. Gans, *ibid.*, 1974, **21**, 53.
10. H. Gampp, M. Maeder, A. D. Zuberbühler and T. A. Kaden, *ibid.*, 1980, **27**, 513.
11. P. M. May, K. Murray and D. R. Williams, *ibid.*, 1985, **32**, 483.
12. R. A. Fisher, *Proc. Cambridge Phil. Soc.*, 1925, **22**, 700.
13. S. Hald, *Statistical Theory with Engineering Applications*, Wiley, New York, 1952.
14. S. Kemény, J. Manczinger, S. Skjold-Jørgensen and K. Toth, *A.I.Ch.E. J.*, 1982, **28**, 20.
15. G. Anderegg, *Critical Survey of Stability Constants of EDTA Complexes*, IUPAC Chemical Series, No. 14, 1975.
16. D. W. Marquardt, *J. Soc. Ind. Appl. Math.*, 1963, **11**, 431.
17. H. H. Rosenbrock, *Computer J.*, 1960, **3**, 175.

APPLICATION OF MODIFIED NORMAL PULSE POLAROGRAPHY AND ITS DIFFERENTIAL MODE TO ALKALINE-EARTH METAL IONS IN ACID SOLUTIONS

MINORU HARA and NOBORU NOMURA

Faculty of Education, Toyama University, Gofuku, Toyama 930, Japan

(Received 7 May 1986. Accepted 11 July 1986)

Summary—The simultaneous determination of alkaline-earth metal ions in acid solution was studied by modified normal pulse polarography. Well-defined waves were recorded for calcium, strontium and barium, but no limiting current was found for magnesium, because of its very negative reduction potential. The differential mode of this method gives peak-type polarograms and is useful for the simultaneous determination of species for which the half-wave potentials lie close together. The interference of dissolved oxygen was eliminated by the use of tetramethylammonium chloride as a supporting electrolyte.

The polarography of the alkaline-earth metal ions in aqueous solution has been the subject of investigation since the introduction of the technique.¹ The d.c. polarographic wave of calcium has a maximum which is not eliminated by any suppressor. Magnesium gives a large reduction current, but shows no limiting current. In a.c. polarography, the peak current for barium is proportional to concentration, but the calibration curve for calcium is concave.² Babrowski *et al.* reported that barium, strontium and calcium could be determined by oscillopolarography if a calibration-graph technique was used.³

In previous papers⁴⁻⁷ we have reported on modified normal pulse polarography (MNPP) in which the electrode potential is applied in a similar manner as in normal pulse polarography (NPP), but the faradaic current is sampled a short time after the end of the pulse, when material reduced during the negative-going pulse and deposited on the mercury drop can be oxidized back into solution. As any reduction product of an irreversible electrode reaction shows no wave in this method, a well-defined polarogram for barium in 0.01M hydrochloric acid/0.1M tetramethylammonium bromide medium was obtained by MNPP, and no hydrogen-ion waves were observed.⁴ Flow polarograms for sodium in air-saturated acid solutions containing sulphate as supporting electrolyte were obtained without interference from dissolved oxygen.⁷

In the study described here, the behaviour of the four principal alkaline-earth metal ions in MNPP and a differential mode of MNPP (DMNPP) was investigated. The elimination of the interference of dissolved oxygen was studied with a view to finding a simple procedure for the determination of these metals.

EXPERIMENTAL

Apparatus

The modified normal pulse polarograph and the other instruments used were those described previously.⁶ They were used for NPP, MNPP and reverse pulse polarography (RPP)⁸ in the present work. The potentiostat has a positive feedback circuit for compensating the iR -drop and can supply up to 60 mA of electrolysis current. The pulse potential was increased at a rate of 10 mV/sec. The flow-rate of the dropping mercury electrode (DME) remained constant at 0.630 mg/sec. The lifetime of the mercury drop was controlled by a mechanical DME-knocker with a solenoid and a plunger, and a lifetime of 2.0 sec was chosen for all work. The potential pulse, with duration t_2 , is applied after an interval of t_1 from the start of a new drop-growth cycle. The pulse potential represented as E_2 is equal to the sum of a constant initial potential, E_1 , and the actual pulse height. Negative-going pulses are added in NPP and MNPP, positive-going pulses in RPP. The pulse height is increased steadily from one pulse to the next. The current in NPP and RPP is sampled after an interval t_3 from the rise of each pulse, and in MNPP at t_3 after the fall of each pulse. In order to perform DMNPP, two sample-hold circuits were connected in series to the output of the polarograph.⁹

Reagents

The standard solutions of alkaline-earth metal ions were made from their chlorides, prepared from hydrochloric acid and the corresponding carbonates. They were standardized by titration with EDTA (Eriochrome Black T as indicator). Reagent-grade tetramethylammonium bromide and chloride were used as supporting electrolytes without further purification. The sample solutions containing bromide were deaerated by the passage of nitrogen in the usual manner.

RESULTS AND DISCUSSION

Polarograms

The three types of pulse polarogram are shown in Fig. 1 for strontium in neutral solution. The normal pulse polarogram, curve 1, has only one wave with a

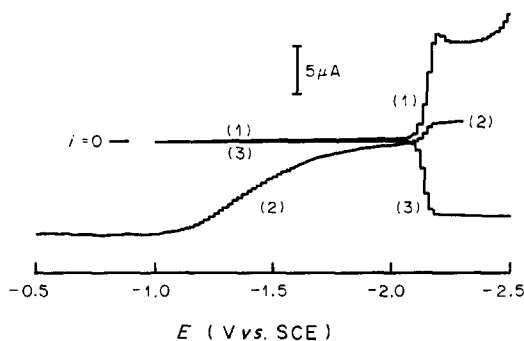


Fig. 1. Three types of pulse polarograms for strontium chloride in a neutral solution: $0.1M$ Me_4NBr , $4.3 \times 10^{-4}M$ $SrCl_2$, $t_1 = 1.111$ sec, $t_2 = 117.6$ msec, $t_3 = 2.3$ msec. E_i : (1) and (3) -1.00 V, (2) -2.30 V. (1) NPP, (2) RPP, (3) MNPP.

small maximum, resulting from the reduction of strontium. The gradual increase in current which appears at more negative potentials may result from the reduction of decomposition products of the tetramethylammonium ion. The effect did not occur for acid solutions. The reverse pulse polarogram has two waves because of the quasi-reversible electrode reaction of strontium at the mercury electrode.¹⁰ The half-wave potentials of the small cathodic waves in RPP for barium, strontium and calcium are -1.94 , -2.14 and -2.24 V, respectively. Ill-defined RPP anodic waves for oxidation of barium, strontium and calcium metals from the mercury drop have limiting current regions at potentials more positive than -1.1 , -1.0 and -0.9 V, respectively. The difference between the half-wave potentials of the cathodic and anodic waves in RPP for a given alkaline-earth metal depends on the reversibility of the electrode reaction, and decreases in the order calcium > strontium > barium. The potential between pulses in MNPP, namely the initial potential E_i , must be set at a potential at which the anodic wave for the alkaline-earth metal in the mercury drop gives a limiting current, so E_i is set at -1.0 V for strontium. The MNPP for strontium has only one oxidation wave, at the same potential as the reduction wave in NPP. Since the limiting current for strontium in MNPP remains steady at more negative potentials it is likely that the gradual increase in the limiting-current region in NPP is due to reduction of decomposition products of the tetramethylammonium salt. Barium and calcium also give well-defined waves in MNPP, and under the same conditions as for strontium (Fig. 1) the wave-heights in MNPP are proportional to the concentrations. Though the MNPP-waves have small maxima for concentrations exceeding $10^{-3}M$, the maxima disappear when the duration of the pulse is shortened. The maxima in MNPP may possibly be due to the high concentration of amalgam in the mercury drop.

It is well-known that magnesium exhibits a large d.c. polarographic current which has no limiting value and accompanies the evolution of hydrogen.¹¹

Magnesium also gives a large NP-polarographic current similar to that of the d.c. polarogram, and shows a small MNP-polarographic current in the potential region more negative than -2.40 V (Fig. 2). Hence it is considered that the cathodic current for magnesium in NPP results from reduction of magnesium ions and from evolution of hydrogen, and is therefore not useful for the determination of magnesium. Magnesium does not, however, interfere in the determination of the other alkaline-earth metals by MNPP, because the potential of the anodic wave for magnesium is considerably more negative than that for the others.

It is very difficult to obtain reproducible RP-polarograms for magnesium because the hydrogen bubbles formed in the period of the initial potential adhere to the DME and interfere in the precise measurement of the currents even in neutral solutions. The RP-polarogram for magnesium has a small anodic wave when the initial potential is set at -2.50 V, and no anodic wave when the initial potential is -2.30 V. As the other alkaline-earth metals give anodic waves in RPP when the initial potential is set at -2.30 V, the anodic wave of the RP-polarogram in Fig. 2 cannot result from the oxidation of the other alkaline-earth metals as impurities, so it must be attributable to the oxidation of amalgamated magnesium, formed at the initial potential.

Simultaneous determination of the alkaline-earth metals

Figure 3 shows the polarograms for a solution at pH 3 containing barium, strontium and calcium. The MNP-polarograms have no hydrogen wave, even in $0.01M$ hydrochloric acid. The wave heights for these metals are proportional to the concentrations at around $10^{-4}M$. The half-wave potentials are quite distinct from one another, so these metals can be determined simultaneously. The determination of these three alkaline-earth metals by NPP suffers interference from the large hydrogen-ion reduction

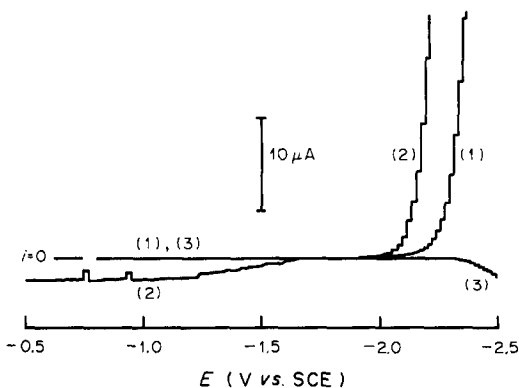


Fig. 2. Three types of pulse polarograms for magnesium chloride in a neutral solution: $0.1M$ Me_4NBr , $3.9 \times 10^{-4}M$ $MgCl_2$, $t_1 = 1.111$ sec, $t_2 = 117.6$ msec, $t_3 = 2.3$ msec. E_i : (1) and (3) -0.80 V, (2) -2.50 V. (1) NPP, (2) RPP, (3) MNPP.

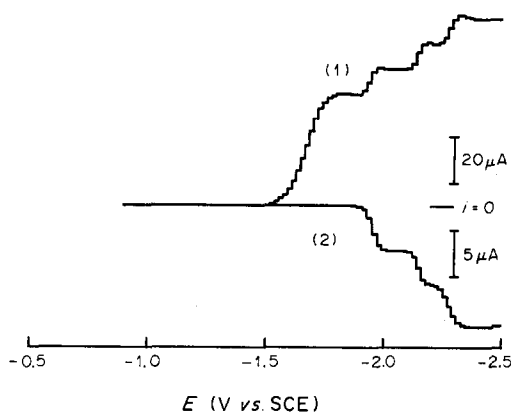


Fig. 3. NP- and MNP-polarograms for chlorides of barium, strontium and calcium in a pH-3 solution: $0.1M$ Me_4NBr , $1 \times 10^{-3}M$ HCl , $4.1 \times 10^{-4}M$ $BaCl_2$, $4.3 \times 10^{-4}M$ $SrCl_2$, $4.2 \times 10^{-4}M$ $CaCl_2$. $E_1 = -0.90$ V, $t_1 = 1.111$ sec, $t_2 = 23.2$ msec, $t_3 = 2.3$ msec. (1) NPP, (2) MNPP.

current in the presence of magnesium, but the determination by MNPP is not affected. Alkali metals other than lithium interfere in the determination of strontium because of the closeness of their half-wave potentials. In such cases, it is convenient to use ion-exchange chromatography for a prior separation.

Polarography without deaeration

Polarographic measurements generally require the deaeration of the sample solution, because dissolved oxygen presents two cathodic waves and thus interferes in the determination of the analyte. If the need for deaeration in polarography can be avoided, then polarographic methods will find a wider range of applicability, particularly in flow systems, in which it is difficult to remove the dissolved oxygen satisfactorily. Three types of pulse polarograms were recorded for barium in an air-saturated acid solution containing tetramethylammonium chloride as supporting electrolyte (Fig. 4). The NP-polarogram has

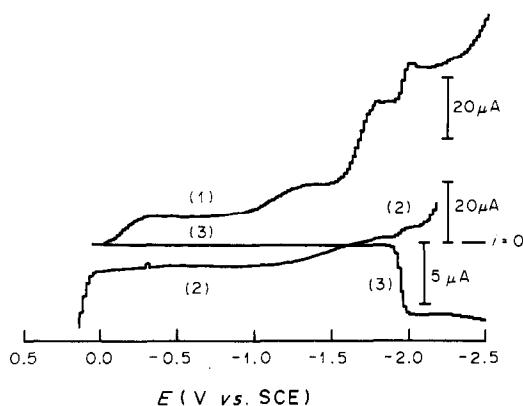


Fig. 4. Three types of pulse polarograms for barium chloride in an air-saturated acid solution: $0.1M$ Me_4NCl , $1 \times 10^{-3}M$ HCl , $4.1 \times 10^{-4}M$ $BaCl_2$. E_1 : (1) and (3) 0.04 V, (2) -2.20 V. $t_1 = 1.111$ sec, $t_2 = 57.3$ msec, $t_3 = 2.3$ msec. (1) NPP, (2) RPP, (3) MNPP.

four reduction waves, namely two oxygen waves, a hydrogen wave and a barium wave in succession at increasingly negative potentials. The RP-polarogram consists of the reduction waves of oxygen, hydrogen ion, and barium and also the oxidation waves of amalgamated barium and mercury. There is a narrow zero-current potential region near 0 V in the RP-polarogram for the blank solution which contains no metals. This potential region has been used for the elimination of the interference by dissolved oxygen in reverse pulse amperometry¹² and flow polarography.⁷ At this potential in RPP, neither the reduction of dissolved oxygen nor the dissolution of mercury occurs but the reduced barium in the amalgam is oxidized back into solution (curve 2). Therefore, when E_1 in MNPP is set at this potential, only one oxidation wave of barium can be obtained for an air-saturated sample, without interference by dissolved oxygen and hydrogen ions. However, the dissolved oxygen in unbuffered neutral solutions affects this method, because hydrogen peroxide and/or hydroxide ions which are generated during the time of the pulse by the reduction of dissolved oxygen give anodic currents even at potentials more negative than 0 V.⁷

When bromide is used as the supporting electrolyte, there is no zero-current region, because the dissolution current for the mercury begins at potentials more negative than 0 V and overlaps the reduction wave of the dissolved oxygen. Though acetate gives a wider zero-current region, it also gives complicated waves for barium. Reagent grade tetramethylammonium nitrate could not be used as a supporting electrolyte because of impurities.

Differential mode of MNPP

MNPP gives a conventional sigmoid polarographic curve, the derivative of which can be obtained by recording the differences between each successive pair of current readings in MNPP, Δi . MNPP and DMNPP polarograms for a mixture of alkaline-earth metals are shown in Fig. 5. The heights of the three peaks are proportional to the metal concentrations. The reduction potentials for strontium and calcium are not far apart, but the simultaneous determination is easy by DMNPP. In MNPP, when the concentrations of the alkaline-earth metals are the same, the wave heights are almost equal but the slopes of the waves decrease in the order barium > strontium > calcium because of the decrease in the reversibility of the electrode reaction. In that order, therefore, the peak heights decrease and the peak widths increase in DMNPP. Other factors which affect the slope of the MNP-polarogram, such as the electron number in an electrode reaction and the magnitude of the iR -drop in the electrolytic cell, influence both the heights and the widths of the peaks in DMNPP. The rapid-scan DMNP-polarogram may be obtained accurately with the aid of a computer and may be applied to three-dimensional detection in flow systems, *i.e.*, the succes-

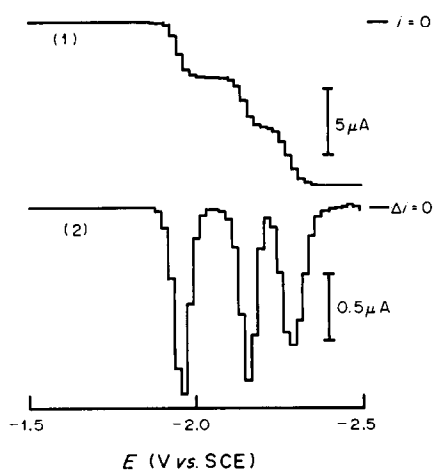


Fig. 5. MNP- and DMNP-polarograms for chlorides of barium, strontium and calcium in a pH-3 solution: conditions as for Fig. 3. (1) MNPP, (2) DMNPP.

sive complete polarograms obtained by rapid-scan DMNPP give information about potential, current and time in a similar manner to that described for

rapid-scan square-wave voltammetry¹³ and may be useful for liquid chromatography and flow-injection analysis.

REFERENCES

1. J. Heyrovský and S. Berezický, *Collection Czech. Chem. Commun.*, 1929, **1**, 19.
2. N. Ishibashi, H. Kohara and T. Haraguchi, *Bunseki Kagaku*, 1965, **14**, 62.
3. A. Babrowski, Z. Kowalski and B. Barchanska, *Chem. Anal. (Warsaw)*, 1978, **23**, 965; *Anal. Abstr.*, 1979, **37**, 5B39.
4. M. Hara and N. Nomura, *Bunseki Kagaku*, 1983, **32**, E185.
5. *Idem*, *Talanta*, 1984, **31**, 105.
6. M. Hara, *ibid.*, 1985, **32**, 41.
7. M. Hara and N. Nomura, *Chem. Lett.*, 1986, 219.
8. J. Osteryoung and E. Kirowa-Eisner, *Anal. Chem.*, 1980, **52**, 62.
9. B. H. Vassos, *ibid.*, 1973, **45**, 1292.
10. H. Matsuda, *Bull. Chem. Soc. Japan*, 1980, **53**, 3439.
11. I. Zlotowski and I. M. Kolthoff, *J. Phys. Chem.*, 1945, **49**, 386.
12. P. Maitoza and D. C. Johnson, *Anal. Chim. Acta*, 1980, **118**, 233.
13. R. Samuelsson, J. O'Dea and J. Osteryoung, *Anal. Chem.*, 1980, **52**, 2215.

SIMULTANEOUS MULTIELEMENT ANALYSIS OF VARIOUS HUMAN TISSUES BY INDUCTIVELY-COUPLED PLASMA ATOMIC-EMISSION SPECTROMETRY

KUNIO SHIRAISHI*, GI-ICHIRO TANAKA and HISAO KAWAMURA

Division of Radioecology, National Institute of Radiological Sciences, 3609 Isozaki, Nakaminato,
Ibaraki 311-12, Japan

(Received 7 April 1986. Accepted 11 July 1986)

Summary—Human soft tissues were analysed by inductively-coupled plasma atomic-emission spectrometry (ICP-AES) for twelve elements. The tissues had been vacuum-dried for storage and were dry-ashed at low temperature and then digested with nitric acid prior to analysis. Accuracy and precision were examined by analysing NBS Standard Reference Material 1577 Bovine Liver. For P, K, Na, Mg, Ca, Fe, Cu, Zn and Cd, the concentrations obtained were within 4% of the certified or informational values. It was found that cerebrum, cerebellum, heart, kidney, liver, pancreas, spleen and muscle samples in portions of less than 1 g dry weight could be conveniently analysed for these elements.

Knowledge of the stable-element contents of human organs and tissues and the distribution of elements in the body is important not only for studies of nutrition but also for estimating internal radiation due to artificial radionuclides released to the environment.¹⁻⁵ Data for Japanese are scarce because tissue samples are difficult to obtain for both religious and cultural reasons. Moreover, most studies have been confined to small numbers of elements and have been done by limited analytical methods. Normal Japanese tissues have been analysed for ten heavy metals by spectrophotometry and flame and flameless atomic-absorption spectroscopy by Sumino *et al.*⁶ for studies of environment pollution. The distributions of twenty-four elements in normal males and metal workers have been compared by Teraoka.⁷ Analysis for trace elements in human organs by neutron-activation analysis was reported by Yukawa *et al.*⁸

Although ICP-IES has recently been used for simultaneous multielement analysis of biological materials,⁹⁻¹¹ its application to human tissue samples has not been found in the literature. In this paper, sequential determination of elements by a scanning emission spectrometer is described. Preliminary analytical results for the concentrations of twelve elements, (potassium, phosphorus, sodium, magnesium, calcium, iron, zinc, copper, cadmium, manganese, strontium and yttrium) in seven types of tissue are described.

EXPERIMENTAL

Apparatus

An internal Plasma Corporation 1101 plasma instrument was used for low-temperature dry-ashing. A Shimadzu ICPQ-1012W inductively-coupled plasma emission spectrometer was used. Operating conditions are summarized in Table 1.

Reagents

Purified water was prepared from tap water with a Barnstead D-2794 outfit. Nitric and hydrochloric acids "for trace element analysis" were obtained from Wako Chemicals, Tokyo. "Specpure" materials containing Ca, Mg, K, Na, Fe, Zn, Cu, Mn or Sr were obtained from Johnson Matthey Chemicals, Royston. Phosphorus, cadmium and yttrium compounds were obtained from Spex Industries, Metuchen, NJ, Research Chemicals, Phoenix, AZ and Kishida Chemicals, Osaka, respectively. Stock solutions (1000 µg/ml) were prepared by dissolving these standard materials as previously described.¹²

Sample preparation

Japanese tissue samples from donors suffering sudden death by heart failure, accidents, *etc.*, were collected in the region of Tokyo from 1975 to 1978. The samples were vacuum-dried by an apparatus designed specifically for trace element determination in human tissue samples and were kept in a large plastic desiccator until required for chemical processing prior to analysis.

The sample preparation was done in a semi-clean room (better than Class 100,000). Portions, weighing approximately 1 g, were taken from the dried tissue samples and placed in fused silica boats with plastic forceps and/or Teflon-coated stainless-steel forceps and re-dried at 80° in a vacuum oven. The samples were transferred to chambers of the low-temperature dry asher and ashed for 24-30 hr at 150 W RF output with a 150-ml/min oxygen flow. In a chemical clean hood (Class 100), the ashed material was dissolved in concentrated nitric acid (approximately 2 ml) and the resultant solution was transferred to a borosilicate glass beaker (50 ml). The beaker was covered with a borosilicate watch-glass and heated on a Thermolyne HP 11415 ceramic hot-plate at 150° in the chemical clean hood. The digested clear solution was then evaporated to dryness. The residue was taken up in acid and transferred to a 25-ml borosilicate glass standard flask and diluted to volume so that the final acid concentration was 0.1M. For most of the tissues the residue was completely soluble in 1.0M nitric acid, but for the residue from liver and spleen samples 0.5M hydrochloric acid had to be used.

Standard reference material

Bovine Liver SRM 1577 was analysed for eleven elements. The bovine liver (approximately 0.7 g) was weighed and treated as above. Six replicate analyses were done.

*Author for correspondence.

Table 1. Operating conditions

Operating frequency	27.120 MHz
Operating power	1.2 kW
Argon flow-rate, carrier	1.0 l./min
coolant	11.5 l./min
plasma	1.5 l./min
Nebulizer	Concentric
Observation height above load coil	1.5 cm (nominal)
Sample uptake rate	2.5 ml/min (demineralized water)
Polychromator	
Grating	Holographic, 2700 grooves/mm
Mount	Paschen-Runge
	1.0 m focal length
Reciprocal linear dispersion	0.37 nm/mm
Entrance slit width	20 μ m
Exit slit width	50 μ m
Integration time	20 sec
Data acquisition system	
Processor	MELCOM 70/L
Program	QC-5D

Determination of five major elements

The sample solutions of human liver and spleen as well as NBS Bovine Liver were diluted before analysis. Calibration curves for each analyte were made by using four different standard solutions (including 0 μ g/ml). The analytical lines used were potassium (I) 766.49 nm, phosphorus (I) 213.62 nm (second order), sodium (I) 589.00 nm, magnesium (I) 383.83 nm and calcium (I) 422.67 nm.

Determination of minor and trace elements

Interference effects of major elements in the ICP-AES measurement were tested for at four levels (0, 250, 500 and 1000 μ g/ml) in solutions containing each of the 7 minor elements at 1- μ g/ml concentration.

Calibration curves were prepared from measurements with different standard solutions (including 0 μ g/ml). The analytical lines were as follows: iron (II) 259.94 nm, zinc 202.55 nm, copper (I) 324.75 nm, cadmium (II) 226.50 nm, manganese (II) 257.61 nm, strontium (II) 407.77 nm and yttrium (II) 371.03 nm.

Seven minor and trace elements in both the NBS Bovine Liver and human tissue samples were determined without dilution.

RESULTS AND DISCUSSION

Determination of major elements

It is considered that the analysis for the five major elements was not subject to chemical interference.¹³

Table 2. Analytical results for NBS Bovine Liver 1577

Element	Concentration (μ g/g dry wt)	
	Present result*	Certified values
P	11340 \pm 60	(11000)†
K	9890 \pm 100	9700 \pm 60
Na	2340 \pm 8	2340 \pm 130
Mg	604 \pm 2	604 \pm 9
Ca	120 \pm 8	124 \pm 6
Fe	264 \pm 4	268 \pm 8
Cu	191 \pm 2	193 \pm 10
Zn	128 \pm 1	130 \pm 13
Mn	9.95 \pm 0.09	10.3 \pm 1.0
Cd	0.26 \pm 0.05	0.27 \pm 0.04
Sr	0.14 \pm 0.02	(0.14)†

*Mean of six determinations.

†Not certified.

These major elements in various human tissues and NBS Bovine Liver were determined prior to the analysis for the seven minor elements. Analytical results for NBS Bovine Liver are shown in Table 2. For all these elements good (within 4%) agreement was obtained with the certified or non-certified values.

Determination of minor and trace elements

Results of the interference study with the model solutions are shown in Table 3. Recoveries of most of the elements (Fe, Cd, Mn and Y) decreased as the concentrations of calcium and magnesium increased. This decrease may be caused mainly by physical interference. Potassium and phosphorus showed little influence on the determination of these elements.

The practical concentrations of the five major elements in the human sample solutions measured in this study were as follows: potassium 110–670 μ g/ml, phosphorus 86–650 μ g/ml, sodium 72–425 μ g/ml, magnesium 5–38 μ g/ml, and calcium 2–43 μ g/ml. Since the concentrations of magnesium and calcium in the sample solutions prepared were lower than about 40 μ g/ml, the minor and trace elements can be determined without interference by Mg and Ca. Interferences are, however, expected to increase when the analyte concentration is lower than the 1- μ g/ml level in our synthetic sample solution.

To check for interferences attributed to the major elements, a recovery test was made with another solution, which was a mixture consisting of equal portions of seven kinds of organ sample solutions. The concentration increments were 0.25–0.5 μ g/ml. All the minor and trace elements, Fe, Zn, Cu, Cd, Mn, Sr and Y, showed good recoveries, ranging from 99 to 105%.

For NBS Bovine Liver 1577 the results for six minor elements showed good agreement with the five certified values and the one tentative value, with relative errors of <4% (Table 2).

Table 3. Effects of matrix elements on 1 µg/ml of minor and trace elements

Matrix element, µg/ml	Relative concentration found*						
	Fe	Zn	Cu	Cd	Mn	Sr	Y
Ca	0	100.0	100.0	100.0	100.0	100.0	100.0
	250	96.9	96.1	100.5	97.6	96.7	98.4
	500	95.2	93.9	102.3	97.4	95.2	99.0
	1000	94.2	93.0	104.4	96.2	93.9	100.0
Mg	0	100.0	100.0	100.0	100.0	100.0	100.0
	250	98.3	101.9	99.0	100.0	99.1	98.1
	500	95.6	102.1	97.6	97.6	95.8	96.1
	1000	95.0	104.0	95.3	95.4	95.9	92.8
P	0	100.0	100.0	100.0	100.0	100.0	100.0
	250	100.1	99.9	101.2	100.5	99.7	101.1
	500	99.6	99.6	100.8	99.3	98.8	100.6
	1000	101.0	99.3	101.1	99.9	99.8	101.0
K	0	100.0	100.0	100.0	100.0	100.0	100.0
	250	101.0	99.0	97.6	99.8	100.2	98.0
	500	98.6	98.9	97.0	99.6	98.3	97.7
	1000	100.3	100.2	96.7	100.7	100.2	97.2
Na	0	100.0	100.0	100.0	100.0	100.0	100.0
	250	100.1	100.0	96.5	100.0	100.1	97.2
	500	99.7	99.8	98.2	100.0	99.5	98.7
	1000	98.0	99.3	94.7	99.1	97.8	94.4

*Mean of three determinations.

Concentrations of major elements in tissues

Although variation in the level of some elements with age¹ and sex⁶ has been reported, it was not considered in this work because of the small number of samples. The water contents¹⁴ of the tissues were as follows: cerebrum 77.5%, cerebellum 80.0%, heart 72.0%, kidney 77.4%, liver 72.2%, muscle 78.5%, pancreas 71.0% and spleen 77.7%. Results for the human tissue samples are shown in Tables 4, 5 and 7-9.

Potassium concentrations in the various tissues were in the narrow range of 2.2-3.5 mg/g wet weight. Relatively wide ranges were found for pancreas and muscle. In other tissues much smaller variations were obtained.

Phosphorus concentrations in the tissues were in the range 1.3-3.2 mg/g. Phosphorus concentrations in cerebrum and cerebellum showed a small variation between subjects. Relatively wide ranges were found for pancreas and spleen.

Sodium concentrations in the tissues were in the

range 1.2-1.9 mg/g, except in muscle. The concentration in muscle was between a quarter and a half of the levels in the other samples. Wide ranges were found in liver, pancreas and spleen.

Calcium concentrations in kidney and pancreas showed high values, which were two or three times those in other tissues. The concentration in muscle was rather low. Concentrations in the other five organs were in the range 38-57 µg/g. Wide ranges were found in liver, pancreas and spleen. The tissue calcium concentration varied considerably, depending on the tissues.

Magnesium concentrations in the tissues were uniformly distributed, ranging from 130 to 190 µg/g, but wide ranges were found in muscle, pancreas, and spleen.

Relative concentrations of major elements

Table 6 shows the relative concentrations of the elements with respect to magnesium, which had the narrowest range of concentration in the various

Table 4. Concentrations of potassium, phosphorus and sodium in various human tissues*

Organ and tissue	Potassium			Phosphorus			Sodium		
	Mean	Range	n†	Mean	Range	n	Mean	Range	n
Cerebrum	2.85	2.00-3.48	7	3.22	3.16-3.31	7	1.72	1.61-2.02	7
Cerebellum	3.26	2.95-3.54	6	3.15	2.94-3.26	6	1.68	1.36-2.04	6
Heart	2.95	2.29-3.54	7	1.86	1.47-2.19	7	1.20	0.91-1.71	7
Kidney	2.20	1.44-2.65	6	1.81	1.01-2.21	6	1.89	1.45-2.44	6
Liver	2.84	2.37-3.33	7	3.08	2.52-3.60	7	1.56	0.76-2.24	7
Muscle	2.37	1.55-3.51	6	1.25	0.85-1.79	7	0.47	0.39-0.61	6
Pancreas	2.91	1.65-4.21	5	2.59	1.70-4.29	5	1.39	0.52-2.84	6
Spleen	3.47	2.95-4.55	7	2.42	1.59-3.53	7	1.19	0.69-1.74	7

*mg/g wet sample.

†Number of samples.

Table 5. Concentrations of calcium and magnesium in various human tissues*

Organ and tissue	Calcium			Magnesium		
	Mean	Range	n†	Mean	Range	n
Cerebrum	50.5	34.0–60.1	7	126	109–143	7
Cerebellum	49.1	40.6–58.0	6	134	120–140	6
Heart	44.9	34.3–55.6	7	193	145–227	7
Kidney	168	124–228	5	125	69–157	6
Liver	38.4	20.5–51.9	7	145	110–189	7
Muscle	22.1	16.5–27.2	6	131	80–208	7
Pancreas	117	63–167	6	173	90–237	5
Spleen	57.1	31.2–90.1	7	117	64–190	7

* $\mu\text{g/g}$ wet sample.

†Number of samples.

tissues. The elemental ratios in the cerebrum and cerebellum were very similar. Another set of similar ratios was obtained in heart and muscle. In the case of liver, pancreas and spleen, the ratios showed similar trends, but each organ had characteristic concentrations of some elements. For example, liver had a lower calcium to magnesium ratio than the other organs. Pancreas had lower phosphorus and sodium ratios than the others. Spleen had the highest potassium ratio. Kidney seemed to be different in type from the other tissues.

Concentrations of minor and trace elements in tissues

Iron concentrations in the tissues had a wide range of 38–260 $\mu\text{g/g}$ (Table 7). High iron concentrations were found in liver and spleen. Low values were

found in muscle, pancreas and cerebellum. Wide ranges in most of the tissues may be attributed to variations in blood content during sampling.

Zinc concentrations in the tissues had a relatively narrow range of 11–64 $\mu\text{g/g}$ (Table 7), but wide ranges in kidney, liver and pancreas were found. The highest zinc content was found in liver.

Copper concentrations in the tissues were in the range 0.6–10 $\mu\text{g/g}$ (Table 7). Wide ranges in heart and liver were found. The high values were found in liver, cerebellum and cerebrum.

Markedly high concentrations of cadmium (Table 8) were found in kidney, liver and pancreas, 10–100 times those in other tissues. Larger variations in each tissue were also found, compared with the other elements.

Manganese concentrations in the tissues (Table 8) were in the wide range of 0.05–1.6 $\mu\text{g/g}$. High concentrations of manganese were found in liver and kidney, and low concentrations in muscle and spleen. Relatively wide ranges in each tissue were found.

Strontium concentrations in the tissues were in the relatively narrow range of 0.013–0.090 $\mu\text{g/g}$ (Table 9). The concentrations in kidney and pancreas were several times higher than in other tissues. Relatively wide ranges in each tissue were found.

Yttrium was uniformly distributed in all the tissues, with concentrations ranging from 0.002 to 0.005 $\mu\text{g/g}$ (Table 9). It is suggested that yttrium might be used as an internal standard element for the analysis of human samples by ICP-AES.

Table 6. Relative w/w concentrations of five major elements in human tissues

Organ and tissue	Element*				
	Calcium	Magnesium	Phosphorus	Potassium	Sodium
Cerebrum	40	100	2560	2260	1260
Cerebellum	37	100	2350	2430	1250
Heart	23	100	960	1530	620
Kidney	134	100	1450	1760	1510
Liver	27	100	2120	1960	1080
Muscle	17	100	950	1810	360
Pancreas	68	100	1500	1680	800
Spleen	49	100	2070	2970	1010

*Values were based on magnesium concentrations in each organ and tissue.

Table 7. Concentrations of iron, zinc and copper in various human tissues*

Organ and tissue	Iron			Zinc			Copper		
	Mean	Range	n†	Mean	Range	n	Mean	Range	n
Cerebrum	49.1	28.4–83.1	7	9.97	6.7–10.8	7	5.01	2.42–6.79	7
Cerebellum	38.4	33.1–47.7	6	10.9	9.3–11.6	6	7.35	6.52–8.81	6
Heart	63.2	31.1–135	7	23.9	14.5–34.0	7	3.39	1.39–6.52	7
Kidney	86.7	64.6–100	6	39.6	21.1–56.9	6	2.39	1.26–3.70	6
Liver	212	110–331	7	63.8	34.9–99.3	7	10.3	4.90–20.2	7
Muscle	25.0	10.4–38.0	7	35.2	23.4–50.6	7	0.64	0.32–0.80	7
Pancreas	37.1	22.8–53.6	5	30.6	15.4–41.3	5	1.53	0.77–2.22	5
Spleen	260	146–346	7	13.5	9.7–16.0	7	1.11	0.90–1.61	7

* $\mu\text{g/g}$ wet sample.

†Number of samples.

Table 8. Concentrations of cadmium and manganese in various human tissues*

Organ and tissue	Cadmium			Manganese		
	Mean	Range	n†	Mean	Range	n
Cerebrum	0.110	0.033–0.269	7	0.231	0.120–0.494	7
Cerebellum	0.183	0.055–0.308	6	0.307	0.273–0.335	6
Heart	0.154	0.066–0.216	7	0.262	0.122–0.747	7
Kidney	18.8	7.2–32.6	6	0.757	0.389–1.08	6
Liver	9.69	1.37–25.8	7	1.58	1.02–2.21	7
Muscle	0.278	0.042–0.606	7	0.046	0.007–0.145	7
Pancreas	5.41	0.61–12.8	6	0.150	0.652–1.62	5
Spleen	0.463	0.049–1.05	7	0.051	0.028–0.085	7

* $\mu\text{g/g}$ wet sample.

†Number of samples.

Table 9. Concentrations of strontium and yttrium in various human tissues*

Organ and tissue	Strontium			Yttrium		
	Mean	Range	n†	Mean	Range	n
Cerebrum	0.0210	0.009–0.033	7	0.0043	0.002–0.008	7
Cerebellum	0.0190	0.012–0.025	6	0.0045	0.004–0.006	6
Heart	0.0321	0.018–0.051	7	0.0034	0.002–0.005	7
Kidney	0.0907	0.042–0.117	6	0.0053	0.002–0.007	7
Liver	0.0199	0.013–0.032	7	0.0059	0.001–0.018	7
Muscle	0.0134	0.008–0.020	7	0.0023	0.001–0.004	7
Pancreas	0.0786	0.053–0.108	5	0.0048	0.002–0.006	6
Spleen	0.0294	0.013–0.048	7	0.0039	0.002–0.005	7

* $\mu\text{g/g}$ wet sample.

†Number of samples.

The cadmium concentrations in most of the tissues were found to be different from the literature values. Lower values than those of the ICRP¹ were found in cerebrum, cerebellum, muscle and heart. Similar low levels for Japanese have been reported elsewhere.⁶ High values were found for the pancreas and liver.¹⁵ This tendency for Japanese has also been reported in detail.¹⁶ Although the average zinc concentrations in muscle and kidney seem to be lower than those for Europeans,¹⁵ the ranges were almost the same. Mean iron and copper concentrations in liver were slightly higher than those for Europeans, but the differences were not significant. Some other differences are apparent between our results and the literature values, including those for major elements (K, P, Na, Ca and Mg), but this preliminary report cannot adequately deal with this problem, owing to the small number of samples analysed.

In conclusion, five major elements and seven minor elements in various human tissues can be determined simultaneously and easily by use of ICP-AES. Although major and minor elements were separately determined in this report, it is possible to measure all twelve elements at the same time.

Acknowledgement—The authors wish to express gratitude to Miss Masako Ouchi for her help in processing the data.

REFERENCES

1. ICRP Task Group of Committee 2, *Report of the Task Group on Reference Man*, ICRP Publication 23, Pergamon Press, Oxford, 1975.
2. G. Tanaka, A. Tomikawa, H. Kawamura and Y. Ohyagi, *Nippon Kagaku Zasshi*, 1968, **89**, 175.
3. G. Tanaka, A. Tomikawa and H. Kawamura, *Bull. Chem. Soc. Japan*, 1977, **50**, 2310.
4. G. Tanaka, H. Kawamura and E. Nomura, *Health Phys.*, 1981, **40**, 601.
5. H. Kawamura, G. Tanaka and K. Shiraishi, *ibid.*, 1986, **50**, 159.
6. K. Sumino, K. Hayakawa, T. Shibata and S. Kitamura, *Arch. Environ. Health*, 1975, **30**, 487.
7. H. Teraoka, *ibid.*, 1981, **36**, 155.
8. M. Yukawa, M. Suzuki-Yasumoto, K. Amano and M. Terai, *ibid.*, 1980, **35**, 36.
9. J. L. M. de Bore and F. J. M. J. Maessen, *Spectrochim. Acta*, 1983, **38B**, 739.
10. K. A. Wolnik, J. I. Rader, C. M. Gaston and F. C. Frick, *ibid.*, 1985, **40B**, 245.
11. A. A. Verbeek, *ibid.*, 1984, **39B**, 599.
12. K. Shiraishi, H. Kawamura and G. Tanaka, *Anal. Sci.*, 1985, **1**, 321.
13. V. A. Fassel, *Science*, 1978, **202**, 183.
14. G. Tanaka, Reference Japanese Man, in *Report of Committee on the Application of ICRP Reference Man to Japanese*, S. Takahashi (ed.) (in Japanese), Japan Radiological Society, April 1980.
15. J. Versieck, *CRC Crit. Rev. Clin. Lab. Sci.*, 1985, **22**, 97.
16. K. Tsuchiya, *Cadmium Studies in Japan: A Review*, p. 37. Kodansha Shuppan, Tokyo, 1979.

FIBRE-OPTIC TITRATIONS—IV

DIRECT COMPLEXOMETRIC TITRATION OF ALUMINIUM(III) WITH DCTA

OTTO S. WOLFBELIS and BERNHARD P. H. SCHAFFAR

Institute of Organic Chemistry, Karl-Franzens-University, 8010 Graz, Austria

R. A. CHALMERS

Department of Chemistry, University of Aberdeen, Old Aberdeen, Scotland

(Received 27 June 1985. Revised 29 April 1986. Accepted 4 July 1986)

Summary—The end-point of the direct complexometric titration of Al^{3+} in pH 4.6 solution can be determined by monitoring the fluorescence intensity of the aluminium–morin complex, by use of a bifurcated fibre-optic light guide. The method allows the determination of aluminium in the 1–800 ppm range with good precision. The procedure is applicable even when the solutions are strongly coloured or turbid, but because of the slow complexation kinetics requires a titration time of about 20 min.

Complexometric titration of Al^{3+} is usually performed at room temperature by addition of excess of chelating agent such as EDTA or DCTA (diaminocyclohexanetetra-acetic acid), followed by back-titration with zinc¹ or lead² with dithizone or Xylenol Orange as indicator at pH 4–6. This procedure is necessary because the complexation is slow, owing to the presence of polymeric aluminium species. DCTA gives a more rapid reaction, but titration of heated solutions is often recommended.

Fluorescent indicators such as morin* are well known, but have found application only in qualitative analysis and in microanalysis.⁴ Thermometric, amperometric, conductometric, or radiometric end-point detection can be used for complexometric determination of aluminium, with various degrees of precision.⁵

Fluorometry appears to be one of the most sensitive techniques and several methods have been published in which morin or a related flavone-type reagent is employed.⁴ The aluminium–morin complex has been studied in great detail^{6,7} with respect to pH effects and interferences resulting from beryllium, zirconium, etc. Though these ions also form complexes with morin, the pH at which they do so is mostly different from that ideal for the aluminium reaction.

Saari and Seitz^{7,8} have immobilized morin at the end of a bifurcated optical fibre to obtain a sensor that responds linearly and reversibly to aluminium in the 1–100 μM concentration range. The detection limit is 1 μM . In subsequent work⁹ another type of

aluminium sensor was obtained by electrostatic immobilization of 8-hydroxyquinoline-5-sulphonic acid. Both sensors display similar characteristics.

However, because of the limited linearity between analyte concentration and optical signal, and the relatively long response time (~ 1 min or more) these sensors are considered not to be ideal for titration purposes. Moreover, they suffer from another type of interference in that the immobilized ligand also forms complexes with transition metal ions such as iron(III). Although the complex thus formed is itself non-fluorescent, there is an interference because of the binding of immobilized morin which otherwise would be available for complexation with aluminium.

In continuation of studies^{1,10} on the potential utility of fibre-optic light guides in place of electrodes for end-point determination in titrimetry we have attempted to solve the old problem of direct complexometric determination of aluminium, by using morin as a fluorogenic indicator. The use of fibre optics, an off-shoot of the communications industry, offers the advantages that the fibres are inexpensive, robust, and allow the determination of ions for which electrodes are not available. Unlike electrodes, fibre sensors are not affected by surface potential and do not have a liquid–liquid junction, which is known to be the most delicate part of potentiometric electrodes. In addition, use of fibre optics allows analyses to be performed in hostile environments and at sites quite remote from the operator. The feasibility of performing optical analyses over distances as great as 1 km has been demonstrated.¹¹

EXPERIMENTAL

The experimental arrangement is shown in Fig. 1. It consists of a 250-W xenon arc lamp as a light-source (L),

*The IUPAC name for morin is 2-(2,4-dihydroxyphenyl)-3,5,7-trihydroxy-4H-benzopyran-4-one. The trivial name is used throughout this paper.

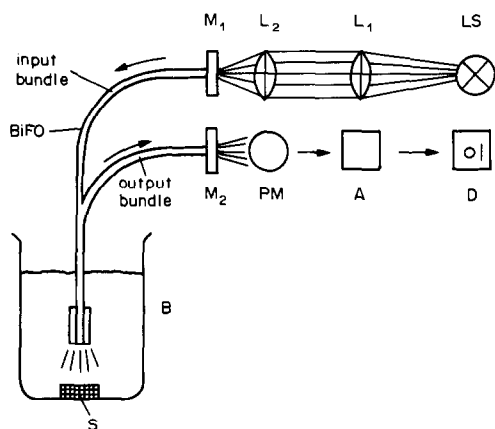


Fig. 1. Experimental arrangement for performing fibre-optic titrations.

and light-collecting lenses L_1 and L_2 . After passing through monochromator M_1 , the excitation light is guided through the input bundle of a bifurcated fibre optic (BiFO) into the titration beaker (B) containing the analyte solution and morin. The fluorescence of the aluminium–morin complex is guided by the output bundle to the photomultiplier (PM) after passage through monochromator M_2 . The signal is amplified in A and displayed on D.

A 150-cm long bifurcated fibre-optic light-guide of 4 mm internal diameter made of poly(methyl methacrylate) was used, with statistically mixed fibre bundles (Faseroptik Henning, 8501 Allersburg, FRG). In some experiments, a 150-cm silica light-guide (internal diameter 2 mm; Moritex Corp., Tokyo) was used. The excitation wavelength was 420 nm and the emission was monitored at 500 nm, with both band-passes set at 8 nm.

It should be noted that the instrumentation, which in this work was part of an Aminco SPF 500 spectrofluorimeter, may be considerably simplified. The light-source can be an inexpensive halogen lamp or a blue light-emitting diode (LED), the monochromators may be replaced by optical filters, and the photodetector may be a rather cheap photodiode.

For performing titrations, an aliquot of the aluminium solution was transferred into a black beaker, adjusted to pH 4.6 with acetate buffer after addition of the indicator solution, and made up to 50 ml. The fibre and the jet of a 10-ml burette were introduced into the beaker through holes in the black cover, the fibre being immersed in the solution, which was continuously stirred.

The DCTA monohydrate (Titriplex IV, Merck) and morin (Sigma) used were of analytical purity. The DCTA solution was standardized by titration with zinc sulphate (Titrisol, Merck) with Eriochrome Black T as indicator in alkaline solution. A standard 1000- $\mu\text{g}/\text{ml}$ aluminium solution (Titrisol, Merck) was used for titrations and the preparation of a dilution series. All operations were performed at room temperature.

RESULTS

To find out the optimum morin concentration, a 10- $\mu\text{g}/\text{ml}$ aluminium solution was titrated with DCTA in the presence of morin in the 0.1–100 μM concentration range. The end-point, characterized by a drop in fluorescence intensity to a low and constant level (Figs. 2 and 3) was sharpest when the morin concentration was 10 μM , but its position

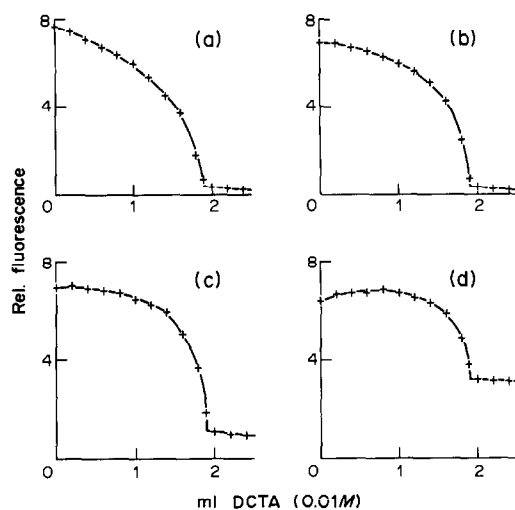


Fig. 2. Typical graphs obtained in the fibre-optic titration of 0.50 mg of aluminium(III) with 0.01M DCTA, and varied morin concentration: (a) 0.1mM morin; (b) 10 μM morin; (c) 1 μM morin; (d) 0.1 μM morin. The end-point is independent of the indicator concentration.

was not affected by the indicator concentration (Fig. 2). This is also the case for other aluminium concentrations.

Aluminium was titrated in the 1–800 $\mu\text{g}/\text{ml}$ range at constant morin concentration. The lower limit was taken as that corresponding to consumption of 2 ml of 0.001M DCTA, though the end-point could still be recognized even at lower concentrations (see Fig. 3). Lower aluminium levels are better determined by one of the conventional fluorimetric methods⁴ or by using a fibre-optic sensor^{8,9} working in the 1–100 μM (0.027–2.7 $\mu\text{g}/\text{ml}$) aluminium range, or should first be preconcentrated.¹² Typical titration graphs are shown

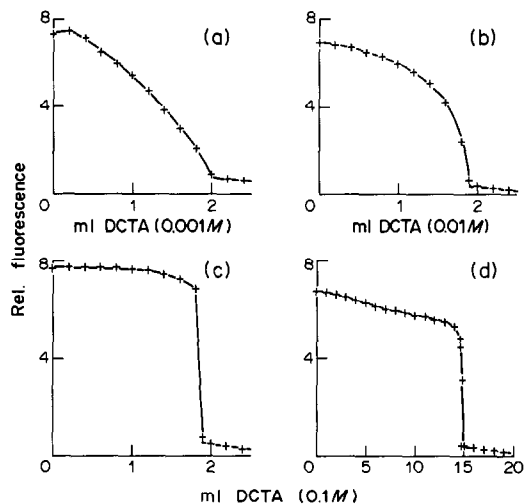


Fig. 3. Typical graphs obtained in the fibre-optic titration of various amounts of aluminium(III) with DCTA. Morin concentration 10 μM . (a) 0.050 mg Al^{3+} with 0.001M DCTA; (b) 0.50 mg of Al^{3+} with 0.01M DCTA; (c) 5.00 mg of Al^{3+} with 0.1M DCTA; (d) 40.0 mg of Al^{3+} with 0.1M DCTA.

in Fig. 3. Initially, the fluorescence is strong since all the morin is present as the highly fluorescent metal complex. With increasing addition of DCTA the fluorescence decreases and drops most distinctly at the very end. The final signal, which remains constant even after further addition of DCTA, results from some stray light from the light-source and any external light passing into the beaker. The experimental results obtained in the complexometric titration of aluminium with DCTA are summarized in Table 1.

In the initial experiments, EDTA was used as the titrant but proved unsuitable, giving a premature end-point and very slow complexation kinetics. DCTA, in contrast, gives a correct end-point even at room temperature and forms the complex fairly quickly, although a single titration still requires about 20 min.

Procedure

Take an aliquot of sample solution containing 0.05–40 mg of aluminium and adjust to pH 4.6 with acetate buffer (0.1M for <25 mg of aluminium, 1M for >25 mg). Add 0.5 ml of 0.03% aqueous solution of morin, dilute to ~50 ml with water, and titrate with 0.1M DCTA for >25 mg of aluminium, 0.01M DCTA for 2.5–25 mg, or 0.001M DCTA for <2.5 mg, using the fibre-optic titrator (Fig. 1) at analytical wavelengths 420 nm (excitation) and 500 nm (emission). Calculate the amount of aluminium in the aliquot titrated, from $Al = 26.99 Vx$ mg, where V is the volume (ml) of xM DCTA consumed.

DISCUSSION

Morin was chosen as indicator since it is itself essentially non-fluorescent, but forms a strongly fluorescent chelate with aluminium. Both the excitation (420 nm) and emission maxima (500 nm) of the complex are in the visible part of the spectrum. This is advantageous because it allows the use of inexpensive plastic fibre-optics having spectral cut-off at around 380–400 nm, instead of the much more expensive and less flexible silica fibres.

Table 1. Experimental results obtained in the fibre-optic titration of 50 ml of aluminium(III) solutions with DCTA

Al taken, mg	DCTA consumed, ml			Al found, mg
	0.1M	0.01M	0.001M	
40.0	14.82			40.0
30.0	11.17			30.2
20.0	7.38			19.9
10.0	3.74			10.1
5.00	1.84			4.97
3.00	1.12			3.03
2.00		7.51		2.02
1.00		3.75		1.01
0.50		1.86		0.50
0.30		1.12		0.30
0.20			7.54	0.20 ₄
0.10			3.77	0.10 ₅
0.05			1.83	0.049

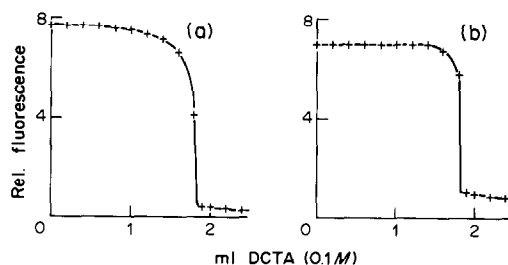


Fig. 4. Fibre-optic titration of 50 ml of 5.0 mg of aluminium(III) in (a) the presence of 20 $\mu\text{g/ml}$ Methylene Blue and (b) a turbid solution produced by adding 50 μg of AgNO_3 and 50 mg of KCl . Morin concentration 10 μM .

A major advantage over conventional colorimetric methods is the possibility of performing the titrations in strongly coloured as well as turbid solutions. Figure 4 shows the titration curves obtained in the presence of 20- $\mu\text{g/ml}$ Methylene Blue. This dye was chosen because of its intense colour and its known adverse effect on potentiometric electrodes. Although the solution is quite dark and not transparent, the end-point is easily detected. The result for a 100- $\mu\text{g/ml}$ aluminium solution was 99.3 $\mu\text{g/ml}$, the same value as that obtained in the absence of the dye. In order to produce a turbid solution, silver chloride was precipitated in the test solution, and again the end-point was recognizable without difficulty (Fig. 4), and the result for a 100- $\mu\text{g/ml}$ aluminium solution was 100.4 $\mu\text{g/ml}$, the difference being accountable for as the error in burette-reading.

The major advantage of this technique results from the minute size of the fibres, which can be as thin as 50 μm per single strand. As shown for acid-base titrations,¹⁰ this enables the titration of very small sample volumes (typically 200–500 μl) with micro-syringe burettes, conditions in which electrodes can be employed only with difficulty. Since fibres are not affected by high radiation doses, titrations in a highly radioactive environment may be performed and followed by remote sensing.

In comparison to the slow-responding aluminium sensors which, in principle, may also be utilized for titration purposes, we note the great versatility of the method presented here. The aluminium sensors are comparatively restricted in scope, whereas the experimental arrangement described here is suitable for a variety of titrations: it is only the indicator and the analytical wavelengths that have to be changed. The indicator is added to the solution in the usual way and the titration is monitored with a plastic fibre.

The method is, of course, not limited to morin as an indicator. Other fluorogenic reagents, *viz.* 8-hydroxyquinoline-5-sulphonic acid, 2-hydroxynaphthoic acid, Lumogallion, Pontachrome Blue-Black R, Solochrome Red ERS, and various others¹³ are also known to form fluorescent aluminium chelates. The fluorescences range from green to yellow and red. These dyes offer a variety of analytical

wavelengths for use when the background fluorescence is too strong for the wavelength combination used in this work, and can also offer selectivity advantages over morin, which at pH 4.6 is complexed by Be^{2+} , Zr^{4+} , Ti^{4+} , Th^{4+} , and many lanthanides.

Other cations can interfere if (a) they form DCTA complexes with conditional stability constants (β') greater than $10^{-3} \times \beta'_{\text{Al-DCTA}}$, or (b) are present in concentrations greater than that of the morin and can form complexes with it that are more stable than the Al-morin complex and "block" the indicator.

Metal ions such as Fe^{3+} , Cu^{2+} and, to a lesser extent, Co^{2+} , can cause fluorescence quenching.⁸ These ions can seriously interfere when direct-response aluminium sensors are used because with these sensors it is the *absolute* fluorescence intensity that is related to the analyte concentration; in the titrimetric procedures, however, it is the *relative* changes in fluorescence intensity that are exploited for recognizing the end-point, so these ions do not have an adverse effect, provided a sufficient amount of indicator is added and the interfering ions can be masked [e.g., by reduction of iron(III) to iron(II), addition of thiourea or thiosulphate to complex copper].

Acknowledgement—Our thanks are due to Y. Morito of the Moritex Corp. (Tokyo) for providing fibre-optic light-guides.

REFERENCES

1. O. S. Wolfbeis and P. Hochmuth, *Mikrochim. Acta*, 1984 **III**, 129.
2. D. T. Pritchard, *Anal. Chim. Acta*, 1986, **32**, 184.
3. R. Přibil and V. Veselý, *Talanta*, 1963, **9**, 23.
4. A. Fernandez-Gutierrez and A. Munoz de la Pena, *Determination of Inorganic Substances by Luminescence Methods*, in *Molecular Luminescence Spectroscopy, Methods and Applications: Part I*, S. G. Schulman (ed.), Wiley, New York, 1985.
5. G. Kraft and J. Fischer, *Indikation von Titrationen*, de Gruyter, Berlin, 1972.
6. M. Katyal, *Talanta*, 1968, **15**, 95.
7. M. Katyal, and S. Prakash, *ibid.*, 1977, **24**, 367.
8. L. Saari and W. R. Seitz, *Anal. Chem.*, 1983, **55**, 667.
9. Z. Zhujun and W. R. Seitz, *Anal. Chim. Acta*, 1985, **171**, 251.
10. O. S. Wolfbeis, B. P. H. Schaffer and E. Kaschnitz, *Analyst*, in press.
11. T. Hirschfeld, T. Deaton, F. Milanovich and S. Klainer, *Opt. Eng.*, 1983, **22**, 527.
12. O. S. Wolfbeis and H. Offenbacher, *Z. Anal. Chem.*, 1984, **319**, 282.
13. Reference 4, Table 4.4.

FLUORESCENCE IN THIN LIQUID FILMS

R. VON WANDRUSZKA* and J. D. WINEFORDNER†

Department of Chemistry, University of Florida, Gainesville, FL 32611, U.S.A.

(Received 28 May 1986. Accepted 27 June 1986)

Summary—The fluorescence properties of Rhodamine B in thin liquid films, formed from a number of anionic, cationic and non-ionic surfactant solutions, were investigated. Laser excitation was used and the emission was monitored over a period of time. Drainage profiles with light and dark fluorescence fringes were recorded with plane-polarized radiation. Change of polarization caused profound changes in the appearance of the profiles. The distribution of dye molecules between surfaces of the film and its interior was assessed and found to be related to the speed of film drainage. Expressions were established for the relation between fluorescence fringes and film thickness at different orientations of the film surface to the emission measurement direction.

Optical studies on thin liquid films (soap lamellae) have dealt mainly with reflectance measurements for the purpose of film-thickness determinations.¹⁻³ Fluorescence of such systems was first reported in 1964,⁴ but has not been studied extensively since then. The scope of that investigation was also limited to average film-thickness determination. More recently, Fromherz and Kotulla⁵ have published a fundamental study on the use of fluorescent dyes as probes of electrical potential in soap lamellae.

The present paper describes further phenomena associated with fluorophores in thin liquid films. Rhodamine B was dissolved in solutions of anionic, cationic and non-ionic surfactants and thin films were formed with these solutions. The films were illuminated with the 514.5 nm line of an argon-ion laser to excite the dye molecules and the fluorescence was measured after dispersion by a double monochromator.

EXPERIMENTAL

Materials

The following surfactants were used to form thin films: sodium lauryl sulphate (SLS) (Fisher Scientific), cetylpyridinium chloride (CPC) (Sigma), tetradecyltrimethylammonium bromide (TMAB) (Sigma), Brij 56 [poly(oxyethylene ether)] (Sigma) and Brij 99 [poly(oxyethylene 20 oleyl ether)] (Sigma). Glycerol was purchased from Mallinckrodt and Rhodamine B (laser grade) from Eastman. Demineralized water, treated with a Barnstead multi-stage water purification system, was used for making all solutions. The surfactant solutions prepared were: 1.7% w/v TMAB, 1.0% CPC, 1.4% SLS, 1% Brij 99 and 0.2% Brij 56. All solutions contained Rhodamine B at $5.6 \times 10^{-5} M$ concentration.

Laser

Fluorescence was excited with an argon-ion laser (Spectra-Physics 171), mode-locked (80 MHz) on the 514.5 nm line. A Spex 1680 0.22-m double-grating monochromator, controlled by a CD2A Compudrive module, was

used for wavelength isolation. The polarization of the laser beam was adjusted with two Glan-Thompson polarizers (Melles Griot) and a Soleil-Babinet compensator (Karl Lambrecht). The system lay-out is shown in Fig. 1.

The fragility of the thin film placed a limit on the laser power that could be used for excitation. It was found that powers in the range 200–600 mW did not unduly shorten the film life.

Sample cell

A diagram of the sample cell is shown in Fig. 2. The cell consists of an upper measurement compartment with two windows and a lower drain compartment. A manually operated valve connects the two compartments. The device is made of brass, painted to a non-reflecting black finish. The thin film is formed in a circular frame attached to the lid of the upper compartment and projecting vertically into it. The frame is a seamless circle 20 mm in diameter and 2 mm thick, milled from stainless steel. A magnetic mechanism is used to open a valve between the two cell compartments; it enters the cell through the lid and is operated from above. The lid is made of Teflon and provides an airtight seal.

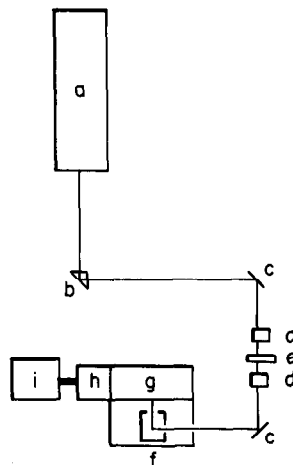


Fig. 1. Diagram of instrument lay-out for thin-film fluorescence measurements; (a) argon-ion laser; (b) right-angle prism; (c) flat mirror; (d) compensator; (e) double monochromator; (f) cell compartment with film; (g) double monochromator; (h) photomultiplier tube; (i) recorder.

*On leave from Department of Chemistry, University of the Witwatersrand, Johannesburg, South Africa.

†Author to whom reprint requests should be sent.

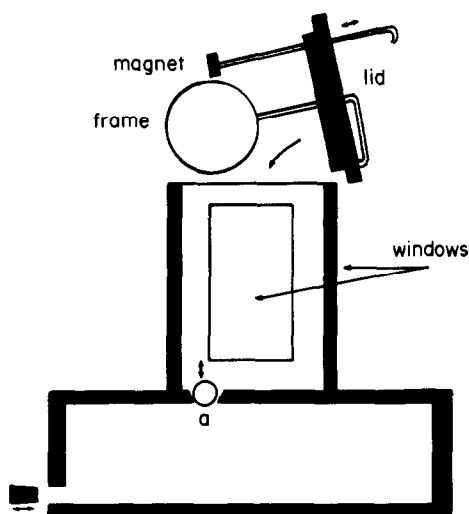


Fig. 2. Diagram of sample cell; (a) drain hole with ball-bearing.

The cell is prepared for measurement by first placing a steel ball-bearing in the tapered drain hole and filling the upper compartment with the surfactant solution. The lid is then closed and the cell is placed in the laser light-path. The ball-bearing is lifted by means of the magnet and the solution drains from the upper cell compartment, leaving a thin film in the frame. This process ensures a minimum of disturbance and allows reproducible film formation. Completion of the film takes from 2 to 4 sec and optical measurements are made virtually from the instant of film formation. Extensive temperature controls are not included in the cell design; temperatures were always in the range 23–25° and no significant variations were observed. The film frame is constructed so as to have two possible orientations with respect to the excitation and emission directions (Fig. 3a); the frame is placed in one of these two positions by means of a notch-and-hole locator in the lid. For vertical illumination ("down" into the film), a frame incorporating the excitation source in its periphery was constructed (light-in-frame) as shown in Fig. 3b. The laser light is brought into the frame by a 600- μm silica optic fibre. Viscosity measurements were made with a Brookfield Synchro-Lectric viscometer.

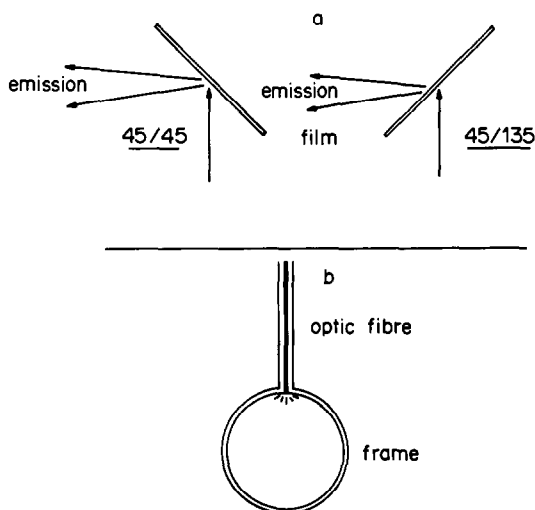


Fig. 3. (a) Measurement orientation of thin film; (b) light-in-frame structure for film formation.

RESULTS AND DISCUSSION

Fluorescence of films

It has been noted by other workers⁵ that fluorescence from thin liquid films exhibits interference effects, which is ascribed to accumulation of dye molecules at the two film surfaces and the interference of the emissions from these two surfaces. The results is a pattern of light and dark fluorescence fringes, varying with the thickness of the film.

In this investigation, the film was illuminated with a laser beam of approximately 1 mm² cross-sectional area, at a point near the centre of the circular film. The fluorescence emission was monitored at 580 nm for periods of time up to 2 hr. As the film thinned through vertical drainage, light and dark fringes appeared. This was because most of the fluorescence emanated from the two surfaces; as the distance between the front and back surfaces decreased with time, the emissions interfered alternately constructively (bright fringe) and destructively (dark fringe). Figure 4 shows the fringe pattern (drainage profile) for Rhodamine B in a number of surfactant solutions. The 45/45 orientation (see Fig. 3) was used.

It is noted in Fig. 4 that the fringes get broader and more widely spaced with time. This arises because the drainage is most rapid at the beginning of film formation and slows down progressively. A similar effect is observed with reflectance fringes. There is, however, an important difference in the appearance of reflectance and fluorescence fringes; the former usually increase in intensity with time (before black film formation), while the latter decrease. This indicates that despite significant localization of dye molecules in the surfaces, they are not strongly held there and flow out as the film drains. The intensities of the dark fringes give an indication of the fluorescence emanating from the region between the film surfaces. The depths of the valleys in the drainage profiles increase with time, suggesting that the fluorophores in the interior of the film drain more rapidly than those contained in the surfaces. This is further borne out by measurements made with the light-in-frame system (Fig. 5). The radiation is incident vertically into the film, so fluorescence will mainly be excited in the central portion of the film. Interference fringes are clearly absent and the fluorescence intensity decreases rapidly, as would be expected for molecules not primarily located at the surfaces.

Polarization effects

The measurements described above were made with use of exciting radiation that was vertically polarized relative to the (horizontal) fringes in the film. No significant differences were observed between results obtained with different surfactants. However, when the direction of polarization was changed to horizontal, no interference fringes were found in the drainage profile of the CPC solution (Fig. 5). The TMAB solution gave weak fringes, the

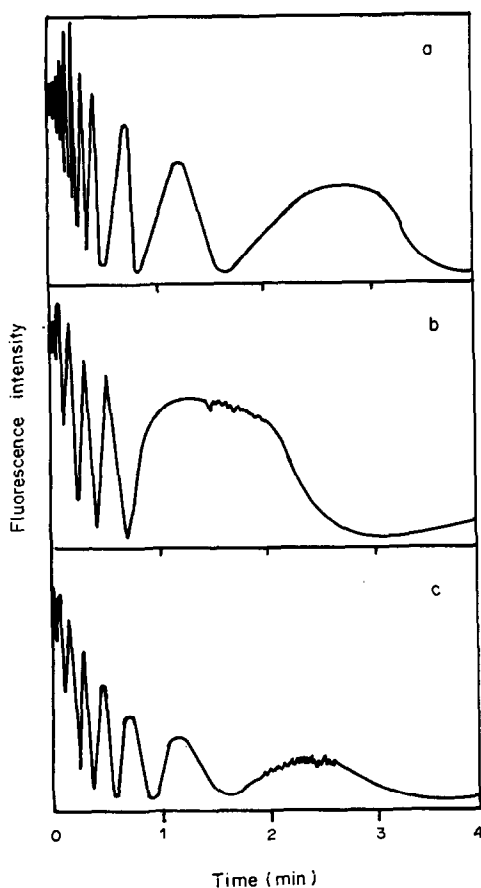


Fig. 4. Drainage profile of Rhodamine B in (a) SLS, (b) TMAB and (c) CPC solutions.

SLS solution slightly stronger ones, and those of the Brij 99 solution were virtually indistinguishable from the ones obtained with vertically polarized excitation. This suggests that the Rhodamine B molecules have very specific anisotropic orientations in the surfaces, especially in the case of the CPC film. This orientation is such that they are excited only by vertically polarized radiation. Horizontal polarization excites only the randomly oriented molecules in the inner portion of the film; the resulting emission decreases rapidly with time (Fig. 5), because the inner film drains quickly. It is noteworthy that the anionic and cationic surfactants all show this effect to some extent, whereas non-ionic Brij 99 does not.

Speed of drainage

Relative speeds of drainage of thin liquid film can be assessed by the number of fringes "passing" a fixed excitation point in a given period of time. Figure 6a shows the first 30 sec in the existence of an SLS film. In this period, 11 fringes are counted, reproducible to ± 2 fringes. The viscosity of the solution is 3.8 cp. When a similar solution, prepared with 1:2 v/v glycerol:water solvent (viscosity 6.2 cp), was used, the drainage rate increased to 23 fringes in 30 sec (Fig. 6b). Despite this approximately 2-fold greater

initial drainage rate, the glycerol-containing film had remarkable stability and could be kept for hours.⁶

The "short exposure" representations in Fig. 6 show another interesting effect; up to 10 sec of film life, the fringes on the SLS/water film increase in intensity, while those on the SLS/water/glycerol film only decrease in amplitude. This effect can be ascribed to differences in the speed of film drainage; in the SLS/water film, there is probably a net movement of fluorophore from the film interior to the surfaces during the first seconds of film life. After this, drainage becomes prevalent. In the SLS/water/glycerol film, initial drainage is too fast to allow for observable surface enrichment by the fluorophore. This is further indicated by the relative shallowness of the fringe pattern; a large proportion of the fluorophore content of the film stays in the interior during the rapid drainage.

All films with sufficiently long lifetimes reached a stage at which fluorescence intensities became very low and relatively invariant with time (Fig. 7). This condition resembles the "black film"⁷ found in reflectance measurements on thin films, but has a different origin. The black film arises because the film thickness has become so small that virtually all optical interference is destructive, whereas the

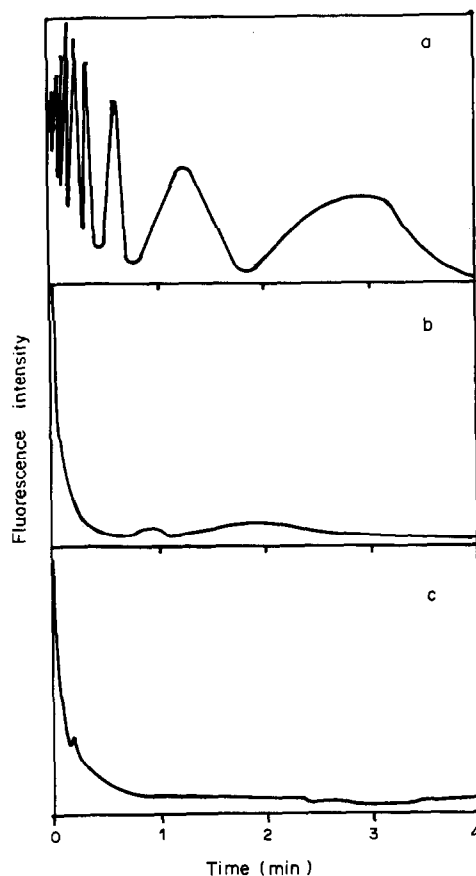


Fig. 5. Fluorescence response in thin films; (a) SLS, vertically polarized, 45/45; (b) SLS, light-in-frame; (c) CPC, horizontally polarized, 45/45.

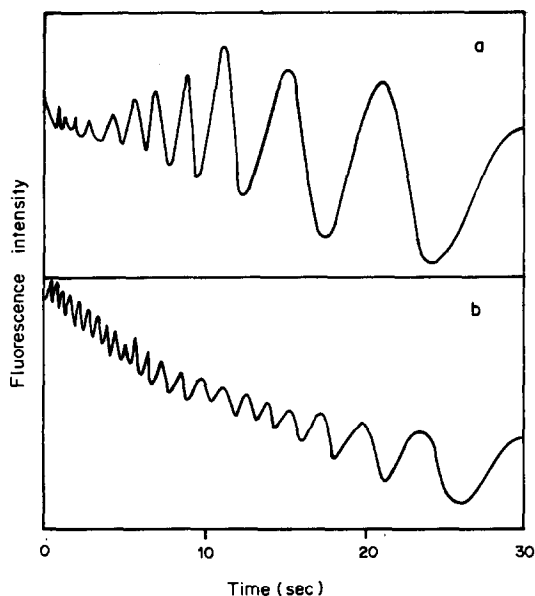


Fig. 6. Rhodamine B fluorescence fringes during initial stages of film life; (a) SLS solution in water; (b) SLS solution in 1:2 glycerol:water.

fluorescent film emits weakly at the later stages primarily because most of the fluorescent molecules have drained out of it.

Film thickness

Geometric considerations allow for the estimation of film thickness from time-resolved measurements of fluorescent fringes. When the film is inclined at 45° to both the excitation and emission directions (45/45), constructive interference (a bright fringe) is obtained when

$$k\lambda = \frac{t(2n - 1)}{n \cos\left(\arcsin \frac{0.707}{n}\right)}$$

where k = fringe number, λ = emission wavelength, t = film thickness and n = refractive index of the film.

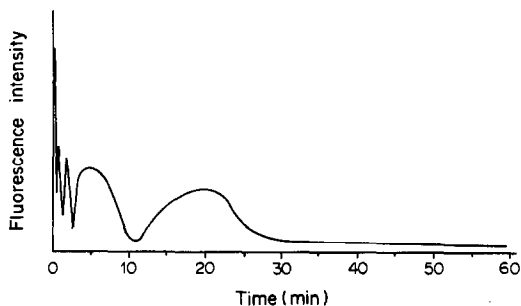


Fig. 7. Extended-period drainage profile of Rhodamine B in SLS solution.

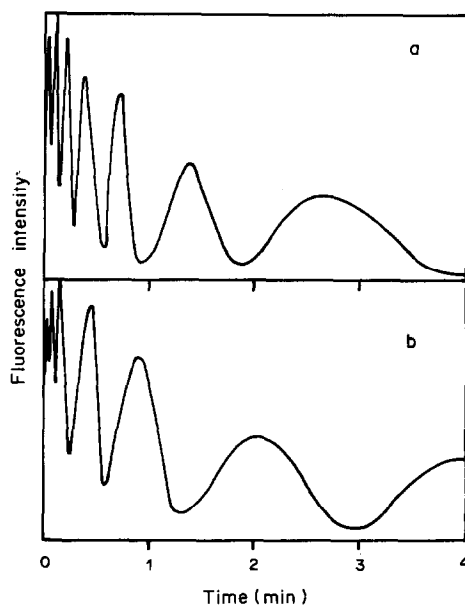


Fig. 8. Drainage profile of Rhodamine B in CPC solution; (a) 45/45 orientation; (b) 45/135 orientation.

If n is taken as approximately 1.33 and $\lambda = 600$ nm, then $t = 407k$. This means that the fringes are approximately 407 nm apart. When the film is inclined at 135° to the emission direction (45/135), the equation becomes

$$k\lambda = \frac{t}{n \cos\left(\arcsin \frac{0.707}{n}\right)}$$

so under the previous conditions $t = 676k$. Therefore, fringes measured at 135° are $676/407 = 1.66$ times farther apart than those measured at 45° . The experimental results are in reasonable agreement with this (Fig. 8). When the film surface was inclined at 90° to the exciting beam, interference fringes were observed, but they were of irregular shape and could not be interpreted.

Acknowledgement—This research was solely supported by NIH No. 5R01-GM11373-23.

REFERENCES

1. J. Lyklema, P. C. Scholten and K. J. Mysels, *J. Phys. Chem.*, 1965, **68**, 116.
2. J. Lyklema and A. J. Mysels, *J. Am. Chem. Soc.*, 1965, **87**, 12.
3. J. B. Rijnbout, *J. Phys. Chem.*, 1970, **74**, 2001.
4. G. F. Hewitt, P. C. Lovegrove and P. Nicholls, *A.E.R.E.*, R4478, 1964.
5. P. Fromherz and R. Kotulla, *Ber. Bunsenges. Phys. Chem.*, 1984, **88**, 1106.
6. W. G. Agterof, *Ph.D. Thesis*, University of Utrecht, 1977.
7. J. T. G. Overbeek, *J. Phys. Chem.*, 1960, **64**, 1178.

SPECTROMETRIC ANALYSIS OF NON-METALS INTRODUCED FROM A GRAPHITE FURNACE INTO A MICROWAVE-INDUCED PLASMA

JAROSLAV P. MATOUSEK, BRIAN J. ORR and MARK SELBY*

School of Chemistry, The University of New South Wales, P.O. Box 1, Kensington, N.S.W. 2033,
Australia

(Received 18 March 1986. Revised 3 June 1986. Accepted 27 June 1986)

Summary—A low-power helium microwave-induced plasma, sustained in a cylindrical TM_{010} cavity, has been used with sample introduction from a graphite furnace. An end-on optical configuration was employed to monitor both atomic and ionic emission from Cl, I, S and P. The operating parameters were optimized with respect to the nature of the plasma background response, the limits of detection, and the shapes and linearity ranges of the log-log analytical working curves. Possible applications were evaluated by determining iodine in milk and analysing a multi-component mixture of sulphur compounds.

Microwave-induced plasmas [MIPs] possess a number of advantages as excitation sources in emission spectrometry.¹ Chief among these is the high plasma-excitation temperature, which makes the MIP more suitable than thermal excitation sources for determining non-metals. Moreover, the power required for the MIP is relatively low, typically 100 W or less, so the need for cooling is minimal and the support-gas flow-rate can be 1 l./min or less. By comparison, the inductively-coupled plasma (ICP) uses power levels greater than 1000 W and large amounts of support gas for cooling.²

In addition, the MIP can be operated with helium which, because of its high excitation potential, enables halogens and other non-metals not readily amenable to ICP detection to be excited efficiently and detected with adequate sensitivity.

The low power requirements of the MIP produce low background emission. However, the low power also results in a relatively low gas temperature (around 2000 K),² limiting the capacity of the plasma to volatilize solid or liquid samples or to atomize the analyte species. This fact, together with the sensitivity of the plasma to changes in impedance when small amounts of foreign material are introduced, causes fundamental problems with sample introduction.

Many of the problems of sample introduction can be circumvented if the sample can be presented in the form of a gas or vapour to the plasma. For this reason, the most extensive use of MIPs has been in combination with gas chromatography as an element-selective detector, especially in the determination of non-metals. This aspect of MIP applications has been reviewed recently.²

The use of an MIP for the determination of non-metals in involatile substances has received relatively little attention. It was only with the introduction of the cylindrical TM_{010} cavity by Beenakker³ that plasmas could be sustained at atmospheric pressure and therefore combined simply with electrothermal (ET) atomizers. ET atomizers provide the necessary thermal energy to convert liquid or solid samples into atoms, requiring the MIP only to excite the analyte atoms. This approach has already been taken by several authors to determine sulphur, chlorine and bromine in samples volatilized from a graphite cord atomizer,⁴ chlorine, bromine, iodine and sulphur by using a tantalum furnace⁵ and halogens in organic compounds with carbon-cup or tantalum-boat sample-introduction.⁶ Recently, the determination of chloride in aqueous solutions by direct nebulization into an atmospheric-pressure helium MIP has been described.⁷ Compared with ET sample introduction, the direct-nebulization approach necessitates far higher power levels, typically approaching 500 W.

We have combined a minifurnace-based ET atomizer with an atmospheric-pressure helium MIP for the determination of chlorine, iodine, phosphorus and sulphur. The plasma discharge is viewed end-on to avoid problems of variable signal-attenuation by the walls of the silica discharge tube. In order to evaluate the potential of the MIP technique for speciation studies, a preliminary investigation with some sulphur-containing compounds has been made.

EXPERIMENTAL

Instrumentation

A Varian Techtron AA-5 atomic-absorption spectrometer equipped with an RCA 1P28 photomultiplier tube was operated in the emission mode by placing a chopper (285 Hz) in the light-path to give an ac signal for

*Present address: Department of Chemistry, Indiana University, Bloomington, Indiana 47405, U.S.A.

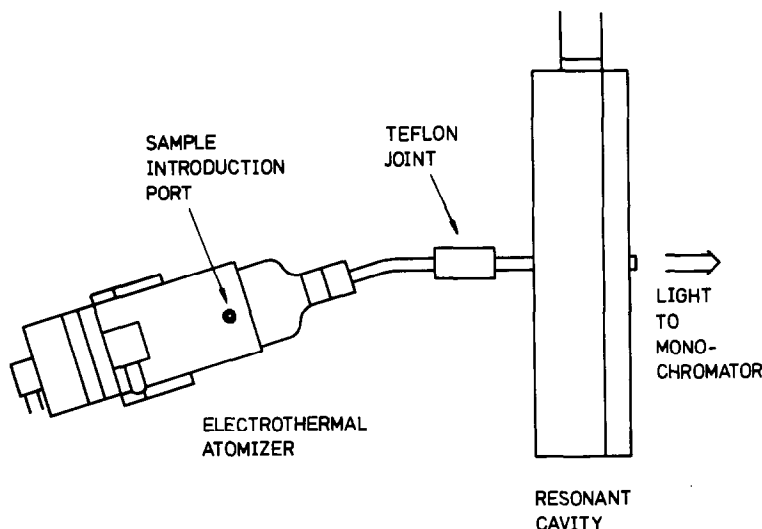


Fig. 1. Diagram of the experimental arrangement, showing coupling of the graphite atomizer with the helium MIP and the end-on viewing configuration employed. A further perspective of this apparatus is shown in Fig. 1 of ref. 8.

amplification. Signals were displayed on a National VP-6541A chart recorder or, for faster time-resolved measurements, the emission signals were recorded with a Tracor Northern TN-1505 signal averager. To achieve fast-response detection, the signal from the photomultiplier was fed directly into the signal averager after processing by a simple current amplifier with an *RC* time-constant of 10 msec.

The helium MIP was sustained within a Beenakker cylindrical cavity³ by use of microwave circuitry based on the Electromedical Supplies Microtron Mark II microwave generator, as described previously.⁸ Samples were volatilized into the plasma from a modified Varian Techtron CRA-63 ET atomizer after being introduced through a small hole drilled along the axis of one of the graphite support rods.⁸ The helium plasma, maintained in silica tubing of 3-mm internal diameter, was confined to the inside of the cavity at all incident power levels. The silica tube was subject to rapid devitrification, which precluded viewing through its walls. Hence, an end-on optical configuration was employed, as shown schematically in Fig. 1. The arrangement contained a Teflon joint to enable quick and convenient replacement of the discharge tubing, and the ET atomizer was mounted slightly off-axis to prevent the continuum radiation emitted by the incandescent furnace from entering the optical system.

Furnace temperatures below 1000° were measured with a chromel–alumel thermocouple, and those above it were monitored with an Ircon series 6000 radiation thermometer capable of covering a temperature range of 1000–3000°.

Reagents

All reagent solutions were prepared from high-purity chemicals. Nitric acid was distilled in an all-Teflon infrared-heated two-bottle still. Ultrapure water was obtained by passing distilled water through a Milli-Q ion-exchange and membrane-filtration system.

Procedure

Standard solutions of metal ions were prepared in 1% v/v nitric acid and stored in high-density polyethylene containers. A 5- μ l syringe with a Teflon capillary-tip extension was used to apply sample volumes of 1–2 μ l to the inner wall of the furnace. Typically, the heating programme consisted of drying for 40 sec at 120°, and atomization for 2.5 sec with a temperature ramp up to 2000°.

Industrial-grade helium was purified by passage through a type 4A molecular sieve in liquid nitrogen.

RESULTS AND DISCUSSION

Optimization of microwave power and gas flow-rate

The emission intensity for I(I), S(I), I(II) and Cl(II) lines was found to increase steadily with applied microwave power between 50 and 100 W. This result is in contrast to earlier results for spatially resolved measurements with an argon MIP,⁸ possibly as a consequence of the end-on viewing configuration now used and due to the fact that the helium plasma is confined to the inside of the cavity. With the plasma located inside the cavity, deposition effects are minimized as the analyte is readily introduced into the most intense region of the plasma. The greatest sensitivity has generally been obtained with the highest possible input power, but devitrification of the silica discharge tube means that input powers higher than 100 W are not practicable.

For each of the P(I), I(I), I(II) and Cl(II) lines observed with a range of helium flow-rates between 0.5 and 3.5 l./min, the maximum emission response occurs at flow-rates around 1.7–2.1 l./min. The optimum flow-rates thus obtained for the range of microwave powers studied are considerably higher than those published for similar furnace–MIP devices,^{5,9} which are generally in the range 0.2–0.5 l./min.

Analytical signal measurement

In contrast to the argon plasma, for which a negative background peak is usually observed during the heating of the graphite furnace,¹⁰ the helium MIP commonly gives a positive background response. Figure 2 illustrates the broad-band nature of the background signal in the helium-supported plasma, with the example of I(I) emission signals at the 206.24 nm line and at 0.2 nm either side of this line. Closer inspection of the wavelength-dependent behaviour of the background in the vicinity of 200 nm

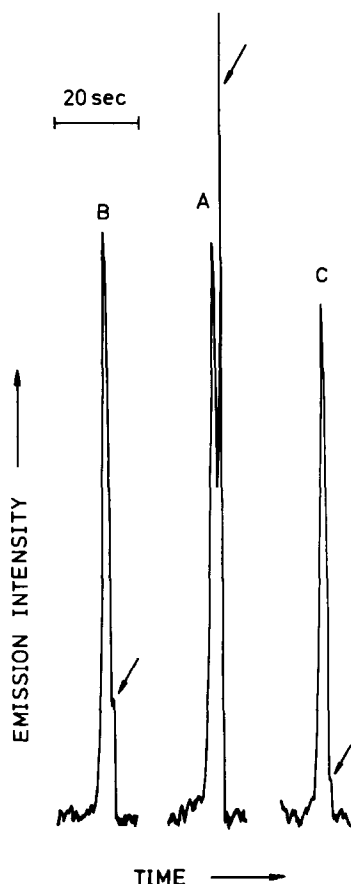


Fig. 2. Time-resolved emission signals for 1.4 μg of iodine (as KI) at the analytical line and at 0.2 nm either side of it: A, 206.24 nm; B, 206.04 nm; C, 206.44 nm. Arrows denote I(I) emission.

revealed a spectrum readily identified with molecular emission from the $A^1\pi - X^1\Sigma$ vibronic transitions of carbon monoxide by comparison with the data of Pearse and Gaydon.¹¹ This gas is produced by reaction of the heated graphite with impurity levels of oxygen in the support gas. In the vicinity of 500 nm, on the other hand, the background signal is made up of the $A^3\pi_g - X^3\pi_u$ vibronic transitions of the C_2 Swan system,¹¹ owing to carbon being vaporized into the plasma during the atomization cycle. It is evident, therefore, that the wavelengths selected to detect a given element will determine whether a background signal, either negative or positive, is observed. In both

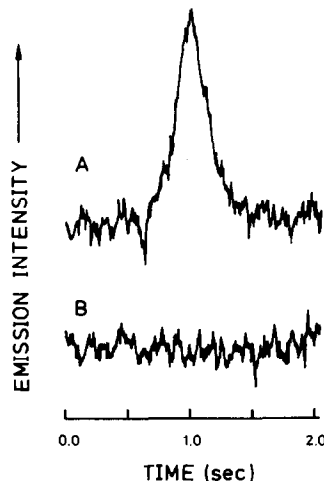


Fig. 3. Time-resolved emission signals at 479.45 nm: A, 35 ng of chlorine (as LiCl); B, blank firing of the graphite furnace.

instances the background emission intensity is a sensitive function of the vaporization temperature and may become so large that it prohibits the detection of the atomic signal for less volatile elements.

From these comments concerning variation of background during vaporization of the analyte, it is clear that a dynamic means of background correction, such as wavelength modulation, would be advantageous for the graphite furnace-MIP system. However, even though instrumentation with wavelength modulation was unavailable during the course of this work, good detectability could still be obtained, as seen in the following section.

Limits of detection

The detection limits shown in Table I represent the quantity of analyte equivalent to twice the standard deviation of the baseline noise of an analytical signal for a concentration close to the detection limit. The signal for Cl(II) (as LiCl) at 479.45 nm for a concentration approximately five times the detection limit is illustrated in Fig. 3.

The strongest emission from chlorine and bromine is from the ionic lines at 479.45 nm and 470.49 nm, respectively. Ionic emission from S at 545.39 nm was also observed but, contrary to the table of relative intensities published by Tanabe *et al.*,¹² was not as

Table I. Detection limits and log-log calibration slopes

Element	Form	Analysis line, nm	Detection limit,* ng	Log-log calibration slope
I	KI	206.24	1.0	1.57
Cl	LiCl	479.45	6.2	1.38
S	MgSO ₄	527.86/527.89	13.0	0.94
S	Thiourea	527.86/527.89	12.0	1.13

*Represents the quantity of analyte equivalent to twice the standard deviation of the baseline noise for an amount of analyte close to the detection limit.

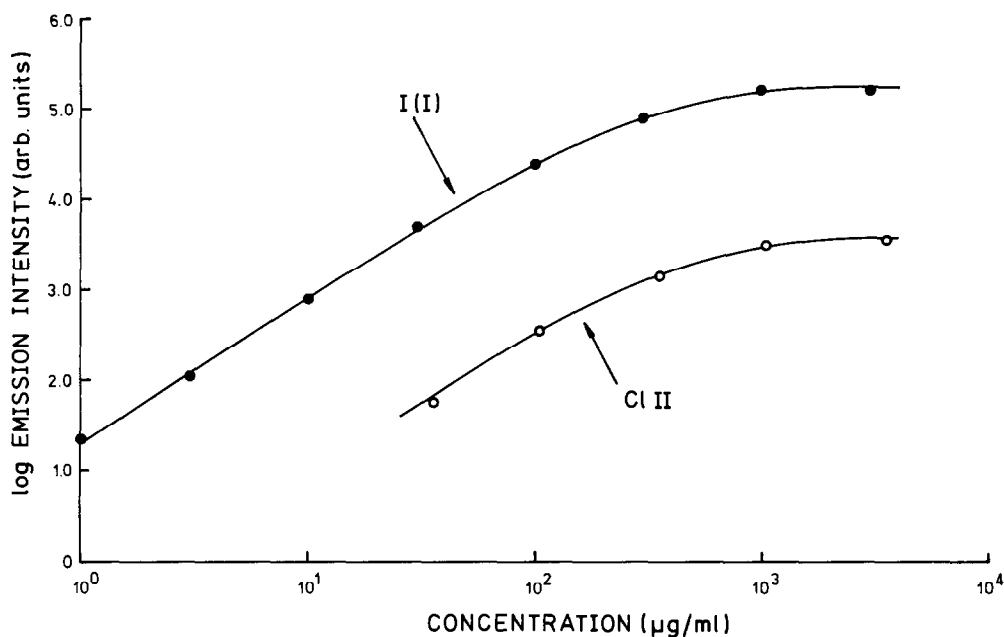


Fig. 4. Log-log analytical working curves for I(I) as KI (at 206.24 nm) and Cl(II) as LiCl (at 479.45 nm). The MIP was operated at 100 W and a helium flow-rate of 1.71./min.

intense as the S(I) emission at 217.05 or 675.71 nm or at the unresolved doublet at 527.86 and 527.89 nm. The 217.05 nm line is ordinarily the most intense emission line for sulphur at wavelengths longer than 200 nm but is accompanied by a large background signal which leads to a poor signal-to-background ratio. However, a favourable signal-to-background ratio has been found at the 527.86/527.89 nm doublet. The 675.71 nm line proves unsuitable for the detection of sulphur in thiourea, owing, apparently, to second-order interference from NH band emission produced during the decomposition of the $(\text{NH}_2)_2\text{CS}$. The detection limits obtained here for chlorine and sulphur are comparable to those reported by Beenakker *et al.*,⁴ but are considerably better than those reported more recently by van Dalen *et al.*⁵ For instance, the latter authors obtained detection limits of 0.80 µg for chlorine, 4.0 µg for iodine and 3.0 µg for sulphur, which are 2–3 orders of magnitude higher than those reported here (Table 1), presumably because van Dalen *et al.*⁵ did not use the optimum analytical lines in their work. Atomic emission from phosphorus (added as NaH_2PO_4) at the unresolved doublet at 213.62 and 213.55 nm and from fluorine (added as KF) at 685.60 nm has also been observed in the helium MIP. On the other hand, atomic emission from nitrogen and oxygen at 746.88 and 777.19 nm, respectively could not be detected from the vaporization of nitrates, such as potassium nitrate. However, NO γ -band emission at 237.0 nm was observed during vaporization of solutions containing potassium nitrate.

Analytical working curves

Log(emission intensity) versus log(concentration)

calibration curves for some of the non-metals studied are illustrated in Figs. 4 and 5. The linear dynamic range of response appears to be limited to 2–3 orders of magnitude by self-absorption effects, which can be expected to be more severe in an end-on optical arrangement than in a side-on configuration because of the greater optical path traversed by the emitted radiation. Sample overloading and partial quenching of the plasma also contribute to non-linearity at higher concentrations. When solutions of potassium iodide were investigated, sample loadings of more than 1 µg were observed to produce distortion in the time-resolved signal shapes, which was not observed at lower concentrations, as seen in Fig. 6. The iodine 206.24 nm emission at the 1.4-µg iodine level was observed to increase initially, then rapidly decrease before reappearing once more (trace A in Fig. 6). This behaviour for high concentrations of iodine (as KI) is consistent with a quenching of I(I) emission during the period in which potassium is coincidentally present with the iodine in large amounts (the effect of large amounts of easily ionized elements has been discussed recently¹³). Similar overloading effects may also account for curvature in the high concentration range of the log-log plots for other elements shown in Figs. 4 and 5. Consequently, the susceptibility of the MIP to sample overloading is a limitation of this technique.

An unusual feature of these log-log calibration curves is that the slopes are generally greater than unity (see Table 1). Only for sulphur does the slope approach unity. In general, the slope of log-log plots in the linear region should be 1.0 within experimental error, indicating that the instrumental response is a simple function of concentration. However, for the

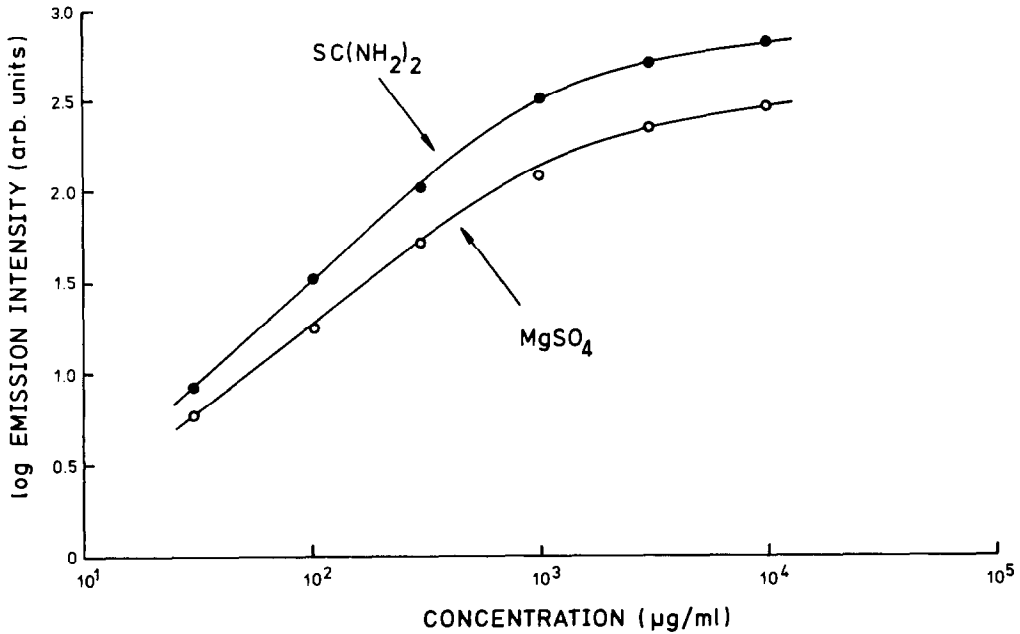


Fig. 5. Log-log analytical working curves for sulphur as MgSO_4 and thiourea at the doublet 527.86/527.89 nm. MIP conditions as for Fig. 4.

MIP technique such a simple relationship does not appear to hold. The possibility that these effects could be due to instrumental factors was investigated with the aid of a source of constant line emission (hollow-cathode lamp) and a set of neutral density filters to vary the emission output by several orders of magnitude. This instrumental calibration demonstrated that the detector/amplifier system was not responsible for the anomalously high slope of the log-log plots.

The results obtained here therefore appear to indicate that there is a complicated relationship between the concentration of the analyte and the emission intensity output when this MIP source is used.

Though the slopes > 1 present difficulties in understanding the nature of the excitation processes in the MIP, they do not lead to major practical difficulties in the use of the MIP for chemical analysis. In fact,

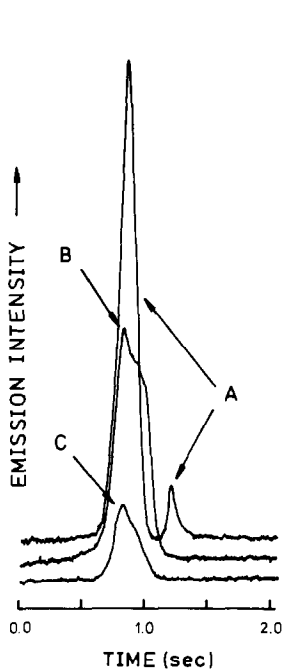


Fig. 6. Time-resolved emission signals for iodine as KI measured at 206.24 nm: A, 1.4 μg ; B, 0.42 μg ; C, 0.14 μg . MIP conditions as for Fig. 4.

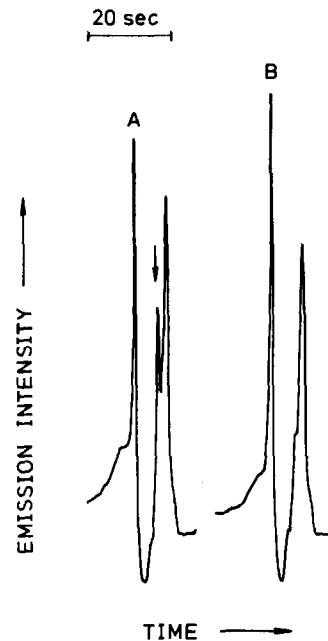


Fig. 7. Time-resolved emission signals for the ramp vaporization of 1.4 μl of untreated milk, measured at 206.24 nm: A, spiked with 0.46 μg of iodine (as KI); B, untreated milk only. The arrow denotes I(I) emission.

a slope of more than 1.0 increases the precision of measurement for a given concentration. It should also be mentioned that log-log plots with slopes differing significantly from unity have been reported by several authors.¹⁴⁻¹⁸ Much disagreement exists from laboratory to laboratory, however, and slopes of unity for log-log working curves have been obtained in some instances.^{4,9}

Potential applications

To assess further the capability of the graphite furnace-MIP technique for the determination of non-metals in different matrices, the determination of iodine in milk and the speciation of a multi-component mixture of sulphur compounds have been investigated. These studies were chosen to illustrate possible areas of application and so are preliminary in nature.

Iodine is a normal component of cow's milk at levels up to 100 $\mu\text{g/l}$. However, the use of iodine-containing detergents as germicidal agents has become widespread for various cleaning tasks in the dairy industry and has led to the risk of iodine contamination of milk supplies. Because of the possibility of iodine-induced thyrotoxicosis, rapid and reliable methods of iodine determination are necessary for quality control. Most available methods¹⁹ suffer from the disadvantage of either not being sufficiently sensitive or being time-consuming and so difficult to apply to a large throughput of samples. Ion-selective electrode methods are adequately sensitive and are suitable for the analysis of large batches of samples, but interferences from chloride and thiol groups in heat-treated milk, long response times and signal drift have been reported.¹⁹ In addition, a separation step is usually necessary to remove milk-fats which otherwise poison the electrode.

Samples of powdered milk were made up to full strength and spiked with potassium iodide but were otherwise untreated. Aliquots of 1.4 μl (containing 0.46 μg of added iodine) were applied to the atomizer, dried and vaporized into the helium MIP with a slow heating ramp. As can be seen from Fig. 7, the iodine signal was readily detected but was accompanied by a large background signal due to band emission produced by species such as carbon monoxide from decomposition of the organic material. Better results were obtained by ashing the sample *in situ* with potassium nitrate at approximately 500° to remove the organic material whilst retaining the iodine as potassium iodide. However, the background signal was still not diminished sufficiently to allow the detection of iodine at the low levels normally found in milk. The use of sample volumes greater than 2 μl produced difficulties in maintaining a stable discharge during vaporization of the sample, owing to the large quantities of organic material present. Sufficient discrimination between the background signal and the iodine signal to facilitate detection at the low levels in milk may be possible by

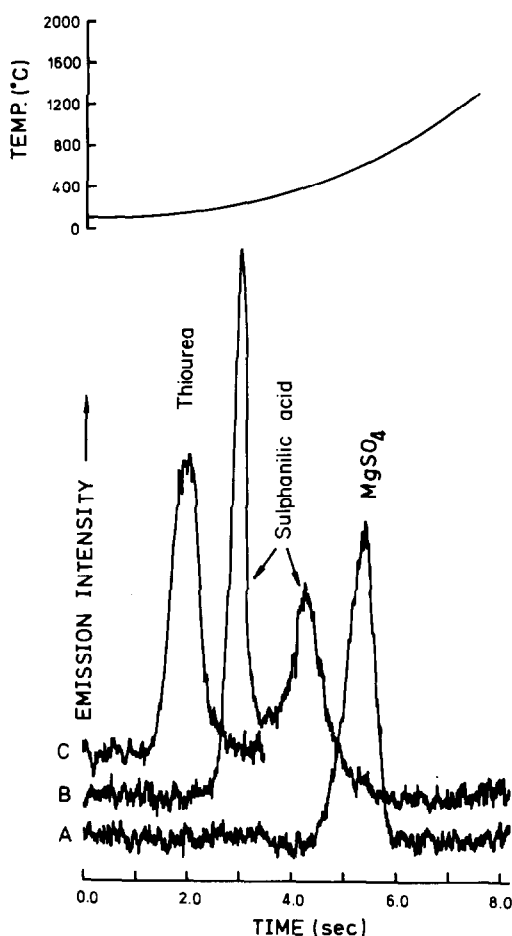


Fig. 8. Time-resolved emission signals for sulphur compounds measured at 527.86/527.89 nm and vaporized separately: A, MgSO_4 ; B, sulphanilic acid; C, thiourea. Amount of sulphur added is 1.4 μg in each case. MIP conditions as for Fig. 4. The correspondence between furnace temperature and time is shown on the accompanying diagram.

using wavelength-modulated detection, which was not available for this study.

In a second example, the MIP technique was applied to the analysis of a mixture of sulphur-containing compounds. The approach adopted employs the helium MIP as an evolved-gas detector which measures the emission signal of the volatilized analyte as a function of temperature.

A three-component mixture of magnesium sulphate, thiourea and sulphanilic acid (*p*-aminobenzenesulphonic acid) was selected for investigation. The unresolved S(I) doublet at 527.86 and 527.89 nm was used as the analysis line. A slow heating ramp was applied to the sample in order to achieve maximum resolution of the peaks. Figure 8 shows the time-resolved profiles for the three sulphur-containing compounds vaporized separately into the helium MIP. For magnesium sulphate and thiourea a single peak is observed, but for sulphanilic acid two peaks are found. The first sulphanilic acid peak (trace B in Fig. 8) proved to be broad-band in nature and

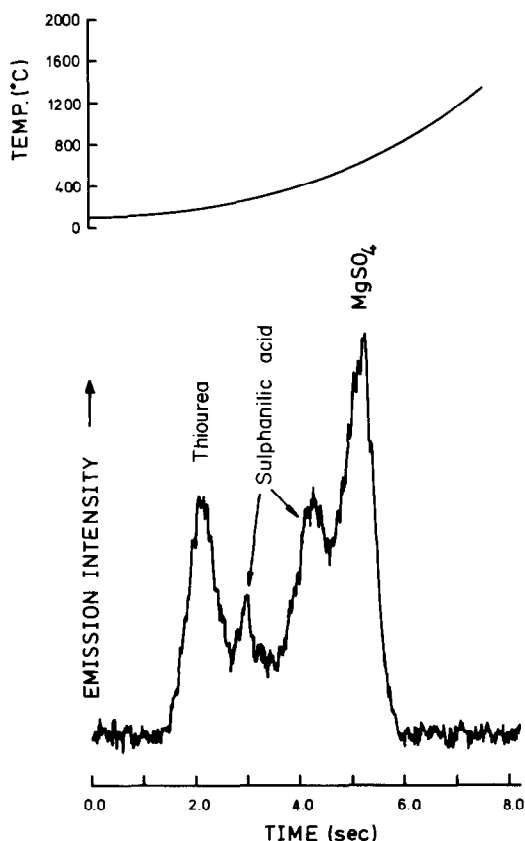


Fig. 9. Time-resolved emission signals for sulphur compounds measured under the conditions of Fig. 8 but vaporized as a mixture.

is likely to be due to C_2 Swan band emission, which is known to be weakly present in this spectral region. If this hypothesis is correct then the first peak in the sulphanic acid trace (trace B in Fig. 8) should be indicative of the decomposition of the benzene-ring part of the sulphanic acid. Figure 9 shows the time-resolved profiles obtained for a mixture containing the three components, equivalent to $1.4 \mu\text{g}$ of sulphur in each case. Four emission peaks can be clearly identified, corresponding to the pattern for the individual components seen in Fig. 8. However, the first peak for sulphanic acid (which does not correspond to emission by sulphur) is reduced in intensity in this trace.

So far, we have demonstrated that it is possible to resolve analytical signals from sulphur in different molecular environments. The time-resolution in this instance results from the fact that the different sulphur compounds possess different volatilization or decomposition temperatures, thus releasing the sulphur-containing analyte species into the plasma gradually. This concept may be extended to obtain discrimination between different atoms of the same element in a single molecular form, provided that the atoms are bonded differently. For example, sodium thiosulphate, $\text{Na}_2\text{S}_2\text{O}_3$, is known to disproportionate on heating, generating a mixture of sulphur-

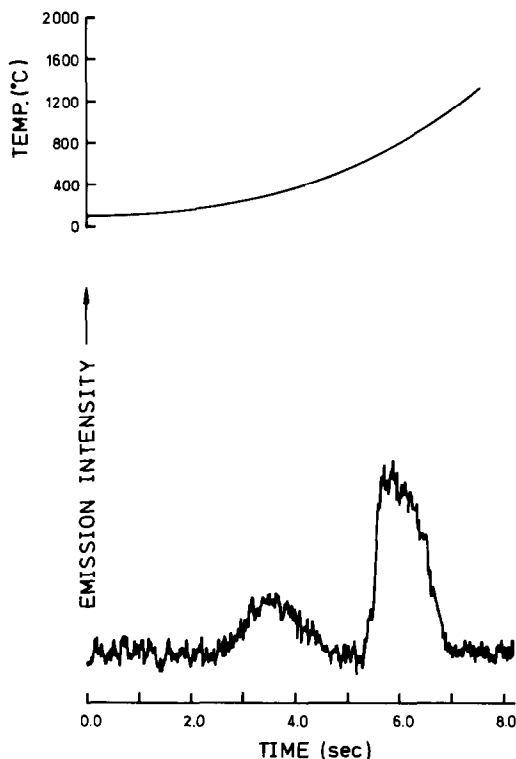


Fig. 10. Time-resolved emission signal for $\text{Na}_2\text{S}_2\text{O}_3$ ($0.9 \mu\text{g}$ of sulphur) measured at $527.86/527.89 \text{ nm}$. MIP conditions as for Fig. 4.

containing products. The time-resolved trace in Fig. 10 is consistent with such a process, the two emission peaks being taken to correspond to sulphur atoms from different environments within the $\text{S}_2\text{O}_3^{2-}$ anion, released in a two-step decomposition reaction.

CONCLUSIONS

The present investigations confirm that the atmospheric-pressure helium MIP is capable of detecting non-metals with appreciable sensitivity and without the need to use resonance emission lines in the vacuum-ultraviolet region. Complications associated with vacuum monochromators and non-absorbing optics, necessary with ICP non-metal detection,⁷ are thus avoided. The MIP approach is less suitable for the determination of metals, since the detection limits lie in the range $10\text{--}100 \text{ pg}$.¹⁰ Potentially, however, simultaneous determination of both metals and non-metals is possible.

Substantial improvement in the detection capability of the helium MIP system is expected to arise from the use of wavelength modulation. The wavelength-modulation technique can discriminate between atomic-emission signals and continuum or band-structure background by a factor of more than 100 in intensity.^{20,21} Judging from the improvement in detection limits reported when wavelength modulation is applied to ET atomic-emission spectrometry (namely, two orders of magnitude),²² similar im-

provement may realistically be expected with the MIP technique.

Our short evaluation of potential applications has demonstrated that the graphite furnace-MIP approach may play a useful role in the determination of chemical form or species. In this regard, the strength of the technique depends on its two-step character: by separately controlling the conditions in the graphite furnace and in the MIP itself, it is possible to optimize the circumstances under which different chemical species may be distinguished. The variety of experimental parameters and their standardization is an inherent complication, but this is offset by the compactness of the apparatus and its low cost compared to ICP and other techniques. So far, liquid samples have been employed but it should also be possible to examine solid samples.

REFERENCES

1. A. T. Zander and G. M. Hieftje, *Appl. Spectrosc.*, 1981, **35**, 357.
2. J. P. Matousek, B. J. Orr and M. Selby, *Prog. Anal. Atom. Spectrosc.*, 1984, **7**, 275.
3. C. I. M. Beenakker, *Spectrochim. Acta*, 1976, **31B**, 483.
4. C. I. M. Beenakker, P. W. J. M. Boumans and P. J. Rommers, *Philips Tech. Rev.*, 1980, **39**, 65.
5. H. P. J. van Dalen, B. G. Kwee and L. de Galan, *Anal. Chim. Acta*, 1982, **142**, 159.
6. J. W. Carnahan and J. A. Caruso, *ibid.*, 1982, **136**, 261.
7. K. G. Michlewicz and J. W. Carnahan, *Anal. Chem.*, 1985, **57**, 1092.
8. J. P. Matousek, B. J. Orr and M. Selby, *Appl. Spectrosc.*, 1984, **38**, 231.
9. M. Zerezhghi, K. J. Mulligan and J. A. Caruso, *Anal. Chim. Acta*, 1983, **154**, 219.
10. M. Selby, *Ph.D. Thesis*, University of New South Wales, 1984.
11. R. W. B. Pearse and A. G. Gaydon, *The Identification of Molecular Spectra*, 3rd Ed., Chapman & Hall, London, 1965.
12. K. Tanabe, H. Haraguchi and K. Fuwa, *Spectrochim. Acta*, 1981, **36B**, 119.
13. J. P. Matousek, B. J. Orr and M. Selby, *ibid.*, 1986, **41B**, 415.
14. J. H. Runnels and J. H. Gibson, *Anal. Chem.*, 1970, **42**, 1569.
15. H. Kawaguchi, I. Atsuya and B. L. Vallee, *ibid.*, 1977, **49**, 266.
16. I. Atsuya, H. Kawaguchi, C. Veillon and B. L. Vallee, *ibid.*, 1977, **49**, 1489.
17. F. L. Fricke, O. Rose and J. A. Caruso, *ibid.*, 1975, **47**, 2018.
18. O. Rose, D. W. Mincey, A. M. Yacynych, W. R. Heineman and J. A. Caruso, *Analyst*, 1976, **101**, 753.
19. S. M. Wheeler, *Aust. J. Dairy Technol.*, 1979, **34**, 169.
20. W. Snelleman, T. C. Rains, K. W. Yee, H. D. Cook and O. Menis, *Anal. Chem.*, 1970, **42**, 394.
21. M. S. Epstein and T. C. O'Haver, *Spectrochim. Acta*, 1975, **30B**, 135.
22. M. S. Epstein, T. C. Rains and T. C. O'Haver, *Appl. Spectrosc.*, 1976, **30**, 324.

EVALUATION OF SINGLE-POINT CALIBRATION IN FLOW POTENTIOMETRIC STRIPPING ANALYSIS

BOY HØYER and LARS KRYGER

Department of Chemistry, Aarhus University, Langelandsgade 140, 8000 Aarhus C, Denmark

(Received 12 March 1986. Revised 17 June 1986. Accepted 27 June 1986)

Summary—The use of a single-point calibration in flow potentiometric stripping analysis has been evaluated. For a number of sample matrices, the results obtained by calibration methods agree with those obtained by using standard addition. The most serious source of systematic error is inhibition in the deposition step, caused by organic surfactants and chelating agents in the sample matrix. Consequently, the use of the calibration method should be restricted to samples which have been totally mineralized. It is shown that most sources of systematic error in the calibration method will result in underestimation of the analyte concentration.

The application of flow-cells and medium-exchange facilities in conjunction with potentiometric stripping analysis (PSA)^{1,2} has two distinct advantages:^{3,4} first, by replacement of the sample solution with a suitable medium prior to the stripping step, strict control of the oxidant concentration in the stripping medium can be achieved.³ Hence inter-sample variations in oxidant concentration do not influence the sensitivity obtained. The second advantage is that the selectivity can be controlled by introduction of suitable complexing agents in the stripping medium.

Recently, in studies of mineralized sediments and biological materials,^{3,4} it was demonstrated that the flow technique permits determination of trace analytes by use of a single calibration. From the practical point of view, the calibration approach makes the determination easier: with the conventional type of flow-cells, each portion of the sample is analysed once and cannot be recovered, and this makes the standard addition method—commonly used in batch analysis—cumbersome in flow PSA because it requires the preparation, exchange and analysis of several batches of unspiked and spiked sample. With the calibration approach, however, a quantitative result can be obtained from two measurements: one on the sample, and one on the standard solution.

The calibration method is, however, only valid if the preconcentration efficiencies are the same for the sample and the calibration solution. Although the major-component composition of the sample and thus the chemical form of the analyte can be controlled to a large extent by the addition of a matrix-modifying solution,³ the rate of deposition may still be affected by non-analyte species in the sample. Furthermore, surface-active compounds accumulated on the electrode during deposition may have a pronounced effect on the stripping process in spite of the medium exchange.

At present, however, no information is available on the general utility of the direct calibration approach. It is the purpose of the present work to identify the most probable causes of systematic error in it and to point out the practical measures available for mitigating them. The discussion is based on results obtained in a study in which a number of substances were examined by PSA and the trace metals were determined by both direct calibration and standard-addition methods.

EXPERIMENTAL

Instrumentation, flow system and electrodes

A computerized instrument⁵ was used for data acquisition and experimental control. During the stripping phase in the PSA, the potential of the working electrode was sampled at constant frequency, 6.7 kHz, and recorded as a potential distribution, the stripping of an amalgamated analyte appearing as a peak. In most cases, the capacitance component of the primary stripping potentiogram was corrected for by subtraction of a background potentiogram obtained in a separate deposition/stripping cycle.⁶ The deposition time chosen in this cycle was sufficiently short (2 sec) for analyte accumulation to be neglected. In a few cases, however (signal/background < 4), a numerical correction—assuming that capacitance was a linear function of potential—was employed. The net signal amplitudes obtained in this manner did not deviate significantly from those obtained by using the experimental correction. The standard deviations, however, were generally lower.

The flow-cell employed was of thin-layer type and consisted of a PTFE bottom and a Perspex top, separated by a cell spacer.^{7,8} The working electrode and the counter-electrode, both fabricated from 3-mm glassy-carbon rods, were placed in the bottom part with the counter-electrode downstream from the working electrode. The top part contained the solution inlet and outlet ports as well as the reference electrode, which was placed in a separate compartment in the solution outlet. The reference electrode was a Radiometer K401 saturated calomel electrode. The flow channel was 0.15 mm deep, 3.5 mm wide and 25 mm long. Solution exchange was provided by means of a 6-way pneumatic valve (Rheodyne 5011P) under microcomputer control.

Table 1. Composition of media employed in the flow PSA

Step	Inlet no.	Medium composition
Film removal	1	1M NaI, 1 mM I ₂
Rinsing	2	50% v/v ethanol in 0.1M HCl
Mercury plating	3	400 µg/g Hg(II) in 0.1M HCl
Rinsing	4	same as for inlet no. 2
Deposition	5	sample
Stripping	6	2.5M CaCl ₂ , 20 µg/g Hg(II)*

*In the determination of tin in tomato juice, 1M acetate buffer spiked with 20 µg/g Hg(II) was used as stripping medium.

Gravitational solution flow was obtained by placing the sample and reagent flasks about 55 cm above the flow-cell. The flow-rates were 1.9 and 1.7 ml/min for sample solutions modified with 0.5M hydrochloric acid and 1M acetate buffer, respectively, and the flow-rate of the 2.5M calcium chloride was 1.1 ml/min.

Chemicals, laboratory equipment and samples

Triply distilled water and analytical-grade chemicals were used except for the mineral acids, sodium acetate and calcium chloride, which were of *Suprapur* grade (Merck). Most stock solutions of the analytes (4 g/l.) were prepared by diluting commercial standards (Merck, Titrisol) with water. The tin standard, however, was prepared by dissolution of tin(II) chloride in 0.5M hydrochloric acid. Dilute solutions of the standards were prepared daily. Polyethylene vessels were used throughout, except for the volumetric glassware needed in the final dilution of decomposed samples. All containers, and the flow-cell, were rinsed thoroughly with 0.5M hydrochloric acid before use. Schleicher & Schüll ashless filters were used.

The food samples investigated were purchased in local supermarkets. The tinned mussels originated from the Limfjord in Denmark, and the canned tomato juice was produced in Italy. The standard kale was obtained from Dr. H. J. M. Bowen,⁹ and the certified coal fly-ash (SRM 1633a) was obtained from the U.S. National Bureau of Standards. The urine samples originated from three members of the laboratory staff and were acidified immediately after sampling.

Composition of media and potential/time sequence employed in flow PSA

Table 1 gives the composition of the media in the cell during each step of the measurement cycle. In the first step, the old mercury film was removed in an iodide medium which allowed oxidation of mercury at a potential where the

supporting glassy-carbon electrode is not affected.¹⁰ After the rinsing step, a new mercury film was plated onto the electrode, and the usual deposition/stripping procedure was started. Table 2 lists the potential-time programme used during the analytical cycle.

Decomposition and pretreatment of samples

Tinned mussels. Approximately 2 g of wet mussel was digested with 2 ml of concentrated nitric acid, 2 ml of water and 0.125 ml of octanol in essentially the same manner as previously described,¹¹ except that the final decomposition took place in a PTFE-lined pressure bomb left overnight at 100°. Finally, the digest was diluted to 50 ml with water. This procedure yielded a slight mineral residue.

Standard kale. One g of dried kale was decomposed with 8 ml of concentrated nitric acid in the PTFE-lined pressure bomb, left overnight at 100°. After decomposition, the sample was diluted to 50 ml with water.

NBS coal fly-ash. The decomposition procedure was that previously described.¹² Thus, approximately 1 g of dried ash was fused with 2 g of a 66+34 mixture of lithium tetraborate and lithium metaborate (Spectromelt A12, Merck) at 900–1000° and subsequently dissolved in hydrochloric acid (1+3) and diluted to a final volume of 100 ml with the same acid.

Red wine and urine. A 2.5-ml sample was acidified with 7.5 ml of 0.5M hydrochloric acid and analysed without further treatment. The urine samples were not analysed quantitatively as the content of lead and cadmium was not significantly higher than the reagent blanks. However, this sample type was included in the study because of the high content of surface-active substances in the matrix.

Tomato juice. A 2-ml portion of juice was mixed with 18 ml of 0.5M hydrochloric acid. The mixture was filtered because suspended organic matter in the juice tended to block the flow system. Owing to the high content of the analyte determined (tin), it was necessary to dilute the

Table 2. Potential-time sequence employed in the flow PSA

Step	Inlet no.	Time, sec	Potential, mV vs. SCE
Film removal	1	7.5	0
Rinsing	2	7.5	0
Mercury plating	3	10	-450
Mercury plating	3	20	-750
Rinsing	4	7.5	0
Sample inlet	5	10	0
Deposition	5	*	*
Stripping solution inlet	6	*	†
Recording of primary signal	6		
Rest period	6	2	0
Deposition for background signal	6	2	†
Recording of background signal	6		

*Dependent on sample analysed.

†Same potential as deposition potential.

Table 3. Instrumental parameters for the flow PSA determinations

Sample	Element(s) determined	Deposition potential, <i>mV</i> vs. <i>SCE</i>	Deposition time, <i>sec</i>	Stripping solution inlet time, <i>sec</i>
Mussel	Pb, Cd	-1000	120	20
Standard kale	Pb, Cd	-1000	90	20
Fly-ash	Pb	-1000	60	20
Red wine	Pb	-1000	60	15
Tomato juice	Sn	-1200	30	15

filtered solution tenfold with 0.5*M* hydrochloric acid to avoid saturation of the mercury film electrode.

Before the PSA, the decomposed samples (mussel, kale and coal fly-ash) were buffered with a medium prepared by adjusting 1*M* sodium acetate to pH 4.8 with concentrated hydrochloric acid. The mussel and kale digests were diluted fivefold (*i.e.*, 1 + 4) with the buffer, whereas the fly-ash solution, the most acidic sample studied, was diluted tenfold. One portion of each substance was decomposed and replicate analyses were done on aqueous subsamples drawn from the same digest.

General analytical procedure

The instrumental parameters used for each type of sample are given in Table 3. Most calibration solutions were prepared in the same manner as the sample solutions, with water instead of the sample, except for the red wine analysis, where the sample was replaced by a 12% v/v ethanol solution corresponding to the alcohol content of the wine. The concentration of analyte in the calibration solution was chosen so that the calibration and the analytical signals were of similar magnitude. In each analysis, to check the validity of the calibration scheme, two standard additions were made, chosen so that the final signal was about three times the analytical signal. All PSA measurements were made in triplicate.

RESULTS

The results obtained for lead, cadmium and tin in the samples investigated are given in Table 4. Generally, the concentrations obtained by standard-addition and direct calibration agree well. Apart from the cadmium determination in the mussel sample, the difference between the concentrations found by the two methods is less than the standard deviation of either value. The results have been corrected for the blank values obtained for the decomposition pro-

cedures, which in all cases were less than 5% of the analyte concentrations found. The reagent blanks of the buffers used for the final preparation of samples and standards were frequently checked and found to be negligible except for the acetate buffer used in the analysis of the standard kale, which showed blank values corresponding to 20 and 10%, respectively, of the cadmium and lead concentrations in the kale. Both the sample signal and the calibration signal were corrected for the background values. The results for the standard materials agree with the certified (or recommended) values within experimental error.

DISCUSSION

During the preliminary optimization of the experimental parameters, it was found that when there was a difference in sensitivity between the sample and the calibration solution, the latter always gave the higher sensitivity. In addition, it was observed that equality of sensitivity for the sample and standard was only achievable by empirical optimization of the experimental conditions. The major factors found to affect the accuracy of the calibration approach are discussed below.

Effects of chelating agents and surface-active compounds in the sample

Although the major-ion composition of both the sample and the calibration solutions may be controlled by the addition of a matrix-modifying solution, the plating efficiency of the sample may also be affected by chelating agents or surface-active organic compounds, particularly if untreated samples are

Table 4. Analytical results of flow PSA determinations.

Sample	Analyte	Concentration found,* $\mu\text{g/g}$		Certified or recommended value, $\mu\text{g/g}$
		Standard addition	Calibration	
Tinned mussels	Pb	1.1 (0.2)	1.06 (0.05)	
	Cd	0.61 (0.04)	0.55 (0.02)	
Standard kale	Pb	2.1 (0.2)	2.0 (0.2)	2.6 (1.6-3.8)†
	Cd	0.9 (0.1)	0.86 (0.05)	0.8 (0.38-1.06)†
Coal fly-ash	Pb	78 (8)	76 (7)	72.4 (0.4)§
Red wine	Pb	0.062 (0.003)	0.060 (0.003)	
Canned tomato juice	Sn	167 (6)	162 (4)	

*Mean and standard deviation based on four determinations.

†Best mean value and range reported by Bowen.⁹

§Certified value and estimated uncertainty (NBS certificate).

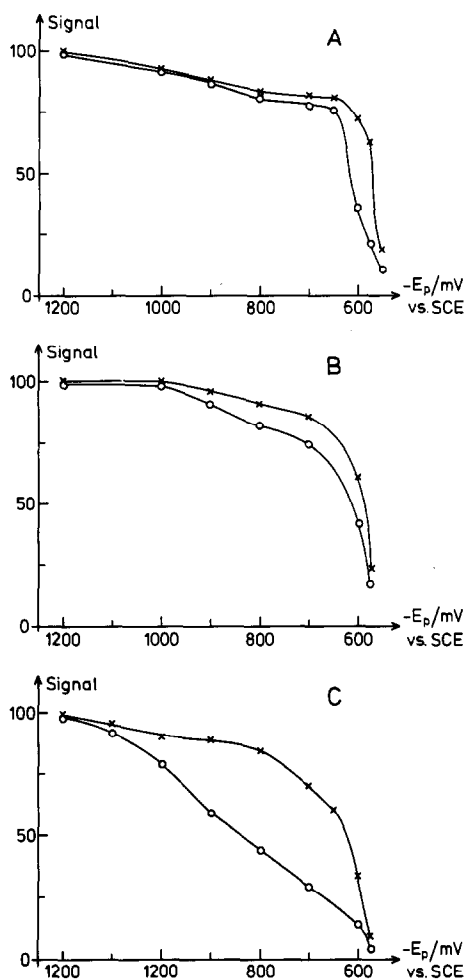


Fig. 1. Stripping signal of lead as function of deposition potential E_p for (A) acid digest of standard kale, (B) red wine, (C) urine. Samples were spiked with (A) 0.2 $\mu\text{g/g}$, (B) 0.2 $\mu\text{g/g}$ and (C) 0.1 $\mu\text{g/g}$ lead(II): (O) signal measured in sample solution, (x) signal measured in calibration solution spiked with same concentration of lead(II) as the samples. The lead signal of the calibration solutions at $E_p = -1200$ mV vs. SCE is set to 100. The lead content of samples prior to spiking and the effect of ethanol in the red wine sample (see text) have been corrected for in the figure. Deposition for 30 sec.

analysed. To determine whether such effects were operative, pseudo-polarograms of lead (*i.e.*, plots of stripping signal as a function of deposition potential) were recorded for three of the sample types investigated (Fig. 1). The experimental conditions were identical to those employed in the quantitative analysis of the samples. Apart from a slight cathodic shift, the pseudo-polarograms of the standard kale digest (Fig. 1A) and of the red wine sample (Fig. 1B) closely resemble those of the calibration solutions and show plateaux due to limited mass-transport rate. Consequently, moderate deposition overpotentials are sufficient to achieve almost identical pre-electrolysis efficiencies for the samples and the standards. However, for the urine sample (Fig. 1C), there are kinetic complications, as the shape of the pseudo-

polarogram for this sample differs from that of the standard solution and, unless a very high plating overpotential ($E_p = -1200$ mV vs. SCE) is applied, the sensitivity obtained for lead in the sample is lower than that obtained for the calibration solution. On the basis of the present data, it is not possible to determine whether the decreased reversibility of the amalgamation process during plating is caused by chelation of the analyte or by adsorption of surface-active compounds on the electrode surface. If the electro-deposition of trace metals from a multi-ligand system is regarded as dissociation of the metal complexes followed by reduction of the free metal ion, it can be shown theoretically¹³ that the general shape of the stripping pseudo-polarogram is independent of the nature of the ligands. Clearly, the stripping pseudo-polarogram of urine is much more drawn out than those of digested kale and of red wine. Thus, a possible explanation of this feature is that the lead in the urine sample, in spite of the acidification, is retained in non-labile complexes, but that direct reduction of the metal from these complexes takes place at very negative deposition potentials.¹⁴

Strong adsorption effects were observed in the analysis of the urine samples, as omission of the film-renewal procedure led to gradual fouling of the electrode surface during consecutive plating/stripping cycles. In the examination of all three urine samples, a very high plating overpotential ($E_p = -1200$ mV vs. SCE) was required in order to obtain equal sensitivities for lead in the sample and the calibration solution. However, even though equal sensitivities could eventually be achieved, it cannot be concluded that the calibration approach will work for all untreated urine samples, as the composition of this sample type varies greatly and spurious interferences in its PSA have been reported, usually associated with a high protein content.¹⁵

Mixed-solvent samples

The plating efficiency is generally dependent on the composition of the solvent system, and, if solvents miscible with water are present in the sample matrix,

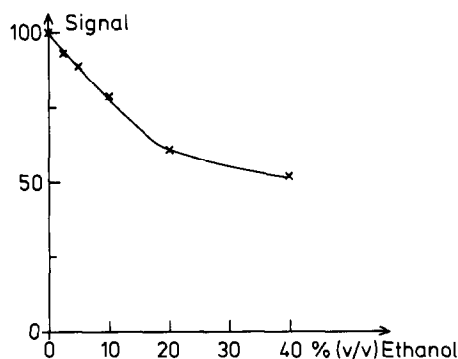


Fig. 2. Effect of ethanol content on the lead signal measured in 0.3M hydrochloric acid spiked with 0.1 $\mu\text{g/g}$ lead(II). Deposition for 45 sec at -850 mV vs. SCE. The signal is scaled to a reference value of 100 at 0% ethanol.

the calibration solution must be modified accordingly. As an example, the sensitivity for lead in hydrochloric acid-ethanol mixtures was recorded as a function of the ethanol content (Fig. 2). At the ethanol concentration corresponding to the acidified red wine sample (3% v/v), the sensitivity for lead decreased by 7%, and the inclusion of a corresponding amount of ethanol in the calibration solution was necessary.

Intermetallic compounds

A calibration procedure will generally be inaccurate if intermetallic effects occur in the analysis of the sample, since no corresponding intermetallic-compound formation will take place when the analyte signal of a synthetic standard is measured. Although standard-addition may partially compensate for the interference effect,¹⁶ it also is likely to fail because the analytical signal is no longer selective. Reliable results can be expected only if the interference is eliminated by one of the various strategies available for this purpose.¹⁶ The flow approach facilitates implementation of some of the elimination methods. In particular, between the plating/stripping cycles, it is possible to remove the electrode film completely and to generate a fresh one under well-defined conditions. In this manner it is possible to control the film thickness and hence the degree of association of plated metals. Furthermore, when the film is always renewed in this way, noble metals and inert intermetallic compounds are not accumulated on the working electrode.

Intermetallic-compound formation usually causes a depression of the analytical signal,¹⁶ and the analyte concentration will consequently be underestimated by a calibration procedure. In the present study, it is probably the formation of one or more of the cadmium-copper intermetallic compounds¹⁷ which causes the discrepancy between the cadmium values found by calibration and by standard-addition for the mussel digest. Indeed, this sample contained a very high ratio of copper to cadmium.

Samples with high concentrations of oxidants

For full control of the re-oxidation rate in the stripping step, the fraction of sample solution remaining in the flow-cell must be negligible when registration of the stripping signal begins. In practice, however, the required degree of completeness of sample flushing is strongly dependent on the composition of the sample matrix. In particular, there is a risk of memory effects when samples with high oxidant concentrations are analysed, and the time required for medium exchange is longer than in the analysis of other samples. For example, in the analysis of the red wine sample, the analytical signal reached its limiting value 10 sec after inlet of the stripping solution, whereas an exchange time of 15 sec was necessary in the analysis of the fly-ash sample. According to the certificate, this material

contains 9.4% iron, which is present as iron(III) after the decomposition step. In practice, it is always advisable to keep the medium exchange-time well above the minimum required.

CONCLUSIONS

The most serious risk of systematic error in the calibration method is from the inhibition of the deposition reaction by surfactant and chelating agents present in the sample matrix. These interference effects are mostly observed in the analysis of samples with an organic matrix that are not subjected to a decomposition procedure. In the present study, sample acidification and renewal of the mercury film between each scan did not eliminate the organic interferences, and equal sensitivity for the sample and calibration solutions could only be achieved by the use of a very high plating potential. However, this measure severely reduces the selectivity of PSA, since elements causing peak overlap or intermetallic interferences with the analytes may be co-plated. The attainment of equal sensitivity for a particular sample and the calibration solution does not necessarily mean that the conditions used will be generally applicable to samples of the same type, since variations in the content of adsorbable species may give rise to considerable variations in analyte deposition efficiency.

In the analysis of samples containing organic solvents (e.g., alcoholic beverages), the preparation of the calibration solution requires prior knowledge of the content of the organic solvent. Consequently, the calibration approach is of limited utility for such analyses.

In conclusion, future attempts to exploit a calibration approach in PSA should be restricted to samples which are totally mineralized.

When applicable, the calibration approach initially requires some effort in searching for appropriate experimental conditions and a suitable composition of the matrix-modifying solution. However, once the optimum conditions have been established, subsequent analyses can be done much more rapidly, and the consumption of sample, solvents and reagents will be considerably reduced.

The drawbacks of the calibration approach are mostly associated with the necessity for addition of concentrated matrix-modifying solution to the sample. In ultratrace analysis, this addition may be a serious source of contamination.

Acknowledgements—The authors are indebted to J. K. Christensen for assistance with sample preparation and to P. Christensen, J. Rokkjær and C. F. Hansen for developing the flow-cell and adapting the microcomputer program to flow PSA. A research fellowship (to B.H.) from the Danish Technical Science Research Council (16-3499K-810) and a grant (511-8032) from the Danish Natural Science Research Council for the computerized instrument are gratefully acknowledged.

REFERENCES

1. D. Jagner and A. Graneli, *Anal. Chim. Acta*, 1976, **83**, 19.
2. D. Jagner, *Anal. Chem.*, 1978, **50**, 1924.
3. L. Anderson, D. Jagner and M. Josefson, *ibid.*, 1982, **54**, 1371.
4. D. Jagner and K. Årén, *Anal. Chim. Acta*, 1982, **141**, 157.
5. H. J. Skov and L. Kryger, *ibid.*, 1980, **122**, 179.
6. L. Kryger and D. Jagner, *ibid.*, 1975, **78**, 251.
7. C. F. Hansen, *M.Sc. Thesis*, Aarhus University, 1984.
8. J. Rokkjær, *M.Sc. Thesis*, Aarhus University, 1984.
9. H. J. M. Bowen, *J. Radioanal. Chem.*, 1974, **19**, 215.
10. D. Jagner, *Trends Anal. Chem.*, 1983, **2**, 53.
11. L.-G. Danielson, D. Jagner, M. Josefson and S. West-erlund, *Anal. Chim. Acta*, 1981, **127**, 147.
12. J. K. Christensen, L. Kryger and N. Pind, *ibid.*, 1982, **141**, 131.
13. D. R. Turner and M. Whitfield, *J. Electroanal. Chem.*, 1979, **103**, 43.
14. T. M. Florence, *Anal. Chim. Acta*, 1982, **141**, 73.
15. M. T. Watts, B. J. Poulsen, L. L. Szabo, M. A. Kenny and W. Y. Lee, *J. Anal. Toxicol.*, 1981, **5**, 231.
16. J. Wang, *Stripping Analysis: Principles, Instrumentation and Applications*, VCH Publishers, Deerfield Beach/Weinheim, 1985.
17. B. W. Woodget and K. R. Franklin, *Analyst*, 1981, **106**, 1017.

FLUORIMETRIC DIFFERENTIAL-KINETIC DETERMINATION OF SILICATE AND PHOSPHATE IN WATERS BY FLOW-INJECTION ANALYSIS

P. LINARES, M. D. LUQUE DE CASTRO and M. VALCARCEL

Department of Analytical Chemistry, Faculty of Sciences, University of Córdoba, Córdoba, Spain

(Received 6 January 1986. Revised 9 June 1986. Accepted 27 June 1986)

Summary—A flow-injection analysis (FIA) method for simultaneous determination of silicate and phosphate, based on the different rates of formation of their molybdate heteropoly acids is suggested. The fluorimetrically monitored product is thiochrome, formed by oxidation of thiamine by the heteropoly acid. The FIA configurations designed allow performance of two measurements at different times on each sample injected. The method permits the determination of these anions in the range 30–600 ng/ml in ratios from 1:10 to 10:1 and can be applied to samples of running and bottled water with good results. The sampling frequency achievable is 60/hr.

Flow-injection analysis, FIA, has been used for determination of silicate or phosphate by formation of their heteropoly acids with molybdate and photometric detection of molybdenum blue¹⁻¹³ or voltammetric detection.¹⁴⁻¹⁷ The analysis of mixtures of both anions has been based on the use of separation (e.g., by precipitation,¹⁸ or extraction¹⁹), masking agents,^{20,21} and differential kinetics.^{22,23} The sensitivity of these methods is low, however, and the methods involving separation are rather slow and laborious. Only one FIA method (based on heteropoly acid formation and voltammetric detection) has been proposed for the determination of silicate and phosphate; it was applied to determination of total phosphate and soluble silicate in commercial washing powders, and used a different sample treatment for determination of each anion (an unhydrolysed sample for silicate and a hydrolysed one for phosphate).⁴

The method suggested in this paper for the simultaneous determination of silicate and phosphate is based on the formation rate of the phosphate heteropoly acid being higher than that of the silicate product. The heteropoly acid is detected by means of its oxidation of thiamine to thiochrome, which is fluorimetrically monitored. The use of a single detection point, which simplifies the instrumentation needed, calls for the design of FIA configurations allowing measurements to be performed at two different residence times. Two such configurations have been used: a manifold with a single injection, and splitting and confluence points before the detector,^{24,25} and a manifold with dual injection, and confluence before the detection system.²⁶

EXPERIMENTAL

Reagents

Stock aqueous solutions of 0.06M ammonium heptamolybdate, $1 \times 10^{-2}M$ silicate, $1 \times 10^{-2}M$ phosphate and

1 g/l. EDTA. Aqueous thiamine solutions of a suitable concentration were prepared daily. The buffer solution was made by dissolving 3.814 g of borax and 37 ml of concentrated ammonia solution in 100 ml of distilled water, and adjusting to the desired pH with concentrated hydrochloric acid.

Apparatus

A Perkin-Elmer LS-1 LC fluorescence detector with 4- μ l flow-cell, and a Perkin-Elmer 56 recorder; Gilson Minipuls-2 and Ismatec S-840 peristaltic pumps; Tecator L100-1 and dual home-made injection valves; a Tecator TM III "Chemifold" and a Selecta S-382 thermostat.

RESULTS AND DISCUSSION

Preliminary studies

The method for simultaneous determination requires knowledge of the behaviour of each individual system: $\text{SiO}_3^{2-}/\text{MoO}_4^{2-}$ /thiamine and $\text{PO}_4^{3-}/\text{MoO}_4^{2-}$ /thiamine. The former was described in a recent paper,²⁸ and the study of the latter constituted a preliminary step in development of the simultaneous determination. The FIA configuration used in both cases is shown in Fig. 1, and Tables 1 and 2 summarize the optimum values of the chemical, physico-chemical and FIA variables and the features of the methods for the individual determination of these species, respectively. Both systems were optimized by the Modified Simplex Method, MSM. The most outstanding features of these studies are discussed below.

The excitation and emission wavelengths of the monitored product—thiochrome—are 375 and 440 nm, respectively.

Whilst the $\text{SiO}_3^{2-}/\text{MoO}_4^{2-}$ /thiamine system is dramatically affected by temperature, this variable exerts almost no influence on the phosphate system.

Nitric acid is the most suitable medium for the phosphate system (in this medium the signal provided

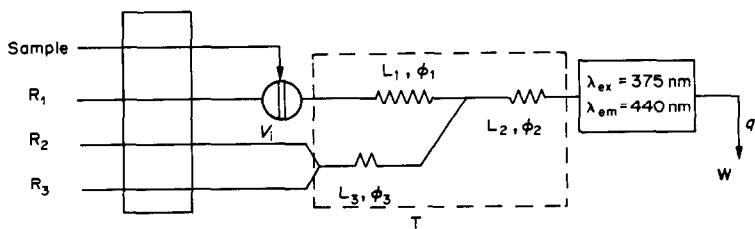


Fig. 1. Manifold for individual determination of silicate and phosphate.

by silicate is only 30% of that corresponding to the same concentration of phosphate) whereas silicomolybdic acid is best formed in perchloric acid medium (in which the signal for phosphate is 54% of that for the same concentration of silicate). A mixture of both acids provides optimum signals for both ions.

Characteristics common to both methods are the low determination limit, wide linear range of calibration, small relative standard deviation (r.s.d.) values and good sampling frequency (Table 2).

Only phosphate and sulphide interfere at the same concentration level as the analyte in the determination of silicate. Hypochlorite and iodide are tolerated in 5:1 and 15:1 ratio to silicate, respectively. Arsenite and sulphite are tolerated in 50:1 ratio to analyte. Up to 30 common ions²⁷ (acetate, citrate, oxalate, tartrate, EDTA, Cl^- , CO_3^{2-} , CrO_4^{2-} , NO_3^- , NO_2^- , SO_4^{2-} , Br^- , F^- , NH_4^+ , Na^+ , K^+ , Al^{3+} , Ca^{2+} , Mg^{2+} , Cd^{2+} , Cr^{3+} , Ni^{2+} , Zn^{2+} , Hg^{2+} , Pb^{2+} , Co^{2+} , Cu^{2+} , Fe^{2+} , Fe^{3+}) are tolerated in at least 100:1 ratio to silicate, though some of them, such as Co^{2+} , Fe^{2+} , Fe^{3+} and Cu^{2+} , must be masked with EDTA. It is worthy of note that EDTA is tolerated in at least 5000:1 ratio.

Table 1. Optimum values of variables for individual determination

Variable	SiO_3^{2-}	PO_4^{3-}
L_1 , cm	150	12
L_2 , cm	10	18
L_3 , cm	5	5
V_1 , μl	71.6	71.6
q_1 , ml/min	4.0	4.7
T , °C	45	30
$[\text{MoO}_4^{2-}]$, M	0.0136	0.0290
$[\text{HNO}_3]$, M		1.33
$[\text{HClO}_4]$, M	0.34	
[Thiamine], M	0.03	0.04
pH	10.8	11.0

Sulphide and copper(II) interfere with the determination of phosphate when present at the same level as the analyte; SiO_3^{2-} , Fe^{2+} and Fe^{3+} are tolerated in a 1:1 ratio and ClO^- and CO_3^{2-} in 25:1 ratio to phosphate. Twenty-six common ions (acetate, citrate, oxalate, tartrate, EDTA, AsO_4^{3-} , Cl^- , CrO_4^{2-} , I^- , Br^- , F^- , NO_3^- , NO_2^- , NH_4^+ , Na^+ , K^+ , Al^{3+} , Ca^{2+} , Mg^{2+} , Cd^{2+} , Zn^{2+} , Ni^{2+} , Pb^{2+} , Co^{2+} , Hg^{2+}) are tolerated at ratios above 100:1 to phosphate, but Co^{2+} and Hg^{2+} require the presence of EDTA. All the tolerances above are expressed as w/w ratios.

Optimization of variables for the simultaneous determination

Measurement of the two analytical signals at two different times, the basis of the kinetic determination, was achieved with the two slightly different configurations shown in Fig. 2. Two peaks are obtained per injection in both cases. Since phosphomolybdic acid is formed faster than silicomolybdic acid, the optimization aimed at achieving complete formation of the former with minimum formation of the latter for the first peak measured and noticeable development of the silicomolybdic acid for the second peak. The optimization was done by examination of the results obtained by injecting each anion separately into the manifolds illustrated in Fig. 2. The response function, F_r , selected for optimization by the MSM was:

$$F_r = \frac{(h_1^p - h_2^p)(h_2^{\text{Si}} - h_1^{\text{Si}})}{(h_1^p - h_2^{\text{Si}})}$$

where h_1^p and h_2^p denote the height of the first and second peaks obtained on injecting phosphate and h_1^{Si} and h_2^{Si} the corresponding heights for the injection of silicate. The higher h_1^p and the lower h_2^p (complete development during the first residence time and high dispersion during the second), the larger is F_r . The

Table 2. Features of the individual determinations

	SiO_3^{2-}	PO_4^{3-}
Equation*	$h = -6.2 + 2.56 \times 10^7 [\text{SiO}_3^{2-}]$	$h = 6.0 + 1.40 \times 10^7 [\text{PO}_4^{3-}]$
Range, ng/ml	30–600	20–1000
Regression coefficient	0.999	0.999
r.s.d.†, %	0.25	0.70
Samples/hr	120	270

* h = analytical signal, mm; concentrations in mole/l.

†For $[\text{SiO}_3^{2-}] = 4 \times 10^{-6} \text{ M}$; $[\text{PO}_4^{3-}] = 6 \times 10^{-7} \text{ M}$ (11 samples).

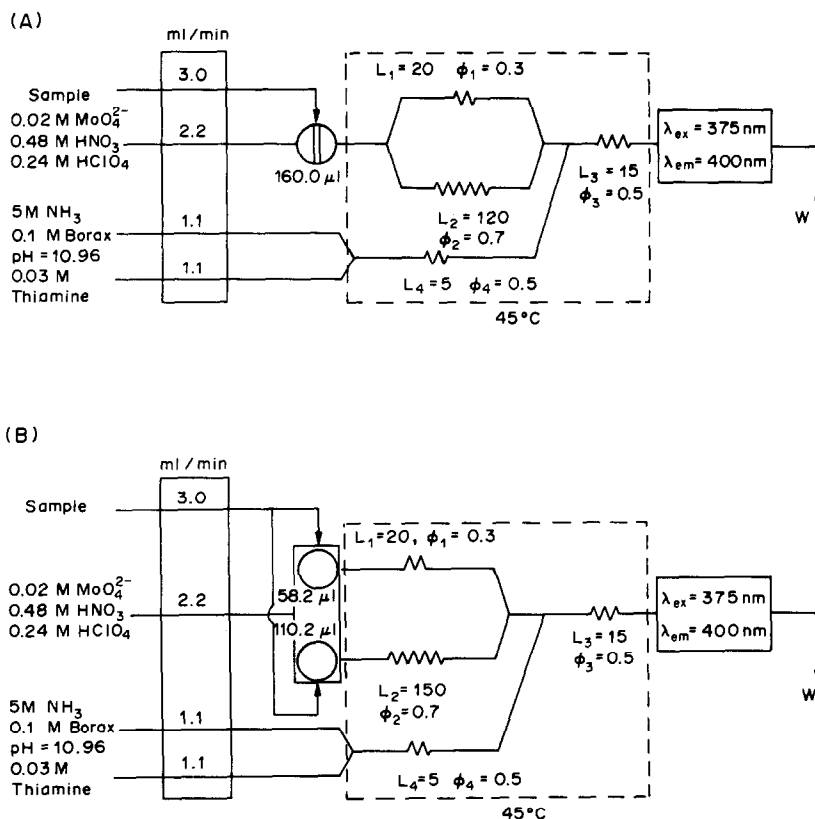


Fig. 2. Manifolds for the simultaneous determination of silicate and phosphate. (A) With splitting and confluence points and single injection. (B) With dual sample injection and confluence point before the detector. L (reactor length) and ϕ (inner diameter) are expressed in cm and mm, respectively.

situation is the opposite for silicate (i.e., F_1 is favoured by minimal degree of reaction for the first peak and high degree of reaction for the second), which is reflected in the numerator of the function.

Configuration with single injection and splitting and confluence of the flow before the detector (Fig. 2A). The MSM was applied to optimization of the chemical (MoO_4^{2-} , HNO_3 and HClO_4 concentrations and sample pH) and FIA variables (reactor diameter and length, injected volume and overall flow-rate). The optimum values found for the variables are those given in Fig. 2A.

The reproducibility of the splitting is appreciably increased by addition of glycerine to increase the viscosity of the sample (optimum concentration 2 g per 100 ml).

Configuration with dual injection and confluence before the detector (Fig. 2B). This configuration has two advantages over the other: (1) the absence of a splitting point, which makes the addition of glycerine unnecessary; (2) the sample volume for each channel is easy to optimize by changing the loops in each valve. As the other variables were optimized in the study of the first configuration, only these loop-sizes remained to be optimized. The optimum values found are those given in Fig. 2B.

Simultaneous determination of silicate and phosphate

Calibration is done by injecting various standard solutions of silicate and phosphate separately into each configuration, to obtain two calibration graphs for each of the two peaks. Table 3 shows the equations of the linear range of these graphs, and other characteristics of the determination. The values of the corresponding blanks, H_1^b and H_2^b , obtained by injecting distilled water at the same pH into each manifold, are also shown.

The analysis of mixtures of both anions is performed with the aid of a system of equations derived from the calibration equations, as shown in Table 3, where H_1^m and H_2^m denote the heights of peaks 1 and 2 for a mixture. Results obtained for mixtures by use of both configurations are listed in Table 4. The sampling rate is 60 per hr in both cases.

Application of the method to real samples

To confirm the performance given by the method, configuration B was applied to the determination of silicate and phosphate in water samples collected from several places in the province of Córdoba, and in a mineral water marketed in plastic and glass bottles. Various sample dilutions were necessary to fit

Table 3. Features of the simultaneous determination of SiO_3^{2-} and PO_4^{3-} (h and H in mm)

Configuration	Analyte	Equations	Regr. coeff.	r.s.d.*, %
A	SiO_3^{2-}	$h_1^{\text{Si}} = 13.0 + 1.36 \times 10^6 [\text{SiO}_3^{2-}]$	0.999	± 0.8
		$h_2^{\text{Si}} = 11.0 + 7.37 \times 10^6 [\text{SiO}_3^{2-}]$	0.999	± 0.6
	PO_4^{3-}	$h_1^{\text{P}} = 12.0 + 7.47 \times 10^6 [\text{PO}_4^{3-}]$	0.999	± 1.0
		$h_2^{\text{P}} = 5.0 + 3.63 \times 10^6 [\text{PO}_4^{3-}]$	0.996	± 1.8
	$\text{SiO}_3^{2-} + \text{PO}_4^{3-}$	$H_1^{\text{M}} = 25.0 + 1.36 \times 10^6 [\text{SiO}_3^{2-}] + 7.47 \times 10^6 [\text{PO}_4^{3-}]$		
		$H_2^{\text{M}} = 16.0 + 7.37 \times 10^6 [\text{SiO}_3^{2-}] + 3.63 \times 10^6 [\text{PO}_4^{3-}]$		
	blank	$h_1^{\text{b}} = 16.0$ $h_2^{\text{b}} = 15.0$		
B	SiO_3^{2-}	$h_1^{\text{Si}} = 3.0 + 3.67 \times 10^6 [\text{SiO}_3^{2-}]$	0.999	± 1.0
		$h_2^{\text{Si}} = 10.0 + 6.00 \times 10^6 [\text{SiO}_3^{2-}]$	0.999	± 1.0
	PO_4^{3-}	$h_1^{\text{P}} = 4.0 + 1.04 \times 10^6 [\text{PO}_4^{3-}]$	0.999	± 0.4
		$h_2^{\text{P}} = 0.0 + 2.64 \times 10^6 [\text{PO}_4^{3-}]$	0.999	± 0.5
	$\text{SiO}_3^{2-} + \text{PO}_4^{3-}$	$H_1^{\text{M}} = 7.0 + 3.67 \times 10^6 [\text{SiO}_3^{2-}] + 1.04 \times 10^6 [\text{PO}_4^{3-}]$		
		$H_2^{\text{M}} = 10.0 + 6.00 \times 10^6 [\text{SiO}_3^{2-}] + 2.64 \times 10^6 [\text{PO}_4^{3-}]$		
	blank	$H_1^{\text{b}} = 17.0$ $h_2^{\text{b}} = 25.0$		

*For $[\text{SiO}_3^{2-}] = [\text{PO}_4^{3-}] = 5 \times 10^{-6} M$ (11 samples).

the analytical signals within the linear range of the calibration equations. The results are given in Table 5 along with recoveries obtained.

CONCLUSIONS

The precision of the proposed method is similar to

that of other differential-kinetic procedures, but the method has certain advantages over earlier methods: (a) the fluorimetric detection gives a lower determination limit than that of the other methods;¹⁸⁻²³ (b) determination of both species in a single injection; (c) freedom from interferences, which allows its application to real samples.

Table 4. Analysis of SiO_3^{2-} and PO_4^{3-} mixtures

Added, M		Found, configuration A, M		Found, configuration B, M	
PO_4^{3-}	SiO_3^{2-}	PO_4^{3-}	SiO_3^{2-}	PO_4^{3-}	SiO_3^{2-}
1.00×10^{-5}	1.00×10^{-5}	1.02×10^{-5}	1.02×10^{-5}	1.03×10^{-5}	1.02×10^{-5}
5.00×10^{-6}	1.00×10^{-5}	5.06×10^{-6}	1.04×10^{-5}	4.96×10^{-6}	1.03×10^{-5}
1.00×10^{-5}	5.00×10^{-6}	1.04×10^{-5}	5.03×10^{-6}	1.03×10^{-5}	5.00×10^{-6}
5.00×10^{-6}	5.00×10^{-6}	5.01×10^{-6}	4.97×10^{-6}	5.08×10^{-6}	5.11×10^{-6}
5.00×10^{-6}	1.00×10^{-6}	4.91×10^{-6}	0.97×10^{-6}	5.09×10^{-6}	0.99×10^{-6}
1.00×10^{-6}	5.00×10^{-6}	0.97×10^{-6}	4.95×10^{-6}	0.96×10^{-6}	4.95×10^{-6}
1.00×10^{-5}	1.00×10^{-6}	0.98×10^{-5}	0.98×10^{-6}	1.05×10^{-5}	0.99×10^{-6}
1.00×10^{-6}	1.00×10^{-5}	1.06×10^{-6}	1.03×10^{-5}	0.96×10^{-6}	0.98×10^{-5}
5.00×10^{-6}	5.00×10^{-7}	5.13×10^{-6}	4.65×10^{-7}	5.04×10^{-6}	5.08×10^{-7}
5.00×10^{-7}	5.00×10^{-6}	4.79×10^{-7}	4.64×10^{-6}	5.22×10^{-7}	5.28×10^{-6}
5.00×10^{-7}	5.00×10^{-7}	5.12×10^{-7}	4.94×10^{-7}	5.04×10^{-7}	5.23×10^{-7}
1.00×10^{-6}	1.00×10^{-6}	1.02×10^{-6}	0.99×10^{-6}	1.04×10^{-6}	0.99×10^{-6}

Table 5. Determination of SiO_3^{2-} and PO_4^{3-} in water samples

Sample	Dilution	Added, $\mu\text{g/ml}$		Found, $\mu\text{g/ml}$	
		PO_4^{3-}	SiO_3^{2-}	PO_4^{3-}	SiO_3^{2-}
La Rambla	1:25			0.14	0.48
		0.47	0.30	0.62	0.79
Sta. Eufemia	2:25			0.06	0.12
		0.47	0.30	0.55	0.45
Lucena	1:25			0.12	0.21
		0.47	0.30	0.60	0.53
well (Córdoba)	1:50			0.20	0.31
		0.47	0.30	0.70	0.61
tap (Córdoba)	1:25			0.13	0.21
		0.47	0.30	0.64	0.53
mineral water (glass bottle)	1:25			0.43	0.74
		0.47	0.30	0.89	1.06
mineral water (plastic bottle)	1:25			0.36	0.53
		0.47	0.30	0.82	0.85

Acknowledgement—The authors wish to acknowledge support for this research from Ministerio de Educación y Ciencia, through a grant from CAICYT No 2012-83.

REFERENCES

1. J. Růžička and J. W. B. Stewart, *Anal. Chim. Acta*, 1975, **79**, 79.
2. Y. Hirai, N. Yoza and S. Ohashi, *ibid.*, 1980, **115**, 269.
3. J. F. van Staden, *J. Assoc. Off. Anal. Chem.*, 1983, **66**, 718.
4. Y. Hirai, N. Yoza and S. Ohashi, *Bunseki Kagaku*, 1981, **30**, 465.
5. H. Bergamin F^o., E. A. G. Zagatto, F. J. Krug and B. Reis, *Anal. Chim. Acta*, 1978, **101**, 17.
6. B. Reis, E. A. G. Zagatto, A. O. Jacintho, F. J. Krug and H. Bergamin F^o., *ibid.*, 1980, **119**, 305.
7. Y. Hirai, N. Yoza and S. Ohashi, *Chem. Lett.*, 1980, 499.
8. Z. Fang, L. Sun, Z. Gao, X. Wang and N. Li, *Turang Tongbao*, 1982, **4**, 40.
9. J. W. B. Stewart and J. Růžička, *Anal. Chim. Acta*, 1976, **82**, 137.
10. K. S. Johnson and R. L. Petty, *Anal. Chem.*, 1982, **54**, 1185.
11. J. Růžička and E. H. Hansen, *Anal. Chim. Acta*, 1975, **78**, 145.
12. T. Yokoyama, Y. Hirai, N. Yoza, T. Tarutani and S. Ohashi, *Bull. Chem. Soc. Japan*, 1982, **55**, 3477.
13. J. Thomsen, K. S. Johnson and R. L. Petty, *Anal. Chem.*, 1983, **55**, 2378.
14. A. G. Fogg and G. C. Cripps, *Analyst*, 1981, **108**, 1485.
15. A. G. Fogg and N. K. Bsebsu, *ibid.*, 1981, **106**, 1288.
16. *Idem*, *ibid.*, 1982, **107**, 566.
17. *Idem*, *ibid.*, 1984, **109**, 19.
18. I. M. Kolthoff, E. B. Sandell, E. J. Meehan and S. Bruckenstein, *Quantitative Chemical Analysis*, Macmillan, London, 1969.
19. M. Sager and H. Puxbaum, *Mikrochim. Acta*, 1984 **I**, 361.
20. H. Friedeberg, *Anal. Chem.*, 1955, **27**, 305.
21. J. A. Allen and D. G. Holloway, *Nature*, 1950, **166**, 274.
22. D. Ingle Jr. and S. R. Crouch, *Anal. Chem.*, 1971, **43**, 7.
23. K. Ohashi, H. Kawaguchi and K. Yamamoto, *Anal. Chim. Acta*, 1979, **111**, 301.
24. A. Fernández, M. A. Gómez-Nieto, M. D. Luque de Castro and M. Valcárcel, *ibid.*, 1984, **165**, 217.
25. A. Fernández, M. D. Luque de Castro and M. Valcárcel, *Anal. Chem.*, 1984, **56**, 1146.
26. F. Lázaro, M. D. Luque de Castro and M. Valcárcel, *Z. Anal. Chem.*, 1985, **320**, 128.
27. P. Linares, M. D. Luque de Castro and M. Valcárcel, *Anal. Chim. Acta*, 1985, **177**, 263.

SEPARATION OF SOME TRANSITION-METAL IONS ON SILICA-IMMOBILIZED 2-PYRIDINECARBOXALDEHYDE PHENYLHYDRAZONE

SURASAK WATANESK and A. A. SCHILT

Department of Chemistry, Northern Illinois University, DeKalb, IL 60115, U.S.A.

(Received 14 May 1985. Accepted 20 June 1986)

Summary—A metal-ion extractant, prepared by chemical binding of 2-pyridinecarboxaldehyde phenylhydrazone on a silica support, is described and shown to be effective for use in separation and determination of trace amounts of iron, cobalt, nickel, and copper. Metal-ion sorption conforms to the Langmuir isotherm. The relative orders of the Langmuir constants K and the column retention-capacity factors k' for the four transition-metal ions are the same as the natural order of the stabilities predicted for their metal chelates: $\text{Fe(II)} < \text{Co(II)} < \text{Ni(II)} < \text{Cu(II)}$.

Use of immobilized ligands on solid supports to separate metal ions has received considerable attention in recent years.¹⁻⁵ Advantageous applications include enrichment of trace concentrations of metal ions to enable more effective measurement, purification of reagents to decrease reagent blanks, and providing the means for attaining greater selectivities in multicomponent determinations.

Our interests in both the chelation properties of *N*-heterocyclic hydrazones and applications of immobilized ligands led us to undertake the present investigation to explore the chelation properties of a surface-bonded pyridylhydrazone ligand and its application to metal-ion separations.

EXPERIMENTAL

Apparatus

Absorbances were measured with either a Varian Model 2290 or a Beckman Model DU spectrophotometer, and 1.00-cm micro or regular size silica cells. All pH measurements and potentiometric titrations were performed with an Orion Ionalyzer pH-meter equipped with a combination pH-SCE electrode. Solutions were agitated at 25° in a constant temperature bath. A mini pump (Milton Roy Model 396) and a fraction collector (Model 328, Instrumentation Specialties Co., Lincoln, NE) were used for column separations.

Reagents and materials

Controlled-pore glass (CPG) (Pierce Chemical Co.) was pretreated by immersing 7 g in 100 ml of a 1:1 mixture of concentrated nitric and sulphuric acids, briefly applying a vacuum and ultrasonic agitation to fill the pores, and then refluxing for 2 hr at atmospheric pressure. After rinsing with demineralized water until the pH of the filtrate was the same as that of the water used, the CPG was dried overnight at 120°.

The aminophenyltrimethoxysilane (Petrarch System, Inc., Bristol, PA) used contained both the *o*- and *p*-isomers. It was vacuum distilled twice and stored in a sealed container under refrigeration before use. The 2-pyridinecarboxaldehyde (Aldrich Chemical Co.) was used as received. The 2,2'-dipyridyl ketone 2-pyridylhydrazone (DPPH) was prepared by the procedure of Case.⁷

Buffer solutions of pH between 3 and 5 were prepared by addition of glacial acetic acid to 1M sodium acetate until the desired pH was attained. The pH-4.5 eluent solution was prepared by adding acetic acid to 0.010M sodium acetate to adjust the pH, and the pH-3 eluent by adding 0.1M nitric acid to 0.1M potassium hydrogen phthalate. The sodium acetate solutions were prepared from a stock solution treated to remove trace metal contamination.⁸

Analytical-reagent grade chemicals were employed in the preparation of all solutions. Stock solutions of metal ions were prepared from the sulphates.

Synthesis of CPG-PAPH

A mixture of 5 g of the dry CPG and 20 ml of a 10% solution of aminophenyltrimethoxysilane in dry toluene was refluxed for 4 hr, filtered under suction through a sintered-glass funnel, rinsed with toluene followed by 2-propanol, and dried in an oven at 80° for 8-12 hr. This arylamine-silica product was then treated with 100 ml of 2% sodium nitrite solution in 2M hydrochloric acid at 0° for 30 min to obtain the diazonium hydrochloride-silica, which was filtered off and quickly washed with three 25-ml portions of cold water. While the diazotization reaction was taking place, a sodium sulphite solution was prepared by dissolving 1.53 g of sodium hydroxide in 100 ml of distilled water and then slowly adding 4.28 g of sodium metabisulphite ($\text{Na}_2\text{S}_2\text{O}_5$); the resulting solution was cooled to approximately 5°. The freshly prepared and washed diazonium hydrochloride-CPG was then added to the cold solution of sodium sulphite, and the temperature of the mixture was slowly raised to 60-70° in a water-bath and maintained at this temperature for 1 hr. The resulting phenylhydrazone-CPG product was filtered off while still warm, washed with 250 ml of 0.1M hydrochloric acid, followed by 250 ml of distilled water, and then added to 100 ml of 2% 2-pyridinecarboxaldehyde solution in ethanol and left to stand for 30 min. The resulting silica-immobilized picolinaldehyde phenylhydrazone (denoted as CPG-PAPH) was collected by filtration and washed with ethanol, then 0.1M hydrochloric acid, and finally water. This material was then air-dried and stored in a desiccator over anhydrous magnesium perchlorate.

Chelation capacity of CPG-PAPH

The amount of ligand immobilized on the silica surface (mole/g) was determined by titration with acid and also by using copper(II) as a metal-ion probe. Potentiometric acid-base titrations in glacial acetic acid medium were

performed on the materials obtained from each major step in the synthesis of CPG-PAPH, including the uncoated controlled-pore glass. For this purpose a 0.20-g sample was added to 25 ml of glacial acetic acid and titrated with standardized 0.1M perchloric acid in glacial acetic acid. The amounts of immobilized aniline and/or PAPH were found from the volumes of standard acid corresponding to the equivalence points evident in each titration curve. Measurements with copper(II) as a metal-ion probe were made as follows. Into 50-ml conical flasks equipped with ground-glass stoppers and containing an accurately weighed quantity (0.15 g) of either CPG-PAPH or untreated CPG were added 20-ml portions of 2.00mM solutions of copper(II) buffered at pH 3, 4 or 5. After stoppering and sealing with paraffin wax, the flasks were agitated for 3 hr at 25° in a shaker/water-bath. To deduce the amount of copper taken up per g of solid, the initial and final copper concentrations were determined spectrophotometrically with DPPH as chromogenic reagent. For confirmation, the copper content of the solid was recovered by agitating the washed solid with 10.0 ml of 0.1M hydrochloric acid for 30 min to extract the copper(II), which was then measured spectrophotometrically with DPPH.

The stability of the CPG-PAPH towards hydrolysis over the pH range from 0 to 11 was evaluated by measuring the copper-ion sorption capacities before and after prolonged treatment with various buffer solutions.

Copper was determined in the various solutions as follows. A 5.00-ml aliquot was pipetted into a standard flask (100 or 250 ml) and treated with 2 ml of 0.01M DPPH in ethanol, 20 ml of distilled water and sufficient 2M sodium hydroxide to adjust the pH to 12. After dilution of the solution to volume the absorbance at 448 nm was measured and compared with the values for standards treated in the same way.

Sorption isotherms

The amount of metal ion taken up by CPG-PAPH as a function of metal-ion concentration was determined for various metal ions as follows. Solutions of different concentrations, buffered at pH 4.5, were pipetted (25.00 ml) into a series of 50-ml glass-stoppered flasks, each containing an accurately weighed amount (50 mg) of CPG-PAPH. After agitation for 3 hr at 25° the metal-ion concentration of the solution in equilibrium with the CPG-PAPH was determined spectrophotometrically with DPPH.

Separations

A stainless-steel column (250 mm long, 4.6 mm bore) was washed sequentially with 0.1M nitric acid, chloroform, detergent solution, and water. It was then oven-dried and dry-packed with CPG-PAPH by the procedure described by Snyder and Kirkland.⁹ After each use the column was flushed with 0.1M nitric acid, followed by demineralized water, to remove any uneluted metal contaminant. Before any sample injection, the column was conditioned by passage of 50–60 ml of the appropriate eluent at a flow-rate of 1 ml/min. Samples were injected by means of a 20- μ l injection loop. Concentrations of metal-ion solutions injected ranged from 1.0 to 5.0mM. The following stepwise elutions were performed to achieve separations: iron(II) and cobalt(II) were eluted with pH 4.5 acetate buffer at a flow-rate of 0.4 ml/min, nickel was eluted with pH-3 potassium hydrogen phthalate/nitric acid buffer at 1 ml/min, and copper(II) with 0.1M nitric acid at 1 ml/min. The eluates were collected by an automatic fraction collector in increments of 5 drops (0.27 ml) per tube. In some special cases, separations were sufficiently complete to permit larger fractions (50 or even 300 drops) to be collected. The metal-ion concentration of each fraction was determined spectrophotometrically with DPPH at pH 12 and appropriate

wavelengths (586 and 490 nm for simultaneous determination of iron and cobalt, 440 nm for nickel or copper).

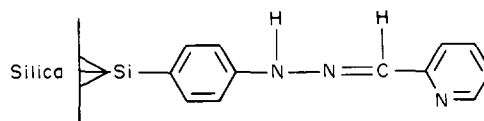
The overall void volume was determined by injecting 20 μ l of 0.1M magnesium chloride and monitoring each drop of eluate for magnesium by adding Eriochrome Black T indicator and for chloride by treatment with silver nitrate solution.

RESULTS AND DISCUSSION

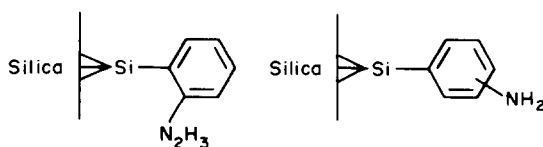
Synthesis and characterization of CPG-PAPH

The four-step sequence of reactions employed to synthesize 2-pyridinecarboxaldehyde phenylhydrazone (PAPH) covalently bonded to controlled-pore glass (CPG) proved successful but low in yield. Analysis of both the silylated product and the final product revealed that only about 60% of the arylamine immobilized in the silylation step was converted into hydrazone groups. Non-aqueous acid-base titrimetry indicated the presence of 250 ± 10 μ moles of basic groups per g of CPG-arylamine before conversion into the hydrazone. Titration of the final CPG-PAPH product yielded a titration curve with two distinct breaks, indicating the presence of a total of 251 ± 10 μ moles of two different basic groups per g of CPG-PAPH. The first of these corresponded to 93 μ moles/g of a weak base and probably represents the number of hydrazine groups that did not or could not condense with the 2-pyridinecarboxaldehyde to form the hydrazone in the final step. The difference between the first and second titration breaks indicated the presence of 158 μ moles of a very weak base per g of CPG-PAPH, believed to correspond to the number of bound hydrazone groups. Undoubtedly a greater yield of hydrazone could have been attained were it not for the fact that the aminophenyltrimethoxysilane contained both *o*- and *p*-isomers. The *o*-isomer should give rise to a diazonium salt which for steric reasons would be expected not to react with 2-pyridinecarboxaldehyde.

Although decidedly yellow in colour, the CPG-PAPH product did not yield any significant infrared or NMR spectra. Considering the relatively small number of organic groups bonded per g of CPG this is perhaps not surprising. The fact that titrimetric determination of the basic groups proved impractical in aqueous medium but satisfactory in glacial acetic acid solutions is consistent with the conclusion that the CPG-PAPH possesses weakly basic phenylhydrazine and very weakly basic hydrazone groups. A schematic structure for CPG-PAPH is depicted as follows:



The silica surface also contains some phenylhydrazine and possibly aniline bonded as follows:



Copper(II) was selected as a probe to determine the number of bound pyridylhydrazone groups available for metal-ion chelation. The results were surprising. Only 25 ± 2 μ moles of copper(II) were taken up per g of CPG-PAPH at pH 5. This amount was confirmed by determination of the bound copper recovered by extraction with dilute acid. Sorption of copper(II) decreased on decreasing the pH: 19 μ moles/g at pH 4 and 7 μ moles/g at pH 3. Untreated CPG did not sorb any detectable amount of copper over the pH range 3–5. Above pH 5 copper can be adsorbed by the silanol groups of CPG and glass vessels.

The stability of covalently bound PAPH on CPG towards hydrolysis proved to be good over the pH range 0–7, as evidenced by measurements of copper(II) sorption capacities before and after 48-hr equilibrations with aqueous solutions of various pH values. At pH 9 and 11 discoloration of the CPG-PAPH and the development of a faint yellow-orange colour in the solution was observed after a few minutes. A faint yellow colour was also observed in solutions of pH 0 and 1 after 48 hr, indicating some loss of PAPH from the silica substrate. Numerical results are given in Table 1. Storage stability proved excellent in the dry state, with no measurable change in copper sorption capacity over a period of 4 months.

Sorption isotherms and chelation of metal ions by CPG-PAPH

The ability of covalently bonded PAPH to extract various metal ions from aqueous solution at pH 4.5 was evaluated by measuring the sorption isotherms. Data treatment revealed that the sorption conformed to the Langmuir rather than the Freundlich isotherm. The isotherms and Langmuir plots are shown in Figs. 1 and 2 for the sorption of iron, cobalt, nickel and copper ions. Langmuir behaviour is reasonable because there is a limited number of chelation sites

Table 1. Stability of CPG-PAPH towards hydrolysis (original capacity 25 μ mole/g)

pH	Fraction of original capacity, %
0	95
1	101
3	98
5	100
7	98
9	82
11	75

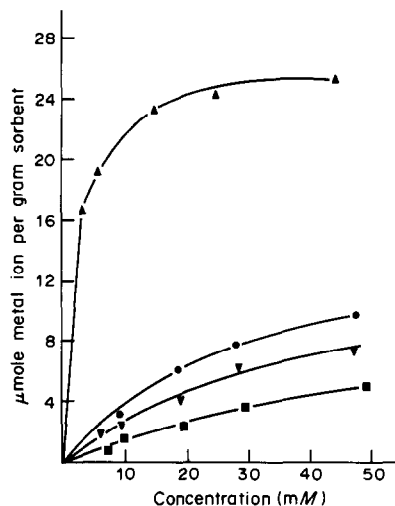


Fig. 1. Isotherms for sorption of metal ions from pH-4.5 aqueous solution on CPG-PAPH at 25°. ■ = Fe(II); ▼ = Co(II); ● = Ni(II); ▲ = Cu(II).

available for metal ions. Evaluation of the slopes and ordinate intercepts of the $1/q$ vs. $1/C$ plots provided values for the Langmuir parameters K and b , which are compiled in Table 2. In general, the capacities and equilibrium sorption constants of the metal ions increase with atomic number of the metal. The trend in K -values is thus consistent with the natural order^{10–12} of stabilities of the metal(II) complexes with the same ligand, *viz.* Fe < Co < Ni < Cu. The rationale for the trend observed in b , the number of moles of chelation or sorption sites per g of solid, is less obvious. One explanation centres on the evidence that both uncoupled phenylhydrazine and PAPH are present on the silica surface. Thus, since copper(II) can readily form complexes with either species the substrate should have a higher capacity for copper(II)

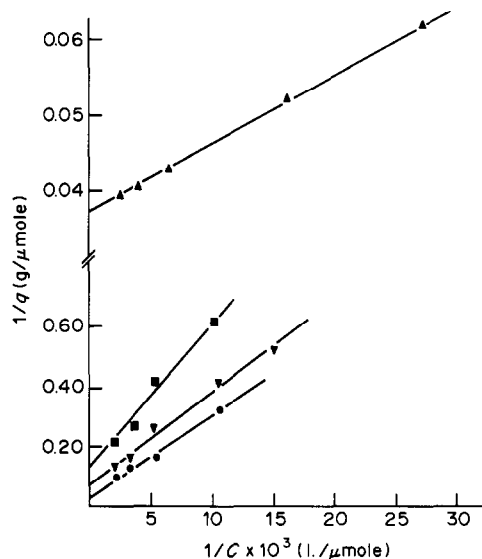


Fig. 2. Langmuir treatment of sorption isotherms of Fig. 1 (same symbols used for the metal ions); q = amount sorbed per g of sorbent; C = concentration in solution.

Table 2. Langmuir parameters for metal-ion sorption

Metal ion	b , $\mu\text{mole/g}$	K , $l./\mu\text{mole}$
Cu(II)	27	0.040
Ni(II)	15	0.036
Co(II)	13	0.025
Fe(II)	8	0.023

than for other metal ions. Also, as the stability of a metal-ion complex decreases, the amount of that metal ion extractable by complex formation also decreases, which may explain the metal-sorption capacities of CPG-PAPH decreasing in the order Ni(II) > Co(II) > Fe(II).

Comparison of the number of PAPH ligands present, as evidenced by acid-base titration, with that found for the Langmuir b -value for copper(II), indicates that only approximately 20% of the immobilized ligands are available for chelation, based on a metal to ligand ratio and 1:1. Formation of complexes with higher ligand to metal ratios is very unlikely, because the immobilized ligands are relatively far apart, being relatively few in number per unit area.

Separations

The elution behaviour of each metal ion of interest was evaluated by determining its column capacity factor k' . Results obtained with 0.05M sodium acetate, adjusted to pH 3 with acetic acid, as eluent are compiled in Table 3, together with a description of the column characteristics. As expected, the relative

Table 3. Retention of metal ions by CPG-PAPH column*

Metal ion	pH-3 elution, k'	Stepwise elution† V_R , ml	k'
Fe(II)	0.84	4.9	0.5
Co(II)	0.93	7.1	1.2
Ni(II)	1.18	32.2	9.1
Cu(II)	(retained)	54.8	16.1

*Column characteristics: 1.79 g of CPG-PAPH (37-74 μm particle size, 130 m^2/g surface area, 240 \AA pore diameter, 142 $\mu\text{mole/g}$ bonded phase, 1.09 $\mu\text{mole}/\text{m}^2$ surface coverage); 250 \times 4.6 (mm) column; 3.22 ml void-volume; 0.4 ml/min flow-rate.

†Corresponding to elution procedure described for Fig. 3.

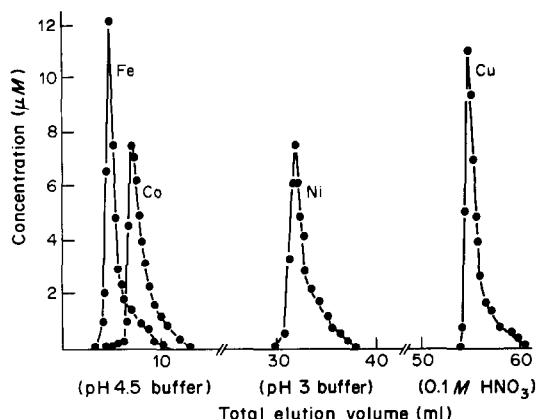


Fig. 3. Resolution of a 20- μl sample of a solution which was 1.00mM each in Fe(II), Co(II), Ni(II) and Cu(II), developed by stepwise elution: pH-4.5 buffer at 0.4 ml/min, followed by pH-3 phthalate buffer at 1 ml/min, and 0.1M nitric acid at 1 ml/min.

order of the capacity factors of the four metal ions is the same as that of their Langmuir K -values, which is that of the natural order¹⁰⁻¹² of stabilities of their complexes. An attempt to resolve a mixture of the four metal ions on the column by using an eluent buffered at pH 3 proved ineffective, owing to co-elution of iron and cobalt, closely followed by elution of nickel; copper(II) was strongly retained at pH 3 and not eluted.

Study of the effect of pH on the elution behaviour of the four metal ions revealed that a stepwise decrease in pH provided the means for resolving their mixtures. Iron(II) and cobalt(II) were eluted at pH 4.5 with partially overlapped bands, but simultaneous spectrophotometric monitoring at two wavelengths provided good resolution. Nickel(II) was eluted next with pH-3 buffer, and copper last with 0.1M nitric acid. Typical separation obtained in this manner is shown in Fig. 3.

It is pertinent to note that cobalt(II) and nickel(II), which could not be completely resolved by a Porasil-8-hydroxyquinoline column,⁴ were successfully resolved on the CPG-PAPH column described here. It is also interesting that neither 0.05M sulphate nor 0.10M nitrate had any significant effect on the elution behaviour.

Table 4. Analysis of metal-ion solutions

Solution	Taken, μmole				Found*, μmole			
	Fe	Co	Ni	Cu	Fe	Co	Ni	Cu
1	30	30	30	30	30	28	30	20
2	—	100	100	—	—	93	101	—
3	100	—	—	100	99	—	—	96
4	20.0	20.0	—	—	20 \pm 0.4	20 \pm 0.6	—	—
5	30.0	30.0	—	—	30 \pm 0.9	29 \pm 0.9	—	—
6	—	—	20.0	20.0	—	—	20 \pm 0.4	21 \pm 0.6
7	—	—	30.0	30.0	—	—	29 \pm 0.9	30 \pm 0.9

*Data for solutions 4-7 are averages of three separate runs with \pm average deviations specified.

Various metal ion mixtures were quantitatively analysed with spectrophotometric determination of each metal ion in separate fractions. The results listed in Table 4 show good agreement between the amounts of metal ion taken and found. The relative average deviations are reasonable. CPG-PAPH thus appears to be a promising stationary phase for metal ion separations and merits further study.

The retention behaviour of other transition metal ions was examined to learn what other mixtures might be successfully resolved on CPG-PAPH with pH-4.5 acetate buffer as eluent. Zinc(II), cadmium(II) and lead(II) were found to be eluted after iron(II) but before cobalt(II), and could not be resolved from one another. Manganese(II), however, was eluted before iron(II) and could be resolved from the others.

REFERENCES

1. S. Ismal, M. Muroi, A. Hamaguchi and M. Koyama, *Anal. Chem.*, 1983, **55**, 1215.
2. J. R. Parrish, *ibid.*, 1982, **54**, 1890.
3. J. L. Lundgren and A. A. Schilt, *ibid.*, 1977, **49**, 974.
4. J. R. Jezorek and H. Freiser, *ibid.*, 1979, **51**, 366.
5. E. M. Moyer and J. S. Fritz, *ibid.*, 1976, **48**, 1117.
6. F. H. Case, A. A. Schilt and N. Simonzadeh, *ibid.*, 1984, **56**, 2860.
7. F. H. Case, *J. Chem. Eng. Data*, 1976, **21**, 124.
8. D. J. Hutchinson and A. A. Schilt, *Anal. Chim. Acta*, 1983, **154**, 159.
9. L. R. Snyder and J. J. Kirkland, *Modern Liquid Chromatography*, Wiley, New York, 1974.
10. D. P. Mellor and L. E. Maley, *Nature*, 1947, **159**, 370.
11. M. Calvin and N. C. Melchior, *J. Am. Chem. Soc.*, 1948, **70**, 3270.
12. H. Irving and R. J. P. Williams, *Nature*, 1948, **162**, 146.

STUDIES ON FLUORESCEIN—III

THE ACID STRENGTHS OF FLUORESCEIN AS SHOWN BY POTENTIOMETRIC TITRATION

HARVEY DIEHL, NAOMI HORCHAK-MORRIS, ALTA J. HEFLEY,
LINDA F. MUNSON and RICHARD MARKUSZEWSKI
Department of Chemistry, Iowa State University, Ames, IA 50011, U.S.A.

(Received 10 May 1985. Revised 3 June 1986. Accepted 20 June 1986)

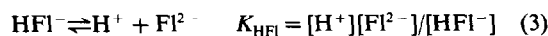
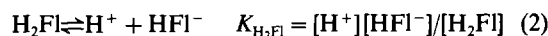
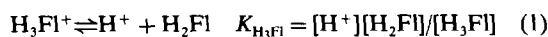
Summary—Potentiometric back-titration of yellow solid fluorescein (H_3FI) and of red solid fluorescein in alkali with acid yielded titration curves that were practically identical in shape and position. The end-points at pH 8.5, 5.40 and 3.3 corresponded, respectively, to titration of the excess of standard alkali, and the successive protonations $FI^{2-} + H^+ = HFI^-$ and $HFI^- + H^+ = H_2FI$. The pH at the mid-point of the first protonation yielded a value of 6.36 for pK_{HFI} (ionic strength 0.10). Because of precipitation of yellow fluorescein during the second protonation step, a value for pK_{H_2FI} could not be obtained. The total concentration of fluorescein at the first appearance of the precipitate fell on the curve for the solubility of yellow fluorescein as a function of pH. The titrations and the pK values found for the three acid groups of protonated fluorescein (H_3FI^+) have been interpreted on the basis that in water fluorescein exists in only one structural form the yellow zwitterion. Similar back-titrations of alkalized solutions of yellow or red fluorescein in 50% aqueous ethanol showed that in this medium fluorescein is present in only one form, presumably the quinonoid structure, with much weaker apparent acid functions, $pK'_1 = 6.38$ and $pK'_2 = 7.16$ (ionic strength 0.10).

The potentiometric titrations of yellow and red solid fluorescein reported in our earlier paper¹ were for the purpose of assay only, such a titration having been used earlier, but in ethanolic medium, by Dolinsky and Jones² for the assay of yellow fluorescein. The results confirmed Bayer's early observation³ that fluorescein is dibasic, and revealed that both acid functions are moderately weak. The second proton comes from a phenol group which would normally be too weakly acidic to give a titration end-point in aqueous medium. We now report titrations of yellow and red fluorescein in water and in 50% aqueous ethanol, done in the hope of evaluating the two pK values and correlating them with structure. Because of the low solubility of both fluoresceins, the titrations were done by dissolving the materials in excess of standard alkali and back-titrating with acid, at ionic strength 0.10, in aqueous medium and in 50% aqueous ethanol (at constant ethanol content). The aqueous titrations yielded a value for K_{HFI} and a very provisional value for pK_{H_2FI} and these values and the characteristics of the titration curves were related to our earlier work⁴ on the solubility of fluorescein as a function of pH. The properties of fluorescein in 50% aqueous ethanol proved quite different from those of fluorescein in water and required a different interpretation.

Earlier,⁴ we proposed that in purely aqueous medium fluorescein exists in only one structural form, the yellow zwitterion, with the positive charge distrib-

uted over the oxygen-bearing ring. The titrations in aqueous media now reported are in conformity with this, but those done in aqueous ethanol indicate that in this medium fluorescein is in a different structural form with much lower acid strength. To interpret these phenomena we draw on supplementary information on the acid-base properties of the related compounds phenolphthalein, dihydroxydimethyl-xanthine, and colourless fluorescein.

The symbolism used is the same as in the earlier paper.⁴



EXPERIMENTAL

Reagents

Diacetylfluorescein, yellow fluorescein and red fluorescein were prepared as described earlier.¹

Apparatus

A Beckman Zeromatic pH-meter was used in conjunction with a Beckman high-alkalinity glass electrode and an S.C.E. The pH-meter was calibrated with at least two standard NBS buffers.

Procedure

A weighed amount, generally ~0.40 g, of the material to be titrated was placed in a beaker containing 45.00 ml of 0.1M sodium hydroxide. The mixture was warmed gently and stirred (magnetic stirring bar) until all the material was dissolved. The solution was removed from the heat-source

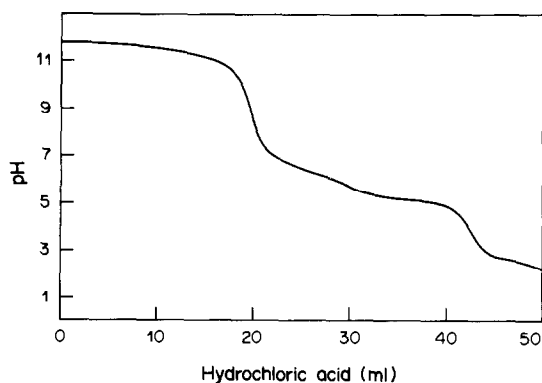


Fig. 1. Back-titration of yellow fluorescein in water, ionic strength ~ 0.08 ; 0.4051 g of yellow fluorescein, 45.00 ml of 0.1024M sodium hydroxide, 100.0 ml of 0.10M potassium chloride, back-titrated with 0.1075M hydrochloric acid. The titration curve for red fluorescein is the same as that for yellow fluorescein.

and 100.0 ml of 0.100M potassium chloride were added. Throughout the back-titration with 0.1M hydrochloric acid the solution was stirred mechanically and the pH was recorded as soon as equilibrium was attained.

In one series of titrations the quantity of yellow fluorescein titrated was varied from 0.1 to 1.2 g, and the volume of 0.100M potassium chloride added was altered so that the total volume at the end of the titration was between 170 and 250 ml. All volumes were carefully recorded so that the total concentration of fluorescein could be calculated for each stage in the titration.

For the titrations in 50% aqueous ethanol (0.100M in potassium chloride), the 0.1M sodium hydroxide and 0.1M hydrochloric acid used were made up in the same solvent.

RESULTS AND DISCUSSION

The undissolved fluorescein present during the early part of direct titration (with alkali) of suspensions of fluorescein in water, made the readings of pH unstable; the titration curves were not smooth, and indicated only that both red and yellow fluorescein are dibasic acids that are sufficiently strong for both protons to be titratable in water. The greater solubility of the fluoresceins in 50% aqueous

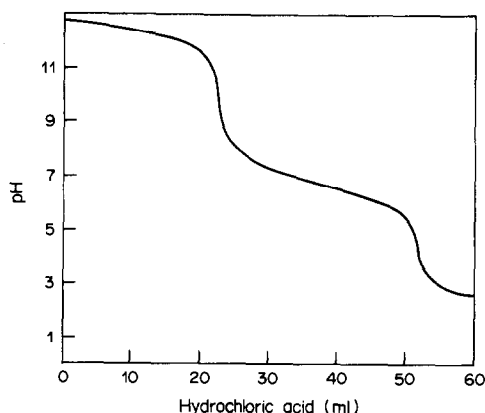


Fig. 2. Back-titration of yellow fluorescein in 50% aqueous ethanol; 0.4056 g of yellow fluorescein; 45.00 ml of 0.0989M sodium hydroxide, 100.0 ml of 0.100M potassium chloride, back-titrated with 0.0860M hydrochloric acid; all solutions contained 50% v/v ethanol.

ethanol made the curves for titration in that solvent a little smoother, but only one end-point was found, at two equivalents of base per mole of fluorescein, starting with either the yellow or red form.

The back-titration curves for the two fluoresceins in aqueous potassium chloride medium, Fig. 1, were identical in shape but differed slightly in position. They were characterized by three breaks (end-points) with the appearance of a yellow precipitate in the neighbourhood of the second. The first end-point, at pH 8.5, corresponded to titration of the excess of sodium hydroxide, the second (at pH 5.4) corresponded to apparent completion of the reaction $\text{Fl}^{2-} + \text{H}^+ = \text{HFl}^-$, and the third (at pH 3.3), to completion of $\text{HFl}^- + \text{H}^+ = \text{H}_2\text{Fl}$. The curves for back-titration of yellow and red fluorescein in 50% aqueous ethanol were identical, Fig. 2, but no precipitate appeared and there were only two end-points, one for neutralization of excess of sodium hydroxide, and the other (at apparent pH 4.5) corresponding to $\text{Fl}^{2-} + 2\text{H}^+ = \text{H}_2\text{Fl}$. The characteristics of the titration curves are detailed in Table 1. Although these

Table 1. Characteristics of the back-titrations of fluorescein (W = weight of fluorescein titrated; $\Delta_1 = \text{pH}_{a=0.25} - \text{pH}_{a=0.75}$; V = total volume at $a = 1.0$; C = total concentration of fluorescein at $a = 1.0$; Cld = pH at which cloudiness appeared; Ppte = pH at which permanent precipitate appeared; $\Delta_2 = \text{pH}_{a=1.25} - \text{pH}_{a=1.75}$)

No.	W, g	Δ_1	$\text{pH}_{a=0.5}$	$\text{pH}_{a=1.0}$	V, ml	C, $10^{-4}M$	Cld	Ppte	Δ_2	$\text{pH}_{a=1.5}$	$\text{pH}_{a=2.0}$	$\text{p}K_{\text{H}_2\text{Fl}}$ [equation (4)]
0.1000M Potassium chloride, yellow fluorescein												
1	0.1036	0.88	6.38	5.50	152.4	20.5	5.10	4.92	0.55	4.80	3.80	4.62
2	0.2034	0.94	6.40	5.45	160.5	38.1	5.62	5.22	0.52	4.90	3.55	4.50
3	0.4051	0.93	6.35	5.40	176.4	69.1	5.65	5.32	0.48	5.10	3.60	4.45
4	0.4033	0.90	6.35	5.45	177.4	68.4	5.35	5.12	0.53	4.82	3.00	4.55
5	0.8040	0.92	6.50	5.60	212.6	113.8	5.78	5.60	0.34	5.28	3.80	4.70
6	1.2055	1.02	6.65	5.80	228.0	159.1	5.88	5.72	0.40	5.45	3.70	4.95
0.1000M Potassium chloride, red fluorescein												
7	0.4101	0.97	6.30	5.35	176.9	69.8	5.42	5.35	0.50	5.10	3.20	4.40
50% ethanol, 0.1000M potassium chloride, yellow fluorescein												
8	0.4056	0.75	7.30	6.70	182.3	67.0	—	—	0.75	6.25	4.48	—
50% ethanol, 0.1000M potassium chloride, red fluorescein												
9	0.4048	0.62	7.31	6.78	182.3	67.0	—	—	0.78	6.25	4.48	—

titrations were performed as protonation titrations, they will be discussed in terms of the dissociation constants of fluorescein as defined by equations (1)–(3). For simplicity, the titration of the excess of alkali will be ignored, and the protonation titration of FI^{2-} will be treated as starting from the first end-point, and will be analysed in terms of the degree of titration a , where a is the molar ratio of protons added to base (FI^{2-}) initially present.

Titrations in aqueous medium

It is obvious that the titration curve from $a = 0.25$ to $a = 0.75$ can be treated as that for a monobasic acid ($\Delta\text{pH} = 0.93$ for yellow fluorescein, 0.97 for red, Table 1, close to the theoretical value^{5,6} of 0.95), and $\text{p}K_{\text{HF1}^-}$ is therefore given by the pH at $a = 0.5$, viz. 6.36 from results 1, 3, 3, 4 and 7 in Table 1, in agreement with that obtained in the earlier solubility work⁴ and again later by fluorimetric measurements.⁷ Treatment of the curve from $a = 1.25$ to $a = 1.75$ is more problematic since it is complicated by the precipitation of undissociated fluorescein, H_2FI , which begins soon after $a = 1.0$.

Theoretically, the pH at $a = 1.0$ for a diacidic base is given by the mean of the $\text{p}K$ values of the conjugate acid:

$$\text{p}H_{a=1} = \frac{1}{2}(\text{p}K_1 + \text{p}K_2) \quad (4)$$

This relationship can be used to estimate $\text{p}K_{\text{H}_2\text{FI}}$ from $\text{p}H_{a=1}$ and $\text{p}K_{\text{HF1}^-}$, and gives the values listed in Table 1. From the nature of the calculation the biggest error will arise from measurement of $\text{p}H_{a=1}$, since it will be doubled. This is clearly shown for

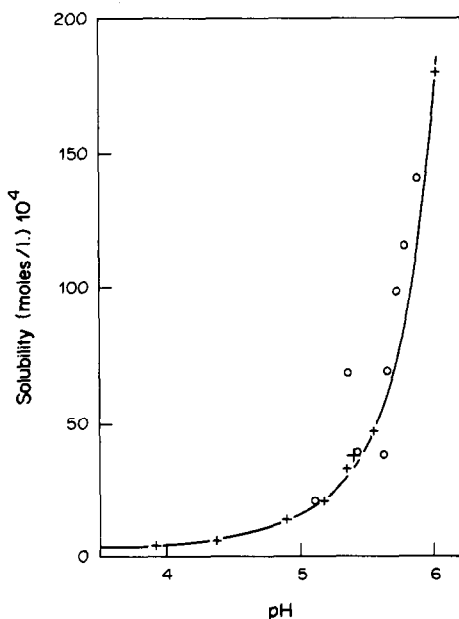


Fig. 3. Solubility of yellow fluorescein: +, as measured by Diehl and Markuszewski;⁴ O, as indicated by the appearance of a cloudiness in the back-titration of fluorescein; +, pH at the "first equivalence-point".

samples 3 and 4. This error will be increased by the effect of the precipitation on the pH vs. a relationship. In principle,⁸ the equilibrium in reaction (2) will be shifted to the left because $[\text{H}_2\text{FI}]$ will be determined by the intrinsic solubility (S_i) of H_2FI , which sets a maximum value for it during the back-titration from $a = 1 + S_i$ to about $a = 1.5 + S_i$ (where protonation of H_2FI begins to set in) and to a first approximation we can write

$$K_{\text{H}_2\text{FI}} = \frac{[\text{H}^+][\text{HF1}^-]}{[\text{H}_2\text{FI}]} \\ = \frac{[\text{H}^+](a-1)C_{\text{H}_2\text{FI}}}{S_i} \quad (5)$$

where $C_{\text{H}_2\text{FI}}$ is the total concentration of fluorescein. For $a = 1.5$ this calculation gives $\text{p}K_{\text{H}_2\text{FI}}$ values ranging from 3.8 to 4.3 for the first six results in Table 1.

The pH of appearance of the precipitate. In the first six titrations in Table 1, in which the amount of fluorescein titrated was varied, the pH at which a definite precipitate appeared shifted to higher pH with increasing concentration of fluorescein in the system. A cloudiness appeared slightly earlier than the first permanent precipitate, presumably because of local precipitation where the drop of hydrochloric acid struck the solution, and slow redissolution. From the record of the volumes added, the concentration of fluorescein at the pH of first cloudiness was calculated and found to fall on the solubility curve⁴ for yellow fluorescein (Fig. 3), confirming that the pH during this protonation step is governed by the solubility of fluorescein as well as the volume of acid added.

Titrations in aqueous ethanol. The conditional pH vs. a curves for back-titration of both yellow and red fluorescein in 50% aqueous ethanol were almost identical, with one end-point (at $a = 2$), indicating that the fluorescein is behaving as a dibasic acid with only a small difference between its two dissociation constants. As a first approximation we took the conditional dissociation constants as equal to the pH values at $a = 0.5$ and $a = 1.5$, which gave $\text{p}K'_{\text{H}_2\text{FI}} = 6.25$ and $\text{p}K'_{\text{HF1}^-} = 7.31$.

To evaluate the results more accurately, we used Yan's method⁹ as adapted for high-precision coulometric titrations¹⁰ and applied with the Iowa State University VAX (Digital Equipment Corporation) system and the Minitab¹¹ statistical system. From the volumes of acid needed to reach the two end-points, 22.35 and 51.63 ml of 0.0860M hydrochloric acid (0.4048 g of fluorescein, 45.0 ml of 0.0989M sodium hydroxide, all media 0.1M potassium chloride in 50% v/v ethanol aqueous), the average number of hydrogen ions n_{exp} added per molecule of fluorescein was calculated from

$$n_{\text{exp}} = 2[(\text{ml}_{\text{HCl}} - 22.35 \text{ ml})/29.28 \text{ ml}]$$

Sixty-one sets of data were entered, and the principal values obtained were

n_{exp}	0	0.50	1.0	1.5	2.0
pH'	10.60	7.31	6.78	6.25	4.48

The theoretical value of n (in the absence of protonation to H_3F1^+) is

$$\bar{n} = \frac{2[H_2F1] + [HF1^-]}{[H_2F1] + [HF1^-] + [F1^{2-}]} \quad (6)$$

which on substitution from equations (1)–(3) and rearrangement yields

$$\bar{n} = \frac{2 + K_{H_2F1}[H^+]}{1 + K_{H_2F1}/[H^+] + K_{H_2F1}K_{HF1}/[H^+]^2} \quad (7)$$

The quantity n was then calculated with $pK'_{HF1} = 7.31$ and pK'_{H_2F1} made successively 6.15, 6.25, 6.35, 6.45, 6.55 and 6.65. The difference $\Delta n = n_{\text{exp}} - n$ at each data point was then calculated and plotted *vs.* n_{exp} , and as criteria of fit the standard deviation, σ_{Δ} , and the sum of squares, $(SSQ)_{\Delta}$, were calculated. Well-defined minima for these criteria gave the best value of pK'_{H_2F1} as 6.35. This value was then used in a similar refinement of pK'_{HF1} by giving it the values 7.02, 7.07, 7.214, 7.18, 7.26 and 7.31, the best value found being 7.19. Iterative refinement was applied in this way to the sum of the pK' values kept constant at 13.54, twice the pH value corresponding to $n_{\text{exp}} = 1.000$, in accordance with equation (4). The final values found were $pK'_{H_2F1} = 6.38$ and $pK'_{HF1} = 7.16$. The drop in conditional pH from $a = 0.5$ to $a = 1.5$ was $7.31 - 6.25 = 1.06$. Setting n at 0.50 and 1.50 in equation (7), and using the two conditional dissociation constants gives $pK'_{a=0.5} = 7.30$ and $pH'_{1.5} = 6.25$ in agreement with the values observed. The ratio of the two dissociation constants is only 6 ($\Delta pK' = 0.78$), which is so low that no break at $a = 1.0$ would be expected.⁵

It should be noted that the effect of the medium on the hydrogen activity measurements will affect both dissociation constants equally so the difference between the ratios of the constants found for the aqueous and ethanolic systems must be attributed to the solubility effect and/or the effect of the change in environment on the structure of the fluorescein species in solution.

Nature of the acid groups in fluorescein

Colourless fluorescein, once dissolved in alkaline water or 50% aqueous ethanol behaves on titration identically with yellow fluorescein. Upon dissolution the lactone ring is opened immediately, as evidenced by the formation of the yellow colour and the behaviour as a dibasic acid on titration.

In our earlier paper⁴ on the solubility of yellow and red fluorescein in water as a function of pH, we pointed out that the two solids are in equilibrium with the same dissolved species, the yellow zwitterion form with the positive charge distributed over the central, oxygen-bearing ring. The potentiometric titrations in water further bear this out; in 50% aqueous ethanol, however, the situation is distinctly different and presumably the quinonoid structure is present.

Because the yellow, amphoteric, zwitterion structure is present throughout the potentiometric titrations in water (direct or reverse titration, starting with either yellow or red fluorescein), it is the two phenolic groups that are involved in titration. The extraordinary acidity of the carboxyl group and these two phenolic groups, (K_a values 2.13, and 4.44, 6.36 respectively) is a consequence of the strong electron-withdrawing power of the positive charge on the central oxygen-bearing ring, and will presumably be due in part to the entropy effect of charge-spreading in the fluoresceinate anions.

Fluorescein dissolved in water, *i.e.*, in the zwitterion form, is thus remarkably different from the closely related compound, phenolphthalein (oxygen bridge missing). Our attempts to titrate phenolphthalein with sodium hydroxide in both water and ethanol were unsuccessful. On addition of the first increment of base the solution became purple and the pH rose into the alkaline region. Back-titrations, both in water and in 50% aqueous ethanol, were distinguishable from titration of sodium hydroxide alone but had no features which could be used to characterize the phenolphthalein, other than that the two phenol groups are both very weak and non-titratable acids. These experiences are quite at odds with the findings of others. Dehn¹² claimed that phenolphthalein can be titrated with up to one equivalent of base without becoming coloured and that only at the start of the addition of the second equivalent of base does the colour arise. Rosenstein¹³ reported the two protons to be typical phenolic protons with pK_a values of 9.64–9.96. It is not quite clear whether the two protons can be differentiated by their dissociation constants; Lalanne,¹⁴ for example, gives one pK value, 9.95, without specifying to which proton it refers.

Attempts to titrate 9,9-dimethylxanthene, synthesized in a pure form by Markuszewski, with sodium hydroxide and with tetrabutylammonium hydroxide in water, 50% aqueous ethanol, acetonitrile, or dimethyl sulphoxide were all unsuccessful. Back-titration in water and 50% aqueous ethanol was also unsuccessful.

The acid character of fluorescein in 50% aqueous ethanol, with conditional pK' values of 6.35 and 7.19, indicates the presence of two acid groups that are barely strong enough to be titratable. Presumably the fluorescein is then present in the quinonoid structure and the titratable groups are the carboxylic acid group and one phenol group.

Note regarding interconversion of the yellow and red forms of fluorescein

Yellow solid fluorescein passes into the red solid form on heating. In a capillary tube this occurs by sublimation but the very small red crystals formed are so highly twinned as to be useless for an X-ray crystal structure study.

A revealing interconversion was observed during a back-titration in water at a temperature just below the boiling point. The titration curve followed that at room temperature to about $a = 1.5$, then the yellow solid which had precipitated was suddenly converted into the red form and the pH rose abruptly from 5.0 to 6.5.

As a confirmatory experiment, a suspension of 0.5 g of yellow fluorescein was boiled for 2 hr; the pH changed from 4.42 before heating to 5.30 after cooling back to room temperature. This behaviour is explicable on the basis that in conversion of the strong acid (zwitterion structure) into the weaker acid (red quinoid structure), hydrogen ions are taken up.

Acknowledgements—The numerous titration curves referred to but not reproduced in this paper will be found in the M.S. thesis of L. A. Freytag¹⁵ and the Ph. D. dissertation of R. Markuszewski.¹⁶ One of us (N. H.) wishes to acknowledge aid from a grant from Mr and Mrs C. C. Hach to Iowa State University for research in analytical chemistry.

REFERENCES

1. R. Markuszewski and H. Diehl, *Talanta*, 1980, **27**, 937.
2. M. Dolinsky and J. H. Jones, *J. Assoc. Off. Agri. Chem.*, 1951, **34**, 114.
3. A. Baeyer, *Annalen*, 1876, **183**, 1.
4. R. Markuszewski and H. Diehl, *Talanta*, 1985, **32**, 159.
5. P. E. Sturrock, *J. Chem. Educ.*, 1968, **45**, 259.
6. A. Tchaplá and C. Fabre, *ibid.*, 1983, **60**, 1030 and references therein.
7. H. Diehl and R. Markuszewski, *Talanta*, in press.
8. H. A. Krebs and J. J. Speakman, *J. Chem. Soc.*, 1945, 593.
9. J. F. Yan, *Anal. Chem.*, 1965, **37**, 1588.
10. W. F. Koch, D. P. Poe and H. Diehl, *Talanta*, 1975, **22**, 609.
11. T. A. Ryan, Jr., B. L. Joiner and B. F. Ryan, *Minitab Student Handbook*, Duxbury Press, 20 Providence Street, Boston, Mass 02116, U.S.A.; *Minitab Reference Manual*, Statistical Laboratory, 215 Pond Laboratory, Pennsylvania State University, University Park, Pennsylvania 16802, U.S.A.
12. W. M. Dehn, *J. Am. Chem. Soc.*, 1932, **54**, 2947.
13. L. Rosenstein, *ibid.*, 1912, **34**, 1117.
14. J. R. Lalanne, *J. Chem. Educ.*, 1971, **48**, 266.
15. L. A. Freytag, *M.S. Thesis*, Iowa State University, Ames, Iowa, 1971.
16. R. Markuszewski, *Ph.D. Dissertation*, Iowa State University, Ames, Iowa, 1976.

MISE EN EVIDENCE DE DEUX NOUVEAUX INDICATEURS ACIDE-BASE DANS L'ACIDE ACETIQUE ANHYDRE

M. SARBAR, S. M. GOLABI et M. H. POURNAGHI-AZAR

Laboratoire de chimie analytique, Faculté des Sciences, Université de Tabriz, Tabriz, Iran

(Reçu le 9 mai 1985. Révisé le 17 mai 1986. Accepté le 28 juin 1986)

Résumé—En traçant les courbes de $A = f(\lambda)$ pour les deux composés organiques 1,5-di[2-furyl] 1,4-pentadiène 3-one (DFPO) et 1,5-di[2-thienyl] 1,4-pentadiène 3-one (DTPO) dans l'acide acétique anhydre et en présence de différentes concentrations d'acide perchlorique, on a montré que ces composés peuvent fonctionner comme les indicateurs acide-base dans ce milieu. Les valeurs de pK_i des réactions $I + \text{HClO}_4 \rightleftharpoons \text{IH}^+ \text{ClO}_4^-$ sont déterminées par la méthode spectrophotométrique. L'efficacité de ces indicateurs dans la détection visuelle et colorimétrique des points finaux a été confirmée en les utilisant dans les titrages acide-base.

Summary—The behaviour of two organic compounds, 1,5-di[2-furyl]-1,4-pentadien-3-one (DFPO) and 1,5-di[2-thienyl]-1,4-pentadien-3-one (DTPO), as acid-base indicators has been studied by plotting the curves $A = f(\lambda)$ in the presence of various concentrations of perchloric acid, in anhydrous acetic acid medium. The values of $pK_i^{\text{HClO}_4}$ have been determined by spectrophotometry. The efficiency of these indicators in visual and colorimetric detection of the end-points of acid-base titrations has been examined.

Depuis longtemps, l'acide acétique anhydre a été utilisé comme un solvant convenable dans la réalisation des réactions chimiques et électrochimiques.¹⁻⁷ L'emploi de ce solvant au cours des titrages acide-base présente de nombreux avantages, dus à son caractère acide par rapport à l'eau. Il en résulte une augmentation de la force des bases qui sont très faibles dans l'eau et un accroissement remarquable de la précision de leurs titrages acidimétriques.^{4,5,7}

La détection visuelle et colorimétrique des points finaux, relatifs aux titrages acidimétriques des bases faibles dans l'acide acétique anhydre, exige l'emploi des indicateurs colorés seulement sensibles aux acides forts, tel que l'acide perchlorique.

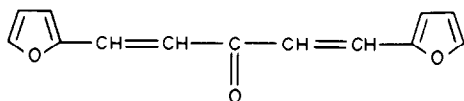
Au cours de ce travail, nous avons étudié d'abord le comportement acido-basique de deux composés organiques dans l'acide acétique anhydre en utilisant une méthode spectrophotométrique. Ensuite, nous avons montré la possibilité de l'emploi de ces deux composés comme indicateurs colorés dans les titrages colorimétriques des bases qui sont très faibles ou insolubles dans l'eau.

PARTIE EXPERIMENTALE

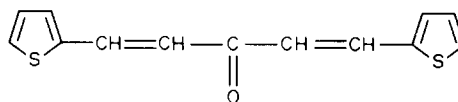
Réactifs

Les composés* étudiés sont les suivants:

(a) 1,5-di[2-furyl] 1,4-pentadiène 3-one (DFPO):



(b) 1,5-di[2-thiényl] 1,4-pentadiène 3-one (DTPO):



Ces composés, en solution $10^{-3}M$ dans l'acide acétique anhydre, se décomposent rapidement à la lumière de jour. Ainsi, il est indispensable de les conserver à l'abri de la lumière et dans des flacons de verre coloré.

Le solvant utilisé est l'acide acétique anhydre 100%.

Acide perchlorique 0,10M dans l'acide acétique anhydre est préparé à partir d'une solution 70% d'acide perchlorique et par addition d'une quantité nécessaire d'anhydride acétique comme déshydratant. Afin d'éviter une influence défavorable de la dilution sur l'activité de l'indicateur au cours de titrages, une concentration $10^{-4}M$ de ce dernier a été ajouté à la solution d'acide perchlorique.

Solution 0,10M de biphthalate de potassium deshydraté dans l'acide acétique anhydre contenant une concentration $10^{-4}M$ de l'indicateur. Cette solution est servie à la correction du titre de la solution d'acide perchlorique.

Solution $10^{-3}M$ de l'indicateur dans l'acide acétique anhydre: 1,1 ml de cette solution ajouté à 10 ml de la solution de base à titrer, constitue un mélange contenant une concentration $10^{-4}M$ de l'indicateur.

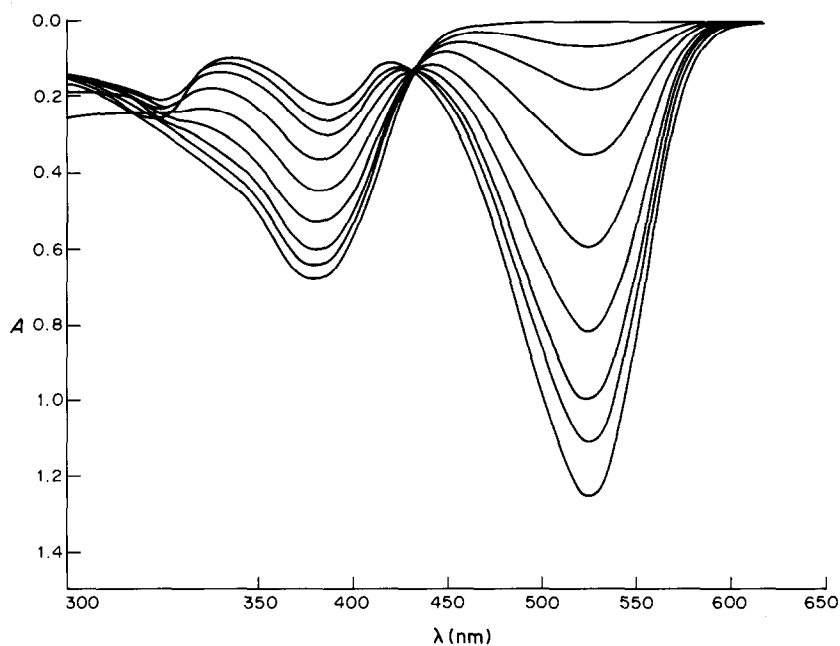
Solution 1,00M de perchlorate de sodium dans l'acide acétique anhydre contenant l'indicateur à $10^{-4}M$ concentration. Cette solution est servie pour la fixation de la force ionique.

Tous les produits chimiques sont de fabrication Merck, grade P.A.

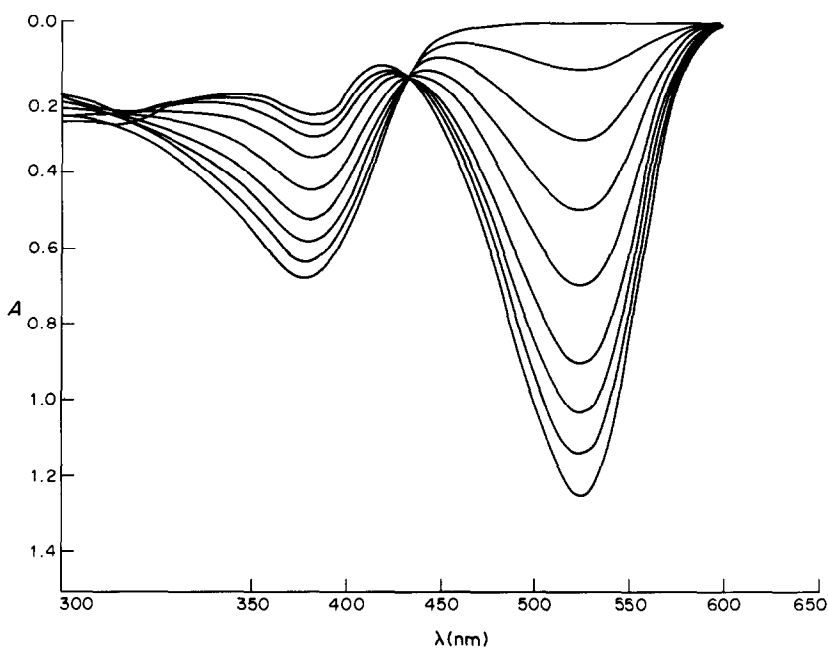
Appareillage

Une spectrophotomètre UV-Visible Perkin-Elmer, modèle 402 a été servie pour tracer les courbes $A = f(\lambda)$. Le tracé des courbes de titrage $A = f(V_{\text{HClO}_4})$ a été réalisé à l'aide d'un titrateur à filtre d'EEL (Evans Electro Selenium Ltd., Angleterre).

*Ces composés sont synthétisés dans la laboratoire de chimie organique, Faculté des Sciences, Tabriz.



(a)



(b)

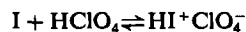
Fig. 1. Les courbes $A = f(\lambda)$ correspondantes à une concentration $5 \times 10^{-5} M$ de: (a) DFPO; (b) DTPO, en présence de différentes concentrations d'acide perchlorique (0,00–0,50M).

RESULTATS ET DISCUSSION

Détermination de pK_i des indicateurs

L'existence d'un équilibre simple entre les deux formes protonées et non protonées des indicateurs a été révélé par le tracé des courbes $A = f(\lambda)$ (Fig. 1).⁸ Pour déterminer les valeurs de pK_i , nous examinons l'équilibre reliant les deux formes acide et base de

l'indicateur en présence d'acide perchlorique:



$$K_i = \frac{[I][\text{HClO}_4]}{[\text{HI}^+ \text{ClO}_4^-]}$$

d'où:

$$p\text{HClO}_4 = pK_i + \log\left(\frac{[I]}{[\text{HI}^+ \text{ClO}_4^-]}\right)$$

La présentation des variations de $\log([I]/[HI^+ClO_4^-])$ en fonction de $pHClO_4$ est une droite dont l'ordonnée à l'origine conduit à la valeur de pK_i . Pour tracer cette droite, nous avons appliqué la méthode spectrophotométrique en utilisant dix séries de solutions pour chacun des indicateurs. Ces solutions contiennent des concentrations variables d'acide perchlorique (de 0,00 à 0,50M) et une concentration constante de $2 \times 10^{-5}M$ de l'indicateur. La force ionique des solutions a été ajustée à 0,50M par $NaClO_4$ 1,00M.

La concentration maximale d'acide perchlorique dans l'acide acétique anhydre est limitée à 0,50M, car:

(a) une concentration supérieure provoque une détérioration progressive du solvant et l'apparition d'une coloration brune;

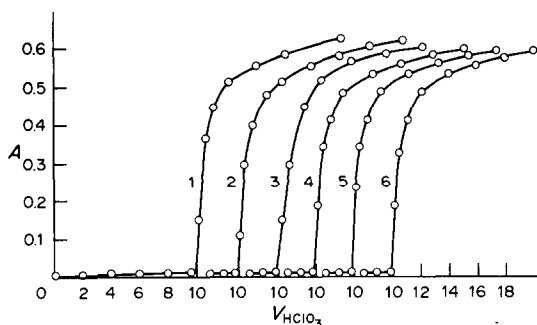
(b) l'indicateur se trouve presque totalement sous forme d'acide, lorsque la concentration d'acide perchlorique atteint 0,50M;

(c) la stabilité de l'indicateur décroît lorsque la concentration en $HClO_4$ dépasse 0,50M.

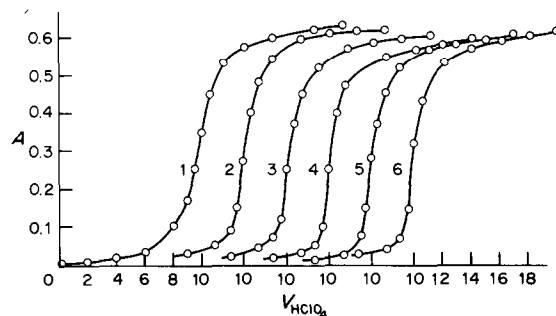
A l'appui des méthodes statistiques, nous avons trouvé les valeurs suivantes pour les pK_i : DFPO $2,26 \pm 0,01$, DTPO $2,09 \pm 0,01$.

Application de DFPO et DTPO dans les titrages acide-base

Détection des points finaux de titrages acidimétriques des bases faibles. Les bases avec un pK_A de l'ordre de 2 dans l'eau ($pK_A = pK_w - pK_B$) ont été déjà titrées avec une précision suffisante dans l'acide acétique anhydre.^{4,5,9,10} Les points finaux de ces titrages sont détectés par les méthodes potentiométriques^{11,12} ou photométriques en présence des indicateurs colorés.^{13,14} Les indicateurs DFPO et DTPO étant presque analogues à Sudan III, nous les avons utilisés pour tracer les courbes de titrages colorimétriques d'un certain nombre de bases organiques et inorganiques rassemblées dans le tableau 1, en prenant l'acide perchlorique 0,10M comme réactif titrant. Les courbes de titrages sélectionnées sont représentées dans Fig. 2. Pour déterminer le point final, nous avons procédé par l'une des méth-



(a)



(b)

Fig. 2. Courbes de titrages colorimétriques des bases organiques et inorganiques de concentration 0,1M environ, par une solution titrée d'acide perchlorique dans l'acide acétique anhydre, en utilisant le DTPO comme l'indicateur coloré: (a): (1) β -picoline, (2) *N*-méthylaniline, (3) aniline, (4) acétate de sodium, (5) nitrate de lithium, (6) fluorure de sodium; (b): (1) chlorure de lithium, (2) urée, (3) caféine, (4) diphenylamine, (5) *p*-nitroaniline, (6) antipyrine.

odes décrites par Rumeau¹⁵ ou Higuchi *et al.*,¹² selon l'allure des courbes de titrages obtenues.

Détection des points finaux de titrages alcalimétriques des acides forts. Nous avons essayé le titrage des acides forts en présence des acides faibles dans l'acide acétique anhydre. Ainsi nous avons montré la possibilité de titrage d'acide perchlorique en présence d'acides nitrique, chlorhydrique et fluorhydrique en utilisant une solution titrée d'acétate de sodium ou biphtalate de potassium dans l'acide acétique anhydre. La détection du point final peut être réalisée visuellement par un virage de rouge au jaune-pâle de l'indicateur. La courbe colorimétrique correspondante à ce titrage a été présentée dans Fig. 3.

Le titrage colorimétrique a été effectué sur une prise de 5 ml d'une solution acétique de concentration 0,10M des acides perchlorique et chlorhydrique. La solution acétique a été obtenue par le traitement d'une aliquote de 5 ml de solution aqueuse contenant de 50 mmoles de chacun des acides pour 32 ml d'anhydride acétique et amené à 50 ml par l'acide acétique.

Conclusion

DFPO et DTPO sont deux cétones conjuguées qui apparaissent sous forme (I) des bases très faibles dans l'acide acétique anhydre. En présence d'un acide fort.

Tableau 1

Bases à titrer	$pK_{H_2O}^*$
β -Picoline	5.5
<i>N</i> -Méthylaniline	5.0
Aniline	4.6
Acétate de sodium	4.8
Fluorure de sodium	3.2
Nitrate de lithium	-1.8
Chlorure de lithium	-3.7
Urée	0.4
Caféine	0.6
Diphénylamine	0.8
<i>p</i> -Nitroaniline	1.0
Antipyrine (phénazone)	1.5

*Réf. 4, p. 81.

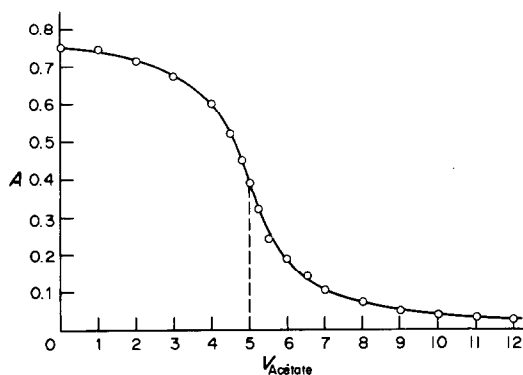
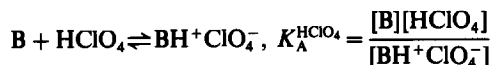


Fig. 3. Courbe de titrage colorimétrique de HClO_4 $0,1M$ en présence de HCl $0,1M$, par une solution d'acétate $0,10M$ dans l'acide acétique anhydre avec $10^{-4}M$ DTPO comme l'indicateur.

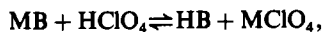
comme HClO_4 , ces formes basiques colorées en jaune-pâle se transforment aux formes acides (H^+ClO_4^-) rouges. La détermination des pK_A de ces deux indicateurs et la comparaison des valeurs obtenues avec celles des indicateurs Sudan III et Sudan IV montre qu'on peut les regrouper sous ces derniers dans le tableau des indicateurs de Higuchi *et al.*¹²

Parmi ces deux indicateurs étudiés, le DTPO est le plus stable; ainsi nous l'avons utilisé dans les titrages acide-base. Nous avons évalué l'efficacité de cet indicateur dans la détermination des points finaux des titrages colorimétriques des bases faibles par une solution titrée d'acide perchlorique, selon les réactions suivantes:

—pour les bases de la forme B:



—pour les bases de la forme MB:



$$K_A^{\text{HClO}_4} = \frac{[\text{MB}][\text{HClO}_4]}{[\text{HB}][\text{MClO}_4]}$$

A partir des travaux de Rumeau,¹⁵ toutes les bases ayant un $pK_A^{\text{HClO}_4}$ égal ou supérieur à 7 et une

concentration de l'ordre de $0,10M$, entrent dans une réaction quantitative avec HClO_4 ($K_A/C_{\text{base}} \leq 10^{-4}$) et en présence de DTPO ($K_i/(K_A C_{\text{base}})^{1/2} \geq 10^2$) montrent une courbe de titrage dont le point final se caractérise par un point angulaire (les courbes 1 à 6, Fig. 2a). Alors que les bases plus faibles ($pK_A \approx 4-5$) avec une concentration environ $0,10M$ font apparaître des courbes de titrage de l'allure S symétrique ou asymétrique (courbes 1 à 6, Fig. 2b), dont les points finaux seront déterminés par les méthodes graphiques¹⁶ ou celles décrites par Rehm et Higuchi.¹⁴

Nous avons utilisé ces deux indicateurs dans le dosage d'acide perchlorique en présence de différents acides faibles. Le point final peut être détecté visuellement par le virage de l'indicateur de rouge à jaune-pâle. L'application de la colorimétrie augmente la précision de la détection du point final.

LITTÉRATURE

1. J. B. Conant et N. F. Hall, *J. Am. Chem. Soc.*, 1927, **49**, 3062.
2. I. M. Kolthoff et S. Bruckenstein, *ibid.*, 1956, **78**, 2974.
3. B. Trémillon, *Bull. Soc. Chim. France*, 1960, 1940.
4. G. Charlot et B. Trémillon, *Les réactions chimiques dans les solvants et les sels fondus*, pp. 211-237. Gauthier-Villars, Paris, 1963.
5. J. Kucharský et L. Šafařík, *Titrations in Non-Aqueous Solvents*, Elsevier, Amsterdam, 1965.
6. G. Durand, *Bull. Soc. Chim. France*, 1970, 1220.
7. B. Trémillon, *La chimie des solvants non-aqueux*, p. 93. Presses universitaires de France, Paris, 1971.
8. L. C. Smith et L. P. Hammett, *J. Am. Chem. Soc.*, 1945, **67**, 23.
9. H. H. Jaffé, *Chem. Rev.*, 1953, **53**, 191.
10. M. Gutterson et T. S. Ma, *Mikrochim. Acta*, 1960, 1.
11. N. F. Hall et T. H. Werner, *J. Am. Chem. Soc.*, 1928, **50**, 2367.
12. T. Higuchi, J. A. Felomann et C. Rehm, *Anal. Chem.*, 1956, **28**, 1120.
13. T. Higuchi, C. Rehm et C. Barnstein, *ibid.*, 1956, **28**, 1506.
14. C. Rehm et T. Higuchi, *ibid.*, 1957, **29**, 367.
15. M. Rumeau, *Thèse de Doctorat ès Sciences*, Paris, 1971.
16. G. Mattock, *pH Measurement and Titration*, Heywood, London, 1961.

SHORT COMMUNICATIONS

COMPARISON OF INORGANIC FILMS AND POLY(4-VINYLPYRIDINE) COATINGS AS ELECTRODE MODIFIERS FOR FLOW-INJECTION SYSTEMS

JAMES A. COX* and KRISHNAJI R. KULKARNI

Department of Chemistry and Biochemistry, Southern Illinois University, Carbondale, IL 62901, U.S.A.

(Received 17 February 1986. Revised 19 June 1986. Accepted 30 June 1986)

Summary—A glassy-carbon electrode modified with a ruthenium-containing inorganic film was used for the flow-injection determination of As(III). The linear working range was 5-100 μ M, and the detection limit was 300 pg. The response was reproducible for periods of several days. A glassy-carbon electrode modified by adsorption of a quaternized poly(4-vinylpyridine) film impregnated with hexachloroiridate(II and III) was used for the oxidation of nitrite. The calibration graphs were non-linear and varied from day to day, and the peak widths were broad. Nitrite determination at a platinum electrode modified by adsorption of iodine gave results analogous to the As(III) study; however, an overlayer of quaternized poly(4-vinylpyridine) decreased the sensitivity.

Amperometric detection is commonly used in flow-injection systems, but the range of analytes and sample types is limited because many compounds cause poisoning of the indicator electrode surface. Such problems have been extensively documented in investigations on voltammetry in static solutions. For example, the oxidation of nitrite at clean platinum electrodes is characterized by a gradual loss of sensitivity, whereas coating the platinum with the monolayer of iodine produces a stable indicator electrode.^{1,2} The oxidation of As(III) at a platinum electrode depends on the presence of an oxide layer on the electrode surface;^{3,4} the oxidation does not occur at a bare carbon electrode.⁵ The determination of nitrite with a flow-injection system employing a glassy-carbon indicator electrode was found to be limited because several ionic species poisoned the electrode; for example, the presence of thiocyanate in a sample resulted in electrode passivation in the first run.⁶

Modification of electrode surfaces provides a means of extending the range of amperometric detection in flow-injection systems, both by alleviating some of the problems associated with stability of the electrode surface and by providing a catalytic surface to increase the number of analytes that can be determined. Electrolysis systems may also be made more selective by use of a coating that passivates the electrode surface towards all but a few species.⁷

Although modified electrodes have frequently been used for voltammetric determinations in static solutions, few applications to flow systems have been reported. Sittampalam and Wilson⁸ demonstrated that in the liquid chromatographic determination of

hydrogen peroxide the interference caused by adsorption of protein or oxidation of ascorbate could be eliminated by coating the electrode with cellulose acetate. This is consistent with our report that the effect of surfactants on the transport of analytes through membranes is significantly less than the effect of surfactants on electrode reactions.⁹ Hydrolysis of the cellulose acetate changes the permeability of the film but protection is still provided against proteins in flow-injection determinations.¹⁰

The first electrocatalytic modified electrode used in a flow-injection system and liquid chromatography was a carbon-paste electrode containing metallophthalocyanine, and was applied in the determination of hydrazine.¹¹

In the present study, we have employed modified electrodes, developed initially for static systems, in flow-injection systems. One type was prepared by anchoring hexacyanoruthenate(II) to glassy carbon by electrochemical deposition from a mixture of ruthenium(III) chloride and potassium hexacyanoruthenate(II).⁵ Because these two species do not react rapidly in solution, the deposit is probably not a true analogue of Prussian Blue, but a highly stable deposit is formed. Arsenic(III) can be oxidized at this modified glassy-carbon electrode whereas it is not electroactive at the uncoated electrode.

A more common means of modifying electrodes is to coat the substrate with an ion-exchange polymer and subsequently impregnate it with a redox mediator. We have demonstrated that platinum or glassy carbon which has been coated with poly(4-vinylpyridine), PVP, in acid solution, or with quaternized PVP over a range of pH, can be used for the oxidative determination of nitrite in static solution when the polymer is impregnated with hexachloroiridate(II, III).¹² Modification of the platinum

*Author for correspondence.

electrode by adsorption of iodine^{1,2,13} also provides an electrode suitable for the oxidation of nitrite.

Our goal was to compare these rather diverse modified electrodes in terms of their suitability for flow-injection systems. The factors of primary concern were the response time and the stability.

EXPERIMENTAL

Apparatus

The flow-injection system comprised a Cole Parmer Master Flex peristaltic pump, a Rheodyne 7010 six-port injection valve with a 20- μ l sample loop, a home-made pulse dampener, and an electrochemical cell which was assembled from Bioanalytical Systems TL5A-glassy carbon and TL10A-Pt transducer cells. An IBM EC/230 system served as the potentiostat.

Electrodes

The electrodes were modified as previously reported. The transducer cell was dismantled and immersed in a static solution for this step. The Ru-containing film was prepared by cycling a clean glassy-carbon electrode between 0.35 and 0.85 V *vs.* SCE at 50 mV/sec in a fresh mixture of 2mM ruthenium(III) chloride, 2mM potassium hexacyanoruthenate(II), and 0.5M sodium chloride at pH 2 for 25 min.⁵ The clean platinum electrode was modified by dipping it in deaerated 2mM sodium iodide.^{1,2} In some cases it was then treated with three drops of a 0.4% methanol solution of quaternized PVP (total of 0.12 mg of polymer), in a manner described elsewhere.¹³ Clean glassy carbon was coated with quaternized PVP in the same manner. Further modification by impregnating the polymer with hexachloroiridate(II, III) was accomplished by cycling the polymer-coated electrode in 2mM potassium hexachloroiridate(II) in pH-4.6 phosphate buffer between 0.4 and 0.85 V *vs.* SCE for 1 hr.¹²

A Kelgraf electrode was prepared as previously reported.^{14,15} A 1 + 3 mixture of Ultra Carbon spectroscopic graphite powder and 32-mesh Kel-F powder (3M Co.) was dispersed in absolute ethanol, the ethanol was evaporated, and the residue was pressed into a rod at 250° and 1000 psig. The rod was sealed into a Plexiglas block with epoxy resin. The block was machined to fit the electrochemical cell.

Reagents

The quaternized PVP was prepared by letting 50 ml of 0.4% methanol solution of PVP (Aldrich) and 5 ml of benzyl chloride react overnight. The water used was distilled and then further treated by passage through a Barnstead Nanopure II system.

RESULTS AND DISCUSSION

Arsenic(III) was determined in a carrier stream of 0.5M sodium chloride acidified to pH 2; the flow-rate was 1.0 ml/min. A seven-point calibration graph prepared over the range 5.0×10^{-6} – 2.0×10^{-4} M As(III) was linear. Five consecutive injections of 3.0×10^{-5} M As(III) yielded a relative standard deviation of 0.5%. The experiments were repeated daily for one week. The average of the seven slopes was $7.4 \pm 0.4 \mu\text{A} \cdot \text{l} \cdot \text{mmole}^{-1}$; the correlation coefficient and intercept calculated on the basis of all data in that range were 0.9999 and -1.5 nA , respectively. The detection limit, expressed as the concentration equivalent to a signal three times the standard deviation of a blank, was 300 pg of As(III) in 20 μ l. The

detectability was limited by the rather high level of fluctuation caused by the pump used. The width of the peak at half-height was 22 sec for a concentration that yielded a 38- μ A peak height. Up to 90 samples per hour could be determined, with return of recorder signal to the baseline between samples. The ruthenium-containing inorganic film therefore provides a suitable electrode for the flow-injection determination of As(III).

A modest improvement in the detection limit is achieved by using the modified Kelgraf electrode. Because the active surface resembles a disordered array of microelectrodes, depletion effects are then not as significant.¹⁶ Hence, the decrease in active surface area does not cause a concomitant loss of signal. The estimated geometric area of the electrode is 25% of that of the glassy-carbon electrode, and the slope of the calibration graph is 30% of that for the glassy-carbon system. If smaller Kel-F particles had been used, the decrease in sensitivity undoubtedly would have been less. Because the noise level is significantly less at the modified Kelgraf surface, the detection limit is improved to 200 pg of As(III) in 20 μ l even though the sensitivity is poorer, as mentioned above.

For the determination of nitrite, various bare and modified electrodes were examined. Because of the well known passivation that occurs when nitrite is oxidized at bare electrodes, especially platinum, the effect of consecutive injections on the response of the electrode was first determined. The results are summarized in Table 1.

As expected, the modified electrodes gave more constant sensitivity, but certain other factors must be considered. The nitrite concentrations were about 10^{-4} M; the passivation effect on the bare electrode will be less pronounced at trace levels. It is also important to note that the electrodes with a quaternized PVP coating are not easily renovated since the cell must be dismantled for the purpose; this point is particularly significant, because these electrodes do not have good day-to-day stability.

Table 1. Stability of various electrodes* during the oxidation of consecutive nitrite samples†

Injection number	Current, nA				
	Pt	C	Pt/I	Pt/I/qPVP	C/qPVP, IrCl ₆ ⁴⁻³⁻
1	60	52	69	44	35
2	58	52	70	44	36
3	55	51	68	44	35
4	52	48	68	43	35
5	51	48	66	43	35

*Electrodes: Pt = clean platinum; C = glassy carbon; Pt/I = platinum modified with NaI; Pt/I/qPVP = Pt/I electrode treated with quaternized PVP; C/qPVP, IrCl₆⁴⁻³⁻ = glassy carbon treated with quaternized PVP and hexachloroiridate (II, III).

†The oxidations were at 0.9 V *vs.* Ag/AgCl in pH-4.6 phosphate buffer. The buffer, flowing at 1.0 ml/min, was the carrier solvent.

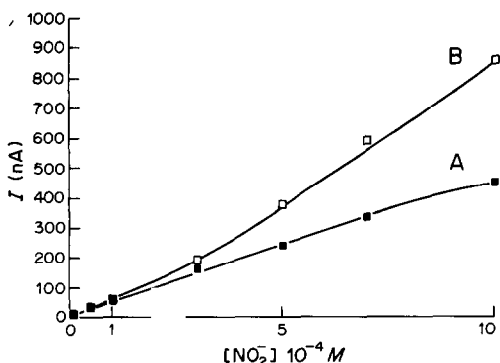


Fig. 1. Effect of time on the oxidation of nitrite at a platinum electrode coated with a quaternized PVP film containing hexachloroiridate(II, III), A, days 1 and 2; B, day 3.

A glassy-carbon electrode modified with a quaternized PVP film containing hexachloroiridate(II, III) was used to prepare nine-point calibration graphs on three consecutive days, for nitrite in the range 10^{-5} – 10^{-3} M in a pH-4.6 phosphate buffer. The plots were non-linear; the first two days yielded convex curves and the third day a concave curve (Fig. 1). The initial slopes were 0.45, 0.48 and 0.86 $\mu\text{A.l.mmole}^{-1}$. The detection limit with a freshly modified glassy-carbon electrode is 1.4 ng of nitrite in a 20- μl injection.

The non-linearity resulted from the fact that the current-limiting step included a contribution from diffusion of nitrite in the polymer instead of being exclusively controlled by mass transport in the solution.¹² The change of slope with time is attributed to loss of the quaternized PVP. As the film became thinner, some oxidation probably occurred at the glassy-carbon substrate.

Two facts support these hypotheses. First, the sensitivity with a bare glassy-carbon electrode is higher than that for the surface modified with quaternized polymer. Secondly, quaternized PVP is known to be somewhat soluble in aqueous solution even when a counter-ion such as phosphate is present to act as a cross-linking agent.

The polymer-coating causes a second problem in the flow-injection system that is not significant in static solution. The peak width is increased because of the effect of diffusion (in the polymer) of the nitrite and of the ions needed to maintain charge balance in the film during the electrolysis. The two-electron oxidation of nitrite at the iodine-coated platinum

electrode has a peak half-width of 20 sec at a 1-ml/min flow-rate, which is comparable to the value for the oxidation of As(III). The current for both of these electrode processes is limited by mass transport of nitrite in the solution of the electrode surface.^{5,12} With the coated glassy-carbon electrode, the half-width was 35 sec.

Our conclusion is that for polymer-coated electrodes to be useful for analytical determinations in systems that do not permit simple reconstitution of the surface, films more stable than the popular poly(4-vinylpyridine) systems will need to be employed. Such polymers are being investigated by several groups, including ours. However, it will also be necessary for the films to be extremely thin or heavily loaded with mediator for them to be practical in a flow system. This may in turn complicate the problem of maintaining a constant load of the mediator couple unless the mediator is bonded to the polymer more strongly than by simple ion-exchange.

Acknowledgement—This work was supported by the National Science Foundation (U.S.A.) under grant CHE-8215371.

REFERENCES

1. R. F. Lane and A. T. Hubbard, *Anal. Chem.*, 1976, **48**, 1287.
2. D. C. Johnson, *J. Electrochem. Soc.*, 1972, **119**, 331.
3. W.-H. Kao and T. Kuwana, *J. Electroanal. Chem.*, 1985, **193**, 145.
4. T. D. Cabelka, D. S. Austin and D. C. Johnson, *J. Electrochem. Soc.*, 1985, **132**, 359.
5. J. A. Cox and P. J. Kulesza, *Anal. Chem.*, 1984, **56**, 1021.
6. J. E. Newbery and M. P. Lopez de Haddad, *Analyst*, 1985, **110**, 81.
7. J. A. Cox and M. Majda, *Anal. Chim. Acta*, 1980, **118**, 271.
8. G. Sittampalam and G. S. Wilson, *Anal. Chem.*, 1983, **55**, 1608.
9. G. L. Lundquist, G. Washinger and J. A. Cox, *ibid.*, 1975, **47**, 319.
10. J. Wang and L. D. Hutchins, *ibid.*, 1985, **57**, 1536.
11. K. M. Korfhage, K. Ravichandran and R. P. Baldwin, *ibid.*, 1984, **56**, 1514.
12. J. A. Cox and P. J. Kulesza, *J. Electroanal. Chem.*, 1984, **175**, 105.
13. *Idem*, *Anal. Chim. Acta*, 1984, **158**, 335.
14. D. J. Chesney, J. L. Anderson, P. E. Weisshaar and D. E. Tallman, *ibid.*, 1981, **124**, 321.
15. J. E. Anderson, D. E. Tallman, D. J. Chesney and J. L. Anderson, *Anal. Chem.*, 1978, **50**, 1051.
16. J. L. Anderson, K. K. Whiten, J. D. Brewster, T.-Y. Ou, and W. K. Nonidez, *ibid.*, 1985, **57**, 1366.

KINETIC FLUORIMETRIC DETERMINATION OF ORGANIC PEROXIDES AND LIPOHYDROPEROXIDES AT THE NANOMOLE LEVEL

J. PEINADO,* F. TORIBIO* and D. PEREZ-BENDITO†

*Departamento de Bioquímica, Facultad de Veterinaria and †Departamento de Química Analítica,
Facultad de Ciencias, Universidad de Córdoba, Córdoba, Spain

(Received 11 February 1986. Revised 24 April 1986. Accepted 19 June 1986)

Summary—A new kinetic fluorimetric method for determination of cumene hydroperoxide, tert-butyl hydroperoxide and lipohydroperoxides is reported. It is based on the manganese(II)-catalysed oxidation of 2-hydroxynaphthaldehyde thiosemicarbazone (HNTS) by a hydroperoxide. Measurements are made by the initial-rate method, which allows determination of as little as 0.1 nmole of peroxide and also permits establishment of the differences in reactivity between the hydroperoxides assayed. The method has been applied to the determination of lipohydroperoxides in six commercial oil samples (grape, corn, sunflower seed, cod-liver and linseed). The results obtained can be expressed as meq of peroxide per kg of oil, and are in close agreement with those obtained by the classical iodometric method.

Several techniques have been used to date for the determination of peroxides, but few have proved suitable or reliable when dealing with peroxides at concentrations as low as 1–10 μM .¹⁻³ One of the most sensitive uses fluorimetric detection and is based on the oxidation of dichlorofluorescein⁴ in the presence of haematin, which allows determination of organic hydroperoxides and lipohydroperoxides at a level of 8nM. This method is suitable for a variety of hydroperoxides: tert-butyl hydroperoxide, cumene hydroperoxide, hydroperoxylinoleate, hydroxy-5 α -cholesterol, hydrogen peroxide, etc. The assay is done at pH 7.2 and the dichlorofluorescein–hydroperoxide mixture is incubated in an argon atmosphere for 50 min.

In this work we propose a new fluorimetric kinetic method for determination of organic hydroperoxides and lipohydroperoxides, based on the manganese(II)-catalysed oxidation of 2-hydroxynaphthaldehyde thiosemicarbazone (HNTS). The oxidation product exhibits intense blue fluorescence ($\lambda_{\text{exc}} = 390$ nm, $\lambda_{\text{em}} = 450$ nm). The method has been applied to the determination of tert-butyl hydroperoxide and cumene hydroperoxide, and the lipohydroperoxide content in six commercial oil samples. The determination ranges for tert-butyl hydroperoxide and cumene hydroperoxide are 0.08–1.56 and 0.13–3.3 μM , respectively. The method allows the determination of lipohydroperoxides in small sample volumes (the sample is diluted 1:20000) with high precision.

EXPERIMENTAL

Reagents

All reagents used were of analytical grade. Solutions (100 $\mu\text{g}/\text{ml}$) of HNTS, cumene and tert-butyl hydroperoxide were prepared in ethanol. These and the ammonia solution

(concentrated solution s.g. 0.88, diluted 1 + 5 with water) were prepared daily. A standard manganese(II) solution (1.0 g/l.) was made by dissolving a suitable amount of the metal in the minimum possible volume of hydrochloric acid (1 + 1) and then diluting with hydrochloric acid (1 + 9). The solutions of oil samples were prepared by dissolving 0.25 g of the oil and diluting accurately to 50 ml with absolute ethanol.

Apparatus

All spectrofluorimetric measurements ($\lambda_{\text{exc}} = 390$ nm, $\lambda_{\text{em}} = 450$ nm) were made with an Aminco-Bowman spectrofluorimeter fitted for kinetic measurements; 16.5-nm band-pass excitation and emission slits, and an 11.0-nm photomultiplier slit were used. Under these conditions, 0.1- $\mu\text{g}/\text{l}$. quinine sulphate solution yielded 16% full-scale deflection.

Procedure for determination of tert-butyl and cumene hydroperoxide, and lipohydroperoxides

To a 10-ml standard flask were added, in the order given, 1.5 ml of HNTS solution, various volumes of hydroperoxide solution (1.5mM) or up to 200 μl of oil sample, 5 ml of ethanol, 0.5 ml of ammonia solution, and redistilled water up to the mark, followed by 2.5 μl of manganese(II) solution. The ethanol and water had been preheated to 30° in a thermostat. A portion of the sample was transferred to a 10-mm quartz cell maintained at 30 \pm 0.1, and the fluorescence intensity was recorded as a function of time after 15 sec. The blank reaction was monitored under similar conditions (no hydroperoxide or oil sample present). The reaction rate was calculated from the difference between the slopes of the fluorescence *vs.* time plots.

RESULTS AND DISCUSSION

HNTS is oxidized by atmospheric oxygen in a manganese-catalysed reaction. The addition of hydrogen peroxide or indeed any hydroperoxide significantly increases the rate of oxidation of HNTS. The oxidation product exhibits intense blue fluorescence ($\lambda_{\text{ex}} 390$ nm, $\lambda_{\text{em}} 450$ nm) in contrast to HNTS ($\lambda_{\text{ex}} 410$ nm, $\lambda_{\text{em}} 475$ nm).

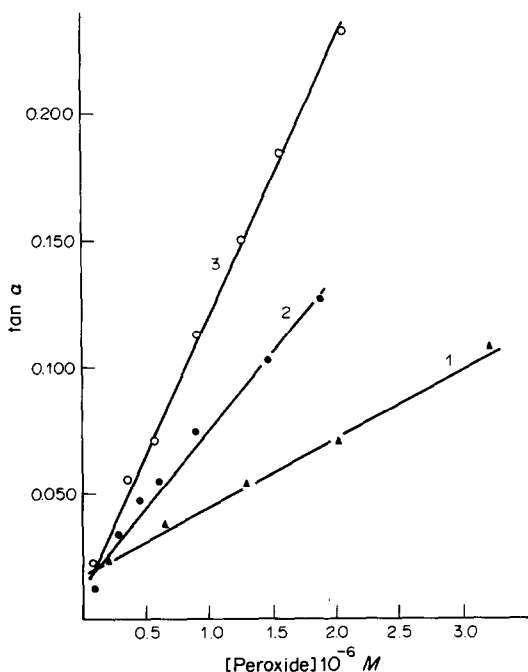


Fig. 1. Range of determination for cumene (1), tert-butyl (2) and hydrogen peroxide (3) by the initial-rate method.

This system is used as the basis for a fast method of determination of organic hydroperoxides (tert-butyl and cumene hydroperoxides) and lipohydroperoxides present in commercial oil samples. The method is quite simple and requires no sample pretreatment. The experimental conditions for determination of these peroxides are identical with those established for the determination of hydrogen peroxide.⁶

Figure 1 shows the calibration graphs for the organic hydroperoxides and hydrogen peroxide. The slopes reveal that the reactivity decreases in the order hydrogen peroxide > tert-butyl hydroperoxide > cumene hydroperoxide.

These differences may be attributed to steric hindrance in the attack by the organic hydroperoxides assayed, and are in agreement with the results of Frew *et al.*,⁵ who found that hydrogen peroxide reacts more rapidly than tert-butyl or cumene hydroperoxide with phenolphthalin and iodide.

Table 1. Determination of tert-butyl and cumene peroxide by the initial-rate method

Peroxide	Linear range, $10^{-6}M$	Sensitivity, $I_F \cdot \text{min}^{-1} \cdot l. \text{mole}^{-1}$	R.s.d., %
Tert-butyl	0.08–1.46	6.2×10^4	2.3
Cumene	0.13–3.30	2.6×10^4	2.5

The ranges of determination found for the organic hydroperoxides by the initial rate method are listed in Table 1, which also includes the relative standard deviations calculated ($n = 11$; 95% confidence limit).

Determination of lipohydroperoxides in oil samples

When HNTS is added to an oil sample in the presence of manganese(II) in ammoniacal medium the lipohydroperoxides present give rise to an oxidation product of HNTS with the same spectral characteristics as that obtained when hydrogen peroxide or indeed any hydroperoxide is added to the HNTS–Mn(II)–NH₃ system.

Thus, by means of the HNTS/Mn(II) indicator system it is possible to determine the lipohydroperoxide content in oil samples: grape, corn, sunflower seed, olive, cod liver and linseed oil samples have been tested. The oil solutions are prepared (5 mg/ml) in absolute ethanol and analysed as described in the experimental section. Since the oxidation medium contains 35% water, to avoid turbidity the volume of oil solution used must not exceed 200 μ l.

In a previous work,⁶ the kinetic–fluorimetric determination of hydrogen peroxide with the HNTS/Mn(II) system was described. It has also been demonstrated that the reactivity of hydroperoxolinoleate in the catalysed oxidation of HNTS is similar to that of hydrogen peroxide.⁷ Thanks to this fact, the calibration graph for hydrogen peroxide determination can be used for the lipohydroperoxides, the values being expressed as “active peroxide concentration” (as meq of peroxide/kg of oil), Table 2 shows the excellent agreement between the results obtained by the HNTS method and the classical iodometric method.⁸

It also follows that hydrogen peroxide can conveniently be used as the standard additive in the determination of low lipohydroperoxide contents in oil samples by the standard-additions method. No

Table 2. Determination of the lipohydroperoxide content of oil samples

Oil	Lipohydroperoxide content, meq/kg		
	Iodometric method	Proposed method	Active peroxide concentration, $10^{-7}M$
Grape	2.5 ₀	2.6 ₀	1.3 ₀
Corn	2.2 ₀	2.1 ₈	1.0 ₉
Sunflower seed	13.2	13.4	6.7
Olive	2.0 ₀	2.2 ₆	1.1 ₃
Cod liver	3.9 ₅	4.1 ₂	2.0 ₆
Linseed	15.2	17.3	8.7

1:20000 dilutions of the oil concerned were used in every case.

Table 3. Lipohydroperoxide determination in oil samples by the method of standard additions

Oil	H ₂ O ₂ added, 10 ⁻⁷ M	Active peroxide concentration, 10 ⁻⁷ M	Recovery, %
Grape	—	1.3	—
	7.57	8.7	98
	10.00	11.3	100
	12.60	13.8	100
Corn	—	1.1	—
	7.57	8.8	101
	10.00	11.2	101
	12.60	14.3	104
Sunflower seed	—	6.7	—
	7.57	14.4	101
	10.00	16.6	99
	12.60	19.3	100
Olive	—	1.1	—
	7.57	8.7	100
	10.00	10.7	96
	12.60	13.5	99
Cod liver	—	2.1	—
	7.57	9.7	100
	10.00	12.0	99
	12.60	14.5	100
Linseed	—	8.7	—
	7.57	16.8	97
	10.00	18.5	99
	12.60	21.0	100

secondary reactions occur since the initial rate is measured over the first three minutes. Table 3 lists the results obtained by this method.

CONCLUSIONS

The new method proposed for the determination of the lipohydroperoxide content in oil samples has high sensitivity and thus requires only very small sample volumes, which minimizes possible interferences. Even smaller samples can be used if the standard-additions method is used, with hydrogen peroxide as the added standard.

In principle the method is also applicable to micro-samples of other foodstuffs, but if sample pretreatment is required (for example, chloroform extraction of fat from bacon, and evaporation of most of the

chloroform to avoid emulsion formation) the method becomes substantially slower.

REFERENCES

1. A. O. Allien, C. J. Hochanadel, J. A. Ghormley and T. W. Davis, *J. Phys. Chem.*, 1952, **56**, 575.
2. H. C. Kelly, D. M. Davies, M. J. King and P. Jones, *Biochemistry*, 1977, **16**, 3543.
3. R. L. Heath and A. L. Tappel, *Anal. Biochem.*, 1976, **76**, 184.
4. R. Cathcart, E. Schwieters and B. N. Ames, *ibid.*, 1983, **134**, 111.
5. J. E. Frew, P. Jones and G. Scholes, *Anal. Chim. Acta*, 1983, **155**, 139.
6. J. Peinado, F. Toribio and D. Pérez-Bendito, *Anal. Chem.*, 1986, **58**, 1725.
7. *Idem*, *Anal. Chim. Acta*, in press.
8. R. D. Mair and R. T. Hall, in *Organic Peroxides*, Vol. II, D. Swern (ed.), pp. 535–635. Wiley-Interscience, New York, 1971.

EFFECTS OF VACUUM ON TETRAKIS-ISOCYANIDE COMPLEXES OF SILVER(I) AND COPPER(I): IMPLICATIONS FOR SIMS ANALYSES

LISA D. DETTER, STEVEN J. PACHUTA, R. G. COOKS* and R. A. WALTON*
Purdue University, Chemistry Department, West Lafayette, IN 47907, U.S.A.

(Received 20 April 1986. Accepted 27 June 1986)

Summary—Vacuum-promoted ligand loss has been detected for the complexes $[\text{Ag}(\text{CNMe})_4]\text{PF}_6$ (Me = methyl), $[\text{Ag}(\text{CN-t-Bu})_4]\text{ClO}_4$ (t-Bu = tert-butyl) and $[\text{Ag}(\text{CNCy})_4]\text{ClO}_4$ (Cy = cyclohexyl). The analogous Cu(I) isocyanide complexes are stable under the same conditions. These conclusions are based on infrared spectroscopy, secondary-ion mass-spectrometry (SIMS) and weight-loss measurements.

A series of silver and copper co-ordination complexes has been studied by secondary-ion mass-spectrometry (SIMS).¹ In extensions of this work, larger samples of these complexes were subjected to ion bombardment under vacuum in an attempt to cause transformations of the monomeric silver(I) complexes $[\text{Ag}(\text{CNR})_4]\text{X}$ (where R = cyclohexyl or tert-butyl for X = ClO_4 , and methyl for X = PF_6). In a similar fashion, the copper(I) complexes $[\text{Cu}(\text{CNR})_4]\text{PF}_6$, where R = methyl, tert-butyl or cyclohexyl, were examined and although the ion beam itself produced no detectable chemical effects under the conditions used, an interesting effect was observed for the silver(I) complexes. It appears that under vacuum the silver(I) complexes undergo rapid loss of up to two isocyanide ligands to form the bis-isocyanide Ag(I) species. Unlike the silver(I) complexes, the copper(I) complexes were stable under the same conditions. These results, and their implications for SIMS analyses, are discussed in this report.

EXPERIMENTAL

This study was undertaken in two different vacuum ranges. The first employed pressures of ca. 10^{-2} mmHg obtained by means of an Edwards model EDSO mechanical vacuum pump connected to a desiccator by a bench-top vacuum line. The rated pumping speed for air was 54 l./min, and the pressure was monitored by a Stokes McLeod gauge. Pressures in the 10^{-5} mmHg range were obtained with an Edwards Diffstack-100 diffusion pump backed by an Edwards E2M12 mechanical pump. The air-pumping speeds were 320 l./sec and 289 l./min, respectively, and pressures were monitored by a Bayard-Alpert ionization gauge. The sample preparation chamber of a Riber Model SQ 156L secondary-ion mass-spectrometer was used to perform these high-vacuum experiments. Typically, between 10 and 50 mg of complex was placed in a vial, which was then inserted in the preparation chamber and subjected to vacuum for several hr. All measurements were made under ambient conditions.

Fourier-transform infrared spectra (nujol mulls) were recorded over the region $4800\text{--}400\text{ cm}^{-1}$ on an IBM IR/32 spectrometer. Positive-ion secondary-ion mass spectra were obtained with the Riber instrument, which consists of an energy selector, a quadrupole mass-filter, a channeltron electron-multiplier and pulse-counting electronics. A 4.5-keV argon primary-ion beam was used at primary-ion current densities of 10^{-9} A/cm² or less. The operating pressure of the analysis chamber was typically less than 1×10^{-8} mmHg. Spectra were obtained at a quadrupole scanning-rate of 3 sec/amu. No charge compensation was necessary.

The isocyanide complexes were prepared by addition of silver hexafluorophosphate or perchlorate to a stirred solution of the appropriate isocyanide ligand.² The analogous copper(I) complexes were prepared in a similar fashion from $[\text{Cu}(\text{NCCH}_3)_4]\text{PF}_6$.³

RESULTS AND DISCUSSION

Synthetic procedures are now well documented for the tetrakis-isocyanide complexes of Ag(I) and Cu(I).^{2,3} Synthetic routes to the bis-isocyanide complexes of Ag(I) and Cu(I) are less well developed. Bell *et al.* have reported the isolation of the $[\text{Ag}(\text{CNCy})_2]\text{ClO}_4$ species,² and the $[\text{Ag}(\text{CN-t-Bu})_2]\text{ClO}_4$ complex was prepared by a similar procedure for use in the present study. The analogous bis-isocyanide Cu(I) complexes have not been prepared. Data for the tert-butyl isocyanide complexes will be discussed first.

The complex $[\text{Ag}(\text{CN-t-Bu})_4]\text{ClO}_4$ showed a 24% weight loss after pumping in the SIMS instrument preparation chamber and a new (C \equiv N) band at 2245 cm^{-1} was observed in the infrared spectrum. This new band corresponds to the (C \equiv N) stretching mode of $[\text{Ag}(\text{CN-t-Bu})_2]\text{ClO}_4$, which is seen at 2243 cm^{-1} in the spectrum of a sample of the authentic complex. The analogous Cu(I) compound, $[\text{Cu}(\text{CN-t-Bu})_4]\text{PF}_6$, showed only a 6% weight loss under similar conditions and its infrared spectrum remained

*Address any correspondence to either of these authors.

Table 1. SIMS study of $[\text{Ag}(\text{CN-t-Bu})_4]\text{ClO}_4^*$

Time, hr	t-Bu ⁺	t-BuNC ⁺	Ag ⁺	Ag(CNH) ⁺	Ag(CNH) ₂ ⁺	AgL ⁺	AgL(CNH) ⁺	AgL ₂ ⁺
0.0	100	0	78	18	10	5	5	3
0.5	100	0	71	19	10	5	8	1
1.0	100	0	62	14	6	3	6	2
2.0	100	0	63	13	5	3	5	0

*All values % relative to t-Bu⁺. L represents the intact isocyanide ligand.

Table 2. SIMS study of $[\text{Ag}(\text{CN-t-Bu})_2]\text{ClO}_4^*$

Time, hr	t-Bu ⁺	t-BuNC ⁺	Ag ⁺	Ag(CNH) ⁺	Ag(CNH) ₂ ⁺	AgL ⁺	AgL(CNH) ⁺	AgL ₂ ⁺
0.0	79	18	100	25	7	11	17	4
0.5	100	7	100	46	15	8	13	5
1.0	96	2	100	45	9	5	5	1
2.0	98	0	100	38	5	5	4	0

*The sample was prepared by the method of Bell *et al.*² All values % relative to Ag⁺. L represents the intact isocyanide ligand.

essentially unchanged. The observation of significant weight losses for the Ag(I) species seems reasonable since both two and four co-ordinate geometries are known for Ag(I) compounds.⁴ However, copper(I) complexes prefer four co-ordination and might therefore be more stable toward vacuum-induced ligand dissociation. In fact, monitoring of the pressure in the preparation chamber during pumping showed that it decreased very slowly (from 4×10^{-5} to 5×10^{-6} mmHg in 12 hr) for the $[\text{Ag}(\text{CN-t-Bu})_4]\text{ClO}_4$ tests, but decreased rapidly (in about 10 min for the same range) for the copper complexes.

To examine vacuum-enhanced ligand dissociation further, a poorer vacuum was employed, namely, 10^{-2} mmHg. A sample of $[\text{Ag}(\text{CN-t-Bu})_4]\text{ClO}_4$ was placed in a desiccator and pumped at 10^{-2} mmHg for 7 days. After 24 hr the pumping was interrupted and the sample examined. No significant weight loss or infrared spectral changes were noted. However, after a week, formation of the bis-isocyanide complex was indicated by the appearance of an infrared band at 2243 cm^{-1} and a 16% weight loss.

A SIMS study of $[\text{Ag}(\text{CN-t-Bu})_4]\text{ClO}_4$ and $[\text{Ag}(\text{CN-t-Bu})_2]\text{ClO}_4$ was undertaken and spectra were recorded after 0.0, 0.5, 1.0 and 2.0 hr of argon ion-bombardment (Tables 1 and 2). The relative abundances of all the fragment ions after 0.5 hr are the same within a factor of 2 or less for both compounds, except for the Ag⁺ and Ag(CNH)⁺ ions. The higher relative abundance of the Ag⁺ ion from the $[\text{Ag}(\text{CN-t-Bu})_2]\text{ClO}_4$ samples could be explained if small amounts of the unreacted starting reagent (AgClO₄) remained after recrystallization of the final product. To check this possibility, a sample of the bis-isocyanide complex was prepared by pumping $[\text{Ag}(\text{CN-t-Bu})_4]\text{ClO}_4$ for 9 hr under high-vacuum conditions. The results of a SIMS study of this sample were very similar to those obtained for $[\text{Ag}(\text{CN-t-Bu})_4]\text{ClO}_4$. The abundance of Ag(CNH)⁺ after 30 min or more ion-bombardment was about

three times greater for the $[\text{Ag}(\text{CN-t-Bu})_2]\text{ClO}_4$ sample than for $[\text{Ag}(\text{CN-t-Bu})_4]\text{ClO}_4$, an effect we believe could result from a greater degree of beam damage experienced by the $[\text{Ag}(\text{CN-t-Bu})_2]\text{ClO}_4$ sample. Overall, the SIMS data suggest that the tetrakis complex rapidly loses two isocyanide ligands to form the bis complex. This dissociation most likely occurs during the 0.5 hr pump-down period in the sample preparation chamber before transfer into the main SIMS chamber.

From the significant weight loss of the silver(I) complexes and from the SIMS results, it is apparent that these complexes are predisposed to dissociate by ligand loss under vacuum. The greatest extent of dissociation occurs within 30 min at 10^{-5} mmHg; longer periods are necessary to achieve the same results at 10^{-2} mmHg.

Considerable weight losses were also recorded for the $[\text{Ag}(\text{CNCy})_4]\text{ClO}_4$ (29%) and $[\text{Ag}(\text{CNMe})_4]\text{PF}_6$ (21%) complexes, but the corresponding copper(I) species showed weight losses of only 2.3 and 3.9%, respectively. The infrared data for the silver(I) complexes after pumping showed (C ≡ N) bands corresponding to the formation of the bis-isocyanide complexes, but these bands were weak in comparison with those observed for $[\text{Ag}(\text{CN-t-Bu})_2]\text{ClO}_4$. The infrared data also showed that the copper(I) complexes were again unchanged under these high-vacuum conditions.

Acknowledgement—This work was supported by the NSF-MRL programme (Grant DMR83-16988).

REFERENCES

1. L. Detter, R. G. Cooks and R. A. Walton, *Inorg. Chim. Acta*, 1986, **115**, 55.
2. A. Bell and D. A. Edwards, *J. Chem. Soc. Dalton Trans.*, 1984, 1317.
3. A. Bell, R. A. Walton, D. A. Edwards and M. A. Poulter, *Inorg. Chim. Acta*, 1985, **104**, 171.
4. F. A. Cotton and G. Wilkinson, *Advanced Inorganic Chemistry*, 4th Ed., p. 969. Wiley, New York, 1980.

ANALYTICAL DATA

SIMULTANEOUS DETERMINATION OF THE ACID AND BASIC IONIZATION CONSTANTS OF IMIDAZOLE

M. TERESA S. D. VASCONCELOS and ADELIO A. S. C. MACHADO
Chemistry Department, Faculty of Science, 4000 Oporto, Portugal

(Received 7 May 1986. Accepted 30 June 1986)

Summary—The acid and base ionization constants of imidazole (LH) have been determined simultaneously by potentiometry. Concentration constants were obtained at 10.0, 15.0, 25.0 and 40.0° with $I = 0.1M$ (KNO_3), the values (and standard deviations) at 25.0° being $pK_{a1}(LH_2^+) = 7.002 \pm 0.006$ and $pK_{a2}(LH_2^+) = 12.588 \pm 0.004$. The following values were obtained for the corresponding thermodynamic parameters: $\Delta H_1 = 38$ and $\Delta H_2 = 38$ kJ/mole; $\Delta S_1 = -8$ and $\Delta S_2 = -112$ J. mole⁻¹. K⁻¹.

Imidazole (Im) is an amphiprotic molecule, with weak basic character and very weak acidic properties. Its basic ionization constant has been measured several times by potentiometry¹⁻⁴ but the acid properties of the compound were ignored. The acid ionization constant has been measured by spectrophotometry in strongly alkaline solution,^{2,5,6} where the basic character of the substance is obscured, or by kinetic methods.⁷ In study of the complexing properties of 1-(2-carbamylethyl)-2-alkylimidazoles,⁸ which also show amphiprotic character, we determined both ionization constants of the compounds by a potentiometric procedure (since the study included the determination of the deprotonation equilibrium constants of the compounds when co-ordinated, we were interested in the acid constants for the purpose of comparison). For the same reason, we decided to extend the determinations to imidazole. Concentration ionization constants were obtained at several temperatures in solutions with ionic strength adjusted to 0.1M and, from the plots of $\log K$ vs. $1/T$, the thermodynamic parameters ΔH and ΔS were obtained.

EXPERIMENTAL

Reagents

Imidazole (BDH or Koch-Light) was recrystallized twice from a mixture of ethanol and acetone. All other chemicals were of analytical grade. Potassium nitrate was recrystallized three times from water. Freshly prepared solutions of this salt were used to prevent problems from the presence of carbon dioxide in solution.

Apparatus

An Orion 801A decimillivoltmeter equipped with a Philips GAH110 glass electrode and an Orion 90-02-00 reference electrode (outer solution 0.1M KNO_3) was used for the potentiometric measurements. The glass electrode was calibrated (E vs. $\log [H^+]$) with buffers (0.01M borax, phosphate [KH_2PO_4 , 0.025M/ Na_2HPO_4 , 0.025M] and 0.05M potassium hydrogen phthalate)⁹ with ionic strength adjusted to 0.1M with potassium nitrate (the second buffer requires no adjustment) by a procedure reported in detail elsewhere.^{8,10}

The titrations were done in Metrohm EA 880T double-walled cells under purified nitrogen, the solutions being kept at 25.0 ± 0.1 , 10.0 ± 0.2 , 15.0 ± 0.2 or $40.0 \pm 0.2^\circ$.

Grade A glassware and demineralized and doubly distilled water (silica still) were used throughout. The water was boiled before preparation of the solutions (under nitrogen). Whenever possible, the solutions were prepared directly in the titration vessel.

Procedure

The experiments consisted of titrations of pure imidazole solutions with nitric acid (concentration $10^{-2}M$ or less) at a constant ionic strength of 0.1M adjusted with potassium nitrate. Typical conditions used in the titrations are listed in Table 1. Different concentrations of imidazole were used so as to detect any influence of the concentration on the values of the equilibrium constants (the data in Table 1 refer to the maximum and minimum values of imidazole concentration). The pH(= $-\log [H^+]$) range in the titrations was ~ 8.5 - 9.5 , in an intermediate position between the pK values of the two acid functions of the system.

Calculations

Experimental data were treated by the program MINQUAD.^{11,12} A value of $R_{im} = 0.0012$ was calculated¹³ for the type of experiments performed in the present work. Protonation concentration constants for systems A and B are

Table 1. Influence of the imidazole concentration on the results (25°, $I = 0.1M$)*

$C_{LH}, M \times 10^2$	pH	n	$R \times 10^4$	χ^2	β_1	β_2
3.772	9.61-8.70	14	0.34	0.57	12.589(7)	19.581(7)
1.594	9.49-8.64	17	0.31	2.71	12.587(5)	19.596(6)

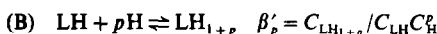
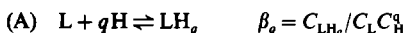
*LH = imidazole; n , number of points; R , χ^2 given by MINQUAD; $\beta(\sigma_i)$ logarithmic values (number in brackets is standard deviation, and refers to last digit of value), model (I).

Table 2. Comparison of the fits with different models*

Model	β_1 or β'_1	β_2	β_1/β_2	χ^2	$R \times 10^4$
		Temperature: 10.0°			
(I)	12.870(10)	20.221(10)	7.351(5)	4.0	0.3
(II)	7.342(2)			34.4	2.5
		Temperature: 15.0°			
(I)	12.734(9)	20.055(9)	7.321(4)	3.3	0.5
(II)	7.319(0.7)			16.3	1.0
		Temperature: 25.0°			
(I)	12.589(7)	19.581(7)	6.992(9)	0.6	0.3
(II)	6.981(5)			24.6	4.2
		Temperature: 40.0°			
(I)	12.132(25)	18.839(24)	6.707(3)	6.2	0.5
(II)	6.696(4)			30.6	4.1

*See note in Table 1; Model (I): $\log(\beta_2/\beta_1) = \text{p}K_{a1}(\text{LH}_2^+)$; $\log \beta_1 = \text{p}K_{a2}(\text{LH}_2^+)$; Model (II): $\log \beta'_1 = \text{p}K_{a1}(\text{LH}_2^+)$.

defined as:



The following models were tried:

(I) L/LH/LH₂ [A, $\log \beta_1 = \text{p}K_{a2}(\text{LH}_2^+)$, $\log(\beta_2/\beta_1) = \text{p}K_{a1}(\text{LH}_2^+)$], which allows for the amphiprotic character of imidazole;

(II) LH/LH₂ [B, $\log \beta_1 = \text{p}K_{a1}(\text{LH}_2^+)$], in which only the basic properties of imidazole are considered.

Typical results are presented in Table 2. Other models were also attempted. For instance, when imidazole was treated as if it were a diprotic acid and a monoprotic base, as might be suggested by the existence of complexes in which the ligand is co-ordinated at C(2) after loss of a proton¹⁴ and by evidence that the reactivity of the same carbon atom in deuteration reactions is explained by a mechanism that includes its deprotonation,¹⁵ the equilibrium constant corresponding to the second acid ionization was systematically rejected, yielding model (I) above.

From $\beta_i(\sigma_i)$ values (standard deviation, σ_i), both in logarithmic form, obtained in different experiments by computer adjustment, the final value of the equilibrium constant, β , was calculated¹⁶ as a weighted average,

$$\bar{\beta} = \left(\frac{\sum \beta_i / \sigma_i^2}{\sum (1/\sigma_i^2)} \right)$$

the standard deviation being calculated as

$$\bar{\sigma} = \left[\frac{1}{\sum (1/\sigma_i^2)} \right]^{1/2}$$

Tests of the procedure

The procedure was tested at 25.0° with substances of known ionization constants. Boric acid, ($\text{p}K_a = 8.98$)¹⁷ and

dipotassium hydrogen phosphate (H_3PO_4 : $\text{p}K_{a2} = 6.638$ and $\text{p}K_{a3} = 11.545$)¹⁸ were used because their ionization constants are close to those to be measured. Good agreement with the literature values was obtained for the ionization constants and non-existent constants were systematically rejected when included in the model.

RESULTS AND DISCUSSION

Influence of K_w on the results

In the determination of acid ionization constants of very weak acids, the final value obtained from computational refinement is strongly influenced by the value of the autoionization constant of water, K_w . In the present work, following a procedure adopted by others,¹⁹ it was attempted to treat K_w as an adjustable parameter like the other ionization constants of the system, but no convergence of iteration was obtained. The influence of K_w on the results was therefore studied by another procedure, in which the same set of experimental data was successively adjusted with several different values of K_w . Literature values for conditions similar to those used in this work,^{20,21} and the value $K_w = 1.398 \times 10^{-14}$ (at 25.0°) obtained in this work from treatment of the results of a titration of strong base with strong acid by Gran's procedure,^{22,23} as well as some arbitrary larger and smaller values were employed (Table 3). The results showed that K_w has no influence on the basic ionization constant of imidazole, but does have a marked

Table 3. Influence of the value of K_w on the ionization constants of imidazole (25.0°, $I = 0.1M$)*

$K_w \times 10^{14}$	β_1	β_2	β_2/β_1	$R \times 10^4$	χ^2	Notes†
0.5	12.304(8)	19.295(7)	6.991	0.36	1.76	a
1.097	12.473(16)	19.465(16)	6.992	0.35	0.56	b, Ref. 20
1.398	12.590(7)	19.581(7)	6.991	0.34	0.57	c
1.68	12.740(6)	19.732(6)	6.992	0.35	0.57	Ref. 21
2	13.020(54)	20.012(54)	6.992	0.33	0.57	a
5						d

*See note in Table 1; $\log(\beta_2/\beta_1) = \text{p}K_{a1}(\text{LH}_2^+)$; $\log \beta_1 = \text{p}K_{a2}(\text{LH}_2^+)$.

†a Arbitrarily fixed value.

b Value at 20°.

c This work.

d No convergence was obtained.

influence on the acid ionization constant, as expected. Except for very low and very large values of K_w , the goodness of fit was practically independent of K_w . This may explain the lack of convergence when K_w was tried as an adjustable parameter, but also prevents the choice of any of the tested values of K_w as the optimum value. However, it was found that, when the data obtained in experiments repeated under the same conditions were adjusted with different values of K_w , the dispersion of the equilibrium constants was smaller for the value of K_w determined by us (Table 4), so this value was used for all subsequent calculations. At 10.0, 15.0 and 40.0° the experimental values of K_w were respectively 0.4468×10^{-14} , 0.6310×10^{-14} and 4.213×10^{-14} .

Ionization constants

The present study shows that both acid-base constants of imidazole can be determined simultaneously by potentiometry, provided that experimental data are collected for a suitable range of pH. Indeed, the results presented in Table 2 show that the fit for model (I), which allows for the amphiprotic character of the compound, is statistically better than that for model (II), in which only the basic properties of imidazole are considered. More specifically, the value of the R -factor for model (I) is the lower at every temperature. As the R -factor is lower than R_{lim} for both models, the R -factor ratio test¹⁶ was used^{13,24} to compare the models. For values obtained at 25.0°

$\mathcal{R} = R_{\text{II}}/R_{\text{I}} = 4.2/0.3 = 14$ (Table 2), and since the number of points is 14 (Table 1) and model (II) involves one constant less than model (I), this value of \mathcal{R} has to be compared²⁴ with $R_{1,12,z}$ [12 = degrees of freedom = number of points - number of constants of model (I)]. At the 99.5% significance level ($\alpha = 0.005$) the value of this parameter is $R_{1,12,0.005} = 1.4 < \mathcal{R}$, which shows that there is a 99.5% probability that model (II) is not correct. Besides, at every temperature, only for model (I) does χ satisfy the χ^2 -test: for model (II), the χ^2 -values are larger than the limiting value, 12.59 at the 95% confidence level¹⁶ for 6 degrees of freedom, as is the case.¹¹

The final values of the ionization constants, obtained as weighted averages of 3 or 4 determinations at each temperature, are presented in Table 5. The values at 25.0° can be compared with literature values obtained in similar conditions. The value $pK_{a1}(\text{LH}_2^+) = 7.002$ compares well with values reported for 25.0° and ionic strength close to the value used in the present work: 7.09 [$I = 0.135M(\text{KCl})$]²⁴, 7.09 [$I = 0.11M$]²⁵ or 6.993 [$I = 0.135M(\text{KCl})$].²⁶ The value of $pK_{a2}(\text{LH}_2^+) = 12.588$ is intermediate between the value found by Krishnamurthy⁷ by a kinetic method, 11.72 [$I = 0.2M(\text{NaClO}_4)$] and the older values obtained by spectrophotometry, for instance 14.44,⁵ or 14.17⁶, corrected to $I = 0$.

Thermodynamic parameters

Values of ΔH and ΔS for both ionization equilibria (Table 5) were obtained by linear-least squares adjustment of $\log K_a(\text{LH}_2^+)$ vs. $1/T$. Acceptable correlation coefficients r were obtained (Table 5). However, their statistical significance is very limited since the data consisted of only four points (for the same reason, standard deviations for the thermodynamic parameters calculated from the linear regression data are considered not to be worth reporting).

The values of ΔH and ΔS corresponding to $K_{a1}(\text{LH}_2^+)$ compare well with those obtained by Datta and Grzybowski²⁷ at the same temperature and ionic strength, also by a potentiometric procedure ($\Delta H = 35 \text{ kJ/mole}$ and $\Delta S = -16 \text{ J.mole}^{-1}.\text{K}^{-1}$), as well as with calorimetric data obtained under several

Table 4. Influence of the value of K_w on the dispersion of the ionization constants of imidazole (25.0°, $I = 0.1M$)*

K_w		Experimental			Range
		1	2	3	
0.5×10^{-14}	β_1	12.304	12.308	12.083	0.225
	β_2	19.295	19.306	19.091	0.215
1.097	β_1	12.473	12.479	12.349	0.130
	β_2	19.465	19.478	19.357	0.121
1.398	β_1	12.590	19.600	12.587	0.013
	β_2	19.581	19.598	19.596	0.017
1.68	β_1	12.740	12.752	13.080	0.340
	β_2	19.732	19.751	19.656	0.095

*See notes in Table 3.

Table 5. Ionization constants of imidazole* and the corresponding thermodynamic parameters† ($I = 0.1M$)

Temp., °C	β_1	β_2	β_2/β_1
10.0	12.846(5)	20.092(5)	7.350(7)
15.0	12.724(6)	20.043(6)	7.319(8)
25.0	12.588(4)	19.590(4)	7.002(6)
40.0	12.160(7)	18.883(7)	6.722(10)
ΔH_i , kJ/mole	38		38
ΔS_i , J.mole ⁻¹ .K ⁻¹	-112		-8
r	0.986		0.990

*Weighted averages of values obtained in 3 or 4 determinations at each temperature; logarithmic values, model (I); $\log \beta_1 = pK_{a1}(\text{LH}_2^+)$, $\log(\beta_2/\beta_1) = pK_{a2}(\text{LH}_2^+)$.

†Referred to equilibria $\text{Acid} \rightleftharpoons \text{Base} + \text{H}^+$; r , correlation coefficient of linear least-squares adjustment.

different conditions,²⁸⁻³¹ which show ΔH values in the range 36–38 kJ/mole and ΔS values in the range from –8 to –12 J.mole⁻¹.K⁻¹. The values corresponding to $K_{a2}(\text{LH}_2^+)$ show poor agreement with the only set of values in the literature, obtained from spectrophotometric measurements⁵ ($\Delta H = 74 \pm 7$ kJ/mole, $\Delta S = -29 \pm 21$ J.mole⁻¹.K⁻¹). This may be a consequence of the inaccuracy in the values of the second acid constant. In both cases, since ΔS is obtained from extrapolation of experimental data (intercept at $1/T = 0$ of the straight line fitted to the points) larger differences in this parameter than in ΔH are not unreasonable.

Acknowledgement—Financial support received from INIC (Lisbon) through Research Line No. 4A of CIQ(UP) is gratefully acknowledged.

REFERENCES

1. L. G. Sillén and A. E. Martell, *Stability Constants of Metal-Ion Complexes*, p. 387. Special Publication No. 17, The Chemical Society, London, 1964.
2. *Idem*, *Stability Constants of Metal-Ion Complexes, Supplement No. 1*, p. 280. Special Publication No. 25, The Chemical Society, London, 1971.
3. D. D. Perrin, *Stability Constants of Metal-Ion Complexes, Part B, Organic Ligands*, p. 104. Pergamon Press, Oxford, 1979.
4. J. Oszczapowicz and M. Czuryłowska, *Talanta*, 1984, **31**, 559.
5. P. George, G. I. H. Hania, D. H. Irvine and I. Abu-Issa, *J. Chem. Soc.*, 1964, 5689.
6. G. Yagil, *Tetrahedron*, 1967, **23**, 2855.
7. M. Krishnamurthy, *Inorg. Chim. Acta*, 1978, **26**, 137.
8. M. T. S. D. Vasconcelos, *Doctoral Thesis*, University of Oporto, Oporto, 1983.
9. R. G. Bates, *Determination of pH, Theory and Practice*, p. 90. Wiley, New York, 1973.
10. M. T. S. D. Vasconcelos and A. A. S. C. Machado, *Rev. Port. Quim.*, in the press.
11. A. Sabatini, A. Vacca and P. Gans, *Talanta*, 1974, **21**, 53.
12. P. Gans, A. Sabatini and A. Vacca, *Inorg. Chim. Acta*, 1976, **18**, 237.
13. A. Vacca, A. Sabatini and M. A. Cristina, *Coord. Chem. Rev.*, 1972, **8**, 45.
14. R. J. Sundberg, R. F. Bryan, I. F. Taylor Jr. and H. Taube, *J. Am. Chem. Soc.*, 1974, **96**, 381.
15. J. D. Vaughan, Z. Mughrabi and E. Chung Wu, *J. Org. Chem.*, 1970, **35**, 1141.
16. W. C. Hamilton, *Statistics in Physical Science*, pp. 41, 157, 207, 216. Ronald Press, New York, 1964.
17. N. Ingri, *Acta Chem. Scand.*, 1962, **16**, 439.
18. A. Vacca, A. Sabatini and L. Bologni, *J. Chem. Soc. Dalton Trans.*, 1981, 1264.
19. M. Wozniak and G. Nowogrocki, *Talanta*, 1978, **25**, 633.
20. G. Anderegg, *Helv. Chim. Acta*, 1967, **50**, 2333.
21. L. C. Thompson, *Inorg. Chem.*, 1962, **1**, 491.
22. G. Gran, *Analyst*, 1952, **77**, 661.
23. F. J. C. Rossotti and H. Rossotti, *J. Chem. Ed.*, 1965, **42**, 375.
24. M. Jaskólski and L. Lomozik, *Talanta*, 1985, **32**, 511.
25. B. L. Mickel and A. C. Andrews, *J. Am. Chem. Soc.*, 1955, **77**, 5291.
26. N. C. Li, P. Tang and R. Mathur, *J. Phys. Chem.*, 1961, **65**, 1074.
27. S. P. Datta and A. K. Grzybowski, *J. Chem. Soc. (B)*, 1966, 136.
28. I. Wadsö, *Acta Chem. Scand.*, 1962, **16**, 479.
29. F. Holmes and D. R. Williams, *J. Chem. Soc. (A)*, 1967, 1256.
30. J. J. Christensen, D. P. Wrathall and R. M. Izatt, *Anal. Chem.*, 1968, **40**, 175.
31. E. M. Woolley, R. W. Wilton and L. G. Hepler, *Can. J. Chem.*, 1970, **48**, 3249.

PHOTOTAUTOMERISM IN THE LOWEST EXCITED SINGLET STATE OF 1-HYDROXY-2-CARBOXYANTHRAQUINONE

F. SALINAS*, A. MUÑOZ DE LA PEÑA and J. A. MURILLO

Department of Analytical Chemistry, Faculty of Sciences, University of Extremadura, 06071 Badajoz, Spain

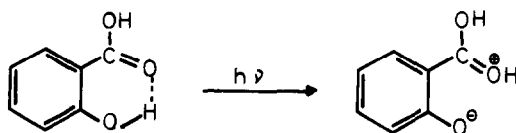
(Received 16 December 1985. Revised 3 June 1986. Accepted 30 June 1986)

Summary—The dependence of the absorption and fluorescence spectra of 1-hydroxy-2-carboxyanthraquinone on pH and Hammett acidity have been studied. This compound exhibits phototautomerism in its uncharged and its singly-charged anionic species in aqueous media. Its ground state (pK_a) and lowest excited singlet-state (pK_a^*) dissociation constants have been determined by absorptometric and fluorimetric titrations and the assignment of the pK_a and pK_a^* values to the equilibria concerned has been carefully considered.

Hydroxy-derivatives of anthraquinone are well known as photometric and fluorimetric reagents for metal ions. Because of our interest in the application of hydroxyanthraquinones as analytical reagents and the photochemistry of these compounds, the present study of the dependence of the absorption and fluorescence of 1-hydroxy-2-carboxyanthraquinone on acidity was undertaken.

This reagent has been synthesized in our laboratory, and has been proposed for the photometric determination of Be(II),¹ Ni(II)² and Co(II)³ and for the fluorimetric determination of Be(II),⁴ Mg(II),⁵ Y(III),⁶ Al(III),⁷ Ga(III)⁸ and La(III),⁹ in previous papers. However, no reference has been found to the values of its protolytic dissociation constants. In fluorimetric analysis, the spectroscopic effects of chemical reactions in the lowest excited singlet-state manifest themselves as interferences in the form of quenching of the fluorescence of the analyte if the product of the photo-reaction is non-fluorescent, or as displacement of the fluorescence spectrum if the photo-product is fluorescent. Consequently, the analyst must be aware of the ways in which excited-state proton transfers can influence the fluorescence spectra of analytical reagents.

In molecules containing electron-withdrawing and electron-donating groups situated *ortho* or *peri* to one another, phototautomerism may occur by proton transfer across an intramolecular hydrogen bond between the two groups as, for example, in salicylic acid.^{10,11}



In molecules where the electron donor and electron acceptor groups are widely separated, intermolecular phototautomerism may occur. This requires, subsequent to excitation, an extremely rapid double proton-transfer, to the solvent by the electron-donor group and from the solvent to the electron-acceptor group. 4-Methyl-7-hydroxycoumarin is an example of a molecule which displays such phototautomerism in the lowest excited singlet-state.¹²

In these types of compounds, the gain in acidity of the electron-donating group and the gain in basicity of the electron-withdrawing group, in the same electronically excited molecule, can be so great that the order of ionization of the two groups is reversed with respect to the normal order observed in the ground-state.¹⁰⁻¹⁴ In the present work, it will be shown that 1-hydroxy-2-carboxyanthraquinone demonstrates phototautomerism in its uncharged and its singly-charged anionic species in aqueous media.

EXPERIMENTAL

Apparatus

Absorption spectra were recorded with a Zeiss DMR-11 spectrophotometer. Fluorescence spectra were recorded with a Perkin-Elmer MPF-43 fluorescence spectrophotometer, equipped with an Osram BO 150-W xenon lamp, excitation and emission grating monochromators, an R-508 photomultiplier and a Perkin-Elmer 056 recorder. A standard fluorescence stick (equivalent to a $3 \times 10^{-4}M$ solution of Rhodamine B) was used daily to adjust the spectrofluorimeter to compensate for changes in source intensity. No correction was made of the instrumental response. A thermostatic water-bath circulator Selecta 382 was used for temperature control. The pH-measurements were made on a Crison digital 74 pH-meter employing a glass saturated-calomel combination electrode.

Reagents

1-Hydroxy-2-carboxyanthraquinone was synthesized by diazotization of 1-amino-2-carboxyanthraquinone, followed by hydrolysis, according to Scholl's method¹⁵ and purified by recrystallization from glacial acetic acid. The purity was

*To whom requests for reprints should be addressed.

Table 1. Features of absorption and fluorescence spectra of 1-hydroxy-2-carboxyanthraquinone and its corresponding cation and singly- and doubly-charged anions in aqueous media

	Long-wavelength absorption maxima, nm	Fluorescence maxima, nm
Cation	455	576
Neutral molecule	400	597
Singly-charged anion	395	593
Doubly-charged anion	500	~500*

*Practically non-fluorescent.

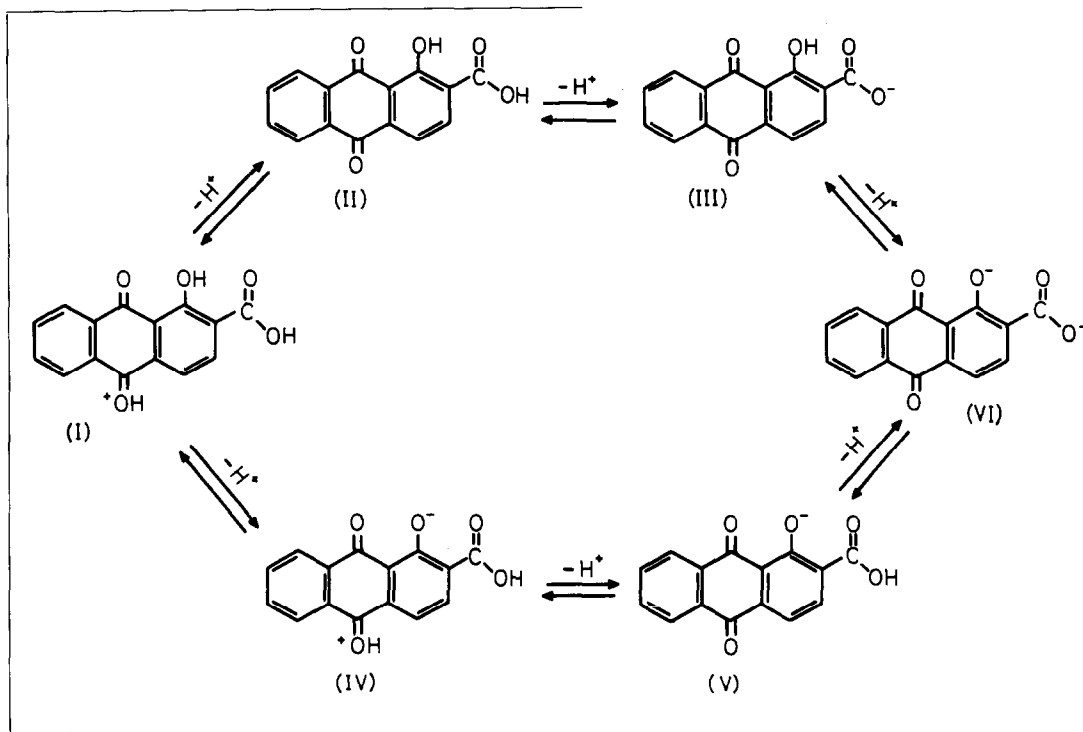
checked by thin-layer chromatography. The melting point of 223–225° was in agreement with that reported in the literature.¹⁵

The concentrations of the solutions examined were 2.8×10^{-5} , 1.0×10^{-4} and $1.0 \times 10^{-3} M$. Their pH was adjusted with sulphuric acid and sodium hydroxide solution. Jorgenson and Hartter's corrected Hammett acidity scale¹⁶ was employed to calibrate the sulphuric acid solutions. Doubly distilled and demineralized water was used throughout.

hibits charge-transfer from the aromatic ring to the electron-withdrawing group in the excited state. As a consequence, there is a shift of the fluorescence of the aromatic molecule to shorter wavelengths on dissociation. Dissociation of a proton from an electron-donor group stabilizes the dissociated excited molecules relative to the excited undissociated molecules because it enhances charge-transfer from the electron-donor group to the aromatic ring in the excited state. This results in a shift of the fluorescence of the molecule to longer wavelengths on dissociation.¹⁸ Similar arguments are generally applicable to the shifts in absorption spectra occurring on protolytic dissociation.^{18,19}

The long-wavelength absorption maxima as well as the fluorescence maxima of 1-hydroxy-2-carboxyanthraquinone and its corresponding cation and singly- and doubly-charged anions are presented in Table 1.

1-Hydroxy-2-carboxyanthraquinone is capable of undergoing three successive protolytic dissociations by either of two paths:



RESULTS AND DISCUSSION

Förster has discussed the relationship between fluorescence and the shifts occurring upon protolytic dissociation and the protolytic equilibrium constants in the ground and lowest excited singlet states.¹⁷ Dissociation of a proton from an electron-withdrawing group in an aromatic molecule destabilizes the dissociated excited molecules relative to the undissociated excited molecules, because it in-

When the acidity of the medium is increased, there is a red-shift in the absorption spectrum, due to protonation of one or other of the three basic groups in the molecule (the quinone groups in positions 9 and 10 and the carboxyl group in position 2). We think that this protonation must occur on the quinone group in position 10, because the other two basic groups are close to electron-withdrawing groups (which diminish their basicities), and also have electron pairs which can be involved in

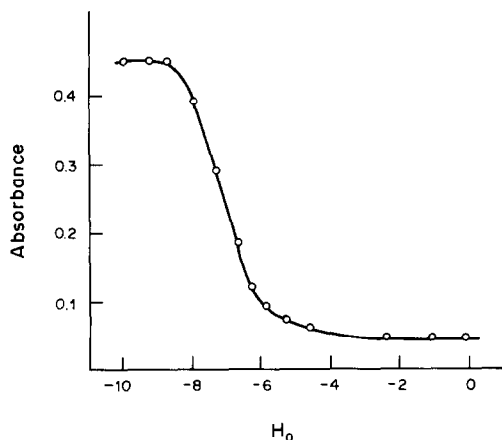


Fig. 1. Absorbance vs. H_0 for $2.8 \times 10^{-5} M$ 1-hydroxy-2-carboxyanthraquinone in sulphuric acid at an analytical wavelength of 455 nm and temperature $20 \pm 0.5^\circ$.

hydrogen-bonding with the phenolic group, which again diminishes their basicities.

The first path entails dissociation of the acid protonated at the quinone group (I) to form the neutral molecule (II). This is followed by dissociation from the carboxyl group, to form the singly-charged anion (III) and then dissociation from the phenolic group to form the doubly-charged anion (VI). This pathway would be expected to be accompanied by two shifts to shorter wavelengths and finally to a longer wavelength for the long-wavelength absorption and fluorescence bands. This is, in fact, the sequence of shifts observed in the long-wavelength absorption maxima, and indicates that these changes correspond to successive ionizations of the ground-state species.

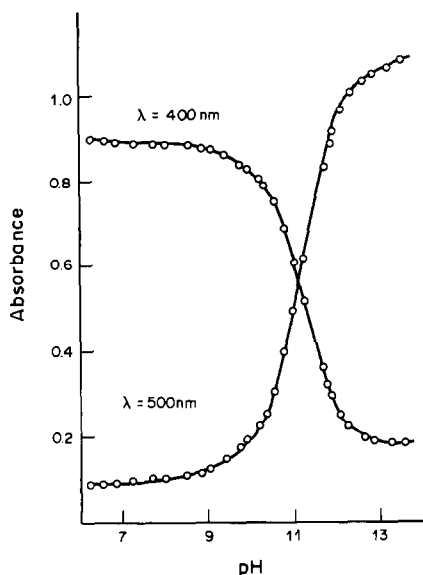


Fig. 2. Absorbance vs. pH for $1.0 \times 10^{-4} M$ 1-hydroxy-2-carboxyanthraquinone in water at two analytical wavelengths (400 and 500 nm) and $20 \pm 0.5^\circ$.

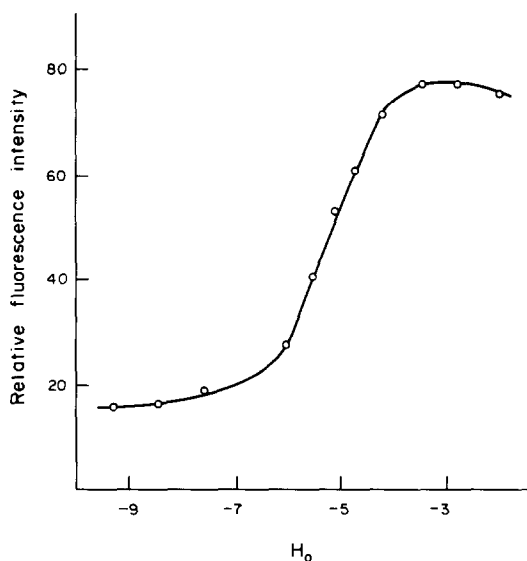


Fig. 3. Dependence on H_0 of the fluorescence intensity for $1.0 \times 10^{-5} M$ 1-hydroxy-2-carboxyanthraquinone (at the emission maximum of 597 nm). Excitation at 405 nm, the isobestic point in the absorption spectra of the neutral molecule and its cation.

However, the sequence of fluorescence shifts is first to longer wavelength, then to shorter wavelengths. Examination of the second pathway from cation to doubly-charged anion (I \rightarrow IV \rightarrow V \rightarrow VI) indicates that this will produce the observed order of fluorescence shifts. This suggests that in the lowest excited singlet state the phenolic group is more acidic than either the protonated carbonyl or undissociated carboxylic groups, a situation opposite to that in the ground state.

Absorptiometric titration curves for 1-hydroxy-2-carboxyanthraquinone are shown in Figs. 1 and 2. The pK_a of protonated 1-hydroxy-2-carboxyanthraquinone was calculated by use of an H_0 acidity scale for the concentrated sulphuric acid solutions employed in the determination.

The variations of the fluorescence intensities at the appropriate band maxima of 1-hydroxy-2-carboxyanthraquinone are shown in Figs. 3 and 4. The protolytic dissociation constants were calculated from eight points in the appropriate absorptiometric or fluorimetric titration, and are shown in Table 2.

The pK_a values found for the ground-state equilibria between species I and II and species III and VI, were -7.08 and 11.13 respectively.

The absorption maxima of the 1-hydroxy-2-carboxyanthraquinone shift only slightly as the neutral molecule is converted into the singly charged anion with increasing pH. The absorbance does not change very much with pH in the H_0 /pH range from -3 to 8 . Because of this, the pK_a value corresponding to the protolytic equilibrium between species II and III cannot be determined by absorption spectrophotometry. Because the solubility of this com-

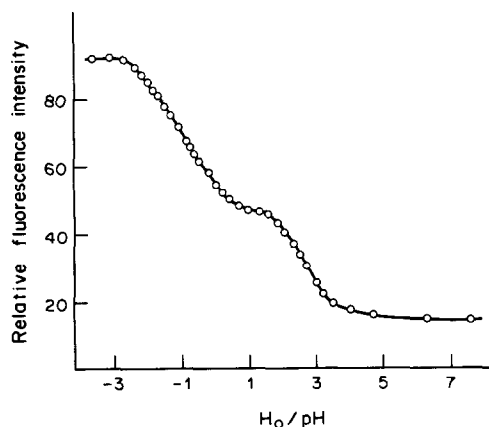


Fig. 4. Dependence on H_0/pH of the fluorescence intensity of $1.0 \times 10^{-5}M$ 1-hydroxy-2-carboxyanthraquinone (at the emission maximum of 597 nm). Excitation at 440 nm, the isosbestic point in the absorption spectra of the singly and doubly charged anions.

pound in water is rather low, a potentiometric titration cannot be used for the calculation, but the value has been found by fluorimetry. We think that the second inflection of the fluorimetric titration plot, between $H_0 = -3$ and $\text{pH} = 7$ (Fig. 4), can be assigned to the ground-state $\text{p}K_a$ corresponding to the equilibrium between species II and III.

Excited-state equilibria are characterized by variations of fluorescence intensity in acidity regions where the absorption spectra are invariant and it is this type of fluorimetric titration curve that was employed to determine the $\text{p}K_a^*$ values given in Table 2.

Table 2. Protolytic dissociation constants of 1-hydroxy-2-carboxyanthraquinone for equilibria occurring in the acidity range from $\text{pH} 14.0$ to $H_0 -9.0$

	$\text{p}K_1$	$\text{p}K_2$	$\text{p}K_3$
$\text{p}K_a$	-7.08 ± 0.11	$-2.74 \pm 0.01^\dagger$	11.13 ± 0.02
$\text{p}K_a^*$	-5.27 ± 0.09	-0.97 ± 0.09	—

† By fluorimetric titration. Assignment of the $\text{p}K_a$ and $\text{p}K_a^*$ values to their respective equilibria is discussed in the text.

Although the $\text{p}K_a$ data of Table 2 reflect all the possible ground-state equilibria represented in the scheme above (studied by absorptiometry and fluorimetry), the $\text{p}K_a^*$ data of Table 2 do not contain all possible excited-state equilibria represented in the scheme. The reason for this is that the ground-state has an infinite mean lifetime with respect to the acid-base equilibria, while the lowest excited singlet-state is often too short-lived for protolytic equilibrium to occur before fluorescence deactivates the lowest excited singlet-state. Thus, the $\text{p}K_a^*$ value of -5.27 corresponds to the excited-state equilibrium between species I and IV and the $\text{p}K_a^*$ value of -0.97 corresponds to the excited-state equilibrium between species IV and V. However, the excited-state protolytic equilibria between species V and VI is not fast enough for the $\text{p}K_a^*$ value to be determined.

Acknowledgement—We thank the Comisión Asesora de Investigación Científica y Técnica del Ministerio de Educación y Ciencia de España for supporting this study (Project No. 2903-83).

REFERENCES

1. F. Salinas and L. M. Franquelo, *Quim. Anal.*, 1975, **29**, 319.
2. F. Capitán, F. Salinas and L. M. Franquelo, *An. Quim.*, 1976, **72**, 529.
3. *Idem*, *Bol. Soc. Quim. Perú*, 1976, **42**, 206.
4. *Idem*, *Anal. Lett.*, 1975, **8**, 753.
5. *Idem*, *Quim. Anal.*, 1977, **31**, 275.
6. F. Salinas, A. Muñoz de la Peña and J. A. Murillo, *Analyst*, 1984, **109**, 1135.
7. *Idem*, *Anal. Lett.*, 1984, **17**, 497.
8. *Idem*, *Mikrochim. Acta*, 1984 **III**, 79.
9. *Idem*, *Microchem. J.*, in the press.
10. A. Weller, *Z. Elektrochem.*, 1956, **60**, 1144.
11. S. G. Schulman and H. Gershon, *J. Phys. Chem.*, 1968, **72**, 3297.
12. G. J. Yakatan, R. J. Juneau and S. G. Schulman, *Anal. Chem.*, 1972, **44**, 1044.
13. *Idem*, *J. Pharm. Sci.*, 1972, **61**, 749.
14. R. E. Ballard and J. W. Edwards, *J. Chem. Soc.*, 1964, 4868.
15. R. Scholl, *Monatsh. Chem.*, 1913, **34**, 1023.
16. M. J. Jorgenson and D. R. Hartter, *J. Am. Chem. Soc.*, 1963, **85**, 878.
17. T. Förster, *Z. Elektrochem.*, 1950, **54**, 42.
18. A. Weller, *Prog. React. Kinet.*, 1961, **1**, 187.
19. S. G. Schulman, *J. Pharm. Sci.*, 1971, **60**, 371.
20. K. Yates and H. Wai, *Can. J. Chem.*, 1965, **43**, 2131.

THE pK_a VALUES OF N,N,N',N' -TETRAKIS-(2-HYDROXYPROPYL)ETHYLENEDIAMINE

R. McMAHON, M. BRENNAN and J. D. GLENNON
 Department of Chemistry, University College, Cork, Ireland

(Received 28 April 1986. Accepted 11 July 1986)

Summary—Aqueous solutions of the industrially important chelating agent N,N,N',N' -tetrakis(2-hydroxypropyl)ethylenediamine exhibit basic properties. The proton dissociation constants were determined to be 8.99 ± 0.04 (pK_1) and 4.30 ± 0.04 (pK_2) by potentiometric titration at 25° in 0.15M sodium chloride.

N,N,N',N' -Tetrakis(2-hydroxypropyl)ethylenediamine (L) is described as a totally hydroxypropylated alkene diamine and has numerous industrial applications as a result of its physical and chemical properties. It is used as a complexing agent in electroplating and is an excellent cross-linking agent and catalyst for use in rigid polyurethane foams. The four hydroxyl groups give multiple cross-linking sites and the two tertiary nitrogen atoms are responsible for the catalysis.

An outstanding property, however, is its remarkable thermal stability, used with great success in conjunction with its sequestering of cations such as Ag^+ , Pb^{2+} , Hg^{2+} , Cd^{2+} , Co^{2+} , Ni^{2+} , Cu^{2+} and Zn^{2+} . The chemical and physical properties suggest, also, possible uses as a colorimetric analytical reagent and as a masking agent or titrant in complex-formation studies. As expected, its aqueous solutions exhibit basic properties but surprisingly the pK_a values for the protonated ligand have not been reported. As part of our investigations into the aqueous coordination chemistry of the ligand, the proton dissociations were studied by potentiometric titration, performed with a Radiometer automatic titration apparatus, with pH readings recorded on a digital pH M64 research pH-meter and the base (sodium hydroxide) added from an ABU 13 autoburette. The electrode pair consisted of a Radiometer G2040C glass electrode and K4040 KCl electrode. Solutions

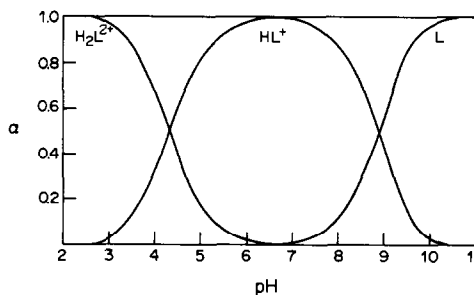
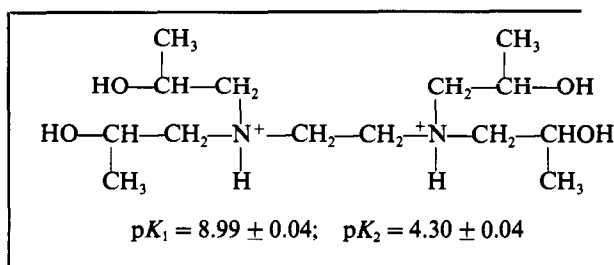


Fig. 1. Distribution diagram for N,N,N',N' -tetrakis(2-hydroxypropyl)ethylenediamine as a function of pH.

calculated \bar{n}_H data were treated in two sections, $0 < \bar{n}_H < 1$ and $1 < \bar{n}_H < 2$; \bar{n}_H is related to pH and pK_a by

$$\log \frac{\bar{n}_H}{(1 - \bar{n}_H)} + pH = pK_a$$

A plot of \bar{n}_H vs. pH showed two distinct dissociation regions. The proton dissociations were found not to overlap, and the refined pK_a values were calculated by taking the averages of the values obtained by using the equation above. The distribution diagram for the alkene diamine species as a function of pH is shown in Fig. 1. The structure of the fully protonated alkene diamine, together with the pK_a values obtained, is shown below.



$$K_1 = \frac{[H^+][L]}{[HL^+]}$$

$$K_2 = \frac{[H^+][HL^+]}{[H_2L^{2+}]}$$

of the alkene diamine at a concentration of $4.83 \times 10^{-3}M$ in 0.029M nitric acid/0.15M sodium chloride were titrated at 25° and the pK_a values determined by the use of formation functions.^{1,2} The

REFERENCES

1. N. Bjerrum, *Z. Anorg. Chem.*, 1921, **119**, 179.
2. H. Irving and H. Rossotti, *Acta Chem. Scand.*, 1956, **72**, 10.

ANNOTATIONS

MATHEMATICAL TREATMENT OF ABSORBANCE VERSUS pH GRAPHS OF POLYBASIC ACIDS

A. G. ASUERO, J. L. JIMENEZ-TRILLO and M. J. NAVAS

Department of Bromatology, Toxicology, and Applied Chemical Analysis, Faculty of Pharmacy,
 The University of Seville, 41012 Seville, Spain

(Received 22 October 1985. Revised 28 May 1986. Accepted 20 June 1986)

Summary—Mathematical relationships determining the shape of absorbance vs. pH graphs of polybasic acids are derived, and new graphical and numerical techniques for evaluating the acidity constants of two-step overlapping equilibria are examined.

The computation of acidity constants is made easier by the use of molar fractions.

For a polybasic acid H_nR , if the Beer-Lambert law holds, the measured absorbance A at a given wavelength (calculated for 1-cm path-length and corrected for absorption by the solvent and any buffering agent that may be present) of a solution containing a total concentration

$$C_R = \sum_{j=0}^n [H_jR]$$

of the acid is given by

$$A = \sum_{j=0}^n \epsilon_j [H_jR] \quad (1)$$

where ϵ_j is the molar absorptivity of the j th species. Thus, the form of a graph of A as a function of pH depends on the relative magnitudes of $(2n + 1)$ parameters. The relationships of the molar absorptivities vary as the wavelength is changed.

In the following treatment, absorbances will be used throughout instead of molar absorptivities, since the cell length, and the molar concentrations at a given pH, are constant throughout the measurements. The ionic strength and temperature are regarded as fixed and constant (because molar absorptivity depends on the medium and the temperature), so conditional constants¹ are involved in the calculations.

If the reagent is entirely in the form H_jR , we can write $A_j = \epsilon_j C_R$. The relationship between the absorbance and composition of a given solution of the acid may then be written as

$$A = \sum_{j=0}^n A_j f_j \quad (2)$$

where $f_j = [H_jR]/C_R$ is the degree of formation² of the species H_jR , and is also referred to as the distribution function³ or the molar fraction⁴ of the j th species. It is related to the overall stability constant β_j by the equation ($j = 0, \dots, n$):

$$f_j = \frac{\beta_j [H]^j}{1 + \beta_1 [H] + \dots + \beta_j [H]^j + \dots + \beta_n [H]^n} \quad (3)$$

with $\beta_0 = 1$ by definition and $\beta_j = [H_jR]/[H]^j [R]$, so

$$f_j = \beta_j [H]^j / f_0 \quad (4)$$

The dissociation constants of the acid H_nR are given by

$$K_{ak} = \frac{\beta_{n-k}}{\beta_{n+1-k}} = \frac{[H][H_{n-k}R]}{[H_{n+1-k}R]} \quad (5)$$

for $k = 1, \dots, n$.

By differentiating the absorbance with respect to pH we have

$$\frac{dA}{d(\text{pH})} = -2.303 [H] \frac{dA}{d[H]} \quad (6)$$

By combining equations (2) and (6) we get

$$\frac{dA}{d(\text{pH})} = -2.303 [H] \sum_{j=0}^n A_j \frac{df_j}{d[H]} \quad (7)$$

A_j is constant in this differentiation since C_R is constant.

From equations (3) and (4) we have

$$\frac{df_j}{d[H]} = j f_0 \beta_j [H]^{j-1} + \beta_j [H]^j \frac{d\beta_j}{d[H]} \quad (8)$$

$$\frac{df_0}{d[H]} = -\frac{f_0}{[H]} (f_1 + 2f_2 + \dots + n f_n) \quad (9)$$

and it follows that

$$\frac{df_j}{d[H]} = \frac{1}{[H]} f_j (j - \bar{n}) \quad (10)$$

where

$$\bar{n} = \sum_{j=0}^n j f_j$$

is the proton number,⁵ the average number of protons bound per entity R , a very useful experimental function.⁶ Equation (9) is essentially identical with that given by Bodländer:^{2,7,8}

$$\frac{d[\log(1/f_0)]}{d(\log[H])} = \bar{n} \quad (11)$$

and equation (10) with those given by Butler³ and Souchay and Lefebvre⁹

$$\frac{d(\ln f_j)}{d(\ln [\text{H}])} = \frac{d(\log f_j)}{d(\log [\text{H}])} = j - \bar{n} \quad (12)$$

Inserting equation (10) into (7) and rearranging gives

$$\frac{dA}{d(\text{pH})} = -2.303 \left(\sum_{j=0}^n j A_j f_j - \bar{n} A \right) \quad (13)$$

Equation (10) may be written in the form

$$\frac{df_j}{d(\text{pH})} = -2.303 f_j (j - \bar{n}) \quad (14)$$

Differentiation with respect to pH yields

$$\begin{aligned} \frac{d^2 f_j}{d(\text{pH})^2} &= \frac{d}{d(\text{pH})} \left(\frac{df_j}{d(\text{pH})} \right) = \frac{d}{d[\text{H}]} \left(\frac{df_j}{d(\text{pH})} \right) \frac{d[\text{H}]}{d(\text{pH})} \\ &= -2.303 [\text{H}] \frac{d}{d[\text{H}]} \left(\frac{df_j}{d(\text{pH})} \right) \\ &= -2.303 [\text{H}] \left((j - \bar{n}) \frac{df_j}{d[\text{H}]} - f_j \frac{d\bar{n}}{d[\text{H}]} \right) \\ &= 2.303^2 f_j \left((j - \bar{n})^2 - \sum_{j=0}^n j (j - \bar{n}) f_j \right) \quad (15) \end{aligned}$$

so

$$\frac{d\bar{n}}{d[\text{H}]} = \frac{d}{d[\text{H}]} \sum_{j=0}^n j f_j = \frac{1}{[\text{H}]} \sum_{j=0}^n j f_j (j - \bar{n}) \quad (16)$$

Since from equation (2)

$$\frac{d^2 A}{d(\text{pH})^2} = \sum_{j=0}^n A_j \frac{d^2 f_j}{d(\text{pH})^2} \quad (17)$$

it follows that

$$\begin{aligned} \frac{d^2 A}{d(\text{pH})^2} &= \\ 2.303^2 \left(\sum_{j=0}^n A_j f_j (j - \bar{n})^2 - \sum_{j=0}^n A_j f_j \sum_{j=0}^n j (j - \bar{n}) f_j \right) \quad (18) \end{aligned}$$

and taking into account equation (2) we finally get

$$2.303^2 \left(\sum_{j=0}^n A_j f_j (j - \bar{n})^2 - A \sum_{j=0}^n j (j - \bar{n}) f_j \right) \quad (19)$$

Expressions (13) and (19) have the advantages of being compact and suitable for programming. The data treatment suggested here in terms of molar fractions is different from, and rather simpler than, the conventional treatment, *e.g.*, that by Irving *et al.*¹⁰

To serve as a practical example, the theory developed above has been applied to monobasic and dibasic acids, in the following.

Monobasic acid

For a monobasic acid we have the equilibrium $\text{H} + \text{R} \rightleftharpoons \text{HR}$ with acidity constant $k_a = [\text{H}][\text{R}]/[\text{HR}]$. In this case, $n = 1$, $\bar{n} = f_1$, $f_0 + f_1 = 1$, $A = A_0 f_0 + A_1 f_1$, and from equation (13), the slope of the graph

of A as a function of pH is given by

$$\begin{aligned} \frac{dA}{d(\text{pH})} &= -2.303(A_1 - A_0)f_1 = -2.303(A - A_0)f_0 \\ &= -2.303(A_1 - A_0)f_0 f_1 \quad (20) \end{aligned}$$

Stationary points are given by the condition $dA/d(\text{pH}) = 0$, and correspond to the trivial solutions $A' = A_0$ and $A' = A_1$, to which the graph tends asymptotically, at high and low pH values, respectively, and also to the case in which $A_0 = A_1 = A'$, *i.e.*, there is no change in the absorbance as pH varies.

From equation (19) we have for a monoprotic acid

$$\begin{aligned} \frac{d^2 A}{d(\text{pH})^2} &= 2.303^2 [A_0 f_0 (-\bar{n})^2 + A_1 f_1 (1 - \bar{n})^2 \\ &\quad - A(1 - \bar{n})f_1] = 2.303^2 A (f_0^2 - f_0 f_1) \quad (21) \end{aligned}$$

and thus the value of the inflexion point in the graph of A vs. pH—which satisfies the condition $d^2 A/d(\text{pH})^2 = 0$ —will be given by $f_0 = f_1$, and so $[\text{H}'] = K_a$, and the value of the absorbance at the inflexion point of the curve will be given by

$$A'' = \frac{A_1 + A_0}{2} \quad (22)$$

Dibasic acid

For a diprotic acid we have the equilibria $\text{H}_2\text{R} \rightleftharpoons \text{H} + \text{HR}$, and $\text{HR} \rightleftharpoons \text{H} + \text{R}$. These equilibria have the acidity constants

$$K_{a1} = \frac{[\text{H}][\text{HR}]}{[\text{H}_2\text{R}]} \quad \text{and} \quad K_{a2} = \frac{[\text{H}][\text{R}]}{[\text{HR}]} \quad (23a,b)$$

The relationship between absorbance and the composition of a given solution of the acid becomes

$$\begin{aligned} A &= A_0 f_0 + A_1 f_1 + A_2 f_2 \\ &= f_0 \left(A_0 + A_1 \frac{f_1}{f_0} + A_2 \frac{f_2}{f_0} \right) \quad (24) \end{aligned}$$

and from equations (4) and (23) the following equation—which provides a starting point for the determination of acidity constants from spectral data—is readily derived:

$$A = \frac{A_0 + A_1 \frac{[\text{H}]}{K_{a2}} + A_2 \frac{[\text{H}]^2}{K_{a2} K_{a1}}}{1 + \frac{[\text{H}]}{K_{a2}} + \frac{[\text{H}]^2}{K_{a2} K_{a1}}} \quad (25)$$

The equation for $dA/d(\text{pH})$ becomes in this specific case

$$\frac{dA}{d(\text{pH})} = -2.303(A_1 f_1 + 2A_2 f_2 - \bar{n} A) \quad (26)$$

The derivative $dA/d(\text{pH})$ is always negative if $A_2 > A_1 > A_0$ and positive if $A_2 < A_1 < A_0$ since f_j cannot (from its definition) ever be either negative or imaginary. The expression (26) is zero for infinitely large or small values of $[\text{H}]$, which correspond to the limiting values A_0 and A_2 , to which the graph of A vs.

pH tends asymptotically. In cases other than these trivial solutions, the absorbance reaches a maximum (or minimum) at a certain value of pH if the following condition is satisfied: $A_0 < A_1 > A_2$ (or $A_0 > A_1 < A_2$).

Equation (26) is especially useful because it can be utilized to deduce several relationships. Maximum or minimum absorbance will occur when $dA/d(\text{pH}) = 0$, whence

$$A' = \left(\frac{A_1 f_1 + 2A_2 f_2}{f_1 + 2f_2} \right)_{\text{pH} = \text{pH}'} \quad (27)$$

On rearrangement, this expression gives

$$\frac{f_1'}{f_2'} = 2 \left(\frac{A_2 - A'}{A' - A_1} \right) \quad (28)$$

and taking into account (23a) and $f_j = [\text{H}_j \text{R}]/C_{\text{R}}$:

$$K_{a1} = 2[\text{H}'] \left(\frac{A_2 - A'}{A' - A_1} \right) \quad (29)$$

Also, since the sum of the molar fractions is unity, from equation (27) we get

$$\frac{f_0'}{f_2'} = \frac{A' - A_2}{A' - A_0} \quad (30)$$

so

$$K_{a1} K_{a2} = [\text{H}']^2 \left(\frac{A' - A_2}{A' - A_0} \right) \quad (31)$$

From equation (29)

$$A_1 = A' + 2 \frac{[\text{H}']}{K_{a1}} (A' - A_2) \quad (32)$$

After introduction of (32) into (25), a simple algebraic rearrangement leads to the following form

$$\left(\frac{A - A_0}{[\text{H}]} \right) K_{a2} + \frac{1}{K_{a1}} \{ (A - A_2)[\text{H}] - 2[\text{H}'](A' - A_2) \} = A' - A \quad (33)$$

Taking into account (31), which allows K_{a1} to be eliminated, the following equation is readily derived:

$$K_{a2} = [\text{H}] \frac{A' - A}{A - A_0 + \frac{(A - A_2)r^2 - 2(A' - A_2)r}{b}} \quad (34)$$

where for clarity we write

$$b = \frac{A' - A_2}{A' - A_0} \quad (35)$$

$$r = \frac{[\text{H}]}{[\text{H}']} \quad (36)$$

The value of K_{a2} can thus be evaluated from experimental data for pH and A , provided that the values of A' , pH' , A_0 and A_2 are available. Once the value of K_{a2} is known, K_{a1} is evaluated from equation (31). Nevertheless, it is always disadvantageous to evaluate an equilibrium constant from only one result.¹¹ It is advisable to make as full use as possible of the measurements.

Equation (34) may be transformed into the more customary pH and $\text{p}K_{a2}$ notation to yield the relation

$$\log U = \text{pH} - \text{p}K_{a2} \quad (37)$$

$$U = \frac{A' - A}{A - A_0 + \frac{(A - A_2)r^2 - 2(A' - A_2)}{b}} \quad (38)$$

A plot of $\log U$ vs. pH yields a straight line with unit slope and intercept on the x -axis equal to $\text{p}K_{a2}$. All reliable points except those near to A_0 , A_2 or A' are used in the calculations.

By combining equations (34) and (31), taking logarithms and substituting for U we get

$$\log [Ur^2] = \text{p}K_{a1} - \text{pH} \quad (39)$$

Plotting the logarithmic term in brackets in equation (39) vs. pH gives a straight line of slope -1 , intersecting the pH axis at $\text{p}K_{a1}$.

In practice, the main difficulty of the method is the accurate location of the maximum or minimum in the A -pH graph, which may not be a simple task,¹² and may lead to inaccurate results. A smooth curve is plotted through experimental values of A obtained at various values of H; as many points as possible are obtained around the maximum (or minimum) value before the best (pH' , A') point is chosen. However, in order to increase the precision in the evaluation of the maximum (or minimum) in the A -pH curve, the ratio

$$\frac{\Delta A}{\Delta \text{pH}} = \frac{A_{n+1} - A_n}{\text{pH}_{n+1} - \text{pH}_n} \quad (40)$$

can be plotted against $(\text{pH}_{n+1} + \text{pH}_n)/2$, where pH_n and A_n denote the pH and A values, respectively, for the n th point. The pH value for which $\Delta A/\Delta \text{pH} = 0$ is taken as pH' . This curve is obtained by graphical differentiation of the A -pH curve, with use of very small increments in pH.

When equation (18) is applied to a dibasic acid, we have

$$\frac{d^2 A}{d(\text{pH})^2} = 2.303^2 \{ A_0 f_0 (-\bar{n})^2 + A_1 f_1 (1 - \bar{n})^2 + A_2 f_2 (2 - \bar{n})^2 - A [(1 - \bar{n})f_1 + 2(2 - \bar{n})f_2] \} \quad (41)$$

Values of $d^2 A/d(\text{pH})^2 = 0$ will locate points of inflexion in the graph of A vs. pH, and thus, from equation (41), ($\text{pH} = \text{pH}''$):

$$A_1 f_1 (1 - 2\bar{n}) + 4A_2 f_2 (1 - \bar{n}) - A'' [\bar{n}(1 - 2\bar{n}) + 2f_2] = 0 \quad (42)$$

By substituting for $A_1 f_1 (= A'' - A_0 f_0 - A_2 f_2)$ and taking into account that

$$4(1 - \bar{n}) = 3 - 2\bar{n} - (2\bar{n} - 1) \quad (43)$$

we have

$$A_2 f_2 (3 - 2\bar{n}) + A_0 f_0 (2\bar{n} - 1) - A'' \times [f_0 (2\bar{n} - 1) + f_2 (3 - 2\bar{n})] = 0 \quad (44)$$

Substituting now for $3 - 2\bar{n}$ and $2\bar{n} - 1$:

$$3 - 2\bar{n} = 3f_0 + f_1 - f_2 \quad (45)$$

$$2\bar{n} - 1 = -f_0 + f_1 + 3f_2 \quad (46)$$

dividing by f_0^2 and rearranging terms, we get

$$(A_2 - A'') \frac{f_2}{f_0} \left(3 + \frac{f_1}{f_0} - \frac{f_2}{f_0} \right) + (A_0 - A'') \left(-1 + \frac{f_1}{f_0} + 3\frac{f_2}{f_0} \right) = 0 \quad (47)$$

After substitution from (4), this expression can conveniently be rearranged to give

$$-c\beta_2^2[H'']^4 + c\beta_1\beta_2[H'']^3 + (3r + 3)\beta_2[H'']^2 + \beta_1[H''] - 1 = 0 \quad (48)$$

where

$$c = \frac{A_2 - A''}{A_0 - A''} \quad (49)$$

Equation (48) has three real roots (three points of inflexion) in cases where $c < 0$ ($A_2 > A_1 > A_0$ or $A_2 < A_1 < A_0$) and two real roots (two points of inflexion) in systems in which $A_0 > A_1 < A_2$ or $A_0 < A_1 > A_2$ ($c > 0$).

Another expression that can readily be derived from equation (47) is

$$\frac{f_0}{f_1} = \frac{(A_2 - A'') \frac{f_2}{f_0} + (A_0 - A'')}{(A_2 - A'') \left\{ \left(\frac{f_2}{f_0} \right)^2 - 3\frac{f_2}{f_0} \right\} + (A_0 - A'') \left(1 - 3\frac{f_2}{f_0} \right)} \quad (50)$$

and taking into account the expressions (4), (31), (35), (36) and (48) we get finally

$$K_{a2} = [H''] \frac{c \frac{p^2}{b} + 1}{c \left(\frac{p^4}{b^2} - 3\frac{p^2}{b^2} \right) + 1 - 3\frac{p^2}{b}} \quad (51)$$

where

$$p = \frac{[H'']}{[H']} \quad (52)$$

Thus, the value of K_{a2} can be calculated from the co-ordinates of the maximum (or minimum) and the inflexion points in the graph of A vs. pH. The inflexion points correspond to the maxima or minima of the graph of the derivative $dA/d(\text{pH})$ vs. pH and so, in many cases, a direct plot of $\Delta A/\Delta(\text{pH})$ against pH allows location of the inflexion points of the A -pH curve.

Applications

The evaluation of acidity constants of two-step overlapping equilibria has been extensively studied. In spite of this, only a limited amount of absorbance vs. pH experimental data has been published. The

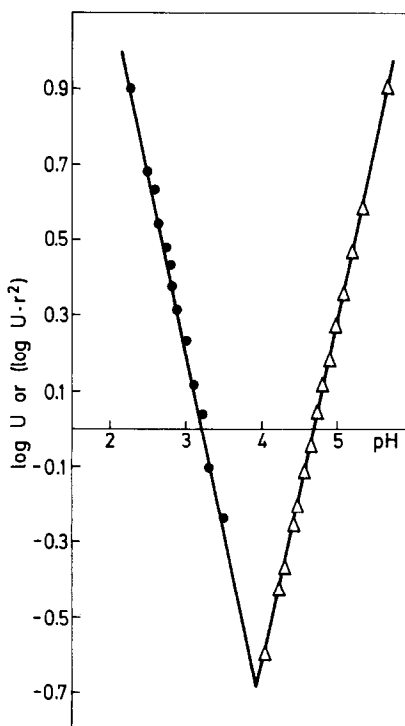


Fig. 1. Determination of pK_a values of *m*-aminobenzoic acid.

data reported by Bryson and Matthews¹³ for *m*-aminobenzoic acid and 3-amino-1-naphthoic acid, and the data reported by Ang¹⁴ for isophthalic acid have been used to check our proposed calculation procedures. Results obtained when the expressions (37) and (39) were applied are depicted in Figs. 1-3. Values of $[H']$ were calculated in all cases from the zero ordinates in the graph of $\Delta A/\Delta(\text{pH})$ vs. pH, as

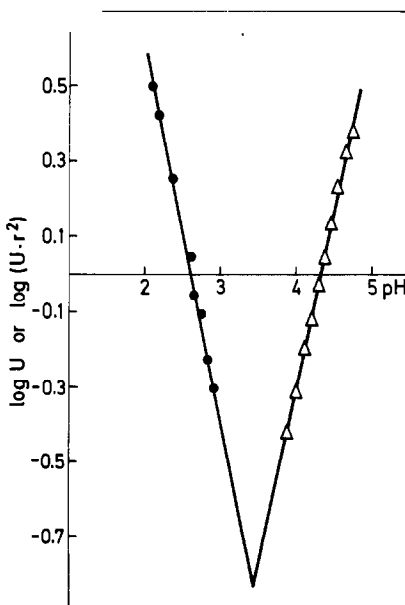


Fig. 2. Determination of pK_a values of 3-amino-1-naphthoic acid.

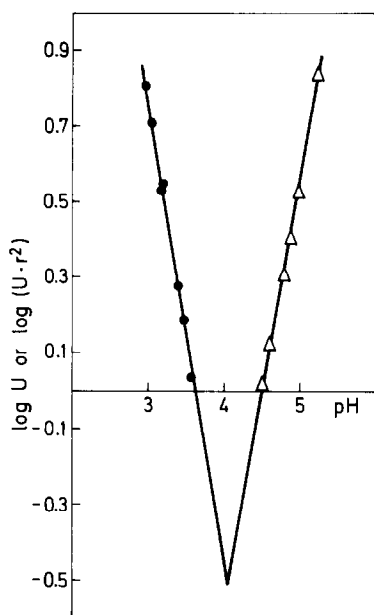


Fig. 3. Determination of pK_a values of isophthalic acid.

shown in Fig. 4 for *m*-aminobenzoic acid. The agreement between the results obtained by means of the logarithmic method proposed in this paper and the ones reported by Bryson and Matthews¹³ and Ang¹⁴ (Table 1) is excellent. For the *m*-aminobenzoic acid system, the pK_a values were also calculated from the co-ordinates of the minimum (3.85, 0.318) and the inflexion points (3.15, 0.400) and (4.65, 0.440). First equation (51) was applied, then once the value of K_{a2} was known, K_{a1} was calculated from equation (31). Data of the highest possible precision are necessary for the full benefits of the second derivative method to be realized, because numerical methods are very sensitive to the choice of points used for the calculations. Values obtained from either the first or the second inflexion point (Table 1) agree well, but differ by 0.08 and 0.15 from the pK_{a1} and pK_{a2} values obtained by the graphical method. However, a three-equation method applied to the points (pH' , A') (pH'_1 , A'_1) and (pH'_2 , A'_2) led to the values of 3.24 and 4.52 for pK_{a1} and pK_{a2} .

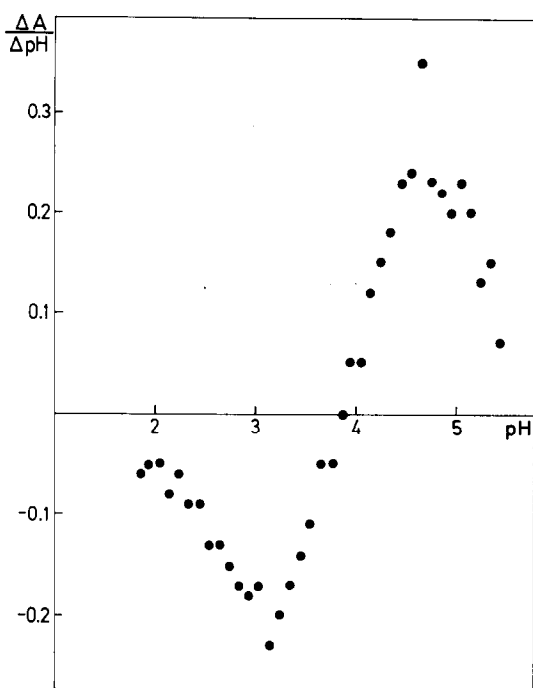


Fig. 4. Derivative curve $\Delta A/\Delta(pH)$ vs. pH, for *m*-aminobenzoic acid.

Conclusion

Attention is first drawn in this paper to the mathematical treatment of the absorbance vs. pH graphs of polybasic acids. Simple expressions are deduced for the first and second derivatives of the A -pH function, which can be calculated directly with a programmable calculator.

Many organic reagents of analytical importance, and many molecules which possess biological significance are derived from dibasic acids. However, in the evaluation of acidity constants of overlapping equilibria, approximations of various sorts are frequently made, and these can lead to inaccurate results.^{15,16} The literature contains a diversity of numerical, graphical and computerized methods for evaluation of acidity constants of diprotic acids from spectrophotometric data.^{17,18} This problem was recently reviewed critically by Meloun and Čermák.¹⁹

Table 1. Acidity constants of several dibasic acid derivatives*

Acid	pK_{a1}	pK_{a2}	Comments
<i>m</i> -aminobenzoic	3.14	4.71	Bryson and Matthews ¹³
	3.223 ± 0.006	4.694 ± 0.004	This paper; logarithmic method, $pH' = 3.85$ and $A' = 0.318$
	3.29	4.56	This paper; from the 1st inflexion point
3-amino-1-naphthoic	3.31	4.54	This paper; from the 2nd inflexion point
	2.67	4.45	Bryson and Matthews ¹³
isophthalic	2.612 ± 0.009	4.316 ± 0.004	This paper; logarithmic method $pH' = 3.45$ and $A' = 0.172$
	3.49 ± 0.08	4.36 ± 0.08	Thamer and Voigt ¹²
	3.51 ± 0.03	4.36 ± 0.08	Ang's method ¹⁴ applied to the data of Thamer and Voigt
	3.65 ± 0.02	4.44 ± 0.02	Ang's method as applied to Ang's data ¹⁴
	3.616 ± 0.012	4.492 ± 0.007	This paper; logarithmic method $pH' = 3.99$ and $A' = 0.414$

*The standard deviations of the pK_a values in the logarithmic method have been evaluated by single linear regression analysis taking into account the covariance between the slope and intercept of the straight lines obtained.

The research field concerning spectrophotometric evaluation of acidity constants of two-step overlapping equilibria may seem to be completely exhausted. Nevertheless, in this report—which forms part of a systematic investigation of overlapping equilibria^{20,21}—the equations derived permit the evaluation of acidity constants of two-step overlapping equilibria in cases in which the absorbance vs. pH graphs have a maximum or a minimum in the region of the curve where the intermediate species (e.g., HR, of the diprotic acid H₂R) predominates; an accurate knowledge of the limit absorbances of the species H₂R and R, A₂ and A₀, is required. It has been shown that the acidity constants can be computed from the co-ordinates of the maximum (or minimum) and the inflexion points of the A–pH graph. In particular, the use of molar fractions in the derivation of equations is highly desirable because this leads to more compact equations.

REFERENCES

1. A. Ringbom, *Complexation in Analytical Chemistry*, Interscience, New York, 1963.
2. J. Bjerrum, *Metal Amine Formation in Aqueous Solution*, Haase, Copenhagen, 1941.
3. J. Butler, *Ionic Equilibrium*, Addison-Wesley, Reading, Mass., 1964.
4. W. A. E. McBryde, *Talanta*, 1974, **21**, 979.
5. W. B. Guenter, *Chemical Equilibrium*, Plenum Press, New York, 1975.
6. H. Rossotti, *Chemical Applications of Potentiometry*, Van Nostrand, London, 1969.
7. G. Bodländer, *Festschrift für R. Dedekind*, Braunschweig, 1901.
8. L. Johansson, *Coord. Chem. Rev.*, 1968, **3**, 293.
9. P. Souchay and J. Lefebvre, *Equilibres et réactivité des complexes en solution*, Masson, Paris, 1969.
10. H. Irving, H. S. Rossotti and G. Harris, *Analyst*, 1955, **80**, 83.
11. H. S. Rossotti, *Talanta*, 1974, **21**, 809.
12. B. J. Thamer and A. F. Voigt, *J. Phys. Chem.*, 1952, **56**, 225.
13. A. Bryson and R. W. Matthews, *Aust. J. Chem.*, 1961, **14**, 237.
14. K. P. Ang, *J. Phys. Chem.*, 1958, **62**, 1109.
15. A. G. Asuero and G. Gonzalez, unpublished work.
16. A. G. Asuero, M. A. Herrador and A. M. Camean, *Anal. Lett.*, in press.
17. F. J. C. Rossotti and H. S. Rossotti, *The Determination of Stability Constants*, McGraw-Hill, New York, 1961.
18. M. T. Beck, *Chemistry of Complex Equilibria*, Van Nostrand Reinhold, New York, 1970.
19. M. Meloun and J. Čermák, *Talanta*, 1979, **26**, 569.
20. A. G. Asuero, J. L. Jimenez-Trillo and M. J. Navas, *Talanta*, 1986, **33**, 531.
21. A. G. Asuero, M. A. Herrador, A. M. Jimenez and M. J. Navas, *Z. Anal. Chem.*, in press.

STUDIES ON FLUORESCEIN—IV*

NOTES ON OBTAINING ACID DISSOCIATION CONSTANTS FROM THE TITRATION CURVES OF DIBASIC ACIDS

HARVEY DIEHL

Department of Chemistry, Iowa State University, Ames, IA 50011, U.S.A.

(Received 10 May 1985. Revised 3 June 1986. Accepted 20 June 1986)

Summary—Equations have been derived by which the dissociation constants of a dibasic acid can be calculated from three points on a titration curve. The equations hold irrespective of the ratio of the dissociation constants, that is, irrespective of whether an end-point break appears at one equivalent of base added per mole of dibasic acid. Conditions have also been established, under which each dissociation constant can be evaluated from a single point on the titration curve.

In the preceding paper¹ a report was given of the titration of sodium fluoresceinate in water and in 50% aqueous ethanol. Only one end-point appeared in the titration curve for the ethanolic medium, corresponding to fluoresceinate being a diacidic base. The curve was linear between $\alpha = 0.5$ and 1.5 ($\alpha =$ molar ratio of protons added to fluoresceinate present), with a pH-drop of 1.06 between these points. For the titration in water, however, break-points were observed for protonation of the fluoresceinate (Fl^{2-}) to HF^- and then to undissociated fluorescein (H_2Fl); this titration was complicated by the formation of a precipitate of yellow fluorescein shortly after the first of these end-points. The problem then was to obtain values for the dissociation constants of fluorescein from the data for the titration in aqueous ethanol.

THEORY

In the titration of a weak dibasic acid with a strong base, the average number of protons bound per mole of acid present, can be calculated from

$$\bar{n} = \frac{2 + K_1/[\text{H}^+]}{1 + K_1/[\text{H}^+] + K_1 K_2/[\text{H}^+]^2} \quad (1)$$

where K_1 and K_2 are the first and second dissociation constants.

This equation has some interesting simplified forms for specific values of \bar{n} . Rearrangement yields a quadratic:

$$(\bar{n} - 2)[\text{H}^+]^2 + (\bar{n} - K_1)[\text{H}^+] + \bar{n}K_1K_2 = 0 \quad (2)$$

the positive root of which,

$$[\text{H}^+] = \frac{(\bar{n}K_1 - K_1) + [(\bar{n}K_1 - K_1)^2 + 4(\bar{n} - 2)\bar{n}K_1K_2]^{1/2}}{2(2 - \bar{n})} \quad (3)$$

reduces for $\bar{n} = 1.0$ to the well-known expression

$$[\text{H}^+]_{\bar{n}=1.0} = [K_1 K_2]^{1/2} \quad (4)$$

or in logarithmic form

$$\text{pH}_{\bar{n}=1.0} = \frac{1}{2}[\text{p}K_1 + \text{p}K_2] \quad (5)$$

For $\bar{n} = 0.5$ equation (3) becomes

$$[\text{H}^+]_{\bar{n}=0.5} = \frac{[(0.5K_1)^2 + 3K_1K_2]^{1/2} - 0.5K_1}{3} \quad (6)$$

and for $\bar{n} = 1.5$

$$[\text{H}^+]_{\bar{n}=1.5} = 0.5K_1 + [(0.5K_1)^2 + 3K_1K_2]^{1/2} \quad (7)$$

Note that the discriminant, $b^2 = 4ac$, is the same in equations (6) and (7).

Of especial interest is the equation obtained by combining equations (5) and (7):

$$[\text{H}^+]_{\bar{n}=1.5} = 0.5K_1 + \{(0.5K_1)^2 + 3[\text{H}^+]_{\bar{n}=1.0}^2\}^{1/2} \quad (8)$$

Algebraic manipulation yields

$$0.25K_1^2 - [\text{H}^+]_{\bar{n}=1.5}K_1 + [\text{H}^+]_{\bar{n}=1.5}^2 = 0.25K_1^2 + 3[\text{H}^+]_{\bar{n}=1.0}^2 \quad (9)$$

The K_1^2 terms cancel, and

$$K_1 = \frac{[\text{H}^+]_{\bar{n}=1.5}^2 - 3[\text{H}^+]_{\bar{n}=1.0}^2}{[\text{H}^+]_{\bar{n}=1.5}} \quad (10)$$

Surprisingly, combination of equations (5) and (6) similarly leads to

$$K_1 = \frac{[\text{H}^+]_{\bar{n}=1.0}^2 - 3[\text{H}^+]_{\bar{n}=0.5}^2}{[\text{H}^+]_{\bar{n}=0.5}} \quad (11)$$

Table 1. Relative errors in the assumptions $K_1 = [H^+]_{\bar{n}=1.5}$ and $K_2 = [H^+]_{\bar{n}=0.5}$ (held constant, $K_1 K_2 = 1.0 \times 10^{-12}$; varied, K_1 and K_2)

pK_1	6.0	5.8	5.6	5.4	5.2	5.0	4.8	4.6	4.4	4.2	4.0
pK_2	6.0	6.2	6.4	6.6	6.8	7.0	7.2	7.4	7.6	7.8	8.0
K_1/K_2	1	2.5	12	16	40	1×10^2	1.2×10^2	1.6×10^2	1.0×10^3	4.0×10^3	1.0×10^4
Rel. error in K_1^*	130	70.2	35.2	16.3	7.0	2.9	1.2	0.47	0.18	0.07	0.03
Rel. error in K_2^\dagger	-56.6	-41.2	-26.0	-14.0	-6.6	-2.8	-1.2	-0.47	-0.18	-0.07	-0.02

*Relative error (%) = $100([H^+]_{\bar{n}=1.5} - K_1)/K_1$.

†Relative error (%) = $100([H^+]_{\bar{n}=0.5} - K_2)/K_2$.

That is, from a pair of selected points on the titration curve, either $pH_{\bar{n}=0.5}$ and $pH_{\bar{n}=1.0}$, or $pH_{\bar{n}=1.0}$ and $pH_{\bar{n}=1.5}$, the first dissociation constant can be calculated, by equations (10) or (11), respectively, and subsequently, by equation (5), the value of the second dissociation constant.

APPLICATION

Titration of fluorescein in 50% aqueous ethanol

The data given previously for the titration¹ were

\bar{n}_{exp}	0	0.50	1.00	1.5	2.00
pH	10.06	7.31	6.78	6.25	4.48

With both equations (10) and (11) these data give $pK_1 = pK_{\text{H}_2\text{FI}} = 6.38$. Equation (5) then gives $pK_2 = pK_{\text{HFI}} = 7.18$. These values for the first dissociation constant are identical with that found by the iteration method in the preceding paper¹ and that for the second dissociation constant is very close to the earlier value of $pK_2 = 7.16$. Insertion of these values into equations (6) and (7) yields $pH_{\bar{n}=0.5} = 7.31$ and $pH_{\bar{n}=1.5} = 6.25$, in exact agreement with the observed values, confirming the correctness of the approach. For this particular titration, in which an end-point break does not appear at $\bar{n} = 1.0$ ($K_1/K_2 = 6.3$) the pK_a values do not equal the pH at the "quarter titration" points $a = 0.5$ and 1.5 , but fall closer to $pH_{a=1.0}$.*

$$\begin{array}{lll} pH_{a=1.5} = 7.31 & pH_{a=1.00} = 6.78 & pH_{a=0.5} = 6.25 \\ pK_2 = 7.18 & & pK_1 = 6.38 \end{array}$$

This problem is examined in more detail below.

Titration of fluorescein in water

Typical data from the earlier paper¹ were

\bar{n}_{exp}	0	0.50	1.00	1.50	2.00
pH	8.50	6.35	5.40	5.10	3.60

The data for \bar{n}_{exp} equal to 0.50 and 1.00, when inserted into equation (11), yield $pK_{\text{H}_2\text{FI}} = 4.47$, in fair agreement with $pK_{\text{H}_2\text{FI}} = 4.44$ found by the solubility method.² Equation (10) is inapplicable owing to the precipitation of yellow undissociated fluorescein dur-

ing the latter part of the titration, which renders the data at $\bar{n} = 1.50$ inappropriate. In the preceding paper,¹ it was assumed that pK_{HFI} was equal to the pH at $\bar{n}_{\text{exp}} = 0.50$ and from the various data the value $pK_{\text{HFI}} = 6.36$ was chosen. For $pH_{\bar{n}=0.5} = 6.36$ and $pH_{\bar{n}=1.0} = 5.40$ equation (5) yields $K_{\text{H}_2\text{FI}} = 4.44$, a not surprising result inasmuch as equation (11) is derived by combining equations (5) and (6).

Further examination of the approximations

$K_1 = [H^+]_{\bar{n}=1.5}$ and $K_2 = [H^+]_{\bar{n}=0.5}$

Although, as pointed out above, values for the dissociation constants of a dibasic acid can be obtained from two points on the titration curve, it becomes possible under certain conditions to obtain each value from a corresponding single point. By using equations (6) and (7) it is possible to calculate the approach of K_2 to $[H^+]_{\bar{n}=0.5}$ and of K_1 to $[H^+]_{\bar{n}=1.5}$ as K_1 and K_2 are varied. Table 1 gives the results of such a calculation for a system in which $K_1 K_2 = 1 \times 10^{-12}$, i.e., $[H^+]_{\bar{n}=1.0} = 1 \times 10^{-6}$ and K_1 and K_2 are varied over two orders of magnitude. Thus, for $K_1/K_2 = 250$, the relative error is about -1% for K_2 and +1% for K_1 , corresponding to a difference of about 0.006 in the pK values.

For $K_1/K_2 = 2500$, the relative error is only about 0.1%. Thus, if the pH values for the $\bar{n} = 0.5$ and $\bar{n} = 1.5$ points differ by 1.2, pK_2 may be taken as equal to $pH_{\bar{n}=0.5}$ and pK_1 equal to $pH_{\bar{n}=1.5}$ with an error of only 1% or so in the dissociation constants.

The same result can be obtained by setting

$$K_1/K_2 = b \quad (12)$$

substituting into equation (6) to remove K_1 , and getting

$$[H^+]_{\bar{n}=0.5} = \frac{-0.5K_2 + K_2(0.5^2b^2 + 3b)^{1/2}}{3} \quad (13)$$

then expanding the square-root term by the binomial theorem and reducing the algebra, which yields

$$[H^+]_{\bar{n}=0.5} = K_2 - K_2(3/b) + K_2(\dots) \quad (14)$$

For values of b so large that all terms but the first are negligible,

$$[H^+]_{\bar{n}=0.5} = K_2 \quad (15)$$

For $b = 100$, $[H^+]_{\bar{n}=0.5} = 0.97K_2$, corresponding to the relative error in the bottom line of Table 1 (but

*Note that these data refer to titration of the fluorescein conjugate base, so $a = 1.5$ corresponds approximately to $\bar{n} = 0.5$, and $a = 0.5$ to $\bar{n} \sim 1.5$.

not quite identical with it because the cubic term in the binomial expansion was dropped).

Similarly, equation (7) gives

$$[H^+]_{\bar{n}=1.5} = 0.5K_1 = K_1[0.5^2 + (3/b)]^{1/2} \quad (16)$$

and hence

$$[H^+]_{\bar{n}=1.5} = K_1 + K_1(3/b) + K_1(\dots) \quad (17)$$

and for very large b ,

$$[H^+]_{\bar{n}=1.50} = K_1 \quad (18)$$

For $b = 100$, $[H^+]_{\bar{n}=1.50} = 1.03K_1$, corresponding to the relative error in the second line from the bottom of Table 1.

Slopes of the first and second parts of the titration curve of a dibasic acid

Starting from equation (4), further formulae can similarly be derived by relating four points ($\bar{n} = 0.25, 0.75, 1.25, 1.75$) on the titration curve of a dibasic acid to the values of the dissociation constants and their ratio, and allow the calculation of the slopes of the mid-regions of the two parts of the titration curve:

$$[H^+]_{\bar{n}=0.25} = (1/3K_2 - (7/27b)K_2 + \dots) \quad (19)$$

$$[H^+]_{\bar{n}=0.75} = 3K_2 - (45/b)K_2 + \dots \quad (20)$$

$$[H^+]_{\bar{n}=1.25} = (1/3)K_1 - (5/b)K_1 + \dots \quad (21)$$

$$[H^+]_{\bar{n}=1.75} = 3K_1 + (7/3b)K_1 + \dots \quad (22)$$

For values of b sufficiently large for the second and subsequent terms to be negligible, the hydrogen-ion concentrations at the four points become simple multiples of the dissociation constants, and the two slopes, as measured by the drop in pH between $\bar{n} = 0.25$ and 0.75 or 1.25 and 1.75 , approach that for the titration of a monobasic acid:

$$\frac{[H^+]_{\bar{n}=0.75}}{[H^+]_{\bar{n}=0.25}} = \frac{3K_2}{\frac{1}{3}K_2} = 9; \quad \frac{[H^+]_{\bar{n}=1.75}}{[H^+]_{\bar{n}=1.25}} = \frac{3K_1}{\frac{1}{3}K_1} = 9 \quad (23)$$

$$\Delta pH = pH_{\bar{n}=0.75} - pH_{\bar{n}=0.25} = pH_{\bar{n}=1.75} - pH_{\bar{n}=1.25} = -\log 9 = -0.954 \quad (24)$$

For the titration of fluorescein in water (data given above, $pK_2 = 6.36$ and $b = K_1/K_2 = 83$), equations (19) and (20) yield $\Delta pH = 0.88$; the experimental value is 0.90 . Equations (21) and (22) are inapplicable because of the precipitation already mentioned.

REFERENCES

1. H. Diehl, N. Horchak-Morris, A. J. Hefley, L. F. Munson and R. Markuszewski, *Talanta*, 1986, **33**, 901.
2. H. Diehl and R. Markuszewski, *ibid.*, 1985, **32**, 159.

RAPID SPECTROPHOTOMETRIC DETERMINATION OF PALLADIUM IN TITANIUM ALLOYS WITH 2-(5-BROMO-2-PYRIDYLAZO)-5- (DIETHYLAMINO)PHENOL

CHANG YUN PO and ZHOU NAN*

Shanghai Research Institute of Materials, MMBI, Shanghai, People's Republic of China

(Received 4 June 1986. Accepted 1 August 1986)

Summary—A rapid spectrophotometric method for the determination of Pd in titanium alloys is proposed. It is based on the reaction of 2-(5-bromo-2-pyridylazo)-5-(diethylamino)phenol with Pd(II) in a sulphuric acid medium in the presence of ethanol. Beer's law is obeyed up to 40 μg of Pd. The molar absorptivity is $4.5 \times 10^4 \text{ l. mole}^{-1} \cdot \text{cm}^{-1}$. The standard deviation is 0.3 μg of Pd and the coefficient of variation varies from 0.8 to 3.3%. The elements ordinarily present in such alloys do not interfere. High selectivity is achieved by using fluoroboric acid as masking agent. Improvements in the method of sample decomposition also contribute to the rapidity of the method.

Palladium may be added to titanium alloys to increase stress corrosion resistance. For its spectrophotometric determination in such alloys only a few methods have been reported in the literature, and are all of the solvent extraction type. The biacetyldioxime method¹ is not sensitive and the 1-nitroso-2-naphthol method² is time-consuming, requiring 2 hr for full colour development and 15 min for layer separation after extraction. In this paper a new method without any separation is proposed. Use is made of the reaction of palladium with 2-(5-bromo-2-pyridylazo)-5-(diethylamino)phenol, 5-Br-PADEP, in an ethanolic aqueous medium of appropriate acidity. The proposed method is simple, rapid and convenient, and gives accurate and reproducible results. Owing to its high selectivity it should find many practical applications.

EXPERIMENTAL

Reagents

Analytical-reagent grade chemicals were used unless otherwise specified.

Fluoroboric acid, 40%, C.P. grade.

Sulphuric acid, 40% v/v.

5-Br-PADEP solution in ethanol, 0.03%.

Pd standard solution A. Dissolve 50.0 mg of palladium powder of spectrally pure grade in a mixture of 8 ml of concentrated hydrochloric acid and 2 ml of concentrated nitric acid by warming. Then add 10 ml of 40% v/v sulphuric acid and heat to strong fumes. Cool to room temperature, carefully add a little water and cool again. Transfer the solution into a 50-ml standard flask, dilute to volume and mix: 1 ml of this solution contains 1.00 mg of Pd. *Note.* Fuming with sulphuric acid may be dispensed with if nitric acid alone is used to dissolve the palladium metal; the presence of a little silver nitrate hastens this dissolution.

Pd standard solution B. Freshly prepared before use as follows. Pipette 1.00 ml of Pd standard solution A into a 100-ml standard flask, add 8 ml of 40% v/v sulphuric acid, dilute to volume and mix; 1 ml of this solution contains 10 μg of Pd.

Procedure

Transfer a 10-mg sample, weighed to the nearest 0.1 mg, into a 25-ml polyethylene beaker. Add 2 ml of fluoroboric acid and 3 or 4 drops of concentrated nitric acid, and warm in a hot water-bath until the sample has dissolved. Cool to room temperature and transfer the solution into a 25-ml standard flask. Add successively, 3 ml of 40% v/v sulphuric acid, 3 ml of fluoroboric acid, 10 ml of ethanol and 1.0 ml of 5-Br-PADEP solution. Dilute to volume and mix. After 5 min measure the absorbance at 620 nm against water as reference, using 1-cm cells, and read the palladium content from the calibration curve.

Preparation of calibration curve

Pipette 0.5, 1.0, 1.5, 2.0, 2.5, 3.0, 3.5 and 4.0 ml of Pd solution B into eight 25-ml standard flasks. Proceed in accordance with the procedure above and plot the absorbance readings vs. μg of Pd.

Note. The procedure above is applicable to titanium alloys containing $\leq 0.4\%$ of Pd. For those with higher content of Pd, an appropriate aliquot of the sample solution should be taken for the determination.

RESULTS AND DISCUSSION

Choice of chromogenic agent

Numerous new chromogenic agents for Pd have been developed, but many of them still require use of solvent extraction,³⁻¹² Reagents not needing use of extraction are more attractive for practical application. These may be further divided into two classes. One class reacts with Pd(II) in weakly acidic medium. Some members of this class form ternary systems either of mixed-ligand type^{13,14} or with a surfactant.¹⁵⁻¹⁹ The other class, which reacts with Pd(II) in a rather acidic medium, is to be preferred, since hydrolysis of titanium(IV), the matrix species, is then

*To whom correspondence and requests of reprints should be sent. Present address: 99 Handan Lu, 200433, Shanghai, People's Republic of China.

avoided. This class includes chlorosulphophenol-azorhodanine,²⁰ *S*-allyldithizone,²¹ 5-(2-hydroxy-3,5-dinitrophenylazo)-8-hydroxyquinoline-*N*-oxide,²² and sulphochlorophenol S,²³ which require a heating period for colour development, and 4-(3,5-dibromopyridylazo)-1,3-diaminobenzene,²⁴ which needs a 15-min standing period for completion of the reaction.

2-(5-Bromo-2-pyridylazo)-5-(diethylamino)phenol is reported by Gusev *et al.*^{25,26} to react with Pd(II) to form a coloured chelate which is extractable into chloroform. Our preliminary experiments with it revealed that this reaction also takes place in a sulphuric acid medium, especially in the presence of ethanol, and goes to completion within 5 min. Hence this reagent would seem a promising one for the rapid, direct determination of Pd.

Choice of medium and effect of acidity

As chloride complexes Pd(II) fairly strongly ($\log \beta_4 = 13.22$),²⁷ hydrochloric acid would seem inappropriate as a medium for the Pd determination. As Ti(IV), the matrix of the alloys to be analysed, hydrolyses readily in nitric or perchloric acid medium, neither of these acids is suitable either. Therefore sulphuric acid of appropriate concentration seems the only choice. The optimum concentration was found to be 0.75–1.5*M* (Table 1).

Effect of ethanol

Preliminary experiments revealed that the presence of ethanol makes the Pd spectrophotometric system more sensitive. The optimum concentration was found to be 25–40% v/v. Hence 10 ml is specified for use in the procedure. Ethanol also stabilizes the colour, the absorbance remaining virtually unchanged for at least 3 days in its presence but for only 110 min in its absence (Table 2).

Effect of 5-Br-PADEP concentration

The optimum amount of 5-Br-PADEP for the determination of Pd was studied and the results are shown in Table 3. Accordingly 0.3 mg is specified in the procedure.

Characteristics of the Pd–5-Br-PADEP chelate

The absorption spectra of 5-Br-PADEP and its Pd-chelate under the specified conditions are shown in Fig. 1. The absorption maximum of 5-Br-PADEP

Table 2. Time dependence of the absorbance reading for 20 μg of Pd

Standing time after colour development		Absorbance*	
<i>min</i>	<i>hr</i>	A	B
5		0.300	0.340
30		0.300	0.340
110		0.300	0.345
200		0.200	0.345
	24	—	0.340
	72	—	0.345
	168	—	0.335

*A—In the absence of ethanol; B—in the presence of 10 ml of ethanol.

lies at 455 nm, and its Pd-chelate has two maxima, at 575 and 620 nm; this is ascribed to the presence of the diethylamino group on the benzene ring, *para* to the azo linkage.²⁸ Measurement at 620 nm was chosen because at this wavelength no absorption by 5-Br-PADEP was found, so water may be used as the reference solution.

Beer's law is obeyed up to 40 μg of Pd and the molar absorptivity of this system is 4.5×10^4 l.mole⁻¹.cm⁻¹. The conditional formation constant $\log K'_f$ of the Pd-chelate is calculated to be 5.65 and its Pd:5-Br-PADEP ratio established as 1:2 by the mole-ratio and slope-ratio methods.

Effect of diverse cations and ligands

The effect of fluoroborate, a hard Lewis base, was first studied (Table 4). As it does not interfere with the determination of Pd, a soft Lewis acid, it is used for masking those cationic species of the hard Lewis acid type, including Ti(IV), the matrix. It should be noted that the method uses a medium sufficiently acidic for only a few cationic species to interfere. No attempt was made to determine tolerance limits. As the method was intended only for analysis of titanium alloys, the effects of those species possibly present in such alloys were studied and the results obtained are summarized in Table 4. The amounts added correspond to the upper limits specified by ASTM.² As shown by Table 4, the presence of fluoroboric acid is absolutely necessary and renders the determination of Pd in titanium alloys highly selective. It is preferable to hydrofluoric acid, which is inconvenient to use owing to its strong tendency to corrode glass vessels even at room temperature.

Table 1. Effect of acidity on determination of 20 μg of Pd(II) with 0.3 mg of 5-Br-PADEP

[H ₂ SO ₄], <i>M</i>	Absorbance*
0.5	0.290
0.75	0.300
1.0	0.305
1.5	0.305

*At 620 nm; 1-cm cell.

Table 3. Effect of 5-Br-PADEP in the presence of ethanol; Pd(II) 20 μg ; 1*M* H₂SO₄

5-Br-PADEP, <i>mg</i>	Absorbance
0.08	0.325
0.16	0.335
0.24	0.340
0.40	0.335
0.56	0.335

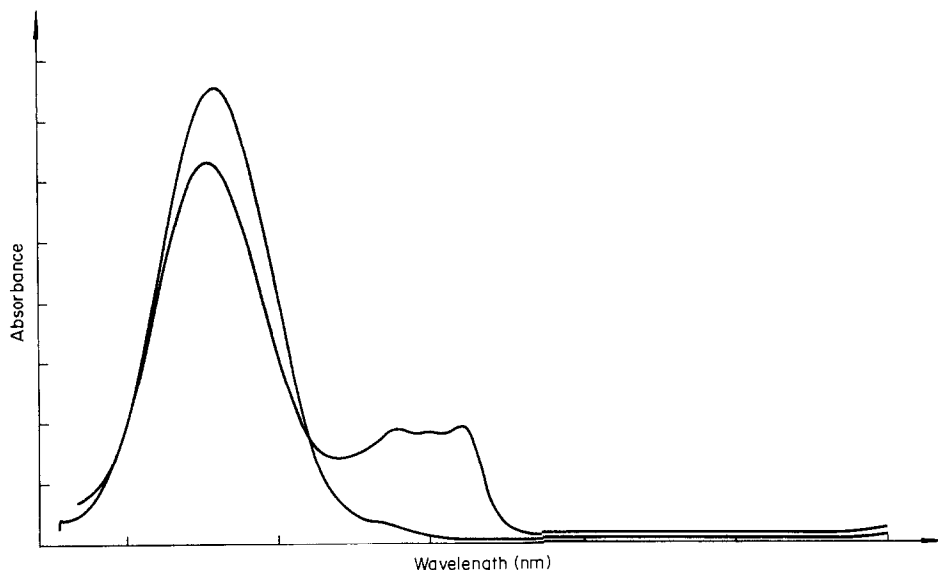


Fig. 1. Absorption spectra of 5-Br-PADEP and its Pd-chelate (1-cm cell). Curve 1, $1.2 \times 10^{-3}\%$ 5-Br-PADEP solution. Curve 2, $1.2 \times 10^{-3}\%$ 5-Br-PADEP and $0.4 \mu\text{g/ml}$ Pd.

Table 4. Effect of diverse cations and ligands on the determination of $20 \mu\text{g}$ of Pd(II)

Species tested	Added		Pd found, μg
	ml	mg	
40% HBF_4	4		20.0
	5		20.0
	10		20.0
NaCl		5	20.0
HNO_3	0.2		20.0
Al(III)		1	20.2
Cr(III)		2	20.0
Cu(II)		0.11	20.0
Fe(III)		2	20.2
Mg(II)		0.1	20.0
Mn(II)		2	19.8
Mo(VI)		0.5	20.2
Nb(V)		0.5	20.2
Si(IV)		0.5	19.7
Sn(IV)		1	19.8
Ta(V)		0.5	20.2
Ti(IV)	10		24.0*
	10		20.0
	20		19.7
V(IV)	2		23.0*
	2		19.7
V(V)		2	19.7
W(VI)		0.1	19.8
Zr(IV)		2	20.2

*In the absence of fluoroboric acid.

Table 5. Determination of Pd in some titanium alloys

Sample	Pd found, %	
	Proposed method	Other method*
Ti wire	0.175	0.170
Ti plate	0.158	0.154

*ASTM E 120-75.

Sample decomposition

It seems advisable to make two successive additions of fluoroboric acid, because the attack on 10-mg samples of titanium alloys by 3 or 4 drops of concentrated nitric acid proceeds readily in the presence of 2 ml of fluoroboric acid on warming, but is slower, probably owing to the dilution of the nitric acid, if 5 ml of fluoroboric acid are used.

To make the preparation of sample solutions as rapid as possible, the following improvements have been made. Fuming with sulphuric acid,² which may cause slightly lower results,¹ is dispensed with. The sample weight, specified as $0.4\text{--}1 \text{ g}^1$ or even 5 g^2 in other methods, is greatly reduced, to 10 mg.

Applications

The proposed method has been validated by analysis of synthetic samples containing 10 mg of Ti(IV), 2 mg each of Cr(III), Fe(III), Mn(II), V(V) and Zr(IV), 1 mg each of Al(III) and Sn(IV), 0.5 mg each of Nb(IV), Mo(VI), Ta(V) and Si(IV) 0.11 mg of Cu(II), 0.1 mg each of Mg(II) and W(VI) and $20 \mu\text{g}$ of Pd(II). The standard deviation was $0.3 \mu\text{g}$ ($n = 18$) and the coefficient of variation varied from 0.8 to 3.3%.

Results for analysis of industrial samples are shown in Table 5.

Acknowledgements—Grateful thanks are due to all members of the Directorate of SRIM for permission to publish this paper.

REFERENCES

1. W. F. Davis, *Talanta*, 1969, **16**, 1330.
2. ASTM, *1978 Annual Book of ASTM Standards*, Part 12, p. 399. ASTM, Philadelphia, 1978.

3. Y. Sasaki, *Anal. Chim. Acta*, 1982, **134**, 407.
4. A. Kumar, M. F. Hussian, M. Satake and B. K. Puri, *Bull. Chem. Soc. Japan*, 1982, **55**, 3455.
5. R. Yoda, K. Akiyama, Y. Yamamoto and Y. Murakami, *Bunseki Kagaku*, 1981, **30**, 160.
6. H. Akaiwa, H. Kawamoto and E. Yoshimatsu, *Nippon Kagaku Kaishi*, 1981, 79.
7. P. W. Beaupré and W. J. Holland, *Mikrochim. Acta*, 1983 **I**, 273.
8. M. Blanco and S. Maspoeh, *ibid.*, 1983 **III**, 11.
9. R. Yoda, Y. Yamamoto and Y. Murakami, *ibid.*, 1983 **I**, 75.
10. J. Cacho, M. A. Lacomá and C. Nerín, *Talanta*, 1985, **32**, 11.
11. A. D. Langade and V. M. Shinde, *Analyst*, 1982, **107**, 708.
12. Z. B. Aneva, *Zavodsk. Lab.*, 1982, **48**, No. 6, 16.
13. K. Kodua, V. K. Akimov and G. Rudzitis, *Latv. PSR Zinat Akad. Vestis, Kim. Ser.*, 1982, No. 1, 63.
14. M. B. Saha and A. K. Chakraborty, *J. Indian Chem. Soc.*, 1982, **59**, 1109.
15. V. N. Tikhonov and N. P. Aleksandrova, *Zh. Analit. Khim.*, 1981, **36**, 242.
16. Z. Gregorowicz, P. Górka, S. Kowalski and J. Cebula, *Mikrochim. Acta*, 1983, **II**, 181.
17. J. Egermaierová, L. Čermáková, V. Suk and L. Klir, *Chem. Listy*, 1982, **76**, 985.
18. R. Kant, O. Prakash and S. P. Mushran, *Analisis*, 1980, **8**, 56.
19. R. Kant, O. Prakash, S. Kumar and S. P. Mushran, *Microchem. J.*, 1983, **28**, 55.
20. M. Gur'eva, S. B. Savvin, L. M. Trutneva, N. N. Chalisova, T. A. Formina and L. K. Shubochin, *Zh. Analit. Khim.*, 1982, **37**, 667.
21. A. V. Kotov, I. Yu. Davydova and N. M. Golovkina, *ibid.*, 1982, **37**, 594.
22. O. K. Kleimenova, A. A. Nemodruk and I. M. Gibalo, *ibid.*, 1980, **35**, 2170.
23. F. Ishikura, *Bunseki Kagaku*, 1982, **31**, 722.
24. N. Motekov, *Z. Anal. Chem.*, 1982, **313**, 141.
25. S. I. Gusev and L. M. Shchurova, *Zh. Analit. Khim.*, 1966, **21**, 1042.
26. S. I. Gusev and V. A. Vin'kova, *ibid.*, 1967, **22**, 552.
27. D. H. Templeton, G. W. Watt and C. S. Garner, *J. Am. Chem. Soc.*, 1943, **65**, 1608.
28. D. J. Johnson and T. M. Florence, *Talanta*, 1975, **22**, 253.

CALCULATION OF EQUILIBRIUM CONSTANTS FROM MULTIWAVELENGTH SPECTROSCOPIC DATA—IV

MODEL-FREE LEAST-SQUARES REFINEMENT BY USE OF EVOLVING FACTOR ANALYSIS

HARALD GAMPP, MARCEL MAEDER, CHARLES J. MEYER
 and ANDREAS D. ZUBERBÜHLER

Institute of Inorganic Chemistry, University of Basel, CH-4056 Basel, Switzerland

(Received 2 June 1986. Accepted 1 August 1986)

Summary—The newly developed algorithm of evolving factor analysis has been supplemented by iterative refinement. It allows the completely model-free calculation of concentration profiles and spectra from spectrophotometric and other spectroscopic data. Not even implicit use is made of the law of mass action. The results are practically identical with those based on a specific chemical model and classical least-squares refinement. Iterative evolving factor analysis is based on applying factor analysis successively to the set of the first 1, 2... M spectra of a spectrometric titration. The analysis is repeated from the opposite end and the eigenvalues thus calculated are combined into "concentration profiles" of completely abstract "species". These "concentration profiles" are iteratively refined by normalization, calculation of the absorption spectra from the normalized concentrations and recalculation of the concentration profiles from the absorption spectra. Evolving factor analysis is not restricted to spectrometric titrations, and can also be applied to peak resolution in chromatography using a multiwavelength (diode array) photometric or mass-spectrometric detection system, or to any other ordered set of multichannel data.

In our continuing efforts to optimize the technique of spectrophotometric titration¹ and its numerical treatment²⁻⁴ we have recently developed a new algorithm which allows a completely model-free semi-quantitative description of the underlying concentration profiles.⁵ After assignment of stoichiometric coefficients to these purely abstract species by chemical reasoning, very good estimates for the corresponding equilibrium constants are obtained. Since this algorithm is based on factor analysis (more specifically, principal component analysis, PCA⁶) and determines the evolution of factors as a function of the progressing titration, we propose to call it evolving factor analysis (EFA).

Evolving factor analysis can be carried much further by iterative refinement, using a variant of target factor analysis (TFA).⁶ Essentially perfect descriptions can be obtained for both concentration profiles and absorption spectra without relying on any specific chemical model and, in fact, without making even implicit use of the law of mass action. First results with this iterative version of EFA have been presented in a short communication.⁷ Here we wish to describe the mathematical details of EFA and to discuss the scope of this powerful algorithm on the basis of selected experimental and model data.

of absorbances Y into two smaller matrices of the concentrations C ($M \times S$) and the molar absorptivities A ($S \times W$), where M , S and W are the numbers of measured spectra, absorbing species and wavelengths (channels), respectively. (An analogous approach can be applied to resolution of chromatographic peaks.) Classically, this decomposition is achieved by obtaining the best non-linear least-squares fit for a given chemical model.^{3,4,8} Principal component analysis (PCA) accomplishes a related task, yielding an abstract $M \times S$ column matrix (score matrix, factor matrix) and an $S \times W$ row matrix (eigenvector matrix, loading matrix),⁶ respectively, together with a diagonal matrix of the eigenvalues Λ of the covariance matrix $M = Y \cdot Y$. In keeping with the notation used previously,^{3,4} we designate the abstract column and row matrices by L and E , respectively, equation (1). An alternative would be

$$\begin{array}{c} S \\ \boxed{C} \\ M \end{array} = \begin{array}{c} W \\ \boxed{A} \\ S \end{array} = \begin{array}{c} W \\ \boxed{Y} \\ M \end{array} = \begin{array}{c} S \\ \boxed{L} \\ M \end{array} = \begin{array}{c} W \\ \boxed{E} \\ S \end{array} \quad (1)$$

CA = Y = LE (1)

THE MATHEMATICAL CONCEPT OF EVOLVING FACTOR ANALYSIS

The primary goal in the analysis of spectrometric titrations is to decompose the original $M \times W$ matrix

the method of singular-value decomposition of Y

into the product of three matrices U , S and V , equation (2).⁹⁻¹²

$$Y = USV \quad (2)$$

The two results are closely related: $L = US$ and $V = E$, S being a diagonal matrix with the positive square roots of the eigenvalues λ in descending order. Columns of U and L , as well as rows of V and E , are orthogonal, equations (3) and (4).

$$U^t U = VV^t = EE^t = I \text{ (identity matrix)} \quad (3)$$

$$L^t L = A = S^2 \quad (4)$$

Recently, several authors dealing mainly with the closely related (and mathematically identical) problem of peak resolution in chromatography have tried a model-free decomposition of Y based on PCA and appropriate transformation of L and E , making use of the non-negativity of C and/or A and sometimes further restrictions based on assumptions with regard to the shape of the peaks.¹³⁻²⁰ Most of these methods seem to be confined to rather simple systems and apparently none has made full use of the information contained in the original data matrix, as we propose to do with EFA.

EFA consists of two more or less independent parts. The first of them, which we now call primary EFA, has been described in the preceding paper,⁵ but has been considerably streamlined since then in order to speed up the algorithm. Primary EFA consists of the following steps.

(i) PCA is performed on the original data matrix Y , equation (1), yielding S , the number of significant factors, L ($M \times S$), E ($S \times W$), and the level of residual noise $\sigma_y(\text{PCA})$, equation (5).

$$R_{\text{PCA}} = Y - LE;$$

$$\sigma_y(\text{PCA}) = \sqrt{\sum_{i=1}^M \sum_{j=1}^W R_{\text{PCA}}^2(i, j) / (M \times W - S)} \quad (5)$$

(ii) The eigenvalues λ_i of the covariance matrices $M_i = L_i^t L_i$ ($i = 1, 2, \dots, M$) are calculated successively. The L_i are $i \times S$ matrices made up of the first i rows of L . Note that the eigenvalues of the $S \times S$ matrices M_i are the same as the S largest eigenvalues associated with the corresponding $W \times W$ matrices $Y_i^t Y_i$ constructed from the original data. The numerical effort is, however, greatly reduced, as typical values are 3-5 for S and 20-40 for W . In addition, both the construction of M_i and the calculation of λ_i have been made very efficient. Starting from the preceding step $i - 1$, each element of M_i , $M_i(j, k)$ is simply obtained from equation (6), $L(i, j)$ and $L(i, k)$ being the j th and k th elements of row i from L .

$$M_i(j, k) = M_{i-1}(j, k) + L(i, j) \times L(i, k) \quad (6)$$

Also, the calculation of λ_i is very fast since the eigenvectors of the previous step $i - 1$ in general provide excellent starting values for their refinement by vector iteration.²¹ This part of the algorithm is

called forward EFA. The eigenvalues λ_i are combined into an $M \times S$ matrix of evolving factors or concentrations, C_f .

(iii) The eigenvalues thus calculated can be plotted as a function of the progressing titration. Since the eigenvalues span several orders of magnitude, their logarithms are more suitable for graphical representation. The evolution of an additional significant factor will indicate the formation of an additional species.

(iv) The analysis is repeated from the opposite direction, *i.e.*, starting with the last measurement and proceeding to the first (backward EFA, producing C_b). This backward evolution of new factors corresponds to the disappearance of factors (or species) with progressing titration.

(v) The j th forward curve (column j of C_f) is merged with the backward curve number $S + 1 - j$ (column $S + 1 - j$ of C_b , $j = 1, 2, \dots, S$), the smaller of the two corresponding eigenvalues always being retained. This combined matrix of abstract concentrations C_a is then normalized with respect to the total (analytical) concentration matrix C_{tot} . The normalized concentration matrix C_n is obtained by simple linear regression, equation (7).

$$C_n = C_a(C_a^t C_a)^{-1} C_a^t C_{\text{tot}} \quad (7)$$

Previously, the logarithms were combined instead of the actual eigenvalues.⁵

Primary EFA fulfils the following tasks. It gives the number of absorbing species (as PCA) and the ranges of existence of the individual species (not available through PCA). EFA indicates the correct number of species through the shape of the eigenvalue plots (forward and backward EFA) even in cases where PCA would not have detected all absorbing species because of linear dependence.⁵ Finally, it yields a semi-quantitative description of the concentration profiles, which allows direct estimation of equilibrium constants after assignment of stoichiometric coefficients to the so far purely abstract "species".

The goal of the second part, iterative EFA, is a quantitative calculation of the concentration profiles and absorption spectra, without making use of the law of mass action and still on a completely model-free basis. Essentially it performs a rotation of L and E into C and A , *cf.* equation (1), by a variant of target factor analysis (TFA).^{6,10,18-20} It does not make any assumptions with respect to the shape of the absorption spectra but uses all information which is available through primary EFA. The fundamental difference between iterative EFA and other approaches using TFA lies in the availability of an $M \times S$ defining or discriminating matrix D containing ones for significant and zeros for insignificant factors (or abstract concentrations C_a). Defining the border between significant and insignificant eigenvalues is to a certain degree arbitrary. It becomes problematic when a given concentration profile or spectrum can

be nearly represented by a linear combination of others and will fail completely if linear independence is not maintained at the level of experimental noise. However, normally this distinction is rather uncritical within reasonable limits. We have adopted the standard procedure of using the $(S + 1)$ th eigenvalue of \mathbf{M} as the discriminatory level, *i.e.*, for the construction of \mathbf{D} . Iterative EFA consists of steps (vi)–(x).

(vi) All concentration profiles are normalized to make their maximum concentration unity. At the end of the iterative process, equation (7) is applied in order to obtain the final concentrations. Obviously, this final use of equation (7) is impossible in the case of peak resolution in chromatography, where the analytical concentrations C_{tot} are unknown.

(vii) The molar absorptivities are calculated from the simple matrix equation (8) which is obtained by premultiplying equation (1) by $(\mathbf{L}^t \mathbf{C}_n)^{-1} \mathbf{L}^t$ and using \mathbf{C}_n in the place of the unknown concentrations \mathbf{C} .

$$\begin{aligned} \mathbf{A} &= (\mathbf{L}^t \mathbf{C}_n)^{-1} \mathbf{L}^t \mathbf{C}_n \mathbf{A} \\ &= (\mathbf{L}^t \mathbf{C}_n)^{-1} \mathbf{L}^t \mathbf{L} \mathbf{E} = (\mathbf{L}^t \mathbf{C}_n)^{-1} \mathbf{A} \mathbf{E} \quad (8) \end{aligned}$$

(viii) The matrix of residuals \mathbf{R} , and thus the sum of squares of errors, can be calculated from equation (9).

$$\begin{aligned} \mathbf{R} &= \mathbf{L} \mathbf{E} - \mathbf{C}_n \mathbf{A} = \mathbf{L} \mathbf{E} - \mathbf{C}_n (\mathbf{L}^t \mathbf{C}_n)^{-1} \mathbf{A} \mathbf{E} \\ &= (\mathbf{L} - \mathbf{C}_n (\mathbf{L}^t \mathbf{C}_n)^{-1} \mathbf{A}) \mathbf{E} \quad (9) \end{aligned}$$

Normally, the actual residuals are not needed and further simplification is possible by dropping the eigenvector matrix \mathbf{E} . The sum of squares Sq is then obtained by equation (10). This is possible because of the orthonormality of rows in \mathbf{E} .³

$$\mathbf{R}' = \mathbf{L} - \mathbf{C}_n (\mathbf{L}^t \mathbf{C}_n)^{-1} \mathbf{A}; \quad Sq = \sum_{i=1}^M \sum_{j=1}^S R'^2(i, j) \quad (10)$$

(ix) Next, the concentrations \mathbf{C}_n are recalculated. This is achieved successively for each row i ($i = 1, \dots, M$) by linear regression, equation (11), using a discriminating spectra matrix \mathbf{A}_d which contains the spectra of only those species j with a non-zero discriminating element $D(i, j)$ of \mathbf{D} .

$$\mathbf{C}_n(i) = \mathbf{L} \mathbf{E} \mathbf{A}_d^t (\mathbf{A}_d \mathbf{A}_d^t)^{-1} \quad (11)$$

Numerous test calculations have shown that the much faster alternative^{10,19,20} of recalculating the entire concentration matrix directly by using the result of singular value decomposition, equation (2), and then treating insignificant concentrations as zero, equation (12), has much inferior converging properties.

$$\mathbf{C}_n = \mathbf{U} \mathbf{U}^t \mathbf{C}_n \quad (12)$$

(x) The iterative cycle is closed by treating all negative concentrations obtained through equation (11) as zero.

Some additional points should be noted. (a) The iterative cycle (vi–x) is rather simple and needs about

1 sec for a data set of 28 spectra at 21 wavelengths for 4 absorbing species, on an HP 9000/310 desk computer. (b) Convergence, while normally very fast at the beginning tends to become sluggish close to the minimum, somewhat similarly to the algorithm of steepest descent in least-squares calculations. The iterative process has been made much faster by calculating a shift matrix from the difference in \mathbf{C}_n in two successive cycles, and obtaining a stretching factor Sf for all shifts, by a normal Newton–Gauss algorithm with Sf as the adjustable parameter. (c) The algorithm described thus far occasionally tends to converge to secondary local minima. Surprisingly, this could be overcome in our calculations by rejecting values below 1 for the stretching factor and using a relatively high value ($Sf = 5\text{--}50$) instead. All calculations to be described below were done with $Sf = 15$ in such cases. Although this iterative strategy may look chaotic, it turns out to be very efficient and quite reliable even in rather tricky cases. (d) As discussed above, the result of primary EFA was normally used as the starting set for the iterative refinement. This is, however, not at all critical. Convergence was equally well obtained by starting from the discriminating matrix \mathbf{D} or from needle-like distribution curves¹⁹ with the maxima of the primary EFA as the only non-zero concentrations. (e) If complexation is very strong and more than one species is present from the beginning, the use of fixed spectra can be helpful. Obviously, the spectrum of the uncomplexed metal ion is normally available independently and is an obvious candidate for the inclusion of fixed spectra. (f) Instead of the eigenvector representation $\mathbf{L} \mathbf{E}$ and equations (8), (10) and (11), the original data matrix \mathbf{Y} and equations (13)–(15) could be used directly.^{7,22}

$$\mathbf{A} = (\mathbf{C}_n^t \mathbf{C}_n)^{-1} \mathbf{C}_n^t \mathbf{Y} \quad (13)$$

$$\mathbf{R} = \mathbf{Y} - \mathbf{C}_n \mathbf{A} \quad (14)$$

$$\mathbf{C}_n = \mathbf{Y} \mathbf{A}^t (\mathbf{A} \mathbf{A}^t)^{-1} \quad (15)$$

As expected, the results obtained with the two algorithms are practically identical, but the second is both slower and more demanding on computer memory. Therefore, the algorithm using standard linear regression, equations (13)–(15), was not retained in the final program.

RESULTS AND DISCUSSION

All calculations were done on an HP 9000/310 desk top computer. The EFA algorithm has been included in the BASIC version of our program SPECFIT⁴ for the calculation of equilibrium constants from spectrophotometric data. Iterative EFA has been successfully tested on roughly a dozen chemical systems of varying complexity, and the results compared with those obtained by using the law of mass action.^{7,23} In the present paper we specifically discuss the complexation of Cu^{2+} with 3,7-diazanonediamide

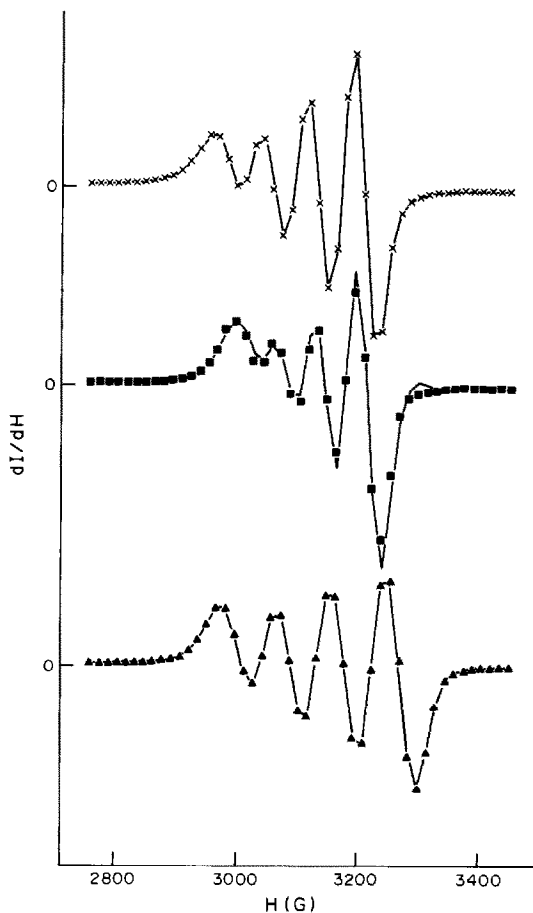


Fig. 1. ESR spectra of Cu^{2+} complexes with DANA. Points calculated by using the law of mass action; \times : CuL^{2+} , \blacksquare : CuLH_{-1}^{+} , \blacktriangle : CuLH_{-2} . — Spectra calculated by using EFA.

(DANA), using spectrophotometric^{7,24} and ESR²⁵ data.

In the first contribution, dealing with primary EFA only,⁵ ESR data for the complexation of Cu^{2+} by DANA (L) were used as one of the test systems. Four species, Cu^{2+} and the three complexes CuL^{2+} , CuLH_{-1}^{+} and CuLH_{-2} contribute to the overall ESR signal. As shown in Fig. 1, the individual ESR spectra of CuL^{2+} , CuLH_{-1}^{+} and CuLH_{-2} calculated by iterative EFA are virtually identical with those obtained by a classical analysis using the law of mass action (LMA). For the analysis presented in Fig. 1, the spectrum of free Cu^{2+} , which of course can be obtained independently in the absence of ligand, was kept constant (entry 2 in Table 1). It may be noted that (i) the final standard deviation of the EFA residuals is less than that of the LMA result (see entries 1 and 2 in Table 1); (ii) there is no independent test to give preference to either the EFA or LMA results; (iii) the EFA result has been obtained not only in a completely model-free way, but also without making any use of the pH-values of the individual solutions. The measurement of pH is thus superfluous with regard to the EFA analysis, *i.e.*, if only the ESR spectra, but not the equilibrium constants, are to be determined.

The same kind of analysis is of course equally possible by use of spectrophotometric data (entries 3 and 4 in Table 1), as discussed in the first note on iterative EFA.⁷ As shown in Figs. 2 and 3, very good agreement between LMA and EFA results is obtained. If the spectrum of uncomplexed Cu^{2+} is again taken as that found experimentally, the two results become almost indistinguishable, as is also indicated by the relative standard deviation of only 0.7%

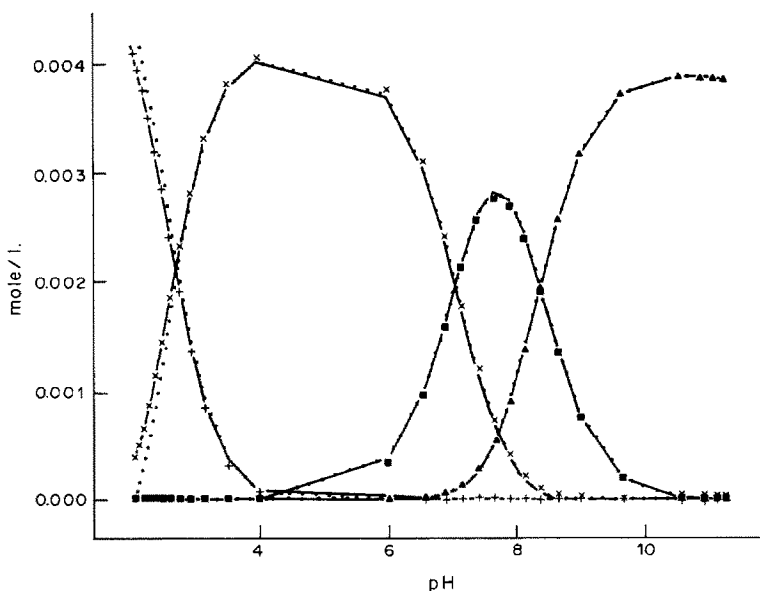


Fig. 2. Concentration profiles of Cu^{2+} complexes with DANA. Data from spectrophotometric measurements, $c_L = 0.005M$, $c_{\text{Cu}} = 0.0045M$. $+$: Cu^{2+} , \times : CuL^{2+} , \blacksquare : CuLH_{-1}^{+} , \blacktriangle : CuLH_{-2} . EFA results with fixed (—) and freely adjustable (····) spectrum for Cu^{2+} .

Table 1. Comparison of results obtained by using the law of mass action (LMA), principal component analysis (PCA) and evolving factor analysis (EFA)

	Stability constants*				pH-range	σ (pH)	$\sigma_y (\times 10^4)$				$\sigma_{C_v} \% \dagger$
	β_{111}	β_{110}	β_{11-1}	β_{11-2}			gen	LMA	PCA	EFA	
1	—	12.18	5.02	-3.27	2.0-11.6	—	—	54.0	43.3	51.8	7.1
2‡	—	12.18	5.02	-3.27	2.0-11.6	—	—	54.0	43.3	51.9	2.0
3	—	12.11	5.02	-3.34	2.0-11.2	—	—	5.6	3.28	3.49	1.4
4‡	—	12.11	5.02	-3.34	2.0-11.2	—	—	5.6	3.28	3.55	0.7
5	—	12.00	5.00	-3.50	2.0-11.0	0.008	2.0	3.4	1.71	1.77	0.8
6‡	—	12.00	5.00	-3.50	2.0-11.0	0.008	2.0	3.4	1.71	1.77	0.2
7	—	10.00	5.00	-0.32	2.0-8.0	0.008	2.0	4.0	1.71	1.78	0.5
8	—	10.00	4.70	-0.32	2.0-8.0	0.008	2.0	4.0	1.71	1.78	0.5
9	—	10.00	4.40	-0.32	2.0-8.0	0.008	2.0	3.9	1.71	1.80	0.8
10	—	10.00	4.00	-0.32	2.0-8.0	0.008	2.0	3.9	1.71	1.80	2.1
11	—	10.00	3.70	-0.32	2.0-8.0	0.008	2.0	3.9	1.71	1.78	3.1
12	—	10.00	3.40	-0.32	2.0-8.0	0.008	2.0	3.9	1.71	1.80	4.8
13	—	10.00	5.00	-0.32	2.3-8.0	0.008	2.0	4.6	1.71	1.77	1.1
14	—	10.00	5.00	-0.32	2.5-8.0	0.008	2.0	5.3	1.71	1.78	0.8
15	—	10.00	5.00	-0.32	2.8-8.0	0.008	2.0	5.5	1.71	1.77	1.0
16	—	10.00	5.00	-0.32	3.0-8.0	0.008	2.0	5.0	1.71	1.77	21.5
17	—	10.00	5.00	-0.32	3.3-8.0	0.008	2.0	4.3	1.71	2.00	20.0
18	—	10.00	5.00	-0.32	3.5-8.0	0.008	2.0	3.8	1.71	1.90	6.8
19‡	—	10.00	5.00	-0.32	2.3-8.0	0.008	2.0	—	1.71	1.77	1.4
20‡	—	10.00	5.00	-0.32	2.5-8.0	0.008	2.0	—	1.71	1.77	1.0
21‡	—	10.00	5.00	-0.32	2.8-8.0	0.008	2.0	—	1.71	1.77	1.2
22‡	—	10.00	5.00	-0.32	3.0-8.0	0.008	2.0	—	1.71	1.81	1.4
23‡	—	10.00	5.00	-0.32	3.3-8.0	0.008	2.0	—	1.71	1.80	1.4
24‡	—	10.00	5.00	-0.32	3.5-8.0	0.008	2.0	—	1.71	1.81	2.3
25	—	10.00	5.00	-0.32	2.0-8.0	0.008	5.0	6.0	4.27	4.50	1.0
26	—	10.00	5.00	-0.32	2.0-8.0	0.008	10.0	10.2	8.53	9.00	1.2
27	—	10.00	5.00	-0.32	2.0-8.0	0.008	20.0	19.2	17.1	17.9	2.7
28	—	10.00	5.00	-0.32	2.0-8.0	0.008	40.0	37.8	34.1	85.5	2.9
29	—	10.00	5.00	-0.32	2.0-8.0	0.002	2.0	2.1	1.71	1.77	0.5
30	—	10.00	5.00	-0.32	2.0-8.0	0.004	2.0	2.6	1.71	1.77	0.5
31	—	10.00	5.00	-0.32	2.0-8.0	0.016	2.0	8.7	1.71	1.77	0.5
32	13.00	7.30	0.00	-8.52	2.0-11.0	0.008	2.0	3.1	1.62	1.69	1.7
33	13.00	7.30	0.00	-8.00	2.0-11.0	0.008	2.0	3.2	1.62	1.70	2.3
34	13.00	7.30	0.00	-7.52	2.0-11.0	0.008	2.0	3.4	1.62	1.86	3.1

*Logarithms of overall formation constants $\beta_{mnh} = [M_m L_n H_n] / [M]^m [L]^n [H]^n$.

†Relative standard deviation between concentrations based on LMA and EFA. For model data, input concentrations were used in place of the LMA results.

‡Results obtained with fixed spectrum for Cu^{2+} .

between the concentration profiles of the LMA and EFA treatments, respectively. As with the ESR data, the residuals for the EFA are smaller than for the LMA counterpart, which is expected because the former is not influenced by any errors in the pH-measurement.

For a more systematic study of the scope and possible limitations of EFA we relied on semi-synthetic data (entries 5–34 in Table 1). This allows analysis under closely controlled conditions. More important, it is necessary because there are relatively few equilibrium systems of sufficient complexity (more than two or three absorbing species) for which the chemical model is absolutely unambiguous, and also these systems cannot be expected to have optimum properties for disclosure of the influence of specific factors such as the range of species co-existence, the pH-range covered by the original data, and experimental errors. The following strategy was adapted for data generation. For the spectral matrix

A of the individual species, the spectra calculated for DANA by classical least-squares analysis (*cf.* Fig. 3) were taken; a concentration matrix **C** was calculated by using the LMA for the model Cu^{2+} , CuL^{2+} , CuLH_{-1}^+ and CuLH_{-2} with variable sets of equilibrium constants at 28 equidistant pH values. From **C** and **A** the original absorbance matrix \mathbf{Y}_{orig} was calculated: $\mathbf{Y}_{\text{orig}} = \mathbf{C}\mathbf{A}$. Random errors were superimposed on \mathbf{Y}_{orig} and on the pH values. The resulting arrays **Y** and **pH** were used as the raw data. Normally, standard errors $\sigma_y = 2 \times 10^{-4}$ and $\sigma_{\text{pH}} = 8 \times 10^{-3}$ were used, *i.e.*, the values which correspond to our experimental work, excluding systematic errors.¹ The values of the stability constants, the pH range, and the levels of the random errors are compiled in Table 1. The results are given in the last four columns: the standard deviations in the absorbance obtained by using the law of mass action $\sigma_y(\text{LMA})$, principal component analysis $\sigma_y(\text{PCA})$, and evolving factor analysis $\sigma_y(\text{EFA})$, respectively, and σ_C , the

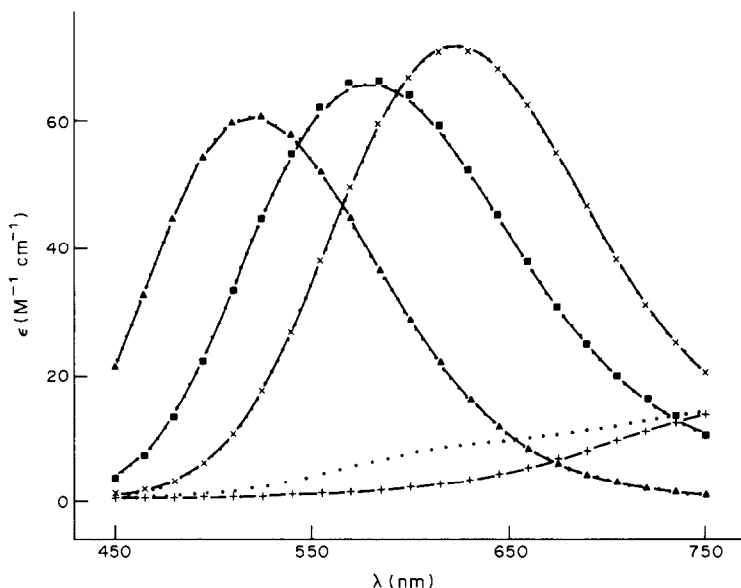


Fig. 3. Absorption spectra of Cu^{2+} complexes with DANA. +: Cu^{2+} , \times : CuL^{2+} , \blacksquare : CuLH^+_{-1} , \blacktriangle : CuLH^-_{-2} . EFA results with fixed (—) and freely adjustable (····) spectrum for Cu^{2+} .

relative standard deviation* between the concentrations used for construction of the data matrix and those calculated by EFA.

$\sigma_y(\text{PCA})$ is the lowest possible error to describe the data with a given number of factors, no restrictions being imposed on the numerical values (of \mathbf{L} and \mathbf{E}). Obviously, errors in \mathbf{Y} and \mathbf{pH} contribute to $\sigma_y(\text{LMA})$. $\sigma_y(\text{EFA})$ is not influenced at all by the errors in \mathbf{pH} , but there are the restrictions of non-negative concentrations and of the concentration windows for the individual species. Therefore, $\sigma_y(\text{EFA})$ must be higher than $\sigma_y(\text{PCA})$, but the difference should be of the order of the experimental noise in \mathbf{Y} alone. It is thus postulated by theory for a successful analysis, that the standard deviation $\sigma_y(\text{EFA})$ lies between the corresponding values of the LMA fit, $\sigma_y(\text{LMA})$, and of the principal component analysis, $\sigma_y(\text{PCA})$, as is found in most cases. It must be realized, however, that a low $\sigma_y(\text{EFA})$ does not *per se* prove that the result gives the correct concentration profiles and spectra. In this respect, the last column in Table 1, σ_c , is more directly relevant. Most of the σ_c values are between 0.5 and 2%, indicating good correlation between the input and calculated concentration profiles.

Entries 5 and 6 closely correspond to the spectrophotometric data for DANA. Equidistant pH values were used and random errors superimposed on \mathbf{Y}_{orig} and \mathbf{pH} as described, but the pH-range and the set of stability constants are as in the experimental

system (entries 3 and 4). Complexation starts at rather low pH with DANA, so for the experimental data (1–4) as well as the model data (5 and 6) significant amounts of CuL^{2+} are present from the beginning of the titration. This is of no consequence with respect to the analysis, as far as $\sigma_y(\text{EFA})$ is concerned (compare 1, 3, 5 with 2, 4, 6). It is, however, important with respect to σ_c and thus to the concentration profile as well as the calculated spectrum of the free metal ion, as is also evident from Figs. 2 and 3.

As can be seen in Fig. 2, overlap of the concentration profiles is relatively weak for DANA. The problem thus was made more demanding by decreasing the stability of CuL^{2+} and assuming deprotonation of the two amide groups of DANA to produce CuLH^+_{-1} and CuLH^-_{-2} at lower pH values. Simultaneously, the pH range was decreased to 2–8. As indicated by entry 7, the analysis is as successful as with the original set for DANA, despite considerable overlap of all the concentration profiles and although CuLH^+_{-1} has a maximum relative concentration of 30%. Entries 8–12 show the effect of successively reducing the stability of CuLH^+_{-1} , keeping all other parameters at the values for entry 7. With an essentially constant $\sigma_y(\text{EFA})$ of 1.8×10^{-4} the fit in σ_c gets gradually poorer, but as seen in Fig. 4 (corresponding to entry 9) even a minor species with a maximum relative concentration of 15% can be successfully identified. In fact the range of species existence, position of concentration maxima and general shape of the profiles are calculated correctly for all species even in the still more critical cases 10–12. The only significant discrepancy is the height of the profile corresponding to CuLH^+_{-1} , which is generally elevated. Even when the maximum relative

$$*\sigma_c = 100 \sqrt{\sum_{i=1}^M \sum_{j=1}^S \{ [C(i,j) - C_n(i,j)] / C_{\text{tot}}(i) \}^2 / \nu}$$

where $C(i,j)$ are the concentrations based on LMA (experimental data) or used for construction of \mathbf{Y} (model data), and ν = number of degrees of freedom.

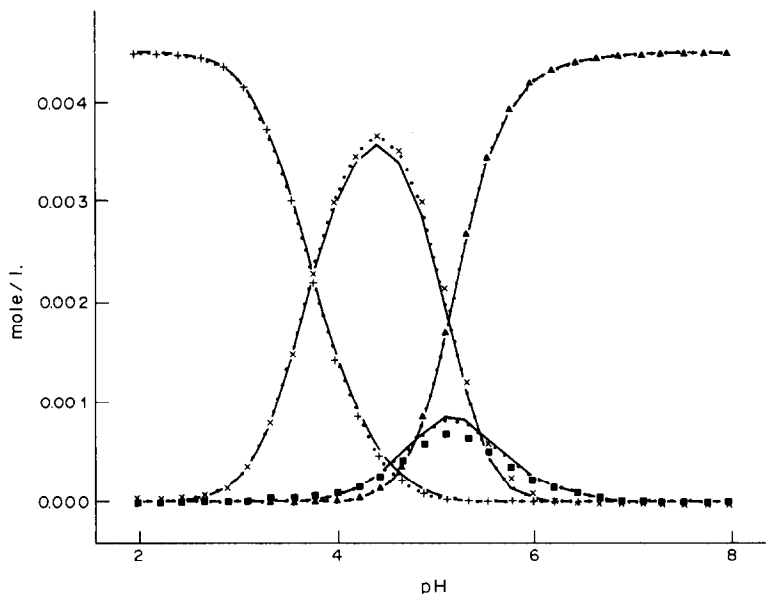


Fig. 4. Concentration profiles of model data using $c_1 = 0.005M$, $c_{Cu} = 0.0045M$, $\log \beta_{110} = 10.00$, $\log \beta_{11-1} = 4.40$, and $\log \beta_{11-2} = -0.32$. Symbols as in Fig. 2.

concentration of $CuLH_{-1}^+$ is reduced to less than 2% (entry 12), EFA still finds four absorbing species and essentially the correct ranges of existence.

The effect of narrowing the pH range in data generation is shown in entries 13–24. With the first cuts, the analysis is still unproblematic with either adjustable (13–15) or fixed (19–21) values for the spectrum of Cu^{2+} , but this is no longer true when the analysis begins at still higher pH values. When such data are used, CuL^{2+} appears to be present in high amounts right from the beginning, and the calculated concentration profiles as well as the spectra of Cu^{2+}

and CuL^{2+} are seriously in error (16–18) unless the spectrum of Cu^{2+} is fixed at the correct value (22–24). Since the present iterative algorithm does not guarantee to yield the real minimum of $\sigma_y(\text{EFA})$, it is not yet clear whether the unsatisfactory results in (16–18) are due to divergence or to truly insufficient information contained in the data matrix.

In entries 25–31 the effect of varying noise levels is analysed. The stability constants and pH range used correspond to the standard set 7. As expected, $\sigma_y(\text{EFA})$ closely parallels the random noise in the absorbances used for data generation, $\sigma_y(\text{gen})$,

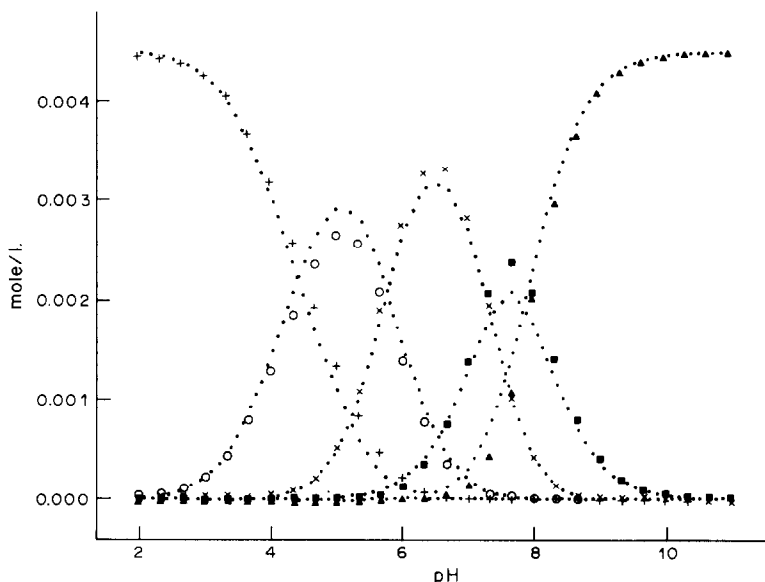


Fig. 5. Concentration profiles with model data for 5 absorbing species, cf. Table 1, entry 33. \circ : $CuLH^{3+}$, other symbols as in Fig. 2.

(25–28) with a less pronounced effect on σ_C . On the other hand, EFA necessarily is completely independent of pH errors, σ_{pH} , which have an effect only on the LMA analysis (29–31).

A few additional calculations were done with data matrices based on a model with 5 absorbing species. CuLH^{3+} ($\lambda_{\text{max}} = 684 \text{ nm}$, $\epsilon_{\text{max}} = 57 \text{ l.mole}^{-1}.\text{cm}^{-1}$) was assumed in addition to the species discussed above. The pH range and equilibrium constants were chosen so that significant overlap of the concentration profiles was obtained. As indicated by entries 32–34 and as shown in Fig. 5, the presence of an additional species does not qualitatively complicate matters: $\sigma_y(\text{EFA})$ is again close to the random noise of the input data and σ_C is still acceptable in all cases. Ranges of species existence, shapes of concentration profiles, peak positions and maximum concentrations are all of similar quality as in the four-component cases and there is no reason to exclude successful resolution of even more complicated systems.

Given the quality of the EFA calculations, equilibrium constants may be obtained directly from the abstract concentration profiles after assigning stoichiometric coefficients to the individual species by chemical reasoning. For the original data with DANA (entry 4), simple linear interpolation gives points of intersection at pH 2.72, 7.06 and 8.39, respectively. With the aid of the protonation constants of the free ligand, $\log K_{\text{LH}}^{\text{H}} = 8.40$ and $\log K_{\text{LH}_2}^{\text{H}} = 6.55$, equilibrium constants are calculated for the copper complexes: CuL^{2+} , $\log \beta_{110} = 12.10$; CuLH_{-1}^+ , $\log \beta_{11-1} = 5.04$; CuLH_{-2} , $\log \beta_{11-2} = -3.35$. These values are virtually identical with those obtained by a least-squares analysis based on the LMA and the same protonation constants for the uncomplexed ligand: $\log \beta_{110} = 12.11$, $\log \beta_{11-1} = 5.02$ and $\log \beta_{11-2} = -3.34$. The EFA result is certainly correct within experimental uncertainty in this case and the same is true for most systems included in Table 1. Therefore, even the final stage of data reduction to a set of equilibrium constants is possible on the basis of EFA.

CONCLUSIONS

The calculations presented here and application of EFA to roughly a dozen real chemical systems^{5,7,23} have convinced us that EFA is an efficient and reliable new method for the completely model-free analysis of spectrophotometric data and, in fact, of any two-dimensional array of ordered data with contiguous ranges of "species" existence along one dimension. The decisive part is primary EFA,⁵ which defines these ranges for all species and also yields reasonable starting values for the concentration matrix. As discussed in the previous paper,⁵ primary EFA can give useful information about the formation of additional species, including estimates of the corresponding stability constants, even in cases where

classical factor analysis would not even have given the correct number of species.

There can be no doubt that EFA can be successfully applied to problems rather different from the analysis of complex equilibria. One most promising field is peak resolution in chromatography, a problem which is extensively discussed in the recent literature.^{26,27} EFA seems to be ideally suited to deal with this problem²² since individual chromatographic peaks normally have rather similar concentration profiles, minimizing the danger of erroneous combination of forward and backward EFA and consequent setting up of wrong ranges for non-zero concentrations of the individual species. This application of EFA may actually be more important than the one discussed here, because there is no other reliable algorithm (such as the LMA) to deal with that problem.

The iterative part of EFA is an application of target factor analysis.^{10,19,20} Similar approaches for iterative refinement starting from a given estimated concentration matrix have been discussed recently.^{19,20} None of the earlier approaches could, of course, make use of the information and restrictions resulting from primary EFA through the discriminating matrix *D*, which is the decisive factor for a successful analysis.

Acknowledgement—This work was supported by the Swiss National Science Foundation (Grant No. 2.213-0.81).

REFERENCES

1. G. Hänisch, Th. A. Kaden and A. D. Zuberbühler, *Talanta*, 1979, **26**, 563.
2. H. Gampp, M. Maeder and A. D. Zuberbühler, *ibid.*, 1980, **27**, 1037.
3. H. Gampp, M. Maeder, C. J. Meyer and A. D. Zuberbühler, *ibid.*, 1985, **32**, 95.
4. *Idem*, *ibid.*, 1985, **32**, 257.
5. *Idem*, *ibid.*, 1985, **32**, 1133.
6. E. R. Malinowski and D. G. Howery, *Factor Analysis in Chemistry*, Wiley, New York, 1980.
7. H. Gampp, M. Maeder, C. J. Meyer and A. D. Zuberbühler, *Chimia*, 1985, **39**, 315.
8. *Computational Methods for the Determination of Formation Constants*, D. J. Leggett (ed.), Plenum Press, New York, 1985.
9. G. H. Golub and C. Reinsch, *J. Numer. Math.*, 1970, **14**, 403.
10. A. Lorber, *Anal. Chem.*, 1984, **56**, 1004.
11. S. D. Frans and J. M. Harris, *ibid.*, 1985, **57**, 1718.
12. E. Sánchez and B. R. Kowalski, *ibid.*, 1986, **58**, 496.
13. M. A. Sharaf and B. R. Kowalski, *ibid.*, 1982, **54**, 1291.
14. D. W. Osten and B. R. Kowalski, *ibid.*, 1984, **56**, 991.
15. A. Meister, *Anal. Chim. Acta*, 1984, **161**, 149.
16. B. Vandeginste, R. Essers, T. Bosman, J. Reijnen and G. Kateman, *Anal. Chem.*, 1985, **57**, 971.
17. S. D. Frans, M. L. McConnell and J. M. Harris, *ibid.*, 1985, **57**, 1552.
18. W. Lindberg, J. Oehman and S. Wold, *ibid.*, 1986, **58**, 299.

19. P. J. Gemperline, *J. Chem. Inf. Comput. Sci.*, 1984, **24**, 206.
20. B. G. M. Vandeginste, W. Derks and G. Kateman, *Anal. Chim. Acta*, 1985, **173**, 253.
21. H. R. Schwarz, H. Rutishauser and E. Stiefel, *Matrizennumerik*, Teubner, Stuttgart, 1972.
22. M. Maeder and A. D. Zuberbühler, *Anal. Chim. Acta*, 1986, **181**, 287.
23. M. Briellmann, Th. A. Kaden, S. Kaderli, C. J. Meyer and A. D. Zuberbühler, in preparation.
24. A. D. Zuberbühler and Th. A. Kaden, *Talanta*, 1979, **26**, 141.
25. H. Gampp, *Inorg. Chem.* 1984, **23**, 1553.
26. I. E. Frank and B. R. Kowalski, *Anal. Chem.*, 1982, **54**, 232R.
27. M. F. Delaney, *ibid.*, 1984, **56**, 261R.

AN ANALYTICAL SCHEME FOR DETERMINING FORMS OF SULPHUR IN OIL SHALES AND ASSOCIATED ROCKS

M. L. TUTTLE and M. B. GOLDBABER

U.S. Geological Survey, MS 916, Box 25046, Denver Federal Center, Denver, CO 80225, U.S.A.

D. L. WILLIAMSON

Department of Physics, Colorado School of Mines, Golden, CO 80401, U.S.A.

(Received 21 December 1985. Accepted 1 August 1986)

Summary—An analytical scheme for determining various forms of sulphur in oil shales and associated rocks is presented. Acid-soluble sulphate, sulphur contained in monosulphide and in disulphide minerals, and organically-bound sulphur are all quantitatively recovered as separate fractions. Finely-ground oil-shale samples are treated in an inert atmosphere with 6*M* hydrochloric acid to dissolve the acid-soluble sulphate minerals and form H₂S from the decomposition of monosulphide minerals. The acid-soluble sulphate is precipitated as barium sulphate and the H₂S is collected and weighed as silver sulphide. Disulphide minerals in the solid residue from the acid treatment are reduced by an acidified Cr(II) solution in an inert atmosphere, releasing the sulphide as H₂S. The H₂S is collected as silver sulphide. An Eschka fusion oxidizes and solubilizes all sulphur remaining within the Cr(II)-treated residue. This sulphate represents organically-bound sulphur and is collected as barium sulphate. The analytical procedures have been verified by using ⁵⁷Fe Mössbauer spectroscopy. Good agreement between the chemical and Mössbauer data substantiated the sequential removal of the forms of sulphur and also demonstrated the ability of Mössbauer spectroscopy to determine the absolute quantities of iron present in specific minerals.

The concentrations of individual forms of sulphur in oil shale provide information that can be applied to studies of (1) the natural cycling of sulphur in oil-shale deposits, (2) the development potential of oil-shale deposits, and (3) the probable partitioning and the effects of sulphur compounds during oil-shale distillation.

The analytical scheme reported in this paper was developed in order to facilitate studies of the sulphur geochemistry of oil shale in the Green River Formation (Eocene) of Colorado, Utah, and Wyoming. Various chemical techniques developed by other researchers are modified and combined. The modified techniques are an improvement on previous versions because they provide for quantitative separation and collection of the major forms of sulphur in the oil shale. In addition, the scheme is readily adaptable to studies on sediment types (*e.g.*, coal, marine or freshwater sediments).

The analytical scheme was specifically designed to detect the sulphur-bearing phases of the Green River Formation. Concentrations of total sulphur range from undetectable in algal carbonates in the Uinta basin, Utah,¹ to 5% in organic-rich marlstones from the saline zone in the Piceance basin, Colorado.² The sulphur is known from previous work to occur as sulphate, monosulphide, disulphide and organically-bound sulphur. The abundance of sulphate in the oil shale is low (less than 4% of the total sulphur^{3,4}) and discrete sulphate minerals have not been identified in

the formation.⁵ Occurrences of monosulphides [pyrrhotite (Fe_{1-x}S) and wurtzite (ZnS)] and disulphides [pyrite (cubic FeS₂) and marcasite (orthorhombic FeS₂)] have been reported.⁵⁻⁹ Monosulphides have not previously been quantified, but are considered to be a minor sulphur phase. Between 50 and 90% of the sulphur in most Green River oil shales resides in pyrite, with the remaining 10-50% occurring as organically-bound sulphur.^{3,10} Sulphur-containing organic compounds in the Green River oil shales include thiophenes, benzothiophenes, and polycyclic thiols.¹¹

Before this study, two different analytical schemes were used to quantify sulphur forms. We chose not to use either of these schemes, for reasons discussed below. One of them³ involves determination of total sulphur by Eschka fusion. Acid-soluble sulphates are dissolved with hydrochloric acid, and pyritic sulphur is quantified by oxidation with nitric acid and subsequent determination of the solubilized iron. Organic sulphur concentrations are determined by difference. Monosulphide sulphur is not separately determined and there is no collection of the sulphur associated with the various forms. Collection of the separate sulphur species is a critical requirement for our geochemical study, because we want to measure the isotopic composition of the sulphur in the various forms. Furthermore, there is some debate regarding the effectiveness of nitric acid in removing pyritic sulphur without removing some organically-bound

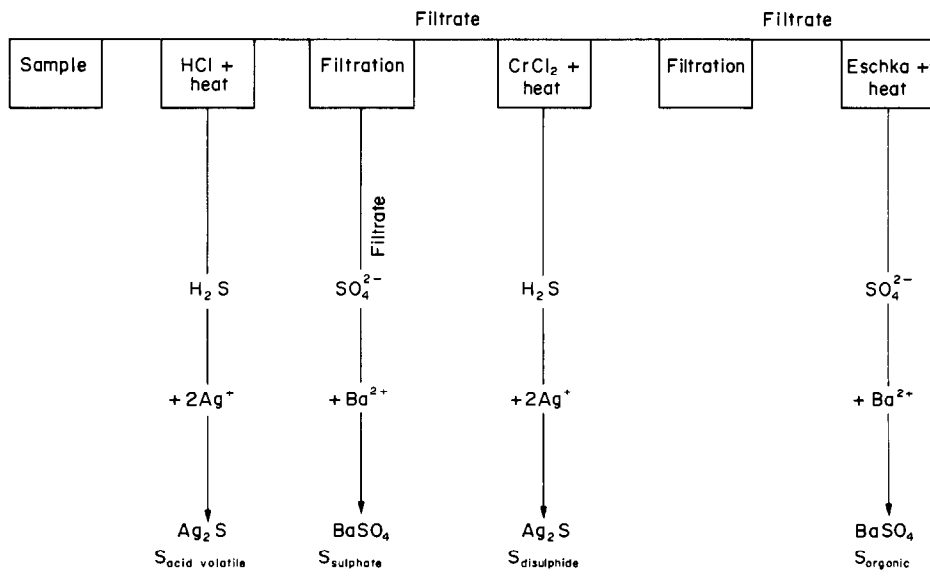


Fig. 1. A diagrammatic representation of the analytical scheme used to separate various forms of sulphur in oil shales and associated rocks.

sulphur. Pyritic sulphur could also be overestimated if non-pyritic iron is released during the nitric acid oxidation.

The second procedure⁴ uses perchloric acid to dissolve the acid-soluble sulphates. Pyritic sulphur is determined by a lithium aluminium hydride (LAH) reduction technique. Organic sulphur is determined by difference or by an Eschka fusion of the residue from the LAH reduction. Again, monosulphide sulphur is ignored. The LAH technique, although commonly used in the analysis of other sedimentary materials, is not used in our scheme because (1) the reagent can be very explosive, and (2) yields for LAH-reduction of pure pyrite are often low. Results from Kuhn *et al.*¹² indicate that the particle size of the sample should be smaller than -400 mesh for quantitative recovery of the pyritic sulphur.

Our analytical scheme is shown diagrammatically in Fig. 1. It is designed to sequentially collect and gravimetrically determine the sulphur species discussed above. The sulphur associated with monosulphide and acid-soluble sulphate minerals is removed first, by treatment of the sample with hydrochloric acid in an inert atmosphere. Monosulphide minerals evolve H_2S when treated with hydrochloric acid and are hence referred to as acid-volatile (av) sulphides (S_{av}). The method we employ in collecting and determining these two forms of sulphur is a modification of ASTM method D2492,¹³ which is generally used in determining sulphate. The H_2S (S_{av}) is collected and weighed as silver sulphide and the acid-soluble sulphate (S_{SO_4}) is precipitated as barium sulphate.

The second step removes disulphide sulphur (S_{di}) bound in the minerals pyrite and marcasite. These minerals are not decomposed during the hydrochloric

acid treatment, so disulphides can be easily separated from the monosulphide minerals. The disulphide method which best fits our needs is a modification of a technique¹⁴ to separate pyritic sulphur in recent marine sediments and rocks. The procedure uses chromium(II) to reduce the disulphides to H_2S , which is then collected as silver sulphide.

The last step in the scheme removes organically-bound sulphur (S_{org}). Organic sulphur concentrations are determined as the total sulphur remaining after removal of the S_{SO_4} , S_{av} , and S_{di} . The method is a modification of ASTM method D3177.¹³ The residue from the chromium(II) treatment is fused with Eschka mixture (magnesium oxide and sodium carbonate). The fusion product is dissolved in water and the organic sulphur precipitated as barium sulphate.

Mössbauer spectroscopy of iron-containing phases, as well as the chemical and/or Mössbauer determination of the iron content of solutions and residues from each step within the scheme, gave the primary data used in validating the techniques. Earlier studies^{9,15,16} of coal and oil shales have demonstrated that Mössbauer spectroscopy can identify a variety of iron-containing compounds in these very complex materials and provide quantitative values of the absolute abundances of such compounds.^{15,16} Sulphur and iron mass-balances, standard addition of pure pyrite to samples, and analyses of pure and mixed sulphur compounds were also used to test the effectiveness of the analytical scheme.

EXPERIMENTAL

Samples

Three samples from the Green River Formation were used for developing and testing the analytical scheme. The

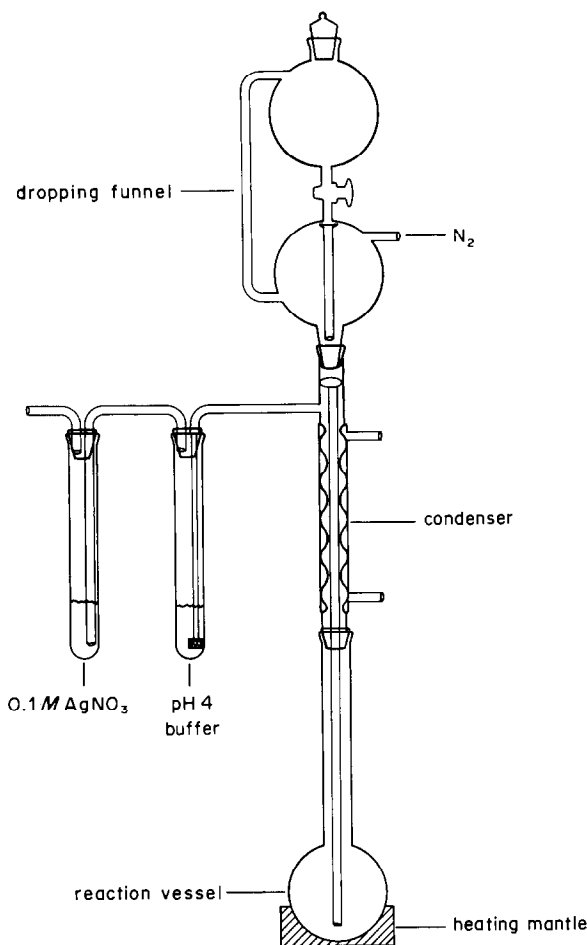


Fig. 2. Apparatus used to analyse for acid-volatile and disulphide sulphur.

samples were chosen to represent different sulphur mineral assemblages, organic carbon contents, and particle sizes. Two rich oil shales from the Mahogany zone (MZ) of the Parachute Creek Member, Rio Blanco County, Colorado were chosen to represent organic-rich samples containing abundant, finely-disseminated sulphides. Sample MZ-1 was collected from a mine at Anvil Points, Colorado and ground to -65 mesh. Pyrite and small amounts of pyrrhotite had previously been identified in this sample.⁹ Sample MZ-2 was collected from the Rulison mine approximately 5 km from Anvil Points and ground to -100 mesh. The third sample was collected from drill core from the Wilkins Peak Member (WP) in Sweetwater County, Wyoming. This sample (WP-1) was ground to -100 mesh and contained low amounts of organic matter and abundant pyrrhotite.

Apparatus

Jones reductor. The Jones reductor¹⁷ contains amalgamated zinc for reduction of chromium(III) to chromium(II).

H₂S apparatus. The decomposition of acid-volatile sulphides and disulphides is done in the apparatus shown in Fig. 2. The H₂S generated in the reaction flask passes through an aqueous wash solution buffered to a pH of 4.0, and is collected as silver sulphide by passage through aqueous 0.1M silver nitrate.

Reagents

Cr(II) solution, 1M. Dissolve 133 g of reagent-grade CrCl₃·6H₂O in 500 ml of 0.1M hydrochloric acid. Pass the solution through the Jones reductor. The colour changes

from bright green to bright blue as the chromium(III) is reduced to chromium(II). The chromium(II) solution is unstable in air and should be prepared every few days.

Eschka mixture. This can be obtained commercially or prepared by mixing three parts by weight of magnesium oxide with two parts of sodium carbonate. We used the commercial reagent-grade mixture.

Sulphur-separation procedure

Introduce a sample of known weight (about 5 g) into the round-bottomed reaction flask (Fig. 2). If the sample contains iron(III) (see Results and Discussion section), add 10–15 g of tin(II) chloride. Connect up the apparatus and flush it for 5 min with high-purity grade nitrogen. Slowly introduce 80 ml of 6M deaerated hydrochloric acid through the dropping funnel. Deaerate the acid beforehand by passage of the pure nitrogen through it. Establish a slow flow of nitrogen through the whole system and allow the reaction to proceed at room temperature for 15 min. Heat slowly until the solution just begins to boil, reduce the heat and continue the reaction until the silver sulphide has coagulated and no H₂S is detected when paper wetted with silver nitrate solution is held in the gas stream issuing from the buffer. Disconnect the apparatus, filter off the residual solids, wash them with water and dry them, saving the filtrate for sulphate (S_{SO₄}) determination. Filter off, wash with water, and dry to constant weight the silver sulphide precipitate (S_{av}).

Return the dried residual solid to the round-bottomed reaction flask and add 10 ml of ethanol. Connect up the apparatus and flush it with nitrogen. Add a mixture of 50 ml of 1M chromium(II) and 20 ml of deaerated concentrated hydrochloric acid through the dropping funnel. Establish a slow flow of nitrogen through the system and allow the reaction to proceed at room temperature for 15–30 min. Heat the sample to boiling and allow the solution to boil slowly until H₂S generation ceases. Filter off, wash with water, and dry the residual solids. Filter off, wash with water, and dry to constant weight the silver sulphide precipitate (S_{di}).

Mix the residual solids with three times their weight of Eschka mixture and place in a porcelain crucible. Cover the mixture with additional Eschka mixture. Fuse the mixture in a muffle furnace at 800° for 2 hr. Remove the crucible from the furnace, let it cool in air, and dissolve the cake in distilled water (10 ml for every 0.1 g of sample). Heat the solution for about 30 min, filter off and discard the solid residue (flux plus the refractory fraction of the sample). Adjust the filtrate to pH < 4.0 with hydrochloric acid and add 10 ml of bromine-saturated distilled water. Boil the solution until the bromine is expelled. Add 10 ml of 10% barium chloride solution and continue boiling for 15 min. Reduce the heat and allow the covered solutions to digest overnight. Filter off, wash with water, and dry to constant weight the barium sulphate precipitate (S_{org}). The acid filtrate reserved from the acid-volatile sulphur step (S_{SO₄}) is treated in the same way as the solution from the Eschka fusion, starting with the addition of the bromine-saturated water. The limit of detection for all the techniques (0.01% S for a 5-g sample) is based on the uncertainty in weighing very small amounts of precipitate.

Mössbauer procedure

Absorbers for transmission Mössbauer measurements were made from the oil-shale samples and from selected chemically-treated [hydrochloric acid or chromium(II)] residues by compressing the powder into disks of accurately known mass per unit area, typically about 0.2 g/cm². Spectra were acquired at room temperature with a conventional constant-acceleration Mössbauer system using a 25-mCi ⁵⁷Co:Rh source. Figures 3–5 show the Mössbauer spectra from the untreated oil shales and chemically-treated residues and indicate the spectral signatures of detected iron

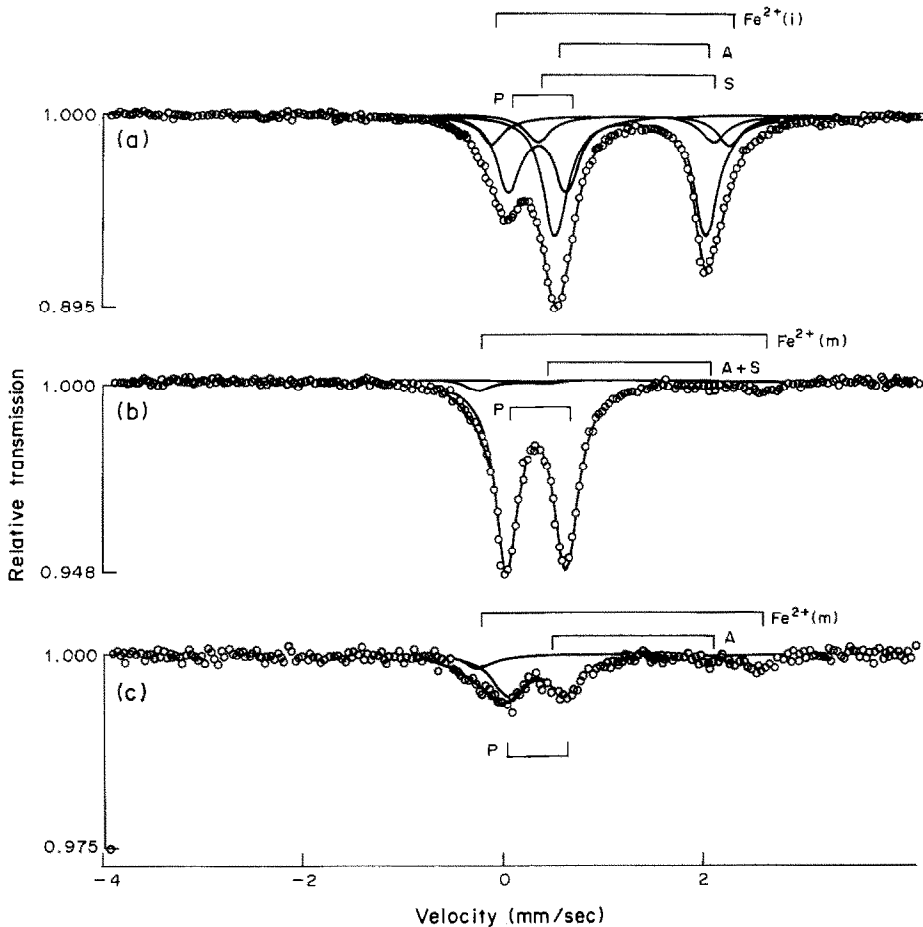


Fig. 3. Mössbauer spectra of sample MZ-1; (a) the untreated sample, (b) HCl-treated sample, (c) HCl- and Cr^{2+} -treated sample. A spectrum of the untreated sample covering a larger velocity range (as in Fig. 5) reveals weak resonance due to troilite. See Table 1 for mineral abbreviations.

minerals by stick diagrams. The computer least-squares deconvolution of each spectrum is aided by the known resonance-line shape (Lorentzian), the known relative splittings and symmetric (pairwise) intensities of a six-line magnetic pattern (*e.g.*, for troilite), and the assumption of equal intensities for both lines of a quadrupole pair (*e.g.*, for pyrite and siderite). This assumption is valid for a powder specimen in which the iron-containing crystallites have a random distribution of orientations.

These minerals were identified by comparing the Mössbauer spectral parameters listed in Table 1 with literature values.¹⁸⁻²⁰ The sample MZ-2 series of spectra in Fig. 4 yields the simplest iron mineralogy of the three shales investigated; pyrite, ankerite and siderite are found in the untreated shale, only pyrite after the hydrochloric acid treatment, and only a very small quantity of iron(III)* (0.01%) after the chromium(II) treatment. The latter iron(III) may be present in the untreated shale and acid-treated residue but is not detectable because of the much larger concentrations of iron present as pyrite and ankerite (note the vertical scale difference in Fig. 4 a, b and c). The strong overlap of iron(III) (*e.g.*, in clays) and pyrite Mössbauer spectra presents a resolution problem, as dis-

cussed by others.¹⁸⁻²⁰ This problem is evident in the analysis of the MZ-1 and WP-1 samples and will be discussed together with the chemical results below.

The quantitative Mössbauer analysis is performed according to the detailed procedure described by Williamson *et al.*¹⁵ as the "Resonance Area Method." Briefly, the integrated absorption intensity (resonance area) corresponding to each mineral, corrected for the thickness saturation effect and background radiation,¹⁵ is directly proportional to the amount of iron present in the form of that mineral. Each mineral (and each crystallographic iron site within a given mineral) has its own proportionality constant, owing to its particular recoil-less fraction, f_s ,^{15,18-20} (*i.e.*, its ability to absorb or emit gamma-rays without recoil). This means that the resonance-area fractions presented in the last column of Table 1 are not generally the fractions of iron present as the given mineral (or at a site within a mineral). The recoil-less fractions used in the analysis are: $f_s = 0.78$ for the Rh source;²¹ $f_{py} = 0.72$ for pyrite;²² $f_{po} = 0.43$ for pyrrhotite;²³ $f = 0.53$ for all other phases.¹⁵ This use of differing f -values represents an improvement over the usual practice of assuming the same f -value for all iron-containing phases.

*The Stock notation [iron(II) and iron(III)] is used in the text in connection with both the solution chemistry and the Mössbauer spectroscopy, but refers solely to the oxidation state and does *not* imply the spin configurations.

RESULTS AND DISCUSSION

The chemical and Mössbauer results for the three Green River Formation samples are shown in Table

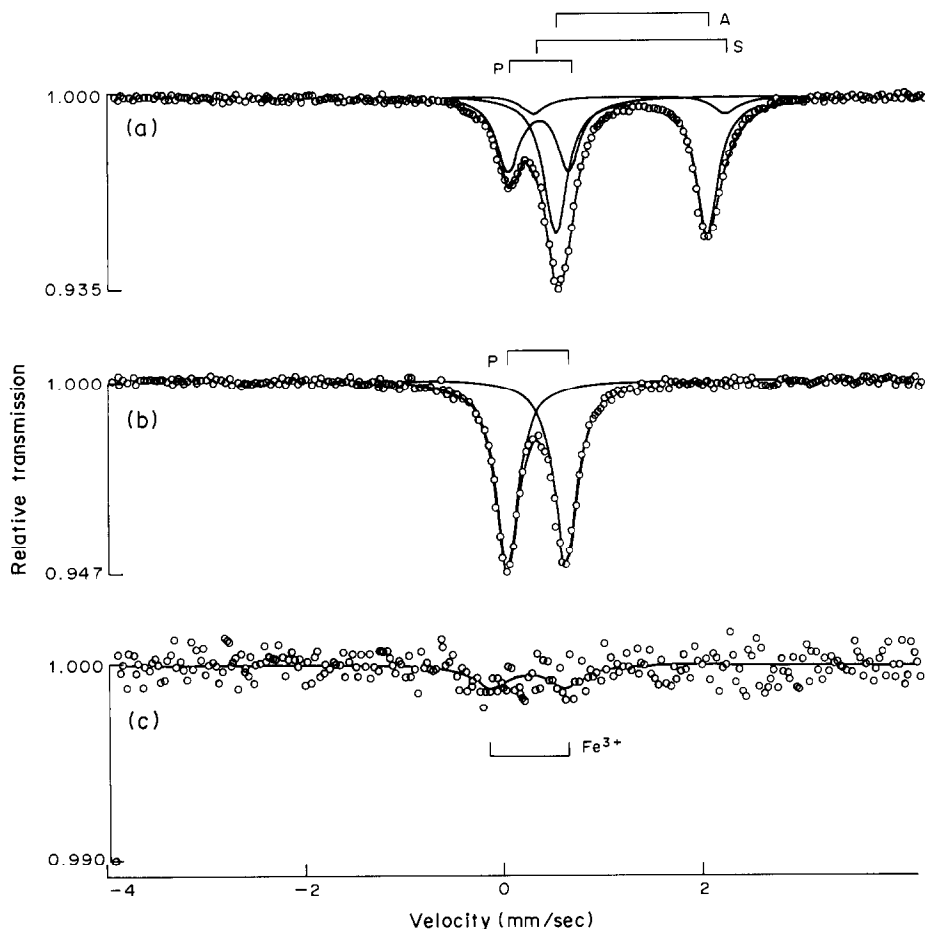


Fig. 4. Mössbauer spectra of sample MZ-2; (a) the untreated sample, (b) HCl-treated sample, (c) HCl- and Cr^{2+} -treated sample. See Table 1 for mineral abbreviations.

2. The precision of the separation techniques is reported as the coefficient of variation (V) of replicate analyses and is calculated as follows:

$$V\% = 100s/\bar{x}$$

where s is the standard deviation for n replicates giving a mean of \bar{x} . As expected, the precisions of determination (V) for all the sulphur forms are highest at, or near, the limit of detection and decrease with increasing sulphur concentrations.

Monosulphide and sulphate sulphur

The values of V for the sulphate and acid-volatile sulphur were judged adequate for our procedures, especially considering the low concentrations of these sulphur forms in some of the samples. The Mössbauer results for acid-volatile sulphur, obtained by using the change in abundances of the iron phases, agree very well with the chemical analyses (Table 2) and confirm the removal of the S_{av} as shown in Fig. 5b by the disappearance of the pyrrhotite resonance.

Two problems are inherent in this technique. First, the amounts of acid-volatile sulphide can be underestimated if acid-soluble iron(III) is present during the evolution of H_2S . The iron(III) oxidizes the H_2S

to elemental sulphur, which remains with the residue and is then separated with the pyritic sulphur. To prevent this oxidation, Pruden and Bloomfield²⁴ added tin(II) chloride to the sample prior to the decomposition of the sulphide minerals. The tin(II) rapidly reduces the iron(III) to iron(II) and thus prevents it from reacting with the H_2S . The first analysis of sample WP-1 indicated the presence of acid-volatile and disulphide sulphur, but the hydrochloric acid solution from the acid-volatile analysis was bright yellow [indicating the presence of acid-soluble iron(III)] and contained small white floating particles (possibly elemental sulphur). Mössbauer data for the untreated and treated samples show the presence of iron(III) in a site similar to that present in the clay illite and some of this iron is probably acid-soluble. The minor difference between Fig. 5b and 5c shows that little or no pyrite was present. Iron(III) and pyrite are difficult to resolve by Mössbauer measurements on the untreated shales. For example, the MZ-2 and WP-1 spectra (Figs. 4a and 5a) are similar, yet the acid residue of MZ-2 (Fig. 4b) clearly contains only pyrite while that of WP-1 (Fig. 5b) contains little or none. Subsequent analyses of WP-1 were done in the presence of added tin(II), which

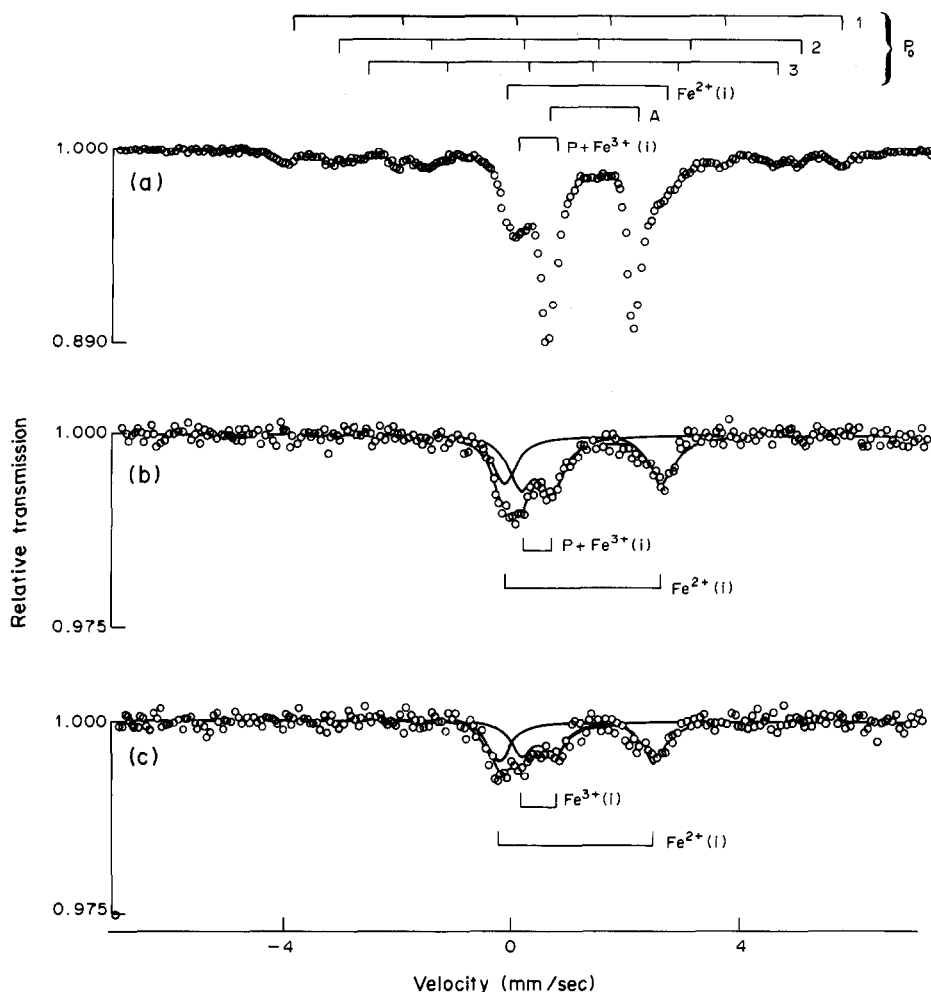


Fig. 5. Mössbauer spectra from sample WP-1; (a) the untreated sample, (b) HCl-treated sample, (c) HCl- and Cr^{2+} -treated sample. A larger relative range was used than those in Figs. 3 and 4, in order to encompass all magnetic pyrrhotite resonance. See Table 1 for mineral abbreviations.

increased the yield of S_{av} and decreased the yield of S_{di} to an undetectable amount. Chanton and Marten's data²⁵ show that a 1-hr exposure to a boiling 20% acid tin(II) chloride solution strips only 0.7% of the sulphur in fine-grained pyrite. Their results indicate that addition of tin(II) chloride is not likely to affect most analyses unless the sample contains a large amount of pyrite, in which case, the amount of monosulphide sulphur found might be in question.

The second problem is only significant when acid-insoluble sulphates occur in the sample (*e.g.*, barite). The insoluble sulphate is unreactive until the Eschka fusion step and, therefore, is determined as if it were organically-bound sulphur. Since barite is generally not present in Green River samples,⁵ no attempt was made to separate this sulphur phase although a procedure for doing so is available.²⁶

Disulphide sulphur

The Mössbauer and chemical results are in excellent agreement. The V value for disulphide sulphur in

sample MZ-2 is very low (3%), but is 23% for sample MZ-1. As mentioned in the sample description, MZ-1 was ground only to -65 mesh. We believe that coarse-grained pyrite in this -65 mesh fraction results in some sample inhomogeneity and possibly incomplete reduction of the disulphide sulphur, causing the higher V value. This hypothesis is supported by (1) inconsistent chemical and Mössbauer values for iron removed during the chromium(II) treatment ($\text{Fe}_{\text{Cr-ex}}$), 0.25 and 0.45%; the Mössbauer and chemical analyses were performed on residues from two separate sample splits, and (2) the presence of some undissolved pyrite, as indicated by the Mössbauer spectrum of the chromium(II)-treatment residue (Fig. 3c). The results for samples MZ-2 and WP-1 indicate that grinding samples to -100 mesh is adequate for our procedures.

Several simple chemical analyses were performed to confirm the Mössbauer indications that S_{di} is not removed during the separation of S_{av} and S_{SO_4} , but is quantitatively removed on treatment with chromium(II). Hydrochloric acid treatment of pure pyrite

Table 1. Mössbauer spectral parameters and phase identification: δ , isomer shift relative to metallic iron; Δ , quadrupole splitting; H, magnetic hyperfine field; Γ , full linewidth at half maximum; M, mineral as indicated by stick diagram in Figs. 3–5; F, fractional resonance area due to indicated minerals (corrected for thickness saturation, see Williamson *et al.*);¹⁵ untr'd, untreated sample; HCl, residue after HCl treatment; Cr²⁺, residue after HCl + Cr²⁺ treatment

Sample	δ , mm/sec	Δ , mm/sec	H, tesla	Γ	M	F, %
MZ-1						
untr'd	0.29 (2) ^a	0.58 (2)	0	0.29 (2)	P ^b	28 (3)
	1.23 (1)	1.52 (1)	0	0.29 (2)	A	48 (3)
	1.17 (3)	1.77 (3)	0	0.29 (2)	S	10 (2)
	1.01 (3)	2.40 (3)	0	0.29 (2)	Fe ²⁺ (i)	11 (2)
	0.5 (1)	0.2 (1) ^c	30.5 (5)	0.4 (1)	Tr	3 (1)
HCl	0.309 (2)	0.598 (3)	0	0.280 (4)	P	92 (1)
	1.22 (5)	1.67 (9)	0	0.280 (4)	A + S	2 (1)
	1.15 (2)	2.88 (3)	0	0.280 (4)	Fe ²⁺ (m)	6 (1)
Cr ²⁺	0.32 (1)	0.58 (2)	0	0.38 (2)	P	68 (3)
	1.2 (1)	1.6 (1)	0	0.38 (2)	A	10 (2)
	1.14 (4)	2.83 (5)	0	0.38 (2)	Fe ²⁺ (m)	22 (3)
MZ-2						
untr'd	0.303 (2)	0.604 (4)	0	0.262 (4)	P	32 (2)
	1.237 (2)	1.502 (4)	0	0.262 (4)	A	61 (2)
	1.22 (2)	1.91 (4)	0	0.262 (4)	S	7 (2)
HCl	0.303 (1)	0.594 (2)	0	0.268 (4)	P	100
Cr ²⁺	0.2 (1)	0.8 (1)	0	0.4 (1)	Fe ³⁺	100
WP-1						
untr'd	0.3 (1)	0.6 (1)	0	0.3 (1)	P + Fe ³⁺ (i)	15 (5)
	1.23 (1)	1.50 (1)	0	0.29 (1)	A	49 (3)
	1.2 (2)	2.7 (2)	0	0.3 (1)	Fe ²⁺ (i)	9 (4)
	0.70 (2)	0.16 (3)	30.0 (2)	0.40 (3)	Po ¹	12 (2)
	0.68 (4)	0.2 (1)	25.2 (3)	0.36 (5)	Po ²	7 (2)
	0.69 (4)	0.2 (1)	22.7 (3)	0.52 (5)	Po ³	8 (2)
HCl	0.34 (4)	0.55 (5)	0	0.50 (4)	P + Fe ³⁺ (i)	50 (5)
	1.15 (2)	2.72 (3)	0	0.48 (4)	Fe ²⁺ (i)	50 (5)
Cr ²⁺	0.44 (4)	0.58 (5)	0	0.47 (4)	Fe ³⁺ (j)	43 (5)
	1.11 (2)	2.70 (3)	0	0.47 (4)	Fe ²⁺ (i)	57 (5)

^aUncertainties based on counting statistics and computer deconvolution are given in parentheses for the last significant figure.

^bP, pyrite (+marcasite); A, ankerite; S, siderite; Fe²⁺(i), ferrous Fe similar to that in illite; Tr, troilite; Fe²⁺(m), ferrous Fe similar to that in montmorillonite; Poⁱ, *i*th Fe site in pyrrhotite.

^cFor magnetic phases, Δ is computed as $[(v_6 - v_5) - (v_2 - v_1)]/2$ where v_1 (v_6) is the lowest (highest) velocity position of the six-line pattern.

in the absence of tin(II) chloride produced no detectable H₂S. Sulphur yields from chromium(II) treatment of pure pyrite ranged from 97.8 to 100.7%. Standard-addition experiments with pure pyrite added to acid-treated MZ-2 showed complete recovery of the pyritic sulphur.

Chromium(II) will reduce elemental sulphur. If samples are suspected of containing elemental sulphur, they should be extracted with acetone before treatment with chromium(II). Prior knowledge regarding sample type is helpful in assessing whether or not the extraction is necessary.

Organic sulphur

V is very low (2%) for sample MZ-2. Again, *V* was highest when the concentration of S_{org} was near the

limit of detection (0.01%). Only one organic-sulphur analysis was performed on sample MZ-1.

Two crude oils were tested for their stability in the presence of the reagents used in this study. These oils contain sulphur-containing organic compounds similar to those reported in the oil shale.¹¹ No H₂S was produced when the oils were treated with hydrochloric acid or chromium(II). Our results confirm those of earlier workers^{14,27} and show that all types of sulphur-containing organic compounds tested to date are unreactive during the acid and chromium(II) treatments.

Additional tests

The effectiveness of silver nitrate as an H₂S-trapping reagent was investigated by calculating the

Table 2. Results of chemical and Mössbauer analyses of samples MZ-1, MZ-2 and WP-1; results are given as the mean (\bar{x}) for n samples with coefficient of variation V ; all concentrations are reported as % w/w in the untreated sample

Sample	Sulphur data							
	Chemical data						Mössbauer Fe data ^a	
	S_{av}	S_{di}	S_{org}	S_{SO_4}	$S_t(\Sigma)^b$	$S_t(L)^c$	S_{av}	S_{di}
MZ-1								
\bar{x} , %	0.08	0.43	0.16	<0.01	0.67	0.68	0.05	0.51
V , %	6	23	—	—	—	10	—	—
n	7	4	1	4	—	4	1	1
MZ-2								
\bar{x} , %	0.01	0.37	0.14	0.05	0.57	0.56	<0.03	0.36
V , %	30	3	2	19	—	12	—	—
n	5	5	4	3	—	11	1	1
WP-1								
\bar{x} , %	0.80	<0.01	0.02	0.06	0.88	0.93	0.75	<0.05
V , %	13	—	33	11	—	4	—	—
n	7	7	4	4	—	4	1	1
Sample	Iron data ^d							
	Fe_t^e , %	Determined on residues ^e			Determined in ex. sol. ^f			
		Fe_{HCl-ex} , %	Fe_{Cr-ex} , %	Fe_{non-ex} , %	Fe_{HCl-ex} , %	Fe_{Cr-ex} , %		
MZ-1								
chem	2.3	1.8	0.45	0.08	1.9	0.46		
Möss	2.0	1.7	0.25	0.07	—	—		
MZ-2								
chem	1.2	0.93	0.28	0.03	0.80	0.45		
Möss	1.2	0.93	0.28	0.01	—	—		
WP-1								
chem	4.2	3.8	0.13	0.23	4.0	0.04		
Möss	4.1	3.9	0.07	0.16	—	—		

^aSulphur values were calculated from Mössbauer pyrrhotitic and disulphide Fe values.

^bSummation of the means of the sulphur forms.

^cTotal sulphur as determined by Leco analysis.

^dThe iron data are for one chemical and one Mössbauer analysis.

^eCalculated differences between Fe in the sequentially-treated solid residues.

Values represent concentrations of Fe removed from the sample during each treatment (Fe_{HCl-ex} represents acid-soluble Fe; Fe_{Cr-ex} represents Fe released upon treatment with HCl + Cr^{2+} ; Fe_{non-ex} represents the Fe remaining in the residue after the HCl + Cr^{2+} treatment, i.e. non-extractable Fe). Chemical (chem) data represent calculated differences of lithium metaborate fusion/atomic-absorption analyses of the sequentially-treated residues and Möss represents calculated differences as determined by Mössbauer analysis of the sequentially-treated residues.

^fFe concentrations measured in the extract solutions (ex. sol.) from the separation analyses (see footnote e above).

^gTotal Fe in the untreated sample as determined by lithium metaborate fusion/atomic-absorption spectrometry (chem) or Mössbauer spectroscopy (Möss).

sulphur yield obtained by combusting the Ag_2S to yield SO_2 . The yields ranged from 95 to 104%, indicating that the precipitate is stoichiometric Ag_2S . Yields (97.8–100.7%) from the pure pyrite analysis also confirm these results.

Reproducibility of isotopic measurements of the various forms of sulphur was an important concern during development of the technique since isotopic compositions are to be used in our study. Isotope analyses of the Ag_2S and $BaSO_4$ from duplicate separations indicate that the sulphur isotopic com-

positions of the various forms of sulphur are indeed reproducible.

Sulphur and iron mass-balances were used as an additional confirmation that the analytical scheme could account for all the sulphur and iron in our samples. The results in Table 2 indicate that the summation of the concentrations of the forms of sulphur agree with the independently determined total sulphur concentrations for the samples. Iron mass-balances indicate that the iron removed from the sample during each step of the analytical scheme

can be determined by either analysing the extract solutions or as the difference in the iron concentrations of the sequentially-treated residues. These chemical data for iron show excellent agreement with the amounts of iron removed, as calculated from the Mössbauer data (Table 2). This substantiates the ability of Mössbauer spectroscopy to determine absolute quantities of iron. Furthermore, these results indicate that iron concentrations determined either in the extract solutions or the solid residues are quantitative and can thus be used in geochemical studies of iron distribution.

CONCLUSIONS

Separation of the forms of sulphur in three Green River Formation samples was efficient and quantitative. Our results indicate that some of the procedures are sensitive to the particle size of the sample. We also illustrate the importance of having some prior knowledge of the mineralogy and chemistry of the samples; information on the presence of acid-soluble iron(III), barite, or elemental sulphur is necessary to ensure the accuracy of results for any suite of rocks or sediments.

Mössbauer spectroscopy is nearly always used for relative iron analyses, e.g., for $\text{Fe}^{3+}/\text{Fe}^{2+}$ ratios. However, in this study, the iron contents determined by Mössbauer spectroscopy agreed well with the chemical results, confirming the ability of Mössbauer spectroscopy to measure absolute quantities of iron. The good agreement of the data also supports the validity of the f -values used in the analyses (e.g., $f_{\text{po}}/f_{\text{py}} = 0.60$).

REFERENCES

1. D. L. Boyer and R. D. Cole, in *Sixteenth Oil Shale Symposium Proceedings*, J. H. Gary (ed.), pp. 160–175. Colorado School of Mines, Golden, 1983.
2. J. R. Dyni, in *Sixteenth Oil Shale Symposium Proceedings*, J. H. Gary (ed.), pp. 144–159. Colorado School of Mines, Golden, 1983.
3. K. E. Stanfield, I. C. Frost, W. S. McAuley and H. N. Smith, *U.S. Bur. Mines Rept. Inv.*, 1951, No. 4825, 27.
4. J. W. Smith, N. B. Young and D. L. Lawlor, *Anal. Chem.*, 1964, **36**, 618.
5. C. Milton and H. P. Eugster, in *Researches in Geochemistry*, P. H. Abelson (ed.), pp. 118–150. Wiley, New York, 1959.
6. A. Pabst, *Am. Mineral.*, 1970, **56**, 133.
7. R. D. Cole, J. H. Liu, G. V. Smith, C. C. Hinckley and M. Saporoschenko, *Fuel*, 1978, **57**, 514.
8. R. D. Cole and M. D. Picard, *Geol. Soc. Am. Bull.*, 1978, **89**, 1441.
9. D. C. Melchior, T. R. Wildeman and D. L. Williamson, *Fuel*, 1982, **61**, 516.
10. J. W. Smith and N. B. Young, in *Sixteenth Oil Shale Symposium Proceedings*, J. H. Gary (ed.), pp. 176–188. Colorado School of Mines, Golden, 1983.
11. L. L. Ingram, J. Ellis, P. T. Crisp and A. C. Cook, *Chem. Geol.*, 1983, **38**, 185.
12. J. K. Kuhn, L. B. Kohlenberger and N. F. Shimp, *Illinois Geol. Survey Environmental Geol. Notes*, 1973, No. 66, 11.
13. *Annual Book of Standards*, Part 26, pp. 322–326. American Society for Testing Materials, Philadelphia, 1977.
14. N. N. Zhabina and I. I. Volkov, in *Environmental Biogeochemistry and Geomicrobiology*, Vol. 3, W. E. Krumbein (ed.), pp. 735–746. Ann Arbor Science Publishers, Ann Arbor, 1978.
15. D. L. Williamson, T. W. Guettinger and D. W. Dickerhoof, in *Mössbauer Spectroscopy and Its Chemical Applications*, J. G. Stevens and G. K. Shenoy (eds.), p. 177. American Chemical Society, Washington, D.C., 1981.
16. J. L. Giulianelli and D. L. Williamson, *Fuel*, 1982, **61**, 1267.
17. D. A. Skoog and D. M. West, *Fundamentals of Analytical Chemistry*, 3rd Ed., p. 750. Holt, Rinehart and Winston, New York, 1976.
18. G. P. Huffman and F. E. Huggins, *Fuel*, 1978, **57**, 592.
19. F. E. Huggins and G. P. Huffman, in *Analytical Methods For Coal and Coal Products*, C. Karr, Jr. (ed.), Vol. 3, p. 371. Academic Press, New York, 1979.
20. P. A. Montano, in *Mössbauer Spectroscopy and Its Chemical Applications*, J. G. Stevens and G. K. Shemoy (eds.), p. 135. American Chemical Society, Washington, D.C., 1981.
21. Z. M. Stadnik, *Mössbauer Effect Ref. Data J.*, 1978, **1**, 217.
22. T. W. Guettinger, *Ph.D. Thesis*, Colorado School of Mines, Golden, Colorado, 1984.
23. D. L. Williamson, 1983, unpublished data based on Mössbauer spectra of known mixtures of Fe_7S_8 and FeS_2 . This gave $f(\text{Fe}_7\text{S}_8)/f(\text{FeS}_2) = 0.60$, so using the recent result of Guettinger, ²² of $f(\text{FeS}_2) = 0.72$, yields $f(\text{Fe}_7\text{S}_8) = 0.43$.
24. G. Pruden and C. Bloomfield, *Analyst*, 1968, **93**, 532.
25. J. P. Chanton and C. S. Martens, *Biogeochemistry*, 1985, **1**, 375.
26. G. N. Breit, E. C. Simmons and M. B. Goldhaber, *Isotope Geology*, 1985, **52**, 333.
27. D. E. Canfield, R. Raiswell, J. T. Westrich, C. M. Reaves and R. A. Berner, *Geochim. Cosmochim. Acta, Chem. Geol.*, 1986, **54**, 149.

CHROMATOGRAPHY OF CHLOROPHYLLS AND BACTERIOCHLOROPHYLLS

JOSE A. S. CAVALEIRO

Departamento de Quimica, Universidade de Aveiro, 3800 Aveiro, Portugal

KEVIN M. SMITH

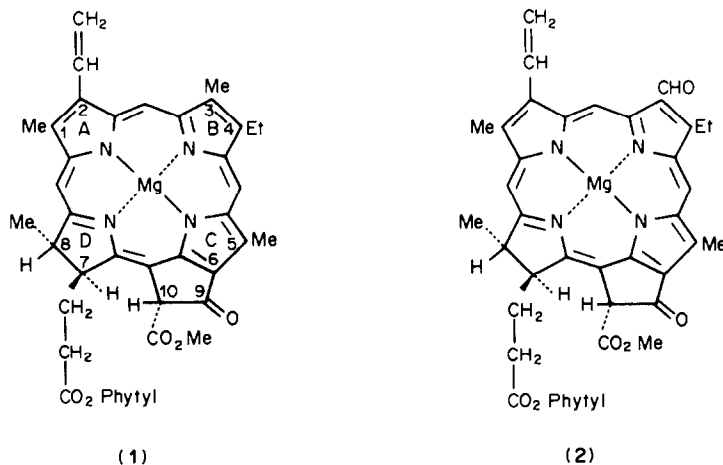
Department of Chemistry, University of California, Davis, CA 95616, U.S.A.

(Received 24 February 1986. Revised 24 June 1986. Accepted 31 July 1986)

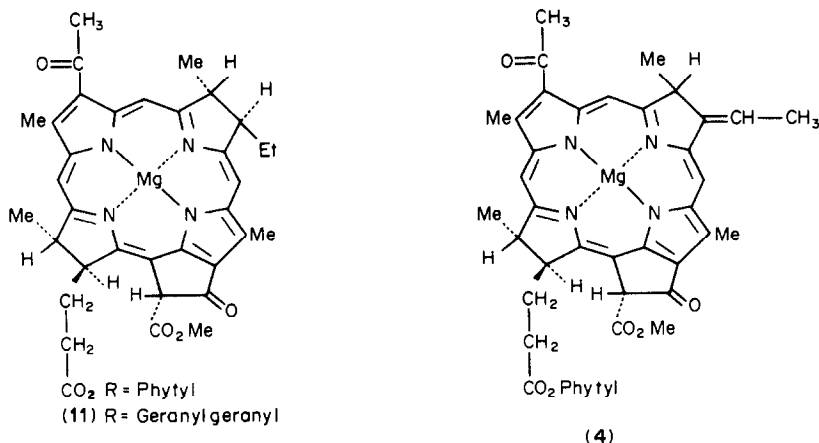
Summary—Recent advances in the paper, thin-layer, column, and high-performance liquid chromatography of chlorophylls, bacteriochlorophylls, and their derivatives, with particular emphasis on high-pressure liquid chromatography, are discussed.

Chlorophylls and bacteriochlorophylls comprise the large group of pigments responsible for photosynthesis in most plants, algae and bacteria.¹ The major plant chlorophylls are (Scheme 1) chlorophyll-a (1) and chlorophyll-b (2), the proportions of

these usually being 3:1. In contrast, most bacterial chlorophylls [e.g., bacteriochlorophyll-a (3) and bacteriochlorophyll-b (4) (Scheme 2)] tend to be "reduced" in both rings B and D, and so are nominally tetrahydroporphyrins, compared with



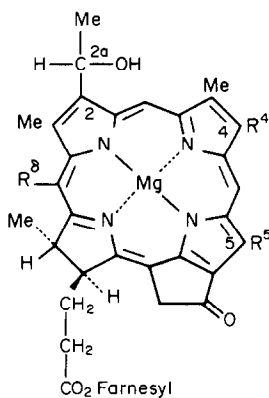
Scheme 1.



Scheme 2.

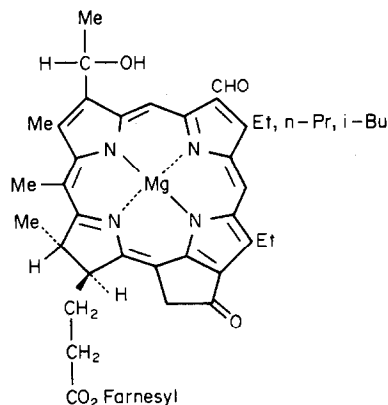
chlorophyll-a, which is reduced only in ring D.² However, in the strictest terms, bacteriochlorophyll-b is only a dihydroporphyrin, because of the tautomeric shift of the ring B double bond. A series of bacteriochlorophylls from green sulphur bacteria, which have proved to be a formidable chromatographic problem owing to the presence of methyl, ethyl, propyl, isobutyl, and neopentyl side-chain homologues, are the bacteriochlorophylls-c, -d, and -e [(5), (6), and (7), respectively, in Schemes 3 and 4; see later]. Though these co-called "*Chlorobium* chlorophylls" are bacteriochlorophylls, they are more akin to chlorophyll-a than to bacteriochlorophyll-a because they are dihydro- rather than tetrahydroporphyrins.³

Leaf, algal, and bacterial extracts contain not only chlorophylls of various sorts, but also ancillary pigments such as carotenes and xanthophylls. Thus, chromatographic purification of pigment extracts from natural sources not only involves separation of, for example, chlorophyll-a from chlorophyll-b, but also separation of these chlorophylls from the accompanying non-pyrrole pigments. A complication in the choice of chromatographic systems is the fact that chlorophylls, as a class of organic compounds, are labile and are thereby subject to a variety of side-reactions and degradative processes. For example, the central magnesium atom can be removed by treatment with the mildest of acids, and transesterification or hydrolysis of the phytyl (or other) ester can cause multiple chromatographic bands to be produced. Treatment with base in the



Scheme 3.

(6) [Bacteriochlorophylls-d]				(5) [Bacteriochlorophylls-c]			
R ⁴	R ⁵	R ⁶	Config. at 2a	R ⁴	R ⁵	R ⁶	Config. at 2a
a	Et	Me	H	R	Et	Me	R
b	Et	Et	H	R	Et	Et	R
c	n-Pr	Me	H	R	n-Pr	Et	R
d	n-Pr	Et	H	R	n-Pr	Et	S
e	i-Bu	Me	H	S	i-Bu	Et	R
f	i-Bu	Et	H	S	i-Bu	Et	S
g	neoPn	Me	H	S			
h	neoPn	Et	H	S			



(7) [Bacteriochlorophylls—e]

Scheme 4.

presence of oxygen causes a large variety of chemical transformations to take place, and accurate analysis and chemical logic was the basis for the assignment of unique molecular structures to the chlorophylls.⁴ As with most natural-product isolation and characterization, it is important to be able to differentiate between truly new compounds and ones produced as artifacts owing to the lability of the natural systems.

As will be seen later, selection of a particular technique (paper, thin-layer, column, high-pressure liquid chromatography *etc.*) will depend on the specific needs of the project. Various workers have their own individual need for information, be it simple detection of a chlorophyll, its determination for environmental purposes in various water samples, its purification on an analytical scale, or large scale isolation in milligram to gram quantities. Paper chromatography, TLC, and analytical HPLC are the methods best suited to detection and determination of chlorophylls, the last of these being particularly simple with the advent of variable-wavelength spectrophotometric and fluorimetric detectors. On the other hand, larger amounts of chlorophylls are required for structure determination, or if a particular chlorophyll is to be used as a starting material for a series of chemical transformations;⁵ in this case, preparative thick layer, column, medium-pressure, or high-pressure liquid chromatography (using an analytical instrument with multiple injection or a dedicated preparative instrument such as the Waters Prep 500A) are required. It should not be forgotten that leaf pigments were the first to be subjected to chromatographic purification in the pioneering work of Tsvett,⁶ and that these same pigments, with their impressive range of structures and colours, were used to optimize the new technique of column chromatography. In this work the properties of the solid support as well as of the solvent were studied in detail.

The importance of chromatography of chlorophylls and plant pigments is emphasized by the existence of several reviews.⁷⁻¹³ It is the objective of this review to update these works with more recent

results, particularly with regard to HPLC, which has been developed as a standard technique since the early 1970s.¹⁴ We shall concentrate mainly on methods for detection, isolation and purification of samples from various sources, and will not deal at all with the rapidly expanding area of isolation and purification of photosynthetic reaction centres and other chlorophyll-protein complexes.

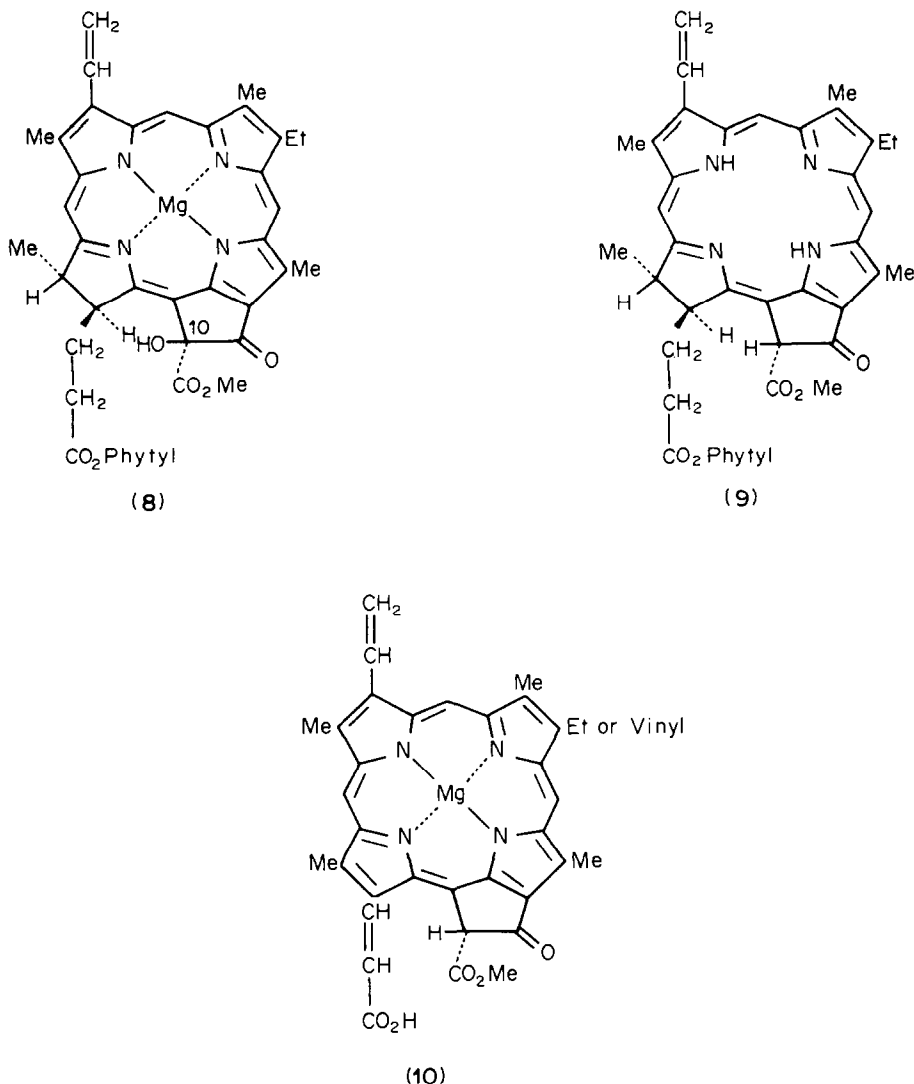
Extraction of chlorophylls from natural materials

Various methods for obtaining crude pigment mixtures from plant material have been reviewed. These usually involve brief scalding of leaves (*e.g.*, spinach) followed by extraction with acetone or methanol in petroleum ether.¹ Alternatively, the scalding can be avoided if the leaves are macerated in a blender with cold organic solvents. Bacteria, for example those producing the *Chlorobium* chlorophylls (*Chlorobium vibrioforme*, *Prosthecochloris aestuarii*, *Chlorobium phaeobacterioides*) tend to liberate their photo-

synthetic pigments merely on washing of the collected (centrifuged) cells with acetone or methanol.¹⁵⁻¹⁷ On the other hand, the alga *Spirulina maxima* holds on tenaciously to its chlorophyll-a, which can only be efficiently liberated by freezing with "dry-ice"/acetone or liquid nitrogen, followed by boiling in acetone.⁵ Considerable care must be exercised to ensure that artifacts are not produced under such vigorous conditions, and particularly that the chlorophyll is not contaminated with the 10-hydroxy derivative [(8) in Scheme 5]. An advantage in the use of *Spirulina maxima* is that it produces only chlorophyll-a, with no chlorophyll-b whatsoever. Thus, pigments of the "a" series can be isolated in abundance, but the vigorous conditions make this alga more suitable for preparation of methyl pheophorbide-a (9) (Scheme 5), the metal-free methyl ester of chlorophyll-a.

Paper chromatography

This subject has been reviewed in detail by Sestak,⁷



Scheme 5.

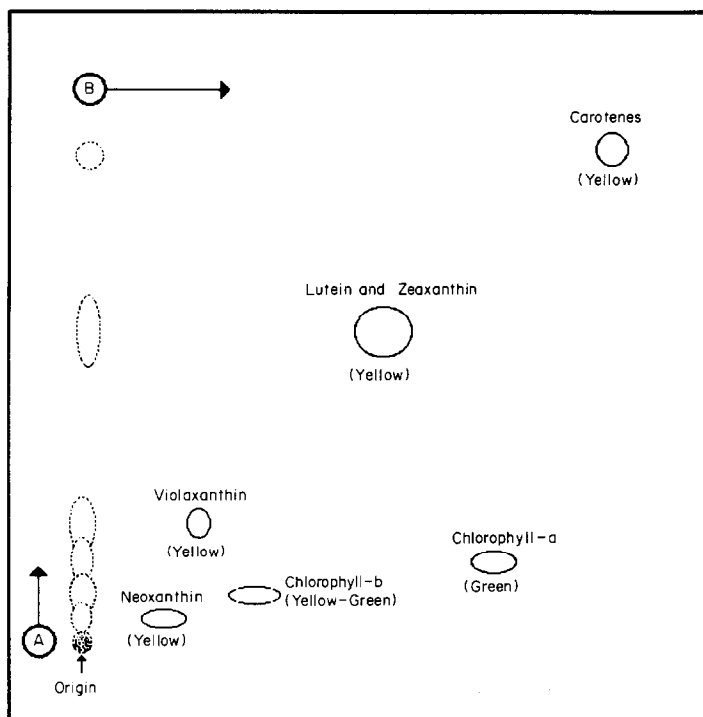


Fig. 1. Two-dimensional paper chromatogram (after Strain and Svec¹²) of chloroplast pigments from leaves. The first solvent was petroleum ether, and the second was petroleum ether + 0.6% 1-propanol.

and more recently by Strain and Svec.¹² With the advent of HPLC, however, interest in paper chromatography, or at least the frequency of appearance of papers on it, has fallen. The principal variable in paper chromatography is the solvent, and the technique as a whole is limited by the small amounts of pigments which can be applied without overloading (which tends to cause serious tailing of the spots). Favoured solvents are petroleum ether, benzene, toluene, xylene, chlorobenzene, carbon tetrachloride, or carbon disulphide containing small amounts of diethyl ether or acetone or various alcohols. Figure 1 shows a two-dimensional paper chromatogram of pigments from leaf chloroplasts, developed first with petroleum ether, and then with the same solvent containing 0.6% v/v 1-propanol.¹⁸ The coloured spots can then be eluted from the paper with alcohols, and determined spectrophotometrically. In a fluorographic method for detection of chlorophyll and derivatives after paper chromatography recently described,¹⁹ the fluorescence of the pigment spots is excited with blue-violet light and recorded by contact printing on panchromatic photographic printing paper. Development of the print gives grey to black spots on a white background, and their size and intensity can be used for estimation of the pigments.

A semiquantitative method for separation of chlorophylls-a and -b has been used²⁰ to demonstrate contamination of chlorophyll-b with oxidation products of chlorophyll-a, and a paper-chromatographic method for separation and quantitative determination of chlorophyll-a and chlorophyll-c (10)

(Scheme 5) from various algae has been reported;²¹ the results were compared with data from spectrophotometry of the original mixture.

Thin-layer chromatography

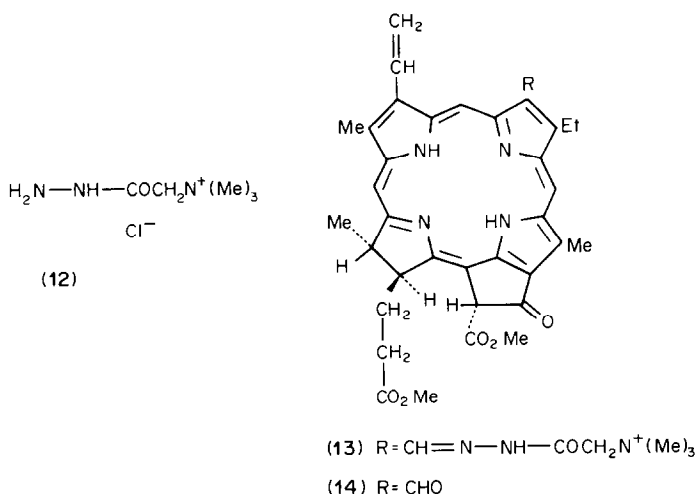
In a detailed review in 1980, Sestak commented⁸ that though this was not a "dead" subject, he believed there would be no future major improvements in TLC methods for chlorophylls, and at least up till 1985 he seems to be correct.

Separations similar to those obtained on paper can be achieved by using thin layers of adsorbents such as cellulose or sugar. Use of silica gel, however, often leads to partial loss of the magnesium atom, resulting in the formation of pheophytins, but this can be used to advantage for indirect determination of chlorophylls-a and -b.²²

Several papers have detailed TLC separations of chlorophylls and derivatives by use of reversed-phase adsorbents.^{23,24} Chlorophyll-a and -b epimers²⁵ and bacteriochlorophylls formed with various esterifying alcohols²⁶ have been separated on cellulose layers impregnated with olive oil or a triglyceride. By combination with reversed-phase C₁₈ HPLC, the existence of seven diastereomers of bacteriochlorophyll-a_{phytol} (3) and bacteriochlorophyll-a_{geranylgeraniol} (11) (Scheme 2), and more than one diastereomer of bacteriochlorophyll-b (4) (Scheme 2) was demonstrated.

Column chromatography

Several types of finely packed adsorbents have



Scheme 6.

been used in column chromatography to provide relatively large quantities of purified or partially purified pigments from plant, bacterial, or algal extracts. The most commonly used adsorbent is powdered sugar, and methods have been reported for preparation of efficient and reproducible columns with this support. Petroleum ether is usually the least polar solvent employed during elution. Addition of benzene or lower alcohols causes the chlorophylls to separate further from the various carotenoids and other ancillary pigments.

If polyethylene is used as the adsorbent in place of sugar, the elution sequence is inverted. When leaf extracts in 80% acetone are chromatographed on polyethylene the carotenes and chlorophylls are strongly adsorbed and the xanthophylls pass through the column. In 90% acetone the chlorophylls-a and -b are poorly separated and eluted before the carotenes.²⁷ Several workers have shown that it is advantageous to partially purify leaf extracts, before column chromatography, by treatment with dioxan to form an insoluble polymeric precipitate, leaving most of the carotenoids still in solution;²⁸⁻³⁰ this procedure facilitates separation of chlorophylls-a and -b. Various other supports used in column chromatography of plant pigments include Spherasorb HP Ultrafine,³¹⁻³³ Sepharose CL 6B,³³⁻³⁵ Bioglas,³⁶ and Sephadex LH-20.^{37,38} All give good purification of chlorophyll-b.

Though multiple liquid-liquid partition has been described for separation of chlorophylls-a and -b,^{39,40} a very interesting early application of liquid-liquid partition on Celite was reported by Purdie and co-workers: partition of metal-free chlorophylls (pheophorbides) from green sulphur bacteria on Celite with ether and hydrochloric acid was successfully used^{41,42} for separation of homologous fractions from bacteriochlorophylls-c and -d (*Chlorobium* chlorophylls). Subsequent degradative analysis,⁴³ however, showed minor contamination of some homologues with others. Strouse and co-workers^{44,45}

subsequently used a reversed-phase system with a polyethylene support and acetone as solvent for separation of the bacteriochlorophylls-c, and achieved separations not only of the bacteriochlorophyll-c homologues themselves, but also of the various series of pigments with the farnesyl and other esters of the 6-propionate side-chain.

A large scale (up to 20 grams) separation⁴⁶ of pheophorbides or pheophytins-a and -b makes use of the Girard's reagent T complex of the 3-formyl group in the b-series to aid chromatographic separation on a column. Thus, the mixture of chlorophylls-a and -b, or of the pheophytins or pheophorbides, is treated⁴⁷ with Girard's reagent T (12) (Scheme 6) to give the complex (13) of the b-series, but the a-series is unaffected. In the subsequent large-scale column chromatography on alumina the a-series pheophytin or pheophorbide passes through the column while the Girard's salt complex is retained. Use of more polar solvents (containing methanol) results in elution of the b-series Girard's salt complex, from which the pheophorbide-b (14) can be regenerated.

High-pressure liquid chromatography

There can be no doubt that the major developments in chromatography of chlorophylls and bacteriochlorophylls, in the past several years, have been in the area of HPLC. Separations obtained with reversed-phase supports, particularly commercially available μ -Bondapak C_{18} columns, have been impressive with respect to both resolution and rapidity.

A simple undergraduate laboratory project has been described⁴⁸ in which β -carotene and chlorophylls-a and -b from collard greens are separated on either microPak silica or reversed-phase C_{18} columns, or even simple SepPak cartridges, and then determined. Separations are achieved in minutes.

Isocratic HPLC on silica gel⁴⁹ has also provided a powerful means for rapid preparative (20-25 mg) isolation of chlorophylls-a, a', -b, and b', and the corresponding pheophytins. Chlorophyll-a can also

be isolated⁵⁰ from the blue-green alga *Anacystis nidulans* by initial precipitation as the dioxan complex (see above), followed by HPLC on a μ -Bondapak C₁₈ column; purity of the chlorophyll-a obtained by this procedure is comparable with that obtained by other standard methods. HPLC of dioxan complexes has also been used⁵¹ for determination and separation of chlorophylls-a and -b.

A C₁₀ reversed-phase column has been used⁵² for separation and determination of radiochemically labelled chlorophylls-a and -b; with the HPLC method minor degradation products of chlorophyll-a (which follow chlorophyll-b) do not overlap and interfere as they do in the comparable TLC and paper chromatographic methods.

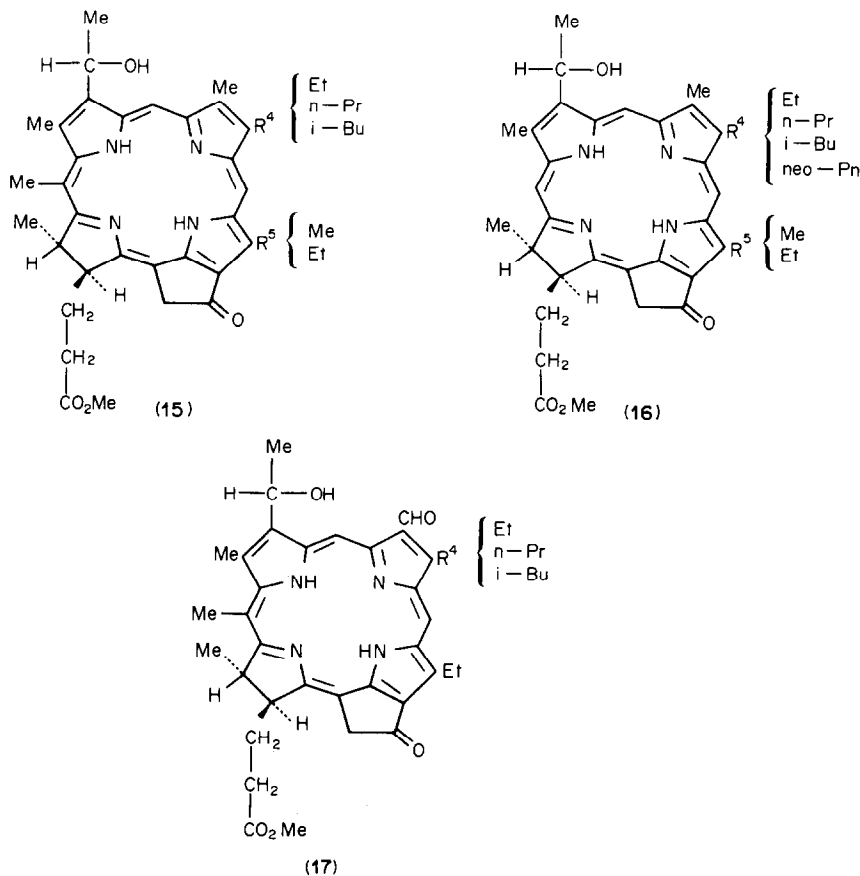
Chlorophylls and their derivatives from various sources (sediments,⁵³ phytoplankton,⁵⁴⁻⁵⁷ marine diatoms,⁵⁸ algal cultures,⁵⁹⁻⁶¹ and spinach⁶²) have been separated and determined by reversed-phase HPLC. In many cases, fluorimetric detection was used to provide exceptional sensitivity. The detection limit for chlorophyll-a in one study⁵⁸ was 0.1 pmole, whereas determination of carotenes and chlorophylls by spectrophotometry⁵⁷ required approximately 5 ng and 80 ng, respectively. Typically, reversed-phase HPLC of pigments containing chlorophylls-a and -b, chlorophyll isomers, pheophytins-a and -b, α -carotene, β -carotene, rutein, violaxanthin, lutein-

5,6-epoxide, antheraxanthin, neoxanthin, and several carotenoids in a single sample were separated in one injection with a short analysis time, the retention-time reproducibility for each pigment being better than 1.5%. Fluorimetric determination has been used⁶² for an extremely sensitive chlorophyll-a isocratic HPLC estimation (C₁₈ column) of some 17 pigments from a natural extract. Here, ten replicate measurements of a 50 μ g/l. standard gave a reproducibility of 3% and a detection limit of 84 pg of chlorophyll-a. To indicate the speed that can be achieved in such separations, with fluorescence sensitivity in the pmole range,^{63,64} resolution on a reversed-phase column of five chlorophyll-a species and four pyrochlorophyll species esterified at the 7-side-chain with different alcohols was achieved in just 22 min in a single experiment. Also, the HPLC (unlike many other analytical methods) did not produce any artifacts, and the variation in retention-time was less than 0.5%.

Bacteriochlorophyll-b has been chromatographed without degradation by reversed-phase HPLC.⁶⁵ As with other chlorophylls mentioned above, pigments differing only in the nature of their esterifying alcohols were resolved.

HPLC of bacteriochlorophylls-c, -d, and -e

As mentioned previously, Strouse and co-



Scheme 7.

workers^{44,45} introduced preparative-scale reversed-phase HPLC of the bacteriochlorophyll-c series with use of polyethylene powder as stationary phase. Extremely difficult separations of the bacteriochlorophyll-c homologues (5) (Scheme 3) were accomplished, along with significant resolution of bands for esters other than the farnesyl compounds. This method was modified by Smith and co-workers^{16,66} to achieve separations of the bacteriopheophorbides (15) (Scheme 7) produced by methanol-sulphuric acid treatment of the chlorophyll pigments from *Prosthecochloris aestuarii*. The acid treatment removes the chelated magnesium ion and transforms the various 7-esters (mainly farnesyl) into methyl esters. Virtually no resolution of the six pheophorbide homologues (15) was obtained on a normal-phase microporasil column, but μ -Bondapak C₁₈ reversed-phase column gave (Fig. 2) quite remarkable separations of the homologues.^{16,66} Even diastereomeric differences between pigments (*e.g.*, bands 3 and 4 in Fig. 2) were efficiently resolved on recycling.

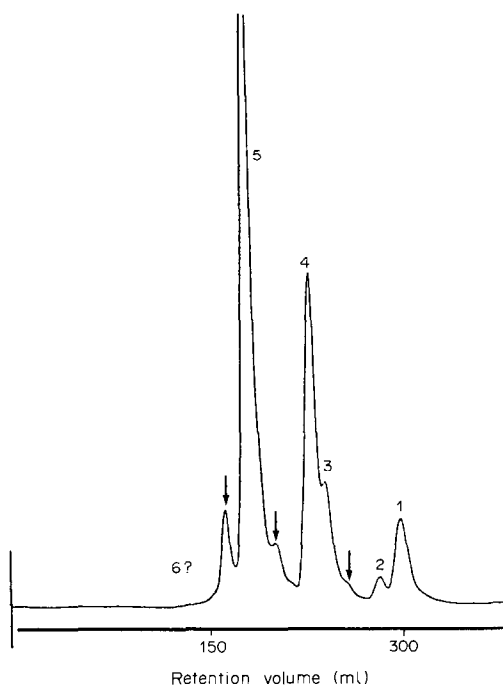


Fig. 2. High-performance liquid chromatogram of the methyl bacteriopheophorbides-c from *Prosthecochloris aestuarii*.¹⁶ Numbers above the peaks represent band numbers according to Holt's nomenclature.^{41,42} The Holt nomenclature is based on a normal-phase elution and therefore in the reversed-phase system shown above, band 6 elutes first. Holt's assignments, modified by Smith *et al.*,¹⁶ are band 6, 2'-(R), R⁴ = Et, R⁵ = Me; band 5, 2'-(R), R⁴ = Et, R⁵ = Et; band 4, 2'-(R), R⁴ = n-Pr, R⁵ = Et; band 3, 2'-(S), R⁴ = n-Pr, R⁵ = Et; band 2, 2'-(R), R⁴ = i-Bu, R⁵ = Et; band 1, 2'-(S), R⁴ = i-Bu, R⁵ = Et. Arrowed peaks emphasize contamination by methyl bacteriopheophorbides-d, also produced by this same bacterium. Flow-rate 3 ml/min; eluent methanol-water (85:15); two μ Bondapak columns were used. Back-pressure was *ca.* 2000 psi.

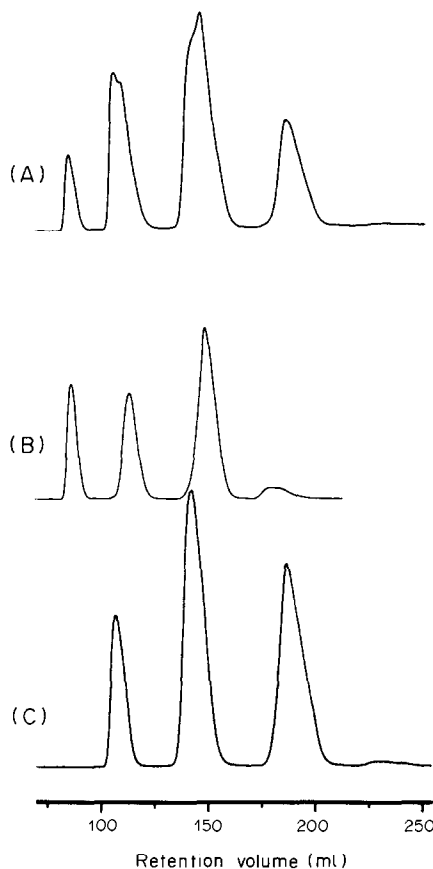


Fig. 3. High-performance liquid chromatograms¹⁵ of (A) the complete mixture of methyl bacteriopheophorbides-d from *Chlorobium vibrioforme* forma *thiosulfatophilum*, (B) the 5-methyl series after pre-separation on a silica column, (C) the 5-ethyl series after the silica pre-separation. A Waters Z-module system, equipped with a 10 μ m C₁₈ reversed-phase column was used; the solvent was methanol-water (85:15).

Similarly, the bacteriochlorophylls-d from *Chlorobium vibrioforme* forma *thiosulfatophilum* can be separated by reversed-phase HPLC on μ -Bondapak C₁₈.^{15,67,68} Figure 3A shows the complete mixture of pheophorbide-d homologues (16) (Scheme 7), which can be separated^{15,67-69} by simple silica-gel thick-layer plates into the 5-methyl (Fig. 3B) and 5-ethyl (Fig. 3C) series. HPLC then gives good resolution of the components of each series. The details presented in Figs. 3A and 3B/C are an excellent demonstration of how chromatographic properties can be altered by switching between normal (silica) and reversed-phase (C₁₈) systems. Remarkably, the HPLC separation also allowed isolation of small amounts of homologues bearing a 4-neopentyl substituent, these being the first natural products bearing neopentyl substituents ever to be isolated and characterized.⁶⁸

Finally, the bacteriopheophorbides-e (17) (Scheme 7) from the homologous mixture of bacteriochlorophylls-e (7) have been studied by HPLC.⁷⁰ Here, the homologous mixture is simpler, consisting only of the

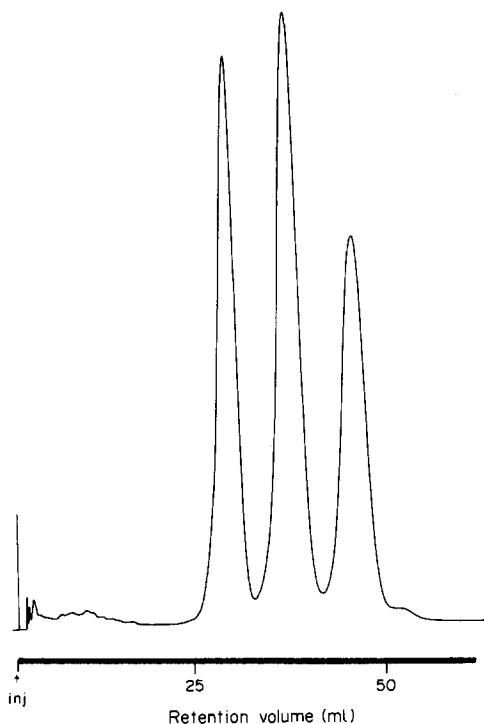


Fig. 4. High-performance liquid chromatogram⁷⁰ of the methyl bacteriopheophorbides-e from *Chlorobium pheobacteroides*. A Waters Z-module system equipped with a 10- μ m C₁₈ reversed-phase column was used; methanol-water solvent.

so-called 5-ethyl series.⁷¹ Once again, however, clear resolution of the three pigments is readily achieved, as shown in Fig. 4.⁷⁰

Acknowledgements—Support from the Calouste Gulbenkian Foundation and the National Science Foundation (CHE-81-20891) during the preparation of this review is gratefully acknowledged.

REFERENCES

- L. R. Vernon and G. R. Seely (eds.), *The Chlorophylls*, Academic Press, New York, 1966.
- K. M. Smith (ed.), *Porphyryns and Metalloporphyryns*, Elsevier, Amsterdam, 1975.
- A. S. Holt, in *Chemistry and Biochemistry of Plant Pigments*, T. W. Goodwin (ed.), 1st Ed., pp. 3–28. Academic Press, New York, 1965.
- H. Fischer and A. Stern, *Die Chemie des Pyrrols*, Vol. II, Part 2, Akademische Verlag, Leipzig, 1940.
- K. M. Smith, D. A. Goff and D. J. Simpson, *J. Am. Chem. Soc.*, 1985, **107**, 4946.
- M. Tsvett, *Ber. Deut. Botan. Ges.*, 1906, **24**, 384.
- Z. Sestak, *Photosynthetica*, 1980, **14**, 239.
- Idem, ibid.*, 1982, **16**, 568.
- H. H. Strain, B. T. Cope and W. A. Svec, *Methods Enzymol.*, 1971, **23**, 452.
- G. Zweig and J. Sherma, *Handbook of Chromatography*, Vols. I and II, Chemical Rubber Co., Cleveland, 1972.
- H. H. Strain and W. A. Svec, in *The Chlorophylls*, L. R. Vernon and G. R. Seely (eds.), Academic Press, New York, 1966.
- H. H. Strain and W. A. Svec, *Chromatography*, 3rd Ed., E. Heftmann (ed), p. 744. Van Nostrand Reinhold, New York, 1975.
- W. A. Svec, in *The Porphyrins*, Vol. V, D. Dolphin (ed.), p. 341. Academic Press, New York, 1978.
- L. R. Snyder and J. J. Kirkland, *Introduction to Modern Liquid Chromatography*, Wiley-Interscience, New York, 1979.
- K. M. Smith and D. A. Goff, *J. Chem. Soc., Perkin Trans. I*, 1985, 1099.
- K. M. Smith, L. A. Kehres, G. W. Craig and N. Pfennig, *J. Chromatog.*, 1983, **281**, 209.
- H. Brockmann, Jr., A. Gloe, N. Risch and W. Trowitzsch, *Ann. Chem.*, 1976, 566.
- H. H. Strain and T. R. Sato, *U.S. At. Energy Comm.*, 1956, TID 7512, p. 175.
- J. L. Wickliff, *Proc. Arkansas Acad. Sci.*, 1981, **35**, 78.
- S. Burke and S. Aronoff, *Anal. Biochem.*, 1979, **101**, 103.
- G. P. Berseneva and Z. Z. Finenko, *Okeanologiya*, 1975, **15**, 176.
- I. Csorba, Z. Buzas, B. Polyak and L. Boross, *J. Chromatog.*, 1979, **172**, 287.
- R. J. Daley, C. B. Gray and S. R. Brown, *ibid.*, 1973, **76**, 175.
- I. D. Jones, L. S. Butler, E. Gibbs and R. C. White, *ibid.*, 1972, **70**, 87.
- B. Scholtz, K. D. Willascheck, H. Mueller and K. Ballschmiter, *ibid.*, 1981, **208**, 156.
- B. Scholtz and K. Ballschmiter, *ibid.*, 1982, **252**, 269.
- A. F. H. Anderson and M. Calvin, *Arch. Biochem. Biophys.*, 1964, **107**, 252.
- K. Iriyama, N. Ogura and A. Takamiya, *J. Biochem. (Tokyo)*, 1974, **76**, 901; K. Iriyama, M. Shiraki and M. Yoshiura, *Chem. Lett.*, 1977, 787; K. Iriyama, *Biochem. Biophys. Res. Commun.*, 1978, **83**, 501.
- P. H. Hynninen, *Acta Chem. Scand.*, 1977, **B31**, 829.
- K. Iriyama, M. Shiraki and M. Yoshiura, *J. Liq. Chromatog.*, 1979, **2**, 255.
- M. Yoshiura, K. Iriyama, M. Shiraki and A. Okada, *Bull. Chem. Soc. Japan*, 1979, **52**, 2383.
- K. Iriyama, M. Yoshiura and M. Shiraki, *J. Chem. Soc., Chem. Commun.*, 1979, 406.
- K. Iriyama and M. Yoshiura, *J. Liq. Chromatog.*, 1982, **5**, 2211.
- K. Iriyama, M. Yoshiura, T. Ishii and M. Shiraki, *ibid.*, 1981, **4**, 533.
- T. Omata and N. Murata, *Plant Cell Physiol.*, 1983, **24**, 1093.
- E. Glynn-Jones, R. Marshall, R. A. Hann and G. Read, *J. Chromatog.*, 1975, **114**, 232.
- K. Iriyama and M. Yoshiura, *ibid.*, 1979, **177**, 154.
- N. Sato and N. Murata, *Biochim. Biophys. Acta*, 1978, **501**, 103.
- H. P. Hynninen and N. Ellfolk, *Acta Chem. Scand.*, 1973, **27**, 1463.
- C.-K. Wun, J. Rho, R. W. Walker and W. Litsky, *Hydrobiologia*, 1980, **71**, 289.
- J. W. Purdie and A. S. Holt, *Can. J. Chem.*, 1965, **43**, 3347.
- A. S. Holt, D. W. Hughes, H. J. Kende and J. W. Purdie, *J. Am. Chem. Soc.*, 1962, **84**, 2835.
- R. A. Chapman, M. W. Roomi, J. C. Norton, D. T. Krazcarski and S. F. MacDonald, *Can. J. Chem.*, 1971, **49**, 3544.
- H.-C. Chow, M. B. Caple and C. E. Strouse, *J. Chromatog.*, 1978, **151**, 357.
- M. B. Caple, H.-C. Chow, R. M. Burns and C. E. Strouse, *Brookhaven Symp. Biol.*, 1976, **28**, 56.
- G. W. Kenner, S. W. McCombie and K. M. Smith, *J. Chem. Soc., Perkin Trans. I*, 1973, 2517.
- H. R. Wetherell and M. J. Hendrickson, *J. Org. Chem.*, 1959, **24**, 710.
- A. Silveira, J. A. Koehler, E. F. Beadel and P. A. Monroe, *J. Chem. Educ.*, 1984, **61**, 264.

49. T. Watanabe, A. Hongu, K. Honda, M. Nakazato, M. Konno and S. Saitoh, *Anal. Chem.*, 1984, **56**, 251.
50. G. Gleixner, V. Karg and P. Kis, *Experientia*, 1982, **38**, 303.
51. B. Scholtz and K. Ballschmiter *J. Chromatog.*, 1981, **208**, 148.
52. S. Burke and S. Aronoff, *Chromatographia*, 1979, **12**, 808.
53. L. M. Brown, B. T. Hargrave and M. D. MacKinnon, *Can. J. Fish Aquat. Sci.*, 1981, **38**, 205.
54. G. Liebezeit, *High Resolut. Chromatog., Chromatog. Commun.*, 1980, **3**, 531.
55. S. W. Wright and J. D. Shearer, *J. Chromatog.*, 1984, **294**, 281.
56. J. Bessiere and A. Montiel, *Water Res.*, 1982, **16**, 987.
57. J. Abaychi and J. P. Riley, *Anal. Chim. Acta*, 1979, **107**, 1.
58. P. G. Falkowski and J. Sucher, *J. Chromatog.*, 1981, **213**, 349.
59. R. F. C. Mantoura and C. A. Llewellyn, *Anal. Chim. Acta*, 1983, **151**, 297.
60. T. Braumann and L. H. Grimme, *Biochim. Biophys. Acta*, 1981, **637**, 8.
61. S. J. Schwartz, S. L. Woo and J. H. von Elbe, *J. Agric. Food Chem.*, 1981, **29**, 533.
62. L. Goeyens, E. Post, A. Vanderhout and W. Baeyens, *Int. J. Environ. Anal. Chem.*, 1982, **12**, 51.
63. Y. Shioi, R. Fukae and T. Sasa, *Biochim. Biophys. Acta*, 1983, **722**, 72.
64. Y. Shioi, M. Doi and T. Sasa, *J. Chromatog.*, 1984, **298**, 141.
65. R. Steiner, H. Wieschhoff and H. Scheer, *ibid.*, 1982, **242**, 127.
66. K. M. Smith, L. A. Kehres and H. D. Tappa, *J. Am. Chem. Soc.*, 1980, **102**, 7149.
67. K. M. Smith, D. A. Goff, J. Fajer and K. M. Barkigia, *ibid.*, 1982, **104**, 3747.
68. *Idem*, *ibid.*, 1983, **105**, 1674.
69. T. Kemmer, H. Brockmann, Jr. and N. Risch, *Z. Naturforsch.*, 1979, **34b**, 633.
70. D. J. Simpson and K. M. Smith, unpublished results.
71. H. Brockmann, Jr., A. Gloe, N. Risch and W. Trowitzsch, *Liebigs Annalen*, 1979, 408.

N,N'-DIPHENYLDITHIOMALONAMIDE AS A GRAVIMETRIC REAGENT FOR NICKEL AND COBALT*

T. PAL†, A. GANGULY and D. S. MAITY

Department of Chemistry, Indian Institute of Technology, Kharagpur 721 302, India

STANLEY E. LIVINGSTONE

School of Chemistry, University of New South Wales, Kensington, N.S.W., 2033, Australia

(Received 11 December 1985. Revised 7 April 1986. Accepted 31 July 1986)

Summary—*N,N'*-Diphenyldithiomalonamide, (C₆H₅.NH.CS)₂CH₂, is found to be a very suitable gravimetric reagent for nickel(II) and cobalt(II). The complexes, of composition Ni(C₁₅H₁₃N₂S₂)₂ and Co(C₁₅H₁₃N₂S₂)₃, are stable and can be weighed after drying at 110°. Separation from base metals has been studied, and the structural interpretation is supported by DTA, TG, infrared and NMR data.

Thioureas,¹ thiols,^{2,3} thio-acids and their derivatives,^{4,5} thiosemicarbazones⁶ and other sulphur-containing ligands⁷ have been widely used for gravimetric determination of nickel, and the determination of cobalt with such compounds has also been reported.^{8,9} Usually nickel and cobalt are determined with dimethylglyoxime¹⁰ and α -nitroso- β -naphthol,¹¹ respectively.

The conditions for the use of *N,N'*-diphenyldithiomalonamide (DPDTM) as a gravimetric reagent for nickel and cobalt were studied in this investigation. The procedure described below is not only very selective but also has good precision and accuracy.

EXPERIMENTAL

Reagents

DPDTM was prepared according to Barnikow *et al.*¹² Sodium (0.01 mole) dissolved in dry absolute alcohol (30 ml) was added to acetylacetone (0.01 mole) with stirring, at room temperature. After 5 min 0.02 mole of phenylisothiocyanate was added. The solution was kept cold for 24 hr, then poured into ice-cold water to give the desired compound, which is lemon yellow and sparingly soluble in alcohol; m.p. 152°.

Nickel nitrate and cobalt nitrate solutions were made in dilute nitric acid, standardised by conventional methods^{10,11} and diluted as desired.

Procedures

Nickel. An amount of stock solution containing 7.3–14.7 mg of nickel was diluted to about 200 ml with water, and heated to 60–65° on a water-bath. A 60% excess of 1% ethanolic solution of the reagent (*i.e.*, 10–20 ml) was added dropwise with constant stirring and the pH was raised to 7.0–8.0 by addition of 1M ammonia solution. After digestion on the water-bath for about 1 hr, the yellowish-brown precipitate was filtered off on a sintered-glass crucible

(porosity No. 4), washed with warm water (~60°), dried at 110° and weighed as Ni(C₁₅H₁₃N₂S₂)₂, which contains 9.33% of nickel (Table 1).

Cobalt. A solution containing 6.8–13.8 mg of cobalt was diluted to 200 ml with water and treated as for the nickel determination except that the pH was adjusted to 6.5–7.0. The chocolate brown precipitate is Co(C₁₅H₁₃N₂S₂)₃, which contains 6.44% of cobalt (Table 1).

Nickel in steel or aluminium alloy. Dissolve the sample in 6M hydrochloric acid with heating. Oxidize iron and carbides with a few drops of concentrated nitric acid. Dilute with water, filter off any silica, and make the filtrate up to volume in a 250-ml standard flask. Take a suitable aliquot containing 7.0–14.0 mg of nickel in a 500-ml beaker, dilute with water to 150 ml, and add 1 g of sodium potassium tartrate (dissolved in 5 ml of water) to the warm solution,

Table 1. Individual determination of nickel and cobalt

	Taken, mg	Weight of ppte, mg	Metal found, mg
Ni(II)	7.30	78.1, 78.2	7.28, 7.30
	10.30	110.1, 110.2	10.28, 10.30
	14.65	155.6, 155.6	14.63, 14.63
Co(II)	6.80	105.5, 105.3	6.80, 6.80
	9.65	150.1, 150.2	9.67, 9.67
	13.80	213.6, 213.8	13.77, 13.80

Table 2. Determination of nickel in a steel and an alloy

Sample composition, %	Nickel found, %
C, 0.39; Mn, 0.79;	7.15
Ni, 7.15; Cr, 0.69	7.14
C, 0.1; Cr, 17.51;	9.50
Ni, 9.48;	9.48
C, 0.06; Cr, 16.47;	16.50
Ni, 16.47; Mo, 2.7;	16.57
Cu, 1.98; Cr, 1.05; Fe, 0.69; Mg, 0.21;	1.09
Ni, 1.10; Si, 10.73; Zn, 0.26;	1.09
Al, 83.98;	
Cu, 2.72; Cr, 0.09; Fe, 0.99;	1.50
Ni, 1.50; Si, 5.56, V, 0.007;	1.51
Zn, 1.76; Al, 87.37	

*This work was accepted for presentation at the International Symposium on Metal Speciation, Separation and Recovery (July 1986), held in Chicago, U.S.A.

†Author for correspondence.

Table 3. Analytical data

Compound		M	C	N	H	S
$(C_6H_5.NH.CS)_2CH_2; LH$	Found, %	—	62.4	9.7	4.8	22.4
	Theory, %	—	62.9	9.8	4.9	22.4
CoL_3	Found, %	6.4	59.0	9.1	4.3	20.6
	Theory, %	6.4	59.1	9.2	4.3	21.0
NiL_2	Found, %	9.3	56.4	8.5	4.2	19.9
	Theory, %	9.3	57.3	8.9	4.1	20.4

Table 4. Thermal decomposition studies of $Ni(DPDTM)_2$ and $Co(DPDTM)_3$

Compound	Decomposition temperature, °C		Final decomposition weight loss, %	
	First	Final	Obsvd.	Calc.
$Ni(DPDTM)_2$	160	500	88.1	88.1
$Co(DPDTM)_3$	150	510	91.6	91.2

followed by 10–20 ml of 1% ethanolic reagent solution, as appropriate. Raise the pH to *ca.* 7.0 with 1M ammonia solution and keep the mixture warm for 45 min. Filter off, wash, dry and weigh, as above. Copper, if present, can be removed by rapid precipitation with H_2S from acid solution. A large excess of Fe(III) (>15-fold ratio to nickel) can be masked with fluoride. Results for the determination of nickel in several samples are given in Table 2.

RESULTS AND DISCUSSION

Nature of the complexes

The complexes are fairly soluble in common organic solvents. They were analysed for nitrogen by the Dumas method and for sulphur by its conversion into sulphate. The metal contents were determined after oxidative decomposition of the complex. The results in Table 3 indicate 1:2 complexation of nickel and 1:3 complexation of cobalt.

The magnetic susceptibilities of the complexes were measured on a Gouy balance; both complexes are diamagnetic. The diamagnetism of nickel chelate supports the assignment of a square-planar structure and low-spin arrangement of the electrons in the split

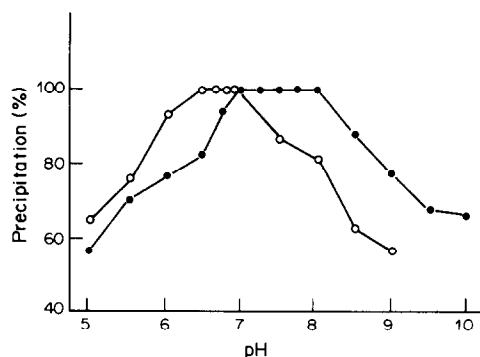


Fig. 1. Variation of degree of precipitation with pH. Nickel —●—; cobalt —○—.

d-orbitals. Cobalt(II) produces the chocolate brown cobalt(III) chelate. The diamagnetism indicates an octahedral low-spin arrangement and also suggests transition from the $^1A_{1g}$ ground state to $^1T_{1g}$ and $^1T_{2g}$ excited states.

Thermogravimetric studies

Oven-dried samples of the chelates (60 mg) were mixed with aluminium oxide and heated at $10^\circ/\text{min}$ in a Metriplex Derivatograph model OD-102, with DTA sensitivity 1/10. The first and final decompositions are recorded in Table 4. The thermogravimetric curves are given in Fig. 2 and show that the thermal stabilities of the two chelates are similar. The complexes are hygroscopic but the uptake of

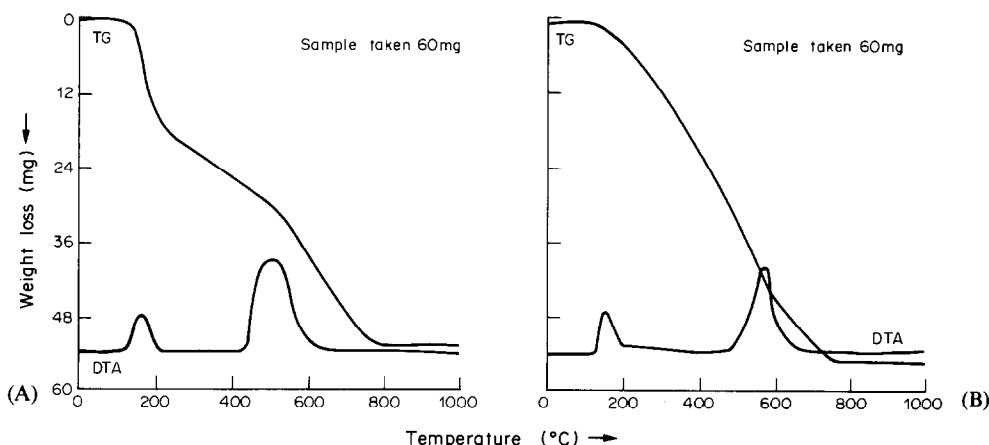


Fig. 2. Thermal decomposition curves of (A) NiL_2 , (B) CoL_3 .

Table 5. Infrared spectra of reagent and its nickel(II) and cobalt(III) complexes

Compound	Maxima, cm^{-1}
LH	226, 255, 310, 352, 389, 410, 436, 459, 549, 592, 618, 850 $\nu(C=S) + \delta(C-H)$, 1115 $\nu(C-S)$, 1525 $\nu(C=C)$, 1590 $\nu(C=S)$.
NiL ₂	202, 230, 254, 277, 352, 387, 480 $\nu(Ni-S)?$, 484, 540 wsh, 605, 616, 645, 790, 850 $\nu(C=S) + \delta(C-H)$, 1115 $\nu(C-S)$, 1175, 1525 $\nu(C=C)$, 1590 $\nu(C=S)$.
CoL ₃	186, 203, 226, 254, 350, 389, 411, 437, 500, (Co-S)?, 549, 593, 617, 850 $\nu(C=S) + \delta(C-H)$, 1115 $\nu(C-S)$, 1525 $\nu(C=C)$, 1590 $\nu(C=S)$.

water over a 24-hr period is too slow to be of significance, and the water may readily be removed by heating at 110°, with no decomposition of the complex. The decomposition starts at 130° in both cases. The final weight losses of 88.1% for nickel and 91.6% for cobalt are in agreement with expectation from the formulae. The DTA curves indicate that the decomposition takes place in two stages, the final products being NiO and Co₃O₄. The thermogram of the nickel complex is slightly different from that of the cobalt complex, probably because of the presence of two isomeric forms of the nickel chelate, whereas cobalt forms a single compound. This was further evidenced by the NMR spectra.

Mass spectra

Owing to the easy pyrolysis of both chelates the mass spectra were unsatisfactory and the molecular ion (M⁺) peaks could not be obtained.

Infrared spectra

The infrared spectra of the chelates and the reagent in a KBr matrix possessed some interesting features, noted in Table 5. The metal-sulphur bond stretching frequency would be expected in the range 360–380 cm^{-1} but was not observed in either case; it is not always observed, as recorded by Martin and co-workers.^{13,14}

NMR spectra

The ¹H NMR spectrum of the ligand was obtained from a solution of the reagent in a mixture of CDCl₃ and DMSO-*d*₆. The spectra of the nickel(II) and cobalt(III) complexes were obtained from CDCl₃ solutions. The data are given in Table 6.

The spectrum of the reagent shows the presence of two methylene signals at 4.4 and 4.3 ppm in *ca.* 9:1 ratio. This suggests that in solution there is a mixture of the tautomeric forms (I) and (II). The small broad signal at 11.24 ppm indicates the presence of a thiol proton as in tautomer (II).

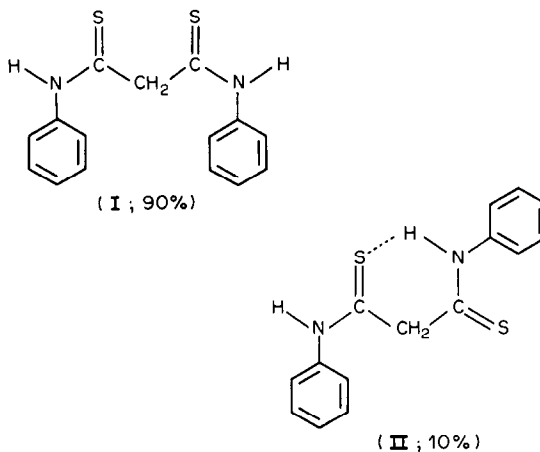
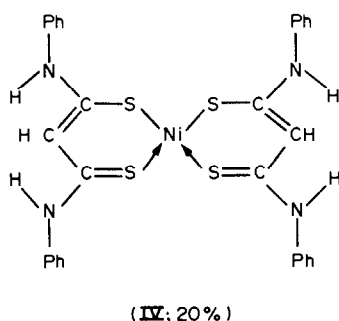
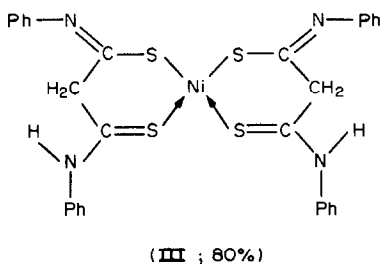


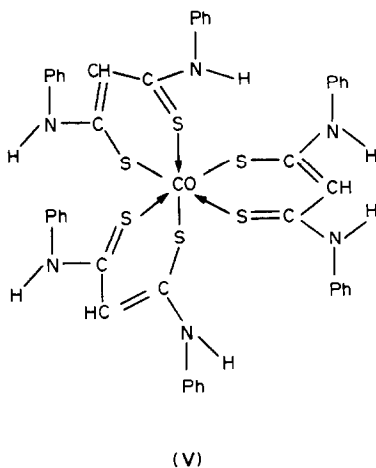
Table 6. NMR signals for the reagent and its nickel(II) and cobalt(III) complexes

Compound	Chemical shift, ppm	No. of protons	Assignment	Structure
LH	4.4 s	2	—CH ₂ —	I
	7.3–7.8 m	10	Ar—H	
	10.16 m	2	—NH—Ph	
	4.3 s		—CH ₂ —	II
	7.2–7.87 m		Ar—H	
	11.24		—SH	
NiL ₂	4.10 s	2	—CH ₂ —	III
	6.95 t	2	Ar.H	
	7.10 t	4		
	7.59 d	4		
	11.0 s	2		
	5.95 s		C=CH—	
6.75–7.10 m		C=CH—		
CoL ₃	6.10 s	1	C=CH	V
	7.10 m	5	Ar—H	
	7.25 m	5		
	7.70 s	2		

The spectrum of the nickel complex indicates the presence of two forms (III) and (IV) in a ratio of *ca.* 4:1. The data suggest that the structures are as shown below.



The spectrum of the cobalt complex indicates the presence of only one isomer, which is considered to have structure (V) which is analogous to the (IV) isomer of the nickel complex. The singlet at 7.7 ppm (multiplicity 2) is tentatively assigned to the PhN-H protons.



Effect of reagent concentration and pH

Approximately 60% excess of reagent was found necessary for quantitative precipitation. Nickel and cobalt start to precipitate at pH 5.0, the ranges for quantitative precipitation being 7.0–8.0 and 6.5–7.0, respectively. At higher pH precipitation is incomplete. The effect of pH is shown in Fig. 1.

Table 7. Tolerance limits for determination of 14.65 mg of Ni and 9.65 mg of Co

Diverse ion, mg	Found, mg	
	Ni	Co
Na ⁺ , 1000	14.66, 14.63	9.68, 9.65
Ca ²⁺ , 1000	14.65, 14.67	9.67, 9.64
Mg ²⁺ , 1000	14.66, 14.68	9.66, 9.65
Zn ²⁺ , 1200	14.65, 14.65	9.64, 9.63
Cd ²⁺ , 100	14.67, 14.63	9.65, 9.64
Cu ²⁺ , 50	14.61, 14.63	9.63, 9.67
Pb ²⁺ , 1000	14.64, 14.67	9.65, 9.67
Bi(III), 1000	14.65, 14.66	9.66, 9.68
As(V), 1000	14.68, 14.64	9.67, 9.65
Sb(V), 1000	14.65, 14.64	9.64, 9.63
Sn(II), 200	14.69, 14.64	9.62, 9.63
Fe ³⁺ *, 1400	14.64, 14.67	9.66, 9.63
Fe ²⁺ *, 1200	14.65, 14.63	9.65, 9.66
Al ³⁺ , 1800	14.63, 14.65	9.65, 9.67
Zr(IV), 1000	14.65, 14.64	9.64, 9.63
Cr ³⁺ , 1000	14.64, 14.61	9.63, 9.67
Mn ²⁺ , 1800	14.68, 14.65	9.65, 9.66
VO ²⁺ , 1000	14.67, 14.65	9.68, 9.65
MoO ₄ ²⁻ , 200	14.60, 14.63	9.62, 9.63
WO ₄ ²⁻ , 1000	14.65, 14.64	9.64, 9.64

*In presence of fluoride.

Effect of sequestering agents

Reasonable amounts of tartrate, ascorbic acid, fluoride and triethanolamine do not hinder quantitative precipitation in either case, so they can be used as sequestering agents, but Na₂EDTA hinders precipitation of both metal ions.

Effect of diverse ions

The precipitation of nickel along with cobalt cannot be avoided when the procedure given above is used. Tests of other metal ions were made on aqueous solutions of the chlorides, sulphates or nitrates, containing small quantities of suitable acids to prevent hydrolysis. For studying the effect of tungstate or molybdate either the sodium or ammonium salt was used. Iron(III) and iron(II) can both be masked with fluoride, but a large excess of copper must be removed by precipitation of CuS with H₂S from acid solution. The results of the tests on potential interferences are given in Table 7.

Precision and accuracy

The relative standard deviations were 0.2% for nickel and 0.6% for cobalt. Typical 95% confidence limits were Ni 14.65 ± 0.01 mg and Co 9.65 ± 0.02 mg (30 determinations).

REFERENCES

1. P. Capitan and F. Salinas, *Bol. Soc. Quim. Peru*, 1967, **33**, 1.
2. E. Domagalina and L. Przyborowski, *Z. Anal. Chem.*, 1965, **207**, 411.
3. J. A. W. Dalziel and A. K. Slawinski, *Talanta*, 1968, **15**, 1385.
4. B. Janik, B. Sawicki and R. Zimon, *Chem. Anal. (Warsaw)*, 1965, **10**, 121.

5. A. K. Majumdar, *J. Ind. Chem. Soc.*, 1941, **18**, 415.
6. S. Stankoviansky, J. Carsky and A. Beno, *Chem. Zvesti*, 1969, **23**, 589.
7. N. K. Dutt and B. K. Bhattacharjee, *Indian J. Appl. Chem.*, 1964, **27**, 195.
8. D. C. Sen, *J. Ind. Chem. Soc.*, 1938, **15**, 473.
9. H. H. Willard and D. Hall, *J. Am. Chem. Soc.*, 1922, **44**, 2226.
10. O. Brunck, *Angew. Chem.*, 1914, **27**, 315.
11. H. Herfeld and O. Gerngross, *Z. Anal. Chem.*, 1934, **98**, 408.
12. V. G. Barnikow, V. Kath and D. Richter, *J. Prakt. Chem.*, 1965, **30**, 63.
13. A. R. Hendrickson and R. L. Martin, *Inorg. Chem.*, 1973, **12**, 2582.
14. T. N. Lockyer and R. L. Martin, *Progr. Inorg. Chem.*, 1980, **27**, 223.

PREPARATION, MESOMORPHIC PROPERTIES AND BEHAVIOUR OF 4,4'-BIPHENYLENEDIBENZOATES AS STATIONARY PHASES IN GAS CHROMATOGRAPHY

GIUSEPPE CHIAVARI, LUCIANA PASTORELLI and GEORGIOS PERRAKIS

Istituto Chimico "G. Ciamician", Università di Bologna, Via Selmi, 2, 40100 Bologna, Italy

(Received 27 March 1986. Revised 26 May 1986. Accepted 27 July 1986)

Summary—This paper describes the preparation, mesomorphic properties and behaviour as stationary phases of a series of biphenylenedibenzoates. These compounds exhibit broad mesomorphic ranges with high solid-crystal-liquid-crystal transition temperatures, and give relatively short retention times in the determination of polynuclear aromatic hydrocarbons. The chromatographic selectivity for linear and planar structures is confirmed.

Liquid crystals¹ are interesting states of matter, intermediate between crystalline solids and isotropic liquids. In the liquid-crystal state, the molecules exhibit some degree of order in that they cannot rotate freely; they are normally rod-shaped and have to lie parallel to each other. These compounds show mechanical properties specific to liquids, but at the same time reveal the anisotropic properties of a solid crystal, such as birefringence.

The ordered arrangement of liquid crystals results in unusual solvent properties; the more easily the solute molecules fit into the ordered liquid crystal lattice, the more easily do they dissolve. In particular, positional isomers exhibit different solubilities in mesomeric phases, owing to differences in their length/breadth ratios and molecular planarity. This selective solubility has been found useful for the gas chromatographic separation of many substances with identical or very similar boiling points (*e.g.*, isomers), which are difficult to separate on conventional stationary phases.

These unusual solvent properties were initially applied to the separation of the positional isomers of various disubstituted benzenes.²⁻⁵ Since then, liquid-crystal stationary phases have been applied successfully in the separation of complex mixtures of aromatic polycyclic hydrocarbons,⁶ steroid epimers,⁷ azaheterocyclic compounds⁸ and monochlorobiphenyls.⁹ Several papers have described the synthesis of liquid crystals suitable for use as stationary phases¹⁰⁻¹² and commercial liquid-crystal stationary phases are also available.

In our earlier papers¹³⁻¹⁵ we described the synthesis and chromatographic properties of some naphthalene diesters with relatively large mesomeric ranges. In the present paper, we report a study on some liquid-crystal structures with biphenyl as the central group. We report the preparation and mesomorphic properties, together with the behaviour as stationary

phases, of eight 4,4'-biphenylene di(*para*-substituted benzoate)s.

EXPERIMENTAL

Preparation of materials

The mesomeric substances were synthesized by a method similar to that of Dewar.⁴ The acid chloride was first prepared by boiling the appropriate *para*-substituted acid (1 mole) with an excess of thionyl chloride (2 moles) for 8 hr. The excess of thionyl chloride was removed by distillation under reduced pressure. To the residual acid chloride (1 mole) dissolved in anhydrous pyridine, was added dropwise a solution of 4,4'-dihydroxybiphenyl (0.5 mole) in pyridine, with stirring. The mixture was maintained at 50° for 30 min and then left at room temperature for 48 hr.

The precipitate was collected and washed with pyridine, water and ethanol. As diesters can be soluble in pyridine, the filtrate (or the reaction solution, if no precipitate was obtained) was acidified to pH 1. The precipitate was washed a few times with water then stirred with 5% sodium carbonate solution for 1 hr and the residual diester was filtered off.

The dibenzoates were recrystallized three times before the determination of their transition temperatures.

The infrared spectrum of the synthesized compounds showed a typical absorption band of aromatic esters, with the C=O stretching band at 1730 cm⁻¹.

Structures, yields, recrystallization solvents and transition temperatures of the synthesized diesters are collected in Table 1.

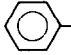
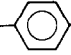
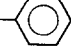
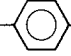
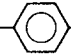
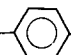
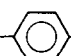
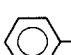
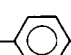
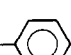
The column packing was prepared with Chromosorb W (80-100 mesh) as the inert support, and solutions of the mesomeric diester in the appropriate solvent, or dry mixtures of support and solid diester. The characteristics of the columns used are listed in Table 2. The columns were heated to about 100° above the solid-liquid crystal transition temperature, before cooling to the temperature chosen for analysis. This heating-cooling cycle was repeated each time the column was used.

The reagents and solvents used for the synthesis and gas-chromatographic studies were the best available and were used as received.

Apparatus

Gas chromatograms were obtained with a Carlo Erba Fractovap 4200 with flame ionization detector and linear

Table 1. Yields, recrystallization solvents and transition temperatures for diesters of the general structure $(\text{RCOOC}_6\text{H}_4\text{---})_2$

Compounds	R	Esterification yield, %	Recrystallization solvent	Transition temperatures,* °C		
				to smectic	to nematic	to isotropic
I	 -CH ₂ -O- 	40	Chloroform		240	310†
II	CH ₂ =CHCH ₂ -O- 	15	Chloroform		184	277
III	C ₃ H ₇ O- 	40	Chloroform	188	214	386
IV	C ₆ H ₁₃ O- 	87	Ethylacetate	158	175	340†
V	N≡C- 	78	Chlorobenzene		242	340†
VI	CH ₃ O- 	89	Pyridine		250	350†
VII	 - 	89	Pyridine		308	390†
VIII	NO ₂ - 	90	Chlorobenzene		254	370†

*Determined by differential thermal analysis (DTA).

†Suffers decomposition.

temperature programmer; the detector output was displayed on a Houston Omniscrite recorder or on a C-R1A Shimadzu data processor. The nitrogen carrier gas flow-rate was 30 ml/min, that of air 250 ml/min and that of hydrogen 30 ml/min.

For the identification of mesomeric compounds and intermediates a Perkin-Elmer 682 infrared spectrophotometer was used.

Transition temperatures were determined by differential scanning calorimetry (Perkin-Elmer DSC2; scan-rate: 10°/min).

The texture of the mesophases was studied by use of a Leitz Wetzlar melting point apparatus with a viewing microscope and provision for observing birefringence.

RESULTS AND DISCUSSION

In our previous investigations on liquid-crystal stationary phases in gas chromatography, we studied the influence of naphthalene, as the central group, on the tendency to form mesophases and on their behaviour as chromatographic solvents. To obtain a better understanding of the effect of the type of central group, we extended the study to the biphenyl group by preparing a series of 4,4'-biphenylenedibenzoates with different *para*-substituents on the benzoic acid.

Thermal analysis (Table 1) shows that all the

Table 2. Chromatographic columns*

Column number	Length, <i>m</i>	Stationary phase	Concentration of stationary phase, %	Stationary phase solvent
1	2	I	15	Chloroform
2	2	II	15	Chloroform
3	2	VI	15	Dry packing
4	1	VI	3	Dry packing
5	2	III	15	Dry packing
6	2	III	15	Chloroform
7	3	III	15	Chloroform
8	2	IV	15	Ethylacetate
9	2	VIII	15	Dry packing
10	2	V	15	Dry packing

*Stainless-steel tubing, 4 mm outer diameter.

compounds exhibit a nematic phase with a broad mesomeric range. However, the mesomorphic range is not completely available for chromatographic use because several substances begin to decompose at a temperature of approximately 350°. Differential scanning calorimetric (DSC) traces were reproducible, from cycle to cycle, provided that the sample was heated to a temperature no higher than 150° above the solid-crystal transition temperature.

This incomplete availability of the mesomeric range for gas chromatographic use is not important, because it is known that the best chromatographic performances are usually obtained at the lowest temperatures of the mesophase or in the supercooled mesophase when its ordering is at its highest.

Table 3. Chromatographic behaviour of pairs of positional isomers

Column number	Compound	t_r , min	α^*	R^\dagger	β^\S
1	<i>m</i> -methyltoluate	3	—	—	—
	<i>p</i> -methyltoluate	3.6	—	—	—
	1-acetylnaphthalene	14.6	1.4	1.0	1.2
	2-acetylnaphthalene	21	—	—	1.6
2	<i>m</i> -methyltoluate	2.1	1.3	0.5	—
	<i>p</i> -methyltoluate	2.8	—	—	—
	1-acetylnaphthalene	17.4	1.7	1.0	1.2
	2-acetylnaphthalene	29	—	—	1.2
3	<i>m</i> -methyltoluate	1.7	1.7	0.8	—
	<i>p</i> -methyltoluate	2.9	—	—	—
	1-acetylnaphthalene	7.8	1.8	1.0	1.0
	2-acetylnaphthalene	14.3	—	—	1.1
5	<i>m</i> -methyltoluate	2.1	1.3	1.0	1.0
	<i>p</i> -methyltoluate	2.8	—	—	1.0
	1-acetylnaphthalene	9.4	1.5	1.0	1.0
	2-acetylnaphthalene	14.6	—	—	1.1
6	<i>m</i> -methyltoluate	5.2	1.2	1.0	1.4
	<i>p</i> -methyltoluate	6.4	—	—	1.8
	1-acetylnaphthalene	14.8	1.5	1.0	1.6
	2-acetylnaphthalene	22.8	—	—	1.8
7	<i>m</i> -methyltoluate	7.2	1.4	1.0	1.0
	<i>p</i> -methyltoluate	10.1	—	—	1.0
	1-acetylnaphthalene	27.6	1.6	1.0	1.0
	2-acetylnaphthalene	43.4	—	—	1.0
8	<i>m</i> -methyltoluate	7.4	1.2	0.8	1.0
	<i>p</i> -methyltoluate	9.1	—	—	1.2
	1-acetylnaphthalene	18	1.4	1.0	1.6
	2-acetylnaphthalene	25.9	—	—	1.3
9	<i>m</i> -methyltoluate	—	—	—	—
	<i>p</i> -methyltoluate	—	—	—	—
	1-acetylnaphthalene	4.9	1.7	1.0	1.3
	2-acetylnaphthalene	7.9	—	—	2.5
10	<i>m</i> -methyltoluate	—	—	—	—
	<i>p</i> -methyltoluate	—	—	—	—
	1-acetylnaphthalene	2.6	1.7	0.9	1.1
	2-acetylnaphthalene	4.5	—	—	3.0

*The separation factor α was determined as the ratio of corrected retention times ($\alpha = t_{r2}/t_{r1}$).

†Resolution was determined by the ratio of the distance between peak maxima and their average peak width at base, as $R = (t_{r2} - t_{r1})/2(w_2 - w_1)$.

§The asymmetry factor β is measured at 10% of peak height as $\beta = B/A$ where A is distance from peak front to peak maximum and B is distance from peak maximum to peak tail.

Table 4. Chromatographic parameters for column 3

Compound	Column 3			
	Column temperature, °C	t_r , min	α	R
<i>m</i> -dimethoxybenzene	200	1.6	1.2	0.4
<i>p</i> -dimethoxybenzene		2.0		
<i>m</i> -methyltoluate	190	1.7	1.7	0.8
<i>p</i> -methyltoluate		2.9		
<i>m</i> -nitritololuene	170	2.3	1.5	0.7
<i>p</i> -nitritololuene		4.6		
<i>m</i> -methylacetophenone	200	2.0	1.5	0.9
<i>p</i> -methylacetophenone		3.0		
<i>m</i> -methoxyacetophenone	200	4.6	2.2	1.0
<i>p</i> -methoxyacetophenone		10.2		
dimethylisophthalate	230	4.5	1.4	1.0
dimethylterephthalate		6.3		
1-bromonaphthalene	220	6.0	1.2	0.7
2-bromonaphthalene		7.4		
1-acetylnaphthalene	230	7.8	1.8	1.0
2-acetylnaphthalene		14.3		
1-methoxynaphthalene	220	4.7	1.4	1.0
2-methoxynaphthalene		6.8		
1-ethylnaphthalene	200	3.3	1.3	0.5
2-ethylnaphthalene		4.3		
phenanthrene	250	12.5	1.3	1.0
anthracene		16.3		

Table 5. Chromatographic parameters for column 7

Compound	Column 7			
	Column temperature, °C	t_r , min	α	R
<i>m</i> -dimethoxybenzene	190	6.8	1.3	1.0
<i>p</i> -dimethoxybenzene		8.2		
<i>m</i> -methyltoluate	175	7.2	1.4	1.0
<i>p</i> -methyltoluate		10.1		
<i>m</i> -nitritololuene	175	7.0	1.4	1.0
<i>p</i> -nitritololuene		9.8		
<i>m</i> -methylacetophenone	190	6.2	1.4	1.0
<i>p</i> -methylacetophenone		9.0		
<i>m</i> -methoxyacetophenone	190	14.0	2.0	1.0
<i>p</i> -methoxyacetophenone		28.8		
<i>m</i> -cresol	170	7.0	1.1	0.5
<i>p</i> -cresol		7.7		
<i>m</i> -methylanisole	170	4.8	1.2	0.8
<i>p</i> -methylanisole		5.8		
<i>m</i> -chloroaniline	210	12.6	1.1	0.9
<i>p</i> -chloroaniline		14.0		
dimethylisophthalate	215	16.3	1.3	1.0
dimethylterephthalate		20.7		
1-bromonaphthalene	210	21.0	1.1	1.0
2-bromonaphthalene		23.8		
1-acetylnaphthalene	200	27.6	1.6	1.0
2-acetylnaphthalene		43.3		
1-methoxynaphthalene	210	16.8	1.3	1.0
2-methoxynaphthalene		21.6		
1-ethylnaphthalene	215	11.6	1.1	0.8
2-ethylnaphthalene		13.2		
1-methylnaphthalene	190	15.2	1.0	0
2-methylnaphthalene		—		
1-naphthylamine	225	10.4	1.2	1.0
2-naphthylamine		13.1		
naphthalene	180	9.0	—	—
tetrahydronaphthalene		4.2		
decahydronaphthalene (<i>cis</i>)	3.0	—	—	—
decahydronaphthalene (<i>trans</i>)	2.6	—	—	—

Table 6. Chromatographic parameters for column 5

Compound	Column 5		
	Column temperature, °C	t_r , min	α R
<i>m</i> -dimethoxybenzene	180	1.8	1.2 0.9
<i>p</i> -dimethoxybenzene		2.2	
<i>m</i> -methyltoluate		2.1	
<i>p</i> -methyltoluate	180	2.8	1.3 1.0
<i>m</i> -nitritololuene		1.9	
<i>p</i> -nitritololuene	175	2.6	1.4 0.9
<i>m</i> -methylacetophenone		2.1	
<i>p</i> -methylacetophenone	180	3.1	1.5 0.9
<i>m</i> -methoxyacetophenone		4.6	
<i>p</i> -methoxyacetophenone	190	8.8	1.9 1.0
<i>m</i> -methylanisole		0.7	
<i>p</i> -methylanisole	170	1.0	1.3 0.3
dimethylisophthalate		6.8	
dimethylterephthalate	210	8.3	1.2 0.9
1-bromonaphthalene		9.8	
2-bromonaphthalene	200	11.0	1.1 0.7
1-acetylnaphthol		6.6	
2-acetylnaphthol	220	9.2	1.4 1.0
1-acetylnaphthalene		9.4	
2-acetylnaphthalene	220	14.6	1.5 1.0
1-methoxynaphthalene		5.2	
2-methoxynaphthalene	210	6.8	1.3 0.9
1-ethylnaphthalene		9.8	
2-ethylnaphthalene	200	11.2	1.1 0.3
1-methylnaphthalene		4.0	
2-methylnaphthalene	190	4.0	1.0 0.0
1-naphthylamine		9.8	
2-naphthylamine	220	12.0	1.2 1.0
phenanthrene		19.6	
anthracene	220	24.6	1.3 1.0

Table 3 lists the measured retention times, together with other chromatographic parameters such as resolution (R), separation factor (α) and symmetry coefficient (β) for two test pairs of benzene positional

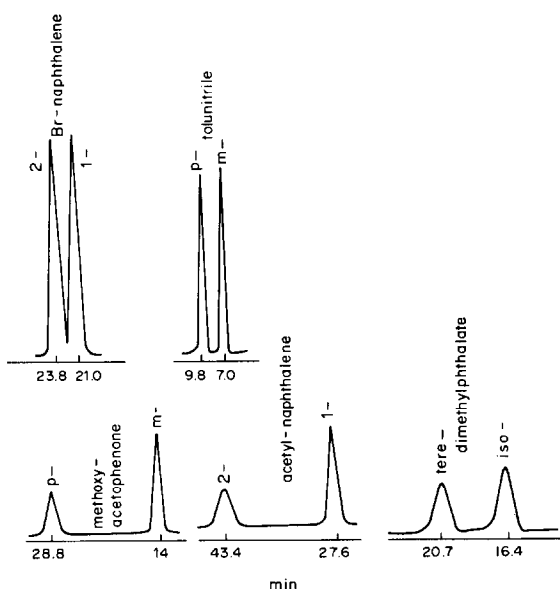


Fig. 1. Gas chromatograms of some isomeric pairs on column 7; separation temperatures are reported in Table 5.

Table 7. Chromatographic parameters for column 4

Compound	Column 4	
	Column temperature, °C	t_r , min
pyrene	240	3.4
benzo(c)phenanthrene	240	6.8
terphenylene	240	10.4
benzo(a)anthracene	240	14.6
benzo(a)phenanthrene	240	18.0
naphthacene	240	42.0
benzo(e)pyrene	280	4.3
benzo(a)pyrene	280	6.3

isomers in columns containing the synthesized compounds as stationary phases.

Tables 4-7 summarize the best performances of these stationary phases. The order of elution in all cases follows the same pattern, *i.e.*, the isomer with the largest length/breadth ratio is retained longer. Thus in the separation of *m*- and *p*-disubstituted

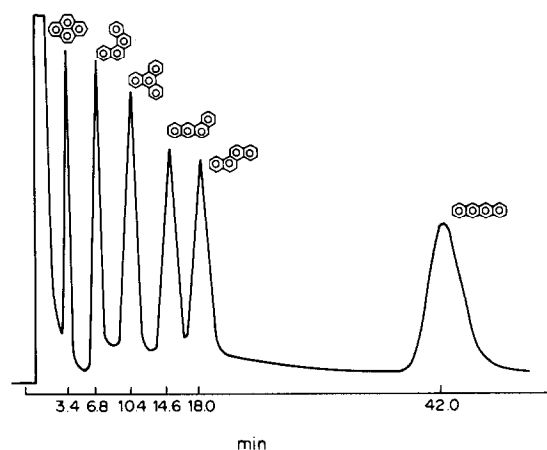


Fig. 2. Gas chromatographic separation of isomeric polynuclear compounds on column 4 at 240°C.

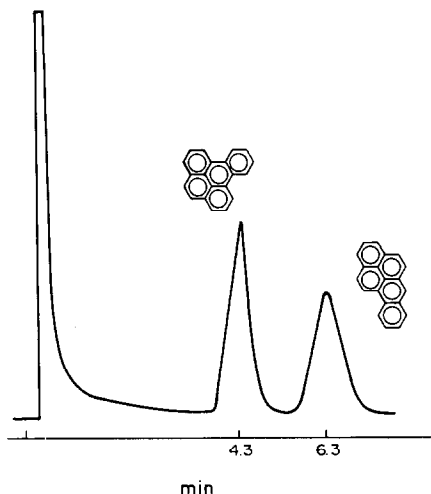


Fig. 3. Separation of benzopyrenes on column 4 at 280°C.

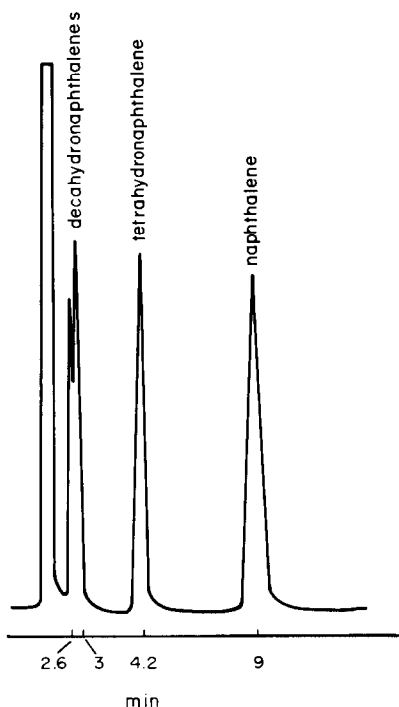


Fig. 4. Gas chromatographic separation of naphthalene and its hydrogenated derivatives on column 7 at 180°C.

benzenes it is the *para*-isomer which is retained longer, while in the separation of isomeric polynuclear hydrocarbons anthracene is eluted after phenanthrene. In addition, there is an effect of the length/breadth ratio and planarity on the selectivity (α). From the data presented in Table 4 for the pairs of *m*- and *p*-isomers of methylacetophenone, dimethoxybenzene and methoxyacetophenone (at the same temperature) we observe an α -value of 2.2 for the methoxyacetophenones (compound with the highest length/breadth ratio and greatest planarity) compared to a value of 1.5 for the methylacetophenones and 1.2 for the dimethoxybenzenes. The relatively low value for dimethoxybenzene isomers, which have a higher length/breadth ratio than methylacetophenone, can be explained by the lower planarity of the molecule.

Figures 1–3 show examples of chromatograms of polyaromatic hydrocarbons and isomeric substituted benzenes.

As reported earlier for biphenylene as the central group in the chromatographic solvent, the best results are obtained with alkyloxy-groups as terminal substituents. We have found that the *p*-propoxybenzoate diester gives the best performance in the separation of benzene and naphthalene positional isomers, while bis-*p*-methoxycinnamate, thanks to its higher solid–nematic transition temperature, permits the analysis of polyaromatic compounds in a relatively short time.

Figure 4 clearly shows the selectivity of the mesomeric solvent for the planar structures in a mixture of decahydronaphthalenes, tetrahydronaphthalene and naphthalene.

The thermal stability under normal working conditions was studied by keeping column 3 for 30 days at 200°. It exhibited no significant loss of efficiency after this treatment.

Acknowledgement—The support of this work by the Ministero della Pubblica Istruzione through Grant 8357 is gratefully acknowledged.

REFERENCES

1. G. W. Gray, *Molecular Structure and the Properties of Liquid Crystals*, Academic Press, New York.
2. H. Kelker, *Ber. Bunsenges. Phys. Chem.* 1963, **67**, 698.
3. *Idem*, *Z. Anal. Chem.*, 1963, **198**, 254.
4. M. J. Dewar and J. P. Schroeder, *J. Am. Chem. Soc.*, 1964, **86**, 5235.
5. *Idem*, *J. Org. Chem.*, 1965, **30**, 3485.
6. G. M. Janini, K. Johnston and W. L. Zielinski Jr., *Anal. Chem.*, 1975, **47**, 670.
7. W. L. Zielinski Jr., K. Johnston and G. M. Muschik, *ibid.*, 1976, **48**, 907.
8. M. Pailer and V. Hlozek, *J. Chromatog.*, 1976, **128**, 163.
9. K. P. Naikwadi, D. G. Panse, B. V. Bapat and B. B. Ghatge, *ibid.*, 1980, **195**, 309.
10. Z. Witkiewicz, *ibid.*, 1982, **251**, 311.
11. G. M. Muschik, T. Kelly and W. B. Manning, *ibid.*, 1980, **202**, 75.
12. S. Sakagami and M. Nakamizo, *ibid.*, 1982, **234**, 357.
13. G. Chiavari, A. Arcelli and A. M. Di Pietra, *Rend. Accad. Naz. Lincei*, 1972, **52**, 381.
14. G. Chiavari and L. Pastorelli, *Chromatographia*, 1974, **7**, 30.
15. *Idem*, *J. Chromatog.*, 1983, **262**, 175.

ACTION DES RAYONNEMENTS BETA ET DES OXYDANTS SUR LE DI-tert.BUTYL- 3,5 HYDROXY-4 TOLUENE

C. MAJCHERCZYK, P. POLGE, D. BAYLOCQ et F. PELLERIN

Laboratoire de Chimie Analytique, Centre d'Etudes Pharmaceutiques Université de Paris XI,
rue J. B. Clément, F92290 Chantenay-Malabry, France

(Reçu le 4 juin 1986. Accepté le 22 juillet 1986)

Résumé—Un procédé d'identification et dosage par HPLC du BHT et des produits de dégradation formés sous l'action des rayonnements beta et des agents d'oxydation est décrit. La structure des produits de dégradation résultant de l'irradiation et de l'oxydation du BHT est établie à l'aide de la spectrométrie de masse. L'irradiation conduit à la formation d'un dimère et d'un trimère de l'antioxydant et l'oxydation à celle d'aryl-cétones oxydées en position 1- (alcool primaire et aldéhydes).

Summary—An HPLC method for the identification and determination of BHT (3,5-di-tert.butyl-4-hydroxytoluene) and the by-products obtained from it by β -ray or oxidative treatment is described. The chemical structure of the by-products is established by mass spectrometry. The irradiation leads to the dimeric and trimeric forms of the antioxidant and the oxidation to a cyclohexa-2,5-dien-1-one with substitution of a hydroxy and a methanol or aldehyde group at position 4.

Le butyl-hydroxy toluène (BHT; di-tert.butyl-3,5 hydroxy-4 toluène) est un agent antioxydant courant de nombreux polymères de synthèse et est également largement utilisé dans le domaine alimentaire. La stérilisation par les rayonnements beta et gamma est le procédé de choix appliqué au matériel médico-chirurgical à usage unique. De nombreux travaux récents concernent l'étude des phénomènes de dégradation des polyoléfines soumis aux traitements d'irradiation; d'une façon générale les altérations se manifestent par des modifications des propriétés physiques des matériaux en relation avec des modifications chimiques (réticulation en particulier).¹⁻⁴

Dans le cas du polychlorure de vinyle plastifié, il se produit un jaunissement, une réticulation du matériau et une libération de produits chlorés.⁵ La dégradation des additifs se manifeste également par des altérations de couleur en particulier. Des essais antérieurs ont montré que certains additifs subissent une modification de leur structure au cours des traitements de stérilisation par les rayonnements beta et gamma. C'est ainsi que l'Irganox Goodrite 3114 donne lieu à la formation du di-tert.butyl-3,5 hydroxy-4 benzaldéhyde. Une précédente étude a permis de révéler l'existence de dégradation du BHT dans des produits radiostérilisés.^{6,7} Le BHT est également susceptible de s'oxyder spontanément à l'air.⁸

L'objet du présent mémoire concerne l'identification et l'étude de la structure des dérivés formes après irradiation et oxydation par voie chimique du BHT.

La chromatographie liquide et la spectrométrie de masse ont été appliquées en reprenant les schémas

d'études décrits dans le mémoire concernant le Goodrite 3114.⁹

PARTIE EXPERIMENTALE

Réactifs

BHT pur pour l'analyse (Merck); échantillons de BHT irradiés à 2,5, 5, et 10 Mrad; isocyanate de phényle R.P.; peroxyde d'hydrogène (30 volumes).

Appareillage

L'ensemble chromatographique est constitué d'une pompe haute pression Chromatem 320 équipée d'un programmeur 420, d'une vanne d'injection (Rhéodyne) munie d'une boucle de 20 μ l, d'un détecteur UV-visible (Kratos), d'une colonne de silice à polarité de phases inversée (C₁₈) de granulométrie 7 μ m, de 250 mm de longueur et de 4 mm de diamètre. La spectrométrie de masse est effectuée par un appareillage Nermag 10-10c.

Le traitement des données est effectué sur un ordinateur PD-P11. L'ionisation a lieu par impact électronique à 20 eV et l'ionisation chimique par l'ammoniaque.

Mise en évidence et analyse structurale des produits de dégradation formés par les traitements ionisants (rayons β)

Analyse par chromatographie liquide HPLC. Les échantillons et les témoins sont en solution à raison de 1 mg/ml dans l'acétonitrile respectivement pour le BHT irradié à 2,5, 5 et 10 Mrad et le BHT pur. Les conditions chromatographiques sont:

- phase mobile, acétonitrile 80, eau 20;
- débit 2 ml/min;
- détection à 280 nm.

Analyse structurale par spectrométrie de masse. Le procédé d'ionisation chimique par l'ammoniaque a été appliqué; l'injection est effectuée directement. L'échantillon soumis à l'analyse est une solution (dans l'acétonitrile) de BHT irradié à 10 Mrad; la solution témoin est préparée à partir de BHT pur.

RESULTATS

Les chromatogrammes obtenus à partir de l'analyse de solutions de BHT irradié révèlent la présence d'un produit de dégradation. Les temps de rétention sont respectivement 7,4 et 9,7 min pour le BHT et le dérivé formé.

L'intégration des réponses permet d'évaluer la teneur relative du dérivé par rapport à la concentration initiale en BHT. Les calculs effectués montrent que les teneurs croissent avec l'intensité du rayonnement: 0,7, 1,7 et 2,4 pour 2,5, 5 et 10 Mrad respectivement.

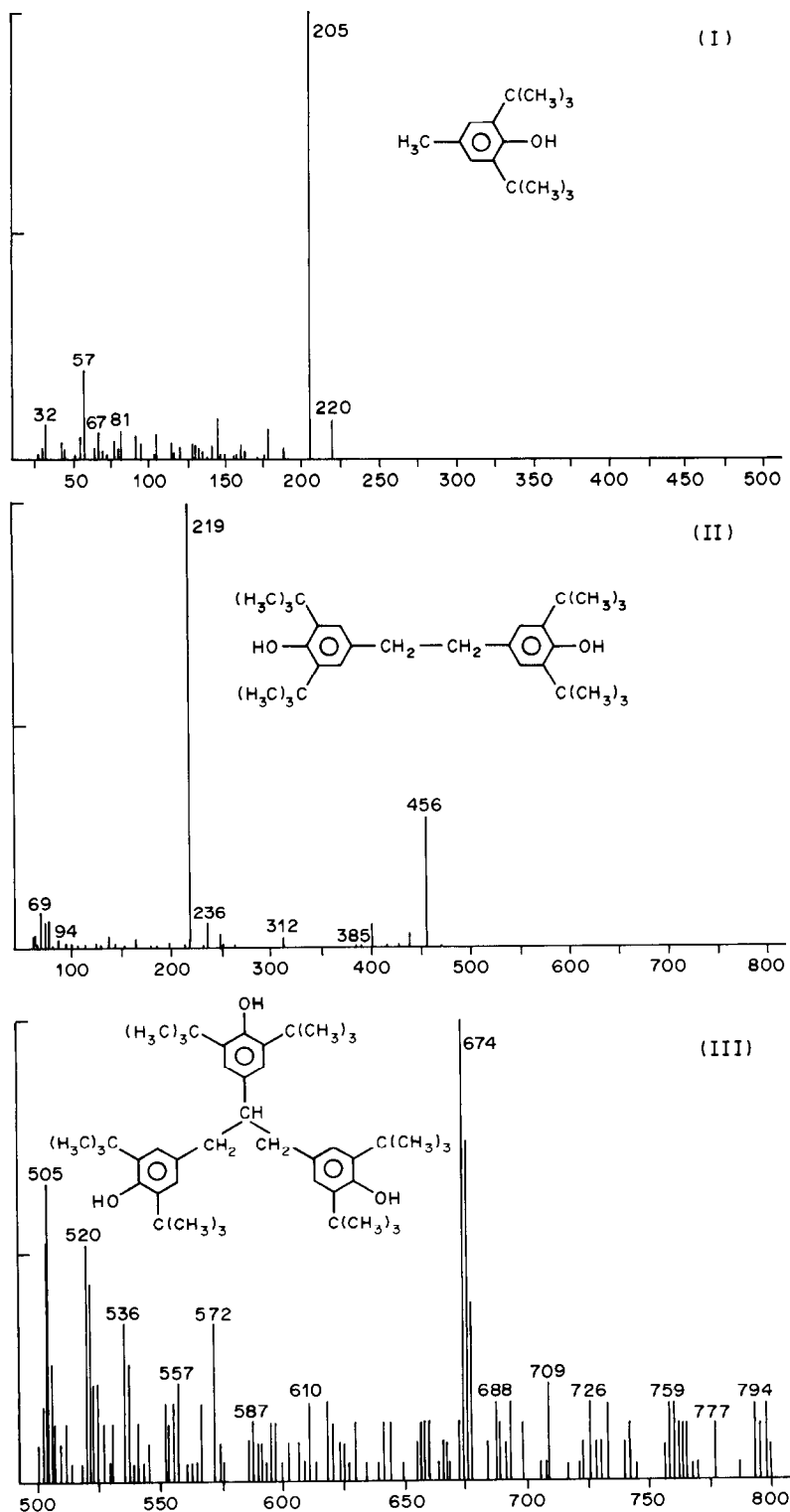


Fig. 1. Spectre de masse du BHT témoin (I) et irradié (II), (III).

Les spectres de masse (Fig. 1, I) révèlent les pics de masse suivants:

	M ⁺	(M + 18) ⁺
Témoin (I.E. 20 eV)	220	—
BHT(10-Mrad), (I.C. NH ₄ ⁺)	—	456, 674

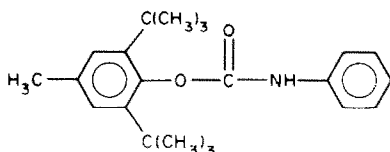
Les masses des produits de dégradation sont en conséquence 438 et 656. Elles caractérisent un dimère du BHT formés par l'irradiation de cet antioxydant aux rayons- β . Les configurations figurent ci-après. Il s'agit du monomère (I), dimère (II) et trimère (III) (Fig. 1).

Confirmation des structures par formation d'un dérivé chimique

La confirmation de la structure énoncée correspondant au dimère du BHT a été établie par formation d'un dérivé spécifique des groupements hydroxyles; celle-ci n'a pu être établie pour le trimère révélé en spectrométrie de masse, sa teneur dans l'échantillon irradié étant trop faible.

La réaction de l'isocyanate de phényle sur les groupements hydroxyles a été retenue pour former le dérivé. La formation de carbamate avec les éthers isocyaniques a été appliquée à la séparation et au dosage des alcools et phénols.

Dans le cas du BHT le dérivé obtenu est:



Dans le cas du dimère formé, une réaction analogue s'effectue sur les groupements hydroxyles. Les dérivés formés présentent une absorbance à 280 nm qui permet leur mise en évidence en HPLC.

Mode opératoire. Préparer une solution témoin (1 mg/ml) de BHT (irradié à 10 Mrad) dans l'acétonitrile. Pour la solution d'essai, introduire 50 mg de BHT dans une fiole jaugée de 50 ml, ajouter 0,5 ml d'isocyanate de phényle, compléter à 50 ml avec de l'acétonitrile pur, détruire l'excès de réactif par l'addition de méthanol dans les proportions suivantes: 4,5 ml de la solution d'essai, 0,5 ml de méthanol. Effectuer l'analyse HPLC sur une colonne à polarité de phase inversée suivant la technique précédemment décrite.

Résultats. La chromatographie de la solution de BHT irradié à 10 Mrad et traitée par l'isocyanate de phényle, révèle les produits dérivés du BHT et du dimère ainsi que la présence du BHT et du dimère résiduel, les temps de rétention étant 2,53 min pour le phénylcarbamate de méthyle (obtenu par réaction du réctif en excès avec le méthanol), 6,15 min pour le dérivé de BHT, 6,8 min pour le BHT, 9,42 min pour le dimère et 13,56 min pour le dérivé du dimère. L'obtention d'un dérivé à partir du dimère présent

dans l'échantillon irradié confirme la présence de groupements hydroxyles dans cette molécule.

Mise en évidence et analyse structurale des produits d'oxydation du BHT

L'irradiation des matières plastiques par les rayonnements β fait apparaître une coloration jaune qui s'atténue progressivement; ceci laisse supposer que les produits de dégradation formés sont instables et que le phénomène d'oxydation se poursuit.

Pour cette raison, il nous est apparu intéressant de poursuivre cette recherche par une comparaison entre les produits d'oxydation dans un échantillon irradié et ceux obtenus après oxydation chimique à partir d'un agent oxydant tel que le peroxyde d'hydrogène.

L'oxydation d'une solution de BHT dans l'acétonitrile a été réalisée par l'addition de peroxyde d'hydrogène; la cinétique de la réaction a été étudiée à température ambiante et à 60°, avec mise en évidence des produits formés, par chromatographie en phase liquide.

Des travaux antérieurs⁸ ont mis à profit cette réaction d'oxydation du BHT pour son dosage dans les polymères sans toutefois préciser l'identité du produit d'oxydation formé.

Cinétique d'oxydation. La cinétique d'oxydation du BHT a été examinée jusqu'à oxydation complète de ce dernier afin de pouvoir soumettre directement la solution obtenue à l'analyse par spectrométrie de masse et d'établir les structures des produits d'oxydation formés dans ces conditions.

Conditions opératoires. Introduire 100 mg de BHT dans une fiole de 100 ml, ajouter 70 ml d'acétonitrile et 30 ml de peroxyde d'hydrogène à 30 volumes; maintenir une partie aliquote à la température ambiante et une partie aliquote à 60°. Analyser ces prélèvements au temps 0 et à intervalles réguliers durant 5 hr selon la technique décrite précédemment.

Résultats. Les chromatogrammes font apparaître nettement des produits d'oxydation dont les concen-

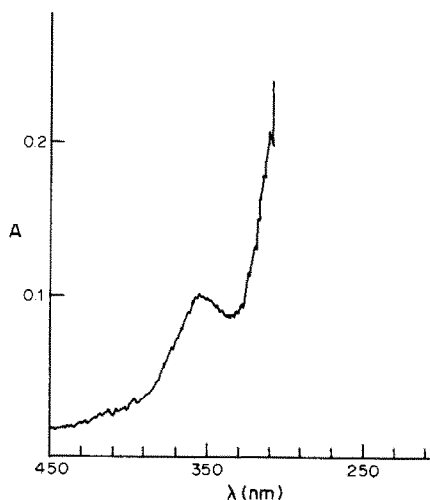


Fig. 2. Spectre d'absorption du dérivé d'oxydation du BHT (oxydation par le peroxyde d'hydrogène).

trations sont relativement faibles dans le cas de l'oxydation à la température ambiante poursuivie durant 4 hr. En revanche la réaction est accélérée par l'élévation de température et est totale après 5 hr à 60°C. Il apparaît alors deux produits d'oxydation formés au détriment du BHT (8 min). Un essai similaire a été effectué dans les mêmes conditions (24 hr, 60°). Il a confirmé la présence des deux produits d'oxydation ainsi que la disparition pratiquement totale du BHT. Le spectre d'absorption dans l'ultra-violet et l'analyse par spectrométrie de masse couplée à la chromatographie gaz-liquide ont été effectués sur cette solution.

Spectrométrie dans l'ultra-violet. Le spectre fait apparaître des maxima d'absorption à 280 et 350 nm. Ce dernier laisse présumer une forme aryl-cétone (Fig. 2).

Spectrométrie de masse (Fig. 3). La spectrométrie de masse a été réalisée par couplage à la chromatographie gaz-liquide. L'ionisation a été obtenue à l'aide d'ammoniac; elle a été appliquée à une solution de BHT dans l'acétonitrile.

Résultats. La chromatographie gaz-liquide couplée à la spectrométrie de masse révèle la présence de deux produits d'oxydation et confirme l'analyse chromatographique en phase liquide (HPLC). Les spectres

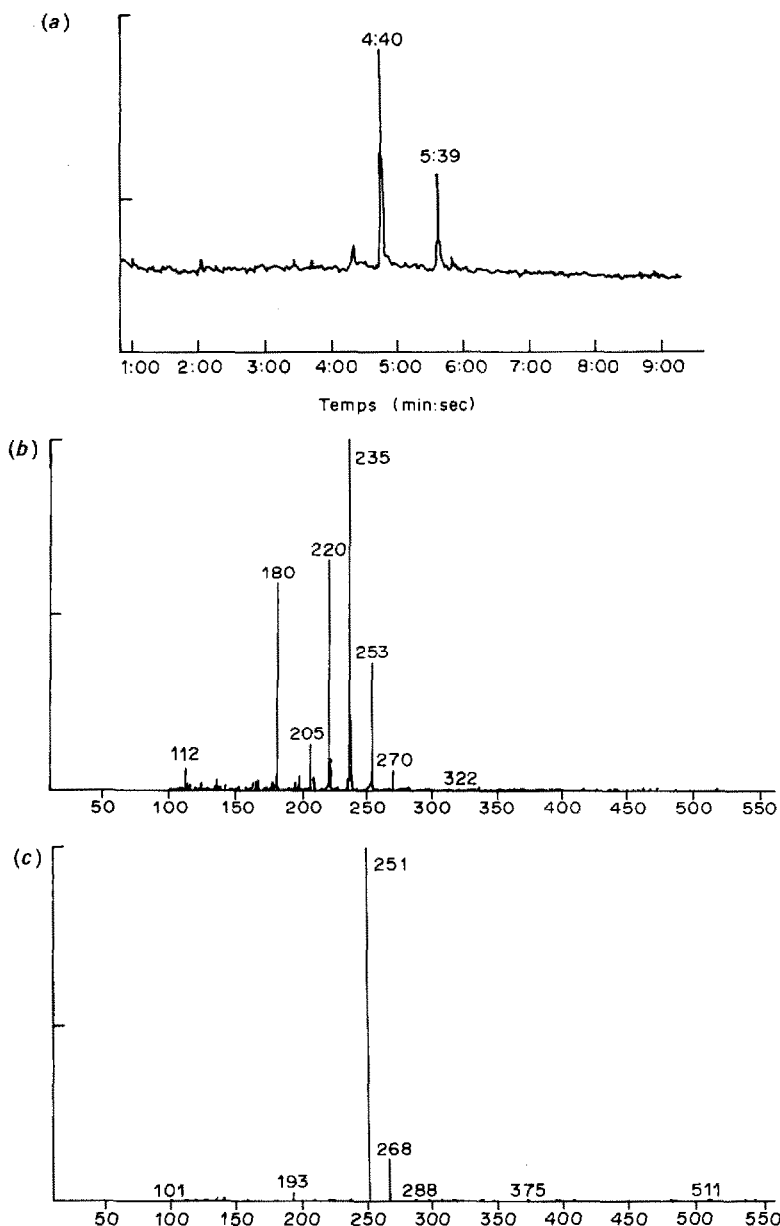
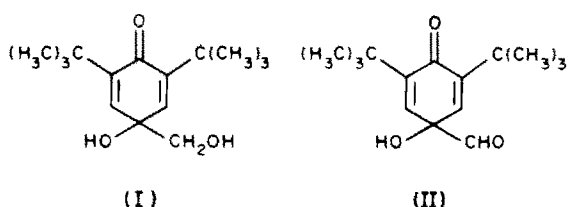


Fig. 3. Spectres de masse de produits d'oxydation du BHT par le peroxyde d'hydrogène. (a) Chromatographie gaz-liquide couplée à la spectrométrie de masse; (b) spectre de masse du produit avec $t_R = 3$ mn; (c) spectre de masse du produit avec $t_R = 3,5$ mn.

obtenus indiquent les pics pseudomoléculaires suivants:

Produit d'oxydation	Temps de rétention, mn:sec	(M + 1) ⁺ (M + 18) ⁺	
1	4:40	253	270
2	5:39	251	268

Les masses de deux produits d'oxydation sont alors I = 252, II = 250. Ceci nous conduit à émettre l'hypothèse de la formation de deux dérivés en position 4 dont l'un serait oxydé en 1 (C-méthyle) sous forme d'alcool primaire (I) et le second (II), dérivé du précédent aurait une fonction aldéhyde.



La confirmation de ces structures par dérivation chimique selon la méthode précédemment décrite n'a pu être obtenue, l'excès de peroxyde d'hydrogène dans la solution d'essai étant incompatible avec le réactif utilisé (isocyanate de phényle).

Il apparaît que les produits d'oxydation du BHT, formés dans les conditions opératoires retenues sont différents de ceux obtenus par l'action des rayonnements. Les dérivés I et II résultant de l'oxydation

chimique par le peroxyde d'hydrogène semblent être des produits intermédiaires d'oxydation du groupement méthyle en position 1. La poursuite de l'oxydation devrait conduire à une fonction acide qui n'a pu être obtenue dans les conditions opératoires retenues, la température de la réaction se trouvant limitée par le choix du solvant.

CONCLUSION

L'étude du comportement du BHT à la stérilisation par les rayonnements β et à l'oxydation par voie chimique, a conduit à la mise en évidence de produits de dégradation, ainsi qu'à l'établissement de leur structure. La connaissance de ces produits doit être prise en compte dans les recherches de compatibilité contenant-contenu entre les formes pharmaceutiques et les récipients, afin d'améliorer le contrôle de qualité des produits finis et assurer la sécurité de leur emploi.

LITTÉRATURE

1. Y. Arnaud, *Pharm. Hosp. Franç.*, 1973, **24**, 90.
2. G. V. Reed, *Brevet Franç.*, 1982, 822892 AI.
3. K. Kogaki, *Brevet Belge*, 1981, 894434 AI.
4. M. Kasai, T. Tchikawa et K. Kosegaki, *ibid.*, 1983, 896275 AI.
5. F. Guillot, *Thèse de Doctorat d'Etat*, Univ. Paris XI (à paraître).
6. D. Baylocq, C. Majcherczyk et F. Pellerin, *Ann. Pharm. Franç.*, 1985, **43**, 329.
7. C. Majcherczyk, *Thèse de Doctorat 3^e cycle*, Univ. Paris XI, 1985.
8. C. Stafford, *Anal. Chem.*, 1964, **36**, 272.
9. F. Pellerin, C. Majcherczyk et D. Baylocq, *Talanta*, 1986, **33**, 89.

DETERMINATION OF CADMIUM, LEAD AND COPPER IN MILK AND MILK POWDER BY MEANS OF FLOW POTENTIOMETRIC STRIPPING ANALYSIS

L. ALMESTRAND, D. JAGNER and L. RENMAN

Department of Technical Analytical Chemistry, Chemical Center, University of Lund, P.O. Box 124,
S-22100 Lund, Sweden

(Received 26 April 1986. Accepted 22 July 1986)

Summary—A flow potentiometric stripping analysis procedure for the determination of cadmium, lead and copper in milk and milk powder samples is described. The instrumental arrangement consists of a glassy-carbon thin-layer cell through which six different solutions may be drawn by means of a peristaltic pump and magnetically operated valves. The glassy-carbon electrode is pre-coated with a film of mercury which can be employed for several analytical runs. The sample, diluted five-fold with Suprapur hydrochloric acid, is electrolysed for 0.5–4 min prior to stripping in Suprapur hydrochloric acid. Pump-rate, electrolysis time and potential, opening and closing of inlet valves and digital evaluation of stripping times are controlled automatically by the computer. The analytical results agree satisfactorily with the certified values for three milk powder reference samples. The detection limit for cadmium, lead and copper in milk samples after 4, 1 and 0.5 min of pre-electrolysis is 0.8, 4 and 8 $\mu\text{g/l.}$, respectively. An analytical procedure for the determination of lead in samples containing high concentrations of tin is described.

Most rapid analytical methods for the determination of toxic trace elements in milk products have hitherto dealt with the determination of lead. For this element both spectroscopic and electroanalytical methods have been issued by the Association of Official Analytical Chemists. The electroanalytical method is based on anodic stripping voltammetry (ASV) applied subsequent to a somewhat time-consuming dry ashing step.¹ In a recent communication Zink *et al.*² reported a modified ASV procedure using the decomplexing reagent Metexchange[®] which made it possible to omit both the dry ashing and the sample deaeration steps. In a collaborative study by thirteen laboratories the Metexchange[®] procedure proved to yield reliable results for the determination of lead in milk powder,³ but the limit of detection was 50 $\mu\text{g/l.}$, which is a somewhat high value for lead in milk.⁴

Another indication that milk can be analysed for lead by electroanalytical methods without prior wet or dry ashing is the recent study by Mannino and Bianco.⁵ These authors used a potentiometric stripping procedure⁶ subsequent to dilution of the milk sample with glacial acetic acid, but in their procedure it is necessary to deaerate the sample in order to reduce the rate of the chemical re-oxidation of the amalgamated lead.

As part of a study on methods for trace metal determination by computerized flow potentiometric stripping analysis,⁷ the suitability of this technique for the determination of lead in milk and milk powder has been investigated. The purpose of the work was to design and evaluate an automated procedure involving a minimum of sample handling.

Furthermore, it was considered imperative to design a method capable of handling samples suspected of containing high concentrations of tin, *e.g.*, canned condensed milk. This problem does not seem to be solved satisfactorily by the stripping methods suggested hitherto.^{1,2,5} During the course of the work it became apparent that the method employed for the determination of lead could, after minor modifications, also be used for the determination of cadmium and copper.

A key problem in the development of a rapid analytical method is to find a simple procedure for the sample pretreatment, preferably involving only dissolution of the sample in a suitable medium modifier. The purpose of the modifier is to change all trace metal analytes into well-defined electrochemically reducible species, *e.g.*, chloride complexes, and, at the same time, to avoid precipitation of the sample proteins. In the Metexchange[®] procedure this is achieved by means of competitive complexation with other metal ions and a suitable choice of pH. In this study we have used concentrated hydrochloric acid as medium modifier. In a parallel study⁸ on trace metal determinations in whole blood it was shown that protein precipitation can be avoided if the hydrochloric acid concentration is higher than approximately 6M. Moreover, in this medium protons compete successfully with cadmium, lead and copper for the complexation sites of the organic constituents and, owing to the high chloride concentration, these metal ions are converted into their chloride complexes. Another advantage of using hydrochloric acid as medium modifier is that it can be purified easily or

obtained commercially in suprapur grade, so the sample pretreatment procedure does not require special reagents.

EXPERIMENTAL

Instrumentation

Flow system. The flow system consisted of a laboratory-constructed thin-layer cell⁷ into which six different solutions could be drawn by means of a peristaltic pump (Gilson Minipulse 2). Unless otherwise stated the flow-rate was 2 ml/min. The six solution inlets were controlled by magnetic valves (Angar Scientific, USA). The glassy-carbon working electrode (Ringsdorff, FRG) in the thin-layer cell had a diameter of 1 mm. A 10-mm long platinum tube with an inner diameter of 0.4 mm (Goodfellow, U.K.) placed downstream from the working electrode, served as counter-electrode. The calomel reference electrode (Radiometer K4040, Denmark) was separated from the flow-cell apartment by a ceramic plug filled with 5M hydrochloric acid. The length, width and thickness of the flow slit in the polyethylene spacer in the thin-layer cell⁷ were 7, 1 and 0.2 mm, respectively.

Computer system. The computer system consisted of an ABC 806 personal computer (Luxor, Sweden) equipped with floppy discs, printer/plotter, A/D and D/A converters and various relay functions. Working-electrode potential, pump flow-rate, and opening and closing of magnetic valves were under computer control. During stripping the computer registered the potential *vs.* time transient signal with a 12-bit A/D converter at a maximum sampling frequency of 16 kHz and a potential resolution of 1 mV. Details of the hardware and software system will be given elsewhere.⁹

Reagents

All reagents used were of analytical grade except the hydrochloric acid, which was of suprapur grade (Merck, FRG). Stock solutions (1000 mg/l.) of cadmium, lead, tin(IV), copper(II) and mercury(II) were prepared from Titrisol (Merck, FRG) ampoules, in 1M hydrochloric acid and diluted further as required.

Milk powder reference samples BCR 63, 150 and 151 were obtained from The Commission of the European Communities, Community Bureau of Reference (Brussels, Belgium).

Sample pretreatment

Milk samples. Add a 4-ml sample of milk to 16 ml of 8M hydrochloric acid containing 50 mg of mercury(II) per litre. Add another 4-ml portion of the milk to 16 ml of 8M hydrochloric acid containing 50 mg of mercury(II) and standard additions of 2.5 µg of cadmium, 25 µg of lead and 50 µg of copper(II) per litre.

Milk powder samples. Add 2 g of milk powder to 8 ml of doubly distilled water and mix by swirling. Treat the mixture as the milk samples above.

Working-electrode pretreatment

Polishing. Before analysis polish the glassy-carbon electrode for 1 min with 3-µm diamond paste, clean it ultrasonically in ethanol for 1 min, polish with 1-µm diamond paste for 1 min and finally clean ultrasonically in ethanol for 2 min.

Mercury film pre-coating. Before the first analytical run after electrode polishing pre-coat the glassy-carbon electrode with a thin film of mercury. Use 8M hydrochloric acid containing 200 mg of mercury(II) per litre and a flow-rate of 0.4 ml/min. A suitable potential *vs.* time sequence in the mercury pre-coating procedure is: -0.5 V for 5 sec, +0.2 V for 4 sec, -0.6 V for 5 sec, +0.2 V for 5 sec, -0.6 V for 10 sec, -0.65 V for 10 sec, -0.70 V for 10 sec and finally -0.80 V for 60 sec. Once pre-coated with mercury the working electrode can be used for 20–50 analytical runs. The results of the first analytical run after the mercury pre-

coating should be ignored, since they may often be too low, and the run should be repeated. When failure of the mercury film is indicated by increasing noise level or inadequate background subtraction, the polishing and mercury pre-coating procedures should be repeated.

Analytical procedures

Determination of cadmium. Allow 8M hydrochloric acid containing 200 mg of mercury per litre into the flow-cell and renew the mercury film surface by electrolysis at -0.8 V *vs.* SCE for 10 sec. Care must be taken that the reducing potential is applied before the mercury-containing solution is allowed into the cell, otherwise the mercury film electrode will be destroyed owing to spontaneous calomel formation. Introduce the sample into the cell and electrolyse for 4 min at -1.15 V *vs.* SCE, then replace the sample by 8M hydrochloric acid. Disconnect the potentiostat 20 sec later and register the potential *vs.* time gradient at a measuring frequency of 16 kHz. When the stripping potential reaches -0.6 V *vs.* SCE apply an electrolysis potential of -1.15 V *vs.* SCE for 1 sec and register a background scan. Finally introduce a cleaning solution of 0.1M hydrochloric acid in 95% ethanol and apply a potential of -0.2 V *vs.* SCE for 10 sec. Repeat the procedure with the cadmium-spiked sample.

Determination of lead. Renew the mercury film surface by electrolysis for 10 sec at -0.8 V *vs.* SCE in 8M hydrochloric acid containing 200 mg of mercury per litre. Introduce the sample and electrolyse at -1.0 V *vs.* SCE for 1 min then switch to 8M hydrochloric acid for 20 sec, registering the stripping curve at a measuring frequency of 16 kHz. When the potential reaches -0.4 V *vs.* SCE apply an electrolysis potential of -1.0 V *vs.* SCE for 1 sec and register the background with the same frequency. Clean the electrodes with ethanol as for cadmium.

In samples suspected of containing more than 50 µg of tin per litre the procedure should be modified so that 2M sodium hydroxide is allowed into the cell for 10 sec after the 8M hydrochloric acid solution has been in the flow-cell for 20 sec, then 8M hydrochloric acid is again allowed into the cell for 20 sec and the stripping and background curves are registered as above.

Determination of copper. Renew the mercury film surface as for cadmium and lead above and electrolyse the sample for 30 sec at -0.8 V *vs.* SCE. Switch to 8M hydrochloric acid for 20 sec and register the stripping transient signal at 16 kHz in the potential interval from -0.8 to -0.3 V *vs.* SCE. Register a background curve and clean the electrodes as for cadmium and lead.

Digital evaluation and graphical display

In the digital evaluation of the potentiometric stripping times the computer program first subtracts the background scan from the analytical scan. After this the program localizes the exact potential of the stripping peak,⁹ the allowed potential regions for cadmium, lead and copper being from -0.90 to -0.80, -0.75 to -0.65 and -0.65 to -0.35 V *vs.* SCE, respectively. The stripping time is then calculated by integrating the dt/dE plot. The potential region used in the evaluation of the cadmium and lead stripping times was ±50 mV around the stripping peak. Since copper is oxidized to copper(I) chloride complexes in the hydrochloric acid medium a potential interval of ±100 mV was used.

Finally the computer program displays the stripping curve, dt/dE *vs.* E , for each peak, on the printer/plotter together with the stripping time. The potential region used for the display was ±100 mV around the stripping peak. In the graphical display experimental data in consecutive 30-mV intervals were averaged arithmetically ("filter 30 mV").

All concentrations were evaluated by means of the normal equations for standard addition.

RESULTS AND DISCUSSION

Cadmium, lead and copper in milk and milk powder samples; accuracy

The results obtained in the determination of cadmium, lead and copper in the three reference samples are shown in Table 1 and Figs. 1-3.

Figures 4-6 show the potentiometric stripping curves obtained in the analysis of spiked and unspiked Swedish milk samples containing 3% fat. The value obtained for copper was 35 $\mu\text{g/l.}$ in the milk sample; the lead and cadmium concentrations were below 5 and 1 $\mu\text{g/l.}$, respectively.

As can be seen from Table 1 the experimental results agree satisfactorily with the certified value for the reference samples, the main exception being cadmium in BCR 63 where the concentration in this sample is below the detection limit of the method.

Table 1. Results of analysis of three reference milk powders

Sample	Element	Certified concentration, $\mu\text{g/g}$	No. of detns.	Range found, $\mu\text{g/g}$
BCR 63	Cd	0.0029 ± 0.0012	4	0.002-0.008
BCR 63	Pb	0.1045 ± 0.0031	6	0.12-0.14
BCR 63	Cu	0.544 ± 0.030	6	0.49-0.58
BCR 150	Cd	0.0218 ± 0.0014	6	0.023-0.028
BCR 150	Pb	1.00 ± 0.04	6	0.98-1.06
BCR 150	Cu	2.23 ± 0.08	6	2.10-2.45
BCR 151	Cd	0.1010 ± 0.008	6	0.11-0.13
BCR 151	Pb	2.002 ± 0.026	6	2.05-2.35
BCR 151	Cu	5.23 ± 0.08	6	5.10-5.65

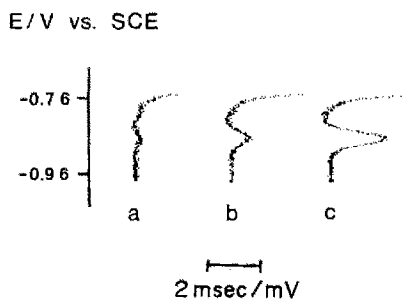


Fig. 1. Potentiometric stripping curves, E vs. dt/dE , obtained in the determination of cadmium in reference samples BCR 63 (a), BCR 150 (b) and BCR 151 (c).

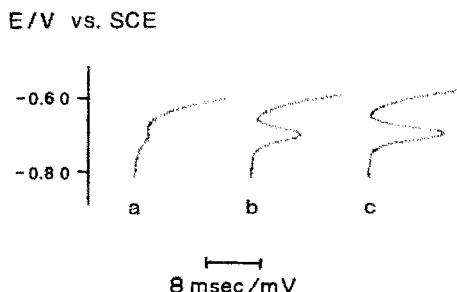


Fig. 2. Potentiometric stripping curves, E vs. dt/dE , obtained in the determination of lead in reference samples BCR 63 (a), BCR 150 (b) and BCR 151 (c).

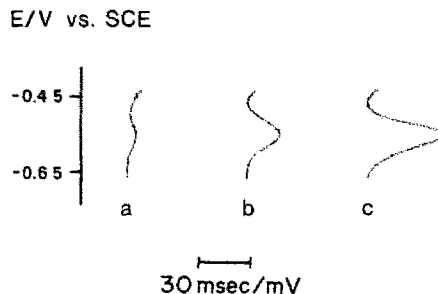


Fig. 3. Potentiometric stripping curves, E vs. dt/dE , obtained in the determination of copper in reference samples BCR 63 (a), BCR 150 (b) and BCR 151 (c).

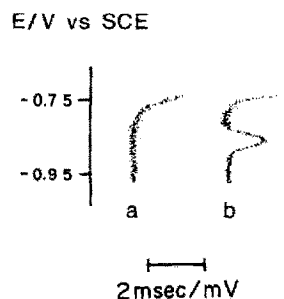


Fig. 4. Potentiometric stripping curves, E vs. dt/dE , obtained in the determination of cadmium in a milk sample (a) and in the sample spiked with 10 $\mu\text{g/l.}$ cadmium (b).

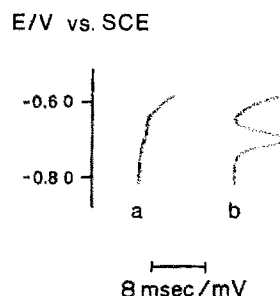


Fig. 5. Potentiometric stripping curves, E vs. dt/dE , obtained in the determination of lead in a milk sample (a) and in the same sample spiked with 100 $\mu\text{g/l.}$ lead (b).

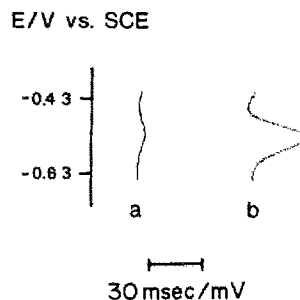


Fig. 6. Potentiometric stripping curves, E vs. dt/dE , obtained in the determination of copper in a milk sample (a) and in the same sample spiked with 200 $\mu\text{g/l.}$ copper (b).

Furthermore, the cadmium results are affected by the different cadmium concentrations in the different Suprapur acid batches used. As is apparent from Table 1, the lead value obtained for BCR 63 is too high. This may be attributed to lead contamination during sample handling and should be avoidable by working in a clean laboratory environment. Since, however, the purpose of this work was to develop a method capable of rapid identification of samples containing elevated trace metal concentrations, clean laboratory techniques were not exploited.

No alternative analytical technique was used to verify the results obtained in the analysis of the milk samples. The results obtained are, however, in good agreement with those normally obtained for Swedish milk samples.¹⁰

Linear range and sensitivity

The linear range was investigated by spiking a milk sample, diluted fivefold with hydrochloric acid, with different amounts of cadmium, lead and copper and analysing by the procedures given above. The stripping signal varied linearly with metal concentration in the ranges investigated, 0.1–5 $\mu\text{g/l.}$ for cadmium, 1–20 $\mu\text{g/l.}$ for lead and 5–100 $\mu\text{g/l.}$ for copper.

The sensitivity of the potentiometric stripping procedure varies from one glassy-carbon electrode to another. Sensitivity variations also occur from one mercury pre-coating to the next on the same glassy-carbon electrode. The relative variations between glassy-carbon electrodes are 0–50% and between different mercury films 0–20%. As can be seen by comparing Figs. 1–3 with Figs. 4–6 there are variations in sensitivity between the different runs. These runs were, however, registered with different glassy-carbon electrodes and do not represent any significant variations in sensitivity in the analyses of the milk powder and the milk samples. Separate experiments on a cream sample containing 40% fat indicate that high fat concentrations do not affect the sensitivity significantly.

Precision and detection limit

The precision was investigated by means of ten consecutive electrolysis/stripping cycles in the spiked milk samples (Figs. 4–6). The relative standard deviation was 5–7% for all three elements, the major source of variation being the pulsation of the peristaltic pump. From the precision the detection limits for cadmium, lead and copper in milk samples can be estimated as 1.0, 4 and 8 $\mu\text{g/l.}$, respectively. The detection limits for lead and copper can be decreased by increasing the time of electrolysis. Electrolysis times of more than 4 min generally resulted in decreased precision and consequently no decrease in detection limit.

Interferences

Interferences in potentiometric stripping analysis are normally due to stripping potential overlap,

intermetallic compound formation or surface adsorption of electroactive organic matter present in the sample. In the highly acidic medium used in the analysis no organic constituents will be adsorbed onto the electrode surface. The elements most likely to cause stripping potential overlap are tin and thallium. The interference with the lead stripping peak by tin is illustrated in Fig. 7. Figure 7(a) shows the potentiometric stripping curve for lead in an acid-diluted milk sample containing 5 $\mu\text{g/l.}$ lead. Figures 7(b) and 7(c) show the potentiometric stripping curves for the same sample after the addition of 0.2 and 1.0 mg of tin per litre, respectively. Finally Fig. 7(d) shows the potentiometric stripping curve for the sample with 1 mg/l. added tin, after removal of tin by 2M sodium hydroxide. As can be seen from Fig. 7 all the amalgamated tin is oxidized in the sodium hydroxide solution, owing to the formation of Sn(OH)_3^- . The amalgamated lead is not oxidized, since the lead(II) hydroxy-complexes are considerably weaker than the corresponding tin(II) complexes.

The potential overlap from thallium on the stripping peaks for cadmium and lead has been investigated by analysing a milk sample spiked with the three elements. The hydrochloric acid used as stripping medium resolved the three stripping peaks, the peak potential for thallium at -0.70 V vs. SCE being almost equidistant from the peak potentials for lead and cadmium. Of cadmium, lead and copper, only copper forms strong intermetallic compounds. Those elements which form intermetallic compounds with copper and at the same time are

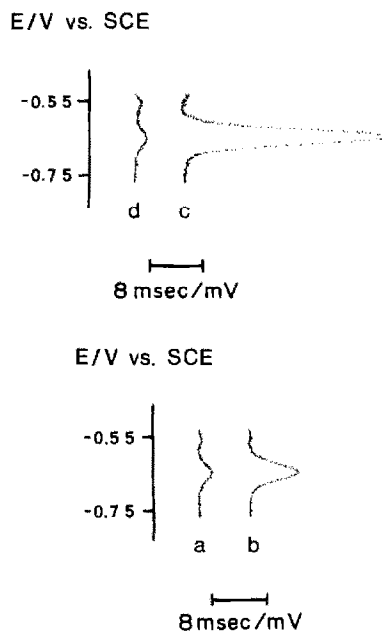


Fig. 7. Potentiometric stripping curves E vs. dI/dE , obtained in a milk sample containing (a) 5 $\mu\text{g/l.}$ Pb(II) (b) 5 $\mu\text{g/l.}$ Pb(II) and 0.2 mg/l. Sn(II) (c) 5 $\mu\text{g/l.}$ Pb(II) and 1.0 mg/l. Sn(II) and (d) same as (c) but after removal of Sn(II) with 2M sodium hydroxide.

likely to be present in milk samples are tin and zinc. At the electrolysis potential used in the determination of copper neither zinc nor tin is reduced and interferences from intermetallic compound formation are thus avoided. At the electrolysis potential used for lead, tin is also reduced (Fig. 7). Part of the reduced tin forms a 1:1 intermetallic compound with copper which is subsequently re-oxidized at a potential very close to that for copper. Consequently, as long as the tin concentration is lower than the copper concentration, tin will not interfere with the lead stripping peak. This explains why small concentrations of tin do not interfere in the batch ASV procedure² nor, of course, in the potentiometric stripping procedure.

Conclusions

Computerized flow potentiometric stripping analysis can be used for rapid determination of, in particular, elevated concentrations of cadmium, lead and copper in milk and milk powder samples. The detection limit for lead, after 1 min of electrolysis, is approximately a fifth of that for lead in the corresponding ASV procedure. In the flow approach, computerized potentiometric stripping analysis is capable of a high degree of automation. If supplemented with a sampler the instrumental arrangement is capable of running several samples unattended. When this is done, the graphical display of the printer/plotter is of considerable importance since it

permits rapid visual inspection of several analytical runs. Possible malfunction of the system will be indicated by, e.g., broadening or absence of stripping peaks for the spiked samples or peak splitting due to the presence of thallium. Inadequate rinsing of the electrodes between consecutive electrolysis/stripping runs will be indicated by continuous decrease in the peak heights of the spiked samples.

Acknowledgements—The authors acknowledge financial support from Carl Tryggers Stiftelse and from the Swedish Natural Science Research Council.

REFERENCES

1. *Official Methods of Analysis*, 13th Ed., AOAC, Arlington, VA, 1980, Method No. 25.074.
2. E. W. Zink, R. A. Moffit and W. E. Matson, *J. Assoc. Off. Anal. Chem.*, 1983, **66**, 1409.
3. E. W. Zink, P. H. Davis, R. M., Griffin, W. E. Matson, R. A. Moffit and D. T. Sakai, *ibid.*, 1983, **66**, 1414.
4. G. K. Murthy and U. S. Rhea, *J. Dairy Sci.*, 1984, **54**, 1001.
5. S. Mannino and M. Bianco, *J. Micronutrient Anal.*, 1985, **1**, 47.
6. D. Jagner and A. Granéli, *Anal. Chim. Acta*, 1976, **83**, 19.
7. L. Anderson, D. Jagner and M. Josefson, *Anal. Chem.*, 1982, **54**, 1371.
8. L. Almqvist, D. Jagner and L. Renman, in preparation.
9. L. Renman, D. Jagner and R. Berglund, in preparation.
10. H. Jönsson, *Thesis*, 1979, University of Lund, Sweden.

DOSAGE DES XANTHIQUES NATURELS PAR CLHP COMPARAISON DES METHODES ET APPLICATIONS

M. F. VERGNES et J. ALARY

Faculté de Pharmacie, Laboratoire de Chimie Analytique et Bromatologie, Domaine de la Merci,
38700 La Trouche, France

(Reçu le 27 janvier 1986. Révisé le 2 juillet 1986. Accepté le 22 juillet 1986)

Résumé—Les trois xanthiques naturels, caféine, théobromine et théophylline, ont été dosés par CLHP soit sur colonne de silice, soit sur phase greffée en C_{18} . Pour l'application au dosage dans les boissons, c'est la CLHP sur silice qui a été retenue. La méthode a alors été appliquée au café, au thé, au maté, à des extraits pour boissons ou aux boissons elles-mêmes. Pour les extraits, une comparaison a été faite avec les autres méthodes de dosage de la caféine. La chromatographie en phase liquide sous pression semble une méthode bien adaptée pour doser les xanthiques dans des milieux complexes.

Summary—The three natural xanthines, caffeine, theobromine and theophylline, have been determined by HPLC on columns of silica gel or a C_{18} -bonded phase. For the determination in beverages, HPLC on silica gel was used. The method was applied to coffee, tea, maté, in extracts or in the drinks themselves. For the extracts a comparison was made with other methods for determining caffeine, HPLC seems a method well suited to analysis of complex matrices for the xanthines.

Découverte en 1819 par Runge, la caféine fut décrite en 1821 par Pelletier et Robiquet. Par la suite, elle a été mise en évidence dans différents végétaux, notamment le thé et le café, mais également dans le cacao, la noix de kola, le guarana et le maté. Les concentrations varient selon l'espèce végétale et la caféine est quelquefois accompagnée de théophylline (thé) ou de théobromine (cacao, guarana, kola, maté). Le café vert renferme en moyenne 1,21% de caféine, alors que le café torréfié en présente 1,40%. Dans le thé, la proportion varie de 1,5 à 4% pour les thés d'Annam et du Tonkin. Ce sont les jeunes feuilles qui sont les plus riches. Dans le cacao, c'est la théobromine qui domine (1,5 à 2%), alors que les concentrations en caféine sont environ dix fois moindres. Pour le guarana, la caféine est seule présente dans l'amande (environ 3,9%) mais la théobromine existe dans d'autres parties de la plante. Les graines de kola renferment en général plus de 2% de caféine, mais également de la théobromine. Enfin, le maté contient de la caféine dans des proportions sensiblement égales à celles du thé, et un peu de théobromine.

Les xanthines sont donc présentes dans de nombreux produits naturels servant à la préparation de boissons toniques, et la caféine fait même partie des molécules les plus consommées dans le monde. Elle figure dans l'alimentation de très nombreux peuples, quel que soit leur niveau de vie. Il nous a donc paru intéressant de trouver une méthode de dosage performante, rapide, et spécifique, pour doser les bases xanthiques dans les boissons. La chromatographie en phase liquide à haute performance (CLHP) en associ-

ation avec un détecteur ultra-violet nous a semblé la méthode de choix par sa sélectivité et sa sensibilité.

Deux techniques ont été étudiées: la chromatographie d'adsorption¹⁻⁵ et la chromatographie de partage en phase inversée.⁶⁻¹² Lorsqu'une bonne séparation a été obtenue, nous avons vérifié la reproductibilité des résultats et la linéarité de la réponse.

Nous avons ensuite sélectionné la technique d'adsorption pour réaliser des dosages dans les aliments: café, thé, maté, extraits pour distributeurs de boissons et boissons manufacturées, en particulier Coca-Cola et Pepsi-Cola. Ce sont en effet des boissons de très grande consommation. Près de 200 millions de petites bouteilles sont vendues quotidiennement dans le monde.¹³

Nous avons en outre comparé les résultats de dosage en CLHP avec ceux obtenus en chromatographie gazeuse et en spectrophotométrie ultra-violet.

PARTIE EXPERIMENTALE

Extraction des bases xanthiques

Cas des échantillons solides (café, thé, maté) Des prises d'essai de 1 g sont mélangées à 50 g de sable de Fontainebleau. Le mélange est introduit dans des cartouches d'extraction, le poudre est imbibée par 20 gouttes d'ammoniaque diluée (20% p/v). Un tampon de coton est alors placé sur la cartouche, qui est abandonnée une nuit avant l'extraction de manière à permettre le gonflement de la poudre. L'extraction est ensuite réalisée en continu pendant 7 hr, par du chloroforme, dans un extracteur de Soxhlet. Au terme de l'extraction, la phase chloroformique est évaporée à sec. Le résidu est redissous dans 100 ml de solvant éluant.

Cas des boissons (Coca-Cola, Pepsi-Cola et guarana). Des volumes de boisson de 50 ml sont alcalinisés jusqu'à pH 9 par de l'ammoniaque diluée (20% p/v). Une extraction liquide-liquide est alors réalisée par le chloroforme, dans un extracteur de Jalade pendant 10 hr. La phase chloroformique est évaporée à sec, le résidu est comme précédemment repris par 100 ml de solvant éluant.

Cas des extraits. Des prises d'essai de 25 ml sont additionnées de 25 ml d'eau distillée. Le mélange est ajusté à pH 9, puis traité comme dans le cas précédent.

CLHP

Technique d'adsorption. Colonne de Sphérisorb 800, 5 μ m, remplie au laboratoire, longueur 15 cm; pompe Chromatem 380; détecteur UV Pye Unicam (mesures faites à 273 nm); vanne d'injection à boucle (20 μ l); éluant dichlorométhane-méthanol (90:10); débit 1,25 ml/mn.

Technique de partage. Colonne Lichrosorb RP 18, remplie au laboratoire, longueur 15 cm; pompe, détecteur et vanne d'injection identiques à ceux décrits pour la technique d'adsorption; éluant acétate de sodium 0,01M à pH 4-acétonitrile (90:10); débit 3 ml/mn.

Le calcul des concentrations a été fait pour les deux méthodes en mesurant la surface des pics (essais et témoins) grâce à un intégrateur Shimadzu CR 1 B. Il est possible également de mesurer les hauteurs de pics.

Chromatographie gaz-liquide

Appareillage. Colonne OV 17 (peu polaire), à 3% sur Chromosorb W-HP 80-100 mesh, longueur 2 m, diamètre 2 mm; températures 220° (du four), 240° (de l'injecteur), 250° (du détecteur); détecteur à ionisation de flamme.

Préparation de l'échantillon. Des volumes de 10 ml (pour l'extrait de café) ou de 50 ml (pour les extraits de thé ou de cola) de solutions chloroformiques d'extraction sont évaporés à sec. Le résidu est redissous dans l'acétate d'éthyle et ajusté à 20 ml dans une fiole jaugée après l'introduction de 1 ml de solution d'étalon interne.

Prise d'essai injectée: 2 μ l.

Absorption dans l'ultra-violet (après purification par la méthode AFNOR)¹⁴

La solution chloroformique d'extraction est purifiée par passage sur deux colonnes de Célite qui fixent la caféine (deux colonnes successives, l'une alcaline, l'autre acide), l'éluant étant réalisée par l'éther éthylique, puis le chloroforme. L'absorption est mesurée à 276 nm, les absorptions avant et après le pic étant soustraites, selon

$$A_{276 \text{ nm}} - (A_{246 \text{ nm}} + A_{306 \text{ nm}})/2.$$

RESULTATS

Les chromatogrammes obtenus dans les deux techniques sont présentés dans les figures 1 et 2. Les courbes d'étalonnage correspondant aux trois bases xanthiques, par la technique d'adsorption, sont linéaires.

Les résultats obtenus pour les applications aux produits solides et aux différentes boissons sont présentés dans le tableau 1. Enfin, le tableau 2 présente les teneurs en caféine obtenues pour les extraits par les différentes méthodes qui ont été comparées.

DISCUSSION

Les deux techniques de CLHP testées permettent une bonne séparation des trois xanthiques, comme en témoignent les figures 1 et 2. Les ordres de sorties

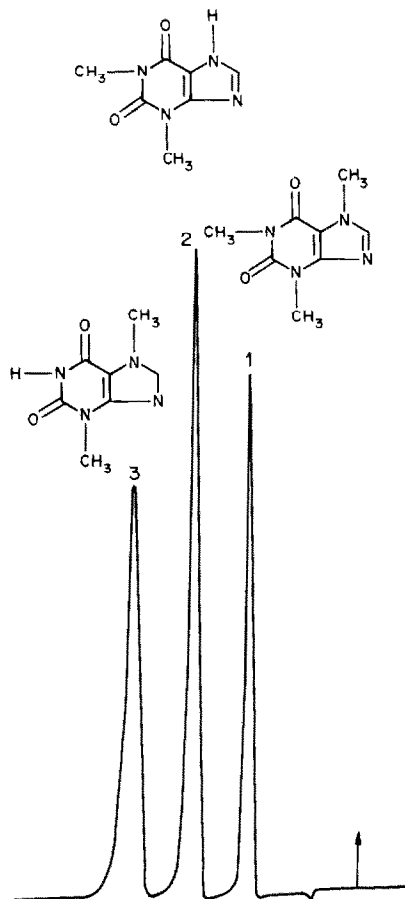


Fig. 1. Mélange de caféine (1), théophylline (2), théobromine (3). CLHP par technique d'adsorption.

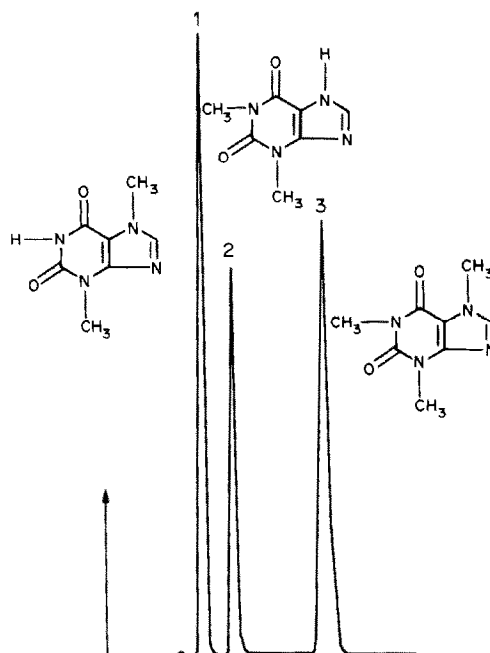


Fig. 2. Mélange de théobromine (1), théophylline (2), caféine (3). CLHP par technique de partage.

Tableau 1. Teneurs en caféine de cafés, thés, maté et différentes boissons

Echantillons	Caféine	Echantillons	Caféine
Café Guadeloupe	1,35%	Thé de Russie	3,29%
"Nectar"	1,26%	Thé de Chine	3,03%
"Régat"	1,41%	Thé du Vietnam	2,99%
CENG (a)	1,2%	Thé de Ceylan	2,58%
CENG (b)	1,19%	Coca-Cola	114 mg/l.
CENG (c)	1,26%	Pepsi-Cola	72 mg/l.
Maté Pampero	0,8%	Boisson à base de Guarana "Antartic"	96 mg/l.

sont simplement inversés en fonction du phénomène mis en jeu.

Cependant, c'est la technique d'adsorption sur silice qui a été sélectionnée pour les applications, car sa reproductibilité et sa précision sont meilleures. Les courbes d'étalonnage sont en effet d'une excellente linéarité.

En ce qui concerne le café, plusieurs variétés ont été analysées:

(1) Café provenant de la Guadeloupe: cet échantillon de café provient d'une des dernières exploitations de café des Antilles françaises; il correspond à la variété Arabica.

(2) Cafés commercialisés en France: l'une des variétés est du pur Arabica, l'autre un mélange de cafés d'origines diverses.

(3) Café cultivé en France sous serre chauffée: en effet, dans l'optique d'une valorisation des rejets thermiques, des cultures de plantes tropicales ont été entreprises au Centre d'Etudes Nucléaires de Grenoble (CENG), sous tunnel plastique. La source de chaleur est l'eau de refroidissement d'un réacteur nucléaire. Celle-ci circule dans le sol de la serre selon le système du paillage radiant.¹⁵ Au bout de trois ans, une récolte a pu être obtenue. Les biologistes responsables de cette expérience de culture ont été intéressés par la composition de leur café, notamment par sa teneur en caféine. Nous avons pu doser la caféine dans un échantillon correspondant à la première année de production (échantillon torréfié) (a), puis sur des échantillons de la deuxième année de production, pour lesquels nous avons comparé la teneur en caféine avant (b) et après torréfaction (c).¹⁵

Les teneurs en caféine des différents cafés torréfiés analysés, qui correspondent tous (un excepté) à des variétés Arabica, sont très proches. Elles sont tout à fait comparables aux valeurs publiées qui sont comprises entre 0,8 et 1,6%

Cette technique de CLHP offre l'avantage de sa bonne spécificité, ce qui n'était pas toujours le cas des techniques spectrales antérieures, ne réalisant pas une séparation très fiable avant la mesure.

Tableau 2. Teneurs en caféine (g/l.) déterminées par différentes méthodes

Echantillons	CLHP	UV	CGL	AFNOR
Extrait de café	3,00	3,35	2,85	2,98
Extrait de thé	0,446	0,445	0,440	0,456
Extrait de cola	0,208	0,237	0,168	0,191

Elle nous a permis de constater que le café cultivé sous serre chauffée avait la même teneur en caféine que les cafés cultivés dans les pays producteurs. Il y a donc une bonne fixité de la composition pour une espèce donnée et une prépondérance des facteurs génétiques sur les caractéristiques de la composition, par rapport aux facteurs climatiques.

Pour les différents thés analysés, nos résultats rejoignent tout à fait ceux qui ont été publiés antérieurement.¹⁶ En effet, les taux de caféine trouvés dans le thé sont compris entre 2,5 et 3,5% et pour le maté entre 0,6 et 1,6%.

Les teneurs en caféine du Coca-Cola et du Pepsi-Cola (respectivement 114 et 72 mg/l), pour des boissons de grande consommation qui peuvent être destinées aux enfants, posent un problème réglementaire. Dans certains pays, la norme a établi un taux maximal de 150 mg/l.¹⁷ Pour la CEE, un texte est en discussion au niveau des commissions compétentes.

La teneur en caféine nettement plus faible dans le Pepsi-Cola semble une remarque générale.¹⁷ Par contre, nos chiffres sont significativement plus élevés que ceux publiés par le laboratoire coopératif,¹⁷ en appliquant la méthode AFNOR.¹⁴ Les différences peuvent s'expliquer par la non-homogénéité de la composition en fonction des lots de fabrication.

Les extraits destinés aux distributeurs de boisson (café, thé, Coca-Cola) sont des concentrés destinés à être dilués à l'eau froide ou chaude selon le cas. La dilution est d'environ 10%. Pour ces extraits, nous avons non seulement réalisé le dosage de la caféine par CLHP mais nous avons aussi comparé les résultats moyens obtenus par différentes techniques: CLHP, chromatographie en phase gazeuse, spectrophotométrie dans l'ultra-violet directe ou après purification selon la technique AFNOR. Cette comparaison figure dans le tableau 2.

En comparant les résultats obtenus pour l'extrait de café par les quatre méthodes, on peut constater qu'un dosage direct en l'ultra-violet donne un chiffre supérieur à celui des autres techniques, ce qui s'explique par des interférences dues aux autres constituants. Pour les trois autres techniques, les résultats sont très proches, ce qui prouve l'efficacité du procédé de purification de la norme AFNOR¹⁴ et l'intérêt des techniques chromatographiques qui séparent avant de doser et sont donc plus sélectives.

Pour l'extrait de thé, les résultats sont extrêmement voisins. Il ne doit pas y avoir dans ce cas de substances interférentes.

Pour l'extrait de cola, les mêmes remarques que précédemment peuvent être faites. Cependant, en ce qui concerne la chromatographie gaz-liquide, les résultats moyens sont nettement inférieurs. Ceci peut s'expliquer par le fait que le taux de caféine de cet extrait est particulièrement bas, ce qui nous place très près des limites de détection de cette technique.

CONCLUSION

La chromatographie en phase liquide à haute performance est une technique bien adaptée à la séparation et au dosage spécifique des bases xanthiques. Cette méthode permet de contrôler les taux de caféine, théobromine ou théophylline dans des produits solides (café, thé, maté) ou des boissons, après une simple extraction par un solvant organique, sans purification particulière. Elle présente l'avantage d'une bonne précision, alliée à une rapidité d'exécution et à une excellente sélectivité.

LITTÉRATURE

1. K. K. Midha, S. Sved, R. D. Hossie et I. J. McGilveray, *Biomed. Mass. Spectrom.*, 1977, **4**, 172.
2. D. S. Sitar, K. M. Piafsky, R. E. Rangno et R. I. Ogilvie, *Clin. Chem.*, 1975, **21**, 1774.
3. A. A. Tin, S. M. Somani, H. S. Bada et N. N. Khanna, *J. Anal. Toxicol.*, 1979, **3**, 36.
4. J. P. Sommadossi, C. Aubert, J. P. Cano, A. Durand et A. Viala, *J. Liq. Chromatog.*, 1981, **4**, 97.
5. W. Wildanger, *Dtsch. Lebensm. Rundsch.*, 1976, **72**, 160.
6. S. H. Ashoor, G. J. Seperich, W. C. Monte et J. Welty, *J. Assoc. Off. Anal. Chem.*, 1983, **66**, 606.
7. J. L. Blauch et S. M. J. Tarka, *J. Food Sci.*, 1983, **48**, 745.
8. W. J. Craig et T. T. Nguyen, *ibid.*, 1984, **49**, 302.
9. M. Dulitzky, E. de la Teja et H. F. Lewis, *J. Chromatog.*, 1984, **317**, 403.
10. Y. Hamann, C. Tisse et J. Estienne, *Ann. Fals. Exp. Chim.*, 1984, **828**, 271.
11. W. J. Hurst et R. A. J. Martin, *J. Liq. Chromatog.*, 1982, **5**, 585.
12. H. Terada et Y. Sakabe, *J. Chromatog.*, 1984, **291**, 453.
13. J. Alary, P. Bertoin et A. Coeur, *Bull. Trav. Soc. Pharm. Lyon*, 1977, **XXI**, 20.
14. *AFNOR Norme V05-251, Détermination de la teneur en caféine.*
15. A. Fourcy, A. Freychet, J. Alary, M. F. Vergnes et C. Grosset, *Ann. Fals. Exp. Chim.*, 1984, **77**, 393.
16. *Manuel suisse des denrées alimentaires*, 5ème édition, Office Central Fédéral des imprimés et du matériel, Berne, 1969.
17. *Bulletin Labo Coopératif*, 1982, **144**, 1.

DESORPTION IONIZATION/TANDEM MASS SPECTROMETRY WITH A CAESIUM ION SOURCE AND A TRIPLE QUADRUPOLE MASS SPECTROMETER

W. B. EMARY, I. ISERN-FLECHA, K. V. WOOD, T. Y. RIDLEY and R. G. COOKS
Department of Chemistry, Purdue University, West Lafayette, IN 47907, U.S.A.

(Received 6 June 1986. Accepted 21 July 1986)

Summary—The coupling of a caesium ion source to a triple quadrupole mass spectrometer is described. The potential of this combination for examining thermally labile, non-volatile molecules, such as thiamine hydrochloride, is examined. Emphasis is placed on the advantages the various scanning modes of tandem mass spectrometry provide in ion structure elucidation and the investigation of desorption ionization mechanisms. Use of the caesium ion source for desorption of neutral molecules which are chemically ionized by an auxiliary gas is demonstrated. This procedure may be especially useful for examining non-volatile, non-ionic samples.

The use of energetic primary particles to desorb thermally labile, high molecular-weight molecules from the solid or liquid phase is a well-established method of ionization.¹⁻⁴ The technique uses a wide variety of primary bombarding species, *e.g.*, fission fragments in plasma desorption (PD), photons in laser desorption (LD), ions in secondary-ion mass spectrometry (SIMS), and neutral atoms in fast-atom bombardment (FAB).

The combination of these desorption (DI) techniques with tandem mass spectrometry (MS/MS)⁵ adds significantly to the individual capabilities of both procedures.⁶⁻⁸ DI/MS/MS has provided valuable results in the analysis of a variety of classes of compounds.⁶⁻¹³ Particularly noteworthy is the quality of the structural information available through collisional activation.⁹⁻¹¹ Structurally diagnostic fragment ions often result when tandem mass spectrometry is used in combination with these ionization methods, for example, to enhance abundances of sequence ions in the FAB spectra of peptides¹⁴ and oligosaccharides.¹⁵ DI/MS/MS has also been useful for lowering the detection limits for constituents in a complex mixture.¹² For example, the combination of laser desorption with tandem mass spectrometry⁶ has been used successfully in a variety of studies, including the discovery of new quaternary alkaloids in complex mixtures.¹⁶ In one study of the DI/MS/MS combination, Glish *et al.* followed the gas-phase chemistry of a variety of simple organic ions generated in secondary-ion mass spectrometry (SIMS) with a multiple sector instrument.¹⁷

One of the newer versions of the DI technique is that which employs a caesium ion source. This primary ion source has been used for the desorption of a variety of biomolecules, *e.g.*, cobalamine and peptides, particularly in Fourier-transform mass spectrometers where the low gas load is an advantage.^{18,19} This paper describes an interface between a triple

quadrupole mass spectrometer and a caesium ion source. The device is simple and easily removed to allow substitution of other accessories. The main thrust of the paper is an exploration of the capabilities provided by this particular combination of the desorption ionization method and tandem mass spectrometry. The results presented concern (1) structural characterization, (2) signal-to-noise enhancement, (3) fragmentation paths for desorbed ions and (4) characterization of desorbed neutral molecules through ion-molecule reactions.

EXPERIMENTAL

Apparatus

An exploded view of the caesium ion gun and the interface to the triple quadrupole mass spectrometer (Finnigan-Mat TSQ) is shown in Fig. 1. The caesium ion source and power supply²⁰ were purchased from Antek Corp. (Palo Alto, CA). The interface secures the caesium ion source and associated lens system in the vacuum system, from which it is electrically isolated, and allows the axis of the caesium ion beam to be oriented with respect to the mass spectrometer ion source. Electrical supplies to the caesium ion gun are provided by high-voltage feed-throughs carried in a flange other than that on which the caesium ion source is mounted. An aperture (3 mm diameter) in the ionization volume allows the caesium ion beam access to the probe on which the sample is loaded. The probe tips were machined so that the probe face was at various angles (45°, 60°, 75° and 90°) with respect to the primary beam. The best results were obtained with an angle of 75°.

The spot size of the caesium ion beam is controlled by focusing lenses. The minimum spot size was *ca.* 2 mm in diameter (measured by means of the image apparent on a silver beam-flag) at a focal length of about 10 mm. Ion currents were also measured on a beam-flag, installed for this purpose in place of the ion volume; a Keithley Model 417 picoammeter was used. The caesium ion current was *ca.* 1 μ A in the energy range 5-6 keV. At lower caesium ion energies, a large decrease in sensitivity was observed, as evidenced by the total ion-current plot for the desorption of silver nitrate in glycerol, shown in Fig. 2. All experiments were performed with the probe grounded.

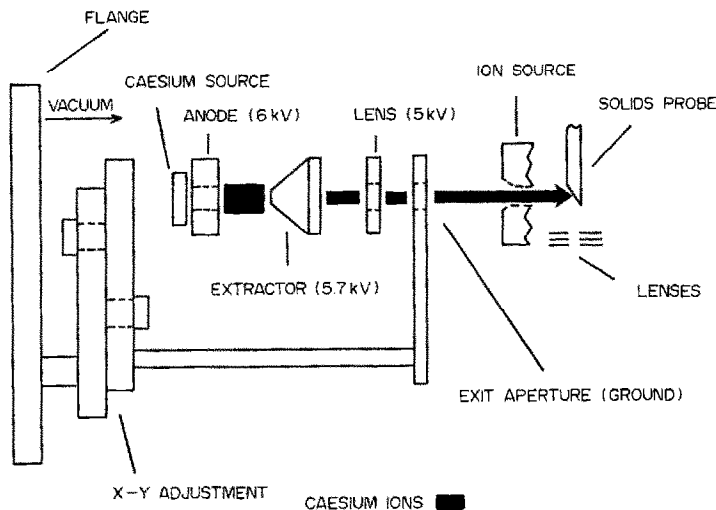


Fig. 1. Exploded view of caesium ion source and interface, with typical lens voltages.

Measurements

Samples were prepared by suspending or dissolving the solid (1–100 μg) on the surface of a glycerol droplet (5–10 μl) which had been placed on the probe tip. Mass spectra (Table 1) were obtained by scanning the third quadrupole, while operating the other two quadrupoles in the radiofrequency-only mode. Daughter spectra (Table 2) were obtained by mass-selection of the parent ion by using the first quadrupole, and subjecting these ions to collision-induced dissociation (CID) in the second quadrupole operated in the radiofrequency-only mode. Parent scans were recorded by setting the third quadrupole to pass ions of a fixed m/z ratio and scanning the first quadrupole. Argon was used as collision gas at a pressure of *ca.* 1.8×10^{-3} mmHg (*viz.*, under multiple collision conditions). The collision energy, as determined from the potential difference between the collision quadrupole and the ion source (ground potential) was 20 eV. The potential of the third quadrupole was set at 2 V more negative than that of the second quadrupole. The ion source temperature was maintained at *ca.* 150°. Glycerol matrix background ions have *not* been removed from the mass spectra presented here; the typical background ions are the protonated gly-

cerol oligomers, *viz.* m/z 93 and 185, and their dehydration products, *viz.* m/z 57, 75, 149 (which can also be due to a phthalate-derived ion) and 167.

Reagent grade thiamine hydrochloride (1) and Woodward's reagent L [2-*tert*-butyl-5-methylisoxazolium perchlorate, (2)] were purchased from Fluka and used without further purification. Ortho (3) and para (4) *N,N'*-dimethyl-2-amino-*N,N,N'*-trimethylanilinium iodide were synthesized by standard methods.

RESULTS AND DISCUSSION

Initial experiments were aimed at evaluating the performance of the combination of caesium ion gun and triple quadrupole mass spectrometer. Particle-induced desorption of thiamine hydrochloride (1) has been studied by use of SIMS, liquid SIMS and plasma desorption,^{17,21} making it a compound of choice for our investigations. The mass spectrum obtained by caesium ion bombardment of thiamine hydrochloride shows ions of m/z 265, 144, 123 and 122 (relative abundances 24, 15, 40 and 100% respectively). These ions are assigned to C^+ , ThH^+ , PyCH_3^+ and PyCH_2^+ , respectively, where Py and Th represent the pyrimidine and thiazolium units and C^+ is the intact cation. The ion at m/z 122 results from homolytic cleavage of the carbon–nitrogen bond between the rings in the intact ion, and m/z 144 corresponds to the product of heterolytic cleavage of the carbon–nitrogen bond, with hydrogen transfer to the thiazolium ring.

The daughter spectrum of the intact cation, 265⁺, generated by using caesium ion desorption of thiamine hydrochloride, contains ions with m/z 122 and 144 (100 and 40% relative abundance, respectively) in excellent agreement with previous reports on high-energy collision-induced dissociation experiments utilizing a sector instrument.¹⁷ The degree of similarity is striking, since the daughter spectra were obtained by employing two desorption methods with

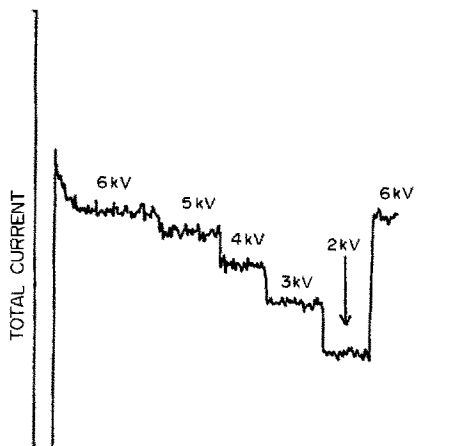
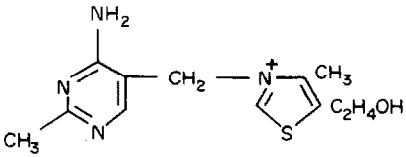
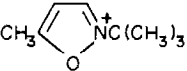
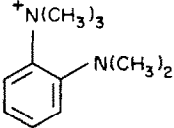
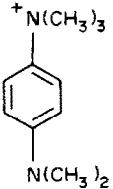


Fig. 2. Plot of the total ion current of silver nitrate in a glycerol matrix *vs.* accelerating voltage of the primary caesium ion beam.

Table 1. Summary of principal ions in mass spectra

Compound	Ions (relative abundance, %)*
(1) 	265 (24, C ⁺), 144 (15), 123 (40), 122 (100), 81 (35)
(2) 	ClO ₄ ⁻ 140 (97, C ⁺), 141 (6), 93 (24), 84 (100), 75 (8), 73 (9), 57 (33), 55 (11)
(3) 	I ⁻ 179 (100, C ⁺) 164 (7), 133 (3), 93 (8), 74 (8), 57 (9)
(4) 	I ⁻ 179 (100, C ⁺), 164 (22), 185 (12), 93 (55), 75 (14), 73 (9), 57 (17)

*Ions with m/z 185, 167, 149, 93, 75, 57 in the mass spectra are typically, but not always, due to protonated glycerol oligomers and their dehydration products; m/z 133 is typically due to reflected caesium primary ions. C⁺ represents the intact cation.

very different collision energies (keV *vs.* eV) and collision gas-pressures (50% *vs.* 90% beam intensity attenuation). Evidently, the internal energy transferred when the selected ion is activated by collision is similar in the two experiments.

The combination of caesium ion desorption and MS/MS utilizes the strengths of both techniques. Desorption ionization methods frequently produce intact molecular or quasi-molecular ions of non-volatile, thermally labile compounds, but MS/MS

Table 2. Summary of desorption ionization daughter spectra

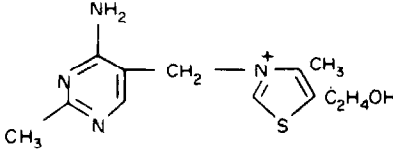
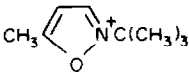
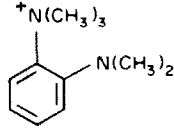
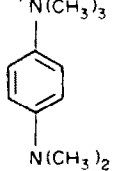
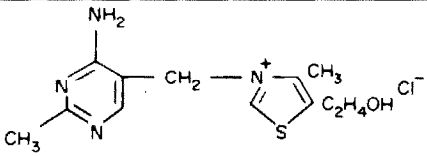
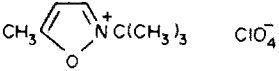
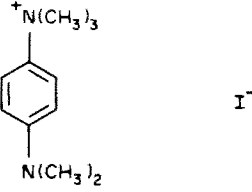
Compound	Parent ion m/z	Daughter ions (relative abundance, %)
(1) 	265 123 122 144	122 (100), 144 (33) 122 (3), 82 (54), 81 (21), 105 (6), 55 (100), 54 (28) 121 (3), 81 (54), 54 (23), 42 (77), 122 (100) 126 (18), 113 (100), 112 (15)
(2) 	140	84 (100), 57 (31)
(3) 	179	164 (25), 149 (41), 134 (34), 133 (60), 132 (100), 120 (50), 118 (32), 117 (9), 106 (30), 91 (26), 77 (8)
(4) 	179 164	164 (98), 149 (100), 122 (22), 121 (6), 120 (10), 107 (12) 159 (56), 122 (64), 121 (24), 120 (70), 107 (100), 106 (27), 79 (10), 77 (9)

Table 3. Summary of desorption ionization parent spectra

Compound	Daughter ion m/z	Parent ions (relative abundance, %)
(1) 	122	265 (100), 266 (9), 267 (6)
	123	266 (23), 267 (6), 268 (5), 123 (100)
	144	164 (72), 266 (19), 144 (100)
(2) 	84	140 (100), 141 (8)
	57	140 (100), 141 (24)
(4) 	149	164 (8), 179 (100), 180 (11)

enhances the structural information to be gained through collisional activation of the parent ion. In addition, MS/MS is analytically useful for reducing chemical noise, enabling detection of minor components in a complex mixture. Examples are demonstrated below.

Background noise due to neutrals is a common problem in desorption ionization experiments utilizing liquid matrices. The selective elimination of undesirable chemical noise in a DI experiment¹² by using tandem mass spectrometry is illustrated with a 50:1 mixture of two salts, the ortho isomer of *N,N'*-dimethyl-2-amino-*N,N,N*-trimethylanilinium iodide (*o*-TMA iodide) (3) and Woodward's reagent L (2). The Cs⁺-bombardment mass spectrum of this mixture in glycerol shows a signal for Woodward's reagent L (m/z 140) which is lost in the background (less than 1% of the base peak m/z 179, which corresponds to the molecular ion of *o*-TMA, Fig. 3a). However, mass selection of m/z 140 from the same mixture, followed by collisional activation, yielded a daughter spectrum (Fig. 3b) which matches that of authentic Woodward's reagent L [major daughter ions of m/z 140 are m/z 84, (100%) and 57 (23%)].

The DI mass spectrum of this mixture contained an abundant 179⁺ molecular ion from *o*-TMA, but few structurally informative fragment ions were present. Similarly, the desorption mass spectrum of *p*-TMA iodide (4) also contained an abundant 179 ion and few fragment ions. The desorption mass spectra of the ortho and para isomers of TMA iodide (shown in Fig. 4) do not allow differentiation between the two compounds. However, striking differences are found in their respective daughter spectra (Fig. 5). The dominant ions in the daughter ion spectrum of the intact para cation (m/z 179) appear at m/z 149 and 164, as shown in Fig. 5a. The same ions, m/z 149 and 164, are also seen, but with different relative abundances, in the daughter spectrum of the ortho

isomer (Fig. 5b). In addition, abundant ions of m/z 132, 133 and 134 are evident in the daughter spectrum of this isomer. These results for the isomers parallel those obtained by other authors using MS/MS but different ionization techniques.²² The structures of the ions in the mass range 132–134 seen in the daughter ion spectrum of m/z 179 from *o*-TMA have not been

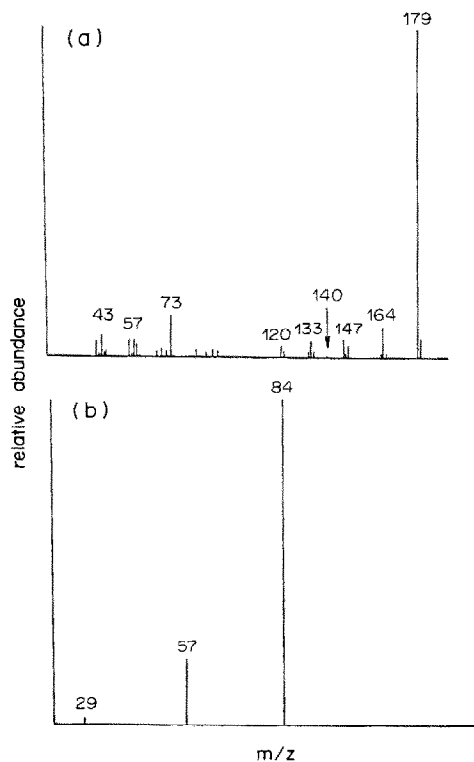


Fig. 3. (a) Desorption ionization mass spectrum of a 50:1 mixture of Woodward's reagent L and *o*-TMA; (b) daughter spectrum of Woodward's reagent L intact cation, m/z 140; collision energy 20 eV, argon collision gas pressure 1.8×10^{-3} mmHg.

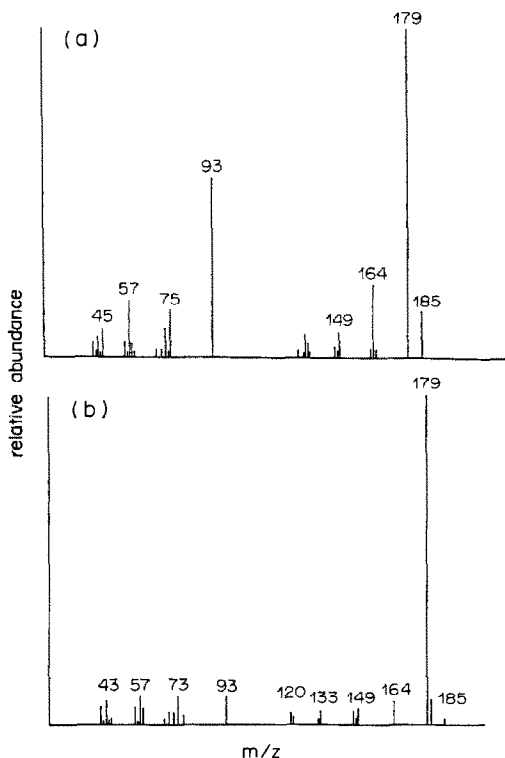


Fig. 4. (a) Desorption ionization mass spectrum of *p*-TMA; (b) desorption ionization mass spectrum of *o*-TMA.

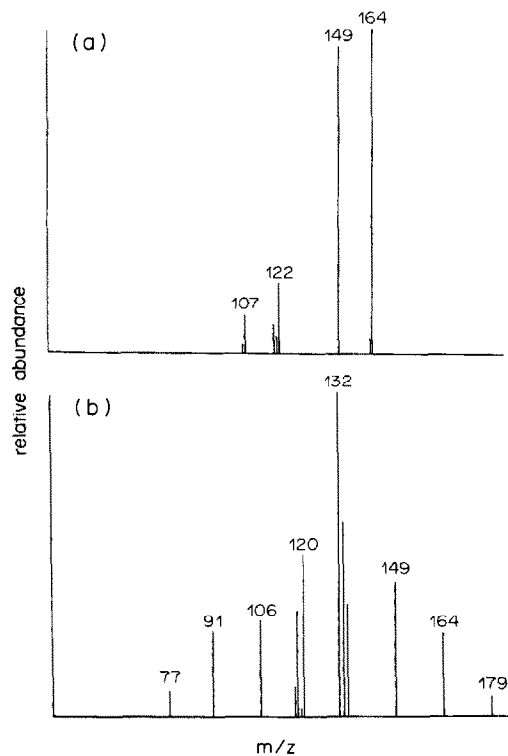
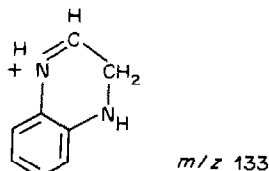


Fig. 5. (a) Daughter ion spectrum of m/z 179 of *p*-TMA; (b) daughter ion spectrum of m/z 179 of *o*-TMA; collision energy 20 eV, argon gas pressure 1.8×10^{-3} mmHg.

determined conclusively, but are suggestive of ring-closure products (possible with the ortho isomer but not the para isomer) produced by collisional excitation of the molecular ion. A daughter spectrum of the proposed ring-closure fragment ion (m/z 133) displays a base peak at m/z 92 corresponding to loss of CH_3CN . The second most abundant peak occurs at m/z 65. A proposed structure for m/z 133 consistent with the data is



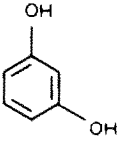
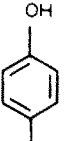
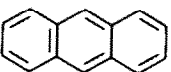
In addition to providing structural information as shown above, collision-induced dissociation of gas-phase ions reveals details about the reaction processes which lead to production of the secondary ions recorded in a desorption ionization mass spectrum. The DI mass spectrum of Woodward's reagent L contains a base peak at m/z 84 (probably loss of butene from the molecular ion), a molecular ion (m/z 140, 97% relative abundance, RA), and a peak at m/z 57 (33% RA) which most likely represents the tert-butyl ion. Formation of the ions with m/z 84 and 57 could be the result of (1) the gas-phase fragmentation of an excited parent ion desorbed from the surface, or (2) desorbed fragment ions generated at

the surface by the primary ions. The occurrence of the former process is supported by the daughter ion spectrum of the intact cation m/z 140. Selection of this ion with the first mass analyser, followed by collision-induced dissociation in the second quadrupole, yields fragments with m/z 57 and 84 and similar relative abundances to those observed in the mass spectrum. This adds to other evidence that gas-phase fragmentation of energetic secondary ions plays a major role in many desorption ionization experiments.^{23,24}

The formation of secondary ions in these experiments can be summarized as the result of direct desorption of preformed ions followed by gas-phase unimolecular fragmentation. In addition, caesium ion beams can be used to form ions by a route different from that discussed so far. To do this, the primary-ion impact region is arranged to fall within the enclosed ion volume, and chemical reagent gases are introduced above the sample surface. The primary ions desorb involatile sample molecules from the condensed phase and concurrently ionize an auxiliary chemical reagent gas. The resulting chemical reagent ions react with the desorbed neutral molecules. Ion-molecule reactions between FAB desorbed species and gaseous reagent ions created by electrons have previously been reported.²⁵

In a typical experiment methyl chloride was introduced as the auxiliary gas and was bombarded by 6 keV primary caesium ions at an ion-current of

Table 4. Summary of DICI daughter spectra*

Compound	Parent ion, m/z	Daughter ions (relative abundance, %)
(5) 	125	110 (100), 125 (40), 107 (22), 93 (5), 79 (23), 77 (47), 65 (4)
	140	123 (100), 95 (17), 77 (7), 67 (29)
(6) 	125	110 (100), 125 (25), 107 (11), 93 (5), 82 (7), 79 (18), 77 (21), 65 (10)
	140	123 (100), 95 (14), 77 (7), 67 (26), 65 (6)
(7) 	193	178 (100), 193 (61), 152 (7), 139 (5)
	227	227 (12), 218 (9), 191 (100), 178 (89)

*Ionization of methyl chloride reagent gas is by Cs^+ . No electron ionization is used.

ca. 1 μA . Predominant ions evident in the mass spectrum of the reagent gas occur at m/z 65 and 67 corresponding to $(\text{CH}_3)_2\text{Cl}^+$, at m/z 99 and 101 corresponding to $\text{ClCH}_3 \dots \text{CH}_2\text{Cl}^+$ and at m/z 49 and 51 ascribed to CH_2Cl^+ . These ions occur with the same relative abundance as those formed under standard chemical ionization (CI) conditions,^{26,27} but with lower absolute yields. The desorption ionization/chemical ionization (DICI) mass spectrum of *m*-dihydroxybenzene (resorcinol), obtained by using methyl chloride as the auxiliary gas, displays a variety of ions characterized as ion-molecule reaction products of methylation (m/z 125), halomethylation (m/z 159), dimethylation (m/z 140), protonation (m/z 111) and charge exchange (m/z 110). It is also possible that the ion at m/z 110 is the result of direct ionization of gaseous resorcinol by the primary caesium ion.

In order to deduce the site of methylation on the desorbed neutral species, daughter spectra were obtained of both methylated (m/z 125) and dimethylated (m/z 140) resorcinol (5) and hydroquinone (6) (see Table 4). Methylated resorcinol products induced by using DICI exhibited predominantly ring methylation²⁶ as evidenced by the daughter spectrum of the parent ion, $\text{C}_7\text{H}_9\text{O}_2^+$. The predominance of ring over substituent methylation was deduced by comparing the daughter spectra of the methylated species with that of protonated model compounds, *viz.* hydroxyanisoles and dihydroxytoluenes, obtained in a previous study. Specifically, the relative abundances of 79^+ and 107^+ (which suggest ring methylation of the model) are much higher than those of 65^+ and 93^+ (suggesting substituent methylation) in the daughter spectra of the methylated species, indicating predominantly ring methylation. Methylation of hydroquinone occurs both in the aromatic ring and in the substituent, as is evident from

the daughter spectrum of the methylated molecular ion (m/z 125), which reveals that ring methylation occurs more frequently than substituent methylation. Analogous results to these were obtained in standard chemical ionization experiments for the gas-phase methylation of the dihydroxybenzenes.^{26,27}

In addition to resorcinol and hydroquinone, a fused-ring aromatic molecule, anthracene (7), was also subjected to DICI with methyl chloride as reagent gas. The base peak in the DICI mass spectrum (Fig. 6) of anthracene occurs at m/z 193 and corresponds to methylated anthracene. Ionization of the neutral molecule (m/z 178) is the next most abundant process, followed by protonation (m/z 179) and halomethylation (m/z 227). Collisional activation of 193^+ resulted in fragmentation with loss of a methyl radical to give m/z 178 (summarized in Table 4) and the daughter spectrum of 227^+ indicated loss of HCl to be the predominant process.

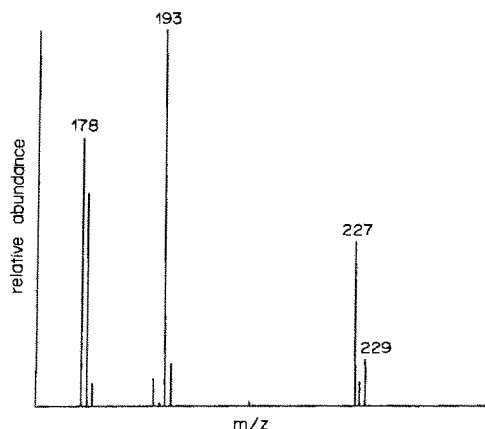


Fig. 6. Desorption ionization/chemical ionization of anthracene.

CONCLUSIONS

Coupling of a caesium ion source to a triple quadrupole mass spectrometer enhances the information obtainable by using these techniques individually. By utilizing the different types of scans available in tandem mass spectrometry (*i.e.*, daughter and parent scans) information can be obtained which assists in isomer distinction, structure elucidation and studies in ion reaction mechanisms. In addition, for this particular apparatus, it was demonstrated that ion-molecule reactions can be induced between desorbed non-volatile neutral molecules and chemical reagent ions, and that this procedure also gives useful MS/MS spectra.

Acknowledgements—We wish to acknowledge support by the National Science Foundation CHE84-08258.

REFERENCES

1. M. Barber, R. S. Bordoli, R. D. Sedgwick and A. N. Tyler, *J. Chem. Soc. Chem. Commun.*, 1981, 325.
2. K. L. Busch and R. G. Cooks, *Science*, 1982, **218**, 247.
3. D. F. Barofsky, U. Giessmann, A. E. Bell and L. W. Swanson, *Anal. Chem.*, 1983, **55**, 1318.
4. C. N. McEwen and J. R. Hass, *ibid.*, 1985, **57**, 890.
5. F. W. McLafferty (ed.), *Tandem Mass Spectrometry*, Wiley-Interscience, New York, 1983.
6. D. Zakett, A. E. Schoen, R. G. Cooks and P. H. Hemberger, *J. Am. Chem. Soc.*, 1981, **103**, 1295.
7. L. G. Wright, R. G. Cooks and K. V. Wood, *Biomed. Mass Spectrom.*, 1985, **12**, 159.
8. I. J. Amster, M. A. Baldwin, M. T. Cheng, C. J. Proctor and F. W. McLafferty, *J. Am. Chem. Soc.*, 1983, **105**, 1654.
9. D. F. Hunt, W. M. Bone, J. Shabanowitz, J. Rhodes and J. M. Ballard, *Anal. Chem.*, 1981, **53**, 1706.
10. D. A. McCrery, D. A. Peake and M. L. Gross, *ibid.*, 1985, **57**, 1181.
11. W. R. Sherman, K. E. Ackerman, R. H. Bateman, B. N. Green and I. Lewis, *Biomed. Mass Spectrom.*, 1985, **12**, 409.
12. R. G. Cooks and K. L. Busch, *J. Chem. Educ.*, 1982, **59**, 926.
13. A. J. Clifford, C. S. Silverman-Hones, K. E. Creek, L. M. DeLuca and Y. Tondeur, *Biomed. Mass Spectrom.*, 1985, **12**, 221.
14. D. L. Lippstreu-Fisher and M. L. Gross, *Anal. Chem.*, 1985, **57**, 1174.
15. S. A. Carr, V. N. Reinhold, B. N. Green and J. N. Hass, *Biomed. Mass Spectrom.*, 1985, **12**, 288.
16. D. V. Davis, R. G. Cooks, B. N. Meyer and J. L. McLaughlin, *Anal. Chem.*, 1983, **55**, 1302.
17. G. L. Glish, P. J. Todd, K. L. Busch and R. G. Cooks, *Int. J. Mass Spectrom. Ion Proc.*, 1984, **56**, 177.
18. D. F. Hunt, J. Shabanowitz, R. T. McIver Jr., R. L. Hunter and J. E. Syka, *Anal. Chem.*, 1985, **57**, 765.
19. M. E. Castro and D. H. Russell, *ibid.*, 1984, **56**, 578.
20. W. Aberth, K. M. Straub, K. M. and A. L. Burlingame, *ibid.*, 1982, **54**, 2029.
21. N. Furstenuau, *Z. Naturforsch.*, 1978, **33A**, 563.
22. D. D. Fetterhoff and R. A. Yost, *Int. J. Mass Spectrom. Ion Phys.*, 1982, **44**, 37; S. Unger, *Int. J. Mass Spec. Ion Proc.*, 1985, **66**, 195.
23. K. L. Busch, B. H. Hsu, K. V. Wood, R. G. Cooks, C. G. Schwarz and A. R. Katritzky, *J. Org. Chem.*, 1984, **49**, 764.
24. J. Michl, *Int. J. Mass Spectrom. Ion Phys.*, 1983, **53**, 255.
25. J. E. Campana and R. B. Freas, *J. Chem. Soc. Chem. Commun.*, 1984, 1414.
26. I. Isern-Flecha, R. G. Cooks and K. V. Wood, *Int. J. Mass Spectrom. Ion Proc.*, 1984, **62**, 73.
27. S. J. Pachuta, I. Isern-Flecha and R. G. Cooks, *Org. Mass Spectrom.*, 1986, **21**, 1.

DETERMINATION OF CHROMATE AND CYANIDE BY ANION-EXCHANGE WITH LEAD IODATE, AND THE ANALYSIS OF MIXTURES OF CYANIDE, THIOCYANATE AND HALIDES

KRISHNA K. VERMA, PRAMILA TYAGI and MARY GRACE PUSHPA EKKA
Department of Chemistry, Rani Durgavati University, Jabalpur 482 001, India

(Received 4 September 1985. Revised 16 May 1986. Accepted 14 July 1986)

Summary—Chromate and cyanide have been determined by their ability to displace iodate from sparingly soluble lead iodate. The released iodate is treated with acidified iodide to give iodine, which is determined either by titration with thiosulphate, or spectrophotometrically as its blue complex with starch. Chromium(III) has been determined as chromate after its oxidation with peroxydisulphate. Sulphate, iodide, bromide, chloride, fluoride, oxalate, tartrate, phosphate and thiocyanate do not interfere. Thiosulphate, sulphite, sulphide, hexacyanoferrate(II) and molybdate ions vitiate the results. Silver, mercury, barium and iron(III) should be masked. Mixtures of cyanide, thiocyanate and halides have been analysed by using complementary procedures that employ the iodates of lead and mercury, and bromine oxidimetry. It has been shown that cyanide or thiocyanate interferes in the determination of iodide by oxidation to iodic acid, because of formation of cyanogen bromide.

An anion can be determined by exchange for the anion of a sparingly soluble compound if it forms a still less soluble or undissociated compound with the cation concerned. This principle has been tested with mercuric iodate¹⁻⁴ for the determination of chloride, bromide, iodide, sulphide, sulphite, thiocyanate, cyanide and thiosulphate, and with barium iodate⁵ for sulphate. The working procedure essentially consists of stirring the test solution with a sparingly soluble metal iodate and determining the iodate liberated, after filtering off the excess of solid reagent, by reaction with acidified iodide to yield iodine, which is either titrated with thiosulphate or measured spectrophotometrically as its blue complex with starch. Since many anions are capable of displacing iodate from these two metal salts, the method lacks specificity.¹ Also, strict adherence to the experimental conditions is necessary to avoid excessive blank values.

The high sensitivity of the metal iodate methods led us to examine the analytical potential of lead iodate (which has not hitherto been used) for the determination of chromate. Chromate does undergo anion-exchange with barium iodate, but there is serious interference by sulphate, which is the reduction product of peroxydisulphate, commonly used for oxidizing chromium(III) to chromate. Several other reagents have been tried for this oxidation, but peroxydisulphate in the presence of silver(I) has been found to be the most effective. Unlike other metal iodate methods, the determination of chromate with lead iodate is not subject to interference by large amounts of a number of ions. The blank values are almost negligible and not sensitive to changes in reaction conditions. Cyanide also reacts quan-

titatively with lead iodate, but relatively slowly, and can be eliminated as hydrogen cyanide from samples that are to be analysed for chromium.

EXPERIMENTAL

Reagents

Lead iodate. Prepared by slowly adding (with constant stirring) a solution of 25.7 g (0.12 mole) of potassium iodate in 250 ml of warm water to a solution of 16.5 g (0.05 mole) of lead nitrate in 200 ml of water, digesting the heavy precipitate of lead iodate on a boiling water-bath for 15 min, cooling to room temperature, and repeatedly washing with water by decantation, then with ethanol followed by diethyl ether. The product was obtained in almost theoretical yield (25 g), and found to be 99.6% pure by iodometric analysis.

Mercuric iodate. Prepared similarly to lead iodate, by using 16.0 g (0.05 mole) of mercuric acetate and 25.7 g (0.12 mole) of potassium iodate. The product was 99.8% pure as determined by iodometry.

Starch-iodide solution. Made by boiling a solution of 4 g of cadmium iodide in 150 ml of water to remove any traces of iodine, then slowly adding a suspension of 5 g of soluble starch in 50 ml of water, continuing the boiling for 10 min, cooling and diluting to 250 ml. Only freshly prepared solutions were used.

Standard solutions of test samples. Prepared by dissolving the stoichiometric amounts of high-purity reagents in distilled water, and standardized, potassium chromate by titration with ammonium iron(II) sulphate,⁶ potassium cyanide and ammonium thiocyanate with mercuric iodate,³ potassium iodide by a bromine amplification method⁷ and potassium bromide and chloride by argentometry.⁸

Standard solution of chromium(III). Made by reducing an appropriate weight of analytical reagent grade potassium dichromate with sodium metabisulphite in dilute sulphuric acid, boiling to remove sulphur dioxide, diluting the cooled solution to a known volume and standardizing.⁹

Less concentrated test solutions were made by diluting the stock solutions with water. All other substances used were of the highest purity available.

Apparatus

A Pye-Unicam SP 8-100 spectrophotometer was used.

Determination of chromate

Titration. To a 5-ml portion of test solution, containing 0.5–5 mg of chromate, in a 20-ml beaker, add 0.5 ml of 1% acetic acid and about 100 mg of finely powdered lead iodate, then stir for 20 min. Filter and wash by decantation, using a Whatman No. 41 filter paper and three successive washes with 5-ml portions of water, mix the combined filtrate and washings with 0.5 g of potassium iodide, 2 ml of 5% sulphuric acid and 25 ml of water, then titrate the liberated iodine with 0.01M thiosulphate (if the test sample contains up to 2 mg of chromate) or with 0.04M titrant (for larger amounts). Concurrently run a blank determination with approximately the same amount of lead iodate (the blank titration is usually 0.10 ml of 0.04M thiosulphate).

$$\text{CrO}_4^{2-} (\text{mg}) = 9.67 \Delta V M$$

where ΔV is the difference in the volume (ml) of thiosulphate (molarity M) used in the sample and blank determinations.

Spectrophotometric determination. A standard solution of potassium iodate is used for construction of the calibration graph. This has the advantage that a single calibration graph can be used for the determination of diverse anions.

Prepare a solution of potassium iodate containing 25.0 mg of iodate (IO_3^-) per litre. Mix 0.5–3.0 ml volumes of this solution with 2 ml of starch-iodide reagent and 1 ml of 1M sulphuric acid, in a 25-ml standard flask, shake and make up to the mark. After 5 min read the absorbance at 580 nm in a 1-cm cell, against water, and plot it against the weight (μg) of iodate present to construct the calibration graph.

Combine a 5-ml aliquot of test solution, containing 10–30 μg of chromate, with 1 drop of 1% acetic acid and 20 mg of lead iodate. Stir for 20 min, filter into a 25-ml standard flask and wash the residue with three 2-ml portions of water. Treat the combined filtrate plus washings with 2 ml of starch-iodide reagent and 1 ml of 1M sulphuric acid, dilute to volume and measure the absorbance after 5 min at 580 nm against a reagent blank. Reference to the calibration graph gives the amount of iodate liberated, which is related to that of chromate in the sample aliquot by the equation

$$\text{CrO}_4^{2-} (\mu\text{g}) = 0.331m$$

where m is the amount of iodate (μg) liberated.

Determination of chromium(III)

Mix a measured volume (5–10 ml) of test solution, containing 0.2–2 mg of chromium(III) for titration and 4–12 μg for spectrophotometric determination, with 2 ml of 1M sulphuric acid and 1 drop of 0.1% silver nitrate solution. Heat on a hot-plate, while adding ammonium peroxydisulphate in small portions with stirring, the amount of oxidant being 0.5 g for visual titration and 0.2 g for spectrophotometric measurement. Boil the solution gently for 15 min (adding water to compensate for evaporation), cool, neutralize the acid with 10% ammonia solution, then acidify with 5% acetic acid, and determine chromate as described before.

$$\text{Cr}^{3+} (\text{mg}) = 4.33\Delta V M$$

$$\text{Cr}^{3+} (\mu\text{g}) = 0.1486m$$

Determination of cyanide

Stir 0.13–3 mg of cyanide and 100 mg of lead iodate (for titration) and 2–8 μg of cyanide and 20 mg of lead iodate (for spectrophotometric determination) in 5–10 ml of water for 2 hr. Filter, wash the residue with water, then analyse the filtrate for iodate by the titration or spectrophotometric procedure

$$\text{CN}^- (\text{mg}) = 4.33\Delta V M$$

$$\text{CN}^- (\mu\text{g}) = 0.1486m$$

Analysis of mixtures of cyanide with thiocyanate, chloride, bromide or iodide. Stir a known volume (5–10 ml) of binary mixture, containing not more than 0.1 mmole total of the determined anions, with 100 mg of lead iodate for 2 hr. Filter, wash with water, combine the filtrate with 0.5 g of potassium iodide and 2 ml of 5% sulphuric acid, then titrate the released iodine with 0.04M thiosulphate. Run a blank determination. Let the difference between the sample and blank titrations be V ml; then

$$\text{CN}^- (\text{mg}) = 4.33VM$$

Combine a separate but equal volume of mixture with an equal volume of 95% ethanol and 100 mg of mercuric iodate, stir for 30 min, filter, wash the residue with three 5-ml portions of 50% ethanol, mix the filtrate with 0.5 mg of potassium iodide and 2 ml of 5% sulphuric acid, and titrate the liberated iodine with 0.04M thiosulphate. Do a blank determination. Let the corrected titration volume be V' ml.

$$\text{Co-existing anion (mg)} = FM(V' - V)$$

where the factor F is 9.67, 5.92, 13.33 and 21.16 for thiocyanate, chloride, bromide and iodide, respectively.

Analysis of mixtures of cyanide, bromide and iodide. Three analyses are necessary on three separate but equal-sized samples of test solution (5–10 ml) containing a total of about 0.1 mmole of the determinands, each analysis accompanied by the appropriate blank. The same thiosulphate solution is used throughout.

Sample 1. Determine cyanide by using lead iodate (titration procedure) as described above; iodide and bromide do not interfere. Let the net titration volume be V ml of thiosulphate of molarity M .

Sample 2. Determine the sum of the three anions by the mercuric iodate method. Let the net volume of thiosulphate be V' ml.

Sample 3. Add a saturated aqueous solution of bromine until the colour of free bromine persists, shake the solution for 5 min, add 0.5 g of sodium acetate, and the formic acid dropwise until the bromine colour disappears. After 2 min, add 1 g of potassium iodide and 5 ml of 5% sulphuric acid and titrate the liberated iodine with thiosulphate. Let the net volume of thiosulphate be V'' ml.

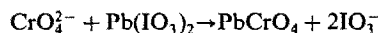
$$\text{CN}^- (\text{mg}) = 4.33VM$$

$$\text{I}^- (\text{mg}) = 21.16M(V'' - V/3)$$

$$\text{Br}^- (\text{mg}) = 13.33M[V' - (V'' + 2V/3)]$$

RESULTS AND DISCUSSION

The anion-exchange reaction that occurs when chromate is stirred with a suspension of lead iodate is:



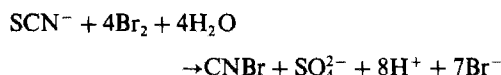
The solubility products (K_{s0}) for the lead iodate and chromate are 1.2×10^{-13} and 1.8×10^{-14} respectively.⁹ The most suitable pH range for the exchange reaction is 4–8. The method can be used to analyse mixtures of chromium(III) and chromate by first determining the chromate, then oxidizing chromium(III) with persulphate (with silver as catalyst) and determining the total chromate, the chromium(III) being obtained by difference. The determinations are not affected by the presence of as much as a 100-fold molar ratio (to chromium) of chloride, bromide, fluoride, iodide, phosphate, oxalate, tartrate, thiocyanate or sulphate. Sulphide, sulphite or

cyanide, if also present with chromium(III), should be removed before the analysis, by boiling the test solution after acidification. Thiosulphate does not undergo anion-exchange with lead iodate but interferes in the iodometric titration. Hexacyanoferrate(II) and molybdate vitiate the analysis by giving analogous exchange reactions. Ammonium, alkali metals, zinc and manganese do not interfere. Iron(III) and mercury(II) should be masked by forming the fluoride and chloride complexes, respectively, and silver and barium by their precipitation as chloride and sulphate respectively.

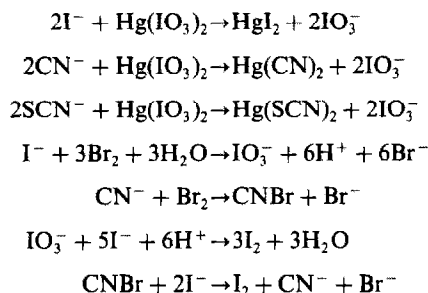
The spectrophotometric determinations with mercuric and barium iodates employ ethanol as a co-solvent to minimize the reagent blank. However, the absorption spectrum of the blue starch-iodine complex is critically dependent on the alcohol concentration, making necessary the construction of a calibration graph under exactly identical conditions. Lead iodate, being much less soluble than the mercuric and barium salts,⁹ gives a negligible blank in aqueous medium, and addition of ethanol is not necessary.

The tolerance for thiocyanate, bromide, iodide and chloride in the lead iodate method suggested that their mixtures with cyanide might be analysed by using mercuric iodate as a complementary reagent to determine the sum of the anions concerned. Iodide is most commonly determined by oxidation with bromine to iodic acid, then iodometry after reduction of excess of bromine with formic acid.^{10,11} Cyanide forms cyanogen bromide with bromine,¹² which is not reduced by formic acid and also liberates iodine on reaction with potassium iodide. Thus, high values for

iodide are obtained if cyanide is an impurity. Thiocyanate behaves similarly.



The analysis of mixtures of iodide with cyanide or thiocyanate is possible by two separate determinations based on bromine oxidation and anion-exchange with mercuric iodate. On bromine oxidation, iodide gives the same amount of iodate as that released in the mercuric iodate reaction, but one mole of cyanide or thiocyanate liberates only one mole of iodine instead of the three moles it gives in the mercuric iodate method:



The equations used for calculation are

$$\text{SCN}^- (\text{mg}) = 14.5M(V - V')$$

$$\text{CN}^- (\text{mg}) = 6.5M(V - V')$$

$$\text{I}^- (\text{mg}) = 21.16M(1.5V' - 0.5V)$$

where V is the net volume (ml) of thiosulphate (molarity M) used in the mercuric iodate method,

Table 1. Spectrophotometric and titrimetric determination of chromate, chromium(III) and cyanide

Ion	Titrimetric determination			Spectrophotometric determination		
	Taken, mg	Found,* mg	CV, %	Taken,† μg	Found,* μg	CV, %
Cr(VI)	0.46	0.45	0.5	9.8	9.9	1.8
	0.78	0.81	0.4	12.5	12.0	1.5
	1.60	1.63	0.4	15.6	15.9	0.9
	2.38	2.36	0.2	19.2	19.5	0.7
	3.42	3.44	0.3	25.0	24.6	1.2
	4.90	4.95	0.4	28.6	28.0	1.6
Cr(III)	0.18	0.20	0.6	3.9	3.7	2.0
	0.45	0.48	0.5	5.5	5.8	1.6
	1.08	1.10	0.5	8.8	8.4	1.5
	1.56	1.58	0.3	10.6	10.2	1.5
	1.79	1.81	0.4	11.8	11.6	1.7
	2.10	2.08	0.5	12.2	12.5	1.8
CN ⁻	0.12	0.11	0.5	2.1	2.0	2.2
	0.32	0.33	0.5	4.5	4.2	1.9
	0.85	0.83	0.6	5.6	5.8	1.6
	1.40	1.38	0.6	6.8	6.4	1.5
	1.83	1.80	0.5	7.2	7.0	1.8
	2.55	2.58	0.6	8.4	8.1	1.9

*Average of six determinations; CV = coefficient of variation.

†Amount found by spectrophotometric reference methods; chromium(VI) by diphenylcarbazide,¹³ chromium(III) by phenylarsenazo¹⁴ and cyanide by palladium(II) 5-phenylazo-8-aminoquinoline.¹⁵

Table 2. Titrimetric analysis of mixtures (mean of 6 determinations CV = coefficient of variation)

Taken, mg			Found, mg					
I	II	III	I	CV, %	II	CV, %	III	CV, %
Cyanide	Bromide	Iodide						
0.457	1.85	6.20	0.461	0.5	1.88	0.8	6.17	0.5
0.680	2.06	5.76	0.659	0.5	2.10	0.6	5.58	0.5
1.22	2.84	3.15	1.20	0.6	2.90	0.8	3.21	0.4
1.40	1.62	2.04	1.46	0.4	1.63	0.5	2.14	0.5
0.65	3.05	3.25	0.63	0.6	3.09	0.6	3.36	0.6
Chromate	Chromium (III)							
2.10	1.52		2.04	0.5	1.46	0.6		
3.42	0.841		3.39	0.2	0.828	0.4		
3.90	0.636		3.85	0.3	0.650	0.4		
4.62	0.458		4.60	0.4	0.482	0.5		
Cyanide	Thiocyanate							
0.620	4.80		0.609	0.5	4.72	0.5		
1.20	3.52		1.22	0.4	3.48	0.4		
1.63	2.65		1.60	0.2	2.69	0.3		
2.01	1.84		2.10	0.5	1.76	0.5		
Cyanide	Bromide							
0.582	5.83		0.556	0.4	5.76	0.5		
1.16	4.42		1.10	0.5	4.45	0.4		
1.52	3.56		1.48	0.5	3.61	0.5		
1.86	2.13		1.78	0.5	2.07	0.6		
Cyanide	Iodide							
0.559	9.82		0.580	0.6	9.75	0.5		
1.21	6.26		1.19	0.5	6.18	0.5		
1.60	4.75		1.65	0.5	4.68	0.4		
1.95	3.00		1.90	0.4	2.95	0.5		
Cyanide	Chloride							
0.656	2.95		0.672	0.6	2.90	0.4		
1.32	2.02		1.36	0.5	2.08	0.5		
1.70	1.67		1.68	0.5	1.73	0.5		
2.03	0.91		2.10	0.4	0.94	0.5		
Thiocyanate	Iodide							
2.86	9.12		2.88	0.6	9.25	0.8		
3.54	8.51		3.50	0.5	8.46	0.7		
4.45	7.33		4.51	0.5	7.23	0.6		
5.21	6.41		5.18	0.4	6.38	0.6		
6.37	4.26		6.32	0.5	4.19	0.8		
6.85	3.14		6.93	0.6	3.20	0.8		

and V' is the net volume of thiosulphate required in the bromine oxidation method.

Results given in Tables 1 and 2 for the determination of various ions suggest that the proposed procedures are accurate and precise.

Chromium occurs widely in the trivalent and hexavalent states in nature and in industrial waste waters. Chromium(III) is an essential element to mammals, but chromium(VI) is harmful to animals and plants, and microdeterminations of these oxidation states are of interest.^{16,17} Several reagents for chromium(III) have been developed,¹⁸ but the most usual method is oxidation to chromium(VI) and either titration with iron(II)⁶ or spectrophotometric determination with diphenylcarbazide.¹³ Recently, sequential determinations of chromium(III) and (VI) have been reported.¹⁹⁻²¹ The lead iodate method given here has a much better stoichiometric ratio of titrant to analyte (by a factor of four) than iron(II) titrations of chromium(VI).

Chloramine-T and dibromamine-T have been used as titrimetric oxidizing agents for the determination of cyanide.²² Thiocyanate also reacts quantitatively with these reagents. After the methyl isocyanate gas tragedy at Bhopal, cyanide and thiocyanate were detected in the local water. Such mixtures have been analysed by separation of the cyanide as zinc cyanide,²² but bromide and iodide interfere severely. Ten organic aromatic halosulphonamides have been prepared and used for thiocyanate determination in its metal salts and complexes.²³

The reaction of halides with mercuric iodate is the most sensitive available method,³ but many other ions also react. The amplification method for iodide involving oxidation to iodic acid (which is iodometrically determined) with bromine^{7,11} tolerates large quantities of bromide, but that using periodate oxidation gives higher blank values if bromide is also present.^{24,25} Determination of bromide in the presence of iodide seems to be troublesome, the best procedure

perhaps being argentometric titration with end-point detection by potentiometry or with adsorption indicators.⁸ Mixtures of iodide and bromide have recently been analysed by using 2-iodosobenzoate, the sequential oxidation to halogens being effected by control of pH.²⁶

Lead iodate is more selective in its action than barium and mercuric iodates, and a suitable combination of methods using these reagents and bromine can profitably be employed for the analysis of mixtures of ions which are otherwise troublesome to determine.²⁷

Acknowledgement—Thanks are due to the Council of Scientific and Industrial Research, New Delhi, for a Senior Research Fellowship to P.T.

REFERENCES

1. F. D. Snell, *Photometric and Fluorometric Methods of Analysis: Non-metals*, p. 254. Wiley-Interscience, New York, 1981.
2. R. E. Humphrey, R. R. Clark, L. Houston and D. J. Kippenberger, *Anal. Chem.*, 1972, **44**, 1299.
3. W. L. Hinze and R. E. Humphrey, *ibid.*, 1973, **45**, 385.
4. R. E. Humphrey and W. L. Hinze, *ibid.*, 1973, **45**, 1747.
5. W. L. Hinze and R. E. Humphrey, *ibid.*, 1973, **45**, 814.
6. J. Bassett, R. C. Denney, G. H. Jeffery and J. Mendham, *Vogel's Text-Book of Quantitative Inorganic Analysis*, 4th Ed., p. 361. Longmans, London, 1978.
7. R. Belcher, S. S. T. Liao and A. Townshend, *Talanta*, 1976, **23**, 541.
8. Ref. 6, p. 339.
9. F. J. Welcher and R. B. Hann, *Semimicro Quantitative Analysis*, p. 212. Van Nostrand, New York, 1969.
10. D. Amin and M. S. Al-Ajely, *Talanta*, 1981, **28**, 955.
11. F. A. Abeer, M. Jasim and D. Amin, *ibid.*, 1983, **30**, 609.
12. E. Schulek, *Z. Anal. Chem.*, 1923, **62**, 337.
13. E. B. Sandell, *Colorimetric Determination of Traces of Metals*, p. 293. Interscience, New York, 1959.
14. S. Fu-Scheng, *Talanta* 1983, **30**, 446.
15. M. Blanco and S. Maspoch, *ibid.*, 1984, **31**, 85.
16. T. M. Florence and G. E. Batley, *CRC Crit. Rev. Anal. Chem.*, 1980, **9**, 219.
17. E. Berman, *Toxic Metals and Their Analysis*, Heyden, London, 1980.
18. Z. Marczenko, *Spectrophotometric Determination of Elements*, Horwood, Chichester, 1976.
19. G. Fang and C. Miano, *Analyst*, 1985, **110**, 65.
20. J. C. de Andrade, J. C. Rocha and N. Baccan, *ibid.*, 1985, **110**, 197.
21. A. G. Cox, I. G. Cook and C. W. McLeod, *ibid.*, 1985, **110**, 331.
22. B. T. Gowda and D. S. Mahadevappa, *Indian J. Chem.*, 1977, **15A**, 938; 1978, **16A**, 635.
23. *Idem*, *Talanta*, 1983, **30**, 359.
24. R. Belcher, J. W. Hamya and A. Townshend, *Anal. Chim. Acta*, 1970, **49**, 570.
25. S. A. Rahim, S. M. Bishara and D. Amin, *Talanta*, 1977, **24**, 681.
26. K. K. Verma and A. K. Gulati, *ibid.*, 1983, **30**, 279.
27. T. S. Ma and R. E. Lang, *Quantitative Analysis of Organic Mixtures*, Wiley, New York, 1979.

AN ALGORITHM AND A FORTRAN PROGRAM (CHEMEQUIL-2) FOR CALCULATION OF COMPLEX EQUILIBRIA

VIJAY S. TRIPATHI

Environmental Sciences Division, Oak Ridge National Laboratory, Oak Ridge, TN 37831, U.S.A.

(Received 6 May 1986. Accepted 11 July 1986)

Summary—A computer program, CHEMEQUIL-2 (CHEMical EQUILibrium), based on interfacing an iterative algorithm with the Newton-Raphson method, for calculating equilibrium compositions in aqueous mixtures of metals and ligands, is described. The program is also capable of simulating acid-base titrations. It has been compared with MINQUAD, COMPLEX and MINEQL with respect to execution time and memory requirements. As a result of algorithm development and program design, CHEMEQUIL-2 offers considerable savings in both execution time (by 1-2 orders of magnitude) and memory requirements, especially for large problems, compared to these programs. The computational efficiency of CHEMEQUIL-2 makes it well suited for use in hydrogeochemical transport models.

In a multicomponent system, metals and ligands may react to form complexes, and calculations of the concentration of free components and complexes is necessary in several contexts, such as analytical chemistry, environmental chemistry, geochemistry, and biochemistry. Given the analytical concentration of metals and ligands and the stability constants for complexes, the task is to compute the concentration of free metals, ligands, and complexes. Various approaches to calculation of chemical equilibria have been described¹ and existing computer programs have been reviewed.^{2,3}

A basic set of reactants are called components. These components, normally metals and ligands, may react to form complexes in aqueous solutions. Concentrations of all species may be calculated from the concentrations of uncomplexed components and the stability constants of the complexes. At equilibrium, the mass-action and mass-balance constraints that must hold may be stated as follows:

Mass-action expression:

$$C_j = \beta_j \prod_{i=1}^m X_i A_{ij} \quad (j = 1, \dots, n) \quad (1)$$

Mass-balance expression:

$$\text{TOT}_i = X_i + \sum_{j=1}^n A_{ij} C_j \quad (i = 1, \dots, m) \quad (2)$$

where the symbols used have the following meanings

- A_{ij} Stoichiometric coefficient of component i in complex j
- β_j Overall stability (formation) constant of the j th complex
- C_j Concentration of complex j
- CALC_i Calculated total concentration at an intermediate iteration (based on guesses for X_i)

- k The iteration number for the iterative algorithm
- m The number of components
- n The number of complexes
- STEP The step size for varying concentration (in log units) of a fixed component
- TOL Convergence tolerance parameter
- TOT_i Total concentration of component i
- X_i Concentration of free component i

According to Brinkley's approach,⁴ the mass-balance equations are solved subject to the constraints of the equilibrium constant (mass-action) equations.

Various iterative methods can be used to solve the system of non-linear algebraic equations obtained by substituting (1) in (2).⁵⁻⁹ The Newton-Raphson method⁶⁻¹⁰ has been widely used in such calculations, and MINQUAD⁵ was found to be the most efficient³ among programs tested. In the Newton-Raphson method, an initial guess is made (X_i^0) for the concentrations of the free components and corresponding C_j values are calculated. The X_i and C_j values are then used to evaluate the mass-balance equations (CALC _{i}). Iterations are continued until the calculated mass-balance (CALC _{i}) is sufficiently close to TOT _{i} for all components.

The principal disadvantage of the Newton-Raphson method^{6,9,11} is that, unless the X_i^0 values are close enough to the actual values for the system, the method may take a large number of iterations to converge, or may even diverge in spite of the existence of a unique real solution.⁶⁻¹¹ The task of choosing a good initial guess is often difficult and is at the root of most of the problems encountered by the Newton-Raphson method.

This paper describes an iterative algorithm for calculating the equilibrium concentration of

free components, and a FORTRAN program, CHEMEQUIL-2, that is based on interfacing the proposed algorithm with the Newton-Raphson method. A comparison of CHEMEQUIL-2 and some existing programs with respect to array requirements and execution times is also presented.

ALGORITHM

The development of the proposed iterative algorithm was influenced by the work of Ginzburg,¹² who wrote the program COMPLEX. The algorithm starts by setting $X_i^0 = \text{TOT}_i$ for all components (without any distinction between metals and ligands), and uses the following iterative formula to calculate successive approximations:

$$X_i^{k+1} = \frac{\text{TOT}_i}{\text{CALC}_i^k} X_i^k \quad (3)$$

in which CALC_i is the value of the right-hand side of equation (2) at $X_i = X_i^k$.

The implementation involves the following steps.

1. Repeat steps 2-5 for all components (except those that are fixed, such as pH or pCl) starting with the component present in the *smallest* number of complexes and ending with the one present in the *largest* number of complexes.

2. If this is the first pass, set $X_i^0 = \text{TOT}_i$.

3. Calculate the concentration of those complexes for which $A_{ij} \neq 0$, using the updated values $X_1^{k+1} - X_{i-1}^{k+1}$ and $X_i^k - X_m^k$ in equation (1).

4. Evaluate CALC_i by using equation (2).

5. Compute X_i^{k+1} , using equation (3).

6. Test for convergence and proceed:

If $|\text{TOT}_i - \text{CALC}_i| < \text{TOT}_i \times \text{TOL}$ for all components, stop; otherwise start again at step 1.

The specification in step 1 that the iterations begin with the component present in the fewest complexes was found to give a substantial reduction in program run-time. Although this method alone is sufficient for solving chemical equilibrium problems, the rate of iterative improvement becomes rather slow when the X_i values approach the true ones. Therefore, a hybrid computer program was developed in which the first phase uses the new algorithm and the second phase uses the multidimensional Newton-Raphson method. Phase I brings the X_i^k values fairly close to the final values ($\text{TOL} = 0.5$), then in phase II the

Newton-Raphson method is invoked to force rapid convergence. This approach eliminates the difficulties of the ordinary Newton-Raphson method, thus ensuring rapid convergence throughout. For the component H^+ , when $\Sigma \text{H}^+ = 0$ and the pH is not fixed, only the Newton-Raphson method is used because equation (3) collapses at $\Sigma \text{H}^+ = 0$.

THE CHEMEQUIL-2 PROGRAM

The algorithm has been implemented in FORTRAN. A complete description of the key variables, options, and input to the program is included in the program listing which is available on request (see *Program availability*). The program has built-in options for varying a fixed ligand or cation concentration, such as pH, and for simulating acid-base titrations. The program has been run on many different computers under various operating systems, including DEC-20, DEC-10, VAX/UNIX, VAX/VMS and IBM 370.

Comparison of storage requirements

Almost all programs for equilibrium calculations utilize a two-dimensional array for storing the stoichiometric coefficients of the i th component in the j th complex (e.g., MINEQL¹³). Because the number of components in a complex seldom exceeds 5, the array (A) is sparse (i.e., most of the A_{ij} values are 0); its sparsity grows with increasing number of components and complexes. This can cause difficulties on smaller computers or for large problems, prompting the suggestion³ that programs such as COMPLEX or COMICS may be preferable to faster programs such as MINQUAD when the memory is limited or the problem to be solved is very large. This is because most programs store zeros as well. Furthermore, storing, referencing, and multiplying by zeros during computation increases the "DO LOOP overhead" and program run-time. CHEMEQUIL-2 exploits the storage algorithm outlined by Tripathi¹⁴ which uses a data structure to store only non-zero coefficients. Table 1 shows the storage requirements for some programs. In CHEMEQUIL-2, a considerable saving (by up to a factor of 5.7) in storage has been achieved by storing only non-zero stoichiometric coefficients; the relative saving grows with problem size. For MINQUAD⁵ and MINEQL¹³ only those arrays required for concentration calculations were counted.

Table 1. Array requirements for some programs as a function of the number of components and complexes

Program	No. of components \times no. of complexes					
	6 \times 20	10 \times 50	20 \times 50	20 \times 100	30 \times 400	50 \times 500
CHEMEQUIL	400	880	1320	1920	6160	9240
COMPLEX	281	825	1435	2635	13,945	27,565
MINQUAD	360	1010	1950	3200	15,340	30,720
COMICS	390	1320	2370	4620	26,170	52,770
MINEQL	744	1328	2178	3378	15,128	30,228

A sample problem

The sample problem consists of calculating the species distribution in a system containing three metal-ion components (UO_2^{2+} , Hg^{2+} , Cd^{2+}), six ligands (CO_3^{2-} , SO_4^{2-} , PO_4^{3-} , F^- , Cl^- , SiO_3^{2-}), and fifty complexes, as a function of pH. Table 2 contains the input data for this problem, with pH STEP = 4.0. A segment of output from CHEMEQUIL-2 for this problem is shown in Table 3.

Comparison of run-times with MINQUAD, COMPLEX and MINEQL

The computational efficiency of CHEMEQUIL-2 was compared with that of MINQUAD,^{3,5} MINEQL¹³ and COMPLEX.¹² For this comparison, the program segments responsible for output in MINQUAD and COMPLEX were rewritten to make their output as similar as possible to that of CHEMEQUIL-2. For MINEQL, only TYPE I, II and III species were printed. Moreover, for MINEQL, TYPE V species were not considered during computation; therefore, the execution time for MINEQL reflects only solution-phase calculations. Some other modifications for MINQUAD are described in the *Appendix*. All programs were run in single precision. The convergence tolerance (TOL or equivalent) was set at 10^{-4} for all programs.

All programs were saved as executable files, so the execution times do not include compilation time. Program testing was done on a DEC-20 computer in a time-sharing environment; therefore, the CPU time includes the time spent by the operating system in swapping jobs. All programs were subject to this overhead. However, the testing was done when few users were on the system and the system "load" was very low, so nearly all of the CPU time reflects execution time.

The example described in the preceding section was solved for pH increments of 0.2, 2.0 and 4.0, and the corresponding execution times shown in Table 4, from which it is evident that CHEMEQUIL-2 is the fastest for the sample problem.

CHEMEQUIL-2 was also compared with the programs studied by Leggett.³ Leggett evaluated seven computer programs on the basis of their run-times on six equilibrium systems (containing at most two metals and three ligands). Using storage requirements and execution time as criteria, he observed the order of efficiency to be MINQUAD > COMPLEX > SPECON II > MINQUAD-75 > EQUIL > COMICS. Table 5 shows a comparison between CHEMEQUIL-2 and MINQUAD, which shows the two programs take almost equal time; however, from Tables 4 and 5, it appears that with a growing number of components and complexes CHEMEQUIL-2 can be faster.

To evaluate the relative efficiency of CHEMEQUIL, MINQUAD, MINEQL and COMPLEX for large systems, a hypothetical system containing 28

components was designed, consisting of metal-ions (UO_2^{2+} , Hg^{2+} , Cd^{2+} , Ca^{2+} , Mg^{2+} , Ba^{2+} , Mn^{2+} , Cu^{2+} , Zn^{2+} , Ni^{2+} , Pb^{2+} , Fe^{3+} , Ag^+ , Al^{3+} , Co^{2+}), twelve

Table 2. Input data for the example problem

Example run for the program CHEMEQUIL									
0.1790E-05 0	0.0000E+00								
0.1500E-03 0	0.0000E+00								
0.1000E-05 0	0.0000E+00								
0.1000E-02 0	0.0000E+00								
0.1580E-04 0	0.0000E+00								
0.2820E-03 0	0.0000E+00								
0.4990E-03 0	0.0000E+00								
0.0000E+00 1	0.1000E-01								
0.1000E-05 0	0.0000E+00								
0.1000E-05 0	0.0000E+00								
0.9990E+03 0	0.0000E+00								
U02	CO3	PO4	SO4	F	CL	SIO3H	HG	CD	
-14.000	8	-1.0	0	0.0	0	0.0	0	0.0	
-5.780	1	1.0	8	-1.0	0	0.0	0	0.0	
-5.630	1	2.0	8	-2.0	0	0.0	0	0.0	
-15.650	1	3.0	8	-5.0	0	0.0	0	0.0	
10.070	1	1.0	2	1.0	0	0.0	0	0.0	
16.980	1	1.0	2	2.0	0	0.0	0	0.0	
21.400	1	1.0	2	3.0	0	0.0	0	0.0	
5.100	1	1.0	5	1.0	0	0.0	0	0.0	
8.960	1	1.0	5	2.0	0	0.0	0	0.0	
11.350	1	1.0	5	3.0	0	0.0	0	0.0	
12.570	1	1.0	5	4.0	0	0.0	0	0.0	
0.240	1	1.0	6	1.0	0	0.0	0	0.0	
2.730	1	1.0	4	1.0	0	0.0	0	0.0	
4.220	1	1.0	4	2.0	0	0.0	0	0.0	
20.750	1	1.0	3	1.0	8	1.0	8	1.0	
43.260	1	1.0	3	2.0	8	2.0	8	2.0	
22.580	1	1.0	3	1.0	8	1.0	8	2.0	
44.570	1	1.0	3	2.0	8	4.0	8	4.0	
65.840	1	1.0	3	3.0	8	6.0	8	6.0	
20.530	1	1.0	7	1.0	8	1.0	8	1.0	
10.330	2	1.0	8	1.0	0	0.0	0	0.0	
16.690	2	1.0	8	2.0	0	0.0	0	0.0	
1.990	4	1.0	8	1.0	0	0.0	0	0.0	
3.180	5	1.0	8	1.0	0	0.0	0	0.0	
12.350	3	1.0	8	1.0	0	0.0	0	0.0	
19.550	3	1.0	8	2.0	0	0.0	0	0.0	
21.700	3	1.0	8	3.0	0	0.0	0	0.0	
13.110	7	1.0	8	1.0	0	0.0	0	0.0	
22.930	7	1.0	8	2.0	0	0.0	0	0.0	
-3.160	9	1.0	8	-1.0	0	0.0	0	0.0	
-5.180	9	1.0	8	-2.0	0	0.0	0	0.0	
-20.260	9	1.0	8	-3.0	0	0.0	0	0.0	
2.400	9	1.0	4	1.0	0	0.0	0	0.0	
3.500	9	1.0	4	2.0	0	0.0	0	0.0	
7.270	9	1.0	6	1.0	0	0.0	0	0.0	
14.000	9	1.0	6	2.0	0	0.0	0	0.0	
14.880	9	1.0	6	3.0	0	0.0	0	0.0	
15.600	9	1.0	6	4.0	0	0.0	0	0.0	
1.600	9	1.0	5	1.0	0	0.0	0	0.0	
4.750	9	1.0	8	-1.0	6	1.0	6	1.0	
3.200	10	1.0	2	1.0	0	0.0	0	0.0	
2.300	10	1.0	4	1.0	0	0.0	0	0.0	
2.000	10	1.0	6	1.0	0	0.0	0	0.0	
2.700	10	1.0	6	2.0	0	0.0	0	0.0	
2.100	10	1.0	6	3.0	0	0.0	0	0.0	
1.100	10	1.0	5	1.0	0	0.0	0	0.0	
3.900	10	1.0	3	1.0	0	0.0	0	0.0	
-9.000	10	1.0	8	-1.0	0	0.0	0	0.0	
-19.100	10	1.0	8	-2.0	0	0.0	0	0.0	
-30.400	10	1.0	8	-3.0	0	0.0	0	0.0	
999.000	0	0.0	0	0.0	0	0.0	0	0.0	
0	1	1							
8	2.000	10.000	4.000						

Table 3. Example run for the program CHEMEQUIL

Concentration of components						
ID	Name	Iteration No. 7 X	Newton No. 1 PX	Tot.	Differ	Type
1	UO2	1.2780E-06	-5.8935E+00	1.7900E-06	8.3844E-13	0
2	CO3	3.0625E-17	-1.6514E+01	1.5000E-04	-2.0009E-11	0
3	PO4	1.1665E-22	-2.1933E+01	1.0000E-06	2.1316E-13	0
4	SO4	5.0553E-04	-3.2963E+00	1.0000E-03	-1.4552E-11	0
5	F	9.6940E-07	-6.0135E+00	1.5800E-05	1.5916E-12	0
6	CL	2.7997E-04	-3.5529E+00	2.8200E-04	2.5466E-11	0
7	SIO3	5.8627E-23	-2.2232E+01	4.9900E-04	-7.2760E-12	0
8	H	1.0000E-02	-2.0000E+00	0.0000E+00	0.0000E+00	1
9	HG	1.2719E-13	-1.2896E+01	1.0000E-06	9.5213E-12	0
10	CD	8.8581E-07	-6.0527E+00	1.0000E-06	5.2580E-13	0

Concentration of complexes						
ID	Beta	C		Name		
1	-14.00	1.0000E-12	H	-1.0		
2	-5.78	2.1210E-10	UO2	2.0	H	-1.0
3	-5.63	3.8289E-14	UO2	2.0	H	-2.0
4	-15.65	4.6732E-24	UO2	3.0	H	-5.0
5	10.07	4.5984E-13	UO2	1.0	CO3	1.0
6	16.98	1.1447E-22	UO2	1.0	CO3	2.0
7	21.40	9.2205E-35	UO2	1.0	CO3	3.0
8	5.10	1.5597E-07	UO2	1.0	F	1.0
9	8.96	1.0953E-09	UO2	1.0	F	2.0
10	11.35	2.6064E-13	UO2	1.0	F	3.0
11	12.57	4.1932E-18	UO2	1.0	F	4.0
12	0.24	6.2181E-10	UO2	1.0	CL	1.0
13	2.73	3.4697E-07	UO2	1.0	SO4	1.0
14	4.22	5.4204E-09	UO2	1.0	SO4	2.0
15	20.75	8.3835E-10	UO2	1.0	PO4	1.0
16	43.26	3.1645E-11	UO2	1.0	PO4	2.0
17	22.58	5.6679E-10	UO2	1.0	PO4	1.0
18	44.57	6.4612E-14	UO2	1.0	PO4	2.0
19	65.84	1.4035E-18	UO2	1.0	PO4	3.0
20	20.53	2.5389E-10	UO2	1.0	SIO3	1.0
21	10.33	6.5475E-09	CO3	1.0	H	1.0
22	16.69	1.4999E-04	CO3	1.0	H	2.0
23	1.99	4.9402E-04	SO4	1.0	H	1.0
24	3.18	1.4672E-05	F	1.0	H	1.0
25	12.35	2.6115E-12	PO4	1.0	H	1.0
26	19.55	4.1389E-07	PO4	1.0	H	2.0
27	21.70	5.8464E-07	PO4	1.0	H	3.0
28	13.11	7.5527E-12	SIO3	1.0	H	1.0
29	22.93	4.9900E-04	SIO3	1.0	H	2.0
30	-3.16	8.7996E-15	HG	1.0	H	-1.0
31	-5.18	8.4036E-15	HG	1.0	H	-2.0
32	-20.26	6.9898E-28	HG	1.0	H	-3.0
33	2.40	1.6151E-14	HG	1.0	SO4	1.0
34	3.50	1.0279E-16	HG	1.0	SO4	2.0
35	7.27	6.6310E-10	HG	1.0	CL	1.0
36	14.00	9.9701E-07	HG	1.0	CL	2.0
37	14.88	2.1175E-09	HG	1.0	CL	3.0
38	15.60	3.1112E-12	HG	1.0	CL	4.0
39	1.60	4.9087E-18	HG	1.0	F	1.0
40	4.75	2.0025E-10	HG	1.0	H	-1.0
41	3.20	4.2994E-20	CD	1.0	CO3	1.0
42	2.30	8.9348E-08	CD	1.0	SO4	1.0
43	2.00	2.4800E-08	CD	1.0	CL	1.0
44	2.70	3.4799E-11	CD	1.0	CL	2.0
45	2.10	2.4473E-15	CD	1.0	CL	3.0
46	1.10	1.0810E-11	CD	1.0	F	1.0
47	3.90	8.2078E-25	CD	1.0	PO4	1.0
48	-9.00	8.8581E-14	CD	1.0	H	-1.0
49	-19.10	7.0362E-22	CD	1.0	H	-2.0
50	-30.40	3.5265E-31	CD	1.0	H	-3.0

Log of conc. of the fixed comp. to be varied (H) = -2.00

Table 4. Execution times of some programs for the example problem at fixed pH (range 2.0–10.0) for different pH increments (ΔpH)

Program	Execution time, sec		
	$\Delta\text{pH} = 0.2$	$\Delta\text{pH} = 2.0$	$\Delta\text{pH} = 4.0$
CHEMEQUIL ⁰	7.55	1.28	0.96
CHEMEQUIL ¹	7.16	1.91	1.81
MINIQUAD	10.15	3.73	3.95
MINIQUAD-II	9.72	3.27	3.45
COMPLEX	23.35	3.61	2.37
MINEQL	32.70	11.89	10.82

CHEMEQUIL⁰: the iterative method and the Newton-Raphson method are both used at each point.

CHEMEQUIL¹: only the Newton-Raphson method is used after the first pH point.

Table 5. Comparison of execution times of CHEMEQUIL and MINIQUAD for systems 1–5 (Leggett³)

Program	Execution time, sec				
	System 1	2	3	4	5
CHEMEQUIL ⁰	1.98	1.59	1.91	2.02	2.72
CHEMEQUIL ¹	1.85	1.50	1.78	1.87	2.51
MINIQUAD	1.79	1.43	1.81	1.91	2.76
MINIQUAD-II	1.80	1.41	1.75	1.90	2.75

Notes. Leggett's system 1 contained 4 components and 12 complexes, and his most complicated system 5 contained 6 components and 21 complexes.

CHEMEQUIL⁰: the iterative method and the Newton-Raphson method are both used at each point.

CHEMEQUIL¹: only the Newton-Raphson method is used after the first pH point.

Table 6. Comparison of execution times of some programs for a system containing 28 components and 282 complexes at fixed pH (range 2–10), for different pH increments (ΔpH)

Program	Execution time, sec					
	$\Delta\text{pH} = 0.2$		$\Delta\text{pH} = 2.0$		$\Delta\text{pH} = 4.0$ pH	
	P	NP	P	NP	P	NP
CHEMEQUIL ⁰	51.78	31.8	9.68	7.2	6.41	4.9
CHEMEQUIL ¹	46.30	26.3	14.13	11.6	13.86	12.4
MINIQUAD	254.83	234.8	155.97	153.4	156.72	155.2
MINIQUAD-II	189.03	169.0	93.15	90.7	92.19	90.7
COMPLEX	864.86	844.9	123.38	120.9	57.94	56.4
MINEQL	1163.49	1143.5	416.10	413.6	366.75	365.3

Notes: P: run time when printing was allowed.

NP: run time when printing was suppressed.

CHEMEQUIL⁰: the iterative method and the Newton-Raphson method are both used at each point.

CHEMEQUIL¹: only the Newton-Raphson method is used after the first pH point.

ligands (CO_3^{2-} , PO_4^{3-} , SO_4^{2-} , F^- , Cl^- , SiO_3^{2-} , Br^- , I^- , NH_3 , $\text{P}_2\text{O}_7^{4-}$, $\text{P}_3\text{O}_{10}^{5-}$, CH_3COO^-), and H^+ , forming 282 complexes, including hydroxo, polynuclear, and mixed-ligand complexes. Distribution of species in this system was calculated for pH 2–10 in increments of 0.2, 2.0 and 4.0 pH units. Execution times for these calculations are shown in Table 6. The results indicate that CHEMEQUIL-2 is 5–25 times faster than MINIQUAD and 25–60 times faster than MINEQL for this problem. In finite-element hydrogeochemical transport models, results of intermediate iterations are not printed. To simulate the effectiveness of CHEMEQUIL as a module in such a transport model, all four programs were rerun for this problem after suppression of printing; the new run-times (Table 6) indicate that CHEMEQUIL-2 is 9–30 times faster than MINIQUAD and 44–75 times faster than MINEQL. From these comparisons the order of program efficiency appears to be CHEMEQUIL-2 > MINIQUAD > COMPLEX > MINEQL.

While such large problems are rarely encountered in analytical chemistry, they are not uncommon in geochemical systems where the possible formation of a large number of aqueous species and minerals must be considered. The computational efficiency of

CHEMEQUIL-2 makes it an ideal candidate for inclusion in hydrogeochemical models in which most of the run-time is spent in the geochemical module.

Program availability

A listing of the program and examples of input and output are available free of charge on request. If an unlabelled 2400-ft (9 track) tape is supplied, the program will be made available, at 1600 BPI, on the tape either using the UNIX tar utility on a VAX 11/780, or as ASCII data at FIXED RECORD LENGTH of 80 and BLOCKSIZE OF 8000.

Acknowledgements—This work is supported by the Ecological Research Division, Office of Health and Environmental Research, Office of Energy Research, U.S. Department of Energy, as part of hydrogeochemical model development (Subsurface Transport Program) under contract No. DE-AC05-84OR21400 with Martin Marietta Energy Systems, Inc. The paper benefited from reviews by R. B. Clapp, G. K. Jacobs, B. P. Spalding and G. T. Yeh. Oak Ridge National Laboratory Environmental Sciences Division Publication No. 2773.

REFERENCES

1. F. Van Zeggeren and S. H. Storey, *The Computation of Chemical Equilibria*, Cambridge University Press, Cambridge, 1970.
2. C. W. Childs, P. S. Hallman and D. D. Perrin, *Talanta*, 1969, **17**, 119.
3. D. J. Leggett, *ibid.*, 1977, **24**, 535.
4. S. R. Brinkley, *J. Chem. Phys.*, 1947, **15**, 107.
5. A. Sabatini, A. Vacca and P. Gans, *Talanta*, 1974, **21**, 53.
6. G. Dahlquist and A. Bjork, *Numerical Methods*, Prentice Hall, Englewood Cliffs, NJ, 1974.
7. G. E. Forsythe, M. A. Malcolm and C. B. Moler, *Computer Methods for Mathematical Computations*, Prentice Hall, Englewood Cliffs, NJ, 1974.
8. J. M. Ortega and M. A. Rheinboldt, *Iterative Solution of Non-linear Equations in Several Variables*, Academic Press, New York, 1970.
9. A. C. Bajpai, I. M. Calus and J. A. Fairley, *Numerical Methods for Engineers and Scientists*, Wiley, New York, 1977.
10. G. M. Phillips and P. J. Taylor, *Theory and Applications of Numerical Analysis*, Academic Press, New York, 1973.
11. F. S. Acton, *Numerical Methods That Work*, Harper & Row, New York, 1970.
12. G. Ginzburg, *Talanta*, 1976, **23**, 149.
13. J. C. Westall, J. L. Zachary and F. M. M. Morel, *MINEQL, A Computer Program for the Calculation of Chemical Composition of Aqueous Systems*, Tech. Note No. 18, Dept. of Civil Engineering, M.I.T., 1976.
14. V. S. Tripathi, *Talanta*, 1983, **30**, 65.
15. J. Inczedy, *Analytical Applications of Complex Equilibria*, Ellis Horwood, Chichester, 1976.
16. D. Langmuir, *Geochim. Cosmochim. Acta*, 1978, **42**, 547.
17. V. S. Tripathi, *Talanta*, 1980, **27**, 1103.

APPENDIX

The purpose of this paper is to present a computational algorithm; no attempt has been made at critical selection of formation constants. Those used were taken mostly from three publications.^{13,15,16}

The original MINQUAD⁵ was adapted for concentration calculations by Leggett³ who provided a program listing. For the present paper, the following additional modifications were made.

1. The program was converted to single precision in order to be comparable to COMPLEX, MINEQL and CHEMEQUIL-2.

2. Program testing was done on a DEC-20, using F-floating numbers on which single-precision floating-point numbers greater than approximately 1.7×10^{38} overflow. For the sample problem and the 28-component problem, three β values exceeded this magnitude. Because MINQUAD deals with β rather than $\log \beta$, the attempt to calculate β (array BABS in MINQUAD) caused overflow. Therefore, for the example problem and the 28-component problem these three complexes were not included in MINQUAD calculations.

3. In Tables 4-6 MINQUAD refers to the original MINQUAD⁵ in which the initial guess for the free concentration for all components was set at 10^{-7} . MINQUAD-II refers to the version that included the correction suggested by Tripathi.¹⁷

For MINEQL, an initial guess of 10^{-7} for the concentration of free components was provided and worked successfully for the example problem. For the 28-component problem, however, this guess did not lead to convergence, and a message, "...SINGULAR Z MATRIX" was printed. MINEQL converged with initial guesses of 10^{-10} for free component concentrations, and produced correct results.

Overflow occurred during execution of COMPLEX, but the final results were correct.

With the advent of G-floating point numbers on the DEC-20 and VAXes, a greater dynamic range of double precision floating-point numbers (approximately from 10^{-308} to 10^{308}) is available. This dynamic range is also recommended in the proposed floating point standard by the Institute of Electrical and Electronics Engineers. To exploit this option dynamically, without user intervention, CHEMEQUIL-2 incorporates a mechanism for automatically setting machine-dependent constants (T and SMALL in the program). On the DEC-20 or the VAX it will be necessary to change all real variables to double precision before the wide dynamic range can be utilized.

STUDY OF THE MIXED-METAL LANTHANUM- MAGNESIUM-PURPURIN COMPLEX: SPECTROPHOTOMETRIC DETERMINATION OF YTTRIUM AND LANTHANIDES

A. ARREBOLA RAMIREZ and C. JIMENEZ LINARES

Department of Analytical Chemistry, Faculty of Sciences, University of Granada, Granada, Spain

F. ALES BARRERO and M. ROMAN CEBAS*

Department of General Chemistry, Faculty of Sciences, University of Granada, Granada, Spain

(Received 25 July 1985. Revised 14 March 1986. Accepted 11 July 1986)

Summary—Mixtures of La(III) and Mg(II) form with purpurin (P; 1,2,4-trihydroxyanthraquinone) the mixed-metal complex LaMg_2P_2 , which is extracted with methyl isobutyl ketone at pH 7.5. The molar absorptivity of the complex is $6.1 \times 10^4 \text{ l. mole}^{-1} \text{ cm}^{-1}$ at 570 nm and its conditional extraction constant $5 \times 10^{13} \text{ l}^4 \text{ mole}^{-4}$. Similar complexes have been found to be formed with yttrium, cerium, praseodymium, neodymium and samarium. The use of these complexes for the spectrophotometric determination of yttrium and lanthanides up to 15 μg has been investigated.

The least studied complexes are those formed by two different metals and one ligand. Some of these are useful in photometric analysis because of their stability, intense colour and frequently their easy extractability.¹⁻⁴ In some of these systems the molar absorptivity of the ternary complexes is three or four times greater than that of the binary complexes from which they are formed.

Few of the various mixed-metal complexes containing lanthanum have been used to determine it photometrically,⁵⁻⁷ although several of them have been described.⁸⁻¹⁰ Certain anthraquinone derivatives, such as Alizarin S and Alizarin Complexone, have also proved to be capable of forming mixed-metal complexes.¹¹⁻¹³

In the present work we have studied the La-Mg-purpurin complex and its extraction with methyl isobutyl ketone, which results in notable increase in sensitivity compared with the binary La-purpurin complex.¹⁴ The spectrophotometric determination of yttrium and lanthanides by formation of similar complexes has also been investigated.

EXPERIMENTAL

Reagents

All solutions were prepared with analytical-reagent grade chemicals.

Purpurin solution (1,2,4-trihydroxyanthraquinone). A 10^{-3} M solution was prepared by dissolving 0.256 g of the Merck product and diluting to 1 litre with methyl isobutyl ketone (MIBK). More dilute solutions were prepared from this.

Standard solutions of yttrium and lanthanides, $5 \times 10^{-3} \text{ M}$. Prepared by dissolving $\text{Y}(\text{NO}_3)_3 \cdot 5\text{H}_2\text{O}$, $\text{La}(\text{NO}_3)_3 \cdot 6\text{H}_2\text{O}$,

$\text{CeCl}_3 \cdot 7\text{H}_2\text{O}$, Pr_6O_{11} , Nd_2O_3 and Sm_2O_3 in dilute nitric acid and standardized by EDTA titration with Xylenol Orange as indicator.

Standard magnesium solution, 0.5M. Prepared by dissolving $\text{Mg}(\text{NO}_3)_2 \cdot 6\text{H}_2\text{O}$ and standardized by EDTA titration.

Buffer solutions (pH 6.5 and pH 7.5). Prepared by dissolving 121 g of tris(hydroxymethyl)aminomethane (Merck) in 600 ml of demineralized water, adjusting to the required pH with hydrochloric acid and diluting to 1 litre with water.

8-Quinolinol solution, 5%. Prepared by dissolving 5.0 g of 8-quinolinol in 10 ml of glacial acetic acid and diluting to 100 ml with water.

Ammonium acetate solution, 3.5M. Made by dissolving 135 g in 500 ml of water.

Recommended procedure

Transfer a measured volume of sample, containing less than 15 μg of yttrium or lanthanide to a 100-ml separating funnel. Add 5 ml of a masking solution, 0.2M in potassium cyanide and 0.1M in ammonium citrate, then 5 ml of 0.5M magnesium nitrate solution, and 5 ml of pH 6.5 buffer and dilute with demineralized water to 50 ml. (Confirm that the pH of the solution is 7.5 ± 0.2 .) Shake the solution for 5 min with 10 ml of 10^{-4} M purpurin solution in MIBK. Leave the mixture for 10 min, separate the organic phase, then centrifuge it, and measure its absorbance at 570 nm against a reagent blank similarly prepared. Prepare a calibration graph by using standard solutions of lanthanum and treating them identically.

RESULTS AND DISCUSSION

Absorption spectra

The absorption spectra of purpurin, Mg-purpurin, La-purpurin and La-Mg-purpurin at pH 7.5 and 1:1 phase-volume ratio are shown in Fig. 1.

The absorption spectra of purpurin and the Mg-purpurin complex are practically identical, which demonstrates the very weak interaction between magnesium and the reagent. The La-purpurin complex

*Author to whom correspondence should be sent.

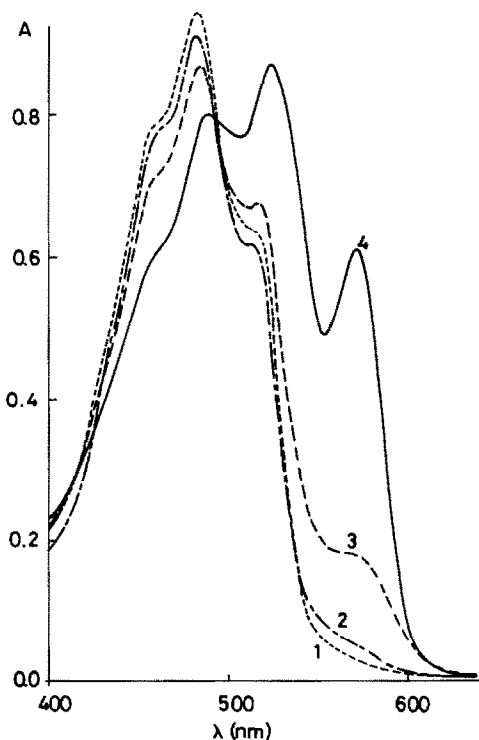


Fig. 1. Absorption spectra at pH 7.5, $C_{\text{purpurin}} = 10^{-4}M$, $C_{\text{La}} = 10^{-5}M$, $C_{\text{Mg}} = 10^{-2}M$. (1) Purpurin, (2) Mg-purpurin complex, (3) La-purpurin complex, (4) La-Mg-purpurin ternary complex.

has a moderate absorption band with a maximum at 570 nm. By contrast, the La-Mg-purpurin complex has a sharp absorption maximum at 570 nm, which has more than three times the sum of the absorbances of the binary complexes for the same metal concentrations, clear evidence of the existence of the mixed-metal La-Mg-purpurin complex.

Among the ions that precipitate as oxalates in acid medium, Y, Ce(III), Pr, Nd and Sm form, with the Mg-purpurin system, mixed-metal complexes with absorption spectra almost identical to that of the La-Mg-purpurin complex.

Effect of pH

The effect of pH at concentrations of La(III) and Mg(II) of 10^{-5} and $0.05M$ respectively, and a purpurin concentration of $10^{-4}M$ in MIBK was established. The final volume of the aqueous phase was always 10 ml. The phase-volume ratio was 1:1 and shaking time 30 min. The absorbance increased with pH and was maximal over the pH range 7.3–7.8.

Influence of purpurin and Mg(II) concentrations

Investigations were made at pH 7.5, a lanthanum concentration of $10^{-5}M$ and various concentrations of purpurin and magnesium. Figure 2 shows the difference in absorbance between the mixed-metal complex and the binary La-purpurin complex as a function of $\log C_{\text{purpurin}}$. The results show that the

extraction is complete when a purpurin concentration of $10^{-4}M$ and a magnesium concentration of $0.05M$ are used. A lower magnesium concentration would make a large increase in the purpurin concentration necessary for extraction to remain complete.

Stoichiometry and extraction constant

The stoichiometry of the binary La-purpurin complex is 1:2 and its conditional extraction constant at pH 7.3 is $\log K_e = 11.7$,¹⁴ indicating a strong complex. Bent and French's method indicates that the composition of the Mg-purpurin complex is 1:1. The conditional stability constant of this complex has been determined by a dilution method¹⁵ at pH 7.3 in a 40% (v/v) ethanol-water mixture and is $\log K = 2.1$, which corresponds to a weak complex. Therefore, we consider that the formation of the mixed-metal complex occurs in accordance with the equilibrium:



Mole-ratio plots showed clearly that the combining ratio of lanthanum to purpurin is 1:5 (Fig. 3). The decreased absorbance observed at mole ratios higher than 1:5 is the result of an increase in the concentration of the stronger La-purpurin complex at the expense of purpurin available to form the ternary complex.

The value of n was determined by the equilibrium-shift method. The plot of $\log([\text{LaMg}_n\text{P}_{(m+2)}]_o/[\text{LaP}_2]_o)$ vs. $\log[\text{Mg}]_a$ at a fixed purpurin concentration and pH 7.5 gives a slope of 1.8, indicating a magnesium/lanthanum ratio of 2:1 in the mixed-metal complex (Fig. 4, curve 4). We conclude therefore that the combining ratio La:Mg:purpurin is 1:2:5, in accordance with the stoichiometry assigned to a similar complex, Er-Ca-Alizarin S.¹¹

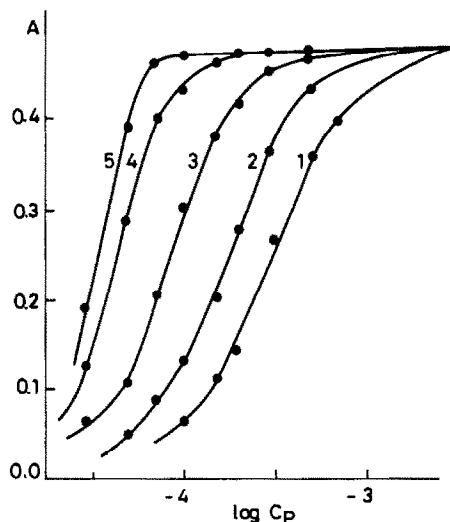


Fig. 2. Influence of purpurin and Mg(II) concentrations. $C_{\text{La}} = 10^{-5}M$: (1) $C_{\text{Mg}} = 5.10^{-4}M$, (2) $10^{-3}M$, (3) $3 \times 10^{-3}M$, (4) $10^{-2}M$, (5) $5 \times 10^{-2}M$.

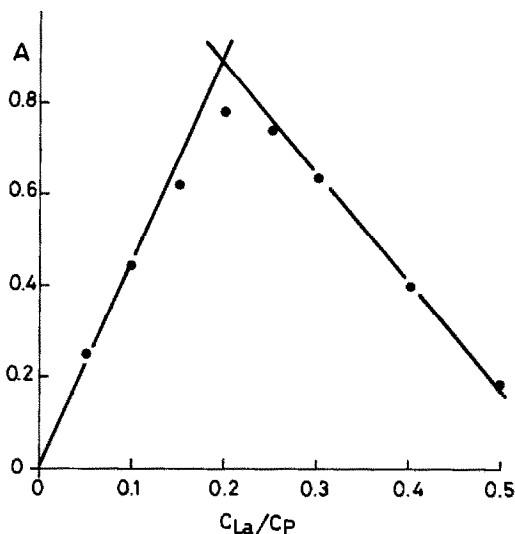


Fig. 3. Mole-ratio plot. $C_{\text{purpurin}} = 10^{-4}M$, $C_{\text{Mg}} = 5 \times 10^{-2}M$.

In order to confirm the value of m , we also used the equilibrium-shift method at pH 7.5 and three constant concentrations of magnesium. The plot of $\log([LaMg_nP_{(m+2)}]_o/[LaP_2]_o)$ vs. $\log[P]_o$, ($[P]_o = C_p - 5[LaMg_2P_5]_o - 2[LaP_2]_o$), gives straight lines with a slope of 1.8. Hence, we conclude that $m = 2$, which ought to correspond to the two purpurin molecules bound to the two magnesium ions (Fig. 4). The equilibrium-shift method shows only weakly bound ligand molecules, so we must assume that a third purpurin molecule is bound strongly to the lanthanum during the formation of the mixed-metal complex, an occasional occurrence in the formation of ternary complexes.¹⁶ The possible structure of the complex is represented in Fig. 5.

The results of the application of the equilibrium-shift method were used to calculate the conditional

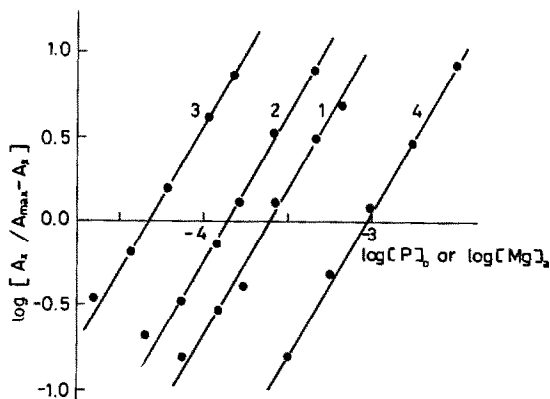


Fig. 4. Equilibrium-shift method. $C_{\text{La}} = 10^{-5}M$. Relationship of purpurin to La: (1) $C_{\text{Mg}} = 5 \times 10^{-4}M$, (2) $10^{-3}M$, (3) $3 \times 10^{-3}M$. Relationship of Mg to La: (4) $C_{\text{purpurin}} = 2 \times 10^{-4}M$. A_x = absorbance of mixture, A_{max} = saturation absorbance with an excess of reagent present.

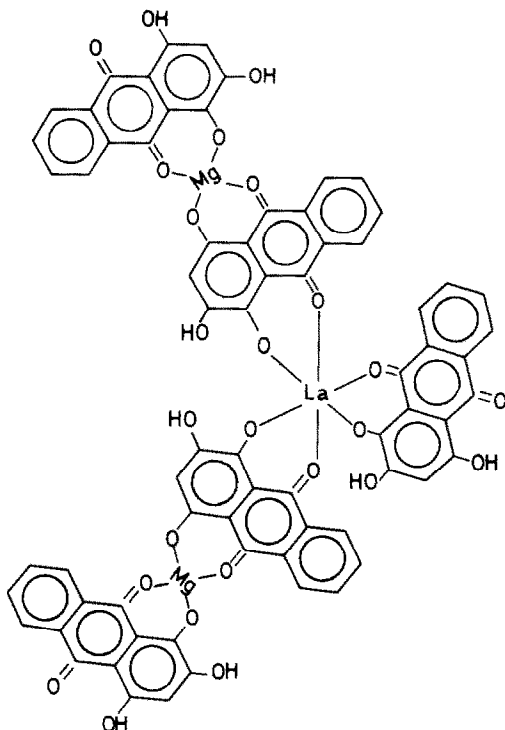
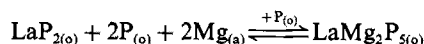


Fig. 5. Postulated structure of the complex.

extraction constant of the complex as defined by the equilibrium:



At pH 7.5, the value of $\log K_e$ was shown to be 13.70 ± 0.06 .

Spectrophotometric determination of yttrium and lanthanides

Lanthanum was chosen to represent the lanthanides. The effect of phase-volume ratio was studied for the optimal conditions: pH 7.5, C_{Mg} 0.05M and C_{purpurin} $10^{-4}M$. The absorbance of the organic phase was practically constant for the range 1:1-5:1, $V_{\text{aq}}/V_{\text{org}}$. We chose the 5:1 ratio as being satisfactory, and found that the absorbance of the solution is constant within 3% over the pH range 7.3-7.8. Beer's law is obeyed between 2.5 and 20 μg of lanthanum in 50 ml of aqueous phase. The molar absorptivity at 570 nm is $6.1 \times 10^4 \text{ l. mole}^{-1} \text{ cm}^{-1}$. A shaking time of 5 min is sufficient for equilibrium to be reached. The absorbance of the complex is constant from 10 min to 8 hr after its formation. The reproducibility of the method was checked by means of three series of 10 solutions having lanthanum concentrations of 0.1, 0.2 and 0.3 ppm. We obtained relative standard deviations of 0.5, 0.4 and 0.3% respectively. The IUPAC detection limit¹⁷ is 0.007 ppm for a value of $k = 3$.

Under the same operating conditions, Y, Ce(III), Pr, Nd and Sm ions also form mixed-metal complexes

Table 1. Interference of foreign species in the determination of 12.5 μg of lanthanum

Species	Tolerance ratio to La(III), w/w
B(III), Ba(II), Ca(II), citrate	400*
Mo(VI), oxalate, Sr(II), tartrate	400†
Ag(I), Cd(II), Co(II), Cu(II), Hg(II), Ni(II), Pd(II), Zn(II)	200
Sb(III), W(VI)	20
Mn(II)	20§
Al(III), Be(II)	4
F, V(V)	4§
Cr(III), Sn(II), Ti(IV)	2§
Fe(III)	2‡
Zr(IV)	1
Th(IV), U(VI)	1‡
Pb(II)	0.04
PO ₄ ³⁻	<1
Bi(III), In(III)	

*Maximum tested.

†Cyanide (30 mg) added.

§Acetylacetone (100 mg) added.

‡Citrate (95 mg) added.

which obey Beer's law. These compounds have molar absorptivities almost identical to that of the La-Mg-purpurin complex (Table 2).

Table 2

Ion	Beer's law maximum,	$\epsilon, l. mole^{-1}. cm^{-1}$
	μg	
Y	12.5	4.5×10^4
Ce(III)	20	6.1×10^4
Pr	20	6.2×10^4
Nd	15	6.3×10^4
Sm	15	6.2×10^4

Effect of foreign ions

The tolerance of the method to foreign ions was investigated with solutions containing 12.5 μg of lanthanum and various amounts of foreign ions. The concentrations indicated in Table 1 caused an

error of not more than 2% in the absorbance measurements.

Ag⁺, Al³⁺, Be²⁺, Cd²⁺, Cu²⁺, Cr³⁺, Fe³⁺, Hg²⁺, Pd²⁺, Sn²⁺, Th⁴⁺, Ti⁴⁺, UO₂²⁺, V⁵⁺ and Zr⁴⁺ interfere by the formation of lakes and by mixed-metal complex adsorption, while Co²⁺, Ni²⁺, Pb²⁺ and Zn²⁺ cause interference by forming binary coloured complexes. The tolerance ratio for many of these ions can be raised by using cyanide, citrate or acetylacetone as masking agents. Bi and In ions give high values by forming mixed-metal complexes with the Mg-purpurin system. Fluoride and phosphate ions interfere by precipitation of lanthanum.

The lanthanides are generally to be found in nature in the form of phosphates, zirconates or titanates and almost always in the company of uranium, thorium, yttrium and variable quantities of iron, aluminium, calcium *etc.* To try out the application of our proposed procedure, we have analysed mixtures of yttrium and lanthanides together with other elements frequently found accompanying them. Any interference caused by iron, aluminium, titanium and vanadium was avoided by the prior extraction of the relevant oxinates with chloroform at pH 4.8 and of the phosphates by ion-exchange according to the following general procedure.

Ion-exchange. Pass through a resin column (cation-exchanger Sephadex SP, 40–120 μm , sodium form), 10 cm in length and 0.6 cm in diameter, a measured volume of sample containing less than 15 μg of yttrium and lanthanides. Wash the resin with 100 ml of water and elute with three 5-ml portions of 1M sodium chloride acidified to pH 2. Determine yttrium and the lanthanides by the recommended procedure, with a blank consisting of an aqueous solution containing 15 ml of 1M sodium chloride as well as the quantities of magnesium and buffer used for the samples.

8-Quinolol-chloroform extraction. Add either to the sample or to the eluate 2 ml of 5% 8-quinolol solution, 2 ml of 3.5M ammonium acetate solution (the pH of the solution should be 4.8) and shake for

Table 3. Determination of yttrium and lanthanides in the presence of other elements

Y	Lanthanides ($\mu\text{g}/50$ ml aqueous phase)					Other species ($\mu\text{g}/50$ ml aqueous phase)							Total lanthanides		
	La	Ce	Pr	Nd	Sm	Th	U	Zr	Fe	Al	V	Ti	PO ₄ ³⁻	Taken, μg	Found, μg
2	4	2	4		3									15	15.7*
	2	2	2	2	2									10	10.6*
1	3	4	3	4										15	15.6*
1	3	4	3	4		30	30							15	13.5*
1	3	4	3	4		15	15							15	15.2*
	2	2	2	2	2			10	20					10	9.9*
1	3	4	3	4					1000	1000	1000			15	15.2‡
1	3	4	3	4					500	500	500			15	15.4‡
1	3	4	3	4						1000		1000		15	15.2‡
1	3	4	3	4		30			1000		1000	1000	1500	15	14.4§

*Recommended procedure.

†8-Quinolol-chloroform extraction.

§General procedure.

1 min with 20 ml of chloroform. Remove the organic phase and repeat the extraction with 1 ml of 5% 8-quinolinol solution and 20 ml of chloroform. Wash the aqueous phase, shaking it with two 10-ml portions of chloroform, and neutralize the aqueous phase with 1.7M ammonia solution. Yttrium and lanthanides can then be determined by the recommended procedure, the blank in this case being prepared with 3.5 ml of 3.5M ammonium acetate solution as well as the corresponding quantities of magnesium and buffer.

The results obtained in the analyses (an average of three determinations) are given in Table 3. They show that the less well tolerated ions such as Th^{4+} , Zr^{4+} and UO_2^{2+} may be present in amounts up to about twice those of the lanthanide ions.

REFERENCES

1. I. P. Alimarin, I. M. Gibalo and A. K. Pigaga, *Zh. Analit. Khim.*, 1970, **25**, 2336; *Dokl. Akad. Nauk, SSSR*, 1969, **186**, 1323.
2. M. Khattak and R. Magee, *Anal. Chim. Acta*, 1966, **35**, 17.
3. A. T. Pilipenko, V. N. Danilova and S. L. Lisitchenok, *Zh. Analit. Khim.*, 1970, **25**, 1154.
4. V. N. Danilova and S. L. Lisitchenok, *ibid.*, 1969 **24**, 1064; *Zavodsk. Lab.*, 1969, **34**, 1284.
5. Shen Hanxi and Xu Guanghi, *Fenxi Huaxue*, 1981, **9**, 17.
6. Shen Hanxi and Wang Zhenquing, *ibid.*, 1981, **9**, 711.
7. P. K. Spitsyn, *Zavodsk. Lab.*, 1982, **48**, 16.
8. Shen Hanxi, Liu Zenguing and Wang Zhenquing, *Fenxi Huaxue*, 1982, **10**, 324.
9. Shen Hanxi and Liu Zenguing, *ibid.*, 1982, **10**, 339.
10. *Idem*, *Huaxue Xuebao*, 1983, **41**, 144.
11. Yu. I. Usatenko, A. I. Tolubara and A. I. Kochubei, *Zh. Neorgan. Khim.*, 1971, **16**, 99.
12. M. A. Leonard and F. J. Nagi, *Talanta*, 1969, **16**, 1104.
13. I. V. Pyatnitskii, A. Kh. Klibus and N. I. Khomich, *Probl. Solvatsii i Kompleksoobraz*, p. 71. Ivanovo, 1982.
14. F. Alés Barrero, M. Román Ceba and A. Arrebola Ramírez, *An. Quim.*, 1985, **81**, 217.
15. J. J. Berzas Nevado, A. Arrebola Ramírez and M. Román Ceba, *Anal. Chim. Acta*, 1981, **124**, 201.
16. M. K. Akhmedli, E. L. Gluschenko and Z. L. Gasanova, *Zh. Analit. Khim.*, 1971, **26**, 1947.
17. IUPAC, *Spectrochim. Acta*, 1978, **33B**, 242.

SHORT COMMUNICATION

TETRABUTYLAMMONIUM BROMIDE/THENOYLTRI- FLUOROACETONE/MIBK EXTRACTION FOR AAS DETERMINATION OF COBALT, NICKEL, AND MANGANESE IN COPPER ORES AND CONCENTRATES

BARBARA RÓŻAŃSKA and ELWIRA LACHOWICZ

Department of Analytical Chemistry, Warsaw University of Technology, PL-00-664 Warsaw,
Noakowskiego 3, Poland

(Received 24 March 1986. Revised 14 July 1986. Accepted 1 August 1986)

Summary—An extraction-AAS method of determination of Co, Ni, and Mn in metallurgical copper materials containing considerable amounts of Cu, Fe, Pb, Zn, and Al has been developed. Good selectivity of group separation of Co, Ni, and Mn has been achieved by (a) the use of tetrabutylammonium bromide to improve extractability of HTTA complexes by ion-pair formation, and (b) the masking of major elements with sodium thiosulphate and sulphosalicylic acid. The extracts are stable for at least 3 weeks.

The analysis of copper ores and concentrates has been extensively investigated. Atomic-absorption methods have been published for determination of noble metals in copper ores,¹ gold and silver in copper intermediates,² platinum metals in Cu-Ni ores,³ bismuth in ores⁴ and concentrates,^{5,6} cobalt, nickel, manganese and chromium in copper ore, concentrate and dust,⁷ silver in ore and concentrate⁸ or ores and tailings,⁹ selenium in copper and lead concentrate,¹⁰ and mercury in copper concentrates.¹¹ Three AAS methods for silver in ores and concentrates have been compared.¹² Microamounts of arsenic and antimony in copper industry materials have been determined by flame AAS,¹³ and gallium in mixed copper ore by graphite furnace AAS,¹⁴ without matrix separation.

Spectrophotometric methods have been developed for the determination of bismuth,¹⁵ arsenic,¹⁶ selenium¹⁷ and tellurium¹⁸ in copper (and other) concentrates, and germanium¹⁹ in ores and concentrates.

Many copper ores and concentrates contain, besides copper, silica, calcium and magnesium, considerable amounts of iron, lead and zinc.

The aim of the present work was to develop a group-extraction separation method for use with AAS determination of cobalt, nickel and manganese in various metallurgical copper materials, such as ores, concentrates and tailings containing considerable and varying amounts of Cu, Fe, Pb, Al, Si, Ca and Mg. The method was designed for $1 \times 10^{-3}\%$ and upwards of cobalt, nickel and manganese.

Although the concentration of Co, Ni and Mn in some materials of this kind is relatively high, it is profitable to extract them into MIBK, which is a suitable medium for the AAS determination, and thus avoid the use of a solution of rather high acid and matrix concentration, for which the standard-addition technique would probably be required.

However, the separation of traces of Co, Ni and Mn from major components (which are often easily hydrolysed and form more stable complexes with most chelating agents) creates serious difficulties. To overcome these, two different approaches were applied simultaneously: (a) enhancement of the extractability of the HTTA-analyte complexes by ion-association complex formation with a quarternary ammonium salt ($\text{TBA}^+ \text{Br}^-$), and (b) masking of the major elements. Iron was separated first by extraction into MIBK from 6M hydrochloric acid medium. The combination of a β -diketone and a tertiary amine (or quarternary ammonium salt) is one of the most frequently investigated synergic systems. Recent examples include extraction of manganese(II) with HTTA in the presence of tribenzylamine,^{20,21} cobalt(II) and nickel with benzoyltrifluoroacetone in presence of tetrabutylammonium,²² iron(III) with HTTA and tribenzylamine,²³ praseodymium with HTTA in the presence of Aliquat-336S and triethylamine,²⁴ and cobalt(II) with acetylacetone and various organic bases.²⁵

EXPERIMENTAL

Apparatus

A Pye Unicam SP 90A series 2 AAS spectrometer was used for the Co (240.7 nm), Ni (232.0 nm), and Mn (279.5 nm) determinations. The air flow-rate was 5 l./min, acetylene flow-rate 0.6 l./min, observation height 10 mm above the burner.

Reagents

Thenoyltrifluoroacetone (HTTA) solution (0.02M) in MIBK. Aqueous tetrabutylammonium bromide ($\text{TBA}^+ \text{Br}^-$) solution (0.2M). Sodium thiosulphate solution (3M), 10% sulphosalicylic acid solution, and 1M sodium hydroxide. Buffer solutions were made from 1M acetic acid and 1M sodium acetate. Cobalt, nickel, and manganese stock solutions were prepared by dissolving appropriate amounts of

the chlorides or sulphates, and standardized. All other reagents were of analytical purity.

Procedures

Ore decomposition. Weigh 1 g of sample into a Teflon-lined bomb, add 15 ml of concentrated hydrofluoric acid and 15 ml of concentrated nitric acid. Seal the bomb and heat at 150° for 4 hr.

Cool, transfer the solution into a Teflon beaker and evaporate it to dryness. Add 5 ml of concentrated nitric acid and evaporate to dryness, and repeat this step. Add 1 ml of concentrated perchloric acid and evaporate to dryness again. Dissolve the dry residue in 40 ml of hot 6*M* hydrochloric acid, cool, transfer the solution to a 50-ml standard flask and dilute to volume with 6*M* hydrochloric acid.

Concentrate decomposition. Weigh 0.5 g of sample into a Teflon-lined bomb. Add 10 ml of concentrated hydrofluoric acid, 10 ml of concentrated nitric acid, and 5 ml of concentrated sulphuric acid. Seal the bomb and heat it at 150° for 6 hr. Cool, transfer the contents to a Teflon beaker, evaporate to dryness, then continue as for the decomposition of ores, starting with the treatment, but omitting the perchloric acid step.

Extractions. Pipette 10 ml of the sample solution into a separatory funnel and shake with two 10-ml portions of MIBK in succession, each for 1 min. Discard the organic phases. Wash the aqueous phase into a beaker and evaporate it almost to dryness. Dissolve the residue in 5 ml of 10% sulphosalicylic acid solution, adjust to pH 3–3.5 with 1*M* sodium hydroxide and add 2 ml of 3*M* sodium thiosulphate. Adjust to pH 5.2 ± 0.1 with 1*M* sodium hydroxide, add 2.5 ml of acetate buffer (pH 5.2), and dilute to ~20 ml. Transfer the solution to a separatory funnel, rinsing the beaker with ~2 ml of water. Add 3 ml of 0.2*M* TBA⁺Br⁻ solution, mix, then shake with 10 ml of 0.02*M* HTTA solution in MIBK for 10 min.

Transfer the organic phase to a suitable standard flask and make up to the mark with MIBK. Measure the concentrations of manganese (after dilution with MIBK, if necessary), cobalt and nickel by AAS.

Calibration graph. Prepare combined aqueous standard solutions containing appropriate amounts of cobalt, nickel and manganese to cover the range 0–1.2 µg/ml, enough sulphosalicylic acid solution to give a final concentration of 2%, and adjusted to pH 5.2 with sodium hydroxide solution and acetate buffer of pH 5.2. For each standard pipette 25 ml into a separatory funnel, add 3 ml of 0.2*M* TBA⁺Br⁻ solution and extract with 10 ml of 0.02*M* HTTA solution in MIBK as for the sample solutions.

RESULTS AND DISCUSSION

Decomposition

According to earlier experiments in this laboratory²⁶ and our current results, dissolution under pressure in a Teflon bomb ensures complete decomposition of various copper ores, concentrates and tailings, and shortens the time required for this operation. The advantage of the closed system is especially distinct for concentrates because of the serious difficulty in open-vessel decomposition of

organic substances present in the concentrates. Decomposition under pressure has been recommended for silicon-containing materials, iron ores and sulphide ores.²⁷

Masking

The masking was studied by extracting synthetic solutions with 0.1*M* HTTA in MIBK (without TBA⁺Br⁻).

Two masking reagents were used to prevent extraction of copper and lead, and precipitation of aluminium, during the chelating extraction of copper, nickel and manganese with HTTA: sodium thio-sulphate and sulphosalicylic acid. Thiosulphate is a powerful masking agent for Cu(I), (log β₁ = 10.35)²⁸ and a much weaker one for Pb (log β₁ = 2.42).²⁸ Sulphosalicylic acid forms a very stable complex with aluminium (log β₁ = 12.3).²⁹ Preliminary experiments showed that the presence of 0.2*M* sodium thio-sulphate prevents extraction of copper (2 mg/ml) with 0.1*M* HTTA in MIBK at pH 7, whereas cobalt, nickel, and manganese (0.1–1 µg/ml) are quantitatively separated under these conditions. Addition of 1 g of sulphosalicylic acid to 25 ml of 1-mg/ml aluminium solution allows adjustment of the pH to 7 without precipitation of aluminium hydroxide.

TBA⁺Br⁻-HTTA/MIBK System

The lowest pH for the quantitative extraction of manganese (which is less well extracted than cobalt or nickel) is 7 with 0.1*M* HTTA as reagent but 5 for 0.02*M* HTTA in the presence of 0.02*M* TBA⁺Br⁻. The use of TBA⁺Br⁻ provides more convenient conditions for the extraction, thereby reducing the masking problems. The effect of TBA⁺Br⁻ on extraction of Co, Ni, and Mn with 0.02*M* HTTA is shown in Fig. 1. The addition of TBA⁺Br⁻ does not influence extraction of lead.

The apparent recovery of 25 µg of Co, Ni and Mn separated at pH 5.2 with 0.02*M* HTTA in MIBK from 25 ml of artificial sample solution containing 75 mg of Cu(II), 25 mg of Fe(III), 25 mg of Al(III) and 5 mg of Pb(II) in the presence of 1 g sulphosalicylic acid, 4.2 ml of 3*M* sodium thiosulphate and 3 ml of 0.2*M* TBA⁺Br⁻ was 100–106%. Only small amounts of copper (~0.01%) and lead (~0.04%) were co-extracted. The AAS signals for the analytes in MIBK medium were 2–3 times as large as those for aqueous medium.

The extracts are very stable. The signal for manganese remained the same for at least 20 days, whereas that for the Mn-HHTA complex in the same solvent decreased by ~5% in 24 hr.

Table 1. Determination of Co, Ni and Mn in copper ore and concentrate samples (*n* = 6)

	Co		Ni		Mn	
	Mean, %	R.s.d., %	Mean, %	R.s.d., %	Mean, %	R.s.d., %
Ore	1.75 × 10 ⁻²	5.0	1.12 × 10 ⁻²	3.1	1.66 × 10 ⁻¹	4.2
Concentrate	7.55 × 10 ⁻²	2.6	4.17 × 10 ⁻²	3.5	1.67 × 10 ⁻¹	4.1

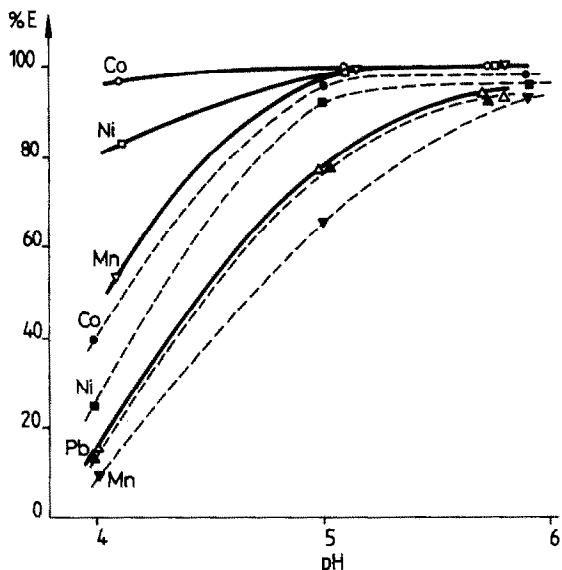


Fig. 1. Degree of extraction of Co, Ni, Mn and Pb complexes vs. pH: 0.02M HTTA in MIBK—dashed lines; 0.02M HTTA in MIBK in the presence of 0.02M TBA⁺Br⁻ in the aqueous phase—solid lines.

Either sulphosalicylic acid or sodium chloride can be added to the standard solutions to improve the separation of the phases, but the former also acts as masking agent for aluminium. There is good separation of the phases in the sample extraction, owing to the high concentration of salts.

Analytical results

The proposed method was applied to copper ore and concentrate samples. Results are listed in Table 1. Six replicate analyses gave relative standard deviations of not more than 5% for each of the three ions. To check the accuracy of the separation, the samples were spiked with appropriate amounts of Co, Ni, and Mn before the acid digestion. Full recoveries were obtained. The amounts of Co, Ni, Mn (and Cr) in the same samples (and in dusts) were also determined by

AAS after matrix-element separation by extraction.⁷ The results were in good agreement.

REFERENCES

1. Yu. M. Yukhin, T. A. Udalova and V. G. Tsimbalist, *Zh. Analit. Khim.*, 1985, **40**, 850.
2. B. W. Buděšinský, *Microchem. J.*, 1984, **29**, 1.
3. I. V. Kubrakova, G. M. Varshal, E. M. Sedykh, G. V. Myasoedova, I. I. Antokolskaya and T. P. Shemarykina, *Zh. Analit. Khim.*, 1983, **38**, 2205.
4. Yu Xian-an, Dong Gao-Xiang and Li Chun-xue, *Talanta*, 1984, **31**, 367.
5. D. J. Howell and B. R. Dohnt, *ibid.*, 1982, **29**, 391.
6. E. M. Donaldson, *ibid.*, 1979, **26**, 1119.
7. E. Lachowicz and A. Kaliszuk, *Z. Anal. Chem.*, 1986, **323**, 54.
8. E. M. Donaldson, *Talanta*, 1984, **31**, 443.
9. Z. Skorko-Trybulowa, Z. Boguszewska and B. Różańska, *Mikrochim. Acta*, 1979 **I**, 151.
10. L. Futekov, R. Partitschkova and H. Specker, *Z. Anal. Chem.*, 1981, **306**, 378.
11. B. Różańska and E. Lachowicz, *Anal. Chim. Acta*, 1985, **175**, 211.
12. E. M. Donaldson, E. Mark and M. E. Leaver, *Talanta*, 1984, **31**, 89.
13. L. A. Kopylova, T. B. Sryvtseva, E. A. Simkin and Yu. Ya. Favinskii, *Zavodsk. Lab.*, 1985, **51**, No. 4, 32.
14. D. C. Barron and B. W. Haynes, *Analyst*, 1986, **111**, 19.
15. E. M. Donaldson, *Talanta*, 1978, **25**, 131.
16. *Idem, ibid.*, 1977, **24**, 105.
17. *Idem, ibid.*, 1977, **24**, 441.
18. *Idem, ibid.*, 1976, **23**, 823.
19. *Idem, ibid.*, 1984, **31**, 997.
20. M. M. Saeed, M. N. Cheema and I. H. Qureshi, *Radiochim. Acta*, 1984, **37**, 33.
21. *Idem, ibid.*, 1985, **38**, 107.
22. T. Sekine, R. Murai and H. Konno, *Solvent Extr. Ion Exch.*, 1984, **2**, 213.
23. M. N. Cheema, M. M. Saeed and S. H. Qureshi, *Radiochim. Acta*, 1980, **27**, 109.
24. I. Dukov and L. Genov, *J. Inorg. Nucl. Chem.*, 1981, **43**, 412.
25. A. M. El-Atrash, E. R. Souaya and W. Georgy, *J. Indian Chem. Soc.*, 1980, **57**, 690.
26. Z. Boguszewska, to be published.
27. E. Jackwerth and S. Gomišček, *Pure Appl. Chem.*, 1984, **56**, 479.
28. R. M. Smith and A. E. Martell, *Critical Stability Constants*, Vol. 4, p. 86. Plenum Press, New York, 1976.
29. A. E. Martell and R. M. Smith, *Critical Stability Constants*, Vol. 3, p. 191. Plenum Press, New York, 1977.

ANALYTICAL DATA

POLAROGRAPHIC STUDIES OF MIXED HYDROXY-COMPLEXES OF MONOETHANOLAMINE WITH CADMIUM AND WITH LEAD

F. ARCE, C. BLANCO* and J. CASADO

Departamento de Química Física, Facultad de Química, Universidad, Santiago de Compostela, Spain

(Received 11 December 1985. Revised 26 June 1986. Accepted 11 July 1986)

Summary—The composition and stability of mixed complexes of cadmium or lead with hydroxide and monoethanolamine have been determined polarographically at 25° in aqueous and aqueous methanol solutions at ionic strength 0.1M. For the aqueous solutions the results agree with those of others. In the methanolic systems the previously unreported complexes $\text{Cd}(\text{MEA})_4(\text{OH})$, $\text{Pb}(\text{MEA})(\text{OH})_3$, $\text{Pb}(\text{MEA})_2(\text{OH})$ and $\text{Pb}(\text{MEA})_2(\text{OH})_2$ were detected.

It is well known that the characteristics of complexes formed in solution depend to a large extent on the nature of the solvent. Thus in an early study of complexes formed by alcoholamines in aqueous alcoholic media Kirson and Barsily¹ found the stability of Cu^{2+} complexes to increase with the concentration of alcohol, and similar results were obtained by Migal and Serova^{2,3} for simple complexes of Cd^{2+} and Pb^{2+} with monoethanolamine. It has likewise been reported²⁻⁴ that co-ordination numbers vary with the alcohol content of the medium. This article describes a study contributing to the little research that has so far been done on such effects in the case of mixed hydroxo-complexes.

In a previous article⁵ we reported a study made to resolve a discrepancy in the literature regarding the existence of mixed complexes of Pb^{2+} with hydroxide and monoethanolamine (MEA) in aqueous solution, for which purpose we developed a regression program (CONSEL) which, when used in conjunction with non-linear optimization programs such as POLAG,⁶ eliminates the need to use graphical methods of data analysis. In the work now described the same methodology was employed to determine the influence of the solvent on metal-MEA-OH⁻ complexes formed by Cd^{2+} and Pb^{2+} in methanol-water media.

EXPERIMENTAL

All reagents were Merck *p.a.* grade, MEA being purified by standard procedures⁷ before use. Solutions of Cd^{2+} ($2 \times 10^{-4}M$) and Pb^{2+} ($1.6 \times 10^{-4}M$) were prepared from the corresponding nitrates. Ionic strength was maintained at 0.1M with potassium nitrate.

Polarograms were obtained with a Beckman Electroscan 30 with an SCE reference electrode and a reaction cell kept

at $25.0 \pm 0.1^\circ$. Oxygen was eliminated from the sample solutions by a current of nitrogen previously passed through a water-methanol mixture of the same composition as the sample solvent.

The pH measurements were made with a precision of ± 0.02 with a Radiometer 26 pH-meter equipped with a GK2401B electrode, calibrated^{8,9} with buffers prepared in the appropriate water-methanol mixture. The pH of the experimental solutions was varied by adding 0.1M sodium hydroxide or nitric acid.

Cd^{2+} complexes were studied for concentrations of MEA in the range 0.10–1.00M in each of three solvents (with 10, 30 and 50% w/w methanol) at each of six pH values (10.60, 10.90, 11.30, 11.70, 12.10 and 12.50). For each of four solvents (with 16.3, 33.3, 52.1 and 68.1% w/w methanol), Pb^{2+} complexes were studied in at least 25 solutions with MEA concentrations of 0.10–0.80M and pH values in the range 10.50–12.80 (it was not necessary to maintain the pH constant throughout a series of experiments when the results were to be analysed only by the CONSEL-POLAG program).

RESULTS AND DISCUSSION

All the systems studied presented well-defined polarograms without peaks. In all cases, plotting E against $\log i/(i_d - i)$ yielded straight lines with slopes of less than 0.034, showing a reversible two-electron reduction process to be involved. Plotting the limiting current against $h^{1/2}$ (h being the height of the mercury column) afforded straight lines passing through the origin, showing the reactions taking place to be diffusion-controlled.

To determine the composition and stability of the complexes formed, two methods were used to analyse the polarographic data. All the systems studied were analysed by the programs CONSEL⁵ and POLAG,⁶ and for the Cd^{2+} -MEA-OH⁻ systems, which were studied in series of experiments in which the pH was kept constant while the concentration of MEA was varied, the graphical method of Schaap and

*Author for correspondence.

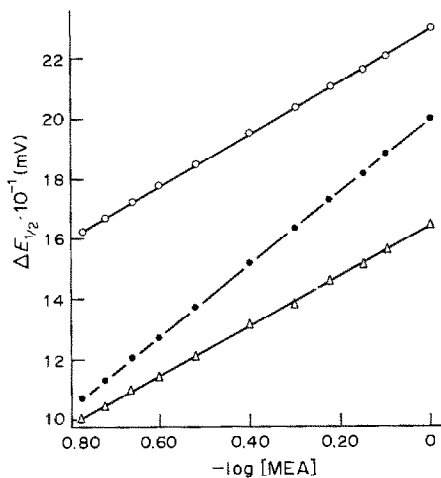


Fig. 1. $\Delta E_{1/2}$ plotted against $\log [\text{MEA}]$. \triangle 10% MeOH, pH 10.60; \bullet 30% MeOH, pH 11.70; \circ 50% MeOH, pH 12.50.

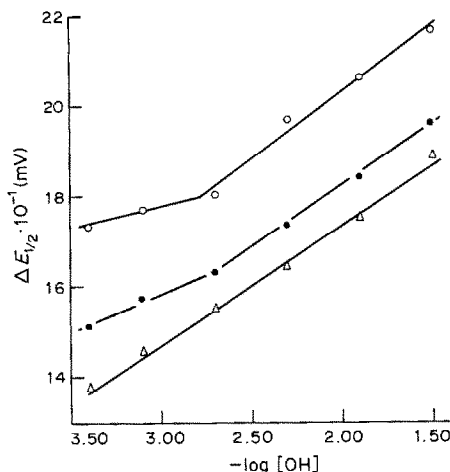


Fig. 2. $\Delta E_{1/2}$ plotted against $\log [\text{OH}^-]$. \triangle 10% MeOH, $[\text{MEA}] = 0.50M$; \bullet 30% MeOH, $[\text{MEA}] = 0.60M$; \circ 50% MeOH, $[\text{MEA}] = 0.70M$.

Table 1. Polarographic data for Pb^{2+} -MEA- OH^- systems in methanol-water media (C_{MEA} = molar concentration of monoethanolamine)

C_{MEA}	16.3		33.3		52.1		68.1	
	pH	$-E_{1/2}$, mV	pH	$-E_{1/2}$, mV	pH	$-E_{1/2}$, mV	pH	$-E_{1/2}$, mV
0.0	—	372	—	366	—	362	—	358
0.100	11.71	547	—	—	—	—	—	—
0.100	11.99	600	—	—	—	—	—	—
0.100	12.38	630	—	—	—	—	—	—
0.100	10.56	512	—	—	—	—	—	—
0.150	11.91	596	—	—	11.14	540	—	—
0.150	11.27	556	—	—	11.86	583	—	—
0.150	10.72	524	—	—	12.56	630	—	—
0.150	12.46	640	—	—	11.57	566	—	—
0.200	11.33	565	—	—	11.18	544	—	—
0.200	10.83	534	—	—	11.16	538	—	—
0.200	—	—	—	—	11.96	591	—	—
0.200	—	—	—	—	12.58	633	—	—
0.250	10.94	544	11.36	529	11.26	553	11.23	546
0.250	11.39	568	10.83	519	10.68	515	12.25	607
0.250	11.94	603	12.12	612	12.09	595	12.74	638
0.250	12.46	640	12.55	639	12.55	634	12.83	581
0.300	10.95	545	10.57	519	11.28	546	11.30	552
0.300	12.46	639	10.93	539	10.96	530	10.94	531
0.300	11.97	608	11.41	567	12.05	597	12.21	605
0.300	—	—	12.07	608	12.57	636	12.69	637
0.400	11.03	553	11.02	548	11.35	557	11.38	560
0.400	11.49	584	11.48	574	11.70	578	11.79	585
0.400	11.98	611	12.52	642	12.24	614	12.36	617
0.400	12.47	642	12.05	612	12.61	641	12.72	641
0.500	12.02	513	11.05	554	11.47	571	11.51	565
0.500	12.40	641	12.04	613	11.18	556	11.21	547
0.500	11.56	593	12.52	644	12.17	613	12.27	614
0.500	11.07	611	—	—	12.63	644	12.74	643
0.600	11.13	567	10.95	550	11.48	579	11.51	571
0.600	11.56	590	11.55	586	10.89	542	11.03	544
0.600	12.00	617	12.08	617	12.16	616	12.26	615
0.600	—	—	12.57	652	12.64	653	12.77	647
0.700	—	—	10.98	555	—	—	11.55	575
0.700	—	—	12.08	622	—	—	11.05	548
0.700	—	—	12.45	645	—	—	12.25	617
0.700	—	—	11.58	589	—	—	12.67	643
0.800	11.05	565	11.63	595	11.54	584	11.54	577
0.800	11.57	595	12.06	623	10.90	547	11.04	550
0.800	12.00	618	12.56	655	12.15	622	12.17	616
0.800	12.51	651	11.00	558	12.75	661	12.70	648

Table 2. Logarithmic stability constants of complexes of Pb^{2+} with monoethanolamine and/or OH^- in aqueous and aqueous methanolic media

Methanol, % w/w	0	16.3	33.3	52.1	68.1
$Pb(MEA)(OH)_2$	12.50 ± 0.02	12.82 ± 0.08		12.64 ± 0.03	
$Pb(MEA)(OH)_3$			14.37 ± 0.08		
$Pb(MEA)_2(OH)$			9.94 ± 0.08		
$Pb(MEA)_2(OH)_2$					12.50 ± 0.07
$Pb(OH)_2$					11.93 ± 0.06

McMasters¹⁰ was also employed (as described previously⁵) and led to the same results. The terms I_{ds}/I_{dc} in the Schaap and McMasters F function was in all cases negligible.

In what follows, the charges of the complexes have been omitted for convenience.

Complexes of Cd^{2+}

Figures 1 and 2 show the change in half-wave potential as the concentration of one ligand is changed while that of the other is kept constant, for each of the three methanol concentrations tested, $\Delta E_{1/2}$ being defined as $E_{s/2} - E_{c/2}$, where $E_{s/2}$ and $E_{c/2}$ are the half-wave potentials of the uncomplexed and complexed cadmium species respectively. A single complex predominates in all the 10% methanol solutions, and analysis of the data shows it to be $Cd(MEA)_3(OH)$, with $\log \beta_{3,1} = 8.96 \pm 0.02$.

In the 30% methanol medium there are two complexes which predominate in different pH ranges and differ in the number of OH^- ions co-ordinated to the metal ion, though both contain the same number of MEA molecules. Analysis of the data reveals these complexes to be $Cd(MEA)_4$ ($\log \beta_{4,0} = 5.85 \pm 0.02$) and $Cd(MEA)_4(OH)$ ($\log \beta_{4,1} = 9.03 \pm 0.01$), the mixed complex predominating at $pH > 10.90$. The value obtained for $\beta_{4,0}$ is similar to that found by others³ for 40% alcohol medium, $\log \beta_{4,0} = 6.4$.

In 50% methanol, two different complexes are again detected, $Cd(MEA)_3$ ($\log \beta_{3,0} = 5.85 \pm 0.07$) and $Cd(MEA)_3(OH)$ ($\log \beta_{3,1} = 9.21 \pm 0.03$), the mixed complex predominating at $pH > 10.90$.

Complexes of Pb^{2+}

In studying the Pb^{2+} systems advantage was taken of the experimental flexibility allowed by the use of CONSEL-POLAG,⁵ which makes it unnecessary to use experiments at constant pH. The experimental data are given in Table 1. Analysis by CONSEL-POLAG revealed the presence of the complexes listed in Table 2, together with their stability constants.

Studies in aqueous media

The results reported above may be compared with those obtained in experiments using aqueous solutions with similar concentrations of metal ion, alcoholamine and OH^- . The complexes of cadmium found in these media were $Cd(MEA)_2(OH)_2$ ($\log \beta_{2,2} = 8.99 \pm 0.09$) and $Cd(MEA)_3(OH)$ ($\log \beta_{3,1} = 8.11 \pm 0.02$), the latter also being found in 10 and 50% water-methanol solutions, but with higher stability constants (Table 3). The value found for $\log \beta_{2,2}$ is similar to the value 8.65 obtained by Subrahmanya,¹¹ who also reported the presence of $Cd(MEA)_3(OH)_2$ (but not the corresponding stability constant). The only Pb^{2+} complex found in water in the present study was $Pb(MEA)(OH)_2$, $\log \beta_{1,2} = 12.50 \pm 0.02$, compatible with the value $\log \beta_{1,2} = 11.83$ found by Subrahmanya at an ionic strength of 1.0M.

DISCUSSION

The results obtained for aqueous solutions are similar to those reported by others.¹¹ In the water-methanol mixtures the previously unreported complexes $Cd(MEA)_4(OH)_3$, $Pb(MEA)(OH)$ and $Pb(MEA)_2(OH)_2$ have been detected.

As the concentration of alcohol in the medium rises, the half-wave potential of the uncomplexed metal ion shifts to less negative values. This has been interpreted as indicating that the energy necessary for the electron-transfer reaction is less in alcoholic media than in water because of solvation effects.² The general tendency for the number of ligands co-ordinated to the metal ion to increase with the proportion of alcohol present also suggests that it is easier for incoming ligands to displace methanol molecules than water molecules because the former must have less capacity for solvation than the latter (the exceptional behaviour in media containing approximately 50% of methanol would appear to be due¹² to the interaction of the two solvents being

Table 3. Logarithmic stability constants of complexes of Cd^{2+} with monoethanolamine and/or OH^- in aqueous and aqueous methanolic media

Methanol, % w/w	0	10	30	50
$Cd(MEA)_2(OH)_2$	8.99 ± 0.09			
$Cd(MEA)_3$				5.85 ± 0.07
$Cd(MEA)_3(OH)$	8.11 ± 0.02	8.96 ± 0.01		9.21 ± 0.03
$Cd(MEA)_4$			5.85 ± 0.02	
$Cd(MEA)_4(OH)$			9.03 ± 0.01	

maximal at these concentrations, as witnessed by the peak values attained in this region by physical properties such as viscosity). Finally, the stability constants of those complexes detected in more than one of the media employed ($\text{Pb}(\text{MEA})(\text{OH})_2$ and $\text{Cd}(\text{MEA})_2(\text{OH})_2$] confirm that the stability is increased by the presence of methanol.

Acknowledgement—We are grateful to F. Rey for his help with this work.

REFERENCES

1. B. Kirson and L. Barsily, *Bull. Soc. Chim. France*, 1959, 1226.
2. P. K. Migal and G. F. Serova, *Russ. J. Inorg. Chem.*, 1962, **7**, 825.
3. *Idem, ibid.*, 1965, **10**, 1366.
4. P. K. Migal and V. A. Tsiplyakova, *ibid.*, 1964, **9**, 333.
5. J. S. Santaballa, C. Blanco, F. Arce and J. Casado, *Talanta*, 1985, **32**, 931.
6. D. J. Leggett, *ibid.*, 1980, **27**, 787.
7. S. Siggia, *Quantitative Organic Analysis Via Functional Groups*, p. 423. Wiley, New York, 1967.
8. C. L. Ligny, *Rec. Trav. Pays Bas*, 1960, **79**, 712.
9. R. G. Bates, M. Paabo and R. Robinson, *J. Phys. Chem.*, 1963, **67**, 1833.
10. W. B. Schaap and D. L. McMasters, *J. Am. Chem. Soc.*, 1961, **83**, 4699.
11. R. S. Subrahmanya, *Advances in Polarography*, Vol. 2, Pergamon Press, London, 1960.
12. R. Andreoli, G. Battistuzzi Gavioli, G. Brandi and P. G. Benedetti, *J. Electroanal. Chem. Interfacial Electrochem.*, 1973, **41**, 439.

ANNOTATION

ACTION DE L'ACIDE CITRIQUE SUR L'ANHYDRIDE ACETIQUE ET LA PYRIDINE

DETERMINATION DU MECANISME REACTIONNEL ET DE LA STRUCTURE DU COMPOSE FORME

D. BAYLOCQ, C. MAJCHERCZYK et F. PELLERIN

Laboratoire de Chimie Analytique, Centre d'Etudes Pharmaceutiques, Université de Paris XI,
Rue J. B. Clément, F 92290 Chatenay-Malabry, France

(Reçu le 9 mai 1985. Révisé le 14 juin 1986. Accepté le 11 juillet 1986)

Résumé—Cette étude met en évidence la structure du dérivé coloré obtenu par l'action de l'acide citrique sur la pyridine, en présence d'anhydride acétique. Les méthodes utilisées sont la résonance magnétique du ^{13}C , la spectrophotométrie infra-rouge, et la spectrométrie de masse. Le schéma réactionnel proposé conduit à l'aconitate de pyridinium, dont la structure est confirmée par la spectrométrie de masse.

Summary—This study outlines the structure of the coloured by-product obtained by the action of citric acid on acetic anhydride and pyridine. The methods used are ^{13}C nuclear magnetic resonance, infrared spectrometry and mass spectrometry. The reaction scheme proposed indicates that the compound is pyridinium aconitate. The chemical structure is corroborated by mass spectrometry.

La réaction de l'acide citrique sur les amines tertiaires en présence d'anhydride acétique a fait l'objet de quelques applications analytiques. Chambon a fondé sur cette réaction le dosage de l'acide citrique dans les médicaments et les produits d'origine biologique.¹ Kalnin² a poursuivi l'application de la réaction par le dosage des amines tertiaires en présence d'acide citrique; Feigl a repris cette réaction sous la forme d'un "Spot test".³

Pesez et Bartos ont mis cette réaction à profit dans la mesure de la fluorescence verte qui apparaît dans la réaction des amines tertiaires sur l'anhydride acétique; ces auteurs ont aussi dosé différents types de composés; cette réaction qui est spécifique des amines tertiaires,³ peut s'appliquer en particulier à l'identification de la caféine, de la cinchonine, de la pilocarpine, de la vitamine B1, de l'acide nicotinique, de la diméthylaniline, etc.

Le mécanisme réactionnel et la structure du produit formé n'ont pas été décrits. L'objet du présent mémoire est la proposition d'un schéma réactionnel confirmé par l'analyse structural du produit obtenu, par les techniques spectrales (spectrophotométrie infra-rouge et de masse).

PARTIE EXPERIMENTALE

Mode opératoire

Les conditions opératoires de la méthode de dosage selon Chambon ont été adaptées en vue d'obtenir une quantité suffisante de produit, compatible avec les différentes techniques analytiques appliquées.

Dans une fiole, introduire 25 mg d'acide citrique et 25 ml

de pyridine, agiter dans un bain de glace durant 15 min, ajouter en agitant 114 ml d'anhydride acétique et laisser la coloration se développer à la température ambiante.

RESULTATS

Spectrophotométrie infra-rouge

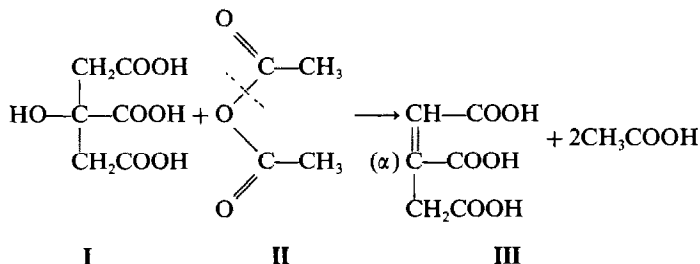
Le spectre infra-rouge du composé obtenu (pastille de bromure de potassium) fait apparaître une large bande à $1800\text{--}1680\text{ cm}^{-1}$ (Fig. 1) suggérant une fonction anhydride cyclique; il révèle une fonction hydroxyle à 3500 cm^{-1} . Toutefois la faible intensité des bandes rend l'interprétation délicate; elle est liée à la nature pâteuse du composé formé et à la difficulté rencontrée dans le pastillage de l'échantillon.

Caractéristiques spectrales

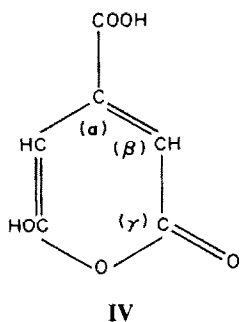
Le composé obtenu s'avère instable et sa purification par évaporation sous vide des réactifs en excès (pyridine, anhydride acétique, acide acétique), entraîne une dégradation du produit, se traduisant par la disparition des bandes d'absorption caractéristiques (λ_{max} 413 et 395 nm, $E_{1\text{cm}}^{1\%}$ 64 et 70).

Résonance magnétique nucléaire du ^{13}C

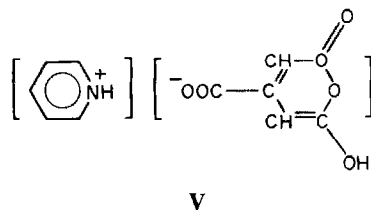
Le tracé du spectre de résonance magnétique nucléaire du ^{13}C , effectué extemporanément, après évaporation des réactifs en excès, révèle le groupement anhydride cyclique qui présente les déplacements chimiques du carbone suivants: 167,1, 168,8 et 172,2 ppm. La mise en évidence du groupement anhydride cyclique nous a conduits à formuler le mécanisme réactionnel suivant:



Dans un premier temps en milieu anhydride acétique, l'acide citrique conduit à l'acide aconitique (III), puis à l'acide α - γ -anhydroaconitique (IV), selon la structure proposée par Groth et Dalhen.⁵



Dans un deuxième temps il se forme en présence de pyridine un sel, dont la formule proposée (V) est un aconitate de pyridinium. En effet, la pyridine en milieu acide se protonne et conduit à l'ion pyridinium.



Spectrométrie de masse

L'analyse structurale a été effectuée sur un spectrophotomètre NERMAG 10-10c. Le traitement des données est réalisé sur un ordinateur PD-P11. Les procédés d'ionisation utilisés sont l'impact électronique à 75 eV et l'ionisation chimique par le méthane; l'injection a été effectuée directement par le procédé "flash" permettant l'élimination spontanée des solvants.

Le pic de masse obtenu correspond à $m/z = 233$, dans le cas de l'ionisation par impact électronique; le pic de masse obtenu par l'ionisation chimique par le méthane, correspond à $(m + 1)/z = 234$. La masse du composé V correspondant à la formule proposée est 235.

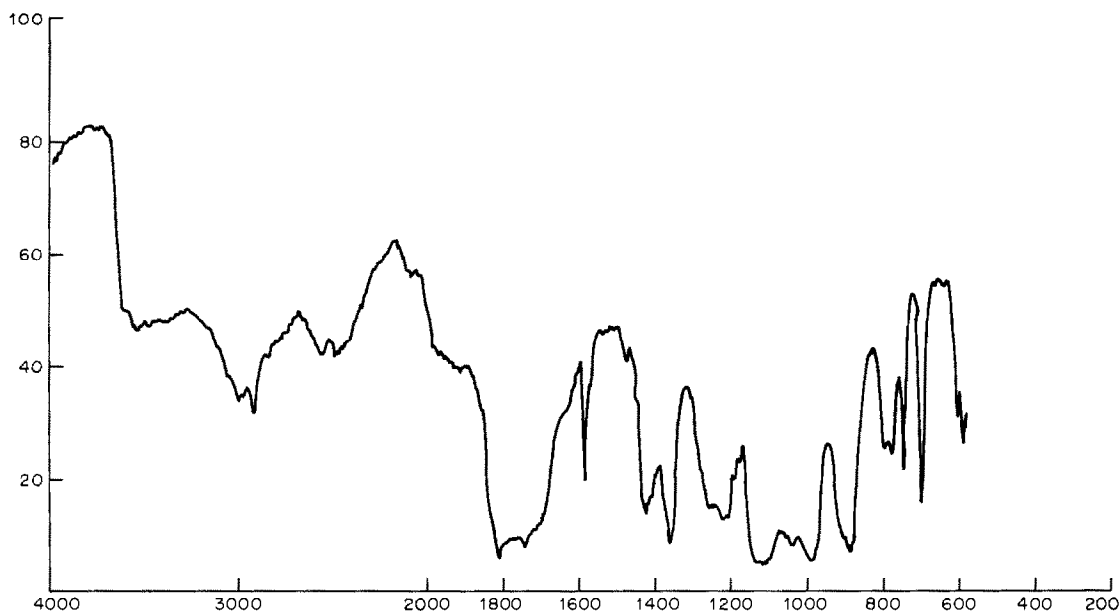


Fig. 1. Spectre infra-rouge du composé coloré.

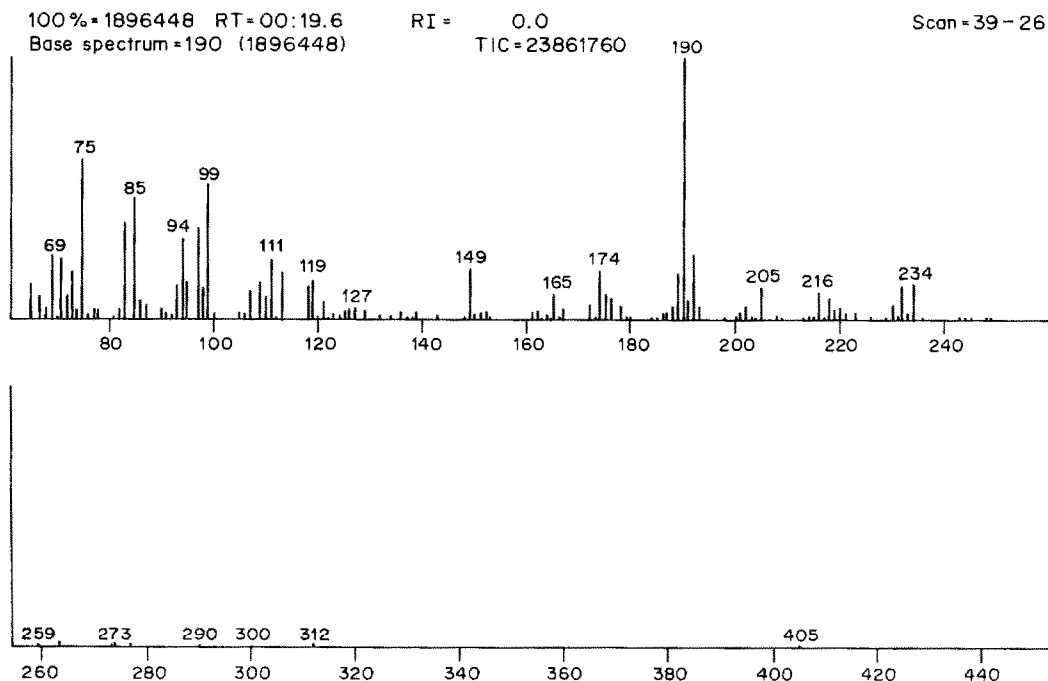
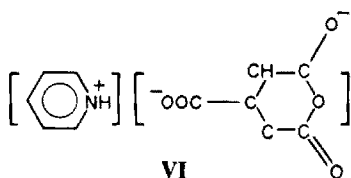


Fig. 2. Spectre de masse obtenu après ionisation chimique par le méthane.

Il apparaît en conséquence un déficit de 2 protons pour le pic de masse $m/z = 233$ par rapport à la formule V. Le pic de masse 233 peut alors être considéré comme un pic pseudomoléculaire. Le déficit de 2 protons peut s'expliquer par la mobilité des ions hydrogène, situés sur le cycle lactonique, lié à l'environnement électronégatif.

Le pic pseudomoléculaire de masse $m/z = 233$ pourrait avoir la structure suivante (VI):



L'analyse fragmentaire (Figs. 2 et 3) conduit aux observations suivantes: le pic de masse 190 correspond à $m - 44$, soit à une perte de masse équivalente à CO_2 , le pic de masse 111 correspond au cycle lactonique. Il apparaît que l'analyse fragmentaire du spectre de masse obtenu par impact électronique et par ionisation chimique révèle des ions moléculaires constitutifs de la structure proposée (V).

Cependant, les procédés d'ionisation appliqués ne font pas apparaître le pic de masse M^+ , mais un pic pseudomoléculaire attribuable à une fragmentation ionique de la molécule, en rapport avec la distribution des charges électroniques.

Alternativement, peut être, peut-on envisager une migration en position 2 ou 4 de la pyridine, donnant avec $R = \text{C}_6\text{H}_3\text{O}_3$:

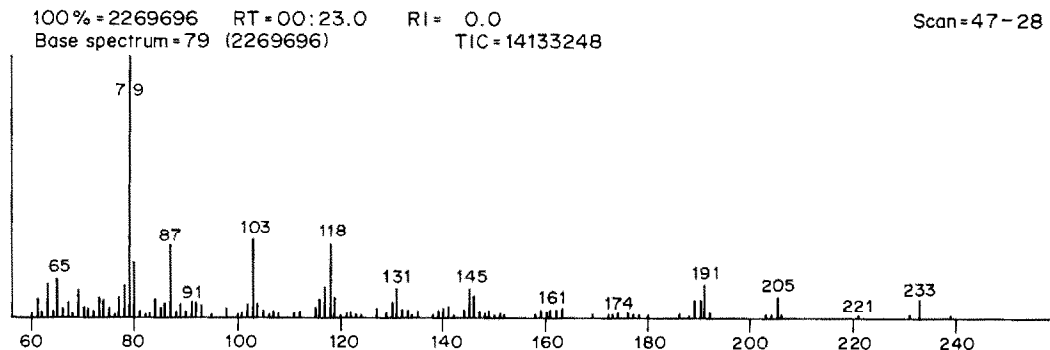
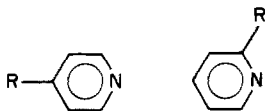


Fig. 3. Spectre de masse obtenu après impact électronique à 75 eV.



Compte tenu des nombreuses possibilités de redistributions dans la phase gazeuse, il apparaît difficile d'aboutir à une conclusion définitive.

Les résultats de la spectrométrie de masse ne permettent pas de vérifier complètement l'hypothèse de la formation du composé (VI). Ce composé est en effet thermolabile et dans les conditions opératoires du procédé de désorption, le produit est susceptible de se décomposer dans la source d'ionisation. Le composé de masse 233 pourrait alors correspondre à un réarrangement à partir des fragments formés. La poursuite de cette étude pourrait aboutir à la vérification de cette hypothèse.

Conclusion

La mise en évidence de la configuration chimique du composé coloré obtenu par l'action de l'acide

citrique sur l'anhydride acétique et la pyridine a pu être réalisé à l'aide de la spectrométrie de masse, permettant par le procédé d'injection "flash", de parvenir directement à l'analyse du produit, dont l'instabilité n'autorise pas la purification par les méthodes traditionnelles.

La spectrométrie infra-rouge, ainsi que la RMN du ^{13}C , apportent des éléments de confirmation à la structure établie.

La connaissance du mécanisme réactionnel renforce la validité du procédé de dosage fondé sur cette réaction, et peut permettre d'envisager d'autres applications aux composés organiques.

LITTÉRATURE

1. P. Chambon, *Ann. Pharm.* 1963, **21**, 617.
2. P. Kalnin, *Helv. Chem. Acta*, 1928, **11**, 977.
3. F. Feigl, *Qualitative Analysis by Spot Tests*, 1st Ed., Elsevier, New York, 1947.
4. M. Pezez et Bartos, *Colorimetric and Fluorimetric Analysis of Organic Compounds and Drugs*, 1st Ed., Dekker, New York, 1974.
5. A. B. Groth et M. Dalhen, *Acta Chem. Scand.*, 1967, **21**, 291.

PRELIMINARY COMMUNICATION

NOVEL FLUORESCENCE REACTION FOR MALONONITRILE

HARVEY W. YUROW

U.S. Army Chemical Research, Development and Engineering Center,
Aberdeen Proving Ground, Maryland 21010-5423, U.S.A.

(Received 8 September 1986. Accepted 12 October 1986)

Although fluorimetric techniques are inherently more sensitive than colorimetric ones, they are utilized far less commonly in analytical chemistry. One reason for this is that when new reactions are investigated, colour is readily discerned, but unless samples are examined routinely under ultraviolet light (even in the presence of colour) the existence of a fluorescent species will not be noted. A case in point is the riot-control agent *o*-chloro-benzylidene malononitrile (CS), which decomposes rapidly at pH >10 to give *o*-chlorobenzaldehyde and malonitrile. Because the latter compound has an active methylene group, it is capable of condensation with various reagents to give highly coloured products. We have observed that reaction of 2-pyridinecarboxaldehyde with malononitrile in aqueous acidic solution gives a magenta colour (λ_{max} 510 nm), with a detection limit of ~ 0.1 $\mu\text{g/ml}$, appreciably higher than that with benzofurazan oxide¹ (0.025 $\mu\text{g/ml}$). However, when viewed under long-wave ultraviolet light, the reaction mixture produces an intense yellow-green fluorescence, measurable down to a nitrile concentration of 0.01 $\mu\text{g/ml}$. The optimum conditions are pH 2.0 (phosphate buffer), reagent concentration 5×10^{-4} M, and heating for 5 min at 100°. The fluorescence spectrum has an excitation maximum at 395 nm and emission peaks at 490 and 590 nm. Because the intensity ratio of product to reagent blank is greater at the longer emission wavelength, the 590 nm peak is selected for use.

The reaction is not given by two other active cyano-compounds, *viz.* ethyl cyanoacetate and 1,1-dicyanoethyl acetate, or by methylene dithiocyanate, and appears to be relatively specific for the test compound. No colour or fluorescence is produced by reaction of malononitrile with the 3- and 4-pyridinecarboxaldehyde isomers, but a blue colour of moderate intensity is given by 2-acetylpyridine.

In acidic solution, 2-pyridinecarboxaldehyde can exist as equilibrium mixtures of three forms:² the unhydrated species, the hydrated aldehyde with the nitrogen atom protonated, and the zwitterion (by loss of a proton from the hydrated aldehyde moiety). At pH 2, the optimum for the condensation reaction with malononitrile, the protonated aldehyde is almost exclusively present, while at pH 6, at which only the other two forms exist, the fluorescence intensity is negligible. Consequently, it may be assumed that the reactive species is the protonated one. In this connection it should be noted that the intensity of the magenta colour produced by reaction of ammonium ion, formaldehyde, and 2-pyridinecarboxaldehyde is also strongly pH-dependent.³

A number of analytically useful and highly sensitive reactions involving the isomeric pyridinecarboxaldehydes have been reviewed,⁴ indicating the versatility of these reagents. Though most of the applications are based on use of the derivatives, a significant number utilize direct condensation with the aldehyde moiety.

REFERENCES

1. M. Haddadin, U. Khalidi, N. Turjuman and R. Ghougassian, Anal. Chem., 1974, 46, 2072.
2. K. Nakamoto and A.E. Martel, J. Am. Chem. Soc., 1959, 81, 5862.
3. H.W. Yurow and I. Master, Talanta, 1978, 25, 423.
4. L.Y. Leitis, R.A. Skolmeistre, K.I. Rubina, D.P. Yansone and N.V. Shimanskaya, Russian J. Anal. Chem., 1985, 40, 308.

PAPERS RECEIVED

- Spectrophotometric determination of piroxicam with 4-aminophenazone and potassium ferricyanide:** C. S. P. SASTRY, AMBATI R. MOHANA RAO and T. N. V. PRASAD. (3 October 1986)
- Spectrophotometric determination of paracetamol in drug formulations by oxidation with potassium dichromate:** SALAH M. SULTAN. (3 October 1986)
- Complexometric-spectrophotometric assay of tetracyclines in drug formulations:** SALAH M. SULTAN, IBRAHIM Z. ALZAMIL and NAWAL A. ALARFAJ. (3 October 1986)
- Rapid spectrophotometric determination of zirconium(IV) with 2-(5-bromo-2-pyridylazo)-5-diethylaminophenol:** G. V. RATHAIAH and M. C. ESHWAR. (3 October 1986)
- Studies on fluorescein—VI: The absorbance of fluorescein in the ultraviolet as a function of pH:** HARVEY KIEHL and NAOMI HORCHAK-MORRIS. (3 October 1986)
- Solvent extraction and spectrophotometric determination of palladium with 3,4-dihydro-4,4,6-trimethyl-2(1H)-pyrimidinethione as a selective reagent:** A. SAFAVI, A. MASSOUMI and M. EDRISSI. (3 October 1986)
- Evaluation of volume and matrix effects for the generalized standard addition method:** JOHN H. KALIVAS. (8 September 1986)
- Determination of hydrogen peroxide with *N,N*-diethylaniline and 4-aminoantipyrine by use of an anion-exchange resin modified with manganese-tetrakis(sulphophenyl)porphine as a mimesis of peroxidase:** YUTAKA SAITO, MASAKI MIFUNE, SUZUYO MAKASHIMA, JUNICHI ODO, YOSHIMASA TANAKA, MASAHIKO CHIKUMA and HISASHI TANAKA. (3 October 1986)
- Fluorescence in thin liquid films: A simple model:** R. VON WANDRUSZKA and J. D. WINEFORDNER. (3 October 1986)
- A simple and rapid fluorimetric method for the microdetermination of isonicotinic acid hydrazide:** P. C. IOANNOU. (3 October 1986)
- Alkalimetric determination of mercury by reaction with 1-mercaptopropane-2,3-diol:** KRISHNA K. VERMA, PRAMILA TYAGI and SUNIL K. SNAGHI. (3 October 1986)
- Extractive-spectrophotometric determination of cobalt with trilaurylamine oxide and thiocyanate:** ABDUL BARI and M. RASHID. (3 October 1986)
- Comparison of hydride generation methods for arsenic and antimony with detection in a long absorption cell:** W. J. WANG, S. HANAMURA and J. D. WINEFORDNER. (3 October 1986)
- The use of 2,3-dichloro-5,6-dicyano-*p*-benzoquinone for the spectrophotometric determination of some cardiovascular drugs:** A. S. ISSA, M. ABDEL SALAM, M. S. MAHROUS and N. SOLIMAN. (9 October 1986)
- Spectrophotometric determination of rhenium with dithio-oxamide (rubeanic acid) in strongly alkaline medium:** O. D. BOZHKOV, L. V. BORISOVA and N. JORDANOV. (10 October 1986)
- High-energy collisional spectroscopy in qualitative and quantitative analysis of diesel particulates:** ANNA MARIA MACCIONI, PIETRO TRALDI and LUCIO DORETTI. (13 October 1986)
- Uranium-Xylidine Blue I complex and its application in linear sweep polarography:** ZOAFAN ZHAO, XIAOHUA CAI and PEIBIAO LI. (16 October 1986)
- Extraction-photometric determination of vanadium in steels with mandelohydroxamic acid:** F. SALINAS, J. L. MARTINEZ-VIDAL and V. GONZALEZ-MURCIA. (14 October 1986)

PAPERS RECEIVED

- Spectrofluorimetric determination of cadmium in PVC stabilizers in non-aqueous media:** JOSE AZNAREZ, JAVIER GALBAN, JUAN CARLOS VIDAL and CARMelo DIAZ. (14 August 1986)
- Adsorptive stripping voltammetric measurements of trace levels of uranium following chelation with Mordant Blue 9:** JOSEPH WANG and JAVAD M. ZADEH. (14 August 1986)
- Simple colorimetric methods for the determination of Diosmin in pharmaceutical preparations:** R. T. SANE, T. G. CHANDRASHEKHAR, C. L. SAWANT, S. J. ACHARYA and N. N. GORE. (1 September 1986)
- Spectrophotometric determination of trace osmium in aqueous medium with a new reagent, 4-sulpho-2-aminobenzenethiol:** ANIL K. CHAKRABARTI. (1 September 1986)
- A graphical derivative approach for the photometric determination of lutetium and praseodymium mixtures:** F. GARCIA SANCHEZ, M. HERNANDEZ LOPEZ and J. C. MARQUEZ GOMEZ. (1 September 1986)
- Analytical properties of 2-nitro-5,6-dimethyl-1,3-indanedione dithiosemicarbazone:** Y. LINGAPPA, K. HUSSAIN REDDY and D. VENKATA REDDY. (1 September 1986)
- A special way of signal processing in multicomponent potentiometric titration:** A. PARCZEWSKI. (1 September 1986)
- An indirect complexometric method for the estimation of tin in alloys:** N. RUKMANI DESIKAN and M. VIKAYAKUMAR. (1 September 1986)
- Polarographic investigation of nickel complexation by morpholine in aqueous medium:** G. VISALAKSHI, S. V. NARASIMHAN and K. S. VENKATESWARLU. (1 September 1986)
- Determination of vanadium and nickel chelates with 2-(5-bromo-2-pyridylazo)-5-diethylaminophenol, with precolumn derivative formation, by reversed-phase liquid chromatography.** CHANG-SHAN LIN, XIAO-SONG ZHANG and YING-FAN YING. (1 September 1986)
- The effect of temperature on single-column ion-chromatography of metal ions:** NANCY E. FORTIER and JAMES S. FRITZ. (1 September 1986)
- Extraction and microdetermination of manganese(II) with Aliquat 336:** SOBHANA K. MENON, YADVENDRA K. AGRAWAL and MAHENDRA N. DESAI. (1 September 1986)
- Complexometric titration of thallium(III) with 4-amino-5-mercapto-3-propyl-1,2,4-triazole as replacing reagent:** NITYANANDA SHETTY A., R. V. GADAG and M. R. GAJENDRAGAD. (1 September 1986)
- Purification of solvents for liquid chromatography:** BOGUSLAW BUSZEWSKI, ROMAN LODKOWSKI and JERZY TROCEWICZ. (3 September 1986)
- Interfacing an analogue IR spectrometer to a microcomputer:** M. J. ADAMS and G. J. EWEN. (17 August 1986)
- Synthesis and analytical characterization of a chelating resin with dithizone:** J. CHWASTOWSKA and E. KOSIARSKA. (5 September 1986)
- Novel fluorescence reaction for malonitrile:** HARVEY W. YUROW. (8 September 1986)
- Kinetics and analytical applications of the ruthenium-catalyzed bromate oxidation of Bordeaux—I: Kinetics of the uncatalysed reaction:** J. T. AYODELE, B. G. COOKSEY and J. W. OTTAWAY (8 September 1986)
- Kinetics and analytical applications of the ruthenium-catalysed bromate oxidation of Bordeaux—II: Kinetics of the catalysed reaction:** J. T. AYODELE, B. G. COOKSEY and J. M. OTTAWAY. (8 September 1986)
- Spectrophotometric determination of primaquine phosphate with potassium iodate, potassium periodate, glucose-phosphoric acid and *p*-dimethylaminobenzaldehyde:** G. VASUDEVA PRASAD, Y. PULLA RAO and N KRISHNA MURTY. (8 September 1986)
- Spectrophotometric determination of microamounts of tantalum with *o*-chlorophenylfluorone and cetyltrimethylammonium bromide:** LUO ZONGMING and SHEN WEI. (8 September 1986)
- Artifacts of the decalin-molecular sieve system in the analysis of mineral waxes:** MUHAMMAD NAZIR, MUHAMMAD KHURSHID BHATTY and FRANK D. GUFFEY. (10 September 1986)
- Extraction of aromatic organic compounds by polyurethane foam:** L. SCHUMACK and A. CHOW. (10 September 1986)
- Co-precipitation of vanadium with iron by sodium tetrahydroborate:** MICHIKO MANIKI and KICHINOSUKE HIROKAWA. (15 September 1986)
- Application of microcomputers in the analytical laboratory—III: ASV analysis:** DRORA KAPLAN, DAN RAPHAELI and SAM BEN-YAAKOV. (15 September 1986)
- Quantitative estimation of substances spotted on filter paper, by photoacoustic spectroscopy:** T. SOMASUNDARAM, SANJAY S. R. RAO and P. GANGULY. (15 September 1986)
- Kinetic and oxidative aspects of treatment of some disaccharides with tetra-amminocuprate(II) in ammoniacal medium:** S. P. PANDEY and C. B. PANDEY. (15 September 1986)
- 1,2-Naphthoquinone-2-thiosemicarbazone as a new acid-base indicator in isopropyl and tert-butyl alcohol media:** ELISABETH BOSCH and MARTI ROSES. (15 September 1986)
- Extraction-spectrophotometric determination of strontium in calcium-rich materials with cryptand (2.2.2):** B. JUSKOWIAK. (15 September 1986)
- Improved microcombustion technique for nitrogen estimation in organotin complexes of *o*-carboxazine:** T. S. BASU BAUL. (15 September 1986)
- Photometric determination of selenium with ferrocene:** MINORI KAMAYA, TETASURO MURAKAMI and EIZEN ISHII. (16 September 1986)
- 2,6-Diacetylpyridine bis(arylhydrazone) derivatives as analytical reagents for uranium:** MARISSA BONILLA-ALVAREZ, MARGO PALMIERI, DEBRA DAVIS and JAMES S. FRITZ. (16 September 1986)

PAPERS RECEIVED

- Spectrofluorimetric determination of cadmium in PVC stabilizers in non-aqueous media:** JOSE AZNAREZ, JAVIER GALBAN, JUAN CARLOS VIDAL and CARMelo DIAZ. (14 August 1986)
- Adsorptive stripping voltammetric measurements of trace levels of uranium following chelation with Mordant Blue 9:** JOSEPH WANG and JAVAD M. ZADEH. (14 August 1986)
- Simple colorimetric methods for the determination of Diosmin in pharmaceutical preparations:** R. T. SANE, T. G. CHANDRASHEKHAR, C. L. SAWANT, S. J. ACHARYA and N. N. GORE. (1 September 1986)
- Spectrophotometric determination of trace osmium in aqueous medium with a new reagent, 4-sulpho-2-aminobenzenethiol:** ANIL K. CHAKRABARTI. (1 September 1986)
- A graphical derivative approach for the photometric determination of lutetium and praseodymium mixtures:** F. GARCIA SANCHEZ, M. HERNANDEZ LOPEZ and J. C. MARQUEZ GOMEZ. (1 September 1986)
- Analytical properties of 2-nitro-5,6-dimethyl-1,3-indanedione dithiosemicarbazone:** Y. LINGAPPA, K. HUSSAIN REDDY and D. VENKATA REDDY. (1 September 1986)
- A special way of signal processing in multicomponent potentiometric titration:** A. PARCZEWSKI. (1 September 1986)
- An indirect complexometric method for the estimation of tin in alloys:** N. RUKMANI DESIKAN and M. VIKAYAKUMAR. (1 September 1986)
- Polarographic investigation of nickel complexation by morpholine in aqueous medium:** G. VISALAKSHI, S. V. NARASIMHAN and K. S. VENKATESWARLU. (1 September 1986)
- Determination of vanadium and nickel chelates with 2-(5-bromo-2-pyridylazo)-5-diethylaminophenol, with precolumn derivative formation, by reversed-phase liquid chromatography.** CHANG-SHAN LIN, XIAO-SONG ZHANG and YING-FAN YING. (1 September 1986)
- The effect of temperature on single-column ion-chromatography of metal ions:** NANCY E. FORTIER and JAMES S. FRITZ. (1 September 1986)
- Extraction and microdetermination of manganese(II) with Aliquat 336:** SOBHANA K. MENON, YADVENDRA K. AGRAWAL and MAHENDRA N. DESAI. (1 September 1986)
- Complexometric titration of thallium(III) with 4-amino-5-mercapto-3-propyl-1,2,4-triazole as replacing reagent:** NITYANANDA SHETTY A., R. V. GADAG and M. R. GAJENDRAGAD. (1 September 1986)
- Purification of solvents for liquid chromatography:** BOGUSLAW BUSZEWSKI, ROMAN LODKOWSKI and JERZY TROCEWICZ. (3 September 1986)
- Interfacing an analogue IR spectrometer to a microcomputer:** M. J. ADAMS and G. J. EWEN. (17 August 1986)
- Synthesis and analytical characterization of a chelating resin with dithizone:** J. CHWASTOWSKA and E. KOSIARSKA. (5 September 1986)
- Novel fluorescence reaction for malonitrile:** HARVEY W. YUROW. (8 September 1986)
- Kinetics and analytical applications of the ruthenium-catalyzed bromate oxidation of Bordeaux—I: Kinetics of the uncatalysed reaction:** J. T. AYODELE, B. G. COOKSEY and J. W. OTTAWAY (8 September 1986)
- Kinetics and analytical applications of the ruthenium-catalysed bromate oxidation of Bordeaux—II: Kinetics of the catalysed reaction:** J. T. AYODELE, B. G. COOKSEY and J. M. OTTAWAY. (8 September 1986)
- Spectrophotometric determination of primaquine phosphate with potassium iodate, potassium periodate, glucose-phosphoric acid and *p*-dimethylaminobenzaldehyde:** G. VASUDEVA PRASAD, Y. PULLA RAO and N KRISHNA MURTY. (8 September 1986)
- Spectrophotometric determination of microamounts of tantalum with *o*-chlorophenylfluorone and cetyltrimethylammonium bromide:** LUO ZONGMING and SHEN WEI. (8 September 1986)
- Artifacts of the decalin-molecular sieve system in the analysis of mineral waxes:** MUHAMMAD NAZIR, MUHAMMAD KHURSHID BHATTY and FRANK D. GUFFEY. (10 September 1986)
- Extraction of aromatic organic compounds by polyurethane foam:** L. SCHUMACK and A. CHOW. (10 September 1986)
- Co-precipitation of vanadium with iron by sodium tetrahydroborate:** MICHIKO MANIKI and KICHINOSUKE HIROKAWA. (15 September 1986)
- Application of microcomputers in the analytical laboratory—III: ASV analysis:** DRORA KAPLAN, DAN RAPHAELI and SAM BEN-YAAKOV. (15 September 1986)
- Quantitative estimation of substances spotted on filter paper, by photoacoustic spectroscopy:** T. SOMASUNDARAM, SANJAY S. R. RAO and P. GANGULY. (15 September 1986)
- Kinetic and oxidative aspects of treatment of some disaccharides with tetra-amminocuprate(II) in ammoniacal medium:** S. P. PANDEY and C. B. PANDEY. (15 September 1986)
- 1,2-Naphthoquinone-2-thiosemicarbazone as a new acid-base indicator in isopropyl and tert-butyl alcohol media:** ELISABETH BOSCH and MARTI ROSES. (15 September 1986)
- Extraction-spectrophotometric determination of strontium in calcium-rich materials with cryptand (2.2.2):** B. JUSKOWIAK. (15 September 1986)
- Improved microcombustion technique for nitrogen estimation in organotin complexes of *o*-carboxazine:** T. S. BASU BAUL. (15 September 1986)
- Photometric determination of selenium with ferrocene:** MINORI KAMAYA, TETASURO MURAKAMI and EIZEN ISHII. (16 September 1986)
- 2,6-Diacetylpyridine bis(arylhydrazone) derivatives as analytical reagents for uranium:** MARISSA BONILLA-ALVAREZ, MARGO PALMIERI, DEBRA DAVIS and JAMES S. FRITZ. (16 September 1986)

PAPERS RECEIVED

- Multiwavelength simultaneous spectrophotometric determination of iron(II) and iron(III) by flow-injection analysis:** M. BLANCO, J. GENE, H. ITURRIAGA, S. MASPOCH and J. RIBA. (30 June 1986)
- Kinetic-thermometric determination of Co(II), based on its catalytic effect on permanganate decomposition in basic media:** F. BORRULL and V. CERDA. (30 June 1986)
- A sub-microlitre two-photon ionization detector for high-performance liquid chromatography:** S. YAMADA, C. SAKANE and T. OGAWA. (25 June 1986)
- The speciation of trace amounts of organometallics in marine organisms by gel-permeation high-pressure liquid chromatography and reaction with PAR:** AMBROGIO MAZZUCOTELLI, ALDO VIARENGO, GABRIELLO MARTINO and ROBERTO FRACHE. (2 July 1986)
- Fluorimetric detection of polyaromatic hydrocarbons in Nigerian crude oil:** O. A. FAKANKUN and S. A. ADEYEMI. (7 July 1986)
- Complexes of nickel(II) with *S*-carboxyalkyl-L-cysteines in aqueous medium: Determination of enthalpies by thermometric titrimetry:** ROBERTO ARUGA. (7 July 1986)
- Determination of polynuclear aromatic hydrocarbons in water by flotation enrichment and HPLC:** BO-XING XU and YU-ZHI FANG. (9 July 1986)
- Speciation of manganese in freshwater—I: Use of EPR studies:** BARRY CHISWELL and MAZLIN BIN MOKHTAR. (9 July 1986)
- New reactions for making derivatives on *N*-nitrosamines:** O. O. P. FABOYA and O. R. IDOWU. (9 July 1986)
- Extraction-spectrophotometric determination of boron with 4,6-di-*tert* butyl-3-methoxycatechol and Ethyl Violet:** MITSUKO OSHIMA, KIYOM SHIBATA, SHOJI MOTOMIZU and KYOJI TÔEI. (9 July 1986)
- Determination of calcium and magnesium in limestone and dolomite by enthalpimetric flow-injection analysis:** WALACE A. DE OLIVEIRA and AFONSO S. MENDES. (11 July 1986)
- The separation of heavy metal chelates by HPLC:** H. J. M. BOWEN and WANNA WIMOLWATTANAPUNT. (14 July 1986)
- Drug determination in biological fluids—approaches to method validation:** ANIL C. MEHTA. (16 July 1986)
- Rapid extractive spectrophotometric determination of yttrium(III) with 1-(2-thiazolylazo)-2-naphthol:** U. G. GAOKAR, J. KRISHNAMA CHARYULU and M. C. ESHWAR. (16 July 1986)
- Extraction behaviour of cobalt(II)-2,4,6-tri-(2'-pyridyl)-1,3,5-triazine-tetraphenylborate complex in molten naphthalene:** B. K. PURI, M. SATAKE, K. ISHIDA and M. KATYAL. (16 July 1986)
- The determination of sulphur content in oil shale and shale oil:** RICHARD C. GRAHAM and ELIZABETH OGDEN. (18 July 1986)
- Uranyl complexes of α -carboxylpolymethylenediaminetetra-acetic acids:** A. MATILLA HERNANDEZ, S. GOLZALEZ GARCIA, J. M. TERCERO MORENO, M. CANDIDA T. A. VAZ and L. VILLAS BOAS. (18 July 1986)
- Analytical properties of *N*-benzothiazolyl-*N'*-alkyl thioureas:** H. GRESCHONIG. (21 July 1986)
- Formation constants for the complexes of 2-mercapto-3-phenylpropanoate with nickel(II) and hydrogen ions:** MONTSERRAT FILLELLA, NURIA GARRIGA and ALVARO IZQUIERDO. (21 July 1986)
- Application of a metallized membrane electrode for the determination of gaseous sulphur compounds after reductive pyrolysis:** JAN LANGMAIER, FRANTIŠEK OPEKAR and VĚRA PACÁKOVÁ. (25 July 1986)
- Microgram detection of aliphatic amines with 2,4-dinitroaniline in dimethylsulphoxide, dimethylformamide and acetone:** SAIDUL ZAFAR QURESHI and SEEMA HAQUE. (25 July 1986)
- Pentacyanoferrate(II) ions as reagents in determining HS-3:** NICOLETTA BURGER. (28 July 1986)
- Spectrophotometric determination of molybdenum with Bromopyrogallol Red sensitized with poly(vinylpyrrolidone):** J. HERNANDEZ MENDEZ, B. MORENO CORDERO and L. GUTIERREZ DAVILA. (28 July 1986)
- Spectrophotometric applications of oximes—a review:** K. SHRAVAH, R. K. SHARMA, SAHADEV and S. K. SINDHWANI. (1 August 1986)
- Acid-base ionization equilibria of 1-(2-carbamylethyl)-2-alkylimidazoles:** M. TERESA, S. D. VASCONCELOS and ADELIO A. S. C. MACHADO. (1 August 1986)
- Microdetermination of some stabilizing additives in propellants:** M. S. ROY, H. C. DWIVEDI, T. K. CHAKRABORTHY and I. C. SHUKLA. (1 August 1986)
- Deconvolution of ultraviolet absorption spectra of tricyclic antidepressant drugs in aqueous solution:** ANA C. MINGUEZ, MA. MERCEDES VELOZQUEZ and LICESIO J. RODRIGUEZ. (31 July 1986)
- Trace metal determination in animal tissues: Interlaboratory and method comparison:** R. WAGEMANN and F. A. J. ARMSTRONG. (6 August 1986)
- Analysis of the platinum group elements—an overview:** SILVE KALLMANN. (6 August 1986)
- Thin-layer chromatography of anions on antimonic acid and mixture of antimonic acid and silica gel 'G':** R. P. S. RAJPUT and ADITYA K. MISRA. (6 August 1986)
- Polarographic adsorptive complex wave of alkaline earths with thymolphthalexon:** ZHANG QING and HAUNG YUYING. (6 August 1986)
- A voltammetric study of the thiazolidine-4-carboxylic acid on mercury electrodes: Analytical applications:** J. L. MUÑIZ ALVAREZ, A. COSTA GARCIA, S. ARRIBAS JIMENO and P. TUÑON BLANCO. (6 August 1986)

PAPERS RECEIVED

- Review of the current status of methods for determining hydrogen in steels:** V. S. SASTRI. (2 June 1986)
- A study on the stability and photoacoustic spectroscopy of mercury(II) dithizonate:** NAI-LIN CHEN and EDWARD P. C. LAI. (2 June 1986)
- Highly sensitive spectrophotometric determination of osmium:** BASILIO MORELLI and PASQUALE PELUSO. (2 June 1986)
- Calculation of equilibrium constants from multiwavelength spectroscopic data—IV: Model-free least-squares refinement using evolving factor analysis:** HARALD GAMPP, MARCEL MAEDER, CHARLES J. MEYER and ANDREAS D. ZUBERBÜHLER. (2 June 1986)
- Amplification reactions: Origins, definitions, progress and present status:** D. THORBURN BURNS and ALAN TOWNSEND. (4 June 1986)
- Rapid spectrophotometric determination of palladium in titanium alloys with 2-(5-bromo-2-pyridylazo)-5-(diethylamino)phenol:** CHANG YUN PO and ZHOU NAN. (4 June 1986)
- A new facile and sensitive method for the spectrophotometric determination of ascorbic acid:** AMIR BESADA. (4 June 1986)
- Etude de la formation des complexes en solution aqueuse—III: Nouvelle méthode d'affinement des constantes de stabilité des complexes et des autres paramètres des titrages photométriques:** ROBERT FOURNAISE and CHRISTIAN PETITFAUX. (4 June 1986)
- Action des rayonnements β et des oxydants sur le B.H.T.; Analyse et structure des produits de dégradation:** C. MAJCHERCZYK, P. POLGE and F. PELLERIN. (4 June 1986)
- Desorption ionization/tandem mass spectrometry with a caesium ion source and a triple quadrupole mass spectrometer:** W. B. EMARY, I. ISERN-FLECHA, K. V. WOOD, T. Y. RIDLEY and R. G. COOKS. (6 June 1986)
- Constant Calcium Blue: An indicator for spectrofluorometric calcium analysis:** GERALDINE M. HUITINK. (6 June 1986)
- Extraction of zirconium and hafnium thiocyanate with polyurethane foam:** LIU JIN-CHUN and ARTHUR CHOW. (6 June 1986)
- A continuous hydride-generation system for direct-current plasma atomic-emission spectrometry (DCP-AES). Determination of arsenic and selenium:** PAUL EK and STIG-GORÄN HULDÉN. (9 June 1986)
- Solvent extraction of metal-4-(2-pyridylazo)-resorcinol complexes with dicyclohexyl-18-crown-6:** ABAJI G. GAIKWAD, HIDEYUKI NOGUCHI and MASAKI YOSHIO. (9 June 1986)
- Transport of alkali-metal picrates through liquid membranes: Coupled action of w/o microemulsion droplets and lipophilic crown-ether carriers:** ARISTOTELIS XENAKIS, CLAUDE SELVE and CHRISTIAN TONDRE. (9 June 1986)
- Liquid-liquid extraction separation and sequential determination of plutonium and americium in environmental samples by alpha spectrometry:** K. SEKINE, T. IMAI and A. KASAI. (9 June 1986)
- Behaviour of a copper ion-selective electrode in solutions of iron(III) ions:** ADAM HULANICKI and TADEUSZ KRAWCZYŃSKI VEL KRAWCZYK. (9 June 1986)
- Determination of rubidium, strontium and barium in barite by atomic-absorption spectrometry after dissolution in disodium ethylenediaminetetra-acetate:** J. G. SEN GUPTA. (9 June 1986)
- Piezoelectric air-pollution detectors with liquid crystal coating materials:** ADAM MIERZWINSKI and ZYGFRYD WITKIEWICZ. (9 June 1986)
- A PVC membrane pH-sensitive electrode based on methyldioctadecylamine (MDODA) as neutral carrier:** HAI-LONG WU and RU-QUIN YU. (9 June 1986)
- Acidity constants of benzidine in aqueous solutions:** G. B. REARTES, S. J. LIBERMAN and M. A. BLESÁ. (17 June 1986)
- Phthalhydrazidylazoacetylacetone as a chemiluminescent acid-base indicator:** N. THANKARAJAN and K. KRISHNANKUTTY. (17 June 1986)
- Anodic stripping voltammetric determination of arsenic at the glassy carbon electrode:** S. JAYA, T. PRASADA RAO and G. PRABHAKARA RAO. (17 June 1986)
- Manganese determination by solvent extraction and atomic-absorption spectroscopy:** F. SALINAS, M. JIMENEZ-ARRABAL and I. DURAN MERAS. (17 June 1986)
- An apparatus for the emission spectrometric determination of nitrogen released into an argon gas stream by chemical reactions in solution:** G. T. ABOU ZEID, J. B. HEADRIDGE and C. WHITE. (20 June 1986)
- Étude de l'adsorption de substances organiques sur l'amiante chrysotile par chromatographie en phase gazeuse:** H. MENARD, Y. LEFEBVRE and J. KHORAMI. (12 June 1986)
- The use of mathematical models in the characterization of ethylene oxide condensate surfactants by infrared and ultraviolet spectroscopy:** M. DE LA GUARDIA, J. E. TRONCH, J. L. CARRION and A. AUCEO. (23 June 1986)
- Electromigration of carrier-free radionuclide ions: Bismuth complexes in aqueous solutions of oxalic, fumaric and succinic acids:** F. RÖSCH, TRAN KIM HUNG, M. MILANOV and V. A. KHALKIN. (23 June 1986)
- The effect of inorganic particulates on the ASV signals of Cd, Pb and Cu:** T. U. AUALIITIA and W. F. PICKERING. (23 June 1986)
- Simultaneous determination of arsenic(III) and arsenic(V) in metallurgical processing media by ion chromatography:** LIANG K. TAN and JOHN E. DUTRIZAC. (24 June 1986)
- Simultaneous determination of histidine and histamine by second-derivative synchronous fluorescence spectroscopy:** M. C. GUTIERREZ, S. RUBIO, A. GOMEZ-HENS and M. VALCARCEL. (24 June 1986)
- Liquid-liquid extraction of metal ions by the 6-membered N-containing macrocycle hexacyclen:** S. ARPADJAN, M. MITEWA and P. R. BONTCHEV. (26 June 1986)
- A graphite-tube furnace for laser-excited atomic-fluorescence:** D. GOFORTH and J. D. WINEFORDNER. (30 June 1986)
- Chemical and electrochemical behaviour of nitric and nitrous acids in sulpholane:** A. BOUGHRIET and M. WARTEL. (30 June 1986)
- Spectrophotometric determination of griseofulvin in raw materials and tablets:** EZZAT M. ABDEL-MOETY and AZZA A. MOUSTAFA. (30 June 1986)

PAPERS RECEIVED

- Pharmacokinetics and the analytical chemist:** ANIL C. MEHTA. (2 May 1986)
- Determination of iodine-bromine numbers of some edible oils with two *N*-bromoimides:** C. MOHANA DAS and P. INDRASENAN. (6 May 1986)
- Spektralphotometrische Bestimmung organischer Verbindungen durch ternäre Komplexbildung I: Das Chelat FeY^- ($\text{H}_2\text{Y} = \text{EDTA}$) als analytisch funktionelle Gruppe für Phenole:** S. KOCH and G. ACKERMANN. (6 May 1986)
- An algorithm and a FORTRAN program CHEMEQUIL-2 for calculation of complex equilibria:** VIJAY S. TRIPATHI. (6 May 1986)
- Separation of iron(III) and iron(II) by polyurethane foam extraction:** K. LEPLA and A. CHOW. (6 May 1986)
- Accurate spectrophotometric determination of arsenic in zinc concentrates and other lead-zinc smelter roasted products:** R. RAGHAVAN, S. S. MURTI and C. S. RAO. (7 May 1986)
- Modified normal pulse polarography and its differential mode for determination of alkaline-earth metal ions in acid solutions:** MINORU HARA and NOBORU NOMURA. (7 May 1986)
- Simple colorimetric methods for the determination of enfenamic acid in pharmaceutical preparations:** R. T. SANE, U. A. GHORPADE and S. J. ACHARYA. (7 May 1986)
- A simultaneous colorimetric method for the determination of diloxanide furoate and tinidazole in combined dosage forms:** R. T. SANE, R. S. SAMANT and V. G. NAYAK. (7 May 1986)
- Simultaneous determination of the acid and basic ionization constants of imidazole:** M. TERES, S. D. VASONCELOS and ADELIO A. S. C. MACHADO. (7 May 1986)
- Physico-chemical properties of $\text{Mn(II)}-1-(2\text{-quinolyloxy})-2,4,5\text{-trihydroxybenzene}$ and spectrophotometric determination of micro amounts of manganese(II) in foodstuffs and chemical reagents:** ABDULHAMEED A. R. LAILA. (7 May 1986)
- Effects of vacuum on tetrakis-isocyanide complexes of silver(I) and copper(I): Implications for SIMS analyses:** LISA D. DETTER, STEVEN J. PACHUTA, R. G. COOKS and R. A. WALTON. (20 April 1986)
- Hydrogen enthalpimetry—I: Methods and apparatus:** D. W. ROGERS and B. J. SIEDMAN. (11 April 1986)
- Derivative spectrophotometric determination of micro amounts of zirconium in rocks and ores with arsenazo III:** CHANG-FA WANG. (24 April 1986)
- Potentiometric titration of aqueous solutions of $(\text{NH}_4)_3\text{TiO}_2\text{F}_5$ and determination of its acid-base constants:** J. HERNANDEZ MENDEZ, L. POLO DIEZ and M. J. ALMENDRAL PARRA. (12 May 1986)
- Spectrophotometric studies on the ion-association complex of palladium-tin(II) chloride-Crystal Violet in the presence of poly(vinyl alcohol):** MINZHENG ZHAO and SHENGWEN HU. (14 May 1986)
- Simple spectrophotometric method for determination of Cu(II) in pharmaceutical raw materials and in lotions, with salicylic acid as colour developer:** U. SAHA, A. K. SEN, J. GANGULY and K. BAKSHI. (14 May 1986)
- Kinetic determination of iodide, based on the chlorpromazine-bromate reaction:** P. VIÑAS, M. HERNANDEZ CORDOBA and C. SANCHEZ-PEDREÑO. (16 May 1986)
- Electron transfer in the systems Cu(II)/Cu(I) and $\text{I}_2/2\text{I}^-$ as the basis of an oxidimetric analytical method:** T. KOPEČ and W. RZESZUTKO. (16 May 1986)
- Separation of some transition metal ions on silica-immobilized 2-pyridinecarboxaldehyde phenylhydrazone:** SURASAK WATANESK and A. A. SCHILT. (14 May 1986)
- Fire-assay collection of gold and silver by copper:** A. DIAMANTATOS. (21 May 1986)
- Pretreatment for extraction-spectrophotometric determination of vanadium in pond sediment:** SADANOBU INOUE, SUWARU HOSHI and MUTSUYA MATSUBARA. (21 May 1986)
- A new chelating ion-exchanger containing *p*-bromophenyl-substituted hydroxamic acid functional groups—IV: Column separations on a hydroxamic acid resin:** AJAY SHAH and SUREKHA DEVI. (21 May 1986)
- Determination of trace manganese through the manganese-catalysed periodate-formaldehyde reaction, monitored by a periodate ion-selective electrode:** RU-QIN YU, YA-PING FENG, WEI-WEN HUANG and ZHEN-YAN GUO. (22 May 1986)
- Direct determination of trace organophosphates in chlorine-containing water by an enzymic method:** TINFA DU and SHIGUANG ZHOU. (22 May 1986)
- Determination of germanium by graphite-furnace atomic-absorption spectrometry:** YOSHIKI SOHRIN, KENJI ISSHIKI, TOORU KUWAMOTO and EIICHIRO NAKAYAMA. (22 May 1986)
- Application of Fourier transform technique to simultaneous resolution enhancement and smoothing of noisy spectra:** SSKO V. PIHLAJAMÄKI. (22 May 1986)
- Determination of the association of trace metals with naturally occurring colloids:** H. E. BJØRNSTAD and B. SALBU. (22 May 1986)
- Separation of selenium(IV) and tellurium(IV) from mixtures by extraction chromatography with trioctylphosphine oxide:** R. B. HEDDUR and S. M. KHOPKAR. (22 May 1986)
- Spectrophotometric determination of nickel in copper-base alloy with 2-(2-thiazolylazo)-*p*-cresol (TAC):** SERGIO LUIS COSTA FERREIRA. (22 May 1986)
- Solvent extraction of lithium and sodium with 4-benzoyl or 4-perfluoroacyl-5-pyrazolone and TOPO:** SHIGEO UMETANI, KOHJI MAEDA, SORIN KIHARA and MASAKAZU MATSUI. (26 May 1986)
- Determination of stability constants for alkaline-earth and alkali-metal ion complexes of glycine by spectrophotometry:** LEO HARJU. (26 May 1986)
- Spectrophotometric determination of tryptophan by a nitrosation reaction:** KRISHNA K. VERMA and ARCHANA JAIN. (28 May 1986)
- Determination of ultratrace amounts of cobalt by the catalysis of the Tiron-hydrogen peroxide reaction, with an improved continuous-flow analysis system:** KENJI ISSHIKI and EIICHIRO NAKAYAMA. (28 May 1986)
- Fluorescence in thin liquid films:** R. VON WANDRUSZKA and J. D. WINEFORDNER. (28 May 1986)

PAPERS RECEIVED

- Preparation, mesomorphic properties and behaviour as gas-chromatographic solvents of 4,4'-bis-biphenylene benzoates:** GIUSEPPE CHIAVARI, LUCIANA PASTORELLI and GEORGIOS PERRAKIS. (27 March 1986)
- Stability constants and molar absorptivities for complexes of copper(II) with *N*-methyldiethanolamine, 1,4-bis-(2-hydroxypropyl)-2-methylpiperazine, and 2-amino-2-methyl-1-propanol:** JOSEPH R. SIEFKER and RODOLFO V. AROC. (31 March 1986)
- Slope estimations from limited data:** G. L. SILVER. (2 April 1986)
- Stability order of the lanthanide chelates of two disubstituted 3-hydrox-4*H*-pyran-4-ones in aqueous solution:** RAJJA PETROLA, PAULA LAMPÉN and SEPPO LINDROOS. (2 April 1986)
- New methods for detection and spectrophotometric determination of submicrogram amounts of copper through redox reactions of the cyanocuprate(I) complex:** AMIR BESADA. (7 April 1986)
- Simultaneous multielement analysis of various human tissues by inductively-coupled plasma atomic-emission spectrometry:** KUNIO SHIRAIISHI, GI-ICHIRO TANAKA and HISAO KAWAMURA. (7 April 1986)
- Synthesis of 2-(3,5-dichloro-2-pyridylazo)-5-dimethylaminophenol and its application to the determination of cobalt by spectrophotometry:** MASAOKI NAKAMURA, YUTAKA SAKANASHI, HIROAKI CHIKUSHI, FUMIAKI KAI, SHIGEYA SATO, TOSHIE SATO and SUMIO UCHIKAWA. (9 April 1986)
- Measurement of the diffusion coefficients of Zr(IV) in aqueous and non-aqueous solutions by use of an analytical ultracentrifuge:** V. FRIEHMELT, CH. FRYDRYCH, M.-L. YE and G. MARX. (24 February 1986)
- 1-(2-Quinolylazo)-2,4,5-trihydroxybenzene as a spectrophotometric reagent for cobalt(II) and copper(II) determination:** ABDULHAMEED A. LAILA. (10 April 1986)
- Colour changes of redox and screened indicators for direct titration of ascorbic acid with Ce(IV):** J. MARTINEZ CALATAYUD, R. MARIN SAEZ and M. PASCUAL MARTI. (14 April 1986)
- Determination of protonation constants by coulometric titration:** STANISŁAW GĘŻB, ELZBIETA SKRZYDLEWSKA and ADAM HULANICKI. (14 April 1986)
- All-solid-state trimethoprim ion-selective electrode:** SHOU-ZHOU YAO, JING SHIAO and LI-HUA NIE. (21 March 1986)
- o*-Dianisidine as a colorimetric reagent for vanadium:** L. P. PANDEY, B. SINGH and K. K. PADHI. (18 April 1986)
- Detection methods in flow-injection analysis—a review:** DAVID J. PASS, S. MARK TROTMAN and JAMES AVRAAMIDES. (18 April 1986)
- Thermodynamics of the formation of Mn(II), Fe(II), Co(II), Ni(II), Cu(II) and Zn(II) complexes with 2,3-dihydroxy-naphthalene and chromotropic acid:** J. K. NEPAL and S. N. DUBEY. (26 April 1986)
- Extraction and spectrophotometric determination of molybdenum(VI) with Malachite Green and *p*-chloromandelic acid:** SHIGEYA SATO, MARI IWAMOTO and SUMIO UCHIKAWA. (26 April 1986)
- Dosage des acides faibles en milieu ammonium quaternaire concentré:** D. BAYLOCOQ, W. KAYATA and F. PELLERIN. (26 April 1986)
- Studies on synthesis of a new colour reagent bromophosphonazo-pSN-BPA-pSn and its colour reactions with rare-earth elements:** BIN-CAI WU, YU-XIN QU, HENG-CHUAN LIU, CHENG WU and XING-QIANG ZHU. (26 April 1986)
- Determination of cadmium, lead and copper in milk and milk powder by means of flow potentiometric stripping analysis:** L. ALMESTRAND, D. JAGNER and L. RENMAN. (26 April 1986)
- pK_a values of *N,N,N',N'*-tetrakis(2-hydroxypropyl)ethylenediamine:** R. MCMAHON, M. BRENNAN and J. D. GLENNON. (28 April 1986)
- Some ion-exchange resins for anion chromatography:** ALI S. AL-OMAIR and SAMUEL J. LYLE. (28 April 1986)
- Continuous-flow determination of chloride in the non-linear response region by using a tubular chloride ion-selective electrode:** HIROKAZU HARA, YOSHIKI WAKIZAKA and SATOSHI OKAZAKI. (28 April 1986)
- Anion-exchange enrichment and spectrophotometric determination of uranium in sea-water:** ROKURO KURODA, KOICHI OGUMA, NORIKO MUKAI and MASATOSHI IWAMOTO. (28 April 1986)
- A vancomycin determination by coulometric generation of copper ions:** D. ANDRE, J. CHASTANG, C. CHABENAT, D. BLANC-CONTINSOUZA and P. BOUCLY. (26 April 1986)
- Simultaneous determination of uranium(IV) and hydrazine—a novel technique:** N. S. B. SINGH, S. V. MOHAN, P. J. UPADHYAYA and G. R. BALASUBRAMANIAN. (28 April 1986)
- Polarographic behaviour of 3-(2'-thiazolylazo)-2,6-diaminopyridine: Effect of a new surfactant:** ALI Z. ABU ZUHRI, SH. M. ZOURB and J. SHALABI. (28 April 1986)
- Ultra-trace molybdenum determinations in biological samples by graphite-furnace atomic-absorption spectrometry:** SCOTT P. ERICSON, MICHAEL L. MCHALSKY and BRUNO JASELSKIS. (28 April 1986)

PAPERS RECEIVED

- Characterization of interferences in analytical methods—I: Computation and application of non-specific coefficients as correction factors:** B. S. FERNANDEZ BAND, E. RUBIO and A. L. ALLAN. (7 March 1986)
- Characterization of interferences in analytical methods—II: Experimental verification on a spectrophotometric direct method:** B. S. FERNANDEZ BAND, E. RUBIO and A. L. ALLAN. (7 March 1986)
- Stabilities of bivalent metal complexes with biologically active 2-hydroxy-1,4-naphthoquinone monosemicarbazone (HNQS) in dioxan-water mixtures:** RAKESH KUMAR SHARMA and SHARWAN KUMAR SINDHWANI. (12 March 1986)
- Electrodeless reduction and colorimetric determination of silver, copper and nickel:** GHAZI AL-JABARI and BRUNO JASELSKIS. (12 March 1986)
- Evaluation of the calibration approach to quantification in flow potentiometric stripping analysis:** BOY HØYER and LARS KRYGER. (12 March 1986)
- Fuzzy linear-weight transformation simplex method and its application in analytical chemistry:** CHEN GUONAN. (17 March 1986)
- Studies of hydrodynamic voltammetry at tubular electrodes—III: Determination of trace amounts of bismuth by differential-pulse anodic-stripping voltammetry at glassy-carbon tubular electrodes with *in situ* mercury plating:** WAN ZHEN and CHEN QIANG. (18 March 1986)
- Spectrometric analysis of non-metals introduced from a graphite furnace into a microwave-induced plasma:** JAROSLAV P. MATOUSEK, BRIAN J. ORR and MARK SELBY. (18 March 1986)
- Trace measurements of the antineoplastic agent methotrexate by adsorptive stripping voltammetry:** JOSEPH WANG, PENG TUZHI, MENG-SHAN LIN and TIM TAPIA. (18 March 1986)
- Rapid solvent extraction and separation of gallium, indium and thallium with *n*-octylaniline:** SHASHIKANT R. KUCHEKAR and MANOHAR B. CHAVAN. (18 March 1986)
- A study of bright Pt electrodes as pH electrodes:** J. M. FERNANDEZ ALVAREZ, A. COSTA GARCIA and P. TUÑON BLANCO. (21 March 1986)
- Effect of speciation on uptake and toxicity of cadmium to *Crangon crangon* I shrimps:** M. L. S. SIMOES GONCALVES, F. M. C. VILHENA, L. M. V. F. MACHADO, C. M. R. PESCADÁ and M. LEGRAND DE MOURA. (21 March 1986)
- Determination of sulphha-drugs with all-solid-state sulphha-drug sensitive electrodes:** SHOU-ZHOU YAO, JING SHIAO and LI-HUA NIE. (21 March 1986)
- Fluorimetric and absorptometric determination of dissociation constants and chromogenic reactions of benzyl-2-pyridyl ketone 2-quinoloylhydrazone:** F. GARCIA SANCHEZ, C. CRUCES BLANCO and J. MEDINILLA. (21 March 1986)
- Spectrophotometric evaluation of acidity constants: Can a diprotic acid be treated as a monoprotic one?:** A. G. ASUERO and A. G. GONZALEZ. (21 March 1986)
- TBA⁺Br⁻-HTTA/MIBK extraction for AAS determination of cobalt, nickel, and manganese in copper ore and concentrate:** BARBARA RÓŻAŃSKA and ELWIRA LACHOWICZ.
- Direct flame atomic-absorption determination of minor elements in argillites:** E. KLAOS, R. TALKOP and V. ODINETS. (24 March 1986)
- Direct determination of metals in milligram amounts and microlitre volumes by direct-current argon-plasma emission-spectrometry with sample introduction by electrothermal vaporization:** PETER G. MITCHELL and JOSEPH SNEDDON. (26 March 1986)
- Spectrophotometric determination of organic matter in soils, plants and organic manures by the dichromate method:** YIN TIAN-SHOU and CHIAO MING-LWEN. (26 March 1986)
- Kinetic-spectrophotometric determination of nanogram levels of manganese by use of salicylaldehyde guanyldiazone-hydrogen peroxide system:** F. SALINAS, J. J. BERZAS NEVADO and P. VALIENTE GONZALEZ. (26 March 1986)
- Spectrophotometric reaction-rate method for the determination of nitrite in waters with pyridine-2-aldehyde 2-pyridylhydrazone:** R. MONTES and J. J. LASERNA. (26 March 1986)
- Identification of twelve 1,4-benzodiazepines by a combination of gas-chromatography and high-performance liquid chromatography:** M. BAKAVOLI and M. M. HERAVI. (26 March 1985)
- Ion-pair extraction study of strontium (2.2.2) cryptate with Erythrosin B: Spectrophotometric determination of Sr(II):** BERNARD JUSKOWIAK. (26 March 1986)
- A wet chemical method for the estimation of carbon in uranium carbides:** V. CHANDRAMOULI, R. B. YADAV and P. R. VASUDEVA RAO. (26 March 1986)

PAPERS RECEIVED

- Spectrophotometric determination of some insecticides with 3-methyl-2-benzothiazolinone hydrazone hydrochloride:** C. S. P. SASTRY and D. VIJAYA. (13 February 1986)
- Comparison of inorganic films and poly(4-vinylpyridine) coatings as electrode modifiers for flow-injection systems.** JAMES A. COX and KRISHNAJI R. KULKARNI. (17 February 1986)
- Solvent extraction of rare-earth elements with hexa-aza-18-crown-6 and Erythrosin A:** WALENTY SZCZEPANIAK, WANDA CISZEWSKA and BERNARD JSUKOWIAK. (17 February 1986)
- Spectrophotometric determination of the light rare earths with a new reagent, arsenazo-DCS:** F. YIN, L. P. HU, Y. R. ZHU and G. W. ZHAO. (18 February 1986)
- A new chemiluminescence system EtOH-H₂O₂-Co(II)-KOH and its analytical application to cobalt:** M. G. LU, M. F. LING, H. CUI and F. YIN. (18 February 1986)
- Determination of trace amounts of the flotation collectors ethylxanthate and diethyldithiophosphate in aqueous solutions by cathodic stripping voltammetry:** ARI IVASKA and JAAKKO LEPPINEN. (21 February 1986)
- Differential-pulse polarographic determination of thiol collector and sulphide ions:** JAAKKO LEPPINEN and SUSANNA VAHTILA. (21 February 1986)
- Chelex 100 for preconcentration of bismuth from sulphide ores, concentrates, metals and alloys:** J. S. ADSUL, C. C. DIAS, S. G. IYER and CH. VENKATESWARLU. (21 February 1986)
- Potentiometric study of silver ion co-ordination with azo dyes:** J. KATONA-BALÁZS, G. MOLNÁR, ZS. NEMES-VETÉSSY and K. BURGER. (21 February 1986)
- The utility of charge-transfer complexation in the spectrophotometric determination of some monosaccharides through their osazones:** MAGDA AYAD, SAEED BELAL, AFAF ABOU EL KHEIR and SOBHI EL ADL. (21 February 1986)
- Spectrophotometric determination of iron by extraction of the iron(II)-5,5-dimethyl-1,2,3-cyclohexanetrione-1,2-dioxime-3-thiosemicarbazone complex: Determination of iron in water:** F. SALINAS, T. GALEANO DIAZ and J. C. JIMENEZ SANCHEZ. (21 February 1986)
- The electrochemical generation of small amounts of hydrogen cyanide:** ZUZANA TOCKSTEINOVÁ and FRANTIŠEK OPEKAR. (24 February 1986)
- Chromatography of chlorophylls and bacteriochlorophylls:** JOSE A. S. CAVALEIRO and KEVIN M. SMITH. (24 February 1986)
- Determination of trace amounts of nickel by atomic-absorption spectrometry after carbonyl generation:** J. ALARY, J. VANDAELE, C. ESCRIEUT and R. HARAN. (25 February 1986)
- Effect of temperature on the determination of aromatic nitro compounds by coulometrically generated chromium(II):** ISMAIL M. AL-DAHER and BYRON KRATOCHVIL. (25 February 1986)
- Spectrophotometric determination of arsenic from an organic phase:** E. N. VASANTA. (25 February 1986)
- Oxidizing and masking agents in volatile covalent hydride-atomic-absorption spectrometry (VCH-AAS): Determination of lead in blood:** J. R. CASTILLO, J. M. MIR, C. MARTINEZ and M. C. RAMIREZ. (26 February 1986)
- Two-phase titration of cationic surfactants in alkaline solution:** MASAHIRO TSUBOUCHI, YOKO NITTA and TAKAHIRO KUMAMARU. (27 February 1986)
- Dissociation constants of arsenazo III:** IRENA NĚMCOVÁ, BOREK METAL and JAROSLAV PODLAHA. (27 February 1986)
- How to measure heavy-atom kinetic isotope effects:** PIOTR PANETH. (4 March 1986)
- Micellar modification of the fluorescence spectral, intensity and lifetime characteristics of fluorescein-labelled phenobarbital:** TERESA L. KEIMIG and LINDA B. MCGOWN. (19 February 1986)
- Analytical applications of the technique of solid-liquid separation after liquid-liquid extraction:** B. K. PURI, M. KATYAL and M. SATAKE. (4 March 1986)

PAPERS RECEIVED

- Non-aqueous titration of hydrochlorides of phenothiazine derivatives, with silver perchlorate:** N. A. ZAKHARI, S. M. AHMED and M. I. WALASH. (10 January 1986)
- Sensitive spectrophotometric determination of nitrogen:** QIU XING-CHU and ZHU YINZ-QUAN. (10 January 1986)
- Fluorimetric determination of pyrimethamine in pharmaceutical preparations:** PYARE PARIMOO. (10 January 1986)
- 4,5-Dibromo-*o*-nitrophenylfluorone, a new reagent for the spectrophotometric determination of micro amounts of tantalum in the presence of niobium:** WU ZHENG, YU CHAO-SHENG and JIA XI-PING. (10 January 1986)
- Four-component computing systems for analysis by infrared spectroscopy:** LONG-BIAO YING and YI-YING LIU. (13 January 1986)
- Dosage colorimétrique des ions cyanures par formation du complexe mixte bis(bathophenanthroline)dicyano fer(II):** M. MARIAUD and P. LEVILLAIN. (15 January 1986)
- Les possibilités réactionnelles de la dichloro-2,6 quinone chlorimine (DC-QC)—I: Considérations théoriques sur la réaction de Gibbs:** BRUNO BADER, JOSYANE LACROIX, ROGER LACROIX and CLAUDE VIEL. (13 January 1986)
- Les possibilités réactionnelles de la dichloro-2,6 quinone chlorimine (DC-QC)—II: Les colorants d'indophénol et les applications de la réaction de Gibbs:** BRUNO BADER, JOSYANE LACROIX, ROGER LACROIX and CLAUDE VIEL. (13 January 1986)
- Nitrate-selective electrode based on bis(triphenylphosphine)iminium salts:** G. WERNER, I. KOLOWOS and J. ŠENKÝŘ. (13 January 1986)
- Construction of a perhenate ion-selective electrode:** K. BENEŠOVÁ, J. ŠENKÝŘ, I. KOLOWOS and G. WERNER. (13 January 1986)
- Direct potentiometric determination of manganese in water by means of a permanganate-selective electrode:** K. BENEŠOVÁ, J. ŠENKÝŘ, Z. GLATZ, M. VRCHLABSKÝ, I. KOLOWOS and G. WERNER. (13 January 1986)
- Oxydation électrochimique de la khelline et de l'amikhelline: Etude par voltammétrie cyclique:** J. M. KAUFFMANN, G. J. PATRIARCHE, M. CHATEAU-GOSSELIN and B. L. GALLO-HERMOSA. (13 January 1986)
- Diffusion coefficients and complex equilibria in solution—V: Limitations to the validity of the diffusion equations:** D. R. CROW. (13 January 1986)
- Use of *N*-benzyl-2-naphthohydroxamic acid as a highly selective reagent for solvent extraction and spectrophotometric determination of vanadium(V):** BASANT SAHU and USHA TANDON. (17 January 1986)
- Evaluation of coupled transport across a liquid membrane as an analytical preconcentration technique:** JAMES A. COX, ATUL BHATNAGAR and ROBERT W. FRANCIS JR. (22 January 1986)
- Rapid distillation of boron in steel as methyl borate for ICP atomic emission spectrometric determination:** MINORU HOSYA, KŌICHI TOZAWA and KUNIO TAKADA. (22 January 1986)
- Microdetermination of copper in brass and water on tin(IV) antimonophosphate by ion-exchanger colorimetry:** P. S. THIND and S. K. MITTAL. (21 January 1986)
- Determination of molybdenum, chromium and vanadium by ion-pair high-pressure liquid chromatography based on precolumn chelation with 4-(2-pyridylazo)resorcinol:** ZHANG XIAO-SONG, ZHU XIANG-PING and LIN CHANG-SHAN. (24 January 1986)
- Interference by aluminium species in fluoride ion determinations: Competing equilibria effects:** W. F. PICKERING. (27 January 1986)
- Dosage des xanthiques naturels par C.L.H.P.: Comparaison des méthodes et applications:** M. F. VERGNES and J. ALARY. (27 January 1986)
- Non-aqueous fluorimetric determination of scandium in silicate rocks:** F. GARCIA SANCHEZ, C. CRUCES BLANCO and A. HEREDIA BAYONA. (27 January 1986)
- Design and evaluation of an electrochemical sensor for dissolved oxygen determination in water:** S. QUINTAR DE GUZMAN, O. M. BAUDINO and V. A. CORTINEZ. (27 January 1986)
- A computer-based flow-injection analysis system for continuous monitoring of trace and macroconcentrations:** LUIS A. FERNANDEZ, JOSE L. APARICIO and MAMOUN MUHAMMED. (28 January 1986)
- Fluorometric determination of nitrite in natural waters with 3-amino-1,5-naphthalenedisulphonic acid by flow-injection analysis:** SHOJI MOTOMIZU, HIROSHI MIKASA and KYOJI TŌEI. (28 January 1986)
- Methods of increasing the efficiency of luminescent analysis of inorganic substances:** L. E. ZEL'TSER, SH. TALIPOV and N. G. VERECHAGINA. (29 January 1986)
- Determination of neodymium concentration from absorption spectra.** CH. GOPINATH, S. V. J. LAKSHMAN and S. BUDDHUDU. (30 January 1986)
- Iodometric determination of aryldialkylamine *N*-oxides:** A. H. KHUTHIER, A. S. AL-KAZZAR and D. AMIN. (31 January 1986)
- Rapid, sensitive spectrophotometric method for the determination of piperazine:** SALWA R. EL-SHABOURI, FARDOUS A. MOHAMED, ABDEL-MABOUD I. MOHAMED. (31 January 1986)
- Determination of optical purity in partially racemized samples of L-aspartic acid by means of liquid crystals:** GIOVANNA BERTOCCHI. (4 February 1986)
- Determination of organically-associated trace metals in estuarine sea-water by solvent extraction and atomic-absorption spectrometry:** KOHJI HAYASE, KIMINOI SHITASHIMA and HIROYUKI TSUBOTA. (7 February 1986)
- Microdetermination of iron in water by chelating ion-exchanger colorimetry:** CHUEN-YING LIU and HUAN-TSUNG CHANG. (11 February 1986)
- Extraction-spectrophotometric determination of vanadium with *N*-*m*-tolyl-*N*-phenylhydroxylamine and its application to coal and coal fly-ash:** SADANOBU INOUE, SUWARU HOSHI and MUTSUYA MATSUBARA. (11 February 1986)
- Kinetic fluorimetric determination of organic peroxides and lipohydroperoxides at the nanomole level:** J. PEINADO, F. TORIBIO and D. PEREZ-BENDITO. (11 February 1986)
- Composite modified simplex optimization of HPLC coupled with photometric detection:** S. AL-NAJAFI, C. A. WELLINGTON, A. P. WADE, T. J. SLY and D. BETTERIDGE. (11 February 1986)

PAPERS RECEIVED

- Extractive spectrophotometric determination of trace amounts of iron(III) with benzyltriethylammonium chloride:** K. C. BAYAN and H. K. DAS. (5 November 1985)
- Studies on some colour reactions of zinc-dye complexes in the presence of surfactants:** WENBIN QI and WEIQIANG GUO. (7 November 1985)
- Preconcentration and determination of ultratraces of lead and bismuth:** CORRADO SARZANINI, EDOARDO MENTASTI, MARIA CARLA GENNARO, VALERIO PORTA and PAOLO VOLPE. (7 November 1985)
- One-point titration of metal ions and ligands by measuring the change in pH:** ANDRZEJ LEWENSTAM, ARI IVASKA and ERKKI WÄNNINEN. (7 November 1985)
- A new method for the voltammetric determination of nitrite:** KURT KALCHER. (7 November 1985)
- Continued investigation of the diazotization-coupling spectrophotometric technique for the determination of aromatic amines with 8-amino-1-hydroxynaphthalene-3,6-disulphonic acid and *N*-(1-naphthyl)ethylenediamine as coupling agents:** GEORGE NORWITZ and PETER N. KELIHER. (1 November 1985)
- Spectrophotometric determination of nitrazepam in tablets:** SALWA RIZK EL-SHABOURI. (11 November 1985)
- Thin-layer chromatography with low-volatility mobile phases:** V. G. BEREZKIN and S. L. BOLOTOV. (11 November 1985)
- Effect of deposited metals on background of a carbosil electrode: Stripping voltammetry:** A. N. DORONIN and S. M. BENIAMINOVA. (11 November 1985)
- Determination of oxygen in fusible metals with solid electrolytic cells:** L. L. KUNIN, A. A. BOGDANOV and V. I. RODIONOV. (11 November 1985)
- Degradation of nitrilotriacetic acid (NTA) by oxidation with lead dioxide suspension:** TOSHIO MATSUDA and TOYOSHI NAGAI. (11 November 1985)
- Determination of the optimum working range in spectrophotometric procedures:** A. G. ASUERO, G. GONZALEZ, F. DE PABLOS and J. L. GOMEZ ARIZA. (11 November 1985)
- Formation constants of some Hg(II) complexes, as determined from their anodic polarographic signals:** M. ESTEBAN, E. CASASSAS and L. FERNANDEZ. (13 November 1985)
- The influence of thiourea on the cation-exchange behaviour of various elements in dilute nitric and hydrochloric acids:** C. H.-SIEGFRIED W. WEINERT, FRANZ W. E. STRELOW and REINHARD G. BÖHMER. (18 November 1985)
- Discussion of distribution of chromium(VI) species in solution:** TONG SHEN-YANG and LI KE-AN. (19 November 1985)
- Spectrophotometric determination of tungsten(VI) with rutin and cetyltrimethylammonium bromide:** MINLIANG XU and GORDON A. PARKER. (19 November 1985)
- Spectrophotometric determination of mercury(II) and silver(I) with copper(II) and diethyldithiocarbamate in the presence of Triton X-100:** M. C. GARCIA ALVAREZ-COQUE, R. M. VILLANUEVA CAMAÑAS, M. C. MARTINEZ VAYA, G. RAMIS RAMOS and C. MONGAY FERNANDEZ. (22 November 1985)
- Direct fluorescent detection of amino-acids separated by TLC, with 9-isothiocyanatoacridine derivatives:** C. SÂRBU, C. MĂRUTOIU, M. VLASSA and C. LITEANU. (24 November 1985)
- Determination of traces of EDTA, EGTA and CDTA by adsorptive accumulation of their complexes with Hg(II), followed by cathodic stripping:** MAŁGORZATA CISZKOWSKA and ZBIGNIEW STOJEK. (24 November 1985)
- The analysis of ferroalloys:** R. S. YOUNG. (24 November 1985)
- Composition and formula of the reagent "basic cupric carbonate":** FREDERICK C. STRONG III and KATIA FERRAZ SANTANA. (27 November 1985)
- Determination analysis of anthranilic acid by liquid chromatography:** THOMAS M. SCHMITT, ROBERT J. ZIEGLER, EAD S. MUZHER, ROBERT J. DOYLE and JAMES L. FREERS. (27 November 1985)
- A new liquid-membrane electrode for selective determination of perchlorate:** SAAD S. M. HASSAN and M. M. ELSAIED. (30 November 1985)
- Spectrophotometric and fluorimetric determination of nomifensine maleate:** ABDEL-AZIZ M. WAHBI, MOHAMMAD A. ABOUNASSIF, EL-RASHEED A. GAD-KARIEM and HASSAN Y. ABOUL-ENEIN. (30 November 1985)
- Spectrophotometric and first derivative spectrophotometric determination of magnesium with 1-hydroxy-2-carboxyanthraquinone:** F. SALINAS, A. MUÑOZ DE LA PEÑA and J. A. MURILLO. (6 December 1985)
- X-Ray diffraction data for six analgesics:** J. E. KOUNTOURELLIS, F. A. UNDERWOOD, P. P. GEORGAKOPOULOS and A. RAPTOULI. (9 December 1985)
- Determination of elemental boron in tetra-arylborates by d.c. argon-plasma emission spectrometry:** AGNES YOO, CARL E. MOORE, RUPERT JONES and AARON SYNSTEBY. (13 November 1985)
- Di-(acetothioacetanilido)methane as a gravimetric reagent for nickel and cobalt:** T. PAL, A. GANGULY, D. S. MAITY and STANLEY E. LIVINGSTONE. (11 December 1985)
- Polarographic studies of mixed hydroxy-complexes of monoethanolamine with cadmium and with lead:** F. ARCE, C. BLANCO and J. CASADO. (11 December 1985)
- Application of a combination of analytical techniques in the multicomponent analysis of metal alloys:** P. KOSCIELNIAK and A. PARCZEWSKI. (11 December 1985)
- The speciation of manganese in freshwaters: (with special reference to the use of EPR spectroscopy):** BARRY CHISWELL and MAZLIN MOKHTAR. (13 December 1985)
- Individual rare-earth element determination in monazites by neutron-activation analysis:** R. PARTHASARATHY, H. B. DESAI and S. R. KAYASTH. (16 December 1985)
- Formation and stability of zinc(II) and cadmium(II) citrate complexes in aqueous solution at different temperatures:** SANTI CAPONE, ALESSANDRO DE ROBERTIS, CONCETTA DE STEFANO and SILVIO SAMMARTANO. (16 December 1985)

- Phototautomerism in the lowest excited singlet state of 1-hydroxy-2-carboxyanthraquinone:** F. SALINAS, A. MUÑOZ DE LA PEÑA and J. A. MURILLO. (16 December 1985)
- The analysis of 1,4-benzodiazepines by capillary-column gas chromatography and HPLC:** I. R. TEBBETT, M. ANDERSON and B. CADDY. (20 December 1985)
- Spectrophotometric determination of nickel by ammonium (5'-chloro-2',3'-dihydropyridyl-4'-azo)benzene-4-arsenate:** SWARAN LATA, Y. S. VARMA and B. S. GARG. (20 December 1985)
- Studies of hydrodynamic voltammetry at tubular electrodes—III: Determination of trace amounts of bismuth by differential-pulse anodic-stripping voltammetry at a glassy-carbon tubular electrode with *in situ* mercury plating:** WAN ZHEN and CHEN QIANG. (20 December 1985)
- ¹H NMR structural study of phosmethylan:** Zs. H.-KOVÁCS. (27 December 1985)
- ETA-AAS investigations of Sc, Tb, Eu and Yb with different metal carbide-coated pyrographite atomizers and matrix modifiers—I:** FADHIL JASIM and NADHUM A. N. AWAD. (31 December 1985)
- Solvent extraction of copper with *N-p*-octyloxybenzoyl-*N*-phenylhydroxylamine:** SADANOBU INOUE, KOUZO MICHITSUJI, SUWARU HOSHI and MUTSUYA MATSUBARA. (31 December 1985)
- Etude de l'interaction ion-ammonium tétramines cycliques par pH-métrie et RMN à l'aide du programme MICMAC:** ELISABETH SUET and ANDRE LAOUEANAN. (31 December 1985)
- Les cristaux d'oxalate de sodium et cuivre: Obtention, identification, détermination de la morphologie et des propriétés optiques:** R. PULOU, C. TRICHE, B. BARBIER and G. PITET. (31 December 1985)
- Selective collection of selenium(IV) and selenium(VI) by the use of anion-exchange resin loaded with bismuthiol-II sulphonic acid:** MORIO NAKAYAMA, TOMOO TANAKA, MOTOKO TANAKA, MASAHIKO CHIKUMA, KAZUO ITOH, HIROMU SAKURAI, HISASHI TANAKA and TERUMICHI NAKAGAWA. (4 January 1986)
- Determination of borate ion-pair stability constants by potentiometry and a non-approximative linearization of titration data:** HOWARD R. ROGERS and CONSTANT M. G. VAN DEN BERG. (6 January 1986)
- Voltammetric determination of benzidine and its derivatives on a glassy carbon electrode:** JIŘÍ BAREK, ANTONÍN BERKA, ZUZANA TOCKSTEINOVÁ and JIŘÍ ZIMA. (6 January 1986)
- Fluorimetric differential-kinetic determination of silicate and phosphate in waters by flow-injection analysis:** P. LINARES, M. D. LUQUE DE CASTRO and M. VALCARCEL. (6 January 1986)

PAPERS RECEIVED

- Adsorption of metals on activated carbon from aqueous solutions:** HIDEKO KOSHIMA and HIROSHI ONISHI. (30 September 1985)
- Extraction and spectrophotometric determination of titanium(IV) with alizarin and fluoride:** R. LOPEZ NUÑEZ, M. CALLEJON MOCHON and A. GUIRAUM PEREZ. (1 October 1985)
- Potentiometric determination of fluorine in silicate rocks with an ion-selective electrode and a novel decomplexing agent:** GILBERTO CALDERONI. (1 October 1985)
- Simple sample-cell positioner for reducing the imprecision due to placement of test-tube shaped sample cells:** J. D. INGLE, JR. (2 October 1985)
- The role of the auxiliary electrode in electrochemical detectors for microbore chromatography:** SAM A. MCCLINTOCK. (3 October 1985)
- Electrochemical behaviour of As on the mercury drop electrode: Development of a procedure to determine micro-amounts of arsenic in natural samples by cathodic stripping voltammetry:** G. GILLAIN, R. MACHIROUX and P. PITTANCE. (4 October 1985)
- Preconcentration of metal ions from natural water samples on a resin modified by SPADNS:** M. L. MARINA, V. GONZALEZ and A. R. RODRIGUEZ. (10 October 1985)
- Adduct formation of nickel chelates of 4-methyl and 2-methyl-8-quinolins with heterocyclic nitrogen bases:** KUMAR S. MATH and T. SURESH. (10 October 1985)
- Determination of inorganic acid content in some industrial organic acids by GPC:** Zs. WITTMANN. (10 October 1985)
- Spectrophotometric determination of paraquat with BiI_4^- in the presence of gum arabic:** P. TAÑEZ-SEDEÑO and L. M. POLO DIEZ. (10 October 1985)
- Spectrophotometric determination of iron in process samples from the chemical cleaning of coal:** COLIN D. CHRISWELL, RICHARD, G. RICHARDSON and RICHARD MARKUSZEWSKI. (15 October 1985)
- Potentiometric titration of fulvic acids from lignite, in dimethylformamide and dimethylsulphoxide:** JOSE M. ANDRES, C. ROMERO and JOSE M. GAVILAN. (9 October 1985)
- Determination of Se in sea-water by pulse cathodic stripping voltammetry of piarselenol:** PH. BREYER and G. GILLAIN. (16 October 1985)
- Multiparametric curve fitting—XII: Resolution capability of two multicomponent spectra analysing programs, SQUAD(84) and PSEQUAD(83):** MILAN MELOUN, MILAN JAVŮREK and ALENA HYNKOVÁ. (18 October 1985)
- Mathematical treatment of absorbance vs. pH graphs of polyprotic acids:** A. G. ASUERO, J. L. JIMENEZ-TRILLO and M. J. NAVAS. (22 October 1985)
- Spectrophotometric evaluation of acidity constants—III: Graphical methods for overlapping two-step equilibria:** A. G. ASUERO, J. L. JIMENEZ-TRILLO and M. J. NAVAS. (22 October 1985)
- The analysis of volatile components of thermodynamically non-equilibrium systems:** R. V. GOLOVNYA. (15 October 1985)
- Concentration, separation and determination of scandium, zirconium, hafnium and thorium with a silica-based sulphonic cation-exchanger:** I. P. ALIMARIN, V. I. FADEEVA, G. V. KUDRYAVTSEV, I. M. LOSKUTOVA and T. I. TIKHOMIROVA. (15 October 1985)
- 5-Azo derivatives of rhodanine and analogues in the analytical chemistry of noble metals:** S. B. SAVVIN and R. F. GUR'eva. (15 October 1985)
- Identification of block copolymers and determination of their purity by thin-layer chromatography:** E. S. GANKINA, I. I. EFIMOVA, J. J. KEVER and B. G. BELENKII. (15 October 1985)
- Determination of molecular-weight distribution and average molecular weights of block copolymers by GPC:** V. V. NESTEROV, O. I. KURENBIN, V. D. KRASIKOV and B. G. BELENKII. (15 October 1985)
- Analytical chemistry in the Soviet Union:** YU. A. ZOLOTOV. (15 October 1985)
- Analytical chemistry teaching in the USSR:** YE. N. DOROKHOVA. (15 October 1985)
- Catalytic methods for the determination of platinum metals:** K. B. YATSIMIRSKII and L. P. TIKHONOVA. (15 October 1985)
- Perspectives in the development of spark and laser plasma-source mass-spectrometry theory:** G. I. RAMENDIK, B. M. MANZON, D. A. TYURIN, N. E. BENYAEV and A. A. KOMLEVA. (15 October 1985)
- Ion-selective electrodes for gold and silver determination:** O. M. PETRUKHIN, E. N. AVDEEVA, YU. V. SHAVNYA, V. P. YANKAUSKAS, R. M. KAZLAUSKAS, A. S. BYCHKOV and YU. A. ZOLOTOV. (15 October 1985)
- Photometric determination of tungsten in rocks with trihydroxyfluorones:** V. A. NAZARENKO, V. P. ANTONOVICH and N. A. VESCHIKOVA. (15 October 1985)
- Spectrophotometric study of ionic equilibria of organic analytic reagents in water and non-aqueous media:** N. O. MCHEDLOV-PETROSSYAN. (15 October 1985)
- Advances in voltammetry:** KH. Z. BRAININA. (15 October 1985)
- Selectivity and sensitivity of metal determination by co-ordination compounds:** A. T. PILIPENKO and L. I. SAVRANSKY. (15 October 1985)
- Electrothermal atomic-absorption and atomic-fluorescence spectrometry with a tungsten coil atomizer:** V. N. MUZGIN, YU. B. ATNASHEV, V. E. KOREPANOV and A. A. PUPYSHEV. (15 October 1985)
- Laser ultramicroscopic method for determination of suspended particles in high-purity liquids:** G. G. DEVYATYKH, YU. A. KARPOV, V. A. KRYLOV and O. P. LAZUKINA. (15 October 1985)
- Electrochemical concentrates on solid electrodes and their application in voltammetric analysis:** A. I. KAMENEV and P. K. AGASYAN. (15 October 1985)
- The effect of thermal sample pretreatment on the absorption signal in graphite furnace AAS:** B. V. L'VOV, L. K. POLZIK and L. P. YATSENKO. (15 October 1985)
- Determination of alkali metals by laser atomic-ionization in flames:** V. I. CHAPLYGIN, YU. YA. KUZYAKOV, O. A. NOVODVORSKY and N. B. ZOROV. (15 October 1985)
- Fluorescence determination of trace amounts of uranium(VI) in different materials by a repetitive laser technique:** G. I. ROMANOVSKAYA, V. I. POGONIN and A. K. CHIBISOV. (15 October 1985)

- Assay of enzyme effectors:** I. F. DOLMANOVA, T. N. SHEKHOVTSOVA and V. V. KUTCHERYAEVA. (15 October 1985)
- Specific features of concentration by complicated electrode processes in anodic stripping voltammetry:** A. G. STROMBERG, A. A. KAPLIN, Y. A. KARBAINOV and B. F. NAZAROV. (15 October 1985)
- The method of pulse circulation gas chromatography on capillary columns, and equipment therefor:** V. P. CHIZHKOV, S. S. PAVLOV, N. V. STERKHOV, V. M. RAVIKOVICH, E. F. LITVIN and E. A. VARYVONCHIK. (15 October 1985)
- Liquid chromatography of palladium and non-ferrous metal chelates with 1-(2-pyridylazo)-2-naphthol:** YU. S. NIKITIN, N. B. MOROZOVA, S. N. LANIN, T. I. BOL'SHOVA, V. M. IVANOV and E. M. BASOVA. (15 October 1985)
- Steric and hydrophobic effects of substituents in the extraction of metal complexes with *O,O*-dialkyldithiophosphoric acids:** V. F. TOROPOVA, A. R. GARIFZYANOV and I. E. PANFILOVA. (15 October 1985)
- Liquid-liquid extraction of elements by antipyrine and diantipyrylmethane salts from non-aqueous solutions or in systems without organic solvent:** B. I. PETROV and V. P. ZHIVOPISTSEV. (15 October 1985)
- Forming organic co-precipitants for preconcentration of micro-amounts of elements:** YU. A. BANKOVSKY, M. V. VIRCAVS, O. E. VEVERIS, A. R. PELNE and D. K. VIRCAVA. (15 October 1985)
- Atomic-absorption methods for analysis of high-purity substances:** I. G. YUDELEVICH, L. V. ZELENTOSOVA and N. F. BEISEL. (15 October 1985)
- The analysis of solid and liquid high-purity materials:** G. G. DEVYATYKH and YU. A. KARPOV. (15 October 1985)
- Recent advances in the analytical chemistry of the transplutonium elements:** B. F. MYASOEDOV. (15 October 1985)
- Electrochemical investigation of palladium complexes with organic sulphides and their use in extraction differential pulse polarography:** H. C. BUDNIKOV, V. N. MAYSTRENKO and YU. I. MURINOV. (15 October 1985)
- Artificial intelligence systems for molecular spectral analysis:** M. E. ELYASHBERG, V. V. SEROV and L. A. GRIBOV. (15 October 1985)
- Electrochemical behaviour of dinitrogen tetroxide in sulpholane:** A. BOUGHRIET, M. WARTEL and J. C. FISCHER. (24 October 1985)
- Kinetic spectrofluorimetric determination of silver based on its catalytic effect on the oxidation of pyrocatechol-1-aldehyde 2-pyridylhydrazone by peroxodisulphate in the presence of 1,10-phenanthroline as activator:** A. M. AFONSO, J. J. SANTANA and F. GARCIA MONTELONGO. (24 October 1985)
- Synergic extraction and spectrophotometric determination of titanium(IV):** C. P. SAVARIAR and K. VIJAYAN. (24 October 1985)
- Optimum conditions for the removal of nitrous acid interference in the dithizone and Volhard methods—peculiar behaviour of mercury(II):** NKEMFULU U. EZEKWE. (24 October 1985)
- A study of the colour reaction of anions with 2-(5-Br-2-pyridylazo)-5-diethylaminophenol (5-Br-PADAP):** ZHAO XINWEI and HU ZHIDE. (24 October 1985)
- Two new spectrophotometric methods of determination of stepwise stability constants, and studies on the molybdenum complex with 2-aminobenzenethiol:** ANIL K. CHAKRABARTI. (24 October 1985)
- A new membrane concept for quantitative separation and determination of metal ions: Studies on the estimation of tungsten(VI) in a ternary system as the tannin-cinchonine complex:** ANIL K. CHAKRABARTI. (24 October 1985)
- A study of the reaction of *N*-chlorosuccinimide with sulphonamides and its analytical application:** IMADUL ISLAM, D. D. MISHRA and J. P. SHARMA. (26 October 1985)
- Determination of levamisole hydrochloride with HgI_4^{2-} by an FIA-turbidimetric method:** J. MARTINEZ CALATAYUD and P. CAMPINS FALCO. (30 October 1985)
- 4-Aminoantipyrine as an analytical reagent for the colorimetric determination of tetracycline and oxytetracycline:** M. AYAD, M. EL-SADEK and S. MOSTAFFA. (30 October 1985)
- Determination of ammonium in a buddingonite sample by ion-chromatography:** PAUL R. KLOCK and PAUL J. LAMOTHE. (16 September 1985)
- Iodimetric determination of organometallic compounds—I: Organolead compounds:** D. AMIN and TALAL A. K. AL-ALLAF. (30 October 1985)
- Kalman filtering for the evaluation of the current-time function in d.c. polarography:** M. BOS. (4 November 1985)

SUBJECT INDEX

Absorbance <i>vs.</i> pH graphs, of polybasic acids	929
Absorption spectroelectrochemistry at grazing incidence	51
Acetophenone, Phosphorescence of	17
Acid-base indicators, new	907
— strength, of fluorescein	901
Acidity constants, Evaluation	195, 531
—, of benzothiadiazines	119
Active carbon, Adsorption of metal ions	391
Aggregation, of Cu(II) and Zn(II) complexes	335
Algorithm and program for calculation of complex equilibria	1015
Alkaline-earth metal ions, Determination, polarographic	857
Aluminium(III), Titration with DCTA	867
Amikhelline, electrochemical oxidation	733
Amines, Determination, spectrophotometric	415
Amine-carbon disulphide reaction, analytical applications	703
<i>p</i> -Aminobenzophenone, Phosphorescence	17
Aminopolycarboxylate ligands bound to cellulose	620
Ammonium, Determination by ion-chromatography	495
— ion, Interaction with cyclic tetramines	721
Analgesics, X-ray diffraction data	631
Analysis, of ferroalloys	561
—, of papers on analytical chemistry	7
—, of variance in potentiometric titrations	471
Analytical applications, of amine-carbon disulphide reaction	703
—, of synchronous fluorescence spectrometry	633
— scheme, for forms of S	953
Anion-exchangers, with SPADNS and Orange II	149
Anthranilic acid, Analysis by HPLC	657
Antibiotics, Determination, spectrophotometric	164
Antihypertensive and antipyretic drugs, Titration	173
Antimalarials, Determination, spectrophotometric	185
Antimony, Determination by AAS	233
—, crystalline, for electrodes	125
Aromatic amines, Determination, spectrophotometric	311
— nitro-compounds, Determination with Cr(II)	751
Arsenic, Determination by FAAS	577
L-Aspartic acid, Determination of optical purity	760
Atomic-absorption spectrometry (AAS), Determination of Bi	233
—, —, — of Co	1027
—, —, — of metals	91, 233
—, —, — of Mn	1027
—, —, — of Ni	1027
—, —, — of Pb	279, 358
—, —, — of Sn	458
—, —, — of W	277
—, —, —, flameless (FAAS), Determination of As	577
—, —, —, — of Ca	61
—, —, —, — of Mo	265
—, —, —, — of Ni	748
—, —, —, — of Se	249
—, —, —, —, — trace metals	754
Benzidine and derivatives, Determination, voltammetric	811
Benzophenone, Phosphorescence of	17
Benzothiadiazines, Acidity constants	119
—, Determination, spectrophotometric	170
Bismuth, Complexes of citric and malic acids	371
—, Determination, by AAS	233
—, —, electrochemical	11
—, —, Electrode, ion-selective	371
—, —, Preconcentration of traces	835
— hydride, Stability	203
Bivalent cations, Interference in Se determination	705

Boron, accurate isotope measurements	291
—, Determination, by plasma AES	691
—, —, fluorimetric	541
Cadmium, Citrate complexes	763
—, Determination, by AAS	233
—, —, by flow potentiometric stripping analysis	991
—, —, polarographic	187
—, —, spectrophotometric	375
—, —, — and fluorimetric	807
—, Extraction by Amberlite LA-2	769
—, polarographic study of complexes	1031
Caesium source for mass spectrometry	1001
Calcium, Determination, by FAAS	61
Calculation, of equilibrium constants	943
Calibration, in flow potentiometric stripping analysis	883
Cation-exchange behaviour, Influence of thiourea	481
Ceftriaxone, Determination, spectrophotometric	363
Cephalosporins, Reaction with Ellman's reagent	366
Chalmers, Robert Alexander	1
Chlorophylls and bacteriochlorophylls, Chromatography of	963
Chlorpromazine, Determination, voltammetric	467
Chromate, Determination, by ion-exchange	1009
Chromatography, of chlorophylls and bacteriochlorophylls	963
—, gas (GC), Determination, of Se	443
—, —, Stationary phases for	979
—, — /Fourier-transform IR, for complex mixtures	299
—, high-pressure liquid (HPLC), Analysis of anthranilic acid	657
—, —, — of Goodrite 3114 antioxidant	85
—, —, —, Detection of purine and pyrimidine compounds	379
—, —, —, Determination of BHT	985
—, —, —, — of natural xanthenes	997
—, —, —, — of serum cortisol	325
—, —, —, of fluoride ion	661
—, —, —, Separation of nitroimidazoles	95
—, —, —, ion-pair, Determination of Cr, Mo and V	838
—, ion-, Determination of ammonium	495
—, thin-layer (TLC), Determination of rare earths	455
Chromium, Determination, by HPLC	838
—, —, spectrophotometric	694
Chromium(II), Determination of aromatic nitro-compounds	751
Chromium(VI) species, Distribution in solution	755
Chromogenic reactions, of benzyl 2-pyridyl ketone 2-quinolyldrazone	847
Citric acid, Reaction with acetic anhydride and pyridine	1035
Cobalt, Determination, by AAS	1027
—, —, gravimetric	973
—, Preconcentration	161
Complex equilibria, Algorithm and program for calculation	1015
Complexes, Determination of stability constants	851
—, Formation in aqueous solution	499
—, mixtures, analysed by GC/Fourier-transform IR	299
Computer program, for analysing multicomponent spectra	513
—, —, for estimation of formation constants	525
Computer-controlled FIA	107
Copper, Determination, by AAS	233
—, —, by flow potentiometric stripping analysis	991
—, —, fluorimetric kinetic	567
—, —, spectrophotometric	617
Copper(I), Tetrakis-isocyanide complexes	917
Copper(II), Complexes, with cyclic tetra-azatetra-acetic acids	285
—, —, with different ligands	768
—, —, with <i>N</i> -cyclohexyl- <i>N</i> -nitrosohydroxylamine	141
—, —, with <i>meso</i> -tetra(<i>p</i> -sulphonatophenyl)porphine	335
Correction factors, for glass electrode	105
<i>o</i> -Cresol Red, Determination, spectrophotometric	341
Cuprous sulphide, as collecting agent	75
Curve fitting, multiparametric	435, 513, 525, 825
Cyanide, Determination, by ion-exchange	1009
—, thiocyanate and halides, Analysis of mixtures	1009
DCTA, Determination, voltammetric	817
Dibasic acids, Dissociation constants	935
Digestion methods, Comparison of	249
Diffusion coefficients and complex equilibria	553
Dissociation, of 5-fluoro- and 3,5-dinitrosalicylic acids	461

— constants, of Arsenazo III	841
—, of benzyl 2-pyridyl ketone 2-quinolylylhydrazone	847
—, of dibasic acids	935
—, of <i>N,N,N',N'</i> -tetrakis(2-hydroxypropyl)ethylenediamine	927
Dodecyl sulphate ion, Titration, thermometric	167
Drugs, Determination of traces	67
Dye-surfactant interactions: a review	255
Dysprosium, Determination, by plasma AES	445
EDTA, EGTA and DCTA, Determination, voltammetric	817
Electrochemical stripping analysis, Determination of Bi	11
Electrode, glass, Correction factors	105
—, glassy-carbon, for voltammetry	811
—, ion-selective, Determination of nafronyl drugs	101
—, —, for Bi	371
—, —, for perchlorate	679
—, Kel-F-graphite, for ergonovine maleate	448
—, mercury-film, Determination of Bi	11
—, pH-sensing	125
— modifiers, for flow-injection systems	911
Elements, Distribution between polyurethane, polyethers and HF solution	219
Equilibrium constants, Calculation of	943
Europium, Determination by plasma AES	445
Extraction, of Cd	769
—, of Cu and Ni	617
—, of Cu(II)	141, 288, 617
—, of metal iodide complexes	35
—, of Mo, W and Tc	315
—, of Pb	769
—, of Pd	411
—, of phenothiazine drugs	352
—, of Ti(IV)	587
—, of Zn	463
—, of Zn(II), Cd(II) and Pb(II)	769
—, with membrane phase separator	119
—, anion-exchange, of Au	349
Ferroalloys, Analysis of	561
Filter papers, for solid-surface fluorimetry	215
Flow cell, for laser fluorimetry	281
Flow-injection analysis (FIA), computer-controlled	107
—, —, Determination, of Fe	547
—, —, —, of levamisole hydrochloride	685
—, —, —, of nitrite	729
—, —, —, of silicate and phosphate	889
—, —, —, for metal speciation	199
—, —, —, of ergonovine maleate	448
—, —, —, Speciation by	45
— systems, Electrode modifiers for	911
— potentiometric stripping analysis, Calibration	883
—, —, —, Determination of Cd, Pb and Cu	991
Flotation collectors, Determination, polarographic	795
—, —, —, voltammetric	801
Fluocortolone esters, Identification by Raman spectrometry	295
Fluorescein, Acid strength	901
Fluorescence, in thin liquid films	871
—, of Zn-morin complex	537
Fluoride ion, Effect of Al on HPLC determination	661
Fluorimetry, Determination, of Ag	779
—, —, of B	541
—, —, of Cu	567
—, —, of nitrite	649
—, —, of perchlorate	274
—, —, of U(VI)	355
—, solid-surface room-temperature	215
—, synchronous derivative, Determination of Zn	785
—, ultramicro flow-cell for	281
5-Fluoro- and 3,5-dinitrosalicylic acids, Dissociation	461
Formation constants, Computer program for estimation	525
—, of Hg(II) complexes	843
Gadolinium, Determination, by plasma AES	445
Generation of HCN, electrochemical	688
Gold, Determination, by anion-exchange extraction	349
—, Sorption, on polythioether foam	182

Goodrite 3114 antioxidant, Analysis by HPLC	85
Group Vb hydrides, Decomposition	203
Hydration of ion-exchange resins, Determination, aquametric	429
Hydrogen cyanide, electrochemical generation	688
— sulphide, Determination, gravimetric	550
1-Hydroxy-2-carboxyanthraquinone, Photoautomerism of	923
Imidazole, Ionization constants	919
Indium, Determination, by AAS	233
—, —, spectrophotometric	607
Indolecarboxylic acids, Phosphorimetry	27
Iodide, Oxidation to iodate	451
Iodine, Determination, polarographic	451
Ion-association complexes, Thermochromism	415
— exchange, Preconcentration of rare earths and Y	601
— membrane, selective for Pb(II) ions	717
Ionization constants, of imidazole	919
Iridium, crystalline, for electrodes	125
Iron, Determination, spectrophotometric	547, 700
— and phosphorus, Fractionation	593
Isotope measurements on boron	291
Kalman filtering, in d.c. polarography	583
Khelline, electrochemical oxidation	733
Lanthanides, Determination, spectrophotometric	1021
Lead, Determination, by AAS	279, 358
—, —, by flow potentiometric stripping analysis	991
—, —, spectrophotometric	407
—, polarographic study of complexes	1031
—, Preconcentration of traces	835
Lead(II), Extraction by Amberlite LA-2	769
— ions, Ion-exchange membrane selective for	717
— alkyls, Behaviour in plumbane generation	401
Levamisole hydrochloride, Determination, by FIA	685
Limitations, to validity of diffusion equations	553
Lipohydroperoxides, Determination, kinetic	914
Louis Gordon Memorial Award	No. 6, III; No. 9, III
Manganese, Determination, by AAS	1027
—, —, kinetic	135
—, Extraction, with 1-phenyl-3-methyl-4-acyl-5-pyrazolone	288
—, Speciation	669
Matrix, Biological fluids, Determination of drugs	61
—, Blood, Determination of metals	55
—, Bovine liver, Determination of Se	249
—, Buddingtonite, Determination of ammonium	495
—, Cadmium telluride, Determination of Cd and Te	187
—, Coal and fly-ash, Determination of V	611
—, — cleaning samples, Determination of Fe	700
—, Copper alloys, Determination of Bi	11
—, — ores and concentrates, Determination of Co, Ni and Mn	1027
—, Fresh water, Speciation of Mn	669
—, Gasoline, Determination of Pb	279, 358
—, Geological materials, Preconcentration of rare earths	601
—, Human tissues, Multielement analysis	861
—, Minerals and rocks, Determination of Ti	209
—, —, — of W	277
—, Monazite sand, Determination of rare earths	455
—, Natural water, Determination of iodine	451
—, —, — of nitrite	729
—, Nickel alloys, Determination of In	607
—, Oil shales, Determination of S forms	953
—, Ores and concentrates, Determination of metals	233
—, Organomercurials, Determination of Hg	329
—, Plant tissue, Determination of Mo	265
—, Sea-water, Determination of metals	754
—, Soil, Determination of Cr	694
—, Solders, Determination of metals	91
—, Steels, Determination of B	691
—, —, — of Ca	61
—, —, — of Ti(IV)	115
—, — and alloys, Determination of Ti	360
—, Surface waters, Determination of Fe and P	593

—, Tablets, Determination of nitrazepan	743
—, Titanium alloys, Determination of Pd	939
—, Uranium products, Determination of metals	445
—, Waste water, Determination of Cr	694
—, Water, Determination of Au	349
—, —, — of flotation collectors and sulphide	795
—, —, — of P	98
—, —, — of silicate and phosphate	889
—, White metals, Determination of metals	91
—, Zinc ores, Determination of In	607
Mercury, Determination, spectrophotometric	329
Mercury(II), Complexes with EDTA, EGTA and DCTA	817
—, Determination, spectrophotometric	697
— complexes, Formation constants	843
Methotrexate, Determination, voltammetric	707
Methyl borate, rapid distillation	691
Metals, biosorption by chitin	225
—, Determination by AAS	91
—, — by ASV	243
—, — by AFS and flame emission spectrometry	55
—, — by FAAS	754
— iodide complexes, Extraction	35
— ions, Adsorption on active carbon	391
—, —, Separation by chelating resins	149
—, —, Single-point titration	739
Michler's ketone, Phosphorescence	17
Mineralization, of organic S compounds	754
Molybdenum, Determination by FAAS and plasma AES	265
—, — by HPLC	838
—, Extraction with polyether foam	314
Multielement analysis, by plasma AES	861
N_2O_4 , Determination, voltammetric	385
Nafronyl drugs, Determination by ion-selective electrode	101
Natural xanthenes, Determination by HPLC	997
Nickel, Determination, by AAS	1027
—, —, by FAAS	748
—, —, gravimetric	973
—, —, spectrophotometric	617
Nitrate, Adsorption on lead dioxide	191
Nitrazepam, Determination, spectrophotometric	743
Nitrioltriacetic acid (NTA), Degradation	614
Nitrite, Determination, fluorimetric	649, 729
—, —, voltammetric	489
Nitroimidazoles, Separation by HPLC	95
Non-metals, Analysis, spectrometric	875
Numerical methods, for two-step overlapping equilibria	531
Non-metals, Analysis, spectrometric	875
Numerical methods, for two-step overlapping equilibria	531
Obituary, Lado Kosta	No. 4, V
—, J. M. Ottaway	No. 12, III
—, Rudolf Přibil	No. 4, III
Optical purity, of L-aspartic acid	761
Organic peroxides, Determination, kinetic	914
Oxidation, electrochemical of khelline and amikhelline	733
Palladium, Determination, complexometric	544
—, —, spectrophotometric	939
—, —, — and fluorimetric	411
—, Sorption on polythioether foam	182
—, crystalline, for electrodes	125
Paper on analytical chemistry, Analysis of	7
Paraquat, Determination, spectrophotometric	745
Perchlorate ions, Determination, fluorimetric	274
—, —, ion-selective electrode for	679
Phenobarbital, micellar modification of spectral characteristics	653
Phenothiazines, Determination with chloranilic acid	111
— drugs, Determination, spectrophotometric	352
Phosphate, Determination by FIA	889
Phosphorescence, of aromatic ketones	17
Phosphorimetry, of indolecarboxylic acids	27
Phosphorus, Determination, by photochemical decomposition	98
Photosensors, for photo-titrations	665
Phototautomerism, of 1-hydroxy-2-carboxyanthraquinone	923
Photo-titrations, acid-base and chelatometric	665

Piperazine, Determination, spectrophotometric	179
Platinum gauze, for adsorption of Ag traces	155
Polarimeters, Signal-to-noise characteristics.	571
Polarography, Determination, of iodine	451
—, —, of Th	623
—, of Cd and Pb complexes.	1031
—, of Cd and Te	187
—, use of Kalman filtering	583
—, differential-pulse, of alkaline-earth metal ions	857
—, —, of flotation collectors and sulphide	795
—, —, of vinca alkaloids	791
Polybasic acids, Absorbance <i>vs.</i> pH graphs.	929
Polythioether foam, for sorption of Ag, Au and Pd.	182
Preconcentration, across liquid membrane	713
—, electrolytic	421
—, of Pb and Bi traces	835
Purine and pyrimidine compounds, Detection by HPLC	379
Quaternary ammonium salts, Determination, spectrophotometric	415
Rare-earth elements, Determination, by TLC	455
—, —, —, voltammetric.	321
—, —, —, Preconcentration by ion-exchange	601
Rational spline functions, Use of	641
Reagent, Alizarin and fluoride, for Ti(IV)	587
—, 8-Amino-1-hydroxynaphthalene-3,6-disulphonic acid, for aromatic amines	311
—, 3-Aminonaphthalene-1,5-disulphonic acid, for nitrite	729
—, Arsenazo III, Dissociation constants.	841
—, <i>p</i> -Benzoquinone, for piperazine	179
—, Benzyl 2-pyridyl ketone 2-quinolyldiazone, Dissociation constants.	847
—, —, —, for Hg	329
—, 2-(5-Bromo-2-pyridylazo)-5-(diethylamino)phenol, for Pd.	939
—, <i>p</i> -Chloranilic acid, for antimalarials	185
—, —, —, for phenothiazines.	111
—, <i>p</i> -Chloromandelic acid, for Ti(IV)	115
—, 2-(5-Chloro-2-pyridylazo)-5-dimethylaminophenol, for Cd	375
—, Cu diethyldithiocarbamate, for Hg(II) and Ag(I)	697
—, Cyclic tetra-azetetracetic acids, Complexes with Cu(II)	285
—, 1,2-Cyclohexanedione bis-benzoylhydrazone, for Ti.	209
—, <i>N</i> -Cyclohexyl- <i>N</i> -nitrosohydroxylamine, Complex with Cu(II)	141
—, DCTA, for Al(III)	867
—, Diazacrown ether dye, for Pb	407
—, 1,4-Dibromo-2,3-diaminonaphthalene, for Se	443
—, 3,5-Di- <i>tert.</i> butyl-4-hydroxytoluene (BHT), Effect of β -rays	985
—, 5,7-Dichloro-2-methyl-8-hydroxyquinoline, for Zn	463
—, 1,5-Di(2-furyl)-1,4-pentadien-3-one (DFPO), as acid-base indicator	907
—, 2,4-Dihydroxyacetophenone thiosemicarbazone, for Cu and Ni	617
—, <i>N,N'</i> -Diphenyldithiomalonamide, for Ni and Co	973
—, 1,5-Di(2-thienyl)-1,4-pentadien-3-one (DTPO), as acid-base indicator	907
—, <i>N</i> -(Dithiocarbonyl)sarcosine, for Co	161
—, 2,6-Di- <i>p</i> -tolyl-4-phenylpyrylium chloride, for perchlorate.	274
—, Ellman's reagent, for cephalosporins.	366
—, Iodine, for antibiotics	164
—, Lead dioxide, for nitrilotriacetic acid	614
—, Malachite Green, for Ti(IV)	115
—, Morin, for Zn	537
—, <i>N</i> -(1-Naphthyl)ethylenediamine, for aromatic amines	311
—, Nitroso-R salt, for phenothiazine drugs	352
—, Periodate, for antibiotics	164
—, 1-Phenyl-3-methyl-4-acyl-5-pyrazolone, for Mn(II)	288
—, 2-Pyridinecarboxaldehyde phenylhydrazone, for transition metal ions	895
—, 2,2'-Pyridyl bis(2-quinolyldiazone), for Zn and Cd	807
—, 1-(2-Pyridylmethylideneamine)-3-(salicylideneamine)thiourea, for In	607
—, Salicylaldehyde-1-phthalazinohydrazone, for metals.	627
—, Tannin and thioglycolic acid, for Ti	360
—, <i>N,N,N',N'</i> -Tetrakis(2-hydroxypropyl)ethylenediamine, dissociation constants	927
—, <i>meso</i> -Tetra(<i>p</i> -sulphonatophenyl)porphine, for Cu(II) and Zn(II)	335
—, <i>N-m</i> -Tolyl- <i>N</i> -phenylhydroxylamine, for V.	611
Resin, Amberlite XAD-4, for preconcentration of Co	161
—, ion-exchange, Determination of hydration.	429
Resolution capability, of SQUAD(84) and PSEQUAD(83) programs	825
Review: Dye-surfactant interactions	255
Ronald Belcher Memorial Award	No. 7, III
Samarium, Determination by plasma AES	445

Sample-cell positioner	271
Selenium, Determination, by AAS	705
—, —, by FAAS	249
—, —, by GC	443
Semi-Xylenol Orange, Determination, spectrophotometric	341
Separation, of transition-metal ions	895
Serum cortisol, Assay of	325
Signal-to-noise characteristics, of polarimeters	571
Silica, NMR spectrometry of	176
Silicate, Determination by FIA	889
Silver, Determination, by AAS	155, 233
—, —, kinetic fluorimetric	779
—, —, spectrophotometric	155
—, Sorption on polythioether foam	182
Silver(I), Determination, spectrophotometric	697
—, Tetrakis-isocyanide complexes	917
Speciation, by FIA	45
—, —, of metals	199
—, of Mn	669
Spectral characteristics, of phenobarbital	653
Spectrometric analysis, of non-metals	875
Spectrometry, atomic fluorescence (AFS), Detector for	401
—, —, of metals	55
—, EPR, Biosorption of metals	225
—, flame-emission, of metals	55
—, mass, with Ca source	1001
—, NMR, of porous silica	176
—, —, IR and mass, of reaction product	1035
—, plasma atomic-emission (AES), Determination of B	691
—, —, —, —, of Dy, Eu, Gd and Sm	445
—, —, —, —, of Fe and P	593
—, —, —, —, of Gd, Sm, Dy and Eu	445
—, —, —, —, of Mo	265
—, —, —, —, of Sm, Eu, Gd and Dy	445
—, —, —, —, for multielement analysis	861
—, Raman, Identification of fluocortolone esters	295
—, secondary-ion mass (SIMS), Study of Ag(I) and Cu(I) complexes	917
—, synchronous-fluorescence, analytical applications	633
SQUAD(84) and PSEQUAD(83) programs, resolution capability	825
Stability, of Zn(II) and Cd(II) citrate complexes	763
— constants, of complexes	435, 499, 851
—, of Cu(II) complexes	768
Stationary phases, for GC	979
Sulphide, Determination, polarographic	795
Sulphur, soluble sulphides and hydrogen sulphide, Determination, gravimetric	550
— compounds, organic, Mineralization	757
— forms, analytical scheme for	953
Sweeps, Analysis of	75
Talanta Advisory Board	No. 2, III
— Medal	No. 10, III
Technetium, Extraction with polythioether foam	315
Tellurium, Determination, polarographic	187
Thermochromism, of ion-association complexes	415
Thin liquid films, Fluorescence	871
Thionidazine, Determination, voltammetric	467
Thiourea, Influence on cation-exchange	481
Thorium, Determination, polarographic	623
Tin, Determination by AAS	458
Titanium, Determination, spectrophotometric	115, 209, 360, 587
Titration, complexometric, of Al(III)	867
—, —, of Pd	544
—, potentiometric, Analysis of variance	471
—, —, finding end-points	641
—, single-point, of metal ions	739
—, thermometric, of dodecyl sulphate ion	167
—, —, of pharmaceuticals	173
Transition-metal ions, Separation of	895
Transport across liquid membrane, as preconcentration technique	713
Tungsten, Determination by AAS	277
—, Extraction with polythioether foam	315
Uranium(VI), Determination, fluorimetric	355
Vanadium, Determination, by HPLC	838

—, —, spectrophotometric	611
Vinca alkaloids, Determination, polarographic	791
Voltammetry, Determination of benzidine and derivatives	811
—, — of nitrite	489
—, of N ₂ O ₄	385
—, Resolution of measurements	397
—, adsorptive stripping, Determination of methotrexate	707
—, —, — of Y, Dy, Ho and Yb	321
—, anodic stripping (ASV), Determination of metals	243
—, cathodic stripping, Determination of EDTA, EGTA and DCTA	817
—, —, Determination of flotation collectors	801
—, differential-pulse, Determination of chlorpromazine and thioridazine	467
X-Ray diffraction data, for analgesics	631
Xylenol Orange, Determination, spectrophotometric	341
Yttrium, Determination, spectrophotometric	1021
—, —, voltammetric	321
—, Proconcentration by ion-exchange	601
Zinc, Determination, fluorimetric	785
—, —, — and spectrophotometric	807
—, Extraction with 5,7-dichloro-2-methyl-8-hydroxyquinoline	463
Zinc(II), Citrate complexes	763
—, Complex of <i>meso</i> -tetra(<i>p</i> -sulphonatophenyl)porphine	335
—, Extraction by Amberlite LA-2	769
Zinc-Morin complex, Enhancement of fluorescence	537

Talanta

The International Journal of Pure and Applied Analytical Chemistry



The illustration of a Greek balance from one of the Hope Vases is reproduced here by kind permission of Cambridge University Press

Editor-in-Chief

DR R.A.CHALMERS, Department of Chemistry, University of Aberdeen, Old Aberdeen, Scotland

Assistant Editors

DR J.R.MAJER, University of Birmingham, England

DR I.L.MARR, University of Aberdeen, Scotland

Computing Editor

DR MARY R.MASSON, University of Aberdeen, Scotland

Regional Editors

PROFESSOR I.P.ALIMARIN, Vernadsky Institute of Geochemistry and Analytical Chemistry, U.S.S.R. Academy of Sciences, Kosygin St., 19, Moscow V-334, U.S.S.R.

PROFESSOR E.BLASIUS, Institut für Analytische Chemie und Radiochemie der Universität des Saarlandes, D-6600 Saarbrücken 15, G.F.R.

MR H.J.FRANCIS JR, Pennwalt Corporation, 900 First Avenue, King of Prussia, PA 19406, U.S.A.

PROFESSOR J.S.FRITZ, Department of Chemistry, Iowa State University, Ames, IA 50010, U.S.A.

PROFESSOR T.HORI, Department of Chemistry, Kyoto University, Kyoto, Japan

DR M.PESEZ, Roussel-Uclaf, 102 et 111 route de Noisy, F-93, Romainville (Seine), France

PROFESSOR E.PUNGOR, Institute for General and Analytical Chemistry, Technical University, Gellért tér 4, 1502 Budapest XI, Hungary

PROFESSOR J.D.WINEFORDNER, Department of Chemistry, University of Florida, Gainesville, FL 32611, U.S.A.

Consulting Editor

DR M.WILLIAMS, Oxford, England

Editorial Board

Chairman: PROFESSOR J. D. WINEFORDNER

DR R.A.CHALMERS

DR M.WILLIAMS

DR I.L.MARR

DR J.R.MAJER

MR H.J.FRANCIS JR

Annual Subscription Rates (1986)

US\$350.00 (2-yr rate US\$665.00)—For libraries, government laboratories, research establishments, manufacturing houses and other multiple-reader institutions. Price includes postage and insurance. Published monthly, 1 volume per annum.

Specially Reduced Rate for Individuals

In the interests of maximizing the dissemination of the research results published in this important international journal we have established a two-tier price structure. Any individual, whose institution takes out a library subscription, may purchase a second or additional subscriptions for personal use at the much reduced rate of US\$75.00 per annum.

Microform Subscriptions and Back Issues

Back issues of all previously published volumes are available in the regular editions and on microfilm and microfiche. Current subscriptions are available on microfiche simultaneously with the paper edition and on microfilm on completion of the annual index at the end of the subscription year.

Publishing Office

Pergamon Press Ltd, Journals Production Unit, Hennock Road, Marsh Barton, Exeter, Devon EX2 8RP, England (Tel. Exeter (0392) 51558; Telex 42749).

Subscription Enquiries and Advertising Offices

North America: Pergamon Press Inc., Maxwell House, Fairview Park, Elmsford, NY 10523, U.S.A.

Rest of the World: Pergamon Press Ltd, Headington Hill Hall, Oxford OX3 0BW, England (Tel. Oxford (0865) 64881).

Copyright © 1986 Pergamon Press Limited

It is a condition of publication that manuscripts submitted to this journal have not been published and will not be simultaneously submitted or published elsewhere. By submitting a manuscript, the authors agree that the copyright for their article is transferred to the publisher if and when the article is accepted for publication. However, assignment of copyright is not required from authors who work for organizations which do not permit such assignment. The copyright covers the exclusive rights to reproduce and distribute the article, including reprints, photographic reproductions, microform or any other reproductions of similar nature and translations. No part of this publication may be reproduced, stored in a retrieval system or transmitted in any form or by any means, electronic, electrostatic, magnetic tape, mechanical, photocopying, recording or otherwise, without permission in writing from the copyright holder.

Photocopying information for users in the U.S.A.

The Item-Fee Code for this publication indicates that authorization to photocopy items for internal or personal use is granted by the copyright holder for libraries and other users registered with the Copyright Clearance Center (CCC) Transactional Reporting Service provided the stated fee for copying beyond that permitted by Section 107 or 108 of the U.S. Copyright Law is paid. The appropriate remittance of \$3.00 per copy per article is paid directly to the Copyright Clearance Center Inc., 21 Congress Street, Salem, MA 01970. The copyright owner's consent does not extend to copying for general distribution, for promotion, for creating new works or for resale. Specific written permission must be obtained from the publisher for such copying. In case of doubt please contact your nearest Pergamon office. *The Item-Fee Code for this publication is:* 0039-9140/86 \$3.00 + 0.00

SOFTWARE SURVEY SECTION

The purpose of the Software Survey Section in TALANTA is to encourage the open exchange of information on software for use in analytical chemistry. Alongside the rapid penetration of computers into academic and industrial institutions has come a parallel increase in the number of scientists and researchers designing their own software. The existence of much of this software remains unknown to many who could greatly benefit from its use. We believe that it would be extremely useful to our readers to have such information made available, and that a professional journal is the best place for doing it. We therefore invite you to consider making a contribution to the Section.

The two-page questionnaire on the following pages is designed to assist you in reporting on software that you have developed or are in the process of developing. The information you supply will then be published; thus it will reach thousands of your colleagues who may benefit from your work and possibly offer suggestions for enhancement of your software. If you are interested, please complete the form and return it to our Computing Editor:

Dr. Mary R. Masson
Department of Chemistry
University of Aberdeen
Meston Walk
Old Aberdeen AB9 2UE, Scotland

We do not intend to comment on or review the material submitted, which will be published "as received" (apart from any editing needed for clarity and uniformity) in order to expedite its publication. Any comments or suggestions you may have will be welcome. The Software Description Form will appear in all future issues.

THE EDITORS

NAME OF JOURNAL TALANTAP E R G A M O N
SOFTWARE DESCRIPTION FORMTitle of software package: _____

_____It is: Application program Utility Other _____Specific area _____
(e.g. stability constants, calibration, pattern recognition, optimization)

Software developed for [name of computer(s)] _____

in [language(s)] _____

to run under [operating system] _____

and available on:

 Floppy disk/diskette.Size _____ Density _____ Single-sided Double-sided Magnetic tape.

Size _____ Density _____ Character set _____

Distributed by: _____

Minimum hardware configuration required: _____

Memory required: _____ User friendly?: Yes NoDocumentation: None Minimal Self-documenting
 Extensive external documentationSource code available: Yes NoLevel of development: Design complete Coding complete
 Fully operational Collaboration would be welcomedIs software being currently used? Yes No
If yes, how long? _____ If yes, how many sites? _____Contributor is willing to deal with enquiries?: Yes No

(continued)

RETURN COMPLETED FORM TO:

Dr. Mary R. Masson
Department of Chemistry
University of Aberdeen
Meston Walk
Old Aberdeen AB9 2UE, Scotland[This Software Description Form may be photocopied without permission]

Description of what software does [200 words maximum; use separate sheet if necessary]:

Potential users: _____

Fields of interest: _____

#####

Name of contributor: _____

Institution: _____

Address: _____

Telephone number: _____

#####

Reference No. [Assigned by Journal Editor] _____

[The information below is not for publication.]

Would you like to have your program:

Reviewed? []Yes []No []Not at this time
Marketed and distributed? []Yes []No []Not at this time

[This Software Description Form may be photocopied without permission]

PUBLICATIONS RECEIVED

Physical and Chemical Characterization of Individual Airborne Particles: edited by K. R. SPURNY. Ellis Horwood, Chichester, 1986. Pages 418. £55.

The recent Chernobyl disaster and the acid rain problem have focused attention on the need for quick and accurate methods of characterizing airborne particles. The publication of a book on the current developments in particle characterization is welcome.

The book is true to its title. It is a compilation of chapters (23 contributors) each dealing with some aspect of particle characterization. The first three chapters deal with the physics and chemistry of aerosols, physical characterization and sampling. Chapter 4 is a short article on deposition in human airways and sets the background for Chapter 12—Particles and fibres in human lungs.

One of the most promising recent developments is laser-microprobe mass analysis—LAMMA. Probably because of its promise three chapters (13–15) are devoted to it. There are descriptions of the apparatus and techniques, and also included are a large number of results. The next 5 chapters are all very similar in construction—a small amount of theory, a description of the apparatus, some applications and results.

The methods covered are

Particle induced X-ray emission analysis (PIXE)
Secondary-ion mass spectroscopy (SIMS)
X-Ray photoelectron spectroscopy (XPS or ESCA)
Micro Raman spectroscopy (MRS)
Mass spectrometry *in situ*.

The classical methods of light scattering, optical microscopy, electron microscopy and chemical analyses have not been neglected and modern aspects (laser light scattering, TEM, SEM, EPMA) are treated in Chapters 5–11.

In my view, the editor has compiled a useful, timely and up-to-date book on current developments in particle characterization.

W. A. J. BRYCE

Atmospheric Chemistry: B. J. FINLAYSON-PITTS and J. N. PITTS JR., Wiley, New York, 1986. Pages xxviii + 1098. £57.45.

This book of some 1100 pages by two experienced workers in their field—placed in the best or worst environment depending upon your point of view!—represents a veritable mine of information with very up-to-date references. These are mainly American and are inevitably somewhat subjective. The book derives greatly from two previous monographs—“Photochemistry of Air Pollution” by Leighton and “Photochemistry” by Calvert and Pitts. Although there are extensive sections on analysis, the main emphasis of this book is on photochemical kinetics and modelling of mechanisms. One might add that the thermochemistry for reactions is not given as much attention as it deserves.

The authors show that they have a fine sense of history. They start with an overview of the natural and polluted atmosphere (troposphere). In particular they emphasize meteorological effects such as temperature inversion which can lead to local high concentrations of pollutants. Just about enough fundamental aspects of photochemistry, spectroscopy and gas kinetics are reviewed. Since many unimolecular and bimolecular reactions are pressure-dependent under atmospheric conditions, this includes the Troe formulation of RRKM theory for these processes. This has distinct advantages over the full treatment although some *ad hoc* assumptions have to be made. In respect of these three topics some effort has been made to define units of concentration, photolysis rate constant *etc.*, which clarifies some confusion in the literature. However in terms of a “fast” or “slow” reaction is would have been desirable to differentiate clearly between rate and rate constant. Condensed phases are also considered. A thorough review of solar radiation is given, once again clearly defining such items as actinic radiation, zenith angle *etc.* Unfortunately only variations as a function of latitude in the Northern Hemisphere are considered. A critical review is given of monitoring techniques for detecting species responsible for air pollution, such as CO, NO₂, O₃, SO₂ and hydrocarbons other than methane. In particular it is concluded that O₂ (¹Δg) and N₂O₃ are *not* important and the source of HONO is unknown. H₂SO₄ and HNO₃ formation in acid rain and fogs is dealt with in some depth. The complex mechanism for the conversion of SO₂ into H₂SO₄ is shown still to be not fully understood. Effects on health, lung cancer in particular, are also considered.

Interaction of the troposphere with the stratosphere is considered in a short chapter. Concentrations of intermediates here would have been useful. There are very useful tables in the appendices.

The test would be useful for a course on atmospheric chemistry although most students would find the cost prohibitive. The authors clearly had in mind beginners and readers with peripheral knowledge. Altogether a very useful book for workers in this important field, with relatively few typographical errors. The hardest thing to do was to cut this review down to size because of the wealth of information.

L. BATT

PUBLICATIONS RECEIVED

Auger Electron Spectroscopy: M. THOMPSON, M. D. BAKER, A. CHRISTIE and J. F. TYSON, Wiley, New York, 1985. Pages vii + 394. £95.00.

The great success of the mass spectrometric technique over the past three decades encouraged basic research in the manipulation of charged particles in vacuum systems and physicists were able to develop sophisticated techniques for the generation and measurement of energy distribution in electron beams. As a result of this increasing sophistication several spectroscopic techniques were transformed from methods for research experiments into routine analytical tools; this family of techniques, which includes electron and photoelectron spectroscopy, as well as Auger spectroscopy, is described in the first chapter of this book. Subsequent chapters deal with the fundamentals of the Auger effect and with the instrumentation required to apply it in the examination of surface properties.

Although the main application of the techniques is in the study of surface chemistry, where it often complements the evidence obtained by X-ray photoelectron spectroscopy, there is a chapter devoted to a discussion of the Auger effect in gases. Because of the large difference in the energies of electrons ejected from different elements and the measurable shifts of these energies caused by the molecular environment, there is considerable potential for the exploitation of the Auger effect in the gas phase for both qualitative and quantitative analysis, and many examples of atomic and molecular spectra are provided.

Subsequent chapters are devoted to the more familiar applications of Auger spectroscopy in metallurgy and materials science where accurate descriptions of surface properties are of fundamental importance. While interest in the past has tended to be largely restricted to these areas, the book is recommended to all practising analytical chemists, who may find in it solutions to future problems in general analysis.

J. R. MAJER

PUBLICATIONS RECEIVED

CLUE: A Microcomputer Program for Hierarchical Clustering: A. THIELEMANS, M. P. DERDE and D. L. MASSART, Elsevier Scientific Software, Amsterdam, 1986. \$295/Dfl.975/£245; manual only \$30/Dfl.100/£25. The introductory part of the manual is available free.

Available for:

IBM-PC, -XT, -AT with PC-DOS 2.x or 3.0 and PC-BASIC, 180/360K 5.25-in disc drive, 128K RAM.

Apple II, II+, IIe, IIc with DOS 3.3, Applesoft BASIC, 140K 5.25-in disc drive, 48K RAM (interpreter), 64K RAM (compiled).

The version tested for this review was for the IBM-PC, and the machine used for testing was an IBM-PC-AT, with PC-DOS 3.0

This microcomputer software package is an implementation of a divisive hierarchical method of clustering, originally proposed by MacNaughton-Smith *et al.* (*Nature*, 1964, **202**, 1034). This particular method of clustering is suitable for implementation on a microcomputer because it operates by starting with all the objects to be clustered, then divides them into two groups, then divides each of these into two more groups, and so on, until each object is in a separate group.

The first part of the package deals with data input and transformation; the data input routines are well protected from crashes that would otherwise be caused by mistypes such as the letter O instead of the figure 0. The second part contains the calculation of the dissimilarity matrix (it can use either the Euclidian distance between objects or the correlation as a measure of dissimilarity) and the clustering algorithm itself. The third part allows display and/or printing of previously stored clustering results.

The package is easy to learn to use, and, overall, it works very well in a way that is friendly to the user. Both compiled and interpreted versions were supplied on the disc: the compiled version was much faster, but otherwise they appeared identical. The manual, too, is nicely produced in a loose-leaf format (to allow updates to be added, presumably), though I did find it rather unwieldy for working with at the computer. The sections are Introduction, User Guide, Scientific Background, and Program Listings. (These listings are not provided if a manual is purchased on its own.)

However, the program is not entirely free from bugs. The manual explains that the initial setting-up program can only be used with a disc that is not write-protected; in fact, none of the package will run with a write-protected disc. If the package is set up for a 2-drive system, the data files on the disc in drive B are saved and loaded without trouble in the first and second parts of the package, but in the third part, files are reported as "not found" (because the machine is trying to read from drive A) unless the filename is preceded by "B:". This problem arises with both the compiled and interpreted versions of the program. Another, rather puzzling, error occurred in the printing of data matrices after a log transformation, in that just two or three spurious data values were printed out, *e.g.*, 9.99 instead of 0.103. The data in memory and on disc did not contain these errors, but they occurred every time the data were printed.

The manual lists some errors trapped by the program, but I found some that were not, and which caused the program to crash, leaving the system in BASIC. The authors did not mention this possibility, and did not give instructions on restarting from within BASIC. This would cause little bother to a user familiar with the machine, but a computer novice wanting just to use the package would be baffled—and the manual does otherwise seem to be aimed at a complete novice.

Despite these problems, I rather liked the package. It offers an easy introduction to clustering methods for the many analytical chemists who have not yet tried them. It is sad and unfortunate that the price is so excessive. Until the advent of microcomputers, programs like this were published in the open scientific literature, and freely exchanged among any workers interested. Is the price so high because IBM customers expect software to be in this price bracket? Many comparable packages for the Acorn BBC microcomputer can be had for £30-40. The only redeeming feature is that the purchaser is permitted to make four copies of the disc for use within the purchasing organization or institution.

MARY R. MASSON

Chromatographic Methods, 4th Ed. A. BRAITHWAITE and F. J. SMITH, Chapman & Hall, London, 1985. Pages x + 414. Hardback £29.00. Paperback £12.95.

This fourth and extended version of "Chromatographic Methods" is the result of the rich experience of both authors. The first two chapters are devoted to fundamental concepts and theories of chromatography, including also a short and interesting historical survey.

Plane (planar) Chromatography, Liquid Phase Chromatography in Open Columns, Gas Chromatography and High Performance Liquid Chromatography make up the main body of the book and are dealt with in four subsequent chapters. The modern approach to the treatment of the material is an outstanding feature of the four chapters.

Chapter 7 deals with procedures which have been developed for identifying compounds separated from a mixture. This chapter covers the coupling of chromatography with infrared and ultraviolet-visible spectrophotometry, mass spectrometry and atomic spectrometry.

Chapter 8 covers important new developments such as computerized data-handling and is devoted to methods of recording the chromatographic signal and data processing.

In the final chapter the authors give a number of examples of model experiments in chromatographic techniques.

In my opinion, the sub-chapter Electrophoresis included in Chapter 3 (Planar Chromatography) does not meaningfully fit into the concept of Chromatography but, on the other hand, it does fit into a book dealing with separation methods. Once there, however, it should be supplemented with further essential electromigration techniques, *e.g.*, isotachopheresis.

Each chapter is abundantly illustrated with figures, diagrams and tables and is concluded with a list of references that is ample though still kept within reasonable limits.

The book can be heartily recommended to all chemists who are interested in analytical chemistry, ranging from research workers in certain branches to biochemists and environmentalists. Chemistry students will also find the book a useful introductory text and a valuable source of information.

J. CHURÁČEK

PUBLICATIONS RECEIVED

CLUE: A Microcomputer Program for Hierarchical Clustering: A. THIELEMANS, M. P. DERDE and D. L. MASSART, Elsevier Scientific Software, Amsterdam, 1986. \$295/Dfl.975/£245; manual only \$30/Dfl.100/£25. The introductory part of the manual is available free.

Available for:

IBM-PC, -XT, -AT with PC-DOS 2.x or 3.0 and PC-BASIC, 180/360K 5.25-in disc drive, 128K RAM.

Apple II, II+, IIe, IIc with DOS 3.3, Applesoft BASIC, 140K 5.25-in disc drive, 48K RAM (interpreter), 64K RAM (compiled).

The version tested for this review was for the IBM-PC, and the machine used for testing was an IBM-PC-AT, with PC-DOS 3.0

This microcomputer software package is an implementation of a divisive hierarchical method of clustering, originally proposed by MacNaughton-Smith *et al.* (*Nature*, 1964, **202**, 1034). This particular method of clustering is suitable for implementation on a microcomputer because it operates by starting with all the objects to be clustered, then divides them into two groups, then divides each of these into two more groups, and so on, until each object is in a separate group.

The first part of the package deals with data input and transformation; the data input routines are well protected from crashes that would otherwise be caused by mistypes such as the letter O instead of the figure 0. The second part contains the calculation of the dissimilarity matrix (it can use either the Euclidian distance between objects or the correlation as a measure of dissimilarity) and the clustering algorithm itself. The third part allows display and/or printing of previously stored clustering results.

The package is easy to learn to use, and, overall, it works very well in a way that is friendly to the user. Both compiled and interpreted versions were supplied on the disc: the compiled version was much faster, but otherwise they appeared identical. The manual, too, is nicely produced in a loose-leaf format (to allow updates to be added, presumably), though I did find it rather unwieldy for working with at the computer. The sections are Introduction, User Guide, Scientific Background, and Program Listings. (These listings are not provided if a manual is purchased on its own.)

However, the program is not entirely free from bugs. The manual explains that the initial setting-up program can only be used with a disc that is not write-protected; in fact, none of the package will run with a write-protected disc. If the package is set up for a 2-drive system, the data files on the disc in drive B are saved and loaded without trouble in the first and second parts of the package, but in the third part, files are reported as "not found" (because the machine is trying to read from drive A) unless the filename is preceded by "B:". This problem arises with both the compiled and interpreted versions of the program. Another, rather puzzling, error occurred in the printing of data matrices after a log transformation, in that just two or three spurious data values were printed out, *e.g.*, 9.99 instead of 0.103. The data in memory and on disc did not contain these errors, but they occurred every time the data were printed.

The manual lists some errors trapped by the program, but I found some that were not, and which caused the program to crash, leaving the system in BASIC. The authors did not mention this possibility, and did not give instructions on restarting from within BASIC. This would cause little bother to a user familiar with the machine, but a computer novice wanting just to use the package would be baffled—and the manual does otherwise seem to be aimed at a complete novice.

Despite these problems, I rather liked the package. It offers an easy introduction to clustering methods for the many analytical chemists who have not yet tried them. It is sad and unfortunate that the price is so excessive. Until the advent of microcomputers, programs like this were published in the open scientific literature, and freely exchanged among any workers interested. Is the price so high because IBM customers expect software to be in this price bracket? Many comparable packages for the Acorn BBC microcomputer can be had for £30-40. The only redeeming feature is that the purchaser is permitted to make four copies of the disc for use within the purchasing organization or institution.

MARY R. MASSON

Chromatographic Methods, 4th Ed. A. BRAITHWAITE and F. J. SMITH, Chapman & Hall, London, 1985. Pages x + 414. Hardback £29.00. Paperback £12.95.

This fourth and extended version of "Chromatographic Methods" is the result of the rich experience of both authors. The first two chapters are devoted to fundamental concepts and theories of chromatography, including also a short and interesting historical survey.

Plane (planar) Chromatography, Liquid Phase Chromatography in Open Columns, Gas Chromatography and High Performance Liquid Chromatography make up the main body of the book and are dealt with in four subsequent chapters. The modern approach to the treatment of the material is an outstanding feature of the four chapters.

Chapter 7 deals with procedures which have been developed for identifying compounds separated from a mixture. This chapter covers the coupling of chromatography with infrared and ultraviolet-visible spectrophotometry, mass spectrometry and atomic spectrometry.

Chapter 8 covers important new developments such as computerized data-handling and is devoted to methods of recording the chromatographic signal and data processing.

In the final chapter the authors give a number of examples of model experiments in chromatographic techniques.

In my opinion, the sub-chapter Electrophoresis included in Chapter 3 (Planar Chromatography) does not meaningfully fit into the concept of Chromatography but, on the other hand, it does fit into a book dealing with separation methods. Once there, however, it should be supplemented with further essential electromigration techniques, *e.g.*, isotachopheresis.

Each chapter is abundantly illustrated with figures, diagrams and tables and is concluded with a list of references that is ample though still kept within reasonable limits.

The book can be heartily recommended to all chemists who are interested in analytical chemistry, ranging from research workers in certain branches to biochemists and environmentalists. Chemistry students will also find the book a useful introductory text and a valuable source of information.

J. CHURÁČEK

PUBLICATIONS RECEIVED

Modern Practice of Gas Chromatography: edited by R. B. GROB, 2nd Ed., Wiley, New York, 1985. Pages xix + 897. £75.20.

This is the best general book on gas chromatography I have read. There is no skimping of detail yet the text is never obscure or cluttered and is always literate and sometimes amusing. The individualistic styles add liveliness and authority to the chapters, all of which are of very high quality. There is a remarkable, almost a missionary, zeal evident in the work of several of the authors—an eagerness to communicate information in depth along with caution, guidance, views, encouragement and excitement. The authors are good teachers who pass on their experience of handling techniques, the need for care when interpreting results, and detailed instruction, and helpful hints on how to improve methods by attention to the multitudinous factors. This is not an elementary text, neither is it one which swamps the reader with its copious detail. All of the information is in well-digested form. Major points about GC are discussed in many books and articles but the “what do you do when” and “I found” points are generally by-passed because wrongly regarded as too trivial. Some of the “minor” comments throughout this book are particularly helpful and illuminating in such areas. The authors are not only good expositors but are, likewise, enthusiastic, and highly experienced bench partners. The driving force is clearly that of Grob but there was also the dynamic of the Chromatography Forum of Delaware Valley behind the creation of the book and the assembly of the team. The illustrations, figures and tables are well chosen. The book will be invaluable to those already experienced in the art of chromatography who are turning this ever-expanding subject even more into a science.

The book is divided into three sections, with the first two, on Theory and Basics and on Techniques and Instrumentation occupying the first half, and the section of Applications the remainder. The introductory chapters by the editor are models of compression, clarity and comprehensiveness. They deal with principles of separation methods in general, and provide a useful GC glossary, before concentrating on the theory. W. R. Supina then guides the reader faced with the problems of selecting, using, and preparing packed columns and considers factors affecting the separation of peaks. M. A. Kaiser extends the description and discussion to cover GC on capillary columns. The first section of the book concludes with a chapter by M. S. Klee on optimizing separations by chromatography, taking into account the selection of columns and the ability to resolve overlapping peaks. The second section is introduced by a highly detailed chapter on detectors by M. J. O'Brien. R. Schill and R. R. Freeman deal with sample inlet systems, column ovens, carrier gas systems, detectors, and with data handling. F. J. Debbrecht is concerned with qualitative and quantitative analysis and gives a salutary reminder to all that “the ‘weakest link’ concept is (nowhere) more pronounced than it is in quantitative GC”. G. R. Umbreit deals with trace analysis and the relevant techniques of sample preparation. In the final section there are chapters on applications of GC to environmental analysis (R. L. Grob), analysis of foods (R. A. Barford and P. Magidman), physicochemical measurements (M. A. Kaiser and C. Dybowski), petrochemical analysis (F. E. Smith and K. E. Paulsen), polymer analysis (J. F. Sullivan) and drug analysis (E. J. McGonigle and F. Bigley) and on clinical applications of GC (J. C. Touchstone and M. F. Dobbins).

This summary of the contents provides an idea of the territory exposed to view and review but attention should focus less on this summary than on the high and worthwhile achievement of all the authors who have contributed to making this such a splendid book. The price is modest compared to the cost of a single capillary column, which in any case, with the aid of this book will be selected with greater skill, be used with enhanced expertise, and have the results interpreted with more intelligence.

K. C. B. WILKIE

Affinity Chromatography: Template Chromatography of Nucleic Acids and Proteins: H. SCHOTT, Dekker, New York, 1984. Pages x + 234. US \$59.25 (\$49.50 U.S. and Canada).

There has been a revolution in the scientists' and technologists' abilities to separate natural and synthetic biopolymers of highly complex structures by selectively abstracting them from solutions containing other compounds of like kind but different sequences of constituent building unit or having different biological functionalities. There are now many elegant, and practical, variations on techniques for immobilizing, say, molecules as diverse in size as nucleotides and nucleic acid, or amino-acids and proteins or peptides, on solid or gel supports such as cellulose, Sephadexes and Sephacryls. Thereafter chromatographic use can be made of the ability of the immobilized ligands to recognize solute molecules, including the many classes of nucleic acids, proteins and their lower molecular-weight chemical counterparts. Such recognition involves the formation of weak, reversible, conformationally possible hydrogen-bonds, leading to the highly selective abstraction of complementary solutes from mixed populations of chemically and biologically similar compounds, including those in dilute solutions. The separated species, after immobilization, could be used in turn to selectively abstract solute molecules having some chemical similarity to those originally employed as immobilized ligands.

The book is concerned with the techniques for immobilizing nucleoside phosphates, nucleosides, oligonucleotides, nucleic acids, and proteins and peptides and with the use of immobilized ligands to separate, characterize, or diagnose the various classes which have complementary bonding relationships with these ligands. It is also a practical guide and deals with what has been achieved and attempted in the field of immobilization chemistry applied to this highly specific field of adsorption chromatography. The technology of immobilizing nucleic acid and protein ligands, and their monomeric or oligomeric constituent units, is thoroughly documented. The author has given a very useful guide through the literature, most of which was published within the past ten years and much, indeed, within the past few years. The book should encourage many to use not only the methods already successfully employed but to develop others of like type to solve problems peculiar

PUBLICATIONS RECEIVED

Modern Practice of Gas Chromatography: edited by R. B. GROB, 2nd Ed., Wiley, New York, 1985. Pages xix + 897. £75.20.

This is the best general book on gas chromatography I have read. There is no skimping of detail yet the text is never obscure or cluttered and is always literate and sometimes amusing. The individualistic styles add liveliness and authority to the chapters, all of which are of very high quality. There is a remarkable, almost a missionary, zeal evident in the work of several of the authors—an eagerness to communicate information in depth along with caution, guidance, views, encouragement and excitement. The authors are good teachers who pass on their experience of handling techniques, the need for care when interpreting results, and detailed instruction, and helpful hints on how to improve methods by attention to the multitudinous factors. This is not an elementary text, neither is it one which swamps the reader with its copious detail. All of the information is in well-digested form. Major points about GC are discussed in many books and articles but the “what do you do when” and “I found” points are generally by-passed because wrongly regarded as too trivial. Some of the “minor” comments throughout this book are particularly helpful and illuminating in such areas. The authors are not only good expositors but are, likewise, enthusiastic, and highly experienced bench partners. The driving force is clearly that of Grob but there was also the dynamic of the Chromatography Forum of Delaware Valley behind the creation of the book and the assembly of the team. The illustrations, figures and tables are well chosen. The book will be invaluable to those already experienced in the art of chromatography who are turning this ever-expanding subject even more into a science.

The book is divided into three sections, with the first two, on Theory and Basics and on Techniques and Instrumentation occupying the first half, and the section of Applications the remainder. The introductory chapters by the editor are models of compression, clarity and comprehensiveness. They deal with principles of separation methods in general, and provide a useful GC glossary, before concentrating on the theory. W. R. Supina then guides the reader faced with the problems of selecting, using, and preparing packed columns and considers factors affecting the separation of peaks. M. A. Kaiser extends the description and discussion to cover GC on capillary columns. The first section of the book concludes with a chapter by M. S. Klee on optimizing separations by chromatography, taking into account the selection of columns and the ability to resolve overlapping peaks. The second section is introduced by a highly detailed chapter on detectors by M. J. O'Brien. R. Schill and R. R. Freeman deal with sample inlet systems, column ovens, carrier gas systems, detectors, and with data handling. F. J. Debbrecht is concerned with qualitative and quantitative analysis and gives a salutary reminder to all that “the ‘weakest link’ concept is (nowhere) more pronounced than it is in quantitative GC”. G. R. Umbreit deals with trace analysis and the relevant techniques of sample preparation. In the final section there are chapters on applications of GC to environmental analysis (R. L. Grob), analysis of foods (R. A. Barford and P. Magidman), physicochemical measurements (M. A. Kaiser and C. Dybowski), petrochemical analysis (F. E. Smith and K. E. Paulsen), polymer analysis (J. F. Sullivan) and drug analysis (E. J. McGonigle and F. Bigley) and on clinical applications of GC (J. C. Touchstone and M. F. Dobbins).

This summary of the contents provides an idea of the territory exposed to view and review but attention should focus less on this summary than on the high and worthwhile achievement of all the authors who have contributed to making this such a splendid book. The price is modest compared to the cost of a single capillary column, which in any case, with the aid of this book will be selected with greater skill, be used with enhanced expertise, and have the results interpreted with more intelligence.

K. C. B. WILKIE

Affinity Chromatography: Template Chromatography of Nucleic Acids and Proteins: H. SCHOTT, Dekker, New York, 1984. Pages x + 234. US \$59.25 (\$49.50 U.S. and Canada).

There has been a revolution in the scientists' and technologists' abilities to separate natural and synthetic biopolymers of highly complex structures by selectively abstracting them from solutions containing other compounds of like kind but different sequences of constituent building unit or having different biological functionalities. There are now many elegant, and practical, variations on techniques for immobilizing, say, molecules as diverse in size as nucleotides and nucleic acid, or amino-acids and proteins or peptides, on solid or gel supports such as cellulose, Sephadexes and Sephacryls. Thereafter chromatographic use can be made of the ability of the immobilized ligands to recognize solute molecules, including the many classes of nucleic acids, proteins and their lower molecular-weight chemical counterparts. Such recognition involves the formation of weak, reversible, conformationally possible hydrogen-bonds, leading to the highly selective abstraction of complementary solutes from mixed populations of chemically and biologically similar compounds, including those in dilute solutions. The separated species, after immobilization, could be used in turn to selectively abstract solute molecules having some chemical similarity to those originally employed as immobilized ligands.

The book is concerned with the techniques for immobilizing nucleoside phosphates, nucleosides, oligonucleotides, nucleic acids, and proteins and peptides and with the use of immobilized ligands to separate, characterize, or diagnose the various classes which have complementary bonding relationships with these ligands. It is also a practical guide and deals with what has been achieved and attempted in the field of immobilization chemistry applied to this highly specific field of adsorption chromatography. The technology of immobilizing nucleic acid and protein ligands, and their monomeric or oligomeric constituent units, is thoroughly documented. The author has given a very useful guide through the literature, most of which was published within the past ten years and much, indeed, within the past few years. The book should encourage many to use not only the methods already successfully employed but to develop others of like type to solve problems peculiar

to their own needs. The techniques described in this book may reasonably be expected rapidly to supersede others which are much less sensitive and selective. The family of techniques had enormous potential not only in genetic engineering, and molecular biology but in chemical studies of structures by use of compounds of known structure as investigative tools. The roles in biochemical investigations and, by a change of scale, in biotechnological and other industrial operations may at present seem to be in the realm of science fiction--but note the word seem.

K. C. B. WILKIE

Microcolumn Separations: edited by M. V. NOVOTNY and D. ISHII, Elsevier, Amsterdam, 1985. Pages xi + 336. \$64.75 (U.S.A. & Canada), Dfl 175.00 (rest of world).

This book originated out of a restricted seminar on microcolumn separation techniques held in Hawaii in 1982. A number of participants were asked to provide a survey-type contribution in their area of expertise and these contributions are in this book. Articles were updated to the end of 1983. The contributions are divided into four sections, namely column studies, miniaturized instrumentation and new techniques, spectroscopic detection and electrochemical detection.

It is stated in the preface that microcolumn techniques offer the following advantages over the commonly used HPLC, (a) increased separation efficiencies, (b) the ability to use expensive mobile phases because of extremely low volumetric flow-rates, (c) increased mass sensitivities with the connection-sensitive detectors, and (d) opportunities for novel detection modes.

Contributions in column studies cover open-tubular micro-HPLC, packed capillary columns, microcolumn size-exclusion HPLC and reversed-phase LC with a packed glass micro-capillary column. The section on miniaturized systems includes articles on sources of extra-column band-broadening in microcolumn LC, component miniaturization in HPLC, microbore HPLC, capillary supercritical fluid chromatography and capillary zone electrophoresis. Under spectroscopic detection the following are considered: optical detectors for microcolumn LC, laser-based chromatographic detectors, micro-HPLC combined with IR spectroscopy, flame-based detection in microcolumn LC, and LC- and micro LC-mass spectrometry. Finally under electrochemical detection, miniaturized ion-chromatography and miniaturized potentiometric and voltammetric detectors are considered.

This is a good book. The articles are well-written and there is a nice blend of theory, instrumentation and applications. All those interested in miniaturized separation systems will benefit from these surveys. Each article is well-referenced and there is a useful subject index.

J. B. HEADRIDGE

Computational Methods for the Determination of Formation Constants: DAVID J. LEGGETT, editor, Plenum Publishing Corporation, New York, 1985. Pages xvi + 478. \$75.00 in USA and Canada, \$90.00 elsewhere.

The distinguished list of contributors to this volume (Avdeef, Havel, Leggett, May, Meloun, Nagypál, Perrin, Sabatini, Stunzi, Vacca, Williams and Zekány) gives an indication of the quality to be expected. Dave Leggett has assembled a comprehensive collection of the most useful computer programs for evaluation of stability constants from experimental potentiometric and spectrophotometric experimental data, and for elucidation of the equilibrium model. An introductory chapter gives an overview of the problems to be solved by the computer in order to evaluate constants, and of the various possible ways in which solutions may be obtained. The second chapter describes the possible experimental strategies for investigating complex equilibria, and gives a brief treatment of the graphical methods of data treatment which, before the use of computers, were the only way to obtain stability constants, and which are still very useful for preliminary evaluations. The other chapters describe particular programs or suites of programs; in each, there is first a discussion of the theory behind the program, followed by details of the implementation, suggestions for applications, and detailed instructions for operation. The programs themselves are also included, and these listings should be accurate, since they have been reproduced photographically from listings of working versions of the programs produced by use of a high quality daisy-wheel printer. Anyone who has struggled to type in programs from inferior listings will appreciate the trouble that has been taken here. The programs included are MAGEC, SCOGS2, MINQUAD, MIQUV, SQUAD, ABLET and related programs, PSEQUAD and STBLTY.

MARY MASSON

Pyrolysis and GC in Polymer Analysis: S. A. LIEBMAN and E. J. LEVY, editors, Dekker, New York, 1985. Pages x + 557. \$89.75 (U.S.A. and Canada), \$107.50 or SFr. 269 (all other countries).

This monograph is a highly specialized contribution to polymer research. It is entirely devoted to pyrolytic analysis of natural and synthetic polymers by modern techniques for characterization of pyrolytic products. The opening chapter is an introduction to polymer characterization, followed by a study of basic analytical pyrolysis instrumental methods, including Pyrolysis Gas Chromatography (PGC) which is a rapidly growing area of GC. Subsequent discussions are focused on advanced pyrolysis instrumentation. There is an extensive coverage of GC columns, types of packing materials, and GC detectors. Other combined characterization techniques such as spectrometry (Mass Spectrometry and Fourier Transform Infrared) have also been undertaken. Discussion is centred on programmed pyrolysis methods and on the mechanism of thermal degradation of organic polymers. The authors have also included a discussion on the microstructure of synthetic polymers, which plays an important role in understanding the mechanism of pyrolysis of polymers.

Analytical PGC has also been used in analysis of biopolymers, e.g., amino-acids, peptides, proteins, carbohydrates and micro-organisms. An interesting inclusion is the forensic aspects of analytical pyrolysis. The combination of pyrolysis and

OBITUARY



PROFESSOR J. M. OTTAWAY
1939–1986

It came as a profound shock to hear on Monday 20 October that John Ottaway had suffered a brain haemorrhage during the week-end, and later that he had died that night. Born in 1939, John had a brilliant career and was at the height of his powers when stricken down. He obtained his B.Sc. (1961), Ph.D. (1965) and D.Sc. (1976) from the University of Exeter, and was elected a Fellow of the Royal Society of Edinburgh in 1982. After three years as an Assistant Lecturer at Exeter, he transferred to the University of Strathclyde, where he was successively Lecturer, Reader, and Professor, and was Head of the Chemistry Department at the time of his death. His research work was originally in the field of kinetic methods of analysis, but at Strathclyde he turned his attention to spectroscopic analysis, and rapidly gained an international reputation for his inventiveness in the field of atomic-absorption spectrometry. His distinction in this field was recognized by the award of the Silver Medal of the Society for Analytical Chemistry (1974) and the Gold Medal (1984) of the Analytical Division of the Royal Society of Chemistry. He also won a Royal Society of Chemistry Sponsored Award in 1983. A long-standing member of these two societies, he served on their Councils and many of their committees, notably the Editorial boards of *The Analyst*, *Analytical Proceedings* and *Journal of Analytical Atomic Spectroscopy*. He also served on the Advisory or Editorial Boards of several other journals, including *Talanta*, *Spectrochimica Acta B*, *Progress in Analytical Spectroscopy* and *Mikrochimica Acta*. A talented, lucid and witty speaker, he was invited to lecture in many countries throughout the world. A man of many interests, full of fun, good-humoured and friendly, he was universally liked and respected. His going at such an early age, full of promise for the future, is a grievous loss to analytical chemistry, his family, and all his many friends, whose memories of him will always be happy and cherished ones.

R. A. CHALMERS

TALANTA MEDAL

PROFESSOR ERNÖ PUNGOR



The Publisher and Editorial Board of *Talanta* take pleasure in announcing that, with the approval of the Advisory Board, the Eleventh Award of the Talanta Medal has been made to Professor Ernő Pungor, of the Institute for General and Analytical Chemistry, Technical University of Budapest.

Professor Pungor has published some 300 papers and written or edited several books in a wide variety of fields in analytical chemistry, including indicator theory and applications, gravimetric analysis, heteropoly acid chemistry, high-frequency titrimetry, flame photometry, atomic-absorption spectrometry, non-aqueous titrimetry, voltammetry, polarography, potentiometric titration, gas analysis, chromatography, continuous-flow analysis, and, above all, ion-selective electrodes. In addition, he has built up a very effective research team and teaching institute, which is exceptionally well equipped, and for many years has played a leading role in the Federation of European Chemical Societies and especially its Working Party on Analytical Chemistry. He is internationally recognized as an authority and innovator in several fields of analytical chemistry, and has played an outstanding role in the development of the subject in Hungary.

The previous winners of the Talanta Medal are as follows:

1961 F. FEIGL	1971 R. PŘIBIL
1963 G. SCHWARZENBACH	1974 B. V. L'VOV
1965 I. P. ALIMARIN	1977 R. BELCHER
1967 E. STAHL	1981 J. RŮŽIČKA
1969 A. WALSH	1983 T. FUJINAGA

NOTICES

SYMPOSIUM ON IMMUNOASSAYS PRESENT STATUS AND FUTURE PERSPECTIVES

Swedish Academy of Pharmaceutical Sciences

STOCKHOLM, 11-13 NOVEMBER 1986

The aim of the Symposium is to increase our understanding of the possibilities presented by immunoassay techniques for more efficient applications to future scientific and practical work.

The Symposium will be organized in sessions covering the following main areas:

1. General Immunology
2. Radioimmunoassays
3. Enzyme Immunoassays
4. Fluorescence and Luminescence Immunoassays
5. Particle-Based Systems
6. New Trends
7. Aspects of Immunoassays for Drug Quantification

In addition, ample scope for presentation of posters will be available. All participants are invited to submit a title or titles with the registration form.

The Proceedings of the Symposium will be published in a Special Issue of the *Journal of Pharmaceutical and Biomedical Analysis*. The cost of the Proceedings of the Symposium is included in the participation fee, so all participants will receive their copy automatically. Persons who are unable to attend the Symposium can obtain further information about the Proceedings on request. Authors of Posters are invited to submit their manuscripts to one of the Editors-in-Chief of the *Journal of Pharmaceutical and Biomedical Analysis* for publication in a consolidated issue.

The Symposium will be held at the SAS Arlandia Hotel, adjacent to Arlanda Airport, 40 km north of Stockholm, and will begin with an informal reception at 7 p.m. on Monday 10 November. The Scientific Programme will start at 9 a.m. on 11 November and end at 2 p.m. on 13 November.

The official language will be English.

Further information and application forms may be obtained by writing to: "Symposium on Immunoassays", The Swedish Academy of Pharmaceutical Sciences, P.O. Box 1136, S-11 81 Stockholm, Sweden.

6TH INTERNATIONAL CONFERENCE

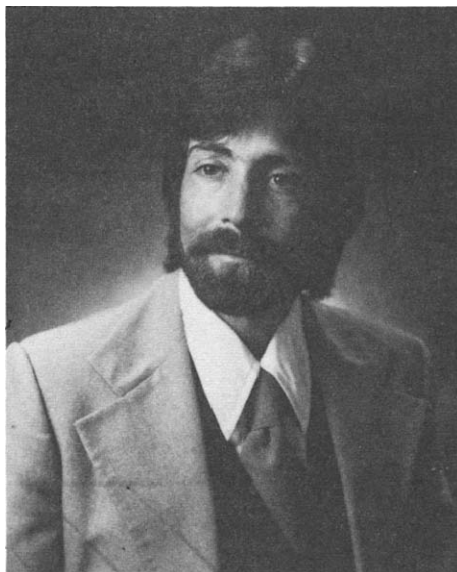
CHEMISTRY FOR PROTECTION OF THE ENVIRONMENT

15-18 September 1987

TORINO, ITALY

This Conference follows those held in Poland (1976, 1979, 1981), France (1983) and Belgium (1985). The Conference will be sponsored by: University of Torino, The Division of Analytical Chemistry of The Italian Chemical Society, EPA U.S., and among others by the Federation of European Chemical Societies. This Conference will provide an international forum for scientists, all chemists, chemical engineers, biologists etc., involved in environmental protection activities. The Conference proceedings will be published by Elsevier.

THE LOUIS GORDON MEMORIAL AWARD



B. S. FREISER

The Editorial Board and Publisher of *Talanta* take great pleasure in announcing that the Louis Gordon Memorial Award for 1985 (for the paper judged to be the best written of those appearing in *Talanta* during the year) will be made to Professor Ben S. Freiser, of Purdue University, for his paper "Investigation of reactions of metal ions and their clusters in the gas phase by laser-ionization Fourier-transform mass spectrometry" (*Talanta*, 1985, **32**, 697).

ERRATUM

Table 1 was accidentally omitted from the paper by Izquierdo, Compañó and Bars, *Talanta*, 1986, **33**, 463, and is printed below.

Table 1. Characteristics of the spectrophotometric determination of zinc with 5,7-dichloro-2-methyl-8-hydroxyquinoline

λ_{\max}	405 nm
Colour stability	5 hr
pH range of maximum absorbance	6.0-9.5
Reagent concentration	$2.4 \times 10^{-4} - 2.0 \times 10^{-2} M^*$
Beer's law range	1.0-23 $\mu\text{g/ml}^*$
Molar absorptivity	$5.9 \times 10^3 \text{ l. mole}^{-1} \text{ cm}^{-1}$
Precision	$\pm 0.6\%$
Detection limit ²⁶	0.05 $\mu\text{g/ml}$

*Higher concentrations were not investigated.

PUBLICATIONS RECEIVED

Selected Methods of Trace Metal Analysis: Biological and Environmental Samples: JON C. VAN LOON, Wiley-Interscience, New York, 1985. Pages xix + 357. £56.25.

This book is volume 80 in *Chemical Analysis*, a series of monographs on analytical chemistry and its applications, edited by J. D. Winefordner and the late P. J. Elving. This is in many ways a personal book, even though the author relies heavily on the work of other people. The bulk of the book consists of a detailed reproduction of a large number of previously published analytical procedures, given mostly in the words of the original authors. The description of reagents and equipment (with figures) is also included; the emphasis is on the practical aspects of each procedure. To have all this information in a single volume is very convenient for the practising analytical chemist.

Only procedures employing atomic-absorption of ICP emission spectrometry have been included. However, some very useful preconcentration techniques are also dealt with throughout the text. The emphasis is on the analysis of real samples, with a preference for standard reference materials.

After introductory chapters on instrumentation and methods of sample decomposition, the chapters are organized according to sample type, covering botanical, zoological, food, clinical, water, air and soil samples. A separate chapter has been devoted to the determination of metal species, *i.e.*, the chemical form of an element, in the various types of samples mentioned above. This chapter contains many interesting examples of the combination of chromatography with atomic absorption spectrometry.

The selection of procedures must necessarily be subjective. However, the book has broad scope, and it is up to date, with references up to 1984, so it should be very useful for a large number of analytical chemists. Thus, I discovered some references that I was not aware of, although I should have been! Further with a book like this the reader may learn a few tricks that can be carried over from one sample type to another.

I could have wished a more thorough discussion of the relative merits of the different procedure given for each type of sample. Also, a colleague of mine was a bit disappointed because his procedures for methylmercury in fish by GC-AAS, which is given in the book, was incorrectly ascribed to someone else, but I suppose that a few misprints are unavoidable.

Everyone who is interested in real trace and ultratrace determinations of metals will like this book. At least I do.

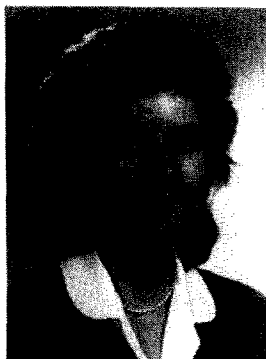
THE RONALD BELCHER MEMORIAL AWARD

The candidates for the first Ronald Belcher Memorial Award were all of very high calibre, which made the task of the selection committee particularly difficult. A great many factors had to be taken into account, and it was finally decided to make the award of as much help as possible by dividing it between two of the younger candidates, Lesley MacDonald and Carmen Cruces Blanco.



L. MACDONALD

Miss MacDonald, from Glasgow, Scotland, has been working on automation of surfactant analysis, which involved her in using a wide variety of analytical techniques, both classical and instrumental, in close collaboration with an industrial laboratory.



C. CRUCES BLANCO

Miss Cruces Blanco, from Málaga, Spain, has been working on synchronous and derivative spectrofluorimetry, with special reference to determination of pesticides and their metabolites in the environment.

LOUIS GORDON MEMORIAL AWARD



Presentation of the Louis Gordon Memorial Award for 1984, to Dr. Lilly Gustafsson, University of Uppsala (see *Talanta*, 1985, No. 3, page V). From left to right, the photograph shows Dr. Åke Olin, Dr. Lilly Gustafsson, Professor Folke Ingman (joint first winner of the Award, with Dr. Ebbe Still, in 1966), Professor Folke Nydahl (winner of the Award in 1976), Dr. Yngve Hermondsson and Professor Bengt Nygård.

to their own needs. The techniques described in this book may reasonably be expected rapidly to supersede others which are much less sensitive and selective. The family of techniques had enormous potential not only in genetic engineering, and molecular biology but in chemical studies of structures by use of compounds of known structure as investigative tools. The roles in biochemical investigations and, by a change of scale, in biotechnological and other industrial operations may at present seem to be in the realm of science fiction--but note the word seem.

K. C. B. WILKIE

Microcolumn Separations: edited by M. V. NOVOTNY and D. ISHII, Elsevier, Amsterdam, 1985. Pages xi + 336. \$64.75 (U.S.A. & Canada), Dfl 175.00 (rest of world).

This book originated out of a restricted seminar on microcolumn separation techniques held in Hawaii in 1982. A number of participants were asked to provide a survey-type contribution in their area of expertise and these contributions are in this book. Articles were updated to the end of 1983. The contributions are divided into four sections, namely column studies, miniaturized instrumentation and new techniques, spectroscopic detection and electrochemical detection.

It is stated in the preface that microcolumn techniques offer the following advantages over the commonly used HPLC, (a) increased separation efficiencies, (b) the ability to use expensive mobile phases because of extremely low volumetric flow-rates, (c) increased mass sensitivities with the connection-sensitive detectors, and (d) opportunities for novel detection modes.

Contributions in column studies cover open-tubular micro-HPLC, packed capillary columns, microcolumn size-exclusion HPLC and reversed-phase LC with a packed glass micro-capillary column. The section on miniaturized systems includes articles on sources of extra-column band-broadening in microcolumn LC, component miniaturization in HPLC, microbore HPLC, capillary supercritical fluid chromatography and capillary zone electrophoresis. Under spectroscopic detection the following are considered: optical detectors for microcolumn LC, laser-based chromatographic detectors, micro-HPLC combined with IR spectroscopy, flame-based detection in microcolumn LC, and LC- and micro LC-mass spectrometry. Finally under electrochemical detection, miniaturized ion-chromatography and miniaturized potentiometric and voltammetric detectors are considered.

This is a good book. The articles are well-written and there is a nice blend of theory, instrumentation and applications. All those interested in miniaturized separation systems will benefit from these surveys. Each article is well-referenced and there is a useful subject index.

J. B. HEADRIDGE

Computational Methods for the Determination of Formation Constants: DAVID J. LEGGETT, editor, Plenum Publishing Corporation, New York, 1985. Pages xvi + 478. \$75.00 in USA and Canada, \$90.00 elsewhere.

The distinguished list of contributors to this volume (Avdeef, Havel, Leggett, May, Meloun, Nagypál, Perrin, Sabatini, Stunzi, Vacca, Williams and Zekány) gives an indication of the quality to be expected. Dave Leggett has assembled a comprehensive collection of the most useful computer programs for evaluation of stability constants from experimental potentiometric and spectrophotometric experimental data, and for elucidation of the equilibrium model. An introductory chapter gives an overview of the problems to be solved by the computer in order to evaluate constants, and of the various possible ways in which solutions may be obtained. The second chapter describes the possible experimental strategies for investigating complex equilibria, and gives a brief treatment of the graphical methods of data treatment which, before the use of computers, were the only way to obtain stability constants, and which are still very useful for preliminary evaluations. The other chapters describe particular programs or suites of programs; in each, there is first a discussion of the theory behind the program, followed by details of the implementation, suggestions for applications, and detailed instructions for operation. The programs themselves are also included, and these listings should be accurate, since they have been reproduced photographically from listings of working versions of the programs produced by use of a high quality daisy-wheel printer. Anyone who has struggled to type in programs from inferior listings will appreciate the trouble that has been taken here. The programs included are MAGEC, SCOGS2, MINQUAD, MIQUV, SQUAD, ABLET and related programs, PSEQUAD and STBLTY.

MARY MASSON

Pyrolysis and GC in Polymer Analysis: S. A. LIEBMAN and E. J. LEVY, editors, Dekker, New York, 1985. Pages x + 557. \$89.75 (U.S.A. and Canada), \$107.50 or SFr. 269 (all other countries).

This monograph is a highly specialized contribution to polymer research. It is entirely devoted to pyrolytic analysis of natural and synthetic polymers by modern techniques for characterization of pyrolytic products. The opening chapter is an introduction to polymer characterization, followed by a study of basic analytical pyrolysis instrumental methods, including Pyrolysis Gas Chromatography (PGC) which is a rapidly growing area of GC. Subsequent discussions are focused on advanced pyrolysis instrumentation. There is an extensive coverage of GC columns, types of packing materials, and GC detectors. Other combined characterization techniques such as spectrometry (Mass Spectrometry and Fourier Transform Infrared) have also been undertaken. Discussion is centred on programmed pyrolysis methods and on the mechanism of thermal degradation of organic polymers. The authors have also included a discussion on the microstructure of synthetic polymers, which plays an important role in understanding the mechanism of pyrolysis of polymers.

Analytical PGC has also been used in analysis of biopolymers, e.g., amino-acids, peptides, proteins, carbohydrates and micro-organisms. An interesting inclusion is the forensic aspects of analytical pyrolysis. The combination of pyrolysis and

to their own needs. The techniques described in this book may reasonably be expected rapidly to supersede others which are much less sensitive and selective. The family of techniques had enormous potential not only in genetic engineering, and molecular biology but in chemical studies of structures by use of compounds of known structure as investigative tools. The roles in biochemical investigations and, by a change of scale, in biotechnological and other industrial operations may at present seem to be in the realm of science fiction--but note the word seem.

K. C. B. WILKIE

Microcolumn Separations: edited by M. V. NOVOTNY and D. ISHII, Elsevier, Amsterdam, 1985. Pages xi + 336. \$64.75 (U.S.A. & Canada), Dfl 175.00 (rest of world).

This book originated out of a restricted seminar on microcolumn separation techniques held in Hawaii in 1982. A number of participants were asked to provide a survey-type contribution in their area of expertise and these contributions are in this book. Articles were updated to the end of 1983. The contributions are divided into four sections, namely column studies, miniaturized instrumentation and new techniques, spectroscopic detection and electrochemical detection.

It is stated in the preface that microcolumn techniques offer the following advantages over the commonly used HPLC, (a) increased separation efficiencies, (b) the ability to use expensive mobile phases because of extremely low volumetric flow-rates, (c) increased mass sensitivities with the connection-sensitive detectors, and (d) opportunities for novel detection modes.

Contributions in column studies cover open-tubular micro-HPLC, packed capillary columns, microcolumn size-exclusion HPLC and reversed-phase LC with a packed glass micro-capillary column. The section on miniaturized systems includes articles on sources of extra-column band-broadening in microcolumn LC, component miniaturization in HPLC, microbore HPLC, capillary supercritical fluid chromatography and capillary zone electrophoresis. Under spectroscopic detection the following are considered: optical detectors for microcolumn LC, laser-based chromatographic detectors, micro-HPLC combined with IR spectroscopy, flame-based detection in microcolumn LC, and LC- and micro LC-mass spectrometry. Finally under electrochemical detection, miniaturized ion-chromatography and miniaturized potentiometric and voltammetric detectors are considered.

This is a good book. The articles are well-written and there is a nice blend of theory, instrumentation and applications. All those interested in miniaturized separation systems will benefit from these surveys. Each article is well-referenced and there is a useful subject index.

J. B. HEADRIDGE

Computational Methods for the Determination of Formation Constants: DAVID J. LEGGETT, editor, Plenum Publishing Corporation, New York, 1985. Pages xvi + 478. \$75.00 in USA and Canada, \$90.00 elsewhere.

The distinguished list of contributors to this volume (Avdeef, Havel, Leggett, May, Meloun, Nagypál, Perrin, Sabatini, Stunzi, Vacca, Williams and Zekány) gives an indication of the quality to be expected. Dave Leggett has assembled a comprehensive collection of the most useful computer programs for evaluation of stability constants from experimental potentiometric and spectrophotometric experimental data, and for elucidation of the equilibrium model. An introductory chapter gives an overview of the problems to be solved by the computer in order to evaluate constants, and of the various possible ways in which solutions may be obtained. The second chapter describes the possible experimental strategies for investigating complex equilibria, and gives a brief treatment of the graphical methods of data treatment which, before the use of computers, were the only way to obtain stability constants, and which are still very useful for preliminary evaluations. The other chapters describe particular programs or suites of programs; in each, there is first a discussion of the theory behind the program, followed by details of the implementation, suggestions for applications, and detailed instructions for operation. The programs themselves are also included, and these listings should be accurate, since they have been reproduced photographically from listings of working versions of the programs produced by use of a high quality daisy-wheel printer. Anyone who has struggled to type in programs from inferior listings will appreciate the trouble that has been taken here. The programs included are MAGEC, SCOGS2, MINQUAD, MIQUV, SQUAD, ABLET and related programs, PSEQUAD and STBLTY.

MARY MASSON

Pyrolysis and GC in Polymer Analysis: S. A. LIEBMAN and E. J. LEVY, editors, Dekker, New York, 1985. Pages x + 557. \$89.75 (U.S.A. and Canada), \$107.50 or SFr. 269 (all other countries).

This monograph is a highly specialized contribution to polymer research. It is entirely devoted to pyrolytic analysis of natural and synthetic polymers by modern techniques for characterization of pyrolytic products. The opening chapter is an introduction to polymer characterization, followed by a study of basic analytical pyrolysis instrumental methods, including Pyrolysis Gas Chromatography (PGC) which is a rapidly growing area of GC. Subsequent discussions are focused on advanced pyrolysis instrumentation. There is an extensive coverage of GC columns, types of packing materials, and GC detectors. Other combined characterization techniques such as spectrometry (Mass Spectrometry and Fourier Transform Infrared) have also been undertaken. Discussion is centred on programmed pyrolysis methods and on the mechanism of thermal degradation of organic polymers. The authors have also included a discussion on the microstructure of synthetic polymers, which plays an important role in understanding the mechanism of pyrolysis of polymers.

Analytical PGC has also been used in analysis of biopolymers, e.g., amino-acids, peptides, proteins, carbohydrates and micro-organisms. An interesting inclusion is the forensic aspects of analytical pyrolysis. The combination of pyrolysis and

PUBLICATIONS RECEIVED

Evaluation of Analytical Methods in Biological Systems, Part B: Hazardous Metals in Human Toxicology: edited by A. VERCRUYSSE, Elsevier, Amsterdam, 1984. Pages x + 338. \$73.00; Dfl. 190.00

This book, arising from the increasing need for understanding the metabolic fate of a number of toxic metals, illustrates the tools available at present to reach that goal. It starts from the fact that reliable analytical data are a prerequisite for the correctness of conclusions about "toxicity" and "essentiality". The book addresses the issue of identifying the right indices for short and long term exposure of the human body to toxic metals and their monitoring. In a very comprehensive, yet concise, summary of literature data, Singerman covers the principles of monitoring biological effects, cautions about uncritical interpretation of data and describes current knowledge on exposure indices for Pb, Hg, Cd, Cr, As, Se, Te, Th, Ni.

A chapter on principles underlying instrumental analytical techniques, as well as general discussion of instrumentation and performance of modern techniques concludes the general introductory first half of the book. The second part is dedicated to an in-depth discussion of the analytical assessment of the individual metals Pb, Hg, Cd, As, Th, Cr, Ni, Se and Te.

The great merit of this book lies not only in the internationally recognized expertise of each of the contributing authors, but in the well balanced and most professional and uniform construction of the chapters. The specific properties of the element are summarized in an introduction along with a brief enumeration of analytical challenges and possible solutions. Sampling, sample-handling and storage of biological materials with respect to each of the target elements receive due attention in each chapter. A critical overview of available methods updates the reader on current beliefs and experience both in terms of analytical performance, potentials and limitations and cost-benefit considerations. Much to the help of the user, attention is paid to aspects of standardization, quality-control and calibration, and not least to interpretation of the data obtained.

The scrutiny of the problems and the systematic approach taken render this book one of the better works of reference for the analyst who needs to decide which techniques to set up for routine analyses. Each of the chapters could exist as a monograph by itself and provides the user with a comprehensive compilation of references to start from. The reader does not get lost in too detailed descriptions.

This book is warmly recommended to everyone involved in biochemical, toxicological or analytical research on trace "elements", be they toxic and/or essential.

MARLEEN VERLINDEN

Characterisation of Spilled Oil Samples: edited by J. A. BUTT, D. F. DUCKWORTH and S. G. PERRY, Wiley, New York, 1985. Pages ix + 95. £17.50.

This book is a relatively broad-based treatise on the analytical and social implications inherent in the qualitative assessment of the source of marine oil spillages. As an update of a previous Institute of Petroleum issue ("Marine pollution by oil") with an expanded discussion on the use of modern analytical approaches, it will prove of interest to both analyst and layman alike.

The first two chapters give a brief insight into the wider aspects of oil pollution. The analyst's role in assessing potential environmental impact and spillage clean-up and the legal dilemmas posed in validating evidence based on the probability matching of samples (*i.e.*, on a "like" or "not like" basis) are examined.

The analytical problem is then outlined in two chapters dealing with the effects of "weathering" on different types of spilled oils and the subsequent sampling of these oils at different types of spill sites. The exposure of spilled oils to prevailing climatic conditions necessarily results in samples which are adulterations of the original "suspect" source oils, while sample "clean-up" prior to presentation for analysis is difficult to standardize.

The next two chapters deal, first, with the particular constituents of crude oils which lend themselves to easiest comparison between different oils and, secondly, with their detection and quantification. Distinguishing between crude oils, residual oils, distillate oils and vegetable oils is easily achieved by measuring physical properties and non-hydrocarbon contents (*e.g.*, density, viscosity, sulphur and trace metal contents, infrared spectra *etc.*). The distinguishability of different types of crude oil is, however, much more affected by sample weathering and, where such weathering is extensive, comparisons can be based on the differing contents of "biological markers" such as steranes, isoprenoids and triterpanes or heavy aromatic species. High and low resolution GLC, computerized CC/MS and ultraviolet fluorescence methods are presented as "front line" instrumental analysis techniques for the identification of oils, and the interpretation of data produced from these methods is discussed. The potential application of other techniques, including TLC, HPLC, ¹³C NMR and soft-ionization MS is also presented.

Where feasible, characterization of oils is best achieved by correlation of results from as many of these analysis techniques as are available and, due to the abundance of numerical data provided by some techniques, the need for statistical interpretation rather than visual "matching" in the identification of the source of marine oil spillages is expected to increase.

D. A. EDWARDS

PUBLICATIONS RECEIVED

Evaluation of Analytical Methods in Biological Systems, Part B: Hazardous Metals in Human Toxicology: edited by A. VERCRUYSSE, Elsevier, Amsterdam, 1984. Pages x + 338. \$73.00; Dfl. 190.00

This book, arising from the increasing need for understanding the metabolic fate of a number of toxic metals, illustrates the tools available at present to reach that goal. It starts from the fact that reliable analytical data are a prerequisite for the correctness of conclusions about "toxicity" and "essentiality". The book addresses the issue of identifying the right indices for short and long term exposure of the human body to toxic metals and their monitoring. In a very comprehensive, yet concise, summary of literature data, Singerman covers the principles of monitoring biological effects, cautions about uncritical interpretation of data and describes current knowledge on exposure indices for Pb, Hg, Cd, Cr, As, Se, Te, Th, Ni.

A chapter on principles underlying instrumental analytical techniques, as well as general discussion of instrumentation and performance of modern techniques concludes the general introductory first half of the book. The second part is dedicated to an in-depth discussion of the analytical assessment of the individual metals Pb, Hg, Cd, As, Th, Cr, Ni, Se and Te.

The great merit of this book lies not only in the internationally recognized expertise of each of the contributing authors, but in the well balanced and most professional and uniform construction of the chapters. The specific properties of the element are summarized in an introduction along with a brief enumeration of analytical challenges and possible solutions. Sampling, sample-handling and storage of biological materials with respect to each of the target elements receive due attention in each chapter. A critical overview of available methods updates the reader on current beliefs and experience both in terms of analytical performance, potentials and limitations and cost-benefit considerations. Much to the help of the user, attention is paid to aspects of standardization, quality-control and calibration, and not least to interpretation of the data obtained.

The scrutiny of the problems and the systematic approach taken render this book one of the better works of reference for the analyst who needs to decide which techniques to set up for routine analyses. Each of the chapters could exist as a monograph by itself and provides the user with a comprehensive compilation of references to start from. The reader does not get lost in too detailed descriptions.

This book is warmly recommended to everyone involved in biochemical, toxicological or analytical research on trace "elements", be they toxic and/or essential.

MARLEEN VERLINDEN

Characterisation of Spilled Oil Samples: edited by J. A. BUTT, D. F. DUCKWORTH and S. G. PERRY, Wiley, New York, 1985. Pages ix + 95. £17.50.

This book is a relatively broad-based treatise on the analytical and social implications inherent in the qualitative assessment of the source of marine oil spillages. As an update of a previous Institute of Petroleum issue ("Marine pollution by oil") with an expanded discussion on the use of modern analytical approaches, it will prove of interest to both analyst and layman alike.

The first two chapters give a brief insight into the wider aspects of oil pollution. The analyst's role in assessing potential environmental impact and spillage clean-up and the legal dilemmas posed in validating evidence based on the probability matching of samples (*i.e.*, on a "like" or "not like" basis) are examined.

The analytical problem is then outlined in two chapters dealing with the effects of "weathering" on different types of spilled oils and the subsequent sampling of these oils at different types of spill sites. The exposure of spilled oils to prevailing climatic conditions necessarily results in samples which are adulterations of the original "suspect" source oils, while sample "clean-up" prior to presentation for analysis is difficult to standardize.

The next two chapters deal, first, with the particular constituents of crude oils which lend themselves to easiest comparison between different oils and, secondly, with their detection and quantification. Distinguishing between crude oils, residual oils, distillate oils and vegetable oils is easily achieved by measuring physical properties and non-hydrocarbon contents (*e.g.*, density, viscosity, sulphur and trace metal contents, infrared spectra *etc.*). The distinguishability of different types of crude oil is, however, much more affected by sample weathering and, where such weathering is extensive, comparisons can be based on the differing contents of "biological markers" such as steranes, isoprenoids and triterpanes or heavy aromatic species. High and low resolution GLC, computerized CC/MS and ultraviolet fluorescence methods are presented as "front line" instrumental analysis techniques for the identification of oils, and the interpretation of data produced from these methods is discussed. The potential application of other techniques, including TLC, HPLC, ¹³C NMR and soft-ionization MS is also presented.

Where feasible, characterization of oils is best achieved by correlation of results from as many of these analysis techniques as are available and, due to the abundance of numerical data provided by some techniques, the need for statistical interpretation rather than visual "matching" in the identification of the source of marine oil spillages is expected to increase.

D. A. EDWARDS

PUBLICATIONS RECEIVED

Analytical Measurement and Information; Advances in the Information Theoretic Approach to Chemical Analyses: K. ECKSCHLAGER and V. ŠTĚPÁNEK, Research Studies Press, Letchworth, Hertfordshire, England; Wiley, New York, 1985. Pp. xii + 140. £25.

This sequel to *Information Theory as Applied to Chemical Analysis* (the same authors, Wiley, New York, 1979) enlarges on all trends and recent developments of this new discipline. In a condensed form it provides the essential theoretical background and reference material for those who want an introduction to this promising field of theoretical thought. Information theory is regarded by some workers as a useful tool to assess experiments, and moreover, this discipline is supposed to become a philosophy much needed to unify various diverging lines of modern analytical chemistry. As can be seen from the literature, which is covered to about 1983, Eckschlager and Štěpánek have published in recent years many original contributions to analytical applications of information theory and so they further develop ideas based upon their own work.

After a brief introductory account of analytical procedures and systems as sources of information, Chapter 2 deals with information measures (Brillouin and Shannon concepts) and also illustrates the divergence measure of the information content of analytical determinations. In Chapter 3 the main topics of the monograph are discussed, namely the theoretical approaches to various analytical procedures (identification of a component, one- and multicomponent determinations, trace analysis). Chapter 4 is aimed more towards the future. The use of information theory in investigation of analytical systems is considered from various aspects (description of analytical systems; mathematical expression of accuracy, selectivity or specificity of a method; sources of uncertainty and their implications in chemical analysis; sampling). In this chapter an interesting treatment of calibration procedures is also given. Various concepts of entropy as amount of information are discussed in the Appendix. The text reflects the present status of information theory in analytical chemistry. The achievements have been mapped and the blank spaces shown for future endeavour. The theoretical approaches outlined are illustrated by solved problems; for some of them the conclusions are more or less evident from the data given. The reader can thus form his own opinion of the feasibility and utility of theoretical calculation. The condensed style and abstract presentation of generally formulated problems require attentive reading and active co-operation of the reader. It is advisable to study the earlier monograph first and to have it at hand. The fundamental concepts of probability calculus and information theory are given there in more detail. The authors refer quite often to this text and a useful list of symbols can also be found there. Reading of the present book is not at all easy and in some places the text is difficult to understand, owing to the style and many special terms (a glossary on terminology may be of great help). The standard of the book could have been much improved by more careful editing of the text, by elimination of mistakes in typing (pp. 54 and 64, values of absorbencies/values of absorbance) and perhaps by the use of typographical setting which allows use of italics for symbols. Let us not forget the tired eyes and weary mind of many of those who want up-to-date information and advice on new developments of science.

STANISLAV KOTRLÝ

Standard Potentials in Aqueous Solution: A. J. BARD, R. PARSONS and J. JORDAN (eds.), Dekker, New York, 1985. Pages xii + 834. \$29.95.

Most analytical chemists must at some time have had occasion to refer to Wendell M. Latimer's *Oxidation Potentials*. This new book aims to provide a text similar to Latimer's (which was last revised in 1952), but using current notation and conventions, and incorporating all the new data now available. The task of producing such a book is now much too great for a single author, so instead, under the auspices of IUPAC Commissions I.3 (Electrochemistry) and V.5 (Electroanalytical Chemistry), chapters were commissioned from specialists in particular fields, then reviewed by named referees. The potentials given are critically selected wherever possible, or at least they are the best estimates available. The potentials are discussed for the elements arranged in periodic-table groups—as in Latimer's book—and many thermodynamic data are included. An enormous amount of valuable information has been collected, and it is presented together with much valuable discussion and background information on industrial processes, etc. Also as in Latimer, an Appendix provides two tables, one for acid and one for basic solutions, of selected half-reaction potentials listed in order of increasingly positive values—a most useful feature. Some 60 authors contributed material, so the editors are to be congratulated on achieving such a remarkably consistent volume. The book has been produced to a very high standard, and at the currently advertised price of \$29.95, it offers outstanding value: buy it as soon as possible—the price is said to be subject to change without notice.

MARY MASSON

PUBLICATIONS RECEIVED

Analytical Measurement and Information; Advances in the Information Theoretic Approach to Chemical Analyses: K. ECKSCHLAGER and V. ŠTĚPÁNEK, Research Studies Press, Letchworth, Hertfordshire, England; Wiley, New York, 1985. Pp. xii + 140. £25.

This sequel to *Information Theory as Applied to Chemical Analysis* (the same authors, Wiley, New York, 1979) enlarges on all trends and recent developments of this new discipline. In a condensed form it provides the essential theoretical background and reference material for those who want an introduction to this promising field of theoretical thought. Information theory is regarded by some workers as a useful tool to assess experiments, and moreover, this discipline is supposed to become a philosophy much needed to unify various diverging lines of modern analytical chemistry. As can be seen from the literature, which is covered to about 1983, Eckschlager and Štěpánek have published in recent years many original contributions to analytical applications of information theory and so they further develop ideas based upon their own work.

After a brief introductory account of analytical procedures and systems as sources of information, Chapter 2 deals with information measures (Brillouin and Shannon concepts) and also illustrates the divergence measure of the information content of analytical determinations. In Chapter 3 the main topics of the monograph are discussed, namely the theoretical approaches to various analytical procedures (identification of a component, one- and multicomponent determinations, trace analysis). Chapter 4 is aimed more towards the future. The use of information theory in investigation of analytical systems is considered from various aspects (description of analytical systems; mathematical expression of accuracy, selectivity or specificity of a method; sources of uncertainty and their implications in chemical analysis; sampling). In this chapter an interesting treatment of calibration procedures is also given. Various concepts of entropy as amount of information are discussed in the Appendix. The text reflects the present status of information theory in analytical chemistry. The achievements have been mapped and the blank spaces shown for future endeavour. The theoretical approaches outlined are illustrated by solved problems; for some of them the conclusions are more or less evident from the data given. The reader can thus form his own opinion of the feasibility and utility of theoretical calculation. The condensed style and abstract presentation of generally formulated problems require attentive reading and active co-operation of the reader. It is advisable to study the earlier monograph first and to have it at hand. The fundamental concepts of probability calculus and information theory are given there in more detail. The authors refer quite often to this text and a useful list of symbols can also be found there. Reading of the present book is not at all easy and in some places the text is difficult to understand, owing to the style and many special terms (a glossary on terminology may be of great help). The standard of the book could have been much improved by more careful editing of the text, by elimination of mistakes in typing (pp. 54 and 64, values of absorbencies/values of absorbance) and perhaps by the use of typographical setting which allows use of italics for symbols. Let us not forget the tired eyes and weary mind of many of those who want up-to-date information and advice on new developments of science.

STANISLAV KOTRLÝ

Standard Potentials in Aqueous Solution: A. J. BARD, R. PARSONS and J. JORDAN (eds.), Dekker, New York, 1985. Pages xii + 834. \$29.95.

Most analytical chemists must at some time have had occasion to refer to Wendell M. Latimer's *Oxidation Potentials*. This new book aims to provide a text similar to Latimer's (which was last revised in 1952), but using current notation and conventions, and incorporating all the new data now available. The task of producing such a book is now much too great for a single author, so instead, under the auspices of IUPAC Commissions I.3 (Electrochemistry) and V.5 (Electroanalytical Chemistry), chapters were commissioned from specialists in particular fields, then reviewed by named referees. The potentials given are critically selected wherever possible, or at least they are the best estimates available. The potentials are discussed for the elements arranged in periodic-table groups—as in Latimer's book—and many thermodynamic data are included. An enormous amount of valuable information has been collected, and it is presented together with much valuable discussion and background information on industrial processes, etc. Also as in Latimer, an Appendix provides two tables, one for acid and one for basic solutions, of selected half-reaction potentials listed in order of increasingly positive values—a most useful feature. Some 60 authors contributed material, so the editors are to be congratulated on achieving such a remarkably consistent volume. The book has been produced to a very high standard, and at the currently advertised price of \$29.95, it offers outstanding value: buy it as soon as possible—the price is said to be subject to change without notice.

MARY MASSON

PUBLICATIONS RECEIVED

Analytical Solution Calorimetry: J. K. GRIME (editor), Wiley-Interscience, Chichester, 1985. Pages 417. £69.40, \$79.80.

The editor accurately summarizes the aim of this book as "providing a guide to the application of calorimetry to analytical chemistry and the determination of thermodynamic parameters". He is responsible for the brief introductory chapter on thermodynamics, thermochemistry and calorimetry, and for the detailed reviews, in the last two chapters, of applications of solution calorimetry to inorganic, organic, environmental, pharmaceutical, biochemical and clinical analysis. In the last two fields, the technique has considerable promise because the robust, inert, easily miniaturized and highly sensitive, thermistor probes have advantages over alternative devices, particularly for the study of proteins and enzyme-catalysed processes.

The fundamentals of the techniques are considered in detail by the recognized authority on solution calorimetry, Professor Jordan, and his colleague Dr. Stahl.

Instrumentation, data reduction and the determination of ΔH and K_{eq} values, with practical examples, are covered by the research group at Brigham Young University, who have been responsible for the development of modern instrumentation and its use in obtaining industrial analytical data and measuring thermodynamic parameters. The industrially-important analytical flow systems based on calorimetric measurement are reviewed by Dr. Schifreen of the Dupont Company.

In analytical solution calorimetry, since temperature is the dependent variable, selectivity is achieved by choice of the analytical reaction. The book, in explaining this approach, can be considered to be the definitive reference text for workers in the field. It makes the case for further evaluation of this relatively neglected analytical technique which, with the instrumentation now available, should find a wider more general use.

The book should find a place in the libraries of research and educational establishments concerned with analytical science, but its price restricts its use as a student text book.

E. J. GREENHOW

Photometric Methods in Inorganic Trace Analysis: E. UPOR, M. MOHAI and GY. NOVÁK (Wilson and Wilson's Comprehensive Analytical Chemistry, edited by G. Svehla, Vol. XX), Elsevier, Amsterdam, 1985. Pages XIII + 404. \$111.00 (U.S.A. and Canada), Dfl. 300.00 (elsewhere).

Though quite strong in its treatment of analysis of "practical samples", and rich in passing on the personal experience of the authors, this book is certainly not comprehensive, since the coverage of methods for certain elements is rather eclectic and many key references to the background chemistry are omitted. Moreover, the literature coverage does not seem to get beyond very early 1983. There are some curious statements, such as that on page 34 about iron(II) complexes; the informed reader will know what was meant, but the words used are misleading. In a book written and edited by Hungarian chemists, it is surprising that accents are given on journal titles, but not on authors' names, and is particularly unfortunate since the omission is equivalent to a mis-spelling of an accentless name, and in some languages can result in a name having a rude meaning. Sometimes useful information is buried in the text and is not traceable from the index; an example is the interference caused by formation of a heteronuclear ligand-bridged complex (pages 31 and 34). The index is, in fact, not much more informative than the contents list; it also has some spelling errors (or undetected printer's errors). On the whole, the book is rather disappointing, and certainly expensive, though useful as a guide to reliable methods.

R. A. CHALMERS

Spot Test Analysis: ERVIN JUNGREIS, Wiley-Interscience, New York, 1985. Pages xi + 315. £76.00.

To the busy industrial or academic analyst receiving a telephone call that begins "I wonder whether you could help me with this problem I have with a water supply (cement, metal, foodstuff, drug, stain . . .)", this book will come as a godsend, being a well-organized, well-indexed mine of information, complete with practical details, on rapid screening of clinical, forensic, geochemical, air, water, soil, plant tissue and food samples. Not cheap, but well worth the price for the time it can save (but the reader should be warned that in the references to Chapter 9, it appears that "See ref. 49" means "See ref. 16", and "See ref. 58" means "See ref. 59", etc.). Should be in all works or university libraries, and will take its place alongside "Feigl".

R. A. CHALMERS

Treatise on Analytical Chemistry, Part I, Vol. 4, 2nd Ed.: edited by PHILIP J. ELVING, VICTOR G. MOSSOTTI and I. M. KOLTHOFF, Wiley-Interscience, New York, 1984. Pages xxix + 675. £86.75.

Like its predecessors in the second edition of what might well be called "the analyst's friend", this volume demonstrates very clearly the enormous development that has taken place in analytical science since the first edition was published. The topics covered are the informational structure of analytical chemistry, analogue electronics, operational amplifiers and analogur circuit analysis, transducers, automation in laboratory and on-line analysis, and the use and interfacing of computer systems. In the context of current thought in organization and practice of analytical science, this volume will undoubtedly prove one of the most useful and significant in the series. Packed with information, it is good value for money.

R. A. CHALMERS

PUBLICATIONS RECEIVED

Analytical Solution Calorimetry: J. K. GRIME (editor), Wiley-Interscience, Chichester, 1985. Pages 417. £69.40, \$79.80.

The editor accurately summarizes the aim of this book as "providing a guide to the application of calorimetry to analytical chemistry and the determination of thermodynamic parameters". He is responsible for the brief introductory chapter on thermodynamics, thermochemistry and calorimetry, and for the detailed reviews, in the last two chapters, of applications of solution calorimetry to inorganic, organic, environmental, pharmaceutical, biochemical and clinical analysis. In the last two fields, the technique has considerable promise because the robust, inert, easily miniaturized and highly sensitive, thermistor probes have advantages over alternative devices, particularly for the study of proteins and enzyme-catalysed processes.

The fundamentals of the techniques are considered in detail by the recognized authority on solution calorimetry, Professor Jordan, and his colleague Dr. Stahl.

Instrumentation, data reduction and the determination of ΔH and K_{eq} values, with practical examples, are covered by the research group at Brigham Young University, who have been responsible for the development of modern instrumentation and its use in obtaining industrial analytical data and measuring thermodynamic parameters. The industrially-important analytical flow systems based on calorimetric measurement are reviewed by Dr. Schifreen of the Dupont Company.

In analytical solution calorimetry, since temperature is the dependent variable, selectivity is achieved by choice of the analytical reaction. The book, in explaining this approach, can be considered to be the definitive reference text for workers in the field. It makes the case for further evaluation of this relatively neglected analytical technique which, with the instrumentation now available, should find a wider more general use.

The book should find a place in the libraries of research and educational establishments concerned with analytical science, but its price restricts its use as a student text book.

E. J. GREENHOW

Photometric Methods in Inorganic Trace Analysis: E. UPOR, M. MOHAI and GY. NOVÁK (Wilson and Wilson's Comprehensive Analytical Chemistry, edited by G. Svehla, Vol. XX), Elsevier, Amsterdam, 1985. Pages XIII + 404. \$111.00 (U.S.A. and Canada), Dfl. 300.00 (elsewhere).

Though quite strong in its treatment of analysis of "practical samples", and rich in passing on the personal experience of the authors, this book is certainly not comprehensive, since the coverage of methods for certain elements is rather eclectic and many key references to the background chemistry are omitted. Moreover, the literature coverage does not seem to get beyond very early 1983. There are some curious statements, such as that on page 34 about iron(II) complexes; the informed reader will know what was meant, but the words used are misleading. In a book written and edited by Hungarian chemists, it is surprising that accents are given on journal titles, but not on authors' names, and is particularly unfortunate since the omission is equivalent to a mis-spelling of an accentless name, and in some languages can result in a name having a rude meaning. Sometimes useful information is buried in the text and is not traceable from the index; an example is the interference caused by formation of a heteronuclear ligand-bridged complex (pages 31 and 34). The index is, in fact, not much more informative than the contents list; it also has some spelling errors (or undetected printer's errors). On the whole, the book is rather disappointing, and certainly expensive, though useful as a guide to reliable methods.

R. A. CHALMERS

Spot Test Analysis: ERVIN JUNGREIS, Wiley-Interscience, New York, 1985. Pages xi + 315. £76.00.

To the busy industrial or academic analyst receiving a telephone call that begins "I wonder whether you could help me with this problem I have with a water supply (cement, metal, foodstuff, drug, stain . . .)", this book will come as a godsend, being a well-organized, well-indexed mine of information, complete with practical details, on rapid screening of clinical, forensic, geochemical, air, water, soil, plant tissue and food samples. Not cheap, but well worth the price for the time it can save (but the reader should be warned that in the references to Chapter 9, it appears that "See ref. 49" means "See ref. 16", and "See ref. 58" means "See ref. 59", etc.). Should be in all works or university libraries, and will take its place alongside "Feigl".

R. A. CHALMERS

Treatise on Analytical Chemistry, Part I, Vol. 4, 2nd Ed.: edited by PHILIP J. ELVING, VICTOR G. MOSSOTTI and I. M. KOLTHOFF, Wiley-Interscience, New York, 1984. Pages xxix + 675. £86.75.

Like its predecessors in the second edition of what might well be called "the analyst's friend", this volume demonstrates very clearly the enormous development that has taken place in analytical science since the first edition was published. The topics covered are the informational structure of analytical chemistry, analogue electronics, operational amplifiers and analogur circuit analysis, transducers, automation in laboratory and on-line analysis, and the use and interfacing of computer systems. In the context of current thought in organization and practice of analytical science, this volume will undoubtedly prove one of the most useful and significant in the series. Packed with information, it is good value for money.

R. A. CHALMERS

PUBLICATIONS RECEIVED

Analytical Solution Calorimetry: J. K. GRIME (editor), Wiley-Interscience, Chichester, 1985. Pages 417. £69.40, \$79.80.

The editor accurately summarizes the aim of this book as "providing a guide to the application of calorimetry to analytical chemistry and the determination of thermodynamic parameters". He is responsible for the brief introductory chapter on thermodynamics, thermochemistry and calorimetry, and for the detailed reviews, in the last two chapters, of applications of solution calorimetry to inorganic, organic, environmental, pharmaceutical, biochemical and clinical analysis. In the last two fields, the technique has considerable promise because the robust, inert, easily miniaturized and highly sensitive, thermistor probes have advantages over alternative devices, particularly for the study of proteins and enzyme-catalysed processes.

The fundamentals of the techniques are considered in detail by the recognized authority on solution calorimetry, Professor Jordan, and his colleague Dr. Stahl.

Instrumentation, data reduction and the determination of ΔH and K_{eq} values, with practical examples, are covered by the research group at Brigham Young University, who have been responsible for the development of modern instrumentation and its use in obtaining industrial analytical data and measuring thermodynamic parameters. The industrially-important analytical flow systems based on calorimetric measurement are reviewed by Dr. Schifreen of the Dupont Company.

In analytical solution calorimetry, since temperature is the dependent variable, selectivity is achieved by choice of the analytical reaction. The book, in explaining this approach, can be considered to be the definitive reference text for workers in the field. It makes the case for further evaluation of this relatively neglected analytical technique which, with the instrumentation now available, should find a wider more general use.

The book should find a place in the libraries of research and educational establishments concerned with analytical science, but its price restricts its use as a student text book.

E. J. GREENHOW

Photometric Methods in Inorganic Trace Analysis: E. UPOR, M. MOHAI and GY. NOVÁK (Wilson and Wilson's Comprehensive Analytical Chemistry, edited by G. Svehla, Vol. XX), Elsevier, Amsterdam, 1985. Pages XIII + 404. \$111.00 (U.S.A. and Canada), Dfl. 300.00 (elsewhere).

Though quite strong in its treatment of analysis of "practical samples", and rich in passing on the personal experience of the authors, this book is certainly not comprehensive, since the coverage of methods for certain elements is rather eclectic and many key references to the background chemistry are omitted. Moreover, the literature coverage does not seem to get beyond very early 1983. There are some curious statements, such as that on page 34 about iron(II) complexes; the informed reader will know what was meant, but the words used are misleading. In a book written and edited by Hungarian chemists, it is surprising that accents are given on journal titles, but not on authors' names, and is particularly unfortunate since the omission is equivalent to a mis-spelling of an accentless name, and in some languages can result in a name having a rude meaning. Sometimes useful information is buried in the text and is not traceable from the index; an example is the interference caused by formation of a heteronuclear ligand-bridged complex (pages 31 and 34). The index is, in fact, not much more informative than the contents list; it also has some spelling errors (or undetected printer's errors). On the whole, the book is rather disappointing, and certainly expensive, though useful as a guide to reliable methods.

R. A. CHALMERS

Spot Test Analysis: ERVIN JUNGREIS, Wiley-Interscience, New York, 1985. Pages xi + 315. £76.00.

To the busy industrial or academic analyst receiving a telephone call that begins "I wonder whether you could help me with this problem I have with a water supply (cement, metal, foodstuff, drug, stain . . .)", this book will come as a godsend, being a well-organized, well-indexed mine of information, complete with practical details, on rapid screening of clinical, forensic, geochemical, air, water, soil, plant tissue and food samples. Not cheap, but well worth the price for the time it can save (but the reader should be warned that in the references to Chapter 9, it appears that "See ref. 49" means "See ref. 16", and "See ref. 58" means "See ref. 59", etc.). Should be in all works or university libraries, and will take its place alongside "Feigl".

R. A. CHALMERS

Treatise on Analytical Chemistry, Part I, Vol. 4, 2nd Ed.: edited by PHILIP J. ELVING, VICTOR G. MOSSOTTI and I. M. KOLTHOFF, Wiley-Interscience, New York, 1984. Pages xxix + 675. £86.75.

Like its predecessors in the second edition of what might well be called "the analyst's friend", this volume demonstrates very clearly the enormous development that has taken place in analytical science since the first edition was published. The topics covered are the informational structure of analytical chemistry, analogue electronics, operational amplifiers and analogur circuit analysis, transducers, automation in laboratory and on-line analysis, and the use and interfacing of computer systems. In the context of current thought in organization and practice of analytical science, this volume will undoubtedly prove one of the most useful and significant in the series. Packed with information, it is good value for money.

R. A. CHALMERS

PUBLICATIONS RECEIVED

Analytical Solution Calorimetry: J. K. GRIME (editor), Wiley-Interscience, Chichester, 1985. Pages 417. £69.40, \$79.80.

The editor accurately summarizes the aim of this book as "providing a guide to the application of calorimetry to analytical chemistry and the determination of thermodynamic parameters". He is responsible for the brief introductory chapter on thermodynamics, thermochemistry and calorimetry, and for the detailed reviews, in the last two chapters, of applications of solution calorimetry to inorganic, organic, environmental, pharmaceutical, biochemical and clinical analysis. In the last two fields, the technique has considerable promise because the robust, inert, easily miniaturized and highly sensitive, thermistor probes have advantages over alternative devices, particularly for the study of proteins and enzyme-catalysed processes.

The fundamentals of the techniques are considered in detail by the recognized authority on solution calorimetry, Professor Jordan, and his colleague Dr. Stahl.

Instrumentation, data reduction and the determination of ΔH and K_{eq} values, with practical examples, are covered by the research group at Brigham Young University, who have been responsible for the development of modern instrumentation and its use in obtaining industrial analytical data and measuring thermodynamic parameters. The industrially-important analytical flow systems based on calorimetric measurement are reviewed by Dr. Schifreen of the Dupont Company.

In analytical solution calorimetry, since temperature is the dependent variable, selectivity is achieved by choice of the analytical reaction. The book, in explaining this approach, can be considered to be the definitive reference text for workers in the field. It makes the case for further evaluation of this relatively neglected analytical technique which, with the instrumentation now available, should find a wider more general use.

The book should find a place in the libraries of research and educational establishments concerned with analytical science, but its price restricts its use as a student text book.

E. J. GREENHOW

Photometric Methods in Inorganic Trace Analysis: E. UPOR, M. MOHAI and GY. NOVÁK (Wilson and Wilson's Comprehensive Analytical Chemistry, edited by G. Svehla, Vol. XX), Elsevier, Amsterdam, 1985. Pages XIII + 404. \$111.00 (U.S.A. and Canada), Dfl. 300.00 (elsewhere).

Though quite strong in its treatment of analysis of "practical samples", and rich in passing on the personal experience of the authors, this book is certainly not comprehensive, since the coverage of methods for certain elements is rather eclectic and many key references to the background chemistry are omitted. Moreover, the literature coverage does not seem to get beyond very early 1983. There are some curious statements, such as that on page 34 about iron(II) complexes; the informed reader will know what was meant, but the words used are misleading. In a book written and edited by Hungarian chemists, it is surprising that accents are given on journal titles, but not on authors' names, and is particularly unfortunate since the omission is equivalent to a mis-spelling of an accentless name, and in some languages can result in a name having a rude meaning. Sometimes useful information is buried in the text and is not traceable from the index; an example is the interference caused by formation of a heteronuclear ligand-bridged complex (pages 31 and 34). The index is, in fact, not much more informative than the contents list; it also has some spelling errors (or undetected printer's errors). On the whole, the book is rather disappointing, and certainly expensive, though useful as a guide to reliable methods.

R. A. CHALMERS

Spot Test Analysis: ERVIN JUNGREIS, Wiley-Interscience, New York, 1985. Pages xi + 315. £76.00.

To the busy industrial or academic analyst receiving a telephone call that begins "I wonder whether you could help me with this problem I have with a water supply (cement, metal, foodstuff, drug, stain . . .)", this book will come as a godsend, being a well-organized, well-indexed mine of information, complete with practical details, on rapid screening of clinical, forensic, geochemical, air, water, soil, plant tissue and food samples. Not cheap, but well worth the price for the time it can save (but the reader should be warned that in the references to Chapter 9, it appears that "See ref. 49" means "See ref. 16", and "See ref. 58" means "See ref. 59", etc.). Should be in all works or university libraries, and will take its place alongside "Feigl".

R. A. CHALMERS

Treatise on Analytical Chemistry, Part I, Vol. 4, 2nd Ed.: edited by PHILIP J. ELVING, VICTOR G. MOSSOTTI and I. M. KOLTHOFF, Wiley-Interscience, New York, 1984. Pages xxix + 675. £86.75.

Like its predecessors in the second edition of what might well be called "the analyst's friend", this volume demonstrates very clearly the enormous development that has taken place in analytical science since the first edition was published. The topics covered are the informational structure of analytical chemistry, analogue electronics, operational amplifiers and analogur circuit analysis, transducers, automation in laboratory and on-line analysis, and the use and interfacing of computer systems. In the context of current thought in organization and practice of analytical science, this volume will undoubtedly prove one of the most useful and significant in the series. Packed with information, it is good value for money.

R. A. CHALMERS

NOTICES

SYMPOSIUM ON IMMUNOASSAYS PRESENT STATUS AND FUTURE PERSPECTIVES

Swedish Academy of Pharmaceutical Sciences

STOCKHOLM, 11-13 NOVEMBER 1986

The aim of the Symposium is to increase our understanding of the possibilities presented by immunoassay techniques for more efficient applications to future scientific and practical work.

The Symposium will be organized in sessions covering the following main areas:

1. General Immunology
2. Radioimmunoassays
3. Enzyme Immunoassays
4. Fluorescence and Luminescence Immunoassays
5. Particle-Based Systems
6. New Trends
7. Aspects of Immunoassays for Drug Quantification

In addition, ample scope for presentation of posters will be available. All participants are invited to submit a title or titles with the registration form.

The Proceedings of the Symposium will be published in a Special Issue of the *Journal of Pharmaceutical and Biomedical Analysis*. The cost of the Proceedings of the Symposium is included in the participation fee, so all participants will receive their copy automatically. Persons who are unable to attend the Symposium can obtain further information about the Proceedings on request. Authors of Posters are invited to submit their manuscripts to one of the Editors-in-Chief of the *Journal of Pharmaceutical and Biomedical Analysis* for publication in a consolidated issue.

The Symposium will be held at the SAS Arlandia Hotel, adjacent to Arlanda Airport, 40 km north of Stockholm, and will begin with an informal reception at 7 p.m. on Monday 10 November. The Scientific Programme will start at 9 a.m. on 11 November and end at 2 p.m. on 13 November.

The official language will be English.

Further information and application forms may be obtained by writing to: "Symposium on Immunoassays", The Swedish Academy of Pharmaceutical Sciences, P.O. Box 1136, S-11 81 Stockholm, Sweden.

6TH INTERNATIONAL CONFERENCE

CHEMISTRY FOR PROTECTION OF THE ENVIRONMENT

15-18 September 1987

TORINO, ITALY

This Conference follows those held in Poland (1976, 1979, 1981), France (1983) and Belgium (1985). The Conference will be sponsored by: University of Torino, The Division of Analytical Chemistry of The Italian Chemical Society, EPA U.S., and among others by the Federation of European Chemical Societies. This Conference will provide an international forum for scientists, all chemists, chemical engineers, biologists etc., involved in environmental protection activities. The Conference proceedings will be published by Elsevier.

TOPICS

The general theme of the topics will be the physicochemical processes and aspects of chemistry and chemical engineering in the science of the aquatic environment. Papers on microbiological aspects or air pollution and solid waste will be considered as well. The sessions will deal more specifically with:

- advanced physicochemical treatment;
- the interaction of biological and physicochemical (sub) processes in combined treatment processes;
- the origin, transfer, fate and effects of chemical pollutants in the environment;
- plants for treatment of effluents;
- methods for the removal of hazardous hydrocarbons and organic materials from aqueous environments;
- advances in environmental monitoring and analytical chemistry.

SUBMISSION OF PAPERS

Papers and abstracts must be in English. They must contain original material not published elsewhere.

Papers will be selected on the basis of extended abstracts. A compilation of these abstracts (together with the full invited papers) will be handed out at the Conference. Beside an introduction they should describe methods, results and conclusions, and must be submitted before 31 October 1986 in a form enabling direct reproduction by the photo-offset process. An abstract should contain ~600 words and one or two figures and/or tables (2-4 pages). It should be single-spaced on DIN A4 format (210-297 mm), white paper with a 12 pitch Gothic or similar letter type and leaving 30 mm margins. Title, name of author(s) and address(es) should be typed within an additional 70 mm spaced at the head of the first page.

SECRETARIAT

All correspondence concerning the Conference should be addressed to:

6th Int. Conference Chemistry for Protection of the Environment

Prof. C. SARZANINI

Dipartimento di Chimica Analitica

Via P. Giuria 5

10125 TORINO (ITALY)

Tel. (natl.) 011/657272

Tel. (internatl.) /39/11/657272

INTERNATIONAL SYMPOSIUM ON PHARMACEUTICAL AND BIOMEDICAL ANALYSIS

Barcelona Congress Centre, Spain

23-25 September 1987

The aim of the meeting is to present and evaluate new trends and developments in, and applications of, analytical methods for the analysis of drugs and endogenous components of human metabolism in biological samples.

The scientific programme will cover, as special topics, Anticancer Drugs, Computer-Aided Analysis (including Robotics), Psychoactive Drugs and New Developments and Applications. These topics as well as any others of interest in the field of Pharmaceutical and Biomedical Analysis will be discussed in invited plenary and keynote lectures, invited and submitted research contributions, and poster presentations. The Proceedings of the Symposium will be published by the *Journal of Pharmaceutical and Biomedical Analysis*. If interested, please provide tentative title(s) for contributed paper(s).

The Symposium will precede the International Symposium on Applied Mass Spectrometry in the Health Sciences, to be held on 28-30 September 1987, also in the Barcelona Congress Centre, which will cover complementary analytical approaches exclusively centred on the application of Mass Spectrometric Techniques.

Exhibition space will be available for manufacturers.

For further information on registration and instrument exhibition facilities please contact:

DR. EMILIO GELPI, Chairman, Organizing Committee, International Symposium on Pharmaceutical and Biomedical Analysis, PALACIO DE CONGRESOS, Avda. Reina Ma Cristina, s/n., 08004 Barcelona, Spain
Phone 325.30.00-223.99.40
Telex 53.117 FOIMB-E

to their own needs. The techniques described in this book may reasonably be expected rapidly to supersede others which are much less sensitive and selective. The family of techniques had enormous potential not only in genetic engineering, and molecular biology but in chemical studies of structures by use of compounds of known structure as investigative tools. The roles in biochemical investigations and, by a change of scale, in biotechnological and other industrial operations may at present seem to be in the realm of science fiction--but note the word seem.

K. C. B. WILKIE

Microcolumn Separations: edited by M. V. NOVOTNY and D. ISHII, Elsevier, Amsterdam, 1985. Pages xi + 336. \$64.75 (U.S.A. & Canada), Dfl 175.00 (rest of world).

This book originated out of a restricted seminar on microcolumn separation techniques held in Hawaii in 1982. A number of participants were asked to provide a survey-type contribution in their area of expertise and these contributions are in this book. Articles were updated to the end of 1983. The contributions are divided into four sections, namely column studies, miniaturized instrumentation and new techniques, spectroscopic detection and electrochemical detection.

It is stated in the preface that microcolumn techniques offer the following advantages over the commonly used HPLC, (a) increased separation efficiencies, (b) the ability to use expensive mobile phases because of extremely low volumetric flow-rates, (c) increased mass sensitivities with the connection-sensitive detectors, and (d) opportunities for novel detection modes.

Contributions in column studies cover open-tubular micro-HPLC, packed capillary columns, microcolumn size-exclusion HPLC and reversed-phase LC with a packed glass micro-capillary column. The section on miniaturized systems includes articles on sources of extra-column band-broadening in microcolumn LC, component miniaturization in HPLC, microbore HPLC, capillary supercritical fluid chromatography and capillary zone electrophoresis. Under spectroscopic detection the following are considered: optical detectors for microcolumn LC, laser-based chromatographic detectors, micro-HPLC combined with IR spectroscopy, flame-based detection in microcolumn LC, and LC- and micro LC-mass spectrometry. Finally under electrochemical detection, miniaturized ion-chromatography and miniaturized potentiometric and voltammetric detectors are considered.

This is a good book. The articles are well-written and there is a nice blend of theory, instrumentation and applications. All those interested in miniaturized separation systems will benefit from these surveys. Each article is well-referenced and there is a useful subject index.

J. B. HEADRIDGE

Computational Methods for the Determination of Formation Constants: DAVID J. LEGGETT, editor, Plenum Publishing Corporation, New York, 1985. Pages xvi + 478. \$75.00 in USA and Canada, \$90.00 elsewhere.

The distinguished list of contributors to this volume (Avdeef, Havel, Leggett, May, Meloun, Nagypál, Perrin, Sabatini, Stunzi, Vacca, Williams and Zekány) gives an indication of the quality to be expected. Dave Leggett has assembled a comprehensive collection of the most useful computer programs for evaluation of stability constants from experimental potentiometric and spectrophotometric experimental data, and for elucidation of the equilibrium model. An introductory chapter gives an overview of the problems to be solved by the computer in order to evaluate constants, and of the various possible ways in which solutions may be obtained. The second chapter describes the possible experimental strategies for investigating complex equilibria, and gives a brief treatment of the graphical methods of data treatment which, before the use of computers, were the only way to obtain stability constants, and which are still very useful for preliminary evaluations. The other chapters describe particular programs or suites of programs; in each, there is first a discussion of the theory behind the program, followed by details of the implementation, suggestions for applications, and detailed instructions for operation. The programs themselves are also included, and these listings should be accurate, since they have been reproduced photographically from listings of working versions of the programs produced by use of a high quality daisy-wheel printer. Anyone who has struggled to type in programs from inferior listings will appreciate the trouble that has been taken here. The programs included are MAGEC, SCOGS2, MINQUAD, MIQUV, SQUAD, ABLET and related programs, PSEQUAD and STBLTY.

MARY MASSON

Pyrolysis and GC in Polymer Analysis: S. A. LIEBMAN and E. J. LEVY, editors, Dekker, New York, 1985. Pages x + 557. \$89.75 (U.S.A. and Canada), \$107.50 or SFr. 269 (all other countries).

This monograph is a highly specialized contribution to polymer research. It is entirely devoted to pyrolytic analysis of natural and synthetic polymers by modern techniques for characterization of pyrolytic products. The opening chapter is an introduction to polymer characterization, followed by a study of basic analytical pyrolysis instrumental methods, including Pyrolysis Gas Chromatography (PGC) which is a rapidly growing area of GC. Subsequent discussions are focused on advanced pyrolysis instrumentation. There is an extensive coverage of GC columns, types of packing materials, and GC detectors. Other combined characterization techniques such as spectrometry (Mass Spectrometry and Fourier Transform Infrared) have also been undertaken. Discussion is centred on programmed pyrolysis methods and on the mechanism of thermal degradation of organic polymers. The authors have also included a discussion on the microstructure of synthetic polymers, which plays an important role in understanding the mechanism of pyrolysis of polymers.

Analytical PGC has also been used in analysis of biopolymers, e.g., amino-acids, peptides, proteins, carbohydrates and micro-organisms. An interesting inclusion is the forensic aspects of analytical pyrolysis. The combination of pyrolysis and

GC is a powerful and sensitive analytical method used for identifying paint marks, fibres and other type of trace evidence necessary in forensic work.

The last chapter is devoted to the theory and application of inverse GC, which is a study of the stationary phase and an important aspect of physical polymer chemistry. Polymer solution thermodynamics is also been reviewed in this chapter.

This volume has brought together experts' contributions in pyrolysis, GC and polymer chemistry. The book is well presented with detailed and helpful indexing and is a significant contribution in the field.

M. YOUNUS QURESHI

Interfacing Your BBC Microcomputer: R. MORGAN, W. McCLEAN and J. ROSELL, Prentice-Hall International, London, 1985. Pages ix + 179. £8.95.

I have read many books on interfacing the BBC Microcomputer, but this is the most useful I have seen, because it combines coverage of the programming techniques required, with descriptions of electronic circuits. The main distinction from other texts is that the circuits are explained and discussed in terms that can be readily understood by a reader who is not an electronics specialist (*i.e.*, someone who can usually read a circuit diagram, but not understand it). As a result, the reader has a chance of being able to adapt circuits to fit a particular situation, and of understanding some of the circuits given in other books. The main topics covered include digital input and output, analogue input and output, and control systems. Direct-addressing techniques are used in the early part of the book, but the "official" OSBYTE routines are introduced later, as are assembler code techniques. Construction projects include driving a lamp and motors, burglar alarms, measurement of light levels, measurement of temperature, controlling the temperature of an enclosure, a light pen, and an external ADC. Highly recommended.

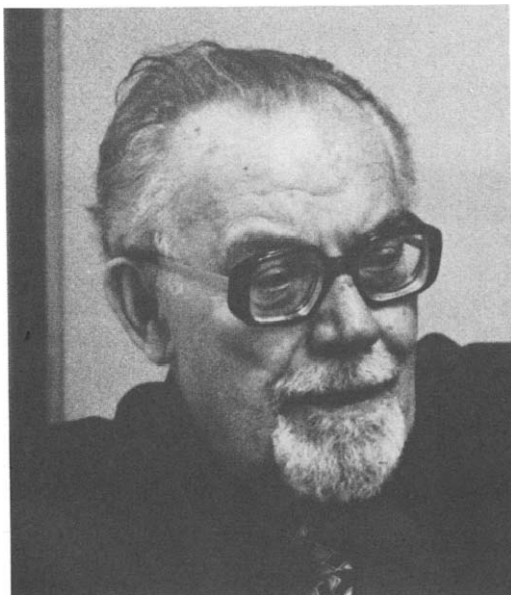
MARY MASSON

The BBC Microcomputer in Control: P. BEVERLEY, N. EAMES and G. OSBORNE, Prentice-Hall International, London, 1985. Pages xi + 150. £7.95.

This is an interesting collection of "Interfacing Projects for Beginners", to quote the sub-title. The book is nicely produced, and is indeed very helpful to a beginner, who may never have assembled an electronic circuit previously. Thus, Appendix I describes the necessary constructional techniques, including soldering, strip board and printed circuit board construction, gives colour codes for resistors and capacitors, and explains how to connect diodes, transistors *etc.* The topics covered include power switching, digital input, use of the analogue-to-digital converter for voltage measurement, resistance measurement, as a logic probe, and for timing, *e.g.*, of a pendulum. Computer communications via the RS423 (Acorn's RS232) serial interface are also discussed.

MARY MASSON

OBITUARIES



RUDOLF PŘIBIL, D.Sc.
(1910–1986)

We have learned with deep regret that Dr. Rudolf Přibil died suddenly on 2 February 1986. This is a great loss to the international chemical community, of a renowned analytical chemist, a pioneer in complexometry and a friend to many analysts throughout the world.

Dr. Přibil was born on 23 July 1910, in Prague. He studied chemistry, mathematics and physics at the Faculty of Natural Sciences, Charles University in Prague. During his university years, in 1930, he became a demonstrator at the Department of Analytical Chemistry under Professor Oldřich Tomíček and since then analytical chemistry was his main interest. In 1933 he graduated with an RNDr. degree (M.Sc.) in natural sciences. He spent short periods as a temporary teacher of chemistry, physics and mathematics at various secondary schools in Prague, but mostly worked with Professor Tomíček at the Department of Analytical Chemistry of his Alma Mater, first as a demonstrator and later as a lecturer, until all the Czech universities were closed by the Germans in 1939. He spent the years of the second world war as an analyst for chemical companies in Pardubice–Rybitví and in Prague.

At the end of the war, in May 1945, he returned to the very badly damaged laboratories of Charles University and devoted all his energy to rapid recommencement of the courses in analytical chemistry that were impatiently awaited by hundreds of students who were deprived of university education during the war. In 1946 he became an associate professor in analytical chemistry and worked as deputy to the head of the Department, Professor Tomíček. In 1948–1950 he acted as the head of the Department of Inorganic and Forensic Chemistry, simultaneously retaining all his teaching duties at the Department of Analytical Chemistry.

In 1950, Dr. Přibil left the University and worked for five years as the head of the Analytical Chemistry Section of the Research Institute of Pharmacy and Biochemistry. In 1955 he moved to the then Polarographic Institute of the Czechoslovak Academy of Sciences where he headed the Analytical Laboratory until his retirement at the end of 1978.

The scientific work of Dr. Přibil is contained in some 350 original and review papers in renowned journals and 25 monographs written in Czech, English, Bulgarian, German, Russian and Rumanian. His early research before the second world war was influenced by Professor Tomíček and dealt mainly with potentiometric titrations, especially cerimetry. After the war, he was one of the first people in the world to recognize the

enormous analytical potential of the class of compounds termed "complexones", introduced by Professor G. Schwarzenbach. With dozens of his pupils he developed numerous practical analytical methods involving the use of EDTA and related compounds, first as masking agents, later mainly as titrants. With his co-workers he introduced a number of new metallochromic indicators, such as Xylenol Orange, Methylthymol Blue, Thymolphthaleincomplexone and Fluoresceincomplexone. These works have had a great impact on analytical chemistry throughout the world. In Czechoslovakia, his outstanding contribution to analytical chemistry was recognized in 1953 by the award of the State Prize and in 1958 by the degree of D.Sc. He was awarded the Talanta Gold Medal in 1971.

Dr. Přibil did much to disseminate knowledge in his excellent lectures, that were renowned for their wit and for his inimitable skill in practical demonstrations. The lecture theatres were always packed by students, as well as practising analysts, who came to listen to him. He was a fanatic at work, with an unerring sense for practical usefulness and with countless original ideas. He asked much of his students, but did not spare himself or his time in helping them. Even after his retirement, he went to work in the analytical laboratory of the Geological Institute, Charles University, until poor health finally prevented him from doing so.

He was a great story-teller and it was a delight listening to him. He made lots of friends in all the continents of the world, with whom he maintained friendly contacts until the end of his life. His many years of service to *Talanta*, as a regional editor, should also not be forgotten.

One of the last classical chemists in the world, a unique personality with a very broad background, has died. He will be greatly missed by all his pupils, friends and other people associated with analytical chemistry.

KAREL ŠTULÍK

RUDOLF PŘIBIL—THE MAN

I first met Rudolf Přibil in 1959 when he came to Aberdeen to give a lecture. An immediate rapport was established and we rapidly became good friends. In the years that followed I came to know him well, as a person as well as a chemist. He had a warm, extrovert and generous personality, and many unsuspected talents. As a young man he had a reputation as a tennis player, but in much later life revealed an unexpected skill at billiards (presumably dating from student days). He was renowned for his sense of humour and very ready wit. During a demonstration lecture in Aberdeen, finding no spatula had been provided, he broke up a firmly caked chemical in a reagent bottle with what he immediately referred to as an "analytically pure finger", a term that at once passed into daily use among students. When asked whether a certain lecture might not be terminated after about 90 minutes of exposition, he replied "Why? My plane doesn't leave till next week". All who have heard him give a lecture in English will recall his habitual opening remark "Please forget all rules of English grammar!", followed by what may best be described as a fluid use of the language in giving a clear and always fascinating account of his newest ideas, illustrated by elegant demonstrations performed with remarkable dexterity.

His extensive travels in the course of lecturing on complexometric analysis led to a fund of stories about his adventures, ranging from breaking light bulbs with his head in Japanese hotel rooms ("I am too tall for Japan") to being marooned for a week in Moscow because of fog at the airport, and a plane missed through a misunderstanding. Like the late Professor Belcher, he seemed to attract problems and happenings when travelling, so that travel with him was always full of surprises.

By those who knew him well he will be remembered with warmth and great affection, for his friendship and the something extra he brought into their lives.

R. A. CHALMERS

TALANTA ADVISORY BOARD

The Editorial Board and the Publisher of *Talanta* take great pleasure in welcoming two new members of the Advisory Board:

M. VALCARCEL H. FALK

and wish them long and fruitful service on it.

At the same time, they are very sorry to be losing the services of Mr. Howard J. Francis, Jr., as Regional Editor in the U.S.A. and as the Editorial Board representative of the Regional Editors, a position he has filled with assiduous care and attention since his appointment as successor to Professor Louis Gordon in 1966. For twenty years Mr. Howard has served the journal well, and has played a considerable part in its success, and it is with regret that his retirement from chemistry and the Board must be accepted. The Board and Publisher wish him a long and happy retirement, and are sure his many interests will keep him fully occupied for many years to come.

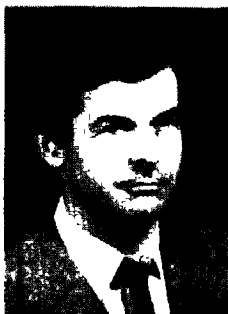


H. J. FRANCIS

MIGUEL VALCARCEL is Professor of Analytical Chemistry at the University of Córdoba (Spain). He was born in 1946 in Barcelona and graduated in Chemistry at the University of Seville, from which he received his Ph.D. in Chemical Sciences in 1971. He became professor in 1976. His fields of activity and interest are automatic methods, with emphasis on unsegmented flow alternatives, simultaneous determinations involving no separation, continuous liquid-liquid extraction, indirect atomic-absorption methods, kinetic methods of analysis, and modern molecular fluorescence spectroscopic techniques. He has written or co-authored about 150 papers and is author of three analytical textbooks published in Spanish, co-author of the monograph "Flow Injection Analysis: Principles and Applications" (currently in press) and co-editor of another monograph, "Kinetic Methods of Analysis", published in Spanish. Since July 1985 Professor Valcárcel has been the President of the Spanish Society of Analytical Chemistry.



M. VALCARCEL



H. FALK

PROFESSOR HEINZ FALK obtained his Diploma in Physics in 1961 and the degrees of Dr. rer. nat. in Physics (1966) and Dr. sci. nat. in Physics (1976) from the Humboldt University of Berlin, and worked as Scientific Assistant and Lecturer in the Physical Institute of that university from 1961 to 1964, then successively as Scientific Assistant (until 1969), Head of the Department of Spectroscopy (until 1980) and Head of the Section of Spectroscopy at the Central Institute for Optics and Spectroscopy of the Academy of Sciences of the German Democratic Republic, where he was appointed Professor of Physics in 1980. His main research interests have been the theoretical and experimental basis of the analytical application of atomic spectroscopy, with special attention to the physical possibilities and limitations of different atomic spectroscopic methods, such as atomic emission, absorption and fluorescence, including the application of tunable lasers. He has also studied the elementary processes in radiation sources used in atomic emission and absorption methods, and has made contributions to the analytical use of the short wavelength spectral range, including development and application of electron-impact excitation sources and photon counters for this range. His research group has developed and applied a novel emission method based on electrothermal atomization in combination with non-thermal excitation. Special attention has been paid to investigation of basic processes in electrothermal atomizers. Besides his involvement in this research in atomic spectroscopy, which has led to 31 publications and 40 lectures at international conferences, Professor Falk has been concerned for several years in the development of spectrometers (especially of Fourier transform type) for space research.

With profound sorrow we record the
sudden and untimely death of a valued
member of the Advisory Board

PROFESSOR LADO KOSTA

on 13 January 1986 at Ljubljana, Yugoslavia.

LIST OF CONTENTS

JANUARY

Special Honour Issue

Editorial	VII
Introduction	IX
Anniversary Greetings	XI
Mary R. Masson	1 Robert Alexander Chalmers
Robert A. Chalmers	7 The analysis of a paper on analytical chemistry
Jiří Lexa and Karel Štulík	11 Determination of bismuth by electrochemical stripping analysis. Elimination of interferences by using a mercury film electrode modified with tri- <i>n</i> -octylphosphine oxide, and application to copper alloys
G. Scharf and J. D. Winefordner	17 Phosphorescence characteristics of acetophenone, benzophenone, <i>p</i> -aminobenzophenone and Michler's ketone in various environments
Marta Andino, J. J. Aaron and J. D. Winefordner	27 Study of pH and substrate effects on room-temperature phosphorimetry of some indolecarboxylic acids
Elsie M. Donaldson and Mohui Wang	35 Methyl isobutyl ketone extraction of iodide complexes from sulphuric acid-potassium iodide media and back-extraction into an aqueous phase
M. D. Luque de Castro	45 Speciation studies by flow-injection analysis
Julian F. Tyson	51 Analytical applications of absorption spectroelectrochemistry at grazing incidence
E. J. Ekanem, C. L. R. Barnard, J. M. Ottaway and G. S. Fell	55 Matrix modification—the use of protein-free solutions in the determination of metals in blood by flame atomic fluorescence and emission spectrometry
Jose Alvarado, Francisco Campos and John M. Ottaway	61 Determination of trace levels of calcium in steels by carbon-furnace atomic-absorption and atomic-emission spectrometry
Anil C. Mehta	67 Sample pretreatment in the trace determination of drugs in biological fluids
Silve Kallmann	75 Analysis of sweeps. The cuprous sulphide collecting system
F. Pellerin, C. Majcherczyk et D. Bayloqç	85 Etude analytique du Goodrite 3114, antioxydant des polyoléfines. Comportement vis à vis des agents de stérilisation
Chow Chong	91 Determination of silver, bismuth, cadmium, copper, iron, nickel and zinc in lead- and tin-base solders and white-metal bearing alloys by atomic-absorption spectrophotometry
<i>Short Communications</i>	
Bishop B. Sithole and Robert D. Guy	95 Separation of nitroimidazoles by reversed-phase high-pressure liquid chromatography
Liu Zaiyou and Wu Limin	98 Determination of total phosphorus in water by photochemical decomposition with ultraviolet irradiation
Mariana S. Ionescu, Veronica Badea, G. E. Baiulescu and V. V. Coşofreţ	101 Nafronyl ion-selective membrane electrodes and their use in pharmaceutical analysis
<i>Analytical Data</i>	
Gustavo González, Daniel Rosales, José L. Gómez Ariza and Alfonso Guiraúm Pérez	105 Correction factors for the glass electrode in aqueous <i>N,N</i> -dimethylformamide solutions

FEBRUARY

- | | |
|---|---|
| <i>Talanta Advisory Board</i> | III |
| F. T. M. Dohmen and P. C. Thijssen | 107 A FORTH package for computer-controlled flow-injection analysis |
| N. A. Zakhari, M. Rizk, F. Ibrahim and M. I. Walsh | 111 Determination of phenothiazines by charge-transfer complex formation with chloranilic acid |
| Shigeya Sato and Sumio Uchikawa | 115 Extraction and spectrophotometric determination of titanium(IV) with Malachite Green and <i>p</i> -chloromandelic acid, with application to mild steels |
| Anjum S. Khan and Frederick F. Cantwell | 119 Measurement of acidity constants of benzothiadiazines by solvent extraction with use of a membrane phase-separator |
| Eita Kinoshita, Folke Ingman, Gunnar Edwall, Sigvard Thulin and Stanislaw Gląb | 125 Polycrystalline and monocrystalline antimony, iridium and palladium as electrode material for pH-sensing electrodes |
| M. Hernández Cordoba, P. Viñas and C. Sánchez-Pedreño | 135 Kinetic determination of traces of manganese in different materials by its catalytic effect on the Methylene Green-periodate reaction |
| G. Rauret, L. Pineda, M. Ventura and R. Compañó | 141 Solvent extraction of <i>N</i> -cyclohexyl- <i>N</i> -nitrosohydroxylamine (cnha) into some organic solvents and of the Cu(II)-cnha complex into methyl isobutyl ketone |
| Krystyna Brajter and Ewa Dąbek-Złotorzyńska | 149 Selective separation of metal ions by use of chelate-forming resins prepared by modification of conventional anion-exchangers with SPADNS and Orange II |
| Zofia Boguszewska, Maria Krasiejko and Bogna Palmowska-Kuś | 155 Application of platinum gauze activated by hydrogen to the adsorption separation of silver traces and their determination by AAS or spectrophotometry |
| <i>Short Communications</i> | |
| Yukio Sakai and Naoko Mori | 161 Preconcentration of cobalt with <i>N</i> -(dithiocarboxyl)sarcosine and Amberlite XAD-4 resin |
| C. S. P. Sastry, T. E. Divakar and U. Viplava Prasad | 164 Indirect spectrophotometric methods for the determination of antibiotics with iodine or periodate, and metol and sulphanilamide |
| Toshiaki Hattori and Hitoshi Yoshida | 167 Thermometric titration of the dodecyl sulphate ion with metal-phenanthroline complexes |
| F. Belal, M. Rizk, F. Ibrahim and M. Sharaf El-Din | 170 Spectrophotometric determination of benzothiadiazines in dosage forms |
| U. M. Abbasi, Fateh Chand, M. I. Bhanger and S. A. Memon | 173 A rapid method for the determination of some antihypertensive and antipyretic drugs by thermometric titrimetry |
| R. K. Gilpin and M. E. Gangoda | 176 Nuclear magnetic resonance spectrometry of chemically and physically altered porous silica surfaces under gas chromatographic conditions |
| Abdel-Aziz M. Wahbi, Mohammad A. Abounassif and E. A. Gad-Kariem | 179 Colorimetric determination of piperazine with <i>p</i> -benzoquinone |
| A. S. Khan and A. Chow | 182 Sorption of silver, gold and palladium with a polythioether foam |
| M. S. Mahrous, M. Abdel Salam, A. S. Issa and M. Abdel-Hamid | 185 Use of <i>p</i> -chloranilic acid for the colorimetric determination of some antimalarials |
| Andrzej Darkowski and Michael Cocivera | 187 Simultaneous polarographic determination of cadmium and tellurium in electro-deposited cadmium telluride thin films |
| <i>Analytical Data</i> | |
| Hiroaki Kawano, Yoshikazu Nakai, Toshio Matsuda and Toyoshi Nagai | 191 Adsorption of univalent and bivalent metal nitrates on hydrous lead dioxide. Adsorption behaviour of potassium, cupric, zinc, cadmium and nitrate ions |
| <i>Annotation</i> | |
| A. G. Asuero, M. J. Navas and J. L. Jimenez-Trillo | 195 Spectrophotometric methods for the evaluation of acidity constants—I. Numerical methods for single equilibria |

<i>Papers Received</i>	i
<i>Publications Received</i>	iii
<i>Notices</i>	iv
<i>Notes for Authors</i>	v
<i>Questionnaire: Software Survey Section</i>	vii

MARCH

J. Ruz, A. Ríos, M. D. Luque de Castro and M. Valcárcel	199	Flow-injection analysis with multidetection as a useful technique for metal speciation
Katsuyuki Fujita and Takeo Takada	203	Effect of temperature on generation and decomposition of the group Vb element hydrides and estimation of the kinetic stability of gaseous bismuth hydride by atomic-absorption spectrometry
M. Garcia-Vargas, S. Trevilla and M. Milla	209	Synthesis and characterization of 1,2-cyclohexanedione bis-benzoyl-hydrazone and its application to the determination of Ti in minerals and rocks
Joëlle Fidanza and Jean-Jacques Aaron	215	Evaluation of filter papers as substrates for solid-surface room-temperature fluorimetry and photochemical fluorimetry
R. Caletka, R. Hausbeck and V. Krivan	219	The distribution of elements between polyether-type polyurethane foam, cyclic polyethers and hydrofluoric acid solution
M. Tsezos and S. Mattar	225	A further insight into the mechanism of biosorption of metals, by examining chitin EPR spectra
Elsie M. Donaldson and Mohui Wang	233	Determination of silver, antimony, bismuth, copper, cadmium and indium in ores, concentrates and related materials by atomic-absorption spectrophotometry after methyl isobutyl ketone extraction as iodides
Clinio Locatelli, Francesco Fagioli, Corrado Bighi and Tibor Garai	243	Trace-metal determination by second-harmonic alternating-current anodic stripping voltammetry
Jean Pettersson, Lena Hansson and Åke Olin	249	Comparison of four digestion methods for the determination of selenium in bovine liver by hydride generation and atomic-absorption spectrometry in a flow system
M. E. Díaz García and A. Sanz-Medel	255	Dye-surfactant interactions: a review
Lauri H. J. Lajunen and Aaro Kubin	265	Determination of trace amounts of molybdenum in plant tissue by solvent extraction-atomic-absorption and direct-current plasma emission spectrometry
<i>Short Communications</i>		
J. D. Ingle, Jr	271	Simple sample-cell positioner for reducing the imprecision due to placement of test-tube type sample cells
Kenichiro Nakashima, Shoko Tomiyoshi, Shin'ichi Nakatsuji and Shuzo Akiyama	274	Development and application of organic reagents for analysis—VII. Extraction and fluorimetric determination of perchlorate ions with 2,6-di- <i>p</i> -tolyl-4-phenylpyrylium chloride
N. K. Roy and A. K. Das	277	Determination of tungsten in rocks and minerals by chelate extraction and atomic-absorption spectrometry
E. Cardarelli, M. Cifani, M. Mecozzi and G. Sechi	279	Analytical application of emulsions. Determination of lead in gasoline by atomic-absorption spectrophotometry
Yuji Kawabata, Totaro Imasaka and Nobuhiko Ishibashi	281	Ultramicro flow-cell for semiconductor laser fluorimetry
<i>Analytical Data</i>		
Rita Delgado, J. J. R. Fraústo da Silva and M. Cândida T. A. Vaz	285	Copper(II) complexes of cyclic tetra-azatetra-acetic acids—unusual features and possible analytical applications
Y. Akama, H. Yokota, K. Sato and T. Nakai	288	Studies on extraction of manganese(II) with 1-phenyl-3-methyl-4-acyl-5-pyrazolone

<i>Papers Received</i>	i
------------------------	---

<i>Publications Received</i>	iii
<i>Notices</i>	iv
<i>Software Survey Section</i>	v Haltafall; Polarog; Miniterm; Gran; Diagrams; Buffer; Simplex; Valpot; CAPU1-1, CAPU1-2, CAPU1-3, CAPU2-1

APRIL

Obituaries	III
Nicolas L. Duchateau, A. Verbruggen, F. Hendrickx and P. De Bièvre	291 Rapid accurate isotopic measurements on boron in boric acid and boron carbide
A. P. Gamot, G. Vergoten, M. Saudemon, G. Fleury et J. Barbillat	295 Microspectrométrie Raman multicanale: application à l'identification du triméthylacétate et du caproate de fluocortolone isolés d'une forme galénique
G. Merlot, B. Lacroix, M. T. Romon, J. P. Huvenne et G. Fleury	299 Analyse de mélanges complexes sur le couplage chromatographie en phase gazeuse/spectrométrie infrarouge par transformée de Fourier équipe de colonnes capillaires
George Norwitz and Peter N. Keliher	311 Continued investigation of the diazotization and coupling spectrophotometric technique for the determination of aromatic amines with 8-amino-1-hydroxynaphthalene-3,6-disulphonic acid and <i>N</i> -(1-naphthyl)-ethylenediamine as coupling agents
R. Caletka, R. Hausbeck and V. Krivan	315 Extraction of Mo, W and Tc with polyurethane foam and with cyclic polyether from SCN ⁻ /HCl medium
Joseph Wang and Javad M. Zadeii	321 Trace determination of yttrium and some heavy rare-earths by adsorptive stripping voltammetry
Aldo Laganà, Mauro Rotatori, Giuliana Vinci, M. Perla Colombini and Roberta Curini	325 Sample-pretreatment procedure for routine liquid chromatographic assay of serum cortisol
J. Medinilla, F. Ales and F. García Sánchez	329 Spectrophotometric and second-derivative spectrophotometric determination of mercury in organomercurials by means of benzyl 2-pyridyl ketone 2-quinolyldrazone
A. Corsini and O. Herrmann	335 Aggregation of <i>meso</i> -tetra-(<i>p</i> -sulphonatophenyl)porphine and its Cu(II) and Zn(II) complexes in aqueous solution
S. Kiciak and H. Gontarz	341 Simultaneous spectrophotometric determination of <i>o</i> -Cresol Red, Semi-Xylenol Orange and Xylenol Orange
<i>Short Communications</i>	
J. B. McHugh	349 Determining gold in water by anion-exchange batch extraction
Jayarama, M. Violet D'Souza, H. S. Yathirajan and Rangaswamy	352 Interaction of phenothiazines with nitroso-R salt and extractive spectrophotometric determination of phenothiazine drugs
Samuel J. Lyle and Nidal A. Za'tar	355 An exploratory study of the indirect fluorimetric determination of uranium(VI) by energy transfer and measurement of fluorescent emission by europium(III)
Samaresh Banerjee	358 A new method for the atomic-absorption determination of lead blended as lead alkyls in motor spirit
Samaresh Banerjee	360 Spectrophotometric determination of titanium with tannin and thioglycollic acid and its application to titanium-treated steels and ferrous and non-ferrous alloys
F. İnci Şengün and Köksal Ulaş	363 Analytical investigations on cephalosporins—I. Spectrophotometric determination of ceftriaxone
F. İnci Şengün and İnci Fedai	366 Analytical investigations on cephalosporins—IV. Application of Ellman's reagent
<i>Analytical Data</i>	
Walenty Szczepaniak and Maria Ren	371 Use of a bismuth ion-selective electrode for investigation of bismuth complexes of citric and malic acids

<i>Papers Received</i>	i
<i>Publications Received</i>	iii
<i>Notices</i>	v
<i>Questionnaire: Software Survey Section</i>	vii

MAY

M. Villarreal, L. Porta, E. Marchevsky and R. Olsina	375	Spectrophotometric determination of cadmium with 2-(5-chloro-2-pyridylazo)-5-dimethylaminophenol
Anna Maria Ghe, Giuseppe Chiavari and Joanis Evgenidis	379	Photometric and electrochemical detection of purine and pyrimidine compounds in reversed-phase and ion-exchange high-pressure liquid chromatography
A. Boughriet, M. Wartel et J. C. Fischer	385	Comportement électrochimique du tétraoxyde de diazote dans le sulfolane
Hideko Koshima and Hiroshi Onishi	391	Adsorption of metal ions on activated carbon from aqueous solutions at pH 1–13
Joseph Wang, Den Bai Luo and Bassam Freiha	397	Evaluation and improvement of the resolution of voltammetric measurements
A. D'Ulivo, R. Fuoco and P. Papoff	401	Behaviour of some dialkyl- and trialkyl-lead compounds in the hydride-generation procedure using a non-dispersive atomic-fluorescence detector
Yukio Sakai, Naoko Kawano, Hiroshi Nakamura and Makoto Takagi	407	Extraction and photometric determination of lead with diazacrown ether dye
I. López García, J. Martínez Aviles and M. Hernández Córdoba	411	Determination of palladium with thiocyanate and Rhodamine B by a solvent-extraction method
Tadao Sakai and Noriko Ohno	415	Simultaneous two- and three-component determinations in multicomponent mixtures by extraction-spectrophotometry and thermochromism of ion-association complexes
Roman E. Sioda, Graeme E. Batley, Walter Lund, Joseph Wang and Steven C. Leach	421	Electrolytic preconcentration in instrumental analysis
F. B. Sherman, B. M. Katz and G. N. Evenko	429	Aquametric microdetermination of hydration of ion-exchange resins
Josef Havel and Milan Meloun	435	Multiparametric curve fitting—IX. Simultaneous regression estimation of stoichiometry and stability constants of complexes
<i>Short Communications</i>		
Ouyang Zheng, Xu Pei-Yi, Xiong Guan-Lan and Liu Yue	443	A new reagent for determining trace selenium by gas chromatography: 1,4-dibromo-2,3-diaminonaphthalene
Frances Flavelle and Alan D. Westland	445	The determination of samarium, europium, gadolinium and dysprosium in uranium products by direct-current plasma emission spectrometry
F. Belal and J. L. Anderson	448	Flow injection determination of ergonovine maleate with amperometric detection at the Kel-F-graphite composite electrode
Kazufumi Takayanagi and George T. F. Wong	451	The oxidation of iodide to iodate for the polarographic determination of total iodine in natural waters
Hsu Zhang-Fa, Jia Xi-Pin and Hu Chao-Sheng	455	Simultaneous determination of light rare earths in monazite sand by densitometry on thin-layer chromatograms
Jose Aznárez, Jose M. Rabadan, Angel Ferrer and Pilar Cipres	458	Atomic-absorption spectrophotometric determination of tin by hydride generation in non-aqueous medium after extraction
<i>Analytical Data</i>		
G. Poulas, N. Papadopoulos and D. Jannakoudakis	461	Dissociation of 5-fluoro- and 3,5-dinitrosalicylic acids in water-methanol mixtures at 25°
A. Izquierdo, R. Compañó and E. Bars	463	Solvent extraction of zinc with 5,7-dichloro-2-methyl-8-hydroxyquinoline into chloroform
<i>Papers Received</i>	i	
<i>Publications Received</i>	ii	
<i>Questionnaire: Software Survey Section</i>	v	

JUNE

Louis Gordon Memorial Award	III	
N. Zimová, I. Němec and J. Zima	467	Determination of chlorpromazine and thioridazine by differential pulse voltammetry in acetonitrile medium
Antonio Braibanti, Claudio Bruschi, Emilia Fisicaro and Marzia Pasquali	471	Analysis of variance in determinations of equivalence volume and of the ionic product of water in potentiometric titrations
C. H.-Siegfried, W. Weinert, Franz W. E. Strelow and Reinhard G. Böhmer	481	The influence of thiourea on the cation-exchange behaviour of various elements in dilute nitric and hydrochloric acids
Kurt Kalcher	489	A new method for the voltammetric determination of nitrite
Paul R. Klock and Paul J. Lamothe	495	Determination of ammonium in a buddingonite sample by ion-chromatography
Robert Fournaise et Christian Petitfaux	499	Etude de la formation des complexes en solution aqueuse—I. Méthode protométrique informatisée de détermination des concentrations des ions libres en solution (méthode CILS) et d'estimation des constantes de stabilité des complexes: choix critique des modalités d'application à partir d'un exemple simulé
Milan Meloun, Milan Javůrek and Josef Havel	513	Multiparametric curve fitting—X. A structural classification of programs for analysing multicomponent spectra and their use in equilibrium-model determination
Josef Havel and Milan Meloun	525	Multiparametric curve fitting—XI. POLET computer program for estimation of formation constants and stoichiometric indices from normalized potentiometric data
A. G. Asuero, J. L. Jimenez-Trillo and M. J. Navas	531	Spectrophotometric methods for the evaluation of acidity constants—II. Numerical methods for two-step overlapping equilibria
<i>Short Communications</i>		
F. Hernández Hernández, J. Medina Escriche and M. T. Gasco Andreu	537	Enhancement of the fluorescence of the zinc-morin complex by a non-ionic surfactant
J. M. Mir and C. Martinez	541	Fluorimetric determination of boron at microgram level
Sarala Raoot and K. N. Raoot	544	Selective complexometric determination of palladium with thiosulphate as masking agent
T. D. Yerian, T. P. Hadjiioannou and G. D. Christian	547	Flow-injection analysis with the iron-induced perbromate-iodide reaction: spectrophotometric determination of iron
Doddaballapur K. Padma	550	A gravimetric procedure for the determination of wet precipitated sulphur, dissolved sulphur, soluble sulphides and hydrogen sulphide
<i>Papers Received</i>	i	
<i>Questionnaire: Software Survey Section</i>	iii	

JULY

The Ronald Belcher Memorial Award	III	
D. R. Crow	553	Diffusion coefficients and complex equilibria in solution—V. Limitations to the validity of the diffusion equations
R. S. Young	561	The analysis of ferroalloys
M. C. Gutiérrez, A. Gomez-Hens and M. Valcárcel	567	Selective kinetic fluorimetric determination of copper at the ng/ml level
Jouko J. Kankare and Roger Stephens	571	The influence of optical design on the signal to noise characteristics of polarimeters
Etsuro Iwamoto, Chan-Huan Chung, Manabu Yamamoto and Yuroku Yamamoto	577	Arsenic determination with graphite-cloth ribbon in graphite-furnace atomic-absorption spectrometry

M. Bos	583	Kalman filtering for the evaluation of the current-time function in d.c. polarography
R. López Núñez, M. Callejón Mochón and A. Guiráu Pérez	587	Extraction and spectrophotometric determination of titanium(IV) with alizarin and fluoride
I. T. Urasa and A. M. O'Reilly	593	The application of direct current plasma spectrometry to the study of the fractionation of iron and phosphorus in surface waters
J. G. Crock, F. E. Lichte, G. O. Riddle and C. L. Beech	601	Separation and preconcentration of the rare-earth elements and yttrium from geological materials by ion-exchange and sequential acid elution
Daniel Rosales, Isabel Millán and José L. Gómez Ariza	607	Spectrophotometric determination of indium in nickel alloys and zinc ores with 1-(2-pyridylmethylideneamine)-3-(salicylideneamine)thiourea
<i>Short Communications</i>		
Sadanobu Inoue, Suwaru Hoshi and Mutsuya Matsubara	611	Extraction-spectrophotometric determination of vanadium with <i>N</i> - <i>m</i> -tolyl- <i>N</i> -phenylhydroxylamine and its application to coal and coal fly-ash
Toshio Matsuda and Toyoshi Nagai	614	Degradation of nitrilotriacetic acid (NTA) by oxidation with lead dioxide suspension
A. Varada Reddy and Y. Krishna Reddy	617	Sequential extraction and determination of copper and nickel with 2,4-dihydroxyacetophenone thiosemicarbazone
M. C. Gennaro, E. Mentasti and C. Sarzanini	620	Binding properties of aminopolycarboxylate ligands bound to cellulose
Zaofan Zhao, Xiaohua Cai, Peibiao Li and Handong Yang	623	Polarographic determination of trace amounts of thorium
<i>Analytical Data</i>		
M. Callejón Mochón, M. Centeno Gallego and A. Guiráu Pérez	627	Salicylaldehyde-1-phthalazinohydrazone as an analytical reagent
J. E. Kountourellis, F. A. Underwood, P. P. Georgakopoulos and A. Raptouli	631	X-ray diffraction data for six analgesics
<i>Papers Received</i>		i
<i>Publications Received</i>		iii
<i>Notice</i>		v
<i>Questionnaire: Software Survey Section</i>		vii

AUGUST

S. Rubio, A. Gómez-Hens and M. Valcárcel	633	Analytical applications of synchronous fluorescence spectroscopy
Krzysztof Ren and Anna Ren-Kurc	641	A new numerical method of finding potentiometric titration end-points by use of rational spline functions
P. Damiani and G. Burini	649	Fluorometric determination of nitrite
Teresa L. Keimig and Linda B. McGown	653	Micellar modification of the spectral, intensity and lifetime characteristics of the fluorescence of fluorescein-labelled phenobarbital
Thomas M. Schmitt, Robert J. Ziegler, Ead S. Muzher, Robert J. Doyle and James L. Freers	657	Analysis of anthranilic acid by liquid chromatography
W. F. Pickering	661	The effect of hydrolysed aluminium species in fluoride ion determinations
Tsutomu Matsuo, Yoshitaka Masuda and Eiichi Sekido	665	Acid-base and chelatometric photo-titrations with photosensors and membrane photosensors

Barry Chiswell and Mazlin B. Mokhtar	669	The speciation of manganese in freshwaters
Saad S. M. Hassan and M. M. Elsaied	679	A new liquid-membrane electrode for selective determination of perchlorate
<i>Short Communications</i>		
J. Martínez Calatayud and Campins Falco	685	Determination of levamisole hydrochloride with HgI_4^{2-} by a turbidimetric method and flow-injection analysis
Zuzana Tocksteinová and František Opekar	688	The electrochemical generation of small amounts of hydrogen cyanide
Minoru Hosoya, Kōichi Tozawa and Kunio Takada	691	Rapid technique for distillation of methyl borate for ICP atomic-emission spectrometric determination of boron in steel
Wen-bin Qi and Li-zhong Zhu	694	Spectrophotometric determination of chromium in waste water and soil
M. C. García Álvarez-Coque, R. M. Villanueva Camañas, M. C. Martínez Vayá, G. Ramis Ramos and C. Mongay Fernández	697	Spectrophotometric determination of mercury(II) and silver(I) with copper(II) and diethyldithiocarbamate in the presence of Triton X-100
Colin D. Chriswell, Richard G. Richardson and Richard Markuszewski	700	Spectrophotometric determination of iron in process samples from the chemical cleaning of coal
B. C. Verma, S. Chauhan, Neelam Sharma, Usha Sharma, D. K. Sharma and Anila Sood	703	Analytical applications of the amine-carbon disulphide reaction in acetonitrile

Annotation

Ragnar Bye	705	Interferences from bivalent cations in the determination of selenium by hydride-generation and atomic-absorption spectrometry. A discussion of the claim that the metal ions are reduced to the metallic state by sodium borohydride
-------------------	-----	--

Papers Received i

Publications Received ii

*Questionnaire: Software
Survey Section* iii

SEPTEMBER

The Louis Gordon Memorial Award	III	
Joseph Wang, Peng Tuzhi, Meng-Shan Lin and Tim Tapia	707	Trace measurements of the antineoplastic agent methotrexate by adsorptive stripping voltammetry
James A. Cox, Atul Bhatnagar and Robert W. Francis Jr.	713	Evaluation of coupled transport across a liquid membrane as an analytical preconcentration technique
Suresh K. Srivastava, Satish Kumar, Chakresh K. Jain and Surender Kumar	717	Studies with an inorganic ion-exchange membrane exhibiting selectivity for Pb(II) ions
Elisabeth Suet et André Laouénan	721	Etude de l'interaction ion-ammonium tétramines cycliques par potentiométrie et RMN à l'aide du programme MICMAC
Shoji Motomizu, Hiroshi Mikasa and Kyoji Tōei	729	Fluorometric determination of nitrite in natural waters with 3-aminonaphthalene-1,5-disulphonie acid by flow-injection analysis
J. M. Kauffmann, G. J. Patriarcho, M. Chateau-Gosselin et B. Gallo Hermosa	733	Oxydation électrochimique de la khelline et de l'amikhelline: étude par voltammétrie cyclique
Andrzej Lewenstam, Ari Ivaska and Erkki Wänninen	739	Single-point titration of metal ions and ligands by measuring change in pH

<i>Short Communications</i>	
Salwa Rizk El-Shabouri	743 Spectrophotometric determination of nitrazepam in tablets
P. Yañez-Sedeño and L. M. Polo Diez	745 Spectrophotometric determination of Paraquat with BiI_4^- in the presence of gum arabic
J. Alary, J. Vandaele, C. Escrieut and R. Haran	748 Determination of trace amounts of nickel by atomic-absorption spectrometry after carbonyl generation
Ismail M. Al-Daher and Byron Kratochvíl	751 Effect of temperature on the determination of aromatic nitro-compounds by coulometrically generated chromium(II)
Kohji Hayase, Kiminori Shitashima and Hiroyuki Tsubota	754 Determination of organically-associated trace metals in estuarine seawater by solvent extraction and atomic-absorption spectrometry
J. V. Gimeno Adelantado and F. Bosch Reig	757 Mineralization of some organic sulphur compounds by fusion with molten alkali
Giovanna Bertocchi	760 Determination of optical purity in partially racemized samples of L-aspartic acid by means of liquid crystals
<i>Analytical Data</i>	
Santi Capone, Alessandro De Robertis, Concetta De Stefano and Silvio Sammartano	763 Formation and stability of zinc(II) and cadmium(II) citrate complexes in aqueous solution at various temperatures
Joseph R. Siefker and Rodolfo V. Aroc	768 Stability constants and molar absorptivities for complexes of copper(II) with <i>N</i> -methyldiethanolamine, 1,4-bis(2-hydroxypropyl)-2-methylpiperazine and 2-amino-2-methyl-1-propanol
Wiesława Zaborska and Maciej Leszko	769 The extraction of Zn(II), Cd(II) and Pb(II) from hydrochloric acid media by Amberlite LA-2 hydrochloride dissolved in 1,2-dichloroethane
<i>Annotation</i>	
Tong Shen-yang and Li Ke-an	775 The distribution of chromium(VI) species in solution as a function of pH and concentration
<i>Papers Received</i>	i
<i>Publications Received</i>	ii
<i>Erratum</i>	iii
<i>Notice</i>	iv
<i>Notes for Authors</i>	v
<i>Questionnaire</i>	vii
OCTOBER	
Talanta Medal	III
A. M. Afonso, J. J. Santana and F. García Montelongo	779 Kinetic spectrofluorimetric determination of silver, based on its catalytic effect on the oxidation of pyrocatechol-1-aldehyde 2-pyridylhydrazone by peroxodisulphate in the presence of 1,10-phenanthroline as activator
F. García Sánchez and M. Hernández López	785 Trace zinc determination by synchronous derivative fluorimetry
Aytekin Temizer	791 Electroanalytical determination of vinca alkaloids used in cancer chemotherapy
Jaakko Leppinen and Susanna Vahtila	795 Differential pulse polarographic determination of thiol flotation collectors and sulphide in waters
Ari Ivaska and Jaakko Leppinen	801 Determination of trace amounts of the flotation collectors ethyl xanthate and diethyl dithiophosphate in aqueous solutions by cathodic stripping voltammetry
Kevin J. West and Ronald T. Pflaum	807 Spectrophotometric and spectrofluorometric determination of zinc and cadmium with 2,2'-pyridil bis(2-quinolyldiazone)

Jiří Barek, Antonín Berka, Zuzana Tocksteinová and Jiří Zima	811	Voltammetric determination of benzidine and its derivatives, at a glassy-carbon electrode
Małgorzata Ciszowska and Zbigniew Stojek	817	Determination of traces of EDTA, EGTA and DCTA by adsorptive accumulation of their complexes with Hg(II) followed by cathodic stripping
Milan Meloun, Milan Javůrek and Alena Hynková	825	Multiparametric curve fitting—XII. Resolution capability of two programs for analysing multicomponent spectra, SQUAD(84) and PSEQUAD(83)
<i>Short Communications</i>		
Corrado Sarzanini, Edoardo Mentasti, Maria Carla Gennaro, Valerio Porta and Paolo Volpe	835	Preconcentration and determination of ultratraces of lead and bismuth
Zhang Xiao-song, Zhu Xiang-ping and Lin Chang-shan	838	Determination of molybdenum, chromium and vanadium by ion-pair high-pressure liquid chromatography based on precolumn chelation with 4-(2-pyridylazo)resorcinol
<i>Analytical Data</i>		
Irena Němcová, Borek Metal and Jaroslav Podlaha	841	Dissociation constants of arsenazo III
M. Esteban, E. Casassas and L. Fernandez	843	Formation constants of some mercury(II) complexes determined from their anodic polarographic signals
F. García Sánchez, C. Cruces Blanco and J. Medinilla	847	Fluorimetric and absorptiometric determination of dissociation constants and chromogenic reactions of benzyl 2-pyridyl ketone 2-quinolyldiazone
<i>Annotation</i>		
Tadeusz Hofman and Małgorzata Krzyżanowska	851	Determination of stability constants of complexes from the titration curve by the maximum likelihood principle
<i>Papers Received</i>	i	
<i>Notices</i>	iii	
<i>Questionnaire: Software Survey Section</i>	v	

NOVEMBER

Minoru Hara and Noboru Nomura	857	Application of modified normal pulse polarography and its differential mode to alkaline-earth metal ions in acid solutions
Kunio Shiraishi, Gi-ichiro Tanaka and Hisao Kawamura	861	Simultaneous multielement analysis of various human tissues by inductively-coupled plasma atomic-emission spectrometry
Otto S. Wolfbeis, Bernhard P. H. Schaffar and R. A. Chalmers	867	Fibre-optic titrations—IV. Direct complexometric titration of aluminium(III) with DCTA
R. von Wandruszka and J. D. Winefordner	871	Fluorescence in thin liquid films
Jaroslav P. Matousek, Brian J. Orr and Mark Selby	875	Spectrometric analysis of non-metals introduced from a graphite furnace into a microwave-induced plasma
Boy Høyer and Lars Kryger	883	Evaluation of single-point calibration in flow potentiometric stripping analysis
P. Linares, M. D. Luque de Castro and M. Valcárcel	889	Fluorimetric differential-kinetic determination of silicate and phosphate in waters by flow-injection analysis
Surasak Wataneski and A. A. Schilt	895	Separation of some transition-metal ions on silica-immobilized 2-pyridinecarboxaldehyde phenylhydrazone
Harvey Diehl, Naomi Horchak-Morris, Alta J. Hefley, Linda F. Munson and Richard Markuszewski	901	Studies on fluorescein—III. The acid strengths of fluorescein as shown by potentiometric titration

M. Sarbar, S. M. Golabi et M. H. Pournaghi-Azar	907	Mise en évidence de deux nouveaux indicateurs acide-base dans l'acide acétique anhydre
<i>Short Communications</i>		
James A. Cox and Krishnaji R. Kulkarni	911	Comparison of inorganic films and poly(4-vinylpyridine) coatings as electrode modifiers for flow-injection systems
J. Peinado, F. Toribio and D. Pérez-Bendito	914	Kinetic fluorimetric determination of organic peroxides and lipo-hydroperoxides at the nanomole level
Lisa D. Detter, Steven J. Pachuta, R. G. Cooks and R. A. Walton	917	Effects of vacuum on tetrakis-isocyanide complexes of silver(I) and copper(I): implications for SIMS analyses
<i>Analytical Data</i>		
M. Teresa S. D. Vasconcelos and Adello A. S. C. Machado	919	Simultaneous determination of the acid and basic ionization constants of imidazole
F. Salinas, A. Muñoz de la Peña and J. A. Murillo	923	Phototautomerism in the lowest excited singlet state of 1-hydroxy-2-carboxyanthraquinone
R. McMahon, M. Brennan and J. D. Glennon	927	The pK_a values of <i>N,N,N',N'</i> -tetrakis-(2-hydroxypropyl)ethylenediamine
<i>Annotations</i>		
A. G. Asuero, J. L. Jimenez-Trillo and M. J. Navas	929	Mathematical treatment of absorbance versus pH graphs of polybasic acids
Harvey Diehl	935	Studies on fluorescein—IV. Notes on obtaining acid dissociation constants from the titration curves of dibasic acids
<i>Papers Received</i>	i	
<i>Questionnaire: Software Survey Section</i>	iii	

DECEMBER

Obituary	III	
Chang Yun Po and Zhou Nan	939	Rapid spectrophotometric determination of palladium in titanium alloys with 2-(5-bromo-2-pyridylazo)-5-(diethylamino)phenol
Harald Gampp, Marcel Maeder, Charles J. Meyer and Andreas D. Zuberbühler	943	Calculation of equilibrium constants from multiwavelength spectroscopic data—IV. Model-free least-squares refinement by use of evolving factor analysis
M. L. Tuttle, M. B. Goldhaber and D. L. Williamson	953	An analytical scheme for determining forms of sulphur in oil shales and associated rocks
José A. S. Cavaleiro and Kevin M. Smith	963	Chromatography of chlorophylls and bacteriochlorophylls
T. Pal, A. Ganguly, D. S. Maity and Stanley E. Livingstone	973	<i>N,N'</i> -Diphenyldithiomalonamide as a gravimetric reagent for nickel and cobalt
Giuseppe Chiavari, Luciana Pastorelli and Georgios Perrakis	979	Preparation, mesomorphic properties and behaviour of 4,4'-biphenylene-dibenzoates as stationary phases in gas chromatography
C. Majcherczyk, P. Polge, D. Baylocq et F. Pellerin	985	Action des rayonnements beta et des oxydants sur le di-tert.butyl-3,5 hydroxy-4 toluène
L. Almestrand, D. Jagner and L. Renman	991	Determination of cadmium, lead and copper in milk and milk powder by means of flow potentiometric stripping analysis
M. F. Vergnes et J. Alary	997	Dosage des xanthiques naturels par CLHP. Comparaison des méthodes et applications
W. B. Emary, I. Isern-Flecha, K. V. Wood, T. Y. Ridley and R. G. Cooks	1001	Desorption ionization/tandem mass spectrometry with a caesium ion source and a triple quadrupole mass spectrometer
Krishna K. Verma, Pramila Tyagi and Mary Grace Pushpa Ekka	1009	Determination of chromate and cyanide by anion-exchange with lead iodate, and the analysis of mixtures of cyanide, thiocyanate and halides

Vijay S. Tripathi	1015	An algorithm and a FORTRAN program (CHEMEQUIL-2) for calculation of complex equilibria
A. Arrebola Ramírez, C. Jiménez Linares, F. Alés Barrero and M. Román Ceba	1021	Study of the mixed-metal lanthanum–magnesium–purpurin complex: spectrophotometric determination of yttrium and lanthanides
<i>Short Communication</i> Barbara Róžańska and Elwira Lachowicz	1027	Tetrabutylammonium bromide/thenoyltrifluoroacetone/MIBK extraction for AAS determination of cobalt, nickel, and manganese in copper ores and concentrates
<i>Analytical Data</i> F. Arce, C. Blanco and J. Casado	1031	Polarographic studies of mixed hydroxy-complexes of mono-ethanolamine with cadmium and with lead
<i>Annotation</i> D. Baylocq, C. Majcherczyk et F. Pellerin	1035	Action de l'acide citrique sur l'anhydride acétique et la pyridine. Détermination du mécanisme réactionnel et de la structure du composé forme
<i>Preliminary Communication</i> Harvey W. Yurow	1039	Novel fluorescence reaction for malononitrile
<i>Papers Received</i>	i	
<i>Publications Received</i>	ii	
<i>Questionnaire: Software Survey Section</i>	iii	

TOPICS

The general theme of the topics will be the physicochemical processes and aspects of chemistry and chemical engineering in the science of the aquatic environment. Papers on microbiological aspects or air pollution and solid waste will be considered as well. The sessions will deal more specifically with:

- advanced physicochemical treatment;
- the interaction of biological and physicochemical (sub) processes in combined treatment processes;
- the origin, transfer, fate and effects of chemical pollutants in the environment;
- plants for treatment of effluents;
- methods for the removal of hazardous hydrocarbons and organic materials from aqueous environments;
- advances in environmental monitoring and analytical chemistry.

SUBMISSION OF PAPERS

Papers and abstracts must be in English. They must contain original material not published elsewhere.

Papers will be selected on the basis of extended abstracts. A compilation of these abstracts (together with the full invited papers) will be handed out at the Conference. Beside an introduction they should describe methods, results and conclusions, and must be submitted before 31 October 1986 in a form enabling direct reproduction by the photo-offset process. An abstract should contain ~600 words and one or two figures and/or tables (2-4 pages). It should be single-spaced on DIN A4 format (210-297 mm), white paper with a 12 pitch Gothic or similar letter type and leaving 30 mm margins. Title, name of author(s) and address(es) should be typed within an additional 70 mm spaced at the head of the first page.

SECRETARIAT

All correspondence concerning the Conference should be addressed to:

6th Int. Conference Chemistry for Protection of the Environment

Prof. C. SARZANINI

Dipartimento di Chimica Analitica

Via P. Giuria 5

10125 TORINO (ITALY)

Tel. (natl.) 011/657272

Tel. (internatl.) /39/11/657272

INTERNATIONAL SYMPOSIUM ON PHARMACEUTICAL AND BIOMEDICAL ANALYSIS

Barcelona Congress Centre, Spain

23-25 September 1987

The aim of the meeting is to present and evaluate new trends and developments in, and applications of, analytical methods for the analysis of drugs and endogenous components of human metabolism in biological samples.

The scientific programme will cover, as special topics, Anticancer Drugs, Computer-Aided Analysis (including Robotics), Psychoactive Drugs and New Developments and Applications. These topics as well as any others of interest in the field of Pharmaceutical and Biomedical Analysis will be discussed in invited plenary and keynote lectures, invited and submitted research contributions, and poster presentations. The Proceedings of the Symposium will be published by the *Journal of Pharmaceutical and Biomedical Analysis*. If interested, please provide tentative title(s) for contributed paper(s).

The Symposium will precede the International Symposium on Applied Mass Spectrometry in the Health Sciences, to be held on 28-30 September 1987, also in the Barcelona Congress Centre, which will cover complementary analytical approaches exclusively centred on the application of Mass Spectrometric Techniques.

Exhibition space will be available for manufacturers.

For further information on registration and instrument exhibition facilities please contact:

DR. EMILIO GELPI, Chairman, Organizing Committee, International Symposium on Pharmaceutical and Biomedical Analysis, PALACIO DE CONGRESOS, Avda. Reina Ma Cristina, s/n., 08004 Barcelona, Spain
Phone 325.30.00-223.99.40
Telex 53.117 FOIMB-E

NOTICE

31st IUPAC CONGRESS

13-18 July 1987

National Palace of Culture, Sofia, Bulgaria
The Bulgarian Academy of Sciences will be
responsible for the organization
of the Congress

The Scientific Programme will include the following Sections and Topics:

1. ANALYTICAL CHEMISTRY

1.1. General Aspects of Analytical Chemistry.

New Theoretical Developments, New Instrumentation and Techniques in Electroanalytical Chemistry, Automation, Application of Microcomputers, Solubility.

1.2. Particular Aspects of Analytical Chemistry.

Participation in Biotechnology, Medicinal, Pharmaceutical and Food Areas. Environmental Analysis, Microchemical and Trace Analysis, Methods of Analysis, etc.

2. EDUCATION

Chemical Education in the Third World. Informing the Public about Chemistry. Teaching of Chemistry.

3. ENGINEERING CHEMISTRY

Chemical Technologies for Energy Production. Electrochemical Hydrogen Production. Fuel Cell Technology. Electrochemical Power Sources. Metal Recovery, including Solvent Extraction, Ion Exchange and Electro-winning. Extraction with Dense Gases.

4. INDUSTRIAL CHEMISTRY

Agrochemistry, Herbicides, Pesticides, Biotechnology. Essential Oils. Pharmaceutical Chemistry.

5. INORGANIC CHEMISTRY

Heterogeneous and Homogeneous Catalysts, including Catalyst Characterization. p-Block Element Chemistry. Semiconductors. Solid State Chemistry. Ultrapure Elements.

6. ORGANIC CHEMISTRY

Asymmetric Synthesis. Bioorganic Chemistry and Biosynthesis. Computer-aided Synthesis and Computer-graphics. Gas Phase Reactions. New Synthons for Organic Reactions.

7. PHYSICAL CHEMISTRY

Electrochemistry: Electrocatalysis, Liquid/Liquid Interfaces, Chemically Modified Electrodes, Spectroscopic Methods in Electrochemistry. Elementary Steps in Kinetic Processes. Liquid Crystals. Surface Science, including Long-range Forces, Colloidal Systems, and Liquid Films.

8. POLYMERS

Biopolymers. Electrically Conducting Organic Polymers. Polymers in Medicine.

9. CLINICAL CHEMISTRY

Congress Circulars containing further details are available from the Secretariat of the 31st IUPAC Congress

c/o Dr R. Vlahov
Institute of Organic Chemistry
Bulgarian Academy of Sciences
1113 Sofia, Bulgaria
Telex: 22729 ECHBAN BG

GC is a powerful and sensitive analytical method used for identifying paint marks, fibres and other type of trace evidence necessary in forensic work.

The last chapter is devoted to the theory and application of inverse GC, which is a study of the stationary phase and an important aspect of physical polymer chemistry. Polymer solution thermodynamics is also been reviewed in this chapter.

This volume has brought together experts' contributions in pyrolysis, GC and polymer chemistry. The book is well presented with detailed and helpful indexing and is a significant contribution in the field.

M. YOUNUS QURESHI

Interfacing Your BBC Microcomputer: R. MORGAN, W. McCLEAN and J. ROSELL, Prentice-Hall International, London, 1985. Pages ix + 179. £8.95.

I have read many books on interfacing the BBC Microcomputer, but this is the most useful I have seen, because it combines coverage of the programming techniques required, with descriptions of electronic circuits. The main distinction from other texts is that the circuits are explained and discussed in terms that can be readily understood by a reader who is not an electronics specialist (*i.e.*, someone who can usually read a circuit diagram, but not understand it). As a result, the reader has a chance of being able to adapt circuits to fit a particular situation, and of understanding some of the circuits given in other books. The main topics covered include digital input and output, analogue input and output, and control systems. Direct-addressing techniques are used in the early part of the book, but the "official" OSBYTE routines are introduced later, as are assembler code techniques. Construction projects include driving a lamp and motors, burglar alarms, measurement of light levels, measurement of temperature, controlling the temperature of an enclosure, a light pen, and an external ADC. Highly recommended.

MARY MASSON

The BBC Microcomputer in Control: P. BEVERLEY, N. EAMES and G. OSBORNE, Prentice-Hall International, London, 1985. Pages xi + 150. £7.95.

This is an interesting collection of "Interfacing Projects for Beginners", to quote the sub-title. The book is nicely produced, and is indeed very helpful to a beginner, who may never have assembled an electronic circuit previously. Thus, Appendix I describes the necessary constructional techniques, including soldering, strip board and printed circuit board construction, gives colour codes for resistors and capacitors, and explains how to connect diodes, transistors *etc.* The topics covered include power switching, digital input, use of the analogue-to-digital converter for voltage measurement, resistance measurement, as a logic probe, and for timing, *e.g.*, of a pendulum. Computer communications via the RS423 (Acorn's RS232) serial interface are also discussed.

MARY MASSON

GC is a powerful and sensitive analytical method used for identifying paint marks, fibres and other type of trace evidence necessary in forensic work.

The last chapter is devoted to the theory and application of inverse GC, which is a study of the stationary phase and an important aspect of physical polymer chemistry. Polymer solution thermodynamics is also been reviewed in this chapter.

This volume has brought together experts' contributions in pyrolysis, GC and polymer chemistry. The book is well presented with detailed and helpful indexing and is a significant contribution in the field.

M. YOUNUS QURESHI

Interfacing Your BBC Microcomputer: R. MORGAN, W. McCLEAN and J. ROSELL, Prentice-Hall International, London, 1985. Pages ix + 179. £8.95.

I have read many books on interfacing the BBC Microcomputer, but this is the most useful I have seen, because it combines coverage of the programming techniques required, with descriptions of electronic circuits. The main distinction from other texts is that the circuits are explained and discussed in terms that can be readily understood by a reader who is not an electronics specialist (*i.e.*, someone who can usually read a circuit diagram, but not understand it). As a result, the reader has a chance of being able to adapt circuits to fit a particular situation, and of understanding some of the circuits given in other books. The main topics covered include digital input and output, analogue input and output, and control systems. Direct-addressing techniques are used in the early part of the book, but the "official" OSBYTE routines are introduced later, as are assembler code techniques. Construction projects include driving a lamp and motors, burglar alarms, measurement of light levels, measurement of temperature, controlling the temperature of an enclosure, a light pen, and an external ADC. Highly recommended.

MARY MASSON

The BBC Microcomputer in Control: P. BEVERLEY, N. EAMES and G. OSBORNE, Prentice-Hall International, London, 1985. Pages xi + 150. £7.95.

This is an interesting collection of "Interfacing Projects for Beginners", to quote the sub-title. The book is nicely produced, and is indeed very helpful to a beginner, who may never have assembled an electronic circuit previously. Thus, Appendix I describes the necessary constructional techniques, including soldering, strip board and printed circuit board construction, gives colour codes for resistors and capacitors, and explains how to connect diodes, transistors *etc.* The topics covered include power switching, digital input, use of the analogue-to-digital converter for voltage measurement, resistance measurement, as a logic probe, and for timing, *e.g.*, of a pendulum. Computer communications via the RS423 (Acorn's RS232) serial interface are also discussed.

MARY MASSON

enormous analytical potential of the class of compounds termed "complexones", introduced by Professor G. Schwarzenbach. With dozens of his pupils he developed numerous practical analytical methods involving the use of EDTA and related compounds, first as masking agents, later mainly as titrants. With his co-workers he introduced a number of new metallochromic indicators, such as Xylenol Orange, Methylthymol Blue, Thymolphthaleincomplexone and Fluoresceincomplexone. These works have had a great impact on analytical chemistry throughout the world. In Czechoslovakia, his outstanding contribution to analytical chemistry was recognized in 1953 by the award of the State Prize and in 1958 by the degree of D.Sc. He was awarded the Talanta Gold Medal in 1971.

Dr. Přibil did much to disseminate knowledge in his excellent lectures, that were renowned for their wit and for his inimitable skill in practical demonstrations. The lecture theatres were always packed by students, as well as practising analysts, who came to listen to him. He was a fanatic at work, with an unerring sense for practical usefulness and with countless original ideas. He asked much of his students, but did not spare himself or his time in helping them. Even after his retirement, he went to work in the analytical laboratory of the Geological Institute, Charles University, until poor health finally prevented him from doing so.

He was a great story-teller and it was a delight listening to him. He made lots of friends in all the continents of the world, with whom he maintained friendly contacts until the end of his life. His many years of service to *Talanta*, as a regional editor, should also not be forgotten.

One of the last classical chemists in the world, a unique personality with a very broad background, has died. He will be greatly missed by all his pupils, friends and other people associated with analytical chemistry.

KAREL ŠTULÍK

RUDOLF PŘIBIL—THE MAN

I first met Rudolf Přibil in 1959 when he came to Aberdeen to give a lecture. An immediate rapport was established and we rapidly became good friends. In the years that followed I came to know him well, as a person as well as a chemist. He had a warm, extrovert and generous personality, and many unsuspected talents. As a young man he had a reputation as a tennis player, but in much later life revealed an unexpected skill at billiards (presumably dating from student days). He was renowned for his sense of humour and very ready wit. During a demonstration lecture in Aberdeen, finding no spatula had been provided, he broke up a firmly caked chemical in a reagent bottle with what he immediately referred to as an "analytically pure finger", a term that at once passed into daily use among students. When asked whether a certain lecture might not be terminated after about 90 minutes of exposition, he replied "Why? My plane doesn't leave till next week". All who have heard him give a lecture in English will recall his habitual opening remark "Please forget all rules of English grammar!", followed by what may best be described as a fluid use of the language in giving a clear and always fascinating account of his newest ideas, illustrated by elegant demonstrations performed with remarkable dexterity.

His extensive travels in the course of lecturing on complexometric analysis led to a fund of stories about his adventures, ranging from breaking light bulbs with his head in Japanese hotel rooms ("I am too tall for Japan") to being marooned for a week in Moscow because of fog at the airport, and a plane missed through a misunderstanding. Like the late Professor Belcher, he seemed to attract problems and happenings when travelling, so that travel with him was always full of surprises.

By those who knew him well he will be remembered with warmth and great affection, for his friendship and the something extra he brought into their lives.

R. A. CHALMERS

Pratique de l'Analyse Organique Colorimétrique et Fluorimétrique: J. BARTOS and M. PESEZ, Masson, Paris, 1984. Pages xiv + 398.

Two very experienced and competent analytical chemists have prepared this working handbook of quantitative colorimetric and fluorimetric methods for determination of a wide range of organic compounds, including alcohols, phenols, alkyl and aryl amines, guanidines and ureas, other diverse nitrogen-containing compounds, carbonyl compounds, carboxylic acids, peroxides, thiols, unsaturation, heterocyclic compounds, sugars, and steroids. The methods presented are those actually used in the laboratories of Roussel-Uclaf: sometimes the procedures are as described in the original literature source (which is cited), but often the details given have been modified from the original in order to obtain optimum reproducibility and sensitivity. Nearly 300 methods are described. For each is given the principle, the reaction, the detailed procedure, and applications, with an indication of the amounts and/or concentrations of the compounds that will yield an absorbance of 0.30 in a 1-cm cell. Frequently, notes are also given on topics such as relative reactivities or sensitivities, applicability to related compounds, interferences, and much other relevant information. There is an admirably comprehensive index to the compounds determined and the reagents utilized.

MARY MASSON

The Professional Touch: ALAN and SUE ROWLEY, Sigma, Wilmslow, Cheshire, 1985. Pages viii + 169. £7.95.

Not very long ago, a scientist wanting to use a computer program expected to have to make some attempt to understand the coding, and to be fully responsible for checking the validity of the input data. The introduction of microcomputers in recent years has led to many new kinds of applications for computers, and to new kinds of programs. One of the main innovations is the "user-friendly" computer package, in which the user need never look at the coding—indeed, it is probably concealed to prevent stealing of ideas, or, in educational programs, cribbing of answers. The data-input operations will be extensively protected to stop program crashes, and error-trapping will be used to help the user and prevent loss of data whenever possible. The price to be paid for such user-friendliness is the much greater programming effort needed to incorporate all the desirable features.

However, user-friendliness should now be much easier to accomplish with the aid of Alan and Sue Rowley's well-produced and thoroughly professional guide on "how to turn your software into a robust commercial product". Besides input protection, concealment of coding and data, and error-trapping, the authors (one of whom is a university lecturer in analytical chemistry) have included sections on Controlling the Program (by menu- or command-driving), Output to screen and printer, Passwords and data encryption, Filing systems, Compatibility, and Documentation. Numerous usable computer listings are included by way of illustration. All the topics are discussed with particular reference to the BBC microcomputer, and listings are presented in BBC Basic, but most of the material should also be useful to users of other types of microcomputer. Any scientist attempting to develop microcomputer programs for use by others should find this book an indispensable aid to current methods.

MARY MASSON

Pratique de l'Analyse Organique Colorimétrique et Fluorimétrique: J. BARTOS and M. PESEZ, Masson, Paris, 1984. Pages xiv + 398.

Two very experienced and competent analytical chemists have prepared this working handbook of quantitative colorimetric and fluorimetric methods for determination of a wide range of organic compounds, including alcohols, phenols, alkyl and aryl amines, guanidines and ureas, other diverse nitrogen-containing compounds, carbonyl compounds, carboxylic acids, peroxides, thiols, unsaturation, heterocyclic compounds, sugars, and steroids. The methods presented are those actually used in the laboratories of Roussel-Uclaf: sometimes the procedures are as described in the original literature source (which is cited), but often the details given have been modified from the original in order to obtain optimum reproducibility and sensitivity. Nearly 300 methods are described. For each is given the principle, the reaction, the detailed procedure, and applications, with an indication of the amounts and/or concentrations of the compounds that will yield an absorbance of 0.30 in a 1-cm cell. Frequently, notes are also given on topics such as relative reactivities or sensitivities, applicability to related compounds, interferences, and much other relevant information. There is an admirably comprehensive index to the compounds determined and the reagents utilized.

MARY MASSON

The Professional Touch: ALAN and SUE ROWLEY, Sigma, Wilmslow, Cheshire, 1985. Pages viii + 169. £7.95.

Not very long ago, a scientist wanting to use a computer program expected to have to make some attempt to understand the coding, and to be fully responsible for checking the validity of the input data. The introduction of microcomputers in recent years has led to many new kinds of applications for computers, and to new kinds of programs. One of the main innovations is the "user-friendly" computer package, in which the user need never look at the coding—indeed, it is probably concealed to prevent stealing of ideas, or, in educational programs, cribbing of answers. The data-input operations will be extensively protected to stop program crashes, and error-trapping will be used to help the user and prevent loss of data whenever possible. The price to be paid for such user-friendliness is the much greater programming effort needed to incorporate all the desirable features.

However, user-friendliness should now be much easier to accomplish with the aid of Alan and Sue Rowley's well-produced and thoroughly professional guide on "how to turn your software into a robust commercial product". Besides input protection, concealment of coding and data, and error-trapping, the authors (one of whom is a university lecturer in analytical chemistry) have included sections on Controlling the Program (by menu- or command-driving), Output to screen and printer, Passwords and data encryption, Filing systems, Compatibility, and Documentation. Numerous usable computer listings are included by way of illustration. All the topics are discussed with particular reference to the BBC microcomputer, and listings are presented in BBC Basic, but most of the material should also be useful to users of other types of microcomputer. Any scientist attempting to develop microcomputer programs for use by others should find this book an indispensable aid to current methods.

MARY MASSON

NOTICES

CHANGE OF DATE FOR SILVER JUBILEE EASTERN ANALYTICAL SYMPOSIUM

The dates of the Silver Jubilee Eastern Analytical Symposium have been changed. The new dates are 20–24 October 1986. A recent scheduling problem at the New York Hilton Hotel, the new home of the Eastern Analytical Symposium, has made available to the EAS this new set of dates, which provide fewer conflicts with other meetings and with religious holidays. It is our hope that these new dates will also prove more convenient for the many thousands who attend the EAS. All other previously announced information pertaining to the Eastern Analytical Symposium and its Silver Jubilee celebration remains unaltered.

1987 (10th) WORLD CHROMATOGRAPHY/ and (8th) WORLD SPECTROSCOPY CONFERENCE

11–12 MAY 1987

HILTON INTERNATIONAL HOTEL DÜSSELDORF, WEST GERMANY

CHROMATOGRAPHY

Papers dealing with any aspect of gas chromatography, liquid chromatography, thin layer chromatography, HPLC, gel permeation, column chromatography, equipment and design, theory and applications, marketing, *etc.* are now being solicited.

SPECTROSCOPY

Papers dealing with any aspect of infrared spectroscopy, emission spectroscopy, spectrochemical analysis, multiplex methods in spectroscopy, molecular spectroscopy, NMR, atomic absorption spectroscopy, separation and vibrational spectroscopy, mass spectroscopy, X-ray spectroscopy, Raman spectroscopy, ESR and special analytical techniques and applications are now being solicited.

Tentative titles must arrive before 15 October 1986. Deadline for submission of abstracts and biographical data of speakers, 15 January 1987. Deadline for complete papers, 15 April 1987.

PLEASE SEND YOUR PAPERS TO:

Dr. V. M. Bhatnagar
Alena Enterprises of Canada
P.O. Box 1779
Cornwall, Ontario K6H 5V7, Canada

NOTICES

INTERNATIONAL SYMPOSIUM ON ELECTROANALYSIS IN BIOMEDICAL, ENVIRONMENTAL AND INDUSTRIAL SCIENCES

6-9 APRIL 1987, UWIST, CARDIFF, WALES

The Electroanalytical Group, together with the Education & Training Group of the Analytical Division of the Royal Society of Chemistry, is organizing an International Symposium on Electroanalysis in Biomedical, Environmental and Industrial Sciences, 6-9 April 1987, at UWIST, Cardiff. The First Circular, calling for papers and expression of interest, is now available from:

Short Courses Section (Electroanalysis Symposium)

UWIST

PO Box 68

Cardiff CF1 3XA

Wales, UK

10th INTERNATIONAL VACUUM CONGRESS (*IVC-10*) 6th INTERNATIONAL CONFERENCE ON SOLID SURFACES (*ICSS-6*) 33rd NATIONAL SYMPOSIUM OF THE AMERICAN VACUUM SOCIETY

27-31 OCTOBER 1986, BALTIMORE, MARYLAND, USA

Sponsored and Organized by: The International Union for Vacuum Science, Technique and Applications (*IUVSTA*) and the American Vacuum Society (*AVS*).

Co-sponsor: International Union of Pure and Applied Physics (*IUPAP*)

Authors are encouraged to submit papers representing original contributions in all related areas. An abstract of 150 words or less prepared in special format will be required for paper submission. Abstract form and preparation information will be included in the call for papers planned for distribution in January-February, 1986. Abstract deadline will be 9 May 1986. Additional information may be obtained from Marion Churchill, Meetings Manager, American Vacuum Society, 335 East 45th Street, New York 10017 or from the programme chairman, Dr. Theodore E. Madey, Surface Science Division, National Bureau of Standards, Gaithersburg, MD 20899.

INTRODUCTION

It is with great pleasure that I dedicate this issue in honour of Bob Chalmers on the occasion of his 20th anniversary as Editor-in-Chief of *Talanta* and his retirement from the University of Aberdeen.

Talanta commenced publication in July 1958 and is today read by many thousands of readers the world over. I thank Bob for his continuing service in maintaining the high standards of publication and join his many friends and colleagues in wishing him a happy anniversary and continued good health.

ROBERT MAXWELL
Publisher

ERRATUM

Table 1 was accidentally omitted from the paper by Izquierdo, Compañó and Bars, *Talanta*, 1986, 33, 463, and is printed below.

Table 1. Characteristics of the spectrophotometric determination of zinc with 5,7-dichloro-2-methyl-8-hydroxyquinoline

λ_{\max}	405 nm
Colour stability	5 hr
pH range of maximum absorbance	6.0-9.5
Reagent concentration	$2.4 \times 10^{-4} - 2.0 \times 10^{-2} M^*$
Beer's law range	1.0-23 $\mu\text{g/ml}^*$
Molar absorptivity	$5.9 \times 10^3 \text{ l. mole}^{-1} \cdot \text{cm}^{-1}$
Precision	$\pm 0.6\%$
Detection limit ²⁶	0.05 $\mu\text{g/ml}$

*Higher concentrations were not investigated.

NOTICE

WORKING PARTY ON ANALYTICAL CHEMISTRY WPAC/FECS

EUROPEAN ANALYTICAL COLUMN 9

(SUMMARY OF WPAC ACTIVITIES IN 1985)

In January 1986 the membership of WPAC remains at the same high levels as the year before (29 chemical societies from 23 European countries, represented by 27 delegates). Spain is now represented by the Spanish Society for Analytical Chemistry in addition to the Spanish Royal Society for Chemistry. Only the Society of Luxembourg Chemists and the Pancyprian Union of Chemists among the members of FECS are not yet active in the WPAC. The chemical societies of Egypt, the German Democratic Republic, Israel and Romania, as well as IUPAC, have observer status.

The 16th meeting of the WPAC was held in Vienna, 24 November, 1985, and attended by 21 delegates (Chairman: Prof. E. Pungor).

The following main activities of the WPAC are brought to your attention.

1. Euroanalysis Conference series

1.1 Euroanalysis V, 1984, Cracow, Poland.

President: Prof. A. Hulanicki. The proceedings of this conference contain all but 1 of the 14 invited lectures and are now available in the series "Reviews on Analytical Chemistry" from Akadémiai Kiadó, Budapest.

1.2 Euroanalysis VI, 7-11 September, 1987, Paris, France.

Presidents: Prof. E. Roth, Prof. A. Hulanicki, Prof. H. Malissa. The first circular including information on selected topics and special sessions is available. Please contact Prof. Roth, or GAMS, 88, Bd. des Malesherbes, F-75008 Paris.

1.3 Euroanalysis VII, 1990, Vienna, Australia.

President: Prof. J. F. K. Huber. Host society: Austrian Society for Microchemistry and Analytical Chemistry.

2. Events sponsored or supported by WPAC in 1985

2.1 4th Scientific Session on Ion-Selective Electrodes, 1984, Matrafüred, Hungary.

Chairman: Prof. E. Pungor. Proceedings containing all plenary, keynote and discussion lectures are available now from Akadémiai Kiadó and Elsevier.

2.2 12th International Competition in Analytical Chemistry, 13-15 May, 1985, Veszprém, Hungary.

Chairman: Prof. J. Inczédy. Students from several European countries participated. The next competition will be in 1986 in Szeged.

2.3 1st International Symposium on Philosophy and History in Analytical Chemistry, 22-23 November, 1985, Vienna/Schallaburg, Austria.

Chairmen: Prof. H. Malissa (Philosophy), Prof. F. Szabadváry (History). Participants from 18 countries discussed, in a stimulating historic environment, the impact and importance of selected time periods and philosophical aspects in the development of Analytical Chemistry. The philosophical papers will be published (for further information please contact the secretary).

2.4 Education in Analytical Chemistry.

The WPAC brochure has been distributed to all 229 participating institutions; a few further copies are available at the secretariat.

3. Further activities sponsored or supported by WPAC

3.1 COBAC IV, 15-19 September, 1986, Graz, Austria.

Chairmen: Doz. W. Wegscheider, Doz. K. Varmuza.

The first circular is available, as well as detailed information on the programme.

3.2 Symposium on Bioelectroanalysis, 6-8 October, 1986, Matrafüred, Hungary, organized by the Electroanalytical Committee of the Hungarian Academy of Sciences.

- 3.3 6th International Conference on Fourier Transform Spectroscopy, 24–28 August, 1987, Vienna, Austria. Chairman: Prof. G. Zerbi, Milan, Italy. Programme Chairman: Dr. G. Guelachvili, Paris. Secretary: Prof. R. Kellner, Technical University Vienna, Institute for Analytical Chemistry, A-1060 Wien, Getreidemarkt 9. The first circular is available from the secretariat.
- 3.4 European Conference on Molecular Spectroscopy (EUCMOS 18), 30 August–4 September 1987, Amsterdam, The Netherlands. President: Prof. Orville-Thomas. The first circular has been sent out recently. Thanks to a coordinative effort by WPAC it is possible to link the FTS-Conference, Vienna (see 3.3), EUCMOS Amsterdam (3.4) and Euroanalysis VI Paris (1.2) without time clashes.
- 3.5 8th European Symposium on Polymer Spectroscopy (ESOPS 8), 1988, Budapest, Hungarian Academy of Sciences.

For any further information related to WPAC activities please contact the secretary, Prof. R. Kellner, Institute for Analytical Chemistry, Technical University Vienna, A-1060 Wien, Getreidemarkt 9.



PROFESSOR LADO KOSTA
(1921–1986)

Born in Kidričevo, near Ptuj in North East Slovenia, on 11 February 1921, the son of a tailor, Lado Kosta graduated in Chemistry in Ljubljana in 1944 and was awarded his doctorate at the same University in 1955. His first positions were as Assistant and then Head of the Toxicology Laboratory of the Institute of Legal Medicine of the Medical Faculty in Ljubljana.

In 1950 he began research work at the Institute of Physics, Ljubljana, soon after renamed the “Jožef Stefan” Institute, and joined its staff in 1952. In the next few years he gathered a wealth of experience during stays at the Badische Anilin und Soda Fabrik in Ludwigshafen, the University of Ghent, the Radioisotope School at Harwell and the Londonderry Radiochemistry Laboratory, University of Durham. In 1961 he was awarded an IAEA Fellowship which he spent profitably in Durham and at Hamilton in Canada.

By 1955 Lado was lecturing in qualitative and quantitative chemistry in the Pharmaceutical Department of the Natural Sciences Faculty at Ljubljana, and in 1962 he became honorary Assistant Professor. From 1963 to 1967 he worked at the IAEA Seibersdorf Laboratory near Vienna, and during this time lectured and organized various courses, including Isotope Schools in Tokyo and Cairo.

After his return to Ljubljana, he became Assistant Professor at the Faculty of Science and Technology, and Head of the Nuclear Chemistry Section of the “J. Stefan” Institute, a position he held until 1980, thereafter remaining as Senior Consultant. In 1970, he was appointed to the Chair of Analytical Chemistry at the University of Ljubljana.

He was frequently invited to serve on IAEA Panels and at Expert Meetings, and as an IAEA Expert worked in Thailand, Sofia and Jamaica. He was a long-standing member of the IUPAC Commission on Radio-analytical Chemistry and Nuclear Materials and the International Committee of the Modern Trends in Activation Analysis Symposium, and of the Advisory Boards of *Talanta*, *Microchimica Acta*, the *Journal of Radioanalytical and Nuclear Chemistry* (and its Letters Edition) and the *Bulletin of the Slovene Chemical Society*. At the time of his death he was also President of the Union of Yugoslav Chemical Societies.

What of his work and the man himself? Lado Kosta was above all an analytical chemist, but one with an exceptionally wide breadth of experience and interests, something that is becoming rarer in these days of specialization. His best known work is in the field of analytical techniques and radioanalytical chemistry, particularly activation analysis (which he was able to exploit after completion of a TRIGA Mk II reactor at the Institute in 1966), but he retained and developed his early interest in toxicology, became expert in environmental chemistry, trace element studies, the analytical chemistry of uranium and the fuel cycle, in electrochemical techniques, flow-injection analysis and gas chromatography, as well as mastering the field of quality control and reference materials.

Lado had an exceptionally good “nose” for new trends and important developments in analytical chemistry, which he often set about investigating in his laboratories at the University or the Institute. He was author of over a hundred papers, and was in demand for plenary and contributed lectures at Conferences.

His work was characterized by elegance and clarity, and a dislike of vagueness or irrelevant material. Throughout his career he was fascinated by the possibilities offered by volatilization techniques, which he

exploited elegantly in methods for determining mercury and selenium by neutron activation analysis, methylmercury by isothermal distillation in Conway dishes, and similar techniques for separation of iodine, fluoride and cyanide. He was stimulated by, and in turn led his co-workers to respond to, the challenge of determining difficult elements or species at ultralow levels, such as As, B, Cd, CN^- , F, Hg, MeHg^+ , I, Ni, Se, Si, V and U. He was in the forefront of those who saw the importance of quality control and the role of reference materials, and in recognizing the importance of element speciation, particularly in assessing the role and influence of metals.

He led many co-operative projects with International or National bodies such as the IAEA, NBS, WHO, the U.S. Department of Agriculture and UNEP; for the last-named he was completing a survey of mercury, methylmercury and selenium levels in exposed Mediterranean populations, a study which characteristically he had insisted should concentrate on development of accurate methodology.

In writing papers, reports or letters, typical of his approach was the care with which he searched for the appropriate English expression or phrase to correspond exactly to his thoughts. As a person, he impressed everyone by his quiet authority and unassertive knowledge. Always polite and correct, rarely flustered, self-effacing, generous in all respects, he was a true gentleman. Though slight in appearance he was "wiry" and enjoyed relaxing with his family and friends, amongst whom his hospitality was proverbial.

He will be greatly missed by his wide international circle of friends and colleagues in analytical and environmental chemistry, and at home where he made great contributions to the post-war development of analytical chemistry in his native Republic of Slovenia. We extend our deepest sympathy to his wife Irena and their three daughters.

A. J. BYRNE
R. A. CHALMERS

NOTICES

29TH OAK RIDGE ANALYTICAL CHEMISTRY CONFERENCE

30 SEPTEMBER–2 OCTOBER 1986, KNOXVILLE, TENNESSEE

“Analytical Directions for the Future” will be the theme for this conference. Major session topics include measurement of trace constituents in hazardous waste (chemical and/or radiochemical), Fourier-transform mass spectrometry, laser spectroscopy, separations, robotics and automation, plasma spectroscopy, and artificial intelligence. Each area will be introduced by invited lecturers, and contributed papers are solicited that fit these categories. An exhibitors’ session and a poster session are planned.

Co-sponsored by the U.S. Department of Energy (DOE), the conference brings together U.S. and foreign analytical chemists representing government laboratories, industry, and educational institutions.

Contributors should submit an abstract of approximately 200 words no later than 10 June 1986, including the title of the presentation, author’s name, time required for presentation and, in the case of multiple authorship, the name of the speaker. Abstracts and inquiries should be directed to: W. R. Laing, Technical Program Chairman, Oak Ridge National Laboratory, P.O. Box X, Oak Ridge, TN 37831. Telephone (615) 574-4852 or FTS 624-4852. Authors will be notified of acceptance of papers by about 15 July.

Facilities will be available to manufacturers’ representatives for exhibits on new developments in analytical instrumentation, equipment, and supplies. Because the theme, “Analytical Directions for the Future,” reflects the interests of many exhibitors, time has been set aside specifically for manufacturers’ representatives to make presentations. Information on availability and rates for exhibit space may be obtained from A. L. Harrod, Oak Ridge National Laboratory (615) 576-7582.

1987 (8th) EUROPEAN CONFERENCE ON ENVIRONMENTAL POLLUTION

13–14 MAY 1987

HILTON HOTEL

DÜSSELDORF, WEST GERMANY

1987 (9th) INTERNATIONAL SYMPOSIUM ON ENVIRONMENTAL POLLUTION

11–12 JUNE 1987

TORONTO, CANADA

Papers dealing with any aspect of the environmental field, *e.g.*, basic concepts and current developments which relate to equipment, materials, design, engineering and construction services, air/water and environmental pollution control, analyses and instrumentation, operation and quality control, noise control, solid waste disposal, industrial waste water, absorbents, catalysts, filter aids, water and waste treatment chemicals, regulations and standards, detoxification or neutralization of residues and wastes, remote sensing, controlled-release energy, protective materials, safe design of plant, *etc.*, are now being solicited.

Also, papers dealing with medical topics such as health effects, risk estimation, epidemiology, mutagenesis and carcinogenesis, heavy metals, pesticides, short-term tests *etc.*, are most welcome.

Tentative titles must arrive before 15 November 1986. Abstracts and biographical data of Speakers by 15 February 1987.

Deadline for complete papers by 15 March 1987:

PLEASE SEND YOUR PAPERS TO:

Dr. V. M. Bhatnagar
Alena Enterprises of Canada
P.O. Box 1779
Cornwall, Ontario K6H 5V7, Canada



DR. R. A. CHALMERS

EDITORIAL

Dr. R. A. Chalmers has been Editor of *Talanta* for two decades. Although he retired in September 1985 from his post as Reader in Analytical Chemistry at Aberdeen University, he will continue as Editor of *Talanta*. At this major point in his career, I, like many others, wish Bob the best in his "retirement" and thank him for his continuation as Editor of *Talanta*. This Special Honour Issue is well-deserved and a small indication of the appreciation of many of us for his dedicated and diligent work as Editor of *Talanta*. Few, if any Editors in all of science take their editorial duties so seriously. Anyone who has submitted a manuscript to *Talanta* realizes that the best review comes from the Editor, himself. Oftentimes, he repeats experiments, checks references, and revises major sections of the manuscript. As a result, *Talanta* has had during the past 20 years, great consistency of high quality science and high quality writing. The international flavour and the quality of each issue of *Talanta* has increased since Dr. Chalmers took the reins.

After September 1985, I am sure Dr. Chalmers will continue to spend most of his days and nights with *Talanta* matters. However, I do hope he'll also be able to enjoy other more personal activities. Dr. R. A. Chalmers, in starting your 21st year as Editor of *Talanta* and in your retirement from Aberdeen University, on behalf of your friends and the scientific community, I thank you for your service to *Talanta* and to analytical chemistry and wish you the very best in the years to come.

JAMES D. WINEFORDNER
Chairman, *Talanta* Editorial Board

ANNIVERSARY GREETINGS

This issue of *Talanta* is a Special Honour Issue dedicated to Dr. R. A. Chalmers, in recognition of the twentieth anniversary of his becoming Editor-in-Chief of the Journal. It is a Special Honour Issue and not an ordinary Honour Issue, because for an ordinary Honour Issue the papers would have been solicited from former research students and associates. This Special Honour Issue includes a brief biography, and a paper written by Dr. Chalmers (reprinted without his prior knowledge) in which he expresses much of his editorial philosophy; but apart from these two, all the papers have been submitted to *Talanta* in the ordinary way, and have been edited and processed by Dr. Chalmers in his usual fashion. What we have been able to do is to manipulate the publishing schedules a little, unknown to Dr. Chalmers, so as to be able to include as many papers as possible written by regular *Talanta* contributors and others closely associated with the Journal and Dr. Chalmers. We invited as many as time permitted of these authors to add dedications to their papers.

Other friends of *Talanta* contributed to this Special Honour Issue by sending anecdotes for inclusion in the biography of Dr. Chalmers. Many more people have expressed a wish to have their greetings included, and we are happy to give the following list of all the friends who send good wishes to Dr. Chalmers:

I. P. Alimarin, Moscow (sends hearty congratulations, and wishes good health and luck); G. E. Baiulescu, Bucharest; Stuart Bark, Salford; D. (Jack) Betteridge, Sunbury-on-Thames; P. R. Bontchev, Sofia; Omortag Budevsky, Sofia; Margaret Campbell, Aberdeen; V. V. Coşofreţ, Bucharest; Malcolm Cresser, Aberdeen; Harvey Diehl, Iowa ("Best wishes to Bob Chalmers for many happy days to come. May he thoroughly enjoy the freedom that release from his university chores will bring. May he relish the opportunity to continue the writing and editing he does so superlatively well."); A. C. Docherty, Stockton-on-Tees; Elsie M. Donaldson, Ottawa; Mahmoud Farooqi, Lahore ("I hope you will get some time to look for the molybdenum reference you lost 30 years ago"); Arnold Fogg, Loughborough; Nancy and Howard Francis, Pennsylvania; R. Gijbels, Antwerp; J. Inczédy, Veszprém; Toshitaka Hori, Kyoto; Lado Kosta, Ljubljana; Stan Kotrlý, Pardubice; J. Kragten, Amsterdam; Larry J. Kricka, Birmingham; Herbert A. Laitinen, Florida; Michael Leonard, Belfast; Sam Lyle, Kent; John Majer, Birmingham; Zygmund Marzenko, Warsaw; Iain and Eva Marr, Aberdeen; Bob and Mary Masson, Aberdeen; Anil Mehta, Leeds; Wolfgang Merz, Ludwigshafen; Frank Miller, Aberdeen; Chrissie Miller, Edinburgh; Briony Moon, Exeter; John Ottaway, Glasgow; F. Pellerin, Paris-Sud; M. Pesez, Romainville; Rudolf Přibil, Prague; E. Pungor, Budapest (I hope that my friend Bob Chalmers will not only enjoy this celebration, but also will prepare himself for the work for the next 20 years and the next celebration, for which I wish him good health); Cameron Ramsay, Aberdeen; S. B. Savvin, Moscow; Alan G. Sinclair, New Zealand; B. Bruce Sithole, Ottawa; John Y. Steel, Pennsylvania; Karel Štulík and all friends at Charles University, Prague; Gyula Svehla, Belfast; G. Tölg, Dortmund; J. D. R. Thomas, Cardiff ("Diolch yn fawr am 20 mlynedd o wasanaeth i'r Gemeg Dadansyddol, a Dymuniadau Da i'r dyfodol"); Alan Townshend, Hull; Julian and Aileen Tyson, Loughborough; Allan M. Ure, Aberdeen; David W. Wells, Pitlochry; J. D. Winefordner, Florida; T. S. West, Aberdeen; John Whitley, East Kilbride; Mo Williams, Oxford; David W. Wilson, Essex; Yuri Zolotov, Moscow; A. Zuberbühler, Basel; and the Committee of the Scottish Region of the Analytical Division of the Royal Society of Chemistry.

AUTHOR INDEX

- Aaron J.-J. 27, 215
 Abbasi U. M. 173
 Abdel-Hamid M. 185
 Abdel Salam M. 185
 Abounassif M. A. 179
 Afonso A. M. 779
 Akama Y. 288
 Akiyama S. 274
 Alary J. 748, 997
 Alcs F. 329
 Alés Barrero F. 1021
 Almestrand L. 991
 Alvarado J. 61
 Al-Daher I. M. 751
 Anderson J. L. 448
 Andino M. 27
 Arce F. 1031
 Aroc R. V. 768
 Arrebola Ramírez A. 1021
 Asuero A. G. 195, 531, 929
 Aznárez J. 458
- Badea V. 101
 Baiulescu G. E. 101
 Banerjee S. 358, 360
 Barbillat J. 295
 Berek J. 811
 Barnard C. L. R. 55
 Bars E. 463
 Batley G. E. 421
 Bayloqç D. 85, 985, 1035
 Beech C. L. 601
 Belal F. 170, 448
 Berka A. 811
 Bertocchi G. 760
 Bhangar M. I. 173
 Bhatnagar A. 713
 Bigli C. 243
 Blanco C. 1031
 Boguszewska Z. 155
 Böhmer R. G. 481
 Bos M. 583
 Bosch Reig F. 757
 Boughriet A. 385
 Braibanti A. 471
 Brajter K. 149
 Brennan M. 927
 Bruschi C. 471
 Burini G. 649
 Bye R. 705
- Cai X. 623
 Calatayud J. M. 685
 Caletka R. 219, 315
 Callejón Mochón M. 587, 627
 Campos F. 61
 Cantwell F. F. 119
 Capone S. 763
 Cardarelli E. 279
 Casado J. 1031
 Casassas E. 843
 Casconcelos M. T. S. D. 919
 Cavalciro J. A. S. 963
 Centeno Gallego M. 627
 Chalmers R. A. 7, 867
 Chand F. 173
 Chang Y. P. 939
 Chateau-Gosselin M. 733
 Chauhan S. 703
 Chiavari G. 379, 979
 Chiswell B. 669
- Chong C. 91
 Chow A. 182
 Christian G. D. 547
 Chriswell C. D. 700
 Chung C-H. 577
 Cifani M. 279
 Cipres P. 458
 Ciszowska M. 817
 Cocivera M. 187
 Colombini M. P. 325
 Compañó R. 141, 463
 Cooks R. G. 917, 1001
 Córdoba M. 135
 Corsini A. 335
 Coşofret V. V. 101
 Cox J. A. 713, 911
 Crock J. G. 601
 Crow D. R. 553
 Cruces Blanco C. 847
 Curini R. 325
- Dąbek-Złotorzyńska E. 149
 Damiani P. 649
 Darkowski A. 187
 Das A. K. 277
 Díaz García M. E. 255
 De Bièvre P. 291
 De Robertis A. 763
 De Stefano C. 763
 Delgado R. 285
 Detter L. D. 917
 Diehl H. 901, 935
 Divakar T. E. 164
 Dohmen F. T. M. 107
 Donaldson E. M. 35, 233
 Doyle R. J. 657
 D'Souza M. V. 352
 Duchateau N. L. 291
 D'Ulivo A. 401
- Edwall G. 125
 Ekanem E. J. 55
 Ekka M. G. P. 1009
 El-Din M. S. 170
 Elsaied M. M. 679
 El-Shabouri S. R. 743
 Emary W. B. 1001
 Escrieut C. 748
 Esteban M. 843
 Evenko G. N. 429
 Evgenidis J. 379
- Fagioli F. 243
 Falco C. 685
 Fedai I. 366
 Fell G. S. 55
 Fernandez L. 843
 Ferrer A. 458
 Fidanza J. 215
 Fischer J.C. 385
 Fiscaro E. 471
 Flavelle F. 445
 Fleury G. 295, 299
 Fournaise R. 499
 Francis R. W. Jr. 713
 Fraústo da Silva J. J. R. 285
 Freers J. L. 657
 Freiha B. 397
 Fujita K. 203
 Fuoco R. 401
- Gad-Kariem E. A. 179
 Gallo Hermosa B. 733
 Gamot A. P. 295
 Gampp H. 943
 Gangoda M. E. 176
 Ganguly A. 973
 Garai T. 243
 Garcia M. E. 255
 García Alvarez-Coque M. C. 697
 García Montelongo F. 779
 García Sánchez F. 329, 785, 847
 Garcia-Vargas M. 209
 Gasco Andreu M. T. 537
 Gennaro M. C. 620, 835
 Georgakopoulos P. P. 631
 Ghe A. M. 379
 Gilpin R. K. 176
 Gimeno Adelantado J. V. 757
 Głęb S. 125
 Glennon J. D. 927
 Golabi S. M. 907
 Goldhaber M. B. 953
 Gómez Ariza J. L. 105, 607
 Gómez-Hens A. 567, 633
 Gontarz H. 341
 González G. 105
 Guiraúm Pérez A. 105, 587, 627
 Gutiérrez M. C. 567
 Guy R. D. 95
- Hadjiioannou T. P. 547
 Hansson L. 249
 Hara M. 857
 Haran R. 748
 Hassan S. S-M. 679
 Hattori T. 167
 Hausbeck R. 219, 315
 Havel J. 435, 513, 525
 Hayase, K. 754
 Hayer B. 883
 Hefley A. J. 901
 Hendrickx F. 291
 Hernández Córdoba M. 135, 411
 Hernández Hernández, F. 537
 Hernández López M. 785
 Herrmann O. 335
 Hofman T. 851
 Horchak-Morris N. 901
 Hoshi S. 611
 Hosoya M. 691
 Hsu Z.-F. 455
 Hu C.-S. 455
 Huvenne J. P. 299
 Hynková A. 825
- Ibrahim F. 170
 Ibrahim F. 111
 Imasaka T. 281
 Ingle J. D. Jr. 271
 Ingman F. 125
 Inoue S. 611
 Ionescu M. S. 101
 Isern-Flécha I. 1001
 Ishibashi N. 281
 Issa A. S. 185
 Ivaska A. 739, 801
 Iwamoto E. 577
 Izquierdo A. 463
- Jagner D. 991
 Jain C. K. 717

- Jannakoudakis D. 461
 Javůrek M. 513, 825
 Jayarama 352
 Jia X.-P. 455
 Jiménez Linares C. 1021
 Jimenez-Trillo J. L. 195, 531, 929
- Kalcher K. 489
 Kallmann S. 75
 Kankare J. J. 571
 Katz B. M. 429
 Kauffmann J. M. 733
 Kawabata Y. 281
 Kawamura H. 861
 Kawano H. 191
 Kawano N. 407
 Keimig T. L. 653
 Keliher P. N. 311
 Khan A. S. 119, 182
 Kiciak S. 341
 Kinoshita E. 125
 Klock P. R. 495
 Koshima H. 391
 Kountourellis J. E. 631
 Krasiejko M. 155
 Kratochvil B. 751
 Krivan V. 219, 315
 Kryger L. 883
 Krzyżanowska M. 851
 Kubin A. 265
 Kulkarni K. R. 911
 Kumar Satish 717
 Kumar Surender 717
- Lachowicz E. 1027
 Lacroix B. 299
 Laganà A. 325
 Lajunen L. H. J. 265
 Lamothe P. J. 495
 Laouénan A. 721
 Leach S. C. 421
 Leppinen J. 795, 801
 Leszko M. 769
 Lewenstam A. 739
 Lexa J. 11
 Li K. 775
 Li P. 623
 Lichte F. E. 601
 Limin W. 98
 Lin C. 838
 Lin M-S 707
 Linares P. 889
 Liu Y. 443
 Livingstone S. E. 973
 Locatelli C. 243
 López García I. 411
 López Núñez, R. 587
 Lund W. 421
 Luo D. B. 397
 Luque de Castro M. D. 45, 199, 889
 Lyle S. J. 355
- Machado A. A. S. C. 919
 Maeder M. 943
 Mahrous M. S. 185
 Maity D. S. 973
 Majcherczyk C. 85, 985, 1035
 Marchevsky E. 375
 Markuszewski R. 700, 901
 Martinez C. 541
 Martinez Vayá M. C. 697
 Martínez Avile J. 411
 Masson M. R. 1
 Masuda Y. 665
- Matousek J. P. 875
 Matsubara M. 611
 Matsuda T. 191, 614
 Matsuo T. 665
 Mattar S. 225
 McGown L. B. 653
 McHugh J. B. 349
 McMahon R. 927
 Mecozzi M. 279
 Medina Escriche J. 537
 Medinilla J. 329, 847
 Mehta A. C. 67
 Meloun M. 435, 513, 525, 825
 Memon S. A. 173
 Mentasti E. 620, 835
 Merlot G. 299
 Metal B. 841
 Meyer C. J. 943
 Mikasa H. 729
 Milla M. 209
 Millán I. 607
 Mir J. M. 541
 Mokhtar M. B. 669
 Mongay Fernández C. 697
 Mori N. 161
 Motomizu S. 729
 Muñoz de la Peña A. 923
 Munson L. F. 901
 Murillo J. A. 923
 Muzher E. S. 657
- Nagai T. 191 614
 Nakai T. 288
 Nakai Y. 191
 Nakamura H. 407
 Nakashima K. 274
 Nakatsuji S. 274
 Navas M. J. 195, 531, 929
 Němcová I. 841
 Němec I. 467
 Nomura N. 857
 Norwitz G. 311
- Ohno N. 415
 Olin Á. 249
 Olsina R. 375
 Onishi H. 391
 Opekar F. 688
 O'Reilly A. M. 593
 Orr B. J. 875
 Ottawa J. M. 55, 61
 Ouyang Z. 443
- Pachuta S. J. 917
 Padma D. K. 550
 Pal T. 973
 Palmowski-Kuś B. 155
 Papadopoulos N. 461
 Papoff P. 401
 Pasquali M. 471
 Pastorelli L. 979
 Patriarche G. J. 733
 Peinado J. 914
 Pellerin F. 85, 985, 1035
 Pérez-Bendito D. 914
 Perrakis G. 979
 Petitfaux C. 499
 Pettersson J. 249
 Pflaum R. T. 807
 Pickering W. F. 661
 Pineda L. 141
 Podlaha J. 841
 Polge P. 985
 Polo Díez L. M. 745
- Porta L. 375
 Porta V. 835
 Poulías G. 461
 Pournaghi-Azar M. H. 907
 Prasad U. V. 164
- Qi W. 694
- Rabadan J. M. 458
 Ramis Ramos G. 697
 Rangaswamy 352
 Raoot K. N. 544
 Raoot S. 544
 Raptouli A. 631
 Rauret G. 141
 Reddy A. V. 617
 Reddy Y. K. 617
 Ren K. 641
 Ren M. 371
 Renman L. 991
 Ren-Kurc A. 641
 Richardson R. G. 700
 Riddle G. O. 601
 Ridley T. Y. 1001
 Ríos A. 199
 Rizk M. 111, 170
 Román Ceba M. 1021
 Romon M. T. 299
 Rosales D. 105, 607
 Rotatori M. 325
 Roy N. K. 277
 Róžańska B. 1027
 Rubio S. 633
 Ruz J. 199
- Sakai T. 415
 Sakai Y. 161, 407
 Safinas F. 923
 Sammartano S. 763
 Sanchez-Pedreño C. 135
 Santana J. J. 779
 Sanz-Medel A. 255
 Sarbar M. 907
 Sarzanini C. 620, 835
 Sastry C. S. P. 164
 Sato K. 288
 Sato S. 115
 Saudemon M. 295
 Schaffar B. P. H. 867
 Scharf G. 17
 Schilt A. A. 895
 Schmitt T. M. 657
 Sechi G. 279
 Sekido E. 665
 Selby M. 875
 Şengün F. I. 363, 366
 Sharma D. K. 703
 Sharma N. 703
 Sharma U. 703
 Sherman F. B. 429
 Shiraishi K. 861
 Shitashima K. 754
 Siefker J. R. 768
 Siegfried C.H. 481
 Sioda R. E. 421
 Sithole B. B. 95
 Smith K. M. 963
 Sood A. 703
 Srivastava S. K. 717
 Stephens R. 571
 Stojek Z. 817
 Strelow F. W. E. 481
 Štulík K. 11
 Suet E. 721
 Szczepaniak W. 371

Takada K. 691
 Takada T. 203
 Takagi M. 407
 Takayanagi K. 451
 Tanaka G. 861
 Tapia T. 707
 Temizer A. 791
 Thijssen P. C. 107
 Thulin S. 125
 Tocksteinová Z. 688, 811
 Tôei K. 729
 Tomiyoshi S. 274
 Tong S. 775
 Toribio F. 914
 Tozawa K. 691
 Trevilla S. 209
 Tripathi V. S. 1015
 Tsezos M. 225
 Tsubota H. 754
 Tuttle M. L. 953
 Tuzhi P. 707
 Tyagi P. 1009
 Tyson J. F. 51

 Uchikawa S. 115
 Ulaş K. 363
 Underwood F. A. 631
 Urasa I. T. 593

 Vahtila S. 795
 Valcárcel M. 199, 567, 633, 889

 Vándaele J. 748
 Vaz M. C. T. A. 285
 Ventura M. 141
 Verbruggen A. 291
 Vergnes I. F. 997
 Vergoten G. 295
 Verma B. C. 703
 Verma K. K. 1009
 Villanueva Camañas R. M. 697
 Villareal M. 375
 Viñas P. 135
 Vinci G. 325
 Volpe P. 835
 von Wandruszka R. 871

 Wahbi A.-A. M. 179
 Walash M. I. 111
 Walton R. A. 917
 Wang J. 321, 397, 421, 707
 Wang M. 35, 233
 Wänninen E. 739
 Wartel M. 385
 Watanesk S. 895
 Weinert W. 481
 West K. J. 807
 Westland A. D. 445
 Williamson D. L. 953
 Winefordner J. D. 17, 27, 871
 Wolfbeis O. S. 867

 Wong G. T. F. 451
 Wood K. V. 1001

 Xiong G.-L. 443
 Xu P.-Y. 443

 Yamamoto M. 577
 Yamamoto Y. 577
 Yañez-Sedeño P. 745
 Yang H. 623
 Yathirajan H. S. 352
 Yerian T. D. 547
 Yokota H. 288
 Yoshida H. 167
 Young R. S. 561
 Yurow H. W. 1039

 Zaborska W. 769
 Zadeii J. M. 321
 Zaiyou L. 98
 Zakhari N. A. 111
 Za'tar N. A. 355
 Zhang X. 838
 Zhao Z. 623
 Zhou N. 939
 Zhu L. 694
 Zhu X. 838
 Ziegler R. J. 657
 Zima J. 467, 811
 Zimová N. 467
 Zuberbühler A. D. 943